TEXTBOOK OF ARTERIAL STIFFNESS AND PULSATILE HEMODYNAMICS IN HEALTH AND DISEASE

Volume 1

Edited by
Julio A. Chirinos

Textbook of Arterial Stiffness and Pulsatile Hemodynamics in Health and Disease

Volume 1

This page intentionally left blank

Textbook of Arterial Stiffness and Pulsatile Hemodynamics in Health and Disease

Volume 1

Edited by

Julio A. Chirinos
Associate Professor of Medicine;
Director,
Arterial Hemodynamics and Cardiac Imaging Quantification Core Laboratory;
Co-Director,
Training Program in Cardiovascular Biology and Medicine, Clinical/Translational Science;
Adjunct Faculty, Center for Magnetic Resonance and Optical Imaging,
University of Pennsylvania Perelman School of Medicine, United States

For information on all Academic Press publications visit our website at
https://www.elsevier.com/books-and-journals

Working together
to grow libraries in
developing countries

www.elsevier.com • www.bookaid.org

Contents of Volume 1

Section III
Biologic pathways leading to arterial stiffness and dysfunctional pulsatile hemodynamics

Contributors

Elena Aikawa, The Center for Excellence in Vascular Biology, Brigham and Women's Hospital, Harvard Medical School, Boston, MA, United States

S.G. Anderson, George Alleyne Chronic Disease Research Centre, University of the West Indies Cave Hill Campus, Barbados; Division of Cardiovascular Sciences, School of Medical Sciences, University of Manchester, United Kingdom; College of Medical, Veterinary and Life Sciences, University of Glasgow, United Kingdom

Livia Silva Araújo Passos, The Center for Excellence in Vascular Biology, Brigham and Women's Hospital, Harvard Medical School, Boston, MA, United States

Samsul Arefin, Division of Renal Medicine, Department of Clinical Science, Intervention & Technology, Karolinska University Hospital, Stockholm, Sweden

Per M. Arvidsson, Clinical Physiology, Department of Clinical Sciences Lund, Faculty of Medicine, Lund University, Lund, Sweden

Alberto Avolio, Macquarie Medical School, Faculty of Medicine, Health and Human Sciences, Macquarie University, Sydney, NSW, Australia

Martin Bachler, Center for Health & Bioresources, Austrian Institute of Technology (AIT), Vienna, Austria

Magnus Bäck, Université de Lorraine, Inserm, DCAC, Nancy, France; Translational Cardiology, Department of Medicine, Karolinska Institutet, and Division of Coronary and Valvular Heart Disease, Karolinska University Hospital, Stockholm, Sweden

Michael J. Bashline, Division of Cardiology, Department of Medicine, University of Pittsburgh, Pittsburgh, PA, United States

Dakota Becker-Greene, The Center for Excellence in Vascular Biology, Brigham and Women's Hospital, Harvard Medical School, Boston, MA, United States

Jamie Bellinge, Royal Perth Hospital, Victoria Square, Perth, WA, Australia; School of Medicine, The University of Western Australia, Crawley, WA, Australia

Amar Bennasroune, UMR CNRS 7369 Matrice Extracellulaire et Dynamique Cellulaire (MEDyC), Team 2: Matrix Aging and Vascular Remodelling, Université de Reims Champagne Ardenne (URCA), UFR Sciences Exactes et Naturelles et UFR Médecine, Reims, France

Sébastien Blaise, UMR CNRS 7369 Matrice Extracellulaire et Dynamique Cellulaire (MEDyC), Team 2: Matrix Aging and Vascular Remodelling, Université de Reims Champagne Ardenne (URCA), UFR Sciences Exactes et Naturelles et UFR Médecine, Reims, France

Barry A. Borlaug, Mayo Clinic, Rochester, MN, United States

Pierre Boutouyrie, Paris University, Assistance-Publique Hôpitaux de Paris, PARCC-INSERM U970, Department of Pharmacology and Hôpital Européen Georges Pompidou, Paris, France

Y. Breet, Hypertension in Africa Research Team; MRC Unit for Hypertension and Cardiovascular Disease, North-West University, South Africa

Jerome W. Breslin, Department of Molecular Pharmacology and Physiology, Morsani College of Medicine, University of South Florida, Tampa, FL, United States

Matthew J. Budoff, David Geffen School of Medicine at UCLA, The Lundquist Institute at Harbor-UCLA, Torrance, CA, United States

Mark Butlin, Macquarie Medical School, Faculty of Medicine, Health and Human Sciences, Macquarie University, Sydney, NSW, Australia

Marina Cecelja, British Heart Foundation Centre, King's College London, Department of Clinical Pharmacology, St Thomas' Hospital, London, United Kingdom

Chen-Huan Chen, Department of Medicine, National Yang Ming Chiao Tung University College of Medicine, Taipei, Taiwan; Institute of Public Health and Community Medicine Research Center, National Yang Ming Chiao Tung University College of Medicine, Taipei, Taiwan; Department of Medical Education, Taipei Veterans General Hospital, Taipei, Taiwan

Hao-Min Cheng, Department of Medicine, National Yang Ming Chiao Tung University College of Medicine, Taipei, Taiwan; Institute of Public Health and Community Medicine Research Center, National Yang Ming Chiao Tung University College of Medicine, Taipei,

Taiwan; Center for Evidence-based Medicine, Taipei Veterans General Hospital, Taipei, Taiwan

Yi-Bang Cheng, National Research Centre for Translational Medicine, Centre for Epidemiological Studies and Clinical Trials, Shanghai Key Laboratory of Hypertension, The Shanghai Institute of Hypertension, Department of Hypertension, Ruijin Hospital, Shanghai Jiao Tong University School of Medicine, Shanghai, Shanghai, China

Julio A. Chirinos, University of Pennsylvania Perelman School of Medicine, Hospital of the University of Pennsylvania and Perelman Center for Advanced Medicine, Philadelphia, PA, United States; Ghent University, Ghent, Belgium

Phil Chowienczyk, British Heart Foundation Centre, King's College London, Department of Clinical Pharmacology, St Thomas' Hospital, London, United Kingdom

Shao-Yuan Chuang, Institute of Population Health Science, National Health Research Institutes, Miaoli, Taiwan

Marie-Annick Clavel, Institut Universitaire de Cardiologie et de Pneumologie de Québec / Québec Heart & Lung Institute, Laval University, Québec City, QC, Canada

Jordana B. Cohen, Renal-Electrolytes and Hypertension Division, Perelman School of Medicine, University of Pennsylvania, Philadelphia, PA, United States; Department of Biostatistics, Epidemiology, and Informatics, Perelman School of Medicine, University of Pennsylvania, Philadelphia, PA, United States

Alexis M. Corcoran, Division of Pulmonary and Critical Care Medicine, Department of Medicine, Brigham and Women's Hospital, Boston, MA, United States

William K. Cornwell, III, Department of Medicine-Cardiology, University of Colorado Anschutz Medical Campus, Aurora, CO, United States

Vicente F. Corrales−Medina, Department of Medicine, Division of Infectious Diseases at the University of Ottawa, The Ottawa Hospital Research Institute, Centre for Infection, Immunity and Inflammation (CI3) at the University of Ottawa, Ottawa, ON, Canada

Nancy Côté, Institut Universitaire de Cardiologie et de Pneumologie de Québec / Québec Heart & Lung Institute, Laval University, Québec City, QC, Canada

Thais Coutinho, Division of Cardiology, Division of Cardiac Prevention & Rehabilitation, University of Ottawa Heart Institute, Ottawa, ON, Canada

James Cox, Macquarie Medical School, Faculty of Medicine, Health and Human Sciences, Macquarie University, Sydney, NSW, Australia

J.K. Cruickshank, Cardiovascular Medicine Group, Division of Life-course/ Nutritional Sciences, Kings College London, United Kingdom

Lu Dai, Division of Renal Medicine, Department of Clinical Science, Intervention & Technology, Karolinska University Hospital, Stockholm, Sweden

Stella S. Daskalopoulou, Fonds de recherche du Québec − Santé − Boursier Clinicien − Senior, Director, Vascular Health Unit, Department of Medicine, Division of Internal Medicine, McGill University Health Centre, McGill University, Montreal, QC, Canada

Kevin P. Davy, Virginia Tech, Blacksburg, VA, United States

Marc L. De Buyzere, Department of Cardiology, Ghent University Hospital, Ghent, Belgium

Paul B. Dieffenbach, Division of Pulmonary and Critical Care Medicine, Department of Medicine, Brigham and Women's Hospital, Boston, MA, United States

Laurent Duca, UMR CNRS 7369 Matrice Extracellulaire et Dynamique Cellulaire (MEDyC), Team 2: Matrix Aging and Vascular Remodelling, Université de Reims Champagne Ardenne (URCA), UFR Sciences Exactes et Naturelles et UFR Médecine, Reims, France

Girish Dwivedi, School of Medicine, The University of Western Australia, Crawley, WA, Australia; Department of Cardiology, Fiona Stanley Hospital, Murdoch, WA, Australia; Department of Advanced Clinical and Translational Cardiovascular Imaging, Harry Perkins Institute of Medical Research, Murdoch, WA, Australia

David G. Edwards, Department of Kinesiology and Applied Physiology, University of Delaware, Newark, DE, United States

William B. Farquhar, Department of Kinesiology and Applied Physiology, University of Delaware, Newark, DE, United States

Bo Fernhall, University of Illinois at Chicago, Chicago, IL, United States

John S. Floras, Toronto General Research Institute, Toronto, ON, Canada; University Health Network and Mount Sinai Hospital, Division of Cardiology, Department of Medicine, University of Toronto, Toronto, ON, Canada

Laura E. Fredenburgh, Division of Pulmonary and Critical Care Medicine, Department of Medicine, Brigham and Women's Hospital, Boston, MA, United States

Masafumi Fukumitsu, Department of Pulmonary Medicine, Amsterdam Universitair Medische Centra, Vrije Universiteit Amsterdam, Amsterdam Cardiovascular Sciences, Amsterdam, the Netherlands

L. Gafane-Matemane, Hypertension in Africa Research Team; MRC Unit for Hypertension and Cardiovascular Disease, North-West University, South Africa

Nestor Gahungu, Royal Perth Hospital, Victoria Square, Perth, WA, Australia

Ahmed K. Ghanem, Department of Cardiology, The Lundquist Institute at Harbor-UCLA, Torrance, CA, United States

Thierry C. Gillebert, Department of Cardiology, Ghent University and Ghent University Hospital, Ghent, Belgium

Philippe Gillery, UMR CNRS 7369 Matrice Extracellulaire et Dynamique Cellulaire (MEDyC), Team 2: Matrix Aging and Vascular Remodelling, Université de Reims Champagne Ardenne (URCA), UFR Sciences Exactes et Naturelles et UFR Médecine, Reims, France; Department of Biochemistry, University Hospital Center, Reims, France

Delphine Gomez, Pittsburgh Heart, Lung, Blood, and Vascular Medicine Institute, University of Pittsburgh, Pittsburgh, PA, United States; Department of Medicine, Division of Cardiology, University of Pittsburgh, Pittsburgh, PA, United States

Ezequiel Guzzetti, Institut Universitaire de Cardiologie et de Pneumologie de Québec / Québec Heart & Lung Institute, Laval University, Québec City, QC, Canada

Bernhard Hametner, Center for Health & Bioresources, Austrian Institute of Technology (AIT), Vienna, Austria

Junichiro Hashimoto, Miyagi University of Education Medical Center, Sendai, Miyagi, Japan

Kevin S. Heffernan, Syracuse University, Syracuse, NY, United States

Brooks A. Hibner, University of Illinois at Chicago, Chicago, IL, United States

Sam Hobson, Division of Renal Medicine, Department of Clinical Science, Intervention & Technology, Karolinska University Hospital, Stockholm, Sweden

Nien-Wen Hu, J. Crayton Pruitt Family Department of Biomedical Engineering, University of Florida, Gainesville, FL, United States

T.M. Hughes, Department of Internal Medicine, Wake Forest School of Medicine, Winston-Salem, NC, United States

Jay D. Humphrey, Department of Biomedical Engineering, School of Engineering and Applied Science, Yale University, New Haven, CT, United States; Vascular Biology and Therapeutics Program, Yale School of Medicine, New Haven, CT, United States

Stéphane Jaisson, UMR CNRS 7369 Matrice Extracellulaire et Dynamique Cellulaire (MEDyC), Team 2: Matrix Aging and Vascular Remodelling, Université de Reims Champagne Ardenne (URCA), UFR Sciences Exactes et Naturelles et UFR Médecine, Reims, France; Department of Biochemistry, University Hospital Center, Reims, France

Nadjia Kachenoura, Sorbonne Université, INSERM, CNRS, Laboratoire d'Imagerie Biomédicale, Paris, France

Kazuomi Kario, Division of Cardiovascular Medicine, Department of Medicine, Jichi Medical University School of Medicine, Shimotsuke, Tochigi, Japan; The Hypertension Cardiovascular Outcome Prevention and Evidence in Asia (HOPE Asia) Network, Tokyo, Japan

Prasad V.G. Katakam, Tulane University School of Medicine, New Orleans, LA, United States

Goro Katsuumi, Department of Cardiovascular Biology and Medicine, Juntendo University Graduate School of Medicine, Tokyo, Japan

Avinash Kondiboyina, Heart Research, Murdoch Children's Research Institute, Parkville, VIC, Australia; Department of Paediatrics, University of Melbourne, Parkville, VIC, Australia

Sándor J. Kovács, Cardiovascular Division, Department of Medicine, Washington University in Saint Louis, School of Medicine, Saint Louis, Missouri, United States

R. Kruger, Hypertension in Africa Research Team; MRC Unit for Hypertension and Cardiovascular Disease, North-West University, South Africa

Karolina Kublickiene, Division of Renal Medicine, Department of Clinical Science, Intervention & Technology, Karolinska University Hospital, Stockholm, Sweden

Patrick Lacolley, Université de Lorraine, Inserm, DCAC, Nancy, France

Muriel Laffargue, INSERM UMR 1048, Institut des Maladies Métaboliques et Cardiovasculaires (I2MC), Toulouse, France

Arinola O. Lampejo, J. Crayton Pruitt Family Department of Biomedical Engineering, University of Florida, Gainesville, FL, United States

Agne Laucyte-Cibulskiene, Division of Renal Medicine, Department of Clinical Science, Intervention & Technology, Karolinska University Hospital, Stockholm, Sweden; Department of Nephrology; Skåne University Hospital, Malmö, Sweden

Stéphane Laurent, Department of Pharmacology and Hôpital Européen Georges Pompidou, Paris, France; INSERM, U970, Paris Cardiovascular Research Center, PARCC, Paris, France; Université de Paris, Paris, France; Assistance Publique, Hopitaux de Paris, Paris, France

Hae-Young Lee, Department of Internal Medicine, Seoul National University College of Medicine, Jongno-Gu, Seoul, South Korea

Wesley K. Lefferts, University of Illinois at Chicago, Chicago, IL, United States; Iowa State University, Ames, IA, United States

Elizabeth C. Lefferts, University of Illinois at Chicago, Chicago, IL, United States; Iowa State University, Ames, IA, United States

Adelino F. Leite-Moreira, Department of Surgery and Physiology, Cardiovascular Research Centre, Faculty of Medicine of the University of Porto, Porto, Portugal; Department of Cardiothoracic Surgery, São João Hospital Centre, Porto, Portugal

Chee H. Liew, National Institute for Prevention and Cardiovascular Health, National University of Ireland Galway, Galway, Ireland

Joao A.C. Lima, Departments of Cardiology/Medicine and Radiology, Johns Hopkins University, Baltimore, MD, United States

André P. Lourenço, Department of Surgery and Physiology, Cardiovascular Research Centre, Faculty of Medicine of the University of Porto, Porto, Portugal; Department of Anaesthesiology, São João Hospital Centre, Porto, Portugal

Kaisa Maki-Petaja, Experimental Medicine and Immunotherapeutics, University of Cambridge, Cambridge, United Kingdom

Marcy Maracle, Schulich School of Medicine and Dentistry, Western University, London, ON, Canada

Laurent Martiny, UMR CNRS 7369 Matrice Extracellulaire et Dynamique Cellulaire (MEDyC), Team 2: Matrix Aging and Vascular Remodelling, Université de Reims Champagne Ardenne (URCA), UFR Sciences Exactes et Naturelles et UFR Médecine, Reims, France

Pascal Maurice, UMR CNRS 7369 Matrice Extracellulaire et Dynamique Cellulaire (MEDyC), Team 2: Matrix Aging and Vascular Remodelling, Université de Reims Champagne Ardenne (URCA), UFR Sciences Exactes et Naturelles et UFR Médecine, Reims, France

Christopher C. Mayer, Center for Health & Bioresources, Austrian Institute of Technology (AIT), Vienna, Austria

Barry J. McDonnell, Cardiovascular Physiology Research Group, Cardiff School of Sport & Health Sciences, Cardiff Metropolitan University, Cardiff, United Kingdom

John W. McEvoy, National Institute for Prevention and Cardiovascular Health, National University of Ireland Galway, Galway, Ireland; Ciccarone Center for the Prevention of Cardiovascular Disease, Johns Hopkins University School of Medicine, Baltimore, MD, United States

M.L. Meyer, Department of Emergency Medicine, School of Medicine, University of North Carolina at Chapel Hill, Chapel Hill, NC, United States

Jean-Baptiste Michel, Inserm UMR_S 1148, CHU X. Bichat, Paris, France

Philip J. Millar, Department of Human Health and Nutritional Sciences, University of Guelph, Guelph, ON, Canada; Toronto General Research Institute, Toronto, ON, Canada

Tohru Minamino, Department of Cardiovascular Biology and Medicine, Juntendo University Graduate School of Medicine, Tokyo, Japan; Japan Agency for Medical Research and Development-Core Research for Evolutionary Medical Science and Technology (AMED-CREST), Japan Agency for Medical Research and Development, Tokyo, Japan

Gary F. Mitchell, Cardiovascular Engineering, Inc., Norwood, MA, United States

Walter L. Murfee, J. Crayton Pruitt Family Department of Biomedical Engineering, University of Florida, Gainesville, FL, United States

Jonathan P. Mynard, Heart Research, Murdoch Children's Research Institute, Parkville, VIC, Australia; Department of Paediatrics, University of Melbourne, Parkville, VIC, Australia; Department of Biomedical Engineering, University of Melbourne, Parkville, VIC, Australia

Massimo Nardone, Department of Human Health and Nutritional Sciences, University of Guelph, Guelph, ON, Canada

Peter M. Nilsson, Lund University, Department of Clinical Sciences, Skane University Hospital, Malmö, Sweden

Kevin O'Gallagher, Department of Clinical Pharmacology, School of Cardiovascular Medicine and Sciences, King's College London British Heart Foundation Centre, St. Thomas' Hospital, London, United Kingdom

Yoshiaki Ohyama, Departments of Cardiology/Medicine and Radiology, Johns Hopkins University, Baltimore, MD, United States; Clinical Investigation and Research Unit, Gunma University Hospital, Maebashi, Japan

Kazunori Omote, Mayo Clinic, Rochester, MN, United States

Jeong Bae Park, Department of Precision Medicine and Biostatistics, Yonsei University Wonju College of Medicine, Seoul, Republic of Korea

Shayn M. Peirce, Department of Biomedical Engineering, University of Virginia, Charlottesville, VA, United States

Philippe Pibarot, Institut Universitaire de Cardiologie et de Pneumologie de Québec / Québec Heart & Lung Institute, Laval University, Québec City, QC, Canada

Gary L. Pierce, University of Iowa, Iowa City, IA, United States

Stuart B. Prenner, University of Pennsylvania Perelman School of Medicine, Hospital of the University of Pennsylvania and Perelman Center for Advanced Medicine, Philadelphia, PA, United States

Athanase Protogerou, Cardiovascular Prevention and Research Unit, Clinic-Laboratory of Pathophysiology, Laiko Hospital, Medical School, National and Kapodistrian University of Athens, Athens, Greece

Reed E. Pyeritz, Perelman School of Medicine, University of Pennsylvania Health System, Philadelphia, PA, United States

Michael A. Quail, Department of Pediatric Cardiology, Great Ormond Street Hospital for Children and University College London, London, United Kingdom

Yogesh N.V. Reddy, Mayo Clinic, Rochester, MN, United States

Alban Redheuil, Sorbonne Université, INSERM, CNRS, Laboratoire d'Imagerie Biomédicale, Paris, France; Cardiovascular and Thoracic Imaging, Hôpital La Pitié-Salpêtrière, AP-HP, Sorbonne Université, Paris, France

Véronique Regnault, Université de Lorraine, Inserm, DCAC, Nancy, France

Rakhshinda Rehman, Division of Pulmonary and Critical Care Medicine, Department of Medicine, Brigham and Women's Hospital, Boston, MA, United States

Ernst R. Rietzschel, Department of Cardiology (Internal Medicine & Pediatrics), Ghent University, Ghent, Belgium; Biobanking and Cardiovascular Epidemiology, Ghent University Hospital, Ghent, Belgium

Béatrice Romier-Crouzet, UMR CNRS 7369 Matrice Extracellulaire et Dynamique Cellulaire (MEDyC), Team 2: Matrix Aging and Vascular Remodelling, Université de Reims Champagne Ardenne (URCA), UFR Sciences Exactes et Naturelles et UFR Médecine, Reims, France

Jasjit Rooprai, Department of Medicine, University of Toronto, Toronto, ON, Canada

Lucia Salvi, Medicina II Cardiovascolare, AUSL-IRCCS di Reggio Emilia, Italy

Paolo Salvi, Istituto Auxologico Italiano, IRCCS, Cardiology Unit, Milan, Italy

Hervé Sartelet, UMR CNRS 7369 Matrice Extracellulaire et Dynamique Cellulaire (MEDyC), Team 2: Matrix Aging and Vascular Remodelling, Université de Reims Champagne Ardenne (URCA), UFR Sciences Exactes et Naturelles et UFR Médecine, Reims, France

Christian E.H. Schmelzer, Institute of Pharmacy, Faculty of Natural Sciences I, Martin Luther University Halle-Wittenberg, Halle (Saale), Germany; Fraunhofer Institute for Microstructure of Materials and Systems IMWS, Halle (Saale), Germany

A.E. Schutte, Hypertension in Africa Research Team; MRC Unit for Hypertension and Cardiovascular Disease, North-West University, South Africa; School of Population Health, University of New South Wales, The George Institute for Global Health, Sydney, Australia

Angelina Schwarz, Division of Renal Medicine, Department of Clinical Science, Intervention & Technology, Karolinska University Hospital, Stockholm, Sweden

Patrick Segers, Faculty of Biomedical Sciences, Institute of Biomedical Engineering and Technology, Ghent University, Ghent, Belgium

James E. Sharman, Menzies Institute for Medical Research, University of Tasmania, Hobart, TAS, Australia

Ippei Shimizu, Department of Cardiovascular Biology and Medicine, Juntendo University Graduate School of Medicine, Tokyo, Japan

Marc A. Simon, Division of Cardiology, Department of Medicine, University of California, San Francisco (UCSF), San Francisco, CA, United States

Piera Sosa, Meharry Medical College, Nashville, TN, United States

Bart Spronck, Department of Biomedical Engineering, School of Engineering and Applied Science, Yale University, New Haven, CT, United States; Department of Biomedical Engineering, CARIM School for Cardiovascular Diseases, Maastricht University, Maastricht, the Netherlands

Peter Stenvinkel, Division of Renal Medicine, Department of Clinical Science, Intervention & Technology, Karolinska University Hospital, Stockholm, Sweden

Eric J. Stöhr, Cardiovascular Physiology Research Group, Cardiff School of Sport & Health Sciences, Cardiff Metropolitan University, Cardiff, United Kingdom; Department of Medicine, Division of Cardiology, Columbia University Irving Medical Center, New York, NY, United States

M. Strauss-Kruger, Hypertension in Africa Research Team; MRC Unit for Hypertension and Cardiovascular Disease, North-West University, South Africa

Ariana Suarez-Martinez, J. Crayton Pruitt Family Department of Biomedical Engineering, University of Florida, Gainesville, FL, United States

Masayoshi Suda, Department of Cardiovascular Biology and Medicine, Juntendo University Graduate School of Medicine, Tokyo, Japan

Shih-Hsien Sung, Department of Medicine, National Yang Ming Chiao Tung University College of Medicine, Taipei, Taiwan; Department of Medicine, Taipei Veterans General Hospital, Taipei, Taiwan

Isabella Tan, Macquarie Medical School, Faculty of Medicine, Health and Human Sciences, Macquarie University, Sydney, NSW, Australia

Dimitrios Terentes-Printzios, First Department of Cardiology, Hippokration Hospital, Medical School, National and Kapodistrian University of Athens, Athens, Greece

Raymond R. Townsend, Perelman School of Medicine, University of Pennsylvania Health System, Philadelphia, PA, United States

Andrew H. Tran, The Heart Center, Nationwide Children's Hospital, Columbus, OH, United States; The Ohio State University, Columbus, OH, United States

Elaine M. Urbina, Division of Cardiology, Cincinnati Children's Hospital Medical Center, Cincinnati, OH, United States; University of Cincinnati, Cincinnati, OH, United States

Bharath Ambale Venkatesh, Departments of Cardiology/Medicine and Radiology, Johns Hopkins University, Baltimore, MD, United States

Charalambos Vlachopoulos, First Department of Cardiology, Hippokration Hospital, Medical School, National and Kapodistrian University of Athens, Athens, Greece

Anton Vonk Noordegraaf, Department of Pulmonary Medicine, Amsterdam Universitair Medische Centra, Vrije Universiteit Amsterdam, Amsterdam Cardiovascular Sciences, Amsterdam, the Netherlands

Amandine Wahart, UMR CNRS 7369 Matrice Extracellulaire et Dynamique Cellulaire (MEDyC), Team 2: Matrix Aging and Vascular Remodelling, Université de Reims Champagne Ardenne (URCA), UFR Sciences Exactes et Naturelles et UFR Médecine, Reims, France; INSERM UMR 1048, Institut des Maladies Métaboliques et Cardiovasculaires (I2MC), Toulouse, France

Ji-Guang Wang, National Research Centre for Translational Medicine, Centre for Epidemiological Studies and Clinical Trials, Shanghai Key Laboratory of Hypertension, The Shanghai Institute of Hypertension, Department of Hypertension, Ruijin Hospital, Shanghai Jiao Tong University School of Medicine, Shanghai, Shanghai, China

Siegfried Wassertheurer, Center for Health & Bioresources, Austrian Institute of Technology (AIT), Vienna, Austria

Andrew James Webb, Department of Clinical Pharmacology, School of Cardiovascular Medicine and Sciences, King's College London British Heart Foundation Centre, St. Thomas' Hospital, London, United Kingdom

Thomas Weber, Cardiology Department, Klinikum Wels-Grieskirchen, Wels, Paracelsus Medical University, Salzburg, Austria

Berend E. Westerhof, Department of Pulmonary Medicine, Amsterdam Universitair Medische Centra, Vrije Universiteit Amsterdam, Amsterdam Cardiovascular Sciences, Amsterdam, the Netherlands

Ian B. Wilkinson, Experimental Medicine and Immunotherapeutics, University of Cambridge, Cambridge, United Kingdom; Addenbrooke's Hopital, Cambridge, United Kingdom

Yohko Yoshida, Department of Cardiovascular Biology and Medicine, Juntendo University Graduate School of Medicine, Tokyo, Japan

Foreword

Ernesto L. Schiffrin, CM, MD, PhD, FRSC, FRCPC, FACP

Physician-in-Chief, Sir Mortimer B. Davis-Jewish General Hospital, Director, Hypertension and Vascular Research, Lady Davis Institute of Medical Research, Distinguished James McGill Professor and Associate Chair, Department of Medicine, McGill University, Montreal, Canada; Editor-in-Chief, The American Journal of Hypertension

Arterial Stiffness and Pulsatile Hemodynamics in Health and Disease, edited by Julio A. Chirinos, MD, PhD, arrives to us at a time when the field of arterial stiffness has come full circle from experimental to clinical and therapeutic implications, including its potential applications to patients in the clinic. It is not an easy area of research and clinical understanding for most physicians, because of the physical and mathematical aspects that tend to be beyond their knowledge and typical clinical training curricula. Therefore, a text that fills the gap between biophysics, biology, physiology, clinical application, epidemiology, and therapeutics applied to a range of vessels throughout the body and different clinical conditions is certainly very welcome. In particular, it is important that the text is accessible to experts in different fields at all these levels, thanks to the ability to explain difficult concepts in detail but with clarity and some degree of simplicity, and that is what *Arterial Stiffness and Pulsatile Hemodynamics in Health and Disease* does throughout its two volumes, with homogenous prose despite being multiauthored. Dr. Chirinos has managed to summon a group of writers for all chapters that comprises the "who's who" of the field of arterial stiffness and pulsatile hemodynamics from North America, Europe, Asia, and Australia.

The book is organized in sections that deal with successive aspects of vascular stiffness and its consequences. The first section addresses biophysical principles of pressure, flow, pulsatile hemodynamics, aortic structure, wall stiffness, and hemodynamic function. This is followed by a section on pulsatile hemodynamics of the arterial vasculature and its impact on the left ventricular function, and the microcirculation. The following section deals with the biology of arterial stiffening including associated effects on elastin, inflammation and calcification, and mechanisms of cellular aging, and dysfunction of smooth muscle and the endothelium. The clinical and epidemiological aspects of arterial stiffness and its role in cardiovascular prevention and different disease conditions, including hypertension, obesity, diabetes, heart failure, coronary artery disease, chronic kidney disease, cognitive decline, and pregnancy among others, follow in the next section. The primary aortopathies and conditions associated with low pulsatility such as use of left ventricular assist devices are described next. The following section addresses therapeutic implications of large artery stiffness and effects of exercise, weight control, and drugs, both presently in use and potential new drugs for the future. The last section addresses stiffening of the pulmonary circulation, including pulmonary hypertension.

Throughout this book the different authors manage to present complex concepts in a way that can be understood by the uninitiated, who could be expert in other aspects of this subject matter. Undoubtedly this is an authoritative textbook that will familiarize the biomedical community with the field, and facilitate the use of the knowledge acquired so far on arterial stiffness to improve patient outcomes.

This page intentionally left blank

Preface

The field of arterial stiffness and pulsatile hemodynamics has significantly expanded over the last few decades. Increasingly, epidemiologists, clinicians, engineers, and biologists recognize the importance of large artery stiffening in various disease states. The role of large artery stiffness and pulsatile hemodynamics in cardiovascular aging is also widely recognized. However, there remains a gap between the biophysical and theoretical concepts and clinical practice. The aim of this textbook is to provide a comprehensive reference on arterial stiffness and pulsatile hemodynamics, covering the intersection of clinical, biologic, epidemiologic, and biophysical concepts.

We intend for the audience of this book to be composed of clinical and basic science investigators interested in arterial stiffness, physicians and other healthcare providers, epidemiologists and biomedical engineers. Whereas excellent books are already available covering various aspects of this field, in many cases, these are highly specialized, are mathematically-oriented, are restricted to specific knowledge areas, or deal exclusively with clinical or biologic aspects without discussing hemodynamic mechanisms linking arterial stiffness and pulsatile hemodynamics with disease pathophysiology. Therefore, we intended to produce a book that introduces the interested reader to this field in relatively simple terms but at the same time covers, with reasonable depth, a broad range of relevant topics in biophysics, biology, epidemiology, and clinical medicine.

Despite the increasing recognition of this field, studies on arterial stiffness and pulsatile hemodynamics are often misinterpreted or underappreciated from a clinical standpoint. I believe that a proper interpretation of the field is nevertheless essential for a better understanding of multiple clinical conditions and disease states. One of the barriers to a better integration and data interpretation is that clinicians and biologists tend to be less familiar with the biophysical aspects of this field, whereas engineers naturally tend to be less familiar with the clinical and biologic aspects. Yet, a basic understanding of both is essential to drive the field forward and to adequately interpret available data. There is a need for a reference that: (a) presents complex engineering concepts in a readable format for individuals trained in clinical medicine, biology, or epidemiology rather than engineering; (b) clearly discusses the clinical implications of pulsatile hemodynamics

and arterial stiffness; and (c) provides a comprehensive review of key biologic pathways involved in arterial stiffening. This textbook intends to fill this gap.

Throughout the textbook, we utilize stand-alone basic concept boxes to deal with: (1) biophysics concepts that clinicians would be either be unlikely to be familiar with, but that would be very useful for understanding the topic; (2) clinical or biologic concepts that nonclinicians or non-biologists (i.e., bioengineers) are unlikely to be familiar but that are essential to understand the topic. We also utilize stand-alone "in-depth" boxes to develop more advanced concepts that clinicians or biologists are unlikely to be eager to study in depth due to relatively complex math or biophysics, even though a mathematically oriented person (such as a bioengineer) would find very useful. Stand-alone boxes are mentioned and are useful to understand the main text in the chapters, but should in general not be absolutely necessary to follow its flow. To the extent possible, mathematical principles are explained in the main text without complicated formulas, in a conceptual manner.

The book is organized into six sections. Section I deals with the biophysical and technical principles involved in the measurements and interpretation of pressure, flow, pulsatile hemodynamics, aortic structure, wall stiffness, and hemodynamic function, and is not considered optional but rather essential to better understand the rest of the book. Most of the content in this section deals with *in vivo* assessments, particularly in humans, but a dedicated chapter in this section deals with animal models and *ex vivo* methods to study arterial stiffness. Section II deals with basic anatomic and physiologic considerations, including the hemodynamic role of the aorta, pulsatile hemodynamics in the arterial tree, ventricular physiology, ventricular–arterial interactions (as they relate to both load and myocardial oxygen supply), and the microcirculation. Section III deals with the biologic pathways leading to arterial stiffening and dysfunctional pulsatile hemodynamics, including elastin breakdown and associated processes, inflammation, aortic wall calcification, smooth muscle dysfunction, endothelial dysfunction, autonomic dysfunction, and cellular mechanisms of aging. Section IV deals with clinical and epidemiologic aspects of arterial stiffness and pulsatile hemodynamics, including normal,

supernormal, and early vascular aging, ethnic differences, and the role of arterial stiffness in cardiovascular prevention strategies and in various disease states, such as hypertension, obesity, diabetes, exercise intolerance, heart failure, aortic valve disease, coronary artery disease, age-related cognitive dysfunction, chronic kidney disease, pregnancy related complications, congenital heart disease, and the cardiovascular complications of infectious diseases. Additional chapters deal with relevant aspects of primary arteriopathies and clinical situations associated with low arterial pulsatility (particularly, implanted left ventricular assist devices). Section V deals with therapeutic approaches to improve arterial stiffness and pulsatile hemodynamics, including discussions of standard vasoactive drugs in current use, as well as novel drugs, nonpharmacologic approaches (exercise training, diet), and personalized medicine strategies. Finally, Section VI deals with the pulmonary circulation, with an emphasis on pulmonary arterial stiffening, right ventricular−pulmonary arterial interactions, and pulmonary hypertension.

Throughout this book, we intend to discuss the relevant biophysics, presenting complex engineering concepts in a simplified format. Similarly, we intend to place the importance of arterial stiffness in the appropriate clinical context, ultimately keeping in mind how this field can aid in patient care and development of novel therapies. I have been extremely fortunate to have the support of a large number of internationally recognized experts, who have selflessly contributed their time, effort, and deep expertise to write the various chapters in this book, providing authoritative reviews about the state-of-the-art in their respective topics. I hope that this textbook will help advance the field, that it will be an aid to educators in this field, and that it will contribute to the training of the next generation of investigators dedicated to the study of arterial stiffness and pulsatile hemodynamics.

Acknowledgments

I want to thank the chapter authors for selflessly contributing their time and expertise for the success of this project. I am forever grateful to Melissa, Gabriella, and Daniel Chirinos for their support throughout this project, and to my parents, Julio Chirinos Pacheco and Josefina Medina, for being such inspirational role models. I also want to acknowledge my academic home, the Cardiovascular Medicine Division at the University of Pennsylvania, for strongly supporting my career and the various academic activities that led to the edition of this book. My very special thanks to my colleagues at the University of Ghent (particularly Ernst Rietzschel, Thierry Gillebert, Patrick Segers, and Marc De Buyzere) for many years of wonderful collaboration, and to the North American Artery, ARTERY, Pulse of Asia, and Latin American Artery societies for providing platforms for the advancement of this important field. I am also grateful to the National Institutes of Health (NIH) which supported my work through multiple awards throughout the years, particularly the National Institutes of Aging which provided me with a mid-career development award to study large artery stiffness and arterial aging (K24-AG070459). I am indebted to Dr. Patrick Segers for going above and beyond his chapter writing, providing critical feedback for several other sections of the book. I also want to acknowledge the essential contributions by the many senior investigators, who although did not participate in the book, inspired or motivated many of us, including but not limited to Wilmer Nichols, Nico Westerhof, Michael O'Rourke and Michel Safar, as well as John Cockcroft, who has worked relentlessly to promote the field in Europe and the US, and Alfonso Bryce, Pedro Forcada, Eduardo Barbosa and Enrique Melgarejo, who have done the same throughout Latin America. Last but not least, my gratitude goes to the editorial team at Elsevier for their guidance and help throughout this project.

Research funding and disclosures

This page intentionally left blank

Biophysical and technical principles

This page intentionally left blank

Chapter 1

Basic principles that determine relationships between pulsatile hemodynamic phenomena and function of elastic vessels

Alberto Avolio[1], Bart Spronck[2,3], Isabella Tan[1], James Cox[1] and Mark Butlin[1]

[1]*Macquarie Medical School, Faculty of Medicine, Health and Human Sciences, Macquarie University, Sydney, NSW, Australia;* [2]*Department of Biomedical Engineering, School of Engineering and Applied Science, Yale University, New Haven, CT, United States;* [3]*Department of Biomedical Engineering, CARIM School for Cardiovascular Diseases, Maastricht University, Maastricht, the Netherlands*

Introduction

The pulsatile nature of blood flow in arteries has been known since antiquity through palpation of the arterial pulse for early diagnosis of disease.[1] However, the inherent function of arterial elasticity in determining the relationship of pulsatile blood pressure and flow was only able to be studied in recent decades following development of techniques for reliable measurement of hemodynamic parameters. Although it was possible to measure arterial pressure accurately under experimental conditions, flow measurement was much more challenging. Hence, biophysical relationships were initially explored by calculating flow from pressure measurements.[2]

The pivotal, and perhaps the most important, work in the application of the fundamental theory of fluid flow to blood flow in arteries was done in the 1950s by John Womersley, an English applied mathematician. The critical contribution of Womersley was to extend basic knowledge of fluid flow to blood flow in compliant tubes, such as arteries, under an oscillating pressure gradient. This then made it possible to compute blood flow from measured pressure (or more specifically, pressure gradient) and from knowledge of physical properties of blood vessels. He did much of this work in the United States (Wright−Patterson Airforce Base, Ohio) in the latter part of his career, and during the post-war period when there was great expansion of the novel machines (early digital computers) used in the war effort to perform rapid computations of missile trajectories. Womersley made use of these facilities to obtain solutions of the fundamental fluid flow (Navier−Stokes) equations with circular boundaries as applied to arteries. The derivation, theory, and tabulation of basic functions appeared in his in-depth technical report[3] (an officially classified document until recently), which has formed the theoretical basis of much of modern hemodynamics. This gave rise to a seminal monograph on *Blood Flow in Arteries* by his physiologist collaborator Donald McDonald in 1960, with a second edition in 1974, and six other subsequent editions of *McDonald's Blood Flow in Arteries* under the stewardship of Wilmer Nichols and Michael O'Rourke. The seventh edition is currently in press.[4]

This chapter addresses the fundamental concepts inherent in pulsatile hemodynamics, with the view that much has already been written for specialists in the field, but more needs to be done to promote the basic conceptual understanding to a wider audience of scientists, early career researchers, and clinicians. This textbook will contribute significantly to such a challenging task and will impact extensively on translation of the knowledge contained in the various chapters to inform and support scientific investigation and advance clinical practice. This chapter presents the underlying concepts inherent in pulsatile hemodynamics and arterial stiffness through a combination of qualitative description and formal mathematical relations. The field is vast, as is evident by the extensive

number of chapters in this book. Thus, this chapter is by necessity not exhaustive, and to avoid excessive repetition, reference is made to other relevant chapters where appropriate.

The relevance of arteries to cardiovascular disease is clear, insofar as the contribution of their function as blood conduits: any blockages in the vessel lumen will cause ischemic events. However, the role of arteries as closed elastic vessels which contain blood, and which are under circumferential wall tension and pulsatile load, is not as clear. It is obvious to physical scientists that arteries are more than just passive conduits for blood distribution. They are a key determinant of arterial blood pressure, the biomarker of the mechanical tension in the arterial wall. A healthy heart, in adapting to a stiffening arterial vasculature while preserving cardiac output, will generate increasingly higher pulse pressure, feeding back to a path of increasing degenerative changes in the heart and other target organs, and in the arteries themselves. The evolution of the recognition of the intrinsic role of arterial elasticity associated with hemodynamic pulsatility might be akin to the trajectory in the understanding of the role of the vascular endothelium. There was a time when the endothelium was thought to be a passive lining of blood vessels, until its role was recast to be the stuff of Nobel Prizes[5]!

The basic hemodynamic concepts described in this chapter will aim to support the large amount of material presented in the subsequent chapters to promote the relevance of pulsatility of arterial blood pressure and flow and the important role of arterial stiffness, with the overall translational goal to have measurement of arterial stiffness done alongside the conventional clinical measurement of blood pressure.

Pulsatile phenomena

Pulsatility as an evolutionary requirement for self-sustaining circulatory systems

Hemodynamic pulsatility and elasticity of blood vessels are fundamental phenomena in the intact circulation of self-sustaining organisms. Since the heart is the power source for motion of blood in the circulation, for a self-regulating and self-contained system, there will necessarily be a requirement for a time period when the heart obtains energy (as an "input" quantity) and a subsequent time period when it delivers energy (as an "output" quantity), that is, in machine parlance, a "duty cycle." The heart receives energy mainly from oxygenated blood in the coronary circulation during the time of ventricular relaxation (including the energy-dependent diastolic filling phase and the atrial kick) and transforms the input (chemical) energy into output (mechanical) work, where blood motion in the systemic arterial vasculature occurs due to ventricular contraction

and opening of the aortic valve. In general usage (ranging from machine operation to digital waveforms and neural circuits), the duty cycle is expressed as a percentage of the time for which the system is active. For the heart, this is the time of ventricular ejection, which constitutes approximately 30% of the cardiac cycle.
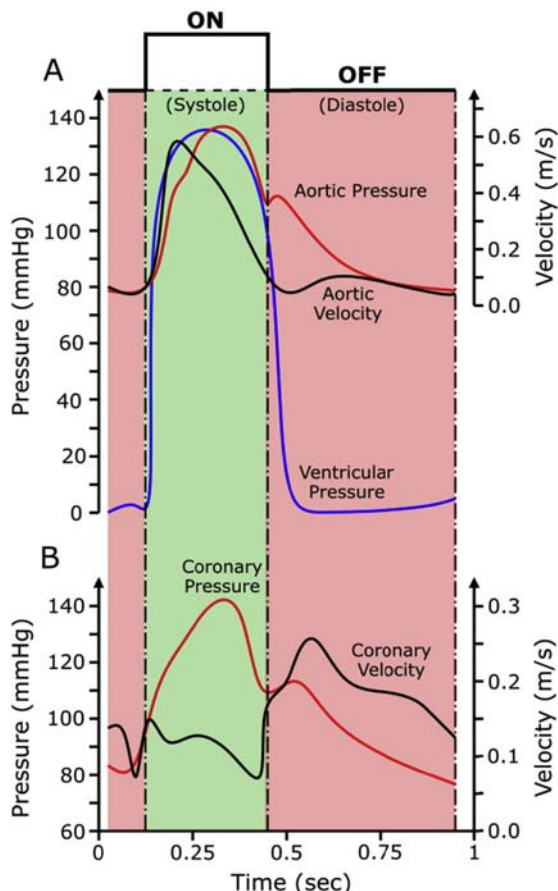
The "self-sustaining" concept requires a continuous repetition of the process of energy conversion and a general regularity of the duty cycle for optimization of mechanical efficiency. The principal function of the heart to operate as a pump is to convert the potential energy developed as tension in the myocardial fibers to kinetic energy, manifesting as movement of blood in the circulatory system. In terms of energy conversion for motion of blood, it is estimated that the heart is a rather inefficient pump, with an overall mechanical efficiency at rest of some 20%.[6] (Note: if there is no movement of blood in the aorta, the heart, while still being able to beat, will have a pump efficiency of 0%.) While this may appear to be a suboptimal design constraint, it could be considered to translate to an evolutionary advantage, enabling the heart to have a substantial "reserve capacity," allowing for a large operating range in terms of the ability to increase cardiac output through increased contractility and increased frequency of repetition of the duty cycle, that is, an increase in heart rate.

Fundamental association of pulsatility and vascular structure and function

The opening of the aortic valve establishes continuity between the contracting left ventricle as the power source and the aorta as the reservoir of blood, enabling blood distribution throughout the systemic vasculature. The branching structure of the aorta and major arteries constitutes a system of conduits distributing blood to the microcirculatory beds, where the large pulsatility of blood flow due to ventricular contraction becomes extremely low. Because of the essential design of the heart as a pump, the aorta and arterial tree as blood conduits, and the evolutionary requirement for organism self-sustainability, the operation of the duty cycle requires closure of the aortic valve, so that the (mammalian) heart can replenish its energy through oxygenated blood flow in the coronary circulation (most of which occurs in diastole for the left ventricle) and fill the ventricle for the subsequent ejection (Fig. 1.1).

The conduit function of the arterial vasculature enables blood distribution to all tissues of the body. The blood volume is compartmentalized by the branching tree structure in which vessel caliber gradually decreases with successive branching generation. The change in cross-sectional area and branch points generally follows principles of optimality to maximize energy transfer at junctions[7,8] (see Section The arterial vasculature as a distributed system of branching distensible tubes).

Cardiac "Duty Cycle"

FIGURE 1.1 Schematic representation of a cardiac "Duty Cycle" (energy in/energy out), with ventricular pressure, aortic pressure, and aortic flow velocity waveforms (panel A) and coronary pressure and coronary flow velocity waveforms (panel B). Pump energy output (stroke volume) mainly occurs during the ON period (systole) and energy input (oxygenated coronary blood flow) mainly occurs during the OFF period (diastole).

In addition to the conduit function, the aorta and major arteries expand during ventricular systole to store a portion of the ejected blood volume. The degree of expansion is determined by the elastic properties of the vessel wall; that is, the distensibility of the vessel wall will determine the storage capacity of an arterial segment, generally referred to as vessel compliance (C; units of mL/mmHg). This property, together with vessel size, determines the pressure pulse (ΔP; units of mmHg) that is generated by an increase in volume (ΔV; units of mL):

$$\Delta P = \frac{\Delta V}{C} \qquad (1.1)$$

This relationship is fundamental to the interaction of hemodynamic pulsatility and arterial stiffness (when total arterial compliance (TAC) is substituted for C, and cardiac

stroke volume (SV) for ΔV, the resulting ΔP corresponds to the pulse pressure *(PP):* the diastolic-to-systolic pressure difference: *PP=SV/TAC).* Since the stiffness of the arterial wall determines the degree of expansion for accommodating the increase in blood volume, a stiffer arterial wall has a lower compliance, i.e.,

$$arterial\ stiffness \propto \frac{1}{C} \qquad (1.2)$$

Hence, from Eqs. (1.1) and (1.2),

$$\Delta P \propto arterial\ stiffness \qquad (1.3)$$

Eq. (1.3) essentially states that for a given stroke volume, the pulse pressure depends on arterial stiffness. Since stroke volume is reasonably well-regulated during normal healthy aging,[9] this association can explain the underlying mechanism of isolated systolic hypertension, the most common form of hypertension in the elderly, where systolic pressure is elevated in the presence of normal diastolic pressure, that is, an increase in *pulse* pressure.[10] The effect of volume on the distension of the arterial vasculature, and so increase in wall tension, which then manifests as arterial pressure, is partly mediated through modification of kidney function affecting plasma volume.[11] This broadly explains why hypertension has traditionally been the domain of nephrologists.
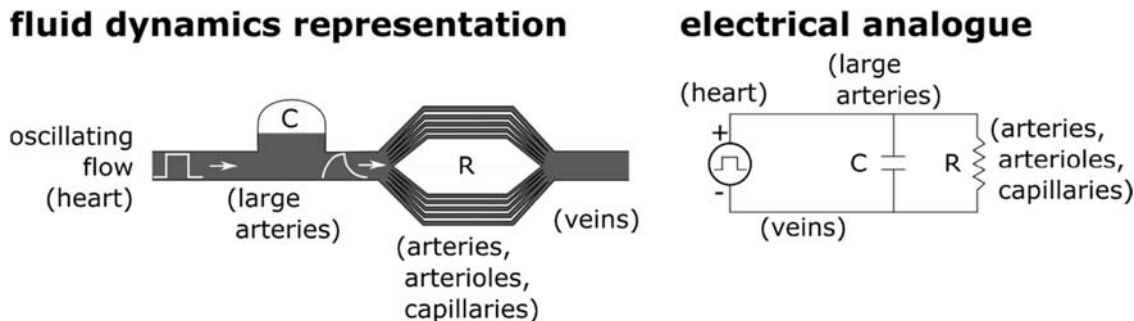
The concepts underpinning the associations expressed in the above equations are based on steady-state quantities of changes in blood volume and blood pressure during a cardiac cycle. Based on the concept of the duty cycle (as described above), it is assumed that changes in volume and pressure occur as average quantities, that is, there is no involvement of instantaneous time-varying quantities in relation to the duty cycle. Clearly, blood is ejected due to the time-varying contraction of the ventricular muscle, and so the stroke volume ($SV = \Delta V$, mL) is the time integral of the ventricular outflow rate ($Q(t)$, mL/s) during the ejection (systolic) period (Ts, seconds) of the cardiac cycle:

$$SV = \int_0^{Ts} Q(t) \cdot dt \qquad (1.4)$$

The volume in a closed compartment is intrinsically associated with the storage property of the vascular compartment, that is, arterial compliance. When the volume moves with time, the rate of flow ($Q_r(t)$) is associated with a component of the system that offers resistance (R) to flow under pressure ($P(t)$). (This is analogous to Ohm's Law in electrical circuits: pressure analogous to voltage and flow rate analogous to current), i.e.,

$$P(t) = Q_r(t) \cdot R \qquad (1.5)$$

Since R is a scalar quantity, Eq. (1.5) suggests that time-varying pressure and flow profile would be identical.

FIGURE 1.2 The Windkessel model of the systemic vasculature represented as a fluid dynamics model and electrical analogue (RC circuit). The heart ejects blood (fluid or flow or current) in an oscillating manner into the systemic vessels that have capacitance (C) and resistance (R). The Windkessel properties (R,C) convert a square wave input to an output wave profile with exponential rise and fall. The Windkessel model can be expanded to capture characteristic impedance and blood inertia (inductance).

However, at steady state and at a given instant of time, the total flow from the left ventricle $(Q(t))$ consists of a component which is stored $(Q_c(t))$ due to the elastic expansion of the arterial wall constituting arterial compliance, and a component $(Q_r(t))$ flowing through the peripheral resistance:

$$Q(t) = Q_c(t) + Q_r(t) \qquad (1.6)$$

If R represents the total peripheral resistance and C the total compliance, or the arterial storage capacity, from Eqs. (1.1)−(1.6), an expression can be obtained where the relationship between aortic pressure and aortic flow is determined by an exponential function (which can be estimated during diastole when flow is zero) and the combination of R and C. That is, for a given time-varying flow profile $(Q(t))$, the resulting time-varying pressure $(P(t))$ is a function of the product of R and C (R times C has units of time (sec) and is related to the exponential time constant τ ($\tau = RC$), the time taken for the pressure to decrease by 63% of an initial value).

For a given value of R and C (and so of the time constant, τ), the pressure decay during diastole $(P_d(t))$ is given as

$$P_d(t) = P_0 \cdot e^{-t/\tau} \qquad (1.7)$$

where P_0 is the value of pressure at the beginning of diastole.

Since during diastole there is no ventricular outflow, arterial pressure is related to $Q_r(t)$ and $Q_c(t)$ and peripheral resistance and arterial compliance, respectively, hence the value of the time constant becomes a determining factor for pulse pressure; for a given peripheral resistance, the smaller the compliance (C), that is, the higher the arterial stiffness, the shorter the time (τ) to release the volume of blood stored during systole, and so pressure drops more rapidly.

A conceptual representation of this storage function of the arterial vasculature has conventionally been related to the inverted dome of a fire engine, where the intermittent input of volume of water is converted to a quasi-steady-state hose outlet due to the storage properties of the dome—a model conventionally known as the Windkessel[12] (Fig. 1.2).

As described in detail in Chapter 3, the Windkessel model offers a useful approach to illustrate basic concepts of the effects of arterial stiffness and peripheral resistance on blood pressure and flow, and can be further formalized to describe the concept of reservoir pressure.[13] However, it is based on a "lumped parameter" approach in which there are no physical dimensions, and the parameters only exist as scalar mathematical quantities; that is, a "zero-dimension" model. Clearly, the distributed structure of the arterial tree will involve the propagation of the ventricle's energy output in terms of blood pressure and flow over different path lengths from the aortic valve to the periphery of the systemic vasculature. Indeed, the true relationship of pressure and flow in the three-dimensional structure of blood vessels as elastic conduits is complex and extremely challenging to be completely and accurately described, as this would require the complete solution of the Navier−Stokes equations of fluid flow (requiring powerful computational algorithms). However, very good approximations can be obtained by considering blood flow in the axial direction and averaged over the entire arterial cross section.[14] This approach has been shown to be adequate to describe the relationship of blood pressure and flow as time-varying quantities traveling in one dimension, that is, along the axial length of arterial segments, resulting in approaches using one-dimensional models.[15]

Basic principles related to hemodynamic pulsatility and arterial stiffness will be addressed in subsequent sections of this chapter using the approach of one-dimensional flow and propagation of pulsatile energy as periodic wave of pressure and flow, with further details addressed in other chapters (Chapters 3, 7 and 11).
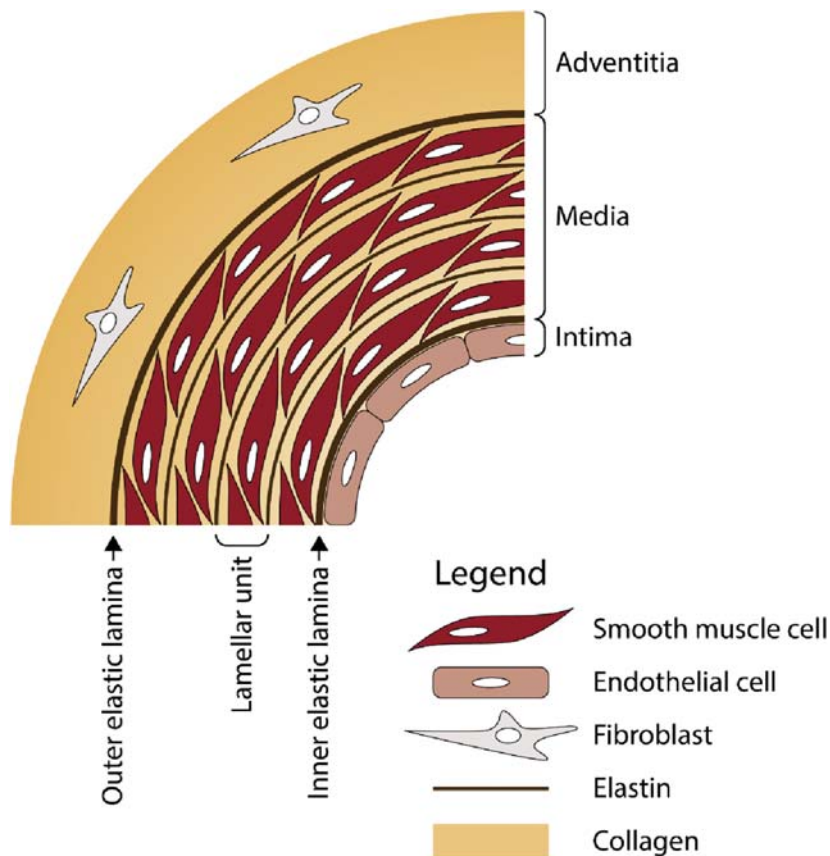
Elastic vessels

Hemodynamic pulsatility and structure of the arterial wall

As distensible conduits, arteries are required to expand and recoil during the cardiac cycle and withstand large ranges of intraluminal pressure (arterial pressure in weightlifters can exceed 480/350 mmHg [systolic/diastolic blood pressure] during a double-leg press[16]). The distensible properties enable the storage function, which determines the degree of pulsatility present throughout the arterial tree, and the tensile properties determine the ability to withstand high pressures. The elastic and tensile properties are largely determined by the two main load-bearing components in the arterial wall: elastin and collagen, respectively.

Elastin and collagen are arranged in concentric layers forming a lamellar structure in the arterial media (Fig. 1.3). In the human aorta, there are approximately 60 lamellae,[17] with the number decreasing with vessel caliber. The lamellar unit has been suggested to be a fundamental entity of arterial structure and function, with the tension per lamellar unit being remarkably constant across a broad range of mammalian species.[17,18]

The mechanical properties of the arterial wall are determined mainly by the material components and are characterized by the conventional material response to an applied force, that is, the *stress/strain (σ/ε)* relationships, (where σ is the applied force/unit area in the same direction, and ε is the relative change in length $(L_1 - L_0)/L_0$) in a given direction). Since elastin and collagen constitute approximately 30% and 50%, respectively, of the (dry) weight of the aortic wall,[19] and this is fairly consistent across a large range of animal species,[20] the stress/strain characteristics will be determined mainly by these two components. Hence, at low levels of resting stress (when the wall is subjected to low loading conditions), the amount of stretch is mainly determined by the elastin protein, whereas at high levels of resting stress, the amount of stretch is determined by the collagen protein. In terms of functional performance of arteries, this property is structurally advantageous since the vessel can expand easily at low pressure due to the distensible properties of elastin (and so have increased storage capacity). It will also have a high yield strength (the material property related to the point when there is plastic deformation of the material) at high pressure due to the strong tensile

FIGURE 1.3 Schematic illustration of the cross section of the arterial wall showing the components of the adventitia, media, and intima. The number of lamellar units vary with size of vessel and species (e.g., human aorta: ∼ 60; rat aorta: ∼ 5); however, the tension per lamellar unit is quite similar.[17,18]

properties pertaining to collagen, but with a reduced storage capacity, since collagen is much less distensible than elastin, being some 100 to 1000 times stiffer than elastin.[21] The structural properties of the artery wall also determine the static and dynamic (frequency-dependent) elastic properties.[22,23] The dynamic elasticity is seen as a phase delay between pressure and diameter signals and is a measure of the viscoelasticity of the arterial wall.[24] Wall viscoelasticity implies that the wall itself has viscosity, whereby stretch causes some friction that dissipates a small amount of energy as heat, whereas a purely elastic vessel would be one that does not dissipate energy.

The stiffness of a material at a given condition of stress and strain can be defined as the incremental elastic modulus or incremental Young's modulus (E_{inc}): the ratio of incremental stress ($\Delta\varepsilon$) and strain ($\Delta\sigma$) when stretched uniaxially (Eq. 1.8). [*Note 1*: E_{inc} quantifies the stiffness of the wall material and is, hence, a material stiffness metric. This contrasts to structural stiffness metrics such as pulse wave velocity, which quantify the structure of the artery as a whole. This important difference is elaborated in Chapter 9, Box 9.1; *Note 2*: Although E_{inc} is the most commonly used material stiffness metric in clinical studies, other material stiffness metrics that exist, especially in engineering/modeling studies, may be more appropriate. See Chapter 9, Box 9.5].

$$E_{inc} = \frac{\Delta\sigma}{\Delta\varepsilon} \qquad (1.8)$$
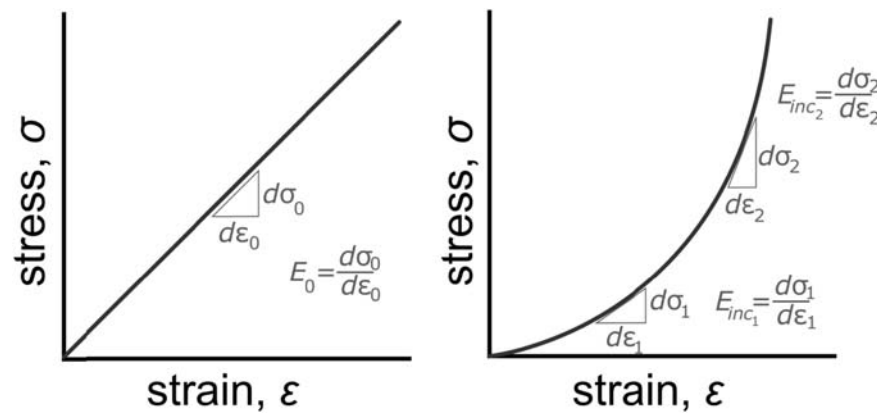
If this ratio is the same for all conditions (i.e., if stress and strain relate linearly), the material has a constant value of E, that is, it is a linear elastic material (or Hookean) (Fig. 1.4). However, given the different structural properties of elastin and collagen, E_{inc} cannot be constant; it is low when the artery is distended at low pressure and high when distended at high pressure. Hence, E_{inc} varies with

loading and depends on where the operating point is on the stress/strain curve; that is, arteries become stiffer with increasing pressure (Fig. 1.4). The implications of this property are profound: for the same blood volume stored in an artery during ventricular ejection, the pulse pressure increases with increasing distending pressure. If this is applied to the concept of hypertension, the higher pulsatility associated with higher intraarterial pressure will lead to further arterial deterioration, which can reduce wall distensibility, increase arterial stiffness, and lead to a further increase in pulse pressure. This, of course, constitutes a type of positive feedback or a vicious cycle potentiating compromised function of the arterial vasculature.[28] In this context, the degree of pulsatility associated with the effect of age on large arteries will increase degeneration of load-bearing components due to increase in peak stress.[21]
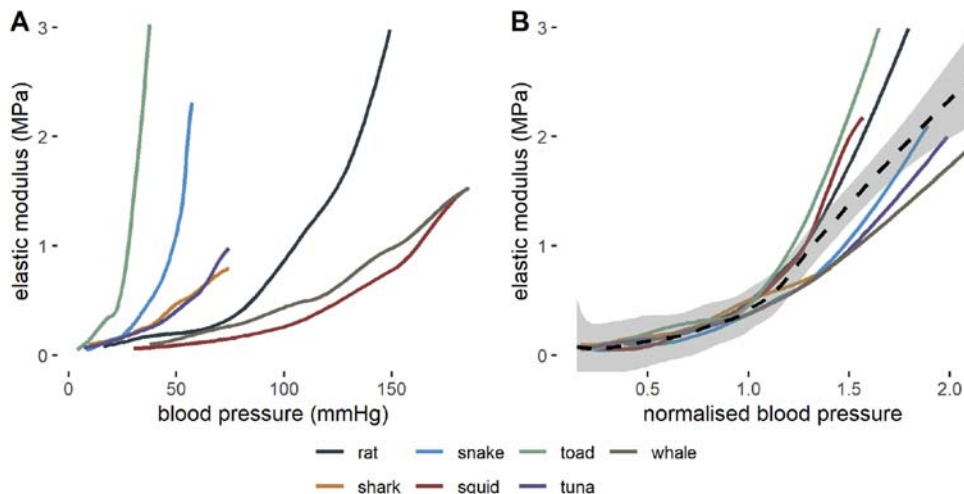
Pressure dependence of arterial stiffness: an essential ingredient for optimal arterial design

The structural characteristics of the load-bearing components of the arterial wall—elastin and collagen—are responsible for the nonlinear (pressure-dependent) stiffness of arteries. Similar to the relatively constant tension per lamellar unit found across a broad range of species,[17] the elegant work conducted by Robert Shadwick in a range of species (from rat (~ 0.45 kg) to whale ($\sim 40,000$ kg)) concluded that pressure dependence of arterial stiffness is a fundamental property of arterial design, and that it is present in all vertebrates and invertebrates with a closed circulatory system.[29] A remarkable similarity is seen when the relationship is normalized for normal operating pressure of different animal species (Fig. 1.5).

This property of blood vessels is a fundamental determinant of the principal function of arteries as conduits to provide a reliable blood supply to peripheral organs and

FIGURE 1.4 Stress (σ) and strain (ε) relationships illustrating linear and nonlinear elasticity. For a linear elastic material, the elastic modulus (E_o, slope of curve) is constant at all level of stress and srain (left panel). For a nonlinear elastic material, the elastic modulus (E_{inc}) increases with higher stress or strain (right panel). The nonlinear elastic properties of arteries are responsible for the pressure dependence of arterial stiffness.

FIGURE 1.5 Pressure dependence of elastic modulus of aortic tissue in a range of species. The degree of dependency (slope) varies with each species (A). However, the slope becomes quite similar and the variation becomes markedly reduced when pressure (units in the *x*-axis) is normalized with the normal operating pressure of each species (B). This suggests a fundamental structural property of arteries that is characteristic of the evolutionary development of the circulation. Black dashed line shows average across the listed species. *Data from Shadwick RE. Mechanical design in arteries.* **J Exp Biol**. *1999; 202(Pt 23):3305−3313.*

body tissue. The property also applies to veins as collapsible tubes (see Section Fundamental importance of pressure-dependent arterial stiffness (nonlinear elasticity) for arteries), with the veins comprising the main capacitive component of the circulatory vasculature where the majority (approximately 75%) of the blood is contained.[30]

Fundamental importance of pressure-dependent arterial stiffness (nonlinear elasticity) for arteries

The word "artery" derives from the original Greek meaning of "αρτηρία" for "air duct." This was probably because when blood vessels were examined postmortem, arterial conduits were generally empty, whereas veins were generally filled with blood or collapsed. The fundamental difference between the two is that arteries never collapse when unloaded and always remain open due to the presence of residual stress in the wall.[31] In terms of evolutionary development, this important property of structure and function ensures reliable movement of blood in the arterial vasculature even with a low transmural pressure. It is of interest to understand how this property is intrinsically related to the obligatory property of nonlinear elasticity, as it is also a basic determinant of the relationship between pulsatile hemodynamic phenomena and arterial stiffness.

Arterial segments can be considered as uniform circular elastic tubes subjected to an internal distending (transmural) pressure (*P*). When inflated to a specific radius (*r*), the distending (radial) force on the wall is balanced by the circumferential tension (*T*) that is supported by the circumferential lamellar structure of elastin and collagen. For a thin-walled vessel, that is, the magnitude of the wall

thickness (*h*) is much smaller than the radius ($h \ll r$; hence *r* can either be the internal or external radius), *P* and *T* are related by Laplace's Law,
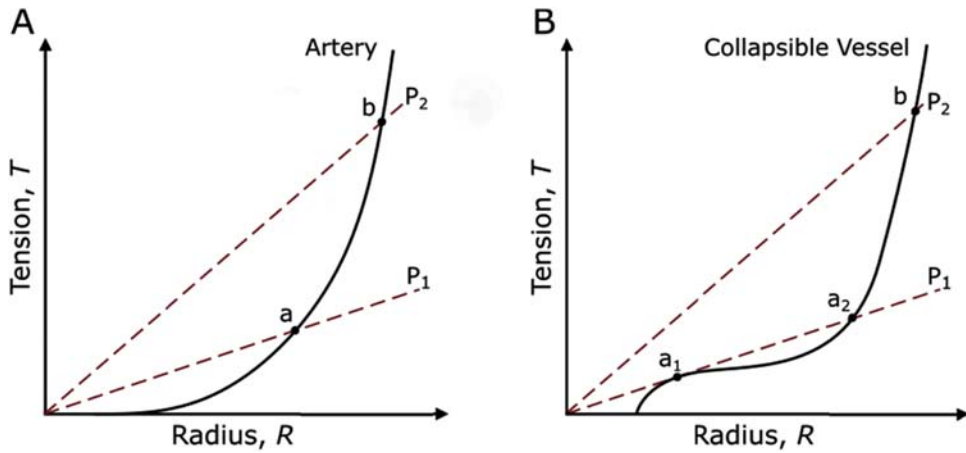
$$T = P \cdot r \qquad (1.9)$$

The circumferential wall stress (*σ*), also known as hoop stress, is the tension per unit wall thickness,

$$\sigma = T/h \qquad (1.10)$$

Eq. (1.9) means that a plot of *T* versus *r* will be a straight line with a slope of *P*. As described previously, the structural attributes of elastin and collagen, the proteins which mainly take up the wall tension, also produce the nonlinear elastic properties of the wall. The plot of *T* versus *r* would thus be curvilinear. Hence, the operating point of the vessel would be the intersection of the straight line (*P*) and the *T*-*r* curve. That is, there is always a unique combination of *P*, *r*, and *T* (Fig. 1.6A). This is not the case for a collapsible tube (such as a vein) where the straight line (*P*) and the *T*-*r* curve can intersect at more than a single point (Fig. 1.6B).

The vascular properties illustrated in Fig. 1.6 indicate that the specific component structure of the arterial wall that gives arteries the property of nonlinear (or pressure-dependent) wall stiffness also endows them with the ability to have a stable operating function (single intersecting point on the *T*-*r* curves, Fig. 1.6A) and thus cannot collapse, as opposed to the instability of collapsible tubes (multiple intersecting points, Fig. 1.6B). [In this context, the notion of "stability" refers to the vessel having only a single possible radius value for a given pressure, whereas "instability" refers to the vessel having more than a possible single value of radius for a given pressure.] It is this
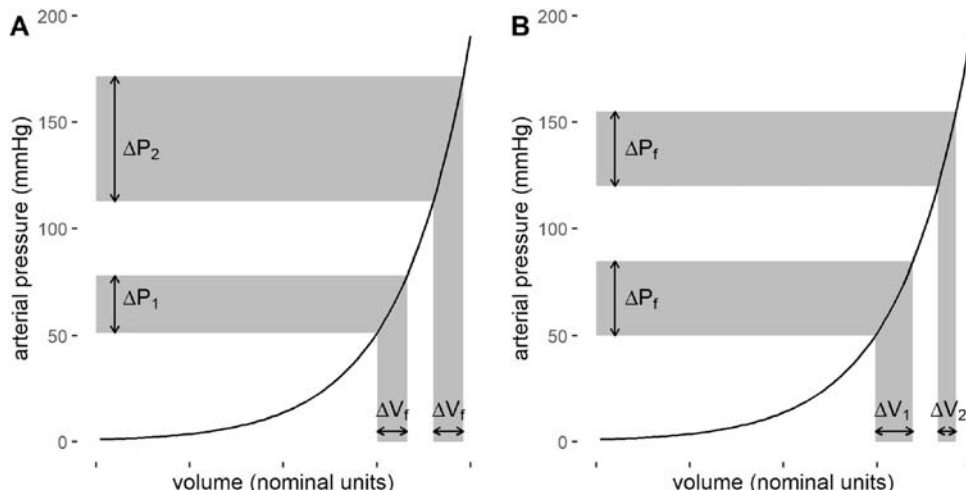
FIGURE 1.6 Schematic illustration of tension/radius relationships for a non-collapsible (A, artery) and collapsible vessel (B). In both cases, the Laplace relationships have linear slopes equivalent to the distending pressures (e.g., P_1 and P_2). However, for the artery, there is always a unique operating point where the pressure curves intersect with the T-R curve (indicating stability of vessel caliber at P_1 and P_2), whereas there can be more than one intersecting point (a_1, a_2) for the same pressure value for the collapsible vessel (indicating stability of vessel caliber at P_2 [with a single possible radius] but instability of vessel caliber at P_1 [with more than one value of radius]).

property of increased stiffness with pressure that also protects arteries from developing aneurysms,[32,33] which of course can develop when the wall tensile properties degenerate.

Influence of pressure-dependent arterial stiffness on hemodynamic pulsatility

From Section Fundamental association of pulsatility and vascular structure and function, it was shown that for an arterial segment, the volume storage capacity (vessel compliance) is inversely related to the structural stiffness of the artery wall. Hence, the increase in structural stiffness with increasing pressure would reduce the storage capacity. Since the normal operating heart can accommodate to

changes in vascular load to eject the required stroke volume for adequate perfusion, the contracting ventricle has sufficient power to force the ejected blood into the vasculature. Although the heart is essentially a power source for the full operating range,[34] under normal operating conditions and to a reasonable approximation, it can be considered a constant flow source (this would strictly apply to a non-diseased heart or in the case where inherent contractility is not reduced). This means that for a constant stroke volume (ΔV) delivered to the arterial vasculature by the ejecting ventricle, the resulting increase in pressure (ΔP) depends on the position of the operating point of the T-R-P curve shown in Fig. 1.6A, or the pressure−volume curve (Fig. 1.7). Hence, the same characteristics of nonlinear

FIGURE 1.7 (A) Schematic illustration of increase in pulse pressure (ΔP) for a fixed change in volume (ΔV_f) on a P-V nonlinear curve at low and high pressure (normal heart). At high pressure, the same fixed volume change causes a larger pulse pressure change ($\Delta P_2 > \Delta P_1$). (B) Schematic illustration of a fixed pulse pressure (ΔP_f) for a change in volume on a P-V nonlinear curve at low and high pressure. ΔV is lower at higher pressure (failing heart, $\Delta V_1 > \Delta V_2$).

elasticity that ensure stability of operation and protect against aneurysm development also have the consequences of increasing pulsatility with increasing pressure throughout the arterial vasculature (Fig. 1.7A).

Although pressure-dependent elasticity is associated with increased pulsatility with a normal heart that does not change its output with increasing arterial pressure, it is not the case for a failing heart, in which myocardial contractility (and therefore ventricular ejection) is sensitive to afterload, and so will decrease with increasing arterial afterload. In this case, the heart cannot be considered a constant flow source, but rather a pressure source, whose output is largely determined by afterload. Thus, for a failing heart, the nonlinear elasticity characteristics do not necessarily result in marked increase in pressure pulsatility (Fig. 1.7B), but may rather result in decreased stroke volume and, hence, tissue perfusion.

The arterial vasculature as a distributed system of branching distensible tubes

Structural implications of arterial branching

The arterial tree, like any branching structure in nature, is subject to fundamental laws underpinning function and form as exquisitely described in D'Arcy Thompson's seminal monograph in the early 20th century.[35] In structures where there is energy transfer across junctions, such as fluid flow, the branching generally obeys principles of optimality, such as minimization of energy losses at branch points. In the vascular system, this principle was developed by Cecil Murray in 1926, where it was applied to the distribution of blood volume[7] and branching angles.[8] This seminal work gave rise to the well-known Murray's Law, which states that the volumetric flow rate (Q) (assumed to be laminar flow) is related to the cube of vessel diameter (D),

$$Q = k \cdot D^3 \qquad (1.11)$$

where k is a proportionality constant.

At branch points, conservation of mass requires that the sum of volumetric flow in the branches ($Q_1 + Q_2$) equals the flow in the parent branch (Q_0). Hence, for a bifurcation,

$$D_0^3 = D_1^3 + D_2^3 \qquad (1.12)$$

For a symmetrical bifurcation defined by Eqs. (1.11) and (1.12), the optimal (and theoretical) branching angle between the daughter branches is 75 degrees.[8]

Murray's Law assumes complete Poiseuille (laminar) flow, which clearly is not always true in real biological systems, where flow might be disturbed at junctions or at irregular surfaces. There has been vigorous activity in theoretical studies of optimality in attempts to understand how much the exponent of 3 in Eqs. (1.11) and (1.12) varies in real bifurcations.[36,37] Some studies suggest a range between 2.33 and 3.0.[38] However, the underlying basic phenomena inherent in Murray's Law are evident where, in broad terms, similar principles of optimality occur in other branching structures in nature with a requirement for maximizing efficiency of fluid transport, as occurs for blood flow in arteries or transport of water in plants.[39] In relation to pulsatility phenomena, the underlying optimality principles of branching are relevant in the context of energy transport at branch points. According to Eq. (1.11), the energy transfer would be optimal and so there would be minimal reflected energy at individual branch points. That is, the closer the exponent in Eq. (1.11) is to 3, the greater the efficiency of energy transfer at minimum energy cost. In blood flow in arteries, the energy is carried by the time-varying quantities of pressure $P(t)$ and flow $Q(t)$, and the total work (W) during a cardiac cycle (of time T_c) can be quantified by the integral of their instantaneous product,

$$W = \int_0^{T_c} P(t) \cdot Q(t) \cdot dt \qquad (1.13)$$

If there are optimal branching conditions, all (or most) of the energy that arrives at the bifurcation is transmitted; that is, the junction is said to be matched. However, if the conditions are not optimal, thus there is mismatch at the junction, not all the energy is transmitted, and some is reflected. This would cause an increase in net W at the upstream end of the junction and would be associated with an increase in pressure and a decrease in flow. Hence, because of the essential pulsatile function of the heart (see Section Pulsatility as an evolutionary requirement for self-sustaining circulatory systems), the phenomenon of reflection of energy at any location of mismatch in the arterial vasculature usually manifests as increases in the pulsatile component of arterial pressure.

Notwithstanding the obligatory branching structure of the arterial vasculature, and the variability around the principles of optimality underlying Murray's Law, it is of interest to quantify the effect of branching on the phenomena of reflection and pulsatility.

The theoretical and analytical aspects of reflection of the propagating arterial pulse are treated in greater detail in a subsequent chapter (Chapter 11) dealing specifically with wave reflection. However, in terms of the relevance of branching, it is useful to consider a major branch point in the aortic trunk: the aortoiliac junction. For a symmetrical junction with two daughter branches, from Eq. (1.12), the theoretical diameter of the branch vessels would be 0.794 times the diameter of the parent branch. Hence, the optimal area ratio is 1.26 (ratio of areas of the sum of individual branch vessels to area of parent branch). [*Note*: These
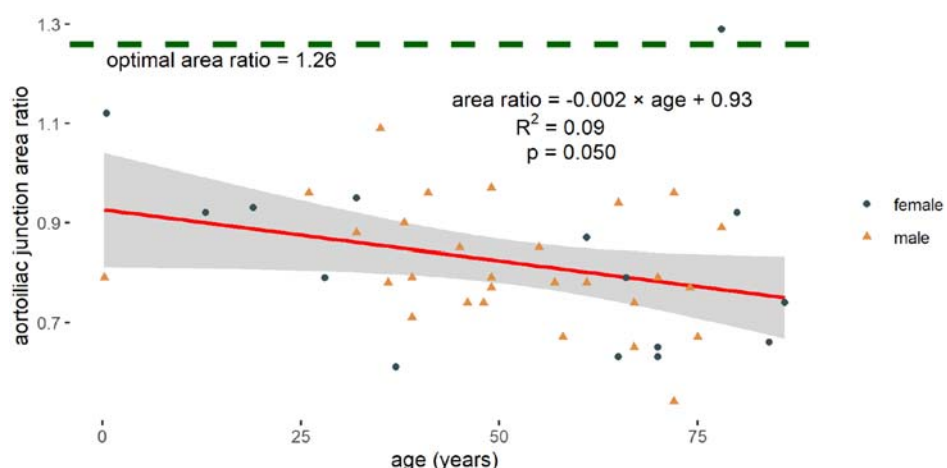
theoretical considerations refer to a branching structure with uniform material properties for parent and daughter vessels, i.e., similar material stiffness and wave speed.] The aortoiliac area ratio (ratio of sum of area of iliac arteries to area of the abdominal aorta) over an age-span of 2 months to 86 years[40] shows that the optimal area ratio of 1.26 is approached only in the very young (Fig. 1.8). The overall trend is a decrease with age from an average of 0.96 in the first decade to 0.77 in the ninth decade, that is, an age-related increase in structural mismatch. These structural changes would imply an increase in impedance mismatch in the human aorta with age. However, this may be explained by compensatory mechanisms of different age-related changes in stiffness of central and peripheral arteries leading to a reduction of stiffness gradient[41,42] resulting in reduced wave reflection. This was confirmed in the same study showing decrease in the magnitude of computed reflection coefficient at the aortoiliac junction with age.[40]

Since arteries are distensible conduits, the degree of matching in relation to energy transfer is determined by the geometric and elastic properties of the parent and branch vessels. Geometric and elastic properties determine vascular impedance, that is, the resistance of the vessel to pulsatile flow (see Section Vascular impedance). So, variability of change in vessel geometry or deviation from the optimal value can be offset by changes in elastic properties to increase the matching properties.[43] This phenomenon has been confirmed by theoretical studies showing that reflections at bifurcations that have large area ratios can only be minimized by larger increases in arterial stiffness of the branches in relation to the parent vessel.[44] This finding

is consistent with the generally accepted phenomenon that arterial stiffness[45] (and so pulse wave velocity,[46] discussed in detail in Section Wave speed and pulse wave velocity) increases with distance along the aortic trunk and peripheral conduit arteries. Although there are other significant factors such as geometric tapering,[45] it is tempting to speculate that, to some extent, the increase of arterial stiffness with distance along the arterial tree might be driven by the underlying optimality principles of minimization of energy cost functions as are inherent in the original concepts of Murray's Law[7,8] and common to branching structures present in nature.[39]

Structural and functional effects of arterial branching on pulsatility phenomena—implications for measurement of blood pressure

In the systemic and pulmonary vasculature, arterial branching generally implies that with each successive generation of branching, there is a decrease in individual vessel caliber, increase in total cross-sectional area, increase in relative wall thickness (ratio of wall thickness to diameter), and increase in structural arterial stiffness. In large conduit vessels, there is also a certain degree of geometric and elastic "tapering," that is, the vessel caliber decreases gradually with axial distance and the arterial wall becomes progressively stiffer.[45] The overall effect of the geometric and material property changes is that there is a graded change in geometric and elastic uniformity from the single uniform segment of the ascending aorta to the peripheral organs and body tissues.

FIGURE 1.8   Change of aortoiliac junction area ratio with age. Dashed line: value of area ratio for optimal branching of a symmetrical bifurcation (area ratio = 1.26). *Data from Greenwald SE, Carter AC, Berry Cl. Effect of age on the in vitro reflection coefficient of the aortoiliac bifurcation in humans. Circulation. 1990; 82(1):114−123.*
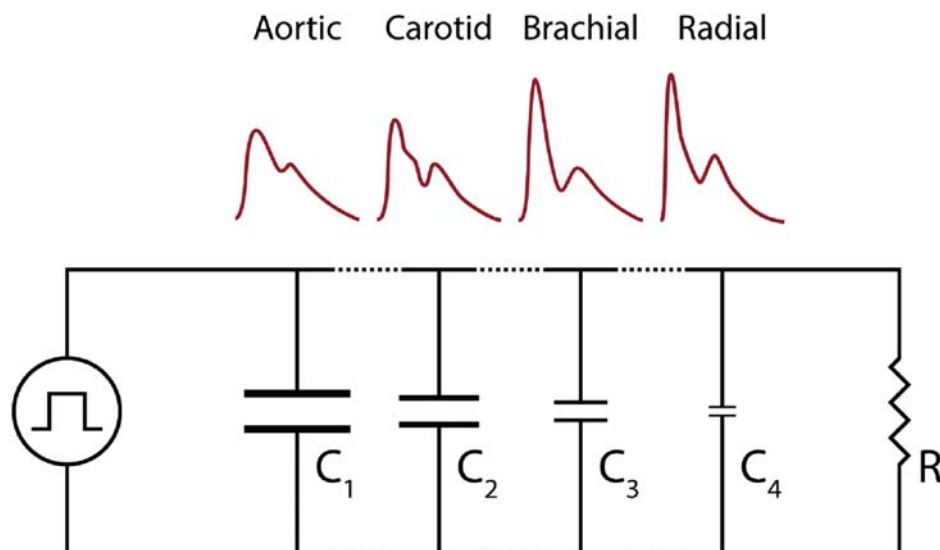
The stroke volume ejected into the aorta will be partitioned throughout the arterial tree according to the branch dimensions. Since the storage capacity of any segment will affect the specific relation of stored volume and associated change in pressure (as expressed by Eq. 1.1), any changes in relative volume at different generations of branching will manifest as a change in pressure. Thus, the relative changes in volume (ΔV) for a given resting volume (V_0) will normalize for the change in vascular caliber, and so the effect of change in relative storage capacity of vessels can be compared along the arterial tree. That is, when the storage capacity of the vessel (compliance, $C = \Delta V/\Delta P$) is normalized for the resting volume (V_0), the relative changes can be compared across different vessel sizes in terms of distensibility. Hence, from Eq. (1.1),

$$distensibility = \frac{\Delta V/V_0}{\Delta P} \qquad (1.14)$$

Given the geometric and material property changes, distensibility decreases from proximal to distal segments along the arterial tree. This reduction in distensibility (i.e., a reduction in the relative storage capacity of the distributed component of stroke volume) will inherently be associated with an increase in pulse pressure. Hence, the implication of this conceptual construct is that, in simple terms of storage capacity of vessels, the pressure pulse generated in the ascending aorta will be amplified along the arterial branching structure toward the periphery. As explained in Section Fundamental association of pulsatility and vascular structure and function, this explanation is confined to a "lumped parameter" representation. However, the distributed system can be represented by a series of essentially uniform segments with altered geometric and elastic properties as illustrated in Fig. 1.9 and still applies when considering effects of wave propagation (analogous to transmission lines, in which case the lumped parameter segments have an infinitesimally small "length").

The arterial vasculature exhibits reducing storage capacity with increasing distance from the heart, as well as changes in geometric and elastic material properties, which in turn affect the speed of the traveling pulse, wave transmission, and reflection. These phenomena constitute the basis of underlying mechanisms for the difference in pulse pressure between the central aorta and peripheral arteries. In large arteries, there is minimal change in mean pressure with distance from the heart. Hence, when there is a change in amplitude of the pressure in the presence of no change in mean pressure, by necessity there needs to be a change in shape of the pressure waveform. This change in waveform morphology can thus be exploited to obtain mathematical associations between central and peripheral pressure with knowledge of the transmission properties of the peripheral arterial vasculature. This has been successfully done to provide a means of estimating central aortic pressure from the calibrated peripheral arterial pulse[47] (see Chapter 2).

FIGURE 1.9 Schematic illustration of the changes in arterial compliance with distance from the heart (nominally aortic, carotid, brachial, and radial artery sites) and the resultant amplification of the pressure pulse $C_1>C_2>C_3>C_4$. This illustrates the concept of a tube in which the compliance per unit length decreases with distance (analogous to a nonuniform electrical transmission line in which characteristic impedance gradually increases with distance from the input). This concept can explain how the pulse pressure can increase with distance from the input while the mean pressure remains essentially the same.

Wave propagation phenomena—pulse wave velocity and arterial stiffness

Wave speed and pulse wave velocity

Wave speed

Pulsatility of pressure and flow in the arterial vasculature can be investigated by considering the role of material properties of a distributed system of elastic tubes on wave propagation. If an elastic tube is filled with fluid and a pressure pulse is applied to the fluid at the input of the tube, the disturbance, produced as a local expansion of the proximal wall, will travel downstream with a speed determined by the bulk modulus of the tube material and the density of the fluid. For any material, the bulk modulus is a description of the deformation characteristics, that is, of the stiffness of the material (volume deformation occurs due to an applied force and conservation of mass). Hence, if an increase in pressure (dP) on a material causes a relative decrease in volume (dV/V), the bulk modulus (K) is defined as

$$K = \frac{dP}{dV/V} \qquad (1.15)$$

[*Note*: this is similar to the ratio of stress/strain for material stiffness].

In an arterial segment, the applied force (dF) which moves the blood obeys Newton's Law of motion, where force is the product of blood mass (m) and acceleration (a),

$$dF = m \cdot a \qquad (1.16)$$

If the force is applied over a very short time interval, effect of movement of the proximal blood mass against the inertia of the downstream blood mass is to expand the size of the tube in the radial direction, and the volume of the blood mass which is accelerated can be assumed to constitute the same volume expansion of the vessel segment (dV).

Hence,

$$dF = \rho \cdot dV \cdot a \qquad (1.17)$$

where ρ is blood density.

Since the force (dF) is applied at the cross-section of the tube with an area A, dF can also be written as $dP \cdot A$. Hence, from Eq. (1.17),

$$a = \frac{dP}{dV} \frac{A}{\rho} \qquad (1.18)$$

If the blood mass is assumed to be accelerated over a small distance Δx, and the blood mass is contiguous with the vessel wall, the wall will have the same acceleration as

the blood mass. Both sides of Eq. (1.18) can also be multiplied by Δx,

$$a \cdot \Delta x = \frac{dP}{dV} \frac{A \cdot \Delta x}{\rho} \qquad (1.19)$$

The product $A \cdot \Delta x$ is the volume (V) of the blood mass being accelerated. Since the material properties are related to the pressure/volume relationships of the elastic tube (arterial segment), Eq. (1.15) can be applied to Eq. (1.19),

$$a \cdot \Delta x = \frac{K}{\rho} \qquad (1.20)$$
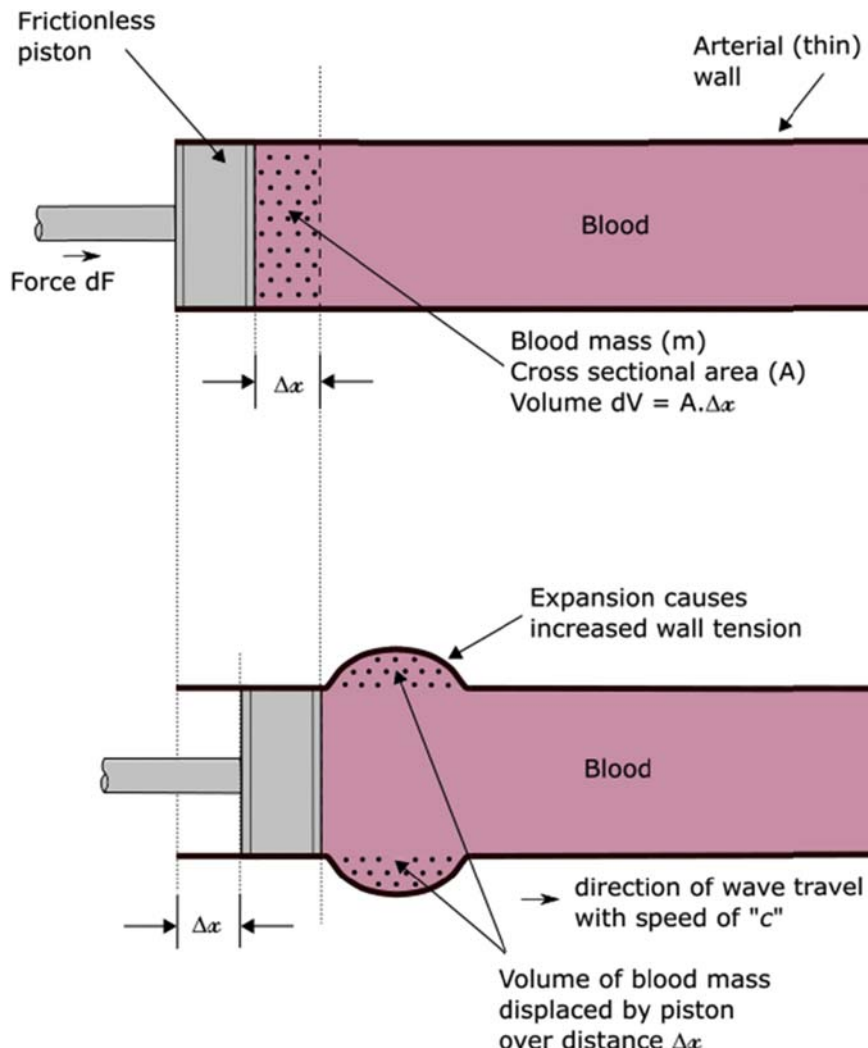
The term $a \cdot \Delta x$ has units of velocity squared. Hence, replacing $a \cdot \Delta x$ by "c^2," and taking the square root of both sides,

$$c = \sqrt{\frac{K}{\rho}} \qquad (1.21)$$

The term c is designated as "wave speed" (c is conventionally used for this quantity as it refers to "celerity," meaning "velocity" or "swiftness of movement"; it is the basis of the term "acceleration"—change in celerity), a scalar quantity determined by the bulk modulus (overall stiffness) of the vessel wall and blood density. The stiffness of the wall will determine the wall tension due to the applied pressure (Laplace's Law, Eq. 1.9). The wall tension in turn determines the restoring force against the fluid mass that consists of the inertial opposition to the same restoring force supplied by the wall tension.

The above conceptual derivation of the origin of wave speed is illustrated in Fig. 1.10.

Eq. (1.21) is the classical representation of wave speed in a medium. In a closed system, such as the elastic arterial conduits, the disturbance (or wave) generated by the applied pressure at the aortic root can travel along the arterial wall (an elastic material) or through the blood (which is an incompressible fluid). In both cases, the value of K is not the same, being much higher for blood ($\sim 2.6 \times 10^8$ N/m^2) than for arteries ($\sim 10.6 \times 10^4$ N/m^2). However, blood is essentially incompressible. This implies that compression waves would involve very little energy (it is much easier for the heart to expand the aorta, than to compress the blood therein). Therefore, for practical purposes, the relevant K for the arteries is that arising from the arterial wall and, hence, the relevant velocities are in the order of 10 m/s. (In the blood the disturbance travels at the speed of sound, approximately 1570 m/s; this high-speed transmission of a system disturbance is a fundamental property of the ballistocardiogram, which can also provide hemodynamic information.[48])

FIGURE 1.10 Schematic illustration of a pulse wave generated in the wall of an elastic vessel (artery). A force (dF) applied by a piston to a small mass of blood (m) that is contiguous with the arterial wall will displace the mass and the wall with the same acceleration. Since blood is incompressible in relation to the elastic wall, and it also has inertia which opposes movement of the total blood column, the displacement (Δx) for the blood mass would be accommodated by expansion of the arterial wall. The amount of expansion is determined by the wall material properties and the wave speed determined by both the wall material properties and the density of the blood mass on which the force acts to displace the wall (see text for details).

When considering blood in an elastic tube, Eq. (1.21) is recast as

$$c = \sqrt{\frac{VdP}{\rho dV}} \qquad (1.22)$$

which is the well-known Bramwell–Hill equation, derived independently by Bramwell and Hill[49] and Frank.[50]

Since arteries mainly expand in the radial direction, changes in volume (dV) are proportional to changes in area or to 2 times change in radius (r) and so the quantity $VdP/$ dV ($dP/(dV/V)$) can be replaced by $dP/(2dr/r)$. From Laplace's Law (Eq. 1.9), pressure changes (dP) can be expressed in terms of circumferential stress (σ) at specific values of wall thickness (h) and r, that its, $dP = d\sigma(h/r)$. The incremental elastic modulus (E_{inc}) is defined as the ratio of the change of stress ($d\sigma$) to change of strain ($d\varepsilon$) at the specific operating point in the stress–strain curve, that is, at the specific value of r. Hence, $d\varepsilon = dr/r$ and so the quantity VdP/dV can be replaced by $E_{inc}.h/2r$. So, the Bramwell–Hill equation of Eq. (1.22) is recast as the well-known Moens–Korteweg equation,

$$c = \sqrt{\frac{E_{inc}h}{2\rho r}} \qquad (1.23)$$

The main assumptions for the above derivation of the wave speed are that the tube is thin walled ($h << r$), that the increase in volume causes small changes in vessel cross-sectional area (A) and wall thickness (h) and that blood is incompressible (no change in density ρ).

As described in Section Pressure dependence of arterial stiffness: an essential ingredient for optimal arterial design, the stiffness of the arterial wall is essentially nonlinear, suggesting that the value of E_{inc} varies with the specific relation of the tension−radius curve and the wall tension determined by the Laplace relation with pressure and radius (Eq. 1.9). Hence, since E_{inc} is a function of pressure, ($E(P)$), c will also depend on pressure ($c(P)$). The implication of this is that the wave speed will change during the time in which pressure changes during the cardiac cycle. Although this can be demonstrated,[51,52] the stress−strain curve during small pressure excursions can be reasonably approximated by a straight line, making E a constant value. This is an important consideration when considering the application of oscillatory analysis for determining vascular impedance from pulsatile pressure and flow wave decomposition (See Sections Oscillatory pressure and flow: impedance and Input impedance), since linearity considerations also take into account that true wave speed is determined by high frequency oscillations.[53]

Pulse wave velocity

At first glance, the distinction between wave speed (c) and pulse wave velocity (PWV) in the context of vascular assessment might seem a semantic exercise. c is a fundamental (scalar) parameter determined from biophysical relationships for wall elastic properties and conduit dimensions at a specific location and under specific loading conditions (particularly pressure), that is, a regional property over an infinitesimally small axial distance (note there is no distance or length quantity in Eq. 1.23). The term "velocity" denotes a vector quantity (with magnitude and direction) whose magnitude is the value of the wave speed. Hence, PWV is strictly a vector quantity, and in vascular assessment it is generally considered as a measured variable of the speed of the traveling pulse along the arterial path

length. It is commonly obtained by measuring the pulse transit time (PTT) over a given distance (d),

$$PWV = \frac{d}{PTT} \qquad (1.24)$$

Clearly, if the arterial segment is uniform over a distance d, then, $c = PWV$ (more specifically, $PWV = U + c$, where U is blood velocity; since $U << c$, particularly at the end of diastole where PTT is usually measured at the foot of the pulse, U is generally ignored). However, PWV is usually measured over long path lengths (e.g., carotid-to-femoral) where there is substantial variability of all arterial quantities in Eq. (1.23). Notwithstanding these caveats, it is generally accepted that in large conduit arteries, the quantity h/r is generally preserved.[17] Furthermore, any irregularity in wall thickness would generally be in intimal changes, and these layers have a much lower stiffness than the arterial media, which is the main vessel component that determines the mechanical properties of the arterial wall. Hence, although an approximation, any measured changes in PWV would indicate that they are mainly due to medial properties that affect arterial stiffness. These concepts have given rise to the important surrogate relationship of

$$arterial\ stiffness \propto PWV \qquad (1.25)$$

Notably, the notion that PWV is a (structural) metric of arterial stiffness does not imply that PWV is the *only* arterial stiffness marker (there is no "=" sign in Eq. 1.25).[54] Hence, care should be taken to always define *which* arterial stiffness metric is reported.

Pulse wave velocity and pressure-independent arterial stiffness index beta (β)

The qualitative relationship of Eq. (1.25) is generally used to quantify changes in arterial stiffness with age, arterial site, or blood pressure. However, because of the pressure dependency of arterial stiffness (and therefore of PWV), it will not be possible to distinguish a difference in stiffness due to structural arterial wall properties (that is, intrinsic arterial stiffness) or due to a change in pressure. It is important to note that a change in stiffness due to pressure would be on the *same* pressure−volume curve, whereas a change in intrinsic stiffness would imply a *different* curve. Detailed analysis is described in Box 1.1.

BOX 1.1 Pressure-independent index of arterial stiffness

To a good approximation, pressure (P) has an exponential relationship with diameter (D) of the form,[25]

$$P = P_{ref}e^{\beta_0(D-D_{ref})/D_{ref}} \tag{1.26}$$

or

$$\ln P = \beta_0\left(\frac{D}{D_{ref}} - 1\right) + \ln P_{ref} \tag{1.27}$$

where β_0 is the index that defines a specific stress–strain curve of the wall stiffness characteristics, and P_{ref} and D_{ref} are reference pressure and diameter, respectively. Hence, if there are two pressure points on the curve (such as systolic (P_s) and diastolic (P_d) pressure associated with systolic (D_s) and diastolic (D_d) diameter), the index β_0 (a measure of intrinsic stiffness) can be obtained by the slope of the logarithmic relationship from Eq. (1.27):

$$\beta_0 = \ln\left(\frac{P_s}{P_d}\right)\bigg/\left(\frac{D_s}{D_d} - 1\right) - \ln\left(\frac{P_d}{P_{ref}}\right) \tag{1.28}$$

This equation is very often simplified by omission of the second term:

$$\beta = \ln\left(\frac{P_s}{P_d}\right)\bigg/\left(\frac{D_s}{D_d} - 1\right) \tag{1.29}$$

Since diameters are not readily measured, use is made of the Bramwell–Hill equation for PWV (Eq. 1.22), and assuming that the volume change occurs only in the radial direction (that is, $\Delta V = 2\Delta D$), where $\Delta D = D_s - D_d$,

$$PWV^2 = \frac{D_s(P_s - P_d)}{2\rho(D_s - D_d)} \tag{1.30}$$

By combining Eqs. 1.29 and 1.30,

$$\beta = \ln\frac{P_s}{P_d} \cdot PWV^2 \cdot \frac{2\rho}{P_s - P_d} \tag{1.31}$$

Hence, since *PWV* can be measured, usually over path lengths from the carotid to the femoral artery, and with measurement of systolic and diastolic pressure, a pressure-independent index of arterial stiffness can be obtained. This has now been accepted in the form of a cardio-ankle vascular index (*CAVI*), where *PWV* is taken along the heart-to-ankle arterial bed.[26] *CAVI* was further improved into $CAVI_0$ by using β_0 instead of β as a starting point (Eq. 1.29 vs. 1.28; $P_{ref} = 100$ mmHg), and by referring the calculations to diastolic pressure (P_d),[27]

$$CAVI_0 = \beta_0 = \frac{PWV^2 \cdot 2\rho}{P_d} - \ln\left(\frac{P_d}{P_{ref}}\right) \tag{1.32}$$

Pulse wave propagation and oscillatory phenomena

The periodic nature of the cardiac cycle enables the analysis of the time-dependent oscillations of pressure and flow in terms of each frequency component of the signal. The fundamental frequency is determined by the time of the cardiac cycle and harmonic components are integer multiples of the fundamental frequency. The complex time-varying signal is considered as a sum of simple time-varying sinusoids at harmonic frequencies with different magnitudes and phase (see Section Oscillatory pressure and flow: impedance). This then allows the quantification of the change in magnitude and time delay of each frequency component. That is, the propagation of the complex wave can be analyzed in terms of propagation coefficients as a function of frequency, consisting of the amount of damping and delay as a function of distance. The delay term is related to the pulse wave velocity of each frequency component. Box 1.2 gives an example of the frequency analysis for a sinusoidal signal of a pressure wave (*P(t)*).

BOX 1.2 Frequency analysis of pulse wave propagation

For description of oscillatory waves as sinusoidal functions, use is frequently made of Euler's formula,

$$e^{-j\omega t} = \cos(j\omega) + j\sin(j\omega) \tag{1.33}$$

where ω is the oscillation frequency in rad/s and $j = \sqrt{-1}$.

Hence, a time-varying sinusoidal frequency component of a pressure wave of amplitude Po is completely described as

$$P(t) = Po \cdot e^{-j\omega t} \tag{1.34}$$

For a uniform arterial segment of length l, the sinusoidal wave from the input of the tube along its length undergoes modification of the amplitude; that is, it is modified in time (t) and space (x).

This can be concisely expressed as

$$P(t, x) = P(t) \cdot e^{-\lambda x} \tag{1.35}$$

where λ is the propagation coefficient, defined as

$$\lambda = a + jb \tag{1.36}$$

where a is the attenuation constant (how much of the traveling amplitude is damped due to viscous losses for blood and wall), and b is the phase constant (the "time delay" of the particular frequency component). [*Note*: with x in meters, $a = 1\ \text{m}^{-1}$ corresponds to an attenuation to $1/e \approx 37\%$ of original amplitude per meter; $b = 1$ rad/m corresponds to a phase shift of 1 rad (~ 57 degrees) per meter.]

Each frequency component will travel at a finite wave speed (c), hence,

$$c = \frac{\omega}{b} \tag{1.37}$$

and

$$P(t) \cdot e^{-\lambda x} = (Po \cdot e^{-ax}) \cdot e^{j\omega\left(t - \left(\frac{x}{c}\right)\right)} \tag{1.38}$$

where Po is the magnitude at the input of the tube and c is the wave velocity of the wave of frequency ω.

The above description is for a uniform arterial segment with no terminal reflection. Hence, the value of the wave speed in Eq. (1.37) is the true wave velocity, which can be reliably estimated from the foot-to-foot time delay of pressure waves.

Forward and backward waves

Pressure (P) and flow (Q) waves can be described as a combination of forward (P_f, Q_f) and backward (reflected) waves (P_b, Q_b), such the reflected waves add to pressure and subtract from flow,

$$P = P_f + P_b \tag{1.39}$$

$$Q = Q_f + Q_b \tag{1.40}$$

The relationship of P_f and Q_f, and P_b and Q_b (Q_b has a negative sign) is determined by the characteristic impedance (Z_c [See Section Vascular impedance and Chapter 3]), such that

$$Z_c = \frac{P_f}{Q_f} = \frac{P_b}{-Q_b} \tag{1.41}$$

This allows calculation of forward and backward arterial pressure waves from measured pressure and flow and

characteristic impedance calculated from frequency- or time-domain analysis of pressure and flow waves (see Chapters 3 and 11),

$$P_f = 0.5(P + Z_c \cdot Q) \tag{1.42}$$

$$P_b = 0.5(P - Z_c \cdot Q) \tag{1.43}$$

Thus, from the above equations, measured pressure and flow waves can be decomposed into forward and back waves. For sampled waveforms, the equations are applied at each sample point.

Vascular impedance

Steady pressure and flow: resistance

The obligatory intermittent ventricular ejection, which occurs for only part of the cardiac cycle, produces pulsatile flow input to the aorta. The elastic properties of the arterial

tree provide a buffer for the intermittent pulsations and storage of blood in the presence of arterial wall tension, such that a positive head of pressure is established in the arterial vasculature to provide potential energy for continuous perfusion of peripheral microvascular beds. At any location in the arterial tree, the flow is determined by the arterial pressure and the resistance to flow due the downstream effects of the blood vessels. (More precisely, the driving pressure is the difference between arterial and central venous pressure, but venous pressure in the systemic vasculature is very much less than in arteries [order of 5%], so it is usually ignored, although this is not the case for the pulmonary vasculature as it operates at lower arterial pressure). Hence, since pulsatility in pressure and flow involves time-varying phenomena, the resistance to flow can be described as the relation of pressure and flow as time-varying quantities.

Since the duty cycle of the heart as a pump can be considered periodic (not all cardiac cycles have the identical duration, but the variability is generally small in normal conditions), the characteristics of the arterial vasculature that determine relationships of pressure and flow can be completely described by the values of pressure and flow as a function of time in a single cardiac cycle. For pressure $P(t)$ and flow $Q(t)$, and a cardiac cycle duration of T_c, the mean values (P_m, Q_m) can be calculated as

$$P_m = \frac{1}{T} \int_0^{T_c} P(t) \cdot dt \qquad (1.44)$$

$$Q_m = \frac{1}{T} \int_0^{T_c} Q(t) \cdot dt \qquad (1.45)$$

The pulsatile component $P_p(t)$ and $Q_p(t)$ can be obtained by subtracting the mean value from the original signal,

$$P_p(t) = P(t) - P_m \qquad (1.46)$$

$$Q_p(t) = Q(t) - Q_m \qquad (1.47)$$

The impedance to flow is calculated as the ratio of pressure and flow. Hence, for the mean values, the resistance (R) is

$$R = \frac{P_m}{Q_m} \qquad (1.48)$$

Arterial properties that determine relationship of steady pressure and flow

Eq. (1.48) gives the value of resistance as the ratio of mean pressure to mean flow. Thus, if pressure and flow are measured at any specific location in the arterial tree, the ratio quantifies the total resistance to flow downstream from the point of measurement. However, this is a computed value and does not describe arterial properties

in an explicit form. The resistance to flow occurs in accordance with the laws of motion of fluid due to an applied force. For a fluid of viscosity μ flowing due to a pressure difference between inlet and outlet of a uniform segment of conduit of length l and internal radius r, the ratio of pressure to flow, designating the resistance (R) of the segment, is given as

$$R = \frac{8\mu l}{\pi r^4} \qquad (1.49)$$

This relation assumes laminar, stationary flow (no turbulence), a Newtonian fluid (constant viscosity), no slip at the wall, and a tube long enough so that the laminar flow is fully developed. Fluid flow can then be calculated for a measured pressure gradient, tube dimensions, and fluid viscosity; this relationship is known as the Hagen−Poiseuille equation[55] (page 10 of Ref. [26]).

Because of the dependency of fluid resistance on the inverse of the fourth power of the radius, the large arteries in the arterial vasculature contribute very little to the resistance to flow. This also illustrates the powerful role of the small vessels in the control of peripheral resistance, such as arterioles being able to modulate vessel caliber under active control of smooth muscle tone[55] (page 36 of Ref. [26]).

For a symmetrical bifurcation obeying Murray's Law of optimality of branching, using Eq. (1.48), the total resistance of the branches increases to 1.26 times the resistance of the parent vessel of equal length. This value is also the optimal area ratio based on maximal energy transmission at branch points (obtained by simple algebraic addition of the individual branch area rations, corresponding to the addition of admittance of the branch, or inverse of resistance). Although not all branch points in the arterial vasculature are theoretically optimally matched, there is still a general increase in cross-sectional area in large vessels with branching generation. However, in small vessels such as arterioles, the caliber is determined by active smooth tone, such that the arteriolar regions become the sites of modulation of maximal resistance, and as a consequence the site of modulation of maximal reflection that would influence pulse pressure.[4]

Oscillatory pressure and flow: impedance

For the pulsatile component, the ratio of the time-varying signals cannot be computed to describe resistance to pulsatile flow. That is, the division of pressure at a particular time point cannot be divided by a flow value at the same time point, as a time-varying resistance does not strictly have any real physiological meaning, and in addition, during diastole, when flow is zero, resistance would be infinite. Furthermore, the rapid changes in flow would cause rapid changes in resistance, and there are no plausible

biological mechanisms that would cause such rapid changes in vascular properties.

For the pulsatile component, use is made of the periodic nature of the signal to decompose the time-varying signal into its sinusoidal harmonic components. From the Fourier theorem, any time-varying signal can be expressed as a sum of a series of sinusoidal waves, whose period depends on the time over which the signal is sampled. Hence, for the cardiac cycle, the first harmonic sinusoid would have the period of the cardiac cycle (T_c), and so the frequency would be ($1/T_c$). For a heart rate of 60 beats, the cycle period would be 1 s and the fundamental (first harmonic) frequency (ω_0) would be 1 Hz. Box 1.3 gives formal expressions for the frequency analysis and its use for calculation of impedance as a function of frequency.

Aortic input impedance is a complete description of the pulsatile load on the left ventricle, and so can also describe the fundamental relationships of ventricular−vascular coupling. Fig. 1.11 shows the comparison between the human and rabbit aortic impedance, with the energy spectrum of aortic flow. The human heart operates against a higher relative impedance than the rabbit heart, suggesting a relatively higher mismatch in ventricular vascular coupling.[56] For further discussion regarding aortic input impedance and its derivation, the reader is referred to Chapter 3.

BOX 1.3 Frequency analysis and impedance calculation

The conversion of the time-varying signals is done by a Fourier transform, which enables the time-varying $P_p(t)$ and $Q_p(t)$ signals to be expressed in the frequency domain.

Any periodic signal $x(t)$, with period T_c, can be expressed as

$$x(t) = \frac{1}{T_c} \sum_{n=-\infty}^{\infty} X_n e^{jn\omega_0 t} \tag{1.50}$$

where

$$X_n = \int_0^{T_c} x(t) e^{-jn\omega_0 t} dt \tag{1.51}$$

$j = \sqrt{-1}$ and $X_n(\omega)$ is a complex quantity which represents a sine wave at a frequency of $n\omega_0$. That is, for the series of harmonics (n = 1, 2, 3 ...), X_n has a magnitude $|X|_n$ and phase angle ($arg(X)_n$).

Hence, for the respective pressure and flow representation,

$$P(\omega) = |P|_n \cdot \angle arg(P)_n \quad (n = 1, 2, 3, ...) \tag{1.52}$$
$$Q(\omega) = |Q|_n \cdot \angle arg(Q)_n \quad (n = 1, 2, 3, ...) \tag{1.53}$$

where the symbol $\angle$ designates the phase angle representation of the complex quantity.

As in the case for the mean value of $P(t)$ and $Q(t)$ to determine resistance, similarly, the ratio of $P(\omega)$ and $Q(\omega)$ is used to determine the resistance at each specific harmonic component. In analogy with electrical circuits for oscillating voltage and current in the frequency domain, the ratio of $P(\omega)$ and $Q(\omega)$ is designated as impedance, $Z(\omega)$, a complex quantity with a modulus ($|Z|_n$) and phase ($arg(Z)_n$),

$$Z(\omega) = \frac{P(\omega)}{Q(\omega)} \tag{1.54}$$
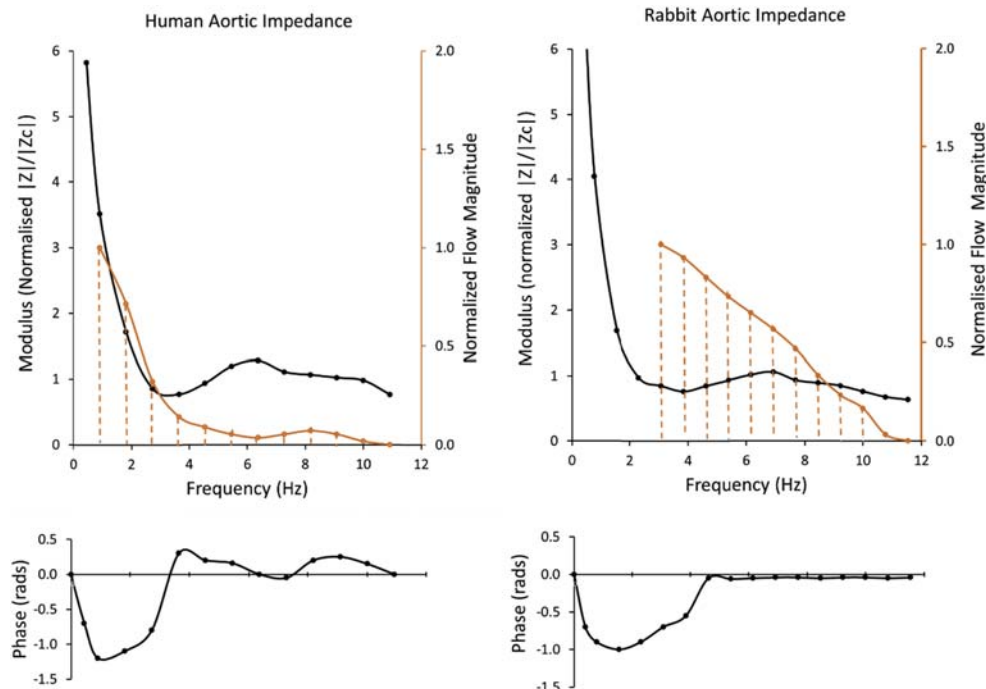
Hence,

$$|Z| = \frac{|P|n}{|Q|n} \tag{1.55}$$
$$arg(Z)_n = arg(P)_n - arg(Q)_n \tag{1.56}$$

The impedance spectrum consists of a plot of $|Z|n$ and $arg(Z)_n$ as a function of frequency for each harmonic (n = 1,2,3, ...). The value of impedance at zero frequency, that is, for steady pressure and flow, is the value of resistance (R) determined from mean pressure and flow and a phase angle of zero (Fig. 1.11).

FIGURE 1.11 Vascular impedance determined from frequency components of aortic pressure and flow (i.e., aortic input impedance) in humans and rabbits and shown as modulus and phase as a function of frequency. The impedance modulus (Z) is normalized by the characteristic impedance (Zc) computed from the average moduli between 6 and 10 Hz. The impedance spectrum is quite similar for the human and rabbit, with the modulus falling rapidly at low frequencies and the phase having a negative value until around the frequency of impedance minimum. Negative phase indicates a capacitive load, such that flow leads pressure. The orange stippled curve shows the energy in the aortic flow normalized by the value for first harmonic. The overlay of these curves on the impedance curves illustrates the different degree of matching of ventricular–vascular coupling. In the rabbit, most of the flow energy is in the low impedance part of the spectrum, whereas in the human it is in the descending limb and at relatively higher impedance value, suggesting a less efficient matching compared to the rabbit. *Human data obtained from Murgo JP, et al. Aortic input impedance in normal man: relationship to pressure wave forms. **Circulation**. 1980; 62(1):105–116; Rabbit data obtained from Avolio, AP, et al. A comparative study of pulsatile arterial hemodynamics in rabbits and Guinea pigs. **Am J Physiol**. 1976; 230(4):868–875.*

Arterial properties that determine relationship of pulsatile pressure and flow

Due to the periodic nature of cardiac contraction, the associated time-varying pressure and flow in arteries can be considered as periodic oscillations. Just as the vessels downstream of point of measurement present a resistance to steady (i.e., nonpulsatile) flow due to a pressure gradient (Eq. 1.48), they also present an opposition to oscillatory flow. For steady flow, the relevant quantities are the magnitudes of means pressure (P_m) and mean flow (Q_m), and for oscillatory flow they are the magnitudes of the oscillations of $P(t)$ and $Q(t)$. Because, by definition, oscillatory flow implies a change of velocity with time, and since a blood mass is accelerated in an elastic conduit with capacity for volume storage due to its compliance (C), the opposition to flow is due to the blood inertia of the mass (L) and also due to the storage capacity. That is, the opposition to flow will be high for a high inertia and low for a high compliance. In analogy with similar conceptual models of

electrical transmission lines, the resistance to oscillatory flow due to the physical properties is defined as the characteristic impedance (Z_c) and (for large vessels and inviscid fluid) is described as

$$Z_c = \sqrt{\frac{L}{C}} \qquad (1.57)$$

For an arterial segment of length *l*, wall thickness *h*, radius *r*, wall material stiffness *E*, and blood density *ρ*, the value of the tube compliance *C* can be computed as

$$C = \frac{3\pi l r^3}{2Eh} \qquad (1.58)$$

Alternatively, *C* can be estimated as *ΔV/ΔP*. When impedance is determined from frequency components of pressure and flow (Eq. 1.54), Z_c is estimated from the average of the high harmonics of the spectrum of impedance modulus. For the human arterial system, usually harmonics 6–10 are used (see Chapter 3).

Effects of blood viscosity and pulsatile flow: Womersley's alpha

When fluid flows in a tube due to a pressure gradient, the rate of flow is determined by the properties of the fluid (density, viscosity) and tube dimensions (diameter, length). For a constant pressure gradient, flow determined by these properties is steady, and for a long tube it will be laminar flow with a parabolic profile. That is, it has maximum velocity at the center of the tube and low velocity close to the wall. In this case, the relation between the steady pressure gradient and flow would be quantified as a resistance (Eq. 1.48). However, if the pressure gradient varies with time, the relationship between the pressure and flow will be determined by the frequency of oscillation and properties of blood and tube dimensions, with the values of impedance converging to Eq. (1.48) for a frequency of zero. This advanced analysis is described in Box 1.4.

Input impedance

For an arterial segment, the input impedance (Z_{in}) would be similar to the characteristic impedance (Z_c) if it were uniform and had a matched terminal impedance (Z_t). This relationship is defined by a reflection coefficient (Γ),

$$\Gamma = \frac{Z_c - Z_t}{Z_c + Z_t} \tag{1.63}$$

Eq. (1.63) suggests that for a uniform arterial segment, the amount of wave reflection is determined by the degree of impedance matching.

An important consideration when addressing vascular impedance is that each frequency component of the pulse wave undergoes transformation of its amplitude along the traveled distance, as described by Eqs. 1.33–1.38, where the change in amplitude and delay on the traveled path is determined by the propagation coefficient λ.

BOX 1.4 Womersley's theory of pulsatile blood pressure and flow in arteries

Womersley's solution of the Navier–Stokes equations of fluid flow in circular boundaries enabled the computation of fluid flow profiles due to an oscillating pressure gradient[3] and by knowledge of vessel mechanical and geometric properties. For a sinusoidal oscillation of frequency ω, the closed-form solutions involved a nondimensional parameter (alpha, α) and a series of Bessel functions, which modify the characteristic impedance as a function of alpha values, Womersley's alpha (α) is defined as

$$\alpha = r\sqrt{\frac{\omega\rho}{\mu}} \tag{1.59}$$

where r is luminal radius, ω is frequency of oscillation, ρ is fluid density, and μ is the fluid viscosity.
    (Note the similarity of the nondimensional parameter (α) with the nondimensional Reynolds number (Re)):

$$R_e = \frac{\rho VD}{\mu} \tag{1.60}$$

where ρ is fluid density; V is fluid velocity; D is linear dimension (diameter for circular boundaries); μ is fluid viscosity.
    "V" in the numerator of the expression for Re corresponds to "ω" in the expression for α. Hence, as Re is a critical parameter for characterization of steady flow phenomena, similarly, α is a critical parameter for characterization of oscillatory flow phenomena.
    The characteristic impedance (Eq. 1.57) is modified as[59]
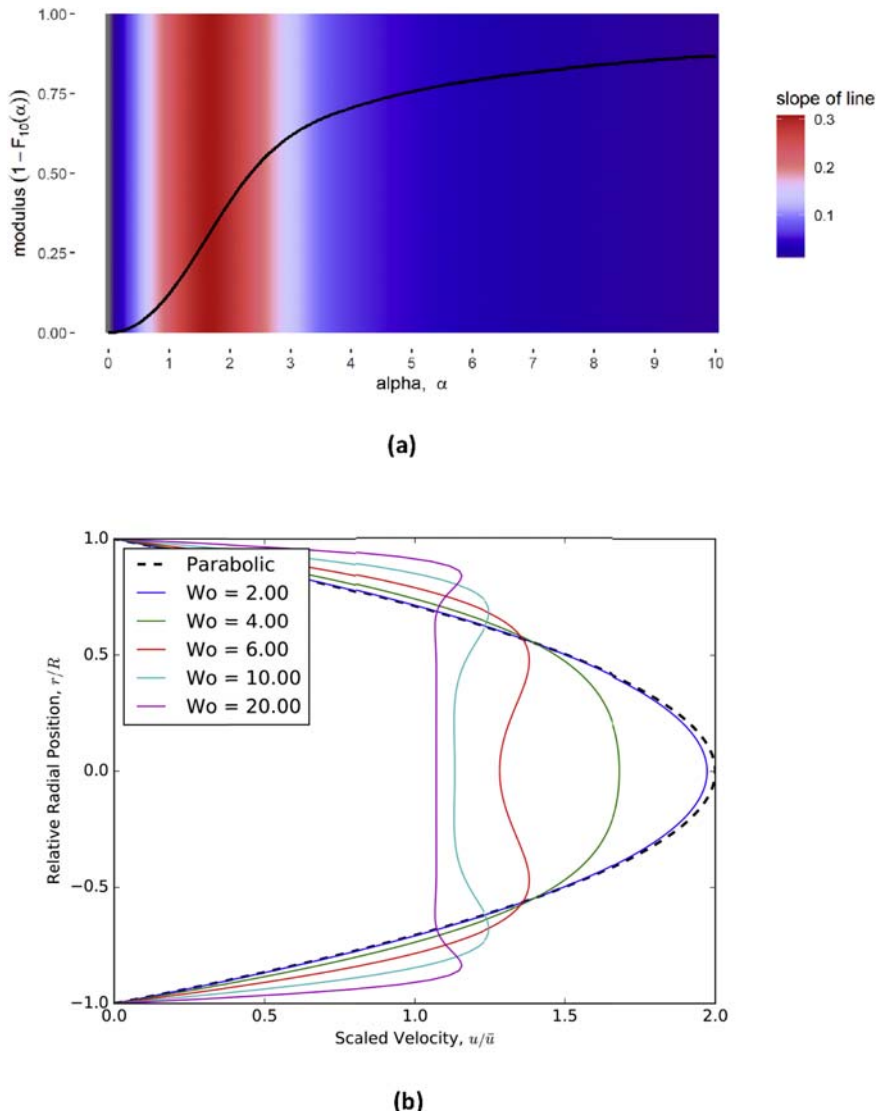
$$Z_c = \left(\frac{L}{C}\right)^{1/2} \cdot (1 - F_{10})^{-1/2} \tag{1.61}$$

where

$$1 - F_{10} = 1 - \frac{2J_1\left(\alpha j^{\frac{3}{2}}\right)}{\alpha j^{\frac{3}{2}} J_0\left(\alpha j^{\frac{3}{2}}\right)} \tag{1.62}$$

and J_0 is Bessel function of the first kind of zero order, J_1 is Bessel function of the first kind of first order, α as in Eq. (1.59); $j = \sqrt{-1}$.
    The values of function $(1-F_{10})$ are plotted as a function of α (Fig. 1.12A), showing that the greatest effect is for range of low values of $\alpha < 3$ and values of α affect the cross-sectional flow profile (Fig. 1.12B).

(a)

(b)

FIGURE 1.12 (A) Function of $1-F_{10}$ as a function of alpha (α). Maximum change occurs for α values below 3. This suggests the combination of vessel size (radius), frequency (heart rate), and blood properties (density and viscosity) that give values of α in the red region will affect the dynamic relationship of pressure and flow. (B) The flow profiles are also affected by the values of α (designated as Womersley's Number [Wo] in the above figure). Profiles are shown for normalized tube radius (r/R) and normalized relative to mean flow ($u/\bar{u}$). The parabolic flow corresponds to $\alpha = 0$, where the viscosity is the main determinant of the flow profile. This is generally maintained for low values of α. As α increases, blood inertia begins to dominate in the central part of the lumen and at high values of α the flow undergoes marked changes to a flat profile, with inertia being the main determinant and the effects of viscosity are seen at the boundary layers adjacent to the wall. Part (B) of the figure is used under Creative Commons License [https://commons.wikimedia.org/w/index.php?curid=54810155 (Rudolf Hellmuth)].

For a tube of length l and with a terminal impedance Z_t, the input impedance Z_{in} is defined by the characteristic impedance (Z_c), the reflection coefficient (Γ), and the wave propagation coefficient (λ),

$$Z_{in} = Z_c \cdot \frac{1 + \Gamma e^{-2\lambda L}}{1 - \Gamma e^{-2\lambda L}} \qquad (1.64)$$

The equations describe the impedance of arterial segments in a closed form in terms of physical geometric and material properties. Thus, with connections of uniform segments in the form of a distributed and branching tree structure, it is possible to investigate spatial and temporal relationships of pulsatile pressure and flow.[59-62]

System linearity

Eq. (1.54) suggests that each frequency component of flow is scaled by a single value of impedance to obtain a single frequency component of pressure. That is, a specific frequency component of flow is uniquely related to the pressure component of the same frequency and no other pressure component. This is an important characteristic of linear systems and is a fundamental assumption for impedance calculation for pulsatile pressure and flow in arteries.[63] The fact that a single frequency component of flow can be related to a single frequency component of pressure assumes that the system is time invariant. That is, during the cardiac cycle (the interval of time for which pulsatile pressure and flow are obtained and analyzed), all properties of the system remain constant. Since a determinant characteristic of pulsatile pressure and flow is arterial stiffness, the implication is that during the cardiac cycle, when pressure increases between the nadir (diastolic pressure) to the peak (systolic pressure), the elastic properties remain constant and there is no change in arterial stiffness. However, as was explained in Section Elastic vessels, the pressure-dependence of arterial stiffness is an inherent property of arterial structure and a fundamental property of arterial design, hence it would seem counterintuitive and contradictory to assume a constant value of arterial stiffness during the time when there is a change in pressure, unless there are justifiable assumptions.

Intermodulation: justification for assumptions of system linearity

The nonlinearity of the system due to a pressure-dependent elastic modulus of the arterial wall would lead to a phenomenon known as intermodulation. That is, if a single sinusoidal frequency of flow were used as the input at the aorta, the resulting pressure would be a single sinusoid at the same frequency but would also include components of differing amplitudes at different frequencies. This important characteristic was examined in some early studies to ascertain whether arterial impedance could indeed be computed from harmonic components of pressure and flow and be able to describe the system with reasonable and meaningful physiological application.[63] When the canine arterial system was perturbed with sinusoidal pumps, power at intermodulation frequencies was found to be very low (around 2%).[64] The fact that it was able to be detected suggests the presence of nonlinearity and it is consistent with the pressure dependency of arterial stiffness. The rather small effect suggests that the excursion of pressure during the cardiac cycle is relatively small compared to the entire range of operating pressure of arteries, and so during this interval, the stress/strain curve of the arterial wall can be approximated with a linear slope.

Nonlinearity in arterial models

Although the assumptions of linearity have been able to facilitate the development of early arterial models using closed-form expressions for hemodynamic relationships[59,61] or physical circuit elements,[62] more recent models that are based on iterative numerical solutions of basic fluid flow equations can readily include features of system nonlinearity by making arterial elasticity dependent on arterial pressure.[60]

Relation between characteristic impedance and pulse wave velocity

If a fluid of density ρ flows with velocity v in a tube and the end is suddenly closed, there will be a change in velocity (Δv) and an associated pressure change (ΔP). The pressure wave will travel in the tube at a wave speed (c) determined by the tube and fluid properties. The relationship is

$$\Delta P = c\rho\Delta v \qquad (1.65)$$

This is the classic water hammer formula (which commonly manifests as a sudden noise in pipes following rapid closure of a tap).

Since volumetric flow $Q = A \cdot v$, where A is cross-sectional area, and characteristic impedance Z_c is the ratio of $\Delta P/\Delta Q$, the relation between impedance and wave speed is

$$c = Z_c A/\rho \qquad (1.66)$$

Eq. (1.66) implies that local wave speed can be determined by computation of impedance by measured pressure and flow. It also implies that if impedance is computed using flow velocity (cm/sec) rather than volume flow (cm^3/sec), (that is, scaled by area), the magnitudes are scaled only by the reciprocal of blood density, and if expressed in CGS units, they are approximately equal (since blood density is 1.06 g/mL). Scaling impedance by area also enables comparisons of impedance spectral patterns in different arterial districts and in different animals of different sizes[58] (since arterial blood pressure and flow velocity do not scale to body size or vessel caliber).

Pressure and flow relationship in the time domain

The periodicity of cardiac contractions has enabled the characterization of the pressure and flow and impedance in the frequency domain, with the assumption of system stationarity. However, since energy is carried by the combination of pressure and flow as time-varying quantities, energy-based analysis can also be used to characterize wave propagation, which does not require any periodicity. The time-domain characterization has been used to describe the reservoir concept[13] and wave intensity analysis.[65] The details of these concepts will be covered in Chapter 3.

Summary

This chapter describes the fundamental biophysical relationships that underpin the physiological understanding of the interaction between pulsatile arterial blood pressure and flow and arterial stiffness. The approach has been to attempt to provide sufficient qualitative background explanation to support the quantitative description of the relationships and to highlight the fundamental significance of pulsatile hemodynamic phenomena. Arterial blood pressure and arterial stiffness are fundamental quantities intrinsic to arterial function (they do not scale to body size as do cardiac output or heart rate) and arterial stiffness is a significant determinant of vascular impedance and wave propagation that form the basis of the interaction of the arterial vasculature and the obligatory action of the heart as a pulsatile pump.

References

1. Leake CD. *The Historical Development of Cardiovascular Physiology* in *Handbook of Physiology: Circulation*. Bethesda, MD, USA: American Physiological Society; 1962:11−22.

2. McDonald DA. The relation of pulsatile pressure to flow in arteries. **J Physiol**. 1955; 127(3):533−552.

3. Womersley JR. **An Elastic Tube Theory of Pulse Transmission and Oscillatory Flow in Mammalian Arteries (WADC-TR-56-614)**. Ohio, USA: Wright Air Development Center, Wright Patterson Air Force Base; 1957.

4. Nichols WW, O'Rourke MF, Vlachopoulos C, Edelman E. **McDonald's Blood Flow in Arteries**. London: Hodder Arnold; 2021.

5. Furchgott RF. Endothelium-derived relaxing factor: discovery, early studies, and identification as nitric oxide. **Biosci Rep**. 1999; 19(4):235−251.

6. ten Velden GH, Elzinga G, Westerhof N. Left ventricular energetics. Heat loss and temperature distribution of canine myocardium. **Circ Res**. 1982; 50(1):63−73.

7. Murray CD. The physiological principle of minimum work: I. The vascular system and the cost of blood volume. **Proc Natl Acad Sci U S A**. 1926; 12(3):207−214.

8. Murray CD. The physiological principle of minimum work applied to the angle of branching of arteries. **J Gen Physiol**. 1926; 9(6):835−841.

9. de Simone G, Roman MJ, Daniels SR, et al. Age-related changes in total arterial capacitance from birth to maturity in a normotensive population. **Hypertension**. 1997; 29(6):1213−1217.

10. Franklin SS, Gustin W 4th, Wong ND, et al. Hemodynamic patterns of age-related changes in blood pressure. The Framingham Heart Study. **Circulation**. 1997; 96(1):308−315.

11. Guyton AC, Coleman TG, Fourcade JC, Navar LG. Physiologic control of arterial pressure. **Bull N Y Acad Med**. 1969; 45(9):811−830.

12. Westerhof N, Lankhaar JW, Westerhof BE. The arterial Windkessel. **Med Biol Eng Comput**. 2009; 47(2):131−141.

13. Wang JJ, O'Brien AB, Shrive NG, Parker KH, Tyberg JV. Time-domain representation of ventricular-arterial coupling as a windkessel and wave system. **Am J Physiol Heart Circ Physiol**. 2003; 284(4):H1358−H1368.

14. Meier D, Maier S, Bosiger P. Quantitative flow measurements on phantoms and on blood vessels with MR. **Magn Reson Med**. 1988; 8(1):25−34.

15. Bikia V, Pagoulatou S, Trachet B, et al. Noninvasive cardiac output and central systolic pressure from cuff-pressure and pulse wave velocity. **IEEE J Biomed Health Inform**. 2020; 24(7):1968−1981.

16. MacDougall JD, Tuxen D, Sale DG, Moroz JR, Sutton JR. Arterial blood pressure response to heavy resistance exercise. **J Appl Physiol**. 1985; 58(3):785−790.

17. Wolinsky H, Glagov S. A lamellar unit of aortic medial structure and function in mammals. **Circ Res**. 1967; 20(1):99−111.

18. Clark JM, Glagov S. Transmural organization of the arterial media. The lamellar unit revisited. **Arteriosclerosis**. 1985; 5(1):19−34.

19. Harkness ML, Harkness RD, McDonald DA. The collagen and elastin content of the arterial wall in the dog. **Proc R Soc Lond B Biol Sci**. 1957; 146(925):541−551.

20. Avolio A, Jones D, Tafazzoli-Shadpour M. Quantification of alterations in structure and function of elastin in the arterial media. **Hypertension**. 1998; 32(1):170−175.

21. Greenwald SE. Ageing of the conduit arteries. **J Pathol**. 2007; 211(2):157−172.

22. Bergel DH. The static elastic properties of the arterial wall. **J Physiol**. 1961; 156(3):445−457.

23. Bergel DH. The dynamic elastic properties of the arterial wall. **J Physiol**. 1961; 156(3):458−469.

24. Valdez-Jasso D, Haider MA, Banks HT, et al. Analysis of viscoelastic wall properties in ovine arteries. **IEEE Trans Biomed Eng**. 2009; 56(2):210−219.

25. Hayashi K, Handa H, Nagasawa S, Okumura A, Moritake K. Stiffness and elastic behavior of human intracranial and extracranial arteries. **J Biomech**. 1980; 13(2):175−184.

26. Shirai K, Hiruta N, Song M, et al. Cardio-ankle vascular index (CAVI) as a novel indicator of arterial stiffness: theory, evidence and perspectives. **J Atherosclerosis Thromb**. 2011; 18(11): 924−938.

27. Spronck B, Avolio AP, Tan I, Butlin M, Reesink KD, Delhaas T. Arterial stiffness index beta and cardio-ankle vascular index inherently depend on blood pressure but can be readily corrected. **J Hypertens**. 2017; 35(1):98−104.

28. Humphrey JD, Harrison DG, Figueroa CA, Lacolley P, Laurent S. Central artery stiffness in hypertension and aging: a problem with cause and consequence. **Circ Res**. 2016; 118(3):379−381.

29. Shadwick RE. Mechanical design in arteries. **J Exp Biol**. 1999; 202(Pt 23):3305−3313.

30. Tucker WD, Arora Y, Mahajan K. **Anatomy, Blood Vessels**. Treasure Island (FL): StatPearls; 2020.

31. Fung YC. What are the residual stresses doing in our blood vessels? **Ann Biomed Eng**. 1991; 19(3):237−249.

32. Burton AC. Relation of structure to function of the tissues of the wall of blood vessels. **Physiol Rev**. 1954; 34(4):619−642.

33. Roach MR, Burton AC. The reason for the shape of the distensibility curves of arteries. **Can J Biochem Physiol**. 1957; 35(8):681−690.

34. Elzinga G, Westerhof N. Matching between ventricle and arterial load. An evolutionary process. **Circ Res**. 1991; 68(6):1495−1500.

35. Thompson DAW. **On Growth and Form - the Complete Revised Edition**. Cambridge, UK: Dover Publications; 1992.

36. Sherman TF. On connecting large vessels to small. The meaning of Murray's law. **J Gen Physiol**. 1981; 78(4):431−453.

37. Kassab GS. Scaling laws of vascular trees: of form and function. **Am J Physiol Heart Circ Physiol**. 2006; 290(2):H894–H903.

38. Uylings HB. Optimization of diameters and bifurcation angles in lung and vascular tree structures. **Bull Math Biol**. 1977; 39(5):509–520.

39. McCulloh KA, Sperry JS, Adler FR. Water transport in plants obeys Murray's law. **Nature**. 2003; 421(6926):939–942.

40. Greenwald SE, Carter AC, Berry CL. Effect of age on the in vitro reflection coefficient of the aortoiliac bifurcation in humans. **Circulation**. 1990; 82(1):114–123.

41. Avolio AP, Chen SG, Wang RP, Zhang CL, Li MF, O'Rourke MF. Effects of aging on changing arterial compliance and left ventricular load in a northern Chinese urban community. **Circulation**. 1983; 68(1):50–58.

42. London GM, Pannier B, Safar ME. Arterial stiffness gradient, systemic reflection coefficient, and pulsatile pressure wave transmission in essential hypertension. **Hypertension**. 2019; 74(6):1366–1372.

43. Mitchell GF, Parise H, Benjamin EJ, et al. Changes in arterial stiffness and wave reflection with advancing age in healthy men and women: the Framingham Heart Study. **Hypertension**. 2004; 43(6):1239–1245.

44. Brown N. Impedance matching at arterial bifurcations. **J Biomech**. 1993; 26(1):59–67.

45. Langewouters GJ, Wesseling KH, Goedhard WJ. The static elastic properties of 45 human thoracic and 20 abdominal aortas in vitro and the parameters of a new model. **J Biomech**. 1984; 17(6):425–435.

46. Nichols WW, McDonald DA. Wave-velocity in the proximal aorta. **Med Biol Eng**. 1972; 10(3):327–335.

47. Karamanoglu M, O'Rourke MF, Avolio AP, Kelly RP. An analysis of the relationship between central aortic and peripheral upper limb pressure waves in man. **Eur Heart J**. 1993; 14(2):160–167.

48. Noordergraaf A. The ballistocardiogram as a source of haemodynamic information. **Proc Roy Soc Med**. 1967; 60(12):1286–1289.

49. Bramwell JC, Hill AV. The velocity of pulse wave in man. **Proc R Soc Lond - Ser B Contain Pap a Biol Character**. 1922; 93(265):298–306.

50. Frank O. Die Elastizitat der Blutegefasse. **Z Biol**. 1920; 71:255–272.

51. Mirault T, Pernot M, Frank M, et al. Carotid stiffness change over the cardiac cycle by ultrafast ultrasound imaging in healthy volunteers and vascular Ehlers-Danlos syndrome. **J Hypertens**. 2015; 33(9):1890–1896. discussion 1896.

52. Spronck B, Heusinkveld MH, Vanmolkot FH, et al. Pressure-dependence of arterial stiffness: potential clinical implications. **J Hypertens**. 2015; 33(2):330–338.

53. Anliker M, Histand MB, Ogden E. Dispersion and attenuation of small artificial pressure waves in the canine aorta. **Circ Res**. 1968; 23(4):539–551.

54. Spronck B, Humphrey J. Arterial stiffness: different metrics, different meanings. **J Biomech Eng**. 2019; 141(9):0910041–09100412. https://doi.org/10.1115/1.4043486. Epub ahead of print. PMID: 30985880; PMCID: PMC6808013.

55. Westerhof N, Stergiopulos N, Noble MI, Westerhof BE. **Snapshots of Hemodynamics: An Aid for Clinical Research and Graduate Education**. London: Springer; 2018.

56. Adji A, O'Rourke MF, Namasivayam M. Arterial stiffness, its assessment, prognostic value, and implications for treatment. **Am J Hypertens**. 2011; 24(1):5–17.

57. Murgo JP, Westerhof N, Giolma JP, Altobelli SA. Aortic input impedance in normal man: relationship to pressure wave forms. **Circulation**. 1980; 62(1):105–116.

58. Avolio AP, O'Rourke MF, Mang K, Bason PT, Gow BS. A comparative study of pulsatile arterial hemodynamics in rabbits and Guinea pigs. **Am J Physiol**. 1976; 230(4):868–875.

59. Taylor MG. The input impedance of an assembly of randomly branching elastic tubes. **Biophys J**. 1966; 6(1):29–51.

60. Alastruey J. Numerical assessment of time-domain methods for the estimation of local arterial pulse wave speed. **J Biomech**. 2011; 44(5):885–891.

61. Avolio AP. Multi-branched model of the human arterial system. **Med Biol Eng Comput**. 1980; 18(6):709–718.

62. Westerhof N, Bosman F, De Vries CJ, Noordergraaf A. Analog studies of the human systemic arterial tree. **J Biomech**. 1969; 2(2):121–143.

63. O'Rourke MF, Taylor MG. Input impedance of the systemic circulation. **Circ Res**. 1967; 20(4):365–380.

64. Dick DE, Kendrick JE, Matson GL, Rideout VC. Measurement of nonlinearity in the arterial system of the dog by a new method. **Circ Res**. 1968; 22(2):101–111.

65. Parker KH. An introduction to wave intensity analysis. **Med Biol Eng Comput**. 2009; 47(2):175–188.

Chapter 2

Measurements of arterial pressure and flow in vivo

James E. Sharman[1], Patrick Segers[2] and Julio A. Chirinos[3,4]

[1]*Menzies Institute for Medical Research, University of Tasmania, Hobart, TAS, Australia;* [2]*Faculty of Biomedical Sciences, Institute of Biomedical Engineering and Technology, Ghent University, Ghent, Belgium;* [3]*University of Pennsylvania Perelman School of Medicine, Hospital of the University of Pennsylvania and Perelman Center for Advanced Medicine, Philadelphia, PA, United States;* [4]*Ghent University, Ghent, Belgium*

Introduction

Cuff-measured blood pressure (BP) is the most widely applied and clinically important measurement used in clinical practice. The principles of cuff BP measurement used in clinical practice today are based on the technique of cuff mercury sphygmomanometry that was refined by Dr Nikolai Korotkoff in 1905. This method relies on estimating the BP within the brachial artery where the cuff is applied by listening to the sounds (auscultation by stethoscope) within the brachial artery as the cuff is slowly deflated and with BP measured on a mercury sphygmomanometer. A distinctive sound occurring at the onset of flow under the cuff denotes systolic BP (Korotkoff phase 1), whereas the point at which sound disappears denotes diastolic BP (Korotkoff phase 5) and occurs with full restitution of blood flow.[1] These brachial artery sounds are separable in time and distinctive from heart sounds.[2]

When measured carefully using a standardized approach, cuff-measured BP provides critical clinical information relating to the risk of high BP-related disease.[3] A spectrum of clinical conditions occur as a consequence of high BP, which are related to stiffening of large central arteries (particularly the aorta) and accelerated atherosclerotic plaque development, both of which ultimately affect the vasculature and perfusion of the brain, heart, and kidneys, and promote heart disease through direct effects on left ventricular afterload (often referred to as "pressure overload"). Thus, the underlying tenet of accurate BP measurement is to determine the pressure loading and consequent vascular risk at the central arterial beds.[4] This measurement has been coined "central BP," as distinct from standard upper arm cuff BP and represents BP at the ascending aorta.[5] The upper arm is the nearest site at which a cuff can safely be inflated to perform mercury auscultation, and even though this is distal to the central arterial beds, the technique can provide a reasonable determination of an individual's true intra-arterial central BP.

The unequivocal clinical importance of cuff BP measurement was demonstrated in many seminal epidemiology studies and clinical trials throughout the 20th and 21st centuries.[6,7] In the 1970s, the first commercially available devices to measure BP using a "modern" automated technique, known as oscillometric BP, became available. Oscillometric BP was developed as an automated way to derive the same BP values as mercury auscultation and is the current mainstay BP measurement technique used worldwide and recommended by hypertension societies for all modalities of BP measurement (office BP, automated unobserved BP, self-measured home BP, and 24-hour ambulatory BP). Many thousands of unique oscillometric BP devices are sold online globally to millions of people each year. A new wave of techniques and cuffless devices asserting to measure BP at different arterial sites have also emerged, which raise many questions about what is being measured and of what additive value will they provide. In seeking to understand this, we must firstly return to the original BP method from which all others have emerged and (most) seek to emulate: cuff mercury sphygmomanometry.

Cuff mercury sphygmomanometry

In his original thesis of 1896 on the measurement of BP using cuff mercury sphygmomanometry, Riva Rocci considered that the technique provided a measurement of

BP (referring to this as the "total charge") at "… a point fairly close to the aorta…" either "…. in the aorta itself or of the brachiocephalic trunk…."[8] This was a reasonable supposition because sphygmomanometry was applied to a large arterial branch of the aorta. However, as an indirect measure, the veracity of these statements could not be assessed until the 1930s with the advent of intra-arterial BP measurement using calibrated manometers. By the 1950s, results from several small experimental studies led a committee of the Scientific Council of the American Heart Association to conclude that cuff mercury sphygmomanometry was error-prone when compared with the true intra-arterial brachial BP, seemingly to systematically underestimate systolic BP but overestimate diastolic BP a mean error of 8 mmHg may be expected in individual readings of systolic and diastolic pressures.[9]

Many investigators have put forward theories on the origin of Korotkoff sounds and possible explanations for systematic errors of systolic BP and diastolic BP.[10−13] The act of cuff occlusion of an artery in itself may cause hemodynamic changes that contribute to systematic error.[11] However, dynamic reactions also occur during cuff deflation, which can additionally influence cuff-measured BP values compared with intra-arterial BP (see Video 1).[10] A possible explanation for systematic overestimation of diastolic BP is that due to incomplete transmission of pressure in the cuff to the compressed brachial artery, the occluded arterial segment opens at an intra-arterial pressure below that exerted by the cuff.[10] Importantly, the size of the cuff relative to the arm of the person having their BP measured, as well as the shape of the arm relative to the cuff,[14] plays a role in the accuracy of cuff mercury sphygmomanometry. Indeed, good "cuff performance" is more likely using an appropriately sized cuff bladder relative to the circumference of the person's upper arm. Current recommendations are that bladder length should be 75%−100%, and bladder width 37%−50%, of the upper arm circumference.[15]

The full extent of the difference of cuff mercury sphygmomanometry BP compared against an intra-arterial reference was only recently appreciated through meta-analyses of individual patient-level data.[16] Even when apparently measured correctly (i.e., with appropriate cuff size) among more than 300 people, on average, cuff systolic BP was underestimated by −3.4 (95% confidence intervals, CI; −6.9 to −0.2) mmHg and diastolic BP overestimated by 6.3 (2.8 to 9.8) mmHg compared with intra-arterial brachial BP. As already mentioned above, the most clinically relevant BP sought to be measured with accuracy is that at the central aorta, but data for this comparison were only available for 21 people using cuff mercury sphygmomanometry (as the majority of available data in this regard is for oscillometric BP).[16]

In any case, the systematic underestimation of brachial systolic BP with cuff mercury sphygmomanometry suggests this cuff method could give a reasonable estimate of intra-arterial central aortic systolic BP, because on average this is lower than intra-arterial brachial systolic BP. But arguing against the consistent accuracy of cuff mercury sphygmomanometry for measuring aortic BP is that: (1) large individual variability in the magnitude of systolic BP difference (>30 mmHg) occurs between the aorta and brachial artery (termed, systolic BP amplification) even among people with similar intra-arterial brachial systolic BP[17]; (2) hemodynamic variations associated with chronological aging, or disease-related vascular aging, create additional error in cuff-measured BP (e.g., greater underestimation of systolic BP and pulse pressure, but overestimation of diastolic BP with advanced vascular aging)[18−20]; and; (3) there is a lack of empirical evidence or biophysical rationale that Kortotkoff sounds denoting systolic BP at the brachial artery directly relate to central aortic systolic BP.[2] Thus, even though cuff mercury sphygmomanometry has been an invaluable clinical tool, it is not always a precise determination of an individual's true intra-arterial central BP.

Together the above observations provide some of the rationale toward efforts to improve the accuracy of cuff-measured BP.[21] But in the meantime, cuff mercury (or mercury-free) sphygmomanometry is still regarded as the reference standard method by which the accuracy (validation) of most other BP measurement techniques are compared.[22] An exception to this is the protocol for the validation of devices that purport to measure central aortic BP, as distinct from standard upper arm cuff BP, whereby intra-arterial central aortic BP is the recommended reference standard (discussed below).[5] Environmental and health concerns associated with using mercury in the manometric column has led to the phasing out of cuff mercury sphygmomanometry from clinical practice, and with replacement mostly by cuff oscillometric BP devices.

Cuff "oscillometric" blood pressure

The automated nature of cuff oscillometric BP is favored for use in clinical practice as it removes the influence of many potential measurement method errors, such as terminal digit preference,[23] but still has a similar "cuff-based" appearance to the widely accepted cuff mercury sphygmomanometry method. Measurement begins with cuff inflation to about 30 mmHg above expected systolic BP and then steady deflation. Miniature piezoelectric pressure transducers are used to record small, so-called "oscillation" waves that are converted from pressure to analog voltage, which is amplified and filtered.[24] The waves first become apparent before registration of systolic BP using the first Korotkoff sound.[25] Initially, the wave amplitude is very small at around systolic BP, reaches maximal amplitude at mean arterial pressure, and then declines in amplitude as the cuff deflates toward and below diastolic BP.

Digital signal processing is used to obtain and analyze the envelope of the recorded "oscillometric" waves using fitting functions and algorithms that may differ between each unique oscillometric BP device and are not publicly
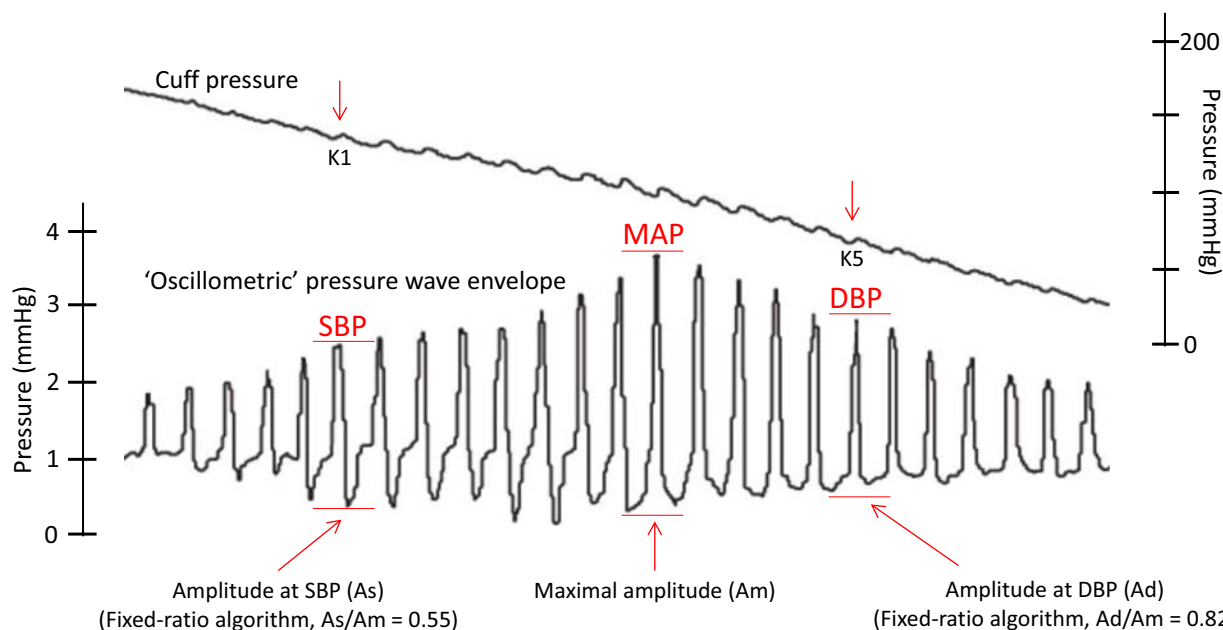
disclosed. Moreover, a clear assessment of wave amplitude at different inflation pressures requires very slow deflation of the cuff, allowing for the acquisition of full cardiac cycles within small pressure inflation ranges; this process is often "abbreviated" and a faster deflation is used to achieve rapid measurements in the clinic, which require indirect algorithm-based inferences regarding the exact amplitude of the oscillometric envelopes at various inflation pressures. Importantly, if different algorithmic approaches are used to construct the wave amplitude envelope, this will result in different estimated BP values.[26] After identifying mean arterial pressure from the point of maximum wave amplitude,[27] systolic and diastolic BPs are estimated often using fixed-ratio algorithms. These algorithms are based on systolic BP and diastolic BP (measured with cuff mercury sphygmomanometry) correlating with points on the envelope where the wave amplitude approximates 55% (0.55) and 82% (0.82) of the maximal amplitude, respectively.[25] Fig. 2.1 illustrates an overview of the technique, highlighting the relations between cuff pressure, Korotkoff sounds, and the wave amplitude trace, as well as example fixed-ratio algorithms to estimate systolic BP and diastolic BP.

The percentage (ratio) estimates to derive BP using this method only represent population averages and have some flaws, including a systematic bias toward greater underestimation of systolic BP as systolic BP increases. This is because the optimal fixed-ratio algorithm required to accurately estimate systolic BP (by comparison with cuff mercury sphygmomanometry) becomes progressively lower as systolic BP increases (e.g., the optimal fixed-ratio for systolic BP approximates 0.57 at 100 mmHg but this falls to 0.45 at 190 mmHg), thus potentially compromising accurate diagnostic assessment of hypertension. A smaller range in the optimal fixed-ratio occurs for diastolic BP (e.g., range approximates 0.86−0.75 across 55−115 mmHg diastolic BP).[25]

Compared with intra-arterial brachial BP, on average, diastolic BP is overestimated by $\approx$ 6 mmHg, whereas systolic BP and pulse pressure are underestimated by −6 and −12 mmHg, respectively, using oscillometric devices. Unsurprisingly, these discrepancies could have a major influence on correct BP classification.[16] The same general oscillometric method to estimate BP has also been developed using wrist cuff BP devices. Whether they be upper arm or wrist cuff BP devices, the failure of these algorithms to provide consistent accuracy across different BP values, nor account for individual variation in waveform morphology related to accurate BP assessment,[17] leaves room for more sophisticated approaches to improve accuracy.

It is worth briefly reviewing the terminology "oscillometric" BP, which implies that the waveforms are oscillations, but this is not the case.[126] Oscillations are periodic waves in which there is repetitive variation of a measure about a central value, such as an alternating current. In fact, the waves are arterial pressure waves generated by the distending and recoiling brachial artery that occurs with each cardiac cycle. The "oscillometric" method gained this name from historical reference to oscillations by investigators from the 19th century, which was then carried on into the 1970s with the invention of the automated

FIGURE 2.1 Example of the "oscillometric" method to estimate blood pressure. The pressure at the maximal amplitude of the pressure wave envelope represents mean arterial pressure (MAP), and fixed-ratio algorithms are used to derive systolic (SBP) and diastolic blood pressure (DBP). Example positions of Korotkoff phase 1 (K1) and phase 5 (K5) are indicated on the cuff pressure waveform.

"oscillometric" method.[24] Part of the terminology confusion may also originate from the process of filtering the waveforms during processing, which dampens typically recognizable features of arterial pressure waves and could give the (false) impression of an oscillometric wave. More appropriate terminology, such as "automatic sphygmomanometer" has been proposed. For the ease of understanding, the term "oscillometric" is used in this chapter.

Determining the accuracy of oscillometric BP devices is recommended to be performed by comparison with cuff mercury (or mercury-free) sphygmomanometry according to standardized, internationally accepted validation protocols,[22] by investigators who are independent from the device manufacturer to avoid potential bias. Currently, this includes the requirement to be tested among at least 85 people comprising men and women, and across a range of low to high BP values.[15,28] Transparency of findings is paramount, and these should be made publicly available by publication in peer-reviewed scientific journals.[29] While these requirements are desired, they are infrequently achieved because BP devices may be cleared for marketing and sale by regulatory authorities without having undergone rigorous accuracy testing or publication of validation studies in peer-reviewed journals.[30,31] Devices that have not undergone such testing likely have greater inaccuracy compared with cuff mercury sphygmomanometry, are widely used and more likely to contribute to suboptimal medical management.[32−36]

At the time of writing this chapter, there were more than 3600 unique BP device models available for consumer purchase, manufactured by more than 450 different companies worldwide, but less than 20% had undergone the necessary validation testing described above.[37] Among BP devices sold by large e-commerce companies with global reach (e.g., Amazon, eBay), only about 5% of the BP devices were validated, which if used for home BP monitoring could seriously undermine best-practice cardiovascular risk management.[38] A project by the Lancet Commission on Hypertension Group[39] is seeking to redress the above issues to improve the global availability of validated BP devices.[40] Even if achieved, there will be room for improvement because validated BP devices can still have sizable differences from carefully measured mercury sphygmomanometry (e.g., ≥ 10 mmHg difference in 36% of systolic or diastolic BP readings,[41] and a range of 6 to 26 mmHg difference for systolic BP).[36]
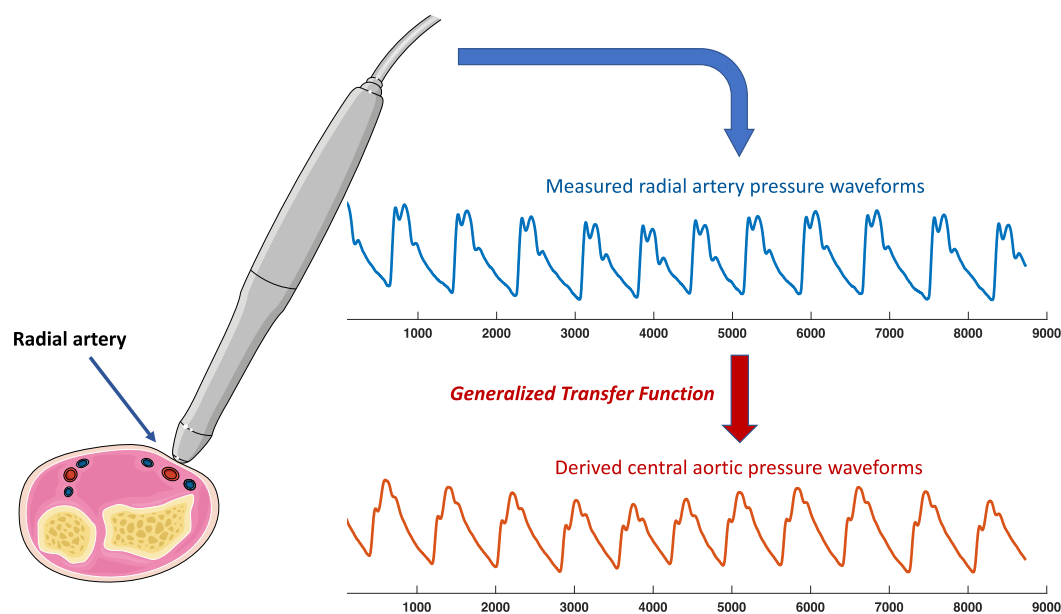
With the advent of more advanced technological capabilities, the principles of oscillometric BP have been redeployed into cuffless methods at arterial beds distal from the brachial artery. For example, in the transverse palmar arch artery of the forefinger via a sensor unit embedded on the face of a smartphone that records pressure signals when the finger is pressed up against the unit.[42] This approach replaces the cuff with the finger as the actuator to apply external pressure and generate the wave envelope for analysis and estimation of BPs. A critical factor for accurate BP measurement at vessels peripheral to the brachial artery is that systolic BP may be substantially amplified, but this amplification is of highly variable magnitude (range 0−40 mmHg), and currently there is no way to know the interindividual variability noninvasively.[43] This, together with the known variability in systolic BP between the aorta and brachial artery,[16] infers that clinically meaningful BP measurement becomes increasingly challenging as distance increases from the ascending aorta. Attempts to improve accuracy of BP measurement at distal arteries have been explored using the technique of applanation tonometry, most notably at the radial artery.

Radial artery applanation tonometry

Noninvasive recording of arterial pressure waveforms can be achieved using applanation tonometry at a palpable peripheral artery, usually applied at the more easily accessible radial or carotid arteries. The technique typically involves use of a pen-like tonometer probe housing a piezoelectric pressure sensor at the tip, but can also be undertaken by servo-controlled devices with piezoelectric arrays to help limit movement artifact.[44] The sensor is lightly applied perpendicular to the artery, partially flattening the wall (applanation), which eliminates tangential forces and exposes the sensor to the pressure within the artery. This enables high-quality recordings of the arterial pulse that are similar to that acquired by intra-arterial measurement.[45−47]

With accurate recording of the radial artery waveform, a central aortic pressure waveform can be generated using a mathematical transfer function (Fig. 2.2), often a generalized function assessed from population data.[48,49] Correct calibration of the radial waveform (scaling using units of pressure) is required to generate an accurate estimation of central aortic BP. Indeed, many investigators have shown that calibration using aortic intra-arterial mean arterial pressure and diastolic BP produces accurate central aortic systolic BP values, even among subjects of different age, heart rate, and BP, but also with major hemodynamic perturbations induced by vasoactive medications, Valsalva maneuver, abdominal compression, and exercise.[44,48−51] However, it should be noted that such validation is present only for peak pressure, rather than the details of the waveform, which are required for more sophisticated hemodynamic analyses. Moreover, some evidence indicates the technique is less accurate among populations at higher risk for vascular disease (i.e., type 2 diabetes, chronic kidney disease),[18,52] implying potential weakness of generalized transfer functions being used in people with extreme vascular aging.[20] This issue probably also applies to cuff oscillometric BP,[19,20] but is incompletely understood and requires further research.

FIGURE 2.2   Estimation of central aortic pressure using radial arterial tonometry.

Carotid arterial tonometry can be used to obtain high-fidelity pressure wave forms from the carotid artery, which is morphologically similar (but not identical) to the aortic pressure waveform.[53] This approach is advantageous because it does not require a transfer function. However, the procedure is more technically demanding than radial tonometry. Anatomic and technical considerations for carotid applanation tonometry are discussed in Box 2.1 and represented in Fig. 2.3.

Two factors reported in 1990, using intra-arterial BP measures in patients undergoing cardiac catheterization, emphasized the potential clinical importance of pursuing measurements of central aortic BP as distinct from brachial BP. Firstly, central aortic systolic BP could be significantly different among patients with similar brachial systolic BP (e.g., brachial ≈ 150 mmHg but aortic $\approx 130-150$ mmHg)[54]; meaning that the true risk related to BP could be missed if only focusing on BP measurement at the upper arm. Secondly, the BP lowering effects of antihypertensive agents could be more pronounced at the central aorta compared with the brachial artery, and it was even possible for large BP lowering effects to only occur at the central aorta[54]; meaning that greater precision of hypertension management could theoretically be achieved with knowledge of an individual's central BP. These observations, summarized in Fig. 2.4, provided rationale to pursue development of noninvasive means to record and calibrate radial waveforms and derive central BP from it.

The first commercial device became available in 1996, was intensively used in clinical research and preceded development of many other similar methods.[55] Operation was based on radial artery tonometry and calibration of the radial waveform with conventional cuff systolic BP and diastolic BP. The method held promise[56] and has enhanced understanding of the differential therapeutic effects on cuff BP compared with derived central aortic BP,[57-60] but the method has failed to integrate into practice and accuracy issues have prevailed.[61,62] Unfortunately, the systematic error intrinsic to cuff-based BP, and especially oscillometric, methods (i.e., underestimation of systolic BP but overestimation of diastolic BP) leads to substantial underestimation of the true central aortic systolic BP and pulse pressure (confirmed with intra-arterial assessment).[63-67] Further calibration error also comes from the assumption there is no systolic BP difference between the brachial and radial artery,[68] when in fact there is large interindividual variability.[43,69-72] This has a major influence on estimation of aortic systolic BP[71,73] and emphasizes yet again how difficult it is to achieve accurate and clinically meaningful BP recordings, particularly from measurement at the wrist artery.
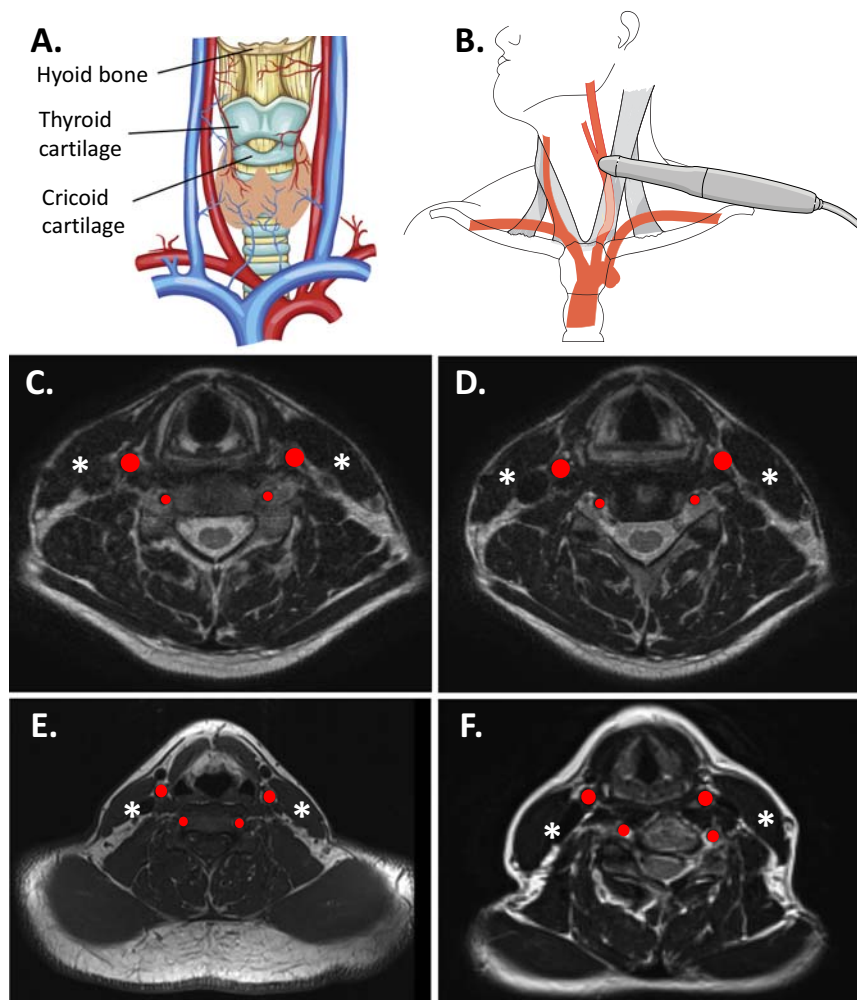
Another factor that adds to the lack of clarity in distinguishing the diagnostic utility of the radial tonometry method above and beyond standard cuff BP[61] is the very high correlation that exists between cuff brachial systolic BP and tonometry-derived central aortic systolic BP (e.g., $R^2 = 0.93$).[74] Slight improvement in accuracy of radial tonometry may be achieved by calibration with cuff BP-derived mean arterial pressure and diastolic BP,[67] but this also has fundamental limitations and does not fully resolve calibration problems.[75,76] In seeking to develop better methods that are also more amenable to integration into daily clinical practice, the last decade has seen the field turned toward estimation of central aortic BP using cuff-based approaches with similar modes of operation to standard automated BP devices already in widespread use.

BOX 2.1 How to perform carotid arterial tonometry

Carotid tonometry is best performed in the supine position. A rolled towel under the neck and slight extension may help bring the carotid artery anteriorly and/or stabilize it between the tonometer and underlying anatomic structures. This maneuver may tighten the skin overlying the artery, particularly among subjects with short necks, impeding adequate flattening of the arterial wall. This can be overcome by relaxation/opening of the jaw.

The goal of carotid tonometry is to record intra-arterial pressure waveforms. This can be accomplished by flattening the artery against underlying hard structures in the neck (cartilage and/or bone tissue). Reviewing anatomic relationships between the common carotid artery and these structures is useful, as shown in Fig. 2.3. The common carotid arteries (large red circles) exhibit roughly consistent relationships with the underlying laryngeal/pharyngeal cartilages, the bony structures in the neck (such as vertebral transverse processes, which surround the vertebral arteries), and the sternocleidomastoid muscle.

Panel A in Fig. 2.3 shows the relationships between the common carotid and the thyroid and cricoid cartilages. Panel B shows its relationship with the sternocleidomastoid muscle. Panels C, D, and E show examples of these relationships in cross section. It can be seen that the common carotid artery is not superficial but lies medial and posterior to the anterolateral part of the sternocleidomastoid muscle, particularly in the lower part of the neck. These relationships are important to approach the artery in an attempt to position the tonometer directly on top of it (without intervening muscle tissue), flattening it against underlying structures.
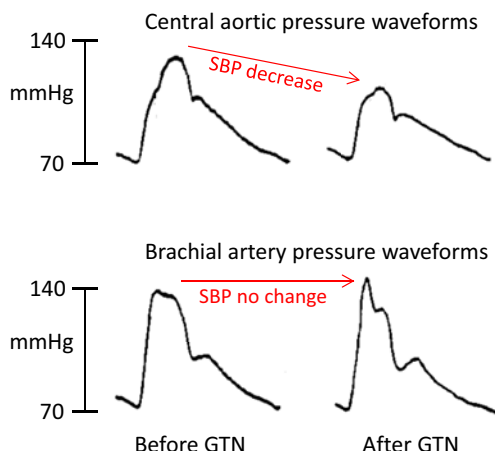
FIGURE 2.3 Anatomic considerations for carotid arterial tonometry. Panel A shows the relationships between the common carotid and the thyroid and cricoid cartilages. Panel B shows its relationship with the sternocleidomastoid muscle. Panels C, D, and E shows its relationship with various anatomic structures in cross section. Panel F shows how the relationship changes with slight rotation of the head. The common carotid arteries are marked by big red circles, whereas the vertebral arteries are marked with small red circles. The asterisks mark the sternocleidomastoid muscle. See Box 2.1 text for details.

Another issue to consider is the level of the carotid bifurcation, since the goal of carotid tonometry is to acquire common carotid waveforms rather than external carotid waveforms. The thyroid cartilage ("Adam's apple") is located at the C4 level and is an easily identifiable landmark. The carotid bifurcation usually occurs at the C3–C4 level (between the thyroid cartilage and the hyoid bone), although a small percentage of people exhibit higher bifurcations (more common among Asians) or lower bifurcations.

In the authors' experience, the best way to "trap" the carotid artery against underlying hard structures to obtain high-fidelity recordings is to approach it from the anterolateral aspect, orienting the tonometer posteromedially (toward the back and the midline), gently pulling the sternocleidomastoid muscle posteriorly (i.e., toward the back of the neck), initially with the hand that is not holding the tonometer and subsequently with the pen-like portion of the tonometer, so that the artery can be flattened without intervening muscle tissue between the sensor and the arterial wall. With slight rotation of the head, the carotid can be positioned anterior to the vertebral transverse process and closer to the vertebral body (Panel F in Fig. 2.3), facilitating applanation.

The amount of pressure exerted by the operator on the tonometer should be high enough to acquire a clear signal, but excessive pressure has the potential to result in subject discomfort, vagal responses, and/or the inability to record the pressure nadir. The latter problem can be detected by the presence of a flat late diastolic pressure profile, rather than the expected asymptotic exponential fall. The latter problem is uncommon with carotid tonometry but sometimes occur with radial tonometry when excessive pressure is applied over the artery, which should be avoided.
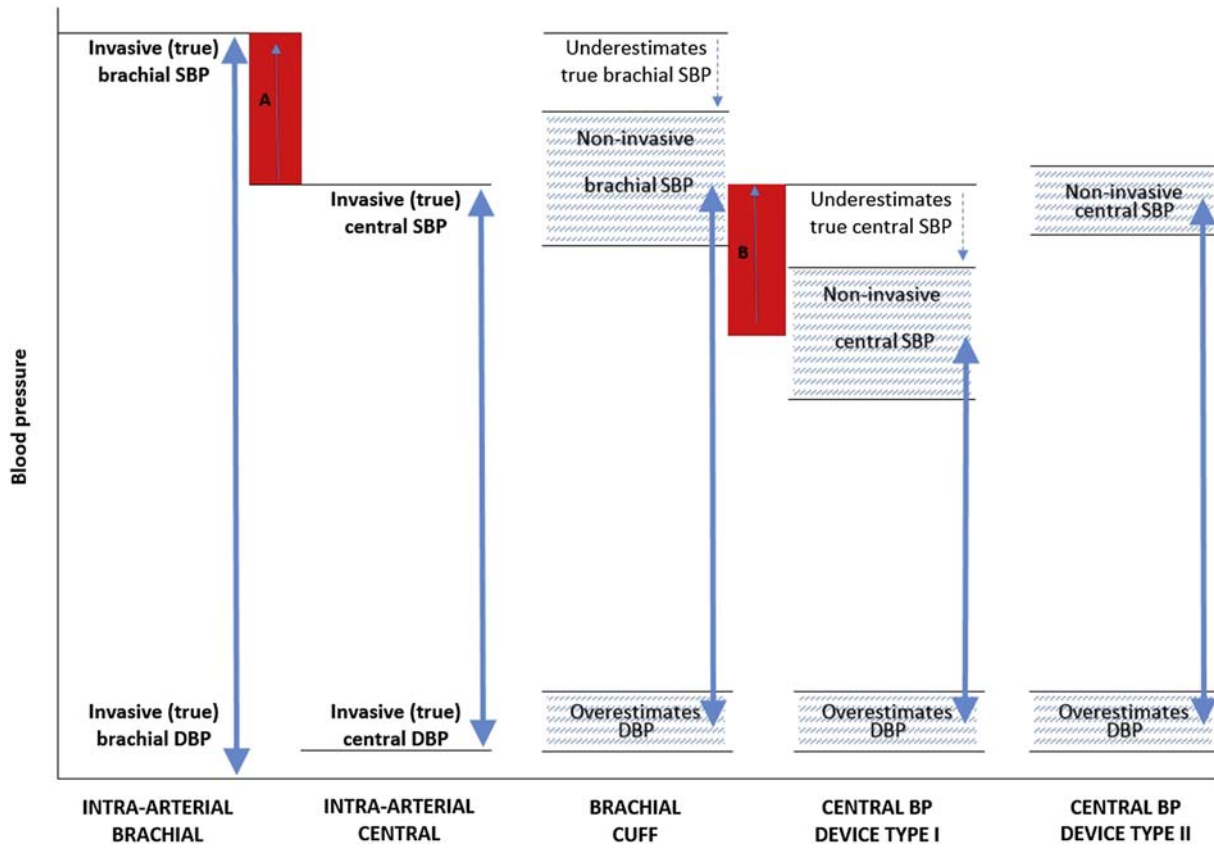
FIGURE 2.4 Intra-arterial central and brachial pressure waveforms before and after 0.3 mg sublingual nitroglycerin (GTN) in a 59-year-old male. Note that the morphology of the pressure waveforms changes after GTN and for this individual there is a marked drop in central systolic blood pressure (SBP) but no accompanying drop in brachial artery SBP. Other people may experience a decrease in both central and brachial BP. *Adapted from Kelly RP, Gibbs HH, O'Rourke MF, et al. Nitroglycerin has more favourable effects on left ventricular afterload than apparent from measurement of pressure in a peripheral artery.* Eur Heart J. 1990;11:138–144 with permission from Oxford University Press.

Cuff central aortic blood pressure

All cuff methods to estimate central aortic BP, as a separate entity from brachial BP, follow similar principles to radial tonometry, with the main distinction being that the first step of peripheral waveform recording is achieved by cuff sensors at the upper arm/brachial artery instead of the radial artery by tonometry.[55,77,78] Brachial waves are recorded as per the oscillometric method previously mentioned, which may also be referred to as some variation of "pulse volume plethysmography." Depending on the device, brachial waveforms may be recorded at variable cuff pressure, anywhere between subdiastolic to suprasystolic BP, but with all devices using brachial cuff oscillometric BP as the mode of calibration. Proprietary generalized transfer functions that differ between manufacturers are used to generate a central aortic BP waveform and estimate central BP. Thus, it is not unexpected that the same underestimation of the true central systolic BP occurs when waveforms are calibrated with brachial systolic BP and diastolic BP.[79–81] An advantage of cuff-based central BP is that automated, repeat measures can be acquired in the office (observed or unobserved), at home or with 24 h ambulatory BP monitoring.

It was only in 2017 when guidelines on standardized validation protocols for testing the accuracy of central BP devices were developed by a task force of the European ARTERY Society.[5] General integration with existing international protocols for brachial cuff device validation in terms of sample size (n = 85) and subject characteristics were advocated, and a key recommendation was for intra-arterial BP measured by catheter at the ascending aorta to be the reference standard by which device performance is compared.[5] Central BP devices were also broadly classified into two categories of operation: type I devices that purport to estimate central BP relative to brachial BP (which may provide relatively accurate systolic BP difference between central and peripheral sites) and type 2 devices that purport to estimate the intra-arterial (true) central BP, despite inaccuracy at the peripheral site (as detailed previously).[5] Illustration of the differences between devices types is depicted in Fig. 2.5.

FIGURE 2.5   Differences in brachial and central blood pressure (BP), between intra-arterial BP, brachial cuff BP and noninvasive central BP devices Types I and II. Double arrows represent BP ranges; red shaded area A represents the true level of central-to-brachial systolic blood pressure (SBP) amplification, and red shaded area B represents the noninvasive estimated central-to-brachial SBP amplification. The noninvasive central SBP estimated using central BP device Type II may be higher than noninvasive brachial cuff SBP, but this is due to underestimation of true (intra-arterial) brachial SBP with the cuff device and, therefore, does not reflect physiological amplification. The hatched areas denote that there will be a degree of variability in estimated BP between devices. *Reproduced from Sharman JE, Avolio AP, Baulmann J, et al. Validation of non-invasive central blood pressure devices: ARTERY Society task force consensus statement on protocol standardization. Eur Heart J. 2017;38:2805−2812 with permission from Oxford University Press.*

International guidelines recommend diagnosis and treatment based on absolute cardiovascular disease risk rather than single risk factor management (i.e., only focusing on BP or lipids).[82−85] Thus, central BP information derived from type I devices may be best applied when brachial cuff BP is borderline or mildly elevated but absolute cardiovascular disease risk is low and there is an absence of target organ damage. In these circumstances, there may be uncertainty as to whether antihypertensive treatment should be initiated, or uptitrated, and knowing central BP relative to brachial BP could be helpful to resolve clinical indecision. However, whether this adds value in terms of reducing cardiovascular events has never been determined in randomized controlled trials, which is a major gap in knowledge that requires additional research.

Type II central BP devices essentially aim to provide a more accurate measure of a clinically relevant (central aortic) BP than either cuff brachial BP or central BP using a

type I device (noting that both function types may be available within a single device).[5] Greater accuracy is achieved by additional proprietary algorithms to recalibrate the peripheral waveform and generate a central systolic BP closer to the intra-arterial measure.[78,86,87] A nationally representative study in Taiwan reported that the prevalence of hypertension would be increased (from 25% to 33%) if central BP using a type II device was employed in favor of standard brachial cuff BP.[88] Others have shown that central BP recorded using type II device elicits stronger associations with cardiovascular endpoints than either brachial BP or central BP estimated in Type I device operation.[89,90] This is not unexpected given that type II device central BP provides a more clinically relevant BP, but still there is no randomized controlled trial data proving clinical superiority beyond best-practice standard cuff BP methods, and these data are desirable. With type II devices, it will be important to determine whether recalibration of peripheral waveforms

(and therefore estimation of true intrabrachial pressures) as opposed to also estimating a more accurate aortic pressure, is a relevant step in enhancing cardiovascular risk prediction and decision-making.

Cuffless blood pressure wearables

Technological capability to measure biometric signals and convert them to apparent BP values from virtually any body part has burgeoned in recent years.[91] Cuffless BP wearables can be embedded into clothing, worn as ear buds, eyeglasses, soft arm bands, watch-type wristbands, or stick on patches, just to name a few.[92-95] The global market size for wearable BP technologies is on the rise and expected to reach USD $2.25 billion in 2023.[96] Increasing demand for wearable BP monitors is due to increased disease prevalence, increased patient monitoring services, and greater interest in self-monitoring of health. Cuffless alternatives to standard inflatable cuff-based BP also offer more convenient and comfortable means of BP measurement. Although it seems that people trust the accuracy of wearables (>70% in one survey),[97] this could be misplaced confidence if the findings of an Australian study are representative of the global marketplace, where >500 unique wristband wearable BP devices were available for purchase but none had proof of accuracy testing.[38]

Some cuffless BP methods acquire a single "snapshot" BP,[42] which is clinically less useful, whereas others have continuous recording capability for nonintrusive data collection (and intelligent analysis) over much longer time periods relative to cuff-based methods.[94] It is beyond this chapter to detail all methods and readers are directed to an electronic book that is dedicated to the topic.[98] Cuffless devices broadly follow measurement principles of conventional cuff-based approaches in terms of recording a peripheral pressure waveform signal (through various techniques), then applying algorithms (again through various techniques) to generate an estimated BP. A critical step that is different from conventional cuff-based approaches, and currently presenting the greatest challenge for achieving accurate cuffless BP measurement, is correct calibration of the recorded peripheral pressure waveforms so that accurate absolute BP values can be derived. Unfortunately, in most cases, conventional cuff-based systolic and diastolic BP is used to calibrate waveforms from cuffless sensors despite all the inherent inaccuracies previously described, and this calibration error is likely transferred to erroneous cuffless BP estimation.

Highly sophisticated methods based on artificial intelligence and machine learning algorithms have been applied to novel BP assessment tools such as transdermal optical imaging of facial blood flow through smartphone videos.[99] These type of approaches allow for possible contactless BP monitoring, but again, calibration and reference comparators for new cuffless BP technologies are almost exclusively based on cuff-based oscillometric BP methods with inherent accuracy flaws. Having said this, relatively small deficiencies regarding BP accuracy could be outweighed by the extra BP information gained with long-term unintrusive continuous BP monitoring and big data analysis (e.g., better understanding/new discovery on the genesis and early detection of hypertension, and advanced tracking of therapeutic responses). Hybrid approaches incorporating less accurate continuous novel measurement devices with more established, accurate, and precise methods seem attractive to overcome the limitations of each group of measurements in isolation.

Integration of BP data with existing health system electronic databases for better clinical decisions and improved quality of care, underpin the rationale for international prioritization on the development, implementation and scaling up of digital health technologies.[100] This recommendation comes with the warning that the enthusiasm for digital health has driven a proliferation of transitory implementations, an overwhelming diversity of tools with limited understanding of the impact on people and health systems,[100] as we currently see with the cuffless BP device sector. Efficacious BP device companies of the future will have considered integration into clinical systems of care in addition to proving accuracy and clinical value.

Medical device regulators are aware of the need to revise regulatory frameworks and create efficient processes governing the use, safety, and effectiveness of digital health technologies.[101] Accuracy concerns have been identified as a factor that will inhibit market growth in wearables technology,[96] and hopefully this will incentivize manufacturers toward better practice. In the meantime, it is important that the medical community and organized societies promote rigorous validation protocols[102,103] prior to endorsing specific devices or strategies. Similarly, the medical community must stay alert to false claims of accuracy, which have potential for harm via overdetection or underdetection of hypertension.

Invasive, intra-arterial blood pressure

The direct physiological measurement of BP can only be achieved with invasive, intra-arterial methods, as such, all the cuff-based and cuffless BP methods mentioned above provide an indirect estimation of BP.[14] Direct measurement involves the intra-arterial introduction of a fluid-filled or micromanometer-tipped catheter in a sterile medical procedure that is not without risk and thus is not sensible, nor ethically acceptable, to be performed unless clinically indicated (e.g., among people with suspected coronary artery disease requiring coronary artery angiography). It is not surprising then, that the evidence on the risk associated with high BP and the importance of therapy to lower BP

has been derived almost exclusively using noninvasive cuff-based BP methods, and there is limited evidence on the prognostic value of invasive BP.[14,104,105]

Despite limitations of invasive BP measurement, this is the gold standard reference to determine accuracy of central BP devices (minimum n = 85)[5] and may also be used in validation protocols of automated brachial cuff BP devices,[15] albeit with caution in this latter protocol where much fewer subjects are allowable (minimum n = 15), which limits the full range and quality of validation testing. Careful attention to handling of monitoring equipment and procedures of measurement are required to avoid errors with invasive BP.[106] Micromanometer-tipped catheters are preferred, especially where waveform morphology is the subject of analysis (not just systolic and diastolic BP), because additional sources of error can occur with incorrect handling of fluid-filled catheters. However, accessibility to micromanometer-tipped catheters is more difficult as they are expensive and not routinely used clinically. Reassuringly, if meticulously handled, fluid-filled catheters are acceptable for accurate intra-arterial BP measurement.

Readers are directed to detailed information on recommended protocols for intra-arterial BP measurement provided in the International Standard ISO 81060-2,[15] the ARTERY Society task force consensus statement,[5] and other sources.[106–108] Adequate dynamic response of the pressure transducer is required for accurate BP recording and maintenance of arterial pressure waveform features. An under- or overdamped system can influence the quality of waveform recording and lead to incorrect BP values (Table 2.1). For example, underdamping causes pressure "overshoot" resulting in overestimated systolic BP (and pulse pressure), underestimated diastolic BP, a pronounced dicrotic notch, and nonphysiological wave fluctuations during diastole. Overdamping, on the other hand, underestimates systolic BP (and pulse pressure),

overestimates diastolic BP, and smooths out arterial waveform features. A common practical approach for assessing the dynamic response and appropriate dampening of fluid-filled catheter systems is the square wave (fast flush) test, described in Box 2.2 (from References 106–109).

Differences between the transducer level of fluid-filled catheters and the level of the measurement site can create significant error from hydrostatic pressure differences (e.g., 10 cm difference = 7.5 mmHg difference). Therefore, the transducer (stopcock) should be kept at the level of the left ventricle (or vessel of interest) during zeroing and BP recording. Many of the technical issues associated with fluid-filled catheters can be overcome using micromanometer-tipped catheters or pressure wires with a pressure transducer in the tip, providing the most accurate quantification of BP.[110] Implantable invasive hemodynamic monitoring of pulmonary artery pressure is also now available for patients with advanced heart failure where it has been shown to improve outpatient management and reduce heart failure-related hospitalizations.[111] The rationale is that worsening symptoms of heart failure congestion may be identified early from increased pulmonary artery pressure via telemonitoring and thereby prompt remediating action and avoidance of costly hospitalizations.[112]

Summary of blood pressure measurement methods

Beyond biophysical principles of BP measurement, this chapter has presented ideas on the clinical advantages and pitfalls of different BP methods (Table 2.2). The accurate measurement of BP not only relies on valid recording equipment but also on making sure to follow correct protocols of measurement.[113] In 2005, Pickering and colleagues lamented that even though BP was one of the most

TABLE 2.1 Comparison of underdamping and overdamping of fluid-filled catheter systems.

	Underdamping (resonance)	Overdamping
Systolic blood pressure	Overestimated	Underestimated
Diastolic blood pressure (BP)	Underestimated	Overestimated
Pulse pressure	Overestimated	Underestimated
Dicrotic notch	Deep	Absent; however, the absence of a dicrotic notch is sometimes observed in systems with an adequate dynamic response, and should not be considered of overdamping by itself
Other	Nonphysiologic diastolic fluctuations	Slurred upstroke and general loss of detail
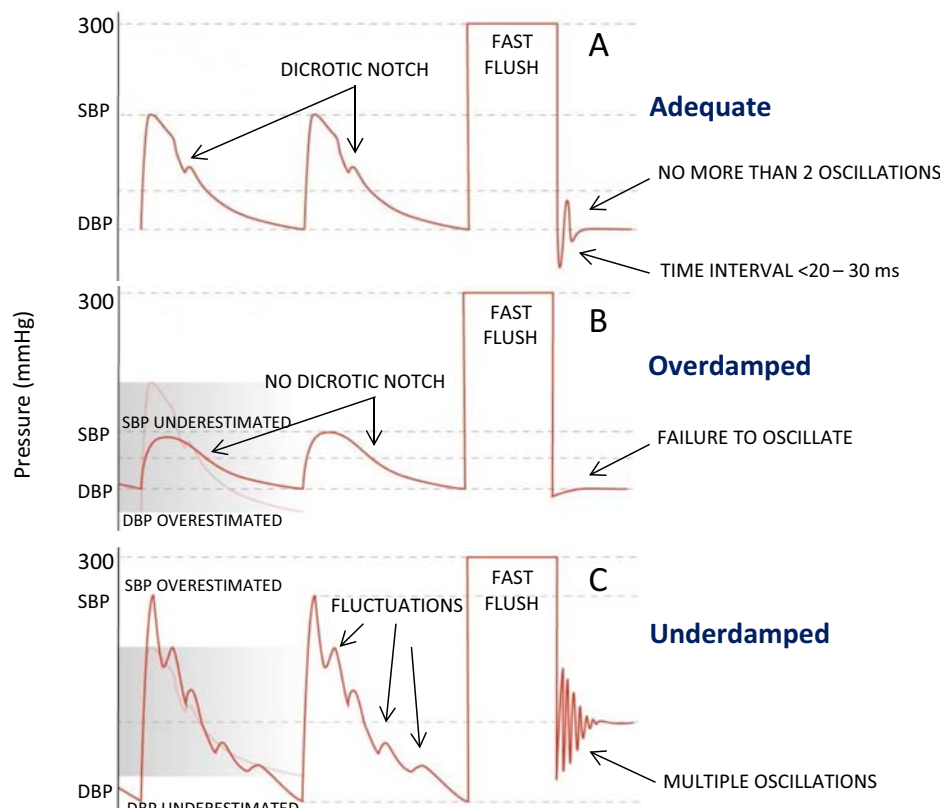
TABLE 2.1 Comparison of underdamping and overdamping of fluid-filled catheter systems.—cont'd

	Underdamping (resonance)	Overdamping
Characteristics in the square wave test	More than two oscillations after the test, high amplitude of oscillations relative to preceding oscillation (as a general rule, the amplitude of each oscillation should be no greater than ~1/3 of the amplitude of the preceding oscillation)	The system does not oscillate after the square wave (there should be one to two "bounce" oscillations)
Reasons	Excessively long and stiff tubing or defective transducer	Low infusion bag pressure, air bubbles or blood clots in the circuit, lose or open connections and kinking or obstruction of the catheter
Strategies to prevent or remediate	• Use of short, stiff tubing • Limit the number of stopcocks • Reduce motion of the catheter in the artery • Adjustable dampening devices	• Avoid kinking • Remove air and blood clots • Replace the catheter as needed

BOX 2.2 How to test the dynamic response of fluid-filled catheter systems?

A dynamic response test determines function of the entire system of recording arterial pressure, from the arterial catheter, tubing, and transducer to the system of recording the arterial pressure waveforms. There are several ways that a dynamic response test may be conducted, and each of which involves perturbing the system with a rapid pressure change, then analyzing the dynamic response to determine the characteristics of the measuring system.

The commonly used fast flush test briefly exposes the transducer to high pressure (i.e., 300 mmHg by a quick turn of a stopcock) from a pressurized saline bag, causing a square wave (a sharp pressure rise followed by a brief plateau then a sharp pressure fall), at the end of which the transducer system returns to baseline. In returning to baseline, the pressure wave briefly oscillates, and analysis of these oscillations is conducted to determine the dynamic response from the natural frequency and damping coefficient.

FIGURE 2.6 Example pressure waveforms from dynamic response testing using the square wave, fast flush test. *Adapted from Deranged Physiology: Arterial line dynamic response testing. https://derangedphysiology.com/main/cicm-primary-exam/required-reading/cardiovascular-system/Chapter%20759/arterial-line-dynamic-response-testing. Accessed October 20, 2020.*
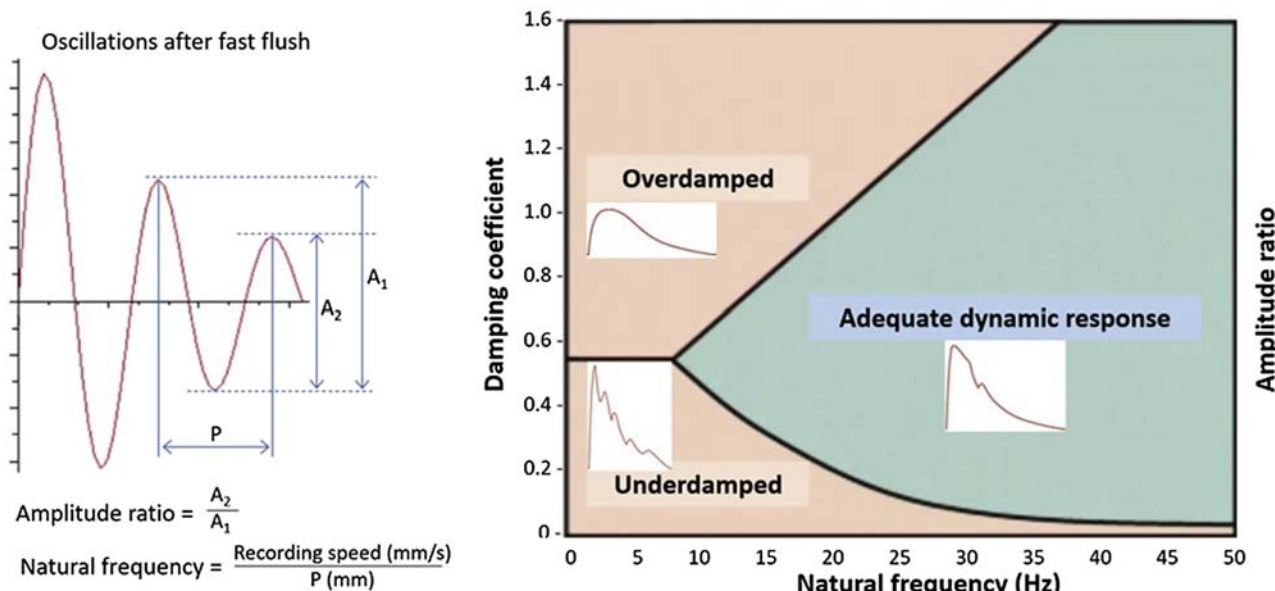
The natural frequency is the frequency of pressure pulse oscillations when not subjected to external force (how rapidly the system oscillates), whereas the damping coefficient is how quickly the oscillations come to rest (the decay of the oscillations).

Fig. 2.6 illustrates the concept of the square wave fast flush test with adequate dynamic response (panel A), as well as example overdamped (panel B) and underdamped (panel C) systems. Key features of a system with adequate dynamic response as per panel A are:

- Short time between oscillations (<20−30 ms)
- At least one oscillation (system is overdamped if it does not oscillate after fast flushing)
- No more than two oscillations (system is underdamped if too many oscillations)
- A distinct dicrotic notch (this is a major waveform feature that can disappear in an overdamped system).

Although there are signs evident in the morphology of the arterial pressure waveform that provide information on the characteristics of the recording system, waveform inspection on its own is inadequate for assessing dynamic response characteristics. For example, there may be no discernable dicrotic notch in the waveforms of some people even in a recording system with adequate dynamic response.

As depicted in Fig. 2.7, the natural frequency of the system is calculated from the quotient of recording speed and the period (P) of one oscillation cycle after the fast flush. The damping coefficient is calculated from the ratio of successive peaks of the oscillations. Note that the dynamic response of the system is determined by a combination of both the natural frequency and the damping coefficient. If the recording system has a high natural frequency (e.g., >24 Hz), it allows for a large leeway in the damping coefficient to achieve adequate dynamic response.

FIGURE 2.7   Determining the dynamic response characteristics of the catheter-transducer measurement system. *Adapted from Gardner RM. Direct blood pressure measurement–dynamic response requirements.* Anesthesiology. *1981;54:227−236; Deranged Physiology: Arterial line dynamic response testing.* https://derangedphysiology.com/main/cicm-primary-exam/required-reading/cardiovascular-system/Chapter%20759/arterial-line-dynamic-response-testing. *Accessed October 20, 2020.*

important measures in clinical medicine, it was still one of the most inaccurately performed.[3] This statement holds true today despite many efforts to redress, and is a key reason for the focus on accuracy within this chapter. Recent initiatives include providing open access to rapid, free, online certificate training courses in accurate BP measurement,[114] demanding better regulatory control on the accuracy of BP devices,[30,40] establishing listings of validated BP devices,[37,115] and developing consumer resources to help find validated BP devices.[116]

The BP measurement with the most profound and longstanding influence on global clinical practice is cuff mercury sphygmomanometry. This was the reference standard that oscillometric BP devices sought to match and remains the reference standard by which cuff-based BP devices are tested for accuracy.[15] Extensive epidemiology and clinical trial prognostic data over many decades firmly establish cuff-based BP as the *gold standard clinical measure*. However, the nontrivial systematic (and random) differences of cuff-based BP from *gold standard*

TABLE 2.2 Summary of advantages and disadvantages of blood pressure measurement methods.

Method	Advantages	Disadvantages
Cuff mercury sphygmomanometry	• Gold standard noninvasive blood pressure (BP) measurement • Low cost • Reproducible results with minimal maintenance requirements • Amenable for use in low resource settings • Randomized controlled trial evidence to support clinical use	• Susceptible to operator-related error (training required) • Less widely available due to phasing out of clinical use • Systematic error in estimating brachial BP (systolic BP underestimated, diastolic BP overestimated) • May not be a precise estimate of central aortic BP
Cuff "oscillometric" BP	• Low cost, widely available • Automated, easy to use • Suitable for home and ambulatory monitoring • Randomized controlled trial evidence to support clinical use	• Susceptible to device-related error (most available for sale are not validated for accuracy) • Susceptible to operator-related error (training required) • Systematic error in estimating brachial BP (systolic BP underestimated, diastolic BP overestimated) • May not be a precise estimate of central aortic BP
Arterial applanation tonometry	• Enables high-quality noninvasive recordings of arterial waveforms • Enables analysis of waveform features • Carotid tonometry can derive central BP estimates without a mathematical transfer function • May be helpful to resolve clinical indecision based on brachial cuff BP	• Requires operator training and skill • Requires dedicated, costly equipment • Radial tonometry requires accurate calibration which is difficult to achieve noninvasively • Carotid tonometry is more technically demanding than radial tonometry • Lacking randomized controlled trial evidence to support clinical use
Cuff central aortic BP (general)	• Widely available • Automated, easy to use • Suitable for home and ambulatory monitoring • Enables analysis of brachial waveforms • May be helpful to resolve clinical indecision based on brachial cuff BP	• Subject to calibration error and underestimation of central aortic systolic BP for Type I devices • Waveform features may be lost using cuff-based recording methods (especially at subdiastolic BP) • Lacking randomized controlled trial evidence to support clinical use
Cuffless BP devices (general)	• Widely available • Automated, nonintrusive, easy to use • Continuous recording over long time periods (big data analysis) is possible • Potential for more information on BP risk and tracking therapy than cuff-based methods • Potential integration with existing health system electronic records for improved quality of care	• Proliferation of diverse technologies with limited understanding of health value or impact • Measurement accuracy is largely uncertain • Peripheral waveforms require accurate calibration which is difficult to achieve • Peripheral recording sites may not reflect clinically relevant BP • Lacking randomized controlled trial evidence to support clinical use
Intra-arterial, invasive BP	• Gold standard invasive BP measure • Enables accurate BP measurement • Enables arterial waveform analysis • Implantable intra-arterial technology available to aid clinical care for high-risk patients	• Invasive medical procedure not amenable for use without clinical indication • Requires significant technical skill and expensive medical resources to perform safely and accurately

physiological measures of intra-arterial BP cannot be ignored and emphasize an unmet need for improving accuracy. This is a key challenge for high-quality BP device manufacturers of the 21st century.

Measurements of arterial flow

The two most widely used techniques for flow measurements in human studies and clinical practice are pulsed wave-Doppler (PW-Doppler) echocardiography and cardiac phase-contrast magnetic resonance imaging (PC-MRI).[117–119] A general comparison of these two techniques is shown in Table 2.3.

Pulsed wave-Doppler

PW-Doppler flow measurements rely on the principle that the Doppler shift of reflected ultrasound waves induced by moving blood particles is proportional to the velocity of those particles.[120] Important considerations for measuring blood flow with PW-Doppler include adequate sample position and volume, gain settings, and Doppler beam orientation, which must be well aligned to the direction of blood flow (zero-insonation angle) to avoid underestimation of flow velocities (although mathematical corrections can be performed for slightly misaligned interrogations).

In practice, flow into the aortic root equals the flow out of the left ventricular outflow tract (LVOT), which is easily visualized with transthoracic echocardiography, allowing for interrogations of LVOT flow velocity and cross-sectional diameter (which in turn is used to compute cross-sectional area), as shown in Fig. 2.8. The latter is important, since volume flow is obtained by multiplying flow velocity times the cross-sectional area of the conduit at the exact point of PW-Doppler interrogation.[120–122] This method assumes a flat flow profile across the vessel lumen and is linearly dependent on cross-sectional area estimations. The latter is generally made from diameter measurements, assuming a circular cross section.
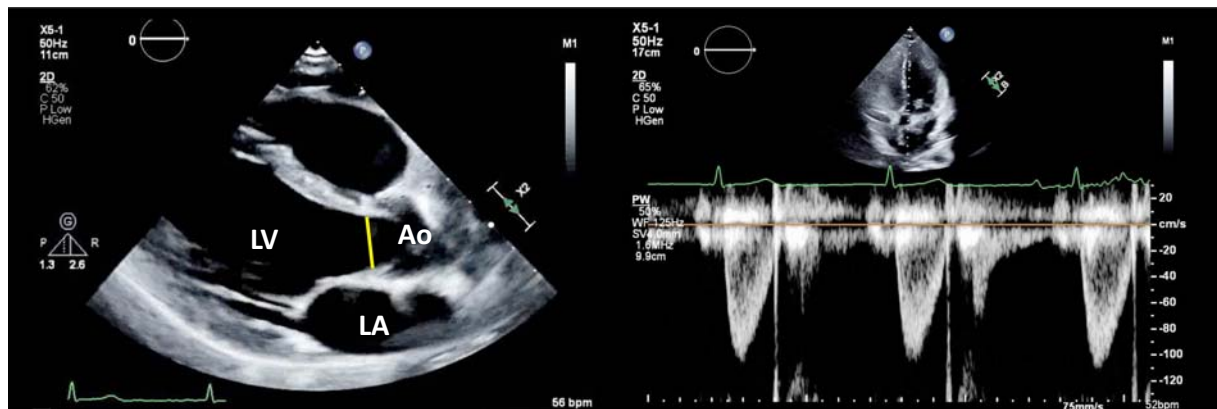
The LVOT tends to be cone-shaped, with the minimal cross-sectional area occurring just below the aortic annulus[122]; often, there is slight widening just underneath the aortic annulus, distal to the narrowest segment, particularly in older patients with septal hypertrophy. When PW-Doppler signals are acquired, the point of maximal flow velocities in the LVOT is identified proximal to the aortic valve, and the velocity signal from that point is recorded; this corresponds to the minimal cross-sectional LVOT area, which is subsequently identified and measured in anatomic images. This is because the continuity principle implies that, in the absence of anatomic defects and assuming a nondeforming LVOT, the volume of blood passing through all points of the LVOT must be equal; since the product of flow velocity and cross-sectional area at any point equals volume flow passing through that point, the point of maximal LVOT flow velocity must correspond to the narrowest area in the LVOT. Another approach is to place the Doppler sample at or immediately below the aortic valve annulus and to measure velocities at precisely this location. Regardless of the approach, the site of flow velocity measurement should always be used along with the diameter measured at the same point, in order to compute volume flow.
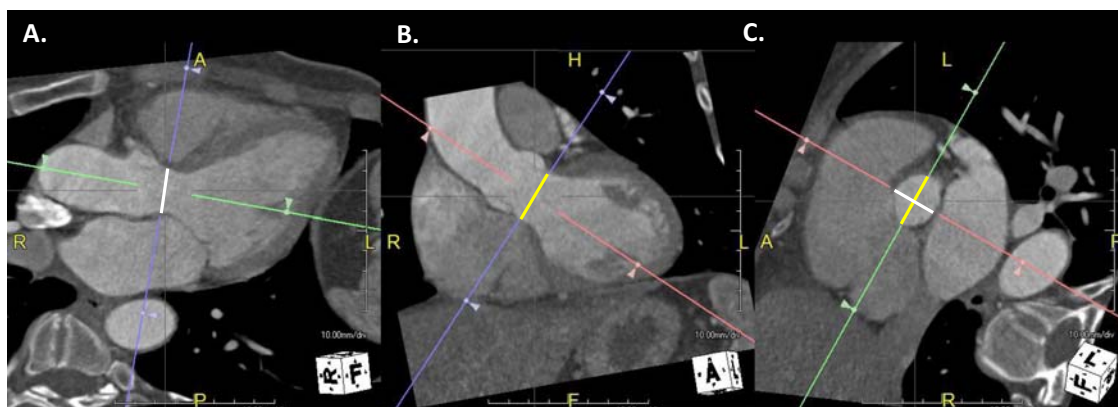
An important limitation of the use of LVOT diameter to compute cross-sectional area is the assumption of a circular

TABLE 2.3 Summary of advantages and disadvantages of blood flow measurement methods.

	Pulsed wave Doppler	Phase-contrast magnetic resonance imaging
Advantages	• Low cost and wide availability • High temporal resolution • Can be performed at the bedside • Can be used simultaneously with acquisitions of pressure wave forms • Can be performed in most patients	• Measures volume flow across the entire cross-sectional area • Not limited by acoustic windows or anatomic planes • Does not assume a flat flow profile
Disadvantages	• Limited by acoustic windows • Assumes a flat flow profile or requires correction to account for an assumed profile • Computation of volume flow requires knowledge of vessel cross-sectional area, which is often based on questionable assumptions • Errors in linear measurements are squared for area computations	• Requires expensive dedicated facility • High cost and less widespread availability/expertise • Inconvenient, since it cannot be performed at the bedside • Lower temporal resolution with standard acquisition times • Difficulties in obtaining simultaneous pressure wave forms due to ferromagnetic components in tonometry equipment • Cannot be performed in claustrophobic patients or patients with certain metallic objects
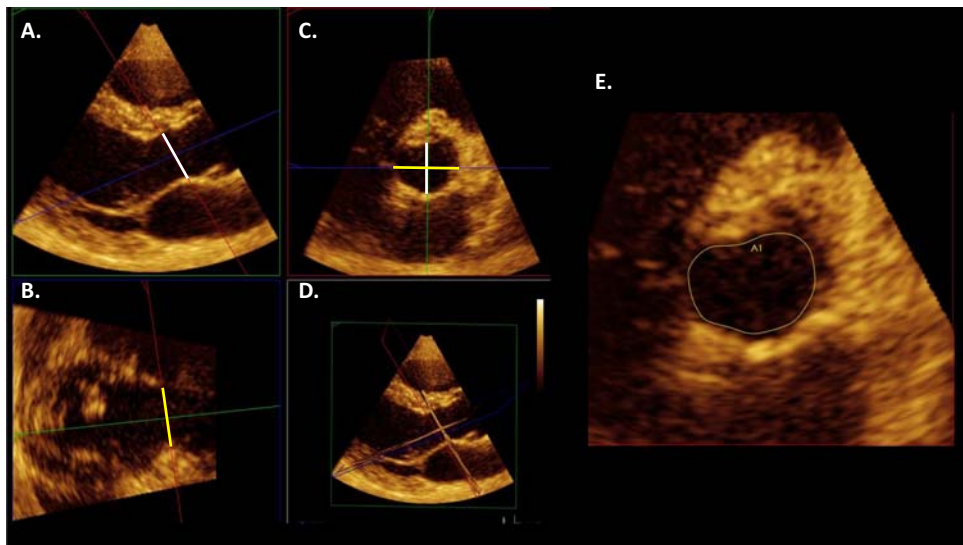
FIGURE 2.8 Measurements of left ventricular outflow tract (LVOT) blood flow with pulsed wave Doppler. The LVOT antero-posterior diameter is typically measured using two-dimensional echocardiography in the parasternal long axis view (left) and the cross-sectional area is computed assuming a circular cross section. LVOT flow velocities are interrogated from the apical five-chamber view, as in this case (right) or from the apical three-chamber view. *Ao*, aorta; *LA*, left atrium; *LV*, left ventricle.

FIGURE 2.9 Example of left ventricular outflow tract (LVOT) cross-sectional geometry using computed tomography three-dimensional reconstruction. Prescription of two orthogonal planes along the long axis of the LVOT (A and B) allows for visualization of a third orthogonal plane (C) which represents the LVOT cross section. An eccentric, rather than circular cross-sectional geometry is present, with the antero-posterior diameter (white line) being shorter than its orthogonal diameter (yellow). Note that the anatomic plane in panel A is similar to the parasternal long axis view (Fig. 2.8A). In cases of LVOT eccentric geometry, the use of this diameter assuming a circular cross-section underestimates the true LVOT cross-sectional area, and thus the volume flow when combined with pulsed wave Doppler flow velocity. *Adapted from Chirinos JA, Segers P. Noninvasive evaluation of left ventricular afterload: part 1: pressure and flow measurements and basic principles of wave conduction and reflection.* Hypertension. *2010;56:555−562.*

LVOT cross-sectional profile (where cross-sectional area equals 0.25π * LVOT diameter2). The LVOT antero-posterior diameter in the parasternal long axis view is typically utilized (Fig. 2.8).[121,122] However, LVOT shape is almost always elliptical, with the antero-posterior diameter usually being shorter than its orthogonal counterpart (Fig. 2.9). Full-volume three-dimensional (3D)-echocardiography with reconstruction of a cross-sectional view can be used for a direct assessment of LVOT cross-sectional area (Fig. 2.10), but it is more technically demanding and time-consuming. With this technique, it is often apparent that the LVOT cross-sectional area can vary throughout systole due to contraction of the basal septum and deformation of the aortomitral continuity (which forms the posterior aspect of the LVOT) during systole.

In a study among 58 adults, we found a mean 2.98 mm-difference between the antero-posterior and its orthogonal diameter and a mean 0.4 cm^2-difference between 3D- and two-dimensional (2D)-derived LVOT area. However, the magnitude of difference varied widely, in some subjects being >1 cm^2. Furthermore, there was only a moderate correlation between 2D- and 3D-measurements ($R^2 = 0.58$).[118] Another limitation of Doppler ultrasound to compute volume flow in vessels is that it assumes a flat flow profile in the vessel lumen (which would result in identical flow velocities at any point in the cross section), a condition that is often not met in arteries in which blood flow exhibits a parabolic profile, or occasionally, highly disorganized profiles (particularly in the distal ascending aorta and aortic arch).

FIGURE 2.10 Example of left ventricular outflow tract (LVOT) cross-sectional geometry assessed with three-dimensional echocardiography. Prescription of two orthogonal planes along the long axis of the LVOT (A and C) allows for visualization of a third orthogonal plane (C) which represents the LVOT cross section. An eccentric, rather than circular cross-sectional geometry is present, with the antero-posterior diameter (*white line*) being shorter than its orthogonal diameter (yellow). Panel D shows representation of the anatomic planes (both orthogonal to the parasternal long axis view). Reconstruction of the LVOT in this manner allows for a direct measurements of cross-sectional area (panel E) that does not assume a circular cross-section. *Adapted from Chirinos JA, Segers P. Noninvasive evaluation of left ventricular afterload: part 1: pressure and flow measurements and basic principles of wave conduction and reflection.* Hypertension. *2010;56:555−562.*

Phase-contrast magnetic resonance imaging
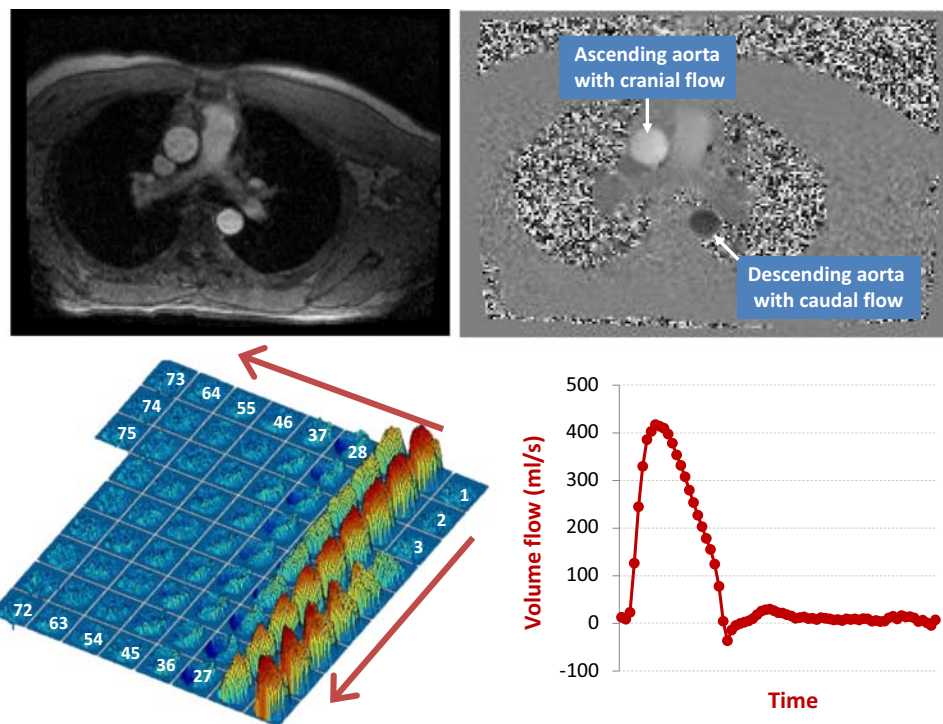
Phase-contrast MRI relies on the fact that, when two opposing magnetic gradient pulses are applied to static nuclei aligned in a magnetic field, the effects of the two pulses on their nuclear spin cancel each other out. However, if a particle moves in the time between the pulses, a shift in the phase of the nuclear spins within the moving particle is accumulated, which is proportional to the velocity of movement along the gradient's direction.[117]

PC-MRI allows for the acquisition of velocity maps along any given anatomical plane. By controlling the gradient direction, velocities can be encoded either "in plane" or "through plane" (in cross section), the latter being particularly useful for assessing flow across an entire vascular cross section without assuming a flat flow profile. With this technique, the anatomic plane should be prescribed exactly perpendicular to the direction of blood flow.

Among other parameters, PC-MRI sequences require a user-defined velocity-encoding sensitivity ("VENC"), which should be as low as possible to maximize the signal from blood flow (thus maximizing the signal-to-noise ratio), yet higher than peak flow velocity in the region of interest to avoid aliasing. VENC should be tailored to individual measurements and iterative PC-MRI acquisitions may be needed, but a good starting point for proximal aortic flow acquisitions is 130−150 cm/s in most cases (unless significant aortic stenosis is present in which case higher velocities are found in some areas of the vessel cross section).

Hyperdynamic LV function or high-output states may also be associated with higher peak flow velocities in some points of the proximal aortic cross section (e.g., 180 cm/s) even in the absence of aortic stenosis, therefore requiring higher VENCs. 2D PC-MRI data are typically acquired over several cardiac cycles and consistent cardiac timing in each cycle is assumed. Prolonged acquisitions may be necessary to accomplish adequate temporal resolution, required for hemodynamic analyses such as pressure-flow analyses.

Limitations of PC-MRI flow measurements include phase-offset errors caused by in-homogeneities of the magnetic field environment (short-term eddy currents).[117] These appear as apparent flow velocities within stationary tissues, typically stable or constant over all frames of a retrospectively gated acquisition.[123] They tend to follow a spatial pattern, such as increasing with distance from the center of the image, which allows for some software correction methods. However, despite correction, even small background velocity offset errors have the potential to result in significant errors in calculated volume flow, due to summation of phase-offset across the entire cross-sectional area of the vessel. Correction for phase-offset can be performed using PC-MRI data acquired from a stationary phantom,[124] but this is not frequently done in practice; moreover, the phase-offset map can change depending on whether the phantom versus the patient is within the bore of the MRI scanner, and therefore the map acquired with a phantom cannot be assumed to be an exact representation of the phase offset present when imaging the

FIGURE 2.11 Measurements of aortic blood flow with through-plane phase-contrast magnetic resonance imaging (MRI). The top left and right panels show magnitude and phase-contrast images of the aortic cross section, respectively. Each pixel in these images represents a voxel (three-dimensional volume with a given thickness). The magnitude image is an anatomic image, whereas the phase-contrast image is essentially a velocity map in which through-plane velocities at each voxel are coded in grayscale in the corresponding pixel. The lower left panel shows the flow velocity profile in the ascending aortic cross-section at each time point in the cardiac cycle (75 time points are recorded in this particular case), and the right lower panel shows the total flow (sum of flow across all individual voxels in the ascending aorta) at each time point. *Adapted from Chirinos JA, Segers P. Noninvasive evaluation of left ventricular afterload: part 1: pressure and flow measurements and basic principles of wave conduction and reflection.* Hypertension. *2010;56:555−562.*

patient. Alternatively, the phase offset can be assessed using information from stationary tissue located in the imaging plane, which generates an error map (including the blood vessel) via interpolation.[125]

Other potential problems in PC-MRI include signal loss due to turbulent flow, partial volume averaging due to limited spatial resolution (since a slice of finite thickness must be interrogated to obtain a sufficient through-plane signal), misregistrations due to in-plane movement of the aorta and pulsatile flow artifacts. PC-MRI is also limited by its high cost, limited availability, incompatibility with patient claustrophobia, and various ferromagnetic objects or implants. The latter also introduces difficulties in truly simultaneous carotid pressure recordings, since available tonometry devices are not MRI-compatible. PC-MRI typically requires breath-hold cooperation for collecting raw data over several cycles, although distal ascending aortic flow can be interrogated during free breathing. An example of through-plane PC-MRI measurements of proximal aortic flow is shown in Fig. 2.11.

Supplementary material

Supplementary data related to this article can be found online at https://doi.org/10.1016/B978-0-323-91391-1.00002-9

References

1. McCutcheon EP, Rushmer RF, Jacobson O, Sandier H. Korotkoff sounds. **Circ Res**. 1967; 20:149−161.
2. Chungcharoen D. Genesis of Korotkoff sounds. **Am J Physiol Legacy Content**. 1964; 207:190−194.
3. Pickering TG, Hall JE, Appel LJ, et al. Recommendations for blood pressure measurement in humans and experimental animals: Part 1: blood pressure measurement in humans: a statement for professionals from the Subcommittee of Professional and Public Education of the American Heart Association Council on High Blood Pressure Research. **Hypertension**. 2005; 45:142−161.
4. Picone DS, Schultz MG, Hughes AD, Sharman JE. Cuff under pressure for greater accuracy. **Curr Hypertens Rep**. 2020; 22:93.
5. Sharman JE, Avolio AP, Baulmann J, et al. Validation of noninvasive central blood pressure devices: ARTERY Society task

force consensus statement on protocol standardization. **Eur Heart J**. 2017; 38:2805−2812.

6. Lewington S, Clarke R, Qizilbash N, Peto R, Collins R. Age-specific relevance of usual blood pressure to vascular mortality: a meta-analysis of individual data for one million adults in 61 prospective studies. **Lancet**. 2002; 360:1903−1913.

7. Ettehad D, Emdin CA, Kiran A, et al. Blood pressure lowering for prevention of cardiovascular disease and death: a systematic review and meta-analysis. **Lancet**. 2016; 387:957−967.

8. Booth J. A short history of blood pressure measurement. **Proc R Soc Med**. 1977; 70:793−799.

9. Bordley 3rd J, Connor CA, Hamilton WF, Kerr WJ, Wiggers CJ. Recommendations for human blood pressure determinations by sphygmomanometers. **Circulation**. 1951; 4:503−509.

10. Freis ED, Sappington RF. Dynamic reactions produced by deflating a blood pressure cuff. **Circulation**. 1968; 38:1085−1096.

11. Bazett HC, Laplace LB, Scott JC. The pressure changes induced in the vascular system as the result of compression of a limb, and their effect on the indirect measurement of lateral pressures. **Am J Physiol Legacy Content**. 1935:112.

12. Wiggers CJ. Dynamic reactions induced by compression of an artery. **Circ Res**. 1956; 4:4−7.

13. Cunningham T. Korotkoff sounds. **BMJ**. 2003; 327:0307234.

14. Palatini P, Asmar R, O'Brien E, Padwal R, Parati G, Sarkis J, Stergiou G, European Society of Hypertension Working Group on Blood Pressure Monitoring CV, International Standardisation OrganisAtion. Recommendations for blood pressure measurement in large arms in research and clinical practice: position paper of the European society of hypertension working group on blood pressure monitoring and cardiovascular variability. **J Hypertens**. 2020; 38:1244−1250.

15. International Organization for Standardization, ISO 81060-2. **Non-invasive Sphygmomanometers - Part 2: Clinical Investigation of Intermittent Automated Measurement Type**; 2018. https:// www.iso.org/standard/73339.html. Accessed December 7, 2018.

16. Picone DS, Schultz MG, Otahal P, et al. Accuracy of cuff-measured blood pressure: systematic reviews and meta-analyses. **J Am Coll Cardiol**. 2017; 70:572−586.

17. Picone DS, Schultz MG, Peng X, et al. Discovery of new blood pressure phenotypes and relation to accuracy of cuff devices used in daily clinical practice. **Hypertension**. 2018; 71:1239−1247.

18. Carlsen RK, Peters CD, Khatir DS, et al. Estimated aortic blood pressure based on radial artery tonometry underestimates directly measured aortic blood pressure in patients with advancing chronic kidney disease staging and increasing arterial stiffness. **Kidney Int**. 2016; 90:869−877.

19. Picone DS, Schultz MG, Otahal P, et al. Influence of age on upper arm cuff blood pressure measurement. **Hypertension**. 2020; 75:844−850.

20. Boutouyrie P, London GM, Sharman JE. Estimating central blood pressure in the extreme vascular phenotype of advanced kidney disease. **Kidney Int**. 2016; 90:736−739.

21. Sharman JE, Marwick TH. Accuracy of blood pressure monitoring devices: a critical need for improvement that could resolve discrepancy in hypertension guidelines. **J Hum Hypertens**. 2018; 33:89−93.

22. Stergiou GS, Alpert B, Mieke S, et al. A universal standard for the validation of blood pressure measuring devices: association for the Advancement of Medical Instrumentation/European Society of Hypertension/International Organization for Standardization (AAMI/ ESH/ISO) collaboration statement. **Hypertens**. 2018; 71:368−374.

23. Alpert BS, Quinn D, Gallick D. Oscillometric blood pressure: a review for clinicians. **J Am Soc Hypertens**. 2014; 8:930−938.

24. Jilek J, Stork M. Cuff pressure pulse waveforms: their current and prospective application in biomedical instrumentation. **In: Biomedical Engineering, Trends in Electronics, Communications and Software**. Intech; 2011:193−210.

25. Geddes LA, Voelz M, Combs C, Reiner D, Babbs CF. Characterization of the oscillometric method for measuring indirect blood pressure. **Ann Biomed Eng**. 1982; 10:271−280.

26. Alvarado Alvarez M, Padwal R, Ringrose J, Jalali A, Hiebert W. Optimum waveform envelopes and amplitude ratios in oscillometric blood pressure estimation. **Blood Press Monit**. 2020; 26(1):53−59.

27. Posey JA, Geddes LA, Williams H, Moore AG. The meaning of the point of maximum oscillations in cuff pressure in the indirect measurement of blood pressure. 1. **Cardiovasc Res Center Bull**. 1969; 8:15−25.

28. Stergiou GS, Palatini P, Asmar R, et al. Recommendations and practical guidance for performing and reporting validation studies according to the universal standard for the validation of blood pressure measuring devices by the association for the Advancement of Medical Instrumentation/European Society of Hypertension/International Organization for Standardization (AAMI/ESH/ISO). **J Hypertens**. 2019; 37:459−466.

29. Muntner P, Einhorn PT, Cushman WC, et al. Blood pressure assessment in adults in clinical practice and clinic-based research: JACC scientific expert panel. **J Am Coll Cardiol**. 2019; 73: 317−335.

30. Campbell NR, Gelfer M, Stergiou GS, et al. A call to regulate manufacture and marketing of blood pressure devices and cuffs: a position statement from the world hypertension league, international society of hypertension and supporting hypertension organizations. **J Clin Hypertens**. 2016; 18:378−380.

31. Alpert BS. Can 'FDA-cleared' blood pressure devices be trusted? A call to action. **Blood Pres Monit**. 2017; 22:179−181.

32. Akpolat T, Dilek M, Aydogdu T, Adibelli Z, Erdem DG, Erdem E. Home sphygmomanometers: validation versus accuracy. **Blood Pres Monit**. 2009; 14:26−31.

33. Erdem DG, Erdem E, Dilek M, et al. Accuracy of sphygmomanometers at pharmacies. **Kidney Blood Press Res**. 2009; 32: 231−234.

34. Dilek M, Adibelli Z, Aydogdu T, Koksal AR, Cakar B, Akpolat T. Self-measurement of blood pressure at home: is it reliable? **Blood Press**. 2008; 17:34−41.

35. Sharman JE, Padwal R, Campbell NRC. Global marketing and sale of accurate cuff blood pressure measurement devices. **Circulation**. 2020; 142:321−323.

36. Jung MH, Kim GH, Kim JH, et al. Reliability of home blood pressure monitoring: in the context of validation and accuracy. **Blood Press Monit**. 2015; 20:215−220.

37. Medaval. **Blood Pressure Monitors**. Dublin, Ireland: Medaval Ltd; 2018 [Internet] https://medaval.ie/blood-pressure-monitors/. Accessed September 29, 2020.

38. Picone DS, Deshpande R, Schultz MG, et al. Non-validated home blood pressure devices dominate the online marketplace in Australia:

major implications for cardiovascular risk management. **Hypertension**. 2020; 75:1593−1599.

39. Olsen MH, Angell SY, Asma S, et al. A call to action and a life-course strategy to address the global burden of raised blood pressure on current and future generations: the Lancet Commission on hypertension. **Lancet**. 2016; 388:2665−2712.

40. Sharman JE, O'Brien E, Alpert B, et al. Lancet Commission on Hypertension group position statement on the global improvement of accuracy standards for devices that measure blood pressure. **J Hypertens**. 2020; 38:21−29.

41. Ringrose JS, Polley G, McLean D, Thompson A, Morales F, Padwal R. An assessment of the accuracy of home blood pressure monitors when used in device owners. **Am J Hypertens**. 2017; 30:683−689.

42. Chandrasekhar A, Kim CS, Naji M, Natarajan K, Hahn JO, Mukkamala R. Smartphone-based blood pressure monitoring via the oscillometric finger-pressing method. **Sci Transl Med**. 2018; 10(431):eaap8674.

43. Armstrong MK, Schultz MG, Picone DS, et al. Brachial and radial systolic blood pressure are not the same. **Hypertension**. 2019; 73:1036−1041.

44. Sharman JE, Lim R, Qasem AM, et al. Validation of a generalized transfer function to noninvasively derive central blood pressure during exercise. **Hypertension**. 2006; 47:1203−1208.

45. Kelly R, Hayward C, Avolio A, O'Rourke M. Noninvasive determination of age-related changes in the human arterial pulse. **Circulation**. 1989; 80:1652−1659.

46. Salvi P, Lio G, Labat C, Ricci E, Pannier B, Benetos A. Validation of a new non-invasive portable tonometer for determining arterial pressure wave and pulse wave velocity: the Pulse Pen device. **J Hypertens**. 2004; 22:2285−2293.

47. Kelly R, Hayward C, Ganis J, Daley J, Avolio AP, O'Rourke MF. Noninvasive registration of the arterial pulse waveform using high fidelity applanation tonometry. **J Vasc Med Biol**. 1989; 1:142−149.

48. Chen CH, Nevo E, Fetics B, et al. Estimation of central aortic pressure waveform by mathematical transformation of radial tonometry pressure. Validation of generalized transfer function. **Circulation**. 1997; 95:1827−1836.

49. Karamanoglu M, O'Rourke MF, Avolio AP, Kelly RP. An analysis of the relationship between central aortic and peripheral upper limb pressure waves in man. **Eur Heart J**. 1993; 14:160−167.

50. Pauca AL, O'Rourke MF, Kon ND. Prospective evaluation of a method for estimating ascending aortic pressure from the radial artery pressure waveform. **Hypertension**. 2001; 38:932−937.

51. Hope SA, Meredith IT, Cameron JD. Effect of non-invasive calibration of radial waveforms on error in transfer-function-derived central aortic waveform characteristics. **Clin Sci**. 2004; 107:205−211.

52. Hope SA, Tay DB, Meredith IT, Cameron JD. Use of arterial transfer functions for the derivation of central aortic waveform characteristics in subjects with type 2 diabetes and cardiovascular disease. **Diabetes Care**. 2004; 27:746−751.

53. Colan SD, Borow KM, Neumann A. Use of the calibrated carotid pulse tracing for calculation of left ventricular pressure and wall stress throughout ejection. **Am Heart J**. 1985; 109:1306−1310.

54. Kelly RP, Gibbs HH, O'Rourke MF, et al. Nitroglycerin has more favourable effects on left ventricular afterload than apparent from measurement of pressure in a peripheral artery. **Eur Heart J**. 1990; 11:138−144.

55. Millasseau S, Agnoletti D. Non-invasive estimation of aortic blood pressures: a close look at current devices and methods. **Curr Pharm Des**. 2015; 21:709−718.

56. Sharman JE, Laurent S. Central blood pressure in the management of hypertension: soon reaching the goal? **J Hum Hypertens**. 2013; 27:405−411.

57. Williams B, Lacy PS, Thom SM, et al. Differential impact of blood pressure-lowering drugs on central aortic pressure and clinical outcomes: principal results of the Conduit Artery Function Evaluation (CAFE) study. **Circulation**. 2006; 113:1213−1225.

58. Borlaug BA, Olson TP, Abdelmoneim Mohamed S, et al. A randomized pilot study of aortic waveform guided therapy in chronic heart failure. **J Am Heart Assoc**. 2014; 3:e000745.

59. Sharman JE, Marwick TH, Gilroy D, Otahal P, Abhayaratna WP, Stowasser M. Randomized trial of guiding hypertension management using central aortic blood pressure compared with best-practice care: principal findings of the BP GUIDE study. **Hypertension**. 2013; 62:1138−1145.

60. Protogerou AD, Papaioannou TG, Lekakis JP, Blacher J, Safar ME. The effect of antihypertensive drugs on central blood pressure beyond peripheral blood pressure. Part I: (Patho)-physiology, rationale and perspective on pulse pressure amplification. **Curr Pharm Des**. 2009; 15:267−271.

61. Mitchell GF. Central pressure should not be used in clinical practice. **Artery Res**. 2015; 9:8−13.

62. Cameron JD. Comparison of noninvasive devices for assessing central blood pressure parameters: what to compare, when and why. **J Hypertens**. 2013; 31:27−31.

63. Cloud GC, Rajkumar C, Kooner J, Cooke J, Bulpitt CJ. Estimation of central aortic pressure by SphygmoCor requires intra-arterial peripheral pressures. **Clin Sci**. 2003; 105:219−225.

64. Davies JI, Band MM, Pringle S, Ogston S, Struthers AD. Peripheral blood pressure measurement is as good as applanation tonometry at predicting ascending aortic blood pressure. **J Hypertens**. 2003; 21:571−576.

65. Smulyan H, Siddiqui DS, Carlson RJ, London GM, Safar ME. Clinical utility of aortic pulses and pressures calculated from applanated radial-artery pulses. **Hypertension**. 2003; 42:150−155.

66. Laugesen E, Rossen NB, Peters CD, et al. Assessment of central blood pressure in patients with type 2 diabetes: a comparison between sphygmocor and invasively measured values. **Am J Hypertens**. 2013; 27:169−176.

67. Papaioannou TG, Karageorgopoulou TD, Sergentanis TN, et al. Accuracy of commercial devices and methods for noninvasive estimation of aortic systolic blood pressure a systematic review and meta-analysis of invasive validation studies. **J Hypertens**. 2016; 34:1237−1248.

68. O'Rourke MF, Takazawa K, Tanaka N. Letter by O'Rourke et al regarding article "Brachial and Radial Systolic Blood Pressure Are Not the Same: evidence to Support the Popeye Phenomenon". **Hypertension**. 2019; 74:e34.

69. Armstrong MK, Schultz MG, Picone DS, et al. Response by Armstrong et al to letter regarding article "Brachial and Radial Systolic Blood Pressure Are Not the Same: evidence to Support the Popeye Phenomenon". **Hypertension**. 2019; 74:e35−e36.

70. Davies JE, Shanmuganathan M, Francis DP, Mayet J, Hackett DR, Hughes AD. Caution using brachial systolic pressure to calibrate radial tonometric pressure waveforms: lessons from invasive study. **Hypertension**. 2010; 55:e4.

71. Verbeke F, Segers P, Heireman S, Vanholder R, Verdonck P, Van Bortel LM. Noninvasive assessment of local pulse pressure: importance of brachial-to-radial pressure amplification. **Hypertension**. 2005; 46:244−248.

72. Segers P, Mahieu D, Kips J, et al. Amplification of the pressure pulse in the upper limb in healthy, middle-aged men and women. **Hypertension**. 2009; 54:414−420.

73. Picone DS, Schultz MG, Peng X, et al. Intra-arterial analysis of the best calibration methods to estimate aortic blood pressure. **J Hypertens**. 2019; 37:307−315.

74. O'Rourke MF, Pauca A, Jiang XJ. Pulse wave analysis. **Br J Clin Pharmacol**. 2001; 51:507−522.

75. Mahieu D, Kips J, Rietzschel ER, et al. Noninvasive assessment of central and peripheral arterial pressure (waveforms): implications of calibration methods. **J Hypertens**. 2010; 28:300−305.

76. Schultz MG, Picone DS, Armstrong MK, et al. The influence of SBP amplification on the accuracy of form-factor-derived mean arterial pressure. **J Hypertens**. 2020; 38:1033−1039.

77. McEniery CM, Cockcroft JR, Roman MJ, Franklin SS, Wilkinson IB. Central blood pressure: current evidence and clinical importance. **Eur Heart J**. 2014; 35:1719−1725.

78. Dorr M, Richter S, Eckert S, et al. Invasive validation of antares, a new algorithm to calculate central blood pressure from oscillometric upper arm pulse waves. **J Clin Med**. 2019; 8.

79. Schultz MG, Picone DS, Armstrong MK, et al. Validation study to determine the accuracy of central blood pressure measurement using the sphygmocor xcel cuff device. **Hypertension**. 2020; 76:244−250.

80. Gotzmann M, Hogeweg M, Seibert FS, et al. Accuracy of fully automated oscillometric central aortic blood pressure measurement techniques. **J Hypertens**. 2020; 38:235−242.

81. Shoji T, Nakagomi A, Okada S, Ohno Y, Kobayashi Y. Invasive validation of a novel brachial cuff-based oscillometric device (SphygmoCor XCEL) for measuring central blood pressure. **J Hypertens**. 2017; 35:69−75.

82. National Vascular Disease Prevention Alliance. **Guidelines for the Management of Absolute Cardiovascular Disease Risk**. 2012.

83. National Institute for Health and Care Excellence, (NICE). **Hypertension in Adults: Diagnosis and Management**; 2019. https://www.nice.org.uk/guidance/ng136.

84. Whelton PK, Carey RM, Aronow WS, et al. 2017 ACC/AHA/AAPA/ACPM/AGS/APhA/ASH/ASPC/NMA/PCNA guideline for the prevention, detection, evaluation, and management of high blood pressure in adults: a report of the American College of Cardiology/American Heart Association Task Force on clinical practice guidelines. **J Am Coll Cardiol**. 2018; 71:e127−e248.

85. Piepoli MF, Hoes AW, Agewall S, et al. 2016 European guidelines on cardiovascular disease prevention in clinical practice: the Sixth Joint Task Force of the European society of Cardiology and Other Societies on Cardiovascular Disease Prevention in Clinical Practice (constituted by representatives of 10 societies and by invited experts) Developed with the special contribution of the European association for cardiovascular prevention & Rehabilitation (EACPR). **Eur Heart J**. 2016; 37:2315−2381.

86. Cheng HM, Sung SH, Shih YT, Chuang SY, Yu WC, Chen CH. Measurement accuracy of a stand-alone oscillometric central blood pressure monitor: a validation report for Microlife WatchBP Office Central. **Am J Hypertens**. 2013; 26:42−50.

87. Weber T, Wassertheurer S, Rammer M, et al. Validation of a brachial cuff-based method for estimating central systolic blood pressure. **Hypertension**. 2011; 58:825−832.

88. Chuang SY, Chang HY, Cheng HM, Pan WH, Chen CH. Prevalence of hypertension defined by central blood pressure measured using a type II device in a nationally representative cohort. **Am J Hypertens**. 2018; 31(3):346−354.

89. Negishi K, Yang H, Wang Y, et al. Importance of calibration method in central blood pressure for cardiac structural abnormalities. **Am J Hypertens**. 2016; 29:1070−1076.

90. Wassertheurer S, Baulmann J. Assessment of systolic aortic pressure and its association to all cause mortality critically depends on waveform calibration. **J Hypertens**. 2015; 33:1884−1888.

91. Goldberg EM, Levy PD. New approaches to Evaluating and monitoring blood pressure. **Curr Hypertens Rep**. 2016; 18:49.

92. Zheng YL, Ding XR, Poon CC, et al. Unobtrusive sensing and wearable devices for health informatics. **IEEE Trans Bio-Med Eng**. 2014; 61:1538−1554.

93. Zheng Y, Leung B, Sy S, Zhang Y, Poon CC. A clip-free eyeglasses-based wearable monitoring device for measuring photoplethysmograhic signals. **Conf Proc IEEE Eng Med Biol Soc**. 2012; 2012:5022−5025.

94. Kamišalić A, Fister Jr I, Turkanović M, Karakatič S. Sensors and functionalities of non-invasive wrist-wearable devices: a review. **Sensors**. 2018; 18.

95. Wang C, Li X, Hu H, et al. Monitoring of the central blood pressure waveform via a conformal ultrasonic device. **Nat Biomed Eng**. 2018; 2:687−695.

96. **Wearable Blood Pressure Monitor Market Global Report 2020: COVID-19 Growth and Change**; June 20, 2020. https://www.thebusinessresearchcompany.com/report/wearable-blood-pressure-monitor-market-global-report-2020-covid-19-growth-and-change. Accessed October 1, 2020.

97. **State of Wearables Today - 2018 Consumer Survey − Slide Share**; November 29, 2018. https://www.slideshare.net/Valencell/state-of-wearables-today-2018-consumer-survey. Accessed October 1, 2020.

98. **The Handbook of Cuffless Blood Pressure Monitoring. A Practical Guide for Clinicians, Researchers, and Engineers**; 2019. https://www.springer.com/gp/book/9783030247003.

99. Luo H, Yang D, Barszczyk A, et al. Smartphone-based blood pressure measurement using transdermal optical imaging technology. **Circ Cardiovasc Imaging**. 2019; 12:e008857.

100. **WHO Guideline: Recommendations on Digital Interventions for Health System Strengthening**. Geneva: World Health Organization; 2019. Licence: CC BY-NC-SA 3.0 IGO.

101. Shuren J, Patel B, Gottlieb S. FDA regulation of mobile medical apps. **J Am Med Assoc**. 2018; 320:337−338.

102. Sharman JE, O'Brien E, Alpert B, et al. Cuffless blood pressure measurement is already here but more validation using specifically developed standards is needed (Reply). **J Hypertens**. 2020; 38:775.

103. BS EN ISO 81060-3. Non-invasive sphygmomanometers. Part 3. Clinical investigation of continuous non-invasive automated measurement type. https://shop.bsigroup.com/ProductDetail?pid=000000000030397676. Accessed November 21, 2019.

104. Fagard RH, Pardaens K, Staessen JA, Thijs L. Prognostic value of invasive hemodynamic measurements at rest and during exercise in hypertensive men. **Hypertension**. 1996; 28:31−36.

105. Fagard RH, Pardaens K, Staessen JA, Thijs L. The pulse pressure-to-stroke index ratio predicts cardiovascular events and death in uncomplicated hypertension. **J Am Coll Cardiol**. 2001; 38:227−231.

106. Gardner RM. Direct blood pressure measurement–dynamic response requirements. **Anesthesiology**. 1981; 54:227−236.

107. Saugel B, Kouz K, Meidert AS, Schulte-Uentrop L, Romagnoli S. How to measure blood pressure using an arterial catheter: a systematic 5-step approach. **Crit Care**. 2020; 24:172.

108. Taylor BC. Frequency response testing in catheter-transducer systems. **J Clin Eng**. 1990; 15:395−406.

109. Deranged Physiology: Arterial line dynamic response testing. https://derangedphysiology.com/main/cicm-primary-exam/required-reading/cardiovascular-system/Chapter%20759/arterial-line-dynamic-response-testing. Accessed October 20, 2020.

110. de Vecchi A, Clough RE, Gaddum NR, et al. Catheter-induced errors in pressure measurements in vessels: an in-vitro and numerical study. **IEEE Trans Bio-Med Eng**. 2014; 61:1844−1850.

111. Abraham WT, Adamson PB, Bourge RC, et al. Wireless pulmonary artery haemodynamic monitoring in chronic heart failure: a randomised controlled trial. **Lancet**. 2011; 377:658−666.

112. Angermann CE, Assmus B, Anker SD, et al. Pulmonary artery pressure-guided therapy in ambulatory patients with symptomatic heart failure: the CardioMEMS European Monitoring Study for Heart Failure (MEMS-HF). **Eur J Heart Fail**. 2020. https://doi.org/10.1002/ejhf.1943.

113. Padwal R, Campbell NRC, Schutte AE, et al. Optimizing observer performance of clinic blood pressure measurement: a position statement from the Lancet Commission on Hypertension Group. **J Hypertens**. 2019; 37(9):1737−1745.

114. Campbell NRC, Khalsa T, Ordunez P, et al. Brief online certification course for measuring blood pressure with an automated blood pressure device. A free new resource to support World Hypertension Day Oct 17, 2020. **J Clin Hypertens**. 2020; 22(10):1754−1756.

115. STRIDE BP https://www.stridebp.org/index.php. Accessed October 2, 2020.

116. Picone DS, Padwal R, Campbell NRC, et al. How to check if a blood pressure monitor has been properly validated for accuracy. **J Clin Hypertens**. 2020; 22(12):2167−2174.

117. Gatehouse PD, Keegan J, Crowe LA, et al. Applications of phase-contrast flow and velocity imaging in cardiovascular MRI. **Eur Radiol**. 2005; 15:2172−2184.

118. Chirinos JA, Segers P. Noninvasive evaluation of left ventricular afterload: part 1: pressure and flow measurements and basic principles of wave conduction and reflection. **Hypertension**. 2010; 56:555−562.

119. Chirinos JA, Segers P. Noninvasive evaluation of left ventricular afterload: part 2: arterial pressure-flow and pressure-volume relations in humans. **Hypertension**. 2010; 56:563−570.

120. Nichols WW, O'Rourke MF. McDonald's blood flow in arteries. **In: Theoretical, Experimental and Clinical Principles**. 5 ed. Oxford University Press; 2005.

121. Segers P, Rietzschel ER, De Buyzere ML, et al. Noninvasive (input) impedance, pulse wave velocity, and wave reflection in healthy middle-aged men and women. **Hypertension**. 2007; 49:1248−1255.

122. Mitchell GF. Clinical achievements of impedance analysis. **Med Biol Eng Comput**. 2009; 47:153−163.

123. Gatehouse PD, Rolf MP, Graves MJ, Hofman MB, Totman J, Werner B, Quest RA, Liu Y, von Spiczak J, Dieringer M, Firmin DN, van Rossum A, Lombardi M, Schwitter J, Schulz-Menger J, Kilner PJ. Flow measurement by cardiovascular magnetic resonance: a multi-centre multi-vendor study of background phase offset errors that can compromise the accuracy of derived regurgitant or shunt flow measurements. **J Cardiovasc Magn Reson**. 2010; 12:5.

124. Chernobelsky A, Shubayev O, Comeau CR, Wolff SD. Baseline correction of phase contrast images improves quantification of blood flow in the great vessels. **J Cardiovasc Magn Reson**. 2007; 9:681−685.

125. Heiberg E, Sjogren J, Ugander M, Carlsson M, Engblom H, Arheden H. Design and validation of segment–freely available software for cardiovascular image analysis. **BMC Med Imaging**. 2010; 10:1.

126. Jilek J, Stork M. Arterial pulsations in the Blood Pressure cuff: are they Hemodynamic Pulses or Oscillations? **Int J Biol Biomed Eng**. 2012; 6(1):35−41.

This page intentionally left blank

Chapter 3

Essential principles of pulsatile pressure-flow relations in the arterial tree

Patrick Segers[1] and Julio A. Chirinos[2,3]

[1]*Faculty of Biomedical Sciences, Institute of Biomedical Engineering and Technology, Ghent University, Ghent, Belgium;* [2]*University of Pennsylvania Perelman School of Medicine, Hospital of the University of Pennsylvania and Perelman Center for Advanced Medicine, Philadelphia, PA, United States;* [3]*Ghent University, Ghent, Belgium*

Introduction

In clinical cardiovascular medicine, arterial wave dynamics are most commonly addressed in terms of arterial pressure, which is understandable given the important role of blood pressure in an individual's cardiovascular risk and the relative ease of accurate arterial pressure measurements. Flow is only seldomly considered in terms of wave dynamics. Rather, the heart is implicitly assumed to be a simple flow source, where only the mean flow (or cardiac output) is typically considered of physiological and clinical relevance. There is, however, an intrinsic inconsistency in this approach, since flow is also pulsatile, and pulsatile hemodynamics affect pressure and flow in a closely interrelated manner.

With each contraction of the heart, the ejection of blood from the ventricles into the aorta and pulmonary arteries initiates both pressure and flow waves traveling down the systemic and pulmonary tree. Along their path, waves undergo complex changes in amplitude and shape. For instance, it is well documented that the amplitude (systolic-diastolic difference) of pressure first increases along large and midsized arteries (the so-called pressure amplification)[1,2] before pulsations get damped in smaller arteries to virtually disappear in the microcirculation.[3]

From a biophysics perspective, one cannot study pressure without also considering the flow.[4−6] Both are tightly coupled, and the relation between pressure and flow is entirely determined by the properties of the arterial tree (i.e., the complete topology and branching structure, vessel dimensions and, importantly, the mechanical properties—and thus the composition—of the arterial wall), as well as the properties of the blood flowing in the arteries. Together, they define the opposition to flow that will be generated by the arterial tree, i.e., the arterial (hydraulic) impedance.[7−9] The term impedance is basically a generalization of the concept of resistance, but while the latter is used to express the relation between mean pressure and mean flow, impedance pertains to pulsatile (time-varying) pressure and flow.[10] Further details on the determinants of impedance are extensively covered in Chapter 1.

The eventual pressure and flow that are observed in an individual's arterial system are therefore the result of what we call ventricular-vascular interactions: as the ventricle ejects, it is hydraulically coupled to the arterial tree and its output will be determined by the performance of the heart on one hand, and by arterial impedance on the other.[11−14] We refer the reader to Chapters 15 and 17 of this textbook for more in depth literature on ventricular-vascular interaction.

In this chapter, we will first introduce the concept of arterial input impedance, which fully characterizes the mathematical relation between pressure and flow in the arterial tree. To do so, we will use the Fourier theorem to transform measured pressure and flow waveforms into families of sinusoidal waves ("harmonics" or "overtones" with frequencies that are natural multiples of the fundamental frequency, which is the heart rate). With this approach, the relation between pressure and flow can be expressed per harmonic, and thus as a function of frequency. We will briefly illustrate that we rely on paradigms—models—for the interpretation of input impedance (which is simply the spectrum of the pressure-

flow relation at various frequencies). These models may or may not consider wave travel and reflection, which may or may not be justifiable under certain conditions. We will then focus on "characteristic impedance" (note the difference with "input impedance"), a fundamental local property of an elastic tube that forms the basis of wave separation analysis. We will illustrate how characteristic impedance relates to and can be estimated from input impedance, but also how it can be estimated directly from measured pressure and flow waveforms. This will lead us to the time domain assessment of pressure-flow relations, making use of wave intensity and wave power analyses, techniques that can be used side by side with impedance analysis for a complete assessment of arterial pulsatile hemodynamics. Illustrations throughout the chapter are based on digitized invasively measured pressure and flow waveforms by Murgo et al.[15] A list of symbols and abbreviations utilized in this chapter is shown in Table 3.1.

TABLE 3.1 Symbols and abbreviations.

dP, dQ, dU	Wavelet as used in the time domain analysis of pressure (P), flow (Q), or flow velocity (U); step change in P, Q, or U from instant t_N to t_{N+1} calculated as $P(t_{N+1}) - P(t_N)$, $Q(t_{N+1}) - Q(t_N)$, or $U(t_{N+1}) - U(t_N)$
dI	Wave intensity calculated as $dU.dP$
f	Frequency (in Hz) of a pressure or flow harmonic.
f_{min}	Frequency at which the first minimum in the input impedance modulus occurs. Used to calculate the effective length of the arterial tree using the quarter wavelength formula
I	Complex constant $\sqrt{-1}$
T	Time
A	Cross-sectional area
C	Total arterial compliance (dV/dP with V volume and P pressure)
C_A	Area compliance (dA/dP with A area and P pressure)
L	In context of windkessel models: parameter in the four-element windkessel model representing the inertia of blood in the arterial tree
L	In context of wave propagation: tube length
L_{eff}	Effective length of the arterial tree as derived from the input impedance spectrum and the quarter wavelength formula
P, Q	Pressure (P), flow (Q)
$\overline{P}$, $\overline{Q}$	Mean arterial pressure (P) or flow (Q); the steady (0 Hz) pressure or flow component that is obtained from Fourier decomposition of the pressure or flow waveform
$\widetilde{P}$, $\widetilde{Q}$	Sinusoidal pressure (P) or flow (Q) harmonic obtained from Fourier decomposition of the pressure or flow waveform, characterized by an amplitude, frequency, and phase angle
$\widetilde{P}_f$, $\widetilde{P}_b$, $\widetilde{Q}_f$, $\widetilde{Q}_b$	Forward (subscript f) and backward (subscript b) components of pressure and flow harmonics
PWV	Pulse wave velocity
R	Total arterial resistance, obtained as $\overline{P}\big/\overline{Q}$
Z	Impedance, calculated at a given frequency as $\widetilde{P}/\widetilde{Q}$ and characterized by an amplitude and phase angle
Z_c	Characteristic impedance, the ratio of pressure and flow in absence of any wave reflections
∂	Differential operator (change in a given variable)
λ	Wavelength
$d\pi$	Wave power calculated as $dQ.dP$
φ_P, φ_Q	Phase lag of pressure (P) or flow (Q) harmonics
φ_Z	Impedance phase angle, calculated as $\varphi_Q - \varphi_P$
ρ	Density of blood
ω	Angular frequency (in rad/s) of a pressure or flow harmonic
Γ	Reflection coefficient
Π	Hydraulic power, approximated as by $P.Q$ (pressure power)

Arterial input impedance: a frequency-domain characterization

Impedance: generalizing resistance for sinusoidal signals

Assume a given systemic or pulmonary arterial tree, in which we position ourselves at its inlet. In order to generate a *constant* flow, $\overline{Q}$, in that system, we would have to generate a *constant* pressure $\overline{P}$. In a linear system (as is usually assumed for the arterial system in vivo), $\overline{P}$ is proportional to $\overline{Q}$ such that $\overline{P} = R\overline{Q}$ (analogous to Ohm's law in electrical theory) with R the total arterial resistance that mainly results from viscous friction forces that the blood exerts on the arterial walls in a normal arterial tree. Note that we hereby assume that venous pressures are small enough to be ignored, and we discard the existence of any zero-flow or critical closing pressure, i.e., a minimal pressure required to generate flow.[16]

If we now impose a *sinusoidally* varying pressure $\widetilde{P}$ (with zero mean value) with a given magnitude and frequency to that same linear(ized) system, this will give rise to a flow $\widetilde{Q}$ that also varies sinusoidally, with the same frequency as the pressure. We call this signal a wave, although we will initially only consider pressure and flow variations in time, and not (yet) in space (thus not considering wave travel for now). Just like resistance represents the ratio of mean pressure and mean flow, the ratio of pressure and flow sine waves represent the impedance at a given frequency. However, sine waves have amplitude and phase (position in time relative to the cardiac cycle). So, for a given frequency, we need two parameters to express the relation between the sinusoidally varying pressure and flow (impedance): the ratio of the amplitude of the harmonics (the impedance modulus) and the phase angle, expressing the phase (time) delay between pressure and flow (Box 3.1).

Calculating impedance at the inlet of the arterial tree

Measured arterial pressure and flow waves are pulsatile, but clearly not sinusoidal (or perfectly oscillatory). Arterial pressure and flow signals are however quasi periodic (i.e., with events consistently occurring at regular intervals) when the cardiovascular system is in steady state. It follows from the Fourier theorem (See basic concept box and Fig. 3.1) that any periodic signal can be decomposed into a steady signal and a series of sine waves (also called harmonics) with frequencies that increase as multiples of the ground frequency of the original signal (in this case, the heart rate). When summed, the result is mathematically identical to the original signal when enough harmonics are taken into consideration. As the Fourier theorem can be applied to measured pressure and flow, the ratio of corresponding harmonics yields impedance for those frequencies present within the spectrum. The value at 0Hz is the ratio of mean pressure and flow ("steady" impedance), which is

---

BOX 3.1 Impedance
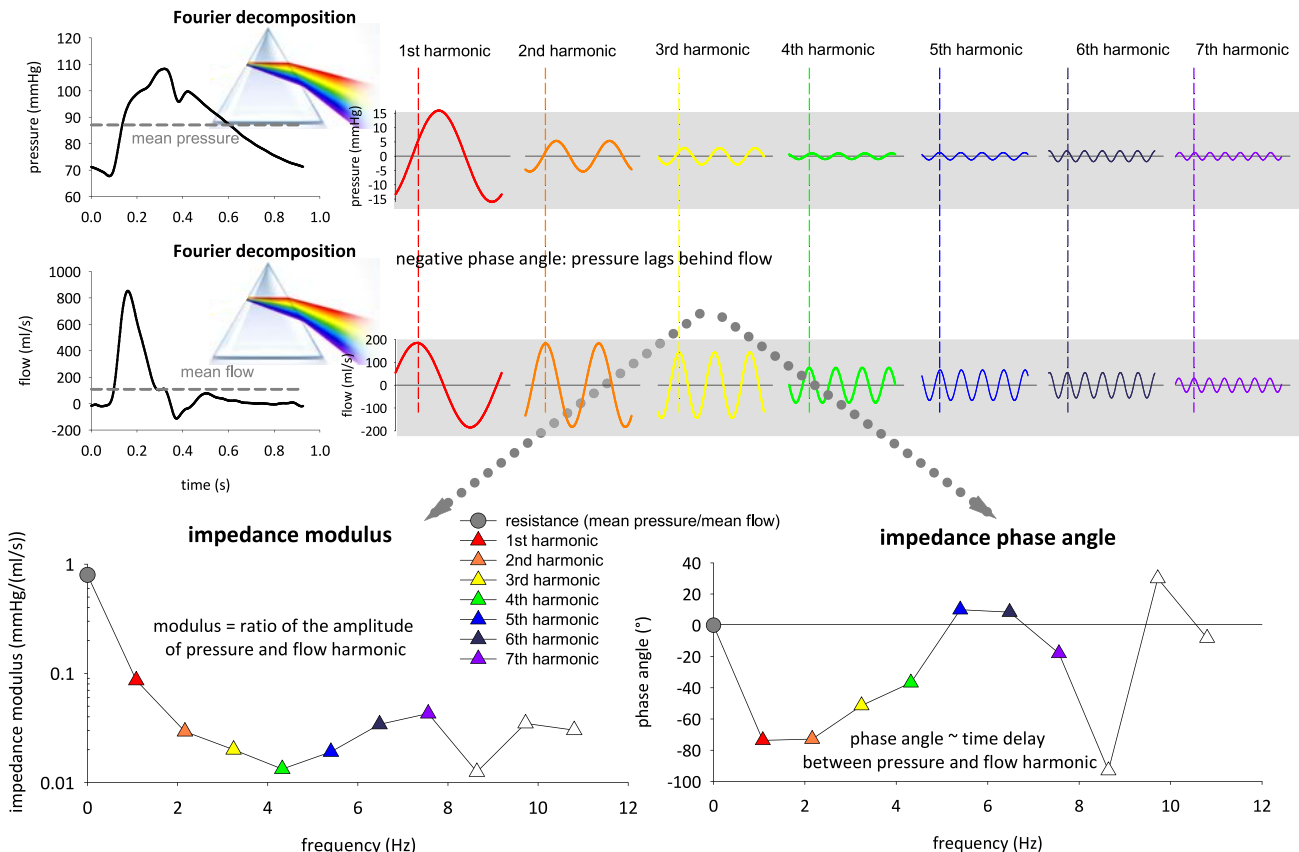
A pressure sine wave can be mathematically represented as $\widetilde{P} = |P|e^{i(\omega t - \varphi_P)}$ with $|P|$ the magnitude of the wave, φ_P the phase *lag* (to position it in time), and ω the angular frequency (in rad/s), being equal to $2\pi f$ with f the frequency in Hz. Similarly, we have $\widetilde{Q} = |Q|e^{i(\omega t - \varphi_Q)}$. We can then generally define impedance, Z, for that frequency as

$$Z = \frac{\widetilde{P}}{\widetilde{Q}} = \frac{|P|e^{i(\omega t - \varphi_P)}}{|Q|e^{i(\omega t - \varphi_Q)}} = \frac{|P|}{|Q|}e^{i(\varphi_Q - \varphi_P)} = |Z|e^{i(\varphi_Z)}$$

So, for a given frequency, we need two parameters to express the relation between the sinusoidally varying pressure and flow (impedance): the ratio of the amplitude of the harmonics (the impedance modulus, $|Z|$) and the phase angle (φ_Z), expressing the phase (time) delay between pressure and flow.

The phase angle, and in particular its sign, is important as it reveals some of the underlying physics and properties of the system we are studying. In our notation, with φ_P and φ_Q being phase delays and $\varphi_Z = \varphi_Q - \varphi_P$,

- $\varphi_Z < 0$ implies that the phase lag of pressure is larger than the phase lag of flow, so flow is ahead of pressure. Such behavior indicates a system that behaves as a capacitor, where flow is needed to load the capacitance and build up pressure.
- $\varphi_Z > 0$ implies that the phase lag of pressure is less than the phase lag of flow, so pressure is ahead of flow. Such behavior indicates a system where inertia dominates, and where a certain pressure build-up is required to generate the flow.
- $\varphi_Z = 0$ implies that pressure and flow are in phase, suggesting a resistive-like behavior (whereby resistance is not to be interpreted in terms of viscous resistance as we will see further).

FIGURE 3.1   Practical guide to calculating input impedance. The pressure and flow waveforms are decomposed into their mean (DC) component signal and harmonics (∼spectral components), sine waves with a frequency at a natural multiple of cardiac frequency and a time lag. For each frequency, impedance represents the ratio of the corresponding pressure and flow harmonic, with the impedance modulus being the ratio of their amplitudes, and the phase angle the difference of their phase angles. Negative phase angle implies that flow is ahead of pressure. The value at 0 Hz is the ratio of mean pressure and flow, i.e., total arterial resistance.

equal to the total arterial resistance. With knowledge of impedance, pressure can be calculated when flow is known, and vice versa.

Fig. 3.1 illustrates the steps that are needed to calculate impedance from aortic pressure and flow waveforms measured at the inlet of the systemic circulation (proximal aorta) of a person exhibiting a "type-A" pressure waveform.[15] The data yield a typical human systemic input impedance pattern characterized by:

- A high value at 0 Hz where phase angle is zero (total arterial resistance);
- A fast drop in impedance in the impedance modulus for the first two to four harmonics, for which the phase angle is negative. This is indicative that, for these frequencies, the system behaves in a capacitive way with flow harmonics peaking before pressure harmonics (see Fig. 3.1);
- Impedance modulus reaches a minimum value, while the phase angle goes up, crossing the horizontal axis

for a frequency that (approximately) coincides with the minimum in the modulus;
- Trend toward a constant impedance modulus for the higher harmonics (from the fifth harmonic on) accompanied by a phase angle that oscillates around zero. As we will discuss later, at these higher frequencies, it is thought that a myriad of reflections arriving from multiple locations in the arterial tree cancel each other out at random. Therefore, the remaining impedance is purely dependent on the local arterial impedance (i.e., the characteristic impedance of the vessel at the measurement site, in this case the proximal aorta).

Impedance can be calculated for any point in the arterial tree, but it is most common to calculate it for the ascending aorta, then representing the arterial input impedance (where arterial denotes the entire arterial tree downstream of the proximal aorta). It therefore includes any possible effect of the downstream vasculature on the pressure and flow waves.

Interpreting input impedance: the windkessel perspective

Input impedance in itself can be a fairly abstract concept that is not easily interpreted. One way to approach input impedance is to discard any effects of wave travel and to consider the arterial tree as a system whose properties are lumped in space, so signals (pressure and flow) only vary in time, not in space. The behavior (i.e., the impedance) of such a system can be modeled by a limited number of discrete lumped parameter model components. It is common to mimic the system as an electrical circuit—using resistors (to represent viscous friction experienced by the blood in resistance vessels), capacitances (representing arterial compliance), and inductances (representing blood inertia) as building blocks—but the system can be equally built using hydraulic components, as was demonstrated by Westerhof et al. who developed an artificial arterial system in their studies on heart-arterial interaction in isolated (cat) heart preparations connected to that artificial system.[17]
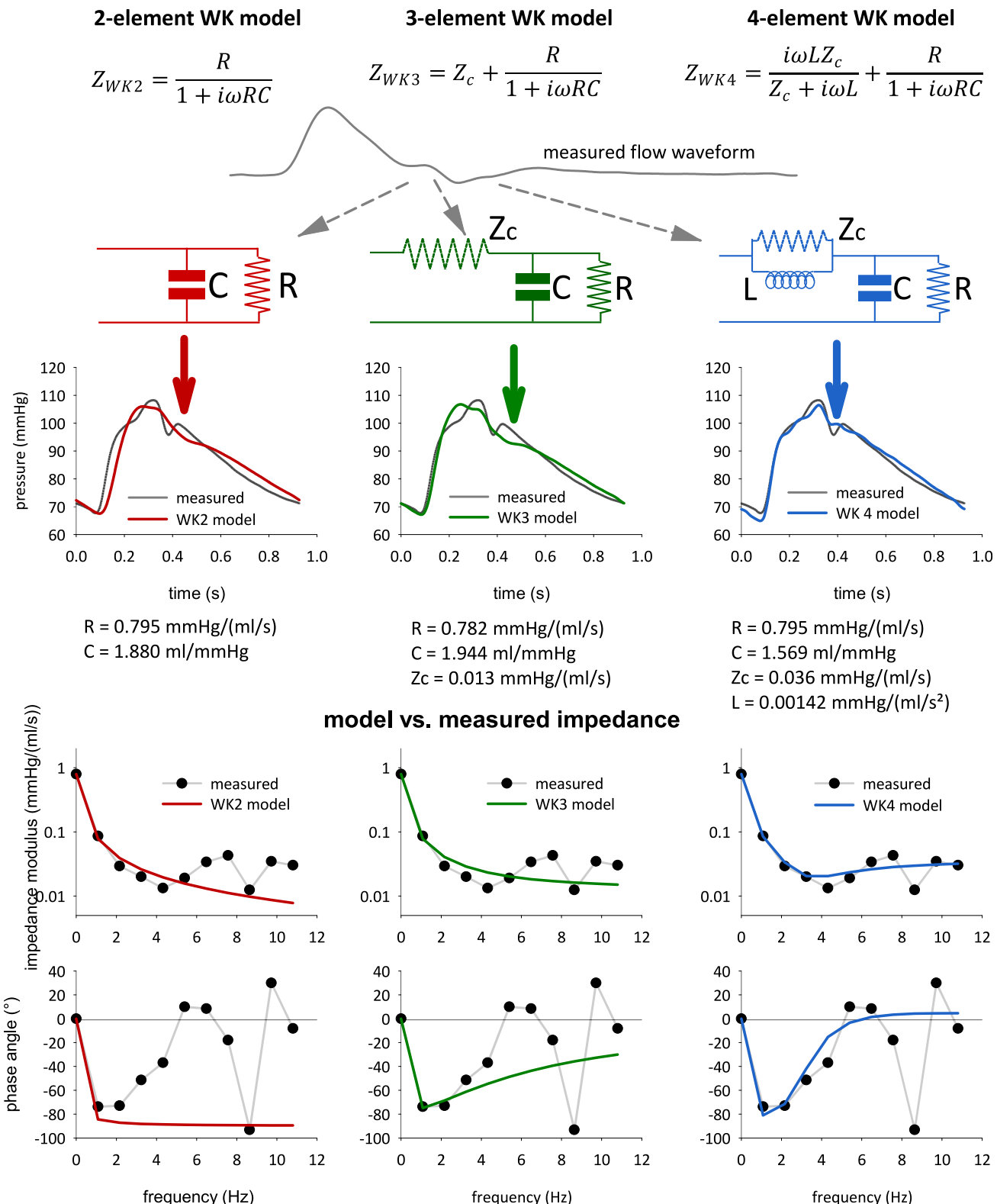
It takes only two components, a resistance (R) and a volume compliance (C) placed in parallel, to mimic the effect of the resistance vessels and the buffering action of the large arteries, a model known as the two-element windkessel model (the terminology referring to the German word for air chamber after Otto Frank who was the first to document the model).[18] The two-element windkessel model can replicate the low frequency features of the pressure waveform fairly well. Indeed, when imposing a measured flow to the model, the pressure predicted by the model has the correct amplitude (pulse pressure) and shows the exponential pressure decay in diastole (with a rate of decline determined by the time constant RC) as shown in Fig. 3.2. The two-element windkessel model forms the basis of compliance estimation methods as the pulse pressure method,[19] decay time or area method[20] as we will discuss further on.

The two-element windkessel model, however, cannot replicate the higher frequency (or "finer detail") behavior of the arterial tree (visible in the filtered and delayed appearance of pressures predicted by the model—see Fig. 3.2), a problem solved by the three-element windkessel model where a resistive element—characteristic impedance, Z_c—is placed in series with the two-element model.[17] Indeed, for higher frequencies, the model impedance now approaches Z_c, generating the desired behavior for those frequencies. However, while solving the problem at the higher frequencies, Z_c introduces problems for the lower frequencies. It is immediately clear from the expression for impedance that the value at zero frequency is $R + Z_c$ which means that—in this model—Z_c accounts for some of the resistance due to viscous friction, a property ascribed to the resistance vessels and that we preferably capture with R (such that mean pressure/mean flow equals R, and not $R + Z_c$). In addition, the effect of Z_c over the complete frequency range also interferes with the effect of compliance. This becomes most obvious when the three-element windkessel model is used to estimate compliance; compared to other models, it will tend to overestimate compliance to compensate for the presence of Z_c that generates an "impedance offset" in the low frequency band.[21] The higher the ratio of Z_c to R, the more prominent this effect becomes. We demonstrated that the three-element windkessel model particularly overestimates compliance in the pulmonary and in the vasodilated systemic circulation, where resistance is low and the ratio of Z_c to R is higher.[22] Fig. 3.2 reports the parameters of the windkessel model fitted to the data from Fig. 3.1. Note that the three-element windkessel model indeed yields the highest value for C of all models included.

Many other model configurations exist, with more parameters usually improving the ability of the model to mimic impedance or improve model fitting, yet with the drawback that model parameters lose their physiological interpretation and the uncertainty on the fitted parameter value increases. A model worth mentioning is an extension of the three-element windkessel model with an inertial element (L) placed in parallel with Z_c, proposed by Stergiopulos and Westerhof.[23] Having the inertial element in parallel with Z_c is not very intuitive, but authors demonstrated that L represents the inertia of the blood present in all arteries. Interestingly, at zero and low frequencies, the low impedance generated by the inertial element L makes that it acts like a bypass of Z_c; while it forces all "current" (blood) through Z_c at the higher frequencies. As such, the model combines the strengths of the two- and three-element windkessel models and corresponds well to measured input impedance of the arterial circulation in vivo. It is clear from Fig. 3.2 that the four-element windkessel model outperforms the other models, with an excellent fit of the measured impedance modulus and phase, and hence an excellent prediction of the measured pressure waveform.

In summary, windkessel models can be elegant tools to concisely parametrize and quantify basic physiological properties of the arterial tree. With an adequate parameter fit, the parameters of the windkessel model provide the same information as a measured impedance spectrum and therefore capture the relation between arterial pressure and flow. What is important to keep in mind is that these models cannot account for wave travel and reflection. They represent the arterial system and its function as a whole, and parameters cannot not be linked to specific anatomical regions. Below, we expand on the use of windkessel models to estimate total arterial compliance.

2-element WK model

$$Z_{WK2} = \frac{R}{1 + i\omega RC}$$

3-element WK model

$$Z_{WK3} = Z_c + \frac{R}{1 + i\omega RC}$$

4-element WK model

$$Z_{WK4} = \frac{i\omega L Z_c}{Z_c + i\omega L} + \frac{R}{1 + i\omega RC}$$

R = 0.795 mmHg/(ml/s)
C = 1.880 ml/mmHg

R = 0.782 mmHg/(ml/s)
C = 1.944 ml/mmHg
Zc = 0.013 mmHg/(ml/s)

R = 0.795 mmHg/(ml/s)
C = 1.569 ml/mmHg
Zc = 0.036 mmHg/(ml/s)
L = 0.00142 mmHg/(ml/s²)

model vs. measured impedance

FIGURE 3.2   The arterial system can be represented as a windkessel model. The top panels display the mathematical expression for the impedance of a two-, three-, and four-element windkessel model and the electrical analog representation. The middle panels display, for each model, the best possible prediction of the measured pressure when imposing the measured flow waveform and fitting the model parameters to the data. It is clear that the four-element windkessel model provides the best fit. This is also reflected in the two lower rows where the model impedance modulus and phase are shown together with the measured impedance. The two-element windkessel model describes measured impedance well for the first two to three harmonics, but the four-element windkessel model has an excellent fit over the complete frequency range.

Estimating total arterial compliance by use of windkessel models

The most direct way of using a windkessel model to estimate total arterial compliance is to fit the model parameters to measured pressure and flow waveform data as was illustrated above for the 2, 3-, and four-element windkessel model (Fig. 3.2). The value obtained for the model compliance then provides an estimate for total arterial compliance. In this chapter, we limit ourselves to models with a constant, pressure-independent compliance. More advanced models incorporating nonlinear[24] or frequency-dependent values of compliance[25] can be fitted to data, but the clinical application of these models has been limited to date. It is important to keep in mind that different models yield (slightly) different values of compliance and to be aware of the susceptibility of the three-element windkessel model to overestimate compliance, which becomes problematic in the pulmonary circulation or in the vasodilated systemic circulation.[22] We end this section with compliance estimation methods that are based on the two-element windkessel model, but do not require time-resolved pressure and flow waveforms.

The decay-time and area method

The decay of measured arterial pressure in (late) diastole resembles an exponential function (especially in older subjects) which is the course predicted by a two-element windkessel model with resistance R and compliance C: $P(t) = P_0 e^{-t/RC}$. The decay time method makes use of this property and fits an exponential relation to the pressure in diastole which then yields the time constant, RC. With R calculated as the ratio of mean pressure and flow, C is directly found as RC/R. Given that the exponential relation requires zero inflow, the method is restricted to the central aorta. Physiological oscillations on the measured pressure due to wave travel and reflection may complicate the decay-time method, even when fitting only the last two-thirds of diastole.[26] An elegant work around these diastolic pressure oscillations is found in the area method of Liu et al.[20] They formulated an integral version of the decay time method and find the time constant as $RC = \frac{\int_{t1}^{t2} P(t)dt}{P(t1)-P(t2)}$. The integral in the numerator is the area under the pressure curve between t_1 and t_2. This area method is typically applied using the dicrotic notch and the end of diastole as t_1 and t_2, respectively.

The pulse pressure method

Whereas the decay-time and area method require time resolved arterial pressure (in diastole) and mean flow (cardiac output), the pulse pressure method is applied with knowledge of systolic and diastolic pressure (i.e., pulse pressure) and time resolved aortic flow. The method is again based on the two-element windkessel model; R is calculated from mean pressure and flow, and a value of C is found in an iterative way such that the pulse pressure predicted by the model is equal to the measured pulse pressure.[19] The method has a simple and stable iterative scheme, and results do not depend on a chosen time interval or initial parameter values. The rationale behind the method is that pulse pressure (as the exponential pressure decay) is a low-frequency feature that is well replicated by the two-element model.

Interpreting input impedance: the wave-system perspective

Characteristic impedance revisited: inertia and compliance combined
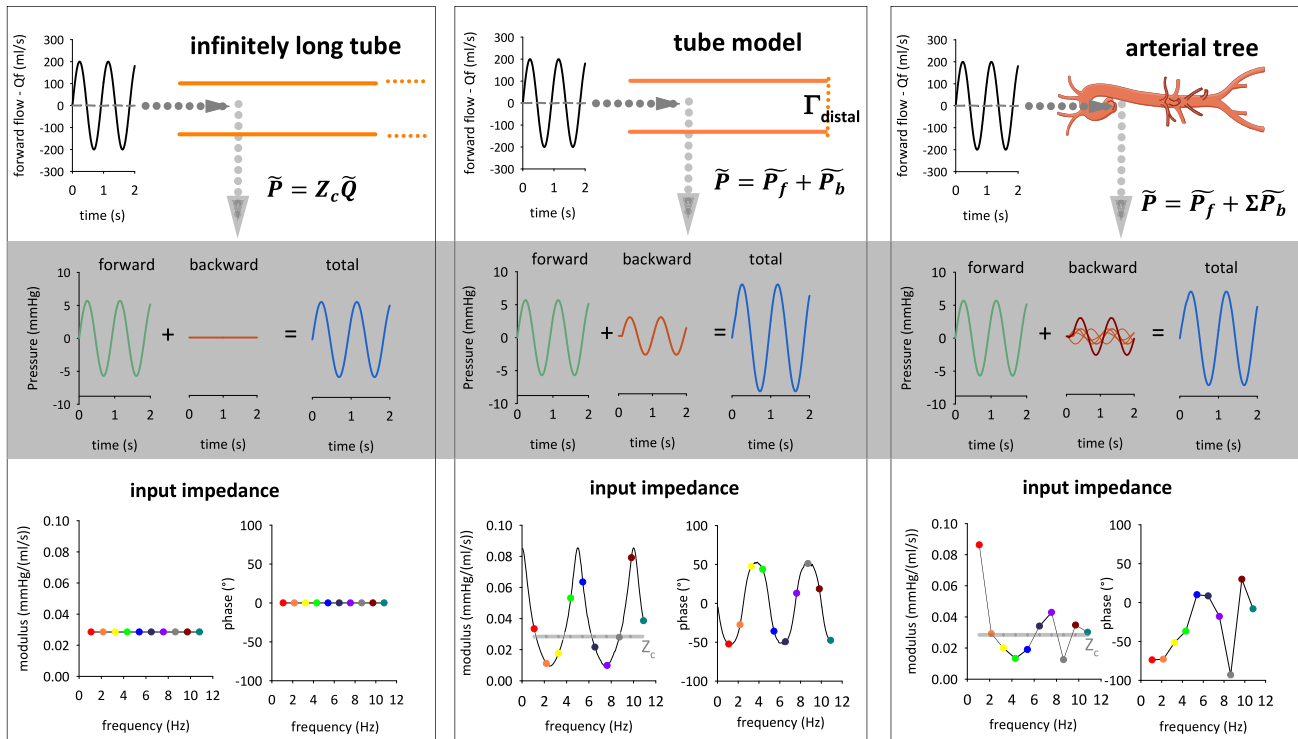
Consider the inlet of a uniform elastic tube that is infinitely long (Fig. 3.3, left panel). The cross-sectional area of the tube is A, and it is filled with a fluid with density ρ. The compliance (C_A) of the tube is given by $C_A = \frac{\partial A}{\partial P}$ (see also Chapter 7). When imposing a (sinusoidal) flow $\widetilde{Q}$ at the inlet, fluid mass has to be displaced along the tube and accelerated, requiring a proportional increase in pressure $\widetilde{P}$. The mass to accelerate, and the associated velocities will on the one hand depend on the density of the fluid and the cross-sectional area (i.e., inertia $\frac{\rho}{A}$), but also on how much mass can be locally stored in the distending tube (mass that is locally stored does not need to be displaced along the tube), and thus on local compliance C_A. If fluid viscosity is neglected, characteristic impedance of the tube can be expressed in terms of these inertial and local compliance properties, $Z_c = \sqrt{\dfrac{\frac{\rho}{A}}{\frac{\partial A}{\partial P}}} = \sqrt{\frac{\rho \partial P}{A \partial A}}$[4–6]. As above, pressure and flow are linked via $\widetilde{P} = Z_c \widetilde{Q}$.

We can further specify the propagation direction of the wave as forward (or positive, e.g., left to right) and backward (negative, from right to left). In this specific setting of the infinitely long uniform tube, reflection sites are absent and only unidirectional waves can exist. By definition, $\widetilde{P_f} = Z_c \widetilde{Q_f}$ and $\widetilde{P_b} = -Z_c \widetilde{Q_b}$ with subscript f referring to forward and b to backward propagating waves. The minus sign accounts for the fact that, in contrast to pressure, flow is not a scalar property but has a direction, with flow considered negative when flowing from right to left.

We deliberately used the same notation as above for characteristic impedance, as it is in essence the same property that we describe, yet from a different perspective. While Z_c emanated as a resistance from a lumped parameter model perspective (and in particular for the three-element

FIGURE 3.3   Left panels: imposing a sinusoidal flow wave (harmonic) to an infinitely long tube gives rise to a sinusoidal pressure wave of the same frequency and in phase with the flow wave of an amplitude equal to Z_c times the amplitude of the flow wave. Backward waves are nonexisting and the input impedance will be equal to the characteristic impedance for all harmonics. Middle: in a tube model with a single reflection site at its distal end, a backward wave will be generated and the measured pressure will consist of a forward and a backward wave. The input impedance modulus is characterized by successive peaks and troughs (and concomitant zero crossings for the phase angle) nonsymmetrically around Z_c that occur at frequencies for which there is maximum destructive (troughs) or constructive (peaks) interference between the forward and backward pressure wave. Right: In the arterial tree, imposing a sinusoidal flow wave will generate a forward pressure wave that gets reflected at innumerable proximal and distal sites along the arterial tree, leading to a scattered and diffuse reflection patterns. All backward waves add up to one resultant backward wave that is retrieved when performing wave separation analysis. The scattered reflections lead to the typical input impedance pattern that resembles that of the single tube for the lower frequencies, but where destructive interference at higher frequencies yields a system that is seemingly free of reflections with input impedance approaching characteristic impedance.

windkessel model), it here becomes clear that it has nothing to do with viscous friction, but rather integrates local inertia and compliance. Note that it can also be written as $Z_c = \frac{\rho PWV}{A}$ with *PWV* pulse wave velocity, the speed at which perturbations propagate along the tube.

Input impedance: fingerprint of arterial wave reflections

The arterial tree is, obviously, much more complex than a uniform elastic tube free of reflection. Therefore, measured pressure and flow waves are in general composed of forward and backward propagating signals. As such, when we decompose measured pressure and flow waves into harmonics using the Fourier theorem, each of these harmonics will be composed of forward and backward propagating components, adding up to $\widetilde{P_f}$ and $\widetilde{P_b}$ for pressure, and $\widetilde{Q_f}$ and $\widetilde{Q_b}$ for flow. By definition, for each harmonic, it applies that $\widetilde{P} = \widetilde{P_f} + \widetilde{P_b}$ and $\widetilde{Q} = \widetilde{Q_f} + \widetilde{Q_b}$.

Making use of the intrinsic relation $\widetilde{P_f} = Z_c\widetilde{Q_f}$ and $\widetilde{P_b} = -Z_c\widetilde{Q_b}$, it is easily shown that

$$\widetilde{P_f} = \frac{\widetilde{P} + Z_c\widetilde{Q}}{2} \;\; ; \;\; \widetilde{P_b} = \frac{\widetilde{P} - Z_c\widetilde{Q}}{2}$$

Thus, each individual harmonic of pressure (and flow) can be decomposed into a forward and backward harmonic of the same frequency.[27] Adding all backward and forward harmonics in the time domain yields the total backward and forward pressure wave, the end result of a wave separation analysis.

For each harmonic frequency, we can define the reflection coefficient Γ as:

$\Gamma = \frac{\widetilde{P_b}}{\widetilde{P_f}} = \frac{-Z_c\widetilde{Q_b}}{Z_c\widetilde{Q_f}} = -\frac{\widetilde{Q_b}}{\widetilde{Q_f}}$. Again, Γ is a complex number where the modulus expresses the ratio of the amplitude of the backward and forward harmonic, while the phase angle expresses the time delay between the backward and forward harmonic. Bringing the above together, it follows that

$$Z = \frac{\widetilde{P}}{\widetilde{Q}} = \frac{\widetilde{P_f} + \widetilde{P_b}}{\widetilde{Q_f} + \widetilde{Q_b}} = \frac{\widetilde{P_f}(1+\Gamma)}{\widetilde{Q_f}(1-\Gamma)} = Z_c \frac{(1+\Gamma)}{(1-\Gamma)}$$

Input impedance is therefore nothing but a mathematical representation of how reflection "disturbs" the relation between pressure and flow, deflecting it from characteristic impedance. It is obvious from this formula that the input impedance always equals characteristic impedance when Γ is zero (in the absence of reflections).

Assuming Γ to be a real number (no phase delays between forward and backward waves), an input impedance higher than Z_c implies $\Gamma > 0$, so the reflected pressure wave adds to the forward wave and increases the amplitude of pressure (constructive interference) (Box 3.2), while total flow will be reduced because of the opposite effect of reflection on the flow wave. Similarly, $Z < Z_c$ implies that $\Gamma < 0$ and reflection now reduces the total pressure (destructive interference) (Box 3.2), while increasing the flow.

It is important to stress that so far we have done nothing but analyze the relation between pressure and flow at a given point in the circulation (usually the ascending aorta or main pulmonary artery) and developed a method that allows us to decompose the measured signals into forward and backward waves with knowledge of Z_c. We did not make any interpretations about the origin or mechanism of wave reflection, which requires further assumptions or the use of models/paradigms. We will discuss several such models/paradigms in the following section.

The arterial system: a network of tubes with distributed reflection sites

The tube model—too simple as a paradigm
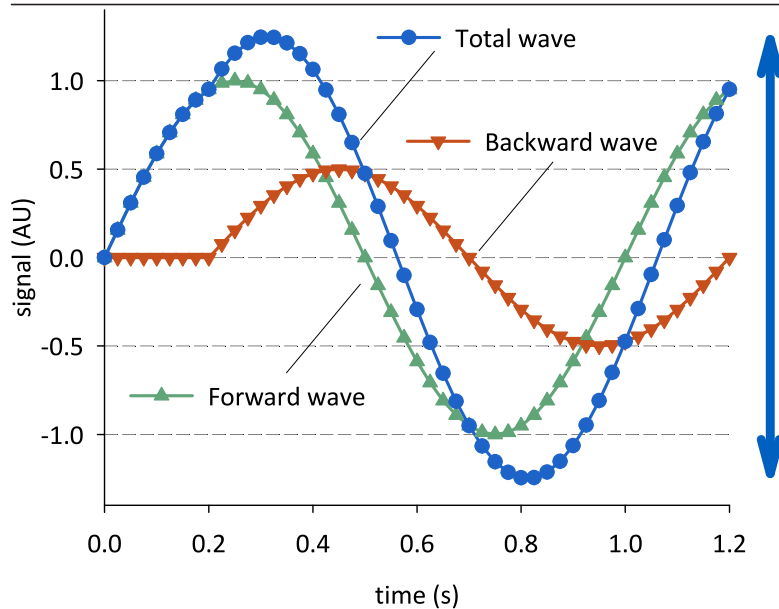
The simplest model of the arterial system that accounts for wave travel and reflection is the tube model (Fig. 3.3, middle panel), whereby the entirety of the arterial tree is conceptualized as a uniform tube of a given length L (e.g., 0.5 m), characterized by characteristic impedance Z_c. The distal end acts as a single discrete reflection site where resistance, impedance, or a reflection coefficient can be prescribed.

Assuming a pulse wave velocity of 5 m/s, it will take 0.2 s for a wave to travel back and forth from the inlet to the distal reflection site (see also basic concept box on constructive and destructive interference). The net effect of the reflection will now largely depend on the timing when the backward wave adds to the forward wave, and this will highly depend on the frequency (f) of the harmonic, the associated wavelength $\lambda = PWV/f$ and the phase delay between the forward and the backward harmonic, given by $\Delta\varphi = \frac{2L}{PWV} 2\pi f$. The maximal impact of the backward wave occurs when $\Delta\varphi = n\pi$, with n an integer. When n is even, the backward pressure wave arrives perfectly in phase
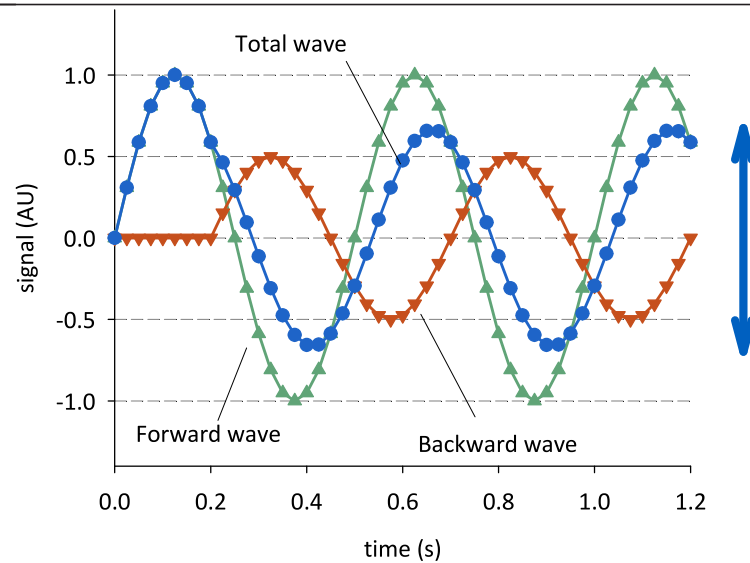
with the forward wave leading to maximal constructive interference. The opposite happens for the flow wave, implying a peak in the impedance spectrum for that frequency. Conversely, when n is odd, the backward pressure wave arrives completely out of phase with the forward wave, leading to maximal destructive interference and a minimum in the impedance spectrum. The first minimum occurs for $n = 1$, for a frequency $f_{min} = \frac{PWV}{4L}$ (2.5 Hz in our example). In a tube model, this leads to a succession of peaks and troughs at these frequencies, as illustrated by the impedance spectrum in the middle panel in Fig. 3.3). As there are no apparent phase delays between the total pressure and flow harmonic, the phase angle will be zero at these frequencies.

The arterial tree—scattered reflections

Most insights on arterial impedance and hemodynamics have been gained from one-dimensional (1D) arterial network models accounting for the Navier−Stokes equations (conservation of mass and momentum) and a relation describing arterial distensibility[28−32] or based on electrical transmission line theory.[7,33] These models demonstrate that reflections arise from discrete impedance mismatch (e.g., at bifurcations) but also as a consequence of progressive changes in impedance (geometric and/or elastic taper) which provoke diffuse, continuous reflections.[34] These reflections also get re-reflected as they propagate toward the heart, adding again to the forward wave. As such, what is conceived as "the" forward and backward wave after wave separation analysis is the integrated effect of all simultaneously coexisting forward and backward propagating contributions, with reflections returning from sites close to the heart and further away.[35] For the lower harmonics, these dispersed reflections still act relatively well in phase with each other. For the first harmonic, the net effect of the added reflections is constructive for pressure waves and destructive for flow waves, leading to an impedance higher than Z_c. Most often, one will find a clear local minimum in the input impedance modulus between the second and fourth harmonic where Z drops below Z_c and where the net effect of reflected waves is to reduce pressure and increase flow. With further increasing frequency, however, phase delays are highly variable, with some reflections arriving in phase, while others arrive out of phase. Reflected waves therefore start canceling each other out, leading to a system that is seemingly free of reflections (comparable to what happens in an acoustic chamber, where the walls are constructed in such a way that sound waves reflect scattered in all directions). The frequency corresponding to the minimum (f_{min}) has been used to estimate an "effective length" of the arterial tree as $L_{eff} = \frac{PWV}{4f_{min}}$. Since wavelength $\lambda = PWV/f$, this is known as the quarter wavelength formula. However, the discrepancy between the real arterial

BOX 3.2 constructive and destructive interference

Constructive interference

Destructive interference

The backward wave (in red) arrives in phase with the forward wave (green), such that the amplitude of the total wave (the summation of both) increases (blue).

The backward wave (in red) arrives out of phase with the forward wave (green), such that the amplitude of the total wave (the summation of both) decreases (blue).

tree and a tube model is large, and the tube model paradigm has led to controversial or incorrect interpretations of arterial hemodynamics.[36]

Estimating Z_c from impedance

Fig. 3.1 displays the modulus and phase of input impedance measured in a human subject exhibiting type-A pressure waveforms.[15] It is indeed observed that for higher harmonics (usually from about the fourth to fifth harmonic), the impedance modulus tends toward a constant value, while also the phase angle is about zero or oscillates around zero. For these harmonics, reflections thus appear absent ($\Gamma \approx 0$), which implies that for these frequencies, $Z \approx Z_c$. Therefore, averaging the higher harmonics of input impedance is one way to estimate characteristic impedance.[4−6] In previous work, analyzing noninvasively measured input impedance in middle-aged subjects, we averaged the fourth to 10th harmonic,[37] but other choices are possible. A good criterion is to select the range where the phase angle is zero or oscillates around zero due to randomly interacting wave reflections, which act as noise at these frequencies.

Pressure-flow relations in the time domain

So far, we addressed pressure-flow relations in the frequency domain, hence considering measured signals as the superposition of a constant value and sinusoidal waves, largely building upon the analogy with electrical circuit theory. This approach assumes linearity of the system (harmonics coexist but to not interact with each other), limits the analysis to steady state situations, and is a somewhat abstract way to analyze the system.

Time domain formulation of wave separation equations

An alternative way to assess pressure-flow relations is to simply analyze them in the time domain. To do so, we need to reconsider the definition of "a wave." In our digital world, measured pressure and flow signals are sampled at discrete moments in time, separated by a given time (sample) interval. We can then define $dP = P(n + 1) - P(n)$ and $dQ = Q(n + 1) - Q(n)$ as the discrete change in pressure and flow, respectively, from time step n to $n + 1$, where dP and dQ are considered as wavelets or wave fronts. This definition of a wave is underlying the wave intensity analysis as introduced for hemodynamic analysis by Parker and Jones[38] and what follows is largely based on work of Parker and colleagues. We will, however, use volume flow (Q in m^3/s) rather than flow velocity (m/s) in the analysis to have an immediate parallel with impedance analysis. One is easily converted into the other via the cross-sectional area of the artery.

Again assuming an infinitely long uniform elastic tube (free of any reflections) characterized by Z_c, it follows from the water hammer equations (see Chapter 1) that under these conditions, $dP_f = Z_c dQ_f$ and $dP_b = -Z_c dQ_b$ with subscripts f and b referring to the forward (positive) and backward (negative) direction, respectively. In the arterial system, just like we previously showed that harmonics consist of a forward and backward component, also dP and dQ will be the result of forward and backward waves, such that $dP = dP_f + dP_b$ and $dQ = dQ_f + dQ_b$. These equations can again be combined and lead to the equations used for wave separation analysis[39]:

$$dP_f = \frac{dP + Z_c dQ}{2} \; ; \; dP_b = \frac{dP - Z_c dQ}{2}$$
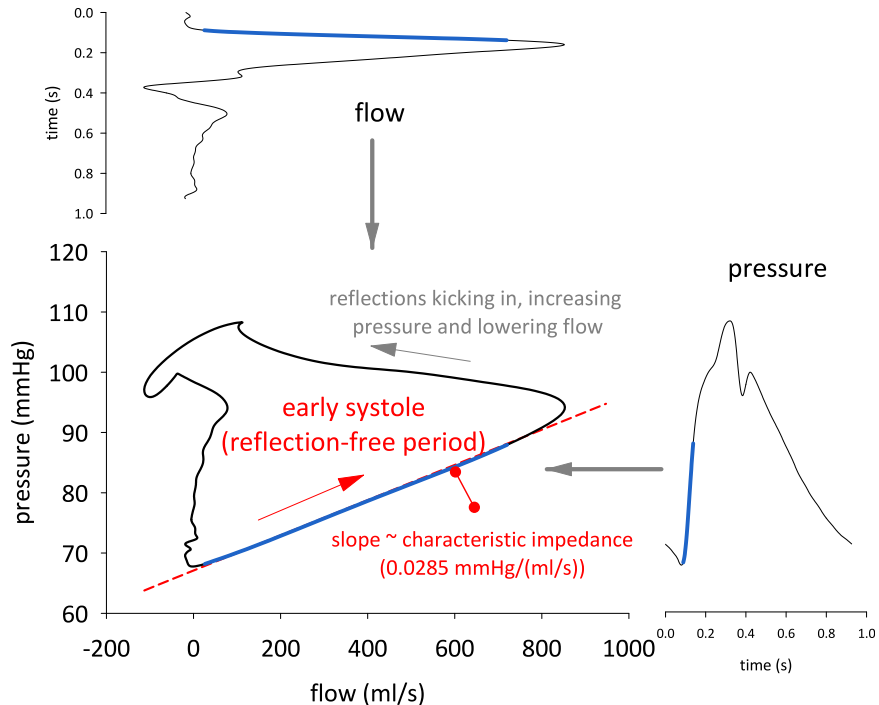
These equations look identical to equations used to separate pressure harmonics,[27] but have an important practical difference: rather than being applied to harmonics of pressure and flow (for which one needs Fourier decomposition), we now decompose pressure and flow wavelets that are easily calculated in any spreadsheet—with knowledge of Z_c.

Estimating characteristic impedance in the time domain

Fig. 3.4 shows a representative aortic pressure-flow pair, whereby instantaneous pressure is plotted as a function of the instantaneous flow level, forming a pressure-flow loop. When the pressure and flow waveforms are well aligned in time, one will observe that the section of the loop that corresponds with early systole (the first $\sim$ 50−100 ms) is linear. Bearing in mind that it should take some time for forward waves to reach reflection sites and return as backward waves, it is a common assumption that early systole provides a time window where aortic pressure and flow waves are free of reflections. In such conditions, we only have forward waves and $dP = Z_c dQ$. Z_c can therefore be estimated as the slope of the linear segment of the pressure-flow loop.[40] Whether that period is really free of reflections is not entirely clear, however, as linearity of the pressure-flow relation as such does not exclude presence of reflections, as has been demonstrated for carotid pressure-flow relations.[41] It cannot be excluded that this also happens in the aorta,[42] at least in some circumstances that lead to very early systolic reflections such as proximal aortic aneurysms, aortic coarctation, or ascending aortic tapering.

Wave separation analysis in practice: an instruction manual

In this section, we will illustrate with a practical example using the same type-A waveforms how to calculate the forward and backward wave from a given pair of pressure (P) and flow (Q) waveforms which have been properly aligned in time (Fig. 3.5). The data in the example represent one heartbeat, but data from longer time recordings can be used as well. The waveform contains $N = 463$ datapoints

FIGURE 3.4   Time-aligned pressure and flow waveforms are combined in a flow-pressure diagram, which displays a loop. It is assumed that early systole (the segment marked in blue) is relatively free of reflections, leading to a linear relationship between flow and pressure. The slope of the line provides an estimate of characteristic impedance.

sampled each 2 ms. Z_c was estimated as the slope of the linear segment of the PQ loop in early systole (Fig. 3.4)

   Step 1—differentiate: calculate $dP(n) = P(n + 1) - P(n)$ and $dQ(n) = Q(n + 1) - Q(n)$ for $n = 1$ to $N - 1$, i.e., the changes in P and Q as a function of time. Note that these arrays will thus consist of one element less than P and Q.
   Step 2—separate: apply the wave separation equations at each instant in time, yielding $dP_f(n)$ and $dP_b(n)$, with $n = 1$ to $N - 1$. if the flow wave is also to be separated, calculate $dQ_f(n) = dP_f(n)/Z_c$; $dQ_b(n) = -dP_b(n)/Z_c$.
   Step 3—integrate: calculate the total forward (P_f, Q_f) and backward (P_b, Q_b) pressure and flow waves as

$$P_f(n) = P_f(n - 1) + dP_f(n); P_b(n) = P_b(n - 1) + dP_b(n); n = 1:N - 1$$

$$Q_f(n) = Q_f(n - 1) + dQ_f(n); Q_b(n) = Q_b(n - 1) + dQ_b(n); n = 1:N - 1$$
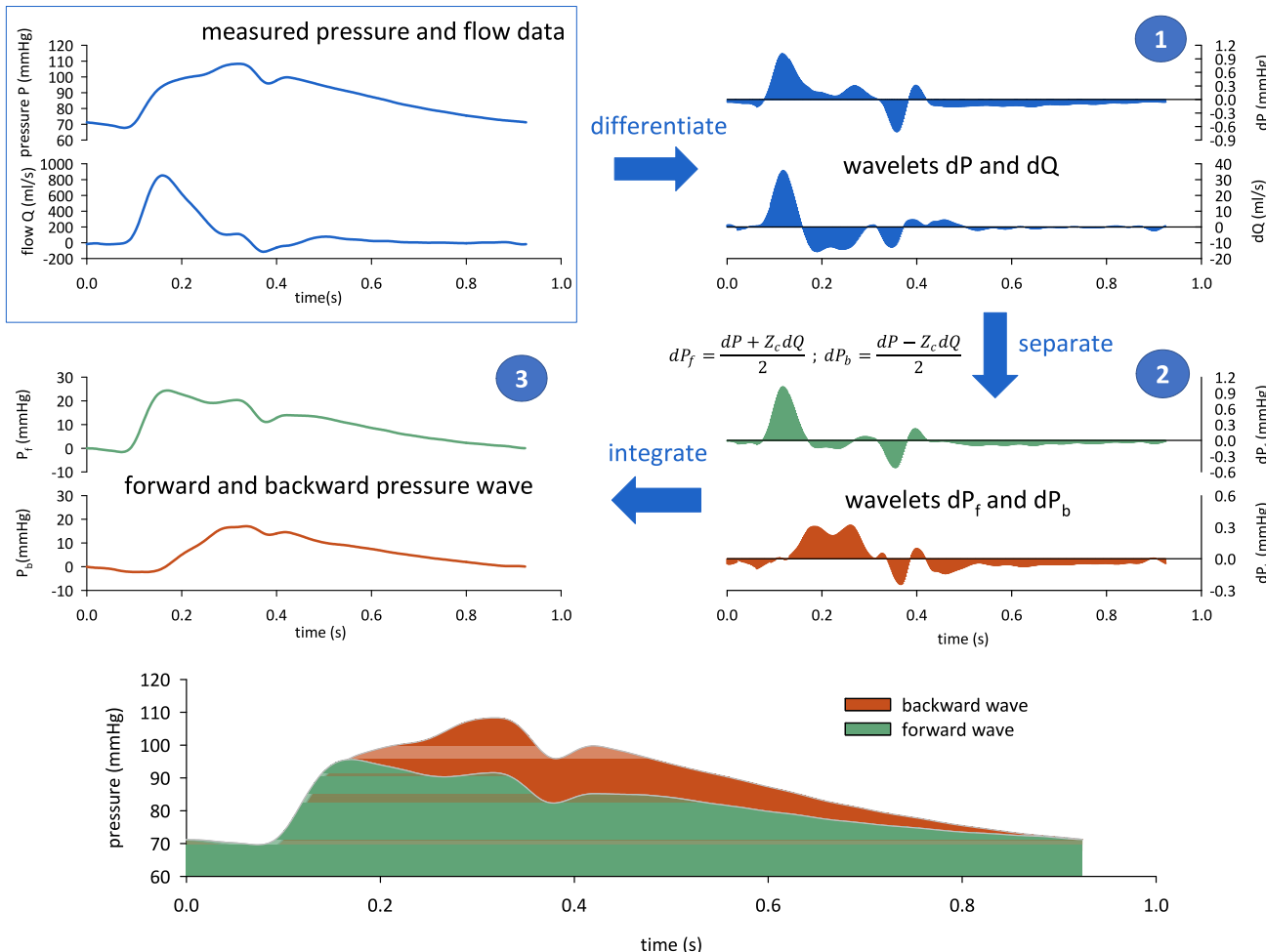
   In this step, we add the contributions of dP_f, dP_b, dQ_f, and dQ_b at the respective timestep, numerically integrating these waveforms. As this is an integration, we can also add an integration constant. By convention, $P_f(0) = P(1)$ and $Q_f(0) = Q(1)$, while $P_b(0) = Q_b(0) = 0$. This ensures that

$P_f + P_b = P$, and $Q_f + Q_b = Q$. Other choices for these integration constants are, however, possible.
   An intuitive way to visually present the results of wave separation analysis is to simultaneously plot the measured and forward pressure wave; the difference between both then represents the contribution of the backward pressure wave (bottom panel Fig. 3.5). A similar presentation can be used for flow. We also stress here that P_f is *not* identical to $Q * Z_c$, because wave reflection also affects the flow wave (the correct statement is $P_f = Q_f * Z_c$).[43] Also, caution is warranted on the strict interpretation of the forward (and backward) wave, as the forward wave in itself includes backward waves that get re-reflected (rectified) at the ventricular-aortic interface, contributing to the forward wave.[27,35,43] As such, P_f is not to be interpreted as the component of pressure that would exist if the heart would eject in a reflection-fee system.

Wave power analysis: energizing hemodynamics

Readers familiar with the literature on arterial hemodynamics will be well acquainted with wave intensity analysis as introduced by Parker and Jones,[38] with wave intensity (dI) at a given measuring location being a time-dependent variable defined as $dI = dP.dU$ with dP a step change in pressure, as previously defined, and dU a step change in

FIGURE 3.5 Practical guideline on how to separate the measured pressure waveform into its forward and backward components in three steps ("differentiate—separate—integrate"), starting from measured pressure and flow waveforms and with knowledge of Z_c. The bottom panel shows the backward and forward components on top of each. The reader is referred to the text for details on the different steps.
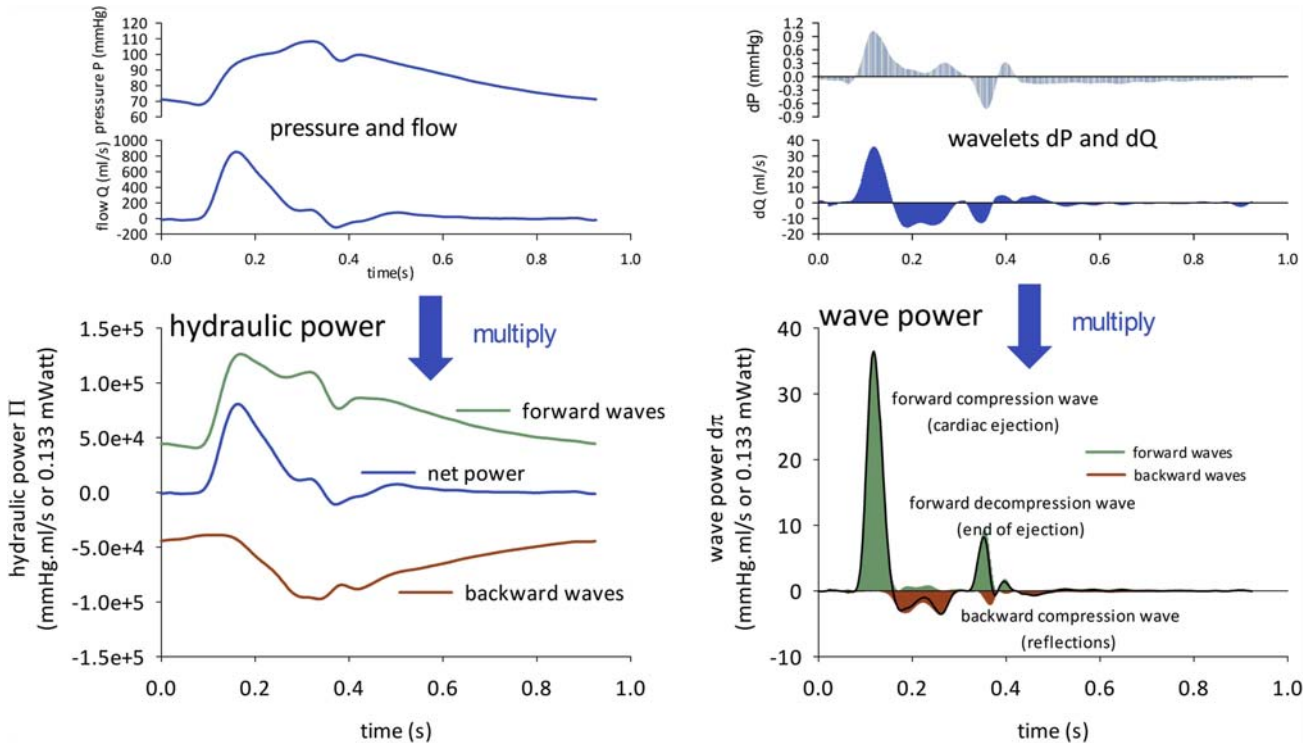
flow velocity. In SI units, dI has the dimension W/m^2 and represents the energy flux carried by the pressure and flow waves. Following Mynard et al., using volumetric flow Q as substitute for U (with $Q = U.A$, A being the cross-sectional area of the artery), one can define wave power $d\pi = dP \cdot dQ$ which is expressed in W (Watt) when using SI units for pressure and flow.[44] Clearly, $d\pi$ closely relates to dI (they scale by a factor A), but has the advantage of representing a conserved quantity, which is not the case for dI (at bifurcations, for instance, $d\pi$ in the mother branch equals the sum of $d\pi$ in the daughter branches, which is not the case for dI).

Wave power to assess the nature and timing of wave reflection

One obvious application of wave power is to just use it as a surrogate of wave intensity, as exemplified in Fig. 3.6 where $d\pi$ was calculated from pressure and flow. With (i)

$d\pi > 0$ indicating forward propagating waves ($d\pi < 0$ indicate backward propagating waves), and (ii) $dP > 0$ indicating compression waves while $dP < 0$ indicates decompression waves, it is immediately clear from $d\pi$ (and dP) which of the four possible wave types dominate at any moment in time: forward compression waves (generated by the heart in early systole), forward decompression (or "suction") waves (generated at end systole due to inertial effects[45]), backward compression waves (as typically observed in the aorta in mid-systole) or backward decompression waves (rarely seen in vivo, but may be observed in case of severe aortic aneurysms, causing the systolic forward compression wave to reflect as a backward decompression wave).[46]

We stressed that $d\pi$ can only reveal the *dominant* wave types. To better appreciate coexisting forward and backward waves, it is recommended to separate $d\pi$ into $d\pi_+$ and $d\pi_-$, the wave power due to the forward and backward pressure and flow waves with $d\pi_+ = dP_+ dQ_+$ and

FIGURE 3.6 Left: hydraulic power Π is calculated as the instantaneous product of pressure and flow. It can be decomposed into contributions of forward and backward waves. Right: wave power $d\pi$ calculated as the instantaneous product of dP and dQ. It is equivalent to wave intensity and can be used to identify the timing and nature of forward and backward waves. Note the difference in y-scale with hydraulic power orders of magnitude higher than wave power.

$d\pi_- = dP_-dQ_-$ and $d\pi = d\pi_+ + d\pi_-$. This is particularly important to reveal early reflections which are easily masked by the dominant systolic forward compression wave. An example of wave power analyses of proximal aortic pressure and flow in a normal adult is shown in Fig. 3.6.

Energetics in the arterial circulation

In their seminal work, Mynard and Smolich elaborated a comprehensive framework on wave energetics and hydraulic power, and how this relates with the wave potential concept (i.e., the potential of a pressurized elastic vessel to generate waves).[44,47] In this final section, we briefly discuss some of their ideas on hydraulic power under the assumption that the undisturbed pressure in the arterial circulation is zero (the equilibrium pressure that is attained when no wave potential or waves exist in the vascular system).

Wave power quantifies the power (energy/unit of time) carried by the waves and due to changes in pressure and flow, irrespective of the absolute pressure level. In the cardiovascular system, however, it is also the absolute pressure and flow levels that matter, as this will largely affect the pressure-volume loop of the heart and hence the

heart's energy expenditure. The quantity to consider then is the hydraulic power Π, which is composed of a pressure component $\Pi_P = PQ$ and a kinetic component which is usually small enough to be ignored in the arterial circulation.[44]

One can then make use of the previously demonstrated wave separation analysis (and with $P_fQ_b + P_bQ_f = 0$) to rewrite $\Pi_P = (P_f + P_b)(Q_f + Q_b) = P_fQ_f + P_bQ_b = \Pi_{P,f} + \Pi_{P,b}$. As such, total hydraulic power can be separated into forward and backward hydraulic power, allowing to quantify the energetic costs of wave reflection.

We repeat that Π_P and $d\pi$—and their forward and backward separated quantities—are pulsatile functions of time with units Watt or Joule/second (J/s) when P is expressed in Pa and flow in m³/s. As such, integration in time (for instance over one heartbeat) of Π_P and $d\pi$ yields the net wave or hydraulic energy (in J) injected into the circulation distal from the point of observation. Separating into forward and backward components allows for the quantification of how wave transmission and reflection contribute to this energy transfer.

As an application of this approach to a clinical problem, we recently utilized these principles to study whether differences of energy transmission into the brain circulation (carotid artery) may play a role in some of the side effects

observed in patients taking organic nitrates (headache and dizziness).[48] In contrast to inorganic nitrates, administration of nitroglycerine, an organic nitrate, led to a significant reduction of aortic hydraulic power, an increase in power penetration to the carotid artery (due to cerebrovascular vasodilation), and an absolute increase in carotid hydraulic power.

The reservoir-wave concept—overarching paradigm or misleading enigma?
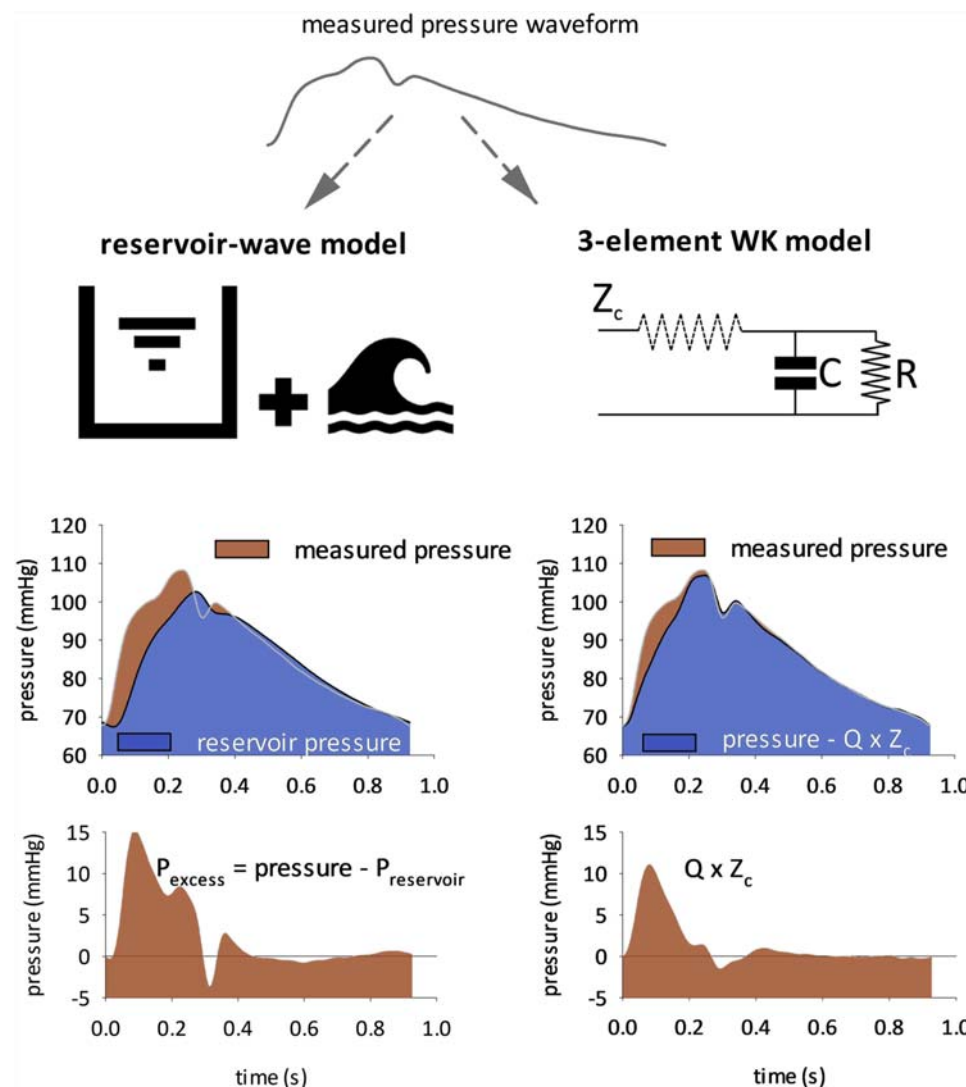
Although the presence of pressure and flow waves in the arterial tree is undisputed, the arterial tree does exhibit a windkessel-like function that is typically approached using lumped parameter models, as discussed extensively in previous sections of this chapter. Lumped parameter (windkessel) models, by definition, contain no space dimension and therefore cannot resolve time and space-dependent wave phenomena. The reservoir-wave concept, introduced by Parker and colleagues, aims to reconcile the arterial windkessel function and wave system. The concept was first introduced by Wang et al.[49] and promoted in subsequent papers in which investigators expanded on the analysis of the wave component.[50–52] Briefly, the arterial pressure waveform is considered as the superposition of a reservoir (windkessel) component and an excess pressure that is ascribed to traveling waves (Fig. 3.7). The concept is intuitively appealing, since one can imagine that rapidly acting wave phenomena superimpose on a slower phenomenon, just like ocean waves generated by the wind superimpose on a tidal wave. To some extent, however, the concept is old wine in new barrels, and a time domain representation of the three-element windkessel model: low frequency (slow phenomena) behavior is described by the RC-component in the model, while the characteristic impedance is needed to describe the high frequency (rapid phenomena) behavior (Fig. 3.7). That also explains why the shape of excess pressure and the flow wave is similar, since the ratio of excess pressure and flow is simply the characteristic impedance. In that sense, it is not surprising that excess pressure carries prognostic information in some patient populations,[53] as it is likely a quantification of the effect of characteristic impedance, which in turn depends on ascending aortic size and stiffness.

An important consequence of the originally introduced concept is that it suppresses the importance of waves and wave reflections.[54] It leads to a drastically different interpretation of arterial hemodynamics with a potential impact on therapeutic strategies. Supporters of the concept reported that application of the reservoir-wave concept yields physiologically more plausible patterns of wave travel and reflection in the aorta than conventional analyses: whereas

traditional wave separation analysis (as applied above on recorded pressure and flow waves) does not lead to a backward wave that travels from the distal to proximal aorta, wave separation analysis on the excess pressure (after subtraction of the reservoir component) does show a backward wave traveling from the bifurcation toward the heart.[51] Also, while conventional wave separation analysis leads to self-canceling forward and backward flow waves in diastole (such that total flow is zero), wave separation analysis on the wave component leads to a wave-free period in diastole.[51]

The reservoir-wave concept—as originally introduced—does carry some inconsistencies. First, invasive pressure recordings immediately demonstrate that the pressure waveform propagates as a whole (including the slow varying component) while the original reservoir-wave concept assumes a steady, nonpropagating reservoir pressure that is uniform over the entire arterial tree. Three-dimensional fluid-structure interaction simulations in an in silico model of aortic coarctation failed to demonstrate that reservoir pressure relates to the volume in the aortic reservoir in systole.[55] Computer model studies in 1D arterial network models, confirmed by in vivo experiments have shown that when wave separation analysis is performed on excess pressure, errors are introduced in the timing, nature, and magnitude of reflected waves, suppressing compression waves and amplifying decompression waves.[54] Also, the argumentation that wave separation analysis applied to excess pressure leads to a more plausible timing of the backward wave has been refuted: in a nonuniform and tapering vessel as the aorta, backward waves are continuously generated along the entire tree as the forward wave propagates.[56] It is only in a uniform tube with a discrete reflection site at the distal end that the backward wave would indeed propagate from distal to proximal. As discussed above, the uniform tube is a poor model for the arterial tree.[36]

Mynard conjectured that the inconsistency in the original reservoir-wave formulation arises from the use of hybrid dimensionality, where zero-dimensional (0D) and 1D formulations are inappropriately combined.[45,57,58] The reservoir-like behavior (with the exponential pressure decay in diastole) is quite bluntly treated as a 0D phenomenon, while such behavior is in essence also the consequence of waves propagating back and forth in the aorta during diastole.[47] The energy carried by these waves is, however, low and it is not trivial to demonstrate their existence in vivo using techniques like wave intensity analysis. These fundamental critiques have been acknowledged by Parker and colleagues, who modified the theory. In recent publications, the reservoir pressure is being treated as a propagating wave (but still of a uniform shape along the aorta)[59] and acknowledged to arise from repeated reflections and re-reflections.[60] This is also consistent with

FIGURE 3.7   Illustration of the parallel between the reservoir-wave and three-element windkessel model using the type A dataset digitized from.[15] In the reservoir-wave concept, the reservoir pressure is determined, and excess pressure is calculated as the difference between measured and reservoir pressure. Reservoir pressure was estimated using a pressure-only approach (courtesy of J. Mynard). In the three-element windkessel model, pressure can equally be seen as the superposition of Q x Z_c and the pressure due to the *RC* components (measured pressure—$Z_c \times Q$).

studies reporting that the reservoir pressure is equal to two times the magnitude of the backward wave as obtained when applying conventional wave separation analysis.[53,61] It is important for the scientific community to get fully aware of these most recent insights, and especially of the highly problematic use of excess pressure for wave separation analysis which leads to incorrect assumptions about therapeutic approaches. As convincingly demonstrated using rigorous computer modeling supported by in vivo experimentation, wave patterns based on wave separation analysis of the excess pressure introduce nonsensical errors and contribute nothing to our understanding on the role of wave reflections in the arterial tree. The reservoir-wave paradigm is still being fine-tuned,[60] but we remain

skeptical about using an intuitive at first sight, but ill-fitting paradigm to help us in understanding the complexity of arterial hemodynamics.

Concluding remarks

In this chapter, we aimed to provide an overview of techniques and methods to analyze and interpret pressure-flow relations using both "classical" frequency domain methods (impedance-based) as well as the more recent time domain methods. Both exist side-by-side and should be used as such, exploring strengths of both. Impedance analysis is an excellent way to characterize the arterial system; time domain methods are more suitable to assess

timing and nature of wave reflections. We particularly wanted to convey the message that interpretation of impedance or wave dynamics is explicitly or implicitly based on an assumed paradigm (model) for the arterial circulation. Correct analysis and interpretation of data can only be built on a solid and full understanding of these paradigms, considering their strengths and limitations.

References

1. Avolio AP, Van Bortel LM, Boutouyrie P, et al. Role of pulse pressure amplification in arterial hypertension: expgerts' opinion and review of the data. **Hypertension**. 2009; 54(2):375−383.

2. Latham R, Westerhof N, Sipkema P, Rubal B, Reuderink P, Murgo J. Regional wave travel and reflections along the human aorta : a study with six simultaneous micromanometric pressures. **Circulation**. 1985; 72:1257−1269.

3. Hall JE. **Guyton and Hall Textbook of Medical Physiology E-Book**. Elsevier Health Sciences; 2010.

4. Milnor WR. **Hemodynamics**. 2nd ed. Baltimore, Maryland: Williams & Wilkins; 1989.

5. Nichols W, O'Rourke M. **McDonald's Blood Flow in Arteries. Theoretical, Experimental and Clinical Principles**. 5th ed. USA: Hodder Arnold - Oxford University Press; 2005.

6. Westerhof N, Stergiopulos N, Noble M. **Snapshots of Hemodynamics. An Aid for Clinical Research and Graduate Education**. New York, NY: Springer Science + Business Media; 2004.

7. Taylor MG. Input impedance of an assembly of randomly branching elastic tubes. **Biophys J**. 1966; 6(1):29−&.

8. Patel DJ, Fry DL, Defreitas FM. Hydraulic input impedance to aorta and pulmonary artery in dogs. **J Appl Physiol**. 1963; 18(1):134.

9. Mills CJ, Gabe IT, Gault JH, et al. Pressure-flow relationships and vascular impedance in man. **Cardiovasc Res**. 1970; 4(4):405−&.

10. Jager GN, Westerhof N, Noordergraaf A. Oscillatory flow impedance in electrical analog of arterial system - representation of sleeve effect and non-Newtonian properties of blood. **Circ Res**. 1965; 16(2):121−&.

11. Elzinga G, Westerhof N. Pressure and flow generated by the left ventricle against different impedances. **Circ Res**. 1973; 32:178−186.

12. Milnor WR. Arterial impedance as ventricular afterload. **Circ Res**. 1975; 36(5):565−570.

13. Sunagawa K, Maughan WL, Burkhoff D, Sagawa K. Left ventricular interaction with arterial load studied in isolated canine ventricle. **Am J Physiol**. 1983; 245:H773−H780.

14. Sunagawa K, Maughan WL, Sagawa K. Optimal arterial resistance for the maximal stroke work studied in isolate canine left ventricle. **Circ Res**. 1985; 56:586−595.

15. Murgo JP, Westerhof N, Giolma JP, Altobelli SA. Aortic input impedance in normal man: relationship to pressure wave forms. **Circulation**. 1980; 62(1):105−116.

16. Burton AC. On the physical equilibrium of small blood vessels. **Am J Physiol**. 1951; 164(2):319−329.

17. Westerhof N, Elzinga G, Sipkema P. An artificial arterial system for pumping hearts. **J Appl Physiol**. 1971; 31(5):776−781.

18. Frank O. Die Grundfurm des arteriellen Pulses. Erste Abhandlung. Mathematische Analyse. **Z Biol**. 1899; 37:483−526.

19. Stergiopulos N, Meister JJ, Westerhof N. Simple and accurate way for estimating total and segmental arterial compliance: the pulse pressure method. **Ann Biomed Eng**. 1994; 22:392−397.

20. Liu Z, Brin K, Yin F. Estimation of total arterial compliance : an improved method and evaluation of current methods. **Am J Physiol**. 1986; 251:H588−H600.

21. Stergiopulos N, Meister JJ, Westerhof N. Evaluation of methods for the estimation of total arterial compliance. **Am J Physiol**. 1995; 268:H1540−H1548.

22. Segers P, Brimioulle S, Stergiopulos N, et al. Pulmonary arterial compliance in dogs and pigs: the three-element windkessel model revisited. **Am J Physiol**. 1999; 277:H725−H731.

23. Stergiopulos N, Westerhof B, Westerhof N. Total arterial inertance as the fourth element of the windkessel model. **Am J Physiol**. 1999; 276:H81−H88.

24. Li J, Cui T, Drzewiecki GM. A nonlinear model of the arterial system incorporating a pressure-dependent compliance. **IEEE Trans Biomed Eng**. 1990; 37(7):673−678.

25. Quick CM, Berger DS, Noordergraaf A. Apparent arterial compliance. **Am J Physiol**. 1998; 274:H1393−H1403.

26. Simon A, Safar L, London G, Levy B, Chau N. An evaluation of large arteries compliance in man. **Am J Physiol**. 1979; 237: H550−H554.

27. Westerhof N, Sipkema P, van den Bos CG, Elzinga G. Forward and backward waves in the arterial system. **Cardiovasc Res**. 1972; 6:648−656.

28. Blanco PJ, Watanabe SM, Passos MA, Lemos PA, Feijóo RA. An anatomically detailed arterial network model for one-dimensional computational hemodynamics. **IEEE Trans Biomed Eng**. 2015; 62(2):736−753.

29. Matthys KS, Alastruey J, Peiró J, et al. Pulse wave propagation in a model human arterial network: assessment of 1-D numerical simulations against in vitro measurements. **J Biomech**. 2007; 40(15): 3476−3486.

30. Mynard J, Nithiarasu P. A 1D arterial blood flow model incorporating ventricular pressure, aortic valve and regional coronary flow using the locally conservative Galerkin (LCG) method. **Commun Numer Methods Eng**. 2008; 24(5):367−417.

31. Olufsen MS. A one-dimensional fluid dynamic model of the systemic arteries. **Stud Health Technol Inform**. 2000; 71:79−97.

32. Reymond P, Merenda F, Perren F, Rufenacht D, Stergiopulos N. Validation of a one-dimensional model of the systemic arterial tree. **Am J Physiol Heart Circ Physiol**. 2009; 297(1):H208−H222.

33. Avolio A. Multi-branched model of the human arterial system. **Med Biol Eng Comp**. 1980; 18:709−718.

34. Segers P, Verdonck P. Role of tapering in aortic wave reflection: hydraulic and mathematical model study. **J Biomech**. 2000; 33:299−306.

35. Berger D, Li J, Laskey W, Noordergraaf A. Repeated reflection of waves in the systemic arterial system. **Am J Physiol**. 1993; 264:H269−H281.

36. Westerhof BE, Westerhof N. Uniform tube models with single reflection site do not explain aortic wave travel and pressure wave shape. **Physiol Meas**. 2018; 39(12):124006.

37. Segers P, Rietzschel ER, De Buyzere ML, et al. Noninvasive (input) impedance, pulse wave velocity, and wave reflection in healthy middle-aged men and women. **Hypertension**. 2007; 49(6):1248−1255.

38. Parker KH, Jones CJ. Forward and backward running waves in the arteries: analysis using the method of characteristics. **J Biomech Eng**. 1990; 112(3):322−326.

39. Khir AW, O'Brien A, Gibbs JS, Parker KH. Determination of wave speed and wave separation in the arteries. **J Biomech**. 2001; 34(9):1145−1155.

40. Dujardin J, Stone D. Characteristic impedance of the proximal aorta determined in the time and frequency domain: a comparison. **Med Biol Eng Comp**. 1981; 19:565−568.

41. Segers P, Swillens A, Taelman L, Vierendeels J. Wave reflection leads to over-and underestimation of local wave speed by the PU-and QA-loop methods: theoretical basis and solution to the problem. **Physiol Meas**. 2014; 35(5):847.

42. Arias DC, Stergiopulos N, Moliner TR, Segers P. Mapping the site-specific accuracy of loop-based local pulse wave velocity estimation and reflection magnitude: a 1D arterial network model analysis. **Physiol Meas**. 2019; 40(7):075002.

43. Phan TS, Li JK, Segers P, Chirinos JA. Misinterpretation of the determinants of elevated forward wave amplitude inflates the role of the proximal aorta. **J Am Heart Assoc**. 2016; 5(2).

44. Mynard JP, Smolich JJ. Novel wave power analysis linking pressure-flow waves, wave potential, and the forward and backward components of hydraulic power. **Am J Physiol Heart Circ Physiol**. 2016; 310(8):H1026−H1038.

45. Mynard JP, Kondiboyina A, Kowalski R, Cheung MMH, Smolich JJ. Measurement, analysis and interpretation of pressure/flow waves in blood vessels. **Front Physiol**. 2020; 11(1085).

46. Swillens A, Lanoye L, De Backer J, et al. Effect of an abdominal aortic aneurysm on wave reflection in the aorta. **IEEE Trans Biomed Eng**. 2008; 55(5):1602−1611.

47. Mynard JP, Smolich JJ. Wave potential and the one-dimensional windkessel as a wave-based paradigm of diastolic arterial hemodynamics. **Am J Physiol Heart Circ Physiol**. 2014; 307(3): H307−H318.

48. Londono-Hoyos F, Zamani P, Beraun M, Vasim I, Segers P, Chirinos JA. Effect of organic and inorganic nitrates on cerebrovascular pulsatile power transmission in patients with heart failure and preserved ejection fraction. **Physiol Meas**. 2018; 39(4):044001.

49. Wang JJ, O'Brien AB, Shrive NG, Parker KH, Tyberg JV. Time-domain representation of ventricular-arterial coupling as a windkessel and wave system. **Am J Physiol Heart Circ Physiol**. 2003; 284(4):H1358−H1368.

50. Hughes A, Wang JJ, Bouwmeester C, et al. The reservoir-wave paradigm. **J Hypertens**. 2012; 30(9):1880−1881. author reply 1-3.

51. Tyberg JV, Bouwmeester JC, Parker KH, Shrive NG, Wang JJ. The case for the reservoir-wave approach. **Int J Cardiol**. 2014; 172(2):299−306.

52. Tyberg JV, Davies JE, Wang Z, et al. Wave intensity analysis and the development of the reservoir-wave approach. **Med Biol Eng Comput**. 2009; 47(2):221−232.

53. Hametner B, Wassertheurer S, Hughes AD, Parker KH, Weber T, Eber B. Reservoir and excess pressures predict cardiovascular events in high-risk patients. **Int J Cardiol**. 2014; 171(1):31−36.

54. Mynard JP, Penny DJ, Davidson MR, Smolich JJ. The reservoir-wave paradigm introduces error into arterial wave analysis: a computer modelling and in-vivo study. **J Hypertens**. 2012; 30(4):734−743.

55. Segers P, Taelman L, Degroote J, Bols J, Vierendeels J. The aortic reservoir-wave as a paradigm for arterial haemodynamics: insights from three-dimensional fluid-structure interaction simulations in a model of aortic coarctation. **J Hypertens**. 2015; 33(3):554−563. discussion 63.

56. Westerhof N, Westerhof BE. Waves and windkessels reviewed. **Artery Res**. 2017; 18:102−111.

57. Mynard JP. Assessment of conceptual inconsistencies in the hybrid reservoir-wave model. **Annu Int Conf IEEE Eng Med Biol Soc**. 2013; 2013:213−216.

58. Mynard JP, Smolich JJ. The case against the reservoir-wave approach. **Int J Cardiol**. 2014; 176(3):1009−1012.

59. Parker KH. The reservoir-wave model. **Artery Res**. 2017; 18:87−101.

60. Hughes AD, Parker KH. The modified arterial reservoir: an update with consideration of asymptotic pressure ($P\infty$) and zero-flow pressure (Pzf). **Proc IME H J Eng Med**. 2020; 234: 0954411920917557.

61. Westerhof N, Segers P, Westerhof BE. Wave separation, wave intensity, the reservoir-wave concept, and the instantaneous wave-free ratio: presumptions and principles. **Hypertension**. 2015; 66(1):93−98.

Chapter 4

MRI for the assessment of aortic stiffness and pulsatile hemodynamics

Yoshiaki Ohyama[1,4], Alban Redheuil[2,3], Nadjia Kachenoura[2], Bharath Ambale Venkatesh[1] and Joao A.C. Lima[1]

[1]*Departments of Cardiology/Medicine and Radiology, Johns Hopkins University, Baltimore, MD, United States;* [2]*Sorbonne Université, INSERM, CNRS, Laboratoire d'Imagerie Biomédicale, Paris, France;* [3]*Cardiovascular and Thoracic Imaging, Hôpital La Pitié-Salpêtrière, AP-HP, Sorbonne Université, Paris, France;* [4]*Clinical Investigation and Research Unit, Gunma University Hospital, Maebashi, Japan*

Introduction

For a comprehensive characterization of changes in aortic morphology, flow, and hemodynamics associated with aging and disease, accurate and reproducible quantitative methods are needed.

Magnetic resonance imaging (MRI) has the unique ability to provide noninvasive, accurate, and reproducible measurements of aortic stiffness measures such as aortic strain, distensibility, and pulse wave velocity (PWV), as well as aortic geometry measures such as aortic diameter, area, or volume,[1,2] length, and curvature.[3] Importantly, MRI allows noninvasive imaging of the proximal aorta and aortic arch that have pivotal roles in the central cardiocirculatory system. Such exploration includes both 2D and 3D anatomy and dynamics as well as time-resolved 2D (2D + t) and 3D (3D + t) flow patterns, allowing for precise local measurements without geometrical assumptions. This chapter describes the methodology and prospects of MRI for the assessment of aortic stiffness and hemodynamics.

Aortic stiffness assessed by MRI

Aortic strain and distensibility

Aortic distensibility—defined as the relative change in aortic lumen area during cardiac cycle (aortic strain) divided by local pulse pressure—is commonly used as a measure of *local* aortic stiffness in population studies[4−6] (Fig. 4.1). Ascending and descending aortic strains are measured using dynamic MRI images acquired in a plane at the mid-ascending aorta perpendicular to the aortic wall at the level of the right pulmonary artery. Validated

semiautomated software can accurately determine changes in the aortic cross-sectional area throughout the cardiac cycle and represent them as area over time curves[4] (Fig. 4.2). Aortic strain is calculated as follows[7]:
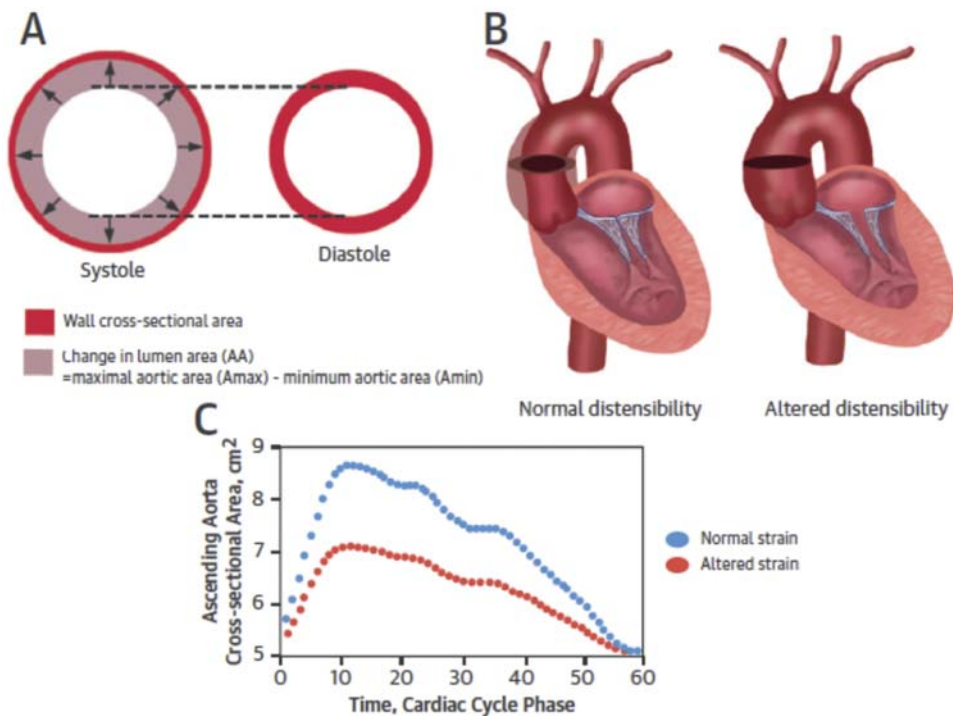
$$\text{Aortic strain } (\%) = [(\text{maximum aortic area} - \text{minimum aortic area})/(\text{minimum aortic area})] \times 100$$

Distensibility is then calculated as aortic strain normalized by the pulse pressure driving systolic wall stretch and diastolic recoil of the aorta.[7]
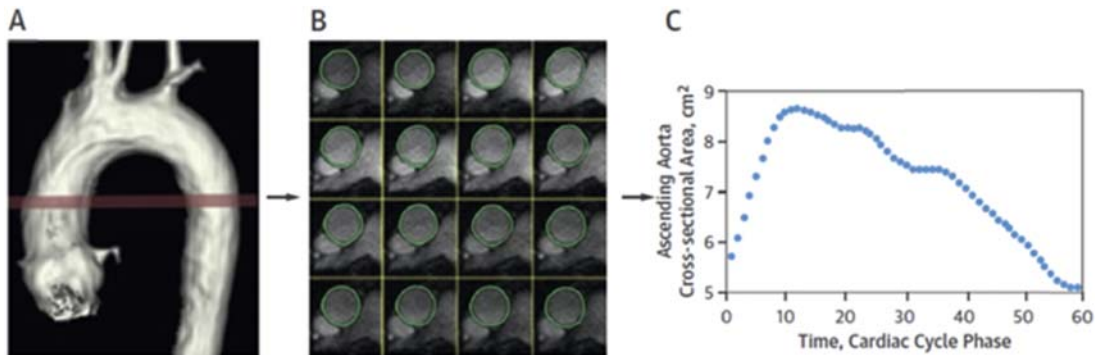
$$\text{Aortic distensibility}\left(\text{mmHg}^{-1}10^{-3}\right) = [\text{aortic strain / pulse pressure}] \times 10$$

Central pulse pressure instead of brachial pulse pressure should be used in the calculation of local distensibility, in order to account for the highly variable pulse pressure amplification phenomenon across the age spectrum. As discussed in detail in Chapter 2, several noninvasive methods have been developed to estimate central blood pressure using pressure waveforms from the carotid, brachial, or radial arteries, and calibrated for brachial cuff pressure, and which can be measured simultaneously to the aortic MRI acquisitions.

SSFP cine imaging is the most commonly used dynamic sequence and is validated for measuring aortic strain and distensibility, due to its high spatial and temporal resolution and effective flow compensation minimizing flow-related artifacts.[8,9] Studies have also demonstrated that phase contrast MRI (PC-MRI) modulus images can be used in place of SSFP imaging. Using PC-MRI images has the practical advantage of reducing scan time since they will be also used for aortic arch PWV

FIGURE 4.1 Principle of local aortic stiffness: ascending aortic distensibility. (A) The ascending aorta is highly distensible and stores most of the stroke volume from the heart during systole, and, thanks to elastic recoil, redistributes part of this volume to downstream during diastole, thus transforming a pulsatile flow into steadier flow. The relative change in aortic lumen area divide by pulse pressure defines the distensibility. (B) Comparative illustration of preserved (left) and altered (right) distensibility of ascending aorta. (C) Corresponding cross-sectional area to cardiac cycle time curves for preserved (blue) and altered (red) aortic distensibility. *Reprinted from Redheuil A, Wu CO, Kachenoura N, et al. Proximal aortic distensibility is an independent predictor of all-cause mortality and incident CV events: the MESA study.* J Am Coll Cardiol. *2014;64:2619−2629 with permission of the publisher.*

FIGURE 4.2 Measurement of aortic distensibility in MRI. (A) Magnetic resonance imaging (MRI) shows three-dimensional reconstruction of the thoracic aorta with the transverse aortic dynamic acquisition plane (red). (B) Results of the semiautomated segmentation of the ascending aorta (green contour). (C) Resulting cross-sectional area to cardiac cycle time curve. *Reprinted from Redheuil A, Wu CO, Kachenoura N, et al. Proximal aortic distensibility is an independent predictor of all-cause mortality and incident CV events: the MESA study.* J Am Coll Cardiol. *2014;64:2619−2629 with permission of the publisher.*

calculation and flow components estimation,[9] without requiring additional scan time. Of note, through-plane motion of the aorta resulting from left ventricular (LV) contraction may impact the assessment of cross-sectional aortic distensibility especially in the proximal aortic segments as it is measured from a fixed acquisition plane. However, this effect, more pronounced closer to the aortic root, can be minimized by measuring aortic strain at the tubular part of the ascending aorta and the descending aorta most often at the level of the center of the right pulmonary artery. In this plane, the ascending aorta is mostly cylindrical with the centerline and aortic walls remaining mostly perpendicular to the acquisition plane with a circular cross section throughout the cardiac cycle.

Interestingly, the longitudinal deformation of the aortic root can be also quantified from sagittal SSFP MRI images and was proven of clinical interest in patients with Marfan syndrome.[10]

Aortic pulse wave velocity

The most widely used measure of aortic stiffness overall is PWV, defined as the speed of propagation of the pulse wave along the arterial path,[11] as discussed in detail in Chapters 1 and 7. PWV is calculated as the ratio of the distance between two anatomical locations along the artery to the transit time required for the pressure or flow wave to cover that distance, commonly expressed in m/s. Arterial PWV is commonly measured using applanation tonometry between the carotid and femoral arteries. Carotid-femoral PWV (cf-PWV) is regarded as the reference method for arterial stiffness evaluations because it is relatively easy to use, available in large populations, and has high reliability.[12] However, cf-PWV, measured by applanation tonometry, is affected by inherent measurement errors associated with using the body surface distance as a surrogate for true arterial path length, which ignores the tortuous vessel routes.[7] Such errors are increased in obese (increased body surface) or elderly (increased aortic tortuosity) individuals.[13] Furthermore, cf-PWV ignores the proximal ascending aorta segment since the proximal point of measure regards the common carotid artery. Since the proximal aorta has the majority of the buffering capacity of the arterial system, this omission may have significant consequences in understanding the impact of age and disease on the aorta.
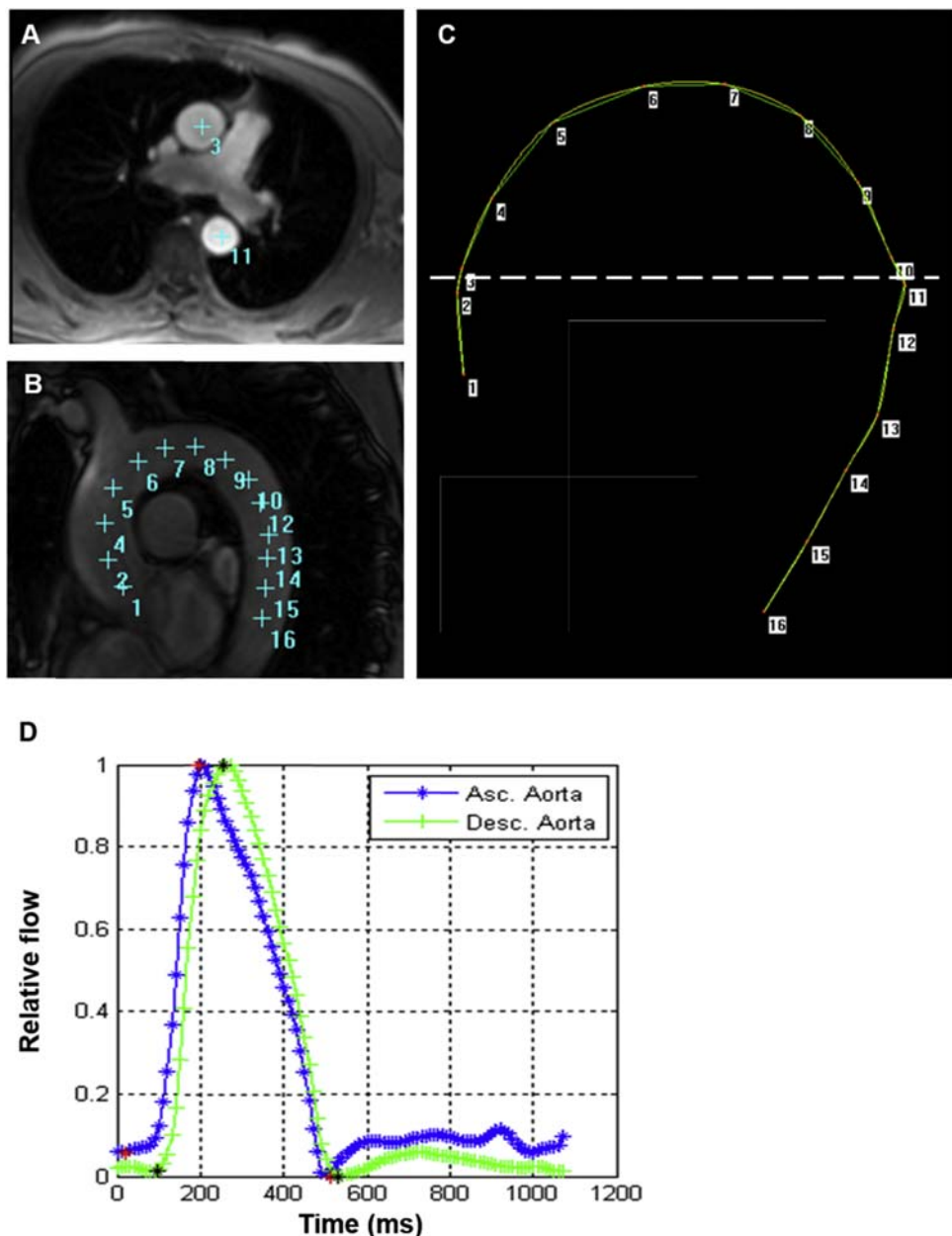
Aortic PWV assessment by MRI is a novel method that reduces measurement error by using accurate aortic length with a three-dimensional imaging approach[1,3] and the corresponding transit time between flow wave measurements[14,15] in precise locations. Aortic PWV assessment using blood flow waves derived from PC-MRI has been well validated in comparison to invasive, intraaortic pressure assessment[14] and to cf-PWV,[16] as well as through the Bramwell—Hill theoretical model.[17] MRI PWV assessment can also provide *regional* aortic stiffness in different segments of the aorta, including the ascending aorta, aortic arch, thoracic descending, and abdominal aorta.[18] Arch PWV is most commonly measured using 2D PC-MRI due to its simple acquisition and high temporal and spatial resolution during a single breath-hold of two PC-MRI planes with a velocity encoding gradient in the through-plane direction,[19,20] making it suitable for routine protocols. To measure aortic arch PWV, images of the ascending and descending aorta are obtained simultaneously in the transverse plane perpendicular to the aortic centerline, at the level of the right pulmonary artery. Specific software for aortic analysis provide an estimate of the transit time between the two flow waves after automated segmentation of the modulus and velocity PC-MRI images[21] (Fig. 4.3).

The disadvantage of MRI for PWV assessment is its relatively lower temporal resolution (10−30 ms, according to breath holding capability and R-R interval) compared to echocardiography and to applanation tonometry. The foot-to-foot method is well established in studies using tonometry to estimate transit time between pressure waves since it avoids the early reflected pressure waves.[7] Transit time estimation using the foot-to-foot method requires high temporal resolution to identify an accurate upstroke time, making this approach unsuitable for flow wave analysis in PC-MRI. Therefore, different methods to estimate the transit time using PC-MRI have been described to overcome such drawback.[14,22−24] In addition to the foot-to-foot approach, the methods to measure transit time by PC-MRI can be classified into two different strategies: (1) point-based methods, using systolic peak-to-systolic peak or maximal upslope acceleration-to-maximal upslope acceleration,[25,26] and (2) wave-based methods using similarity criteria such as cross-correlation as well as Fourier or wavelet analysis to calculate phase differences between two flow curves from different aortic sites.[27,28] While point-based methods have been shown to be robust on pressure waves, it has the disadvantage in MRI of the relatively low temporal resolution of PC-MRI flow curves.[24] Applying the wave-based methods to the whole cardiac cycle can be plagued by the presence of wave reflections that occur in late systole, affecting the morphology of the systolic downslope.[7] To overcome these issues, recent wave-based techniques have been proposed that focus only on the systolic upslope of the PC-MRI flow curves.[14,19,24] These methods have been shown to be more robust for low temporal resolution, especially when performed in the frequency domain using a wavelet approach.[27] Nevertheless, a limited temporal resolution remains the main limitation of MRI, particularly for short arterial path lengths and for patients with highly stiff aortas (and thus very short transit times).

Aging and aortic stiffness measurements in MRI
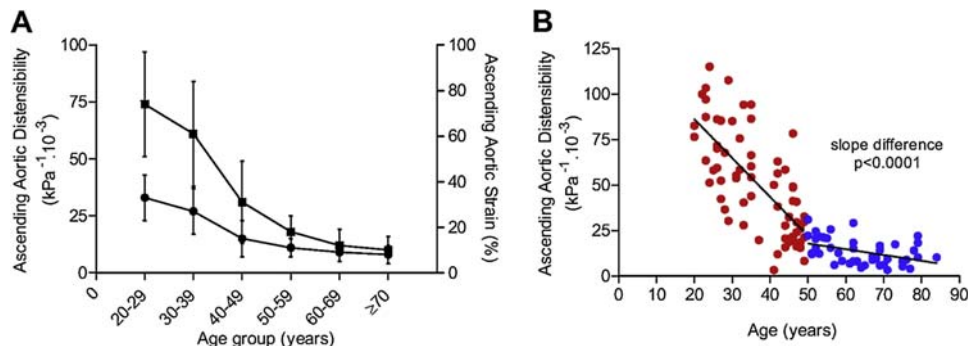
The relationship of aortic distensibility with age is nonlinear.[19] Recent MRI studies have demonstrated a marked decrease in local aortic strain and distensibility before the fifth decade among asymptomatic general population volunteers.[19] Ascending aortic distensibility measured using central pulse pressure was on average 7.4 ± 2.3 mmHg$^{-1} \cdot 10^{-3}$ between 20 and 30 years of age, 1.8 ± 0.7 mmHg$^{-1} \cdot 10^{-3}$ between 50 and 60 years of age, and 1.0 ± 0.6 mmHg$^{-1} \cdot 10^{-3}$ after 70 years (Fig. 4.4). Furthermore, aortic distensibility was the most sensitive

FIGURE 4.3 Measurement of arch PWV in MRI using ARTFUN software (LIB, INSERM 1146, France). (A) Phase contrast cine transverse view. (B) Aortic arch view with steady-state free precession sequence. (C) Measurement of the transit distance in the aortic arch. Numbers correspond to those in A and (B) (D) Flow wave curves of ascending aorta and descending aorta after peak flow normalization. Transit time is measured as the average time shift that minimizes the least squares difference between systolic upslope data points of the ascending and descending aortic flow curves. *Reprinted from Ohyama Y, Ambale-Venkatesh B, Noda C, et al. Association of aortic stiffness with left ventricular remodeling and reduced left ventricular function measured by magnetic resonance imaging: the Multi-Ethnic Study of Atherosclerosis.* Circ Cardiovasc Imaging. *2016;9:pii: e004426 with permission of the publisher.*

and strongest marker of age compared to the following peripheral aortic stiffness measures: carotid distensibility, cf-PWV, and augmentation Index (AIx, which is a surrogate marker of wave reflection).[7] This interesting finding of a dramatic decrease in aortic strain and distensibility—when changes in blood pressure are not yet apparent—is consistent with the mechanical hypothesis of a decline in aortic elasticity in the third decade of life, which results from thinning and fragmentation of elastin fibers caused by repeated deformation and stretch induced by pulsatile stress, among various other biologic processes (discussed in Chapters 19—25).[29]

FIGURE 4.4 The change in ascending aortic distensibility with aging. (A) Ascending aorta strain (dot) and distensibility (squares) by decades of age. (B) Ascending aortic distensibility (age <50 = red dots and >50 years = blue dots). *Reprinted from Redheuil A, Yu WC, Wu CO, et al. Reduced ascending aortic strain and distensibility: earliest manifestations of vascular aging in humans.* Hypertension. *2010;55:319−326 with permission of the publisher.*

cf-PWV increases progressively with aging, from approximately 7 m/s at 30 years of age to 12 m/s at 70 years of age.[11] A recent study from the Multi-Ethnic Study of Atherosclerosis (MESA) reports arch PWV assessed by MRI in a multiethnic population aged 45−85 years.[30] MESA is a prospective study designed to evaluate risk factors and mechanisms that underlie the development and progression of subclinical CVD among asymptomatic individuals using MRI to assess cardiovascular structure and function.[31] In that study, arch PWV assessed by PC-MRI increased pronouncedly between participants aged 45−54 years and those aged 54 years and older. Another recent study using PC-MRI has shown that age has different impacts on regional aortic stiffness.[18] The distal aorta exhibited the greatest age-related increase in regional PWV and the aortic arch had the least, whereas the aortic arch had the greatest increase in aortic diameter and length, which may, in part, help offset an increase in wall stiffness by maintaining the capacity of the aorta to store volume during systole. Heterogeneity of structural and functional changes with aging as well as of atherosclerotic burden throughout the arterial tree causes differential regional aortic stiffening.

Cardiovascular risk factors, left ventricular function, and aortic stiffness

Longitudinal studies from MESA have shown that age, high blood pressure at baseline, increase in blood pressure during follow-up, and smoking history were independently associated with the increase over 10 years in aortic stiffness, with a decrease in aortic distensibility, and an increase in arch PWV.[20] In this study, reduction of blood pressure to an adequate level during the follow-up period was associated with less aortic stiffening. In addition, the use of calcium channel blockers was associated with less decrease in ascending aortic distensibility, while other drugs including ACE-I/ARB, beta-blockers, and diuretics did not have the same relationship with aortic stiffness. Recent data

demonstrated an improvement in aortic distensibility in first-time marathon trainers and completers including older participants, shedding light on the possibility to partially reverse this age-related vascular aging phenotype.[32] Future investigations are needed to assess the beneficial effects of different pharmacological and nonpharmacological interventions on aortic function.

MRI has the ability to assess ventricular geometry and myocardial deformation as well as central aortic stiffness simultaneously in a single examination. A recent study on vascular−ventricular interaction has shown the relationship between aortic arch PWV assessed by MRI and LV deformation assessed by tagged MRI as well as LV structure in the MESA cohort. In that study, higher arch PWV was associated with LV remodeling and reduced LV systolic and diastolic function, and this association had a significant gender interaction.[21] In women, greater arch PWV was associated with LV concentric remodeling, worse LV diastolic function, and preserved ejection fraction (EF) with maintained torsion. In contrast, reduced LV systolic function demonstrated as impaired LV circumferential strain and torsion as well as reduced LV concentric remodeling were related to elevated arch PWV in men. This gender difference in the relationship between aortic arch stiffness and LV structure and function may be mediated by hormonal factors and may explain the higher incidence of heart failure with preserved EF among women.

Prognostic value of proximal aortic stiffness measures

A recent study from MESA showed that decreased ascending aortic distensibility assessed by MRI significantly predicted hard CV events including myocardial infarction, resuscitated cardiac arrest, stroke, and cardiovascular death, and all-cause mortality in individuals without overt CV disease.[4] The hazard ratio for death and hard CV events over 8.5 years was 2.7 and 2.2 for the 20%

of individuals with the stiffest aortas, independent of traditional risk factors. The predictive value of ascending aortic distensibility for CV events was highest in those with low-to-moderate baseline individual risk.

Another study using the MESA cohort showed that arch PWV had incremental predictive value for incident CVD events above traditional CVD risk factors in participants aged 45−54 years in the general population. Arch PWV was not associated with incident CVD events in those aged above 55 years.[30] These findings on the age interaction between arch PWV and events were somewhat consistent with those previously documented regarding the association between PWV and age in metaanalyses.[33] Indeed, the marked increase in predictive power among MESA participants aged 45−54 years compared to those aged over 54 years may reflect the greater predictive value of arch PWV in younger compared to older populations, similar to distensibility. Furthermore, considering the regional heterogeneity of aortic structure, differences in prognostic values may be related to regional differences in the material properties of the aortic wall components and their evolution over time; however, outcome data on such regional differences are lacking.

Advanced methodology to assess pulsatile aortic properties using MRI

Flow analysis

PC-MRI analysis can separate global aortic flow into two components: forward and backward flow. It should be noted that here, we refer to the direction of blood flow in a given region of an aortic cross section due to vortical flow, rather than forward or backward traveling waves which impact net measured pressure and flow (as discussed in Chapters 1, 3, and 11). It has been shown that the magnitude of ascending aorta backward flow increases with age and its onset during a cardiac cycle occurs earlier with aging.[34] Such changes are strongly associated with geometric changes of the aortic arch such as dilation and elongation, that lead to changes in local pressure gradients and local rotating blood vortices.[34] These flow modifications, which might lead to increased LV load and a loss in circulatory system efficiency, partially explain age-related vascular alterations and their potential clinical implications regarding increased CVD risk.
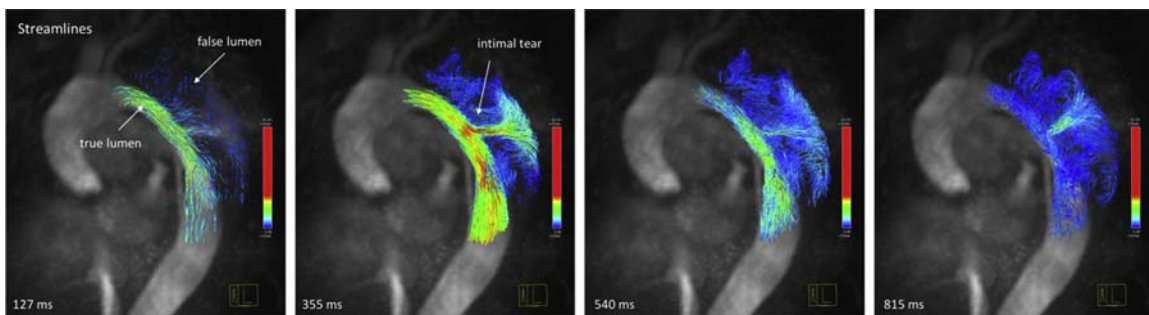
It is also important to note that in PC-MRI through-plane velocity data, the backward flow crossing the ascending aorta section for a single phase of the cardiac cycle includes both backward flow going back toward the heart and locally rotating blood vortices, which reorganize into forward flow in the following phases. These flow patterns can be confirmed using 4D-flow MRI, as further discussed in this chapter.

Combining pressure and flow
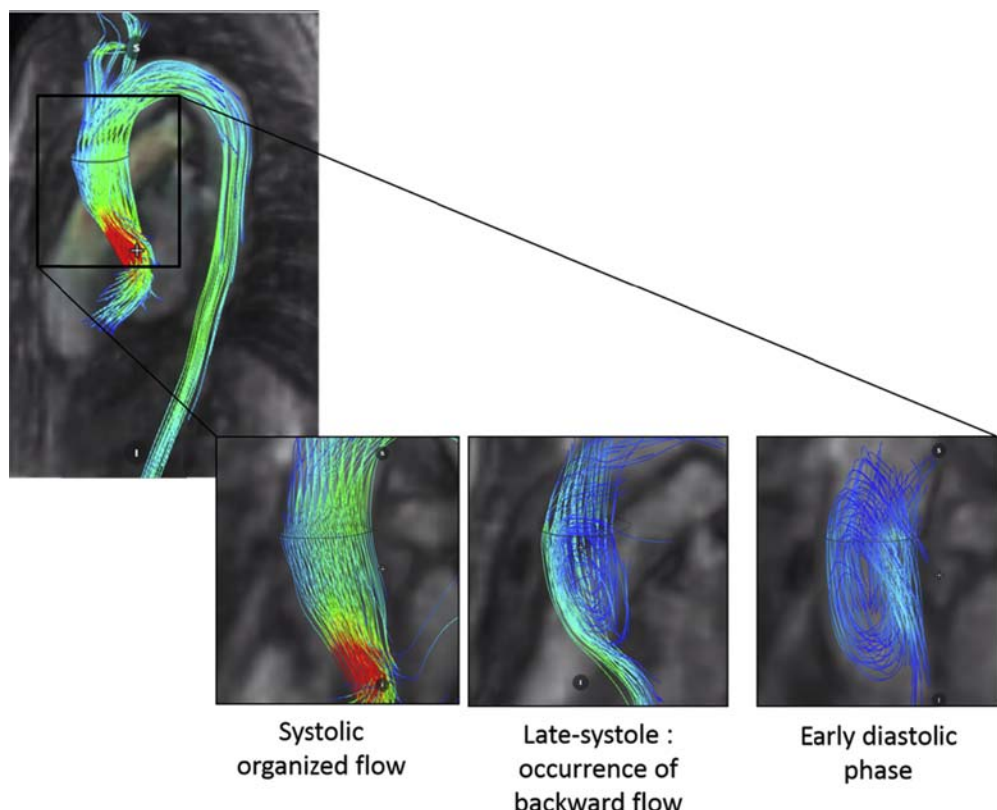
According to the American Heart Association's statement on scientific principles of arterial stiffening, the ascending aortic input impedance (Z_{in}) spectrum is the most comprehensive measurement of vascular load in relation to aortic stiffness.[35] Analyses of pressure flow relations are discussed in detail in Chapters 1, 3, 11, and 17. Z_{in} is derived from simultaneous pressure and flow assessments, and characteristic impedance (Z_c) can be estimated in the either frequency or time domain using tonometry and PC-MRI[36,37] or Doppler echocardiography velocity data. Flow assessment by MRI with noninvasive pressure assessment can provide more accurate aortic Zc compared to measures derived using ultrasound flow assessment, which samples the LV outflow tract instead of the ascending aortic flow. In aging, MRI could demonstrate that stiffening of the ascending aorta was related to increased Z_c, concentric LV remodeling, decreased strain, and augmented cardiac work to preserve the vascular–ventricular coupling in asymptomatic individuals.[38] The ability to more accurately measure ascending aortic flow and Z_c would likely provide new insights into aortic function and vascular/ventricular interactions, and the opportunity to clarify the differences and similarities between patients with systolic and diastolic LV dysfunction as the cause of heart failure.[39]

4D flow

More comprehensive 3D cine techniques in combination with three-directional encoding of blood flow velocities (known as 3D cine PC or 4D-flow MRI) over the cardiac cycle (3D + t = 4D) have recently been reported and have greatly expanded clinical and research possibilities regarding the aorta.[40−45] Immediate applications have been toward the visualization and understanding of complex aortic diseases such as aneurysms and complications such as aortic dissection with discernible multilumen flows (Fig. 4.5). The most interesting feature of 4D-flow MRI is its full 4D (3D + t) spatial–temporal coverage of the vessel of interest and the acquisition of multidirectional flow at all locations in a predefined volume (Fig. 4.6). Such volume can also include the aorta and the heart for the evaluation of their coupling when they share the same hemodynamic and loading conditions. Taking into account the unique anatomy of the thoracic aorta in individuals with complex aortic geometry without a priori is one of the advantages of the 4D-flow technique, which enables any desired a posteriori slicing of the acquired volume for local quantitative measures. 4D flow can also evaluate regional PWV at any location of interest in the aorta[41,44,46] and 4D-magnitude images could allow the estimation of local distensibility at multiple locations with adequate postprocessing software. Therefore, 4D-flow MRI could provide a comprehensive assessment of aortic structure, function, and flow

FIGURE 4.5 4D-flow streamlines depicting aortic dissection Stanford type B with a local intimal tear responsible for a false lumen entry of the flow in the proximal descending aorta. *Image: Dubourg B., Redheuil A. (ICT PSL).*

FIGURE 4.6 4D-flow images of an 80-year-old subject free from overt cardiovascular disease. *Reprinted from Ohyama Y, Redheuil A, Kachenoura N, Ambale Venkatesh B and Lima JAC. Imaging insights on the aorta in aging.* Circ Cardiovasc Imaging. *2018;11:e005617 with permission of the publisher.*

simultaneously, and further elucidate the combined age-related effects of altered aortic geometry, compliance, and pressure on changes in local flow patterns, and partly explain aortic complications.

One of the main drawbacks of 4D flow is its currently low temporal resolution (30−40 ms). Low precision in the assessment of timing has an impact on the precision of the PWV estimate, especially in short aortic segments. To compensate for the low temporal resolution, the time of travel between two planes is routinely calculated by including all intermediate analysis planes, and by linear fitting of the systolic upslope of the resulting series of flow curves to derive the PWV.[41] Several studies have been dedicated to methods comparison for an optimal estimation of aortic PWV from 4D-flow data while comparing to tonometric PWV as well as to the Bramwell−Hill model−derived PWV,[42] corroborating the value of considering all intermediate planes rather than two extreme planes, and also the 2D PC-MRI findings in terms of robustness of transit time estimation.[47]

The 4D flow also provides complex hemodynamic measures, such as helical and vortical blood flow,[48] flow

eccentricity,[49] estimates wall shear stress (WSS),[50] and intraaortic pressure gradients.[51] Abnormal blood flow patterns, flow eccentricity, and increased WSS have been reported in patients with aortic stenosis and may be associated with LV remodeling.[52,53] These hemodynamic measures could also provide useful quantitative description of aortic hemodynamics in patients with other cardiovascular diseases including aortic aneurysm[54] or congenital heart disease.[55] Especially, WSS, that is the tangential force exerted by blood flow on the vessel wall acting on the endothelial cells,[56] can be readily estimated through 4D-flow MRI.[57,58] WSS direction and magnitude can be obtained from spatial derivatives of 3D spatial velocities at the vessel wall from 4D-flow MRI.[57] Recent studies have shown that regions of aortic wall with an elevated estimated WSS correlate with dysregulation of the extracellular matrix and degeneration of the elastic fibers in patients with bicuspid aortic valve.[59−61] Other studies have shown that patients with Marfan syndrome have differences in estimated WSS despite similar aortic dimensions compared to controls. Together with the fact that aortic distensibility is also reduced in such patients irrespective of aortic dimensions,[62] these novel findings implicate that estimated WSS might be useful in prediction of disease progression even in earlier and less severe stages.

It should be noted that current methods of 4D-flow acquisition require rather long, although rapidly improving, scan times (5−20 min), in addition to the complexity of postprocessing that requires specific software, resulting in its still limited use in large populations. However, recent studies showed that compressed sensing could shorten 4D-flow scan times drastically to less than half.[63,64] Furthermore, deep learning enables fast and automated 3D aortic segmentation form 4D-flow MRI angiograms.[65] Such parallel improvements in both 4D-flow pulse sequences and postprocessing methods with expanded calculation power can lead to rapid increase in clinical research use and potential translation to routine clinical use.

Conclusions

MRI has recently been optimized to enable quantification of aortic function and structure with the aim of improving medical diagnosis and risk prediction. The precision and excellent reproducibility of MRI measurements could allow for the assessment of longitudinal variations of aortic parameters with aging as well as the effect of pharmacological and nonpharmacological interventions on aortic function. In practice, aortic flow and functional assessment both visual and quantitative could be added to clinical routine cardiovascular MRI as a comprehensive imaging modality performed primarily for the noninvasive evaluation of LV geometry and function. Advanced imaging such as 4D flow

could further provide noninvasive access to elucidate aortic properties. Further methodological developments and research including acceleration in acquisition sequences, large population studies with normative values with longitudinal follow-up, fast and robust image processing tools possibly relying on machine learning are needed for a more complete understanding of changes in aortic stiffness and hemodynamics in response to aging and disease processes.

Disclosures

None.

References

1. Dietenbeck T, Craiem D, Rosenbaum D, et al. 3D aortic morphology and stiffness in MRI using semi-automated cylindrical active surface provides optimized description of the vascular effects of aging and hypertension. **Comput Biol Med**. 2018; 103:101−108.
2. Dietenbeck T, Houriez-Gombaud-Saintonge S, Charpentier E, et al. Quantitative magnetic resonance imaging measures of three-dimensional aortic morphology in healthy aging and hypertension. **J Magn Reson Imag**. 2021; 53:1471−1483.
3. Noda C, Ambale Venkatesh B, Ohyama Y, et al. Reproducibility of functional aortic analysis using magnetic resonance imaging: the MESA. **Eur Heart J Cardiovasc Imaging**. 2016; 17:909−917.
4. Redheuil A, Wu CO, Kachenoura N, et al. Proximal aortic distensibility is an independent predictor of all-cause mortality and incident CV events: the MESA study. **J Am Coll Cardiol**. 2014; 64:2619−2629.
5. Malayeri AA, Natori S, Bahrami H, et al. Relation of aortic wall thickness and distensibility to cardiovascular risk factors (from the Multi-Ethnic Study of Atherosclerosis [MESA]). **Am J Cardiol**. 2008; 102:491−496.
6. Turkbey EB, Jain A, Johnson C, et al. Determinants and normal values of ascending aortic diameter by age, gender, and race/ethnicity in the Multi-Ethnic Study of Atherosclerosis (MESA). **J Magn Reson Imag**. 2014; 39:360−368.
7. Laurent S, Cockcroft J, Van Bortel L, et al. Expert consensus document on arterial stiffness: methodological issues and clinical applications. **Eur Heart J**. 2006; 27:2588−2605.
8. Herment A, Kachenoura N, Lefort M, et al. Automated segmentation of the aorta from phase contrast MR images: validation against expert tracing in healthy volunteers and in patients with a dilated aorta. **J Magn Reson Imag**. 2010; 31:881−888.
9. Herment A, Lefort M, Kachenoura N, et al. Automated estimation of aortic strain from steady-state free-precession and phase contrast MR images. **Magn Reson Med**. 2011; 65:986−993.
10. Guala A, Teixidó-Tura G, Rodríguez-Palomares J, et al. Proximal aorta longitudinal strain predicts aortic root dilation rate and aortic events in Marfan syndrome. **Eur Heart J**. 2019; 40:2047−2055.
11. Reference Values for Arterial Stiffness C. Determinants of pulse wave velocity in healthy people and in the presence of cardiovascular risk factors: 'establishing normal and reference values. **Eur Heart J**. 2010; 31:2338−2350.
12. Mancia G, Fagard R, Narkiewicz K, et al. 2013 ESH/ESC guidelines for the management of arterial hypertension: the Task Force for the Management of Arterial Hypertension of the European Society of

Hypertension (ESH) and of the European Society of Cardiology (ESC). **Eur Heart J**. 2013; 34:2159−2219.

13. Joly L, Perret-Guillaume C, Kearney-Schwartz A, et al. Pulse wave velocity assessment by external noninvasive devices and phase-contrast magnetic resonance imaging in the obese. **Hypertension**. 2009; 54:421−426.

14. Grotenhuis HB, Westenberg JJ, Steendijk P, et al. Validation and reproducibility of aortic pulse wave velocity as assessed with velocity-encoded MRI. **J Magn Reson Imag**. 2009; 30:521−526.

15. Cavalcante JL, Lima JA, Redheuil A, Al-Mallah MH. Aortic stiffness: current understanding and future directions. **J Am Coll Cardiol**. 2011; 57:1511−1522.

16. Dogui A, Kachenoura N, Frouin F, et al. Consistenc of aortic distensibility and pulse wave velocity estimates with respect to the Bramwell-Hill theoretical model: a cardiovascular magnetic resonance study. **J Cardiovasc Magn Reson**. 2011; 13:11.

17. Westenberg JJM, van Poelgeest EP, Steendijk P, Grotenhuis HB, Jukema JW, de Roos A. Bramwell-Hill modeling for local aortic pulse wave velocity estimation: a validation study with velocity-encoded cardiovascular magnetic resonance and invasive pressure assessment. **J Cardiovasc Magn Reson**. 2012; 14:2.

18. Hickson SS, Butlin M, Graves M, et al. The relationship of age with regional aortic stiffness and diameter. **JACC Cardiovasc Imaging**. 2010; 3:1247−1255.

19. Redheuil A, Yu WC, Wu CO, et al. Reduced ascending aortic strain and distensibility: earliest manifestations of vascular aging in humans. **Hypertension**. 2010; 55:319−326.

20. Ohyama Y, Teixido-Tura G, Ambale-Venkatesh B, et al. Ten-year longitudinal change in aortic stiffness assessed by cardiac MRI in the second half of the human lifespan: the multi-ethnic study of atherosclerosis. **Eur Heart J Cardiovasc Imaging**. 2016; 17:1044−1053.

21. Ohyama Y, Ambale-Venkatesh B, Noda C, et al. Association of aortic stiffness with left ventricular remodeling and reduced left ventricular function measured by magnetic resonance imaging: the Multi-Ethnic Study of Atherosclerosis. **Circ Cardiovasc Imaging**. 2016; 9. pii: e004426.

22. Boonyasirinant T, Rajiah P, Setser RM, et al. Aortic stiffness is increased in hypertrophic cardiomyopathy with myocardial fibrosis: novel insights in vascular function from magnetic resonance imaging. **J Am Coll Cardiol**. 2009; 54:255−262.

23. Zhao X, Pratt R, Wansapura J. Quantification of aortic compliance in mice using radial phase contrast MRI. **J Magn Reson Imag**. 2009; 30:286−291.

24. Dogui A, Redheuil A, Lefort M, et al. Measurement of aortic arch pulse wave velocity in cardiovascular MR: comparison of transit time estimators and description of a new approach. **J Magn Reson Imag**. 2011; 33:1321−1329.

25. Groenink M, de Roos A, Mulder BJ, Spaan JA, van der Wall EE. Changes in aortic distensibility and pulse wave velocity assessed with magnetic resonance imaging following beta-blocker therapy in the Marfan syndrome. **Am J Cardiol**. 1998; 82:203−208.

26. Kraft KA, Itskovich VV, Fei DY. Rapid measurement of aortic wave velocity: in vivo evaluation. **Magn Reson Med**. 2001; 46:95−102.

27. Bargiotas I, Mousseaux E, Yu WC, et al. Estimation of aortic pulse wave transit time in cardiovascular magnetic resonance using complex wavelet cross-spectrum analysis. **J Cardiovasc Magn Reson**. 2015; 17:65.

28. Meloni A, Zymeski H, Pepe A, Lombardi M, Wood JC. Robust estimation of pulse wave transit time using group delay. **J Magn Reson Imag**. 2014; 39:550−558.

29. O'Rourke MF, Hashimoto J. Mechanical factors in arterial aging: a clinical perspective. **J Am Coll Cardiol**. 2007; 50:1−13.

30. Ohyama Y, Ambale-Venkatesh B, Noda C, et al. Aortic arch pulse wave velocity assessed by magnetic resonance imaging as a predictor of incident cardiovascular events. **Hypertension**. 2017; 70:524−530.

31. Bild DE, Bluemke DA, Burke GL, et al. Multi-ethnic study of atherosclerosis: objectives and design. **Am J Epidemiol**. 2002; 156:871−881.

32. Bhuva AN, D'Silva A, Torlasco C, et al. Training for a first-time marathon reverses age-related aortic stiffening. **J Am Coll Cardiol**. 2020; 75:60−71.

33. Ben-Shlomo Y, Spears M, Boustred C, et al. Aortic pulse wave velocity improves cardiovascular event prediction: an individual participant meta-analysis of prospective observational data from 17,635 subjects. **J Am Coll Cardiol**. 2014; 63:636−646.

34. Bensalah MZ, Bollache E, Kachenoura N, et al. Geometry is a major determinant of flow reversal in proximal aorta. **Am J Physiol Heart Circ Physiol**. 2014; 306:H1408−H1416.

35. Townsend RR, Wilkinson IB, Schiffrin EL, et al. Recommendations for improving and standardizing vascular research on arterial stiffness: a scientific statement from the American Heart Association. **Hypertension**. 2015; 66:698−722.

36. Bollache E, Kachenoura N, Bargiotas I, et al. How to estimate aortic characteristic impedance from magnetic resonance and applanation tonometry data? **J Hypertens**. 2015; 33:575−582. discussion 583.

37. Bargiotas I, Bollache E, Mousseaux E, et al. MR and applanation tonometry derived aortic impedance: association with aging and left ventricular remodeling. **J Magn Reson Imag**. 2015; 41:781−787.

38. Redheuil A, Kachenoura N, Bollache E, et al. Left ventricular and proximal aorta coupling in magnetic resonance imaging: aging together? **Am J Physiol Heart Circ Physiol**. 2019; 317:H300−h307.

39. Nichols WW, O'Rourke MF, Vlachopoulos C. **McDonald's Blood Flow in Arteries : Theoretical, Experimental and Clinical Principles**. 2011.

40. Wentland AL, Wieben O, Francois CJ, et al. Aortic pulse wave velocity measurements with undersampled 4D flow-sensitive MRI: comparison with 2D and algorithm determination. **J Magn Reson Imag**. 2013; 37:853−859.

41. Markl M, Wallis W, Strecker C, Gladstone BP, Vach W, Harloff A. Analysis of pulse wave velocity in the thoracic aorta by flow-sensitive four-dimensional MRI: reproducibility and correlation with characteristics in patients with aortic atherosclerosis. **J Magn Reson Imag**. 2012; 35:1162−1168.

42. Dyverfeldt P, Ebbers T, Lanne T. Pulse wave velocity with 4D flow MRI: systematic differences and age-related regional vascular stiffness. **Magn Reson Imaging**. 2014; 32:1266−1271.

43. Markl M, Wallis W, Brendecke S, Simon J, Frydrychowicz A, Harloff A. Estimation of global aortic pulse wave velocity by flow-sensitive 4D MRI. **Magn Reson Med**. 2010; 63:1575−1582.

44. Harloff A, Mirzaee H, Lodemann T, et al. Determination of aortic stiffness using 4D flow cardiovascular magnetic resonance - a population-based study. **J Cardiovasc Magn Reson**. 2018; 20:43.

45. Dyverfeldt P, Bissell M, Barker AJ, et al. 4D flow cardiovascular magnetic resonance consensus statement. **J Cardiovasc Magn Reson**. 2015; 17:72.

46. Soulat G, Gencer U, Kachenoura N, et al. Changes in segmental pulse wave velocity of the thoracic aorta with age and left ventricular remodelling. An MRI 4D flow study. **J Hypertens**. 2020; 38.

47. Houriez-Gombaud-Saintonge S, Mousseaux E, Bargiotas I, et al. Comparison of different methods for the estimation of aortic pulse wave velocity from 4D flow cardiovascular magnetic resonance. **J Cardiovasc Magn Reson**. 2019; 21:75.

48. von Spiczak J, Crelier G, Giese D, Kozerke S, Maintz D, Bunck AC. Quantitative analysis of vortical blood flow in the thoracic aorta using 4D phase contrast MRI. **PLoS One**. 2015; 10:e0139025.

49. Sigovan M, Hope MD, Dyverfeldt P, Saloner D. Comparison of four-dimensional flow parameters for quantification of flow eccentricity in the ascending aorta. **J Magn Reson Imag**. 2011; 34:1226−1230.

50. Barker AJ, Markl M, Bürk J, et al. Bicuspid aortic valve is associated with altered wall shear stress in the ascending aorta. **Circ Cardiovasc Imaging**. 2012; 5:457−466.

51. Bouaou K, Bargiotas I, Dietenbeck T, et al. Analysis of aortic pressure fields from 4D flow MRI in healthy volunteers: associations with age and left ventricular remodeling. **J Magn Reson Imag**. 2019; 50:982−993.

52. von Knobelsdorff-Brenkenhoff F, Karunaharamoorthy A, Trauzeddel RF, et al. Evaluation of aortic blood flow and wall shear stress in aortic stenosis and its association with left ventricular remodeling. **Circ Cardiovasc Imaging**. 2016; 9:e004038.

53. Garcia J, Barker AJ, Markl M. The role of imaging of flow patterns by 4D flow MRI in aortic stenosis. **JACC Cardiovasc Imaging**. 2019; 12:252−266.

54. Ziegler M, Welander M, Lantz J, et al. Visualizing and quantifying flow stasis in abdominal aortic aneurysms in men using 4D flow MRI. **Magn Reson Imaging**. 2019; 57:103−110.

55. Vasanawala SS, Hanneman K, Alley MT, Hsiao A. Congenital heart disease assessment with 4D flow MRI. **J Magn Reson Imag**. 2015; 42:870−886.

56. Reneman RS, Arts T, Hoeks APG. Wall shear stress — an important determinant of endothelial cell function and structure — in the arterial system in vivo. **J Vasc Res**. 2006; 43:251−269.

57. Potters WV, van Ooij P, Marquering H, vanBavel E, Nederveen AJ. Volumetric arterial wall shear stress calculation based on cine phase contrast MRI. **J Magn Reson Imag**. 2015; 41:505−516.

58. van Ooij P, Potters WV, Nederveen AJ, et al. A methodology to detect abnormal relative wall shear stress on the full surface of the thoracic aorta using four-dimensional flow MRI. **Magn Reson Med**. 2015; 73:1216−1227.

59. Bollache E, Guzzardi DG, Sattari S, et al. Aortic valve-mediated wall shear stress is heterogeneous and predicts regional aortic elastic fiber thinning in bicuspid aortic valve-associated aortopathy. **J Thorac Cardiovasc Surg**. 2018; 156:2112−2120 e2.

60. Guzzardi DG, Barker AJ, van Ooij P, et al. Valve-related hemodynamics mediate human bicuspid aortopathy: insights from wall shear stress mapping. **J Am Coll Cardiol**. 2015; 66:892−900.

61. Rodriguez-Palomares JF, Dux-Santoy L, Guala A, et al. Aortic flow patterns and wall shear stress maps by 4D-flow cardiovascular magnetic resonance in the assessment of aortic dilatation in bicuspid aortic valve disease. **J Cardiovasc Magn Reson**. 2018; 20:28.

62. Teixido-Tura G, Redheuil A, Rodríguez-Palomares J, et al. Aortic biomechanics by magnetic resonance: early markers of aortic disease in Marfan syndrome regardless of aortic dilatation? **Int J Cardiol**. 2014; 171:56−61.

63. Pathrose A, Ma L, Berhane H, et al. Highly accelerated aortic 4D flow MRI using compressed sensing: performance at different acceleration factors in patients with aortic disease. **Magn Reson Med**. 2021; 85:2174−2187.

64. Cheng JY, Hanneman K, Zhang T, et al. Comprehensive motion-compensated highly accelerated 4D flow MRI with ferumoxytol enhancement for pediatric congenital heart disease. **J Magn Reson Imag**. 2016; 43:1355−1368.

65. Berhane H, Scott M, Elbaz M, et al. Fully automated 3D aortic segmentation of 4D flow MRI for hemodynamic analysis using deep learning. **Magn Reson Med**. 2020; 84:2204−2218.

66. Ohyama Y, Redheuil A, Kachenoura N, Ambale Venkatesh B, Lima JAC. Imaging insights on the aorta in aging. **Circ Cardiovasc Imaging**. 2018; 11:e005617.

Chapter 5

Computed tomography of the aorta

Ahmed K. Ghanem[1] and Matthew J. Budoff[2]

[1]*Department of Cardiology, The Lundquist Institute at Harbor-UCLA, Torrance, CA, United States;* [2]*David Geffen School of Medicine at UCLA, The Lundquist Institute at Harbor-UCLA, Torrance, CA, United States*

Introduction

The aorta is the largest artery in the body. It originates from the left ventricle and conducts oxygenated blood to the rest of the body through a network of smaller arteries and arterioles. To perform such function efficiently, the aorta has unique features in its distinct three wall layers, which provide elasticity to the aortic wall. Various changes in this structure can result in disruption of the cushioning function of the aorta. Aging is a natural process affecting the aortic function; meanwhile, pathological factors can take the form of atherosclerosis and arteriosclerosis of the arterial wall.

Aging and pathological processes cause changes in aortic characteristics like shape, length, diameter, and elasticity.[1] These changes affect cardiovascular health in a negative way.

There are many imaging modalities for the detection of aortic changes with aging and disease, including magnetic resonance imaging and computed tomography (CT), plain radiography, ultrasonography (US), and echocardiography. Currently, CT is the modality of choice for aortic anatomic assessment. With the new generations of CT scanners, the time needed for scans as well as the radiation dose have been minimized.

CT is currently used for the diagnosis of wide variety of pathological conditions related to the heart and vascular tree. It is the first choice in diagnosing aortic aneurisms, dissection, coronary and aortic calcification, and many other disease states. The applications of CT scans expanded from its diagnostic ability into prognostic and predictive abilities. A large number of studies have shown a strong correlation of the presence of certain pathologic processes in the aorta or coronary arteries, detected by CT scan, with the development of cardiac and cerebrovascular adverse events as well as increased mortality. Vascular calcifications, which occur in different vascular beds, including coronary arteries and aorta, can be easily detected by the CT scans in an accurate, noninvasive way and its presence reflects the cardiovascular health status.

Basics of CT and physics

Sir Godfrey Hounsfield invented the first CT scanner in 1967 at EMI Central Research Laboratories, England. It was initially used for brain scanning but was later used for scanning the whole body.

The origin of the word "tomography" is from the Greek word "Tomos" meaning "slice or section" and "Graphe" meaning "drawing." The name itself gives a pretty good idea about the whole concept of the CT.

The idea of CT is based on using an X-ray source emitting thin, fan-shaped beams through the body "slice" in many angles and detectors receiving these X-rays on the opposite side. The X-ray source and the detectors are placed on a circular, rotating frame called "the gantry" (Table 5.1). X-rays are absorbed by different atoms at different rates depending on their physical density and atomic number. This absorption of the X-ray beams while passing through different tissues in the body is detected and represented by brightness on a gray scale in the resulting cross-sectional image where the higher the density, the higher the absorption, and the brighter the structure on the CT image (contrast resolution).

Unlike the conventional CT scanners, electron beam computed tomography (EBCT) does not have a rotating X-rays source and detector. It has a fixed electron beam gun at the back of the machine generating an electron beam directed to four tungsten targets covering 210 degrees of the gantry beneath the patient leading to generation of a 30 degrees fanlike X-ray beams. The X-rays penetrate the patient's body perpendicular to its z-axis. Attenuation of the X-rays is detected by two fixed detector segments on the opposite direction of the tungsten targets covering 210 degrees of the gantry above the patient.

77

TABLE 5.1 Important terms used in the CT scan.

1	Gantry	The circular skeleton containing the rotating X-ray tube and detectors. It has a central opening where the patient is moved in and out for the scan.
2	Matrix	Two-dimensional grid of pixels used to compose images on a display monitor. Numbers of rows and columns in this grid determine the matrix.
3	Pitch	The pitch is defined as the distance traveled by the table inside the gantry in one 360° gantry rotation divided by the total thickness of all simultaneously acquired slices.
4	Scan Field of View (SFOV)	The anatomical area got scanned from the patient's body.
5	Display Field of View (DFOV)	The area of the SFOV reconstructed into images. It can be equal or less than the SFOV.
6	Z-axis	The cranio-caudal axis of the patient.
7	Helical acquisition	The data obtained from the rotating X-ray source and detectors set while the table is moving inside the gantry resulting in a helical path of the X-rays penetrating the patient.
8	Reconstruction	Converting scan data into image data using complicated mathematical formulas and algorithms.
9	Retrospective reconstruction	Creating images from the raw date after the scan when needed.
10	Prospective reconstruction	Automatically creating images from the raw data during the scan.
11	Multiple segments reconstruction	Reconstruction of the combined data obtained for the same view of interest from different gantry rotations in different heart beats.

Data recorded by the detectors are digitized into picture elements called pixels (in 2D) or voxels (in 3D), with known dimensions. A high quality of the resulting CT images is very important for accurate diagnosis. Many factors affect the quality of the images including the following provided below.

Spatial resolution

This is the ability to discriminate small high-contrast objects next to each other as two distinct entities. The size and the number of detectors determine the spatial resolution of the CT scan. With thinner slices, the resolution will increase but so will the radiation dose. The pixels size in the axial view is determined by the ratio of the display field of view to the image matrix. The current multidetector computed tomography (MDCT) scanners use a matrix of 512×512 allowing a spatial resolution in x- and y-axis of 0.35 mm (in axial view). However, the best resolution available in the z-axis for current scanners ranges between 0.5 and 0.625 mm (the width of each detector or the slice thickness) depending on the type of the scanner, which has always been a limitation of the spatial resolution of CT scanners because thinner detectors are not available yet. For 3D images, voxels with equal dimensions in x, y, and z axes (isotropic) are ideal, but cannot be obtained with current scanners due to the slice thickness (z-axis) being greater than resolution in x- and y-axis. However, the x and y dimensions can be adjusted to the resolution in z-axis to get the isotropic voxels required for the 3D images reconstruction but the resolution will be inferior to the axial view

resolution. The area covered with each gantry rotation in the z-axis depends on the number of detector rows, the width of each detector, the pitch at which the table is moving, and the speed of the gantry rotation. Newer scanners like 320 slice-MDCTs can cover large volumes in one rotation. For example, if the detector width is 0.625 mm and the number of detectors is 320, then the area covered in the z-axis with each gantry rotation is 200 mm (0.625 mm $\times$ 320 slices = 200 mm). The whole aorta from the most cranial segment of the arch to the end of abdominal aorta can be scanned within a few seconds.

Flat-panel volume CT scanners, where the detector rows are replaced by an area of detector, have a higher spatial resolution than MDCT scanners, but they are inferior regarding temporal and contrast resolution.[2] Spatial resolution can be increased by decreasing the field of view and using a lower pitch, as usually applied in cardiac CT; however, utilization of a lower pitch increases the radiation dose. The standard CT matrix is 512×512, limiting the number of pixels or voxels which can be represented. Increasing matrix size to 1024×1024 and 2048×2048 in new ultra-high resolution CT scanners have improved the image quality and spatial resolution.[3] Flat-panel volume and ultra-high resolution CT scanners are under development now and have not been used in clinical practice yet.

Temporal resolution

This is the ability to freeze the motion during data acquisition. For most applications of CT, it is not that important,

because of the limited motion of organs such as the abdominal aorta. However, in cardiac CT, temporal resolution is critical because the heart, coronary arteries, and thoracic aorta are in continuous motion from the cardiac cycle. This motion creates artifacts in CT images especially during the scan of ascending aorta and aortic valve which can interfere with accurate characterization of them. This can be problematic during assessment of complex aortic anatomy like in case of ascending aortic aneurysm or in the case of interventional procedures depending on accurate scan readings like transcatheter aortic valve replacement. Such problem decreased dramatically with the increased speed of image acquisition in new-generation scanners and with the use of electrocardiographic(ECG)-gating, which synchronizes the acquisition with the cardiac cycle.[4]

Temporal resolution can be improved by using multiple segment reconstruction,[5,6] lower pitch, and higher gantry rotation speed, which is, however, limited due to the G force generated with higher rotation speeds.[6] The limitation of achieving higher rotation speeds led to the appearance of dual-source CT scanners where the gantry has two X-ray sources with corresponding two detector rows perpendicular on each other so that they can cover the whole thickness in a half rotation of the gantry, dramatically decreasing the time needed for the scan. This improves temporal resolution and image quality.[7]

ECG-gated versus non–ECG-gated CTA

ECG gating means that there is synchronization of the CT scanner to the cardiac cycle of the patient, allowing for data acquisition during phases of cardiac cycle where heart motion is minimal. These phases are end systole, early diastole, i.e., (40% phase), or mid-diastole, i.e., (75% phase).[8] There are two methods for gating.
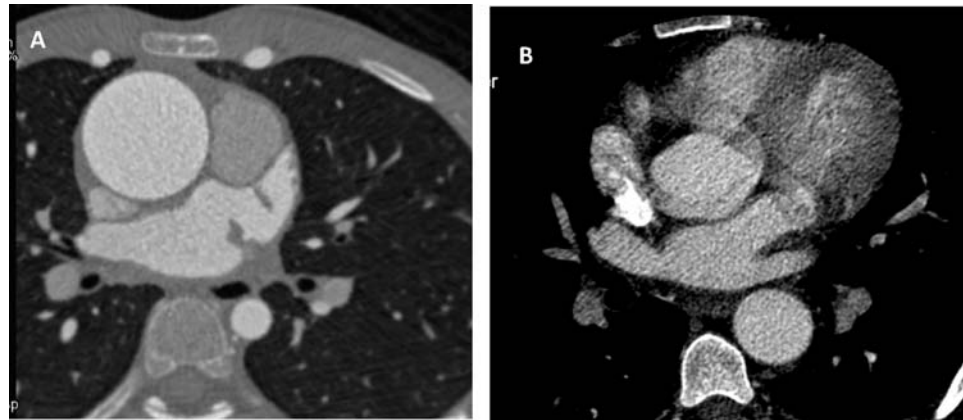
With retrospective gating helical acquisition, data acquisition occurs during the whole cardiac cycle and then the computer chooses the images obtained during specific phases of the cardiac cycle for the image reconstruction. This method is used when the heart rate is irregular because we cannot predict the timing of the relevant phases (typically from 40% to 75% of the cycle). It is also used with higher heart rates since it provides more images and a higher chance to get rid of motion artifacts. It also can detect cardiac motion abnormalities and study the heart during the systole. The downside of this acquisition modality is a higher radiation exposure, which can be reduced in ways we will discuss later.

The second technique is prospective gating (step and shoot), in which the acquisition occurs only during a predetermined time in the cardiac cycle (75% or 40%) and the gantry is moved for a second rotation in a different heartbeat. This method is used in the presence of regular and slower heart rates, because we can predict the phases of the cardiac cycle. This technique takes a longer time depending on the number of rotations and the length needed to be imaged, but it has the advantage of decreasing the radiation dose by up to 80% (15 mSv down to 3 mSv).[9]

The importance of ECG-gated computed tomography angiography (CTA) is not limited to decreasing the radiation exposure in prospective gating[10] but also to eliminating image artifacts which can be misinterpreted as pseudo-dissection of the ascending aorta (image of pseudoaneurysm). It is well known that an intimal flap constitutes one of the main findings on CTA seen in aortic dissection. With non–ECG-gated acquisitions, misalignment of the reconstructed images can mimic intimal flaps, leading to the wrong diagnosis[11] (Fig. 5.1).

ECG-gated CTA requires a longer time for acquisition compared to non–ECG-gated. To overcome this situation in aortic imaging, a combination of ECG-gated imaging for the thoracic aorta and non–ECG-gated imaging for the abdominal aorta can be used to decrease the time of the scan (Fig. 5.1).

FIGURE 5.1 Noncontrast CTA of ascending aorta with ECG gated in (A) versus non-ECG gated in (B).

Contrast resolution

This is the ability of the CT scanner to identify different tissues based on the absorption or the attenuation of the X-rays passing through these tissues. Gray scale values of the pixels within the reconstructed tomogram are defined with reference to the value of water and are called Hounsfield units (HUs) or simply "CT numbers."

There are more than 5000 shades of this gray scale represented on CT centered around zero (water). Each pixel is assigned a value between -1000 (air, black) and $+3000$ (dense bone, white). Typical CT densities of types of structures or tissue are shown in Table 5.2.

Blood and soft tissue (in the absence of vascular contrast enhancement) have similar density, since they consist of similar proportions of the same atoms (hydrogen, oxygen, carbon) thus appearing gray on CT. Bone is rich in calcium and is thus brighter (white) on CT. Fat has an abundance of hydrogen. Lung tissue contains air, which is of extremely low physical density and appears black on CT (HU -1000). CT, therefore, can distinguish blood from air, fat, and bone, but not readily from muscle or other soft tissue (i.e., the intrinsic contrast resolution of the CT is not high for soft tissues).

To identify and differentiate tissues with similar HU we use intravenous nonionic iodinated contrast media (enhanced CT scan) which absorb and attenuate X-rays more than the blood pool and soft tissue, resulting in higher brightness on the gray scale.

The iodine concentration in the contrast media, the rate of contrast injection, and the duration of the injection (resulting in a stable flow rate of the contrast media during data acquisition) play a critical role in achieving optimal arterial enhancement and better diagnostic images on CTA of the aorta. The contrast volume needed for the scan decreased after the new generation of the scanners with increased number of detectors and greater z-axis coverage abilities per each gantry rotation. With injection rates of $4-6$ mL/s in most of the modern scanners and moderate iodine concentration in the contrast media,[12] individualized protocols are important for taking in consideration the patient's body weight, cardiac output, and disease status.[13]

There are two ways to know the perfect timing to start CTA scanning after injecting the contrast. One is called the "test bolus," in which we give a small bolus of the contrast media and watch the increase in HU in the aorta in order to measure the time to reach the peak enhancement; we then give the rest of the contrast and start acquisition after this time delay. The second way is called "bolus tracking" in which the region of interest is placed in the aorta. This area is monitored during contrast injection and the scan acquisition is triggered when a certain density of contrast is detected (usually $110-180$ HU).[14] Injection of a saline flush following the contrast injection is important to washout the contrast from the peripheral circulation, for optimizing contrast delivery in the aorta and for decreasing the required contrast volume[15] (Fig. 5.2).

3D reconstruction

The optimal spatial resolution of the current MDCT scanners, while not perfect isotropic voxels, allows creating 3D volumes of data, which is in turn used to reconstruct true 3D images like multiplanar reformats (MPRs), maximum intensity projections (MIPs), volume renderings (VRs), and visual reality representations (Fig. 5.2).[16] These 3D modalities of CT are crucial for diagnosing various aortic diseases and assessing anatomical variations and abnormalities before interventions in many diseases (such as the diagnosis of aortic aneurysms and planning aortic repairs). Two important modalities in aortic diseases are

(1) MIP where only the voxels of the highest HU will be displayed. With enhanced CT scans where the contrast media will have the highest HU in aortic imaging using MIP, the whole aorta can be assessed for any stenosis, occlusion, aneurysms, etc., but it cannot be used to assess aortic calcifications because the contrast media and calcium can have similar HU, preventing visualization if calcifications.
(2) VR, in which unlike MIP, every voxel is used to create the image. This technique is superior to MIP in detecting aortic calcifications and overviewing the complex anatomical structures in real 3D representations.[17] (Fig. 5.3)

Challenges

Radiation exposure and contrast use limit the applications of CTA. That is why decreasing the radiation dose and

TABLE 5.2 Typical Hounsfield units for different types of structures or tissues.

Metal	+1000 or greater
Enhanced blood pools (lumen, aorta, LV)	+300 to +600
Calcium	> +130 to about +1000
Enhanced myocardium	+80 to +150
Nonenhanced myocardium and blood	+40 to +50
Water	0
Fat	−100 to −40
Air	∼ −1000 HU

FIGURE 5.2 ECG-gated CTA with contrast of normal aorta. (A) Volume rendering (VR) view showing complex anatomy of the whole aorta, and (B) maximum intensity projections (MIPs) view of descending aorta.

FIGURE 5.3 Centerline extraction steps and applications. (A) Showing seeding points (arrows) used to draw centerline in the aorta (arrowheads). (B, C) Volume rendering view of aorta that was extracted using centerline. (D) Cross section perpendicular to the centerline of the aorta giving accurate estimation of aortic diameter. (E) Centerline is used to measure accurate aortic length in curved and straightened MPR views.

contrast became critical to using CTA to its full potential. Ways to decrease radiation and contrast doses include the following:

1 Modulating the milliamperage of the tube current (mA) in retrospectively gated studies according to the cardiac cycle (i.e., decrease the mA dose from the phase corresponding to 80% until the phase corresponding to 40% of the cardiac cycle, and increase it between 40% and 80% to have better images during the phases with the least cardiac motion).
2 Performing prospectively gated studies (on and off).[9,10]
3 Decreasing the kilovoltage (KV) from 120 to 100 when possible.[9] However, this should not be done at the expense of diagnostic image quality.
4 Administering a saline flush after the contrast injection.[15]
5 Using bolus tracking and test bolus methods.[14]
6 Using the new generations of scanners, with higher number of detectors, which also results in a better image quality.[18]

Over the last few years, with the appearance newer scanners with higher speed, greater coverage in the z-axis, iterative reconstruction techniques, and dual-source scanners, the scanning time and radiation exposure has decreased dramatically.[19]

Anatomy of aorta

The aorta is the biggest artery in the body. It originates from the left ventricle and ends at its bifurcation into right and left common iliac arteries at the level of the fourth lumbar vertebra. The aorta is an elastic artery which conducts blood from the heart to the rest of the body and works as a cushion to buffer the pulsatile cardiac ejection. The aortic wall is composed of three distinct layers: the innermost layer is the intima, which contains endothelial cells arranged on a basement membrane and subendothelial loose connective tissue. The outermost layer is the adventitia, which contains connective tissue, some elastic fibers, collagen, and fibroblasts; it also contains nerve fibers and small blood vessels called *vasa vasorum*, which supply the arterial wall with blood. The middle layer is the media, which contains elastic fibers, vascular smooth muscle cells (VSMCs), and collagenous tissue. Changes in the normal histology of these three layers affect the aortic function. The aorta can be divided into two main parts: the thoracic aorta above the diaphragm and the abdominal aorta below the diaphragm. The thoracic aorta is further divided into three parts starting from the aortic root. By drawing an imaginary line between the angle of Louis of the sternum and the lower border of the body of the forth-thoracic vertebra, we can divide the thoracic aorta into (1) The ascending aorta, from the root until this line; (2) The aortic

arch, which is the segment of the aorta cranial to this line; (3) The descending thoracic aorta, below this line and the diaphragm. The aortic arch usually gives three main branches, which supply the upper body: the brachiocephalic, left common carotid, and left subclavian arteries. Normal populations have variations in the origin of these three branches. The most common variation is the "bovine aortic arch," in which the left common carotid artery originates from the brachiocephalic artery instead of the aortic arch itself.[20] Identifying the anatomy of the aorta is critical in treating many aortic diseases like aneurisms or dissections. Whether normal aortic anatomic variations have an effect on pulsatile hemodynamics in the aorta and the brain is unknown.

Aortic assessment using CT for characterizing aortic geometry, diameter, centerline length, and shape

Given the noninvasive nature and high accuracy of the new generations of CT scanners, CT has become the gold standard imaging technique for aortic evaluation in many centers. Aortic assessments depend on the clinical condition and hemodynamic stability of the patient, as well as the underlying pathology and its location in the aorta. CTA of the aorta is used to diagnose different aortic diseases like aortic dissection, aneurysms, intramural hematoma, aortitis, and atherosclerosis, aortic injuries from either trauma or penetrating ulcers and any wall or luminal pathology. In addition, CT is critical in choosing management plans and for patient follow-up.

Aortic imaging is performed using either contrast or noncontrast CTA, depending on the purpose of the scan and the clinical scenario. Noncontrast scans assess aortic calcification and some pathologies like intramural hematoma. Some studies also suggested using noncontrast scan to assess the aortic diameter. Contrast-enhanced, ECG-gated CTA provides an accurate assessment of the aortic geometry. The supervision of an experienced radiographer during the scan is needed to track the contrast peak in the aorta using either the bolus tracking or the test bolus method and to overcome the automated data acquisition if any error occurred for any reason, like abnormal anatomy.

For an accurate assessment of aortic geometry, the acquisition of clear images is important. The use of 3D reconstruction algorithms and centerline extraction and analysis allow for an accurate assessment of various aortic characteristics.[21] An accurate assessment of aortic geometric features is important especially during the preoperative planning of endovascular aortic procedures, because critical decisions in the treatment plan depend on it.

Thanks to the high temporal and spatial resolution of the CT scans and the wide variety of image post processing

techniques, CTA gained the superiority over other modalities used for aortic assessment. One of the important techniques for aortic characterization using CT is centerline extraction and analysis.

Aortic centerline is a thin line drawn in the center of the aorta and used to segment the aortic lumen and to identify the aortic diameter, length, shape, and branches.[22] Many reconstruction software packages can be used to detect the aortic centerline.[23] Many seed points are placed along the course or the aorta. Complex anatomy, angulation, kinking, and tortuosity require the use of more seed points. The software then segments the lumen at the level of the seed point depending on the contrast gradient between the lumen and the aortic wall and the surrounding tissues determining the central point of the lumen. The software then connects all the central points creating a centerline automatically.
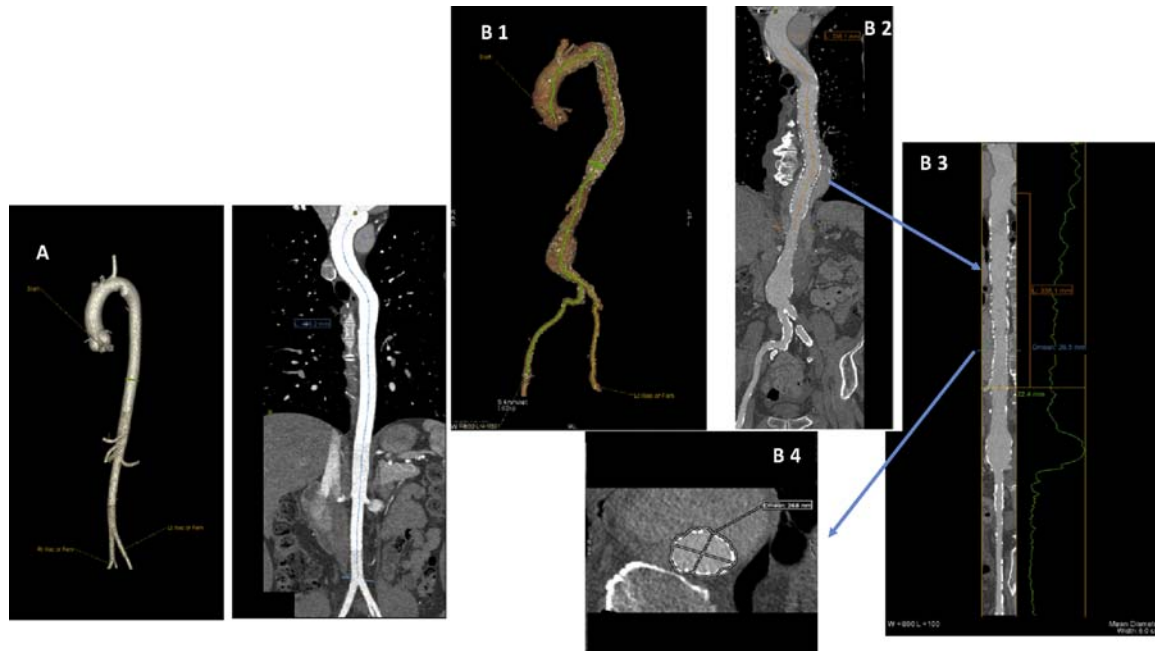
Any error of the centerline extraction and measurements will result in inaccurate measurements. That is why a vascular imaging expert should verify the resultant centerline for any errors of the calculation and deviation from the visually correct center of the aortic lumen, especially at the site of angulation and tortuosity. Control points along the centerline is used for manually editing and for correction of the position of the centerline.

After the verification of the centerline, measurements are completed. Cross sections perpendicular to this centerline can be obtained at any point along the vessel course to accurately assess the minimum, maximum, and average diameters, in addition to the wall area of the vessel. These cross sections can be obtained automatically or manually, especially to include the aortic wall or to optimize the measurement in cases of thrombus or calcifications.[24] Centerline analysis also detects the aortic length accurately with the option to display the centerline in a stretched or curved multiplanar reconstruction (MPR).[25] (Fig. 5.4). Tortuous aortas (typical with advanced age and hypertension) can be straightened by use of MPR to accurately evaluate cross sections, aneurysms, and diameters (Fig. 5.5).
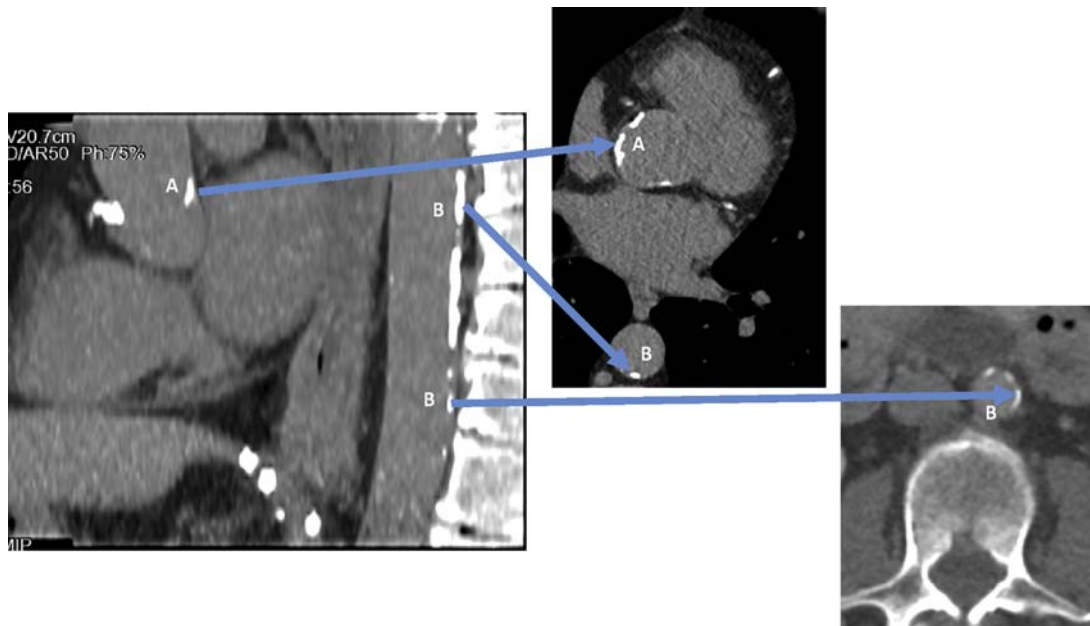
The axial view of aortic CT images does not reflect the actual diameter of the aorta because of the oblique course and the tortuosity of the aorta in the body. However, MPR reconstruction of these axial data can be used to "straighten" the aorta in reformatted images to create a plane perpendicular to the aortic lumen giving more accurate measurements correcting for the shape distortion due to the tortuosity.[26,27] (Fig. 5.2).

Many researchers investigated the accuracy and variability of these measurement techniques of the aorta and found that centerline analysis with VR is a more accurate and faster technique than manual interpretation, and it is associated with less interobserver variability compared to other modalities.[28,29]

FIGURE 5.4   (A) Aorta of a 38-year-old patient in volume rendering and curved MPR view appears less tortuous compared to the aorta of a 79-year-old patient in (B). (B 1) Volume rendering image of the tortuous aorta obtained by centerline extraction, showing a stent in the proximal descending part of the aorta and an aneurysm in the infrarenal part. (B 2, B 3) curved and straightened MPR images used to measure aortic length despite increased tortuosity. (B 4) Cross section of the aorta showing the stent and giving an accurate diameter measurement.

FIGURE 5.5   ECG-gated CTA of the aorta without contrast showing aortic calcification in the ascending (A) and descending (B) thoracic aorta.

Changes in aortic geometry with aging

The aortic diameter, wall thickness, wall composition, length, and shape change with aging,[30−32] gender, and various disease states. Many investigators have attempted to establish normal aortic diameters and the changes in aortic diameter associated with aging. Mao et al. evaluated the ascending thoracic aortic diameter of 1442 healthy men and women (mean age of 55 years) referred for CTA and coronary artery calcium (CAC) scoring, using 64 MDCT and EBCT. The investigators found that the ascending aortic diameter increases with age and male gender, with very low variability in measurements between MDCT and EBCT.[33]

Pearce et al. evaluated CT scans performed for clinical patients for nonvascular diagnoses of 389 men and women and measured aortic diameters at four anatomic levels: thoracic aorta and abdominal aorta at the celiac axis, renal arteries, and midway between the renal arteries and the aortic bifurcation. They found that at all levels, the aortic diameter increases with age and male gender; there was also a positive correlation between aortic diameter and body surface area (BSA).[34]

The same results of progressive increase in abdominal aortic diameter with age and male gender was observed by Dixon et al. based on an analysis of CT scans obtained for a variety of clinical indications other than known or suspected aortic disease from 257 male and female participants aged 30−60 years.[35] It was found that different segments of the aorta increase in diameter with aging at different rates. Fleischmann et al. evaluated CT scans of 77 healthy

potential renal donors (33 men and 44 women) aged between 19 and 67 years, to determine age-related geometric changes in the normal abdominal aorta. They assessed the diameter of abdominal aorta using centerline analysis in six consecutive anatomic segments (supraceliac, supramesenteric, suprarenal, interrenal, proximal infrarenal, and distal infrarenal). A significant effect of male gender, BSA, and age was noticed. They also found that the age-related increased aortic diameter is strongly associated with the relative anatomic position along the abdominal aorta where it was highest (0.14 mm/year) in the most proximal segment and diminished gradually when moving distally to (0.03 mm/year) near the bifurcation, causing an increase of tapering of the entire abdominal aorta from proximal to distal with age. However, they found that this proximal-to-distal tapering is not universal in all segments. Diameter increase in infrarenal aorta was absent or mild that caused "negative tapering." They suggested that this age-related tapering in aortic diameter does not occur in people older than 60 years unlike younger people.[22] In the population-based Rotterdam study, which included 5419 men and women aged 55 years and older, Pleumeekers et al. assessed the abdominal aorta using ultrasound. They found that age-related increases in proximal and distal abdominal aortic diameters are (0.07 mm/year) and (0.03 mm/year), respectively.[36] The difference in the segmental growth rate between the two studies might relate to the different age group of the study population.

CTA can also detect changes in aortic distensibility.[37,38] Ganten et al. evaluated changes in aortic distensibility with age among 31 patients without known or suspected aortic

disease aged between 28 and 85 years using retrospective, ECG-gated, time-resolved CT images to detect the change in the aortic cross-sectional area during the cardiac cycle. The authors found a linear decrease in aortic distensibility with aging with greater decrease in the suprarenal versus infrarenal aorta.[39]

Aortic calcification

The mechanisms of arterial calcification are discussed in detail in Chapter 21, but a brief overview will be provided here. It is now well established that aortic calcification is an important predictor of cardiovascular risk. For this reason, early detection and quantification of aortic calcification could be used as a tool for cardiovascular prevention strategies. For a long time, vascular calcifications were thought to represent a passive degenerative process resulting from advancing age. Recent studies demonstrate that vascular calcification is an active process triggered and regulated via different biologic pathways. Calcifications in the vascular tree occur in either the media or the intima of the arterial wall. It is hard to differentiate between these two locations with standard imaging techniques. The mechanisms by which these two types of calcification occur are different.

Intimal calcifications: This type of calcification occurs within atherosclerotic plaques. It is the dominant type of calcification in coronary arteries but also occurs in the aorta. It starts as early as childhood as a part of the atherosclerotic process. Calcification is an active process, rather than passive as believed in the past. Intimal calcification starts as microcalcifications also known as spotty, which coalesce to form larger and more diffuse calcifications, while the atherosclerotic plaques progress forming calcified plaque. Intimal calcification occurs as a result of an imbalance between factors stimulating and inhibiting calcification. The atherosclerotic process causes inflammation in the arterial intima which increases the level of extracellular calcium released from dead cells, favoring calcification. Calcification, in turn, increases the inflammatory process, creating a vicious circle of inflammation and calcification. Bone-forming pathways are involved in this calcification process. VSMCs exhibit transformation into an osteogenic phenotype in atherosclerosis, with expression of many calcium regulating proteins which cause calcification similar to what happens in bone tissue.[40] Macrophages involved in the inflammatory process also initiate and regulate this phenotypic transformation of VSMCs. Apoptosis of VSMCs and macrophages and the formation of apoptotic bodies and matrix vesicles are believed to play a role in initiation of the calcifications.[41] In atherosclerosis, the accumulated lipids in the intima are believed to initiate calcifications in different ways, including stimulation of osteogenic differentiation of VSMCs. In addition, oxidized fatty acids interfere with the clearance of apoptotic cells by macrophages.[42,43]

Intimal calcification plays an important role in plaque stability and rupture. In early stages of atherosclerosis, the heterogeneous nature of the plaques with partial calcifications makes it less stable and more vulnerable to rupture under the effect of mechanical stress. However, it has been noticed that plaques become more stable in the late stages of atherosclerosis when extensive calcification of the fibrous cap of the plaque occurs. On the other hand, well-developed calcified plaques can cause stenosis in the arterial lumen and change the normal hemodynamics of the blood flow, although this is less likely to occur in large arteries like the aorta.

Traditional cardiovascular risk factors that cause endothelial dysfunction and increase the risk of atherosclerosis also increase the risk of intimal calcification. These risk factors include advanced age, male gender, white race, hypertension, diabetes, smoking, hyperlipidemia, and renal failure.

Medial calcification: This type of calcification occurs with or without atherosclerosis or intimal calcification. Medial calcification has a different morphology than intimal calcification. Medial calcification occurs in the elastic layer of the arterial media and appears early as a linear deposit. Later on, it progresses to form circumferential dense calcified layers in the middle of the artery. Medial calcification does not cause arterial occlusion but increases the stiffness of the arterial wall, which alters pulsatile hemodynamics, increasing the pulse pressure. Medial calcification is more common in peripheral arteries and in the aorta. Apoptosis of VSMCs and failure of clearance of apoptotic bodies in the media increases extracellular calcium. In addition, the breakdown of elastin during aging and the production of elastin-derived peptides increase calcium intake into endothelial cells, which participate in the induction of medial calcification. In medial calcification, VSMCs in the media showed activation of many bone-associated genes with expression of bone-regulating proteins.[42,44] The prevalence and severity of medial calcification increases with age; however, it can occur in otherwise healthy young individuals, supporting a role of genetics in the pathophysiology of medial calcification. Medial calcification is more frequently observed in metabolic diseases with electrolyte and pH abnormalities, particularly diabetes and end-stage renal disease (ESRD).

Quantification of aortic calcification

Many imaging modalities can detect aortic calcification, including US and plain X-ray films, but only CT scanning can quantify it in an accurate noninvasive way (Fig. 5.3). The protocol used in CAC scoring is the Agatston method, in which noncontrast, ECG-gated acquisitions of 3 mm-thick

consecutive slices without gaps in between are performed. Voxels having >130 HU with an area >1 mm^2 are included and the intensity of each voxel is weighted using a grading system from 1 to 4. The calcium score of each slice is calculated by multiplying the intensity grade and the area. The total calcium score is calculated as the sum of the scores of all the slices.[45] Calcification and contrast overlap in their HU. Theoretically this overlap can cause unreliable grading and inaccurate calcium scoring using the Agatston method in the setting of intravenous contrast. However, there have been trials of detection calcium scoring in the setting of contrast using the Agatston method.[46]

The quantification is usually performed in a semi-automated manner in which an observer verifies the calcification selection for accuracy. The same protocol is used for the detection of aortic calcification. Noncontrast, ECG-gated studies are used for the ascending aorta to decrease motion artifacts from the heart. For the abdominal aorta, ECG gating is not required because the motion is limited. Another method comparable to the Agatston method is using the volume of the calcified spots. In this method, the amount of voxels above certain cutoff point is multiplied by the volume of each voxel.[47] Many studies have assessed whether automated aortic calcification quantification is as accurate as the semiautomated or the manual methods and found that automated quantification is possible, time-saving and can be used as a risk marker for cardiovascular disease (CVD).[48–50] With deep learning artificial intelligence, the algorithm detecting calcification improved with very high sensitivity and specificity.[48] The first method detected 73.8% of coronary calcifications at the expense of on average 0.1 false positives, and assigned the correct risk category to 93.4% of all scans. In the second study,[50] the authors detected 209 calcifications (sensitivity 83.9%) at the expense of on average 1.0 false-positive objects per scan. The correct category label was assigned to 30 scans and only 2 scans were off by more than one category. Most incorrect classifications can be attributed to the presence of contrast material in the scans. Overall the sensitivity and positive predictive value for the volume of detected calcifications are 0.989 and 0.948. Only one patient out of 40 patients had been assigned to the wrong risk category defined according to Agatston scores.

Tsushima et al. developed a new image analysis software program to quantify aortic calcification volume (ACV) and aortic wall and calcification volume using plain CT images.[51] Few years later, Miwa et al. calculated the percentage of calcified aortic volume against the whole vascular volume (%ACV) using a new image color analysis program.[52] Lindholt et al. also used the aortic cross sections to quantify the calcification as a percentage above or below 50% of the maximal aortic wall circumference based on visual inspection.[53] Hashiba et al. used aortic calcification area to quantify aortic calcification in ESRD patients undergoing hemodialysis.[54]

Other less quantitative scoring systems have been used to quantify aortic calcifications. Kauppila et al. developed a semiquantitative calcium scoring system called Abdominal Aortic Calcification 24-score (AAC-24) among 617 Framingham heart study participants. They included participants who had two lateral lumbar radiographic films acquired at baseline and after 25 years follow-up. The aim was to classify the location, progression, and severity of abdominal aortic calcification and to evaluate the calcification system they used. After they identified the abdominal aorta alongside the first through the fourth lumbar vertebrae, they divided the aorta into three segments per vertebra, and each segment was divided into anterior and posterior, resulting in 24 segments. Each segment was evaluated for the presence or the absence of calcification with a score of 1 or 0, respectively. The final score ranges between 0 and 24. They found that this method is reproducible.[55]

Another simplified scoring system based on the same principle was developed and is called Abdominal Aortic Calcification 8-score (AAC-8). The abdominal aorta alongside lumbar vertebrae L1-L4 was divided into four segments corresponding to each vertebra, with further diving each segment into anterior and posterior, resulting in eight segments. Each segment was scored either 0 or 1 depending on the presence or absence of calcification with a total score ranging from 0 to 8.[56] These two scoring systems are performed manually in a fast way without the need of measurement algorithms. Many studies validated the reproducibility and the predictive value of these scores regarding cardiovascular risk.[57,58]

Other approaches based on radiography to quantify aortic calcifications were investigated over the years.[59–61]

In conclusion, many aortic calcification scoring systems have been used. The Agatston method and volumetric scoring methods using CT scans are more accurate than other methods, but more studies are needed to assess their reproducibility, inter- and intraobserver and scanner variability on a larger number of patients.

Progression of aortic calcification

Aortic calcification is related to increased cardiovascular risk and coronary artery disease (CAD). Detection of the changes in aortic calcification over time may be a valuable cardiovascular risk predictor. CT scan is an excellent tool to detect the progression of aortic calcification over time. Different studies evaluated the progression of aortic calcification using different quantification methods based on serial CT scans to assess the associated risk factors with the calcification progression and to assess the relationship between aortic and coronary calcification.

Kälsch et al. evaluated aortic calcification incidence, progression, and its association with CAC in a population-based cohort study. A total of 3270 participants aged 45−74 years (53.1% women) underwent two cardiac CT scans, at a baseline and after a mean follow-up of 5.1 + 0.3 years. The Agatston method was used to quantify the calcium score in the ascending aorta, descending aorta, and coronary arteries. The authors reported that in patients with a calcium score of zero in the thoracic aorta at baseline, 41.6% developed calcification after 5 years of follow-up and this incidence was associated with age, blood pressure, low-density lipoprotein (LDL) cholesterol levels, and smoking. They also found that participants with elevated initial thoracic aortic calcification, especially in the ascending aorta, tended to have an increased risk of CAC progression and vice-versa.[62]

In Multi-Ethnic Study of Atherosclerosis (MESA), Youssef et al. evaluated thoracic aorta calcification (TAC) incidence and progression over a period of 2.4 + 0.8 years. The Agatston method was used to measure the TAC scores of 5886 participants (mean age of 62 years; 48% male) of four different ethnicities at a baseline and a follow-up second scans. For the follow-up scan measurements, the participants were randomly divided into two groups so that one group had the CTA measurements after 1.6 years and the other group had the CTA measurements after 3.2 years with a mean time between the two scans of 2.4 + 0.8 years. They found that age, systolic blood pressure, lipid lowering medications, diabetes, and smoking were associated with TAC progression.[63]

Pham et al. investigated the relationship between smoking and coronary and aortic calcification among 781 Japanese men aged 40−79 years and free of CVD. The Agatston method was used to measure both aortic and CAC scores. At baseline, the scores were measured using either a 16-MDCT or an EBCT scan. After 5 years of follow-up, the scores were measured using a 64-MDCT scan. With a multivariable analyses controlling for age and other cardiovascular risk factors, they found that current smokers had 147% higher odds of aortic calcification progression compared to never smokers. They also found that the residual adverse effect of smoking on the aorta and coronary arteries is present for at least 10 years after smoking cessation.[64]

Miwa et al. used the %ACV to investigate the relationship between pulse pressure and abdominal aortic calcification progression in 116 patients (74 men and 42 women, mostly middle aged). They included participants who showed aortic calcification in the baseline scan and followed them up for a period of 6.3 + 3.2 years. All participants had well-controlled lipid levels with either statins or other medications. They found that 89% of the participants had calcification progression reflected by increase in the %ACV over the study period. This progression was related to age, body mass index, systolic blood pressure, and pulse pressure, which was the strongest predictor of calcification progression.[52]

Using the Agatston method, Sutton-Tyrrell et al. evaluated the changes in coronary artery and aortic calcification in 80 healthy postmenopausal women by EBCT over an average of 18 months. They found that aortic calcification progression was associated with an increased baseline calcification score, total cholesterol, LDL cholesterol, and elevated pulse pressure. They also noticed that aortic calcification progression correlated with the CAC score.[65]

In a study of 281 kidney transplant recipients, 197 participants had 2 CT scans, 4.4 + 0.28 years apart. The Agatston method was used to measure CAC and TAC scores. Aortic calcification progression was associated with higher baseline aortic calcification score, higher pulse pressure, statin use, older age, higher serum phosphate level, aspirin use, and male sex.[66]

In a randomized clinical trial of 18 ESRD patients undergoing hemodialysis, Hashiba et al. investigated the effect of etidronate, a medication used for the treatment of osteoporosis, on aortic calcification progression. Patients were randomly divided into an etidronate-treated group of 8 patients and a control group of 10 patients. The treatment period was 6 months. The patients had CT scans at baseline, after 6 months and after 12 months to quantify aortic calcification. They found that the progression of calcification in participants treated with etidronate was lower than among patients who did not receive it.[54] This study confirms the role of osteogenic proteins involved in vascular calcification.

From these studies, we conclude that risk factors for aortic calcification include risk factors for atherosclerosis and vascular calcification in vascular beds. Aortic calcification is independently associated with increasing severity of coronary atherosclerosis as measured by CAC. These studies also demonstrated the close relationship between aortic and coronary calcification.

Studies about the progression of aortic calcification using CT scans are relatively scarce. New cohort studies like MESA study will provide further insights about the nature of aortic calcification and its progression. More studies on a larger number of community-based participants for a longer time are needed to better understand the progression of aortic calcification.

The importance of aortic calcification detection

In the recent guidelines issued by the American Heart Association and the American College of Cardiology, CAC score was recommended in asymptomatic adults at low and low-to-intermediate cardiovascular risk to stratify these patients into low-, moderate-, or high-risk patients in order

to implement appropriate preventive strategies. The results of the studies conducted on aortic calcification and atherosclerosis showed that aortic calcification is an independent predictor of CVD. Available data also demonstrate a correlation of aortic atherosclerosis and calcification with cerebrovascular accidents and mortality.[67–71]

As discussed previously, several studies found an association between aortic calcification and CAC.[62,65] On a population of 6807 included in the MESA study, Budoff et al. evaluated that the prevalence of TAC and CAC detected by CT scan using the Agatston method. Over a period of $4.5 + 0.9$ years, the investigators assessed the incidence of coronary heart disease (CHD) events, including hard events (myocardial infarction, resuscitated cardiac arrest and CHD death), in the study population. The investigators found that TAC was an independent predictor of future coronary events only in women.[72] Another study found similar results using plain radiography in which the presence of abdominal aortic calcification in older women was associated with increased mortality.[73]

Takasu et al. found that descending thoracic aortic calcification in the MESA study population is associated with increasing CAC and cardiovascular risk independent of cardiovascular risk factors.[74] In another study, Takasu et al. found that independent of age, descending aortic calcification detected with nonenhanced CT scan was associated with a 3.8-fold increase in the risk for obstructive CAD.[75] Criqui et al. evaluated the association between AAC and CVD in 1974 men and women included in the MESA cohort. He found that AAC was an independent predictor of hard CHD, CVD events, and mortality.[76]

Despite emerging data regarding the prognostic value of aortic calcification detected by CT scanning, the role of aortic calcification on routine risk stratification requires further study.

References

1. Komutrattananont P, Mahakkanukrauh P, Das S. Morphology of the human aorta and age-related changes: anatomical facts. **Anat Cell Biol**. 2019; 52:109−114.
2. Gupta R, Cheung AC, Bartling SH, et al. Flat-panel volume CT: fundamental principles, technology, and applications. **Radiographics**. 2008; 28:2009−2022.
3. Hata A, Yanagawa M, Honda O, et al. Effect of matrix size on the image quality of ultra-high-resolution CT of the lung: comparison of 512×512, 1024×1024, and 2048×2048. **Acad Radiol**. 2018; 25:869−876.
4. Roos JE, Willmann JK, Weishaupt D, Lachat M, Marincek B, Hilfiker PR. Thoracic aorta: motion artifact reduction with retrospective and prospective electrocardiography-assisted multi−detector row CT. **Radiology**. 2002; 222:271−277.
5. Herzog C, Nguyen SA, Savino G, et al. Does two-segment image reconstruction at 64-section CT coronary angiography improve image quality and diagnostic accuracy? **Radiology**. 2007; 244:121−129.
6. Mahesh M, Cody DD. Physics of cardiac imaging with multiple-row detector CT. **Radiographics**. 2007; 27:1495−1509.
7. Achenbach S, Anders K, Kalender WA. Dual-source cardiac computed tomography: image quality and dose considerations. **Eur Radiol**. 2008; 18:1188−1198.
8. Seifarth H, Wienbeck S, Püsken M, et al. Optimal systolic and diastolic reconstruction windows for coronary CT angiography using dual-source CT. **AJR Am J Roentgenol**. 2007; 189:1317−1323.
9. Gopal A, Mao SS, Karlsberg D, et al. Radiation reduction with prospective ECG-triggering acquisition using 64-multidetector computed tomographic angiography. **Int J Cardiovasc Imaging**. 2009; 25:405−416.
10. Blanke P, Bulla S, Baumann T, et al. Thoracic aorta: prospective electrocardiographically triggered CT angiography with dual-source CT−feasibility, image quality, and dose reduction. **Radiology**. 2010; 255:207−217.
11. Qanadli SD, El Hajjam M, Mesurolle B, et al. Motion artifacts of the aorta simulating aortic dissection on spiral CT. **J Comput Assist Tomogr**. 1999; 23:1−6.
12. Behrendt FF, Pietsch H, Jost G, Palmowski M, Günther RW, Mahnken AH. Identification of the iodine concentration that yields the highest intravascular enhancement in MDCT angiography. **AJR Am J Roentgenol**. 2013; 200:1151−1156.
13. Murphy DJ, Aghayev A, Steigner ML. Vascular CT and MRI: a practical guide to imaging protocols. **Insights Imaging**. 2018; 9:215−236.
14. Bae KT. Intravenous contrast medium administration and scan timing at CT: considerations and approaches. **Radiology**. 2010; 256:32−61.
15. Haage P, Schmitz-Rode T, Hübner D, Piroth W, Günther RW. Reduction of contrast material dose and artifacts by a saline flush using a double power injector in helical CT of the thorax. **AJR Am J Roentgenol**. 2000; 174:1049−1053.
16. Dalrymple NC, Prasad SR, Freckleton MW, Chintapalli KN. Introduction to the language of three-dimensional imaging with multidetector CT. **Radiographics**. 2005; 25:1409−1428.
17. Fishman EK, Ney DR, Heath DG, Corl FM, Horton KM, Johnson PT. Volume rendering versus maximum intensity projection in CT angiography: what works best, when, and why. **Radiographics**. 2006; 26:905−922.
18. Rezvanizadeh V, Nezarat N, Dahal S, et al. Lower utilization of contrast media and beta-blocker in 256-detector Ge revolution ct scanner: the converge registry. **J Cardiovasc Comput Tomogr**. 2020; 14:S38−S39.
19. Raff GL. Radiation dose from coronary CT angiography: five years of progress. **J Cardiovasc Comput Tomogr**. 2010; 4:365−374.
20. Berko NS, Jain VR, Godelman A, Stein EG, Ghosh S, Haramati LB. Variants and anomalies of thoracic vasculature on computed tomographic angiography in adults. **J Comput Assist Tomogr**. 2009; 33:523−528.
21. Boskamp T, Rinck D, Link F, Kümmerlen B, Stamm G, Mildenberger P. New vessel analysis tool for morphometric quantification and visualization of vessels in CT and MR imaging data sets. **Radiographics**. 2004; 24:287−297.
22. Fleischmann D, Hastie TJ, Dannegger FC, et al. Quantitative determination of age-related geometric changes in the normal abdominal aorta. **J Vasc Surg**. 2001; 33:97−105.
23. Paik DS, Beaulieu CF, Jeffrey RB, Rubin GD, Napel S. Automated flight path planning for virtual endoscopy. **Med Phys**. 1998; 25:629−637.

24. Sedghi Gamechi Z, Bons LR, Giordano M, et al. Automated 3D segmentation and diameter measurement of the thoracic aorta on non-contrast enhanced CT. **Eur Radiol**. 2019; 29:4613−4623.

25. Rengier F, Weber TF, Giesel FL, Böckler D, Kauczor H-U, von Tengg-Kobligk H. Centerline analysis of aortic CT angiographic examinations: benefits and limitations. **Am J Roentgenol**. 2009; 192:W255−W263.

26. Agarwal PP, Chughtai A, Matzinger FRK, Kazerooni EA. Multidetector CT of thoracic aortic aneurysms. **Radiographics**. 2009; 29:537−552.

27. Boll DT, Lewin JS, Duerk JL, Smith D, Subramanyan K, Merkle EM. Assessment of automatic vessel tracking techniques in preoperative planning of transluminal aortic stent graft implantation. **J Comput Assist Tomogr**. 2004; 28:278−285.

28. Müller-Eschner M, Rengier F, Partovi S, et al. Accuracy and variability of semiautomatic centerline analysis versus manual aortic measurement techniques for TEVAR. **Eur J Vasc Endovasc Surg**. 2013; 45:241−247.

29. Rengier F, Weber TF, Partovi S, et al. Reliability of semiautomatic centerline analysis versus manual aortic measurement techniques for TEVAR among non-experts. **Eur J Vasc Endovasc Surg**. 2011; 42:324−331.

30. Xu X, Wang B, Ren C, et al. Age-related impairment of vascular structure and functions. **Aging Dis**. 2017; 8:590−610.

31. Virmani R, Avolio AP, Mergner WJ, et al. Effect of aging on aortic morphology in populations with high and low prevalence of hypertension and atherosclerosis. Comparison between Occidental and Chinese communities. **Am J Pathol**. 1991; 139:1119−1129.

32. Collins JA, Munoz J-V, Patel TR, Loukas M, Tubbs RS. The anatomy of the aging aorta. **Clin Anat**. 2014; 27:463−466.

33. Mao SS, Ahmadi N, Shah B, et al. Normal thoracic aorta diameter on cardiac computed tomography in healthy asymptomatic adults: impact of age and gender. **Acad Radiol**. 2008; 15:827−834.

34. Pearce WH, Slaughter MS, LeMaire S, et al. Aortic diameter as a function of age, gender, and body surface area. **Surgery**. 1993; 114:691−697.

35. Dixon AK, Lawrence JP, Mitchell JR. Age-related changes in the abdominal aorta shown by computed tomography. **Clin Radiol**. 1984; 35:33−37.

36. Pleumeekers HJ, Hoes AW, van der Does E, et al. Aneurysms of the abdominal aorta in older adults. The Rotterdam Study. **Am J Epidemiol**. 1995; 142:1291−1299.

37. Li N, Beck T, Chen J, et al. Assessment of thoracic aortic elasticity: a preliminary study using electrocardiographically gated dual-source CT. **Eur Radiol**. 2011; 21:1564−1572.

38. Ganten M, Boese JM, Leitermann D, Semmler W. Quantification of aortic elasticity: development and experimental validation of a method using computed tomography. **Eur Radiol**. 2005; 15:2506−2512.

39. Ganten M, Krautter U, Hosch W, et al. Age related changes of human aortic distensibility: evaluation with ECG-gated CT. **Eur Radiol**. 2007; 17:701−708.

40. Proudfoot D, Skepper JN, Shanahan CM, Weissberg PL. Calcification of human vascular cells in vitro is correlated with high levels of matrix Gla protein and low levels of osteopontin expression. **Arterioscler Thromb Vasc Biol**. 1998; 18:379−388.

41. Proudfoot D, Skepper JN, Hegyi L, Bennett MR, Shanahan CM, Weissberg PL. Apoptosis regulates human vascular calcification in vitro. **Circ Res**. 2000; 87:1055−1062.

42. Shanahan CM, Cary NRB, Salisbury JR, Proudfoot D, Weissberg PL, Edmonds ME. Medial localization of mineralization-regulating proteins in association with mönckeberg's sclerosis. **Circulation**. 1999; 100:2168−2176.

43. Parhami F, Morrow AD, Balucan J, et al. Lipid oxidation products have opposite effects on calcifying vascular cell and bone cell differentiation. **Arterioscler Thromb Vasc Biol**. 1997; 17:680−687.

44. Doherty TM, Fitzpatrick LA, Inoue D, et al. Molecular, endocrine, and genetic mechanisms of arterial calcification. **Endocr Rev**. 2004; 25:629−672.

45. Agatston AS, Janowitz WR, Hildner FJ, Zusmer NR, Viamonte M, Detrano R. Quantification of coronary artery calcium using ultrafast computed tomography. **J Am Coll Cardiol**. 1990; 15:827−832.

46. van der Bijl N, Joemai RMS, Geleijns J, et al. Assessment of Agatston coronary artery calcium score using contrast-enhanced CT coronary angiography. **Am J Roentgenol**. 2010; 195:1299−1305.

47. Išgum I, Rutten A, Prokop M, van Ginneken B. Detection of coronary calcifications from computed tomography scans for automated risk assessment of coronary artery disease. **Med Phys**. 2007; 34:1450−1461.

48. Isgum I, Rutten A, Prokop M, et al. Automated aortic calcium scoring on low-dose chest computed tomography. **Med Phys**. 2010; 37:714−723.

49. Yang G, Chen Y, Ning X, Sun Q, Shu H, Coatrieux J-L. Automatic coronary calcium scoring using noncontrast and contrast CT images. **Med Phys**. 2016; 43:2174−2186.

50. Isgum I, van Ginneken B, Olree M. Automatic detection of calcifications in the aorta from CT scans of the abdomen. 3D computer-aided diagnosis. **Acad Radiol**. 2004; 11:247−257.

51. Tsushima M, Koh H, Suzuki M, et al. Noninvasive quantitative evaluation of early atherosclerosis and the effect of monatepil, a new antihypertensive agent an interim report. **Am J Hypertens**. 1994; 7:154S−160S.

52. Miwa Y, Tsushima M, Arima H, Kawano Y, Sasaguri T. Pulse pressure is an independent predictor for the progression of aortic wall calcification in patients with controlled hyperlipidemia. **Hypertension**. 2004; 43:536−540.

53. Lindholt JS. Aneurysmal wall calcification predicts natural history of small abdominal aortic aneurysms. **Atherosclerosis**. 2008; 197:673−678.

54. Hashiba H, Aizawa S, Tamura K, Shigematsu T, Kogo H. Inhibitory effects of etidronate on the progression of vascular calcification in hemodialysis patients. **Ther Apher Dial**. 2004; 8:241−247.

55. Kauppila LI, Polak JF, Cupples LA, Hannan MT, Kiel DP, Wilson PWF. New indices to classify location, severity and progression of calcific lesions in the abdominal aorta: a 25-year follow-up study. **Atherosclerosis**. 1997; 132:245−250.

56. Schousboe JT, Wilson KE, Kiel DP. Detection of abdominal aortic calcification with lateral spine imaging using DXA. **J Clin Densitom**. 2006; 9:302−308.

57. Buijs RVC, Willems TP, Tio RA, et al. Calcification as a risk factor for rupture of abdominal aortic aneurysm. **Eur J Vasc Endovasc Surg**. 2013; 46:542−548.

58. Schousboe JT, Taylor BC, Kiel DP, Ensrud KE, Wilson KE, McCloskey EV. Abdominal aortic calcification detected on lateral spine images from a bone densitometer predicts incident myocardial infarction or stroke in older women. **J Bone Miner Res**. 2008; 23:409−416.

59. Mitchell JR, Cranston WI. A simple method for the quantitative assessment of aortic disease. **J Atheroscler Res**. 1965; 5:135−144.

60. Witteman JCM, Grobbee DE, Valkenburg HA, et al. J-shaped relation between change in diastolic blood pressure and progression of aortic atherosclerosis. **Lancet**. 1994; 343:504−507.

61. Hak AE, Pols HAP, Hemert AMV, Hofman A, Witteman JCM. Progression of aortic calcification is associated with metacarpal bone loss during menopause. **Arterioscler Thromb Vasc Biol**. 2000; 20:1926−1931.

62. Kälsch H, Lehmann N, Moebus S, et al. Aortic calcification onset and progression: association with the development of coronary atherosclerosis. **J Am Heart Assoc**. 2017; 6:e005093.

63. Youssef G, Guo M, McClelland RL, et al. Risk factors for the development and progression of thoracic aorta calcification: the multi-ethnic study of atherosclerosis. **Acad Radiol**. 2015; 22:1536−1545.

64. Pham T, Fujiyoshi A, Hisamatsu T, et al. Smoking habits and progression of coronary and aortic artery calcification: a 5-year follow-up of community-dwelling Japanese men. **Int J Cardiol**. 2020; 314:89−94.

65. Sutton-Tyrrell K, Kuller LH, Edmundowicz D, et al. Usefulness of electron beam tomography to detect progression of coronary and aortic calcium in middle-aged women. **Am J Cardiol**. 2001; 87:560−564.

66. Maréchal C, Coche E, Goffin E, et al. Progression of coronary artery calcification and thoracic aorta calcification in Kidney transplant recipients. **Am J Kidney Dis**. 2012; 59:258−269.

67. Santos RD, Rumberger JA, Budoff MJ, et al. Thoracic aorta calcification detected by electron beam tomography predicts all-cause mortality. **Atherosclerosis**. 2010; 209:131−135.

68. Iribarren C, Sidney S, Sternfeld B, Browner WS. Calcification of the aortic ArchRisk factors and association with coronary heart disease, stroke, and peripheral vascular disease. **J Am Med Assoc**. 2000; 283:2810−2815.

69. Dávila-Román VG, Barzilai B, Wareing TH, Murphy SF, Schechtman KB, Kouchoukos NT. Atherosclerosis of the ascending aorta. Prevalence and role as an independent predictor of cerebrovascular events in cardiac patients. **Stroke**. 1994; 25:2010−2016.

70. Atherosclerotic disease of the aortic arch as a risk factor for recurrent ischemic stroke. **N Engl J Med**. 1996; 334:1216−1221.

71. Rennenberg RJ, Kessels AG, Schurgers LJ, van Engelshoven JM, de Leeuw PW, Kroon AA. Vascular calcifications as a marker of increased cardiovascular risk: a meta-analysis. **Vasc Health Risk Manag**. 2009; 5:185−197.

72. Budoff MJ, Nasir K, Katz R, et al. Thoracic aortic calcification and coronary heart disease events: the multi-ethnic study of atherosclerosis (MESA). **Atherosclerosis**. 2011; 215:196−202.

73. Rodondi N, Taylor BC, Bauer DC, et al. Association between aortic calcification and total and cardiovascular mortality in older women. **J Intern Med**. 2007; 261:238−244.

74. Takasu J, Budoff MJ, O'Brien KD, et al. Relationship between coronary artery and descending thoracic aortic calcification as detected by computed tomography: the Multi-Ethnic Study of Atherosclerosis. **Atherosclerosis**. 2009; 204:440−446.

75. Takasu J, Mao S, Budoff MJ. Aortic atherosclerosis detected with electron-beam CT as a predictor of obstructive coronary artery disease. **Acad Radiol**. 2003; 10:631−637.

76. Criqui MH, Denenberg JO, McClelland RL, et al. Abdominal aortic calcium, coronary artery calcium, and cardiovascular morbidity and mortality in the multi-ethnic study of atherosclerosis. **Arterioscler Thromb Vasc Biol**. 2014; 34:1574−1579.

Chapter 6

Radionuclide-based imaging of the aortic wall

Nestor Gahungu[1], Jamie Bellinge[1,2] and Girish Dwivedi[2,3,4]

[1]*Royal Perth Hospital, Victoria Square, Perth, WA, Australia;* [2]*School of Medicine, The University of Western Australia, Crawley, WA, Australia;* [3]*Department of Cardiology, Fiona Stanley Hospital, Murdoch, WA, Australia;* [4]*Department of Advanced Clinical and Translational Cardiovascular Imaging, Harry Perkins Institute of Medical Research, Murdoch, WA, Australia*

Introduction
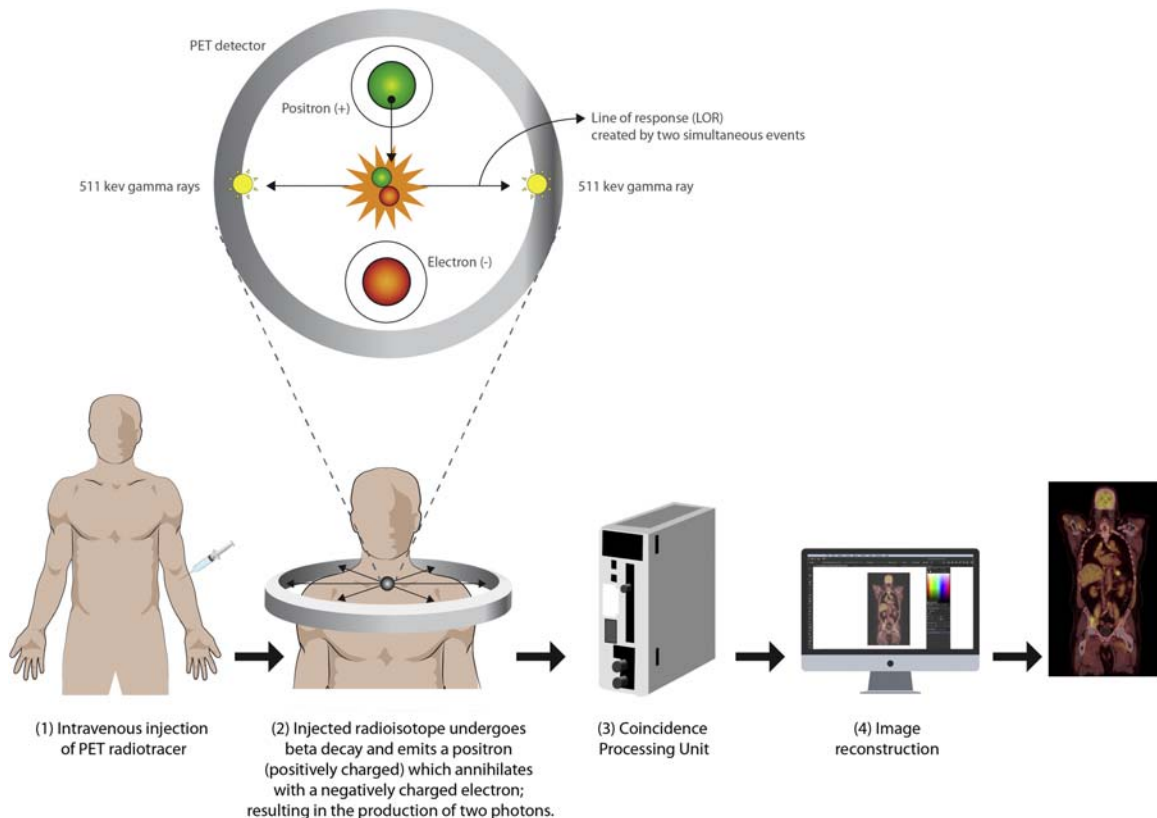
Increased large artery stiffness (LASt) is thought to result predominantly from a degenerative process that affects the tunica media of the arterial wall system (arteriosclerosis). LASt is associated with traditional cardiovascular (CV) risk factors and is independently associated with an increased risk of incident CV events.[1-3] The mechanisms of LASt involve a complex interplay between various pathological processes, including elastin degradation, collagen deposition and cross-linking, endothelial dysfunction, inflammation, and medial calcification.[4,5] This eventually results in impaired arterial compliance, a diminished Windkessel effect, and increased pulse wave velocity (PWV) with premature arrival of arterial wave reflections to the proximal aorta, further potentiating systolic hypertension, left ventricular hypertrophy, and heart failure.[6]

Various imaging modalities have been developed for imaging of LASt but are only able to detect the late stages or the hemodynamic consequences of LASt, and do not provide information about biologic activity of the aortic wall. Computed tomography (CT) or X-ray imaging may detect established calcification (macrocalcification) of the arterial wall which is only present at a late stage of the disease process whereby hemodynamic compromise is likely already present.[7] The rising incidence of cardiovascular diseases (CVDs) and associated CV events have stimulated an interest in the understanding of the earliest pathological processes of CVD as well as novel targeted methods for detecting these processes to enable the development of preventative therapies.

As discussed in Chapters 20 and 21, respectively, inflammation and microcalcification often occur in the early stages of vascular remodeling and play an integral role in the development and progression of LASt.[8,9] Local and systemic inflammation is associated with LASt through complex and poorly understood mechanisms and may promote vascular calcification.[8,10] Inflammation may result in destruction and alteration of the extracellular matrix architecture, thereby potentially contributing to LASt.[11,12] Medial aortic wall calcification occurs when calcium and phosphate crystallize in the form of hydroxyapatite in the extracellular matrix of the aortic wall.[13] Both mechanisms are ideal targets for noninvasive molecular imaging modalities.

^{18}F-fluorodeoxyglucose (^{18}F-FDG) and ^{18}F-sodium fluoride (^{18}F-NaF) positron emission tomography (PET) in combination with anatomical imaging using CT (PET/CT) or magnetic resonance imaging (PET/MRI) have emerged as promising modalities for quantitative noninvasive assessment of vascular inflammation and microcalcification, respectively.[10,14-16] PET imaging of the aortic wall using these radiotracers may provide significant insights into the pathogenesis of LASt, prove useful as risk stratification tools and may serve as specific endpoints in the trial of novel pharmaceuticals targeting LASt.[17,18] Both modalities were initially introduced for oncological imaging and were subsequently found to be useful in vascular imaging, predominantly in the context of atherosclerosis. However, their role in imaging aortic disease is becoming increasingly recognized, in part due to common mechanisms (inflammation and calcification) and shared risk factors between atherosclerosis and LASt, and in part due to the independent relationship between medial arterial inflammation and calcification and aortic wall diseases.

FIGURE 6.1 Mechanisms of positron emission tomography (PET) imaging. Upon injection of a radiotracer, the radioisotope undergoes beta-decay and emits a positively charged electron (positron). The emitted positron interacts with a free electron resulting in an annihilation reaction and production of two 511-keV annihilation photons in opposite directions. The annihilation photons strike scintillation crystals and are detected by the PET detectors placed around the patient, creating a line of response (LOR). The distribution of radioactivity within the body is determined by obtaining multiple LORs after a reconstruction of the images in three-dimension while the direction of the annihilation photons helps to localize the origin of the photons.

In this chapter, we discuss the application of ^{18}F-FDG PET/CT and ^{18}F-NaF PET/CT for imaging of inflammation and active calcification of the vascular wall, respectively. These modalities are discussed both in the context of atherosclerosis and LASt, with a greater focus on LASt. The advantages and disadvantages of applying PET imaging to the medial arterial wall are presented. Other potential radiotracers and molecular imaging probes that could be explored for specific targeting of the medial wall pathology are also briefly discussed.

Positron emission tomography imaging

PET is a form of molecular imaging which employs radionuclides or radiolabeled isotopes to visualize, characterize, and measure various biological processes at the molecular and cellular levels.[19] PET imaging is performed by intravenous injection of a radioisotope (e.g., ^{18}F) that binds, via various mechanisms, to its target tissue. In time, the radioisotope undergoes beta-decay and emits a positron (a positively charged electron) from the central nucleus of

the molecular structure. The emitted positron annihilates with free or loosely bound electrons resulting in the production of two photons: 511 keV each.[20] These photons travel in opposite directions and are simultaneously detected by PET detectors placed around the patient (Fig. 6.1), creating a line of response (LOR). The distribution of radioactivity within the body is determined by obtaining multiple LORs after a reconstruction of the images in three-dimension as well as corrections for attenuation, dead time, scatter, and random coincidences.[21]

Positron emission tomography radionuclides

Many PET radionuclides have short half-lives that decay at predictable rates following administration. ^{18}F is the most frequently used PET nuclide in clinical practice and has a long half-life of 109 min, which allows for a higher positron yield and a short positron range, allowing for injection of lower dose of radioactivity, a higher spatial-temporal resolution in tissues, delayed imaging protocols, and for easy transportation over long distances.[20,22] Nuclides with

TABLE 6.1 Characteristics of typical positron emission tomography radionuclides with potential utility in vascular imaging.[23–25]

Nuclide	Decay (%)	Half-life	Maximum β^+ energy	γ energy (keV)	Examples of positron emission tomography radiotracers	Potential clinical applications
[11]C	β^+ (99.8) EC (0.2)	20.4 min	960 keV	511	^{11}C-choline[11]C-PK11195	Vascular inflammation[26,27]
[18]F	β^+ (97) EC (3)	109.8 min	635 keV	511	^{18}F-NaF ^{18}F-FDG	Vascular calcification, vascular inflammation
[64]Cu	β^+ (18) β^- (37) (45)	12.7 h	653 keV	511	^{64}Cu-TNP	Vascular inflammation[28]
[68]Ga	β^+ (90) EC (10)	68.3 min	1.9 MeV	511	^{68}Ga-DOTATATE; ^{68}Ga-NOTA-RGD	Vascular inflammation[29–31]
[89]Zr	β^+ (22.7) EC (77)	78.5 h	2.8 MeV	511 909	[89]Zr-DNP	Vascular inflammation[32]

[64]Cu, copper-64; *[64]Cu-TNP*, ^{64}Cu-tri-reporter nanoparticle; *[68]Ga*, gallium-68; *[68]Ga-NOTA-RDG*, ^{68}Ga-labeled 1,4,7- triazacyclononane-1,4,7-triacetic acid (NOTA) - Arg-Gly-Asp (RGD); *[89]Zr*, zirconium-89; *[89]Zr-DNP*, zirconium-89-labeled dextran nanoparticles; *DOTATATE*, Dodecanetetraacetic acid-DPhe1, Tyr3-octreotate.

significantly shorter half-lives, such as carbon-11 (^{11}C; 20 min), nitrogen-13 (^{13}N; 10 min), and oxygen-15 (^{15}O; 2 min) can also be used, but often require local availability of a cyclotron.[23,24] The characteristics of typical PET radionuclides with a potential role in vascular imaging are summarized in Table 6.1. Two ^{18}F-based radiotracers, ^{18}F-FDG and ^{18}F-NaF, are of significant interest in vascular imaging and are further described.
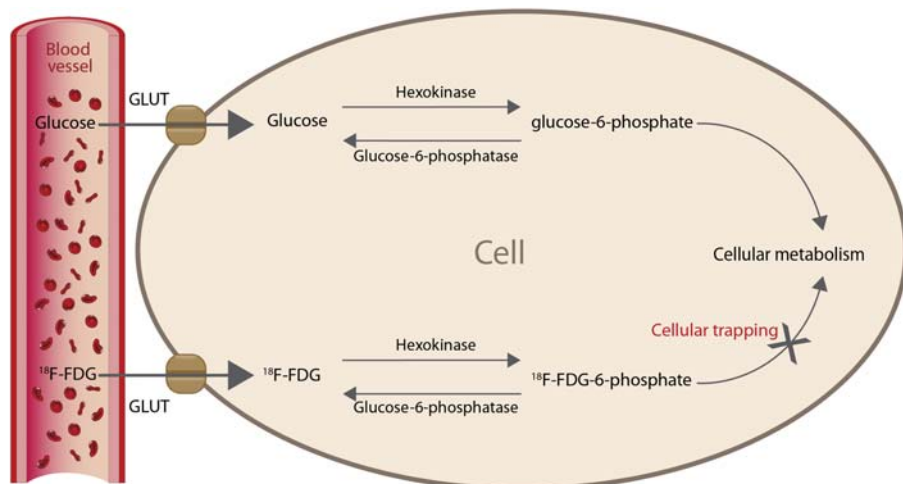
Positron emission tomography/computed tomography fusion imaging

A key advantage of PET over other molecular imaging modalities, including single-photon emission computerized tomography (SPECT), is its higher spatial resolution (4–5 vs. 10–16 mm for clinical PET vs. SPECT, respectively).[33] However, the 4–5 mm resolution is often insufficient to localize regions of small activity in the absence of established anatomical imaging tools.[34,35] Most modern PET scanners are combined with CT (PET/CT) or MRI (PET/MRI) to overcome this limitation, allowing same time-point acquisition of anatomical information.[21,36] These functional and anatomical images can be obtained simultaneously in a single study and automatically co-registered, allowing for more precise identification of PET tracer uptake by the multimodality scanners (PET/CT; PET/MRI).[36] This has revolutionized PET imaging both in oncological and CV medicine and is particularly useful in the identification of small, arterial regions of radiotracer activity.

[18]F-fluorodeoxyglucose positron emission tomography

Historical background and mechanisms

^{18}F-FDG is a radiolabeled analog of glucose which binds to glucose transporters (GLUT) to enter cells that use glucose as a source of energy.[37] This was first discovered by researchers at the University of Pennsylvania in the early 1970s who demonstrated that ^{14}C deoxyglucose (DG) crossed the blood–brain barrier and could be used to image brain's metabolic activity.[38] These investigators were the first to show that DG could be phosphorylated by hexokinase enzyme to DG-6-phosphate in a similar manner to glucose, as depicted in Fig. 6.2.[39] They observed that DG-6-phosphate could not undergo further metabolism, which made radiolabeled DG an attractive candidate for imaging of the brain metabolic activity. Further collaboration between the University of Pennsylvania and the Brookhaven National laboratory in 1973 led to a joint pursuit for radionuclides that could be used in humans, and by 1975, ^{18}F-FDG had been successfully synthesized at the Brookhaven National laboratory.[38] In a series of animal studies that followed, preferential ^{18}F-FDG uptake was demonstrated in animal models of malignant tumors.[37,40] It was later demonstrated that ^{18}F-FDG uptake correlated with the grade of tumor. In modern clinical practice, ^{18}F-FDG-PET has become a well-established modality for noninvasive imaging of cancer metastasis, prognostication, and for early detection of cancer recurrence after treatments.[38]

FIGURE 6.2   Mechanism of cellular ^{18}F-fluorodeoxyglucose (F-FDG) uptake and metabolism. Both glucose and [18]FDG enter metabolic cells via GLUT receptors. Upon entry, they both undergo phosphorylation by hexokinase to form glucose-6-phosphate and ^{18}F-FDG-6-phosphate, respectively. However, only glucose-6-phosphate undergoes further metabolism to its final products via glycolysis, whereas ^{18}F-FDG-6-phosphate becomes trapped within the cells.

Over a decade ago, it was observed that vascular areas with atherosclerotic disease had increased ^{18}F-FDG uptake compared to nonatherosclerotic segments.[41] This exciting discovery led to further exploration of this modality for potential imaging of vascular inflammation. In 2002, Rudd et al. performed the first prospective clinical study of ^{18}F-FDG-PET imaging in atherosclerosis, and demonstrated that ^{18}F-FDG accumulated in symptomatic atherosclerotic carotid artery disease compared to asymptomatic carotid lesions.[14] Since then, multiple retrospective and prospective studies have shown that ^{18}F-FDG uptake is a strong predictor of atherosclerotic plaque rupture and poor CV outcomes in atherosclerotic CVD.[18,42] ^{18}F-FDG-PET has become the most established molecular imaging modality used in atherosclerosis, although its use predominates in research settings. Its application to the imaging of aortic wall stiffness is still emerging.

Interpretation of ^{18}F-fluorodeoxyglucose signal

The rate of ^{18}F-FDG update tends to be proportional to the cells' metabolic activity and is increased in malignant tumors, brain tissue, myocytes, and inflammatory cells. This is in part due to the upregulation of GLUT receptors and enzymes involved in glucose metabolism owing to the cells' increased metabolic needs.[40,43] In inflammatory conditions such as atherosclerosis, increased ^{18}F-FDG uptake reflects accumulation of activated macrophages, which are the major driver of vascular inflammation.[21] However, the interpretation of vascular ^{18}F-FDG uptake can be challenging because other metabolically active cells such as neutrophils, lymphocytes, endothelial cells, and smooth muscle cells can also uptake glucose.[44,45] In

particular, smooth muscle cells and endothelial cells can markedly increase their glycolytic activity when exposed to proinflammatory cytokines.[45] Increased vascularity in atherosclerotic plaques may also result in increased ^{18}F-FDG uptake due to enhanced ^{18}F-FDG delivery to the resident cells.[21]

Furthermore, hypoxia has been shown to influence ^{18}F-FDG uptake through various mechanisms. While both M1 (proatherogenic) and M2 (atheroprotective and antiinflammatory) macrophages are observed in atherosclerotic plaques, M1 macrophages are the predominant subtype in the early stages of atherosclerosis and preferentially uptake ^{18}F-FDG.[46,47] *In vitro* studies have shown that increased ^{18}F-FDG uptake correlates with hypoxia-inducible factor 1α (*HIF1A*) gene expression, which may be related to an upregulation of GLUT receptors.[43,45,48] Hypoxia can also influence the polarization toward M1 macrophages and can stimulate glycolysis in M1 macrophages by stimulating overexpression of hexokinases.[43,47,49] Taken together, these factors complicate the interpretation of vascular ^{18}F-FDG uptake and may potentially reduce its specificity for imaging of inflammation. It remains unclear to what extent hypoxia rather than inflammation, influences ^{18}F-FDG uptake by macrophages.

Practical considerations in ^{18}F-fluorodeoxyglucose imaging

When studying arterial ^{18}F-FDG uptake, a pre-scan plasma glucose concentration ≤ 7 mmol/L (126 mg/dL) is recommended because higher blood glucose levels are associated with falsely low target-to-background ratios (TBRs) partly due to an increase in blood pool activity.[50] ^{18}F-FDG PET

imaging of the coronary arteries is particularly influenced by hyperglycemia because background myocardial uptake is often greater than ^{18}F-FDG signals originating from coronary plaques.[51]

Compared to ^{18}F-FDG PET imaging in oncology, longer ^{18}F-FDG circulation times of 2−3 h are also required in vascular imaging to allow enough time for ^{18}F-FDG accumulation into the arterial wall while permitting decay and excretion of background levels of ^{18}F-FDG before image acquisition. This is a critical step because a shorter time interval between ^{18}F-FDG injection and image acquisition will result in underestimation of arterial ^{18}F-FDG uptake.[50,52] When image acquisition is performed at 3 h after ^{18}F-FDG injection, the intensity of arterial ^{18}F-FDG uptake correlates with histological macrophage density.[52] Some experts believe that a circulation time of 2 h is likely to be sufficient and potentially more acceptable to patients.[53] Delaying image acquisition by >3 h does not offer any additional benefit.

The dose of ^{18}F-FDG required for imaging of aortic wall inflammation can be influenced by the sensitivity of the scanner, patient's body habitus, and the circulation time. It is recommended that the dose be minimized to reduce the exposure to ionizing radiation, particularly among patients undergoing serial ^{18}F-FDG PET imaging.[53] At least one study has previously demonstrated that a low ^{18}F-FDG dose does not significantly affect the image quality or quantification of ^{18}F-FDG uptake.[50] The recommended dose is between 3 and 4 MBq/kg body weight.[53]

[18]F-fluorodeoxyglucose positron emission tomography imaging of the arterial wall

^{18}F-FDG PET is a well-established modality for the imaging of vascular inflammation of the intimal wall in the context of atherosclerosis.[14,41] This reflects the pivotal role of ^{18}F-FDG in the detection of intimal macrophages, the key drivers in the inflammatory cascade of atherogenesis. This is further demonstrated in both ex vivo and in vivo studies in which ^{18}F-FDG accumulates in macrophage-dense areas of atherosclerotic plaques.[14,41] In patients with severe carotid stenosis, ^{18}F-FDG PET signal correlates strongly with macrophage staining on corresponding histologic sections after carotid endarterectomy.[52]

In contrast, the application of ^{18}F-FDG PET to the imaging of the medial layer of the arterial wall is less established, perhaps due to the differences in the histology between the tunica intima and the tunica media, and the pathophysiological differences between atherosclerosis and arteriosclerosis. Vascular smooth muscle cells (VSMCs) are the predominant cell types present in the avascular tunica media, and the balance between the proinflammatory and antiinflammatory properties of the VSMCs determines the extent and severity of medial arterial wall inflammation.[11]

While inflammation plays an essential role in the pathophysiology of atherosclerosis, LASt has a complex pathophysiology that differs from atherosclerosis, and involving elastic fragmentation and degradation, collagen deposition, collagen and elastin cross-linking, VSMC stiffening, endothelial dysfunction, medial calcification, and indeed, a component of inflammation.[4,5] The association between vascular inflammation and LASt is itself complex and multifaceted. On the one hand, the tunica media is considered an "immune-privileged" site, being spared of resident and infiltrating inflammatory cells in normal and atherosclerotic disease states.[11] On the other hand, medial immunoprivilege breakdown can be observed in the form of intense leukocyte infiltration associated with certain aortic aneurysms and vasculitides, which may result in loss of VSMCs, and destruction of the extracellular matrix architecture.[11] How this inflammation affects LASt is not well understood, but it may promote the trans-differentiation of VSMCs into an osteoblastic phenotype, resulting in active calcium deposition within the arterial media.[8,54,55] Vascular inflammation can also activate matrix metalloproteinases, resulting in degradation of elastin and collagen.[12]

Although LASt is mostly determined by factors affecting the medial arterial wall, it remains unclear whether medial arterial wall inflammation can be imaged in isolation because pathologies affecting any of the three layers of the arterial wall can result in aortic wall stiffness,[4] and differentiating these layers noninvasively is difficult.[9,56] Indeed, traditional CV risk factors and endothelial dysfunction which cause atherosclerosis are also associated with LASt.[4,57,58] Unsurprisingly, a recent study performed by Al-Mashhadi et al., demonstrated that arterial ^{18}F-FDG PET signal accumulates equally in intimal wall and other arterial wall tissues, including the arterial media,[56] supporting the notion that aortic wall inflammation may be associated with both atherosclerosis and arteriosclerosis.[9] It is theoretically possible that some of the ^{18}F-FDG uptake in the medial arterial wall may be mediated through VSMCs, rather than or in addition to the macrophages, because VSMCs can exhibit proinflammatory properties and have the ability to upregulate GLUT receptors under stress.[45,59] Detecting such processes would be possible with ^{18}F-FDG PET but would rely upon global methods of analysis whereby entire aortic ^{18}F-FDG burden would be of greater importance than localized regions of activity.[39,60]

While the mechanisms of inflammation in LASt remain poorly defined, many studies have shown that measures of aortic wall stiffness are associated with markers of active inflammation in patients with chronic inflammatory conditions such as rheumatoid diseases,[10] chronic obstructive pulmonary disease,[61,62] and vasculitides.[63] In a small study

of patients with rheumatoid arthritis (RA), Mäki-Petäjä et al. demonstrated an increased aortic wall stiffness in RA patients as determined by aortic PWV, which is strongly correlated with raised inflammatory markers.[10] In a cohort of patients with ANCA-associated small vessel vasculitis (systemic inflammation), Booth et al. showed that subjects with active inflammation had increased measures of aortic stiffness whereas PWV did not differ in individuals with disease in remission compared to control subjects.[63] The relationship between inflammation and LASt is discussed in detail in Chapter 20.

The potential utility of ^{18}F-FDG PET imaging in LASt can be observed in small studies of older patients and individuals with diabetes mellitus, and other CV risk factors. In a cohort of 44 patients with type 2 diabetes without established CV disease and who were not on hypoglycaemic medications, De Boer et al. found a significant independent correlation between subclinical arterial inflammation assessed with ^{18}F-FDG PET and arterial stiffness.[9] Furthermore, systemic low-grade inflammation exists among older individuals and is associated with aortic wall stiffness. In a study of 149 subjects who were stratified by age group, it was observed that the percentage of visible large artery segments with ^{18}F-FDG uptake increased with age (27% for the first decade, 38% for the second decade, 67% for the third decade, and 77% for the fourth decade).[64] In a cohort of 30 patients aged over 65 years with and without hypertension, Joly et al. observed a positive correlation between aortic ^{18}F-FDG uptake and aortic stiffness at the level of ascending aorta.[65] Stiffness was increased among individuals with raised inflammatory markers and this correlated well with ^{18}F-FDG uptake. Compared to older individuals who were normotensive, hypertensive older patients of matched age had higher thoracic aortic PWV and increased ^{18}F-FDG uptake.[65] Taken together, these early observations may suggest a role for ^{18}F-FDG PET imaging of the aortic wall to detect early markers of aortic stiffness, but further research is needed.

^{18}F-fluorodeoxyglucose positron emission tomography imaging in prognostic assessment

Increased vascular ^{18}F-FDG-PET activity may correlate with future clinical events, suggesting that it may have a role in the identification of a subset of patients who may benefit from intensive medical therapies.[52] Indeed, macrophages tend to accumulate in unstable atherosclerotic plaques, which are associated with a risk of rupture and future CV events.[14,42] In a cohort of cancer patients who were followed up for 29 months after undergoing a whole body ^{18}F-FDG-PET, Rominger et al. observed a strong correlation between ^{18}F-FDG uptake in large arteries and

subsequent vascular events.[18] Other studies have also demonstrated a prognostic value of ^{18}F-FDG PET imaging in predicting CV events.[42,66] Figueroa et al. evaluated whether arterial inflammation measured by ^{18}F-FDG-PET could predict CV events beyond traditional risk factors. In this study, 513 individuals with treated cancers and who had no history of CVD underwent ^{18}F-FDG-PET and were followed up for 4.2 years. The study demonstrated that TBR (quantified in the ascending aorta) was a strong and an independent predictor of subsequent CV events (incident stroke, transient ischaemic attack, acute coronary syndrome, revascularization, new-onset angina, peripheral arterial disease, heart failure, or CV-related death).[42] Furthermore, the addition of ^{18}F-FDG measurements to Framingham risk scores resulted in incremental improvement in ^{18}F-FDG-PET being able to predict future CVD events.

These findings suggest that increased vascular ^{18}F-FDG uptake is associated with active inflammation and is, at least in coronary atherosclerotic plaques, a predictor of plaque instability and increased risk of adverse CV events.[14,21] This is particularly relevant from a clinical standpoint because inflammation is now a key target for therapeutic interventions in CVD. The Canakinumab Antiinflammatory Thrombosis Outcome Study showed that antiinflammatory therapy targeting the interleukin-1β pathway with a fully humanized monoclonal antibody, canakinumab 150 mg every three months, significantly reduced the rate of recurrent CV events, among patients with previous myocardial infarction and a high-sensitivity C-reactive protein level.[67] However, this benefit occurred at the expense of increased risk of fatal infections, making Canakinumab a less desirable treatment option for coronary disease. In the low-dose colchicine for secondary prevention of CVD (LoDoCo and LoDoCo2 trials), colchicine 0.5 mg compared to placebo, significantly reduced the rates of CV events among patients with stable coronary disease.[68,69] The Colchicine Cardiovascular Outcomes Trial showed that colchicine compared to placebo was effective at preventing major adverse CV events after a myocardial infarction.[70] These results provide strong evidence for the potential benefits of antiinflammatory therapies in patients with coronary artery disease, perhaps by stabilizing atherosclerotic plaques.

The prognostic value of vascular ^{18}F-FDG uptake in relation to aortic stiffness and future CV events remains unclear. It is unlikely that high-risk plaques in the aorta are of great clinical importance, but global aortic inflammation, assessed with ^{18}F-FDG PET, may represent an increased propensity to develop further arterial disease (both intimal and medial) and subsequent CVD events.[18] Data from small studies indicate that both vascular inflammation and

aortic stiffness may be reduced by antitumor necrosis factor-α (anti-TNF) therapies,[10] but there is currently no direct evidence to suggest that this is associated with reduced CV events.

^{18}F-fluorodeoxyglucose positron emission tomography in translational research and clinical trials

There is substantial interest in using ^{18}F-FDG PET as a surrogate endpoint in clinical trials evaluating the treatment effects of anti-atherosclerotic and antiinflammatory drugs. It is expected that this tool may serve as a bridge between phase I/II and phase III clinical trials by providing early in vivo evidence of molecular benefits of new pharmaceuticals. Absence of improvement in ^{18}F-FDG uptake after treatment with a new pharmaceutical may indicate that the new drug is unlikely to have significant clinical effects and may argue against the need to embark on expensive and potentially futile phase III clinical trials.[71] However, these studies should be interpreted with caution since other factors such as duration of follow up, and methods of quantification of ^{18}F-FDG uptake are likely to influence the results.[71,72]

In the first randomized trial evaluating this concept, 43 patients undergoing ^{18}FDG-PET imaging for cancer screening and who had demonstrable ^{18}FDG uptakes in the thoracic aorta and/or the carotid arteries were randomized to either statin group receiving simvastatin (n = 21) or diet group receiving dietary management only. After 3 months of follow up, attenuated ^{18}F-FDG standardized uptake value (SUV) was observed among statin-treated individuals compared to the individuals in the diet control group, which paralleled improvement in lipid profiles.[73] In a study of Japanese adults with dyslipidaemia undergoing percutaneous coronary intervention for stable angina, Ishii et al. showed that 6 months of treatment with atorvastatin 20 mg compared to 5 mg was associated with a significant reduction in TBR in the ascending aorta and femoral artery, mirroring improvement in lipid profile and a decrease in inflammatory biomarkers.[74] Other trials have also shown improvement in ^{18}F-FDG uptake after statin treatment, which may be dose-dependent,[75] and correlates with improvement in inflammatory biomarkers.[76] In RA patients, Mäki-Petäjä et al. showed that anti-TNF therapy could reduce aortic inflammation, and this effect correlated with the decrease in aortic stiffness.[10] In this study, 17 patients with RA underwent ^{18}F-FDG PET before and after 8 weeks of anti-TNF therapy. Additional 34 patients with stable CVD were imaged concurrently and used as positive control at baseline. Both groups underwent assessment of aortic ^{18}F-FDG TBRs and aortic PWV. At baseline, RA patients had higher aortic TBRs than patients with CVD (2.02 ± 0.22 vs. 1.74 ± 0.22, P = .0001). At follow up, aortic TBR fell significantly to 1.90 ± 0.29, and the proportion of inflamed slices decreased from 50 ± 33% to 33 ± 27%. Furthermore, TBR in the most diseased segment of the aorta also improved. These improvements in TBR values after treatment with anti-TNF therapies correlated with reduction in aortic PWV. The results suggest that ^{18}F-FDG PET may be useful as surrogate endpoint in clinical trials of therapies for atherosclerosis and may potentially have a role in evaluation of therapies for aortic stiffness.

^{18}F-fluorodeoxyglucose uptake in aortic aneurysms and large vessel vasculitis

^{18}F-FDG PET is a very useful modality in certain aortic aneurysms and large vessel vasculitis where medial inflammation is typical.[77] Rupture of abdominal aortic aneurysmal (AAA) is associated with high mortality and although imaging modalities such as CT and ultrasound can be used to monitor for progression and risk of rupture, these modalities are imprecise and unable to provide information about biologic activity within the aortic wall. Aortic wall inflammation may be associated with an increased risk of aneurysmal rupture. Biopsy of aneurysmal walls with ^{18}F-FDG uptake has increased inflammatory cells, and a marked reduction of VSMCs in the medial wall compared with PET negative sites.[78] ^{18}F-FDG uptake in aneurysmal walls may also be associated with increased activity of matrix metallopeptidase 1 and 13, which could suggest active remodeling and a potential risk of rupture.[78] Ex vivo studies have shown an association between pre-rupture ^{18}F-FDG uptake on micro-PET imaging and inflammation in the ruptured AAA wall,[79] suggesting that it may be possible to use ^{18}F-FDG PET imaging to monitor inflammatory changes before AAA rupture. However, although these ex-vivo observations have been corroborated in small human studies, the results have been contradictory and there remains insufficient data to conclusively determine the association between aneurysm growth and rupture and ^{18}F-FDG uptake.[80]

Large vessel vasculitis (LVV), including Takayasu arteritis and giant cell arteritis are associated with intense aortic wall inflammation which may promote vascular calcification.[8] While ^{18}F-NaF remains an investigational tool in this context, ^{18}F-FDG PET can currently be used in clinical practice for assessment of suspected giant cell arteritis when the diagnosis cannot be excluded on basis of biomarkers, other imaging modalities, and temporal artery biopsy.[81] It may have a greater role in the diagnosis of extracranial vascular involvement in patients with LVV, but this is yet to be further elucidated in randomized clinical trials. If combined with CT angiography, ^{18}F-FDG PET may help to detect LVV-associated complications such as stenosis, aneurysmal formation, and dissection.[82] ^{18}F-FDG PET may also have a role in monitoring for therapeutic

response after treatment initiation for LVV although data to support this use are scarce.[81] At present, there is no internationally accepted definition of LVV based on ^{18}F-FDG uptake, but expert recommendations have been published.[82]

[18]F-sodium fluoride positron emission tomography

Historical background and mechanisms

[18]F-NaF is an established radiotracer that was first introduced and purposed for the detection of osteolytic and osteoblastic disease in the 1960s.[83] The radiotracer had limited clinical utility initially due to its high-energy nature and limited imaging modalities at the time and was subsequently superseded by 99 mTc—methylene diphosphonate scintigraphy.[84] However, recent improvements in molecular imaging, notably the evolution of PET, has seen the resurgence of ^{18}F-NaF as a bone-specific agent that has enhanced diagnostic accuracy in the detection of metastatic bony disease.[85] The improved image resolution of PET imaging occasioned the observation of nonosseous ^{18}F-NaF uptake, the most intriguing of such reflecting arterial calcification activity.[86] This has led to a growing interest in the role of this tracer for imaging of vascular calcification.

Upon intravenous injection, ^{18}F-NaF rapidly binds to hydroxyapatite $(Ca_{10}(PO_4)_6(OH)_2)$, the predominant mineral present in bone.[13] This involves the ^{18}F-ion exchanging for a hydroxyl group in the mineral matrix, thereby resulting in fluorapatite $(Ca_{10}(PO_4)_4F_2)$ formation.[87] This exchange process is rapid, reflecting the high affinity of this radiotracer for hydroxyapatite structures.[87,88] The ^{18}F-ion undergoes radioactive decay as previously described, and like ^{18}F-FDG, the resulting positron emission allows targeted identification of regions of radiotracer binding within the vascular and osseous structures.

Interpretation of ^{18}F-sodium fluoride- signal

The two major factors influencing the uptake of ^{18}F-NaF into vascular calcifications are (1) the surface area of hydroxyapatite available for binding and (2) the delivery of radiotracer to the area of binding. These features have been studied mostly in the setting of atherosclerotic calcification,[88] though similar principles are likely to apply to all types of calcification within the vasculature. Irkle et al. studied extracted carotid artery atherosclerotic specimens incubated with ^{18}F-NaF then imaged with spectroscopy, autoradiography, histology, and immunohistochemistry.[88] In the absence of calcification, no ^{18}F-accumulation was detected. ^{18}F-NaF radiotracer uptake was greater in the presence of microcalcifications (nodules <50 μm) more so than macrocalcification (nodules ≥ 50 μm). When carotid artery specimens were dissected prior incubation in ^{18}F-NaF, the radiotracer uptake was much higher than in specimens that were not dissected prior to incubation. These findings are secondary to the increase in surface area of hydroxyapatite available for ^{18}F-binding and ultimately translate to an increased signal intensity of such regions, on PET imaging.

The role of blood flow and delivery of radiotracer to hydroxyapatite crystals is surprisingly important, even in vascular calcification. In the study of carotid specimens interrogated by Irkle et al., the nondissected regions of carotid lesions had less radiotracer uptake, likely secondary to the inability for radiotracer to reach the inner core of the calcified plaque.[88] Therefore, delivery to the core of such plaques would likely increase radiotracer uptake in that region. Calcifications in close proximity to the vessel lumen may have a higher affinity for radiotracer activity, than those situated nearer to the adventitia, owing to the increased delivery of radiotracer to this area.[88,89] Regions of progressive atherosclerotic disease, of which calcification forms an important component, are often associated with the presence of microvessels, or vasa vasorum, that penetrate from the adventitia into the intima[90,91] and in atherosclerotic plaques with high ^{18}F-NaF binding, the presence of vasa vasorum is almost twice as much compared to ^{18}F-NaF negative arteries.[92] The presence of vasa vasorum may ultimately assist in the delivery of ^{18}F-NaF to regions of otherwise "walled off" calcification. While it is proposed that almost all of ^{18}F-NaF binds to regions of calcifications on first pass of blood,[93] it is very likely that regions of low blood flow may result in increased radiotracer binding capabilities because of pooling and a resulting increase in time to bind. This belief, albeit not entirely understood, may be of particular importance in aortic wall diseases including dissection, aneurysm, and coarctation.

In the pathophysiology of calcification within the vasculature, actively depositing calcifications often begin in the microscopic form, with high surface area available for binding and in the absence of locally impaired blood flow.[94] These key features promote increased binding of the ^{18}F-NaF radiotracer in the early and active stages of the disease process supporting its role in the detection of metabolically active disease. Furthermore, other histological and imaging data support the role of ^{18}F-NaF in the detection of calcification activity.

An ex-vivo analysis by Joshi et al. observed regions of radiotracer activity in explanted carotid specimens were positively associated with other histological and

immunological markers of calcification activity, increased alkaline phosphatase, osteocalcin, inflammation (CD68), necrotic core, and cell death.[95] A different study of carotid plaques also described an inverse relationship between ^{18}F-NaF activity and α-smooth muscle actin,[96] supporting a role for VSMC transdifferentiation,[55] or even apoptosis,[97] in the pathophysiological development of arterial calcification. In animal studies, ^{18}F-NaF binds to early intimal disease, perhaps even before the development of histologically identifiable macroaggregates of calcification.[98]

Imaging data from both prospective and retrospective studies have described the role of ^{18}F-NaF activity, detected using PET imaging, in predicting new CT-detectable calcification in the same anatomical location, years later. In the aortic valve, baseline ^{18}F-NaF activity is associated with the rate of change of calcification.[99] Within the femoral arteries, baseline ^{18}F-NaF activity is positively associated with the development of new calcifications after almost six months.[16] Within the aorta, retrospective studies have observed high radiotracer activity within the aortic wall go on to develop new calcifications in the same area.[100,101] Taken together, these observations support the role of ^{18}F-NaF PET in the detection of calcification activity within the vasculature. The utility of such an imaging tool is further described.

[18]F-sodium fluoride- positron emission tomography imaging of the aortic calcification activity

Intimal calcification activity

From a pathophysiological perspective, intimal aortic calcification differs greatly from medial arterial calcification. However, in severe intimal calcification, the functional impact on arterial wall stiffness is likely to be similar to that of medial arterial disease, at least at a local level.[7] Therefore, the prediction of severe intimal calcifications using ^{18}F-NaF PET is likely to be of great clinical importance when considering LASt. Within the aorta, calcified atherosclerotic plaque develops in a similar mechanism to other vascular territories; however, the prevalence of aortic calcification is generally lower than the coronary arteries.[17,102]

The role of ^{18}F-NaF imaging in intimal aortic calcifications is not well understood, though a significant proportion of our understanding can be extrapolated from invasive coronary imaging techniques. Atherosclerotic plaques with increased ^{18}F-NaF PET uptake display increased prevalence of positive remodeling, necrotic core and microcalcification, and vasa vasorum.[92,95] Additionally, ^{18}F-NaF positive plaques have a greater burden of atherosclerosis compared to ^{18}F-NaF negative plaques.[92] However, ^{18}F-NaF PET activity is higher in partially calcified plaques than fully calcified plaques, representing

its capacity to differentiate between active ongoing disease and burnt out, established calcifications.[103] In the coronary arteries, the role of this imaging modality may serve to function as a tool to identify high-risk plaques noninvasively, which may be associated with increased risk of CVD events. In the aorta, the role of high-risk plaque features is less clinically relevant and the ability to detect disease activity is of more importance. Increased aortic wall ^{18}F-NaF uptake can be observed many years before the onset of CT-detectable calcification,[104] which may subsequently precede the development of clinically relevant aortic wall stiffness.[7]

Intimal calcification activity within the aorta was first described by Derlin et al. in a retrospective analysis of patients undergoing ^{18}F-NaF PET imaging for oncological purposes.[86] In this study, the prevalence of thoracic aortic ^{18}F-NaF PET positive disease was 36%, and 48% in the abdominal aorta. In contrast, a different study of high CVD risk patients described ^{18}F-NaF PET positive disease in more than 90% of patients.[105] Though, it is important to recognize the difference in thresholds of ^{18}F-NaF PET positivity between different studies. Intimal aortic calcification activity is positively related to already established calcification burden,[106,107] but is inversely related to plaque density,[108] suggesting that densely calcified plaques have a reduced surface area for binding and probably represent burnt out, inactive sites. Retrospective studies have described the relationship between ^{18}F-NaF PET being more associated with the rate of change of CT calcium score than the baseline calcium score itself[100] and may be most predictive of disease processes at 1 year follow-up.[101] Prospective data have demonstrated a role of ^{18}F-NaF PET in predicting new calcifications.[109] This is of particular importance in the arterial media, whereby predicting calcification prior to its macroscopic development may identify those patients who go on to develop clinically significant LASt.

Medial arterial calcification activity

X-ray and CT imaging modalities have provided some insight into the differentiation between intimal and medial arterial disease using noninvasive imaging. X-ray imaging has described medial calcifications as uniform, linear "railroad track" like appearance and intimal calcifications as discrete, interrupted plaque-like lesions.[7,110]CT imaging has more recently established alternative quantitative methods to differentiate intimal from medial calcifications, using circularity, thickness, and morphology of the calcifications.[111] Translating these to ^{18}F-NaF PET is possible but must be considered in light of the reduced spatial resolution of the imaging technique.

Generally speaking, medial arterial calcifications are more common than intimal calcifications, in the lower

limbs.[112] In contrast, medial calcification is rare in the coronary arteries where intimal calcification predominates. In the aorta, the prevalence of medial calcifications is not well described, though the prevalence likely sits somewhere between the coronary arteries and the aorta will vary depending on age and other traditional CVD risk factors.[113,114] Medial arterial calcifications begin as fine, powdery deposits and can develop to severe calcifications containing osteocytes and features consistent with bone marrow formation.[55,115] Situated in the tunica media, often with sufficient supply of blood, early stages of these calcifications are likely to display great ^{18}F-NaF uptake. In comparison to their intimal counterparts, the effect of a heavily calcified "walled off" effect is probably less prominent.[88]

Imaging of medial arterial calcification with ^{18}F-NaF PET is possible when applying the X-ray and CT guided imaging principles to the interpretation. Indeed, the prevalence of medial calcification detected on ^{18}F-NaF PET is associated with hypertension, diabetes, and other clinical risk factors frequently associated with medial arterial calcification detected using CT and X-ray.[116,117] Indeed, medial arterial ^{18}F-NaF PET activity is positively associated with established medial arterial calcification burden detected using CT.[118] This is important, because using current technologies, the single biggest predictor of developing vascular calcifications is the burden of calcification at baseline[119] and any modality that can provide additional prognostic information is likely to be of good clinical utility. Interestingly, smoking is inversely associated with reduced medial arterial calcification activity detected with ^{18}F-NaF PET,[116] and this is a phenomenon witnessed in other vascular territories examining medial arterial calcification.[120,121]

Compared to intimal pathologies, the medial arterial wall is less influenced by inflammation[121] whereas the calcification of the medial arterial wall is a well-established process in medial arterial pathologies.[118] These differences have important implications both in the selection of appropriate imaging modalities and in the prognostic assessment. In prospective studies of heterogenous cohorts directly comparing ^{18}F-FDG and ^{18}F-NaF, aortic ^{18}F-NaF activity was strongly related to CV risk, while aortic ^{18}F-FDG activity was not.[106] However, as previously discussed, other studies have observed a strong relationship between aortic ^{18}F-FDG activity and increased CV risk.[14,21] This may be partly explained by the dynamic and temporal relationship between the pathophysiological mechanisms underlying inflammation and calcification, which may occur at different time points in a patient's disease progression, but still contributing to the development of CV risk.[8,10]

By detecting arterial calcification activity, ^{18}F-NaF PET may have an important role in CVD risk stratification, beyond its role in identifying early medial-specific arterial calcifications. Firstly, ^{18}F-NaF PET activity is related to traditional CVD risk factors; age,[15] gender,[122] diabetes mellitus,[123] hypercholesterolemia,[124] hypertension,[125] and Framingham risk score,[106,126] and may provide additional prognostic information over clinical risk scores. Secondly, in the abdominal aorta, calcification burden is a strong predictor of CV events,[127] even after adjusting for traditional CVD risk factors and current observations support the positive relationship between ^{18}F-NaF PET activity at baseline and subsequent aortic macrocalcification development.[100,101] Finally, the progression of aortic calcification, likely to be predicted by ^{18}F-NaF PET, is positively associated with the risk of incident coronary calcification development; the single best available independent predictor of CVD events.[102,128,129]
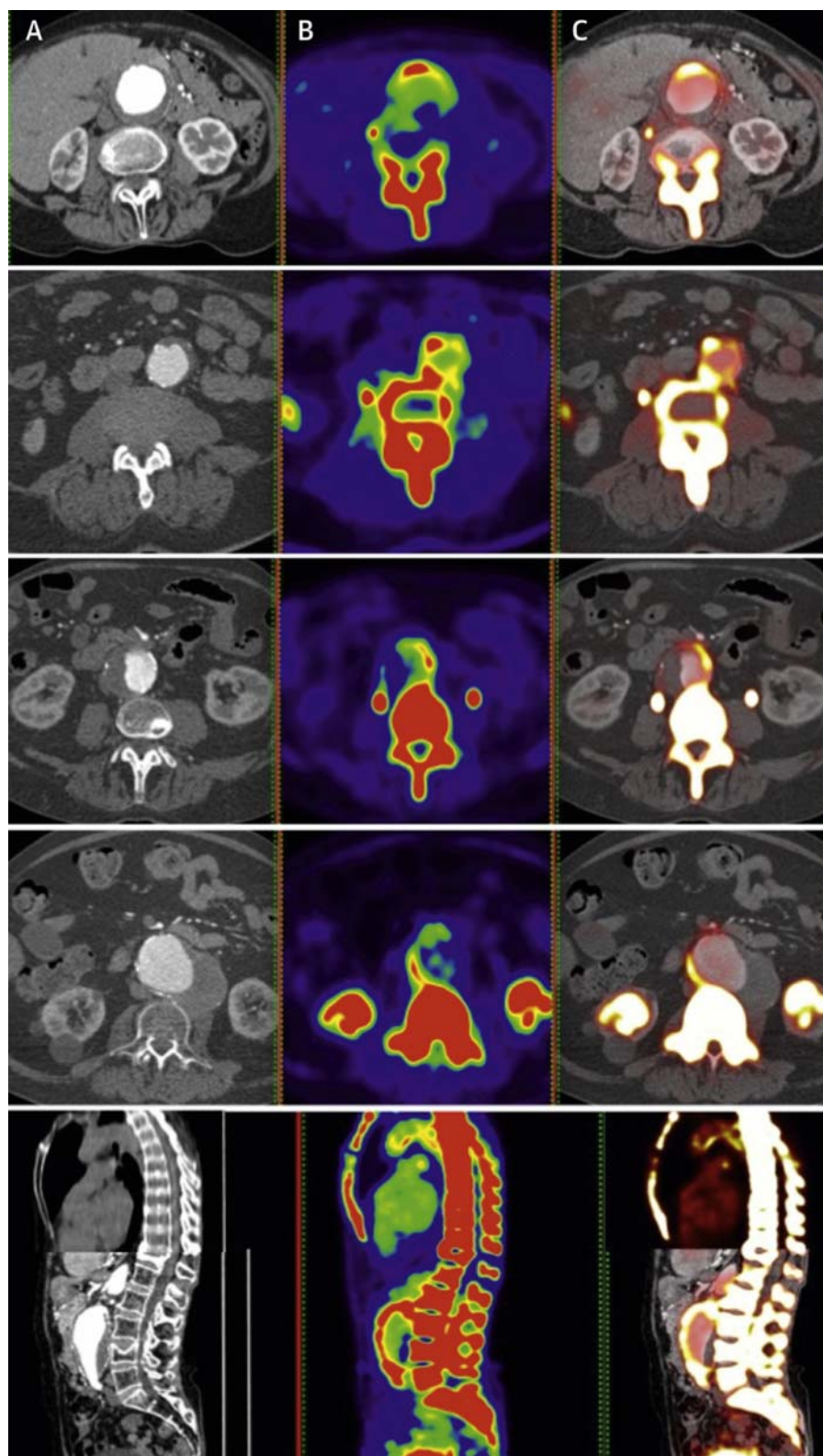
[18]F-sodium fluoride- positron emission tomography in aortic aneurysms, large vessel vasculitis, and other aortic pathologies

The interaction between aortic calcification and corresponding impairment in arterial compliance is becoming increasingly understood. However, the relationship between calcification and aortic-specific pathologies, such as aortic aneurysms is less well understood. Some suggest that calcification in the presence of an aortic aneurysm is protective in a nature.[130] This may particularly be the case if the calcifications exist on the outer medial-adventitia border thereby limiting the progression of arterial wall expansion.[131] It has also been proposed that the presence of calcification within the aortic wall may prevent the worsening proteolysis within the aortic wall, further preventing the degradation of arterial integrity and progression of disease.[131,132]

In contrast, some studies have suggested that the presence of calcification within the aortic wall is an important contributor to isolated disruption of already pathological wall stressors and may increase the risk of rupture of an existing aortic aneurysm.[133,134] The region at the edge of partially calcified aortic wall within an aorta is at specifically susceptible to failure.[135] Notably, the edges of partially calcified regions are likely susceptible active calcification processes which may therefore be detectable using ^{18}F-NaF PET imaging.

[18]F-NaF PET imaging provides unique biological information about the calcification activity developing within an already existent aneurysm and may subsequently serve to determine who may go on to be at risk of aneurysm rupture. While such prospective data are not yet available, ^{18}F-NaF PET activity appears to be positively associated with the rate of change of aortic aneurysm expansion and likelihood of aneurysmal repair (Fig. 6.3).[136] Furthermore, histological analyses of ^{18}F-NaF uptake within aortic regions correspond well with regions of

FIGURE 6.3 Positron emission tomographic and computed tomographic images of abdominal aortic aneurysms. (A) Structural image of computed tomographic angiography, (B)[18]F-sodium fluoride uptake on positron emission tomography, and (C) fused positron emission tomographic−computed tomographic images colocalizing ^{18}F-sodium fluoride uptake with the skeleton and abdominal aortic aneurysm. *Reproduced from Forsythe RO, Dweck MR, McBride OMB, et al. (18)F-sodium fluoride uptake in abdominal aortic aneurysms: the SoFIA(3) study.* J Am Coll Cardiol. *2018;71(5):513−523.*

microcalcifications.[136] It is also possible that the presence of vasa vasorum, also associated with increased risk of aneurysm rupture, supplements ^{18}F-NaF delivery to the vessel media and results in increased ^{18}F-NaF signal intensity.[137]

The relationship between aortic calcification, stress, and subsequent impairment of arterial integrity is also relevant in the development of aortic dissections. Regions of intimal tearing, the initiating factor in an aortic dissection, appear to develop near to or just on regions of aortic calcification.[138] Coupled with computational fluid dynamics and traditional CT imaging, detecting early stages of this disease process may be possible with ^{18}F-NaF PET. Though, the low prevalence of the dissections and the high incidence of aortic calcifications, the positive predictive value of such a tool must be much higher than CT to have clinical utility. In high-risk subpopulations, ^{18}F-NaF PET may be more useful.

In patients with Marfan syndrome, early intervention of aortic aneurysms may be required.[139] The disease is characterized by impaired fibrillin formation and subsequently compromised elastin integrity. The presence of elastic fragmentation co-localizes with regions of aortic wall microcalcification deposition and this may further predispose to the development of structural aortic wall diseases.[12,140] It is possible that early detection of calcification activity with ^{18}F-NaF PET may discriminate between those who require more intensive monitoring, or even intervention, and those who can continue regular monitoring.

Other large vessel vascular diseases have a calcific component that may warrant dedicated imaging with ^{18}F-NaF PET. Pseudoxanthoma elasticum involves extensive calcification of elastic fibers in connective tissues of the vasculature and prognostication could be assisted with the use of metabolic imaging.[141] Though further research is needed to understand whether ^{18}F-NaF PET can guide novel therapies in this population.[142]

Patients with Takayasu arteritis experience granulomatous large vessel inflammation, and it is traditionally considered that the resulting calcification is a sequela of inflammation[8] and may present as the chronic component of the disease process.[139] ^{18}F-NaF PET can assist in identifying regions of metabolically active disease,[143] as opposed to metabolically indolent disease, and may perhaps further assist in identifying regions of the aorta at risk of life-threatening complications (i.e., Aneurysm formation or dissection).

Finally, it is possible that ^{18}F-NaF PET may be useful for the identification of those patients in whom interventional therapies, such as endovascular aneurysmal repair, are failing. In other vascular territories ^{18}F-NaF PET activity is related to the risk of in-stent complications[144] and prosthetic valvular complications.[145] However, in these settings, calcification may be more related to stenosis, which is less likely within the aorta.
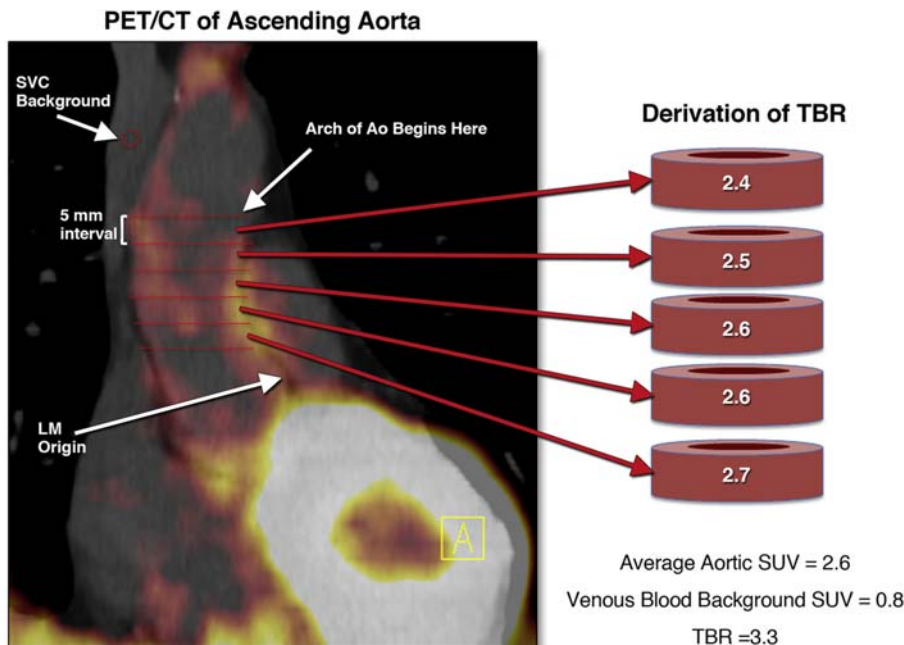
Methods of analysis and limitations of positron emission tomography imaging

In vivo visualization of molecular and cellular processes is achievable with PET imaging but relies heavily on the availability of discriminating radiotracers that can be detected with high-resolution PET imaging hardware. The quantification of the signal emitted by radionuclides can be affected by signal-to-noise ratio, which necessitates that radionuclides exhibit good contrast against normal tissue surrounding the area of interest. This can be achieved by selecting radiotracers with a high specificity for its target (to minimize off-target effects), and a rapid clearance from nontarget tissues.[146] Ideal radiotracers should also be able to overcome biological barriers while exerting low toxicities to human tissues.[25]

Many techniques are used to quantify radiotracer uptake in PET imaging. A relatively common method involves the segmentation of a region of interest (ROI) and measurements or estimation of radiotracer uptake in the ROI to determine the mean and maximum SUV.[147] SUV is a dimensionless value and is calculated by dividing radiotracer uptake in a ROI by the injected dose per body weight. Maximal SUV (SUVmax) is the SUV of the most radiotracer-avid voxel within a ROI while mean SUV (SUVmean) is the mean SUV within the ROI.[53] SUV can also be normalized for lean body mass, known as SUL, which provides less variation in the calculated value. However, SUVmax is preferred in clinical practice due to its superior reproducibility.[60]

The accurate quantification of PET radiotracer uptake is very challenging particularly in the arterial system where lesions are of small sizes compared to the spatial resolution of PET.[147] While the SUV is commonly used for quantification of radiotracer uptake in oncology, it has many limitations when applied to vascular imaging. It can be markedly influenced by blood glucose in ^{18}F-FDG PET, the time between injection and image acquisition, spatial resolution of the PET scanner, partial volume effects, activity spill in and spill out, attenuation correction, and image reconstruction parameters.[147,148] PET imaging of the vasculature is particularly susceptible to partial volume effects which can significantly underestimate the true radiotracer uptake.[148]

TBR measurements are preferred in vascular inflammation as they have been shown to better correlate with macrophage density.[52] TBRmax corrects for blood pool uptake and is calculated by dividing SUVmax measured in an arterial vessel wall by the venous blood pool (Fig. 6.4).[42] TBR quantification of ^{18}F-FDG uptake in atherosclerotic plaques can be performed using three different approaches. In the assessment of global vascular inflammation (whole vessel analysis), the average TBR is measured in all the axial segments of the target vessel (TBRmax; TBRmean). This allows for signals to be

FIGURE 6.4 **Fluorodeoxyglucose (FDG) uptake measurement.** In this example, FDG uptake was evaluated within the wall of the aorta on axial images. At each axial section, a region of interest (ROI) was drawn around the wall of the aorta and the maximum standardized FDG uptake value (SUV_{max}) was recorded. The thickness of each axial slice was approximately 5 mm. Subsequently, the target-to-background ratio (TBR) was calculated by dividing the mean of all axial slice SUV_{max} (approximately six to eight slices per patient) by the venous blood SUV_{max} obtained from the superior vena cava (average of 10 ROIs) to correct for the blood compartment contribution. *Ao*, aorta; *LM*, left main artery; *SVC*, superior vena cava. *Reprinted With permission from Elsevier from Figueroa AL, Abdelbaky A, Truong QA, et al. Measurement of arterial activity on routine FDG PET/CT images improves prediction of risk of future CV events.* JACC Cardiovasc Imaging. *2013;6(12):1250−1259.*

averaged over many arterial segments and is therefore thought to be less sensitive to image noise and ^{18}F-FDG signal from surrounding structures.[60] The trade-off is reduced sensitivity for detecting small changes in ^{18}F-FDG uptake in focal areas of atherosclerotic plaques.[60,72] In contrast, the most diseased segment (MDR) approach measures the average TBR across a small segment of the index vessel and has been shown to be useful when assessing the degree of inflammation in a specific atherosclerotic plaque.[10,75] Finally, the active segment (AS) analysis is most useful in clinical trials where only lesions with increased ^{18}F-FDG uptake are monitored overtime to evaluate the effects of therapeutic interventions on ^{18}F-FDG uptake.[73]

Both TBRmax and TBRmean demonstrate excellent reproducibility and are less influenced by radiotracer circulation times, acquisition times, and reconstruction filters, which is of particular importance when analyzing radiotracer uptake within arterial structures where circulating radiotracer may influence readings.[60] However, factors that affect blood pool activity such as ^{18}F-FDG uptake in the circulating blood cells can significantly impact TBR measurements. Similarly, blood pool ^{18}F-NaF PET activity is a critical regulating factor in the analysis of vascular ^{18}F-NaF PET and is often adjusted for by taking measurements from

either within the vena cava or the right atria.[89] Not surprisingly, the dose of radiotracer injected and PET/CT imaging system used are important predictors of blood pool radiotracer activity and should be consistent in serial imaging, or in person−person comparisons.[149] Furthermore, the role of renal function is important, with a lower glomerular filtration rate being associated with a higher thoracic aortic ^{18}F-NaF activity.[149] This relationship is likely related to the clinical impact of renal failure on arterial calcification but should also be considered in its role in the possibly delayed excretion of radiotracer.[22,115]

In the analysis of aortic ^{18}F-NaF PET, the proximity of the aorta to the vertebra can cause significant disruption to the analysis of aortic activity, owing to the effect of radiotracer overspill from vertebral bone into the aortic lumen. This impairs the accuracy of aortic ^{18}F-NaF PET analysis, mostly owing to a reduced specificity of perceived aortic measurements. Approaches to improve analysis include the manual extraction of regions with vertebral overspill,[150] or semiautomated extraction of vertebral ^{18}F-NaF activity.[151] The former method is time consuming and highly dependent on clinician experience.

Finally, patient motion artifact is a significant limitation of all imaging modalities and may be particularly undesirable in the temporal acquisition techniques employed in

PET imaging. The risk of patient motion is likely higher in PET imaging due to prolonged acquisition times (up to 30 min) and may be influenced by breathing and the cardiac cycle. Several strategies are used to improve image quality, including motion-compensation techniques,[21] and software incorporating patient motion correction algorithms, which display considerable success.[152] Other prospective acquisition techniques, such as respiratory and cardiac gating may also be useful, although are likely to serve a greater utility in the analysis of the coronary arteries moreso than the aorta.[153]

Future directions

Various strategies are being pursued to improve the diagnostic utility of PET imaging, including the search for novel radiotracers with improved specificity for molecular targets, developments in whole body PET imaging, and ongoing research in automated data analysis technologies such as artificial intelligence.

Novel PET radiotracers in the current research pipeline are focused on assessment of atherosclerosis and seek to improve the specificity of vascular imaging by targeting specific receptors and proteins that are overexpressed by activated macrophages. This includes ^{68}Ga-DOTATATE, a novel PET tracer with specificity for somatostatin receptor 2, which is overexpressed by macrophages in response to inflammation.[29] Several studies have demonstrated its potential utility in PET imaging of vascular inflammation in atherosclerotic disease.[29,30] Other radiotracers that have shown promise in atherosclerotic imaging include ^{11}C-PK11195, a selective ligand of the translocator protein that is commonly used in PET imaging of neuro-inflammation but also shows promise in vascular inflammation.[26] Tracers that target tissue hypoxia such as ^{18}F-Fluoromisonadazole are also being studied,[154] and may be particularly helpful because hypoxia probably precedes and may promote vascular calcification.[155] PET imaging with ^{18}F-labeled fluoromethylcholine or ^{11}C-choline is used in cancer imaging but shows promise in atherosclerosis.[27] Choline is taken up by activated macrophages, phosphorylated by choline kinase, and is then incorporated into cell membranes after further metabolism to phosphatidylcholine.[156] ^{68}Ga-NOTA-RGD is a radiotracer that targets integrin $\alpha\nu\beta3$, expressed in angiogenic endothelial cells and macrophages.[31] PET imaging of neoangiogenesis using this tracer appears feasible in atherosclerotic disease and may be a useful marker of plaque vulnerability.[31] These novel radiotracers are still in research settings, and although their use in LASt is theoretically possible, there is currently no direct evidence of such utility and further research is needed.

Molecular targeting of the extracellular matrix such as elastin degradation and collagen deposition is a feasible future direction in LASt. This approach has been evaluated in the context of atherosclerosis[157] and in patients with lung and hepatic fibrosis[158]; however, its application to aortic wall stiffness remains to be seen. If validated for LASt, it could lead to imaging modalities specific for aortic fibrosis, which would be useful in both research and clinical settings.

Finally, whole body PET imaging techniques that are under development,[159] along with improved analysis techniques, incorporating manual and automated processes,[160] will further assist in the full utilization of PET imaging, allowing mass analysis of data to be extracted from single datasets, reducing the manual time required for analysis and improving accuracy.

Conclusion

Vascular inflammation and microcalcification occur in the earliest stages of vascular remodeling and often precede the development of detrimental LASt. Both processes are detectable using ^{18}F-FDG and ^{18}F-NaF PET imaging, respectively, though the direct role of each radiotracer in detecting the early stages of LASt needs further research. Most existing studies have assessed the utility of ^{18}F-FDG PET imaging of the aortic wall in the context of atherosclerosis and only a few small studies have examined the role of ^{18}F-FDG PET imaging in dedicated LASt. Because vascular inflammation tends to be associated with both arteriosclerosis and atherosclerosis and may indeed play a role in medial arterial calcification, it is reasonable to consider that ^{18}F-FDG PET could play an important role in the imaging of early LASt. In contrast, although ^{18}F-NaF remains primarily a research tool, it may serve a greater purpose in the imaging of LASt than ^{18}F-FDG PET, as calcification of the medial arterial wall is better understood than medial wall inflammation and its relationship with LASt is well established. ^{18}F-NaF PET has a unique capability to localize and quantify arterial calcification within the aortic wall, at an early stage in its development, prior to the established calcifications detectable on CT imaging.

Overall, PET imaging of the aortic wall could be used for CVD risk stratification and subsequent implementation of preventative therapies prior to irreversible disease development, in those patients with high disease activity. It may assist in determining response to established therapeutics or as a useful tool for the trial of novel therapeutics, reducing the time required to reach a comparable endpoint of CT-detectable changes or hard CV outcomes. Finally, PET imaging of the aortic wall can dramatically improve our understanding of the complex pathophysiological processes of aortic wall stiffness along with their associated clinical and physiological effects on the aorta.

Acknowledgments

References

1. Meaume S, Benetos A, Henry OF, Rudnichi A, Safar ME. Aortic pulse wave velocity predicts cardiovascular mortality in subjects >70 years of age. **Arterioscler Thromb Vasc Biol**. 2001; 21(12):2046−2050.

2. Laurent S, Boutouyrie P, Asmar R, et al. Aortic stiffness is an independent predictor of all-cause and cardiovascular mortality in hypertensive patients. **Hypertension (Dallas, Tex : 1979)**. 2001; 37(5):1236−1241.

3. Blacher J, Guerin AP, Pannier B, Marchais SJ, Safar ME, London GM. Impact of aortic stiffness on survival in end-stage renal disease. **Circulation**. 1999; 99(18):2434−2439.

4. Chirinos JA, Segers P, Hughes T, Townsend R. Large-artery stiffness in health and disease. **JACC**. 2019; 74(9):1237−1263.

5. Lyle AN, Raaz U. Killing me unsoftly: causes and mechanisms of arterial stiffness. **Arterioscler Thromb Vasc Biol**. 2017; 37(2):e1−e11.

6. Demer LL, Tintut Y. Vascular calcification: pathobiology of a multifaceted disease. **Circulation**. 2008; 117(22):2938−2948.

7. Cecelja M, Hussain T, Greil G, et al. Multimodality imaging of subclinical aortic atherosclerosis: relation of aortic stiffness to calcification and plaque in female twins. **Hypertension (Dallas, Tex : 1979)**. 2013; 61(3):609−614.

8. Abdelbaky A, Corsini E, Figueroa AL, et al. Focal arterial inflammation precedes subsequent calcification in the same location: a longitudinal FDG-PET/CT study. **Circ Cardiovasc Imaging**. 2013; 6(5):747−754.

9. de Boer SA, Hovinga-de Boer MC, Heerspink HJ, et al. Arterial stiffness is positively associated with ^{18}F-fluorodeoxyglucose positron emission tomography-assessed subclinical vascular inflammation in people with early type 2 diabetes. **Diabetes Care**. 2016; 39(8):1440−1447.

10. Mäki-Petäjä KM, Hall FC, Booth AD, et al. Rheumatoid arthritis is associated with increased aortic pulse-wave velocity, which is reduced by anti-tumor necrosis factor-alpha therapy. **Circulation**. 2006; 114(11):1185−1192.

11. Tellides G, Pober JS. Inflammatory and immune responses in the arterial media. **Circ Res**. 2015; 116(2):312−322.

12. Basalyga DM, Simionescu DT, Xiong W, Baxter BT, Starcher BC, Vyavahare NR. Elastin degradation and calcification in an abdominal aorta injury model: role of matrix metalloproteinases. **Circulation**. 2004; 110(22):3480−3487.

13. Clarke B. Normal bone anatomy and physiology. **Clin J Am Soc Nephrol**. 2008; 3(Suppl. 3):S131−S139.

14. Rudd JH, Warburton EA, Fryer TD, et al. Imaging atherosclerotic plaque inflammation with [^{18}F]-fluorodeoxyglucose positron emission tomography. **Circulation**. 2002; 105(23):2708−2711.

15. Beheshti M, Saboury B, Mehta NN, et al. Detection and global quantification of cardiovascular molecular calcification by fluoro18-fluoride positron emission tomography/computed tomography–a novel concept. **Hellenic J Nucl Med**. 2011; 14(2):114−120.

16. den Harder AM, Wolterink JM, Bartstra JW, et al. Vascular uptake on 18 F-sodium fluoride positron emission tomography: precursor of vascular calcification? **J Nucl Cardiol**. 2020:1−11.

17. Budoff MJ, Nasir K, Katz R, et al. Thoracic aortic calcification and coronary heart disease events: the multi-ethnic study of atherosclerosis (MESA). **Atherosclerosis**. 2011; 215(1):196−202.

18. Rominger A, Saam T, Wolpers S, et al. ^{18}F-FDG PET/CT identifies patients at risk for future vascular events in an otherwise asymptomatic cohort with neoplastic disease. **J Nucl Med**. 2009; 50(10):1611−1620.

19. Jaffer FA, Libby P, Weissleder R. Molecular imaging of cardiovascular disease. **Circulation**. 2007; 116(9):1052−1061.

20. Kapoor V, McCook BM, Torok FS. An introduction to PET-CT imaging. **Radiographics**. 2004; 24(2):523−543.

21. Tarkin JM, Joshi FR, Rudd JH. PET imaging of inflammation in atherosclerosis. **Nat Rev Cardiol**. 2014; 11(8):443−457.

22. Czernin J, Satyamurthy N, Schiepers C. Molecular mechanisms of bone ^{18}F-NaF deposition. **J Nucl Med**. 2010; 51(12):1826−1829.

23. Miele E, Spinelli GP, Tomao F, et al. Positron Emission Tomography (PET) radiotracers in oncology–utility of ^{18}F-fluoro-deoxyglucose (FDG)-PET in the management of patients with non-small-cell lung cancer (NSCLC). **J Exp Clin Cancer Res**. 2008; 27(1):52.

24. Kazuma SM, Sultan D, Zhao Y, et al. Recent advances of radionuclide-based molecular imaging of atherosclerosis. **Curr Pharm Des**. 2015; 21(36):5267−5276.

25. Correia JD, Paulo A, Raposinho PD, Santos I. Radiometallated peptides for molecular imaging and targeted therapy. **Dalton Trans**. 2011; 40(23):6144−6167.

26. Pugliese F, Gaemperli O, Kinderlerer AR, et al. Imaging of vascular inflammation with [11C]-PK11195 and positron emission tomography/computed tomography angiography. **J Am Coll Cardiol**. 2010; 56(8):653−661.

27. Kato K, Schober O, Ikeda M, et al. Evaluation and comparison of 11C-choline uptake and calcification in aortic and common carotid arterial walls with combined PET/CT. **Eur J Nucl Med Mol Imaging**. 2009; 36(10):1622−1628.

28. Nahrendorf M, Zhang H, Hembrador S, et al. Nanoparticle PET-CT imaging of macrophages in inflammatory atherosclerosis. **Circulation**. 2008; 117(3):379−387.

29. Dalm VA, van Hagen PM, van Koetsveld PM, et al. Expression of somatostatin, cortistatin, and somatostatin receptors in human monocytes, macrophages, and dendritic cells. **Am J Physiol Endocrinol Metab**. 2003; 285(2):E344−E353.

30. Rominger A, Saam T, Vogl E, et al. In vivo imaging of macrophage activity in the coronary arteries using 68Ga-DOTATATE PET/CT: correlation with coronary calcium burden and risk factors. **J Nucl Med**. 2010; 51(2):193−197.

31. Paeng JC, Lee YS, Lee JS, et al. Feasibility and kinetic characteristics of (68)Ga-NOTA-RGD PET for in vivo atherosclerosis imaging. **Ann Nucl Med**. 2013; 27(9):847−854.

32. Majmudar MD, Yoo J, Keliher EJ, et al. Polymeric nanoparticle PET/MR imaging allows macrophage detection in atherosclerotic plaques. **Circ Res**. 2013; 112(5):755−761.

33. Saraste A, Nekolla SG, Schwaiger M. Cardiovascular molecular imaging: an overview. **Cardiovasc Res**. 2009; 83(4):643−652.

34. Chen IY, Wu JC. Cardiovascular molecular imaging: focus on clinical translation. **Circulation**. 2011; 123(4):425−443.

35. Levin CS, Hoffman EJ. Calculation of positron range and its effect on the fundamental limit of positron emission tomography system spatial resolution. **Phys Med Biol**. 1999; 44(3):781−799.

36. Izquierdo-Garcia D, Davies JR, Graves MJ, et al. Comparison of methods for magnetic resonance-guided [18-F]fluorodeoxyglucose positron emission tomography in human carotid arteries: reproducibility, partial volume correction, and correlation between methods. **Stroke**. 2009; 40(1):86−93.

37. Kubota R, Yamada S, Kubota K, Ishiwata K, Tamahashi N, Ido T. Intratumoral distribution of fluorine-18-fluorodeoxyglucose in vivo: high accumulation in macrophages and granulation tissues studied by microautoradiography. **J Nucl Med**. 1992; 33(11):1972−1980.

38. Alavi A, Reivich M. Guest editorial: the conception of FDG-PET imaging. **Semin Nucl Med**. 2002; 32(1):2−5.

39. Rudd JH, Narula J, Strauss HW, et al. Imaging atherosclerotic plaque inflammation by fluorodeoxyglucose with positron emission tomography: ready for prime time? **J Am Coll Cardiol**. 2010; 55(23):2527−2535.

40. Som P, Atkins HL, Bandoypadhyay D, et al. A fluorinated glucose analog, 2-fluoro-2-deoxy-D-glucose (F-18): nontoxic tracer for rapid tumor detection. **J Nucl Med**. 1980; 21(7):670−675.

41. Lederman RJ, Raylman RR, Fisher SJ, et al. Detection of atherosclerosis using a novel positron-sensitive probe and 18-fluorodeoxyglucose (FDG). **Nucl Med Commun**. 2001; 22(7).

42. Figueroa AL, Abdelbaky A, Truong QA, et al. Measurement of arterial activity on routine FDG PET/CT images improves prediction of risk of future CV events. **JACC Cardiovasc Imaging**. 2013; 6(12):1250−1259.

43. Satomi T, Ogawa M, Mori I, et al. Comparison of contrast agents for atherosclerosis imaging using cultured macrophages: FDG versus ultrasmall superparamagnetic iron oxide. **J Nucl Med**. 2013; 54(6):999−1004.

44. Rosenbaum D, Millon A, Fayad ZA. Molecular imaging in atherosclerosis: FDG PET. **Curr Atherosclerosis Rep**. 2012; 14(5):429−437.

45. Folco EJ, Sheikine Y, Rocha VZ, et al. Hypoxia but not inflammation augments glucose uptake in human macrophages: implications for imaging atherosclerosis with [18]fluorine-labeled 2-deoxy-D-glucose positron emission tomography. **J Am Coll Cardiol**. 2011; 58(6):603−614.

46. Bartlett B, Ludewick HP, Misra A, Lee S, Dwivedi G. Macrophages and T cells in atherosclerosis: a translational perspective. **Am J Physiol Heart Circ Physiol**. 2019; 317(2):H375−H386.

47. Pello OM, Silvestre C, De Pizzol M, Andrés V. A glimpse on the phenomenon of macrophage polarization during atherosclerosis. **Immunobiology**. 2011; 216(11):1172−1176.

48. Pedersen SF, Græbe M, Hag AM, Højgaard L, Sillesen H, Kjær A. (18)F-FDG imaging of human atherosclerotic carotid plaques reflects gene expression of the key hypoxia marker HIF-1α. **Am J Nucl Med Mol Imaging**. 2013; 3(5):384−392.

49. Marsch E, Sluimer JC, Daemen MJ. Hypoxia in atherosclerosis and inflammation. **Curr Opin Lipidol**. 2013; 24(5):393−400.

50. Bucerius J, Mani V, Moncrieff C, et al. Optimizing ^{18}F-FDG PET/CT imaging of vessel wall inflammation: the impact of ^{18}F-FDG circulation time, injected dose, uptake parameters, and fasting blood glucose levels. **Eur J Nucl Med Mol Imaging**. 2014; 41(2):369−383.

51. Dunphy MP, Freiman A, Larson SM, Strauss HW. Association of vascular ^{18}F-FDG uptake with vascular calcification. **J Nucl Med**. 2005; 46(8):1278−1284.

52. Tawakol A, Migrino RQ, Bashian GG, et al. In vivo ^{18}F-fluorodeoxyglucose positron emission tomography imaging provides a noninvasive measure of carotid plaque inflammation in patients. **J Am Coll Cardiol**. 2006; 48(9):1818−1824.

53. Bucerius J, Hyafil F, Verberne HJ, et al. Position paper of the cardiovascular Committee of the European Association of Nuclear Medicine (EANM) on PET imaging of atherosclerosis. **Eur J Nucl Med Mol Imaging**. 2016; 43(4):780−792.

54. Yildiz M. Arterial distensibility in chronic inflammatory rheumatic disorders. **Open Cardiovasc Med J**. 2010; 4:83−88.

55. Shanahan CM, Cary NR, Salisbury JR, Proudfoot D, Weissberg PL, Edmonds ME. Medial localization of mineralization-regulating proteins in association with Mönckeberg's sclerosis: evidence for smooth muscle cell-mediated vascular calcification. **Circulation**. 1999; 100(21):2168−2176.

56. Al-Mashhadi RH, Tolbod LP, Bloch LØ, et al. [18]Fluorodeoxyglucose accumulation in arterial tissues determined by PET signal analysis. **J Am Coll Cardiol**. 2019; 74(9):1220−1232.

57. Kinlay S, Creager MA, Fukumoto M, et al. Endothelium-derived nitric oxide regulates arterial elasticity in human arteries in vivo. **Hypertension (Dallas, Tex : 1979)**. 2001; 38(5):1049−1053.

58. Wilkinson IB, Qasem A, McEniery CM, Webb DJ, Avolio AP, Cockcroft JR. Nitric oxide regulates local arterial distensibility in vivo. **Circulation**. 2002; 105(2):213−217.

59. Gardner SE, Humphry M, Bennett MR, Clarke MC. Senescent vascular smooth muscle cells drive inflammation through an interleukin-1α-dependent senescence-associated secretory phenotype. **Arterioscler Thromb Vasc Biol**. 2015; 35(9):1963−1974.

60. Rudd JH, Myers KS, Bansilal S, et al. Atherosclerosis inflammation imaging with ^{18}F-FDG PET: carotid, iliac, and femoral uptake reproducibility, quantification methods, and recommendations. **J Nucl Med**. 2008; 49(6):871−878.

61. Fisk M, Cheriyan J, Mohan D, et al. Vascular inflammation and aortic stiffness: potential mechanisms of increased vascular risk in chronic obstructive pulmonary disease. **Respir Res**. 2018; 19(1):100.

62. Mills NL, Miller JJ, Anand A, et al. Increased arterial stiffness in patients with chronic obstructive pulmonary disease: a mechanism for increased cardiovascular risk. **Thorax**. 2008; 63(4):306−311.

63. Booth AD, Wallace S, McEniery CM, et al. Inflammation and arterial stiffness in systemic vasculitis: a model of vascular inflammation. **Arthritis Rheum**. 2004; 50(2):581−588.

64. Bural GG, Torigian DA, Chamroonrat W, et al. FDG-PET is an effective imaging modality to detect and quantify age-related atherosclerosis in large arteries. **Eur J Nucl Med Mol Imaging**. 2008; 35(3):562−569.

65. Joly L, Mandry D, Verger A, et al. Influence of thoracic aortic inflammation and calcifications on arterial stiffness and cardiac function in older subjects. **J Nutr Health Aging**. 2016; 20(3):347−354.

66. Marnane M, Merwick A, Sheehan OC, et al. Carotid plaque inflammation on ^{18}F-fluorodeoxyglucose positron emission tomography predicts early stroke recurrence. **Ann Neurol**. 2012; 71(5):709−718.

67. Ridker PM, Everett BM, Thuren T, et al. Antiinflammatory therapy with canakinumab for atherosclerotic disease. **N Engl J Med**. 2017; 377(12):1119−1131.

68. Nidorf SM, Eikelboom JW, Budgeon CA, Thompson PL. Low-dose colchicine for secondary prevention of cardiovascular disease. **J Am Coll Cardiol**. 2013; 61(4):404−410.

69. Nidorf SM, Fiolet ATL, Mosterd A, et al. Colchicine in patients with chronic coronary disease. **N Engl J Med**. 2020; 383(19):1838−1847.

70. Tardif J-C, Kouz S, Waters DD, et al. Efficacy and safety of low-dose colchicine after myocardial infarction. **N Engl J Med**. 2019; 381(26):2497−2505.

71. Potter K, Lenzo N, Eikelboom JW, Arnolda LF, Beer C, Hankey GJ. Effect of long-term homocysteine reduction with B vitamins on arterial wall inflammation assessed by fluorodeoxyglucose positron emission tomography: a randomised double-blind, placebo-controlled trial. **Cerebrovasc Dis**. 2009; 27(3):259−265.

72. Elkhawad M, Rudd JH, Sarov-Blat L, et al. Effects of p38 mitogen-activated protein kinase inhibition on vascular and systemic inflammation in patients with atherosclerosis. **JACC Cardiovasc Imaging**. 2012; 5(9):911−922.

73. Tahara N, Kai H, Ishibashi M, et al. Simvastatin attenuates plaque inflammation: evaluation by fluorodeoxyglucose positron emission tomography. **J Am Coll Cardiol**. 2006; 48(9):1825−1831.

74. Ishii H, Nishio M, Takahashi H, et al. Comparison of atorvastatin 5 and 20 mg/d for reducing F-18 fluorodeoxyglucose uptake in atherosclerotic plaques on positron emission tomography/computed tomography: a randomized, investigator-blinded, open-label, 6-month study in Japanese adults scheduled for percutaneous coronary intervention. **Clin Therapeut**. 2010; 32(14):2337−2347.

75. Tawakol A, Fayad ZA, Mogg R, et al. Intensification of statin therapy results in a rapid reduction in atherosclerotic inflammation: results of a multicenter fluorodeoxyglucose-positron emission tomography/computed tomography feasibility study. **J Am Coll Cardiol**. 2013; 62(10):909−917.

76. Wu YW, Kao HL, Huang CL, et al. The effects of 3-month atorvastatin therapy on arterial inflammation, calcification, abdominal adipose tissue and circulating biomarkers. **Eur J Nucl Med Mol Imaging**. 2012; 39(3):399−407.

77. Shen YH, LeMaire SA. Molecular pathogenesis of genetic and sporadic aortic aneurysms and dissections. **Curr Probl Surg**. 2017; 54(3):95−155.

78. Courtois A, Nusgens BV, Hustinx R, et al. ^{18}F-FDG uptake assessed by PET/CT in abdominal aortic aneurysms is associated with cellular and molecular alterations prefacing wall deterioration and rupture. **J Nucl Med**. 2013; 54(10):1740−1747.

79. English SJ, Piert MR, Diaz JA, et al. Increased ^{18}F-FDG uptake is predictive of rupture in a novel rat abdominal aortic aneurysm rupture model. **Ann Surg**. 2015; 261(2):395−404.

80. Jalalzadeh H, Indrakusuma R, Planken RN, Legemate DA, Koelemay MJ, Balm R. Inflammation as a predictor of abdominal aortic aneurysm growth and rupture: a systematic review of imaging biomarkers. **Eur J Vasc Endovasc Surg**. 2016; 52(3):333−342.

81. Blockmans D, de Ceuninck L, Vanderschueren S, Knockaert D, Mortelmans L, Bobbaers H. Repetitive ^{18}F-fluorodeoxyglucose positron emission tomography in giant cell arteritis: a prospective study of 35 patients. **Arthritis Rheum**. 2006; 55(1):131−137.

82. Slart RHJA, Writing G, Reviewer G, et al. FDG-PET/CT(A) imaging in large vessel vasculitis and polymyalgia rheumatica: joint procedural recommendation of the EANM, SNMMI, and the PET Interest Group (PIG), and endorsed by the ASNC. **Eur J Nucl Med Mol Imaging**. 2018; 45(7):1250−1269.

83. Blau M, Nagler W, Bender MA. Fluorine-18: a new isotope for bone scanning. **J Nucl Med**. 1962; 3:332−334.

84. Bastawrous S, Bhargava P, Behnia F, Djang DS, Haseley DR. Newer PET application with an old tracer: role of ^{18}F-NaF skeletal PET/CT in oncologic practice. **Radiographics**. 2014; 34(5):1295−1316.

85. Langsteger W, Rezaee A, Pirich C, Beheshti M. (18)F-NaF-PET/CT and (99m)Tc-MDP bone scintigraphy in the detection of bone metastases in prostate cancer. **Semin Nucl Med**. 2016; 46(6):491−501.

86. Derlin T, Richter U, Bannas P, et al. Feasibility of ^{18}F-sodium fluoride PET/CT for imaging of atherosclerotic plaque. **J Nucl Med**. 2010; 51(6):862−865.

87. Grynpas MD. Fluoride effects on bone crystals. **J Bone Miner Res**. 1990; 5(Suppl 1):S169−S175.

88. Irkle A, Vesey AT, Lewis DY, et al. Identifying active vascular microcalcification by (18)F-sodium fluoride positron emission tomography. **Nat Commun**. 2015; 6:7495.

89. Bellinge JW, Francis RJ, Majeed K, Watts GF, Schultz CJ. In search of the vulnerable patient or the vulnerable plaque: (18)F-sodium fluoride positron emission tomography for cardiovascular risk stratification. **J Nucl Cardiol**. 2018; 25(5):1774−1783.

90. Kolodgie FD, Gold HK, Burke AP, et al. Intraplaque hemorrhage and progression of coronary atheroma. **N Engl J Med**. 2003; 349(24):2316−2325.

91. Virmani R, Kolodgie FD, Burke AP, et al. Atherosclerotic plaque progression and vulnerability to rupture: angiogenesis as a source of intraplaque hemorrhage. **Arterioscler Thromb Vasc Biol**. 2005; 25(10):2054−2061.

92. Lee JM, Bang JI, Koo BK, et al. Clinical relevance of (18)F-sodium fluoride positron-emission tomography in noninvasive identification of high-risk plaque in patients with coronary artery disease. **Circ Cardiovasc Imaging**. 2017; 10(11).

93. Wootton R. The single-passage extraction of ^{18}F in rabbit bone. **Clin Sci Mol Med**. 1974; 47(1):73−77.

94. Roijers RB, Debernardi N, Cleutjens JPM, Schurgers LJ, Mutsaers PHA, van der Vusse GJ. Microcalcifications in early intimal lesions of atherosclerotic human coronary arteries. **Am J Pathol**. 2011; 178(6):2879−2887.

95. Joshi NV, Vesey AT, Williams MC, et al. ^{18}F-fluoride positron emission tomography for identification of ruptured and high-risk coronary atherosclerotic plaques: a prospective clinical trial. **Lancet**. 2014; 383(9918):705−713.

96. Zhang Y, Li H, Jia Y, et al. Noninvasive assessment of carotid plaques calcification by (18)F-sodium fluoride accumulation: correlation with pathology. **J Stroke Cerebrovasc Dis**. 2018; 27(7):1796−1801.

97. Proudfoot D, Skepper JN, Hegyi L, Bennett MR, Shanahan CM, Weissberg PL. Apoptosis regulates human vascular calcification in vitro: evidence for initiation of vascular calcification by apoptotic bodies. **Circ Res**. 2000; 87(11):1055−1062.

98. McKenney-Drake ML, Territo PR, Salavati A, et al. (18)F-NaF PET imaging of early coronary artery calcification. **JACC Cardiovasc Imaging**. 2016; 9(5):627−628.

99. Jenkins WS, Vesey AT, Shah AS, et al. Valvular (18)F-fluoride and (18)F-fluorodeoxyglucose uptake predict disease progression and clinical outcome in patients with aortic stenosis. **J Am Coll Cardiol**. 2015; 66(10):1200−1201.

100. Ishiwata Y, Kaneta T, Nawata S, Hino-Shishikura A, Yoshida K, Inoue T. Quantification of temporal changes in calcium score in

active atherosclerotic plaque in major vessels by (18)F-sodium fluoride PET/CT. **Eur J Nucl Med Mol Imaging**. 2017; 44(9):1529−1537.

101. Nakahara T, Narula J, Fox JJ, Jinzaki M, Strauss HW. Temporal relationship between (18)F-sodium fluoride uptake in the abdominal aorta and evolution of CT-verified vascular calcification. **J Nucl Cardiol**. 2019:1−10.

102. Detrano R, Guerci AD, Carr JJ, et al. Coronary calcium as a predictor of coronary events in four racial or ethnic groups. **N Engl J Med**. 2008; 358(13):1336−1345.

103. Kitagawa T, Yamamoto H, Toshimitsu S, et al. (18)F-sodium fluoride positron emission tomography for molecular imaging of coronary atherosclerosis based on computed tomography analysis. **Atherosclerosis**. 2017; 263:385−392.

104. Høilund-Carlsen PF, Sturek M, Alavi A, Gerke O. Atherosclerosis imaging with ^{18}F-sodium fluoride PET: state-of-the-art review. **Eur J Nucl Med Mol Imaging**. 2020; 47(6):1538−1551.

105. Oliveira-Santos M, Castelo-Branco M, Silva R, et al. Atherosclerotic plaque metabolism in high cardiovascular risk subjects - a subclinical atherosclerosis imaging study with (18)F-NaF PET-CT. **Atherosclerosis**. 2017; 260:41−46.

106. Blomberg BA, de Jong PA, Thomassen A, et al. Thoracic aorta calcification but not inflammation is associated with increased cardiovascular disease risk: results of the CAMONA study. **Eur J Nucl Med Mol Imaging**. 2017; 44(2):249−258.

107. Derlin T, Tóth Z, Papp L, et al. Correlation of inflammation assessed by ^{18}F-FDG PET, active mineral deposition assessed by ^{18}F-fluoride PET, and vascular calcification in atherosclerotic plaque: a dual-tracer PET/CT study. **J Nucl Med**. 2011; 52(7):1020−1027.

108. Fiz F, Morbelli S, Piccardo A, et al. ^{18}F-NaF uptake by atherosclerotic plaque on PET/CT imaging: inverse correlation between calcification density and mineral metabolic activity. **J Nucl Med**. 2015; 56(7):1019−1023.

109. Bellinge JW, Francis RJ, Lee SC, et al. ^{18}F-sodium fluoride positron emission tomography activity predicts the development of new coronary artery calcifications. Arteriosclerosis, thrombosis, and vascular biology. **ATVBAHA**. 2020; 120:315364.

110. Lehto S, Niskanen L, Suhonen M, Rönnemaa T, Laakso M. Medial artery calcification. A neglected harbinger of cardiovascular complications in non-insulin-dependent diabetes mellitus. **Arterioscler Thromb Vasc Biol**. 1996; 16(8):978−983.

111. Kockelkoren R, Vos A, Van Hecke W, et al. Computed tomographic distinction of intimal and medial calcification in the intracranial internal carotid artery. **PLoS One**. 2017; 12(1):e0168360.

112. O'Neill WC, Han KH, Schneider TM, Hennigar RA. Prevalence of nonatheromatous lesions in peripheral arterial disease. **Arterioscler Thromb Vasc Biol**. 2015; 35(2):439−447.

113. Tanimura A, McGregor DH, Anderson HC. Calcification in atherosclerosis. I. Human studies. **J Exp Pathol**. 1986; 2(4):261−273.

114. Desai MY, Cremer PC, Schoenhagen P. Thoracic aortic calcification: diagnostic, prognostic, and management considerations. **JACC Cardiovasc Imaging**. 2018; 11(7):1012−1026.

115. Lanzer P, Boehm M, Sorribas V, et al. Medial vascular calcification revisited: review and perspectives. **Eur Heart J**. 2014; 35(23):1515−1525.

116. Janssen T, Bannas P, Herrmann J, et al. Association of linear ^{18}F-sodium fluoride accumulation in femoral arteries as a measure of diffuse calcification with cardiovascular risk factors: a PET/CT study. **J Nucl Cardiol**. 2013; 20(4):569−577.

117. Zwakenberg SR, de Jong PA, Hendriks EJ, et al. Intimal and medial calcification in relation to cardiovascular risk factors. **PLoS One**. 2020; 15(7):e0235228.

118. Zwakenberg SR, de Jong PA, Bartstra JW, et al. The effect of menaquinone-7 supplementation on vascular calcification in patients with diabetes: a randomized, double-blind, placebo-controlled trial. **Am J Clin Nutr**. 2019; 110(4):883−890.

119. Yoon HC, Emerick AM, Hill JA, Gjertson DW, Goldin JG. Calcium begets calcium: progression of coronary artery calcification in asymptomatic subjects. **Radiology**. 2002; 224(1):236−241.

120. Vos A, Kockelkoren R, de Vis JB, et al. Risk factors for atherosclerotic and medial arterial calcification of the intracranial internal carotid artery. **Atherosclerosis**. 2018; 276:44−49.

121. Lee SC, Phillips M, Bellinge J, Stone J, Wylie E, Schultz C. Is breast arterial calcification associated with coronary artery disease?-a systematic review and meta-analysis. **PLoS One**. 2020; 15(7):e0236598.

122. Blomberg BA, Thomassen A, de Jong PA, et al. Coronary fluorine-18-sodium fluoride uptake is increased in healthy adults with an unfavorable cardiovascular risk profile: results from the CAMONA study. **Nucl Med Commun**. 2017; 38(11):1007−1014.

123. Raggi P, Senior P, Shahbaz S, et al. (18)F-Sodium fluoride imaging of coronary atherosclerosis in ambulatory patients with diabetes mellitus. **Arterioscler Thromb Vasc Biol**. 2019; 39(2):276−284.

124. Takx RAP, van Asperen R, Bartstra JW, et al. Determinants of (18) F-NaF uptake in femoral arteries in patients with type 2 diabetes mellitus. **J Nucl Cardiol**. 2020:1−6.

125. Morbelli S, Fiz F, Piccardo A, et al. Divergent determinants of ^{18}F-NaF uptake and visible calcium deposition in large arteries: relationship with Framingham risk score. **Int J Cardiovasc Imaging**. 2014; 30(2):439−447.

126. Dweck MR, Chow MW, Joshi NV, et al. Coronary arterial ^{18}F-sodium fluoride uptake: a novel marker of plaque biology. **J Am Coll Cardiol**. 2012; 59(17):1539−1548.

127. Bastos Gonçalves F, Voûte MT, Hoeks SE, et al. Calcification of the abdominal aorta as an independent predictor of cardiovascular events: a meta-analysis. **Heart**. 2012; 98(13):988−994.

128. Budoff MJ, Hokanson JE, Nasir K, et al. Progression of coronary artery calcium predicts all-cause mortality. **JACC Cardiovasc Imaging**. 2010; 3(12):1229−1236.

129. Kälsch H, Lehmann N, Moebus S, et al. Aortic calcification onset and progression: association with the development of coronary atherosclerosis. **J Am Heart Assoc**. 2017; 6(4).

130. Taguchi E, Nishigami K, Miyamoto S, Sakamoto T, Nakao K. Impact of shear stress and atherosclerosis on entrance-tear formation in patients with acute aortic syndromes. **Heart Ves**. 2014; 29(1):78−82.

131. Michel JB, Martin-Ventura JL, Egido J, et al. Novel aspects of the pathogenesis of aneurysms of the abdominal aorta in humans. **Cardiovasc Res**. 2011; 90(1):18−27.

132. Bäck M, Gasser TC, Michel JB, Caligiuri G. Biomechanical factors in the biology of aortic wall and aortic valve diseases. **Cardiovasc Res**. 2013; 99(2):232−241.

133. Speelman L, Bohra A, Bosboom EM, et al. Effects of wall calcifications in patient-specific wall stress analyses of abdominal aortic aneurysms. **J Biomech Eng**. 2007; 129(1):105−109.

134. Li ZY, J UK-I, Tang TY, Soh E, See TC, Gillard JH. Impact of calcification and intraluminal thrombus on the computed wall stresses of abdominal aortic aneurysm. **J Vasc Surg**. 2008; 47(5):928−935.

135. O'Leary SA, Mulvihill JJ, Barrett HE, et al. Determining the influence of calcification on the failure properties of abdominal aortic aneurysm (AAA) tissue. **J Mech Behav Biomed Mater**. 2015; 42:154−167.

136. Forsythe RO, Dweck MR, McBride OMB, et al. (18)F-sodium fluoride uptake in abdominal aortic aneurysms: the SoFIA(3) study. **J Am Coll Cardiol**. 2018; 71(5):513−523.

137. Choke E, Thompson MM, Dawson J, et al. Abdominal aortic aneurysm rupture is associated with increased medial neovascularization and overexpression of proangiogenic cytokines. **Arterioscler Thromb Vasc Biol**. 2006; 26(9):2077−2082.

138. Yang C-J, Tsai S-H, Wang J-C, et al. Association between acute aortic dissection and the distribution of aortic calcification. **PLoS One**. 2019; 14(7):e0219461.

139. Erbel R, Aboyans V, Boileau C, et al. 2014 ESC Guidelines on the diagnosis and treatment of aortic diseases: document covering acute and chronic aortic diseases of the thoracic and abdominal aorta of the adult. The Task Force for the Diagnosis and Treatment of Aortic Diseases of the European Society of Cardiology (ESC). **Eur Heart J**. 2014; 35(41):2873−2926.

140. Wanga S, Hibender S, Ridwan Y, et al. Aortic microcalcification is associated with elastin fragmentation in Marfan syndrome. **J Pathol**. 2017; 243(3):294−306.

141. Mention PJ, Lacoeuille F, Leftheriotis G, Martin L, Omarjee L. ^{18}F-flurodeoxyglucose and ^{18}F-sodium fluoride positron emission tomography/computed tomography imaging of arterial and cutaneous alterations in Pseudoxanthoma Elasticum. **Circ Cardiovasc Imaging**. 2018; 11(1):e007060.

142. Kranenburg G, de Jong PA, Bartstra JW, et al. Etidronate for prevention of ectopic mineralization in patients with Pseudoxanthoma Elasticum. **J Am Coll Cardiol**. 2018; 71(10):1117−1126.

143. Alexanderson-Rosas E, Monroy-Gonzalez AG, Juarez-Orozco LE, et al. [(18)F]-Sodium fluoride uptake in Takayasu arteritis. **J Nucl Cardiol**. 2017; 24(5):1674−1679.

144. Chowdhury MM, Tarkin JM, Albaghdadi MS, et al. Vascular positron emission tomography and restenosis in symptomatic peripheral arterial disease: a prospective clinical study. **JACC Cardiovasc Imaging**. 2020; 13(4):1008−1017.

145. Cartlidge TRG, Doris MK, Sellers SL, et al. Detection and prediction of bioprosthetic aortic valve degeneration. **J Am Coll Cardiol**. 2019; 73(10):1107−1119.

146. Chen K, Chen X. Design and development of molecular imaging probes. **Curr Top Med Chem**. 2010; 10(12):1227−1236.

147. Adams MC, Turkington TG, Wilson JM, Wong TZ. A systematic review of the factors affecting accuracy of SUV measurements. **AJR Am J Roentgenol**. 2010; 195(2):310−320.

148. Huet P, Burg S, Le Guludec D, Hyafil F, Buvat I. Variability and uncertainty of ^{18}F-FDG PET imaging protocols for assessing inflammation in atherosclerosis: suggestions for improvement. **J Nucl Med**. 2015; 56(4):552−559.

149. Blomberg BA, Thomassen A, de Jong PA, et al. Impact of personal characteristics and technical factors on quantification of sodium ^{18}F-fluoride uptake in human arteries: prospective evaluation of healthy subjects. **J Nucl Med**. 2015; 56(10):1534−1540.

150. Bellinge JW, Schultz CJ. Optimizing arterial (18)F-sodium fluoride positron emission tomography analysis. **J Nucl Cardiol**. 2019.

151. Akerele MI, Karakatsanis NA, Forsythe RO, et al. Iterative reconstruction incorporating background correction improves quantification of [(18)F]-NaF PET/CT images of patients with abdominal aortic aneurysm. **J Nucl Cardiol**. 2019.

152. Lassen ML, Kwiecinski J, Cadet S, et al. Data-driven gross patient motion detection and compensation: Implications for coronary 18F-NaF PET imaging. **J Nucl Med**. 2019; 60(6):830−836.

153. Lassen ML, Kwiecinski J, Dey D, et al. Triple-gated motion and blood pool clearance corrections improve reproducibility of coronary 18 F-NaF PET. **Eur J Nucl Med Mol Imaging**. 2019; 46(12):2610−2620.

154. Mateo J, Izquierdo-Garcia D, Badimon JJ, Fayad ZA, Fuster V. Noninvasive assessment of hypoxia in rabbit advanced atherosclerosis using ^{18}F-fluoromisonidazole positron emission tomographic imaging. **Circ Cardiovasc Imaging**. 2014; 7(2):312−320.

155. Balogh E, Tóth A, Méhes G, Trencsényi G, Paragh G, Jeney V. Hypoxia triggers osteochondrogenic differentiation of vascular smooth muscle cells in an HIF-1 (Hypoxia-Inducible Factor 1)-dependent and reactive oxygen species-dependent manner. **Arterioscler Thromb Vasc Biol**. 2019; 39(6):1088−1099.

156. HAEFFNER EW. Studies on choline permeation through the plasma membrane and its incorporation into phosphatidyl choline of Ehrlich-Lettré-Ascites tumor cells in vitro. **Eur J Biochem**. 1975; 51(1):219−228.

157. Reimann C, Brangsch J, Colletini F, et al. Molecular imaging of the extracellular matrix in the context of atherosclerosis. **Adv Drug Deliv Rev**. 2017; 113:49−60.

158. Montesi SB, Désogère P, Fuchs BC, Caravan P. Molecular imaging of fibrosis: recent advances and future directions. **J Clin Invest**. 2019; 129(1):24−33.

159. Badawi RD, Shi H, Hu P, et al. First human imaging studies with the EXPLORER total-body PET scanner. **J Nucl Med**. 2019; 60(3):299−303.

160. Nensa F, Demircioglu A, Rischpler C. Artificial intelligence in nuclear medicine. **J Nucl Med**. 2019; 60(Suppl. 2):29s−37s.

This page intentionally left blank

Arterial wall stiffness: basic principles and methods of measurement in vivo

Patrick Segers[1] and Julio A. Chirinos[2, 3]

[1]Faculty of Biomedical Sciences, Institute of Biomedical Engineering and Technology, Ghent University, Ghent, Belgium; [2]University of Pennsylvania Perelman School of Medicine, Hospital of the University of Pennsylvania and Perelman Center for Advanced Medicine, Philadelphia, PA, United States; [3]Ghent University, Ghent, Belgium

Introduction

"Arterial stiffness" is an intuitive general term that refers to the arterial mechanical properties, particularly of large elastic arteries. In this chapter, we first cover the constitution of the arterial wall, and focus on the role of extracellular structural proteins and vascular smooth muscle cells (VSMCs) as drivers of the mechanical behavior of arteries. We briefly introduce concepts from material science and soft tissue biomechanics, highlighting the complexity in quantifying material properties of complex composite tissues as the arteries. In the in vivo setting, however, one often has to settle with functional indices that encompass material properties as well as the geometrical of the artery. To many, arterial stiffness may have become synonymous to pulse wave velocity (PWV), the speed at which the arterial pulse travels over the arterial wall. We outline how PWV relates to the pressure-area relation of the artery and cover transit-time methods to measure PWV in the clinical setting and briefly touch upon the strengths and weaknesses of more recent and emerging methods to assess arterial stiffness.

Arteries—what's inside?

The primary role of arteries is the transport of blood from the heart toward the organs and tissues (systemic circulation) or the lungs (pulmonary circulation). To that end, the arterial tree forms a magnificent branching network of progressively smaller yet more numerous vessels, encompassing the aorta/pulmonary artery with a diameter >2 cm close to the heart, down to capillaries measuring ∼8 μm in diameter inside the tissues where the exchange of nutrients and waste products takes place. With the exception of capillaries, all arteries exhibit a three-layer structure. In healthy arteries, the innermost layer—the intima—is a thin, confluent monolayer of endothelial cells on a basal membrane, forming the interface between the blood and the surrounding tissues.[1] Its physiological importance and biological function are vital, but the intima does not directly contribute to the mechanical properties of the healthy artery. The middle layer, the media, is delineated by the internal and external elastic membrane, with matrix proteins (collagen fibers oriented in different directions and elastic lamellae), VSMCs, and other matrix components such as glycosaminoglycans as major constituents. The outermost layer, called the adventitia, is mainly composed of connective tissue, and connects the artery to its surroundings. It is especially the collagen within the media and adventitia that provide the artery its mechanical strength, while elastin in the media provides its resilience and distensibility.

Besides simply distributing blood, the arterial system (together with the heart) also has a key role in active and passive blood pressure regulation. Mean arterial pressure (the average pressure over a heartbeat) is driven by cardiac output, on the one hand, and the total resistance that the viscous blood experiences because of friction as it pumped through the arterial network. It is known from Poiseuille's law that the flow resistance of a vessel with diameter D is proportional to $1/D^4$, so it is clear that arterial resistance is mainly driven by the smaller arteries. It is important to keep in mind that, as vessels bifurcate, they individually decrease in diameter but increase in number with an increase in the net cross-sectional area after each new vessel generation. In the circulation, it is the arterioles with diameters of 30−100 μm that play a role in controlling resistance and blood distribution through active

regulation of their diameters via contraction/relaxation of the vascular smooth muscle in the media. In addition to arteriolar constriction, microvascular rarefaction can significantly increase resistance in a given vascular bed.[2]

Pulse pressure (PP), the difference between systolic and diastolic pressure, on the other hand, is driven by the properties of the large central arteries that have the ability to distend when pressurized and to buffer part of the stroke volume (SV) with each cardiac contraction. Elastic energy is stored upon distension in systole, which is released to promote blood flow in diastole (the "windkessel" function).[3] The more blood stored locally in the proximal aorta, the less blood has to be transported over longer distances in systole. This limits the "inertial load," the required driving pressure (and energy demands for the heart) and limits the diastolic-systolic pressure differences.
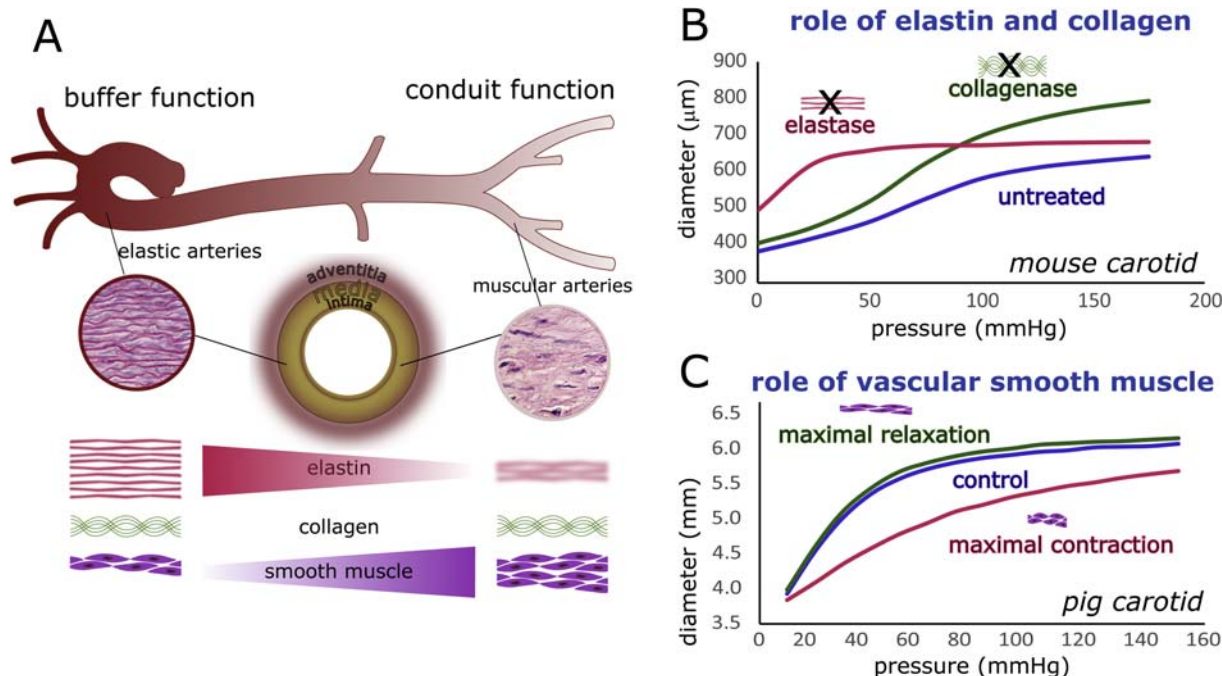
The physiological function of arteries thus differs along the arterial tree, which also translates into gradual changes in their structure and composition along with their size (and the mechanical load acting on the artery). This difference in structure and composition is especially visible in the media as observed from histological images. The media of large central arteries is characterized by an ultrastructure of concentric elastic lamellae (up to 60—80 in the human ascending aorta), interdigitated by connective tissue layers that contain VSMCs. This layered microstructure gradually vanishes in peripheral vessels as the number of elastic lamellae decreases while the smooth muscle cell contents increases.[4] Arteries thus undergo a spatial central-to-peripheral transition from elastic to muscular arteries, in line with their functional transition of vessels contributing to buffering to conduit vessels contributing to pressure regulation.

Large artery stiffness and stiffening—a tale of elastin and collagen

As any organ and tissue in the human body, arteries are not immune to disease or effects of aging. In this chapter, we do not consider focal disease as atherosclerosis (that may lead to stenosis) or pathologies affecting locally the structural integrity of the artery (e.g., aortic aneurysm, aortic dissection), but rather focus on the consequences of diffuse processes affecting the overall arterial structure and function, particularly of large elastic arteries, leading to what is known as large artery stiffening. As a consequence of large artery stiffening, large arteries gradually lose their windkessel function with a widening of PP, imposing higher mechanical stress on the vessels and organs that may result in organ damage in the heart, kidney, brain, and other organs.[7] At the same time, peripheral arteries (possibly because of their much lower elastin content) are less susceptible to stiffening, and the "stiffness gradient" between the central and peripheral arteries decreases. These processes alter hemodynamics, affect the magnitude and timing of forward and backward traveling pressure and flow waves in the circulation, and the

physiological amplification of the pressure pulse from the heart to the periphery.[7,8] All in all, arterial stiffness is considered as a key biomarker of vascular health, believed to integrate the accumulated effect of aging and exposure of the arterial system to insults and mechanochemical stressors, and has repeatedly been demonstrated to predict cardiovascular mortality and morbidity above and beyond conventional cardiovascular risk factors.[9–11]

To understand the mechanical behavior of arteries, it is important to understand the role of the matrix proteins elastin and collagen. The distensibility of young, healthy arteries at physiological pressures arises first from the intrinsic distensibility of the vessel's elastin (having a Young elasticity modulus that increases with strain up to values of about 600 kPa[12]) and from the wavy, undulating nature of the stiffer collagen fiber families (Young modulus in the order of 10 MPa[12]) that helically spiral along the artery and allow for vessel expansion as intra-arterial pressure rises. It is then the elastic nature of elastin that provides resilience and allows for arterial recoil as pressure decreases. The undulation and dispersion of collagen fibers ensures that collagen is only progressively recruited with increasing pressure/stretch levels, ensuring smooth progressive functional stiffening of the artery at higher pressures (Fig. 7.1B, left panel). The Achilles heel of the artery, however, is elastin. In contrast to collagen—continuously degraded and deposited in a process of mechanobiological homeostasis[13]—elastin is believed to (a) be only deposited in the media of the arterial wall during fetal growth and infancy, without the ability to renew[14] and (b) degrade with a reported half-life of 40—50 years.[15] Both have important consequences for large artery function. With somatic growth, elastin within the arterial wall becomes progressively stretched, subjecting the elastic arteries to a permanent tensional load in the circumferential and longitudinal direction (explaining why the arterial wall retracts after surgical incision). Much like worn out rubber, elastin degradation in later life in arteries gradually relaxes arterial prestretch, leading to dilation, elongation, and increased tortuosity with age.[16] In the process, arteries progressively lose their low-stretch bearing component, shifting load from elastin to stiffer matrix components (collagen). Obviously, other constituents can contribute to or modulate arterial stiffness, including smooth muscle cell stiffness and tone, fibrosis, cross-linking of elastin and collagen, and calcification of the media, which interact with each other and with overarching pathways (such as inflammation and endothelial dysfunction). We refer to Reference 7 for an overview. Although stiffness is generally considered a "passive" property of an artery, smooth muscle tone does play a significant role in the mechanical behavior of the arterial wall, whereby the level of smooth muscle cell contraction seems to modulate the transition point at which collagen takes over the load bearing from elastin as demonstrated in pressure-inflation tests on perfused arterial

FIGURE 7.1 (A) There is a gradual transition in the composition of arteries along the arterial tree. Large elastic arteries, close to the heart, have the characteristic lamellar structure with layers of elastin interdigitated by layers of collagen and vascular smooth muscle. These arteries contribute to buffer function. Further away from the heart, arteries lose the elastic lamellar structure and evolve into muscular-type arteries with a decrease in elastin and increase in smooth muscle contents. (B) pressure-diameter relation of the untreated mouse carotid artery (dark blue) and after removal of elastin (red) or collagen (green). (C) pressure-diameter relation of the pig carotid under control conditions (dark blue) and after modulation of smooth muscle tone to maximal contraction (red) and relaxation (green). *(A, B) Reconstructed from Gabriela Espinosa M, Catalin Staiculescu M, Kim J, Marin E, Wagenseil JE. Elastic fibers and large artery mechanics in animal models of development and disease. J Biomech Eng. 2018;140:0208031−02080313; (C) Reconstructed from Zulliger MA, Kwak NT, Tsapikouni T and Stergiopulos N. Effects of longitudinal stretch on VSM tone and distensibility of muscular conduit arteries. Am J Physiol Heart Circ Physiol. 2002;283:H2599−H2605 (data at stretch 1.4).*

segments. This may lead to a perhaps unexpected behavior, with muscle contraction leading to a functionally more distensible artery than a vessel under normal tone in the higher pressure range. Indeed, complete muscle contraction shifts the elastin-collagen load-bearing transition to higher pressure levels, implying a more distensible artery as the contracted muscle becomes the dominant load-bearing component at lower pressure (Fig. 7.1C, right panel).
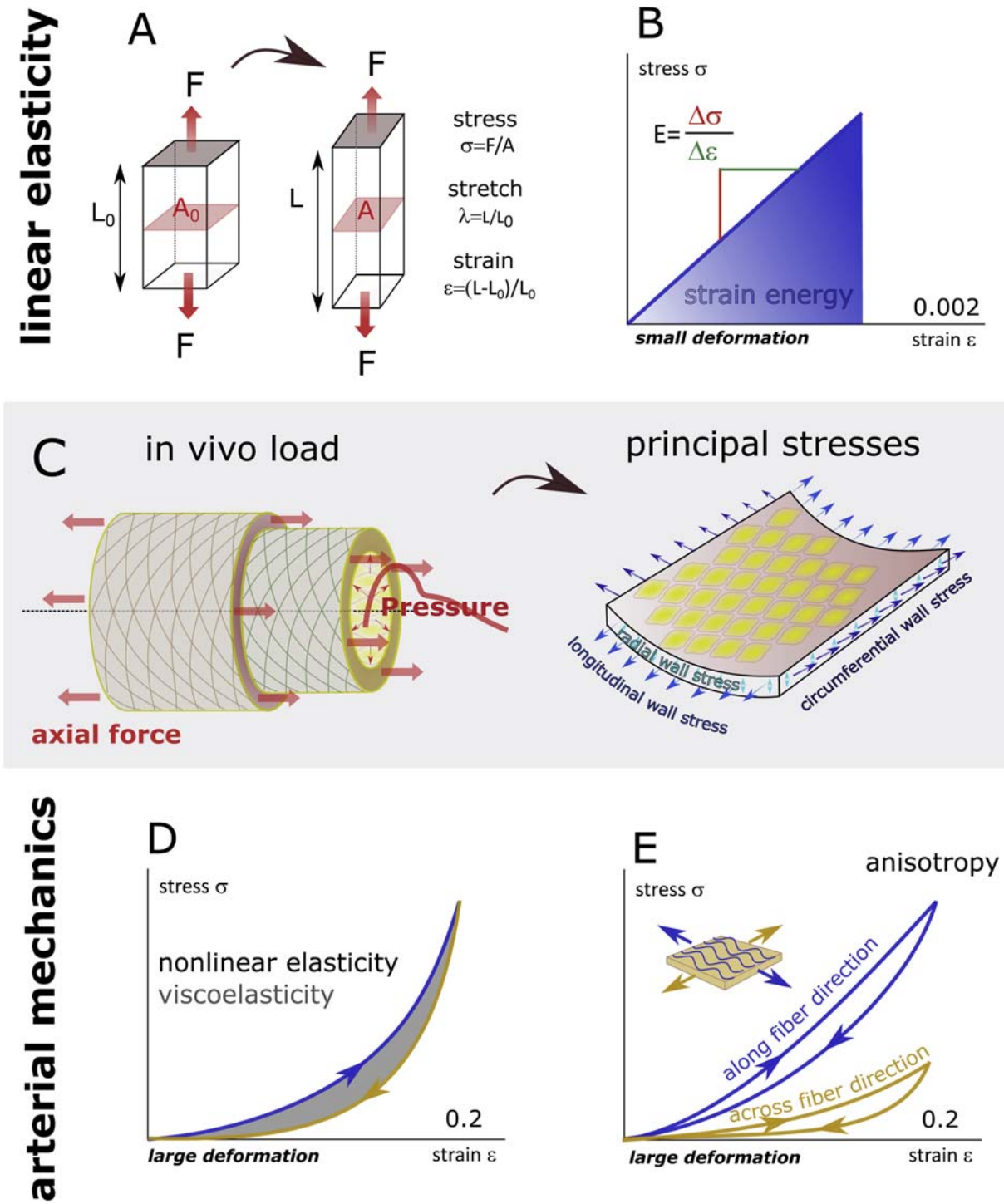
Mechanics of arterial tissues: bioengineering principles and perspective

In this section, we briefly discuss some bioengineering principles to characterize the mechanical behavior of materials and tissues. The main motivation is to sketch the complexity of arterial biomechanics and confront it with the prevalent simplistic approach of arterial stiffness characterization in vivo. Rather than formulating equations and mathematical expressions, we will attempt to illustrate principles and complexity making use of data that has been acquired from *ex-vivo* testing on arterial tissue.

Stress and strain—what's in a name?

We all have at least an intuitive notion of the concepts of stress and strain. Stress, with SI units N/m^2 (also called Pa), is generally defined as force divided by surface (noted here as σ). Strain (noted as ε) is the deformation of material relative to a reference state and is dimensionless.

In material science, materials are characterized from the relation between stress and strain, i.e., a constitutive relation describing the response of the material to a stimulus. The simplest example is a metal rod with unloaded length L_0 and cross-sectional area A_0 subjected to a force F (Fig. 7.2, panel A) that leads to small deformation (lengthening) of the rod, say 0.2%, to its new deformed length L (stretch $\lambda = L/L_0$) and cross-section A. Stress is then simply calculated as F/A, and strain ε (in this case, 0.2%) is calculated as $(L - L_0)/L_0 = \lambda - 1$. The relation between stress and strain is linear (the material is called linear elastic or Hookean) and the ratio of stress and strain is the Young elasticity modulus E (in Pa), such that $\sigma = E\varepsilon$. If the material is isotropic, i.e., its mechanical properties are the same in all directions, E fully characterizes the material (Fig. 7.2B).

FIGURE 7.2   (A) and (B) concepts from linear elasticity. (A) Definition of stress, strain, and stretch based on simple extension; (B) stress-strain plot for small deformations (much less than 1%) with the slope yielding the Young elasticity modulus. The area under the stress-strain curve is the elastic energy stored in the material. (C) in vivo loads acting on an arterial segment and resulting principal strains acting in the radial, circumferential and longitudinal direction. (D) and (E) concepts from arterial mechanics, characterized by large deformations with nonlinear stress-strain relations and appearance of hysteresis loops in loading-unloading experiments indicating viscoelasticity (D). The tissue is anisotropic, with much stiffer behavior when a load is applied along the fiber direction than across the fiber direction (E).

This simple example with uniaxial loading of an isotropic linear elastic material undergoing small deformations is, however, of little relevance when studying arterial mechanics, and the concepts of stress and strain become much more complex and ambiguous.

Stresses acting on the arterial wall

Let us approximate an arterial segment in the circulation as a cylinder with radius R and wall thickness h. The blood pressure, P, will induce stresses that, for a thin-walled cylinder ($h/R < 0.1$), are given by Laplace law yielding PR/h (tensile) in the circumferential and $-P/2$ (compressive) in the radial direction. In the arterial tree, however, the cylinder is not isolated and axial stresses of unknown magnitude will act on the segment due to axial prestretch (that can be as high as 1.6 or higher), effects of tethering, anchoring, or other factors (e.g., cardiac motion). Arterial pulsations induce diameter changes in the order of 10%, but these are superimposed on the much larger deformation that already exists at the diastolic blood pressure level. As such, to understand the effective stress and strain levels that the artery is subjected to, one should first consider the segment in its unloaded configuration (depressurized and disconnected from its surroundings). The stresses that are needed to deform the unloaded segment to its diastolic in vivo configuration are called the initial stresses. Assessing these initial stresses involves solving a complex inverse problem. Note that the unloaded arterial segment will generally not be totally stress-free: arterial remodeling will lead to the development of residual stresses that are evidenced when further cutting up the arterial segment in ring segments, cutting these ring segments that will typically open up to a certain angle.

The above demonstrates that (i) arterial tissue is simultaneously loaded in multiple directions; (ii) deformations are very large and approximations based on small deformation theory should be used with caution; (iii) initial stresses are present on which the diastolic-to-systolic loading is superimposed.

Arteries consist of anisotropic, viscoelastic, nonlinear tissue

Arterial biomechanics is further complicated by the composition of the artery, directing its mechanical behavior. The concentric layering of large elastic arteries and especially the specific orientation of different collagen fiber families render arterial tissue anisotropic, meaning that its behavior will depend on the loading direction. Also, loading the tissue in one direction will interfere with its behavior in another direction and induce a complex stress field with principal stresses in the circumferential, axial, and radial direction (Fig. 7.2C). The undulation, dispersion, and

progressive recruitment of collagen fibers as the artery is stretched will lead to a nonlinear relationship between stress and strain. Arteries will also exhibit some degree of viscoelasticity, which manifests itself in hysteresis (energy losses due to internal friction) in stress-strain plots of cyclic loading experiments (Fig. 7.2D),[17] but its effects on arterial hemodynamics are relatively small.[18] For ex vivo testing of arterial segments or tissue specimens to be relevant and insightful, it is important that experiments are conducted in line with the loading as experienced by the vessel in vivo. In particular, data from pressure-inflation tests on prestretched segments and multiaxial testing on tissue specimens have been instrumental for the arterial biomechanics community (Fig. 7.2E).

A glimpse on strain energy functions

It is clear that the complex behavior of arterial tissue cannot be described by the linear elasticity theory with the Young modulus as single material parameter. One has to rely on large deformation theory of nonlinear materials, simultaneously considering stress, strain, and stretch and their relations in all directions in a three-dimensional (3D) setting making use of tensor notations for stress and strain. It is also important to realize that different definitions for strain and stress exist, and that caution is warranted when interpreting stress-strain data (one can, however, always convert one into the other). The reader is referred to specialized literature on the topic for more details.[19−21] In (computational) soft tissue biomechanics, it is most common to express deformation using the Green−Lagrange strain tensor, **E**, and stress by the so-called second Piola Kirchhoff stress tensor, **S** (with **E** and **S** being 3×3 tensors with nine components).

What is still missing is a constitutive relation that relates **S** to **E**, thus describing the material behavior. In soft tissue biomechanics, that relation is typically expressed making use of a so-called "strain energy density" function Ψ, such that $\mathbf{S} = \frac{\partial \Psi}{\partial \mathbf{E}}$. The function Ψ yields a positive scalar value, representing the energy stored in the material for a given deformation status, and with value 0 in the undeformed state. As the material deforms, energy is stored (or, conversely, it requires a certain amount of energy to deform the material). Applying the concept to the example of the linear elastic rod loaded along its axis, $\Psi = \frac{1}{2}E\varepsilon^2$ such that $\sigma = \frac{\partial \Psi}{\partial \varepsilon} = E\varepsilon$. Ψ represents the area under the stress-strain curve (Fig. 7.2B).

In arterial biomechanics, strain energy functions as the Holzapfel-Gasser-Ogden model (called after the researchers proposing the model) are probably most widely used, describing the anisotropic nonlinear behavior of arterial tissues, accounting for fiber orientation. Models are phenomenological in the sense that material constants are

derived after fitting the model to experimental data. As denoted in Chapter 9, it is essential that experimental data are acquired under conditions that are representative for the in-vivo loading.

Mechanics of arterial tissues: clinical/in vivo perspective

In the previous sections, we highlighted the complex architecture and microstructure of arterial tissue. Structural and mechanical properties of individual matrix constituents and smooth muscle cells, their 3D organization, interconnectivity, and smooth muscle tone drive the functional behavior of the artery. Ex-vivo experimentation on arteries have demonstrated nonlinear, nonisotropic properties (mainly induced by the orientation and distribution of collagen fiber families), with stress-strain relations that highly depend on the loading direction. Given the spatial variation of the size and composition of arteries throughout the arterial tree, and the permanent pathophysiological mechanobiological processes of matrix degradation and synthesis leading to arterial growth and remodeling, arterial properties vary from one location to another and are not constant in time. The mathematical formulation of the mechanical behavior of such materials is nontrivial and still mainly restricted to a phenomenological approach where the parameters of constitutive laws—under the form of strain energy functions—are determined by fitting data from experiments to these models.

To date, however, this biomechanical approach has been of little direct diagnostic or prognostic value to the clinical community. Conversely, the clinical community—besides being the provider of tissue samples—has been of relatively limited value to the biomechanical community (at least to those members of the community performing fundamental biomechanical research). This is regretful, as recent work in mouse models of arterial aging—with availability of in-vivo and ex-vivo testing—has demonstrated that concepts arising from a fundamental biomechanics approach can lead to important insights in the pathophysiology of arteries. In particular, stored elastic energy seems to be a sensitive biomarker of microstructural damage as demonstrated in fibulin-5 deficient mice. Advanced computational models also pinpoint an important role of perivascular tethering in arterial biomechanics.[22]

The fundamental problem that is faced when applying some of the more advanced biomechanical concepts in vivo is that the data that can be acquired in vivo are simply insufficient to reliably determine the parameters needed to feed into constitutive relations. Limiting factors are not so much imaging or measuring limitations, but rather the confined loading of the in vivo vessel. Indeed, the artery at interest is subjected to a given (unknown) level of axial prestretch, and deforms mainly in the radial direction under the pulsatile loading of blood pressure, varying between diastolic and systolic blood pressure. Typical datasets such as pressure-diameter relations over the in vivo pressure range are simply insufficient to reliably fit the multiple parameters of constitutive models without making stringent assumptions on the in situ configuration[23] and factors such as perivascular tissue and tethering and presence of unknown residual stresses that will have an effect on model fitting and the parameter values obtained.[24]
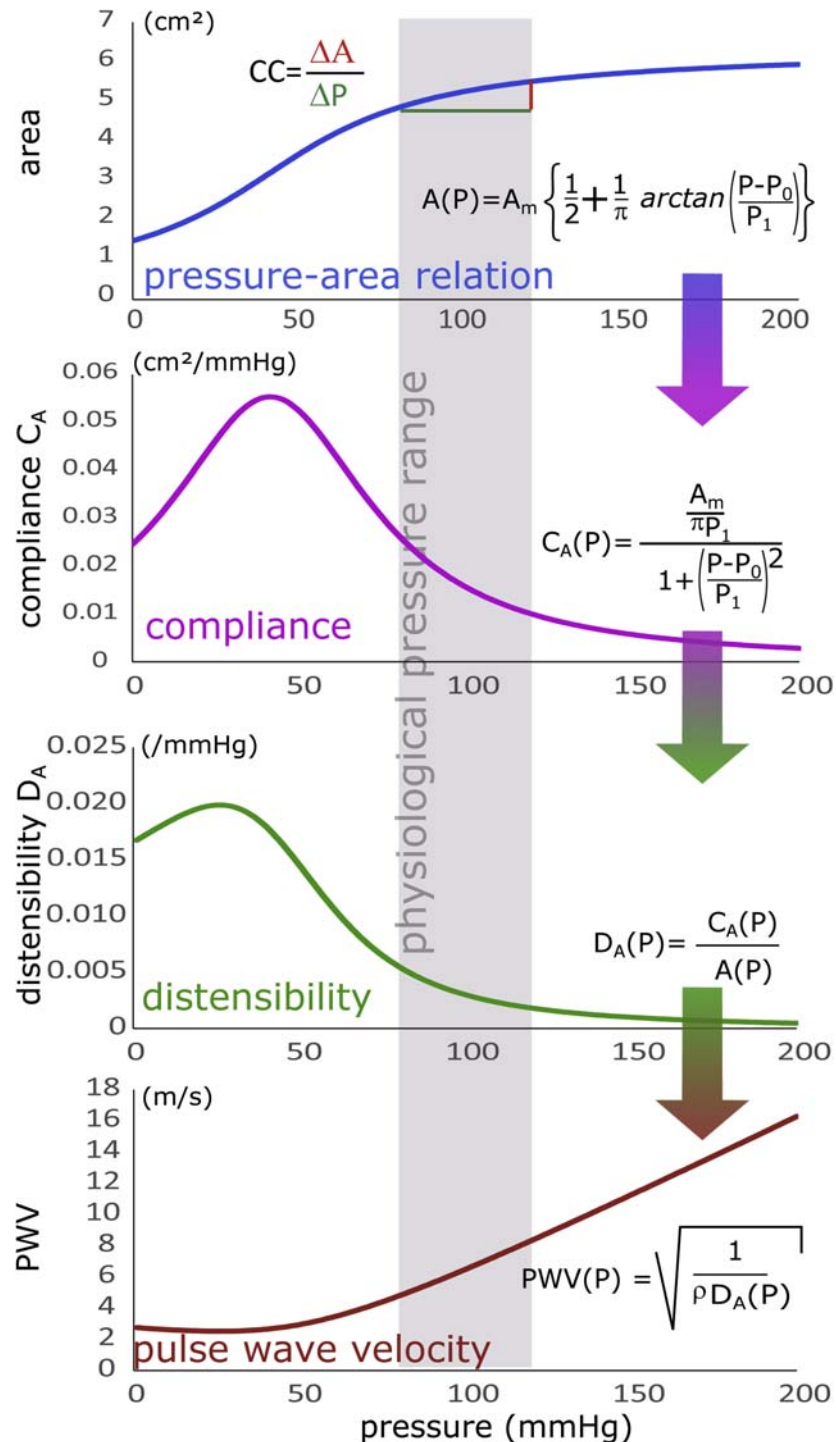
The clinical perspective on arterial stiffness, therefore, rather focusses on quantifying arterial function and assessing functional indices—biomarkers—that are, ideally, easy to measure with an acceptable accuracy and sensitivity that allows to discern pathology from normal physiology and carry prognostic information beyond standard clinical data (such as age, blood pressure, plasma lipids, etc). The remaining part of this chapter will focus on the in-vivo measurement of such functional indices. We will first cover *locally* measured functional indices that come closest to the biomechanical perspective—yet most often making abstraction of the continuum mechanics complexity. We will next discuss PWV as an elegant way to regionally phenotype arterial stiffness indices and conclude with methods that aim to quantify the buffering capacity of the entire arterial tree (or arterial territories) through measurement of (total) arterial compliance.

Local functional indices from pressure-area data: compliance and distensibility

As previously described, there is a nonlinear relation between intra-arterial pressure and lumen cross-sectional area (or diameter), which becomes particularly visible when testing arterial segments over a wide pressure range. This is best illustrated using seminal work done by Langewouters et al., who performed pressure-inflation tests on human excised, perfused thoracic, and abdominal aortic segments.[25] Testing over a 0−200 mmHg pressure range, they observed a typical nonlinear pressure (P)-area (A) relation that they analytically described using an arc-tangent relation as illustrated in the top panel of Fig. 7.3. We can now use this data-based analytical expression to study well-known functional indices as (area) compliance and distensibility.

(Area) compliance and distensibility

Area compliance, C_A, is defined as the ratio of the change in area, ∂A, in response to the change in pressure ∂P, C_A (in m2/Pa in SI units) is the local slope of the pressure-area curve. Using the arc-tangent relation, C_A is equally a function of pressure as illustrated in the second panel of Fig. 7.3. Normalizing C_A to cross-sectional are yields the

FIGURE 7.3 The top panel displays a pressure-area plot that is analytically described by an arc-tangent relation. A_m, P_0, and P_1 are obtained via curve-fitting on experimental data of the thoracic aorta of a 39-year old ($A_m = 6.4$ cm^2, $P_0 = 41.3$, and $P_1 = 36.8$ mmHg)[17]. A_m is the maximal cross-section at high pressures, P_0 the pressure corresponding to the inflection point of $A(P)$ where the vessel reaches its maximal compliance, and P_1 is a measure for the steepness of the pressure-area relation. The pressure-area relation forms the basis for the computation of compliance and distensibility, which can be converted into pulse wave velocity using the Bramwell–Hill equation[26].

distensibility, D_A (in Pa^{-1}), defined as $\partial A/A/\partial P$. It is the ratio of the relative change in cross-sectional area ($\partial A/A$) and change in pressure ∂P and is obtained as $C_A(P)/A(P)$.

Clearly, compliance is pressure-dependent and reaches its maximal value for infraphysiological pressures (at P_0). Within the physiological pressure range of 80–120 mmHg,

C_A is reduced by 62% when pressure increases from 80 to 120 mmHg, a phenomenon known as pressure-dependent stiffening. As C_A, distensibility is maximal at infraphysiological pressures, but not at the same pressure as C_A. Distensibility is reduced by 67% when pressure increases from 80 to 120 mmHg.

Compliance coefficient and distensibility coefficient

It is not uncommon in clinical studies to discard the pressure dependency of C_A and distensibility, and to calculate the compliance coefficient (CC) and distensibility coefficient (DC) from diastolic and systolic values differences in cross-sectional area (ΔA) and pressure (ΔP) as

$$CC = \frac{\Delta A}{\Delta P} \approx \frac{\pi D \Delta D}{2\Delta P}; \ DC = \frac{\Delta A/A}{\Delta P} \approx \frac{2\Delta D}{D\Delta P}$$

Cross-sectional area (change) is obviously easily derived from diameter (D) measurements and assuming circularity of the cross-sectional area. This approach implies a linearization of the pressure-area relation between diastolic and systolic pressure, with CC the slope of this line yielding a value in between the diastolic and systolic value (Fig. 7.3).

C_A and D_A (or CC and DC) quantify the functional mechanical properties of the blood vessel. They depend not only on intrinsic wall tissue properties but also on wall thickness and vessel dimensions (especially C_A). Indices are best calculated using local blood pressure, which may differ substantially from brachial cuff values due to pulse amplification as the pulse travels from the heart to the periphery.[27] Arterial area and diameter can be obtained using ultrasound for superficial vessels (typically the carotid and femoral arteries); magnetic resonance imaging (MRI) can in principle provide such data all along the systemic and pulmonary vasculature, but the spatial resolution sets limits in practice to the larger vessels where changes in area can still be measured with reasonable accuracy. Obviously, pulmonary artery pressure cannot be obtained in a noninvasive way. Of note is that in ultrasound, some algorithms (especially wall tracking algorithms) may measure the diameter using the media-to-adventitia transitions rather than lumen diameter. As this yields smaller ΔD and larger D, DC will be somewhat underestimated.[28]

Stiffness moduli

Although the bioengineering perspective provides many arguments against doing so, the linear elasticity theory (assuming infinitesimal changes in diameter) applied to a pressurized thin-walled (with thickness h) cylinder does

provide a Young elasticity modulus (E, SI units Pa) given as

$$E = \frac{\Delta P}{\Delta D} D^2 \frac{(1 - \nu^2)}{2h}$$

with ΔD the diameter variation corresponding the pressure variation ΔP, h wall thickness, and ν the Poisson ratio of the wall material (0.5 for biological tissue).[29]

A better approach, given the high nonlinearity of the vessel wall and the large deformations, is to use the "incremental" elasticity modulus E_{inc}, derived from stepwise variations of pressure (and diameter).[29] Assuming no external pressure, E_{inc} is given by:

$$E_{inc} = \frac{\Delta P}{\Delta D_o/D_o} \frac{2D_i^2(1 - \nu^2)}{D_o^2 - D_i^2}$$

with indices o and i for outer and inner wall, respectively. E_{inc} increases with intraluminal pressure; for a blood pressures of 100 mmHg, it is about 400 kPa for the aorta, while reaching 2000 kPa or more for peripheral arteries.[29]

Lastly, it is worth mentioning the sometimes reported Peterson incremental elasticity modulus E_P, which does not require knowledge of arterial wall thickness. It is defined as[30]:

$$E_P = \frac{\Delta P}{\Delta D_o/D_o}$$

The reader should, anyhow, be aware that none of the above indices should be seen as constitutive material parameters describing the intrinsic nonlinear mechanical properties of an artery. At best, they provide a single number quantification of the functional stiffness of the artery in the circumferential direction. The reader is referred to Chapter 9 for further advanced reading on this topic.

Shear wave elastography—an in-vivo bioengineering perspective?

Shear wave elastography for soft tissue characterization is receiving a lot of attention in the ultrasound community[31] and may provide a clinically feasible way to effectively apply bioengineering principles in vivo. The working principle is that (i) small amplitude mechanical perturbations are induced locally within the tissue (typically micrometer displacements generated using mechanical energy from the focused ultrasound beam), and (ii) the propagation of the generated shear waves is tracked. As the shear wave speed is proportional to the stiffness of the tissue, shear wave elastography is potentially a direct stiffness measuring technique. Initially mainly used for liver fibrosis staging or breast tumor characterization, shear wave elastography is now fully being explored for the quantification of stiffness of the heart and arteries.[32] Methods are still under investigation,

and the complex anisotropic and layered nature of the thin-walled tissues pose extra challenges, but initial results are highly promising.[33] In addition, given that shear waves can be tracked in 3D and propagation characteristics are sensitive to the tissues microstructure and anisotropy, shear wave elastography may provide in vivo assessment of arterial anisotropy.[34] Applications would be mainly directed toward the superficial carotid artery (whose properties may not always change in tandem with those of the aortic wall). Clearly, this technique is under development and any clinical and prognostic value remains to be established.

From local pressure-diameter to pulse wave velocity

Local stiffness measurements have the merit of phenotyping functional properties at a specific arterial site, but measurements and postprocessing—one has to combine pressure and diameter/area data—may be tedious and local properties not necessarily reflect the overall vascular health of a person. Above methods are therefore less frequently applied in clinical research whereby more global markers of vascular health may be more relevant. In the vast majority of these studies, PWV will be used as biomarker of arterial stiffness.

PWV is the speed at which the arterial pulse travels through the arterial tree, leading to easily observed time delays when the pulse is measured at two distinct locations (try, for instance, simultaneous palpation of the carotid and radial artery). The theoretical grounds that relate PWV to the stiffness of the distensible tube that the pulse travels in were established by Moens in 1877[35] and Korteweg in 1878[36] leading to the Moens–Korteweg equation $\text{PWV} = \sqrt{\frac{Eh}{\rho D}}$ with E the Young elasticity modulus, h wall thickness, ρ the density of the liquid inside the tube, and D the tube diameter. It were Bramwell and Hill in 1922, who reformulated this equation avoiding the necessity to measure E, h, and D into $\text{PWV} = \sqrt{\frac{V}{\rho}\frac{\partial P}{\partial V}}$ with V the volume within a tube segment of a given length.[37] Assuming a fixed length, one finds $\text{PWV} = \sqrt{\frac{A}{\rho}\frac{\partial P}{\partial A}}$ with ∂A the change in lumen area in response to a change in pressure ∂P. With $\frac{\partial A}{A\partial P}$ representing the distensibility (D_A) of the tube, $\text{PWV} = \sqrt{\frac{1}{\rho D_A}}$. High vessel stiffness (lower D_A) thus translates into a higher PWV. Note that, as the relation between pressure and area is nonlinear (as is the case in arteries), PWV will equally depend on operating pressure. As such, when using the foot of the wave as the fiducial point to assess transit time, one obtains PWV at diastolic pressure. The interrelations between the pressure-area diagram, distensibility, and PWV are illustrated in Fig. 7.3. It is important to realize that the

theoretical Moens–Korteweg and Bramwell–Hill relations hold for a uniform elastic tube, free of reflections (presumed infinitely long), which are conditions that not met in vivo, with arterial size and properties permanently changing across the arterial tree and with pressure and flow waves shaped by transmission and reflection. As such, despite generally considered the clinical gold standard to assess arterial stiffness, PWV may not be the most sensitive biomarker to detect changes in arterial wall material stiffness, as shown by modeling studies.[38]
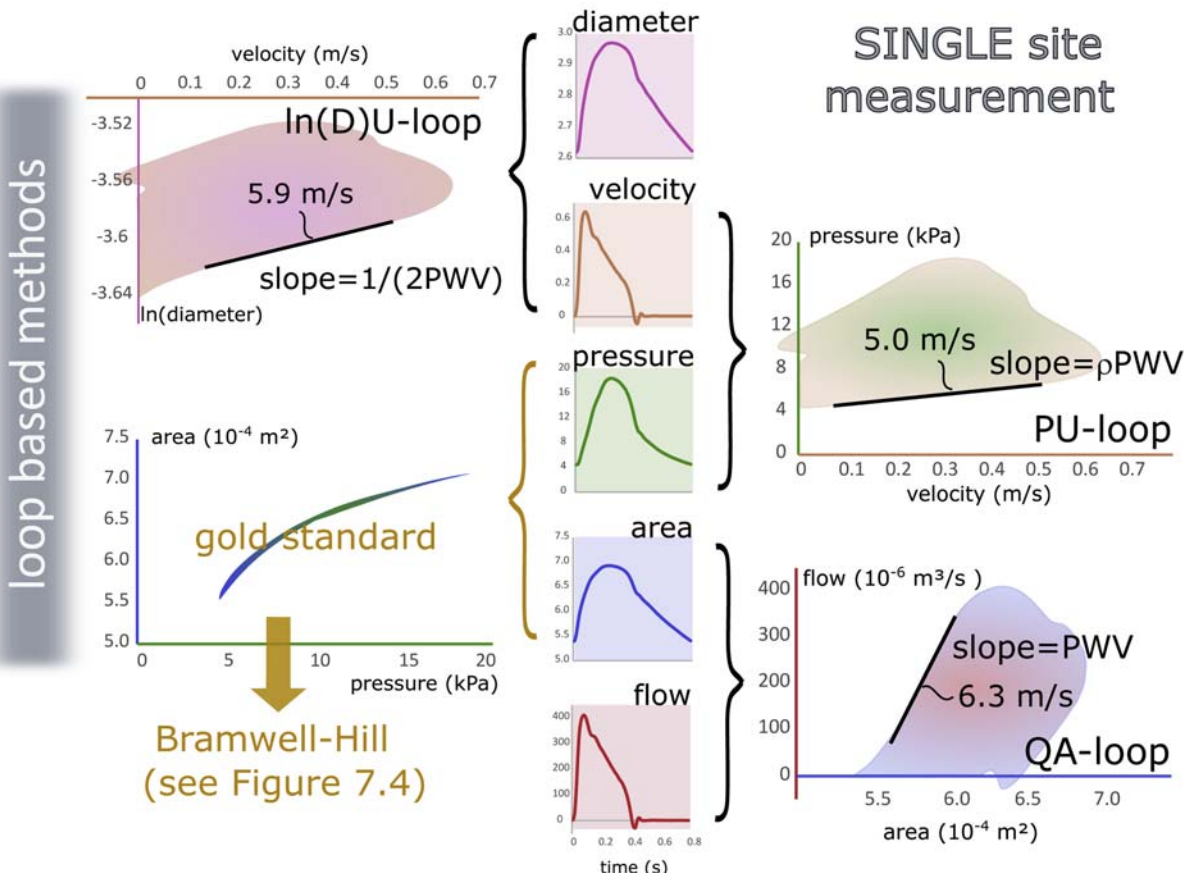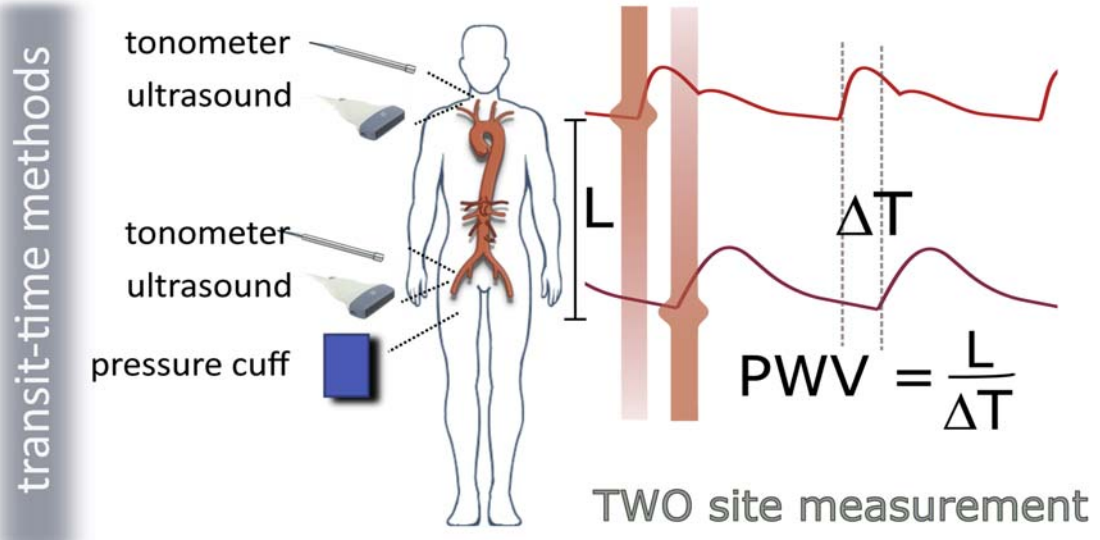
Measuring (aortic) pulse wave velocity in vivo

Transit-time methods

In clinical practice, PWV is most commonly calculated as $\text{PWV} = \Delta L/\Delta T$, with ΔL the distance between two measuring sites, and ΔT the time it takes for the arterial pulse to travel from the proximal to the distal measuring site[42] (Fig. 7.4). With "pulse," we refer to measurable physiological signals that all propagate as a wave along the arterial tree at the same PWV such as pressure, flow or velocity waves, and arterial distension. With the aorta the largest elastic artery in the body, contributing to over 60% of the arterial buffer capacity,[43] most methods aim to measure aortic PWV which is ideally based on measurement locations within the aorta itself. The absolute reference is PWV from invasive pressure catheter recordings, but it is clear that such protocols are typically confined to technical validation studies (see e.g., Reference 44). More feasible, though probably not for large scale studies, is MRI which provides the 3D aorta and path length from anatomical imaging, while transit times can be assessed from flow measurements in specific cross-sections using phase contrast sequences.[45] Keep in mind, however, the temporal resolution of MRI which may not be sufficient to resolve transit times of a few tens of milliseconds, particularly when assessing regional PWV over shorter segments as the aortic arch.[46] Besides MRI, also two-dimensional ultrasound holds promise as a widely available technique to assess thoracic aortic PWV (from the aortic root to the diaphragmatic hiatus).[7]

To date, the closest proxy for aortic PWV is carotid-femoral PWV, with transit times assessed from "fiducial points" that are identified on signals measured at the carotid and femoral arteries.[42] These sites provide superficial arteries, still relatively close to the aorta, and accessible to measure pressure (applanation tonometry), flow velocity (ultrasound), arterial distension (ultrasound), or even skin-measured acceleration or vibrations (Fig. 7.4). These measuring techniques are embedded in commercially available systems such as Complior,[47] Sphygmocor,[48] Pulsepen,[49] and others, as well as custom-built data acquisition systems (as

FIGURE 7.4   Left: illustration of the concept of carotid-femoral pulse wave velocity. The transit-time time (ΔT) of the pulse from the carotid to femoral is measured, together with an estimated travel path length L. The ratio of L and ΔT yields PWV. Right: illustration of the various loop-based methods that have been proposed to estimate local pulse wave velocity. The PU-loop method was first introduced by Khir et al.,[39] who reformulated the method to the $ln(D)U$ method to avoid the use of pressure.[40] The QA method was introduced by Rabben et al.[41] The absolute reference and gold standard, however, is to use the pressure-area relation from which one can get PWV as a function of pressure as illustrated in Fig. 7.3. Methods have been shown susceptible to wave reflection (see text).

used in the Framingham[11] and Asklepios[50] population studies). Measurements are best performed simultaneously, but ECG-gated sequential measurements are common practice.[51] The availability of a large reference value database acquired from data across Europe[52] and studies demonstrating its prognostic power[10,53] have given carotid-femoral PWV a reference status of reference for clinical studies in Europe and the United States. The biomarker has, however, some important drawbacks as phenotype of large artery stiffness as the method bypasses the ascending aorta and part of the aortic arch, discarding the properties of the aortic section that contributes most its buffering function. Besides the difficulty in assessing the carotid-femoral pathlength (the current consensus being to simply calculate PWV using 0.8 times the distance between the carotid and femoral measuring site), there is ambiguity in its definition since the pulse does not directly travel along a single path from the carotid to the femoral measuring site. Also, computer modeling studies have shown that carotid-femoral PWV strongly correlates with, but differs substantially from theoretical PWV values derived from the Bramwell−Hill equation due to nonlinearities in arterial elasticity and the nonhomogeneity of the arterial tree.[54]

Several other devices have been developed over the past decades (see Reference 55 for a recent review), recording signals at more peripheral locations using cuffs at the brachial, ankle, and thigh or photoplethysmograph devices on the finger and toe.[56] As can be expected and confirmed by an invasive validation study, the further measuring sites move away from the aorta, the lesser the correlation and agreement with invasively measured aortic PWV.[44] Nonetheless, brachial-ankle PWV is frequently used in Asia, with large studies demonstrating the prognostic ability of this metric to assess cardiovascular risk.[57] The very large distance of the measuring sites to the aorta leads to an uninterpretable ambiguity in the path traveled by the wave along elastic and muscular arteries, making it virtually impossible to reconcile how derived values effectively relate to aortic PWV.[58] It may be more sensible to aim for heart-femoral PWV, detecting the time delay between closure of the aortic valve (detectable via a microphone) and arrival of the pressure wave picked up by a femoral cuff.

An index closely related to PWV is CAVI, the cardio-ankle vascular index. CAVI assumes a nonlinear (exponential) pressure-diameter relation[59] and provides a pressure-independent stiffness metric (after correcting the original formulation).[60] However, the arterial path used for the underlying measurement of PWV will largely impact its physiological meaning and interpretation.

As extensively discussed in a recent review,[58] we discourage the use of devices estimating PWV from a single brachial cuff pressure recording. It is physically impossible to *measure* PWV from only a pressure tracing at one single measuring site, and devices only provide some estimate that may or may not be based on legitimate underlying models, and involve algorithms trained on datasets to ensure that plausible PWV values are provided by the device.

Loop-based methods to measure local pulse wave velocity

An appealing class of methods to assess arterial stiffness are the so-called loop-based methods that exist in several formulations, depending on the combined signals (Fig. 7.4). All methods rely on the (reformulated) water hammer equations that state that—in a uniform elastic tube and in absence of wave reflections—changes in pressure (dP) and flow velocity (dU) relate as[61] $dP_\pm = \pm\rho\mathrm{PWV}dU_\pm$ with the $\pm$ sign indicating the direction of propagation of the wave, ρ the density of the liquid inside the tube (about 1050 kg/m^3 for blood), and PWV the local PWV. To illustrate: for an arterial segment with a PWV of 5 m/s, a step increase in flow velocity of 1 m/s would give rise to a step increase in pressure of 5250 Pa (36.4 mmHg).

Khir et al. demonstrated that, when plotting simultaneously measured and properly time-aligned in-vivo pressure as a function of flow velocity, a loop is obtained that will typically display a linear segment that corresponds in time with the first few tens of milliseconds in early systole.[39] As also discussed in Chapters 3 and 17, when describing a time-domain method to estimate characteristic impedance, it seems plausible that wave reflection is minimal during that particular window in time, which would fulfill the conditions of the water hammer equation. In other words, the slope of the linear segment of the PU-loop in early systole equals ρPWV from which PWV is directly calculated. Reformulations of the method have led to more easily noninvasively applicable methods such as the flow-area method (QA method[41]) and the $ln(D)U$ method, D being diameter.[40] Especially the QA-loop method is alluring as both variables are fairly easily measured with MRI and can also be applied to the pulmonary artery.[62]

The presence of a linear segment in the PU-loop (or QA or $ln(D)U$ loops), however, does not guarantee absence of reflections, and these most appealing methods have proven to be susceptible to error induced by wave reflections.[63] This has been demonstrated in hydraulic bench set-ups,[64] in silico[65,66] and in vivo.[66] The impact of reflections on the accuracy of the method is variable and differs from one location to the other.[65,67] In the vicinity of a reflection of the closed type as in the carotid artery, the PU loop tends to overestimate effective PWV, while the QA and $ln(D)U$ method tend to underestimate. The opposite happens in the vicinity of open-type reflections.[65,67] Attempts to correct for the error have been undertaken, but without real applicable success to date.

Pulse wave imaging

An interesting ultrasound technique that holds the middle between a transit time and a local PWV measurement is pulse wave imaging. The use of unfocused plane waves enables measurements with a temporal resolution of several kHz that are thus fast enough to monitor the propagation of a pulse within the artery over the width of the imaging window.[68] Pulse wave imaging visualizes the propagating wave front using spatiotemporal plots of wall displacement, velocity, or acceleration indeed, with PWV given by the slope of the propagating wave front.[69] The technique, applicable to superficial vessels as the carotid artery, captures PWV throughout time, and it is possible to track the wave front in early systole (PWV at diastolic pressure) as well as the wave front arising from aortic valve closure (at the dicrotic notch pressure).[33]

Total arterial compliance

As explained before, the "windkessel" function refers to the ability of the arterial tree to partly buffer SV in systole, keeping pressure pulsations within physiological limits preventing excessive systolic pressures as well as a steep pressure decline in diastole, preserving perfusion pressure. That overall function is best quantified by the total arterial compliance (C). C, defined as dV/dP with V intra-arterial volume and P pressure, is expressed in m^3/Pa in SI units (or in mL/mmHg). A simple estimate of total arterial compliance is the ratio of SV and PP.[70,71] SV/PP could be thought of as the total arterial compliance if the complete SV were buffered in the large elastic arteries in systole, without any peripheral outflow (and discarding, among others, wave reflection and viscoelastic effects). As there is a continuous run-off of blood, the volume increase during ejection is only a fraction of SV and SV/PP should overestimate true compliance.[72,73] The reader is referred to Chapter 3 (Essential Principles of Pulsatile Pressure-flow relations in the arterial tree) for windkessel model–based methods to estimate total arterial compliance.

Total arterial compliance versus arterial stiffness and pulse wave velocity

Despite the physiological significance of total arterial compliance, it is only seldomly used in clinical research. Besides the necessity to measure pressure and flow (SV), an important drawback of compliance is that it depends on stroke volume and pressure. While pressure can be assumed to be intrinsically independent of body height, SV clearly is not. This necessitates normalization, implies different values for men and women, and complicates comparison between groups. In addition, arterial aging encompasses changes in arterial stiffness and aortic enlargement, which

may compensate and lead to little changes in volume compliance, making it a rather insensitive biomarker to follow up on arterial changes. This stands in contrast with most (not all) aforementioned metrics of local stiffness and PWV which are insensitive to body size in humans and have similar values in mammals. This also facilitates translational research, with a straightforward adoption and translation of findings in animal models to the human setting.

Total arterial compliance versus effective arterial elastance

Effective arterial elastance (E_A), defined as the ratio of SV and end-systolic pressure, is a parameter frequently used in studies on ventriculo-arterial coupling. It is, however, occasionally reported as a measure of arterial stiffness. We have shown theoretically[74] and in vivo[75] that E_A is simply a function of systemic vascular resistance and heart rate and is negligibly influenced by (and insensitive to) changes in pulsatile afterload in humans. It should therefore not be used to quantify arterial stiffness or compliance.

Concluding remarks

Arterial stiffness (or rather the inverse, arterial distensibility) is a key physiological property of the organism which is, unfortunately, not easily quantified in a simple, tangible metric. The complex composite nature of the arterial wall yields a soft tissue with highly nonlinear anisotropic and viscoelastic properties that are site-dependent and further modulated by arterial tone and adaptations driven by mechanobiological interactions. It is therefore almost surprising that crude in vivo functional measurements as carotid-femoral PWV (and alternatives) have been proven such strong prognostic biomarkers. The urge for quick and easy assessment of stiffness (PWV) in larger (general) populations has stimulated the development of devices—some more trustworthy than others—though without really advancing the field or facilitating standardization. In the research setting, the further exploration of MRI for aortic assessment, and developments in ultrasound imaging may open up new, reliable methods for targeted functional phenotyping of the proximal aorta and large central arteries and material characterization using elastography. The further integration of imaging, advanced computational biomechanics, and most likely artificial intelligence, will, no doubt, further unravel the complex biomechanical axial-circumferential interactions in arteries and how these evolve in an aging aorta that dilates and elongates while being exposed to mechanical and biological/metabolic insults. At a macroscale, such studies should include the interaction of the aorta with its surroundings—the heart at its inlet, and its anchoring and

tethering. At the microscale, they should increase our understanding of mechanobiological interplay and the interaction of cells within the arterial wall and the extracellular matrix that it maintains and synthesizes. Ultimately, these insights should lead to novel methods for an easy assessment of vascular health in the general public, and to therapies for an optimal preservation of vascular health within an individual's lifetime.

References

1. Rhodin JA. Architecture of the vessel wall. In: Terjung R, ed. **Comprehensive Physiology**. 2014:1−31.
2. Greene AS, Tonellato PJ, Lui J, Lombard JH, Cowley Jr AW. Microvascular rarefaction and tissue vascular resistance in hypertension. **Am J Physiol**. 1989; 256:H126−H131.
3. Westerhof N, Lankhaar JW, Westerhof BE. The arterial Windkessel. **Med Biol Eng Comput**. 2009; 47:131−141.
4. Lacolley P, Regnault V, Segers P, Laurent S. Vascular smooth muscle cells and arterial stiffening: relevance in development, aging, and disease. **Physiol Rev**. 2017; 97:1555−1617.
5. Gabriela Espinosa M, Catalin Staiculescu M, Kim J, Marin E, Wagenseil JE. Elastic fibers and large artery mechanics in animal models of development and disease. **J Biomech Eng**. 2018; 140:0208031−02080313.
6. Zulliger MA, Kwak NT, Tsapikouni T, Stergiopulos N. Effects of longitudinal stretch on VSM tone and distensibility of muscular conduit arteries. **Am J Physiol Heart Circ Physiol**. 2002; 283:H2599−H2605.
7. Chirinos JA, Segers P, Hughes T, Townsend R. Large-artery stiffness in health and disease: JACC state-of-the-art review. **J Am Coll Cardiol**. 2019; 74:1237−1263.
8. Mitchell GF, van Buchem MA, Sigurdsson S, et al. Arterial stiffness, pressure and flow pulsatility and brain structure and function: the age, gene/environment susceptibility–Reykjavik study. **Brain**. 2011; 134:3398−3407.
9. Laurent S, Boutouyrie P, Asmar R, et al. Aortic stiffness is an independent predictor of all-cause and cardiovascular mortality in hypertensive patients. **Hypertension**. 2001; 37:1236−1241.
10. Vlachopoulos C, Aznaouridis K, Stefanadis C. Prediction of cardiovascular events and all-cause mortality with arterial stiffness a systematic review and meta-analysis. **J Am Coll Cardiol**. 2010; 55:1318−1327.
11. Mitchell GF, Hwang SJ, Vasan RS, et al. Arterial stiffness and cardiovascular events the Framingham heart study. **Circulation**. 2010; 121:505−511.
12. Bergel DH. Arterial viscoelasticity. In: Attinger EO, ed. **Pulsatile Blood Flow**. New York, NY: McGraw-Hill; 1964:275−292.
13. Humphrey JD. Vascular adaptation and mechanical homeostasis at tissue, cellular, and sub-cellular levels. **Cell Biochem Biophys**. 2008; 50:53−78.
14. Sherratt MJ. Tissue elasticity and the ageing elastic fibre. **Age**. 2009; 31:305−325.
15. Arribas SM, Hinek A, González MC. Elastic fibres and vascular structure in hypertension. **Pharmacol Ther**. 2006; 111:771−791.
16. Horny L, Adamek T, Zitny R. Age-related changes in longitudinal prestress in human abdominal aorta. **Arch Appl Mech**. 2013; 83:875−888.
17. Langewouters GJ. **Visco-elasticity of the Human Aorta in Vitro in Relation to Pressure and Age**. 1982.
18. Milnor WR. **Hemodynamics**. 2nd ed. Baltimore, Maryland: Williams & Wilkins; 1989.
19. Fung Y-c. **Biomechanics: Mechanical Properties of Living Tissues**. Springer Science & Business Media; 2013.
20. Holzapfel GA, Ogden RW. **Biomechanics of Soft Tissue in Cardiovascular Systems**. Springer; 2014.
21. Humphrey JD. **Cardiovascular Solid Mechanics: Cells, Tissues, and Organs**. Springer Science & Business Media; 2013.
22. Ferruzzi J, Bersi MR, Uman S, Yanagisawa H, Humphrey JD. Decreased elastic energy storage, not increased material stiffness, characterizes central artery dysfunction in fibulin-5 deficiency independent of sex. **J Biomech Eng**. 2015; 137.
23. Smoljkić M, Vander Sloten J, Segers P, Famaey N. Non-invasive, energy-based assessment of patient-specific material properties of arterial tissue. **Biomech Model Mechanobiol**. 2015; 14:1045−1056.
24. Masson I, Beaussier H, Boutouyrie P, Laurent S, Humphrey JD, Zidi M. Carotid artery mechanical properties and stresses quantified using in vivo data from normotensive and hypertensive humans. **Biomech Model Mechanobiol**. 2011; 10:867−882.
25. Langewouters G, Wesseling K, Goedhard W. The static elastic properties of 45 human thoracic and 20 abdominal aortas in vitro and the parameters of a new model. **J Biomech**. 1984; 17:425−435.
26. Bramwell CJ, Hill A. The velocity of the pulse wave in man. **Proc R Soc Lond**. 1922; 93:298−306.
27. Avolio AP, Van Bortel LM, Boutouyrie P, et al. Role of pulse pressure amplification in arterial hypertension: experts' opinion and review of the data. **Hypertension**. 2009; 54:375−383 (Dallas, Tex: 1979).
28. Segers P, Rabben SI, De Backer J, et al. Functional analysis of the common carotid artery: relative distension differences over the vessel wall measured in vivo. **J Hypertens**. 2004; 22:973−981.
29. Bergel HD. The properties of blood vessels. In: Fung Y, Perrone N, Anliker M, eds. **Biomechanics, its Foundations and Objectives**. Englewood Cliffs, New Jersey: Prentice Hall; 1972:105−139.
30. Peterson LH, Jensen RE, Parnell J. Mechanical properties of arteries in vivo. **Circ Res**. 1960; 8:622−639.
31. Bercoff J, Tanter M, Fink M. Supersonic shear imaging: a new technique for soft tissue elasticity mapping. **IEEE Trans Ultrason Ferroelectr Freq Control**. 2004; 51:396−409.
32. Couade M, Pernot M, Prada C, et al. Quantitative assessment of arterial wall biomechanical properties using shear wave imaging. **Ultrasound Med Biol**. 2010; 36:1662−1676.
33. Marais L, Pernot M, Khettab H, et al. Arterial stiffness assessment by shear wave elastography and ultrafast pulse wave imaging: comparison with reference techniques in normotensives and hypertensives. **Ultrasound Med Biol**. 2019; 45:758−772.
34. Caenen A, Knight AE, Rouze NC, Bottenus NB, Segers P, Nightingale KR. Analysis of multiple shear wave modes in a nonlinear soft solid: experiments and finite element simulations with a tilted acoustic radiation force. **J Mech Behav Biomed Mater**. 2020; 107:103754.
35. Moens A. **Over de voortplantingssnelheid van den pols**. 1877 [On the speed of propagation of the pulse].
36. Korteweg DJ. **Over Voortplantings-Snelheid Van Golven in Elastische Buizen**. Van Doesburgh; 1878.
37. Bramwell JC, Hill AV. The velocity of pulse wave in man. **Proc R Soc Lond - Ser B Contain Pap a Biol Character**. 1922; 93:298−306.
38. Cuomo F, Roccabianca S, Dillon-Murphy D, Xiao N, Humphrey JD, Figueroa CA. Effects of age-associated regional changes in aortic

stiffness on human hemodynamics revealed by computational modeling. **PLoS One**. 2017; 12:e0173177.

39. Khir AW, O'Brien A, Gibbs JS, Parker KH. Determination of wave speed and wave separation in the arteries. **J Biomech**. 2001; 34:1145–1155.

40. Feng J, Khir AW. Determination of wave speed and wave separation in the arteries using diameter and velocity. **J Biomech**. 2010; 43:455–462.

41. Rabben SI, Stergiopulos N, Hellevik LR, et al. An ultrasound-based method for determining pulse wave velocity in superficial arteries. **J Biomech**. 2004; 37:1615–1622.

42. Laurent S, Cockcroft J, Van Bortel L, et al. Expert consensus document on arterial stiffness: methodological issues and clinical applications. **Eur Heart J**. 2006; 27:2588–2605.

43. Stergiopulos N, Meister JJ, Westerhof N. Simple and accurate way for estimating total and segmental arterial compliance: the pulse pressure method. **Ann Biomed Eng**. 1994; 22:392–397.

44. Salvi P, Scalise F, Rovina M, et al. Noninvasive estimation of aortic stiffness through different approaches. **Hypertension**. 2019; 74:117–129 (Dallas, Tex: 1979).

45. Grotenhuis HB, Westenberg JJ, Steendijk P, et al. Validation and reproducibility of aortic pulse wave velocity as assessed with velocity-encoded MRI. **J Magn Reson Imaging**. 2009; 30:521–526.

46. Ohyama Y, Ambale-Venkatesh B, Noda C, et al. Aortic arch pulse wave velocity assessed by magnetic resonance imaging as a predictor of incident cardiovascular events. **Hypertension**. 2017; 70:524–530.

47. Asmar R, Benetos A, Topouchian J, et al. Assessment of arterial distensibility by automatic pulse-wave velocity-measurement - validation and clinical-application studies. **Hypertension**. 1995; 26:485–490.

48. Wilkinson IB, Fuchs SA, Jansen IM, et al. Reproducibility of pulse wave velocity and augmentation index measured by pulse wave analysis. **J Hypertens**. 1998; 16:2079–2084.

49. Salvi P, Lio G, Labat C, Ricci E, Pannier B, Benetos A. Validation of a new non-invasive portable tonometer for determining arterial pressure wave and pulse wave velocity: the PulsePen device. **J Hypertens**. 2004; 22:2285–2293.

50. Segers P, Rietzschel ER, De Buyzere ML, et al. Noninvasive (input) impedance, pulse wave velocity, and wave reflection in healthy middle-aged men and women. **Hypertension**. 2007; 49:1248–1255.

51. Van Bortel LM, Laurent S, Boutouyrie P, et al. Expert consensus document on the measurement of aortic stiffness in daily practice using carotid-femoral pulse wave velocity. **J Hypertens**. 2012; 30:445–448.

52. Mattace-Raso FUS, Hofman A, Verwoert GC, et al. Determinants of pulse wave velocity in healthy people and in the presence of cardiovascular risk factors: 'establishing normal and reference values. **Eur Heart J**. 2010; 31:2338–2350.

53. Ben-Shlomo Y, Spears M, Boustred C, et al. Aortic pulse wave velocity improves cardiovascular event prediction: an individual participant meta-analysis of prospective observational data from 17,635 subjects. **J Am Coll Cardiol**. 2014; 63:636–646.

54. Trachet B, Reymond P, Kips J, et al. Numerical validation of a new method to assess aortic pulse wave velocity from a single recording of a brachial artery waveform with an occluding cuff. **Ann Biomed Eng**. 2010; 38:876–888.

55. Milan A, Zocaro G, Leone D, et al. Current assessment of pulse wave velocity: comprehensive review of validation studies. **J Hypertens**. 2019; 37:1547–1557.

56. Alivon M, Phuong TVD, Vignon V, et al. A novel device for measuring arterial stiffness using finger-toe pulse wave velocity: validation study of the pOpmetre (R). **Arch Cardiovasc Dis**. 2015; 108:227–234.

57. Yamashina A, Tomiyama H, Takeda K, et al. Validity, reproducibility, and clinical significance of noninvasive brachial-ankle pulse wave velocity measurement. **Hypertens Res**. 2002; 25:359–364.

58. Segers P, Rietzschel ER, Chirinos JA. How to measure arterial stiffness in humans. **Arterioscler Thromb Vasc Biol**. 2020; 40:1034–1043.

59. Shirai K, Utino J, Otsuka K, Takata M. A novel blood pressure-independent arterial wall stiffness parameter; cardio-ankle vascular index (CAVI). **J Atherosclerosis Thromb**. 2006; 13:101–107.

60. Spronck B, Avolio AP, Tan I, Butlin M, Reesink KD, Delhaas T. Arterial stiffness index beta and cardio-ankle vascular index inherently depend on blood pressure but can be readily corrected. **J Hypertens**. 2017; 35:98–104.

61. Parker KH, Jones CJ. Forward and backward running waves in the arteries: analysis using the method of characteristics. **J Biomech Eng**. 1990; 112:322–326.

62. Quail MA, Knight DS, Steeden JA, et al. Noninvasive pulmonary artery wave intensity analysis in pulmonary hypertension. **Am J Physiol Heart Circ Physiol**. 2015; 308:H1603–H1611.

63. Segers P, Swillens A, Taelman L, Vierendeels J. Wave reflection leads to over- and underestimation of local wave speed by the PU- and QA-loop methods: theoretical basis and solution to the problem. **Physiol Meas**. 2014; 35:847–861.

64. Borotti A, Li Y, Parker KH, Khir AW. Experimental evaluation of local wave speed in the presence of reflected waves. **J Biomech**. 2014; 47:87–95.

65. Alastruey J. Numerical assessment of time-domain methods for the estimation of local arterial pulse wave speed. **J Biomech**. 2011; 44:885–891.

66. Swillens A, Taelman L, Degroote J, Vierendeels J, Segers P. Comparison of non-invasive methods for measurement of local pulse wave velocity using FSI-simulations and in vivo data. **Ann Biomed Eng**. 2013; 41:1567–1578.

67. Campos Arias D, Stergiopulos N, Rodríguez Moliner T, Segers P. Mapping the site-specific accuracy of loop-based local pulse wave velocity estimation and reflection magnitude: a 1D arterial network model analysis. **Physiol Meas**. 2019; 40:075002.

68. Tanter M, Fink M. Ultrafast imaging in biomedical ultrasound. **IEEE Trans Ultrason Ferroelectr Freq Control**. 2014; 61:102–119.

69. Luo J, Li RX, Konofagou EE. Pulse wave imaging of the human carotid artery: an in vivo feasibility study. **IEEE Trans Ultrason Ferroelectr Freq Control**. 2012; 59:174–181.

70. Chemla D, Hébert J-L, Coirault C, et al. Total arterial compliance estimated by stroke volume-to-aortic pulse pressure ratio in humans. **Am J Physiol**. 1998; 274:H500–H505.

71. Randall OS, Westerhof N, van den Bos GC, Alexander B. Reliability of stroke volume to pulse pressure ratio for estimating and detecting changes in arterial compliance. **J Hypertens**. 1986; 4:S293–S296.

72. Liu Z, Brin K, Yin F. Estimation of total arterial compliance : an improved method and evaluation of current methods. **Am J Physiol**. 1986; 251:H588–H600.

73. Segers P, Verdonck P. Principles of vascular physiology. In: Lanzer P, Topol EJ, eds. **Pan Vascular Medicine Integrated Clinical Management**. Heidelberg: Springer-Verlag; 2002.

74. Segers P, Stergiopulos N, Westerhof N. Relation of effective arterial elastance to arterial system properties. **Am J Physiol Heart Circ Physiol**. 2002; 282:H1041–H1046.

75. Chirinos JA, Rietzschel ER, Shiva-Kumar P, et al. Effective arterial elastance is insensitive to pulsatile arterial load. **Hypertension**. 2014; 64:1022–1031 (Dallas, Tex: 1979).

Ambulatory measurement of pulsatile hemodynamics

Thomas Weber[1], Siegfried Wassertheurer[2], Bernhard Hametner[2], Christopher C. Mayer[2], Martin Bachler[2], Athanase Protogerou[3] and James E. Sharman[4]

[1]Cardiology Department, Klinikum Wels-Grieskirchen, Wels, Paracelsus Medical University, Salzburg, Austria; [2]Center for Health & Bioresources, Austrian Institute of Technology (AIT), Vienna, Austria; [3]Cardiovascular Prevention and Research Unit, Clinic-Laboratory of Pathophysiology, Laiko Hospital, Medical School, National and Kapodistrian University of Athens, Athens, Greece; [4]Menzies Institute for Medical Research, University of Tasmania, Hobart, TAS, Australia

Ambulatory 24-h measurement of brachial blood pressure and heart rate

Although office blood pressure (BP), admittedly through its time-honored wealth of outcome data, particularly related to drug treatment of hypertension, is still the basis of the management of high BP,[1,2] out-of-office measurement of BP (24 h ambulatory BP monitoring—24 h ABPM and home BP monitoring) is increasingly recognized and recommended in current guidelines.[1,2] Compared to office BP, 24 h ABPM has numerous advantages,[3] including but not limited to the following: 24 h ABPM provides a much larger number of readings for a better assessment of an individual's BP level, with reproducible average 24 h, daytime and nighttime values, identifies white coat and masked phenomena in untreated and—less reproducible—in treated individuals,[4] provides a BP profile in the individual's usual daily environment, demonstrates nocturnal hypertension and dipping patterns, assesses BP variability over 24 h, and assesses the efficacy of antihypertensive drugs over 24 h. These benefits translate into a superior prognostic value of 24 h ABPM, as compared to office BP, as studies, beginning in the 1960s[5] and up to the present,[6] have repeatedly shown. Recently, an analysis of the International Database on Ambulatory Blood Pressure in Relation to Cardiovascular Outcome (IDACO), including 13 population studies in Europe, Asia, and South America and 11,135 participants,[6] provided compelling evidence that 24 h ABPM provides additive prognostic information to office BP, corroborating previous findings.[7] Accordingly, 24 h ABPM is recommended in the most recent versions of Guidelines on the Management of Hypertension globally, for instance, in Europe,[1] in the US,[2] and Japan.[8] Within this context, nocturnal BP and the daytime/nighttime ratio ("dipping") seems to be particularly important.[3,6,9] During healthy nocturnal sleep, a marked shift in autonomic balance occurs, with an increase in parasympathetic activity and a reduction in sympathetic cardiac/cardiovascular modulation, giving rise to a decrease in BP and heart rate by 10%−20% compared with daytime average.[3,10]

Although regularly assessed during 24 h ABPM, 24 h heart rate and daytime/nighttime ratio of heart rate have been investigated less often than BP. In an analysis from the IDACO registry,[11] 24 h and nighttime heart rate as well as night/day ratio of heart rate independently predicted all-cause mortality. The results regarding the prognostic relevance of heart rate "dipping" were confirmed in the Spanish ABPM registry on data from 56,901 patients.[12] Interestingly, in most studies investigating the prognostic role of 24 h ABPM, heart rate was not taken into consideration in the statistical models.[6,13,14]

Pulsatile and steady state hemodynamics

Due to the nature of the pump in the human circulation (the heart), pressure and flow in the arterial circulation are pulsatile, rather than steady. During the first decades of BP research, the focus was mean arterial pressure (MAP) and diastolic BP (DBP), with the very first successful trial in patients with high DBP (averaging 115−129 mm Hg) published in 1967.[15] At that time, hemodynamic phenomena were often simplified (ignoring atrial pressure) as "cardiac output = MAP/systemic vascular resistance

(SVR)," assuming a steady-state circulation. This approach is not only widely used in clinical medicine but also has a long track record in hypertension research,[16] up to recent years.[17]

However, for a more comprehensive view, one has to take the pulsatile phenomena, arising from the pulsatile pump and its interaction with the arterial system, into account. The simplest measurement is *brachial pulse pressure (bPP)*, the difference between brachial systolic (SBP) and DBP. bPP is convenient and available with every single BP measurement, but only a crude measurement of pulsatile hemodynamics. Brachial PP increases with age and with stiffening of the aorta and the large arteries, and with increasing wave reflections.[18] Brachial PP is more closely related to cardiovascular risk in middle-aged and elderly individuals than other BP components,[19] and can be used in the diagnostic workup of patients with unexplained exertional dyspnea.[20] Brachial PP > 60 mm Hg indicates asymptomatic hypertension-mediated organ damage in older people, according to the 2018 European Society of Hypertension (ESH)/European Society of Cardiology (ESC) guidelines for the management of arterial hypertension.[1] However, bPP has several limitations: it depends not only on arterial (PP increases with increased arterial stiffness/wave reflections) but also on cardiac function (PP decreases with severely impaired systolic function),[21] which leads to an inverse relationship (i.e., a lower PP is associated with a worse prognosis) with outcomes in patients with severely impaired systolic function[22]; PP measured at the brachial artery does not exactly reflect PP at the ascending aorta (*aortic = central PP—cPP*), with bPP being higher ("amplified") than aoPP in most people. The *pulse pressure amplification (PPA)*,[23] expressed as a difference or ratio between aoPP and bPP, depends among other factors on aortic stiffness, cardiac function, heart rate, and arterial geometry, as discussed below.
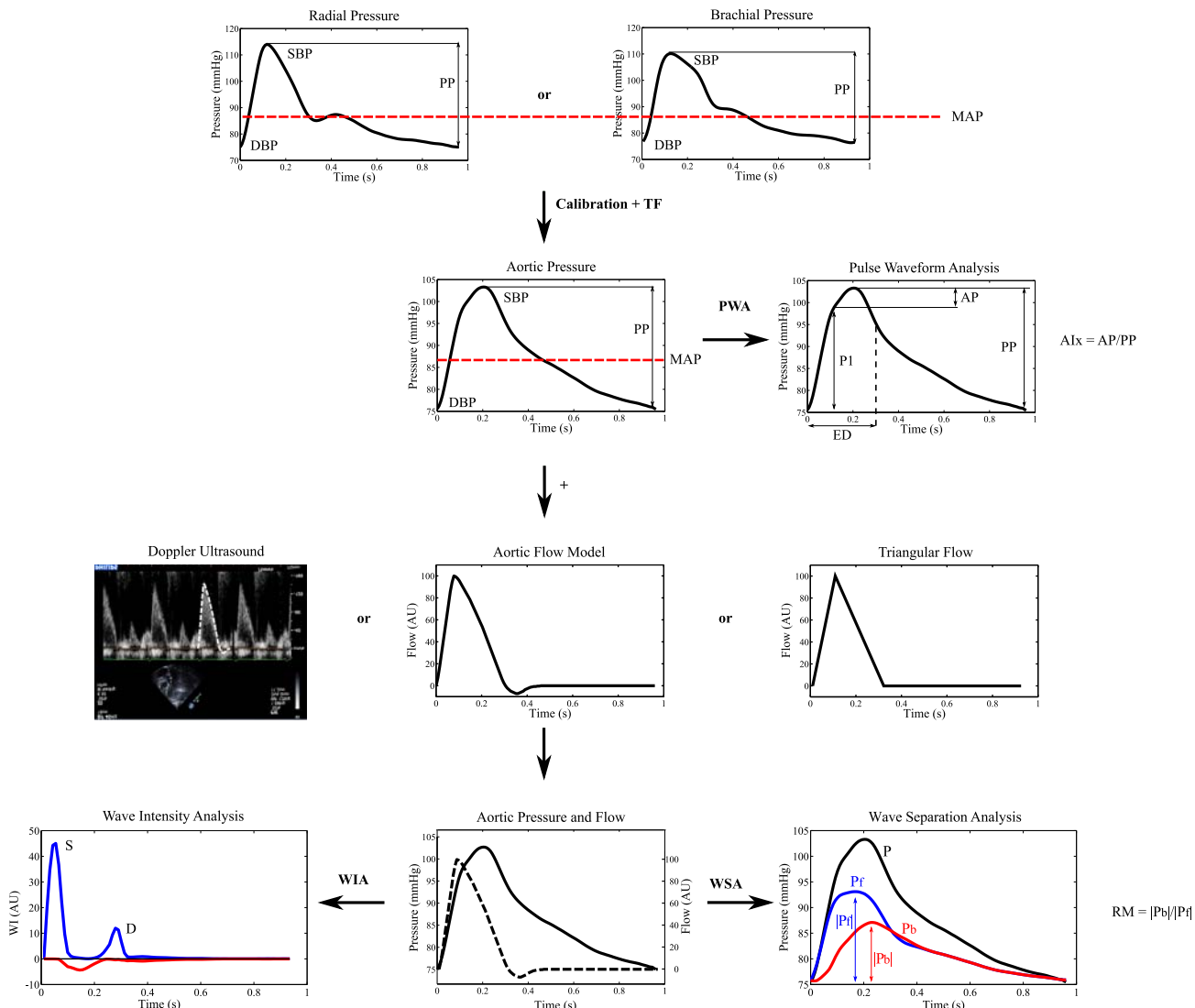
More sophisticated measurements of pulsatile hemodynamics beyond brachial and central pressures (cSBP, cPP) have become available, e.g., estimates of forward and reflected waves, and measures of arterial stiffness. A wide array of more complex models of the circulation are discussed in depth in other chapters of this book and elsewhere,[24] but below we focus on measurements available from current 24 h ABPM techniques.

The classical theory of pulsatile hemodynamics, i.e., the Windkessel model, fails to take into consideration the concept of pressure wave reflections, which is essential for the understanding of the peripheral circulation. Indeed, whereas *cSBP* and *cPP* are lower than their brachial counterparts (by anywhere up to 30+ mm Hg),[25] MAP and DBP decrease by only 1−2 mm Hg from the aorta to peripheral arteries.[24] As a consequence, cSBP and cPP are—compared to bSBP and bPP—more relevant to vital organs like the heart, brain, and kidney, and have been

closer associated with cardiovascular outcomes in some,[26,27] but not all studies.[28,29] These are direct consequences of the fact that pressure and flow waves, which are generated with each heartbeat and propagate toward peripheral sites, are also reflected backwards (toward the heart) for a combination of reasons (impedance mismatch, stiffness gradient, presence of bifurcations, abrupt diameter gradient in arterioles). Reflected waves merge with the antegrade waves at various phases during the cardiac cycle,[24] with pressure waves adding to the antegrade wave, and flow waves subtracting from the incident wave.[24] With aging, waves travel faster due to an increase in arterial stiffness. With vasoconstriction, the amplitude of the reflected pressure waves increases. As a net result of both of these processes, cardiac load and oxygen consumption is increased, resulting in an imbalance toward myocardial ischemia and an impairment of (mainly diastolic) left ventricular function.[30]

Wave reflection can be quantified from pressure waveforms (pulse waveform analysis—PWA), or from simultaneous analysis of pressure and flow waves (wave separation analysis—WSA)—Fig. 8.1. The technique of PWA is based on the mathematical identification of an inflection point on the pressure waveform, which is thought to represent the beginning of the arrival of reflected waves at the ascending aorta.[24] The pressure rise from the inflection point to the systolic peak of the pressure curve is named "*Pressure Augmentation—AP*," and the ratio AP/cPP is named "*Augmentation Index—AIx*." Thus, AP and AIx are thought to reflect and quantify the influence of wave reflection on the central aortic waveform. Using WSA, the amplitudes of the *forward wave* (*Pf*; the pressure wave generated by the heart) and the *backward wave* (*Pb*; the reflected pressure wave) can be derived, as well as their ratio (*Reflection Magnitude RM*; Pb/Pf).

Arterial stiffness (particularly *aortic stiffness*) can be measured in vivo because the speed of propagation of pulse waves (pressure or flow or distension) in an artery is directly related to the mechanical properties of the vessel (the stiffer the vessel, the higher the velocity).[31] Therefore, when the time delay between the arrival of a pulse wave at two locations (commonly the carotid artery and the femoral artery), and the distance between both locations are measured, *pulse wave velocity (PWV)* as the most robust measure of arterial stiffness[31] can easily be calculated. As the effects of the aging process (i.e., loss of elasticity, increased stiffening) are most pronounced in the human aorta as opposed to the muscular arteries,[32] the aortic pathway should be included in the measurement. In addition, the prognostic value is largely limited to pathways including the aorta,[33] such as carotid-femoral PWV (cfPWV). cfPWV is a strong independent predictor of cardiovascular events in different groups of high and low-risk patients and in the general population.[34] Obviously,

FIGURE 8.1 Methods to quantify pulsatile hemodynamics. *Top line*: recording of signal-averaged radial or brachial pressure waveforms with tonometry or brachial cuff. *Second line*: following calibration with brachial pressures, aortic waveforms are calculated with a TF. Pulse waveform analysis, based on pressure signals alone, yields measures of the first (P1) and second (P2) systolic peaks for computation of augmented pressure and augmentation index (AP, AIx). *Third line*: flow waveforms are obtained, either with Doppler recording of LV outflow (which equals aortic inflow), or as model-driven flow or triangular flow as a proxy. *Bottom line*: combined and time-aligned analysis of a pressure-flow pair is used for wave separation analysis, wave intensity analysis, and other analytical approaches. *AIx*, augmentation index; *AP*, augmented pressure; *DBP*, diastolic blood pressure; *MAP*, mean arterial pressure; *Pb*, amplitude backward wave; *Pf*, amplitude forward wave; *PP*, pulse pressure; *PWA*, pulse waveform analysis; *RM*, reflection magnitude; *SBP*, systolic blood pressure; *TF*, transfer function; *WIA*, wave intensity analysis; *WSA*, wave separation analysis. WSA, wave separation analysis. Courtesy of Bernhard Hametner, reproduced with permission from Weber T, Chirinos J. Pulsatile haemodynamics in heart failure. Eur Heart J 2018;39:3847−3854.

24 h ambulatory measurement of cfPWV is not feasible. Technical[35,36] and mathematical[37] solutions to provide estimates of aortic PWV, based on brachial cuff recordings, have been developed. Although smaller preliminary studies in patients with chronic kidney disease, showing a relationship with cardiovascular events,[38,39] are promising, there is no consensus regarding the potential value of these aoPWV estimates at present.[40]

Techniques and devices for 24-h ambulatory measurement of pulsatile (and steady state) hemodynamics

For office measurements of cBP and wave reflections, most often brachial or radial tonometry was the basis (Fig. 8.1) of the next steps (calibration, transfer functions, PWA, WSA, etc). In one study, the daytime variability of parameters

related to wave reflection has been assessed with tonometry,[41] and shown that it is the main cause of circadian variability of PPA.[42] However, in general, the feasibility of tonometry for ambulatory recordings is quite limited. Therefore, alternatives have been developed, which rely on acquisition of waveforms with a brachial cuff[35,43–45] or with a wrist-watch like tonometer.[46] Table 8.1 provides an overview of current devices.

24-h variability ("dipping") of pulsatile and steady state hemodynamics

Brachial BP and heart rate in healthy individuals are higher during daytime and decrease during nocturnal sleep ("dipping").[47] Circadian variations in steady-state hemodynamics have been repeatedly assessed, using invasive[48–50] and noninvasive[51–54] methods, in healthy individuals,[49,52,54] in patients with so-called essential hypertension,[48–51,53] and in patients with chronic kidney disease.[54] In general, it was observed that SBP, DBP, MAP, and heart rate decreased during nighttime.[48–54] CO decreased during nighttime in most studies,[48,50,52,54] and was unchanged in some.[49,53,54] Results

for SVR were more variable and showed an increase,[51,52] a decrease,[48,49,53,54] or no consistent changes[54] with a peak value at 08.00 a.m.[50]. These differences may be related to measurement techniques or the influence of disease.[54]

Most interestingly, the diurnal variability, i.e., "dipping," of bSBP and cSBP are different to a smaller or larger amount. Using the BPro device, in a trial of two different drugs for BP lowering,[55] 24 h curves for bSBP and cSBP were largely parallel with preserved nocturnal dipping. However, the amount of nocturnal dip in SBP was 8.2% for bSBP and 6.9% for cSBP, respectively. Adjustment for the nocturnal change in heart rate attenuated the difference. In a trial in normotensives and hypertensives, using the same device, the nocturnal decrease of amplification (the difference between cSBP and bSBP) was mainly driven by the day-night difference in heart rate.[56] Similar results were obtained with the BPLab device in a multicenter registry,[57] with SBP amplification being 11.6 mm Hg at daytime and 8.8 mm Hg at nighttime.

When the Mobilograph device is used, a particular technical aspect needs to be taken into account: for calibration of the initially acquired waveforms, brachial BP is used. Due to the well-established systematic underestimation

TABLE 8.1 Commercially available device for 24 h measurement of central hemodynamics.

Name of device	Manufacturer	Type of device	Algorithms used	Parameters displayed (selection) and technical validation studies	FDA 510(k) clearance
Arteriograph 24	Tensiomed, Budapest, Hungary	Brachial cuff	Suprasystolic signals	Brachial SBP and DBP, heart rate,[88] MAP, central SBP,[89] central PP, AIx,[90,91] aoPWV[35]	No
Bpro	Healthstats, Singapore	Wrist-worn tonometer	Tonometry, n-point moving average algorithm	Brachial SBP and DBP,[92] MAP, cSBP[46,93]	Yes
Mobilograph PWA	IEM, Stolberg, Germany	Brachial cuff	Transfer function, PWA, WSA, nonlinear regression (estimated aoPWV)	Brachial SBP and DBP,[94–96] heart rate,[88] MAP,[43] central SBP,[43,97,98] central PP, AIx,[99,100] AP, Pb,[101] Pf, RM, SV,[102] CO,[103] SVR, estimated aoPWV[36,104]	Yes
Oscar 2 with SphygmoCor inside	AtCormedical, Naperville, IL, and SunTech Medical, Morrisville, NC, USA	Brachial cuff	Transfer function, PWA	Brachial SBP and DBP,[105,106] heart rate, MAP, central SBP, central PP, AIx, AP	Yes
Vasotens BPlab	Petr Telegin Ltd, Nizhny Novgorod, Russia	Brachial cuff	Transfer function, PWA, transition time between first and second wave (PWV)	Brachial SBP and DBP,[107] heart rate, MAP, central SBP,[108] central PP, AIx,[108] AP, Pb, Pf, RM, PP amplification, aoPWV[109]	No

Aix, augmentation index; *AP*, augmented pressure; *CO*, cardiac output; *DBP*, diastolic blood pressure; *estimated aoPWV*, estimated aortic pulse wave velocity; *MAP*, mean arterial pressure; *Pb*, backward wave amplitude; *Pf*, forward wave amplitude; *PP*, pulse pressure; *RM*, reflection magnitude; *SBP*, systolic blood pressure; *SV*, stroke volume; *SVR*, systemic vascular resistance.

of true (i.e., invasive) bSBP by noninvasive cuff-based measurement,[25] waveform calibration with noninvasive bSBP will most often result in underestimation of cSBP, as compared to true (invasively measured) cSBP, whereas SBP and PP amplification will be preserved. In contrast, MAP can be determined directly with oscillometry as the point of maximal oscillations of cuff pressure during gradual cuff deflation.[43,58,59] As a consequence, waveform calibration with MAP (and DBP) may result in a better estimate of true (=invasive) cSBP.[60–62] With MAP/DBP calibration, the true level of SBP amplification can be *apparently* distorted (i.e., negative/inverse) because usually cuff-measured bSBP (and not invasive bSBP) is the comparator. In other words, the apparent inverse amplification is the result of a correct measurement of cSBP and an underestimation of bSBP by cuff measurement.[60] Theoretically, true (=invasive) bSBP can be calculated from MAP/DBP calibrated cSBP and SBP/DBP calibrated amplification,[63] but this approach has never been tested clinically. Preliminary results suggest that this technical issue translates into clinical outcomes (see below), favoring MAP/DBP calibration. It has to be acknowledged, however, that the concept does not hold for all cuff-based devices.[64]

Data from the SAFAR study, using the Mobilograph device and SBP/DBP calibration, show that SBP amplification is higher during daytime, as compared to nighttime.[65] In a random sample of 167 participants from Uruguay, the difference between bSBP and cSBP was 14 mm Hg at daytime and 9.7 mm Hg at nighttime.[66] In 136 untreated adolescents and young adults from Greece,[67] virtually the same results were obtained, with a difference between bSBP and cSBP of 16.3 mm Hg at daytime and 10.5 mm Hg at nighttime. In the same population, also the results of MAP/DBP calibration were reported: due to the different calibration, cSBP was apparently *higher* than bSBP, particularly during nighttime, and dipping of cSBP (MAP/DBP) was absent (even slightly reversed). In a preliminary analysis[68] from a global academic research consortium (international 24 h aortic BP consortium—i24abc), based on measurements in more than 2500 healthy individuals from 20 centers in 14 countries, analysis of nocturnal "dipping" was stratified across age groups. For bSBP, daytime-nighttime difference was between 10% and 20% in the youngest age group (i.e., normal[3]), and smaller in the oldest age groups. In contrast, cSBP (MAP/DBP calibration) displayed only minor daytime-nighttime changes. Fig. 8.2 shows 24 h profiles of bSBP and cSBP in a random sample of 500 individuals from the authors' institutions.

Apart from SBP, most other hemodynamic parameters exhibit circadian variability. Using the Mobilograph device, Boggia et al. were among the first to describe diurnal profiles of pulsatile hemodynamics, using a sample of 167 middle-aged and elderly Latin Americans. During nighttime, a decrease of cSBP, DBP, heart rate, and PPA, and an increase
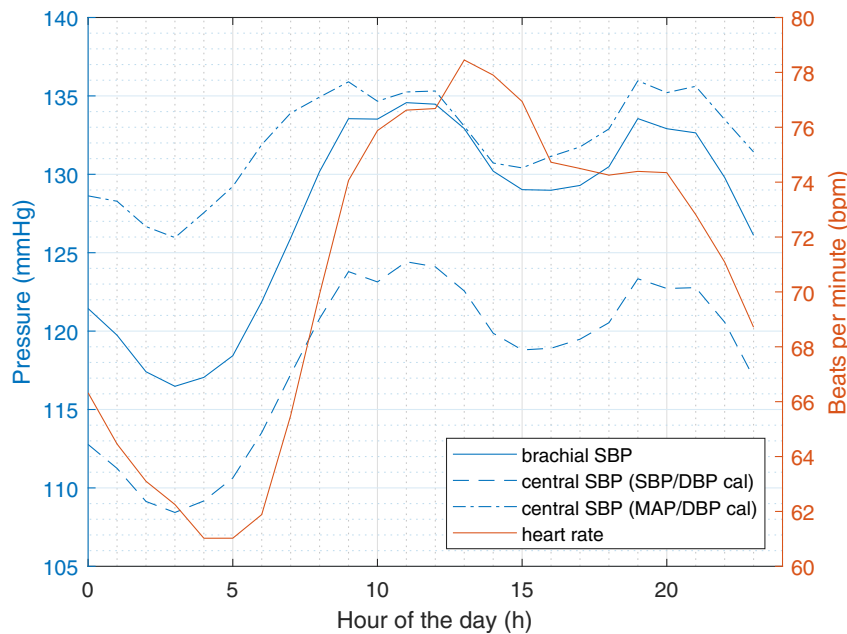
of cPP and AIx were observed. These findings were later verified and further extended by data published from the SAFAR study.[69] Moreover, in 136 adolescents and young adults from Greece, Ntineri et al.[67] confirmed the results for pulsatile hemodynamics, and extended them to steady-state hemodynamics: they observed an increase in SV and a decrease on SVR and CO at nighttime. Fig. 8.3 shows 24 h profiles of selected steady-state and pulsatile hemodynamics in a random sample of 500 individuals from the authors' institutions.

As the change in body position is one of the obvious differences between daytime and nighttime, the changes in 24 h ABPM profiles are contrasted to those during active standing[70] and head-up tilt test.[71] It appears that daytime-nighttime variability of most hemodynamic measures indeed mirrors changes induced by active or passive (tilt-test) standing—Table 8.2. These results were confirmed and extended in a randomized cross over study with assessment of bBP and aortic pressure waveforms in the sitting and supine position in randomized order in 61 subjects. Whereas MAP did not change upon changing of body position, bPP, cPP, AIx, and AIx75 significantly increased in the supine position, whereas PPA decreased. The decrease in PPA was mainly driven by changes in pressure wave reflections.[72]
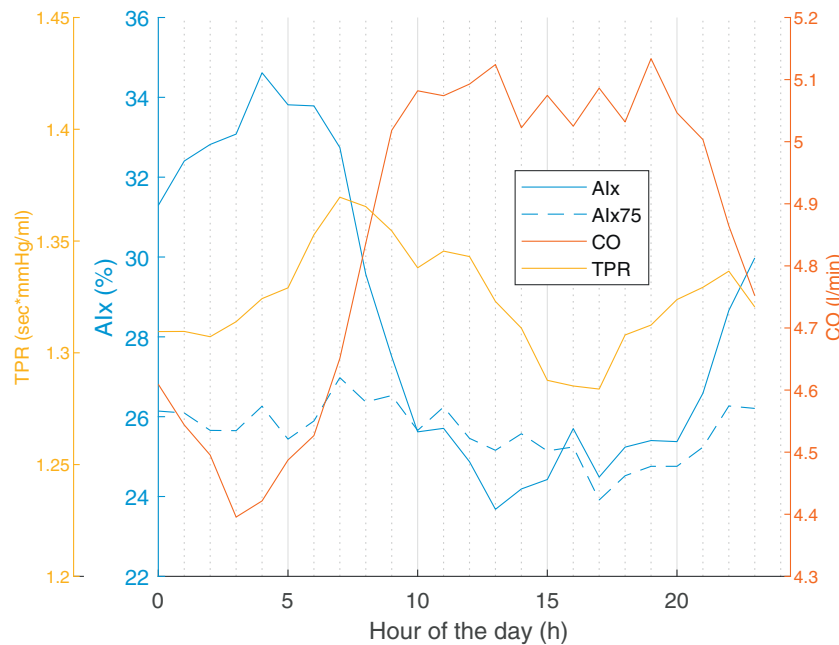
24-h ambulatory measurement of pulsatile (and steady state) hemodynamics—clinical studies

Regarding office-based measurements, a recent meta-analysis suggested that cBP is more strongly related to hypertension-mediated organ damage (left ventricular mass, carotid intima media thickness, and PWV) than bBP.[73] Along the same lines, 24 h cSBP was more closely associated with left ventricular mass and left ventricular hypertrophy in the SAFAR study (a single center study from Greece)[65] and in a multicenter study,[74] performed in seven European centers, as compared to brachial office and brachial 24 h SBP. The same trend, albeit without reaching statistical significance, was available in another small single center study from Spain.[75] In all studies, the same device (Mobilograph), has been used, and in all three studies, the superiority of 24 h cSBP was dependent on a technical issue, i.e., MAP/DBP calibration. Virtually the same results (a closer association with 24 h cSBP, as compared to 24 h bSBP; the results are confined to the MAP/DBP calibration method) have been obtained for left ventricular diastolic dysfunction.[76] Moreover, central BP variability, investigated with the Mobilograph device, has been shown to be superior to brachial BP variability in terms of association either with cardiac[77] or carotid[78] damage. In a multicenter registry using the BPLab device,[79] 24 h cSBP and cPP

FIGURE 8.2 24-h profiles of brachial and central systolic blood pressure as well as heart rate in a random sample of 500 adults. Daytime-nighttime difference ("dipping") can be easily seen for brachial systolic blood pressure (SBP) and heart rate. Central SBP (systolic-diastolic BP calibration) by and large parallels brachial SBP, whereas "dipping" is much smaller for central SBP (mean-diastolic BP calibration).


FIGURE 8.3 24-h profiles of steady-state and pulsatile hemodynamics in a random sample of 500 adults. During nighttime, there is a clear increase in AIx, a small increase in AIx75, and a decrease in CO, as compared to daytime. There are no consistant daytime-nighttime changes for TPR, with peak values in the morning hours. *AIx*, Augmentation Index; *AIx75*, Augmentation Index, normalized for heart rate 75; *CO*, cardiac output; *TPR*, total peripheral resistance.

showed a numerically closer association with LV hypertrophy, as compared to 24 h bSBP and bPP.

In patients with end-stage renal disease undergoing hemodialysis, ambulatory 48 h aoPWV, estimated with a nonlinear regression which includes age, central SBP, and waveform characteristics, was an independent predictor of cardiovascular events and all-cause mortality.[39] These results were confirmed in another small study in dialysis patients.[38]

24-h ambulatory measurement of pulsatile (and steady state) hemodynamics—drug trials

Office-based studies successfully demonstrated that drug-induced changes in cSBP may be different from changes in bSBP.[80−82] For 24 h cBP, such results are currently missing. Changes in 24 h cSBP in most trials paralleled

TABLE 8.2 Comparison of hemodynamic changes (brachial and central blood pressure, steady-state and pulsatile hemodynamics) during 24 h ambulatory monitoring, passive (tilt table test[71]) and active standing.[70]

Parameter	Change ABPM from daytime to nighttime	Change TT from supine to standing	Change AS from supine to standing Y/O
Brachial (radial–tilt test) systolic blood pressure (SBP)	⇓⇓	↓	↓/⇔
Diastolic blood pressure (DBP)	⇓⇓	↑	↑/↑
Mean arterial pressure (MAP)	⇓⇓		↑/⇑
Brachial (radial–tilt test) pulse pressure (PP)	⇔	⇓	⇓/↓
Heart rate	⇓⇓	⇑⇑	⇑⇑/⇑
Aortic SBP (SBP/DBP calibration)	⇓	↓	
Aortic SBP (MAP/DBP calibration)	⇔/↓		
SBP amplification (SBP/DBP calibration)	↓		
SBP amplification (MAP/DBP calibration)	⇓⇓		
Aortic PP (SBP/DBP calibration)	⇑	⇓	⇓
Aortic PP (MAP/DBP calibration)	⇑⇑		
Augmentation index (AIx)	↑/⇑	⇓⇓	⇓⇓/⇓
AIx75	↓/⇔	⇓	
Augmentation pressure (AP)	⇑⇑	⇓⇓	
Forward wave amplitude (Pf)	⇑/↑		↓/⇔
Backward wave amplitude (Pb)	⇑⇑/⇑		⇓/↓
Reflection magnitude (RM)	⇑/↑		↓/↓
Stroke volume (SV)	⇑/↑	⇓	⇓⇓/⇓
Cardiac output (CO)	↓/⇔	⇓	⇓/↓
Systemic vascular resistance (SVR)	↓/⇔	⇑	↑/↑

O, old; Y, young; other abbreviations see Table 8.1.

changes in bSBP, for instance, in a study comparing Sacubitril/Valsartan and Olmesartan in elderly patients with isolated systolic hypertension,[83] in a study comparing Nebivolol and Olmesartan in patients with acute ischemic stroke,[84] or in a study comparing the hemodynamic effects of Empagliflozin with placebo in patients with type 2 diabetes mellitus.[85]

Summary and outlook

Recent advances in technology enable 24 h measurement not only of brachial BP and heart rate but also of steady-state and pulsatile hemodynamics, the latter including central hemodynamics, antegrade and reflected waves. With technical validation rapidly progressing, these measurements can be performed in daily routine and even under unusual conditions, like long-term space flights.[86] 24 h hemodynamics may find their way into physiological, pharmacological, and clinical research and, finally, clinical routine, if important prerequisites can be fulfilled: (1) proof of (added) prognostic value; (2) establishment of reference values, which are currently only available for office-based measurements[87]; (3) development of treatment strategies, based on the 24 h ambulatory hemodynamic measurements (personalized medicine); and (4) proof of medical and economic superiority of these strategies.

References

1. Williams B, Mancia G, Spiering W, et al. 2018 practice guidelines for the management of arterial hypertension of the European Society of Hypertension and the European Society of Cardiology: ESH/ESC task force for the management of arterial hypertension. **J Hypertens**. 2018; 36:2284−2309.
2. Whelton PK, Carey RM, Aronow WS, et al. 2017 ACC/AHA/AAPA/ABC/ACPM/AGS/APhA/ASH/ASPC/NMA/PCNA guideline for the prevention, detection, evaluation, and management of high blood pressure in adults: a report of the American College of Cardiology/American Heart Association task force on clinical practice guidelines. **J Am Coll Cardiol**. 2018; 71:e127−e248.
3. Parati G, Stergiou G, O'Brien E, et al. European Society of Hypertension practice guidelines for ambulatory blood pressure monitoring. **J Hypertens**. 2014; 32:1359−1366.
4. Mancia G, Facchetti R, Cuspidi C, Bombelli M, Corrao G, Grassi G. Limited reproducibility of MUCH and WUCH: evidence from the ELSA study. **Eur Heart J**. 2020; 41:1565−1571.
5. Sokolow M, Werdegar D, Kain HK, Hinman AT. Relationship between level of blood pressure measured casually and by portable recorders and severity of complications in essential hypertension. **Circulation**. 1966; 34:279−298.
6. Yang WY, Zhang ZY, Staessen JA, International Database on Ambulatory Blood Pressure in Relation to Cardiovascular Outcomes Investigators. Blood pressure indexes associated with mortality and cardiovascular outcomes-reply. **J Am Med Assoc**. 2019; 322:2343−2344.
7. Dolan E, Stanton A, Thijs L, et al. Superiority of ambulatory over clinic blood pressure measurement in predicting mortality: the Dublin outcome study. **Hypertension**. 2005; 46:156−161.
8. Umemura S, Arima H, Arima S, et al. The Japanese Society of Hypertension Guidelines for the Management of Hypertension (JSH 2019). **Hypertens Res**. 2019; 42:1235−1481.
9. Hansen TW, Li Y, Boggia J, Thijs L, Richart T, Staessen JA. Predictive role of the nighttime blood pressure. **Hypertension**. 2011; 57:3−10.
10. Mancia G, Ferrari A, Gregorini L, et al. Blood pressure and heart rate variabilities in normotensive and hypertensive human beings. **Circ Res**. 1983; 53:96−104.
11. Hansen TW, Thijs L, Boggia J, et al. Prognostic value of ambulatory heart rate revisited in 6928 subjects from 6 populations. **Hypertension**. 2008; 52:229−235.
12. Bohm M, Schwantke I, Mahfoud F, et al. Association of clinic and ambulatory heart rate parameters with mortality in hypertension. **J Hypertens**. 2020; 38:2416−2426.
13. Boggia J, Li Y, Thijs L, Hansen TW, Kikuya M, Bjorklund-Bodegard K, Richart T, Ohkubo T, Kuznetsova T, Torp-Pedersen C, Lind L, Ibsen H, Imai Y, Wang J, Sandoya E, O'Brien E. Staessen JA and International Database on Ambulatory blood pressure monitoring in relation to Cardiovascular Outcomes investigators. Prognostic accuracy of day versus night ambulatory blood pressure: a cohort study. **Lancet**. 2007; 370:1219−1229.
14. Ohkubo T, Hozawa A, Yamaguchi J, Kikuya M, Ohmori K, Michimata M, Matsubara M, Hashimoto J, Hoshi H, Araki T, Tsuji I, Satoh H, Hisamichi S, Imai Y. Prognostic significance of the nocturnal decline in blood pressure in individuals with and without high 24-h blood pressure: the Ohasama study. **J Hypertens**. 2002; 20, 2183-1289.
15. Effects of treatment on morbidity in hypertension. Results in patients with diastolic blood pressures averaging 115 through 129 mm Hg. **J Am Med Assoc**. 1967; 202:1028−1034.
16. Eich RH, Cuddy RP, Smulyan H, Lyons RH. Hemodynamics in labile hypertension. A follow-up study. **Circulation**. 1966; 34:299−307.
17. Park C, Fraser A, Howe LD, et al. Elevated blood pressure in adolescence is attributable to a combination of elevated cardiac output and total peripheral resistance. **Hypertension**. 2018; 72:1103−1108.
18. Namasivayam M, McDonnell BJ, McEniery CM, O'Rourke MF. Does wave reflection dominate age-related change in aortic blood pressure across the human life span? **Hypertension**. 2009; 53:979−985.
19. Franklin SS, Larson MG, Khan SA, et al. Does the relation of blood pressure to coronary heart disease risk change with aging? The Framingham Heart Study. **Circulation**. 2001; 103:1245−1249.
20. Weber T, Wassertheurer S, O'Rourke MF, et al. Pulsatile hemodynamics in patients with exertional dyspnea: potentially of value in the diagnostic evaluation of suspected heart failure with preserved ejection fraction. **J Am Coll Cardiol**. 2013; 61:1874−1883.
21. Weber T, Chirinos JA. Pulsatile arterial haemodynamics in heart failure. **Eur Heart J**. 2018; 39:3847−3854.
22. Regnault V, Lagrange J, Pizard A, et al. Opposite predictive value of pulse pressure and aortic pulse wave velocity on heart failure with reduced left ventricular ejection fraction: insights from an Eplerenone Post-Acute Myocardial Infarction Heart Failure Efficacy and

Survival Study (EPHESUS) substudy. **Hypertension**. 2014; 63:105−111.

23. Avolio AP, Van Bortel LM, Boutouyrie P, et al. Role of pulse pressure amplification in arterial hypertension: experts' opinion and review of the data. **Hypertension**. 2009; 54:375−383.

24. Nichols WW, ORourke MF, Vlachopoulos C. **McDonald's Blood Flow in Arteries**. London: Hodder Arnold; 2011.

25. Picone DS, Schultz MG, Otahal P, et al. Accuracy of cuff-measured blood pressure: systematic reviews and meta-analyses. **J Am Coll Cardiol**. 2017; 70:572−586.

26. Safar ME, Blacher J, Pannier B, et al. Central pulse pressure and mortality in end-stage renal disease. **Hypertension**. 2002; 39:735−738.

27. Pini R, Cavallini MC, Bencini F, et al. Cardiovascular remodeling is greater in isolated systolic hypertension than in diastolic hypertension in older adults: the Insufficienza Cardiaca negli Anziani Residenti (ICARE) a Dicomano Study. **J Am Coll Cardiol**. 2002; 40:1283−1289.

28. McEniery CM, Cockcroft JR, Roman MJ, Franklin SS, Wilkinson IB. Central blood pressure: current evidence and clinical importance. **Eur Heart J**. 2014; 35:1719−1725.

29. Huang QF, Aparicio LS, Thijs L, et al. Cardiovascular end points and mortality are not closer associated with central than peripheral pulsatile blood pressure components. **Hypertension**. 2020; 76:350−358.

30. Vlachopoulos C, Xaplanteris P, Aboyans V, et al. The role of vascular biomarkers for primary and secondary prevention. A position paper from the European Society of Cardiology working group on peripheral circulation: Endorsed by the Association for Research into Arterial Structure and Physiology (ARTERY) Society. **Atherosclerosis**. 2015; 241:507−532.

31. Laurent S, Cockcroft J, Van Bortel L, et al. Expert consensus document on arterial stiffness: methodological issues and clinical applications. **Eur Heart J**. 2006; 27:2588−2605.

32. O'Rourke MF, Hashimoto J. Mechanical factors in arterial aging: a clinical perspective. **J Am Coll Cardiol**. 2007; 50:1−13.

33. Pannier B, Guerin AP, Marchais SJ, Safar ME, London GM. Stiffness of capacitive and conduit arteries: prognostic significance for end-stage renal disease patients. **Hypertension**. 2005; 45:592−596.

34. Ben-Shlomo Y, Spears M, Boustred C, et al. Aortic pulse wave velocity improves cardiovascular event prediction: an individual participant meta-analysis of prospective observational data from 17,635 subjects. **J Am Coll Cardiol**. 2014; 63:636−646.

35. Horvath IG, Nemeth A, Lenkey Z, et al. Invasive validation of a new oscillometric device (Arteriograph) for measuring augmentation index, central blood pressure and aortic pulse wave velocity. **J Hypertens**. 2010; 28:2068−2075.

36. Weber T, Wassertheurer S, Hametner B, Parragh S, Eber B. Noninvasive methods to assess pulse wave velocity: comparison with the invasive gold standard and relationship with organ damage. **J Hypertens**. 2015; 33:1023−1031.

37. Greve SV, Blicher MK, Kruger R, et al. Estimated carotid-femoral pulse wave velocity has similar predictive value as measured carotid-femoral pulse wave velocity. **J Hypertens**. 2016; 34:1279−1289.

38. Matschkal J, Mayer CC, Sarafidis PA, et al. Comparison of 24-hour and office pulse wave velocity for prediction of mortality in hemodialysis patients. **Am J Nephrol**. 2019; 49:317−327.

39. Sarafidis PA, Loutradis C, Karpetas A, et al. Ambulatory pulse wave velocity is a stronger predictor of cardiovascular events and all-cause mortality than office and ambulatory blood pressure in hemodialysis patients. **Hypertension**. 2017; 70:148−157.

40. Chirinos JA, Segers P, Hughes T, Townsend R. Large-artery stiffness in health and disease: JACC state-of-the-art review. **J Am Coll Cardiol**. 2019; 74:1237−1263.

41. Papaioannou TG, Karatzis EN, Papamichael CM, et al. Circadian variation of arterial pressure wave reflections. **Am J Hypertens**. 2006; 19:259−263.

42. Protogerou ADPT, Sfikakis PP, Blacher J, et al. Differences in pulse pressure day variability between the brachial artery and the aorta in healthy subjects. **Artery Res**. 2012:34−40.

43. Weber T, Wassertheurer S, Rammer M, et al. Validation of a brachial cuff-based method for estimating central systolic blood pressure. **Hypertension**. 2011; 58:825−832.

44. Omboni S, Posokhov IN, Rogoza AN. Evaluation of 24-hour arterial stiffness indices and central hemodynamics in healthy normotensive subjects versus treated or untreated hypertensive patients: a feasibility study. **Int J Hypertens**. 2015; 2015:601812.

45. Burns MJ, Seed JD, Incognito AV, Doherty CJ, Notay K, Millar PJ. Comparison of laboratory and ambulatory measures of central blood pressure and pulse wave reflection: hitting the target or missing the mark? **J Am Soc Hypertens**. 2018; 12:275−284.

46. Williams B, Lacy PS, Yan P, Hwee CN, Liang C, Ting CM. Development and validation of a novel method to derive central aortic systolic pressure from the radial pressure waveform using an n-point moving average method. **J Am Coll Cardiol**. 2011; 57:951−961.

47. Pickering TG, Harshfield GA, Kleinert HD, Blank S, Laragh JH. Blood pressure during normal daily activities, sleep, and exercise. Comparison of values in normal and hypertensive subjects. **J Am Med Assoc**. 1982; 247:992−996.

48. Kawano Y, Tochikubo O, Minamisawa K, Miyajima E, Ishii M. Circadian variation of haemodynamics in patients with essential hypertension: comparison between early morning and evening. **J Hypertens**. 1994; 12:1405−1412.

49. Bristow JD, Honour AJ, Pickering TG, Sleight P. Cardiovascular and respiratory changes during sleep in normal and hypertensive subjects. **Cardiovasc Res**. 1969; 3:476−485.

50. Tochikubo O, Kawano Y, Miyajima E, Toshihiro N, Ishii M. Circadian variation of hemodynamics and baroreflex functions in patients with essential hypertension. **Hypertens Res**. 1997; 20:157−166.

51. Mori H. Circadian variation of haemodynamics in patients with essential hypertension. **J Hum Hypertens**. 1990; 4:384−389.

52. Diamant M, Harms MP, Immink RV, Van Lieshout JJ, Van Montfrans GA. Twenty-four-hour non-invasive monitoring of systemic haemodynamics and cerebral blood flow velocity in healthy humans. **Acta Physiol Scand**. 2002; 175:1−9.

53. Sherwood A, Hill LK, Blumenthal JA, Hinderliter AL. Circadian hemodynamics in men and women with high blood pressure: dipper vs. nondipper and racial differences. **J Hypertens**. 2018; 36:250−258.

54. Voogel AJ, Koopman MG, Hart AA, van Montfrans GA, Arisz L. Circadian rhythms in systemic hemodynamics and renal function in healthy subjects and patients with nephrotic syndrome. **Kidney Int**. 2001; 59:1873−1880.

55. Williams B, Lacy PS, Baschiera F, Brunel P, Dusing R. Novel description of the 24-hour circadian rhythms of brachial versus central aortic blood pressure and the impact of blood pressure treatment in a randomized controlled clinical trial: the ambulatory central aortic pressure (AmCAP) study. **Hypertension**. 2013; 61:1168−1176.

56. Jankowski P, Bednarek A, Olszanecka A, Windak A, Kawecka-Jaszcz K, Czarnecka D. Twenty-four-hour profile of central blood pressure and central-to-peripheral systolic pressure amplification. **Am J Hypertens**. 2013; 26:27−33.

57. Omboni S, Posokhov I, Parati G, et al. Ambulatory blood pressure and arterial stiffness web-based telemonitoring in patients at cardiovascular risk. First results of the VASOTENS (Vascular health ASsessment of the hypertENSive patients) Registry. **J Clin Hypertens**. 2019; 21:1155−1168.

58. Alpert BS, Quinn D, Gallick D. Oscillometric blood pressure: a review for clinicians. **J Am Soc Hypertens**. 2014; 8:930−938.

59. Smulyan H, Sheehe PR, Safar ME. A preliminary evaluation of the mean arterial pressure as measured by cuff oscillometry. **Am J Hypertens**. 2008; 21:166−171.

60. Sharman JE, Avolio AP, Baulmann J, et al. Validation of non-invasive central blood pressure devices: ARTERY Society task force consensus statement on protocol standardization. **Eur Heart J**. 2017; 38:2805−2812.

61. Picone DS, Schultz MG, Peng X, et al. Intra-arterial analysis of the best calibration methods to estimate aortic blood pressure. **J Hypertens**. 2019; 37:307−315.

62. Papaioannou TG, Karageorgopoulou TD, Sergentanis TN, et al. Accuracy of commercial devices and methods for noninvasive estimation of aortic systolic blood pressure a systematic review and meta-analysis of invasive validation studies. **J Hypertens**. 2016; 34:1237−1248.

63. Wassertheurer S, Hametner B, Sharman J, Weber T. Systolic blood pressure amplification and waveform calibration. **Hypertens Res**. 2017; 40:518.

64. Schultz MG, Picone DS, Armstrong MK, et al. Validation study to determine the accuracy of central blood pressure measurement using the sphygmocor xcel cuff device. **Hypertension**. 2020; 76:244−250.

65. Protogerou AD, Argyris AA, Papaioannou TG, et al. Left-ventricular hypertrophy is associated better with 24-h aortic pressure than 24-h brachial pressure in hypertensive patients: the SAFAR study. **J Hypertens**. 2014; 32:1805−1814.

66. Boggia J, Luzardo L, Lujambio I, et al. The diurnal profile of central hemodynamics in a general Uruguayan population. **Am J Hypertens**. 2016; 29:737−746.

67. Ntineri A, Kollias A, Zeniodia MA, Vazeou A, Soldatou A, Stergiou GS. Insight into the 24-hour ambulatory central blood pressure in adolescents and young adults. **J Clin Hypertens**. 2020; 22:1789−1796.

68. Weber T, Wassertheurer S, Agharazii M, et al. International academic 24 hour pulsatile hemodynamics research consortium (i24abc.org). 24-hour central blood pressure: reference values for healthy individuals. The international 24 hour ambulatory aortic blood pressure consortium (i24ABC). **J Hypertens**. 2019; 37:e85.

69. Argyris AA, Nasothimiou E, Aissopou E, et al. Mechanisms of pulse pressure amplification dipping pattern during sleep time: the SAFAR study. **J Am Soc Hypertens**. 2018; 12:117−127.

70. Davis SC, Westerhof BE, van den Bogaard B, et al. Active standing reduces wave reflection in the presence of increased peripheral resistance in young and old healthy individuals. **J Hypertens**. 2011; 29:682−689.

71. Tikkakoski AJ, Tahvanainen AM, Leskinen MH, et al. Hemodynamic alterations in hypertensive patients at rest and during passive head-up tilt. **J Hypertens**. 2013; 31:906−915.

72. Vrachatis D, Papaioannou TG, Konstantopoulou A, et al. Effect of supine versus sitting position on noninvasive assessment of aortic pressure waveform: a randomized cross-over study. **J Hum Hypertens**. 2014; 28:236−241.

73. Kollias A, Lagou S, Zeniodi ME, Boubouchairopoulou N, Stergiou GS. Association of central versus brachial blood pressure with target-organ damage: systematic review and meta-analysis. **Hypertension**. 2016; 67:183−190.

74. Weber T, Wassertheurer S, Schmidt-Trucksass A, et al. Relationship between 24-hour ambulatory central systolic blood pressure and left ventricular mass: a prospective multicenter study. **Hypertension**. 2017; 70:1157−1164.

75. Blanch P, Armario P, Oliveras A, et al. Association of either left ventricular hypertrophy or diastolic dysfunction with 24-hour central and peripheral blood pressure. **Am J Hypertens**. 2018; 31:1293−1299.

76. Zhang Y, Kollias G, Argyris AA, Papaioannou TG, Tountas C, Konstantonis GD, Achimastos A, Blacher J, Safar ME, Sfikakis PP, Protogerou AD. Association of left ventricular diastolic dysfunction with 24-h aortic ambulatory blood pressure: the SAFAR study. **J Human Hypertens**. 2015; 29:442−448.

77. Chi C, Yu SK, Auckle R, et al. Association of left ventricular structural and functional abnormalities with aortic and brachial blood pressure variability in hypertensive patients: the SAFAR study. **J Hum Hypertens**. 2017; 31:633−639.

78. Yu S, Chi C, Protogerou AD, et al. 24-hour aortic blood pressure variability showed a stronger association with carotid damage than 24-hour brachial blood pressure variability: the SAFAR study. **J Clin Hypertens**. 2018; 20:499−507.

79. Omboni S, Posokhov I, Parati G, et al. Variable association of 24-h peripheral and central hemodynamics and stiffness with hypertension-mediated organ damage: the VASOTENS Registry. **J Hypertens**. 2020; 38:701−715.

80. Boutouyrie P, Achouba A, Trunet P, Laurent S. Amlodipine-valsartan combination decreases central systolic blood pressure more effectively than the amlodipine-atenolol combination: the EXPLOR study. **Hypertension**. 2010; 55:1314−1322.

81. Williams B, Lacy PS, Thom SM, et al. Differential impact of blood pressure-lowering drugs on central aortic pressure and clinical outcomes: principal results of the Conduit Artery Function Evaluation (CAFE) study. **Circulation**. 2006; 113:1213−1225.

82. Asmar RG, London GM, O'Rourke ME, Safar ME. Improvement in blood pressure, arterial stiffness and wave reflections with a very-low-dose perindopril/indapamide combination in hypertensive patient: a comparison with atenolol. **Hypertension**. 2001; 38:922−926.

83. Williams B, Cockcroft JR, Kario K, et al. Effects of Sacubitril/Valsartan versus Olmesartan on central hemodynamics in the elderly with systolic hypertension: the PARAMETER study. **Hypertension**. 2017; 69:411−420.

84. Georgianou EGP, Petidis K, Markakis K, Zografou I, Karagiannis A. Effect of Nebivolol and Olmesartan on 24-hour

brachial and aortic blood pressure in the acute stage of ischemic stroke. **Int J Hypertens**. 2019; 2019.

85. Striepe K, Jumar A, Ott C, et al. Effects of the selective sodium-glucose cotransporter 2 inhibitor Empagliflozin on vascular function and central hemodynamics in patients with type 2 diabetes mellitus. **Circulation**. 2017; 136:1167−1169.

86. Hoffmann FMS, Luchitskaya E, Funtova I, Jordan J, Baevsky R, Tank J. An oscillometric approach in assessing early vascular ageing biomarkers following long-term space flights. **Int J Cardiol Hypertens**. 2019; 2:100013.

87. Paiva AMG, Mota-Gomes MA, Brandao AA, et al. Reference values of office central blood pressure, pulse wave velocity, and augmentation index recorded by means of the Mobil-O-Graph PWA monitor. **Hypertens Res**. 2020; 43:1239−1248.

88. Lauder L, Scholz SS, Ewen S, et al. Accuracy of pulse rate derived from 24-h ambulatory blood pressure monitoring compared with heart rate from 24-h Holter-ECG. **J Hypertens**. 2020; 38:2387−2392.

89. Echeverri D, Pizano A, Cabrales J, Moreno K. Validation of central and peripheral non-invasive hemodynamic variables using an oscillometric method. **High Blood Press Cardiovasc Prev**. 2018; 25:65−77.

90. Jatoi NA, Mahmud A, Bennett K, Feely J. Assessment of arterial stiffness in hypertension: comparison of oscillometric (Arteriograph), piezoelectronic (Complior) and tonometric (SphygmoCor) techniques. **J Hypertens**. 2009; 27:2186−2191.

91. Baulmann J, Schillings U, Rickert S, et al. A new oscillometric xmethod for assessment of arterial stiffness: comparison with tonometric and piezo-electronic methods. **J Hypertens**. 2008; 26:523−528.

92. Nair D, Tan SY, Gan HW, et al. The use of ambulatory tonometric radial arterial wave capture to measure ambulatory blood pressure: the validation of a novel wrist-bound device in adults. **J Hum Hypertens**. 2008; 22:220−222.

93. Ott C, Haetinger S, Schneider MP, Pauschinger M, Schmieder RE. Comparison of two noninvasive devices for measurement of central systolic blood pressure with invasive measurement during cardiac catheterization. **J Clin Hypertens**. 2012; 14:575−579.

94. Franssen PM, Imholz BP. Evaluation of the Mobil-O-Graph new generation ABPM device using the ESH criteria. **Blood Press Monit**. 2010; 15:229−231.

95. Jones CR, Taylor K, Chowienczyk P, Poston L, Shennan AH. A validation of the Mobil O Graph (version 12) ambulatory blood pressure monitor. **Blood Press Monit**. 2000; 5:233−238.

96. Wei W, Tolle M, Zidek W, van der Giet M. Validation of the mobil-O-Graph: 24 h-blood pressure measurement device. **Blood Press Monit**. 2010; 15:225−228.

97. Hoshide S, Komori T, Ogata Y, Eguchi K, Kario K. Evaluation of central blood pressure in an Asian population: comparison between brachial oscillometry and radial tonometry methods. **Pulse**. 2018; 6:98−102.

98. Gotzmann M, Hogeweg M, Seibert FS, et al. Accuracy of fully automated oscillometric central aortic blood pressure measurement techniques. **J Hypertens**. 2020; 38:235−242.

99. Wassertheurer S, Kropf J, Weber T, et al. A new oscillometric method for pulse wave analysis: comparison with a common tonometric method. **J Hum Hypertens**. 2010; 24:498−504.

100. Papaioannou TG, Thymis J, Benas D, et al. Measurement of central augmentation index by three different methods and techniques: agreement among Arteriograph, Complior, and Mobil-O-Graph devices. **J Clin Hypertens**. 2019; 21:1386−1392.

101. Weber T, Wassertheurer S, Rammer M, Haiden A, Hametner B, Eber B. Wave reflections, assessed with a novel method for pulse wave separation, are associated with end-organ damage and clinical outcomes. **Hypertension**. 2012; 60:534−541.

102. Weber T, Middlemiss J, McEniery CM, et al. Validation of a method to estimate stroke volume from brachial-cuff derived pressure waveforms. **Artery Res**. 2020; 26:42−47.

103. Papaioannou TG, Xanthis D, Argyris A, et al. Accuracy and precision of cardiac output estimation by an automated, brachial cuff-based oscillometric device in patients with shock. **Proc Inst Mech Eng H**. 2019, 954411919888321.

104. Feistritzer HJ, Reinstadler SJ, Klug G, et al. Comparison of an oscillometric method with cardiac magnetic resonance for the analysis of aortic pulse wave velocity. **PLoS One**. 2015; 10:e0116862.

105. Jones SC, Bilous M, Winship S, Finn P, Goodwin J. Validation of the OSCAR 2 oscillometric 24-hour ambulatory blood pressure monitor according to the International Protocol for the validation of blood pressure measuring devices. **Blood Press Monit**. 2004; 9:219−223.

106. Goodwin J, Bilous M, Winship S, Finn P, Jones SC. Validation of the Oscar 2 oscillometric 24-h ambulatory blood pressure monitor according to the British Hypertension Society protocol. **Blood Press Monit**. 2007; 12:113−117.

107. Koudryavtcev SA, Lazarev VM. Validation of the BPLab((R)) 24-hour blood pressure monitoring system according to the European standard BS EN 1060-4:2004 and British Hypertension Society protocol. **Med Devices**. 2011; 4:193−196.

108. Rogoza ANKA. Central aortic blood pressure and augmentation index: comparison between Vasotens® and SphygmoCor® technology. **Res Rep Clin Cardiol**. 2012; 3:27−33.

109. Salvi P, Scalise F, Rovina M, et al. Noninvasive estimation of aortic stiffness through different approaches. **Hypertension**. 2019; 74:117−129.

This page intentionally left blank

Chapter 9

Animal models and methods to study arterial stiffness

Bart Spronck[1,2] and Jay D. Humphrey[1,3]

[1]*Department of Biomedical Engineering, School of Engineering and Applied Science, Yale University, New Haven, CT, United States;* [2]*Department of Biomedical Engineering, CARIM School for Cardiovascular Diseases, Maastricht University, Maastricht, the Netherlands;* [3]*Vascular Biology and Therapeutics Program, Yale School of Medicine, New Haven, CT, United States*

Introduction

As emphasized throughout this textbook, increased arterial stiffness is an initiator and indicator of diverse cardiovascular, renovascular, and neurovascular conditions, and thus all-cause mortality. It is increasingly important, therefore, to measure arterial stiffness in at-risk patients, though typically such measurements are limited to in vivo metrics. Complementary studies in animal models therefore remain important for identifying the underlying molecular and mechanical mechanisms of arterial stiffening. These preclinical studies can also be useful for evaluating new measurement methods as well as potential drug efficacy. In this chapter, we first review key mechanical concepts related to arterial stiffness and its measurement, including common in vivo and ex vivo methods. We then discuss representative mouse models and conclude with a comparison of techniques and a set of brief recommendations.

Mechanical concepts

As discussed in Chapter 7 and various other sections of this textbook, pulse wave velocity (PWV)—the speed at which the blood pressure wave travels along a vascular path—has come to be regarded as the gold standard metric for arterial stiffness in the clinical setting. A much broader range of measurements and metrics are possible in animal studies, however, and an overall standard in animal models has yet to emerge. Toward this end, it is important to remember that the different metrics have different meanings, and thus different utilities.[1]
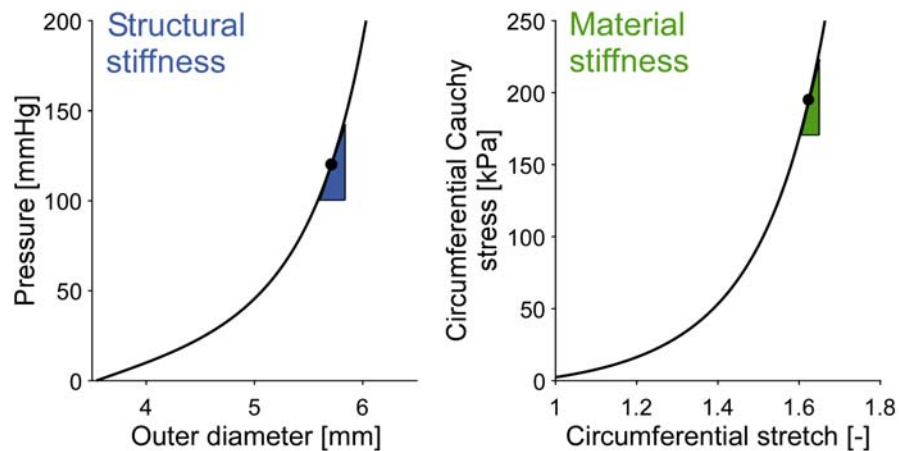
Briefly, stiffness is a measure of the change in loading needed to cause a particular deformation; compliance is the inverse of stiffness. The different metrics of stiffness thus emerge depending on the definitions of "load" and "deformation" as well as the conditions of loading. Importantly, material stiffness refers to an intrinsic property of the material; structural stiffness depends on both the material stiffness and geometry (Box 9.1). As an example, if the deformation is taken as an in vivo change in luminal cross-sectional area over the cardiac cycle and the load is the corresponding change in blood pressure, one obtains a structural measure of compliance—the coefficient $CC = (A_s - A_d)/(P_s - P_d)$, with A_s and A_d the systolic and diastolic luminal cross-sectional area, and P_s and P_d the systolic and diastolic blood pressure, respectively. An overview of different metrics of arterial stiffness commonly used in animal research is given in Table 9.1, which delineates structural and material metrics.

Measurements of arterial stiffness thus depend strongly on the loading conditions.[1] The most variable loading determinant in vivo is the blood pressure at the time of measurement, followed by heart rate (Box 9.2). In vivo, an artery is also subjected to a significant degree of axial stretch that is induced largely during somatic growth; it helps to ensure that the artery does not bend during blood pressure fluctuations. In addition, this *axial* stretch influences the *circumferential* stiffness of the arterial tissue. Whereas the axial stretch of an artery is dictated by the prevalent physiologic conditions in vivo, it is highly modifiable ex vivo, though often not reported or emphasized. For an ex vivo measure of stiffness to mimic in vivo conditions, the artery should be stretched axially to its in vivo length, as well as pressurized to its in vivo value. Box 9.3 illustrates some effects of different ex vivo loading conditions on stiffness measurements.

BOX 9.1 Arterial stiffness—material versus structural

Metrics of arterial stiffness can be divided into *structural* and *material* (Fig. 9.1). Metrics of structural stiffness quantify the stiffness of the artery as a whole, that is, as a structure. Examples include pulse wave velocity (PWV), compliance coefficient (CC), and distensibility coefficient (DC) (equations in Table 9.1). Metrics of material stiffness, on the other hand, quantify the intrinsic stiffness of the wall material, reflecting its composition, which is necessarily defined at a point. Examples include the incremental Young's modulus (E_{inc})[14] and the small-on-large metric $C_{\theta\theta\theta\theta}$.[49] Differences between structural and material metrics can be appreciated through an illustrative example of vascular hypertrophy. Suppose, for example, that the arterial wall begins to thicken in incident hypertension. If this thickening occurs via deposition of the same type of material as was already present, the *material* stiffness does not change although the thickening necessarily increases the *structural* stiffness.

- Structural property
- Geometry-**dependent**
- Changes when material changes (e.g. collagen cross-linking) and/or when geometry changes (e.g. wall thickening)
- (conceptually) the slope of the pressure-diameter curve
- Typical metrics: PWV, CC, DC

- Material property
- Geometry-**independent**
- Changes when material changes (e.g. collagen cross-linking); **not** when geometry changes

- (conceptually) the slope of the stress-strech curve
- Typical metrics: E_{inc}, $C_{\theta\theta\theta\theta}$

FIGURE 9.1 Structural versus material stiffness. *Source data from Spronck B, Humphrey J. Arterial stiffness: different metrics, different meanings.* **J Biomech Eng**. *2019.*

Finally, as can be seen from the Moens–Korteweg equation, PWV (a structural metric) incorporates both material (through E_{inc}) and geometric (wall thickness h and internal radius r_i) information:

$$\mathrm{PWV} = \sqrt{\frac{E_{inc} \cdot h}{2 \cdot \rho \cdot r_i}},$$ (9.1)

with ρ the mass density of the fluid, namely blood in vivo. It is thus structural metrics of stiffness that dictate the hemodynamics. By contrast, material metrics are important to the local mechanobiology, that is, the response of the cells to changes in their local mechanical environment.
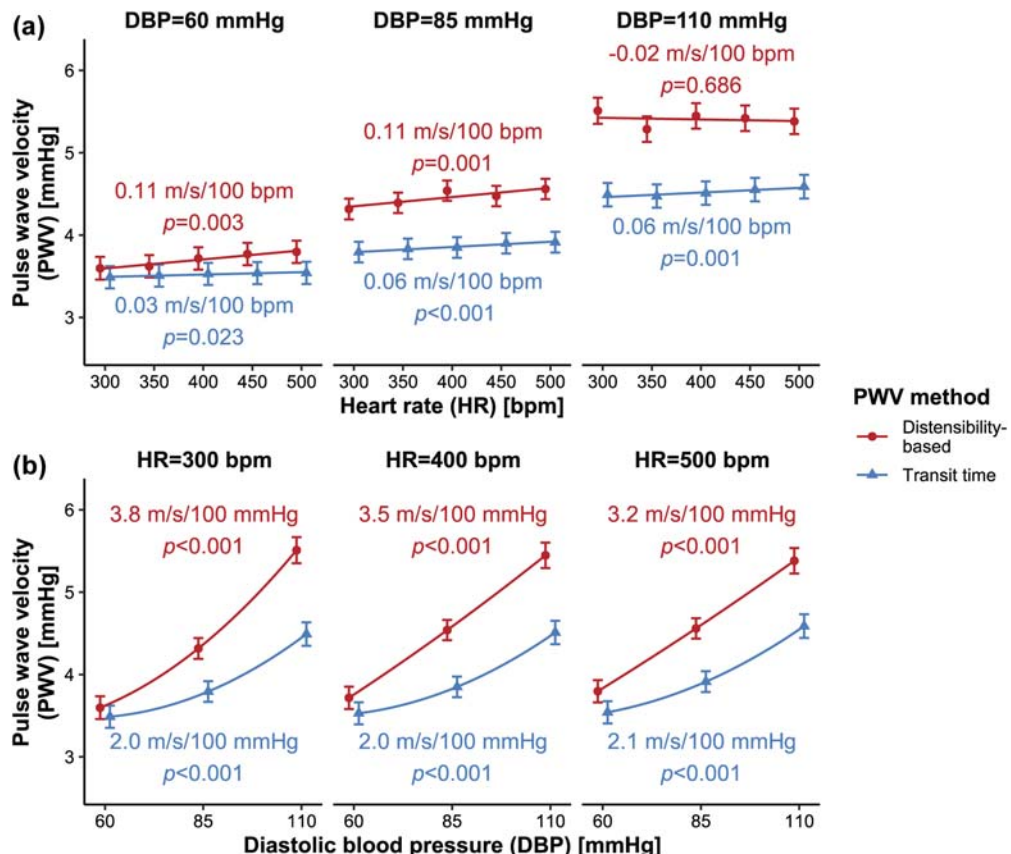
TABLE 9.1 Overview of commonly used formulas for arterial stiffness calculation in animal research.

Name	Equation	Eq.	Structural/ material?	Description
Compliance coefficient (CC)	$CC = \frac{A_s - A_d}{SBP - DBP}$	(9.2)	Structural	Absolute change in area for a given change in intraluminal pressure
Distensibility coefficient (DC)	$DC = \frac{A_s - A_d}{(SBP - DBP) \cdot A_d} = \frac{CC}{A_d}$	(9.3)	Structural	Relative change in area for a given change in intraluminal pressure
Pulse wave velocity (PWV)	$PWV = \frac{\Delta s}{TT}$	(9.4)	Structural	Propagation speed of the blood pressure wave along the arterial tree
	$PWV = \sqrt{\frac{1}{\rho \cdot DC}}$	(9.5)	Structural	
Incremental (circumferential) Young's modulus (E_{inc})*	$E_{inc} = \frac{2 \cdot \rho \cdot r_i \cdot PWV^2}{h}$	(9.6)	Material	Linearized, approximate increase in Cauchy stress per unit increase in stretch*
	$E_{inc} = \frac{d\sigma_{\vartheta\vartheta}}{d\lambda_{\vartheta}}$	(9.7)	Material	
Small-on-large material stiffness ($\mathbb{C}$) *,**	$\mathbb{C}_{ijkl} = \delta_{ik}\widehat{t}_{lj}^{\,o} + \widehat{t}_{il}^{\,o}\delta_{jk} + 4F_{iA}^{o}F_{jB}^{o}F_{kP}^{o}F_{lQ}^{o}\frac{\partial^2 W}{\partial C_{AB}\partial C_{PQ}}\Big|_{\mathbf{C}^o}$	(9.8)	Material	Linearized increase in Cauchy stress per unit increase in strain*
Referential material stiffness (**K**)*	$\mathbf{K} = \frac{\partial \mathbf{S}}{\partial \mathbf{E}} = \frac{\partial^2 W}{\partial \mathbf{E}\partial \mathbf{E}} = 4\frac{\partial^2 W}{\partial \mathbf{C}\partial \mathbf{C}}$	(9.9)	Material	Increase in second Piola—Kirchhoff stress per unit increase in Green—Lagrange strain*

A_s and A_d, systolic and diastolic cross-sectional area; SBP and DBP, systolic and diastolic blood pressures; Δs, transit distance; TT, transit time; ρ, blood mass density; r_i, inner radius; h wall thickness; $\sigma_{\vartheta\vartheta}$, circumferential Cauchy stress; λ_{ϑ}, circumferential stretch; **F**, deformation gradient tensor; W, stored strain energy function; $\widehat{t}$, extra (deformation-dependent) part of Cauchy stress tensor; δ, Kronecker tensor; **S**, second Piola—Kirchhoff tensor; **E**, Green—Lagrange strain tensor; and **C**, right Cauchy-Green tensor (**C** = $\mathbf{F}^{\mathsf{T}}\mathbf{F}$). * for more details on material stiffness metrics and their differences, see Box 9.5. ** a detailed derivation of $\mathbb{C}$ can be found in Reference 49.

BOX 9.2 Effect of loading conditions: in vivo

The nonlinear material behavior of the artery wall renders measurements of arterial stiffness strongly dependent on the loading conditions, especially transmural pressure (Fig. 9.2). These dependences are of particular relevance during in vivo studies due to changes in blood pressure and heart rate, which are highly variable in rodents; emotional stress due to handling quickly raises blood pressure while anesthesia decreases heart rate and blood pressure. Therefore, when reporting arterial stiffness metrics measured in vivo, the blood pressure at which those measurements were taken should always be reported.

FIGURE 9.2   Influence of heart rate (HR, A) and diastolic blood pressure (DBP, B) on pulse wave velocity (PWV) measurements in rats.[10] Numbers in red/blue denote average HR and BP dependencies, respectively. BP dependencies are calculated for DBP = 85 mmHg. Distensibility-based measurements are derived from ultrasound echotracking-based measurement of diameter and catheter-based measurement of blood pressure. Transit time PWVs are derived from the time difference between two catheter-based measurements taken simultaneously a fixed distance apart. *Figure reproduced from Spronck B, Tan I, Reesink KD, et al. Heart rate and blood pressure dependence of aortic distensibility in rats: comparison of measured and calculated pulse wave velocity.* **J Hypertens**. *2020, with permission.*

In vivo methods to study arterial stiffness

In principle, most methods for measuring arterial stiffness in vivo in humans (discussed in detail in Chapter 7) can be used in animals. In some cases, however, size/resolution
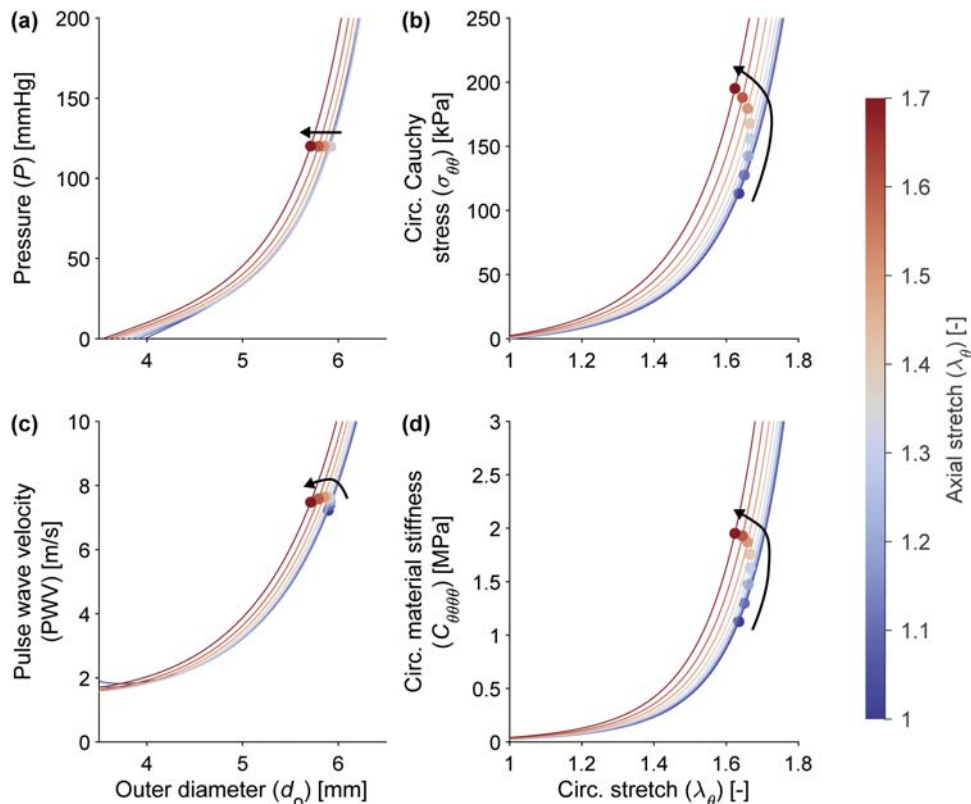
may be a limiting factor. We will therefore review the most appropriate methods.

Blood pressure measurements

Blood pressure is a strong determinant of the measured value of arterial stiffness (Box 9.2). Therefore, ideally,

BOX 9.3 Effect of loading conditions: ex vivo

The influence of loading conditions on measurements of arterial stiffness is not limited to the in vivo case (Box 9.2). While an artery is (by definition) at its in vivo length/stretch in the body, the researcher is free to stretch the artery to any length ex vivo. Fig. 9.3 illustrates the influence of axial stretch on a structural (PWV) and a material (small-on-large stiffness, $C_{\theta\theta\theta\theta}$) metric of stiffness (see Table 9.1).


FIGURE 9.3 Effects of pressure and axial stretch on arterial stiffness ex vivo. Panels a and b show typical arterial pressure-diameter (structural) and circumferential (circ.) stress-stretch (material) curves. Individual lines correspond to values of axial stretch (λ_z), increasing from $\lambda_z = 1$ to $\lambda_z = 1.7$ in steps of 0.1. Dots correspond to a pressure of 120 mmHg. Panels c and d illustrate effects of increasing λ_z on pulse wave velocity and small-on-large material stiffness, typical structural and material stiffness metrics, respectively. *Source data from Spronck B, Humphrey J. Arterial stiffness: different metrics, different meanings.* J Biomech Eng. 2019. *A theoretical analysis of the PWV can be found elsewhere Demiray H. Wave propagation through a viscous fluid contained in a prestressed thin elastic tube.* **Int J Eng Sci**. 1992; 30:1607−1620.

every in vivo study measuring arterial stiffness should also measure (or estimate) blood pressure at the site(s) of interest. Methods have been developed, for example, to transform peripheral measurements (e.g., via sphygmomanometer) to central measurements. In mice, peripheral blood pressure can be measured similarly using a tail-cuff device, as well as invasively using a catheter, either indwelling or during a surgical procedure. Both fluid-filled and (solid state) pressure-tip catheters are used, though given the fast heart rate and correspondingly high-frequency content of the mouse blood pressure signal, pressure-tip catheters are preferable. When measured by acute catheterization, it is important to remember that anesthesia generally reduces blood pressure from its ambulatory value.[2,3] By contrast, when measured by telemetry, with the pressure catheters connected to a radio

transmitter that is implanted under the skin, one measures ambulatory pressures under conscious conditions—currently considered the gold standard. Nevertheless, due to the small size of the mouse vasculature, catheterization can alter blood flow and pressure.[4] Whereas the tail-cuff measurement does not affect the blood flow and pressure directly, the required animal restraint can result in highly variable results in mice due to differences in emotional distress.[5]

Invasive blood pressure to measure arterial stiffness by transit time

If blood pressure is measured invasively and simultaneously at two locations along the arterial tree in mice, a diastolic foot-to-foot transit time can be obtained which, given a distance measurement, yields a transit time PWV (Eq. (9.4), Table 9.1).[3,6] Distance can be measured by leaving both catheters in place after euthanasia, dissecting the (intact) artery free, and measuring the distance using a small suture or, when straight, directly with a ruler or caliper.[7] This technique can also be performed using a single, dual-tip catheter, which removes the necessity to measure the distance between measurement sites and thus removes any measurement error in such distance measurement. Alternatively, when an ECG is recorded together with the BP signal, the time difference between the R-wave on the ECG and the diastolic foot on the BP signal can be obtained. By performing this in duplicate, for two BP measurement locations, one also obtains a transit time.

Different methods are available to determine the time difference between two blood pressure waves. Similar to the human case, the diastolic foot of the waveform provides a reliable fiducial point for transit time determination in murine models.[8] Both second derivative−based and intersecting tangent−based methods provide robust foot detection.[9,10]

High-resolution ultrasound

Several other methods exist for measuring structural stiffness in mice.[11] Ultrasound tracking of arterial wall motion can be used to measure in vivo changes in diameter. Together with pressure measurements, this yields the structural stiffness metrics of compliance and distensibility, the latter of which can be converted into a *local* estimate of PWV (Eqs. (9.2), (9.3), and (9.5), Table 9.1), for a given artery (e.g., carotid). Alternatively, ultrasound can be used to obtain *regional*, point-to-point (over finite lengths) PWVs by measuring the velocity waveform at two points along the artery and determining the time difference between those points. Division of the effective distance between these points by the transit time yields a transit time PWV (Eq. (9.4), Table 9.1). Because PWV varies along the

arterial tree, such transit time PWV represents a regionally averaged metric.

Applanation tonometry

In humans, transit time PWV is commonly estimated using applanation tonometry, where a tonometer is pressed against (superficial) arteries, typically at the carotid and femoral locations. This approach is also feasible in mice.[12] As with all in vivo methods for measuring stiffness in rodents, the animal has to be sedated, thus potentially influencing blood pressure (Box 9.2) and, thereby, the measured PWV.

Ex vivo methods to study arterial stiffness

In vivo measurements of arterial stiffness are necessarily limited to in vivo loading conditions, namely, with blood pressure fluctuating but axial stretch fixed. In contrast, ex vivo measurements offer much greater experimental control, and thus freedom, to test a sample over a wide range of loading conditions. Yet, the choice of these loading conditions has important consequences for the obtained results.[13]

Atomic force microscopy

Atomic force microscopy (AFM) allows measurement of material stiffness (Box 9.1) at the nano- and microscales, thus enabling stiffness to be inferred for individual components of the arterial wall (e.g., cells, elastic laminae, and collagen fibrils) or locally. Typically, the AFM tip is used to indent (i.e., push into) an otherwise unloaded sample while measuring the indentation depth and corresponding force. In this mode, AFM yields a (radial) *compressive* stiffness under nearly unloaded conditions (near the traction-free state, implying no external forces acting upon the sample) typically inferred as an (estimated) Young's modulus.[14] In contrast, physiologically, the dominant relevant loads within the arterial wall are typically *tensile*, oriented in the circumferential and axial directions. These differences in loading, radial compression rather than in-plane tensile, leads to Young's moduli that typically differ by multiple orders of magnitude between AFM and the in vivo loading state (Table 9.2).[1] Other methodological confounders are the indenter tip size and diameter, and the algorithm/model (e.g., Hertz) used to convert measured data into a Young's modulus.

Wire myography

Wire myography involves the circumferential stretching of a short arterial ring between two wires while

TABLE 9.2 Values of aortic stiffness (mouse) depend strongly on methodology.

Vessel/Mouse	Modality	Definition/State	Value, units, age	References
Thoracic aorta, C57BL/6J (age 2–18 mo)	AFM	In vitro, unloaded, cut open, radially indented from luminal side (endothelium intact)/compressive	$E = 3.1$ kPa (2 mo) $E = 3.6$ kPa (6 mo) $E = 16.9$ kPa (12 mo) $E = 21.8$ kPa (18 mo)	77
Suprarenal abdominal aorta, C57/Sv129 (age 10–13 mo)	AFM	In vitro, unloaded or pressurized to 100 mmHg and elongated to in vivo axial stretch, ring, axially indented/compressive	$E = 18.7$ kPa (unloaded) $E = 12.3–76.4$ kPa (loaded; bimodal distribution)	78
Aorta, C57BL/6J (age 11 mo)	AFM	In vitro, unloaded, cut open, radially indented from luminal side (endothelium removed)/compressive	$E = 24$ kPa	32
Ascending thoracic aorta, C57BL/6J (age 0.5–3.5 mo)	AFM	In vitro, unloaded, cut open, radially indented from luminal side (endothelium intact)/compressive	$E = 2.8–12.7$ kPa (0.5 mo)[a] $E = 5.0–38.8$ kPa (2 mo)[a] $E = 4.4–36.7$ kPa (3.5 mo)[a]	79
Ascending thoracic aorta, C57BL/6J (age 15.2 ± 0.1 wks)	Biaxial testing	In vitro, loaded, intact, pressurized to 128 mmHg, elongated to in vivo axial stretch/tensile	$\mathbb{C}_{\theta\theta\theta\theta} = 2.76$ MPa $\mathbb{C}_{zzzz} = 2.26$ MPa	80
Suprarenal abdominal aorta, C57BL/6J (age 5–6 mo)	Biaxial testing	In vitro, loaded, intact, pressurized to 100 mmHg, elongated to in vivo axial stretch/tensile	$\partial S_{\theta\theta}/\partial E_{\theta\theta} = 1.33$ MPa $\partial S_{zz}/\partial E_{zz} = 0.082$ MPa	81
Carotid-to-femoral arterial bed, C57BL/6J (age 5.6 ± 0.2 mo)	Applanation tonometry	In vivo, 4%–5% sevoflurane or 75 mg/kg sodium pentobarbital anesthesia, noninvasive/PWV	PWV = 3.96 m/s (sevoflurane)[b] PWV = 2.89 m/s (sodium pentobarbital)[b]	12
Abdominal aorta, C57BL/6 (age 3–4 mo)	Ultrasound echotracking	In vivo, 125 mg/kg tribromoethanol anesthesia, noninvasive/PWV	PWV = 2.70 m/s[c]	82
Aorta (regionally dependent), C57BL/6J (age 3 mo)	Ultrasound echotracking/pressure catheter	In vivo, 1.5% isoflurane anesthesia, noninvasive (ultrasound), invasive (catheter)/PWV	PWV = 5.2 m/s[d] PWV = 3.0 m/s[e] PWV = 3.5 m/s[f]	11

E, Young's modulus
[a]*Computationally separated, numbers denote intimal/medial moduli. AFM, atomic force microscopy; PWV, pulse wave velocity; $\mathbb{C}_{\theta\theta\theta\theta}$ and $\mathbb{C}_{zzzz}$, linearized circumferential and axial spatial material stiffness obtained using the theory of small-on-large. $\partial S_{\theta\theta}/\partial E_{\theta\theta}$ and $\partial S_{zz}/\partial E_{zz}$, referential material stiffness defined as the derivative of second Piola–Kirchhoff stress with respect to Green strain.*
[b]*Carotid-to-femoral transit time PWV.*
[c]*PWV in the window of an ultrasound probe.*
[d]*Aortic arch-to-femoral bifurcation transit time PWV (ultrasound).*
[e]*Abdominal transit time PWV (blood pressure catheter, 2 cm path length).*
[f]*Distensibility-based local abdominal PWV obtained from Bramwell–Hill equation. In studies where interventions were performed, control groups are displayed here.*
Table adapted from Spronck B, Humphrey J. Arterial stiffness: different metrics, different meanings. **J Biomech Eng**. 2019.

Models and methods to study arterial stiffness **Chapter | 9**   **143**

Wire myography

Uniaxial (circumferential) extension/force

Pressure myography

Inflation/diameter measurement

Biaxial testing

Axial extension/ force measurement

Inflation/diameter measurement

Panoramic digital image correlation

Camera capturing full displacement field from top

Variable axial stretch

Inflation/diameter measurement

Conical mirror below specimen

FIGURE 9.4   Schematic comparison of ex vivo methods for whole-artery stiffness testing: from top to bottom: wire myography, pressure myography, biaxial biomechanical testing, and panoramic digital image correlation (pDIC).

simultaneously measuring the associated force (Fig. 9.4). Wire myography is typically performed with the artery at a physiological level of circumferential stretch, but the axial direction is left unloaded, allowing it to move freely during testing and thus shorten via a Poisson effect (the phenomenon in which a material tends to compress in directions perpendicular to the direction of extension, and vice versa). In vivo, however, arteries are typically tethered axially and *prestretched* (elongated). The effect of axial stretch on circumferential mechanics is elaborated in Box 9.3. For a more detailed review about wire myography, the reader is referred to Reference 7.

Pressure myography

In pressure myography, an arterial segment (preferred length ∼5 times its unloaded diameter) is mounted between cannulae and pressurized, which necessitates that

all side branches are ligated (Fig. 9.4). The artery is typically maintained at a fixed length, which is often chosen as the minimum length at which the vessel does not buckle visually during inflation. Yet, the length (axial stretch) at which the artery is distended influences its circumferential behavior (Box 9.3). Hence, the artery should be mounted at its in vivo length, thus ensuring that the loading conditions mimic those in vivo. This can be accomplished for some arteries by measuring the length in situ prior to excision. Identifying the proper in situ length can be difficult for many arteries, however, including the ascending aorta and coronary arteries (which change length over a cardiac cycle), the common carotids (if the neck is extended to enable the requisite cut-down), and smaller arteries (which have significant adherent perivascular tissue).

Some pressure myographs allow measurement of axial force. If such measurement is available, the in vivo length of the artery can be estimated without measuring an actual in situ length. This method exploits the observation that the axial force remains approximately constant when an artery is pressurized at its in vivo length.[15] When held at a greater or shorter length, the force increases or decreases, respectively, with increased pressure. Using this knowledge, one can estimate the axial stretch that corresponds to the in vivo situation by repeatedly inflating/deflating an artery while measuring axial force.

Biaxial biomechanical testing

Biaxial biomechanical testing is similar to pressure myography. These two techniques differ, however, in that a biaxial test does not only involve distension (while keeping the artery at a fixed *length* or axial *force*) but also extension (while keeping the artery at a fixed *diameter* or *pressure*; Fig. 9.4). By combining these two loading modes, biaxial testing assesses arterial behavior along the two primary directions or axes.[16,17] Hence, one can quantify both the circumferential and the axial material stiffness, thus revealing potentially coupled behaviors (Box 9.3). Although beyond the current scope, such biaxial data allow one to quantify the nonlinear anisotropic behavior in terms of appropriate constitutive relations.[18]

Digital image correlation

Panoramic digital image correlation (pDIC) is a relatively new technique that provides spatially resolved material properties under biaxially loaded conditions.[19,20] For pDIC, the artery is typically first tested biaxially (see previous paragraph) to estimate the in vivo axial stretch and to determine the bulk biaxial properties. Optical coherence tomography (OCT) can also be used to measure local wall thickness for the full sample. Thereafter, a speckle pattern is created on the sample, which is then mounted vertically within a conical mirror (Fig. 9.4). Imaging via this mirror from the top yields the full surface deformation pattern,

which is repeated for different pressures and axial stretches. The OCT and pDIC data can then be used together to identify constitutive properties locally, which can be particularly important in cases of complex geometry, such as aneurysms.

Mouse models to study arterial stiffness

Many different animal models continue to contribute to our understanding of arterial stiffening, both its presentation and potential reversal. Nevertheless, the mouse has emerged as the model of choice for multiple reasons. The many different genetically modified mouse models available allow one to delineate effects of individual cell phenotypes, proteins, receptors, etc., on overall vascular structure, function, and properties. The many different surgical models enable one to focus on the effects that altered hemodynamics have on subsequent vascular and cardiac changes. The many different possible pharmacological interventions allow one to study both disease progression and its treatment. Perhaps most importantly, technological advances now allow one to collect extensive cell biological, biomechanical, and physiological data that, in turn, can be correlated with (immuno)histological information given the many antibodies available in the mouse. Finally, the short gestational period, the ease of handling, and the lower cost of mice are particularly advantageous for performing longitudinal studies over periods of weeks or months. Box 9.4 discusses key differences and similarities between the mouse and human aorta. In the following sections, we briefly discuss a few studies representative of the large number of papers available on arterial stiffness in diverse mouse models.

Aging

Among others, Sir William Osler, one of the four founding fathers of Johns Hopkins Medicine, remarked at the beginning of the 20th century that we (humans) are as old as our arteries. Natural aging is now a well-known contributor to arterial stiffening and thus a strong, inevitable risk factor for many cardiovascular diseases. In humans, extreme aging results in many vascular changes, including endothelial cell dysfunction, increased inflammation, and fibrosis. Importantly, aging also results in progressive decreases in elastic fiber integrity, since functional elastic fibers are only deposited early in life, though with a normal half-life in the order of 50 years. In mice, with much shorter lifespans than humans, the elastic lamellar structure appears to change little with natural aging. If the effects of reduced elastic fiber integrity are of interest in a particular study, mice deficient in the elastin-associated glycoprotein fibulin-5 can be useful, which mechanically phenocopy human aging,[21] enabling their use, for example, in studies on the combined effects of

aging and hypertension.[22] Despite the minor changes in elastic lamellar structure in mice, other effects of aging do manifest therein. Careful measurements of blood flow and pressure reveal changes in characteristic impedance in aged mice,[23] thus reflecting underlying stiffening. At least in some mice, such age-induced stiffening associates with arterial inflammation and adventitial fibrosis, which is partially reversible with aerobic exercise.[24] Again remembering the different definitions and metrics, such stiffening appears to be due primarily to changes in wall thickness, due to increased accumulation of fibrillar collagen and glycosaminoglycans, rather than marked changes in material stiffness[21] (that is, it is the structural stiffness that increases). Similarly, a paradoxical increase in arterial stiffness, and thus PWV, emerges in progeria, an extremely rare, highly accelerated aging disorder. In this condition, decreases in material stiffness are far outweighed by increases in wall thickness, again due to accumulating collagen and especially glycosaminoglycans, thus increasing structural stiffness and PWV.[25] These changes can be slightly greater in the abdominal than in the thoracic aorta, causing regional differences in PWV, but nevertheless augmenting central pulse pressures as would be expected of aortic stiffening.

Connective tissue disorders

Marfan syndrome results from a mutation in the *Fbn1* (mouse) gene, which codes for the elastin-associated glycoprotein fibrillin-1. This syndrome affects many different tissues, though aortic root aneurysms are the most common cause of morbidity. In addition to aneurysms, Marfan syndrome results in a stiffening of many central arteries, as first inferred via measurements of PWV.[26] In mice, Marfan syndrome is also associated with endothelial cell dysfunction and compromised nitric oxide signaling, which can have myriad effects on wall composition and thus properties.[27] Biaxial mechanical testing reveals further that it is an increase in material stiffness in the thoracic aorta that associates with Marfan syndrome in the $Fbn1^{mgR/mgR}$ mouse model,[28] consistent with a reduced ability of the smooth muscle cells to mechanosense and mechanoregulate wall stiffness in genetically predisposed thoracic aortopathies.[29] Material stiffness otherwise appears to be mechanoregulated well in many cases,[30] hence suggesting that measurements of intrinsic stiffness are also important indicators of the ability of the intramural cells to sense and regulate their local mechanical environment, which is crucial for maintaining proper structure and function via mechanical homeostasis.[31] Although most findings herein derive from mouse studies, the mouse and human aorta are, despite their size difference, structurally very similar. Controversy, however, exists about the role of smooth muscle tone in the human aorta, whereas this is well established in the mouse aorta (Box 9.4).

BOX 9.4 The mouse aorta versus the human aorta

When choosing the mouse as a model animal for arterial stiffness research, one should be aware that, necessarily, differences exist between murine and human large arteries. Table 9.3 lists key structural and functional metrics for both species. Most structural metrics come from the seminal work by Wolinsky and Glagov,[56] in which they showed that, despite major size differences across species from mouse to human, the medial lamellar unit is remarkably well conserved. Indeed, though the number of lamellar units in the human aorta is ∼12 times that of the mouse, lamellar thickness and especially tension per unit is similar across species.

TABLE 9.3 Structural and functional metrics for mouse and human aortas.

Metric		Mouse	Human	References
Diameter (loaded) (mm)		1.2	17	56
Medial thickness (mm)		0.03	1.1	56
Number of lamellar units		5	60	56
Interlamellar distance (lamellar thickness) (μm)		6	18	56
Medial circumferential wall tension (N/m)	Total	7.8	110	56
	Per lamellar unit	1.6	2.2	56
Material stiffness ($\mathbb{C}_{\theta\theta\theta\theta}$, Eq. (9.8), Table 9.1) [MPa]		1.89	0.65−1.71	48,57
Structural stiffness (cfPWV*, Eq. (9.4), Table 9.1) [m/s]		4.0	6.6	12,58
Wall shear stress [Pa]		9−30	0.5−1.5	59,60
Vasa vasorum		Absent	Present	61
Subendothelial connective tissue		Absent	Varies**	61

Typical murine and human body weights are 30 and 75,000 g, respectively.[56]
*cfPWV: carotid-femoral PWV from applanation tonometry. Murine measurements were performed in ∼5.5-month old mice under sevoflurane anesthesia.[12] Human values are for 30−39 year old normotensives.[58] **Varies with age/disease.

The human aorta is often said to possess little vascular tone, in contrast to the murine aorta which contracts strongly to vasoactive substances.[62] Despite these claims, direct measurements (e.g., myography) of human aortic contractility remain wanting. "Indirect" evidence suggests, however, some vascular tone in the human aorta. Stefanadis et al., for example, showed a shift in the aortic pressure-diameter *relationship* shortly after smoking, suggesting involvement of vascular tone.[63] In addition, several studies investigated effects of sympathetic activation on PWV with disparate results, which may be attributable to the concomitant changes in blood pressure that often occur with sympathetic stimulation[64−68] (review in Reference 69). To overcome this limitation, Nardone et al. used lower-body pressure changes to elicit sympathetic activation, and showed significant increases in carotid-femoral PWV after mild lower-body negative pressure, without changes in blood pressure.[70]

When arteries distal to the aorta are studied, the influence of vascular tone becomes stronger and clearer. Vascular tone is well known to modulate human brachial artery diameter, as used in flow-mediated dilation measurements.[71] In addition, transit time PWV measurements that (also) involve more distal arteries have shown a vascular tone dependency.[72,73] Finally, cardio-ankle PWV as used in cardio-ankle vascular index (CAVI)/CAVI$_0$ changes markedly with alpha-1 adrenergic receptor blockade,[74,75] independent of blood pressure.

Diabetes and obesity

Obesity and diabetes are increasingly responsible for many sequelae, including cardiovascular disease. They also have significant effects on large artery stiffness. Importantly, it was shown that increases in arterial stiffness, as inferred via the PWV, in obese mice can precede the development of hypertension,[32] consistent with general findings in humans.[33] That is, it is now clear that increased large artery stiffness can be both a cause and consequence of

hypertension, thus revealing potentially insidious positive feedback loops that drive disease.[34,35] Recent data also indicate a bidirectional relationship between diabetes and large artery stiffness, since the latter can predict new-onset diabetes[36] and conversely, diabetes increases arterial stiffness, largely via fibrosis,[37] though also via changes in advanced glycation end-products.[38] We are reminded, therefore, that it is both changes in arterial wall composition and organization that dictate the material stiffness. Indeed, increasing evidence points to a critical role of tissue transglutaminases in arterial stiffening, which are important in matrix cross-linking.[39,40] The reader is also referred to a study that showed that obesity-induced arterial stiffening can be prevented with low-dose mineralocorticoid receptor blockage in mice, with arterial stiffness assessed using ultrasound (in vivo) as well as pressure myography and AFM (in vitro), hence emphasizing the different metrics having different meanings, though with overall consistent implications.[41]

Hypertension

Uncontrolled hypertension is one of the most common risk factors for myriad cardiovascular diseases; it, too, associates with marked increases in arterial stiffness. There are many different ways to induce hypertension in mice, including salt-loading, blocking endothelial-derived nitric oxide synthase using N(G)-Nitro-L-arginine methyl ester (L-NAME), surgically introducing constrictions, and chronic infusion of angiotensin II (AngII) or norepinephrine. Each model provides important, complementary insights. The so-called transverse aortic constriction model is particularly useful for it introduces proximal hypertension mainly via a mechanical perturbation. Nevertheless, it elicits infiltration of inflammatory cells and engages a local AngII response, both contributing to a structural stiffening of the wall.[42,43] Because of the central role of the renin-angiotensin system, chronic infusion of AngII is very common, with diverse arterial phenotypes being possible.[44] Again emphasizing the importance of matrix cross-linking in arterial stiffness, blocking the effects of lysyl oxidase (using β-amino-propionitrile, BAPN) in AngII-induced hypertension prevents the expected increase in PWV in mice.[45] The important dependence of mechanosensing in hypertensive arterial remodeling was demonstrated directly by showing attenuated remodeling in mice lacking the α1-integrin subunit[46]; integrins are, of course, key components of mechanotransduction in arteries. At least in the AngII-infused model, aortic stiffening depends both on elevated pressure-induced wall stress and inflammatory cell burden, which was demonstrated clearly using mice deficient in T-cells or interleukin 17a.[47] Again, however, it was structural, not material, stiffening that emerged,[48] suggesting yet again that the intramural cells try to mechanoregulate material stiffness. It is, nonetheless, the structural stiffness that affects the hemodynamics (see Eq. (9.1), Box 9.1), hence

reinforcing the importance of measurements of wall thickness, though this should ideally be total wall thickness, not just intimal-medial thickness, since adventitial fibrosis is evident in many cases of arterial stiffening, ranging from aging to hypertension.

Comparison of methods

In the preceding sections, we reviewed the primary methods available for measuring arterial stiffness, both in vivo and ex vivo, and illustrated their use via brief discussions of diverse mouse models. As elaborated in Boxes 9.2 and 9.3, loading conditions significantly influence such measurements.[1] Table 9.2 illustrates how differences in loading conditions and methodologies can potentially lead to large differences in calculated values of stiffness for the mouse aorta. As an example, note that reported values of material stiffness obtained from AFM (radial compressive in the traction-free state) and biaxial testing (circumferential and axial tensile in the in vivo stressed state) can differ by three *orders of magnitude* (i.e., 1000×). Clearly, such metrics cannot be compared directly. Although we did not detail appropriate constitutive relations, they are essential to the interpretation of measurements. Given that the arterial wall exhibits strongly nonlinear, anisotropic behaviors over finite deformations, appropriate theoretical frameworks should be employed.[18] We emphasize further that the associated reference state should be chosen carefully noting that stress-free (approximated via a series of judicious cuts), traction-free (in the absence of applied loads), and in vivo (e.g., in vivo value of axial stretch and diastolic pressure) can each be appropriate, indeed convenient, depending on the metric of interest. When using the in vivo state as a reference, however, one must ensure that the state of "prestress" is accounted for appropriately, which can be achieved in different ways depending on the application. As an example, our group has used three different approaches simply when considering the in vivo reference, with applications to quantifying the hemodynamics, the mechanobiological state, or a reference for complex subject-specific geometries.[49–51] One approach is not necessarily better than another, they are simply different with different utilities.

Recommendations

In this section, we offer a few recommendations for choosing an appropriate method to study arterial stiffness. First, if a direct comparison/translation is to be made to human studies, in vivo measurement of PWV may be an appropriate choice. We emphasize again, however, the importance of the associated loading conditions: blood pressure at the time of measurement strongly influences the value of the calculated in vivo stiffness. Therefore, care must be taken to ensure that measured effects are not due to anesthesia and/or emotional stress influencing blood

pressure. Another potential factor that mandates in vivo studies is the requirement for follow-up measurements. If follow-up measurements are not required and excised tissue can be obtained, ex vivo measurements—not affected by the large confounding influence of blood pressure—may be more appropriate. Importantly, PWV can be approximated from ex vivo measurements of pressure and diameter (when performed under loading conditions similar to in vivo) using the Bramwell—Hill equation (Eqs. (9.3) and (9.5), Table 9.1),[10,52] without the need to take into account the effects of anesthesia or emotional stress, while allowing direct comparisons between in vivo and ex vivo. In this regard, note that perivascular tissue typically exerts a radial load on the adventitial surface, thus affecting the transmural pressure that distends the wall. Such perivascular effects can be significant and should be accounted for.[53]

Ex vivo methods come in many varieties. Indentation methods such as AFM provide extremely detailed maps ("images") of spatially resolved stiffness values. Yet, often performed as an indentation test, AFM measures compressive—not tensile—stiffness, often in the excised traction-free state. Hence, translation of such measurements to whole-artery, in vivo—relevant arterial stiffness values is cumbersome.

Myography has become a well-established method to functionally test arterial responses to vasoactive stimuli. In particular, wire myography (requiring only small ring-like samples) allows simultaneously testing of responses to various stimuli. Wire myography also has the advantage that side branches, if present, do not have to be ligated (pressure myography does require this, in order for the artery under test to hold pressure). Smooth muscle

---

BOX 9.5 Different material stiffness metrics

Many different metrics of material stiffness are used in arterial stiffness research. Often encountered is Young's modulus (E), a measure of the extensional stiffness (i.e., change of stress with respect to strain) of a material, which can be inferred by plotting normal stress versus extensional strain in a *uniaxial* stress test.[76] E is defined for LEHI (linear, elastic, homogeneous, isotropic) material behavior. The artery wall material, however, is strongly nonlinear and anisotropic, limiting the appropriateness of E in arterial mechanics.

The linearity assumption of E is commonly "overcome" by estimating an *incremental* Young's modulus (E_{inc}) as the local tangent of the circumferential Cauchy stress-stretch curve obtained during inflation (Eq. (9.7), Table 9.1). However, such loading is not uniaxial but rather biaxial (with lateral contraction due to a Poisson effect in standard "uniaxial" tests and, with strong biaxial coupling present due to the axial (pre)stretch in pressurized vessels (Box 9.3). The local tangent, hence, is influenced by both circumferential and axial behaviors and cannot be interpreted as an "independent," circumferential, material stiffness.

Strictly speaking, (material) stiffness is defined as a change in stress with respect to a change in conjugate strain (or stretch).[76] Common stress-strain pairs are given in Table 9.4, below. Note that E_{inc} when obtained from Cauchy stress and stretch ratio (a component of the deformation gradient or the left stretch tensor), violates this definition.

TABLE 9.4 Conjugate stress-strain measures.

Stress measure	Conjugate strain measure	Volume	Integral of stress-strain product over volume
Cauchy ($\boldsymbol{\sigma}$)	—	Deformed/current	—
First Piola—Kirchhoff ($\mathbf{P}$)	Deformation gradient ($\mathbf{F}$)[a]	Original/material	Stored energy
Second Piola—Kirchhoff ($\mathbf{S}$)	Green—Lagrange ($\mathbf{E}$)	Original/material	Stored energy

[a]*which has stretch ratios λ on diagonal in the absence of rigid body rotations.*

Commonly observed (circumferential) stiffness metrics that obey conjugacy are $\partial P_{\theta\theta}/\partial\lambda_\theta$ and $\partial S_{\theta\theta}/\partial E_{\theta\theta}$. Both, however, are defined with respect to the original volume. Typically, one wants a (material) stiffness metric to reflect how a material will deform if it is loaded in the *current* configuration. Baek et al. invoked the theory of small-on-large to arrive at such a metric that is useful in fluid—solid interaction simulations over a cardiac cycle ($\mathbb{C}$; Eq. (9.8), Table 9.1),[49] which has the advantage that it can be intuitively used to directly operate on a small strain tensor ($\boldsymbol{\varepsilon}$; the *small* strain in small-on-large theory), yielding the associated change in Cauchy stress ($\boldsymbol{\sigma} = \mathbb{C} : \boldsymbol{\varepsilon}$).

contraction in wire myography occurs under non-physiological axial loading, however, and may not be directly comparable to the physiological case.[54] This issue is resolved in pressure myography, where the artery can be held at its in vivo length. When the main study of interest is to quantify structural stiffness (Box 9.1) under reproducible, in vivo relevant conditions, pressure myography is a good compromise. When constitutive behavior and material stiffness (Box 9.1) are of particular interest, biaxial testing has a clear advantage.

Biaxial testing enables parameterization of an anisotropic *constitutive* model of the arterial wall material. Such a constitutive model enables calculation of true material stiffness parameters (Box 9.5), which have been shown to be particularly relevant in aneurysm mechanobiology,[28] and which are essential in informing finite element formulations.[49] pDIC, finally, extends biaxial testing to account for nontubular/nonuniform geometries. This is also particularly relevant in aneurysm research, yielding detailed maps of material parameters along the entire aneurysmal surface. As such, it allows properties to be compared, as, for example, at the neck and in the dome regions of an aneurysm. pDIC is, however, a highly specialized technique, typically requiring the combination of three measurement modalities ("normal" biaxial testing, OCT, and pDIC imaging) as well as inverse finite element modeling. As such, its use is practically limited to dedicated engineering labs.

References

1. Spronck B, Humphrey J. Arterial stiffness: different metrics, different meanings. **J Biomech Eng**. 2019; 141:0910041−09100412.
2. Field KJ, White WJ, Lang CM. Anaesthetic effects of chloral hydrate, pentobarbitone and urethane in adult male rats. **Lab Anim**. 1993; 27:258−269.
3. Kuo MM, Barodka V, Abraham TP, et al. Measuring ascending aortic stiffness in vivo in mice using ultrasound. **J Vis Exp**. 2014;(94):52200.
4. Cuomo F, Ferruzzi J, Humphrey JD, Figueroa CA. An experimental-computational study of catheter induced alterations in pulse wave velocity in anesthetized mice. **Ann Biomed Eng**. 2015; 43:1555−1570.
5. Wilde E, Aubdool AA, Thakore P, et al. Tail-cuff technique and its influence on central blood pressure in the mouse. **J Am Heart Assoc**. 2017; 6.
6. Cosson E, Herisse M, Laude D, et al. Aortic stiffness and pulse pressure amplification in Wistar-Kyoto and spontaneously hypertensive rats. **Am J Physiol Heart Circ Physiol**. 2007; 292:H2506−H2512.
7. Butlin M, Tan I, Spronck B, Avolio AP. Measuring arterial stiffness in animal experimental studies. **Arterioscler Thromb Vasc Biol**. 2020; 40:1068−1077.
8. Mitchell GF, Pfeffer MA, Finn PV, Pfeffer JM. Comparison of techniques for measuring pulse-wave velocity in the rat. **J Appl Physiol**. 1997; 82:203−210.
9. Chiu YC, Arand PW, Shroff SG, Feldman T, Carroll JD. Determination of pulse wave velocities with computerized algorithms. **Am Heart J**. 1991; 121:1460−1470.
10. Spronck B, Tan I, Reesink KD, et al. Heart rate and blood pressure dependence of aortic distensibility in rats: comparison of measured and calculated pulse wave velocity. **J Hypertens**. 2021; 39:117−126.
11. Trachet B, Fraga-Silva RA, Londono FJ, Swillens A, Stergiopulos N, Segers P. Performance comparison of ultrasound-based methods to assess aortic diameter and stiffness in normal and aneurysmal mice. **PLoS One**. 2015; 10:e0129007.
12. Leloup AJ, Fransen P, Van Hove CE, Demolder M, De Keulenaer GW, Schrijvers DM. Applanation tonometry in mice: a novel noninvasive technique to assess pulse wave velocity and arterial stiffness. **Hypertension**. 2014; 64:195−200.
13. Bennett RT. **The Light in the Heart**. Roy Bennett; 2016.
14. Na S, Sun Z, Meininger GA, Humphrey JD. On atomic force microscopy and the constitutive behavior of living cells. **Biomech Model Mechanobiol**. 2004; 3:75−84.
15. Brossollet LJ, Vito RP. An alternate formulation of blood vessel mechanics and the meaning of the in vivo property. **J Biomech**. 1995; 28:679−687.
16. Ferruzzi J, Bersi MR, Humphrey JD. Biomechanical phenotyping of central arteries in health and disease: advantages of and methods for murine models. **Ann Biomed Eng**. 2013; 41:1311−1330.
17. Gleason RL, Gray SP, Wilson E, Humphrey JD. A multiaxial computer-controlled organ culture and biomechanical device for mouse carotid arteries. **J Biomech Eng**. 2004; 126:787−795.
18. Humphrey JD. **Cardiovascular Solid Mechanics: Cells, Tissues, and Organs**. NY: Springer; 2002.
19. Genovese K, Lee YU, Lee AY, Humphrey JD. An improved panoramic digital image correlation method for vascular strain analysis and material characterization. **J Mech Behav Biomed Mater**. 2013; 27:132−142.
20. Bersi MR, Bellini C, Di Achille P, Humphrey JD, Genovese K, Avril S. Novel methodology for characterizing regional variations in the material properties of murine aortas. **J Biomech Eng**. 2016; 138.
21. Ferruzzi J, Madziva D, Caulk AW, Tellides G, Humphrey JD. Compromised mechanical homeostasis in arterial aging and associated cardiovascular consequences. **Biomech Model Mechanobiol**. 2018; 17:1281−1295.
22. Spronck B, Ferruzzi J, Bellini C, Caulk AW, Murtada SI, Humphrey JD. Aortic remodeling is modest and sex-independent in mice when hypertension is superimposed on aging. **J Hypertens**. 2020; 38:1312−1321.
23. Reddy AK, Li YH, Pham TT, et al. **Measurement of Aortic Input Impedance in Mice: Effects of Age on Aortic Stiffness**. Vol. 285. 2003:H1464−H1470.
24. Lesniewski LA, Durrant JR, Connell ML, et al. **Aerobic Exercise Reverses Arterial Inflammation with Aging in Mice**. Vol. 301. 2011:H1025−H1032.
25. Murtada SI, Kawamura Y, Caulk AW, et al. Paradoxical aortic stiffening and subsequent cardiac dysfunction in Hutchinson-Gilford progeria syndrome. **J R Soc Interface**. 2020; 17:20200066.
26. Marque V, Kieffer P, Gayraud B, Lartaud-Idjouadiene I, Ramirez F, Atkinson J. Aortic wall mechanics and composition in a transgenic mouse model of Marfan syndrome. **Arterioscler Thromb Vasc Biol**. 2001; 21:1184−1189.
27. Chung AW, Au Yeung K, Cortes SF, et al. Endothelial dysfunction and compromised eNOS/Akt signaling in the thoracic aorta during the progression of Marfan syndrome. **Br J Pharmacol**. 2007; 150:1075−1083.
28. Bellini C, Bersi MR, Caulk AW, et al. Comparison of 10 murine models reveals a distinct biomechanical phenotype in thoracic aortic aneurysms. **J R Soc Interface**. 2017; 14.

29. Humphrey JD, Milewicz DM, Tellides G, Schwartz MA. Cell biology. Dysfunctional mechanosensing in aneurysms. **Science**. 2014; 344:477−479.

30. Shadwick RE. Mechanical design in arteries. **J Exp Biol**. 1999; 202:3305−3313.

31. Humphrey JD, Dufresne ER, Schwartz MA. Mechanotransduction and extracellular matrix homeostasis. **Nat Rev Mol Cell Biol**. 2014; 15:802−812.

32. Weisbrod RM, Shiang T, Al Sayah L, et al. Arterial stiffening precedes systolic hypertension in diet-induced obesity. **Hypertension**. 2013; 62:1105−1110.

33. Kaess BM, Rong J, Larson MG, et al. Aortic stiffness, blood pressure progression, and incident hypertension. **J Am Med Assoc**. 2012; 308:875−881.

34. Laurent S, Boutouyrie P. The structural factor of hypertension: large and small artery alterations. **Circ Res**. 2015; 116:1007−1021.

35. Humphrey JD, Harrison DG, Figueroa CA, Lacolley P, Laurent S. Central artery stiffness in hypertension and aging: a problem with cause and consequence. **Circ Res**. 2016; 118:379−381.

36. Muhammad IF, Borne Y, Ostling G, et al. Arterial stiffness and incidence of diabetes: a population-based cohort study. **Diabetes Care**. 2017; 40:1739−1745.

37. Raaz U, Schellinger IN, Chernogubova E, et al. Transcription factor Runx2 promotes aortic fibrosis and stiffness in type 2 diabetes mellitus. **Circ Res**. 2015; 117:513−524.

38. Zieman SJ, Kass DA. Advanced glycation endproduct crosslinking in the cardiovascular system: potential therapeutic target for cardiovascular disease. **Drugs**. 2004; 64:459−470.

39. Oh YJ, Pau VC, Steppan J, et al. Role of tissue transglutaminase in age-associated ventricular stiffness. **Amino Acids**. 2017; 49:695−704.

40. Steppan J, Sikka G, Jandu S, et al. Exercise, vascular stiffness, and tissue transglutaminase. **J Am Heart Assoc**. 2014; 3:e000599.

41. DeMarco VG, Habibi J, Jia G, et al. Low-dose mineralocorticoid receptor blockade prevents western diet-induced arterial stiffening in female mice. **Hypertension**. 2015; 66:99−107.

42. Kuang SQ, Geng L, Prakash SK, et al. Aortic remodeling after transverse aortic constriction in mice is attenuated with AT1 receptor blockade. **Arterioscler Thromb Vasc Biol**. 2013; 33:2172−2179.

43. Eberth JF, Gresham VC, Reddy AK, Popovic N, Wilson E, Humphrey JD. Importance of pulsatility in hypertensive carotid artery growth and remodeling. **J Hypertens**. 2009; 27:2010−2021.

44. Bersi MR, Khosravi R, Wujciak AJ, Harrison DG, Humphrey JD. Differential cell-matrix mechanoadaptations and inflammation drive regional propensities to aortic fibrosis, aneurysm or dissection in hypertension. **J R Soc Interface**. 2017; 14:20170327.

45. Eberson LS, Sanchez PA, Majeed BA, Tawinwung S, Secomb TW, Larson DF. Effect of lysyl oxidase inhibition on angiotensin II-induced arterial hypertension, remodeling, and stiffness. **PLoS One**. 2015; 10:e0124013.

46. Louis H, Kakou A, Regnault V, et al. Role of α1β1-integrin in arterial stiffness and angiotensin-induced arterial wall hypertrophy in mice. **Am J Physiol Heart Circ Physiol**. 2007; 293:H2597−H2604.

47. Wu J, Thabet SR, Kirabo A, et al. Inflammation and mechanical stretch promote aortic stiffening in hypertension through activation of p38 mitogen-activated protein kinase. **Circ Res**. 2014; 114:616−625.

48. Bersi MR, Bellini C, Wu J, Montaniel KRC, Harrison DG, Humphrey JD. Excessive adventitial remodeling leads to early aortic maladaptation in angiotensin-induced hypertension. **Hypertension**. 2016; 67:890−896.

49. Baek S, Gleason RL, Rajagopal K, Humphrey J. Theory of small on large: potential utility in computations of fluid−solid interactions in arteries. **Comput Methods Appl Mech Eng**. 2007; 196:3070−3078.

50. Bellini C, Ferruzzi J, Roccabianca S, Di Martino ES, Humphrey JD. A microstructurally motivated model of arterial wall mechanics with mechanobiological implications. **Ann Biomed Eng**. 2014; 42:488−502.

51. Rausch MK, Genet M, Humphrey JD. An augmented iterative method for identifying a stress-free reference configuration in image-based biomechanical modeling. **J Biomech**. 2017; 58:227−231.

52. Bramwell JC, Hill AV. The velocity of the pulse wave in man. **Proc R Soc Lond B**. 1922; 93:298−306.

53. Ferruzzi J, Di Achille P, Tellides G, Humphrey JD. Combining in vivo and in vitro biomechanical data reveals key roles of perivascular tethering in central artery function. **PLoS One**. 2018; 13:e0201379.

54. Caulk AW, Humphrey JD, Murtada SI. Fundamental roles of axial stretch in isometric and isobaric evaluations of vascular contractility. **J Biomech Eng**. 2019; 141.

55. Demiray H. Wave propagation through a viscous fluid contained in a prestressed thin elastic tube. **Int J Eng Sci**. 1992; 30:1607−1620.

56. Wolinsky H, Glagov S. A lamellar unit of aortic medial structure and function in mammals. **Circ Res**. 1967; 20:99−111.

57. Roccabianca S, Figueroa CA, Tellides G, Humphrey JD. Quantification of regional differences in aortic stiffness in the aging human. **J Mech Behav Biomed Mater**. 2014; 29:618−634.

58. Reference Values for Arterial Stiffness Collaboration. Determinants of pulse wave velocity in healthy people and in the presence of cardiovascular risk factors: ’establishing normal and reference values. **Eur Heart J**. 2010; 31:2338−2350.

59. Weinberg PD, Ross Ethier C. Twenty-fold difference in hemodynamic wall shear stress between murine and human aortas. **J Biomech**. 2007; 40:1594−1598.

60. Greve JM, Les AS, Tang BT, et al. Allometric scaling of wall shear stress from mice to humans: quantification using cine phase-contrast MRI and computational fluid dynamics. **Am J Physiol Heart Circ Physiol**. 2006; 291:H1700−H1708.

61. Treuting PM, Dintzis SM, Frevert CW, Liggitt HD, Montine KS. **Comparative Anatomy and Histology : A Mouse and Human Atlas**. 1st ed. Amsterdam ; Boston: Elsevier/Academic Press; 2012.

62. Leloup AJA, Van Hove CE, De Moudt S, De Meyer GRY, De Keulenaer GW, Fransen P. Vascular smooth muscle cell contraction and relaxation in the isolated aorta: a critical regulator of large artery compliance. **Physiol Rep**. 2019; 7:e13934.

63. Stefanadis C, Vlachopoulos C, Tsiamis E, et al. Unfavorable effects of passive smoking on aortic function in men. **Ann Intern Med**. 1998; 128:426−434.

64. Phillips AA, Bredin SS, Cote AT, Drury CT, Warburton DE. Aortic distensibility is reduced during intense lower body negative pressure and is related to low frequency power of systolic blood pressure. **Eur J Appl Physiol**. 2013; 113:785−792.

65. Lydakis C, Momen A, Blaha C, Herr M, Leuenberger UA, Sinoway LI. Changes of elastic properties of central arteries during acute static exercise and lower body negative pressure. **Eur J Appl Physiol**. 2008; 102:633−641.

66. Sonesson B, Vernersson E, Hansen F, Lanne T. Influence of sympathetic stimulation on the mechanical properties of the aorta in humans. **Acta Physiol Scand**. 1997; 159:139−145.

67. Maki-Petaja KM, Barrett SM, Evans SV, Cheriyan J, McEniery CM, Wilkinson IB. The role of the autonomic nervous system in the regulation of aortic stiffness. **Hypertension**. 2016; 68:1290−1297.

68. Harvey RE, Barnes JN, Hart EC, Nicholson WT, Joyner MJ, Casey DP. Influence of sympathetic nerve activity on aortic hemodynamics and pulse wave velocity in women. **Am J Physiol Heart Circ Physiol**. 2017; 312:H340−H346.

69. Nardone M, Floras JS, Millar PJ. Sympathetic neural modulation of arterial stiffness in humans. **Am J Physiol Heart Circ Physiol**. 2020; 319:H1338−H1346.

70. Nardone M, Incognito AV, Millar PJ. Evidence for pressure-independent sympathetic modulation of central pulse wave velocity. **J Am Heart Assoc**. 2018; 7.

71. Celermajer DS, Sorensen KE, Gooch VM, et al. Non-invasive detection of endothelial dysfunction in children and adults at risk of atherosclerosis. **Lancet**. 1992; 340:1111−1115.

72. Bia D, Armentano R, Pessana F, Zocalo Y, Lluberas S, Avolio AP. Non-symmetrical double-logistic analysis of 24 hour arterial stiffness profile in normotensive and hypertensive subjects. **Annu Int Conf IEEE Eng Med Biol Soc**. 2008; 2008:809−812.

73. Liu Q, Yan BP, Yu CM, Zhang YT, Poon CC. Attenuation of systolic blood pressure and pulse transit time hysteresis during exercise and recovery in cardiovascular patients. **IEEE Trans Biomed Eng**. 2014; 61:346−352.

74. Shirai K, Shimizu K, Takata M, Suzuki K. Independency of the cardio-ankle vascular index from blood pressure at the time of measurement. **J Hypertens**. 2017; 35:1521−1523.

75. Shirai K, Song M, Suzuki J, et al. Contradictory effects of beta1- and alpha1- aderenergic receptor blockers on cardio-ankle vascular stiffness index (CAVI)–CAVI independent of blood pressure. **J Atherosclerosis Thromb**. 2011; 18:49−55.

76. Humphrey JD, O'Rourke SL. **An Introduction to Biomechanics : Solids and Fluids, Analysis and Design**. 2nd ed. New York: Springer; 2015.

77. Liu SL, Bae YH, Yu C, et al. Matrix metalloproteinase-12 is an essential mediator of acute and chronic arterial stiffening. **Sci Rep**. 2015; 5:17189.

78. Hayenga HN, Trache A, Trzeciakowski J, Humphrey JD. Regional atherosclerotic plaque properties in ApoE-/- mice quantified by atomic force, immunofluorescence, and light microscopy. **J Vasc Res**. 2011; 48:495−504.

79. Lee JJ, Galatioto J, Rao S, Ramirez F, Costa KD. Losartan attenuates degradation of aorta and lung tissue micromechanics in a mouse model of severe Marfan syndrome. **Ann Biomed Eng**. 2016; 44:2994−3006.

80. Bellini C, Caulk AW, Li G, Tellides G, Humphrey JD. Biomechanical phenotyping of the murine aorta: what is the best control? **J Biomech Eng**. 2017; 139:0445011.

81. Haskett D, Speicher E, Fouts M, et al. The effects of angiotensin II on the coupled microstructural and biomechanical response of C57BL/6 mouse aorta. **J Biomech**. 2012; 45:772−779.

82. Fujikura K, Luo J, Gamarnik V, et al. A novel noninvasive technique for pulse-wave imaging and characterization of clinically-significant vascular mechanical properties in vivo. **Ultrason Imaging**. 2007; 29:137−154.

This page intentionally left blank

Section II

Basic and applied physiology

This page intentionally left blank

Chapter 10

Hemodynamic role of the aorta

Julio A. Chirinos[1,2]

[1]University of Pennsylvania Perelman School of Medicine, Hospital of the University of Pennsylvania and Perelman Center for Advanced Medicine, Philadelphia, PA, United States; [2]Ghent University, Ghent, Belgium

Introduction

The aorta, a large elastic artery, exerts important hemodynamic role beyond its conduit function. A healthy aorta exerts a powerful cushioning function, contributing to the delivery of nearly steady flow to the microvasculature despite the intermittent left ventricular (LV) ejection. Increased large artery stiffness (LAS), which occurs with aging and various disease states, causes an impairment in this cushioning function, leading to multiple deleterious consequences on pulsatile arterial hemodynamics, and ultimately on target organs (Fig. 10.1). LAS causes isolated systolic hypertension,[1] an endemic condition characterized by increased systolic blood pressure with normal or low diastolic blood pressure (i.e., increased pulse pressure [PP]), responsible for a large proportion of the global burden of cardiovascular morbidity and mortality. Second, LAS reduces coronary perfusion pressure and increases LV afterload, promoting LV remodeling, dysfunction, and failure, as discussed in Chapters 15, 16, 17 and 36.[2] Third, by promoting increased arterial pressure and flow pulsatility, LAS leads to increased penetration of pulsatile energy into the microvasculature of target organs, particularly those that require high blood flow and therefore must operate at low arteriolar resistance.[3] Interestingly, target organ failure (such as chronic kidney disease and diabetes) can lead to further arterial stiffening,[4] creating a vicious cycle of hemodynamic dysfunction that ultimately contributes to the pathogenesis of heart failure (HF), impaired coronary perfusion, kidney disease, and cerebrovascular disease. Recent data also support a potential role for LAS in metabolic dysfunction and diabetes. Consistent with the central role of LAS in human health, measures of LAS (such as carotid-femoral pulse wave velocity, CF-PWV) independently predict the risk of incident cardiovascular

events in various populations including clinical and community-based cohorts.[5-7]
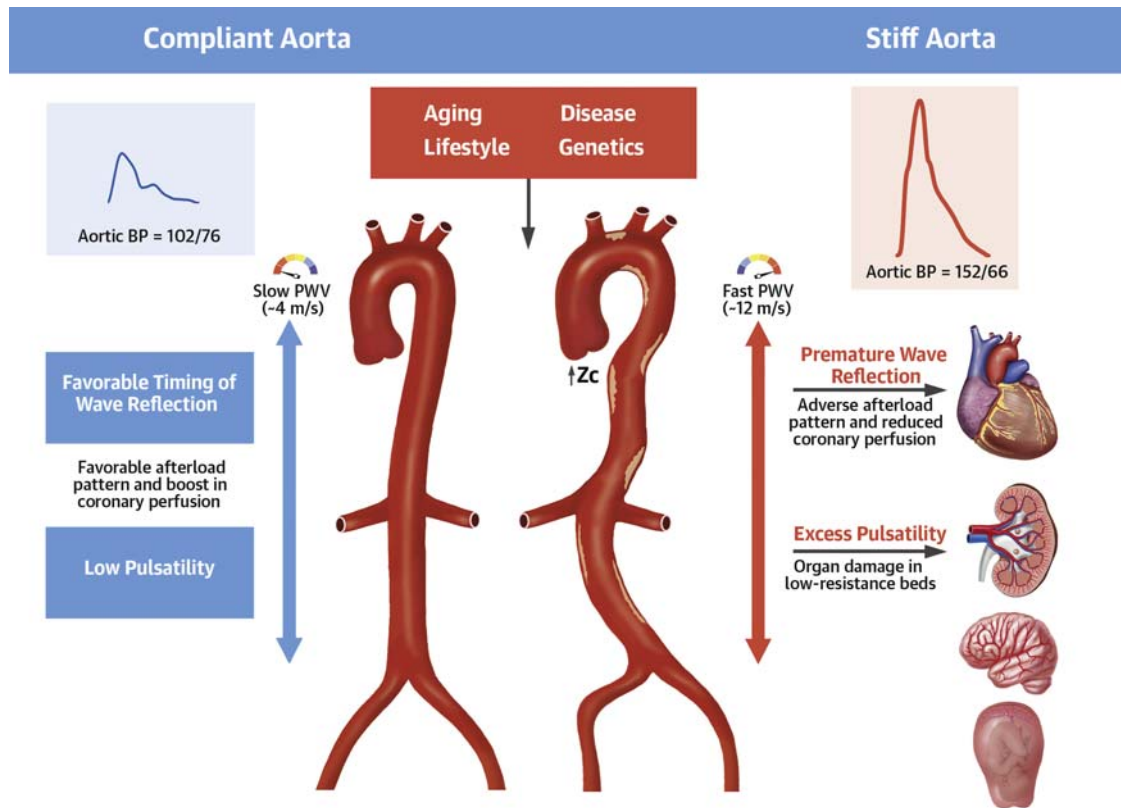
This chapter, largely based on a recent review of aortic stiffness by the author and collaborators,[7] provides an overview of key principles related to the hemodynamic role of the aorta, the impact of aortic stiffening on target organs. Specific aspects of the hemodynamic role of the aorta will be developed in dedicated chapters throughout this textbook. This chapter also provides a brief description of key mechanisms leading to aortic stiffening, which are developed in detail in subsequent chapters.

Hemodynamic consequences of large artery stiffness

The hemodynamic consequences of LAS are variable and relatively complex, but can be conceptually described from: (1) The effects of LAS on the early aortic systolic pressure rise; (2) The effects of LAS on the speed at which the cardiac pulse travels in the arterial wall[2,8]; (3) The effects of LAS on wave reflections at first-order bifurcations.

Effect on the early systolic aortic pulse pressure rise

As described in detail in Chapters 1 and 3, at the beginning of each cardiac cycle, the left ventricle generates a forward-traveling pulse that increases pressure and flow in the proximal aorta. The amount of pressure increase required to push the pulse flow through the aortic root in early systole depends on the local impedance offered by the proximal aorta. This local impedance, called the *characteristic impedance* (Zc), is a measurable property that increases due to aortic root wall stiffening, a small aortic cross-sectional area, or both.[2] Interestingly, Zc is much more sensitive to size (i.e., cross-

FIGURE 10.1   Role of large artery stiffness in health and disease. In young healthy adults, a compliant aorta: (A) effectively buffers excess pulsatility due to the intermittent left ventricular ejection; (B) exhibits a slow pulse wave velocity (PWV), which allows pulse wave reflections to arrive to the heart during diastole, effectively increasing diastolic coronary perfusion pressure but not systolic ventricular load. A number of factors increase aortic wall stiffness, which leads to several adverse hemodynamic consequences. Aortic stiffening leads to increased forward wave amplitude on one hand and premature arrival of wave reflections to the heart on the other. This leads to increased pulsatile load to the left ventricle in systole and a reduced coronary perfusion pressure in diastole, ultimately promoting myocardial remodeling, dysfunction, failure, and a reduced perfusion reserve (even in the absence of epicardial coronary disease). This adverse hemodynamic pattern also results in excessive pulsatility in the aorta, which is transmitted preferentially to low-resistance vascular beds (such as the kidney, placenta and brain), because in these organs, microvascular pressure is more directly coupled with aortic artery pressure and flow fluctuations. *Reproduced from Chirinos JA, Segers P, Hughes T, Townsend R., Large-artery stiffness in health and disease: JACC state-of-the-art review. **J Am Coll Cardiol**. 2019; 74(9):1237−1263, with permission from Elsevier.*
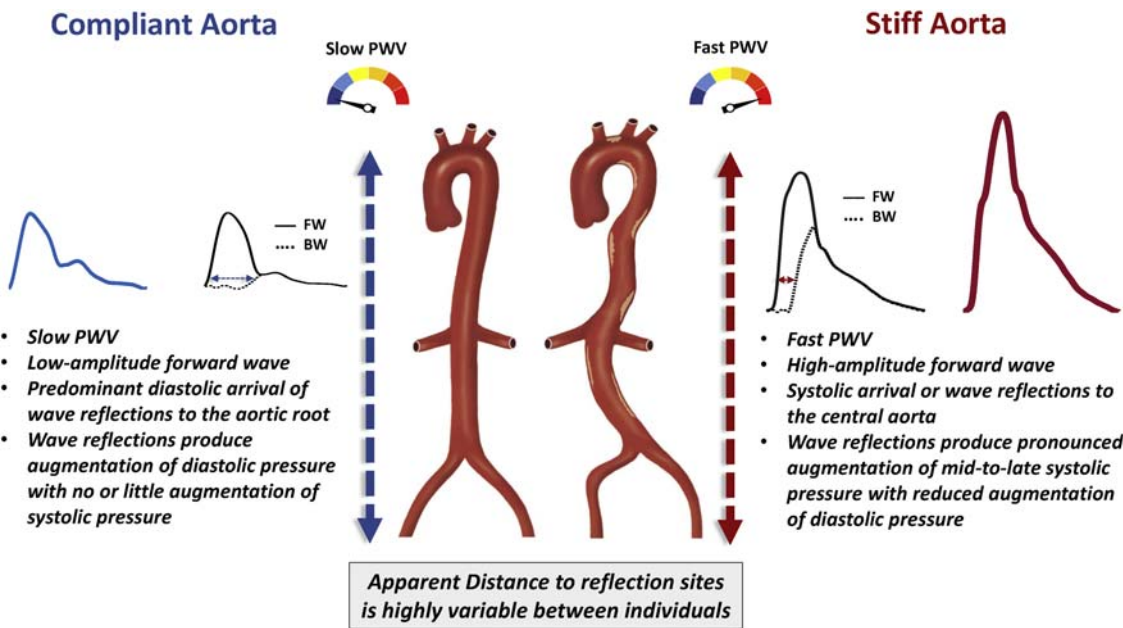
sectional area) than to the stiffness of the aortic wall material. Therefore, aortic dilation may partially overcome the hemodynamic consequences of aortic root stiffening, and conversely, wall stiffening in the absence of eccentric remodeling of the root can have particularly pronounced effects on PP. However, excessive aortic dilation with aneurysm formation is clearly deleterious and associated with a risk of aortic rupture. Although the physical principles governing PP are well understood, the causal interrelationships between aortic dilation, aortic wall stiffening, and pressure pulsatility are likely multidirectional and incompletely understood from a biologic standpoint.

Effect on wave speed (Fig. 10.2)

As discussed in detail in Chapter 11, the energy wave generated by the LV (incident wave) is transmitted by conduit vessels and partially reflected at innumerable sites of impedance mismatch throughout the arterial tree, including

points of change in wall diameter, change in material properties along the artery wall, and points of branching. A myriad of scattered tiny reflections from individual reflection sites are conducted back to the proximal aorta and merge into a net reflected wave. The timing of arrival of reflected waves to the proximal aorta is strongly influenced by the pulse wave velocity (PWV) of conduit vessels, particularly the aorta, which transmits both forward and backward traveling waves. Stiffer aortas conduct waves at greater PWV, and therefore promote an earlier arrival of the reflected waves for any given distance to reflection sites.

In the presence of a slow PWV, as occurs in young, healthy adults with elastic aortas, wave reflections arrive at the aorta predominantly during diastole, augmenting diastolic pressure. In contrast, when PWV increases due to aortic wall stiffening, wave reflections return to the proximal aorta in mid-to-late systole, producing systolic pressure augmentation, with loss of diastolic pressure augmentation and widening of the aortic PP (Fig. 10.2).

FIGURE 10.2   Consequences of increased aortic stiffness on the central pressure waveform. The left side represents what occurs with a highly compliant aorta, as occurs in young healthy adults; the right side represents a very stiff aorta, as occurs in the elderly and/or in the presence of various disease states. A stiff aorta is associated with a high-amplitude forward wave and a faster pulse wave velocity (PWV), determining a faster forward and backward (reflected) wave speeds. This determines an earlier arrival of wave reflections to the aorta, with progressive loss of diastolic pressure augmentation and increased late systolic augmentation. The figure illustrates two rather extreme situations, with most people falling "in between." Moreover, it should be emphasized that the apparent distance to reflection sites is highly variable between individuals and may become a dominant determinant of the timing of wave reflections in populations that exhibit stiff aortas or in the setting of hypertension. The term "apparent" is used because reflection sites can modify the morphology of reflected waves making it appear "shifted" in time (i.e., a shift to the right appears as if a reflection site is further away from the heart, for any given PWV). *BW*, backward wave; *FW*, forward wave. *Reproduced from Chirinos JA, Segers P, Hughes T, Townsend R., Large-artery stiffness in health and disease: JACC state-of-the-art review.* **J Am Coll Cardiol**. *2019; 74(9):1237−1263, with permission from Elsevier.*

Interestingly, this phenomenon cannot be measured via brachial PP measurements because the reflected wave tends to augment central systolic pressure to a greater degree than brachial pressure. Moreover, even at the central aorta, the reflected wave not only increases central peak pressure but also has a predominant effect on the morphology of the pressure waveform, with a pronounced mid-to-late systolic component relative to early systolic and diastolic pressure. Therefore, individuals with identical central PP values can have markedly different central pressure profiles and for any given absolute blood pressure level, late systolic loading from wave reflections determines abnormal ventricular−vascular interactions and an adverse LV loading sequence,[9−11] as will be discussed in detail in Chapter 16.

Although forward and backward traveling waves are often seen as having different determinants, they are in fact highly interrelated. First, the amplitude of the reflected wave is highly dependent on the amplitude of the forward wave. In turn, wave reflections can re-reflect at the LV, becoming rectified and thus contributing to the amplitude of the forward wave.[12] In the presence of very high PWV, as occurs with advanced age and/or disease, multiple reflections and re-reflections occur in a single cardiac cycle, and forward and backward waves are highly dependent on each other.

Some caveats to the simplified description above are worth mentioning. First, although the reflected wave appears discrete and is often referred as a single wave, it is important to keep in mind that the net reflected wave measured in at the aortic root is the net sum of innumerable tiny reflections. Accordingly, the reflected wave does not arise from a single reflection site, and the concept of the "effective" length of the arterial tree (i.e., distance to the reflection site) is an unrealistic concept. As discussed in detail in Chapter 11, given the highly distributed nature of wave reflections, individual reflection sites have little importance relative to the bulk of reflections originating elsewhere (except for strong reflection sites in specific conditions, such as aortic coarctation or complete distal aortic occlusion). Finally, it is important to note that wave reflections and arterial stiffness do not necessarily vary in the same direction. In general, arterial stiffness *modulates* the effects of wave reflections on the central pressure profile by affecting the timing of their arrival to the proximal aorta. However, wave reflections also vary independently

of arterial stiffness due to modulation of muscular artery stiffness and size,[13] as well as microvascular tone. Although the timing of wave reflections is correlated with aortic PWV, there is also great variability in the distance to reflection sites, such that this relationship is not perfect. Moreover, the variability in the distance to reflection sites can become the dominant determinant of the timing of wave reflections within patient populations that in general exhibit stiff aortas (such as older, diseased populations), in the setting of hypertension or in the setting of specific pharmacologic interventions that modulate muscular artery properties.[13]

Effect of aortic stiffness on wave reflections in first-order bifurcations
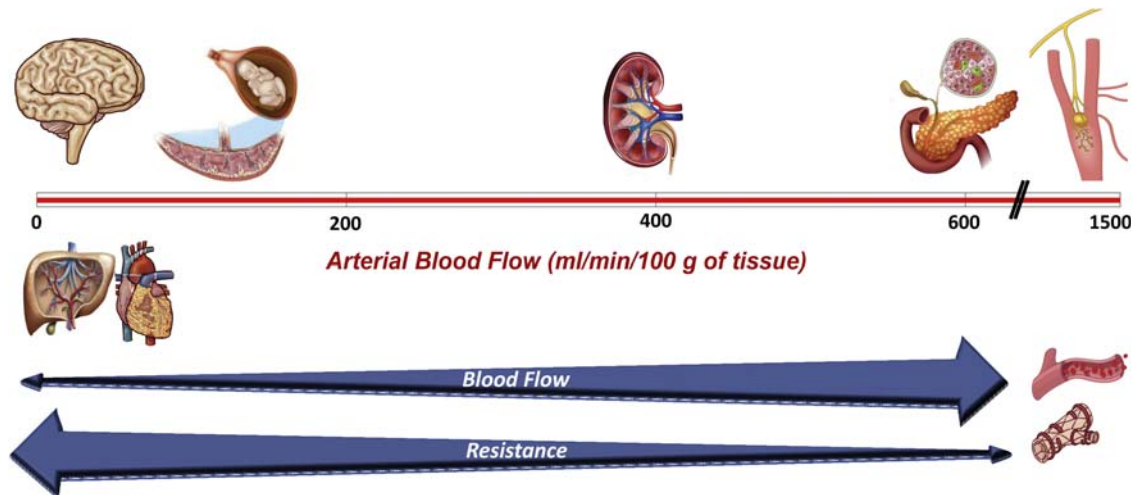
In young adults, aortic PWV is much lower than the PWV of intermediate-sized muscular arteries. With aging, aortic PWV increases and matches the PWV of these more distal segments. This has led to the controversial proposition that increased PWV with aging produces "impedance matching" with the stiffer muscular arterial segments, reducing wave reflections at first-order bifurcations (such as the aortic-femoral or aortic-carotid interfaces).[14] This principle has been extended to propose protective reflections at first-order branches of target organs such as the brain and the kidney. Several aspects of this concept are inconsistent with physiologic considerations. First, wave reflections at the inlet of target organs amplify the PP, and thus increase it in daughter branches to a much greater degree than they prevent energy penetration. This is because PP amplification into the branches is linearly related to the local reflection coefficient, whereas prevention of energy penetration is related to its square root; for example, a local reflection coefficient at the aortic-carotid interface of 0.10 would prevent only 1% of energy penetration but would increase carotid PP by 10%. Second, *impedance matching* does not equal *PWV matching* between parent and daughter vessels, but largely depends on vessel size (specifically, the ratio of the area of the parent vessels to the sum of the areas of the daughter vessels). This is due to the fact that characteristic impedance of a vessel is much more dependent on its caliber than on its stiffness. The geometry of vessels at first-order bifurcations tends to be already optimized for forward energy transmission,[15] such that impedances are relatively well-matched even before the aorta stiffens with age. Third, due to this matched geometry, reflections at single bifurcations are rather small relative to the composite reflected wave arising from the sum of innumerable tiny reflections elsewhere. For example, reflection coefficients as small as 0−0.15 have been reported for the aorta-carotid interface,[14] which would prevent only up to ~2.25% of energy transmission into the carotid artery. This contrasts with systemic reflection coefficients of ~0.5 or higher,

which in sum return as much as ~25% of the energy contained in the pulse to the central aorta. Fourth, the bulk of reflections originating outside the target organs (such as the brain and kidney) and returning to the aorta, penetrate these organs as forward waves. This may be particularly important for reflected wave returning from the lower body and traveling up the carotid arteries as forward waves into the brain vasculature. Moreover, arteries upstream of the carotid appear to be more effective at attenuating high-frequency flow pulsations (such as those produced by the initial cardiac contraction) than low-frequency oscillations (contained in the reflected wave from the lower body),[16] suggesting that the latter wave more effectively penetrates the cerebral microvasculature. Therefore, a protective effect of wave reflections at the inlet of target organs is not substantiated from a theoretical standpoint, not clearly demonstrated from a clinical standpoint, and its quantitative importance remains to be determined by rigorous studies that account for the complexity of whole-system hemodynamics. Clearly, further work is required regarding this important issue, which has implications for common disease states such as age-related dementias and chronic kidney disease. The reader is also referred to discussions of this topic with somewhat different points of view by various experts in Chapters 11, 17, and 40.

Aortic stiffening and its role in target organ damage

When aortic stiffness increases, the resulting increase in arterial pressure and flow pulsatility can exert deleterious effects in various systemic organs, particularly those that exhibit richly perfused low-resistance vascular beds such as the kidney, the placenta, and the brain (Fig. 10.3). Both increased pulsatile pressure (barotrauma) and pulsatile flow (with excessive shear forces from increased pulsatile flow velocity) can result in microvascular damage in these organs. Similarly, pancreatic islets are characterized by a low-resistance, torrential flow, dense glomerular vascular network. Through effects on pancreatic islets and the liver, increased LAS may also contribute to metabolic dysfunction, and accumulating evidence links increased LAS to incident new-onset diabetes. Although myocardial vessels also exhibit low resistance, but are protected during systole by the myocardial contraction, which extrinsically compresses intramyocardial blood vessels.

However, increased LAS does result in increased pulsatile load to the left ventricle (which directly interacts with the pulsatile load imposed by aorta and downstream wave reflections) and a reduction in diastolic perfusion pressure. It is useful to discuss the cardiac consequences of arterial stiffening (derived from its effects on load and the diastolic pressure decay) separately from consequences in peripheral high-flow, low-resistance target organs. A list of potential

FIGURE 10.3   Arterial blood flow per unit of tissue mass in various organs. The kidney, placenta-fetal unit, heart, brain, pancreatic islets, liver, and testicle are shown. Although liver blood flow is much higher than shown, most of it is from the portal vein (not accounted for in the graph, which represents only arterial flow). For the pancreas, flow rates represent islet blood flow, rather than combined endocrine and exocrine pancreatic blood flow. *Modified from Chirinos JA, Segers P, Hughes T, Townsend R. Large-artery stiffness in health and disease: JACC state-of-the-art review.* **J Am Coll Cardiol***. 2019; 74(9):1237−1263, with permission from Elsevier.*

consequences of arterial stiffening on various target organs is shown in Fig. 10.4.

Arterial stiffness and the heart
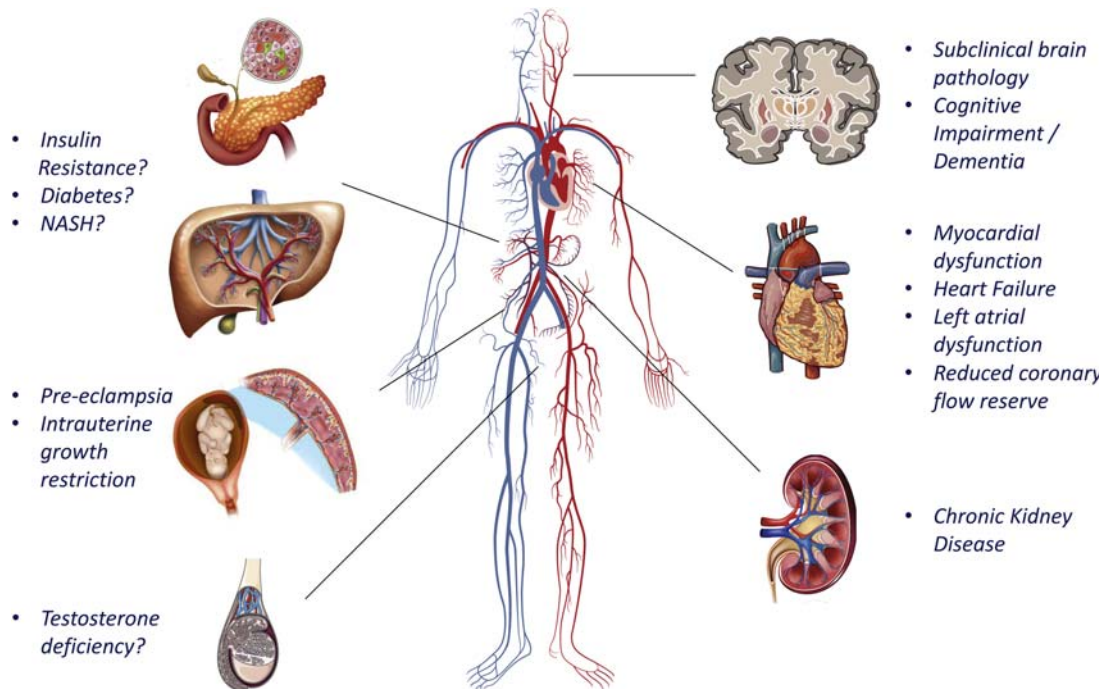
The adverse consequences of aortic stiffening and abnormal pulsatile hemodynamics on the heart are discussed in detail in Chapters 13−18. Only a brief description will be provided here. The aorta affects ventricular−arterial interactions via: (1) Its impact on the early systolic pressure rise, which is a key determinant of peak myocardial wall stress in early systole; (2) Its impact on the timing of arrival of wave reflections to the LV, which increases late systolic load, promoting LV remodeling, fibrosis, diastolic dysfunction, and reduces coronary perfusion pressure in diastole.[9]

During early ejection, the characteristic impedance of the proximal aorta (Zc) governs the aortic and LV pressure rise for any given blood flow from the LV into the aorta. Peak myocardial wall stress occurs in early systole, when systolic pressure coexists with quasi-diastolic LV geometry (thinner wall and larger cavity), consistent with Laplace's law.[17] Therefore, aortic Zc impacts peak myocardial wall stress in early systole. Interestingly, although absolute levels of wall stress in early systole are high, in the absence of ischemia, the LV myocardium seems to adapt relatively well to increased load during this early period of contraction.[18] However, peak myocardial wall stress is a key determinant of myocardial oxygen consumption,[19] implying that a high aortic root characteristic impedance increases myocardial oxygen demand.

As discussed above, another important consequence of aortic stiffening is an increase in aortic PWV, which favors an earlier arrival of reflected waves to the heart. Wave reflections arriving at the heart during mid-to-late systole rather than diastole determine an increase in mid-to-late systolic load on one hand, and a reduction in the area under the pressure curve in diastole (i.e., coronary perfusion pressure) on the other (Figs. 10.1 and 10.2).

As discussed in detail in Chapter 16, pulsatile afterload during mid- and late-systole has adverse consequences on LV remodeling and function.[9,20,21] A prohypertrophic and profibrotic effect of late systolic load has been demonstrated in experimental studies in animal models,[20] and is also supported by human studies[22−24] Similarly, experimental animal data demonstrate that late systolic load has a profound effect on LV relaxation and systolic−diastolic coupling,[21] which is supported by human studies demonstrating that late systolic load is independently associated with diastolic dysfunction in clinical and community-based cohorts[25−27] and strongly predicts new-onset HF in the general population.[28,29] Late systolic load is also associated with atrial dysfunction[30] and independently predicts the risk of atrial fibrillation.[31] Interestingly, adverse consequences of impaired pulsatile hemodynamics on the LV seem to be more directly related to late systolic load and the timing of wave reflections to the proximal aorta, rather than to aortic stiffness per se. Hence, measures of LAS (such as CF-PWV) predicted incident HF in some studies,[6,32] but not others,[33] whereas measures of late systolic hypertension seem to be more robustly associated with adverse left heart quantitative phenotypes, incident HF, and incident atrial fibrillation. It should be noted that the timing of wave reflection is not only dependent on aortic PWV but also on muscular artery function, which can impact the apparent distance to reflection sites. In general, direct measurements

FIGURE 10.4   Potential consequences of large artery stiffness on target organs. LAS can impact the heart through effects on afterload (particularly, modulation of the timing of wave reflections) and may damage low-resistance organs via excess arterial pulsatility. Importantly, not all these potential consequences are similarly well-established. In general, there is a large body of evidence supporting deleterious effects on the kidney and heart, moderate evidence for the brain and the placenta, and early/limited evidence for the pancreas, liver, and testicles (see text for details). *ASH*, Nonalcoholic steatohepatitis. *Modified from Chirinos JA, Segers P, Hughes T, Townsend R. Large-artery stiffness in health and disease: JACC state-of-the-art review.* **J Am Coll Cardiol**. *2019; 74(9):1237−1263, with permission from Elsevier.*

of LV pulsatile afterload and late systolic load (which can be accomplished with analyses of time-resolved aortic pressure and flow waveforms),[9] rather than measurements of LAS per se, appear to most informative for the assessment of ventricular afterload, ventricular−arterial interactions, and for predicting incident HF and atrial fibrillation. The assessment of ventricular−arterial interactions is discussed in detail in Chapters 15−17.

A premature arrival of wave reflections to the proximal aorta also determines a loss of diastolic pressure augmentation by wave reflections (Figs. 10.1 and 10.2). The reduction in aortic compliance by aortic stiffness along with premature wave reflections determines a steep diastolic pressure decay, reducing coronary perfusion pressure.[34] The increase in systolic load along with the reduction in coronary perfusion pressure induced by aortic stiffening and premature wave reflections adversely impact myocardial supply/demand, which may partially exhaust the coronary perfusion reserve at rest, particularly in women.[35] This has implications exercise tolerance due to impaired coronary perfusion even in the absence of epicardial coronary stenoses, a topic that requires further research in specific populations.

Arterial stiffness and the kidney

The relationship between the aorta and the kidney is bidirectional. On one hand, aortic stiffness may promote progressive declines in kidney function due to glomerular damage, whereas established kidney disease promotes further aortic stiffening.

The kidney exhibits high-flow, low-resistance arterial physiology, rendering glomerular capillaries susceptible to trauma from pulsatile pressure and blood flow.[36] Therefore, aortic stiffness may contribute to the pathogenesis of albuminuria and reduced glomerular filtration capacity over time.

Patients with established chronic kidney disease (CKD) (particularly diabetic CKD) exhibit increased CF-PWV, which worsens as kidney function declines.[37,38] Once established, CKD enhances aortic stiffening due to several mechanisms, including dysregulated bone and mineral metabolism with vascular calcification,[39−41] inflammation,[42] neurohormonal dysregulation, (including increased renin-angiotensin-aldosterone axis activation),[43] and sympathetic hyperactivity.[44] LAS independently predicts adverse cardiovascular outcomes in CKD patients, including incident hospitalized HF,[6] progression to end-stage

kidney disease, and all-cause death, independent of office blood pressure.[45] LAS is also predictive of all-cause death among patients with end-stage kidney disease on hemodialysis.[46] The relationship between arterial stiffness, pulsatile hemodynamics, and renal disease is discussed in detail in Chapter 40.

Arterial stiffness and the brain

Given its high metabolic demand, the brain also exhibits low-resistance, high-flow physiology,[47] thus being susceptible to pulsatile microvascular trauma.[3] Although on average, the brain receives a lower blood flow per gram of tissue compared to the kidney, activation of specific areas of the brain are associated with sharp regional increases in blood flow. Therefore, the fine regulation of regional arteriolar resistance is a key aspect of neurovascular function.

Maintaining consistent and well-regulated cerebral perfusion is essential for proper cognitive and physical function, and abnormalities in regional perfusion may be key for the progression of cognitive impairment and dementia. Microvascular dysfunction in the brain may lead to impaired neurovascular coupling and regional hypoperfusion, particularly in the white matter, which receives less perfusion than the gray matter. An increased LAS with consequent increased pulsatility in the cerebral circulation may promote brain microvascular remodeling, impaired oxygen delivery, and impaired blood flow autoregulation (a multifactorial process of the cerebral circulation which regulates vascular resistance and perfusion through myogenic, autonomic, and metabolic mechanisms).[48] A growing body of evidence links LAS with age-related cognitive dysfunction and dementia,[49−51] as well as imaging phenotypes of regional brain atrophy, cerebral small vessel disease, including white matter hyperintensities, lacunar infarcts, cerebral microbleeds, and enlarged perivascular spaces.[52,53] The relationship between LAS, pulsatile arterial hemodynamics, and cognitive dysfunction and dementia is discussed in detail in Chapter 41.

In addition, emerging data suggest that arterial stiffness also increases the risk for subclinical brain infarction and incident stroke.[5] This may be due to common risk factors between atherosclerosis and aortic stiffening and/or to an increased risk of plaque rupture induced by excessive pressure and flow pulsatility. For a detailed discussion regarding the relationship between arterial stiffness and atherosclerosis, the reader is referred to Chapter 38.

Arterial stiffness and the placental circulation

Given the fetal metabolic needs, the placenta also operates at very high-flow/low vascular resistance, particularly as pregnancy progresses toward late stages. LAS has been implicated in placentofetal pathology, particularly preeclampsia (a late pregnancy complication characterized by hypertension and proteinuria) and intrauterine growth restriction (a condition in which the fetus is smaller than expected for gestational age) (Fig. 10.4).

Preeclampsia is associated with increased LAS.[54] More importantly, differences in LAS and pulsatile hemodynamics appear to precede the development of late pregnancy complications. A high PP early in pregnancy is predictive of subsequent preeclampsia, but not of uncomplicated gestational hypertension.[55] A meta-analysis[56] demonstrated that CF-PWV is increased in women who subsequently develop preeclampsia or intrauterine growth restriction. Whether LAS and/or adverse pulsatile hemodynamics causally contribute to these pregnancy complications, whether LAS measurements have clinical value to predict these complications to facilitate early interventions, and whether pulsatile hemodynamics can be a target for preventive therapeutic interventions in this setting remains to be determines. Similarly, it is unknown whether women who develop preeclampsia exhibit long-term alterations in LAS and whether an increased LAS may lead to an increased cardiovascular risk in this population. Chapter 42 discusses the role of arterial stiffness and pulsatile hemodynamics in pregnancy-related complications.

Aortic stiffness, metabolic dysfunction, and diabetes mellitus

It has long been known that diabetes mellitus (DM) and obesity are important risk factors for accelerated large artery stiffening. However, recent data indicate that increased LAS precedes the development of overt DM, suggesting a bidirectional relationship.[57−61]

As discussed in detail in Chapter 30, there are several potential mechanisms that could explain the relationship between LAS and new-onset diabetes. LAS may contribute to the pathogenesis of insulin resistance and DM through its hemodynamic effects. The endocrine pancreas, which comprises only $\sim 1\%-2\%$ of the pancreatic mass, receives $\sim 10\%-20\%$ of its blood supply. Therefore, in contrast to the exocrine pancreatic circulation, pancreatic islet blood flow is among the highest in the body when normalized for tissue mass (Fig. 10.3).[7,62] Like in other high-flow, low-resistance vascular beds, increased LAS has the potential to impact microvascular health in pancreatic islets, leading to dysfunctional or dysregulated endocrine function. Pancreatic islets exhibit a dense glomerular capillary network, which mediates chemical signaling between various endocrine cell types. Vascular integrity may be essential to maintain an order of sequential perfusion of β, δ, and α cells, which appears to allow for an adequate inhibition of glucagon secretion by insulin.[63] Moreover, hyperglycemia and the associated beta cell activation result in islet arteriolar dilation, capillary dilation, and increased

islet capillary pressure, suggesting that local hemodynamics participate in endocrine responses[64] Therefore, pancreatic islet microvascular dysfunction may contribute to the pathogenesis of type 2 DM via impaired insulin secretion and/or an imbalance between insulin/glucagon secretion.

Additional mechanisms may mediate the relationship between LAS and new-onset DM, as discussed in Chapter 30. These include elastin degradation in the aortic wall with production of elastin-related peptides (which can block insulin signaling), neurohormonal dysregulation (increased sympathetic tone and renin-angiotensin-aldosterone system activation), liver dysfunction, and skeletal muscle dysfunction.

The liver receives ∼25% of the cardiac output and exhibits a high-flow, low-resistance arterial circulation, since the hepatic artery provides approximately one-third of the liver blood flow.[7] The hepatic arterial circulation constantly regulates arterial flow to maintain total liver blood flow constant, regardless of changes in portal vein flow (hepatic arterial buffer response), which contributes to metabolic homeostasis.[65] Multiple studies have demonstrated an association between nonalcoholic fatty liver disease (NAFLD) and LAS.[66] Furthermore, among patients with NAFLD, LAS may be associated with liver fibrosis.[67] Given the important intersection of hemodynamic arterial function and metabolic function in the liver, it is possible that LAS contributes to the progression of NAFLD and hepatic insulin resistance, but further studies are required to assess whether a causal relationship between LAS and liver fibrosis exists. Finally, abnormal pulsatile hemodynamics due to LAS may impair normal postprandial vasodilation of skeletal muscle,[68–70] further promoting insulin resistance.[71,72] In general, it remains to be seen whether LAS causally contributes to pancreatic islet, skeletal muscle, or liver microvascular dysfunction, a question that should be pursued in future studies.

Once DM ensues, LAS may favor the development of diabetic complications. Diabetic individuals exhibit much higher CF-PWV than their nondiabetic counterparts,[73] even in the setting of established CKD[37,38] or heart failure with preserved ejection fraction.[74] Among patients with existing DM, increased LAS is associated with rapid progression of microvascular complications including diabetic retinopathy, nephropathy, and neuropathy. Further research is needed to clarify the mechanisms linking LAS and accompanying pulsatile hemodynamic changes with DM. Novel strategies that target arterial stiffness may help to prevent and slow the progression of complications of DM. The bidirectional relationship between LAS and DM appears to be highly clinically relevant, may offer novel therapeutic avenues, and should be the focus of further research.

Arterial stiffness and testicular dysfunction

Several considerations also suggest a bidirectional relationship between testicular function and LAS. Androgen receptors can modulate vascular function and conversely, LAS with excess pulsatility may impact testicular microvascular function. Lower androgen levels are independently associated with greater LAS in older men.[75] The testicles exhibit Doppler features of a low-resistance vascular bed, suggesting that increased pulsatile energy in conduit vessels may damage the testicular microcirculation. An intact testicular microvascular network is required to maintain oxygen delivery and uptake by testicular tissue.[76] Abnormal vasoactive responses and structural degeneration of the testicular microvasculature occurs with aging, which is thought to play an active role in promoting aging of the testis. In animal models, a reduced capacity to regulate testicular blood flow is sufficient to impact testosterone secretion, even in the presence of intact Leydig cell function.[77] Although hemodynamic considerations and limited observational data suggest that LAS may contribute to microvascular damage in the testicles, further mechanistic research is required in this area.

Mechanisms of arterial stiffening and therapeutic approaches

The arterial wall has three main layers (intima, tunica media, and adventitia), which vary according to the artery type (Basic concept Box 10.1; Fig. 10.5 and Table 10.2).

Various processes in the aortic wall layers can affect LAS (Fig. 10.6). The medial layer is the main determinant of LAS, via its various constituents: the extracellular matrix proteins elastin and collagen, vascular smooth muscle cells (VSMCs), cell-matrix connections, and matrix constituents such as glycosaminoglycans interconnecting the extracellular matrix. In large arteries, these elements are organized in concentric elastin sheets, intertwined by smooth muscle cells and matrix material, along with collagen fibers running both in the axial and circumferential directions, providing mechanical strength to the artery. With progressive distance from the heart, arteries evolve from elastic (rich in elastin) to muscular (rich in VSMCs). The abdominal aorta, in particular, exhibits transitional ultrastructure, with a significant amount of both elastic elements and VSMCs.

Multiple pathologic processes related to elastin fragmentation/degradation, collagen deposition, collagen and elastin cross-linking by advanced glycation end-products, VSMC stiffening, medial calcification, endothelial dysfunction, and inflammation can impact LAS. These processes are briefly summarized in Fig. 10.6 and Table 10.2, but are discussed in great detail in subsequent chapters of this textbook.
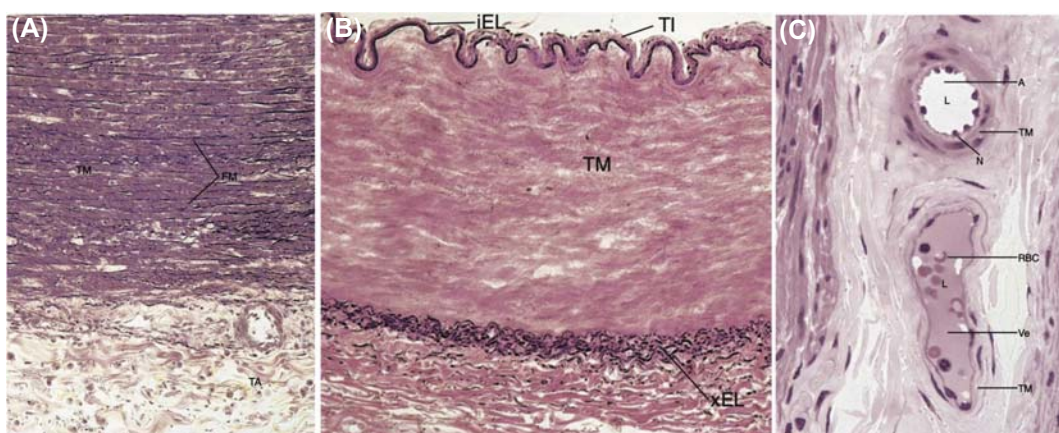
BASIC CONCEPT BOX 10.1 Types of systemic arteries

Arteries are classified into three major types based on their size and morphology; these 3 types are: elastic arteries (conducting arteries), muscular arteries (distributing arteries), and arterioles. Key structural characteristics and differences between these artery types are shown in Table 10.1. Light micrographs of each type of artery are shown in Fig. 10.5.

TABLE 10.1 Main types of systemic arteries.

Artery	Tunica intima	Tunica media	Tunica adventitia	Hemodynamic role/effect
Elastic artery (conduction; e.g., aorta)	Endothelium with weibel-palade bodies, basal lamina, subendothelial layer, incomplete internal elastic lamina	40-70 fenestrated elastic membranes, smooth muscle cells interspersed between elastic membranes; thin external elastic lamina; vasa vasorum in outer half	Thin layer of fibroelastic connective tissue, vasa vasorum, lymphatic vessels, never fibers	Conduit function and compliance (major source of compliance in healthy adults)
Muscular artery (distributing; e.g., femoral artery)	Endothelium with weibel-palade bodies, basal lamina, subendothelial layer, thick internal elastic lamina	Up to 40 layers of smooth muscle cells; thick external elastic lamina	Think layer of fibroelastic connective tissue; vasa vasorum not very prominent; lymphatic vessels, nerve fibers	Distributive conduit function, some compliance, modulation of wave reflections
Arteriole	Endothelium with weibel-palade bodies, basal lamina, subendothelial layer not very prominent, some elastic fibers instead of an internal elastic lamina	One to three layers of smooth muscle cells	Loose connective tissue, nerve fibers	Provide resistance and regulate blood flow distribution through modulation of local tone

Modified from Gartner LP, Hiatt JL. *Color Textbook of Histology*. 3rd ed. Saunders Elsevier; 2007.

FIGURE 10.5   Light micrographs of an elastic artery (A), muscular artery (B), and arteriole (C). *A*, arteriole; *FM*, fenestrated membranes; *iEL*, internal elastic lamina; *N*, nuclei of endothelial cells bulging into the arteriole lumen; *RBC*, red blood cell; *TA*, tunica adventitia; *TI*, tunica intima; *TM*, tunica media; *Ve*, venule; *xEL*, external elastic lamina. The degree magnification is not uniform across the various micrographs and is ∼4 times greater for panel C compared to panel A. *Reproduced from Gartner LP, Hiatt JL.* Color Textbook of Histology. *3rd ed. Saunders Elsevier; 2007.*

In *elastic arteries*, the tunica intima is composed of endothelial cells supported by a narrow layer of underlying connective tissue containing a few fibroblasts, smooth muscle cells, and collagen fibers. Thin laminae of elastic fibers, the internal elastic laminae, are also present. Endothelial cells are oriented parallel to the longitudinal axis of the vessel and like those in other types of arteries, exhibit Weibel-Palade bodies (small vesicles that contain von Willebrand factor and various other proteins involved in hemostasis, inflammation, angiogenesis, and tissue repair). The tunica media of the elastic arteries consists of many fenestrated lamellae of elastin, known as fenestrated membranes, alternating with circularly oriented layers of smooth muscle cells, which are less abundant in elastic arteries than in muscular arteries. An external elastic lamina is also present in the tunica media. The tunica adventitia of elastic arteries is relatively thin and is composed of loose fibroelastic connective tissue housing some fibroblasts. Vasa vasorum also are abundant throughout the adventitia and extend to the tissues of the tunica media, where they supply the connective tissue and smooth muscle cells. The aorta is the main source of compliance in the normal arterial tree.

Muscular arteries are characterized by a relatively thick tunica media composed mostly of smooth muscle cells arranged in 3−40 layers (depending on the size of the artery). The tunica intima in the muscular arteries is thinner than that in the elastic arteries. In contrast, the internal elastic lamina is more prominent than in elastic arteries and displays an undulating surface. Most smooth muscle cells in the tunica media are oriented circularly, with few bundles arranged longitudinally close to the in the tunica adventitia. Small muscular arteries have three or four layers of smooth muscle cells, whereas larger muscular arteries may have as many as 40 layers of circularly arranged smooth muscle cells. Interspersed within the layers of smooth muscle cells are elastic fibers, type III collagen fibers, and chondroitin sulfate. The tunica adventitia of muscular arteries consists of elastic and collagen fibers, and proteoglycans, with vasa vasorum and unmyelinated nerve endings in its outer region. From a hemodynamic standpoint, the tone of muscular arteries modulates arterial wave reflections.

Arterioles are arteries with a diameter <0.1 mm. The cross-sectional width of the wall of an arteriole is approximately equal to the diameter of its lumen. The tunica media of arterioles consists of 1-3 layers of smooth muscle cells. Arterioles do not have an external elastic lamina, whereas the tunica adventitia is scant and composed by fibroelastic connective tissue housing a few fibroblasts. The terminal arterioles that supply blood to capillary beds are called metarterioles. The smooth muscle layer of meta-arterioles is not continuous; rather, individual muscle cells are spaced apart, and each encircles the endothelium of a capillary arising from the meta-arteriole, allowing them to act as a sphincter upon contraction, controlling blood flow into the capillary bed.

It is important to note that changes in morphological characteristics as arteries transition from one type to another are gradual, such that some vessels have characteristics of two categories (for example, the most distal part of the abdominal aorta has a relatively high content of smooth muscle cells, whereas the carotid arteries exhibit mixed characteristics of muscular and elastic arteries as they morph from proximal to distal segments).

The role of elastin and elastin-derived peptides is discussed in detail in Chapter 19. Chapter 20 deals with the role of inflammation on arterial stiffening. Chapter 21 provides a detailed discussion of mechanisms of aortic wall calcification. The role of vascular smooth muscle dysfunction on arterial stiffening is discussed in Chapter 22, whereas chapter 23 deals with endothelial cell dysfunction and senescence. Finally, Chapter 24 discussed autonomic and neuroendocrine modulation of arterial stiffness, and Chapter 25 deals with cellular aging.

Whereas the various processes leading or contributing to aortic stiffening are discussed separately for didactic purposes, it should be noted that these processes do not occur in isolation, but rather interact to promote LAS. For example, elastin fragmentation is often followed by collagen accumulation, and the generation of elastin degradation products (elastin-related peptides) may activate signaling pathways that promote VSMC osteogenic differentiation and vascular calcification.[78] Similarly, inflammatory pathways can lead to endothelial cell dysfunction and activation, and to the release of bone morphogenetic protein-2 by endothelial cells, which in turn promotes VSMC osteogenic differentiation and vascular calcification. Given the complex interrelationships in various processes listed in Fig. 10.6 and Table 10.2, it is not surprising that pleiotropic mediators, such as various micro-RNAs[79] and *Klotho*[80] appear to exert a coordinated regulation of various processes involved in LAS, providing opportunities for therapeutic interventions.
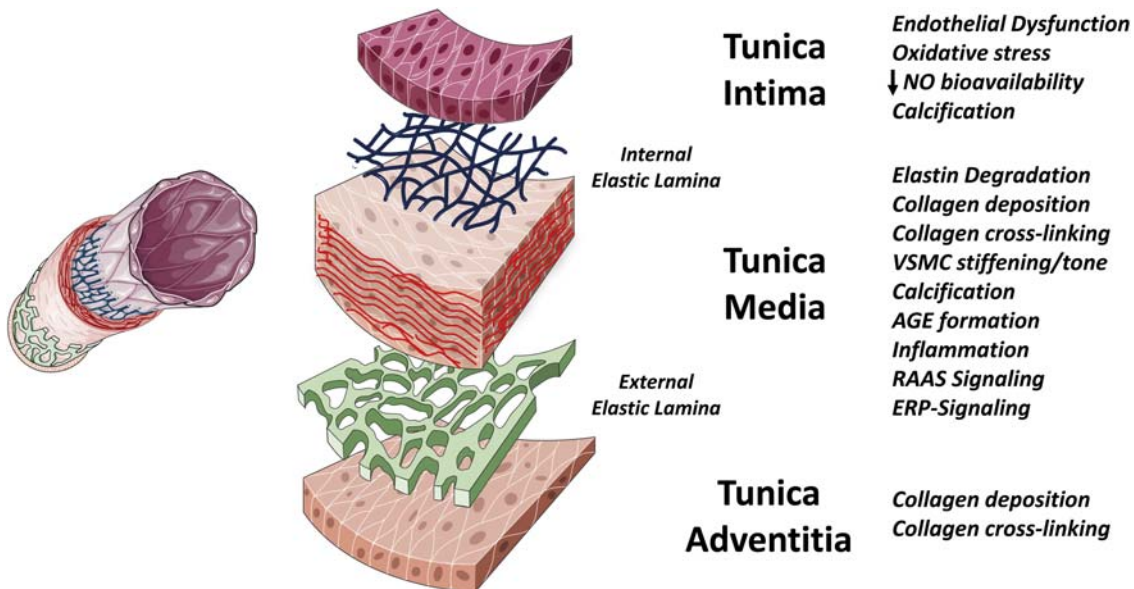
Understanding mechanisms of arterial stiffening can inform therapeutic approaches. Although a detailed description of potential therapeutic approaches to LAS is outside of the scope of this chapter, these will be discussed in detail in subsequent chapters. Chapter 50 deals with various pharmacologic approaches to reduce arterial stiffness. Chapter 51 discusses the role of organic nitrates, dietary (i.e., inorganic) nitrates and nitric oxide donor therapy to modulate pulsatile arterial hemodynamics. Chapters 52 and 53 discuss the role of lifestyle factors interventions (exercise training and weight loss, and salt restriction, respectively) to reduce LAS. Finally, antihypertensive medications that largely act through reductions in vascular resistance or cardiac output do not necessarily change the intrinsic material properties of the arterial wall, but may lead

TABLE 10.2 General mechanisms of large artery stiffening.

Mechanism	General Description	Key Molecular Mediators
Elastin fragmentation	Elastin deposition in the arterial is limited to the fetal development period and infancy and is subsequently turned off; therefore, in adulthood, elastin fiber damage is essentially irreparable. Progressive elastin fragmentation/loss occurs due to: (a) Mechanical fatigue over the lifetime (cyclic stress); (b) elastase-mediated proteolysis.	• MMP-1, MMP-2, MMP-9, MMP-12, MMP-14, cathepsins, neutrophil elastase, other elastases. • Elastin glycation, carbamylation and peroxidation may increase its mechanical fragility and/or susceptibility to proteolysis. • Elastin degradation products (elastin-related peptides) may promote arterial damage, calcification and systemic metabolic dysregulation.
Collagen deposition	Collagen deposits occur at the arterial wall (predominantly the media), including sites of elastin breakdown	• VSMC angiotensin-II type 1 receptor activation • VSMC mineralocorticoid receptor activation
AGE-mediated collagen and elastin cross-linking	Glucose cross-links develop and AGEs form between proteins with a long half-life (such as collagen). Cross-linked collagen is more resistant to enzymatic proteolysis. Glycated elastin is more susceptible to degradation. Hyperglycemia leads to AGE formation, whereas renal dysfunction leads to reduced AGE elimination	• Glucose, uremic toxins • AGEs can activate the receptor of AGEs (RAGEs), inducing inflammation, oxidative stress and calcification pathways (via sodium phosphate co-transporter PiT-1 expression). The functional significance of AGE-RAGE interactions in vivo is unclear.
VSMC stiffening/tone	Alterations in the VSMC cytoskeleton and integrin interactions with the extracellular matrix. Likely to be more important in distal aortic segments, which are richer in VSMCs.	• Increased α-smooth muscle actin and β1-integrin expression • Increased adhesiveness to fibronectin (primate models)
Calcification	Medial calcification is predominantly mediated by the osteochondrogenic differentiation of VSMCs. This process is different from the intimal calcification associated with atherosclerosis, which is predominantly mediated by chondrocyte-like cells of bone marrow origin. Adventitial calcification may also occur, which involves myofibroblasts and/or microvascular pericytes.	• Imbalance between calcification inhibitors (MGP, fetuin A, pyrophosphate, osteopontin, osteoprotegerin, klotho) and activators (FGF-23, inflammatory cytokines, vitamin D). • BMP-2 signaling • ALP activation (degrades pyrophosphate, a calcification inhibitor) • Osteogenic transcription factors (Msx2-Wnt signaling)
Endothelial dysfunction	Reduced NO production by the endothelium may play a role in regulating VSMC stiffness/tone in distal aortic segments like the abdominal aorta. Increased stiffness of the endothelial cell cytoskeleton that is in close to the membrane (cortical cytoskeleton) may also play a role in modulating stiffness	• Oxidative stress • Nitric oxide deficiency • proinflammatory pathways
Inflammation	There are interconnections between inflammatory pathways and various mechanisms of large artery stiffening (elastin degradation, medial calcification, calcification, endothelial dysfunction)	• TNF-alpha (can activate calcification pathways via Msx2-Wnt signaling and release of BMP-2 within endothelial microparticles) • Various elastases are produced by inflammatory cells • Inflammatory cascades lead to endothelial dysfunction

AGEs, advanced glycation end-products; *ALP*, alkaline phosphatase; *BMP-2*, Bone morphogenetic protein 2; *FGF-23*, fibroblast growth factor 23; *MGP*, matrix Gla protein; *MMP*, matrix metalloproteinase; *Msx2*, Homeobox Protein Hox-8; *NO*, nitric oxide.; *PiT-1*, phosphate transporter 1; *RAGEs*, receptor of AGEs; *VSMC*, vascular smooth muscle cell; *Wnt*, willingness Int.
Reproduced from Chirinos JA, Segers P, Hughes T, Townsend R. Large-artery stiffness in health and disease: JACC state-of-the-art review. *J Am Coll Cardiol*, 2019;74(9):1237−1263, with permission from Elsevier.

FIGURE 10.6   General mechanisms of arterial stiffness. (A) Various mechanisms can increase the stiffness of the intima, media, and adventitia. The media is, however, the most important layer in large arteries. See text for details. *AGE*, advanced glycation end-products; *ERP*, elastin-related peptides; *NO*, nitric oxide; *RAAS*, renin-angiotensin-aldosterone system. *Reproduced from Chirinos JA, Segers P, Hughes T, Townsend R. Large-artery stiffness in health and disease: JACC state-of-the-art review.* **J Am Coll Cardiol**, *2019; 74(9):1237−1263, with permission from Elsevier.*

to a reduction in operating stiffness, given the nonlinear arterial compliance curve, as discussed is Chapter 1.

Conclusions

LAS has profound consequences for cardiovascular health and is likely responsible for a large proportion of the global chronic cardiovascular disease burden. This burden will likely increase as the lifespan of the general population increases, even in the absence of atherosclerotic cardiovascular disease. Given the important consequences of aortic stiffening and excess pulsatility on target organs, a better understanding of molecular mechanisms that contribute to LAS should be aggressively pursued, in order to design effective pharmacologic interventions. Mechanical approaches to reduce pulsatility in the presence of irreversible aortic stiffening should also be pursued. Aortic stiffening represents an unmet, high-priority therapeutic target to ameliorate the global burden of cardiovascular disease.

Acknowledgments

References

1. Kaess BM, Rong J, Larson MG, et al. Aortic stiffness, blood pressure progression, and incident hypertension. **JAMA**. 2012; 308:875−881.
2. Chirinos JA, Segers P. Noninvasive evaluation of left ventricular afterload: part 2: arterial pressure-flow and pressure-volume relations in humans. **Hypertension**. 2010; 56:563−570.
3. O'Rourke MF, Safar ME. Relationship between aortic stiffening and microvascular disease in brain and kidney: cause and logic of therapy. **Hypertension**. 2005; 46:200−204.
4. Payne RA, Wilkinson IB, Webb DJ. Arterial stiffness and hypertension: emerging concepts. **Hypertension**. 2010; 55:9−14.
5. Ben-Shlomo Y, Spears M, Boustred C, et al. Aortic pulse wave velocity improves cardiovascular event prediction: an individual participant meta-analysis of prospective observational data from 17,635 subjects. **J Am Coll Cardiol**. 2014; 63:636−646.
6. Chirinos JA, Khan A, Bansal N, et al. Arterial stiffness, central pressures, and incident hospitalized heart failure in the chronic renal insufficiency cohort study. **Circ Heart Fail**. 2014; 7:709−716.
7. Chirinos JA, Segers P, Hughes T, Townsend R. Large-artery stiffness in health and disease: JACC state-of-the-art review. **J Am Coll Cardiol**. 2019; 74:1237−1263.

8. Chirinos JA, Segers P. Noninvasive evaluation of left ventricular afterload: part 1: pressure and flow measurements and basic principles of wave conduction and reflection. **Hypertension**. 2010; 56:555−562.

9. Weber T, Chirinos JA. Pulsatile arterial haemodynamics in heart failure. **Eur Heart J**. 2018; 39:3847−3854.

10. Chirinos JA. Deep phenotyping of systemic arterial hemodynamics in HFpEF (Part 2): clinical and therapeutic considerations. **J Cardiovasc Transl Res**. 2017; 10:261−274.

11. Chirinos JA, Segers P, Gillebert TC, et al. Arterial properties as determinants of time-varying myocardial stress in humans. **Hypertension**. 2012; 60:64−70.

12. Phan TS, Li JK, Segers P, Chirinos JA. Misinterpretation of the determinants of elevated forward wave amplitude inflates the role of the proximal aorta. **J Am Heart Assoc**. 2016; 5.

13. Chirinos JA, Londono-Hoyos F, Zamani P, et al. Effects of organic and inorganic nitrate on aortic and carotid haemodynamics in heart failure with preserved ejection fraction. **Eur J Heart Fail**. 2017; 19:1507−1515.

14. Mitchell GF, van Buchem MA, Sigurdsson S, et al. Arterial stiffness, pressure and flow pulsatility and brain structure and function: the age, gene/environment susceptibility–Reykjavik study. **Brain**. 2011; 134:3398−3407.

15. Li JK. Dominance of geometric over elastic factors in pulse transmission through arterial branching. **Bull Math Biol**. 1986; 48:97−103.

16. Hirata K, Yaginuma T, O'Rourke MF, Kawakami M. Age-related changes in carotid artery flow and pressure pulses: possible implications for cerebral microvascular disease. **Stroke**. 2006; 37:2552−2556.

17. Chirinos JA, Segers P, Gupta AK, et al. Time-varying myocardial stress and systolic pressure-stress relationship: role in myocardial-arterial coupling in hypertension. **Circulation**. 2009; 119:2798−2807.

18. Chirinos JA. Deciphering systolic-diastolic coupling in the intact heart. **Hypertension**. 2017; 69:575−577.

19. Strauer BE. Myocardial oxygen consumption in chronic heart disease: role of wall stress, hypertrophy and coronary reserve. **Am J Cardiol**. 1979; 44:730−740.

20. Kobayashi S, Yano M, Kohno M, et al. Influence of aortic impedance on the development of pressure-overload left ventricular hypertrophy in rats. **Circulation**. 1996; 94:3362−3368.

21. Gillebert TC, Lew WY. Influence of systolic pressure profile on rate of left ventricular pressure fall. **Am J Physiol**. 1991; 261:H805−H813.

22. Zamani P, Bluemke DA, Jacobs Jr DR, et al. Resistive and pulsatile arterial load as predictors of left ventricular mass and geometry: the multi-ethnic study of atherosclerosis. **Hypertension**. 2014; 65(1):85−92.

23. Hashimoto J, Westerhof BE, Westerhof N, Imai Y, O'Rourke MF. Different role of wave reflection magnitude and timing on left ventricular mass reduction during antihypertensive treatment. **J Hypertens**. 2008; 26:1017−1024.

24. Chirinos JA, Akers SR, Schelbert E, et al. Arterial properties as determinants of left ventricular mass and fibrosis in severe aortic stenosis: findings from ACRIN PA 4008. **J Am Heart Assoc**. 2019; 8:e03742.

25. Fukuta H, Ohte N, Wakami K, et al. Impact of arterial load on left ventricular diastolic function in patients undergoing cardiac catheterization for coronary artery disease. **Circ J**. 2010; 74:1900−1905.

26. Weber T, O'Rourke MF, Ammer M, Kvas E, Punzengruber C, Eber B. Arterial stiffness and arterial wave reflections are associated with systolic and diastolic function in patients with normal ejection fraction. **Am J Hypertens**. 2008; 21:1194−1202.

27. Chirinos JA, Segers P, Rietzschel ER, et al. Early and late systolic wall stress differentially relate to myocardial contraction and relaxation in middle-aged adults: the asklepios study. **Hypertension**. 2013; 61:296−303.

28. Chirinos JA, Segers P, Duprez DA, et al. Late systolic central hypertension as a predictor of incident heart failure: the multi-ethnic study of Atherosclerosis. **J Am Heart Assoc**. 2015; 4:e001335.

29. Chirinos JA, Kips JG, Jacobs Jr DR, et al. Arterial wave reflections and incident cardiovascular events and heart failure: MESA (Multi-ethnic Study of Atherosclerosis). **J Am Coll Cardiol**. 2012; 60:2170−2177.

30. Chirinos JA, Phan TS, Syed AA, et al. Late systolic myocardial loading is associated with left atrial dysfunction in hypertension. **Circ Cardiovasc Imaging**. 2017; 10:e006023.

31. Shaikh AY, Wang N, Yin X, et al. Relations of arterial stiffness and brachial flow-mediated dilation with new-onset atrial fibrillation: the framingham heart study. **Hypertension**. 2016; 68:590−596.

32. Tsao CW, Lyass A, Larson MG, et al. Relation of central arterial stiffness to incident heart failure in the community. **J Am Heart Assoc**. 2015; 4.

33. Pandey A, Khan H, Newman AB, et al. Arterial stiffness and risk of overall heart failure, heart failure with preserved ejection fraction, and heart failure with reduced ejection fraction: the health ABC study (health, aging, and body composition). **Hypertension**. 2017; 69:267−274.

34. Hoffman JI, Buckberg GD. The myocardial oxygen supply: demand index revisited. **J Am Heart Assoc**. 2014; 3:e000285.

35. Coutinho T, Mielniczuk LM, Srivaratharajah K, deKemp R, Wells GA, Beanlands RS. Coronary artery microvascular dysfunction: role of sex and arterial load. **Int J Cardiol**. 2018; 270:42−47.

36. Hashimoto J, Ito S. Central pulse pressure and aortic stiffness determine renal hemodynamics: pathophysiological implication for microalbuminuria in hypertension. **Hypertension**. 2011; 58:839−846.

37. Townsend RR, Wimmer NJ, Chirinos JA, et al. Aortic PWV in chronic kidney disease: a CRIC ancillary study. **Am J Hypertens**. 2010; 23:282−289.

38. Briet M, Boutouyrie P, Laurent S, London GM. Arterial stiffness and pulse pressure in CKD and ESRD. **Kidney Int**. 2012; 82:388−400.

39. Scialla JJ, Leonard MB, Townsend RR, et al. Correlates of osteoprotegerin and association with aortic pulse wave velocity in patients with chronic kidney disease. **Clin J Am Soc Nephrol**. 2011; 6:2612−2619.

40. Coban M, Inci A, Yilmaz U, Asilturk E. The association of fibroblast growth factor 23 with arterial stiffness and atherosclerosis in patients with autosomal dominant polycystic kidney disease. **Kidney Blood Press Res**. 2018; 43:1160−1173.

41. Raggi P, Bellasi A, Ferramosca E, Islam T, Muntner P, Block GA. Association of pulse wave velocity with vascular and valvular calcification in hemodialysis patients. **Kidney Int**. 2007; 71:802−807.

42. Peyster E, Chen J, Feldman HI, et al. Inflammation and arterial stiffness in chronic kidney disease: findings from the CRIC study. **Am J Hypertens**. 2017; 30:400−408.

43. Mehdi UF, Adams-Huet B, Raskin P, Vega GL, Toto RD. Addition of angiotensin receptor blockade or mineralocorticoid antagonism to maximal angiotensin-converting enzyme inhibition in diabetic nephropathy. **J Am Soc Nephrol**. 2009; 20:2641−2650.

44. Converse Jr RL, Jacobsen TL, Toto RD, et al. Sympathetic over-activity in patients with chronic renal failure. **N Engl J Med**. 1992; 327:1912−1918.

45. Townsend RR, Anderson AH, Chirinos JA, et al. Association of pulse wave velocity with chronic kidney disease progression and mortality: findings from the CRIC study (chronic renal insufficiency cohort). **Hypertension**. 2018; 71:1101−1107.

46. Guerin AP, Blacher J, Pannier B, Marchais SJ, Safar ME, London GM. Impact of aortic stiffness attenuation on survival of patients in end-stage renal failure. **Circulation**. 2001; 103:987−992.

47. Attwell D, Laughlin SB. An energy budget for signaling in the grey matter of the brain. **J Cerebr Blood Flow Metabol : Official Journal of the International Society of Cerebral Blood Flow and Metabolism**. 2001; 21:1133−1145.

48. Yang SH, Liu R. Chapter 10 − Cerebral autoregulation. In: Caplan LR, Biller J, Leary MC, et al., eds. **Primer on Cerebro-vascular Diseases**. 2nd ed. San Diego: Academic Press; 2017:57−60.

49. Meyer ML, Palta P, Tanaka H, et al. Association of central arterial stiffness and pressure pulsatility with mild cognitive impairment and dementia: the atherosclerosis risk in communities study-neurocognitive study (ARIC-NCS). **J Alzheim Dis**. 2017; 57:195−204.

50. Pase MP, Beiser A, Himali JJ, et al. Aortic stiffness and the risk of incident mild cognitive impairment and dementia. **Stroke**. 2016; 47(9):2256−2261.

51. Rabkin SW. Arterial stiffness: detection and consequences in cognitive impairment and dementia of the elderly. **J Alzheimers Dis**. 2012; 32:541−549.

52. Henskens LH, Kroon AA, van Oostenbrugge RJ, et al. Increased aortic pulse wave velocity is associated with silent cerebral small-vessel disease in hypertensive patients. **Hypertension**. 2008; 52:1120−1126.

53. Poels MM, Zaccai K, Verwoert GC, et al. Arterial stiffness and cerebral small vessel disease: the Rotterdam scan study. **Stroke**. 2012; 43:2637−2642.

54. Tan I, Butlin M, Avolio A. Does increase in arterial stiffness and wave reflection precede development of placental-mediated complications in pregnancy? **J Hypertens**. 2018; 36:1029−1031.

55. Thadhani R, Ecker JL, Kettyle E, Sandler L, Frigoletto FD. Pulse pressure and risk of preeclampsia: a prospective study. **Obstet Gynecol**. 2001; 97:515−520.

56. Osman MW, Nath M, Breslin E, et al. Association between arterial stiffness and wave reflection with subsequent development of placental-mediated diseases during pregnancy: findings of a systematic review and meta-analysis. **J Hypertens**. 2018; 36:1005−1014.

57. Muhammad IF, Borne Y, Ostling G, et al. Arterial stiffness and incidence of diabetes: a population-based cohort study. **Diabetes Care**. 2017; 40:1739−1745.

58. Zhang Y, He P, Li Y, et al. Positive association between baseline brachial-ankle pulse wave velocity and the risk of new-onset diabetes in hypertensive patients. **Cardiovasc Diabetol**. 2019; 18:111.

59. Chirinos JA. Large artery stiffness and new-onset diabetes. **Circ Res**. 2020; 127:1499−1501.

60. Zheng M, Zhang X, Chen S, et al. Arterial stiffness preceding diabetes: a longitudinal study. **Circ Res**. 2020; 127:1491−1498.

61. Yasuno S, Ueshima K, Oba K, et al. Is pulse pressure a predictor of new-onset diabetes in high-risk hypertensive patients?: a subanalysis of the Candesartan Antihypertensive Survival Evaluation in Japan (CASE-J) trial. **Diabetes Care**. 2010; 33:1122−1127.

62. Tsushima Y, Miyazaki M, Taketomi-Takahashi A, Endo K. Feasibility of measuring human pancreatic perfusion in vivo using imaging techniques. **Pancreas**. 2011; 40:747−752.

63. Stagner JI, Samols E. The vascular order of islet cellular perfusion in the human pancreas. **Diabetes**. 1992; 41:93−97.

64. Almaca J, Weitz J, Rodriguez-Diaz R, Pereira E, Caicedo A. The pericyte of the pancreatic islet regulates capillary diameter and local blood flow. **Cell Metabol**. 2018; 27:630−644 e4.

65. Eipel C, Abshagen K, Vollmar B. Regulation of hepatic blood flow: the hepatic arterial buffer response revisited. **World J Gastroenterol**. 2010; 16:6046−6057.

66. Villela-Nogueira CA, Leite NC, Cardoso CR, Salles GF. NAFLD and increased aortic stiffness: parallel or common physiopathological mechanisms? **Int J Mol Sci**. 2016; 17.

67. Sunbul M, Agirbasli M, Durmus E, et al. Arterial stiffness in patients with non-alcoholic fatty liver disease is related to fibrosis stage and epicardial adipose tissue thickness. **Atherosclerosis**. 2014; 237:490−493.

68. Lee JJ, Tyml K, Menkis AH, Novick RJ, McKenzie FN. Evaluation of pulsatile and nonpulsatile flow in capillaries of goat skeletal muscle using intravital microscopy. **Microvasc Res**. 1994; 48:316−327.

69. Vincent MA, Dawson D, Clark AD, et al. Skeletal muscle microvascular recruitment by physiological hyperinsulinemia precedes increases in total blood flow. **Diabetes**. 2002; 51:42−48.

70. Emanuel AL, Meijer RI, Muskiet MH, van Raalte DH, Eringa EC, Serne EH. Role of insulin-stimulated adipose tissue perfusion in the development of whole-body insulin resistance. **Arterioscler Thromb Vasc Biol**. 2017; 37:411−418.

71. Serne EH, de Jongh RT, Eringa EC, IJzerman RG, Stehouwer CD. Microvascular dysfunction: a potential pathophysiological role in the metabolic syndrome. **Hypertension**. 2007; 50:204−211.

72. Potenza MA, Marasciulo FL, Chieppa DM, et al. Insulin resistance in spontaneously hypertensive rats is associated with endothelial dysfunction characterized by imbalance between NO and ET-1 production. **Am J Physiol Heart Circ Physiol**. 2005; 289:H813−H822.

73. Townsend RR, Wilkinson IB, Schiffrin EL, et al. Recommendations for improving and standardizing vascular research on arterial stiffness: a scientific statement from the American heart association. **Hypertension**. 2015; 66:698−722.

74. Chirinos JA, Bhattacharya P, Kumar A, et al. Impact of diabetes mellitus on ventricular structure, arterial stiffness, and pulsatile hemodynamics in heart failure with preserved ejection fraction. **J Am Heart Assoc**. 2019; 8:e011457.

75. Dockery F, Bulpitt CJ, Donaldson M, Fernandez S, Rajkumar C. The relationship between androgens and arterial stiffness in older men. **J Am Geriatr Soc**. 2003; 51:1627−1632.

76. Dominguez 2nd JM, Davis 3rd RT, McCullough DJ, Stabley JN, Behnke BJ. Aging and exercise training reduce testes microvascular PO_2 and alter vasoconstrictor responsiveness in testicular arterioles. **Am J Physiol Regul Integr Comp Physiol**. 2011; 301:R801−R810.

77. Damber JE, Bergh A, Daehlin L. Testicular blood flow, vascular permeability, and testosterone production after stimulation of unilaterally cryptorchid adult rats with human chorionic gonadotropin. **Endocrinology**. 1985; 117:1906−1913.

78. Duca L, Blaise S, Romier B, et al. Matrix ageing and vascular impacts: focus on elastin fragmentation. **Cardiovasc Res**. 2016; 110:298−308.

79. Nanoudis S, Pikilidou M, Yavropoulou M, Zebekakis P. The role of MicroRNAs in arterial stiffness and arterial calcification. An update and review of the literature. **Front Genet**. 2017; 8:209.

80. Pierce GL. Mechanisms and subclinical consequences of aortic stiffness. **Hypertension**. 2017; 70:848−853.

Wave reflection in the arterial tree

Jonathan P. Mynard[1,2,3] and Avinash Kondiboyina[1,2]

[1]*Heart Research, Murdoch Children's Research Institute, Parkville, VIC, Australia;* [2]*Department of Paediatrics, University of Melbourne, Parkville, VIC, Australia;* [3]*Department of Biomedical Engineering, University of Melbourne, Parkville, VIC, Australia*

Introduction

The pulsatility of arterial blood pressure and flow is a fundamental feature of the cardiovascular system. Although clearly arising from the ventricle's design as a pulsatile pump, the evolution of pressure and flow over time (i.e., pulse waveform during systole and diastole) and space (i.e., from central to peripheral arteries) depends not only on the properties of this pump, but also to a large extent on the properties of the vascular network. Ever since Thomas Young studied "the laws of the propagation of an impulse through the fluid contained in an elastic tube" and concluded that "application of this theory to the motion of the blood in the arteries is very obvious,"[1] it has been recognized that the initial ventricular impulse produces a wave that propagates at finite speed from proximal to distal arteries. That this "forward-running" wave is not perfectly absorbed by the arterial network, but undergoes some degree of reflection, became the subject of many pioneering studies in the 20th century that form the basis of work that continues to this day.[2–11] As with electromagnetic waves or acoustic waves, wave reflection in arteries occurs when a wave encounters an impedance mismatch, that is, a change in the wave propagation properties of the medium.

Because the impedance of the arterial network as a whole (input impedance) is greater than the local impedance of the proximal aorta (characteristic impedance), where the incident wave originates, reflected waves returning to the heart tend to augment blood pressure. Importantly, the time delay between incident and reflected waves at a given location (e.g., the heart) is determined by the distance to the reflection site(s) and the propagation speed ["pulse wave velocity (PWV)"]. Pressure-increasing reflected waves that return during diastole make an advantageous contribution to coronary perfusion pressure (as discussed in detail in Chapter 18), whereas waves that return during systole present an additional afterload to the

ventricle, which reduces pump energy efficiency.[12,13] A transition from the former to the latter situation is thought to occur with aging because the progressive loss of aortic compliance leads to a two- to threefold increase in aortic PWV,[14,15] leading to characteristic changes in the shape of pulse waveforms.[16] As will be described throughout this chapter, although various aspects of this "standard" view have been debated over multiple decades, many of the controversies relate to limitations in the way arterial wave reflection has been modeled (i.e., conceived of) and measured (i.e., quantified).

This chapter starts by introducing basic concepts around the propagation and reflection of pressure and flow waves in elastic tubes. After covering the fundamental (patho) physiological sources of impedance mismatching, we critically review the various models that have been used to "make sense" of wave reflection in the arterial system. We then explore some key complexities of the real system (re-reflections and the "horizon effect," ventricular wave reflection, and the interplay between wave dynamics and windkessel function) that render many simplistic notions of arterial wave reflection ineffective at best and misleading at worst. With these principles in mind, we then introduce and critically assess the methods that are commonly used to quantify the magnitude and timing of reflected waves.

Pressure and flow in the absence of wave reflection

To understand the impact of wave reflection, it is useful to first consider what the relationship between blood pressure and blood flow would be in a theoretically reflectionless scenario—an infinitely long distensible vessel with uniform mechanical properties. If a pulse of fluid is injected into the vessel, a change in flow (ΔQ_f) and pressure (ΔP_f) is produced that travels as a wave in the forward direction

("*f*" subscript). The mathematical description of wave travel in a distensible vessel was originally formulated by Euler in 1775, although published later.[17] Von Kries identified that ΔQ_f and ΔP_f in an elastic tube are intrinsically linked via a simple equation, now known as the "water hammer" equation[18,19] (Fig. 11.1A):

$$\Delta P_f = Z_c \Delta Q_f \qquad (11.1)$$

where Z_c is called characteristic impedance, a term that is borrowed from electrical transmission line theory,[20] noting that voltage and current are the electrical equivalents of pressure and flow, respectively. Assuming no leakage of blood through the vessel wall, characteristic impedance is determined by the inertance of the fluid (L), compliance of the vessel (C), and viscous resistance to flow (R) per unit length,[21]

$$Z_c(\omega) = \sqrt{\frac{R + j\omega L}{j\omega C}} \qquad (11.2)$$

where $j = \sqrt{-1}$ and ω is the angular frequency of the wave, with higher frequencies corresponding to faster changes in pressure and flow. The parameters L, C, and R can be related to measurable quantities as follows:

$$L = \frac{\rho}{A} \qquad (11.3)$$

$$C = \frac{A}{\rho c^2} \qquad (11.4)$$

$$R = \frac{8\pi\eta}{A^2} \qquad (11.5)$$

where ρ is blood density, η is blood viscosity, A is lumen cross-sectional area, and c is wave speed (which increases with vessel stiffness, see Chapter 1). Importantly, resistance is negligible in large vessels but becomes significant in smaller vessels because it is inversely proportional to the square of A, and hence the fourth power of radius (Eq. 11.5). By ignoring resistance in large vessels, Eq. (11.2) reduces to $Z_c = \sqrt{L/C}$, which is frequency-independent and, via Eqs. (11.3) and (11.4), becomes:
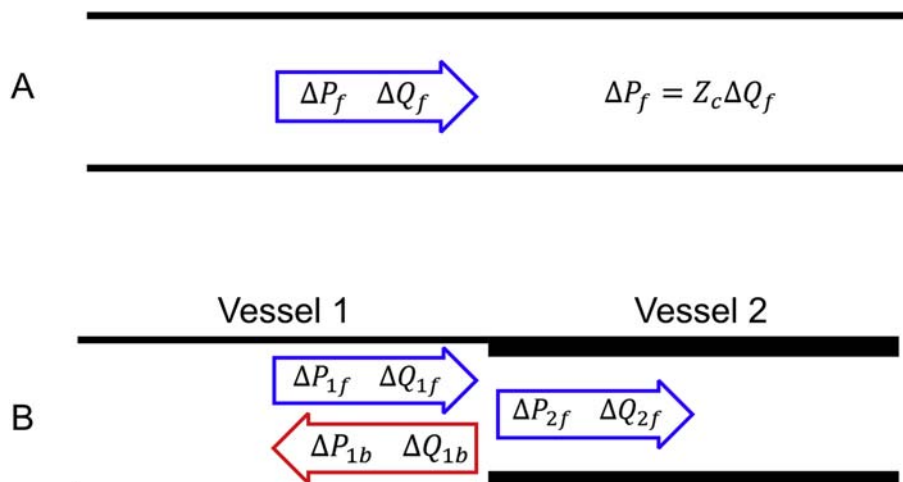
$$Z_c = \frac{\rho c}{A} \qquad (11.6)$$

This equation implies that a higher c (e.g., due to increased vessel stiffness) will be associated with a higher Z_c, causing a larger pressure rise for a given flow (Eq. 11.1). Indeed, this principle is thought to be the major factor underlying the hypertensive effect of aortic stiffening with advancing age,[22,23] although the approximately 100% increase in Z_c starting in middle age[22,24] is tempered by an increasing aortic area.[25]

To summarize the key points in this section, in the absence of wave reflection (1) pressure and flow waveforms will have the same shape; (2) the ratio of pressure and flow is called characteristic impedance (Z_c); and (3) Z_c is essentially independent of wave frequency in large vessels and depends on vessel size and stiffness (via A and c).

The basis of wave reflection: impedance mismatching

Given the intrinsic link between pressure and flow in a reflectionless tube, *any differences* in the shape of measured pressure and flow waveforms must arise due to wave reflection. Consider two connected vessels of finite length with differing characteristic impedances (Z_1 and Z_2, Fig. 11.1B); an "impedance mismatch" therefore exists at the interface between them. If a pulse of fluid is injected

FIGURE 11.1 (A) In a uniform tube with infinite length, a forward-traveling pressure change (ΔP_f) is intrinsically linked to an accompanying forward-traveling flow change (ΔQ_f) via characteristic impedance (Z_c). (B) At the interface between two vessels that have differing Z_c, a site of impedance mismatch exists. The incident forward wave produces pressure and flow changes in vessel 1 (ΔP_{1f} and ΔQ_{1f}) and the transmitted wave produces respective changes in vessel 2 (ΔP_{2f} and ΔQ_{2f}). A reflected wave produced at the site of impedance mismatch produces further changes in pressure (ΔP_{1b}) and flow (ΔQ_{1b}) in vessel 1.

BOX 11.1 Origin of wave reflection

Wave reflection must arise at sites of impedance mismatch to satisfy the fundamental laws of conservation of energy and mass. To understand this requirement, imagine a theoretical scenario where wave reflection does not occur at the interface between vessel 1 and 2 (Fig. 11.1B). If this were so, the only pressure and flow changes would be ΔP_{1f} and ΔQ_{1f} in vessel 1 and ΔP_{2f} and ΔQ_{2f} in vessel 2, respectively. Assuming no viscous dissipation, conservation of energy requires "continuity of pressure," which means that the total pressure change in both vessels must be the same ($\Delta P_{1f} = \Delta P_{2f}$). Rewriting both sides with the water hammer equation (Eq. 11.1) would then imply that $Z_1 \Delta Q_{1f} = Z_2 \Delta Q_{2f}$. If the two vessels had the same characteristic impedance ($Z_1 = Z_2$), i.e., no impedance mismatch, then we see that $\Delta Q_{1f} = \Delta Q_{2f}$, which satisfies conservation of mass. However, if there is an impedance mismatch ($Z_1 \neq Z_2$), then the water hammer equation requires that $\Delta Q_{1f} \neq \Delta Q_{2f}$, which would violate conservation of mass. Therefore, where an impedance mismatch is present, the only way for mass and energy to be conserved, while upholding the water hammer equation in both vessels, is for a reflected wave to arise in vessel 1; this leads to Eqs. (11.7) and (11.8).

---

into the first vessel, a forward-traveling wave ("*f*" subscript) is produced that causes a change in pressure and flow in vessel 1 (ΔP_{1f} and ΔQ_{1f}, respectively). A portion of the wave energy is transmitted into vessel 2 (ΔP_{2f} and ΔQ_{2f}, respectively), but a reflected wave is also produced because of the impedance mismatch. This is akin to light or sound waves being partially reflected when they travel from one medium to another with different refractive indices or densities. The reflected wave travels in the backward direction ("*b*" subscript) and also produces a change in pressure (ΔP_{1b}) and flow (ΔQ_{1b}) in vessel 1 (Fig. 11.1B). Hence, the overall pressure change in vessel 1 is $\Delta P_{1f} + \Delta P_{1b}$ and overall change in flow is $\Delta Q_{1f} + \Delta Q_{1b}$ (Fig. 11.1). As discussed in Box 11.1, wave reflection must arise at sites of impedance mismatch to ensure that the laws of conservation of mass and (assuming no viscous dissipation) conservation of energy are fulfilled. These require that the changes in pressure and flow in both vessels be equal, hence:

$$\Delta P_{1f} + \Delta P_{1b} = \Delta P_{2f} \tag{11.7}$$

$$\Delta Q_{1f} + \Delta Q_{1b} = \Delta Q_{2f} \tag{11.8}$$

Impact of wave reflection on arterial pressure and flow

To understand how reflected waves affect pressure and flow, a critical principle is that the water hammer equation for backward-traveling waves includes a negative sign (in contrast to Eq. (11.1) for forward-traveling waves):

$$\Delta P_b = -Z_c \Delta Q_b \tag{11.9}$$

Where both forward and backward waves are present at a particular measurement site, the observed pressure (ΔP) and flow (ΔQ) changes are equal to the sum of the respective forward and backward waves ($\Delta P = \Delta P_f + \Delta P_b$ and $\Delta Q = \Delta Q_f + \Delta Q_b$), if the generally small influence of nonlinearities is neglected.[26,27] These water hammer

equations (Eqs. 11.1 and 11.9) have two very important implications for interpreting arterial hemodynamics. First, forward waves cause pressure and flow to change in the same direction (a pressure-increasing forward wave will accompany a flow increase). However, backward waves cause pressure and flow to change in opposite directions (a pressure-increasing backward wave will accompany a flow decrease). Consequently, it is backward waves that cause measured pressure and flow waveforms in arteries to differ (Fig. 11.2). With the exception of coronary arteries, where some backward waves are actively generated in the intramyocardial circulation,[28,29] wave reflection is therefore ultimately responsible for the well-known differences in the shape of arterial pressure and flow waveforms. These differences are virtually abolished by reducing wave reflection via infusion of vasodilators, whereas the differences are accentuated when wave reflection is increased via the infusion of vasoconstrictors.[9,30–33]

Reflection and transmission coefficients
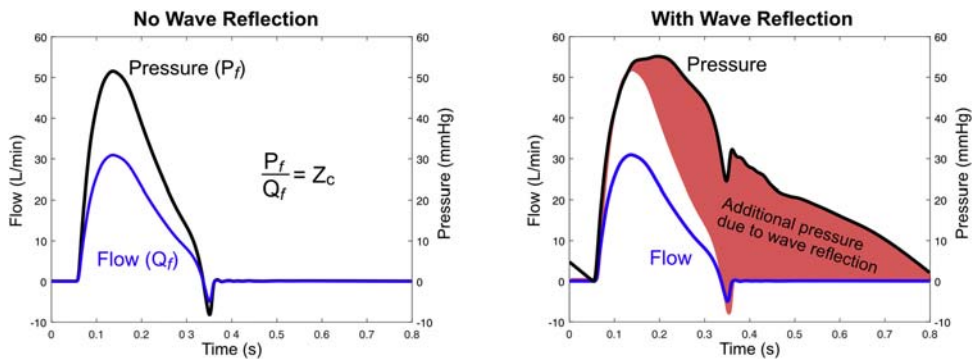
The degree to which a pressure wave is reflected at the boundary between vessel 1 and vessel 2 in Fig. 11.1B can be quantified as the ratio of the reflected pressure wave (ΔP_{1b}) to the incident pressure wave (ΔP_{1f}). This is called the local reflection coefficient (Γ_P) and can be expressed in terms of the mismatch in characteristic impedance using Eqs. (11.7)–(11.9):[20,34]

$$\Gamma_P = \frac{\Delta P_{1b}}{\Delta P_{1f}} = \frac{Z_2 - Z_1}{Z_2 + Z_1} \tag{11.10}$$

Similarly, the pressure transmission coefficient (T_P) is defined as

$$T_P = \frac{\Delta P_{2f}}{\Delta P_{1f}} = \frac{2Z_2}{Z_2 + Z_1} \tag{11.11}$$

By combining Eqs. (11.8) and (11.9), it can also be shown that T_P and Γ_P are related via $T_P = 1 + \Gamma_P$. At first this may seem counterintuitive because one might

FIGURE 11.2   In the absence of wave reflection (left), flow and pressure waveforms have the same shape, scaled by the characteristic impedance (1.67 mmHg min/L in this case). In the presence of wave reflection (right), the pressure waveform diverges from the flow waveform. The red shading indicates the total pressure contributed by wave reflection above what would exist in the theoretical absence of wave reflection. Note: the diastolic pressure in both cases is assumed to be zero for simplicity of representation.

expect that a 40% reflection would be accompanied by 60% transmission. However, this intuition only applies to conserved quantities like flow and energy, whereas pressure is not a conserved quantity. On the other hand, pressure is essentially *continuous* at arterial junctions, which means that pressure does not exhibit large changes over very short distances; it can be shown that the relation $T_P = 1 + \Gamma_P$ is required to ensure such continuity of pressure.[34]

Reflection and transmission coefficients for flow (Γ_Q and T_Q) can also be defined and expressed in terms of Γ_P (Table 11.1). In addition, the coefficients of composite measures that combine pressure and flow (hydraulic power and wave intensity) can also be found by combining the respective coefficients in the same manner (Table 11.1).

To understand reflection and transmission coefficients, it is instructive to highlight three limiting scenarios:

1. *Well-matched junctions*. When there is no impedance mismatch ($Z_2 = Z_1$), no reflected wave arises ($\Gamma_P = 0$ and $\Gamma_Q = 0$) and a pressure/flow wave is transmitted forward unaltered ($T_P = 1$ and $T_Q = 1$).

2. *Closed-ended or "positive" reflection* (i.e., $\Gamma_P > 0$) occurs when a wave encounters an impedance increase ($Z_1 < Z_2$ in Fig. 11.3). If vessel 2 were progressively occluded (area approaches zero, i.e., $A_2 \rightarrow 0$), Z_2 would progressively increase. As $Z_2 \rightarrow \infty$ (i.e., complete occlusion), $\Gamma_P \rightarrow 1$ and $T_P \rightarrow 2$, which means that an incident pressure-increasing ("compression") wave will be reflected as a compression wave that further increases pressure. On the other hand, $\Gamma_Q \rightarrow -1$ and $T_Q \rightarrow 0$, which means that (as expected) transmission of flow approaches zero and therefore the reflected flow wave must totally cancel out the incident flow wave (i.e., $\Gamma_Q = -1$). *One may therefore consider positive reflection as a conversion from kinetic energy (flow) to potential energy (pressure).*
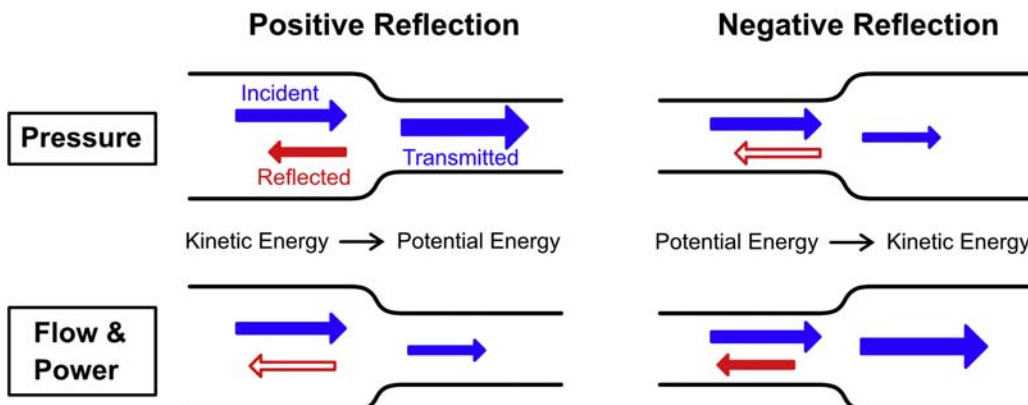
3. *Open-end or "negative" reflection* (i.e., $\Gamma_P < 0$) occurs when a wave encounters an impedance decrease ($Z_1 > Z_2$ in Fig. 11.3). If vessel 2 were progressively enlarged ($A_2 \rightarrow \infty$), $Z_2 \rightarrow 0$, $\Gamma_P \rightarrow -1$ and transmission of pressure falls toward zero ($T_P \rightarrow 0$). Hence, the reflected pressure wave entirely cancels the incident pressure wave, so that pressure at the interface does not change (just as flow does not change for a complete occlusion). The concept of negative reflection may be understood when considering the analogy of a wave propagating along a river (vessel 1) that meets the sea (vessel 2). A wave that increases water level in the river (analogous to an increase in pressure) cannot also raise sea level because the sea is effectively an infinite reservoir compared with the river. Hence to ensure continuity of pressure at the interface, the reflected pressure wave must cancel the pressure effect of the incident wave. *Negative reflection therefore involves a conversion from potential energy (pressure) to kinetic energy (flow)*, since as $Z_2 \rightarrow 0$, we see that $\Gamma_Q \rightarrow 1$ and $T_Q \rightarrow 2$; hence, the reflected wave augments flow in the same direction as the incident wave.

Although we have considered a single reflection site between two vessels, the same principles apply when considering wave reflection that is distributed through an arterial network. Positive reflection ($\Gamma_P > 0$) is well-recognized to occur in systemic arteries, causing systolic pressure augmentation and a less dome-like, and more triangular-shaped flow waveform observed with advancing age. However, as discussed in a later section, negative wave reflection ($\Gamma_P < 0$), although less widely recognized, also occurs throughout the arterial network, mainly in relation to re-reflection of backward-running waves at arterial junctions; however, negative reflection of forward traveling waves does occur in specific pathologies, such as aortic aneurysms.[35,36]

TABLE 11.1 Reflection and transmission coefficients.

	Coefficient	Expressions	Positive reflection example	Negative reflection example
Pressure reflection	Γ_P	$\frac{\Delta P_{1b}}{\Delta P_{1f}} = \frac{Y_1 - (Y_2 + Y_3)}{Y_1 + Y_2 + Y_3}$	$\Gamma_P = 0.2$ $\Delta P_{1f} = 10$ $\Delta P_{1b} = 2$	$\Gamma_P = -0.2$ $\Delta P_{1f} = 10$ $\Delta P_{1b} = -2$
Pressure transmission	T_P	$\frac{\Delta P_{2f}}{\Delta P_{1f}} = \frac{\Delta P_{3f}}{\Delta P_{1f}} = \frac{2Y_1}{Y_1 + Y_2 + Y_3} = 1 + \Gamma_P$	$T_P = 1.2$ $\Delta P_{2f} = \Delta P_{3f} = 12$	$T_P = 0.8$ $\Delta P_{2f} = \Delta P_{3f} = 8$
Flow reflection	Γ_Q	$\frac{\Delta Q_{1b}}{\Delta Q_{1f}} = \frac{Y_2 + Y_3 - Y_1}{Y_1 + Y_2 + Y_3} = -\Gamma_P$	$\Gamma_Q = -0.2$ $\Delta Q_{1f} = 10$ $\Delta Q_{1b} = -2$	$\Gamma_Q = 0.2$ $\Delta Q_{1f} = 10$ $\Delta Q_{1b} = 2$
Flow transmission	T_Q	$T_{Q2} = \frac{\Delta Q_{2f}}{\Delta Q_{1f}} = \frac{2Y_2}{Y_1 + Y_2 + Y_3}$ $T_{Q3} = \frac{\Delta Q_{3f}}{\Delta Q_{1f}} = \frac{2Y_3}{Y_1 + Y_2 + Y_3}$	$T_{Q2} = 0.72$ $\Delta Q_{2f} = 7.2$ $T_{Q3} = 0.08$ $\Delta Q_{3f} = 0.8$	$T_{Q2} = 0.8$ $\Delta Q_{2f} = 8$ $T_{Q3} = 0.4$ $\Delta Q_{3f} = 4$
Power reflection	Γ_Π	$\frac{\Delta \Pi_{1b}}{\Delta \Pi_{1f}} = \Gamma_P \Gamma_Q$	$\Gamma_\Pi = -0.04$ $\Delta \Pi_{1f} = \Delta P_{1f} \Delta Q_{1f} = 100$ $\Delta \Pi_{1b} = 4$	$\Gamma_\Pi = -0.04$ $\Delta \Pi_{1f} = \Delta P_{1f} \Delta Q_{1f} = 100$ $\Delta \Pi_{1b} = 4$
Power transmission	T_Π	$T_{\Pi2} = \frac{\Delta \Pi_{2f}}{\Delta \Pi_{1f}} = T_P T_{Q2}$ $T_{\Pi3} = \frac{\Delta \Pi_{3f}}{\Delta \Pi_{1f}} = T_P T_{Q3}$	$\Delta \Pi_{2f} = 86.4$ $\Delta \Pi_{3f} = 9.6$	$\Delta \Pi_{2f} = 64$ $\Delta \Pi_{3f} = 32$

The positive reflection example involves a bifurcation with three branches having admittances $Y_1 = 3$, $Y_2 = 1.8$, and $Y_3 = 0.2$. The negative reflection example involves a bifurcation with three branches having admittances $Y_1 = 3$, $Y_2 = 3$, and $Y_3 = 1.5$. Assumes an incident wave in vessel 1 with a nominal pressure effect $\Delta P_{1f} = 10$ and nominal flow effect $\Delta Q_{1f} = 10$ (units neglected).

FIGURE 11.3 Positive reflection occurs when an incident wave encounters an impedance increase ($Z_1 < Z_2$). The reflected wave changes pressure in the same direction as the incident wave (*filled arrows*), but changes flow in the opposite direction as the incident wave (*unfilled arrows*). The reverse is true for negative reflection.

We now consider the specific features of the arterial system that are thought to give rise to impedance mismatching and hence wave reflection, namely junctions, tapering, resistance vessels, stenoses, aneurysms, and stents.

Arterial junctions

Wave reflection at junctions can be analyzed by extending Eq. (11.10) to include two daughter vessels. For simplicity,

we now write the equation in terms of characteristic admittance, which is the inverse of characteristic impedance (i.e., $Y = 1/Z_c = A/\rho c$ in large vessels).

$$\Gamma_P = \frac{Y_1 - (Y_2 + Y_3)}{Y_1 + (Y_2 + Y_3)} \qquad (11.12)$$

where the subscripts 1, 2, and 3 refer to the parent and two daughters, respectively. Additional daughter branches could be included as additional terms in the brackets (Y_4, Y_5, etc.), but we here only consider a bifurcation. As in

the previous section, the pressure transmission coefficient is $T_P = 1 + \Gamma_P$, and the same pressure change is transmitted into both daughter vessels, regardless of the degree of asymmetry in daughter radii (assuming that pressure losses that depend on branch angle are negligible).
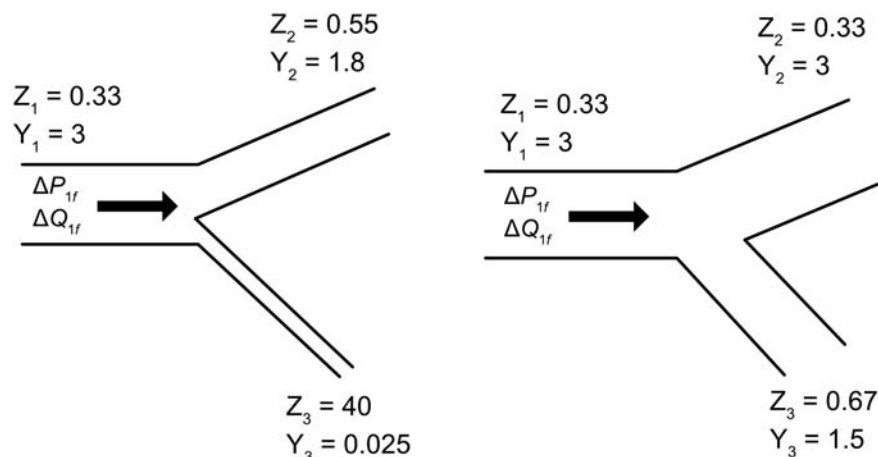
Expressions for calculating reflection and transmission coefficients for flow and hydraulic power (i.e., $\Pi = PQ$) are provided in Table 11.1; this table includes worked examples of reflected and transmitted pressure, flow, and power waves for the bifurcations shown in Fig. 11.4 ($\Gamma_P = 0.2$ and -0.2 for the incident wave in vessel 1). It is instructive to note that, unlike pressure, flow and power are transmitted unequally between branches for an asymmetric bifurcation, with less flow and power transmitted to higher impedance/smaller branches (in vivo, this means, for example, that less flow and power from the ascending aorta are transmitted into the smaller supra-aortic branches vs. the larger descending aorta). Interestingly, both examples in Fig. 11.4 involve the same degree of power reflection ($\Delta\Pi_{1b}$) and total power transmission ($\Delta\Pi_{2f} + \Delta\Pi_{3f}$), highlighting that any degree of wave reflection (whether positive or negative) reduces power transmission, compared with a well-matched junction.

Having covered the basic theory, we now consider how much wave reflection generally occurs at arterial junctions. Assuming symmetrical daughter vessels ($A_2 = A_3$) and that $c \propto 1/A^4$ (as per the Moens-Korteweg equation), it can be shown that a bifurcation will be well-matched ($\Gamma_P = 0$) when the daughter-to-parent ratio ($\alpha = (A_2 + A_3)/A_1$) is approximately 1.15.[19,37] For asymmetric bifurcations, the optimal area ratio is slightly lower.[19] Interestingly, extensive measurements of area ratios of the arterial tree in humans found that (with the notable exception of the aortoiliac bifurcation),[38,39] in general $\alpha = 1.14 \pm 0.03$, suggesting that the arterial tree is indeed very well-matched,

facilitating the efficient transmission of forward waves from the heart to organs and tissues, with minimal reflection.[40] This principle has been a key design feature of computational models of arterial haemodynamics, where it has been found that well-matched junctions are required to produce realistic pressure/flow waveforms.[41–43] Some earlier studies suggested that bifurcations provided sites of wave reflection.[44] However, it was later found that wave reflections can be almost entirely abolished by vasodilators, which directly increase the diameter of high resistance arterioles but have little to no effect on branching patterns.[30] Hence, although wave reflection can occur at junctions if not well-matched, it is unlikely that this is the major source of wave reflection in the healthy arterial system.

Tapering

Arterial tapering refers to the gradual decrease in area (geometric tapering) or change in wall properties (elastic tapering) along the length of the vessel. Both kinds of tapering lead to a continuous change in Z_c and consequently, wave reflection also occurs in a continuous manner along the entire length of the vessel instead of at a discrete point.[45] Interestingly, Segers et al. found that such continuous reflections had similar effects on measured pressure and flow signals as discrete reflections, thus making them indiscernible with measurements at a single site.[46] Arterial tapering (which involves decreasing area and increasing stiffness) has been hypothesized to play a role in pulse amplification because the continuously increasing Z_c produces reflected waves that increasingly add to the pressure waveform as waves travel from the heart to the periphery, as per the consequences of wave reflection on pressure transmission discussed earlier in this chapter.[47–49] Tapering may also attenuate the power transmission of

FIGURE 11.4 Bifurcations with a positive reflection coefficient ($\Gamma_P = 0.2$, left) and negative reflection coefficient ($\Gamma_P = -0.2$, right) for the incident pressure wave (ΔP_f). Calculation of reflection and transmission coefficients for pressure, flow, and power, for the given nominal characteristic impedance (Z) and characteristic admittance ($Y = 1/Z$) values of vessels 1, 2, and 3, are provided in Table 11.1.

reflected waves traveling back toward the heart, since such waves see a continuous impedance decrease. The actual contribution of tapering to arterial wave reflection is uncertain, however, as tapering may be predominantly an impedance-preserving feature due to the presence of side branches.[50]

Resistance vessels

Viscous resistance is negligible in large arteries but becomes significant in smaller vessels such as arterioles. In these smaller vessels, resistance makes an appreciable or even dominant contribution to Z_c (Eq. 11.2). This abrupt increase in resistance occurs over a very short length.[51] Several lines of evidence support the view that high resistance arterioles serve as the major sites of wave reflection.[52,53] First, as mentioned above, arterial bifurcations tend to be well-matched and tapering of large conduit arteries is likely impedance-preserving,[50] both of which appear to be good design features of the arterial network. Second, vascular beds have been shown to have a relatively high reflection coefficient, with a value of 0.8 estimated for the canine femoral vascular bed[30]; there is also evidence of a relatively large backward compression wave (BCW) in the distal radial artery in humans.[54] Third, vasodilation of resistance vessels markedly reduces or even abolishes wave reflection, whereas vasoconstriction increases wave reflection.[30,32,55-57]

These observations notwithstanding, the role of peripheral resistance in generating wave reflection is still debated, primarily because changes in wave reflection may be induced without a parallel change in systemic vascular resistance.[58] For example, administration of inorganic nitrate results in a clear reduction in wave reflection, even when peripheral resistance is unchanged.[55] However, Yaginuma et al.[59] suggested that a similar phenomenon observed in several studies after administration of glyceryl trinitrate[59,60] could be explained by negative reflection arising at the interface between larger parent arteries and the dilated muscular arteries, which would offset the unchanged positive reflection occurring at the arteriolar level.

Stenosis

Stenosis is the focal narrowing of an artery, typically caused by congenital defects or atherosclerosis. While the severity of a stenosis nonlinearly determines its effective resistance to flow,[61] the associated local increase in impedance also produces positive wave reflection.[62,63] The impedance mismatch occurring at a stenosis is influenced by (1) the characteristic impedance of the parent vessel, (2) the stenotic cross-sectional area, (3) the stiffness of the stenosis vessel wall, and (4) the viscous resistance arising from complex or turbulent flow downstream to the vena contracta. Importantly, based on computational and in vitro studies, Stergiopulos et al.[64] concluded that the reflection coefficient of a stenosis rises more steeply than its resistance, suggesting that even hemodynamically insignificant stenoses (i.e., those that cause a clinically insignificant increase in resistance) may produce substantial wave reflection.

Aneurysms

Aneurysm is the localized enlargement of an artery caused by weakening of the arterial wall. In vitro and computational studies have demonstrated that negative reflection occurs at fusiform aneurysms due to the local increase in area and resultant decrease in characteristic impedance (Eq. 11.6).[35,65] Negative reflection of the initial forward compression wave (FCW) produces a backward decompression wave (BDW) that has a pressure-decreasing and flow-increasing effect. A small BDW was detected in one patient in a pilot study before (and not after) repair of an abdominal aortic aneurysm. All three patients studied exhibited an increased (i.e., more positive) reflection coefficient after repair, suggesting that local negative reflection at the aneurysm may not always be detectable if it is overwhelmed by positive reflection from other sites.[35]

Stents

Stents are mesh-like structures made of stainless steel that eventually integrate with the vessel wall. Since the stent is stiffer than the vessel wall, two sites of impedance mismatch are created, one at the proximal end (impedance increase) and one at the distal end (impedance decrease), associated with positive and negative Γ_P, respectively. For a short stent, one might expect the reflected compression and decompression waves arising from these two sites to be almost in phase and thus cancel each other out. Indeed, a theoretical analysis by Crespo et al.[66] suggested that wave reflection from a stent is directly proportional to its length and inversely proportional to the wave speed of the parent artery (assuming very high wave speed in the rigid stent itself). A shorter stent may therefore cause less hemodynamic perturbation and contribute to a lower risk of restenosis.[67] Although not confirmed in vivo, computational studies by Papathanasiou et al.[68] predicted that the structure of a stent mesh affects wave reflection in a frequency-dependent manner, and that placement of two stents may lead to high levels of wave reflection.

Models of arterial wave reflection

When attempting to understand wave reflection in the arterial system as a whole, conceptual models are unavoidable. Mathematical models provide the blessing of

analytical precision and conceptual robustness, but also the curse of assumptions. Since the concepts and indices used to describe and quantify arterial wave reflection are based on one or another model, awareness of model limitations is crucial to avoid misinterpretation and thinking "inside the box" (e.g., only conceiving of physiological processes in terms of one specific limited model).
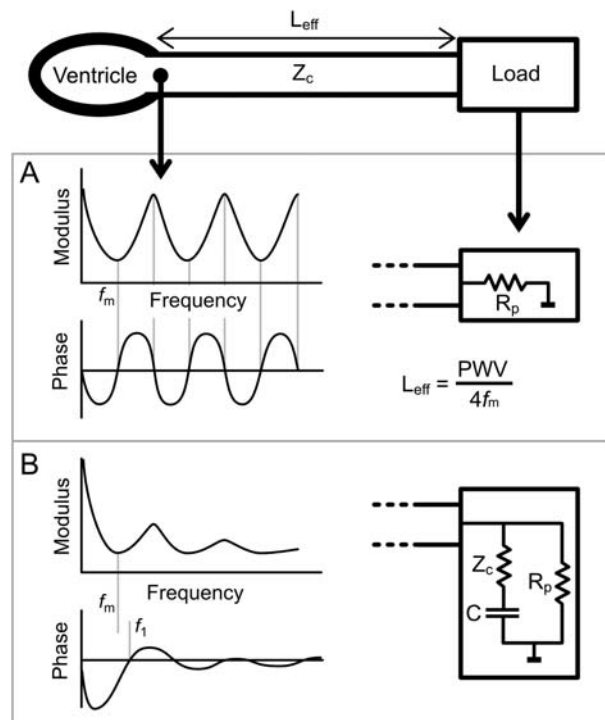
Broadly speaking, models of waves in arteries are generally founded on three pillars. The first is the Navier—Stokes equations that express the basic laws of fluid dynamics. Although these are derived from the unassailable laws of conservation of mass and momentum, when addressing the phenomenon of waves, these equations are usually reduced to a one-dimensional (1D) form with the aid of several simplifying assumptions—for example, long cylindrical geometry.[69,70] The second is a constitutive relation that describes the distensibility of the arterial wall (i.e., how transmural pressure relates to cross-sectional area). Due to the complex composition and mechanical properties of the arterial wall, all constitutive relations are empirical and approximate. When neglecting nonlinearities in the combined system of equations, the telegraph (or transmission line) equations are obtained. These form the basis for concepts such as characteristic impedance and impedance mismatching.

In addition to these basic model constructs regarding waves in elastic tubes, a third (and pivotal) aspect of wave reflection models is how the systemic arterial network is represented. Historically, a frequently pursued goal has been to reduce the very complex wave reflection properties of the arterial network to a model form that is as simple as possible, in the hope that a model with few parameters may provide both conceptual clarity and clinical utility. We here briefly review the most prominent wave reflection models.

Single tube model

The simplest model of arterial wave reflection is a uniform tube, with characteristic impedance Z_c, terminated in a load that creates a single reflection site (Fig. 11.5). According to Campbell et al.,[71] the origins of this model appear to extend back to Otto Frank, who proposed that one "effective" reflection site might be used to represent the lumped effect of the many actual reflection sites distributed around the body. An "effective length" (L_{eff}) refers to the distance from a measurement site to the apparent "location" of this reflection site, while "effective reflection time" (T_{eff}) refers to the time taken for a wave to travel to this effective reflection site and back. Although long-recognized to be a simplification of reality, estimation of T_{eff} and L_{eff} has been a frequent topic of investigation over the past 80 years.[2,72—78]

An overview of the various methods used to estimate T_{eff} is provided in a later section. L_{eff} can then be calculated as PWV/T_{eff}, where PWV is pulse wave velocity. When applying these methods, it is important to keep in mind that

FIGURE 11.5 Input impedance of the single tube model with (A) resistive load, and (B) complex load (in this example, a modified windkessel).

all of them are (either explicitly or implicitly) based on the single tube model. For example, pulse wave analysis and wave separation analysis involve analysis of waveform features and are not explicitly tied to a single tube model, but when singular L_{eff} or T_{eff} are calculated, a single effective reflection site is implied. Other techniques are explicitly linked to a specific mathematical form of the single tube model. The earliest of these involved a perfectly elastic tube and purely resistive load,[75] with L_{eff} calculated via the "quarter wavelength formula" (see Fig. 11.5). However, this model exhibits unphysiological oscillations in the impedance spectrum (see Box 11.2), and so subsequent investigators variably employed tubes with pulse attenuation (i.e., viscous friction) and/or a complex load (standard or modified 3-element windkessel).[72—74] L_{eff} was estimated from the first local minimum in impedance modulus or first zero crossing of the phase, or through fitting a computational model to measured waveforms.

Importantly, given the same input data, different models and techniques lead to different values of L_{eff}, e.g., with resistive loads producing larger values than complex loads.[72,73,79] Moreover, it has been shown that the "location" of the effective reflection site (i.e., the end position of the tube) depends on where measurements are taken.[53,80,81] For example, when impedance is measured at the thoracic aorta, an apparently discrete reflection site is found at the aortic bifurcation, whereas when measured from the abdominal aorta, the discrete reflection site appears more
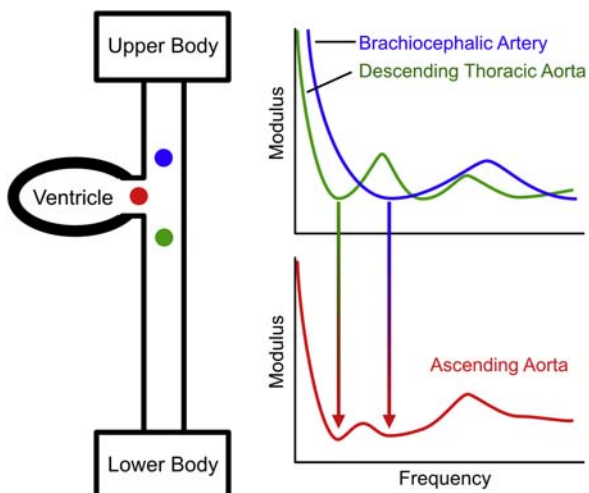
BOX 11.2 Impedance analysis of the single tube and asymmetric T-tube models

The input impedance defines the relationship between pressure and flow (see also Chapters 1 and 3). The impedance spectrum at the inlet of the single tube model depends on the assumptions adopted, primarily on: (1) whether the tube has uniform properties along its length, or incorporates geometric and/or elastic tapering; (2) whether the model includes lossless wave propagation, or attenuation due to viscoelasticity in the vessel wall and/or viscous friction of flowing blood, and; (3) whether the load is represented as a pure resistance, a three-element windkessel, or a modified windkessel.

Fig. 11.5A shows the input impedance of a lossless tube with a resistive load. The impedance spectrum exhibits minima and maxima that are equally spaced at frequencies kf_m, where f_m is the frequency of the first minima and $k = 1,2,3$ .... The impedance phase also crosses zero at these frequencies. The length of the tube determines f_m via the quarter wavelength formula: $f_m = c/4L_{eff}$, where c is the phase velocity (frequency-dependent wave speed). By rearranging this formula, and approximating c via a measured PWV, L_{eff} can be estimated after obtaining f_m from a measured input impedance spectrum.

This model has been criticized because the oscillations in measured impedance spectra are damped at higher frequencies. A more realistic representation of impedance is obtained by including a complex load, such as the modified windkessel shown in Fig. 11.5B (similar damping at high frequencies is obtained by including tapering or viscous attenuation in the tube, but these are not considered further here). At low frequencies, the impedance of the load approaches peripheral resistance (R_p), whereas at high frequencies, impedance approaches characteristic impedance (Z_c). Unlike the resistive load, the wave reflection properties of this load (which appear as oscillations in the input impedance) are frequency-dependent and are modulated by the load compliance (C).[85] In addition, f_m no longer necessarily aligns with the frequency of the first zero crossing of phase (f_1),[72] which means that L_{eff} is no longer uniquely defined (as it could be calculated via either f_m or f_1 using the quarter wavelength formula). To avoid this issue, L_{eff} is often equated with the length of a transmission line (i.e., single tube) that is obtained after a parameter optimization process that fits computed to measured pressure waveforms for a given measured flow waveform.[84,86] Note, however, that the L_{eff} value obtained is less than that obtained via f_m and the quarter wavelength formula, because the complex load introduces a frequency-dependent phase lag at the distal end; in other words, confusingly, the load itself has its own "effective length" that is frequency-dependent.[87] These issues have led some to conclude that attempting to define a singular effective length for the arterial system is ultimately a futile exercise.[87]

The principles underlying calculation of two effective reflection sites from the asymmetric T-tube model are the same as those for the single tube model, except that we now consider the combined effect of those two reflection sites (roughly corresponding to upper and lower bodies), when viewed from the ascending aorta (Fig. 11.6). Thus, one can estimate the distance to the two effective reflection sites via the quarter wavelength formula using the frequency of each impedance minimum and PWV at the root of each branch.[88] Since this approach implies resistive loads, an alternative is to fit a computational model (consisting of two transmission lines terminated in complex loads) to measured pressure and flow data.[89]

FIGURE 11.6 (Left) Asymmetric T-tube model consisting of one short tube approximately representing arteries feeding the upper body, and one long tube representing arteries feeding the lower body. (Right) Impedance patterns seen at the entrance of the short and long tubes combine to produce two distinct impedance minima in the ascending aorta. (Note: illustration only).

distally in the upper thigh, an effect that has been likened to chasing the end of a rainbow.[82] Thus, any statements about the main reflection site occurring at a specific anatomical location, such as the aortic bifurcation[83] or renal arteries,[80,84] should be interpreted notionally.

Other limitations of the single tube model are widely recognized. First, the large conduit arteries form a complex branching network with varying diameters and mechanical properties; therefore, the intrinsic premise that waves propagate to and from a reflection site along a uniform tube is fundamentally unrealistic. Second, wave reflection does not occur at a single location, but many. Third, L_{eff} is usually calculated from a single PWV value; since PWV is not the same in all vessels (tending to be higher in smaller vessels), the length is generally underestimated compared with a value that would be obtained if accounting for the true propagation speed. Finally, a key prediction of the single tube model is that the reflected wave will arrive earlier in more distal locations; however, this is not found to be the case in vivo, as will be discussed later in this chapter.

Asymmetric T-tube model

Seminal modeling work by Taylor[90] showed that an arterial network with an asymmetric branching pattern produces two adjacent local minima in the impedance spectrum, implying the presence of not one but two effective reflection sites. Evidence of two effective reflection sites was reported from data in the ascending aorta of dogs,[11,91] humans,[88] and other species.[53] An impedance minimum seen in the brachiocephalic trunk occurred at a higher frequency than that seen in the descending thoracic aorta, implying shorter and longer distances to effective reflection sites, respectively. These impedance patterns appeared to combine from the viewpoint of the ascending aorta, with two minima implying two reflection sites. This led to the concept that the input impedance seen at the ascending aorta resembles that expected from the asymmetric T-tube shown in Fig. 11.6.

An important concept related to the T-tube model is that the input impedances of upper and lower bodies interact in such a way that fluctuations in ascending aortic impedance are lower than in any other artery. In other words, the arterial tree is designed in such a way as to minimize the return of reflected waves to the left ventricle, thus optimizing afterload.[82] This optimization appears to decrease with aging, however, because aortic stiffening primarily lowers arrival time of lower body reflections, causing a rightward shift in the first impedance minimum and a merging of the two reflection sites.[24,82,92]

Although potentially useful as a means of describing system-level impedance patterns, it has long been recognized that the asymmetric T-tube model represents a marked oversimplification of the arterial system.[11] It shares many of the same limitations as the single tube model in that any calculation of effective lengths should be treated notionally, and not corresponding to some actual discrete reflection

site. The T-tube model better represents the input impedance of the ascending aorta compared with the single tube model,[89,93] but this is not surprising given its greater complexity. The better fit does not "validate" the model in terms of its physical implications (i.e., the actual existence of two reflecting sites), despite these making intuitive sense. From a mathematical point of view, whether the parameters in a T-tube model can be uniquely determined based on input impedance has been questioned.[74] Finally, Murgo et al.[83] argued that the T-tube model implies that one should see two inflection points in the aortic pressure waveform, whereas in most cases only one is visible; similarly, it may be difficult to reliably identify distinct impedance minima and maxima due to limitations in signal fidelity.

Tapered tube models

Whereas the models considered so far involve uniform tubes, some have argued that wave reflection in the real arterial system is affected by geometric and elastic taper, and this property should be accounted for in model representations. Einav et al.[94] explored the impedance properties of a transmission line composed of many small transmission line segments, with characteristic impedance increasing progressively with distance from the inlet. It was shown that even with a well-matched (reflectionless) distal load, the input impedance of the tapered tube exhibited oscillations suggestive of wave reflection, and these oscillations were damped at high frequencies as in the real system. Fogliardi et al.[95] showed that a single tube model incorporating tapering provided a better fit to descending aortic impedance than a uniform tube. However, the parameters providing the optimal fit overestimated proximal characteristic impedance and did not predict other key physical quantities; it was concluded that the introduction of tapering did not show any identifiable benefits regarding the physiological interpretation.[95] An exponentially tapered T-tube model was also explored,[96] but heavily criticized.[97]

Branching network models
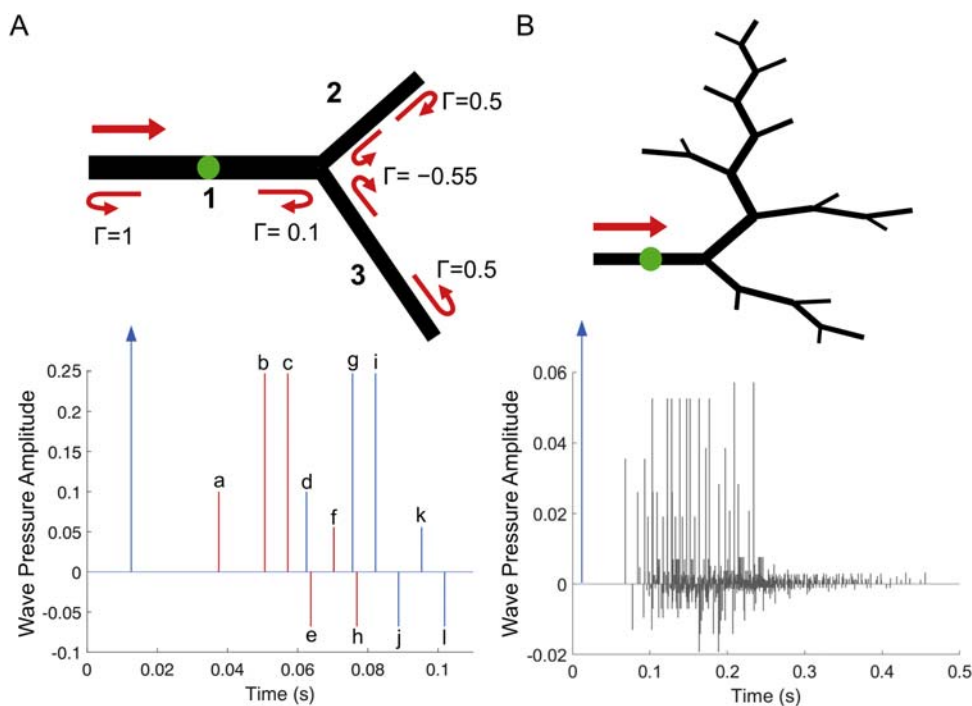
The single tube and T-tube models attempt to derive salient information about the arterial network from measured pressure and flow waveforms using the minimum possible number of parameters, a process known as the "inverse problem." By contrast, branching network models address the "forward problem," where knowledge about the complex structure and mechanical properties of the arterial network is prescribed in a model and pressure and/or flow waveforms are *predicted* via solution of reduced-order forms of the Navier−Stokes equations. This approach is useful for exploring the dynamics of wave propagation and reflection in models with realistic properties and can be used as a platform for virtual experiments. We here briefly review the commonly used types of branching network models and some of the insights they have provided about arterial wave reflection.

Linear wave tracking was originally described by Taylor[90] using a frequency domain approach applied to a randomly branching network, and by Remington and O'Brien[8] using a time domain approach applied to the dog aorta and its main branches. As the name implies, any nonlinearities in the system (such as the pressure-dependence of wave speed) must be neglected to allow individual waves to be treated independently of each other. A single "parent" wave (defined as a single sine wave in the frequency domain or a pressure-flow perturbation in the time domain) is prescribed at the inlet of the model and all reflected and transmitted "daughter" waves that are generated at sites of impedance mismatch in the system are tracked. With a unit impulse function as the parent wave, one can then build up an impulse response function.[43,98] Fig. 11.7 provides examples of the impulse response for a simple bifurcation model and a more complex branching network; convolution of the impulse response with a realistic input wave can then be used to predict hemodynamic waveforms.[43]

Using linear wave tracking, it has been shown that (1) asymmetry of a fractal network and inclusion of pulse attenuation leads to a more realistic input impedance (and thus wave reflection properties) than a symmetric, lossless fractal tree[99,100]; (2) very complex wave patterns arise in the arterial network due to multiple re-reflections,[43] as is evident in Fig. 11.7; (3) wave reflection in the periphery makes a greater contribution to aortic pressure than wave reflection in the large conduit arteries[98]; and (4) wave reflection in conduit arteries promotes transmission of pulse pressure to the microvasculature, and therefore does not protect it from excessive pulse pressure.[34]

With *1D models*, the reduced-order equations governing pressure and flow for compliant tubes are solved computationally. Individual segments are connected together to form anatomically realistic networks, and boundary conditions for the heart and microvascular beds are provided at the proximal inlet and distal outlets. The first anatomical model of the major systemic arteries, constructed physically with analog electronics by Westerhof et al.,[101] was a particular type of 1D model known as a *transmission line model*. These models involve certain linearizing assumptions: cyclical diameter changes are much smaller than the diameter itself, and similarly, variations of wave speed with
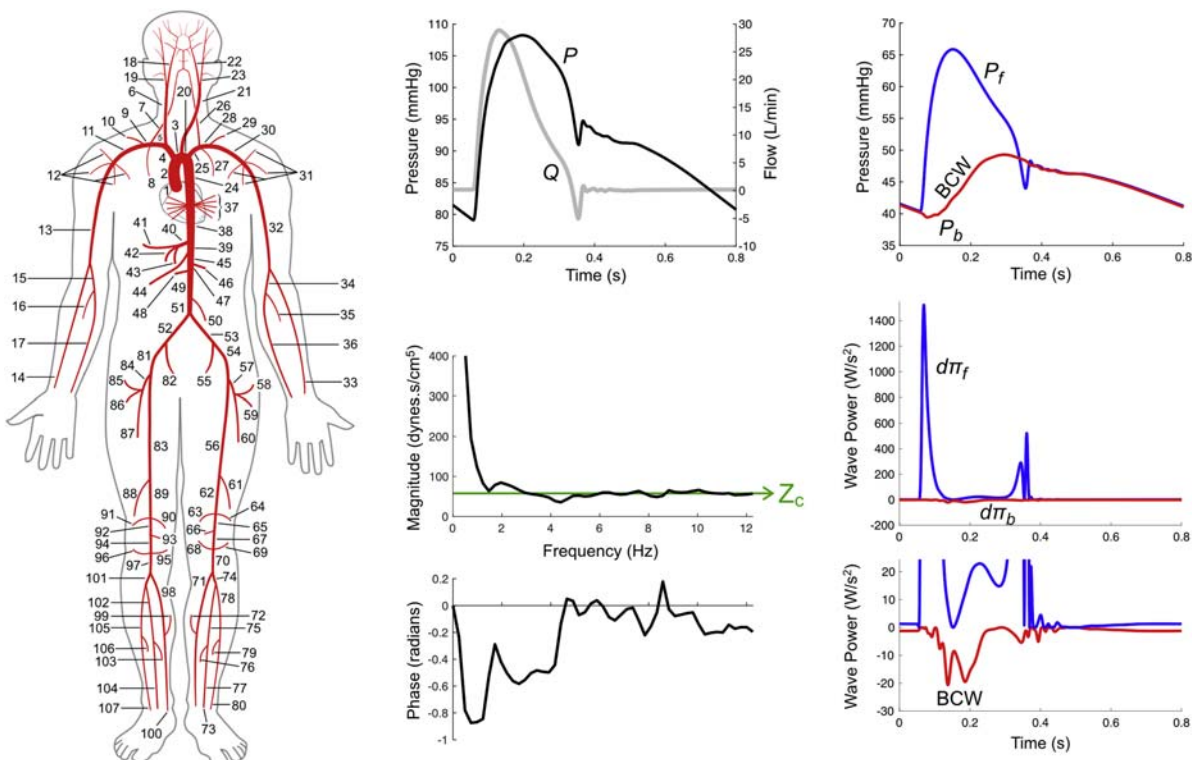
FIGURE 11.7 (A) The linear wave-tracking process is illustrated in a simple bifurcation with a unit impulse sent forward from the inlet. The impulse is transmitted, reflected, and re-reflected at the bifurcation and terminal vessels. This produces multiple waves that arrive at the monitoring point (*green circle*) at different times—modulated by the length and wave speed of each vessel, and at different amplitudes—modulated by the proximal and distal reflection coefficients (Γ) at the inlet and outlet of each vessel. The pressure amplitude of individual waves is depicted by the impulse response, with forward waves in blue and backward waves in red. The input forward wave has an amplitude of 1 (represented by an *arrow*) and arrives at the monitoring site at 0.01 s. It is then reflected at the junction, producing wave "a," having traversed vessel 1 in the forward then backward directions (hence the "wave history" is 1-1). Wave "b" arises from reflection at the outlet of vessel 2, hence its wave history is 1-2-2-1. Wave "c" arises from reflection at the outlet of vessel 3 (1-3-3-1). Wave "d" is from total re-reflection of "a" at the inlet (i.e., 1-1-1). The other waves arise from multiple re-reflections as follows: e, 1-2-2-2-2-1; f, 1-3-3-2-2-1 (also 1-2-2-3-3-1); g, 1-2-2-1-1; h, 1-3-3-3-3-1; i, 1-3-3-1-1; j, 1-2-2-2-2-1-1; k, 1-3-3-2-2-1-1 (also 1-2-2-3-3-1-1); l, 1-3-3-3-3-1-1. (B) Wave tracking in a relatively small branching network produces a multitude of reflected and re-reflected waves (in this case, forward/backward waves are not differentiated with color).

changes in blood pressure are negligible. The resulting equations are mathematically equivalent to those that govern electrical transmission lines. Four elements describe a basic transmission line segment (per unit length): (1) series inductance representing blood inertia (L), (2) series resistor representing energy dissipation due to blood viscosity (R_v), (3) parallel resistor representing leakage through the vessel wall (R_l, often taken to be zero), and (4) parallel capacitor representing local wall compliance (C). Equations for calculating characteristic impedance and reflection coefficients discussed elsewhere in this chapter are based on this model.
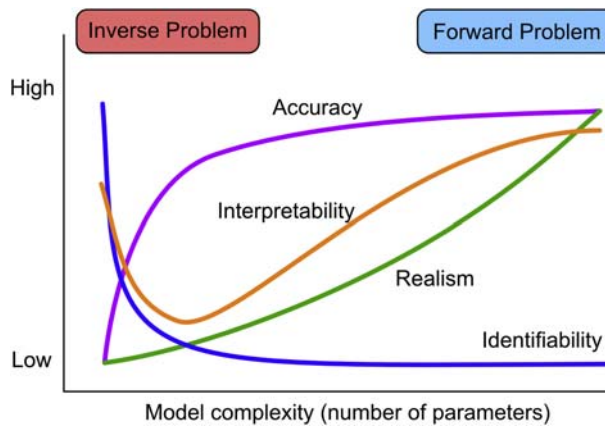
Nonlinear 1D models provide the greatest level of realism (for a reduced-order model) in terms of describing arterial hemodynamics, as they account for the nonlinear behavior of the arterial wall and many other physiological phenomena that will not be reviewed here. These models have undergone extensive refinement and validation over the past 40 years and are now widely used as an in silico research platform in the arterial hemodynamics field.[41,70,102–107] These models provide pressure and flow waveforms, an input impedance spectrum, and wave patterns that closely resemble those seen in vivo (Fig. 11.8).

Synthesis

Fig. 11.9 displays the tradeoffs that exist when modeling arterial wave reflection in terms of *accuracy* (can the model predict measured hemodynamics?), *identifiability* (is there a unique set of optimal model parameters?), *interpretability* (can we correlate model parameters with physical properties of the system?), and *realism* (does the model representation and its interpretation correspond with reality?). We suggest that any model may be useful for certain purposes, but every model has limits in scope and utility. Simple models, such as the single tube or asymmetric T-tube (and windkessel models that do not account for wave travel), are suited to estimating bulk or effective properties of the arterial system (inverse problem), but these lack realism and can therefore lead to false conclusions if interpreted literally rather than notionally.[58,108] With increasing model complexity, there is a steep incline in the ability of even simple models to accurately predict pressure-flow patterns at a specific arterial location, but this is not matched by high levels of realism. Complex models, such as anatomically realistic 1D models, are suited to studying the mechanisms underlying arterial wave

FIGURE 11.8   Schematic of a nonlinear one-dimensional model of the systemic arteries and the predicted pressure (P) and flow (Q) waveforms, input impedance (magnitude and phase), and forward (green) and backward (red) components of pressure (P_f and P_b, respectively) and wave power ($d\pi_f$ and $d\pi_b$, respectively) in the ascending aorta. Wave reflection produces a backward compression wave (BCW) seen with wave separation and wave power analysis, and, in the input impedance, a departure from characteristic impedance (Z_c, blue line) at nonzero frequencies. This model is an updated and adapted version of that reported by Reference 41; segment numbers for cerebral arteries are not shown.

FIGURE 11.9 Relationship between the complexity of the models of wave reflection and their accuracy, realism, interpretability, and identifiability. Low complexity models, such as the single tube model, are typically used for the inverse problem (estimating system properties from haemodynamics), but these have limited accuracy and realism. High complexity models, such as one-dimensional network models, are used for the forward problem (predicting haemodynamics from system properties) but have poor identifiability.
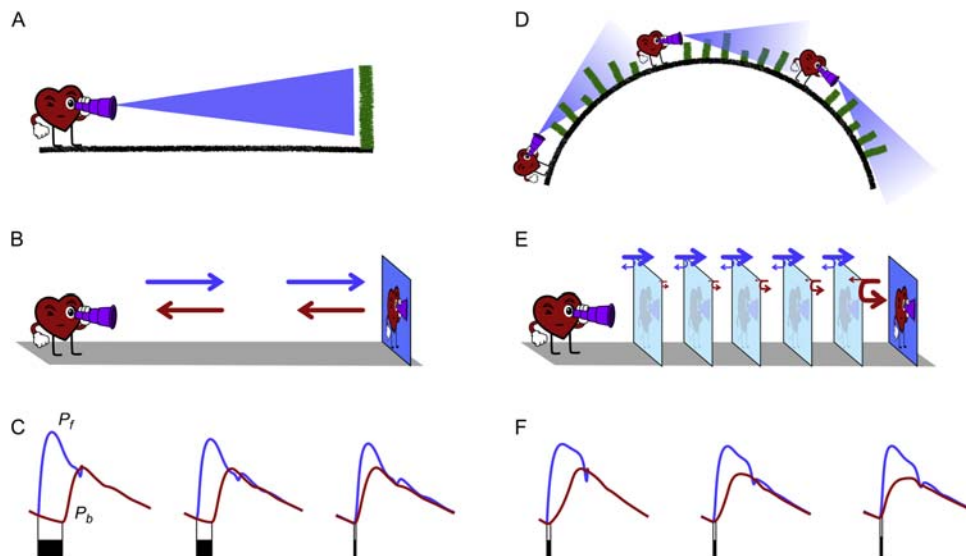
dynamics (forward problem) and attain high levels of accuracy, realism and interpretability. However, due to the large number of parameters involved, identifying a unique set of parameters describing an individual is extremely challenging. Very simple models (for the inverse problem) and very realistic models (for the forward problem) can be

readily interpreted; however, although adding a few additional parameters to a simple model improves accuracy, the physiological meaning of those extra parameters (interpretability) is often unclear. Our understanding of arterial wave reflection is entrenched in model descriptions; these models are most useful when their properties, strengths, and limitations are kept clearly in sight.
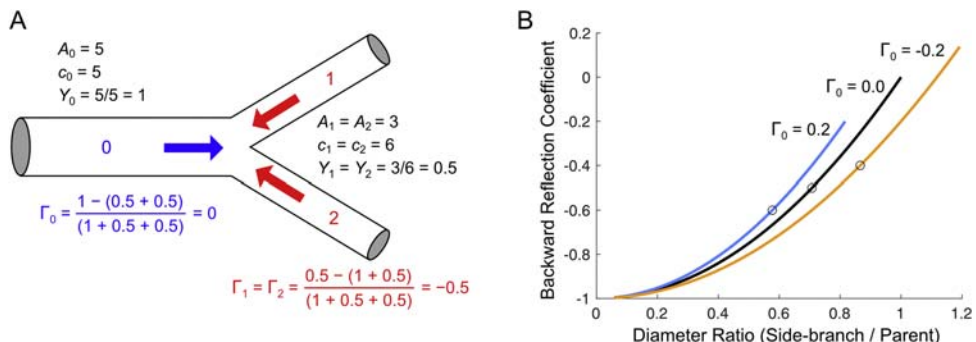
Re-reflections and the horizon effect

It is often incorrectly assumed that the delay between backward (reflected) and forward (incident) waves should decrease with greater distance from the heart, which would occur if the arterial system were a tube terminated with a single reflection site. Fig. 11.10 shows two analogies of this situation, an observer viewing a single object (panel A) or light waves propagating unhindered to a single mirror and back again (panel B). In these scenarios, the delay between forward and backward waves will decrease as the observer approaches the reflection site, as in Fig. 11.10C, which shows forward and backward components of pressure from a 1D model of a single uniform tube.

In reality, however, calculated L_{eff} has been found to be approximately constant relative to the measurement point, when assessed at different points along the aorta.[53,80,81] This may be explained on the basis of two key properties of the arterial system. First, wave reflection is distributed throughout the network; although some uncertainty exists

FIGURE 11.10 Viewing the arterial network as uniform tube with a single major reflection site may be likened to (A) observing a single landmark (green bar) from a distance, or (B) seeing one's reflection in a single mirror. (C) The delay between forward and backward waves (here shown as blood pressure components P_f and P_b) decreases progressively as the observer moves toward the reflection site (*black boxes*); however, this phenomenon is not observed in vivo. Better analogies of arterial wave reflection involve (D) many reflections sites distributed through space and a "horizon" effect, or (E) a series of "one-way" mirrors that efficiently transmit forward waves and produce only minor reflection (*blue arrows*), but that strongly reflect backward waves (*red arrows*); (F) the delay between P_f and P_b onset is then relatively constant regardless of observer location because the reflected waves that are seen mainly arise from the reflection sites nearest to the observer.

FIGURE 11.11 (A) Reflection coefficient (Γ) for a forward-traveling wave (*blue arrow*) or backward traveling waves (*red arrows*) approaching a symmetrical bifurcation, calculated from characteristic admittance ($Y = A/(\rho c)$, where A is area, c is wave speed, and blood density $\rho = 1$ for simplicity). The junction is well-matched in the forward direction ($\Gamma_0 = 0$), but there is strong negative reflection ($\Gamma_1 = \Gamma_2 = -0.5$) in the backward direction. (B) Reflection coefficient in the backward direction in a daughter branch of a bifurcation for a range of daughter/parent diameter ratios, given specified parent vessel reflection coefficients in the forward direction ($\Gamma_0 = 0.2$, 0, and -0.2). *Circles* indicate the case of a symmetric bifurcation.

as to the relative contribution of bifurcations, tapering, and resistance vessels to reflection, all of these sources are spatially distributed throughout the body. Second, the main conduit arteries are well-matched in the forward direction, but not the backward direction.[109,110] For a symmetrical bifurcation that has a reflection coefficient of 0 for forward waves, backward waves in the daughter branches face a reflection coefficient of -0.5 at the junction (Fig. 11.11A). This can be shown by swapping Y_2 or Y_3 with Y_1 in Eq. (11.12), for waves in vessel 1 and 2, respectively. Given fixed forward reflection coefficients, Fig. 11.11A plots the backward reflection coefficients for different daughter-to-parent diameter ratios. These coefficients approach -1 for very small branches, which means that the backward wave is totally re-reflected and has a minimal effect on pressure in the parent branch.
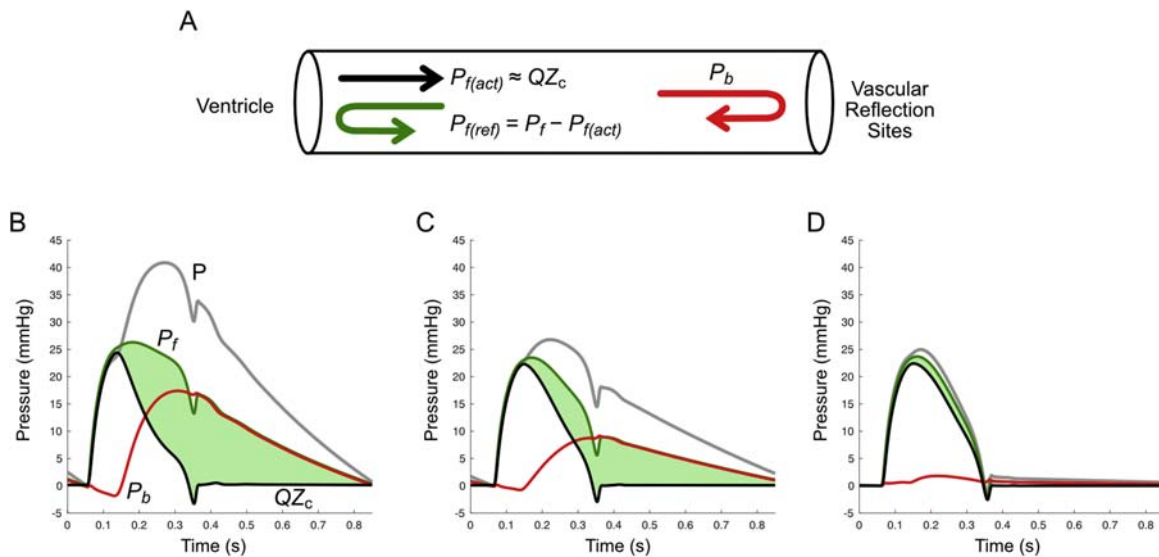
Hardung[10] first described the consequences of this strong negative reflection in the backward direction as follows (translated from German): "The side branch represents a kind of trap for the incoming wave, from which it can only emerge very weakly." For a network with multiple generations of branching, the situation is therefore something like that depicted in Fig. 11.10E. Here junctions are represented as one-way mirrors (mostly transparent in the forward direction and mostly reflective in the backward direction). Forward waves (blue arrows) are efficiently transmitted, with only minor reflection at each junction. By contrast, backward waves (red arrows) returning from the peripheral reflection sites (last mirror) are strongly reflected at each junction, such that very little wave energy returns to the observer. The importance of this phenomenon in the arterial system was evidenced by the finding that distal aortic occlusion in dogs (which introduced a large reflected wave at that site) had an almost imperceptible effect on hemodynamics in the ascending aorta (Westerhof et al.[150]; Van den Bos et al.[151]).

The process of "wave-trapping" in a branching network leads to the so-called wave horizon effect, in which the return time of reflected waves is about the same regardless of where measurements are performed.[81] As depicted in Fig. 11.11D, only waves reflected from relatively nearby sites are observable, because waves originating more distally are progressively attenuated by re-reflection at junctions. Furthermore, the view seen by the observer is similar regardless of the viewpoint. Fig. 11.11F shows results from a tapered tube simulation; because reflection occurs at each point along the vessel, and backward waves are partially trapped by negative re-reflection, the delay between the onset of forward and backward pressure waves is almost the same at different monitoring points.

An interesting avenue for future research may be to investigate the circumstances under which wave-trapping is reduced and transmission of backward waves increased, for example, the effect of changes in aortic tapering or stiffness with age. One example of a situation where reflected waves from apparently diffuse/peripheral sites appear to be strongly transmitted back to the ventricle is in the fetal lamb, where a very large BCW is observed in the proximal pulmonary arteries.[111,112] The resulting abrupt flow decrease during mid-systole is also seen in adult humans with pulmonary arterial hypertension,[113] where the reflected wave can also cause partial closure of the pulmonary valve well before the onset of ventricular relaxation.[114,115] In these cases, strong reflection occurs throughout the peripheral vascular bed, rather than in one branch, so although the backward transmission of individual waves may be small, the combined effect of many waves in concert appears to be large.

Ventricular wave re-reflection

The ventricle is often described as the active source of forward waves and the vasculature as the passive locale of

FIGURE 11.12 (A) The ventricle actively produces forward-running pressures waves ($P_{f(act)}$), which are approximately equal to flow (Q) times characteristic impedance (Z_c). Backward-running waves are also re-reflected at the ventricle ($P_{f(ref)}$), contributing to the overall forward component of pressure (P_f), which undergoes reflection in the vasculature (P_b). (B–D) Pressure waveforms from simulations of a ventricle-tube-load model, as in panel A, with different load impedances causing (B) high, (C) medium, and (D) low levels of vascular wave reflection, similar to that presented by Phan et al.[116] The shaded green area represents $P_{f(ref)}$. For clarity, end-diastolic pressure is offset to zero for each waveform.

wave reflection. However, the ventricle is also a major source of wave reflection. Consider what reflected waves approaching the ventricle encounter—a relatively stiff, closed chamber during systole and a closed aortic valve during diastole. The ventricle is therefore essentially a "dead-end" from the perspective of backward-running waves, with a reflection coefficient close to one.[74] The caveats to this are that (1) a small amount of wave energy is likely transmitted into the coronary arteries and (2) the ventricle constitutes a time-varying complex impedance, so the ventricular reflection coefficient (Γ_v) will be lower for high-frequency waves.[74]

There are several important implications of ventricular wave reflection. First, the forward component of pressure (P_f) is formed by the combination of two quite separate mechanisms, (1) active ventricular contraction ($P_{f(act)}$) and (2) re-reflection of backward waves that arise from vascular wave reflection ($P_{f(ref)}$, Fig. 11.12). Second, the backward wave (P_b) does not represent the total effect of vascular wave reflection on pulse pressure; rather, its effect is better represented by $P_b + P_{f(ref)}$, which is equivalent to $P - Q \times Z_c$ (i.e., the difference between measured pulsatile pressure and the product of flow and Z_c). Third, the forward wave should not be considered independent of the reflected wave, nor equated with "ventricular function" per se (in contradistinction to vascular wave reflection), as elegantly demonstrated by Phan et al.[116] Findings that the forward wave contributes to central pressure augmentation[22,117] are not inconsistent with the principle that this augmentation ultimately arises from vascular wave reflection, and that
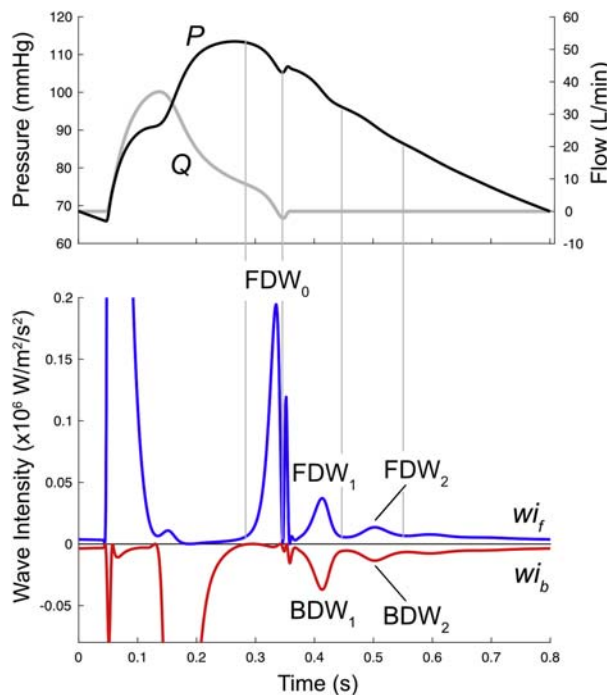
vascular wave reflection is responsible for differences in arterial pressure and flow waveforms.

Wave reflection, windkessel function, and diastolic pressure decay

The principle that wave reflection underlies all differences in pressure and flow waveforms holds when considering what is perhaps the most obvious difference: during diastole, pressure decays in an approximately exponential fashion while flow remains zero due to the closed aortic valve. This phenomenon is usually interpreted as the decline in pressure of the compliant arterial "chamber" that is discharging its volume through a peripheral resistance. This windkessel model assumes infinite wave speed, which is problematic during systole when wave phenomena dominate but is a reasonable assumption during diastole when waves are highly dispersed (i.e., the wavelengths of waves remaining in the system are long compared with the physical length of the body, so pressure gradients within the large arteries are small and the spatial dimension can be ignored). While the windkessel and wave theories have sometimes been considered "opposing" models, the windkessel model can in fact be derived from (and can be seen as a mathematical reduction of) the wave model.[118] It is therefore instructive to consider how diastolic hemodynamics can be explained in terms of the more general wave theory.

Early work in this area includes that of Singer,[119] who showed that "the major contribution of the reflected wave is

the maintenance of the diastolic pressure" and Sipkema et al.[91] who noted that "the exponential decay is due to diffuse reflection." More recently, Mynard and Smolich[118] showed that the diastolic pressure decay arises specifically from repeated and diffuse reflection of the late-systolic forward decompression wave (FDW). The FDW drives the late-systolic flow deceleration and pressure fall preceding the dicrotic notch. While most discussion around wave reflection revolves around reflection of the early systolic FCW as a BCW, it stands to reason that the FDW is also reflected in the vasculature. Positive reflection of the FDW gives rise to a BDW that further reduces pressure (Fig. 11.13). This wave is further re-reflected at the closed aortic valve giving rise to another FDW, which undergoes further reflection in the vasculature, and so on (Fig. 11.13). Although a series of discrete FDWs and BDWs can sometime be observed in vivo with wave intensity analysis,[45,118] the diffuse nature of wave reflection generally leads to low (albeit nonzero) wave intensity and a lack of distinct wave peaks during this time.

FIGURE 11.13 The diastolic pressure decay arises from repeated reflections of the late-systolic forward decompression wave (FDW$_0$). This wave undergoes positive reflection in the vasculature, returning as a backward decompression wave (BDW$_1$), which is then totally re-reflected at the closed aortic valve, producing an FDW$_1$ of equal magnitude. This forward wave is further reflected in the vasculature (BDW$_2$) and re-reflected at the valve (FDW$_2$) and so on. Data taken from a one-dimensional model of a single tube terminated with a single reflection site (a three-element windkessel). With in vivo data, discrete decompression wave peaks (such as FDW$_1$ and FDW$_2$) are often not visible due to the distributed/diffuse nature of wave reflection.

Methods for assessing the magnitude and timing of arterial wave reflection

This section describes the various methods that are available for quantifying the magnitude and timing of reflected waves, both of which hold important clinical significance. The focus here is on "global" reflection, that is, the combined effect of all wave reflections throughout the arterial network, in contrast to "local" reflection that relates to a single site of impedance mismatch as discussed earlier in this chapter (e.g., single bifurcation). A summary of these techniques is provided in Tables 11.2 and 11.3.

Pulse wave analysis

Aortic pressure waveforms typically display an initial rise that accompanies early systolic flow acceleration, followed by a secondary pressure "augmentation," as shown in Fig. 11.14.[83] Two fiduciary points used to separate these two pressure rises are the "shoulder" point and the "inflection" point, detected via derivatives of the pressure waveform (Fig. 11.14). Kelly et al.[16] found that the shoulder point generally coincided with the time of peak flow, implying that the following augmented pressure, which occurs when flow is decreasing, must be due to reflected waves. However, the inflection point is thought to better correspond with the arrival time of reflected waves and is now more widely used[51]; it should be noted that, confusingly, some papers refer to the "inflection" point as the "shoulder" point.

Augmentation pressure (AP) is defined as AP $= P_{pk} - P_i$, where P_{pk} is peak systolic pressure and P_i is the pressure at the inflection point.[83] Augmentation index (AIx) is then defined as:

$$\text{AI}x = \frac{\text{AP}}{\text{PP}} \tag{11.13}$$

where PP is pulse pressure. AIx increases with age but tends to plateau or even decrease after middle age.[16,77,120,121] Although caused by wave reflection, the limitations of AIx as a measure of reflection magnitude are widely recognized. Negative values of AIx occur in young adults but these do not imply negative wave reflection. AIx is strongly influenced by factors that are not related to reflection magnitude per se, such as heart rate,[122] ventricular function,[123–125] and the arrival time of reflected waves.[126,127]

Arrival time is calculated as the delay between the onset of the initial pressure rise and the inflection point (T_i in Fig. 11.14). T_i was proposed to be a surrogate marker of arterial stiffness, under the principle that the reflected wave will return earlier as PWV increases. A meta-analysis by Baksi et al.[120] showed that T_i decreased only modestly with age and the inflection point always

TABLE 11.2 Summary of techniques for quantifying global wave reflection magnitude.

Method	Definition	Advantages	Disadvantages
Augmentation index	$AIx = AP/PP$	Requires a pressure waveform only	Modulated by various factors other than wave reflection (e.g., heart rate, forward waves, reflection arrival time) Negative values do not indicate negative reflection
Reflection magnitude (time domain)	$RM = \Delta P_b / \Delta P_f$	Intuitive interpretation, scalar index of global reflection	Requires pressure and flow/velocity waveforms; re-reflection contributes to ΔP_f
Global reflection coefficient	$\Gamma_P(\omega) = \frac{Z_{in}(\omega) - Z_c}{Z_{in}(\omega) + Z_c}$	Comprehensive representation of arterial reflection properties for all wave frequencies	Complex quantity (not single number), frequency domain analysis less intuitive than time domain analysis
Terminal reflection coefficient	$\Gamma_0 = \frac{R_p - Z_c}{R_p + Z_c}$	Quantifies contribution of resistance vessels	Neglects pulsatile haemodynamics, physical meaning of reflection at zero frequency is unclear
Reflection coefficient (real part of first harmonic)	$Re(\Gamma_1) = \left\|\frac{Z_{in}(\omega_1) - Z_c}{Z_{in}(\omega_1) + Z_c}\right\|$	Scalar summary of reflection coefficient for the largest harmonic	Neglects contribution of other harmonics, requires frequency domain analysis
Reflection coefficient (real part of multiple harmonics)	$Re(\Gamma_i) = \left\|\frac{Z_{in}(\omega_i) - Z_c}{Z_{in}(\omega_i) + Z_c}\right\|$ where $i = 1,2,3 \ldots$	Provides information about reflection for different frequencies	Provides multiple metrics of reflection; interpretation is not intuitive
Normalized reflection coefficient	$\Gamma_{norm} = \sum_{i=1}^{N} w_i \Gamma_i$, where $w_i = H_i / \sum_{j=1}^{N} H_j$	Scalar summary of global reflection coefficient, accounts for all (nonzero) harmonics	Complex calculation requiring frequency domain analysis
Wave reflection index (frequency domain)	$WRI = \Gamma_P(\omega)_{max} - \Gamma_P(\omega)_{min}$ for harmonics >2 Hz	Scalar summary of global reflection	Based on the single tube model, conceptually difficult
Wave reflection index (wave intensity)	$WRI_{peak} = BCW_{peak}/FCW_{peak}$ $WRI_{area} = BCW_{area}/FCW_{area}$ $WRI_{centroid} = BCW_{centroid}/FCW_{centroid}$	Intuitive time domain approach	Emphasizes high-frequency reflection. Prone to error due to nonlinear amplification effects

AP, augmentation pressure; *BCW*, backward compression wave; *FCW*, forward compression wave; H_i, modulus of the i–th harmonic of the pressure spectrum; *PP*, pulse pressure; Z_{in}, input impedance; Z_c, characteristic impedance; ΔP_f, amplitude of forward component of pressure ("f"); ΔP_b, backward component of pressure ("b"); Γ_i, modulus of the i–th harmonic of the reflection coefficient spectrum; ω_i, angular frequency of the i-th harmonic.

occurred in the first two thirds of systole. It was suggested that these data conflicted with the concept that reflected waves arrive mainly during diastole in youth, and that a progressive shift to earlier reflection time is a key factor underlying isolated systolic hypertension.[128] Moreover, calculated effective reflection distance computed using T_i ($L_{eff} = PWV \times T_i/2$) increases with age, implying a distal shift in reflection sites.[77] However, it has been shown that neither the shoulder nor inflection points align with reflected wave arrival time determined by wave separation analysis, and that L_{eff} calculated with the latter does not change with age.[76,129] The use of T_i to estimate L_{eff} assumes that the arterial system behaves as a single tube and that a single reflected site produces a reflected

wave that has the same morphology over the life course. Simulation studies in a realistic network model showed that T_i is relatively insensitive to arterial stiffness changes and, conversely, is sensitive to proximal reflections produced by aortic tapering, suggesting that it may not provide a satisfactory representation of "global" reflection time.[126]

In summary, despite the widespread use of AIx and T_i to estimate the magnitude and timing of reflected waves, these should be used with caution as their limitations are well-recognized.[76,125,129–131] Many of these limitations have been revealed by comparison to wave separation analysis, which is considered the "gold standard" for assessing reflected waves.

TABLE 11.3 Summary of techniques for quantifying effective return time of reflected waves.

Method	Definition	Advantages	Disadvantages
Pulse wave analysis			
Time to shoulder point	T_s (Fig. 11.14)	Requires only a pressure waveform	Represents time of peak ejection, not arrival time of reflected waves
Time to inflection point	T_i (Fig. 11.14)	Requires only a pressure waveform	Not always detectable, sensitive to noise (depends on second derivative), does not agree with wave separation
Wave separation			
Foot-to-foot time	T_r (Fig. 11.15B and C)	Uses forward/backward components of pressure	Foot time may not be clearly defined, especially for backward wave
Zero-crossing method	T_r (Fig. 11.15D)	Uses forward/backward components of pressure	Wave separation performed in frequency domain
Frequency domain analysis			
First minimum in impedance modulus	$T_m = \frac{1}{2f_m}$ (Fig. 11.5)	–	Based on uniform tube model with resistive load. Complex analysis, not intuitive.
First zero crossing in impedance phase	$T_1 = \frac{1}{2f_m}$ (Fig. 11.5)	–	Based on uniform tube model with resistive load. Not intuitive. Does not align with T_m in real system.
Model-based analysis			
Fit waveforms to single tube model	$2L/PWV$	Simple representative model	Value obtained depends on modeling assumptions and boundary conditions
Wave intensity analysis			
Foot-to-foot (FCW-BCW)	T_{foot} (Fig. 11.17)	Intuitive time-domain method	Foot of the BCW often not well-defined.
Peak-to-peak (FCW-BCW)	T_{peak} (Fig. 11.17)	Intuitive time-domain method	BCW may not have single well-defined peak.
Centroid-to-centroid (FCW-BCW)	$T_{centroid}$ (Fig. 11.17)	Accounts for the whole morphology of each wave	WI emphasizes high-frequency reflection.

BCW, backward compression wave; *FCW*, forward compression wave; f_m, frequency of the first minimum in the impedance modulus; f_1, frequency of the first zero-crossing of impedance phase; *L*, length of the single tube model; *PWV*, pulse wave velocity.

Wave separation

Considerable insights into the wave reflection properties of the arterial tree can be gathered by "separating" the measured pressure and flow waveforms into their forward and backward components, noting that, as mentioned earlier, the forward component also includes re-reflections from the ventricle (Fig. 11.12). Both frequency-domain and time-domain methods of wave separation have been developed, with both giving comparable results.[9,132−134] Wave separation requires pressure and flow waveforms at a particular site, with forward (*f*) and backward (*b*) components obtained in the time-domain as:

$$P_f = \frac{1}{2}(P - P_{ud} + Z_c Q) \qquad (11.14)$$

$$P_b = \frac{1}{2}(P - P_{ud} - Z_c Q) \qquad (11.15)$$

$$Q_f = \frac{1}{2}(Q + (P - P_{ud})/Z_c) \qquad (11.16)$$
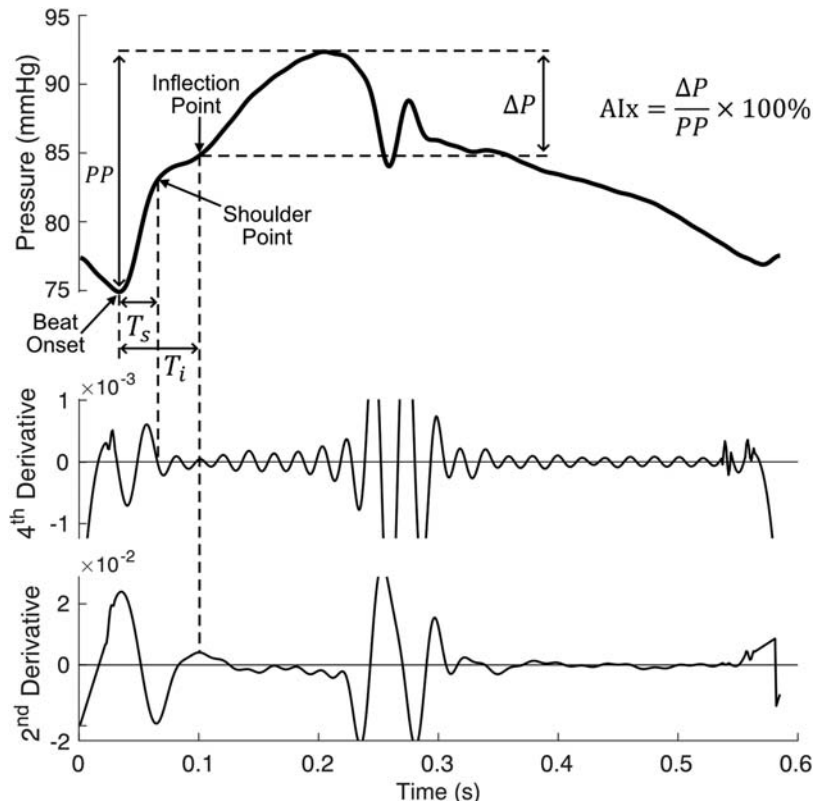
$$Q_b = \frac{1}{2}(Q - (P - P_{ud})/Z_c) \qquad (11.17)$$

where Z_c is characteristic impedance. Undisturbed pressure (P_{ud}) enables assessment of wave potential (absolute values of P_f, P_b, Q_f, and Q_b),[118,135] but can be neglected if only investigating pulsatile aspects of the waveforms (e.g., wave reflection).

Reflection magnitude is calculated from the pressure or flow components as:

$$RM = \frac{\Delta P_b}{\Delta P_f} = -\frac{\Delta Q_b}{\Delta Q_f} \qquad (11.18)$$

where Δ here refers to the overall amplitude of the respective waveform (Fig. 11.15B). Advantages of this approach

FIGURE 11.14   The shoulder point is identified by the second zero-crossing of the fourth derivative of the pressure waveform in the direction from above to below zero. The inflection point is identified by the second peak of the second derivative of the pressure waveform. The shoulder point or the inflection point can be used to estimate reflection time (T_s and T_i, respectively) by their time difference to beat onset time. ΔP is the pressure difference between the systolic pressure and the inflection point. Dividing ΔP by the pulse pressure (PP) gives the augmentation index (AIx), an index of reflection magnitude.
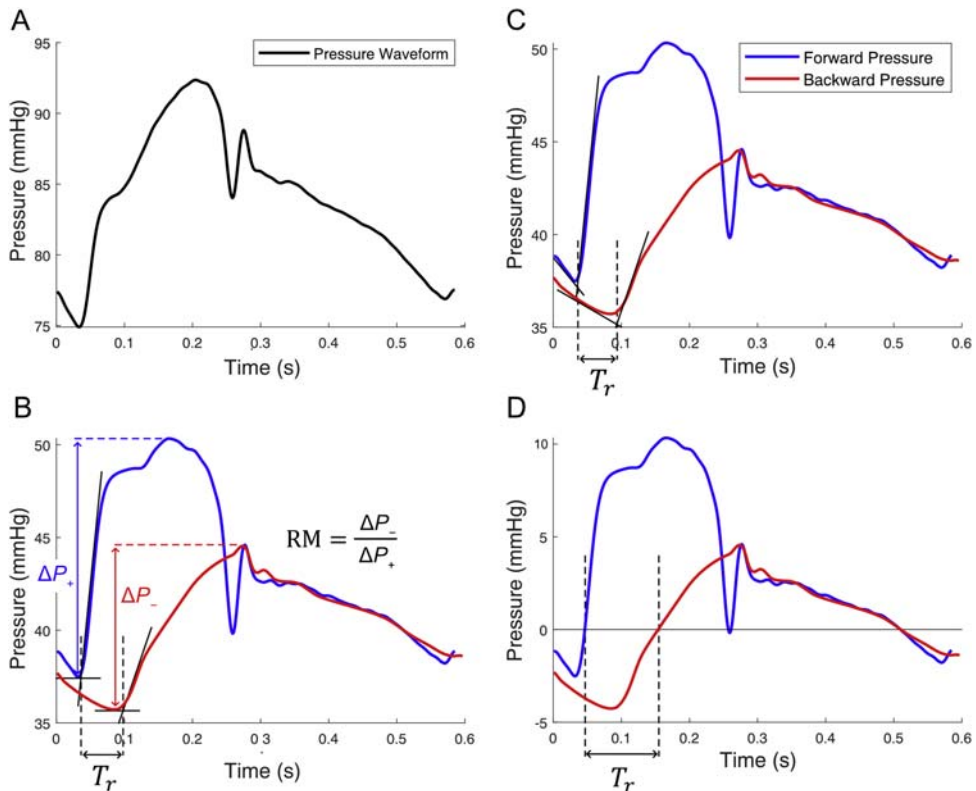
(in contrast to AIx) are that (1) it can correctly attribute pressure changes to backward and forward waves even if they occur simultaneously, and (2) it can capture wave reflection effects that span both systole and diastole.

Compared with RM, there is less consensus regarding the best method for estimating reflection time using wave separation. The most common method takes the difference between the onset (foot) of the backward and forward pressure waveforms as reflection time (T_r). While the foot can be found by visual inspection, Chiu et al.[136] developed the "intersecting tangents" method, in which a tangent is drawn at the point of maximum gradient on the upstroke of the pressure waveform and a horizontal tangent is drawn through the point of minimum pressure at the foot; the point of intersection of the tangents is taken as the foot (Fig. 11.15B). One variant of this approach is to replace the horizontal line with a line of best fit between the minimum and a few preceding points (Fig. 11.15C).[126,137] However, Segers et al.[129] noted that the "foot" is often not clearly defined by a single point, especially for backward waveforms, and instead proposed the zero-crossing method. Here, mean pressure is subtracted from the pressure waveform before wave

separation (essentially, setting $P_{ud} = \text{mean}(P)$ in Eq 11.14). This results in P_f and P_b waveforms that cross the time axis; the difference between the first zero crossing of these waveform is then taken as T_r (Fig. 11.15D). Another study took the difference between the time of peak backward and forward pressure[138]; however, this is likely to be confounded by re-reflections from the ventricle.

Frequency domain analysis

A number of frequency domain or impedance-based techniques have been used to evaluate the magnitude and timing of wave reflection. These provide insight into the frequency-dependence of wave reflection, although they are not commonly used in clinical studies as they can be difficult to grasp for the nonmathematician. Frequency domain analysis is covered in Chapter 3; in brief, pressure and flow are expressed as a series of sinusoidal harmonics, $P(\omega)$ and $Q(\omega)$ (where $\omega = 2\pi f$ and f is frequency) and can be used to calculate an input impedance spectrum $Z_{in}(\omega) = P(\omega)/Q(\omega)$. The following indexes of reflection have been proposed:

FIGURE 11.15   Using wave separation, a pressure waveform (A) can be separated into the forward and backward wave components (B). From this, the reflection magnitude (RM) is calculated as the ratio of the backward pressure amplitude (ΔP_b) to the forward pressure amplitude (ΔP_f). Reflection time (T_r) is calculated as the time between the foot of the backward and forward pressure components, found using the intersection of a tangent line through the pressure upstroke at the point of maximum gradient, and (B) a horizontal line from the minimum pressure, or (C) a line of best fit between minimum pressure and a few preceding points. T_r can also be calculated by subtracting the mean pressure before wave separation and taking the time difference between the first zero crossing of the backward and forward pressures (D).

The *reflection coefficient spectrum*, or "global reflection coefficient,"[9] expresses Eq. (11.10) in the frequency domain and considers the impedance mismatch between characteristic impedance (Z_c) at the measurement site and the lumped frequency-dependent input impedance of the downstream circulation (Z_{in}).

$$\Gamma_P(\omega) = \frac{Z_{in}(\omega) - Z_c}{Z_{in}(\omega) + Z_c} \qquad (11.19)$$

When plotted versus frequency, the modulus of $\Gamma_P(\omega)$ exhibits a peak at the fundamental frequency and falls at higher frequencies (Fig. 11.16). At low frequencies, $\Gamma_P(\omega)$ approaches the zero-order or "terminal reflection coefficient" (Γ_T), or the impedance mismatch between Z_c and peripheral resistance[56]; however, the physical meaning of this coefficient is unclear since mean pressure and flow are not considered waves that could be reflected. A more common metric of reflection magnitude is Γ_1, or reflection coefficient for the fundamental frequency (i.e., heart rate), noting that this harmonic holds the most pulsatile energy (Fig. 11.16 inset).[24,139] Although $\Gamma_P(\omega)$ is frequency-dependent, and hence not a single number, Xiao et al.[140]
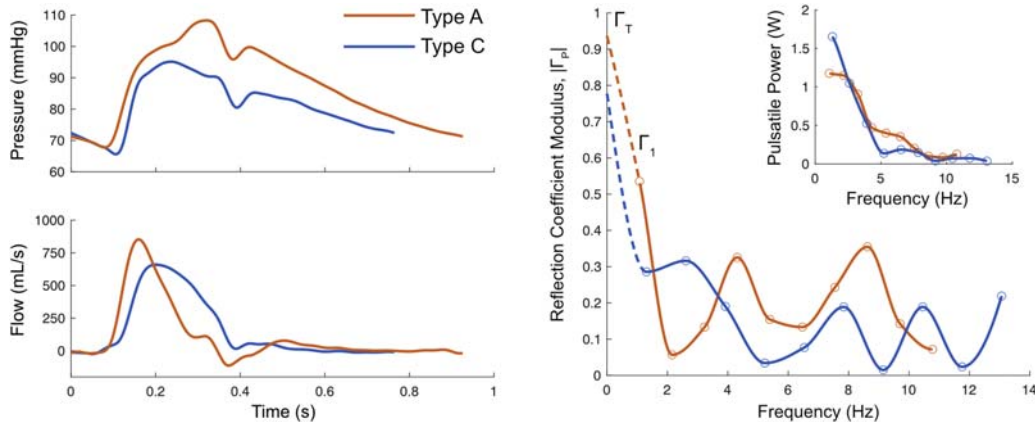
proposed a scalar (i.e., single number) normalized reflection coefficient (Γ_{norm}) equal to the sum of $\Gamma_P(\omega)$ moduli weighted to the normalized pressure moduli, which was considered analogous to reflection magnitude obtained via wave separation analysis.

Another approach for assessing wave reflection in the frequency domain involves directly analyzing the impedance spectrum. Noting that wave reflection causes oscillations in the impedance spectrum around Z_c (Fig. 11.5), the "wave reflection index (WRI)" is defined as the difference between maxima and minima of impedance spectra in the mid-to-high frequency range, which Nichols et al.[141] defined as >2 Hz.

Frequency domain methods for assessing reflection time (and hence, L_{eff}) are covered in Box 11.2 and summarized in Table 11.3.

Wave intensity

Parker and Jones[142] introduced wave intensity analysis as an intuitive time-domain method of analyzing forward and backward waves. While covered in more detail in

FIGURE 11.16 Frequency-dependent reflection coefficient modulus $|\Gamma_P(\omega)|$ for Type A and Type C aortic waveforms taken from Murgo et al.[83] (with thanks to Prof. Patrick Segers). Open circles indicate reflection coefficient for the first 10 harmonics. The dashed lines indicate that reflection coefficient approaches the "terminal reflection coefficient" (Γ_T, i.e., the nominal mismatch between Z_c and peripheral resistance) at very low frequencies. Γ_1 refers to reflection coefficient at the fundamental frequency (i.e., first harmonic), which contains the most pulsatile power (see inset) but is dependent on heart rate. Less pulsatile power resides in high-frequency harmonics, which also undergo generally minor reflection.

Chapter 3, briefly, time-corrected wave intensity (wi) is defined as:

$$wi = \frac{dP}{dt}\frac{dU}{dt} \tag{11.20}$$

where dP/dt and dU/dt are the derivatives of pressure and velocity. As for pressure and flow, wave intensity can be separated into forward and backward components as follows:

$$
\begin{aligned}
wi_f &= +\frac{1}{4\rho c}\left(\frac{dP}{dt} + \rho c\frac{dU}{dt}\right)^2 \\
wi_b &= -\frac{1}{4\rho c}\left(\frac{dP}{dt} - \rho c\frac{dU}{dt}\right)^2
\end{aligned}
\tag{11.21}
$$
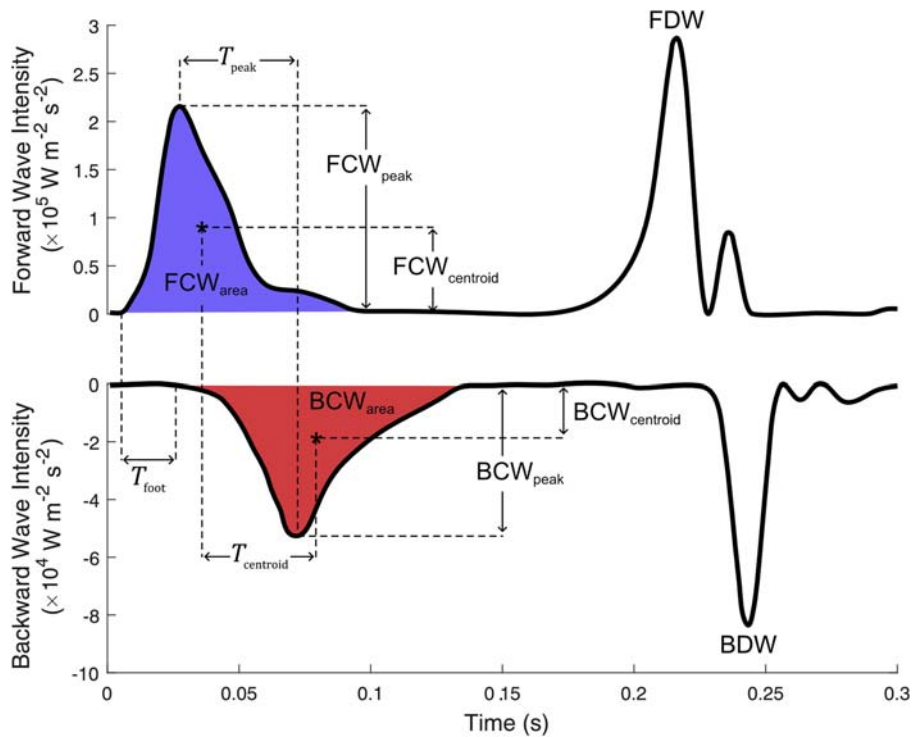
which has the convenient property that forward waves have positive wi and backward waves have negative wi. Wave power, proposed by Mynard and Smolich,[143] uses flow in place of velocity and has the benefit that it is conserved at junctions, allowing the proportion of reflected and transmitted wave power (in Watts) to be quantified. However, when measured at a single site, the two techniques are essentially equivalent. Fig. 11.17 shows a typical wave intensity profile in the aorta and identifies four different types of waves, a FCW reflected as a BCW and a FDWs reflected as a BDW.

In studies of wave intensity, reflection magnitude is estimated as the ratio of the BCW to FCW amplitude, termed the WRI (Fig. 11.17). While peak intensity may seem the logical choice for quantifying wave amplitude, in some instances, the BCW is relatively diffuse and may not contain a single distinct peak; moreover, although peak

intensity relates to the maximum rate of change of pressure and velocity, it does not represent the overall effect of the wave on these signals (which relates to the height *and* width of the wave). WRI is therefore more often calculated as the ratio of the area under the BCW and FCW[29,144] or, less commonly, as the ratio of their centroids (Fig. 11.17).[145]

Mynard et al.[146] showed that the dependence of wave speed on pressure causes both the peak and area of the FCW and BCW to amplify as these waves propagate. This can cause errors in estimating reflection magnitude, even leading to a WRI that exceeds the theoretical limit of 1.[111,147] Importantly, Mynard et al.[146] found that the reflection magnitude obtained by wave separation of the pressure waveform (Eq. 11.18) was not susceptible to this issue and accurately quantified reflection.

It is also important to note that WRI is generally much smaller than RM. This is partly because WRI is theoretically equivalent to the power reflection coefficient (Γ_Π in Table 11.1), which is equal to the square of the pressure or flow coefficients (Γ_P and Γ_Q).[146] In addition, the multiplication of pressure and velocity derivatives acts as a high pass filter, suppressing low frequency reflection and emphasizing high-frequency reflection. However, as discussed above, due to the relatively efficient transmission of forward waves, and distributed nature of arterial wave reflection, the high-frequency components of pressure and flow are minimally reflected, while the majority of reflection occurs in the low frequency range. Indeed, the aortic BCW is often observed to be very small,[148,149] which can lead to the false impression that very little wave reflection occurs in the arterial system.

FIGURE 11.17 From the wave intensity profile, a wave reflection index can be obtained by taking the ratio of backward compression wave (BCW) to forward compression wave (FCW) peak intensity (BCW$_{peak}$/FCW$_{peak}$), intensity at wave centroid (BCW$_{centroid}$/FCW$_{centroid}$), or area under the wave (BCW$_{area}$/FCW$_{area}$). Reflection time can be obtained using the difference of the foot (T_{foot}), peak (T_{peak}), or centroid ($T_{centroid}$) of the BCW and FCW. The forward decompression wave (FDW) and backward decompression wave (BDW) are also shown, but generally not used to quantify reflection. Note the different Y-scales for forward and backward wave intensity plots.

Alastruey et al.[145] investigated several methods for calculating reflection time using wave intensity, namely, defining BCW and FCW time via the (1) peak, (2) foot, and (3) centroid (Fig. 11.17). Using a single tube computational model with a discrete reflection site, they found that the foot method produced the closest estimate of theoretical reflection time. However, the accuracy of these methods in a more realistic network model was less clear owing to the diffuse nature of reflections. Although not specifically investigated, the aforementioned emphasis of high-frequency reflection in wave intensity analysis may mean that the timing of global wave reflection is not adequately captured.

Summary

Wave reflection arises due to impedance mismatching in the arterial network. Although the exact locations of reflection are uncertain, the well-matched design of the conduit arterial network appears to facilitate efficient transmission of forward waves to vascular beds. However, wave reflection necessarily occurs because of the high impedance of smaller vascular beds compared with the low impedance of conduit arteries. Wave reflection occurs at a myriad of spatially distributed sites, and methods that quantify a reflection distance or reflected wave arrival time relate to the lumped or "effective" reflection properties of the network, which should be applied and interpreted with extreme caution. Simplified models of wave reflection capture these lumped properties but provide limited insight into the complex nature of arterial wave dynamics. At arterial junctions, forward waves undergo minimal reflection, whereas backward waves undergo strong negative reflection, limiting the transmission of reflected wave power to the heart. The resulting horizon effect leads to an approximately constant delay between forward and backward waves, regardless of the measurement site. Backward-running waves are also re-reflected by the ventricle during systole and closed aortic valve during diastole, with the resulting forward-running waves contributing to the forward component of pressure. Forward pressure is therefore not generated solely by active ventricular contraction, and the total impact of arterial wave reflection on blood pressure is greater than the commonly used indices of reflection magnitude imply.

References

1. Young T. Hydraulic investigations, subservient to an intended Croonian Lecture on the motion of the blood. **Phil Trans Roy Soc Lond**. 1808:164−186.

2. Hamilton WF, Dow P. An experimental study of the standing waves in the pulse propagated through the aorta. **Am J Physiol Legacy Content**. 1938; 125:48−59.

3. Frank O. Die theorie der pulswellen. **Z Biol**. 1926; 85:91−130.

4. McDonald DA. The relation of pulsatile pressure to flow in arteries. **J Physiol**. 1955; 127:533−552.

5. Taylor MG. An approach to an analysis of the arterial pulse wave I. Oscillations in an attenuating line. **Phys Med Biol**. 1957; 1:258−269.

6. Wetterer E. Die Wirkung der Herztatigkeit auf die Dynamik des Arteriensystems. **Verh Dtsch Ges Kreislaufforsch**. 1956; 34, 609-609.

7. Remington JW, Wood EH. Formation of peripheral pulse contour in man. **J Appl Physiol**. 1956; 9:433−442.

8. Remington JW, O'Brien LJ. Construction of aortic flow pulse from pressure pulse. **Am J Physiol**. 1970; 218:437−447.

9. Westerhof N, Sipkema P, van den Bos GC, Elzinga G. Forward and backward waves in the arterial system. **Cardiovasc Res**. 1972; 6:648−656.

10. Hardung V. Zur mathematischen behandlung der dampfung und reflection der pulswellen. **Arch Kreislaufforsch**. 1952; 18:167−172.

11. O'Rourke MF. Pressure and flow waves in systemic arteries and the anatomical design of the arterial system. **J Appl Physiol**. 1967; 23:139−149.

12. Zannoli R, Schiereck P, Celletti F, Branzi A, Magnani B. Effects of wave reflection timing on left ventricular mechanics. **J Biomech**. 1999; 32:249−254.

13. O'Rourke MF, Kelly RP. Wave reflection in the systemic circulation and its implications in ventricular function. **J Hypertens**. 1993; 11:327−337.

14. McEniery CM, Yasmin, Hall IR, Qasem A, Wilkinson IB, Cockcroft JR. Normal vascular aging: differential effects on wave reflection and aortic pulse wave velocity: the Anglo-Cardiff Collaborative Trial (ACCT). **J Am Coll Cardiol**. 2005; 46:1753−1760.

15. The Reference Values for Arterial Stiffness Collaboration. Determinants of pulse wave velocity in healthy people and in the presence of cardiovascular risk factors: 'establishing normal and reference values'. **Eur Heart J**. 2010; 31:2338−2350.

16. Kelly R, Hayward C, Avolio A, O'Rourke M. Noninvasive determination of age-related changes in the human arterial pulse. **Circulation**. 1989; 80:1652−1659.

17. Euler L. Principia pro motu sanguinis per arterias determinando. **Opera Postuma**. 1862:814−823.

18. Tijsseling AS. Johannes von Kries and the history of water hammer. **J Hydraul Eng**. 2007; 133:1.

19. Parker KH. An introduction to wave intensity analysis. **Med Biol Eng Comput**. 2009; 47:175−188.

20. Karakash JJ. **Transmission Lines and Filter Networks**. 1950.

21. Pollack GH, Reddy RV, Noordergraaf A. Input impedance, wave travel, and reflections in the human pulmonary arterial tree: studies using an electrical analog. **IEEE Trans Biomed Eng**. 1968; 15:151−164.

22. Mitchell GF, Wang N, Palmisano JN, et al. Hemodynamic correlates of blood pressure across the adult age spectrum: noninvasive evaluation in the Framingham Heart Study. **Circulation**. 2010; 122:1379−1386.

23. Nichols WW, O'Rourke MF, Avolio AP, et al. Effects of age on ventricular-vascular coupling. **Am J Cardiol**. 1985; 55:1179−1184.

24. Segers P, Rietzschel ER, De Buyzere ML, et al. Verdonck PR and on behalf of the asklepios i. Noninvasive (input) impedance, pulse wave velocity, and wave reflection in healthy middle-aged men and women. **Hypertension**. 2007; 49:1248−1255.

25. Redheuil A, Yu W-C, Mousseaux E, et al. Age-related changes in aortic arch geometry relationship with proximal aortic function and left ventricular mass and remodeling. **J Am Coll Cardiol**. 2011; 58:1262−1270.

26. Mynard JP, Davidson MR, Penny DJ, Smolich JJ. Non-linear separation of pressure, velocity and wave intensity into forward and backward components. **Med Biol Eng Comput**. 2012; 50:641−648.

27. Pythoud F, Stergiopulos N, Meister JJ. Separation of arterial pressure waves into their forward and backward running components. **J Biomech Eng**. 1996; 118:295−301.

28. Mynard JP, Penny DJ, Smolich JJ. Major influence of a 'smoke and mirrors' effect caused by wave reflection on early diastolic coronary arterial wave intensity. **J Physiol**. 2018; 596:993−1017.

29. Davies JE, Whinnett ZI, Francis DP, et al. Evidence of a dominant backward-propagating "suction" wave responsible for diastolic coronary filling in humans, attenuated in left ventricular hypertrophy. **Circulation**. 2006; 113:1768−1778.

30. O'Rourke MF, Taylor MG. Vascular impedance of the femoral bed. **Circ Res**. 1966; 18:126−139.

31. Murgo JP, Westerhof N, Giolma JP, Altobelli SA. Manipulation of ascending aortic pressure and flow wave reflections with the Valsalva maneuver: relationship to input impedance. **Circulation**. 1981; 63:122−132.

32. van den Bos GC, Westerhof N, Randall OS. Pulse wave reflection: can it explain the differences between systemic and pulmonary pressure and flow waves? A study in dogs. **Circ Res**. 1982; 51:479−485.

33. Condos Jr WR, Latham RD, Hoadley SD, Pasipoularides A. Hemodynamics of the Mueller maneuver in man: right and left heart micromanometry and Doppler echocardiography. **Circulation**. 1987; 76:1020−1028.

34. Kondiboyina A, Smolich JJ, Cheung MMH, Westerhof BE, Mynard JP. Conduit arterial wave reflection promotes pressure transmission, but impedes hydraulic energy transmission, to the microvasculature. **Am J Physiol Heart Circ Physiol**. 2020; 319:H66−H75.

35. Swillens A, Lanoye L, De Backer J, et al. Effect of an abdominal aortic aneurysm on wave reflection in the aorta. **IEEE Trans Biomed Eng**. 2008; 55:1602−1611.

36. Chirinos JA, Lee J, Segers P. Mechanism of pulsus bisferiens in thoracoabdominal thoracic aneurysms: insights from wave intensity analysis. **J Clin Hypertens**. 2021; 23:193−196.

37. Womersley JR. Oscillatory flow in arteries. II: the reflection of the pulse wave at junctions and rigid inserts in the arterial system. **Phys Med Biol**. 1958; 2:313−323.

38. Munk A, Darge K, Wiesel M, Troeger J. Diameter of the infrarenal aorta and the iliac arteries in children: ultrasound Measurements. **Transplantation**. 2002; 73.

39. Horejs D, Gilbert PM, Burstein S, Vogelzang RL. Normal aortoiliac diameters by CT. **J Comput Assist Tomogr**. 1988; 12:602−603.

40. Papageorgiou GL, Jones BN, Redding VJ, Hudson N. The area ratio of normal arterial junctions and its implications in pulse wave reflections. **Cardiovasc Res**. 1990; 24:478−484.

41. Mynard JP, Smolich JJ. One-dimensional haemodynamic modeling and wave dynamics in the entire adult circulation. **Ann Biomed Eng**. 2015; 43:1443−1460.

42. Willemet M, Alastruey J. Arterial pressure and flow wave analysis using time-domain 1-D hemodynamics. **Ann Biomed Eng**. 2014; 43:190−206.

43. Wang JJ, Parker KH. Wave propagation in a model of the arterial circulation. **J Biomech**. 2004; 37:457−470.

44. Alexander RS. The genesis of the aortic standing wave. **Circ Res**. 1953; 1:145−151.

45. Mynard JP, Kondiboyina A, Kowalski R, Cheung MMH, Smolich JJ. Measurement, analysis and interpretation of pressure/flow waves in blood vessels. **Front Physiol**. 2020; 11:1085.

46. Segers P, Verdonck P. Role of tapering in aortic wave reflection: hydraulic and mathematical model study. **J Biomech**. 2000; 33:299−306.

47. Belardinelli E, Cavalcanti S. Theoretical analysis of pressure pulse propagation in arterial vessels. **J Biomech**. 1992; 25:1337−1349.

48. Gaddum N, Alastruey J, Chowienczyk P, Rutten MCM, Segers P, Schaeffter T. Relative contributions from the ventricle and arterial tree to arterial pressure and its amplification: an experimental study. **Am J Physiol Heart Circ Physiol**. 2017; 313:H558.

49. Abdullateef S, Mariscal-Harana J, Khir AW. Impact of tapering of arterial vessels on blood pressure, pulse wave velocity, and wave intensity analysis using one-dimensional computational model. **Int J Numer Method Biomed Eng**. 2020:e3312.

50. Papageorgiou GL, Jones NB. Arterial system configuration and wave reflection. **J Biomed Eng**. 1987; 9:299−301.

51. Nichols WW, O'Rourke MF. **Wave Reflections McDonald's Blood Flow in Arteries: Theoretical, Experimental, and Clinical Principles**. Boca Raton, FL: CRC Press; 2011:195−223.

52. Hamilton WF. The patterns of the arterial pressure pulse. **Am J Physiol**. 1944; 141:235−241.

53. O'Rourke MF, Yaginuma T. Wave reflections and the arterial pulse. **Arch Intern Med**. 1984; 144:366.

54. Zambanini A, Cunningham SL, Parker KH, Khir AW, Mc GTSA, Hughes AD. Wave-energy patterns in carotid, brachial, and radial arteries: a noninvasive approach using wave-intensity analysis. **Am J Physiol Heart Circ Physiol**. 2005; 289:H270−H276.

55. Chirinos JA, Londono-Hoyos F, Zamani P, et al. Effects of organic and inorganic nitrate on aortic and carotid haemodynamics in heart failure with preserved ejection fraction. **Eur J Heart Fail**. 2017; 19:1507−1515.

56. Brin K, Yin F. Effect of nitroprusside on wave reflections in patients with heart failure. **Ann Biomed Eng**. 1984; 12:135−150.

57. Jones CJH, Parker KH. The Role of Wave Reflections in the Ascending Aorta of Man. **The Role of Wave Reflections in the Ascending Aorta of Man. Biofluid Mech**. 1990:451−454. Springer.

58. Westerhof BE, Westerhof N. Uniform tube models with single reflection site do not explain aortic wave travel and pressure wave shape. **Physiol Meas**. 2018; 39:124006.

59. Yaginuma T, Avolio A, O'Rourke M, et al. Effect of glyceryl trinitrate on peripheral arteries alters left ventricular hydraulic load in man. **Cardiovasc Res**. 1986; 20:153−160.

60. Fitchett DH, Simkus GJ, Beaudry JP, Marpole DG. Reflected pressure waves in the ascending aorta: effect of glyceryl trinitrate. **Cardiovasc Res**. 1988; 22:494−500.

61. Young DF, Tsai FY. Flow characteristics in models of arterial stenoses - II. Unsteady flow. **J Biomech**. 1973; 6:547−559.

62. Newman DL, Greenwald SE, Denyer HT. Impulse propagation in normal and stenosed vessels. **Cardiovasc Res**. 1981; 15:190−195.

63. Hacham WS, Khir AW. The speed, reflection and intensity of waves propagating in flexible tubes with aneurysm and stenosis: experimental investigation. **Proc Inst Mech Eng Part H J Eng Med.** 2019; 233:979−988.

64. Stergiopulos N, Spiridon M, Pythoud F, Meister JJ. On the wave transmission and reflection properties of stenoses. **J Biomech**. 1996; 29:31−38.

65. Sazonov I, Khir AW, Hacham WS, et al. A novel method for non-invasively detecting the severity and location of aortic aneurysms. **Biomech Model Mechanobiol**. 2017; 16:1225−1242.

66. Crespo A, García J, Manuel F. Wave reflection at a stent. **Proc Inst Mech Eng Part H J Eng Med.** 2013; 227:72−77.

67. Alderson H, Zamir M. Effects of stent stiffness on local haemodynamics with particular reference to wave reflections. **J Biomech**. 2004; 37:339−348.

68. Papathanasiou TK, Movchan AB, Bigoni D. Wave reflection and transmission in multiply stented blood vessels. **Proc R Soc A Math Phys Eng Sci**. 2017; 473:20170015.

69. Barnard ACL, Hunt WA, Timlake WP, Varley E. A theory of fluid flow in compliant tubes. **Biophys J**. 1966; 6:717−724.

70. Sherwin SJ, Franke V, Peiró J, Parker K. One-dimensional modelling of a vascular network in space-time variables. **J Eng Math**. 2003; 47:217−250.

71. Campbell KB, Lee LC, Frasch HF, Noordergraaf A. Pulse reflection sites and effective length of the arterial system. **Am J Physiol Heart Circ Physiol**. 1989; 256:H1684−H1689.

72. Sipkema P, Westerhof N. Effective length of the arterial system. **Ann Biomed Eng**. 1975; 3:296−307.

73. Burattini R, Burattini R, Di Carlo S. Effective length of the arterial circulation determined in the dog by aid of a model of the systemic input impedance. **IEEE Trans Biomed Eng**. 1988; 35:53−61.

74. Berger DS, Li JK, Laskey WK, Noordergraaf A. Repeated reflection of waves in the systemic arterial system. **Am J Physiol Heart Circ Physiol**. 1993; 264:H269−H281.

75. McDonald DA, Taylor MG. The hydrodynamics of the arterial circulation. **Prog Biophys Biophys Chem**. 1959; 9:105−173.

76. Phan TS, Li JKJ, Segers P, et al. Aging is associated with an earlier arrival of reflected waves without a distal shift in reflection sites. **J Am Heart Assoc**. 2016; 5.

77. Mitchell GF, Parise H, Benjamin EJ, et al. Changes in arterial stiffness and wave reflection with advancing age in healthy men and women. **Hypertension**. 2004; 43:1239−1245.

78. Laxminarayan S, Sipkema P, Westerhof N. Characterization of the arterial system in the time domain. **IEEE Trans Biomed Eng**. 1978:177−184.

79. Westerhof N. **Snapshots of Hemodynamics**. Springer; 2018.

80. Latham RD, Westerhof N, Sipkema P, Rubal BJ, Reuderink P, Murgo JP. Regional wave travel and reflections along the human

aorta: a study with six simultaneous micromanometric pressures. **Circulation**. 1985; 72:1257−1269.

81. Davies JE, Alastruey J, Francis DP, et al. Attenuation of wave reflection by wave entrapment creates a "horizon effect" in the human aorta. **Hypertension**. 2012; 60:778−785.

82. Nichols WW, O'Rourke MF. **Vascular Impedance McDonald's Blood Flow in Arteries: Theoretical, Experimental, and Clinical Principles**. Boca Raton, FL: CRC Press; 2011.

83. Murgo JP, Westerhof N, Giolma JP, Altobelli SA. Aortic input impedance in normal man: relationship to pressure wave forms. **Circulation**. 1980; 62:105−116.

84. Burattini R, Campbell KB. Physiological relevance of uniform elastic tube-models to infer descending aortic wave reflection: a problem of identifiability. **Ann Biomed Eng**. 2000; 28:512−523.

85. Berger DS, Li JK, Noordergraaf A. Differential effects of wave reflections and peripheral resistance on aortic blood pressure: a model-based study. **Am J Physiol Heart Circ Physiol**. 1994; 266:H1626−H1642.

86. Burattini R, Gnudi G. Computer identification of models for the arterial tree input impedance: comparison between two new simple models and first experimental results. **Med Biol Eng Comput**. 1982; 20:134−144.

87. Westerhof BE, van den Wijngaard JP, Murgo JP, Westerhof N. Location of a reflection site is elusive: consequences for the calculation of aortic pulse wave velocity. **Hypertension**. 2008; 52:478−483.

88. O'Rourke MF, Avolio AP. Pulsatile flow and pressure in human systemic arteries. Studies in man and in a multibranched model of the human systemic arterial tree. **Circ Res**. 1980; 46:363−372.

89. Burattini R, Campbell KB. Modified asymmetric T-tube model to infer arterial wave reflection at the aortic root. **IEEE Trans Biomed Eng**. 1989; 36:805−814.

90. Taylor MG. Wave transmission through an assembly of randomly branching elastic tubes. **Biophys J**. 1966; 6:697−716.

91. Sipkema P, Westerhof N, Randall OS. The arterial system characterised in the time domain. **Cardiovasc Res**. 1980; 14:270−279.

92. Burattini R, Knowlen GG, Campbell KB. Two arterial effective reflecting sites may appear as one to the heart. **Circ Res**. 1991; 68:85−99.

93. Campbell KB, Burattini R, Bell DL, Kirkpatrick RD, Knowlen GG. Time-domain formulation of asymmetric T-tube model of arterial system. **Am J Physiol Heart Circ Physiol**. 1990; 258:H1761−H1774.

94. Einav S, Aharoni S, Manoach M. Exponentially tapered transmission line model of the arterial system. **IEEE Trans Biomed Eng**. 1988; 35:333−339.

95. Fogliardi R, Burattini R, Campbell KB. Identification and physiological relevance of an exponentially tapered tube model of canine descending aortic circulation. **Med Eng Phys**. 1997; 19:201−211.

96. Chang KC, Tseng YZ, Lin YJ, Kuo TS, Chen HI. Exponentially tapered t-tube model of systemic arterial system in dogs. **Med Eng Phys**. 1994; 16:370−378.

97. Burattini R, Fogliardi R, Gobbi R. Comments on "Exponentially tapered T-tube model of systemic arterial system in dogs". **Med Eng Phys**. 1996; 18:333−338.

98. Alastruey J, Parker K, Peiró J, Sherwin S. Analysing the pattern of pulse waves in arterial networks: a time-domain study. **J Eng Math**. 2009; 64:331−351.

99. Brown DJ. Input impedance and reflection coefficient in fractal-like models of asymmetrically branching compliant tubes. **IEEE Trans Biomed Eng**. 1996; 43:715−722.

100. Taylor MG. The input impedance of an assembly of randomly branching elastic tubes. **Biophys J**. 1966; 6:29−51.

101. Westerhof N, Bosman F, De Vries CJ, Noordergraaf A. Analog studies of the human systemic arterial tree. **J Biomech**. 1969; 2:121−134.

102. Avolio A. Multi-branched model of the human arterial system. **Med Biol Eng Comput**. 1980; 18:709−718.

103. Stergiopulos N, Young DF, Rogge TR. Computer simulation of arterial flow with applications to arterial and aortic stenoses. **J Biomech**. 1992; 25:1477−1488.

104. Alastruey J, Khir AW, Matthys KS, et al. Pulse wave propagation in a model human arterial network: assessment of 1-D visco-elastic simulations against in vitro measurements. **J Biomech**. 2011; 44:2250−2258.

105. Blanco P, Watanabe S, Passos M, Lemos P, Feijoo R. An anatomically detailed arterial network model for one-dimensional computational hemodynamics. **IEEE Trans Biomed Eng**. 2014; 62:736−753.

106. Olufsen MS, Peskin CS, Kim WY, Pedersen EM, Nadim A, Larsen J. Numerical simulation and experimental validation of blood flow in arteries with structured-tree outflow conditions. **Ann Biomed Eng**. 2000; 28:1281−1299.

107. Reymond P, Bohraus Y, Perren F, Lazeyras F, Stergiopulos N. Validation of a patient-specific one-dimensional model of the systemic arterial tree. **Am J Physiol Heart Circ Physiol**. 2011; 301:H1173−H1182.

108. Segers P, Mynard J, Taelman L, Vermeersch S, Swillens A. Wave reflection: myth or reality? **Artery Res**. 2012; 6:7−11.

109. Greenwald S, Newman D. Impulse propagation through junctions. **Med Biol Eng Comput**. 1982; 20:343−350.

110. Li JK, Melbin J, Noordergraaf A. Directional disparity of pulse reflection in the dog. **Am J Physiol Heart Circ Physiol**. 1984; 247:H95−H99.

111. Smolich JJ, Mynard JP, Penny DJ. Dynamic characterization and hemodynamic effects of pulmonary waves in fetal lambs using cardiac extrasystoles and beat-by-beat wave intensity analysis. **Am J Physiol Regul Integr Comp Physiol**. 2009; 297:R428−R436.

112. Smolich JJ, Mynard JP, Penny DJ. Ductus arteriosus wave intensity analysis in fetal lambs: midsystolic ductal flow augmentation is due to antegrade pulmonary arterial wave transmission. **Am J Physiol Regul Integr Comp Physiol**. 2009; 297:R1171−R1179.

113. Forfia PR, Vachiéry J-L. Echocardiography in pulmonary arterial hypertension. **Am J Cardiol**. 2012; 110:S16−S24.

114. Meltzer RS, Valk NK, ten Cate F, Visser CA, Roelandt J. Contrast echocardiography in pulmonary hypertension: observations explaining the early closure of the pulmonic valve. **Am Heart J**. 1983; 106:1394−1398.

115. Weyman AE, Dillon JC, Feigenbaum H, Chang S. Echocardiographic patterns of pulmonic valve motion with pulmonary hypertension. **Circulation**. 1974; 50:905−910.

116. Phan TS, Li JKJ, Segers P, Chirinos JA. Misinterpretation of the determinants of elevated forward wave amplitude inflates the role of the proximal aorta. **J Am Heart Assoc**. 2016; 5:e003069.

117. Torjesen AA, Wang N, Larson MG, et al. Forward and backward wave morphology and central pressure augmentation in men and

women in the framingham heart study. **Hypertension**. 2014; 64:259−265.

118. Mynard JP, Smolich JJ. Wave potential and the one-dimensional windkessel as a wave-based paradigm of diastolic arterial hemodynamics. **Am J Physiol Heart Circ Physiol**. 2014; 307:H307−H318.

119. Singer A. Systems engineering analysis of aortic root blood pressure. **Bull Math Biophys**. 1969; 31:453−471.

120. Baksi AJ, Treibel TA, Davies JE, et al. A meta-analysis of the mechanism of blood pressure change with aging. **J Am Coll Cardiol**. 2009; 54:2087−2092.

121. Fantin F, Mattocks A, Bulpitt CJ, Banya W, Rajkumar C. Is augmentation index a good measure of vascular stiffness in the elderly? **Age Ageing**. 2006; 36:43−48.

122. Wilkinson IB, MacCallum H, Flint L, Cockcroft JR, Newby DE, Webb DJ. The influence of heart rate on augmentation index and central arterial pressure in humans. **J Physiol**. 2000; 525:263−270.

123. van de Velde L, Schattenkerk DWE, Venema PAHT, et al. Myocardial preload alters central pressure augmentation through changes in the forward wave. **J Hypertens**. 2017; 36:544−551.

124. Cheng K, Cameron JD, Tung M, Mottram PM, Meredith IT, Hope SA. Association of left ventricular motion and central augmentation index in healthy young men. **J Hypertens**. 2012; 30:2395−2402.

125. Heusinkveld MHG, Delhaas T, Lumens J, et al. Augmentation index is not a proxy for wave reflection magnitude: mechanistic analysis using a computational model. **J Appl Physiol**. 2019; 127:491−500.

126. Westerhof BE, Westerhof N. Magnitude and return time of the reflected wave: the effects of large artery stiffness and aortic geometry. **J Hypertens**. 2012; 30:932.

127. O'Rourke MF, Mancia G. Arterial stiffness. **J Hypertens**. 1999; 17:1−4.

128. O'Rourke MF. Mechanical principles. Arterial stiffness and wave reflection. **Pathol Biol**. 1999; 47:623−633.

129. Segers P, Rietzschel ER, De Buyzere ML, et al. Assessment of pressure wave reflection: getting the timing right!. **Physiol Meas**. 2007; 28:1045−1056.

130. Hughes AD, Park C, Davies J, et al. Limitations of augmentation index in the assessment of wave reflection in normotensive healthy individuals. **PLoS One**. 2013; 8:e59371.

131. Segers P, Kips J, Trachet B, et al. Limitations and pitfalls of non-invasive measurement of arterial pressure wave reflections and pulse wave velocity. **Artery Res**. 2009; 3:79−88.

132. Laxminarayan S. The calculation of forward and backward waves in the arterial system. **Med Biol Eng Comput**. 1979; 17, 130-130.

133. Li JK. Time domain resolution of forward and reflected waves in the aorta. **IEEE Trans Biomed Eng**. 1986; 33:783−785.

134. Hughes A, Parker K. Forward and backward waves in the arterial system: impedance or wave intensity analysis? **Med Biol Eng Comput**. 2009; 47:207−210.

135. Mynard JP, Smolich JJ. Wave potential: a unified model of arterial waves, reservoir phenomena and their interaction. **Artery Res**. 2017; 18:55−63.

136. Chiu YC, Arand PW, Shroff SG, Feldman T, Carroll JD. Determination of pulse wave velocities with computerized algorithms. **Am Heart J**. 1991; 121:1460−1470.

137. Mitchell GF, Pfeffer MA, Finn PV, Pfeffer JM. Comparison of techniques for measuring pulse-wave velocity in the rat. **J Appl Physiol**. 1997; 82:203−210.

138. Gatzka CD, Cameron JD, Dart AM, et al. Correction of carotid augmentation index for heart rate in elderly essential hypertensives. **Am J Hypertens**. 2001; 14:573−577.

139. Li JK, Noordergraaf A. Similar pressure pulse propagation and reflection characteristics in aortas of mammals. **AJP Regul Integr Comp Physiol**. 1991; 261:R519−R521.

140. Xiao H, Tan I, Butlin M, Li D, Avolio AP. Mechanism underlying the heart rate dependency of wave reflection in the aorta: a numerical simulation. **Am J Physiol Heart Circ Physiol**. 2018; 314:H443−H451.

141. Nichols WW, O'Rourke MF, Avolio AP, et al. **Age-related Changes in Left Ventricular/arterial Coupling**. Springer; 1987:79−114.

142. Parker KH, Jones CJ. Forward and backward running waves in the arteries: analysis using the method of characteristics. **J Biomech Eng**. 1990; 112:322−326.

143. Mynard JP, Smolich JJ. Novel wave power analysis linking pressure-flow waves, wave potential and the forward and backward components of hydraulic power. **Am J Physiol Heart Circ Physiol**. 2016; 310:H1026−H1038.

144. Penny DJ, Mynard JP, Smolich JJ. Aortic wave intensity analysis of ventricular-vascular interaction during incremental dobutamine infusion in adult sheep. **Am J Physiol Heart Circ Physiol**. 2008; 294:H481−H489.

145. Alastruey J, Hunt AAE, Weinberg PD. Novel wave intensity analysis of arterial pulse wave propagation accounting for peripheral reflections. **Int J Numer Method Biomed Eng**. 2014; 30:249−279.

146. Mynard J, Penny DJ, Smolich JJ. Wave intensity amplification and attenuation in non-linear flow: implications for the calculation of local reflection coefficients. **J Biomech**. 2008; 41:3314−3321.

147. Smolich JJ, Mynard JP, Penny DJ. Simultaneous pulmonary trunk and pulmonary arterial wave intensity analysis in fetal lambs: evidence for cyclical, midsystolic pulmonary vasoconstriction. **Am J Physiol Regul Integr Comp Physiol**. 2008; 294:R1554−R1562.

148. Jones CJ, Sugawara M, Kondoh Y, Uchida K, Parker KH. Compression and expansion wavefront travel in canine ascending aortic flow: wave intensity analysis. **Heart Ves**. 2002; 16:91−98.

149. Khir AW, Parker KH. Wave intensity in the ascending aorta: effects of arterial occlusion. **J Biomech**. 2005; 38:647−655.

150. Westerhof N, Elzinga G, Van den Bos GC. Influence of central and peripheral changes on the hydraulic input impedance of the systemic arterial tree. **Med Biol Eng**. 1973; 11(6):710−723.

151. Van den Bos GC, Westerhof N, Elzinga G, Sipkema P. Reflection in the systemic arterial system: effects of aortic and carotid occlusion. **Cardiovasc Res**. 1976; 10(5):565−573.

Chapter 12

Linking arterial stiffness to microvascular remodeling

Arinola O. Lampejo[1], Nien-Wen Hu[1], Ariana Suarez-Martinez[1], Prasad V.G. Katakam[2], Jerome W. Breslin[3], Shayn M. Peirce[4] and Walter L. Murfee[1]

[1]*J. Crayton Pruitt Family Department of Biomedical Engineering, University of Florida, Gainesville, FL, United States;* [2]*Tulane University School of Medicine, New Orleans, LA, United States;* [3]*Department of Molecular Pharmacology and Physiology, Morsani College of Medicine, University of South Florida, Tampa, FL, United States;* [4]*Department of Biomedical Engineering, University of Virginia, Charlottesville, VA, United States*

Motivation
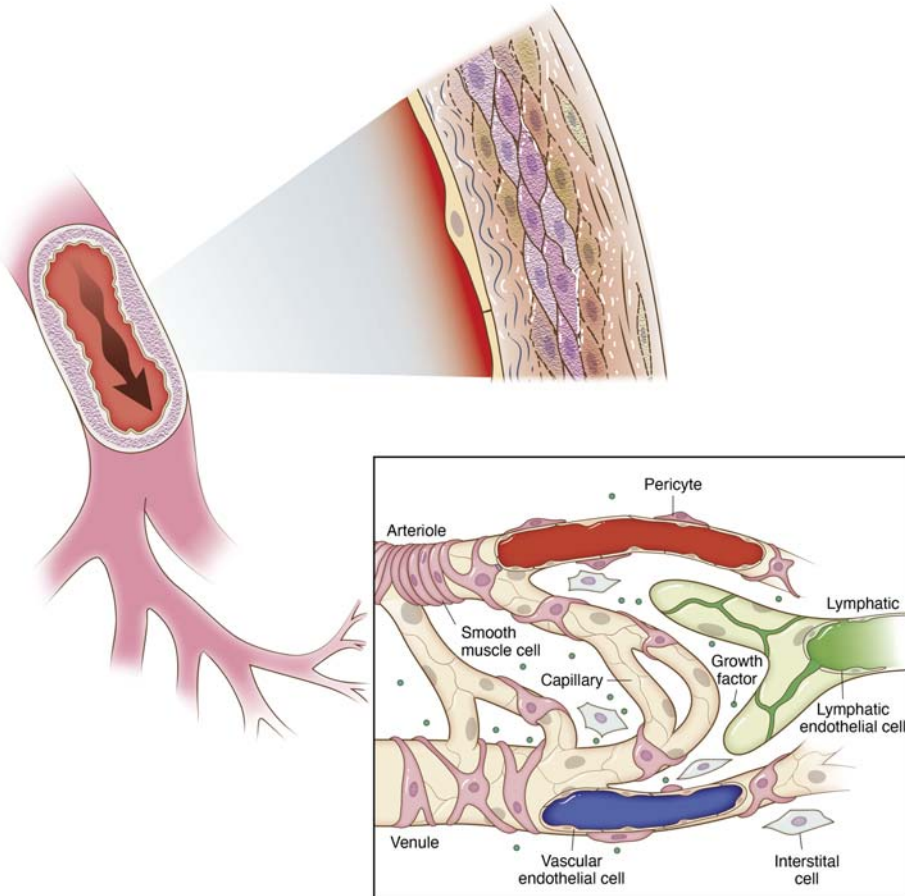
Large artery stiffening (LAS) and more generally arterial stiffening are associated with aging and numerous age-related pathologies including diabetes, atherosclerosis, chronic kidney disease, hypertension, and cerebrovascular disease. Vessel wall remodeling across pathologies involves a concert of cellular and molecular mechanisms, which have been comprehensively reviewed[1−8] and are further detailed in the accompanying book chapters. Consideration of these mechanisms emphasizes that arterial wall stiffening may have implications beyond just a decrease in wall compliance related to changes in the local extracellular matrix. The fact that microvascular dysfunction occurs in the same disease states and is caused by similar, if not overlapping mechanisms, suggests there are more direct linkages between LAS and microvascular remodeling that may be important to consider in the progression of disease.[9,10] Signals that may transmit pathology between macro- and microvessels fall into two categories: circulating factors and hemodynamics. Whether and to what extent arterial stiffening and specifically LAS directly influences downstream functional adaptations of microvascular networks remains unclear because the presence and effects of these signals at the microvascular level are largely undetermined. However, a review of the literature reveals putative mechanisms of communication between arteries and the microcirculation that may contribute to both LAS and downstream abnormalities in microvascular structure and function, creating feedback loops that may further exacerbate disease.

The objective of this chapter is to explore the links between LAS and microvascular remodeling. The chapter first offers a view of arterial wall stiffening from a microvascular remodeling perspective, focused on overlapping cell types. As microvascular remodeling encompasses the growth of new capillaries, capillary acquisition of perivascular wrapping cells, and patterning alterations, the major roles of overlapping cell types involved in arterial stiffening will then be described for the multiple subprocesses that coordinate microvascular remodeling. Next, known microvascular remodeling alterations associated with hypertension and aging will be used to highlight how gaps in our current understanding make links to the macrocirculation less clear. The chapter will culminate with a discussion of how circulating factors may be coupled with hemodynamic changes in LAS. In light of our incomplete understanding, the challenge of linking blood vessel remodeling across the macro- and microvascular systems serves to identify important knowledge gaps for future research.

A microvascular remodeling view of large arterial stiffening

LAS is related to aging, insulin resistance, preeclampsia, cognitive impairment, myocardial dysfunction, kidney disease, and stroke.[1−6,11] From a remodeling perspective, the causes and consequences of LAS can be associated with age or age-related changes in altered cell behavior. Moreover, the same cellular players involved in LAS and more generally arterial stiffening are implicated at the microvascular level (Fig. 12.1). Dynamics associated with the interplay between smooth muscle cells (SMCs), pericytes, endothelial cells, fibroblasts,

FIGURE 12.1 Basic structure of microvessels. All microvessels are lined with endothelial cells and are wrapped by perivascular cells, including smooth muscle cells and pericytes. The spectrum of cell morphologies and phenotypes present along the different vessel types emphasizes the importance of cell−cell interaction and coordination for maintaining microvascular function. The overlap of these cell dynamics with those involved in large artery stiffening (LAS) highlight the need to interrogate common mechanisms of dysfunction. *Printed with permission from Anita Impagliazzo.*

and macrophages are critical to microvascular function and adaptation. Despite the prognostic importance of cell responses in both large and small vessel remodeling, little is known regarding how and why these mechanisms are triggered to manifest integrated pathology in one patient versus another. Patient-specific phenotypic signatures undoubtedly depend on phenotypic variabilities in the local microenvironment and motivate the need to better understand cell dynamics from a systems level view.

While common cellular and molecular alterations have been identified across the macro- and microvessel levels, there still remains a question about whether the common signals represent mechanistic links. Are the effects also common? Does LAS trigger microvascular dysfunction and remodeling? Do imbalances generated by improper microvascular function contribute to LAS? A difficulty in answering these questions is that stiffening is associated with disease states, and it is difficult to delineate cause and effect relationships. Hence, microvascular remodeling

might be a cause of the disease state rather than a direct consequence of increased arterial stiffness. What is apparent is that the hallmark characteristics of LAS (elastin breakdown and degeneration, increases in fibrinogen and collagen content), tell just part of the story.[11−13] Increases in circulating factors like transforming growth factor beta (TGF-β), tumor necrosis factor alpha (TNF-α), and interleukin-6 (IL-6) highlight a proinflammatory shift, which is also known to have direct effects on the microvasculature.[14−16] The milieu of circulating inflammatory factors can be attributed to endothelial cell dysfunction characterized by oxidative stress, decreased nitric oxide (NO) bioavailability, increased proinflammatory factors, and mitochondrial oxidative stress.[1] In larger vessels, inflammation is linked to elastin breakdown and matrix remodeling which are key to wall stiffening. The inflammatory environment can trigger vascular SMCs to adopt a more synthetic phenotype, exhibit shape changes, proliferate, migrate, and increase integrin expression levels.[12,13] Whether microvascular SMCs and
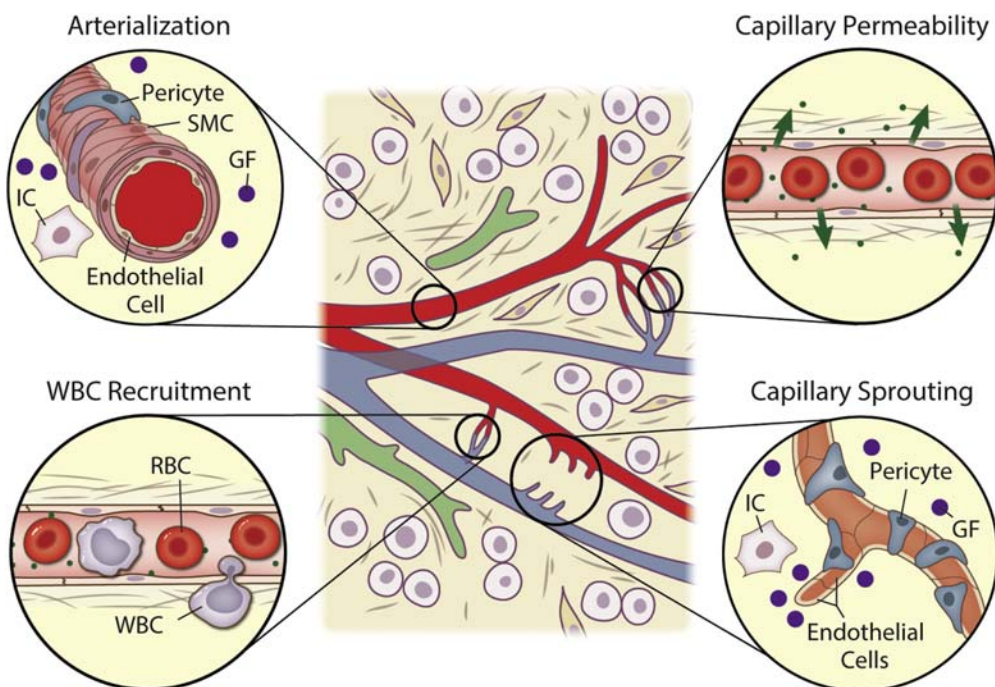
pericytes experience phenotypic changes that are similar to SMCs in larger arteries remains under-investigated; however, proinflammatory cytokines are known to invoke these behaviors in the perivascular cells of the microcirculation in diseases such as diabetes.[17]

A general thought is that increased pulse waves due to LAS are transmitted to the level of the microcirculation, especially in tissues with low-resistance vascular beds such as the kidney, brain, and placenta.[1,6] The increase in elastic modulus of stiffened arteries results in increased pulsatility, which can translate into increased pressure and altered flow velocity profiles in the microcirculation. These altered hemodynamics are often assumed to include increased shear stress, a regulator of endothelial cell function. However, as we consider later in this chapter, the actual velocity profiles, and thus, shear stress levels, are currently not known. Moreover, shear stress ranges depend on the specific microvascular network patterning and specific vessel geometries. Evidence suggesting that microvascular network patterns are specific to the type of tissue, and that blood flow regulation can be controlled at the capillary level, complicate our intuition and motivate the need for more careful thinking (and perhaps quantitative modeling[18]) about how hemodynamics and circulating factors are transmitted across the hierarchy of the vasculature.[19]
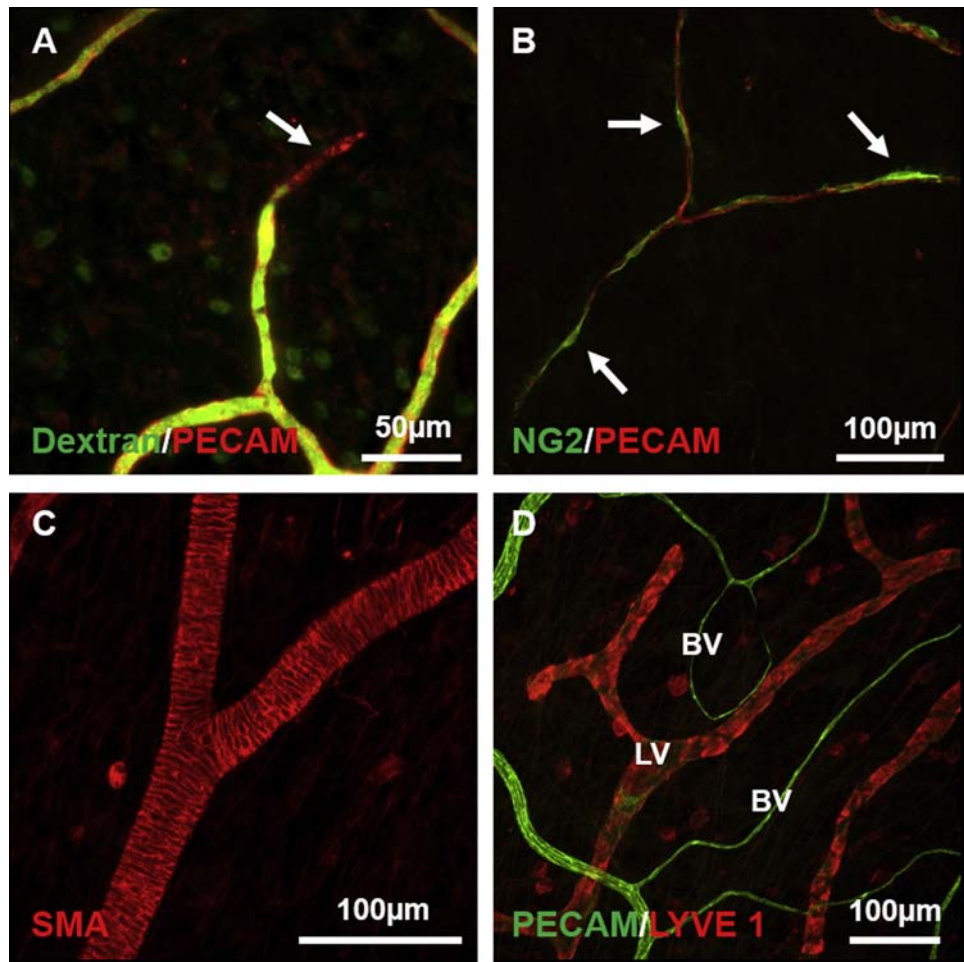
Cell dynamics involved in microvascular growth and remodeling

In order to appreciate the links between large vessel wall remodeling and remodeling of the microcirculation, it is helpful to identify common cell players. This section provides an overview of cell types involved in microvascular growth and remodeling, which also play a role in LAS. Thus, linking LAS with the microvasculature should involve the recognition that remodeling at the microvascular level is an amalgamation of subprocesses involving the same cell types involved in arterial stiffening: endothelial cells, pericytes, SMCs, and macrophages (Figs. 12.2 and 12.3).[20–24] It should be noted for the sake of clarity that the direct role of endothelial cells and pericytes in large vessel wall remodeling can be debated depending on the remodeling scenario. In particular, pericytes are included in the list because they can phenotypically resemble dedifferentiated SMCs or adventitial fibroblasts and both of these cell populations can be associated with atherosclerosis and aspects of large vessel wall remodeling.

Microvascular remodeling is traditionally characterized by three subprocesses: vasculogenesis, angiogenesis, and arteriogenesis (Table 12.1). It has been suggested that vasculogenesis, or the formation of blood vessels from endothelial progenitors, is driven by endothelial cell and pericyte

FIGURE 12.2 Microvascular network function and remodeling. Microvascular remodeling can be thought of as a continuum of subprocesses interrelated across space and time. For example, angiogenesis involves the sprouting of new capillaries from existing ones and is achieved via the interactions of endothelial cells, pericytes, and interstitial cell populations that secrete and respond to local growth factors. The differentiation of pericytes into smooth muscle cells and associated vessel maturation is termed "arterialization," which leads to functional vasoreactivity. Other cell dynamics related to these microvascular processes include permeability and white blood cell trafficking, or recruitment. *Printed with permission from Anita Impagliazzo.*

FIGURE 12.3   Cell types associated with the microvascular networks. (A) Endothelial cells: Platelet endothelial cell adhesion molecule-1 (PECAM)-positive labeling (red) identifies endothelial cells along capillaries and a capillary sprout. Intraluminal labeling with a fixable dextran (green) identifies vessels and the stalk of the capillary sprout, but does not label the extending tip cell (arrow). (B) Pericytes: Example of neuron-glial antigen 2−positive pericytes (green, arrows) wrapping along PECAM-positive endothelial cells at the capillary level (red). (C) Smooth muscle cells: Smooth muscle α-actin labeling (red) identifies tightly wrapped cells oriented circumferentially around an arteriole. (D) Lymphatic endothelial cells: LYVE1 labeling (red) identifies lymphatics near PECAM-positive blood vessels (green). "BV" identifies blood vessels and "LV" identifies lymphatic vessels. Images were obtained by immunolabelling adult rat mesenteric tissues.

recruitment of precursor cells.[25] Angiogenesis is defined as the growth of new endothelial cell-lined vessels from existing ones, and arteriogenesis refers to the process of enlarging existing collateral arterioles to form functional arteries and involves, in part, the recruitment of perivascular cells and their subsequent differentiation into SMCs.[20,24,26] These processes cause the structural adaptations of microvascular networks that are characterized by new vessels and altered network patterning (Fig. 12.4), which can profoundly impact key microvascular functions including, vascular permeability, vasoreactivity, and leukocyte adhesion.

Endothelial cells

In addition to preventing thrombosis and being a physical barrier between blood and tissue compartments, endothelial cells have specific roles that aid in maintaining normal vascular function. These additional roles include regulating vascular tone for dilation and constriction, regulating passage of all molecules and proteins across the vascular wall, appropriately responding to shear stress, being integral participants in inflammation, and lastly, being one of the most critical cell types involved in angiogenesis.[27,28] Numerous biomarkers, including vascular endothelial growth factor (VEGF), TGF-β, and TNF-α, are involved in the regulation of endothelial cell dynamics.[29]
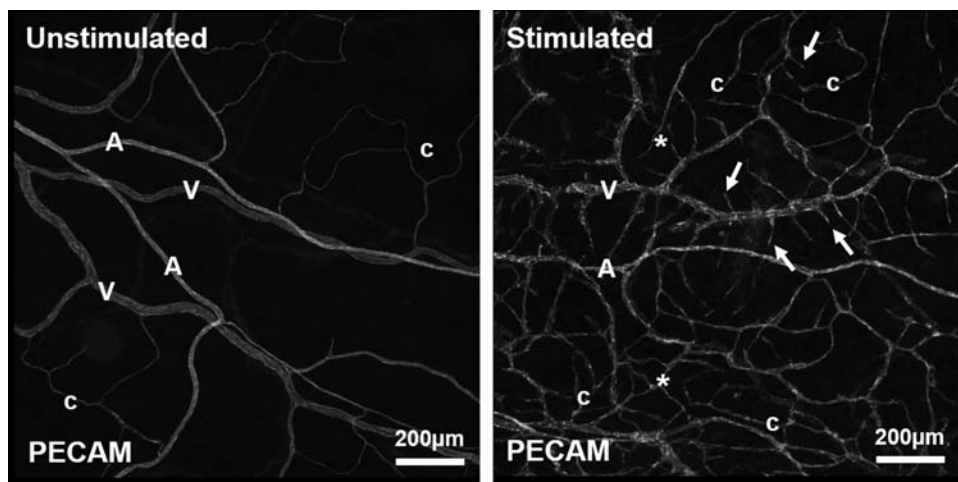
Capillary sprouting seen during angiogenesis is characterized by the proliferation and migration of endothelial cells. Capillary sprouting begins with the degradation of the basement membrane and weakening of nearby endothelial cell adhesions.[23] From this destabilized location in the

TABLE 12.1 Traditional microvascular remodeling processes.

	Angiogenesis	Vasculogenesis	Arteriogenesis
Definition	Angiogenesis is defined as the growth of new blood vessels from existing vessels.	Vasculogenesis is defined as the formation of new vessels from progenitor cells.	Arteriogenesis involves the remodeling of preexisting vessels and can be classified into two categories: (1) enlargement of collateral arterioles and (2) capillary acquisition of smooth muscle cell coverage (i.e., arterialization).
Key cell types	Endothelial cells, pericytes, and macrophages	Endothelial progenitor cells	Endothelial cells, pericytes, smooth muscle cells, and macrophages
Key characteristics	Angiogenesis is characterized by endothelial cell or capillary sprouting.	Vasculogenesis is most commonly associated with development. Vasculogenesis in the adult is less common and potentially involves the integration of vascular progenitor cells into new vessels remodeled by angiogenesis or arteriogenesis.	Collateral vessel enlargement triggered by increased flow and involves wall remodeling. Arterialization involves with pericyte recruitment is interrelated with angiogenesis.

The full understanding of how new vessels form in the adult remains incomplete. For example, intussusception and vascular island incorporation represent nontraditional processes (either understudied or underappreciated) that can contribute to microvascular growth. For descriptions of the information in this Basic Science Box, see References. 23,24.

FIGURE 12.4 Comparison of an unstimulated and stimulated angiogenic microvascular network from adult rat mesenteric tissue. Immunolabeling against Platelet endothelial cell adhesion molecule-1 (PECAM) identifies endothelial cells throughout the hierarchy of microvascular networks. (A) Unstimulated adult rat mesenteric microvascular network. (B) Angiogenic networks are characterized by increased vessel density (*) and increased capillary sprouting (*arrows*) off existing venules and capillaries. "A" identifies arterioles. "V" identifies venules. "c" identifies capillaries.

endothelial membrane, an endothelial tip cell equipped with specialized filopodia can branch out into the extracellular matrix (ECM), providing directional guidance for the continued migration of the sprout.[30] The tip cell, which does not form a lumen or proliferate, is followed by another specialized endothelial cell known as the stalk cell. The stalk cell forms a lumen and proliferates behind the tip cell, further elongating the sprout by pushing the sprout further from its vessel of origin.[31] Tip cells and stalk cells are not only different in function but in phenotype as well. Stalk cells possess high levels of Notch signaling while tip cells have low Notch activity but high platelet-derived growth factor-b (PDGF-β), vascular endothelial growth factor receptor-2, delta-like ligand 4, and unc-5 homolog b expression.[32–34] As the sprout extends, further ECM is degraded and pericytes are recruited to the sprout extension to provide support and stabilization.[35] These elongated vascular sprouts eventually anastomose with neighboring mature vessels or other capillary sprout extensions originating from neighboring vessels.

Recent evidence implicates cellular energetics in new blood vessel formation independent of angiogenic signaling.[36] Specifically, endothelial cell glycolysis has been shown to drive vessels sprouting in multiple vascular beds except brain, as endothelial cells are considered to be glycolysis addicted even though they are exposed to the highest oxygen levels in the blood.[37−39]

Factors such as alterations in wall shear stress levels can have a significant impact on various endothelial dynamics. Shear stress has been shown to regulate microvascular permeability, growth factor secretion, growth factor receptor expression, and endothelial dynamics during capillary sprouting.[40−42] Increases in vascular wall shear stress can also affect the function and phenotype of perivascular cells, which in turn can affect how they interact with and are recruited to vessels. The study of these dynamics at the microvascular level can provide a new way to investigate relevant pathologies and discover new connections between cellular behaviors and the dynamics of larger vessels.

In order to link endothelial cell function at the microvascular level to LAS, consider the microenvironment of a single endothelial cell. As endothelial cells line the inner interface of blood vessels, they are involved in several key cellular and physiological functions including vessel permeability, cell trafficking, and hemostasis. This is the case regardless of the vessel level. Along arterioles at the entrance of the microcirculation, endothelial cells play a role in regulating blood flow through controlling vessel diameter. Then in capillaries and postcapillary venules, endothelial function is more associated with basal permeability, which can be generally characterized as continuous flux of plasma components from the blood into the interstitial space. Permeability can become elevated when agonists such as VEGF, bradykinin, histamine, or serotonin activate their respective membrane receptors on endothelial cells. Elevated permeability is common in inflamed tissues, and is also frequently accompanied by increased leukocyte rolling, adhesion, and diapedesis into surrounding tissues which further amplifies inflammatory signals. For example, TNF-α can contribute to elevated microvascular permeability indirectly by activating neutrophil recruitment into local tissues.[43,44] Activated neutrophils cause conformational changes in endothelial cells that allow increased paracellular diffusion of fluid and solutes.[45,46] Elevated permeability, combined with other inflammatory signals from neutrophils, alters the local tissue environment by increasing diffusion distance for oxygen to reach local parenchymal cells, thus impairing normal tissue homeostasis.[47] In turn, resident cells adapt to the new tissue environment to limit tissue and organ dysfunction. In many cases, the resulting changes include signals that promote angiogenesis, tissue remodeling, and fibrosis. The accumulation of these types of adaptive events reflects the aging process of tissues and organs, and parallels the slow, creeping development of increased arterial stiffness with age.

Pericytes

Another very important type of supporting cell involved in angiogenesis is the pericyte.[20,21] These perivascular cells wrap around and have direct cell-to-cell contact with endothelial cells comprising capillaries and express markers including PDGFR-β, smooth muscle α-actin (SMA), desmin, and neuron-glial antigen 2.[20,21] Pericytes in the microcirculation have been shown to have the following roles: control of capillary diameter via direct contact and paracrine signaling, stabilization and maturation of microvasculature, control of vessel permeability, and promotion of endothelial cell survival and proliferation.[31,48−52]

During angiogenesis, pericytes are recruited to blood vessels in response to PDGF-β, where they aid in stabilizing endothelial cell proliferation and migration.[31] After pericytes have been recruited and there is direct contact with endothelial cells, the assembly of the basement membrane matrix begins with the deposition of laminin, fibronectin, and collagen IV as the sprout elongates.[53] The basement membrane is assembled and maintained by both endothelial cells and pericytes. Importantly, pericytes can promote or inhibit angiogenesis by manipulating the local growth factor environment. For example, pericytes secrete VEGF to signal endothelial cell sprouting or activate angiopoietin 1 (Ang1)/Tie2 signaling to stabilize endothelial cells, respectively.[53]

Dynamics implicated in arterial stiffening include SMC differentiation and matrix deposition. Intriguingly, the altered smooth muscle behavior resembles in many ways pericyte recruitment, pericyte differentiation from fibroblasts or SMCs, and a similar local matrix deposition. For example, consider fibrosis and hyperplasia of the intima and media. Fibrosis and hyperplasia involves SMC to myofibroblast transitions and overlaps the process related to fibroblast and vascular pericyte interactions associated with fibrosis in the lung during chronic kidney disease. Thus, the interconnected nature of different vascular systems and the importance of both macro- and microvessel remodeling emphasizes a value in attempting to understand cell mechanisms on different levels.

Smooth muscle cells

SMCs also make up a key component of blood vasculature in both large and small vessels. SMCs regulate several key processes including vasoconstriction, vasodilation, and maintenance of vessel structure and function.[13] SMCs are commonly identified based on SMA expression, though

other markers such as smooth muscle-myosin heavy chain are also expressed and are indicative of a more contractile phenotype.[54]

While pericytes are involved in stabilizing the new sprout, SMC destabilization is critical along pre- and postcapillary vessels to allow for endothelial sprouting. Destabilization of the adhesions with endothelial cells is triggered by vasodilation, which results in an increase in local vascular permeability.[55] Hence, alterations in vaso-reactivity and endothelial cell barrier function will influence new vessel growth. Like pericytes, SMCs are regulated by Tie2 signaling, which upon stimulation with the inhibitor Angiopoietin 2, induces SMCs to detach from vessels prior to angiogenesis.[29]

Common characteristics of LAS are decreased NO bioavailability and endothelial oxidative stress,[1] both of which are interrelated and influence SMC behavior at the microvascular level. For example, reduced NO bioavailability is the hallmark of cardiovascular disease. Increased oxidative stress from excessive production of reactive oxygen species (ROS) results in the degradation of NO to form peroxynitrite. This oxidative-nitrative stress is the major instigator of vascular remodeling in pathological states.[56−59] Recent evidence also implicates altered cellular energetics in vascular smooth muscle remodeling and microvascular dysfunction.[60,61] For example, glycolytic enzyme activity in SMCs has been shown to promote vascular remodeling in pulmonary hypertension.[60] Furthermore, mitochondria-mediated mechanisms have also been implicated in the macro- and microvascular dysfunction that accompanies aging,[61] ischemic heart disease,[56] and diabetes.[62−64]

Macrophages

Often occurring in conjunction with inflammation, angiogenesis is a common response to injury, which is why macrophages are a key cell of interest in understanding microvascular remodeling. Macrophages affect their surroundings by secreting growth factors, chemokines, and modulatory enzymes as well as by undergoing phagocytosis to remove apoptotic cells. They can also be affected by their local microenvironment, raising the question of how they impact microvascular remodeling processes.[22] Macrophages can be divided into at least two distinct subpopulations based on the mechanisms underpinning their activation. M1 macrophages, or classically activated macrophages, are stimulated by interferon gamma, TNF-α, and lipopolysaccharide, while alternatively activated (M2) macrophages are stimulated by interleukin-4 and interleukin-10.[22] M1 macrophages are known to secrete cytotoxic and proinflammatory agents, while M2 macrophages more commonly secrete growth promoting factors and anti-inflammatory signals that stimulate angiogenesis.[65−67] Though the specific roles of the macrophage subtypes are still unclear, it has been suggested because of the differences in the agents they secrete that M1 macrophages may help stimulate capillary sprouting while M2 macrophages, along with pericytes, may play a role in stabilization of new vessels.[22,68]

In addition to regulating angiogenesis via paracrine mechanisms, macrophages have also been suggested to directly interact with the other key cell types involved in the pruning of vascular networks.[22] Like pericytes, macrophages can form bridges between neighboring capillary sprouts, thus enhancing anastomoses.[17,22] Macrophages interact with SMCs by mediating arteriogenesis through enlargement of collateral arteries.[68] It has also been suggested that macrophages can transdifferentiate into endothelial cells, pericytes, and SMCs, enabling them to participate directly as building blocks in microvessel networks.[22]

Given that circulating monocytes can give rise to macrophages, the suggested roles of macrophages in microvascular remodeling also highlight the importance of leukocyte trafficking, including leukocyte adhesion. The adhesion cascade first occurs in three key steps: rolling, activation, and arrest.[69] After the leukocyte is tethered to the endothelium, rolling is controlled by transiently binding to selectins, such as E-selectin and P-selectin. Rolling eventually transitions to the slow rolling phase until the leukocyte arrests through increased β_1- and β_2-integrin binding. This transition from rolling to arrest is known as activation and is mediated by chemokines including chemokine ligand 5 (CCL5), c-x-c motif chemokine 4 (CXCL4), and CXCL5. The leukocyte then undergoes adhesion strengthening, spreading, and begins crawling on the blood vessel wall to macrophage antigen-1- and intercellular adhesion molecule-1−rich emigration sites. Finally, during paracellular and transcellular transmigration, the leukocyte will penetrate the endothelial cell barrier and begin migrating through the basement membrane. Leukocyte transmigration is regulated by expression of various junctional molecules, including platelet endothelial cell adhesion molecule-1, endothelial cell-selective adhesion molecule, junctional adhesion molecule, and CD99, all of which can also affect vascular permeability through numerous molecular interactions. Thus, as we have described before, each dynamic cellular process influences another cell type or cellular process. So, when considering the impacts of transmitted signals from the macro- to microcirculation levels, it is critical to identify how each of the subprocesses is influenced by disease and ask whether the responses may be integrated.

Lymphatic endothelial cells

While not often a primary focus of study in the field of microvascular remodeling, lymphatic endothelial cells also

participate in structural remodeling of lymphatic microvessels in response to many of the chemical and mechanical stimuli mentioned above. Lymphatic microvascular networks consist of lymphatic capillaries, which are also termed initial lymphatic vessels. Initial lymphatic vessels are lined with endothelial cells, void of wrapping SMCs or pericytes, are spatially coordinated with blood microvascular networks, and can even form junctional connections with these networks.[70,71] Importantly, along with the blood microvessels, lymphatic microvessels are responsible for maintaining tissue homeostasis. Lymphangiogenesis, or the growth of new lymphatic endothelial segments that participate in lymphatic fluid uptake, is linked to inflammatory states which could also persist in settings of LAS. Thus, lymphatic endothelial cells could be affected by the same disease processes that cause LAS. Furthermore, alterations in lymphatic microvascular structure and function as a direct result of LAS should not be ruled out, although little is known about this intersection. We do know that lymphangiogenic and angiogenic signaling often overlap with one another, and that the presence of lymphatic vessels influences blood vessel growth, and vice versa.[72] Recently, lymphangiogenesis has been implicated as a characteristic of hypertension and age-related renal injury.[73,74] Given the interrelationships between lymphatic endothelial cells, blood endothelial cells, and macrophages, they represent an under-investigated aspect of the microcirculation that warrants future investigation in the context of overlapping cell dynamics with those involved in larger vessel stiffening. For example, one particular phenomenon that involves arterial endothelial cells, macrophages, and lymphatic vessels is the formation of atherosclerotic plaques. It has been long known that lymphatic vessels play a key role in reverse cholesterol transport.[71] The loss of lymphatic clearance capacity impairs local tissue homeostasis and results in the buildup of cholesterol, which is usually taken up by macrophages. This leads to the formation of atherosclerotic plaques in the arterial walls.[75] This pathology remains an ongoing clinical problem, and how other risk factors, such as hypertension or inflammatory states associated with chronic diseases impact the coordination of microvascular delivery and lymphatic clearance to maintain optimal homeostasis in the arterial wall remains an area that requires more thorough investigation.

Consideration of microvascular patterning alterations associated with hypertension and aging

The integration of cell dynamics involved in microvascular remodeling subprocesses leads to network level patterning changes that then influence network resistance and local hemodynamics. As pulsatility and altered hemodynamics are potentially transmitted from arteries to the microcirculation, consideration of the patterns in age-related pathologies is warranted.[1,6] This section will provide an overview of microvascular pattern alterations associated with hypertension and aging (two key conditions associated with macrovessel wall remodeling).

Structural rarefaction, defined as the anatomical loss of microvessels, is commonly associated with hypertension and other age-related diseases and is attributed to impaired angiogenesis.[76] Based on the logic that fewer parallel vessels result in increased microvascular resistance, structural rarefaction has also been linked to increased systemic resistance, which increases mean arterial pressure for any given cardiac output.[77] In some cases, microvessel rarefaction has been reported to precede increases in systemic blood pressure, further implicating its role as a causal contributor to hypertension.[78,79] Concurrent with rarefaction, microvascular networks in hypertension are characterized by increased oxidative stress, elevated circulating leukocytes, and endothelial cell apoptosis.[80] The connections between rarefaction and hemodynamics raise questions about relationships between altered pressures and pulsatile blood flow velocity due to LAS. The answers, of course, are unknown and not straightforward because any assumptive links are based on knowledge gaps. Recent evidence suggests that microvessel rarefaction, at least in hypertension, is more complex than vessel loss. Microvascular networks in spontaneously hypertensive rats display patterning alterations highlighted by increased arterial/venous anastomoses that serve to normalize resistance.[81] In addition, while increased microvascular tone has been reported in hypertensive networks,[82–84] the diameters of individual vessels might not necessarily be decreased.[85] Indeed, vasoconstriction is not present along all arterioles. Even the concept of impaired angiogenesis is challenged by evidence that hypertensive networks can undergo normal levels of angiogenesis.[86] Hence, emerging evidence challenges the paradigms that have shaped our understanding. Relating these newer findings to traditional paradigms has caused a reconsideration of how the microcirculation is altered during hypertension and an evolving understanding about how this impacts hemodynamics.

Aging is also associated with microvascular dysfunction characterized by impaired vasoreactivity, increased oxidative stress, and reduced blood flow.[76] Aging is characterized by impaired angiogenesis, vessel loss attributed to decreases in growth factor levels (i.e., PDGF and VEGF), decreases in NO bioavailability, increases in mitochondrial stress.[76] Further influenced by alterations in other pro- and antiangiogenic factors, the aged environment is generally thought to invoke microvascular rarefaction. Still, rarefaction might be tissue-specific, and the hemodynamic implications of microvessel rarefaction remain under investigation.[87,88] For example, as in the case of

hypertension, the evidence for decreased angiogenesis or rarefaction can be assumed to associated with increases in microvascular network resistance. Interestingly, an increase in resistance would increase the pressure drop across a network, raising questions about how this might influence vessel specific stress levels and local velocity profiles. Moreover, work by Sweat et al. suggests (at least in mesentery networks) that aging alone does not increase microvessel resistance.[87]

The need for further characterization of tissue-specific microvascular alterations in hypertension and aging is also highlighted at the cellular level. As indicated in a previous section, vascular pericytes play a critical role in regulating microvascular remodeling. However, there is a lack of information about how pericytes adapt during aging and in response to hypertension.[77] For aging, pericyte presence, structure, and function remains under investigation. While studies support a loss of pericyte coverage in the aged brain and kidney,[89,90] other evidence suggests that in specific tissues aging results in an increase in pericyte number and that aged pericytes can display increased expression of SMA.[91,92] These findings are supported by RNA sequencing data indicating increased PDGF-β receptor expression despite decreased PDGF growth factor levels.[87] In the setting of hypertension, even less is known about whether pericyte phenotype and function is altered. For example, the number of SMA-positive pericytes was reported to be increased in brain tissue harvested from SHR versus in normotensive control WKY strain rats.[93] On the other hand, in the hypertensive retina, pericyte numbers have been reported to be decreased relative to normotensive controls.[94] Considering the impact of perivascular cell presence, structure, and phenotype on vessel function, such cellular adaptations during aging, hypertension, or other pathologies ultimately modulate local and systemic hemodynamics. Thus, linking any changes in hemodynamics at the macrocirculation level down to the microcirculation necessitates identification of microvascular network patterns and altered cellular dynamics along specific vessel types within a network.

Circulating factors and hemodynamics as putative links between arterial stiffness and the microcirculation

Thinking about links between macro- and microvessels parallels the identification of links between different organs during disease states. Consider the links between cardiac dysfunction and chronic kidney disease.[11] Is one related to the other? Are there mechanistic links? The superficial answers are yes, but there is probably more than one single contributor. Just as numerous circulating factors and hemodynamic parameters may link two organ systems

together in health and disease, they may also link structure and function across the macro- and microcirculations and coordinate adaptations in both systems in response to pathology.

Indeed, serum levels of inflammatory biomarkers, such as TGF-β, high-sensitivity C-reactive protein, TNF-α, and IL-6 are associated with LAS across numerous pathological environments.[1,16,95] Each chemical cue can influence microvascular function. For example, increased levels of TNF-α can interfere with endothelial nitric oxide synthase, leading to a decrease in NO, which could prevent angiogenesis. Some inflammatory mediators that are present in hypertension,[96] such as thrombospondin-1 (which is released by endothelial cells exposed to elevated shear stress levels) are antiangiogenic[97] and could provide a direct mechanism by which hemodynamic changes in large vessels impact structural adaptations in microvessels. Other factors, such as angiopoietin 2, have been identified as causal regulators of both hypertension and stiffness.[14,15] Angiopoietin 2 in the context of stiffening can have upstream effects on monocyte chemoattractant protein-1, matrix metalloproteinases (MMPs), nuclear factor kappa-light-chain-enhancer of activated B cells (NF-kB), ROS, and NO. Angiopoietin 2−induced hypertension is also characterized by a loss of microvessels, or rarefaction, which has been linked to increased MMP levels. It is important to point out that MMP inhibition is generally associated with increased matrix deposition in large vessels, whereas MMP increases are present in the microcirculation. Furthermore, broad spectrum MMP inhibition with doxycycline is sufficient to normalize blood pressure and reverse microvascular rarefaction and growth factor receptor cleavage in spontaneously hypertensive rats.[98,99] The effects of doxycycline on large vessel remodeling remain unclear, yet the role of MMPs in the microcirculation during stiffening emphasizes the importance of evaluating potentially differential effects of these circulating factors and drugs used to impact MMP levels in both large and small vessels. It is not as simple as recognizing that the circulating cues can moderate cell macro- and microvascular cell dynamics. Elucidation of common mechanisms requires comprehensive comparison of local effects.

Consistent with the theme of this chapter, the question remains whether these biochemical links are secondary to vessel wall stiffening, implicating hemodynamic changes as the more critical link between large vessels and the microcirculation. A more direct link is the increased pulsatility attributed to changes in artery wall elasticity.[100−106] Undoubtedly, altered flow profiles at the microcirculation level can influence red blood cell passage, local hematocrit, local effects on viscosity, endothelial cell function, and leukocyte adhesion.[23,40] However, more preeminent questions should focus on the actual altered flow profile within a

microvascular network due to upstream arterial stiffening and whether local mechanotransduction mechanisms are altered. Cell mechanotransduction sensing elements include cell—cell junctional proteins, integrins, the cytoskeleton, growth factor receptors, and even ion channels. Thus, any changes to these sensing elements along the microvascular endothelium could influence shear responses.

Increased pulsatile shear stress is thought to be crucial in high flow/low-resistance tissues like the brain and kidney.[1,6,100] These tissues are susceptible to pulsatility and altered hemodynamics because of the lack of upstream vasoconstrictor vessels. However, the actual microvascular flow profiles in these tissues remain to be determined, making it difficult to appreciate the transmitted effects, especially given emerging evidence for a role of vascular pericytes in regulating capillary diameters.[20,21,107—109] Microvascular network flow regulation is more complex than arteriole vasoregulation and can involve diameter control at lower caliber vessel levels and network repatterning. With that being said, increased pulsatility and shear stress are definitive regulators of endothelial cell behavior.

Wall shear stress is due to viscous forces associated with fluid flow and is dependent on velocity gradient, viscosity, and vessel geometry. Endothelial cells along a microvascular network experience levels of shear stress of $\sim 5-150$ dyne/cm^2, with capillaries experiencing closer to the 10 dyne/cm^2 level.[40] But, as noted above, the actual shear stresses experienced by angiogenic vessels are not clear.[110] Even more so, the thresholds for influencing cell behavior remains unclear. Work by Song et al. suggested that shear stresses below 3 dyne/cm^2 inhibited endothelial sprouting.[111] In contrast, work by Galie and colleagues also using a microfluidic based assay suggested that stresses above 10 dyne/cm^2 increase sprouting.[112]

Interestingly, most of the initial evidence implicating shear stress as a regulator of angiogenesis is based on in vitro experiments.[40,113,114] The in vivo link is supported by evidence of increases in the number of capillaries after treatments that result in increased perfusion. For example, seminal work treated animals with prazosin and then quantified vessel numbers in the skeletal muscles.[41,115] Complicating the interpretation of the results, prazosin increased vessel diameter therefore causing more than just an increase in shear stress.

In addition to shear stress, wall shear stress gradients can also play a role in angiogenesis by influencing endothelial proliferation, cell matrix adhesion, migration, and soluble factor production.[116—118] Consideration of the effect of flow pulsatility on local shear stress values and stress gradients further complicates our understanding. With shear stress being dependent on the velocity derivatives, a time-dependent velocity gradient suggests a changing or pulsatile shear stress profile few studies address. The knowledge gap related to increased pulsatility and microvascular remodeling is probably best highlighted by a lack of literature search results. Searching for "pulsatile shear stress microcirculation", "pulsatile shear stress capillary", and "pulsatile shear stress angiogenesis" resulted in 30, 36, and 10 papers, respectively (search done in January 2021). In one example, pulsatile shear stress was shown to induce a significance increase in PECAM-1 phosphorylation, ICAM-1 expression, and NF-kB activation.[119] These results are consistent with evidence that increased pulsatility and potential higher shear stress can cause decreased microvascular diameters and can reduce permeability via increases in tight junction protein expression. On the other hand, pulsatile shear stress has been suggested to promote NO production, increase NO bioavailability, and even endothelial cell proliferation.[120—123] Finally, in another report, high shear stresses (40 dyne/cm^2) and pulsatility decreased junctional morphologies.[121]

Reflection on what is known regarding shear stress and the microcirculation exposes an important knowledge gap—local shear stresses along specific vessel types in a microvascular network, especially due to altered flow conditions that might be attributed to upstream macrovessel remodeling, are unknown. The lack of measurements of shear stress values in vivo has resulted in the mechanistic role of shear stress in angiogenesis remaining ambiguous.

Conclusions and future opportunities

LAS is a hallmark of aging and numerous disease states. While it is obvious that the macro- and microcirculations are coupled both mechanically and biochemically, how the presence of disease impacts the content and transmission of information flowing between these two vascular environments is not well understood. Given the similarities in cell types, cellular dynamics, ECM remodeling, and the role of hemodynamic forces across the entire circulatory tree, it stands to reason that pathological stiffening of large vessels could adversely impact the structure and function of downstream microvessels and, conversely, that alterations in the structure and function of the microcirculation could contribute to stiffening of large vessels. In addition, overarching cellular and molecular mechanisms could simultaneously affect macrovascular and microvascular function. Hence, studying the cross-talk between large and small vessels in diseases characterized by pathological wall stiffening will undoubtedly yield a more comprehensive understanding and suggest novel therapeutic targets. Advances in noninvasive in vivo measurement techniques will provide more comprehensive, accurate, and dynamic assessments of large and small vessel hemodynamics and biomarkers.[124,125] In addition, applications of computational modeling and analysis can provide a more robust platform for systematically integrating, interpreting, and therapeutically manipulating cause and effect relationships that span spatial and temporal scales.[18,126—128] Measurement and modeling of LAS and microvascular adaptations

simultaneously (within the same experimental systems and to the extent that is possible clinically) will also likely reveal new mechanisms of chemomechanical cross-talk and their local and systemic contributions to disease. Finally, numerous reports have established the role of biological sex and sex hormones in the vascular function in health and disease states. Sex differences impact all cell types associated with the vascular wall at both the macro- and microvasculature levels,[129−131] further highlighting how cellular dynamics associated with stiffening and microvascular remodeling might be heterogeneous across groups or individuals. Looking forward, our lack of understanding represents an opportunity for comprehensively linking how cellular dynamics can influence transmitted links throughout the vasculature.

Acknowledgments

References

1. Chirinos JA, Segers P, Hughes T, Townsend R. Large-artery stiffness in health and disease: JACC state-of-the-art review. **J Am Coll Cardiol**. 2019; 74(9):1237−1263. https://doi.org/10.1016/j.jacc.2019.07.012.

2. Oh YS, Berkowitz DE, Cohen RA, et al. A special report on the NHLBI initiative to study cellular and molecular mechanisms of arterial stiffness and its association with hypertension. **Circ Res**. 2017; 121(11):1216−1218. https://doi.org/10.1161/CIRCRESAHA.117.311703.

3. Lacolley P, Regnault V, Laurent S. Mechanisms of arterial stiffening: from mechanotransduction to epigenetics. **Arterioscler Thromb Vasc Biol**. 2020; 40(5):1055−1062. https://doi.org/10.1161/ATVBAHA.119.313129.

4. Lacolley P, Regnault V, Segers P, Laurent S. Vascular smooth muscle cells and arterial stiffening: relevance in development, aging, and disease. **Physiol Rev**. 2017; 97(4):1555−1617. https://doi.org/10.1152/physrev.00003.2017.

5. Zanoli L, Lentini P, Briet M, et al. Arterial stiffness in the heart disease of CKD. **J Am Soc Nephrol**. 2019; 30(6):918−928. https://doi.org/10.1681/ASN.2019020117.

6. Chen Y, Shen F, Liu J, Yang GY. Arterial stiffness and stroke: de-stiffening strategy, a therapeutic target for stroke. **Stroke Vasc Neurol**. 2017; 2(2):65−72. https://doi.org/10.1136/svn-2016-000045.

7. Cecelja M, Chowienczyk P. Molecular mechanisms of arterial stiffening. **Pulse**. 2016; 4(1):43−48. https://doi.org/10.1159/000446399.

8. Shirwany NA, Zou MH. Arterial stiffness: a brief review. **Acta Pharmacol Sin**. 2010; 31(10):1267−1276. https://doi.org/10.1038/aps.2010.123.

9. van de Wouw J, Broekhuizen M, Sorop O, et al. Chronic kidney disease as a risk factor for heart failure with preserved ejection fraction: a focus on microcirculatory factors and therapeutic targets. **Front Physiol**. 2019; 10:1108. https://doi.org/10.3389/fphys.2019.01108.

10. Yannoutsos A, Levy BI, Safar ME, Slama G, Blacher J. Pathophysiology of hypertension: interactions between macro- and microvascular alterations through endothelial dysfunction. **J Hypertens**. 2014; 32(2):216−224. https://doi.org/10.1097/HJH.0000000000000021.

11. Jia G, Aroor AR, Sowers JR. Arterial stiffness: a nexus between cardiac and renal disease. **Cardiorenal Med**. 2014; 4(1):60−71. https://doi.org/10.1159/000360867.

12. Sehgel NL, Vatner SF, Meininger GA. "Smooth muscle cell stiffness syndrome"-revisiting the structural basis of arterial stiffness. **Front Physiol**. 2015; 6:335. https://doi.org/10.3389/fphys.2015.00335.

13. Jaminon A, Reesink K, Kroon A, Schurgers L. The role of vascular smooth muscle cells in arterial remodeling: focus on calcification-related processes. **Int J Mol Sci**. 2019; 20(22):5694. https://doi.org/10.3390/ijms20225694.

14. Park S, Lakatta EG. Role of inflammation in the pathogenesis of arterial stiffness. **Yonsei Med J**. 2012; 53(2):258−261. https://doi.org/10.3349/ymj.2012.53.2.258.

15. Wang M, Monticone RE, Lakatta EG. Proinflammation of aging central arteries: a mini-review. **Gerontology**. 2014; 60(6):519−529. https://doi.org/10.1159/000362548.

16. Mozos I, Malainer C, Horbańczuk J, et al. Inflammatory markers for arterial stiffness in cardiovascular diseases. **Front Immunol**. 2017; 8:1058. https://doi.org/10.3389/fimmu.2017.01058.

17. Corliss BA, Ray HC, Doty RW, et al. Pericyte bridges in homeostasis and hyperglycemia. **Diabetes**. 2020; 69(7):1503−1517. https://doi.org/10.2337/db19-0471.

18. Hashambhoy YL, Chappell JC, Peirce SM, Bautch VL, Mac Gabhann F. Computational modeling of interacting VEGF and soluble VEGF receptor concentration gradients. **Front Physiol**. 2011; 2:62. https://doi.org/10.3389/fphys.2011.00062.

19. Bosetti F, Galis ZS, Bynoe MS, et al. "Small blood vessels: Big health problems?": scientific recommendations of the national institutes of health workshop. **J Am Heart Assoc**. 2016; 5(11):e004389. https://doi.org/10.1161/JAHA.116.004389.

20. Stapor PC, Sweat RS, Dashti DC, Betancourt AM, Murfee WL. Pericyte dynamics during angiogenesis: new insights from new identities. **J Vasc Res**. 2014; 51(3):163−174. https://doi.org/10.1159/000362276.

21. Kelly-Goss MR, Sweat RS, Stapor PC, Peirce SM, Murfee WL. Targeting pericytes for angiogenic therapies. **Microcirculation**. 2014; 21(4):345−357. https://doi.org/10.1111/micc.12107.

22. Corliss BA, Azimi MS, Munson JM, Peirce SM, Murfee WL. Macrophages: an inflammatory link between angiogenesis and lymphangiogenesis. **Microcirculation**. 2016; 23(2):95−121. https://doi.org/10.1111/micc.12259.

23. Murfee WL. Implications of fluid shear stress in capillary sprouting during adult microvascular network remodeling. **Mechanobiol Endothel**. 2015:166−184. https://doi.org/10.1201/b18060.

24. Carmeliet P. Angiogenesis in life, disease and medicine. **Nature**. 2005; 438(7070):932−936. https://doi.org/10.1038/nature04478.

25. Lyden D, Hattori K, Dias S, et al. Impaired recruitment of bone-marrow-derived endothelial and hematopoietic precursor cells blocks tumor angiogenesis and growth. **Nat Med**. 2001; 7(11):1194−1201. https://doi.org/10.1038/nm1101-1194.

26. Mac Gabhann F, Peirce SM. Collateral capillary arterialization following arteriolar ligation in murine skeletal muscle. **Microcirculation**. 2010; 17(5):333−347. https://doi.org/10.1111/j.1549-8719.2010.00034.x.

27. Chien S. Mechanotransduction and endothelial cell homeostasis: the wisdom of the cell. **Am J Physiol Heart Circ Physiol**. 2007; 292(3):H1209−H1224. https://doi.org/10.1152/ajpheart.01047.2006.

28. Michiels C. Endothelial cell functions. **J Cell Physiol**. 2003; 196(3):430−443. https://doi.org/10.1002/jcp.10333.

29. Carmeliet P. Mechanisms of angiogenesis and arteriogenesis. **Nat Med**. 2000; 6(4):389−395. https://doi.org/10.1038/74651.

30. Eichmann A, Le Noble F, Autiero M, Carmeliet P. Guidance of vascular and neural network formation. **Curr Opin Neurobiol**. 2005; 15(1):108−115. https://doi.org/10.1016/j.conb.2005.01.008.

31. Gerhardt H, Golding M, Fruttiger M, et al. VEGF guides angiogenic sprouting utilizing endothelial tip cell filopodia. **J Cell Biol**. 2003; 161(6):1163−1177. https://doi.org/10.1083/jcb.200302047.

32. Jakobsson L, Franco CA, Bentley K, et al. Endothelial cells dynamically compete for the tip cell position during angiogenic sprouting. **Nat Cell Biol**. 2010; 12(10):943−953. https://doi.org/10.1038/ncb2103.

33. Chappell JC, Wiley DM, Bautch VL. Regulation of blood vessel sprouting. **Semin Cell Dev Biol**. 2011; 22(9):1005−1011. https://doi.org/10.1016/j.semcdb.2011.10.006.

34. Ribatti D, Crivellato E. "Sprouting angiogenesis", a reappraisal. **Dev Biol**. 2012; 372(2):157−165. https://doi.org/10.1016/j.ydbio.2012.09.018.

35. Gerhardt H, Betsholtz C. Endothelial-pericyte interactions in angiogenesis. **Cell Tissue Res**. 2003; 314(1):15−23. https://doi.org/10.1007/s00441-003-0745-x.

36. Li X, Sun X, Carmeliet P. Hallmarks of endothelial cell metabolism in health and disease. **Cell Metab**. 2019; 30(3):414−433. https://doi.org/10.1016/j.cmet.2019.08.011.

37. Cantelmo AR, Conradi LC, Brajic A, et al. Inhibition of the glycolytic activator PFKFB3 in endothelium induces tumor vessel normalization, impairs metastasis, and improves chemotherapy. **Cancer Cell**. 2016; 30(6):968−985. https://doi.org/10.1016/j.ccell.2016.10.006.

38. Xu Y, An X, Guo X, et al. Endothelial PFKFB3 plays a critical role in angiogenesis. **Arterioscler Thromb Vasc Biol**. 2014; 34(6):1231−1239. https://doi.org/10.1161/ATVBAHA.113.303041.

39. De Bock K, Georgiadou M, Schoors S, et al. Role of PFKFB3-driven glycolysis in vessel sprouting. **Cell**. 2013; 154(3):651−663. https://doi.org/10.1016/j.cell.2013.06.037.

40. Skalak TC, Price RJ. The role of mechanical stresses in microvascular remodeling. **Microcirculation**. 1996; 3(2):143−165. https://doi.org/10.3109/10739689609148284.

41. Milkiewicz M, Brown MD, Egginton S, Hudlicka O. Association between shear stress, angiogenesis, and VEGF in skeletal muscles *in vivo*. **Microcirculation**. 2001; 8(4):229−241. https://doi.org/10.1038/sj/mn/7800074.

42. Secomb TW. Hemodynamics. **Compr Physiol**. 2016; 6(2):975−1003. https://doi.org/10.1002/cphy.c150038.

43. Lo SK, Everitt J, Gu J, Malik AB. Tumor necrosis factor mediates experimental pulmonary edema by ICAM-1 and CD18-dependent mechanisms. **J Clin Invest**. 1992; 89(3):981−988. https://doi.org/10.1172/JCI115681.

44. Gibbs LS, Lai L, Malik AB. Tumor necrosis factor enhances the neutrophil-dependent increase in endothelial permeability. **J Cell Physiol**. 1990; 145(3):496−500. https://doi.org/10.1002/jcp.1041450315.

45. Breslin JW, Yuan SY. Involvement of RhoA and Rho kinase in neutrophil-stimulated endothelial hyperpermeability. **Am J Physiol Heart Circ Physiol**. 2004; 286(3):H1057−H1062. https://doi.org/10.1152/ajpheart.00841.2003.

46. Breslin JW, Sun H, Xu W, et al. Involvement of ROCK-mediated endothelial tension development in neutrophil-stimulated microvascular leakage. **Am J Physiol Heart Circ Physiol**. 2006; 290(2):H741−H750. https://doi.org/10.1152/ajpheart.00238.2005.

47. Breslin JW. Cellular cross talk, inflammatory signals, and enhanced microvascular permeability. **Microcirculation**. 2017; 24(3). https://doi.org/10.1111/micc.12368.

48. Bergers G, Song S. The role of pericytes in blood-vessel formation and maintenance. **Neuro Oncol**. 2005; 7(4):452−464. https://doi.org/10.1215/S1152851705000232.

49. Hamilton NB, Attwell D, Hall CN. Pericyte-mediated regulation of capillary diameter: a component of neurovascular coupling in health and disease. **Front Neuroenergetics**. 2010; 2(5). https://doi.org/10.3389/fnene.2010.00005.

50. Saunders WB, Bohnsack BL, Faske JB, et al. Coregulation of vascular tube stabilization by endothelial cell TIMP-2 and pericyte TIMP-3. **J Cell Biol**. 2006; 175(1):179−191. https://doi.org/10.1083/jcb.200603176.

51. Stratman AN, Davis GE. Endothelial cell-pericyte interactions stimulate basement membrane matrix assembly: influence on vascular tube remodeling, maturation, and stabilization. **Microsc Microanal**. 2012; 18(1):68−80. https://doi.org/10.1017/S1431927611012402.

52. Winkler EA, Sengillo JD, Bell RD, Wang J, Zlokovic BV. Blood-spinal cord barrier pericyte reductions contribute to increased capillary permeability. **J Cereb Blood Flow Metab**. 2012; 32(10):1841−1852. https://doi.org/10.1038/jcbfm.2012.113.

53. Ribatti D, Nico B, Crivellato E. The role of pericytes in angiogenesis. **Int J Dev Biol**. 2011; 55(3):261−268. https://doi.org/10.1387/ijdb.103167dr.

54. Rensen SS, Doevendans PA, van Eys GJ. Regulation and characteristics of vascular smooth muscle cell phenotypic diversity. **Neth Heart J**. 2007; 15(3):100−108. https://doi.org/10.1007/BF03085963.

55. Conway EM, Collen D, Carmeliet P. Molecular mechanisms of blood vessel growth. **Cardiovasc Res**. 2001; 49(3):507−521. https://doi.org/10.1016/s0008-6363(00)00281-9.

56. Escobales N, Crespo MJ. Oxidative-nitrosative stress in hypertension. **Curr Vasc Pharmacol**. 2005; 3(3):231−246. https://doi.org/10.2174/1570161054368643.

57. Rajendran S, Shen X, Glawe J, Kolluru GK, Kevil CG. Nitric oxide and hydrogen sulfide regulation of ischemic vascular growth and remodeling. **Compr Physiol**. 2019; 9(3):1213−1247. https://doi.org/10.1002/cphy.c180026.

58. Katakam PV, Snipes JA, Steed MM, Busija DW. Insulin-induced generation of reactive oxygen species and uncoupling of nitric oxide synthase underlie the cerebrovascular insulin resistance in obese rats. **J Cereb Blood Flow Metab**. 2012; 32(5):792−804. https://doi.org/10.1038/jcbfm.2011.181.

59. Katakam PV, Tulbert CD, Snipes JA, Erdös B, Miller AW, Busija DW. Impaired insulin-induced vasodilation in small coronary

arteries of Zucker obese rats is mediated by reactive oxygen species. **Am J Physiol Heart Circ Physiol**. 2005; 288(2):H854−H860. https://doi.org/10.1152/ajpheart.00715.2004.

60. Kovacs L, Cao Y, Han W, et al. PFKFB3 in smooth muscle promotes vascular remodeling in pulmonary arterial hypertension. **Am J Respir Crit Care Med**. 2019; 200(5):617−627. https://doi.org/10.1164/rccm.201812-2290OC.

61. Sure VN, Sakamuri SSVP, Sperling JA, et al. A novel high-throughput assay for respiration in isolated brain microvessels reveals impaired mitochondrial function in the aged mice. **Geroscience**. 2018; 40(4):365−375. https://doi.org/10.1007/s11357-018-0037-8.

62. Busija DW, Rutkai I, Dutta S, Katakam PV. Role of mitochondria in cerebral vascular function: energy production, cellular protection, and regulation of vascular tone. **Compr Physiol**. 2016; 6(3):1529−1548. https://doi.org/10.1002/cphy.c150051.

63. Katakam PV, Domoki F, Snipes JA, Busija AR, Jarajapu YP, Busija DW. Impaired mitochondria-dependent vasodilation in cerebral arteries of Zucker obese rats with insulin resistance. **Am J Physiol Regul Integr Comp Physiol**. 2009; 296(2):R289−R298. https://doi.org/10.1152/ajpregu.90656.2008.

64. Katakam PV, Gordon AO, Sure VN, Rutkai I, Busija DW. Diversity of mitochondria-dependent dilator mechanisms in vascular smooth muscle of cerebral arteries from normal and insulin-resistant rats. **Am J Physiol Heart Circ Physiol**. 2014; 307(4):H493−H503.

65. Martinez FO, Gordon S. The M1 and M2 paradigm of macrophage activation: time for reassessment. **F1000Prime Rep**. 2014; 6:13. https://doi.org/10.12703/P6-13.

66. Mills CD, Lenz LL, Ley K. Macrophages at the fork in the road to health or disease. **Front Immunol**. 2015; 6:59. https://doi.org/10.3389/fimmu.2015.00059.

67. Rőszer T. Understanding the mysterious M2 macrophage through activation markers and effector mechanisms. **Mediators Inflamm**. 2015; 2015:816460. https://doi.org/10.1155/2015/816460.

68. Bruce AC, Kelly-Goss MR, Heuslein JL, Meisner JK, Price RJ, Peirce SM. Monocytes are recruited from venules during arteriogenesis in the murine spinotrapezius ligation model. **Arterioscler Thromb Vasc Biol**. 2014; 34(9):2012−2022. https://doi.org/10.1161/ATVBAHA.114.303399.

69. Ley K, Laudanna C, Cybulsky MI, Nourshargh S. Getting to the site of inflammation: the leukocyte adhesion cascade updated. **Nat Rev Immunol**. 2007; 7(9):678−689. https://doi.org/10.1038/nri2156.

70. Robichaux JL, Tanno E, Rappleye JW, et al. Lymphatic/Blood endothelial cell connections at the capillary level in adult rat mesentery. **Anat Rec**. 2010; 293(10):1629−1638. https://doi.org/10.1002/ar.21195.

71. Breslin JW, Yang Y, Scallan JP, Sweat RS, Adderley SP, Murfee WL. Lymphatic vessel network structure and physiology. **Compr Physiol**. 2018; 9(1):207−299. https://doi.org/10.1002/cphy.c180015.

72. Sweat RS, Stapor PC, Murfee WL. Relationships between lymphangiogenesis and angiogenesis during inflammation in rat mesentery microvascular networks. **Lymphat Res Biol**. 2012; 10(4):198−207. https://doi.org/10.1089/lrb.2012.0014.

73. Lopez Gelston CA, Balasubbramanian D, Abouelkheir GR, et al. Enhancing renal lymphatic expansion prevents hypertension in mice. **Circ Res**. 2018; 122(8):1094−1101. https://doi.org/10.1161/CIRCRESAHA.118.312765.

74. Kneedler SC, Phillips LE, Hudson KR, et al. Renal inflammation and injury are associated with lymphangiogenesis in hypertension. **Am J Physiol Renal Physiol**. 2017; 312(5):F861−F869. https://doi.org/10.1152/ajprenal.00679.2016.

75. Martel C, Li W, Fulp B, et al. Lymphatic vasculature mediates macrophage reverse cholesterol transport in mice. **J Clin Invest**. 2013; 123(4):1571−1579. https://doi.org/10.1172/JCI63685.

76. Ungvari Z, Tarantini S, Kiss T, et al. Endothelial dysfunction and angiogenesis impairment in the ageing vasculature. **Nat Rev Cardiol**. 2018; 15(9):555−565. https://doi.org/10.1038/s41569-018-0030-z.

77. Murfee WL, Schmid-Schönbein GW. Chapter 12. Structure of microvascular networks in genetic hypertension. **Methods Enzymol**. 2008; 444:271−284. https://doi.org/10.1016/S0076-6879(08)02812-7.

78. Hutchins PM, Darnell AE. Observations of a decreased number of small arterioles in spontaneously hypertensive rats. **Circ Res**. 1974; 34−35(suppl 1):161−165.

79. Noon JP, Walker BR, Webb DJ, et al. Impaired microvascular dilatation and capillary rarefaction in young adults with a predisposition to high blood pressure. **J Clin Invest**. 1997; 99(8):1873−1879. https://doi.org/10.1172/JCI119354.

80. Suematsu M, Suzuki H, Delano FA, Schmid-Schönbein GW. The inflammatory aspect of the microcirculation in hypertension: oxidative stress, leukocytes/endothelial interaction, apoptosis. **Microcirculation**. 2002; 9(4):259−276. https://doi.org/10.1038/sj.mn.7800141.

81. Yang M, Murfee WL. The effect of microvascular pattern alterations on network resistance in spontaneously hypertensive rats. **Med Biol Eng Comput**. 2012; 50(6):585−593. https://doi.org/10.1007/s11517-012-0912-x.

82. Schmid-Schönbein GW, Zweifach BW, DeLano FA, Chen PC. Microvascular tone in a skeletal muscle of spontaneously hypertensive rats. **Hypertension**. 1987; 9(2):164−171. https://doi.org/10.1161/01.hyp.9.2.164.

83. Suzuki H, Zweifach BW, Schmid-Schönbein GW. Dependence of elevated mesenteric arteriolar tone on glucocorticoids in spontaneously hypertensive rats. **Int J Microcirc Clin Exp**. 1995; 15(6):309−315. https://doi.org/10.1159/000179080.

84. Suzuki H, Zweifach BW, Schmid-Schönbein GW. Glucocorticoid modulates vasodilator response of mesenteric arterioles in spontaneously hypertensive rats. **Hypertension**. 1996; 27(1):114−118. https://doi.org/10.1161/01.hyp.27.1.114.

85. Henrich H, Hertel R, Assmann R. Structural differences in the mesentery microcirculation between normotensive and spontaneously hypertensive rats. **Pflugers Arch**. 1978; 375(2):153−159. https://doi.org/10.1007/BF00584238.

86. Yang M, Aragon M, Murfee WL. Angiogenesis in mesenteric microvascular networks from spontaneously hypertensive versus normotensive rats. **Microcirculation**. 2011; 18(7):574−582. https://doi.org/10.1111/j.1549-8719.2011.00117.x.

87. Sweat RS, Sloas DC, Stewart SA, et al. Aging is associated with impaired angiogenesis, but normal microvascular network structure, in the rat mesentery. **Am J Physiol Hear Circ Physiol**. 2017; 312(2):H275−H284. https://doi.org/10.1152/ajpheart.00200.2016.

88. Hodges NA, Suarez-Martinez AD, Murfee WL. Understanding angiogenesis during aging: opportunities for discoveries and new models. **J Appl Physiol**. 2018; 125(6):1843−1850. https://doi.org/10.1152/japplphysiol.00112.2018.

89. Bell RD, Winkler EA, Sagare AP, et al. Pericytes control key neurovascular functions and neuronal phenotype in the adult brain and during brain aging. **Neuron**. 2010; 68(3):409−427. https://doi.org/10.1016/j.neuron.2010.09.043.

90. Toth P, Tucsek Z, Sosnowska D, et al. Age-related autoregulatory dysfunction and cerebromicrovascular injury in mice with angiotensin II-induced hypertension. **J Cereb Blood Flow Metab**. 2013; 33(11):1732−1742. https://doi.org/10.1038/jcbfm.2013.143.

91. Hughes S, Gardiner T, Hu P, Baxter L, Rosinova E, Chan-Ling T. Altered pericyte-endothelial relations in the rat retina during aging: implications for vessel stability. **Neurobiol Aging**. 2006; 27(12):1838−1847. https://doi.org/10.1016/j.neurobiolaging.2005.10.021.

92. Kador PF, Takahashi Y, Akagi Y, Blessing K, Randazzo J, Wyman M. Age-dependent retinal capillary pericyte degeneration in galactose-fed dogs. **J Ocul Pharmacol Ther**. 2007; 23(1):63−69. https://doi.org/10.1089/jop.2006.0069.

93. Herman IM, Jacobson S. In situ analysis of microvascular pericytes in hypertensive rat brains. **Tissue Cell**. 1988; 20(1):1−12. https://doi.org/10.1016/0040-8166(88)90002-x.

94. Wallow IH, Bindley CD, Reboussin DM, Gange SJ, Fisher MR. Systemic hypertension produces pericyte changes in retinal capillaries. **Invest Ophthalmol Vis Sci**. 1993; 34(2):420−430.

95. Peyster E, Chen J, Feldman HI, et al. Inflammation and arterial stiffness in chronic kidney disease: findings from the CRIC study. **Am J Hypertens**. 2017; 30(4):400−408. https://doi.org/10.1093/ajh/hpw164.

96. Kaiser R, Frantz C, Bals R, Wilkens H. The role of circulating thrombospondin-1 in patients with precapillary pulmonary hypertension. **Respir Res**. 2016; 17(1):96. https://doi.org/10.1186/s12931-016-0412-x.

97. Anderson CR, Hastings NE, Blackman BR, Price RJ. Capillary sprout endothelial cells exhibit a CD36 low phenotype: regulation by shear stress and vascular endothelial growth factor-induced mechanism for attenuating anti-proliferative thrombospondin-1 signaling. **Am J Pathol**. 2008; 173(4):1220−1228. https://doi.org/10.2353/ajpath.2008.071194.

98. Tran ED, Yang M, Chen A, Delano FA, Murfee WL, Schmid-Schönbein GW. Matrix metalloproteinase activity causes VEGFR-2 cleavage and microvascular rarefaction in rat mesentery. **Microcirculation**. 2011; 18(3):228−237. https://doi.org/10.1111/j.1549-8719.2011.00082.x.

99. Fukuda M, Miyamoto K, Hasegawa Y, et al. Isolation of bovine follicular fluid inhibin of about 32 kDa. **Mol Cell Endocrinol**. 1986; 44(1):55−60. https://doi.org/10.1016/0303-7207(86)90105-x.

100. Climie RE, Gallo A, Picone DS, et al. Measuring the interaction between the macro- and micro-vasculature. **Front Cardiovasc Med**. 2019; 6:169. https://doi.org/10.3389/fcvm.2019.00169.

101. Mitchell GF. Effects of central arterial aging on the structure and function of the peripheral vasculature: implications for end-organ damage. **J Appl Physiol**. 2008; 105(5):1652−1660. https://doi.org/10.1152/japplphysiol.90549.2008.

102. Laurent S, Boutouyrie P. The structural factor of hypertension: large and small artery alterations. **Circ Res**. 2015; 116(6):1007−1021. https://doi.org/10.1161/CIRCRESAHA.116.303596.

103. Climie RED, Picone DS, Blackwood S, et al. Pulsatile interaction between the macro-vasculature and micro-vasculature: proof-of-concept among patients with type 2 diabetes. **Eur J Appl Physiol**. 2018; 118(11):2455−2463. https://doi.org/10.1007/s00421-018-3972-2.

104. Urbancic-Rovan V, Bernjak A, Stefanovska A, Azman-Juvan K, Kocijancic A. Macro- and microcirculation in the lower extremities–possible relationship. **Diabetes Res Clin Pract**. 2006; 73(2):166−173. https://doi.org/10.1016/j.diabres.2006.01.002.

105. Mitchell GF, van Buchem MA, Sigurdsson S, et al. Arterial stiffness, pressure and flow pulsatility and brain structure and function: the age, gene/environment susceptibility–Reykjavik study. **Brain**. 2011; 134(Pt 11):3398−3407. https://doi.org/10.1093/brain/awr253.

106. Ganesan P, He S, Xu H. Modelling of pulsatile blood flow in arterial trees of retinal vasculature. **Med Eng Phys**. 2011; 33(7):810−823. https://doi.org/10.1016/j.medengphy.2010.10.004.

107. Gonzales AL, Klug NR, Moshkforoush A, et al. Contractile pericytes determine the direction of blood flow at capillary junctions. **Proc Natl Acad Sci USA**. 2020; 117(43):27022−27033. https://doi.org/10.1073/pnas.1922755117.

108. Alarcon-Martinez L, Yilmaz-Ozcan S, Yemisci M, et al. Capillary pericytes express α-smooth muscle actin, which requires prevention of filamentous-actin depolymerization for detection. **Elife**. 2018; 7:e34861. https://doi.org/10.7554/eLife.34861.

109. O'Farrell FM, Mastitskaya S, Hammond-Haley M, Freitas F, Wah WR, Attwell D. Capillary pericytes mediate coronary no-reflow after myocardial ischaemia. **Elife**. 2017; 6:e29280. https://doi.org/10.7554/eLife.29280.

110. Stapor PC, Wang W, Murfee WL, Khismatullin DB. The distribution of fluid shear stresses in capillary sprouts. **Cardiovasc Eng Technol**. 2011; 2(2):124−136. https://doi.org/10.1007/s13239-011-0041-y.

111. Song JW, Munn LL. Fluid forces control endothelial sprouting. **Proc Natl Acad Sci USA**. 2011; 108(37):15342−15347. https://doi.org/10.1073/pnas.1105316108.

112. Galie PA, Nguyen DH, Choi CK, Cohen DM, Janmey PA, Chen CS. Fluid shear stress threshold regulates angiogenic sprouting. **Proc Natl Acad Sci USA**. 2014; 111(22):7968−7973. https://doi.org/10.1073/pnas.1310842111.

113. Dai G, Kaazempur-Mofrad MR, Natarajan S, et al. Distinct endothelial phenotypes evoked by arterial waveforms derived from atherosclerosis-susceptible and -resistant regions of human vasculature. **Proc Natl Acad Sci USA**. 2004; 101(41):14871−14876. https://doi.org/10.1073/pnas.0406073101.

114. Davies PF. Flow-mediated endothelial mechanotransduction. **Physiol Rev**. 1995; 75(3):519−560. https://doi.org/10.1152/physrev.1995.75.3.519.

115. Zhou A, Egginton S, Hudlická O, Brown MD. Internal division of capillaries in rat skeletal muscle in response to chronic vasodilator treatment with alpha1-antagonist prazosin. **Cell Tissue Res**. 1998; 293(2):293−303.

116. Tardy Y, Resnick N, Nagel T, Gimbrone Jr MA, Dewey Jr CF. Shear stress gradients remodel endothelial monolayers in vitro via a cell proliferation-migration-loss cycle. **Arterioscler Thromb Vasc Biol**. 1997; 17(11):3102−3106. https://doi.org/10.1161/01.atv.17.11.3102.

117. Chen BP, Li YS, Zhao Y, et al. DNA microarray analysis of gene expression in endothelial cells in response to 24-h shear stress. **Physiol Genomics**. 2001; 7(1):55−63. https://doi.org/10.1152/physiolgenomics.2001.7.1.55.

118. DePaola N, Gimbrone Jr MA, Davies PF, Dewey Jr CF. Vascular endothelium responds to fluid shear stress gradients. **Arterioscler**

Thromb. 1992; 12(11):1254−1257. https://doi.org/10.1161/01.atv.12.11.1254 [Published correction appears in Arterioscler Thromb 1993 Mar;13(3):465].

119. Meza D, Musmacker B, Steadman E, Stransky T, Rubenstein DA, Yin W. Endothelial cell biomechanical responses are dependent on both fluid shear stress and tensile strain. **Cell Mol Bioeng**. 2019; 12(4):311−325. https://doi.org/10.1007/s12195-019-00585-0.

120. Colgan OC, Ferguson G, Collins NT, et al. Regulation of bovine brain microvascular endothelial tight junction assembly and barrier function by laminar shear stress. **Am J Physiol Heart Circ Physiol**. 2007; 292(6):H3190−H3197. https://doi.org/10.1152/ajpheart.01177.2006.

121. Garcia-Polite F, Martorell J, Del Rey-Puech P, et al. Pulsatility and high shear stress deteriorate barrier phenotype in brain microvascular endothelium. **J Cereb Blood Flow Metab**. 2017; 37(7):2614−2625. https://doi.org/10.1177/0271678X16672482.

122. Gongol B, Marin T, Zhang J, et al. Shear stress regulation of miR-93 and miR-484 maturation through nucleolin. **Proc Natl Acad Sci USA**. 2019; 116(26):12974−12979. https://doi.org/10.1073/pnas.1902844116.

123. Kadohama T, Nishimura K, Hoshino Y, Sasajima T, Sumpio BE. Effects of different types of fluid shear stress on endothelial cell proliferation and survival. **J Cell Physiol**. 2007; 212(1):244−251. https://doi.org/10.1002/jcp.21024.

124. Sun N, Ning B, Bruce AC, et al. *In vivo* imaging of hemodynamic redistribution and arteriogenesis across microvascular network. **Microcirculation**. 2020; 27(3):e12598. https://doi.org/10.1111/micc.12598.

125. Keller 4th TC, Butcher JT, Broseghini-Filho GB, et al. Modulating vascular hemodynamics with an alpha globin mimetic peptide (HbαX). **Hypertension**. 2016; 68(6):1494−1503. https://doi.org/10.1161/HYPERTENSIONAHA.116.08171.

126. Murfee WL, Sweat RS, Tsubota K, Mac Gabhann F, Khismatullin D, Peirce SM. Applications of computational models to better understand microvascular remodelling: a focus on biomechanical integration across scales. **Interface Focus**. 2015; 5(2):20140077.

127. Walpole J, Chappell JC, Cluceru JG, Mac Gabhann F, Bautch VL, Peirce SM. Agent-based model of angiogenesis simulates capillary sprout initiation in multicellular networks. **Integr Biol**. 2015; 7(9):987−997. https://doi.org/10.1039/c5ib00024f.

128. Walpole J, Mac Gabhann F, Peirce SM, Chappell JC. Agent-based computational model of retinal angiogenesis simulates microvascular network morphology as a function of pericyte coverage. **Microcirculation**. 2017; 24(8). https://doi.org/10.1111/micc.12393.

129. Miller VM. Sex-based differences in vascular function. **Womens Health**. 2010; 6(5):737−752. https://doi.org/10.2217/whe.10.53.

130. Docherty CK, Harvey KY, Mair KM, Griffin S, Denver N, MacLean MR. The role of sex in the pathophysiology of pulmonary hypertension. **Adv Exp Med Biol**. 2018; 1065:511−528. https://doi.org/10.1007/978-3-319-77932-4_31. PMID: 30051404.

131. Ogola BO, Zimmerman MA, Clark GL, et al. New insights into arterial stiffening: does sex matter? **Am J Physiol Heart Circ Physiol**. 2018; 315(5):H1073−H1087. https://doi.org/10.1152/ajpheart.00132.2018.

This page intentionally left blank

Chapter 13

Myocardial function: from myofilaments to cardiac pump

André P. Lourenço[1,2], Thierry C. Gillebert[3] and Adelino F. Leite-Moreira[1,4]

[1]Department of Surgery and Physiology, Cardiovascular Research Centre, Faculty of Medicine of the University of Porto, Porto, Portugal;
[2]Department of Anaesthesiology, São João Hospital Centre, Porto, Portugal; [3]Department of Cardiology, Ghent University and Ghent University
Hospital, Ghent, Belgium; [4]Department of Cardiothoracic Surgery, São João Hospital Centre, Porto, Portugal

The heart is an amazing organ. The heart and cardiovascular system have evolved to overcome the limitations of diffusion ensuring adequate supply of nutrients and oxygen to tissues while providing a route for homeostatic communication between major organ systems. From ontogenesis and embryogenesis, the heart's structure has progressively evolved to fully match *the organism's functional needs* as a highly resilient and enduring pump system that not only ensures its self-supply but also extensive communication with all bodily systems through the vasculature. *Self-supply* through the coronary circulation is closely matched to requirements through local metabolic regulation. In homeothermic air-breathing animals, the cardiovascular system has evolved to a system in series circulation, with the heart fully divided into left and right sides, for systemic and pulmonary pumping, respectively. The highly compliant and vast low-pressure pulmonary circulation interacts with the lungs for achieving full oxygenation and continuous renewal of oxygen carrying capacity. Cardiac output is the main driver of renal filtration and urine output, while renal feedback guarantees effective circulating volume through regulation of sodium balance. The heart provides *steady perfusion to all systems*, in particular the gastrointestinal tract from which it retrieves nutrients, the musculoskeletal and nervous systems to which it provides oxygen and nutrients and from which it effectively clears catabolites, and the kidneys which are perfused in order to promote glomerular filtration. As an efficient system that overcomes the limitations of diffusion, the cardiovascular system not only carries oxygen, nutrients, and catabolites but also brings all organs and tissues into close proximity as carrier of endocrine mediators and intercellular signaling molecules such as cytokines, growth factors, and adipokines. Unsurprisingly, the heart itself is quite active as an *endocrine organ*, and its function and structure are extensively influenced by endocrine mechanisms.[1] The heart integrates neural input through vagal and sympathetic fibers. Finally, the cardiovascular system provides an entry port and means of spread to the hematopoietic system.

The heart is an adaptive pump

The heart as a pump adapts and remodels to meet body demands throughout lifetime but eventually fails with aging and lifelong insults. All these mechanisms are finely tuned and enable *extraordinary adaptions throughout lifetime*. The fetal-to-neonatal transition courses with fast structural, metabolic, and functional changes that suddenly enable adaption to an active respiratory system while pregnancy and long-term adaptions to exercise training also involve slower but substantial structural and functional remodeling. Acute adaptions to various forms of stress are also outstanding and further highlight the role of regulatory mechanisms, such as neurohumoral adaptations.

Despite their remarkable durability, the cardiac pump and the cardiovascular system eventually wear out with aging. Atherosclerosis, loss of elastic content, altered and increasing fibrosis, decreased metabolic flexibility and impaired organelle, cell and tissue repair, and turnover mechanisms ultimately have a toll on the ability to cope with demands. *Decreased cardiovascular reserve* is one of the major components of human senescence. In today's developed world societies, improved healthcare has sustainedly increased longevity while work and social habits dictated sedentary lifestyles and unhealthy diets. Predictably, the population ages and the prevalence of obesity, systemic arterial hypertension, and diabetes mellitus are

higher. These and other comorbidities drive adverse cardiovascular remodeling, further impairing cardiovascular reserve in a growing number of individuals. *Heart failure with preserved ejection fraction (HFpEF)* is an example of impaired cardiovascular reserve, combined with alterations of renal, muscular, and pulmonary function (among various other abnormalities).[2] In the aging population, the health toll of HFpEF now outweighs that of classical heart failure with reduced ejection fraction (HFrEF). Improved health care and prompt interventions for ischemic heart disease substantially reduced the number of patients that overcome extensive myocyte loss due to ischemic insults with left ventricular (LV) dilation and decreased ejection fraction.

Cardiac structure is tightly coupled to function

The heart is composed of *intertwined sheaths of myocardial tissue* interspersed with coronary vessels. Myocardial tissue is mainly composed of striated muscle cast into a thin mold of connective support tissue. Unlike skeletal myocytes, cardiomyocytes act like a *functional syncytium* both in electrical and mechanical terms; cardiomyocytes show complex branching patterns and (mainly) top-to-top mechanical and electrical connections between themselves through specialized cell membrane domains, the intercalated disks, where gap junctions concentrate. Highly organized high-order macromolecular structures arranged in tandem, with top-to-top connections at Z-lines, the sarcomeres, confer the typical striated appearance to cardiomyocytes on histological examination. Sarcomere length under physiological conditions ranges from 1.6 to 2.2 μm. Sarcomeres are composed by partly overlapping thin and thick filaments essentially formed by *actin and myosin* proteins, respectively, combined with other structural and regulator proteins. One of these proteins, *titin*, stands out because of its giant size and filamentous structure that bridges the span of half a sarcomere, connecting thick filaments to Z-lines. It constitutes an essential structural scaffold that stabilizes actin-myosin interaction as well as a key regulator of myocardial passive properties, namely compliance.[3]

Action potentials and contraction arise at an intrinsic pace, which is modulated by the autonomic nervous system and neuroendocrine influences but is fully independent from central somatic neural input. A small subset of cardiomyocytes, the *conduction system*, specializes to evoke and convey action potentials eliciting synchronized patterns of myocardial contraction that maximize cardiac chamber pump performance.

Moreover, a specialized connective tissue structure, the *fibrous skeleton*, completely separates thin-walled highly compliant chambers, the left and right atria (that receive venous return from the pulmonary and systemic circulations,
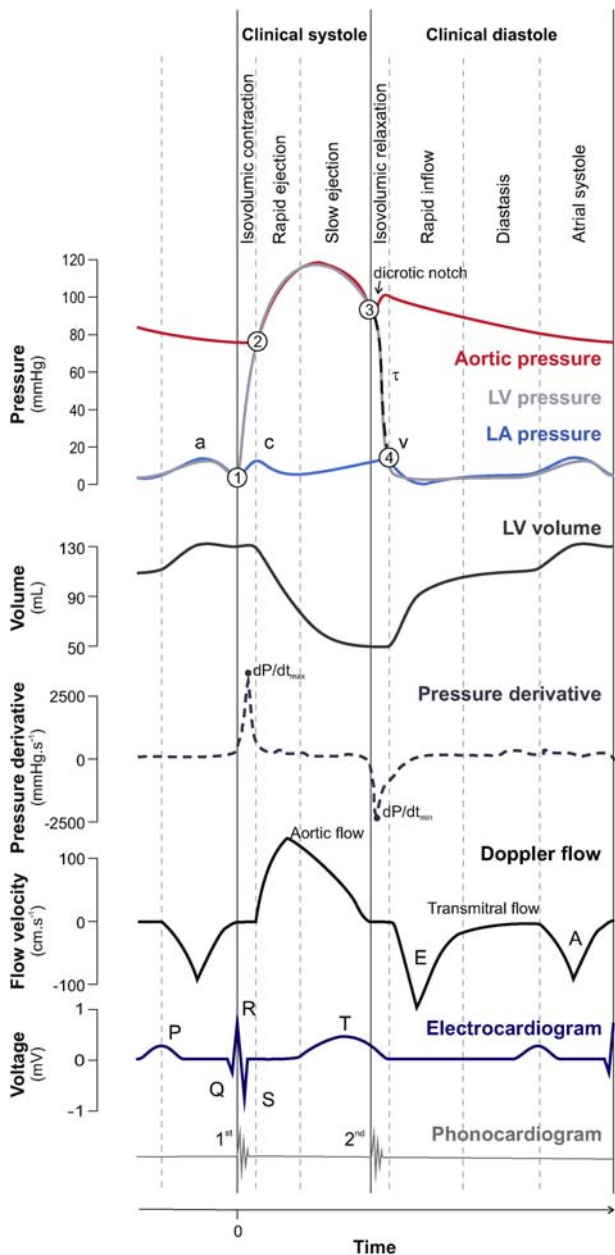
respectively), from thicker-walled LV and right ventricular (RV) chambers (that do most of the pumping into the systemic and pulmonary arteries). Atrial and ventricular contraction are coordinated so that ventricular contraction only starts upon maximal filling following atrial ejection. Indeed, atria contract upon spreading of action potentials generated at the sinus node, the natural highest-frequency pacemaker in cardiac conduction tissue, but transmission to the ventricles is delayed at the unique gateway connecting atria and ventricles through the fibrous skeleton, the atrioventricular node. The spread of the action potential within ventricles is governed by fast-conducting Purkinje cells arranged in thick bundles that ramify throughout the endocardial surface. The fast and sequential pattern of activation ensures maximal performance by first activating the interventricular septum and subendocardial papillary muscles (the myocardial extensions that connect through chordae tendineae to the atrioventricular valves), and only then producing synchronous torsional free-wall contraction of both ventricles from the apex toward the base. This provides a stable support axis and prevents valve prolapse.

The RV is thinner and more compliant than the LV, and is well adapted to accommodate fluctuations in venous return and to pump blood into a low resistance and likewise highly compliant pulmonary circulation. RV geometry clearly distinguishes a saccular body reservoir and an outflowtract infundibulum. The saccular body contracts first through a bellows-like movement that brings the free-wall close to the interventricular septum ejecting through the outflow tract infundibulum, which contracts in a peristaltic-like movement.[4] Quite distinctly, the LV's shape is close to elliptical and its wall is thicker, holding an extra layer of obliquely oriented myocardial fibers. LV contraction proceeds from apex to base, toward the aortic valve, and is aided by a twisting movement that further helps to reduce circumference and longitudinal axis against the high-resistance systemic circulation. Upon ventricular contraction, thin semilunar aortic and pulmonary valves prevent reflow from the arteries back to the heart.

The cardiac cycle

In this chapter, we provide a general review of the cardiac cycle and mechanisms of myocardial contraction and relaxation. Chapter 14 deals with these processes, more specifically as they relate to systolic-diastolic coupling.

The cardiac cycle (Fig. 13.1) is the sequence of events in each heartbeat.[5] The normal cardiac cycle relies on repeated and sequential twitch activations of cardiac chambers' muscle cells and competent cardiac valves for directing flow and for separating low from high pressures. The LV swiftly alternates organ perfusion at high pressures with filling from pulmonary vessels at low pressures. When the sinus node fires, a wave of depolarization is spread through the atria, which is captured on the

FIGURE 13.1 The cardiac cycle according to Wiggers. Synchronous electrical, hemodynamic, and auscultatory features of a cardiac cycle illustrated for the left ventricle (LV). Timings of valve opening and closure are represented by: (1) mitral valve closure, (2) aortic valve opening, (3) aortic valve closure, and (4) mitral valve opening. Signals are color coded. Main features of each signal are represented: the dicrotic notch in aortic pressure tracing, the a (atrial contraction), c (ventricular contraction), and v (venous filling) waves in the left atrial (LA) pressure tracing, the peak rates of LV pressure rise (dP/dt_{max}) and fall (dP/dt_{min}), the E (early) and A (atrial) waves in transmitral flow, the P, QRS and T waves of the electrocardiogram and the first and second heart sounds. Transaortic and transmitral Doppler flow signals are aligned and merged. The dashed region of LV pressure fall between (3) and (4) is used to derive the time constant of LV relaxation, τ.

electrocardiogram as the P wave; this depolarization leads to *atrial contraction*, extra flow to and filling of the ventricles through the atrioventricular valves (identified as an A, or atrial, wave on transmitral or transtricuspid Doppler flow), leading to maximum end-diastolic ventricular volume. The fourth heart sound S_4 (not shown) is due to deceleration of blood flow after atrial contraction.[6] Conduction is delayed at the atrioventricular node, for allowing ventricular contraction to be delayed till completion of priming by atrial contraction.
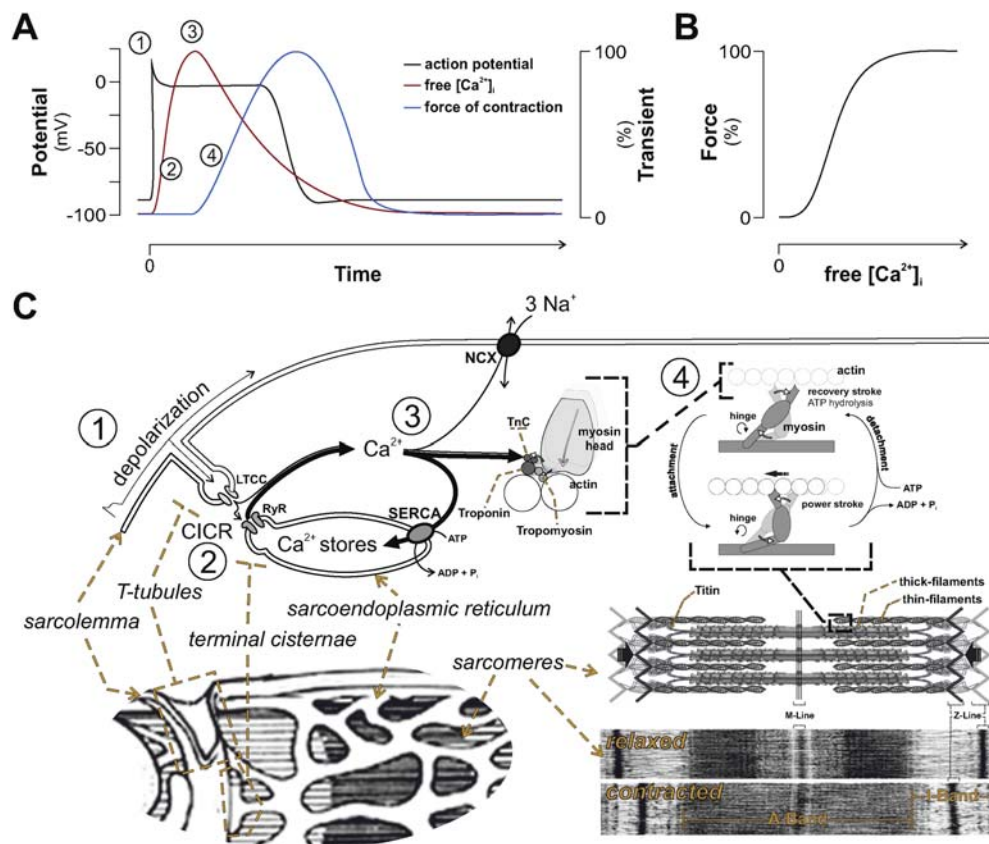
Systole follows atrial contraction. Depolarization quickly spreads through the specialized conduction system to both ventricles in a typical pattern that yields the QRS wave complex in the electrocardiogram and elicits ventricular contraction; atrioventricular valve closure prevents reflow to the atria and ventricular pressure briskly rises (electromechanical coupling). This pressure rise marks the beginning of mechanical systole and a distinctive sound related to atrioventricular valve closure can be heard on cardiac auscultation as the first heart sound (S_1). The upstroke in ventricular pressure initially proceeds without ejection. As soon as ventricular pressure exceeds arterial pressure, fast ejection into the aortic root is initiated. Ejection work and arterial flow carry on while active crossbridges keep cycling and even beyond the start of active relaxation and crossbridge inactivation. The transition from muscular contraction to relaxation occurs early during the ejection phase (see later).[7] At mid-ejection, the pressure gradient reverses, aortic pressure exceeds LV pressure, but flow into the aortic root still continues. This continuing flow results from inertia or kinetic energy imparted to blood flow by ventricular contraction, and is known as the momentum of blood flow.[8] During systole, ventricular volumes decrease from maximal end-diastolic to minimum end-systolic volume. The volume ejected during each systole, which is stroke volume, is transferred to the arterial side of the circulation. While part of it flows to tissues, another part is accommodated by the elastic components of big arteries with pressure build-up and storage of volume. Flow velocity however decreases during the late and slow ejection phase. The build-up in arterial pressure that now surpasses decaying ventricular pressure soon offsets the kinetic energy (inertia) of ejection and eventually leads to semilunar valve closure to prevent reflow to the ventricles. This marks end-systole and the transition to clinical diastole, which is signaled by a distinctive second heart sound on cardiac auscultation (S_2). While the heart sounds S_1 and S_2 are commonly believed to be caused by closing of valves, most investigators now agree that cardiac sounds result from vibrations of cardiac structures produced by acceleration or deceleration of blood flow.[6,9]

Then comes *diastole*. Upon semilunar valve closure, which is characterized by a dicrotic notch on arterial pulse, flow to peripheral circulation continues, being driven by inertia of blood flow combined with elastic recoil of big arteries. Pressure and flow decay to diastolic blood pressure levels, until next atrial contraction and ventricular ejection. Diastole proceeds in the ventricles and active relaxation mechanisms steeply decrease pressure during isovolumic relaxation. Nevertheless, ventricular filling only starts when atrial pressure overcomes ventricular pressure thereby opening the atrioventricular valves. Active relaxation forces fuel a strong atrioventricular pressure gradient that promotes a rapid-ventricular filling phase (sometimes termed suction) which can be tracked by a distinctive dominant E (early) wave in transmitral Doppler flow measurements and is responsible for most of ventricular filling.[10] Initial rapid filling is driven by a pressure gradient from atrium to ventricle. Thereafter, fast filling keeps occurring despite a slight reversed gradient and is driven by inertia.[11] This is quite similar to what happens during ejection. The third heart sound S_3 (not shown) is caused by deceleration of blood flow at the end of rapid filling.[6] This is usually followed by a period of pressure equalization between atria and ventricle and a slow filling phase of passive filling (diastasis), until a new atrial contraction originates from pacemaker activity. These events take place in right and LV chambers but not entirely synchronously. Since the sinus node is in the right atrium, right atrial systole slightly precedes left atrial systole. In contrast, there is a minor delay in RV contraction compared with LV contraction. As afterload is much lower in the pulmonary circulation, the onset of relaxation occurs earlier in the RV.

Electromechanical coupling

Within the cardiomyocyte, action potentials propagate through sarcolemmal invaginations, the T (transverse) tubules. L(long-lasting) calcium channels in the T-tubules mediate a brisk minor calcium inflow. In close vicinity with the T-tubules, type II ryanodine receptors calcium channels in terminations from the sarcoendoplasmic reticulum, the terminal cisternae, release large sarcoendoplasmic reticulum calcium stores open upon sensing calcium inflow (calcium-induced). This calcium transient activates the myofilaments, eliciting force development and cell-shortening (*electromechanical transduction*).[12] Fig. 13.2

FIGURE 13.2   Subcellular mechanisms underlying myocardial electromechanical coupling and contraction. A graphical presentation of the time sequence of cardiomyocyte action potential, calcium transient and twitch is depicted in panel (A) Events 1−4 correspond to: (1) initial depolarization, (2) calcium-induced calcium release (CICR), (3) calcium reuptake, and (4) crossbridge cycles. The close interrelationship between cytosolic calcium levels and force of contraction is highlighted in panel (B) An illustration of molecular players in relation to ultrastructure and to events 1−4 from panel A is given in panel C, for further details refer to text. *LTCC*, L(long-lasting)-type calcium channels; *NCX*, sodium-calcium exchanger; *RyR*; ryanodine receptors; *SERCA*, sarcoendoplasmic reticulum calcium ATPase; *TnC*, troponin (C)

summarizes the mechanisms of electromechanical coupling and contraction as well as the underlying structural organization of cardiomyocytes.

Mechanisms of myocardial contraction

Reversible *multilinking between actin and myosin* is the molecular mechanism underlying contraction during calcium transients. At low cytosolic calcium concentrations, the tropomyosin-troponin complex binds to actin through troponin-I, preventing interaction with myosin whereas at high concentrations, calcium reversibly binds troponin-C inducing conformational changes that expose actin to myosin and enable activation of crossbridges. Active bridges constantly cycle from attached to detached state due to myosin's ATPase activity. Energy consumption is partly converted into conformational changes that promote myofilament sliding and sarcomere shortening.
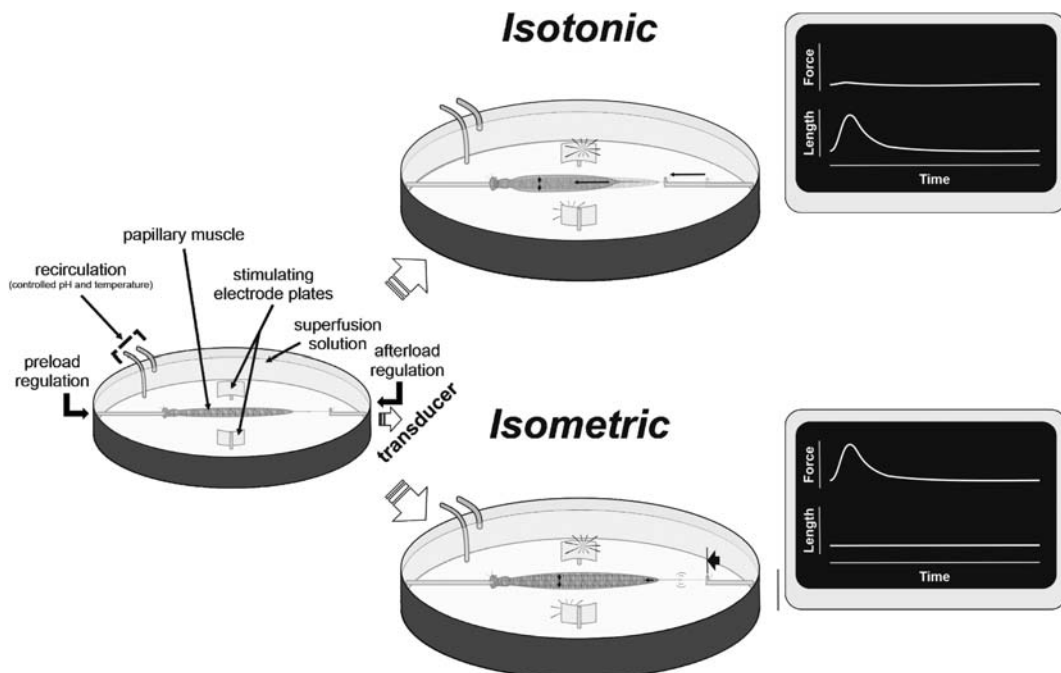
Under experimental conditions, cardiac muscle may be completely unstretched (slack length). Upon activation, when cardiac muscle is experimentally activated and unloaded, the myocardium achieves maximum shortening velocities. *In vivo*, however, cardiac chambers hold volume and thus cardiac muscle is stretched to some degree; this is usually called preload, the load that precedes contraction. Moreover, during contraction load is never null and

myofilament sliding is counteracted by load imposed on crossbridges and muscle force develops; this is called afterload, the load the muscle must bear after contraction starts. Indeed, if the muscle is not allowed to shorten at all (which occurs if for example, papillary muscles, muscle strips, or single myocytes are pinned in an experimental ex vivo setup), crossbridge cycling becomes futile and all the energy is wasted into force development; this is called an isometric contraction. Isotonic contractions are those in which shortening occurs against a constant load. The concept is illustrated in Fig. 13.3.

The major determinant of force development and myocardial shortening is the *number of actively cycling crossbridges* which in turn is dependent on the magnitude of the calcium transient, myofilament sensitivity to calcium, myosin's ATPase rate, and sarcomere length. The latter dictates both the extent of actin and myosin interaction and three-dimensional lattice spacing between them.[13]

Mechanisms of myocardial relaxation and ventricular filling

While calcium release is triggered by the action potential, repolarization by itself cannot restore cytosolic calcium levels to the relaxed state. The key determinant of calcium transient decay is sarcoendoplasmic reticulum
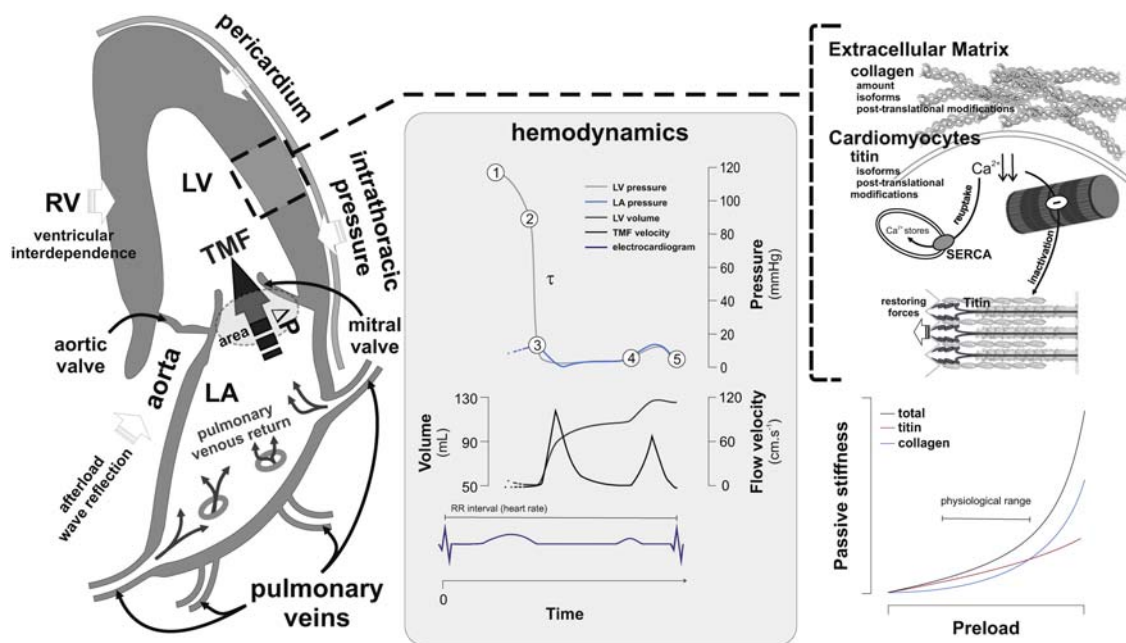
FIGURE 13.3 Isotonic and isometric contractions illustrated in the papillary muscle experimental setup. A papillary muscle quickly excised from a euthanized small laboratory animal can sustain mechanical activity ex vivo if it is provided an oxygenated nourishing superfusion solution with constant temperature and pH as well as electrical stimulation (usually set to a desired frequency). Upon fixation to connecting pins (in the picture by suture wires), its length (preload) can be adjusted. In each contraction, the transducers record both shortening (upward shift on the length tracing) and force development. If the setup is programmed with free pins, contraction approximates pure isotonic (no afterload) whereas with fixed pins contraction is purely isometric (maximum afterload, no shortening).

calcium ATPase which actively restores sarcoendoplasmic reticulum stores while resetting cytosolic calcium levels.[14] Calcium transient decay promotes crossbridge inactivation and myocardial relaxation. Of note, this starts well before the termination of ejection and semilunar valve closure that denote transition from clinical systole to diastole. Therefore, paradoxically, relaxation is an active process that already begins during early ejection well before end-systole. The mechanisms of relaxation, filling, and LV compliance are depicted in Fig. 13.4.

Although the main driver of calcium transient decay is the sarcoendoplasmic reticulum calcium ATPase, we must acknowledge that its activity is highly regulated by phospholamban along with many intracellular-signaling pathways. Likewise, other transporters such as the cell membrane sodium-calcium and sodium hydrogen exchangers, cell energy and acid-base status, molecular and mechanical determinants of crossbridge detachment, titin

and mechanical restoring forces after contraction all dictate the speed and extent of relaxation. *Ventricular filling* is not simply governed by relaxation; active relaxation prepares cardiac chambers to accommodate incoming blood flow, but the extent of inflow itself is dictated by *the completion of myocardial relaxation, the time available for diastolic filling and chamber compliance*. Chamber compliance is dependent on geometry and material properties (myocardial compliance). Myocardial compliance in turn is a function of the properties of extracellular matrix and of cardiomyocytes themselves, with titin assuming a predominant role. Additionally, external mechanical determinants such as intrathoracic pressure, pericardial restraint, and ventricular interdependence also determine filling in vivo. Indeed, ventricles demonstrate a high degree of interdependence because of their shared interventricular septum and the restraining influence of the surrounding pericardium, whose volume remains fairly constant throughout the cardiac

FIGURE 13.4 Mechanisms underlying diastole. The left hand illustration highlights *extrinsic determinants* of left ventricular (LV) diastole: (i) afterload and wave reflection that influence relaxation, (ii) the right ventricle (RV), pericardium and intrathoracic pressure that exert their influence mostly in late diastole (iii) venous return from the pulmonary circulation that acts as driving pressure for filling, (iv) the left atrium (LA) whose function as a reservoir and conduit but also as a pump late in diastole plays a crucial part in diastole as well, and, finally, (v) it is the varying pressure gradient (ΔP) throughout diastole and the area for transmitral flow (TMF) that dictates filling. The *hemodynamic aspects of diastole* are summarized in the central panel as an excerpt of Fig. 13.1. Key events are numbered: 1 is the beginning of myofilament inactivation after calcium reuptake and marks the start of physiological diastole, although no filling as yet occurred, 2 is aortic valve closure and signals the start of clinical diastole (according to heart sounds), 3 indicates mitral valve opening and actual start of LV filling, as can be tracked by TMF velocity tracings, 4 denotes the start of atrial contraction ("atrial kick"), a final contribution to LV filling, and, finally, 5 stands for end-diastole, when all forces must balance to settle LV compliance. It is between 2 and 3, during isovolumic relaxation that pressure decay without concomitant changes in volume is modeled by fitting to derive an index of myocardial relaxation, time constant τ. In this central panel, it becomes clear how tachycardia can shorten diastole with a detrimental impact on LV filling. Lastly, the *major determinants intrinsic to the myocardium* are underscored in the right panel. Briefly, while calcium reuptake by sarcoendoplasmic reticulum calcium ATPase (SERCA), myofilament inactivation, and restoring forces play a key role in relaxation and early filling, titin and collagen are the fundamental determinants of end-diastolic LV compliance. Within the physiological working range titin from cardiomyocytes plays the principal role whereas collagen may determine a steep rise in filling pressures in sudden overfilling. The incremental role of titin and collagen in determination of LV compliance and their interplay is graphically summarized in the lower right panel. Both changes in titin and collagen have been implicated in increased LV stiffness in HFpEF.

cycle. Interdependence occurs in parallel because the interventricular septum shifts toward the other cavity when pressure or volume builds-up during either systole or diastole. Interdependence also occurs in series because each ventricle's input is the other ventricle's output.

Cardiac metabolism

Cardiomyocytes sustain cyclic contraction throughout the lifespan without fatigue because their physiology is strictly adapted to aerobic metabolism favoring fatty-acids as stable energy substrates. Increased tissue demands raise cardiac power yield which raises energy expenditure but also enhances cardiac output and coronary flow. Coronary flow is further raised due to coronary arterial vasodilation mediated by catabolite build-up and endothelial mechanisms.

Cardiac performance is governed by heart rate and loading conditions

Independently from neurohumoral influences, increased heart rate enhances systolic performance, which is partly ascribed to incomplete calcium reuptake, expansion of calcium stores, and enhanced calcium transients. This is known as the *Bowditch effect* or force-frequency relationship.[15] A positive force-frequency relationship is typical of healthy myocardium and will hold for high stimulation rates ex vivo as long as metabolic needs are assured and experimental conditions sustain optimal calcium handling. *In vivo*, however, while at moderate heart rates increases, this enhances active relaxation and restoring forces enabling optimal filling, at heart rates higher than 150−160/min, this adaptation is offset by decrease in *time available to relax and fill*. When the sinus node fires rapidly, as an adaption to increased demands, cycle time decreases, but as calcium transient and contraction show only minor changes with heart rate, it is diastole that shortens. Slow filling may be substantially curtailed and atrial contraction, which normally makes a minor contribution to ventricular filling, then becomes more important because the time available for ventricular filling is limited. At rapid heart rates, atrial contraction is even superposed on rapid LV filling. This is a powerful coordination for maximizing filling during exercise. When heart rate further increases, cardiac performance gets impaired with lower output and with congestion.

Increased ventricular filling volume or preload enhances systolic performance through the *Frank−Starling* mechanism, which is partly explained by extra crossbridge recruitment due to increased calcium sensitivity and higher thin and thick filament overlap. Likewise, increased afterload, or resistance to ejection due to arterial impedance and vascular resistance also raises crossbridge activity and

cardiac performance, which is known as the *Anrep effect* or cooperative activity. Accordingly, lower afterload and decreased resistance to ejection will lead to *shortening inactivation* and enhanced myocardial relaxation. Myocardial stretch, however, also elicits a lagging slower secondary response, the slow force response, that is mediated by autocrine/paracrine mechanisms and leads to amplification of calcium transients.[16,17] Within moderate physiological ranges, increased preload or afterload also enhance relaxation and possibly compliance in the healthy myocardium.[17]

All the aforementioned feedback responses, which help increase cardiac output to meet demands, are modulated by many signaling pathways. While heart rate, preload, and afterload do have an impact on cardiac performance, myocardial functional and energetical status also determine the overall response to sudden hemodynamic stress.[18] Indeed, the failing myocardium may decrease contractile performance at higher load or higher stimulation frequency. Impaired Frank−Starling and negative force-frequency relationships are hallmarks of myocardial failure. Accordingly, relaxation may become impaired and end-diastolic pressures may rise under even moderate loading conditions in the failing heart.
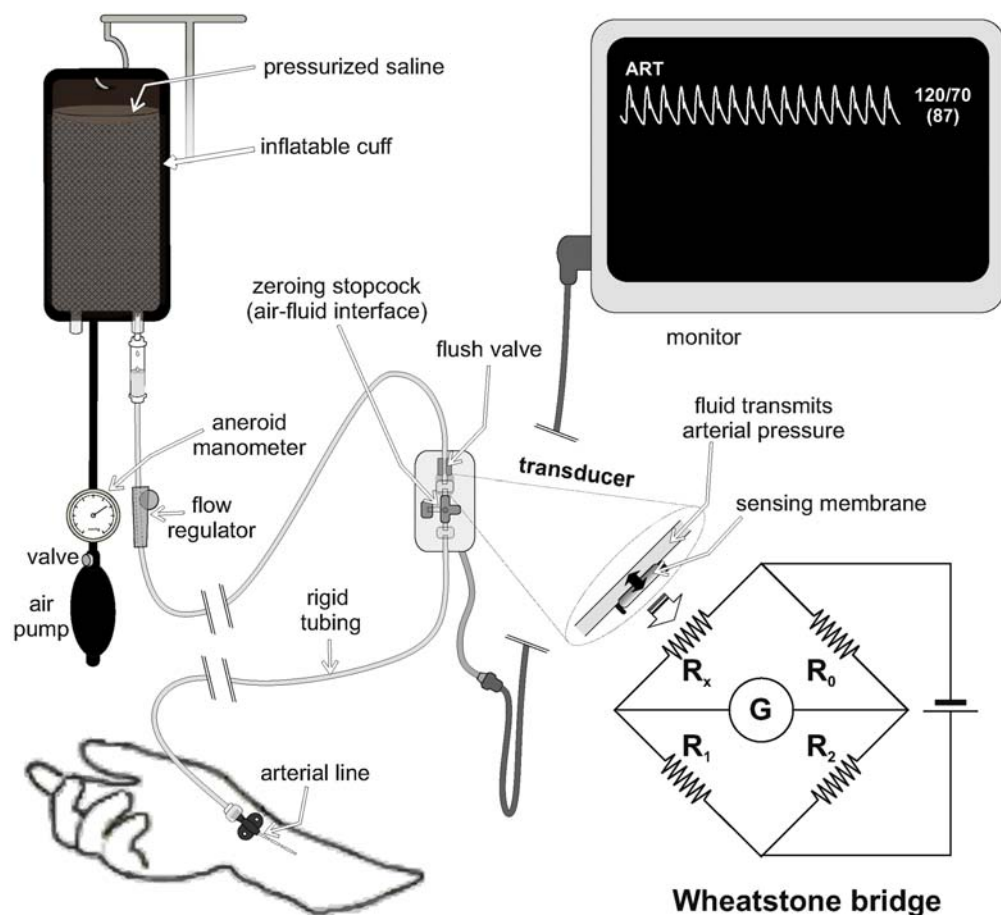
Functional assessment of the cardiovascular system

Most experimental observations underlying our knowledge on fundamental principles of cardiac function regulation derive from experimental setups with ex vivo assessment of *single fibers, muscle strips, and papillary muscles* (such as the one illustrated in Fig. 13.3), which were translated to in vivo *animal cardiovascular function studies*. While experiments enable straightforward assessments of myocardial contractility (for instance, by assessing isometric force at constant heart rate with varying preload, or conversely assessing response to stepwise increases in heart rate at constant preload), achieving the same goal in vivo remains challenging. In *clinical practice* and *clinical research*, monitoring the electrical activity of the heart and measuring blood pressure is relatively straightforward. A surface electrocardiogram and noninvasive intermittent blood pressure readings with oscillometry are widely available at every clinical scenario. When it comes to assessing cardiac volumes, blood flow, cardiac output, and continuous intracavitary or intravascular pressure, however, the invasiveness of procedures, technical expertise, and specialized equipment required constrain the application to specific settings such as cardiology, intensive care medicine, or anesthesiology practice.

Most of the mechanical processes inherent to cardiac physiology can be understood by measuring *chamber volumes and geometry, blood pressure and flow*.

Echocardiography is the most straightforward approach to estimate cardiac volumes, but ventriculography or advanced imaging methods, such as cardiac magnetic resonance, can also be employed. Likewise, ultrasound Doppler can assess flow velocity and upon determination of cross-sectional area flow can be computed from echocardiography. This enables determination of cardiac output at various anatomic locations, e.g., the LV or RV outflow tracts. While the variability in estimation of cross-sectional area and to a minor extent the angle of alignment with Doppler flow raises some concern which led many to consider the direct Fick method or thermodilution as the gold standard, echocardiography is a reasonable means to estimate cardiac output for most purposes. Fick's method is a simple consequence of the law of preservation of mass. Cardiac output to the organism is derived by matching tissue oxygen extraction as assessed by differential oxygen content between arterial and venous blood with oxygen

uptake by the respiratory system. If oxygen consumption cannot be measured directly, estimation by nomograms (indirect Fick method) leads to substantial error, unfortunately this is the current clinical standard in most hemodynamic laboratories. Thermodilution relies on pulmonary artery catheter (Swan-Ganz) and analysis of temperature recordings obtained when a cold marker solution is injected (intermittent readings) or the catheter warms blood in pulses (continuous recording). Finally, intravascular pressure monitoring requires placement of a catheter and intracardiac pressure readings require guidance of the catheter to the specific location, be it by echocardiography or fluoroscopy. In clinical practice, intracardiac and intravascular pressures are usually recorded with fluid-filled catheters coupled to rigid tubing and an external transducer in which a membrane is deflected by pressure oscillations varying one of the resistances in a Wheatstone bridge circuit (Fig. 13.5).

FIGURE 13.5   Continuous pressure recording with fluid-filled catheter. The diagram depicts standard preparation for invasive arterial pressure monitoring in the clinical setting. A radial artery is catheterized in the diagram, but other sites of arterial or venous cannulation follow the same scheme. A pressurized saline solution that fills a rigid tubing system of standard dimensions transmits pressure fluctuations to a transducer which consists of a sensing membrane (usually silicone based) and an electric circuit which is usually a Wheatstone bridge (or any modification of it). Briefly, the branching circuit consists of 4 resistances (R), one of which varies according to the pressure sensed at the membrane (R_x). Current flows either through R_x and R_1 or R_0 and R_2. These two arms are interconnected by a galvanometer (G). Current measured by G correlates with fluid pressure. The circuit must be zeroed by opening the system to atmosphere pressure at the level of the heart, at which point R_0 is set equal to R_x which means no current flows through G (0 mmHg). Pressure in the tubing system keeps a very low flow-rate that prevents the system from clotting.

Upon zeroing, pressures are calibrated and displayed in a monitor. Usually, the temporal resolution of clinical recordings goes up to 250 Hz and these are prone to damping, artifacts, and external wave reflection from tubing. In research settings, micromanometer tip catheters can provide high-fidelity recordings with high-temporal resolution, without damping and other artifacts. Please refer to Chapter 2 for a more extensive discussion of methods to assess intra-arterial pressure.

Assessing intrinsic cardiac performance: contractility, relaxation, and compliance

None of the abovementioned methods can accurately capture cardiac performance in terms of contraction, relaxation, and compliance, as these are intrinsic myocardial properties that can only be gauged acceptably if we minimize confounding by external determinants such as heart rate and loading conditions. To illustrate this concept, we resource to *ejection fraction*, the most commonly (mis)used contractility estimator in clinical practice. Ejection fraction is appraised by imaging methods, usually the echocardiogram, as stroke volume/end-diastolic volume. By simple inspection of the mathematical formula, it becomes clear that we statically estimate the amount of shortening (stroke volume) at a given preload (end-diastolic volume). Furthermore, we know that during ejection, the cardiac pump performs work not only in the form of shortening but also as force. In point of fact, force development (pressure throughout systole, or afterload) and shortening (stroke volume) are inversely related. Ejection fraction is therefore both preload and afterload dependent and cannot reliably be used to gauge contractility. When we consider diseased hearts, stroke volume remains well preserved until advanced stages of the disease. In these circumstances, EF predominantly reflects enlargement of the LV (low EF, HFrEF) or LV volume reduction (high EF, HFpEF), rather than contractility.[19]

Myocardial contractility (*inotropy*) relates to the ability of the myocardium to perform mechanical work (i.e., to generate force and shorten), independently of changes in preload, afterload or heart rate. Likewise, myocardial relaxation (*lusitropy*) relates to the ability to lengthen and relief force development; finally, ventricular *compliance* relates to the ability to accommodate blood at low pressures despite these same determinants and other external mechanical influences. LV relaxation and compliance are also usually estimated by echocardiography in clinical practice. Various measurements and indices obtained from transmitral flow Doppler and tissue Doppler recordings at the myocardium adjoining the mitral ring. It is good practice to take blood pressure and heart rate into account for interpreting data. A more extensive discussion of the relationship between diastolic function and mitral inflow characteristics is presented in Chapter 14.
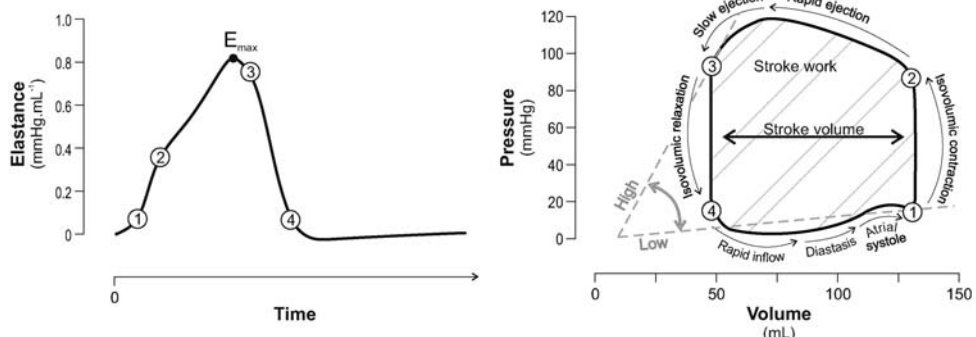
From catheter-derived pressure recordings, contractility can be estimated by measuring peak rate of pressure rise, the maximum of pressure derivative, dP/dt_{max}, which occurs during isovolumic contraction and is dependent on preload. An LV pressure derivative and corresponding dP/dt_{max} is illustrated in Fig. 13.4. Pressure decay is usually less steep and better modeled in research settings by nonlinear fitting methods applied to high-fidelity pressure recordings. Relaxation can be assessed from pressure fall by monoexponential decay, exponential decay to pressure asymptote, or logistic fittings. These methods optimize fitting of pressure decay during isovolumic relaxation as a function of time from aortic valve closure onwards, or from peak pressure fall (dP/dt_{min}) as a surrogate to aortic valve closure. A time constant, τ, is derived such that lower values translate to steeper pressure fall and faster relaxation while higher values mean slower relaxation. This is illustrated as the dashed region in LV pressure decline in Fig. 13.4. The simple monoexponential method first proposed by Weiss assumes pressure fall to zero pressure, whereas the later extension by Glantz introduces a more physiological pressure fall to a positive pressure asymptote. Further refinement by Matsubara provides more robust fits in the extremes of cardiac performance where a clear deviation from exponential decay is observed.[20] Of note, the time resolution of fluid-filled catheters is usually not enough for accurate τ estimation, which warrants solid-state catheters (see below).

As for compliance, even static end-diastolic pressure acquisitions coupled with end-diastolic volume determination can only provide a rough estimate of compliance because the end-diastolic pressure-volume relationship is nonlinear. Titin's elastic behavior within the physiological range and connective tissue at higher sarcomere lengths dictate a steeper rise of pressure at higher volumes.

The pressure-volume loop

Suga and Sagawa developed in ex vivo isolated heart preparations the construct of pressure-volume loops, which conceives the heart as a constantly moving spring with time-varying elastance (pressure/volume) that alternates between high-elastance and low-elastance states during systole and diastole, respectively[21] (Fig. 13.6).

Combined with the development of technology for continuous real-time monitoring of ventricular volume, the pressure-volume construct allowed in vivo assessment of intrinsic myocardial performance, but mostly restricted to animal research due to the invasive nature of the methods. Pressure-volume loops inform us on pressures, volumes, chamber elastance, and stroke work. The same approach can also be applied to regional function by constructing "pressure (or wall stress)—segment length" loops.[22]

FIGURE 13.6   The pressure-volume loop according to Suga and Sagawa. The ventricles are viewed as elastic springs that alternate between low and high-elastance states while performing pump work. Elastance varies with time (E_t) as a function of pressure (P_t) and volume (V_t) as depicted in the left panel according to the equation $E_t = P_t/(V_t-V_0)$ where V_0 is the volume at zero pressure, which can be either extrapolated or determined ex vivo in the unloaded chamber. An alternative view is the pressure-volume loop plotted on the right panel, where the alternance between high and low-elastance states is highlighted as well as the stages of the cardiac cycle and timings of valve opening and closure (see Fig. 13.2). The pressure-volume loop is a highly informative visual representation of the cardiac cycle. Indeed, stroke work (the area within the loop), stroke volume (volume range), end-diastolic volume and ejection fraction (stroke volume/end-diastolic volume) can easily be appraised. Maximal elastance (E_{max}) is a load-independent index of pump function, rather than contractility.
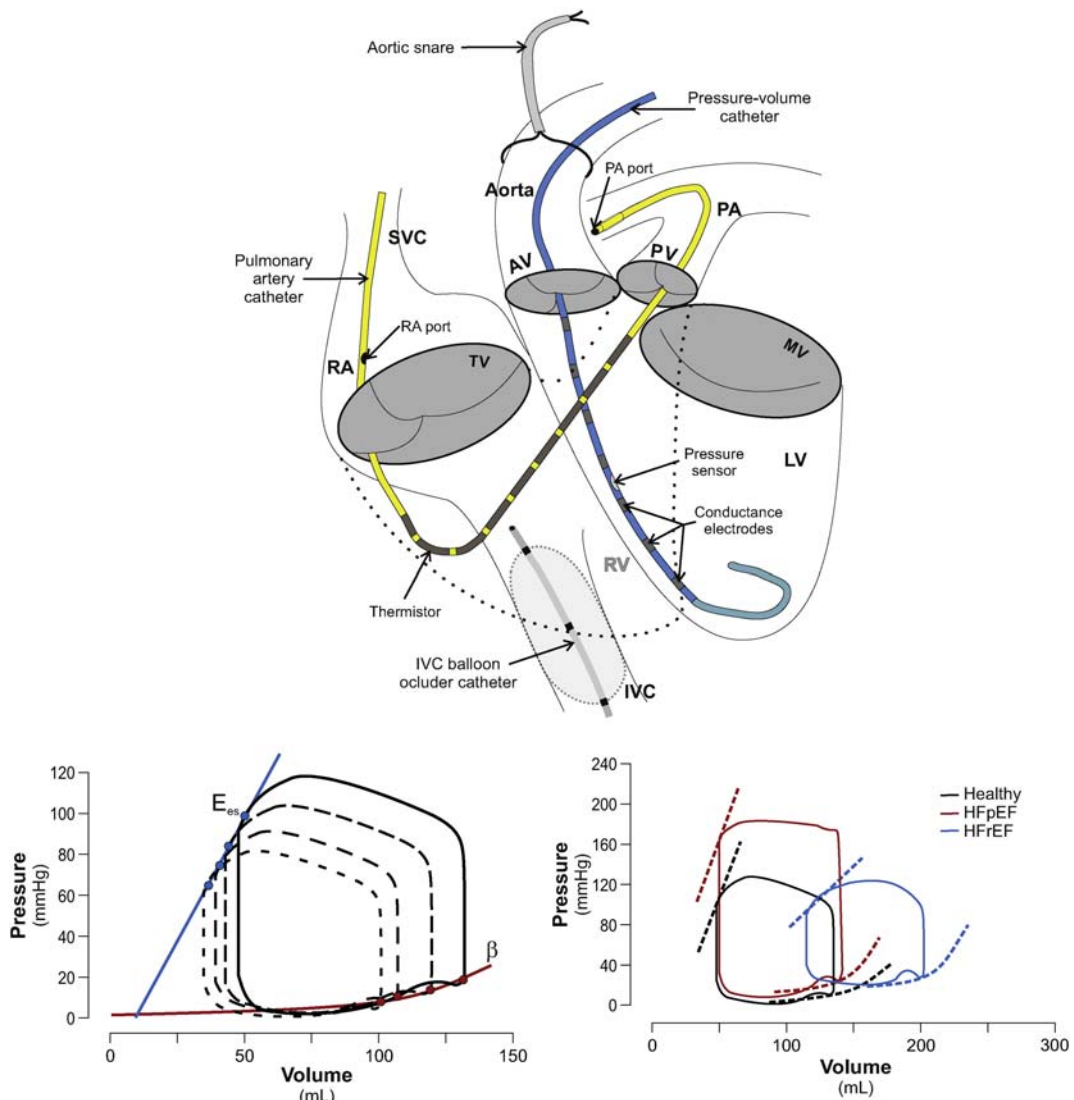
Admittedly, this approach looks at the heart or the segment as a pump and excludes by its design the analysis of time-varying phenomena. As a consequence, it is not suited for evaluating time-varying myocardial contractility and lusitropy. In the research setting, solid-state transducers bring the membrane from the Wheatstone bridge circuit inside the patient, at the tip of the catheter, enabling high-fidelity and high-temporal resolution recordings with minimal artifacts. These measurements, however, still are subject to zero-line shifting. Volume recordings are achieved by applying alternate low voltage currents to cardiac chambers and recording conductance or impedance readings that, upon suitable calibration, estimate cavity volumes continuously in real-time and with high-temporal resolution. The pressure-volume plane has also been used to assess ventricular-arterial coupling, although this approach has significant limitations for this purpose, as discussed in detail in Chapter 15.

Deriving performance indexes from acute load manipulation

High-fidelity pressure recordings with solid-state micro-manometers coupled to synchronous real-time recordings of chamber volume enable gauging intrinsic myocardial performance by indices derived from multiple heartbeats at constant heart rates and varying preload and afterload. This is usually achieved with short *transient inferior vena cava occlusions* either with a snare or an intravascular balloon occluder, or, alternatively, by imposing *transient afterload increases* with aortic clamping. Intrinsic performance can only be appraised if these load interventions are very transient, optimally spanning one or just a few more beats, to avoid influences from neural and endocrine responses.[23] The experimental setup along with an inferior vena cava

occlusion recording and representative tracings of HFpEF and HFrEF are illustrated in Fig. 13.7.

Still, we must underscore that external forces such as *ventricular interdependence*, intrathoracic pressure, and pericardial restraint can only be minimized in open-chest and wide-pericardiotomy experimental preparations which clearly deviates from physiology. Indeed, with intact pericardium, sudden preload reductions will show a biphasic course. First a decrease of RV volume and pressure, distorting LV end-diastolic pressure-volume relationship, will show an initial decrease in LV pressure without LV volume reduction (due to reduced pressure transmission across the interventricular septum) and only later, at lower pressures, will conform to the usual exponential fit. Fitting end-systolic pressure-volume relationships or stroke-work end-diastolic volume relationships at varying preloads provides indices of overall myocardial contractile performance whereas end-diastolic pressure-volume relationships provide indices of myocardial compliance. Some of these indices may be refined by normalization to ventricular mass or cardiomyocyte cross-sectional area. These have been considered for decades to be the gold standards for in vivo evaluation of cardiac function. Nevertheless, from the previous discussion, it becomes obvious that a clear-cut distinction between the effects of any physiological response, pharmacological or mechanical intervention on *heart rate, preload, afterload, and intrinsic myocardial performance* is not possible because these are all highly interdependent. Moreover, responses may vary with time from intervention. Additionally, complexity increases when we consider that pump performance is also governed by perfusion and that regions within the myocardium may behave quite distinctly (nonuniformity). Actually, overall performance is merely the sum of contributions from each myocardial region and ultimately each cardiomyocyte.

FIGURE 13.7   Pressure-volume loop acquisition of an inferior vena cava occlusion recording. The complex invasive set-up is depicted in the upper panel, namely a pulmonary artery (Swan-Ganz) catheter for continuous cardiac output monitoring through a thermistor (yellow), a pressure-volume catheter with solid-state high-fidelity pressure sensor and multiple electrodes for conductance recording (blue), a balloon occluder catheter placed in the inferior vena cava to enable sudden preload decreases and a snare in the ascending aorta for sudden or beat-to-beat afterload elevations. An inferior vena cava occlusion recording in a healthy heart is shown in the lower left panel. Cardiac performance indexes can be derived from the end-systolic and end-diastolic pressure-volume relationships. Contractility is appraised by the slope of the end-systolic relationship, end-systolic elastance (E_{es}), while compliance is quantified by the chamber stiffness constant (β) derived from fitting the end-diastolic relationship. In the lower right panel, pressure-volume loops and end-systolic and end-diastolic relationships are depicted in the healthy heart, HFpEF and HFrEF). HFpEF is characterized by diastolic stiffness (upward shift in end-diastolic pressure-volume relationship) with preserved E_{es} and ejection fraction whereas HFrEF shows decreased Ees and ejection fraction, higher compliance but steep elevations of end-diastolic pressure for further end-diastolic volume elevation. *AV*, aortic valve; *IVC*, inferior vena cava; *LV*, left ventricle; *MV*, mitral valve; *PA*, pulmonary artery; *PV*, pulmonary valve; *RA*, right atrium; *RV*, right ventricle; *SVC*, superior vena cava; *TV*, tricuspid valve.

As mentioned, transient afterload elevations by beat-to-beat or single-beat aortic occlusions have been employed to assess both systolic and diastolic performance as an alternative to sudden preload reduction.[24] They enable assessing relaxation (by pressure decay) at varying load conditions as well as the impact of afterload on end-diastolic pressure. These interventions provide insight on intrinsic myocardial properties. A healthy heart swiftly develops an elevated and early peak wall stress[25] and will have an elevated first-phase ejection fraction.[26] As a consequence of rapid early ejection and according to Laplace's law, systolic fiber stress quickly drops early in systole. This leads to shortening deactivation and fast relaxation. The young and healthy heart has an extraordinary reserve capacity for matching

challenges such as stress and exercise. Even independently from increased heart rate, increased venous return and filling volume (preload), increased contractility and neurohumoral adjustments, the heart has an intrinsic and readily available capacity for facing increased afterload. At rest, the young and healthy works up to 30% of its peak isovolumetric afterload. This heart can develop beat-to-beat pressures up to 300 mm Hg and more, without delaying relaxation and without increasing filling pressures.[24] This is the *afterload reserve* of the healthy heart.

In aged or diseased hearts, afterload reserve will decrease, closely reflecting impaired contractility.[27] When cardiac function deteriorates and/or when filling pressures are higher, load dependence of diastolic function increases, leading to more congestion.[7] Hypertensive patients with diastolic dysfunction exhibit reduced first-phase ejection fraction (i.e., ejection fraction during the initial 1/3 of systole), which may impair shortening deactivation and sustain myocardial contraction, preserving systolic ejection fraction at the expense of impaired diastolic function.[26] In an experimental model of HFpEF with combined obesity and hypertension, dependence of diastolic function on afterload similarly is enhanced.[28] A heart with diastolic function impairment will show slower relaxation and end-diastolic pressure elevation, or afterload-induced diastolic dysfunction, even following mild increases in afterload. In HFrEF, even a slight increase in systolic blood pressure will delay relaxation and increase filling pressures,[7] while a decrease in blood pressure will accelerate relaxation and improve congestion.[29] The behavior of the healthy and failing heart are depicted in Fig. 13.8.
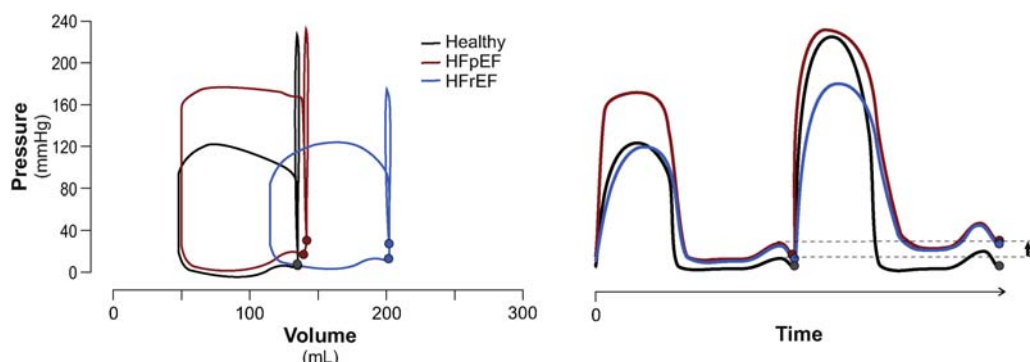
Time-varying afterload, wave reflection, and their toll in the heart

Preload in vivo easily equates with concepts from experimental settings. Preload is the volume in the chamber (length of a muscle segment, fiber, sarcomere) immediately before contraction starts. Afterload, however, assumes further complexity in vivo. While ex vivo it is the constant load the myocardium must bear during shortening, in vivo, because of changing geometry, arterial properties and resulting pressures, afterload continuously varies throughout systole. Thus, afterload is a time-varying function, which cannot be reduced to a single number. Cardiovascular filling, contractile properties of the LV, geometry of the outflow, aortic and arterial elasticity, vasomotor tone, peripheral vascular resistance, forward and backward traveling pressure waves all contribute to *time-varying afterload*. The effects of afterload on myocardial function are therefore also time-dependent.
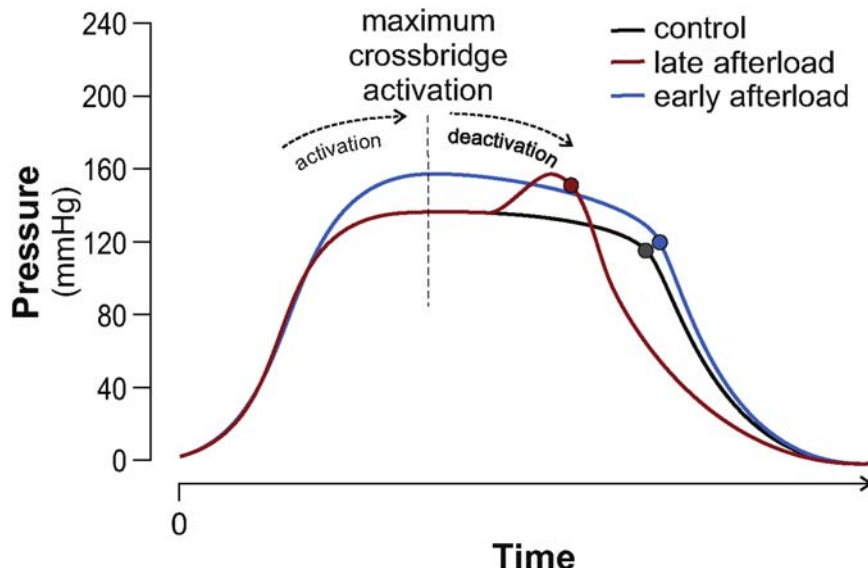
A clamp-increase in systolic pressure, applied early, accelerates relaxation. A similar intervention timed later during ejection (and occurring after the transition from contraction to relaxation) delays relaxation.[30,31] The later in time a given load challenge is applied to the heart, the more it delays myocardial relaxation. This behavior is based on the molecular interaction between actin, myosin, troponin, and titin. In the healthy heart, the calcium transient, activating crossbridge formation and cycling, is over soon after aortic valve opening. This corresponds to the transition from muscular contraction to relaxation. Before the transition, calcium availability is adequate to permit recruitment of additional crossbridge formation so that the resultant stress on individual crossbridges remains physiological. After the transition, the availability of calcium is reduced, limiting the formation of additional crossbridges so that the stress on individual crossbridges increases, causing back-rotation of the myosin head[27,32] and delayed crossbridge inactivation. The effects of early and late systolic load on diastolic function are depicted in Fig. 13.9.

When afterload delays relaxation in the diseased heart, this points toward elevated load beyond the transition to

FIGURE 13.8 **Afterload-induced diastolic dysfunction.** When the aortic snare in the upper panel of Fig. 13.3 is occluded for a single beat, an isovolumetric beat is achieved. Acquisitions can be depicted either as pressure-volume loop, left panel, or simply as a pressure tracing, right panel. While the healthy heart can develop high isometric pressures with enhanced relaxation and no elevation in end-diastolic pressures, the failing heart will show delayed relaxation and an upward shift in end-diastolic pressure (marked by an arrow) both with HFpEF and HFrEF. Distinctively, in HFrEF maximum developed isometric pressure is decreased denoting markedly impaired contractility.
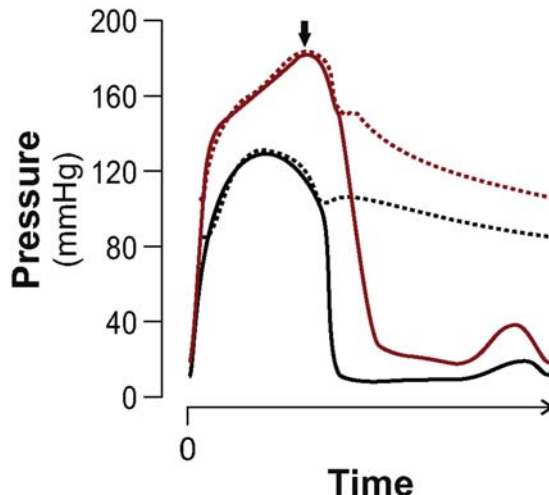
FIGURE 13.9 Differential effects of early and late afterload on diastole. The image displays a control beat and subsequent test beats where the same afterload magnitude was imposed either during early and late left ventricular pressure development (before and after maximum crossbridge recruitment, respectively, as signaled by the dashed vertical line). An early pressure clamp increases the number of interacting crossbridge, by cooperative activity, thereby matching systolic load, lengthening active pressure development and delaying left ventricular pressure fall (marked with a circle) while accelerating relaxation whereas a late pressure clamp induces a mismatch between load and available crossbridges with additional stress imposed on crossbridge, anticipation of left ventricular pressure fall (marked with a circle) and delayed relaxation due to slower crossbridge inactivation.

muscular relaxation. In HFrEF, this transition may even occur before aortic valve opening. As a consequence, in severe HFrEF, afterload inevitably contributes to load-dependent diastolic dysfunction[29] The time-dependent response of relaxation to load is a marker of diastolic dysfunction and of long-term effects of load on the myocardium. Timing of load modulates the hypertrophic response of the myocardium. While early systolic load (contraction load) triggers *physiological hypertrophy*, late systolic load (relaxation-load) is more likely to induce *maladaptive hypertrophy*.[25,33]

Throughout the ejection, the LV interacts with the vascular tree. The time-varying mechanical load (wall stress) on the myocardium is determined by complex interactions between myocardial contractile elements, instantaneous LV geometry, and the time-varying hydraulic load imposed by the arterial tree.[34] Early versus late systolic myocardial wall stress demonstrates finite relationships with specific arterial properties.[35] Systemic vascular resistance is a strong determinant of both early and late wall stress, aortic characteristic impedance determines ejection phase systolic wall stress, whereas wall stress at the end of systolic is also related to reflection magnitude. *Reflected waves* in patients with a stiff vascular tree may contribute to impaired LV relaxation and worsening diastolic dysfunction, which is illustrated in Fig. 13.10.

This underlies the relationship between wave reflections and late-ejection wall stress with systolic and diastolic dysfunction,[25] with left atrial function, maladaptive

FIGURE 13.10 Incremental impact of hypertension and wave reflection on diastolic function. The image displays superimposed aortic pressure (dashed) and left ventricular pressures (solid) from a healthy patient (black) and a hypertensive patient (red) with increased late systolic pressure (marked by arrow). This late systolic increase in pressure is attributable to stronger and earlier wave reflections. Note the delayed onset and slower rate of relaxation, the increased filling pressures and the big atrial contraction wave. Increased afterload delays the onset of relaxation. We may assume that decreased first 1/3 EF contributes as well to delayed relaxation and increased sensitivity to wave reflections (Gu). Late systolic afterload due to faster and enhanced wave reflections from a stiff vascular system further delays relaxation, as appraised by the less steep drop in left ventricular pressure during isovolumic relaxation. In HFpEF, this may jeopardize early filling thereby raising the importance of atrial contraction. During effort, when both left ventricular loading and heart rate increase congestive symptoms and fatigue arise.

hypertrophy, and outcomes. The impact of early and late systolic load on the myocardium is discussed in more detail in Chapter 16.

Conclusions

The heart is a biological pump with complex active ejection and filling. These functions are achieved with phased activation of atria and ventricles, contraction and relaxation of myocardial cells. The tight balance between intracellular molecular mechanisms, metabolism, and bodily needs implies close functional coupling between the heart and the arteries. This cardiovascular system interacts with renal, pulmonary, hematopoietic, and endocrine systems for achieving extraordinary adaptions throughout lifetime and to performant responses to various forms of stress. Aging and lifelong insults form systemic arterial hypertension, atherosclerosis, coronary artery disease, diabetes mellitus, and many other risk factors and pathologies will nevertheless threaten this highly resilient pump of the young healthy human. Unsurprisingly cardiovascular health and research remain among the major front battles in medicine and healthcare.

References

1. Zhao J, Pei L. Cardiac endocrinology: heart-derived hormones in physiology and disease. **JACC Basic Transl Sci**. 2020; 5(9):949−960.

2. Lourenco AP, Leite-Moreira AF, Balligand JL, et al. An integrative translational approach to study heart failure with preserved ejection fraction: a position paper from the Working Group on Myocardial Function of the European Society of Cardiology. **Eur J Heart Fail**. 2018; 20(2):216−227.

3. Linke WA. Titin gene and protein functions in passive and active muscle. **Annu Rev Physiol**. 2018; 80:389−411.

4. Leite-Moreira AF, Lourenco AP, Balligand JL, et al. ESC Working Group on Myocardial Function Position Paper: how to study the right ventricle in experimental models. **Eur J Heart Fail**. 2014; 16(5):509−518.

5. Wiggers CJ. Basic hemodynamic principles essential to interpretation of cardiovascular disorders: the Ludwig Kast Lecture. **Bull N Y Acad Med**. 1942; 18(1):3−17.

6. Van de Werf F, Minten J, Carmeliet P, De Geest H, Kesteloot H. The genesis of the third and fourth heart sounds. A pressure-flow study in dogs. **J Clin Invest**. 1984; 73(5):1400−1407.

7. Gillebert TC, Leite-Moreira AF, De Hert SG. Load dependent diastolic dysfunction in heart failure. **Heart Fail Rev**. 2000; 5(4):345−355.

8. Noble MI. The contribution of blood momentum to left ventricular ejection in the dog. **Circ Res**. 1968; 23(5):663−670.

9. Abrams J. Current concepts of the genesis of heart sounds. I. First and second sounds II. Third and fourth sounds. **J Am Med Assoc**. 1978; 239(26):2787−2791.

10. Leite-Moreira AF. Current perspectives in diastolic dysfunction and diastolic heart failure. **Heart**. 2006; 92(5):712−718.

11. Nagueh SF, Appleton CP, Gillebert TC, et al. Recommendations for the evaluation of left ventricular diastolic function by echocardiography. **Eur J Echocardiogr**. 2009; 10(2):165−193.

12. Aronsen JM, Louch WE, Sjaastad I. Cardiomyocyte Ca^{2+} dynamics: clinical perspectives. **Scand Cardiovasc J**. 2016; 50(2):65−77.

13. Sweeney HL, Hammers DW. Muscle contraction. **Cold Spring Harb Perspect Biol**. 2018; 10(2).

14. Luo M, Anderson ME. Mechanisms of altered Ca^{2+} handling in heart failure. **Circ Res**. 2013; 113(6):690−708.

15. Endoh M. Force-frequency relationship in intact mammalian ventricular myocardium: physiological and pathophysiological relevance. **Eur J Pharmacol**. 2004; 500(1−3):73−86.

16. Dowrick JM, Tran K, Loiselle DS, et al. The slow force response to stretch: controversy and contradictions. **Acta Physiol**. 2019; 226(1):e13250.

17. Leite-Moreira AM, Almeida-Coelho J, Neves JS, et al. Stretch-induced compliance: a novel adaptive biological mechanism following acute cardiac load. **Cardiovasc Res**. 2018; 114(5):656−667.

18. Bertero E, Maack C. Metabolic remodelling in heart failure. **Nat Rev Cardiol**. 2018; 15(8):457−470.

19. Katz AM. Influence of altered inotropy and lusitropy on ventricular pressure-volume loops. **J Am Coll Cardiol**. 1988; 11(2):438−445.

20. Ogilvie LM, Edgett BA, Huber JS, et al. Hemodynamic assessment of diastolic function for experimental models. **Am J Physiol Heart Circ Physiol**. 2020; 318(5):H1139−H1158.

21. Suga H, Sagawa K, Shoukas AA. Load independence of the instantaneous pressure-volume ratio of the canine left ventricle and effects of epinephrine and heart rate on the ratio. **Circ Res**. 1973; 32(3):314−322.

22. Smiseth OA, Donal E, Penicka M, Sletten OJ. How to measure left ventricular myocardial work by pressure-strain loops. **Eur Heart J Cardiovasc Imaging**. 2021; 22(3):259−261.

23. Burkhoff D. Pressure-volume loops in clinical research: a contemporary view. **J Am Coll Cardiol**. 2013; 62(13):1173−1176.

24. Leite-Moreira AF, Lourenco AP, Roncon-Albuquerque Jr R, et al. Diastolic tolerance to systolic pressures closely reflects systolic performance in patients with coronary heart disease. **Basic Res Cardiol**. 2012; 107(2):251.

25. Chirinos JA, Segers P, Rietzschel ER, et al. Early and late systolic wall stress differentially relate to myocardial contraction and relaxation in middle-aged adults: the Asklepios study. **Hypertension**. 2013; 61(2):296−303.

26. Gu H, Li Y, Fok H, et al. Reduced first-phase ejection fraction and sustained myocardial wall stress in hypertensive patients with diastolic dysfunction: a manifestation of impaired shortening deactivation that links systolic to diastolic dysfunction and preserves systolic ejection fraction. **Hypertension**. 2017; 69(4):633−640.

27. Leite-Moreira AF, Gillebert TC. Nonuniform course of left ventricular pressure fall and its regulation by load and contractile state. **Circulation**. 1994; 90(5):2481−2491.

28. Leite S, Rodrigues S, Tavares-Silva M, et al. Afterload-induced diastolic dysfunction contributes to high filling pressures in experimental heart failure with preserved ejection fraction. **Am J Physiol Heart Circ Physiol**. 2015; 309(10):H1648−H1654.

29. Eichhorn EJ, Willard JE, Alvarez L, et al. Are contraction and relaxation coupled in patients with and without congestive heart failure? **Circulation**. 1992; 85(6):2132−2139.

30. Gillebert TC, Lew WY. Influence of systolic pressure profile on rate of left ventricular pressure fall. **Am J Physiol**. 1991; 261(3 Pt 2):H805−H813.

31. Gillebert TC, Sys SU, Brutsaert DL. Influence of loading patterns on peak length-tension relation and on relaxation in cardiac muscle. **J Am Coll Cardiol**. 1989; 13(2):483−490.

32. Housmans PR, Brutsaert DL. Three-step yielding of load-clamped mammalian cardiac muscle. **Nature**. 1976; 262(5563):56−58.

33. Gillebert TC, Chirinos JA. Left ventricular geometry, blood pressure, arterial hemodynamics, and mortality after ischemic stroke. **JACC Cardiovasc Imaging**. 2018; 11(3):383−385.

34. Chirinos JA, Rietzschel ER, De Buyzere ML, et al. Arterial load and ventricular-arterial coupling: physiologic relations with body size and effect of obesity. **Hypertension**. 2009; 54(3):558−566.

35. Chirinos JA, Segers P, Gillebert TC, et al. Arterial properties as determinants of time-varying myocardial stress in humans. **Hypertension**. 2012; 60(1):64−70.

This page intentionally left blank

Chapter 14

Systolic−diastolic coupling

Per M. Arvidsson[1] and Sándor J. Kovács[2]

[1]Clinical Physiology, Department of Clinical Sciences Lund, Faculty of Medicine, Lund University, Lund, Sweden; [2]Cardiovascular Division, Department of Medicine, Washington University in Saint Louis, School of Medicine, Saint Louis, Missouri, United States

Historical background

In this chapter, we will delve into the previously introduced features of ventricular and myocardial physiology to cover the functional interplay between the ventricles and their immediate surroundings, including the entire content of the pericardial sac. We will review cardiac embryology and examine a set of functional propositions relating the macroscopic structure of the heart to its purpose in the circulatory system, evaluate these propositions using the best available data, and finally incorporate the systolic and diastolic properties of the heart including systolic−diastolic coupling, into a model capable of explaining commonly observed cardiac phenomena.

The understanding of the cardiovascular system as a closed-loop system is fundamental, and was first proposed by William Harvey in his 1628 landmark book *De Motu Cordis*. Before Harvey, many anatomists and physicians had unsuccessfully attempted to uncover the role of the heart in maintaining a proper balance of spirits *(pneumata)* in the body, typically reasoning within a fundamentally Platonic framework. Harvey was able to break through such barriers by incorporating a translational approach to cardiovascular research; he successfully combined hypotheses, experiments, observations, interspecies comparisons, and interpretations to produce a rudimentary closed-loop model of the circulatory system. Following on these observations, Richard Lower in 1669 excised strips of cardiac muscle from animals and demonstrated that the contractile feature of cardiac tissue remained for a while even in the absence of blood. Lower also described that the muscular cells of the heart had a weave, and were arranged in a spiral-like pattern whose direction varied with its location within the ventricular wall. He suggested that this arrangement was responsible for the observed "wringing" contractile pattern of the open chest, beating heart.
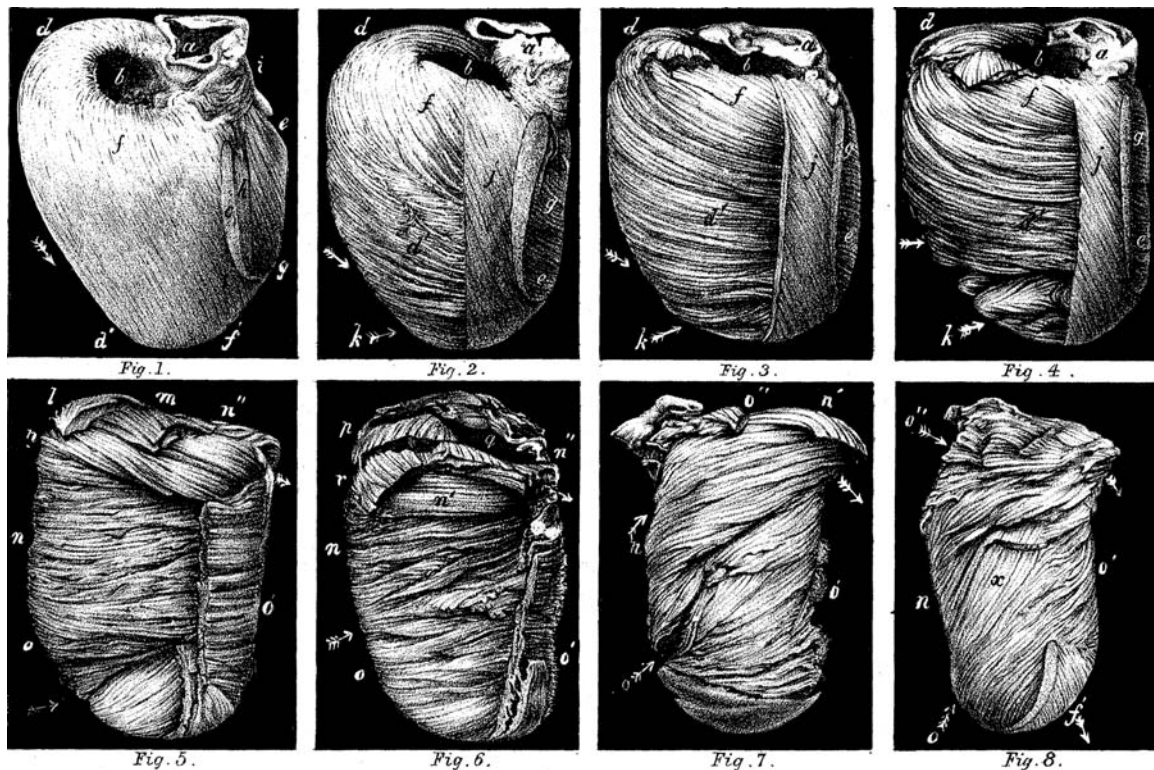
Building on this finding, James Bell Pettigrew studied the structural arrangement of the heart in fish, birds, mammals (including baleen whale, armadillo, and giraffe), and humans. Through a series of meticulous dissections carried out around 1858, he described a gradual change of directional alignment of muscle fibers in the ventricular myocardium, from the endocardium to the epicardium. An example of his findings is shown in Fig. 14.1. The helical and progressive arrangement of cardiomyocytes would later turn out to be crucial both for generation of the blood pressure (pressure pumping) needed in the systemic circulation,[1] and for efficient emptying and filling of the ventricles (volume pumping) despite limited shortening of the individual myocytes.[2] Indeed, the combination of longitudinally and circumferentially aligned myocytes in the human heart enables it to pressure- and volume-pump blood with remarkable efficiency, and elegantly solves what are potentially the two most difficult conceptual physiologic problems in cardiac pumping: (1) how does the chamber achieve an left ventricular (LV) ejection fraction of 60%−70% while individual myocytes shorten by only 10%−15% and (2) how does the chamber achieve adequate (optimal, low pressure) filling over the physiologic range of heart rates and loads that defines diastolic function. To understand how this is achieved, we must examine the anatomy of the heart from a functional and kinematic perspective.

Gross cardiac anatomy, ventricular myocyte orientation, and mechanism of contraction

Anatomy of the heart

Embryologically, the heart evolves from the heart tube that requires looping and development of septa and valves that ultimately establish a four-chamber configuration (Fig. 14.2). The human heart begins to beat at about 22−23 days, with blood flow commencing in the fourth week. By the end of the ninth week, the fetal heart has

FIGURE 14.1   Posterior view of sheep heart dissected by James Bell Pettigrew. Note the transition in the alignment of cardiac muscle fibers from the left-handed epicardial layer (top left), via the circumferential middle layer, to the right-handed endocardial layer (bottom right). *Image courtesy of The Royal Society.*
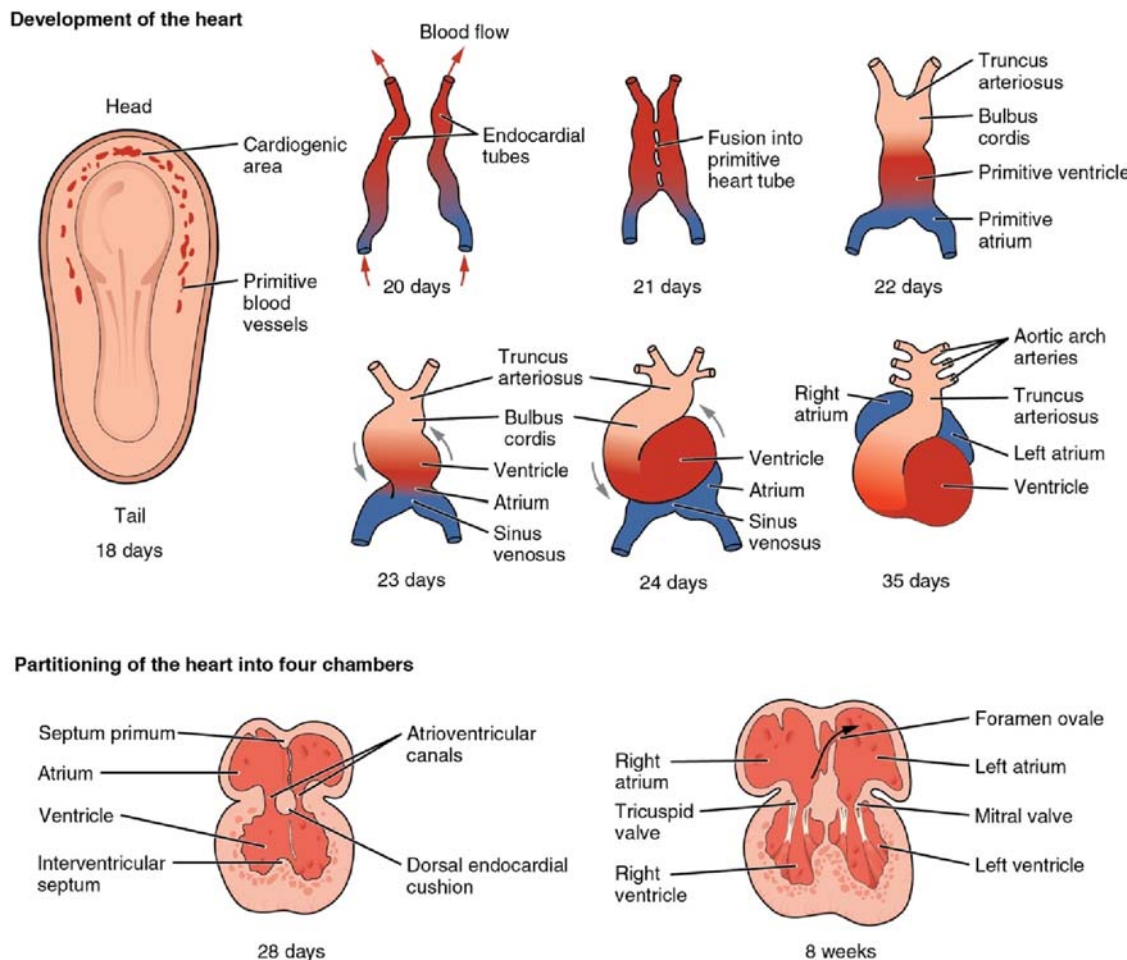
developed septa, valves, and has four chambers. Typical heart rates at this stage of development are 155−195 bpm. Suitable preprogrammed developmental features assure initial establishment of the fetal circulation that obtains nutrition and oxygen through the placenta, while eliminating metabolic waste and CO_2. The fetal circulation diminishes within a few days after delivery, resulting in the complete separation of venous and arterial circulations. Accordingly, circulation proceeds in series, involving the left heart, the periphery, venous return, right heart pumping to the lungs, and arrival of oxygenated blood in the left atrium for systemic perfusion. Therefore, the heart is one of the earliest organs to differentiate and function.

The human heart with pericardium removed, shown in Fig. 14.3, is located in the mediastinum within the thoracic cavity, above the diaphragm and enclosed in the pericardial sac. The pericardium is a soft but essentially nondistensible serous membrane that contains a small amount of pericardial fluid, which acts as a lubricant and permits the surface of the beating heart (visceral pericardium) to contract freely and slide essentially without resistance relative to anatomically fixed pericardial sac (parietal pericardium). The visceral side of the pericardium adheres to the left ventricle, left atrium, right ventricle, and right atrium, as well as the aortic root. The sum of these parts (the contents of the pericardial sac) constitutes the *total heart volume*.

The left ventricle supplies the systemic circulation with oxygenated and pressurized blood, and the right ventricle feeds oxygen-depleted venous blood through the pulmonary circulation to enable gas exchange with the surrounding air. Flow is generated when the systolic pressure of the contracting right ventricle overcomes the pulmonary vascular impedance (such of resistive and pulsatile load). For detailed descriptions of the steady and pulsatile components of arterial load, the reader is referred to (Chapters 1, 3, 17). For a specific detailed discussion of the pulmonary arterial load, the reader is referred to Chapter 57. Here, we will provide a simplified discussion related to vascular resistance only (steady components of load), which can be expressed by the analog of Ohm's Law,

$$Q = \frac{\Delta P}{R}, \tag{14.1}$$

where Q is the flow [ml/sec], ΔP is the pressure difference (mmHg) between the inflow and outflow locations of the resistive circuit, and R is the resistance [mmHg/(mL/ sec)]. Under normal conditions, the resistance in the pulmonary circulation is approximately one-fifth of that in the systemic circulation. For the two ventricles to pump the same volume of blood—in a time-averaged sense—the left ventricle therefore has to apply a driving force (systolic pressure) that is about five times greater than the driving

FIGURE 14.2 Development of the human, four-chambered heart is essentially complete by the eighth week, when the embryo is about 10—12 mm in size.
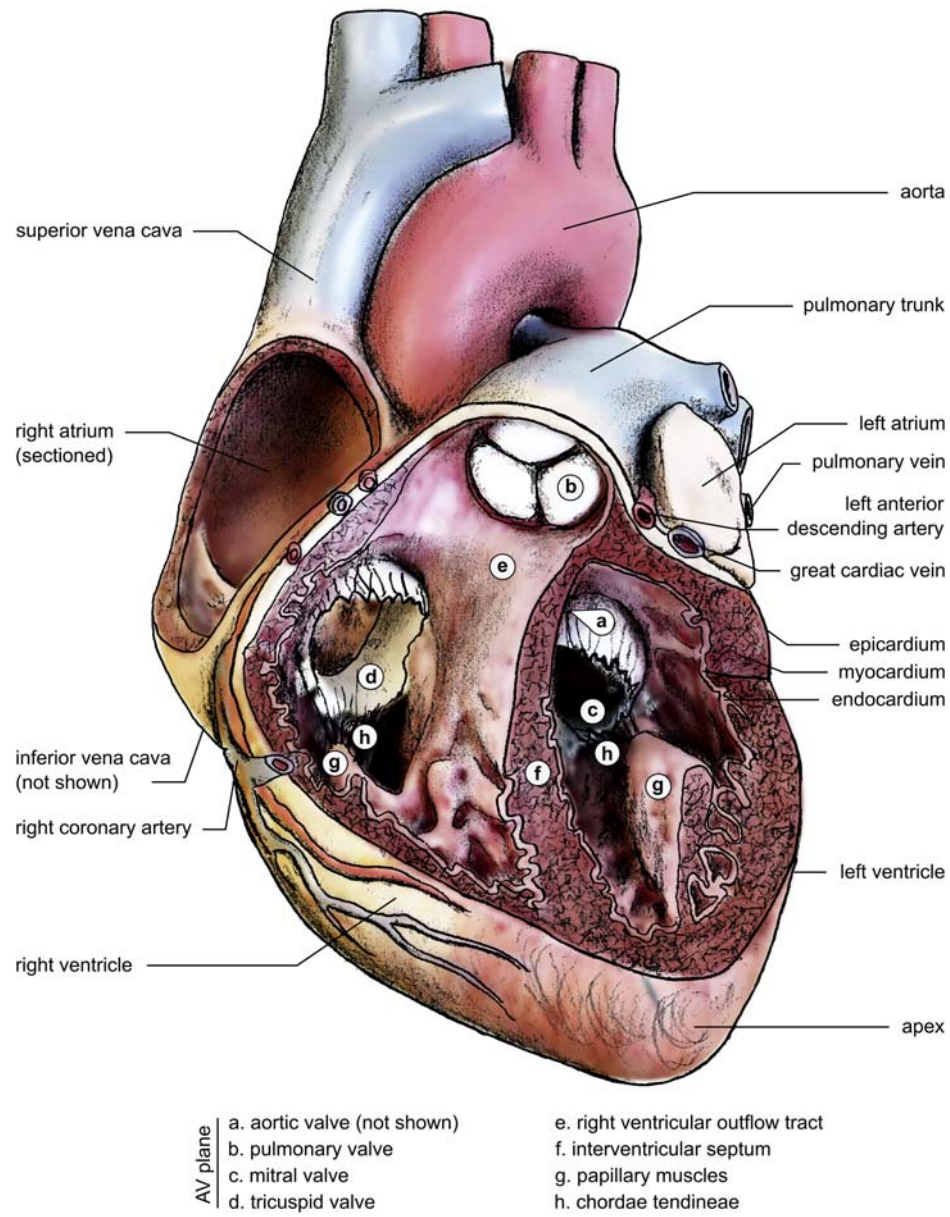
force generated by the right ventricle. This difference in LV versus right ventricular (RV) workload and wall tension requirement is reflected anatomically in that the left ventricle has a significantly thicker (about 1—1.5 cm) myocardium than the right ventricle (0.3—0.8 cm). Cardiac pumping is an energy-demanding process, and oxygenated blood is supplied to both ventricles and atria via the coronary arteries, which originate in the left and right aortic cusps in the aortic root.

Forward flow is ensured by the valve apparatus, i.e., the aortic and pulmonary valves (also called *semilunar valves*), and the mitral and tricuspid valves (*atrioventricular valves*) that separate the ventricles from the atria.

The atria receive blood from the pulmonary and caval veins, which also serve as anchor points for the posterior (basal) aspect of the heart. The left and right sides of the heart are separated by the interventricular septum and the

atrial septum (see Figs. 14.2 and 14.3). The ventricles are separated from the atria by a fibrous structure known as the *atrioventricular plane* (AV plane). This effectively means that the atria and ventricles are functionally interconnected: whenever the ventricles contract, this will affect the atria and vice versa. As we shall see, this is of great importance for cardiac pumping.

The AV plane serves as the anchoring point for the AV valves as well as the aortic root and aortic valve. The AV valves are also connected to the ventricular myocardium via the chordae tendineae, which together with the papillary muscles prevent the valve leaflets from prolapsing into the atria during ventricular contraction. The atrioventricular valves must resist the systolic blood pressure without allowing any backward, regurgitant flow, and they must be compliant enough to permit fast and unobstructed inflow during cardiac filling, which normally occurs at low blood pressure.

a. aortic valve (not shown)
b. pulmonary valve
c. mitral valve
d. tricuspid valve

e. right ventricular outflow tract
f. interventricular septum
g. papillary muscles
h. chordae tendineae

FIGURE 14.3   Anatomy of the heart, anterior view, drawn from an anatomical model. The pericardium and anterior parts of the ventricles have been removed.
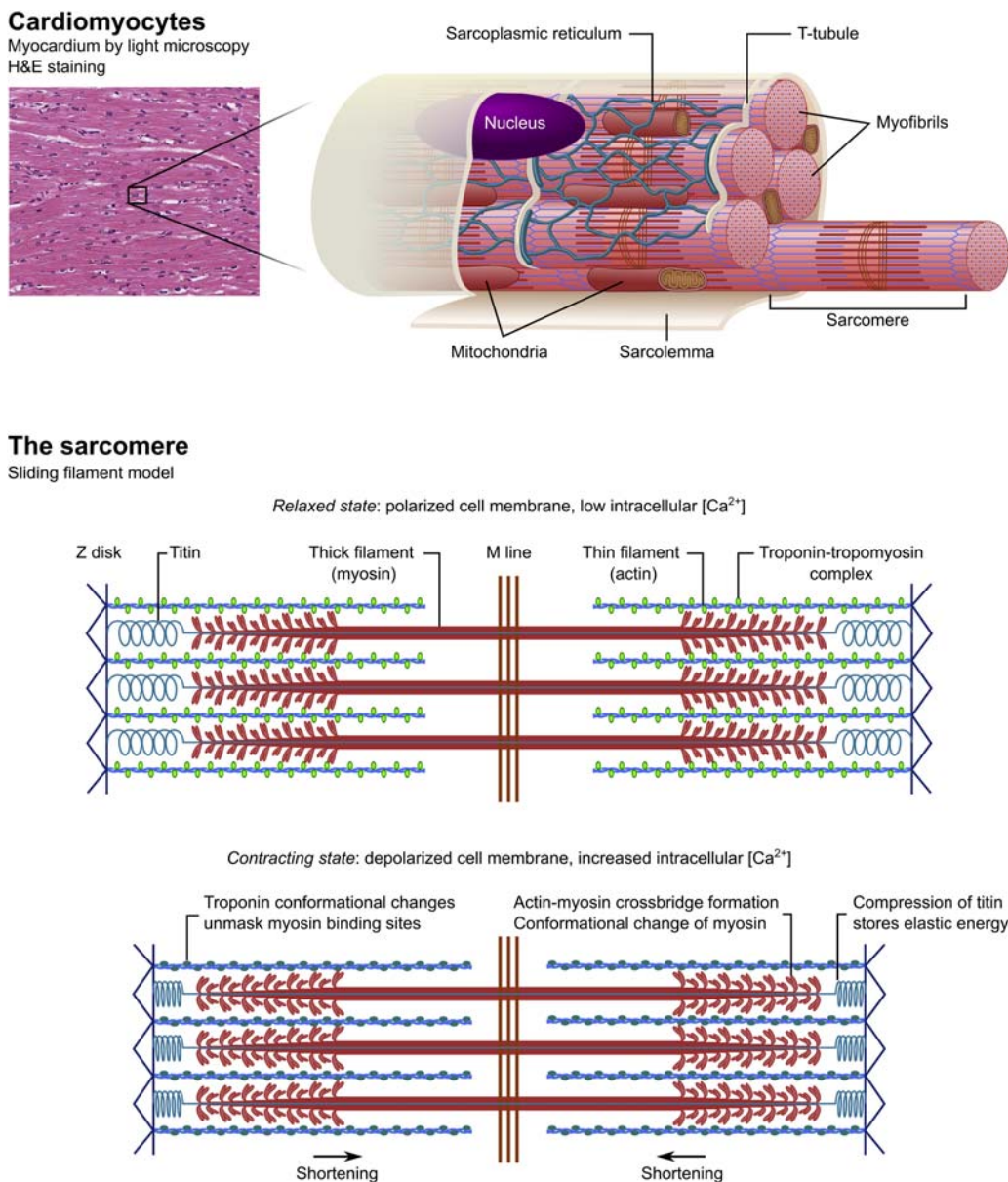
When functioning properly, cardiac valves can be thought of as physiological rectifiers or diodes. It is important to understand that all cardiac valve leaflets are entirely passive structures, and their motion is dictated by the motion of the surrounding blood. While intraventricular, ventriculoaortic, and atrioventricular pressure gradients accelerate the blood, this acceleration force is always opposed by the inertia of the blood. Recall that flow occurs only when resistance is overcome by a force, i.e., a pressure gradient, which develops gradually (over tens of msecs). Valve states (open/closed) therefore always lag behind pressure changes and are ultimately effected by actual blood and tissue motion.[4] It also follows that all valves have some degree of insufficiency (leakiness), as they only begin to close—i.e., coaptation of leaflets to form a leakproof seal—when subjected to retrograde flow, and the closing is gradual (msecs) as opposed to instantaneous. Whether a valve is considered leaky (regurgitant) or not depends on the severity of the insufficiency (quantified as the regurgitation fraction, 0%—100% of forward flow, the latter figure being incompatible with life) and on the clinical consequences (atrial distension, pulmonary edema, and exercise intolerance, to name a few).

Contractile function of myocytes

Let us now briefly turn to the basic function of the *myocyte*, described in greater detail in the preceding chapter. The contractile function of each individual cell arises from the interaction of two sets of intracellular filaments, composed of *thin filaments* (composed of *actin*, *tropomyosin*, and *troponin*) and *thick filaments* (*myosin*), respectively. These filaments are arranged in an interlocking pattern within

each sarcomere along the long axis of each myocyte. Myocyte shortening occurs because within each sarcomere myosin "walks" along the actin filaments, pulling the ends of the myocyte toward its center (Fig. 14.4).

Whenever a cardiomyocyte is depolarized, i.e., its membrane potential is lost, it will respond by increasing its permeability for Ca^{2+}, leading to influx of such ions. Through the ryanodine receptor system, this triggers additional rapid calcium-dependent release of stored

FIGURE 14.4 Structural layout of an individual cardiomyocyte and its contractile subunit, the sarcomere—a molecular motor. Cardiomyocytes are dominated by the contractile elements which are arranged in myofibrils. Myofibrils are surrounded by mitochondria and the sarcoplasmatic reticulum, which is coupled to the exterior of the cell through the T-tubules. Bottom: the sarcomere is understood as a system of sliding filaments, which alternate between relaxed (crossbridges are essentially uncoupled) and contracting (crossbridges are mostly coupled) states depending on the Ca^{2+} concentration—which varies by about a factor of 1000 during each cardiac cycle. Titin is anchored to the Z disk and M line and is a *bidirectional spring*; it is compressed—and stores elastic energy—because of contraction; it then provides a restoring (recoil) force upon cessation of contraction (crossbridge uncoupling) and onset of relaxation.
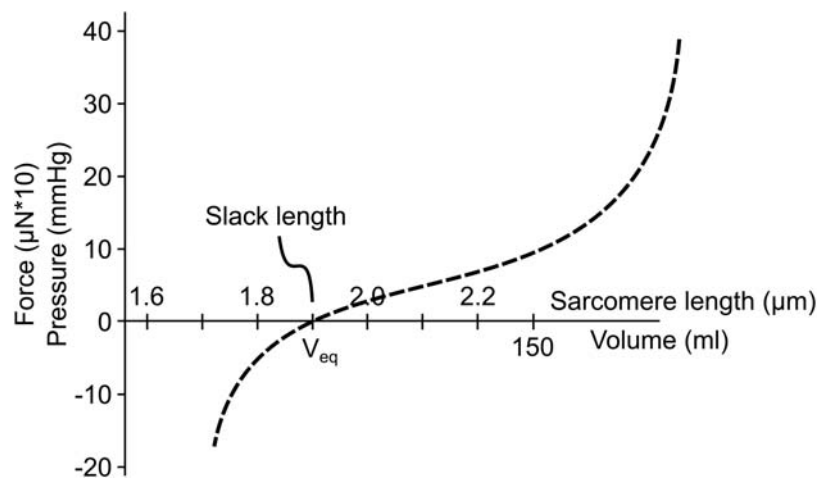
intracellular Ca^{2+} from the sarcoplasmic reticulum—a storage compartment for Ca^{2+} ions. Part of this Ca^{2+} binds to troponin, a protein coupled to the actin filaments, causing it to undergo conformational changes which unmask myosin binding sites in the actin filaments. The subsequent attachment of myosin to actin is called *crossbridge formation*. In the presence of adenosine triphosphate (ATP), myosin then undergoes additional conformational changes causing it to exert a "pull" on actin. This leads to shortening of the sarcomere. During systole, sarcomeres shorten by about 15% from 2.1 to 1.7 microns. ATP is also required to break the actin-myosin crossbridge and restore myosin to its relaxed state, preparing it for repeated crossbridge cycling. Cycles continue for as long as the intracellular space is flooded with Ca^{2+} and while ATP remains available. During a single systolic contraction, an individual sarcomere attaches, shortens, and detaches multiple times (crossbridge cycling). Sliding filament dynamics should be viewed as the result of an astronomical number of crossbridges cycling, governed by a probability distribution modulated by Ca^{2+} concentration.

As the sarcomeres shorten, the cell also thickens, since the intact cellular membrane implies volume conservation at the individual cell level. Total shortening is dependent on the contractile (inotropic) state but is usually in the 15% to 20% range; thickening is markedly less, since the myocyte is longer (≈ 100 microns) than it is thick ($10-25$ microns in diameter).

Importantly, a third filament-like protein is also present within the sarcomere: the giant protein *titin* connects the M line with the Z disk, providing structural continuity along the entire sarcomere. Apart from acting as a scaffold for the contractile elements, titin also contains several spring-like domains which modulate the physical tensile properties of the sarcomere. During systolic contraction, the spring is gradually compressed, storing elastic energy. Once relaxation commences, the titin springs release their stored strain energy and restore the myocyte to its slack length.[5] In other words, during diastole myocytes can actually push! Conversely, titin also resists stretching of the sarcomere during diastole, and is the major intracellular contributor to myocardial passive tension at physiological sarcomere lengths.[6] Taken together, this means *titin acts as a bidirectional spring*. In simple physical terms, titin has an equilibrium length say Lo, (likely during diastasis); if compressed below Lo (LV at end-systolic volume), it stores elastic strain energy, and when crossbridges detach, it lengthens the sarcomere toward Lo. If it is stretched beyond Lo (likely, in normal sinus rhythm, at end diastole after the atrial kick), titin is stretched beyond Lo, and if no systolic contraction ensues, it shortens toward Lo. Recall that *tension* is defined as the amount of force resisting length changes of the relaxed myocyte. In the experimental setting, this can be measured by attaching a relaxed and isolated myocyte to a force measurement device and gradually extending it from its slack length (equilibrium). This produces a highly nonlinear force-length curve (Fig. 14.5), representing the cell-specific stiffness which can be understood as the sum of forces acting to restore the cell to its slack length.

The concept of passive tension can be translated to the three-dimensional organ level, where the sarcomere length is replaced with ventricular volume, and force is replaced with pressure. The sarcomere length is thus equivalent to

FIGURE 14.5 Passive and active tension properties of myocardium. Myocytes resist length changes due to their elastic properties. When stretched from slack length, the amount of restoring force is initially small. At the organ level, this facilitates filling of the ventricle. As the cell becomes more stretched, the restoring force becomes more pronounced, which prevents overstretching of the ventricle. Note that in the 1.8 to 2.1 micron (physiological) range, the curvilinear relationship is essentially linear, justifying the approximation that the system behaves kinematically as a linear, bidirectional spring. During systole, sarcomeres shorten by about 15% from 2.1 to 1.7 microns. Conversely, shortening below slack length results in a restoring force acting to lengthen the cell.

cardiac preload; slack length is equivalent to the *equilibrium volume* (V_{eq}), which is attained during diastasis when the myocardium is fully relaxed, and wall motion ceases. Total stress on the ventricular wall is minimized, but not completely eliminated, at V_{eq}.[7] It therefore follows that the passive tension curve describes the tendency of the ventricle to resist volume change away from V_{eq} (Fig. 14.5). Whenever ventricular volume is below V_{eq}, the *restoring forces contribute to filling of the ventricle* by facilitating ventricular expansion toward its resting (diastatic) volume. On the organ level, titin-mediated passive tension is further compounded by intermediate filaments, extracellular collagen, and external mechanical factors which will be discussed later.

Active tension describes the capacity of the myocyte to generate force by contraction. Cardiomyocytes will generate different amounts of contractile force depending on the initial conditions of the sliding filaments. If cells are stretched, the contractile elements become more sensitive to Ca^{2+}. The mechanisms are unclear, but the result (within limits) is a stronger contractile force for initiation of shortening when starting from increased sarcomere lengths. On the organ level, this has the effect of providing an instantaneous compensatory mechanism for handling different ventricular filling volumes (preload). Increased inflow to the heart is responded to by a stronger contraction, i.e., the heart pumps what it receives. This is called the *Frank—Starling law of the heart*. The potential to generate force is maximized at sarcomere lengths around 2.2 μm. At even higher lengths, the filaments start to slide apart, and fewer active sites are available for crossbridge formation, leading to decreased active tension.

The active tension curve describes the maximum attainable force for a certain level of sarcomere stretch or ventricular filling. This explains why atrial fibrillation leads to decreased ejection fraction. Under normal conditions, atrial contraction (Doppler A-wave of transmitral flow) leads to additional filling of the ventricle, i.e., presystolic stretching of myocytes. The most important contribution, however, is the added stretching of the myocardium because the atria pull the AV plane up toward the base, thereby increasing the subsequent force of ventricular contraction. When atrial contraction is lost, as in atrial fibrillation, the ventricle does not fill beyond V_{eq}, and ventricular contraction occurs at a lower level of precontractile stretch. As a result, ventricular ejection fraction is diminished. Since ventricular contraction pulls at the AV plane and is opposed by it structurally, it also follows that increased stiffness of elastic structures being tugged at—predominantly the atria and great vessels—will likely affect both the end-systolic position and the diastolic return to V_{eq}. Increased stiffness may result from fibrosis, calcification, and other disease processes.

The shape of the active tension curve can also be altered, by adjusting the level of sympathetic tone from the autonomic nervous system and the presence of cathecholamines (primarily adrenaline). The capacity to regulate the contractile force for a given preload is called *inotropy*. Importantly, this differs from the Frank—Starling mechanism by altering the slope of the active tension curve instead of responding to variations in preload.

For a fixed afterload (vascular resistance), increasing the force of contraction (positive inotropy) will lead to more complete emptying of the ventricle. The end-systolic volume will therefore be further below the V_{eq}, resulting in a stronger restoring force of recoil (titin) during early diastole. This is one of the key physical mechanisms of systolic—diastolic coupling, by which systolic function directly influences diastolic performance. Indeed, it is impossible to optimize diastolic function in the presence of systolic dysfunction.

Physiologically, the Frank—Starling mechanism and inotropic regulation address fundamentally different challenges. The Frank—Starling mechanism ensures a steady output of blood flow (volume pumping) under varying preload levels, while inotropy is adjusted to ensure a sufficient ejection force to overcome the peripheral resistance (pressure pumping), equal to different afterloads. Increasing inotropy at rest therefore only lowers the end-systolic volume and increases the ejection fraction but does not increase cardiac output. In contrast, during vigorous exercise, the increase in heart rate and cardiac output is greater than the decrease in peripheral resistance resulting from compensatory vasodilation in working skeletal muscle; as a result, blood pressure (afterload) typically increases by at least 50%. The ability to increase the contractile force is crucial to overcome this increased afterload, which is continuously generated by the working heart. Inotropy is therefore not a mechanism by which cardiac output is increased, but rather maintained at varying afterloads. The utility of the association between increased contractile force and augmented diastolic function will become apparent in the following section.

Ventricular myocyte orientation and function

When examining myocardial tissue, the myocytes exhibit an obvious weave, a directionality. The commonly used term "fiber direction" is somewhat misleading because there are no continuous fibers of myocytes in the myocardium, unlike in skeletal muscle; cardiomyocytes instead branch and interconnect continuously, creating a syncytium (a functional unit of cells). Furthermore, the myocytes are embedded in a three-dimensional extracellular matrix composed primarily of collagen and elastin. Despite this, we can appreciate directional patterns which are visible to

the naked eye, as evidenced by the aforementioned experiments by Lower and Pettigrew.

The overall arrangement of cardiomyocytes is commonly described as helical, albeit with a gradual and smooth change in alignment as a function of their position between the epicardial and endocardial aspects of the myocardial wall. The angle between the myocyte long-axis direction and the LV equatorial (short-axis) plane constitutes the primary pattern of organization in the myocardium, and is referred to as the *helix angle* (HA, Fig. 14.6). Multiple modalities have been used to demonstrate that the endocardial myocytes follow a left-handed helix, while midmural cells are circumferentially aligned, and epicardial cells are arranged in a right-handed helix; the difference in HA between the extremes is around 120 degrees.[9,10] Taken together, the shortening of individual myocytes will therefore cause ventricular long-axis shortening (due to the epicardial and endocardial cells), narrowing (due to the midmural cells), and twisting (torsion) of the ventricle (due to the differences in HA between as one traverses the wall, from endocardium to epicardium).[11]
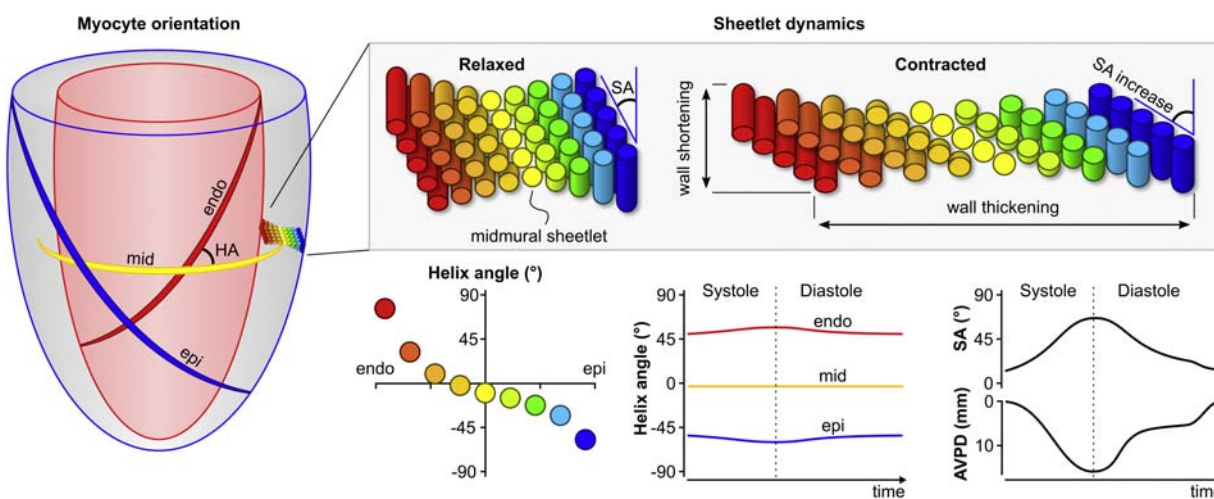
Cardiomyocytes are secondarily organized in microstructures termed *sheetlets*. A sheetlet is a laminar group of parallel myocytes, 5–10 cells in thickness. While the HA describes the relationship between the individual cellular shortening direction and the ventricle, the *sheetlet angle* refers to the cross-sectional alignment of sheetlets in relation to the local epicardial aspect of the ventricle (SA, Fig. 14.6). The sheetlet angle drastically increases during systolic contraction, implying that the myocardium undergoes a significant shear deformation. Indeed, this constitutes the predominant mechanism causing systolic LV wall thickening[12] in contrast with the HA, which changes very little over the cardiac cycle.
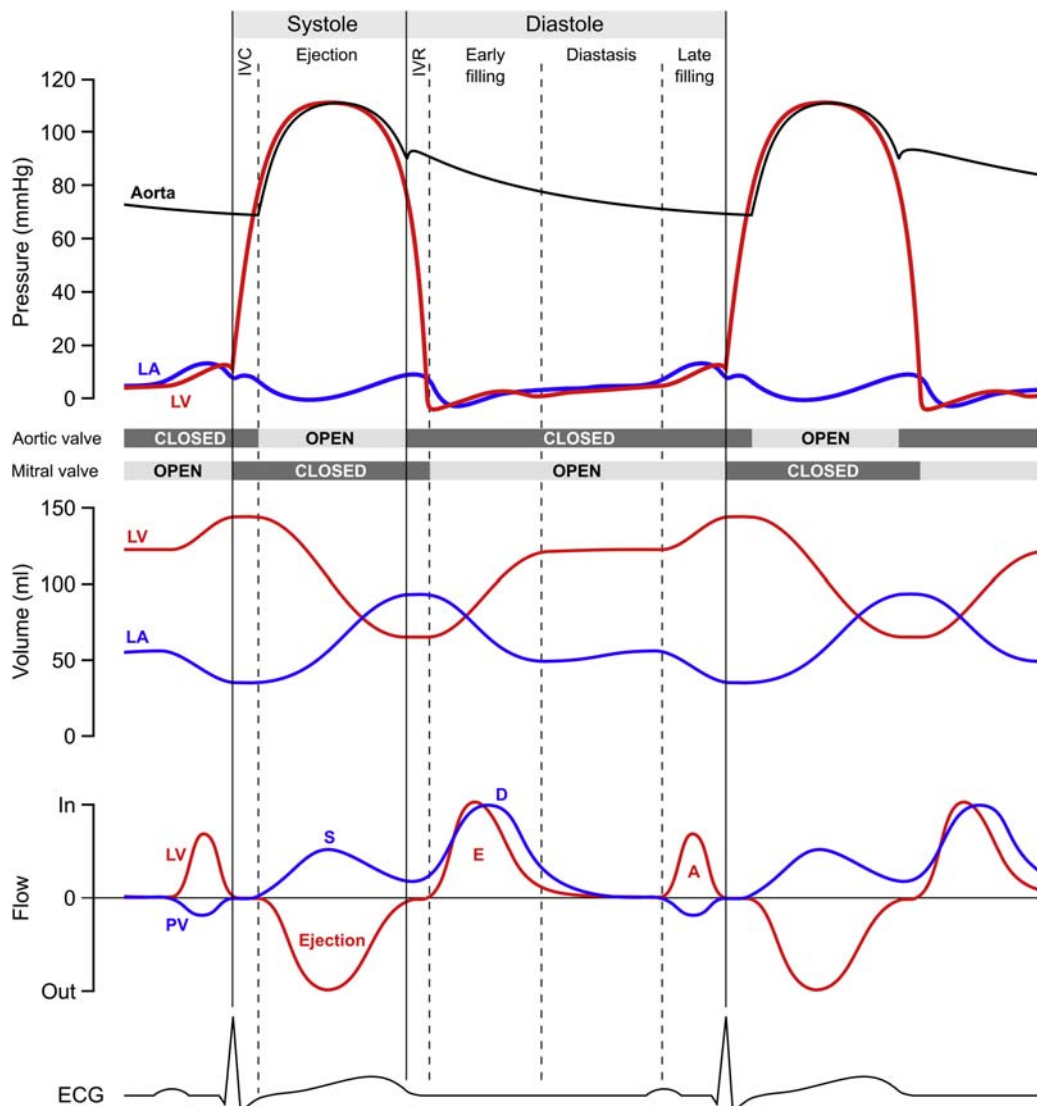
The cardiac cycle

Having established the principal modes of action of the myocardium, let us now consider the filling and emptying dynamics of the heart. The cardiac cycle can be visualized using a Wiggers diagram (Fig. 14.7), named after its inventor, Carl J Wiggers. For simplicity, we will only consider the left side (LA and LV) of the heart; the principles discussed below apply to the right heart (RA and RV) as well, with variations mainly in pressure levels.

The cardiac cycle begins with the spontaneous depolarization of the sinus node (P-wave in the ECG). This causes the atrium to contract and pull the mitral annulus upward, lengthening the chamber and ejecting atrial blood. The atrium has five orifices, four inlets (pulmonary veins, about 1 cm^2 cross-sectional area for each of the veins) and one outflow orifice (mitral valve having a cross-sectional area of 5–6 cm^2). Atrial contraction inscribes the Doppler echocardiographic A-wave of transmitral flow, and pushes blood into all five orifices! Blood flows into the relaxed LV via the large open mitral valve and simultaneously, a small amount of blood is pushed back into each of the pulmonary veins. It is self-evident that the duration of antegrade (into the LV) versus retrograde (back into the PVs) flow and the antegrade versus retrograde volumes are determined by the relative compliance of the LV chamber relative to the compliance of the pulmonary veins themselves. Indeed,

FIGURE 14.6 Patterns of myocyte organization. The primary pattern of myocyte organization is that of a helix whose angle varies across the ventricular wall. The epicardial and endocardial layers are longitudinally arranged, resulting in a systolic long-axis shortening of the ventricle. Relative to a spatially fixed epicardial apex, this is quantifiable as atrioventricular plane displacement (AVPD). Secondarily, myocytes are arranged in sheetlets which undergo systolic shear deformation; this is the main mechanism for wall thickening. Recall total tissue volume is conserved between systole and diastole. The shear deformation also implies cyclical alterations to the space surrounding the myocytes, where the capillaries are situated, which may contribute to perfusion of the myocardium.[8]

FIGURE 14.7 Modified Wiggers diagram, showing pressure, volume, and flow variations over the cardiac cycle. Note that while the atrioventricular and ventriculoaortic pressure gradients are small (1−3 mmHg) in comparison to the absolute pressures, they are sufficient for diastolic volume pumping, i.e., to drive flow.[13] Also note the temporal matching of inflows and outflows, visible both in the volume and flow curves. Note that LV ejection (aortic stroke volume) is not fully compensated by the simultaneous pulmonary vein S wave entering the left atrium. This discrepancy between left heart outflow and simultaneous inflow causes slight (about 5%−8%) total heart volume variation, which is restored by the pulmonary vein D wave.

the duration of antegrade flow (duration of Doppler A-wave in msec) compared to the duration of retrograde PV flow is a measure of end-diastolic LV chamber stiffness.[14]

Atrial contraction pumps blood into the LV while simultaneously pulling the AV valve plane upward, lengthening the chamber, whose epicardial apex remains spatially fixed. This action generates a prestretch of myocytes and "primes" the ventricles for more efficient subsequent ejection through the Frank−Starling mechanism.

After atrial depolarization, the atrioventricular node introduces a slight temporal delay (P-Q interval in the ECG, equivalent to duration of the transmitral Doppler A-wave) before the Purkinje fiber network's depolarization wavefront reaches the ventricles. Once the ventricle starts to depolarize (QRS complex in the ECG), its contraction causes ventricular pressure to increase sharply. The increase in pressure forces blood toward the base of the ventricle, causing the mitral valve to close. Due to the closed mitral and aortic valves, ventricular volume remains constant—this period (30−60 ms) is referred to as isovolumic contraction and is characterized by rapid pressure buildup, usually quantitated by the peak slope of the rising pressure, denoted peak + dP/dt. Once ventricular pressure exceeds aortic pressure, (LVP > AoP) the aortic valve opens, LV pressure continues to rise for a brief interval as blood is accelerated into the aorta—the ejection phase begins.

After opening of the aortic valve, rate of LV pressure increase slows, and approximately halfway through ejection, LVP starts to decrease. The ventricle has now started its repolarization process (T wave on ECG). Aortic pressure now exceeds ventricular pressure and flow starts to decelerate; however, outflow continues for a while due to the inertia of the outflowing blood.[4] In healthy hearts, ejection imparts enough momentum on the outflowing blood to significantly contribute to emptying of the ventricle even in late systole, when contraction has ceased.[15] This leads to a smaller end-systolic volume and hence stronger restoring (recoil) forces, improving subsequent filling.

Eventually the pressure gradient between aorta and ventricle changes sign (LVP < AoP) and causes flow reversal, which quickly closes the aortic valve, ending ejection. The period from closure of the mitral valve to closure of the aortic valve is one definition of (mechanical) *systole*, the ejection phase. The duration of mechanical systole closely corresponds to the QT interval on the normal ECG and is a function of heart rate.[16]

As the ventricle repolarizes, its pressure continues to decrease through the process of isovolumic relaxation (IVR = 70−100 msec) to a point where it undershoots (LVP < LAP) the atrial pressure.[13] This causes the mitral valve to open and the LV begins to fill, while pressure is still decreasing. Because pressure continues to drop as the chamber volume increases, the wall must be springing apart faster than the chamber can fill, which effectively turns the ventricle into a mechanical suction pump that opens the mitral valve and aspirates blood from the atrium.[17,18] Therefore, after mitral valve opening, dP/dV is briefly <0! The "early rapid filling phase" of the LV commences, usually echocardiographically quantified as the transmitral Doppler E-wave. During the acceleration portion of the E-wave, LVP < LAP (suction), after the peak of the E-wave, at pressure crossover, when LVP = LAP, blood continues to flow into the LV due to inertia and continued relaxation of the myocardium, but eventually flow decelerates because LVP > LAP.

Once the pressure gradient between atrium and ventricle is eliminated after the E-wave, and the myocardium is fully relaxed, the chamber enters a temporary state of equilibrium where tissue motion ceases, all forces are balanced (but not zero), and there is no wall motion. The forces balanced interval is called the *diastasis*. Diastasis corresponds to the aforementioned equilibrium volume V_{eq} and therefore conveys information regarding the passive stiffness of the ventricle.[19] Diastasis is concluded when the sinus node depolarizes anew, which again leads to atrial contraction, inscription of the transmitral Doppler A-wave, and the end of the A-wave marks the beginning of a new cardiac cycle. The time spent by the relaxing and filling ventricle, from the isovolumic relaxation until the end of the late filling phase, is collectively called *diastole*. Expressions for the duration of diastole, and its phases (E-wave, diastasis, A-wave) or equivalently on the ECG
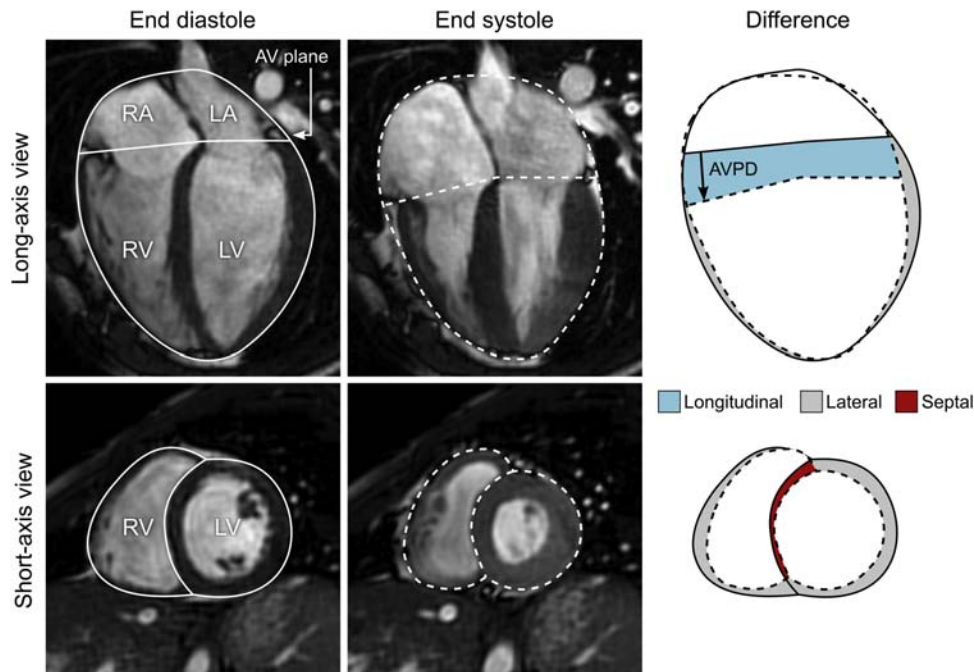
(RR duration minus the QT duration), as a function of heart rate have been proposed and validated.[16]

Atrioventricular valve plane displacement: give and take

With the Wiggers diagram fresh in mind, let us now revisit the anatomy of the heart from a functional perspective. During systole, myocyte shortening will lead to ejection of ventricular blood and subsequent long-axis shortening and short-axis (transverse) narrowing of the ventricles. Due to the predominantly longitudinal arrangement of the myocardium, long-axis shortening will dominate over transverse narrowing. The epicardial apex of the heart remains spatially stationary, since the pericardium is attached to the thoracic wall. Similarly, the base of the heart is anchored to the pulmonary and caval veins, the mediastinum as well as the great arteries. Therefore, ventricular long-axis shortening acts to pull the AV valve plane toward the fixed apex, simultaneously enlarging the atria whose posterior portion is anchored by the PVs. Hence the apically directed motion of the AV plane and its closed valves mechanically acts much like a plunger on a syringe, creating a pressure gradient which aspirates pulmonary and caval venous blood into the atria. Ventricular ejection is therefore temporally and mechanically coupled to atrial filling (Fig. 14.7). This reciprocal action is the main example of *systolic−diastolic coupling* reflected in the ventricular and atrial volume curves: as the LV empties, the LA fills, and vice versa.[20] The only exception to this rule may be during diastasis, when atrial filling may slowly continue due to the pressure head from the pulmonary veins.

In this view, the four-chambered heart acts as a piston (volume) pump that ejects blood through atrioventricular plane displacement (AVPD), a mode of pumping which simultaneously leads to atrial filling, ensuring that an adequate amount of blood is available for the subsequent filling phase. In fact, this effect extends beyond the confines of the heart: venous return to the heart is amplified by AVPD even in distal parts of the vasculature.[21] Now, if AVPD was the only mechanism for cardiac pumping, we should expect a 1:1 relationship between ventricular stroke volume leaving the pericardial space via the aorta and simultaneous atrial filling (pulmonary vein S wave). We should also expect a perfectly constant total heart volume, since the volume removed from the ventricles should be balanced by a corresponding increase in atrial volume. This is an appealing concept since it means no work is wasted displacing adjacent tissues.[22]

How significant, then, is the longitudinal contribution to stroke volume, compared to radial contribution? Studies using cardiac MRI have found that the healthy LV produces approximately 60% of its stroke volume by AVPD, while the rest results from radial narrowing (Fig. 14.8).[23,24] The right ventricle has a larger proportion of longitudinally

FIGURE 14.8   Principles of cardiac pumping require systolic—diastolic coupling. Left: MR images of a normal heart at end diastole shown in long-axis and short-axis views. The atrioventricular plane and epicardial boundaries have been delineated. Middle: end-systolic phase. Note that the AV plane has been pulled downwards toward the apex. Right: superposition of end-diastolic and end-systolic epicardial contours reveals the three principal modes of pumping. The longitudinal contribution to ventricular stroke volume is shown in blue. Note that RV AVPD exceeds LV AVPD. The lateral component is shown in gray. Note that this area corresponds to the outer volume changes of the heart. The septal component is shown in red. Normally, septal contraction contributes to LV pumping, and detracts slightly from RV pumping. The radial contribution to pumping is calculated as the sum of lateral and septal pumping.

oriented myocytes and lacks the midmural circumferential layer needed to generate high pressures, i.e., its primary role is to be a volume-pump. As a result, AVPD produces approximately 80% of RV stroke volume.

Radial pumping ejects a volume that will not be reciprocally filled into the atria, and explains why the pulmonary vein S wave filling the atrium is always smaller than the simultaneous stroke volume.[25,26] Total heart volume reaches its lowest point just before end-systole,[27] and the volume is largely recovered during early diastole through the pulmonary vein D wave. Additional total heart volume variation arises from a slight venous backflow in late diastole, resulting from atrial contraction.
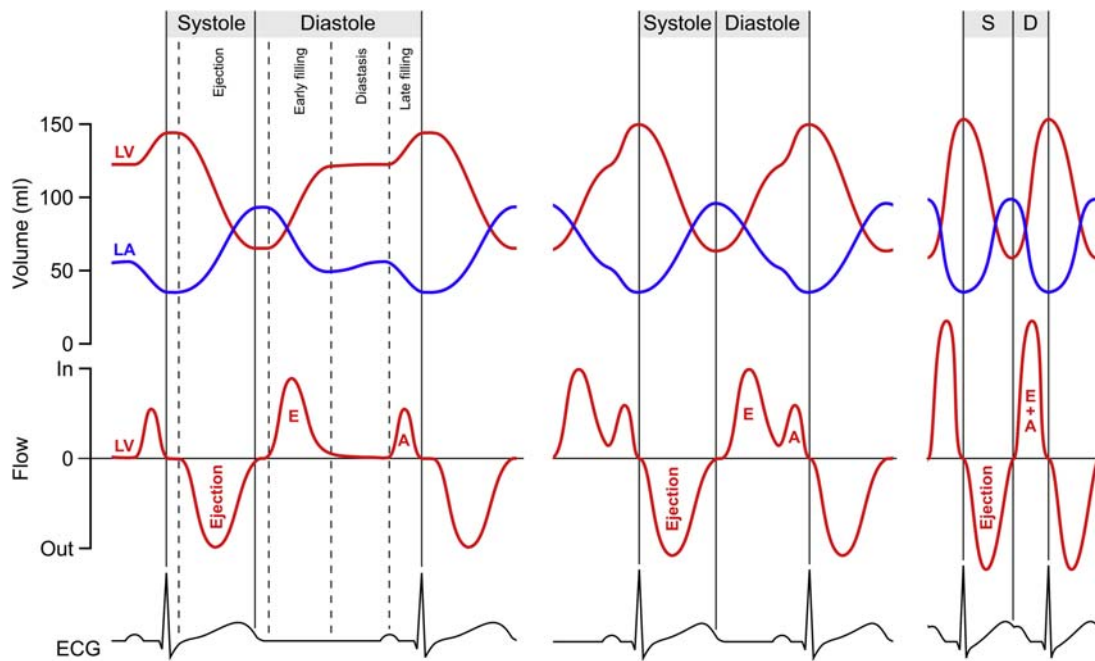
In summary, the four-chambered heart can be described as a *near*-constant volume pump whose total volume (about 800 mL) changes by 5%—8% (40—60 mL) over the cardiac cycle, and whose mode of operation is mainly through longitudinal shortening.[25,28]

Locked and loaded: recovering elastic energy during diastole

Thus far we have concentrated on how ventricular contraction manages to eject blood, but let us now turn to the problem of filling the ventricle. At rest, approximately one-third of the cardiac cycle is spent ejecting blood, a process which accounts for the vast majority of the heart's energy expenditures. The remaining time is spent filling the heart (in normal sinus rhythm) in a biphasic pattern: the E-wave (early rapid filling) is followed by the A-wave (atrial kick, late filling), separated by diastasis. With increasing heart rate, diastasis is gradually shortened and disappears completely at moderately elevated heart rates.[16] At even higher heart rates, the E- and A-waves merge to form a single filling wave, and diastole is *shorter* than systole (Fig. 14.9). Filling (volume pumping) must therefore involve higher levels of acceleration than emptying, despite occurring at much lower pressures. How is this possible?

Recall that systolic contraction below the equilibrium volume V_{eq} results in restoring forces building up in the myocardium. These forces are released upon cessation of systolic contraction, releasing the restoring forces and creating what is known as *diastolic recoil*. Diastolic recoil means that the ventricle rapidly springs back toward V_{eq}, seen in the Wiggers diagram as a rapid pressure decrease during isovolumic relaxation. The pressure decline continues briefly after mitral valve opening during the initial, early rapid phase (Doppler E-wave). As long as ventricular pressure drops while the ventricle fills, the chamber must be mechanically expanding faster than it can fill, hence, the

FIGURE 14.9 Gradual changes in filling dynamics with increasing exercise intensity. Left: At rest, the transmitral E- and A-waves are separated by diastasis. Middle: At moderate exercise, diastasis disappears, but E- and A-waves remain discernible. Right: At intense exercise, E- and A-waves merge into a uniphasic filling wave. The uniphasic waveform means that the LV is sucking at the same time that the atrium is pushing! The result is a sinusoidal filling/emptying pattern, reflected in the reciprocal LA/LV volume curves. Note also that at high heart rates, diastole is shorter than systole.

ventricle by definition functions as a mechanical diastolic *suction pump*. This fulfills the original criterion for ventricular suction defined by Katz:

$$\frac{dP}{dV} < 0,$$

regardless of absolute pressure level. Recall that the definition of chamber stiffness is *dP/dV*, the instantaneous slope of the pressure-volume relation. When the ventricle sucks *dP/dV* is negative, and the LV has negative stiffness! It is important to recall that the definition of suction is that LVP drop below the pressure in the chamber that is the source for filling, i.e., the left atrium. Diastolic suction therefore does not mean that the pressure in the LV is below atmospheric pressure, rather, suction is defined relative to the source pressure for filling. Also note that transmural wall pressure gradients are immaterial to this kinematic definition and need not be considered, as long as atrial pressure is known. This *dP/dV* < 0 definition for suction is also valid regardless of heart rate; ventricular suction contributes to filling even with a simultaneously contracting atrium. In fact, the basally directed "pull" of the atria serve to amplify the relaxation and expansion of the ventricle.

Diastolic relaxation is an active process, dependent on at least three critical events at the cellular level: quick removal of intracellular Ca^{2+}, thin filament deactivation, and crossbridge cycling.[29] To complicate matters further,

these processes are interdependent and influenced by many intracellular processes and factors such as the presence of ATP, changes in gene expression, intracellular sodium levels, and so on. And finally, the modulation of diastolic relaxation (*lusitropy*) occurs through organ-level changes in heart rate, preload, and sympathetic tone, which in turn are also interconnected. When relaxation works properly, it enables quick release of stored elastic strain energy; whenever it is impaired, diastolic suction will be attenuated, and filling impaired as a result.

Impaired diastolic function is a typical finding in heart failure and may precede systolic impairment. As such, it is often seen in heart failure with preserved ejection fraction. Conversely, whenever systolic dysfunction is manifest, as a result of *systolic–diastolic coupling*, it follows *by necessity* that diastolic function is also disturbed. Clinical quantitation of diastolic function seeks to determine whether relaxation abnormality or increased stiffness is present, and whether cardiac filling pressures have become elevated as a compensatory mechanism. In concise terms, the determinants of diastolic function are stiffness, relaxation, and load.

The evidence for diastolic suction has accrued gradually. Early studies in animal models found that clamping the mitral valve at end-systole resulted in negative (subatmospheric) LV pressures, in the open chest, pericardial cradle experiments.[18,30] Using invasive pressure-volume catheters, later studies (closed chest) have demonstrated

the presence of early diastolic intracavitary and atrioventricular pressure gradients whose properties match the dynamics of the E-wave.[13] These pressure gradients are attenuated in myocardial ischemia, with increasingly diminished diastolic suction seen with worsening systolic function.[31] To further underscore the significance of *systolic—diastolic coupling*, incorporating the spring-like characteristics of diastolic function, the effects of the relaxing myocardium on the resulting inflow patterns have been formulated kinematically, and viewed as an inertial cardiohemic oscillation. Accordingly, E-wave contours are generated by this process and must obey the laws of motion. It can be described using a mathematical framework in analogy to damped harmonic oscillatory motion as detailed in the *parametrized diastolic filling formalism*.[32] This model that employed a linear, bidirectional spring was introduced many years before the actual linear, bidirectional molecular spring—titin[14]—was uncovered, demonstrating the fundamental predictive utility of kinematic modeling of the heart.[5]

The presence of a pulmonary venous D wave is key to understanding diastolic suction. It tells us that whichever mechanism normally causes blood to flow from the atrium into the ventricle must reside at the ventricular level. If ventricular filling is increasingly driven by elevated atrial pressure, and diastolic suction is impeded, we expect a diminished D wave, which is exactly what is observed. Furthermore, the volume displaced by radial pumping (epicardial volume change) corresponds to the D wave and atrial conduit volume, as evidenced using both echocardiography and MRI.[33—35] This volume is also equivalent to the difference between the stroke volume exiting the pericardial volume and the simultaneously entering pulmonary S wave volume.[36] Ventricular suction must be present whenever ventricular volume is below V_{eq}, since this implies the presence of restoring forces acting to lengthen the myocytes. In the overstretched ventricle (as in congestive heart failure or acute volume overload), restoring forces may actually counteract ventricular filling since adding more volume implies moving further away from V_{eq}.

Summary

In this chapter, we have examined the functional consequences of both cardiac anatomy, with a focus on atrioventricular interactions, and of the filament model of the myocyte, especially with regards to the spring-like protein titin. Through the helical arrangement of myocytes, systolic contraction mainly leads to shortening of the ventricles, a longitudinal motion of the AV plane which ensures simultaneous filling of the atria. The reciprocation is not perfect, and while the discrepancy between inflow and outflow during systole is caused by radial narrowing of the ventricle, it

also gives rise to the pulmonary vein D wave which is explained by ventricular diastolic suction. At the cellular level, all motion away from slack length or equilibrium will be opposed by restoring forces primarily generated by the spring-like protein titin. It follows that systolic shortening will prime the ventricle for subsequent release of elastic energy—diastolic suction—which serves to bring the ventricle back toward equilibrium. Increasing the deviation from the equilibrium volume, such as after a more forceful contraction, therefore augments diastolic filling both by release of more elastic energy, and by improved atrial inflow during systole. It also follows that patients with systolic dysfunction must always have some degree of diastolic disturbance—but the opposite is not necessarily true.

Supplementary data

Supplementary data to this chapter can be found online at https://doi.org/10.1016/B978-0-323-91391-1.00014-5.

See cardiac MRI cine loop of four-chamber and short-axis views (Online material).

References

1. Coghlan C, Hoffman J. Leonardo da Vinci's flights of the mind must continue: cardiac architecture and the fundamental relation of form and function revisited. **Eur J Cardio Thoracic Surg**. 2006; 29:S4—S17.
2. Sallin EA. Fiber orientation and ejection fraction in the human left ventricle. **Biophys J**. 1969; 9:954—964.
3. Pettigrew J. On the arrangement of the muscular fibres in the ventricles of the vertebrate heart, with physiological remarks. **Philos Trans R Soc Lond**. 1864; 154:445—500.
4. Noble MIM. The contribution of blood momentum to left ventricular ejection in the dog. **Circ Res**. 1968; 23:663—670.
5. Helmes M, Trombitás K, Granzier HL. Titin develops restoring force in rat cardiac myocytes. **Circ Res**. 1996; 79:619—626.
6. Granzier HL, Irving TC. Passive tension in cardiac muscle: contribution of collagen, titin, microtubules, and intermediate filaments. **Biophys J**. 1995; 68:1027—1044.
7. Omens JH, Fung YC. Residual strain in rat left ventricle. **Circ Res**. 1990; 66:37—45.
8. Kilner PJ, McCarthy K, Murillo M, et al. Histology of human myocardial laminar microstructure and consideration of its cyclic deformations with respect to interpretation of in vivo cardiac diffusion tensor imaging. **J Cardiovasc Magn Reson**. 2015; 17:1—3.
9. Hsu EW, Muzikant AL, Matulevicius SA, Penland RC, Henriquez CS. Magnetic resonance myocardial fiber-orientation mapping with direct histological correlation. **Am J Physiol Heart Circ Physiol**. 1998; 274:1627—1634.
10. Streeter DD, Spotnitz HM, Patel DP, Ross J, Sonnenblick EH. Fiber orientation in the canine left ventricle during diastole and systole. **Circ Res**. 1969; 24:339—347.
11. Notomi Y, Popovic ZB, Yamada H, et al. Ventricular untwisting: a temporal link between left ventricular relaxation and suction. **Am J Physiol Heart Circ Physiol**. 2008; 294:H505—H513.

12. Nielles-Vallespin S, Khalique Z, Ferreira PF, et al. Assessment of myocardial microstructural dynamics by in vivo diffusion tensor cardiac magnetic resonance. **J Am Coll Cardiol**. 2017; 69:661−676.

13. Courtois M, Kovács SJ, Ludbrook PA. Transmitral pressure-flow velocity relation. Importance of regional pressure gradients in the left ventricle during diastole. **Circulation**. 1988; 78:661−671.

14. Rossvoll O, Hatle LK. Pulmonary venous flow velocities recorded by transthoracic Doppler ultrasound: relation to left ventricular diastolic pressures. **J Am Coll Cardiol**. 1993; 21:1687−1696.

15. Yoshida T, Ohte N, Narita H, et al. Lack of inertia force of late systolic aortic flow is a cause of left ventricular isolated diastolic dysfunction in patients with coronary artery disease. **J Am Coll Cardiol**. 2006; 48:983−991.

16. Chung CS, Karamanoglu M, Kovács SJ. Duration of diastole and its phases as a function of heart rate during supine bicycle exercise. **Am J Physiol Heart Circ Physiol**. 2004; 287:H2003−H2008.

17. Katz LN. The role played by the ventricular relaxation process in filling the ventricle. **Am J Physiol**. 1930; 95:542−553.

18. Brecher GA. Experimental evidence of ventricular diastolic suction. **Circ Res**. 1956; 4:513−518.

19. Zhang W, Kovács SJ. The diastatic pressure-volume relationship is not the same as the end-diastolic pressure-volume relationship. **Am J Physiol Heart Circ Physiol**. 2008; 294:H2750−H2760.

20. Steding-Ehrenborg K, Carlsson M, Stephensen S, Arheden H. Atrial aspiration from pulmonary and caval veins is caused by ventricular contraction and secures 70% of the total stroke volume independent of resting heart rate and heart size. **Clin Physiol Func Imaging**. 2013; 33:233−240.

21. Abu-Yousef MM, Mufid M, Woods KT, Brown BP, Barloon TJ. Normal lower limb venous Doppler flow phasicity: is it cardiac or respiratory? **Am J Roentgenol**. 1997; 169:1721−1725.

22. Hamilton W, Rompf J. Movements of the base of the ventricle and the relative constancy of the cardiac volume. **Am J Physiol**. 1932; 102:559−565.

23. Carlsson M, Ugander M, Mosen H, Buhre T, Arheden H. Atrioventricular plane displacement is the major contributor to left ventricular pumping in healthy adults, athletes, and patients with dilated cardiomyopathy. **Am J Physiol Heart Circ Physiol**. 2007; 292:H1452−H1459.

24. Stephensen S, Steding-Ehrenborg K, Munkhammar P, Heiberg E, Arheden H, Carlsson M. The relationship between longitudinal, lateral, and septal contribution to stroke volume in patients with pulmonary regurgitation and healthy volunteers. **Am J Physiol Heart Circ Physiol**. 2014; 306:H895−H903.

25. Bowman AW, Kovács SJ. Assessment and consequences of the constant-volume attribute of the four-chambered heart. **Am J Physiol Heart Circ Physiol**. 2003; 285:H2027−H2033.

26. Waters EA, Bowman AW, Kovács SJ. MRI-determined left ventricular "crescent effect": a consequence of the slight deviation of contents of the pericardial sack from the constant-volume state. **Am J Physiol Heart Circ Physiol**. 2005; 288:H848−H853.

27. Carlsson M, Ugander M, Kanski M, Borgquist R, Ekelund U, Arheden H. Heart filling exceeds emptying during late ventricular systole in patients with systolic heart failure and healthy subjects - a cardiac MRI study. **Clin Physiol Funct Imaging**. 2018:1−9.

28. Carlsson M, Cain P, Holmqvist C, Ståhlberg F, Lundbäck S, Arheden H. Total heart volume variation throughout the cardiac cycle in humans. **Am J Physiol Heart Circ Physiol**. 2004; 287:H243−H250.

29. Biesiadecki BJ, Davis JP, Ziolo MT, Janssen PML. Tri-modal regulation of cardiac muscle relaxation; intracellular calcium decline, thin filament deactivation, and cross-bridge cycling kinetics. **Biophys Rev**. 2014; 1:273−289.

30. Kraner JC, Ogden E. Ventricular suction in the turtle. **Circ Res**. 1956; 4:724−726.

31. Courtois M, Kovács SJ, Ludbrook PA. Physiological early diastolic intraventricular pressure gradient is lost during acute myocardial ischemia. **Circulation**. 1990; 81:1688−1696.

32. Kovács SJ, Barzilai B, Perez JE. Evaluation of diastolic function with Doppler echocardiography: the PDF formalism. **Am J Physiol Heart Circ Physiol**. 1987; 252:H178−H187.

33. Bowman AW, Kovács SJ. Left atrial conduit volume is generated by deviation from the constant-volume state of the left heart: a combined MRI-echocardiographic study. **Am J Physiol Heart Circ Physiol**. 2004; 286:H2416−H2424.

34. Riordan MM, Kovács SJ. Elucidation of spatially distinct compensatory mechanisms in diastole: radial compensation for impaired longitudinal filling in left ventricular hypertrophy. **J Appl Physiol**. 2008; 104:513−520.

35. Riordan MM, Kovács SJ. Relationship of pulmonary vein flow to left ventricular short-axis epicardial displacement in diastole: model-based prediction with in vivo validation. **Am J Physiol Heart Circ Physiol**. 2006; 291:H1210−H1215.

36. Arvidsson PM, Töger J, Heiberg E, Carlsson M, Arheden H. Quantification of left and right atrial kinetic energy using four-dimensional intracardiac magnetic resonance imaging flow measurements. **J Appl Physiol**. 2013; 114:1472−1481.

Chapter 15

Ventricular–arterial coupling: the pressure–volume plane

Julio A. Chirinos[1,2]

[1]University of Pennsylvania Perelman School of Medicine, Hospital of the University of Pennsylvania and Perelman Center for Advanced Medicine, Philadelphia, PA, United States; [2]Ghent University, Ghent, Belgium

Introduction

Detailed phenotyping of ventricular–arterial (VA) coupling and arterial hemodynamics provides important insights into the pathophysiology of left ventricular (LV) energetics, remodeling and fibrosis, systolic and diastolic dysfunction in various disease states.[1–6]
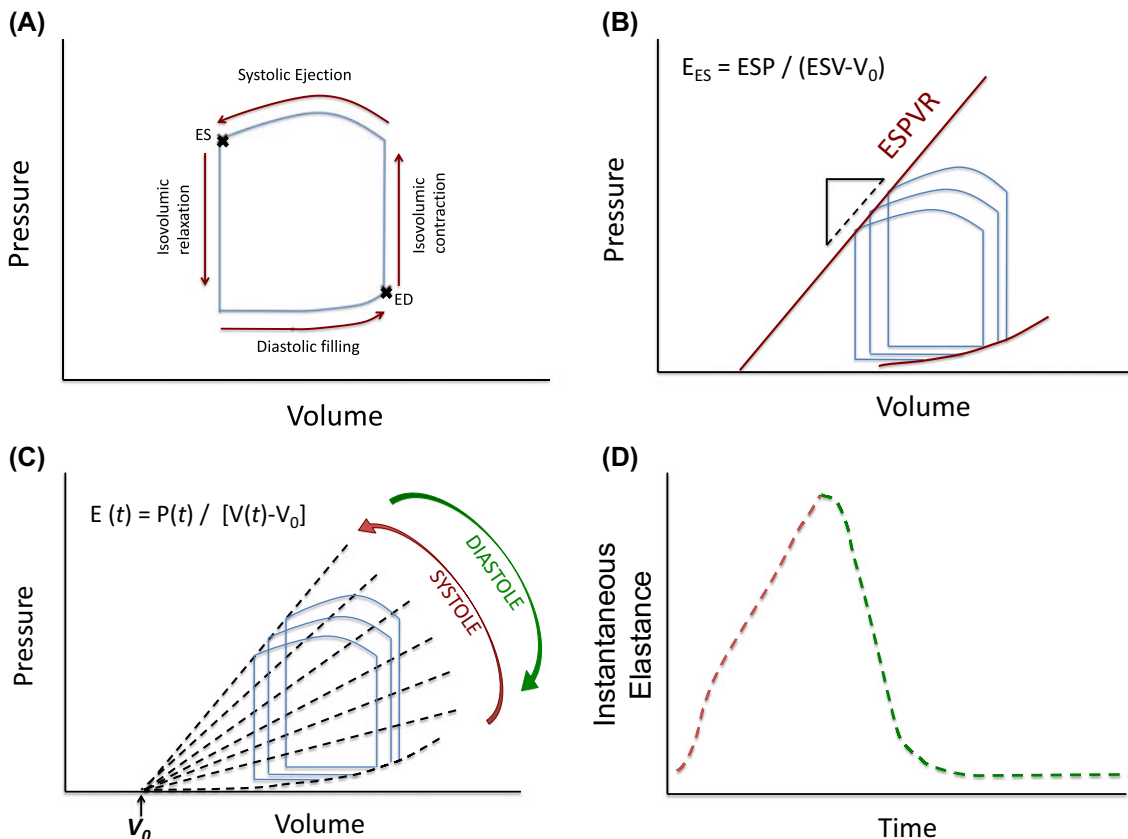
The interactions between the LV and systemic arteries are key determinants of cardiovascular function and encompass a broad and complex set of hemodynamic phenomena. VA coupling, defined narrowly to encompass the determinants of stroke volume and the energetic coupling of the LV and the arterial system, has been most frequently assessed in the pressure–volume plane. This approach is widely taught in formal cardiovascular physiology courses, and provides useful information regarding the operating mechanical efficiency and performance of the VA system when the LV ejection fraction (EF) is frankly abnormal (such as in Heart Failure with Reduced EF, HFrEF). However, analyses in the pressure–volume plane have important limitations and are much less informative in the presence of a normal LV EF, such as in Heart Failure with Preserved EF (HFpEF). More importantly, analyses in the pressure–volume plane do not characterize broader aspects of VA cross-talk, particularly those related to pulsatile arterial load, which are highly clinically relevant both among patients at risk for HF and for patients with established HFrEF or HFpEF. Assessment of arterial load and VA coupling via analysis of time-varying pressure-flow relations and myocardial wall stress (MWS) provides important incremental physiologic information about the cardiovascular system. In particular, the systolic loading sequence (early vs. late systolic load), an important aspect of VA coupling, is neglected by pressure–volume

analyses, and can profoundly impact LV function, remodeling, and progression to heart failure.

This chapter deals with relevant technical and physiologic aspects regarding VA coupling assessments in the pressure–volume plane, and is largely based on previous reviews by the author.[1,3,4] Subsequent chapters in this textbook discuss other informative approaches to characterize VA interactions, including time-varying MWS (Chapter 16) and time-varying pressure-flow analyses (Chapters 17; please also refer to Chapters 1, 3, 11). This chapter does not address pulmonary arterial load and right ventricular–pulmonary vascular interactions, which are discussed in section VI of this textbook (Chapters 55 and 56).

The pressure volume plane

As shown in Fig. 15.1, the pressure volume plane is a two-dimensional plot in which pressure is represented in the vertical axis, whereas volume is represented in the horizontal axis. The LV pressure-volume loop is a plot of instantaneous LV cavity pressure and volume data points throughout a full cardiac cycle. When instantaneous pressure–volume data points are plotted from the beginning of systole to the end of diastole, they proceed in a counterclockwise manner, defining a loop, commonly called the LV pressure–volume loop (Fig. 15.1A). The lower right "corner" of this loop represents end-diastole. Isovolumic LV contraction results in an increase in LV pressure without an increase in LV volume (vertical line). After aortic valve opening, LV volume decreases as the LV ejects blood, which results in a leftward shift of the instantaneous pressure–volume points. At the end of ejection, aortic valve closure is normally followed by a drop in LV pressure at constant volume before mitral valve

FIGURE 15.1 (A) Left ventricular pressure–volume relation in a single beat; (B) end-systolic and end-diastolic pressure–volume relations obtained from a "family" or pressure–volume loops; (C) Instantaneous isochrones during the cardiac cycle (note the assumption of a common volume-axis intercept, V_0 for all isochrones); (D) Time-varying elastance curve, obtained from plotting the slope of the isochrones over time. E, elastance; E_{ES}, end-systolic elastance; ESP, end-systolic pressure; P, pressure; (t), point in time; V_0, volume intercept of the pressure volume relation. *Modified from Chirinos JA. Ventricular-arterial coupling: invasive and non-invasive assessment. **Artery Res**. 2013;7.*

opening (isovolumic relaxation), resulting in a vertical line in the PV loop. After mitral valve opening, diastolic suction continues until the end of relaxation, which is followed by passive filling of the cavity with increasing pressure until end-diastole. Late diastolic passive filling follows a nonlinear pattern in the pressure volume plane.

The LV chamber as a time-varying elastance

The concept of the time-varying LV elastance and its role in LV pump function and myocardial energetics were first formulated by Suga and Sagawa.[7–10] When a family of pressure–volume loops are obtained from the same subject during acute preload or afterload alterations *at a constant inotropic state*, the left upper loop corners (end-systolic pressure–volume points) describe the end-systolic pressure–volume relation (ESPVR). The LV end-systolic elastance (E_{ES}) is quantified as the slope of the ESPVR, which is considered to be linear or quasi-linear in the physiologic range. E_{ES} represents an index of LV end-systolic stiffness and contractility. Fig. 15.1B shows a schematic representation of PV loops from a hypothetical subject, obtained during three beats under different preload

conditions. The points corresponding to end-systole can be connected with a line, the slope of which is E_{ES}. V_0 is the volume-axis intercept of the ESPVR, which represents a purely theoretical volume at zero pressure, assuming a linear ESPVR. E_{ES} is an index of the contractility and systolic stiffness of the LV. As such, it is affected by the inotropic state of the myocardium and in the long-term, by geometric remodeling and biophysical myocardial tissue properties (which in turn depend on stiffness of myocardial cells, fibrosis, and various other factors).[11,12]

The end-systolic elastance concept is intuitive because it is based on an easily recognizable, well-defined time point in the cardiac cycle. However, it should be noted that a pressure–volume relationship exists at each instant during the cardiac cycle, giving rise to the concept of the "time-varying" elastance (Fig. 15.1C and D). Fig. 15.1C shows a representative family of the LV instantaneous pressure–volume relationships based on joining instantaneous pressure–volume points that occur at similar times during the cardiac cycle in different beats (which are referred to as "isochrones"). The slope of these isochrones increases during systole as the chamber stiffness increases, becoming steepest (i.e., stiffest) toward the end of systole (red arrow),

to then decrease during diastole (green arrow). If the slope of these isochrones is plotted over time (with slope in the vertical axis and time in the horizontal axis), a time-varying elastance [E(t)] curve is obtained (Fig. 15.1D). As will be discussed later, the normalized shape of the time-varying elastance curve tends to be conserved between individuals and disease states, such that the linear E(t) model treats the LV as a spring that stiffens and relaxes along a predictable time course during the cardiac cycle.[9,13] Although the maximal value (i.e., steepest isochrone) of E(t) does not always occur in end-systole (due to inertial influences on pressure and LV outflow before aortic valve closure), in practice this issue is usually ignored and the maximal value of E(t) is considered to be equivalent to E_{ES}.[14]

Key requisites and/or proposed features of the linear E(t) model are:

(**1**) A linear shape of all isochrones (lines connecting equal time points in a P-V diagram of different beats (acquired under different loading conditions);
(**2**) A common intercept of these isochrones with the volume axis (Fig. 15.1C);
(**3**) E(t) is a function of time only, independent of instantaneous and past pressure and volume under a stable contractile state;
(**4**) When normalized for amplitude and time to peak amplitude, the shape of the E(t) curve has a relatively constant shape despite variations in underlying cardiac disease, contractility, loading, and heart rate, particularly during early systole (first 25% to 35% of contraction).

These features and assumptions are important to understand because they are central to the E(t) theory and underlie its main strengths and limitations, which will be discussed later in this chapter. In addition, these features allowed for the development of commonly used methods to approximate E_{ES}, which are based on the derivation of V_0 and E_{ES} from measurements performed in a single heartbeat, without the need for preload alterations.[15,16]

Relationship between the pressure—volume area and LV energetics
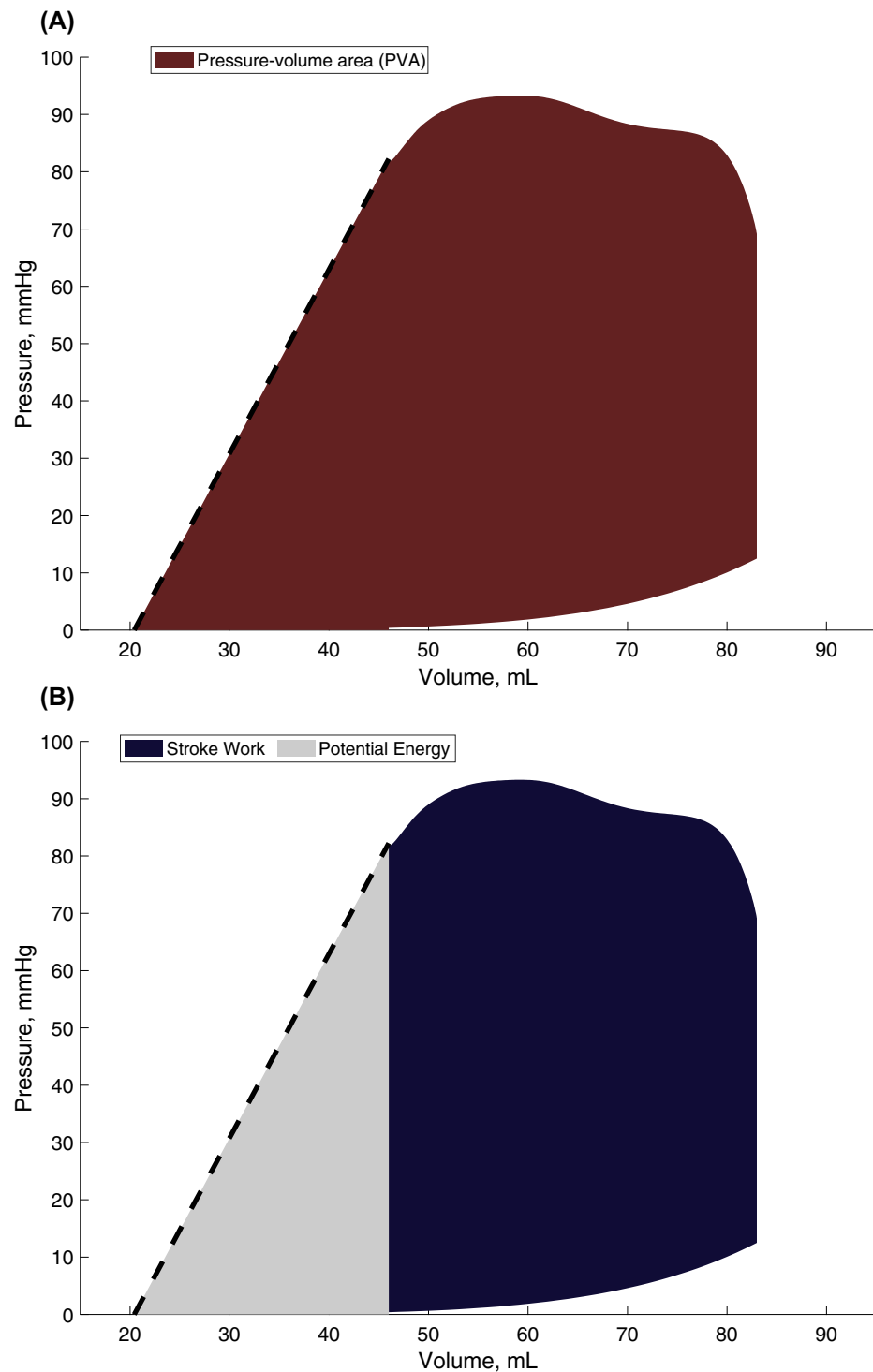
For a given beat, the pressure—volume area (PVA) is the area circumscribed by three sides: (1) the end-diastolic pressure—volume relation curve; (2) the end-systolic P-V relation line, and; (3) the systolic portion of the pressure—volume loop trajectory (Fig. 15.2A).[8,17]

The PVA in an ejecting contraction can be divided in two parts: (1) The area enclosed within the pressure—volume loop trajectory, which represents the LV *external work* or *stroke work*; (2) The approximately triangular area enclosed by the linear ESPVR, the left border of a single pressure—volume loop and the end-diastolic pressure—

volume relation (Fig. 15.2B). The latter area has been proposed to represent the end-systolic elastic potential energy built up and stored in the LV wall during systole.

According to the time varying-elastance theory, the PVA represents the total mechanical energy generated by the LV contraction until end-systole. Experiments in excised canine heart preparations cross-circulated with a support dog have shown that, when a single excised heart operates *at a stable contractile state* under various preload and afterload conditions, PVA correlates strongly and linearly with myocardial oxygen consumption (MVO_2) per beat.[8,17,18] (Fig. 15.3). Based on these experiments, it was proposed and it is now widely accepted that the ratio of stroke work (SW) to PVA (the latter considered in this context a surrogate of MVO_2 per beat) represents an index of mechanical efficiency *under specific operating conditions in a given heart*.
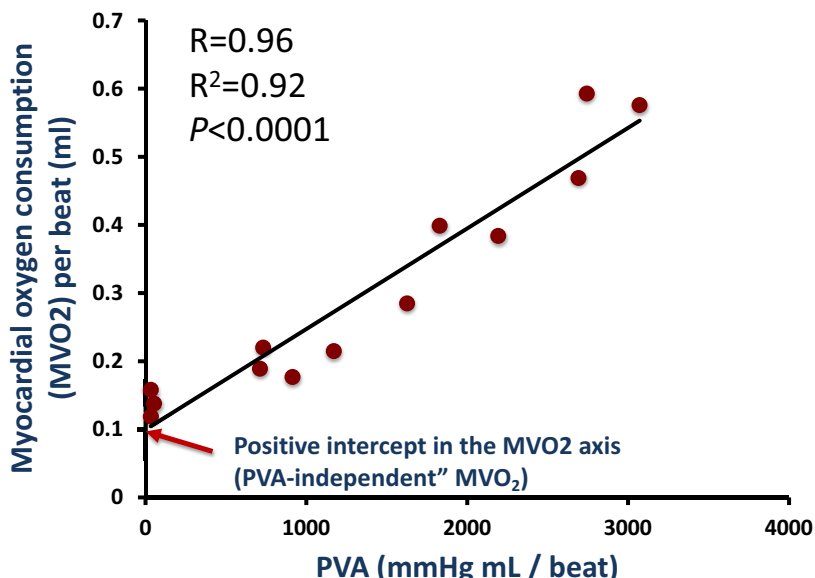
An important point of caution should be considered regarding the use of PVA as a surrogate of MVO_2 in clinical studies, which has become popular due to the relative case of estimating the PVA as opposed to MVO_2 in vivo. Whereas the strong linear relation between PVA and MVO_2 within a given heart is unquestionable, the relationship between measured MVO_2 and PVA within a group of human hearts in vivo is actually much weaker. This can be understood by more closely assessing the nature of the PVA-MVO_2 relation. Within a given heart (Fig. 15.3), the line that relates MVO_2 to PVA demonstrates: (1) A finite slope, which characterizes the efficiency of cardiac chemomechanical conversion in that particular heart in the setting of varying preload and afterload states; (2) A positive intercept with the MVO_2 axis (Fig. 15.3), which can be seen as the "PVA-independent" MVO_2 of that particular heart under that particular inotropic state. The "PVA-independent" MVO_2 is likely related to the energetic costs of excitation—contraction coupling and basal myocardial cellular metabolism. It is important to note that both the slope and particularly, the intercept of this relation are highly variable between different hearts or even in the same heart operating at different inotropic states[19] (for example, positive inotropic interventions generally, but not universally, increase the intercept of the relation and thus shift the entire relation "upward," and vice-versa). Although the variability in the slope and intercept of the PVA-MVO_2 relation appears to be limited between excised hearts operating ex vivo under highly controlled conditions, a more recent reanalysis of invasive human in vivo data[1] reported by Kameyama et al.[19] revealed that the relationship between MVO_2 and PVA is actually much weaker, either at rest ($R^2 = 0.35$) of after phenylephrine administration ($R^2 = 0.16$).[1] This was due to high variability in both the slope and the intercept of the PVA-MVO_2 relation *between* individual hearts, with the slope varying from 2.08 to 3 J/beat, and the MVO_2-axis intercept variability varying

FIGURE 15.2 (A) Representation of the pressure−volume area (PVA) of a single beat; (B) Breakdown of the PVA into stroke (external) work (blue) and potential energy (gray). In both panels, the end-systolic pressure−volume relation is represented by the *black dashed line*. *Modified from Chirinos JA. Ventricular-arterial coupling: invasive and non-invasive assessment.* **Artery Res**. *2013;7.*

over a span greater that an order of magnitude (from 0.04 to 1 J/beat).[19] Therefore, a great deal of caution should be undertaken when using the PVA to assess mechanical efficiency (when the latter is defined as the MVO_2 required to generate a given stroke work), within populations or even within individuals in the setting of interventions that may change the intercept or the slope of the PVA-MVO_2 relation.

FIGURE 15.3 Panel A shows the strong, linear PVA-MVO$_2$ relation in a single excised heart at a stable contractile state operating under various preload and afterload conditions, as initially reported by Khalafbeigui, Suga and Sagawa. *Modified from Chirinos JA. Ventricular-arterial coupling: invasive and non-invasive assessment.* **Artery Res.** 2013;7.

The concept of effective arterial elastance and assessment of ventricular−arterial coupling in the pressure−volume plane

After the pressure−volume paradigm was developed to characterize LV chamber contractility/stiffness and LV energetics, it was extended to the assessment of VA coupling, primarily to understand the determinants of stroke volume, based on the concept of matching elastances (ventricular and arterial).[20−22] This required expressing the arterial load as a single parameter in units of elastance that could be plotted or readily represented in the pressure− volume plane. The concept was based on the premise that, provided that heart rate, diastolic and systolic duration remain constant, arterial end-systolic pressure changes with stroke volume in a roughly linear fashion (the greater the stroke volume ejected into the arterial system, the greater the generated end-systolic pressure will be). Making multiple simplifying assumptions, Sunagawa et al. derived an equation that relates the slope of this relation to arterial properties and proposed that this slope can be used as a lumped parameter of the impedance that the arterial tree offers to the stroke flow (that is, a lumped parameter of arterial load).[20,23] This slope was called effective arterial elastance (E_A), since it treats the arterial system as an elastic chamber that has a volume elastance (and thus has units of elastance, allowing for an easy comparison to LV end-systolic elastance). With such representation, both the LV and the arterial system are thus treated as elastances and quantified in the same units (change in pressure for a given change in volume; or mm/mL).
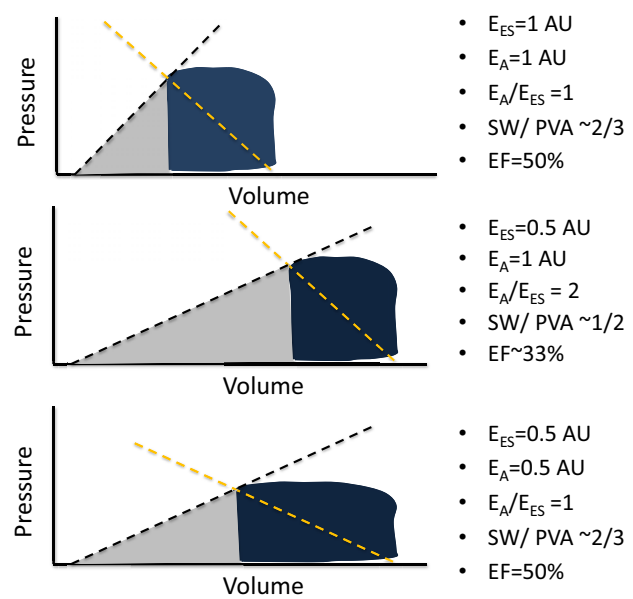
Despite the several important limitations of this approach, discussed later in this chapter, some important aspects of VA coupling can indeed be assessed in the pressure−volume plane using the ratio of E_A to LV E_{ES}. Due to geometric considerations, the E_A/E_{ES} ratio roughly correlates with the ratio of stroke work to PVA. Since the stroke work represents the total mechanical energy transferred from the LV to the arterial elastance, whereas the PVA represents the total mechanical energy generated by ventricular contraction (which in turn correlates with MVO$_2$ per beat within a given heart at a specific contractile state as described above), this ratio relates to the operating energetic and mechanical efficiency of the LV in single hearts operating at different loading conditions. It was predicted analytically and shown experimentally in isolated canine heart preparations that the stroke work is maximal when the slopes of LV E_{ES} and E_A are approximately equal to one another (i.e., roughly matched LV and arterial elastances).[23] It should be noted that the E_A/E_{ES} ratio is intimately related to the "effective" EF (ratio of stroke volume to the effective end-diastolic volume, where "effective" end-diastolic volume equals measured end-diastolic volume minus V_0), and this relationship is represented by the following equation: Effective EF = 1/[1+E_A/ E_{ES}]). A value of E_A/E_{ES} equal to 1 implies that the effective EF is ∼50%. The "effective" EF defined in this manner equals the actual LV EF (stroke volume/end-diastolic volume) only when V_0 is zero. Given that V_0 usually has a small positive value, rather than a zero value, this operating state would correspond to actual EF values slightly lower than 50%, which are clearly not the norm in healthy humans, imposing a fundamental problem on the entire paradigm. It was subsequently predicted that, whereas stroke work is maximized when E_A/E_{ES} ∼1, the energetic efficiency (ratio of stroke work to PVA) is

maximized at lower E_A/E_{ES} ratios (which correspond to higher LV EF values).[24] De Tombe et al. studied the dependence of stroke work and mechanical efficiency on the E_A/E_{ES} ratio in isolated blood-perfused canine hearts[25] over a broad range of E_A values. It was shown that on average, stroke work was maximized at $E_A/E_{ES} \sim 0.80$, whereas efficiency was maximal at $E_A/E_{ES} \sim 0.70$. Interestingly, mean E_A/E_{ES} ratios reported in large cohorts of normal humans are $\sim 0.62-0.82$.[26,27] More importantly, De Tombe et al.[25] showed that both stroke work and efficiency were $\geq 90\%$ of their optimal values over a broad range of E_A/E_{ES} ratios (0.3–1.3), which corresponded to a wide range of EFs ($\sim 40-80\%$). The authors concluded that precise optimization of either stroke work of mechanical efficiency is of little consequence in the absence of severe abnormalities in E_{ES} or E_A and that in such circumstances, regulatory systems likely center on control of blood pressure, circulating volume and oxygenation, and can ignore ventricular stroke work or efficiency.[25] In severely abnormal coupling states, however, this homeostasis is lost. In particular, given the close relationship between the E_A/E_{ES} ratio and effective LV EF as described above, markedly "inefficient" E_A/E_{ES} ratios are closely associated with the presence of important reductions in LV EF. In patients with HFrEF, these ratios may rise to as high as 4.0 due to the relative decline in ventricular contractile function (lower E_{ES}) and concomitant rise in E_A. Such coupling is clearly suboptimal from the standpoint of ventricular performance and metabolic efficiency.[1,20,22,25,28,29]

Assessing the consequences of primary LV dysfunction, changes in arterial load and their consequences in the pressure−volume plane
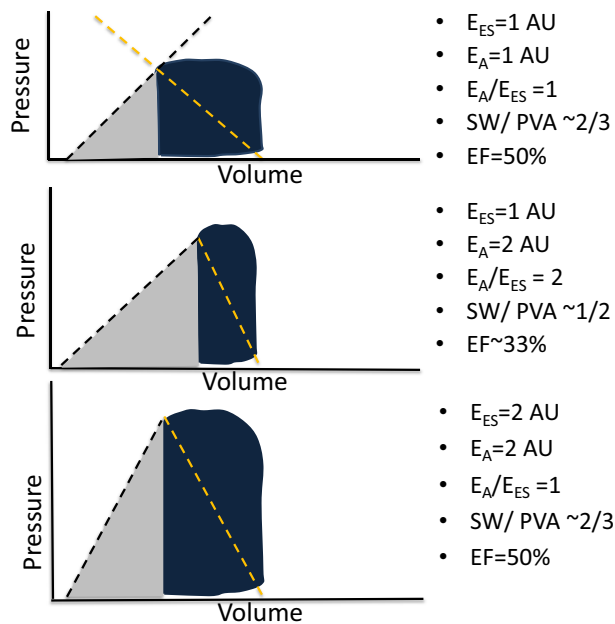
The principles discussed above can be intuitively applied to understand the consequences of primary arterial or myocardial disease on VA coupling. Fig. 15.4 demonstrates some potential consequences of a "primary" reduction in E_{ES}. The top panel represents a normal physiologic state. For simplicity, an E_A/E_{ES} ratio of 1 is assumed to represent "normal" elastance coupling. In this situation, a large proportion ($\sim 2/3$) of the PVA corresponds to stroke work and the LV operates at an effective EF of $\sim 50\%$. The middle panel represents a situation in which, all other factors being equal, E_{ES} has decreased to $\sim 50\%$ of its nominal value and end-diastolic volume has increased, which may occur, for instance, in the setting of a dilated cardiomyopathy. In this situation, a high E_A/E_{ES} ratio is observed, which is accompanied by an increased proportion of the PVA ($\sim 50\%$) corresponding to potential energy, and a reduced proportion (the remaining $\sim 50\%$) corresponding to external work, denoting an unfavorable energetic efficiency state. The high E_A/E_{ES} ratio in this scenario implies that the ventricle operates at an effective EF of $\sim 33\%$, although in

- E_{ES}=1 AU
- E_A=1 AU
- E_A/E_{ES} =1
- SW/ PVA ~2/3
- EF=50%

- E_{ES}=0.5 AU
- E_A=1 AU
- E_A/E_{ES} = 2
- SW/ PVA ~1/2
- EF~33%

- E_{ES}=0.5 AU
- E_A=0.5 AU
- E_A/E_{ES} =1
- SW/ PVA ~2/3
- EF=50%

FIGURE 15.4 Potential consequences of a primary reduction of E_{ES} in energetic aspects of ventricular-arterial coupling. *AU*, arbitrary units. See text for details. *Modified from Chirinos JA. Ventricular-arterial coupling: invasive and non-invasive assessment.* **Artery Res**. *2013;7.*

this particular example, stroke volume is relatively preserved due to the increased end-diastolic volume. The bottom panel corresponds to what may occur with an intervention that, under these circumstances, reduces E_A to 50% of its nominal value. This would theoretically result in normalization of the E_A/E_{ES} ratio, a restoration of the proportions of the PVA corresponding to external work and potential energy, and a normalization of the effective EF. However, this situation is unlikely to be realistic in vivo since the reduction in the intersection point between E_A and E_{ES} in the pressure axis (i.e., end-systolic pressure) is limited by the minimum arterial pressures required for perfusion of peripheral organs. Thus, in hearts with markedly decreased E_{ES}, conditions of near-optimal mechanical efficiency are only achievable at a lower end-systolic pressures than those required to maintain adequate systemic hemodynamics; operating efficiency is thus necessarily decreased relative to the maximally attainable efficiency, in order to maintain acceptable perfusion pressures.

Fig. 15.5 represents the consequences of a "primary" increase in E_A. The top panel again represents a simplified normal physiologic state, with a "normal" E_A/E_{ES} ratio, resulting in a high stroke work relative to PVA and an effective EF of $\sim 50\%$. The middle panel represents a situation in which E_A has increased to twice its nominal value (middle panel), without a change in E_{ES}. A high E_A/E_{ES} ratio is again observed, which is accompanied by an increased proportion of the PVA ($\sim 50\%$) corresponding to potential energy and a reduced proportion (the remaining

- E_{ES}=1 AU
- E_A=1 AU
- E_A/E_{ES} =1
- SW/ PVA ~2/3
- EF=50%

- E_{ES}=1 AU
- E_A=2 AU
- E_A/E_{ES} = 2
- SW/ PVA ~1/2
- EF~33%

- E_{ES}=2 AU
- E_A=2 AU
- E_A/E_{ES} =1
- SW/ PVA ~2/3
- EF=50%

FIGURE 15.5 Potential consequences of a primary increase in E_A on ventricular–arterial coupling. *AU*, arbitrary units. See text for details. *Modified from Chirinos JA. Ventricular-arterial coupling: invasive and non-invasive assessment.* **Artery Res**. *2013;7.*

~50%) corresponding to external work, denoting an unfavorable energetic efficiency state. In this situation, the LV operates at an effective EF of ~33% and systemic arterial pressure is increased. The bottom panel represents an alternative (and more common) situation, in which, in response to the increased E_A, E_{ES} has increased (i.e., the LV demonstrates increased systolic stiffness, due to increased contractility, wall thickness or both). In this situation, the E_A/E_{ES} ratio is normalized, with restoration of the proportions of the PVA corresponding to external work and potential energy and a normalization of the effective EF. However, despite an apparently "favorable" coupling between E_A and E_{ES}, this can be accompanied by systolic hypertension, impaired LV chamber contractile reserve and high sensitivity of blood pressure to preload, thus resulting in blood pressure lability.[28,30] These features tend to be present in older adults with systolic hypertension.

Strengths and limitations of the pressure–volume plane

Analyses of LV and arterial interactions in the pressure–volume plane are valuable and have facilitated our understanding of various physiologic and pathophysiologic states. This simplified approach to VA coupling enables an intuitive evaluation of the specific contributions of ventricular end-systolic properties and some arterial system parameters as determinants of stroke volume and its relation to the overall mechanical energetic cost to the LV (Table 15.1).

Advantages of the pressure–volume plane (Table 15.2) include its well-established relatively intuitive framework, with extensive published data and its ability to represent the LV and arterial systems in the same plane, thus characterizing important mechanical indices that have physiologic relevance from an energetic standpoint. Moreover, although E_{ES} is ideally assessed invasively using data from a family of pressure–volume loops obtained during an acute preload or afterload alterations, "single-beat" methods have also been developed and have undergone limited validation,[15,16] allowing for noninvasive E_{ES} estimations using simple echocardiographic measurements.

Despite its advantages, the pressure–volume approach also has serious limitations (Table 15.2). In particular, E_A has critical disadvantages as an index of arterial load. E_A has been shown to be highly sensitive to heart rate (a cardiac, rather than a ventricular property) and is thus not a pure index of arterial properties.[31,32] More importantly, the commonly made assumption that E_A is a lumped parameter of resistive and pulsatile arterial load, is factually incorrect.[1,31,33,34] Despite its name, E_A is not a true elastance (i.e., the inverse of a compliance) and is mostly dependent on vascular resistance (a microvascular, rather than a conduit artery property),[31,32] while being relatively insensitive to changes in pulsatile arterial load.[31,32] Its strong dependence on resistance is readily explained by the fact that arterial pressure does not increase from zero to end-systolic pressure (as represented in the PV plane) when the stroke volume is injected into the arterial tree, because arterial pressure hovers around a nonzero value (mean arterial pressure, which is in turn entirely determined by peripheral resistance, heart rate and stroke volume).

The almost exclusive dependence of E_A on resistance is a critical limitation of the former, given the importance of pulsatile hemodynamics in the arterial tree. Due to the pulsatile nature of the LV as a pump, arterial load is time-varying, complex, and an attempt to represent it with a single number is unrealistic.[1,35] In fact, E_A has been shown to be minimally sensitive to changes in arterial compliance or to various specific parameters of pulsatile arterial load within physiologically/clinically relevant ranges.[1,31,33,34] Moreover, since the E_A/E_{ES} ratio does not account for time-varying phenomena during ejection,[1] it intrinsically neglects the LV loading sequence (late vs. early systolic load), which is an important determinant of maladaptive remodeling, hypertrophy, diastolic dysfunction, and heart failure risk.[36–43] In particular, E_A was derived using major simplifying assumptions, among which was a "square-shaped" pressure curve in systole, with its upper side corresponding to end-systolic pressure, thus ignoring the contribution of pulsatile phenomena to the contour of the arterial pressure curve above end-systolic pressure. Sunagawa et al. appropriately raised caution regarding the fact that the contribution of these phenomena can become

TABLE 15.1 Key physiologic parameters of in the pressure—volume plane.

Parameter	Definition and interpretation
LV end-systolic elastance (E_{ES})	Slope of the end-systolic pressure—volume relation (ESPVR), obtained by joining end-systolic pressure—volume points from a "family" of left ventricular (LV) pressure—volume loops obtained from the same subject during acute preload or afterload alterations at a constant inotropic state. It can be estimated using single-beat noninvasive methods. Determined by LV contractility and stiffness.
Effective arterial "elastance" (E_A)	Ratio of end-systolic pressure/stroke volume. It is not a true elastance (i.e., inverse of a compliance). It correlates poorly with arterial compliance, but is a quasi-perfect function of the product of systemic vascular resistance (a microvascular property) and heart rate (a cardiac property). Does not capture conduit artery properties, such as stiffness or pulsatile load and does not correlate with large artery stiffness.
Stroke work (SW)	The area enclosed within the LV pressure—volume loop trajectory in a cardiac cycle. Represents the external work provided by the LV to the systemic circulation.
Potential energy (PE)	Approximately triangular area enclosed by the linear end-systolic pressure—volume relation, the left border of a single pressure—volume loop, and the end-diastolic pressure—volume relation. Proposed to represent the end-systolic elastic potential energy built up and stored in the LV wall during systole.
Pressure—volume area (PVA)	Sum of stroke work and potential energy. A surrogate of the total mechanical energy generated by the LV contraction until end-systole. In a single heart a stable contractile state under, PVA correlates strongly and linearly with myocardial oxygen consumption (MVO_2) per beat as preload and afterload varies. However, this correlation does not hold under different contractile states or between different hearts.
SW/PVA	Ratio of external work to PVA, the latter considered in this context a surrogate of MVO_2 per beat. Therefore, this ratio is considered an index of the mechanical energetic efficiency at a given contractile state *specific operating conditions in a given heart.*

important, with a relatively large error in this coupling model when the area under the systolic area of the curve becomes a large fraction of the overall pressure curve (such as occurs with fast heart rates) or when the pulsatile phenomena lead to an increase in the area under the pressure curve above end-systolic pressure, which occurs in the presence of prominent wave reflections.[20,39] The LV pressure curve also markedly deviates from a square-shaped curve in systole in the presence of significant aortic stenosis, which E_A fails to account for (since the transvalvular aortic gradient in end-systole is close to zero). Furthermore, the derivation of E_A as an index of arterial load assumed a constant ejection time, regardless of the loading conditions, whereas it is well known that ejection time can vary with afterload.[39] Even is these simplifications are overseen, the derivation of E_A was performed using a three-element Windkessel model, which does not account for wave reflection.[37,39,44—47]

In a more recent study that aimed to assess the relationship between E_A and pulsatile arterial load,[34] time-resolved central pressure and flow measurements were used to E_A and detailed various parameters of pulsatile arterial load: (1) In a large community-based sample of

middle-aged adults; (2) In a diverse clinical population of older adults; and (3) In response to the handgrip maneuver, a physiologic intervention known to induce pronounced changes in pulsatile arterial load.[48] This series of studies consistently demonstrated that E_A is a quasi-perfect function of the product of systemic vascular resistance and heart rate, with weak, inconsistent and in some cases, erratic/paradoxical relationships with proper measures of pulsatile load, such as aortic root characteristic impedance (Zc), measures of wave reflections, and total arterial compliance. These findings are in full agreement with previous modeling studies,[31] and demonstrate that E_A depends almost entirely on SVR and heart rate, and has very poor sensitivity to the human pathophysiological ranges of pulsatile afterload observed in vivo. Finally, there was no correlation between E_A and carotid-femoral pulse wave velocity, the current reference method to quantify large artery stiffness.[49,50] Current American Heart Association guidelines specifically recommend against utilizing E_A as a measure of arterial stiffness.[49] Given the considerations above, it is incorrect to interpret E_A as an index of arterial "stiffening" or, by extension, to equate a parallel increase in E_A and E_{ES} as a state of "VA stiffening."

TABLE 15.2 Advantages and disadvantages of assessments of ventricular-arterial coupling in the pressure—volume plane.

Advantages

- Widely used, well-established framework
- Extensive published animal and human data
- Relatively simple and intuitive.
- Quantifies left ventricular (LV) chamber contractility/stiffness and arterial load in the same units
- Characterizes mechanical indices that relate to energetics:
  - External mechanical energy
  - Potential energy
  - Energetic efficiency
- Allows us to understand consequences of abnormalities in E_A and E_{ES} on stroke volume, ejection fraction, pressure lability, and some aspects of cardiovascular reserve during exercise.
- Can be assessed noninvasively

Disadvantages

Disadvantages of E_A:
- Is not a pure index of arterial load because it is prominently influenced by heart rate (a cardiac property)
- It is not a true elastance
- Correlates poorly with arterial compliance
- Does not account for time-varying phenomena and neglects the influence of wave transmission and reflections
- Is a quasi-perfect function of resistance (a microvascular property) and heart rate
- Bears no relationship to validated indices of large artery stiffness (i.e., carotid-femoral pulse wave velocity)
- Neglects aortic valvular load in the presence of aortic valve stenosis
- In contrast to metrics of pulsatile arterial load, does not relate to heart failure risk

Disadvantages of E_{ES}:
- Nonlinearity of the end-systolic pressure—volume relation
- E_{ES} demonstrates afterload and some preload dependency
- It does not assess myocardial properties

Disadvantages in the assessment of ventricular—arterial coupling:
- E_A/E_{ES} does not characterize (and indeed neglects) the LV loading sequence
- E_A/E_{ES} and the "mechanical" energetic optimization in the PV plane has unclear relevance in the absence of a frankly reduced ejection fraction, thus providing little unique insights in this situation
- Stroke work does not dissect the importance of systolic pressure versus flow output
- Considers stroke work the only "useful" energy (neglects the value of potential energy deposition in the myocardium that favors diastolic suction)
- The entire paradigm centers of stroke work as "the" variable to be optimized. Yet, stroke work is a limited index of performance and optimization of other factors likely supersede optimization of stroke work in various pathophysiologic situations
- There is a poor correlation between myocardial O_2 consumption (MVO_2) and the pressure—volume area (PVA) in a given population of patients (i.e., between individuals)

To the degree that E_A does not properly characterize arterial pulsatile load, the E_A/E_{ES} ratio is a limited index of VA coupling, even if the important limitations of this approach to assess LV energetics are ignored. This issue is particularly problematic in patients with or at risk for HFpEF, because pulsatile load is highly relevant for VA interactions in these populations. VA coupling encompasses multiple different physiologic aspects that require characterization beyond the pressure—volume plane. These considerations are not purely theoretical, but translate into important limitations to the application of this approach in clinical studies. For example, Goto et al. demonstrated that measures of wave reflection, but not E_A or peripheral vascular resistance, were significantly correlated with the invasively measured time constant of isovolumic relaxation, the gold standard index of diastolic relaxation.[51] Similarly, a recent study demonstrated that E_A did not predict incident HF in the Multiethnic Study of Atherosclerosis (MESA) cohort,[52] whereas indices of reflection magnitude and late systolic load were strong predictors of incident HF in this cohort.[46,53] Finally, a single dose of inorganic nitrate, which has been recently shown to improve aerobic capacity in patients with HFpEF, did not reduce E_A, but substantially reduced wave reflections,[54] and this reduction significantly correlated with the degree of improvement in peak VO_2 in these patients.[55] These findings are consistent with the need to time-resolve arterial load in order to gain clinically relevant insights into VA coupling and the effects of pharmacologic interventions.

Shortcomings of E_{ES} should also be taken into account when interpreting the results of published studies that

applied the pressure–volume paradigm. When subjected to rigorous examination, some fundamental principles of the LV E(t) theory do not hold in vivo. It has been shown that the ESPVR is nonlinear and the degree of nonlinearity depends upon the inotropic state.[56–60] The presence of a V_0 common to all isochrones, a key assumption of the time-varying elastance concept, has also been disproven.[57,61–63] It has been shown that the peak value of the ESPVR decreases with an increase in LV size (preload), even if myocardial contractility is unchanged, which can be accounted for by the lower generated pressure corresponding to a given wall stress in the presence of greater cavity volumes.[64] Furthermore, the ESPVR demonstrates afterload dependency[65,66] and has been shown to be greater on ejecting beats than on isovolumic beats, which is accompanied by a reduced slope of the MVO_2-PVA relation, indicating an increase in metabolic efficiency in ejecting versus nonejecting beats despite an increase in E_{ES}.[56] Both of these phenomena may be related, at least in part, to the greater amount of pressure generation, at identical levels of wall stress, made possible by a greater late systolic wall volume/cavity volume ratio during ejecting beats as opposed to isovolumic beats, as would be predicted by derivations of Laplace's law (see Chapter 16 for a more comprehensive discussion of time-resolved MWS). Another important limitation of the E(t) theory is that it assumes a load-invariant time course of contraction, whereas in reality, the time-course of contraction is load-dependent.[67] Indeed, a fundamental assumption of E_{ES} is that the end-systolic point is reached independently of instantaneous and past pressure and volume.[7–10] This intrinsically neglects the systolic loading sequence, an important determinant of LV dysfunction, LV hypertrophy and failure.[38,40,41,68–75] An additional important limitation is of this approach is that, to the degree that, as shown by De Tombe et al.,[25] nonsevere abnormalities in E_A/E_{ES} are of little consequence to optimization of stroke work and mechanical efficiency, the value of E_{ES}/E_A as a relevant coupling index in the absence of severe disease may be questioned, since it is precisely these energetic aspects of VA coupling that E_A/E_{ES} is meant to characterize. However, E_{ES}/E_A does provide insight into the energetic aspects of VA coupling in the presence of important systolic dysfunction and it is in this situation where it may prove particularly useful in clinical populations. Another important consideration is that, whereas the pressure–volume plane offers insights regarding the energetic efficiency of the system (when the latter is defined as the stroke work generated for any given MVO_2), they are much less reliable to compare the energetic efficiency of the LV-arterial system between individuals or disease populations because, as discussed above, the function that relates the PVA to MVO_2 is highly variable between individuals.[1,8,17,18,76] This results in weak relationships between the PVA and

MVO_2 (and by extension, between PVA-derived efficiency the true underlying efficiency) between individuals. The weak correlation between the PVA and MVO_2 between individuals is in sharp contrast with peak MWS (Chapter 16), which can be evaluated noninvasively and in a large human study, was shown to correlate strongly with MVO_2.[77]

Another weakness of the pressure–volume paradigm is that the use of the stroke work to PVA ratio as an index of energetic efficiency considers the stroke work as the only "useful" energy, thus undermining the value of energy deposition in the myocardium, which favors diastolic suction. An additional limitation of energetic optimization assessed in the pressure–volume plane is that stroke work does not directly dissect the physiologic importance of the flow versus pressure generation. A high stroke volume at normal levels of systemic arterial pressure and a normal stroke volume and high levels of systemic arterial pressure, may thus be characterized by identical stroke work values, despite their vastly different clinical and pathophysiologic implications. Indeed, the latter point leads to more fundamental questions about the role of regulatory processes in cardiovascular status as they relate to the pressure–volume plane. It is likely that the normal cardiovascular control system uses a unique combination of ventricular output, systemic perfusion pressure, heart rate, arterial flow, and impedance patterns, which optimize ventricular performance, energetics, and/or various other cellular processes. However, the pressure–volume scheme treats external stroke work (and its relation to the PVA) as the central coupling variable to be optimized. This does not intrinsically consider the vast differences between different pressure and flow states that may lead to identical stroke work values nor does it address many other cellular of mechanical processes that may require primary optimization on both the ventricle and the arteries. Indeed, Sunagawa et al. pointed out in their early reports from isolated heart preparation studies[20] that their criteria for coupling optimization may not be valid for normally functioning animals or various pathologic states and raised the question of whether the maximum external stroke work is really the crucial criterion that an organism uses for optimizing the operation of the cardiovascular system in physiological circumstances, which likely depends on specific pathophysiologic conditions.

Conclusions

Afterload and VA interactions are important and that they can be characterized with noninvasive techniques. Assessments of afterload and VA interactions offer the potential for a greater mechanistic understanding of normal physiology, early stages of heart and vascular disease, and established heart disease at various clinical stages,

TABLE 15.3 Comparison of the pressure—volume plane versus analyses of pressure-flow relations and myocardial wall stress to assess various aspects of arterial load and ventricular—arterial coupling.

	Pressure—volume plane	Pressure-flow relations and myocardial wall stress
Able to assess left ventricular (LV) pump function in a load-independent manner	Yes	Potentially, but requires further development and validation
Can assess the energetic efficiency of a single heart at various loading conditions	Yes	Yes
Reliable to compare the energetic efficiency between individuals or disease populations	No, although often utilized in this context	Yes
Characterizes and quantifies pulsatile arterial load	No	Yes
Accounts for the time-varying nature of afterload and the LV loading sequence (early vs. late systolic load)	No	Yes
Relationship to diastolic dysfunction	+/−	++
Independently predictive of heart failure risk in the general population	No	Yes
Detects abnormalities in heart failure with preserved ejection fraction compared to age-matched hypertensive controls	No or inconsistently	Yes
Equally useful for heart failure with preserved and heart failure with reduced ejection fraction	No	Likely, although further clinical studies are required
Reliable in the presence of segmental wall motion abnormalities	Yes	Pressure-flow relations are reliable. Myocardial wall stress estimations are unreliable in this situation.
Able to characterize combined arterial and valvular load in aortic stenosis	Not intrinsically, although the paradigm can be partially adapted (see Chapter 37)	Yes, as long as the transvalvular pressure gradient is measured (see Chapter 16)

particularly the continuum of LV remodeling associated with epidemic conditions such as hypertension and obesity and its progression to heart failure. Given the importance of LV afterload and its impact on the heart, afterload and impaired VA interactions should be carefully considered or ruled out as potential mediators or confounders in a wide variety of observed relationships or therapeutic and adverse effects of interventions. The pressure—volume plane remains the reference standard for assessments of LV chamber pump function, and its extension for the assessment of VA coupling is useful as long as the paradigm is adequately interpreted and its significant limitations taken into account. It should be recognized that VA coupling is a broad term that encompasses different physiologic aspects, many of which are not characterized (or are frankly mischaracterized) in the pressure—volume plane. Analyses of VA coupling should thus be complemented by more specific analyses of arterial and myocardial load that can provide additional physiologic information in various disease states, as discussed in the two subsequent chapters. In

particular, analyses of time-resolved proximal aortic pressure-flow relations and time-resolved MWS offer significant advantages to characterize clinically relevant aspects of VA interactions, as shown in Table 15.3 and developed in more detail in Chapters 16 and 17. Despite the apparent complexity of these analyses, they can be readily implemented with contemporary software from signals that can be acquired quickly and noninvasively at the bedside.

Acknowledgments

and Abbott. He is named as inventor in a University of Pennsylvania patent for the use of inorganic nitrates/nitrites for the treatment of Heart Failure and Preserved Ejection Fraction and for the use of biomarkers in heart failure with preserved ejection fraction. He has received payments for editorial roles from the American Heart Association, the American College of Cardiology, and Wiley. He has received research device loans from Atcor Medical, Fukuda-Denshi, Unex, Uscom, NDD Medical Technologies, Microsoft, and Micro-Vision Medical.

References

1. Chirinos JA. Ventricular-arterial coupling: invasive and non-invasive assessment. **Artery Res**. 2013; 7.
2. Chirinos JA. Deep phenotyping of systemic arterial hemodynamics in hfpef (part 2): clinical and therapeutic considerations. **J Cardiovasc Transl Res**. 2017; 10:261−274.
3. Chirinos JA. Deep phenotyping of systemic arterial hemodynamics in hfpef (part 1): physiologic and technical considerations. **J Cardiovasc Transl Res**. 2017; 10:245−259.
4. Chirinos JA, Sweitzer N. Ventricular-arterial coupling in chronic heart failure. **Card Fail Rev**. 2017; 3:12−18.
5. Pandey A, Shah SJ, Butler J, et al. Exercise intolerance in older adults with heart failure with preserved ejection fraction: Jacc state-of-the-art review. **J Am Coll Cardiol**. 2021; 78:1166−1187.
6. Shah SJ, Borlaug BA, Kitzman DW, et al. Research priorities for heart failure with preserved ejection fraction: national heart, lung, and blood institute working group summary. **Circulation**. 2020; 141:1001−1026.
7. Suga H. Theoretical analysis of a left-ventricular pumping model based on the systolic time-varying pressure-volume ratio. **IEEE Trans Biomed Eng**. 1971; 18:47−55.
8. Suga H. Total mechanical energy of a ventricle model and cardiac oxygen consumption. **Am J Physiol**. 1979; 236:H498−H505.
9. Suga H, Sagawa K, Shoukas AA. Load independence of the instantaneous pressure-volume ratio of the canine left ventricle and effects of epinephrine and heart rate on the ratio. **Circ Res**. 1973; 32:314−322.
10. Suga H, Sagawa K. Mathematical interrelationship between instantaneous ventricular pressure-volume ratio and myocardial force-velocity relation. **Ann Biomed Eng**. 1972; 1:160−181.
11. Borlaug BA, Kass DA. Ventricular-vascular interaction in heart failure. **Heart Fail Clin**. 2008; 4:23−36.
12. Chantler PD, Lakatta EG. Arterial-ventricular coupling with aging and disease. **Front Physiol**. 2012; 3:90.
13. Suga H, Sagawa K. Instantaneous pressure-volume relationships and their ratio in the excised, supported canine left ventricle. **Circ Res**. 1974; 35:117−126.
14. Kass DA, Maughan WL. From 'emax' to pressure-volume relations: a broader view. **Circulation**. 1988; 77:1203−1212.
15. Senzaki H, Chen CH, Kass DA. Single-beat estimation of end-systolic pressure-volume relation in humans. A new method with the potential for noninvasive application. **Circulation**. 1996; 94:2497−2506.
16. Chen CH, Fetics B, Nevo E, et al. Noninvasive single-beat determination of left ventricular end-systolic elastance in humans. **J Am Coll Cardiol**. 2001; 38:2028−2034.
17. Khalafbeigui F, Suga H, Sagawa K. Left ventricular systolic pressure-volume area correlates with oxygen consumption. **Am J Physiol**. 1979; 237:H566−H569.
18. Suga H. Ventricular energetics. **Physiol Rev**. 1990; 70:247−277.
19. Kameyama T, Asanoi H, Ishizaka S, Yamanishi K, Fujita M, Sasayama S. Energy conversion efficiency in human left ventricle. **Circulation**. 1992; 85:988−996.
20. Sunagawa K, Maughan WL, Burkhoff D, Sagawa K. Left ventricular interaction with arterial load studied in isolated canine ventricle. **Am J Physiol**. 1983; 245:H773−H780.
21. Sunagawa K, Maughan WL, Friesinger G, Guzman P, Chang MS, Sagawa K. Effects of coronary arterial pressure on left ventricular end-systolic pressure-volume relation of isolated canine heart. **Circ Res**. 1982; 50:727−734.
22. Sunagawa K, Sagawa K, Maughan WL. Ventricular interaction with the loading system. **Ann Biomed Eng**. 1984; 12:163−189.
23. Sunagawa K, Maughan WL, Sagawa K. Optimal arterial resistance for the maximal stroke work studied in isolated canine left ventricle. **Circ Res**. 1985; 56:586−595.
24. Burkhoff D, Sagawa K. Ventricular efficiency predicted by an analytical model. **Am J Physiol**. 1986; 250:R1021−R1027.
25. De Tombe PP, Jones S, Burkhoff D, Hunter WC, Kass DA. Ventricular stroke work and efficiency both remain nearly optimal despite altered vascular loading. **Am J Physiol**. 1993; 264:H1817−H1824.
26. Redfield MM, Jacobsen SJ, Borlaug BA, Rodeheffer RJ, Kass DA. Age- and gender-related ventricular-vascular stiffening: a community-based study. **Circulation**. 2005; 112:2254−2262.
27. Chirinos JA, Rietzschel ER, De Buyzere ML, et al. Arterial load and ventricular-arterial coupling: physiologic relations with body size and effect of obesity. **Hypertension**. 2009; 54:558−566.
28. Kass DA. Ventricular arterial stiffening: integrating the pathophysiology. **Hypertension**. 2005; 46:185−193.
29. Chantler PD, Lakatta EG, Najjar SS. Arterial-ventricular coupling: mechanistic insights into cardiovascular performance at rest and during exercise. **J Appl Physiol**. 2008; 105:1342−1351.
30. Chen CH, Nakayama M, Nevo E, Fetics BJ, Maughan WL, Kass DA. Coupled systolic-ventricular and vascular stiffening with age: implications for pressure regulation and cardiac reserve in the elderly. **J Am Coll Cardiol**. 1998; 32:1221−1227.
31. Segers P, Stergiopulos N, Westerhof N. Relation of effective arterial elastance to arterial system properties. **Am J Physiol Heart Circ Physiol**. 2002; 282:H1041−H1046.
32. Chemla D, Antony I, Lecarpentier Y, Nitenberg A. Contribution of systemic vascular resistance and total arterial compliance to effective arterial elastance in humans. **Am J Physiol Heart Circ Physiol**. 2003; 285:H614−H620.
33. Maughan WL, Sunagawa K, Burkhoff D, Sagawa K. Effect of arterial impedance changes on the end-systolic pressure-volume relation. **Circ Res**. 1984; 54:595−602.
34. Chirinos JA, Rietzschel ER, Shiva-Kumar P, et al. Effective arterial elastance is insensitive to pulsatile arterial load. **Hypertension**. 2014; 64:1022−1031.
35. Nichols WW, OR M, Vlachopoulos C. **Mcdonald's Blood Flow in Arteries: Theoretical, Experimental and Clinical Principles**. 6th ed. Hodder Arnold; 2011.
36. Fukuta H, Ohte N, Wakami K, et al. Impact of arterial load on left ventricular diastolic function in patients undergoing cardiac catheterization for coronary artery disease. **Circ J**. 2010; 74:1900−1905.
37. Weber T, O'Rourke MF, Ammer M, Kvas E, Punzengruber C, Eber B. Arterial stiffness and arterial wave reflections are associated

with systolic and diastolic function in patients with normal ejection fraction. **Am J Hypertens**. 2008; 21:1194−1202.

38. Kobayashi S, Yano M, Kohno M, et al. Influence of aortic impedance on the development of pressure-overload left ventricular hypertrophy in rats. **Circulation**. 1996; 94:3362−3368.

39. Nichols WW, OR M, Vlachopolous C. **Mcdonald's Blood Flow in Arteries. Theoretical, Experimental and Clinical Principles**. Hodder Arnold; 2011.

40. Hashimoto J, Westerhof BE, Westerhof N, Imai Y, O'Rourke MF. Different role of wave reflection magnitude and timing on left ventricular mass reduction during antihypertensive treatment. **J Hypertens**. 2008; 26:1017−1024.

41. Gillebert TC, Lew WY. Influence of systolic pressure profile on rate of left ventricular pressure fall. **Am J Physiol**. 1991; 261:H805−H813.

42. Chirinos JA, Segers P, Rietzschel ER, et al. Early and late systolic wall stress differentially relate to myocardial contraction and relaxation in middle-aged adults: the asklepios study. **Hypertension**. 2013; 61:296−303.

43. Quail MA, Short R, Pandya B, et al. Abnormal wave reflections and left ventricular hypertrophy late after coarctation of the aorta repair. **Hypertension**. 2017; 69.

44. Nichols WW, O'Rourke MF, Avolio AP, et al. Effects of age on ventricular-vascular coupling. **Am J Cardiol**. 1985; 55:1179−1184.

45. Nichols WW, Denardo SJ, Wilkinson IB, McEniery CM, Cockcroft J, O'Rourke MF. Effects of arterial stiffness, pulse wave velocity, and wave reflections on the central aortic pressure waveform. **J Clin Hypertens**. 2008; 10:295−303.

46. Chirinos JA, Kips JG, Jacobs Jr DR, et al. Arterial wave reflections and incident cardiovascular events and heart failure: mesa (multiethnic study of atherosclerosis). **J Am Coll Cardiol**. 2012; 60:2170−2177.

47. Chirinos JA, Segers P. Noninvasive evaluation of left ventricular afterload: part 2: arterial pressure-flow and pressure-volume relations in humans. **Hypertension**. 2010; 56:563−570.

48. Chirinos JA, Segers P, Raina A, et al. Arterial pulsatile hemodynamic load induced by isometric exercise strongly predicts left ventricular mass in hypertension. **Am J Physiol Heart Circ Physiol**. 2010; 298:H320−H330.

49. Townsend RR, Wilkinson IB, Schiffrin EL, et al. Recommendations for improving and standardizing vascular research on arterial stiffness: a scientific statement from the american heart association. **Hypertension**. 2015; 66:698−722.

50. Marwick TH, Gillebert TC, Aurigemma G, et al. Recommendations on the use of echocardiography in adult hypertension: a report from the european association of cardiovascular imaging (eacvi) and the american society of echocardiography (ase)dagger. **Eur Heart J Cardiovasc Imaging**. 2015; 16:577−605.

51. Goto T, Ohte N, Fukuta H, Wakami K, Tani T, Kimura G. Relationship between effective arterial elastance, total vascular resistance, and augmentation index at the ascending aorta and left ventricular diastolic function in older women. **Circ J**. 2013; 77:123−129.

52. Zamani P, Lilly SM, Segers P, et al. Pulsatile load components, resistive load and incident heart failure: the multi-ethnic study of atherosclerosis (mesa). **J Card Fail**. 2016; 22:988−995.

53. Chirinos JA, Segers P, Duprez DA, et al. Late systolic central hypertension as a predictor of incident heart failure: the multi-ethnic study of atherosclerosis. **J Am Heart Assoc**. 2015; 4:e001335.

54. Zamani P, Rawat D, Shiva-Kumar P, et al. Effect of inorganic nitrate on exercise capacity in heart failure with preserved ejection fraction. **Circulation**. 2015; 131:371−380. discussion 380.

55. Chirinos JA, Beraun M, Townsend RR, Varakantam S, Zamani P. Effect of inorganic nitrate on wave reflections vs. Microvascular dilatory reserve: role in improving aeobic capacity in heart failure with preserved ejection fraction. **Circulation**. 2016; 134:A15786.

56. Burkhoff D, Sugiura S, Yue DT, Sagawa K. Contractility-dependent curvilinearity of end-systolic pressure-volume relations. **Am J Physiol**. 1987; 252:H1218−H1227.

57. Claessens TE, Georgakopoulos D, Afanasyeva M, et al. Nonlinear isochrones in murine left ventricular pressure-volume loops: how well does the time-varying elastance concept hold? **Am J Physiol Heart Circ Physiol**. 2006; 290:H1474−H1483.

58. Lee S, Ohga Y, Tachibana H, et al. Effects of myosin isozyme shift on curvilinearity of the left ventricular end-systolic pressure-volume relation of in situ rat hearts. **Jpn J Physiol**. 1998; 48:445−455.

59. van der Velde ET, Burkhoff D, Steendijk P, Karsdon J, Sagawa K, Baan J. Nonlinearity and load sensitivity of end-systolic pressure-volume relation of canine left ventricle in vivo. **Circulation**. 1991; 83:315−327.

60. Kass DA, Beyar R, Lankford E, Heard M, Maughan WL, Sagawa K. Influence of contractile state on curvilinearity of in situ end-systolic pressure-volume relations. **Circulation**. 1989; 79:167−178.

61. Kind T, Westerhof N, Faes TJ, Lankhaar JW, Steendijk P, Vonk-Noordegraaf A. Cardiac phase-dependent time normalization reduces load dependence of time-varying elastance. **Am J Physiol Heart Circ Physiol**. 2009; 296:H342−H349.

62. Drzewiecki GM, Karam E, Welkowitz W. Physiological basis for mechanical time-variance in the heart: special consideration of nonlinear function. **J Theor Biol**. 1989; 139:465−486.

63. Segers P, Tchana-Sato V, Leather HA, et al. Determinants of left ventricular preload-adjusted maximal power. **Am J Physiol Heart Circ Physiol**. 2003; 284:H2295−H2301.

64. Nakano K, Sugawara M, Ishihara K, et al. Myocardial stiffness derived from end-systolic wall stress and logarithm of reciprocal of wall thickness. Contractility index independent of ventricular size. **Circulation**. 1990; 82:1352−1361.

65. Baan J, Van der Velde ET. Sensitivity of left ventricular end-systolic pressure-volume relation to type of loading intervention in dogs. **Circ Res**. 1988; 62:1247−1258.

66. Freeman GL, Little WC, O'Rourke RA. The effect of vasoactive agents on the left ventricular end-systolic pressure-volume relation in closed-chest dogs. **Circulation**. 1986; 74:1107−1113.

67. Burkhoff D, De Tombe PP, Hunter WC. Impact of ejection on magnitude and time course of ventricular pressure-generating capacity. **Am J Physiol**. 1993; 265:H899−H909.

68. Leite-Moreira AF, Gillebert TC. Nonuniform course of left ventricular pressure fall and its regulation by load and contractile state. **Circulation**. 1994; 90:2481−2491.

69. Borlaug BA, Melenovsky V, Redfield MM, et al. Impact of arterial load and loading sequence on left ventricular tissue velocities in humans. **J Am Coll Cardiol**. 2007; 50:1570−1577.

70. Fujimoto N, Onishi K, Tanabe M, et al. Nitroglycerin improves left ventricular relaxation by changing systolic loading sequence in patients with excessive arterial load. **J Cardiovasc Pharmacol**. 2005; 45:211−216.

71. Gillebert TC, Sys SU, Brutsaert DL. Influence of loading patterns on peak length-tension relation and on relaxation in cardiac muscle. **J Am Coll Cardiol**. 1989; 13:483−490.

72. Yano M, Kohno M, Kobayashi S, et al. Influence of timing and magnitude of arterial wave reflection on left ventricular relaxation. **Am J Physiol Heart Circ Physiol**. 2001; 280:H1846−H1852.

73. Hashimoto J, Watabe D, Hatanaka R, et al. Enhanced radial late systolic pressure augmentation in hypertensive patients with left ventricular hypertrophy. **Am J Hypertens**. 2006; 19:27−32.

74. Chirinos JA, Kips J, Jacobs Jr DR, et al. Arterial wave reflections and incident cardiovascular events and heart failure: : the multi-ethnic study of atherosclerosis. **J Am Coll Cardiol**. 2012; 60.

75. Shah SJ, Wasserstrom A. Increased arterial wave reflection magnitude. A novel form of stage b heart failure? **J Am Coll Cardiol**. 2012; 60.

76. Takaoka H, Takeuchi M, Odake M, Yokoyama M. Assessment of myocardial oxygen consumption (vo2) and systolic pressure-volume area (pva) in human hearts. **Eur Heart J**. 1992; 13(Suppl E):85−90.

77. Strauer BE. Myocardial oxygen consumption in chronic heart disease: role of wall stress, hypertrophy and coronary reserve. **Am J Cardiol**. 1979; 44:730−740.

Chapter 16

Myocardial wall stress and the systolic loading sequence

Julio A. Chirinos[1,2]

[1]University of Pennsylvania Perelman School of Medicine, Hospital of the University of Pennsylvania and Perelman Center for Advanced Medicine, Philadelphia, PA, United States; [2]Ghent University, Ghent, Belgium

Introduction

Afterload is an important determinant of myocardial function. At the myocardial level, afterload is often expressed as myocardial wall stress (MWS). MWS is directly related to left ventricular (LV) cavity pressure and cavity size and inversely related to wall thickness. Instantaneous MWS during ejection is determined by complex interactions between myocardial contractile elements, instantaneous LV geometry and the time-varying hydraulic load imposed by the arterial tree.[1] All key determinants of MWS, including wall thickness, cavity size, and ventricular pressure (which in turn depends on arterial properties for any given flow delivered against the input impedance of the systemic circulation) exhibit marked variations during ejection. Therefore, although LV/aortic pressure during systole is related to MWS, LV geometric changes that occur during ejection determine profound changes in the relationship between LV/aortic pressure and MWS.[1] Consequently, time-varying MWS estimations need to account for both time-varying pressure and time-varying geometry and are poorly represented by any single time-point measurement (such as end-systolic wall stress, which has been frequently utilized in the literature).

Late systolic load represents an increasingly recognized mechanistic abnormality that can contribute to LV maladaptive remodeling, LV dysfunction, and impaired systolic–diastolic coupling in experimental models. Similarly, multiple studies demonstrate a relationship between late systolic myocardial load and/or arterial wave reflections and LV remodeling, myocardial fibrosis, reduced LV diastolic relaxation, LV and left atrial (LA) dysfunction, and an increased risk of HF in humans. This chapter discusses basic principles regarding time-varying MWS,

the utilization of time-resolved MWS to assess the myocardial systolic loading sequence, and the adverse consequences of late systolic load on the LV.

The chapter is largely based on previous reviews by the author.[2–4] Chapter 15 deals with the pressure–volume plane, whereas Chapter 17 deals with the assessment of ventricular–arterial interactions using time-varying pressure–flow analyses (also refer to Chapters 1, 3, and 11). This chapter does not address right ventricular wall stress, pulmonary arterial load or right ventricular–pulmonary vascular interactions, which are discussed in section VI of this textbook (Chapters 55 and 56).

Myocardial afterload versus ventricular afterload

Although the terms "myocardial afterload" and "ventricular afterload" are often used interchangeably, the relationship between LV and myocardial afterload is influenced by the time-varying LV geometry during ejection, which in turn affects the MWS for any given LV chamber pressure. LV afterload is the hydraulic load imposed by the systemic circulation (aortic input impedance), which depends on the pressure required to generate flow (ejection) into the proximal aorta. In contrast, myocardial afterload is defined as the MWS required to generate fiber shortening. MWS thus reflects the time-varying mechanical load experienced by the contractile elements in the myocardium and the amount of force and work that the myocardial fibers generate during a contraction.

Although MWS is clearly not equivalent to LV afterload, there is a close interaction between the two. As mentioned above, MWS is intimately related to instantaneous LV geometry (cavity size, wall thickness) and LV cavity pressure.

LV afterload is determined by vascular properties (i.e., aortic input impedance; see Chapters 1, 3 and 17) which govern aortic root pressure−flow relations. In the absence of LV outflow tract obstruction or aortic valve stenosis, other than relatively small differences due to acceleration and deceleration of blood in early and late systole, respectively, aortic pressure and LV cavity pressure during ejection are almost identical. Given that, for a given end-diastolic geometry, instantaneous LV geometry during ejection depends on the amount of ejected volume, whereas aortic (and thus LV cavity) pressure depends on aortic input impedance, MWS and aortic input impedance are intimately related. For instance, arterial wave reflections arriving at the LV prematurely (i.e., in mid-to-late systole, rather than diastole), can profoundly impact time-varying MWS (increasing mid-to-late systolic MWS relative to early systolic MWS).

Despite the logical relationship between LV afterload and MWS, end-diastolic LV geometry (wall and cavity volumes) and the LV contraction pattern have an independent impact on MWS, due to their influence on ejection-phase LV geometry. Given the important role of adaptive and maladaptive LV geometric remodeling in health and disease, a careful study of MWS holds promise to better understand myocardial ventricular−arterial coupling in various conditions.

Quantification of myocardial wall stress

The precise quantification of LV MWS is challenging and in general, MWS in vivo can only be approximated, even in the presence of normal ventricular geometry. In ventricles with more complex geometry (such as the right ventricle, and LVs with regional wall motion abnormalities), the assessment of MWS is even more challenging and often uncertain. For axisymmetric ventricles, a relatively simple formula for the computation of average LV ejection-phase MWS was developed by Arts et al.[5] and can be readily applied using noninvasive measurements of central pressure and LV geometry[3,6,7] (Fig. 16.1). This method does not neglect radially directed forces or forces generated within the wall that oppose fiber shortening, which vary significantly with cavity and wall thickness and can interfere with direct comparisons of myocardial fiber stress at different times during ejection. The formula is based on LV cavity volume (V_{LV}), LV wall volume (V_W), and pressure:

$$Fiber\ \sigma = \frac{P}{\frac{1}{3}\ln\left(1 + \frac{V_W}{V_{LV}}\right)}$$

where P = pressure, ln = natural logarithm, V_W = wall volume and V_{LV} = ventricular cavity volume (computed at each time point).

Time-resolved LV cavity volumes can be measured throughout ejection using various methods, including:

(1) 2D-echocardiography with myocardial speckle tracking, combining apical long axis and parasternal short axis views, and with the application of the area-length method for LV volumes[1,8,9]; this method is generally valid in the absence of important distortions in LV geometry.
(2) 3D-echocardiography, which although widely available, remains challenging due to myocardial endocardial dropout from apical views;
(3) Cardiac MRI cine steady-state free precession (SSFP) images, in which each phase of ejection is carefully segmented.
(4) A practical method to obtain the time-resolved LV cavity volume curve throughout ejection relies on the integration of the proximal aortic systolic flow waveform (Figs. 16.2 and 16.3).[6] The time-integral of the systolic flow waveform represents the cumulative ejected volume at each time point. To improve the correspondence with geometric stroke volume, the ejection-phase flow time-integral can be calibrated to measured stroke volume (computed as end-diastolic minus end-systolic LV cavity volume measured with cardiac imaging). This calibrated flow-time integral can in turn be used to compute the cumulative ejected volume from the onset of ejection to each time point during ejection. The latter value is subtracted from the measured end-diastolic LV cavity volume to compute the time-resolved LV cavity volume at various times points during ejection. LV wall volume can be assumed to be constant throughout ejection,[6,10] and therefore does not need to be measured in every cardiac phase.

Central pressure can be readily measured with arterial tonometry, as discussed in detail in Chapter 2. The pressure and flow waveforms can be aligned to synchronize pressure and geometric measurements at each time point in ejection, and the Arts formula can be readily applied to obtain a time-resolved MWS curve (Fig. 16.3).
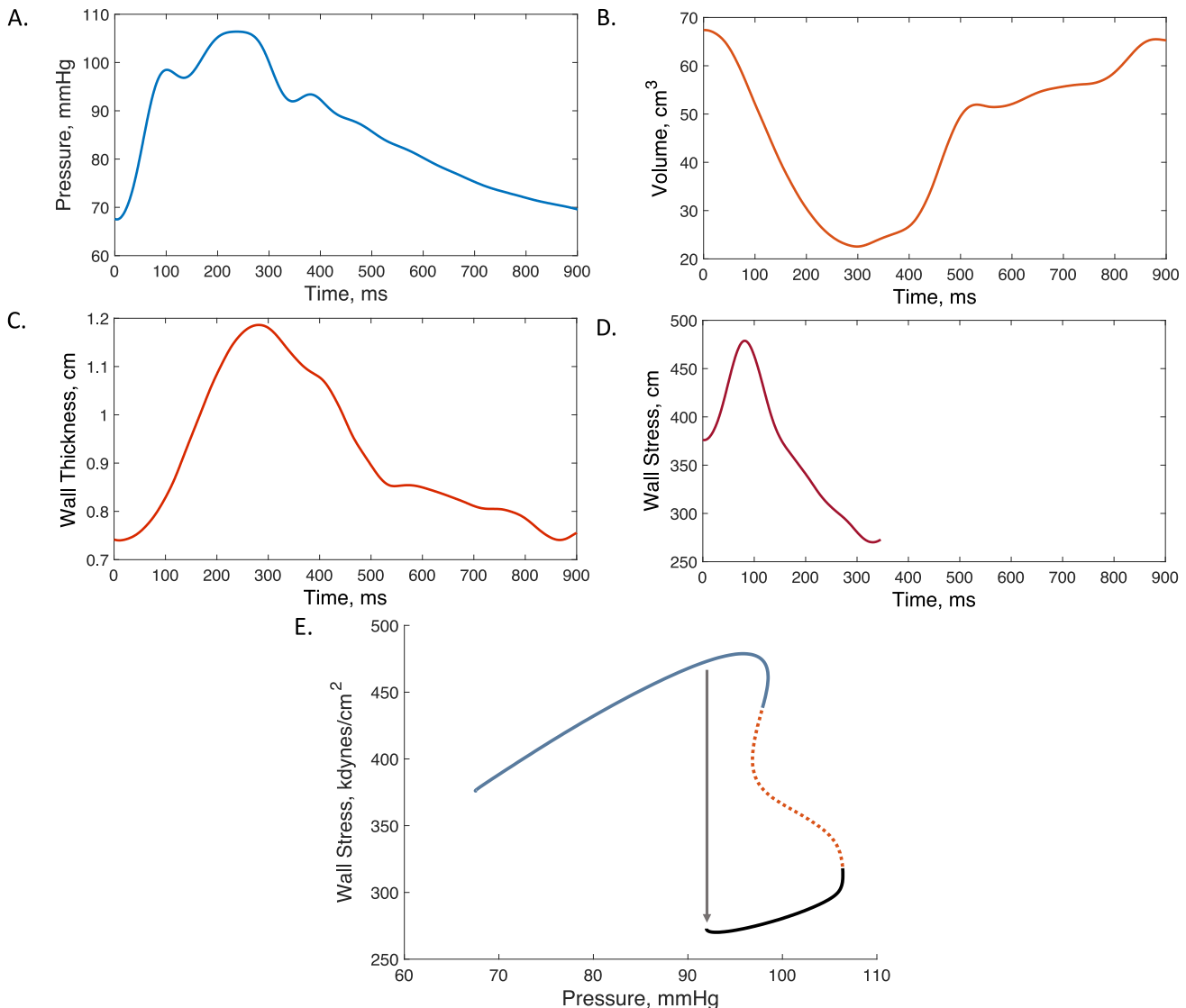
The method above assumes that LV pressure and aortic pressure are similar during ejection. This is true only in the absence of aortic stenosis or LV outflow tract obstruction. Interestingly, in the presence of aortic valve stenosis, the time-resolved transvalvular pressure gradient can be derived with continuous wave Doppler acquisitions to measure transvalvular flow velocities and with the use of the modified Bernoulli equation:

$$\Delta P = 4\left(V_2^2 - V_1^2\right)$$

where V_1 is velocity preorifice and V_2 is velocity postorifice. When proximal velocities are low (such as aortic valvular stenosis in the absence of LV outflow tract obstruction), they can be neglected and the equation can be simplified to:

$$\Delta P = 4V^2$$

In aortic valvular stenosis, the derived transvalvular pressure gradient can be added to the aortic pressure at each point in time during ejection to derive the LV instantaneous pressure, allowing for a noninvasive approximation of
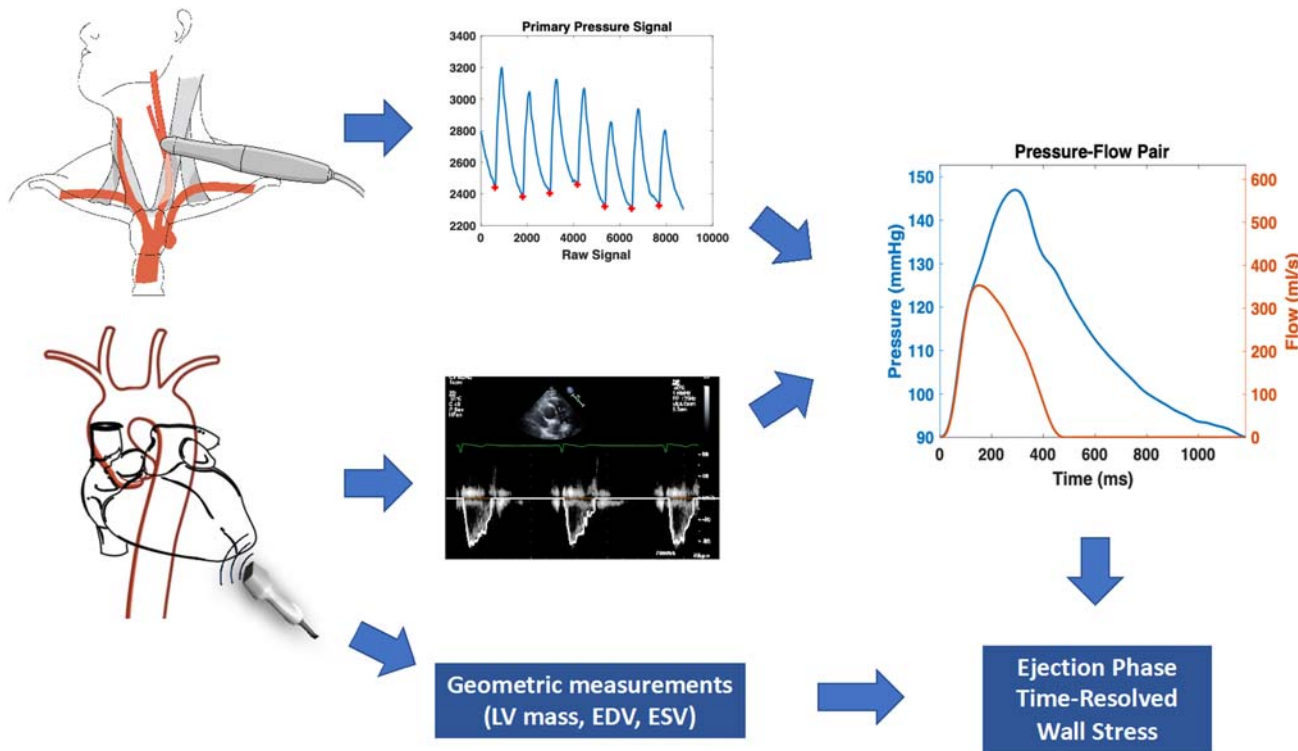
FIGURE 16.1   Example of assessments of time-resolved ejection-phase myocardial wall stress. Arterial tonometry can provide a time-resolved pressure curve (A), whereas speckle-tracking echocardiography and other imaging techniques can provide time-resolved LV geometry (B: cavity volume; C: wall thickness). One can thus compute myocardial wall stress at each time point and generate a time-resolved stress curve (D). Normally, brisk force development and fiber shortening occur in early systole, resulting in an early peak in MWS and shortening rate, followed by continued LV ejection and a dynamic reconfiguration of LV geometry that results in a mid-systolic reduction in MWS relative to LV pressure. Notice the early systolic MWS peak followed by a rapid decline in wall stress despite rising pressure. Panel E shows a pressure−stress plot, demonstrating a mid-systolic shift of the pressure−stress relation (*gray arrow*) which favors lower stress values in late systole despite rising pressure. This mechanism tends to protect the myocardium against excessive load in mid-to-late systole (a period of increased vulnerability), but may be overcome by pronounced wave reflections during this period and/or intrinsic myocardial dysfunction leading to an abnormal ejection pattern. The mid-systolic reduction in MWS, relative to pressure, is impaired in the presence of a lower LV EF (even within the "normal" EF range), concentric LV remodeling or hypertrophy, and/or reduced early systolic ejection (despite a preserved overall EF).

time-resolved LV pressure (Fig. 16.4), in turn allowing for assessments of time-resolved MWS (Fig. 16.5).

The time course of ejection-phase MW

It is important to recognize the advantages of assessing time-resolved ejection-phase MWS as opposed to end-systolic wall MWS. The latter has been widely utilized in clinical studies due to the relative ease of identification of end-systole with echocardiography, but is not representative

of peak force development or other important events that occur during ejection (Table 16.1). Once a time-resolved ejection-phase MWS curve is derived, various key parameters can be readily computed, including peak (maximum) MWS, the MWS time-integral (i.e., area under the time-resolved wall stress curve) during ejection, and the mid-systolic shift in the pressure−stress relation (Fig. 16.2).[9] A time-resolved MWS curve also allows for characterization of the *myocardial* loading sequence, which can be expressed as a ratio of the stress-time integral in late versus early systole.
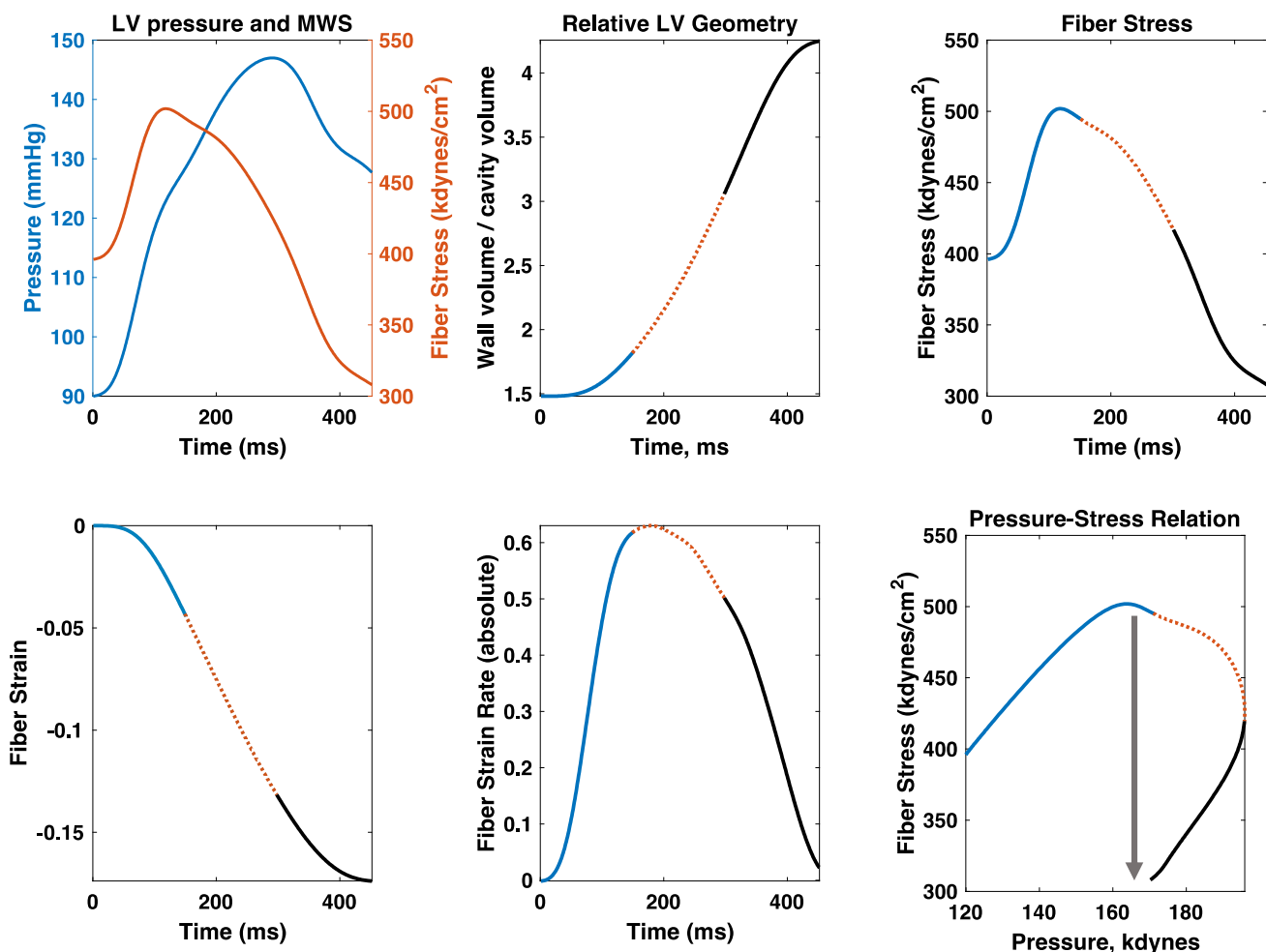
FIGURE 16.2 **Assessment of time-resolved wall stress based on arterial tonometry and Doppler echocardiography.** As an alternative to time-resolved geometric left ventricular (LV) measurements, integration of the time-resolved aortic or left ventricular outflow tract flow curve can provide the cumulative ejected volume until any given time point during ejection, therefore allowing for the computation of a time-resolved LV cavity volume curve during ejection. Wall volume can be assumed to be constant. This method can be readily applied using only the pressure−flow pair and basic LV geometric measurements in end-systole and diastole (end-diastolic cavity volume, end-systolic cavity volume, and LV mass).

In order to better interpret the time-resolved MWS curve, it is useful to review the events that take place at the myocardial, ventricular, and arterial levels during early systole, mid-systole, and late systole.

Throughout systole, myocardial fiber activation results in the development of tension (stress) and shortening of myocardial segments, which results in progressive ejection of blood from the LV cavity and wall thickening (Fig. 16.1). During *early* ejection, active development of fiber cross-bridges occurs in the electrically activated myocardium and peak MWS occurs,[1] at a time when systolic pressure co-exists with quasi-diastolic geometry (relatively thin wall and relatively large cavity) (Fig. 16.1A−D). Myocardial fiber shortening and ejection of blood determine a progressive change in LV geometry, which causes a drop in myocardial stress (despite rising pressure) during mid-to-late systole. This can be quantified as a clear "shift" in the pressure−stress relation (Fig. 16.1E) and appears to be ideal for the myocardium to handle the additional load imposed by systolic wave reflections, which are present in most older adults. This shift, however, may be insufficient and/or compromised in the setting of wave reflections of very early onset or of large magnitude[8,12,13] and in the presence of a lower LV ejection fraction.[1,12]

Various indices of LV afterload derived from pressure−flow relations are useful because they characterize the hydraulic load on the LV pump and can provide indices that are purely reflective of arterial properties.[14] However, arterial load should always be interpreted by considering not only the interactions between arteries and the LV as a pump[14,15] but also between myocardial elements and instantaneous LV geometry and the time-varying load imposed by the systemic circulation. As expected from physiologic principles, various arterial properties affect time-varying MWS differently.[8] SVR is a very important determinant of MWS throughout systole, whereas aortic root characteristic impedance (Zc) selectively affects early systolic and peak systolic MWS. In contrast, wave reflections and total arterial compliance correlate with MWS in mid and late systole and significantly influence the area under the stress-curve generated for any given flow output.[8] Interestingly, women seem to demonstrate greater peak and end-systolic wall stress as well as a higher ejection-phase stress-time integral, even after adjustment for arterial properties, which might relate to the differential susceptibility of women to heart failure.[8]

Interestingly, whereas wave reflections selectively increase late systolic wall stress, the LV contraction pattern
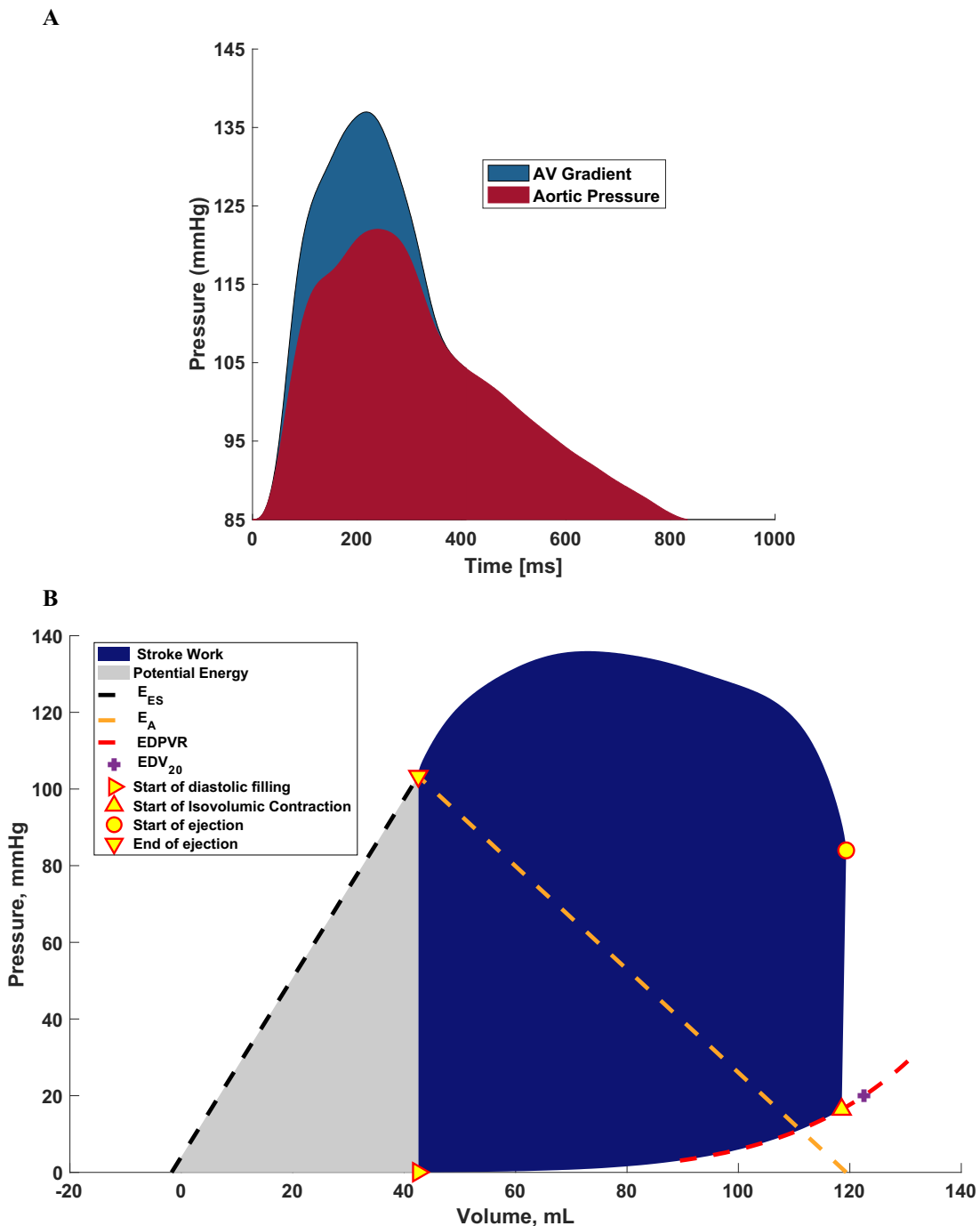
FIGURE 16.3 **Assessment of ejection-phase time-resolved wall stress based on arterial tonometry and Doppler echocardiography, using the method depicted in Fig. 16.2.** Time resolved LV cavity pressure (which in the absence of aortic stenosis or LV outflow tract obstruction is very similar to aortic pressure, blue curve in top left panel) and the relative LV geometry (wall volume/cavity volume ratio) are used to compute time-resolved fiber stress (top right panel and red curve in top left panel). The Arts model can also be used to compute average time-resolved fiber strain and strain rate (bottom left and middle panels). The bottom right panel shows the mid-systolic shift of the pressure—stress relation (*gray arrow*) demonstrating a reduction in fiber stress in mid-systole despite rising pressure. In the top left panel, pressure is represented by the blue line, whereas myocardial wall fiber stress is represented by the red line. In other panels, early systole (first third), mid-systole (middle third), and late systole (last third) are represented by the blue continuous line, the *red dotted line*, and the black continuous line, respectively.
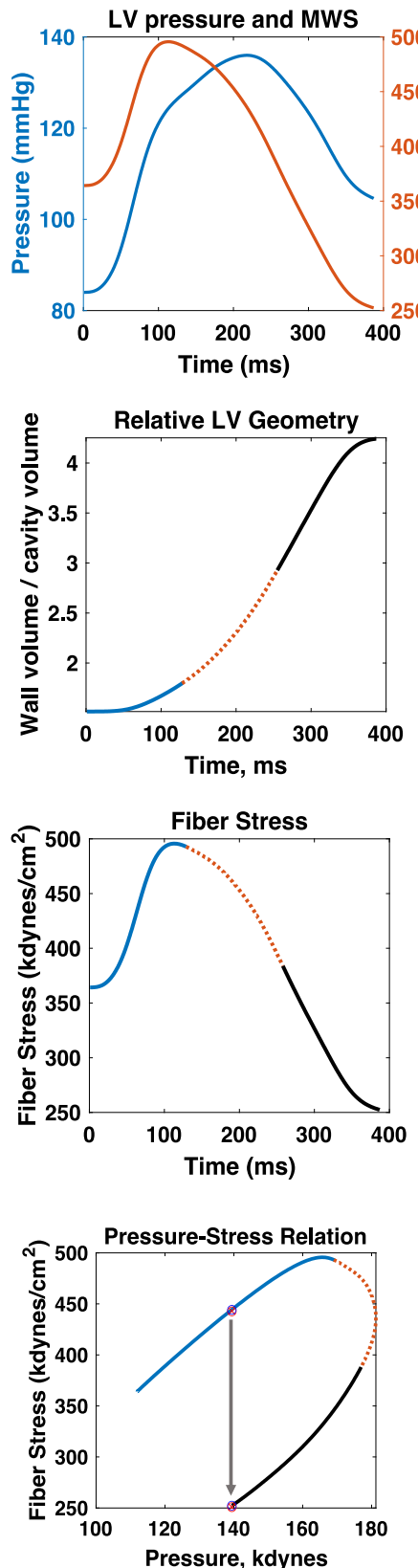
can modulate the influence of wave reflections on late systolic myocardial load. As mentioned above, normally, a marked mid-systolic shift in the pressure—stress relation occurs as a result of LV contraction (Figs. 16.1, 16.3 and 16.5). This shift effectively protects LV cardiomyocytes against excessive wall stress in late systole, a period of increased vulnerability to the ill effects of load. Abnormalities such as reduced early phase ejection, a lower LV ejection fraction, and concentric hypertrophy/remodeling can impair the mid-systolic shift in the pressure—MWS relation, making the LV more susceptible to the effects of wave reflections on the myocardium.[1,12]

Arterial wave reflection

As discussed in detail elsewhere in this book (Chapters 1, 3, 11), wave reflections occur at multiple sites of impedance mismatch, such as points of branching or change in wall diameter or material properties along the arterial tree. Innumerable reflections merge into a discrete reflected wave, which travels back to the heart.[16-18] The time of arrival of the reflected wave to the proximal aorta is strongly dependent on the pulse wave velocity (PWV) of conduit vessels, particularly the aorta, which transmits forward and backward traveling waves from and toward the

FIGURE 16.4 **Example of non-invasive estimation of LV pressure assessments of LV ventricular−arterial coupling in the pressure−volume plane in the presence of aortic stenosis using arterial tonometry and Doppler echocardiography.** Panel A illustrates how the aortic transvalvular gradient measured with continuous wave Doppler can be readily added to the aortic pressure waveform to compute the time-resolved LV intracavitary pressure. Panel B shows the LV pressure volume loop constructed with synchronized pressure and volume measurements, along with an estimation of the LV end-systolic elastance slope using a single beat method (see Chapter 15). The additional pressure above end-systolic pressure from aortic stenosis, wave reflections and other hemodynamic phenomena are not accounted for by the ratio of effective arterial elastance to LV end-systolic elastance (E_A/ E_{ES}). The latter ratio only uses end-systolic pressure and assumes a square shaped pressure−volume loop for assessments of energetic efficiency (see Chapter 15). A more direct assessment of stroke work and potential energy (and thus energetic efficiency) can be made using time resolved pressure and volume and the areas of stroke work and potential energy (shown in blue and gray). In addition, time-resolved pressure and volume allow for straightforward computations of time-resolved fiber stress (Fig. 16.5).

FIGURE 16.5   Assessment of time-resolved ejection-phase myocardial wall fiber stress (MWS) in a patient with aortic valvular stenosis.

LV, respectively.[14,18−20] Stiffer aortas exhibit greater PWV and conduct forward and backward traveling waves at greater velocities and therefore promote an earlier arrival of wave reflections to the LV.[16,18,21,22] As a consequence of the aortic stiffening that occurs with aging and various disease states, the hemodynamic effects of wave reflections shift from diastole to systole (Fig. 16.6), with prominent effects during mid-to-late systole in older adults,[18,21] particularly in women[16,17,21,24−27] and in patients with heart failure and preserved ejection fraction (HFpEF).[28−30] The shift of wave reflection arrival from diastole to systole favors a loss of coronary perfusion pressure on one hand, and increased mid-to-late systolic load on the other. When premature, wave reflections increase aortic pressure and reduce forward flow, therefore increasing the LV pressure while impeding the outflow of blood from the LV in mid-to-late systole. Since this outflow reduces LV cavity size and thus the ratio of cavity to wall volume, premature wave reflections increase mid-to-late systolic MWS by impacting the relationship between LV pressure and LV geometry during this phase of ejection. Therefore, wave reflections can have a substantial impact on the LV loading sequence (increasing mid/late relative to early systolic load).

Wave reflections are typically quantified via wave separation analysis, using the ratio of forward to backward wave amplitude. This approach is discussed in detail in other chapters of this textbook. Pronounced and/or premature wave reflections can have important deleterious effects on the myocardium (Fig. 16.7) as discussed in subsequent sections of this chapter. Importantly, wave reflections may be susceptible to modification by pharmacologic interventions, which could have important implications for the prevention and treatment of HF (as discussed in more detail in Chapters 36 and 51).

LV loading sequence and its role in LV hypertrophy

For any given level of systolic (peak) blood pressure, prominent mid-to-late systolic loading has been shown to

---
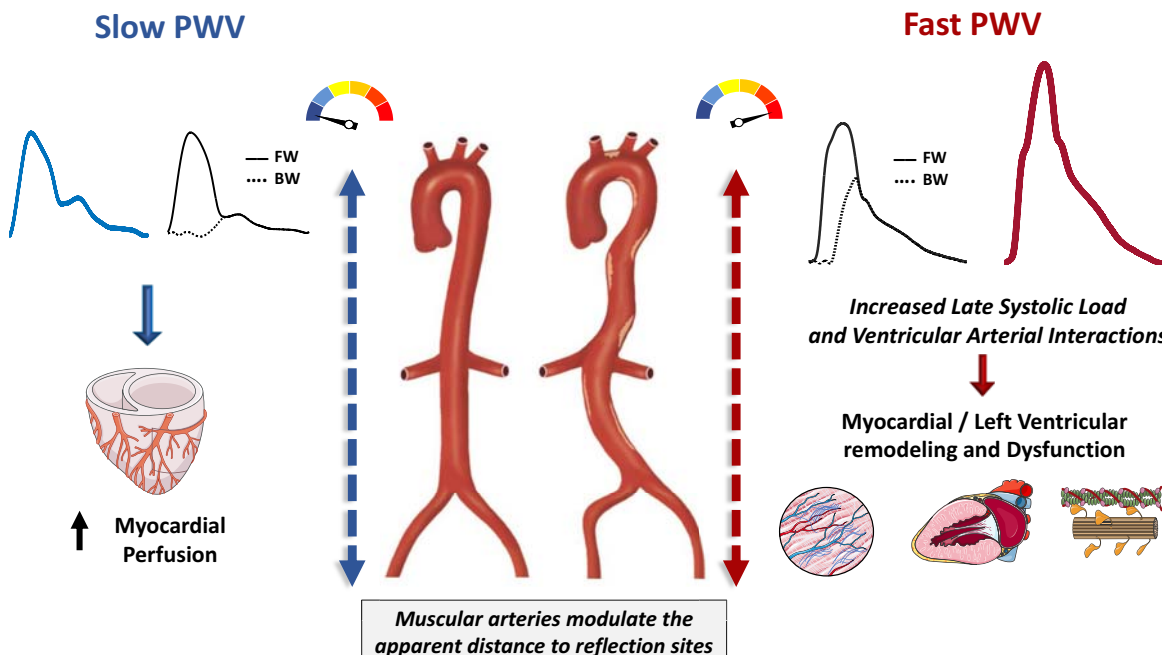
Using an aortic pressure waveform (arterial tonometry) and the transvalvular pressure gradient derived from Doppler echocardiography (Fig. 16.4), the LV pressure waveform (top panel) is computed. The LV outflow waveform can also be used to compute time-resolved LV wall volume, and thus relative LV geometry (second panel). The third panel shows the time-resolved ejection-phase fiber stress. The bottom panel shows the mid-systolic shift of the pressure−stress relation (*gray arrow*) demonstrating a reduction in fiber stress in mid-systole despite rising pressure. In the top left panel, pressure is represented by the blue line, whereas myocardial wall fiber stress is represented by the red line. In other panels, early systole (first third), mid-systole (middle third), and late systole (last third) are represented by the *blue continuous line*, the red dotted line, and the *black continuous line*, respectively.

TABLE 16.1 Key events during early, mid, and late systole relevant for understanding the impact of the LV systolic loading sequence on the myocardium.

Early ejection (∼First third of ejection)	Mid-systole (∼2nd third of ejection)	Late systole (∼Last third of ejection)
• Prior to ejection, the myocardium develops force without significant shortening. The initiation of ejection allows the myocardium to shorten as it ejects blood. The point at which the valve opens is dependent on diastolic blood pressure (which in turn varies directly with mean arterial pressure and inversely with pulse pressure). • As the aortic valve opens, the myocardium transitions from isometric contraction to the early ejection-phase, during which peak myocardial wall stress develops (typically ∼70–100 ms after aortic valve opening in humans), followed by the onset of myocardial relaxation. • Prior to the onset of myocardial relaxation, active cross-bridge formation occurs. During this phase, myocytes can partially adapt to increased load by increasing the number of interacting cross-bridges (cooperative activity). • Fiber shortening during this period results in: (1) Initiation of length-dependent deactivation ("shortening-deactivation") of cardiomyocytes; (2) Dynamic changes in LV geometry that favor a subsequent reduction in myocardial wall stress relative to LV pressure. • Pulsatile arterial load in early ejection is governed by aortic root characteristic impedance (Zc). The net load from wave reflections during this phase is small.	• Sustained LV ejection determines a progressive shift in the pressure–stress relation, such that myocardial wall stress progressively decreases for any given LV cavity pressure. • This shift is quite pronounced in normal circumstances but can be reduced in the presence of LV hypertrophy and/or reduced myocardial contractility. • Shortening-deactivation reduces the force of contraction and wall stress decreases. Despite this, increasing pressure can occur, given the shifting pressure–stress relation mentioned above. • This is a period of particularly increased vulnerability to load, because: (1) it follows the onset of relaxation (and cross-bridges can no longer adapt to load); (2) It precedes the full development of the shift in the pressure–stress relation (which "protects" cardiomyocytes from excessive wall stress). • If present (i.e., due to their premature arrival back at the LV), wave reflections exert significant hemodynamic load on the cardiomyocytes during this period.	• Under normal conditions: (1) The shift in the pressure–stress relationship has fully developed; (2) Myocardial wall stress/force development and the velocity of fiber shortening continue to decrease; (3) The end of the action potential promotes full relaxation. • Wave reflections exert significant hydraulic load on the LV, but if a pronounced shift in the pressure–stress relation occurred earlier in systole, LV wall stress is low (cardiomyocytes are "protected" from wave reflections). • However, when earlier systolic phenomena are abnormal (i.e., impaired early phase ejection from decreased contractility or increased load, impaired mid-systolic shift in the pressure–stress relation due to LV concentric hypertrophy/remodeling or decreased contractility), cardiomyocytes continue to be vulnerable to the effects of wave reflections. Moreover, in the absence of a pronounced shift in the pressure–stress relation in mid-systole, persistently increased force development may be necessary to sustain LV pressure and promote continued ejection. • A sustained contraction pattern may be present (as a result of deficient shortening-deactivation), tending to preserve the overall EF on one hand, but impairing myocardial and LV relaxation on the other.

Modified from reference Chirinos JA. Deep phenotyping of systemic arterial hemodynamics in hfpef (part 2): clinical and therapeutic considerations. **J Cardiovasc Transl Res**. 2017; 10:261–274.

FIGURE 16.6   Cardiac consequences of arterial stiffening and premature wave reflection. Earlier arrival of wave reflections favor a loss of coronary perfusion pressure on one hand, and increased mid-to-late systolic load on the other, due to a shift of wave reflection arrival from diastole to systole. In populations with stiff aortas, muscular artery function may become a key determinant of the apparent distance to reflection sites and thus the effects of wave reflections on the central aorta, for any given PWV. *BW*, backward wave; *FW*, forward wave; *PWV*, pulse wave velocity. *Reproduced from Chirinos JA, Segers P, Hughes T, Townsend R. Large-artery stiffness in health and disease: Jacc state-of-the-art review.* ***J Am Coll Cardiol****. 2019; 74:1237—1263.*

exert deleterious effects on LV structure and function in animal models and has been associated with LV hypertrophy in humans.[18,31,32] Kobayashi et al.[31] used a Wistar rat model and performed constriction of either the ascending aorta or suprarenal abdominal aorta. Constriction of the ascending aorta increased LV load in early systole (which mimics an increased proximal aortic characteristic impedance), whereas constriction of the descending aorta caused prominent mid-to-late systolic loading from a large reflected wave that originated at the distal aortic constriction site.[31] In this study, despite identical peak LV pressure levels in both groups, rats that underwent descending aortic banding (and were thus exposed to greater mid-to-late systolic load) demonstrated much greater LV hypertrophy than those undergoing ascending aortic banding (which were exposed to increased early systolic load).[31].

These findings are supported by observational human data. Hashimoto et al.[33] assessed changes in wave reflection magnitude occurring during antihypertensive therapy and observed that the reduction in wave reflections predicted regression of LV mass independently of blood pressure reduction. The association between reflected wave magnitude reduction and LV mass reduction was also independent of age, sex, and use of renin-angiotensin system inhibitors, and was particularly strong in patients with LV hypertrophy at baseline. Of note, despite the fact that standard antihypertensive therapy reduced wave reflections

on average, the change was highly variable, with reflection magnitude actually increasing in some subjects. In agreement with Hashimoto's findings, a relationship between reflection magnitude (approximated from measured pressure and an assumed physiologic flow waveform) and LV mass has been reported in large community-based studies that included normotensive and hypertensive individuals.[25,34] Similarly, Quail et al. recently demonstrated that in patients with repaired aortic coarctation, reflection magnitude assessed from the ascending aortic distension waveform (a surrogate of the aortic pressure waveform) and measured aortic flow (using phase-contrast MRI) was independently associated with LV hypertrophy.[35] When interpreted in the context of available animal data, available human studies support a role for wave reflections and late systolic load in the development of LV hypertrophy, independent of absolute blood pressure levels.

LV loading sequence and its role in LV fibrosis

Available studies also suggest a role for wave reflections and mid-to-late systolic load on LV fibrosis. In the previously mentioned study by Hashimoto et al.,[33] the banding intervention that increased wave reflections, resulting in mid-to-late systolic LV loading also caused more LV subendocardial fibrosis, compared to the intervention that increased load in early systole. A study assessed the role of

FIGURE 16.7 Effect of late systolic load from arterial wave reflections on the myocardium. Increases in mid-to-late systolic load from prominent and/or premature wave reflections can lead to left ventricular concentric remodeling or hypertrophy, myocardial fibrosis, T-tubule dysfunction, contractile dysfunction, and slow relaxation. At the pump level, this may result in systolic and diastolic dysfunction, and consequent left atrial remodeling and dysfunction.

wave reflections on diffuse LV fibrosis (measured by MRI T1 mapping sequences) among patients with severe aortic stenosis undergoing aortic valve replacement. In this study, patients with symptomatic severe aortic stenosis scheduled to undergo surgical aortic valve replacement underwent measurements of aortic root characteristic impedance, wave reflection parameters (reflection magnitude, reflected wave transit time), and myocardial extracellular mass (a validated surrogate of diffuse myocardial fibrosis) using cardiac magnetic resonance imaging (MRI) and arterial tonometry. Patients with higher extracellular mass exhibited greater reflection magnitude and lower aortic root characteristic impedance, the latter being likely a consequence of aortic dilation. Interestingly, in this study, reflection magnitude was a significant predictor of a smaller improvement in the quality of life (Kansas City Cardiomyopathy Questionnaire score) assessed six months after aortic valve replacement. This study demonstrated that arterial wave reflections are associated with interstitial fibrosis and a worse clinical response to surgical aortic valve replacement, suggesting that the loading sequence is important regardless of the presence of overt pressure overload from aortic stenosis.

Effect of mid-to-late systolic load on LV diastolic dysfunction

Multiple animal studies have demonstrated the deleterious effect of mid-to-late systolic load on LV relaxation.[32,36−41] An early study by Hori et al. was performed using a canine model to impose increased afterload by either: (a) clamping

the ascending aorta to induce early systolic load; (b) clamping the descending aorta to induce mid-to-late systolic load; (c) intermittently clamping the ascending aorta in late systole. The authors demonstrated that, for a given increase in peak systolic LV pressure, clamps that resulted in mid-to-late systolic loading prolonged *tau* (the gold standard index of diastolic relaxation) much more than early loading. In a subsequent study, Gillebert et al.[32] studied the effect of the timing of systolic load on LV relaxation in dogs, by inflating balloons in the ascending aorta at different times during ejection (inducing either early systolic load or mid-to-late systolic load). This study elegantly demonstrated that, for a given increase in peak systolic LV pressure, mid-to-late systolic loading prolonged *tau* much more than early systolic inflation, further demonstrating a cause-effect relationship between mid-to-late systolic load and diastolic dysfunction.[32] These results are consistent with several other animal studies[37,40,42,43] Interestingly, one study[44] did not find slowing of relaxation when load was applied selectively in very late systole (∼20−50 ms before aortic valve closure), whereas load applied in mid-systole (∼80−110 ms before aortic valve closure) significantly slowed relaxation. These results suggest that the effects of wave reflections are not necessarily deleterious in very late systole, unless the bulk of their effect "advances" into mid-systole (as occurs in the setting of markedly increased aortic PWV and premature wave reflections). This is consistent with our understanding of the importance of mid-systole as a critical time during which LV contraction progressively shifts the pressure−

stress relation and "protects" cardiomyocytes from the deleterious effects of wave reflection during late ejection[1,2,8,45] (Table 16.1 and Fig. 16.2).

In support of the large body of animal experimental findings demonstrating a cause-effect relationship between mid-to-late systolic load and impaired LV relaxation, several human studies demonstrate that indices of wave reflections and/or mid-to-late systolic MWS are independently associated with diastolic dysfunction,[9,28,41,42,45−52] LA remodeling,[48,53,54] decreased longitudinal systolic function (despite preserved EF),[9,55] and elevated brain natriuretic peptide levels.[41,51,56,57]

Myocardial loading sequence and atrial dysfunction

LA dysfunction has been associated with an increased risk of cardiovascular morbidity and mortality in population-based and hypertensive cohorts.[58,59] LA function is also important to regulate and promote LV filling during diastole, contributing to cardiac output adaptations to changes in loading conditions, inotropic stimulation, and heart rate. We assessed the relationship between the myocardial loading sequence (early vs. late MWS) and LA dysfunction in 260 adults with hypertension referred for a cardiac MRI study.[6] LA function was assessed from classic phasic LA volumes as well as measurements of LA myocardial deformation (strain) using tissue-tracking algorithms applied to cine-MRI SSFP images. Time-resolved central pressure and time-resolved LV geometry were measured with carotid tonometry and cardiac MRI, respectively, for computation of time-resolved ejection-phase MWS. The MWS time-integral (area under the MWS curve) in the first half of ejection (early systole) and the second half of ejection (late systole) were computed. In this study, an LV myocardial loading sequence characterized by prominent late systolic MWS (relative to early systolic MWS) was independently associated with impaired reservoir, conduit, and booster pump LA function. Interestingly, in models that adjusted for late systolic load, early systolic load was associated with better LA function, indicating that it is not only the absolute load but also the myocardial loading sequence that determines LA dysfunction in hypertension. In the context of available experimental data, these findings further support the deleterious effects of late systolic LV loading on systolic−diastolic coupling.

Late systolic load and heart failure risk

Consistent with the effects of wave reflections on LV remodeling, fibrosis and dysfunction, wave reflection magnitude[12,60] and late systolic hypertension[61] have been shown to be strong independent predictors of incident HF in the Multi-Ethnic Study of Atherosclerosis (MESA), as discussed in more detail in Chapter 36.

Cellular processes in the myocardium

The cellular processes that mediate the deleterious effects of wave reflections on the myocardium are poorly understood. The effect of mid-to-late systolic load on diastolic relaxation and chronic LV remodeling are likely due to intrinsic differences in cellular processes at different phases of systole, as summarized in Table 16.1. During early ejection, active development of fiber cross-bridges occurs in the electrically activated myocardium and peak MWS occurs,[1] which is followed by a transition from contraction to relaxation. The transition from contraction to relaxation occurs very early during ejection in dogs (∼34% after the initiation of mechanical systole and ∼16% into the duration of ejection).[62] In humans, the time to peak MWS, which reflects the time of peak force development (and after which force first starts to decline), has been proposed as a marker of the time to the onset of relaxation.[50] This normally occurs ∼70−100 msec into ejection.[1,8,9]

The immediate effects of afterload on diastolic relaxation have been explained on the basis of the differential effect of early versus mid-to-late systolic load on the number of interacting cross-bridges. Loading during active cross-bridge formation in early systole increases the number of interacting cross-bridges (cooperative activity), a physiological mechanism that favors matching of the number of cross-bridges with systolic load.[32,63] However, when increased load occurs after the onset of myocardial relaxation, the number of interacting cross-bridges can no longer adapt. Under these circumstances, a mismatch between the number of cross-bridges and load may occur, increasing the stress imposed on individual cross-bridges and decreasing cross-bridge cycling.

However, a more complex interplay between cross-bridge recruitment, cooperative activity, cross-bridge inactivation, and cross-bridge cycling rate are likely at play.[45,50,62,63] Recently, the course of ejection in early systole (which depends at least partially on myocardial contractility) has been shown to correlate with the subsequent course of MWS.[50] As mentioned earlier in this chapter, under normal conditions, brisk force development and fiber shortening occur in early systole, resulting in LV ejection and a dynamic reconfiguration of LV geometry that results in a mid-systolic reduction in MWS relative to LV pressure,[1] thus protecting the cardiomyocytes against excessive load in mid-to-late systole (a period of increased vulnerability). The phenomenon of shortening-deactivation (which is associated with reduced calcium sensitivity of the contractile apparatus), decreases force development after early systolic rapid shortening, and increases the relaxation rate of muscle.[45,50] This represents a perfect "match" to this normal physiology, because sustained myocardial force development in mid-to-late systole is unnecessary to preserve fiber shortening and LV ejection against the load imposed by wave reflections. However, in the presence of

contractile abnormalities that compromise early ejection, the mid-systolic dynamic geometric reconfiguration of the LV that favors a reduced MWS relative to pressure is impaired. In these conditions, shortening-deactivation may not operate fully, such that force development continues or increases in mid-to-late systole, tending to preserve the overall EF on one hand, but impairing relaxation on the other.[45,50] Disorganization and disruption of transverse (T-) tubules, which are important for the spatial alignment between L-type calcium channels and the sarcoplasmic reticulum, has also been suggested.[12] Disrupted T-tubules lead to inefficient calcium cycling, myocardial dysfunction, and calcium overload in cardiomyocytes due to deficient calcium reuptake.[12,64] These abnormalities are deleterious in their own right, but may also conspire with impaired shortening-deactivation to sustain contraction and prolong relaxation.

The differential effect of time-varying myocardial afterload on cellular and molecular processes taking place in early versus mid-to-late ejection should be a focus of further research. In particular, the molecular mediators of the long-term effects of mid-to-late systolic load on maladaptive remodeling, and the pharmacologic effects of common drugs that may affect the time course of myocardial contraction require further study. In addition, the role of comorbidities is not well understood and requires further research. Long-standing hypertension, and comorbidities such as coronary artery disease, obesity, and chronic kidney disease, may affect the normal contraction pattern that normally protects myocytes from the effects of wave reflection.[1,12]

Conclusions

Substantial evidence from animal and human studies strongly suggest that a systolic loading sequence characterized by late systolic load can cause maladaptive LV remodeling, fibrosis, diastolic dysfunction and failure, thus representing a highly clinically relevant cardiovascular phenotype. The myocardial loading sequence is not assessed through conventional cardiac imaging methods and is not captured in the pressure−volume plane. However, assessments of time-resolved MWS and arterial wave reflections can be accomplished via noninvasive methods, which should be utilized more broadly. The adverse effects of late systolic load on the myocardium provides an opportunity for therapeutic interventions designed to ameliorate these effects, which could in turn reduce the risk of maladaptive LV remodeling, fibrosis dysfunction and failure. This can, in principle, be accomplished independently of effects on microvascular resistance or mean arterial pressure, as discussed in Chapters 36 and 49−51.

References

1. Chirinos JA, Segers P, Gupta AK, et al. Time-varying myocardial stress and systolic pressure-stress relationship: role in myocardial-arterial coupling in hypertension. **Circulation**. 2009; 119:2798−2807.
2. Chirinos JA. Ventricular-arterial coupling: invasive and non-invasive assessment. **Artery Res**. 2013; 7.
3. Chirinos JA. Deep phenotyping of systemic arterial hemodynamics in hfpef (part 1): physiologic and technical considerations. **J Cardiovasc Transl Res**. 2017; 10:245−259.
4. Chirinos JA, Sweitzer N. Ventricular-arterial coupling in chronic heart failure. **Card Fail Rev**. 2017; 3:12−18.
5. Arts T, Bovendeerd PH, Prinzen FW, Reneman RS. Relation between left ventricular cavity pressure and volume and systolic fiber stress and strain in the wall. **Biophys J**. 1991; 59:93−102.
6. Chirinos JA, Phan TS, Syed AA, et al. Late systolic myocardial loading is associated with left atrial dysfunction in hypertension. **Circ Cardiovasc Imaging**. 2017; 10:e006023.
7. Weber T, Chirinos JA. Pulsatile arterial haemodynamics in heart failure. **Eur Heart J**. 2018; 39:3847−3854.
8. Chirinos JA, Segers P, Gillebert TC, et al. Arterial properties as determinants of time-varying myocardial stress in humans. **Hypertension**. 2012; 60:64−70.
9. Chirinos JA, Segers P, Rietzschel ER, et al. Early and late systolic wall stress differentially relate to myocardial contraction and relaxation in middle-aged adults: the asklepios study. **Hypertension**. 2013; 61:296−303.
10. Swingen C, Wang X, Jerosch-Herold M. Evaluation of myocardial volume heterogeneity during end-diastole and end-systole using cine mri. **J Cardiovasc Magn Reson**. 2004; 6:829−835.
11. Chirinos JA. Deep phenotyping of systemic arterial hemodynamics in hfpef (part 2): clinical and therapeutic considerations. **J Cardiovasc Transl Res**. 2017; 10:261−274.
12. Shah SJ, Wasserstrom JA. Increased arterial wave reflection magnitude: a novel form of stage b heart failure? **J Am Coll Cardiol**. 2012; 60:2178−2181.

13. Chowienczyk P, Shah A. Myocardial wall stress: from hypertension to heart tension. **Hypertension**. 2012; 60:10−11.
14. Nichols WW, O'Rourke MF. **Mcdonald's Blood Flow in Arteries. Theoretical, Experimental and Clinical Principles**. Oxford University Press; 2005.
15. Kawaguchi M, Hay I, Fetics B, Kass DA. Combined ventricular systolic and arterial stiffening in patients with heart failure and preserved ejection fraction: implications for systolic and diastolic reserve limitations. **Circulation**. 2003; 107:714−720.
16. Chirinos JA, Segers P. Noninvasive evaluation of left ventricular afterload: part 1: pressure and flow measurements and basic principles of wave conduction and reflection. **Hypertension**. 2010; 56:555−562.
17. Chirinos JA, Segers P. Noninvasive evaluation of left ventricular afterload: part 2: arterial pressure-flow and pressure-volume relations in humans. **Hypertension**. 2010; 56:563−570.
18. Nichols WW, OR M, Vlachopolous C. **Mcdonald's Blood Flow in Arteries. Theoretical, Experimental and Clinical Principles**. Hodder Arnold; 2011.
19. Mitchell GF. Arterial stiffness and wave reflection in hypertension: pathophysiologic and therapeutic implications. **Curr Hypertens Rep**. 2004; 6:436−441.
20. Mitchell GF. Clinical achievements of impedance analysis. **Med Biol Eng Comput**. 2009; 47:153−163.
21. Phan TS, Li JK, Segers P, et al. Aging is associated with an earlier arrival of reflected waves without a distal shift in reflection sites. **J Am Heart Assoc**. 2016; 5.
22. Chirinos JA. Arterial stiffness: basic concepts and measurement techniques. **J Cardiovasc Transl Res**. 2012; 5:243−255.
23. Chirinos JA, Segers P, Hughes T, Townsend R. Large-artery stiffness in health and disease: Jacc state-of-the-art review. **J Am Coll Cardiol**. 2019; 74:1237−1263.
24. Townsend RR, Wilkinson IB, Schiffrin EL, et al. Recommendations for improving and standardizing vascular research on arterial stiffness: a scientific statement from the american heart association. **Hypertension**. 2015; 66:698−722.
25. Zamani P, Bluemke DA, Jacobs Jr DR, et al. Resistive and pulsatile arterial load as predictors of left ventricular mass and geometry: the multi-ethnic study of atherosclerosis. **Hypertension**. 2015; 65:85−92.
26. Zamani P, Jacobs Jr DR, Segers P, et al. Reflection magnitude as a predictor of mortality: the multi-ethnic study of atherosclerosis. **Hypertension**. 2014; 64:958−964.
27. Chirinos JA, Kips JG, Roman MJ, et al. Ethnic differences in arterial wave reflections and normative equations for augmentation index. **Hypertension**. 2011; 57:1108−1116.
28. Weber T, O'Rourke MF, Ammer M, Kvas E, Punzengruber C, Eber B. Arterial stiffness and arterial wave reflections are associated with systolic and diastolic function in patients with normal ejection fraction. **Am J Hypertens**. 2008; 21:1194−1202.
29. Weber T, Wassertheurer S, O'Rourke MF, et al. Pulsatile hemodynamics in patients with exertional dyspnea: potentially of value in the diagnostic evaluation of suspected heart failure with preserved ejection fraction. **J Am Coll Cardiol**. 2013; 61:1874−1883.
30. Marechaux S, Samson R, van Belle E, et al. Vascular and microvascular endothelial function in heart failure with preserved ejection fraction. **J Card Fail**. 2016; 22:3−11.
31. Kobayashi S, Yano M, Kohno M, et al. Influence of aortic impedance on the development of pressure-overload left ventricular hypertrophy in rats. **Circulation**. 1996; 94:3362−3368.
32. Gillebert TC, Lew WY. Influence of systolic pressure profile on rate of left ventricular pressure fall. **Am J Physiol**. 1991; 261:H805−H813.
33. Hashimoto J, Westerhof BE, Westerhof N, Imai Y, O'Rourke MF. Different role of wave reflection magnitude and timing on left ventricular mass reduction during antihypertensive treatment. **J Hypertens**. 2008; 26:1017−1024.
34. Booysen HL, Woodiwiss AJ, Sibiya MJ, et al. Indexes of aortic pressure augmentation markedly underestimate the contribution of reflected waves toward variations in aortic pressure and left ventricular mass. **Hypertension**. 2015; 65:540−546.
35. Quail MA, Short R, Pandya B, et al. Abnormal wave reflections and left ventricular hypertrophy late after coarctation of the aorta repair. **Hypertension**. 2017; 69:501−509.
36. Hori M, Inoue M, Kitakaze M, et al. Loading sequence is a major determinant of afterload-dependent relaxation in intact canine heart. **Am J Physiol**. 1985; 249:H747−H754.
37. Gaasch WH, Blaustein AS, Adam D. Myocardial relaxation iv: mechanical determinants of the time course of left ventricular pressure decline during isovolumic relaxation. **Eur Heart J**. 1980; 1:7.
38. Yano M, Kohno M, Konishi M, Takahashi T, Seki K, Matsuzaki M. Influence of left ventricular regional nonuniformity on afterload-dependent relaxation in intact dogs. **Am J Physiol**. 1994; 267:H148−H154.
39. Wu MS, Chang CY, Chang RW, Chang KC. Early return of augmented wave reflection impairs left ventricular relaxation in aged Fisher 344 rats. **Exp Gerontol**. 2012; 47:680−686.
40. Schafer S, Fiedler VB, Thamer V. Afterload dependent prolongation of left ventricular relaxation: importance of asynchrony. **Cardiovasc Res**. 1992; 26:631−637.
41. Goto T, Ohte N, Fukuta H, Wakami K, Tani T, Kimura G. Relationship between effective arterial elastance, total vascular resistance, and augmentation index at the ascending aorta and left ventricular diastolic function in older women. **Circ J**. 2013; 77:123−129.
42. Yano M, Kohno M, Kobayashi S, et al. Influence of timing and magnitude of arterial wave reflection on left ventricular relaxation. **Am J Physiol Heart Circ Physiol**. 2001; 280:H1846−H1852.
43. Ishizaka S, Asanoi H, Wada O, Kameyama T, Inoue H. Loading sequence plays an important role in enhanced load sensitivity of left ventricular relaxation in conscious dogs with tachycardia-induced cardiomyopathy. **Circulation**. 1995; 92:3560−3567.
44. Zile MR, Gaasch WH. Load-dependent left ventricular relaxation in conscious dogs. **Am J Physiol**. 1991; 261:H691−H699.
45. Chirinos JA. Deciphering systolic-diastolic coupling in the intact heart. **Hypertension**. 2017; 69.
46. Fukuta H, Ohte N, Wakami K, et al. Impact of arterial load on left ventricular diastolic function in patients undergoing cardiac catheterization for coronary artery disease. **Circ J**. 2010; 74:1900−1905.
47. Borlaug BA, Melenovsky V, Redfield MM, et al. Impact of arterial load and loading sequence on left ventricular tissue velocities in humans. **J Am Coll Cardiol**. 2007; 50:1570−1577.
48. Peterson VR, Woodiwiss AJ, Libhaber CD, Raymond A, Sareli P, Norton GR. Cardiac diastolic dysfunction is associated with aortic wave reflection, but not stiffness in a predominantly young-to-middle-aged community sample. **Am J Hypertens**. 2016; 29:1148−1157.
49. Fujimoto N, Onishi K, Tanabe M, et al. Nitroglycerin improves left ventricular relaxation by changing systolic loading sequence in patients with excessive arterial load. **J Cardiovasc Pharmacol**. 2005; 45:211−216.

50. Gu H, Li Y, Fiok H, et al. Reduced first-phase ejection fraction and sustained myocardial wall stress in hypertensive patients with diastolic dysfunction: a manifestation of impaired shortening deactivation that links systolic to diastolic dysfunction and preserves systolic ejection fraction. **Hypertension**. 2017; 69(4):633−640.

51. Kaji Y, Miyoshi T, Doi M, et al. Augmentation index is associated with b-type natriuretic peptide in patients with paroxysmal atrial fibrillation. **Hypertens Res**. 2009; 32:611−616.

52. Canepa M, Alghatrif M, Strait JB, et al. Early contribution of arterial wave reflection to left ventricular relaxation abnormalities in a community-dwelling population of normotensive and untreated hypertensive men and women. **J Hum Hypertens**. 2014; 28:85−91.

53. Jaroch J, Rzyczkowska B, Bociaga Z, et al. Arterial-atrial coupling in untreated hypertension. **Blood Pres**. 2015; 24:72−78.

54. Jaroch J, Rzyczkowska B, Bociaga Z, et al. Relationship of carotid arterial functional and structural changes to left atrial volume in untreated hypertension. **Acta Cardiol**. 2016; 71:227−233.

55. Russo C, Jin Z, Takei Y, et al. Arterial wave reflection and subclinical left ventricular systolic dysfunction. **J Hypertens**. 2011; 29:574−582.

56. Kimura K, Tomiyama H, Matsumoto C, et al. Correlations of arterial stiffness/central hemodynamics with serum cardiac troponin t and natriuretic peptide levels in a middle-aged male worksite cohort. **J Cardiol**. 2015; 66:135−142.

57. Sakuragi S, Maruo T, Taniguchi M, et al. Radial augmentation index associated with increase in b-type natriuretic peptide in patients with hypertension. **Int J Cardiol**. 2008; 130:414−419.

58. Hoit BD. Left atrial size and function: role in prognosis. **J Am Coll Cardiol**. 2014; 63:493−505.

59. Benjamin EJ, Dagostino RB, Belanger AJ, Wolf PA, Levy D. Left atrial size and the risk of stroke and death - the framingham heart-study. **Circulation**. 1995; 92:835−841.

60. Chirinos JA, Kips JG, Jacobs Jr DR, et al. Arterial wave reflections and incident cardiovascular events and heart failure: mesa (multiethnic study of atherosclerosis). **J Am Coll Cardiol**. 2012; 60:2170−2177.

61. Chirinos JA, Segers P, Duprez DA, et al. Late systolic central hypertension as a predictor of incident heart failure: the multi-ethnic study of atherosclerosis. **J Am Heart Assoc**. 2015; 4:e001335.

62. Solomon SB, Nikolic SD, Frater RW, Yellin EL. Contraction-relaxation coupling: determination of the onset of diastole. **Am J Physiol**. 1999; 277:H23−H27.

63. Gillebert TC, Leite-Moreira AF, De Hert SG. Load dependent diastolic dysfunction in heart failure. **Heart Fail Rev**. 2000; 5:345−355.

64. Shah SJ, Aistrup GL, Gupta DK, et al. Ultrastructural and cellular basis for the development of abnormal myocardial mechanics during the transition from hypertension to heart failure. **Am J Physiol Heart Circ Physiol**. 2014; 306:H88−H100.

Assessment of ventricular arterial interactions via arterial pressure-flow relations in humans

Gary F. Mitchell

Cardiovascular Engineering, Inc., Norwood, MA, United States

Overview of arterial pressure-flow relations

The heart and arterial system represents a flow distribution system that has an ultimate goal of supplying required mean blood flow to the organs. Because the heart is a pulsatile pump, delivery of mean flow is necessarily accompanied by a variable amount of pulsatile overhead. The arterial system is designed to optimize delivery of mean flow with minimal pulsatile overhead. In order to minimize pulsatile overhead, the system design includes a highly compliant aorta coupled to the left ventricle (LV) and followed by a branching network of muscular arteries that arise from the aorta and supply the regional vasculature of various organs. Mean flow (Q_0) in that network interacts with peripheral resistance (Z_0) to produce mean arterial pressure (MAP), where $Z_0 = MAP/Q_0$. During early systole, the LV is exposed to MAP and the load imposed by the proximal aorta, which has a characteristic impedance (Z_c) that is a small fraction of peripheral resistance (Z_0). Z_c is analogous to Z_0, but represents the pressure-flow relations for the pulsatile component only of pressure and flow and can be approximated as $Z_c = dP/dQ$, where dP is the peak time-derivative of pressure and dQ is the peak time-derivative of volumetric flow in early systole. Z_c is normally a small fraction (5%−10%) of Z_0. As a result, whereas peak aortic flow is approximately fivefold higher than mean flow, pulse pressure (PP) (40 mm Hg) is a fraction of MAP (90 mm Hg) in a young healthy person.

In addition to the foregoing forward traveling waves, there are reflected waves in the arterial system that are attributable to impedance mismatch at branch points and other segments of differing physical properties. With advancing age, the aorta stiffens, resulting in an increase in Z_c and the amplitude of forward traveling pressure waves (P_f) produced by a given forward flow wave (Q_f). In addition, pulse wave velocity (PWV), which is the velocity at which these waves travel along the aorta, increases, meaning that reflected waves return to the proximal aorta sooner, resulting in progressive overlap between forward and backward pressure (P_f, P_b) and flow (Q_f, Q_b) waves during systole. These factors combine to increase PP and pulsatile overhead on the LV, resulting in LV remodeling and hypertrophy and leading to wide PP hypertension, which may be isolated systolic or mixed systolic and diastolic hypertension, depending on whether MAP is also increased (mixed hypertension). The resulting increase in pressure pulsatility and pulsatile load also has adverse implications for the periphery, where it triggers remodeling and loss of small vessels, resulting in blunted reactivity and an increase in resting Z_0. The increase in Z_0 can drive up MAP, which will passively stiffen the aorta, resulting in a potential vicious cycle. The loss of reactivity can have adverse effects on perfusion of target organs, especially in autoregulated high-flow organs like the brain and kidneys.[1−3] Similarly, diminished reactivity in muscular beds may limit vasodilatory reserve during exercise, which contributes to diminished exercise tolerance and hypertensive response to exercise.[4]

Noninvasive assessment of aortic pressure-flow relations

When pressure-flow relations in the arterial system were first assessed in the mid-1900s, invasive pressure and flow measurements were required.[5,6] Subsequent work demonstrated the possibility to acquire impedance measurements noninvasively by using carotid artery tonometry and

Doppler flow measurements in the LV outflow tract (LVOT).[7−9] The latter technique allowed investigators to perform large-scale, epidemiologic studies of pulsatile hemodynamics that have greatly expanded our understanding of aortic structure and function and ventricular-vascular interaction.[10−13]

Assessment of aortic input impedance requires measurement of time-resolved proximal aortic pressure and flow waveforms. Pressure can be obtained by performing carotid artery tonometry. The carotid artery waveform is not identical to the central aortic waveform because it is located downstream from the aortic inlet, meaning that there will be modestly more overlap between forward and reflected waves. In addition, there are branch points along the path from aorta to carotid, which will have additional modest effects on the shape of the waveform. However, invasive studies have shown that a properly calibrated carotid tonometry waveforms generally provides an adequate surrogate for central aortic pressure.[14]
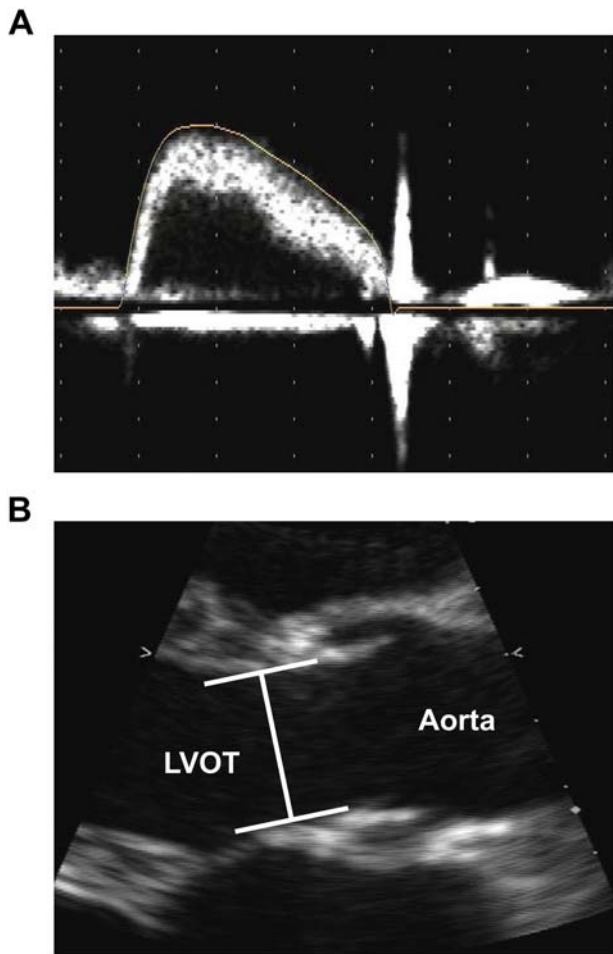
Proper calibration of the carotid pressure waveform is also required. Because of differences in relative timing of forward and reflected waves at various locations in the arterial system, systolic blood pressure (SBP) differs between sites. Therefore, brachial cuff blood pressure cannot be used to calibrate a carotid pressure waveform.[15−18] However, MAP and diastolic blood pressure (DBP) are reasonably consistent along the large arteries in the arterial tree, assuming there are no flow-limiting stenoses between the measurement sites. Therefore, brachial artery MAP and DBP can be used to calibrate the carotid pressure waveform. Note that brachial MAP should be based on a brachial waveform that has been calibrated to cuff SBP and DBP and then integrated to assess MAP. Some have used a formula to compute MAP based on a largely erroneous assumed shape factor of 33%, meaning that MAP is equal to DBP plus one-third of PP. However, the foregoing shape factor is highly variable, with values that are related to arterial stiffness, among other things. In addition, some have advocated for using a radial pressure waveform to derive an estimated central pressure waveform by using a generalized transfer function.[19] The foregoing radial waveform is often calibrated by using cuff SBP and DBP. The latter approach ignores pressure amplification between brachial and radial arteries and thereby markedly underestimates central PP.[16] In addition, the transfer function approach is dependent on the assumption that the transformation of a central pressure waveform into a peripheral pressure waveform is consistent across age, sex, and various risk factor exposures, which is known not to be the case based on the marked variability in higher frequencies of the specific transfer functions between participants, which influence some important morphologic details of the pressure waveform.[20,21] While the transfer function approach may result in an estimate of central pressure that correlates with invasive measures, the features of the reconstructed waveform are not suitable for detailed waveform analysis as too much high frequency content is lost as a result of the filtering that is required.[22]

Central aortic flow can be assessed either by Doppler ultrasound or by phase contrast magnetic resonance imaging (pcMRI). Most large-scale studies have utilized Doppler ultrasound because of lower cost, greater convenience, and better ability to minimize time delay between assessment of tonometry pressure and flow, which can readily be done simultaneously or a few seconds apart with Doppler ultrasound, whereas pcMRI flows are generally separated from pressure measurements by 20 min or more due to logistical difficulties in acquiring tonometry waveforms on a participant who is in the bore of the MR machine.

When using Doppler ultrasound to measure proximal aortic flow, it is important to measure flow velocity and cross-sectional area in the LVOT, where it is relatively straightforward to acquire a stable signal, using pulsed Doppler from an apical five-chamber view, and identify the relevant cross-sectional area required to convert flow velocity to volumetric flow (Fig. 17.1). Assuming continuity of flow, LVOT flow will be equal to proximal aortic flow. Attempts to measure flow directly in the proximal aorta, per se, rather than the LVOT, are confounded by acceleration of flow due to the vena contracta effect, which will result in marked overestimation of volumetric flow if paired with the aortic cross-sectional area at the location of the sample volume. In addition, a high-quality measurement of the proximal aortic diameter is not always technically feasible. Methodologic and technical considerations regarding arterial pressure and flow measurements are discussed in detail in Chapter 2.

Once properly calibrated central aortic pressure and flow waveforms are obtained, pressure-flow analyses can be performed. Analytic methods for the assessment of pressure-flow relations are discussed in detail in Chapter 3, but some key aspects are discussed below. When evaluating pressure-flow relations in the arterial system, one cannot use simple circuit theory because there are finite propagation delays and reflections that alter the shape of the traveling waveforms. One approach that has been used is frequency domain analysis. Propagation delays and reflected waves render arterial load frequency dependent because the implications of a given delay in reflected wave timing varies directly with wavelength and therefore frequency. Frequency domain analysis decomposes the pressure and flow waveforms into a series of sine and cosine waves by using a Fourier transform. Calculation of the first 15 or so harmonics of physiologic waveforms will provide most of the waveform variance and is acceptable. Impedance at each harmonic (Z_i) is then calculated by taking the ratio of pressure (P_i) and flow (Q_i) at harmonics 0 to $\sim$15,
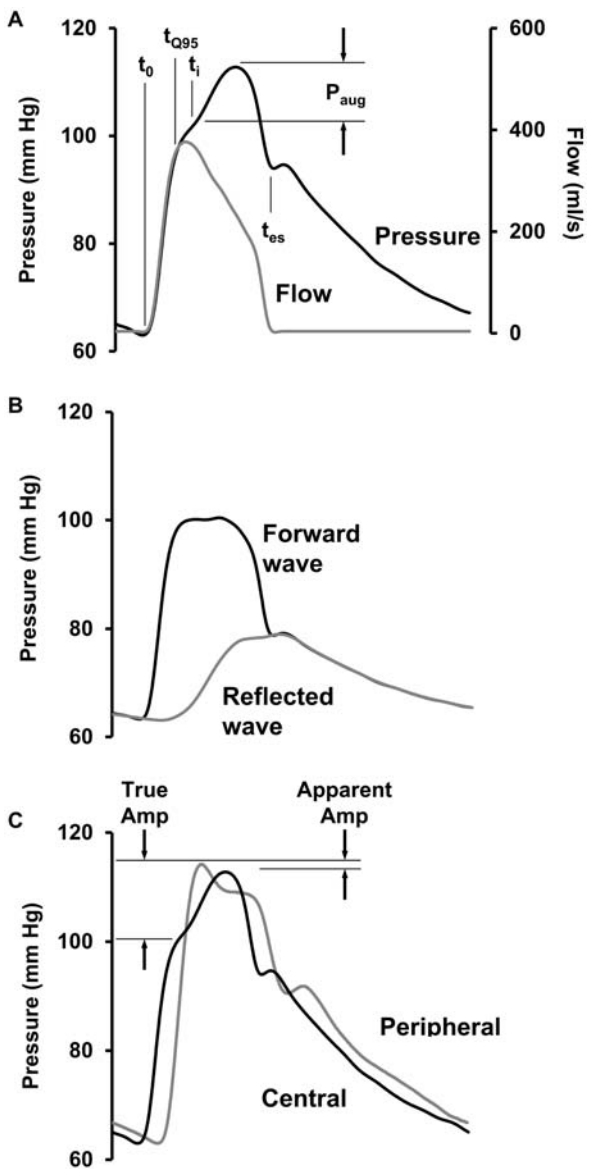
FIGURE 17.1 Measurement of flow rate in the left ventricular outflow tract (LVOT). When performing pressure-flow analysis in the proximal aorta, flow into the aorta is assessed as flow out of the ventricle through the LVOT. LVOT is easily measured by using pulsed Doppler (A) from a standard apical five-chamber view of the heart. If possible, it is preferable to measure Doppler audio and perform signal averaging of the spectral analysis in order to avoid bias due to single beat selection. The sample volume should be placed just proximal to the leaflet attachment point, high enough in the LVOT to be consistent with the measured LVOT diameter (B) but not so high that one begins to capture flow acceleration because of the vena contracta effect.

where harmonic 0 is the mean term and the first harmonic is equivalent to the heart rate, which is normally around 1 Hz in humans (at a heart rate of 60 beats/min). Z_c can be estimated by averaging the higher harmonics of Z_i across a band of frequencies where the effects of wave reflection cancel and provide an estimate of pulsatile pressure-flow relations in the absence of reflections. While frequency domain techniques are important in some settings and can be readily applied to digitized pressure and flow waveforms with contemporary software platforms, the approach is inaccessible or unintuitive to most clinicians and researchers.

Time domain analysis of aortic pressure-flow relations represents an easily understood alternative to the traditional frequency domain approach and has emerged as a frequently used approach.[12,13,23] Time domain assessment of Z_c is based on evaluation of pressure-flow relations in early systole, prior to arrival of the dominant P_b wave. One approach that has been used for proximal aortic pressure and flow involves finding the time point at which flow reaches 95% (Q95) of maximum flow (Fig. 17.1C). The early change in pressure (dPZ$_c$) attributable to interaction of early systolic flow and Z_c during this same time window is then assessed and time domain Z_c (Z_cTD) is computed as Z_cTD = dPZ$_c$/Q95. Peripheral resistance, Z_0, is computed as noted above. Wave separation is performed (Fig. 17.2) by taking the average of the measured pressure waveform (P_m) and the flow waveform scaled by Z_c (Q*Z_c). This average waveform represents the net forward traveling wave (P_f) in the proximal aorta. The point-by-point difference between P_m and P_f represents the net reflected or backward traveling wave, P_b. The foregoing calculations can be performed in any large artery bed where local pressure and flow can be assessed, such as the common carotid arteries, where pressure is assessed by using tonometry and flow is assessed by using Doppler or pcMRI. When using pcMRI, however, it is important to ensure that the scan sequence employs adequate spatial and temporal resolution.

An alternative method for computing Z_c that does not require pressure measurement is based on the water hammer equation, $Z_c = PWV * \rho/\pi r^2$, where PWV is local pulse wave velocity, ρ is the density of blood, which is generally assumed constant at 1.06 g/cm^3, and r is the lumen radius of the vessel. Local PWV can be measured by MRI. For example, one can assess PWV in the aortic arch by using a pcMRI slice positioned at approximately the level of the right main pulmonary artery. However, there are two important caveats to consider when performing these measurements. First, the transit distance is relatively short and therefore the transit time will be proportionally short, particularly in older participants with a stiff aorta. Therefore, care must be taken to ensure that the temporal resolution of the sequence is as high as possible, e.g., 100 phases/cardiac cycle. Second, it is important to note that all methods for measuring Z_c are sensitive to wave reflections. If there are very early reflected waves that encroach on the Q95 window, they will augment pressure and reduce flow, leading to overestimation of Z_c. The same is true for PWV-based measurements. If PWV is assessed by using two pressure waveforms, the error will be overestimation as wave reflection steepens the upstroke of the distal pressure waveform and appears to accelerate the wave velocity. The opposite error is seen, however, when PWV is assessed by measuring transit time from two flow waveforms because

FIGURE 17.2 Pressure waveform analysis and wave separation analysis. The central (carotid) pressure waveform (A) can be analyzed to determine the time lag between the pressure foot (t_0) and the inflection point (t_i) corresponding to the roundtrip reflected wave transit time (RWTT). The rise in pressure after t_i represents late systolic pressure augmentation (P_{aug}) due to the reflected wave, which increases central pulse pressure (PP) and late systolic load on the left ventricle. The timing of end-systole (t_{es}) relative to t_0 represents the systolic ejection period. Flow (Q) is rescaled by characteristic impedance ($Q*Z_c$) and aligned with the pressure foot. The average of these two waveforms represents the forward wave (B) and the difference between the forward wave and measured pressure represents the backward (reflected) wave. There are two types of pressure amplification that are seen in the arterial system. True amplification represent amplification of the first pressure peak as the forward traveling wave encounter regions of impedance mismatch. Apparent amplification represents the overall difference in PP between central (carotid) and peripheral (brachial or radial) sites. An increase in central pressure augmentation has no effect on true amplification but reduces apparent amplification nearly to zero by midlife, meaning that differences in central and peripheral PP abate as augmentation increases.

distal reflection blunts the upstroke of the distal flow waveform and appears to delay the waveform and reduce wave velocity. Therefore, when comparing aortic Z_c assessed by using pressure-flow analysis versus Z_c assessed by pcMRI using the water hammer equation, it is important to note that the former values will be substantially greater than the latter. In contrast, when comparing Z_c based on pressure-flow analysis using Doppler as compared to pcMRI to measure flow, the values for Z_c should be comparable.

One important corollary of the water hammer equation is that it underscores the differing relations of PWV and Z_c with vessel diameter. Relations of PWV with basic material properties of the artery are expressed in the Moens—Korteweg equation: $PWV = \sqrt{(Eh/2\rho r)}$, where E is Young's modulus, h is wall thickness, and r is lumen radius. Thus, PWV has square root sensitivities to wall stiffness (Eh) (direct) and lumen radius (inverse). Substituting the Moens—Korteweg equation into the water hammer equation: $Z_c = \sqrt{(Eh/2\rho r)} * \rho/\pi r^2$, one can show that $Z_c = \sqrt{(Eh/2\rho r)} *\rho/\pi r^2 = \sqrt{(Eh\rho/2\pi^2 r^5)}$. Thus, Z_c has the same direct relation with the square root of wall stiffness (Eh), but the inverse relation with lumen radius is now raised to a power of $5/2 = 2.5$ rather than a simple square root (power = 0.5).[24] Thus, PWV and Z_c will change concordantly if the vessel wall stiffness changes. However, if lumen radius changes, the effect on Z_c will be $5\times$ greater than the effect on PWV. For example, a 10% increase in lumen radius will produce a 5% reduction in PWV but a 25% reduction in Z_c.

When considering remodeling of the aorta during growth and development or in response to weight gain or other factors that increase blood flow, it is important to note that the mass of elastic fibers in the aorta is relatively fixed.[25,26] Elastic fiber assembly results from the complex and carefully orchestrated expression of a number of components in addition to elastin. Elastic fibers in the aorta and elsewhere in the body (lungs, skin) are formed early in life, beginning during fetal development and ending at around the equivalent of the toddler stage in most mammals, when the gene program for creating elastic fibers is permanently silenced.[27] As a result, the pool of elastic fibers created during this critical period of development must last an entire lifetime. Given that the mass of elastic fibers is fixed, when the aorta remodels to a larger diameter, for example, during post-toddler growth, the pool of elastic fibers is effectively thinned. In addition, the fibers are placed under greater load because of the increase in lumen area, which will increase wall stress (σ) according to the Laplace equation: $\sigma = Pr/h$. Increased stress on elastic fibers will transfer some of the load to stiffer elements in the wall, such as collagen, resulting in an increase in effective wall stiffness (E). As a result, PWV, which is relatively
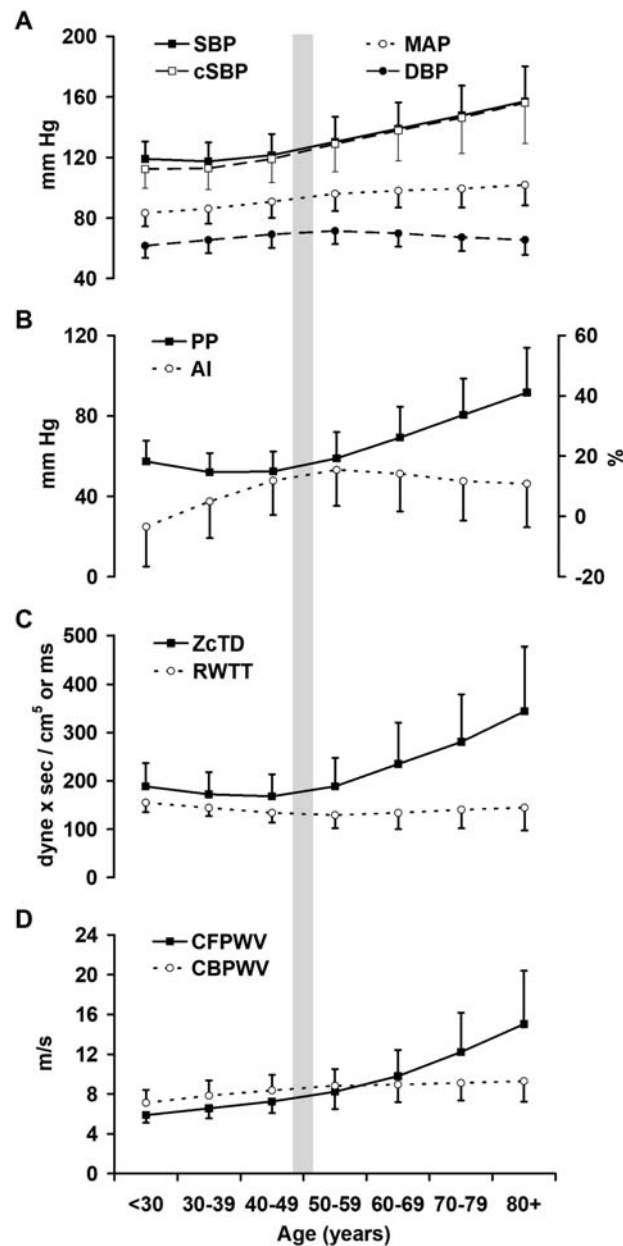
insensitive to lumen radius, may increase whereas Z_c generally will fall unless the increase in Eh is markedly (5×) greater than the increase in lumen radius. Thus, remodeling of the aorta in response to changes in blood flow or other factors can have markedly differing effects on PWV and Z_c.

Age relations of pressure-flow variables across the lifespan

Numerous large cross-sectional studies have examined the complex age relations of various measures of aortic stiffness and aortic pressure-flow relations.[12,13,28] Most studies have revealed markedly differing age relations of various stiffness measures before and after midlife (Fig. 17.3). The standard appearance of blood pressure-age relations in Westerners is presented in Fig. 17.3A,B. PP falls modestly between young adulthood and midlife, whereas MAP increases moderately. After midlife, PP increases rapidly whereas MAP increases modestly. As a result, SBP is relatively flat in young adults but increases rapidly after midlife, whereas DBP increases moderately before midlife and falls moderately thereafter, with the combination resulting in the aforementioned marked increase in PP.

Aortic wall stiffness, assessed as carotid-femoral pulse wave velocity (CFPWV), increases throughout life although the rate of increase accelerates at midlife (Fig. 17.3D). For example, in Framingham Heart Study (FHS) participants, CFPWV increased at a modest rate of 0.52 ± 0.04 m/s per decade of age prior to 50 years and a markedly (4×) higher rate of 2.05 ± 0.03 m/s per decade thereafter. In contrast, Z_c fell modestly prior to 50 years of age, at a rate of -8.4 ± 1.3 dyne*s/cm^5 per decade, and rose markedly thereafter at a rate of 51.1 ± 1.1 dyne*s/cm^5 per decade. The pattern of discordant change in CFPWV (increasing) and Z_c (decreasing) prior to midlife is consistent with remodeling of the aorta to a larger diameter.[12,13,29] Furthermore, the observation that Z_c increases rapidly after midlife, particularly in women, is consistent with the hypothesis that aortic remodeling to a larger diameter is no longer able to compensate for, and may even be contributing to, increasing aortic wall stiffness.

The hemodynamic basis for an increase in PP with advancing age is often debated. An early hypothesis posited that degradation of elastic elements in the aorta led to dilation of the aorta and transferred load to stiffer collagen fibers, resulting in an increase in PWV. The increase in PWV led to premature arrival of P_b during systole rather than diastole, resulting in augmentation of the proximal pressure wave. This late systolic augmentation, which is often assessed by computing the augmentation index (AI), was thought to be the basis for the increase in PP and SBP.[30] However, the foregoing hypothesis is not consistent with empirical observations. While it is true that CFPWV and AI increase prior to midlife that increase in AI occurs in the setting of a fall in PP (Fig. 17.3B). After midlife, AI falls at a time when PP increases dramatically, suggesting

FIGURE 17.3 Age relations of key hemodynamic variables across the full lifespan in the Framingham Heart Study second and third generation cohorts. Systolic blood pressure (SBP) is relatively flat through midlife and increases markedly thereafter (A). Mean arterial pressure (MAP) and diastolic blood pressure (DBP) increase modestly prior to midlife, after which MAP increases modestly and DBP falls. Because of constant SBP and rising DBP, pulse pressure (PP) falls prior to midlife and increases markedly thereafter. Augmentation index (AI) increases markedly prior to midlife, when PP is falling, and falls modestly after midlife, when PP increases markedly, indicating that early wave reflection and increased pressure augmentation are not the reason for rising pulse pressure after midlife. In contrast, characteristic impedance of the aorta (Z_c) parallels the change in pulse pressure across the full lifespan, indicating that changes in PP are attributable to changes in Z_c and forward wave amplitude. Central aortic wall stiffness, assessed by carotid-femoral pulse wave velocity (CFPWV), increases moderately prior to midlife and markedly thereafter (D). In contrast, muscular artery wall stiffness, assessed as carotid-brachial pulse wave velocity (CBPWV) remains relatively constant across the lifespan. Since muscular artery lumen diameter tends to increase with age, peripheral impedance will fall as central impedance (Z_c) increases, resulting in impedance matching between aorta and muscular arteries, reduced global wave reflection and increased transmission of damaging pulsatility into the periphery.
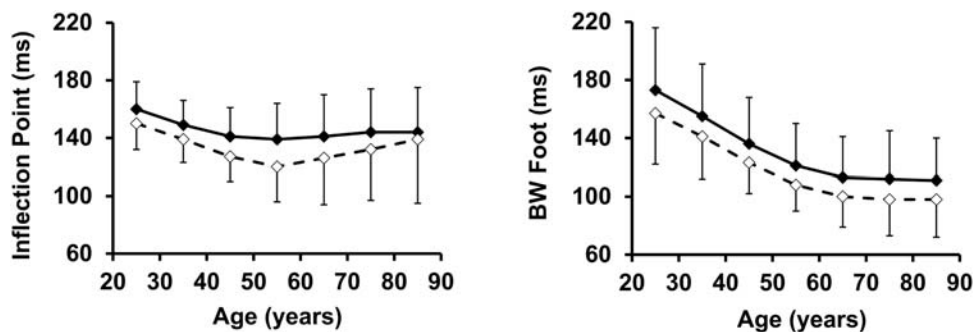
that early P_b and higher AI are not the basis for increasing PP after midlife. In FHS participants, an overwhelming proportion of variance in central and peripheral PP is attributable to variance in P_f, with modest amounts attributable to relative wave reflection (P_b/P_f) and timing of the reflected wave. Furthermore, several studies have shown that higher PP is associated with smaller rather than larger aortic diameter.[24,31,32] For example, in the AGES-Reykjavik study of older adults, markedly higher PP in women was attributable to smaller aortic diameter in women in models that adjusted for body size and other measures of wall stiffness.[11] Furthermore, in a subsequent study that examined aortic structure and function in detail by using MRI, PP was shown to be related directly to aortic wall stiffness and thickness and inversely to aortic lumen area.[33]

The basis for stable or falling AI after midlife despite an accelerated increase in CFPWV has also generated considerable concern and confusion in the literature. One might think that a progressive increase in CFPWV would be associated with proportionally earlier arrival of P_b and greater AI after midlife. However, if one looks at reflected wave arrival time, assessed as either the timing of the inflection point in the central pressure waveform or as the timing of the P_b foot following wave separation, it is evident that an early fall in the roundtrip time prior to midlife gives way to a plateau after midlife (Fig. 17.4). Since CFPWV is increasing and roundtrip time is unchanged after midlife, the distance to the effective aggregate reflection site seems to increase after midlife.[10] Furthermore, the global reflection factor (P_b/P_f) falls modestly with age after midlife.[12] The combination of a modest increase in roundtrip time and a modest decrease in global reflection factor accounts for the fall in AI.

The basis for the fall in global reflection and AI has been attributed by some investigators to impedance matching in the arterial system.[10] In young, healthy adults, aortic stiffness (CFPWV) is markedly lower than peripheral artery stiffness (CBPWV). In addition, the aorta is much larger than the first-generation muscular arteries that arise

from the aorta and supply various regional vascular beds. Smaller diameter and higher stiffness combine to produce markedly higher Z_c in the muscular arteries as compared to the aorta. This steep impedance gradient, due to impedance mismatch between aorta and first-generation muscular arteries, creates wave reflection that limits transmission of pulsatile power into the muscular arteries. With advancing age, the normally compliant aorta stiffens while the normally stiff muscular arteries dilate and possibly become less stiff,[34] leading to impedance matching between aorta and first-generation branch vessels. The progressive increase in CFPWV and unchanged CBPWV results in a crossing of those values at midlife, coinciding with the timing of the transition from rising to flat or falling AI, falling global reflection factor and rising RWTT despite increasing CFPWV (Fig. 17.3). The most straightforward interpretation of this pattern of changes is that impedance mismatch between aorta and first-generation muscular arteries has diminished, leading to a reduction in wave reflection.[10,12] Furthermore, if proximal wave reflection at the origin of first-generation arteries decreases, wave reflection from more distal sites in the vasculature will become more prominent, resulting in an increase in the average distance to reflecting sites and an increase in effective reflection distance computed from RWTT and CFPWV.[10] However, it has also been pointed out that (for reasons described above), impedance matching is highly dependent on vessel size (rather than just PWV), such that PWV matching does not necessarily imply impedance matching, and vice versa. Indeed, impedance matching tends to occur even at younger ages due to well-matched area ratios of parent and daughter vessels; therefore, in general, the magnitude of wave reflection at individual bifurcations (including first order aortic bifurcations) is relatively small. More complex phenomena are likely at play, which will require further detailed study across the lifespan in health and disease. Theoretical and practical considerations regarding the determinants of wave reflections in the arterial tree are discussed in detail in Chapter 11.
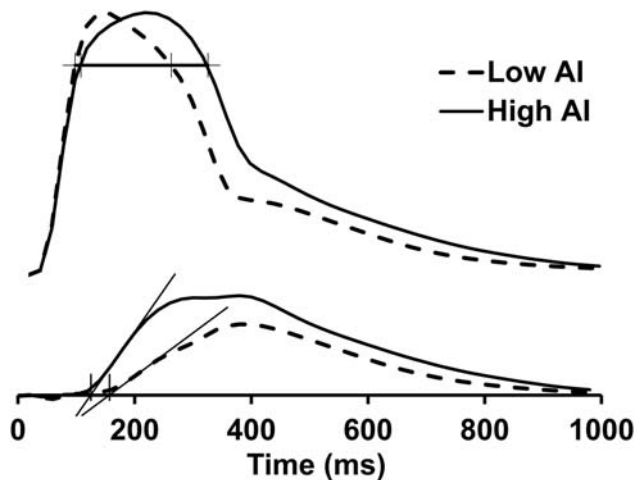
FIGURE 17.4 Comparison of reflected wave transit time assessed by the timing of the inflection point on the carotid pressure waveform (A) or by the timing of the backward wave (BW) foot following wave separation analysis (B). The fall in BW foot time is more pronounced than inflection point time, but nevertheless approaches an asymptote at midlife that is well above zero. As a result, the distance to the "effective" reflecting site increases markedly as pulse wave velocity increases.

One might question why the early increase in CFPWV, prior to midlife, is associated with a reduction in RWTT and a marked increase in AI. During this age range, aortic Z_c is falling whereas peripheral artery wall stiffness, assessed as CBPWV, increases modestly (Fig. 17.3). Thus, it is reasonable to assume that the aorta-peripheral impedance gradient increases with age through midlife. The greater impedance mismatch will increase the amplitude of individual reflected waves occurring at the origins of various branch arteries arising from the aorta. Furthermore, shortening of the transit time will tend to synchronize timing of wave reflection from these distributed reflecting sites, steepening the slope of the rising edge of the aggregate reflected wave and adding to apparent augmentation of the central pressure waveform (Fig. 17.5). In light of potential adverse effects on the heart and brain of central pressure augmentation, additional research is needed to elucidate factors that contribute to constructive and destructive interference between reflected waves arising from various regions in the arterial system.[35]

Aortic pressure-flow measures and the heart

The normal arterial system is designed to isolate the heart, which is a pulsatile pump, from the high impedance peripheral resistance. This isolation is achieved by interposing

FIGURE 17.5 Comparison of ensemble averaged forward (solid line) and backward (dashed line) waveforms for individuals with lowest quartile as compared to highest quartile values for augmentation index (AI). Higher augmentation index is associated with a wider forward wave peak and earlier arrival of a backward wave that has a steeper rising edge. Overlap of the rising edges of the forward and backward waves in the high AI group results in marked augmentation of the measured pressure waveform. In contrast, overlap of the falling edge of the forward wave with the blunted and delayed rising edge of the backward wave results in minimal or negative augmentation of the measured pressure waveform. Vertical lines represent the timing of the foot of the backward wave.

the normally compliant aorta, with a low Z_c and PWV, between the heart and the network of conduit and resistance vessels. Low Z_c ensures low P_f amplitude in response to a given forward flow wave. Low PWV is associated with later return of a reflected P_b wave that has a blunted upstroke, leading to limited or negative pressure augmentation, meaning the late systolic pressure peak does not determine central systolic pressure. As the aorta stiffens, diffuse reflected waves return to the central aorta sooner and are more synchronized, resulting in a steeper P_b upstroke and greater late systolic pressure augmentation, which increases load on the LV and reduces stroke volume. However, it is important to note that a normal LV is protected from the effects of late systolic pressure augmentation because late systolic LV geometry (small chamber volume, high relative wall thickness) favors the heart, leading to low end-systolic wall stress even if AI is high.[36] Consistent with this protected late systolic geometry, in the FHS, higher AI was not associated with LV mass or wall thickness in models that adjusted for standard demographics and CVD risk factors, including MAP.[37] Similarly, P_b amplitude was not associated with LV mass or wall thickness in models that adjusted for forward wave amplitude, indicating that relative wave reflection was not related to LV mass. In contrast, higher P_f, which is closely related to aortic Z_c, was associated with higher LV mass and wall thickness. P_f peaks early in systole, when LV geometry is unfavorable (near diastolic volume, low wall thickness), resulting in an early peak in wall stress that is directly proportional to P_f amplitude and Z_c. Higher AI was associated with lower fractional shortening and higher LV filling pressures, assessed as mitral inflow early velocity divided by mitral annulus tissue Doppler early velocity, E/e', suggesting that an AI-related reduction in stroke volume was associated with a compensatory increase in filling pressure.[37] This is also consistent with the effect of wave reflection and late systolic loading on diastolic relaxation demonstrated in animal models[38] and supported by previous observations in the Asklepios study.[39] Such effects may explain the association between AI and incident AF in the FHS cohort.[40] For a more detailed discussion regarding the impact of the loading sequence on the LV, the reader is referred to Chapter 16.

Pressure-flow measures and cardiovascular disease events

Various aortic stiffness and pressure-flow measures have been related to incident hypertension and CVD events.[41−44] The relation between hypertension and aortic stiffness is often debated. Early studies suggested that arterial stiffness was a consequence of longstanding hypertension that increased stress and strain on the arterial wall and accelerated the aging process, leading to irreversible aortic

damage and stiffening. However, more recent studies have examined blood pressure and stiffness measures at two points in time and demonstrated that abnormal aortic stiffness precedes the development of hypertension.[43] In contrast, in FHS participants, once baseline stiffness was considered, blood pressure did not predict progressive stiffening of the aorta. Thus, aortic stiffness is now viewed as a cause rather than a consequence of hypertension, which remains the leading cause of premature death and disability in the world.
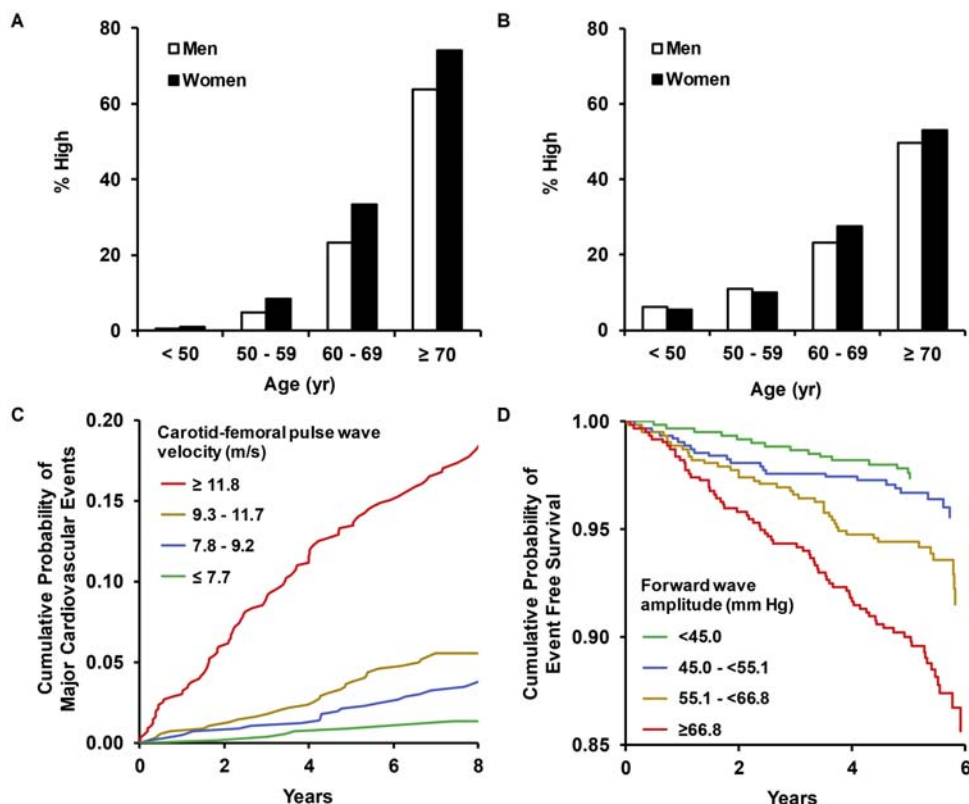
Higher aortic wall stiffness, as assessed by CFPWV, the current reference standard measure of stiffness, is associated with greater risk for a major CVD event and reclassifies risk in individuals at intermediate risk.[44,45] The relative risk associated with higher CFPWV is particularly high in younger individuals,[45] suggesting that CFPWV may represent an ideal risk screening measure at an age when aortic damage can still be mitigated or reversed with lifestyle modification and other interventions. Greater PP, P_f amplitude and higher aortic Z_c are also associated with higher CVD risk in models that adjust for standard risk factors, including CFPWV (Fig. 17.6).[41] In contrast, relative wave reflection, as assessed by AI or the global reflection factor (P_b/P_f), is not associated with higher risk. Aortic stiffness and excessive pressure pulsatility can damage small vessels, leading to dropout and impaired reactivity.[46] The latter damage to small vessels has been shown to partially mediate relations between aortic stiffness and CVD events.[42] Thus, stiffness of specifically the aorta has emerged as a novel CVD risk factor that requires consideration in risk prediction and management.

A number of studies have attempted to demonstrate that central systolic or PP provides incremental risk prediction over peripheral PP. However, several recent studies have shown that in middle-aged and older adults, central and peripheral systolic and PP are very highly correlated ($R \geq 0.9$).[16] In light of the overwhelmingly strong relation between the variables, it will be difficult to demonstrate that one provides incremental risk prediction over the other when both are considered in a single risk model.[17,37] However, as noted earlier, directly assessed central waveform features, such as AI derived by using carotid tonometry, have been related to reduced LV fractional shortening, elevated LV filling pressure, as assessed by the mitral E/e' ratio, and incident atrial fibrillation, suggesting that greater late systolic loading of the LV by a premature reflected wave may have important functional implications.[37,40]

A few studies have derived surrogate pressure-flow measures from pressure waveforms only by using a Windkessel model of the arterial system. By optimizing a normalized flow into a three-element Windkessel model, it

FIGURE 17.6 Prevalence of high values for carotid-femoral pulse wave velocity (A) and the primary (P1) peak of central pressure, a surrogate for forward wave amplitude (B) in the Framingham Offspring cohort. Kaplan—Meier plot of cumulative probability of a major cardiovascular disease event for groups defined by quartiles of carotid-femoral pulse wave velocity (C). Kaplan—Meier plot of cumulative probability of event free survival for groups defined according to quartiles of true forward wave amplitude assessed by using waveform separation analysis (D). For both measures of aortic stiffness, prevalence increases markedly with age and is associated with very high relative risk, indicating that disease burden attributable to aortic stiffness will increase dramatically over the next two decades as the population ages.

is possible to estimate a Windkessel or reservoir pressure as well as an excess pressure. The shape of the Windkessel pressure is closely related to the reflected pressure wave derived by using wave separation analysis on pressure and flow waveforms, although the amplitude is doubled.[47] The associated excess pressure is a surrogate for central aortic flow scaled by aortic Z_c, i.e., $Q*Z_c$. In theory, the combination of $Q*Z_c$ and half of the Windkessel pressure would represent P_f derived from pressure-flow analysis and the other half of the Windkessel pressure would represent P_b. Studies have variably shown that amplitudes of the excess pressure or Windkessel pressure are or are not related to incident CVD events.[48−50]

The foregoing Windkessel model has a few limitations that require additional work to determine whether the values have clear physiologic relevance. For example, a standard Windkessel model has a monoexponential pressure decay during diastole, when inflow is zero and outflow occurs with a time constant equal to the product of peripheral resistance and total arterial compliance. However, the decay of pressure is asymptotic on a terminal pressure (P_{inf}) that is unknown but thought to be related to critical closing pressure, which is the nonzero pressure at which flow through the vascular bed stops because the resistance vessels have occluded. Since the value for P_{inf} is unknown, it is optimized based on the shape of the pressure waveform in diastole. The problem that emerges is that optimized values for P_{inf}, which nearly equal to DBP in many cases, are much higher than physiologic values for critical closing pressure, which should be 20 mm Hg or less.[48] The reason for the model converging on such a high value for P_{inf} is quite straightforward. A monoexponential decay appears relatively linear at values for P that are moderately removed from the asymptote. So, if diastolic pressure is 80 mm Hg and the true asymptotic pressure is 20 mm Hg, the fitted diastolic pressure will appear linear and will not fit the true, concave diastolic pressure adequately. By increasing P_{inf}, the model can add concavity to modeled diastolic pressure decay, resulting in a close fit with observed pressure.[48] However, we know that an estimated P_{inf} that is nearly equal to DBP is unrealistic.

An alternative interpretation of the foregoing P_{inf} dilemma is that the diastolic time constant is not actually constant. If peripheral resistance (R_p) and total arterial compliance (C) are not constant, the time constant of pressure decay (R_p*C) will not be constant. We know that both R_p and C are sensitive to distending pressure, with both values (C and R_p) increasing as pressure falls in the physiologic range encountered during diastole. As a result, the diastolic time "constant" will continuously increase during diastole and the diastolic pressure decay will therefore appear more concave than predicted from a linear Windkessel model, resulting in excellent fitted pressures even when P_{inf} is fixed at a low physiologic value. A recent study that accounted for potential nonlinear relations of R_p or C with distending pressure confirmed that excellent waveform fits were possible and demonstrated relations of Windkessel measures with events.[48] In contrast, measures derived from the standard linear Windkessel model were not related to events. Thus, while a pressure-only approach has considerable appeal for straightforward point-of-care evaluation, it may be important to consider nonlinearities when performing pressure-only analysis of central aortic pressure-flow relations using a Windkessel approach.

Summary

Investigations of arterial stiffness and aortic pressure-flow relations have advanced our knowledge considerably over the past two decades. Studies have elucidated the remarkable ability of a normal, highly compliant aorta to limit simultaneously the pulsatile load on the heart as well as the small vessels. They have also demonstrated that aortic stiffening begins early in adulthood and can be associated with considerable excess risk well before the onset of a marked increase in PP and SBP that occurs after midlife, leading to the current epidemic of wide PP hypertension. Future research will define optimal approaches to detect and correct abnormal trajectories of arterial stiffness and pressure pulsatility and reduce the growing burden of disease that would otherwise be attributable to adverse effects of excessive arterial stiffness.

References

1. Mitchell GF. Effects of central arterial aging on the structure and function of the peripheral vasculature: implications for end-organ damage. **J Appl Physiol**. 2008; 105:1652−1660.

2. Mitchell GF, van Buchem MA, Sigurdsson S, et al. Arterial stiffness, pressure and flow pulsatility and brain structure and function: the Age, Gene/Environment Susceptibility–Reykjavik study. **Brain**. 2011; 134:3398−3407.

3. Mitchell GF. Aortic stiffness, pressure and flow pulsatility, and target organ damage. **J Appl Physiol (1985)**. 2018; 125:1871−1880.

4. Dipla K, Triantafyllou A, Koletsos N, et al. Impaired muscle oxygenation and elevated exercise blood pressure in hypertensive patients: links with vascular stiffness. **Hypertension**. 2017; 70:444−451.

5. O'Rourke MF. Pressure and flow waves in systemic arteries and the anatomical design of the arterial system. **J Appl Physiol**. 1967; 23:139−149.

6. Patel DJ, Defreitas FM, Fry DL. Hydraulic input impedance to aorta and pulmonary artery in dogs. **J Appl Physiol**. 1963; 18:134−140.

7. Kelly R, Fitchett D. Noninvasive determination of aortic input impedance and external left ventricular power output: a validation and repeatability study of a new technique. **J Am Coll Cardiol**. 1992; 20:952−963.

8. Mitchell GF, Tardif JC, Arnold JM, et al. Pulsatile hemodynamics in congestive heart failure. **Hypertension**. 2001; 38:1433−1439.

9. Mitchell GF, Izzo Jr JL, Lacourciere Y, et al. Omapatrilat reduces pulse pressure and proximal aortic stiffness in patients with systolic hypertension: results of the conduit hemodynamics of omapatrilat international research study. **Circulation**. 2002; 105:2955−2961.

10. Mitchell GF, Parise H, Benjamin EJ, et al. Changes in arterial stiffness and wave reflection with advancing age in healthy men and women: the Framingham Heart Study. **Hypertension**. 2004; 43:1239−1245.

11. Mitchell GF, Gudnason V, Launer LJ, Aspelund T, Harris TB. Hemodynamics of increased pulse pressure in older women in the community-based Age, Gene/Environment Susceptibility-Reykjavik Study. **Hypertension**. 2008; 51:1123−1128.

12. Mitchell GF, Wang N, Palmisano JN, et al. Hemodynamic correlates of blood pressure across the adult age spectrum: noninvasive evaluation in the Framingham Heart Study. **Circulation**. 2010; 122:1379−1386.

13. Segers P, Rietzschel ER, De Buyzere ML, et al. Noninvasive (input) impedance, pulse wave velocity, and wave reflection in healthy middle-aged men and women. **Hypertension**. 2007; 49:1248−1255.

14. Chen CH, Ting CT, Nussbacher A, et al. Validation of carotid artery tonometry as a means of estimating augmentation index of ascending aortic pressure. **Hypertension**. 1996; 27:168−175.

15. Davies JE, Shanmuganathan M, Francis DP, Mayet J, Hackett DR, Hughes AD. Caution using brachial systolic pressure to calibrate radial tonometric pressure waveforms: lessons from invasive study. **Hypertension**. 2010; 55:e4.

16. Mitchell GF. Central pressure should not be used in clinical practice. **Artery Res**. 2015; 9:8−13.

17. Mitchell GF, Hwang SJ, Larson MG, et al. Transfer function-derived central pressure and cardiovascular disease events: the Framingham Heart Study. **J Hypertens**. 2016; 34:1528−1534.

18. Segers P, Mahieu D, Kips J, et al. Amplification of the pressure pulse in the upper limb in healthy, middle-aged men and women. **Hypertension**. 2009; 54:414−420.

19. Karamanoglu M, O'Rourke MF, Avolio AP, Kelly RP. An analysis of the relationship between central aortic and peripheral upper limb pressure waves in man. **Eur Heart J**. 1993; 14:160−167.

20. Hope SA, Tay DB, Meredith IT, Cameron JD. Comparison of generalized and gender-specific transfer functions for the derivation of aortic waveforms. **Am J Physiol Heart Circ Physiol**. 2002; 283:H1150−H1156.

21. Hope SA, Meredith IT, Cameron JD. Reliability of transfer functions in determining central pulse pressure and augmentation index. **J Am Coll Cardiol**. 2002; 40:1196−1197.

22. Chen CH, Nevo E, Fetics B, et al. Estimation of central aortic pressure waveform by mathematical transformation of radial tonometry pressure. Validation of generalized transfer function. **Circulation**. 1997; 95:1827−1836.

23. Dujardin JP, Stone DN. Characteristic impedance of the proximal aorta determined in the time and frequency domain: a comparison. **Med Biol Eng Comput**. 1981; 19:565−568.

24. Mitchell GF, Lacourciere Y, Ouellet JP, et al. Determinants of elevated pulse pressure in middle-aged and older subjects with uncomplicated systolic hypertension: the role of proximal aortic diameter and the aortic pressure-flow relationship. **Circulation**. 2003; 108:1592−1598.

25. Davis EC. Stability of elastin in the developing mouse aorta: a quantitative radioautographic study. **Histochemistry**. 1993; 100:17−26.

26. Powell JT, Vine N, Crossman M. On the accumulation of D-aspartate in elastin and other proteins of the ageing aorta. **Atherosclerosis**. 1992; 97:201−208.

27. Ott CE, Grunhagen J, Jager M, et al. MicroRNAs differentially expressed in postnatal aortic development downregulate elastin via 3' UTR and coding-sequence binding sites. **PLoS One**. 2011; 6:e16250.

28. McEniery CM, Yasmin, Hall IR, Qasem A, Wilkinson IB, Cockcroft JR. Normal vascular aging: differential effects on wave reflection and aortic pulse wave velocity: the Anglo-Cardiff Collaborative Trial (ACCT). **J Am Coll Cardiol**. 2005; 46:1753−1760.

29. Lam CS, Xanthakis V, Sullivan LM, et al. Aortic root remodeling over the adult life course: longitudinal data from the Framingham Heart Study. **Circulation**. 2010; 122:884−890.

30. O'Rourke MF, Nichols WW. Aortic diameter, aortic stiffness, and wave reflection increase with age and isolated systolic hypertension. **Hypertension**. 2005; 45:652−658.

31. Agmon Y, Khandheria BK, Meissner I, et al. Is aortic dilatation an atherosclerosis-related process? Clinical, laboratory, and trans-esophageal echocardiographic correlates of thoracic aortic dimensions in the population with implications for thoracic aortic aneurysm formation. **J Am Coll Cardiol**. 2003; 42:1076−1083.

32. Vasan RS, Larson MG, Levy D. Determinants of echocardiographic aortic root size. The Framingham Heart Study. **Circulation**. 1995; 91:734−740.

33. Torjesen AA, Sigurdsson S, Westenberg JJ, et al. Pulse pressure relation to aortic and left ventricular structure in the age, gene/environment susceptibility (AGES)-Reykjavik study. **Hypertension**. 2014; 64:756−761.

34. van der Heijden-Spek JJ, Staessen JA, Fagard RH, Hoeks AP, Boudier HA, Van Bortel LM. Effect of age on brachial artery wall properties differs from the aorta and is gender dependent: a population study. **Hypertension**. 2000; 35:637−642.

35. Haidar MA, van Buchem MA, Sigurdsson S, et al. Wave reflection at the origin of a first-generation branch artery and target organ protection: the AGES-reykjavik study. **Hypertension**. 2021; 77:1169−1177.

36. Chirinos JA, Segers P, Gillebert TC, et al. Arterial properties as determinants of time-varying myocardial stress in humans. **Hypertension**. 2012; 60:64−70.

37. Kaess BM, Rong J, Larson MG, et al. Relations of central hemodynamics and aortic stiffness with left ventricular structure and function: the Framingham Heart Study. **J Am Heart Assoc**. 2016; 5:e002693.

38. Gillebert TC, Lew WY. Influence of systolic pressure profile on rate of left ventricular pressure fall. **Am J Physiol**. 1991; 261:H805−H813.

39. Chirinos JA, Segers P, Rietzschel ER, et al. Early and late systolic wall stress differentially relate to myocardial contraction and relaxation in middle-aged adults: the Asklepios study. **Hypertension**. 2013; 61:296−303.

40. Shaikh AY, Wang N, Yin X, et al. Relations of arterial stiffness and brachial flow-mediated dilation with new-onset atrial fibrillation: the Framingham Heart Study. **Hypertension**. 2016; 68:590−596.

41. Cooper LL, Rong J, Benjamin EJ, et al. Components of hemodynamic load and cardiovascular events: the Framingham Heart Study. **Circulation**. 2015; 131:354−361.

42. Cooper LL, Palmisano JN, Benjamin EJ, et al. Microvascular function contributes to the relation between aortic stiffness and

cardiovascular events: the Framingham Heart Study. **Circ Cardiovasc Imaging**. 2016; 9:e004979.

43. Kaess BM, Rong J, Larson MG, et al. Aortic stiffness, blood pressure progression, and incident hypertension. **J Am Med Assoc**. 2012; 308:875−881.

44. Mitchell GF, Hwang SJ, Vasan RS, et al. Arterial stiffness and cardiovascular events: the Framingham Heart Study. **Circulation**. 2010; 121:505−511.

45. Ben-Shlomo Y, Spears M, Boustred C, et al. Aortic pulse wave velocity improves cardiovascular event prediction: an individual participant meta-analysis of prospective observational data from 17,635 subjects. **J Am Coll Cardiol**. 2014; 63:636−646.

46. Mitchell GF, Vita JA, Larson MG, et al. Cross-sectional relations of peripheral microvascular function, cardiovascular disease risk factors,

and aortic stiffness: the Framingham Heart Study. **Circulation**. 2005; 112:3722−3728.

47. Westerhof N, Segers P, Westerhof BE. Wave separation, wave intensity, the reservoir-wave concept, and the instantaneous wave-free ratio: presumptions and principles. **Hypertension**. 2015; 66:93−98.

48. Behnam V, Rong J, Larson MG, et al. Windkessel measures derived from pressure waveforms only: the Framingham Heart Study. **J Am Heart Assoc**. 2019; 8:e012300.

49. Davies JE, Lacy P, Tillin T, et al. Excess pressure integral predicts cardiovascular events independent of other risk factors in the conduit artery functional evaluation substudy of Anglo-Scandinavian Cardiac Outcomes Trial. **Hypertension**. 2014; 64:60−68.

50. Narayan O, Davies JE, Hughes AD, et al. Central aortic reservoir-wave analysis improves prediction of cardiovascular events in elderly hypertensives. **Hypertension**. 2015; 65:629−635.

This page intentionally left blank

Chapter 18

Hemodynamic determinants of myocardial oxygen demand and supply

Lucia Salvi[1] and Paolo Salvi[2]

[1]Medicina II Cardiovascolare, AUSL-IRCCS di Reggio Emilia, Italy; [2]Istituto Auxologico Italiano, IRCCS, Cardiology Unit, Milan, Italy

Myocardial ischemia results from an imbalance between oxygen supply and demand. The ischemic myocardial damage or acute myocardial infarction (MI) related to atherosclerotic plaque rupture, ulceration, or erosion with resulting intraluminal thrombus in coronary arteries is certainly the best known and most studied type of cardiac ischemic event (Type 1 MI).[1] However, often ischemic myocardial damage or acute MI does not correspond to a significant hemodynamic obstruction of the coronary arteries, and can be caused by a functional imbalance between myocardial oxygen supply and demand (Type 2 MI).[1,2] The latter type of myocardial ischemic damage occurs due to numerous and very different etiopathogenetic mechanisms (Fig. 18.1), such as a fall in arterial oxygen content (severe anemia or hypoxemia), an insufficient blood flow to the myocardium in relation to the myocardial oxygen needs, arrhythmias, hypotension, coronary artery spasm, coronary microvascular dysfunction, or spontaneous coronary artery dissection.[3−5] All these above conditions can also lead to myocardial ischemic cell injury—detected as an increase in circulating biomarkers of myocardial damage—without however resulting in cardiomyocyte necrosis: these cases are referred to as myocardial injury, rather than MI.[1] Type 2 MI and myocardial injury are rather frequently seen in clinical practice and both are related to a poor outcome. Both are due to the same pathogenetic mechanism: the presence of a mismatch between myocardial oxygen supply and its consumption.

The heart is a muscular organ similar to a volumetric pump, as it develops its action through the alternative filling and emptying of a closed volume. During the cardiac cycle, a lower amount of energy is used to ensure the ventricular pump function; most of the energy consumption develops tension in the myocardial fibers and keeps them in this state, in addition to the occurrence of the reactions of the basal metabolism and the excitation-contraction processes.[6] The medium total myocardial oxygen consumption (MVO$_2$) under basal conditions is 250 mL/min, and may rise up to 3−4 L/min during physical activity. The greater the energy demands of the myocardium, the greater the blood flow must be, vice versa, the discrepancy between the two factors may lead to MI or myocardial damage.
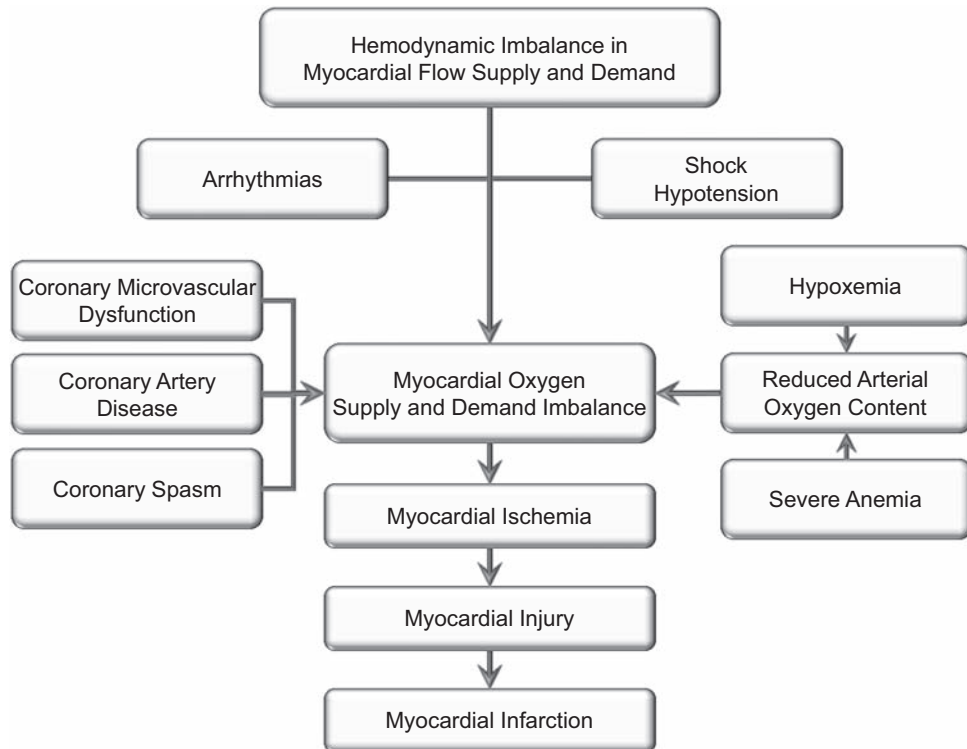
In this chapter, we discuss the determinants of myocardial supply, demand and the balance between the two. The reader is referred to Chapter 39 for a discussion of the role of arterial stiffness and pulsatile hemodynamics in coronary artery disease.

Myocardial O$_2$ demand

The heart muscle needs oxygen for two reasons: an external, volumetric work, that is the mechanical activity that allows the pumping of an adequate amount of blood into the aorta, and an internal work, given both by the set of metabolic processes required for muscle metabolism and by the energy needed to develop the tension of the cardiomyocytes. About 75% of myocardial energy is used in processes to ensure the myocardial muscle contraction.[7,8] This mostly reflects ATP splitting associated with cross-bridge splitting during the isovolumic contraction and ejection phases of the cardiac cycle. A smaller amount of ATP is also consumed for calcium confiscation at the end of each contraction. The largest part (approximately 50%) of the MVO$_2$, occurs during the isovolumic contraction phase of the cardiac cycle, which has high energy demand.[9]

The amount of energy, and therefore oxygen, needed to perform both functions depends on:

— left ventricular afterload,
— systolic wall stress,
— heart rate,

FIGURE 18.1 Factors responsible for myocardial ischemia.

- contractility,
- depolarization,
- shortening against load (Fenn effect),
- supporting the state of activity,
- maintenance of cell viability in basal conditions.

Among these, heart rate, systolic pressure (or more specifically, myocardial wall stress which depends on both left ventricular pressure and instantaneous geometry), and left ventricular contractility are the major determinants of myocardial oxygen consumption. If any of these determinants doubled, coronary flow would need to increase by approximately 50%.[10] We next analyze these factors in detail.

Left ventricular afterload

Work (W), in physics, is the product of the component of the force (F) in the direction of the displacement and the magnitude of the displacement (d) caused by the force (W = F × d). The energy used to perform cardiac work is evaluated by measuring the consumption of O_2. In rest condition, an average O_2 consumption of 0.08–0.10 mL/g/min can be considered: in practice, a heart weighing 300 g consumes $\sim$24–30 mL O_2/min, only for volumetric work. Since pressure (P) is defined as a force acting on a surface (A), work is defined as the product of the volume of fluid (V) and the pressure required to move the fluid

$$Work = F \times d = P \times A \times d = P \times V$$

Therefore, ventricular stroke work can be estimated as the product of mean intraventricular systolic pressure during ejection and stroke volume (SV). In a normal heart, mean intraventricular systolic pressure can be approximated by the mean aortic systolic pressure (MAP). Thus:

$$Left\ Ventricular\ Stroke\ Work = MAP \times SV$$

Stroke work is thus best represented by the ventricular pressure-volume diagrams, where stroke work is the area within the pressure-volume loop. This area represents the external ventricular work to eject blood into the aorta. The mean arterial pressure therefore represents one of the major elements on which cardiac work depends, so much so that arterial pressure is taken as a useful surrogate of left ventricular afterload in clinical practice.[11] However, the pulsatile aspect of afterload, and the pressure distribution in systole versus diastole (both of which impact MAP) also has an important effect on afterload, particularly in situations of aortic stiffening with high pulse pressure. Myocardial afterload is also highly related to the stress on myocardial cells. The afterload on individual muscle fibers can be expressed as ventricular wall stress.

Systolic wall stress

Myocardial wall stress is another major critical determinant of MVO_2, so much so that if the tension of the myocardial wall doubles, MVO_2 doubles. The wall stress is the intensity of the force on the muscular wall which, extended

by the volume it contains, would tend to shorten the ventricular circumferences. Being determined by the volume from which the ventricle is extended in end-diastole, wall stress is an expression of preload. It is proportional to the state of deformation to which the parietal myocardium is subjected, therefore it depends on endoventricular pressure, radius of the circumference, and thickness of the wall itself.[12] From a mathematical point of view, the relationship between these components is described by the Laplace law:[9–14]

Contractility

Together with preload and afterload, contractility constitutes the third determinant of cardiac output. The ability to develop muscular tension depends on the efficiency of the sarcomere, originating from the number of actin-myosin interactions present simultaneously and the speed with which the interactions occur.

As in the other striated muscles, these processes are mainly regulated by calcium (Ca^{++}): at the passage of

$$\text{Myocardial Wall Stress} = \frac{\text{Left Ventricular Cavity Pressure}}{\frac{1}{3}\ln\left(1 + \frac{\text{Ventricular Wall Volume}}{\text{Ventricular Cavity Volume}}\right)}$$

From this formula, it can be deduced that the moment of maximum wall stress in the cardiac cycle is the protosystole (i.e., early systole): in fact, at that point of the cardiac cycle, there are the largest endocavitary dimensions, and the smallest wall thickness (as discussed in more detail in Chapter 16).[15] From the above formula, we can derive another concept: the origin of concentric hypertrophy in the presence of chronic overload. If the wall stress per unit of myocardial mass is reduced with increasing wall thickness, the consumption of oxygen per unit of myocardial mass is also reduced. However, this is only an apparently compensatory mechanism. Actually, if the consumption of oxygen per unit of myocardial mass decreases, on the other hand, there is an increase in the global mass, therefore—due to the mechanisms discussed in the next paragraphs—an increase in global O_2 consumption results.

Heart rate

The factors previously described provide their contribution in determining the myocardial oxygen need for each cardiac contraction. It is therefore intuitive that the greater the number of contractions the heart performs per minute, the greater the energy required. Moreover, heart rate is inversely proportional to the diastolic time, which, as we will see below, is the interval in which subendocardial perfusion occurs. Therefore, paradoxically, the increase in heart rate, even though it requires a higher MVO_2 per minute, is inevitably associated with a lower oxygen supply to the heart muscles. In athletes and individuals trained to perform sustained aerobic activity, the heart develops different mechanisms to support the increased demand without such a marked increase in heart rate, such as increasing cardiac contractility.

the action potential that depolarizes the cell, there is an impressive entry of Ca^{++}, which constitutes up to 10%–50% of the intracytoplasmic pool; to this quantity is added the Ca^{++} released by the sarcoplasmic reticulum mediated by concentration-sensitive Ca^{++} channels (ryanodine receptors, RyR2). This "calcium wave" gives rise to an endergonic reaction: the chemical energy, supplied by ATP, is converted into mechanical energy, activating the actin-myosin lever system. A repetitive interaction of the transverse bridges with the actin filaments is required to achieve appreciable shortening during contraction. Then, each transverse bridge must attach, rotate, detach, and then reattach at a more distant point of the thin filament. The contractile cycle therefore requires at least four stages, each of which is accompanied by the hydrolysis of one or more ATP molecules, a reaction that requires the consumption of oxygen to take place. Relaxation also requires ATP hydrolysis, in the dissociation of actin-myosin bridges.

From all these elements, it can be understood how much the oxygen consumption necessary for the hydrolysis of ATP that allows the muscle contraction itself to function is not a negligible energy expenditure in sustaining the heart pump. Luckily for us, the heart muscle is a machine with a good performance, in fact no more than 30%–50% of this energy is dissipated as heat. Importantly, the relative amount of O_2 consumed during the cardiac cycle that is not transformed into mechanical activity is highly variable between individuals, which has important implications for our understanding of the limitations of the left ventricular pressure-volume area as an indicator of myocardial O_2 consumption when comparisons are made between individuals (as discussed in more detail in Chapter 15).

Depolarization

The action potential wave triggers the entry of Ca^{++} into the cell, but also the propagation of the action potential itself requires a certain energy requirement, and therefore oxygen consumption. In fact, the passage of the depolarization wave occurs upon activation of the voltage-dependent counter-concentration channels that pump Ca^{++} out of the myocyte. It has been studied that in a cardiac cycle the amount of oxygen necessary for the depolarization of the whole heart is approximately 0.5% of the MVO_2 consumed by a healthy heart.[16]

Shortening against load (Fenn effect)

When a muscle contracts isometrically, it produces a certain amount of heat, which increases if the contraction occurs against a load: this effect is called the Fenn effect.[17] Cardiac mechanics is an example of a contraction against load, consisting of the blood volume that must be pumped into the aorta. During shortening, the force exerted and the energy it consumes are greater when there is a greater load; the muscles will therefore have to mobilize a greater amount of energy, or a greater MVO_2. More heat than expected in vitro is actually produced in vivo at the end of a contraction against load. This heat is called "recovery heat" and is due to the metabolic processes that regenerate the compounds used for contraction, which essentially depend on oxidation reactions.

Supporting the state of activity

The energy we discussed in the previous paragraphs can only be released from the sites where muscle tension is generated. In other words, it is necessary that a certain number of ATP-dependent reactions occur that allow the persistence of a minimum number of bridges between thick and thin filaments for the contractile elements to exert a certain constant tension.

Maintenance of cell viability in basal conditions

As in all animal tissues, chemical reactions continuously occur in the myocardium, which serve to maintain cellular integrity. Among these there is, for example, cellular respiration, which is associated with a certain production of heat, defined as resting heat, or internal work. This oxygen consumption cannot be reduced: the efficiency of internal work is the first element on which the well-being of the entire organ depends. MVO_2 represents 5%−8% of resting metabolism, equivalent to about 10 mL of oxygen per 100 g of ventricular mass.

Myocardial O_2 supply

In general, tissue perfusion is kept constant to ensure a quick and efficient transport of oxygen, nutrients, and waste material between the intravascular and extravascular space. However, tissue perfusion in the myocardium is not constant and depends on the cardiac phase and the thickness of tissue considered. Coronary flow occurs mostly during ventricular diastole (Fig. 18.2), as during ventricular systole, it is severely diminished by vessel compression from the myocardial contraction and other factors discussed below.
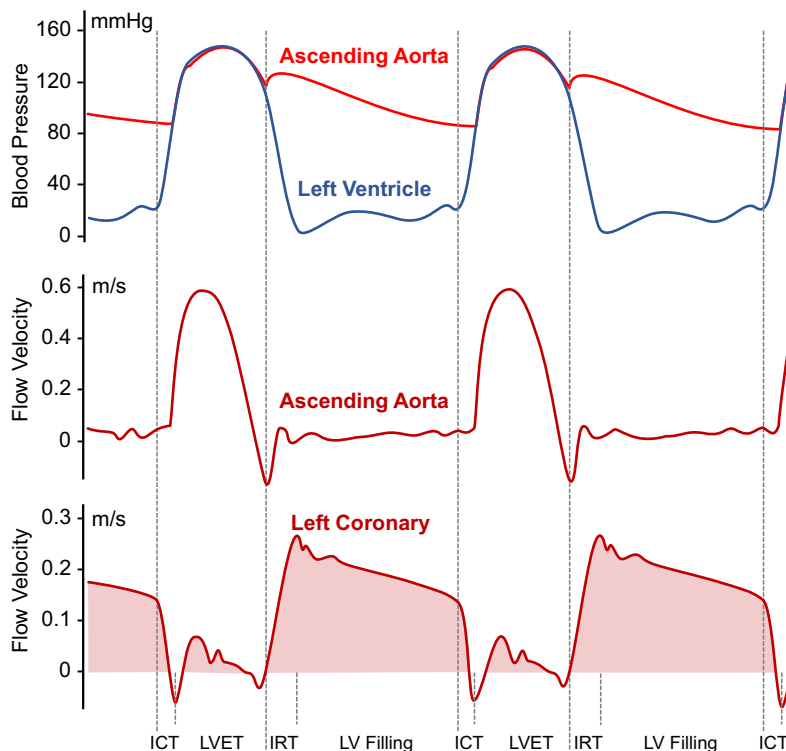
In undamaged coronary artery condition, the blood supply to the myocardium mainly depends on four factors:

- the coronary diastolic blood pressure, which in the absence of coronary artery disease is equal to the diastolic pressure in the ascending aorta,
- the intra-vessel pressure gradient present in diastole between the coronary ostium and their terminal branches at the subendocardial level,
- the left ventricular intracavitary pressure,
- the duration of diastole.

At the beginning of the isovolumic systole, there is a sudden and rapid rise of the ventricular pressure curve, and, at the same time, an instantaneous interruption of the coronary flow, as the semilunar valves are still closed. This systolic flow stop is due to the sum of two extravascular compressive forces: (a) the pressure caused by the contraction of myocardial muscle on the intracardiac vessels and (b) the intraventricular pressure transmitted to the myocardial wall. This compressive pressure is maximum at the subendocardial layers, reaching values close to zero at the subepicardium.

As such, blood flow to subendocardial layers is virtually absent in systole, even though subepicardial layers remain perfused. Subendocardial perfusion therefore occurs mostly, if not completely, during diastole. It is therefore easy to understand the crucial role of two factors in maintaining the viability of the subendocardium and an efficient contractile function of left ventricle: (i) the duration of the diastolic phase and (ii) the perfusion (aortic) pressure in diastole. Diastolic time is close related to heart rate,[18] so, in conditions of hemodynamic instability, a rapid increase in heart rate can cause a dramatic fall in myocardial perfusion.

For a given heart rate, subendocardial perfusion largely depends on the coronary diastolic pressure. In absence of coronary hemodynamically significant stenosis, the diastolic pressure in coronary arteries is equal to diastolic pressure in the ascending aorta. At the level of the subendocardial layers, perfusion is however opposed by the intracavitary pressure of the left ventricle. Therefore, subendocardial

FIGURE 18.2 Relationships between left ventricular pressure and aortic pressure (upper panel), aortic blood flow velocity (medium panel) and left coronary flow velocity related. The close relationship between coronary flow and the area between the aortic and ventricular pressure curve in diastole is evident. *ICT*, isovolumic contraction time; *IRT*, isovolumic relaxation time; *LV*, left ventricular; *LVET*, left ventricular ejection time.

coronary flow depends on the pressure gradient in diastole between the coronary artery intravascular pressure and left ventricular diastolic pressure.

The wave intensity analysis (WIA) seems to be a promising tool in clarifying the dynamics in coronary blood flow and to characterize the interaction between myocardium and coronary blood flow at each point within the cardiac cycle. The wave intensity is defined as the product of the change in pressure (dP) times the change in flow velocity (dU), at a particular point in the cardiac cycle, during a defined time interval (dt); i.e., $WI = (dP/dt) \times (dU/dt)$. WIA is a time-domain analysis. On the basis of recordings of coronary arterial pressure and velocity, WIA correlates pressure and flow in the aorta and in the coronary artery instant by instant, through the analysis of direction, intensity and type of waves present in a given point of the coronary circulation,[19] estimating the role of forward and backward waves at every time during the cardiac cycle.[20]

WIA helps to better understand the different flow waveform between the ascending aorta and coronary arteries, as evident in Fig. 18.2. The coronary flow velocity waveform has a particular and original feature. Left ventricular systolic contraction greatly increases coronary resistance to antegrade flow, thereby preventing a significant increase in coronary flow velocity during systole and inducing backward compression waves. During early

diastole, the re-expansion of the intramyocardial blood vessels, which are compressed by ventricular contraction during systole, generates a backward decompression wave sucking blood into the coronary artery from the distal vessel, causing an accelerative force on blood flow, coinciding with the fall in intracoronary pressure.[21]

Bender et al.,[22] studying variations of coronary blood flow during exercise in large-sized animals, supported the diastolic nature of coronary flow and showed two moments of retrograde flow. The first of these is present at rest and is named early retrograde coronary blood flow, as it is located at the isovolumic systole; at this point in the cardiac cycle, the inversion of flow increases with cardiac contractility and coronary blood volume and decreases as the aortic pressure (coronary perfusion pressure) rises. The second moment, named late retrograde coronary blood flow, appears during moderate exercise (walking at 5 km/h) and is concomitant with the widening of the anterograde aortic decompression wave. Both the early and the late retrograde coronary blood flow increase with the intensity of physical exercise.

Diastolic pressure decay

In addition to the value of the telediastolic (i.e., late diastolic) pressure, a fundamental determinant of the subendocardial flow is the decay of blood pressure during diastole[23]: the speed and the mode by which the pressure

decreases during the diastolic phase of cardiac cycle. The gradual reduction of blood pressure during diastole may be described using an exponential decay curve, by the equation:

$$P(t) = P_0 e^{-\lambda t},$$

where P_0 is the diastole starting pressure, t is the interval from the beginning of the diastole, and λ is the exponential decay constant. The shape of this hypothetical decay is related with aortic characteristics.

Arterial stiffening affects the decay in blood pressure during diastole in at least two ways. Reducing the Windkessel effect results in a rapid reduction in diastolic blood pressure, so in a rapid diastolic decay.[24] On the other hand, the early arrival of backward (reflected) waves to the ascending aorta during the systolic phase leads to a further rapid decay of blood pressure in diastole. A rapid diastolic pressure decay is associated with lower values of mean diastolic blood pressure. Since subendocardial oxygen supply depends on the area below the diastolic phase of arterial pulse waveform in ascending aorta, a rapid decay of blood pressure in diastole is associated with lower subendocardial oxygen supply.[25]

Coronary blood flow regulation

The ATP consumption to provide energy to the myocardium is reconstituted by oxidative phosphorylation from different energy substrates, especially fatty acids. The myocardium possesses a high aerobic metabolism, demonstrable by the large number of mitochondria present in the tissue. Actually, it is not able to use anaerobic glycolysis, except for short periods of time, and therefore the myocardial metabolism depends on an adequate and continuous supply of O_2. In the myocardium, the extraction of O_2 is, under basal conditions, about $8-10$ mL/min/100 g of tissue, which corresponds to $\sim 75\%$ of the amount contained in the arterial blood. Since extraction is particularly high, increases in myocardial O_2 consumption must be met mainly by an increase in coronary flow.

Different mechanisms affect the regulation of blood flow to the myocardium, depending on the increased or reduced energy needs. We now mention the most relevant elements among these:

Coronary self-regulation

First, the coronary circulation is able to respond to rapid and abrupt hemodynamic changes in the cardiovascular system while maintaining organ perfusion at constant levels, despite changes in thrust pressure present in the ascending aorta: this flow stabilization capability is called self-regulation.[26] Perfusion in normal myocardium can be kept relatively constant over a wide range of mean pressure values in the aorta, ranging from about 130 to 40 mmHg. Exceeding the lower or upper limit of this range, the flow respectively decreases or increases very quickly, exposing tissues to a considerable risk of ischemia, even at rest.[27]

In the case of chronic hypertension and left ventricular hypertrophy, the pressure range in which it is present effective self-regulation is strongly reduced, especially at the subendocardium. In the second case, the limitation is also due to the reduction of the capillary density, which reduces the absolute maximum increase in blood supply for each gram of heart tissue in the setting of increased oxygen demand.[10]

Endothelial vasoactive mediators

The endothelium is one of the main elements regulating the supply of oxygen to the heart tissue. It performs this function by producing both powerful vasodilators (EDRF, NO, and EDHF) and vasoconstrictors (ET-1). Under physiological conditions, the endothelium produces vasodilators when the metabolic demands are elevated, such as during physical exercise, cold, tachycardia, and mental stress. An altered vasomotor response characterized by a lack of increase or even a decrease due to paradoxical vasoconstriction occurs with endothelial dysfunction. Endothelial dysfunction is very common in subjects with increased cardiovascular risk, such as systemic arterial hypertension. In fact, endothelium-dependent vasodilation is particularly important in the smaller vessels, that is, in the resistance vessels: these, although normally not directly affected by atherosclerotic processes, are strongly compromised in endothelial dysfunction.[10] A number of studies suggest that endothelial dysfunction and acute microcirculatory dysfunction may play a central role in Takotsubo syndrome.[28]

Metabolic regulation

The products of the cardiac aerobic metabolism released by the myocardium are other indicators of the muscle's need for oxygen. Adenosine is the main myocardial signal: its accumulation indicates a lack of substrates for mitochondrial oxidative phosphorylation; therefore, it is a signal of the need to increase the oxygen supply, and indeed exhibits potent vasodilatatory activity. Other vasoactive factors with similar action released by the myocardium are nitrogen monoxide, prostaglandins, and potassium ions.

Arterial oxygen content

Myocardial oxygen supply depends not only on coronary blood flow but also on the arterial oxygen content.[29,30] Even in the presence of satisfactory subendocardial flow, a reduction in the amount of oxygen in the blood due to

severe anemia or hypoxemia can compromise the oxygen supply to the subendocardium. When considering the myocardial oxygen supply, it is therefore always necessary to consider the two components: the flow supply and the oxygen supply.

The arterial oxygen content (CaO_2) is the total amount of oxygen in 1 dL of blood. Considering that each g/dL hemoglobin (Hb) can carry 1.34 mL of O_2 and 0.0031 mL of O_2 are dissolved in 1 dL of blood for every 1 mmHg of arterial O_2 tension (pO_2), CaO_2 can be estimated by:

The resulting alterations in the viscoelastic properties of the arterial system cause a stiffening in the arterial wall and a distensibility reduction in the aorta and large arteries. Under these conditions, the amount of SV stored by the aorta during the systolic ejection time decreases, even drastically whereas most of the blood ejected at each systole is "pushed" directly toward the periphery of the vascular system. However, hemodynamic phenomena in the arterial tree are more complicated, since they include the effects of wave travel through the arterial wall at a finite wave

$$CaO_2(mL\ O_2\ /\ dL) = (O_2\ carried\ by\ Hb) + (O_2\ in\ solution) = 1.34\ Hb \times O_2 saturation + 0.003\ pO_2$$

Aortic stiffness

In the previous paragraph we described the hemodynamic cardiac components that play a direct role in determining the O_2 supply and demand ratio at myocardial muscle. Now it is necessary to consider another key determinant in the process: the aorta. Aortic function and cardiac-aortic coupling in fact profoundly influence the subendocardial MVO_2 balance, both in healthy subjects and with cardiovascular pathologies.

Watanabe et al.[31] described clear signs of regional myocardial dysfunction and a reduction in coronary flow reserve following a mechanical increase in aortic stiffness. These researchers reduced aortic distensibility in dogs by banding the thoracic aorta with adjustable plastic rings and studied the changes in coronary flow. Even in the absence of coronary stenosis, decreased aortic compliance was shown to be associated with inadequate subendocardial oxygenation, which could be further impaired in the presence of coronary stenosis.[32] Indeed, as discussed throughout this textbook, the aorta and large arteries play a major role in the regulation of blood pressure and peripheral blood flow (Fig. 18.3). It is well known that large arteries not only have a passive function in relation to the transfer of oxygenated blood from the heart to the periphery but also exert an important buffering function, as they are able to "cushion" left ventricular SV due to their viscoelastic properties. Aorta and large arteries have the task of damping the pulsatile output of the left ventricle and switch the intermittent systolic ejection into continuous blood flow at the capillary level. This be intuitively explained with the "Windkessel phenomenon": after ejection of SV and closure of the aortic valves, a great quantity of blood remains "stored" in the aorta and large arteries; the potential energy stored in the walls of the aorta in systole then turns into kinetic energy in diastole, pushing the stored blood into the bloodstream: the aorta behaves like a sort of "diastolic pump" after the aortic valve closure.

velocity, as well as wave reflections throughout the arterial tree.

In general, increased aortic stiffness has three consequences that impact coronary supply/demand:

- increase in systolic blood pressure,
- decrease in diastolic blood pressure,
- increase in pulse wave velocity.

Increase in systolic blood pressure

Increase aortic stiffness leads to increased pulsatile load and an increase in systolic blood pressure (when left ventricular function is normal). If systolic load is elevated, the left ventricle must contract more energetically to maintain adequate SV, which can only be generated at a higher systolic pressure. Thus, an increase in systolic blood pressure related to an increase in left ventricular afterload is intimately linked to a rise in cardiac work and consequently to an increase in MVO_2. The development of left ventricular hypertrophy and progression toward the resulting left ventricular failure predispose to an increase in left ventricular diastolic pressure and to a prolongation in isovolumic contraction time, further reducing the diastolic subendocardial pressure gradient and perfusion time: this lead to a reduction in subendocardial oxygen supply.

Decrease in diastolic blood pressure

A reduced diastolic pressure in the ascending aorta may lead to a reduction in subendocardial diastolic blood flow.[33] In the absence of coronary hemodynamically significant coronary stenosis, the diastolic pressure in coronary arteries is equal to diastolic pressure in the ascending aorta. In fact, subendocardial coronary flow does not depend only on diastolic time but also on aortic diastolic pressure and on the pressure gradient in diastole between coronary arteries intravascular pressure and left ventricular pressure.
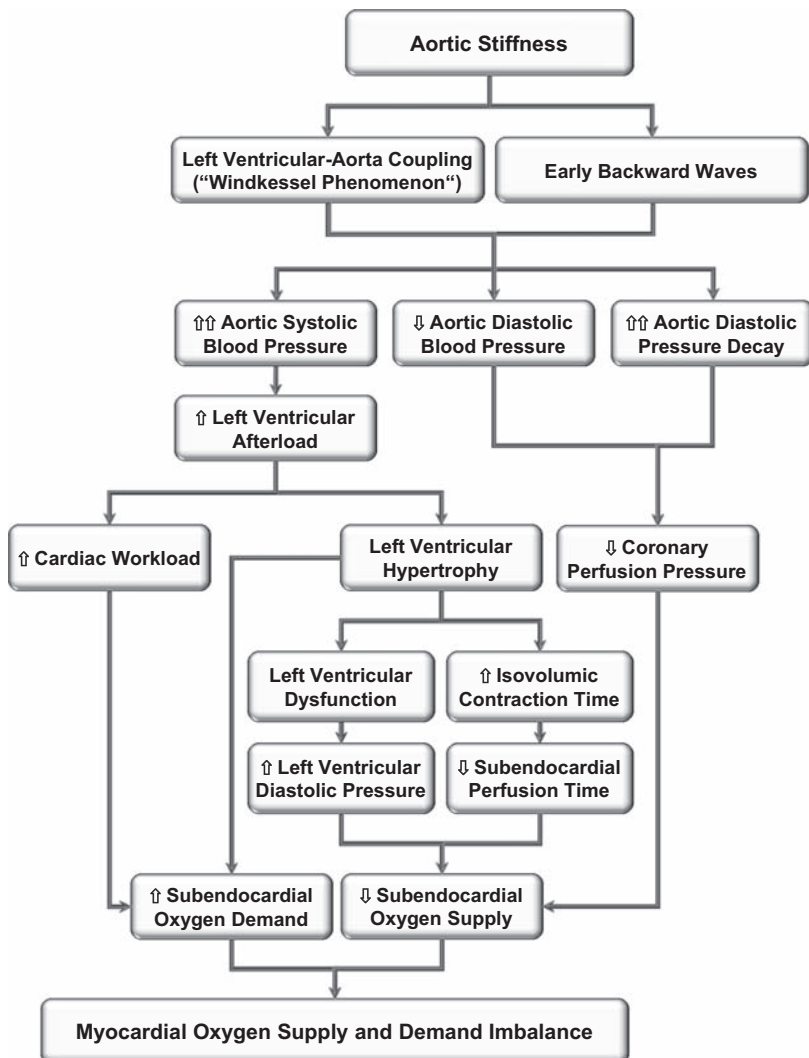
FIGURE 18.3   From arterial stiffening to myocardial ischemia.

Increase in pulse wave velocity
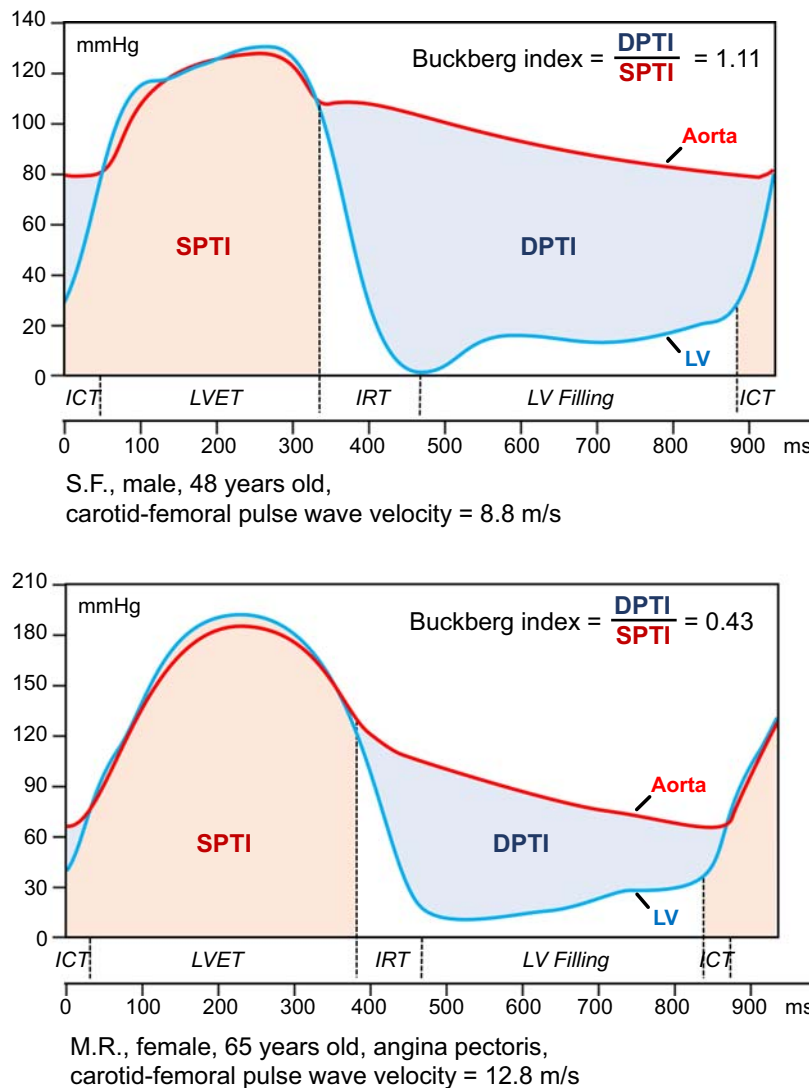
The pressure and flow at the ascending aorta are the result of two main components: a forward and a backward (reflected) component, given numerous reflection sites present at the periphery of the tree arterial tree. In the presence of high aortic stiffness, there is an earlier superimposition of the two waves, in early-to-mid systole, producing a further increase in systolic blood pressure and pulse pressure values.

The myocardial oxygen supply: demand index

Currently, for the diagnosis of myocardial ischemia, we have specific and sensitive biomarkers available and diagnostic investigations are more and more accurate. While the diagnostic imaging ensures an accurate identification of obstructive coronary artery disease, oxygen arterial content is clearly quantifiable and arrhythmias can be easily recorded, we have few tools available readily assess hemodynamic imbalances between myocardial oxygen supply and demand.

At the beginning of the 70 s, G.D. Buckberg and J.I.E. Hoffman introduced a useful index to assess cardiac ischemic risk that reflects the relationship between subendocardial oxygen supply and demand, also known as the Buckberg index or SEVR (subendocardial viability ratio). This index was defined by analyzing left ventricular and aortic pressure curves during invasive studies on large animals and humans. In truth, already in the late 1950s, S.J. Sarnoff and E. Braunwald focused their studies on oxygen consumption of canine heart, highlighting how the product of the aortic mean pressure during the systolic phase and the duration of systole (TTI, the tension time index) represents a reliable index of total tension developed by the

FIGURE 18.4 Systolic pressure-time index (SPTI, salmon area) and diastolic pressure-time index (DPTI, light blue area) in adult with preserved viscoelastic properties of the aorta (upper panel), and in old hypertensive patient with increased aortic stiffness (lower panel). Left ventricular (LV) pressure (blue line) and aortic arterial pressure (red line) were recorded by invasive catheterization. Buckberg index was calculated as DPTI and SPTI ratio. *ICT*, isovolumic contraction time; *IRT*, isovolumic relaxation time; *LVET*, left ventricular ejection time.

myocardium per beat. The area beneath the systolic portion of the aortic pressure curve was then used as an index of the actual myocardial fiber tension, showing a close correlation with myocardial O_2 utilization.[34,35] Buckberg and Hoffman, taking advantage of these previous studies, tried to formulate an index capable of helping the clinician in the diagnosis of subendocardial ischemia in the absence of anatomical obstruction of the coronary arteries, resulting from a discrepancy between metabolic needs and available blood supply.

Whereas the analysis of the systolic phase of the ventricular pressure curve provides an indication on the myocardial oxygen requirement, the analysis of the diastolic phase provides indications on the oxygen supply to the myocardium (Fig. 18.4).

As stated above, the area below the ventricle pressure curve during the whole systolic phase, from the onset of ventricular systole to the dicrotic notch, is closely related to myocardial oxygen demand.[29] This area is known as systolic pressure-time index (SPTI, analogous to the Sarnoff's TTI) and includes both isovolumic contraction time and left ventricular ejection time.[29] SPTI mainly depends on left ventricular ejection time, ejection pressure, and myocardial contractility. If we multiply SPTI by the heart rate, we obtain a surrogate of the left ventricular oxygen requirement per minute.

The area between aortic and ventricular pressure curve during the diastolic phase DPTI (SPTI) is closely related to the blood supply to the subendocardium. DPTI mainly depends on the coronary arterial diastolic pressure,[36] the

pressure gradient in diastole between coronary arteries and left ventricular pressure, and the duration of diastole.[37]

These two areas therefore reflect subendocardial oxygen supply (DPTI) and demand (SPTI), and their ratio is a useful index of supply/demand:

$$\frac{DPTI}{SPTI} = \frac{Supply}{Demand}$$

Buckberg index corrected for cardiac mass

In the presence of myocardial hypertrophy, it is to be noticed a reduction of capillary density, that in an oxygen supply/demand ratio inevitably increases the denominator, resulting in a reduction of the final outcome. In order to improve the estimation of SPTI, recently Hoffmann and Buckberg[38] suggested to multiply SPTI by the relative left ventricular mass index (rel.LVMI) as determined by echocardiography. Thus, Buckberg index can be rewrite as follows:

$$Buckberg\ index = \frac{DPTI}{SPTI \times rel.LVMI}$$

Buckberg index corrected for arterial O_2 content

In the evaluation of the oxygen supply to the sub-endocardium, it has been taken in account the oxygen content of in arterial blood: the blood flow, being equal, the supply of oxygen can be significantly reduced in hypoxic hypoxia conditions as in the case of anemia, hypoxemic respiratory failure, or hypobaric hypoxia. Under these conditions, it is appropriate to correct the Buckberg index multiplying DPTI for arterial O_2 content (CaO_2).[30] Therefore the Buckberg index should be rewritten more correctly as:

$$Buckberg\ index = \frac{DPTI \times CaO_2}{SPTI \times rel.LVMI}$$

Reference values for the Buckberg index

For Buckberg index values less than 0.45, the ratio between subendocardial flow and subepicardial flow, per gram, is reduced in the left ventricle as a signal of insufficient sub-endocardial vascularization.[29,30,39] However, due to the coronary autoregulation, above this value, a linear relationship between Buckberg index and coronary blood flow does not exist. Indeed, for values greater than 0.45, the degree of subendocardial vascularization remains almost constant and the ratio between subendocardial flow and subepicardial flow, per gram, remains within the reference range.

Since oxygen supply to the subendocardium depends not only on coronary blood flow but also on the arterial oxygen content, it is also necessary to consider the critical threshold of Buckberg index in relation to the arterial oxygen content (Buckberg index $\times CaO_2$). According to this formula, the "critical" value for Buckberg index corresponds to 9.0. Buckberg index $\times CaO_2$ values are associated with insufficient oxygen supply to the sub-endocardium, in relation to its needs.

Buckberg index estimated by arterial tonometry

Evaluation of the myocardial oxygen supply and demand ratio, as described by Buckberg and Hoffmann, however, requires invasive catheterization, and this has been the most important limitation to its application in clinical practice. The introduction of transcutaneous arterial tonometry provides a useful approach to noninvasively determine the subendocardial oxygen supply:demand ratio through a simple, fast, well tolerated by the patient, reproducible, and extensively validated procedure.[40–42]

A reliable pressure waveform of the ascending aorta can be directly recorded from the common carotid artery waveform, or estimated from the radial artery waveform, using a transfer function. At present, transcutaneous applanation tonometry is considered the reference method for the noninvasive estimation of central blood pressure and for central pulse wave analysis.[43] All devices available on the market using the method of applanation tonometry provide values of Buckberg's index on the basis of the analysis of the central pulse waveform. DPTI is evaluated by these tonometric system as the area under the diastolic portion of the blood pressure wave and is obtained by multiplying the mean value of blood pressure during the diastolic phase of cardiac cycle by the diastolic time. SPTI is evaluated as the area under the systolic portion of the pressure wave, obtained by multiplying the mean value of blood pressure during the systolic phase of cardiac cycle by the left ventricular ejection time.[44]

In summary:

$$Buckberg\ index\ by\ arterial\ tonometry = \frac{Aortic\ Mean\ Diastolic\ Blood\ Pressure \times Diastolic\ Time}{Aortic\ Mean\ Systolic\ Blood\ Pressure \times Ejection\ Time}$$
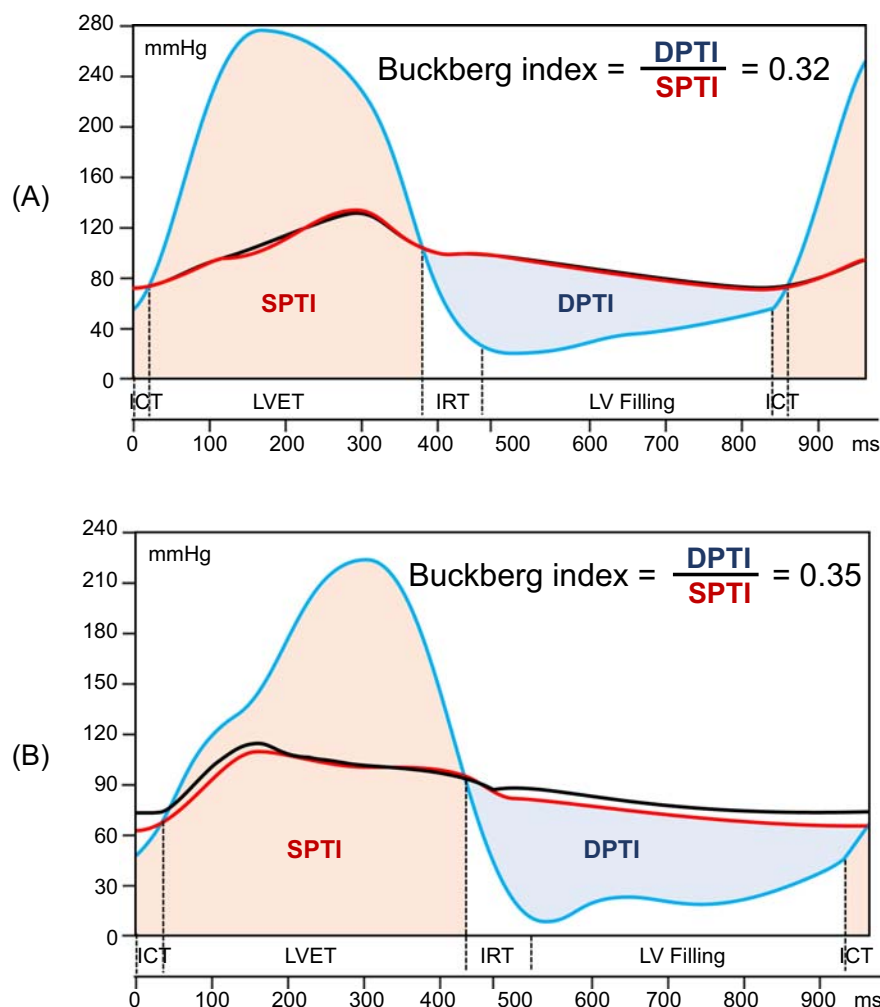
The noninvasive estimation of Buckberg index by means of tonometric analysis of the central pressure waveform is unable in the presence of a stenosis to the aortic valve outflow. Fig. 18.5 shows examples of unreliable estimation of Buckberg index in the presence of aortic stenosis and obstructive cardiomyopathy.

Limits in Buckberg index estimation by arterial tonometry
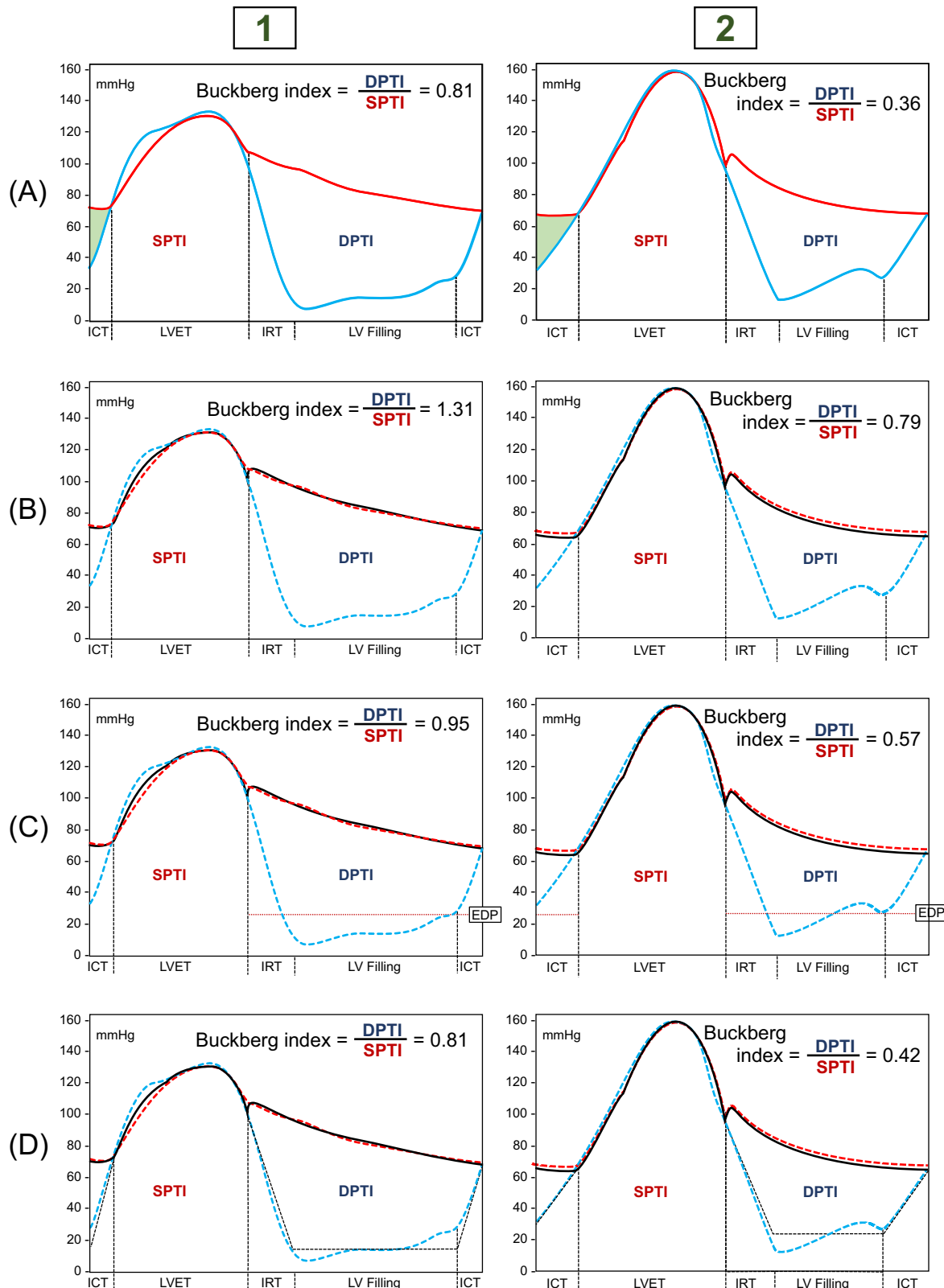
However, the method used by arterial tonometry to assess Buckberg index provides an unreliable estimate of the balance between subendocardial oxygen supply and demand.[39] A recent study, comparing invasive and noninvasive method to assess Buckberg index, showed an average overestimation of tonometric Buckberg index values of 0.44 ± 0.11 (limits of agreement of differences: $0.23-0.65$).[45] A number of factors can cause this discrepancy (Fig. 18.6).

First, the estimation of subendocardial flow supply (DPTI) by the tonometric approach leaves out left ventricular diastolic pressure. The true estimation of diastolic myocardial O_2 supply involves the inclusion of the area between aortic and left ventricular pressure curve during the diastolic phase of the cardiac cycle. Indeed, intraventricular pressure, which is fully transmitted to the

FIGURE 18.5   Unreliable estimation of Buckberg index in the presence of severe aortic stenosis (upper panel) and obstructive cardiomyopathy (lower panel). Left ventricular (LV) pressure (blue line) and aortic arterial pressure (red line) were recorded by invasive catheterization; carotid arterial pressure (black line) was recorded by applanation tonometry. The light blue area shows diastolic pressure-time index (DPTI) and the salmon area shows systolic pressure-time index (SPTI). Buckberg index was calculated as DPTI and SPTI ratio. *ICT*, isovolumic contraction time; *IRT*, isovolumic relaxation time; *LVET*, left ventricular ejection time.

FIGURE 18.6 Representative recordings of diastolic pressure-time index (DPTI, light blue area) and systolic pressure-time index (SPTI, salmon area). Buckberg index was calculated as DPTI and SPTI ratio. Left ventricular pressure (blue line) and aortic arterial pressure (red line) were recorded by invasive catheterization; carotid arterial pressure (black line) was recorded by applanation tonometry. Drawings on the left (1) were recorded on an adult

subendocardial layers, opposes the flow in the sub-endocardial microcirculation during the whole diastole. While in young healthy individuals, the weight of left ventricular diastolic pressure may be negligible due to the low values of intracardiac pressure; on the other hand, in patients with valve disease, diastolic dysfunction or heart failure, characterized by increased left ventricular diastolic pressure, neglecting intraventricular diastolic pressure causes an overestimation of the DPTI, therefore of the Buckberg index values.

Second, the estimation of myocardial oxygen demand (SPTI) requires analyzing the blood pressure curve during the entire systolic phase. This presupposes the analysis of both periods that make up systole: isovolumic contraction time and ventricular ejection time. Conversely, the tono-metric estimation of myocardial oxygen demand takes into account only the left ventricular ejection time, totally ignoring the isovolumic contraction time, with a conse-quent underestimation of SPTI. On the other hand, isovolumic contraction time is considered in DPTI deter-mination, with a consequent overestimation of DPTI. Actually, during isovolumic contraction, time left ventricle develops an important contractile activity, which results in a significant consumption of O_2. It is therefore evidently incorrect to consider this time as a period of oxygen supply to the subendocardium. If in young healthy individuals the weight of ventricular activity during isovolumic contraction time may be negligible due to the low ratio between isovolumic contraction time and ejection time, on the contrary, a misleading evaluation of the isovolumic contraction time induces a significant overestimation of the Buckberg index in the elderly and in patients with heart failure. Indeed, these patients are characterized by high isovolumic contraction time/ejection time ratio.

Third, the tonometric Buckberg index inappropriately includes the isovolumic relaxation time in the assessment of the DPTI. However, blood flow to the subendocardium during this phase of diastole is limited and increases very gradually. The full insertion of the isovolumic relaxation time within the analysis of the oxygen supply to the subendocardium can generate an overestimation of the DPTI, therefore of the Buckberg index.

Fourth, the close dependence of Buckberg index is estimated by tonometry on the diastolic time and ejection time ratio.[46,47] The formula used by tonometers to assess Buckberg index can be rewritten as follows:

$$\text{Buckberg index} = \frac{\text{Aortic Mean Diastolic BP}}{\text{Aortic Mean Systolic BP}} \times \frac{\text{Diastolic Time}}{\text{Ejection Time}}$$

However, the ratio between mean diastolic and mean systolic blood pressure in the aorta presents a limited interindividual variability which makes this parameter insignificant in determining interindividual differences in Buckberg index values.[46] In a large population, our research group found values of this ratio between 0.60 (fifth percentile) and 0.80 (95th percentile). This misleading simplification of the supply and demand ratio therefore implies that tonometry systems provide Buckberg index values between 60% and 80% of the diastolic time/ejection time ratio, i.e., Buckberg index = diastolic time/ejection time × (0.60 ÷ 0.80). These data may erroneously lead to the conclusion that the evaluation of the tonometric Buckberg index can reasonably be replaced by the simple measurement of the diastolic time/ejection time ratio.[29] Actually, interin-dividual variability in hemodynamics induces marked variations in the mean pressure during both the systolic and diastolic phases of the cardiac cycle and the relationship between myocardial oxygen supply and demand is strongly affected by these different blood pressure levels.

Buckberg index estimated by arterial tonometry and echocardiography

Evaluation of the myocardial oxygen supply and demand ratio by means of tonometry associated with echocardiog-raphy can theoretically be useful in overcoming the limits in the estimation of Buckberg index by means of arterial tonometry alone. Echocardiography can in fact offer useful information on ventricular diastolic pressure, providing the value of the end-diastolic pressure. However, the values of the ventricular end-diastolic pressure do not correspond to the values of the ventricular mean diastolic pressure,[45] and the overestimation of Buckberg index values by tonometry is only partially due to the neglect of the role of

---

male (Do.St.), 62 years old. Aortic pulse wave velocity = 10.4 m/s. Drawings on the right (2) were recorded on an adult female (Ma.EL.), 80 years old. Aortic pulse wave velocity = 25.0 m/s. First line (A): invasive Buckberg index assessment. DPTI represents the area between the aortic and left ventricular pressure curves in diastole; SPTI represents the area under the systolic left ventricular pressure curve, including left ventricular isovolumic contraction time. Second line (B): "traditional" tonometric Buckberg index: DPTI is the area below the carotid pressure curve during diastole, including also the left ventricular isovolumic contraction and relaxation times; SPTI is the area below the carotid pressure curve during systole, excluding the left ventricular isovolumic contraction time. Third line (C): Buckberg index estimated by applanation tonometry associated with echocardiography. DPTI is the area below the carotid pressure curve during diastole to which the area corresponding to the left ventricular end-diastolic pressure (EDP, evaluated by echocardiography) is subtracted. Fourth line (D): modified tonometric Buckberg index[45]: DPTI is estimated from the area below the diastolic phase of the carotid pulse pressure curve, after subtracting the ventricular diastolic pressure area, isovolumic contraction, and isovolumic relaxation times; SPTI is estimated from the area below the systolic phase of the carotid pulse pressure curve, to which the area related to the isovolumic contraction time is added. *ICT*, isovolumic contraction time; *IRT*, isovolumic relaxation time; *LVET*, left ventricular ejection time.

ventricular mean diastolic pressure. Other factors, such as isovolumic contraction and relaxation times, play an important role in this discrepancy between real and tonometric Buckberg index values.

New perspectives in Buckberg index estimated by arterial tonometry

Arterial tonometry can provide reliable Buckberg index values only when all the main factors determining myocardial oxygen supply and demands are taken into consideration, including left ventricular diastolic pressure, isovolumic contraction, and relaxation times.

Recently, an original and reliable method to estimate systolic time intervals with arterial tonometry has been proposed,[45,48] by combining analysis of the carotid pressure waveform with pulse wave velocity assessment. The measurement of isovolumic contraction time evaluated with this approach showed good agreement with that performed with conventional echocardiography.[48] The possibility of obtaining measurements of the systolic times intervals from the analysis of the carotid pressure waveform has allowed to develop an algorithm for a more reliable estimation of Buckberg index by carotid tonometry.[45]

DPTI is estimated from the area below the diastolic phase of the carotid pulse pressure curve, defined by the integral of the pressure curve in diastole, from which the following areas are subtracted: (i) the area related to the left ventricular diastolic pressure. The estimate of left ventricular mean diastolic pressure is based on parameters deduced by the pulse waveform analysis, on brachial blood pressure values and on anthropometric variables[45]; (ii) the area related to isovolumic contraction time, according to a validated formula[48]; (iii) the area related to isovolumic relaxation time, based on morphological analysis of the central pulse pressure and the degree of vascular stiffness.[45] SPTI is estimated from the area below the systolic phase of the carotid pulse pressure curve, defined by the integral of the pressure curve in systole, to which the area related to isovolumic contraction time is added.

Buckberg index assessed with this approach, based on carotid tonometry, showed good agreement with measurements performed with invasive catheterization,[45] thus setting the scene for a possible wide use in clinical practice. The reliable noninvasive estimation of the subendocardial oxygen supply and demand balance could be a useful parameter to assess the risk of myocardial ischemia, particularly in those forms of myocardial damage that are not justified by overt coronary artery disease.

References

1. Thygesen K, Alpert JS, Jaffe AS, et al. Fourth universal definition of myocardial infarction (2018). **Eur Heart J**. 2019; 40:237−269.

2. Collet JP, Thiele H, Barbato E, et al. 2020 ESC guidelines for the management of acute coronary syndromes in patients presenting without persistent ST-segment elevation. **Eur Heart J**. 2021; 42:1289−1367.

3. Chapman AR, Shah ASV, Lee KK, et al. Long-term outcomes in patients with type 2 myocardial infarction and myocardial injury. **Circulation**. 2018; 137:1236−1245.

4. Nestelberger T, Boeddinghaus J, Badertscher P, et al. Effect of definition on incidence and prognosis of type 2 myocardial infarction. **J Am Coll Cardiol**. 2017; 70:1558−1568.

5. Neumann JT, Sorensen NA, Rubsamen N, et al. Discrimination of patients with type 2 myocardial infarction. **Eur Heart J**. 2017; 38:3514−3520.

6. Katz A, Konstam M. **Heart Failure: Pathophysiology, Molecular Biology, and Clinical Managment**. 2nd ed. Philadelphia, USA: Lippincott Williams & Wilkins; 2008.

7. Moret P. Hypoxia and the heart. In: Bourne G, ed. **Hearts and Heart-Like Organs**. New York: Academic Press; 1980:333−387.

8. Ferrari R. Healthy versus sick myocytes: metabolism, structure and function. **Eur Heart J**. 2002; 4:G1−G12.

9. Tousoulis D. **Coronary Artery Disease: From Biology to Clinical Practice**. London: Elsevier/Academic Press; 2017.

10. Zipes D, Libby P, Bonow R, Mann D, Tomaselli G. **Braunwald's Heart Disease: A Textbook of Cardiovascular Medicine**. 11th ed. Elsevier; 2019.

11. Chirinos JA, Segers P. Noninvasive evaluation of left ventricular afterload: part 1: pressure and flow measurements and basic principles of wave conduction and reflection. **Hypertension**. 2010; 56:555−562.

12. Chirinos JA, Segers P, Gillebert TC, et al. Arterial properties as determinants of time-varying myocardial stress in humans. **Hypertension**. 2012; 60:64−70.

13. Arts T, Reneman RS, Veenstra PC. A model of the mechanics of the left ventricle. **Ann Biomed Eng**. 1979; 7:299−318.

14. Chirinos JA, Segers P, Rietzschel ER, et al. Early and late systolic wall stress differentially relate to myocardial contraction and relaxation in middle-aged adults: the Asklepios study. **Hypertension**. 2013; 61:296−303.

15. Chirinos JA, Segers P, Gupta AK, et al. Time-varying myocardial stress and systolic pressure-stress relationship: role in myocardial-arterial coupling in hypertension. **Circulation**. 2009; 119:2798−2807.

16. Klocke FJ, Braunwald E, Ross Jr J. Oxygen cost of electrical activation of the heart. **Circ Res**. 1966; 18:357−365.

17. Gibbs C. Cardiac energetics and the Fenn effect. In: Jacob R, Just H, Holubarsch C, eds. **Cardiac Energetics**. Heidelberg: Steinkopff; 1987:61−68.

18. Salvi P, Palombo C, Salvi GM, Labat C, Parati G, Benetos A. Left ventricular ejection time, not heart rate, is an independent correlate of aortic pulse wave velocity. **J Appl Physiol**. 2013; 115:1610−1617.

19. Sun YH, Anderson TJ, Parker KH, Tyberg JV. Wave-intensity analysis: a new approach to coronary hemodynamics. **J Appl Physiol**. 2000; 89:1636−1644.

20. Parker KH. An introduction to wave intensity analysis. **Med Biol Eng Comput**. 2009; 47:175−188.

21. Sen S, Petraco R, Mayet J, Davies J. Wave intensity analysis in the human coronary circulation in health and disease. **Curr Cardiol Rev**. 2014; 10:17−23.

22. Bender SB, van Houwelingen MJ, Merkus D, Duncker DJ, Laughlin MH. Quantitative analysis of exercise-induced enhancement of early- and late-systolic retrograde coronary blood flow. **J Appl Physiol (1985)**. 2010; 108:507−514.

23. Chirinos JA, Segers P. Noninvasive evaluation of left ventricular afterload: part 2: arterial pressure-flow and pressure-volume relations in humans. **Hypertension**. 2010; 56:563−570.

24. Hashimoto J, Ito S. Central diastolic pressure decay mediates the relationship between aortic stiffness and myocardial viability: potential implications for aortosclerosis-induced myocardial ischemia. **J Hypertens**. 2017; 35.

25. Salvi P, Salvi L, Parati G. Central diastolic pressure exponential decay constant and subendocardial flow supply. **J Hypertens**. 2017; 35:1958−1962.

26. Braunwald E. Control of myocardial oxygen consumption: physiologic and clinical considerations. **Am J Cardiol**. 1971; 27:416−432.

27. Buckberg GD, Fixler DE, Archie JP, Hoffman JI. Experimental subendocardial ischemia in dogs with normal coronary arteries. **Circ Res**. 1972; 30:67−81.

28. Ghadri JR, Wittstein IS, Prasad A, et al. International expert consensus document on Takotsubo syndrome (part I): clinical characteristics, diagnostic criteria, and pathophysiology. **Eur Heart J**. June 7, 2018; 39(22):2032−2046.

29. Hoffmann JI, Buckberg GD. Pathophysiology of subendocardial ischaemia. **Br Med J**. 1975; 1:76−79.

30. Brazier J, Cooper N, Buckberg G. The adequacy of subendocardial oxygen delivery: the interaction of determinants of flow, arterial oxygen content and myocardial oxygen need. **Circulation**. 1974; 49:968−977.

31. Watanabe H, Ohtsuka S, Kakihana M, Sugishita Y. Decreased aortic compliance aggravates subendocardial ischaemia in dogs with stenosed coronary artery. **Cardiovasc Res**. 1992; 26:1212−1218.

32. Watanabe H, Ohtsuka S, Kakihana M, Sugishita Y. Coronary circulation in dogs with an experimental decrease in aortic compliance. **J Am Coll Cardiol**. 1993; 21:1497−1506.

33. O'Rourke MF. How stiffening of the aorta and elastic arteries leads to compromised coronary flow. **Heart**. 2008; 94:690−691.

34. Sarnoff SJ, Braunwald E, Welch Jr GH, Case RB, Stainsby WN, Macruz R. Hemodynamic determinants of oxygen consumption of the heart with special reference to the tension-time index. **Am J Physiol**. 1958; 192:148−156.

35. Braunwald E, Sarnoff SJ, Case RB, Stainsby WN, Welch Jr GH. Hemodynamic determinants of coronary flow: effect of changes in aortic pressure and cardiac output on the relationship between myocardial oxygen consumption and coronary flow. **Am J Physiol**. 1958; 192:157−163.

36. Fokkema DS, VanTeeffelen JW, Dekker S, Vergroesen I, Reitsma JB, Spaan JA. Diastolic time fraction as a determinant of subendocardial perfusion. **Am J Physiol Heart Circ Physiol**. 2005; 288:H2450−H2456.

37. Indolfi C, Ross Jr J. The role of heart rate in myocardial ischemia and infarction: implications of myocardial perfusion-contraction matching. **Prog Cardiovasc Dis**. 1993; 36:61−74.

38. Hoffman JI, Buckberg GD. The myocardial oxygen supply: demand index revisited. **J Am Heart Assoc**. 2014; 3:e000285.

39. Salvi P, Parati G. Aortic stiffness and myocardial ischemia. **J Hypertens**. 2015; 33:1767−1771.

40. Chen CH, Ting CT, Nussbacher A, et al. Validation of carotid artery tonometry as a means of estimating augmentation index of ascending aortic pressure. **Hypertension**. 1996; 27:168−175.

41. Salvi P, Lio G, Labat C, Ricci E, Pannier B, Benetos A. Validation of a new non-invasive portable tonometer for determining arterial pressure wave and pulse wave velocity: the pulsepen device. **J Hypertens**. 2004; 22:2285−2293.

42. Salvi P. **Pulse Waves. How Vascular Hemodynamics Affects Blood Pressure**. 2nd ed. Heidelberg, Germany: Springer Nature; 2017.

43. Laurent S, Cockcroft J, Van Bortel L, et al. Expert consensus document on arterial stiffness: methodological issues and clinical applications. **Eur Heart J**. 2006; 27:2588−2605.

44. Chemla D, Nitenberg A, Teboul JL, et al. Subendocardial viability ratio estimated by arterial tonometry: a critical evaluation in elderly hypertensive patients with increased aortic stiffness. **Clin Exp Pharmacol Physiol**. 2008; 35:909−915.

45. Salvi P, Baldi C, Scalise F, et al. Comparison between invasive and noninvasive methods to estimate subendocardial oxygen supply and demand imbalance. **J Am Heart Assoc.** 2021; 10:e021207.

46. Chemla D, Antony I, Lecarpentier Y, Nitenberg A. Contribution of systemic vascular resistance and total arterial compliance to effective arterial elastance in humans. **Am J Physiol Heart Circ Physiol**. 2003; 285:H614−H620.

47. Chemla D, Nitenberg A, Teboul JL, et al. Subendocardial viability index is related to the diastolic/systolic time ratio and left ventricular filling pressure, not to aortic pressure: an invasive study in resting humans. **Clin Exp Pharmacol Physiol**. 2009; 36:413−418.

48. Salvi P, Grillo A, Tan I, et al. Systolic time intervals assessed from analysis of the carotid pressure waveform. **Physiol Meas**. 2018; 39:084002.

This page intentionally left blank

Biologic pathways leading to arterial stiffness and dysfunctional pulsatile hemodynamics

This page intentionally left blank

Chapter 19

Role of elastin and elastin-derived peptides in arterial stiffness: from synthesis to potential therapeutic interventions

Amandine Wahart[1,4], Amar Bennasroune[1], Christian E.H. Schmelzer[2,3], Muriel Laffargue[4], Sébastien Blaise[1], Béatrice Romier-Crouzet[1], Hervé Sartelet[1], Laurent Martiny[1], Philippe Gillery[1,5], Stéphane Jaisson[1,5], Pascal Maurice[1] and Laurent Duca[1]

[1]UMR CNRS 7369 Matrice Extracellulaire et Dynamique Cellulaire (MEDyC), Team 2: Matrix Aging and Vascular Remodelling, Université de Reims Champagne Ardenne (URCA), UFR Sciences Exactes et Naturelles et UFR Médecine, Reims, France; [2]Institute of Pharmacy, Faculty of Natural Sciences I, Martin Luther University Halle-Wittenberg, Halle (Saale), Germany; [3]Fraunhofer Institute for Microstructure of Materials and Systems IMWS, Halle (Saale), Germany; [4]INSERM UMR 1048, Institut des Maladies Métaboliques et Cardiovasculaires (I2MC), Toulouse, France; [5]Department of Biochemistry, University Hospital Center, Reims, France

Elastic fibers and elastin

Function and composition

A key step in the evolution of vertebrates was conversion from an open to a high-pressure closed circulatory system. The required mechanical stability and elasticity of the blood vessels were achieved in particular by structural changes of the vessel walls. The extracellular assemblies that account for the necessary elasticity and extensibility are the elastic fibers, which are highly abundant in large and small arteries. Individual fibers have a very low Young's modulus of between 0.3 and 1.5 MPa[1] and can be linearly stretched to ~150% of their original length before they tear.[2] Elastic fibers store the potential energy required to maintain blood flow during diastole thus enabling proper cardiovascular function. They are also essential for the physiological function of many other organs such as skin, tendons, or lungs, which undergo reversible and repetitive deformation. Elastic fibers consist of two morphologically distinguishable components: a mantle of longitudinally aligned fibrillin-based microfibrils and a dense core of cross-linked elastin, which accounts for over 90% of the fiber content.

The microfibrils are 10−12 nm wide filaments, which have a beads-on-a-string appearance.[3] They provide the tissues with long-range elasticity, especially with participation of elastin when it is deposited on a microfibrillar scaffold. Microfibrils are formed mainly from fibrillins, which are ~350 kDa large modular glycoproteins secreted from mesenchymal cells. In humans, there are three fibrillin isoforms of which each comprises 43 Ca^{2+}-binding epidermal growth factor (EGF)-like domains, five EGF-like domains, seven eight-cysteine-containing domains and two so-called hybrid domains.[4] Several other proteins are known to be associated with microfibrils.[3] Among them are the microfibril-associated glycoproteins,[5] elastin microfibril interfaces (EMILINs),[6] a disintegrin and metalloproteinase with thrombospondin motifs (ADAMTS), and ADAMTS-like proteins,[7] and latent transforming growth factor-β binding proteins (LTBPs).[8]

The other major component, elastin, is an insoluble biopolymer made up of units of its soluble precursor tropoelastin (TE). TE's primary structure is characterized by alternating hydrophobic and hydrophilic domains, which are encoded by distinct exons, and thus TE's domain structure maps the exon organization of the gene. The hydrophilic domains are involved in covalent cross-linking and contain either Lysyl-Alanine (KA) or Lysyl-Proline (KP) motifs. In the KA domains, Lys residues occur as pairs or triplets separated by two or three Ala residues and sometimes by another residue. The KA motifs are often

299
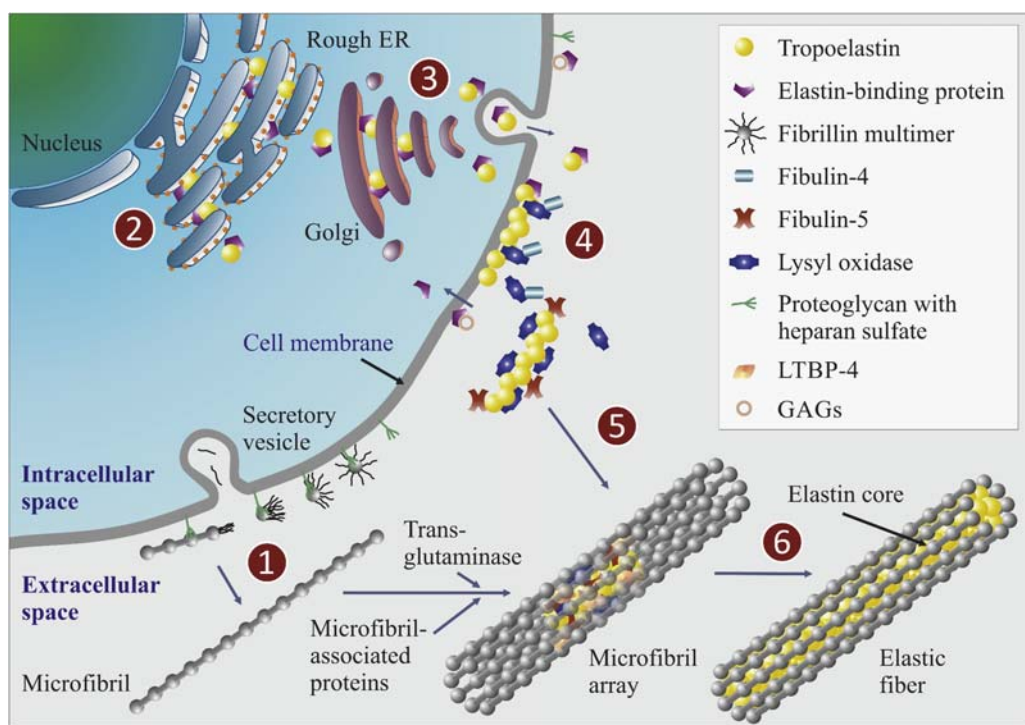
embedded in stretches of poly-Ala. In KP domains, the lysine residues are separated by at least one proline residue. Human TE consists of up to 34 domains of which 5 are KP and 11 are KA domains.[9] In contrast to other vertebrates, the human gene lacks exons 34 and 35, which have been lost during primate evolution.[10] Elastin's primary transcript undergoes extensive alternative splicing resulting in numerous isoforms. For human TE, 18 isoforms ranging from 49 to 69 kDa have been described. At least seven exons have been reported to be alternatively spliced: 3, 10, 11, 13, 22, 23, and 32.[11] The splicing occurs in phase without affecting the reading frame and hence an exon is either included, extended, shortened or removed. The expression of several of these isoforms in human tissues has been proven in some studies.[12] The functional consequences are still elusive, but it has been suggested that splicing may be tissue-specific or related to developmental changes in cells.[13]

Under healthy conditions, mature elastin is metabolically stable over the species' lifespan. Its half-life in humans has been determined to be greater than 70 years.[14] One of the reasons for this exceptional durability is elastin's high resistance to proteolysis, which is mainly caused by its vastly cross-linked nature and the extremely dense packing of the molecules. In its mature form, elastin is hydrophobic and completely insoluble, but its hydrophobic hydration is required for its elastic properties.[15]

Elastogenesis

The in vivo process that leads to the formation of functional elastic fibers, also known as elastogenesis, is a complex and yet not fully understood process involving numerous proteins. Elastogenesis time course has been studied in animals (mouse, chicken, sheep, and bovine) and starts at midgestation. It reaches its maximum around birth and completes during postnatal development, until adolescence. In the aorta, expression decreases rapidly when the physiological rise in blood pressure stabilizes postnatally.[16,17] Virtually no new functional fibers are assembled in adult tissues with the exception of the uterus, where they are rapidly removed after parturition and the fiber formation starts again with every new pregnancy.[16] The main stages of elastogenesis are shown in Fig. 19.1 and discussed below.

FIGURE 19.1   The elastic fiber assembly: (1) Fibrillin and microfibril-associated proteins are secreted into the extracellular space, multimerize, and form the microfibrillar array. (2) TE is synthesized on the rough endoplasmic reticulum (ER) where it binds to the chaperone EBP. (3) The EBP-TE complex is transported through the Golgi apparatus and secreted to the cell membrane. (4) TE is released from the chaperone and forms globules at the cell surface, while EBP dissociates as result of the interaction with glycosaminoglycans. Fibulin-4 is important for the chain alignment of TE mediating the interplay with lysyl oxidases. The oxidation of Lys residues is followed by various condensation reactions leading to the formation of covalent intra- and intermolecular cross-links. (5) After the cluster of TE molecules reaches a critical size, it is moved from the plasma membrane through the extracellular space. Fibulin-5 is thought to direct the premature elastin to fibrillin microfibrils. (6) The elastin aggregates fuse into larger assemblies with support by LTBP-4 and are subsequently further cross-linked. *EBP*, elastin-binding protein; *ER*, endoplasmic reticulum; *LTBP*, latent TGFβ-binding protein; *TE*, tropoelastin.

Microfibrils deposition

Elastogenesis is initiated with the expression of fibrillins and their assembly into microfibrils, which serve as a scaffold for the subsequent TE deposition. During or after secretion of the fibrillin precursors, they undergo N- and C-terminal cleavages by furin/PACE-like proprotein convertases at the consensus motif RXK/RR resulting in ∼320 kDa mature forms. This process is a prerequisite for the subsequent linear multimerization through the C-terminal domain and their assembly at the cell surface.[18] The fibrillin network can undergo cross-linking, which further stabilizes the three-dimensional bundle structure. The cross-links reported to date are intermolecular disulfide bonds[19] and ε(γ-glutamyl)lysine cross-links that are catalyzed by members of the transglutaminase family.[20]

Synthesis and secretion of tropoelastin

With the known exceptions of teleosts and frogs, a single gene encodes TE in vertebrate species.[21] The human gene (ELN) is located on the long arm of chromosome 7 (7q11.23).[22] The expression of the monomer takes place in elastogenic cells, which include vascular smooth muscle cells or fibroblasts. After the mRNA is exported from the nucleus, translation occurs on the surface of the rough endoplasmic reticulum (ER) where the N-terminal signal peptide is cleaved off. Before TE is transported through the Golgi apparatus to the cell surface, many proline residues are partially hydroxylated by prolyl 4-hydroxylase.[23] TE is transported along the secretory pathways together with a chaperone, the elastin-binding protein (EBP). EBP is a 67 kDa large inactive β-galactosidase splice variant that prevents intracellular degradation and aggregation of TE. When the EBP-TE complex is secreted, it associates with the other subunits of the elastin receptor complex (ERC): the membrane-associated proteins cathepsin A/protective protein (PPCA) and neuraminidase-1 (Neu-1).[24] EBP is thought to interact with glycosaminoglycans, which probably causes conformational changes in EBP and leads to the release of TE from its chaperone.[25] The EBP is recycled back into the intracellular endosomal compartments and associated with newly synthesized TE.[24]

Microassembly

TE subsequently undergoes rapid self-association in an endothermic, entropically driven process of liquid−liquid phase separation referred to as coacervation.[26] During this key process of microassembly, hydrophobic domains of TE, especially the domains 17−27, interact with each other[27] leading to the formation of distinct globular aggregates on the cell membrane.[28] It has been further suggested that interactions of the C-terminal region of TE, especially domain 30, with microfibrillar proteins are required for the assembly of elastic fibers.[29] Another

important sequence comprises the polybasic motif KXXXRKRK located in the C-terminal domain, which is encoded by the across-species highly conserved exon 36. It has been shown that TE lacking this sequence is less efficiently incorporated into mature elastin and shows abnormal cross-linking.[30] Proteoglycans may interact with this domain facilitating the correct alignment of the TE monomers.[31] The alignment of TE and the subsequent cross-linking is further promoted by fibulin-4, which mediates the association between TE and the extracellular Cu^{2+}-dependent amine oxidase, lysyl oxidase (LOX).[32]

Cross-linking and macromolecular assembly

LOX and LOX-like enzymes catalyze the oxidative deamination of the ε-amino group of Lys residues to the highly reactive α-aminoadipic acid-δ-semialdehyde, termed allysine (Lya).[33] Intra- and intermolecular cross-links are then formed spontaneously by nonenzymatic condensation reactions. The aldol condensation of two Lya residues results in the formation of an allysine aldol (AA) cross-link. The Schiff base reaction of a Lya residue with the ε-amino group of another Lys residue, however, yields dehydrolysinonorleucine (Δ-LNL). These reducible bifunctional cross-links further condense with each other, partly with participation of unmodified Lys residues or with other intermediates, to form the trifunctional cross-links dehydromerodesmosine and cyclopentenosine as well as the tetrafunctional cross-links desmosine (DES) and its isomer isodesmosine (IDES).[12] While some cross-links such as Δ-LNL and AA are also found in collagen, DES and IDES are unique to elastin in mammals.[34] In-depth characterizations of the cross-links in bovine[35] and human[12] elastin revealed that mature elastin is composed of an unordered network of TE molecules and that the cross-linking pattern is very complex and heterogeneous.[9]

Over time, the clusters formed at the cell surface grow in size by the addition and cross-linking of newly secreted TE molecules. When enough TE is secreted and accumulated, the formed globules are released from the cell surface and move through the extracellular matrix (ECM). Fibulin-5 and fibulin-4 are able to interact with fibrillin and are thought to play central roles in controlling the deposition of the premature elastin aggregates onto the microfibril scaffold.[32] The globules associate with fibrillin-containing microfibrils and readily coalesce into larger aggregates and eventually form functional fibers. Another contributing protein is LTBP-4, which does not directly interact with TE but with the fibulin-5-fibulin-4-TE complex and is apparently required for the proper linear deposition on the microfibril network.[36] Over time, deposited elastin is further oxidized by LOX and/or condensation reactions take place until elastin has been fully integrated into the microfibrillar scaffold.[37]

Elastin role in arterial function

Elastin: a major functional vascular wall component of vertebrate's arteries

The closed circulatory system is made up of a set of branching vessels (arteries, veins, and capillaries). The walls of arteries and veins have, to varying degrees, two fundamental properties: the first one is elasticity, due to the presence of constituents of elastic fibers called elastic lamellae. They transform the pulsatile flow imposed by the blood into permanent laminar flow. The second property concerns contractility, due to a smooth musculature whose role is essential in controlling the caliber of the vessel. Unlike arteries and veins, the extremely branched capillary network which constitutes the zone of exchanges between the vascular system and the tissues, presents a thin wall, more permeable, reduced to a single layer of cells, without muscular or elastic elements. The presence of elastin within these different vessels was first depicted at the end of the 19th century, notably through the work of Unna and colleagues using dyes such as orcein or Weigert's dye to allow the individualization of elastin.[38]

Elastin role in normal hemodynamics

Distributed concentrically and interconnected by structures that could be described as "pillars," elastic lamellae ensure the propulsion of blood throughout the arterial tree when the ventricles are in diastole. Indeed, elastic lamellae transform the pulsatile flow leaving the heart into a continuous flow in arteries. As reviewed in detail in Chapters 3 and 10, when blood is ejected from the heart during ventricular contraction and enters the large elastic arteries, their walls stretch under the pressure of the blood. As they stretch, the elastic fibers temporarily store mechanical energy and thus become reservoirs of pressure of the so-called systolic pressure. When the aortic valve is closed during cardiac systole, and in the absence of blood pressure at the exit of the heart, the elastic lamellae resume their initial degree of stretch and convert the stored potential into kinetic energy, thus propelling the blood. This kinetic energy thus allows blood to flow through the microcirculation while the ventricles are in diastolic phase. Therefore, elastic fibers, under heart systolic-diastolic cycle influence, alternate between stretched and relaxed states approximately 3 billion times during human lifetime.

As discussed in detail in Chapter 7, elastin ensures the elasticity of the vessel at the lower range of vessel stretch, while collagen provides rigidity at the higher range of vessel stretch. The capacity of fibers to return to their initial shape after stopping the stretching, is named elasticity (recoil ability).[39–41] Stiffness is the resistance offered by an elastic body to deformation. The stiffness of elastin is 1000 times lower than that of collagen.[42]
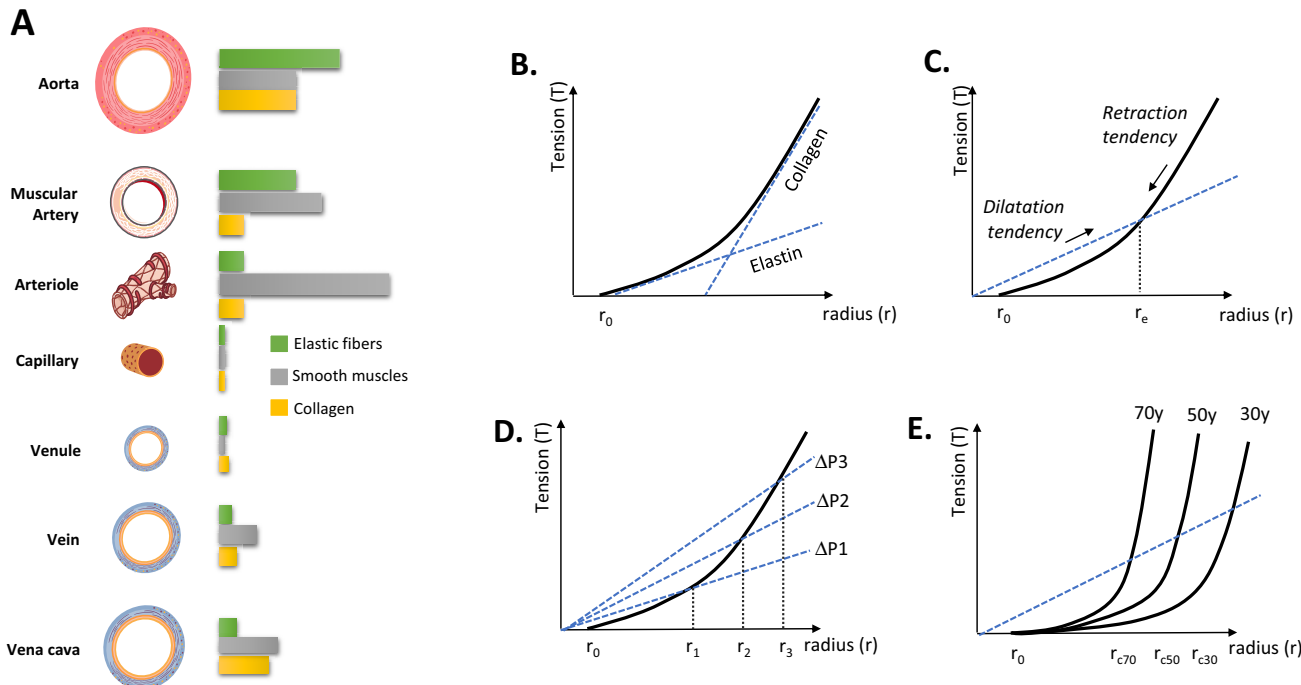
The large amount of elastic fibers in the aorta, especially in its proximal part, influences vascular flow. In fact, the rise of blood pressure during systole distends the aortic wall, increasing its volume. This volume is restored at the time of diastole. As a result, aortic output increases and decreases less quickly than ventricular output during cardiac cycles. This phenomenon transforms a discontinuous flow at the exit of the left ventricle into continuous flow at the capillary level (Fig. 19.2). Taking into account the mechanical properties of the arteries, in order to achieve an identical flow rate, the heart of a young subject (with a much more elastic aorta) must perform significantly less work than that of an older person in whom the integrity of the elastic fibers of the aorta is already compromised by stiffness and fragmentation.

Elastin modifications during aging and pathophysiological consequences

Nonenzymatic posttranslational modifications of elastin

Due to its long half-life, elastin is subjected to various chemical reactions which induce a molecular aging responsible for progressive alterations of its structural and functional properties. These chemical reactions, commonly called nonenzymatic posttranslational modifications (NEPTMs), are characterized by the binding of small metabolites to functional groups of proteins, especially amino groups of lysine and arginine residue side chains.[43] Among these reactions, the best known is glycation, corresponding to the reaction of reducing sugars (or their metabolites) to protein amino groups, followed by complex molecular rearrangements resulting in the formation of advanced glycation end-products (AGEs). However, other NEPTMs have been described to contribute to protein molecular aging such as oxidation and carbonylation, which share similar features. As another example, carbamylation, which is a more recently described NEPTM, is triggered by the reactive metabolite cyanate.[44] Cyanate mainly derives from the spontaneous dissociation of urea or from the myeloperoxidase-dependent metabolism of thiocyanate. Its reactive form, isocyanic acid, binds to the ε-amino groups of lysine residues, leading to the formation of homocitrulline, the most characteristic carbamylation-derived product.

Elastin molecular aging is concomitant to organism chronological aging but can also be intensified during chronic diseases such as diabetes mellitus, end-stage renal disease (ESRD), or atherosclerosis. For instance, the investigation of age-related changes of human aortic elastin in healthy subjects showed a significant increase of elastin

FIGURE 19.2 Role of elastin and collagen fibers on the mechanical properties of blood vessels. (A), Distribution of elastin (green bar), collagen (yellow bar), and myocytes (gray bar) within the vascular wall of various types of blood vessels. (B−E), Impact of elastin/collagen proportions in the tension-radius relationship. (B), Tension-radius curve, for an elastic artery, dependent of elastin and collagen components. r0 is the base radius of the artery when there is no transmural pressure gradient. (C), Laplace line (*dashed blue line*; its slope is equal to the transmural pressure gradient) and tension-radius curve (*black solid line*) for an elastic artery. The artery will have a radius such that both relationships (Laplace and tension-radius relations) are verified simultaneously. This ray is called the balance ray (re). (D), When the transmural pressure gradient varies, the slope of the relation $T = \Delta P.r$ changes, inducing a variation of the equilibrium radius. (E), For the same pressure gradient, when the elastic properties of the arteries decrease with age (30, 50, 70 years), the equilibrium radius of the aorta decreases (rc70, rc50, rc30).

glycation rate with age.[45] In patients with ESRD, levels of glycation and carbonylation of aortic elastin are also increased in comparison with control subjects.[46] Finally, skin elastic fibers are carbamylated during aging,[47] suggesting that vascular elastic fibers could also be susceptible to this modification.

The consequences of elastin molecular aging are multiple, ranging from direct impacts on structural and mechanical properties of this matrix protein to inappropriate effects on vascular cells. In vitro experiments have shown that glycation of elastin was responsible for a drastic loss of its elastic and biomechanical functions.[48,49] In the same way, cross-linking AGEs produced by glycation reactions contribute to limitation of the elastic and resilience properties of elastic fibers.[50] In addition, elastin glycation is responsible for an increased deposit of calcium on elastic fibers in ESRD patients.[51] Taken together, these combined effects contribute to the global increase of arterial stiffening and progression of arteriosclerosis.[50] Finally, elastin-bound AGEs may trigger inappropriate cellular effects such as alteration of migration properties of smooth muscle cells or induction of local oxidative stress mediated by the receptor for AGEs.[52]

Mechanical fatigue and enzymatic fracture of elastin

The breakdown of elastin is a multifactorial process, which can lead to stiffening of tissues and strongly affects vascular remodeling. One important cause is the mechanical fatigue of elastin lamellae due to the billions of repetitive cycles of stretching caused by pulsatile changes in blood pressure as well as shear stress within and between the elastic fibers.[53,54] The impairments or even ruptures lead to a decrease of elastic fiber function, and to a transfer of mechanical stress to other extracellular components such as collagen fibers.[55] The failure of elastic fibers is further induced by the action of members of several classes of extracellular proteases. Elastin-cleaving proteases are collectively termed elastases, although this description does not indicate that elastin degradation is the only physiological function of the enzymes. The known elastases belong to three classes of families: serine proteinases with cathepsin G, proteinase-3 and human leukocyte elastase,[56−58] matrix metalloproteinases (MMPs) including MMP-2, -7, -9, -12, and -14[59−61] and the cysteine proteinases cathepsins K, L, S, and V.[62,63] These proteinases

are primarily produced by fibroblasts, mesenchymal cells, platelets, macrophages, and leukocytes. All these enzymes are capable of irreversibly damaging elastin in vivo, either alone or in concert. Despite their different catalytic mechanisms, all elastases have in common that they cleave elastin in a relatively nonspecific manner at various locations of the molecule. Besides this mechanical impairment, elastin degradation leads to the release of bioactive peptides named elastokines and belonging to the matrikines family.[64,65]

Pathophysiological consequences of elastin modifications

Elastin modifications are involved in the development of several vascular wall–related diseases such as atherosclerosis, abdominal aortic aneurysms (AAAs), or hypertension, processes that can be related to arterial stiffness.

It has been shown during atherosclerosis that both the synthesis and degradation of elastic fibers are increased.[66] Degradation of elastic fibers allows infiltration of lipids and immune cells into the aortic wall participating to plaque formation and disruption.[67] The involvement of elastin degradation in atherosclerosis has moreover been confirmed using animal models and especially by cross-breeding mice deficient in MMP (-2, -7, -9, and -12) or in cathepsins (K, L, and S) with atherogenic models (LDLR$^{-/-}$ and ApoE$^{-/-}$).[68] These results clearly demonstrate that degradation of elastic lamellae is a prerequisite for the development of the disease.

AAA is a chronic degenerative vascular disease that accounts for 1.3% of all deaths in men aged 65 to 85 in developed countries.[69] It corresponds to a localized dilation of the abdominal aorta, usually asymptomatic until the often-fatal outcome, exceeding the normal diameter by more than 50%. Aneurysmal degradation is greatly reduced in genetic models of elastolytic enzymes MMP-2 and MMP-9 knockdown.[70] Comparable results were found in mouse models of AAA deficient in cathepsin L (decrease in elastic fibers fragmentation and decrease in proliferation, apoptosis and infiltration of inflammatory cells) confirming that in this vascular disease too, the degradation of the elastic network is crucial for the progression of AAA.[71]

On the hypertension side, the modulation of TGF-β availability by emilin-1, a protein associated with elastic fibers, determines systolic blood pressure in mice and thereby demonstrates a role for elastic fiber integrity and TGF-β signaling in hypertension.[17] It was shown, in a mouse model deficient in elastin (Eln$^{-/-}$),[72] that the arteries appear similar to the control until day E17.5. After that, however, a significant increase in the number of cells obstructing the arterial lumen is observed. At the postnatal stage, the arterial pressure of Eln$^{-/-}$ mice is doubled compared to wild-type mice and the stiffness is significantly

increased. Smooth muscle cells are disorganized and proliferate. The arteries show local dilations and narrowing and the mice die soon after birth. Heterozygous Eln$^{+/-}$ mice feature hypertension, aortic stenosis, and heart dysfunctions. In these mice, vascular stiffness is observed from the seventh day of birth but hypertension does not appear until the 14th day: the change in mechanical properties therefore seems to precede the change in blood pressure. The team of Hirano et al. generated an elegant mouse model expressing human elastin in a bacterial artificial chromosome (BAC-ELN) which they crossed with Eln$^{+/+}$, Eln$^{+/-}$, and Eln$^{-/-}$ mice to produce a spectrum of mice expressing from 30% to 120% of normal elastin level. Data from these mice show that the level of elastin is inversely related to arterial stiffness and blood pressure, clearly showing the pivotal role of elastin in these processes.[72]

Elastin-derived peptides signaling, elastin receptor complex, and pathophysiological consequences

Elastin-derived peptides

Besides its fundamental importance for the mechanics and function of arteries, elastin is also involved in other biological processes through the production of elastin-derived peptides (EDPs) upon its degradation. As mentioned previously, insoluble elastin can undergo mechanical fragmentation or degradation by elastases. The released bioactive EDPs, also called elastokines due to their cytokine-like properties,[64,73] induce a variety of biological activities including cell adhesion, chemotaxis, migration, proliferation, proteinase activation, angiogenesis, and apoptosis.[74] They are involved in vascular diseases progression, and are now considered central modulators of the cardiovascular continuum.[24]

The typical elastokine is the VGVAPG peptide, which is repeated several times within exon 24-encoding sequence.[75] Longer peptides were shown to be also bioactive[76] and recent analysis of fragments generated by the atherosclerosis-related elastases, leukocyte elastase, cathepsin G, and proteinase-3, brought into light new bioactive GxxPG-related peptides: GVYPG, GFGPG, and GVLPG.[57] Moreover, studies using MMP-7, -9, and -12 showed that GxxPG-containing peptides, such as YTTGKLPYGYGPGG, YGARPGVGVGGIP, and PGFGAVPGA, have also biological activities.[61]

Structural studies on VGVAPG using nuclear magnetic resonance and circular dichroism spectroscopies suggested that the peptide exhibited folded conformations in organic solvents.[77] In later studies, it was found that the GxxPG sequence adopts a type VIII β-turn conformation, which is required for binding of elastokines to EBP in order to mediate biological activities.[75] For note, the β-turn is the third most important secondary structure after helices and

β-strands and belongs to the turn structure family, defined as a type of nonregular secondary structure in proteins causing a change in direction of the polypeptide chain. β-turns have been classified according to the values of the dihedral angles φ and ψ of the central residue and type VIII is one subtype of this family.[78] Then, molecular dynamics simulations on VGVAPG, (VGVAPG)$_2$ and (VGVAPG)$_3$ showed that VGVAPG exists in an equilibrium between different conformations including extended polyproline II and folded conformations such as the type VIII β-turn.[79] The repetition of VGVAPG leads to the formation of additional structures very close to a type VIII β-turn, and the authors hypothesized that the repeated VGVAPG sequence in domain 24 may favor elastin−cell interactions as VGVAPG is more likely to bind to EBP if it occurs in the TE sequence multiple times.[73] With respect to other elastokines, it has been described that GxxP sequences, in which X is not Gly, are well able to adopt the type VIII β-turn conformation.[75,80] Pro following a Gly (GPxPG) has been reported to stabilize the type VIII β-turn owing to its unique heterocyclic pyrrolidine ring structure.[80]

There are 17 GxxPG sequences in elastin, which of nine have been shown to display biological activities while eight have not been investigated except for GGVPG, which has been shown to not be chemotactic to monocytes.[81] In addition to GxxPG-based elastokines, further peptides display biological activities, including VPGVG,[82] VGVPG,[81] PGVGVA,[83] and the nonapeptides GLGVGAGVP[76] and AGVPGLGVG.[84]

All known bioactive peptides are derived from the noncross-linked hydrophobic domains, whose building blocks are Gx, Px, GGx, and PGx with x being either G, A, V, L, or I. Domains 17−27, which contain the four biggest hydrophobic domains encrypting various elastokines, have been described to be key regions for coacervation of TE molecules during elastic fiber formation.[27,85] These domains are solvent-exposed and it is, hence, likely that they are cleaved by elastases during ECM turnover, tissue aging and elastic fiber diseases, resulting in the release of elastokines.

Elastin receptor complex−dependent cell signaling
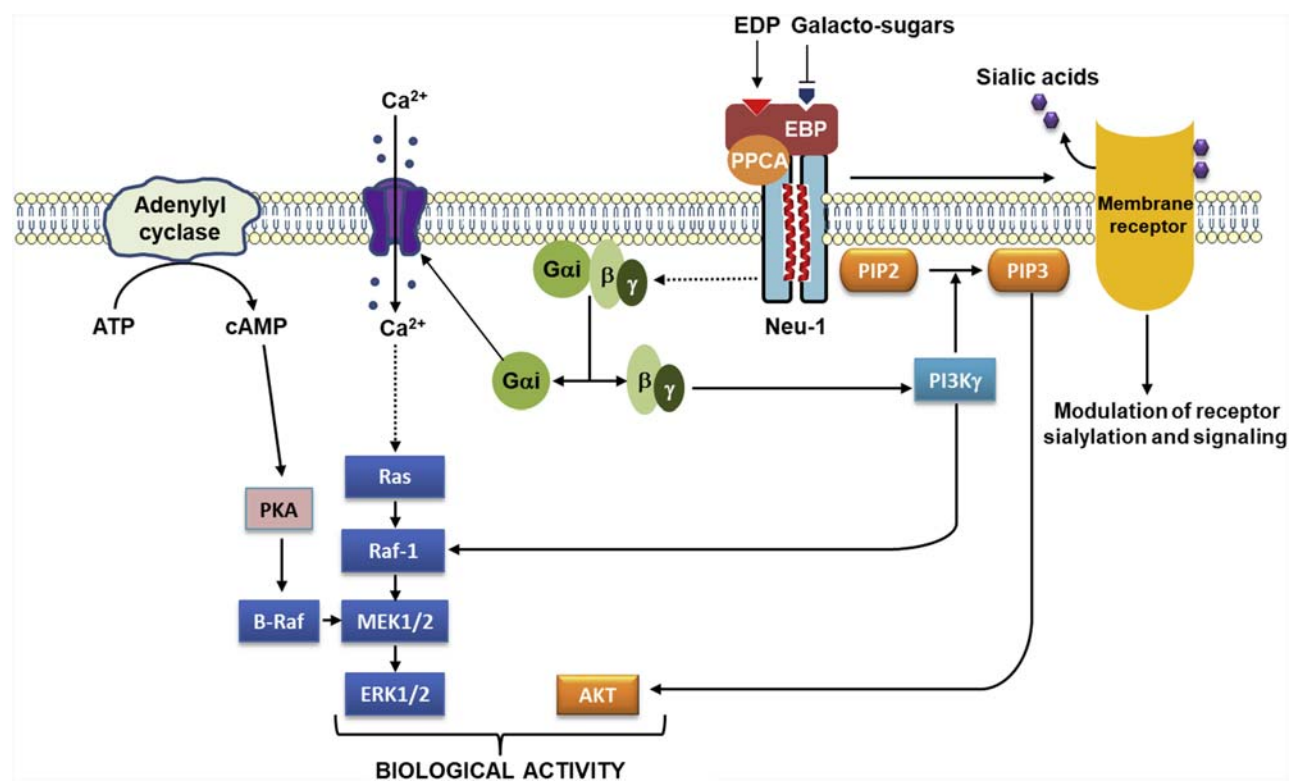
EDPs are able to bind several membrane receptors. So far, the most described is undoubtedly the ERC. The human elastin receptor was originally identified as a 67 kDa peripheral membrane protein called EBP that binds to elastin and laminin fragments.[86] EBP interacts with the 55 kDa (PPCA and the 61 kDa) membrane-bound Neu-1 to form a ternary complex called the ERC.[87] The EBP subunit[88] displays two functional-binding sites comprising (i) the elastin site on which EDPs binding is directly involved in the generation of intracellular signal transmission and (ii) the galactolectin site whose occupation by galactosugars leads to EDPs release and ERC dissociation.[89] EDPs

binding to EBP leads to Neu-1 activation which locally catalyzes the conversion of the GM3 ganglioside into lactosylceramide (LacCer), an essential second messenger of ERC signaling pathways.[90,91] Many intracellular signaling pathways induced by EDPs depending on the cell type have been described: for instance, EDPs induce the activation of multiple tyrosine kinases including MEK1/2 and ERK1/2 through a signal dependent on protein kinase A and phosphoinositide 3-kinase γ (PI3Kγ) in fibroblasts.[92] In endothelial cells, EDPs activate ERK1/2 by a PI3Kγ/Akt/ endothelial nitric oxide synthase/nitric oxide/protein kinase G pathway.[93] Finally, it has been shown in smooth muscle cells that EDP binding on ERC triggers the activation of Gi-proteins, the opening of L-type calcium channels, and then cell proliferation.[94] Neu-1 plays a key role in these signaling pathways and several studies have been conducted to further elucidate its involvement in ERC signaling. In addition to its role in the production of the second messenger LacCer, our group has demonstrated that a distinctive dimerization process is responsible of its catalytic activity. Indeed, two potential dimerization sequences, corresponding to two transmembrane domains (148−168 and 316−333 residues), have been found within human Neu-1. Point mutations in the 316−333 transmembrane domain inhibit significantly dimerization and sialidase activity of Neu-1.[95] Moreover, an increasing number of studies also indicate that Neu-1 plays an important role in modulating the activation of numerous membrane receptors such as the insulin receptor (IR), c-Met, IGFR, PDGFR, or CD36 by desialylation.[96−99] As a whole, these data imply that Neu-1 may be one of the crucial factors of the membrane signalosome from the lipids but also the protein points of view (Fig. 19.3).

Pathophysiological roles of elastin-derived peptides

Elastin remodeling during aging and disease clearly affects vascular events linked to arterial stiffness. It is however important to consider both the protein elastin and EDPs to have a better view of their respective participation. As previously mentioned in this chapter, elastin alteration leads to a loss of function impacting the mechanics and stiffness of arteries.[100] Genetic diseases due to mutations in the elastin gene such as Williams−Beuren syndrome and supravalvular aortic stenosis exhibit clear consequences such as arterial hypertension. Animal models like haploinsufficient murine models (Eln$^{+/-}$) confirmed these observations showing a higher arterial pressure (25−30 mmHg higher than their wild-type counterparts), whereas elastogenesis induction in the same murine model limits arterial hypertension.[100−103]

Besides, it has been shown that EDPs trigger a vasodilatation effect in an isolated organ model.[104] However, due to the uncoupling between the ERC and its intracellular targets during aging, this protective effect is progressively

FIGURE 19.3 Signaling pathways mediated by EDPs through the elastin receptor complex. The binding of EDPs on EBP triggers Neu-1 activation responsible for the induction of signaling pathways. Besides, Neu-1 subunit is able to modulate the sialylation level of other membrane receptors and their signaling. *EBP*, elastin-binding protein; *EDPs*, elastin-derived peptides; *ERK1/2*, extracellular-regulated protein kinases ½; *MEK1/2*, mitogen-activated protein kinase kinases ½; *Neu-1*, neuraminidase-1; *PI3K*, phosphoinositide 3-kinase; *PIP2*, phosphatidylinositol (4,5)-bisphosphate; *PIP3*, phosphatidylinositol (3,4,5)-trisphosphate; *PKA*, protein kinase A; *PPCA*, protective protein/cathepsin A.

lost.[105,106] Moreover, the net production of NO has been shown to drastically decrease during aging. Consequently, despite the positive effect of EDPs on the regulation of the vascular tone, the resulting endothelial dysfunction along with elastin loss of function clearly contribute to vascular stiffness. Nevertheless, the role of EDPs in the regulation of NO production is more complex as EDPs directly participate to the regulation of the vascular tone through their involvement in IR signaling blockade. Indeed, IR which is also present at the surface of endothelial cells, is known as an activator of NO pathway.[107] The blockade of IR signaling by EDPs could thus decrease NO production contributing to vascular dysfunction.

The role of elastin and EDPs in atherosclerosis and its link with arterial stiffness have been also widely studied. The Wagenseil's group evaluated if elastin deficiency and the consequent increase in arterial stiffness could play a role in atherosclerotic plaque formation. Using $Eln^{+/-}$ mice bred with atherosclerosis-prone mice presenting 60% of wild-type elastin levels, they showed that the observed reduced aortic compliance and the associated increased blood pressure were not directly linked to plaque appearance suggesting that other processes are required.[17,108,109] In this way, EDPs are drastically involved in atherosclerosis development as shown using proatherosclerotic $ApoE^{-/-}$ and $LDLR^{-/-}$ mice. The chronic administration of EDPs to such mice leads to an important increase in atherosclerotic plaques through the recruitment of inflammatory cells. Additionally, the use of chimeric $LDLR^{-/-}$ mice devoid of Neu-1 sialidase activity in hematopoietic cells obtained by bone marrow transplant from CathA/Neu-1-deficient mice to irradiated $LDLR^{-/-}$-recipient mice, showed a decrease in atherosclerosis development and in monocyte and lymphocyte infiltration.[110] Moreover, Dale et al. reported that EDPs induced an M1 macrophage polarization that could participate in the disease.[111] Finally, recent data from our group demonstrated that EDPs stimulation of macrophages leads to an increase in oxidized LDL uptake by CD36 involving the Neu-1 subunit of the ERC.[99] It is worthy to note that degraded elastic fibers are not repaired or renewed, but replaced by collagens and proteoglycans. This molecular switching contributes to the stiffening of arteries. In addition, the TE molecules produced by smooth muscle cells and/or macrophages during atherosclerosis development, are not cross-linked into mature and functional elastin, reinforcing the absence of elastic compensation processes.[112,113]

Finally, due to its mineral scaffolding function, elastin can suffer from calcification during atherosclerosis, but also during aging or other pathologies. This has been observed in human carotid arteries obtained by endarterectomy.[114] In human and several animal models, a clear correlation

between elastin degradation and vascular calcification has been demonstrated[115,116] in addition to an osteogenic differentiation of vascular SMCs induced by EDPs which may contribute to vascular calcification and aortic stiffening.[117]

Elastin biology-derived therapeutic options

Targeting elastin synthesis

Elastin production is regulated in a specific temporal and tissue manner and reinduction of functional elastic fibers is of high difficulty. This requires to target the TE production restoration.

The TE promoter contains response elements to TGF-β1,[17] to insulin[118] and to glucocorticoids.[119] However, the regulation of TE expression is also believed to be under control of the binding of regulatory microRNAs (miRs) in the 3′UTR and the coding sequences of TE mRNA.[120] Indeed, a strong expression of miRs-29 and -15 is thought to be responsible for the posttranscriptional repression of elastin in the adult aorta,[121] causing a degradation of the TE mRNA. Insulin-like growth factor-1, vitamin D, and interleukin-1β also modulate the expression of TE either at the promoter level or through the increase of mRNA stability.[22] The regulation of TE production by cytokines includes pro- and antielastogenic cytokines which control the biosynthesis/degradation of TE by transcriptional and posttranscriptional mechanisms, and depends on how these cytokines influence cell cycle actors.[122] Finally, exogenous molecules, whether medicinal or bioactive dietary compounds, can also influence the level of expression of the TE gene. Indeed, in different models of human skin, it has been shown that resveratrol, 4′-acetoxyresvereatrol as well as equol and R-equol are able to increase the expression level of TE mRNA. This effect is correlated with an augmentation of the corresponding protein expression level.[123] In mice receiving minoxidil, an antihypertensive and peripheral vasodilator for two weeks, the TE gene is induced when the drug is withdrawn. Interestingly, this is associated with functional elastic fibers presence.[103] This induction was also found in 24-month aged mice treated for 10 weeks, suggesting the high potential of this molecule in the induction of elastogenesis.[102]

Targeting proteolysis and nonenzymatic posttranslational modifications

Strategies aiming at limiting elastin proteolysis generally rely on the use of elastase inhibitors. However, many enzymes are able to degrade elastin, ranging from neutrophil elastase to MMPs and cathepsins. Thus, global inhibition is not conceivable because of their role in the regulation of multiple useful tissue functions and the potential side

effects such a strategy could cause.[124] However, several synthetic inhibitors have been tested with often disappointing results. Strategies based on the use of natural inhibitors, such as elafin, could give better results but a chronic administration seems necessary to obtain a significant reduction of elastolysis.[125–127]

The limitation of elastic fiber molecular aging may consist of global therapeutic strategies aiming at limiting NEPTMs at the body level without being elastin-specific. The first approaches are based on the administration of small molecules, which compete with the reactive groups of proteins for the binding of reactive metabolites and thus scavenge these metabolites. Numerous studies have been conducted with aminoguanidine, which has provided good results in vitro and in vivo in rodents, for reducing glycation-mediated complications including arterial stiffening.[128,129] Unfortunately, this molecule failed at the stage of clinical trials due to safety concerns. These trials were limited to its action on diabetic nephropathy,[130] and to our knowledge, there is no report about its potential role in the improvement of arterial stiffening. Similar strategies have been considered for limiting carbamylation reaction. Thus, amino acid solutions were used in patients with ESRD, which significantly reduced the level of protein carbamylation.[131] Since oxidative stress favors glycation and carbonylation reactions, the administration of antioxidants may also be considered an interesting therapeutic strategy.[132]

Other approaches have targeted generated products such as AGEs. For example, molecules called "AGE breakers" have been developed, the most studied being alagebrium (ALT-711).[133,134] This compound has given interesting results (even though no specific data on the reduction of elastin glycation are available), particularly in several conclusive clinical studies on cardiovascular diseases. Despite these encouraging data, this molecule has not yet become a commercially viable drug because of the lack of sufficient financial supports and the difficulty to license as a drug.[135]
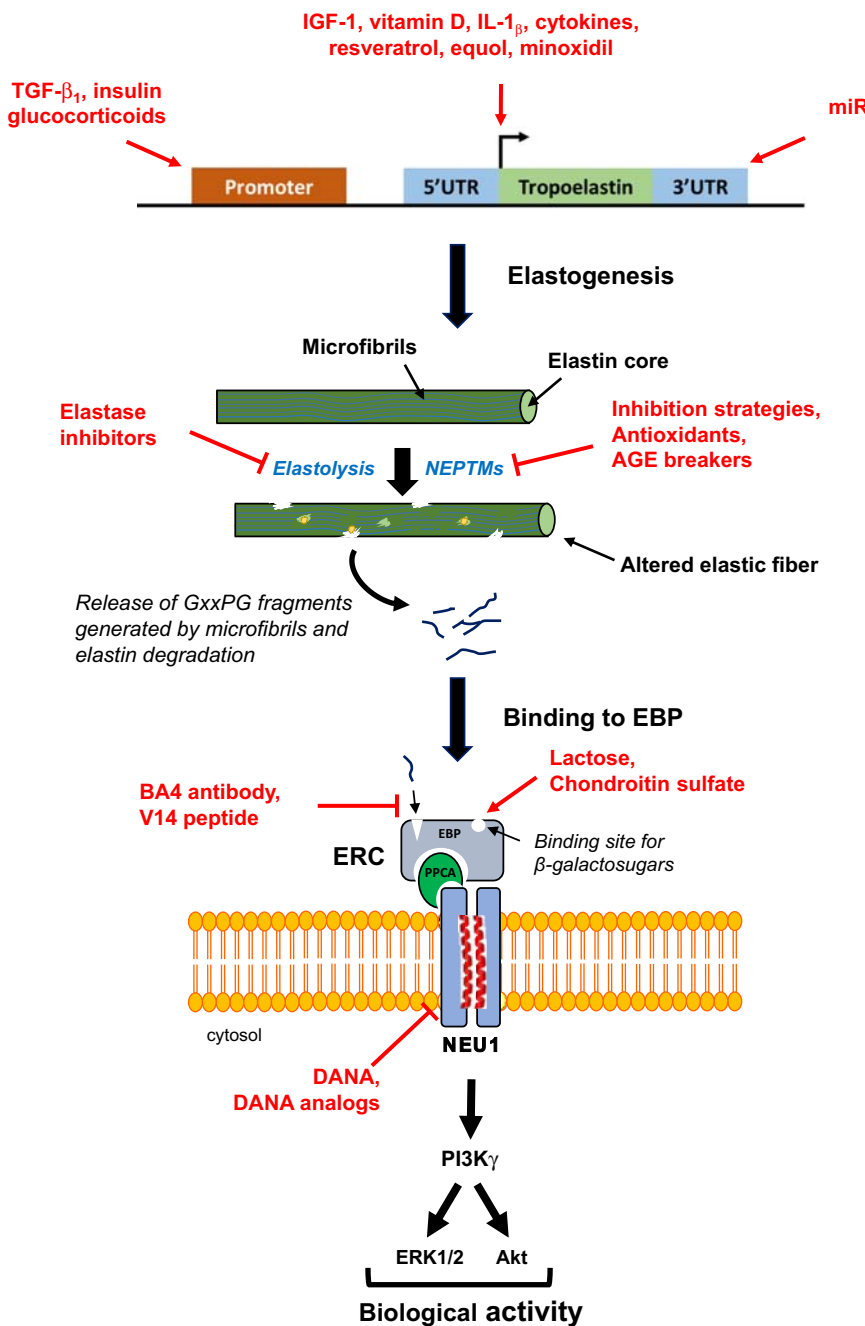
The combination of different strategies could be considered, as recently proposed for chronic obstructive pulmonary disease.[136] However, the major problem with these therapeutic approaches is that their effectiveness will only be guaranteed by long-term preventive treatments, which constitutes a barrier for their regular use in clinical practice, especially because of the cost such treatments would represent.

Elastin-derived peptides and elastin receptor complex modulators

Beside the use of elastase inhibitors, modulation of the pathophysiological effects related to EDPs can be achieved by either modulating the interaction between elastokines

and the ERC and/or by blocking ERC-mediated signaling pathways (Fig. 19.4). EDPs binding to the ERC can be hampered by using two strategies: a blocking antibody (BA4 antibody) targeting the GxxPG motifs located in elastin[70,111,137−140] or a 14-mer peptide (V14 peptide) that encompasses the ligand binding domain on the EBP subunit.[98,99,141,142] EBP also contains a binding site for β-galactosugars, and binding of lactose or chondroitin sulfate to EBP has been shown to change the conformation of the protein such that it loses its ability to bind to elastin

FIGURE 19.4 The different elastin-associated therapeutic strategies. This scheme illustrates the different therapeutic options that could be used to either simulate tropoelastin synthesis, decrease proteolysis and nonenzymatic posttranslational modifications of elastin occurring during aging and/or under pathophysiological conditions, or reduce elastin-derived peptides cell signaling. *AGE*, advanced glycation end-products; *DANA*, 2-deoxy-2,3-dehydro-N-acetylneuraminic acid; *EBP*, elastin-binding protein; *ERC*, elastin receptor complex, *ERK*, extracellular-regulated protein kinases; *IGF*, insulin-like growth factor; IL, interleukine; *NEPTMs*, nonenzymatic posttranslational modifications; Neu-1, neuraminidase-1; *PI3K*, phosphoinositide 3-kinase; *PPCA*, protective protein/cathepsin A; *TGF*, transforming growth factor; *UTR*, untranslated region.

and EDPs and can be shed from the cell surface.[86,89,143] Another valuable strategy relies on the blocking of the activation of key signaling proteins involved in ERC signaling pathways, such as Neu-1. Due to the lack of selective Neu-1 inhibitors, the majority of studies reported so far have used the broad-spectrum sialidase inhibitor DANA (2,3- dehydro-2-deoxy-N-acetylneuraminic acid) or inhibitors of bacterial or viral neuraminidases, such as zanamivir or oseltamivir. However, these bacterial or viral inhibitors were shown to have broad or weak activities against human neuraminidases.[144,145] To date, two selective inhibitors of human Neu-1 have been reported, based on modifications of the DANA scaffold: the C9-amido analog (16) and the C5-hexanamido-C9-acetamido analog.[146] As mentioned previously, recent findings from our group have shown that human Neu-1 contains a dimerization interface located within a transmembrane domain that is involved in membrane Neu-1 dimerization and sialidase activity.[95] These data should open new avenues for selective inhibition of this sialidase.

Conclusion

This chapter aimed at summarizing the role of elastin and elastokines in arterial stiffness. Besides its fundamental role in arterial mechanics, when degraded, elastin leads to the production of highly bioactive EDPs, also named elastokines, able to modulate vascular events and now seen as crucial modulators of the cardiovascular continuum. It is consequently clear that the extensive understanding of elastin biology, through its dual mechanics/elastokines role, could lead to the development of an innovative therapy based on matrix biology with an important potential.

References

1. Koenders MM, Yang L, Wismans RG, et al. Microscale mechanical properties of single elastic fibers: the role of fibrillin-microfibrils. **Biomaterials**. 2009; 30:2425−2432.
2. Gosline J, Lillie M, Carrington E, Guerette P, Ortlepp C, Savage K. Elastic proteins: biological roles and mechanical properties. **Philos Trans R Soc Lond Series B Biol Sci**. 2002; 357:121−132.
3. Thomson J, Singh M, Eckersley A, Cain SA, Sherratt MJ, Baldock C. Fibrillin microfibrils and elastic fibre proteins: functional interactions and extracellular regulation of growth factors. **Semin Cell Dev Biol**. 2019; 89:109−117.
4. Baldwin AK, Simpson A, Steer R, Cain SA, Kielty CM. Elastic fibres in health and disease. **Expert Rev Mol Med**. 2013; 15:e8.
5. Mecham RP, Gibson MA. The microfibril-associated glycoproteins (MAGPs) and the microfibrillar niche. **Matrix Biol**. 2015; 47:13−33.
6. Bressan GM, Daga-Gordini D, Colombatti A, Castellani I, Marigo V, Volpin D. Emilin, a component of elastic fibers preferentially located at the elastin-microfibrils interface. **J Cell Biol**. 1993; 121:201−212.
7. Brocker CN, Vasiliou V, Nebert DW. Evolutionary divergence and functions of the ADAM and ADAMTS gene families. **Hum Genomics**. 2009; 4:43−55.
8. Isogai Z, Ono RN, Ushiro S, et al. Latent transforming growth factor beta-binding protein 1 interacts with fibrillin and is a microfibril-associated protein. **J Biol Chem**. 2003; 278:2750−2757.
9. Schmelzer CEH, Hedtke T, Heinz A. Unique molecular networks: formation and role of elastin cross-links. **IUBMB Life**. 2020; 72:842−854.
10. Szabo Z, Levi-Minzi SA, Christiano AM, et al. Sequential loss of two neighboring exons of the tropoelastin gene during primate evolution. **J Mol Evol**. 1999; 49:664−671.
11. Reichheld SE, Muiznieks LD, Lu R, Sharpe S, Keeley FW. Sequence variants of human tropoelastin affecting assembly, structural characteristics and functional properties of polymeric elastin in health and disease. **Matrix Biol**. 2019; 84:68−80.
12. Hedtke T, Schrader CU, Heinz A, et al. A comprehensive map of human elastin cross-linking during elastogenesis. **FEBS J**. 2019; 286:3594−3610.
13. Heim RA, Pierce RA, Deak SB, Riley DJ, Boyd CD, Stolle CA. Alternative splicing of rat tropoelastin mRNA is tissue-specific and developmentally regulated. **Matrix**. 1991; 11:359−366.
14. Shapiro SD, Endicott SK, Province MA, Pierce JA, Campbell EJ. Marked longevity of human lung parenchymal elastic fibers deduced from prevalence of d-aspartate and nuclear weapons-related radiocarbon. **J Clin Invest**. 1991; 87:1828−1834.
15. Li B, Alonso DO, Bennion BJ, Daggett V. Hydrophobic hydration is an important source of elasticity in elastin-based biopolymers. **J Am Chem Soc**. 2001; 123:11991−11998.
16. Wagenseil JE, Mecham RP. Vascular extracellular matrix and arterial mechanics. **Physiol Rev**. 2009; 89:957−989.
17. Cocciolone AJ, Hawes JZ, Staiculescu MC, Johnson EO, Murshed M, Wagenseil JE. Elastin, arterial mechanics, and cardiovascular disease. **Am J Physiol Heart Circ Physiol**. 2018; 315:H189−H205.
18. Hubmacher D, El-Hallous EI, Nelea V, Kaartinen MT, Lee ER, Reinhardt DP. Biogenesis of extracellular microfibrils: multimerization of the fibrillin-1 c terminus into bead-like structures enables self-assembly. **Proc Natl Acad Sci USA**. 2008; 105:6548−6553.
19. Reinhardt DP, Gambee JE, Ono RN, Bachinger HP, Sakai LY. Initial steps in assembly of microfibrils. Formation of disulfide-cross-linked multimers containing fibrillin-1. **J Biol Chem**. 2000; 275:2205−2210.
20. Qian RQ, Glanville RW. Alignment of fibrillin molecules in elastic microfibrils is defined by transglutaminase-derived cross-links. **Biochemistry**. 1997; 36:15841−15847.
21. Chung MI, Miao M, Stahl RJ, Chan E, Parkinson J, Keeley FW. Sequences and domain structures of mammalian, avian, amphibian and teleost tropoelastins: clues to the evolutionary history of elastins. **Matrix Biol**. 2006; 25:492−504.
22. Vrhovski B, Weiss AS. Biochemistry of tropoelastin. **Eur J Biochem/FEBS**. 1998; 258:1−18.
23. Schmelzer CEH, Nagel MB, Dziomba S, Merkher Y, Sivan SS, Heinz A. Prolyl hydroxylation in elastin is not random. **Biochim Biophys Acta**. 2016; 1860:2169−2177.
24. Wahart A, Hocine T, Albrecht C, et al. Role of elastin peptides and elastin receptor complex in metabolic and cardiovascular diseases. **FEBS J**. 2019; 286:2980−2993.

25. Blanchevoye C, Floquet N, Scandolera A, et al. Interaction between the elastin peptide VGVAPG and human elastin binding protein. **J Biol Chem**. 2013; 288:1317−1328.

26. Muiznieks LD, Sharpe S, Pomes R, Keeley FW. Role of liquid-liquid phase separation in assembly of elastin and other extracellular matrix proteins. **J Mol Biol**. 2018; 430:4741−4753.

27. Dyksterhuis LB, Baldock C, Lammie D, Wess TJ, Weiss AS. Domains 17-27 of tropoelastin contain key regions of contact for coacervation and contain an unusual turn-containing crosslinking domain. **Matrix Biol J Int Soc Matrix Biol**. 2007; 26:125−135.

28. Kozel BA, Rongish BJ, Czirok A, et al. Elastic fiber formation: a dynamic view of extracellular matrix assembly using timer reporters. **J Cell Physiol**. 2006; 207:87−96.

29. Sato F, Wachi H, Ishida M, et al. Distinct steps of cross-linking, self-association, and maturation of tropoelastin are necessary for elastic fiber formation. **J Mol Biol**. 2007; 369:841−851.

30. Kozel BA, Wachi H, Davis EC, Mecham RP. Domains in tropoelastin that mediate elastin deposition in vitro and in vivo. **J Biol Chem**. 2003; 278:18491−18498.

31. Broekelmann TJ, Kozel BA, Ishibashi H, et al. Tropoelastin interacts with cell-surface glycosaminoglycans via its COOH-terminal domain. **J Biol Chem**. 2005; 280:40939−40947.

32. Nakamura T. Roles of short fibulins, a family of matricellular proteins, in lung matrix assembly and disease. **Matrix Biol**. 2018; 73:21−33.

33. Schmelzer CEH, Heinz A, Troilo H, et al. Lysyl oxidase-like 2 (loxl2)-mediated cross-linking of tropoelastin. **FASEB J**. 2019; 33:5468−5481.

34. Mithieux SM, Weiss AS. Elastin. **Adv Protein Chem**. 2005; 70:437−461.

35. Schräder CU, Heinz A, Majovsky P, et al. Elastin is heterogeneously cross-linked. **J Biol Chem**. 2018; 293:15107−15119.

36. Bultmann-Mellin I, Conradi A, Maul AC, et al. Modeling autosomal recessive cutis laxa type 1c in mice reveals distinct functions for ltbp-4 isoforms. **Dis Models Mech**. 2015; 8:403−415.

37. Partridge SM, Elsden DF, Thomas J, Dorfman A, Telser A, Ho PL. Incorporation of labelled lysine into the desmosine cross-bridges in elastin. **Nature**. 1966; 209:399−400.

38. Shadwick RE, Gosline JM. Elastic arteries in invertebrates: mechanics of the octopus aorta. **Science**. 1981; 213:759−761.

39. Rocco PR, Negri EM, Kurtz PM, et al. Lung tissue mechanics and extracellular matrix remodeling in acute lung injury. **Am J Respir Crit Care Med**. 2001; 164:1067−1071.

40. Nollen GJ, Westerhof BE, Groenink M, Osnabrugge A, van der Wall EE, Mulder BJ. Aortic pressure-area relation in marfan patients with and without beta blocking agents: a new non-invasive approach. **Heart**. 2004; 90:314−318.

41. Boyce TT, Roach MR. The canine tail artery as a model for cerebral aneurysm studies. **Can J Physiol Pharmacol**. 1989; 67:34−39.

42. Chirinos JA. Arterial stiffness: basic concepts and measurement techniques. **J Cardiovasc Trans Res**. 2012; 5:243−255.

43. Gillery P, Jaisson S. Post-translational modification derived products (PTMDPS): toxins in chronic diseases? **Clin Chem Lab Med**. 2014; 52:33−38.

44. Jaisson S, Pietrement C, Gillery P. Protein carbamylation: chemistry, pathophysiological involvement, and biomarkers. **Adv Clin Chem**. 2018; 84:1−38.

45. Konova E, Baydanoff S, Atanasova M, Velkova A. Age-related changes in the glycation of human aortic elastin. **Exp Gerontol**. 2004; 39:249−254.

46. Yamamoto Y, Sakata N, Meng J, et al. Possible involvement of increased glycoxidation and lipid peroxidation of elastin in atherogenesis in haemodialysis patients. **Nephrol Dial Transplant**. 2002; 17:630−636.

47. Gorisse L, Pietrement C, Vuiblet V, et al. Protein carbamylation is a hallmark of aging. **Proc Natl Acad Sci USA**. 2016; 113:1191−1196.

48. Wang Y, Zeinali-Davarani S, Davis EC, Zhang Y. Effect of glucose on the biomechanical function of arterial elastin. **J Mech Behav Biomed Mater**. 2015; 49:244−254.

49. Winlove CP, Parker KH, Avery NC, Bailey AJ. Interactions of elastin and aorta with sugars in vitro and their effects on biochemical and physical properties. **Diabetologia**. 1996; 39:1131−1139.

50. Sell DR, Monnier VM. Molecular basis of arterial stiffening: role of glycation - a mini-review. **Gerontology**. 2012; 58:227−237.

51. Sakata N, Noma A, Yamamoto Y, et al. Modification of elastin by pentosidine is associated with the calcification of aortic media in patients with end-stage renal disease. **Nephrol Dial Transplant**. 2003; 18:1601−1609.

52. Stirban A, Gawlowski T, Roden M. Vascular effects of advanced glycation endproducts: clinical effects and molecular mechanisms. **Mol Metabol**. 2014; 3:94−108.

53. O'Rourke MF. Arterial aging: pathophysiological principles. **Vasc Med**. 2007; 12:329−341.

54. Fonck E, Feigl GG, Fasel J, et al. Effect of aging on elastin functionality in human cerebral arteries. **Stroke**. 2009; 40:2552−2556.

55. Hodis S, Zamir M. Mechanical events within the arterial wall: the dynamic context for elastin fatigue. **J Biomech**. 2009; 42:1010−1016.

56. Owen CA, Campbell EJ. The cell biology of leukocyte-mediated proteolysis. **J Leukoc Biol**. 1999; 65:137−150.

57. Heinz A, Jung MC, Jahreis G, et al. The action of neutrophil serine proteases on elastin and its precursor. **Biochimie**. 2012; 94:192−202.

58. Schmelzer CE, Jung MC, Wohlrab J, Neubert RH, Heinz A. Does human leukocyte elastase degrade intact skin elastin? **FEBS J**. 2012; 279:4191−4200.

59. Senior RM, Griffin GL, Fliszar CJ, Shapiro SD, Goldberg GI, Welgus HG. Human 92- and 72-kilodalton type iv collagenases are elastases. **J Biol Chem**. 1991; 266:7870−7875.

60. Gronski Jr TJ, Martin RL, Kobayashi DK, et al. Hydrolysis of a broad spectrum of extracellular matrix proteins by human macrophage elastase. **J Biol Chem**. 1997; 272:12189−12194.

61. Heinz A, Jung MC, Duca L, et al. Degradation of tropoelastin by matrix metalloproteinases–cleavage site specificities and release of matrikines. **FEBS J**. 2010; 277:1939−1956.

62. Bromme D, Okamoto K, Wang BB, Biroc S. Human cathepsin O_2, a matrix protein-degrading cysteine protease expressed in osteoclasts. Functional expression of human cathepsin O_2 in spodoptera frugiperda and characterization of the enzyme. **J Biol Chem**. 1996; 271:2126−2132.

63. Panwar P, Hedtke T, Heinz A, et al. Expression of elastolytic cathepsins in human skin and their involvement in age-dependent elastin degradation. **Biochim Biophys Acta Gen Subj**. 2020; 1864:129544.

64. Maquart FX, Pasco S, Ramont L, Hornebeck W, Monboisse JC. An introduction to matrikines: extracellular matrix-derived peptides which regulate cell activity. Implication in tumor invasion. **Crit Rev Oncol-Hematol**. 2004; 49:199−202.

65. Maurice P, Blaise S, Gayral S, et al. Elastin fragmentation and atherosclerosis progression: the elastokine concept. **Trends Cardiovasc Med**. 2013; 23:211−221.

66. Akima T, Nakanishi K, Suzuki K, Katayama M, Ohsuzu F, Kawai T. Soluble elastin decreases in the progress of atheroma formation in human aorta. **Circ J**. 2009; 73:2154−2162.

67. Van der Donckt C, Van Herck JL, Schrijvers DM, et al. Elastin fragmentation in atherosclerotic mice leads to intraplaque neovascularization, plaque rupture, myocardial infarction, stroke, and sudden death. **Eur Heart J**. 2015; 36:1049−1058.

68. Lafarge JC, Naour N, Clement K, Guerre-Millo M. Cathepsins and cystatin c in atherosclerosis and obesity. **Biochimie**. 2010; 92:1580−1586.

69. Sakalihasan N, Limet R, Defawe OD. Abdominal aortic aneurysm. **Lancet**. 2005; 365:1577−1589.

70. Guo G, Munoz-Garcia B, Ott CE, et al. Antagonism of GXXPG fragments ameliorates manifestations of aortic disease in marfan syndrome mice. **Hum Mol Genet**. 2013; 22:433−443.

71. Sun J, Sukhova GK, Zhang J, et al. Cathepsin l activity is essential to elastase perfusion-induced abdominal aortic aneurysms in mice. **Arterioscler Thromb Vasc Biol**. 2011; 31:2500−2508.

72. Hirano E, Knutsen RH, Sugitani H, Ciliberto CH, Mecham RP. Functional rescue of elastin insufficiency in mice by the human elastin gene: implications for mouse models of human disease. **Circ Res**. 2007; 101:523−531.

73. Duca L, Floquet N, Alix AJ, Haye B, Debelle L. Elastin as a matrikine. **Crit Rev Oncol-Hematol**. 2004; 49:235−244.

74. Antonicelli F, Bellon G, Debelle L, Hornebeck W. Elastin-elastases and inflamm-aging. **Curr Top Dev Biol**. 2007; 79:99−155.

75. Brassart B, Fuchs P, Huet E, et al. Conformational dependence of collagenase (matrix metalloproteinase-1) up-regulation by elastin peptides in cultured fibroblasts. **J Biol Chem**. 2001; 276: 5222−5227.

76. Long MM, King VJ, Prasad KU, Freeman BA, Urry DW. Elastin repeat peptides as chemoattractants for bovine aortic endothelial cells. **J Cell Physiol**. 1989; 140:512−518.

77. Bisaccia F, Morelli MA, De Biasi M, Traniello S, Spisani S, Tamburro AM. Migration of monocytes in the presence of elastolytic fragments of elastin and in synthetic derivates. Structure-activity relationships. **Int J Pept Protein Res**. 1994; 44:332−341.

78. de Brevern AG. Extension of the classical classification of beta-turns. **Sci Rep**. 2016; 6:33191.

79. Floquet N, Hery-Huynh S, Dauchez M, Derreumaux P, Tamburro AM, Alix AJ. Structural characterization of VGVAPG, an elastin-derived peptide. **Biopolymers**. 2004; 76:266−280.

80. Moroy G, Alix AJ, Hery-Huynh S. Structural characterization of human elastin derived peptides containing the GXXP sequence. **Biopolymers**. 2005; 78:206−220.

81. Castiglione Morelli MA, Bisaccia F, Spisani S, De Biasi M, Traniello S, Tamburro AM. Structure-activity relationships for some elastin-derived peptide chemoattractants. **J Pept Res**. 1997; 49:492−499.

82. Wachi H, Seyama Y, Yamashita S, et al. Stimulation of cell proliferation and autoregulation of elastin expression by elastin peptide

83. VPGVG in cultured chick vascular smooth muscle cells. **FEBS Lett**. 1995; 368:215−219.

83. Hauck M, Seres I, Kiss I, et al. Effects of synthesized elastin peptides on human leukocytes. **Biochem Mol Biol Int**. 1995; 37:45−55.

84. Maeda I, Mizoiri N, Briones MP, Okamoto K. Induction of macrophage migration through lactose-insensitive receptor by elastin-derived nonapeptides and their analog. **J Pept Sci**. 2007; 13:263−268.

85. Jensen SA, Vrhovski B, Weiss AS. Domain 26 of tropoelastin plays a dominant role in association by coacervation. **J Biol Chem**. 2000; 275:28449−28454.

86. Hinek A, Wrenn DS, Mecham RP, Barondes SH. The elastin receptor: a galactoside-binding protein. **Science**. 1988; 239:1539−1541.

87. Hinek A, Pshezhetsky AV, von Itzstein M, Starcher B. Lysosomal sialidase (neuraminidase-1) is targeted to the cell surface in a multiprotein complex that facilitates elastic fiber assembly. **J Biol Chem**. 2006; 281:3698−3710.

88. Privitera S, Prody CA, Callahan JW, Hinek A. The 67-kda enzymatically inactive alternatively spliced variant of beta-galactosidase is identical to the elastin/laminin-binding protein. **J Biol Chem**. 1998; 273:6319−6326.

89. Mecham RP, Whitehouse L, Hay M, Hinek A, Sheetz MP. Ligand affinity of the 67-kd elastin/laminin binding protein is modulated by the protein's lectin domain: visualization of elastin/laminin-receptor complexes with gold-tagged ligands. **J Cell Biol**. 1991; 113:187−194.

90. Duca L, Blanchevoye C, Cantarelli B, et al. The elastin receptor complex transduces signals through the catalytic activity of its neu-1 subunit. **J Biol Chem**. 2007; 282:12484−12491.

91. Rusciani A, Duca L, Sartelet H, et al. Elastin peptides signaling relies on neuraminidase-1-dependent lactosylceramide generation. **PLoS One**. 2010; 5:e14010.

92. Duca L, Lambert E, Debret R, et al. Elastin peptides activate extracellular signal-regulated kinase 1/2 via a ras-independent mechanism requiring both p110gamma/raf-1 and protein kinase a/ b-raf signaling in human skin fibroblasts. **Mol Pharmacol**. 2005; 67:1315−1324.

93. Fahem A, Robinet A, Cauchard JH, et al. Elastokine-mediated up-regulation of mt1-mmp is triggered by nitric oxide in endothelial cells. **Int J Biochem Cell Biol**. 2008; 40:1581−1596.

94. Mochizuki S, Brassart B, Hinek A. Signaling pathways transduced through the elastin receptor facilitate proliferation of arterial smooth muscle cells. **J Biol Chem**. 2002; 277:44854−44863.

95. Maurice P, Baud S, Bocharova OV, et al. New insights into molecular organization of human neuraminidase-1: transmembrane topology and dimerization ability. **Sci Rep**. 2016; 6:38363.

96. Blaise S, Romier B, Kawecki C, et al. Elastin-derived peptides are new regulators of insulin resistance development in mice. **Diabetes**. 2013; 62:3807−3816.

97. Hinek A, Bodnaruk TD, Bunda S, Wang Y, Liu K. Neuraminidase-1, a subunit of the cell surface elastin receptor, desialylates and functionally inactivates adjacent receptors interacting with the mitogenic growth factors PDGF-bb and IGF-2. **Am J Pathol**. 2008; 173:1042−1056.

98. Romier B, Ivaldi C, Sartelet H, et al. Production of elastin-derived peptides contributes to the development of nonalcoholic steatohepatitis. **Diabetes**. 2018; 67:1604−1615.

99. Kawecki C, Bocquet O, Schmelzer CEH, et al. Identification of cd36 as a new interaction partner of membrane neu1: potential implication in the pro-atherogenic effects of the elastin receptor complex. **Cell Mol Life Sci**. 2019; 76:791−807.

100. Wagenseil JE, Mecham RP. Elastin in large artery stiffness and hypertension. **J Cardiovasc Trans Res**. 2012; 5:264−273.

101. Faury G, Pezet M, Knutsen RH, et al. Developmental adaptation of the mouse cardiovascular system to elastin haploinsufficiency. **J Clin Investig**. 2003; 112:1419−1428.

102. Coquand-Gandit M, Jacob MP, Fhayli W, et al. Chronic treatment with minoxidil induces elastic fiber neosynthesis and functional improvement in the aorta of aged mice. **Rejuvenation Res**. 2017; 20:218−230.

103. Knutsen RH, Beeman SC, Broekelmann TJ, et al. Minoxidil improves vascular compliance, restores cerebral blood flow, and alters extracellular matrix gene expression in a model of chronic vascular stiffness. **Am J Physiol Heart Circ Physiol**. 2018; 315:H18−H32.

104. Faury G, Ristori MT, Verdetti J, Jacob MP, Robert L. Effect of elastin peptides on vascular tone. **J Vasc Res**. 1995; 32:112−119.

105. Faury G, Robert L, Verdetti J. The age-dependent vasodilatation and endothelial calcium influx induced by elastin peptides are modulated by extracellular glucose level. **Biomed Pharm**. 2003; 57:216−222.

106. Scandolera A, Rabenoelina F, Chaintreuil C, et al. Uncoupling of elastin complex receptor during in vitro aging is related to modifications in its intrinsic sialidase activity and the subsequent lacto-sylceramide production. **PLoS One**. 2015; 10:e0129994.

107. Yu Q, Gao F, Ma XL. Insulin says no to cardiovascular disease. **Cardiovasc Res**. 2011; 89:516−524.

108. Stoka KV, Maedeker JA, Bennett L, et al. Effects of increased arterial stiffness on atherosclerotic plaque amounts. **J Biomech Eng**. 2018:140.

109. Maedeker JA, Stoka KV, Bhayani SA, et al. Hypertension and decreased aortic compliance due to reduced elastin amounts do not increase atherosclerotic plaque accumulation in ldlr-/- mice. **Atherosclerosis**. 2016; 249:22−29.

110. Gayral S, Garnotel R, Castaing-Berthou A, et al. Elastin-derived peptides potentiate atherosclerosis through the immune neu1-pi3kgamma pathway. **Cardiovasc Res**. 2014; 102:118−127.

111. Dale MA, Xiong W, Carson JS, et al. Elastin-derived peptides promote abdominal aortic aneurysm formation by modulating m1/m2 macrophage polarization. **J Immunol**. 2016; 196:4536−4543.

112. Nikkari ST, Jarvelainen HT, Wight TN, Ferguson M, Clowes AW. Smooth muscle cell expression of extracellular matrix genes after arterial injury. **Am J Pathol**. 1994; 144:1348−1356.

113. Kielty CM, Sherratt MJ, Shuttleworth CA. Elastic fibres. **J Cell Sci**. 2002; 115:2817−2828.

114. Bobryshev YV. Calcification of elastic fibers in human atherosclerotic plaque. **Atherosclerosis**. 2005; 180:293−303.

115. Khavandgar Z, Roman H, Li J, et al. Elastin haploinsufficiency impedes the progression of arterial calcification in MGP-deficient mice. **J Bone Miner Res**. 2014; 29:327−337.

116. Aikawa E, Aikawa M, Libby P, et al. Arterial and aortic valve calcification abolished by elastolytic cathepsin s deficiency in chronic renal disease. **Circulation**. 2009; 119:1785−1794.

117. Simionescu A, Philips K, Vyavahare N. Elastin-derived peptides and tgf-beta1 induce osteogenic responses in smooth muscle cells. **Biochem Biophys Res Commun**. 2005; 334:524−532.

118. Shi J, Wang A, Sen S, et al. Insulin induces production of new elastin in cultures of human aortic smooth muscle cells. **Am J Pathol**. 2012; 180:715−726.

119. Del Monaco M, Covello SP, Kennedy SH, Gilinger G, Litwack G, Uitto J. Identification of novel glucocorticoid-response elements in human elastin promoter and demonstration of nucleotide sequence specificity of the receptor binding. **J Invest Dermatol**. 1997; 108:938−942.

120. Duque Lasio ML, Kozel BA. Elastin-driven genetic diseases. **Matrix Biol J Int Soc Matrix Biol**. 2018; 71−72:144−160.

121. Ott CE, Grunhagen J, Jager M, et al. Micrornas differentially expressed in postnatal aortic development downregulate elastin via 3' UTR and coding-sequence binding sites. **PLoS One**. 2011; 6:e16250.

122. Sproul EP, Argraves WS. A cytokine axis regulates elastin formation and degradation. **Matrix Biol J Int Soc Matrix Biol**. 2013; 32:86−94.

123. Lephart ED. Resveratrol, 4' acetoxy resveratrol, r-equol, racemic equol or s-equol as cosmeceuticals to improve dermal health. **Int J Mol Sci**. 2017:18.

124. Duca L, Blaise S, Romier B, et al. Matrix ageing and vascular impacts: focus on elastin fragmentation. **Cardiovasc Res**. 2016; 110:298−308.

125. Alam SR, Lewis SC, Zamvar V, et al. Perioperative elafin for ischaemia-reperfusion injury during coronary artery bypass graft surgery: a randomised-controlled trial. **Heart**. 2015; 101:1639−1645.

126. Alam SR, Newby DE, Henriksen PA. Role of the endogenous elastase inhibitor, elafin, in cardiovascular injury: from epithelium to endothelium. **Biochem Pharmacol**. 2012; 83:695−704.

127. Shaw L, Wiedow O. Therapeutic potential of human elafin. **Biochem Soc Trans**. 2011; 39:1450−1454.

128. Chang KC, Tseng CD, Wu MS, et al. Aminoguanidine prevents arterial stiffening in a new rat model of type 2 diabetes. **Eur J Clin Invest**. 2006; 36:528−535.

129. Thomas MC, Baynes JW, Thorpe SR, Cooper ME. The role of ages and age inhibitors in diabetic cardiovascular disease. **Curr Drug Targets**. 2005; 6:453−474.

130. Bolton WK, Cattran DC, Williams ME, et al. Randomized trial of an inhibitor of formation of advanced glycation end products in diabetic nephropathy. **Am J Nephrol**. 2004; 24:32−40.

131. Kalim S, Ortiz G, Trottier CA, et al. The effects of parenteral amino acid therapy on protein carbamylation in maintenance hemodialysis patients. **J Ren Nutr**. 2015; 25:388−392.

132. Lee IS, Jung SH, Kim JS. Polyphenols from euphorbia pekinensis inhibit ages formation in vitro and vessel dilation in larval zebrafish in vivo. **Planta Medica**. 2018; 84:176−181.

133. Bakris GL, Bank AJ, Kass DA, Neutel JM, Preston RA, Oparil S. Advanced glycation end-product cross-link breakers. A novel approach to cardiovascular pathologies related to the aging process. **Am J Hypertens**. 2004; 17:23S−30S.

134. Susic D. Cross-link breakers as a new therapeutic approach to cardiovascular disease. **Biochem Soc Trans**. 2007; 35:853−856.

135. Toprak C, Yigitaslan S. Alagebrium and complications of diabetes mellitus. **Eur J Med**. 2019; 51:285−292.

136. Janssen R, Piscaer I, Wouters EF. Inhalation therapy for repairing damaged elastin fibers and decelerating elastinolysis in chronic

obstructive pulmonary disease. **Expet Rev Respir Med**. 2018; 12:349−360.

137. Houghton AM, Quintero PA, Perkins DL, et al. Elastin fragments drive disease progression in a murine model of emphysema. **J Clin Investig**. 2006; 116:753−759.

138. Grosso LE, Scott M. Peptide sequences selected by ba4, a tropoelastin-specific monoclonal antibody, are ligands for the 67-kilodalton bovine elastin receptor. **Biochemistry**. 1993; 32:13369−13374.

139. Hance KA, Tataria M, Ziporin SJ, Lee JK, Thompson RW. Monocyte chemotactic activity in human abdominal aortic aneurysms: role of elastin degradation peptides and the 67-kd cell surface elastin receptor. **J Vasc Surg**. 2002; 35:254−261.

140. Guo G, Booms P, Halushka M, et al. Induction of macrophage chemotaxis by aortic extracts of the MGR marfan mouse model and a GXXPG-containing fibrillin-1 fragment. **Circulation**. 2006; 114:1855−1862.

141. Coquerel B, Poyer F, Torossian F, et al. Elastin-derived peptides: matrikines critical for glioblastoma cell aggressiveness in a 3-d system. **Glia**. 2009; 57:1716−1726.

142. Robinet A, Millart H, Oszust F, Hornebeck W, Bellon G. Binding of elastin peptides to s-gal protects the heart against ischemia/reperfusion injury by triggering the risk pathway. **FASEB J**. 2007; 21:1968−1978.

143. Hinek A, Boyle J, Rabinovitch M. Vascular smooth muscle cell detachment from elastin and migration through elastic laminae is promoted by chondroitin sulfate-induced "shedding" of the 67-kda cell surface elastin binding protein. **Exp Cell Res**. 1992; 203:344−353.

144. Hata K, Koseki K, Yamaguchi K, et al. Limited inhibitory effects of oseltamivir and zanamivir on human sialidases. **Antimicrob Agents Chemother**. 2008; 52:3484−3491.

145. Richards MR, Guo T, Hunter CD, Cairo CW. Molecular dynamics simulations of viral neuraminidase inhibitors with the human neuraminidase enzymes: insights into isoenzyme selectivity. **Bioorg Med Chem**. 2018; 26:5349−5358.

146. Guo T, Heon-Roberts R, Zou C, Zheng R, Pshezhetsky AV, Cairo CW. Selective inhibitors of human neuraminidase 1 (neu1). **J Med Chem**. 2018; 61:11261−11279.

This page intentionally left blank

Chapter 20

Inflammation and arterial stiffness

Kaisa Maki-Petaja[1] and Ian B. Wilkinson[1,2]

[1]*Experimental Medicine and Immunotherapeutics, University of Cambridge, Cambridge, United Kingdom;* [2]*Addenbrooke's Hopital, Cambridge, United Kingdom*

Introduction

Inflammation is a key element in atheroma formation, playing a pivotal role in the initiation, progression, and propagation of the disease.[1] Circulating levels of several cytokines are elevated in subjects with atherosclerosis, and correlate with disease burden. Levels of the acute phase reactant C-reactive protein (CRP) also predict the risk of future cardiovascular events both in subjects with known cardiovascular disease (CVD),[2] and in apparently healthy individuals.[3] Moreover, the incidence of CVD is increased in patients with chronic systemic inflammatory diseases such as rheumatoid arthritis (RA),[4,5] systemic lupus erythematosus (SLE),[6] psoriasis,[7] chronic obstructive pulmonary disease (COPD),[8] and polymyalgia rheumatica (PMR).[9] The mechanism by which inflammation leads to increased CV risk remains unclear and numerous potential mechanisms have been proposed, including acceleration of the atherosclerosis process, destabilization of plaques, direct inflammation of the vasculature, endothelial dysfunction, or premature stiffening of large arteries.

Arterial stiffness is regulated by numerous factors. Traditionally, mean arterial pressure (MAP) and structural changes in the components of arterial wall were thought to be main determinants of arterial stiffness. With aging, the neat arrangement of the elastin fibers within the media is lost, the elastin fibers become thinner and fragmented, the stiffer collagen fibers become the load bearing ones, and arterial calcification occurs.[10] Moreover, a disrupted balance between elastin synthesis and breakdown, the latter mediated by matrix metalloproteinases (MMPs), contributes toward arterial stiffening.[10] Arterial stiffness is also regulated by smooth muscle tone, and endothelium-derived mediators, such as NO and endothelin-1, contribute to the functional regulation of arterial stiffness.[11] More recently, the role of inflammation in large arterial stiffening has been recognized,[12] possibly via changes in the composition of the arterial wall, due to inflammatory cell infiltration or via endothelial dysfunction.[13]

Arterial stiffness and low-grade inflammation

Cross-sectional studies

The largest community-based cross-sectional study investigating the association between inflammatory markers and aortic stiffness by Schnabel et al. demonstrated an association between interleukin-6 (IL-6) and aortic pulse wave velocity (PWV); importantly, this association remained significant after adjusting for traditional CV risk factors.[14] A number of studies in healthy individuals and in patients with isolated systolic hypertension indicated an association between arterial stiffness and serum levels of CRP,[13,15−17] suggesting that inflammation plays a role in the regulation of arterial stiffening. However, these studies do not provide information about the causality between inflammation and CVD. By adapting Koch's "Postulates" and using surrogate markers of CV risk, this could be done by answering the following questions; (1) Does inflammation cause arterial stiffening? (2) Does a reduction in inflammation reduce arterial stiffness?

Prospective studies

There have only been very few prospective studies assessing the association between inflammatory markers and arterial stiffness, and data from these studies are conflicting. Data from the Caerphilly Prospective Study showed that both current CRP and CRP at the beginning of the 20-year follow-up period were strongly associated with aortic PWV.[12] Likewise, The Whitehall study demonstrated that baseline inflammatory markers CRP, IL-6, and IL-1Ra predicted aortic PWV measured at 10-year follow-up visit.[18]

Taking another approach, Schumacher et al. investigated the relationship between three single nucleotide polymorphisms in the CRP gene and aortic PWV and found no relationship between any of the CRP genotypes and aortic stiffness, despite these genotypes having an impact on CRP levels, suggesting that CRP is a simply a marker of vascular damage/inflammation, rather than a causal molecule.[19] Furthermore, a large genome-wide association study by Elliott et al. concluded that the lack of concordance between the effect of CRP genotypes on coronary heart disease risk and its effect on CRP levels argues against a causal association of CRP with coronary heart disease.[20]

Experimental models of inflammation

Another approach to study the role of inflammation in arterial stiffening is to induce inflammation in healthy people, and study changes in arterial properties. In these acute experimental models of inflammation, *Salmonella typhi* vaccination was used to induce acute inflammation and shown to lead to an increase in PWV.[21,22] These studies are hypothesis generating, and they suggest a causal role of inflammation in the pathogenesis of large artery stiffening. However, the limitation of this model is that it is not known whether these acute changes reflect "a real-life" situation. After all, healthy volunteers cannot be made chronically inflamed; therefore, an alternative approach to assess the role of inflammation in arterial stiffening is to study patients with existing inflammatory conditions.

Arterial stiffness in patients with primary vasculitides

Booth et al. conducted a series of studies in patients with antibody-associated systemic vasculitis to establish the role of systemic inflammation on arterial stiffness. These studies demonstrated that patients with active disease had a significantly higher carotid femoral pulse wave velocity (CF-PWV) and augmentation index (AIx) than those in remission or matched healthy control subjects.[23] More recently, Chanouzas et al. demonstrated that T-cell expansion is independently associated with increased arterial stiffness in ANCA-associated vasculitis. They showed that the $CD4^+CD28^{null}$ T-cell percentage was associated with increased systolic blood pressure (rho = 0.305, P = .026), pulse pressure (rho = 0.428, P = .001), and CF-PWV (rho = 0.371, P = .006).[24] A metaanalysis performed by Upala et al. extracted data from four observational studies, resulting in 303 subjects with Behçet's disease. They found that CF-PWV is significantly higher in patients with Behçet's disease compared with controls (MD = 0.74; 95%, CI: 0.28−1.20, P = .002, I(2) = 63%).[25]

Vasculitis is an interesting model of systemic inflammation, but the use of this model also has a limitation; these patients have a direct vascular disease, which complicates the interpretation of the results, such that what is seen in vasculitis patients may not necessarily reflect changes in arterial stiffness seen in other conditions. Therefore, other conditions with chronic, systemic inflammation may provide a better model to study the role of systemic inflammation and the effect of circulating cytokines and acute phase proteins in the process of arterial stiffening.

Arterial stiffness in chronic inflammatory diseases

Chronic, systemic inflammatory diseases represent an ideal model to study effect of inflammation on arterial stiffness, especially as they are associated with increased CV mortality, which cannot be fully explained by the traditional CV risk factors.[5] There are numerous studies in various chronic systemic inflammatory conditions that demonstrate that patients with these conditions exhibit increased arterial stiffness.[13]

Perhaps the largest study to investigate the role of inflammation in aortic stiffening was the study by Dregan.[26] This study tested the hypothesis that arterial stiffness is elevated in inflammatory disorders in comparison to the inflammation-free control group. In total, 171,125 adults from the UK Biobank who did not have CVD and have had arterial stiffness measurements performed were included in the analysis. A total of 5976 (3%) participants diagnosed with inflammatory disorders had data on arterial stiffness. However, it is important to note that the stiffness as not assessed using the gold standard measurement of large artery stiffness, (CF-PWV), but was based on waveform analysis. Participants diagnosed with RA, SLE, Sjogren syndrome, psoriasis, ankylosing spondylitis (AS), systemic vasculitis, or inflammatory bowel disease (IBD) represented the exposed group. Participants free of these diagnoses represent the comparison group. Adjusted linear regression analyses revealed 14% increase in mean arterial stiffness for chronic inflammatory disorders (beta coefficient (β) 1.14, 95% CI 1.05 to 1.24, P = .002) compared with the control group. Moreover, the association appeared to increase with the severity of chronic inflammation, as assessed by leukocytes count and granulocytes count.[26]

Rheumatoid arthritis

Numerous small studies have concluded that patients with RA[27−29] exhibit increased aortic CF-PWV which correlates, independently of blood pressure, age, and gender, with the degree of active inflammation.[27] A recent, large

metaanalysis by Ambrosino et al. evaluated the relationship between RA and arterial stiffness across 25 studies (1472 RA patients, 1583 controls). They demonstrated that RA patients had a significantly higher CF-PWV in comparison to controls with a mean difference (MD 1.32 m/s; 95% CI 0.77, 1.88; $P < .00001$); ankle-brachial-PWV (MD 198.42 cm/s; 95% CI 45.79, 342.76; $P = .01$), AIx (MD 11.50%; 95% CI 5.15, 17.86; $P = .0004$), and AIx@75 (MD 6.99%; 95% CI 4.92, 9.06; $P < .00001$) were also increased in RA patients. Furthermore, this metaanalysis demonstrated that there is an association between the severity of inflammation and stiffness, and that increased arterial stiffening is present even in early-stage disease.[30]

Inflammatory bowel disease

A recent metaanalysis by Zanoli et al. used data from four cohorts in three countries, which included 151 patients with ulcerative colitis, 159 with Crohn's disease, and 227 control patients. The results demonstrated CF-PWV was increased in patients with Crohn's disease (mean difference 0.78 z-score; 95% confidence interval, 0.56−1.00 z-score, $P < .001$) and ulcerative colitis (mean difference 0.75 z-score; 95% confidence interval, 0.52−0.97 z-score, $P < .001$).[31]

In a linear regression model adjusted for prespecified confounders, aortic PWV was associated with disease duration and white blood cell count but not with CRP and erythrocyte sedimentation rate, cardiovascular risk factors, or therapy.

Systemic lupus erythematosus

A metaanalysis of data from 14 studies in SLE patients was performed by Wang et al. They used fixed-effect or random-effect models to estimate the pooled standardized mean difference (SMD) and 95% confidence intervals (CIs) between patients and controls. This study demonstrated that patients with SLE had significantly higher CF-PWV levels than the control group (SMD = 0.56; 95% CI: 0.30−0.82). They also showed that body mass index and disease duration were associated with increased CF-PWV.[32]

Systemic sclerosis

A large metaanalysis was performed comprising a total of 1292 patients with systemic sclerosis (SSc) from 35 individual studies. Arterial stiffness, assessed by both CF-PWV and ankle-augmentation index, was found to be higher in SSc patients in comparison to controls. The SMD for CF-PWV was 0.62 (95% CI: 0.35, 0.88, $P < .001$), whereas the standardized difference for AIx was 0.96 (95%CI: 0.45, 1.47, $P < .001$).[33]

Chronic obstructive pulmonary disease

Despite being primarily a chronic lung condition, patients with COPD exhibit an increased risk of CV events. A large metaanalysis of 32 studies (3198 patients and 13867 controls) reported that COPD patients had significantly higher CF-PWV (SMD: 0.70; 95% CI: 0.52, 0.88; $P < .0001$), AIx normalized to a heart rate (MD: 4.59%; 95% CI: 2.80, 6.38; $P < .0001$). Metaregression analysis revealed that the severity of lung disease (as expressed by FEV_1%predicted) was associated with PWV. In the subgroup analysis, the authors showed that COPD patients with even mild airway obstruction had increased arterial compared with controls subjects, suggesting that subclinical vascular changes occur prematurely and increase with declining lung function.[34]

Human immunodeficiency virus infection

Whether patients with human immunodeficiency virus (HIV) have increased arterial stiffness is contentious. A recent review evaluated 18 observational studies which compared individuals with HIV infection and controls, and found that 55% of studies showed no difference in aortic stiffness between HIV+ and age-matched HIV− control groups. The main reported determinants of aortic stiffness in the reviewed studies were age, blood pressure, smoking, metabolic syndrome, and HIV-related variables, including CD4/CD8 ratio, current T-CD4 count $<200/mm^3$, and nadir T-CD4+ count $<200/mm^3$. These findings suggest that HIV and associated immune dysfunction may be associated with large artery stiffness.[35] The impact of HIV infection on arterial stiffness and hemodynamics will be discussed in detail in Chapter 47.

Antiinflammatory treatment for arterial stiffness

Numerous studies in both healthy individuals and in patients with inflammatory conditions have demonstrated that inflammatory markers are independently associated with arterial stiffening, suggesting that stiffening may be modifiable by antiinflammatory treatments. This part of this chapter aims to explore the studies investigating the effect of antiinflammatory drugs for arterial stiffness reduction.

Only few relatively small studies have investigated the effect of traditional antiinflammatory drugs on arterial stiffness. Pieringer et al. demonstrated a reduction in AIx in patients with PMR following corticosteroid treatment; from $28 \pm 9\%$ to $25 \pm 10\%$, $P = .006$.[36] Schillaci et al. demonstrated in patients with PMR that 4-week treatment with prednisolone reduced aPWV (from 11.8 ± 3 to 10.5 ± 3 m/s, $P = .015$) and AIx (from $34 \pm 7\%$ to $29 \pm 8\%$, $P = .01$). These changes were independent of BP

and heart rate and the change in CF-PWV correlated with change in plasma CRP (r = 0.40, P = .037).[37] The results of these studies are contradicted by a study by Wong et al. who found that antiinflammatory therapy with cyclooxygenase (COX) inhibitors indomethacin and rofecoxib did not improve endothelial function or reduce arterial stiffening.[38] It is important to recognize that some of the conventionally used antiinflammatory drugs may actually increase CV risk. Corticosteroids cause dyslipidemia, hypertension, impaired glucose tolerance, and imbalances in thrombosis and fibrinolysis.[39] Methotrexate use can lead to hyperhomocysteinemia, which is an independent predictor of CV events, although this problem can be overcome by concomitant supplementation of folic acid.[40] Selective COX-2 inhibitors and also nonselective NSAIDs increase mortality and CV events in numerous patient groups due to an imbalance of thromboxane A2 and prostacyclin.[41] However, these drugs may also have an ameliorating effect on the vasculature by the reduction of inflammation and hence oxidative stress.

Due to their high specificity, biological immunomodulatory drugs may represent a better pharmacological tool to investigate the role of inflammation on stiffness. Maki-Petaja et al. demonstrated in 17 RA patients that following 8 weeks of antitumor necrosis factor-α (TNF-α) therapy, CF-PWV was reduced from 9.09 ± 1.77 m/s to 8.63 ± 1.42 m/s (P = .04). Also, aortic inflammation assessed by tissue to background ratio of (18)F-fluorodeoxyglucose uptake within the aortic wall decreased from 2.02 ± 0.22 to 1.90 ± 0.29, which correlated with the reduction of CF-PWV (R = 0.60, P = .01).[28] Similarly, Angel at al. demonstrated in 55 patients inflammatory arthropathies that a 1-year treatment course with anti-TNF-α therapy, but not placebo, led to a reduction of CF-PWV (-0.54 ± 0.79 m/s vs. 0.06 ± 0.61 m/s, respectively; P = .004) and carotid intima-media thickness (cIMT) progression was reduced in the treatment group in comparison to the control group.[42] Tam et al. demonstrated in 40 RA patients that after a 6-month treatment period, there was a significantly greater reduction in CF-PWV in those patients receiving both methotrexate and the anti-TNF-α agent, infliximab compared to those receiving methotrexate only (-0.78 ± 1.13 m/s vs. 0.18 ± 1.59 m/s; P = .04), which was accompanied by significantly greater reduction in CRP and disease activity.[43] This suggested that a greater reduction in inflammation and disease activity may in turn lead to a greater reduction in PWV. Contrary to the encouraging findings seen in RA patients with anti-TNF-α agents, McInnes et al. found in a randomized double blind phase III trial, that interleukin-6 receptor (IL-6R) blocker tocilizumab was not beneficial in reducing CF-PWV in 132 patients with RA.[44] Opposing their

hypothesis, they found that reduction in CF-PWV was greater in the placebo group in comparison to tocilizumab group at 12 weeks posttreatment (adjusted mean difference 0.79 m/s; 95% CI 0.22 to 1.35; P = .007). This could be due to the observed increase in total cholesterol, LDL-cholesterol, and triglyceride levels in tocilizumab recipients. However, they demonstrated that tocilizumab led to a reduction of lipoprotein(a), as well as inflammatory and thrombotic markers. And as such the net effect of cardiovascular benefits and/or risks of tocilizumab remains unclear.

Another recent study explored the effect of IL-12/23 inhibition with ustekinumab in patients with psoriasis. In this study by Ikonomidis et al., 150 psoriasis patients were randomized to receive ustekinumab, anti-TNF-α treatment (etanercept), or cyclosporine, and CF-PWV, as well as a host of left ventricular (LV) function tests and inflammatory markers were assessed at baseline and 4 months posttreatment. Data from all three treatment arms demonstrated an improvement in global longitudinal strain, LV twisting, and coronary flow reserve, as well as reduced inflammatory markers, but the greatest improvements were seen in the ustekinumab group. Interestingly, CF-PWV and central augmentation index were only improved by ustekinumab.[45] This could potentially be explained by the fact that IL-12 signaling plays integral part in the pathogenesis of psoriasis, and hence inhibition of IL-12 would had a greater benefit in the vasculature in this particular patient cohort. Pina et al. conducted a prospective study in 29 patients with moderate to severe psoriasis to determine the effect of anti-TNF-α monoclonal antibody adalimumab on endothelial function and CF-PWV[46]. In contrast to the findings of Ikonomidis et al. demonstrated 6-month treatment with anti-TNF-α agent led to an improvement of endothelial function as measured by flow-mediated dilatation (from $6.19 \pm 2.44\%$ to $7.46 \pm 2.43\%$; P = .008) and reduction of CF-PWV (from 6.28 ± 1.04 m/s to 5.69 ± 1.31 m/s; P = .03).

A follow-up study by Zanoli et al. provided important novel data on the longitudinal changes in CF-PWV by after commencement of antiinflammatory therapy.[47] Longitudinal study changes in CF-PWV were observed for 3.4 ± 0.5 years in IBD subjects receiving mixed antiinflammatory therapies: 14 were treated with salicylates; 11, with steroids and azathioprine; 7, with anti-TNF-alpha and 30 matched healthy controls were also studied. Interestingly, the results showed that CF-PWV increased during follow-up in both control and IBD subjects treated with salicylates, whereas CF-PWV remained unchanged in those treated with steroids and azathioprine or anti-TNF-α therapy. Therefore, the annual increase of CF-PWV was significantly higher in subjects treated with salicylates than in those treated with steroids and azathioprine or anti-TNF-alpha (P = .004 and P = .001,

respectively). These data suggest that a better control of inflammation by the use of more potent antiinflammatory drugs may help to slow down aortic stiffening over time.

Although many studies have shown in numerous different chronic inflammatory conditions that antiinflammatory treatments lead to a reduction of arterial stiffening, this does not necessarily seem to be the case in patients with AS. Capkin et al. showed in a prospective trial of 28 AS patients that despite significant improvement in markers of disease activity and inflammation, anti-TNF-α therapy did not improve CF-PWV after 24 weeks of therapy (7.9 ± 1.3 m/s vs. 7.7 ± 1.3 m/s; $P = .4$).[48] Mathieu et al. came to very similar conclusions by demonstrating that there were no changes in CF-PWV or central augmentation index after 6 or 12 months following anti-TNF-α therapy in 49 patients with AS, despite the treatment leading to a significant reduction of inflammation and disease activity.[49] These somewhat unexpected results could potentially be due to a low baseline CF-PWV in these relatively young subjects; after all, number of studies have shown that the greatest change in CF-PWV is seen in those with highest baseline values.

Only very few studies have investigated the effect of antiinflammatory drugs on arterial stiffness in healthy individuals. Vlachopoulos et al. used *S. typhi* vaccination to induce acute inflammation healthy subjects.[22] Interestingly, they demonstrated that there was no change in CF-PWV following the vaccination in those subjects that were randomized to receive aspirin pretreatment, whereas CF-PWV significantly increased in the placebo group. Using the same model of acute inflammation, Wallace et al. similarly demonstrated that pretreatment with Simvastatin also prevents inflammation-induced aortic stiffening.[21]

Antilipidemic drugs

Numerous studies have reported so-called "pleiotropic effects" of HMG-CoA reductase inhibitors (statins). These include improvements of endothelial function,[54] increased nitric oxide bioavailability,[55,56] antioxidant[57] and antiinflammatory[58] or immunomodulatory effects.[59] Therefore, it comes as no surprise that numerous studies have investigated statins as a means to reduce arterial stiffness.

In the late 1990s, Tomochika et al. first suggested in a small prospective study that arterial stiffness, as measured by Beta stiffness index, can be reduced with a strict cholesterol-lowering therapy with pravastatin, probucol, and diet.[50] A year later, Muramatsu et al. demonstrated in 59 patients with hypercholesterolemia, that those patients who had 15% or more reduction in total cholesterol following pravastatin therapy also had a significant decrease in CF-PWV and total peripheral resistance.[51]

Since these first two studies in the 1990s, numerous groups have studied the effect of different statins in various patient groups. Indeed, statins have now been shown to reduce arterial stiffness in patients' hypercholesterolemia, hypertension, CVD, chronic kidney disease, diabetes, RA, and in obese individuals.[52]

Mechanisms of inflammation-induced arterial stiffening

Although there is plenty of evidence to demonstrate that inflammation has a causal effect on arterial stiffening and that treatment of inflammation leads to reductions in stiffness, the mechanisms behind inflammation-induced stiffness remain incompletely understood. Numerous potential mechanisms have been suggested, some of which are discussed below.

Endothelial dysfunction

Endothelial function can regulate arterial stiffness via changes in smooth muscle tone. Both basal and stimulated nitric oxide (NO) production can regulate muscular artery distensibility. There is also an inverse correlation between endothelial function, as measured by flow-mediated dilatation response, and CF-PWV, which appears independent of potential confounding factors, including age and MAP.[53] Furthermore, local arterial distensibility is reduced by blockade of endogenous NO synthesis with the NO synthase inhibitor NG-monomethyl-L-arginine in the human iliac artery.[11] However, the role of nitric oxide in regulating stiffness of the more elastic thoracic aorta remains controversial. A detailed discussion of endothelial dysfunction and its hemodynamic consequences can be found in Chapter 23.

The association between acute and chronic inflammation and endothelial dysfunction has been demonstrated in numerous studies.[54] However, the mechanisms behind this are incompletely understood. One possibility is that certain cytokines induce expression of inducible nitric oxide synthase (iNOS) leading to a production of reactive oxygen species with subsequent uncoupling of endothelial NOS (eNOS) and reduction in nitric oxide (NO) production.[55] Moreover, the acute phase reactant CRP may also decrease eNOS expression and thus reduce NO bioavailability directly.[56] Production of myeloperoxidase (MPO) is another potential key mediator in inflammation-induced endothelial dysfunction. MPO is released from activated neutrophils during inflammation. MPO can catalytically degrade NO, thus reducing NO bioavailability. Furthermore, MPO has the unique ability to produce hypochlorous acid and subsequently lead to uncoupling of eNOS,[57]

oxidation tetrabiopterin (BH_4),[58] and further superoxide (O_2^-) production. Tetrahydrobiopterin (BH_4), a naturally occurring essential co-factor for eNOS, is thought to play an important role. Recent in vitro studies suggest that activation of iNOS may lead to endothelial dysfunction by depleting the bioavailability of BH_4 from eNOS and subsequently uncouple eNOS, resulting to production of superoxide (O_2^-) rather than NO.[59] When O_2^- reacts with NO in vivo, peroxynitrite is formed, leading to oxidation of BH_4 and a reduction in the allosteric stability of eNOS, further uncoupling of eNOS. Furthermore, increased levels of adhesion molecules may damage endothelial cells and lead to altered endothelial function.[60] Activation of neutrophils by antineutrophil cytoplasm antibodies within the vascular lumen may contribute to endothelial cell injury.[61] Finally, oxidation of LDL promoted by inflammation may lead to direct endothelial cell toxicity[62] and disturbed eNOS function.

Increased synthesis of matrix metalloproteinases

Another mechanism that may contribute to arterial stiffening during inflammation is an accelerated elastin breakdown by matrix MMPs. MMP synthesis is induced by CRP, and the release of MMPs from the leukocytes can degrade elastin within the media. Yasmin et al. demonstrated in mixed cohort of 677 hypertensive and normotensive subjects that MMP-9 levels are independently associated with CF-PWV.[63] In a further study, Yasmin et al. demonstrated that aortic stiffness and elastase activity are influenced by MMP-9 gene polymorphisms, suggesting that the genetic variation in this protein may have a causal role in the process of large artery stiffening.[64] Although elastin degradation may play an important role in arterial stiffness over long periods of time, it is unlike to explain more acute changes or how antiinflammatory therapies are able to reduce stiffness. After all very little, if any, elastin is synthesized beyond the first year of life.[65]

Calcification

Calcification is another potential mechanism behind inflammation-induced arterial stiffness. Several mediators of inflammation such as oxidation, carbonyl stress, CRP, and cytokines may directly stimulate vascular calcification.[66] This can lead to a phenotypic transformation of vascular smooth muscle cells (VSMCs), which increases bioapatite formation and therefore calcification, as well as a transformation of VSMCs to osteoblast-like cells. Also,

fetuin-A, an endogenous inhibitor of vascular calcification, is downregulated during inflammation, and recently it has been demonstrated that fetuin-A is an independent risk factor for progressive arterial stiffness[67] in patients with chronic kidney disease. A study in children on dialysis, demonstrated that fetuin-A and another physiological inhibitor of calcification (osteoprotegerin) are associated with increased aortic stiffness and calcification.[68] The role of inflammation on arterial stiffening and mechanisms of aortic wall calcification will be further discussed in Chapter 21.

Smooth muscle proliferation and changes in the composition of extracellular matrix

The inflammatory response initiates an accumulation of leukocytes into the vascular endothelium. This can lead to a complex cascade of VSMC activation, migration, and proliferation. The role of vascular smooth muscle dysfunction on arterial stiffness will be discussed in detail in Chapter 22. Activated VSMC can synthesize and secrete biologically active mediators such as endothelin, angiotensin II, cytokines, proteases, collagen, and proteoglycans (PGs) that regulate contraction, relaxation, inflammation, proliferation, apoptosis, and matrix alterations[69] and can therefore subsequently lead to arterial stiffening. Alternatively, inflammation can alter the extracellular matrix (ECM).

ECM is a complex collection of fibrous proteins and glycoproteins, which are embedded in a hydrated ground substance of PGs, proteins with glycosaminoglycan (GAG) chain attached to them.[70] PGs have numerous specific roles within the vascular ECM, such as hydration, filtration, and regulation of various cellular activities as well as inflammatory processes.[71] During atherosclerosis and inflammation arterial GAGs accumulate within the intima, and inflammatory cytokines have the capacity to alter GAGs both quantitatively and qualitatively.[72] In intermediate and advanced atherosclerotic lesions, GAGs such as decorin, versican, biglycan, and hyaluronan (HA) are upregulated, and alterations in HA metabolism, distribution, and function have been documented in various inflammatory disease states.[73] Tissue enriched with HA tends to trap water and swell, forming a viscous hydrate gel which allows the ECM to resist compression forces,[73] making the wall stiffer. In addition, overproduction of HA in the aorta results in stiffening of the arterial wall by thinning of elastic lamellae in animal models.[74] In vitro findings indicate that upregulation of hydrating GAGs leads to an increased water content of the vessel wall.[75]

Direct vascular inflammation
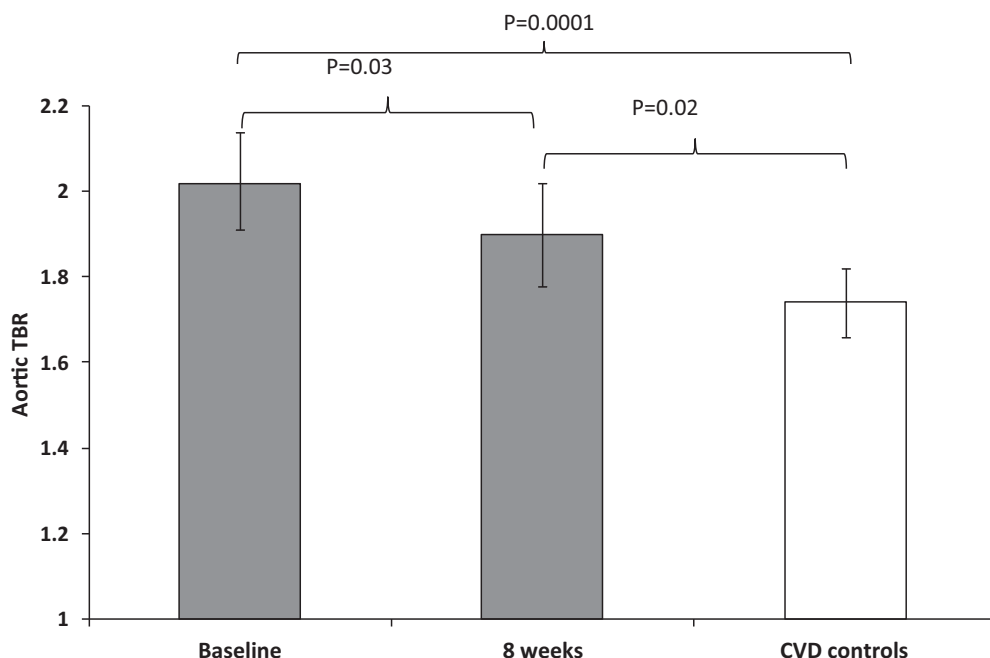
Aortic stiffness in chronic inflammatory conditions may, at least in RA, be driven by direct vascular inflammation. Although the prevalence of clinical vasculitis in RA is low,[76] the results of an autopsy series[77] and histological studies[78] suggest that subclinical vasculitis in RA is may be relatively common. However, it is rarely recognized in clinical practice due to the difficulty in its noninvasive diagnosis.[79] A recent study in patients with severe RA, but without clinically manifest CVD, demonstrated increased aortic inflammation using 18F-FDG PET/CT imaging, in comparison to subjects with established, stable CVD.[28] Additionally, the study demonstrated a reduction in inflammation along the whole aorta (Fig. 20.1A and B), as well as in its most diseased segment following anti-TNF-α therapy, and that the reduction in aortic inflammation correlates with the reduction in CF-PWV. Interestingly, RA patients exhibited a generalized increase in aortic inflammation, rather than focal uptake, suggesting that RA patients exhibit a subclinical vasculitis, rather than increased atherosclerosis, which could provide a potential mechanism for the increased CVD risk seen in RA.[80]

Conclusion

Large number of studies have suggested that inflammation plays a role in arterial stiffening; however, many of these studies are observational studies in patients with inflammatory conditions, whereas the cause–effect studies and placebo-control trials are not as numerous. There are several potential mechanisms which may explain this association, including endothelial dysfunction with subsequent changes in smooth muscle tone, smooth muscle proliferation and activation, changes in the composition of the ECM, and direct vascular inflammation, but further studies are required to ascertain these mechanisms.
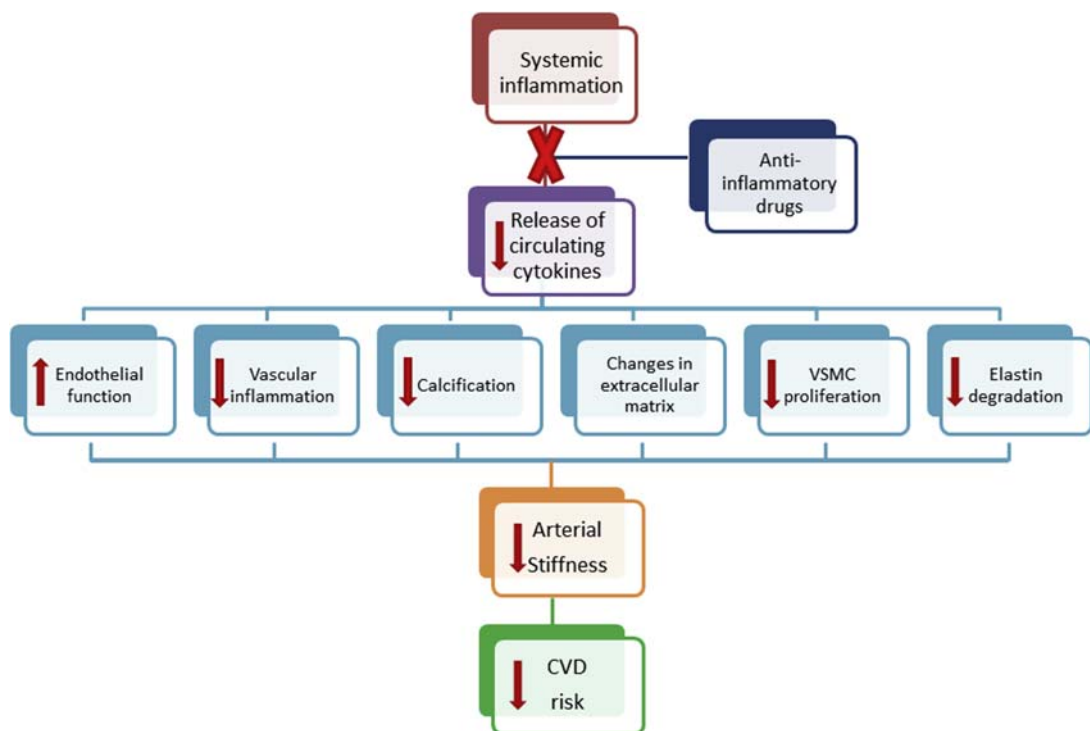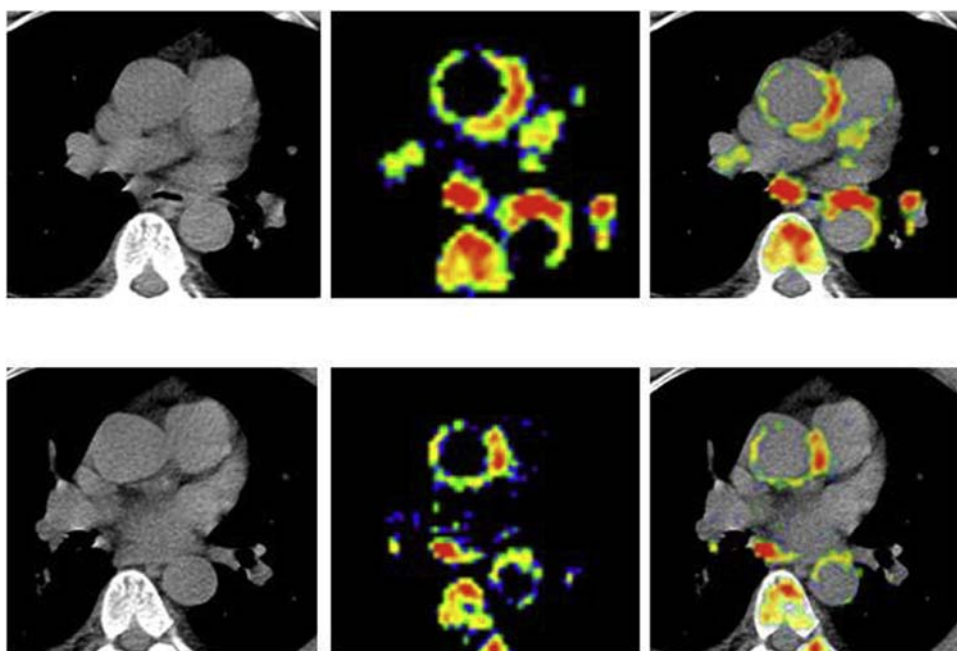
Similarly, the mechanisms by which antiinflammatory therapies lead to a reduction of arterial stiffness are speculative at present (Fig. 20.2). Potentially, treatment with antiinflammatory drugs, leading to reductions in cytokine release, could lead to beneficial changes in the arterial wall composition via improvement of endothelial function, or via reductions of vascular inflammation, and hence, a reduction of the number of inflammatory cells present within the aortic wall. Other potential mechanisms include inhibition of smooth muscle cell proliferation, changes in glycosaminoglycan content of the ECM, reduction of calcification, and inhibition of elastin degrading matrix MMP synthesis. However, studies addressing these possible mechanisms need to be done to ascertain the role of these processes in inflammation-induced arterial stiffening, and large randomized placebo-controlled trials are needed to establish the true effect of antiinflammatory therapies on arterial stiffness, especially in healthy individuals.

FIGURE 20.1A   Effect of anti-TNF-α therapy on ^{18}F-FDG uptake: Tissue to background ratio (TBR) in the whole aorta. Bars represent means and 95% confidence intervals of means. n = 17 RA subjects and n = 34 age-matched controls with stable CVD. *From Mäki-Petäjä et al.* Circulation *2012; 126: 2473−80.*

FIGURE 20.1B   Typical ^{18}F-FDG PET/CT images before and after anti-TNF-α therapy: Axial images of ascending and descending aorta from a typical RA patient. Left to right: CT, ^{18}F-FDG PET, and fused PET/CT images. Baseline images are shown on the top row and after intervention on the bottom row. *From Mäki-Petäjä et al.* Circulation *2012; 126: 2473−80.*

FIGURE 20.2   Potential mechanisms by which antiinflammatory therapies could lead to a reduction of arterial stiffness and the risk of cardiovascular disease.

References

1. Libby P. Inflammation in atherosclerosis. **Nature**. 2002; 420:868−874.

2. Liuzzo G, Biasucci LM, Gallimore JR, et al. The prognostic value of C-reactive protein and serum amyloid a protein in severe unstable angina. **N Engl J Med**. 1994; 331:417−424.

3. Ridker PM, Rifai N, Rose L, Buring JE, Cook NR. Comparison of C-reactive protein and low-density lipoprotein cholesterol levels in the prediction of first cardiovascular events. **N Engl J Med**. 2002; 347:1557−1565.

4. Wolfe F, Mitchell DM, Sibley JT, et al. The mortality of rheumatoid arthritis. **Arthritis Rheum**. 1994; 37:481−494.

5. del Rincon ID, Williams K, Stern MP, Freeman GL, Escalante A. High incidence of cardiovascular events in a rheumatoid arthritis cohort not explained by traditional cardiac risk factors. **Arthritis Rheum**. 2001; 44:2737−2745.

6. Knight JS, Kaplan MJ. Cardiovascular disease in lupus: insights and updates. **Curr Opin Rheumatol**. 2013; 25:597−605.

7. Samarasekera EJ, Neilson JM, Warren RB, Parnham J, Smith CH. Incidence of cardiovascular disease in individuals with psoriasis: a systematic review and meta-analysis. **J Invest Dermatol**. 2013; 133:2340−2346.

8. Sin DD, Man SF. Chronic obstructive pulmonary disease as a risk factor for cardiovascular morbidity and mortality. **Proc Am Thorac Soc**. 2005; 2:8−11.

9. Hancock AT, Mallen CD, Belcher J, Hider SL. Association between polymyalgia rheumatica and vascular disease: a systematic review. **Arthritis Care Res**. 2012; 64:1301−1305.

10. Zieman SJ, Melenovsky V, Kass DA. Mechanisms, pathophysiology, and therapy of arterial stiffness. **Arterioscler Thromb Vasc Biol**. 2005; 25:932−943.

11. Schmitt M, Avolio A, Qasem A, et al. Basal NO locally modulates human iliac artery function in vivo. **Hypertension**. 2005; 46:227−231.

12. McEniery CM, Spratt M, Munnery M, et al. An analysis of prospective risk factors for aortic stiffness in men: 20-year follow-up from the Caerphilly prospective study. **Hypertension**. 2010; 56:36−43.

13. Jain S, Khera R, Corrales-Medina VF, Townsend RR, Chirinos JA. Inflammation and arterial stiffness in humans. **Atherosclerosis**. 2014; 237:381−390.

14. Schnabel R, Larson MG, Dupuis J, et al. Relations of inflammatory biomarkers and common genetic variants with arterial stiffness and wave reflection. **Hypertension**. 2008; 51:1651−1657.

15. Yasmin, McEniery CM, Wallace S, Mackenzie IS, Cockcroft JR, Wilkinson IB. C-reactive protein is associated with arterial stiffness in apparently healthy individuals. **Arterioscler Thromb Vasc Biol**. 2004; 24:969−974.

16. Lieb W, Larson MG, Benjamin EJ, et al. Multimarker approach to evaluate correlates of vascular stiffness: the Framingham Heart Study. **Circulation**. 2009; 119:37−43.

17. Mattace-Raso FU, van der Cammen TJ, van der Meer IM, et al. C-reactive protein and arterial stiffness in older adults: the Rotterdam Study. **Atherosclerosis**. 2004; 176:111−116.

18. Johansen NB, Vistisen D, Brunner EJ, et al. Determinants of aortic stiffness: 16-year follow-up of the Whitehall II study. **PLoS One**. 2012; 7:e37165.

19. Schumacher W, Cockcroft J, Timpson NJ, et al. Association between C-reactive protein genotype, circulating levels, and aortic pulse wave velocity. **Hypertension**. 2009; 53:150−157.

20. Elliott P, Chambers JC, Zhang W, et al. Genetic Loci associated with C-reactive protein levels and risk of coronary heart disease. **J Am Med Assoc**. 2009; 302:37−48.

21. Wallace SM, Maki-Petaja KM, Cheriyan J, et al. Simvastatin prevents inflammation-induced aortic stiffening and endothelial dysfunction. **Br J Clin Pharmacol**. 2010; 70:799−806.

22. Vlachopoulos C, Dima I, Aznaouridis K, et al. Acute systemic inflammation increases arterial stiffness and decreases wave reflections in healthy individuals. **Circulation**. 2005; 112:2193−2200.

23. Booth AD, Wallace S, McEniery CM, et al. Inflammation and arterial stiffness in systemic vasculitis: a model of vascular inflammation. **Arthritis Rheum**. 2004; 50:581−588.

24. Chanouzas D, Dyall L, Dale J, Moss P, Morgan M, Harper L. CD4+CD28- T-cell expansions in ANCA-associated vasculitis and association with arterial stiffness: baseline data from a randomised controlled trial. **Lancet**. 2015; 385(Suppl 1):S30.

25. Upala S, Yong WC, Sanguankeo A. Increased arterial stiffness in Behçet's disease: a systematic review and meta-analysis. **Korean Circ J**. 2017; 47:477−482.

26. Dregan A. Arterial stiffness association with chronic inflammatory disorders in the UK Biobank study. **Heart**. 2018; 104:1257−1262.

27. Maki-Petaja KM, Hall FC, Booth AD, et al. Rheumatoid arthritis is associated with increased aortic pulse-wave velocity, which is reduced by anti-tumor necrosis factor-alpha therapy. **Circulation**. 2006; 114:1185−1192.

28. Maki-Petaja KM, Elkhawad M, Cheriyan J, et al. Anti-tumor necrosis factor-alpha therapy reduces aortic inflammation and stiffness in patients with rheumatoid arthritis. **Circulation**. 2012; 126:2473−2480.

29. Angel K, Provan SA, Gulseth HL, Mowinckel P, Kvien TK, Atar D. Tumor necrosis factor-alpha antagonists improve aortic stiffness in patients with inflammatory arthropathies: a controlled study. **Hypertension**. 2010; 55:333−338.

30. Ambrosino P, Lupoli R, Di Minno A, Tasso M, Peluso R, Di Minno MN. Subclinical atherosclerosis in patients with rheumatoid arthritis. A meta-analysis of literature studies. **Thromb Haemost**. 2015; 113:916−930.

31. Zanoli L, Boutouyrie P, Fatuzzo P, et al. Inflammation and aortic stiffness: an individual participant data meta-analysis in patients with inflammatory bowel disease. **J Am Heart Assoc**. 2017; 6.

32. Wang P, Mao YM, Zhao CN, et al. Increased pulse wave velocity in systemic lupus erythematosus: a meta-analysis. **Angiology**. 2018; 69:228−235.

33. Meiszterics Z, Tímár O, Gaszner B, et al. Early morphologic and functional changes of atherosclerosis in systemic sclerosis-a systematic review and meta-analysis. **Rheumatology**. 2016; 55:2119−2130.

34. Wang LY, Zhu YN, Cui JJ, Yin KQ, Liu SX, Gao YH. Subclinical atherosclerosis risk markers in patients with chronic obstructive pulmonary disease: a systematic review and meta-analysis. **Respir Med**. 2017; 123:18−27.

35. Leite LHM, Cohen A, Boccara F. HIV infection and aortic stiffness. **Arch Cardiovasc Dis**. 2017; 110:495−502.

36. Pieringer H, Stuby U, Hargassner S, Biesenbach G. Treatment with corticosteroids reduces arterial stiffness in patients with polymyalgia rheumatica as measured with pulse wave analysis. **Ann Rheum Dis**. 2008; 67:279.

37. Schillaci G, Bartoloni E, Pucci G, et al. Aortic stiffness is increased in polymyalgia rheumatica and improves after steroid treatment. **Ann Rheum Dis**. 2012; 71:1151−1156.

38. Wong M, Jiang BY, McNeill K, Farish S, Kirkham B, Chowienczyk P. Effects of selective and non-selective cyclo-oxygenase inhibition on endothelial function in patients with rheumatoid arthritis. **Scand J Rheumatol**. 2007; 36:265−269.

39. Maxwell SR, Moots RJ, Kendall MJ. Corticosteroids: do they damage the cardiovascular system? **Postgrad Med J**. 1994; 70:863−870.

40. Slot O. Changes in plasma homocysteine in arthritis patients starting treatment with low-dose methotrexate subsequently supplemented with folic acid. **Scand J Rheumatol**. 2001; 30:305−307.

41. Gislason GH, Jacobsen S, Rasmussen JN, et al. Risk of death or reinfarction associated with the use of selective cyclooxygenase-2 inhibitors and nonselective nonsteroidal antiinflammatory drugs after acute myocardial infarction. **Circulation**. 2006; 113:2906−2913.

42. Mitchell GF, Verwoert GC, Tarasov KV, et al. Common genetic variation in the 3'-BCL11B gene desert is associated with carotid-femoral pulse wave velocity and excess cardiovascular disease risk: the AortaGen Consortium. **Circ Cardiovasc Genet**. 2012; 5:81−90.

43. Tam LS, Shang Q, Li EK, et al. Infliximab is associated with improvement in arterial stiffness in patients with early rheumatoid arthritis – a randomized trial. **J Rheumatol**. 2012; 39:2267−2275.

44. McInnes IB, Thompson L, Giles JT, et al. Effect of interleukin-6 receptor blockade on surrogates of vascular risk in rheumatoid arthritis: MEASURE, a randomised, placebo-controlled study. **Ann Rheum Dis**. 2015; 74:694−702.

45. Ikonomidis I, Papadavid E, Makavos G, et al. Lowering interleukin-12 activity improves myocardial and vascular function compared with tumor necrosis factor-a antagonism or cyclosporine in psoriasis. **Circ Cardiovasc Imaging**. 2017; 10.

46. Pina T, Corrales A, Lopez-Mejias R, et al. Anti-tumor necrosis factor-alpha therapy improves endothelial function and arterial stiffness in patients with moderate to severe psoriasis: a 6-month prospective study. **J Dermatol**. 2016; 43:1267−1272.

47. Zanoli L, Rastelli S, Inserra G, et al. Increased arterial stiffness in inflammatory bowel diseases is dependent upon inflammation and reduced by immunomodulatory drugs. **Atherosclerosis**. 2014; 234:346−351.

48. Capkin E, Karkucak M, Kiris A, et al. Anti-TNF-α therapy may not improve arterial stiffness in patients with AS: a 24-week follow-up. **Rheumatology**. 2012; 51:910−914.

49. Mathieu S, Pereira B, Couderc M, Rabois E, Dubost JJ, Soubrier M. No significant changes in arterial stiffness in patients with ankylosing spondylitis after tumour necrosis factor alpha blockade treatment for 6 and 12 months. **Rheumatology**. 2013; 52:204−209.

50. Tomochika Y, Okuda F, Tanaka N, et al. Improvement of athero-sclerosis and stiffness of the thoracic descending aorta with cholesterol-lowering therapies in familial hypercholesterolemia. **Arterioscler Thromb Vasc Biol**. 1996; 16:955−962.

51. Muramatsu J, Kobayashi A, Hasegawa N, Yokouchi S. Hemody-namic changes associated with reduction in total cholesterol by treatment with the HMG-CoA reductase inhibitor pravastatin. **Atherosclerosis**. 1997; 130:179−182.

52. Maki-Petaja KM, Wilkinson IB. Anti-inflammatory drugs and statins for arterial stiffness reduction. **Curr Pharm Des**. 2009; 15:290−303.

53. Wallace SM, Yasmin, McEniery CM, et al. Isolated systolic hyper-tension is characterized by increased aortic stiffness and endothelial dysfunction. **Hypertension**. 2007; 50:228−233.

54. Hingorani AD, Cross J, Kharbanda RK, et al. Acute systemic inflammation impairs endothelium-dependent dilatation in humans. **Circulation**. 2000; 102:994−999.

55. Gunnett CA, Lund DD, McDowell AK, Faraci FM, Heistad DD. Mechanisms of inducible nitric oxide synthase-mediated vascular dysfunction. **Arterioscler Thromb Vasc Biol**. 2005; 25:1617−1622.

56. Fichtlscherer S, Breuer S, Schachinger V, Dimmeler S, Zeiher AM. C-reactive protein levels determine systemic nitric oxide bioavail-ability in patients with coronary artery disease. **Eur Heart J**. 2004; 25:1412−1418.

57. Xu J, Xie Z, Reece R, Pimental D, Zou MH. Uncoupling of endo-thelial nitric oxidase synthase by hypochlorous acid: role of NAD(P) H oxidase-derived superoxide and peroxynitrite. **Arterioscler Thromb Vasc Biol**. 2006; 26:2688−2695.

58. Laursen JB, Somers M, Kurz S, et al. Endothelial regulation of vasomotion in apoE-deficient mice: implications for interactions be-tween peroxynitrite and tetrahydrobiopterin. **Circulation**. 2001; 103:1282−1288.

59. Kinoshita H, Tsutsui M, Milstien S, Tetrahydrobiopterin KZS. Nitric oxide and regulation of cerebral arterial tone. **Prog Neuro Biol**. 1997; 52:295−302.

60. Wallberg-Jonsson S, Cvetkovic JT, Sundqvist KG, Lefvert AK, Rantapaa-Dahlqvist S. Activation of the immune system and in-flammatory activity in relation to markers of atherothrombotic disease and atherosclerosis in rheumatoid arthritis. **J Rheumatol**. 2002; 29:875−882.

61. Savage CO, Pottinger BE, Gaskin G, Pusey CD, Pearson JD. Auto-antibodies developing to myeloperoxidase and proteinase 3 in sys-temic vasculitis stimulate neutrophil cytotoxicity toward cultured endothelial cells. **Am J Pathol**. 1992; 141:335−342.

62. Morel DW, Hessler JR, Chisolm GM. Low density lipoprotein cytotoxicity induced by free radical peroxidation of lipid. **J Lipid Res**. 1983; 24:1070−1076.

63. Yasmin WS, McEniery CM, Dakham Z, et al. Matrix metalloproteinase-9 (MMP-9), MMP-2, and serum elastase activity are associated with systolic hypertension and arterial stiffness. **Arterioscler Thromb Vasc Biol**. 2005; 25:372.

64. Yasmin, McEniery CM, O'Shaughnessy KM, et al. Variation in the human matrix metalloproteinase-9 gene is associated with arterial stiffness in healthy individuals. **Arterioscler Thromb Vasc Biol**. 2006; 26:1799−1805.

65. Martyn CN, Greenwald SE. Impaired synthesis of elastin in walls of aorta and large conduit arteries during early development as an initiating event in pathogenesis of systemic hypertension. **Lancet**. 1997; 350:953−955.

66. Moe SM, Chen NX. Inflammation and vascular calcification. **Blood Purif**. 2005; 23:64−71.

67. Ford ML, Tomlinson LA, Smith ER, Rajkumar C, Holt SG. Fetuin-A is an independent determinant of change of aortic stiffness over 1 year in non-diabetic patients with CKD stages 3 and 4. **Nephrol Dial Transplant**. 2010; 25:1853−1858.

68. Shroff RC, Shah V, Hiorns MP, et al. The circulating calcification inhibitors, fetuin-A and osteoprotegerin, but not matrix Gla protein, are associated with vascular stiffness and calcification in children on dialysis. **Nephrol Dial Transplant**. 2008; 23:3263−3271.

69. Dzau VJ, Braun-Dullaeus RC, Sedding DG. Vascular proliferation and atherosclerosis: new perspectives and therapeutic strategies. **Nat Med**. 2002; 8:1249−1256.

70. Raines EW. The extracellular matrix can regulate vascular cell migration, proliferation, and survival: relationships to vascular disease. **Int J Exp Pathol**. 2000; 81:173−182.

71. Jacob MP. Extracellular matrix remodeling and matrix metalloproteinases in the vascular wall during aging and in pathological conditions. **Biomed Pharmacother**. 2003; 57:195−202.

72. Kaji T, Hiraga S, Yamamoto C, et al. Tumor necrosis factor alpha-induced alteration of glycosaminoglycans in cultured vascular smooth-muscle cells. **Biochim Biophys Acta**. 1993; 1176:20−26.

73. Toole BP, Wight TN, Tammi MI. Hyaluronan-cell interactions in cancer and vascular disease. **J Biol Chem**. 2002; 277:4593−4596.

74. Chai S, Chai Q, Danielsen CC, et al. Overexpression of hyaluronan in the tunica media promotes the development of atherosclerosis. **Circ Res**. 2005; 96:583−591.

75. Li D, Fayad ZA, Bluemke DA. Can contrast-enhanced cardiac magnetic resonance assess inflammation of the coronary wall? **JACC Cardiovasc Imaging**. 2009; 2:589−591.

76. Watts RA, Mooney J, Lane SE, Scott DG. Rheumatoid vasculitis: becoming extinct? **Rheumatology**. 2004; 43:920−923.

77. Gravallese EM, Corson JM, Coblyn JS, Pinkus GS, Weinblatt ME. Rheumatoid aortitis: a rarely recognized but clinically significant entity. **Medicine (Baltim)**. 1989; 68:95−106.

78. Hollan I, Prayson R, Saatvedt K, et al. Inflammatory cell infiltrates in vessels with different susceptibility to atherosclerosis in rheumatic and non-rheumatic patients: a controlled study of biopsy specimens obtained at coronary artery surgery. **Circ J**. 2008; 72:1986−1992.

79. Hollan I, Meroni PL, Ahearn JM, et al. Cardiovascular disease in autoimmune rheumatic diseases. **Autoimmun Rev**. 2013; 12:1004−1015.

80. Fayad ZA, Greenberg JD, Bucerius J. Subclinical vasculitis as a potential mechanism to explain the heightened cardiovascular risk in rheumatoid arthritis. **Circulation**. 2012; 126:2449−2451.

This page intentionally left blank

Mechanisms of calcification in the aortic wall and aortic valve

Livia Silva Araújo Passos, Dakota Becker-Greene and Elena Aikawa
The Center for Excellence in Vascular Biology, Brigham and Women's Hospital, Harvard Medical School, Boston, MA, United States

Cardiovascular events associated with calcification in the aortic wall and aortic valve

Increased life expectancy over the past several decades has caused a surge in the burden of cardiovascular diseases (CVDs), leading to high mortality, morbidity, and overall healthcare costs.[1] The heart and vasculature undergo numerous alterations during the aging process, primarily as a result of deregulation of molecular longevity pathways, causing impaired vascular structure and function.[2] Age-related CVDs include coronary heart disease, peripheral arterial disease, valvular heart diseases, heart failure, stroke, and vascular dementia.[1,3] In general, the relationship between the average human lifespan and the occurrence of CVDs can be related to two pathologic processes: atherosclerosis (which leads to atherothrombotic events, including myocardial infarction) and large artery stiffening (a general reduction of elasticity in large arteries over time), which causes isolated systolic hypertension and contributes to the development of heart failure, age-related cognitive dysfunction, and chronic renal disease, among others. In children and young adults, CVDs are uncommon due to high tissue durability and elasticity; however, those become weakened with age due to pathologic matrix remodeling, which results in fibrosis and calcification.[4,5] Epidemiological studies have shown extensive age-associated vascular changes that constitute a central etiologic component of CVDs.[5] Among these changes are an individual's immune response, genetic background, comorbidities, environmental exposures, and overall lifestyle.[6–8] These factors can strongly influence the variability and severity of CVD.

Among CVDs, atherosclerosis, aortic wall calcification, and calcific aortic valve disease (CAVD) remain the primary contributors to mortality worldwide, with ectopic mineralization as the central condition.[9] Although these diseases share several risk factors, they cannot be generalized as the same disorder. Only ∼25%−50% of patients with CAVD also present with significant coronary artery disease, suggesting divergent pathological processes.[10] Similarly, large artery stiffening and calcification of the medial layer of the aorta can occur in the absence of atherosclerosis. Aortic wall calcification, CAVD, and large artery stiffening manifest clinically in middle to late adulthood, with increasing severity over time.[11] Similar to many progressive disorders, it has a long subclinical phase, hampering early diagnosis that could reduce future complications.[12]

Advanced calcification in the intimal layer of atherosclerotic plaques has been associated with stable atheroma.[13] However, the link between calcification and plaque rupture, while predicted computationally, is still clinically unproved and an ongoing topic of debate in the field. While macrocalcification can act as a biomechanical stabilizer, microcalcifications have a predisposition of susceptibility to rupture.[14–16] Moreover, calcification reduces aortic wall elasticity.[17] Atherosclerotic plaque rupture can cause subsequent acute events, such as myocardial infarction and stroke.[5] Nonatherosclerotic calcification, common in chronic kidney disease (CKD), affects the medial layer of the ascending aorta and aortic arch; therefore, impacting the efficacy of aortic valve replacement and most treatments of severe aortic stenosis.[18,19]

In aortic valves, calcification reduces leaflet compliance and fails to maintain directionality of blood flow from the left ventricle to systemic circulation.[20–22] Additionally, calcium deposits damage the structural integrity of aortic leaflets, therefore, interfering with the biomechanical functionality.[23] As a risk factor, arterial calcification leads to a fourfold increase in cardiovascular events.[2,24] The size and density of calcification reflects disease stage, since it usually progresses from small calcium deposits to large and dense calcific masses.[25,26]

This chapter will outline the pathogenic mechanisms of aortic wall and aortic valve stiffness. In addition, it will go in depth into the role that calcification plays in these mechanisms, as well as the important factors associated with the role of hemodynamic shear stress throughout all stages of disease. Furthermore, the synergistic effects of risk factors in vascular endothelial dysfunction will be delineated.

Calcification is a result of multiple synergistic pathogenic processes

Several interconnected cellular and a cellular processes are involved in the nucleation and crystallization of calcium/phosphate, resulting in the formation of hydroxyapatite within the cardiovascular system.[22] As a multifaceted disorder, many factors play a role in disease manifestation and calcification extent, thus influencing the overall clinical outcome.[27] Initial mechanisms of mineralization often overlap among different types of cardiovascular calcification, especially initial vascular endothelial injury caused by mechanical alterations of blood flow. However, mechanisms of pathogenesis secondary to hemodynamic abnormalities differ depending on the localization of ectopic mineralization. In this section, we will first discuss the pathological mechanisms of aortic wall calcification and CAVD, followed by the role of hemodynamic shear stress as an instigator and propagator of disease.

Atherosclerosis and intimal calcification of the aortic wall

The endothelium is a major regulator of arterial vasculature homeostasis, thereby, playing an important role in the pathobiology of atherosclerosis.[28] Many of the risk factors that predispose patients to atherosclerosis cause endothelial damage, which is an early marker of disease.[17,29] Endothelial cell dysfunction in lesion-prone areas leads to alterations in vascular tone, redox balance, and permeability, therefore, trapping low-density cholesterol in the subendothelial space. Endothelial dysfunction will be further discussed in the following topic.
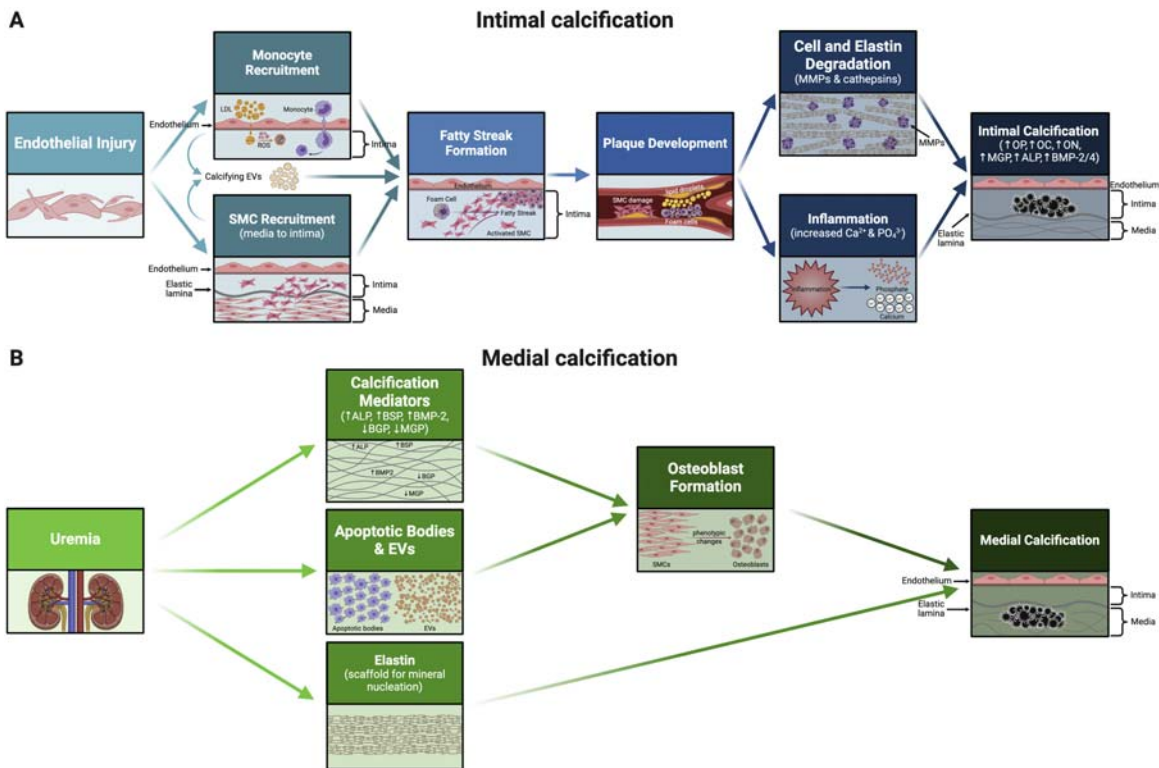
Leukocytes are recruited into the intimal and medial layers of the vessel wall (Fig. 21.1). Circulating monocytes differentiate into macrophages, which internalize modified lipoprotein and become foam cells (lipid-laden macrophages).[30] The breakdown of local homeostasis modifies cytokines, chemokines, and growth factor production, thereby, fueling the recruitment of circulating cells and neighboring vascular smooth muscle cells (SMCs) into arterial wall layers (Fig. 21.1).[31,32] Vascular SMCs are nonstriated, nonvoluntary, contractile cells that are essential for maintaining the blood pressure of vessels through contraction and relaxation in opposition to the heart.[33] In addition, SMCs participate in remodeling the extracellular matrix (ECM).[34]

Inflammatory milieu favors structural remodeling through synthesis and degradation of ECM components and cell proliferation.[35,36] Progressive tissue remodeling results in the formation of a fibrous cap, rich in oxidized lipids, cholesterol crystals, and cellular debris, referred to as the necrotic core. Other immune cell types, including dendritic cells, T cells, and natural killer T-cells, are also abundant in fibroadipose plaques, where they contribute to a proinflammatory environment and production of proteases.[22] Foam cells release proinflammatory cytokines, such as TNF-α, that contribute to arterial calcification (Fig. 21.1).[37] TNF-α induces SMC differentiation into an osteogenic phenotype, which releases calcifying extracellular vesicles (EVs).[32] Furthermore, TNF-α upregulates endothelial cell production of bone morphogenetic protein (BMP), a soluble factor associated with the formation of bone and cartilage.[38] An abundance of proinflammatory macrophages was associated with the presence of calcification in the arterial wall.[26,39]

SMC phenotype differentiation in atherosclerosis involves downregulation of contractile proteins, increased proliferation, and ECM remodeling capacity to facilitate migration of the cells to sites within tissue.[32] Calcific vascular SMC phenotypes include osteogenic, chondrocytic, and osteoclastic. An osteo/chondrogenic phenotype is characterized by the ability to release calcifying vesicles and the gain of osteochondrogenic markers, such as RUNX2, osteopontin (OP), osteocalcin (OC), and alkaline phosphatase (ALP).[40,41] In addition, SMCs can assume adipogenic and macrophagic phenotypes.[42] Therefore, arterial plaque calcification is best conceptualized as a convergence of vascular inflammatory pathobiology and bone biology.

Arterial wall calcification demonstrates bone-like organization with lamellar structure.[43] Intimal calcification leads to arterial obstruction and plaque rupture, while medial calcification is linked to vessel stiffness, systolic hypertension, and increased pulse wave velocity favoring left ventricular hypertrophy and multiple other cardiovascular disorders (as discussed in Chapter 10).[44] Microcalcifications (<15 μm particles) are observed throughout the lesion, but become harmful when located within the fibrous cap, whereas macrocalcifications are found in the deep intima adjacent to the internal elastic lamella and tunica media. While macrocalcification contributes to vessel stiffness and potentially to plaque stabilization, it can also lead to devastating organ dysfunction depending on its location and extent, which can culminate in myocardial infarction, stroke, and valve incompetence.[45]

FIGURE 21.1 Mechanisms of different types of aortic calcification: intimal atherosclerotic calcification versus medial nonatherosclerotic calcification. (A) Intimal calcification. Endothelial injury initiates the transport of monocytes and low-density lipoprotein (LDL) into the intima, as well as the migration and proliferation of vascular smooth muscle cells (SMCs) from the media to the intima. Additionally, calcifying extracellular vesicles (EVs) contribute to fatty streak formation. Layers of foam cells and activated SMCs form fatty streaks in the intima. Intermediate lesions contain scattered collections of lipid droplets with damaged SMCs that experience phenotype trans differentiation. As this process progresses, elastin and cell degradation, along with MMPs and cathepsins, acts as a scaffold for mineral deposition and inflammation that may elevate extracellular calcium (Ca^{2+}) and phosphate (PO_4^{3-}), followed by intimal calcification. SMCs and intimal macrophages produce many calcification-regulating proteins commonly found in bone, such as osteopontin (OP), osteocalcin (OC), osteonectin (ON), matrix Gla protein (MGP), alkaline phosphatase (ALP), and bone morphogenetic protein 2 (BMP-2). (B) Medial calcification. Uremia induces a change in a number of bone-associated proteins not normally expressed in the vessel wall, including ALP, bone sialoprotein (BSP), and BMP-2. There is also evidence of downregulation of MGP bone Gla protein (BGP), which is known to inhibit medial calcification. Apoptotic bodies derived from dying SMCs and calcifying extracellular vesicles (EVs) released from SMCs are also essential contributors. Both of these cause phenotypic changes in smooth muscle cells (SMCs) forming osteoblasts, which lead to medial calcification. Separately, elastin acts as a scaffold for mineral nucleation, ultimately leading to medial calcification.

Nonatherosclerotic medial aortic wall calcification

Calcification can occur independently of atherosclerosis, thereby, affecting the medial layer of the arterial media in the ascending aorta and aortic arch, often affecting patients with CKD and diabetes.[46,47] In those cases, hydroxyapatite crystals deposit in the media along elastin fibers directly neighboring SMCs in the absence of cholesterol deposits.[48] Elastin degradation is mediated by metalloproteinases (MMPs) and serves as an initiation nidus for medial calcification (Fig. 21.1).[47] In addition, it is possible for elastic lamellae to create a barrier between SMCs, limiting calcification in the medial layer.[49] While a strong inflammatory component is sufficient to create the conditions for nucleating calcium phosphates in the absence of hypophosphatemia in atherosclerosis and CAVD, a localized inflammatory response has not been observed in medial calcification.[39] In this type of calcification both intra- and extracellular calcium deposits are present. Intracellular deposits are located in SMCs and extracellular deposits are largely associated with damaged elastic fibers embedded within the ECM[46] and other ECM components, including collagen. Even though atherosclerotic and medial calcification might be two separate entities, their pathogenesis have considerable overlap.

As medial calcification has been frequently associated with type 2 diabetes, end-stage renal disease, and is commonly associated with osteoporosis, demonstrating the central role of mineral metabolism in the pathogenesis of this disorder,[50–52] this disorder is considered a process of metabolite-induced vascular changes. However, the pathophysiological mechanisms contributing to the formation of medial calcification are not fully understood. Experimental

models are widely used to study medial calcification. The rabbit model of CKD shows early morphologic changes in the aortic media with rupture of elastic lamellae and increased ECM in the absence of a high-cholesterol diet. After 3 months of follow-up in these animals, they maintain media degeneration with calcification, but not in the intima.[53] Arteries taken from humans with CKD show calcification of the arterial media, but not the intima, even in patients with a moderate increase of serum creatinine.[48] Additionally, no lipid or cholesterol deposits were observed in the vicinity of the medial calcification in these patients.[48] In type 2 diabetes, patients' medial calcification is the most common form of vascular calcification, mostly affecting the media of peripheral arteries and is more severe in hemodialysis patients.[54,55] Elastin degradation occurs because of SMC proliferation, leading to collagen becoming the principal ECM component of the arterial wall. Collagen can be glycated in patients with diabetes, thereby, promoting arterial wall stiffening.[56,57]

Alterations in mineral metabolism and vascular inflammation induce phenotypic changes of SMCs into osteoblasts in the medial layer (Fig. 21.1). Transformed osteoblasts produce bone-associated proteins, such as ALP, bone sialoprotein (BSP), and BMP-2.[49,58] Apoptotic bodies and EVs from SMCs also contribute to medial calcification by facilitating mineral nucleation.[59]

Aside from CKD, mediastinal radiation can cause medial and intimal calcification in the aortic wall.[60,61] The cumulative incidence of radiation that leads to heart disease is between 10% and 30% and occurs on average 5–10 years after initial treatment.[62] Current radiotherapy techniques, such as those used to treat breast cancer, have measures in place that protect the heart and ascending aorta in order to minimize cardiac and aortic damage.

Medial calcification induces stiffening of the vessel, increased pulse pressure, and left ventricular hypertrophy, which can result in heart failure. The differentiation between intimal (atherosclerotic) and medial (non-atherosclerotic) calcification may have clinical implications, especially because it can complicate surgical aortic valve replacement and treatment of severe aortic stenosis since it is accessed via the ascending aorta.[18,19] Furthermore, large calcification in the medial layer may induce secondary changes in the intima. Medial calcification in the ascending aorta and aortic arch interferes with aortic cannulation, clamping, aortotomy, and central coronary bypass anastomosis.[63] Therefore, medial calcification increases the morbidity and mortality, especially as a result of increased operative risk. Vascular stiffness of the aorta may lead to congestive heart failure, left ventricular hypertrophy, elevated pulse pressure, coronary ischemia, or sudden death resulting from arrhythmia.

Arterial medial calcification is commonly diagnosed by manual palpation performed after sternotomy and exposure of the aorta at the time of cardiac surgery. Chest X-ray and fluoroscopy during coronary angiography might reveal a calcific outline of the ascending aorta. However, there is no accurate imaging modality to differentiate intimal and medial calcification or assess its extent.

Calcific aortic valve disease

Despite the similarities in the mechanisms of intimal and aortic valve calcification, fewer than 50% of patients develop calcification of both atherosclerotic plaques and aortic valve, indicating that those disorders involve different pathogenic mechanisms.[64] The normal aortic valve maintains unidirectional blood flow from the left ventricle into the aorta. In CAVD, the leaflets become thick, stiff, scarred, and calcified, leading to decreased pliability and narrowing of the valve orifice.[65] Early disease is characterized by aortic sclerosis, where ventricular outflow remains intact and progresses to aortic stenosis, which includes ventricular outflow obstruction.[66] Calcium nodular deposits develop within the fibrosa layer at the base of the leaflet.[67] For decades, this disease was thought to be a passive process in which the valve degenerates with age.[27] It is a fact that CAVD has a higher prevalence in the elderly population; however, is not exclusively a "senile" or "degenerative" disorder, suggesting pathological influences other than age play a role.[66]

As with atherosclerosis, valve endothelial cells (VECs) play a key role in the initiation of tissue injury, since they are positioned to sense hemodynamic forces and encounter circulating factors.[68] Oxidative stress is also an early disease event associated with inactivation of endothelial nitric oxide synthase (eNOS), contributing to an abnormal oxidative state.[69] Levels of superoxide and hydrogen peroxide are markedly increased in calcified stenotic human valves.[70]

VECs are phenotypically different from other vascular endothelial cells.[71] The role of hemodynamic forces in valvular endothelial dysfunction and its impact on cardiovascular calcification will be discussed further in the following topic. Located below the endothelium, VICs are the most abundant and diverse valve resident cells, responsible for synthesis of the ECM and expression of matrix degrading enzymes.[72] VECs interact with VICs to maintain the integrity of valve tissue, therefore, this connection may mediate disease.
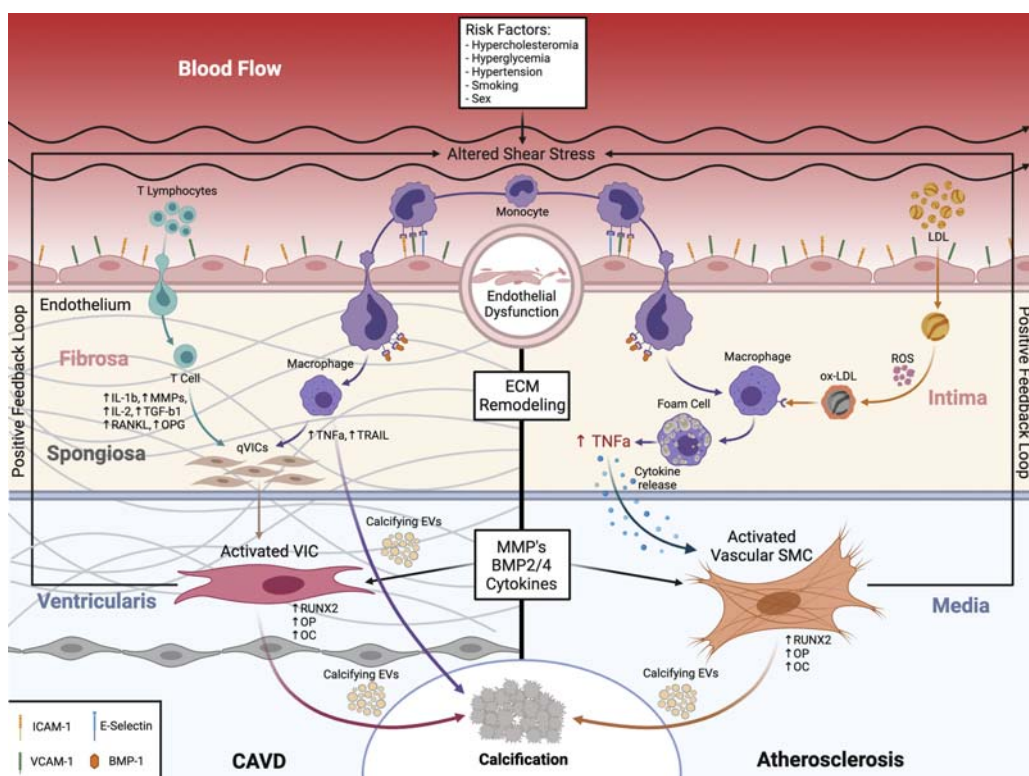
Endothelium damage favors infiltration of inflammatory cells, lipid oxidation, and deposition on the valve surface.[23] Studies have shown that among VICs, there are a small number of circulating progenitors and mesenchymal progenitor-like cells, which likely form after transitioning from endothelial cells.[73,74] The local cytokine environment promotes the activation of VICs, which are a very plastic population that can differentiate into several phenotypes. In

pathological circumstances, VICs shift from quiescent resting fibroblasts to a variety of activated cell types, including myofibroblasts and osteoblasts.[75] Valve myofibroblasts express alpha-smooth muscle actin, leading to an increase in proliferative and ECM remodeling capacity.[75] Additionally, valve myofibroblasts migrate to injured sites and develop angiogenic activity.[76] VICs expressing an osteoblast-like phenotype secrete ALP, OC, OP, BMP-2, 4, and BSP (Fig. 21.2).[66] Different VIC phenotypes may exhibit plasticity and convert from one form to another. In vitro VICs undergo osteoblastic differentiation in the presence of TGF-β and BMPs.[77]

Matrix Gla protein (MGP), a γ-carboxyglutamic acid−rich and vitamin K-dependent protein, is a well-known ectopic calcification inhibitor.[78,79] MGP is a small secretory protein produced by chondrocytes and SMCs. Studies show that MGP antagonizes BMP-2 and protects against vascular calcification.[80] Treatment of VICs isolated from CAVD patients with TNF-α induces calcification and increases BMP-2 expression, accompanied by a strong decrease of MGP.[81] Experimental mouse models of MGP deficiency show early valve calcification, whereas transgenic mice that overexpress MGP are protected.[82] The MGP pathway is also implicated in atherosclerosis.[80]

Human histological studies have shown that CAVD specimens demonstrate rich lymphocytic infiltrates that are composed of macrophages, B cells, and T cells found near osteoblast-like cells and calcified areas.[23,83] Previously, Aikawa E. et al. showed an association between macrophage burden and osteogenesis in experimental early-stage CAVD and atherosclerosis by using near-infrared optical fluorescence molecular imaging. Those findings reinforce the inflammation-dependent mechanisms of calcification and identified the stages of disease progression.[25,26,39] Immune cells secrete inflammatory cytokines, including IL-2, IL-6, IL-1β, TNF-α, and MMPs, which promote the expression of genes involved in osteogenesis by VICs.[22,84] Altogether, it is a consensus in the field that many

FIGURE 21.2 Major pathogenic events underlying the mechanisms of calcification in intimal, medial, and aortic valve calcification. Altered shear stress leads to endothelial dysfunction denoted by increased expression of adhesion molecules, ICAM-1, VCAM-1, and E-Selectin, as well as trapping of low-density lipoprotein (LDL) cholesterol. The recruited LDL takes up reactive oxygen species (ROS), becoming oxidized-LDL (ox-LDL). In turn, ox-LDL binds to macrophages binding high levels of BMP-1, and become foam cells. Foam cells increase TNFα expression, releasing cytokines. Activation of quiescent VICs (qVICs) occurs through T cells overexpressing IL-1β, IL-2, TGFβ1, RANKL, OPG, and releasing MMPs. In addition, macrophages overexpressing TNFα and TRAIL contribute to qVIC activation. Taken together, these changes stimulate the differentiation of VICs and SMCs into an osteogenic phenotype, identified primarily by overexpression of RUNX2, osteopontin (OP), and osteocalcin (OC). These osteoblast-like cells release active vesicles capable of nucleating hydroxyapatite. The inflammatory process is associated with extensive remodeling of the ECM. Calcification causes a positive feedback loop of changes in the tissue affecting its architecture, cell biology, and hemodynamic parameters, which maintain a self-perpetuating pathogenic cycle.

pathogenic factors are centered on an inflammatory process affecting the valve and leading to calcification, supporting that CAVD is an inflammatory disease. Overall, recent studies support the notion that inflammation occurs secondarily in injured tissue, and CAVD is a manifestation of an inflammatory disease.

The role of hemodynamic shear stress in vascular calcification

One of the most discussed and intriguing questions in the field of vascular calcification is how the promoters of pathological cascade culminate in fibrosis and mineralization within the cardiovascular system. As a multifaceted disorder of unclear etiology, it is a very difficult question to be answered. Several studies have shown that shear stress alterations trigger vascular endothelial lesions that ultimately calcify.[85-88] Changes in tissue biology and architecture associated with calcium deposition sustain a self-perpetuating vicious cycle, as this worsens mechanical stress.[89]

The flow of blood, by virtue of viscosity, exerts force on the luminal vessel wall and endothelial surface per unit area, known as hemodynamic shear stress.[29] Physiologic, laminar shear stress is crucial for normal vascular function, as it regulates vascular caliber, acts as a protective barrier, and inhibits proliferation, thrombosis, and inflammation of the vessel wall.[89] In pathological conditions, blood flow is disturbed and/or is nonlaminar, creating force that is mechanically transduced into a biochemical signal that changes vascular behavior.[88] Systemic hypertension and stiffness of the aortic root associated with aging processes may cause abnormal mechanical stress, a common denominator of several vascular pathologies.[3] Cohort studies have demonstrated that systolic blood pressure is related to the risk of atherosclerosis and aortic stenosis, supporting the causality of hypertension and cardiovascular calcification.[90,91] Initial endothelial vascular injury has a distinctive, nonrandom pattern, which matches with points of altered hemodynamics.[68]

In the aorta, arterial branch ostia and bifurcations are prone to lesion development, since this curvature slows blood flow, creating low or oscillatory shear stress. In contrast, vessel regions that are exposed to steady blood flow generally do not develop disease.[89] Decreased shear stress leads to the reduction of eNOS production by vascular endothelial cells, therefore, impacting vasodilatation and endothelial cell repair, accompanied by an increase of reactive oxygen species (ROS).[68] *In vivo* studies show that vascular SMCs are also responsive to shear stress.[92] Furthermore, the level of shear stress is inversely correlated with intimal SMC density, whereas exposure to physiologic flow did not influence cell density.[92] It is likely that shear stress acts through the endothelium to modulate SMC gene expression. Moreover, oxidized low-density lipoprotein (LDL) uptake in the intimal layer is favored during decreased flow conditions.[93]

Large DNA array-based genomic analysis studies in endothelial cells have shown gene sets regulated in response to either physiological or mechanical altered blood flow.[87,94] Furthermore, many of the shear-regulated factors fall into functional classes directly related to endothelial cell biology, including nitric oxide (NO) and TGF-β. It was also shown that altered shear stress can prime endothelial cells through the proinflammatory transcription factor, NF-κB.[95] Decreased shear on endothelial cells enhance adhesion molecules' expression, such as ICAM-1, VCAM-1, MCP-1, and E-selectin, thereby, promoting leukocyte recruitment into the aortic wall.[88]

Endothelial-to-mesenchymal transition (EndMT) is another important pathogenic mechanism in atherosclerosis and is observed in abnormal shear stress.[85] It is also well described in valve pathology, specifically in mitral valves.[96-98] In this biological process, endothelial cells lose cell polarity, gain increased migratory capability through disruption of intercellular junctions, in addition to having higher proliferative capacity.[99] Furthermore, these cells migrate to intimal and medial aortic wall layers, where the cells become highly proinflammatory, releasing high levels of cytokines and growth factors.

Endothelial damage resulting from altered shear stress also contributes to triggering events of CAVD, as in aortic wall calcification. Pulsatile hemodynamic shear stress affects VICs through VEC mechanical transduction.[100] In normal conditions, shear stress contributes to endothelial cell alignment and homeostasis by regulating valvular biosynthetic activity.[100] However, it remains unknown the amount of disturbance needed to trigger pathological events. Valves and vasculature are different in gross morphology and cellular structure; therefore, they demonstrate specific particularities in their pathogenic processes. The cardiac cycle involves both systole and diastole, which impart different forces on the leaflets.[101] Aortic valve shear stress occurs on the ventricularis layer of the valve when blood flows past the leaflets during systole and on the fibrosa when blood pools into the sinuses during diastole. Blood flow is unidirectional and pulsatile on the ventricularis, while bidirectional and oscillatory on the fibrosa.[102] VICs are found to respond to shear stress by altering their biosynthesis of ECM components, including collagen and collagen-processing enzymes, such as lysyl oxidase and prolyl 4-hydroxylase.[103,104] The amount of collagen deposition is dependent on the degree and duration of mechanical stress.[104]

Among the three cusps, noncoronary leaflets experience more oscillatory shear forces than the coronary leaflets, which experience more laminar shear stress. Therefore, noncoronary leaflets are more prone to develop

calcification.[105] Additionally, noncoronary VICs have shown increased expression of calcific markers and mineralization potential. Another example indicating the influence of hemodynamic factors on calcification are patients with a bicuspid aortic valve, the most common congenital heart anomaly, which is found in 0.5%−1.4% of the US population.[106] The bicuspid aortic valve has more rapid progression of stenosis and calcification than in the tricuspid aortic valve.[106]

Endothelial cells that are exposed to oscillatory shear stress in vitro are more prone to increased EndMT and inflammatory capacity, as gauged by high expression of αSMA and NFKβ1, respectively.[107] Altered shear stress in the early stages of disease and increased expression of adhesion molecules (VCAM-1, ICAM1) stimulate leukocyte recruitment. This can lead to endothelial rupture, facilitating even more inflammatory cell infiltration.[23,108] Alignment and juxtaposition of endothelial cells worsen in later stages of the disease due to increased local stiffness associated with fibrosis and calcification.[109] Furthermore, endothelial disruption allows calcium from the blood to get into the tissue. Similar to atherosclerosis, altered shear stress propagates lipid infiltration, especially LDL that becomes oxidized by ROS action (Fig. 21.2).[110] Inflammatory infiltrate releases factors that differentiate VICs to an osteogenic phenotype.[66] Endothelial damage, followed by VIC activation, leads to calcium deposition in CAVD (Fig. 21.2).[111] Trilayered leaflet structures become indistinguishable in the end stage of disease and are associated with intense collagen deposition. Leaflet structure has a very important role in tissue biomechanics and, once calcified, cannot be dissipated evenly across the leaflets, thereby, worsening mechanical stress and propagating pathogenic stimuli.[112]

Mechanical stress and subsequent endothelial injury are early common events of aortic wall calcification and CAVD. Then, secondary downstream events promote activation of vascular SMCs and VICs, which have a central role in aortic wall calcification and CAVD, respectively (Fig. 21.2).[32,39,66] Crosstalk between inflammatory infiltrates and SMCs or VICs culminates in mineralization. Calcium deposits cause tissue stiffening, aortic valve stenosis, and narrowing of the aorta lumen. This, in turn, may cause even greater mechanical stress, thereby, causing disease propagation.

The major cellular events underlying aortic wall and aortic valve calcification are represented in Fig. 21.2.

Synergistic effects of risk factors in vascular endothelial dysfunction

As presented in previous topics, the vascular endothelium is a dynamically mutable interface responsive to a variety of stimuli, both biomechanical and/or biochemical and local and/or systemic. Phenotypic modulation of endothelial cells constitutes the major risk factor for vascular diseases. While the exact causes of vascular calcification are still not well understood, certain conditions and lifestyles may raise someone's likelihood of obtaining either disease through synergistic effects with endothelial shear stress.

Systemic risk factors, such as hypercholesterolemia with increased LDL serum levels, have motivated researchers to find the mechanistic link with cardiovascular calcification. *In vivo* studies conducted with a porcine model demonstrated how hyperlipidemic swine that had intense hypercholesterolemia favored rapid atheroma progression.[113] In addition, a hyperlipidemic environment increases transcytosis of cholesterol to the subendothelial matrix and reduces its efflux from the vessel wall.[114,115] Lipid accumulation in subendothelium alters structure and functionality of endothelial cells.[115] Patients who have the diagnosis of familial hypercholesterolemia have a higher probability to develop atherosclerosis and CAVD, as well as peripheral vascular disease and coronary artery disease.[116,117]

Diabetes is defined by hyperglycemia condition and can predispose atherosclerosis and aortic valve calcification.[118,119] Both diabetes type 1 and 2 show similar implications in CVD development; however, type 2 diabetes demonstrates enhanced atherosclerotic plaque burden when compared to type 1 diabetes.[120] Because type 2 diabetes involves several aspects of metabolic syndrome, the isolated role of hyperglycemia on atherosclerotic plaque formation and calcification development is difficult to determine. In type 1 diabetes, the postmortem study of young patients and children shows enhanced fatty streak formation in the absence of dyslipidemia, suggesting that hyperglycemia is an independent risk factor for early plaque development.[121] Moreover, children with type 1 diabetes show enhanced carotid intimal−medial thickness compared to nondiabetics.[122] The mechanism through which a hyperglycemic environment affects endothelial function was determined in vitro by exposing endothelial cells to high glucose cell culture media, which led to a decrease in NO production. In turn, this gave rise to the activation of NF-κB transcriptional activity, thereby, increasing inflammatory gene expression and leukocyte recruitment.[123−125] Kawakami et al. recently demonstrated that human primary macrophages stimulated with S100A9 in culture conditions mimicking diabetes release calcifying EVs contributing to the formation of microcalcifications.[126] Similar phenomenon has been previously demonstrated in mouse macrophages triggered with high levels of Ca/P, recapitulating environment of CKD.[15] CKD often results from hypertension and diabetes. Dysmetabolic patients with CKD have both intimal and medial calcification as a common pathological process.[127]

CAVD occurs in up to 45% of patients with type 2 diabetes and is associated with an increased cardiovascular mortality, independently of other established risk factors.[128] High glucose induces enhanced monocyte adhesion to VECs through the increase of cell adhesion molecules: ICAM-1, VCAM-1, and CD18.[129] A study evaluating VECs and VICs exposed to high glucose medium showed induction of BMP-2 and 4 expression in VECs and other osteogenic markers, RUNX2 and OP were expressed in VICs.[130] In addition, this same study showed that TGF-β and BMP-2 signaling pathways are triggered by high glucose levels and contribute to bone formation in valve calcification.[130] VICs exposed to high glucose cell culture media increased expression of ECM proteins and MMPs.[130]

Since unhealthy diet and lack of physical activity directly influence cholesterol and glucose serum levels, those also constitute risk factors for the development of cardiovascular calcification. In patients with obesity, adipocyte hypertrophy is accompanied by changes in its derived cytokines and adipokines, leading to a systemic proinflammatory state that can disturb the vascular endothelium.[131] This constitutes an additional mechanism of vascular endothelial damage, apart from cholesterol pathways. Increase of proinflammatory cytokine secretion by adipocytes is considered to be the link between obesity-induced inflammation and endothelial dysfunction.[131] Moreover, a high-fat diet can alter human gut microbiota, leading to gut dysbiosis. An inflamed gastrointestinal tract can impact endothelial dysfunction by systemically releasing inflammatory mediators.[132]

As mentioned in previous topics, hypertension is an age-associated disorder that shows higher prevalence in patients with obesity.[133] This disorder is not commonly a cited risk factor for calcification; however, the majority of patients with atherosclerosis and CAVD have hypertension as a clinical manifestation.[134,135] High blood pressure generates hemodynamic disturbances, impacting vascular endothelium function.[136]

Smoking represents another risk factor for CVD. Because cigarette smoke contains roughly 4000 different chemicals, it is the least understood risk factor.[137] Vascular dysfunction induced by smoking is initiated by reduced NO bioavailability and increased expression of adhesion molecules, leading to endothelial dysfunction.[138] Numerous studies have shown that exposure to cigarette smoke activates platelets, stimulates the coagulation cascade, and reduces fibrinolysis.[139] Additionally, a study showed a positive correlation between smoking and increased total serum cholesterol, very−low-density lipoprotein, LDL, and triglyceride serum concentrations.[140] Effects of smoking in CAVD and atherosclerosis are well documented throughout the literature.[141−144]

Sex differences represent important health disparities. Those differences result from a complex interaction among genetic and hormonal factors and impacts CVDs morbidity and mortality.[144] The vascular endothelium expresses estrogen receptors (ERα and ERβ), progesterone receptors, androgen receptors, and aromatase, therefore, making it susceptible to hormonal regulation.[145] Atherosclerosis and CAVD have a much higher prevalence in males.[146,147] More men die from atherosclerosis than women and at a younger age.[148] On the other hand, women develop atherosclerosis more frequently after menopause, suggesting hormones play an important role in cardiovascular calcification. However, this mechanism is better explained by differences in immune responsive cells themselves than the hormone direct effects on vascular endothelium.[146] Additionally, women who are diagnosed with an autoimmune disease (e.g., systemic lupus erythematous, rheumatoid arthritis, and systemic sclerosis) have a higher risk for atherosclerosis development.[146,149] Therefore, differences in the immune response between males and females are linked to differences in CVD disease phenotype. Risk factors can promote endothelial dysfunction since they modify vascular microenvironment. Mutual influence of risk factors and endothelial cells constitute synergistic interrelationship that feed disease onset. The endothelial response to aggressive factors is gradual and dependent on its intensity.

Experimental approaches in cardiovascular calcification

There are many challenges with creating models to study cardiovascular calcification. Because atherosclerosis and CAVD are multifaceted disorders, experimental designs reproducing them, both in vitro and in vivo, are very difficult. Interpreting data obtained from those studies is complex and hinders its translation into clinic. New experimental methods and new tools of analysis are crucial for scientific advances in this field.

Ex vivo assays using explanted aortic tissue from patients with vascular calcification bring important pathological aspects of natural context of disease. However, end-stage disease specimens may not provide accurate information about early disease processes, thereby, presenting a large biological variability and interindividual confounding risk factors. Calcification can be induced using in vitro culture models through utilizing SMCs to study atherosclerosis or VICs to investigate CAVD and cultivating them in cell culture media containing organic and/or inorganic phosphate and/or other inducers, promoting mineralization development.[150,151]

3D cell culture models have been used to produce complex tissue-like structures of aortic valve leaflets,

mimicking their layered structure.[88,152−155] *In vitro* models offer well-controlled conditions, allowing for a better understanding of the role of certain mediators and pathogenic pathways of interest. Thus, these experiments offer data with less complicating factors and variability, as compared to in vivo assays. *In vitro* simulation of mechanical stress has been used to replicate its role in the pathogenesis of atherosclerosis and CAVD through the production of physiologic and abnormal shear stresses.[155,156] *In vivo* models allow study initiation and progression of the disease and also evaluate the effectiveness of therapeutic interventions.[126,157] The most common species used for experimental atherosclerosis and CAVD are mice, rats, rabbits, and swine.[158] Calcification induction can be accelerated by diet-induced hypercholesterolemia.[159] Cost-effectiveness and small size make mice the most used model. In addition, greater ease of genetic manipulations allows specific investigation of key molecular mediators of calcification.[158,160] Mice deficient in the LDL receptor (*Ldlr−/−*) are often used. *Ldlr−/−* mice containing apolipoprotein B (ApoB) (*Ldlr−/−;Apob*) spontaneously develop hypercholesterolemia.[159] However, mice do not have the trilayer aortic valve tissue morphology characteristic of humans; therefore, they are not ideal to study CAVD.[161] Different experimental approaches have different limitations, and the choice of model varies depending on the questions being answered in a given study. More recently, multiomics approaches have been applied in cardiovascular calcification studies using different experimental models.[162] A multiomics approach includes techniques investigating genome, proteome, transcriptome, epigenome, metabolome, that can be integrated, generating a massive amount of information.[2] Large data sets can be analyzed through computational tools and development of algorithms. Thus, more recently, artificial intelligence and machine learning have been used as a strategy for data processing, which would not be feasible through a manual approach. These strategies broaden the informative capacity of the data obtained in different models, expanding the informative capacity and accelerating research translation into the clinic.

Therapeutic target discovery in cardiovascular calcification

While involving similar risk factors, both vascular and valvular calcifications have sheer stress alteration and subsequent endothelial dysfunction as a disease promoter. However, atherosclerosis and CAVD pathogenesis seems to be different.[64] Treatments that help reduce inflammation in vasculature have been shown to have no effect on valvular calcification.[111] Moreover, currently, no approved drug has shown prophylactic or therapeutic effectiveness on ectopic calcification. Therefore, cardiovascular system mineralization provides an important field for drug discovery.[2] Similarly, as in the bone, calcification is subject to remodeling and this can be explored in order to regress already established injuries. Thus, finding therapeutic targets that inhibit or slow the progression of the disease may guide research efforts in this field. Conventional diagnostic imaging is currently the best method for detecting, measuring, and assisting calcification progression and therapeutic effects on it.[25,163] This research strategy could vastly improve therapeutic discovery; however, the formation of microcalcification lay below the resolution of current imaging modalities. Positron emission tomography (PET) combined with computed tomography (CT) is a noninvasive imaging technique that allows the identification and quantification of calcium deposits and inflammation on aorta and carotid arteries.[164] However, the common PET/CT tracers usually cannot detect microcalcifications.[25] 18F-Flurodeoxyglucose is an alternative PET tracer that is directly incorporated into exposed hydroxyapatite crystals able to assess spotty cardiovascular calcification.[164] Artificial intelligence and machine learning are great allies in drug discovery for allowing the integration of image data from human long-term studies with clinical information.

Final considerations

The lack of effective therapy to treat or prevent cardiovascular calcification reflects the complexity of the disease. Influence of individual risk factors, genetic predisposition, and lifestyle directly impact its outcome besides hindering the pathogenic mechanisms. Cardiovascular calcification implicates endothelial injury as an initiating point of the disease, which in turns leads to VIC and SMC phenotypic changes that culminate in fibrosis and calcification. Hemodynamic shear stress drives initial tissue injury and continuously stimulates pathogenic processes. As demonstrated in this review, cardiovascular calcification is the result of a crosstalk between different signaling pathways and pathologic processes that reciprocally affect each other. Thus, once initiated, calcification causes a positive feedback loop of changes in the tissue affecting its architecture, cell biology, and hemodynamic parameters, which altogether sustains a self-perpetuating pathologic vicious cycle.

Funding

References

1. Yazdanyar A, Newman AB. The burden of cardiovascular disease in the elderly: morbidity, mortality, and costs. **Clin Geriatr Med**. 2009; 25(4):563−577 (vii).

2. Rogers MA, Aikawa E. Cardiovascular calcification: artificial intelligence and big data accelerate mechanistic discovery. **Nat Rev Cardiol**. 2019; 16(5):261−274.

3. North BJ, Sinclair DA. The intersection between aging and cardiovascular disease. **Circ Res**. 2012; 110(8):1097−1108.

4. Erbel R, Churzidse S. Calcification of the aortic wall indicates risk but not beyond current clinically used risk factors assessment. **Atherosclerosis**. 2017; 257:256−258.

5. Hutcheson JD, Blaser MC, Aikawa E. Giving calcification its due: recognition of a diverse disease: a first attempt to standardize the field. **Circ Res**. 2017; 120(2):270−273.

6. Head T, Daunert S, Goldschmidt-Clermont PJ. The aging risk and atherosclerosis: a fresh look at arterial homeostasis. **Front Genet**. 2017; 8:216.

7. Zieske AW, Malcom GT, Strong JP. Natural history and risk factors of atherosclerosis in children and youth: the PDAY study. **Pediatr Pathol Mol Med**. 2002; 21(2):213−237.

8. Libby P, Buring JE, Badimon L, et al. Atherosclerosis. **Nat Rev Dis Primers**. 2019; 5(1):56.

9. Janssen CH, Kuijpers D, Vliegenthart R, et al. Coronary artery calcification score by multislice computed tomography predicts the outcome of dobutamine cardiovascular magnetic resonance imaging. **Eur Radiol**. 2005; 15(6):1128−1134.

10. Rapp AH, Hillis LD, Lange RA, Cigarroa JE. Prevalence of coronary artery disease in patients with aortic stenosis with and without angina pectoris. **Am J Cardiol**. 2001; 87(10):1216−1217. A7.

11. Chen MA, Kawakubo M, Colletti PM, et al. Effect of age on aortic atherosclerosis. **J Geriatr Cardiol**. 2013; 10(2):135−140.

12. Jaffer FA, O'Donnell CJ, Larson MG, et al. Age and sex distribution of subclinical aortic atherosclerosis: a magnetic resonance imaging examination of the Framingham Heart Study. **Arterioscler Thromb Vasc Biol**. 2002; 22(5):849−854.

13. Shi X, Gao J, Lv Q, et al. Calcification in atherosclerotic plaque vulnerability: friend or foe? **Front Physiol**. 2020; 11:56.

14. Ehara S, Kobayashi Y, Yoshiyama M, et al. Spotty calcification typifies the culprit plaque in patients with acute myocardial infarction: an intravascular ultrasound study. **Circulation**. 2004; 110(22):3424−3429.

15. New SE, Aikawa E. Role of extracellular vesicles in de novo mineralization: an additional novel mechanism of cardiovascular calcification. **Arterioscler Thromb Vasc Biol**. 2013; 33(8):1753−1758.

16. Hutcheson JD, Maldonado N, Aikawa E. Small entities with large impact: microcalcifications and atherosclerotic plaque vulnerability. **Curr Opin Lipidol**. 2014; 25(5):327−332.

17. Koskinas KC, Chatzizisis YS, Baker AB, Edelman ER, Stone PH, Feldman CL. The role of low endothelial shear stress in the conversion of atherosclerotic lesions from stable to unstable plaque. **Curr Opin Cardiol**. 2009; 24(6):580−590.

18. Coselli JS, Crawford ES. Aortic valve replacement in the patient with extensive calcification of the ascending aorta (the porcelain aorta). **J Thorac Cardiovasc Surg**. 1986; 91(2):184−187.

19. Fukuda I, Daitoku K, Minakawa M, Fukuda W. Shaggy and calcified aorta: surgical implications. **Gen Thorac Cardiovasc Surg**. 2013; 61(6):301−313.

20. Otto CM, Burwash IG, Legget ME, et al. Prospective study of asymptomatic valvular aortic stenosis. Clinical, echocardiographic, and exercise predictors of outcome. **Circulation**. 1997; 95(9):2262−2270.

21. Writing Group M, Mozaffarian D, Benjamin EJ, et al. Heart disease and stroke statistics-2016 update: a report from the American Heart Association. **Circulation**. 2016; 133(4):e38−360.

22. Passos LSA, Lupieri A, Becker-Greene D, Aikawa E. Innate and adaptive immunity in cardiovascular calcification. **Atherosclerosis**. 2020; 306:59−67.

23. Otto CM, Kuusisto J, Reichenbach DD, Gown AM, O'Brien KD. Characterization of the early lesion of 'degenerative' valvular aortic stenosis. Histological and immunohistochemical studies. **Circulation**. 1994; 90(2):844−853.

24. Wasilewski J, Mirota K, Wilczek K, Glowacki J, Polonski L. Calcific aortic valve damage as a risk factor for cardiovascular events. **Pol J Radiol**. 2012; 77(4):30−34.

25. Aikawa E, Otto CM. Look more closely at the valve: imaging calcific aortic valve disease. **Circulation**. 2012; 125(1):9−11.

26. New SE, Aikawa E. Molecular imaging insights into early inflammatory stages of arterial and aortic valve calcification. **Circ Res**. 2011; 108(11):1381−1391.

27. Yutzey KE, Demer LL, Body SC, et al. Calcific aortic valve disease: a consensus summary from the alliance of investigators on calcific aortic valve disease. **Arterioscler Thromb Vasc Biol**. 2014; 34(11):2387−2393.

28. Davignon J, Ganz P. Role of endothelial dysfunction in atherosclerosis. **Circulation**. 2004; 109(23 Suppl 1):III27−32.

29. Gimbrone Jr MA, Topper JN, Nagel T, Anderson KR, Garcia-Cardena G. Endothelial dysfunction, hemodynamic forces, and atherogenesis. **Ann N Y Acad Sci**. 2000; 902:230−239. discussion 239-40.

30. Simionescu N, Vasile E, Lupu F, Popescu G, Simionescu M. Prelesional events in atherogenesis. Accumulation of extracellular cholesterol-rich liposomes in the arterial intima and cardiac valves of the hyperlipidemic rabbit. **Am J Pathol**. 1986; 123(1):109−125.

31. Swirski FK, Nahrendorf M. Do vascular smooth muscle cells differentiate to macrophages in atherosclerotic lesions? **Circ Res**. 2014; 115(7):605−606.

32. Durham AL, Speer MY, Scatena M, Giachelli CM, Shanahan CM. Role of smooth muscle cells in vascular calcification: implications in atherosclerosis and arterial stiffness. **Cardiovasc Res**. 2018; 114(4):590−600.

33. Metz RP, Patterson JL, Wilson E. Vascular smooth muscle cells: isolation, culture, and characterization. **Methods Mol Biol**. 2012; 843:169−176.

34. Ponticos M, Smith BD. Extracellular matrix synthesis in vascular disease: hypertension, and atherosclerosis. **J Biomed Res**. 2014; 28(1):25−39.

35. Libby P. Inflammation in atherosclerosis. **Nature**. 2002; 420(6917):868−874.

36. Pedrigi RM, de Silva R, Bovens SM, Mehta VV, Petretto E, Krams R. Thin-cap fibroatheroma rupture is associated with a fine interplay of shear and wall stress. **Arterioscler Thromb Vasc Biol**. 2014; 34(10):2224−2231.

37. Westhorpe CL, Dufour EM, Maisa A, Jaworowski A, Crowe SM, Muller WA. Endothelial cell activation promotes foam cell formation by monocytes following transendothelial migration in an in vitro model. **Exp Mol Pathol**. 2012; 93(2):220−226.

38. Hruska KA, Mathew S, Saab G. Bone morphogenetic proteins in vascular calcification. **Circ Res**. 2005; 97(2):105−114.

39. Aikawa E, Nahrendorf M, Figueiredo JL, et al. Osteogenesis associates with inflammation in early-stage atherosclerosis evaluated by molecular imaging in vivo. **Circulation**. 2007; 116(24):2841−2850.

40. Krohn JB, Hutcheson JD, Martinez-Martinez E, Aikawa E. Extracellular vesicles in cardiovascular calcification: expanding current paradigms. **J Physiol**. 2016; 594(11):2895−2903.

41. Rogers MA, Buffolo F, Schlotter F, et al. Annexin A1-dependent tethering promotes extracellular vesicle aggregation revealed with single-extracellular vesicle analysis. **Sci Adv**. 2020; 6(38).

42. Davies JD, Carpenter KL, Challis IR, et al. Adipocytic differentiation and liver x receptor pathways regulate the accumulation of triacylglycerols in human vascular smooth muscle cells. **J Biol Chem**. 2005; 280(5):3911−3919.

43. Dalager S, Paaske WP, Kristensen IB, Laurberg JM, Falk E. Artery-related differences in atherosclerosis expression: implications for atherogenesis and dynamics in intima-media thickness. **Stroke**. 2007; 38(10):2698−2705.

44. Marchais SJ, Guerin AP, London GM. Arterial calcinosis, chronic renal failure and calcium antagonism. **Drugs**. 1992; 44(Suppl 1):119−122.

45. Giachelli CM, Speer MY, Li X, Rajachar RM, Yang H. Regulation of vascular calcification: roles of phosphate and osteopontin. **Circ Res**. 2005; 96(7):717−722.

46. Lanzer P, Boehm M, Sorribas V, et al. Medial vascular calcification revisited: review and perspectives. **Eur Heart J**. 2014; 35(23):1515−1525.

47. Abramowitz Y, Jilaihawi H, Chakravarty T, Mack MJ, Makkar RR. Porcelain aorta: a comprehensive review. **Circulation**. 2015; 131(9):827−836.

48. Amann K. Media calcification and intima calcification are distinct entities in chronic kidney disease. **Clin J Am Soc Nephrol**. 2008; 3(6):1599−1605.

49. Proudfoot D, Shanahan CM. Biology of calcification in vascular cells: intima versus media. **Herz**. 2001; 26(4):245−251.

50. Johnson RC, Leopold JA, Loscalzo J. Vascular calcification: pathobiological mechanisms and clinical implications. **Circ Res**. 2006; 99(10):1044−1059.

51. London GM, Guerin AP, Marchais SJ, Metivier F, Pannier B, Adda H. Arterial media calcification in end-stage renal disease: impact on all-cause and cardiovascular mortality. **Nephrol Dial Transplant**. 2003; 18(9):1731−1740.

52. Lehto S, Niskanen L, Suhonen M, Ronnemaa T, Laakso M. Medial artery calcification. A neglected harbinger of cardiovascular complications in non-insulin-dependent diabetes mellitus. **Arterioscler Thromb Vasc Biol**. 1996; 16(8):978−983.

53. Buzello M, Tornig J, Faulhaber J, Ehmke H, Ritz E, Amann K. The apolipoprotein E knockout mouse: a model documenting accelerated atherogenesis in uremia. **J Am Soc Nephrol**. 2003; 14(2):311−316.

54. Yahagi K, Kolodgie FD, Lutter C, et al. Pathology of human coronary and carotid artery atherosclerosis and vascular calcification in diabetes mellitus. **Arterioscler Thromb Vasc Biol**. 2017; 37(2):191−204.

55. Taniwaki H, Ishimura E, Tabata T, et al. Aortic calcification in haemodialysis patients with diabetes mellitus. **Nephrol Dial Transplant**. 2005; 20(11):2472−2478.

56. Clarke MC, Littlewood TD, Figg N, et al. Chronic apoptosis of vascular smooth muscle cells accelerates atherosclerosis and promotes calcification and medial degeneration. **Circ Res**. 2008; 102(12):1529−1538.

57. Sims TJ, Rasmussen LM, Oxlund H, Bailey AJ. The role of glycation cross-links in diabetic vascular stiffening. **Diabetologia**. 1996; 39(8):946−951.

58. Shanahan CM, Cary NR, Salisbury JR, Proudfoot D, Weissberg PL, Edmonds ME. Medial localization of mineralization-regulating proteins in association with Monckeberg's sclerosis: evidence for smooth muscle cell-mediated vascular calcification. **Circulation**. 1999; 100(21):2168−2176.

59. Reynolds JL, Joannides AJ, Skepper JN, et al. Human vascular smooth muscle cells undergo vesicle-mediated calcification in response to changes in extracellular calcium and phosphate concentrations: a potential mechanism for accelerated vascular calcification in ESRD. **J Am Soc Nephrol**. 2004; 15(11):2857−2867.

60. Coblentz C, Martin L, Tuttle R. Calcified ascending aorta after radiation therapy. **AJR Am J Roentgenol**. 1986; 147(3):477−478.

61. Mesurolle B, Qanadli SD, Merad M, et al. Unusual radiologic findings in the thorax after radiation therapy. **Radiographics**. 2000; 20(1):67−81.

62. Carver JR, Shapiro CL, Ng A, et al. American Society of Clinical Oncology clinical evidence review on the ongoing care of adult cancer survivors: cardiac and pulmonary late effects. **J Clin Oncol**. 2007; 25(25):3991−4008.

63. Blauth CI, Cosgrove DM, Webb BW, et al. Atheroembolism from the ascending aorta. An emerging problem in cardiac surgery. **J Thorac Cardiovasc Surg**. 1992; 103(6):1104−1111. ; discussion 1111-2.

64. Blaser MC, Buffolo F, Halu A, et al. **Conserved and Divergent Modulation of Calcification in Atherosclerosis and Aortic Valve Disease by Tissue Extracellular Vesicles**. 2020, 2020.04.02.022525.

65. Yetkin E, Waltenberger J. Molecular and cellular mechanisms of aortic stenosis. **Int J Cardiol**. 2009; 135(1):4−13.

66. O'Brien KD. Pathogenesis of calcific aortic valve disease: a disease process comes of age (and a good deal more). **Arterioscler Thromb Vasc Biol**. 2006; 26(8):1721−1728.

67. Yabusaki K, Hutcheson JD, Vyas P, et al. Quantification of calcified particles in human valve tissue reveals asymmetry of calcific aortic valve disease development. **Front Cardiovasc Med**. 2016; 3:44.

68. Gimbrone Jr MA, Garcia-Cardena G. Endothelial cell dysfunction and the pathobiology of atherosclerosis. **Circ Res**. 2016; 118(4):620−636.

69. Rajamannan NM, Subramaniam M, Stock SR, et al. Atorvastatin inhibits calcification and enhances nitric oxide synthase production in the hypercholesterolaemic aortic valve. **Heart**. 2005; 91(6):806−810.

70. Miller JD, Chu Y, Brooks RM, Richenbacher WE, Pena-Silva R, Heistad DD. Dysregulation of antioxidant mechanisms contributes to increased oxidative stress in calcific aortic valvular stenosis in humans. **J Am Coll Cardiol**. 2008; 52(10):843−850.

71. Davies PF, Passerini AG, Simmons CA. Aortic valve: turning over a new leaf(let) in endothelial phenotypic heterogeneity. **Arterioscler Thromb Vasc Biol**. 2004; 24(8):1331−1333.

72. Liu AC, Joag VR, Gotlieb AI. The emerging role of valve interstitial cell phenotypes in regulating heart valve pathobiology. **Am J Pathol**. 2007; 171(5):1407−1418.

73. Chen JH, Yip CY, Sone ED, Simmons CA. Identification and characterization of aortic valve mesenchymal progenitor cells with robust osteogenic calcification potential. **Am J Pathol**. 2009; 174(3):1109−1119.

74. Paranya G, Vineberg S, Dvorin E, et al. Aortic valve endothelial cells undergo transforming growth factor-beta-mediated and non-transforming growth factor-beta-mediated transdifferentiation in vitro. **Am J Pathol**. 2001; 159(4):1335−1343.

75. Rabkin E, Aikawa M, Stone JR, Fukumoto Y, Libby P, Schoen FJ. Activated interstitial myofibroblasts express catabolic enzymes and mediate matrix remodeling in myxomatous heart valves. **Circulation**. 2001; 104(21):2525−2532.

76. Kaden JJ, Dempfle CE, Grobholz R, et al. Inflammatory regulation of extracellular matrix remodeling in calcific aortic valve stenosis. **Cardiovasc Pathol**. 2005; 14(2):80−87.

77. Osman L, Yacoub MH, Latif N, Amrani M, Chester AH. Role of human valve interstitial cells in valve calcification and their response to atorvastatin. **Circulation**. 2006; 114(1 Suppl):I547−I552.

78. O'Young J, Liao Y, Xiao Y, et al. Matrix GLA protein inhibits ectopic calcification by a direct interaction with hydroxyapatite crystals. **J Am Chem Soc**. 2011; 133(45):18406−18412.

79. Chirinos JA, Segers P, Hughes T, Townsend R. Large-artery stiffness in health and disease: JACC state-of-the-art review. **J Am Coll Cardiol**. 2019; 74(9):1237−1263.

80. Yao Y, Bennett BJ, Wang X, et al. Inhibition of bone morphogenetic proteins protects against atherosclerosis and vascular calcification. **Circ Res**. 2010; 107(4):485−494.

81. Chiyoya M, Seya K, Yu Z, et al. Matrix GLA protein negatively regulates calcification of human aortic valve interstitial cells isolated from calcified aortic valves. **J Pharmacol Sci**. 2018; 136(4):257−265.

82. Luo G, Ducy P, McKee MD, et al. Spontaneous calcification of arteries and cartilage in mice lacking matrix GLA protein. **Nature**. 1997; 386(6620):78−81.

83. Mohler 3rd ER, Gannon F, Reynolds C, Zimmerman R, Keane MG, Kaplan FS. Bone formation and inflammation in cardiac valves. **Circulation**. 2001; 103(11):1522−1528.

84. Mathieu P, Bouchareb R, Boulanger MC. Innate and adaptive immunity in calcific aortic valve disease. **J Immunol Res**. 2015; 2015:851945.

85. Mahmoud MM, Serbanovic-Canic J, Feng S, et al. Shear stress induces endothelial-to-mesenchymal transition via the transcription factor Snail. **Sci Rep**. 2017; 7(1):3375.

86. Balachandran K, Sucosky P, Yoganathan AP. Hemodynamics and mechanobiology of aortic valve inflammation and calcification. **Int J Inflam**. 2011; 2011:263870.

87. Brooks AR, Lelkes PI, Rubanyi GM. Gene expression profiling of human aortic endothelial cells exposed to disturbed flow and steady laminar flow. **Physiol Genomics**. 2002; 9(1):27−41.

88. Cunningham KS, Gotlieb AI. The role of shear stress in the pathogenesis of atherosclerosis. **Lab Invest**. 2005; 85(1):9−23.

89. Resnick N, Yahav H, Shay-Salit A, et al. Fluid shear stress and the vascular endothelium: for better and for worse. **Prog Biophys Mol Biol**. 2003; 81(3):177−199.

90. Rahimi K, Mohseni H, Kiran A, et al. Elevated blood pressure and risk of aortic valve disease: a cohort analysis of 5.4 million UK adults. **Eur Heart J**. 2018; 39(39):3596−3603.

91. Bermejo J. The effects of hypertension on aortic valve stenosis. **Heart**. 2005; 91(3):280−282.

92. Liu SQ, Tang D, Tieche C, Alkema PK. Pattern formation of vascular smooth muscle cells subject to nonuniform fluid shear stress: mediation by gradient of cell density. **Am J Physiol Heart Circ Physiol**. 2003; 285(3):H1072−H1080.

93. Niwa K, Kado T, Sakai J, Karino T. The effects of a shear flow on the uptake of LDL and acetylated LDL by an EC monoculture and an EC-SMC coculture. **Ann Biomed Eng**. 2004; 32(4):537−543.

94. Passerini AG, Polacek DC, Shi C, et al. Coexisting proinflammatory and antioxidative endothelial transcription profiles in a disturbed flow region of the adult porcine aorta. **Proc Natl Acad Sci U S A**. 2004; 101(8):2482−2487.

95. Hajra L, Evans AI, Chen M, Hyduk SJ, Collins T, Cybulsky MI. The NF-kappa B signal transduction pathway in aortic endothelial cells is primed for activation in regions predisposed to atherosclerotic lesion formation. **Proc Natl Acad Sci U S A**. 2000; 97(16):9052−9057.

96. Kovacic JC, Dimmeler S, Harvey RP, et al. Endothelial to mesenchymal transition in cardiovascular disease: JACC state-of-the-art review. **J Am Coll Cardiol**. 2019; 73(2):190−209.

97. Bischoff J. Endothelial-to-Mesenchymal transition. **Circ Res**. 2019; 124(8):1163−1165.

98. Shapero K, Wylie-Sears J, Levine RA, Mayer Jr JE, Bischoff J. Reciprocal interactions between mitral valve endothelial and interstitial cells reduce endothelial-to-mesenchymal transition and myofibroblastic activation. **J Mol Cell Cardiol**. 2015; 80:175−185.

99. Lim J, Thiery JP. Epithelial-mesenchymal transitions: insights from development. **Development**. 2012; 139(19):3471−3486.

100. Weston MW, Yoganathan AP. Biosynthetic activity in heart valve leaflets in response to in vitro flow environments. **Ann Biomed Eng**. 2001; 29(9):752−763.

101. Sacks MS, David Merryman W, Schmidt DE. On the biomechanics of heart valve function. **J Biomech**. 2009; 42(12):1804−1824.

102. Yap CH, Saikrishnan N, Yoganathan AP. Experimental measurement of dynamic fluid shear stress on the ventricular surface of the aortic valve leaflet. **Biomech Model Mechanobiol**. 2012; 11(1−2):231−244.

103. Merryman WD, Youn I, Lukoff HD, et al. Correlation between heart valve interstitial cell stiffness and transvalvular pressure: implications for collagen biosynthesis. **Am J Physiol Heart Circ Physiol**. 2006; 290(1):H224−H231.

104. Ku CH, Johnson PH, Batten P, et al. Collagen synthesis by mesenchymal stem cells and aortic valve interstitial cells in response to mechanical stretch. **Cardiovasc Res**. 2006; 71(3):548−556.

105. Masjedi S, Amarnath A, Baily KM, Ferdous Z. Comparison of calcification potential of valvular interstitial cells isolated from individual aortic valve cusps. **Cardiovasc Pathol**. 2016; 25(3):185−194.

106. Sabet HY, Edwards WD, Tazelaar HD, Daly RC. Congenitally bicuspid aortic valves: a surgical pathology study of 542 cases (1991 through 1996) and a literature review of 2,715 additional cases. **Mayo Clin Proc**. 1999; 74(1):14−26.

107. Mahler GJ, Frendl CM, Cao Q, Butcher JT. Effects of shear stress pattern and magnitude on mesenchymal transformation and invasion

of aortic valve endothelial cells. **Biotechnol Bioeng**. 2014; 111(11):2326−2337.

108. Sucosky P, Balachandran K, Elhammali A, Jo H, Yoganathan AP. Altered shear stress stimulates upregulation of endothelial VCAM-1 and ICAM-1 in a BMP-4- and TGF-beta1-dependent pathway. **Arterioscler Thromb Vasc Biol**. 2009; 29(2):254−260.

109. Cote N, Mahmut A, Bosse Y, et al. Inflammation is associated with the remodeling of calcific aortic valve disease. **Inflammation**. 2013; 36(3):573−581.

110. Alushi B, Curini L, Christopher MR, et al. Calcific aortic valve disease-natural history and future therapeutic strategies. **Front Pharmacol**. 2020; 11:685.

111. Gomel MA, Lee R, Grande-Allen KJ. Comparing the role of mechanical forces in vascular and valvular calcification progression. **Front Cardiovasc Med**. 2018; 5:197.

112. Hutson HN, Marohl T, Anderson M, Eliceiri K, Campagnola P, Masters KS. Calcific aortic valve disease is associated with layer-specific alterations in collagen architecture. **PLoS One**. 2016; 11(9):e0163858.

113. Koskinas KC, Chatzizisis YS, Papafaklis MI, et al. Synergistic effect of local endothelial shear stress and systemic hypercholesterolemia on coronary atherosclerotic plaque progression and composition in pigs. **Int J Cardiol**. 2013; 169(6):394−401.

114. Mundi S, Massaro M, Scoditti E, et al. Endothelial permeability, LDL deposition, and cardiovascular risk factors-a review. **Cardiovasc Res**. 2018; 114(1):35−52.

115. Khatana C, Saini NK, Chakrabarti S, et al. Mechanistic insights into the oxidized low-density lipoprotein-induced atherosclerosis. **Oxid Med Cell Longev**. 2020; 2020:5245308.

116. Kim YR, Han KH. Familial hypercholesterolemia and the atherosclerotic disease. **Korean Circ J**. 2013; 43(6):363−367.

117. Ten Kate GR, Bos S, Dedic A, et al. Increased aortic valve calcification in familial hypercholesterolemia: prevalence, extent, and associated risk factors. **J Am Coll Cardiol**. 2015; 66(24):2687−2695.

118. Chait A, Bornfeldt KE. Diabetes and atherosclerosis: is there a role for hyperglycemia? **J Lipid Res**. 2009; 50(Suppl):S335−S339.

119. Natorska J, Wypasek E, Grudzien G, et al. Does diabetes accelerate the progression of aortic stenosis through enhanced inflammatory response within aortic valves? **Inflammation**. 2012; 35(3):834−840.

120. Burke AP, Kolodgie FD, Zieske A, et al. Morphologic findings of coronary atherosclerotic plaques in diabetics: a postmortem study. **Arterioscler Thromb Vasc Biol**. 2004; 24(7):1266−1271.

121. McGill Jr HC, McMahan CA, Zieske AW, Malcom GT, Tracy RE, Strong JP. Effects of nonlipid risk factors on atherosclerosis in youth with a favorable lipoprotein profile. **Circulation**. 2001; 103(11):1546−1550.

122. Jarvisalo MJ, Raitakari M, Toikka JO, et al. Endothelial dysfunction and increased arterial intima-media thickness in children with type 1 diabetes. **Circulation**. 2004; 109(14):1750−1755.

123. Ding Y, Vaziri ND, Coulson R, Kamanna VS, Roh DD. Effects of simulated hyperglycemia, insulin, and glucagon on endothelial nitric oxide synthase expression. **Am J Physiol Endocrinol Metab**. 2000; 279(1):E11−E17.

124. Hamuro M, Polan J, Natarajan M, Mohan S. High glucose induced nuclear factor kappa B mediated inhibition of endothelial cell migration. **Atherosclerosis**. 2002; 162(2):277−287.

125. Piconi L, Quagliaro L, Da Ros R, et al. Intermittent high glucose enhances ICAM-1, VCAM-1, E-selectin and interleukin-6 expression in human umbilical endothelial cells in culture: the role of poly(ADP-ribose) polymerase. **J Thromb Haemost**. 2004; 2(8):1453−1459.

126. Kawakami R, Katsuki S, Travers R, et al. S100A9-RAGE Axis Accelerates formation of macrophage-mediated extracellular vesicle microcalcification in diabetes mellitus. **Arterioscler Thromb Vasc Biol**. 2020; 40(8):1838−1853.

127. Disthabanchong S. Vascular calcification in chronic kidney disease: pathogenesis and clinical implication. **World J Nephrol**. 2012; 1(2):43−53.

128. Rossi A, Targher G, Zoppini G, et al. Aortic and mitral annular calcifications are predictive of all-cause and cardiovascular mortality in patients with type 2 diabetes. **Diabetes Care**. 2012; 35(8):1781−1786.

129. Manduteanu I, Voinea M, Serban G, Simionescu M. High glucose induces enhanced monocyte adhesion to valvular endothelial cells via a mechanism involving ICAM-1, VCAM-1 and CD18. **Endothelium**. 1999; 6(4):315−324.

130. Vadana M, Cecoltan S, Ciortan L, et al. Molecular mechanisms involved in high glucose-induced valve calcification in a 3D valve model with human valvular cells. **J Cell Mol Med**. 2020; 24(11):6350−6361.

131. Kwaifa IK, Bahari H, Yong YK, Noor SM. Endothelial dysfunction in obesity-induced inflammation: molecular mechanisms and clinical implications. **Biomolecules**. 2020; 10(2).

132. Jonsson AL, Backhed F. Role of gut microbiota in atherosclerosis. **Nat Rev Cardiol**. 2017; 14(2):79−87.

133. Landi F, Calvani R, Picca A, et al. Body mass index is strongly associated with hypertension: results from the longevity check-up 7+ study. **Nutrients**. 2018; 10(12).

134. Alexander RW. Theodore Cooper Memorial Lecture. Hypertension and the pathogenesis of atherosclerosis. Oxidative stress and the mediation of arterial inflammatory response: a new perspective. **Hypertension**. 1995; 25(2):155−161.

135. Iwata S, Russo C, Jin Z, et al. Higher ambulatory blood pressure is associated with aortic valve calcification in the elderly: a population-based study. **Hypertension**. 2013; 61(1):55−60.

136. Lu D, Kassab GS. Role of shear stress and stretch in vascular mechanobiology. **J R Soc Interface**. 2011; 8(63):1379−1385.

137. Burns DM. Cigarettes and cigarette smoking. **Clin Chest Med**. 1991; 12(4):631−642.

138. Messner B, Bernhard D. Smoking and cardiovascular disease: mechanisms of endothelial dysfunction and early atherogenesis. **Arterioscler Thromb Vasc Biol**. 2014; 34(3):509−515.

139. Csordas A, Bernhard D. The biology behind the atherothrombotic effects of cigarette smoke. **Nat Rev Cardiol**. 2013; 10(4):219−230.

140. Craig WY, Palomaki GE, Haddow JE. Cigarette smoking and serum lipid and lipoprotein concentrations: an analysis of published data. **BMJ**. 1989; 298(6676):784−788.

141. Dudzinski DM, O'Gara PT. Association of cigarette smoking with degenerative aortic valve disease. **Circ Cardiovasc Imaging**. 2019; 12(8):e009441.

142. Michael Pittilo R. Cigarette smoking, endothelial injury and cardiovascular disease. **Int J Exp Pathol**. 2000; 81(4):219−230.

143. Stewart BF, Siscovick D, Lind BK, et al. Clinical factors associated with calcific aortic valve disease. Cardiovascular Health Study. **J Am Coll Cardiol**. 1997; 29(3):630−634.

144. Yamaura Y, Watanabe N, Shimaya M, Tomita Y, Fukaya T, Yoshida K. Impact of cumulative smoking exposure on subclinical degenerative aortic valve disease in apparently healthy male workers. **Circ Cardiovasc Imaging**. 2019; 12(8):e008901.

145. Villablanca AC, Jayachandran M, Banka C. Atherosclerosis and sex hormones: current concepts. **Clin Sci (Lond)**. 2010; 119(12):493−513.

146. Fairweather D. Sex differences in inflammation during atherosclerosis. **Clin Med Insights Cardiol**. 2014; 8(Suppl 3):49−59.

147. Porras AM, McCoy CM, Masters KS. Calcific aortic valve disease: a battle of the sexes. **Circ Res**. 2017; 120(4):604−606.

148. Roger VL, Go AS, Lloyd-Jones DM, et al. Heart disease and stroke statistics–2012 update: a report from the American Heart Association. **Circulation**. 2012; 125(1):e2−e220.

149. Fairweather D, Petri MA, Coronado MJ, Cooper LT. Autoimmune heart disease: role of sex hormones and autoantibodies in disease pathogenesis. **Expert Rev Clin Immunol**. 2012; 8(3):269−284.

150. Jono S, McKee MD, Murry CE, et al. Phosphate regulation of vascular smooth muscle cell calcification. **Circ Res**. 2000; 87(7):E10−E17.

151. Shioi A, Nishizawa Y, Jono S, Koyama H, Hosoi M, Morii H. Beta-glycerophosphate accelerates calcification in cultured bovine vascular smooth muscle cells. **Arterioscler Thromb Vasc Biol**. 1995; 15(11):2003−2009.

152. Hjortnaes J, Goettsch C, Hutcheson JD, et al. Simulation of early calcific aortic valve disease in a 3D platform: a role for myofibroblast differentiation. **J Mol Cell Cardiol**. 2016; 94:13−20.

153. van der Valk DC, van der Ven CFT, Blaser MC, et al. Engineering a 3D-bioprinted model of human heart valve disease using nanoindentation-based biomechanics. **Nanomaterials (Basel)**. 2018; 8(5).

154. Estrada R, Giridharan GA, Nguyen MD, Prabhu SD, Sethu P. Microfluidic endothelial cell culture model to replicate disturbed flow conditions seen in atherosclerosis susceptible regions. **Biomicrofluidics**. 2011; 5(3):32006−3200611.

155. Sun L, Rajamannan NM, Sucosky P. Defining the role of fluid shear stress in the expression of early signaling markers for calcific aortic valve disease. **PLoS One**. 2013; 8(12):e84433.

156. Heo KS, Fujiwara K, Abe J. Shear stress and atherosclerosis. **Mol Cells**. 2014; 37(6):435−440.

157. Aikawa E. Extracellular vesicles in cardiovascular disease: focus on vascular calcification. **J Physiol**. 2016; 594(11):2877−2880.

158. Sider KL, Blaser MC, Simmons CA. Animal models of calcific aortic valve disease. **Int J Inflam**. 2011; 2011:364310.

159. Weiss RM, Ohashi M, Miller JD, Young SG, Heistad DD. Calcific aortic valve stenosis in old hypercholesterolemic mice. **Circulation**. 2006; 114(19):2065−2069.

160. Fazio S, Linton MF. Mouse models of hyperlipidemia and atherosclerosis. **Front Biosci**. 2001; 6:D515−D525.

161. Hinton Jr RB, Alfieri CM, Witt SA, et al. Mouse heart valve structure and function: echocardiographic and morphometric analyses from the fetus through the aged adult. **Am J Physiol Heart Circ Physiol**. 2008; 294(6):H2480−H2488.

162. Schlotter F, Halu A, Goto S, et al. Spatiotemporal multi-omics mapping generates a molecular atlas of the aortic valve and reveals networks driving disease. **Circulation**. 2018; 138(4):377−393.

163. Nakahara T, Dweck MR, Narula N, Pisapia D, Narula J, Strauss HW. Coronary artery calcification: from mechanism to molecular imaging. **JACC Cardiovasc Imaging**. 2017; 10(5):582−593.

164. Dweck MR, Jones C, Joshi NV, et al. Assessment of valvular calcification and inflammation by positron emission tomography in patients with aortic stenosis. **Circulation**. 2012; 125(1):76−86.

Chapter 22

Vascular smooth muscle cell dysfunction: role in arterial stiffening and cardiovascular disease

Patrick Lacolley[1], Jean-Baptiste Michel[2], Delphine Gomez[3,4], Magnus Bäck[1,5] and Véronique Regnault[1]

[1]Université de Lorraine, Inserm, DCAC, Nancy, France; [2]Inserm UMR_S 1148, CHU X. Bichat, Paris, France; [3]Pittsburgh Heart, Lung, Blood, and Vascular Medicine Institute, University of Pittsburgh, Pittsburgh, PA, United States; [4]Department of Medicine, Division of Cardiology, University of Pittsburgh, Pittsburgh, PA, United States; [5]Translational Cardiology, Department of Medicine, Karolinska Institutet, and Division of Coronary and Valvular Heart Disease, Karolinska University Hospital, Stockholm, Sweden

Arterial blood pressure was the last acquired hemodynamic parameter in the evolution of the structure and functions of the cardiovascular system, integrated into species' evolution.[1] This parameter is directly related to the frictional forces which progressively appeared in the arterial part of the circulation during species' life on earth, as closed "in parallel" circulations associated with cardiac septation and arterial arborescence. These important frictional forces are the fact of structural muscularization and functional tonic contraction of the arterial wall (peripheral resistances), which transfer kinetic energy generated by the beating heart into potential energy. These relations were physically defined by the Hagen–Poiseuille laws in which pressure is proportional to the blood viscosity and inversely proportional to the artery radius at power 4. The teleonomy of the arterial system is to allow localized vasodilation directly adapted to the specific biochemical energetic demand of each functioning organ, by local inhibition of the systemic arterial tone. This paradigm implies numerous bifurcations for distribution, which modify the arterial geometries and impede kinetic energy. Similarly to phylogenesis, vascular development is characterized by the presence of limited frictional forces during fetal life, which are considerably enhanced by sympathetic activation at birth, leading to high arterial pressure, in mammalian development, including humans. Therefore, the arterial circulation in mammals remains essentially a longitudinal conductance at high pressure, but frictional forces also initiate both potential energy dissipation within the wall (radial convection) and kinetic energy transfer to reflection pressure waves, a circulating cell wall colliding on arterial bifurcations.

An increase in arterial stiffening is an independent predictor of all-cause mortality and affects the cardiovascular system both globally and locally.[2] Stiffening is essentially a feature of large proximal conductance arteries, whereas control of mean arterial pressure is a feature of distal resistance arteries. Arterial stiffening has been commonly attributed to changes in extracellular matrix (ECM) proteins, mainly collagen accumulation and elastin fragmentation.[3] Beyond the cellular and molecular mechanisms that remain to be identified, one emerging concept is that vascular smooth muscle cells (VSMCs) are major contributors to arterial stiffness. Cells of the aortic wall are exquisitely sensitive to their local environment including mechanical forces, oxidative and proteolytic injuries, often inducing changes in VSMC functional properties, particularly mechanotransduction, vasomotricity, phagocytosis, efferocytosis (the process by which apoptotic cells are removed by phagocytic cells), proliferation, synthesis, and other phenotypic switching (Table 22.1). In addition, the contribution of VSMCs to arterial stiffening has been extended from aortic stiffness to include the concept of VSMC stiffness depending mainly on the architecture of cytoskeletal proteins and focal contacts to the ECM. In this chapter, we discuss molecular pathways pertaining to VSMC tone, membrane and nuclear mechanotransduction, endocytosis and phagocytosis abilities, differentiation, and immunoinflammatory activation. Fig. 22.1 shows an integrative view of signaling pathways in VSMCs underlying arterial stiffening. Fig. 22.2 is a schematic of the interactions among VSMCs, endothelial cells, platelets, and immune cells. The increasing number of studies based on

TABLE 22.1 Typical smooth muscle cell function-related markers.

Phenotype	Triggers	Markers
Contractile	Transforming growth factor (TGF)-β signaling, serum response factor (SRF)/myocardin	α-SMA, SMMHC, smoothelin, calponin-1, caldesmon, desmin, transgelin, metavinculin, α-tropomyosin, cofilin, actinin, SRF, myocardin
Synthetic and proliferative	Platelet-derived growth factor (PDGF), interleukin (IL)-1β, NADPH oxidases	Matrix metalloproteinases, calmodulin, connexin 43, cytokines (IL-6, TNF-α, MCP-1), S100 calcium binding protein A4, osteopontin, UHRF1
Endocytic—phagocytic	Convection-enhanced deliveries of blood molecules [modified low-density lipoprotein (LDL), zymogens], collision of blood cells with the wall	Scavenger receptors (SR-AI/II, LOX1, CD36, LRP-1, CD68), serpins (PN-1, plasminogen activator inhibitor-1), tissue inhibitors of metalloproteinases
Osteoblastic	Calcium phosphate crystals	Runt-related transcription factor 2 (RUNX2), bone morphogenetic protein 2 (BMP2), matrix Gla protein,
Organizer of the adventitial responses	Lipid-stimulated Peroxisome proliferator-activated receptor-γ (PPAR-γ), class II major histocompatibility complex (MHC)	VEGF, chemokines, antigen presentation, immune adaptive response

single-cell imaging and lineage tracing supports the crucial role of VSMC plasticity at the interface between mechanotransduction and epigenetic mechanisms.
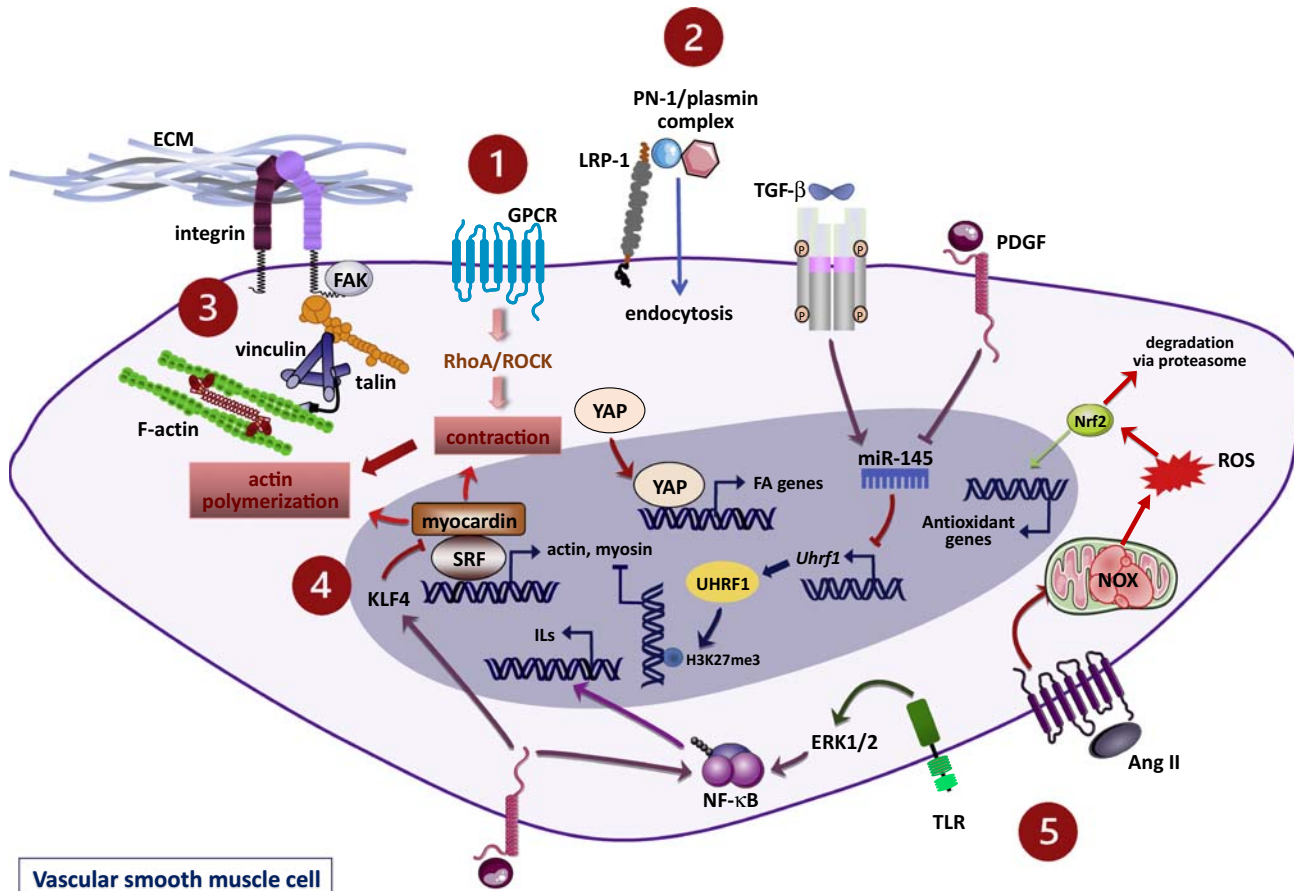
Contractile tone of vascular smooth muscle cells

VSMCs are the stromal cells of the arterial wall, continually exposed to mechanical signals, biochemical and cellular components generated in the blood compartment.[4] From the aorta to distal muscular arteries, there is a progressive reduction of the number of musculo-elastic complexes and ECM together, with an increase in the density of VSMCs. Elastic large arteries have a strong elastic potential whereas small-size muscular arteries control vasomotor tone and myogenic tone. VSMCs are involved in all the physiological functions and the pathological changes taking place in the vascular wall. Owing to their contractile tone, VSMCs of resistance vessels (small-sized muscular arteries and arterioles) participate in the regulation of blood pressure and arterial diameter, thereby protecting the capillaries from any acute increase in mechanical strength. Larger nonresistance vessels also exhibit a baseline tone, which may substantially impact pulsatile hemodynamics (such as wave reflection phenomena) but have a much less prominent role in resistance (given that resistance is strongly dependent on vessel size). VSMC contractile tone is mainly dependent on sympathetic nervous system signaling, which is involved in regional blood flow changes in accordance with organ-specific metabolic demands.

Vascular tone

Arterial tone in conductance arteries is an extrinsic level of tension, mainly depending on sympathetic system signaling, also defined as tensegrity (the internal tension of VSMCs), generated within the cytoskeleton by actin/myosin interactions, inducing arterial wall compaction by binding to ECM via integrins. In contrast, abolition of VSMC tone using potassium cyanide increases in situ carotid arterial compliance in rats. The spatial organization of VSMCs is ensured by a change in their directions in the media and by attachments to each other and to the ECM microenvironment. Indeed, there is an optimal short-term regulation of the distribution of mechanical stresses in the wall that contributes to maintaining a permanent and adapted state of tensional integrity. A stiff ECM material produces a large postload to VSMC contraction. In the longer term, functional regulation of arterial diameter requires structural changes. Elastic arteries are characterized by slow changes in contractile tone unlike muscular arteries where rapid changes in contraction allow fine regulation of regional blood flow.

Actin/myosin interactions in VSMCs are dependent on ionized calcium (Ca^{2+}) mobilization in the cells. This entry is dependent on both the initial release of Ca^{2+} from its sarcoplasmic stores by inositol 3 phosphate and the opening of calcium channels by membrane depolarization (extra- to intracellular entry and plateau). This mobilization of calcium is dependent on the interaction of extracellular ligands (catecholamines, angiotensin II, serotonin, endothelin, etc.) with G protein—coupled receptors (GPCRs), able to
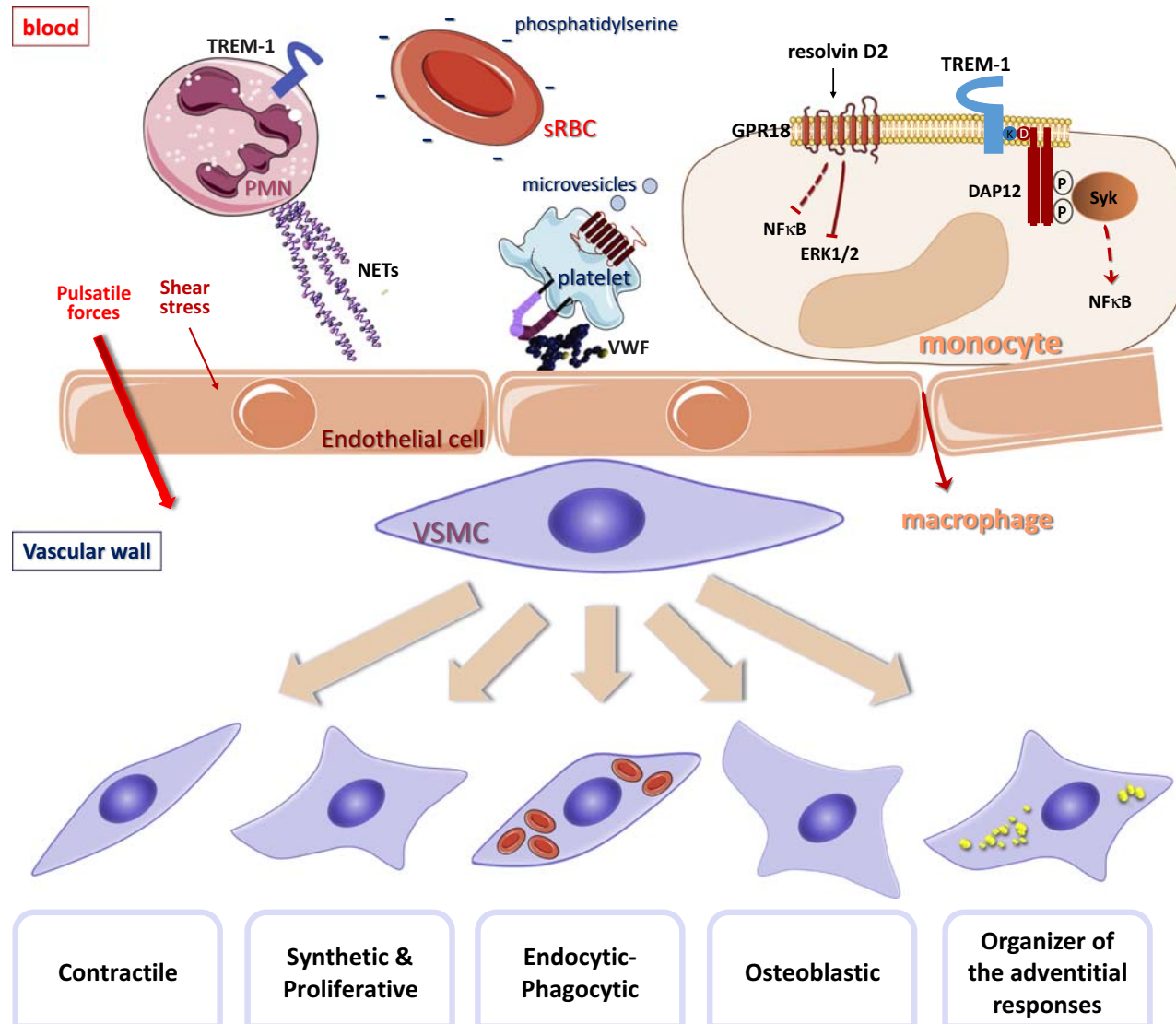
FIGURE 22.1 Molecular signaling pathways involved in vascular smooth muscle cell (VSMC) functions. ❶ Contractile tone of VSMC: activation of G protein−coupled receptors (GPCRs) and downstream effectors, RhoA/Rho kinase (ROCK) increases actomyosin interaction and contraction. ❷ Endocytosis and phagocytosis abilities of VSMCs: protease nexin-1 (PN-1) forms a complex with serine proteases such as plasmin, which is endocytosed via the low-density lipoprotein receptor-related protein 1 (LRP-1). ❸ Integrin-mediated and nuclear mechanotransduction: the local mechanical environment provided by the extracellular matrix (ECM) is transmitted via integrins, focal adhesion kinase (FAK), talin, and vinculin to the actin cytoskeleton. ❹ VSMC plasticity: platelet-derived growth factor (PDGF) induces VSMC phenotypic switching via its action on Krüppel-like factor 4 (KLF4), which disrupts the binding of myocardin to serum response factor (SRF), and binding to microRNA-145 (miR-145). ❺ Participation of inflammation and immunity in VSMC functions: angiotensin II (Ang II) increases the production of reactive oxygen species (ROS) via NADPH oxidases (NOX). In response to oxidative stress, nuclear factor-erythroid-derived 2-related factor 2 (Nrf2) drives the expression of antioxidant genes. Toll-like receptors (TLRs) activate the translocation of nuclear factor κB (NF-κB) into the nucleus, leading to the expression of proinflammatory genes such as interleukins (ILs).

activate phospho lipase-C, and promote release of both cytosolic soluble inositol triphosphate from the polar head of membranous phospholipids and hydrophobic diacyl glycerol (DAG) which remains membrane bound. Calcium binds calmodulin and activates myosin light chain (MLC) kinase. Phosphorylation of MLC promotes the binding of myosin heavy chain to actin and shortening of the actomyosin complex. In contrast with myocardium, there is no direct action of Ca^{2+} on the smooth muscle contractile apparatus. All tonic contraction is directly linked to kinase-dependent phosphorylation. In VSMC tonic contracting biology, the time of contraction is largely longer than the time of calcium mobilization. The sustained contraction is the consequence of other kinases, involving protein kinase

C translocation to membranous DAG, and phosphorylation of calponin and of caldesmon and the inhibition of MLC phosphatase (MLCP).

The Ras protein superfamily, and in particular the RhoA family of proteins, plays an essential role in the contraction and ultimately in the regulation of blood pressure.[5] Phosphorylation of MLC is a key event in contraction. MLC is dephosphorylated by calcium-independent MLCP. Genetic and pharmacological studies have shown that RhoA activation is involved in the pathophysiology of hypertension. This involves the stimulation of its target, Rho kinase (ROCK) which phosphorylates the myosin phosphatase target subunit 1 (MYPT1), a regulatory molecule of MLCP, and inhibit the activity of MLCP. There are both fast and slow forms of

FIGURE 22.2 Intercellular communications in driving vascular smooth muscle cell (VSMC) phenotypic changes. The triggering receptor expressed on myeloid cell (TREM)-1 expressed on neutrophils and monocytes promotes inflammatory pathways enhancing NF-κB nuclear translocation. Excessive release of neutrophil extracellular traps (NETs) by neutrophils leads to endothelial dysfunction and VSMC lysis. Senescent red blood cells (sRBC) exposing phosphatidylserine can be phagocytosed by VSMCs. Adhesion of platelets to the vessel wall via von Willebrand factor (VWF) and collagens disrupts the anticoagulant properties of endothelial cells and favors the expression of the prothrombotic properties of VSMCs. The interplay between immune cells and VSMCs drives the resolution of inflammation via interaction of resolvins with their receptors.

these MLC and MYPT1 molecules that accelerate contraction or promote cyclic-dependent guanosine monophosphate (GMP) relaxation. Exchange factors regulate the activation of RhoA in response to vasoconstrictor agents via GPCRs such as the angiotensin II receptor type 1 receptor. Activation of the RhoA/ROCK pathways sensitizes contractile proteins to Ca^{2+} and produces muscle tone (Fig. 22.1). An imbalance between vasoconstrictive agents, in particular those of the renin-angiotensin-aldosterone system, and vasodilating agents, in particular nitric oxide (NO) released by endothelial cells in response to flow-induced wall shear

stresses, is largely responsible for the increase in hemodynamic resistance during hypertension.

Myogenic tone

Myogenic tone is an intrinsic property of smooth muscle in resistance arteries that contracts in response to stretching (elevated blood pressure) independently of any nervous or humoral influence and contributes to dissipation of blood flow and pressure mainly in small-sized muscular arteries before the capillary system. It is only in the smallest arterioles

of the order of 100 μm that myogenic tone can significantly reduce arterial lumen in response to an increase in blood pressure. Generation of myogenic tone involves different mechanosensors which are cell membrane proteins (ion channels, GPCRs), cell-ECM interactions via integrins connected to the cytoskeleton, and intercellular junctions through cadherin-catenin complexes. Nonselective stretch-activated cation channels are key players of the myogenic response via the opening of voltage-dependent calcium channels. In VSMCs, stretch-activated cation channels opening is negatively regulated by polycystin-2, which acts by binding to filamin-A to induce actin cross-linking and to reduce the tension applied on microdomains in the VSMC membrane for a given level of blood pressure.[6] Myogenic constriction occurs mainly in small-size muscular arteries and is enhanced by integrins $\alpha_v\beta_3$ and $\alpha_5\beta_1$ and nicotinamide adenine dinucleotide phosphate oxidase (NOX)-induced production of reactive oxygen species (ROS) mainly from mitochondria (Fig. 22.1). Alterations in myogenic response cause microvascular disorders (mainly cerebral and coronary vasospasms) and may be enhanced by ECM stiffening.

Chronic low-grade inflammation is an important cause of remodeling at the macro- and microcirculatory levels, particularly in hypertension, pertaining to vascular tone. This relationship is highly dependent on activation of the renin-angiotensin-aldosterone and endothelial systems. Muscle artery remodeling is induced by increased oxidative stress and the production of growth factors such as transforming growth factor (TGF)-β, platelet-derived growth factor (PDGF), and insulin-like growth factor. The synthesis and activation of adhesion molecules leads to a reorganization of cell-matrix interactions and phenotypic changes in VSMCs. Communications between intravascular cells (endothelial cells, VSMCs, and fibroblasts) and circulating cells such as platelets, immune cells, and progenitor cells play a key role in vascular remodeling. Numerous inflammatory molecules such as cytokines controlling both innate and adaptive immune responses (monocytes, macrophages, lymphocytes, etc.) are involved in this process (see below).

Inflammation is more correlated to the elasticity parameters of the large arteries than those of the muscular arteries. It is considered to be one of the main causes of remodeling of large arterial trunks. Arterial stiffness is increased in many systemic inflammatory diseases such as rheumatoid arthritis (RA), lupus erythematosus, vasculitis, acquired immunodeficiency syndrome, and Crohn's disease. A wide variety of mechanisms are involved such as endothelial dysfunction, induction of metalloproteinases, activation of the mineralocorticoid receptor, accumulation of proteoglycans, and finally colonization of the media by inflammatory cells from the vasa-vasorum of the adventitia.

Vascular smooth muscle cell relaxation

VSMC relaxation is responsible for in vivo vasodilation. The main physiological molecule able to induce relaxation of VSMC is NO. NO is essentially produced by the endothelial cells, in which NO synthase produces NO from arginine. In large arteries, the endothelial release of NO is under the control of shear stress (increasing flow velocity increases shear stress) and Ca^{2+} entry in endothelial cells. Coupling Ca^{2+} with calmodulin displaces caveolin from NO synthase, promoting convection/diffusion of NO to subjacent VSMCs where it activates soluble guanylate cyclase, cyclic-GMP production (second messenger) and G-kinase activation, which produce relaxation by targeting numerous molecules able to inhibit all the contraction pathways. In distal resistance arteries, the relaxation mediator could also be cyclic adenosine monophosphate (AMP), generated by adenosine triphosphate (ATP) metabolism, adenosine, which interacts with its receptor, and activates the production of cyclic AMP via adenylate cyclase. Cyclic AMP (as cGMP) binds to G-kinase and inhibits all the contraction pathways, coupling vasodilation with the metabolic demand in particular in striated muscle. Endothelial NO also acts in cerebral resistance arteries, exactly coupling vasodilation with electric (depolarizing wave) neuronal activity. In the wall of large arteries (mainly aorta), VSMC relaxation is associated with increased permeability to plasma components.

In summary, systemic contraction of VSMCs determines frictional forces which define the arterial tone (peripheral resistances) which transfers flow (kinetic energy) into potential energy (arterial pressure). Local relaxation of arterial VSMCs by inhibition of the arterial tone dynamically defines the territorial tissue coupling between an organ's function and its metabolic support. Whatever the functional sense, the long-term regulation of arterial diameter requires structural changes.

Endocytosis and phagocytosis abilities of vascular smooth muscle cells

Convection is a physiological outward hydraulic conductance from the blood through the wall, corresponding to radial dissipation of potential energy (blood/adventitia pressure gradient = 100 mmHg, fluctuating within the cardiac cycle). This conveys more or less all the soluble components present in blood, including oxygen and glucose, and microparticles suspended within the blood, through the wall. Convection intensity is dependent on physicochemical properties of the conveyed molecules, arterial wall permeability, and arterial pressure. In the great majority of tissues, metabolic support delivery is the fact of diffusion from capillaries.[7] Since convection enhances

metabolic deliveries, a complete vasculature, involving capillaries, is not mandatory for the arterial wall (except the external part of the aorta in humans). The physiological principle of convection-enhanced deliveries of blood molecules, potentially explains why the arterial wall tissue is avascular. Since capillaries and venules are the privileged site of leukocyte diapedesis, the avascular character of arterial media explains also why the arterial wall is an immune privileged site, in which the tissue penetration of leukocytes is limited to the capillaries and venules-rich adventitia.[8]

In laminar conditions of flow, the particulate components of blood remain in the central axis, whereas the peripheral position of blood favors its interface with the wall. In a laminar rheological environment, red blood cells (RBCs) concentrate in the core of the stream, whereas small platelets are expelled toward the periphery, close to the endothelium. The "in parallel" evolution of the circulation, and the numerous bifurcations of the arterial tree, cause localized mechanical impairment of kinetic energy in dissipation and transfer to potential energy. These changes in arterial geometry induce collision of circulating cells with the wall due to the loss of laminarity, microscopic dissipation of circulating cells within the wall, and an increase in internal entropy of the particulate part of the blood. Collision of blood cells with the wall are mainly due to the angulation of bifurcations or the presence of luminal narrowing, but also depend on the rheology of the circulating cells. Since RBCs and platelets are the most abundant circulating cells, therefore they represent the main blood particulate elements colliding with the arterial wall in regions where biomechanical stress drives the formation of intimal tears and of small intimal hematomas.[9]

Endocytosis

In regards to the physiological convection-enhanced delivery of blood components to the wall, VSMCs acquire the capacity to endocytose or not these blood components.[10] This endocytic ability is initiated by the convection, but is also related to the ability of ECM or to cell membrane to promote retention of these soluble molecular components within the wall, at close proximity to VSMCs. For instance, blood albumin or high-density lipoproteins are convected through the wall as all soluble blood components but are not retained by interactions with the wall. Therefore these components could be used as tracers for measuring arterial wall permeability[11] and its dependency on numerous parameters: for instance, endothelial functional and structural integrity, intraluminal pressure, elastic internal lamina integrity and hydrophobicity.[12] Wall retention requires VSMC endocytosis of blood components.

The most classical example of this paradigm is physiological convection-enhanced delivery of low-density lipoproteins (LDL) to the arterial wall, their retention by interaction with glycosaminoglycans synthetized by VSMCs,[13] their potential transformation including acetylation, oxidation, aggregation, and their endocytosis after transformation, mainly by VSMCs,[14] leading to foam cell formation, containing lipid microvesicles in their cytosol.[15] Lipids internalized by endocytosis are transported to late endosomes/lysosomes, where lysosomal acid lipase digests cholesteryl esters releasing free cholesterol. Free cholesterol in turn is processed by acetyl-CoA acetyltransferase that transforms cholesterol into cholesteryl esters. Free cholesterol is exocytosed and partly recycled by ATP-binding cassette transporter A1[16] in reverse transport.[17]

Convection-enhanced delivery to the arterial wall is not limited to lipoproteins. All the blood molecules transit and could be or not retained within the arterial wall. Circulating zymogens are outwardly convected through the wall where they can be activated. For instance plasminogen, which circulates in the blood at a μmolar range is convected to the wall and retained on lysine residues of several proteins of the VSMC membrane, where it interacts with tissue and urokinase plasminogen activators forming active plasmin. Plasmin has numerous targets in the arterial wall, involving proteolytic attack of pericellular adhesive proteins, such as fibronectin and fibrillin provoking VSMC detachment and death (a process named anoikis),[18] activation of the TGF−β release[19] from its ECM storage sites, and matrix metalloproteinase activation.[20] But these proteolytic activities are challenged by the ability of VSMCs to synthetize antiproteases, able to form protease/antiproteases complexes. Due to its powerful proteolytic activities, plasmin cannot be endocytosed by VSMCs, but the complex plasmin/protease nexin-1 (PN-1, serpin E2, a tissue serpin, highly expressed by VSMCs[21]) could be endocytosed, via the low-density lipoprotein receptor-related protein 1 (LRP-1) scavenger receptor (SR),[22] which has the ability to bind and to internalize protease/antiprotease complexes (Fig. 22.1).[23] VSMCs are rich in LRP-1 and antiproteases, including tissue inhibitor of matrix metalloproteinases. The formation of complexes and their ability to be endocytosed by VSMCs represent the main defense system against the proteolytic injury of the arterial wall. Other complexes such as hemopexin/heme bind to LRP-1 are then internalized and degraded in the lysosome, representing an important defense system against hemolytic-dependent oxidation within the arterial wall.[24]

Phagocytosis

Since Brown and Goldstein's early work with macrophages, the phagocytic function in the arterial wall is canonically assumed by professional phagocytes of myeloid origin. The team of Martin Bennett was the first to show that VSMCs could assume phagocytosis of

homotypic apoptotic bodies in the arterial wall.[25] A large amount of data exists showing that the presence of nonprofessional phagocytes (VSMCs in the arterial wall) is a general feature in most tissues.[26] This point is important in pathophysiology because it suggests that professional phagocytes, macrophages for instance, are not mandatory for tissue debridement by efferocytosis.[27] For instance, primary cultures of VSMCs are able to clear (and metabolize) a load of 10^6 senescent RBCs in 5 days, whereas fresh RBCs remain intact.[28] Senescent RBCs are characterized by phosphatidylserine exposure (Fig. 22.2). Senescent RBCs are more prone to hemolysis and Fe^{2+}-derived oxidative stress, both participating to the initial stages of atheromata in the human aorta. This phagocytic capacity is not limited to dying cell but also includes crystals such as cholesterol crystals[29] or hydroxyapatite microcrystals. This ability was mainly tested on macrophages, and synoviocytes, but not yet in VSMCs. In this context, crystal phagocytosis provokes inflammasome activation, interleukin (IL)-1 release, neutrophil attraction, and cell death.[30]

Scavenger receptors and eat me signaling

The first SR of modified LDL (but not native LDL) was reported by Brown and Goldstein in 1979. They bind also numerous other ligands, including polyanionic ligands, such as high glycated proteins. An important consensus review on SRs was published in 2017.[31] This review identifies 12 classes and more than 30 SR types in human and mouse. These SRs are able to bind more or less diverse ligands including lipids, phospholipids, sugar, microvesicles, protease/antiprotease complexes, and pathogens. These endocytic schemes are essentially explored in professional phagocytes of myeloid origin, but far less in the arterial physiology and its corresponding stromal cells (endothelial cells and VSMCs). SR-AI/II are expressed by VSMCs, and their expression is enhanced by oxidation and oxidized (ox) LDL.[14] CD36 is essentially expressed by macrophages, but also in VSMCs in which its activity could be stimulated by oxLDL and fatty acids, but this effect is challenged by clinical epidemiology in humans.[32] Similarly lectin-like oxLDL receptor-1 (LOX-1) expression is upregulated in response to oxLDL exposure, oxidative stress, activation of nuclear factor κB (NF-κB), and jun-kinase pathways.[33] Nevertheless, in our own experience, LOX-1 is less expressed than other SRs in cultured human VSMCs in response to oxLDL. In contrast, LRP-1 is more expressed in cultured VSMCs in response to oxLDL and is more specific for aggregated LDL.[34] As cited above, VSMC LRP-1 plays a major role in the VSMC defense against proteolytic injury. *In vivo*, selective deletion of LRP-1 in mouse VSMCs leads to aortic aneurysm development, due to ECM degradation.[23,35]

Interesting enough is the story of CD68 and its mouse ortholog macrosialin. CD68 is a transmembrane glycoprotein essentially associated with the endosomal/lysomal compartment, through a lysosomal-associated membrane protein domain.[36] In bone-marrow leukopoiesis, CD68 expression is restricted to myeloid progenitors, but absent of lymphoid development. CD68 is an SR for oxLDL, exposed phosphatidylserine, and malaria sporozoite.[37] CD68 was mainly used (and abused) as a monocyte/macrophage lineage histochemical tracing in human atherosclerosis, but CD68 is a functional marker of lysosomal and phagosomal activity whatever the cell lineage. CD68 expression is highly regulated by powerful transcription factors, E26 transformation−specific sequence-1 and friend leukemia integration-1, which upregulate its expression in myeloid cells, whereas interferon (IFN)-regulatory factor 4 represses its expression in lymphoid lineage.[38] CD68 expression is also governed by a cell lineage differential splicing, using alternative promoters related to chromatin remodeling in the promoter region.[39] This is usually observed in arterial VSMCs forming foam cells in mice.[40] In VSMCs, expressed CD68 can quickly shuttle from the cell membrane to the lysosome/phagosome. Therefore, in VSMC foam cells, CD68 staining is essentially intracellular, associated with lysosome/phagosome in α-actin-positive vesicles, suggesting important interactions with the cytoskeleton. Therefore, CD68 could participate in the link between endo/phagocytosis, cytosolic microvesiculation, and exosome release.

Exposed phosphatidylserine is the most frequent "eat me" signal for phagocytosis. Some SRs are directly involved in phosphatidylserine exposure. Other diverse phagocytosis biological schemes have been described including phosphatidylserine multiple ligand-mediated engulfment of apoptotic bodies, senescent living cells, or parts of the cell and extracellular vesicles (EVs).[41] Recently another paradigm was published concerning too large biological objects such as large deposits of aggregated lipoproteins (fatty streaks) or dead adipocytes. Contrasting with engulfment, exophagy is characterized by a tight contact with large targets, followed by release of lysosomal acidic enzymes in the near environment of the target, sharing similarities with osteoclastic process.[42] Nevertheless, these biological procedures were experimentally described always with macrophages. The activity or not of such processes, associated with VSMC phagocytic activities remains to be explored in the cardiovascular tissues and cells.

One important point is the direct link between these intracellular inputs of endocytosed and/or phagocytosed activities and the exosomal output releasing activity. Schematically, there are two important pathways for the biological waste metabolism, the lysosomal pathway leading to complete degradation and recycling of the waste

input by lysosomal and phagosomal activity, and exosomal activity, EV and exosome releases, protecting cells against excessive intracellular stress.[43] Because of the physiological convection of blood components through the wall, as described above, these endocytic activities of VSMCs are mandatory for arterial tissue homeostasis. In pathological conditions, these activities could be overloaded in nonprofessional phagocytes, such as VSMCs, leading to death or to an excessive vesiculation and exosomal activities, participating in the pathology through the ability of exosomes to signal to the immune system, particularly to adventitia,[8] and/or to serve as phospholipids, phosphate-rich substrates for calcifications (Fig. 22.2).

In summary, the role of VSMCs in all vascular diseases cannot be interpreted independently of their endocytosis and phagocytosis abilities, as a physiological consequence of arterial blood pressure.

Integrin-mediated and nuclear mechanotransduction in vascular smooth muscle cells

VSMC−matrix interactions are key molecular/cellular mechanisms contributing to vascular stiffness and are controlled by mechanotransduction and mechanosensing.[44] Numerous cardiovascular complications where VSMC dysfunction compromises cell-ECM homeostasis can thus be envisioned as mechanotransduction disorders.

Membrane mechanotransduction

The biological responses of VSMCs to mechanical stimuli include the transduction of the signal ensured by mechanosensitive molecules and the epigenetic control of genes encoding structural components of the ECM (e.g., collagen, fibronectin, fibrillin, and proteoglycans), chemokines [e.g., monocyte chemoattractant protein (MCP)-1], cytokines (e.g., TGF-β, cardiotrophin-1, and ILs), and proteases (e.g., matrix metalloproteinases or serine proteinases) and their inhibitors (e.g., tissue inhibitor of metalloproteinases and tissue serpins). VSMCs sense their local mechanical environment mainly through an ECM fibrillar components—integrins—cytoskeletal axis. Integrins are αβ-heterodimeric transmembrane receptors highly present on the surface of VSMCs in an inactive folded conformation. Many constituents of the ECM have motifs that are binding sites for different members of the integrin family. The specificity of the binding depends on both the motifs in the ECM protein sequence and the type of α and β subunits of the integrin; as an example, integrin $\alpha_1\beta_1$ preferentially binds collagen and integrin $\alpha_5\beta_1$ binds fibronectin. In this way, integrins enable cells to evaluate both the mechanical state and the specific composition of the local ECM.

Clustering of integrins at specific sites of the VSMC membrane form focal adhesions (FAs) serving as hubs for mechanotransduction. FA formation and turnover are highly regulated in a dynamic way that can be divided into three phases: assembly, stability, and disassembly. FAs provide the bidirectional link between extracellular constituents and intracellular actomyosin cytoskeleton through the integrin receptors for the outside-in or inside-out transduction of mechanical and biological signals (Fig. 22.1). Associated integrin linker proteins [e.g., actinin, talin, vinculin, and focal adhesion kinase (FAK)] are responsible for integrin activation and the anchoring of actin filaments to the integrin intracellular domains. Integrin activation and clustering is triggered by ligand binding and recruitment of talin that binds F-actin through actin-binding or vinculin-binding sites. Talin-to-vinculin binding forms a so-called molecular clutch which increases actin polymerization and promotes cell sensing of its mechanical environment.

FA recruitment and strengthening ended by FA protein recycling, defining their lifetime (from 10 s up to a few minutes), depend on intracellular FAK phosphorylation and matrix stiffness. On a compliant ECM, dynamic interactions between integrins, talin, and actin are short-lived and exhibit a slip-bond behavior that does not require vinculin. In contrast, on a stiff ECM, low exchange rates of FA proteins (high association and low dissociation constants) reinforce vinculin-dependent binding of talin to F-actin and activate catch bonds. Such catch bonds are currently thought to be key actors of the stiffening of the wall components. Lifetimes also depend on the direction of the applied force (pointed end−directed and barbed end−directed loads). In addition, levels of adhesion exerted by FAs are spatially regulated with higher levels in periphery at cell edges than near the nucleus. Mechanical stresses enhance ROS production and signaling, which can regulate FA turnover. Indeed, increased expression of NOX4, a main source of ROS localized to FAs and in mitochondria, fosters arterial stiffness, at least in part, by increasing the number of persistent FAs. Actin polymerization-depolymerization and adhesive properties of FAs also contribute to cell stiffness. The FAK/Src signaling network has been reported to control VSMC stiffness.[45] There is, therefore, a need to elucidate the contribution of cellular stiffness to vascular wall stiffening.

Increased arterial stiffness has been attributed to a coupling between the integrin pathway and the mechanosensitive pathways involving GPCRs and their effectors that trigger VSMC contraction. GPCR activation and downstream signaling via RhoA/ROCK pathways maintain a high degree of phosphorylation of MLC by decreasing MLCP activity. In support of a role of ROS on integrin activity, lysophosphatidic acid has been shown to increase integrin-fibronectin adhesion via activation of β_1 and β_3 integrins. This is mediated by

GPCRs and the production of ROS, and controls the myogenic tone in resistance vessels. Intermediate filaments also participate in force transmission between FAs and the actomyosin network. It has been shown, for example, that genetic deletion of vimentin in mice increases carotid stiffness through increased FA turnover and VSMC contractility. It should thus be anticipated that acting on FAs or G-protein—coupled contractility could modulate arterial stiffness.

Nuclear mechanotransduction

The mechanical environment of VSMCs not only impacts the ECM—integrin—cytoskeletal axis but also the nuclear membrane, which becomes physically linked to some FAs through the cytoskeleton and can act as a mechanosensor. The nuclear pore complex, which form a stable scaffold embedded in the nuclear envelope where the inner and outer membranes are fused and decorated with intermediate filaments, serves as the primary gateway regulating the macromolecular traffic between the nucleus and cytoplasm. The linker of nucleoskeleton and cytoskeleton (LINC) complex also couples actomyosin with the lamina scaffold. These two networks ensure the nuclear transmission of the tensile forces in the VSMC microenvironment, thereby affecting gene expression by altering chromatin organization and regulating epigenetic pathways via lamin A and emerin. Highly compacted inactive chromatin (heterochromatin) is associated closely with the lamina scaffold at the periphery of the nucleus (inaccessibility of promoters of genes) while the loosely compacted active chromatin (euchromatin) is present at the center of the nucleus (increased accessibility). In response to matrix stiffening, forces transmitted via assembled actin filaments increase recruitment of FAs and LINC complex proteins, and stabilization of lamin A. In addition, it induces phosphorylation of emerin, which contributes to reinforce the LINC complex. Taken together, this balances outside and inside forces. In support of the key role of lamin A, a mutation in the gene encoding lamin A is responsible for Hutchinson—Gilford progeria syndrome (HGPS), a disease hallmarked by altered mechanotransduction and the inability of the nucleus to respond dynamically to mechanical stress together with disappearance of VSMCs. The consequences are an acceleration of vascular aging and arterial stiffening leading to premature death. HGPS VMSCs exhibit increased phosphorylation of histone H2A.X, which is required for activation of the DNA damage response.

Recently, the Hippo pathway effectors Yes-associated protein (YAP) and transcriptional coactivator with PDZ-binding motif (TAZ) have been shown to act as downstream sensors of ECM stiffness to regulate FA assembly following nuclear shuttling.[46] YAP/TAZ nuclear localization activates RhoA/ROCK signaling and increases the expression of several FA genes (Fig. 22.1), including α_v
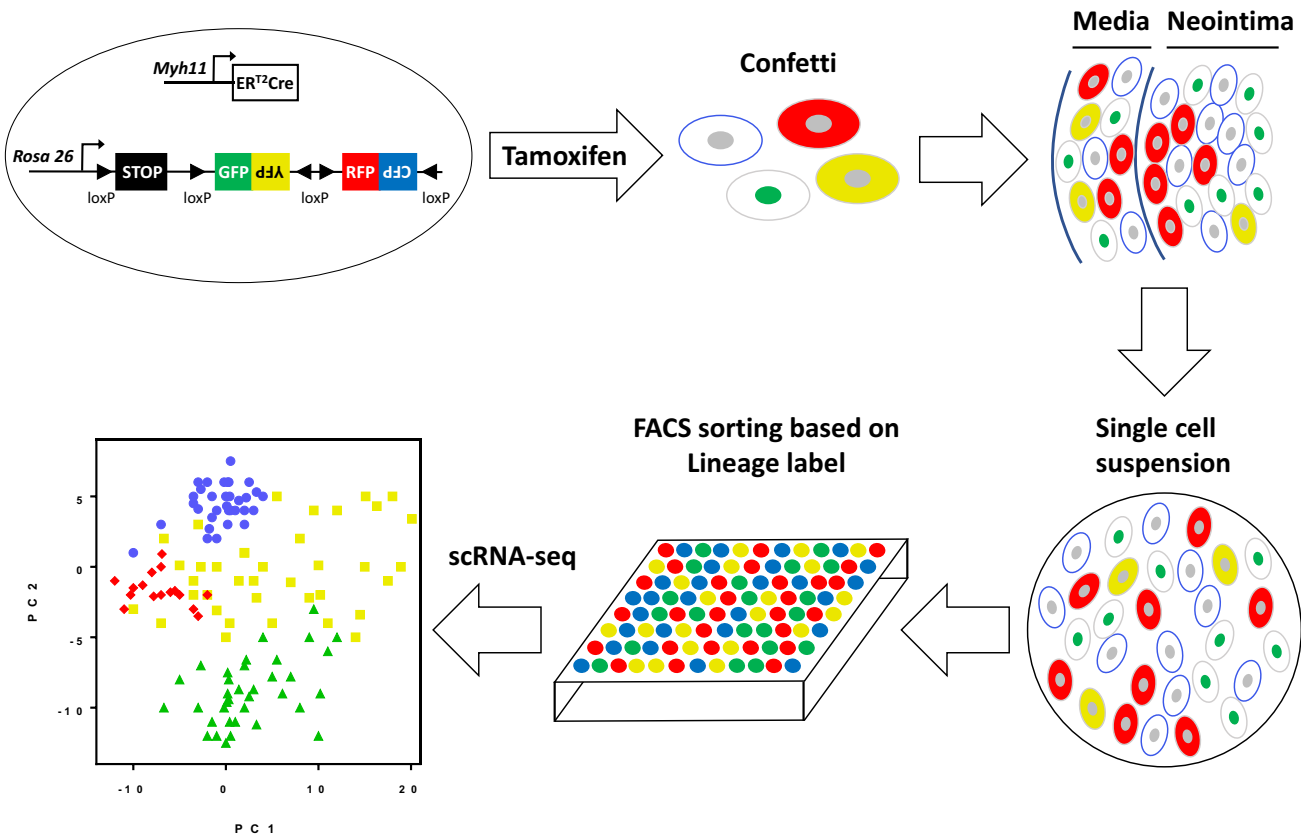
and β_3 genes. YAP and TAZ drive VSMC migration and proliferation, as well as cell renewal. The YAP/TAZ pathway also regulates arterial stiffness as a target of Rac-GTPase involved in TGF-β1—induced fibrotic signaling.

Epigenetic mechanisms are involved centrally in arterial diseases. Classically, the dynamics of the epigenetic code are mainly orchestrated by DNA damage and oxidative stress, causing changes in chromatin regulatory elements (DNA methylation and histone acetylation, methylation, and phosphorylation) as well as in nonprotein-coding RNAs (microRNAs and long noncoding RNAs). Hypomethylation of the promoter region of the integrin-binding protein 2 gene has been reported to be associated with decreased arterial stiffness in the TwinsUK cohort, thus supporting the contribution of epigenetic regulation of arterial stiffness. Hypomethylation of the microRNA-203 promoter induces decreased expression of FA proteins and altered FAK signaling resulting in increased VSMC stiffness.

In summary, mechanotransduction in VSMCs can be resolved into extrinsic (hemodynamic dependent) and intrinsic (actomyosin activation) mechanisms. Outside-in transduction refers to the transmission of the initial stretch of the ECM to the cytoskeleton and nuclear envelope via integrins, FAK et GPCRs. This process drives chromatin remodeling and changes in gene expression. Inside-out transduction, which is initiated by the sliding of myosin onto actin, leads to VSMC shortening and thus compaction of the vascular wall. The effects on cell and tissue physiology can be recapitulated as stretch versus shortening and distension versus compaction.

Vascular smooth muscle cell plasticity

Despite being highly specialized, VSMCs retain the remarkable capacity to modulate their phenotype in response to changes in their environment. These phenotypic modulations drive the functional diversity of VSMCs and their role in arterial physiology and vascular disease. The plastic nature of VSMCs has been extensively studied in vitro for the past 30 years.[47,48] From these studies, Gordon and Julie Campbell established the concept of VSMC phenotypic switching, a model in which VSMCs shift from a differentiated, contractile phenotype to a dedifferentiated, "synthetic" phenotype (Table 22.1). Yet, the investigation of VSMC phenotype and function in vivo has been a decade long challenge in the field due to the inner difficulty and ambiguity to identify dedifferentiated VSMCs because of a strong repression of traditional VSMC marker gene expression (e.g., *MYH11*, *ACTA2*, and *TAGLN*).[49] This major limitation motivated the development of reliable in vivo fate mapping system, based on the specific and stable labeling of medial VSMCs, first developed in the early 2000s by Robert Feil's group.[50—52]

FIGURE 22.3   Schematic showing strategies for lineage labeling of vascular smooth muscle cells (VSMCs) and single-cell RNA-sequencing. Tamoxifen treatment activates Myh11-driven inducible Cre-recombinase resulting in VSMC-specific excision of the stop codon in the multicolor Confetti reporter inserted into the Rosa26 locus. VSMC lineage cells, randomly labeled with one of four fluorescent proteins (GFP, YFP, RFP, and CFP), can be tracked in medial and neointimal layers. After preparation of a single-cell suspension and fluorescence-activated cell sorting (FACS) based on the expression of lineage label, transcriptional profiling is performed by scRNA-seq and principal component analysis.

VSMC fate mapping combined with immunofluorescent staining and high-resolution confocal microscopy have demonstrated the significant contribution of VSMCs in the development and progression of vascular disease and their remarkable phenotypic plasticity (For details, see the basic concept box and Fig. 22.3).[53]

Unbiased analysis of the heterogeneity between VSMCs within and between different healthy vascular beds was enabled with the development of single-cell RNA-sequencing combined with VSMC lineage tracing.[54] For example, such an approach has been used to track subsets of cells expressing the mesenchymal stem cell marker Sca1 among distinct VSMC clusters (Myh11-lineage) identified by single-cell RNA-sequencing on whole aorta and to evaluate their potential contribution in atherosclerotic lesions.[55,56] Thus, VSMC phenotypic characterization and identification of a particular signature at the level of single-cell profiling may provide insight into disease predisposition and response.

The age- or disease-related phenotypic modulation of VSMCs often manifests as a change from a mature quiescent contractile phenotype (differentiated) to a more migratory, proliferative phenotype (dedifferentiated). Dedifferentiation to synthetic and proliferative states leads to ECM accumulation or hypertrophy of the vascular wall, which affects directly arterial stiffness. The differentiated or intermediate states of VSMCs are classically hallmarked by a repertoire of markers including smooth muscle-specific contractile proteins [e.g., α-smooth muscle actin (SMA), smooth muscle myosin heavy chain (SM-MHC) and calponin], cytoskeletal molecules (e.g., actin and actinin), transcription factors [e.g., serum response factor (SRF) and ETS-like transcription factor 1 (Elk-1)], inflammatory-related factors [e.g., phospho-extracellular signal-regulated kinases (ERK) 1/2, intercellular adhesion molecule 1, TGF-β, and pro-collagen 1], epigenetic factors [e.g., sirtuins (SIRTs)], and ECM stiffness.

Environmental molecular changes drive a phenotypic modulation characterized by reduced expression of SMC-specific contractile proteins as well as increased cell proliferation and production of proinflammatory cytokines. These phenotypic changes contribute to intimal thickening

and calcifications. Additional phenotypic changes are common in diseases, including differentiation of VSMCs toward myofibroblast-like, macrophage-like, and mesenchymal stem cell—like cells, among others. Aberrant phenotypic transitions are exemplified in arterial calcification where VSMCs undergo an osteo/chondrocytic conversion with active release of matrix vesicles triggering the mineralization process. Another new concept is that of progenitor cell transition. Differentiated VSMCs can migrate from the outer media into the inner adventitia and express progenitor cell markers on induction of the transcription factor, Kruppel-like factor 4 (KLF4). Resident SMC-derived progenitor cells contribute to medial repair by differentiating into medial VSMCs.[57] A key question is to determine whether phenotypic modulation occurs in all VSMCs (polyclonal hypothesis) or only in subsets of VSMCs (monoclonal/oligoclonal hypothesis). Another challenge is to develop an integrated dynamic analysis of the early (reversible) and late (irreversible) phenoconversion of VSMCs, particularly in relation to arterial stiffening development.

Regulation of vascular smooth muscle cell differentiation by growth factors and transcriptional factors

PDGF and TGF-β are master regulators of VSMC phenotypic plasticity. PDGF-BB and PDGF-DD promote downregulation of VSMC-specific contractile genes by activation of their receptor PDGFR-β. Canonically, the action of PGDF-BB depends on the transcription factors KLF4 and Elk-1. Alternatively, PDGF-BB has been reported to degrade contractile proteins by activation of autophagy which also elicits cytoprotective effects through removal of proteins damaged by increase in oxidative stress. VSMC phenotypic modulation is hallmarked by the inflammatory state of VSMCs. While both IL-1β and PDGF-DD repress SMC differentiation marker genes and upregulate proinflammatory genes, the transcription factor NF-κB is a critical mediator of the effects of IL-1β. PDGF-DD primarily induces downregulation of the proinflammatory chemokine (C—C motif) ligand 20 (CCL20) and upregulation of the regulator of G-protein signaling 17 (RGS17) involved in cell proliferation and migration.

In contrast to PDGF, TGF-β promotes the contractile phenotype through phosphorylation of Smad2/3 and Smad1/5/8 signaling. This increases phosphoSmad2/3 binding to α-SMA, calponin, and SM22α promoters. The opposite effects of PDGF and TGF-β on VSMC phenotype switching is tightly regulated by microRNAs, in particular microRNA-143/145, microRNA-221 and microRNA-222, microRNA-21 and microRNA-24. In the context of intimal proliferation, elevated TGF-β/Smad3 upregulates

canonical Wnt/β-catenin signaling thereby promoting VSMC proliferation.

The SRF/myocardin-dependent control of VSMC plasticity illustrates the role of transcriptional pathways.[58] Binding of the trans-acting factor SRF to a DNA sequence called the CArG box (cis-acting element) induces transcription of VSMC marker genes of differentiation. Interaction of SRF with VSMC coactivators including myocardin and myocardin-related transcription factors A and B strongly enhances its affinity for the CArG elements of specific contractile genes. In contrast, interaction with members of the ternary complex factor family of Ets domain proteins such as Elk-1 increases the expression of immediate-early genes (e.g., c-fos) and VSMC dedifferentiation. Stimulation of the mitogen-activated protein kinase (MAPK) pathway by growth factors shifts the binding of SRF toward Elk-1 and thereby represses VSMC gene expression by disrupting myocardin-SRF interactions. KLF4 has also been identified as a potent repressor of contractile genes through interaction with phosphorylated Elk-1, modifications of chromatin structure of CArG box-containing promoters, sequestration of SRF, and reduction of myocardin expression (Fig. 22.1). VSMC stiffness mechanisms occurring in hypertension depend on the activation of SRF co-factors. An inhibitor of SRF activity normalizes VSMC stiffness paralleled by an improvement of aortic elasticity that precedes the reduction of blood pressure in spontaneous hypertensive rats.

Exaggerated production of ROS and cell senescence are hallmarks of vascular aging. The transcription factor, nuclear factor-erythroid-derived 2-related factor 2 (Nrf2) orchestrates the transcriptional response of cells to oxidative stress by driving the expression of antioxidant genes via its binding to antioxidant response elements in their promoters (Fig. 22.1). Age-related downregulation of vascular Nrf2 expression as well as dysfunction of the nucleocytoplasmic shuttling of Nrf2 sensitize VSMCs to oxidative stress-induced damage.

Altogether, aging and hypertension are associated with a shift toward VSMC dedifferentiation mainly orchestrated by PDGF and SRF/Elk-1 in parallel with a lower activity of the differentiation program triggered by SRF/myocardin and TGF-β. Decrease in Nrf2 with aging acts additionally by reducing the expression of antioxidant genes leading to loss of VSMC plasticity and increased senescence.

Epigenetic determinants of vascular smooth muscle cell plasticity

While VSMC phenotypic switching appears as a causal mechanism responsible for arterial stiffening, characterization of VSMC plasticity at the epigenetic level is a new

area in this topic. Epigenetic regulation directly affects expression of differentiation genes by modulating chromatin remodeling, DNA methylation or histone modifications, and noncoding RNAs.

SIRTs have emerged as the first epigenetic modifiers of arterial stiffness. It has been demonstrated that SIRT-1, an oxidized nicotinamide adenine dinucleotide (NAD$^+$)-dependent class III protein deacetylase, slows down the development of arterial stiffness in the presence of neointimal formation after vascular injury or diet-induced obesity. The mechanisms are likely due to its antiinflammatory and antioxidant effects. SIRT-1 inhibition is caused by disruption of zinc binding that is critical for the enzymatic activity of SIRT-1. In nonhuman primates, the SIRT-1 activator resveratrol prevents the increase in pulse wave velocity in response to Western diet. Increased peroxynitrite-mediated SIRT-1 inhibition in response to nicotine contributes to arterial stiffness in mice. In further support of this protective role, the decline in SIRT-1 protein levels with age drives increased inflammation and premature VSMC senescence. The predominant localization of SIRT-1 in the nucleus confers it the means to exert its effects through transcriptional mechanisms and epigenetic pathways. For example, the antiinflammatory action has been described to be dependent on casein kinase II-mediated phosphorylation of SIRT-1, which promotes its deacetylase activity on the methyltransferase enhancer of zeste homolog 2 (EZH2) and thereby suppresses the EZH2-mediated H3K27 trimethylation of the SM22α promoter region and subsequent gene silencing.

In addition, noncoding RNAs can control the expression of epigenetic regulators. For example, the ubiquitin-like containing PHD and RING finger domains 1 (UHRF1) binds to promoters of genes that govern VSMC differentiation (*MYH11*, *ACTA2*, and *SM22*) and inhibitors of the cell cycle (*CDKN1A* and *CDKN1B*), leading to repression of these genes via DNA and histone methylation (increase in H3K27me3) (Fig. 22.1). In addition, microRNA-145, upregulated by PDGF-BB and downregulated by TGF-β, decreases UHRF1 expression. Inhibition of UHRF1 has been seen to reduce aneurysm severity in experimental models.[59] Altogether, these mechanisms indicate that the Hippo pathway YAP/TAZ as well as UHRF1 may be positioned at the crossroads of nuclear mechanotransduction and epigenetic regulation of arterial stiffness. Finally, the maintenance of the progenitor phenotype dependent on KLF4 and progenitor cells are characterized by loss of the H4Ac chromatin mark and retention of the H3K4Me2 mark. This demonstration suggests that this physiological in situ VSMC reprogramming could be critical in determining the trajectories of vascular aging, normal vascular aging, or early vascular aging.

Cell senescence

As described in detail in Chapter 23, cell senescence is a durable, irreversible, cell cycle arrest of replication with cells which remain metabolically active and become resistant to apoptosis due to the upregulation of antiapoptotic proteins.[60] VSMC senescence with that of endothelial cells is one of the common and early mechanisms that produce reduced vasodilation and increased vasoconstriction, oxidative stress and inflammatory cytokine production in vascular aging.[61] The most highly expressed markers are senescence-associated β-galactosidase (SaβG), a lysosomal enzyme present in endothelial cells, VSMCs and fibroblasts, and the senescence-associated secretory phenotype (SASP) cytokines: IL-6, tumor necrosis factor (TNF)-α, and MCP-1. The presence of telomere-associated DNA damage foci (markers of double stranded DNA breaks) consecutive to SASP appears to be a more specific marker than SAβG because it provides information on the senescent cell and its environment. Indeed, persistent activation of DNA damage and ROS production via the SASP impact adjacent cells, leading to an increased senescence burden. The others, also nonspecific, are those related to irreversible growth arrest with telomere shortening, loss of proliferation markers, and of specific microRNA or proteins, such as lamin B1, CDKN2A (p16), CDKN1A (p21), and TP53 (p53). Leukocyte telomere length, a marker of cell senescence, is inversely correlated with increased arterial stiffness.[62]

The change in expression of a marker in VSMCs in physiopathology is also difficult to interpret because the markers are not lineage specific. Cell senescence is also dependent of epigenetic regulation. Therefore, the combination of markers of the epigenetic signature of VSMCs (dimethylation and acetylation of promoters of the smooth muscle-specific genes, e.g., *SM-MHC* gene) with classical senescence markers is of major interest to determine the origin of the different cells and the stage of progress of vascular senescence. For example, replicative senescence of VSMCs is linked with their propensity to undergo transdifferentiation toward an osteochondrogenic or macrophagic lineage. The age-induced decline in SIRT1, a key epigenetic regulator of TP53 which induces its degradation via deacetylation, reinforces age-related VSMC phenotypic changes. Recent work also indicates that noncoding RNAs play a key role in SASP cytokine release at the interface between cell senescence and vascular aging.[63]

In summary, phenotypic regulation governs the functional diversity of VSMCs and their role in cellular stiffness and arterial stiffness. Changes in their local mechanical environment regulate their gene expression through transcriptional regulatory pathways and epigenetic programming. VSMC senescence can lead to arterial stiffening but

ECM stiffening can also lead to VSMC senescence. In view of the multiple roles of VSMCs and feedback controls, computational models can be used to build protein networks in relation to epigenetic factors.

Participation of inflammation and immunity in vascular smooth muscle cell functions

Increased systemic inflammation, as seen in e.g. in RA, systemic lupus erythematosus, systemic vasculitis, human immunodeficiency virus, and inflammatory bowel disease, is associated with an elevated cardiovascular risk and also with increased arterial stiffness,[64] even in the absence of prevalent cardiovascular comorbidities.[65] Since a longer disease duration of RA is an independent predictor of vascular stiffness, the notion emerges that exposure to chronic inflammation may be causally linked to arterial stiffening. This is further supported when considering that each year of life with RA contributes to a higher rate of vascular stiffening than a patient's year of life without RA.

Arterial stiffening goes hand in hand with chronic inflammation promoting the interactions of different innate and adaptive immune cells and platelets with the vessel wall. This contributes to the immunoinflammatory response by multifactorial mechanisms, including endowing the vascular wall with a proinflammatory phenotype, fostering leukocyte recruitment and infiltration, promoting alterations in intracellular metabolic pathways, and amplifying close interplay between macrophages and VSMCs. Increased proliferation and migration, production of proinflammatory mediators and loss of contractile phenotype hallmark VSMC changes in an inflammatory environment.

Cytokines et chemokines

VSMCs express toll-like receptors that play a critical role in the production of components of the inflammasome associated with the innate immune response (e.g., IL-1β. IL-6, and IL-18) (Fig. 22.1). Angiotensin II acts on T-helper lymphocytes to produce IL-2, TNF-α, and IFN-γ, and Th2 lymphocytes for the cytokines IL-4, IL-5, IL-6, and IL-10. In this context, IL-6 produced by adaptive immune cells and VSMCs contributes to angiotensin II-induced hypertension through the phosphorylation of Janus kinase 2 and signal transducer and activator of transcription 3. Accumulation of IL-17 in the medial layer in thoracic aorta causes vascular dysfunction. The mechanisms involve a synergistic effect with TNF-α to trigger the expression of VSMC proinflammatory genes. IL-18 enhances the angiotensin-II-induced NOX1-dependent VSMC proliferation and migration. Disruption of IL-1β signaling induces a change in cell composition in atherosclerosis characterized by a reduction of VSMCs and an increased proliferation of resident macrophages. Recently, the long noncoding RNA H19, which is located in VSMCs and infiltrating aortic macrophages has been shown to increase IL-6 expression in VSMCs via competition with let-7a target gene IL-6, thus promoting vascular inflammation and cell senescence.

Increased adhesiveness of platelets at the vessel wall and vascular leukocyte infiltration elicit an endothelial dysfunction (Fig. 22.2). This results in a loss of anticoagulant role of endothelial cells together with the expression of the prothrombotic properties of VSMCs that express high levels of tissue factor, which in turn generates various proteases, including activated factor X (factor Xa) and thrombin. Factor Xa acts on protease-activated receptor (PAR)1 to control VSMC proliferation and migration while thrombin-mediated mitogenic effects on VSMCs were found to be dependent on integrin $\alpha_v\beta_3$ via activation of FAs. Activation of PARs by thrombin also promote the proinflammatory phenotype of VSMCs by enhancing the synthesis and release of cytokines and chemokines (e.g., IL-6, C-X-C motif chemokine ligand 8) via activation of MAPK pathways.

Innate immunity and extracellular vesicles

Infiltrating macrophages, EVs, and neutrophil extracellular traps (NETs) are key mediators of vascular inflammation (Fig. 22.2). Activated macrophages exhibit increased glycolysis enhancing cytokine production. Changes in metabolism control macrophage polarization. While several intermediate phenotypes exist that modulate the innate immunity, enhanced glycolysis and tricarboxylic acid cycle activity hallmark proinflammatory M1 macrophage activation while antiinflammatory M2 macrophages show enhanced oxidative phosphorylation, including fatty acid β-oxidation. It has become increasingly evident that EVs mediate cell−cell interactions and could stimulate immune responses. Macrophage-derived EVs have been reported to transport α_5 and β_1 integrins to the surface of VSMCs, which in turn activates the ERK and Akt pathways and fosters VSMC adhesion and migration. VSMC reprogramming has also been found to initiate inflammation. Expression of progenitor cell markers by VSMC migrating into the adventitia, a process regulated by KLF4, potentially results in differentiation into macrophages. NETs are histone-DNA components of dying cells involved in the defense of the host against pathogens. Excessive release of NETs can cause vascular tissue lesions and triggers thrombotic events, particularly in systemic autoimmune diseases.[66] In addition, the release of NETs induces endothelial cell death leading to infiltration of neutrophils and VSMC lysis in atheroma.

Among the potential candidates acting as amplifiers of the innate immune response, the triggering receptor expressed on myeloid cells (TREM)-1 appears to play a central role.[67] TREM-1 is expressed by neutrophils,

macrophages, and mature monocytes (CD14high), as well as by hypoxic dendritic cells, platelets, endothelial cells, and VSMCs. The cytoplasmic tail of TREM-1 associates with the adaptor molecule DNAX activation protein of 12 kDa (DAP12), which becomes phosphorylated and thereby provides a docking site for the spleen tyrosine kinase that promotes signal transduction via several pathways including NF-κB (Fig. 22.2). The engagement of TREM-1 with agonist monoclonal antibodies has been shown to stimulate the production of proinflammatory cytokines and chemokines such as IL-8, MCP-1, MCP-3, and macrophage inflammatory protein-1α, along with rapid neutrophil degranulation and oxidative burst. The activation of TREM-1 in presence of toll-like receptor-2, -4, or nod-like receptors ligands amplifies the production of proinflammatory cytokines (TNF-α, IL-1β, granulocyte-macrophage colony−stimulating factor), as well as the inhibition of IL-10 release. In response to inflammatory stimuli, the expression of TREM-1 is increased, and this mediates proliferation and migration, and shift toward a proinflammatory phenotype of VSMCs.

Failure in the resolution of inflammation

Inflammation is a recognized risk factor and therapeutic target in cardiovascular disease.[68] Chronic cardiovascular inflammation results from both a continuous immune activation and a failure in the resolution of inflammation.[69] Lowering LDL cholesterol decreases inflammatory markers such as C-reactive protein, emphasizing the close interplay between lipids and inflammation.[70] Furthermore, direct antiinflammatory treatments have shown additional beneficial effects in studies of secondary prevention in high risk patients. As an alternative to inhibiting proinflammatory signaling, cardiovascular inflammation could potentially be disrupted by actively promoting an effective resolution of inflammation.[69] Importantly, omega-3 fatty acid−derived lipid mediators called resolvins promote the resolution of inflammation.[71] In addition to their effects on immune cells (Fig. 22.2), resolvin receptors are expressed on VSMCs[72] and may contribute to slow down arterial aging.[58] For example, resolvins, and other specialized proresolving mediators, decrease proliferation, collagen deposition, and phosphate-induced calcification in VSMCs in vitro.[73] These direct inhibitory actions of resolvins on VSMC maladaptive responses indicate potential beneficial effects on vascular stiffness from actively promoting the resolution of chronic vascular inflammation.

Present at the physiological level in the resolution of inflammation, the interactions between blood components with matrix and/or cellular elements associated with mechanical stress are main determinants in the early phase of vascular diseases for atheroma development. In addition to this, the vascularization of the adventitia (capillary- and postcapillary venules) in the aorta allows the lymphocytes diapedesis able to promote locally adaptive immunity and endothelial cell sprouting to form neoangiogenesis in the media. The neovessels formed are partly immature and thus highly susceptible to foster rupture and intraplaque hemorrhage.

Inhibition of immunoinflammatory signaling without immune-suppressive side effects is thus clearly warranted in vascular pathologies. Tailored disruption of intercellular communications or targeting of immune checkpoint proteins [e.g., cluster of differentiation 40 (CD40) and CD40 ligand, TNF receptor superfamily member 18 (TNFRSF18) and TNF ligand superfamily member 18 (TNFSF18)] expressed by VSMCs could be a promising approach.[74]

In summary, infiltration of inflammatory molecules and immune cells in the vascular wall can cause VSMC migration and proliferation as well as the induction of oxidative stress. Other cellular mechanisms more involved in the resolution of inflammation at the VSMC level in addition to other cells may also play a key role in vascular disease priming.

Conclusion

The emergence of VSMCs in the understanding of cellular and molecular mechanisms of vascular diseases highlights the role of hemodynamics factors and the links between VSMCs and ECM in which they reside and also that of other specific cells in the arterial wall including endothelial cells, inflammatory and immune cells, fibroblasts, and progenitor cells. It appears difficult to discriminate atherosclerosis and accelerated arterial aging since they evolve in parallel with hemodynamic changes, calcification, and arterial stiffening, all involving VSMC plasticity. Hemodynamics, structural factors, and signaling pathways are now considered in a single complex biology network (mechanobiology) where the interactions between the different compounds are ordered according to highly variable dynamics of action over time.[75] This field has benefited from new methodologies, in particular lineage tracing, single-cell RNA-sequencing associated with single-cell genome-wide DNA methylation, and high-precision microscopic techniques such as atomic force microscopy or velocity protein mapping, which allows to visualize in real time the location of individual proteins in the assembly and disassembly processes of FAs in relation with actomyosin coupling.

A new direction will also be to correlate these fundamental results with those of genetics, for example, how rare or common variants of certain genes or loci interfere with the differentiation of VSMCs or the viscoelastic response of the arterial wall, and to integrate epigenetic markers and the effects of noncoding RNAs. At a more clinical level, the prevention or treatment of

arterial stiffness requires the transfer of information from cell-matrix interactions and genetics into biomarkers of vascular remodeling and tissue homeostasis. The multiplicity of regulatory or counter-regulatory loops makes this biomarker search difficult. In this sense, proteomic analyses offer new possibilities. The development of biobanks open to the entire scientific community and the constitution of large, perfectly targeted populations strengthen the research continuum in this field. Finally, in addition to VSMC markers (mainly senescence markers and inflammatory molecules) that are measurable in blood, human-induced pluripotent stem cells as a source of well-controlled VSMCs or for creating models of mechanotransduction have therapeutic promise in the dynamics of vascular aging and diseases.

Basic concept box—SMC lineage tracing and single-cell RNA-sequencing

Genetically modified mouse models to fate map VSMCs should combine (1) the efficient and definitive labeling of VSMCs and their progeny with reporter systems (e.g., fluorescent proteins, LacZ); (2) its conditional expression with high specificity for the VSMC lineage; and (3) an inducible system permitting activation of the tracking system in mature VSMCs at a given time upon treatment with tamoxifen.[50–52] Recent VSMC lineage tracing studies have employed tamoxifen-inducible *Myh11*-CreER[T2] mouse model crossed with loxP-STOP-loxP-reporter mouse models to track the fate and phenotype of VSMCs expressing smooth muscle myosin heavy chain (SM-MHC).[76–78] The R26R-Confetti mouse (LoxP site in the *Rosa26* locus) shows a stochastic recombination of four fluorescent markers (nuclear GFP, cytoplasmic YFP or RFP, or membrane CFP) upon Cre activation (Fig. 22.3).

These conditional and inducible Cre recombinase systems allow for the labeling of mature VSMCs (single-cell resolution by Z-stack confocal analysis or multiphoton microscopy) prior to injury or development of vascular disease and the ability to follow their fate independently of marker gene expression while critically avoiding the labeling of cells acquiring the expression of these marker genes during disease or injury.

Cell isolation (enzymatic digestion followed by sorting based on lineage label) leads to the selection of VSMC clusters by single-cell RNA-sequencing. Principal component (PC) analysis allows the identification of differential gene expression between clusters (Fig. 22.3).

References

1. Michel JB. Phylogenic determinants of cardiovascular frailty, focus on hemodynamics and arterial smooth muscle cells. **Physiol Rev**. 2020; 100:1779−1837.

2. Safar ME, Asmar R, Benetos A, et al. Interaction between hypertension and arterial stiffness. **Hypertension**. 2018; 72:796−805.

3. Chirinos JA, Segers P, Hughes T, Townsend R. Large-artery stiffness in health and disease: JACC state-of-the-art review. **J Am Coll Cardiol**. 2019; 74:1237−1263.

4. Lacolley P, Regnault V, Segers P, Laurent S. Vascular smooth muscle cells and arterial stiffening: relevance in development, aging, and disease. **Physiol Rev**. 2017; 97:1555−1617.

5. Loirand G. Rho kinases in health and disease: from basic science to translational research. **Pharmacol Rev**. 2015; 67:1074−1095.

6. Sharif-Naeini R, Folgering JH, Bichet D, et al. Polycystin-1 and -2 dosage regulates pressure sensing. **Cell**. 2009; 139:587−596.

7. Crystal GJ, Pagel PS. The physiology of oxygen transport by the cardiovascular system: evolution of knowledge. **J Cardiothorac Vasc Anesth**. 2020; 34:1142−1151.

8. Michel JB, Thaunat O, Houard X, Meilhac O, Caligiuri G, Nicoletti A. Topological determinants and consequences of adventitial responses to arterial wall injury. **Arterioscler Thromb Vasc Biol**. 2007; 27:1259−1268.

9. Franck G, Even G, Gautier A, et al. Haemodynamic stress-induced breaches of the arterial intima trigger inflammation and drive atherogenesis. **Eur Heart J**. 2019; 40:928−937.

10. Lacolley P, Regnault V, Nicoletti A, Li Z, Michel JB. The vascular smooth muscle cell in arterial pathology: a cell that can take on multiple roles. **Cardiovasc Res**. 2012; 95:194−204.

11. Meyer G, Merval R, Tedgui A. Effects of pressure-induced stretch and convection on low-density lipoprotein and albumin uptake in the rabbit aortic wall. **Circ Res**. 1996; 79:532−540.

12. Tada S, Tarbell JM. Internal elastic lamina affects the distribution of macromolecules in the arterial wall: a computational study. **Am J Physiol Heart Circ Physiol**. 2004; 287:H905−H913.

13. Tabas I, Garcia-Cardena G, Owens GK. Recent insights into the cellular biology of atherosclerosis. **J Cell Biol**. 2015; 209:13−22.

14. Pryma CS, Ortega C, Dubland JA, Francis GA. Pathways of smooth muscle foam cell formation in atherosclerosis. **Curr Opin Lipidol**. 2019; 30:117−124.

15. Chaabane C, Coen M, Bochaton-Piallat ML. Smooth muscle cell phenotypic switch: implications for foam cell formation. **Curr Opin Lipidol**. 2014; 25:374−379.

16. Choi HY, Rahmani M, Wong BW, et al. ATP-binding cassette transporter A1 expression and apolipoprotein A-I binding are impaired in intima-type arterial smooth muscle cells. **Circulation**. 2009; 119:3223−3231.

17. Bowden KL, Dubland JA, Chan T, et al. LAL (lysosomal acid lipase) promotes reverse cholesterol transport in vitro and in vivo. **Arterioscler Thromb Vasc Biol**. 2018; 38:1191−1201.

18. Michel JB. Anoikis in the cardiovascular system: known and unknown extracellular mediators. **Arterioscler Thromb Vasc Biol**. 2003; 23:2146−2154.

19. Borges LF, Gomez D, Quintana M, et al. Fibrinolytic activity is associated with presence of cystic medial degeneration in aneurysms of the ascending aorta. **Histopathology**. 2010; 57:917−932.

20. Ishida T, Tsukada H, Hasegawa T, Yoshizawa H, Gejyo F. Matrix metalloproteinase-1 activation via plasmin generated on alveolar epithelial cell surfaces. **Lung**. 2006; 184:15−19.

21. Bouton MC, Boulaftali Y, Richard B, Arocas V, Michel JB, Jandrot-Perrus M. Emerging role of serpinE2/protease nexin-1 in hemostasis and vascular biology. **Blood**. 2012; 119:2452−2457.

22. Strickland DK, Muratoglu SC, Antalis TM. Serpin-enzyme receptors LDL receptor-related protein 1. **Methods Enzymol**. 2011; 499: 17–31.

23. Boukais K, Borges LF, Venisse L, et al. Clearance of plasmin-PN-1 complexes by vascular smooth muscle cells in human aneurysm of the ascending aorta. **Cardiovasc Pathol**. 2018; 32:15–25.

24. Tolosano E, Fagoonee S, Morello N, Vinchi F, Fiorito V. Heme scavenging and the other facets of hemopexin. **Antioxid Redox Signal**. 2010; 12:305–320.

25. Bennett MR, Gibson DF, Schwartz SM, Tait JF. Binding and phagocytosis of apoptotic vascular smooth muscle cells is mediated in part by exposure of phosphatidylserine. **Circ Res**. 1995; 77: 1136–1142.

26. Seeberg JC, Loibl M, Moser F, et al. Non-professional phagocytosis: a general feature of normal tissue cells. **Sci Rep**. 2019; 9:11875.

27. Morioka S, Maueroder C, Ravichandran KS. Living on the edge: efferocytosis at the interface of homeostasis and pathology. **Immunity**. 2019; 50:1149–1162.

28. Kolb S, Vranckx R, Huisse MG, Michel JB, Meilhac O. The phosphatidylserine receptor mediates phagocytosis by vascular smooth muscle cells. **J Pathol**. 2007; 212:249–259.

29. Donat C, Thanei S, Trendelenburg M. Binding of von Willebrand factor to complement C1q decreases the phagocytosis of cholesterol crystals and subsequent IL-1 secretion in macrophages. **Front Immunol**. 2019; 10:2712.

30. Baggio C, Sfriso P, Cignarella A, et al. Phagocytosis and inflammation in crystal-induced arthritis: a synovial fluid and in vitro study. **Clin Exp Rheumatol**. 2021; 39:494–500.

31. PrabhuDas MR, Baldwin CL, Bollyky PL, et al. A consensus definitive classification of scavenger receptors and their roles in health and disease. **J Immunol**. 2017; 198:3775–3789.

32. Choromanska B, Mysliwiec P, Choromanska K, Dadan J, Chabowski A. The role of CD36 receptor in the pathogenesis of atherosclerosis. **Adv Clin Exp Med**. 2017; 26:717–722.

33. Sun Y, Chen X. Ox-LDL-induced LOX-1 expression in vascular smooth muscle cells: role of reactive oxygen species. **Fundam Clin Pharmacol**. 2011; 25:572–579.

34. Costales P, Fuentes-Prior P, Castellano J, et al. Domain CR9 of low density lipoprotein (LDL) receptor-related protein 1 (LRP1) is critical for aggregated LDL-induced foam cell formation from human vascular smooth muscle cells. **J Biol Chem**. 2015; 290: 14852–14865.

35. Boucher P, Gotthardt M, Li WP, Anderson RG, Herz J. LRP: role in vascular wall integrity and protection from atherosclerosis. **Science**. 2003; 300:329–332.

36. Chistiakov DA, Killingsworth MC, Myasoedova VA, Orekhov AN, Bobryshev YV. CD68/macrosialin: not just a histochemical marker. **Lab Invest**. 2017; 97:4–13.

37. Cha SJ, Park K, Srinivasan P, et al. CD68 acts as a major gateway for malaria sporozoite liver infection. **J Exp Med**. 2015; 212: 1391–1403.

38. O'Reilly D, Quinn CM, El-Shanawany T, Gordon S, Greaves DR. Multiple Ets factors and interferon regulatory factor-4 modulate CD68 expression in a cell type-specific manner. **J Biol Chem**. 2003; 278:21909–21919.

39. Gottfried E, Kunz-Schughart LA, Weber A, et al. Expression of CD68 in non-myeloid cell types. **Scand J Immunol**. 2008; 67:453–463.

40. Allahverdian S, Chaabane C, Boukais K, Francis GA, Bochaton-Piallat ML. Smooth muscle cell fate and plasticity in atherosclerosis. **Cardiovasc Res**. 2018; 114:540–550.

41. Lemke G. How macrophages deal with death. **Nat Rev Immunol**. 2019; 19:539–549.

42. Maxfield FR, Barbosa-Lorenzi VC, Singh RK. Digestive exophagy: phagocyte digestion of objects too large for phagocytosis. **Traffic**. 2020; 21:6–12.

43. Hessvik NP, Llorente A. Current knowledge on exosome biogenesis and release. **Cell Mol Life Sci**. 2018; 75:193–208.

44. Lacolley P, Regnault V, Laurent S. Mechanisms of arterial stiffening: from mechanotransduction to epigenetics. **Arterioscler Thromb Vasc Biol**. 2020; 40:1055–1062.

45. Canugovi C, Stevenson MD, Vendrov AE, et al. Increased mitochondrial NADPH oxidase 4 (NOX4) expression in aging is a causative factor in aortic stiffening. **Redox Biol**. 2019; 26:101288.

46. Nardone G, Oliver-De La Cruz J, Vrbsky J, et al. YAP regulates cell mechanics by controlling focal adhesion assembly. **Nat Commun**. 2017; 8:15321.

47. Campbell JH, Campbell GR. Smooth muscle phenotypic modulation–a personal experience. **Arterioscler Thromb Vasc Biol**. 2012; 32:1784–1789.

48. Chamley-Campbell J, Campbell GR, Ross R. The smooth muscle cell in culture. **Physiol Rev**. 1979; 59:1–61.

49. Gomez D, Owens GK. Smooth muscle cell phenotypic switching in atherosclerosis. **Cardiovasc Res**. 2012; 95:156–164.

50. Feil R, Brocard J, Mascrez B, LeMeur M, Metzger D, Chambon P. Ligand-activated site-specific recombination in mice. **Proc Natl Acad Sci U S A**. 1996; 93:10887–10890.

51. Kuhbandner S, Brummer S, Metzger D, Chambon P, Hofmann F, Feil R. Temporally controlled somatic mutagenesis in smooth muscle. **Genesis**. 2000; 28:15–22.

52. Wolfsgruber W, Feil S, Brummer S, Kuppinger O, Hofmann F, Feil R. A proatherogenic role for cGMP-dependent protein kinase in vascular smooth muscle cells. **Proc Natl Acad Sci U S A**. 2003; 100:13519–13524.

53. Shankman LS, Gomez D, Cherepanova OA, et al. KLF4-dependent phenotypic modulation of smooth muscle cells has a key role in atherosclerotic plaque pathogenesis. **Nat Med**. 2015; 21:628–637.

54. Liu M, Gomez D. Smooth muscle cell phenotypic diversity. **Arterioscler Thromb Vasc Biol**. 2019; 39:1715–1723.

55. Dobnikar L, Taylor AL, Chappell J, et al. Disease-relevant transcriptional signatures identified in individual smooth muscle cells from healthy mouse vessels. **Nat Commun**. 2018; 9:4567.

56. Wang H, Zhao H, Zhu H, et al. Sca1(+) cells minimally contribute to smooth muscle cells in atherosclerosis. **Circ Res**. 2021; 128: 133–135.

57. Majesky MW, Horita H, Ostriker A, et al. Differentiated smooth muscle cells generate a subpopulation of resident vascular progenitor cells in the adventitia regulated by Klf4. **Circ Res**. 2017; 120: 296–311.

58. Lacolley P, Regnault V, Avolio AP. Smooth muscle cell and arterial aging: basic and clinical aspects. **Cardiovasc Res**. 2018; 114:513–528.

59. Elia L, Kunderfranco P, Carullo P, et al. UHRF1 epigenetically orchestrates smooth muscle cell plasticity in arterial disease. **J Clin Invest**. 2018; 128:2473–2486.

60. Grootaert MOJ, Moulis M, Roth L, et al. Vascular smooth muscle cell death, autophagy and senescence in atherosclerosis. **Cardiovasc Res**. 2018; 114:622−634.

61. Ungvari Z, Tarantini S, Sorond F, Merkely B, Csiszar A. Mechanisms of vascular aging, a geroscience perspective: JACC focus seminar. **J Am Coll Cardiol**. 2020; 75:931−941.

62. Benetos A, Toupance S, Gautier S, et al. Short leukocyte telomere length precedes clinical expression of atherosclerosis: the blood-and-muscle model. **Circ Res**. 2018; 122:616−623.

63. Jae N, Dimmeler S. Noncoding RNAs in vascular diseases. **Circ Res**. 2020; 126:1127−1145.

64. Sarajlic P, Friden C, Lund LH, et al. Enhanced ventricular-arterial coupling during a 2-year physical activity programme in patients with rheumatoid arthritis: a prospective substudy of the physical activity in rheumatoid arthritis 2010 trial. **J Intern Med**. 2018; 284:664−673.

65. Vazquez-Del Mercado M, Gomez-Banuelos E, Chavarria-Avila E, et al. Disease duration of rheumatoid arthritis is a predictor of vascular stiffness: a cross-sectional study in patients without known cardiovascular comorbidities: a STROBE-compliant article. **Medicine (Baltim)**. 2017; 96:e7862.

66. Doring Y, Libby P, Soehnlein O. Neutrophil extracellular traps participate in cardiovascular diseases: recent experimental and clinical insights. **Circ Res**. 2020; 126:1228−1241.

67. Tammaro A, Derive M, Gibot S, Leemans JC, Florquin S, Dessing MC. TREM-1 and its potential ligands in non-infectious diseases: from biology to clinical perspectives. **Pharmacol Ther**. 2017; 177:81−95.

68. Back M, Hansson GK. Anti-inflammatory therapies for atherosclerosis. **Nat Rev Cardiol**. 2015; 12:199−211.

69. Back M, Yurdagul Jr A, Tabas I, Oorni K, Kovanen PT. Inflammation and its resolution in atherosclerosis: mediators and therapeutic opportunities. **Nat Rev Cardiol**. 2019; 16:389−406.

70. Tunon J, Badimon L, Bochaton-Piallat ML, et al. Identifying the anti-inflammatory response to lipid lowering therapy: a position paper from the working group on atherosclerosis and vascular biology of the European Society of Cardiology. **Cardiovasc Res**. 2019; 115:10−19.

71. Serhan CN, Levy BD. Resolvins in inflammation: emergence of the pro-resolving superfamily of mediators. **J Clin Invest**. 2018; 128:2657−2669.

72. Pirault J, Back M. Lipoxin and resolvin receptors transducing the resolution of inflammation in cardiovascular disease. **Front Pharmacol**. 2018; 9:1273.

73. Carracedo M, Artiach G, Arnardottir H, Back M. The resolution of inflammation through omega-3 fatty acids in atherosclerosis, intimal hyperplasia, and vascular calcification. **Semin Immunopathol**. 2019; 41:757−766.

74. Lutgens E, Atzler D, Doring Y, Duchene J, Steffens S, Weber C. Immunotherapy for cardiovascular disease. **Eur Heart J**. 2019; 40:3937−3946.

75. Irons L, Humphrey JD. Cell signaling model for arterial mechanobiology. **PLoS Comput Biol**. 2020; 16:e1008161.

76. Nemenoff RA, Horita H, Ostriker AC, et al. SDF-1alpha induction in mature smooth muscle cells by inactivation of PTEN is a critical mediator of exacerbated injury-induced neointima formation. **Arterioscler Thromb Vasc Biol**. 2011; 31:1300−1308.

77. Gomez D, Shankman LS, Nguyen AT, Owens GK. Detection of histone modifications at specific gene loci in single cells in histological sections. **Nat Methods**. 2013; 10:171−177.

78. Herring BP, Hoggatt AM, Burlak C, Offermanns S. Previously differentiated medial vascular smooth muscle cells contribute to neointima formation following vascular injury. **Vasc Cell**. 2014; 6:21.

This page intentionally left blank

Chapter 23

Endothelial cell dysfunction and senescence: biologic mechanisms and hemodynamic consequences

Masayoshi Suda[1], Ippei Shimizu[1], Yohko Yoshida[1], Goro Katsuumi[1] and Tohru Minamino[1,2]

[1]*Department of Cardiovascular Biology and Medicine, Juntendo University Graduate School of Medicine, Tokyo, Japan;* [2]*Japan Agency for Medical Research and Development-Core Research for Evolutionary Medical Science and Technology (AMED-CREST), Japan Agency for Medical Research and Development, Tokyo, Japan*

Introduction

The prevalence of chronic, noncommunicable diseases, including atherosclerosis, diabetes, heart failure, dementia, and kidney dysfunction, increases with aging, and these diseases tend to cluster in older individuals.[1] The diseases shorten the healthy lifespan and increase the burden on healthcare systems in many societies.[2,3] Geriatric syndromes, including frailty, immobility, and cognitive impairment, also increase with aging and reduce quality of life by limiting daily activities. Aging is a physiological biological process and not pathogenic itself, however, it is closely connected to pathologies in age-related diseases, and our understanding of the respective processes remains limited.

Back in the 1960s, Hayflick et al. demonstrated that fibroblasts have limited potential to replicate.[4] This finding indicated that aging also occurs at the cellular level, a process that is currently described as "cellular senescence." Interestingly, most of the molecules involved in aging phenotypes also regulate cellular senescence, suggesting a causative link between the two. In age-related disorders and chronological aging, senescent cells have central roles for the development and progression of tissue remodeling. Several studies reported that senescent cells accumulate in atherosclerotic arteries[5] and in adipose tissue in diabetes and age-related metabolic dysfunction.[6–8] In mouse experiments, transplantation of senescent cells reduced activity levels and lifespan.[9] Recent studies in a transgenic mice system revealed that elimination of senescent cells—a process called senolysis—can alleviate multiple phenotypes in progeroid mice, naturally aged mice, and mice with age-related diseases, such as atherosclerosis.[8,10–12] Thomas Sydenham, a 17th century physician, wrote that "Man is as old as his arteries," and evidence has accumulated for an involvement in endothelial cell (EC) senescence not only in vascular dysfunction and atherosclerosis but also in diabetes, obesity, and heart failure. In this review article, we introduce pathological aspects of EC senescence and discuss therapies for vascular diseases that target senescent ECs.

In vivo evidence of cellular senescence in age-related diseases

Aging is a major risk factor for many diseases,[13] including cardiovascular disease,[14] dementia,[15] cancer,[16] type 2 diabetes,[17] and idiopathic pulmonary fibrosis.[18] Since the discovery of replicative senescence by Hayflick and Moorhead in the early 1960s (4), studies have indicated a close connection between cellular senescence and aging (4). However, identifying and isolating senescent cells in vivo remains challenging because of the lack of specific markers for senescent cells. Increased senescence-associated β-galactosidase (SA-β-gal) activity and elevated levels of p16Ink4a and p53/p21 are representative markers for cellular senescence, but the lack or presence of these markers does not necessarily indicate that cells are actually senescent in the classical meaning of the term. Similar to primary cultured cells undergoing cellular senescence, vascular cells

in human atherosclerotic coronary arteries were previously shown to have strong staining for SA-β-gal.[19] These cells are predominately localized at the luminal surface of the plaque and have been identified as ECs. Interestingly, in the same patients, SA-β-gal—positive cells were not detected in the internal mammary arteries that were exhibiting minimal atherosclerotic changes.[19]

Senescent cells have been found in various organs of animal models, as well as in elderly humans and individuals with age-related disorders. In addition to adipose tissues in type 2 diabetes and age-related metabolic dysfunction, as mentioned above, cells expressing markers for cellular senescence are also found in the aorta in aged or atherosclerotic animals,[10] and in lung in idiopathic pulmonary fibrosis.[12] These findings suggest the presence of cellular senescence in aging and age-related diseases in vivo. Senescent cells themselves are dysfunctional cells, and by acquiring the senescence-associated secretory phenotype (SASP) phenotype, they induce chronic inflammation and vascular remodeling. For this reason, senescent cells are now well recognized to have causal roles for the progression of vascular disorders.[19]

Molecular mechanism of cellular senescence

Since the initial identification of cellular senescence, significant progress has been made in our understanding of this biological process. Cellular senescence is triggered primarily in response to damage and becomes a defense system for suppressing uncontrolled proliferation and expansion of dysfunctional cells. Cell cycle arrest in the G1 phase develops when DNA is damaged and is thought to give cells sufficient time for DNA repair, thereby avoiding the proliferation of abnormal cells. This process is the first defense mechanism against tumorigenesis. The cell cycle resumes once the damage has been repaired; however, if the damage is extensive the cell will undergo apoptosis as a second defense. In the third defense system, cells that did not undergo apoptosis eventually enter a state of irreversible growth arrest termed cellular senescence. Cellular senescence is indeed a well-designed, ingenious system for tumor suppression. However, senescent cells acquire the SASP phenotype and become antiapoptotic, so they contribute to the development of chronic sterile inflammation and tissue remodeling, making animals or humans prone to cardiovascular-metabolic diseases.

One widely accepted driver of cellular senescence is telomere attrition.[20] Telomeres are non-nucleosomal DNA-protein complexes located at the end of chromosomes. They serve as protective caps and contribute to stabilizing chromatin structure. In somatic cells, the telomeres are shortened as a result of cell replication; once this shortening has reached a critical level, it is recognized as DNA damage, which initiates replicative cellular senescence. Another type of cellular senescence is described as stress-induced premature senescence; it develops in response to various stress stimuli, such as DNA damage induced by irradiation; reagents, including DNA synthesis inhibitors; exposure to high levels of reactive oxygen species (ROS); and oncogenic and metabolic stress. Although various stimuli can induce cellular senescence, it is mediated mainly by either the p53/p21 or p16^{Ink4a}/pRb(rRb; retinoblastoma) pathway, depending on the species or type of cells.

Mechanism of cell cycle arrest in senescent cells

The basic mechanisms for the induction of senescence cell cycle arrest have been well documented.[21] The eukaryotic cell cycle consists of four distinct phases: G1, S (synthesis), G2, and M (mitosis and cytokinesis); phases G1, S, and G2 are collectively known as the interphase (Fig. 23.1). Cell cycle events are monitored at cell cycle checkpoints that occur at the G1/S boundary, in the S phase, and during the G2/M phases. These checkpoints are a series of control systems that enable proliferation only in the presence of stimulatory signals, such as growth factors. The checkpoints are also activated by DNA damage stimuli; this activation stops growth, allowing the cell to repair the damage. In mammalian cells, the p53/p21 or p16^{Ink4a}/Rb pathways are activated by DNA damage and induce cell cycle arrest, which is mediated by cyclin-dependent kinase inhibitors (CDKI), the cyclin-dependent kinase (CDK) interacting protein/kinase inhibitory protein (KIP/CIP) family CDKI (p21^{Cip1}, p27^{Kip1}, and p57^{KipII}), and the inhibitor of CDK4 (INK4) family CDKI (p16^{Ink4a}, p15^{Ink4b}, p18^{Ink4c}, and p19^{Ink4d}).[22] In proliferating cells, CDKI expression is low; however, in response to DNA damage, *p21^{Cip1}* and *p16^{Ink4a}* gene expression significantly increases and the cell cycle is arrested.[23,24] In the case of persistent DNA damage, such as telomere shortening, p21^{Cip1}and p16^{Ink4a} expression are simultaneously upregulated and all CDKs, including CDK2, CDK4, and CDK6, are inactivated. Both p53/p21 and p16^{Ink4a}/Rb play a critical role in tumor suppression and cellular senescence.
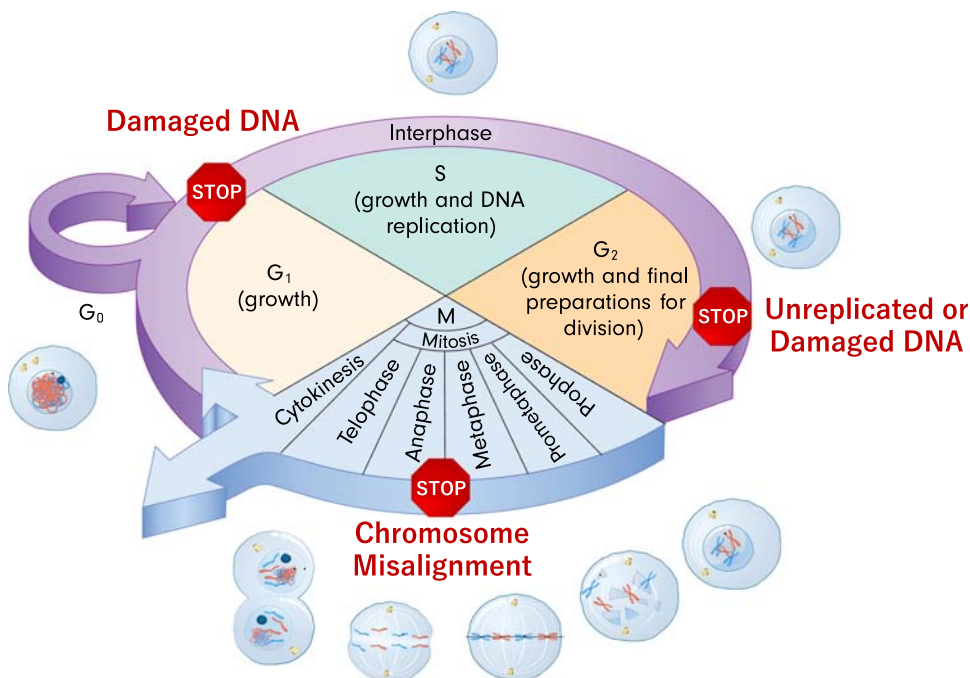
FIGURE 23.1 Phases of the eukaryotic cell cycle.

Endothelial cell senescence in age-related disorders
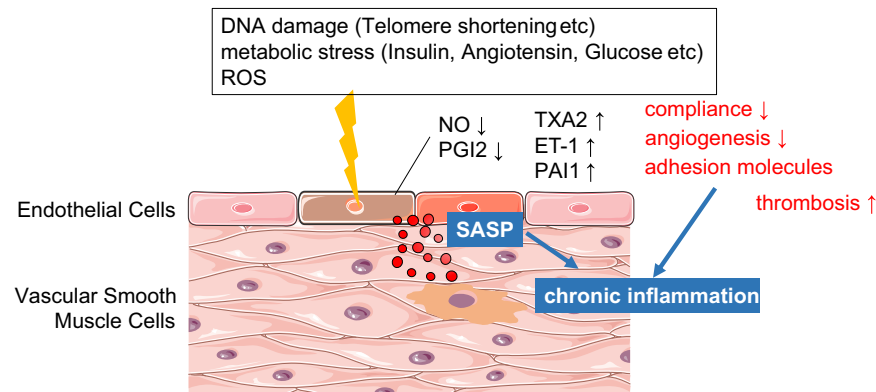
Senescent ECs exhibit various functional abnormalities, such as decreased expression of endothelial nitric oxide (NO) synthase; incremental production of ROS; and increased expression of proinflammatory molecules, including intercellular adhesion molecule-1,[19,25−27] IL-1,[28] IL-6,[29] IL-8,[30] MCP-1.[30] These abnormalities lead to decreased bioavailability of NO and increased formation of peroxynitrite.[31] Furthermore, production of prostacyclin (prostaglandin I2; PGI2) is significantly decreased, whereas production of thromboxane A2 and endothelin-1 is significantly increased.[32−34] Senescent vascular ECs also show an upregulation of plasminogen activator inhibitor-1.[28,35,36] All of these changes are likely to be involved in both the impaired endothelium-dependent vasodilation and the increased trend for thrombogenesis that occur in human atherosclerosis (Fig. 23.2). As described above, a number of studies reported that many of the changes in senescent vascular cells are consistent with those seen in human atherosclerosis and vascular dysfunction, suggesting a critical role of cellular senescence in vascular disorders. Both NO production and endothelial NO synthase (eNOS) activity were reduced in senescent human vascular ECs.[19] Interaction between monocytes and vascular ECs promotes atherogenesis, and this interaction is also enhanced by EC senescence.[37] This process appears to be mediated by upregulation of adhesion molecules and proinflammatory cytokines and decreased production of NO and prostacyclin by senescent ECs.[6,26,29] Senescent ECs have been reported to show diminished capacity for angiogenesis. In addition to the impaired capacity of senescent ECs to form capillaries, bone marrow−derived circulating endothelial progenitor cells (EPCs) show reduced growth and ability to form capillaries in vitro.[38] EPCs are known to participate in postnatal neovascularization and vascular repair.[39−41] Indeed, the function, proliferation capacity, and telomere length of EPCs show a negative correlation with various risk factors for coronary atherosclerosis, including age and circulating vascular ECs, resulting in decreased neovascularization and vascular homeostasis.[42,43]

As described above, EC senescence is induced by a range of factors. A number of studies indicated that telomere shortening occurs also in human vessels and may be related to age-associated vascular diseases. Telomere length in ECs from abdominal aorta and iliac arteries was previously reported to show a strong inverse correlation with age.[44,45] Telomere shortening develops faster in ECs of iliac arteries than in those of internal mammary arteries, suggesting that exposure to higher hemodynamic stress may enhance the rate of EC turnover and induce cellular senescence. Telomere attrition is also more advanced in ECs from coronary arteries in patients with ischemic heart

FIGURE 23.2 Endothelial senescence. Various stimuli that cause DNA damage such as metabolic stress promote endothelial cell senescence. Senescent endothelial cells exhibit functional abnormalities such as decreased production of nitric oxide and increased expression of inflammatory molecules (senescence-associated secretory phenotype [SASP] factors), both of which could accelerate atherogenesis.

disease than in ECs from healthy individuals.[46] Loss of telomere function induces EC dysfunctions in aged arteries, and inhibition of telomere shortening suppresses these senescence-driven alterations in vitro.[19]

The length of telomeres in white blood cells from healthy people showed an inverse correlation with pulse pressure, and this correlation was independent of the person's chronological age.[47] Telomere shortening in white blood cells may increase adhesion or proinflammatory molecules in senescent ECs.[47]

Both premature EC senescence induced by metabolic stress and telomere shortening were also found in lifestyle-related diseases.[25,46,48,49] Insulin/insulin-like growth factor-1/phosphatidylinositol 3-kinase (PI3K)/Akt signaling is preserved in organisms ranging from yeast to mammals. This signaling is well described to regulate the longevity pathway. Genetic studies demonstrated that loss-of-function mutants of this signaling extended the lifespan of *Caenorhabditis elegans*.[50] In contrast, treatment with high-dose insulin resulted in increased Akt phosphorylation and p53/p21 expression, which reduced the lifespan of human ECs, suggesting that insulin/Akt signaling induces EC senescence.[25] Conversely, restriction of calorie intake is known to extend longevity and prevent various age-dependent changes, including atherosclerosis, a decline of immunity, and an increase of inflammatory parameters.[50–52] The plasma level of glucose, insulin, and insulin-like growth factor-1 decreases with calorie restriction, which may contribute to extend the lifespan.[51] Oxidative stress is the chief driving force for human aging and cellular senescence.[53] Oxidized low-density lipoprotein was shown to inactivate telomerase by suppressing the PI3K/Akt pathway in vascular ECs[5] and to induce premature senescence.[29]

Lifestyle-related diseases, including hypertension, diabetes, and dyslipidemia, synergistically enhance the accumulation of senescent cells in systemic organs. The angiotensin II (Ang II) signaling cascade increases with aging and contributes to the pathogenesis of atherosclerosis. Inhibition of Ang II activity has been demonstrated to improve morbidity and mortality in cardiovascular disease.[54] Recently, Ang II was reported to induce premature senescence in human vascular smooth muscle cells via the p53/p21-dependent pathway.[55] Inhibition of this signaling effectively ameliorated the premature senescence and proinflammatory cytokine production caused by Ang II.

Antisenescence therapy

Studies have indicated the critical role of EC senescence in aging and various age-related diseases, and antisenescence therapy is now emerging as a novel strategy for the treatment of such diseases, including atherosclerosis, diabetes, and heart failure. Currently, three approaches are available for antisenescence therapy: (1) inhibition of cellular senescence; (2) suppression of SASP; and (3) elimination of senescent cells (senolysis). These approaches are discussed below.

Inhibition of cellular senescence

Activation of p53 has been observed in aged vessels and failing hearts and has been implicated in atherosclerosis and heart failure.[56] Furthermore, in mice excessive calorie intake caused p53-induced inflammation in adipose tissue, leading to systemic insulin resistance. Suppression of cellular senescence in adipose tissue in adipocyte-specific p53 knockout mice markedly ameliorated the senescence-like phenotypes and improved insulin resistance and glucose tolerance in obese mice.[6] A murine left ventricular pressure overload model exhibited p53-induced chronic sterile inflammation in visceral fat, which enhanced systemic metabolic dysfunction.[57] Inhibiting p53 in adipose tissue suppressed inflammatory processes in visceral fat and ameliorated systemic insulin resistance and cardiac dysfunction.[57] These data indicate that the p53/p21 pathway has a crucial role in age-related diseases and that

inhibition of cellular senescence targeting these pathways could become a novel therapy for age-related disorders.

Studies in EC-specific p53 KO (EC-p53 KO) mice revealed that endothelial senescence is involved in the pathophysiology of aging and age-related diseases.[58,59] In the diabetic state, endothelial-p53 expression was significantly upregulated and endothelium-dependent vasodilatation was impaired in wild-type mice, whereas eNOS-mediated vasodilatation was markedly improved in EC-p53 KO mice. In addition, inhibition of EC senescence by targeting p53 also significantly enhanced angiogenesis in a hind limb ischemia model. Conversely, activation of endothelial p53 reduced both endothelium-dependent vasodilatation and ischemia-induced angiogenesis. The beneficial effect of EC-p53 inactivation on endothelial function was abolished in eNOS-deficient EC-p53 KO mice. These results indicate that EC-p53 negatively regulates endothelium-dependent vasodilatation and ischemia-induced angiogenesis, suggesting that inhibition of endothelial p53 could be a novel therapeutic target in patients with metabolic disorders.[58]

In another report, EC-p53 KO mice fed a high-calorie diet showed improved insulin sensitivity and less fat accumulation and vascular dysfunction. EC-p53 negatively regulated glucose uptake into skeletal muscle by down-regulating glucose transporter 1 expression. Conversely, p53 activation ameliorated metabolic abnormalities. These results indicate that inhibition of endothelial p53 could be a novel therapeutic target to block the vicious cycle of vascular dysfunction and metabolic abnormalities in obesity.[59]

In addition, p53 signaling has been implicated in mediating the pathogenesis of heart failure. In response to pressure overload, the expression of p53 was upregulated in cardiac ECs and bone marrow cells. This upregulation was followed by an upregulation of both ICAM1 expression in ECs and integrin expression in bone marrow cells. Inhibition of EC-p53 and bone marrow cells markedly down-regulated ICAM1 and integrin expression, which ameliorated cardiac inflammation and systolic dysfunction during left ventricular pressure overload. Norepinephrine markedly increased p53 expression in ECs and macrophages. Reducing β2-adrenergic receptor expression in ECs or bone marrow cells attenuated cardiac inflammation and systolic dysfunction during left ventricular pressure overload. These results suggest that activation of the sympathetic nervous system induces cardiac inflammation by upregulating ICAM1 and integrin expression via p53 signaling, thus promoting cardiac systolic dysfunction. Inhibition of p53-induced inflammation could be a novel therapeutic strategy for heart failure.[60]

These reports indicate that inhibition of EC senescence by targeting p53 could improve age-related diseases such as hypertension, atherosclerosis, diabetes, and heart failure. p53 antagonists are available[61]; however, p53, p21, and p16 systemic knockout mice have a high prevalence of cancer and therefore a shorter lifespan than wild type control mice. As already mentioned, cellular senescence is an antitumorigenic system, so suppression of cellular senescence will not become a first-line therapy.
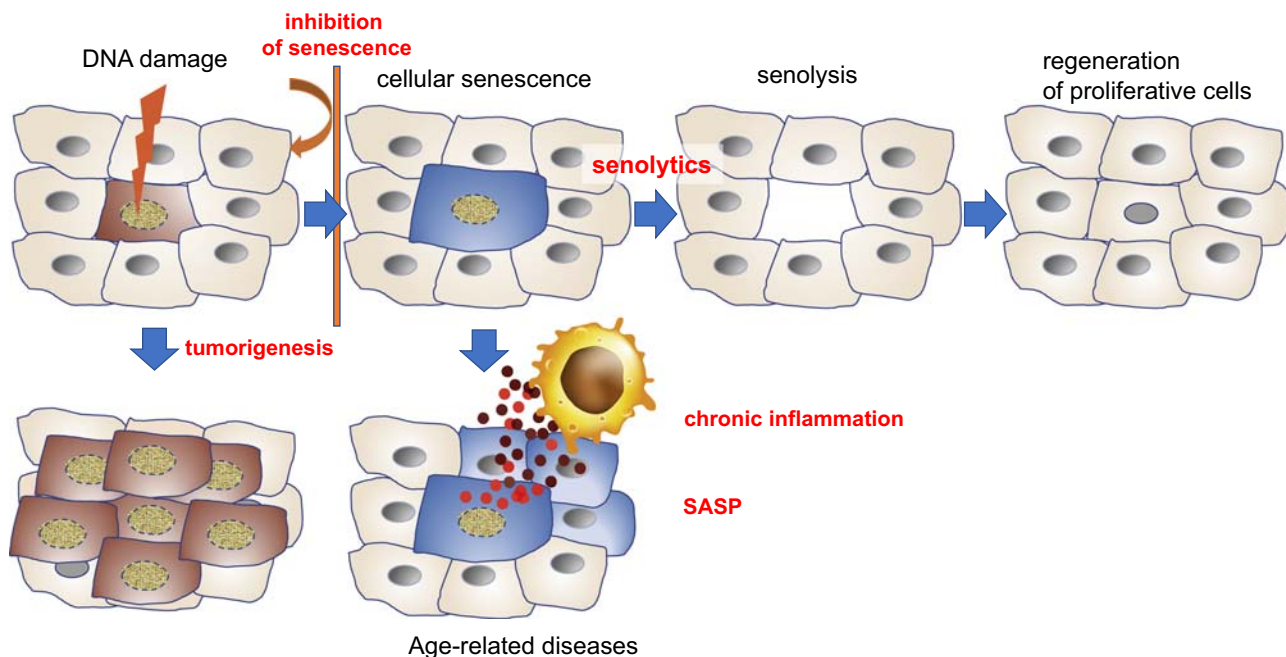
Inhibition of senescence-associated secretory phenotype

Because SASP has a crucial role in inducing chronic inflammation and progression of age-related disorders, it could become another target for antisenescence therapy. Several reagents, including metformin, rapamycin, and ruxolitinib (a JAK1/2 inhibitor), were reported to attenuate SASP. Metformin ameliorated a series of age-related disorders, including cardiovascular disease, cancer development, cognitive dysfunction, and diabetes.[62] It may even increase five-year survival in elderly humans.[63] Rapamycin and related agents increased lifespan and delayed age-related phenotypes, including frailty, heart failure, cancers, cognitive impairment, and immune dysfunction.[64,65] Ruxolitinib alleviated age-related diseases, such as insulin resistance, and stem cell dysfunction.[8] These reports indicate that SASP inhibitors suppress aging and cellular senescence in humans (62−65). However, potential issues related to the specificity of these inhibitors and off-target effects could lead to serious side effects, so SASP inhibitors must have specific targets.

Elimination of senescent cells (senolysis)

In 2011, a breakthrough occurred in aging research: Baker and colleagues reported that removal of senescent cells can prevent or delay tissue dysfunction and extend the healthy lifespan.[11] As explained above, cellular senescence is a state in which damaged and dysfunctional cells irreversibly stop proliferating. The group hypothesized that eliminating senescent cells, termed senolysis, would be a more promising approach for counteracting aging and treating age-related diseases than suppressing cellular senescence (Fig. 23.3). Furthermore, because senolysis eliminates damaged cells, the risks for cancers would also diminish. To establish proof of concept, the researchers made a genetic mouse model with senolysis (INK-ATTAC), enabling inducible elimination of p16Ink4a-positive senescent cells upon administration of a drug. Elimination of senescent cells alleviated multiple phenotypes in progeroid mice, naturally aged mice, and mice with age-related diseases.[8,10−12] Another group showed by transplanting senescent cells that senescent cells caused the aging phenotype.[9] Transplanting relatively small numbers of senescent cells into young mice was sufficient to cause persistent physical dysfunction. Under this condition, senescent cells spread to host tissues, which then also showed reduced survival. In contrast, the senolytic approach improved the physical function of the mice in this implantation model.[9]

FIGURE 23.3   Scheme of antisenescence therapy. Cells with DNA damage develop tumors. Cellular senescence could protect against tumorigenesis, but accumulation of senescent cells causes chronic inflammation that leads to the onset and progression of age-related diseases. Senolytic treatment eliminates senescent cells and rejuvenate aged tissues.

The finding that senescent cells are more resistant to apoptosis than young cells indicated that senolytics could be useful drugs.[66] To find such drugs, Zhu et al. analyzed senescent cells and revealed that they have increased expression of prosurvival pathways, named senescent cell antiapoptotic pathways (SCAPs). Studies with small interfering RNAs showed that ephrins (EFNB1 or 3), the phosphatidylinositol- 4,5-bisphosphate 3-kinase delta catalytic subunit (PI3KCD), the cyclin-dependent kinase inhibitor 1A (p21), BCL-xL, and plasminogen-activated inhibitor-2 could become candidates for SCAP suppression by mediating cell death in senescent cells.[67] The tyrosine kinase inhibitor dasatinib is also known to inhibit EFNB-dependent suppression of apoptosis, and this inhibition eliminated senescent human fat cell progenitors.[68,69] Another compound, quercetin (a natural flavonoid that is known to interfere with PI3K), induced cell death in senescent ECs.[67] A combination of dasatinib and quercetin successfully reduced senescent cell burden in chronologically aged mice.[67] Another group reported that navitoclax, which targets components of the antiapoptotic molecule Bcl-2, also exhibited senolytic ability and alleviated age-related disorders.[70] So far, several reagents have been confirmed as senolytics, as follows: the specific BCL-XL inhibitors A1331852 and A1155463,[71] fisetin,[72] piperlongumine,[73] and FOXO4-related peptide.[74] Several reagents are also effective at causing cell death in senescent ECs (Table 23.1).

TABLE 23.1 List of senolytics.

Senolytics	Target molecules
Dasatinib	Src kinase, tyrosine kinase, etc
Quercetin	Bcl-2 family, p53/p21/serpine, PI3K/AKT
Navitoclax (ABT-263)	Bcl-2 family (Bcl-2, Bcl-xl, Bcl-w)
TW-37	Bcl-2 family (Bcl-2, Bcl-xl, Mcl-1)
ABT-737	Bcl-xl, Bcl-w
Fisetin	PI3K/AKT
A1331852	Bcl-2 family (Bcl-xl)
A1155463	Bcl-2 family (Bcl-xl)
FOXO4-DRI	FOXO-p53 interaction
Alvespimycin (17-DMAG)	HSP90
Tanespimycin (17-AAG)	HSP90
Geldanamycin	HSP90
Piperlongumine	p53/p21, Bcl-2 family (PUMA)
Panobinostat	Histon deacetylase
UBX0101	p53-MDM2/p21
Ruxolitinib (INCB18424)	Selective JAK1/2 inhibitor
CD153 vaccine	CD153

Transgenic and pharmacological approaches to eliminate senescent cells improved atherosclerosis in low-density lipoprotein receptor-deficient (LDL-R) knockout mice. Navitoclax administration alleviated atherogenesis and stabilized plaques in LDL-R knockout mice,[75] and dasatinib and quercetin led to clearance of senescent cells from multiple tissues in apolipoprotein E knockout mice, another model of atherosclerosis.[10] Dasatinib and quercetin also enhanced aortic vascular reactivity, i.e., they caused a modest improvement in endothelium-dependent relaxation elicited by acetylcholine and substantially improved vascular smooth muscle cell relaxation in response to nitroprusside in old mice.[10] Senolytics could become a promising next-generation therapy for atherosclerotic disorders. It is well known that the process of arterial aging involves elastase-mediated proteolysis, inflammation and fibrosis, and senolytic treatment also could delay this process.

Conclusion

This chapter summarizes the undesirable aspects of EC senescence in aging and age-related diseases. In many societies, age-related diseases, including heart failure, diabetes, and atherosclerotic disorders, have become major healthcare problems that reduce the healthy lifespan. Accumulating evidence indicates that EC senescence has central roles in the pathogenesis of these age-related disorders. Senescent ECs have limited capacity to produce vasculoprotective factors, including NO and PGI2; in contrast, they produce vasoconstrictors and prooxidants and promote prothrombotic properties, leading to chronic inflammation and vascular remodeling. Three strategies are suggested to target senescent cells: inhibition of cellular senescence, suppression of SASP, and senolysis. Senolysis is a promising strategy that aims to clear the burden stemming from senescent cells, and several clinical studies on senolytics are underway. In 2019, two pilot studies were reported that showed that dasatinib and quercetin treatment improved physical function in patients with idiopathic pulmonary fibrosis[76] and eliminated senescent cells from adipose tissue and skin in patients with diabetic kidney disease.[77] Whether this approach will be useful in cardiovascular diseases in humans remains to be explored.

References

1. St Sauver JL, Boyd CM, Grossardt BR, et al. Risk of developing multimorbidity across all ages in an historical cohort study: differences by sex and ethnicity. **BMJ Open**. 2015; 5:e006413.
2. Kirkland JL. Translating the science of aging into therapeutic interventions. **Cold Spring Harb Perspect Med**. 2016; 6:a025908.
3. Goldman DP, Cutler D, Rowe JW, et al. Substantial health and economic returns from delayed aging may warrant a new focus for medical research. **Health Aff**. 2013; 32:1698−1705.
4. Hayflick L, Moorhead PS. The serial cultivation of human diploid cell strains. **Exp Cell Res**. 1961; 25:585−621.
5. Breitschopf K, Zeiher AM, Dimmeler S. Pro-atherogenic factors induce telomerase inactivation in endothelial cells through an Akt-dependent mechanism. **FEBS Lett**. 2001; 493:21−25.
6. Minamino T, Orimo M, Shimizu I, et al. A crucial role for adipose tissue p53 in the regulation of insulin resistance. **Nat Med**. 2009; 15:1082−1087.
7. Tchkonia T, Morbeck DE, Von Zglinicki T, et al. Fat tissue, aging, and cellular senescence. **Aging Cell**. 2010; 9:667−684.
8. Xu M, Palmer AK, Ding H, et al. Targeting senescent cells enhances adipogenesis and metabolic function in old age. **Elife**. 2015; 4:e12997.
9. Xu M, Pirtskhalava T, Farr JN, et al. Senolytics improve physical function and increase lifespan in old age. **Nat Med**. 2018; 24:1246−1256.
10. Roos CM, Zhang B, Palmer AK, et al. Chronic senolytic treatment alleviates established vasomotor dysfunction in aged or atherosclerotic mice. **Aging Cell**. 2016; 15:973−977.
11. Baker DJ, Wijshake T, Tchkonia T, et al. Clearance of p16Ink4a-positive senescent cells delays ageing-associated disorders. **Nature**. 2011; 479:232−236.
12. Schafer MJ, White TA, Iijima K, et al. Cellular senescence mediates fibrotic pulmonary disease. **Nat Commun**. 2017; 8:14532.
13. Niccoli T, Partridge L. Ageing as a risk factor for disease. **Curr Biol**. 2012; 22:R741−R752.
14. North BJ, Sinclair DA. The intersection between aging and cardiovascular disease. **Circ Res**. 2012; 110:1097−1108.
15. Querfurth HW, LaFerla FM. Alzheimer's disease. **N Engl J Med**. 2010; 362:329−344.
16. Magalhães JP. How ageing processes influence cancer. **Nat Rev Cancer**. 2013; 13:357−365.
17. Gunasekaran U, Gannon M. Type 2 diabetes and the aging pancreatic beta cell. **Aging**. 2011; 3:565−575.
18. Nalysnyk L, Ruzafa JC, Rotella P, Esser D. Incidence and prevalence of idiopathic pulmonary fibrosis: review of the literature. **Eur Respir Rev**. 2012; 21:355−361.
19. Minamino T, Miyauchi H, Yoshida T, Ishida Y, Yoshida H, Komuro I. Endothelial cell senescence in human atherosclerosis: role of telomere in endothelial dysfunction. **Circulation**. 2002; 105:1541−1544.
20. Campisi J, Kim SH, Lim CS, Rubio M. Cellular senescence, cancer and aging: the telomere connection. **Exp Gerontol**. 2001; 36:1619−1637.
21. Shay JW, Smith OMP, Wright WE. A role for both RB and p53 in the regulation of human cellular senescence. **Exp Cell Res**. 1991; 196:33−39.
22. Sherr CJ, Roberts JM. CDK inhibitors: positive and negative regulators of G1-phase progression. **Genes Dev**. 1999; 13:1501−1512.
23. Ohtani N, Zebdee Z, Huot TJ, et al. Opposing effects of Ets and Id proteins on p16INK4a expression during cellular senescence. **Nature**. 2001:1067−1070.
24. El-Deiry WS, Tokino T, Velculescu VE, et al. WAF1, a potential mediator of p53 tumor suppression. **Cell**. 1993; 75:817−825.
25. Miyauchi H, Minamino T, Tateno K, Kunieda T, Toko H, Komuro I. Akt negatively regulates the in vitro lifespan of human endothelial cells via a p53/p21-dependent pathway. **Embo J**. 2004; 23:212−220.
26. Shelton DN, Chang E, Whittier PS, Choi D, Funk WD. Microarray analysis of replicative senescence. **Curr Biol**. 1999; 9:939−945.

27. Grillari J, Hohenwarter O, Grabherr RM, Katinger H. Subtractive hybridization of mRNA from early passage and senescent endothelial cells. **Exp Gerontol**. 2000; 35:187−197.

28. Garfinkel S, Brown S, Wessendorf JH, Maciag T. Post-transcriptional regulation of interleukin 1 alpha in various strains of young and senescent human umbilical vein endothelial cells. **Proc Natl Acad Sci USA**. 1994; 91:1559−1563.

29. Maier JA, Voulalas P, Roeder D, Maciag T. Extension of the life-span of human endothelial cells by an interleukin-1 alpha antisense oligomer. **Science**. 1990; 249:1570−1574.

30. Minamino T, Yoshida T, Tateno K, et al. Ras induces vascular smooth muscle cell senescence and inflammation in human atherosclerosis. **Circulation**. 2002; 108:2264−2269.

31. van der Loo B, Labugger R, Skepper JN, et al. Enhanced peroxynitrite formation is associated with vascular aging. **J Exp Med**. 2000; 192:1731−1744.

32. Nakajima M, Hashimoto M, Wang F, et al. Aging decreases the production of PGI2 in rat aortic endothelial cells. **Exp Gerontol**. 1997; 32:685−693.

33. Sato I, Kaji K, Morita I, Nagao M, Murota S. Augmentation of endothelin-1, prostacyclin and thromboxane A2 secretion associated with in vitro ageing in cultured human umbilical vein endothelial cells. **Mech Ageing Dev**. 1993; 71.

34. Neubert K, Haberland A, Kruse I, Wirth M, Schimke I. The ratio of formation of prostacyclin/thromboxane A2 in HUVEC decreased in each subsequent passage. **Prostaglandins**. 1997; 54:447−462.

35. Comi P, Chiarmonte R, Maier JA. Senescence-dependent regulation of type 1 plasminogen activator inhibitor in human vascular endothelial cells. **Exp Cell Res**. 1995; 219:304−308.

36. West MD, Shay JW, Wright WE, Linskens MH. Altered expression of plasminogen activator and plasminogen activator inhibitor during cellular senescence. **Exp Gerontol**. 1996; 31:175−193.

37. Maier JA, Statuto M, Ragnotti G. Senescence stimulates U937-endothelial cell interactions. **Exp Cell Res**. 1993; 208:270−274.

38. Yang J, Chang E, Cherry AM, et al. Human endothelial cell life extension by telomerase expression. **J Biol Chem**. 1999; 274:26141−26148.

39. Asahara T, Murohara T, Sullivan A, et al. Isolation of putative progenitor endothelial cells for angiogenesis. **Science**. 1997; 275:964−967.

40. Takahashi T, Kalka C, Masuda H, et al. Ischemia- and cytokine-induced mobilization of bone marrow-derived endothelial progenitor cells for neovascularization. **Nat Med**. 1999; 5:434−438.

41. Werner N, Nickenig G. Clinical and therapeutical implications of EPC biology in atherosclerosis. **J Cell Mol Med**. 2006; 10:318−332.

42. Hill JM, Zalos G, Halcox JP, et al. Circulating endothelial progenitor cells, vascular function, and cardiovascular risk. **N Engl J Med**. 2003; 348:593−600.

43. Vasa M, Fichtlscherer S, Aicher A, et al. Number and migratory activity of circulating endothelial progenitor cells inversely correlate with risk factors for coronary artery disease. **Circ Res**. 2001; 89:e1−e7.

44. Chang E, Harley C. Telomere length and replicative aging in human vascular tissues. **Proc Natl Acad Sci USA**. 1995; 92:11190−11194.

45. Aviv H, Khan MY, Skurnick J, et al. Age dependent aneuploidy and telomere length of the human vascular endothelium. **Atherosclerosis**. 2001; 159:281−287.

46. Ogami M, Ikurs Y, Ohsawa M, et al. Telomere shortening in human coronary artery diseases. **Arterioscler Thromb Vasc Biol**. 2004; 24:546−550.

47. Benetos A, Okuda K, Lajemi M, et al. Telomere length as an indicator of biological aging: the gender effect and relation with pulse pressure and pulse wave velocity. **Hypertension**. 2001; 37:381−385.

48. Rosso A, Balsamo A, Gambino R, et al. p53 Mediates the accelerated onset of senescence of endothelial progenitor cells in diabetes. **J Biol Chem**. 2006; 281:4339−4347.

49. Jeanclos E, Krolewski A, Skurnick J, et al. Shortened telomere length in white blood cells of patients with IDDM. **Diabetes**. 1998; 47:482−486.

50. Kenyon. C. The plasticity of aging: insights from long-lived mutants. **Cell**. 2005; 120:449−460.

51. Longo VD, Finch CE. Evolutionary medicine: from dwarf model systems to healthy centenarians? **Science**. 2003; 299:1342−1346.

52. Koubova J, Guarente L. How does calorie restriction work? **Genes Dev**. 2003; 17:313−321.

53. Finkel T, Holbrook NJ. Oxidants, oxidative stress and the biology of ageing. **Nature**. 2000; 408:239−247.

54. Najjar SS, Scuteri A, Lakatta EG. Arterial aging: is it an immutable cardiovascular risk factor? **Hypertension**. 2005; 46:454−462.

55. Kunieda T, Minamino T, Nishi J, et al. Angiotensin II induces premature senescence of vascular smooth muscle cells and accelerates the development of atherosclerosis via a p21-dependent pathway. **Circulation**. 2006; 114:953−960.

56. Sano M, Minamino T, Toko H, et al. p53-induced inhibition of Hif-1 causes cardiac dysfunction during pressure overload. **Nature**. 2007; 446:444−448.

57. Shimizu I, Yoshida Y, Katsuno T, et al. p53-induced adipose tissue inflammation is critically involved in the development of insulin resistance in heart failure. **Cell Metab**. 2012; 15:51−64.

58. Yokoyama M, Shimizu I, Nagasawa A, et al. p53 plays a crucial role in endothelial dysfunction associated with hyperglycemia and ischemia. **J Mol Cell Cardiol**. 2019; 129:105−117.

59. Yokoyama M, Okada S, Nakagomi A, et al. Inhibition of endothelial p53 improves metabolic abnormalities related to dietary obesity. **Cell Rep**. 2014; 7:1691−1703.

60. Yoshida Y, Shimizu I, Katsuumi G, et al. p53-Induced inflammation exacerbates cardiac dysfunction during pressure overload. **J Mol Cell Cardiol**. 2015; 85:183−198.

61. Komarov PG, Komarova EA, Kondratov RV, et al. A chemical inhibitor of p53 that protects mice from the side effects of cancer therapy. **Science**. 1999; 285:1733−1737.

62. Huffman DM, Justice JN, Stout MB, Kirkland JL, Barzilai N, Austad SN. Evaluating health span in preclinical models of aging and disease: guidelines, challenges, and opportunities for geroscience. **J Gerontol Ser A Biol Sci Med**. 2016; 71:1395−1406.

63. Bannister CA, Holden SE, Jenkins-Jones S, et al. Can people with type 2 diabetes live longer than those without? A comparison of mortality in people initiated with metformin or sulphonylurea monotherapy and matched, non-diabetic controls. **Diabetes Obes Metab**. 2014; 16:1165−1173.

64. Harrison DE, Strong R, Sharp ZD, Nelson JF, Astle CM, Flurkey K, Nadon NL, Wilkinson JE, Frenkel K, Carter CS, Pahor M, Javors MA, Fernandez E, Miller RA. Rapamycin fed late in life extends lifespan in genetically heterogeneous mice. **Nature**. 2009; 460:392−395.

65. Li J, Kim SG, Blenis J. Rapamycin: one drug, many effects. **Cell Metab**. 2014; 19:373−379.

66. Wang E. Senescent human fibroblasts resist programmed cell death, and failure to suppress bcl2 is involved. **Cancer Res**. 1995; 55:2284−2292.

67. Zhu Y, Tchkonia T, Pirtskhalava T, et al. The Achilles' heel of senescent cells: from transcriptome to senolytic drugs. **Aging Cell**. 2015; 14:644−658.

68. Chang QJC, Pawson T, Hedley DW. Effects of dasatinib on EphA2 receptor tyrosine kinase activity and downstream signalling in pancreatic cancer. **Br J Cancer**. 2008; 99:1074−1082.

69. Xi HQ, Wu X-S, Wei B, Chen L. Eph receptors and ephrins as targets for cancer therapy. **J Cell Mol Med**. 2012; 16:2894−2909.

70. Chang J, Wang Y, Shao L, et al. Clearance of senescent cells by ABT263 rejuvenates aged hematopoietic stem cells in mice. **Nat Med**. 2016; 22:78−83.

71. Zhu Y, Doornebal EJ, Pirtskhalava T, et al. New agents that target senescent cells- the flavone, fisetin, and the BCL-XL inhibitors, A1331852 and A1155463. **Aging**. 2017; 9:1−9.

72. Yousefzadeh MJ, Zhu Y, McGowan SJ, et al. Fisetin is a senotherapeutic that extends health and lifespan. **EBioMedicine**. 2018; 36:18−28.

73. Zhu Y, Doornebal EJ, Pirtskhalava T, et al. New agents that target senescent cells: the flavone, fisetin, and the BCL-XL inhibitors, A1331852 and A1155463. **Aging**. 2017; 9:955−963.

74. Baar MP, Brandt RMC, Putavet DA, et al. Targeted apoptosis of senescent cells restores tissue homeostasis in response to chemotoxicity and aging. **Cell**. 2017; 169:132−147 e16.

75. Childs BG, Baker DJ, Wijshake T, Conover CA, Campisi J, van Deursen JM. Senescent intimal foam cells are deleterious at all stages of atherosclerosis. **Science**. 2016; 354:472−477.

76. Justice JN, Nambiar AM, Tchkonia T, et al. Senolytics in idiopathic pulmonary fibrosis: results from a first-in-human, open-label, pilot study. **EBioMedicine**. 2019; 40:554−563.

77. Hickson LJ, Langhi Prata LGP, Bobart SA, et al. Senolytics decrease senescent cells in humans: preliminary report from a clinical trial of Dasatinib plus Quercetin in individuals with diabetic kidney disease. **EBioMedicine**. 2019; 47:446−456.

This page intentionally left blank

Chapter 24

Autonomic and neuroendocrine modulation of arterial stiffness and hemodynamics

Philip J. Millar[1,2], Massimo Nardone[1] and John S. Floras[2,3]

[1]*Department of Human Health and Nutritional Sciences, University of Guelph, Guelph, ON, Canada;* [2]*Toronto General Research Institute, Toronto, ON, Canada;* [3]*University Health Network and Mount Sinai Hospital, Division of Cardiology, Department of Medicine, University of Toronto, Toronto, ON, Canada*

Compliant blood vessels are a fundamental characteristic of the cardiovascular system, enabling pulsatile synchronization between blood ejected from the heart and the arterial tree. Large elastic vessels, such as the aorta, are responsible for dampening the pulsatile pressure caused by left ventricular ejection (i.e., Windkessel effect) and enable anterograde blood flow throughout the cardiac cycle.[1] Large-artery stiffness is gaining clinical recognition as an important measure for patient risk stratification.[2] Such stiffness can impair ventricular-arterial coupling, increasing pulse pressure, ventricular afterload, and downstream microvascular perfusion pressure, which can facilitate end-organ damage,[3,4] and associate independently with major adverse cardiovascular events and mortality in a range of patient cohorts.[5]

The autonomic nervous system maintains tonic and reflex control of arterial pressure through parasympathetic and sympathetic regulation of neural outflow to the heart and circulation. In developed societies, elevations in efferent sympathetic nerve activity and large-artery stiffness occur with healthy aging and are amplified in many cardiovascular disease states (e.g., hypertension and heart failure).[6–10] Whether these observations represent a causal relationship or epiphenomenon has remained controversial. A major reason for this uncertainty remains the inherent difficulty of altering neural outflow independent of changes in arterial pressure and thus the mechanical stress-strain relationship of the vasculature. This chapter will discuss the controversies stimulated by human cross-sectional data and recent evidence supporting the concept that acute increases in muscle sympathetic outflow can augment central and peripheral arterial stiffness. The moderating effects of neuroendocrine factors on arterial stiffness, including the
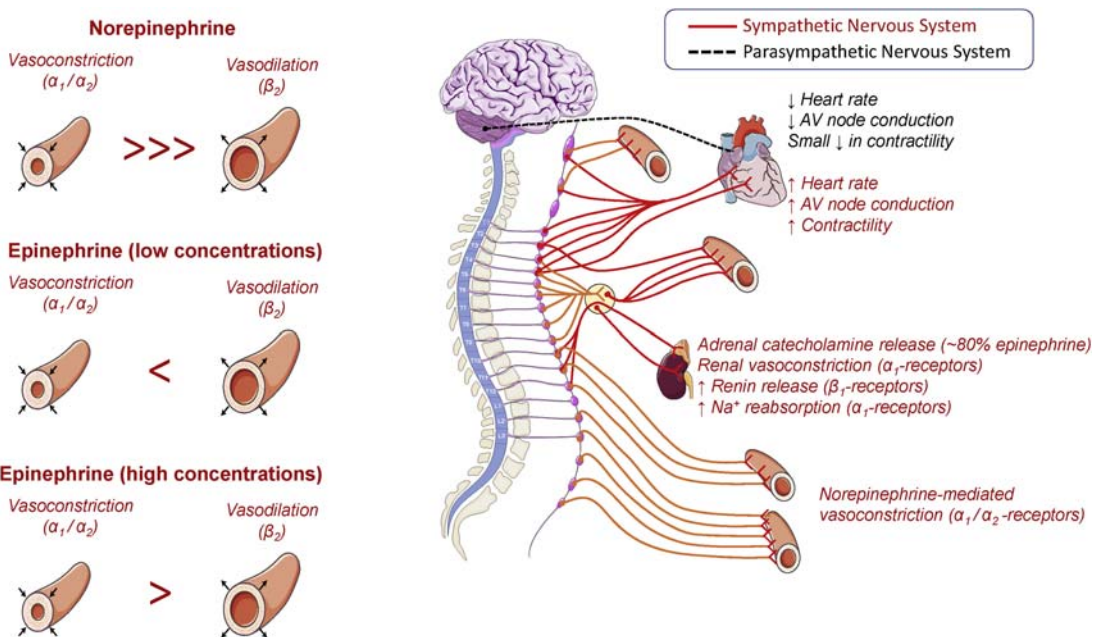
influence of sex hormones on the relationship between sympathetic outflow and pulse wave characteristics, will also be reviewed. Preference has been given to human work unless such data are unavailable.

Autonomic control of the cardiovascular system

Neural control of the cardiovascular system is mediated primarily by parasympathetic innervation of the heart and sympathetic innervation of the heart, kidneys, vasculature, and adrenal medulla (Fig. 24.1).

Parasympathetic nervous system

Parasympathetic (vagal) projections to the heart innervate the sinoatrial and atrioventricular node.[11] Efferent vagal discharge stimulates postsynaptic release of acetylcholine, which binds to muscarinic (M_2) receptors and ultimately decreases sinoatrial membrane potential by altering ionic flux via inhibitory G-protein−coupled mechanisms.[12,13] The resultant hyperpolarization decreases sinoatrial node firing rates (i.e., heart rate) and atrioventricular node action potential conduction velocity.[14,15] Tonic sinoatrial parasympathetic activity produces a lower resting heart rate compared to the intrinsic heart rate; blocking vagal activity increases heart rate.[16] A key feature of parasympathetic modulation is its rapidity of onset and offset; heart rate slows within milliseconds of vagal stimulation and rises a few seconds after the onset of external stress or exercise due to brisk parasympathetic withdrawal and acetylcholinesterase kinetics.[17] Parasympathetic neurons also

FIGURE 24.1 Neurohumoral regulation of the cardiovascular system. Left side: Humoral regulation of resistance vessels. Norepinephrine possesses a higher affinity for α adrenergic receptors causing vasoconstriction. The effects of epinephrine on vascular smooth muscle cell adrenergic receptors are concentration dependent. At low concentrations, epinephrine possesses a higher affinity for β2 adrenergic receptors promoting vasodilation, while a high concentrations epinephrine stimulates α adrenergic receptors causing vasoconstriction. Right side: Neural cardiovascular regulation. Schematic of the sympathetic and parasympathetic divisions of the autonomic nervous system involved in the control of the heart and circulation. Parasympathetic outflow is directed principally at the heart, whereas the sympathetic nervous system innervated the heart, kidney, adrenal medulla, and vascular smooth muscle.

innervate cardiac myocytes[11] and when stimulated can cause small reductions in cardiac contractility.[18,19]

Sympathetic nervous system

In the heart, postganglionic sympathetic neurons densely innervate the sinoatrial and atrioventricular node, and ventricular cardiac myocytes.[20,21] Efferent sympathetic outflow stimulates the translocation and release of norepinephrine which binds to β-adrenergic receptors causing an excitatory G-protein−coupled increase in intracellular cyclic adenosine monophosphate (cAMP). This increases sinoatrial node membrane potential and ultimately firing rate (i.e., heart rate) and atrioventricular node action potential conduction velocity.[13,14] Increased intracellular cAMP also increases intracellular $[Ca^{2+}]$ within cardiac myocytes to enhance contractility.[13,22]

The sympathetic nervous system also innervates vascular smooth muscle, where released norepinephrine can bind to α_1, α_2, and β_2 adrenergic receptors. Stimulation of α_1 and α_2 adrenergic receptors initiates a signaling cascade that increases intracellular $[Ca^{2+}]$, which binds to calmodulin (to create a Ca^{2+}-calmodulin complex) to activate myosin light chain kinase.[23,24] This in turn increases myosin ATPase activity, initiating myosin power strokes on actin to elicit vasoconstriction.[23,24] Stimulation of β_2 adrenergic receptors activate cAMP, inhibiting myosin light chain kinase causing vascular smooth muscle vasodilation.[25,26] Norepinephrine has a higher affinity for α

compared to β adrenergic receptors, and therefore the net vasomotor response to sympathetic outflow is vasoconstriction.[27] Sympathetic nerve terminals also contain presynaptic α_2 adrenergic receptors which inhibit norepinephrine by negative feedback.[27] Sympathetic innervation of the kidneys not only initiates α adrenergic-mediated renal vasoconstriction[28] but also β_1 adrenergic-mediated release of renin from juxtaglomerular cells[29−31] and α adrenergic-mediated sodium reabsorption at the renal tubule.[31−33] There is evidence, as well, for co-release of both neuropeptide Y and ATP with norepinephrine under conditions of intense sympathetic stimulation.[34−38] The importance of sympathetic outflow for maintaining tonic vasoconstriction can be appreciated by the substantial reductions in peripheral vascular resistance and arterial pressure following ganglionic blockade.[16] Lastly, sympathetic innervation of the adrenal medulla is responsible for the release of circulating catecholamines, primarily epinephrine.[39] As the principal endogenous ß2 agonist, epinephrine induces vasodilation, but when administered exogenously to achieve higher plasma concentrations it elicits predominantly α_2−mediated vasoconstriction.[27]

Overall, the control of tonic and reflex parasympathetic and sympathetic outflow directed to these end-organs are influenced by a combination of central rhythm generators within the brainstem, and input from higher order cortical regions and a variety of peripheral afferents (e.g., baroreceptors, arterial and muscle chemoreceptors, and muscle mechanoreceptors) to govern cardiovascular homeostasis.[8,40]

Assessing autonomic modulation of large-artery stiffness: methodological considerations

The curvilinear nature of the stress–strain relationship implies that arterial stiffness progressively increases at higher levels of vascular deformation.[41] For example, increased circumferential stress caused by higher arterial pressure alters vascular loading patterns and increases arterial stiffness.[42] In humans, direct measurements of intra-arterial pressure and carotid-femoral pulse wave velocity (PWV), the in vivo noninvasive gold standard assessment of arterial stiffness,[43] have demonstrated independent associations between static or distending (i.e., mean arterial pressure) and pulsatile (i.e., pulse pressure) components of arterial pressure and large-artery stiffness.[44–47] It is also relevant to note that pacing-induced elevations in heart rate can increase large-artery stiffness in rats,[48–50] independent of the sympathetic nervous system.[49] This may be caused by alterations in the frequency dependence of the viscoelastic components of the arterial wall and diminished time to recoil.[48,51] The influence of heart rate on aortic PWV is arterial pressure–dependent in rats, with the largest effects at higher levels of mean arterial pressure.[50] Similar findings in humans have found that atrial pacing can increase carotid-femoral PWV,[52,53] and decrease radial and carotid artery distensibility[54,55] and the augmentation index (AI$_x$),[56] while ivabradine-mediated reductions in heart rate can decrease carotid-femoral PWV.[57] It should be noted that carotid-femoral PWV possesses stronger associations with left ventricular contractility and ejection time than heart rate.[58] Nonetheless, given that the autonomic nervous system is important to the beat-to-beat regulation of arterial pressure, through the modulation of cardiac chronotropy and inotropy, and vascular smooth muscle tone, this presents an inherent challenge in determining whether the effects of neural modulation on large-artery stiffness are the result of hemodynamic changes or represent a pressure-independent effect on mechanical elements of the vessel wall.

Parasympathetic modulation of large-artery stiffness

There is currently no direct method for measuring parasympathetic activity in humans. Instead, tonic parasympathetic modulation is commonly estimated using heart rate variability (*See Basic Concept Box—What is heart rate variability?*). This method involves the computation of time- and frequency-domain indices based on the variability in electrocardiogram-derived R-R intervals.[59] Indirect assessments of reflex parasympathetic modulation involve examining the changes in R-R interval for a given change in systolic arterial pressure, also known as cardiac baroreflex sensitivity.[60,61] Both methods represent sinoatrial parasympathetic modulation[62] and have shown the capacity to predict poor outcomes after myocardial infarction.[63–65]
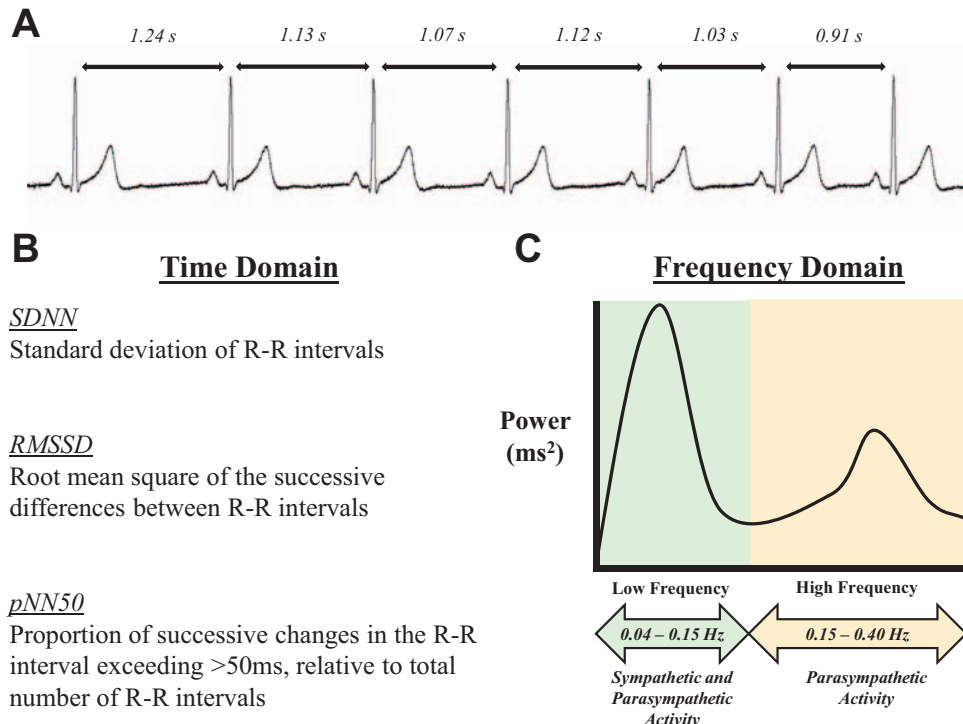
Several cross-sectional studies have evaluated the association between heart rate variability measures associated with sinoatrial parasympathetic modulation and large-artery stiffness in healthy participants[66–68] and patients with cardiometabolic diseases.[69–72] In healthy participants, greater high frequency power (i.e., higher sinoatrial parasympathetic modulation) is correlated with a lower brachial-ankle PWV[66] and carotid-femoral PWV.[67,68] However, in subsequent multiple linear regression analyses, controlling for arterial pressure failed to identify high frequency power as an independent predictor of PWV.[66–68] In this case, heart rate variability may act as a cardiovascular marker and not a causal determinant of arterial stiffness. For example, Mäki-Petäjä and colleagues[68] observed that participants in the highest tertile of high frequency power also had the lowest resting mean arterial pressure. Additional studies in clinical populations have found associations between heart rate variability and carotid artery wall stiffness[69] or carotid-femoral PWV[72] but have mostly failed to adjust for arterial pressure. An independent association between carotid-femoral PWV and high frequency power was observed in patients with orthostatic intolerance but explained only 1.5% of the variability in high frequency power.[71]

Overall, it remains difficult to reconcile how differences in sinoatrial parasympathetic modulation are causally related to large-artery stiffness independent of changes in heart rate, stroke volume, or arterial pressure. A more biologically plausible hypothesis is that chronic changes in large-artery stiffness modify mechanosensitive baroreceptive inputs leadings to alterations in tonic parasympathetic modulation. Such a hypothesis is supported by several cross-sectional studies showing strong pressure-independent relationships between carotid-femoral PWV and cardiac baroreflex sensitivity,[73–75] as well as, prospective work demonstrating correlations between reductions in carotid-femoral PWV or increases in carotid artery compliance and increased cardiac baroreflex sensitivity following endurance exercise training.[75,76]

Basic concept box—What is heart rate variability?

Heart rate variability represents a noninvasive method of indirectly assessing cardiac sympathetic and parasympathetic modulation through the analysis of the spontaneous fluctuations in R-R interval from the electrocardiogram (typically 5–10 min [short-term] or 24 h [long-term] in recording length).[59] The most common methods of assessing heart rate variability involve quantification of time and frequency domain variables (Fig. 24.2), though nonlinear metrics have also been employed.[77] In the time domain, common assessments include the measurement of the standard deviation of normal R-R intervals, a measure of overall variability influenced by both parasympathetic and sympathetic factors, and the root mean square of the successive differences between adjacent normal R-R intervals, the primary time-domain index of sinoatrial parasympathetic modulation.[77] In the frequency domain, a fast Fourier transformation is applied to continuous recordings of spontaneous R-R intervals to calculate the spectral power within the very low frequency (0.0033–0.04 Hz), low-frequency (0.04–0.15 Hz), and high-frequency (0.15–0.4 Hz) bands. In general, the high frequency power spectrum is considered to reflect sinoatrial parasympathetic modulation,[78,79] with data showing a positive correlation with integrated vagal nerve activity in dogs.[80] The low frequency power band is thought to reflect modulation by both the parasympathetic and sympathetic nervous systems[81–83] and more recently has been suggested to reflect baroreflex control of neural outputs.[77,84] The ratio of low frequency to high frequency power has been frequently considered to represent an index of sympathovagal balance,[59] although the assumptions underlying this assertion have been proven false.[85] The heart rate variability spectrum incorporates also broad-band nonharmonic noise that exhibits fractal characteristics, with greatest spectral power within the very low frequency range.[86,87] In addition, the very low frequency band can be modulated by the renin-angiotensin system, physical activity, thermoregulation, and endothelial factors[77] and in healthy individuals attenuated markedly by parasympathetic blockade with atropine sulfate.[88] Despite its widespread adoption, heart rate variability has several limitations that preclude its clinical application as a measure of sinoatrial autonomic modulation. These include its being affected by the mechanical effects of atrial stretch, respiration, and the prevailing heart rate,[85,89,90] which are often not controlled for when data are acquired, and the lack of a precise understanding of the relative proportion of autonomic and nonautonomic contributions to frequency- or time-domain indices of interest in health or specific disease states.

FIGURE 24.2 Representative electrocardiographic (ECG) tracing showing beat-to-beat variability in heart period (Panel A). Heart rate variability is commonly calculated across two different quantitative domains: the time domain (Panel B) and the frequency domain (Panel C). The principal representations of physiological or clinical interest are high frequency (HF; 0.15–0.40 Hz) and low frequency (LF; 0.04–0.15 Hz) spectral power, less so very low frequency power (<0.04 Hz). *Credit: Authors' original work.*

Sympathetic modulation of large-artery stiffness

Several lines of evidence link sympathetic tone to arterial stiffness. *In vitro* experiments show that cytoskeletal proteins involved in contraction within vascular smooth muscle cells stiffen in models of aging and hypertension.[91,92] Canine and rabbit models have shown that α-adrenergic vascular smooth muscle cell activation can produce acute increases in descending thoracic aorta, abdominal aorta, and carotid artery stiffness,[51,93–97] while in humans, altering the contractile state of vascular smooth muscle cells using norepinephrine and nitroglycerin can increase and decrease brachial artery stiffness, respectively.[98–101] The effects of α-adrenergic vascular smooth muscle contraction on artery stiffness are lower in the elastic thoracic aorta compared to more distal segments (or conduit vessels),[93] which would be considered more muscular[102] and densely innervated.[103–106] This distinction between elastic and muscular vessels is important as carotid-femoral PWV predicts morbidity and mortality,[5] whereas the stiffness of the brachial artery does not.[107,108]

Chronic sympathetic outflow can also alter muscular and elastic artery stiffness through vascular smooth muscle cell remodeling. In rats, sympathetic activity can increase contractile protein expression within vascular smooth muscle cells,[109] while α adrenergic stimulation can upregulate pathways associated with vascular smooth muscle cell hypertrophy.[110–112] In a porcine model, thoracic sympathectomy decreased smooth muscle density in the ascending aorta, arch, descending thoracic aorta, with smaller changes in the abdominal aorta, in parallel with increases in collagen and elastin. The result was an increase in stiffness in the ascending aorta, arch, and descending thoracic aorta at low and physiological stress levels.[113] In healthy humans, sympathetic activity is associated positively (with the exception of premenopausal women) with increased femoral[114] and carotid[115] intima-media thickness. These data do not provide insight into whether the changes are mediated by atherosclerotic changes in the intima layer or physiological remodeling of the media layer. However, relative wall thickness is inversely proportional to the compliance of the vessel,[41] and thus stiffer arteries generally have increased intima-media thickness and decreased compliance.[43] Similar to measures of arterial stiffness, carotid artery intima-media thickness is positively associated with systolic arterial pressure.[116] Finally, endothelial cells are involved in regulating vascular smooth muscle tone and extracellular matrix composition through the release of nitric oxide.[117–119] Increases in sympathetic outflow to blood vessels can reduce endothelium-dependent vasodilation.[120–122] Collectively, these studies provide evidence supporting the hypothesis that acute and chronic changes in sympathetic activity can produce vascular smooth muscle cell-mediated alterations in arterial stiffness.
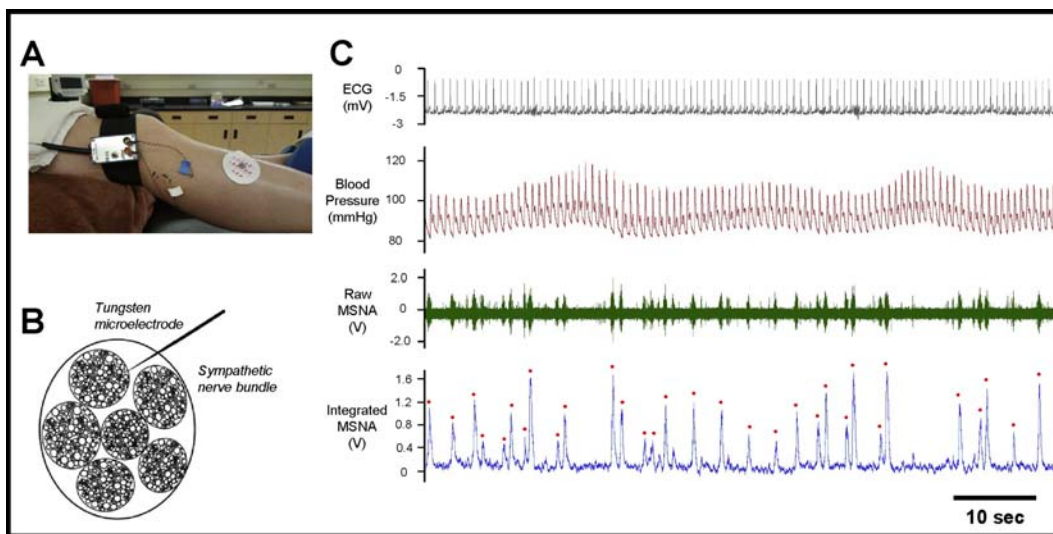
Based on this knowledge, the majority of work has examined associations between arterial stiffness and sympathetic outflow directed toward skeletal muscle resistance vessels (termed muscle sympathetic nerve activity [MSNA]) (*See Basic Concept Box—What is muscle sympathetic nerve activity?*). The strengths of this method are that nerve firing is highly reproducible within an individual over time[123,124] and that it permits instantaneous detection and beat-by-beat quantitation of changes in nerve firing in response to acute interventions designed to perturb sympathetic activity. Although MSNA does not measure the quanta of norepinephrine released from the nerve terminal, correlations with plasma norepinephrine have been reported at rest[125,126] and during exercise.[126] Other studies report indirect measures of sympathetic activity, including plasma norepinephrine, heart rate variability, and spectral analysis of systolic blood pressure.[68,127–130]

Basic concept box—What is muscle sympathetic nerve activity?

Using a technique called microneurography,[131,132] a high impedance, finely tipped tungsten microelectrode is inserted percutaneously into a superficial peripheral nerve (typically the ulnar, radial, or fibular nerves), while a low impedance ground microelectrode is placed 1–2 cm away (Fig. 24.3A and 24.3B). The raw MSNA neurogram is amplified (x75-100,000), bandpass filtered (e.g., 0.7–2.0 kHz), rectified, and integrated using a 0.1-s time constant to produce "bursts" of multiunit MSNA (Fig. 24.3C). Careful examination of the action potential discharge in response to a startling response, light skin stroking, and an end-expiratory apnea are necessary to confirm the recording from postganglionic muscle sympathetic nerve fibers as opposed to skin sympathetic fibers.[131,132] The most distinctive feature of multiunit MSNA is its phase-locked nature to the cardiac cycle, highlighting the strong regulatory influence of the arterial baroreflex (each sympathetic burst occurs ∼1.1–1.3 s after the preceding R-wave of the electrocardiogram), and which ultimately limits the number of potential sympathetic bursts to the prevailing heart rate.[133] The multiunit signal is analyzed using a minimum 3:1 signal-to-noise ratio threshold for burst discrimination. Bursts thus identified are then used to calculate MSNA burst frequency (number of bursts per minute), burst incidence (number of bursts per 100 heartbeats), burst amplitude or area (most commonly normalized to an individual's largest burst in order to reduce the bias of electrode distance to the discharging fibers, and presented as a percent), and total MSNA (the product of burst frequency and normalized burst amplitude or area).[131,132,134,135] The majority of cross-sectional work relies solely on measures of MSNA burst frequency and incidence as these are considered less biased by potential interindividual differences in microelectrode placement.[132] Within the present context, MSNA burst frequency is the principal variable of interest, in so far as neurovascular transduction is proportionate to the quanta of norepinephrine released per unit of time.

FIGURE 24.3   Panel A: Representative image of a microneurography set-up involving a tungsten microelectrode inserted into the fibular nerve (white flag) and a corresponding ground microelectrode (blue flag). Panel B: Schematic illustration of a tungsten microelectrode inserted into a peripheral nerve and manipulated until positioned near clusters of postganglionic muscle sympathetic neurons. Panel C: Representative tracing of heart rate, arterial pressure, and the raw and integrated muscle sympathetic nerve activity (MSNA) signals. Multiunit bursts are identified by red dots within the integrated signal. Noteworthy, it can be observed that MSNA is decreased during periods with elevations in arterial pressure and reflexively increased during falls in arterial pressure supporting strong arterial baroreflex regulation. *Credit: (Panel B) Image used with permission from Macefield VG.* **Handb Clin Neurol.** *2013;117:353−364. doi: 10.1016/B978-0-444-53491-0.00028-6.*

Relationships between sympathetic activity and arterial stiffness: cross-sectional studies
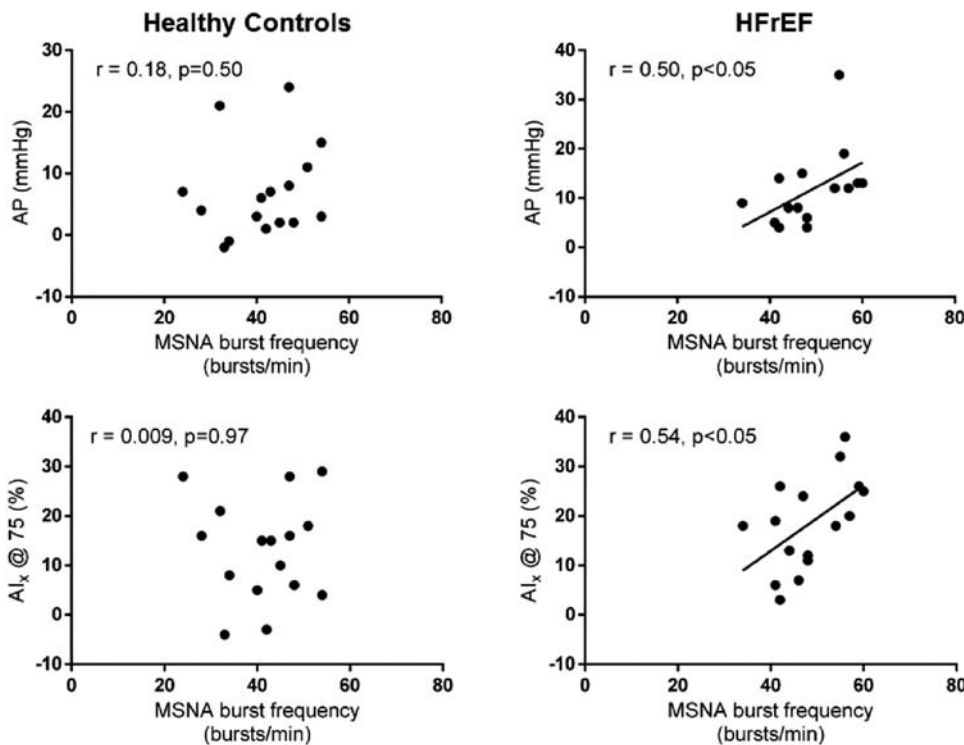
A growing number of cross-sectional studies in healthy cohorts have identified bivariate associations between resting MSNA and measures of arterial stiffness, including carotid-femoral PWV,[129,136,137] carotid-brachial PWV,[129] AI$_x$,[138] AI$_x$ at a controlled heart rate of 75 bpm (AI$_{x@75}$),[139,140] or carotid artery compliance.[129,141] Similar bivariate relationships have been found between MSNA and radial artery compliance[130] and augmentation pressure or AI$_{x@75}$ in patients with heart failure with reduced ejection fraction (Fig. 24.4),[142] while in renal transplant patients, MSNA correlated negatively with brachial but not carotid artery distensibility.[143] In contrast, MSNA was unrelated to central or peripheral PWV in a cohort of premenopausal women with a history of healthy or preeclamptic pregnancy.[144] It is plausible that the relationship between MSNA and arterial stiffness can be modulated by the presence of sex hormones (discussed in greater detail later in this chapter), as premenopausal women demonstrate a negative association between MSNA and AI$_x$[139] compared to positive associations found in postmenopausal women[138] and men.[139] However, arterial stiffness is only one determinant of AI$_x$,[10,43,145] and in the largest study to date, the positive association between MSNA and carotid-femoral PWV was similar in both men and women.[129]

One consideration of current cross-sectional work has been the exclusivity of examining MSNA-arterial stiffness associations using measures of MSNA burst occurrence

without deliberation of the contributions of burst strength. This is relevant as both occurrence and strength can influence the quanta of norepinephrine release, and shown to be regulated differently in older men and women.[146] Several cross-sectional studies employed multivariate analyses to control for confounding factors, including arterial pressure, and demonstrate MSNA to be an independent predictor of carotid-femoral and carotid-brachial PWV,[129,136] brachial artery distensibility,[143] and carotid artery compliance.[129] For example, the relationship between MSNA burst frequency and carotid-femoral PWV was maintained following adjustment for mean arterial pressure, heart rate, sex, and the waist-to-hip ratio but lost once age was included in the model (Fig. 24.5). The moderating effects of age in the model are expected as MSNA and arterial stiffness both increase over the lifespan.[147−149] A similar finding has been reported for 24 h urine norepinephrine content and carotid-femoral PWV.[150]

It is necessary to highlight the reciprocal nature of neural−vascular interactions, with increased carotid and aortic stiffness being associated with reduced sensitivity of arterial baroreflex control of MSNA.[151] Thus, stiffer central vessels permit less transduction of the mechanical stimulus needed to evoke reflex changes in sympathetic outflow in response to arterial pressure fluctuations—similar to reports involving cardiac baroreflex sensitivity.[73−75]

In contrast to the consistent relationships with MSNA, the majority of studies have failed to detect a significant correlation between plasma norepinephrine and arterial

FIGURE 24.4 The relationship between muscle sympathetic nerve activity (MSNA) burst frequency and the augmentation pressure (AP; top panels) and the augmentation index at a heart rate of 75 bpm (AI$_x$@75; bottom panels) in healthy controls (left panels) and patients with heart failure with reduced ejection fraction (HFrEF; right panels). *Credit: Millar PJ, et al. **J Card Fail**. 2019;25(5):404−408. doi: 10.1016/j.cardfail.2019.03.005.*

stiffness,[130,143] while those that have, display weaker associations than observed with MSNA.[129] These findings are unsurprising based on the knowledge that plasma norepinephrine measurements exhibit lower reproducibility than MSNA,[123,152] can be influenced by norepinephrine reuptake and clearance independent of release,[153] and are not specific to sympathetic outflow directed toward the skeletal muscle vasculature.[154] Urinary norepinephrine (but not epinephrine) has been correlated with carotid-femoral PWV,[150,155] but this relationship is unlikely to have causal relevance, since, relative to its plasma concentration, a greater proportion of this catecholamine is of renal origin.

Can acute modulation of sympathetic activity alter large-artery stiffness?

Studies aimed at addressing this question have utilized a variety of well-known provocations to modify sympathetic activity, including both sympathoexcitatory (lower body negative pressure, cold stress, mental stress, isometric handgrip exercise, lower leg venous occlusion, and adrenergic agonists) and sympathoinhibitory (ganglionic blockade, anesthesia, and guided-breathing) maneuvers. As mentioned earlier, it must be acknowledged that the majority of these stressors produce changes in heart rate,

stroke volume, and arterial pressure which themselves could be responsible for changes in large-artery stiffness. Table 24.1 provides an overview of the effects of common laboratory stressors on MSNA and hemodynamic responses.

One sympathoexcitatory maneuver with the capacity to overcome this limitation is lower body negative pressure. This stimulus commonly involves sealing the lower body up to the iliac crest in a custom-made chamber. Supine exposure to a select negative pressure level (e.g., −10 to −60 mmHg) causes the translocation of blood from the upper body compartment.[156] The result is a graded reduction in central venous pressure, which can unload mechanically sensitive baroreceptors located in the cardiopulmonary and arterial circuits causing net reflex activation of MSNA[156,157] to maintain mean arterial pressure. Low levels of lower body negative pressure (e.g., −5 mmHg), simulating upright or standing posture, can increase MSNA without decreasing arterial pressure, while a greater lower body negative pressure stimulus (e.g., ≤ −15 mmHg) can increase MSNA and may also decrease mean arterial pressure concurrently.[156,158,159] The subsequent sections will discuss the diverse experimental models that have been utilized to evaluate the neural contributions to muscular and elastic large-artery stiffness.

A Carotid-femoral PWV

Control variables: R=0.60, P<0.001
[1] MAP, HR [1] R=0.43, P<0.001
[2] Sex, waist/hip, MAP, HR [2] R=0.44, P<0.001
[3] Age, sex, waist/hip, MAP, HR [3] R=0.12, P=0.291
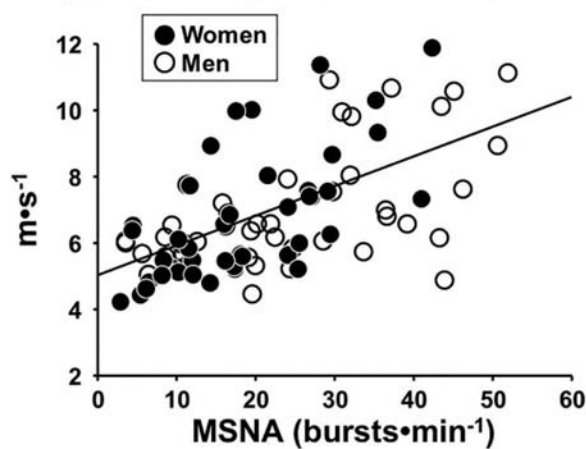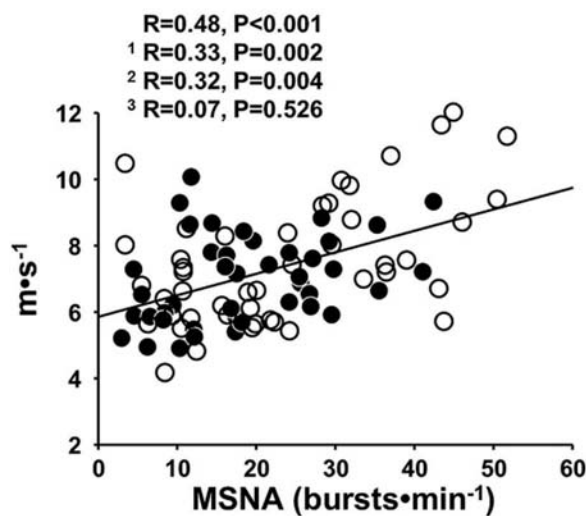
B Carotid-brachial PWV

R=0.48, P<0.001
[1] R=0.33, P=0.002
[2] R=0.32, P=0.004
[3] R=0.07, P=0.526

FIGURE 24.5 The association between muscle sympathetic nerve activity (MSNA) and carotid-femoral (Panel A) and carotid-brachial (Panel B) pulse wave velocity (PWV) in 88 healthy normotensive participants. Multiple linear regression analyses identified MSNA as an independent predictor of PWV following inclusion of mean arterial pressure and heart rate (model 1), model 1 plus sex and waist/hip ratio (model 2). The relationship between MSNA and PWV was abolished following the inclusion of age (model 3). *Credit: Holwerda SW, et al.* **Hypertension.** *2019;73(5):1025−1035. doi: 10.1161/HYPERTENSIONAHA.118.12462. Permission granted.*

Evidence from muscular arteries

Initial human work demonstrated that radial artery compliance was reduced during sympathetic activation using mental stress and the cold pressor test.[160] Similarly, both cigarette smoking and low-dose intravenous infusion of the α_1 adrenergic agonist phenylephrine were observed to decrease radial artery compliance independent of changes in arterial pressure.[130] These results are consistent with observations showing that −15 mmHg lower body negative pressure or a cold pressor test can both decrease brachial artery distensibility.[161,162] More recently, −30 mmHg lower body negative pressure was also found to increase carotid-brachial PWV.[129] Complimentary work has examined the effects of acute sympathoinhibition following brachial plexus or subarachnoid anesthesia and found increased radial and femoral artery compliance, respectively.[130,163] In disagreement, cold pressor stress was also shown to increase radial artery compliance.[164]

Importantly, relative to elastic vessels, these arteries contain a higher proportion of vascular smooth muscle,[46,165] exhibit denser adrenergic innervation,[166,167] and are less subject to stiffening with age.[148,168] When specifically studied with lower body negative pressure, this sympathoexcitatory stimulus did not alter the distensibility of the elastomuscular proximal brachial artery.[169]
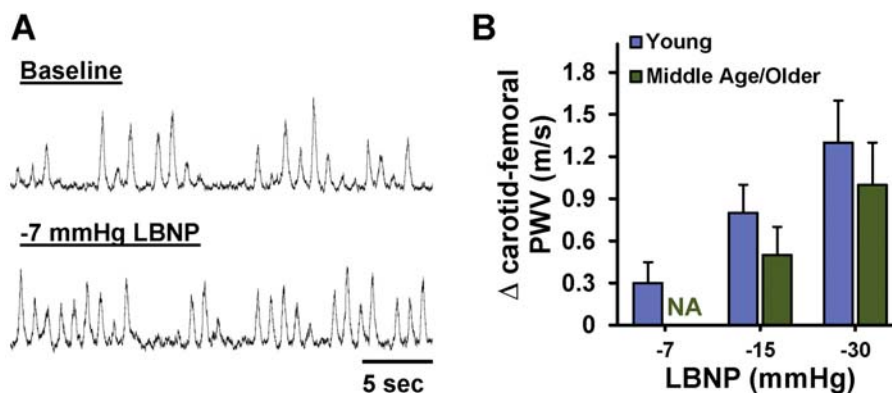
Evidence from elastic arteries

In contrast to brachial artery stiffness, which lacks prognostic significance,[107,108,170] carotid-femoral PWV is a strong independent predictor of major adverse cardiovascular events and mortality.[5] The first studies examining acute sympathetic modulation of elastic artery stiffness reported that sympathoexcitation evoked by lower body negative pressure did not alter compliance or distensibility of the abdominal aorta[171] or common carotid artery or carotid arterial bulb[172] (i.e., local stiffness). More recent work demonstrated that isometric handgrip exercise and lower body negative pressure, two sympathoexcitatory stressors, produced divergent effects on AI_x, timing of the reflected wave, and pulse pressure amplification, caused by underlying differences in heart rate and arterial pressure responses rather than a direct effect of sympathetic activation on vascular smooth muscle per se.[173]

In contrast, work relying on measures of carotid-femoral PWV, a more global assessment of elastic large-artery stiffness, has produced more consistent support for a relationship with sympathetic vasoconstrictor drive. A high (~ -68 mmHg) but not moderate (~ -34 mmHg) lower body negative pressure stress was found to increase carotid-femoral PWV in young healthy men.[128] A strong bivariate correlation was demonstrated between changes in PWV and systolic blood pressure variability, an indirect estimate of sympathetic vasomotor modulation;[82] however, it should be noted that substantial reductions in pulse pressure and increases in heart rate and total peripheral resistance were also noted during the severe hypovolemia.[128] Subsequent studies using larger sample sizes and more modest levels of lower body negative pressure confirmed increases in MSNA and noted parallel rises in carotid-femoral PWV without alteration of arterial pressure, pulse pressure, or heart rate.[129,174] In these studies, lower

TABLE 24.1 Neural and hemodynamic responses to sympathoexcitatory and sympathoinhibitory interventions.

	MSNA	MAP	SV	HR
Sympathoexcitatory interventions				
Low-level lower body negative pressure	↑	↔	↔	↔
≤ −15 mmHg lower body negative pressure	↑ ↑	↓/↔	↓	↑
Cold stress	↑ ↑	↑ ↑	↓/↔	↑/↔
Mental stress	↔	↑ ↑	↔	↑
Isometric handgrip exercise	↑ ↑	↑ ↑	↔	↑ ↑
60° head-up tilt	↑	↑/↔/↓	↓	↑
Lower-limb venous occlusion	↑	↓	↓	↔
Phenylephrine (α_1 adrenergic agonist)	↓ ↓	↑ ↑	↑/↔	↓ ↓
Sympathoinhibitory interventions				
Ganglionic blockade	↓ ↓	↓ ↓	↓ ↓	↑ ↑
+10−20 mmHg lower body positive pressure	↓	↑/↔	↔	↔
6−10° head-down tilt	↓	↔	↑	↔
Device-guided breathing	↓	↓	↑/↔	↓/↔

General responses in muscle sympathetic nerve activity (MSNA), mean arterial pressure (MAP), stroke volume (SV), and heart rate (HR) during commonly used sympathoexcitatory and sympathoinhibitory laboratory interventions. Single arrows reflect mild responses, while double arrows reflect larger responses. Note: the responsiveness of these variables can be influenced by the dose, duration, or intensity of the intervention. This table is meant to highlight the difficulty in separating the neural sympathetic and hemodynamic actions during routine stressors.
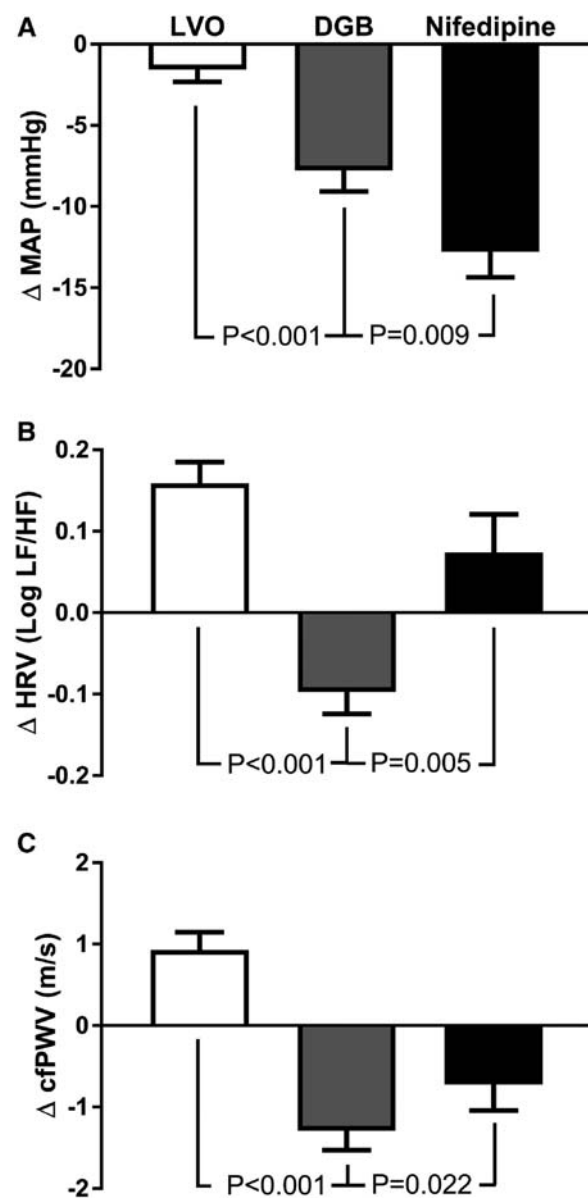
FIGURE 24.6 Panel A: Representative tracings showing an increase in muscle sympathetic nerve activity (MSNA) during −7 mmHg lower body negative pressure (LBNP). Panel B: Change in carotid-femoral pulse wave velocity (PWV) during acute elevations in MSNA using increasing levels of LBNP in young and/or middle to older healthy individuals. NA, represents no data available for the middle to older age range at −7 mmHg LBNP. *Credit: Panel B. Re-drawn from Nardone M, et al.* **J Am Heart Assoc**. *2018;7(3):e007971. doi: 10.1161/JAHA.117.007971 and Holwerda SW, et al. Hypertension. 2019;73(5):1025−1035. doi: 10.1161/HYPERTENSIONAHA.118.12462.*

body negative pressure at −7 mmHg, −15 mmHg, and −30 mmHg increased carotid-femoral PWV by Δ+0.3 m/s, Δ+0.8 m/s, and Δ+1.3 m/s, respectively, in young healthy men and women (Fig. 24.6).[129,174] A similar dose-response pattern for carotid-femoral PWV was observed in middle-aged/older healthy adults, though −15 mmHg and −30 mmHg only reduced carotid artery compliance in young adults.[129] MSNA burst frequency was also positively associated with carotid-femoral

PWV at baseline and during lower body negative pressure stress.[129] In another comparison of young versus older healthy individuals, −20 mmHg lower body negative pressure was associated with a Δ+0.3−0.5 m/s increase in carotid-femoral PWV and a decrease in AI_x despite a small reduction in systolic arterial pressure.[175] This study also investigated responses to the cold pressor test, noting larger increases in carotid-femoral PWV and AI_x in young individuals which were mediated by a greater pressor

response.[175] Isometric handgrip exercise was found to increase carotid-femoral PWV, but the statistical significance of this change was lost after adjusting for the rise in mean arterial pressure.[68] Head-up tilt, another sympathoexcitatory stimulus, caused a reduction in mean arterial pressure and carotid-femoral PWV in patients with severe autonomic failure but an increase in carotid-femoral PWV in healthy controls which was not explained by changes in mean arterial pressure.[176] In a large cohort of hypertensive middle-aged men and women, administering lower-limb venous distention, to reduce cardiac preload and stimulate reflex sympathetic activation, caused an acute increase in ultrasound-derived aortic PWV and tonometric carotid-femoral PWV despite small reductions in mean arterial pressure and pulse pressure.[127] Collectively, these studies support the capacity of acute sympathetic activation to increase elastic large-artery PWV, independent of age.

An alternative approach has been to determine whether acute suppression of sympathetic outflow leads to reductions in large-artery stiffness. Bolus infusion of the ganglionic blocker pentolinium in young adults failed to alter carotid-femoral PWV.[68] However, in these experiments, pentolinium reduced heart rate variability but caused an unexplained increase in mean arterial pressure,[68] suggesting incomplete blockade of ganglionic neurotransmission and paradoxical pressor effects via other mechanisms. In contrast, infusion of the ganglionic blocker trimethaphan reduced central and peripheral arterial pressure and lowered carotid-femoral PWV (Δ-1.3 m/s)—but only in postmenopausal, not premenopausal women.[137] This discordance may reflect the lower sympathetic firing rates of the latter.[147] However, subsequent analysis showed that the differences in carotid-femoral PWV responses between pre- and postmenopausal women were abolished after adjusting for mean arterial pressure responses to trimethaphan.[137] Postmenopausal women also exhibited reductions in augmentation pressure and $AI_x@75$; the change in augmentation pressure correlated negatively with the change in MSNA burst incidence.[137] A single dose of clonidine, a α_2 adrenergic agonist which reduces central sympathetic outflow, was associated with reductions in carotid-femoral PWV, but the independence from parallel reductions in arterial pressure was not tested in that study.[177] Finally, a recent study attempted to separate the neural and pressure-mediated effects on large-artery stiffness by comparing the effects of lower leg venous occlusion, device-guided breathing, and device-guided breathing plus the calcium channel blocker nifedipine (shown previously to increase MSNA[178]) on carotid-femoral PWV.[127] As shown in Fig. 24.7, despite larger reductions in mean arterial pressure with device-guided breathing plus nifedipine, the changes in

FIGURE 24.7   Change from baseline in mean arterial pressure (MAP, A), heart rate variability (HRV, B) and carotid-femoral pulse wave velocity (cfPWV, C) after lower-limb venous occlusion (LVO), device-guided breathing (DGB), and nifedipine (10 mg). *Used with permission from Faconti L, et al. **J Am Heart Assoc**. 2019;8(15):e012601. doi: 10.1161/ JAHA.119.012601.*

carotid-femoral PWV were smaller, coincident with elevations in the low frequency to high frequency ratio of spectral heart rate variability, interpreted by these authors as indicating sympathetic activation.[127] Caveats acknowledged,[85] such data are concordant with the concept that sympathetic activation can impede pressure-mediated reductions in elastic large-artery stiffness.

Does chronic sympathetic modulation contribute to large-artery stiffness?

The majority of clinical conditions associated with exaggerated sympathetic outflow also possess increased large-artery stiffness; these include healthy aging, hypertension, heart failure with reduced ejection fraction, renal failure, chronic obstructive pulmonary disease, obstructive sleep apnea, and others.[8–10,179] If sympathetic activation contributes to the mechanical properties of the vasculature, it would support treatments that specifically target central sympathetic outflow for improving large-artery stiffness.

Evidence from muscular arteries

Radial artery distensibility was increased in two men following hand transplantation and returned toward values similar to the contralateral control hand after ∼four months coincident with qualitative signs of neural reinnervation.[180] Similarly, femoral artery distensibility was increased one month following unilateral lumbar ganglionectomy (but unchanged in the contralateral leg) in five patients with peripheral artery disease.[163] Thus, the stiffness of muscular arteries appears to be mediated by tonic levels of sympathetic outflow.

Evidence from elastic arteries

Patients suffering from pheochromocytoma, a condition characterized by catecholamine-secreting tumors commonly found in the adrenal medulla, exhibit chronic elevations in plasma and urine norepinephrine.[150,181] These patients demonstrate elevated carotid-femoral PWV (but not $AI_{x@75}$) compared to age- and sex-matched controls, even following the adjustment of heart rate, arterial pressure, and fasting plasma glucose.[150] Patients with the greatest catecholamine excess also possess the highest brachial-ankle PWV.[182] With respect to the chronic implications, one year after successful tumor resection, patients with pheochromocytoma demonstrate similar 24-hr urine norepinephrine, arterial pressure, heart rate, and carotid-femoral PWV compared to controls.[150] In patients with chronic obstructive pulmonary disease, inhibiting the carotid chemoreceptors with dopamine infusion reduced MSNA, mean arterial pressure, and carotid-femoral and carotid-radial PWV, but the interdependence of these changes were not evaluated.[183]

The recent development of device-based therapies to target sympathetic overactivation has offered insight into the potential relationships with large-artery stiffness, though these interventions are tested on patient groups with severe disease progression and likely vascular remodeling. In a small cohort of patients with heart failure with reduced ejection fraction, six months of chronic baroreflex activation using carotid sinus electrical stimulation decreased MSNA by ∼30%[184] but did not alter arterial pressure, carotid-femoral PWV or AI_x.[185] In contrast, an uncontrolled trial in resistant hypertensives reported that six months of chronic baroreflex activation reduced carotid-femoral PWV and AI_x.[186] Renal artery denervation in resistant hypertensives has also been found to reduce carotid-femoral PWV to a greater extent than predicted by reductions in arterial pressure,[187] while in another series arterial pressure, MSNA and finger-derived AI_x were reduced concurrently—but the individual changes were not related.[188]

Pharmacologically, several common antihypertensive drugs, namely angiotensin converting enzyme (ACE) inhibitors and angiotensin receptor blockers, have been found to reduce MSNA.[189] These classes have also been shown to decrease elastic large-artery stiffness despite similar reductions in arterial pressure as other drug classes.[190,191] One explanation for these interdrug discrepancies could involve the potential for some antihypertensive medications to cause reflex-mediated increases in MSNA,[178,192] which may attenuate pressure-mediated reductions in artery stiffness.[127] For example, concurrent angiotensin II receptor blocker and diuretic (losartan-hydrochlorothiazide) therapy produce larger reductions in arterial pressure than losartan monotherapy, but similar magnitude changes in AI_x and the cardio-ankle vascular index.[193] Losartan-hydrochlorothiazide has been shown to cause reflex-mediated increases in resting MSNA.[192] Losartan can produce greater reductions in carotid-femoral PWV and AI_x compared to hydrochlorothiazide despite similar blood pressure−lowering capacities.[194] The mineralocorticoid receptor antagonist spironolactone can reduce MSNA and carotid-femoral PWV.[189] Centrally acting sympathoinhibitory medications, such as moxonidine, can reduce large-artery stiffness when used concurrently with the angiotensin II blocker valsartan,[195] but eight week moxonidine monotherapy, which lowered MSNA burst frequency by ∼6 bursts/minute without changing arterial pressure, did not alter carotid-radial PWV or AI_x in obesity-related hypertensives.[196] In the latter study, moxonidine also led to an increase in plasma aldosterone.[196] Peripherally acting sympathoinhibitory medications such as doxazosin can reduce carotid-femoral PWV[197] and AI_x[198] in hypertensive patients. Finally, lipophilic statins (e.g., atorvastatin and simvastatin) have also been shown to be capable of lowering MSNA[199,200] and improving carotid-femoral PWV.[201]

Neuroendocrine modulation of arterial stiffness

Renin-angiotensin-aldosterone system

Experimental and human work consistently support an association between activation of the renin-angiotensin-aldosterone system (RAAS) and increased large-artery stiffness.[202,203] Recall that renal sympathetic activation

promotes the release of renin[29–31] (Fig. 24.1). Animal studies have shown that upregulating ACE activity can increase vascular smooth muscle hypertrophy,[204] while elevated angiotensin II can increase oxidative stress in vascular smooth muscle cells[205] and stimulate adverse remodeling of the extracellular matrix and vascular smooth muscle cells.[206–208] Spontaneously hypertensive rats treated with ACE inhibitors possess greater aortic elastin density and lower aortic PWV than controls.[209,210] Aldosterone has also been shown to increase carotid artery hypertrophy and stiffness in aldosterone-salt treated rats.[211] Importantly, the crosstalk between angiotensin II and aldosterone can upregulate genomic and nongenomic signaling cascades that synergistically increase vascular smooth muscle proliferation, fibrosis, and inflammation.[212] Local tissue RAAS systems are also likely to be involved in mediating arterial stiffness.[117,213]

In normotensive humans, a higher aldosterone-to-renin ratio was associated positively with carotid-femoral PWV but not arterial pressure.[214] Intravenous angiotensin II infusion increases carotid-femoral PWV,[215,216] which was abolished following administration of the angiotensin receptor blocker valsartan.[216] Subsequent analysis found that blunting the angiotensin II–mediated arterial pressure rise explained only 30% of the change in carotid-femoral PWV, suggesting pressure-independent mechanisms are also involved.[216] Normotensive participants demonstrate increased radial artery compliance following ACE inhibition,[217] while in patients with hypertension, ACE inhibitors, angiotensin receptor blockers, and aldosterone antagonists have consistently been shown to reduce carotid-femoral PWV and the AI_x.[190,191,202,218] The concurrent arterial pressure reductions with these drug therapies play a large role in passively attenuating arterial stiffness, though evidence suggests that reductions in arterial stiffness following RAAS inhibition are in part pressure-independent.[219] In coronary artery disease patients, ACE inhibition decreased carotid-femoral PWV independent of the change in mean arterial pressure.[220] Treatment with hydrochlorothiazide or losartan produce similar arterial pressure reductions in hypertensives, but only losartan reduced carotid-femoral PWV and the AI_x.[194] Captopril and valsartan produce similar reductions in arterial pressure and carotid-femoral PWV, yet in combination they produce synergistic reductions in carotid-femoral PWV after correction for arterial pressure.[221] Lastly, spironolactone reduced both mean arterial pressure and carotid-femoral PWV, while bendroflumetazide decreased MAP but was unable to alter carotid-femoral PWV in hypertensive patients.[222] These studies highlight that therapeutically targeting RAAS can reduce arterial stiffness, including through mechanisms beyond the passive unloading of the arterial tree.

Lastly, animal work has highlighted that angiotensin II plays a significant role in modulating central and peripheral sympathetic outflow.[223] It is plausible that RAAS-mediated sympathoexcitation or inhibition can indirectly alter arterial stiffness through neural mechanisms. However, the influence of activation or inhibition of RAAS components in humans has yielded inconsistent findings regarding its neuromodulatory role in healthy, hypertensive, or heart failure populations.[224–232] Therefore, future work is required to delineate the role of RAAS-mediated sympathetic modulation, and whether it can influence large-artery stiffness.

Endothelin-1

Endothelin-1 is a potent endothelial-derived vasoconstrictor.[233] Its over-expression leads to increased collagen deposition and arterial stiffening.[234] Endothelin-1 can also increase inflammation and reduce nitric oxide bioavailability leading to stiffening.[235] Endothelin-A receptor antagonism in normotensive and hypertensives blunts the baroreflex-mediated increase in MSNA to reductions in arterial pressure activity,[236] supporting the concept that endothelin-1 is involved in regulating tonic sympathetic vasoconstrictor activity. Cross-sectional work has shown a pressure-independent association between endothelin-1 and carotid-femoral PWV in young men,[237] with a similar bivariate relationship found in middle-aged patients with coronary artery disease.[238]

Experimental work in anesthetized sheep found that intra-arterial infusion of endothelin-1 increases iliac artery PWV and endothelin-A receptor antagonism decreases iliac artery PWV.[239] Similar findings have been observed in young healthy men, such that: (1) intravenous infusion of endothelin-1 increases carotid-femoral PWV and the AI_x; (2) endothelin-A receptor antagonism decreases carotid-femoral PWV and the AI_x; and (3) arterial stiffness responses are unchanged following co-infusion of endothelin-1 and endothelin-A receptor antagonist.[240] Carotid artery compliance is also increased following endothelin-A/B receptor blockade before, but not after, aerobic exercise training suggesting a role of decreased ET-1 on exercise-mediated changes in arterial stiffness.[241] In patients with chronic kidney disease, acute[242] and chronic[243] endothelin-A receptor antagonism decreases carotid-femoral PWV. Although parallel changes in arterial pressure and arterial stiffness are observed during infusion of endothelin-1 agonists or antagonists, these findings highlight a potential physiological role for modulating elastic large-artery stiffness in humans.

Insulin

Patients with type 1 and 2 diabetes demonstrate increased arterial stiffness,[244–246] while insulin sensitivity and plasma insulin concentrations are independently associated with markers of central and peripheral arterial stiffness.[247–254] In addition, euglycemic hyperinsulinemia attenuates AI_x in healthy humans,[255–257] suggesting that insulin can acutely reduce arterial stiffness. These responses are mediated in part through insulin-mediated endothelial-dependent vasodilation.[258] Patients with type 2 diabetes have attenuated insulin-mediated reductions in AI_x,[257] likely driven by impaired insulin-mediated endothelial nitric oxide production,[259] and adverse remodeling of vascular smooth muscle cells and extracellular matrix.[260] Lastly, in healthy normoglycemic participants, euglycemic hyperinsulinemia increases MSNA,[261–264] highlighting a sympathoexcitatory role of insulin. Indeed, type 2 diabetics have elevated MSNA which is related positively to insulin levels.[265] Insulin-mediated sympathoexcitation may contribute, in part, to the observations of increased arterial stiffness in this population.

Testosterone

Cross-sectional and experimental work has highlighted that sex hormones can modulate arterial stiffness. For example, in healthy middle-aged and older men without cardiovascular disease, serum testosterone was negatively correlated with carotid-femoral PWV[266,267] and carotid artery stiffness,[268] independent of mean arterial pressure and age.[267,268] Similar negative correlations have been reported in men undergoing hemodialysis and may underlie the relationship between low testosterone and cardiovascular mortality.[269] Participants with testosterone deficiencies also demonstrate increased carotid-femoral PWV compared to controls,[267,270–272] while 90 days of testosterone replacement therapy can decrease total systemic arterial compliance.[273] In conflict with human work, animal studies have shown that testosterone can increase collagen protein expression and increase arterial stiffness.[274–276] The mechanisms responsible for a testosterone-mediated benefit to arterial stiffness are poorly understood but may relate to its role as a vasodilator or atheroprotective and antiinflammatory factor.[277] It is unlikely that a neural mechanism is involved given the positive relationship between androgens and MSNA.[278,279]

Estrogen

Women demonstrate increased arterial stiffness compared to men before menarche and after menopause suggesting a vascular protective effect of sex hormones.[45,280,281] Estrogen-mediated signaling cascades can inhibit cellular processes that cause adverse remodeling of the extracellular matrix[282] and medial layer[283] of the aorta. Incubating human aortic cells with estrogen or progesterone increased elastin and decreased collagen protein expression.[274–276] Estrogen can increase nitric oxide bioavailability[284] and decrease oxidative stress,[285] both of which can reduce arterial stiffness.[286] Temporal investigations across the menstrual cycle have found higher radial arterial distensibility,[287] whole body arterial compliance,[288] or carotid compliance[289] during ovulation (i.e., when estrogen is first rising), while AI_x@75 is lowest during the luteal phase (i.e., when estrogen and progesterone are both elevated).[290,291] In contrast, a growing number of studies have reported that carotid-femoral PWV,[288,291–294] AI_x,[293,295] carotid artery stiffness,[294] or carotid and femoral artery compliance[296] are unchanged throughout the menstrual cycle. A similar lack of responsiveness in elastic large-artery stiffness has been reported across different phases of oral contraceptive use,[293,294] while active hypoestrogenic premenopausal women with functional hypothalamic amenorrhea have lower resting systolic arterial pressure, pulse pressure, and AI_x@75 compared to fitness-matched eumenorrheic controls[297] in spite of their exaggerated MSNA responses to graded lower body negative pressure.[298] Numerous randomized controlled trials have sought to determine prospectively the effects of estrogen or combined hormone replacement therapy on arterial stiffness in postmenopausal women. However, the overall results have been equivocal.[299]

Do sex hormones modify the relationship between muscle sympathetic nerve activity and arterial stiffness?

Several lines of evidence suggest that female sex hormones can modify the association between sympathetic vasoconstrictor drive and large-artery stiffness. First, premenopausal women have a smaller drop in arterial pressure following ganglionic blockade supporting a reduced reliance on sympathetic vasoconstrictor tone.[300] This aligns with data showing lower MSNA in premenopausal women versus men[147] and likely reflects the role of estrogen as a central sympatholytic.[301] Second, compared to men, premenopausal women have attenuated reductions in peripheral vascular conductance during graded norepinephrine infusions,[302] which is the result of greater β_2 adrenergic vasodilation.[26,302] The latter findings may explain the positive relationship between MSNA and AI_x in men and postmenopausal women[138,139] but negative association in premenopausal women.[139] However, the positive relationships between MSNA and carotid-femoral PWV or carotid artery compliance were similar in men and women[129] suggesting that sex differences in pulse wave reflection are likely caused downstream of the aorta.

Summary

Greater conduit artery stiffness and central sympathetic outflow have each been identified as an independent marker of increased cardiovascular risk. There is accumulating evidence from many, but not all studies in humans, for a bidirectional relationship between these alterations, with increased sympathetic outflow inducing acute or chronic arterial stiffening and with decreased compliance, in turn, diminishing stimulation by stretch of sympatho-inhibitory arterial baroreceptors. There is, however, little evidence thus far that therapeutic attenuation of sympathetic discharge can reduce cardiovascular risk by improving arterial elasticity. Trials of such interventions will be required to affirm this concept.

References

1. Belz GG. Elastic properties and Windkessel function of the human aorta. **Cardiovasc Drugs Ther**. 1995; 9:73−83.

2. Mancia G, Fagard R, Narkiewicz K, et al. 2013 ESH/ESC guidelines for the management of arterial hypertension the task force for the management of arterial hypertension of the European Society of Hypertension (ESH) and of the European Society of Cardiology (ESC). **Eur Heart J**. 2013; 34:2159−2219.

3. Antonini-Canterin F, Carerj S, Bello VD, et al. Arterial stiffness and ventricular stiffness: a couple of diseases or a coupling disease? A review from the cardiologist's point of view. **Eur Heart J Cardiovasc Imag**. 2009; 10:36−43.

4. Safar ME, Nilsson PM, Blacher J, Mimran A. Pulse pressure, arterial stiffness, and end-organ damage. **Curr Hypertens Rep**. 2012; 14:339−344.

5. Vlachopoulos C, Aznaouridis K, Stefanadis C. Prediction of cardiovascular events and all-cause mortality with arterial stiffness: a systematic review and meta-analysis. **J Am Coll Cardiol**. 2010; 55:1318−1327.

6. Lakatta EG, Levy D. Arterial and cardiac aging: major shareholders in cardiovascular disease enterprises: Part I: aging arteries: a "set up" for vascular disease. **Circulation**. 2003; 107:139−146.

7. Lakatta EG, Levy D. Arterial and cardiac aging: major shareholders in cardiovascular disease enterprises: Part II: the aging heart in health: links to heart disease. **Circulation**. 2003; 107:346−354.

8. Malpas SC. Sympathetic nervous system overactivity and its role in the development of cardiovascular disease. **Physiol Rev**. 2010; 90:513−557.

9. Grassi G, Esler M. The sympathetic nervous system alterations in human hypertension. **Circ Res**. 2015; 116:976−990.

10. Chirinos JA, Segers P, Hughes T, Townsend R. Large-artery stiffness in health and disease: JACC State-of-the-Art Review. **J Am Coll Cardiol**. 2019; 74:1237−1263.

11. Kent KM, Epstein SE, Cooper T, Jacobowitz DM. Cholinergic innervation of the canine and human ventricular conducting system: anatomic and electrophysiologic correlations. **Circulation**. 1974; 50:948−955.

12. Higgins CB, Vatner SF, Braunwald E. Parasympathetic control of the heart. **Pharmacol Rev**. 1973; 25:119−155.

13. Brodde O-E, Michel MC. Adrenergic and muscarinic receptors in the human heart. **Pharmacol Rev**. 1999; 51:651−690.

14. Martin P. The influence of the parasympathetic nervous system on atrioventricular conduction. **Circ Res**. 1977; 41:593−599.

15. Irisawa H, Brown HF, Giles W. Cardiac pacemaking in the sinoatrial node. **Physiol Rev**. 1993; 73:197−227.

16. Jones PP, Shapiro LF, Keisling GA, et al. Altered autonomic support of arterial blood pressure with age in healthy men. **Circulation**. 2001; 104:2424−2429.

17. White DW, Raven PB. Autonomic neural control of heart rate during dynamic exercise: revisited. **J Physiol**. 2014; 592:2491−2500.

18. Landzberg JS, Parker JD, Gauthier DF, Colucci WS. Effects of intra-coronary acetylcholine and atropine on basal and dobutamine-stimulated left ventricular contractility. **Circulation**. 1994; 89:164−168.

19. Lewis ME, Al-Khalidi AH, Bonser RS, et al. Vagus nerve stimulation decreases left ventricular contractility in vivo in the human and pig heart. **J Physiol**. 2001; 534:547−552.

20. Geis W, Kaye M, Randall W. Major autonomic pathways to the atria and S-A and A-V nodes of the canine heart. **Am J Physiol**. 1973; 224:202−208.

21. Forsgren S. The distribution of sympathetic nerve fibres in the AV node and AV bundle of the bovine heart. **Histochem J**. 1986; 18:625−638.

22. Lee WC, Shideman FE. Role of myocardial catecholamines in cardiac contractility. **Science**. 1959; 129:967−968.

23. Somlyo AP, Somlyo AV. Signal transduction and regulation in smooth muscle. **Nature**. 1994; 372:231−236.

24. Horowitz A, Menice CB, Laporte R, Morgan KG. Mechanisms of smooth muscle contraction. **Physiol Rev**. 1996; 76:967−1003.

25. Kuriyama H, Ito Y, Suzuki H, Kitamura K, Itoh T. Factors modifying contraction-relaxation cycle in vascular smooth muscles. **Am J Physiol Heart Circ Physiol**. 1982; 243:H641−H662.

26. Kneale BJ, Chowienczyk PJ, Brett SE, Coltart DJ, Ritter JM. Gender differences in sensitivity to adrenergic agonists of forearm resistance vasculature. **J Am Coll Cardiol**. 2000; 36:1233−1238.

27. Tank AW, Wong DL. Peripheral and central effects of circulating catecholamines. **Comp Physiol**. 2015; 5:1−15.

28. DiBona GF, Rios LL. Renal nerves in compensatory renal response to contralateral renal denervation. **Am J Physiol Ren Physiol**. 1980; 238:F26−F30.

29. Coote JH, Johns EJ, Macleod VH, Singer B. Effect of renal nerve stimulation, renal blood flow and adrenergic blockade on plasma renin activity in the cat. **J Physiol**. 1972; 226:15−36.

30. La Grange RG, Sloop CH, Schmid HE. Selective stimulation of renal nerves in the anesthetized dog: effect on renin release during controlled changes in renal hemodynamics. **Circ Res**. 1973; 33:704−712.

31. Osborn JL, Holdaas H, Thames MD, DiBona GF. Renal adreno-ceptor mediation of antinatriuretic and renin secretion responses to low frequency renal nerve stimulation in the dog. **Circ Res**. 1983; 53:298−305.

32. Bello-Reuss E, Trevino DL, Gottschalk CW. Effect of renal sympathetic nerve stimulation on proximal water and sodium reabsorption. **J Clin Invest**. 1976; 57:1104−1107.

33. Gesek FA. α1- and α2-adrenoceptor control of sodium transport reverses in developing hypertension. **Hypertension**. 1999; 33:524−529.

34. Kasakov L, Ellis J, Kirkpatrick K, Milner P, Burnstock G. Direct evidence for concomitant release of noradrenaline, adenosine 5′-triphosphate and neuropeptide Y from sympathetic nerve supplying the Guinea-pig vas deferens. **J Auton Nerv Syst**. 1988; 22:75−82.

35. Lundberg JM, Martinsson A, Hemsén A, et al. Co-release of neuropeptide Y and catecholamines during physical exercise in man. **Biochem Biophys Res Commun**. 1985; 133:30−36.

36. Pernow J, Schwieler J, Kahan T, et al. Influence of sympathetic discharge pattern on norepinephrine and neuropeptide Y release. **Am J Physiol Heart Circ Physiol**. 1989; 257:H866−H872.

37. Todorov LD, Bjur RA, Westfall DP. Temporal dissociation of the release of the sympathetic co-transmitters ATP and noradrenaline. **Clin Exp Pharmacol Physiol**. 1994; 21:931−932.

38. Qureshi NU, Dayao EK, Shirali S, Zukowska-Grojec Z, Hauser GJ. Endogenous neuropeptide Y mediates vasoconstriction during endotoxic and hemorrhagic shock. **Regul Pept**. 1998; 75−76:215−220.

39. Ramey ER, Goldstein MS. The adrenal cortex and the sympathetic nervous system. **Physiol Rev**. 1957; 37:155−195.

40. Shoemaker JK, Badrov MB, Al-Khazraji BK, Jackson DN. Neural control of vascular function in skeletal muscle. **Comp Physiol**. 2015; 6:303−329.

41. Chirinos JA. Arterial stiffness: basic concepts and measurement techniques. **J Cardiovasc Transl Res**. 2012; 5:243−255.

42. Cox R. Pressure dependence of the mechanical properties of arteries in vivo. **Am J Physiol**. 1975; 229:1371−1375.

43. Laurent S, Cockcroft J, Van Bortel L, et al. Expert consensus document on arterial stiffness: methodological issues and clinical applications. **Eur Heart J**. 2006; 27:2588−2605.

44. Kim EJ, Park CG, Park JS, et al. Relationship between blood pressure parameters and pulse wave velocity in normotensive and hypertensive subjects: invasive study. **J Hum Hypertens**. 2006; 21:141−148.

45. AlGhatrif M, Strait JB, Morrell CH, et al. Longitudinal trajectories of arterial stiffness and the role of blood pressure. **Hypertension**. 2013; 62:934−941.

46. Nichols WW, O'Rourke MF, Vlachopoulos C. **McDonald's Blood Flow in Arteries, Sixth Edition: Theoretical, Experimental and Clinical Principles**. 6th ed. 1990.

47. Cecelja M, Chowienczyk P. Dissociation of aortic pulse wave velocity with risk factors for cardiovascular disease other than hypertension: a systematic review. **Hypertension**. 2009; 54:1328−1336.

48. Mangoni AA, Mircoli L, Giannattasio C, Mancia G, Ferrari AU. Effect of sympathectomy on mechanical properties of common carotid and femoral arteries. **Hypertension**. 1997; 30:1085−1088.

49. Mircoli L, Mangoni AA, Giannattasio C, Mancia G, Ferrari AU. Heart rate-dependent stiffening of large arteries in intact and sympathectomized rats. **Hypertension**. 1999; 34:598−602.

50. Tan I, Butlin M, Liu YY, Ng K, Avolio AP. Heart rate dependence of aortic pulse wave velocity at different arterial pressures in rats. **Hypertension**. 2012; 60:528−533.

51. Armentano RL, Barra JG, Levenson J, Simon A, Pichel RH. Arterial wall mechanics in conscious dogs. **Circ Res**. 1995; 76:468−478.

52. Lantelme P, Mestre C, Lievre M, Gressard A, Milon H. Heart rate: an important confounder of pulse wave velocity assessment. **Hypertension**. 2002; 39:1083−1087.

53. Millasseau SC, Stewart AD, Patel SJ, Redwood SR, Chowienczyk PJ. Evaluation of carotid-femoral pulse wave velocity: influence of timing algorithm and heart rate. **Hypertension**. 2005; 45:222−226.

54. Albaladejo P, Copie X, Boutouyrie P, et al. Heart rate, arterial stiffness, and wave reflections in paced patients. **Hypertension**. 2001; 38:949−952.

55. Giannattasio C, Vincenti A, Failla M, et al. Effects of heart rate changes on arterial distensibility in humans. **Hypertension**. 2003; 42:253−256.

56. Wilkinson IB, MacCallum H, Flint L, Cockcroft JR, Newby DE, Webb DJ. The influence of heart rate on augmentation index and central arterial pressure in humans. **J Physiol**. 2000; 525:263−270.

57. Hohneck AL, Fries P, Ströder J, et al. Effects of heart rate reduction with ivabradine on vascular stiffness and endothelial function in chronic stable coronary artery disease. **J Hypertens**. 2019; 37:1023−1031.

58. Salvi P, Palombo C, Salvi GM, Labat C, Parati G, Benetos A. Left ventricular ejection time, not heart rate, is an independent correlate of aortic pulse wave velocity. **J Appl Physiol**. 2013; 115:1610−1617.

59. Malik M, Bigger JT, Camm AJ, et al. Heart rate variability: standards of measurement, physiological interpretation, and clinical use. **Eur Heart J**. 1996; 17:354−381.

60. deBoer RW, Karemaker JM, Strackee J. Hemodynamic fluctuations and baroreflex sensitivity in humans: a beat-to-beat model. **Am J Physiol Heart Circ Physiol**. 1987; 253:H680−H689.

61. Blaber AP, Yamamoto Y, Hughson RL. Methodology of spontaneous baroreflex relationship assessed by surrogate data analysis. **Am J Physiol Heart Circ Physiol**. 1995; 268:H1682−H1687.

62. Chiou C-W, Zipes DP. Selective vagal denervation of the atria eliminates heart rate variability and baroreflex sensitivity while preserving ventricular innervation. **Circulation**. 1998; 98:360−368.

63. La Rovere MT, Specchia G, Mortara A, Schwartz PJ. Baroreflex sensitivity, clinical correlates, and cardiovascular mortality among patients with a first myocardial infarction. A prospective study. **Circulation**. 1988; 78:816−824.

64. Stein PK, Domitrovich PP, Huikuri HV, Kleiger RE. Traditional and nonlinear heart rate variability are each independently associated with mortality after myocardial infarction. **J Cardiovasc Electrophysiol**. 2005; 16:13−20.

65. De Ferrari GM, Sanzo A, Bertoletti A, Specchia G, Vanoli E, Schwartz PJ. Baroreflex sensitivity predicts long-term cardiovascular mortality after myocardial infarction even in patients with preserved left ventricular function. **J Am Coll Cardiol**. 2007; 50:2285−2290.

66. Nakao M, Nomura K, Karita K, Nishikitani M, Yano E. Relationship between brachial-ankle pulse wave velocity and heart rate variability in young Japanese men. **Hypertens Res**. 2004; 27:925−931.

67. Perkins GM, Owen A, Swaine IL, Wiles JD. Relationships between pulse wave velocity and heart rate variability in healthy men with a range of moderate-to-vigorous physical activity levels. **Eur J Appl Physiol**. 2006; 98:516−523.

68. Mäki-Petäjä KM, Barrett SML, Evans SV, Cheriyan J, McEniery CM, Wilkinson IB. The role of the autonomic nervous system in the regulation of aortic stiffness. **Hypertension**. 2016; 68:1290−1297.

69. Jensen-Urstad K, Reichard P, Jensen-Urstad M. Decreased heart rate variability in patients with type 1 diabetes mellitus is related to arterial wall stiffness. **J Intern Med**. 1999; 245:57−61.

70. Chandra P, Sands RL, Gillespie BW, et al. Relationship between heart rate variability and pulse wave velocity and their association

with patient outcomes in chronic kidney disease. **Clin Nephrol**. 2014; 81:9−19.

71. Lu D-Y, Sung S-H, Yu W-C, Cheng H-M, Chuang S-Y, Chen C-H. Wave reflections, arterial stiffness, heart rate variability and orthostatic hypotension. **Hypertens Res**. 2014; 37:1056−1061.

72. Germano-Soares AH, Cucato GG, Leicht AS, et al. Cardiac autonomic modulation is associated with arterial stiffness in patients with symptomatic peripheral artery disease. **Ann Vasc Surg**. 2019; 61:72−77.

73. Mattace-Raso FU, van den Meiracker AH, Bos WJ, et al. Arterial stiffness, cardiovagal baroreflex sensitivity and postural blood pressure changes in older adults: the Rotterdam Study. **J Hypertens**. 2007; 25:1421−1426.

74. Michas F, Manios E, Stamatelopoulos K, et al. Baroreceptor reflex sensitivity is associated with arterial stiffness in a population of normotensive and hypertensive patients. **Blood Pres Monit**. 2012; 17:155−159.

75. Pierce GL, Harris SA, Seals DR, Casey DP, Barlow PB, Stauss HM. Estimated aortic stiffness is independently associated with cardiac baroreflex sensitivity in humans: role of ageing and habitual endurance exercise. **J Hum Hypertens**. 2016; 30:513−520.

76. Monahan KD, Dinenno FA, Seals DR, Clevenger CM, Desouza CA, Tanaka H. Age-associated changes in cardiovagal baroreflex sensitivity are related to central arterial compliance. **Am J Physiol Heart Circ Physiol**. 2001; 281:H284−H289.

77. Shaffer F, Ginsberg JP. An overview of heart rate variability metrics and norms. **Front Publ Health**. 2017; 5:258.

78. Akselrod S, Gordon D, Ubel FA, Shannon DC, Berger AC, Cohen RJ. Power spectrum analysis of heart rate fluctuation: a quantitative probe of beat-to-beat cardiovascular control. **Science**. 1981; 213:220−222.

79. Hedman AE, Hartikainen JEK, Tahvanainen KUO, Hakumäki MOK. The high frequency component of heart rate variability reflects cardiac parasympathetic modulation rather than parasympathetic 'tone'. **Acta Physiol Scand**. 1995; 155:267−273.

80. Piccirillo G, Ogawa M, Song J, et al. Power spectral analysis of heart rate variability and autonomic nervous system activity measured directly in healthy dogs and dogs with tachycardia-induced heart failure. **Heart Rhythm**. 2009; 6:546−552.

81. Saul JP, Rea RF, Eckberg DL, Berger RD, Cohen RJ. Heart rate and muscle sympathetic nerve variability during reflex changes of autonomic activity. **Am J Physiol Heart Circ Physiol**. 1990; 258:H713−H721.

82. Pagani M, Montano N, Porta A, et al. Relationship between spectral components of cardiovascular variabilities and direct measures of muscle sympathetic nerve activity in humans. **Circulation**. 1997; 95:1441−1448.

83. Malpas SC. Neural influences on cardiovascular variability: possibilities and pitfalls. **Am J Physiol Heart Circ Physiol**. 2002; 282:H6−H20.

84. Goldstein DS, Bentho O, Park M-Y, Sharabi Y. LF power of heart rate variability is not a measure of cardiac sympathetic tone but may be a measure of modulation of cardiac autonomic outflows by baroreflexes. **Exp Physiol**. 2011; 96:1255−1261.

85. Billman GE. The LF/HF ratio does not accurately measure cardiac sympatho-vagal balance. **Front Physiol**. 2013; 4.

86. Kobayashi M, Musha T. 1/f fluctuation of heartbeat period. **IEEE Trans Biomed Eng**. 1982; 29:456−457.

87. Butler GC, Ando S-I, Floras JS. Fractal component of variability of heart rate and systolic blood pressure in congestive heart failure. **Clin Sci**. 1997; 92:543−550.

88. Taylor JA, Carr DL, Myers CW, Eckberg DL. Mechanisms underlying very-low-frequency RR-interval oscillations in humans. **Circulation**. 1998; 98:547−555.

89. Sacha J, Pluta W. Alterations of an average heart rate change heart rate variability due to mathematical reasons. **Int J Cardiol**. 2008; 128:444−447.

90. Horner SM, Murphy CF, Coen B, et al. Contribution to heart rate variability by mechanoelectric feedback. **Circulation**. 1996; 94:1762−1767.

91. Qiu H, Zhu Y, Sun Z, et al. Short communication: vascular smooth muscle cell stiffness as a mechanism for increased aortic stiffness with aging. **Circ Res**. 2010; 107:615−619.

92. Sehgel NL, Zhu Y, Sun Z, et al. Increased vascular smooth muscle cell stiffness: a novel mechanism for aortic stiffness in hypertension. **Am J Physiol Heart Circ Physiol**. 2013; 305:H1281−H1287.

93. Peterson LH, Jensen RE, Parnell J. Mechanical properties of arteries in vivo. **Circ Res**. 1960; 8:622−639.

94. Barnett GO, Mallos AJ, Shapiro A. Relationship of aortic pressure and diameter in the dog. **J Appl Physiol**. 1961; 16:545−548.

95. Aars H. Diameter and elasticity of the ascending aorta during infusion of noradrenaline. **Acta Physiol Scand**. 1971; 83:133−138.

96. Cox R. Effects of norepinephrine on mechanics of arteries in vitro. **Am J Physiol**. 1976; 231:420−425.

97. Barra JG, Armentano RL, Levenson J, Fischer EI, Pichel RH, Simon A. Assessment of smooth muscle contribution to descending thoracic aortic elastic mechanics in conscious dogs. **Circ Res**. 1993; 73:1040−1050.

98. Bank AJ, Wilson RF, Kubo SH, Holte JE, Dresing TJ, Wang H. Direct effects of smooth muscle relaxation and contraction on in vivo human brachial artery elastic properties. **Circ Res**. 1995; 77:1008−1016.

99. Bank AJ, Wang H, Holte JE, Mullen K, Shammas R, Kubo SH. Contribution of collagen, elastin, and smooth muscle to in vivo human brachial artery wall stress and elastic modulus. **Circulation**. 1996; 94:3263−3270.

100. Bank AJ, Kaiser DR, Rajala S, Cheng A. In vivo human brachial artery elastic mechanics: effects of smooth muscle relaxation. **Circulation**. 1999; 100:41−47.

101. Bank AJ, Kaiser DR. Smooth muscle relaxation: effects on arterial compliance, distensibility, elastic modulus, and pulse wave velocity. **Hypertension**. 1998; 32:356−359.

102. Shadwick RE. Mechanical design in arteries. **J Exp Biol**. 1999; 202:3305−3313.

103. Pagani M, Mirsky I, Baig H, Manders WT, Kerkhof P, Vatner SF. Effects of age on aortic pressure-diameter and elastic stiffness-stress relationships in unanesthetized sheep. **Circ Res**. 1979; 44:420−429.

104. Pagani M, Schwartz P, Bishop V, Malliani A. Reflex sympathetic changes in aortic diastolic pressure-diameter relationship. **Am J Physiol**. 1975; 229:286−290.

105. Tebbs BT. The sympathetic innervation of the aorta and intercostal arteries. **J Anat Physiol**. 1898; 32:308−311.

106. Kienecker EW, Knoche H. Sympathetic innervation of the pulmonary artery, ascending aorta, and coronar glomera of the rabbit. A fluorescence microscopic study. **Cell Tissue Res**. 1978; 188:329−333.

107. Pannier B, Guérin AP, Marchais SJ, Safar ME, London GM. Stiffness of capacitive and conduit arteries: prognostic significance for end-stage renal disease patients. **Hypertension**. 2005; 45:592−596.

108. van Sloten TT, Schram MT, van den Hurk K, et al. Local stiffness of the carotid and femoral artery is associated with incident cardiovascular events and all-cause mortality: the Hoorn Study. **J Am Coll Cardiol**. 2014; 63:1739−1747.

109. Damon DH. Sympathetic innervation promotes vascular smooth muscle differentiation. **Am J Physiol Heart Circ Physiol**. 2005; 288:H2785−H2791.

110. Okazaki M, Hu ZW, Fujinaga M, Hoffman BB. Alpha 1 adrenergic receptor-induced c-fos gene expression in rat aorta and cultured vascular smooth muscle cells. **J Clin Invest**. 1994; 94:210−218.

111. Zhang H, Faber JE. Trophic effect of norepinephrine on arterial intima-media and adventitia is augmented by injury and mediated by different α1-adrenoceptor subtypes. **Circ Res**. 2001; 89:815−822.

112. Zhang H, Facemire CS, Banes AJ, Faber JE. Different α-adrenoceptors mediate migration of vascular smooth muscle cells and adventitial fibroblasts in vitro. **Am J Physiol Heart Circ Physiol**. 2002; 282:H2364−H2370.

113. Angouras DC, Dosios TJ, Dimitriou CA, et al. Surgical thoracic sympathectomy induces structural and biomechanical remodeling of the thoracic aorta in a porcine model. **J Surg Res**. 2012; 172:68−76.

114. Dinenno FA, Jones PP, Seals DR, Tanaka H. Age-associated arterial wall thickening is related to elevations in sympathetic activity in healthy humans. **Am J Physiol Heart Circ Physiol**. 2000; 278:H1205−H1210.

115. Holwerda SW, Luehrs RE, DuBose LE, Majee R, Pierce GL. Sex and age differences in the association between sympathetic outflow and central elastic artery wall thickness in humans. **Am J Physiol Heart Circ Physiol**. 2019; 317:H552−H560.

116. Ferreira JP, Girerd N, Bozec E, et al. Intima−media thickness is linearly and continuously associated with systolic blood pressure in a population-based cohort (STANISLAS Cohort Study). **J Am Heart Assoc**. 2016; 5.

117. Aroor AR, DeMarco V, Jia G, et al. The role of tissue renin-angiotensin-aldosterone system in the development of endothelial dysfunction and arterial stiffness. **Front Endocrinol**. 2013; 4.

118. Lyle AN, Raaz U. Killing me unsoftly: causes and mechanisms of arterial stiffness. **Arterioscler Thromb Vasc Biol**. 2017; 37.

119. Wilkinson IB, Franklin SS, Cockcroft JR. Nitric oxide and the regulation of large artery stiffness: from physiology to pharmacology. **Hypertension**. 2004; 44:112−116.

120. Thijssen DHJ, Atkinson CL, Ono K, et al. Sympathetic nervous system activation, arterial shear rate, and flow-mediated dilation. **J Appl Physiol**. 2014; 116:1300−1307.

121. Tymko MM, Lawley JS, Ainslie PN, et al. Global reach 2018 heightened α-adrenergic signaling impairs endothelial function during chronic exposure to hypobaric hypoxia. **Circ Res**. 2020; 127.

122. Hijmering ML, Stroes ESG, Olijhoek J, Hutten BA, Blankestijn PJ, Rabelink TJ. Sympathetic activation markedly reduces endothelium-dependent, flow-mediated vasodilation. **J Am Coll Cardiol**. 2002; 39:683−688.

123. Grassi G, Bolla G, Seravalle G, Turri C, Lanfranchi A, Mancia G. Comparison between reproducibility and sensitivity of muscle sympathetic nerve traffic and plasma noradrenaline in man. **Clin Sci**. 1997; 92:285−289.

124. Floras JS, Hara K. Sympathoneural and haemodynamic characteristics of young subjects with mild essential hypertension. **J Hypertens**. 1993; 11:647−655.

125. Wallin BG, Sundlöf G, Eriksson B-M, Dominiak P, Grobecker H, Lindblad LE. Plasma noradrenaline correlates to sympathetic muscle nerve activity in normotensive man. **Acta Physiol Scand**. 1981; 111:69−73.

126. Leimbach WN, Wallin BG, Victor RG, Aylward PE, Sundlöf G, Mark AL. Direct evidence from intraneural recordings for increased central sympathetic outflow in patients with heart failure. **Circulation**. 1986; 73:913−919.

127. Faconti L, Farukh B, McNally R, Webb AJ, Chowienczyk PJ. Arterial stiffness can be modulated by pressure-independent mechanisms in hypertension. **J Am Heart Assoc**. 2019; 8:e012601.

128. Phillips AA, Bredin SSD, Cote AT, Drury CT, Warburton DER. Aortic distensibility is reduced during intense lower body negative pressure and is related to low frequency power of systolic blood pressure. **Eur J Appl Physiol**. 2012; 113:785−792.

129. Holwerda SW, Luehrs RE, DuBose L, et al. Elevated muscle sympathetic nerve activity contributes to central artery stiffness in young and middle-age/older adults. **Hypertension**. 2019; 73:1025−1035.

130. Grassi G, Giannattasio C, Failla M, et al. Sympathetic modulation of radial artery compliance in congestive heart failure. **Hypertension**. 1995; 26:348−354.

131. Hagbarth K-E, Vallbo ÅB. Mechanoreceptor activity recorded percutaneously with semi-microelectrodes in human peripheral nerves. **Acta Physiol Scand**. 1967; 69:121−122.

132. Hart EC, Head GA, Carter JR, et al. Recording sympathetic nerve activity in conscious humans and other mammals: guidelines and the road to standardization. **Am J Physiol Heart Circ Physiol**. 2017; 312:H1031−H1051.

133. Sundlöf G, Wallin BG. Human muscle nerve sympathetic activity at rest. Relationship to blood pressure and age. **J Physiol**. 1978; 274:621−637.

134. Floras JS. Sympathoinhibitory effects of atrial natriuretic factor in normal humans. **Circulation**. 1990; 81:1860−1873.

135. Notay K, Seed JD, Incognito AV, et al. Validity and reliability of measuring resting muscle sympathetic nerve activity using short sampling durations in healthy humans. **J Appl Physiol**. 2016; 121:1065−1073.

136. Świerblewska E, Hering D, Kara T, et al. An independent relationship between muscle sympathetic nerve activity and pulse wave velocity in normal humans. **J Hypertens**. 2010; 28:979−984.

137. Harvey RE, Barnes JN, Hart ECJ, Nicholson WT, Joyner MJ, Casey DP. Influence of sympathetic nerve activity on aortic hemodynamics and pulse wave velocity in women. **Am J Physiol Heart Circ Physiol**. 2016; 312:H340−H346.

138. Hart EC, Charkoudian N, Joyner MJ, Barnes JN, Curry TB, Casey DP. Relationship between sympathetic nerve activity and aortic wave reflection characteristics in postmenopausal women. **Menopause**. 2013; 20:967−972.

139. Casey DP, Curry TB, Joyner MJ, Charkoudian N, Hart EC. Relationship between muscle sympathetic nerve activity and aortic wave reflection characteristics in young men and women. **Hypertension**. 2011; 57:421−427.

140. Smith MM, Tony Buffington CA, Hamlin RL, Devor ST. Relationship between muscle sympathetic nerve activity and aortic wave

reflection characteristics in aerobic- and resistance-trained subjects. **Eur J Appl Physiol**. 2015; 115:2609−2619.

141. Tanaka H, Dinenno FA, Seals DR. Reductions in central arterial compliance with age are related to sympathetic vasoconstrictor nerve activity in healthy men. **Hypertens Res**. 2017; 40:493−495.

142. Millar PJ, Notarius CF, Haruki N, Floras JS. Heart failure-specific relationship between muscle sympathetic nerve activity and aortic wave reflection. **J Card Fail**. 2019; 25:404−408.

143. Kosch M, Barenbrock M, Kisters K, Rahn KH, Hausberg M. Relationship between muscle sympathetic nerve activity and large artery mechanical vessel wall properties in renal transplant patients. **J Hypertens**. 2002; 20:501−508.

144. Usselman CW, Adler TE, Coovadia Y, Leone C, Paidas MJ, Stachenfeld NS. A recent history of preeclampsia is associated with elevated central pulse wave velocity and muscle sympathetic outflow. **Am J Physiol Heart Circ Physiol**. 2020; 318:H581−H589.

145. Kelly RP, Millasseau SC, Ritter JM, Chowienczyk PJ. Vasoactive drugs influence aortic augmentation index independently of pulse-wave velocity in healthy men. **Hypertension**. 2001; 37:1429−1433.

146. Okada Y, Galbreath MM, Jarvis SS, et al. Broader adaptive range of sympathetic burst size in response to blood pressure change in older women with greater arterial stiffness. **J Physiol**. 2020; 598:3331−3341.

147. Keir DA, Badrov MB, Tomlinson G, et al. Influence of sex and age on muscle sympathetic nerve activity of healthy normotensive adults. **Hypertension**. 2020; 76:997−1005.

148. McEniery CM, Yasmin, Hall IR, Qasem A, Wilkinson IB, Cockcroft JR. Normal vascular aging: differential effects on wave reflection and aortic pulse wave velocity: the Anglo-Cardiff Collaborative Trial (ACCT). **J Am Coll Cardiol**. 2005; 46:1753−1760.

149. The Reference Values for Arterial Stiffness' Collaboration. Determinants of pulse wave velocity in healthy people and in the presence of cardiovascular risk factors: 'establishing normal and reference values'. **Eur Heart J**. 2010; 31:2338−2350.

150. Petrák O, Štrauch B, Zelinka T, et al. Factors influencing arterial stiffness in pheochromocytoma and effect of adrenalectomy. **Hypertens Res**. 2010; 33:454−459.

151. Okada Y, Galbreath MM, Shibata S, et al. Relationship between sympathetic baroreflex sensitivity and arterial stiffness in elderly men and women. **Hypertension**. 2012; 59:98−104.

152. Grassi G, Seravalle G, Dell'Oro R, Arenare F, Facchetti R, Mancia G. Reproducibility patterns of plasma norepinephrine and muscle sympathetic nerve traffic in human obesity. **Nutr Metabol Cardiovasc Dis**. 2009; 19:469−475.

153. Esler M, Jennings G, Lambert G, Meredith I, Horne M, Eisenhofer G. Overflow of catecholamine neurotransmitters to the circulation: source, fate, and functions. **Physiol Rev**. 1990; 70:963−985.

154. Folkow B, DiBona GF, Hjemdahl P, Torén PH, Wallin BG. Measurements of plasma norepinephrine concentrations in human primary hypertension. A word of caution on their applicability for assessing neurogenic contributions. **Hypertension**. 1983; 5:399−403.

155. Hwang C-L, Piano MR, Thur LA, Peters TA, da Silva ALG, Phillips SA. The effects of repeated binge drinking on arterial stiffness and urinary norepinephrine levels in young adults. **J Hypertens**. 2020; 38:111−117.

156. Goswami N, Blaber AP, Hinghofer-Szalkay H, Convertino VA. Lower body negative pressure: physiological effects, applications, and implementation. **Physiol Rev**. 2018; 99:807−851.

157. Sundlöf G, Wallin BG. Effect of lower body negative pressure on human muscle nerve sympathetic activity. **J Physiol**. 1978; 278:525−532.

158. Floras JS, Butler GC, Ando S-I, Brooks SC, Pollard MJ, Picton P. Differential sympathetic nerve and heart rate spectral effects of nonhypotensive lower body negative pressure. **Am J Physiol Regul Integr Comp Physiol**. 2001; 281:R468−R475.

159. Stevens PM, Lamb LE. Effects of lower body negative pressure on the cardiovascular system. **Am J Cardiol**. 1965; 16:506−515.

160. Boutouyrie P, Lacolley P, Girerd X, Beck L, Safar M, Laurent S. Sympathetic activation decreases medium-sized arterial compliance in humans. **Am J Physiol Heart Circ Physiol**. 1994; 267:H1368−H1376.

161. Lafleche AB, Pannier BM, Laloux B, Safar ME. Arterial response during cold pressor test in borderline hypertension. **Am J Physiol Heart Circ Physiol**. 1998; 275:H409−H415.

162. Salzer DA, Medeiros PJ, Craen R, Shoemaker JK. Neurogenic-nitric oxide interactions affecting brachial artery mechanics in humans: roles of vessel distensibility vs. diameter. **Am J Physiol Regul Integr Comp Physiol**. 2008; 295:R1181−R1187.

163. Failla M, Grappiolo A, Emanuelli G, et al. Sympathetic tone restrains arterial distensibility of healthy and atherosclerotic subjects. **J Hypertens**. 1999; 17:1117−1123.

164. Joannides R, Richard V, Moore N, Godin M, Thuillez C. Influence of sympathetic tone on mechanical properties of muscular arteries in humans. **Am J Physiol Heart Circ Physiol**. 1995; 268:H794−H801.

165. Pease DC, Paule WJ. Electron microscopy of elastic arteries; the thoracic aorta of the rat. **J Ultrastruct Res**. 1960; 3:469−483.

166. Cowen T, Burnstock G. Quantitative analysis of the density and pattern of adrenergic innervation of blood vessels. **Histochemistry**. 1980; 66:19−34.

167. Stassen FR, Maas RG, Schiffers PM, Janssen GM, De Mey JG. A positive and reversible relationship between adrenergic nerves and alpha-1A adrenoceptors in rat arteries. **J Pharmacol Exp Therapeut**. 1998; 284:399−405.

168. Bortolotto LA, Hanon O, Franconi G, Boutouyrie P, Legrain S, Girerd X. The aging process modifies the distensibility of elastic but not muscular arteries. **Hypertension**. 1999; 34:889−892.

169. Bjarnegård N, Ahlgren ÅR, Sonesson B, Länne T. The effect of sympathetic stimulation on proximal brachial artery mechanics in humans − differential behaviour within the length of the brachial artery? **Acta Physiol Scand**. 2004; 182:21−27.

170. Yu S, McEniery C. Central versus peripheral artery stiffening and cardiovascular risk. **Arterioscler Thromb Vasc Biol**. 2020; 40:1028−1033.

171. Sonesson B, Vernersson E, Hansen F, Länne T. Influence of sympathetic stimulation on the mechanical properties of the aorta in humans. **Acta Physiol Scand**. 1997; 159:139−145.

172. Pannier B, Slama MA, London GM, Safar ME, Cuche JL. Carotid arterial hemodynamics in response to LBNP in normal subjects: methodological aspects. **J Appl Physiol**. 1995; 79:1546−1555.

173. Lydakis C, Momen A, Blaha C, Herr M, Leuenberger UA, Sinoway LI. Changes of elastic properties of central arteries during acute static exercise and lower body negative pressure. **Eur J Appl Physiol**. 2008; 102:633−641.

174. Nardone M, Incognito AV, Millar PJ. Evidence for pressure-independent sympathetic modulation of central pulse wave velocity. **J Am Heart Assoc**. 2018; 7.

175. Bock JM, Hughes WE, Casey DP. Age-associated differences in central artery responsiveness to sympathoexcitatory stimuli. **Am J Hypertens**. 2019; 32:564−569.

176. Huijben AMT, Mattace-Raso FUS, Deinum J, Lenders J, van den Meiracker AH. Aortic augmentation index and pulse wave velocity in response to head-up tilting: effect of autonomic failure. **J Hypertens**. 2012; 30:307−314.

177. Mitchell A, Bührmann S, Saez AO, et al. Clonidine lowers blood pressure by reducing vascular resistance and cardiac output in young, healthy males. **Cardiovasc Drugs Ther**. 2005; 19:49−55.

178. Wenzel RR, Allegranza G, Binggeli C, et al. Differential activation of cardiac and peripheral sympathetic nervous system by nifedipine: role of pharmacokinetics. **J Am Coll Cardiol**. 1997; 29:1607−1614.

179. Bruno RM, Ghiadoni L, Seravalle G, Dell'Oro R, Taddei S, Grassi G. Sympathetic regulation of vascular function in health and disease. **Front Physiol**. 2012; 3.

180. Giannattasio C, Failla M, Lucchina S, et al. Arterial stiffening influence of sympathetic nerve activity. **Hypertension**. 2005; 45:608−611.

181. Lenders JW, Eisenhofer G, Mannelli M, Pacak K. Phaeochromocytoma. **Lancet**. 2005; 366:665−675.

182. Yokomoto-Umakoshi M, Umakoshi H, Ogata M, et al. Coexistence of osteoporosis and atherosclerosis in pheochromocytoma: new insights into its long-term management. **Osteoporos Int**. 2020; 31:2151−2160.

183. Phillips DB, Steinback CD, Collins SÉ, et al. The carotid chemoreceptor contributes to the elevated arterial stiffness and vasoconstrictor outflow in chronic obstructive pulmonary disease. **J Physiol**. 2018; 596:3233−3244.

184. Gronda E, Seravalle G, Brambilla G, et al. Chronic baroreflex activation effects on sympathetic nerve traffic, baroreflex function, and cardiac haemodynamics in heart failure: a proof-of-concept study. **Eur J Heart Fail**. 2014; 16:977−983.

185. Gronda E, Brambilla G, Seravalle G, et al. Effects of chronic carotid baroreceptor activation on arterial stiffness in severe heart failure. **Clin Res Cardiol**. 2016; 105:838−846.

186. Wallbach M, Lehnig L-Y, Schroer C, et al. Effects of baroreflex activation therapy on arterial stiffness and central hemodynamics in patients with resistant hypertension. **J Hypertens**. 2015; 33:181−186.

187. Brandt MC, Reda S, Mahfoud F, Lenski M, Böhm M, Hoppe UC. Effects of renal sympathetic denervation on arterial stiffness and central hemodynamics in patients with resistant hypertension. **J Am Coll Cardiol**. 2012; 60:1956−1965.

188. Hering D, Lambert EA, Marusic P, et al. Renal nerve ablation reduces augmentation index in patients with resistant hypertension. **J Hypertens**. 2013; 31:1893−1900.

189. Grassi G. Sympathomodulatory effects of antihypertensive drug treatment. **Am J Hypertens**. 2016; 29:665−675.

190. Liu M, Li G-L, Li Y, Wang J-G. Effects of various antihypertensive drugs on arterial stiffness and wave reflections. **Pulse**. 2013; 1:97−107.

191. Ghiadoni L. The effects of antihypertensive drugs on arterial stiffness. **Artery Res**. 2016; 14:1−5.

192. Fu Q, Zhang R, Witkowski S, et al. Persistent sympathetic activation during chronic antihypertensive therapy. **Hypertension**. 2005; 45:513−521.

193. Kinouchi K, Ichihara A, Sakoda M, Kurauchi-Mito A, Itoh H. Safety and benefits of a tablet combining losartan and hydrochlorothiazide in Japanese diabetic patients with hypertension. **Hypertens Res**. 2009; 32:1143−1147.

194. Mahmud A, Feely J. Effect of angiotensin II receptor blockade on arterial stiffness: beyond blood pressure reduction. **Am J Hypertens**. 2002; 15:1092−1095.

195. Ripley DP, Negrou K, Oliver JJ, et al. Aortic remodelling following the treatment and regression of hypertensive left ventricular hypertrophy: a cardiovascular magnetic resonance study. **Clin Exp Hypertens**. 2015; 37:308−316.

196. Dorresteijn JAN, Schrover IM, Visseren FLJ, Scheffer PG, Oey PL, Danser AH, Spiering W. Differential effects of renin−angiotensin−aldosterone system inhibition, sympathoinhibition and diuretic therapy on endothelial function and blood pressure in obesity-related hypertension: a double-blind, placebo-controlled cross-over trial. **J Hypertens**. 2013; 31:393−403.

197. Komai N, Ohishi M, Moriguchi A, et al. Low-dose doxazosin improved aortic stiffness and endothelial dysfunction as measured by noninvasive evaluation. **Hypertens Res**. 2002; 25:5−10.

198. Deary AJ, Schumann AL, Murfet H, Haydock S, Foo RS, Brown MJ. Influence of drugs and gender on the arterial pulse wave and natriuretic peptide secretion in untreated patients with essential hypertension. **Clin Sci**. 2002; 103:493−499.

199. McGowan CL, Murai H, Millar PJ, Notarius CF, Morris BL, Floras JS. Simvastatin reduces sympathetic outflow and augments endothelium-independent dilation in non-hyperlipidaemic primary hypertension. **Heart**. 2013; 99:240−246.

200. Millar PJ, Floras JS. Statins and the autonomic nervous system. **Clin Sci**. 2014; 126:401−415.

201. Upala S, Wirunsawanya K, Jaruvongvanich V, Sanguankeo A. Effects of statin therapy on arterial stiffness: a systematic review and meta-analysis of randomized controlled trial. **Int J Cardiol**. 2017; 227:338−341.

202. Mahmud A, Feely J. Review: arterial stiffness and the renin-angiotensin-aldosterone system. **J Renin-Angiotensin-Aldosterone Syst**. 2004; 5:102−108.

203. Wang M, Khazan B, Lakatta EG. Central arterial aging and angiotensin II signaling. **Curr Hypertens Rev**. 2010; 6:266−281.

204. Morishita R, Gibbons GH, Ellison KE, et al. Evidence for direct local effect of angiotensin in vascular hypertrophy. In vivo gene transfer of angiotensin converting enzyme. **J Clin Invest**. 1994; 94:978−984.

205. Griendling KK, Minieri CA, Ollerenshaw JD, Alexander RW. Angiotensin II stimulates NADH and NADPH oxidase activity in cultured vascular smooth muscle cells. **Circ Res**. 1994; 74:1141−1148.

206. Wang M, Takagi G, Asai K, et al. Aging increases aortic MMP-2 activity and angiotensin II in nonhuman primates. **Hypertension**. 2003; 41:1308−1316.

207. Wang M, Zhang J, Spinetti G, et al. Angiotensin II activates matrix metalloproteinase type II and mimics age-associated carotid arterial remodeling in young rats. **Am J Pathol**. 2005; 167:1429−1442.

208. Spinetti G, Wang M, Monticone R, Zhang J, Zhao D, Lakatta EG. Rat aortic MCP-1 and its receptor CCR2 increase with age and alter vascular smooth muscle cell function. **Arterioscler Thromb Vasc Biol**. 2004; 24:1397−1402.

209. Benetos A, Levy BI, Lacolley P, Taillard F, Duriez M, Safar ME. Role of angiotensin II and bradykinin on aortic collagen following converting enzyme inhibition in spontaneously hypertensive rats. **Arterioscler Thromb Vasc Biol**. 1997; 17:3196−3201.

210. Ng K, Butlin M, Avolio AP. Persistent effect of early, brief angiotensin-converting enzyme inhibition on segmental pressure dependency of aortic stiffness in spontaneously hypertensive rats. **J Hypertens**. 2012; 30:1782−1790.

211. Lacolley P, Labat C, Pujol A, Delcayre C, Benetos A, Safar M. Increased carotid wall elastic modulus and fibronectin in aldosterone-salt−treated rats: effects of eplerenone. **Circulation**. 2002; 106:2848−2853.

212. Rautureau Y, Paradis P, Schiffrin EL. Cross-talk between aldosterone and angiotensin signaling in vascular smooth muscle cells. **Steroids**. 2011; 76:834−839.

213. Jia G, Aroor AR, Hill MA, Sowers JR. Role of renin-angiotensin-aldosterone system Activation in promoting cardiovascular fibrosis and stiffness. **Hypertension**. 2018; 72:537−548.

214. Shapiro Y, Boaz M, Matas Z, Fux A, Shargorodsky M. The association between the renin−angiotensin−aldosterone system and arterial stiffness in young healthy subjects. **Clin Endocrinol**. 2008; 68:510−512.

215. Rehman A, Rahman AR, Rasool AH, Naing NN. The effects of angiotensin II on pulse wave velocity in healthy humans. **Int J Clin Pharmacol Ther**. 2001; 39:423−430.

216. Rehman A, Rahman ARA, Rasool AHG. Effect of angiotensin II on pulse wave velocity in humans is mediated through angiotensin II type 1 (AT1) receptors. **J Hum Hypertens**. 2002; 16:261−266.

217. Perret F, Mooser V, Hayoz D, et al. Evaluation of arterial compliance-pressure curves. Effect of antihypertensive drugs. **Hypertension**. 1991; 18:II77−83.

218. Koumaras C, Tzimou M, Stavrinou E, et al. Role of antihypertensive drugs in arterial 'De-stiffening' and central pulsatile hemodynamics. **Am J Cardiovasc Drugs**. 2012; 12:143−156.

219. Lacolley P, Safar ME, Regnault V, Frohlich ED. Angiotensin II, mechanotransduction, and pulsatile arterial hemodynamics in hypertension. **Am J Physiol Heart Circ Physiol**. 2009; 297:H1567−H1575.

220. Mitchell GF, Dunlap ME, Warnica W, et al. Long-term trandolapril treatment is associated with reduced aortic stiffness: the prevention of events with angiotensin-converting enzyme inhibition hemodynamic substudy. **Hypertension**. 2007; 49:1271−1277.

221. Mahmud A, Feely J. Reduction in arterial stiffness with angiotensin II antagonist is comparable with and additive to ACE inhibition. **Am J Hypertens**. 2002; 15:321−325.

222. Mahmud A, Feely J. Aldosterone-to-renin ratio, arterial stiffness, and the response to aldosterone antagonism in essential hypertension. **Am J Hypertens**. 2005; 18:50−55.

223. Reid IA. Interactions between ANG II, sympathetic nervous system, and baroreceptor reflexes in regulation of blood pressure. **Am J Physiol Endocrinol Metab**. 1992; 262:E763−E778.

224. Matsukawa T, Gotoh E, Minamisawa K, et al. Effects of intravenous infusions of angiotensin II on muscle sympathetic nerve activity in humans. **Am J Physiol Regul Integr Comp Physiol**. 1991; 261:R690−R696.

225. Goldsmith SR, Hasking GJ, Miller E. Angiotensin II and sympathetic activity in patients with congestive heart failure. **J Am Coll Cardiol**. 1993; 21:1107−1113.

226. Lang CC, Stein CM, He HB, Wood AJJ. Angiotensin converting enzyme inhibition and sympathetic activity in healthy subjects. **Clin Pharmacol Ther**. 1996; 59:668−674.

227. Grassi G, Cattaneo BM, Seravalle G, et al. Effects of chronic ACE inhibition on sympathetic nerve traffic and baroreflex control of circulation in heart failure. **Circulation**. 1997; 96:1173−1179.

228. Rongen GA, Brooks SC, Ando S, Dajani HR, Abramson BL, Floras JS. Neural and hypotensive effects of angiotensin II receptor blockade. **Hypertension**. 1998; 31:378−383.

229. Lee CC, Sidani MA, Hogikyan RV, Supiano MA. The effects of ramipril on sympathetic nervous system function in older patients with hypertension. **Clin Pharmacol Ther**. 1999; 65:420−427.

230. Ruzicka M, Floras JS, McReynolds AJG, et al. Do high doses of AT1-receptor blockers attenuate central sympathetic outflow in humans with chronic heart failure? **Clin Sci**. 2013; 124: 589−595.

231. Azevedo ER, Mak S, Floras JS, Parker JD. Acute effects of angiotensin-converting enzyme inhibition versus angiotensin II receptor blockade on cardiac sympathetic activity in patients with heart failure. **Am J Physiol Regul Integr Comp Physiol**. 2017; 313:R410−R417.

232. Wijeysundera HC, Parmar G, Rongen GA, Floras JS. Reflex systemic sympatho-neural response to brachial adenosine infusion in treated heart failure. **Eur J Heart Fail**. 2011; 13:475−481.

233. Yanagisawa M, Kurihara H, Kimura S, et al. A novel potent vasoconstrictor peptide produced by vascular endothelial cells. **Nature**. 1988; 332:411−415.

234. Amiri F, Virdis A, Neves MF, et al. Endothelium-restricted overexpression of human endothelin-1 causes vascular remodeling and endothelial dysfunction. **Circulation**. 2004; 110:2233−2240.

235. Böhm F, Pernow J. The importance of endothelin-1 for vascular dysfunction in cardiovascular disease. **Cardiovasc Res**. 2007; 76:8−18.

236. Bruno RM, Sudano I, Ghiadoni L, Masi L, Taddei S. Interactions between sympathetic nervous system and endogenous endothelin in patients with essential hypertension. **Hypertension**. 2011; 57:79−84.

237. Otsuki T, Maeda S, Iemitsu M, et al. Vascular endothelium-derived factors and arterial stiffness in strength- and endurance-trained men. **Am J Physiol Heart Circ Physiol**. 2007; 292:H786−H791.

238. Heintz B, Dörr R, Gillessen T, et al. Do arterial endothelin 1 levels affect local arterial stiffness? **Am Heart J**. 1993; 126:987−989.

239. McEniery CM, Qasem A, Schmitt M, Avolio AP, Cockcroft JR, Wilkinson IB. Endothelin-1 regulates arterial pulse wave velocity in vivo. **J Am Coll Cardiol**. 2003; 42:1975−1981.

240. Vuurmans TJL, Boer P, Koomans HA. Effects of endothelin-1 and endothelin-1 receptor blockade on cardiac output, aortic pressure, and pulse wave velocity in humans. **Hypertension**. 2003; 41:1253−1258.

241. Maeda S, Sugawara J, Yoshizawa M, et al. Involvement of endothelin-1 in habitual exercise-induced increase in arterial compliance. **Acta Physiol**. 2009; 196:223−229.

242. Dhaun N, MacIntyre IM, Melville V, et al. Blood pressure−independent reduction in proteinuria and arterial stiffness after acute endothelin-A receptor antagonism in chronic kidney disease. **Hypertension**. 2009; 54:113−119.

243. Dhaun N, MacIntyre IM, Kerr D, et al. Selective endothelin-A receptor antagonism reduces proteinuria, blood pressure, and arterial stiffness in chronic proteinuric kidney disease. **Hypertension**. 2011; 57:772−779.

244. Wahlqvist ML, Lo CS, Myers KA, Simpson RW, Simpson JM. Putative determinants of arterial wall compliance in NIDDM. **Diabetes Care**. 1988; 11:787−790.

245. Lehmann ED, Gosling RG, Sönksen PH. Arterial wall compliance in diabetes. **Diabet Med**. 1992; 9:114−119.

246. Stehouwer CDA, Henry RMA, Ferreira I. Arterial stiffness in diabetes and the metabolic syndrome: a pathway to cardiovascular disease. **Diabetologia**. 2008; 51:527.

247. Neutel JM, Smith DHG, Graettinger WF, Weber MA. Dependency of arterial compliance on circulating neuroendocrine and metabolic factors in normal subjects. **Am J Cardiol**. 1992; 69:1340−1344.

248. Kupari M, Hekali P, Keto P, Poutanen VP, Tikkanen MJ, Standerstkjöld-Nordenstam CG. Relation of aortic stiffness to factors modifying the risk of atherosclerosis in healthy people. **Arterioscler Thromb J Vasc Biol**. 1994; 14:386−394.

249. Salomaa V, Riley W, Kark JD, Nardo C, Folsom AR. Non−insulin-dependent diabetes mellitus and fasting glucose and insulin concentrations are associated with arterial stiffness indexes: the ARIC study. **Circulation**. 1995; 91:1432−1443.

250. Emoto M, Nishizawa Y, Kawagishi T, et al. Stiffness indexes β of the common carotid and femoral arteries are associated with insulin resistance in NIDDM. **Diabetes Care**. 1998; 21:1178−1182.

251. Dijk RAJMV, Bakker SJL, Scheffer PG, Heine RJ, Stehouwer CDA. Associations of metabolic variables with arterial stiffness in type 2 diabetes mellitus: focus on insulin sensitivity and postprandial triglyceridaemia. **Eur J Clin Invest**. 2003; 33:307−315.

252. Sengstock DM, Vaitkevicius PV, Supiano MA. Arterial stiffness is related to insulin resistance in nondiabetic hypertensive older adults. **J Clin Endocrinol Metab**. 2005; 90:2823−2827.

253. Webb DR, Khunti K, Silverman R, et al. Impact of metabolic indices on central artery stiffness: independent association of insulin resistance and glucose with aortic pulse wave velocity. **Diabetologia**. 2010; 53:1190−1198.

254. Fu S, Lin Y, Luo L, Ye P. Relationship between central arterial stiffness and insulin resistance in Chinese community-Dwelling population without diabetes mellitus. **Int J Endocrinol**. 2017; 2017:1073919.

255. Westerbacka J, Wilkinson I, Cockcroft J, Utriainen T, Vehkavaara S, Yki-Järvinen H. Diminished wave reflection in the aorta: a novel physiological action of insulin on large blood vessels. **Hypertension**. 1999; 33:1118−1122.

256. Westerbacka J, Seppälä-Lindroos A, Yki-Järvinen H. Resistance to acute insulin induced decreases in large artery stiffness accompanies the insulin resistance syndrome. **J Clin Endocrinol Metab**. 2001; 86:5262−5268.

257. Tamminen M, Westerbacka J, Vehkavaara S, Yki-Jarvinen H. Insulin-induced decreases in aortic wave reflection and central systolic pressure are impaired in type 2 diabetes. **Diabetes Care**. 2002; 25:2314−2319.

258. Scherrer U, Randin D, Vollenweider P, Vollenweider L, Nicod P. Nitric oxide release accounts for insulin's vascular effects in humans. **J Clin Invest**. 1994; 94:2511−2515.

259. Aroor AR, Jia G, Sowers JR. Cellular mechanisms underlying obesity-induced arterial stiffness. **Am J Physiol Regul Integr Comp Physiol**. 2018; 314:R387−R398.

260. Jia G, Aroor AR, DeMarco VG, Martinez-Lemus L, Meininger GA, Sowers JR. Vascular stiffness in insulin resistance and obesity. **Front Physiol**. 2015; 6.

261. Anderson EA, Hoffman RP, Balon TW, Sinkey CA, Mark AL. Hyperinsulinemia produces both sympathetic neural activation and vasodilation in normal humans. **J Clin Invest**. 1991; 87:2246−2252.

262. Anderson EA, Balon TW, Hoffman RP, Sinkey CA, Mark AL. Insulin increases sympathetic activity but not blood pressure in borderline hypertensive humans. **Hypertension**. 1992; 19:621−627.

263. Berne C, Fagius J, Pollare T, Hjemdahl P. The sympathetic response to euglycaemic hyperinsulinaemia. **Diabetologia**. 1992; 35:873−879.

264. Vollenweider P, Tappy L, Randin D, et al. Differential effects of hyperinsulinemia and carbohydrate metabolism on sympathetic nerve activity and muscle blood flow in humans. **J Clin Invest**. 1993; 92:147−154.

265. Grassi G, Biffi A, Dell'Oro R, et al. Sympathetic neural abnormalities in type 1 and type 2 diabetes: a systematic review and meta-analysis. **J Hypertens**. 2020; 38:1436−1442.

266. Dockery F, Bulpitt CJ, Donaldson M, Fernandez S, Rajkumar C. The relationship between androgens and arterial stiffness in older men. **J Am Geriatr Soc**. 2003; 51:1627−1632.

267. Vlachopoulos C, Ioakeimidis N, Miner M, et al. Testosterone deficiency: a determinant of aortic stiffness in men. **Atherosclerosis**. 2014; 233:278−283.

268. Hougaku H, Fleg JL, Najjar SS, et al. Relationship between androgenic hormones and arterial stiffness, based on longitudinal hormone measurements. **Am J Physiol Endocrinol Metab**. 2006; 290:E234−E242.

269. Kyriazis J, Tzanakis I, Stylianou K, et al. Low serum testosterone, arterial stiffness and mortality in male haemodialysis patients. **Nephrol Dial Transplant**. 2011; 26:2971−2977.

270. Smith JC, Bennett S, Evans LM, et al. The effects of induced hypogonadism on arterial stiffness, body composition, and metabolic parameters in males with prostate cancer. **J Clin Endocrinol Metab**. 2001; 86:4261−4267.

271. Dockery F, Bulpitt CJ, Agarwal S, Donaldson M, Rajkumar C. Testosterone suppression in men with prostate cancer leads to an increase in arterial stiffness and hyperinsulinaemia. **Clin Sci**. 2003; 104:195−201.

272. Canpolat U, Tokgözöğlu L, Aydin K, et al. Impaired aortic elastic properties in patients with adult-onset hypogonadism. **Blood Pres**. 2013; 22:114−119.

273. Yaron M, Greenman Y, Rosenfeld JB, et al. Effect of testosterone replacement therapy on arterial stiffness in older hypogonadal men. **Eur J Endocrinol**. 2009; 160:839−846.

274. Fischer GM, Swain ML. Effect of sex hormones on blood pressure and vascular connective tissue in castrated and noncastrated male rats. **Am J Physiol Heart Circ Physiol**. 1977; 232:H617−H621.

275. Fischer GM, Swain ML. Effects of estradiol and progesterone on the increased synthesis of collagen in atherosclerotic rabbit aortas. **Atherosclerosis**. 1985; 54:177−185.

276. Natoli AK, Medley TL, Ahimastos AA, et al. Sex steroids modulate human aortic smooth muscle cell matrix protein deposition and matrix metalloproteinase expression. **Hypertension**. 2005; 46: 1129−1134.

277. Kelly DM, Jones TH. Testosterone: a vascular hormone in health and disease. **J Endocrinol**. 2013; 217:R47−R71.

278. Sverrisdóttir YB, Mogren T, Kataoka J, Janson PO, Stener-Victorin E. Is polycystic ovary syndrome associated with high

sympathetic nerve activity and size at birth? **Am J Physiol Endocrinol Metab**. 2008; 294:E576−E581.

279. Nunes Alves MJN, Dos Santos MR, Dias RG, et al. Abnormal neurovascular control in anabolic androgenic steroids users. **Med Sci Sports Exerc**. 2010; 42:865−871.

280. Waddell TK, Dart AM, Gatzka CD, Cameron JD, Kingwell BA. Women exhibit a greater age-related increase in proximal aortic stiffness than men. **J Hypertens**. 2001; 19:2205−2212.

281. Ahimastos AA, Formosa M, Dart AM, Kingwell BA. Gender differences in large artery stiffness pre- and post puberty. **J Clin Endocrinol Metab**. 2003; 88:5375−5380.

282. Liu S, Bajpai A, Hawthorne EA, et al. Cardiovascular protection in females linked to estrogen-dependent inhibition of arterial stiffening and macrophage MMP12. **JCI Insight**. 2019; 4.

283. Liu L, Kashyap S, Murphy B, et al. GPER activation ameliorates aortic remodeling induced by salt-sensitive hypertension. **Am J Physiol Heart Circ Physiol**. 2016; 310:H953−H961.

284. Chen Z, Yuhanna IS, Galcheva-Gargova Z, Karas RH, Mendelsohn ME, Shaul PW. Estrogen receptor α mediates the nongenomic activation of endothelial nitric oxide synthase by estrogen. **J Clin Invest**. 1999; 103:401−406.

285. Xing D, Nozell S, Chen Y-F, Hage F, Oparil S. Estrogen and mechanisms of vascular protection. **Arterioscler Thromb Vasc Biol**. 2009; 29:289−295.

286. Schmitt M, Avolio A, Qasem A, et al. Basal NO locally modulates human iliac artery function in vivo. **Hypertension**. 2005; 46:227−231.

287. Giannattasio C, Failla M, Grappiolo A, et al. Fluctuations of radial artery distensibility throughout the menstrual cycle. **Arterioscler Thromb Vasc Biol**. 1999; 19:1925−1929.

288. Williams MRI, Westerman RA, Kingwell BA, et al. Variations in endothelial function and arterial compliance during the menstrual cycle. **J Clin Endocrinol Metab**. 2001; 86:5389−5395.

289. Hayashi K, Miyachi M, Seno N, et al. Variations in carotid arterial compliance during the menstrual cycle in young women. **Exp Physiol**. 2006; 91:465−472.

290. Robb AO, Mills NL, Din JN, et al. Influence of the menstrual cycle, pregnancy, and preeclampsia on arterial stiffness. **Hypertension**. 2009; 53:952−958.

291. Adkisson EJ, Casey DP, Beck DT, Gurovich AN, Martin JS, Braith RW. Central, peripheral and resistance arterial reactivity: fluctuates during the phases of the menstrual cycle. **Exp Biol Med**. 2010; 235:111−118.

292. Ounis-Skali N, Mitchell GF, Solomon CG, Solomon SD, Seely EW. Changes in central arterial pressure waveforms during the normal menstrual cycle. **J Invest Med**. 2006; 54:321−326.

293. Yu A, Giannone T, Scheffler P, et al. The effect of oral Contraceptive pills and the natural menstrual cYCLe on arterial stiffness and hemodynamICs (CYCLIC). **J Hypertens**. 2013; 32:100−107.

294. Priest SE, Shenouda N, MacDonald MJ. Effect of sex, menstrual cycle phase, and monophasic oral contraceptive pill use on local and central arterial stiffness in young adults. **Am J Physiol Heart Circ Physiol**. 2018; 315:H357−H365.

295. Papaioannou TG, Stamatelopoulos KS, Georgiopoulos G, et al. Arterial wave reflections during the menstrual cycle of healthy women: a reproducibility study. **Hypertension**. 2009; 54:1021−1027.

296. Willekes C, Hoogland HJ, Keizer HA, Hoeks AP, Reneman RS. Female sex hormones do not influence arterial wall properties during the normal menstrual cycle. **Clin Sci**. 1997; 92:487−491.

297. O'Donnell E, Goodman JM, Floras JS, Harvey PJ. Indexes of aortic wave reflection are not augmented in estrogen-deficient physically active premenopausal women. **Scand J Med Sci Sports**. 2020; 30:1054−1063.

298. O'Donnell E, Goodman JM, Mak S, et al. Discordant orthostatic reflex renin−angiotensin and sympathoneural responses in premenopausal exercising-hypoestrogenic women. **Hypertension**. 2015; 65: 1089−1095.

299. Boutouyrie P, Lacolley P, Briet M, et al. Pharmacological modulation of arterial stiffness. **Drugs**. 2011; 71:1689−1701.

300. Christou DD, Jones PP, Jordan J, Diedrich A, Robertson D, Seals DR. Women have lower tonic autonomic support of arterial blood pressure and less effective baroreflex buffering than men. **Circulation**. 2005; 111:494−498.

301. Wyss JM, Carlson SH. Effects of hormone replacement therapy on the sympathetic nervous system and blood pressure. **Curr Hypertens Rep**. 2003; 5:241−246.

302. Hart EC, Charkoudian N, Wallin BG, Curry TB, Eisenach J, Joyner MJ. Sex and ageing differences in resting arterial pressure regulation: the role of the β-adrenergic receptors. **J Physiol**. 2011; 589:5285−5297.

Chapter 25

Cellular mechanisms of aging and their impact on the aortic/arterial wall

Samsul Arefin[1,*], Agne Laucyte-Cibulskiene[1,2,*], Sam Hobson[1], Angelina Schwarz[1], Lu Dai[1], Karolina Kublickiene[1] and Peter Stenvinkel[1]

[1]*Division of Renal Medicine, Department of Clinical Science, Intervention & Technology, Karolinska University Hospital, Stockholm, Sweden;*

[2]*Department of Nephrology; Skåne University Hospital, Malmö, Sweden*

Introduction

Vascular aging is characterized by a gradual loss in vascular integrity. The latter is characterized by a combination of structural and functional properties of the cardiovascular system designed to meet the demands of blood delivery to target organs at pressures that allow distribution through the capillaries on metabolic demand. Accelerated vascular aging is associated with an increased risk for premature cardiovascular disease (CVD), the leading cause of death worldwide.[1] From a clinical point of view, vascular aging can be defined as a gradually developing process characterized by age-related alterations in both quantitative and qualitative structural properties of passive elements of the vascular wall accompanied by the decline in endothelial-dependent dilatation resulting in an increased vascular tone, the loss of arterial elasticity, and increased arterial stiffness. Vascular aging is significantly exaggerated when accompanied by the presence of certain risk factors and/or disease states, which are primarily related to metabolic disorders, hormonal imbalance, uremic toxin accumulation, nutritional characteristics, and/or obesity, physical inactivity, smoking habits, cholesterol and glucose levels, among other factors.[2,3]

Normal aging affects various organs and processes in the body, including the vascular tree. Experimental animal models and human studies have identified interconnected processes driving aging, which primarily include genomic instability, telomere attrition, epigenetic alterations, loss of proteostasis, dysregulated nutrient-sensing, mitochondrial dysfunction, cellular senescence, stem cell exhaustion, and altered intercellular communication. Common factors triggering the aforementioned processes include oxidative stress, vascular inflammation, endothelial dysfunction, and calcification. The processes described contribute to early vascular aging (EVA), which is primarily characterized by accelerated vascular remodeling, followed by functional decline of target organs such as heart, brain, and kidney.[4] Therefore, in some conditions (such as chronic kidney disease (CKD), diabetes mellitus, obesity, etc.), the biological vascular age is discrepant from the chronological age.[5] Arterial aging processes launch early in the life course and are either accelerated (regarded as EVA[6,7]), normal (so called Healthy Vascular Aging),[8] or slower than usual (SUPER normal Vascular Aging).[9] The latter is characterized by very low carotid−femoral pulse wave velocity (cfPWV) for an individual's chronological age and sex. As reviewed in several other chapters of this book, accelerated vascular aging has been related to CVD, cognitive dysfunction and dementia, CKD, and adverse pregnancy outcomes, such as preeclampsia.[4,7]

During aging, the arterial wall undergoes complex structural changes that affect its hemodynamic function, and in the presence of comorbidities and/or additional toxic milieu (such as uremic toxins), those processes will be gradually exaggerated. The structural changes are primarily related to loss of wall elasticity with accumulation of collagen, elastin fragmentation in the media, which result in reduced arterial compliance and adverse pulsatile hemodynamics.[10] The importance of vascular aging as an indicator of biological aging in humans is increasingly recognized.[5]

review the effect of aging on arterial structure and hemodynamic function. This chapter deals primarily with the fundamental cellular biologic processes that contribute to aging of the arterial wall.

---

* Authors contributed equally.

Effects of aging on the arterial tree

Endothelial dysfunction

Endothelial dysfunction has been responsible for initiating vascular remodeling. Endothelial cells sense the flow-mediated shear stress or frictional force of tensile stress and release vasodilating nitric oxide (NO) in addition to other vasoactive factors to preserve vascular homeostasis including vascular tone, coagulation, inflammation, and proliferation of vascular smooth muscle cells (VSMCs). A number of studies show that in the presence of conditions that increase the risk of CVD, endothelial cells switch from a protective to a proatherosclerotic phenotype with reduced NO availability and increased release of other substances important for arterial wall remodeling, including endothelin-1, thromboxane A2, prostaglandin H2, and reactive oxygen species (ROS).[11] Thus, endothelial dysfunction is seen as an early and major promoter for arterial aging. Interestingly, endothelial function in vivo can be assessed in muscular arteries by using flow-mediated dilation or in the microcirculation using techniques such as laser Doppler flowmetry.[12] There are also other available in vitro methods, such as endothelial cell culture, isolated small artery bioassays to assess endothelium-derived relaxing factors, and analysis of circulating biomarkers related to endothelial dysfunction. However, the lack of standardization limits the clinical applicability of endothelial function assessments.[12]

Elastic arteries

As described in detail in Chapters 19–24, multiple mechanisms contribute to the changes in the structure and function of the elastic arteries seen with aging and disease.[13] Due to aging-induced imbalance between vasoconstrictors and vasodilators, and changes in the quality and quantity of passive elements of the vascular wall, elastic arteries lose their "cushioning" function and slowly become stiff, tortuous, and elongated. In addition to elastic breakdown, collagen deposition in all layers of the artery wall and decreased elastin-to-collagen ratio accompanied by VSMCs phenotypical switching and increased stiffness[14] promote an adverse vascular remodeling process.[15,16] It has also been suggested that at some point VSMCs become senescent[17] and cell division of cells residing at the arterial wall diminishes.[16] In addition to the adverse remodeling process, calcification in the media and local calcification of plaques further contribute to increased arterial stiffness.[15]

Accumulating evidence indicates the presence of regional heterogeneity within the descending aorta[18] determined during embryogenesis[19] by the different thoracic and abdominal aortic developmental origins, neural crest-derived precursor cells, and mesodermal ancestors,

respectively. Moreover, the thoracic aorta has more elastic fibers compared to the abdominal aorta (especially the infrarenal part, where a decrease in elastin relative to collagen has been observed).[20] Aortic remodeling gradually starts in childhood and becomes more accelerated in middle age,[21] with more pronounced intimal thickening and slower enlargement in diameter of the distal aorta compared to the proximal aorta.[22]

Thoracic aortic aneurysms and dissections (TAADs) are two highly lethal aortic disorders, originating from molecular disorders that impair the aortic wall and which also relate to arterial wall aging.[23] The etiology of TAAD can be divided into genetic, biomechanical, and inflammatory subgroups. A genetic example is Marfan syndrome, where a mutation in FBN1 leads to abnormal metabolism of fibrillin1, a glycoprotein of the aortic medial wall extracellular matrix (ECM).[24,25] As an example for metabolic disease origin, oxidative stress can affect telomere attrition. Several studies showed that telomeres in endothelial cells and VSMCs of patients with TAA or abdominal aorta aneurysms are shortened compared to endothelial cells and VSMCs of cadaveric control aortas.[26–28] Biomechanically, the degeneration of arterial media ECM components like collagen, fibronectin, and laminin and the pooling of glycosaminoglycans leave the aorta predisposed to aneurysm formation and dissection.[29,30] Additionally, deficiency of integrins, transmembrane proteins anchoring cells to the ECM, leads to an overall reduction in contractile force and resistance to injury.[31]

The underlying trigger for inflammatory pathophysiology within the aorta is still debated, from autoimmunity to antibody reactions against excess lipids. Nevertheless, the immune reaction involves the presence of apoptotic VSMCs and the consequential influx of lymphocytes and macrophages to the tunica media via the adventitia.[24,32] The aforementioned mechanisms predispose the arterial wall of the aorta to development of aneurysms and dissections, which until rupture are painless and unless not readily detected.

Furthermore, physiological aortic aging is connected to high aortic systolic and pulse pressures, early return of wave reflections, decreased coronary perfusion pressure, degeneration of the arterial wall through elastolysis, increased cfPWV (i.e., arterial stiffening), and abnormal microcirculation.[33] As demonstrated through magnetic resonance imaging, elongation and dilatation of the thoracic aorta, especially the ascending aorta, changes the appearance from a "candy-cane"-like shape in young adults (<30 years) to an "ear"-like shape in senior adults (>60 years).[13] During systole, a healthy adult proximal aorta alone stores about 60% of stroke volume, releasing it through elastic recoil to more peripheral arteries during diastole. Due to decreased elasticity and thus reduced aortic compliance in an aged and stiffened aorta, a higher aortic

pulse pressure in the ascending aorta has been shown to be associated with eventual elongation and widening of the descending aorta.[34−36]

Muscular arteries

Muscular arteries (e.g., common femoral artery, coronary arteries, internal carotid artery, radial artery, etc.) have been hypothesized to be less affected by aging.[37] However, muscular arteries are the main target of systemic calcification (i.e., arteriosclerosis) mainly driven by VSMCs switching from a contractile to synthetic phenotype by transformation to osteoblast-like cells.[38] The medial calcification phenomenon is independent from atherosclerosis and rarely results in narrowing of the arterial lumen[39] as an intramembranous ossification process.[38] Interestingly, intimal calcification (more prominent in elastic vessels) is also prevalent in coronary arteries and mimics the characteristics of endochondral bone formation. Medial sclerosis has been attributed to CKD, aging, diabetes mellitus, and obstructive sleep apnea.[40] Calcium depositions are found in both the intima and media. Calcification of tunica media in coronary arteries is an independent predictor of cardiovascular morbidity and mortality.[41]

The measurement of muscular arterial stiffness (e.g., carotid-radial PWV,[6] femoral-ankle PWV,[42] etc.) has a limited application to assess vascular aging.[43−45] A more accepted index of vascular aging in muscular arteries is carotid intima media thickness[46] and coronary artery calcification score, both of which are predictors of cardiovascular events and mortality.[46−48]

Small arteries

During aging, small arteries exhibit impaired endothelial function. Aging is related to senescence-associated endothelial damage as a result of increased apoptosis and diminished regenerative capacity of the endothelium.[49] Small arteries also undergo an increase in the wall-to-lumen ratio, due to increased wall thickness with hypertrophic or eutrophic remodeling. In animal models, aging is usually accompanied with an outward hypertrophic remodeling (i.e., expanded lumen diameter, increased wall cross-sectional area, and an unaltered internal lumen to tunica media ratio).[50,51] On the other hand, in human hypertension, an inward eutrophic remodeling has been reported.[52,53] In secondary forms of hypertension, such as in diabetes mellitus, an inward hypertrophic remodeling is generally observed.[54] When the lumen diameter decreases and media thickness increases, the circumferential tension decreases and reduces media stress, such that the artery wall is protected from elevated blood pressure. Small reductions in lumen diameter increase the resistance to blood flow significantly.[55] The myogenic response of VSMCs also contributes to these processes, particularly due to altered integrin expression.[56] Integrin receptor subtype forms complexes with fibronectin and therefore may play a pivotal role in VSMCs adhesion to ECM and thus regulating VSMCs tone.[56]

Aging also results in a loss of arteriolar density and a central role of the microcirculation in aging has been proposed[57] (i.e., long-term defects in the microcirculation resulting in ischemic tissue damage and target organ damage). VSMCs may contribute to these processes due to altered integrin expression, as, for example, integrin subunit β1 is predominantly expressed on the surface of VSMCs.[58] In addition, integrin receptor subtype complexes with fibronectin play a pivotal role in VSMCs adhesion to ECM and thus regulating VSMC tone.[56] Some available methods for the evaluation of resistant arteries, not yet applied in clinical practice, include measurements of retinal pulse wave velocity,[59] nailfold capillaroscopy,[60] isolated vessel analysis,[61] laser speckle contrast imaging,[62] and plethysmographic techniques to assess microvascular dilation in response to ischemia (such as cuff inflation).[63−65]

The role of the adventitia in vascular remodeling

The role of the outer layer of the arteries, the adventitia, is often forgotten. It contains fibroblasts, adipocytes, pericytes, immune cells, vasa vasorum microvessels, lymphatics, and perivascular nerves. Whereas the separation between media and adventitia is easily distinguishable in elastic arteries, it is less distinct in small arteries.[66] Collagen fibrils, synthesized by adventitial fibroblasts, are one of the main components of the adventitia. In human studies, the nanoscale elastic modulus of the adventitia in the internal mammary artery correlated with arterial stiffness measured as cfPWV, which may reflect shared mechanisms of aortic wall and mammary artery adventitial stiffening.[67] Additionally, the adventitial inflammatory response is responsible for atherosclerotic plaque instability in coronary arteries.[68]

Furthermore, since the adventitia serves as a niche for progenitor cells,[69] it creates a dynamic environment of interacting cell types that have a specific functional capacity for the control of vascular wall growth, remodeling, and disease. Exhaustion of progenitor cells during the aging process affects the biological function of vessels.[70] Importantly, although it has been shown that compromised function of highly proliferative endothelial progenitor cells (EPCs) contributes to atherosclerosis,[71] the role of EPCs in the genesis of vascular aging phenotypes in humans is not well understood and needs further investigation.

Cellular and molecular mechanisms of vascular aging

Arterial aging is described by age-related deterioration and sclerosis of the media and intimal layers within the vascular tree that will result in age-associated changes in functional and structural properties. Research into aging at a cellular level in vasculature has increased our understanding of causes and consequences of aging at this level, particularly in clinical conditions associated with increased cardiovascular risk. It is now largely acknowledged that age-associated cellular damage predominantly influences cell membrane lipids, proteins involved in metabolic and structural roles, nuclear and mitochondrial DNA, and intracellular signaling processes. In the following paragraphs, we summarize the pathophysiology and contributing factors that lead to vascular aging. In the final paragraph, we present CKD, as a clinical model for studies of EVA with following clinical implications for patients.

Vascular inflammation

It is well established that inflammation plays an important role as a driving force for the development of EVA. Experimental evidence indicates that chronic, low-grade inflammation ("inflammaging") is strongly associated with the aging process. Activation of the inflammatory process with aging plays a key role in micro- and macrovascular pathogenesis and dysfunction in a number of CVD complications,[72,73] in addition to other pathologies like blood–brain barrier disruption or Alzheimer's disease. Experimental rodent and primate studies have shown that aging, particularly EVA, coincides with a proinflammatory shift in the gene expression profile in both vascular endothelial and smooth muscle cells, which involves multiple cytokines such as tumor necrosis factor (TNF), interleukins (IL-1β, IL-6), intracellular adhesion molecule 1 (ICAM1), vascular cell adhesion protein 1 (VCAM1), chemokines, and other proinflammatory mediators.[74–76] In particular, proinflammatory IL-6 has been shown to strongly associate with age-related vascular disease.[77] In middle age and in elderly populations, C-reactive protein associates with increased arterial stiffness.[78] In addition, arteries from older adults exhibit higher expression of monocyte chemoattractant protein-1 (MCP-1) and metalloproteinase in the thickened intima layer compared with younger adults.[75] The proinflammatory microenvironment of the vascular wall ultimately leads to vascular malfunction[79] and to the pathogenesis of vascular diseases.[80] In the aging vasculature, the contribution of inflammation seems multifaceted. The activation of transcription factor nuclear factor kappa (NF-κB) in inflammation is considered as the master regulator among inflammatory molecules including IL-1β, IL-2, IL-6, TNF, chemokines, and enzymes iNOS and COX-2.[81] The increase in inflammatory markers is independently associated with CVD risk factors with arterial thickening and stiffness.[82] Moreover, an increase of inflammatory markers may also occur independently of CVD risk factors independently of age.[83]

It is important to stress that in the aged vascular wall there is a critical crosstalk between elevated oxidative stress and inflammatory processes.[84] For example, ROS activate proinflammatory signaling pathways, including NF-κB,[85] which has been suggested to be an important player for endothelial cell maintenance and even production of angiostatic agents and consequently expression of proinflammatory paracrine mediators that may promote atherogenesis.[86] Importantly endothelial and smooth muscle cells in aging exhibit significant NF-κB activation[85,87] and inhibition of NF-κB in the vasculature has been shown to restore blood flow regulation, decrease systemic inflammation, and exert beneficial metabolic effects.[88] On the other hand, inflammatory mediators may also act as potent inducers of cellular oxidative stress.[79]

TNF acts as an important inflammatory mediator, as, for example, aged coronary arteries are characterized by increased expression of TNF gene expression profile assessed in rats.[80] In addition, application of external TNF has been shown to increase oxidative stress via stimulation of endothelial dysfunction, NADPH oxidase, endothelial apoptosis, and stimulation of proatherogenic inflammatory mediators.[80,89] Administration of TNF upregulates superoxide production in human retinal endothelial cell mitochondria.[90] Moreover, TNF antagonism improves the endothelial-mediated dilatation in resistance arteries of aged animals.[91] Overall, it appears that prolonged TNF exposure could have detrimental consequences to endothelial cells by causing senescence and, therefore, chronically increased TNF levels might contribute to the pathology of chronic inflammatory diseases by driving premature endothelial senescence.[92] The endothelium performs a crucial role to maintain the vascular tone by producing vasoconstrictor and vasodilator molecules, hence regulating blood flow to vital organs. Studies have demonstrated that senescence in human endothelial cells may cause the impairment of shear stress–mediated vascular relaxation.[93] In addition aging populations display reduced endothelial-mediated dilation with decreased NO generation.[94] Hence, an aging-related proinflammatory phenotype is likely to be associated with impaired endothelial function.

Moreover, there is increasing evidence that senescence in endothelium is linked with the release of a broad spectrum of inflammatory cytokines and chemokines,[95] more specifically the "senescence-associated secretory phenotype," or SASP. Since senescent cells are an important source of local, chronic, low-grade inflammation and plaque destabilization, they are a promising upstream therapeutic target. Developing evidence shows that in the aged vasculature, senescence significantly contributes to trigger
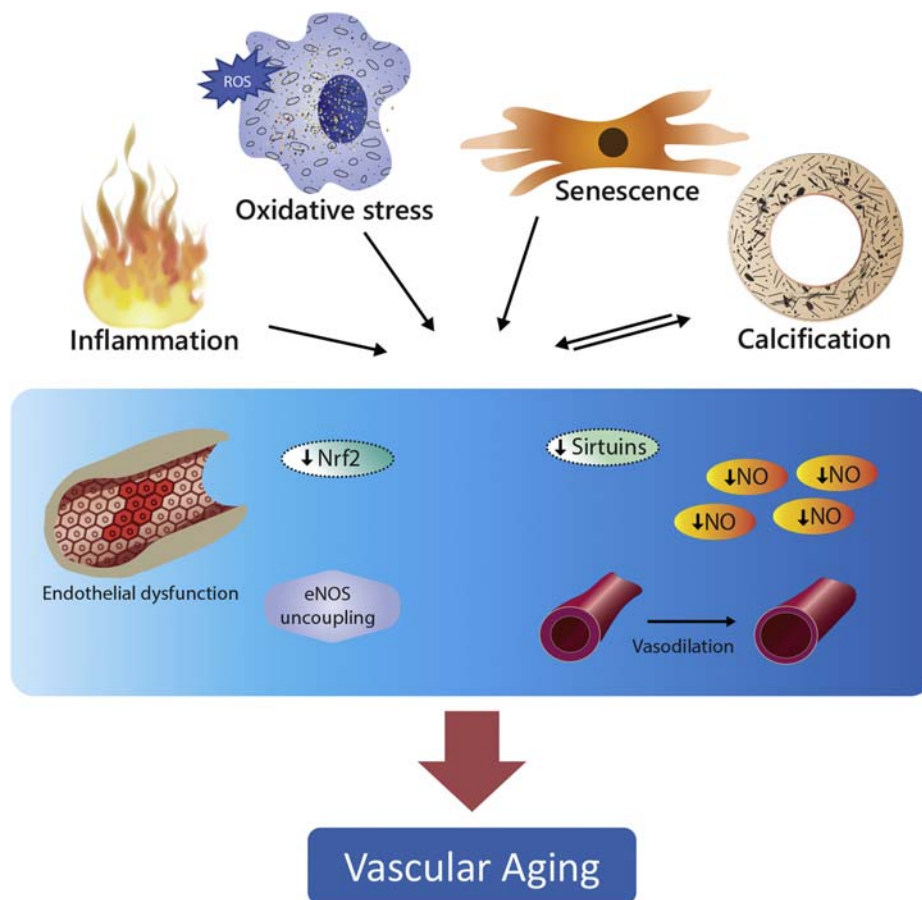
the inflammatory process.[96] Targeting of senescent cells and aging processes therefore holds unexplored potential to ameliorate vascular aging.

The role of inflammation in arterial stiffening is discussed in detail in Chapter 20. Endothelial cell senescence is discussed in detail in Chapter 23.

Oxidative stress

The formation of ROS is a normal part of cellular metabolism, principally the oxidative phosphorylation that takes place in mitochondria for the generation of ATP. Since Harman suggested the free radical theory of aging in the 1950s,[97] many studies have been published connecting oxidative stress with vascular aging. It is now widely appreciated that ROS accumulate with age, ultimately resulting in oxidative damage of genomic DNA, cellular components, and proteins.[97] Specifically, there is a strong indication that aging is associated with elevated production of ROS by NAD(P)H oxidases[98] and mitochondria,[99,100] and those events are linked to endothelial dysfunction and stiffening of elastic arteries as shown both in laboratory animals[85,101] and humans.[102] While oxidative stress has the

capacity to affect numerous aspects of vascular function during aging, such as induction of redox-sensitive transcription factors or oxidation of vital proteins, one of its most powerful impacts is related to the inactivation of endothelium-derived NO.[103] Defective bioavailability of NO is responsible for the age-related decrease in endothelium-dependent dilation, increased vasoconstriction, and tissue perfusion dysregulation (Fig. 25.1).[104−106] Several studies indicate that oxidative stress-mediated endothelial dysfunction is responsible for defective dilation of coronary arteries,[107] stimulating myocardial ischemia and neurovascular uncoupling, and diminishing the moment-to-moment adjustment of cerebral blood flow.[108,109] NO plays potent antiinflammatory, antithrombotic, and antileukocyte adhesion effects; therefore, a decrease in NO stimulates a proatherogenic vascular phenotype in aging.[110,111] Free oxygen radicals ($\bullet O^-_2$) from increased ROS bind to NO and form highly reactive and toxic peroxynitrite ($ONOO^-$), which in turn penetrates cell membranes and leads to DNA damage and protein oxidation.[112] Indeed, increased ($ONOO^-$) staining has been demonstrated in number of pathological conditions, all associated with EVA.[113,114]

FIGURE 25.1 Proposed scheme for mechanisms involved in vascular aging. The model predicts that increased oxidative stress, inflammation, senescence, and calcification accelerate vascular aging process through mediating reduced NO bioavailability due to an eNOS uncoupling event, endothelial dysfunction, reduced vasodilation, and disrupting antioxidant mechanisms, i.e., Nrf2 and sirtuins. *eNOS*, nitric oxide synthase; *NO*, nitric oxide; *Nrf2*, nuclear factor erythroid 2−related factor 2.

It has been suggested that mitochondria act as a seed for aging.[97] The mitochondria serve as a source for endogenous oxidants. An increase in free radicals (i.e., $\bullet O^-_2$ or $ONOO^-$) in mitochondria is positively associated with tissue dysfunction.[115] Molecular oxygen and electrons from the respiratory chain can generate free radicals and ROS inside mitochondria.[116] Mitochondria are organized by heterogeneous flexible networks, which are highly sensitive to metabolic changes (i.e., high glucose) and can react to boost free ROS formation.[116] During aging, mitochondrial physiology and reactive free radical production is altered, which in turns affects ATP synthesis via interrupting the enzymes of the citric acid cycle, respiratory chain components, and mutation of mitochondrial DNA leading to enhanced apoptosis.[115] Another major alteration of mitochondria in aging includes decreased antioxidant capacity. A cytoprotective transcription factor nuclear factor-erythroid-2-related factor 2 (Nrf2) acts as a defense against oxidative stress, as discussed in the following section. Age-associated increased formation of ($\bullet O^-_2$) and (ONOO-) triggers nuclear and mitochondrial DNA damage,[117] which could accelerate mutation and dysfunction of respiratory chain segments, leading to even more ($\bullet O^-_2$) and ($ONOO^-$) generation and vascular dysfunction.[118] Increased generation of reactive ($\bullet O^-_2$) and ($ONOO^-$) are considered major contributors to EVA and endothelial dysfunction.[114,119]

Adaptation to oxidative stresses: role of Nrf2 and sirtuins

Vascular aging is characterized by elevated ROS-mediated chronic oxidative stress, which is accompanied by failure to switch on antioxidant response elements—driven gene expression.[120] Age-associated increases in oxidative stress have been shown to inactivate antioxidative defense mechanisms, in particular Nrf2 and its associated pathways of signaling. Redox homeostasis, comprising a balance between a prooxidative ROS generation and concomitant antioxidant protection, is vital for protection against oxidative stress.[121] Nrf2 is a redox-sensitive transcription factor, which regulates the antioxidant response, including upregulation of enzymes that detoxify ROS and reconstruct ROS-mediated macromolecular casualty.[122] In various cell types including vascular cells[87,120] and cardiomyocytes,[123] an impairment of Nrf2-dependent defense associates with aging. Nrf2 adaptive homeostatic mechanisms are involved in young organisms for the protection of vascular endothelial and VSMCs against increased ROS generation. Growing evidence demonstrates that Nrf2 is a key player in those events and that modulation of its action could promote both regulating the cellular redox homeostasis and physiological homeostasis in pathways associated to the maintenance of cardiovascular health.[124−126]

Aged and transcriptionally Nrf2-deficient mice show similar imbalance of antioxidative activity in experimental models,[122] suggesting that Nrf2 could act as a key modulator in the aging process. Apart from the role of Nrf2 as a master controller of oxidative defense, this cytoprotective transcription factor prevents upregulation of proinflammatory cytokine genes, regulating proteostasis and metabolism.[127,128] In addition, Calvert et al.[129] have suggested that hydrogen sulfide (H_2S)-mediated Nrf2 upregulation has cardioprotective effects. Moreover, TNF, IL-1β, VCAM1, and MCP-1 expression was decreased in endothelial cells when Nrf2 was overexpressed,[130,131] supporting its antioxidant capacity. Nrf2 is also able to regulate and ameliorate the inflammatory response. Diminished Nrf2 action leads to elevated expression of adhesion molecules and proinflammatory chemokines in endothelial cells.[132] In addition, activation of Nrf2 counterbalances the effect of ROS in T-lymphocytes and inhibits acutely induced kidney injury.[133] Boosting the Nrf2 antioxidant pathway decreases oxidative stress and improves the renal function of mice.[134] Several experimental approaches have evaluated the scope of Nrf2 to increase the expression of oxidative stress protective genes and preserve vascular health.[134,135]

The pathophysiological significance of Nrf2 in aging may go beyond maintaining the redox homeostasis. The association between aging and cardiovascular events indicates that the vasculature seems to be the prime target for Nrf2-induced protection during aging. Importantly, Nrf2 conserves the functional endothelial phenotype.[136] As aging and senescence may cause the deterioration of endothelial function, the endothelium may develop both proatherogenic and prothrombotic phenotypes.[137] Hence, in aging, Nrf2-mediated defense of endothelial cell dysfunction might be of particular importance. Since Nrf2 deficiency or inactivation associates with hypertensive kidney disease,[138] renal fibrosis,[139] atherosclerosis development,[140] and hypertension[141] in experimental animals and humans, this further supports a role of Nrf2 in prevention of EVA. Moreover, during caloric restriction, the antiaging effects are linked with induction of Nrf2-mediated pathways.[99,142] Natural and dietary compounds, such as phytosterols, resveratrol, polyphenols, and terpenoids, could be used as physiological activators for Nrf2 to improve vascular function[143] and alleviate the actions of oxidative stress and inflammation in preclinical models of CKD.[144] However, the role and mode of action of Nrf2 within the complicated vascular aging phenotype (i.e., EVA) is not fully understood. How Nrf2 expression is regulated in return to the functional and structural distortion in the cardiovascular system remains to be resolved.

Growing evidence suggests the role of sirtuins (SIRT1−7) for the control of cellular homeostasis, especially against metabolism and inflammation, and reduced action of SIRT1 possibly causes vascular inflammation in

aging.[145,146] Sirtuins are regulated by a preserved group of the cofactor nicotinamide adenine dinucleotide (NAD)-associated protein deacylases, that perform important roles in response to environmental and nutritional factors, e.g., oxidative stress, fasting, DNA damage. Primarily, their activation prompts nuclear transcriptional preparations that increase metabolic capability and boost oxidative metabolism of mitochondria with an ultimate resistance to oxidative stress.[147] Sirtuins stimulate this resistance by enhancing antioxidant processes promoting DNA damage restoration by deacetylation of repair proteins.[148]

In general, SIRT1 plays a broad spectrum of biological roles including antioxidative stress and antiinflammatory responses, DNA repair, glucose and lipid metabolism.[149] Oxidative stress can influence the activity of sirtuins in several ways, including changes in SIRT gene expression, NAD levels, protein−protein interactions, and post-translational modifications.[150] Mild oxidative stress could be beneficial by inducing the sirtuins as a compensatory system, on the other hand, severe or chronic oxidative stress could cause dysfunctional sirtuins by affecting its posttranslational modification.[151] The levels of NAD drop during the course of aging and could be an Achilles' heel, generating nuclear and mitochondrial malfunction leading to many age-related pathologies.[152] Interestingly, pharmacological use of a SIRT1 activator reduces vascular inflammation in an experimental model of aged mice.[153] In addition, elevating SIRT1, particularly in dorsomedial and lateral hypothalamic areas of the brain, lingers aging and prolongs life span in both male and female mice.[154] Promoting NAD activity by supplementing NAD intermediates could alleviate age-related functional defects. Hence, stimulation of sirtuins and NAD supplementation together may be an efficient antiaging intervention. This remains to be proven in clinical trials.

Senescence

By definition, senescence is an antioncotic mechanism, characterized as irreversible cellular arrest, although still with metabolic activity. This specifically refers to SASP, a phenotype of senescence whereby cells secrete a plethora of proinflammatory cytokines, growth factors, and proteases. In addition, senescent cells can initiate antiapoptotic pathways to protect themselves from their own SASP, thereby not allowing effective removal by the immune system. While senescent cell burden is associated with many age-related pathologies (e.g., atherosclerosis, vascular calcification (VC), type-2 diabetes, etc.), and often accumulates at the site of etiology, senescence also plays a beneficial role in physiological processes, such as embryogenesis and wound healing. Therefore, therapeutically targeting senescence to treat age-related diseases must be treated with caution.[155] In short, stressors activate either p^{53} (further activating p21) or $p^{16INK4a}$, which act to inhibit Rb, thus inhibiting the cell's ability to enter the S phase of the cell cycle. The p53/p^{21} and p16 pathways can act synergistically or alone depending on the stressor.[156]

Senescence is often classified as stress/oncogene-induced or acute/developmental senescence. Differences relating to temporal regulation exist between classes: the former is transiently present and effectively removed by apoptosis, while restricted to predefined cell types in specific processes; the latter class accumulates in tissue over time in an unprogrammed manner and can inflict similar injury on neighboring cells through their SASP, a phenomenon termed the "bystander effect." Thus, senescence is not a single static state, but rather a series of phenotypically different states, which reflects its diverse range of functions both physiologically and pathophysiologically.[157] Characteristics of stress-induced senescence includes, but is not limited to, increased senescence associated beta-galactosidase activity, telomere shortening, elevated expression of p16/p^{21}/p53, and SASP activity.[158] Experimental studies have demonstrated that SASP activity is highly heterogeneous between different cell types, thereby secreting different inflammatory components. However, IL-1α/β, IL-6, IL-8, TGF-β, TNF, plasminogen activator inhibitor 1, and monocyte chemoattractant protein 1 are among the best characterized.[159]

Since a single universal biomarker of senescence is not available, a variety of techniques are implemented experimentally to detect the presence of senescent cells. Emerging evidence indicates that senescent cells accumulate in humans and animal models with age and persist at sites of etiology in age-related diseases. Consequences of aging include exposure to increased senescence stressors, and reduced efficiency of senescent cell clearance, which may partially explain why senescent cell burden is associated with age.[160]

Numerous stressors have been linked to triggering senescence, most notably oxidative stress, cytotoxic stress, and telomere shortening. However, discovery of the bystander effect, genetic studies investigating the role of senescence-associated aging processes, and interventional studies in animal models demonstrate that senescent cell burden can, in specific organs and under certain conditions, drive disease. How senescence drives age-related disease is unknown, but is likely to be largely heterogeneous, and dependent on a plethora of factors including cell type, the pathology (or cluster of pathologies) in question, and stressors involved. Many SASP-related hypotheses have been postulated: proteases from senescent cells disrupt tissue structure and integrity, proinflammatory cytokines and chemokines attract immune cells associated with chronic tissue inflammation, such as macrophages and lymphocytes, etc.[157]

In respect to arterial aging, senescent cells accumulate in atherosclerotic plaques[161] and in the medial layer of

vessels such as heavily calcified uremic epigastric arteries, implying a casual role in promoting VC and thus an increase in vessel stiffness.[162] This is associated with depleted Nrf2, the master regulator of antioxidant genes; however, the relationship between senescence and Nrf2 may be bidirectional and warrants further research. Disease-specific stressors also promote VC, such as uremic toxins (e.g., indoxyl sulfate, p-cresyl sulfate, TMAO, etc.) in end-stage kidney disease (ESKD) patients.[163] Furthermore, endothelial cell senescence is a risk factor for age-associated CVD, mediated through disturbances in renin angiotensin–aldosterone system, sirtuin 1 and FGF21 pathways; however, these processes are not fully understood.[164]

By therapeutically earmarking processes which underpin aging, a cohort of age-related pathologies can be targeted simultaneously, as opposed to treating each disease as a single entity. Such a strategy may not only increase life span but also health span.[165] Since cellular senescence is a hallmark of aging, targeting senescent cells has gained much attention in recent years with the use of senolytic agents, SASP inhibitors, or immunosurveillance agents. In a landmark senolytic study, quercetin and dasatinib (in combination) prolonged life span in mice by up to 36%.[166] In addition, the same combination of senolytics attenuated VC in the aorta of aged and hypercholesterolemic mice when administered long term, and it improved endothelial function.[167] Furthermore, studies using genetic and pharmacological approaches to eliminate senescent cells in $Ldlr^{-/-}$ mice suggest that senescent cells promote atherogenesis, contributing to plaque instability by increasing vascular inflammation[168] or upregulation of matrix metalloproteases,[169] while irradiation-induced senescence in mice affects neurovascular units associated with cerebral microvascular dysfunction, resembling the aging phenotype.[170]

These findings, along with other promising preclinical studies, have led to the initiation of clinical trials using agents to target senescent cells in different patient cohorts in an attempt to exert athero-protective and antiaging effects, e.g., phase 1 study using quercetin and dasatinib senolytic cocktail in diabetic nephropathy patients.[171] However, many unknowns remain, including the required dosage and duration of therapy, the long-term effects of such treatment and whether targeting senescent cells hinders the ability of acute senescent cells to carry out their physiological functions.[172]

Chronic kidney disease as a model of early vascular aging and role of calcification

CKD is characterized by an allostatic overload due to excessive oxidative stress, uremic inflammation, and defective antiaging (e.g., decreased Klotho expression and fetuin A) systems, resulting in a large discrepancy between biological and chronological age in this patient group.[173,174] Indeed, as compared to the general population, CKD patients exhibited accelerated aging-related pathological clusters including multiple cardiovascular complications, muscle wasting, osteoporosis, frailty, depression, and cognitive decline, even before the onset of ESKD necessitating renal replacement therapy.[173–176] EVA is an evolving concept elaborating the abnormal and premature vascular aging phenomenon, with arterial stiffness as an intermediate end-point and independent predictor of cardiovascular morbidity and mortality.[4] EVA, as one of the most evident premature aging phenotypes in advanced CKD, contributes to the high risk of cardiovascular morbidity and mortality in ESKD. While the exact underlying mechanisms of EVA remain to be elucidated, DNA damage–induced cellular senescence and "inflammaging" seems to be fundamentally involved in its pathological initiation and progression.[159,177–180] Furthermore, growing evidence indicates that repressed Nrf2 signaling and vitamin K may play a critical role in the interplay between oxidative stress, DNA damage, senescence, and "inflammaging," whereby Nrf2 activation and vitamin K supplementation may provide a novel treatment target for EVA.[180]

Large-scale studies have demonstrated that coronary atherosclerotic calcification increases with age.[181] The presence of calcified arteries, in addition to osteoporosis, is typical in aged populations. Nevertheless, this condition is exaggerated in CKD patients. In CKD, the predominant EVA and arterial stiffness is largely characterized by media VC, a cell-mediated process primarily driven by VSMCs osteogenic differentiation due to excessive DNA damage, and the extent of VC may be used as a measure of the biological vascular age.[38,39] Though VSMCs calcification shares similarities with developmental osteogenesis and chondrogenesis, it is an active and pathological alteration rather than a physiological process.[182] Under normal physiological conditions, a profound defensive pathway protects VSMCs from phenotypic differentiation and ectopic calcification.[183] The inhibitory defense systems in CKD are, however, overwhelmingly declined due to excessive allostatic load resulting from oxidative stress, inflammation, and retention of toxins in the uremic milieu.[174,182] Moreover, the common coexistence of hyperphosphatemia, and hypercalcemia, in combination with hyperparathyroidism, hypomagnesemia, and vitamin K deficiency, further worsen the VC inhibitory mechanism in CKD.[184,185] For instance, fetuin-A, a circulating glycoprotein produced by liver and adipose tissue, acts as a potent inhibitor of VC through the binding of calcium and phosphate into calciprotein particles (CPPs) preventing its crystallization.[186,187] A recent study demonstrated that decreased fetuin-A in extracellular vehicles and CPPs from uremic serum could promote VC in vitro.[188] Consequently, stressed VSMCs lose their capacity to secret sufficient VC inhibitors (e.g., Matrix Gla protein
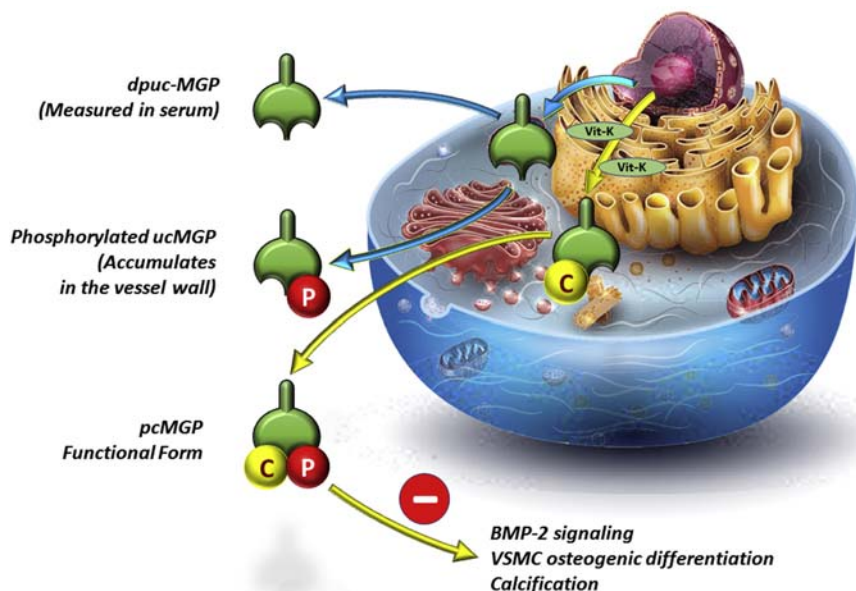
(MGP) and are predisposed to undergo phenotypic differentiation from a contractile to synthetic VSMCs phenotype).[189] Of note, MGP is a vitamin K−dependent protein primarily synthesized by VSMCs.[190] Evidence from preclinical studies has established the role of vitamin K in VC. This occurs mainly through the carboxylation of MGP, whereby it can inhibit VC by directly binding the hydroxyapatite in the arterial walls and by downregulating the function of bone morphogenetic proteins (BMPs) (Fig. 25.2).[191,192] Another culprit of deficient anti-VC system is Nrf2 signaling, which has been shown to be critical in response to various inducers in phenotypic remodeling of VSMCs. Recent studies have reported that butylhydroquinone (a Nrf2 agonist) reduces high phosphate-induced calcification of VSMCs via activation of KEAP1/NRF2/P62 signaling and hydrogen sulfide—another Nrf2 agonist—reduces circulating CPP-induced VSMCs calcification via NRF2/KEAP1 signaling and by increasing NQO1 expression in vitro.[193,194]

Given the overwhelming proatherogenic milieu in CKD, if the above-mentioned dysregulated signaling is not compensated, the activation of essential osteogenic/chondrogenic transcription factors could further induce the expression of osteogenic/chondrogenic proteins in VSMCs, such as osteocalcin, BMP-2, and type I collagen, in the context of high circulating levels of calcium and phosphate, which would eventually promote uremic VSMCs to undergo osteochondrocytic differentiation and vessel ossification.[195,196] In fact, even in the absence of hyperphosphatemia and hypercalcemia, increased phosphate

and calcium load drive a calcification process in both CKD and the general population.[197] In patients with CKD, gut dysbiosis could promote VC.[198] In addition, a recent study showed that protein-bound uremic toxins indoxyl sulfate and p-cresyl sulfate could promote VC in the aorta and peripheral vessels possibly via inflammatory and coagulation pathways.[199] For a detailed discussion regarding mechanisms of arterial wall calcification, the reader is referred to Chapter 21.

Summary

Aging affects the function and structure of the vasculature. All layers of the arterial wall are affected during aging-induced vascular remodeling. The aged tunica intima is characterized by endothelial dysfunction, whereas the tunica media is characterized by the presence of elastin degradation, collagen accumulation, proteoglycan aggregation, and the switching of the physiological contractile phenotype of VSMCs toward a synthetic VSMC phenotype, which induces VC. Furthermore, the inflammatory response of the outer adventitia that also serves as a niche for progenitor cells plays an important role in atherosclerosis. EVA develops when comorbidities emerge and a combination of various factors such as oxidative stress, inflammation, senescence, and calcification trigger exaggerated aging of the vasculature with ultimate development of cardiovascular and/or renal disease. Imbalanced redox homeostasis due to failure of master regulators of antioxidant responses, such as Nrf2 or sirtuins, results in vascular

FIGURE 25.2 Matrix Gla protein (MGP) maturation. MGP maturation requires vitamin K, the inactive form of MGP (dephosphorylated-uncarboxylated MGP, dp-ucMGP) undergoes serial posttranslational carboxylation and phosphorylation to form active pc-MGP. Carboxylation of MGP is dependent upon the availability of vitamin K in the vascular wall. The active form of MGP inhibits bone morphogenetic protein-2-induced osteogenic differentiation of VSMCs and calcification. *BMP-2*, bone morphogenetic protein 2; *dpuc-MGP*, dephosphorylated-uncarboxylated MGP; *MGP*, Matrix Gla protein; *pc-MGP*, phosphorylated-carboxylated MGP; *Vit-K*, vitamin K; *VSMC*; vascular smooth muscle cells.

damage and accelerated aging. Vascular aging causes a systemic, progressive loss of endothelial function, due to downregulation of vasodilator pathways and/or upregulation of vasoconstrictor pathways. Elevated oxidative stress and inflammation enhance the progression of cellular senescence and apoptosis, and this further exaggerates age-related deterioration of vascular health. In respect to arterial aging, senescence may also promote VC and thus an increase in vessel stiffness, in addition with depleted Nrf2 activity. All of the above-mentioned phenomena ultimately lead to increased arterial stiffness, characterized by quantitative and qualitative alterations in passive and active elements of the vascular wall. The changes in functional and structural features of vascular wall ultimately affect blood pressure and blood flow to target organs such as the brain, heart, and kidney.

The EVA concept represents a process of accelerated vascular aging. CKD may represent a suitable clinical model of EVA, because CKD is characterized by chronic inflammation and oxidative stress followed by progressive intimal and medial VC. Accelerated EVA is a hallmark of senescence and a strong predictor of cardiovascular morbidity and mortality in CKD. The cellular and molecular mechanisms that lead to arterial aging may serve as targets for interventions to delay or counter the effects of vascular aging on health and disease.

References

1. Thijssen DH, Carter SE, Green DJ. Arterial structure and function in vascular ageing: are you as old as your arteries? **J Physiol**. 2016; 594:2275−2284.

2. Jani B, Rajkumar C. Ageing and vascular ageing. **Postgrad Med J**. 2006; 82:357−362.

3. Bisbal F, Baranchuk A, Braunwald E, Bayés de Luna A, Bayés-Genís A. Atrial failure as a clinical entity: JACC review topic of the week. **J Am Coll Cardiol**. 2020; 75:222−232.

4. Cunha PG, Boutouyrie P, Nilsson PM, Laurent S. Early vascular ageing (EVA): definitions and clinical applicability. **Curr Hypertens Rev**. 2017; 13:8−15.

5. Hamczyk MR, Nevado RM, Barettino A, Fuster V, Andrés V. Biological versus chronological aging: JACC focus seminar. **J Am Coll Cardiol**. 2020; 75:919−930.

6. McEleavy OD, McCallum RW, Petrie JR, et al. Higher carotid-radial pulse wave velocity in healthy offspring of patients with Type 2 diabetes. **Diabet Med**. 2004; 21:262−266.

7. M Nilsson P. Early vascular ageing - a concept in development. **Eur Endocrinol**. 2015; 11:26−31.

8. Nilsson PM, Laurent S, Cunha PG, et al. Characteristics of healthy vascular ageing in pooled population-based cohort studies: the global Metabolic syndrome and Artery Research Consortium. **J Hypertens**. 2018; 36:2340−2349.

9. Laurent S, Boutouyrie P, Cunha PG, Lacolley P, Nilsson PM. Concept of extremes in vascular aging. **Hypertension**. 2019; 74:218−228.

10. Benetos A, Salvi P, Lacolley P. Blood pressure regulation during the aging process: the end of the 'hypertension era'? **J Hypertens**. 2011; 29:646−652.

11. Versari D, Daghini E, Virdis A, Ghiadoni L, Taddei S. Endothelial dysfunction as a target for prevention of cardiovascular disease. **Diabetes Care**. 2009; 32(Suppl 2):S314−S321.

12. Flammer AJ, Anderson T, Celermajer DS, et al. The assessment of endothelial function: from research into clinical practice. **Circulation**. 2012; 126:753−767.

13. Ohyama Y, Redheuil A, Kachenoura N, Ambale Venkatesh B, Lima JAC. Imaging insights on the aorta in aging. **Circ Cardiovasc Imaging**. 2018; 11:e005617.

14. Lacolley P, Regnault V, Avolio AP. Smooth muscle cell and arterial aging: basic and clinical aspects. **Cardiovasc Res**. 2018; 114:513−528.

15. Lyle AN, Raaz U. Killing me unsoftly: causes and mechanisms of arterial stiffness. **Arterioscler Thromb Vasc Biol**. 2017; 37:e1−e11.

16. Jaminon A, Reesink K, Kroon A, Schurgers L. The role of vascular smooth muscle cells in arterial remodeling: focus on calcification-related processes. **Int J Mol Sci**. 2019; 20.

17. Chi C, Li DJ, Jiang YJ, et al. Vascular smooth muscle cell senescence and age-related diseases: state of the art. **Biochim Biophys Acta Mol Basis Dis**. 2019; 1865:1810−1821.

18. Ruddy JM, Jones JA, Spinale FG, Ikonomidis JS. Regional heterogeneity within the aorta: relevance to aneurysm disease. **J Thorac Cardiovasc Surg**. 2008; 136:1123−1130.

19. Gadson PF, Dalton ML, Patterson E, et al. Differential response of mesoderm- and neural crest-derived smooth muscle to TGF-beta1: regulation of c-myb and alpha1 (I) procollagen genes. **Exp Cell Res**. 1997; 230:169−180.

20. Halloran BG, Davis VA, McManus BM, Lynch TG, Baxter BT. Localization of aortic disease is associated with intrinsic differences in aortic structure. **J Surg Res**. 1995; 59:17−22.

21. Greenwald SE. Ageing of the conduit arteries. **J Pathol**. 2007; 211:157−172.

22. Komutrattananont P, Mahakkanukrauh P, Das S. Morphology of the human aorta and age-related changes: anatomical facts. **Anat Cell Biol**. 2019; 52:109−114.

23. Milewicz DM, Ramirez F. Therapies for thoracic aortic aneurysms and acute aortic dissections. **Arterioscler Thromb Vasc Biol**. 2019; 39:126−136.

24. Harky A, Fan KS, Fan KH. The genetics and biomechanics of thoracic aortic diseases. **Vasc Biol**. 2019; 1:R13−R25.

25. Tan L, Li Z, Zhou C, et al. FBN1 mutations largely contribute to sporadic non-syndromic aortic dissection. **Hum Mol Genet**. 2017; 26:4814−4822.

26. Blunder S, Messner B, Aschacher T, et al. Characteristics of TAV- and BAV-associated thoracic aortic aneurysms–smooth muscle cell biology, expression profiling, and histological analyses. **Atherosclerosis**. 2012; 220:355−361.

27. Dimitroulis D, Katsargyris A, Klonaris C, et al. Telomerase expression on aortic wall endothelial cells is attenuated in abdominal aortic aneurysms compared to healthy nonaneurysmal aortas. **J Vasc Surg**. 2011; 54:1778−1783.

28. Cafueri G, Parodi F, Pistorio A, et al. Endothelial and smooth muscle cells from abdominal aortic aneurysm have increased oxidative stress and telomere attrition. **PLoS One**. 2012; 7:e35312.

29. Humphrey JD. Possible mechanical roles of glycosaminoglycans in thoracic aortic dissection and associations with dysregulated transforming growth factor-β. **J Vasc Res**. 2013; 50:1−10.

30. Humphrey JD, Schwartz MA, Tellides G, Milewicz DM. Role of mechanotransduction in vascular biology: focus on thoracic aortic aneurysms and dissections. **Circ Res**. 2015; 116:1448−1461.

31. Lu H, Fagnant PM, Bookwalter CS, Joel P, Trybus KM. Vascular disease-causing mutation R258C in ACTA2 disrupts actin dynamics and interaction with myosin. **Proc Natl Acad Sci U S A**. 2015; 112:E4168−E4177.

32. Jia LX, Zhang WM, Zhang HJ, et al. Mechanical stretch-induced endoplasmic reticulum stress, apoptosis and inflammation contribute to thoracic aortic aneurysm and dissection. **J Pathol**. 2015; 236:373−383.

33. London GM, Safar ME, Pannier B. Aortic aging in ESRD: structural, hemodynamic, and mortality implications. **J Am Soc Nephrol**. 2016; 27:1837−1846.

34. London GM, Guerin AP. Influence of arterial pulse and reflected waves on blood pressure and cardiac function. **Am Heart J**. 1999; 138:220−224.

35. Sugawara J, Hayashi K, Yokoi T, Tanaka H. Age-associated elongation of the ascending aorta in adults. **JACC Cardiovasc Imaging**. 2008; 1:739−748.

36. O'Rourke M, Farnsworth A, O'Rourke J. Aortic dimensions and stiffness in normal adults. **JACC Cardiovasc Imaging**. 2008; 1:749−751.

37. Leloup AJ, Van Hove CE, Heykers A, Schrijvers DM, De Meyer GR, Fransen P. Elastic and muscular arteries differ in structure, basal NO production and voltage-gated Ca(2+)-channels. **Front Physiol**. 2015; 6:375.

38. Shroff R, Long DA, Shanahan C. Mechanistic insights into vascular calcification in CKD. **J Am Soc Nephrol**. 2013; 24:179−189.

39. Shanahan CM. Mechanisms of vascular calcification in CKD-evidence for premature ageing? **Nat Rev Nephrol**. 2013; 9:661−670.

40. Ho CY, Shanahan CM. Medial arterial calcification: an overlooked player in peripheral arterial disease. **Arterioscler Thromb Vasc Biol**. 2016; 36:1475−1482.

41. Karwowski W, Naumnik B, Szczepański M, Myśliwiec M. The mechanism of vascular calcification - a systematic review. **Med Sci Monit**. 2012; 18:RA1−11.

42. Tsuchikura S, Shoji T, Kimoto E, et al. Central versus peripheral arterial stiffness in association with coronary, cerebral and peripheral arterial disease. **Atherosclerosis**. 2010; 211:480−485.

43. Niiranen TJ, Kalesan B, Larson MG, et al. Aortic-brachial arterial stiffness gradient and cardiovascular risk in the community: the Framingham Heart Study. **Hypertension**. 2017; 69:1022−1028.

44. Fortier C, Agharazii M. Arterial stiffness gradient. **Pulse (Basel)**. 2016; 3:159−166.

45. Fortier C, Desjardins MP, Agharazii M. Aortic-brachial pulse wave velocity ratio: a measure of arterial stiffness gradient not affected by mean arterial pressure. **Pulse (Basel)**. 2018; 5:117−124.

46. Nilsson Wadström B, Fatehali AH, Engström G, Nilsson PM. A vascular aging index as independent predictor of cardiovascular events and total mortality in an elderly urban population. **Angiology**. 2019; 70:929−937.

47. Hermann DM, Gronewold J, Lehmann N, et al. Coronary artery calcification is an independent stroke predictor in the general population. **Stroke**. 2013; 44:1008−1013.

48. Folsom AR, Kronmal RA, Detrano RC, et al. Coronary artery calcification compared with carotid intima-media thickness in the prediction of cardiovascular disease incidence: the Multi-Ethnic Study of Atherosclerosis (MESA). **Arch Intern Med**. 2008; 168:1333−1339.

49. Seals DR, Jablonski KL, Donato AJ. Aging and vascular endothelial function in humans. **Clin Sci (Lond).** 2011; 120:357−375.

50. Safar ME, Struijker-Boudier HA. Cross-talk between macro- and microcirculation. **Acta Physiol**. 2010; 198:417−430.

51. Agabiti-Rosei AloopSLaE. The Cross-Talk between the Macro- and the Microcirculation.

52. Mulvany MJ, Aalkjaer C. Structure and function of small arteries. **Physiol Rev**. 1990; 70:921−961.

53. Rizzoni D, Castellano M, Porteri E, Bettoni G, Muiesan ML, Agabiti Rosei E. Delayed development of hypertension after short-term nitrendipine treatment. **Hypertension**. 1994; 24:131−139.

54. Rizzoni D, Porteri E, Guelfi D, et al. Structural alterations in subcutaneous small arteries of normotensive and hypertensive patients with non-insulin-dependent diabetes mellitus. **Circulation**. 2001; 103:1238−1244.

55. Savoia C, Battistoni A, Calvez V, Cesario V, Montefusco G, Filippini A. Microvascular alterations in hypertension and vascular aging. **Curr Hypertens Rev**. 2017; 13:16−23.

56. Hong Z, Reeves KJ, Sun Z, Li Z, Brown NJ, Meininger GA. Vascular smooth muscle cell stiffness and adhesion to collagen I modified by vasoactive agonists. **PLoS One**. 2015; 10:e0119533.

57. Jin K. A microcirculatory theory of aging. **Aging Dis**. 2019; 10:676−683.

58. Harburger DS, Calderwood DA. Integrin signalling at a glance. **J Cell Sci**. 2009; 122:159−163.

59. Li Q, Li L, Fan S, Dai C, Chai X, Zhou C. Retinal pulse wave velocity measurement using spectral-domain optical coherence tomography. **J Biophot**. 2018; 11.

60. Klein-Weigel PF, Sunderkötter C, Sander O. Nailfold capillaroscopy microscopy - an interdisciplinary appraisal. **Vasa**. 2016; 45:353−364.

61. Mason JC, Lidington EA, Yarwood H. Isolation and analysis of large and small vessel endothelial cells. **Methods Mol Med**. 2007; 135:305−321.

62. Tew GA, Klonizakis M, Crank H, Briers JD, Hodges GJ. Comparison of laser speckle contrast imaging with laser Doppler for assessing microvascular function. **Microvasc Res**. 2011; 82:326−332.

63. Moerland M, Kales AJ, Schrier L, van Dongen MG, Bradnock D, Burggraaf J. Evaluation of the EndoPAT as a tool to assess endothelial function. **Int J Vasc Med**. 2012; 2012:904141.

64. Hansen AS, Butt JH, Holm-Yildiz S, Karlsson W, Kruuse C. Validation of repeated endothelial function measurements using Endo-PAT in stroke. **Front Neurol**. 2017; 8:178.

65. Aozasa N, Hatano M, Saigusa R, et al. Clinical significance of endothelial vasodilatory function evaluated by EndoPAT in patients with systemic sclerosis. **J Dermatol**. 2020; 47:609−614.

66. Tinajero MG, Gotlieb AI. Recent developments in vascular adventitial pathobiology: the dynamic adventitia as a complex regulator of vascular disease. **Am J Pathol**. 2020; 190:520−534.

67. Chang Z, Paoletti P, Barrett SD, et al. Nanomechanics and ultrastructure of the internal mammary artery adventitia in patients with low and high pulse wave velocity. **Acta Biomater**. 2018; 73:437−448.

68. Campbell KA, Lipinski MJ, Doran AC, Skaflen MD, Fuster V, McNamara CA. Lymphocytes and the adventitial immune response in atherosclerosis. **Circ Res**. 2012; 110:889−900.

69. Majesky MW, Dong XR, Hoglund V, Daum G, Mahoney WM. The adventitia: a progenitor cell niche for the vessel wall. **Cells Tissues Organs**. 2012; 195:73−81.

70. Timmermans F, Plum J, Yöder MC, Ingram DA, Vandekerckhove B, Case J. Endothelial progenitor cells: identity defined? **J Cell Mol Med**. 2009; 13:87−102.

71. Du F, Zhou J, Gong R, et al. Endothelial progenitor cells in atherosclerosis. **Front Biosci (Landmark Ed)**. 2012; 17:2327−2349.

72. Ungvari Z, Tarantini S, Donato AJ, Galvan V, Csiszar A. Mechanisms of vascular aging. **Circ Res**. 2018; 123:849−867.

73. Ferrucci L, Fabbri E. Inflammageing: chronic inflammation in ageing, cardiovascular disease, and frailty. **Nat Rev Cardiol**. 2018; 15:505−522.

74. Csiszar A, Ungvari Z, Koller A, Edwards JG, Kaley G. Aging-induced proinflammatory shift in cytokine expression profile in coronary arteries. **FASEB J**. 2003; 17:1183−1185.

75. Wang M, Zhang J, Jiang LQ, et al. Proinflammatory profile within the grossly normal aged human aortic wall. **Hypertension**. 2007; 50:219−227.

76. Song Y, Shen H, Schenten D, Shan P, Lee PJ, Goldstein DR. Aging enhances the basal production of IL-6 and CCL2 in vascular smooth muscle cells. **Arterioscler Thromb Vasc Biol**. 2012; 32:103−109.

77. Tyrrell DJ, Goldstein DR. Ageing and atherosclerosis: vascular intrinsic and extrinsic factors and potential role of IL-6. **Nat Rev Cardiol**. 2021; 18:58−68.

78. Nakhai-Pour HR, Grobbee DE, Bots ML, Muller M, van der Schouw YT. C-reactive protein and aortic stiffness and wave reflection in middle-aged and elderly men from the community. **J Hum Hypertens**. 2007; 21:949−955.

79. Csiszar A, Labinskyy N, Smith K, Rivera A, Orosz Z, Ungvari Z. Vasculoprotective effects of anti-tumor necrosis factor-alpha treatment in aging. **Am J Pathol**. 2007; 170:388−398.

80. Csiszar A, Ungvari Z, Koller A, Edwards JG, Kaley G. Proinflammatory phenotype of coronary arteries promotes endothelial apoptosis in aging. **Physiol Genomics**. 2004; 17:21−30.

81. Liu T, Zhang L, Joo D, Sun SC. NF-κB signaling in inflammation. **Signal Transduct Target Ther**. 2017; 2.

82. Scuteri A, Orru M, Morrell C, et al. Independent and additive effects of cytokine patterns and the metabolic syndrome on arterial aging in the SardiNIA Study. **Atherosclerosis**. 2011; 215:459−464.

83. Miles EA, Rees D, Banerjee T, et al. Age-related increases in circulating inflammatory markers in men are independent of BMI, blood pressure and blood lipid concentrations. **Atherosclerosis**. 2008; 196:298−305.

84. Csiszar A, Wang M, Lakatta EG, Ungvari Z. Inflammation and endothelial dysfunction during aging: role of NF-kappaB. **J Appl Physiol (1985)**. 2008; 105:1333−1341.

85. Ungvari Z, Orosz Z, Labinskyy N, et al. Increased mitochondrial H_2O_2 production promotes endothelial NF-kappaB activation in aged rat arteries. **Am J Physiol Heart Circ Physiol**. 2007; 293:H37−H47.

86. Tabruyn SP, Mémet S, Avé P, et al. NF-kappaB activation in endothelial cells is critical for the activity of angiostatic agents. **Mol Cancer Ther**. 2009; 8:2645−2654.

87. Ungvari Z, Bailey-Downs L, Gautam T, et al. Age-associated vascular oxidative stress, Nrf2 dysfunction, and NF-{kappa}B activation in the nonhuman primate *Macaca mulatta*. **J Gerontol A Biol Sci Med Sci**. 2011; 66:866−875.

88. Hasegawa Y, Saito T, Ogihara T, et al. Blockade of the nuclear factor-κB pathway in the endothelium prevents insulin resistance and prolongs life spans. **Circulation**. 2012; 125:1122−1133.

89. Vila E, Salaices M. Cytokines and vascular reactivity in resistance arteries. **Am J Physiol Heart Circ Physiol**. 2005; 288:H1016−H1021.

90. Busik JV, Mohr S, Grant MB. Hyperglycemia-induced reactive oxygen species toxicity to endothelial cells is dependent on paracrine mediators. **Diabetes**. 2008; 57:1952−1965.

91. Arenas IA, Xu Y, Davidge ST. Age-associated impairment in vasorelaxation to fluid shear stress in the female vasculature is improved by TNF-alpha antagonism. **Am J Physiol Heart Circ Physiol**. 2006; 290:H1259−H1263.

92. Khan SY, Awad EM, Oszwald A, et al. Premature senescence of endothelial cells upon chronic exposure to TNFα can be prevented by N-acetyl cysteine and plumericin. **Sci Rep**. 2017; 7:39501.

93. Ishibazawa A, Nagaoka T, Takahashi T, et al. Effects of shear stress on the gene expressions of endothelial nitric oxide synthase, endothelin-1, and thrombomodulin in human retinal microvascular endothelial cells. **Invest Ophthalmol Vis Sci**. 2011; 52:8496−8504.

94. Lantz J, Renner J, Länne T, Karlsson M. Is aortic wall shear stress affected by aging? An image-based numerical study with two age groups. **Med Eng Phys**. 2015; 37:265−271.

95. Ungvari Z, Podlutsky A, Sosnowska D, et al. Ionizing radiation promotes the acquisition of a senescence-associated secretory phenotype and impairs angiogenic capacity in cerebromicrovascular endothelial cells: role of increased DNA damage and decreased DNA repair capacity in microvascular radiosensitivity. **J Gerontol A Biol Sci Med Sci**. 2013; 68:1443−1457.

96. Morgan RG, Ives SJ, Lesniewski LA, et al. Age-related telomere uncapping is associated with cellular senescence and inflammation independent of telomere shortening in human arteries. **Am J Physiol Heart Circ Physiol**. 2013; 305:H251−H258.

97. Harman D. Aging: a theory based on free radical and radiation chemistry. **J Gerontol**. 1956; 11:298−300.

98. Jacobson A, Yan C, Gao Q, et al. Aging enhances pressure-induced arterial superoxide formation. **Am J Physiol Heart Circ Physiol**. 2007; 293:H1344−H1350.

99. Csiszar A, Gautam T, Sosnowska D, et al. Caloric restriction confers persistent anti-oxidative, pro-angiogenic, and anti-inflammatory effects and promotes anti-aging miRNA expression profile in cerebromicrovascular endothelial cells of aged rats. **Am J Physiol Heart Circ Physiol**. 2014; 307:H292−H306.

100. Csiszar A, Sosnowska D, Wang M, Lakatta EG, Sonntag WE, Ungvari Z. Age-associated proinflammatory secretory phenotype in vascular smooth muscle cells from the non-human primate *Macaca mulatta*: reversal by resveratrol treatment. **J Gerontol A Biol Sci Med Sci**. 2012; 67:811−820.

101. Francia P, delli Gatti C, Bachschmid M, et al. Deletion of p66shc gene protects against age-related endothelial dysfunction. **Circulation**. 2004; 110:2889−2895.

102. Donato AJ, Eskurza I, Silver AE, et al. Direct evidence of endothelial oxidative stress with aging in humans: relation to impaired endothelium-dependent dilation and upregulation of nuclear factor-kappaB. **Circ Res**. 2007; 100:1659−1666.

103. Förstermann U. Nitric oxide and oxidative stress in vascular disease. **Pflugers Arch**. 2010; 459:923−939.

104. Sun D, Huang A, Yan EH, et al. Reduced release of nitric oxide to shear stress in mesenteric arteries of aged rats. **Am J Physiol Heart Circ Physiol**. 2004; 286:H2249−H2256.

105. Donato AJ, Gano LB, Eskurza I, et al. Vascular endothelial dysfunction with aging: endothelin-1 and endothelial nitric oxide synthase. **Am J Physiol Heart Circ Physiol**. 2009; 297:H425−H432.

106. Novella S, Dantas AP, Segarra G, et al. Aging enhances contraction to thromboxane A2 in aorta from female senescence-accelerated mice. **Age (Dordr)**. 2013; 35:117−128.

107. Csiszar A, Ungvari Z, Edwards JG, et al. Aging-induced phenotypic changes and oxidative stress impair coronary arteriolar function. **Circ Res**. 2002; 90:1159−1166.

108. Park L, Anrather J, Girouard H, Zhou P, Iadecola C. Nox2-derived reactive oxygen species mediate neurovascular dysregulation in the aging mouse brain. **J Cereb Blood Flow Metab**. 2007; 27:1908−1918.

109. Toth P, Tarantini S, Tucsek Z, et al. Resveratrol treatment rescues neurovascular coupling in aged mice: role of improved cerebromicrovascular endothelial function and downregulation of NADPH oxidase. **Am J Physiol Heart Circ Physiol**. 2014; 306:H299−H308.

110. Ganz P, Vita JA. Testing endothelial vasomotor function: nitric oxide, a multipotent molecule. **Circulation**. 2003; 108:2049−2053.

111. Moncada S, Palmer RM, Higgs EA. Nitric oxide: physiology, pathophysiology, and pharmacology. **Pharmacol Rev**. 1991; 43:109−142.

112. Phaniendra A, Jestadi DB, Periyasamy L. Free radicals: properties, sources, targets, and their implication in various diseases. **Indian J Clin Biochem**. 2015; 30:11−26.

113. Luksha N, Luksha L, Carrero JJ, Hammarqvist F, Stenvinkel P, Kublickiene K. Impaired resistance artery function in patients with end-stage renal disease. **Clin Sci (Lond)**. 2011; 120:525−536.

114. Pacher P, Beckman JS, Liaudet L. Nitric oxide and peroxynitrite in health and disease. **Physiol Rev**. 2007; 87:315−424.

115. Bachschmid MM, Schildknecht S, Matsui R, et al. Vascular aging: chronic oxidative stress and impairment of redox signaling-consequences for vascular homeostasis and disease. **Ann Med**. 2013; 45:17−36.

116. Zorov DB, Juhaszova M, Sollott SJ. Mitochondrial reactive oxygen species (ROS) and ROS-induced ROS release. **Physiol Rev**. 2014; 94:909−950.

117. Balaban RS, Nemoto S, Finkel T. Mitochondria, oxidants, and aging. **Cell**. 2005; 120:483−495.

118. Finkel T, Holbrook NJ. Oxidants, oxidative stress and the biology of ageing. **Nature**. 2000; 408:239−247.

119. D'Oria R, Schipani R, Leonardini A, et al. The role of oxidative stress in cardiac disease: from physiological response to injury factor. **Oxid Med Cell Longev**. 2020; 2020:5732956.

120. Ungvari Z, Bailey-Downs L, Sosnowska D, et al. Vascular oxidative stress in aging: a homeostatic failure due to dysregulation of NRF2-mediated antioxidant response. **Am J Physiol Heart Circ Physiol**. 2011; 301:H363−H372.

121. Sinha N, Dabla PK. Oxidative stress and antioxidants in hypertension-a current review. **Curr Hypertens Rev**. 2015; 11:132−142.

122. Suh JH, Shenvi SV, Dixon BM, et al. Decline in transcriptional activity of Nrf2 causes age-related loss of glutathione synthesis, which is reversible with lipoic acid. **Proc Natl Acad Sci U S A**. 2004; 101:3381−3386.

123. Gounder SS, Kannan S, Devadoss D, et al. Impaired transcriptional activity of Nrf2 in age-related myocardial oxidative stress is reversible by moderate exercise training. **PLoS One**. 2012; 7:e45697.

124. Cui T, Lai Y, Janicki JS, Wang X. Nuclear factor erythroid-2 related factor 2 (Nrf2)-mediated protein quality control in cardiomyocytes. **Front Biosci (Landmark Ed)**. 2016; 21:192−202.

125. Alfieri A, Srivastava S, Siow RC, Modo M, Fraser PA, Mann GE. Targeting the Nrf2-Keap1 antioxidant defence pathway for neuro-vascular protection in stroke. **J Physiol**. 2011; 589:4125−4136.

126. Arefin S, Buchanan S, Hobson S, et al. Nrf2 in early vascular ageing: calcification, senescence and therapy. **Clin Chim Acta**. 2020; 505:108−118.

127. Hayes JD, Dinkova-Kostova AT. The Nrf2 regulatory network provides an interface between redox and intermediary metabolism. **Trends Biochem Sci**. 2014; 39:199−218.

128. Kobayashi EH, Suzuki T, Funayama R, et al. Nrf2 suppresses macrophage inflammatory response by blocking proinflammatory cytokine transcription. **Nat Commun**. 2016; 7:11624.

129. Calvert JW, Jha S, Gundewar S, et al. Hydrogen sulfide mediates cardioprotection through Nrf2 signaling. **Circ Res**. 2009; 105:365−374.

130. Teasdale JE, Hazell GG, Peachey AM, et al. Cigarette smoke extract profoundly suppresses TNFα-mediated proinflammatory gene expression through upregulation of ATF3 in human coronary artery endothelial cells. **Sci Rep**. 2017; 7:39945.

131. Chen LH, Huang Q, Wan L, et al. Expression, purification, and in vitro refolding of a humanized single-chain Fv antibody against human CTLA4 (CD152). **Protein Expr Purif**. 2006; 46:495−502.

132. Takabe W, Warabi E, Noguchi N. Anti-atherogenic effect of laminar shear stress via Nrf2 activation. **Antioxid Redox Signal**. 2011; 15:1415−1426.

133. Noel S, Martina MN, Bandapalle S, et al. Lymphocyte-specific activation of Nrf2 protects from AKI. **J Am Soc Nephrol**. 2015; 26:2989−3000.

134. Yang SM, Ka SM, Wu HL, et al. Thrombomodulin domain 1 ameliorates diabetic nephropathy in mice via anti-NF-κB/NLRP3 inflammasome-mediated inflammation, enhancement of NRF2 antioxidant activity and inhibition of apoptosis. **Diabetologia**. 2014; 57:424−434.

135. Zheng H, Whitman SA, Wu W, et al. Therapeutic potential of Nrf2 activators in streptozotocin-induced diabetic nephropathy. **Diabetes**. 2011; 60:3055−3066.

136. Florczyk U, Jazwa A, Maleszewska M, et al. Nrf2 regulates angiogenesis: effect on endothelial cells, bone marrow-derived proangiogenic cells and hind limb ischemia. **Antioxid Redox Signal**. 2014; 20:1693−1708.

137. Erusalimsky JD. Vascular endothelial senescence: from mechanisms to pathophysiology. **J Appl Physiol (1985)**. 2009; 106:326−332.

138. Chang J, Ma JZ, Zeng Q, et al. Loss of GSTM1, a NRF2 target, is associated with accelerated progression of hypertensive kidney disease in the African American Study of Kidney Disease (AASK). **Am J Physiol Renal Physiol**. 2013; 304:F348−F355.

139. Oh CJ, Kim JY, Choi YK, et al. Dimethylfumarate attenuates renal fibrosis via NF-E2-related factor 2-mediated inhibition of transforming growth factor-β/Smad signaling. **PLoS One**. 2012; 7:e45870.

140. Mimura J, Itoh K. Role of Nrf2 in the pathogenesis of atherosclerosis. **Free Radic Biol Med**. 2015; 88:221−232.

141. Gao L, Zimmerman MC, Biswal S, Zucker IH. Selective Nrf2 gene deletion in the rostral ventrolateral medulla evokes hypertension and sympathoexcitation in mice. **Hypertension**. 2017; 69:1198−1206.

142. Pearson KJ, Lewis KN, Price NL, et al. Nrf2 mediates cancer protection but not prolongevity induced by caloric restriction. **Proc Natl Acad Sci U S A**. 2008; 105:2325−2330.

143. Ungvari Z, Bagi Z, Feher A, et al. Resveratrol confers endothelial protection via activation of the antioxidant transcription factor Nrf2. **Am J Physiol Heart Circ Physiol**. 2010; 299:H18−H24.

144. Li D, Shi G, Wang J, et al. Baicalein ameliorates pristane-induced lupus nephritis via activating Nrf2/HO-1 in myeloid-derived suppressor cells. **Arthritis Res Ther**. 2019; 21:105.

145. Chen HZ, Wang F, Gao P, et al. Age-associated sirtuin 1 reduction in vascular smooth muscle links vascular senescence and inflammation to abdominal aortic aneurysm. **Circ Res**. 2016; 119:1076−1088.

146. Sebastián C, Satterstrom FK, Haigis MC, Mostoslavsky R. From sirtuin biology to human diseases: an update. **J Biol Chem**. 2012; 287:42444−42452.

147. Haigis MC, Sinclair DA. Mammalian sirtuins: biological insights and disease relevance. **Annu Rev Pathol**. 2010; 5:253−295.

148. Tennen RI, Chua KF. Chromatin regulation and genome maintenance by mammalian SIRT6. **Trends Biochem Sci**. 2011; 36:39−46.

149. Zhou B, Margariti A, Zeng L, Xu Q. Role of histone deacetylases in vascular cell homeostasis and arteriosclerosis. **Cardiovasc Res**. 2011; 90:413−420.

150. Jones DP. Redefining oxidative stress. **Antioxid Redox Signal**. 2006; 8:1865−1879.

151. Santos L, Escande C, Denicola A. Potential modulation of sirtuins by oxidative stress. **Oxid Med Cell Longev**. 2016; 2016:9831825.

152. Imai S, Guarente L. NAD+ and sirtuins in aging and disease. **Trends Cell Biol**. 2014; 24:464−471.

153. Gano LB, Donato AJ, Pasha HM, Hearon CM, Sindler AL, Seals DR. The SIRT1 activator SRT1720 reverses vascular endothelial dysfunction, excessive superoxide production, and inflammation with aging in mice. **Am J Physiol Heart Circ Physiol**. 2014; 307:H1754−H1763.

154. Satoh A, Brace CS, Rensing N, et al. Sirt1 extends life span and delays aging in mice through the regulation of Nk2 homeobox 1 in the DMH and LH. **Cell Metab**. 2013; 18:416−430.

155. Hobson S, Arefin S, Kublickiene K, Shiels PG, Stenvinkel P. Senescent cells in early vascular ageing and bone disease of chronic kidney disease-a novel target for treatment. **Toxins**. 2019; 11.

156. Ben-Porath I, Weinberg RA. The signals and pathways activating cellular senescence. **Int J Biochem Cell Biol**. 2005; 37:961−976.

157. van Deursen JM. The role of senescent cells in ageing. **Nature**. 2014; 509:439−446.

158. Herranz N, Gil J. Mechanisms and functions of cellular senescence. **J Clin Invest**. 2018; 128:1238−1246.

159. Sturmlechner I, Durik M, Sieben CJ, Baker DJ, van Deursen JM. Cellular senescence in renal ageing and disease. **Nat Rev Nephrol**. 2017; 13:77−89.

160. Hernandez-Segura A, Nehme J, Demaria M. Hallmarks of cellular senescence. **Trends Cell Biol**. 2018; 28:436−453.

161. Gorenne I, Kavurma M, Scott S, Bennett M. Vascular smooth muscle cell senescence in atherosclerosis. **Cardiovasc Res**. 2006; 72:9−17.

162. Stenvinkel P, Luttropp K, McGuinness D, et al. CDKN2A/p16INK4(a) expression is associated with vascular progeria in chronic kidney disease. **Aging (Albany NY)**. 2017; 9:494−507.

163. Rapp N, Evenepoel P, Stenvinkel P, Schurgers L. Uremic toxins and vascular calcification-missing the forest for all the trees. **Toxins**. 2020; 12.

164. Jia G, Aroor AR, Jia C, Sowers JR. Endothelial cell senescence in aging-related vascular dysfunction. **Biochim Biophys Acta Mol Basis Dis**. 2019; 1865:1802−1809.

165. Stenvinkel P, Meyer CJ, Block GA, Chertow GM, Shiels PG. Understanding the role of the cytoprotective transcription factor nuclear factor erythroid 2-related factor 2-lessons from evolution, the animal kingdom and rare progeroid syndromes. **Nephrol Dial Transplant**. 2020; 35:2036−2045.

166. Xu M, Pirtskhalava T, Farr JN, et al. Senolytics improve physical function and increase lifespan in old age. **Nat Med**. 2018; 24:1246−1256.

167. Roos CM, Zhang B, Palmer AK, et al. Chronic senolytic treatment alleviates established vasomotor dysfunction in aged or atherosclerotic mice. **Aging Cell**. 2016; 15:973−977.

168. Gardner SE, Humphry M, Bennett MR, Clarke MC. Senescent vascular smooth muscle cells drive inflammation through an interleukin-1α-dependent senescence-associated secretory phenotype. **Arterioscler Thromb Vasc Biol**. 2015; 35:1963−1974.

169. Childs BG, Durik M, Baker DJ, van Deursen JM. Cellular senescence in aging and age-related disease: from mechanisms to therapy. **Nat Med**. 2015; 21:1424−1435.

170. Ungvari Z, Tarantini S, Hertelendy P, et al. Cerebromicrovascular dysfunction predicts cognitive decline and gait abnormalities in a mouse model of whole brain irradiation-induced accelerated brain senescence. **Geroscience**. 2017; 39:33−42.

171. Hickson LJ, Langhi Prata LGP, Bobart SA, et al. Senolytics decrease senescent cells in humans: preliminary report from a clinical trial of Dasatinib plus Quercetin in individuals with diabetic kidney disease. **EBioMedicine**. 2019; 47:446−456.

172. von Kobbe C. Targeting senescent cells: approaches, opportunities, challenges. **Aging (Albany NY)**. 2019; 11:12844−12861.

173. Stenvinkel P, Larsson TE. Chronic kidney disease: a clinical model of premature aging. **Am J Kidney Dis**. 2013; 62:339−351.

174. Kooman JP, Kotanko P, Schols AM, Shiels PG, Stenvinkel P. Chronic kidney disease and premature ageing. **Nat Rev Nephrol**. 2014; 10:732−742.

175. Kooman JP, Broers NJ, Usvyat L, et al. Out of control: accelerated aging in uremia. **Nephrol Dial Transplant**. 2013; 28:48−54.

176. Girndt M, Seibert E. Premature cardiovascular disease in chronic renal failure (CRF): a model for an advanced ageing process. **Exp Gerontol**. 2010; 45:797−800.

177. Valentijn FA, Falke LL, Nguyen TQ, Goldschmeding R. Cellular senescence in the aging and diseased kidney. **J Cell Commun Signal**. 2018; 12:69−82.

178. McGlynn LM, Stevenson K, Lamb K, et al. Cellular senescence in pretransplant renal biopsies predicts postoperative organ function. **Aging Cell**. 2009; 8:45−51.

179. Zhu Y, Armstrong JL, Tchkonia T, Kirkland JL. Cellular senescence and the senescent secretory phenotype in age-related chronic diseases. **Curr Opin Clin Nutr Metab Care**. 2014; 17:324−328.

180. Dai L, Schurgers LJ, Shiels PG, Stenvinkel P. Early vascular ageing in chronic kidney disease: impact of inflammation, vitamin K, senescence and genomic damage. **Nephrol Dial Transplant**. 2020; 35:ii31−ii37.

181. McClelland RL, Jorgensen NW, Budoff M, et al. 10-year coronary heart disease risk prediction using coronary artery calcium and traditional risk factors: derivation in the MESA (multi-ethnic study of atherosclerosis) with validation in the HNR (heinz nixdorf recall) study and the DHS (dallas heart study). **J Am Coll Cardiol**. 2015; 66:1643−1653.

182. Dai L, Qureshi AR, Witasp A, Lindholm B, Stenvinkel P. Early vascular ageing and cellular senescence in chronic kidney disease. **Comput Struct Biotechnol J**. 2019; 17:721−729.

183. Moe SM, Chen NX. Mechanisms of vascular calcification in chronic kidney disease. **J Am Soc Nephrol**. 2008; 19:213−216.

184. Shanahan CM, Crouthamel MH, Kapustin A, Giachelli CM. Arterial calcification in chronic kidney disease: key roles for calcium and phosphate. **Circ Res**. 2011; 109:697−711.

185. Kaesler N, Goettsch C, Weis D, et al. Magnesium but not nicotinamide prevents vascular calcification in experimental uraemia. **Nephrol Dial Transplant**. 2020; 35:65−73.

186. Holt SG, Smith ER. Fetuin-A-containing calciprotein particles in mineral trafficking and vascular disease. **Nephrol Dial Transplant**. 2016; 31:1583−1587.

187. Eleftheriadou I, Grigoropoulou P, Kokkinos A, et al. Association of plasma Fetuin-A levels with peripheral arterial disease and lower extremity arterial calcification in subjects with type 2 diabetes mellitus. **J Diabet Complicat**. 2017; 31:599−604.

188. Viegas CSB, Santos L, Macedo AL, et al. Chronic kidney disease circulating calciprotein particles and extracellular vesicles promote vascular calcification: a role for GRP (Gla-Rich protein). **Arterioscler Thromb Vasc Biol**. 2018; 38:575−587.

189. Vervloet M, Cozzolino M. Vascular calcification in chronic kidney disease: different bricks in the wall? **Kidney Int**. 2017; 91:808−817.

190. Price PA, Urist MR, Otawara Y. Matrix Gla protein, a new gamma-carboxyglutamic acid-containing protein which is associated with the organic matrix of bone. **Biochem Biophys Res Commun**. 1983; 117:765−771.

191. Yao Y, Zebboudj AF, Shao E, Perez M, Boström K. Regulation of bone morphogenetic protein-4 by matrix GLA protein in vascular endothelial cells involves activin-like kinase receptor 1. **J Biol Chem**. 2006; 281:33921−33930.

192. Zebboudj AF, Imura M, Boström K. Matrix GLA protein, a regulatory protein for bone morphogenetic protein-2. **J Biol Chem**. 2002; 277:4388−4394.

193. Wei R, Enaka M, Muragaki Y. Activation of KEAP1/NRF2/P62 signaling alleviates high phosphate-induced calcification of vascular smooth muscle cells by suppressing reactive oxygen species production. **Sci Rep**. 2019; 9:10366.

194. Aghagolzadeh P, Radpour R, Bachtler M, et al. Hydrogen sulfide attenuates calcification of vascular smooth muscle cells via KEAP1/NRF2/NQO1 activation. **Atherosclerosis**. 2017; 265:78−86.

195. Cai T, Sun D, Duan Y, et al. WNT/β-catenin signaling promotes VSMCs to osteogenic transdifferentiation and calcification through directly modulating Runx2 gene expression. **Exp Cell Res**. 2016; 345:206−217.

196. Voelkl J, Lang F, Eckardt KU, et al. Signaling pathways involved in vascular smooth muscle cell calcification during hyperphosphatemia. **Cell Mol Life Sci**. 2019; 76:2077−2091.

197. Giachelli CM. The emerging role of phosphate in vascular calcification. **Kidney Int**. 2009; 75:890−897.

198. Evenepoel P, Dejongh S, Verbeke K, Meijers B. The role of gut dysbiosis in the bone-vascular axis in chronic kidney disease. **Toxins**. 2020; 12.

199. Opdebeeck B, Maudsley S, Azmi A, et al. Indoxyl sulfate and p-cresyl sulfate promote vascular calcification and associate with glucose intolerance. **J Am Soc Nephrol**. 2019; 30:751−766.

This page intentionally left blank

TEXTBOOK OF
ARTERIAL STIFFNESS AND PULSATILE HEMODYNAMICS IN HEALTH AND DISEASE

VOLUME 1

Edited by

Julio A. Chirinos, MD, PhD, FAHA, FESC

Associate Professor of Medicine; Director, Arterial Hemodynamics and Cardiac Imaging Quantification Core Laboratory; Co-Director, Training Program in Cardiovascular Biology and Medicine, Clinical/Translational Science; Adjunct Faculty, Center for Magnetic Resonance and Optical Imaging. University of Pennsylvania Perelman School of Medicine, USA

Most biology-oriented books misinterpret or lack an in-depth discussion of key biophysical aspects of arterial stiffness and pulsatile arterial hemodynamics. A proper understanding of the field requires both biologic/clinical and biophysical/bioengineering knowledge which *Textbook of Arterial Stiffness and Pulsatile Hemodynamics in Health and Disease* provides in a comprehensive yet simplified manner. The resource is organized into five parts covering principles, physiology, biologic pathways, clinical implications, and therapeutics and provides a thorough overview of the field, presenting complex engineering concepts in a way that those in life science and medicine can more easily understand.

Textbook of Arterial Stiffness and Pulsatile Hemodynamics in Health and Disease includes detailed illustrations and advanced bioengineering concepts presented in boxes for the reader who wants more in-depth biophysical knowledge. This is a must-have reference for students, researchers, and clinicians interested in learning more about this rapidly growing field.

Key features

- Provides a comprehensive review of the clinical implications of arterial stiffness and pulsatile hemodynamics and its role in human disease
- Incorporates mathematical principles explained in a conceptual manner without complicated formulas
- Features chapter contributions from leading international researchers and clinicians

TEXTBOOK OF ARTERIAL STIFFNESS AND PULSATILE HEMODYNAMICS IN HEALTH AND DISEASE

Volume 2

Edited by

Julio A. Chirinos

Textbook of Arterial Stiffness and Pulsatile Hemodynamics in Health and Disease

Volume 2

This page intentionally left blank

Textbook of Arterial Stiffness and Pulsatile Hemodynamics in Health and Disease

Volume 2

Edited by

Julio A. Chirinos
Associate Professor of Medicine;
Director,
Arterial Hemodynamics and Cardiac Imaging Quantification Core Laboratory;
Co-Director,
Training Program in Cardiovascular Biology and Medicine, Clinical/Translational Science;
Adjunct Faculty, Center for Magnetic Resonance and Optical Imaging,
University of Pennsylvania Perelman School of Medicine, United States

Working together
to grow libraries in
developing countries

ELSEVIER Book Aid International

www.elsevier.com • www.bookaid.org

Contents of Volume 2

30. Arterial stiffness and pulsatile hemodynamics in diabetes and obesity

Jordana B. Cohen, Stuart B. Prenner and Julio A. Chirinos

31. Cardiovascular risk prevention in clinical medicine: current guidelines in the United States and in Europe

Chee H. Liew and John W. McEvoy

36. Arterial stiffness and pulsatile hemodynamics in heart failure

Julio A. Chirinos

37. Ventricular—arterial coupling and arterial load in aortic valve disease

Ezequiel Guzzetti, Nancy Côté, Marie-Annick Clavel and Philippe Pibarot

38. Arterial stiffness and atherosclerosis: mechanistic and pathophysiologic interactions

Kazuomi Kario

39. Arterial stiffness and pulsatile hemodynamics in coronary artery disease and other forms of atherosclerotic vascular diseases

Junichiro Hashimoto

46. Arterial stiffness and pulsatile hemodynamics in congenital heart disease

Michael A. Quail

47. Infection and arterial stiffness

Vicente F. Corrales—Medina and Julio A. Chirinos

48. Arterial stiffness, hemodynamics, and microvascular complications in conditions characterized by low arterial pulsatility

Barry J. McDonnell, William K. Cornwell, III and Eric J. Stöhr

Section VI
Arterial stiffness and pulsatile hemodynamics in the pulmonary circulation

55. Pulsatile hemodynamics and ventricular–arterial interactions in the pulmonary circulation: physiologic concepts

*Berend E. Westerhof, Anton Vonk
Noordegraaf and Masafumi Fukumitsu*

Contributors

Elena Aikawa, The Center for Excellence in Vascular Biology, Brigham and Women's Hospital, Harvard Medical School, Boston, MA, United States

S.G. Anderson, George Alleyne Chronic Disease Research Centre, University of the West Indies Cave Hill Campus, Barbados; Division of Cardiovascular Sciences, School of Medical Sciences, University of Manchester, United Kingdom; College of Medical, Veterinary and Life Sciences, University of Glasgow, United Kingdom

Livia Silva Araújo Passos, The Center for Excellence in Vascular Biology, Brigham and Women's Hospital, Harvard Medical School, Boston, MA, United States

Samsul Arefin, Division of Renal Medicine, Department of Clinical Science, Intervention & Technology, Karolinska University Hospital, Stockholm, Sweden

Per M. Arvidsson, Clinical Physiology, Department of Clinical Sciences Lund, Faculty of Medicine, Lund University, Lund, Sweden

Alberto Avolio, Macquarie Medical School, Faculty of Medicine, Health and Human Sciences, Macquarie University, Sydney, NSW, Australia

Martin Bachler, Center for Health & Bioresources, Austrian Institute of Technology (AIT), Vienna, Austria

Magnus Bäck, Université de Lorraine, Inserm, DCAC, Nancy, France; Translational Cardiology, Department of Medicine, Karolinska Institutet, and Division of Coronary and Valvular Heart Disease, Karolinska University Hospital, Stockholm, Sweden

Michael J. Bashline, Division of Cardiology, Department of Medicine, University of Pittsburgh, Pittsburgh, PA, United States

Dakota Becker-Greene, The Center for Excellence in Vascular Biology, Brigham and Women's Hospital, Harvard Medical School, Boston, MA, United States

Jamie Bellinge, Royal Perth Hospital, Victoria Square, Perth, WA, Australia; School of Medicine, The University of Western Australia, Crawley, WA, Australia

Amar Bennasroune, UMR CNRS 7369 Matrice Extracellulaire et Dynamique Cellulaire (MEDyC), Team 2: Matrix Aging and Vascular Remodelling, Université de Reims Champagne Ardenne (URCA), UFR Sciences Exactes et Naturelles et UFR Médecine, Reims, France

Sébastien Blaise, UMR CNRS 7369 Matrice Extracellulaire et Dynamique Cellulaire (MEDyC), Team 2: Matrix Aging and Vascular Remodelling, Université de Reims Champagne Ardenne (URCA), UFR Sciences Exactes et Naturelles et UFR Médecine, Reims, France

Barry A. Borlaug, Mayo Clinic, Rochester, MN, United States

Pierre Boutouyrie, Paris University, Assistance-Publique Hôpitaux de Paris, PARCC-INSERM U970, Department of Pharmacology and Hôpital Européen Georges Pompidou, Paris, France

Y. Breet, Hypertension in Africa Research Team; MRC Unit for Hypertension and Cardiovascular Disease, North-West University, South Africa

Jerome W. Breslin, Department of Molecular Pharmacology and Physiology, Morsani College of Medicine, University of South Florida, Tampa, FL, United States

Matthew J. Budoff, David Geffen School of Medicine at UCLA, The Lundquist Institute at Harbor-UCLA, Torrance, CA, United States

Mark Butlin, Macquarie Medical School, Faculty of Medicine, Health and Human Sciences, Macquarie University, Sydney, NSW, Australia

Marina Cecelja, British Heart Foundation Centre, King's College London, Department of Clinical Pharmacology, St Thomas' Hospital, London, United Kingdom

Chen-Huan Chen, Department of Medicine, National Yang Ming Chiao Tung University College of Medicine, Taipei, Taiwan; Institute of Public Health and Community Medicine Research Center, National Yang Ming Chiao Tung University College of Medicine, Taipei, Taiwan; Department of Medical Education, Taipei Veterans General Hospital, Taipei, Taiwan

Hao-Min Cheng, Department of Medicine, National Yang Ming Chiao Tung University College of Medicine, Taipei, Taiwan; Institute of Public Health and Community Medicine Research Center, National Yang Ming Chiao Tung University College of Medicine, Taipei,

Taiwan; Center for Evidence-based Medicine, Taipei Veterans General Hospital, Taipei, Taiwan

Yi-Bang Cheng, National Research Centre for Translational Medicine, Centre for Epidemiological Studies and Clinical Trials, Shanghai Key Laboratory of Hypertension, The Shanghai Institute of Hypertension, Department of Hypertension, Ruijin Hospital, Shanghai Jiao Tong University School of Medicine, Shanghai, Shanghai, China

Julio A. Chirinos, University of Pennsylvania Perelman School of Medicine, Hospital of the University of Pennsylvania and Perelman Center for Advanced Medicine, Philadelphia, PA, United States; Ghent University, Ghent, Belgium

Phil Chowienczyk, British Heart Foundation Centre, King's College London, Department of Clinical Pharmacology, St Thomas' Hospital, London, United Kingdom

Shao-Yuan Chuang, Institute of Population Health Science, National Health Research Institutes, Miaoli, Taiwan

Marie-Annick Clavel, Institut Universitaire de Cardiologie et de Pneumologie de Québec / Québec Heart & Lung Institute, Laval University, Québec City, QC, Canada

Jordana B. Cohen, Renal-Electrolytes and Hypertension Division, Perelman School of Medicine, University of Pennsylvania, Philadelphia, PA, United States; Department of Biostatistics, Epidemiology, and Informatics, Perelman School of Medicine, University of Pennsylvania, Philadelphia, PA, United States

Alexis M. Corcoran, Division of Pulmonary and Critical Care Medicine, Department of Medicine, Brigham and Women's Hospital, Boston, MA, United States

William K. Cornwell, III, Department of Medicine-Cardiology, University of Colorado Anschutz Medical Campus, Aurora, CO, United States

Vicente F. Corrales−Medina, Department of Medicine, Division of Infectious Diseases at the University of Ottawa, The Ottawa Hospital Research Institute, Centre for Infection, Immunity and Inflammation (CI3) at the University of Ottawa, Ottawa, ON, Canada

Nancy Côté, Institut Universitaire de Cardiologie et de Pneumologie de Québec / Québec Heart & Lung Institute, Laval University, Québec City, QC, Canada

Thais Coutinho, Division of Cardiology, Division of Cardiac Prevention & Rehabilitation, University of Ottawa Heart Institute, Ottawa, ON, Canada

James Cox, Macquarie Medical School, Faculty of Medicine, Health and Human Sciences, Macquarie University, Sydney, NSW, Australia

J.K. Cruickshank, Cardiovascular Medicine Group, Division of Life-course/ Nutritional Sciences, Kings College London, United Kingdom

Lu Dai, Division of Renal Medicine, Department of Clinical Science, Intervention & Technology, Karolinska University Hospital, Stockholm, Sweden

Stella S. Daskalopoulou, Fonds de recherche du Québec − Santé − Boursier Clinicien − Senior, Director, Vascular Health Unit, Department of Medicine, Division of Internal Medicine, McGill University Health Centre, McGill University, Montreal, QC, Canada

Kevin P. Davy, Virginia Tech, Blacksburg, VA, United States

Marc L. De Buyzere, Department of Cardiology, Ghent University Hospital, Ghent, Belgium

Paul B. Dieffenbach, Division of Pulmonary and Critical Care Medicine, Department of Medicine, Brigham and Women's Hospital, Boston, MA, United States

Laurent Duca, UMR CNRS 7369 Matrice Extracellulaire et Dynamique Cellulaire (MEDyC), Team 2: Matrix Aging and Vascular Remodelling, Université de Reims Champagne Ardenne (URCA), UFR Sciences Exactes et Naturelles et UFR Médecine, Reims, France

Girish Dwivedi, School of Medicine, The University of Western Australia, Crawley, WA, Australia; Department of Cardiology, Fiona Stanley Hospital, Murdoch, WA, Australia; Department of Advanced Clinical and Translational Cardiovascular Imaging, Harry Perkins Institute of Medical Research, Murdoch, WA, Australia

David G. Edwards, Department of Kinesiology and Applied Physiology, University of Delaware, Newark, DE, United States

William B. Farquhar, Department of Kinesiology and Applied Physiology, University of Delaware, Newark, DE, United States

Bo Fernhall, University of Illinois at Chicago, Chicago, IL, United States

John S. Floras, Toronto General Research Institute, Toronto, ON, Canada; University Health Network and Mount Sinai Hospital, Division of Cardiology, Department of Medicine, University of Toronto, Toronto, ON, Canada

Laura E. Fredenburgh, Division of Pulmonary and Critical Care Medicine, Department of Medicine, Brigham and Women's Hospital, Boston, MA, United States

Masafumi Fukumitsu, Department of Pulmonary Medicine, Amsterdam Universitair Medische Centra, Vrije Universiteit Amsterdam, Amsterdam Cardiovascular Sciences, Amsterdam, the Netherlands

L. Gafane-Matemane, Hypertension in Africa Research Team; MRC Unit for Hypertension and Cardiovascular Disease, North-West University, South Africa

Nestor Gahungu, Royal Perth Hospital, Victoria Square, Perth, WA, Australia

Ahmed K. Ghanem, Department of Cardiology, The Lundquist Institute at Harbor-UCLA, Torrance, CA, United States

Thierry C. Gillebert, Department of Cardiology, Ghent University and Ghent University Hospital, Ghent, Belgium

Philippe Gillery, UMR CNRS 7369 Matrice Extracellulaire et Dynamique Cellulaire (MEDyC), Team 2: Matrix Aging and Vascular Remodelling, Université de Reims Champagne Ardenne (URCA), UFR Sciences Exactes et Naturelles et UFR Médecine, Reims, France; Department of Biochemistry, University Hospital Center, Reims, France

Delphine Gomez, Pittsburgh Heart, Lung, Blood, and Vascular Medicine Institute, University of Pittsburgh, Pittsburgh, PA, United States; Department of Medicine, Division of Cardiology, University of Pittsburgh, Pittsburgh, PA, United States

Ezequiel Guzzetti, Institut Universitaire de Cardiologie et de Pneumologie de Québec / Québec Heart & Lung Institute, Laval University, Québec City, QC, Canada

Bernhard Hametner, Center for Health & Bioresources, Austrian Institute of Technology (AIT), Vienna, Austria

Junichiro Hashimoto, Miyagi University of Education Medical Center, Sendai, Miyagi, Japan

Kevin S. Heffernan, Syracuse University, Syracuse, NY, United States

Brooks A. Hibner, University of Illinois at Chicago, Chicago, IL, United States

Sam Hobson, Division of Renal Medicine, Department of Clinical Science, Intervention & Technology, Karolinska University Hospital, Stockholm, Sweden

Nien-Wen Hu, J. Crayton Pruitt Family Department of Biomedical Engineering, University of Florida, Gainesville, FL, United States

T.M. Hughes, Department of Internal Medicine, Wake Forest School of Medicine, Winston-Salem, NC, United States

Jay D. Humphrey, Department of Biomedical Engineering, School of Engineering and Applied Science, Yale University, New Haven, CT, United States; Vascular Biology and Therapeutics Program, Yale School of Medicine, New Haven, CT, United States

Stéphane Jaisson, UMR CNRS 7369 Matrice Extracellulaire et Dynamique Cellulaire (MEDyC), Team 2: Matrix Aging and Vascular Remodelling, Université de Reims Champagne Ardenne (URCA), UFR Sciences Exactes et Naturelles et UFR Médecine, Reims, France; Department of Biochemistry, University Hospital Center, Reims, France

Nadjia Kachenoura, Sorbonne Université, INSERM, CNRS, Laboratoire d'Imagerie Biomédicale, Paris, France

Kazuomi Kario, Division of Cardiovascular Medicine, Department of Medicine, Jichi Medical University School of Medicine, Shimotsuke, Tochigi, Japan; The Hypertension Cardiovascular Outcome Prevention and Evidence in Asia (HOPE Asia) Network, Tokyo, Japan

Prasad V.G. Katakam, Tulane University School of Medicine, New Orleans, LA, United States

Goro Katsuumi, Department of Cardiovascular Biology and Medicine, Juntendo University Graduate School of Medicine, Tokyo, Japan

Avinash Kondiboyina, Heart Research, Murdoch Children's Research Institute, Parkville, VIC, Australia; Department of Paediatrics, University of Melbourne, Parkville, VIC, Australia

Sándor J. Kovács, Cardiovascular Division, Department of Medicine, Washington University in Saint Louis, School of Medicine, Saint Louis, Missouri, United States

R. Kruger, Hypertension in Africa Research Team; MRC Unit for Hypertension and Cardiovascular Disease, North-West University, South Africa

Karolina Kublickiene, Division of Renal Medicine, Department of Clinical Science, Intervention & Technology, Karolinska University Hospital, Stockholm, Sweden

Patrick Lacolley, Université de Lorraine, Inserm, DCAC, Nancy, France

Muriel Laffargue, INSERM UMR 1048, Institut des Maladies Métaboliques et Cardiovasculaires (I2MC), Toulouse, France

Arinola O. Lampejo, J. Crayton Pruitt Family Department of Biomedical Engineering, University of Florida, Gainesville, FL, United States

Agne Laucyte-Cibulskiene, Division of Renal Medicine, Department of Clinical Science, Intervention & Technology, Karolinska University Hospital, Stockholm, Sweden; Department of Nephrology; Skåne University Hospital, Malmö, Sweden

Stéphane Laurent, Department of Pharmacology and Hôpital Européen Georges Pompidou, Paris, France; INSERM, U970, Paris Cardiovascular Research Center, PARCC, Paris, France; Université de Paris, Paris, France; Assistance Publique, Hopitaux de Paris, Paris, France

Hae-Young Lee, Department of Internal Medicine, Seoul National University College of Medicine, Jongno-Gu, Seoul, South Korea

Wesley K. Lefferts, University of Illinois at Chicago, Chicago, IL, United States; Iowa State University, Ames, IA, United States

Elizabeth C. Lefferts, University of Illinois at Chicago, Chicago, IL, United States; Iowa State University, Ames, IA, United States

Adelino F. Leite-Moreira, Department of Surgery and Physiology, Cardiovascular Research Centre, Faculty of Medicine of the University of Porto, Porto, Portugal; Department of Cardiothoracic Surgery, São João Hospital Centre, Porto, Portugal

Chee H. Liew, National Institute for Prevention and Cardiovascular Health, National University of Ireland Galway, Galway, Ireland

Joao A.C. Lima, Departments of Cardiology/Medicine and Radiology, Johns Hopkins University, Baltimore, MD, United States

André P. Lourenço, Department of Surgery and Physiology, Cardiovascular Research Centre, Faculty of Medicine of the University of Porto, Porto, Portugal; Department of Anaesthesiology, São João Hospital Centre, Porto, Portugal

Kaisa Maki-Petaja, Experimental Medicine and Immunotherapeutics, University of Cambridge, Cambridge, United Kingdom

Marcy Maracle, Schulich School of Medicine and Dentistry, Western University, London, ON, Canada

Laurent Martiny, UMR CNRS 7369 Matrice Extracellulaire et Dynamique Cellulaire (MEDyC), Team 2: Matrix Aging and Vascular Remodelling, Université de Reims Champagne Ardenne (URCA), UFR Sciences Exactes et Naturelles et UFR Médecine, Reims, France

Pascal Maurice, UMR CNRS 7369 Matrice Extracellulaire et Dynamique Cellulaire (MEDyC), Team 2: Matrix Aging and Vascular Remodelling, Université de Reims Champagne Ardenne (URCA), UFR Sciences Exactes et Naturelles et UFR Médecine, Reims, France

Christopher C. Mayer, Center for Health & Bioresources, Austrian Institute of Technology (AIT), Vienna, Austria

Barry J. McDonnell, Cardiovascular Physiology Research Group, Cardiff School of Sport & Health Sciences, Cardiff Metropolitan University, Cardiff, United Kingdom

John W. McEvoy, National Institute for Prevention and Cardiovascular Health, National University of Ireland Galway, Galway, Ireland; Ciccarone Center for the Prevention of Cardiovascular Disease, Johns Hopkins University School of Medicine, Baltimore, MD, United States

M.L. Meyer, Department of Emergency Medicine, School of Medicine, University of North Carolina at Chapel Hill, Chapel Hill, NC, United States

Jean-Baptiste Michel, Inserm UMR_S 1148, CHU X. Bichat, Paris, France

Philip J. Millar, Department of Human Health and Nutritional Sciences, University of Guelph, Guelph, ON, Canada; Toronto General Research Institute, Toronto, ON, Canada

Tohru Minamino, Department of Cardiovascular Biology and Medicine, Juntendo University Graduate School of Medicine, Tokyo, Japan; Japan Agency for Medical Research and Development-Core Research for Evolutionary Medical Science and Technology (AMED-CREST), Japan Agency for Medical Research and Development, Tokyo, Japan

Gary F. Mitchell, Cardiovascular Engineering, Inc., Norwood, MA, United States

Walter L. Murfee, J. Crayton Pruitt Family Department of Biomedical Engineering, University of Florida, Gainesville, FL, United States

Jonathan P. Mynard, Heart Research, Murdoch Children's Research Institute, Parkville, VIC, Australia; Department of Paediatrics, University of Melbourne, Parkville, VIC, Australia; Department of Biomedical Engineering, University of Melbourne, Parkville, VIC, Australia

Massimo Nardone, Department of Human Health and Nutritional Sciences, University of Guelph, Guelph, ON, Canada

Peter M. Nilsson, Lund University, Department of Clinical Sciences, Skane University Hospital, Malmö, Sweden

Kevin O'Gallagher, Department of Clinical Pharmacology, School of Cardiovascular Medicine and Sciences, King's College London British Heart Foundation Centre, St. Thomas' Hospital, London, United Kingdom

Yoshiaki Ohyama, Departments of Cardiology/Medicine and Radiology, Johns Hopkins University, Baltimore, MD, United States; Clinical Investigation and Research Unit, Gunma University Hospital, Maebashi, Japan

Kazunori Omote, Mayo Clinic, Rochester, MN, United States

Jeong Bae Park, Department of Precision Medicine and Biostatistics, Yonsei University Wonju College of Medicine, Seoul, Republic of Korea

Shayn M. Peirce, Department of Biomedical Engineering, University of Virginia, Charlottesville, VA, United States

Philippe Pibarot, Institut Universitaire de Cardiologie et de Pneumologie de Québec / Québec Heart & Lung Institute, Laval University, Québec City, QC, Canada

Gary L. Pierce, University of Iowa, Iowa City, IA, United States

Stuart B. Prenner, University of Pennsylvania Perelman School of Medicine, Hospital of the University of Pennsylvania and Perelman Center for Advanced Medicine, Philadelphia, PA, United States

Athanase Protogerou, Cardiovascular Prevention and Research Unit, Clinic-Laboratory of Pathophysiology, Laiko Hospital, Medical School, National and Kapodistrian University of Athens, Athens, Greece

Reed E. Pyeritz, Perelman School of Medicine, University of Pennsylvania Health System, Philadelphia, PA, United States

Michael A. Quail, Department of Pediatric Cardiology, Great Ormond Street Hospital for Children and University College London, London, United Kingdom

Yogesh N.V. Reddy, Mayo Clinic, Rochester, MN, United States

Alban Redheuil, Sorbonne Université, INSERM, CNRS, Laboratoire d'Imagerie Biomédicale, Paris, France; Cardiovascular and Thoracic Imaging, Hôpital La Pitié-Salpêtrière, AP-HP, Sorbonne Université, Paris, France

Véronique Regnault, Université de Lorraine, Inserm, DCAC, Nancy, France

Rakhshinda Rehman, Division of Pulmonary and Critical Care Medicine, Department of Medicine, Brigham and Women's Hospital, Boston, MA, United States

Ernst R. Rietzschel, Department of Cardiology (Internal Medicine & Pediatrics), Ghent University, Ghent, Belgium; Biobanking and Cardiovascular Epidemiology, Ghent University Hospital, Ghent, Belgium

Béatrice Romier-Crouzet, UMR CNRS 7369 Matrice Extracellulaire et Dynamique Cellulaire (MEDyC), Team 2: Matrix Aging and Vascular Remodelling, Université de Reims Champagne Ardenne (URCA), UFR Sciences Exactes et Naturelles et UFR Médecine, Reims, France

Jasjit Rooprai, Department of Medicine, University of Toronto, Toronto, ON, Canada

Lucia Salvi, Medicina II Cardiovascolare, AUSL-IRCCS di Reggio Emilia, Italy

Paolo Salvi, Istituto Auxologico Italiano, IRCCS, Cardiology Unit, Milan, Italy

Hervé Sartelet, UMR CNRS 7369 Matrice Extracellulaire et Dynamique Cellulaire (MEDyC), Team 2: Matrix Aging and Vascular Remodelling, Université de Reims Champagne Ardenne (URCA), UFR Sciences Exactes et Naturelles et UFR Médecine, Reims, France

Christian E.H. Schmelzer, Institute of Pharmacy, Faculty of Natural Sciences I, Martin Luther University Halle-Wittenberg, Halle (Saale), Germany; Fraunhofer Institute for Microstructure of Materials and Systems IMWS, Halle (Saale), Germany

A.E. Schutte, Hypertension in Africa Research Team; MRC Unit for Hypertension and Cardiovascular Disease, North-West University, South Africa; School of Population Health, University of New South Wales, The George Institute for Global Health, Sydney, Australia

Angelina Schwarz, Division of Renal Medicine, Department of Clinical Science, Intervention & Technology, Karolinska University Hospital, Stockholm, Sweden

Patrick Segers, Faculty of Biomedical Sciences, Institute of Biomedical Engineering and Technology, Ghent University, Ghent, Belgium

James E. Sharman, Menzies Institute for Medical Research, University of Tasmania, Hobart, TAS, Australia

Ippei Shimizu, Department of Cardiovascular Biology and Medicine, Juntendo University Graduate School of Medicine, Tokyo, Japan

Marc A. Simon, Division of Cardiology, Department of Medicine, University of California, San Francisco (UCSF), San Francisco, CA, United States

Piera Sosa, Meharry Medical College, Nashville, TN, United States

Bart Spronck, Department of Biomedical Engineering, School of Engineering and Applied Science, Yale University, New Haven, CT, United States; Department of Biomedical Engineering, CARIM School for Cardiovascular Diseases, Maastricht University, Maastricht, the Netherlands

Peter Stenvinkel, Division of Renal Medicine, Department of Clinical Science, Intervention & Technology, Karolinska University Hospital, Stockholm, Sweden

Eric J. Stöhr, Cardiovascular Physiology Research Group, Cardiff School of Sport & Health Sciences, Cardiff Metropolitan University, Cardiff, United Kingdom; Department of Medicine, Division of Cardiology, Columbia University Irving Medical Center, New York, NY, United States

M. Strauss-Kruger, Hypertension in Africa Research Team; MRC Unit for Hypertension and Cardiovascular Disease, North-West University, South Africa

Ariana Suarez-Martinez, J. Crayton Pruitt Family Department of Biomedical Engineering, University of Florida, Gainesville, FL, United States

Masayoshi Suda, Department of Cardiovascular Biology and Medicine, Juntendo University Graduate School of Medicine, Tokyo, Japan

Shih-Hsien Sung, Department of Medicine, National Yang Ming Chiao Tung University College of Medicine, Taipei, Taiwan; Department of Medicine, Taipei Veterans General Hospital, Taipei, Taiwan

Isabella Tan, Macquarie Medical School, Faculty of Medicine, Health and Human Sciences, Macquarie University, Sydney, NSW, Australia

Dimitrios Terentes-Printzios, First Department of Cardiology, Hippokration Hospital, Medical School, National and Kapodistrian University of Athens, Athens, Greece

Raymond R. Townsend, Perelman School of Medicine, University of Pennsylvania Health System, Philadelphia, PA, United States

Andrew H. Tran, The Heart Center, Nationwide Children's Hospital, Columbus, OH, United States; The Ohio State University, Columbus, OH, United States

Elaine M. Urbina, Division of Cardiology, Cincinnati Children's Hospital Medical Center, Cincinnati, OH, United States; University of Cincinnati, Cincinnati, OH, United States

Bharath Ambale Venkatesh, Departments of Cardiology/ Medicine and Radiology, Johns Hopkins University, Baltimore, MD, United States

Charalambos Vlachopoulos, First Department of Cardiology, Hippokration Hospital, Medical School, National and Kapodistrian University of Athens, Athens, Greece

Anton Vonk Noordegraaf, Department of Pulmonary Medicine, Amsterdam Universitair Medische Centra, Vrije Universiteit Amsterdam, Amsterdam Cardiovascular Sciences, Amsterdam, the Netherlands

Amandine Wahart, UMR CNRS 7369 Matrice Extracellulaire et Dynamique Cellulaire (MEDyC), Team 2: Matrix Aging and Vascular Remodelling, Université de Reims Champagne Ardenne (URCA), UFR Sciences Exactes et Naturelles et UFR Médecine, Reims, France; INSERM UMR 1048, Institut des Maladies Métaboliques et Cardiovasculaires (I2MC), Toulouse, France

Ji-Guang Wang, National Research Centre for Translational Medicine, Centre for Epidemiological Studies and Clinical Trials, Shanghai Key Laboratory of Hypertension, The Shanghai Institute of Hypertension, Department of Hypertension, Ruijin Hospital, Shanghai Jiao Tong University School of Medicine, Shanghai, Shanghai, China

Siegfried Wassertheurer, Center for Health & Bioresources, Austrian Institute of Technology (AIT), Vienna, Austria

Andrew James Webb, Department of Clinical Pharmacology, School of Cardiovascular Medicine and Sciences, King's College London British Heart Foundation Centre, St. Thomas' Hospital, London, United Kingdom

Thomas Weber, Cardiology Department, Klinikum Wels-Grieskirchen, Wels, Paracelsus Medical University, Salzburg, Austria

Berend E. Westerhof, Department of Pulmonary Medicine, Amsterdam Universitair Medische Centra, Vrije Universiteit Amsterdam, Amsterdam Cardiovascular Sciences, Amsterdam, the Netherlands

Ian B. Wilkinson, Experimental Medicine and Immunotherapeutics, University of Cambridge, Cambridge, United Kingdom; Addenbrooke's Hopital, Cambridge, United Kingdom

Yohko Yoshida, Department of Cardiovascular Biology and Medicine, Juntendo University Graduate School of Medicine, Tokyo, Japan

Foreword

Ernesto L. Schiffrin, CM, MD, PhD, FRSC, FRCPC, FACP

Physician-in-Chief, Sir Mortimer B. Davis-Jewish General Hospital, Director, Hypertension and Vascular Research, Lady Davis Institute of Medical Research, Distinguished James McGill Professor and Associate Chair, Department of Medicine, McGill University, Montreal, Canada; Editor-in-Chief, The American Journal of Hypertension

Arterial Stiffness and Pulsatile Hemodynamics in Health and Disease, edited by Julio A. Chirinos, MD, PhD, arrives to us at a time when the field of arterial stiffness has come full circle from experimental to clinical and therapeutic implications, including its potential applications to patients in the clinic. It is not an easy area of research and clinical understanding for most physicians, because of the physical and mathematical aspects that tend to be beyond their knowledge and typical clinical training curricula. Therefore, a text that fills the gap between biophysics, biology, physiology, clinical application, epidemiology, and therapeutics applied to a range of vessels throughout the body and different clinical conditions is certainly very welcome. In particular, it is important that the text is accessible to experts in different fields at all these levels, thanks to the ability to explain difficult concepts in detail but with clarity and some degree of simplicity, and that is what *Arterial Stiffness and Pulsatile Hemodynamics in Health and Disease* does throughout its two volumes, with homogenous prose despite being multiauthored. Dr. Chirinos has managed to summon a group of writers for all chapters that comprises the "who's who" of the field of arterial stiffness and pulsatile hemodynamics from North America, Europe, Asia, and Australia.

The book is organized in sections that deal with successive aspects of vascular stiffness and its consequences. The first section addresses biophysical principles of pressure, flow, pulsatile hemodynamics, aortic structure, wall stiffness, and hemodynamic function. This is followed by a section on pulsatile hemodynamics of the arterial vasculature and its impact on the left ventricular function, and the microcirculation. The following section deals with the biology of arterial stiffening including associated effects on elastin, inflammation and calcification, and mechanisms of cellular aging, and dysfunction of smooth muscle and the endothelium. The clinical and epidemiological aspects of arterial stiffness and its role in cardiovascular prevention and different disease conditions, including hypertension, obesity, diabetes, heart failure, coronary artery disease, chronic kidney disease, cognitive decline, and pregnancy among others, follow in the next section. The primary aortopathies and conditions associated with low pulsatility such as use of left ventricular assist devices are described next. The following section addresses therapeutic implications of large artery stiffness and effects of exercise, weight control, and drugs, both presently in use and potential new drugs for the future. The last section addresses stiffening of the pulmonary circulation, including pulmonary hypertension.

Throughout this book the different authors manage to present complex concepts in a way that can be understood by the uninitiated, who could be expert in other aspects of this subject matter. Undoubtedly this is an authoritative textbook that will familiarize the biomedical community with the field, and facilitate the use of the knowledge acquired so far on arterial stiffness to improve patient outcomes.

This page intentionally left blank

Preface

The field of arterial stiffness and pulsatile hemodynamics has significantly expanded over the last few decades. Increasingly, epidemiologists, clinicians, engineers, and biologists recognize the importance of large artery stiffening in various disease states. The role of large artery stiffness and pulsatile hemodynamics in cardiovascular aging is also widely recognized. However, there remains a gap between the biophysical and theoretical concepts and clinical practice. The aim of this textbook is to provide a comprehensive reference on arterial stiffness and pulsatile hemodynamics, covering the intersection of clinical, biologic, epidemiologic, and biophysical concepts.

We intend for the audience of this book to be composed of clinical and basic science investigators interested in arterial stiffness, physicians and other healthcare providers, epidemiologists and biomedical engineers. Whereas excellent books are already available covering various aspects of this field, in many cases, these are highly specialized, are mathematically-oriented, are restricted to specific knowledge areas, or deal exclusively with clinical or biologic aspects without discussing hemodynamic mechanisms linking arterial stiffness and pulsatile hemodynamics with disease pathophysiology. Therefore, we intended to produce a book that introduces the interested reader to this field in relatively simple terms but at the same time covers, with reasonable depth, a broad range of relevant topics in biophysics, biology, epidemiology, and clinical medicine.

Despite the increasing recognition of this field, studies on arterial stiffness and pulsatile hemodynamics are often misinterpreted or underappreciated from a clinical standpoint. I believe that a proper interpretation of the field is nevertheless essential for a better understanding of multiple clinical conditions and disease states. One of the barriers to a better integration and data interpretation is that clinicians and biologists tend to be less familiar with the biophysical aspects of this field, whereas engineers naturally tend to be less familiar with the clinical and biologic aspects. Yet, a basic understanding of both is essential to drive the field forward and to adequately interpret available data. There is a need for a reference that: (a) presents complex engineering concepts in a readable format for individuals trained in clinical medicine, biology, or epidemiology rather than engineering; (b) clearly discusses the clinical implications of pulsatile hemodynamics

and arterial stiffness; and (c) provides a comprehensive review of key biologic pathways involved in arterial stiffening. This textbook intends to fill this gap.

Throughout the textbook, we utilize stand-alone basic concept boxes to deal with: (1) biophysics concepts that clinicians would be either be unlikely to be familiar with, but that would be very useful for understanding the topic; (2) clinical or biologic concepts that nonclinicians or non-biologists (i.e., bioengineers) are unlikely to be familiar but that are essential to understand the topic. We also utilize stand-alone "in-depth" boxes to develop more advanced concepts that clinicians or biologists are unlikely to be eager to study in depth due to relatively complex math or biophysics, even though a mathematically oriented person (such as a bioengineer) would find very useful. Stand-alone boxes are mentioned and are useful to understand the main text in the chapters, but should in general not be absolutely necessary to follow its flow. To the extent possible, mathematical principles are explained in the main text without complicated formulas, in a conceptual manner.

The book is organized into six sections. Section I deals with the biophysical and technical principles involved in the measurements and interpretation of pressure, flow, pulsatile hemodynamics, aortic structure, wall stiffness, and hemodynamic function, and is not considered optional but rather essential to better understand the rest of the book. Most of the content in this section deals with *in vivo* assessments, particularly in humans, but a dedicated chapter in this section deals with animal models and *ex vivo* methods to study arterial stiffness. Section II deals with basic anatomic and physiologic considerations, including the hemodynamic role of the aorta, pulsatile hemodynamics in the arterial tree, ventricular physiology, ventricular–arterial interactions (as they relate to both load and myocardial oxygen supply), and the microcirculation. Section III deals with the biologic pathways leading to arterial stiffening and dysfunctional pulsatile hemodynamics, including elastin breakdown and associated processes, inflammation, aortic wall calcification, smooth muscle dysfunction, endothelial dysfunction, autonomic dysfunction, and cellular mechanisms of aging. Section IV deals with clinical and epidemiologic aspects of arterial stiffness and pulsatile hemodynamics, including normal,

supernormal, and early vascular aging, ethnic differences, and the role of arterial stiffness in cardiovascular prevention strategies and in various disease states, such as hypertension, obesity, diabetes, exercise intolerance, heart failure, aortic valve disease, coronary artery disease, age-related cognitive dysfunction, chronic kidney disease, pregnancy related complications, congenital heart disease, and the cardiovascular complications of infectious diseases. Additional chapters deal with relevant aspects of primary arteriopathies and clinical situations associated with low arterial pulsatility (particularly, implanted left ventricular assist devices). Section V deals with therapeutic approaches to improve arterial stiffness and pulsatile hemodynamics, including discussions of standard vasoactive drugs in current use, as well as novel drugs, nonpharmacologic approaches (exercise training, diet), and personalized medicine strategies. Finally, Section VI deals with the pulmonary circulation, with an emphasis on pulmonary arterial stiffening, right ventricular—pulmonary arterial interactions, and pulmonary hypertension.

Throughout this book, we intend to discuss the relevant biophysics, presenting complex engineering concepts in a simplified format. Similarly, we intend to place the importance of arterial stiffness in the appropriate clinical context, ultimately keeping in mind how this field can aid in patient care and development of novel therapies. I have been extremely fortunate to have the support of a large number of internationally recognized experts, who have selflessly contributed their time, effort, and deep expertise to write the various chapters in this book, providing authoritative reviews about the state-of-the-art in their respective topics. I hope that this textbook will help advance the field, that it will be an aid to educators in this field, and that it will contribute to the training of the next generation of investigators dedicated to the study of arterial stiffness and pulsatile hemodynamics.

Acknowledgments

I want to thank the chapter authors for selflessly contributing their time and expertise for the success of this project. I am forever grateful to Melissa, Gabriella, and Daniel Chirinos for their support throughout this project, and to my parents, Julio Chirinos Pacheco and Josefina Medina, for being such inspirational role models. I also want to acknowledge my academic home, the Cardiovascular Medicine Division at the University of Pennsylvania, for strongly supporting my career and the various academic activities that led to the edition of this book. My very special thanks to my colleagues at the University of Ghent (particularly Ernst Rietzschel, Thierry Gillebert, Patrick Segers, and Marc De Buyzere) for many years of wonderful collaboration, and to the North American Artery, ARTERY, Pulse of Asia, and Latin American Artery societies for providing platforms for the advancement of this important field. I am also grateful to the National Institutes of Health (NIH) which supported my work through multiple awards throughout the years, particularly the National Institutes of Aging which provided me with a mid-career development award to study large artery stiffness and arterial aging (K24-AG070459). I am indebted to Dr. Patrick Segers for going above and beyond his chapter writing, providing critical feedback for several other sections of the book. I also want to acknowledge the essential contributions by the many senior investigators, who although did not participate in the book, inspired or motivated many of us, including but not limited to Wilmer Nichols, Nico Westerhof, Michael O'Rourke and Michel Safar, as well as John Cockcroft, who has worked relentlessly to promote the field in Europe and the US, and Alfonso Bryce, Pedro Forcada, Eduardo Barbosa and Enrique Melgarejo, who have done the same throughout Latin America. Last but not least, my gratitude goes to the editorial team at Elsevier for their guidance and help throughout this project.

This page intentionally left blank

Clinical significance of arterial stiffness and pulsatile hemodynamics

This page intentionally left blank

Normal aging: arterial stiffness and remodeling over the life course

Ernst R. Rietzschel[1,2] and Marc L. De Buyzere[3]

[1]Department of Cardiology (Internal Medicine & Pediatrics), Ghent University, Ghent, Belgium; [2]Biobanking and Cardiovascular Epidemiology, Ghent University Hospital, Ghent, Belgium; [3]Department of Cardiology, Ghent University Hospital, Ghent, Belgium

Preamble

In the absence of a single "true and comprehensive" measure of this phenomenon, a plethora of parameters have been put forward, all very partially and incompletely describing different aspects of the underlying process of "arterial aging," While this chapter describes the insights gleaned from some of the more well-studied of these parameters, these limitations are best kept in mind to avoid the pitfall of reductionism of the aging process toward a single imperfect parameter.

Insights from cross-sectional epidemiological and cohort data

Blood pressure and pulse wave velocity

Aging is complex, and although many mechanisms are implicated, fragmentation of elastin, one of the most abundant extracellular matrix proteins in the arterial wall (representing 50% of its dry weight) is certainly a key process.[1] Elastogenesis is restricted to fetal life and infancy, and any damage—be it proteolytic, mechanical, or other—that does occur with age and disease is essentially irreparable. Elastin in the arterial wall has an estimated half-life of approximately 40 years.

Unsurprisingly, it is a common belief in physiology that from the fourth decade of human life, aging of the arterial tree takes a direction from which it does not recover anymore, neither in the apparently healthy individual nor in the diseased.

Aortic strain and distensibility sharply decline from the third to the fifth decade; a process mirrored by a rather steep increase in carotid-femoral pulse wave velocity (cf-PWV) which however lags by one or two decades (i.e., steep rise beyond age 50). In concert, albeit not necessarily causally linked, peripheral resistance and DBP increase.
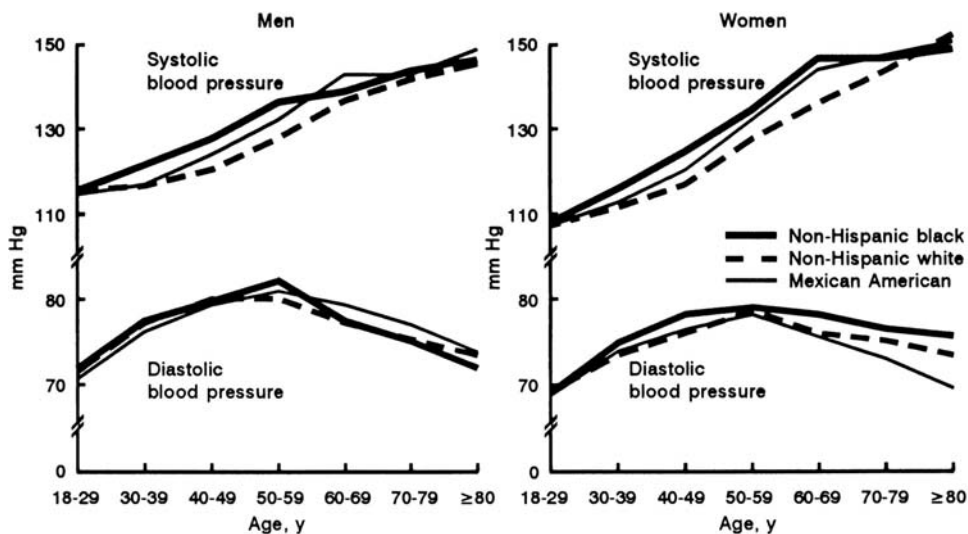
Observations from the different cohorts of the Framingham Heart Study, which have been consistently confirmed in other settings, convincingly demonstrated that after the fifth decade an (increased) diastolic blood pressure (DBP) is no longer a leading blood pressure marker of arterial aging, but that systolic blood pressure (SBP) and pulse pressure (PP) rather aggressively take the lead, because DBP tends to decrease as aortic stiffness increases (Fig. 26.1).[2,3]

Pulse wave velocity (PWV) is—besides blood pressure—one of easiest to measure and most studied parameters for which data are available from early childhood until old age.
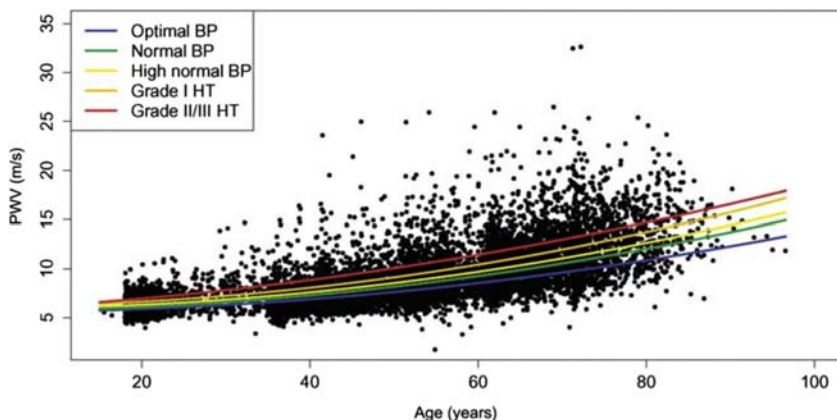
The Reference Values for Arterial Stiffness' Collaboration pooled data on 16,867 subjects from 13 different research samples across eight European countries.[4] Of these, some 11,000 subjects were free from overt cardiovascular disease (CVD), nondiabetic, and untreated either for hypertension or dyslipidemia. This collaboration was sufficiently powered to provide robust reference values for adults within the age range of below 30 years to above 70 years, and across blood pressure strata including subjects with optimal/normal blood pressures.

The increase of cf-PWV with age could best be modeled by a quadratic function with the importance of the quadratic term increasing at higher age and at higher levels of operating blood pressure. To illustrate, the increase in average cf-PWV between the ages of 30 and 40 years was ∼0.3 m/s, while between the ages of 60 and 70 years, this was roughly double (∼0.6 m/s). PWV at any age is linearly related to BP and correspondingly at any BP level is dependent on the quadratic age. The slope of the relation between age (and MBP) and PWV increases by 1.5-fold between the younger/lower BP and the elderly/higher BP, a finding which was already previously well described (Fig. 26.2).[5,6]

FIGURE 26.1 Blood pressure profiles in the US adult population from the Third National Health and Nutrition Examination Survey (NHANES III). *From Burt VL, Whelton P, Roccella EJ, et al. Prevalence of Hypertension in the US Adult Population: Results From the Third National Health and Nutrition Examination Survey, 1988–1991.* **Hypertension**. *1995; 25:305–313.*

FIGURE 26.2 Pulse wave velocity increases with age in the Reference Values for Arterial Stiffness' Collaboration. *From The Reference Values for Arterial Stiffness' Collaboration. Determinants of pulse wave velocity in healthy people and in the presence of cardiovascular risk factors: 'establishing normal and reference values.'* **Eur Heart J.** *2010; 31:2338–2350.*

Modeling of the data could be greatly simplified because in the models there was no important residual influence of either smoking, dyslipidemia, or sex (a 0.1 m/s higher average in men) after correction for age, quadratic age, and mean blood pressure. This lack of a sex difference in cross-sectional data is in striking contrast to the longitudinal data (see below) (Fig. 26.3).[7,8]

There are some limitations to these reference data; a major limitation of this collaborative effort was the almost entirely Caucasian race of the subjects. Furthermore, data described above refer to carotid-femoral PWV, and might not be easily extrapolated to other PWV measures encompassing arterial path lengths substantially beyond the aorta (e.g., brachial-ankle PWV, cardiac-ankle vascular index, etc). Recent insights from magnetic resonance imaging (MRI) are highly informative in this regard, as MRI allows not only for precise calculation of arterial path lengths but also opens the possibility of measuring segmental PWV over various subsections of the aorta,

including sites less easily accessible by ultrasound. In a sample of healthy volunteers aged 20 to 80 years, thoracic aortic PWV (the more elastin-rich segment of the aorta from the heart to above the diaphragm) showed a far steeper age increase in PWV than the more muscular abdominal aorta (see Fig. 26.4).[9]

Cross-sectional wave reflection data
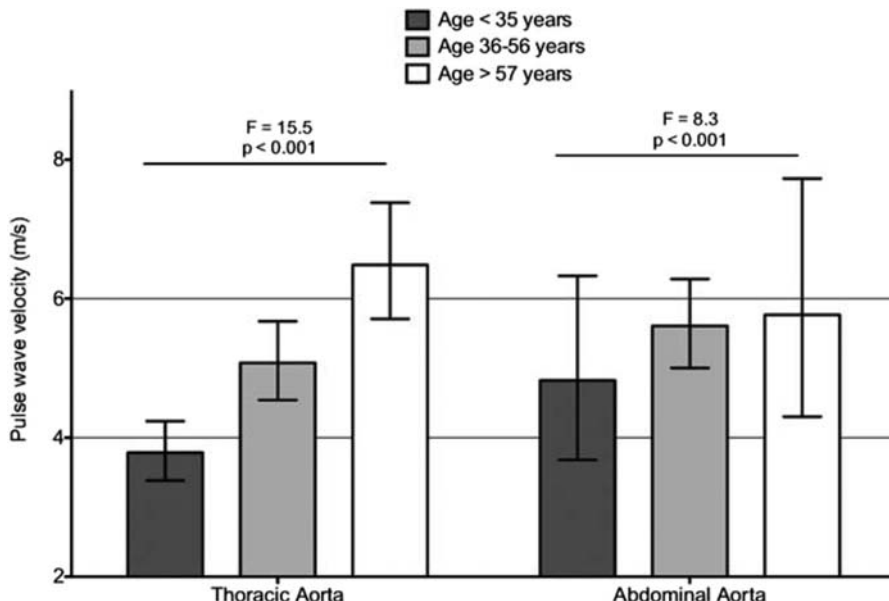
Mitchell et al. and Torjesen et al. have described cross-sectional sex-specific evolutions with aging of reflection-related parameters within the framework of the Framingham Heart Study.[10,11] In their 2004 data, with advancing age (>50) the forward wave amplitude increased in contrast to the reflected wave amplitude which remained rather stable. These cross-sectional observations may suggest (cave: see also longitudinal trajectory studies below) that the forward pressure wave drives the age-related increase in (central) SBP and PP. Moreover, with aging the role of

Table 5 Distribution of pulse wave velocity (PWV) values (m/s) in the reference value population (11 092 subjects) according to age and blood pressure category

Age category (years)	Blood pressure category				
	Optimal	Normal	High normal	Grade I HT	Grade II/III HT
PWV as mean (± 2 SD)					
<30	6.1 (4.6–7.5)	6.6 (4.9–8.2)	6.8 (5.1–8.5)	7.4 (4.6–10.1)	7.7 (4.4–11.0)
30–39	6.6 (4.4–8.9)	6.8 (4.2–9.4)	7.1 (4.5–9.7)	7.3 (4.0–10.7)	8.2 (3.3–13.0)
40–49	7.0 (4.5–9.6)	7.5 (5.1–10.0)	7.9 (5.2–10.7)	8.6 (5.1–12.0)	9.8 (3.8–15.7)
50–59	7.6 (4.8–10.5)	8.4 (5.1–11.7)	8.8 (4.8–12.8)	9.6 (4.9–14.3)	10.5 (4.1–16.8)
60–69	9.1 (5.2–12.9)	9.7 (5.7–13.6)	10.3 (5.5–15.1)	11.1 (6.1–16.2)	12.2 (5.7–18.6)
≥ 70	10.4 (5.2–15.6)	11.7 (6.0–17.5)	11.8 (5.7–17.9)	12.9 (6.9–18.9)	14.0 (7.4–20.6)
PWV as median (10–90 pc)					
<30	6.0 (5.2–7.0)	6.4 (5.7–7.5)	6.7 (5.8–7.9)	7.2 (5.7–9.3)	7.6 (5.9–9.9)
30–39	6.5 (5.4–7.9)	6.7 (5.3–8.2)	7.0 (5.5–8.8)	7.2 (5.5–9.3)	7.6 (5.8–11.2)
40–49	6.8 (5.8–8.5)	7.4 (6.2–9.0)	7.7 (6.5–9.5)	8.1 (6.8–10.8)	9.2 (7.1–13.2)
50–59	7.5 (6.2–9.2)	8.1 (6.7–10.4)	8.4 (7.0–11.3)	9.2 (7.2–12.5)	9.7 (7.4–14.9)
60–69	8.7 (7.0–11.4)	9.3 (7.6–12.2)	9.8 (7.9–13.2)	10.7 (8.4–14.1)	12.0 (8.5–16.5)
≥ 70	10.1 (7.6–13.8)	11.1 (8.6–15.5)	11.2 (8.6–15.8)	12.7 (9.3–16.7)	13.5 (10.3–18.2)

SD, standard deviation, 10 pc, the upper limit of the 10th percentile, 90 pc, the lower limit of the 90th percentile; HT, hypertension.

FIGURE 26.3 Distribution of pulse wave velocity (PWV) values according to age and blood pressure categories in a reference population of 11,092 subjects free from overt cardiovascular disease (CVD), nondiabetic, and untreated either for hypertension or dyslipidemia. *From The Reference Values for Arterial Stiffness' Collaboration. Determinants of pulse wave velocity in healthy people and in the presence of cardiovascular risk factors: 'establishing normal and reference values.'* **Eur Heart J.** *2010; 31:2338−2350.*

FIGURE 26.4 Pulse wave velocity shows a steeper increase with age in the thoracic compared to the abdominal aorta. *From Devos DGH, Rietzschel E, Heyse C, et al. MR pulse wave velocity increases with age faster in the thoracic aorta than in the abdominal aorta: MRPWV Shows Faster Aging Thoracic Aorta.* **J Magn Reson Imag.** *2015; 41:765−772.*

central arterial stiffness seems to be more prominent (no steep rise in carotid-brachial PWV with aging). Reasoning with the concept of a "theoretical single effective reflecting site," effective reflective distance increased with aging in both sexes but was minimally determined by height in women. This is however a controversial issue (see studies by Phan et al.[12,13]) which is further complicated by their sex-specific evolution of reflected wave transit time (RWTT) (increasing in women after age 50 and decreasing in men).

In the 2014 cross-sectional Framingham data, after age 50, the increase of the forward wave amplitude has been confirmed with relatively small variations in the timing of the inflection point and a sharp decline of the timing for the backward wave foot. As a consequence, after

midlife, the timing of the inflection point was later than that of the backward wave foot. Sex differences could be partially explained by the characteristics of the LV ejection phase and morphology of the backward wave (cave: see studies by Phan et al. for a different interpretation of the data, below).

In the framework of the ASKLEPIOS Study, Segers et al.[14] described the cross-sectional effects of sex and age on wave reflection parameters. Both the wave reflection coefficient derived from impedance analysis and the ratio of backward to forward pressure wave amplitude increased from age 35 to 55 with little or no sex differences. However, evolution of the reflection parameters over a 10-y trajectory (Round 2 ASKLEPIOS) revealed more accentuated sex differences with even opposing trends in the evolution of wave reflection! (see below).[15] Thus, the effective impact of aging on arterial system properties, in a middle-aged population, might not be well reflected by cross-sectional studies, which implies a compelling need for longitudinal studies and for reasoning in early and adult life trajectories (Fig. 26.5).
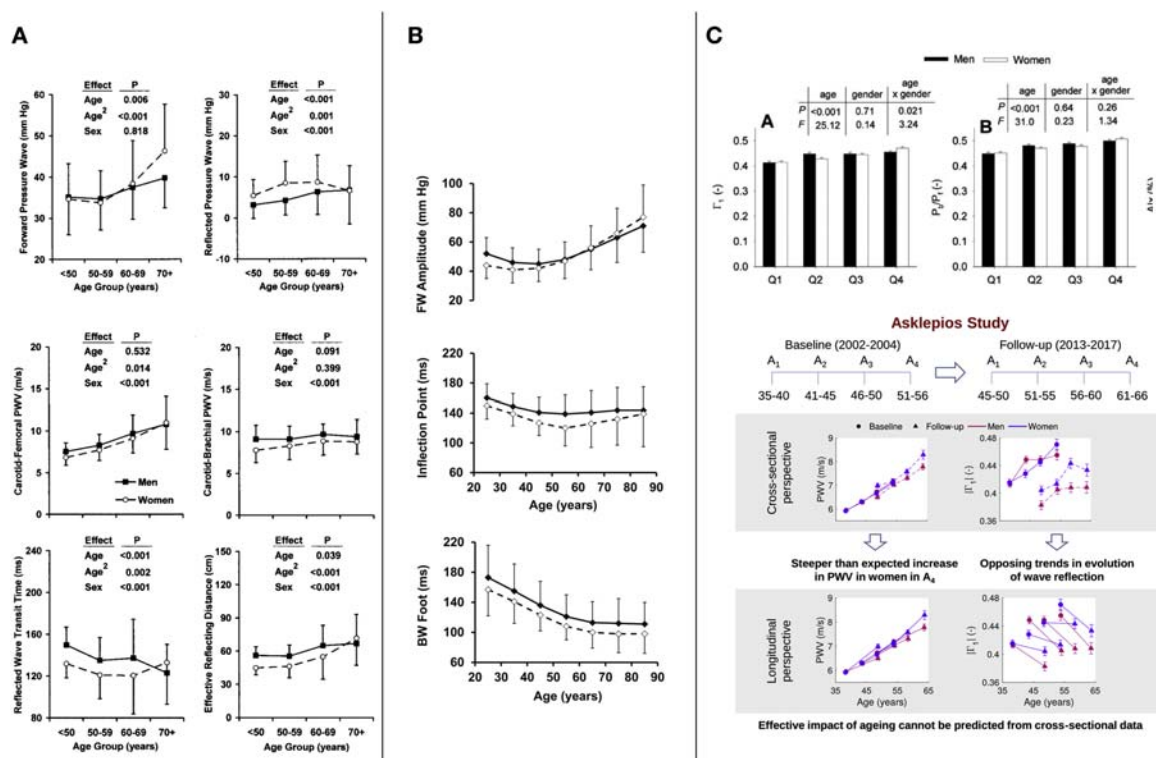
Insights from longitudinal cohort data: the early life trajectory

There is a substantial wealth of epidemiological data studying children which are subsequently reexamined in (young) adulthood suggesting that genetics, the fetal phase, and childhood risk factor burden jointly determine a blood pressure/arterial stiffening trajectory that persists later in life above and beyond the adult risk factor burden.

Beyond the impact of birth weight, gestational diabetes and hypertensive disorders of pregnancy have been implicated in programming higher offspring blood pressure trajectories.[16] The differences in blood pressure between offspring of hypertensive pregnancies and offspring of normotensive pregnancies persisted across childhood and through adolescence. Importantly, higher maternal blood pressure early in the pregnancy was found to have a larger impact than pregnancy related blood pressure changes.[17] Furthermore, higher offspring blood pressure in childhood was present in the absence of other vascular alterations or metabolic derangements, suggesting shared mother-offspring risk factors for higher blood pressure rather than the additional cardiometabolic abnormalities of hypertensive pregnancies being causal for the long-term consequences for the offspring.[18]

Tantalizing trajectory evidence also comes from genetic data looking at the fundamental question whether "blood pressure begets (increasing) blood pressure," i.e., whether higher blood pressure is associated with the higher *rate of change* of blood pressure over time. Ference at al. evaluated the effect of 12 polymorphisms associated with lower SBP on the age-related rate of rise in SBP in a series of

FIGURE 26.5   Panel A and B depict Framingham data adapted, respectively, from Mitchell et al.[10] and from Torjesen et al.[11] Panel C depicts Asklepios data from Segers et al. (upper part)[14] and Campos-Arias et al. (lower part)[15] *BW,* Backward wave; *FW,* Forward wave; P_b/P_f, the ratio of backward to forward pressure wave amplitude; Γ_1, wave reflection coefficient derived from impedance analysis.

meta-regression analyses involving 199,477 participants in 63 studies.[19] Evaluating the effect of higher or lower SBP mediated by polymorphisms provided a naturally randomized (Mendelian) and therefore unconfounded estimate of the causal effect of SBP on the usual age-related rise in SBP. The authors found that randomly receiving polymorphisms associated with lower SBP was also independently associated with a slower rise in SBP over time, suggesting that SBP is causally related to the rate of rise in SBP with age. Fig. 26.6 illustrates that the blood pressure lowering effect increases with age at which the cohort is investigated. These findings are quite distinct from the genetics of other cardiovascular risk factors such as, for example, low-density lipoprotein (LDL) cholesterol where genetics provide a "set point" which does not evolve over time. The findings by Ference at al. suggest that we are inherently genetically programmed to be on a blood pressure (and very likely arterial aging/stiffening) trajectory by default.

A number of pivotal studies, among which (but not limited to) the Bogalusa Heart Study, the Atherosclerosis Risk in Young Adults (ARYA) Study, Childhood Determinants of Adult Health, Muscatine Study, and the Cardiovascular Risk in Young Finns Study provided major insights between childhood exposure to risk factors an adult arterial status.
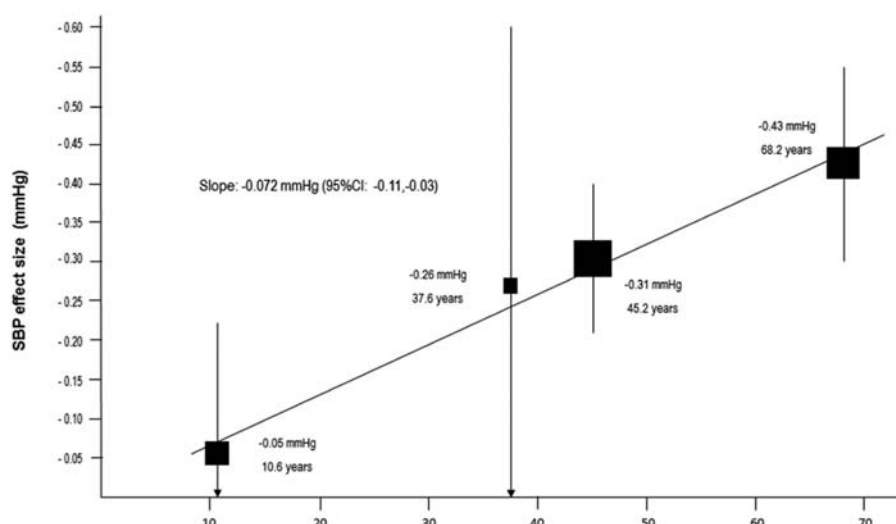
The Cardiovascular Risk in Young Finns Study investigated the cohort of 3696 children, initially investigated in 1980 when they were between the ages of 3 and 18 years. Follow-up studies were conducted in childhood in 1983 and 1986 and in adulthood in 2001 and 2007, respectively, 21 and 27 years after the initial examination. This pivotal cohort was phenotyped in depth and comprised a broad spectrum of markers of arterial aging comprising (but not limited to) intima-media thickness, cf-PWV, and carotid

distensibility, thereby often linking, confirming, and extending results from other cohorts.

Childhood risk factor burden, defined by exceeding the age- and sex-specific 80th percentiles of, respectively, LDL cholesterol, blood pressure, or BMI, or cigarette smoking, was associated with adult intima-media thickness 21 years later even after adjustment for adult risk factors.[22] Subsequently this finding was extended using a broader childhood risk factor construct, adding low HDL cholesterol, diabetes, low physical activity, and infrequent food consumption to the previous four risk factors. Juonala et al. demonstrated a persisting accelerated IMT progression in adulthood related to the childhood risk factor burden, independent of the adult risk factor burden.[23]

Interestingly, a more in-depth analysis of the impact of the age at which the childhood risk factors were measured on adult IMT was conducted by pooling data from the Cardiovascular Risk in Young Finns, Childhood Determinants of Adult Health, Bogalusa Heart Study, and Muscatine Study. In these pooled analyses on 4380 subjects, adjusted odds ratios for elevated intima-media thickness progressively increased with the childhood age at which the risk factor burden was measured, becoming significant from the age of 9 years onwards and failing to reach statistical significance for risk factor burden measured at ages six or below.[24]

Childhood risk factor burden (such as high LDL cholesterol, low HDL cholesterol, elevated blood pressure, skinfold thickness or BMI, high triglycerides, smoking, and glucose levels) and lifestyle factors such as lower childhood fruit and vegetable intake and lower levels of childhood physical activity have been linked to higher adult cf-PWV[25−27] and carotid stiffness measures.[28,29] However, these findings were not universally replicated, e.g., in the ARYA Study, no association between adolescent blood

FIGURE 26.6 Association between effect of exposure alleles and systolic blood pressure (SBP) measured at different ages. Boxes represent the combined weighted mean effect of 10 exposure alleles on SBP (mm Hg) measured at four different ages: 10.7 and 38.7 years in the Young Finns Cohort[20] and 45 and 68 years in the Malmö Preventive Project.[21] Vertical lines represent 95% confidence interval (CI). The line represents the absolute increase in the combined effect of these 10 polymorphisms on SBP per year of increasing age. *From Ference BA, Julius S, Mahajan N, Levy PD, Williams KA, Flack JM. Clinical effect of naturally random allocation to lower systolic blood pressure beginning before the development of hypertension.* **Hypertension**. *2014; 63:1182−1188.*

pressure and adult PWV was observed. This controversial result could be at least partly explained by differences in blood pressure measurement methods as they used only single measurement from school health records rather than measured blood pressure using the same protocol in the entire cohort.[30]

Beyond traditional cardiovascular risk factors, and lifestyle, socioeconomic status and adverse childhood experiences (ACEs), have also shown to have a long-term deleterious impact. In the Georgia Stress and Heart Study, ACEs such as emotional, physical or sexual abuse, physical or emotional neglect, household dysfunction (substance abuse, mental illness, domestic violence, presence of a criminal household member, and parental marital discord) before the age of 18 years were collected in a cohort where blood pressures were measured 13 times on average over a 23 year period.[31] Individual growth curve modeling within a multilevel framework was used to examine the relation between exposure to ACEs and BP development. The authors observed that participants who were exposed to multiple ACEs displayed a graded and greater increase in BP levels in young adulthood compared with their counterparts without ACEs. Interestingly, Kivimäki et al. suggested that early socioeconomic disadvantage influences later blood pressure in part through an effect on blood pressure in early life, which tracks into adulthood, but also in part through an effect on BMI.[32]

Finally, in the Cardiovascular Risk in Young Finns Study, better childhood socioeconomic status was linked to lower arterial stiffness (lower cf-PWV and higher carotid distensibility) in adulthood independent from childhood cardiometabolic risk factor burden[33]
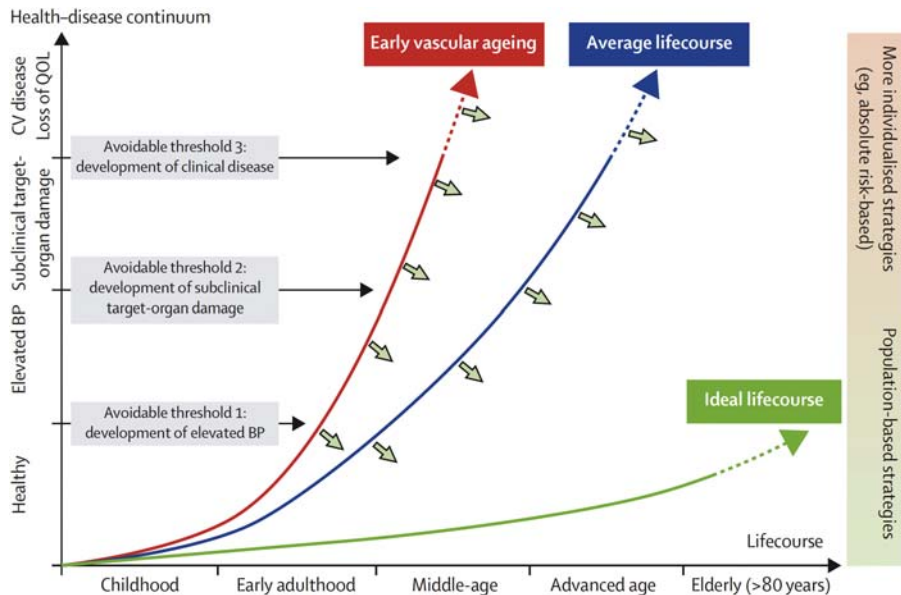
All in all, the long-term follow-up of these childhood cohorts produced a remarkably broad and consistent set of findings which show a persistent and *ongoing* effect of a broad spectrum of childhood risk factors in (early) adulthood above and beyond the risk factor burden in adulthood.

In summary, exposure to risk factors, major life stresses or an unhealthy lifestyle in childhood results in a clear, persistent, and likely progressive adverse effects on vascular health in adulthood. Similarly, a lifelong striving to achieve and maintain the lowest possible cardiovascular risk factor burden (ideal cardiovascular health) is likely to translate into a substantially "better" arterial aging trajectory.

These concepts form part of the underpinnings of the vision from the Lancet Commission on hypertension which envisages a life course strategy to address the global burden of raised blood pressure.[34] Focusing on the life course of an individual, the sum of preventive measures is to try to shift an individual toward an ideal life course, starting with population-based strategies (public health approaches) from birth (e.g., every child should ideally leave school as a health literate adult). Based on the life course of the individual crossing a number of avoidable thresholds such as the development of elevated blood pressure, development of subclinical target organ damage, or the development of clinical disease, these population-based strategies are then augmented by individualized strategies tailored to the individual's needs and risk (Fig. 26.7).

FIGURE 26.7 The life course approach in the Lancet Commission on Hypertension. *From Olsen MH, Angell SY, Asma S, et al. A call to action and a lifecourse strategy to address the global burden of raised blood pressure on current and future generations: the Lancet Commission on hypertension.* **Lancet**. *2016; 388:2665–2712.*

Insights from longitudinal cohort data: the adult life trajectory

Manifestations in middle-aged and aged individuals

One of the many merits of BLSA Study is that it drew the attention of the Hypertension Society that a prediction model of incident hypertension by a greater aging-induced cf-PWV and an increased SBP is a far too simple a model.[7] The BLSA authors' linear-mixed models and also those from the SardiNIA Study based on trajectories of repeated measurements of cf-PWV and SBP clearly revealed sex-specific diverging trajectories over time of rates of SBP (PP) versus rates of PWV.[8] In women the rate of change of SBP with age is merely constant, whereas the rate of change of PWV is steadily increasing. Men show a completely different course; an initially increasing rate of change of SBP which rapidly slows down during the fourth decade. The inversed U-shaped form for the rate of change of SBP is not mirrored by the trajectory for the rate of change of PWV. The latter showing little or no sex dependency.[35]

Whether or not the sex differences in rates of change of SBP have long-term consequences on the development of heart failure and hard CV events is a matter of debate. Nonetheless preliminary data from BLSA suggest that there is a progressive arterial–ventricular uncoupling (ratio of arterial elastance and end-systolic LV elastance) with aging that is more pronounced in women. More specifically, over time the rate of change (increase) of the arterial component was faster than the rate of increase of the ventricular component.[36] The trajectory of change of the arterial component was largely sex-independent whereas in women the trajectory of change of the ventricular component was at a slower pace. AlGhatrif et al. (BLSA data) further concluded that loss of arterial compliance (TAC) was the main determinant of subject-specific rate of change of AV uncoupling.[36] Moreover, progressive AV uncoupling occurred with aging and was more pronounced in women and was inversely associated with rates of changes of end-diastolic volume and stroke volume and directly associated with rate of change of end-systolic volume. As the ratio of the elastances can be approximated by ESV/SV, maintained coupling is mostly associated with a longitudinal increase of SV and a smaller increase of LV end-systolic volume. However, the smaller increase of end-diastolic volume over time is all but intuitive as one could expect commensurate increases with end-systolic volume to maintain a favorable position on the Frank–Starling curve (maintenance of cardiac output).[37] AlGhatrif et al. considered failure of end-diastolic volume to sufficiently increase a pivotal early consequence of AV uncoupling.[36] Thus, the uncoupling might be a sign of deviation from normal physiology preceding (diastolic) heart failure.

Ejection fraction

E_a/E_{es} can* also be written as (EDV-SV)/SV or (1/EF)-1, from which

$$EF = \frac{1}{1 + \dfrac{E_a}{E_{es}}}$$

Most energy-efficient coupling happens when $E_a/E_{es} = 0.5$ giving an $EF = 0.67$; with progressive uncoupling and increase of E_a/E_{es}, EF declines. Many clinicians usually misinterpret ejection fraction (EF) as a cardiac function parameter while it rather reflects coupling.

* with the assumption of the intercept of end-systolic pressure-volume relationship being zero.

Obviously, the ventricle can no longer match the increase in arterial elastance at a certain stage of aging.[38] Of interest, conflicting results have been published with even a longitudinal decline of the arterial component.[39] The physiology underlying arterial and ventricular aging might be counteracted by pharmacological interventions. As a consequence, analysis of cross-sectional data might not be the best way to get insights into the natural history of arterial stiffness, and longitudinal studies might come up with different results (See also below, insights from the second round in the ASKLEPIOS Study).[14,15,40] In BLSA, this is nicely illustrated by sex differences in baseline coupling (ratio usually lower in women) but a higher rate of increase in the ratio, mainly driven by smaller increase of ventricular component, among women.

Data from the first round[14] and recent novel insights from the second round[15] of the Belgian ASKLEPIOS Study may reconcile those apparently diverging sex-specific trajectories. Characteristic impedance (Zc) expressing "impedance to flow" and integrating the concepts of proximal aortic stiffness (PWV) and aortic diameter (dilatation) might be the key to the enigma. Given the comparable rates of change of PWV between the sexes and lower Zc in men versus women, sex-specific changes in aortic diameters with age are very likely involved (in concert with the water hammer principle; please refer to Chapters 1 and 3 for a discussion of this principle). The lower Zc in men has been confirmed in the first round of the ASKLEPIOS Study whereas BLSA has documented steeper increases of aortic diameters with age in men.

Effects of aging on wave reflections

In the Framingham Heart Study, increased forward wave (Pf) amplitude has been incriminated as a major determinant of increasing PP with aging whereas wave reflections were supposed to play a less prominent role. An expert group headed by Mitchell[10,41,42] have introduced mismatch

between peak aortic flow and proximal aortic root properties (geometry and function) as one of the possible explanations for those findings (impedance matching and mismatching).[43,44] Their concept started with observations in systolic hypertension: elevated PP independent of mean arterial pressure and attributable primarily to elevated Zc and reduced effective diameter of the proximal aorta. In the Framingham cohort, an age-related increase in aortic stiffness, as compared with peripheral arterial stiffness, was associated with increasing forward wave amplitude and PP and reversal of the arterial stiffness gradient. Subsequently higher forward pressure wave amplitude (a measure of proximal aortic geometry and stiffness) was associated with increased risk for incident CVD, whereas mean arterial pressure and relative wave reflection (correlates of resistance vessel structure and function) were not associated with increased risk for incident CVD. Also in the multiracial population-based Dallas Heart Study, evidence for a mismatch between proximal aortic stiffness and diameter in young and middle-aged adults with isolated systolic hypertension could be documented.[45]

An important limitation of using the "stiffness gradient" as to support the concept of impedance matching with aging is that vessel impedance is dependent more prominently on vessel size rather than vessel stiffness (as discussed in Chapters 1, 3 and 11). Moreover, the impedance matching at bifurcations is highly influenced by the area of the parent vessel versus the summed area of the daughter branches, which tends to minimize wave reflections in first order (aortic) bifurcations even before age-related aortic stiffening ensues.[46,47]

However, in 2016 Phan et al. revisited some of the prevailing hypotheses.[12,13]

First, they started from earlier literature data of earlier return of reflected waves contributing to elevated PPs.[14] They emphasized the uttermost importance of the so-called rectified wave reflections defined as backward waves that re-reflect at cardiac structures and thereafter will propagate as forward waves. They demonstrated that with increasing arterial stiffness (in essence a higher PWV) rectified reflections should play a more dominant role. Thus, in the natural history of aging, rectified waves may contribute beyond and above the concept of classically defined forward waves. However, one should bear in mind that in reality forward waves should comprise part of the rectified propagating waves. In their experiments at low amounts of reflections in humans, indeed Pf nearly approximates the product of aortic flow and Zc. At more realistic and higher amounts of reflections, the divergence between Pf and this

product becomes larger and larger. Moreover, the backward traveling waves also harbor both impedance matches and mismatches. Phan et al. concluded that elevated (and even earlier, see below) wave reflections contribute to increase of PP with aging without the compelling need to introduce the concept of altered proximal aortic properties. In addition, with increasing stiffness (PWV) even repeated re-reflection will occur resulting in a wider and more peaked forward wave. Thus, one should not overestimate the role of proximal aortic morphology and function in the natural history of aging of the arterial tree and more particularly one should not underestimate the role of rectified waves.

The major limitation for the validation of the work of Phan et al. is the absence of sex-specific results and experiments. Do the observed sex-specific interactions between changes of PWV and SBP (PP) with aging in the linear-mixed modeling of the SardiNIA and BLSA trajectories invalidate the experiments by Phan et al.?[12,13] (Data from the second round of the ASKLEPIOS Study might be key to reconcile available data, as discussed below).

Second, the same authors (Phan et al.[12,13]) further extended their insights into the physiology behind reflected waves in the natural history of aging. They demonstrated that the aging process is characterized by an earlier arrival of reflected waves without a distal shift in reflection sites. It is at odds with a common belief[48] and some observations in the Framingham Study of a shift of the reflection sites to more distal locations at advanced age. Those researchers further assumed an impedance matching of central and muscular peripheral arteries allowing swift albeit deleterious energy transfers to the smaller arteries and the microcirculation. The distal shift hypothesis has arisen from an unproven assumption (suspicion) that the RWTT should remain closely associated with the timing of the inflection point (Tinf) during the natural history of aging. However, there is little evidence from the point-of-view of physiology that the assumption would hold true.[49,50]

Phan et al. studying unselected adults and some elderly CVD patients reported on a remarkable expanding dissociation with both age and stiffening of arteries (increasing PWV) between Tinf (nearly constant over time) and RWTT (dramatic decrease).[12,13] Further application of basic rules of physiology infers that effective reflection distance (ERD = 0.5 × RWTT × PWV) should not increase. On the contrary there was a tendency that in both healthy and unhealthy individuals, the apparent ERD was moving into the direction of the heart with aging! It should be noted, however, that the ERD is a purely theoretical construct (a single reflection site), and not anatomically valid, given the

prominent phase shifts at reflection sites, as reviewed in Chapters 1, 3 and 11.

What are the consequences?
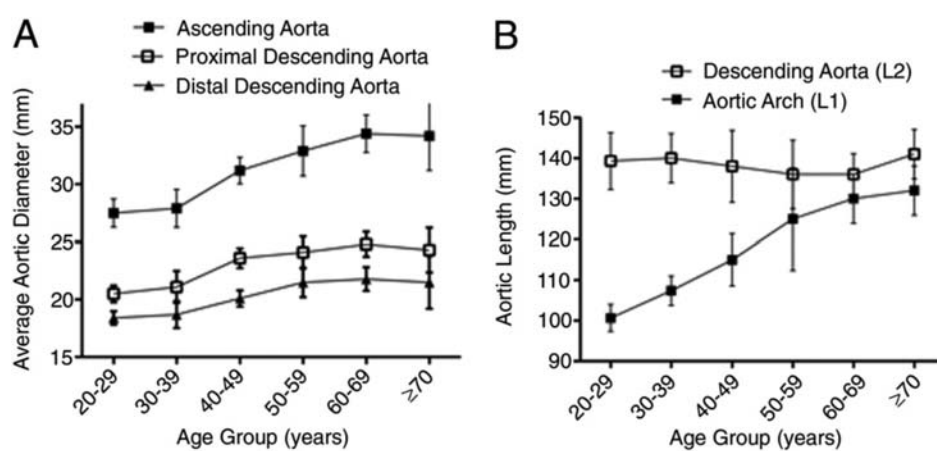
-   Wave reflections will increase the pulsatile load with aging, which might translate into diastolic dysfunction, left ventricular hypertrophy/remodeling, and new-onset (diastolic) heart failure. Thus, earlier arrival of wave reflections at the proximal aorta might be deleterious for the heart and the brain.
-   From an epidemiological point-of-view, the earlier return of reflected waves is in line with earlier described characteristics of input impedance with increasing age: (i) shift of the modulus minimum, (ii) shift of the phase zero-crossings to increasing frequency, and (iii) impedance modulus setting around Zc with increasing frequency.

Is there agreement or disagreement between the ASKLEPIOS Study data and trajectories of PWV and SBP (PP) in BLSA and SardiNIA? In the second round of the ASKLEPIOS Study, overall, the effective 10-year increase in cf-PWV was less than expected from first round cross-sectional data, and cf-PWV was found to accelerate more in women than in men.[15] Interestingly, the increase in PWV was not paralleled by a decrease in arterial volume compliance, particularly in younger males. Aortic root characteristic impedance decreased with age in younger subjects while it increased for the older subjects in the study. These changes suggest that aortic dilation and elongation may play an important role determining the longitudinal age-related changes in impedance parameters in middle-age. Wave reflection decreased with aging, whereas resistance increased in women and decreased in men (Fig. 26.8).

Conclusions

One of largest paradigm shifts over the last decades in epidemiology and preventive medicine is that unsuccessful aging does not start in middle-aged individuals with an already accumulated risk factor burden heralding "the eve of destruction": prevalent target organ damage and incident hard cardiovascular events. Unsuccessful aging starts earlier, much earlier. Accumulation of risk starts intra-uterine and progressively continues during childhood and adulthood. Therefore, the Lancet Commission on hypertension has launched the idea of a lifelong striving to achieve and maintain the lowest possible cardiovascular risk burden. A considerable part of the evidence comes from early life trajectories obtained in childhood cohorts (e.g., Young Finns, Bogalusa Heart Study, Muscatine, and CDAH) all pointing into the same direction that childhood risk factors add up over and above the risk factor burden accumulated in adulthood.

Separate population-based studies (e.g., NHANES III) and adult life trajectories (e.g., BLSA, SardiNIA) over decades allowed for mixed linear modeling and identified some sex-specific longitudinal changes of SBP and PWV (two parameters of particular interest for the description of normal aging and with well-documented reference values). In this chapter, from physiology point-of-view, we discussed the contributions of ventriculo-arterial coupling, characteristic impedance and wave reflection parameters (forward, backward, and rectified waves) in some large population-based cohorts (e.g., Framingham, Dallas Heart, Asklepios). Moreover, we tried to understand and rectify two misunderstandings in the field of aortic stiffness: (i) the overestimated role of the geometry and function of

FIGURE 26.8 Panel A depicts average aortic diameters (ascending, proximal descending, distal descending) for age groups by decade. Panel B depicts estimated aortic lengths for age groups by decade. *L1*, length of the aortic arch; *L2*, length of the descending aorta. *From Redheuil A, Yu W-C, Mousseaux E, et al. Age-Related Changes in Aortic Arch Geometry. **J Am College Cardiol.** 2011; 58:1262–1270.*

the proximal aorta in the process of normal aging and (ii) the unrealistic shift away from the heart of reflection sites during normal aging. Finally, we tried to reconcile the apparently conflicting data from observational studies by more unifying suggestions derived from recently published novel insights from round two of the Asklepios Study.

References

1. Duca L, Blaise S, Romier B, et al. Matrix ageing and vascular impacts: focus on elastin fragmentation. **Cardiovasc Res**. 2016; 110:298−308.
2. Franklin SS, Gustin W, Wong ND, et al. Hemodynamic patterns of age-related changes in blood pressure: the Framingham heart study. **Circulation**. 1997; 96:308−315.
3. Burt VL, Whelton P, Roccella EJ, et al. Prevalence of hypertension in the US adult population: results from the Third National Health and Nutrition Examination Survey, 1988-1991. **Hypertension**. 1995; 25:305−313.
4. The Reference Values for Arterial Stiffness' Collaboration. Determinants of pulse wave velocity in healthy people and in the presence of cardiovascular risk factors: 'establishing normal and reference values'. **Eur Heart J**. 2010; 31:2338−2350.
5. Bramwell JC, Hill AV. Velocity of transmission of the pulse wave. **Lancet**. 1922; 199:891−892.
6. McEniery CM, Yasmin, Hall IR, Qasem A, Wilkinson IB, Cockcroft JR. Normal vascular aging: differential effects on wave reflection and aortic pulse wave velocity. **J Am Coll Cardiol**. 2005; 46:1753−1760.
7. AlGhatrif M, Strait JB, Morrell CH, et al. Longitudinal trajectories of arterial stiffness and the role of blood pressure: the Baltimore longitudinal study of aging. **Hypertension**. 2013; 62:934−941.
8. Scuteri A, Morrell CH, Orrù M, et al. Longitudinal perspective on the conundrum of central arterial stiffness, blood pressure, and aging. **Hypertension**. 2014; 64:1219−1227.
9. Devos DGH, Rietzschel E, Heyse C, et al. MR pulse wave velocity increases with age faster in the thoracic aorta than in the abdominal aorta: MRPWV Shows Faster Aging Thoracic Aorta. **J Magn Reson Imag**. 2015; 41:765−772.
10. Mitchell GF, Parise H, Benjamin EJ, et al. Changes in arterial stiffness and wave reflection with advancing age in healthy men and women: the Framingham heart study. **Hypertension**. 2004; 43:1239−1245.
11. Torjesen AA, Wang N, Larson MG, et al. Forward and backward wave morphology and central pressure augmentation in men and women in the Framingham heart study. **Hypertension**. 2014; 64:259−265.
12. Phan TS, Li JK-J, Segers P, et al. **Aging Is Associated with an Earlier Arrival of Reflected Waves without a Distal Shift in Reflection Sites**. JAHA [Internet]; 2016 [cited 2021 Mar 24];5. Available from: https://www.ahajournals.org/doi/10.1161/JAHA.116.003733.
13. Phan TS, Li JK, Segers P, Chirinos JA. **Misinterpretation of the Determinants of Elevated Forward Wave Amplitude Inflates the Role of the Proximal Aorta**. JAHA [Internet]; 2016 [cited 2021 Mar 24];5. Available from: https://www.ahajournals.org/doi/10.1161/JAHA.115.003069.
14. Segers P, Rietzschel ER, De Buyzere ML, et al. Noninvasive (input) impedance, pulse wave velocity, and wave reflection in healthy middle-aged men and women. **Hypertension**. 2007; 49:1248−1255.
15. Campos-Arias D, De Buyzere ML, Chirinos JA, Rietzschel ER, Segers P. Longitudinal changes of input impedance, pulse wave velocity, and wave reflection in a middle-aged population: the Asklepios study. **Hypertension**. 2021; 77:1154−1165.
16. Aris IM, Rifas-Shiman SL, Li L-J, Belfort MB, Hivert M-F, Oken E. Early-life predictors of systolic blood pressure trajectories from infancy to adolescence: findings from project viva. **Am J Epidemiol**. 2019; 188:1913−1922.
17. Staley JR, Bradley J, Silverwood RJ, et al. Associations of blood pressure in pregnancy with offspring blood pressure trajectories during childhood and adolescence: findings from a prospective study [Internet] **J Am Heart Assoc**; 2015 [cited 2019 Jan 16];4. Available from: https://www.ahajournals.org/doi/10.1161/JAHA.114.001422.
18. Lawlor DA, Macdonald-Wallis C, Fraser A, et al. Cardiovascular biomarkers and vascular function during childhood in the offspring of mothers with hypertensive disorders of pregnancy: findings from the Avon Longitudinal Study of Parents and Children. **Eur Heart J**. 2012; 33:335−345.
19. Ference BA, Julius S, Mahajan N, Levy PD, Williams KA, Flack JM. Clinical effect of naturally random allocation to lower systolic blood pressure beginning before the development of hypertension. **Hypertension**. 2014; 63:1182−1188.
20. Oikonen M, Tikkanen E, Juhola J, et al. Genetic variants and blood pressure in a population-based cohort: the cardiovascular risk in young Finns study. **Hypertension**. 2011; 58:1079−1085.
21. Fava C, Sjögren M, Montagnana M, et al. Prediction of blood pressure changes over time and incidence of hypertension by a genetic risk score in Swedes. **Hypertension**. 2013; 61:319−326.
22. Raitakari OT, Juonala M, Kähönen M, et al. Cardiovascular risk factors in childhood and carotid artery intima-media thickness in adulthood: the Cardiovascular Risk in Young Finns Study. **J Am Med Assoc**. 2003; 290:2277−2283.
23. Juonala M, Viikari JSA, Kahonen M, et al. Life-time risk factors and progression of carotid atherosclerosis in young adults: the Cardiovascular Risk in Young Finns study. **Eur Heart J**. 2010; 31:1745−1751.
24. Juonala M, Magnussen CG, Venn A, et al. Influence of age on associations between childhood risk factors and carotid intima-media thickness in adulthood: the Cardiovascular Risk in Young Finns Study, the Childhood Determinants of Adult Health Study, the Bogalusa Heart Study, and the Muscatine Study for the International Childhood Cardiovascular Cohort (i3C) Consortium. **Circulation**. 2010; 122:2514−2520.
25. Aatola H, Hutri-Kähönen N, Juonala M, et al. Lifetime risk factors and arterial pulse wave velocity in adulthood: the cardiovascular risk in young Finns study. **Hypertension**. 2010; 55:806−811.
26. Aatola H, Koivistoinen T, Hutri-Kähönen N, et al. Lifetime fruit and vegetable consumption and arterial pulse wave velocity in adulthood: the cardiovascular risk in young Finns study. **Circulation**. 2010; 122:2521−2528.
27. Li S, Chen W, Srinivasan SR, Berenson GS. Childhood blood pressure as a predictor of arterial stiffness in young adults: the Bogalusa heart study. **Hypertension**. 2004; 43:541−546.
28. Pälve KS, Pahkala K, Magnussen CG, et al. Association of physical activity in childhood and early adulthood with carotid artery elasticity 21 Years later: the cardiovascular risk in young Finns study [Internet] **JAHA**; 2014 [cited 2021 Mar 15];3. Available from: https://www.ahajournals.org/doi/10.1161/JAHA.113.000594.

29. Juonala M, Järvisalo MJ, Mäki-Torkko N, Kähönen M, Viikari JSA, Raitakari OT. Risk factors identified in childhood and decreased carotid artery elasticity in adulthood: the cardiovascular risk in young Finns study. **Circulation**. 2005; 112:1486−1493.

30. Oren A, Vos LE, Uiterwaal CS, Gorissen WH, Grobbee DE, Bots ML. Adolescent blood pressure does not predict aortic stiffness in healthy young adults. The Atherosclerosis Risk in Young Adults (ARYA) study. **J Hypertens**. 2003; 21:321−326.

31. Su S, Wang X, Pollock JS, et al. Adverse childhood experiences and blood pressure trajectories from childhood to young adulthood: the Georgia stress and heart study. **Circulation**. 2015; 131:1674−1681.

32. Kivimäki M, Lawlor DA, Smith GD, et al. Early socioeconomic position and blood pressure in childhood and adulthood: the cardiovascular risk in young Finns study. **Hypertension**. 2006; 47:39−44.

33. Puolakka E, Pahkala K, Laitinen TT, et al. Childhood socioeconomic status and arterial stiffness in adulthood: the cardiovascular risk in young Finns study. **Hypertension**. 2017; 70:729−735.

34. Olsen MH, Angell SY, Asma S, et al. A call to action and a lifecourse strategy to address the global burden of raised blood pressure on current and future generations: the Lancet Commission on hypertension. **Lancet**. 2016; 388:2665−2712.

35. AlGhatrif M, Wang M, Fedorova OV, Bagrov AY, Lakatta EG. The pressure of aging. **Med Clin**. 2017; 101:81−101.

36. AlGhatrif M, Morrell CH, Becker LC, et al. Longitudinal uncoupling of the heart and arteries with aging in a community-dwelling population [Internet] **GeroScience**; 2021 [cited 2021 Mar 24];Available from: http://link.springer.com/10.1007/s11357-020-00321-x.

37. Renlund DG, Gerstenblith G, Fleg JL, Becker LC, Lakatta EG. Interaction between left ventricular end-diastolic and end-systolic volumes in normal humans. **Am J Physiol Heart Circ Physiol**. 1990; 258:H473−H481.

38. Redfield MM, Jacobsen SJ, Borlaug BA, Rodeheffer RJ, Kass DA. Age- and gender-related ventricular-vascular stiffening: a community-based study. **Circulation**. 2005; 112:2254−2262.

39. Borlaug BA, Redfield MM, Melenovsky V, et al. Longitudinal changes in left ventricular stiffness: a community-based study. **Circ Heart Fail**. 2013; 6:944−952.

40. Rietzschel E-R, De Buyzere ML, Bekaert S, et al. On behalf of the Asklepios investigators. Rationale, design, methods and baseline characteristics of the Asklepios Study. **Eur J Cardiovasc Prev Rehabil**. 2007; 14:179−191.

41. Mitchell GF, Wang N, Palmisano JN, et al. Hemodynamic correlates of blood pressure across the adult age spectrum: noninvasive evaluation in the Framingham heart study. **Circulation**. 2010; 122:1379−1386.

42. Mitchell GF, Conlin PR, Dunlap ME, et al. Aortic diameter, wall stiffness, and wave reflection in systolic hypertension. **Hypertension**. 2008; 51:105−111.

43. Redheuil A, Yu W-C, Mousseaux E, et al. Age-related changes in aortic arch geometry. **J Am Coll Cardiol**. 2011; 58:1262−1270.

44. Craiem D, Chironi G, Redheuil A, et al. Aging impact on thoracic aorta 3D morphometry in intermediate-risk subjects: looking beyond coronary arteries with non-contrast cardiac CT. **Ann Biomed Eng**. 2012; 40:1028−1038.

45. Yano M, Kohno M, Kobayashi S, et al. Influence of timing and magnitude of arterial wave reflection on left ventricular relaxation. **Am J Physiol Heart Circ Physiol**. 2001; 280:H1846−H1852.

46. Li JK-J. Pulse wave reflections at the aorto-iliac junction. **Angiology**. 1985; 36:516−521.

47. Greenwald SE, Carter AC, Berry CL. Effect of age on the in vitro reflection coefficient of the aortoiliac bifurcation in humans. **Circulation**. 1990; 82:114−123.

48. Sugawara J, Hayashi K, Tanaka H. Distal shift of arterial pressure wave reflection sites with aging. **Hypertension**. 2010; 56:920−925.

49. Segers P, Rietzschel ER, De Buyzere ML, et al. Assessment of pressure wave reflection: getting the timing right!. **Physiol Meas**. 2007; 28:1045−1056.

50. Westerhof BE, Westerhof N. Magnitude and return time of the reflected wave: the effects of large artery stiffness and aortic geometry. **J Hypertens**. 2012; 30:932−939.

This page intentionally left blank

Chapter 27

Early vascular aging and supernormal vascular aging: genetics, epigenetics, and the environment

Peter M. Nilsson[1] and Stéphane Laurent[2,3,4,5]

[1]Lund University, Department of Clinical Sciences, Skane University Hospital, Malmö, Sweden; [2]INSERM, U970, Paris Cardiovascular Research Center, PARCC, Paris, France; [3]Université de Paris, Paris, France; [4]Assistance Publique, Hopitaux de Paris, Paris, France; [5]Department of Pharmacology and Hôpital Européen Georges Pompidou, Paris, France

The background and characteristics of early vascular aging

The vascular tree, its morphology and function, is shaped by evolution and subject to different positive or negative influences during the life course of an individual reaching senescence.[1] Factors acting early in life, even before birth, are of importance for the development and structure of the vascular system, most notably for the wall of the large elastic arteries,[2] but also for smaller arteries and the capillary density, both influencing central hemodynamics.[3] This programming effect, that involves postnatal growth patterns,[4] may also be relevant for metabolic function and the risk of insulin resistance and later on type 2 diabetes, factors that are often linked to vascular changes and increased cardiovascular disease (CVD) risk. As this risk in general is clearly age-related, it is of interest to understand if these factors acting early in life could also be instrumental, or mirror, processes that regulate the aging of organs and the body as a whole. One argument to support this is that the increasing longevity of people in western populations are influenced not only by habits, economy, and social factors but also to a large extent by improved conditions for pregnant women, better birth outcomes, and lower perinatal mortality during the 20th century. In fact, fatal cardiovascular events are now becoming less prevalent. The burden on nonfatal events has increased and thus the prevalence rate of CVD as more patients survive into old age. Still, however, some individuals suffer from early onset cardiovascular events and early biological versus chronological aging,[5] a process that is relevant to the early vascular aging (EVA) concept.[6] Of special relevance is the postnatal catch up growth[4] when small babies grow to become overweight or obese adults when the risk of vascular aging (VA) is increased.[7]
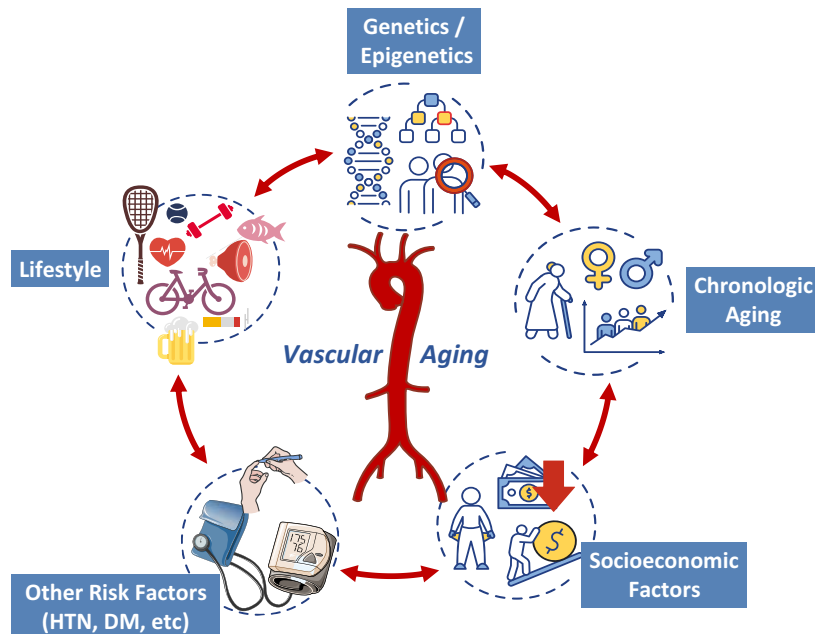
Atherosclerosis versus arteriosclerosis

Genetic factors affect the development of the arterial system and the regulation of blood pressure that is a driving force behind hypertension, and this may in turn interact with vascular remodeling, i.e., functional and structural changes of the large and small arteries. Later on *atherosclerosis* may develop, starting in the arterial intima and leading to plaque formation and risk of thromboembolism and cardiovascular events, a well-described pathophysiological process.[10] This process is enhanced by lipid accumulation, hyperglycemia, oxidative stress, and chronic inflammation besides the influence of hypertension. Another process is the age-dependent stiffening of large elastic arteries caused by changes starting in the arterial media but later on involving also other layers of the arterial wall (endothelium, adventitia), a process named arterial stiffening or *arteriosclerosis*.[11,12] For some individuals the combination of genetic susceptibility, early life programming, unhealthy lifestyle, adverse social conditions, and the burden of cardiovascular risk factors (Fig. 27.1) will lead to earlier than expected, i.e. early vascular aging (EVA), for which arteriosclerosis is the hallmark. This is an effect that is measurable through the stiffness of large elastic arteries, for example, via the measurement of carotid-femoral pulse wave velocity (c-f PWV), the gold standard for large artery wall stiffness.[13,14]

The EVA concept was first developed in 2008,[15,16] but several earlier researchers have discussed arterial aging in general with a focus on endothelial dysfunction and

morphological changes.[17,18] However, following the introduction of new technical devices for a more accurate measurement of PWV, be it c-f PWV or brachial-ankle (b-a) PWV, or in other ways, the interest in arterial stiffness (arteriosclerosis) has rapidly increased. This interest has been sparked by two consensus documents published in 2006[13] and 2012,[14] as well as several longitudinal studies in populations[19−24] that have repeatedly documented that increased PWV, the hallmark of EVA, is independently predictive of cardiovascular events (nonfatal and fatal) as well as total mortality. Two meta-analyses,[25,26] including one on individual data,[26] clearly demonstrated the predictive value of c-f PWV for cardiovascular (CV) events. In parallel, several observational studies linked arterial stiffness with CV risk factors.[27−29] These data were summarized in another consensus document published by the European Society of Cardiology and the ARTERY society in 2015, endorsing the concept of EVA and guiding on how to measure arterial stiffness, an integrated biomarker of cardiovascular risk.[30] The Lancet Commission on Hypertension also supported the EVA concept in 2016 and applied it in a life course perspective for prevention and treatment of vascular changes associated with hypertension.[31] It was suggested that early intervention for prevention had greater opportunities to reverse EVA as compared to prevention starting in mid or later life.

Further studies have looked into other characteristics of EVA, such as hyperglycemia, insulin resistance, chronic inflammation, impaired renal function, or other features.[32−34] Still it has been difficult to fully define the process of EVA and its contributing factors, as discussed in several previous publications.[35,36]

Structural components of arterial wall aging

Aortic stiffening accompanying age and cardiovascular risk factors is caused by common mechanisms including reduced elastin/collagen ratio, production of elastin cross-linking, reactive oxygen species (ROS)-induced inflammation, calcification, vascular smooth muscle cell stiffness, and endothelial dysfunction.[11,12]

It is important to highlight the link between energy balance, metabolic function, and regulatory systems of longevity. A lower calorie intake, for example, has been linked to increased survival in mammals such as rodents and monkeys. Mitochondria and transmembrane nicotinamide adenine dinucleotide phosphate (NADPH) oxidases (NOXs) are involved in the energy metabolism of the cell and represent the two main sources of ROS that may enhance the aging process, also linked to chronic inflammation. Increased NOX4 expression/activity in vascular smooth muscle cells (VSMC) mitochondria results in increased mitochondrial oxidative stress inducing an accelerated VA characterized by increased aortic pulse wave velocity (PWV) and VSMC stiffening.[37] Several novel data suggest a role for the mitochondria in the process of VA and therefore a potential future drug target.[38]

Cross-talk between the micro- and macrocirculation

Small and large artery alterations are closely interdependent in response to aging and CV risk factors, particularly hypertension and type 2 diabetes. Thus, any pathophysiological approach of aortic stiffening should be paralleled by considering the remodeling of small resistance arteries. We previously suggested the existence of a cross-talk (as opposed to a linear sequence) whereby changes in small arteries affect the phenotype of larger arteries, and changes in large arteries affect the phenotype of small arteries.[8] Indeed, it is difficult to establish a temporal relationship between small and large artery changes. The cross-talk between the micro- and the macrocirculation[8] promotes a vicious circle, which can begin either from large vessels or at the site of small arteries. This is well illustrated by the effects of VA in hypertensive patients. Increased resistance in small arteries increases mean BP, and then increases arterial stiffness in the large elastic arteries, which concomitantly with more pressure wave reflections increases central SBP and 24-hour ambulatory brachial BP variability, ultimately leading to target organ damage.[8,9] The increased central BP pulsatility is in turn a factor of small resistance artery damage, i.e., increased media-to-lumen ratio of small resistance arteries and concomitant reduction in lumen diameter, leading to a rise in mean BP, and thus prolonging the vicious circle.

Vascular aging and target organ damage

The small/large artery cross-talk has a synergistic effect on the heart, brain, and kidney, in large part through a high pulsatile energy that is delivered as central systolic or pulse pressure. This aspect, which is well illustrated by hypertension, is detailed in other chapters of this book. Briefly, there is a large amount of evidence that central systolic and pulse pressures are the most deleterious elements of the BP load on the heart, brain, and kidney in hypertensives. Their increase is better correlated with hypertension-mediated organ damage than either brachial systolic and pulse pressures or mean BP.[9,39,40]

Particularly, an interesting line of research has linked arterial stiffness and VA to brain aging and the risk of cognitive decline and dementia, at least for vascular dementia.[41] Several studies have shown that hypertension in poor control is a risk factor not only for stroke but also for white matter intensities and microbleeds,[42] factors that may further impair cognition. It may well be that a neurocognitive reserve protects the brain from the effects of VA (arterial stiffness) until it reaches high levels of c-f PWV when cognitive impairment may become more visible.[43]

Poor sleep, for example, linked to obstructive sleep apnea, is another aspect of brain function that may impact on VA in a bidirectional way.[44]

Genetics and epigenetics

There are some rare genetic syndromes associated with premature aging including vascular changes such as Hutchinson−Gilford Progeria in children[45] and Werner's syndrome in middle-aged subjects,[46] caused by dominant genetic mutations. Another genetic syndrome affecting large arteries is the vascular Ehlers−Danlos syndrome[47] presenting with very lax joints, arterial changes, and increased risk of stroke.

From a genetic perspective, a few studies have specifically focused on genetic markers of arterial stiffness as such.[48−55] For example, Fibrillin-1 genetic deficiency leads to pathological aging of arteries in mice[49] and the Wnt pathway gene expression is associated with arterial stiffness.[53] In one study from Sweden, it was reported that a genetic risk score for hyperglycemia as a trait in a nondiabetic elderly population was independently associated with increased c-f PWV, and thus of VA.[56] This proves a causal link that opens up for interventions on hyperglycemia to counteract VA. Other studies have investigated the role of epigenetics.[57]

Recently a new focus has been to describe the profile of metabolomics associated with VA as one way to deepen our understanding of the metabolic fingerprint that is supposed to influence EVA and its consequences.[58,59] This is part of an approach to develop "personalized medicine" with tailored therapy id data from genomics and other omics can be used to map a certain pathophysiological process and pave the way to find new treatment opportunities.

Finally, a well-known marker associated with biological aging, i.e., telomere length, has also been investigated in relation to VA.[60,61] Telomere length is regulated by genetic factors but also influenced according to telomere attrition rate by factors in early life as well as adverse lifestyle and cardiovascular risk factors in adult life. However, telomere length has not developed into a useful tool for clinical practice to estimate biological aging and more research is needed.

Low socioeconomic status and vascular aging

People live different lives and this translates into resilience to or susceptibility for health problems as influenced by unhealthy lifestyle and adverse background factors such as poor income, low educational level, unemployment, poor housing or lack of social support and networks. This has

been shown to influence the development of VA as mirrored by time-trends in c-f PWV, shown in the Whitehall II study of civil servants in London[62] as well as in a cohort of young Finnish men[63] and with carotid stiffness in the PPS3 study.[64] One consequence of these adverse factors could be the development of depression, a mental state that is also associated with increased arterial stiffness and thus VA.[65,66]

Intervention studies on vascular aging and early vascular aging

Several studies have tried to use improvement of lifestyle as a way to favorably influence VA [by aggressive decrease of arteriosclerosis modifiers (ADAM)], as discussed in a review on EVA and ADAM,[67] and even more are underway, even in the young.[68] One problem is to disentangle the more general effects on cardiovascular risk factor levels from that more specific effect on arterial stiffness that was aimed for. A Mediterranean diet is believed to be protective of the cardiovascular system in general and also used for treatment of hyperglycemia.[69] This could be one feasible way to counteract VA as the ultimate consequence of that is prevention of cardiovascular events, as shown in the randomized, controlled PREDIMED trial based on Mediterranean diet for primary prevention of CVD in more than 9000 Spanish subjects.[70]

The control of hypertension and other cardiovascular risk factors is a cornerstone in cardiovascular prevention and documented in several national and international guidelines from the United States[71] and from Europe.[72] It has been shown that some classes of antihypertensive drugs, i.e., renin-angiotensin-aldosterone system blockers exert beneficial effects on reduction of markers of arterial stiffness beyond the impact of blood pressure lowering per se.[73] Even some of the newer antidiabetes drugs for treatment of type 2 diabetes, so called sodium-glucose cotransporter 2 inhibitors, have been shown to improve markers of arterial stiffness such as augmentation index or c-f PWV.[74] It remains, however, an open question whether this is a specific effect or if it depends on the concomitant lowering of body weight, blood pressure, and HbA$_{1c}$, or the diuretic effect with volume depletion induced by these drugs.[75]

A new treatment option on the horizon is to positively influence the receptor of adiponectin, a biomarker associated with better insulin sensitivity and lower cardiovascular risk, developed by Japanese colleagues.[76]

In the randomized intervention study on c-f PWV (SPARTE study) that has been conducted in France, the goal was to compare a guidelines-based strategy to control cardiovascular risk in hypertensive patients versus a strategy based on repeated measurement of c-f PWV followed by adjustment of drug therapy based on the results.[77] The SPARTE study has recruited 544 patients from 25 centers and was published in 2021.[78]
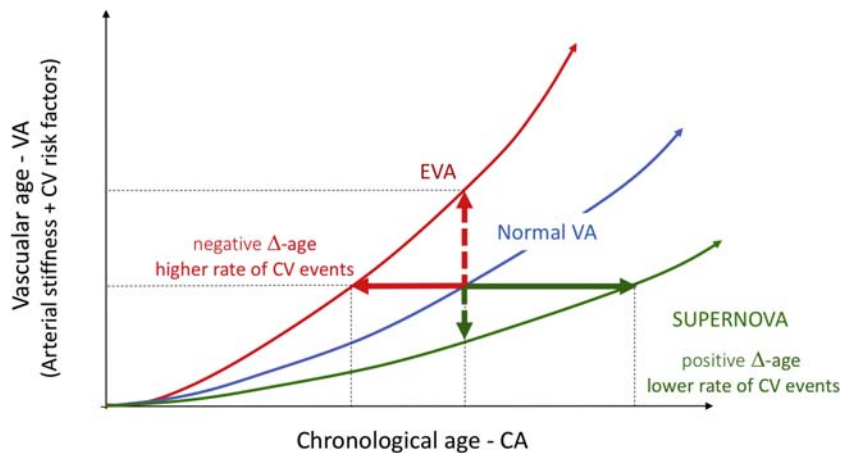
The concept and usefulness of supernormal vascular aging

Some studies have focused on people at the lower end of the distribution of PWV to find out more about vascular protection and healthy vascular aging (HVA) phenotype.[79−81] However, this approach is suboptimal as it does not fully account for the fact that some people seem to be protected from VA in spite of a similar cardiovascular risk factor burden as seen in other subjects with higher PWV.

In fact, the search-light is now directed to patients who seem to survive chronic disease and risk factors for a long duration with no or few complications, the true extremes of phenotypes linked to disease.[82] For instance, as we reported in our concept paper in 2019,[82] a minority of patients with long-standing type-1 diabetes of more than 40 to 50 years duration and daily insulin regimen, seem to escape major cardiovascular complications. In addition, patients with metabolically healthy obesity, a disputed condition normally defined by absence of variables linked to the metabolic syndrome, can remain hospitalization-free during long periods of midlife. Finally, a minority of patients with end-stage renal disease on peritoneal dialysis for a number of years may not exhibit cardiovascular complications.

We thus suggested the concept of SUPERNOVA that stands for Supernormal Vascular Aging.[82] Using arterial stiffness as the best proxy for the cumulative effect of known and unknown risk factors damaging the arterial wall throughout life, i.e., a measure of VA as discussed above, it was possible to suggest that subjects who present very low values of c-f PWV, whatever the level of CV risk factors, define a protective phenotype and we proposed to call this phenotype SUPERNOVA (Fig. 27.2). The difference between SUPERNOVA and HVA is that CV risk factors are generally absent in HVA. SUPERNOVA subjects are protected against the influence of CV risk factors, despite being exposed to them, i.e., CV risk factors are not translated into subclinical organ damage and CV complications.

To make proof of concept, we had to show in a longitudinal study that SUPERNOVA individuals underwent less CV complications than EVA subjects, despite a similar amount of CV risk factors.[83] For this purpose, we had first to identify SUPERNOVA individuals exhibiting a similar level of CV risk factors as EVA subjects.[83] We chose to compare chronological age with vascular age, and defined vascular age as the predicted age in the best fitting

FIGURE 27.2 **Early vascular aging and supernormal vascular aging.** For a substantially similar vascular age and cardiovascular (CV) risk profile (solid arrows), early vascular aging (EVA) individuals are significantly younger, and SUPERNOVA individuals are significantly older than the normal VA aging group. As a consequence, SUPERNOVA subjects have the largest difference (Δ-age, VA < CA) between chronological and vascular age; conversely, EVA subjects have negative difference (Δ-age, CA < VA) between chronological and vascular age. This translates into a lower rate of CV events in SUPERNOVA subjects, and a higher rate in EVA subjects; in other words, Δ-age is inversely associated with CV events. *From Bruno RM, Nilsson PM, Engström G, et al. Early and supernormal vascular aging: clinical characteristics and association with incident cardiovascular events. Hypertension. 2020. https://doi.org/10.1161/HYPERTENSIONAHA.120.14971. [published online ahead of print, 2020 Sep 8], with permission.*

multivariable regression model including classical CV risk factors and treatment and PWV. A large difference between chronological aging and VA means that, despite being "older," subjects have "younger" arteries. These are SUPERNOVA individuals. By contrast, when the difference is negative, it means that chronological aging is well below VA, in other words, that subjects have much "older" arteries than expected from their chronological age. These are EVA subjects. The multivariate analysis was performed in a subset of the cross-sectional Reference Values for Arterial stiffness Collaboration Database.[84] We used the 10th and 90th percentiles of the distribution of the difference between chronological age and vascular age, as cut-offs to define three categories of VA categories: EVA (below the 10th percentile), normal VA (between the 10th and the 90th percentiles), and SUPERNOVA (above the 90th percentile). The first part of the proof of concept was obtained by the following finding: while mean age significantly increased from EVA to normal VA and then to SUPERNOVA, the distribution of CV factors, PWV, and vascular age was similar among the three groups. The second part of the proof of concept was to show that SUPERNOVA individuals would undergo the lowest rate of CV events. For that purpose, the risk of fatal and nonfatal CV events in EVA and SUPERNOVA groups as compared to normal VA was investigated by Cox proportional hazard models in the longitudinal Malmö Diet and Cancer Study Cardiovascular Arm cohort that included 2642 subjects with a 6.6-year follow-up and 286 events.[85] The main finding was that the difference between chronological age and vascular age was significantly and inversely associated with CV events.

Compared to subjects with normal VA, SUPERNOVA individuals had half the risk of CV events, whereas EVA individuals had a 2.7 higher risk, in particular coronary events.

Conclusion

The EVA and SUPERNOVA concepts have led to the search of new models to understand protection from VA. In addition to a large number of studies testing drugs that may favorably influence EVA, a major issue is whether a treatment strategy based on targeting the normalization of arterial stiffness could be more beneficial than conventional treatment based on the normalization of blood pressure levels. Another therapeutic promising approach may use data from genomics and other omics to map specific pathophysiological processes through "personalized medicine." Finally, in clinical practice, it may be useful to detect SUPERNOVA subjects since they do not represent a clinical problem and should not necessarily be followed with the same intensity as EVA patients or even subjects with average VA. They represent, on the contrary, a challenge for academic research to better understand pathways for vascular protection, and if any identified, consider it as a potential therapeutic target in the future.

Acknowledgments

References

1. Ungvari Z, Tarantini S, Sorond F, Merkely B, Csiszar A. Mechanisms of vascular aging, a geroscience perspective: JACC focus seminar. **J Am Coll Cardiol**. 2020; 75(8):931−941.

2. Martyn CN, Greenwald SE. Impaired synthesis of elastin in walls of aorta and large conduit arteries during early development as an initiating event in pathogenesis of systemic hypertension. **Lancet**. September 27, 1997; 350(9082):953−955.

3. Sperling J, Nilsson PM. Does early life programming influence arterial stiffness and central hemodynamics in adulthood? **J Hypertens**. March 2020; 38(3):481−488.

4. Gluckman PD, Hanson MA, Cooper C, Thornburg KL. Effect of in utero and early-life conditions on adult health and disease. **N Engl J Med**. July 3, 2008; 359(1):61−73.

5. Hamczyk MR, Nevado RM, Barettino A, Fuster V, Andrés V. Biological versus chronological aging: JACC focus seminar. **J Am Coll Cardiol**. 2020; 75(8):919−930.

6. Nilsson PM, Boutouyrie P, Cunha P, et al. Early vascular ageing in translation: from laboratory investigations to clinical applications in cardiovascular prevention. **J Hypertens**. 2013; 31(8):1517−1526.

7. van Sloten TT, Boutouyrie P, Lisan Q, et al. Body silhouette trajectories across the lifespan and vascular aging. **Hypertension**. November 2018; 72(5):1095−1102.

8. Laurent S, Briet M, Boutouyrie P. Large and small artery cross talk and recent morbidity-mortality trials in hypertension. **Hypertension**. 2009; 54:388−392.

9. Laurent S, Boutouyrie P. The structural factor of hypertension: large and small artery alterations. **Circ Res**. 2015; 116:1007−1021.

10. Lechner K, McKenzie AL, Kränkel N, et al. High-risk atherosclerosis and metabolic phenotype: the roles of ectopic adiposity, atherogenic dyslipidemia, and inflammation. **Metab Syndr Relat Disord**. 2020; 18(4):176−185.

11. Lacolley P, Regnault V, Segers P, Laurent S. Vascular smooth muscle cell and arterial stiffening: relevance in development, ageing and disease. **Phys Rev**. 2017; 97:1555−1617.

12. Lacolley P, Regnault V, Laurent S. Mechanisms of arterial stiffening: from mechanotransduction to epigenetics. **Arterioscler Thromb Vasc Biol**. 2020; 40:1055−1062.

13. Laurent S, Cockcroft J, Van Bortel L, et al. Expert Consensus Document on arterial stiffness: methodological aspects and clinical applications. **Eur Heart J**. 2006; 27:2588−2605.

14. Van Bortel LM, Laurent S, Boutouyrie P, et al. Expert consensus document on the measurement of aortic stiffness in daily practice using carotid-femoral pulse wave velocity. **J Hypertens**. 2012; 30:445−448.

15. Nilsson PM, Lurbe E, Laurent S. The early life origins of vascular ageing and cardiovascular risk: the EVA syndrome. **J Hypertens**. 2008; 26(6):1049−1057.

16. Nilsson PM. Early vascular aging (EVA): consequences and prevention. **Vasc Health Risk Manag**. 2008; 4(3):547−552.

17. Ooyama T, Sakamoto H. [Arterial ageing of aorta and atherosclerosis–with special reference to elastin]. **Nihon Ronen Igakkai Zasshi**. May 1995; 32(5):326−331 (Japanese).

18. Lajemi M, Labat C, Gautier S, et al. Angiotensin II type 1 receptor-153A/G and 1166A/C gene polymorphisms and increase in aortic stiffness with age in hypertensive subjects. **J Hypertens**. March 2001; 19(3):407−413.

19. Laurent S, Boutouyrie P, Asmar R, et al. Aortic stiffness is an independent predictor of all-cause and cardiovascular mortality in hypertensive patients. **Hypertension**. 2001; 37:1236−1241.

20. Boutouyrie P, Tropeano AI, Asmar R, et al. Aortic stiffness is an independent predictor of primary coronary events in hypertensive patients: a longitudinal study. **Hypertension**. 2002; 39:10−15.

21. Cruickshank K, Riste L, Anderson SG, Wright JS, Dunn G, Gosling RG. Aortic pulse-wave velocity and its relationship to mortality in diabetes and glucose intolerance: an integrated index of vascular function? **Circulation**. 2002; 106:2085−2090.

22. Laurent S, Katsahian S, Fassot C, Tropeano AI, Laloux B, Boutouyrie P. Aortic stiffness is an independent predictor of fatal stroke in essential hypertension. **Stroke**. 2003; 34:1203−1206.26.

23. Mattace-Raso FU, van der Cammen TJ, Hofman A, et al. Arterial stiffness and risk of coronary heart disease and stroke: the Rotterdam Study. **Circulation**. February 7, 2006; 113(5):657−663.

24. Nilsson Wadström B, Fatehali AH, Engström G, Nilsson PM. A vascular aging index as independent predictor of cardiovascular events and total mortality in an elderly urban population. **Angiology**. November 2019; 70(10):929−937.

25. Vlachopoulos C, Aznaouridis K, Stefanadis C. Prediction of cardiovascular events and all-cause mortality with arterial stiffness: a systematic review and meta-analysis. **J Am Coll Cardiol**. March 30, 2010; 55(13):1318−1327.

26. Ben-Shlomo Y, Spears M, Boustred C, et al. Aortic pulse wave velocity improves cardiovascular event prediction: an individual participant meta-analysis of prospective observational data from 17,635 subjects. **J Am Coll Cardiol**. February 25, 2014; 63(7):636−646.

27. Cunha PG, Cotter J, Oliveira P, et al. Pulse wave velocity distribution in a cohort study: from arterial stiffness to early vascular aging. **J Hypertens**. 2015; 33(7):1438−1445.

28. Danninger K, Hafez A, Binder RK, et al. High prevalence of hypertension and early vascular aging: a screening program in pharmacies in Upper Austria. **J Hum Hypertens**. April 2020; 34(4):326−334.

29. Gomez-Sanchez M, Gomez-Sanchez L, Patino-Alonso MC, et al. Vascular aging and its relationship with lifestyles and other risk factors in the general Spanish population: early Vascular Ageing Study. **J Hypertens**. 2020; 38(6):1110−1122.

30. Vlachopoulos C, Xaplanteris P, Aboyans V, et al. The role of vascular biomarkers for primary and secondary prevention. A position paper from the European society of Cardiology Working Group on peripheral circulation: endorsed by the Association for Research into Arterial Structure and Physiology (ARTERY) Society. **Atherosclerosis**. 2015; 241(2):507−532.

31. Olsen MH, Angell SY, Asma S, et al. A call to action and a lifecourse strategy to address the global burden of raised blood pressure on current and future generations: the Lancet Commission on hypertension. **Lancet**. 2016; 388(10060):2665−2712, 26.

32. Liberale L, Montecucco F, Tardif JC, Libby P, Camici GG. Inflammageing: the role of inflammation in age-dependent cardiovascular disease. **Eur Heart J**. 2020; 41(31):2974−2982.

33. Dai L, Schurgers LJ, Shiels PG, Stenvinkel P. Early vascular ageing in chronic kidney disease: impact of inflammation, vitamin K, senescence and genomic damage. **Nephrol Dial Transplant**. 2020; 35(Suppl 2):ii31−ii37.

34. Nilsson PM. Early vascular aging in hypertension. **Front Cardiovasc Med**. 2020; 7:6.

35. Nilsson PM. Early vascular ageing - a concept in development. **Eur Endocrinol**. April 2015; 11(1):26−31.

36. Cunha PG, Boutouyrie P, Nilsson PM, Laurent S. Early vascular ageing (EVA): definitions and clinical applicability. **Curr Hypertens Rev**. 2017; 13(1):8−15.

37. Canugovi C, Stevenson MD, Vendrov AE, et al. Increased mitochondrial NADPH oxidase 4 (NOX4) expression in aging is a causative factor in aortic stiffening. **Redox Biol**. 2019; 26:101288.

38. Forte M, Stanzione R, Cotugno M, Bianchi F, Marchitti S, Rubattu S. Vascular ageing in hypertension: focus on mitochondria. **Mech Ageing Dev**. 2020; 189:111267.

39. O'Rourke MF, Safar ME. Relationship between aortic stiffening and microvascular disease in brain and kidney. Cause and Logic of therapy. **Hypertension**. 2005; 46:200−204.

40. Roman MJ, Devereux RB. Association of central and peripheral blood pressures with intermediate cardiovascular phenotypes. **Hypertension**. 2014; 63:1148−1153.

41. Scuteri A, Tesauro M, Di Daniele N. Preventive geriatrics the cross-talk between arterial and brain aging: a lifelong condition. **Exp Gerontol**. January 2017; 87(Pt B):148−150.

42. Sierra C, López-Soto A, Coca A. Connecting cerebral white matter lesions and hypertensive target organ damage. **J Aging Res**. 2011; 2011:438978.

43. Nilsson ED, Elmståhl S, Minthon L, et al. Nonlinear association between pulse wave velocity and cognitive function: a population-based study. **J Hypertens**. November 2014; 32(11):2152−2157.

44. Mahalakshmi AM, Ray B, Tuladhar S, et al. Sleep, brain vascular health and ageing. **Geroscience**. 2020. https://doi.org/10.1007/s11357-020-00235-8 [published online ahead of print, 2020 Aug 3].

45. Liu GH, Barkho BZ, Ruiz S, et al. Recapitulation of premature ageing with iPSCs from Hutchinson-Gilford progeria syndrome. **Nature**. 2011; 472(7342):221−225.

46. Oshima J, Sidorova JM, Monnat Jr RJ. Werner syndrome: clinical features, pathogenesis and potential therapeutic interventions. **Ageing Res Rev**. January 2017; 33:105−114.

47. Miller AJ, Schubart JR, Sheehan T, Bascom R, Francomano CA. Arterial elasticity in Ehlers-Danlos syndromes. **Genes**. 2020; 11(1):55.

48. Pucci G, Tarnoki AD, Medda E, et al. Genetic and environmental determinants of longitudinal stability of arterial stiffness and wave reflection: a twin study. **J Hypertens**. 2018; 36(12):2316−2323.

49. Mariko B, Pezet M, Escoubet B, et al. Fibrillin-1 genetic deficiency leads to pathological ageing of arteries in mice. **J Pathol**. 2011; 224(1):33−44.

50. Cardus A, Uryga AK, Walters G, Erusalimsky JD. SIRT6 protects human endothelial cells from DNA damage, telomere dysfunction, and senescence. **Cardiovasc Res**. 2013; 97(3):571−579.

51. Cecelja M, Keehn L, Ye L, Spector TD, Hughes AD, Chowienczyk P. Genetic aetiology of blood pressure relates to aortic stiffness with bi-directional causality: evidence from heritability, blood pressure polymorphisms, and Mendelian randomization. **Eur Heart J**. 2020. ehaa238. [published online ahead of print, 2020 May 1].

52. Åström Malm I, Alehagen U, Blomstrand P, Dahlström U, De Basso R. Higher blood pressure in elderly hypertensive females, with increased arterial stiffness and blood pressure in females with the Fibrillin-1 2/3 genotype. **BMC Cardiovasc Disord**. 2020; 20(1):180.

53. Kuipers AL, Miljkovic I, Barinas-Mitchell E, et al. Wnt pathway gene expression is associated with arterial stiffness. **J Am Heart Assoc**. 2020; 9(3):e014170.

54. Logan JG, Yun S, Bao Y, Farber E, Farber CR. RNA-sequencing analysis of differential gene expression associated with arterial stiffness. **Vascular**. 2020; 28(5):655−663.

55. Shimizu S, Mimura J, Hasegawa T, et al. Association of single nucleotide polymorphisms in the NRF2 promoter with vascular stiffness with aging. **PLoS One**. 2020; 15(8):e0236834 [Published 2020 Aug 11].

56. Gottsäter M, Hindy G, Orho-Melander M, Nilsson PM, Melander O. A genetic risk score for fasting plasma glucose is independently associated with arterial stiffness: a Mendelian randomization study. **J Hypertens**. 2018; 36(4):809−814.

57. Wallace RG, Twomey LC, Custaud MA, et al. The role of epigenetics in cardiovascular health and ageing: a focus on physical activity and nutrition. **Mech Ageing Dev**. 2018; 174:76−85.

58. Mels CM, Delles C, Louw R, Schutte AE. Central systolic pressure and a nonessential amino acid metabolomics profile: the African Prospective study on the Early Detection and Identification of Cardiovascular disease and Hypertension. **J Hypertens**. 2019; 37(6):1157−1166.

59. Polonis K, Wawrzyniak R, Daghir-Wojtkowiak E, et al. Metabolomic signature of early vascular aging (EVA) in hypertension. **Front Mol Biosci**. 2020; 7:12.

60. McDonnell BJ, Yasmin, Butcher L, et al. The age-dependent association between aortic pulse wave velocity and telomere length. **J Physiol**. 2017; 595(5):1627−1635.

61. Chiriacò M, Georgiopoulos G, Duranti E, et al. Inflammation and vascular ageing: from telomeres to novel emerging mechanisms. **High Blood Press Cardiovasc Prev**. 2019; 26(4):321−329.

62. Trudel X, Shipley MJ, McEniery CM, Wilkinson IB, Brunner EJ. Socioeconomic status, education, and aortic stiffness progression over 5 years: the Whitehall II prospective cohort study. **J Hypertens**. 2016; 34(10):2038−2044.

63. Puolakka E, Pahkala K, Laitinen TT, et al. Childhood socioeconomic status and arterial stiffness in adulthood: the cardiovascular risk in young Finns study. **Hypertension**. 2017; 70(4):729−735.

64. Climie RE, Boutouyrie P, Perier MC, et al. Individual and neighborhood deprivation and carotid stiffness. **Hypertension**. June 2019; 73(6):1185−1194.

65. Onete V, Henry RM, Sep SJS, et al. Arterial stiffness is associated with depression in middle-aged men - the Maastricht Study. **J Psychiatry Neurosci**. March 2018; 43(2):111−119.

66. van Sloten TT, Boutouyrie P, Tafflet M, et al. Carotid artery stiffness and incident depressive symptoms: the Paris prospective study III. **Biol Psychiatry**. March 15, 2019; 85(6):498−505.

67. Nilsson PM, Boutouyrie P, Laurent S. Vascular aging: a tale of EVA and ADAM in cardiovascular risk assessment and prevention. **Hypertension**. 2009; 54(1):3−10.

68. Staudt A, Stock K, Gande N, et al. Impact of lifestyle and cardiovascular risk factors on early atherosclerosis in a large cohort of healthy adolescents: the Early Vascular Ageing (EVA)-Tyrol Study. **Atherosclerosis**. 2020; 305:26−33.

69. Accardi G, Aiello A, Gambino CM, Virruso C, Caruso C, Candore G. Mediterranean nutraceutical foods: strategy to improve vascular ageing. **Mech Ageing Dev**. 2016; 159:63−70.

70. Estruch R, Ros E, Salas-Salvadó J, et al. PREDIMED study investigators. Primary prevention of cardiovascular disease with a

mediterranean diet supplemented with extra-virgin olive oil or nuts. **N Engl J Med**. June 21, 2018; 378(25):e34.

71. Whelton PK, Carey RM, Aronow WS, et al. 2017 ACC/AHA/AAPA/ABC/ACPM/AGS/APhA/ASH/ASPC/NMA/PCNA guideline for the prevention, detection, evaluation, and management of high blood pressure in adults: executive summary: a report of the American College of Cardiology/American Heart Association Task Force on Clinical Practice Guidelines. **Circulation**. October 23, 2018; 138(17):e426−e483.

72. Williams B, Mancia G, Spiering W, et al. 2018 ESC/ESH guidelines for the management of arterial hypertension: the task force for the management of arterial hypertension of the European society of Cardiology and the European society of hypertension: the task force for the management of arterial hypertension of the European society of Cardiology and the European Society of Hypertension. **Eur Heart J**. 2018; 39:3021−3104.

73. Ong KT, Delerme S, Pannier B, et al. Aortic stiffness is reduced beyond blood pressure lowering by short-term and long-term anti-hypertensive treatment: a meta-analysis of individual data in 294 patients. **J Hypertens**. June 2011; 29(6):1034−1042.

74. Batzias K, Antonopoulos AS, Oikonomou E, et al. Effects of newer antidiabetic drugs on endothelial function and arterial stiffness: a systematic review and meta-analysis. **J Diabetes Res**. December 4, 2018; 2018:1232583.

75. Prattichizzo F, La Sala L, Rydén L, et al. Glucose-lowering therapies in patients with type 2 diabetes and cardiovascular diseases. **Eur J Prev Cardiol**. December 2019; 26(2_suppl):73−80.

76. Okada-Iwabu M, Iwabu M, Yamauchi T, Kadowaki T. Drug development research for novel adiponectin receptor-targeted antidiabetic drugs contributing to healthy longevity. **Diabetol Int**. September 19, 2019; 10(4):237−244.

77. Laurent S, Chatellier G, Azizi M, et al. Protocol of the SPARTE study: a strategy for preventing cardiovascular and renal events based on ARTErial stiffness. **Artery Res**. 2020; 26:250−260.

78. Laurent S, Chatellier G, Azizi M, et al. SPARTE Investigators. SPARTE study: Normalization of arterial stiffness and cardiovascular events in patients with hypertension at medium to very high risk. **Hypertension**. August 2021; 78(4). HYPERTENSIONAHA12 117579. https://doi.org/10.1161/HYPERTENSIONAHA.121.17579. Epub ahead of print. PMID: 34455813; PMCID: PMC8415523.

79. Niiranen TJ, Lyass A, Larson MG, et al. Prevalence, correlates, and prognosis of healthy vascular aging in a western community-swelling cohort: the Framingham heart study. **Hypertension**. August 2017; 70(2):267−274.

80. Nilsson PM, Laurent S, Cunha PG, et al. Characteristics of healthy vascular ageing in pooled population-based cohort studies: the global Metabolic syndrome and Artery REsearch Consortium. **J Hypertens**. 2018; 36(12):2340−2349.

81. Nilsson Wadström B, Engström G, Nilsson PM. Exploring and comparing definitions of healthy vascular ageing in the population: characteristics and prospective cardiovascular risk. **J Hum Hypertens**. 2020. https://doi.org/10.1038/s41371-020-0353-1.

82. Laurent S, Boutouyrie P, Cunha PG, Lacolley P, Nilsson PM. Concept of extremes in vascular aging. **Hypertension**. 2019; 74(2):218−228.

83. Bruno RM, Nilsson PM, Engström G, et al. Early and supernormal vascular aging: clinical characteristics and association with incident cardiovascular events. **Hypertension**. 2020; 76(5):1616−1624.

84. Herbert A, Cruickshank K, Laurent S, et al. Establishing reference values for central blood pressure and amplification in a general healthy population and according to cardiovascular risk-factors. **Eur Heart J**. 2014; 32:3122−3133.

85. Gottsäter M, Östling G, Persson M, Engström G, Melander O, Nilsson PM. Non-hemodynamic predictors of arterial stiffness after 17 years of follow-up: the Malmö Diet and Cancer study. **J Hypertens**. 2015; 33:957−965.

Further reading

1. Rizzoni D, Rizzoni M, Nardin M, et al. Vascular aging and disease of the small vessels. **High Blood Press Cardiovasc Prev**. 2019; 26(3):183−189.

Chapter 28

Ethnic differences in arterial stiffness and central aortic hemodynamics

J.K. Cruickshank[1], S.G. Anderson[2,3,4], M. Strauss-Kruger[5], L. Gafane-Matemane[5], R. Kruger[5], Y. Breet[5] and A.E. Schutte[5,6]

[1]Cardiovascular Medicine Group, Division of Life-course/ Nutritional Sciences, Kings College London, United Kingdom; [2]George Alleyne Chronic Disease Research Centre, University of the West Indies Cave Hill Campus, Barbados; [3]Division of Cardiovascular Sciences, School of Medical Sciences, University of Manchester, United Kingdom; [4]College of Medical, Veterinary and Life Sciences, University of Glasgow, United Kingdom; [5]Hypertension in Africa Research Team; MRC Unit for Hypertension and Cardiovascular Disease, North-West University, South Africa; [6]School of Population Health, University of New South Wales, The George Institute for Global Health, Sydney, Australia

This chapter introduces why ethnic influences on arterial function are relevant, what questions related to ethnicity may be useful and do apparent effects indicate ways to improve vascular outcomes in particular ethnic groups.

Is studying ethnic differences in vascular or any physiological feature or disease useful?

We naturally answer "yes" for three major reasons:

i. If one population group compared with another develops excess rates of cardiovascular events or death, it seems reasonable to examine how and why.
ii. Uncovering general causes of such differences calls into doubt frequent tendencies to consider genetic polymorphic or "inherent" variations as "causes." That is until gene variants, or more likely their products, when expressed by adverse influences, are shown to drive these conditions.
iii. Discovering specific environmental or life-course factors between one group and another offers both preventive and therapeutic opportunity.

Reduced access to diagnosis, intervention, and health care leads to persistent, intergenerational social inequalities in health and plays a major role of in the health status of African-Americans (AfAms) and other minority populations in the United States. Some 150 years since the end of slavery in the United States and less than a century since the same for peonage (the practice of holding persons in servitude or partial slavery, to work off a "debt"[1]) is short phylogenetic (the evolutionary history of a species) and epigenetic time. Similar issues hold for African-Caribbean (AfC) populations. We try here to avoid skin color designation as it is the basis of major discrimination, also preferring ethnicity to "race" which has no biological definition.[2–4] Yet that historical or political perspective seems inadequate in some instances, for example, to account for excess coronary heart disease (CHD) in South Asian people, in the Indian subcontinent itself, in those who migrated, or whose forebears were settled elsewhere under "indentured labor" schemes.[5] The emergence of obvious excess type 2 diabetes in South Asian people, and higher blood pressure (BP) in the last ±30 years, shows these to be dynamic issues which science struggles to keep up with. More recently CHD and diabetes have become epidemic in the subcontinent itself. Less recognized are similar excess rates among indigenous peoples worldwide, especially in their migrants to cities (e.g., in Brazil).

How is this relevant to arterial function and particularly stiffness, still mainly measured as carotid-femoral pulse wave velocity (cfPWV)? We use examples of available data to illustrate how and why cfPWV in particular helps to pinpoint not only risk/prognosis but should become the focus of preventive and therapeutic effort in randomized clinical trials (RCTs). Several studies and meta-analyses demonstrate the value of cfPWV for prognosis independently of ambient BP.[6]
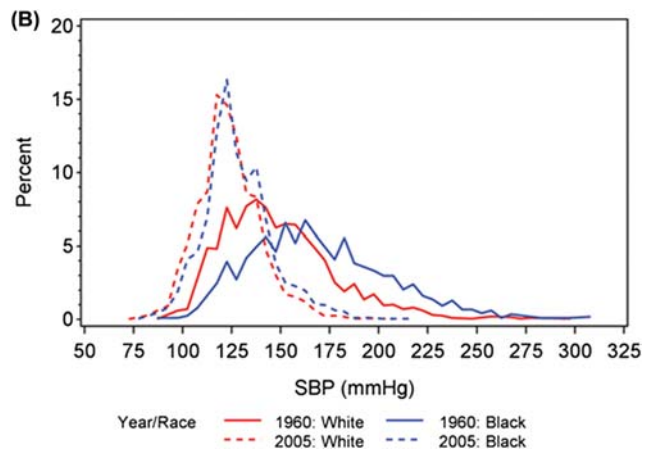
Relationships to blood pressure

A key component for examining ethnic issues in (cardio) vascular function is how much morbidity/mortality apparently

due to (high) BP is in part related to greater arterial stiffening *independently of BP* in one group compared with another.
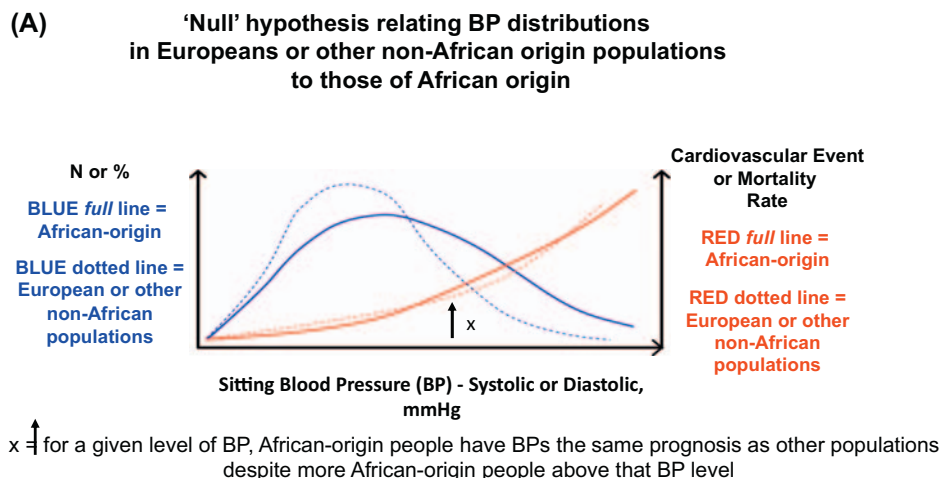
A hypothesis one of us promoted 40 years ago, based on pre-1980s data then, was that for *given levels of BP* in "Black" AfAm or AfC populations, prognosis was not "worse" or "more severe" than in European origin people, just that high BP *prevalence* was greater; so *at given levels of BP*, complications from high BP were no different from those in Europeans[7]—see Fig. 28.1A.

Fig. 28.1B shows how considerably BP distributions improved in the "stroke" belt of the South-East USA over a period of 50 years, greatly diminishing AfAm-white differences, so these can be at least partially reversed.[9] The challenge is to detect how much of any residual difference is due to the pathology of stiffening (medial replacement by collagen, etc., thought to be reversible) independently of BP. Can it be measured better by change in underlying large artery stiffening than by BP—whether true aortic (to bifurcation), as cfPWV, or local carotid PWV or carotid dynamics? Earlier outcome data from the "REasons for Geographic And Racial Differences in Stroke" (REGARDS) study included a much larger area of the south-east US "stroke belt" beyond those in.[9] Stroke risk was three times greater in AfAm than white adults—for a 10mmHg difference in systolic BP (SBP), risk increased 24% for AfAm but 8% for whites. However, adjusting for the two- to threefold excess diabetes nearly eliminated the excess.[8] Could that excess be due to large and small arterial stiffening in type 2 diabetes?

FIGURE 28.1B From: "40-Year Shifting Distribution of Systolic BP with Population Hypertension Treatment and Control." Lackland DT et al.: Circulation 2020; 142, 16: 1524—1531, DOI: (10.1161/CIRCULATION AHA.120.048,063).[8]

Our earlier work had shown the change in aortic PWV across the glucose tolerance (GT) spectrum. Between 1987 and 90 we had measured aortic PWV with a simple Doppler method decoded on a spectrum analyzer, (Fig. 28.2) as developed by Gosling (photo).[10] (He had taken the famous "photo 51" of DNA, as a PhD student with Rosalind Franklin, published beside Watson, Crick, and Wilkins' Nature paper, 1953. After her death from leukemia, Gosling moved into ultrasound). Note this was real "descending aortic" PWV from the aortic arch at the left brachial artery junction to just above the bifurcation. Participants were a

FIGURE 28.1A The "null hypothesis": more (High) blood pressure in African-Americans, African-Caribbeans, and west Africans than Europeans but for given BP levels, no difference in outcomes. *Redrawn and adapted from Cruickshank JK. Natural History of Blood Pressure in Blacks and Whites, Ch.31, pt D, p274 in: Ethnic Factors in Health and Disease, Ed JK Cruickshank, DG Beevers, publ.Wright, Butterworth-Heinemann, 1989/1994.*

Pulse-Wave Velocity Signals

PWV = separation distance/ pulse transit time

x = transit time/time delay of pulse wave
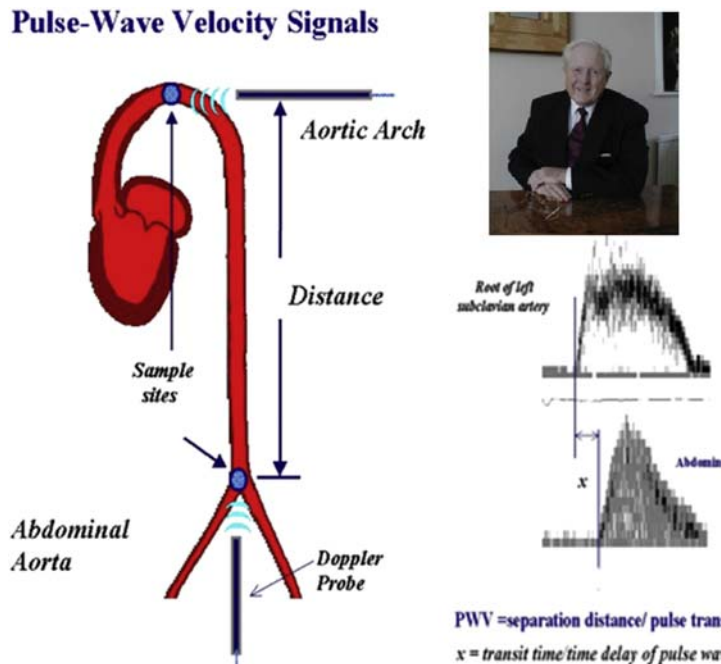
FIGURE 28.2 Doppler measurement of PWV, with length.

cohort of three specific ethnic groups, people of AfC, Gujarati Indian, and European white residents in North West London, England, defined by three of four grandparents in the same ethnic group, all of whom underwent glucose tolerance testing. We followed them for vital status for a mean of 11 years (Table 28.1).[11]

People there with diabetes had an adjusted hazard ratio (HR) of mortality 2.3 greater than those in the "normoglycemic" group, with a similar twofold excess in the intermediate glucose (in)tolerance group. To our surprise at that time, baseline aortic PWV displaced any index of BP, systolic, diastolic, mean or pulse, as a mortality predictor, and risk was *lower* for AfCs or Gujeratis than Europeans (Table). For those still alive 11 years later, intriguingly mean (95% CI) baseline PWV was no different across those 3 GT categories at 9.7 (9.2−10.2), 9.8 (9.1−10.5), and 10.4 (10−10.8) m/s. While BP treatment then was not started until >160 or 95 mmHg, which changed to 140/90 during follow-up, a key point was that between 140 and 160 mmHg, 17% of those with diabetes had baseline PWV >15 m/s compared with only 2% of controls.[11]

The role of early blood vessel pathology underlying and developing earlier than the hyperglycemia currently used to define "Type 2 diabetes" is beyond the scope of the review here.

Other British data continue to show clear differences in stroke rates in AfCs compared with "whites," partly related to less CHD allowing by competing cause more people to be at risk of stroke.[12,13] However, earlier, better BP control is vital.

Arterial stiffness through the life-course across different ethnic/geographic groups

What follows is a summary of data presented by the authors in a review article,[14] with its extensive Tables. Detailed accounts of molecular and mechanical mechanisms of arterial wall stiffening were published by Lacolley et al.[15] and Shadwick,[16] as was an excellent detailed review of aortic microstructure, collagen and elastin content or concentration by Tsamis et al.[17]

We cover studies comparing arterial stiffness, the main evidence-based component of early vascular aging,[18] between ethnic groups over the life-course, but the examples are neither exhaustive nor systematic reviews, which are referenced if available. For instance, only recent reports are quoted from the major US multiethnic cohorts (e.g., ARIC, Dallas, Multiethnic Study of Atherosclerosis [MESA], etc—see the Life-course section below). Their reports which incorporated, generally latterly, a range of arterial stiffness-related indices are cited. For a detailed review of the various metrics of arterial stiffness and pulsatile hemodynamics, the reader is referred to Chapters 3, 4, 7 and 8.

Fetal life, infancy, childhood, and adolescence (see Table 1)[14]

The onset of arterial stiffening starts even in-utero due to continuous adaptations in molecular structure and

TABLE 28.1 Final cox model of factors predicting mortality in a cohort of population-based control and type 2 diabetes participants.

	Hazard ratio	95% CI	*P*
Age (per 1 year older)	1.07	1.04−1.09	<.0001
Sex (female)	0.66	0.48−0.89	0.007
BP treated	1.10	0.82−1.48	0.54
Systolic BP (per 5 mm Hg)	1.02	0.98−1.06	0.34
GTT status (normoglycemia)	1		
Glucose intolerant[a]	2.12	1.11−4.01	0.021
Known diabetes	2.34	1.50−3.74	<0.0001
PWV (per 1 m/s)	1.08	1.03−1.14	0.001
Smoking status (never)	1		
Current	1.57	1.10−2.23	0.012
Ex-smoker	1.16	0.81−1.66	0.42
Ethnicity (European)	1		
Gujerati	0.68	0.49−0.94	0.02
African-Caribbean	0.41	0.25−0.69	0.001
Other	1.34	0.80−2.33	0.25

n = 565. Six people without smoking data were omitted.
[a]*Baseline fasting glucose ≥6.1 mmol/L or 2-h glucose ≥11.1 mmol/L.*
From Cruickshank J, Riste L, Anderson SG, Wright JS, Dunn G, Gosling RG. Aortic pulse-wave velocity and its relationship to mortality in diabetes and glucose Intolerance. **Circulation**. 2002; 106:2085−2090.

biomechanical responsiveness of blood vessels. Perhaps the best example is in monozygotic twins with varying degrees of twin-twin transfusion syndrome, where the donor twin shows increased aortic stiffening postnatally which may subside by 10 years of follow-up, while the recipient twin also develops higher BP.[19,20] Increased aortic stiffness occurs in premature infants as measured by aortic wall thickness and vasomotor function.[21] Together with excess systemic hypertension in preterm infants,[22] low birth weight and other complications such as bronchopulmonary dysplasia[21] all contribute to the early onset of arterial stiffening. Explanations for higher large artery stiffness in preterm infants include impaired elastin synthesis in the aortic wall[23] which alter mechanical properties, reduce arterial compliance,[24] and create higher or premature pulse wave reflections.[25]

As shown in Table 1 of our review,[14] several studies investigated the impact of maternal risk factor. In UK infants, mainly European and Pakistani origin, we reported an inverse possibly adaptive link between maternal BP and neonatal aortic PWV.[26] Another could find no such association[27] although it used routinely measured antenatal BPs taken by clinic staff rather than by specifically trained personnel. That UK study suggested a weaker link between infant PWV and maternal anemia/iron status.[27] The

youngest South African children studied to date (mean age 7.3 years)[28] were boys aged 6−8 years, with regional PWV, arterial PP, as well as carotid ultrasound indices of local vascular stiffness measured. PWV (in all regions) and intima media thickness (IMT) were highest in African compared with white boys. Carotid stiffness indices were similar between groups.

In slightly older children, cfPWV was also higher in African compared with white Brazilian adolescents (mean age, 11.9 years; n = 771),[29] as also found in the United States. In Syracuse, New York state, cfPWV measured using arterial tonometry was higher in AfAm than white adolescents (mean age 10.7 years; n = 107), with no differences in PP, carotid IMT, and central SBP after adjustment for confounders.[30] A study in Memphis, Tennessee of white, AfAm and Hispanic adolescents (age 13.7 years) measured the cardiac-ankle vascular index (CAVI), with higher values indicating stiffer arteries.[31] Despite no univariate differences in CAVI, after adjusting for body mass index (BMI), AfAm boys had higher CAVI than both white and Hispanic boys with normal weight but CAVI was lowest in obese AfAm boys suggesting early vascular adaptations to obesity. Another study indicated higher brachial-ankle PWV in older AfAm than white US adolescents (n = 205, mean age, 15.9 years), with no

difference in PP.[32] In other American studies, socioeconomic disparities and carotid-femoral[33,34] as well as aorto-radial and aorto-dorsalis pedis PWV were higher in AfAm than white adolescents. Augmentation index corrected for heart rate (AI_{75}), which predicts mortality and CVD events,[35] was also higher among young type 2 diabetic AfAm than white American patients,[33] likely indicating more prominent pulse wave reflections.
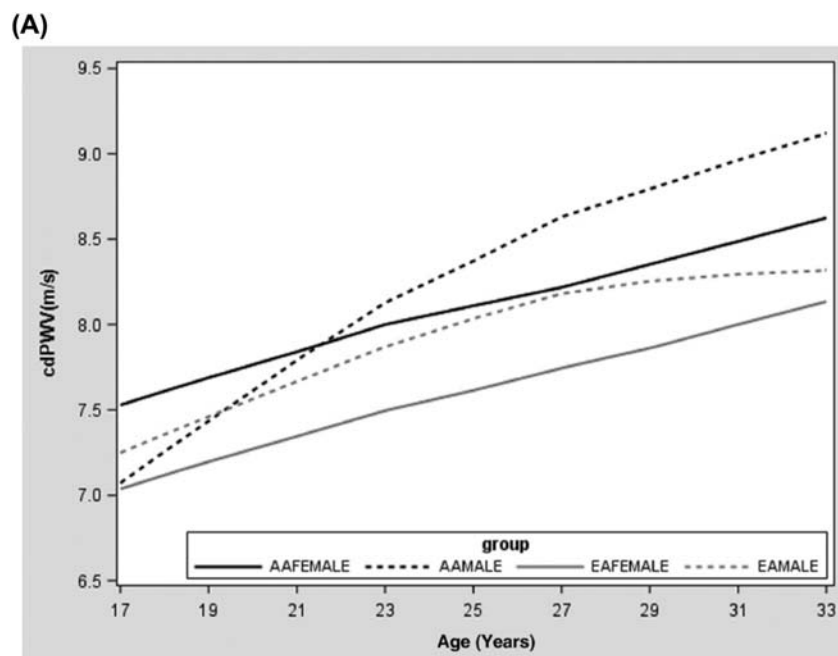
Young adults (see Table 2)[14]

Even within age bands, age and BP, and hypertensive status/treatment, need to be accounted for as major contributors to stiffening when investigating ethnic differences. Here, cross-sectional or longitudinal studies again generally compared AfAm and white populations, with some studies including Hispanics and other minority ethnic groups (Table 2).[14] Most were from the United States, but also Brazil, South Africa, and the United Kingdom, as below. African origin samples, particularly men, had greater arterial stiffness compared with African (origin) women, and men or women of other ethnicities. In one UK study, only augmentation index (AIx) and not PWV was higher.[36] In the South African "Predict" study, neither PWV nor AIx were greater in African participants.[37] Increased PWV in African-origin samples has been related to sociodemographic and psychosocial factors in the United Kingdom and the United States.[36,38]
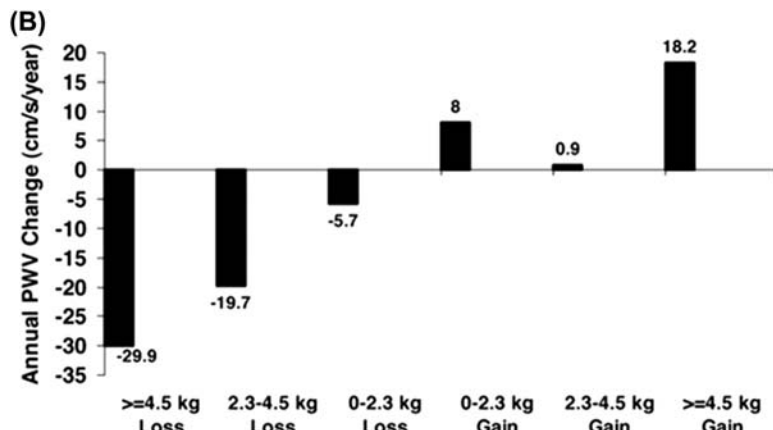
US studies are generally consistent: healthy AfAm men had higher central BP, AI_{75}, augmentation pressure, cfPWV, carotid β-stiffness index, carotid IMT, and lower pulse pressure amplification (PPA) despite younger mean age than whites, 21.7 versus 23.6 years, and after adjustments for heart rate, body fat, and cardiorespiratory fitness.[39] Group differences were not significant comparing brachial structure and function,[40] where routine BP is taken, confirming that early arterial alterations occur in central elastic vessels. Another mechanistic US study compared just 26 AfAm adults (mean age 32 years) who had higher AI_{75} than 10 Hispanics (28 years) and 26 white adults (28 years). cfPWV was also higher in the AfAm versus white group after post hoc analysis.[41]

In important longitudinal work, Liang et al. reported higher carotid-dorsalis pedis PWV over seven years in apparently healthy, normotensive African than white Americans from late childhood to early adulthood (Fig. 28.3A).[38] AfAm men had higher PWV with aging than AfAm women or white men and women.

Further longitudinal work came from follow-up in Allegheny County, Pennsylvania, if in a small sample of 67 AfAm and 85 white Americans there. These carefully measured and analyzed data clearly showed the continuing impact of weight gain on BP-adjusted PWV across ethnic groups in these 20−40 years old participants followed for a period of two years (Fig. 28.3B).[42] A 2019 meta-analysis compared cfPWV in AfAm and white samples aged 18−49 years

FIGURE 28.3A Mean unadjusted carotid-dorsalis pedis pulse wave velocity by age for younger African (AA) and European American (EA) women and men. *From Liang X, Su S, Hao G, et al. Determinants of pulse wave velocity trajectories from youth to young adulthood.* **J Hypertens**. *2019; 37:563−571.*

FIGURE 28.3B Annual carotid-femoral pulse wave velocity (cfPWV) change by weight change, adjusted for baseline cfPWV, age, race—ethnicity, sex, baseline mean arterial pressure (MAP), MAP change, and baseline weight. *From Wildman RP, Farhat GN, Patel AS, et al. Weight change is associated with change in arterial stiffness among healthy young adults.* **Hypertension**. *2005; 45:187−192.* https://doi.org/10.1161/01.HYP.0000152200.10578.5d.

with apparent excess rates among AfAm men and women; however, that analysis was not adjusted for BP.[43]

Outside the United States, in our Determinants of Adolescent, now Young Adult, Social Wellbeing, and Health (DASH) study in London, the United Kingdom, unadjusted aortic PWVs were similar in young (21−23 years) Black Caribbean and white men, but higher than in other groups (Black African, Pakistani/Bangladeshi, and others).[36] Models were then adjusted for age, BP, current and adolescent SES indices (employment, education, and perceived racism). Women had lower stiffness than men, as did Black African, Black Caribbean, and Indian origin young people than white youth, with current BP, current and adolescent waist/height ratio, and perceived racism effects increasing arterial stiffness.[36] In slightly smaller samples of participants who wore five-day physical activity monitors, both number of steps/day and time walking >100steps/min were negative determinants of aortic PWV (i.e., more exercise, lower aortic PWV), independently of all other factors (Fig. 28.4).[36]

In the same study population, unadjusted AI was higher in Caribbean, West African, Indian and Pakistani/Bangladeshi groups compared with white young adults (with some borderline significant). In multivariate models including SBP, AI was marginally but not significantly higher in West Africans and Caribbeans than in whites.[44]
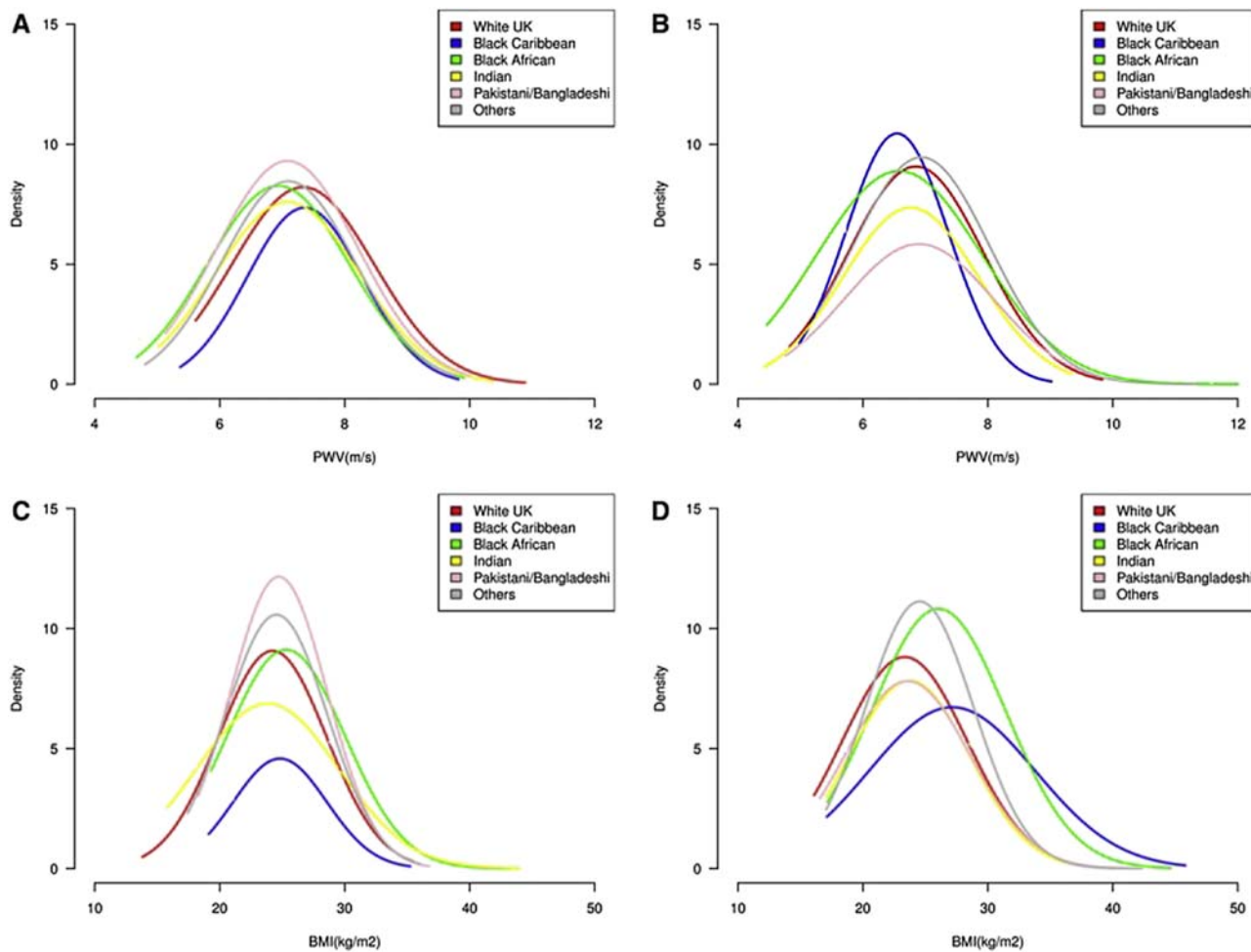
The key issue from all these data is that for given levels of BP, some people have stiffer blood vessels than others—as shown in the large middle-older aged European dataset, Fig. 28.5A,[45] p2338, and the same dataset of the London "DASH" cohort above, Fig. 28.5B (Reference 36, p1055).

Effects of age and BP on PWV were examined in African origin and white, Brazilian-born young men (mean age 26 years). In normotensives, white men had higher PWV than African, but in hypertensives, African men had higher PWV than white. The slope of the age-adjusted PWV-SBP regression was steeper in Black than white men.[46] A cross-sectional study in urban Vitoria, Brazil, included 2015 people (aged 36−47 years) from four different ethnic groups: Amerindians (29.2%), white (26.7%), Mulatto (38.3%), and Black (5.8%). (Note still the color-based classification, as in the more "detailed" UK 2011 census list, or the simplistic Black/white/(Hispanic) US list). cfPWV was higher in the Black group after adjustment for traditional covariates including age, sex, and mean BP.[47]
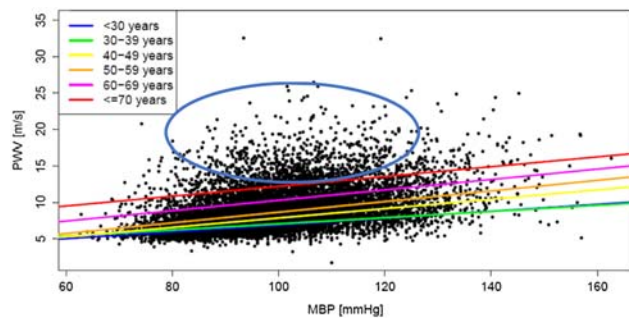
The African-PREDICT study in South Africa included only normotensive young healthy African and white adults (mean 24.4 years, range 20−30 y), reporting no ethnic differences in cfPWV, AI_{75}, or PPA, *adjusted for mean arterial pressure*. Although there were no ethnic differences in stiffness indices between normotensives, African adults showed a steeper decline in PPA between ages 20−30 years, similar to findings in African American men.[37] A subgroup of these young people in African-PREDICT had metabolomic analyses done on two groups either in the lower or higher halves of the PWV range. No associations were found with PWV but several urinary nonessential amino acids with roles in collagen metabolism were independently and inversely related to the 3 mmHg higher central SBP in the African origin young adults.[48]

In summary, cross-sectional US and South African studies report higher cfPWV in African origin men than women and in both, higher cfPWV than other ethnic groups. In younger adults (20−40 years) in England and in Brazil, at lower BP levels and to the surprise of some, European-origin ("white") people had higher cfPWV in fully adjusted analyses as above. Data on women were fewer. However, the slope of the PWV-BP relationship was
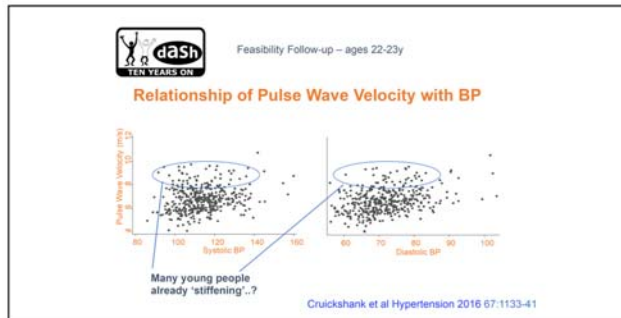
FIGURE 28.4 (A) men and (B) women. Density (frequency distribution) plots for pulse wave velocity by ethnic group and gender. *From Cruickshank J, Silva MJ, Molaodi OR, et al. Ethnic differences in and childhood influences on early adult pulse wave velocity.* **Hypertension***. 2016; 67:1133−1141.*

FIGURE 28.5 Apparent arterial stiffening across the Blood Pressure range: For any level of BP and adult age, some people are stiffer than others (A) European Reference Value Collaboration. (B) The London Multi-Ethnic "DASH" study. *From Reference Values for Arterial Stiffness' Collaboration. Determinants of pulse wave velocity in healthy people and in the presence of cardiovascular risk factors: establishing normal and reference values.* **Eur Heart J***. 2010; 31:2338−2350; Cruickshank J, Silva MJ, Molaodi OR, et al. Ethnic differences in and childhood influences on early adult pulse wave velocity.* **Hypertension***. 2016; 67:1133−1141.*

steeper in African Brazilians. In the London data, Af-Caribbean-origin young men had slighter higher aortic PWV than directly West African origin men. BMI had direct elevating effects on aortic cfPWV in all the studies above, as did waist/height ratios in the London cohort in adolescence and in youth, with additional effects from perceived racism.

Middle-aged and elderly populations

Arterial stiffness in middle-older ages has been extensively investigated. Large population-based, cross-sectional studies in different world regions consistently found that "Black" African origin participants had increased arterial stiffness than the comparison group(s) (Table 3).[14]

Another South African study of African and white adults (40.7 years; n = 750) showed carotid-radial (cr) and carotid-dorsalis-pedis (cdp) PWVs were elevated in Black adults, with normal or elevated BP.[49] Using the cr/cdp PWV ratio could at least estimate its BP independence.[50]

In our study of a multiethnic sample of older middle-aged men (in Manchester, England,[51] mean [SE] aPWV in South Asians [n = 68; age 55 ± 10 years]), at known higher coronary disease risk than other groups, was 0.5 (±0.2) m/s higher than in AfCs (n = 67; 55 ± 10 years), at lowest coronary disease risk here, and than in Europeans (n = 63; 57 ± 8 years), adjusted for age, SBP, and diabetes (P = .01). By magnetic resonance in a subsample of these men balanced by ethnicity, PWV over the descending aorta in South Asians was 0.7 m/s (0.3 m/s) and 0.8 m/s (0.3 m/s) higher than in AfCs and Europeans, respectively; PWV over the aortic arch was not different. We found close approximation of transit times between MR and the aortic measure, and using more precise, MR-measured length for the aortic PWV greatly improved its precision.[52]

In a US community sample from metropolitan Atlanta (48 years; n = 855), cfPWV, central and peripheral AI were higher in the AfAm group compared to white counterparts, after adjustment for traditional risk factors. These differences persisted in a subgroup free of conventional risk factors.[53]

In the large US cohorts, ethnic factors are becoming clearer. In a subsample of ARIC from North Carolina (in the "stroke belt" as above, Fig.28.1B), 268 AfAm and 2459 white men and women aged 45−64 years with no history of CHD or stroke were studied.[54] The size of the AfAm sample is only ±10% of the white sample, but remains sizable compared with other studies (Table 3).[14] After adjustment for CV risk factors, mean β *carotid* stiffness was 9% higher for Black adults (mean ± SE: 11.3 ± 0.3) than for whites (10.3 ± 0.1).

These carotid measures are important because *carotid arterial function* plays a key role in stroke,[55] cerebral white matter lesions (WMLs)[56,57] and cognitive decline,[58]

independent of both ambient BP but also *aortic PWV*. Of those three studies, only in the 303 people in the Healthy Brain subcohort of the Health ABC study,[57] by then elderly at 83 years, was there an AfAm group (41%, N-±124). cfPWV was independently associated with incident WML, together with only sysBP and prevalent stroke in the model adjusted for demographic, cardiovascular risk factors, and diseases over 10 years. Age and ethnicity were not significant predictors of WML, but the study had inadequate power to do so in such survivors. In those with specific MRI brain lesions, AfAm had somewhat higher cfPWV than whites.[57]
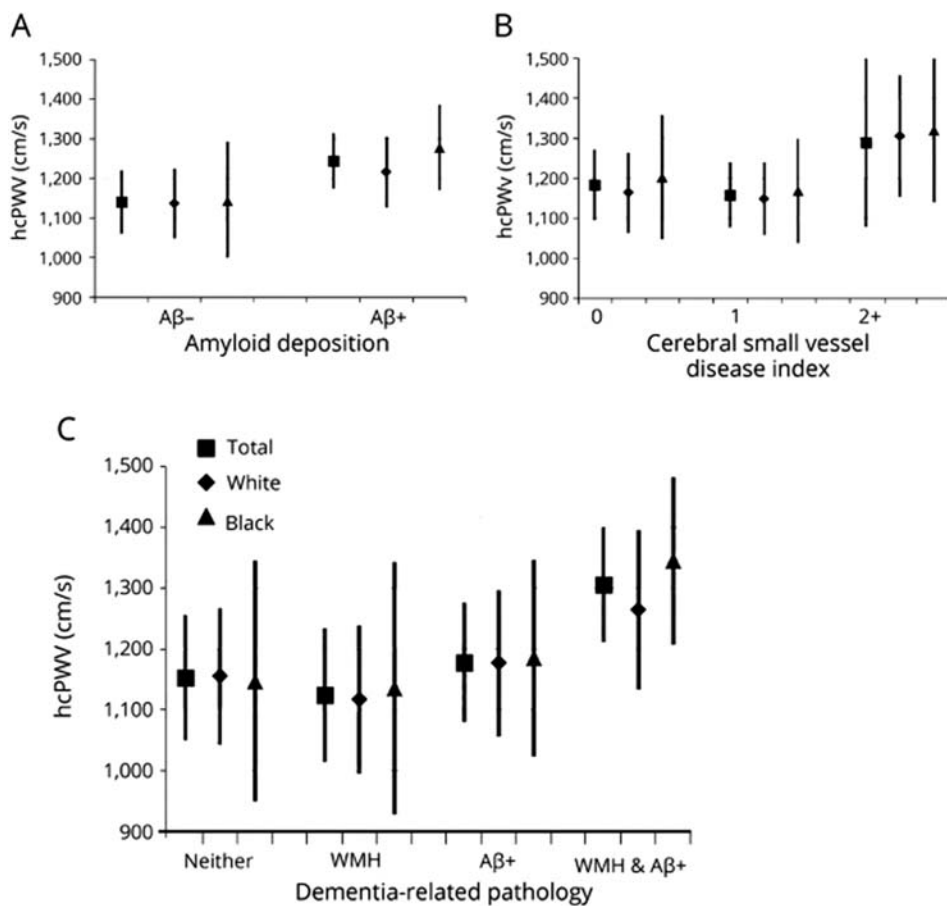
The only sub-Saharan study of carotid features compared 351 hypertensives known for >5 years, aged 59 years, with 241 normotensives, aged 53 years, among HIV-free African South Africans, 63% women in both samples.[59] Any index of carotid distensibility was reduced as expected, but these all remained significantly more so after adjusting for mean BP, but not central sysBP. However, the central SysBP was measured by a radial tonometry device, which probably underestimates SBP.[60]

The value of detailed PET-scan data for showing the impact of heart-*carotid* (hc)PWV in ethnic comparisons came from the recent small ARIC "PET" scan substudy. This substudy included 141 older AfAm and 180 white participants, with a mean age of 76 years, and without dementia.[61] The analysis related "central" heart-carotid PWV to cerebral small vessel disease and to ±30% excess fibrillar amyloid-beta (Aβ) deposition via a fluoride marker and white matter hyperintensities.[61] Oddly, at least by that age, SBP was not related to hcPWV. No ethnic effects were apparent on these cortical brain indices, adjusted for central BP or not, shown in Fig. 28.6 below:
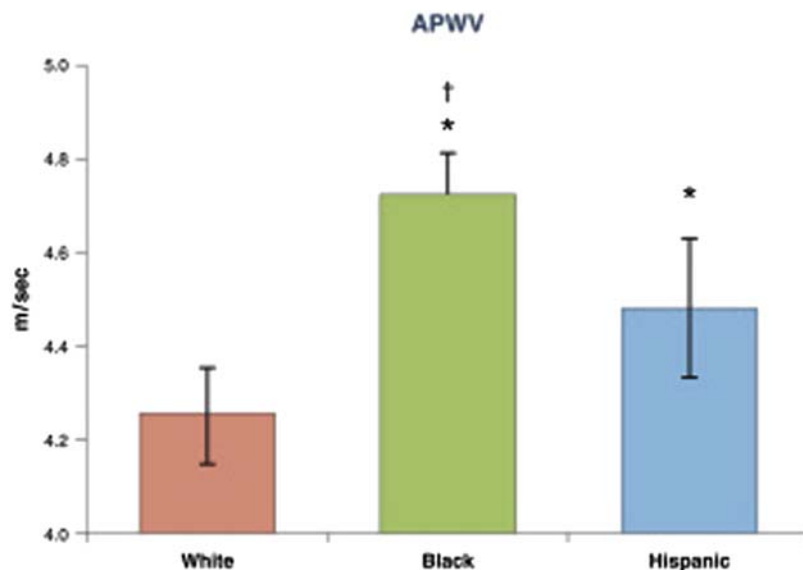
While finding cerebral vessel disease was not associated with Aβ, especially adjusted for usual risk factors, presence of Aβ was somewhat if not significantly greater in white than in AfAM people, who carry a higher ApoEe4 allele frequency.[62] Small sample sizes in these substudies (due to the high cost of PET) and survivor bias may be relevant.

Retinal vessels

A vital additional small vessel site is the eye, particularly for diabetes and risk of retinopathy, perhaps in sickle cell disease but also to indicate smaller cerebral vessel status. In a middle-aged Flemish population sample, cfPWV and estimated *forward and backward pressure waves* are related to retinal arteriolar and venular diameter and their ratios.[64] Further, cfPWV was also found related to mean retinal capillary blood flow, independently of age, sex, SBP, and BMI in a Polish study of hypertensive patients and controls.[65]There were also borderline effects on retinal vessels in the older ARIC study using the Omron VP

FIGURE 28.6 From ref.57 Hughes TM et al. Arterial stiffness and Dementia pathology. ARIC-PET study. Neurology 2018; 90(14):e1248−56 (hcPWV = heart-carotid)[61].

FIGURE 28.7A Proximal Aortic pulse wave velocity adjusted for all major cardiovascular risk factors including mean blood pressure—*from the Dallas Heart Study*[63].

1000+ device: none on arterioles but of cfPWV in relation to wider retinal *venules*, greater in those without high BP and independent of BP.[66] These relationships are clearly worth exploring further across ethnic groups, especially in T2 diabetes.

Pulse wave velocity measures in AORTIC segments by Magnetic Resonance Imaging (MRI)

In the multiethnic, population-based *Dallas Heart Study* (43.7 years; n = 2544)[63] Black and Hispanic compared with white participants had greater *proximal* aortic stiffness, measured either as aortic arch PWV or as characteristic impedance, in fully adjusted models. Although AfAm had a higher prevalence of numerous CV risk factors, none accounted for ethnic differences in aortic arch PWV and characteristic impedance. Different regional aortic components of stiffness each predicted cardiovascular outcomes, but as yet with insufficient events to examine those ethnic differences (Fig. 28.7).[67]

The MESA, another major US multiethnic study with modern imaging, also provides novel results on regional aortic stiffening.[68] Its CVD outcomes distinguished effects of aortic arch stiffening between middle-aged and older adults. A 1SD increase in log arch PWV was associated with incident CVD events in younger middle-age, but not in older people, with a multivariate CVD risk factor-adjusted HR of 1.47 (1.1−1.97) $P < .009$, at 45−54 years. That adjustment included ethnic group (*not independently significant*) and SBP. Arch PWV remained separately significant at 45−54 years after also including left ventricular (LV) mass, carotid IMT (both NS) and coronary artery calcium score ($P = .098$). Only ankle-brachial index (ABI) remained a significant predictor of events ($P = .026$), suggesting that general PWV was adding to prediction by arch PWV.[68] Whether with more events ethnic group will be separately significant is awaited. An important limitation of aortic arch PWV measurements in MESA is the very low temporal resolution achieved by the phase contrast sequences used in this study, which is unlikely to resolve fast PWV ranges as seen in older participants.
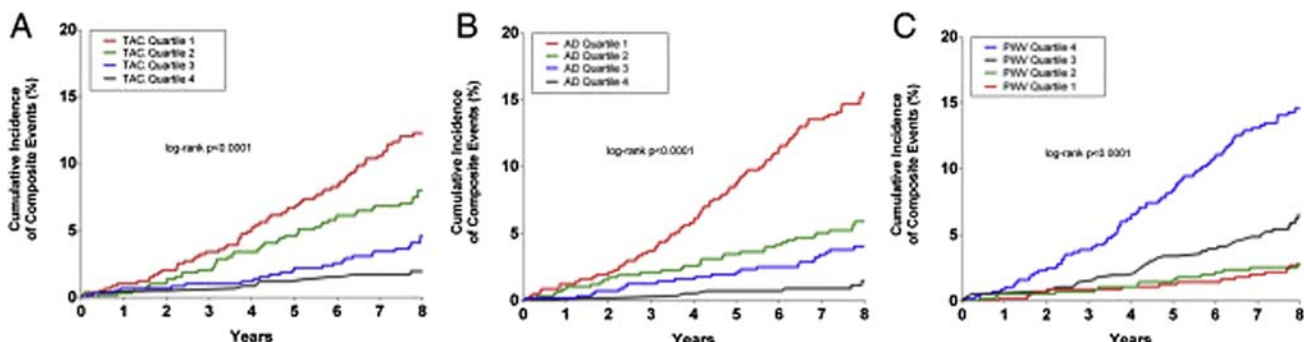
In South Africa, among 309 randomly sampled, untreated people of African ancestry, there was a marked gender divergence in the cross-sectional cfPWV−LV relationships, being found only in women.[69] cfPWV measured with arterial tonometry was closely related in simple correlation to LV mass index at r = 0.67, but rather oddly not at all in men. In multivariate analysis, adjusting for either standard brachial systolic or mean BP, independent relations between LV mass and cfPWV persisted, more strongly so with 24hr systolic ambulatory BP. Including other standard confounders also, with 63% overweight or obese and 17% with poor GT, the partial r, 0.37, for cfPWV was exactly equivalent to, but again independent of, that from SBP. These were cross-sectional data but clearly illustrate the potential impact of ventricular-arterial coupling, which generally we continue to ignore. Longitudinal data and perhaps explanations for the major gender difference so far will be invaluable in this at-risk population.

HIV

Finally, now in a relatively controlled epidemic, the world has near forgotten, a case-control cohort study in South Africa has started, comparing 278 HIV-infected, aged 43 years, and 104 HIV-negative people, aged 39 years, only some 28% men in each.[70] Some 80% were taking their ART, 47 had been for >5 years. Intriguingly in an apparently inflammatory disease, PWV was no different nor was forearm vasodilatation at baseline, with follow-up monitoring ongoing.

Ethnicity and the menopausal transition

A key part of women's life-course is the apparent perimenopausal change in cardiovascular function and risk.

FIGURE 28.7B   Cumulative incidence of cardiovascular events by quartile of: (A) Total Arterial Compliance; (B) Ascending aorta distensibility; (C) Arch pulse wave velocity. *Maroules CD, Khera A, Ayers C, et al. Cardiovascular outcome associations among cardiovascular magnetic resonance measures of arterial stiffness: the Dallas heart study.* **J Cardiovasc Magn Reson**. *2014; 16(1):33.* PMC4031496.
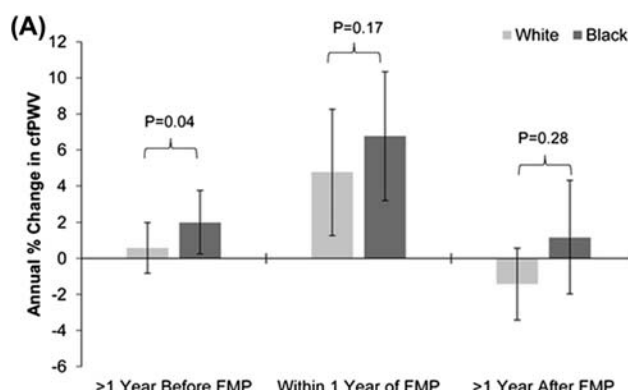
Two studies compared between the United States and China illustrate potential ethnic or geographic issues for arterial stiffening as an end point for standard risk factor impact during this phase. The US "Swan" Heart Study, a sub-study of the full Swan study, enrolled 554 women at baseline,[71] on whom a further analysis was reported recently of 123 AfAm, 216 white women—Fig. 28.8A.[72]

AfAm women had greater progression in cfPWV than did white US women but in the baseline-follow-up, that greater progression was not independent of SBP.[71] However, in the recent report, where the regression "time-oriented" modeling was more complex and the final model included SBP, annual change in cfPWV was significantly greater in AfAm women at 6.8%, and highly so comparing segments during and after the menopause.[72] Only AfAm women had a statistically significant increase in cfPWV up to the menopause (Fig. 28.8A). Adjusting for blood levels of reproductive hormones FSH, estradiol, or CRP, did not alter the analyses.
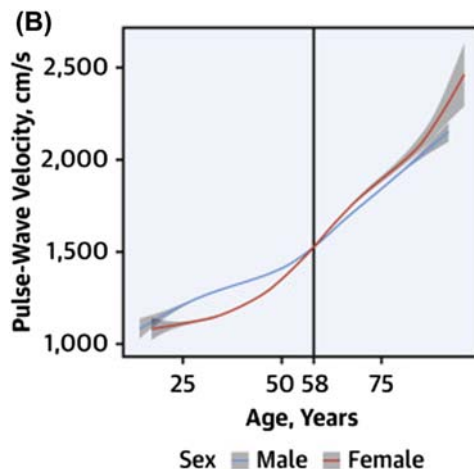
The study from Changsha, central China, combined two large cross-sectional studies (n = 66,058) with a smaller longitudinal one (n = 1724) and included measurements of brachial-ankle PWV (baPWV).[73] The crossover age, ±58 years, where women have equal or higher PWV to men thereafter is very close to that obtained by using MRI-based aortic regional PWV and distensibility in 777 Europeans, 408 women, in Britain.[74]

The elderly

Much less data are available for ethnic effects on arterial stiffness in, and especially from younger ages to, older age. An early example is the Northern Manhattan Study (NOMAS)[75] which compared carotid artery diameter and stiffness in 1536 Black, white, and Hispanic participants at

FIGURE 28.8A Ethnic difference between African and white American Women in carotid-femoral pulse wave velocity before, during, and after the menopause at ±53 years. *From Samargandy S, Matthews KA, Brooks MM, et al. Arterial stiffness accelerates within 1 year of the final menstrual period.* **Arterioscler Thromb Vasc Biol**. 2020; 40:1001−1008.

FIGURE 28.8B Cross-sectional + longitudinal data in China; brachial-ankle pulse wave velocity in women = or > men at ± age 58 years. *From Lu Y, Pechlaner R, Cai J, et al. Trajectories of age-related arterial stiffness in Chinese men and women.* **J Am Coll Cardiol**. 2020; 75: 870−880.
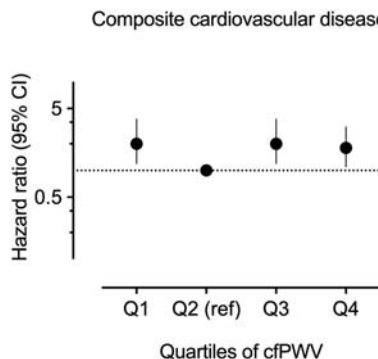
age 70 years, and showed greater carotid stiffness among the AfAm and Hispanic groups compared to whites.[75]

Further comparisons by ethnic group for cfPWV across different arterial paths again come from ARIC in a large sample all aged ∼75 years at their visit 5.[76] Unadjusted mean ± SD cfPWVs were 1163 ± 297 (n = 1694 white men), 1247 ± 344 (363 AfAm men), 1120 ± 282 (2208 white women), and 1222 ± 332 (708 AfAm women) cm/s (note this population sample has a relatively high mean value at this age of ±12 m/s, the usual units for carotid-aortic-femoral PWV). Those "significant" cfPWV differences were accompanied by respective mean arterial pressure values of 86.5 ± 11, 90.9 ± 12, and 86.9 ± 11, 91.5 ± 11 mmHg, but cfPWV adjusted for mean pressure was not presented.[77] baPWV however did not differ by ethnic group because femoral-ankle PWV, which is not prognostic of major outcomes, was *higher* in white groups. At this age in this cohort, prognosis was "J-shaped" for cfPWV, with the lowest quartile at twofold higher risk than quartile 2 as reference, with twofold excess risk also present in quartiles 3 and 4 (see Fig. 28.9).[77]

Renal impairment/failure (end-stage renal disease)

Ethnicity is highly relevant for renal disease because decline into and overt chronic renal disease/end-stage renal disease (ESRD) is much commoner among AfAms, driven by inadequately treated or managed high BP.

Townsend recently reviewed the powerful role of cfPWV in renal disease progression, based on follow-up of 2795 participants in the CRIC study.[78] The 1088 AfAms had a 45(14−84)% excess progression to ESRD. The

FIGURE 28.9 J-shaped relationship of carotid-femoral pulse wave velocity to composite of CHD, stroke and heart failure events in the older ARIC cohort. *From HHS version of Kim ED, Ballew SH, Tanaka H, Heiss G, Coresh J, Matsushita K. Short-term prognostic impact of arterial stiffness in older adults without prevalent cardiovascular disease.* **Hypertension**. *2019; 74(6):1373−1382 open access.*

adjusted risk for halving eGFR or ESRD itself was only "significant" with cfPWVs >10.3 m/s, with mean BP still significant for ESRD or eGFR decline, while mortality risk with cfPWV was continuous and independent of mean BP which no longer predicted mortality.[79] A similar pattern was found for heart failure risk. CRIC investigators also examined relationships between eGFR decline and retinal vessel changes,[80] but the likely role of cfPWV is not yet analyzed.

In the full older ARIC cohort (n = 3424, mean age 75 years), an increase in cfPWV of ±17 cm/s or more (∼0.17 m/s) was associated with a fall in eGFR of 15 mL/min/1.73m,[2] adjusted for age, sex, and ethnicity ("Black" v "white").[81] That reduced to 10 cm/s, (0.1 m/s) additionally adjusted for major risk factors and ABI. So, the 72 people with fully adjusted cfPWV higher by 0.7 m/s had eGFRs down to <30 ml/min/1.73m[2]; vice versa, those in that lowest eGFR group had ±twofold risk of being in the highest quartile of cfPWV.[81] Intriguingly, the effect was most prominent in European rather than in African-Americans (see their Fig. 28.2A). As perhaps expected, much of the impact was on the amount of albumin/creatinine excreted. Other measures of PWV (Ba, heart-carotid, femoral-ankle) had no effect.

Other ethnic differences in arterial function, excepting AfAm populations highlighted above in detail, are evident in middle age, specifically among South Asians, who have a high prevalence/incidence of coronary, stroke, and small vessel disease.[82] These populations have been greatly under-represented in studies on arterial function. A small Canadian study[83] recruited just 22 South Asian 71 years old participants and compared them with age-/sex-matched European-origin participants. South Asians had higher carotid PP and lower compliance, therefore exhibiting stiffer vessels. Similarly, central PP and AI were elevated in an older South Asian sample (69 ± 6.1 years) compared with

AfC and European-origin population samples in the UK Southall and Brent REvisited (SABRE) study.[84] Despite being uniquely valuable to date in Britain, note the study shares the limitation of all long-term adult cohorts of "survivor bias" affecting conclusions. We had found both these groups to have similar central aortic PWV relative to Europeans 25 years earlier, and PWV higher in those with T2 diabetes, despite some differences in BP and outcomes (Table and Fig. 28.2 above Reference 12). The Healthy Life in an Urban Setting (HELIUS) study,[85] a large prospective cohort in Amsterdam, had similar findings. Dutch European (n = 1797), South Asian Surinamese (n = 1846), African-Surinamese (n = 1840), and Ghanaian origin (n = 1673) participants were included in this study. Unadjusted aortic PWV was higher in African and South Asian groups compared with those of European Dutch descent, but these differences disappeared after adjusting for BP. The authors concluded that increased PWV in some groups was driven mainly by conventional risk factors.

Unanswered questions include whether genetic differences underlie these ethnic patterns, for which the evidence is slight so far. A study from Georgia, US of 702 twins, 40% AfAm, suggested heritability but could do no linkage.[86] GWAS studies in European-origin population samples suggest some effects on PWV, originally in 1480 Framingham participants of 817 pedigrees,[87] then meta-analyzed for 20,634, validated in a separate 5306, people of just European ancestry, and adjusted for BP.[88] Some of these variants were also replicated for cfPWV in a separate sample of 7669 Europeans from the LIFE-Adult study of Leipzig, Germany.[89] A small Korean study (n = 400) found no linkage,[90] perhaps illustrating how GWAS studies require very large samples but remain just associations.

It seems that the most likely external causal factors are social, economic, and their intergenerational and psychological effects, including reactions to racism[34,36] which may include obesity.

Summary and conclusions

Studies of ethnic-specific comparisons in physiology and disease provide a focus to understand and act on excess morbidity and mortality in particular groups. Most report that populations of African descent, and more recently also Hispanic populations, often living in western societies as ethnic "minorities," have greater arterial stiffness indices than white populations from very early life (e.g., 6 to 70 years of age). The South African context is interesting where populations and circumstances have changed rapidly in a generation. Yet AfCs and recently West Africans in the United Kingdom, both groups with long experience of excess stroke, have not yet experienced much obstructive coronary, but rather hypertensive heart disease. Raised BP often accompanies arterial stiffness in Black populations

but as above in Fig. 28.1A and B, for given BP levels some people have stiffer vessels than others, and those individuals have a poorer prognosis. Similarly, in analyses of normotensive or healthy subgroups, increased arterial stiffness may co-exist,[51] including in studies of children or young normotensive adults where African origin participants may already have elevated arterial stiffness but "normal," or BPs similar to, their comparison groups. When tracking arterial stiffness with increasing age, it becomes clear that early vascular aging already occurring in adolescence or young adulthood predisposes African origin individuals to excess CV risk throughout the life-course.

Identifying early vascular aging across all ethnic groups throughout the life-course by assessments of aortic PWV will add greater precision to BP alone to define those at risk for early onset of CVD and future events. Trials of specific treatments targeting blood vessel stiffening beyond BP are sorely needed, and some current vascular drugs may be excellent candidates.

There seems to be no doubt that once again continuing physical activity is the major opportunity for preventing early vascular aging, as shown in studies of individuals with differing, near life-long degrees of such activity.[91]

It is certainly clear that whatever the differences or similarities in arterial function by ethnic group and at any given ages and levels of peripheral or central BP, some individuals have stiffer vessels than others, and so are at higher CV risk.

References

1. Blackmon D. **The Re-enslavement of Black Americans from the Civil War to World War II**. Doubleday; 2008.

2. Cooper R, David R. The biological concept of race and its application to public health and epidemiology. **J Health Polit Policy Law**. 1986; 11:97−116.

3. Cruickshank J, Beevers D. Preface to 'ethnic factors in health and disease'. In: Cruickshank J, Beevers D, eds. **Ethnic Factors in Health and Disease**. London: Butterworth-Heinemann; 1989:pvii−ix.

4. Cooper RS, Kaufman JS, Ward R. Race and genomics. **N Engl J Med**. 2003; 348:1166−1170.

5. Laurence K. **A Question of Labour: Indentured Immigration into Trinidad and British Guiana, 1875−1917**. Jamaica: Ian Randle Publishers; 1994.

6. Ben-Shlomo Y, Spears M, Boustred C, et al. Aortic pulse wave velocity improves cardiovascular event prediction. **J Am Coll Cardiol**. 2014; 63:636−646.

7. Cruickshank J. Is blood pressure really "worse" in black people? **Lancet**. 1980; 316:371−372.

8. Howard G, Lackland DT, Kleindorfer DO, et al. Racial differences in the impact of elevated systolic blood pressure on stroke risk. **JAMA Int Med**. 2013; 173, 46-46.

9. Lackland DT, Howard VJ, Cushman M, et al. Forty-year shifting distribution of systolic blood pressure with population hypertension treatment and control. **Circulation**. 2020; 142:1524−1531.

10. Wright JS, Cruickshank JK, Kontis S, Doré C, Gosling RG. Aortic compliance measured by non-invasive Doppler ultrasound: description of a method and its reproducibility. **Clin Sci**. 1990; 78:463−468.

11. Cruickshank J, Riste L, Anderson SG, Wright JS, Dunn G, Gosling RG. Aortic pulse-wave velocity and its relationship to mortality in diabetes and glucose intolerance. **Circulation**. 2002; 106:2085−2090.

12. Harding S, Rosato M, Teyhan A. Trends for coronary heart disease and stroke mortality among migrants in England and Wales, 1979-2003: slow declines notable for some groups. **Heart**. 2007; 94:463−470.

13. Tillin T, Hughes AD, Mayet J, et al. The relationship between metabolic risk factors and incident cardiovascular disease in Europeans, South Asians, and African Caribbeans. **J Am Coll Cardiol**. 2013; 61:1777−1786.

14. Schutte AE, Kruger R, Gafane-Matemane LF, Breet Y, Strauss-Kruger M, Cruickshank JK. Ethnicity and arterial stiffness. **Arterioscler Thromb Vasc Biol**. 2020; 40:1044−1054.

15. Lacolley P, Regnault V, Segers P, Laurent S. Vascular smooth muscle cells and arterial stiffening: relevance in development, aging, and disease. **Physiol Rev**. 2017; 97:1555−1617.

16. Shadwick RE. Mechanical design in arteries. **J Exp Biol**. 1999; 202:3305−3313.

17. Tsamis A, Krawiec JT, Vorp DA. Elastin and collagen fibre microstructure of the human aorta in ageing and disease: a review. **J R Soc Interface**. 2013; 10:20121004.

18. Nilsson PM, Boutouyrie P, Cunha P, et al. Early vascular ageing in translation. **J Hypertens**. 2013; 31:1517−1526.

19. Wohlmuth C, Gardiner HM, Diehl W, Hecher K. Fetal cardiovascular hemodynamics in twin-twin transfusion syndrome. **Acta Obstet Gynecol Scand**. 2016; 95:664−671.

20. Wohlmuth C, Osei FA, Moise KJ, et al. Aortic distensibility as a surrogate for intertwin pulse pressure differences in monochorionic pregnancies with and without twin-twin transfusion syndrome. **Ultrasound Obstet Gynecol**. 2016; 48:193−199.

21. Sehgal A, Malikiwi A, Paul E, Tan K, Menahem S. Systemic arterial stiffness in infants with bronchopulmonary dysplasia: potential cause of systemic hypertension. **J Perinatol**. 2016; 36:564−569.

22. Tauzin L, Rossi P, Giusano B, et al. Characteristics of arterial stiffness in very low birth weight premature infants. **Pediatr Res**. 2006; 60:592−596.

23. Cattell MA, Anderson JC, Hasleton PS. Age-related changes in amounts and concentrations of collagen and elastin in normotensive human thoracic aorta. **Clin Chim Acta**. 1996; 245:73−84.

24. Martyn CN, Greenwald SE. Impaired synthesis of elastin in walls of aorta and large conduit arteries during early development as an initiating event in pathogenesis of systemic hypertension. **Lancet**. 1997; 350:953−955.

25. Lurbe E, Torro MI, Carvajal E, Alvarez V, Redon J. Birth weight impacts on wave reflections in children and adolescents. **Hypertension**. 2003; 41:646−650.

26. Koudsi A, Oldroyd J, McElduff P, Banerjee M, Vyas A, Cruickshank JK. Maternal and neonatal influences on, and reproducibility of, neonatal aortic pulse wave velocity. **Hypertension**. 2007; 49:225−231.

27. Alwan NA, Cade JE, McArdle HJ, et al. Infant arterial stiffness and maternal iron status in Pregnancy: a UK birth cohort (Baby VIP study). **Neonatology**. 2015; 107:297−303.

28. Mokwatsi GG, Schutte AE, Kruger R. Ethnic differences regarding arterial stiffness of 6-8-year-old black and white boys. **J Hypertens**. 2017; 35:960−967.

29. Zaniqueli D, Alvim RO, Luiz SG, Oliosa PR, de Sá Cunha R, Mill JG. Ethnicity and arterial stiffness in children and adolescents from a Brazilian population. **J Hypertens**. 2017; 35:2257−2261.

30. Lefferts WK, Augustine JA, Spartano NL, Atallah-Yunes NH, Heffernan KS, Gump BB. Racial differences in aortic stiffness in children. **J Pediatr**. 2017; 180:62−67.

31. Philip R, Alpert BS, Schwingshackl A, et al. Inverse relationship between cardio-ankle vascular index and body mass index in healthy children. **J Pediatr**. 2015; 167:361−365.e1.

32. Collins RT, Somes GW, Alpert BS. Differences in arterial compliance among normotensive adolescent groups: collins arterial compliance in adolescents. **Pediatr Cardiol**. 2008; 29:929−934.

33. Shah AS, Dolan LM, Gao Z, Kimball TR, Urbina EM. Racial differences in arterial stiffness among adolescents and young adults with type 2 diabetes. **Pediatr Diabetes**. 2011; 13:170−175.

34. Thurston RC, Matthews KA. Racial and socioeconomic disparities in arterial stiffness and intima media thickness among adolescents. **Soc Sci Med**. 2009; 68:807−813.

35. Janner JH, Godtfredsen NS, Ladelund S, Vestbo J, Prescott E. High aortic augmentation index predicts mortality and cardiovascular events in men from a general population, but not in women. **Eur J Prev Cardiol**. 2013; 20:1005−1012.

36. Cruickshank J, Silva MJ, Molaodi OR, et al. Ethnic differences in and childhood influences on early adult pulse wave velocity. **Hypertension**. 2016; 67:1133−1141.

37. Breet Y, Huisman HW, Kruger R, et al. Pulse pressure amplification and its relationship with age in young, apparently healthy black and white adults: the African-PREDICT study. **Int J Cardiol**. 2017; 249:387−391.

38. Liang X, Su S, Hao G, et al. Determinants of pulse wave velocity trajectories from youth to young adulthood. **J Hypertens**. 2019; 37:563−571.

39. Heffernan K, Jae SY, Fernhall B. Racial differences in arterial stiffness after exercise in young men. **Am J Hypertens**. 2007; 20:840−845.

40. Heffernan KS, Jae SY, Wilund KR, Woods JA, Fernhall B. Racial differences in central blood pressure and vascular function in young men. **Am J Physiol Heart Circ Physiol**. 2008; 295:H2380−H2387.

41. Ashraf AP, Fisher G, Alvarez J, et al. Associations of C-reactive protein to indices of vascular health and the influence of serum 25(OH)D status in healthy adults. **J Nutr Metab**. 2012; 2012:1−6.

42. Wildman RP, Farhat GN, Patel AS, et al. Weight change is associated with change in arterial stiffness among healthy young adults. **Hypertension**. 2005; 45:187−192.

43. Buie JNJ, Stanley A, Nietert PJ, Logan A, Adams RJ, Magwood GS. Racial disparities in arterial stiffness between healthy whites and African Americans in the United States: a meta-analysis. **J Natl Med Assoc**. 2019; 111:7−17.

44. Faconti L, Silva MJ, Molaodi OR, et al. Can arterial wave augmentation in young adults help account for variability of cardiovascular risk in different British ethnic groups? **J Hypertens**. 2016; 34:2220−2226.

45. Reference Values for Arterial Stiffness' Collaboration. Determinants of pulse wave velocity in healthy people and in the presence of cardiovascular risk factors: `establishing normal and reference values. **Eur Heart J**. 2010; 31:2338−2350.

46. Ferreira AVL, Viana MC, Mill JG, Asmar RG, Cunha RS. Racial differences in aortic stiffness in normotensive and hypertensive adults. **J Hypertens**. 1999; 17:631−637.

47. de Lima Santos PCJ, de Oliveira Alvim R, Ferreira NE, et al. Ethnicity and arterial stiffness in Brazil. **Am J Hypertens**. 2011; 24:278−284.

48. Mels CM, Delles C, Louw R, Schutte AE. Central systolic pressure and a nonessential amino acid metabolomics profile: the African Prospective study on the Early Detection and Identification of Cardiovascular disease and Hypertension. **J Hypertens**. 2019; 37:1157−1166.

49. Schutte AE, Huisman HW, Schutte R, et al. Arterial stiffness profiles: investigating various sections of the arterial tree of African and caucasian people. **Clin Exp Hypertens**. 2011; 33:511−517.

50. Fortier C, Sidibé A, Desjardins M-P, et al. Aortic−brachial pulse wave velocity ratio. **Hypertension**. 2017; 69:96−101.

51. Rezai M-R, Wallace AM, Sattar N, Finn JD, Wu FCW, Cruickshank JK. Ethnic differences in aortic pulse wave velocity occur in the descending aorta and may Be related to vitamin D. **Hypertension**. 2011; 58:247−253.

52. Rezai M-R, Cowan BR, Sherratt N, Finn JD, Wu FCW, Cruickshank JK. A magnetic resonance perspective of the pulse wave transit time by the Arteriograph device and potential for improving aortic length estimation for central pulse wave velocity. **Blood Pres Monit**. 2013; 18:111−118.

53. Morris AA, Patel RS, Binongo JNG, et al. Racial differences in arterial stiffness and microcirculatory function between black and white Americans. **J Am Heart Assoc**. 2013; 2.

54. Din-Dzietham R, Couper D, Evans G, Arnett DK, Jones DW. Arterial stiffness is greater in African Americans than in whites: evidence from the Forsyth County, North Carolina, ARIC cohort. **Am J Hypertens**. 2004; 17:304−313.

55. van Sloten TT, Sedaghat S, Laurent S, et al. Carotid stiffness is associated with incident stroke. **J Am Coll Cardiol**. 2015; 66:2116−2125.

56. Brisset M, Boutouyrie P, Pico F, et al. Large-vessel correlates of cerebral small-vessel disease. **Neurology**. 2013; 80:662−669.

57. Rosano C, Watson N, Chang Y, et al. Aortic pulse wave velocity predicts focal white matter hyperintensities in a Biracial cohort of older adults. **Hypertension**. 2013; 61:160−165.

58. Chiesa ST, Masi S, Shipley MJ, et al. Carotid artery wave intensity in mid- to late-life predicts cognitive decline: the Whitehall II study. **Eur Heart J**. 2019; 40:2300−2309.

59. Maritz M, Fourie CM, van Rooyen JM, Huisman HW, Schutte AE. Carotid characteristics of black South Africans with five-year sustained hypertension. **Cardiovasc J Afr**. 2016; 27:262−269.

60. Sharman JE, Avolio AP, Baulmann J, et al. Validation of non-invasive central blood pressure devices: ARTERY Society task force consensus statement on protocol standardization. **Eur Heart J**. 2017; 38:2805−2812.

61. Hughes TM, Wagenknecht LE, Craft S, et al. Arterial stiffness and dementia pathology. **Neurology**. 2018; 90:e1248−e1256.

62. Gottesman RF, Schneider ALC, Zhou Y, et al. Association between midlife vascular risk factors and estimated brain amyloid deposition. **J Am Med Assoc**. 2017; 317, 1443-1443.

63. Goel A, Maroules CD, Mitchell GF, et al. Ethnic difference in proximal aortic stiffness. **JACC Cardiovasc Imag**. 2017; 10:54−61.

64. Wei F-F, Thijs L, Yu C-G, et al. Retinal microvasculature in relation to central hemodynamics in a flemish population. **Hypertension**. 2019; 74:606−613.

65. Dąbrowska E, Harazny JM, Miszkowska-Nagórna E, et al. Aortic stiffness is not only associated with structural but also functional parameters of retinal microcirculation. **Microvasc Res**. 2020; 129:103974.

66. Meyer ML, Klein BE, Klein R, et al. Central arterial stiffness and retinal vessel calibers. **J Hypertens**. 2020; 38:266−273.

67. Maroules CD, Khera A, Ayers C, et al. Cardiovascular outcome associations among cardiovascular magnetic resonance measures of arterial stiffness: the Dallas heart study. **J Cardiovasc Magn Reson**. 2014; 16.

68. Ohyama Y, Ambale-Venkatesh B, Noda C, et al. Aortic arch pulse wave velocity assessed by magnetic resonance imaging as a predictor of incident cardiovascular events. The MESA (Multi-Ethnic study of Atherosclerosis). **Hypertension**. 2017; 70:524−530.

69. Libhaber E, Woodiwiss AJ, Libhaber C, et al. Gender-specific brachial artery blood pressure-independent relationship between pulse wave velocity and left ventricular mass index in a group of African ancestry. **J Hypertens**. 2008; 26:1619−1628.

70. Fourie CMT, Botha-Le Roux S, Smith W, et al. Vascular function and cardiovascular risk in a HIV infected and HIV free cohort of African ancestry: baseline profile, rationale and methods of the longitudinal EndoAfrica-NWU study. **BMC Infect Dis**. 2020; 20:473.

71. Birru MS, Matthews KA, Thurston RC, et al. African-American ethnicity and cardiovascular risk factors are related to aortic pulse-wave velocity progression. **Am J Hypertens**. 2011; 24:809−815.

72. Samargandy S, Matthews KA, Brooks MM, et al. Arterial stiffness accelerates within 1 year of the final menstrual period. **Arterioscler Thromb Vasc Biol**. 2020; 40:1001−1008.

73. Lu Y, Pechlaner R, Cai J, et al. Trajectories of age-related arterial stiffness in Chinese men and women. **J Am Coll Cardiol**. 2020; 75:870−880.

74. Nethononda RM, Lewandowski AJ, Stewart R, et al. Gender specific patterns of age-related decline in aortic stiffness: a cardiovascular magnetic resonance study including normal ranges. **J Cardiovasc Magn Reson**. 2015; 17, 20-20.

75. Markert MS, Della-Morte D, Cabral D, et al. Ethnic differences in carotid artery diameter and stiffness: the Northern Manhattan Study. **Atherosclerosis**. 2011; 219:827−832.

76. Meyer ML, Tanaka H, Palta P, et al. Correlates of segmental pulse wave velocity in older adults: the Atherosclerosis Risk in Communities (ARIC) study. **Am J Hypertens**. 2015; 29:114−122.

77. Kim ED, Ballew SH, Tanaka H, Heiss G, Coresh J, Matsushita K. Short-term prognostic impact of arterial stiffness in older adults without prevalent cardiovascular disease. **Hypertension**. 2019; 74:1373−1382.

78. Townsend RR, Anderson AH, Chirinos JA, et al. Association of pulse wave velocity with chronic kidney disease progression and mortality. **Hypertension**. 2018; 71:1101−1107.

79. Townsend RR. Arterial stiffness in CKD: a review. **Am J Kidney Dis**. 2019; 73:240−247.

80. Grunwald JE, Pistilli M, Ying G-S, et al. Association between progression of retinopathy and concurrent progression of kidney disease. **JAMA Ophthalmol**. 2019; 137, 767-767.

81. Kim ED, Tanaka H, Ballew SH, et al. Associations between kidney disease measures and regional pulse wave velocity in a large community-based cohort: the Atherosclerosis Risk in Communities (ARIC) study. **Am J Kidney Dis**. 2018; 72:682−690.

82. Gunarathne A, Patel JV, Gammon B, Gill PS, Hughes EA, Lip GYH. Ischemic stroke in South Asians. **Stroke**. 2009; 40:e415−e423.

83. Brar I, Robertson AD, Hughson RL. Increased central arterial stiffness and altered cerebrovascular haemodynamic properties in South Asian older adults. **J Hum Hypertens**. 2015; 30:309−314.

84. Park CM, Tillin T, March K, et al. Adverse effect of diabetes and hyperglycaemia on arterial stiffness in Europeans, South Asians, and African Caribbeans in the SABRE study. **J Hypertens**. 2016; 34:282−289.

85. Snijder MB, Stronks K, Agyemang C, Busschers WB, Peters RJ, van den Born B-JH. Ethnic differences in arterial stiffness the Helius study. **Int J Cardiol**. 2015; 191:28−33.

86. Ge D, Young TW, Wang X, Kapuku GK, Treiber FA, Snieder H. Heritability of arterial stiffness in black and white American youth and young adults. **Am J Hypertens**. 2007; 20:1065−1072.

87. Mitchell GF, DeStefano AL, Larson MG, et al. Heritability and a genome-wide linkage scan for arterial stiffness, wave reflection, and mean arterial pressure: the Framingham Heart Study. **Circulation**. 2005; 112:194−199.

88. Mitchell GF, Verwoert GC, Tarasov KV, et al. Common genetic variation in the 3'-BCL11B gene desert is associated with carotid-femoral pulse wave velocity and excess cardiovascular disease risk: the AortaGen Consortium. **Circ Cardiovasc Genet**. 2012; 5:81−90.

89. Rode M, Teren A, Wirkner K, et al. Genome-wide association analysis of pulse wave velocity traits provide new insights into the causal relationship between arterial stiffness and blood pressure. **PLoS One**. 2020; 15:e0237237.

90. Park S, Lee JY, Kim BK, et al. Lack of association between arterial stiffness and genetic variants by genome-wide association scan. **Blood Press**. 2015; 24:258−261.

91. Shibata S, Fujimoto N, Hastings JL, et al. The effect of lifelong exercise frequency on arterial stiffness. **J Physiol**. 2018; 596:2783−2795.

This page intentionally left blank

Arterial stiffness and pulsatile hemodynamics in systemic hypertension

Stéphane Laurent[2,3,4,5] and Pierre Boutouyrie[1]

[1]Paris University, Assistance-Publique Hôpitaux de Paris, PARCC-INSERM U970, Department of Pharmacology and Hôpital Européen Georges Pompidou, Paris, France; [2]Department of Pharmacology and Hôpital Européen Georges Pompidou, Paris, France; [3]INSERM, U970, Paris Cardiovascular Research Center, PARCC, Paris, France; [4]Université de Paris, Paris, France; [5]Assistance Publique, Hopitaux de Paris, Paris, France

Introduction

Arterial stiffness refers to the loss of arterial compliance, i.e., its change if volume in response to changes in blood pressure (BP).[62] The major hemodynamic consequence of elevated arterial stiffness is illustrated by increased central systolic and pulse pressures. In systemic hypertension, arterial stiffening is a consequence of the aging of the large artery wall, which is accelerated by long-term high BP.[54,79] Pathophysiological studies have extensively investigated the structural factor in hypertension, including large and small artery remodeling and functional changes. Here, we review the recent literature on the alterations in large arteries in hypertension. We discuss the possible mechanisms underlying the relationship between arterial stiffness and increased central pressure pulsatility. We explain how hypertension is both a cause and a consequence of central arterial stiffening. Finally, we propose an integrated pathophysiological approach in order to better understand how the cross-talk between large and small artery changes interacts in the transmission of pressure pulsatility, exaggerates cardiac, brain, and kidney damage, and lead to cardiovascular and renal complications. We focus on patients with essential hypertension since this is the most prevalent form of hypertension.

Consequence of arterial stiffness on pressure pulsatility

The wording "arterial stiffness" is a general term that refers to the loss of arterial compliance and/or changes in vessel wall properties.[41,63] The classical view is that compliance of large arteries, including the thoracic aorta that has the major role, represents their ability to dampen the pulsatility of ventricular ejection and to transform a pulsatile pressure (and flow) at the site of the ascending aorta into a continuous pressure (and flow) downstream at the site of arterioles. This allows to lower the energy expenditure during organ perfusion and to protect small arteries of target organs (mainly the brain and the kidney) from the damaging effects of pressure pulsatility.[54] Indeed, during ventricular contraction, part of the stroke volume is forwarded directly to the peripheral tissues and part of it is momentarily stored in the aorta and central arteries stretching the arterial walls and raising local BP.[18]

A more contemporary view is that arterial compliance is a key thermodynamic optimization of cardiovascular energetics. Part of the heart energy is reoriented to the distension of the arterial wall. This energy is thus "stored" in the vessel walls during systole, and recoils the aorta during diastole. This phenomenon squeezes the accumulated blood forward into the peripheral tissues, ensuring a subsequent diastolic flow. The stiffness and geometry of the arteries make this phenomenon effective in young, healthy subjects and less effective in older, hypertensive patients.[54,79]

When the stiffness is low (young healthy subject), a large amount of cardiac energy is redistributed during diastole and helps decreasing postload and improving organ perfusion during diastole (especially "torrential" circulations such as brain, kidney, and coronary arteries).[55] In hypertensives, arterial stiffness is higher[47] and a higher pressure is necessary to stretch a more rigid arterial system. Thus, this is mainly during systole that a larger proportion of the stroke volume flows through the arterial system and peripheral tissues. The main consequences are an intermittent flow and pressure, an exaggerated flow and pressure pulsatility at the site of distal small resistance, and a shorter

capillary transit time. The later reduces metabolic exchanges. Altogether, these mechanisms damage target organs.

Arterial stiffness and wave reflection in systemic hypertension

The pulsatility of BP is exaggerated in hypertensives by the phenomenon of wave reflection.[54,79] With hypertension, the large arteries stiffen and pulse pressure (PP = systolic *minus* diastolic) increases at the site of central and peripheral arteries. Because the arterial tree can be approximated to a viscoelastic tube with numerous branches and a high level of impedance (resistance in oscillatory conditions) of the tube end, retrograde waves, due to wave reflection, are generated. The higher the arterial stiffness, the higher the transmission velocity of both forward and reflected waves, thus the reflected wave arrives earlier in the central aorta and augments pressure in late systole, increasing central PP.[62,54]

To better understand the mechanisms leading to wave reflection and augmented central pulse pressure in systemic hypertension, it is important to take into account the heterogeneity of elastic properties along the arterial tree, resulting in a stiffness gradient or mismatch. In young normotensive subjects, the stiffness gradient is illustrated by the progressive increase in arterial stiffness from upstream proximal large arteries to downstream distal medium-size arteries (Fig. 29.1A). Although all of the large artery walls are constituted by three layers (intima, media, and adventitia), there is a difference between large proximal elastic arteries and medium-size distal muscular arteries regarding the relative amount of vascular smooth muscle cells (VSMCs) and extracellular matrix (especially elastin) in their media. In humans, pulse wave velocity increases from 4 to 5 m/s in the ascending aorta to 5−6 m/s in the abdominal aorta then 8−9 m/s in the iliac and femoral arteries.[35,54] In middle-aged normotensive subjects, the cross-sectional distensibility, assessed with echotracking systems, decreases from $40 \, kPa^{-1} \, 10^{-3}$ in the thoracic aorta[26] to $15-25 \, kPa^{-1} \, 10^{-3}$ in the carotid[37,28,5] and brachial[5,70] arteries, $10-15 \, kPa^{-1} \, 10^{-3}$ in the common femoral artery to $5 \, kPa^{-1} \, 10^{-3}$ in the radial artery.[36,38,5] Indeed, both VSMCs and many elastic lamellae are present in the media of large proximal artery, whereas VSMCs prevail in the media of medium-size distal artery.[54] In healthy subjects, the stiffness gradient between proximal elastic arteries and distal muscular arteries may lead to an impedance mismatch, generating pressure wave reflection upwards that limits the transmission of pressure pulsatility downward to the small arteries of target organs (Fig. 29.1A). The reflected pulsatile energy travels at low velocity along elastic arteries, thus do not superimpose on incident pressure wave and central systolic blood pressure (SBP) remains normal.
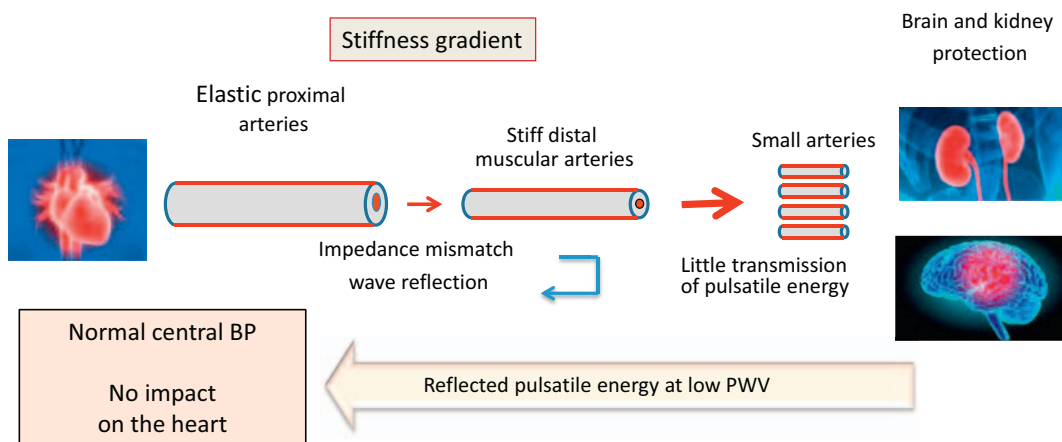
By contrasts, stiff elastic proximal arteries lose their ability to dampen the pulsatility of ventricular ejection. Thus, small arteries of target organ are damaged (Fig. 29.1B). Because distal muscular arteries do not stiffen with age,[43] the stiffness gradient between proximal elastic arteries and distal muscular arteries is reduced (and sometime inverted), and there is more transmission of pressure pulsatility toward small arteries of target organs. Most of the reflected pulsatile energy that return to the heart travels at high velocity along stiff arteries, and superimposes on incident pressure wave, thus increasing central SBP and PP. In parallel, the pulsatile pressure is not sufficiently attenuated and is transmitted downwards, damaging the microcirculation.

Whereas the paradigm described above takes into account the stiffness gradient, it should be noted that the main determinant of reflection at any given interface is the impedance gradient, rather than the stiffness gradient per se. As discussed in Chapters 1−3 and 11, impedance is more prominently influenced by size than stiffness. Therefore, the stiffness gradient does not equal impedance gradient, and indeed, the matching between the size of the aortic lumen and daughter vessels at bifurcations tends to match impedances even in young people with marked stiffness gradients. Conversely, in older people, aortic dilation may impact reflections at first order bifurcations, and may favor impedance mismatch despite stiffness matching (i.e., absence of a stiffness gradient). Clearly, more research is needed to better understand the role of stiffness and impedance matching at first order bifurcations as a determinant of target organ damage.
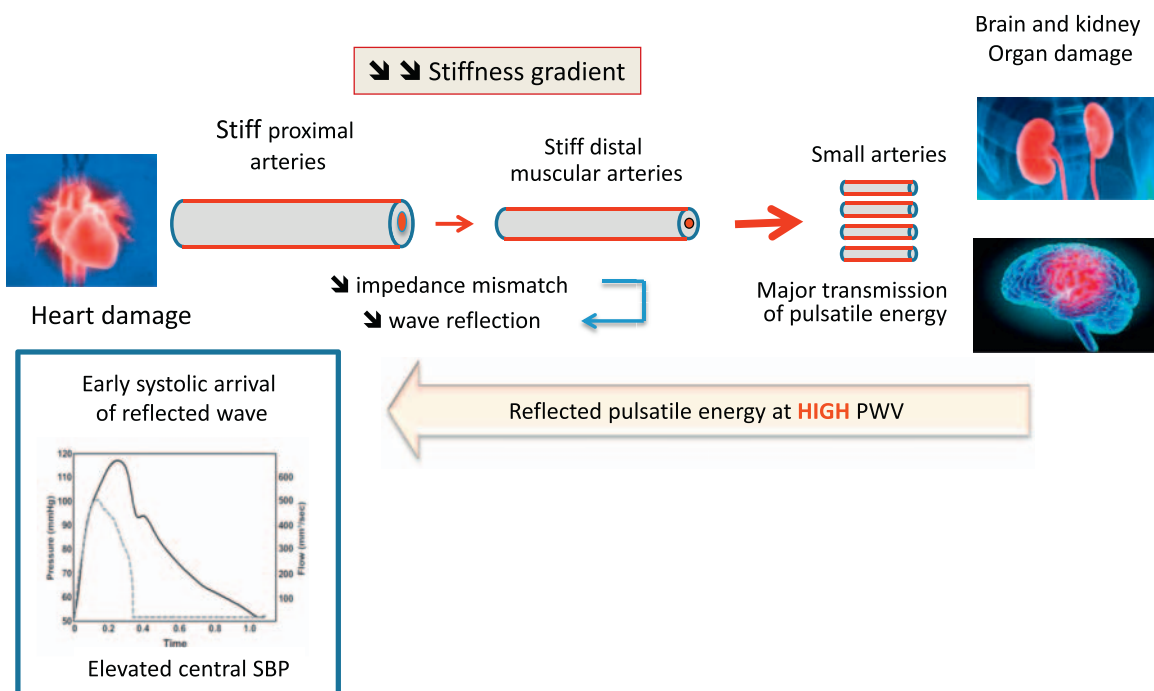
The wave reflection phenomenon also explains why the central systolic and pulse pressures are elevated in hypertensives. The main explanation resides in the "amplification phenomenon." The "central-to-peripheral amplification" means that central SBP increases from the central artery compartment to the peripheral arteries. Indeed, under resting conditions in healthy humans, brachial SBP is in average 10% higher than aortic SBP, sometimes up to 30%. In the presence of physiological arterial stiffness gradient (aortic PWV lower than peripheral PWV), reflection sites are closer to peripheral sites and reflection superimposes on forward wave, leading to amplification of pulse pressure. Because PWV is low, reflection comes late, in late systole or early diastole in central arteries, limiting pulse pressure. By contrast, when the stiffness gradient disappears or is inverted (aortic PWV higher than peripheral PWV), apparent reflection sites are much closer to central arteries, and pulsatile pressure is not sufficiently dampened at central level, and the central-to-peripheral pressure amplification is attenuated.[23]

The physiological amplification phenomenon is attenuated by aging because of arterial stiffening. Indeed, by favoring early wave reflections, arterial stiffening increases
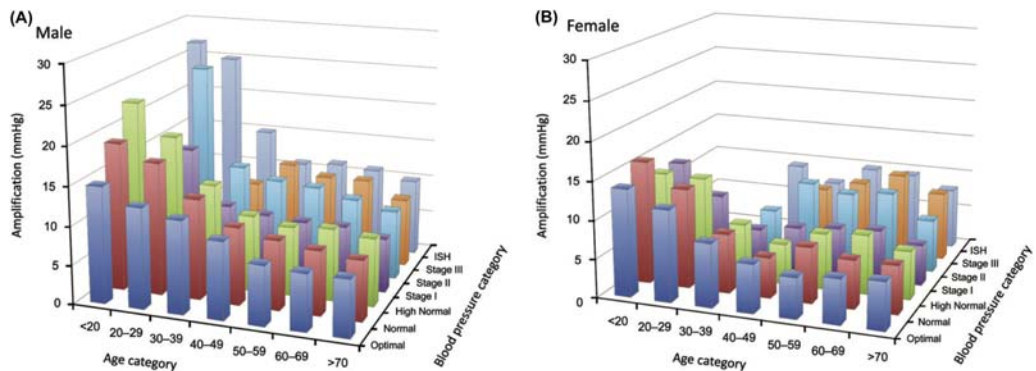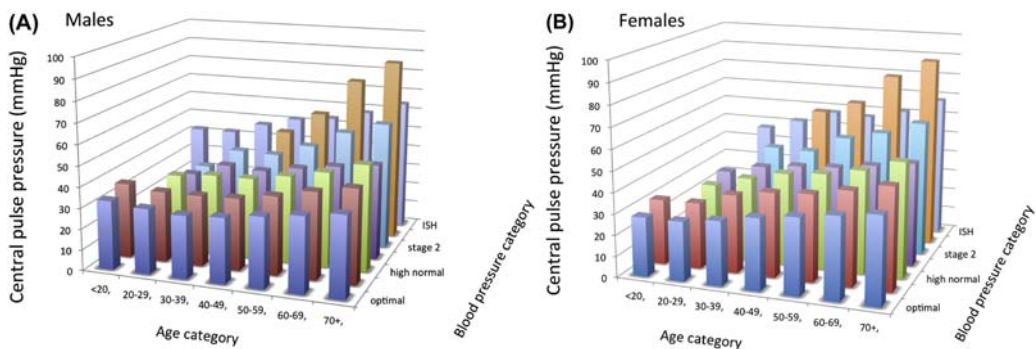
FIGURE 29.1 (A) Healthy aging is a means to retard brain, kidney, and heart damage. Indeed, in healthy subjects, an impedance mismatch occurs in response to the stiffness gradient between proximal elastic arteries and distal muscular arteries. This phenomenon generates pressure wave reflection, limiting the transmission of pressure pulsatility to target organs. The largest part of the reflected pulsatile energy that propagates backward, toward the heart, travels indeed at low velocity along elastic arteries, thus do not superimpose on incident pressure wave. Thus, central BP remains normal. (B) Wave reflections in elderly subjects and hypertensive patients. When the aorta stiffens with aging or hypertension, it loses its ability to dampen the pulsatility of ventricular ejection. Small arteries of the heart, brain, and kidney are damaged by the hyperpulsatility. Because the stiffness of distal muscular arteries does not change with age, there is a reduction of the stiffness gradient between proximal elastic arteries and distal muscular arteries. Thus, pressure pulsatility is transmitted to a larger extent toward small arteries of target organs. The largest part of the reflected pulsatile energy that propagates backward, toward the heart, travels at high velocity along stiff arteries. Thus, it superimposes on incident pressure wave and increase central systolic blood pressure. *(A) From Laurent S, Cunha P. Large vessels in hypertension: central blood pressure. In* **Hypertension in Children and Adolescents***, Ed. Lurbe E, Wuhl E Springer publisher 2019 with permission; (B) From Laurent S, Cunha P. Large vessels in hypertension: central blood pressure. In* **Hypertension in Children and Adolescents***, Ed. Lurbe E, Wuhl E Springer publisher 2019 with permission.*

FIGURE 29.2 (A) and (B): Loss of amplification phenomenon with aging and hypertension. Tridimensional bar-graphs representing amplification according to sex (A, males; B, females), age categories, and blood pressure categories. The value represented here is the median of the group. Some categories are not represented because there were less than 50 observations. *From Herbert A, Cruickshank K, Laurent S, Boutouyrie P, On behalf of the reference values for arterial measurements collaboration. Establishing reference values for central blood pressure and amplification in a general healthy population and according to cardiovascular risk-factors.* **Eur Heart J**. *2014; 32:3122−3133 with permission.*

FIGURE 29.3 A and B: Tridimensional bar-graphs representing central pulse pressure (peripheral *minus* central systolic blood pressures) according to sex (A, males; B, females), age categories, and blood pressure categories. The value represented here is the median of the group. Some categories are not represented because there were less than 50 observations. *From Herbert A, Cruickshank K, Laurent S, Boutouyrie P, On behalf of the reference values for arterial measurements collaboration. Establishing reference values for central blood pressure and amplification in a general healthy population and according to cardiovascular risk-factors.* **Eur Heart J**. *2014; 32:3122−3133 with permission.*

peak- and end-systolic pressures in the ascending aorta. Thus, central systolic and pulse pressures are higher in elderly subjects than in young subjects and closer to the brachial SBP value, reducing the difference[23] (Figs. 29.2A,B and 29.3A,B). Excessive amplification leads to high SBP or PP in peripheral arteries, so called spurious systolic hypertension, often in young males, with various interpretations.[23]

Influence of lumen area on compliance, wave reflection, and pressure pulsatility

There is a bidirectional relationship between aortic root lumen area and pressure pulsatility.[49] The higher the central PP, the larger the aortic root diameter, suggesting a major role of pressure pulsatility on aortic root enlargement, through a fatigue phenomenon. Magnetic resonance imaging, which precisely investigates the geometry of aorta in hypertensives, showed that ascending aortic diameter and increased aortic arch length and width, as well as decreased aortic arch curvature were highly correlated with increased central PP.[57] Conversely the consequences of aortic remodeling on central BP remain less clear.[54,33,49] By contrast to studies in hypertensives, studies in normotensives[33,28] reported a negative relationship between central PP and aortic root diameter, i.e., the smaller the lumen diameter, the higher the central PP.[33] Thus suggested that the lack of aortic root dilatation, increasing characteristic impedance (Z_c) and wave reflection, would be the cause of high central PP and SBP. Altogether, these data suggest that excessive pulsatility favors aortic enlargement when the arterial wall is already damaged, for instance, by the hypertensive disease.[49] In turn, the enlargement of large proximal arteries can be viewed as a compensating phenomenon that enables to maintain a certain level of arterial compliance (expressed as $\Delta V/\Delta P$, i.e., the product of volumic distensibility $\Delta V/V.\Delta P$, and volume (V) despite aortic stiffening).[54] By contrast, when the aortic wall is healthy, a

reduced volume of the aorta can increase characteristic impedance (Z_c) and generate wave reflection, and thus elevate central PP and SBP.

A second factor of complexity is represented by the changes in lumen area along the arterial pathway. Indeed, any change in lumen area (tapering or branching) can generate an impedance mismatch which may act in addition to the stiffness gradient between proximal elastic arteries and distal muscular arteries, as we have seen above. Points of arterial branching leading to changes in lumen area between daughter and parent vessels are sites of impedance mismatch.[13] Thus, given the innumerable sites of impedance mismatch throughout the arterial tree, individual reflection sites have little importance relative to the bulk of reflections originating elsewhere. In addition, all the reflected waves originating from thousands of reflection sites merge into a net reflected wave which appears discrete but is not due to a single reflection site, and can penetrate target organs as forward waves.[13]

Peripheral and central blood pressure in aging hypertensives

Cross-sectional and longitudinal population studies have shown that both peripheral SBP and DBP trajectories increase progressively between adolescence and adulthood.[12,21] Before 50 years of age, the increase in both brachial DBP and SBP can be explained by the increase in peripheral vascular resistance. DBP plateaus around age 50 years, and then decreases. By contrast, SBP continues to rise even after the age of 50 in response to the continuous age-induced increase in arterial stiffness, as explained above. After age 60, the divergent trajectories of SBP and DBP explains why PP begins to increase markedly after age 50. The rapid widening of PP is considered as caused by arterial stiffening.

For these reasons, isolated systolic hypertension, defined as SBP $\geq$140 and DBP <90 mmHg, represents the most frequent subtype of hypertension after age 60.[21] Men and women have different trajectories. The prevalence of hypertension in young women is lower than in men of the same age. And then, BP in women reaches men's values around the fourth decade of life. By the seventh decade, BP in women is higher than in men. Since hypertension is more frequent in the elderly, and elderly women have higher BP than men, it is not surprising that 60% of all hypertensive individuals now are women.[21]

Reference values for central SBP have been reported according to sex, age, and BP categories.[23] According to age, central SBP was higher in men than in women until age 50−59, after which the tendency was reversed. According to BP categories, central SBP was lower in men than in women within each peripheral BP category, except
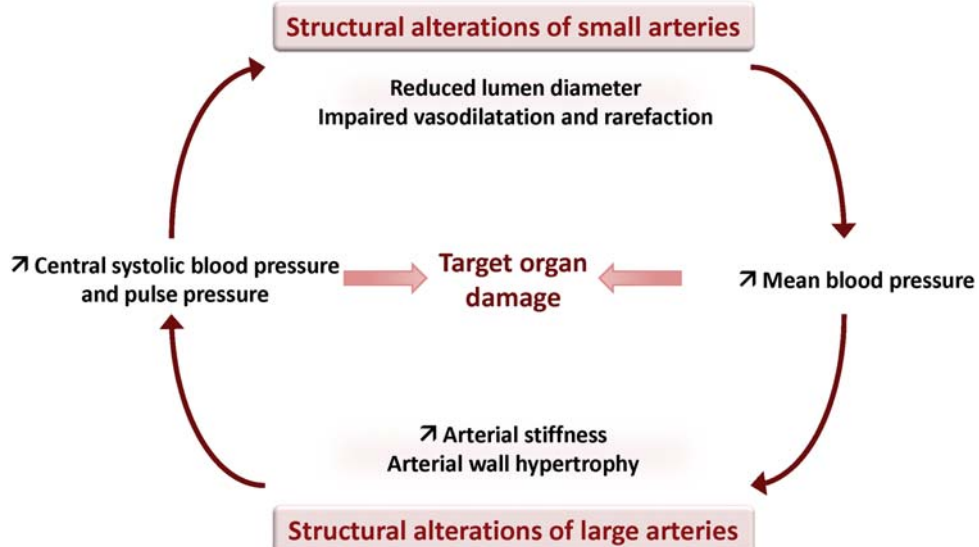
"optimal." Amplification between central and peripheral BP, calculated as peripheral SBP minus central SBP, was higher in males than in females at any given age or BP value.[23] The difference between sexes becomes smaller with increasing age and values of BP. Amplification is very little influenced by BP categories. Amplification decreases gradually with aging without clearly reaching a plateau, except in those with optimal brachial BP.[23] (Figs. 29.2A,B and 29.3A,B).

Interaction between hypertension and arterial stiffness

Whether arterial stiffness is a cause or a consequence of hypertension, and whether large or small arteries are damaged first, have long been considered as major issues. The relationships between arterial stiffness, small artery damage, and BP are rendered more complex by two characteristics of hemodynamics and biomechanics.[63]

First, an insidious positive feedback loop between local mechanobiological responses and global hemodynamics may explain why central artery stiffening is at the same time a cause of hypertension and one of its consequences.[25] For instance, arterial stiffening in early phases of prehypertension may be a major determinant of elevated systolic BP on the long term.[44] Indeed, the longitudinal assessment of the temporal relationship between carotid and aortic stiffness[29] on the one side and incident hypertension on the other side suggests a precursor role of arterial stiffening in future altered systolic hemodynamic load. However, the reverse occurs when hypertension is installed, even at the lower grade of prehypertension. Indeed, arterial stiffening can be a consequence of the rise in mean BP. Early work, in the 1950s to 1970s, suggested that sustained increases in BP stimulate matrix synthesis and thus vascular thickness and structural stiffness. In addition, high BP loads the stiff components of the arterial wall and changes the spatial organization between smooth muscle cells and extracellular matrix[32] and eventually increases arterial stiffness.

Second, arterial stiffening may be paralleled by a remodeling of small resistance arteries. Small and large artery alterations are indeed closely interdependent in sustained grade I hypertension, and likely during the early phases of prehypertension. A temporal relationship is difficult to establish, and we previously suggested that a cross-talk, by which small artery alterations influence larger artery phenotype, and conversely large artery alterations influence small artery phenotype, is more likely than a linear sequence.[42] Both small and large artery damages contribute to the rise in central BP, by favoring the generation of wave reflections and their propagation, respectively. This is exemplified by the fact that, in hypertensive

FIGURE 29.4 Schematic representation of the large/small artery cross-talk: a vicious circle of aggravation between large and small artery alterations in essential hypertension. *From Safar ME, Asmar R, Benetos A, et al. French study group on arterial stiffness. Interaction between hypertension and arterial stiffness.* **Hypertension**. *2018; 72:796−805 with permission.*

patients, media-to-lumen ratio of subcutaneous small resistance arteries and carotid-femoral PWV are both independent determinants of central SBP. The cross-talk between the micro- and the macrocirculation[42] promotes a vicious circle which can be described by starting at the site of small arteries (Fig. 29.4). An increased resistance in small arteries increases mean BP, and then increases arterial stiffness in the large elastic arteries, which in parallel with more pressure wave reflections increases central systolic BP, variability of 24-h ambulatory brachial BP, and ultimately damages target organs.[42,43] The increased central BP pulsatility in turn is a factor of small resistance artery damage, i.e., increased media-to-lumen ratio of subcutaneous small resistance arteries. This has initially been reported in hypertensive animals,[14] and then in hypertensive patients with brachial pulse pressure[27] and more recently with central systolic and pulse pressures measured with applanation tonometry.[53] Interestingly, the wall-to-lumen ratio of retinal arteries is significantly correlated with 24-h systolic BP, and retinal microcirculation changes can already be found in prehypertensive subjects.[64] Eventually, increased media-to-lumen ratio of subcutaneous small resistance arteries, which is associated with reduced lumen diameter, represents the largest part of the structural part of increased total peripheral resistance, leading to a rise in mean BP, and thus continuing the vicious circle (Fig. 29.4). This may also apply to the interactions between diabetes and hypertension.[15]

Thus, whether hypertension causes or is caused by central arterial stiffening and whether large or small arteries are damaged first, can be considered irrelevant. The main issue is that a progressive worsening can ensue in either case, thus any onset of large artery stiffening or small artery remodeling merits early intervention.

High central blood pressure, hypertension-mediated organ damage, and cardiovascular complication

The small/large artery cross-talk has a synergistic effect on the heart, brain, and kidney, in large part through a high pulsatile energy that is delivered as central systolic or pulse pressure. There is a large amount of evidence that central systolic and pulse pressures are the most deleterious elements of the BP load on the heart, brain, and kidney in hypertensives. Their increase is better correlated with hypertension-mediated organ damage (HMOD) than either brachial systolic and pulse pressures or mean BP.[62,42,59] Because the effects of pulsatile hemodynamics on the heart, brain, and kidney are described in details in other chapters of this book, we only address here the main mechanisms and consequences related to systemic hypertension.

Cardiac damage

A higher correlation has been observed with central SBP and PP than with brachial SBP and PP for left ventricular hypertrophy (LVH),[6,56,78] systolic dysfunction,[34] and diastolic dysfunction[77] that can be considered as characteristics of cardiac damage in hypertensive patients. This is also the case for new onset of atrial fibrillation and left atria enlargement.[50] Central SBP increases the load on the left ventricle thus the myocardial oxygen demand. In addition, arterial stiffness is correlated to LVH,[6] a known risk factor

for coronary events.[31] High central PP and low diastolic BP can cause subendocardial ischemia. Indeed, a high central pulsatility reduces large epicardial coronary vascular tree perfusion during diastole, thus decreases coronary flow reserve because of lesser BP during early diastole.[19] Rarefaction and remodeling of intramyocardial coronary artery, as well as LVH and left ventricular diastolic dysfunction also contribute to a reduction in microcirculatory flow reserve, an impairment of tissue perfusion and a higher susceptibility to ischemia during high levels of metabolic and oxygen demand.[19] Atherosclerosis at the site of epicardial coronary arteries increases the damaging effects of above damages and the risk of ischemic heart disease.

Brain damage

The damage of large and small arteries can increase the risk of ischemic stroke, and, likely in parallel, white matter lesions, lacunar infarcts, and cognitive decline.[11,67] High pulse pressure can be transmitted into cerebral arteries, thus leading to an inward remodeling reducing lumen diameter aiming at protecting the microcirculation from pulsatile stress. The cerebral (as well as renal) circulation is particularly susceptible to pressure damage, since this is a high flow/low resistance circulation. Under such condition, mean and pulse pressures are easily transmitted from the aorta to small cerebral (and renal) arteries.[55] An increased arterial pulsatility due to large artery stiffening can thus be transmitted to cerebral small vessels and associated with white matter lesions.[76,52] Indeed, the pulsatility of the carotid flow, measured with Doppler, and pressure, and the carotid-femoral pulse wave velocity (cfPWV), are related with silent subcortical infarcts or white matter lesions,[76,52] and lower scores in various cognitive domains.[52] There is also a relationship between carotid stiffness and large white matter hyperintensity volume, independently of vascular risk factors and carotid plaque,[11] and with stroke.[71]

Several mechanisms can explain why an increased arterial stiffness can increase the risk of stroke: an elevated central PP, remodeling extracranial and intracranial arteries, in association with an increased carotid wall thickness and the development of stenosis and plaques[43] and the prevalence and severity of cerebral white matter lesions.[11,66] Aortic stiffening may also express damages at the site of the cerebral vasculature. Thus, it is not surprising that aortic stiffness can to predict not only incident stroke,[40] but also the functional outcome after stroke, independently of classical cardiovascular risk factors.[22] Another explanation is given by the differential physiological behavior of brain small arteries compared with other systemic vascular beds.[62] In elderly hypertensives, the inward remodeling of small cerebral arteries and associated increased myogenic

tone impairs vasomotor reactivity, limits the autoregulation of cerebral blood flow, and increases susceptibility to focal ischemia when BP is transiently and/or acutely low. Patients with exaggerated visit-to-visit variability of BP, namely SBP, are at increased risk of stroke,[60] which suggests that repeated episodes of hypoperfusion and microvascular ischemia resulting from excessive variability coupled with reduced autoregulation, could favor tissue damage and stroke. Similar findings can result from exaggerated short-term BP variability, detected with ambulatory BP monitoring, that is associated with arterial stiffness.[65] Finally, a high central PP may remodel the arterial system not only at the site of the intracranial arteries, but also in extracranial arteries, thickening the carotid wall, leading to the development of atherosclerotic plaques.[7,82]

Renal damage

Myogenic tone in the renal circulation is impaired in the elderly hypertensive. The consequence is a loss of the autoregulation capacity and an increase in barotrauma due to high systolic BP, leading to glomerular injury. Because of its torrential nature (very low resistances), even small increases in peripheral BP are transformed into high pulsatile energy that is transmitted to the kidney and dissipated in the microcirculation, leading to hyperfiltration and glomerulosclerosis. Clinical data are consistent with this pathophysiological approach. Significant relationships have been demonstrated between brachial pulse pressure and either glomerular filtration rate (GFR) or microalbuminuria[20]; between arterial stiffness and either GFR[9,24] or urinary albumin[24]; between carotid stiffness and GFR[24]; and between central PP and incident end-stage renal disease.[10] Although confounding factors may not be fully excluded, there is a large amount of evidence for linking the pulsatility of BP to renal damage.

Cardiovascular and renal outcome

Because the small/large artery cross-talk exerts a synergistic damaging effect on the heart, brain, and kidney, it is not surprising that arterial stiffness[39,8]; Vlachopoulos et al. 2010,[30,51] central systolic and pulse pressures[10]; Vlachopoulos et al. 2010,[61] and media-to-lumen ratio of small resistance arteries,[58] have independent predictive value for CV events and renal complications in hypertensive patients.

Predictive value of arterial stiffness and wave reflection in hypertensives
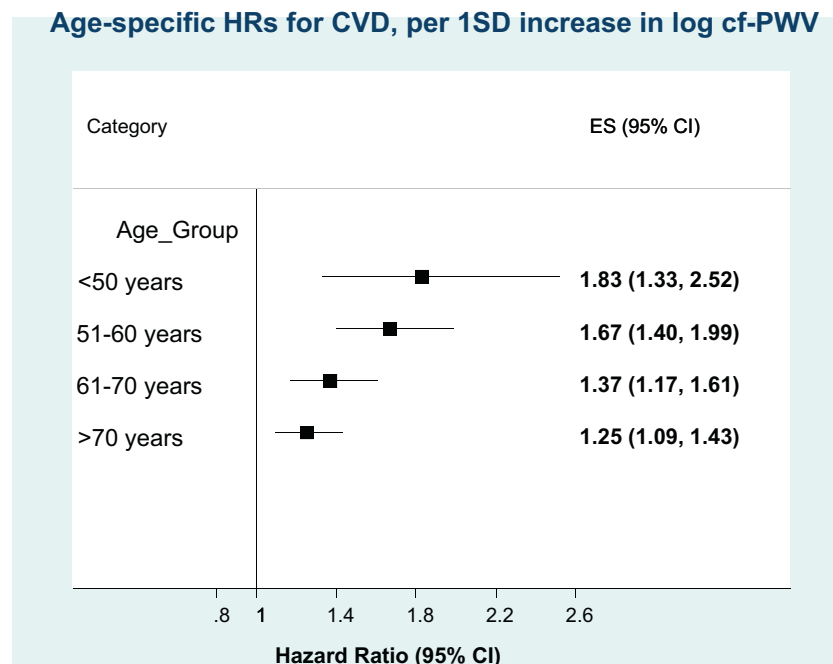
The measurement of arterial stiffness and wave reflections in clinical practice in hypertensives is comforted by the repeated demonstration that arterial stiffness has an independent predictive value for CV events.[41,69]

Several longitudinal epidemiological studies have demonstrated the predictive value of arterial stiffness for CV events. The largest amount of evidence has been given for aortic stiffness, measured through carotid-femoral PWV. Aortic stiffness has independent predictive value for all-cause and CV mortality, fatal and nonfatal coronary events, and fatal strokes not only in patients with uncomplicated essential hypertension,[39,8,40] but also in patients with type 2 diabetes,[17] end-stage renal disease,[4] in elderly subjects[48] and in the general population.[46,51]

Two meta-analyses[72,3] consistently showed the independent predictive value of aortic stiffness, measured by carotid-femoral PWV, for fatal and nonfatal CV events in various populations, as well as two meta-analyses on carotid stiffness.[71,81] Brachial-ankle PWV has also demonstrated a predictive value for CV events.[73] This amount of evidence led the European Society of Hypertension and the European Society of Cardiology, in their 2013[45] and 2018[80] common guidelines for the management of hypertension, to include carotid-femoral PWV in the list of measurements in order to assess HMOD. The measurement of brachial-ankle PWV is recommended by the 2019 Japanese Society of Hypertension guidelines for the management of hypertension.[68] A 2015 position statement from the European Society of Cardiology working group on peripheral circulation ranked the carotid-femoral PWV and the brachial-ankle PWV as top biomarkers for assessing the CV risk in clinical practice.[74]

Aortic stiffness has demonstrated an independent predictive value for CV events after adjustment to classical CV risk factors, including brachial pulse pressure. These data show that aortic stiffness predicts CV events to a larger extent than each of classical risk factors. In addition, aortic stiffness retains its predictive value for CHD events after adjustment to the Framingham risk score, demonstrating an added value to a combination of CV risk factors.[8] Aortic and carotid stiffness have additive predictive value.[71] As discussed above, one reason may be that aortic stiffness is an integrator of the cumulative damage of CV risk factors on the aortic wall over a long period of time, whereas the classical CV risk factors, such as BP, glycemia, and lipids can fluctuate over time. Thus, their values, measured at the time of risk assessment, may not reflect the true values damaging the arterial wall.

An important issue is whether arterial stiffness retains its independent predictive value in elderly hypertensives[3] undertook a systematic review and obtained individual participant data from 16 studies gathering 17,635 participants. cfPWV demonstrated predictive value for coronary heart disease, stroke, and CVD. Associations stratified according to sex, diabetes, and hypertension were similar but decreased in intensity with age: 1.89, 1.77, 1.36, and 1.23 for age <50, 51–60, 61 to 70, and >70 years, respectively, for one standard deviation, with a significant interaction (Fig. 29.5). Thus, although the predictive value of arterial stiffness for CV events is higher in adults less than 50 years, it is still significant in elderly.

Age-specific HRs for CVD, per 1SD increase in log cf-PWV

FIGURE 29.5 Individual participant systematic review of the predictive value of arterial stiffness (carotid-femoral pulse wave velocity) for cardiovascular disease. Associations stratified according to sex, diabetes, and hypertension were similar but decreased with age, with a significant interaction. *HR*, hazard ratio; *CVD*, cardiovascular disease; *SD*, standard deviation; *cfPWV*, carotid-femoral pulse wave velocity. *From Ben-Shlomo Y, Spears M, Boustred C, et al. Aortic pulse wave velocity improves cardiovascular event prediction: an individual participant meta-analysis of prospective observational data from 17,635 subjects.* **J Am Coll Cardiol**. *2014; 63:636–646 with permission.*

The particular case of very elderly hypertensives

Subjects older than 80 years represent a particular population since they are often frail, with several comorbidities. Very few studies have been done in very elderly hypertensives. The HYVET study,[1] one of the rare large randomized clinical trial performed so far in very old hypertensives (average 84 years), showed that antihypertensive treatment with indapamide, with or without perindopril, can be beneficial. This was confirmed by Corrao et al.,[16] in a nested case-control study on a cohort of patients aged 85 years or older (average 88 years). These patients were newly treated with antihypertensive drugs and the level of drug adherence was available. Compared with patients with very low adherence, patients with high adherence[16] showed a significant risk reduction for death and all the outcomes combined. The risk of heart failure and stroke was also reduced, whereas the risk of MI was not affected by adherence with antihypertensive drugs. Interestingly, similar findings were obtained in the cohort of patients aged 70–84 years.

Very few studies addressed the particular case of very elderly individuals. The PARTAGE study is an observational one[2,75] that followed 682 individuals aged older than 80 during 2 years, and showed that arterial stiffness as evaluated by cfPWV was associated with a more pronounced cognitive decline over a one-year period in very old frail institutionalized individuals. These data suggest that even in very old, frail individuals, arterial stiffness remains a determinant of cognitive decline, morbidity, and mortality.[63]

Conclusion

In this chapter, we have discussed the various mechanisms underlying the relationship between arterial stiffness and increased central pressure pulsatility. We addressed the issue that hypertension is both a cause and a consequence of central arterial stiffening. Finally, we suggested an integrated pathophysiological approach through which the cross-talk between large and small artery changes interacts in the transmission of pressure pulsatility, exaggerates cardiac, brain and kidney damage, and lead to cardiovascular and renal complications in hypertensive patients.

Acknowledgments

References

1. Beckett NS, Peters R, Fletcher AE, et al, HYVET Study Group. Treatment of hypertension in patients 80 years of age or older. **N Engl J Med**. 2008; 358:1887−1898.

2. Benetos A, Gautier S, Labat C, et al. Mortality and cardiovascular events are best predicted by low central/peripheral pulse pressure amplification but not by high blood pressure levels in elderly nursing home subjects: the PARTAGE (Predictive Values of Blood Pressure and Arterial Stiffness in Institutionalized Very Aged Population) study. **J Am Coll Cardiol**. 2012; 60:1503−1511.

3. Ben-Shlomo Y, Spears M, Boustred C, et al. Aortic pulse wave velocity improves cardiovascular event prediction: an individual participant meta-analysis of prospective observational data from 17,635 subjects. **J Am Coll Cardiol**. 2014; 63:636−646.

4. Blacher J, Pannier B, Guerin A, Marchais SJ, Safar ME, London GM. Carotid arterial stiffness as a predictor of cardiovascular and all-cause mortality in end-stage renal disease. **Hypertension**. 1998; 32:570−574.

5. Boutouyrie P, Laurent S, Benetos A, Girerd X, Hoeks A, Safar M. Opposite effects of ageing on distal and proximal large arteries in hypertensives. **J Hypertens**. 1992; 10(suppl 6):S87−S92.

6. Boutouyrie P, Laurent S, Girerd X, Beck L, Abergel E, Safar M. Common carotid artery distensibility and patterns of left ventricular hypertrophy in hypertensive patients. **Hypertension**. 1995; 25(part 1):651−659.

7. Boutouyrie P, Bussy C, Lacolley P, Girerd X, Laloux B, Laurent S. Local steady and pulse pressure and arterial remodeling. **Circulation**. 1999; 100:1387−1393.

8. Boutouyrie P, Tropeano AI, Asmar R, et al. Aortic stiffness is an independent predictor of primary coronary events in hypertensive patients: a longitudinal study. **Hypertension**. 2002; 39:10−15.

9. Briet M, Bozec E, Laurent S, et al. Arterial stiffness and enlargement in mild to moderate chronic kidney disease. **Kidney Int**. 2006; 96:350−357.

10. Briet M, Collin C, Karras A, et al. Maladaptive remodeling of large artery has a predictive value for chronic kidney disease progression. **J Am Soc Nephrol**. 2011; 22:967−974.

11. Brisset M, Boutouyrie P, Pico F, et al. Large-vessel correlates of cerebral small-vessel disease. **Neurology**. 2013; 80:662−669.

12. Burt VL, Whelton P, Roccella EJ, et al. Prevalence of hypertension in the US adult population: results from the third national health and nutrition examination survey, 1988-1991. **Hypertension**. 1995; 25:305−313.

13. Chirinos JA, Segers P, Hughes T, Townsend R. Large-artery stiffness in health and disease: JACC state-of-the-art review. **J Am Coll Cardiol**. 2019; 74:1237−1263.

14. Christensen KL. Reducing pulse pressure in hypertension may normalize small artery structure. **Hypertension**. 1991; 18:722−727.

15. Climie RE, van Sloten TT, Bruno RM, et al. Macrovasculature and microvasculature at the crossroads between type 2 diabetes mellitus and hypertension. **Hypertension**. 2019; 73:1138−1149.

16. Corrao G, Rea F, Monzio Compagnoni M, Merlino L, Mancia G. Protective effects of antihypertensive treatment in patients aged 85 years or older. **J Hypertens**. 2017; 35:1432−1441.

17. Cruickshank K, Riste L, Anderson SG, Wright JS, Dunn G, Gosling RG. Aortic pulse-wave velocity and its relationship to mortality in diabetes and glucose intolerance: an integrated index of vascular function? **Circulation**. 2002; 106:2085−2090.

18. Dobrin P. Vascular mechanics. In: Shepherd JT, Abboud FM, eds. **Handbook of Physiology, Section 2: The Cardiovascular System, Volume III: Peripheral Circulation and Organ Blood Flow**. Baltimore, Md: American Physiology Society; 1983:65−102.

19. Erdogan D, Yildirim I, Ciftci O, et al. Effects of normal blood pressure, prehypertension, and hypertension on coronary microvascular function. **Circulation**. 2007; 115:593−599.

20. Fesler P, Safar ME, du Cailar G, Ribstein J, Mimran A. Pulse pressure is an independent determinant of renal function decline during treatment of essential hypertension. **J Hypertens**. 2007; 25:1915−1920.

21. Franklin SS, Gustin 4th W, Wong ND, et al. Hemodynamic patterns of age-related changes in blood pressure. The Framingham Heart Study. **Circulation**. 1997; 96:308−315.

22. Gasecki D, Rokek A, Kwarciany M, Kubach M, Boutouyrie P, Nyka V, Laurent S, Narkiewicz K. Pulse wave velocity predicts functional outcome in patients after ischemic stroke. **Stroke**. 2012; 43(2):543−544.

23. Herbert A, Cruickshank K, Laurent S, Boutouyrie P. On behalf of the reference values for arterial measurements collaboration. Establishing reference values for central blood pressure and amplification in a general healthy population and according to cardiovascular risk-factors. **Eur Heart J**. 2014; 32:3122−3133.

24. Hermans MM, Henry R, Dekker JM, et al. Estimated glomerular filtration rate and urinary albumin excretion are independently associated with greater arterial stiffness: the Hoorn Study. **J Am Soc Nephrol**. 2007; 18:1942−1952.

25. Humphrey JD, Harrison DG, Figueroa CA, Lacolley P, Laurent S. Central artery stiffness in hypertension and aging: a problem with cause and consequence. **Circ Res**. 2016; 118:379−381.

26. Isnard RN, Pannier BM, Laurent S, London GM, Diebold B, Safar ME. Pulsatile diameter and elastic modulus of the aortic arch in essential hypertension: a non-invasive study. **J Am Coll Cardiol**. 1989; 13:399−405.

27. James MA, Watt PAC, Potter JF, Thurston H, Swales JD. Pulse pressure and resistance artery structure in the elderly. **Hypertension**. 1995; 26:301−306.

28. Jondeau G, Boutouyrie P, Lacolley P, et al. Central aortic pulse pressure is a major determinant of aortic dilatation in Marfan syndrome. **Circulation**. 1999; 99:2677−2681.

29. Kaess BM, Rong J, Larson MG, et al. Aortic stiffness, blood pressure progression, and incident hypertension. **J Am Med Assoc**. 2012; 308:875−881.

30. Karras A, Haymann JP, Bozec E, et al. Briet M on behalf of the NephroTest study group. Large artery stiffening and remodeling are independently associated with all-cause mortality and cardiovascular events in chronic kidney disease. **Hypertension**. 2012; 60:1451−1457.

31. Koren MJ, Devereux RB, Casale PN, Savage DD, Laragh JH. Relation of left ventricular mass and geometry to morbidity and mortality in uncomplicated essential hypertension. **Ann Intern Med**. 1991; 114:345−352.

32. Lacolley P, Regnault V, Segers P, Laurent S. Vascular smooth muscle cell and arterial stiffening: relevance in development, ageing and disease. **Phys Rev**. 2017; 97:1555−1617.

33. Lam CS, Xanthakis V, Sullivan LM, et al. Aortic root remodeling over the adult life course: longitudinal data from the Framingham Heart Study. **Circulation**. 2010; 122:884−890.

34. Laskey WK, Kussmaul WG. Arterial wave reflection in heart failure. **Circulation**. 1987; 75:711−722.

35. Latham RD, Westerhof N, Sipkema P, Rubal BJ, Reuederink P, Murgo JP. Regional wave travel and reflections along the human aorta: a study with six simultaneous micromanometric pressures. **Circulation**. 1985; 72:1257−1269.

36. Laurent S, Hayoz D, Trazzi S, et al. Isobaric compliance of the radial artery is increased in patients with essential hypertension. **J Hypertens**. 1993; 11:89−98.

37. Laurent S, Caviezel B, Beck L, et al. Carotid artery distensibility and distending pressure in hypertensive humans. **Hypertension**. 1994; 23(part 2):878−883.

38. Laurent S, Girerd X, Mourad JJ, et al. Elastic modulus of the radial artery wall is not increased in patients with essential hypertension. **Arterioscler Thromb**. 1994; 14:1223−1231.

39. Laurent S, Boutouyrie P, Asmar R, et al. Aortic stiffness is an independent predictor of all-cause and cardiovascular mortality in hypertensive patients. **Hypertension**. 2001; 37:1236−1241.

40. Laurent S, Katsahian S, Fassot C, Tropeano AI, Laloux B, Boutouyrie P. Aortic stiffness is an independent predictor of fatal stroke in essential hypertension. **Stroke**. 2003; 34:1203−1206.

41. Laurent S, Cockcroft J, Van Bortel L, et al. Expert consensus document on arterial stiffness: methodological aspects and clinical applications. **Eur Heart J**. 2006; 27:2588−2605.

42. Laurent S, Briet M, Boutouyrie P. Large/small artery cross talk and recent morbidity mortality trials in hypertension. **Hypertension**. 2009; 54:388−392.

43. Laurent S, Boutouyrie P. The structural factor in hypertension: large and small artery alterations. **Circ Res**. 2015; 116:1007−1021.

44. Laurent S, Cunha P. Large vessels in hypertension: central blood pressure. In: Lurbe E, Wuhl E, eds. **Hypertension in Children and Adolescents**. Springer publisher; 2019.

45. Mancia G, Fagard R, Narkiewicz K, et al. ESH/ESC guidelines for the management of arterial hypertension: the task force for the management of arterial hypertension of the European Society of Hypertension (ESH) and of the European Society of Cardiology (ESC). **Eur Heart J**. 2013; 34:2159−2219.

46. Mattace-Raso FU, van der Cammen TJ, Hofman A, et al. Arterial stiffness and risk of coronary heart disease and stroke: the Rotterdam Study. **Circulation**. 2006; 113:657−663.

47. Mattace-Raso FUS, Hofman A, Verwoert GC, et al. Reference values for carotid-femoral pulse wave velocity in the reference values for arterial stiffness' collaboration database. **Eur Heart J**. 2010; 31:2338−2350.

48. Meaume S, Benetos A, Henry OF, Rudnichi A, Safar ME. Aortic pulse wave velocity predicts cardiovascular mortality in subjects > 70 years of age. **Arterioscler Thromb Vasc Biol**. 2001; 21:2046−2050.

49. Milan A, Tosello F, Caserta M, et al. Aortic size index enlargement is associated with central hemodynamics in essential hypertension. **Hypertens Res**. 2011; 34:126−132.

50. Mitchell GF, Vasan RS, Keyes MJ, et al. Pulse pressure and risk of new-onset atrial fibrillation. **J Am Med Assoc**. 2007; 297:709−715.

51. Mitchell GF, Hwang SJ, Vasan RD, et al. Arterial stiffness and cardiovascular events. The Framingham Heart Study. **Circulation**. 2010; 121:505−511.

52. Mitchell GF, van Buchem MA, Sigurdsson S, et al. Arterial stiffness, pressure and flow pulsatility and brain structure and function: the age, gene/environment susceptibility-Reykjavik study. **Brain**. 2011; 134:3398−3407.

53. Muiesan ML, Salvetti M, Rizzoni D, et al. Pulsatile hemodynamics and microcirculation: evidence for a close relationship in hypertensive patients. **Hypertension**. 2013; 61:130−136.

54. Nichols WW, O'Rourke MF. **In: McDonald's Blood Flow in Arteries; Theoretical, Experimental and Clinical Principles**. 6th ed. Hodder Arnold ed.; 2011, 755 pages.

55. O'Rourke MF, Safar ME. Relationship between aortic stiffening and microvascular disease in brain and kidney. Cause and logic of therapy. **Hypertension**. 2005; 46:200−204.

56. Protogerou AD, Argyris AA, Papaioannou TG, et al. Left-ventricular hypertrophy is associated better with 24-h aortic pressure than 24-h brachial pressure in hypertensive patients: the SAFAR study. **J Hypertens**. 2014; 32:1805−1810.

57. Redheuil A, Yu WC, Mousseaux E, et al. Age-related changes in aortic arch geometry: relationship with proximal aortic function and left ventricular mass and remodeling. **J Am Coll Cardiol**. 2011; 58:1262−1270.

58. Rizzoni D, Porteri E, Boari GE, et al. Prognostic significance of small-artery structure in hypertension. **Circulation**. 2003; 108:2230−2235.

59. Roman MJ, Devereux RB. Association of central and peripheral blood pressures with intermediate cardiovascular phenotypes. **Hypertension**. 2014; 63:1148−1153.

60. Rothwell PM, Howard SC, Dolan E, et al. Prognostic significance of visit-to-visit variability, maximum systolic blood pressure, and episodic hypertension. **Lancet**. 2010; 375:895−905.

61. Safar ME, Blacher J, Pannier B, et al. Central pulse pressure and mortality in end-stage renal disease. **Hypertension**. 2002; 39:735−738.

62. Safar ME, O'Rourke MF. **Handbook of Hypertension, Volume 23: Arterial Stiffness in Hypertension**. Elsevier; 2006, 598 pages.

63. Safar ME, Asmar R, Benetos A, et al. French study group on arterial stiffness. Interaction between hypertension and arterial stiffness. **Hypertension**. 2018; 72:796−805.

64. Salvetti M, Agabiti Rosei C, Paini A, et al. Relationship of wall-to-lumen ratio of retinal arterioles with clinic and 24-hour blood pressure. **Hypertension**. 2014; 63:1110−1115.

65. Schillaci G, Bilo G, Pucci G, et al. Relationship between short-term blood pressure variability and large-artery stiffness in human hypertension: findings from two large databases. **Hypertension**. 2012; 60:369−377.

66. Scuteri A, Nilsson P, Tsourio C, Redon J, Laurent S. Microvascular brain damage: pathophysiological consideration and clinical implications. **J Hypertens**. 2011; 29:1469−1477.

67. Tzourio C, Laurent S, Debette S. Is hypertension associated with an accelerated ageing of the brain? **Hypertension**. 2014; 63:894−903.

68. Umemura S, Arima H, Arima S, et al. The Japanese Society of Hypertension guidelines for the management of hypertension (JSH 2019). **Hypertens Res**. 2019; 42:1235−1481.

69. Van Bortel LM, Laurent S, Boutouyrie P, et al. Expert consensus document on the measurement of aortic stiffness in daily practice using carotid-femoral pulse wave velocity. **J Hypertens**. 2012; 30:445−448.

70. Van der Heijden-Spek JJ, Staessen JA, Fagard RH, Hoeks AP, Boudier HA, van Bortel LM. Effect of age on brachial artery wall properties differs from the aorta and is gender dependent: a population study. **Hypertension**. 2000; 35:637−642.

71. Van Sloten TT, Sedaghat S, Laurent S, et al. Carotid stiffness is associated with incident stroke: a systematic review and meta-analysis. **J Am Coll Cardiol**. 2015; 66:2116−2125.

72. Vlachopoulos C, Aznaouridis K, Stefanadis C. Prediction of cardiovascular events and all-cause mortality with arterial stiffness: a systematic review and meta-analysis. **J Am Coll Cardiol**. 2010a; 55:1318−1327.

73. Vlachopoulos C, Aznaouridis K, Terentes-Printzios D, Ioakeimidis N, Stefanadis N. Prediction of cardiovascular events and all-cause mortality with brachial-ankle elasticity index: a systematic review and meta-analysis. **Hypertension**. 2012; 60:556−562.

74. Vlachopoulos C, Xaplanteris P, Aboyans V, et al. The role of vascular biomarkers for primary and secondary prevention. A position statement from the European Society of Cardiology working group on peripheral circulation. **Atherosclerosis**. 2015; 241:507−532.

75. Watfa G, Benetos A, Kearney-Schwartz A, et al. Do arterial hemodynamic parameters predict cognitive decline over a period of 2 years in individuals older than 80 years living in nursing homes? The PARTAGE study. **J Am Med Dir Assoc**. 2015; 16:598−602.

76. Webb AJ, Simoni M, Mazzucco S, Kuker W, Schulz U, Rothwell PM. Increased cerebral arterial pulsatility in patients with leukoaraiosis: arterial stiffness enhances transmission of aortic pulsatility. **Stroke**. 2012; 10:2631−2636.

77. Weber T, Auer J, O'Rourke MF, Punzengruber C, Kvas E, Eber B. Prolonged mechanical systole and increased arterial wave reflections in diastolic dysfunction. **Heart**. 2006; 92:1616−1622.

78. Weber T, Wassertheurer S, Schmidt-Trucksäss A, et al. Relationship between 24-hour ambulatory central systolic blood pressure and left ventricular mass: a prospective multicenter study. **Hypertension**. 2017:1157−1164.

79. Westerhof N, Sipkema P, van den Bos CG, Elzinga G. Forward and backward waves in the arterial system. **Cardiovasc Res**. 1972; 6:648−656.

80. Williams B, Mancia G, Spiering W, et al. ESC/ESH guidelines for the management of arterial hypertension: the task force for the management of arterial hypertension of the European Society of Cardiology and the European Society of Hypertension: the Task Force for the management of arterial hypertension of the European Society of Cardiology and the European Society of Hypertension. **Eur Heart J**. 2018; 39:3021−3104.

81. Zhong Q, Hu MJ, Cui YJ, et al. Carotid-femoral pulse wave velocity in the prediction of cardiovascular events and mortality: an updated systematic review and meta-analysis. **Angiology**. 2018; 69:617−629.

82. Zureik M, Bureau JM, Temmar M, et al. Echogenic carotid plaques are associated with aortic arterial stiffness in subjects with subclinical carotid atherosclerosis. **Hypertension**. 2003; 41:519−527.

This page intentionally left blank

Chapter 30

Arterial stiffness and pulsatile hemodynamics in diabetes and obesity

Jordana B. Cohen[1,2], Stuart B. Prenner[3] and Julio A. Chirinos[3,4]

[1]*Renal-Electrolytes and Hypertension Division, Perelman School of Medicine, University of Pennsylvania, Philadelphia, PA, United States;*
[2]*Department of Biostatistics, Epidemiology, and Informatics, Perelman School of Medicine, University of Pennsylvania, Philadelphia, PA, United States; [3]University of Pennsylvania Perelman School of Medicine, Hospital of the University of Pennsylvania and Perelman Center for Advanced Medicine, Philadelphia, PA, United States; [4]Ghent University, Ghent, Belgium*
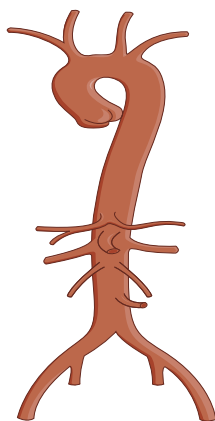
Introduction

Increased large artery stiffness (LAS) contributes to isolated systolic hypertension, increases cardiac afterload, and promotes increased pressure and flow pulsatility in the arterial tree.[1-3] Diabetes mellitus (DM), hypertension, obesity, and chronic kidney disease accelerate vascular aging, promoting LAS.[4,5] Furthermore, as the aorta stiffens over time, the increased pressure pulsatility is preferentially transferred to low-resistance microvascular beds such as the brain, kidney, liver, and pancreatic islets.[6-8] The resulting microvascular dysfunction may contribute to the development of insulin resistance and DM,[9-12] suggesting a bidirectional relationship between arterial stiffness and metabolic diseases (Fig. 30.1). There is a strong association of elevated carotid-femoral pulse wave velocity (CF-PWV; the reference standard measurement of arterial stiffness)[13-16] and measures of adverse pulsatile hemodynamics (e.g., increase and/or premature wave reflection)[17,18] with adverse cardiovascular outcomes. The bidirectional relationship of arterial stiffness with DM likely plays a distinctive role in mediating adverse cardiovascular outcomes in this patient population.

The goal of this chapter is to provide a translational overview of the pathophysiology and epidemiology of the relationship arterial stiffness with DM and obesity, and to identify important areas for future investigation.

Large Artery Stiffness

- *Elastin-derived peptides*
- *Pancreatic islet microvascular dysfunction*
- *Liver dysfunction*
- *Neuroendocrine mechanisms*

- *Advanced glycation end-products*
- *nitric oxide dysregulation*
- *large artery calcification and atherosclerosis*
- *chronic inflammation*
- *Neuroendocrine mechanisms*

Diabetes Mellitus

142

FIGURE 30.1 **Bidirectional relationship between large artery stiffening and diabetes mellitus**. On one hand, large artery stiffening may contribute to the pathogenesis of diabetes mellitus. On the other hand, established diabetes mellitus may contribute to accelerated large artery stiffening. Some potential mechanisms are listed.

Pathophysiologic role of diabetes mellitus in the development of increased arterial stiffness

Multiple mechanisms contribute to accelerated vascular aging and arterial wall stiffening in patients with type 2 DM, including (1) excess collagen deposition and cross-linking due to advanced glycation end-products (AGEs)[19]; (2) nitric oxide dysregulation resulting in oxidative stress and endothelial dysfunction[20]; (3) large artery calcification and atherosclerosis[21]; (4) chronic inflammation[22]; and (5) increased sympathetic tone.[22] In this section, we will highlight proposed pathophysiologic mechanisms of vascular stiffness particularly as they relate to AGEs and nitric oxide dysregulation (Fig. 30.2).

The role of advanced glycation end-products in the development of arterial stiffness

AGEs are proteins or lipids that develop in hyperglycemic environments and during aging.[23] AGEs are glycated and oxidized after exposure to sugars, and are commonly found in the vasculature of patients with diabetes.[19] AGEs have been demonstrated to contribute to the development of several microvascular and macrovascular complications in both diabetic and nondiabetic populations.[24] The main mechanism of arterial stiffness due to AGEs is attributed to the accumulation of AGEs in the arterial vessel wall, resulting in changes to structure and function of the blood vessel.

The AGE formation process begins when the carbonyl group of a reducing sugar moiety (glucose, fructose, glycolytic adductions) interacts with proteins, lipids, and nucleic acid amino groups in a reaction first described by Louis Maillard in the early 20th century. This reaction leads to the formation of two intermediate products, Schiff bases and Amadori products. Over the course of several months, Amadori products accumulate and react with amino, sulfhydryl, and guanidine groups of targeted proteins, promoting the denaturation, fragmentation, and cross-linking of these proteins which ultimately leads to the irreversible formation of AGEs.[24-27] These reactions are enhanced in carbonyl-enriched states such as DM (which increases AGE formation) and end stage kidney disease (which reduces AGE degradation).[3,28] They are also promoted via other intermediates, such as glyoxal and methylglyoxal, through lipid oxidation, inflammation, and environmental pollutant exposure, such as cigarette smoke.[29] Glycated hemoglobin (HbA1c) is an example of a clinically familiar and relevant Amadori product that is used for the diagnosis of diabetes and reflects blood glucose levels over an approximate 90-day period.[30-32]

AGEs can accumulate in arterial walls, where they disrupt normal vascular structure and function. Arterial walls are largely composed of collagen, which provides structural support, and elastin, which provides distensibility.[33] Fragmentation of elastin fibers in the arterial wall occurs during aging. In large arteries, fragmentation and loss of elastin fibers can also be associated with increased collagen deposition.[34,35] AGEs preferentially cross-link
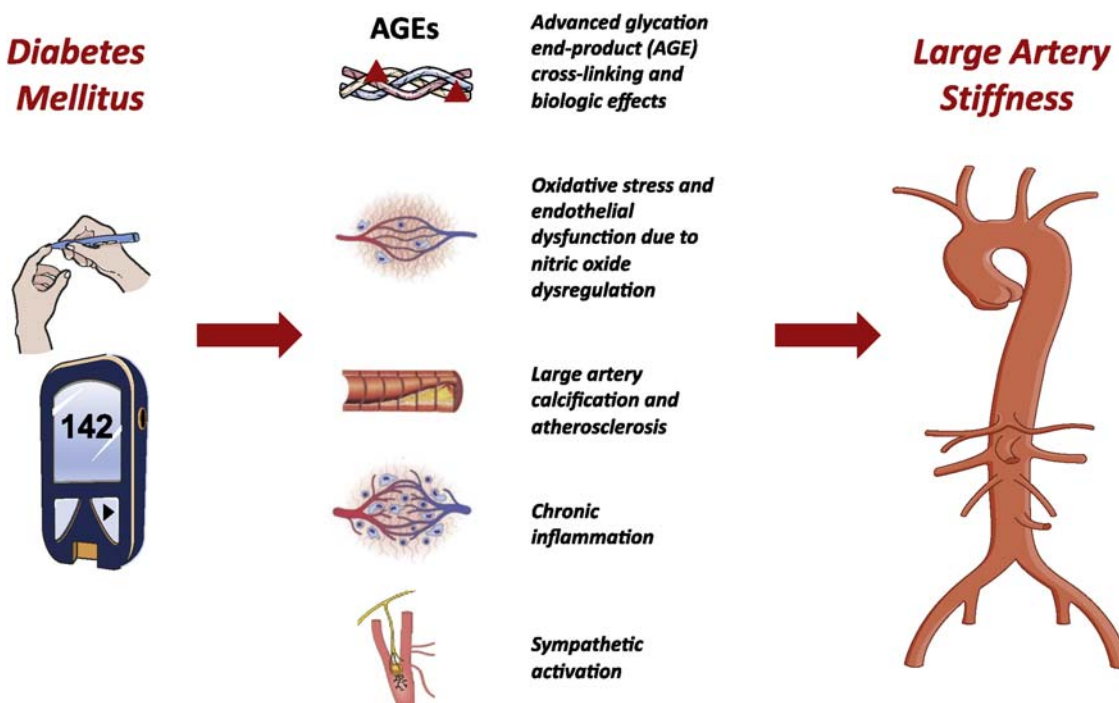
FIGURE 30.2   Pathophysiologic relationship between diabetes mellitus (DM) and large artery stiffness. Mechanistic factors that promote large artery stiffness in patients with DM are shown.

collagen over elastin, potentially due to a relatively higher content of lysine residues on collagen compared with elastin.[34] Normally, cross-links occur at two discrete sites at the N-terminal and C-terminal ends of collagen. However, AGEs can form cross-links at any site on collagen.[36] AGE-mediated cross-links confer increased resistance to enzymatic proteolysis of collagen and decreased rate of collagen degradation, promoting accumulation of collagen in large artery walls.[37] In contrast, glycated elastin is more susceptible to degradation.

In addition to collagen and elastin cross-linking, AGEs may promote vascular stiffness via several alternative mechanisms, including (1) activation of transcription factor NF-κB, which alters cellular adhesion molecule expression and promotes cytokine activation[38,39]; (2) glycosylation and oxidation of lipoproteins and increased foam cell formation[40]; and (3) glycosylation of reactive intermediates that inactivate nitric oxide and mediate endothelial dysfunction.[41] AGEs can activate the receptor of AGEs (RAGEs), inducing inflammation, oxidative stress, and calcification pathways (via sodium phosphate co-transporter PiT-1 expression). However, the functional significance of AGE-RAGE interactions in vivo is unclear.[3]

Several human studies have demonstrated a relationship between collagen cross-linking, AGE accumulation, and elevated CF-PWV. In a study of 41 subjects with long-standing type 1 DM compared with 25 controls, Monnier et al. observed that collagen-linked fluorescence was positively correlated with CF-PWV (r = 0.41, $P < .01$).[42] Subsequently, accumulation of specific AGEs in aortic tissue, such as pentosidine and glyoxal/methylglyoxal hydroimidazolones, has been correlated with aortic stiffness in subjects both with and without DM.[43]

Serum levels of AGE have also been cross-sectionally associated with markers of LAS, though this is not consistent across all studies. In a nested case-control study of 543 type 1 diabetic participants of the EURODIAB Prospective Complications Study, Schram et al. demonstrated that serum levels of two AGEs, Nε-(carboxymethyl)lysine and Nε-(carboxyethyl)lysine, were significantly associated with wider pulse pressure in models adjusted for several demographic, anthropomorphic, and clinical characteristics.[44] Similarly, in 423 diabetic and nondiabetic adult participants of the Baltimore Longitudinal Study of Aging, Semba et al. observed that every standard deviation higher serum level of Nε-(carboxymethyl)lysine was associated with a 0.16 m/s higher CF-PWV in multivariable-adjusted models.[45] Alternatively, in a cohort of 145 patients referred for coronary angiography for assessment of suspected coronary artery disease, Won et al. observed an association of serum levels of AGE with obstructive coronary artery disease, but not with brachial-ankle PWV.[46] The lack of association

may be due to the limitations of brachial-ankle PWV as a metric of LAS.

A number of longitudinal studies have also demonstrated a relationship between AGEs and the development and progression of microvascular complications of DM.[47] In a prospective study of 211 participants of the Diabetes Control and Complications Trial who underwent skin biopsy, skin AGEs independently predicted the 10-year risk of diabetic retinopathy and nephropathy.[48,49] Similarly, in a study of 30 patients with type 1 or type 2 DM and age- and sex-matched controls, skin pentosidine and fluorescence were associated with the six-year risk of progression of retinopathy and nephropathy.[50] In a case-control study of subgroup of 134 participants of the Collaborative Study Group's Trial of captopril in type 1 diabetic nephropathy, Weiss et al. observed that individuals who experienced doubling of serum creatinine during follow-up had higher serum levels of pentosidine compared with those who did not experience progressive nephropathy.[51]

Elevated serum AGE levels have also been linked to all-cause mortality and cardiovascular mortality in several cohorts. For example, in a longitudinal cohort study of 974 Finnish patients with type 2 DM followed for 18 years, the highest sex-specific quartile of serum AGE levels was associated with a 51% higher risk of all-cause mortality [hazard ratio (HR) 1.51, 95% confidence interval (CI) 1.14−1.99] and a 68% higher risk of cardiovascular mortality compared with the lowest quartile (HR 1.68, 95% CI 1.11−2.52) among women, which persisted after robust adjustment for multiple demographic and physiologic parameters.[52] However, the relationship of AGEs with mortality was not significant among men in the cohort. In a cohort of 339 men and women with type 1 DM followed for a median of 12.3 years, every standard deviation increase in serum levels of AGEs was associated with a 30% increased risk of incident fatal and nonfatal cardiovascular disease (adjusted HR 1.30, 95% CI 1.03−1.66) and a 34% increased risk of all-cause mortality (adjusted HR 1.28, 95% CI 1.01−1.64).[53] In the same cohort, higher plasma levels of soluble receptor for AGEs were also strongly and independently associated with increased risk of incident fatal and nonfatal cardiovascular disease and all-cause mortality.[54]

Nitric oxide, oxidative stress, and arterial stiffness

Nitric oxide (NO) has vasodilatory, antiplatelet, anti-inflammatory, and antioxidant properties, impaired nitric oxide synthesis and bioavailability promotes endothelial dysfunction and arterial stiffness.[20] Reduced NO production by the endothelium may play a role in regulating VSMC stiffness/tone in distal aortic segments like the

abdominal aorta.[3] Hyperglycemia and insulin resistance contribute to endothelial dysfunction and arterial stiffness by interfering with NO-mediated vasodilatation. In patients with insulin resistance, impaired NO synthase activation and increased superoxide production lead to increased NO inactivation and decreased endothelial NO production, reducing its overall bioavailability.[55,56] Chronically elevated blood glucose is associated with enhanced polyol, protein kinase C, and pentose phosphate pathways, further contributing to increased oxidative stress and endothelial apoptosis.[57,58]

Abnormalities in the NO pathway in type 2 DM contribute to endothelial progenitor cell dysregulation.[55] Circulating levels of endothelial progenitor cells, which are responsible for the normal development of new endothelial cells, are lower in patients with type 2 DM compared with normal controls.[59] In a cross-sectional study of 234 patient with type 2 DM and 121 age- and sex-matched nondiabetic controls, Yue et al. observed that circulating levels of endothelial progenitor cells were inversely proportional to glycemic control as well as brachial-ankle PWV[60]; patients with DM and better glycemic control, measured using HbA1c, exhibited lower arterial stiffness and higher circulating levels of endothelial progenitor cells than those with poorer glycemic control. However, these associations may represent epiphenomena related to the multiple biologic changes associated with poor glycemic control, and the causal relationship between endothelial progenitor cells and arterial stiffening was not established.

Epidemiologic association of diabetes mellitus with the development of increased arterial stiffness

DM is a well-established risk factor for accelerated large artery stiffening, as measured by pulse pressure, CF-PWV, and aortic characteristic impedance (Zc). The breadth of studies demonstrating cross-sectional and longitudinal associations of DM with LAS and pulsatile hemodynamics has grown substantially over time with ongoing improvements in the techniques used to noninvasively measure these parameters. The aim of this section is to highlight key studies that have evaluated arterial stiffness and pulsatile hemodynamics in patients with DM.

Risk of increased arterial stiffness and adverse cardiovascular events in patients with diabetes mellitus type 2

Cross-sectional data consistently demonstrate a strong association of DM with elevated PWV.[61−69] For example, in a cross-sectional study of 169 patients with type 2 DM (n = 57) and nondiabetic controls (n = 112), Cameron et al. observed that patients with type 2 DM exhibited

CF-PWV, carotid-radial PWV, and aortic-finger PWV values that were similar, on average, to those among nondiabetic patients who were 15 year older.[61] In a population-based study of 571 patients in London, United Kingdom, Cruickshank et al. showed that at any level of systolic blood pressure, aortic PWV was higher in patients with type 2 DM compared with nondiabetic controls.[62,63] Kimoto et al. measured four arterial segments of PWV in 434 patients with type 2 DM and 192 nondiabetic controls. The authors observed that patients with diabetes had greater PWV in all four arterial segments compared with nondiabetic controls. However, after multivariable adjustment, diabetes was significantly associated with higher PWV in larger-sized arterial segments representing aortic PWV, but not in medium-sized arterial segments (heart-brachial and femoral-ankle).[64]

Although most data are cross-sectional, prospective data support that type 2 DM is a risk factor for the development of arterial stiffening over time. For example, in a prospective analysis of 508 community-dwelling participants of the Maine−Syracuse Longitudinal Study, Elias et al. observed that prior type 2 DM was associated with higher subsequent CF-PWV and that uncontrolled DM was associated with a ninefold higher risk of elevated PWV (defined by the authors as $\geq$12 m/s).[70]

There is a strong relationship between arterial stiffness and the risk of cardiovascular events and mortality that is particularly robust in patients with type 2 DM.[71,72] In the Hoorn Study, a population-based cohort study of 2484 Dutch patients including 208 patients with type 2 DM, pulse pressure was associated with cardiovascular mortality among diabetic, but not nondiabetic patients.[73] In a longitudinal, population-based cohort study of 140 patients with impaired fasting glucose, van Dijk et al. showed that every standard deviation increase in brachial artery pulse pressure was associated with a 70% increase in all-cause mortality, with similar results after multivariable adjustment for several demographic, anthropomorphic, and clinical parameters.[74] In a prospective cohort study of 2308 patients with type 2 DM followed for a median of 8.6 years, Kim et al. observed that the highest quartile of brachial-ankle PWV was associated with a 2.5-fold increased risk of all-cause mortality (adjusted HR 2.55, 95% CI 1.49−4.35) and a 5.6-fold increased risk of cardiovascular mortality (adjusted HR 5.57, 95% CI 1.19−26.18) compared with the lowest quartile.

Risk of increased arterial stiffness and adverse cardiovascular events in patients with diabetes mellitus type 1

The relationship between PWV and type 1 DM is less consistently demonstrated than in type 2 DM, which may be due to smaller sample sizes in studies of patients with

type 1 DM as well as generally lower rates of other metabolic diseases and obesity. In a study of 17 patients with type 1 DM compared with age- and sex-matched nondiabetic controls, Sweitzer et al. observed that patients with type 1 DM exhibited wider central and peripheral pulse pressure, despite similar mean blood pressure, compared with nondiabetic controls. Although CF-PWV was similar between diabetics and nondiabetics, aortic characteristic impedance (Zc) was higher in type 1 diabetics compared with diabetics, and was particularly elevated among those with albuminuria.[75] Similarly, in a study of 35 patients with type 1 DM compared with 35 nondiabetic matched controls, Wilkinson et al. observed that aortic augmentation index, a metric of pulse wave reflection, and estimated PWV, were significantly higher in patients with diabetes compared with controls using peripheral pulse waveforms.[76] In contrast, in a cross-sectional study of 89 subjects with type 1 DM compared with 95 nondiabetic controls, Brooks observed that aortic augmentation index was increased in men, but not women, with type 1 DM compared with controls.[77]

Limited evidence exists regarding the association between hyperglycemia and measures of arterial stiffness and pulsatile hemodynamics in type 1 DM. In a mechanistic study of 22 men with type 1 DM and 13 nondiabetic men, Gordin et al. evaluated the effect of acute hyperglycemia on arterial stiffness by measuring carotid-radial PWV, CF-PWV, and aortic augmentation index before and after a 2-h hyperglycemic clamp.[78] At baseline, the authors observed that patients with diabetes had higher aortic augmentation index, but similar carotid-radial and CF-PWV, compared with nondiabetic controls. After the 2-h clamp, acute hyperglycemia increased the carotid-radial PWV in patients with but not those without diabetes, and increased the aortic augmentation index similarly in patients both with and without diabetes.

Risk of increased arterial stiffness and adverse cardiovascular events in patients with prediabetes

Several studies have evaluated the cross-sectional association between prediabetes and vascular stiffness to better understand the temporal relationship between arterial stiffness, impaired glucose tolerance, and DM. In the Hoorn Study, a population-based cohort study of 2484 Dutch patients, Schram et al. observed a dose-response relationship of normal blood glucose, impaired fasting glucose, and DM with regard to carotid-femoral transit time.[79] A number of studies have demonstrated that levels of plasma glucose at the upper limit of normal are associated with increased arterial stiffness,[80–83] but these observations are not consistent across all studies. For example, in the Asklepios Study, a population-based study of 1927 middle-aged

middle-aged adults, after adjustment for age, sex, and mean arterial pressure, impaired fasting glucose was not associated with elevated arterial stiffness.[65] Thus, the temporal relationship between prediabetes and arterial stiffness requires further investigation, particularly in studies that evaluate PWV and changes in glucose tolerance and diabetes status longitudinally.

The role of arterial stiffness in the promotion of diabetic microvascular disease

In the Asklepios Study, after adjustment for age, sex, and mean arterial pressure, type 2 DM was associated with higher CF-PWV, lower total arterial compliance and decreased reflection magnitude.[65] The reduced reflection magnitude arriving at the proximal aorta suggests increased penetration of pulsatile energy to distal vascular beds in patients with type 2 diabetes, as also suggested by previous studies.[84–86] This selective aortic stiffening without stiffening of more distal arteries may facilitate increased penetration of potentially harmful pulsatile energy into the microvasculature of target organs, promoting the microvascular damage observed in patients with DM including retinopathy, nephropathy, peripheral neuropathy, autonomic dysfunction, and cognitive dysfunction. Microvascular damage in DM is consistently associated with elevated mortality risk.[87–90] Thus, more research is needed to identify ways to prevent and slow the progression of microvascular disease in this population.

Arterial stiffness and diabetic retinopathy

Several studies have demonstrated a consistent correlation of arterial stiffness with diabetic retinopathy.[89,91–95] In a cross-sectional analysis of 600 randomly selected subjects with type 2 DM from the Chennai Urban Rural Epidemiology Study, Rema et al. observed that aortic augmentation index was significantly higher in subjects with retinopathy compared with those without retinopathy (27.9 vs. 25.8 mm, $P = .031$), which persisted after multivariable adjustment for age, duration of diabetes, HbA1c, serum cholesterol, serum triglycerides, and microalbuminuria.[91] Similarly, in a cross-sectional study of 494 participants of the Seoul Metro-City Diabetes Prevention Program with type 2 DM, Kim et al. showed that the highest quartile of heart-femoral PWV was independently associated with a fivefold higher odds of diabetic retinopathy than the lowest quartile (adjusted odds ratio 5.02, 95% CI 1.69–14.91).[92] A number of studies have demonstrated similar cross-sectional associations between LAS and pulsatile hemodynamics with diabetic retinopathy.[93–95] Moreover, in a cross-sectional analysis of 689 patients with type 2 DM in Japan, Tanaka et al. observed a positive association between the stages of diabetic retinopathy and higher brachial-ankle PWV.[89]

Arterial stiffness and diabetic nephropathy

DM is the foremost cause of chronic kidney disease and end-stage kidney disease.[96,97] Correspondingly, the development of microvascular disease in the kidney, as evidenced by, albuminuria, is strongly associated with increased risk of progression to end stage kidney disease, cardiovascular disease, and all-cause mortality.[98] Mild albuminuria often precedes the development of clinically evident renal dysfunction, or reduction in glomerular filtration rate, in patients with DM by several years.[99]

Several studies have investigated the relationship between arterial stiffness and diabetic nephropathy.[5,90,100−105] In a cross-sectional analysis of 2564 participants of the Chronic Renal Insufficiency Cohort (CRIC) Study with mild to moderate chronic kidney disease, Townsend et al. observed that DM (β coefficient 1.51, standard error 0.13) and fasting blood glucose (β coefficient 0.04 per 10 mg/dL, standard error 0.01) were independently associated with increased CF-PWV.[5] In multivariable models stratified by diabetes status, carotid-femoral PWV explained a significant portion of the variation in urinary protein excretion among diabetic, but not among nondiabetic, participants.[100] In longitudinal analyses of the full 2795 CRIC Study participants who ultimately underwent CF-PWV measurements and were followed for a mean of 5.4 years, those in the highest tertile of CF-PWV exhibited a 37% higher risk of end stage kidney disease (adjusted HR 1.37, 95% CI 1.05−1.80) and 72% higher risk of all-cause mortality (adjusted HR 1.72, 95% CI 1.24−2.38) compared with those in the lowest tertile.[90]

Smith et al. measured CF-PWV in 134 patients with type 2 DM, normal serum creatinine, and varying severity of albuminuria,[104] and demonstrated that an elevated albumin to creatinine ratio (defined by the authors as ≥3 mg/mmol) was associated with higher CF-PWV and that PWV was higher in patients with lower glomerular filtration rate. Additionally, the authors estimated that a 10-year period of longer duration of DM was associated with PWV to the same extent as 10 mmHg higher pulse pressure or 6.5-year older age.[104] In a case-control study of 122 patients with type 2 DM compared with 122 matched controls, a decline in glomerular filtration rate over time was associated with increased aortic stiffness, independent of baseline level of kidney function.[106] Moreover, in a longitudinal cohort study of 461 patients with type 2 DM followed over a median of 5.9 years, Bouchi et al. demonstrated that CF-PWV was associated with incident albuminuria (HR 1.23, 95% CI 1.13−1.33) and rate of decline in estimated glomerular filtration rate.[107]

In their study measuring four arterial segments of PWV in 434 patients with type 2 DM and 192 nondiabetic controls, Kimoto et al. observed that increased PWV in each segment was associated with advancing stage of chronic

kidney disease, respectively.[64] However, after multivariable adjustment, lower GFR was only independently associated with higher heart-femoral PWV.[64] The authors' findings suggest an association between LAS, but not medium-sized (muscular) artery stiffness, with poorer kidney function,[64] which has also been supported by other studies.[106] Furthermore, aortic PWV, but not brachial or femorotibial PWV, predict all-cause mortality in patients with end stage kidney disease.[67] For an extensive discussion regarding the relationship between arterial stiffness and renal disease, the reader is referred to Chapter 40.

Arterial stiffness and diabetic neuropathy and autonomic dysfunction

Longstanding DM is associated with a high incidence of neuropathy, which can manifest as peripheral neuropathy or autonomic dysfunction. Arterial stiffness and adverse pulsatile hemodynamics have been associated with both peripheral neuropathy and autonomic dysfunction in patients with DM.

In a cross-sectional analysis of 692 patients with type 2 DM, patients with brachial-ankle PWV ≥16 m/s were more likely to have abnormal monofilament testing (14.9% vs. 6.6%) and elevated peripheral neuropathy total symptom score (36.8% vs. 28.3%) compared with those with brachial-ankle PWV <1.6 m/s.[108] A study of 100 patients with DM who underwent nerve conduction studies demonstrated a significant negative correlation between brachial-ankle PWV and superficial peroneal and sural sensory nerve action potential and nerve conduction velocity.[109] Similarly, in 294 patients with type 2 diabetes, Yokoyama et al. observed that brachial-ankle PWV (odds ratio 1.002, 95% CI 1.001−1.003 per cm/s increase) and pulse pressure (odds ratio 1.05, 95% CI 1.02−1.08 per mmHg increase) were independently associated with neuropathy determined by symptoms, absence of ankle tendon reflexes, vibratory perception, and heart rate variability.[110]

Several studies have demonstrated a correlation between elevated PWV and autonomic dysfunction.[111,112] For example, in 2004, Meyer et al. assessed autonomic function in 45 patients with type 2 diabetes and 45 age-, sex-, and BMI-matched nondiabetic controls by assessing heart rate variability during breathing, Valsalva, and postural maneuvers. The authors showed that CF-PWV and femoral-dorsalis pedis PWV were positively correlated with autonomic dysfunction.[112]

Arterial stiffness and cognitive dysfunction in patients with diabetes mellitus

Similar to other markers of microvascular disease in patients with DM, several studies have demonstrated an

independent association of arterial stiffness with cognitive dysfunction and white matter lesions. For example, in a study of 89 patients with recently diagnosed type 2 DM and 89 age- and sex-matched nondiabetic controls, Laugesen et al. observed that CF-PWV was higher in patients with diabetes compared with controls, and that higher PWV was associated with higher volume of white matter lesions.[113] In patients with type 2 DM, LAS is associated with poorer cognitive function on neuropsychiatric testing.[114] Brachial-ankle PWV is higher among patients with type 2 DM with a prior history of ischemic stroke compared to those without stroke.[115] For an extensive discussion regarding the relationship between arterial stiffness and cognitive dysfunction, the reader is referred to Chapter 41.

Epidemiologic association of obesity and the metabolic syndrome with the development of increased arterial stiffness

The stronger association of type 2 DM, versus type 1 DM, with arterial stiffness may in part be due to higher rates of obesity and other metabolic diseases that promote vascular aging in patients with type 2 DM. Several studies have demonstrated an independent association between LAS and both obesity and the metabolic syndrome.[116-120] For example, in a cross-sectional study of 806 asymptomatic adults aged 24−44 years, Li et al. demonstrated that brachial-ankle PWV increased significantly as number of metabolic syndrome components increased.[116] Similarly, in a prospective cohort study of 476 patients classified by number metabolic syndrome components, Safar et al. observed that CF-PWV was higher in the group with multiple components of the metabolic syndrome at baseline compared with those without any components of the metabolic syndrome. Additionally, over six years of follow-up, CF-PWV increased most among those with more components of the metabolic syndrome.[117] These findings have been corroborated by several other longitudinal studies that have demonstrated an association of additional components of the metabolic syndrome with increase in CF-PWV over time.[119,120]
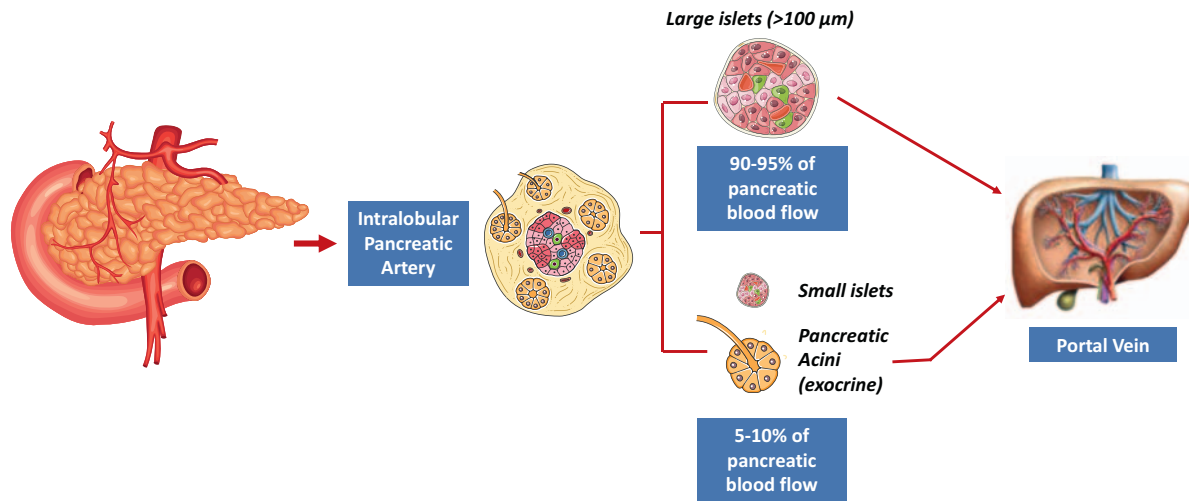
Increased arterial stiffness as a potential contributor to the development of diabetes mellitus

A number of recent studies suggest a relationship of LAS with new onset DM. For example, in 2450 Swedish participants of the Malmo Diet and Cancer Cardiovascular cohort study followed for a mean of 4.4 years, Muhammad

et al. observed that the highest tertile of CF-PWV was associated with a 3.2-fold higher risk of new onset DM than the lowest tertile (adjusted HR 3.24, 95% CI 1.51−6.97).[11] This association was independent of various potential confounders. Similarly, in an analysis of 2429 participants of the China Stroke Primary Prevention Trial, Zhang et al. demonstrated that every standard deviation increase in brachial-ankle PWV was associated with a 33% increased odds (adjusted odds ratio 1.33%, 95% 1.13−1.56) of new-onset DM.[12] Additionally, Zheng et al. observed that elevated brachial-ankle PWV ($\geq$18 m/s) was associated with a twofold increased risk of new onset DM (adjusted HR 2.11, 95% CI 1.71−2.61) over a mean of 3.7 years of follow-up compared with brachial-ankle PWV <14 m/s.[121] Moreover, the authors used cross-lagged regression, which estimates directional relationships from one variable to another and vice versa (hence the term "crossed") using longitudinal data recorded at multiple time points (hence the term "lagged"). In these analyses, baseline baPWV was associated with follow-up FBG, but there was no significant relationship between baseline FBG and follow-up baPWV. Similarly, pulse pressure independently predicted new-onset DM among 2685 hypertensive patients enrolled in the Candesartan Antihypertensive Survival Evaluation in Japan (CASE-J) trial.[122]

Whether LAS contributes to the pathogenesis of future new-onset DM remains to be determined. LAS may contribute to the pathogenesis of insulin resistance and DM through its hemodynamic effects. As discussed throughout this textbook, LAS has ill-effects in various organs, particularly those that require torrential blood flow and must operate at very low vascular resistance. While the relationship between LAS and microvascular disease in high-flow, low-resistance organs such as the kidneys and the brain have been the focus of many studies, little is known about the relationship between increased aortic stiffness and pancreatic microvascular disease. Interestingly, the endocrine pancreas, which comprises only $\sim$1−2% of the pancreatic mass, receives $\sim$10−20% of its blood supply, implying that pancreatic islet blood flow is among the highest in the body and actually higher than renal and cerebral blood flow when normalized for tissue mass.[3,123] Therefore, LAS has the potential to impact microvascular health in pancreatic islets, which may lead to dysfunctional or dysregulated endocrine function (Fig. 30.3).

Pancreatic islets (islets of Langerhans) are supplied by up to $\sim$5 arterioles per islet, which branch into a dense glomerular capillary network. Endocrine cells reside within this network and receive chemical signals across the capillary endothelium. Pancreatic islets are made up of five major endocrine cell types: β-cells (which secrete insulin),

FIGURE 30.3   **Microstructure and blood flow distribution in pancreatic lobules**. Pancreatic islets (endocrine) and their anatomic relationship with exocrine pancreatic tissue (acini) are shown. See text for details.
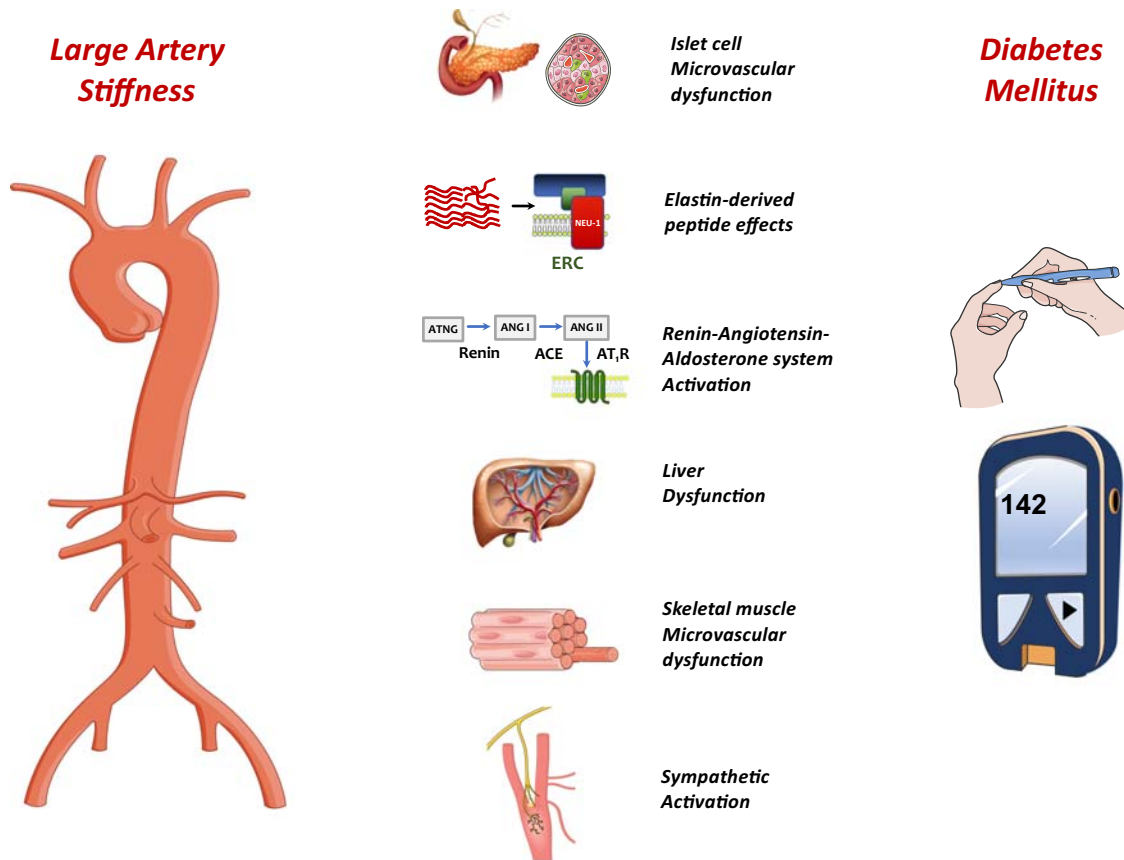
α-cells (which secrete glucagon), δ-cells (which secrete somatostatin), PP-cells (which produce pancreatic polypeptide), ε-cells (which produce ghrelin). Although type 2 DM is primarily associated with insulin resistance, insufficient insulin secretion and an imbalance in insulin versus glucagon secretion play a key role in its pathogenesis. Islet blood flow is a highly regulated process under complex metabolic, autonomic, and paracrine dynamic control. Hyperglycemia and the associated beta cell activation result in islet arteriolar dilation, capillary dilation, and increased islet capillary pressure.[124] Moreover, vascular integrity may be essential to maintain an order of sequential perfusion of β, δ, and α cells, which appears to allow for an adequate inhibition of glucagon secretion by insulin.[125] Given the key role of the pancreatic microvasculature, pancreatic islet microvascular dysfunction is thought to contribute to the pathogenesis of type 2 DM, providing a plausible mechanistic causal link between LAS and the pathogenesis of DM.

In addition to its potential effect on the pancreatic islet microvasculature, other potential mechanisms could be involved in the relationship between LAS and new-onset DM (Fig. 30.4). Elastin degradation in the aortic wall may impact insulin sensitivity via the production of elastin-related peptides, which block insulin signaling, likely by triggering an interaction between the insulin receptor and the neuraminidase-1 subunit of the elastin receptor complex. Increased sympathetic tone, a modulator of arterial stiffness, can lead to renin-angiotensin-aldosterone system activation, which influences insulin sensitivity via multiple mechanisms in skeletal muscle, adipocytes, and pancreas. Finally, the

liver (which receives ∼25% of the cardiac output) also exhibits a high-flow, low-resistance arterial circulation, since the hepatic artery provides approximately one-third of the liver blood flow.[3] The hepatic arterial circulation constantly regulates arterial flow to maintain total liver blood flow constant, regardless of changes in portal vein flow (hepatic arterial buffer response), which contributes to metabolic homeostasis.[126] Additionally, abnormal pulsatile hemodynamics due to LAS may impair normal postprandial vasodilation of skeletal muscle,[127−129] further promoting insulin resistance.[9,10] However, it remains to be seen whether LAS contributes to skeletal muscle or liver microvascular dysfunction. The bidirectional association between LAS and DM requires further study.

Conclusions and future directions

A growing body of literature supports a strong pathophysiologic and epidemiologic link between LAS and microvascular complications due to DM, as well as cardiovascular disease and mortality risk. Furthermore, emerging evidence suggests that LAS may also contribute to the pathogenesis of new onset DM. CF-PWV is an important prognostic marker for adverse outcomes among patients with DM, and may be an important indicator of future diabetes risk. Further investigations are needed to clarify the underlying mechanisms and temporal relationship of arterial stiffness with new onset DM. Therapies targeting mechanisms of arterial stiffness may be critical in preventing the development and progression of target organ damage in this patient population.

FIGURE 30.4 **Mechanisms that underlie the relationship between large artery stiffness and new-onset diabetes mellitus (DM)**. *ACE*, angiotensin converting enzyme; *ANG II*, angiotensin II; *ATNG*, angiotensinogen; *ATR1*, angiotensin II receptor type 1; *ERC*, elastin receptor complex.

Acknowledgments

References

1. Mitchell GF. Effects of central arterial aging on the structure and function of the peripheral vasculature: implications for end-organ damage. **J Appl Physiol (1985)**. 2008; 105:1652−1660.
2. Chirinos JA. Arterial stiffness: basic concepts and measurement techniques. **J Cardiovasc Transl Res**. 2012; 5:243−255.
3. Chirinos JA, Segers P, Hughes T, Townsend R. Large-artery stiffness in health and disease: JACC state-of-the-art review. **J Am Coll Cardiol**. 2019; 74:1237−1263.
4. Gusbeth-Tatomir P, Covic A. Causes and consequences of increased arterial stiffness in chronic kidney disease patients. **Kidney Blood Press Res**. 2007; 30:97−107.
5. Townsend RR, Wimmer NJ, Chirinos JA, et al. Aortic PWV in chronic kidney disease: a CRIC ancillary study. **Am J Hypertens**. 2010; 23:282−289.
6. Jain S, Khera R, Corrales-Medina VF, Townsend RR, Chirinos JA. Inflammation and arterial stiffness in humans. **Atherosclerosis**. 2014; 237:381−390.
7. Payne RA, Wilkinson IB, Webb DJ. Arterial stiffness and hypertension: emerging concepts. **Hypertension**. 2010; 55:9−14.
8. Nichols WW, O'Rourke M, Vlachopoulos C. **McDonald's Blood Flow in Arteries: Theoretical, Experimental and Clinical Principles**. 6th ed. Hodder Arnold; 2011.
9. Serne EH, de Jongh RT, Eringa EC, RG IJ, Stehouwer CD. Microvascular dysfunction: a potential pathophysiological role in the metabolic syndrome. **Hypertension**. 2007; 50:204−211.
10. Potenza MA, Marasciulo FL, Chieppa DM, et al. Insulin resistance in spontaneously hypertensive rats is associated with endothelial dysfunction characterized by imbalance between NO and ET-1 production. **Am J Physiol Heart Circ Physiol**. 2005; 289:H813−H822.
11. Muhammad IF, Borne Y, Ostling G, et al. Arterial stiffness and incidence of diabetes: a population-based cohort study. **Diabetes Care**. 2017; 40:1739−1745.

12. Zhang Y, He P, Li Y, et al. Positive association between baseline brachial-ankle pulse wave velocity and the risk of new-onset diabetes in hypertensive patients. **Cardiovasc Diabetol**. 2019; 18:111.

13. Laurent S, Cockcroft J, Van Bortel L, et al. Expert consensus document on arterial stiffness: methodological issues and clinical applications. **Eur Heart J**. 2006; 27:2588−2605.

14. Ben-Shlomo Y, Spears M, Boustred C, et al. Aortic pulse wave velocity improves cardiovascular event prediction: an individual participant meta-analysis of prospective observational data from 17,635 subjects. **J Am Coll Cardiol**. 2014; 63:636−646.

15. Willum-Hansen T, Staessen JA, Torp-Pedersen C, et al. Prognostic value of aortic pulse wave velocity as index of arterial stiffness in the general population. **Circulation**. 2006; 113:664−670.

16. Mattace-Raso FU, van der Cammen TJ, Hofman A, et al. Arterial stiffness and risk of coronary heart disease and stroke: the Rotterdam Study. **Circulation**. 2006; 113:657−663.

17. Manisty C, Mayet J, Tapp RJ, et al. Wave reflection predicts cardiovascular events in hypertensive individuals independent of blood pressure and other cardiovascular risk factors: an ASCOT (Anglo-Scandinavian Cardiac Outcome Trial) substudy. **J Am Coll Cardiol**. 2010; 56:24−30.

18. Chirinos JA, Kips JG, Jacobs Jr DR, et al. Arterial wave reflections and incident cardiovascular events and heart failure: MESA (Multiethnic Study of Atherosclerosis). **J Am Coll Cardiol**. 2012; 60:2170−2177.

19. Goldin A, Beckman JA, Schmidt AM, Creager MA. Advanced glycation end products: sparking the development of diabetic vascular injury. **Circulation**. 2006; 114:597−605.

20. Kawashima S. The two faces of endothelial nitric oxide synthase in the pathophysiology of atherosclerosis. **Endothelium**. 2004; 11:99−107.

21. Takasu J, Katz R, Nasir K, et al. Relationships of thoracic aortic wall calcification to cardiovascular risk factors: the Multi-Ethnic Study of Atherosclerosis (MESA). **Am Heart J**. 2008; 155:765−771.

22. Weber T. Arterial stiffness, wave reflections, and diabetes: a bidirectional relationship? **Am J Hypertens**. 2010; 23:1047−1048.

23. Garay-Sevilla ME, Regalado JC, Malacara JM, et al. Advanced glycosylation end products in skin, serum, saliva and urine and its association with complications of patients with type 2 diabetes mellitus. **J Endocrinol Invest**. 2005; 28:223−230.

24. Sell DR, Monnier VM. Molecular basis of arterial stiffening: role of glycation - a mini-review. **Gerontology**. 2012; 58:227−237.

25. Meerwaldt R, Links T, Zeebregts C, Tio R, Hillebrands JL, Smit A. The clinical relevance of assessing advanced glycation endproducts accumulation in diabetes. **Cardiovasc Diabetol**. 2008; 7:29.

26. Tessier FJ. The Maillard reaction in the human body. The main discoveries and factors that affect glycation. **Pathol Biol**. 2010; 58:214−219.

27. Prasad A, Bekker P, Tsimikas S. Advanced glycation end products and diabetic cardiovascular disease. **Cardiol Rev**. 2012; 20:177−183.

28. Baynes JW, Thorpe SR. Role of oxidative stress in diabetic complications: a new perspective on an old paradigm. **Diabetes**. 1999; 48:1−9.

29. Rabbani N, Thornalley PJ. Glycation research in amino acids: a place to call home. **Amino Acids**. 2012; 42:1087−1096.

30. International Expert C. International Expert Committee report on the role of the A1C assay in the diagnosis of diabetes. **Diabetes Care**. 2009; 32:1327−1334.

31. Peters AL, Davidson MB, Schriger DL, Hasselblad V. A clinical approach for the diagnosis of diabetes mellitus: an analysis using glycosylated hemoglobin levels. Meta-analysis Research Group on the Diagnosis of Diabetes Using Glycated Hemoglobin Levels. **J Am Med Assoc**. 1996; 276:1246−1252.

32. Koenig RJ, Peterson CM, Jones RL, Saudek C, Lehrman M, Cerami A. Correlation of glucose regulation and hemoglobin AIc in diabetes mellitus. **N Engl J Med**. 1976; 295:417−420.

33. Powell JT, Vine N, Crossman M. On the accumulation of D-aspartate in elastin and other proteins of the ageing aorta. **Atherosclerosis**. 1992; 97:201−208.

34. Greenwald SE. Ageing of the conduit arteries. **J Pathol**. 2007; 211:157−172.

35. Fonck E, Feigl GG, Fasel J, et al. Effect of aging on elastin functionality in human cerebral arteries. **Stroke**. 2009; 40:2552−2556.

36. Brownlee M, Vlassara H, Kooney A, Ulrich P, Cerami A. Aminoguanidine prevents diabetes-induced arterial wall protein cross-linking. **Science**. 1986; 232:1629−1632.

37. Schnider SL, Kohn RR. Effects of age and diabetes mellitus on the solubility and nonenzymatic glucosylation of human skin collagen. **J Clin Invest**. 1981; 67:1630−1635.

38. Schmidt AM, Hori O, Chen JX, et al. Advanced glycation endproducts interacting with their endothelial receptor induce expression of vascular cell adhesion molecule-1 (VCAM-1) in cultured human endothelial cells and in mice. A potential mechanism for the accelerated vasculopathy of diabetes. **J Clin Invest**. 1995; 96:1395−1403.

39. Vlassara H, Fuh H, Donnelly T, Cybulsky M. Advanced glycation endproducts promote adhesion molecule (VCAM-1, ICAM-1) expression and atheroma formation in normal rabbits. **Mol Med**. 1995; 1:447−456.

40. Bucala R, Makita Z, Koschinsky T, Cerami A, Vlassara H. Lipid advanced glycosylation: pathway for lipid oxidation in vivo. **Proc Natl Acad Sci U S A**. 1993; 90:6434−6438.

41. Bucala R, Tracey KJ, Cerami A. Advanced glycosylation products quench nitric oxide and mediate defective endothelium-dependent vasodilatation in experimental diabetes. **J Clin Invest**. 1991; 87:432−438.

42. Monnier VM, Vishwanath V, Frank KE, Elmets CA, Dauchot P, Kohn RR. Relation between complications of type I diabetes mellitus and collagen-linked fluorescence. **N Engl J Med**. 1986; 314:403−408.

43. Sims TJ, Rasmussen LM, Oxlund H, Bailey AJ. The role of glycation cross-links in diabetic vascular stiffening. **Diabetologia**. 1996; 39:946−951.

44. Schram MT, Schalkwijk CG, Bootsma AH, et al. Advanced glycation end products are associated with pulse pressure in type 1 diabetes: the EURODIAB Prospective Complications Study. **Hypertension**. 2005; 46:232−237.

45. Semba RD, Najjar SS, Sun K, Lakatta EG, Ferrucci L. Serum carboxymethyl-lysine, an advanced glycation end product, is associated with increased aortic pulse wave velocity in adults. **Am J Hypertens**. 2009; 22:74−79.

46. Won KB, Chang HJ, Park SH, Hong SY, Jang Y, Chung N. High serum advanced glycation end-products predict coronary artery disease irrespective of arterial stiffness in diabetic patients. **Korean Circ J**. 2012; 42:335−340.

47. Monnier VM, Sell DR, Genuth S. Glycation products as markers and predictors of the progression of diabetic complications. **Ann N Y Acad Sci**. 2005; 1043:567−581.

48. Genuth S, Sun W, Cleary P, et al. Glycation and carboxymethyllysine levels in skin collagen predict the risk of future 10-year progression of diabetic retinopathy and nephropathy in the diabetes control and complications trial and epidemiology of diabetes interventions and complications participants with type 1 diabetes. **Diabetes**. 2005; 54:3103−3111.

49. Genuth S, Sun W, Cleary P, et al. Skin advanced glycation end products glucosepane and methylglyoxal hydroimidazolone are independently associated with long-term microvascular complication progression of type 1 diabetes. **Diabetes**. 2015; 64:266−278.

50. Sternberg M, M'Bemba J, Urios P, et al. Skin collagen pentosidine and fluorescence in diabetes were predictors of retinopathy progression and creatininemia increase already 6years after punch-biopsy. **Clin Biochem**. 2016; 49:225−231.

51. Weiss MF, Rodby RA, Justice AC, Hricik DE. Free pentosidine and neopterin as markers of progression rate in diabetic nephropathy. Collaborative Study Group. **Kidney Int**. 1998; 54:193−202.

52. Kilhovd BK, Juutilainen A, Lehto S, et al. Increased serum levels of advanced glycation endproducts predict total, cardiovascular and coronary mortality in women with type 2 diabetes: a population-based 18 year follow-up study. **Diabetologia**. 2007; 50:1409−1417.

53. Nin JW, Jorsal A, Ferreira I, et al. Higher plasma levels of advanced glycation end products are associated with incident cardiovascular disease and all-cause mortality in type 1 diabetes: a 12-year follow-up study. **Diabetes Care**. 2011; 34:442−447.

54. Nin JW, Jorsal A, Ferreira I, et al. Higher plasma soluble Receptor for Advanced Glycation End Products (sRAGE) levels are associated with incident cardiovascular disease and all-cause mortality in type 1 diabetes: a 12-year follow-up study. **Diabetes**. 2010; 59:2027−2032.

55. Creager MA, Luscher TF, Cosentino F, Beckman JA. Diabetes and vascular disease: pathophysiology, clinical consequences, and medical therapy: Part I. **Circulation**. 2003; 108:1527−1532.

56. Du X, Edelstein D, Obici S, Higham N, Zou MH, Brownlee M. Insulin resistance reduces arterial prostacyclin synthase and eNOS activities by increasing endothelial fatty acid oxidation. **J Clin Invest**. 2006; 116:1071−1080.

57. Gabbay KH. Hyperglycemia, polyol metabolism, and complications of diabetes mellitus. **Annu Rev Med**. 1975; 26:521−536.

58. Baumgartner-Parzer SM, Wagner L, Pettermann M, Grillari J, Gessl A, Waldhausl W. High-glucose–triggered apoptosis in cultured endothelial cells. **Diabetes**. 1995; 44:1323−1327.

59. Hamed S, Brenner B, Roguin A. Nitric oxide: a key factor behind the dysfunctionality of endothelial progenitor cells in diabetes mellitus type-2. **Cardiovasc Res**. 2011; 91:9−15.

60. Yue WS, Lau KK, Siu CW, et al. Impact of glycemic control on circulating endothelial progenitor cells and arterial stiffness in patients with type 2 diabetes mellitus. **Cardiovasc Diabetol**. 2011; 10:113.

61. Cameron JD, Bulpitt CJ, Pinto ES, Rajkumar C. The aging of elastic and muscular arteries: a comparison of diabetic and nondiabetic subjects. **Diabetes Care**. 2003; 26:2133−2138.

62. Safar ME, Czernichow S, Blacher J. Obesity, arterial stiffness, and cardiovascular risk. **J Am Soc Nephrol**. 2006; 17:S109−S111.

63. Cruickshank K, Riste L, Anderson SG, Wright JS, Dunn G, Gosling RG. Aortic pulse-wave velocity and its relationship to mortality in diabetes and glucose intolerance: an integrated index of vascular function? **Circulation**. 2002; 106:2085−2090.

64. Kimoto E, Shoji T, Shinohara K, et al. Regional arterial stiffness in patients with type 2 diabetes and chronic kidney disease. **J Am Soc Nephrol**. 2006; 17:2245−2252.

65. Chirinos JA, Segers P, Gillebert TC, et al. Central pulse pressure and its hemodynamic determinants in middle-aged adults with impaired fasting glucose and diabetes: the Asklepios study. **Diabetes Care**. 2013; 36:2359−2365.

66. Kimoto E, Shoji T, Shinohara K, et al. Preferential stiffening of central over peripheral arteries in type 2 diabetes. **Diabetes**. 2003; 52:448−452.

67. Pannier B, Guerin AP, Marchais SJ, Safar ME, London GM. Stiffness of capacitive and conduit arteries: prognostic significance for end-stage renal disease patients. **Hypertension**. 2005; 45:592−596.

68. Briet M, Bozec E, Laurent S, et al. Arterial stiffness and enlargement in mild-to-moderate chronic kidney disease. **Kidney Int**. 2006; 69:350−357.

69. Strain WD, Chaturvedi N, Dockery F, et al. Increased arterial stiffness in Europeans and African Caribbeans with type 2 diabetes cannot be accounted for by conventional cardiovascular risk factors. **Am J Hypertens**. 2006; 19:889−896.

70. Elias MF, Crichton GE, Dearborn PJ, Robbins MA, Abhayaratna WP. Associations between type 2 diabetes mellitus and arterial stiffness: a prospective analysis based on the Maine-syracuse study. **Pulse (Basel)**. 2018; 5:88−98.

71. Cockcroft JR, Wilkinson IB, Evans M, et al. Pulse pressure predicts cardiovascular risk in patients with type 2 diabetes mellitus. **Am J Hypertens**. 2005; 18:1463−1467. discussion 1468-9.

72. Schram MT, Chaturvedi N, Fuller JH, Stehouwer CD, Group EPCS. Pulse pressure is associated with age and cardiovascular disease in type 1 diabetes: the Eurodiab Prospective Complications Study. **J Hypertens**. 2003; 21:2035−2044.

73. Schram MT, Kostense PJ, Van Dijk RA, et al. Diabetes, pulse pressure and cardiovascular mortality: the Hoorn Study. **J Hypertens**. 2002; 20:1743−1751.

74. van Dijk RA, Dekker JM, Nijpels G, Heine RJ, Bouter LM, Stehouwer CD. Brachial artery pulse pressure and common carotid artery diameter: mutually independent associations with mortality in subjects with a recent history of impaired glucose tolerance. **Eur J Clin Invest**. 2001; 31:756−763.

75. Sweitzer NK, Shenoy M, Stein JH, et al. Increases in central aortic impedance precede alterations in arterial stiffness measures in type 1 diabetes. **Diabetes Care**. 2007; 30:2886−2891.

76. Wilkinson IB, MacCallum H, Rooijmans DF, et al. Increased augmentation index and systolic stress in type 1 diabetes mellitus. **QJM**. 2000; 93:441−448.

77. Brooks B, Molyneaux L, Yue DK. Augmentation of central arterial pressure in type 1 diabetes. **Diabetes Care**. 1999; 22:1722−1727.

78. Gordin D, Ronnback M, Forsblom C, Heikkila O, Saraheimo M, Groop PH. Acute hyperglycaemia rapidly increases arterial stiffness in young patients with type 1 diabetes. **Diabetologia**. 2007; 50:1808−1814.

79. Schram MT, Henry RM, van Dijk RA, et al. Increased central artery stiffness in impaired glucose metabolism and type 2 diabetes: the Hoorn Study. **Hypertension**. 2004; 43:176−181.

80. Li CH, Wu JS, Yang YC, Shih CC, Lu FH, Chang CJ. Increased arterial stiffness in subjects with impaired glucose tolerance and newly diagnosed diabetes but not isolated impaired fasting glucose. **J Clin Endocrinol Metab**. 2012; 97:E658−E662.

81. Shin JY, Lee HR, Lee DC. Increased arterial stiffness in healthy subjects with high-normal glucose levels and in subjects with pre-diabetes. **Cardiovasc Diabetol**. 2011; 10:30.

82. Ohnishi H, Saitoh S, Takagi S, et al. Pulse wave velocity as an indicator of atherosclerosis in impaired fasting glucose: the Tanno and Sobetsu study. **Diabetes Care**. 2003; 26:437−440.

83. Lukich E, Matas Z, Boaz M, Shargorodsky M. Increasing derangement of glucose homeostasis is associated with increased arterial stiffness in patients with diabetes, impaired fasting glucose and normal controls. **Diabetes Metab Res Rev**. 2010; 26:365−370.

84. O'Rourke MF, Hashimoto J. Mechanical factors in arterial aging: a clinical perspective. **J Am Coll Cardiol**. 2007; 50:1−13.

85. Chirinos JA, Kips JG, Roman MJ, et al. Ethnic differences in arterial wave reflections and normative equations for augmentation index. **Hypertension**. 2011; 57:1108−1116.

86. Mitchell GF. Arterial stiffness and wave reflection: biomarkers of cardiovascular risk. **Artery Res**. 2009; 3:56−64.

87. Ewing DJ, Campbell IW, Clarke BF. The natural history of diabetic autonomic neuropathy. **Q J Med**. 1980; 49:95−108.

88. Chen HS, Hwu CM, Kuo BI, et al. Abnormal cardiovascular reflex tests are predictors of mortality in Type 2 diabetes mellitus. **Diabet Med**. 2001; 18:268−273.

89. Tanaka K, Kawai T, Saisho Y, et al. Relationship between stage of diabetic retinopathy and pulse wave velocity in Japanese patients with type 2 diabetes. **J Diabetes Res**. 2013; 2013:193514.

90. Townsend RR, Anderson AH, Chirinos JA, et al. Association of pulse wave velocity with chronic kidney disease progression and mortality: findings from the CRIC study (chronic renal insufficiency cohort). **Hypertension**. 2018; 71:1101−1107.

91. Rema M, Mohan V, Deepa R, Ravikumar R, Chennai Urban Rural Epidemiology S. Association of carotid intima-media thickness and arterial stiffness with diabetic retinopathy: the Chennai Urban Rural Epidemiology Study (CURES-2). **Diabetes Care**. 2004; 27:1962−1967.

92. Kim WJ, Park CY, Park SE, et al. The association between regional arterial stiffness and diabetic retinopathy in type 2 diabetes. **Atherosclerosis**. 2012; 225:237−241.

93. Yun YW, Shin MH, Lee YH, Rhee JA, Choi JS. Arterial stiffness is associated with diabetic retinopathy in Korean type 2 diabetic patients. **J Prev Med Public Health**. 2011; 44:260−266.

94. Ogawa O, Hiraoka K, Watanabe T, et al. Diabetic retinopathy is associated with pulse wave velocity, not with the augmentation index of pulse waveform. **Cardiovasc Diabetol**. 2008; 7:11.

95. Ogawa O, Hayashi C, Nakaniwa T, Tanaka Y, Kawamori R. Arterial stiffness is associated with diabetic retinopathy in type 2 diabetes. **Diabetes Res Clin Pract**. 2005; 68:162−166.

96. Centers for Disease Control and Prevention. **Chronic Kidney Disease in the United States**. US Department of Health and Human Services, Centers for Disease Control and Prevention; 2019. Accessed August 12, 2019.

97. United States Renal Data System. **USRDS Annual Data Report: Epidemiology of Kidney Disease in the United States**. 2020.

98. Levey AS, de Jong PE, Coresh J, et al. The definition, classification, and prognosis of chronic kidney disease: a KDIGO Controversies Conference report. **Kidney Int**. 2011; 80:17−28.

99. Molitch ME, Steffes M, Sun W, et al. Development and progression of renal insufficiency with and without albuminuria in adults with type 1 diabetes in the diabetes control and complications trial and the epidemiology of diabetes interventions and complications study. **Diabetes Care**. 2010; 33:1536−1543.

100. Weir MR, Townsend RR, Fink JC, et al. Hemodynamic correlates of proteinuria in chronic kidney disease. **Clin J Am Soc Nephrol**. 2011; 6:2403−2410.

101. Townsend RR. Arterial stiffness in CKD: a review. **Am J Kidney Dis**. 2019; 73:240−247.

102. Yokoyama H, Aoki T, Imahori M, Kuramitsu M. Subclinical atherosclerosis is increased in type 2 diabetic patients with micro-albuminuria evaluated by intima-media thickness and pulse wave velocity. **Kidney Int**. 2004; 66:448−454.

103. Yokoyama H, Hirasawa K, Aoki T, Ishiyama M, Koyama K. Brachial-ankle pulse wave velocity measured automatically by oscillometric method is elevated in diabetic patients with incipient nephropathy. **Diabet Med**. 2003; 20:942−945.

104. Smith A, Karalliedde J, De Angelis L, Goldsmith D, Viberti G. Aortic pulse wave velocity and albuminuria in patients with type 2 diabetes. **J Am Soc Nephrol**. 2005; 16:1069−1075.

105. Ishimura E, Taniwaki H, Tsuchida T, et al. Urinary albumin excretion associated with arterial wall stiffness rather than thickness in type 2 diabetic patients. **J Nephrol**. 2007; 20:204−211.

106. Aoun S, Blacher J, Safar ME, Mourad JJ. Diabetes mellitus and renal failure: effects on large artery stiffness. **J Hum Hypertens**. 2001; 15:693−700.

107. Bouchi R, Babazono T, Mugishima M, et al. Arterial stiffness is associated with incident albuminuria and decreased glomerular filtration rate in type 2 diabetic patients. **Diabetes Care**. 2011; 34:2570−2575.

108. Ha BK, Kim BG, Kim DH, et al. Relationships between brachial-ankle pulse wave velocity and peripheral neuropathy in type 2 diabetes. **Diabetes Metab J**. 2012; 36:443−451.

109. Suh BC, Chung PW, Moon HS, et al. Association between pulse wave velocity and nerve conduction study in diabetic patients. **Eur Neurol**. 2010; 64:219−223.

110. Yokoyama H, Yokota Y, Tada J, Kanno S. Diabetic neuropathy is closely associated with arterial stiffening and thickness in Type 2 diabetes. **Diabet Med**. 2007; 24:1329−1335.

111. Theilade S, Lajer M, Persson F, Joergensen C, Rossing P. Arterial stiffness is associated with cardiovascular, renal, retinal, and autonomic disease in type 1 diabetes. **Diabetes Care**. 2013; 36:715−721.

112. Meyer C, Milat F, McGrath BP, Cameron J, Kotsopoulos D, Teede HJ. Vascular dysfunction and autonomic neuropathy in Type 2 diabetes. **Diabet Med**. 2004; 21:746−751.

113. Laugesen E, Hoyem P, Stausbol-Gron B, et al. Carotid-femoral pulse wave velocity is associated with cerebral white matter lesions in type 2 diabetes. **Diabetes Care**. 2013; 36:722−728.

114. Mehrabian S, Raycheva M, Gateva A, et al. Cognitive dysfunction profile and arterial stiffness in type 2 diabetes. **J Neurol Sci**. 2012; 322:152−156.

115. Ogawa O, Onuma T, Kubo S, Mitsuhashi N, Muramatsu C, Kawamori R. Brachial-ankle pulse wave velocity and symptomatic cerebral infarction in patients with type 2 diabetes: a cross-sectional study. **Cardiovasc Diabetol**. 2003; 2:10.

116. Li S, Chen W, Srinivasan SR, Berenson GS. Influence of metabolic syndrome on arterial stiffness and its age-related change in young

adults: the Bogalusa Heart Study. **Atherosclerosis**. 2005; 180:349−354.

117. Safar ME, Thomas F, Blacher J, et al. Metabolic syndrome and age-related progression of aortic stiffness. **J Am Coll Cardiol**. 2006; 47:72−75.

118. Sipila K, Koivistoinen T, Moilanen L, et al. Metabolic syndrome and arterial stiffness: the health 2000 survey. **Metabolism**. 2007; 56:320−326.

119. Tomiyama H, Hirayama Y, Hashimoto H, et al. The effects of changes in the metabolic syndrome detection status on arterial stiffening: a prospective study. **Hypertens Res**. 2006; 29:673−678.

120. Nakanishi N, Suzuki K, Tatara K. Clustered features of the metabolic syndrome and the risk for increased aortic pulse wave velocity in middle-aged Japanese men. **Angiology**. 2003; 54: 551−559.

121. Zheng M, Zhang X, Chen S, et al. Arterial stiffness preceding diabetes: a longitudinal study. **Circ Res**. 2020; 127:1491−1498.

122. Yasuno S, Ueshima K, Oba K, et al. Is pulse pressure a predictor of new-onset diabetes in high-risk hypertensive patients?: a subanalysis of the Candesartan Antihypertensive Survival Evaluation in Japan (CASE-J) trial. **Diabetes Care**. 2010; 33:1122−1127.

123. Tsushima Y, Miyazaki M, Taketomi-Takahashi A, Endo K. Feasibility of measuring human pancreatic perfusion in vivo using imaging techniques. **Pancreas**. 2011; 40:747−752.

124. Almaca J, Weitz J, Rodriguez-Diaz R, Pereira E, Caicedo A. The pericyte of the pancreatic islet regulates capillary diameter and local blood flow. **Cell Metab**. 2018; 27:630−644 e4.

125. Stagner JI, Samols E. The vascular order of islet cellular perfusion in the human pancreas. **Diabetes**. 1992; 41:93−97.

126. Eipel C, Abshagen K, Vollmar B. Regulation of hepatic blood flow: the hepatic arterial buffer response revisited. **World J Gastroenterol**. 2010; 16:6046−6057.

127. Lee JJ, Tyml K, Menkis AH, Novick RJ, McKenzie FN. Evaluation of pulsatile and nonpulsatile flow in capillaries of goat skeletal muscle using intravital microscopy. **Microvasc Res**. 1994; 48:316−327.

128. Vincent MA, Dawson D, Clark AD, et al. Skeletal muscle microvascular recruitment by physiological hyperinsulinemia precedes increases in total blood flow. **Diabetes**. 2002; 51:42−48.

129. Emanuel AL, Meijer RI, Muskiet MH, van Raalte DH, Eringa EC, Serne EH. Role of insulin-stimulated adipose tissue perfusion in the development of whole-body insulin resistance. **Arterioscler Thromb Vasc Biol**. 2017; 37:411−418.

This page intentionally left blank

Cardiovascular risk prevention in clinical medicine: current guidelines in the United States and in Europe

Chee H. Liew[1] and John W. McEvoy[1,2]

[1]National Institute for Prevention and Cardiovascular Health, National University of Ireland Galway, Galway, Ireland; [2]Ciccarone Center for the Prevention of Cardiovascular Disease, Johns Hopkins University School of Medicine, Baltimore, MD, United States

Epidemiology of hypertension

Elevated blood pressure (BP), or hypertension, is a well-established and modifiable driver of cardiovascular disease (CVD),[1] with more than 1.13 billion adults worldwide diagnosed with hypertension in 2015.[2] The first report of increased CVD risk associated with hypertension came from the Framingham Heart Study.[3] Abundant evidence has since demonstrated the benefit of hypertension treatment in reducing important adverse health outcomes.[4–9] In this chapter, we will compare and contrast the 2017 American College of Cardiology (ACC)/American Heart Association (AHA) guidelines for the prevention, detection, evaluation, and management of high BP in adults[10] with the 2018 European Society of Cardiology (ESC)/European Society of Hypertension (ESH) guidelines for the management of arterial hypertension.[11] We will also highlight key areas in CVD risk assessment that are relevant to the management of hypertension. Particular attention will be placed on aspects of these hypertension guidelines that relate to the assessment and management of large artery stiffness (LAS) and pulsatile hemodynamics.[12] Where pertinent, we also provide suggestions for future iterations of hypertension guidelines with a view to better integrating the assessment and management of LAS into the management of hypertension.

Definition and classification of hypertension

It goes without saying that the epidemiology of hypertension is heavily influenced by its definition, particularly because BP itself is a continuous physiologic variable while hypertension is defined based on a binary BP threshold.

The 2017 ACC/AHA BP guidelines[10] altered the definition of hypertension from a cutoff of $\geq$140/90 mm Hg (i.e., the previous 2003 threshold from the Joint National Committee [JNC] 7 guideline[13]) to a lower threshold of $\geq$130/80 mm Hg. This seismic change in the clinical approach to millions of US adults was motivated in large part by results from the Systolic BP Intervention Trial (SPRINT).[14] By contrast, the 2018 ESC/ESH BP guidelines[11] maintain the level of BP that defines hypertension at $\geq$140/90 mm Hg (Table 31.1) and also recommend that most adults not receive antihypertensive drug treatment until their BP exceeds this level. However, for persons at very high cardiovascular risk due to established CVD, the ESC/ESH guidelines recommend that drug treatment be considered (Class 2b) at 130–139/85–89 mm Hg (i.e., high normal BP) because these individuals appear to benefit from further BP-lowering treatment.[15] In addition, and more in line with US guidelines, the ESC/ESH document recommends that, once drug treatment has commenced and is well tolerated, a systolic BP target of 130 mm Hg or lower be applied to most patients.

The landmark SPRINT,[14] which comprised 9361 nondiabetic hypertensive individuals aged 50 years or older at high cardiovascular risk, reported a 25% reduction in the primary composite cardiovascular outcome and a 27% reduction in all-cause mortality among those randomized to an intensive target (systolic BP <120 mm Hg), compared with the standard target (systolic BP <140 mm Hg). The mean systolic BP achieved in SPRINT was 121.4 mm Hg in the intensive arm versus 136.2 mm Hg in the standard arm. Interestingly, the ACC/AHA decided on a more conservative systolic threshold to redefine hypertension (i.e., a systolic of $\geq$130 mm Hg), rather than the threshold directly

TABLE 31.1 Blood pressure classification in the ACC/AHA[a] and ESC/ESH[b] guidelines.

ACC/AHA 2017				ESC/ESH 2018			
Category	SBP[c] (mm Hg)		DBP[d] (mm Hg)	Category	SBP (mm Hg)		DBP (mm Hg)
Normal	<120	and	<80	Optimal	<120	and	<80
Elevated	120−129	and	<80	Normal	120−129	and/or	80−84
Stage 1 hypertension	130−139	or	80−89	High normal	130−139	and/or	85−89
Stage 2 hypertension	≥140	or	≥90	Grade 1 hypertension	140−159	and/or	90−99
				Grade 2 hypertension	160−179	and/or	100−109
				Grade 3 hypertension	≥180	and/or	≥110
				Isolated systolic hypertension	≥140	and	<90

[a]*American College of Cardiology/American Heart Association.*
[b]*European Society of Cardiology/European Society of Hypertension.*
[c]*Systolic blood pressure.*
[d]*Diastolic blood pressure.*

supported by SPRINT (≥120 mm Hg). This more conservative threshold of 130 mm Hg accounts primarily for the technique of BP measurement in SPRINT (which was often unattended compared to the attended measurements usually performed in routine care[10,16−18]), as well as the fact that BP values from research studies tend to be lower than the corresponding values from clinical measurements (with the latter often being done without the recommended delay of 5 min rest and without adherence to standardized measurement protocols[19]).

According to the new ACC/AHA definition, approximately 46% of adults in the United States now meet diagnostic criteria for hypertension—a 14% increase in prevalence based on the prior JNC 7 definition.[20] It is worth noting that the decision to lower the ACC/AHA diastolic threshold for hypertension from 90 to 80 mm Hg was based on expert opinion and not on randomized clinical trial (RCT) data,[10] which is an important consideration because almost one in three of those newly diagnosed with hypertension using 2017 ACC/AHA guidelines are eligible due to a diastolic BP ≥80 mm Hg despite a systolic BP <130 mm Hg.[21]

Cardiovascular risk assessment in the management of hypertension

Blood pressure measurement

The recommended approach to BP measurement is consistent between the ACC/AHA and ESC/ESH guidelines. To confirm the diagnosis of hypertension and for treatment recommendations, both guidelines endorse greater use of out-of-office BP measurements, obtained by either home BP monitoring (HBPM) or ambulatory BP monitoring (ABPM).

Similar to the differences in office BP, both guidelines propose different out-of-office BP thresholds to define hypertension (Table 31.2). Both guidelines state that ABPM, performed over 24 h, provides useful information on 24-h mean BP and nighttime BP (both of which appear to be the best BP measures for accessing cardiovascular risk[22]). Out-of-office monitoring is also useful for the detection of white-coat hypertension and masked hypertension. The latter refers to untreated patients with normal BP values in the office but with elevated BP readings on either HBPM or ABPM. Endorsement of more widespread use of out-of-office BP measurements has important clinical implications, given that masked (and to a lesser extent white-coat) hypertension is associated with increased cardiovascular morbidity and mortality.[23] There are also cost implications that remain understudied.

Risk assessment tools

For primary prevention, the 2017 ACC/AHA guideline recommends the estimation of 10-year atherosclerotic CVD (ASCVD) risk when considering drug treatment among adults with stage 1 hypertension (i.e., office systolic BP 130−139 and/or office diastolic BP 80−89 mm Hg). Specifically, drug treatment for stage 1 hypertension is recommended only among persons with a 10-year CVD risk of greater than 10%. To this end, the ACC/AHA endorse the pooled cohort equations (PCEs) to estimate 10-year CVD risk,[24,25] which have been validated for US adults aged 40−79 years. Irrespective of CVD risk estimates, all adults with confirmed stage 2 hypertension by US definitions are recommended for drug therapy according to US guidelines.

By contrast, European guidelines do not endorse the use of risk assessment tools in deciding on specific BP

TABLE 31.2 Comparison of ACC/AHA[a] and ESC/ESH[b] definitions of hypertension.

Level of BP[c] defining hypertension	ACC/AHA 2017			ESC/ESH 2018		
	Systolic (mm Hg)	and/or	Diastolic (mm Hg)	Systolic (mm Hg)	and/or	Diastolic (mm Hg)
Office/clinic BP[d]	≥130		≥80	≥140		≥90
Home BP mean	≥130		≥80	≥135		≥85
Daytime mean, ABPM[e]	≥130		≥80	≥135		≥85
24-h mean, ABPM[e]	≥125		≥75	≥130		≥80
Nighttime mean, ABPM[e]	≥110		≥65	≥120		≥70

[a]American College of Cardiology/American Heart Association.
[b]European Society of Cardiology/European Society of Hypertension.
[c]Blood pressure.
[d]Refers to conventional office blood pressure rather than unattended office blood pressure.
[e]Ambulatory blood pressure monitor.

thresholds or targets for drug therapy, instead recommending that drugs only be initiated once BP ≥140/90 mm Hg (irrespective of 10-year CVD risk). However, European guidance does incorporate assessment of CVD risk into the timing of antihypertensive drug initiation. Specifically, for persons with BP 140−159/90−99 mm Hg, immediate commencement of drug therapy is recommended only among those with evidence of target organ damage (see section directly below) or those with high or very high risk. Patients at lower risk are advised lifestyle modifications and to wait three−six months prior to initiating drug treatment. To this end, the ESC/ESH recommend the use of Systematic COronary Risk Evaluation (SCORE),[26,27] which is based on a large, representative European population, for patients between 40 and 65 years of age. High or very high risk according to SCORE is defined as a 10-year risk of ≥5% using this tool.

The SCORE system allows for calibration for different cardiovascular risk levels across European countries. Notably, risk classification by SCORE is based on the risk of fatal events only, whereas the PCEs predict risk of both fatal and nonfatal (i.e., total) ASCVD events. Given that the main goal of primary prevention should be on preventing the first ASCVD event,[28] exclusion of nonfatal ASCVD events from risk assessment tools seems counterintuitive and future iterations of SCORE are planned to incorporate these outcomes. Development of a SCORE algorithm specifically for patients aged 65 or older (i.e., SCORE Older Persons [SCORE OP]) is also underway.[29,30]
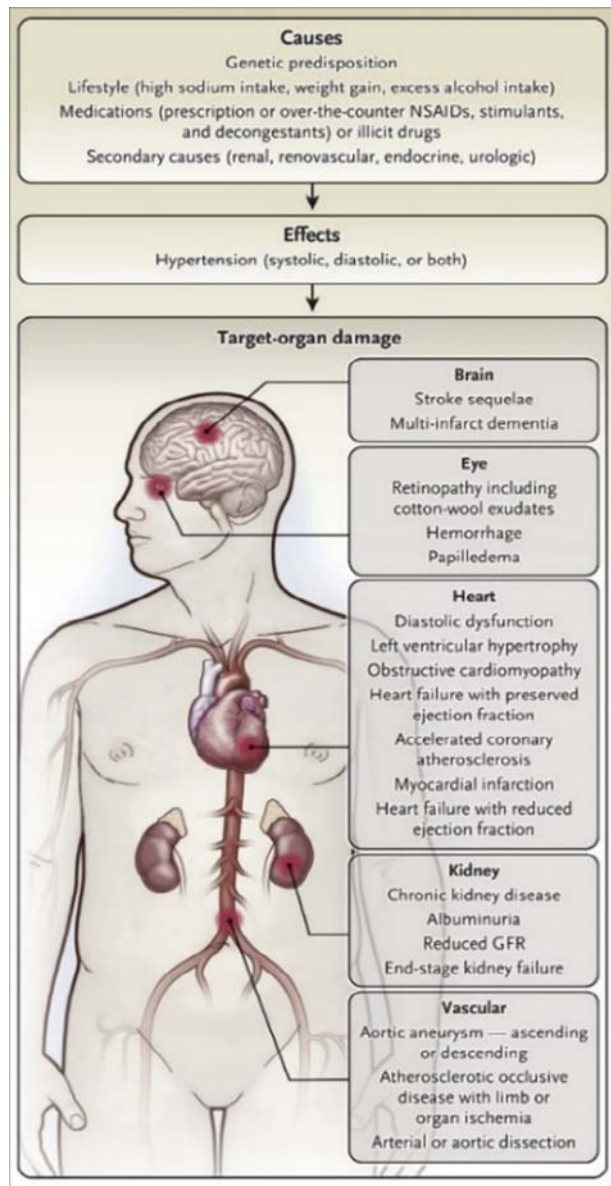
However, it must be acknowledged that risk estimation using either PCE or SCORE is not perfect[31] and both provide modest discrimination for ASCVD events at best, as they can overestimate or underestimate 10-year ASCVD risk at the individual level.[25,30,32−36] These equations also do not assess risk for heart failure (HF) for which intensive BP control is especially beneficial.[14,37] Recognizing the imprecision of ASCVD risk prediction scores,[31] both guidelines recommend consideration of additional testing to support cardiovascular risk stratification. Assessment of LAS and pulsatile hemodynamics may both be particularly suitable to this effort.

Hypertension-mediated organ damage and risk modifiers

The 2018 ESC/ESH, and to a lesser extent the 2017 ACC/AHA BP guidelines, recommend that risk estimation be complemented by assessment of hypertension-mediated organ damage (HMOD), which includes hypertension-induced structural and/or functional changes in major organs (e.g., the heart, brain, and kidney, Fig. 31.1). This helps to identify asymptomatic hypertensive patients at increased cardiovascular risk who may otherwise be misclassified as having a lower level of risk by PCE or by SCORE. Furthermore, European guidelines include the assessment of carotid-femoral pulse wave velocity (PWV), as a surrogate for LAS, in their definition of HMOD. Given the focus of this book on LAS, we have allocated a dedicated section, below, to the use of LAS and pulsatile hemodynamics as risk modifiers in the management of hypertension.

In terms of non-HMOD risk modifiers, the ESC/ESH guidelines cite resting heart rate (RHR) greater than 80 beats per minute (bpm) as one example. The Valsartan Antihypertensive Long-term Use Evaluation (VALUE) trial reported that increased heart rate predicted future cardiovascular events among high-risk patients with hypertension.[38] An analysis of the Henry Ford Hospital Exercise Testing (FIT) Project demonstrated increased risk of hypertension among traditionally normotensive individuals with a RHR greater than 85 bpm.[39] A Multi-Ethnic Study of Atherosclerosis (MESA) analysis showed that a higher

FIGURE 31.1 Target organ damage in hypertension. *From Taler SJ. Initial treatment of hypertension.* **N Engl J Med.** *2018; 378(7):636−644; with permission.*

RHR was associated with increased arterial stiffness independent of atrioventricular nodal blocker use and physical activity level in an asymptomatic multiethnic population.[40] Whether therapeutic RHR reduction is useful for reducing incident hypertension or cardiovascular events is unknown and warrants further study.

Risk modifiers not specifically endorsed in US/EU hypertension guidelines but with emerging data suggesting promise in guiding hypertension management include coronary artery calcium (CAC), measured by noncontrast cardiac computerized tomography (CT), and cardiac biomarkers measured in blood. For example, CAC is associated with incident hypertension[41] and is a strong independent predictor of future cardiovascular events.[42−45] Selective use of CAC measurement coupled with ASCVD risk scores[46,47] may help guide cardiovascular risk stratification and support a personalized approach to initiation and intensification of antihypertensive therapy.[48−50] According to CVD prevention guidelines, CAC should be considered to guide preventive therapies among adults at borderline (5%) or intermediate (7.5%) 10 year risk by the PCEs (2019 ACC/AHA)[51] or, in Europe, those with calculated SCORE risks close to the 5% or 10% risk thresholds (2016 ESC/ ESH).[26] However, these broad prevention guidelines focus much of the discussion around CAC on allocating statin therapy and make little reference to modulating antihypertensive drug intensity according to CAC. Forthcoming evidence may address the potential use of CAC scoring to guide treatment decisions in high-risk primary prevention patients, inclusive of antihypertensive therapy.[52−54]

Related to CAC, thoracic aortic calcium (TAC) is also quantifiable on noncontrast chest CT imaging and may offer indirect insights into the LAS status of a given individual that could inform treatment decisions regarding hypertension. Among Framingham Heart Study Third Generation and Offspring Cohort participants who were free of CVD, TAC was associated with both higher values of carotid-femoral PWV and central pulse pressure (PP).[55] There is also evidence that TAC is associated with incident hypertension[41] and with other important cardiovascular outcomes.[56,57] Nonetheless, the use of TAC in guiding treatment in stage 1 hypertension and in providing incremental prognostic value for risk assessment (particularly when CAC is available) remains under debate.[50,58]

Additional biomarker candidates that have demonstrated promise for risk stratification in the management of hypertension include high-sensitivity cardiac troponin T (hs-cTnT) and N-terminal pro-brain natriuretic peptide (NT-proBNP).[59,60] Like CAC, these biomarkers are associated with incident hypertension and they also indicate subclinical structural damage to the heart.[61,62] Elevations in hs-cTnT or NT-proBNP may help identify individuals not currently recommended for antihypertensive medication who are at higher risk for CVD events and thus may benefit from initiation of BP-lowering medication. Further research is needed to assess the potential for combined use of different biomarkers to improve CVD risk assessment.[63,64]

Arterial stiffness and cardiovascular risk

Measurement of carotid-femoral PWV[65−67] for evaluating LAS as part of HMOD assessment received a Class 2b recommendation in the 2018 ESC/ESH hypertension guidelines. A meta-analysis including 15,877 participants showed that those in the higher tertiles of carotid-femoral PWV had increased risk of future cardiovascular events

and all-cause mortality.[68] A subsequent participant-level meta-analysis of prospective studies including 17,635 participants found that each standard deviation increase in carotid-femoral PWV was associated with a 35%, 54%, and 45% increase in the risk of coronary artery disease (CAD), stroke, and overall CVD, respectively.[69] Carotid-femoral PWV was an independent predictor of risk across multiple subpopulations, with a more pronounced effect among those aged 60 or younger.[69] Accordingly, LAS may add incremental prognostic information to CVD risk estimates derived from traditional risk factors.[70]

The European Reference Values for Arterial Stiffness' Collaboration reported a marked increase in carotid-femoral PWV across BP categories at any particular age (Fig. 31.2).[71] According to the ESC/ESH, a PWV more than 10 m/s is a conservative estimate of significant alterations of aortic function in middle-aged hypertensive patients. The 2017 ACC/AHA BP guidelines consider carotid-femoral PWV a noninvasive estimate of vascular target organ injury and atherosclerosis without further elaboration.

A prospective study of 34,649 adults showed that large- and small-artery disease/stiffness (as measured by cardio-ankle vascular index [CAVI] and retinal fundoscopy, respectively) were independently associated with incident hypertension,[72] suggesting their distinct implications on the pathway to hypertension. CAVI is a derived measure of LAS that includes PWV in the calculation but that is reportedly influenced less by the BP at the time of estimation than the PWV is.
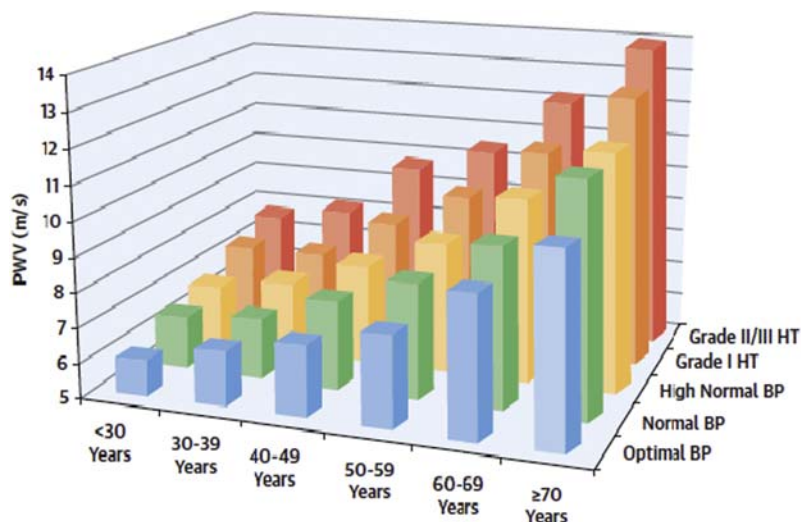
Another useful and easily measured surrogate of LAS is PP, which is the simple difference between systolic BP and diastolic BP. Accordingly, PP may serve as an independent prognostic marker of cardiovascular risk, particularly in middle-aged and older hypertensive patients.[11,73,74] In the international Reduction of Atherothrombosis for Continued Health (REACH) registry, a higher PP quartile was associated with increased risk of adverse CVD outcomes.[75] The prognostic utility of PP has also been demonstrated in other studies.[76–80] Furthermore, studies have shown associations of isolated systolic hypertension (ISH) and wide PP with abnormalities in biomarkers such as hs-cTnT and NT-proBNP, findings that may potentially guide personalized antihypertensive treatment of older patients with these BP aberrations.[81] This comes with the caveat that PP is not just influenced by LAS, but also cardiac output and other important physiologic parameters. It is important to also acknowledge that PP remains a relatively poorly studied parameter in trials of BP management compared to other BP parameters or risk-modifiers.

Therapeutic goals in the management of hypertension

Blood pressure treatment thresholds and targets in US/EU guidelines

As noted earlier, the BP threshold for a diagnosis of hypertension recommended by guidelines has changed over the years. An early Framingham report in 1957 defined hypertension as BP $\geq$160/95 mm Hg.[3] Subsequent observational studies and BP treatment trials (initially focusing on diastolic BP targets[82–84] then transitioning to systolic BP targets[85–87]) provided further insights into BP treatment effects that resulted in hypertension being redefined at lower BP values. The safety of treating systolic BP to <140 mm Hg was first demonstrated in the Antihypertensive and Lipid-Lowering Treatment to Prevent Heart Attack Trial (ALLHAT).[88] More recently, SPRINT was the

FIGURE 31.2 Mean reference values for pulse wave velocity according to age and blood pressure categories. Note that blood pressure categories correspond to European guidelines, rather than to 2017 AHA/ACC categories. *From Reference Values for Arterial Stiffness' Collaboration. Determinants of pulse wave velocity in healthy people and in the presence of cardiovascular risk factors: 'establishing normal and reference values'.* **Eur Heart J.** *2010; 31(19):2338–2350; with permission.*

first trial to suggest a benefit to treating high-risk individuals to even lower BP targets, in the case of this trial, a systolic BP of <120 mm Hg.

The Heart Outcomes Prevention Evaluation (HOPE)-3 trial provides additional insight beyond persons at high risk by evaluating the use of antihypertensive therapy among intermediate-risk hypertensive individuals with mean BP of 138/82 mm Hg at baseline.[89] While the trial did not show any significant benefit in the composite endpoints, a prespecified subgroup analysis of HOPE-3 demonstrated lower rates of both first and second composite outcomes among those in the highest tertile of baseline SBP (above 143.5 mm Hg). Taken together, both SPRINT and HOPE-3 suggest that benefits from BP reduction to lower values than previously recommended may be related to baseline estimated CVD risk. Indeed, the recent published STEP (Strategy of Blood Pressure Intervention in the Elderly Hypertensive Patients) trial also confirmed that the benefit seen in the arm randomized to a more intensive SBP target (<130 mm Hg) appeared to be limited to those with (15% 10-year risk of CVD.[90] This ever-evolving evidence base has informed the recommendations in the most recent BP treatment guidelines.

In this context, and for the first time, the ACC/AHA guidelines recommend a target BP of less than 130/80 mm Hg for all hypertensive patients across all age groups.[10] This class I recommendation applies to all secondary prevention patients, as well as to primary prevention patients with either (1) an estimated 10-year ASCVD risk ≥10% and BP ≥ 130/80 mm Hg or (2) an estimated 10-year ASCVD risk <10% and BP ≥140/90 mm Hg. In other words, US guidelines state that BP treatment should be initiated once BP ≥130/80 mm Hg and treated to <130/80 mm Hg among persons with a history of prior CVD or among primary prevention adults with 10-year CVD risk estimates ≥10%. For primary prevention, adults with 10-year CVD risk estimates <10%, treatment initiation is not recommended until a BP ≥140/90 mm Hg; however, the target of treatment remains <130/80 mm Hg. As discussed earlier, SPRINT[14] was among the major drivers of the new lower BP therapeutic target. A meta-analysis of 144,220 patients in 42 trials showed a linear association between mean achieved SBP and risk of CVD mortality with the lowest risk at 120−124 mm Hg.[91]

The lower SBP target in the 2017 ACC/AHA BP guidelines is justified by a number of lines of evidence, not just SPRINT alone.[90] However, the new ACC/AHA diastolic target of <80 mm Hg is more debatable. Indeed, in the Hypertension Optimal Treatment (HOT) trial, there was no difference in outcomes between the groups who were allocated to a DBP target of ≤90 mm Hg, 85 mm Hg, or 80 mm Hg.[92] Whether this lower 2017 US diastolic target is justifiable remains to be proven in future outcomes trials of antihypertensive drug treatments. Nevertheless, the new BP goal of 130/80 mm Hg recommended by the ACC/AHA enables earlier execution of preventive lifestyle efforts than ever before (which can only be a good thing), as well as resulting in the eradication of the vague "prehypertension" category that was used in previous US BP guidelines.[13]

Although the 2018 ESC/ESH BP guidelines have seemingly taken a more restrained stance on BP treatment, their core recommendations are in fact not too dissimilar to those endorsed by the 2017 ACC/AHA BP guidelines. Nonetheless, there are clear differences in BP thresholds above which treatment initiation is recommended in EU guidelines. Specifically, the BP threshold above which treatment initiation is recommended by the ESC/ESH is ≥140/90 mm Hg for all patients. The only exception to this treatment initiation threshold is a weaker recommendation that treatment initiation may be considered at BP 130−139/85−89 mm Hg those with established CVD or primary prevention adults with a >5% 10-year risk of fatal CVD by the SCORE equation.

In contrast to the differences between guidelines in recommended BP thresholds above which to initiate drug therapy, similarities begin to emerge between the US and EU guidelines when considering treatment targets. The general recommendation for treatment targets by the ESC/ESH comprises two parts. To start, the guidelines mention that the first therapeutic objective should be to reduce BP to a target of <140/90 mm Hg in all patients,[11] rendering the ACC/AHA recommended target of <130/80 mm Hg appear "aggressive" at first glance. However, a second objective, which may not be readily apparent to some and is important to stress, then recommends a treatment target BP of 130/80 mm Hg or lower in most patients, provided that antihypertensive therapy is well tolerated. Indeed, for persons under 65 years, ESC/ESH recommend that a systolic BP target of 120−129 mm Hg be pursued as long as treatment is tolerated (which is arguably more intensive than the US recommendation). Notably, the 2018 ESC/ESH BP guidelines also recommend against a target BP of <120/70 mm Hg (a stipulation that not in the 2017 ACC/AHA BP guidelines). There are several other key differences between the transatlantic BP guidelines that deserve further attention.

Blood pressure goals in older adults

BP increases predictably with age and as many as 70% of adults over the age of 70 develop hypertension.[93] Consistent with the 2017 ACC/AHA BP guidelines, there is acknowledgment by the 2018 ESC/ESH BP guidelines of the difference between biological versus chronological age. However, in contrast to the "one-size-fits-all" approach by the ACC/AHA (who recommend the same BP target of <130/80 mm Hg irrespective of age), the ESC/ESH propose a target BP of 130−139/80 mm Hg for adults aged 65 or older (note that the previous 2013 ESC/ESH target for

this age group was 140−149/90 mm Hg[94]). As such, European guidance recommends a lower systolic BP limit of 130 mm Hg below which treatment should be de-escalated among those ≥65 years, contrasting with the lower systolic BP limit of 120 mm Hg recommended for adults below 65 years.

Active treatment of systolic BP among older adults is well supported by evidence. A prespecified subgroup analysis of SPRINT involving 2636 ambulatory adults aged 75 years or older showed that intensive systolic BP treatment was associated with lower rates of total cardiovascular events and all-cause mortality.[95] Although event rates were higher with increasing frailty in both treatment groups, within each frailty stratum absolute event rates were lower for the intensive treatment group. The Hypertension in the Very Elderly Trial (HYVET), which included 3845 individuals aged 80 years or older, demonstrated risk reductions in all-cause mortality and HF with antihypertensive therapy,[96] and that the benefit on outcomes was not influenced by frailty status.[97] The SPRINT Memory and Cognition in Decreased Hypertension (SPRINT MIND) trial reported a lower risk of mild cognitive impairment[98] with more intensive BP treatment despite not meeting the primary endpoint of risk of dementia. Intensive antihypertensive therapy also delayed the progression of white matter lesions on brain imaging.[99] A subsequent meta-analysis of 12 RCTs found a lower risk of incident dementia or cognitive impairment with antihypertensive medication use.[100]

The new and lower BP targets in both guidelines raise several age-related concerns. First, based on observational data, the heightened possibility of a J-curve for diastolic BP in older persons[93] may signify potential harm with intensive BP treatment, particularly when applying the ACC/AHA guidelines (which do not provide lower bounds for BP level below which treatment should be de-escalated). However, this J-curve concern is allayed in analyses that adjust for competing risk comorbidities[101] and by the randomized data from SPRINT.[102] Second, orthostatic hypotension (OH) is a major concern with more intensive BP treatment and, importantly, prevails among individuals aged >65 or with increased LAS.[103] Data from analyses evaluating the association of intensive BP treatment with OH-related adverse outcomes such as falls are mixed.[104−106] A SPRINT study found no association between intensive BP treatment and risk of cardiovascular events, syncope, electrolyte abnormalities, injurious falls, or acute renal failure, irrespective of baseline OH status.[107] An important caveat; however, is that SPRINT excluded persons with a standing systolic BP <110 mm Hg at baseline. Finally, third, with intensive BP treatment comes greater polypharmacy and associated repercussions (e.g., cost,[108] medication errors, nonadherence, interactions, and side effects[109−111])—a key consideration for older patients who, by and large, are more prone to polypharmacy due to underlying medical comorbidities. In SPRINT, the intensive arm required a mean of three medications compared with 1.9 in the standard arm.[14] In the Action to Control Cardiovascular Risk in Diabetes (ACCORD) trial, the mean number of medications was 3.4 and 2.1 in the intensive and standard arms, respectively.[112]

The more cautious approach to the treatment of older adults taken by the ESC/ESH hypertension guideline may reflect some of these concerns. Nonetheless, results from SPRINT, STEP and HYVET reinforce the concept that risk reductions in CVD events and mortality from hypertension treatment are evident regardless of frailty status, and suggest that older independent patients perhaps should not be treated any differently than their younger counterparts. However, benefit-risk assessment and personalization remain integral to the intensity of antihypertensive therapy in older patients.

Chronic kidney disease

For hypertensive patients with chronic kidney disease (CKD), the 2018 ESC/ESH hypertension guidelines contend that there is insufficient evidence to support a target systolic BP <130 mm Hg (Table 31.3), despite the fact that this target is endorsed by the 2017 ACC/AHA hypertension guidelines in persons with CKD. In SPRINT, among those with CKD at baseline, there was no significant difference in adverse renal outcomes between treatment groups with a caveat that the number of adverse renal events was small.[14] Indeed, analyses of SPRINT focusing on patients with CKD demonstrated lower rates of all-cause mortality and potential reductions in major cardiovascular events with intensive BP treatment,[113] and that this benefit was evident across the spectrum of kidney function and albuminuria.[114,115] Notably, the majority of CKD participants in SPRINT had relatively mild CKD (baseline estimated glomerular filtrate rate ≥45 mL/min/1.73 m^2).

Diabetes

The target BP of <130/80 mm Hg for diabetic adults recommended by the ACC/AHA (all age groups) and ESC/ESH (age less than 65 years) has come into question because: (1) no trial has specifically proven a benefit for a target BP of 130/80 mm Hg or lower among diabetics[112], and (2) SPRINT did not include diabetic patients. Of note, a factorial trial showed that intensive BP treatment in ACCORD Blood Pressure (ACCORD BP) was beneficial among those randomized to standard (but not to intensive) glycemic control.[116] A post hoc observational analysis of the Examination of Cardiovascular Outcomes with Alogliptin versus Standard of Care (EXAMINE) trial showed that among type 2 diabetes patients with recent acute

TABLE 31.3 Office blood pressure targets for patients with hypertension according to clinical conditions.

Category	ACC/AHA[a] 2017		ESC/ESH[b] 2018	
	SBP[c] (mm Hg)	DBP[d] (mm Hg)	SBP (mm Hg)	DBP (mm Hg)
Age ≥ 65 years	<130	<80	130–139 if tolerated	70–79
Chronic kidney disease[e]	<130	<80	130–139 if tolerated	70–79
Diabetes	<130	<80	130 or lower if tolerated Not <120	70–79
Coronary artery disease	<130	<80	130 or lower if tolerated Not <120	70–79
Post-stroke/transient ischemic attack	<130	<80	130 or lower if tolerated Not <120	70–79

[a]*American College of Cardiology/American Heart Association.*
[b]*European Society of Cardiology/European Society of Hypertension.*
[c]*Systolic blood pressure.*
[d]*Diastolic blood pressure.*
[e]*Defined as an estimated glomerular filtration rate <60 mL/min/1.73 m² with or without proteinuria.*

coronary syndromes, BP <130/80 mm Hg was associated with worse cardiovascular outcomes.[117] This analysis is subject to the same potential biases mentioned earlier for other observational analysis suggesting a BP J-curve. Contradicting this finding, and lending indirect evidence that supports the assertion by the ACC/AHA and ESC/ESH, an analysis from the Action in Diabetes and Vascular disease: preterAx and diamicroN-Modified Release Controlled Evaluation (ADVANCE) trial[118] found that the benefit of more intensive BP treatment, seen in the ADVANCE trial overall, also extended to the subgroup of diabetics with baseline systolic BP between 120 and 140 mm Hg. Moreover, this benefit was largely independent of baseline cardiovascular risk. Consistent with this evidence and the 2017 ACC/AHA recommendations, the American Diabetes Association endorses the lower BP target of <130/80 mm Hg for high-risk diabetic patients (defined as existing ASCVD or 10-year ASCVD risk ≥15%) in their 2020 recommendation document (Grade C evidence), provided that this target can be safely attained.[119]
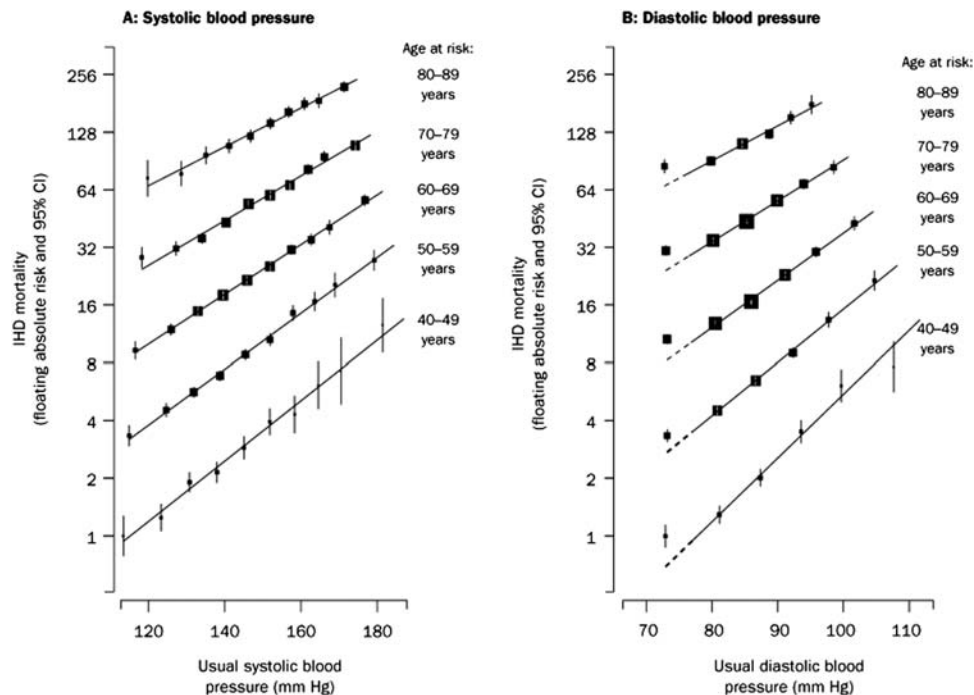
Blood pressure J-curve: role of large artery stiffness and implications for treatment targets

In a meta-analysis of one million individuals without CVD at baseline who were enrolled in prospective observational studies, the risk of CVD death increased at systolic BP above 115 mm Hg and diastolic BP above 75 mm Hg.[120] However, this meta-analysis also signaled a potential J-curve for diastolic BP with a trend for increased ischemic heart disease (IHD) events, but not stroke, among those with diastolic BP <70 mm Hg (Fig. 31.3)—a finding supported by subsequent observational studies[121−123]. This
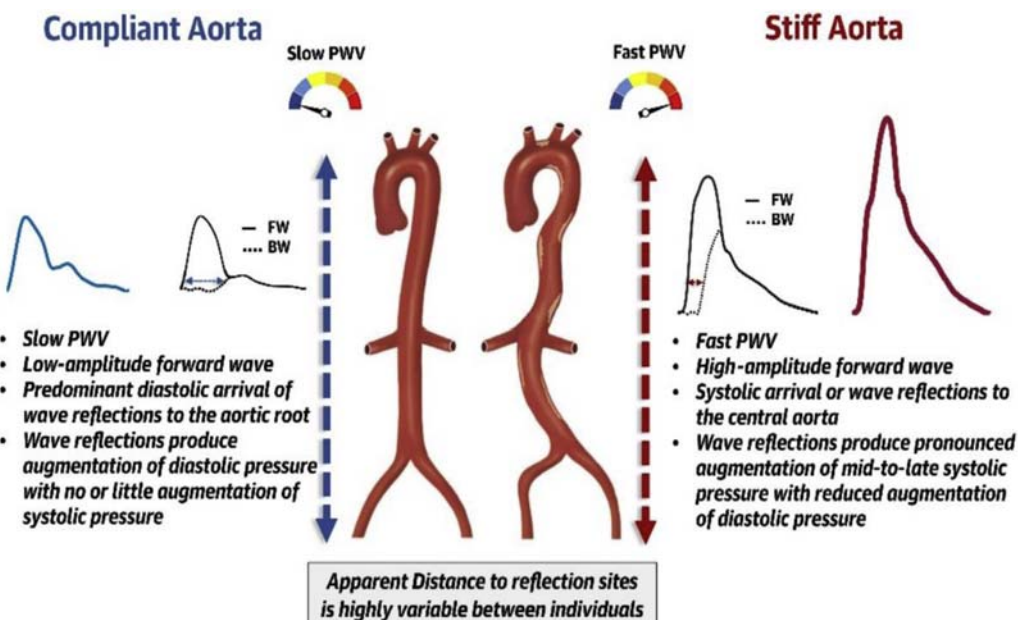
J-curve finding is thought to be attributable in part to impaired coronary perfusion to the myocardium at low diastolic BP.[124] Nonetheless, post hoc analyses of SPRINT[102] and ACCORD[125] have shown no evidence that the benefit of intensive systolic BP lowering differed across quintiles of baseline diastolic BP, suggesting that the diastolic BP J-curve seen in observational studies is confounded and that, when studied in the context of a randomized trial, further BP reduction among individuals with low diastolic BP but elevated systolic BP is not harmful. A potential weakness of the post hoc SPRINT analysis was that increased PP, as a marker of LAS, was not adjusted for.[126]

Some if not most of the diastolic BP J-curve may be confounded by LAS or PP. Wave reflections arrive at the aorta predominantly during diastole in young, healthy adults, augmenting diastolic pressure.[70] As PWV increases due to wall stiffening, reflections arrive at the aorta in mid-to-late systole instead. This results in systolic pressure augmentation, with loss of diastolic pressure augmentation and widening of the aortic PP (Fig. 31.4). These important physiologic changes may explain why a low diastolic BP is a marker of risk in observational studies (specifically because it is correlated with LAS) and also why treatment of elevated systolic BP appears beneficial irrespective of baseline diastolic BP; highlighting the fact that the diastolic BP J-curve may be mostly due to confounding by LAS and that naturally occurring low diastolic BP may not directly cause harm in the vast majority of adults.[101]

It is worth briefly noting that some observational data have suggested a systolic BP J-curve also, though this is more controversial (and not anticipated to be related to LAS) so will not be covered in detail in this chapter. In brief, several studies have reported either lack of reduction

FIGURE 31.3 Ischemic heart disease mortality rate in each decade of age versus blood pressure at the start of each decade. *From Lewington S, Clarke R, Qizilbash N, Peto R, Collins R. Age-specific relevance of usual blood pressure to vascular mortality: a meta-analysis of individual data for one million adults in 61 prospective studies. **Lancet.** 2002; 360(9349):1903−1913; with permission.*

FIGURE 31.4 Effects of increased large artery/aortic stiffness on central pressure waveform. *From Chirinos JA, Segers P, Hughes T, Townsend R. Large-artery stiffness in health and disease: JACC State-of-the-Art Review. **J Am Coll Cardiol.** 2019; 74(9):1237−1263; with permission.*

in major CVD events or increased risk of events/mortality with "excessive" systolic BP lowering.[112,123,127−129] For example, results from the Prospective Observational Longitudinal Registry of Patients with Stable CAD (CLARIFY)[123] study suggest that a systolic target around 120 mm Hg is probably safe, but that further reductions may lead to adverse outcomes, particularly among individuals with preexisting restrictions to coronary blood flow. However, these prior observational reports are contradicted by SPRINT[14] and by analyses of BP studies that

comprehensively adjusted for confounding variables.[101,130,131] Comprehensive adjustment of potential confounders is critical because individuals with worse health status may have lower systolic BP and therefore reverse causation is a major concern with observational reports suggesting a systolic BP J curve. Indeed, a recent MESA study including 1457 individuals free of baseline ASCVD and without any other ASCVD risk factors found no evidence of a J-curve for systolic BP levels as low as 90 mm Hg.[132] Nonetheless, because of concerns around a diastolic and systolic BP J-curve, 2018 ESC/ESH hypertension guidelines introduced for the first time lower limits of recommended BP levels (specifically to not reduce BP with medication to lower than 120/70 mm Hg).

Additional therapeutic considerations for hypertension management in current guidelines

Nonpharmacologic and pharmacologic interventions

Lifestyle modifications remain the cornerstone of hypertension prevention and treatment, regardless of cardiovascular risk,[133] with strong endorsement from both 2017 ACC/AHA and 2018 ESC/ESH guidelines (Table 31.4). Among patients in whom pharmacologic antihypertensive therapy is needed, concurrent lifestyle efforts should continue to be advocated. There is general consensus on the pharmacological approaches to hypertension management between guidelines, including significant emphasis on medication adherence. Because of their slightly weaker BP lowering effects, both guidelines now restrict the use of beta blockers for the treatment of hypertension to patients with other specific and compelling clinical indications, such as IHD or HF.

Notably, the ESC/ESH strongly recommend the use of an initial single pill combination (SPC) therapy comprising a renin-angiotensin system blocker (either an angiotensin-converting enzyme inhibitor or an angiotensin receptor blocker) with either a thiazide diuretic or a calcium channel blocker, for all stages of hypertension. In the United States, according to the ACC/AHA guideline, this recommendation pertains to patients with stage 2 hypertension and BP >20/10 mm Hg above their BP target (i.e., 150/90 mm Hg). There is little doubt that initial SPC therapy, as proposed by EXC/ESH, improves medication adherence, increases likelihood of achieving BP goals, is more cost effective, and has fewer adverse effects,.[134–136] However, the inherent risk of therapeutic inertia with SPC should not be overlooked, nor should the more limited titration and combination options.[137] Of interest, recent reports have suggested there is potential for an initial triple combination therapy to improve BP control,[138,139] a possibility that calls for further outcomes trials.

Other considerations in the approach to hypertension management

Available evidence suggests that nocturnal BP may be a stronger predictor of cardiovascular outcomes than daytime BP.[140,141] Taking antihypertensive medications at nighttime is neither endorsed nor opposed by the ACC/AHA and ESC/ESH. In 2019, the Hygia Chronotherapy Trial (open label) of 19,084 hypertensive patients reported significant reductions in the primary CVD outcome, CVD death, and all-cause mortality among those randomized to bedtime dosing compared with upon awakening dosing[142]—a finding that requires further trial replication. Unfortunately, concerns have been expressed about the conduct and reporting of Hygia[143] and, as such, nocturnal dosing of antihypertensive medications should not be endorsed routinely at this time.

Resistant hypertension, defined as either above-goal elevated BP despite concomitant use of three antihypertensive drug classes (one of which must be a thiazide diuretic) or BP that achieves target values on four or more antihypertensive medications, affects approximately 15% of treated adults with hypertension (when considering a traditional cutoff of 140/90 mm Hg).[144] In the REACH registry, among patients with resistant hypertension and BP above target, an increasing number of antihypertensive medications were associated with an increased risk for a composite of cardiovascular death, myocardial infarction, or stroke over 4 years in a dose-response fashion (Fig. 31.5), though the association between number of antihypertensives and outcomes was attenuated after adjustment for BP.[145]

Various device-based therapies have emerged for the treatment of hypertension, although both 2017 ACC/AHA and 2018 ESC guidelines do not endorse their routine use at present due to insufficient clinical evidence regarding their safety and efficacy. Despite early setbacks,[146] renal denervation, which involves catheter ablation of renal sympathetic nerves, has shown promising results in more recent trials and global registry using a circumferential renal denervation system (SPYRAL).[147–151] There is evidence that ISH (which is typically present in the setting of LAS) is associated with an attenuated or blunted therapeutic response to renal denervation with older technologies.[152,153] Future studies of the new denervation technologies in patients with ISH are warranted.

How do isolated systolic hypertension, pulse pressure, and LAS factor into current guideline recommendations for the treatment of hypertension and what gaps exist that could be filled in future guideline iterations?
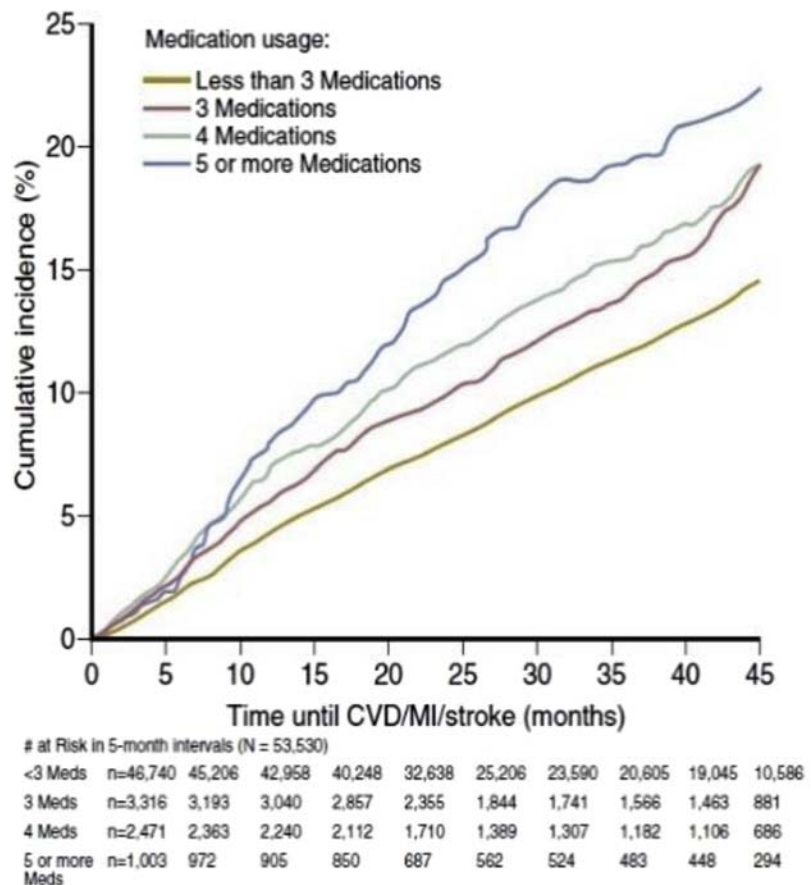
ISH, defined as BP that meets the systolic (but not diastolic) threshold for hypertension, is the predominant BP

TABLE 31.4 Lifestyle modifications for prevention and treatment of hypertension.

Nonpharmacologic intervention	Dose	Approximate impact on SBP	
		Hypertension (mm Hg)	Normotension (mm Hg)
Physical activity			
Aerobic	• 90—150 min/week • 65%—75% heart rate reserve	−5 to −8	−2 to −4
Dynamic resistance	• 90—150 min/week • 50%—80% 1 repetition maximum • 6 exercises, 3 sets/exercise, 10 repetitions/set	−4	−2
Isometric resistance	• 4 × 2 min (hand grip), 1 min rest between exercises, 30%—40% maximum voluntary contraction, 3 sessions/weeks. • 8—10 weeks	−5	−4
Healthy diet DASH dietary pattern	Diet rich in fruits, vegetables, whole grains, and low-fat dairy products with reduced content of saturated and total fat	−11	−3
Weight loss weight/body fat	Ideal body weight is best goal but ≥1 kg reduction in body weight for most adults who are overweight	−5	−2 to −3
Reduced intake of dietary [Na^+] Dietary sodium	<1500 mg/day is optimal goal but ≥1000 mg/day reduction in most adults	−5 to −6	−2 to −3
Enhanced intake of dietary [K^+] Dietary potassium	3500—5000 mg/day, preferably by consumption of a diet rich in potassium	−4 to −5	−2
Moderation in alcohol intake and alcohol consumption	In individuals who drink alcohol, reduce alcohol to • Men: <2 drinks/day • Women: <1 drink/day	−4	−3

DASH, dietary approaches to stop hypertension; *SBP*, systole blood pressure.
From Bakris G, Ali W, Parati G. ACC/AHA versus ESC/ESH on hypertension guidelines: JACC Guideline Comparison. **J Am Coll Cardiol**. 2019; 73(23):3018—3026; with permission.

FIGURE 31.5   Cumulative hazard curves for the primary endpoint and nonfatal strokes based on number of antihypertensive agents (<3, 3, 4, ≥5). *From Kumbhani DJ, Steg PG, Cannon CP, Eagle KA, Smith SC, Jr., Crowley K et al. Resistant hypertension: a frequent and ominous finding among hypertensive patients with atherothrombosis. **Eur Heart J.** 2013; 34(16):1204−1214; with permission.*

phenotype in older adults due to age-related LAS.[154] Both 2017 US and 2018 EU BP guidelines recommend BP lowering in ISH to reduce risk of major cardiovascular events.[10,11] The EU BP guidelines also uniquely outline suggestions for the management of ISH in younger adults (age less than 50 years), which comprise of lifestyle modification (particularly smoking cessation) and maintenance of longer-term follow up, noting that the role of drug therapy in these individuals remains unclear. With ISH comes increased PP.[154] Again, both guidelines acknowledge the additional prognostic significance of increased PP (≥60 mm Hg), particularly in middle-aged and older people. However, compared with SBP and DBP, the guideline writing committees felt the evidence base for using PP in making hypertension treatment decisions is not as robust.

In addition to the importance of LAS in understanding a given hypertensive patient's physiology, PWV, a marker of HMOD, may be sensitive to treatment-induced BP changes.[155,156] This might be particularly useful to indicate a given antihypertensive medication is being taken and is working, with a caveat that the correlation between carotid-femoral PWV and BP changes seems to diminish after six months of initiating therapy.[157,158] The 2018 EU (but not the 2017 US) BP guidelines appreciate the incremental value of PWV above and beyond traditional cardiovascular risk factors. In a secondary analysis of SPRINT,[159] intensive treatment to SBP <120 mm Hg was superior to standard treatment SBP <140 mm Hg only when it was accompanied by a temporal reduction in estimated PWV (derived from an equation that incorporates age and mean BP). Furthermore, within the standard treatment group,

TABLE 31.5 Suggested clinical applications of measurements of large artery stiffness in primordial and primary prevention of cardiovascular disease.

Clinical scenario	Rationale	Impact on clinical management
Hypertension		
ACC/AHA Stage 1 Hypertension (130–139/80–89 mm Hg) with PCE-calculated 10-year ASCVD risk ~10% without diabetes or CKD	LAS can be useful to refine risk stratification when PCE-calculated 10-year ASCVD risk is close to the threshold for treatment, after an informed clinician-patient discussion.	• Initiation of pharmacologic antihypertensive therapy
Stage 2 isolated systolic hypertension (>140 mm Hg) in very young adults with paucity of other cardiovascular risk factors	The combination of high pulse pressure amplification (with normal central systolic pressure) and low or normal LAS for age support a low CV risk.	• Withholding of pharmacologic antihypertensive therapy
Nonhypertensive adults <40 yrs of age with family histories of ISH	LAS is partially heritable. LAS precedes and predicts the development of ISH, a potentially avoidable threshold in the life course of cardiovascular disease. A high PWV for age is consistent with early vascular aging.	• Guide clinician-patient risk discussions • Intensification of lifestyle interventions • More frequent assessments of cardiovascular risk before age 40 (<4 to 6 yrs)
Other CV risk-assessment scenarios		
Refinement of cardiovascular risk assessment in nondiabetic adults 40–75 years of age at intermediate PCE-calculated 10-year ASCVD risk	In this group of patients, risk-based decisions for preventive interventions may be uncertain and LAS measurements can be used to refine risk assessment (particularly if various "risk-enhancing" clinical parameters do not clearly favor a specific course of action).	• Guide clinician-patient risk discussion • Guide decision making regarding initiation of pharmacologic therapy (i.e., statins)
Refinement of cardiovascular risk assessment in middle-aged nondiabetic adults at borderline PCE-calculated 10-yr risk of ASCVD (5%–<7.5%) who also have other factors that increase their ASCVD risk ("risk enhancers")	In this group of patients, LAS measurements may be useful to improve risk-based deepens as an alternative or as a "gate keeper" for coronary calcium score testing, particularly when concerns about radiation exposure (younger age, overweight/obese) or about cost are present.	• Guide clinician-patient risk discussion • Guide decision making regarding further testing (coronary calcium score) or initiation of therapy (i.e., statins)
Assessment of CV risk in special populations	PCE-calculated 10-year risk estimations can provide miscalibrated estimates in non-US populations, particularly those at earlier stages of the epidemiologic transition. This may also apply to immigrants from those populations in the United States.	• Guide clinician-patient risk discussions and various interventions • An abnormal PWV for age indicates subclinical arterial damage and suggests a higher-risk. Expert clinical judgment must guide result interpretation and decision making depending on the specific clinical scenario.

ACC/AHA, American College of Cardiology/American Heart Association; *ASCVD*, atherosclerotic cardiovascular disease; *CKD*, chronic kidney disease; *CV*, cardiovascular; *ISH*, isolated systolic hypertension; *LAS*, large artery stiffness; *PCE*, pulled cohort equations.
From Chirinos JA, Segers P, Hughes T, Townsend R. Large Artery Stiffness in Health and Disease: JACC State-of-the-Art Review. **J Am Coll Cardiol**. 2019; 74(9):1237–1263; with permission.

individuals in whom estimated PWV responded to antihypertensive treatment at 1 year demonstrated a 42% lower risk of death compared with nonresponders; noting that effects were independent of changes in systolic BP.

We appreciate the limitations with deploying LAS/PWV assessment more broadly in clinical practice. These include cost, technical difficulties, operator dependency, and the need to uncover the groin for femoral assessment in the case of carotid-femoral PWV. It is likely that future technologies will be designed to overcome these limitations. Additionally, methods that use cardiac imaging modalities commonly used in clinical practice may enable more widespread assessment of LAS by clinicians. One example is the echocardiographic assessment of thoracic aortic PWV.[70]

How do large artery stiffness and pulsatile hemodynamics factor into guideline recommendations for the treatment of other cardiovascular risk factors?

Because measures of LAS (like PP and PWV, for example) provide prognostic information over and above traditional risk factors alone, they may also have utility in guiding the therapeutic approach to other CVD risk factors, not just the management of hypertension (Table 31.5). For example, the 2018 AHA/ACC/Multisociety guidelines[160] and the 2019 ESC/European Atherosclerosis Society (EAS) guidelines[161] for lipid management both stress the importance of an accurate assessment of CVD risk in allocating the intensity of lipid reduction therapies. In this section, we briefly discuss the similarities and differences between the two major society lipid guidelines, acknowledging that LAS assessment is not as germane to this aspect of CVD prevention as it is for hypertension.

Risk enhancers

The use of risk-enhancing factors is supported in patients at borderline/intermediate risk by the PCE (AHA/ACC) or at low/moderate risk by SCORE (ESC/EAS), because they can reclassify individual risk and therefore might up-classify or down-classify risk sufficiently to make the therapeutic decision to treat or not treat with statins and other lipid lowering therapies more clear for the patient and health-care provider. There are several risk-modifying or risk-enhancing factors highlighted in both guideline documents; carotid-femoral PWV is specifically mentioned as a marker of excess risk by ESC guidelines.

Risk groups

One notable difference between the US and EU lipid guideline documents relates to the definition of the very high-risk group (those considered to benefit from the most aggressive lipid-lowering therapy). The 2019 ESC/EAS lipid guidelines define this group more broadly and include patients with not only clinical ASCVD but also selected patients with peripheral arterial disease and those with subclinical CVD (arguably this could be extrapolated to include measures of abnormal LAS). This very high-risk ESC group also encompasses primary prevention patients, including those with severe CKD, certain patients with diabetes, and patients with an estimated risk by SCORE $\geq 10\%$. The definition of very high-risk by ESC guidance has implications for lipid treatment goals as well as lipid therapies that should be considered. For example, the 2019 ESC/EAS guidelines recommend PCSK9 inhibitor as an add-on for primary prevention for those at very high risk if LDL-C goals are not met (class IIb). In contrast, only patients with clinical ASCVD (classic secondary prevention) are included in the very high-risk group by the 2018 AHA/ACC lipid treatment guidelines (with the caveat that US guidelines do recommend PCSK9 inhibitors where necessary for primary prevention patients with genetic familial hypercholesterolemia).

Summary

The 2017 ACC/AHA and 2018 ESC/ESH hypertension guidelines find more common ground than major key differences. The perceived discordance between guidelines may stem from incompatible definitions of hypertension and, to a lesser extent, BP treatment targets. A closer inspection reveals the same target BP <130/80 mm Hg for most adults in both guidelines. Admittedly, the ESC/ESH approach this more gently and, notably, with a few exceptions. With an appreciable downward trend in the target "normal" BP over time, a thorough understanding of guideline documents, ideally allied with an open mind, is crucial. Personalization is key to help clinicians concentrate intensity of therapy in patients who are most likely to benefit. Arterial stiffness may allow for better risk estimation in addition to quantitative ASCVD risk scores (which applies to both the treatment of elevated BP but also other risk factors like hyperlipidemia). Further studies will help

refine our individualized approach to hypertension management so as to yield "as low as reasonably achievable" BP, thereby maximizing CVD risk reduction.

References

1. Lim SS, Vos T, Flaxman AD, et al. A comparative risk assessment of burden of disease and injury attributable to 67 risk factors and risk factor clusters in 21 regions, 1990-2010: a systematic analysis for the Global Burden of Disease Study 2010. **Lancet**. 2012; 380(9859):2224−2260.

2. Worldwide trends in blood pressure from 1975 to 2015: a pooled analysis of 1479 population-based measurement studies with 19·1 million participants. **Lancet**. 2017; 389(10064):37−55.

3. Dawber TR, Moore FE, Mann GV. Coronary heart disease in the Framingham study. **Am J Public Health Nation's Health**. 1957; 47(4 Pt 2):4−24.

4. Collaboration NCDRF. Worldwide trends in blood pressure from 1975 to 2015: a pooled analysis of 1479 population-based measurement studies with 19.1 million participants. **Lancet**. 2017; 389(10064):37−55.

5. Emdin CA, Rahimi K, Neal B, Callender T, Perkovic V, Patel A. Blood pressure lowering in type 2 diabetes: a systematic review and meta-analysis. **J Am Med Assoc**. 2015; 313(6):603−615.

6. Ettehad D, Emdin CA, Kiran A, et al. Blood pressure lowering for prevention of cardiovascular disease and death: a systematic review and meta-analysis. **Lancet**. 2016; 387(10022):957−967.

7. O'Donnell MJ, Chin SL, Rangarajan S, et al. Global and regional effects of potentially modifiable risk factors associated with acute stroke in 32 countries (INTERSTROKE): a case-control study. **Lancet**. 2016; 388(10046):761−775.

8. Tsai WC, Wu HY, Peng YS, et al. Association of intensive blood pressure control and kidney disease progression in nondiabetic patients with chronic kidney disease: a systematic review and meta-analysis. **J Am Med Assoc Int Med**. 2017; 177(6):792−799.

9. Staessen JA, Wang JG, Thijs L. Cardiovascular protection and blood pressure reduction: a meta-analysis. **Lancet**. 2001; 358(9290):1305−1315.

10. Whelton PK, Carey RM, Aronow WS, et al. 2017 ACC/AHA/AAPA/ABC/ACPM/AGS/APhA/ASH/ASPC/NMA/PCNA guideline for the prevention, detection, evaluation, and management of high blood pressure in adults: executive summary: a report of the American College of Cardiology/American Heart Association Task Force on Clinical Practice Guidelines. **J Am Coll Cardiol**. 2018; 71(19):2199−2269.

11. Williams B, Mancia G, Spiering W, et al. 2018 ESC/ESH Guidelines for the management of arterial hypertension. **Eur Heart J**. 2018; 39(33):3021−3104.

12. Kaess BM, Rong J, Larson MG, et al. Aortic stiffness, blood pressure progression, and incident hypertension. **J Am Med Assoc**. 2012; 308(9):875−881.

13. Chobanian AV, Bakris GL, Black HR, et al. Seventh report of the Joint national committee on prevention, detection, evaluation, and treatment of high blood pressure. **Hypertension**. 2003; 42(6):1206−1252.

14. Wright Jr JT, Williamson JD, Whelton PK, et al. A randomized trial of intensive versus standard blood-pressure control. **N Engl J Med**. 2015; 373(22):2103−2116.

15. Thomopoulos C, Parati G, Zanchetti A. Effects of blood-pressure-lowering treatment on outcome incidence. 12. Effects in individuals with high-normal and normal blood pressure: overview and meta-analyses of randomized trials. **J Hypertens**. 2017; 35(11):2150−2160.

16. Bakris GL. The implications of blood pressure measurement methods on treatment targets for blood pressure. **Circulation**. 2016; 134(13):904−905.

17. Johnson KC, Whelton PK, Cushman WC, et al. Blood pressure measurement in SPRINT (systolic blood pressure intervention trial). **Hypertension**. 2018; 71(5):848−857.

18. Salvetti M, Paini A, Aggiusti C, et al. Unattended versus attended blood pressure measurement. **Hypertension**. 2019; 73(3):736−742.

19. Drawz PE, Agarwal A, Dwyer JP, et al. Concordance between blood pressure in the systolic blood pressure intervention trial and in routine clinical practice. **J Am Med Assoc Int Med**. 2020; 180(12):1655−1663.

20. Muntner P, Carey RM, Gidding S, et al. Potential U.S. population impact of the 2017 ACC/AHA high blood pressure guideline. **J Am Coll Cardiol**. 2018; 71(2):109−118.

21. McEvoy JW, Daya N, Rahman F, et al. Association of isolated diastolic hypertension as defined by the 2017 ACC/AHA blood pressure guideline with incident cardiovascular outcomes. **J Am Med Assoc**. 2020; 323(4):329−338.

22. Yang WY, Melgarejo JD, Thijs L, et al. Association of office and ambulatory blood pressure with mortality and cardiovascular outcomes. **J Am Med Assoc**. 2019; 322(5):409−420.

23. Franklin SS, O'Brien E, Staessen JA. Masked hypertension: understanding its complexity. **Eur Heart J**. 2017; 38(15):1112−1118.

24. Goff Jr DC, Lloyd-Jones DM, Bennett G, et al. 2013 ACC/AHA guideline on the assessment of cardiovascular risk: a report of the American College of Cardiology/American Heart Association Task Force on Practice Guidelines. **Circulation**. 2014; 129(25 Suppl 2):S49−S73.

25. Lloyd-Jones DM, Braun LT, Ndumele CE, et al. Use of risk assessment tools to guide decision-making in the primary prevention of atherosclerotic cardiovascular disease: a special report from the American Heart Association and American College of Cardiology. **J Am Coll Cardiol**. 2019; 73(24):3153−3167.

26. Piepoli MF, Hoes AW, Agewall S, et al. 2016 European Guidelines on cardiovascular disease prevention in clinical practice: the Sixth Joint Task Force of the European Society of Cardiology and Other Societies on Cardiovascular Disease Prevention in Clinical Practice (constituted by representatives of 10 societies and by invited experts) Developed with the special contribution of the European Association for Cardiovascular Prevention & Rehabilitation (EACPR). **Eur Heart J**. 2016; 37(29):2315−2381.

27. Conroy RM, Pyörälä K, Fitzgerald AP, et al. Estimation of ten-year risk of fatal cardiovascular disease in Europe: the SCORE project. **Eur Heart J**. 2003; 24(11):987−1003.

28. Mortensen MB, Falk E. Limitations of the SCORE-guided European guidelines on cardiovascular disease prevention. **Eur Heart J**. 2017; 38(29):2259−2263.

29. SCORE2 working group and ESC Cardiovascular risk collaboration. SCORE2 risk prediction algorithms: new models to estimate 10-year risk of cardiovascular disease in Europe. **Eur Heart J**. 2021; 42(25):2439−2454.

30. SCORE2-OP working group and ESC Cardiovascular risk collaboration. SCORE2-OP risk prediction algorithms: estimating incident cardiovascular event risk in older persons in four geographical risk regions. **Eur Heart J**. 2021; 42(25):2455−2467.

31. McEvoy JW, Diamond GA, Detrano RC, et al. Risk and the physics of clinical prediction. **Am J Cardiol**. 2014; 113(8):1429−1435.

32. DeFilippis AP, Young R, Carrubba CJ, et al. An analysis of cali- bration and discrimination among multiple cardiovascular risk scores in a modern multiethnic cohort. **Ann Intern Med**. 2015; 162(4):266−275.

33. Kavousi M, Leening MJ, Nanchen D, et al. Comparison of appli- cation of the ACC/AHA guidelines, Adult Treatment Panel III guidelines, and European Society of Cardiology guidelines for car- diovascular disease prevention in a European cohort. **J Am Med Assoc**. 2014; 311(14):1416−1423.

34. Rana JS, Tabada GH, Solomon MD, et al. Accuracy of the athero- sclerotic cardiovascular risk equation in a large contemporary, multiethnic population. **J Am Coll Cardiol**. 2016; 67(18):2118−2130.

35. Amin NP, Martin SS, Blaha MJ, Nasir K, Blumenthal RS, Michos ED. Headed in the right direction but at risk for miscalcu- lation: a critical appraisal of the 2013 ACC/AHA risk assessment guidelines. **J Am Coll Cardiol**. 2014; 63(25 Pt A):2789−2794.

36. DeFilippis AP, Young R, McEvoy JW, et al. Risk score over- estimation: the impact of individual cardiovascular risk factors and preventive therapies on the performance of the American Heart Association-American College of Cardiology-Atherosclerotic Car- diovascular Disease risk score in a modern multi-ethnic cohort. **Eur Heart J**. 2017; 38(8):598−608.

37. Upadhya B, Rocco M, Lewis CE, et al. Effect of intensive blood pressure treatment on heart failure events in the systolic blood pressure reduction intervention trial. **Circ Heart Fail**. 2017; 10(4).

38. Julius S, Palatini P, Kjeldsen SE, et al. Usefulness of heart rate to predict cardiac events in treated patients with high-risk systemic hypertension. **Am J Cardiol**. 2012; 109(5):685−692.

39. Aladin AI, Al Rifai M, Rasool SH, et al. The association of resting heart rate and incident hypertension: the Henry Ford Hospital Ex- ercise Testing (FIT) Project. **Am J Hypertens**. 2016; 29(2):251−257.

40. Whelton SP, Blankstein R, Al-Mallah MH, et al. Association of resting heart rate with carotid and aortic arterial stiffness: multi-ethnic study of atherosclerosis. **Hypertension**. 2013; 62(3):477−484.

41. Aladin AI, Al Rifai M, Rasool SH, et al. Relation of coronary artery calcium and extra-coronary aortic calcium to incident hypertension (from the multi-ethnic study of atherosclerosis). **Am J Cardiol**. 2018; 121(2):210−216.

42. Blaha M, Budoff MJ, Shaw LJ, et al. Absence of coronary artery calcification and all-cause mortality. **JACC Cardiovasc Imaging**. 2009; 2(6):692−700.

43. Detrano R, Guerci AD, Carr JJ, et al. Coronary calcium as a pre- dictor of coronary events in four racial or ethnic groups. **N Engl J Med**. 2008; 358(13):1336−1345.

44. Keelan PC, Bielak LF, Ashai K, et al. Long-term prognostic value of coronary calcification detected by electron-beam computed tomog- raphy in patients undergoing coronary angiography. **Circulation**. 2001; 104(4):412−417.

45. Joshi PH, Blaha MJ, Budoff MJ, et al. The 10-year prognostic value of zero and minimal CAC. **JACC Cardiovasc Imaging**. 2017; 10(8):957−958.

46. Silverman MG, Blaha MJ, Krumholz HM, et al. Impact of coronary artery calcium on coronary heart disease events in individuals at the extremes of traditional risk factor burden: the Multi-Ethnic Study of Atherosclerosis. **Eur Heart J**. 2014; 35(33):2232−2241.

47. Yeboah J, McClelland RL, Polonsky TS, et al. Comparison of novel risk markers for improvement in cardiovascular risk assessment in intermediate-risk individuals. **J Am Med Assoc**. 2012; 308(8):788−795.

48. McEvoy JW, Martin SS, Dardari ZA, et al. Coronary artery calcium to guide a personalized risk-based approach to initiation and inten- sification of antihypertensive therapy. **Circulation**. 2017; 135(2):153−165.

49. Uddin SMI, Mirbolouk M, Kianoush S, et al. Role of coronary artery calcium for stratifying cardiovascular risk in adults with hyperten- sion. **Hypertension**. 2019; 73(5):983−989.

50. Elshazly MB, Abdellatif A, Dargham SR, et al. Role of coronary artery and thoracic aortic calcium as risk modifiers to guide anti- hypertensive therapy in stage 1 hypertension (from the multiethnic study of atherosclerosis). **Am J Cardiol**. 2020; 126:45−55.

51. Arnett DK, Blumenthal RS, Albert MA, et al. 2019 ACC/AHA guideline on the primary prevention of cardiovascular disease: a report of the American College of Cardiology/American Heart As- sociation Task Force on Clinical Practice Guidelines. **Circulation**. 2019; 140(11):e596−e646.

52. van der Aalst CM, Denissen S, Vonder M, et al. Screening for cardiovascular disease risk using traditional risk factor assessment or coronary artery calcium scoring: the ROBINSCA trial. **Eur Heart J Cardiovasc Imaging**. 2020; 21(11):1216−1224.

53. McEvoy JW, Martin SS, Blaha MJ, et al. The case for and against a coronary artery calcium trial: means, motive, and opportunity. **JACC Cardiovasc Imaging**. 2016; 9(8):994−1002.

54. Denissen SJ, van der Aalst CM, Vonder M, et al. Screening for coronary artery calcium in a high-risk population: the ROBINSCA trial. **Eur J Prev Cardiol**. 2020.

55. Tsao CW, Pencina KM, Massaro JM, et al. Cross-sectional relations of arterial stiffness, pressure pulsatility, wave reflection, and arterial calcification. **Arterioscler Thromb Vasc Biol**. 2014; 34(11):2495−2500.

56. Cho IJ, Chang HJ, Cho I, et al. Association of thoracic aorta calcium score with Exercise blood pressure response and clinical outcomes in elderly individuals: differential impact of aorta calcification compared with coronary artery calcification. **J Am Heart Assoc**. 2016; 5(4).

57. Tison GH, Guo M, Blaha MJ, et al. Multisite extracoronary calci- fication indicates increased risk of coronary heart disease and all- cause mortality: the Multi-Ethnic Study of Atherosclerosis. **J Cardiovasc Comput Tomogr**. 2015; 9(5):406−414.

58. Kim J, Budoff MJ, Nasir K, et al. Thoracic aortic calcium, cardio- vascular disease events, and all-cause mortality in asymptomatic individuals with zero coronary calcium: the Multi-Ethnic Study of Atherosclerosis (MESA). **Atherosclerosis**. 2017; 257:1−8.

59. Pandey A, Patel KV, Vongpatanasin W, et al. Incorporation of biomarkers into risk assessment for allocation of antihypertensive medication according to the 2017 ACC/AHA high blood pressure guideline: a pooled cohort analysis. **Circulation**. 2019; 140(25):2076−2088.

60. Paget V, Legedz L, Gaudebout N, et al. N-terminal pro-brain natriuretic peptide: a powerful predictor of mortality in hyperten- sion. **Hypertension**. 2011; 57(4):702−709.

61. Bower JK, Lazo M, Matsushita K, et al. N-terminal pro-brain natriuretic peptide (NT-proBNP) and risk of hypertension in the

Atherosclerosis Risk in Communities (ARIC) study. **Am J Hypertens**. 2015; 28(10):1262−1266.

62. McEvoy JW, Chen Y, Nambi V, et al. High-sensitivity cardiac troponin T and risk of hypertension. **Circulation**. 2015; 132(9):825−833.

63. de Lemos JA, Ayers CR, Levine BD, et al. Multimodality strategy for cardiovascular risk assessment: performance in 2 population-based cohorts. **Circulation**. 2017; 135(22):2119−2132.

64. Berry JD, Nambi V, Ambrosius WT, et al. Associations of high-sensitivity troponin and natriuretic peptide levels with outcomes after intensive blood pressure lowering: findings from the SPRINT randomized clinical trial. **J Am Med Assoc Cardiol**. 2021. https://doi.org/10.1001/jamacardio.2021.3187.

65. Laurent S, Cockcroft J, Van Bortel L, et al. Expert consensus document on arterial stiffness: methodological issues and clinical applications. **Eur Heart J**. 2006; 27(21):2588−2605.

66. Townsend RR, Wilkinson IB, Schiffrin EL, et al. Recommendations for improving and standardizing vascular research on arterial stiffness: a scientific statement from the American Heart Association. **Hypertension**. 2015; 66(3):698−722.

67. Van Bortel LM, Laurent S, Boutouyrie P, et al. Expert consensus document on the measurement of aortic stiffness in daily practice using carotid-femoral pulse wave velocity. **J Hypertens**. 2012; 30(3):445−448.

68. Vlachopoulos C, Aznaouridis K, Stefanadis C. Prediction of cardiovascular events and all-cause mortality with arterial stiffness: a systematic review and meta-analysis. **J Am Coll Cardiol**. 2010; 55(13):1318−1327.

69. Ben-Shlomo Y, Spears M, Boustred C, et al. Aortic pulse wave velocity improves cardiovascular event prediction: an individual participant meta-analysis of prospective observational data from 17,635 subjects. **J Am Coll Cardiol**. 2014; 63(7):636−646.

70. Chirinos JA, Segers P, Hughes T, Townsend R. Large-artery stiffness in health and disease: JACC state-of-the-art review. **J Am Coll Cardiol**. 2019; 74(9):1237−1263.

71. Determinants of pulse wave velocity in healthy people and in the presence of cardiovascular risk factors: 'establishing normal and reference values. **Eur Heart J**. 2010; 31(19):2338−2350.

72. Kario K, Kanegae H, Oikawa T, Suzuki K. Hypertension is predicted by both large and small artery disease. **Hypertension**. 2019; 73(1):75−83.

73. Blacher J, Staessen JA, Girerd X, et al. Pulse pressure not mean pressure determines cardiovascular risk in older hypertensive patients. **Arch Intern Med**. 2000; 160(8):1085−1089.

74. Staessen JA, Gasowski J, Wang JG, et al. Risks of untreated and treated isolated systolic hypertension in the elderly: meta-analysis of outcome trials. **Lancet**. 2000; 355(9207):865−872.

75. Selvaraj S, Steg PG, Elbez Y, et al. Pulse pressure and risk for cardiovascular events in patients with atherothrombosis: from the REACH registry. **J Am Coll Cardiol**. 2016; 67(4):392−403.

76. Chae CU, Pfeffer MA, Glynn RJ, Mitchell GF, Taylor JO, Hennekens CH. Increased pulse pressure and risk of heart failure in the elderly. **J Am Med Assoc**. 1999; 281(7):634−639.

77. Franklin SS, Khan SA, Wong ND, Larson MG, Levy D. Is pulse pressure useful in predicting risk for coronary heart disease? The Framingham heart study. **Circulation**. 1999; 100(4):354−360.

78. Verdecchia P, Schillaci G, Reboldi G, Franklin SS, Porcellati C. Different prognostic impact of 24-hour mean blood pressure and pulse pressure on stroke and coronary artery disease in essential hypertension. **Circulation**. 2001; 103(21):2579−2584.

79. Bangalore S, Messerli FH, Franklin SS, Mancia G, Champion A, Pepine CJ. Pulse pressure and risk of cardiovascular outcomes in patients with hypertension and coronary artery disease: an INternational VErapamil SR-trandolapril STudy (INVEST) analysis. **Eur Heart J**. 2009; 30(11):1395−1401.

80. Domanski M, Norman J, Wolz M, Mitchell G, Pfeffer M. Cardiovascular risk assessment using pulse pressure in the first national health and nutrition examination survey (NHANES I). **Hypertension**. 2001; 38(4):793−797.

81. Madan N, Lee AK, Matsushita K, et al. Relation of isolated systolic hypertension and pulse pressure to high-sensitivity cardiac troponin-T and N-terminal pro-B-type natriuretic peptide in older adults (from the atherosclerosis risk in communities study). **Am J Cardiol**. 2019; 124(2):245−252.

82. Effects of treatment on morbidity in hypertension. Results in patients with diastolic blood pressures averaging 115 through 129 mm Hg. **J Am Med Assoc**. 1967; 202(11):1028−1034.

83. Effects of treatment on morbidity in hypertension. II. Results in patients with diastolic blood pressure averaging 90 through 114 mm Hg. **J Am Med Assoc**. 1970; 213(7):1143−1152.

84. Five-year findings of the hypertension detection and follow-up program. I. Reduction in mortality of persons with high blood pressure, including mild hypertension. Hypertension Detection and Follow-up Program Cooperative Group. **J Am Med Assoc**. 1979; 242(23):2562−2571.

85. The Australian therapeutic trial in mild hypertension. Report by the Management Committee. **Lancet**. 1980; 1(8181):1261−1267.

86. Prevention of stroke by antihypertensive drug treatment in older persons with isolated systolic hypertension. Final results of the Systolic Hypertension in the Elderly Program (SHEP). SHEP Cooperative Research Group. **J Am Med Assoc**. 1991; 265(24):3255−3264.

87. Amery A, Birkenhäger W, Brixko P, et al. Mortality and morbidity results from the European Working Party on High Blood Pressure in the Elderly trial. **Lancet**. 1985; 1(8442):1349−1354.

88. Major cardiovascular events in hypertensive patients randomized to doxazosin vs chlorthalidone: the antihypertensive and lipid-lowering treatment to prevent heart attack trial (ALLHAT). ALLHAT Collaborative Research Group. **J Am Med Assoc**. 2000; 283(15):1967−1975.

89. Lonn EM, Bosch J, López-Jaramillo P, et al. Blood-pressure lowering in intermediate-risk persons without cardiovascular disease. **N Engl J Med**. 2016; 374(21):2009−2020.

90. Zhang W, Zhang S, Deng Y, et al. Trial of intensive blood-pressure control in older patients with hypertension. **N Engl J Med**. 2021. https://doi.org/10.1056/NEJMoa2111437.

91. Bundy JD, Li C, Stuchlik P, et al. Systolic blood pressure reduction and risk of cardiovascular disease and mortality: a systematic review and network meta-analysis. **J Am Med Assoc Cardiol**. 2017; 2(7):775−781.

92. Hansson L, Zanchetti A, Carruthers SG, et al. Effects of intensive blood-pressure lowering and low-dose aspirin in patients with hypertension: principal results of the Hypertension Optimal Treatment (HOT) randomised trial. HOT Study Group. **Lancet**. 1998; 351(9118):1755−1762.

93. Burt VL, Whelton P, Roccella EJ, et al. Prevalence of hypertension in the US adult population. Results from the third national health and

nutrition examination survey, 1988-1991. **Hypertension**. 1995; 25(3):305−313.

94. Mancia G, Fagard R, Narkiewicz K, et al. 2013 ESH/ESC guidelines for the management of arterial hypertension: the task force for the management of arterial hypertension of the European Society of Hypertension (ESH) and of the European Society of Cardiology (ESC). **J Hypertens**. 2013; 31(7):1281−1357.

95. Williamson JD, Supiano MA, Applegate WB, et al. Intensive vs standard blood pressure control and cardiovascular disease outcomes in adults aged ≥75 years: a randomized clinical trial. **J Am Med Assoc**. 2016; 315(24):2673−2682.

96. Beckett NS, Peters R, Fletcher AE, et al. Treatment of hypertension in patients 80 years of age or older. **N Engl J Med**. 2008; 358(18):1887−1898.

97. Warwick J, Falaschetti E, Rockwood K, et al. No evidence that frailty modifies the positive impact of antihypertensive treatment in very elderly people: an investigation of the impact of frailty upon treatment effect in the HYpertension in the Very Elderly Trial (HYVET) study, a double-blind, placebo-controlled study of anti-hypertensives in people with hypertension aged 80 and over. **BMC Med**. 2015; 13:78.

98. Williamson JD, Pajewski NM, Auchus AP, et al. Effect of intensive vs standard blood pressure control on probable dementia: a ran-domized clinical trial. **J Am Med Assoc**. 2019; 321(6):553−561.

99. Group SMISR, Nasrallah IM, Pajewski NM, et al. Association of intensive vs standard blood pressure control with Cerebral white matter lesions. **J Am Med Assoc**. 2019; 322(6):524−534.

100. Hughes D, Judge C, Murphy R, et al. Association of blood pressure lowering with incident dementia or cognitive impairment: a sys-tematic review and meta-analysis. **J Am Med Assoc**. 2020; 323(19):1934−1944.

101. Arvanitis M, Qi G, Bhatt DL, et al. Linear and nonlinear Mendelian randomization analyses of the association between diastolic blood pressure and cardiovascular events: the J-curve revisited. **Circula-tion**. 2021; 143(9):895−906.

102. Beddhu S, Chertow GM, Cheung AK, et al. Influence of baseline diastolic blood pressure on effects of intensive compared with standard blood pressure control. **Circulation**. 2018; 137(2):134−143.

103. Wolters FJ, Mattace-Raso FU, Koudstaal PJ, Hofman A, Ikram MA. Orthostatic hypotension and the long-term risk of dementia: a population-based study. **PLoS Med**. 2016; 13(10):e1002143.

104. Sexton DJ, Canney M, O'Connell MDL, et al. Injurious falls and syncope in older community-dwelling adults meeting inclusion criteria for SPRINT. **J Am Med Assoc Int Med**. 2017; 177(9):1385−1387.

105. Sink KM, Evans GW, Shorr RI, et al. Syncope, hypotension, and falls in the treatment of hypertension: results from the randomized clinical systolic blood pressure intervention trial. **J Am Geriatr Soc**. 2018; 66(4):679−686.

106. Shimbo D, Barrett Bowling C, Levitan EB, et al. Short-term risk of serious fall injuries in older adults initiating and intensifying treat-ment with antihypertensive medication. **Circ Cardiovasc Qual Outcomes**. 2016; 9(3):222−229.

107. Juraschek SP, Taylor AA, Wright Jr JT, et al. Orthostatic hypo-tension, cardiovascular outcomes, and adverse events: results from SPRINT. **Hypertension**. 2020; 75(3):660−667.

108. Bress AP, Bellows BK, King JB, et al. Cost-Effectiveness of intensive versus standard blood-pressure control. **N Engl J Med**. 2017; 377(8):745−755.

109. Cooney D, Pascuzzi K. Polypharmacy in the elderly: focus on drug interactions and adherence in hypertension. **Clin Geriatr Med**. 2009; 25(2):221−233.

110. Mukete BN, Ferdinand KC. Polypharmacy in older adults with hypertension: a comprehensive review. **J Clin Hypertens**. 2016; 18(1):10−18.

111. Thomopoulos C, Parati G, Zanchetti A. Effects of blood pressure lowering treatment in hypertension: 8. Outcome reductions vs. dis-continuations because of adverse drug events - meta-analyses of randomized trials. **J Hypertens**. 2016; 34(8):1451−1463.

112. Cushman WC, Evans GW, Byington RP, et al. Effects of intensive blood-pressure control in type 2 diabetes mellitus. **N Engl J Med**. 2010; 362(17):1575−1585.

113. Cheung AK, Rahman M, Reboussin DM, et al. Effects of intensive BP control in CKD. **J Am Soc Nephrol**. 2017; 28(9):2812−2823.

114. Chang AR, Kramer H, Wei G, et al. Effects of intensive blood pressure control in patients with and without albuminuria: post hoc analyses from SPRINT. **Clin J Am Soc Nephrol**. 2020; 15(8):1121−1128.

115. Vaduganathan M, Pareek M, Kristensen AMD, Biering-Sørensen T, Byrne C, Almarzooq Z, et al. Prevention of heart failure events with intensive versus standard blood pressure lowering across the spec-trum of kidney function and albuminuria: a SPRINT substudy. **Eur J Heart Fail**. 2021; 23(3):384−392.

116. Beddhu S, Chertow GM, Greene T, et al. Effects of intensive sys-tolic blood pressure lowering on cardiovascular events and mortality in patients with type 2 diabetes mellitus on standard glycemic control and in those without diabetes mellitus: reconciling results from ACCORD BP and SPRINT. **J Am Heart Assoc**. 2018; 7(18):e009326.

117. White WB, Jalil F, Cushman WC, et al. Average clinician-measured blood pressures and cardiovascular outcomes in patients with type 2 diabetes mellitus and ischemic heart disease in the EXAMINE trial. **J Am Heart Assoc**. 2018; 7(20):e009114.

118. Rahman F, McEvoy JW, Ohkuma T, et al. Effects of blood pressure lowering on clinical outcomes according to baseline blood pressure and cardiovascular risk in patients with type 2 diabetes mellitus. **Hypertension**. 2019; 73(6):1291−1299.

119. 10. Cardiovascular disease and risk management: standards of medical care in diabetes-2020. **Diabetes Care**. 2020; 43(Suppl 1). S111−s34.

120. Lewington S, Clarke R, Qizilbash N, Peto R, Collins R. Age-specific relevance of usual blood pressure to vascular mortality: a meta-analysis of individual data for one million adults in 61 prospective studies. **Lancet**. 2002; 360(9349):1903−1913.

121. Cruickshank JM. Antihypertensive treatment and the J-curve. **Car-diovasc Drugs Ther**. 2000; 14(4):373−379.

122. McEvoy JW, Chen Y, Rawlings A, et al. Diastolic blood pressure, subclinical myocardial damage, and cardiac events: implications for blood pressure control. **J Am Coll Cardiol**. 2016; 68(16):1713−1722.

123. Vidal-Petiot E, Ford I, Greenlaw N, et al. Cardiovascular event rates and mortality according to achieved systolic and diastolic blood pressure in patients with stable coronary artery disease: an interna-tional cohort study. **Lancet**. 2016; 388(10056):2142−2152.

124. Bhatt DL. Troponin and the J-curve of diastolic blood pressure: when lower is not better. **J Am Coll Cardiol**. 2016; 68(16):1723−1726.

125. Ilkun OL, Greene T, Cheung AK, et al. The influence of baseline diastolic blood pressure on the effects of intensive blood pressure lowering on cardiovascular outcomes and all-cause mortality in type 2 diabetes. **Diabetes Care**. 2020; 43(8):1878−1884.

126. Rahman F, McEvoy JW. Letter by Rahman and McEvoy regarding article, "influence of baseline diastolic blood pressure on effects of intensive compared with standard blood pressure control". **Circulation**. 2018; 137(24):2666−2667.

127. Mancia G, Schumacher H, Redon J, et al. Blood pressure targets recommended by guidelines and incidence of cardiovascular and renal events in the Ongoing Telmisartan Alone and in Combination with Ramipril Global Endpoint Trial (ONTARGET). **Circulation**. 2011; 124(16):1727−1736.

128. Cooper-DeHoff RM, Gong Y, Handberg EM, et al. Tight blood pressure control and cardiovascular outcomes among hypertensive patients with diabetes and coronary artery disease. **J Am Med Assoc**. 2010; 304(1):61−68.

129. Ovbiagele B, Diener HC, Yusuf S, et al. Level of systolic blood pressure within the normal range and risk of recurrent stroke. **J Am Med Assoc**. 2011; 306(19):2137−2144.

130. Böhm M, Schumacher H, Teo KK, et al. Achieved blood pressure and cardiovascular outcomes in high-risk patients: results from ONTARGET and TRANSCEND trials. **Lancet**. 2017; 389(10085):2226−2237.

131. D'Agostino RB, Belanger AJ, Kannel WB, Cruickshank JM. Relation of low diastolic blood pressure to coronary heart disease death in presence of myocardial infarction: the Framingham Study. **BMJ**. 1991; 303(6799):385−389.

132. Whelton SP, McEvoy JW, Shaw L, et al. Association of normal systolic blood pressure level with cardiovascular disease in the absence of risk factors. **J Am Med Assoc Cardiol**. 2020; 5(9):1011−1018.

133. Olsen MH, Angell SY, Asma S, et al. A call to action and a life-course strategy to address the global burden of raised blood pressure on current and future generations: the Lancet Commission on hypertension. **Lancet**. 2016; 388(10060):2665−2712.

134. Gupta AK, Arshad S, Poulter NR. Compliance, safety, and effectiveness of fixed-dose combinations of antihypertensive agents: a meta-analysis. **Hypertension**. 2010; 55(2):399−407.

135. Wald DS, Law M, Morris JK, Bestwick JP, Wald NJ. Combination therapy versus monotherapy in reducing blood pressure: meta-analysis on 11,000 participants from 42 trials. **Am J Med**. 2009; 122(3):290−300.

136. Lung T, Jan S, de Silva HA, et al. Fixed-combination, low-dose, triple-pill antihypertensive medication versus usual care in patients with mild-to-moderate hypertension in Sri Lanka: a within-trial and modelled economic evaluation of the TRIUMPH trial. **Lancet Glob Health**. 2019; 7(10):e1359−e1366.

137. Wang N, Salam A, Webster R, et al. Association of low-dose triple combination therapy with therapeutic inertia and prescribing patterns in patients with hypertension: a secondary analysis of the TRIUMPH trial. **J Am Med Assoc Cardiol**. 2020; 5(11):1219−1226.

138. Volpe M, Gallo G, Tocci G. New approach to blood pressure control: triple combination pill. **Trends Cardiovasc Med**. 2020; 30(2):72−77.

139. Webster R, Salam A, de Silva HA, et al. Fixed low-dose triple combination antihypertensive medication vs usual care for blood pressure control in patients with mild to moderate hypertension in Sri Lanka: a randomized clinical trial. **J Am Med Assoc**. 2018; 320(6):566−579.

140. Dolan E, Stanton A, Thijs L, et al. Superiority of ambulatory over clinic blood pressure measurement in predicting mortality: the Dublin outcome study. **Hypertension**. 2005; 46(1):156−161.

141. Salles GF, Reboldi G, Fagard RH, et al. Prognostic effect of the nocturnal blood pressure fall in hypertensive patients: the ambulatory blood pressure collaboration in patients with hypertension (ABC-H) meta-analysis. **Hypertension**. 2016; 67(4):693−700.

142. Hermida RC, Crespo JJ, Domínguez-Sardiña M, et al. Bedtime hypertension treatment improves cardiovascular risk reduction: the Hygia Chronotherapy Trial. **Eur Heart J**. 2020; 41(48): 4565−4576.

143. Turgeon RD, Althouse AD, Cohen JB, et al. Lowering nighttime blood pressure with bedtime dosing of antihypertensive medications: controversies in hypertension - con side of the argument. **Hypertension**. 2021; 78(3):871−878.

144. Carey RM, Calhoun DA, Bakris GL, et al. Resistant hypertension: detection, evaluation, and management: a scientific statement from the American Heart Association. **Hypertension**. 2018; 72(5): e53−e90.

145. Kumbhani DJ, Steg PG, Cannon CP, et al. Resistant hypertension: a frequent and ominous finding among hypertensive patients with atherothrombosis. **Eur Heart J**. 2013; 34(16):1204−1214.

146. Bhatt DL, Kandzari DE, O'Neill WW, et al. A controlled trial of renal denervation for resistant hypertension. **N Engl J Med**. 2014; 370(15):1393−1401.

147. Böhm M, Kario K, Kandzari DE, et al. Efficacy of catheter-based renal denervation in the absence of antihypertensive medications (SPYRAL HTN-OFF MED Pivotal): a multicentre, randomised, sham-controlled trial. **Lancet**. 2020; 395(10234):1444−1451.

148. Kandzari DE, Böhm M, Mahfoud F, et al. Effect of renal denervation on blood pressure in the presence of antihypertensive drugs: 6-month efficacy and safety results from the SPYRAL HTN-ON MED proof-of-concept randomised trial. **Lancet**. 2018; 391(10137): 2346−2355.

149. Azizi M, Schmieder RE, Mahfoud F, et al. Endovascular ultrasound renal denervation to treat hypertension (RADIANCE-HTN SOLO): a multicentre, international, single-blind, randomised, sham-controlled trial. **Lancet**. 2018; 391(10137):2335−2345.

150. Mahfoud F, Mancia G, Schmieder R, et al. Renal denervation in high-risk patients with hypertension. **J Am Coll Cardiol**. 2020; 75(23):2879−2888.

151. Mahfoud F, Azizi M, Ewen S, et al. Proceedings from the 3rd European clinical consensus conference for clinical trials in device-based hypertension therapies. **Eur Heart J**. 2020; 41(16): 1588−1599.

152. Mahfoud F, Bakris G, Bhatt DL, et al. Reduced blood pressure-lowering effect of catheter-based renal denervation in patients with isolated systolic hypertension: data from SYMPLICITY HTN-3 and the Global SYMPLICITY Registry. **Eur Heart J**. 2017; 38(2):93−100.

153. Ewen S, Ukena C, Linz D, et al. Reduced effect of percutaneous renal denervation on blood pressure in patients with isolated systolic hypertension. **Hypertension**. 2015; 65(1):193−199.

154. Franklin SS, Jacobs MJ, Wong ND, L'Italien GJ, Lapuerta P. Predominance of isolated systolic hypertension among middle-aged and elderly US hypertensives: analysis based on National Health and Nutrition Examination Survey (NHANES) III. **Hypertension**. 2001; 37(3):869−874.

155. Asmar R, Topouchian J, Pannier B, Benetos A, Safar M. Pulse wave velocity as endpoint in large-scale intervention trial. The complior study. Scientific, quality control, coordination and investigation committees of the complior study. **J Hypertens**. 2001; 19(4):813−818.

156. Protogerou A, Blacher J, Stergiou GS, Achimastos A, Safar ME. Blood pressure response under chronic antihypertensive drug therapy: the role of aortic stiffness in the REASON (Preterax in Regression of Arterial Stiffness in a Controlled Double-Blind) study. **J Am Coll Cardiol**. 2009; 53(5):445−451.

157. Fernandes LA, Cestario ED, Cosenso-Martin LN, Vilela-Martin JF, Yugar-Toledo JC, Fuchs FD. Chlorthalidone plus amiloride reduces the central systolic blood pressure in stage 1 hypertension patients. **Cardiol Res**. 2016; 7(6):196−201.

158. Lacourcière Y, Béliveau R, Conter HS, et al. Effects of perindopril on elastic and structural properties of large arteries in essential hypertension. **Can J Cardiol**. 2004; 20(8):795−799.

159. Vlachopoulos C, Terentes-Printzios D, Laurent S, et al. Association of estimated pulse wave velocity with survival: a secondary analysis of SPRINT. **J Am Med Assoc Netw Open**. 2019; 2(10):e1912831.

160. Grundy SM, Stone NJ, Bailey AL, et al. 2018 AHA/ACC/ AACVPR/AAPA/ABC/ACPM/ADA/AGS/APhA/ASPC/NLA/ PCNA guideline on the management of blood cholesterol: a report of the American College of Cardiology/American Heart Association Task Force on Clinical Practice Guidelines. **Circulation**. 2019; 139(25):e1082−e1143.

161. Mach F, Baigent C, Catapano AL, et al. 2019 ESC/EAS Guidelines for the management of dyslipidaemias: lipid modification to reduce cardiovascular risk. **Eur Heart J**. 2020; 41(1):111−188.

Chapter 32

Cardiovascular risk prevention in clinical medicine: current guidelines in Asia

Hae-Young Lee[1] and Jeong Bae Park[2]

[1]*Department of Internal Medicine, Seoul National University College of Medicine, Jongno-Gu, Seoul, South Korea;* [2]*Department of Precision Medicine and Biostatistics, Yonsei University Wonju College of Medicine, Seoul, Republic of Korea*

Cardiovascular risk prevention in clinical practice: current guidelines in Asia

Sociodemographic factors and an increase in average life expectancy have dramatically increased the burden of cardiovascular (CV) disease in Asia. There are important differences in the characteristics of CV risk factors in Asia compared to populations in the United States and Europe. In general, the Asian population has a lower body mass index (BMI) but higher salt intake compared with European and North American populations. Although the prevalence of hypertension is similar, large artery stiffness in Asian hypertensive patients is more elevated, possibly due to aging and high salt intake. Higher forward pulse wave and its reflection to the central aorta can cause higher systolic blood pressure (BP) and pulse pressure, which are critical in target organ damage. These differences may explain a higher prevalence of stroke in Asian and more non-atherosclerotic CV disease with aging. Although CV risk prediction tools developed in Europe and North America are used in Asians, many reports suggest overestimation of risk and low performance for risk prediction in Asians. However, Asians might be more susceptible to hypertension-mediated organ damage such as stroke,[1] requiring more sophisticated risk calculation and management for the intermediate- and high-risk population.

Characteristics of cardiovascular risks in Asia, in comparison to the United States, Europe, and other populations

The CV risk in the Asian population is stiffly increased with increased BP, which is different from that seen in patients from Western regions.[2] In an analysis of data from the Asia Pacific Cohort Studies Collaboration, Asian patients with hypertension had a 4.5-fold higher risk of cardiovascular disease (CVD) compared with those with normal BP.[3] Moreover, the relationship between overall CV risk and hypertension was shown to be significantly stronger for Asian patients. Overall, stroke is generally more common than coronary artery diseases in Asians, whereas the converse is seen in Western subjects.[4,5]

Accurate CV risk stratification presents a major challenge for Asian populations. Still there were no established CV risk prediction models for Asians. The Pooled Cohort Equation is used to estimate 10-year ASCVD risk and determine BP targets in US guidelines.[6] The Pooled Cohort Equation is known to overestimate risk in Asian populations and is not a universal risk calculator for all ethnicities.[7,8] Similarly, the Framingham General CVD Risk Prediction Score overestimated especially for Asian women.[9] In the 2018 European Society of Cardiology (ESC)/ European Society of Hypertension (ESH) guideline, the Systematic COronary Risk Evaluation (SCORE) system is used to estimate risk of the first fatal atherosclerotic event. Unlike the Pooled Cohort Equation, SCORE includes a correction factor for first-generation immigrants to Europe based on their country of origin[10]. In this regard, the potential of vascular measures to enhance estimation of global risk could be made. For instance, the presence or absence of prevalent subclinical vascular disease (such as arterial stiffening) could better calibrate risk estimations especially in intermediate risk group.[11]

Current Asian guidelines on cardiovascular prevention

Hypertension

Hypertension is a global public health issue, reported to be responsible for almost 13% of all deaths and 3.7% of total

disability-adjusted life-years.[12] The worldwide prevalence of hypertension in adults was estimated to be approximately 40% in 2008. The prevalence of hypertension is similarly high across different Asian countries, ranging from 30% in South Korea to 47% in Mongolia. Moreover, the prevalence also increases with advancing age.[13] With a rapidly aging population, the prevalence of hypertension and related CV morbidity in Asian patients continues to rise, placing a substantial and escalating social and economic burden on this region.[14]

The risk of coronary artery disease and stroke increases linearly as levels of systolic BP increase.[15] In particular, the linear relationship between BP and stroke risk is markedly more pronounced in Asian patients than in Caucasian populations.[16] This may be attributable to the higher proportion of hemorrhagic versus ischemic strokes reported in the Asian population, as hemorrhagic strokes correlate more closely with BP than do ischemic strokes.[3]

The prevalence of isolated systolic hypertension in Asians, which is reported to be 3.9%−12.5%, is age dependent.[17,18] A meta-analysis of 41 cohort studies conducted by the Asia Pacific Cohort Studies Collaboration clearly illustrated the progressive increase in systolic BP with advancing age in Asian patients.[19] The increasing proportion of older patients across Asia means that the burden of systolic hypertension is continuously growing. It is also anticipated that this increase will be more pronounced than in the Western countries, primarily as a result of lifestyle changes such as consuming Western-style diets and undertaking less physical activity.

Although it was previously reported that there was no difference in prognosis between BP targets of 140 and 150 mmHg,[20] SPRINT trial showed clear evidence of BP lowering effects in elderly patients with HYPERTEN-SION.[21] Therefore, the target systolic BP is below 140 mmHg with a diastolic BP that is not excessively low, i.e., less than approximately 60 mmHg.[20,22]

Since 2017 American College of Cardiology (ACC)/ American Heart Association (AHA) BP guideline, there were discrepancy in the definition of hypertension between ≥130/80 mmHg in ACC/AHA BP guidelines and ≥140/90 in other countries including European guidelines. Most Asian society hypertension guidelines, including Korea, Japan, and China, define hypertension as BP ≥ 140/90 mmHg.[13,23,24] The Japanese Society of Hypertension recommends a target BP of <130/80 mmHg, while the Korean and Chinese guidelines recommend a target BP of <140/90 mmHg or <130/80 mmHg if treatment is well-tolerated especially for high-risk patients such as chronic kidney disease and diabetes. The evaluation of subclinical organ damage including vascular stiffness may be valuable in excluding masked hypertension and correlates with the variability of 24 h BP.[25] If increased vascular stiffness is detected or even worsened during follow up, it may be a clue to the presence of masked hypertension, which can be detected by home BP or ambulatory BP monitoring.[26]

Dyslipidemia

The distribution of serum lipid concentrations varies according to sex and age, and there is a notable difference among women before and after menopause.[27] Generally, the total blood cholesterol concentration is higher among men, but women actually have a higher total cholesterol concentration after the mid-50s. The distribution of low density lipoprotein-cholesterol (LDL-C) concentration is similar to that of total cholesterol. Triglyceride concentrations rapidly increase from the age of 10 to 40 years, are maintained at a high level between ages 40 and 60, and gradually decrease after the age of 60 in men. Conversely, in women, triglyceride concentrations are very low until the ages of 30−40, begin to increase after the mid-40s, and peak after the age of 65.[28] HDL-C concentration is higher among women than men in across all age groups, and the gap is greater in the 20- to 30-year-old group.[28]

The prevalence of hypercholesterolemia in adults aged 30 years or older in South Korea (total cholesterol ≥240 mg/dL or use of cholesterol-lowering drugs) has risen consistently, from 7% to 8% in men and women, respectively, in 2005, to 19% and 20%, respectively, in 2016. The prevalence of dyslipidemia was more than double that of hypercholesterolemia at 40.5%. Sex and age differences indicate that the prevalence of dyslipidemia in men is the highest between the ages of 55 and 59 years (49%) and gradually declines thereafter, while prevalence in women is low between the ages of 20 and 44 years, after which it rapidly increases to 50% between the ages of 60 and 64 years, eventually exceeding that of male counterparts. The prevalence of dyslipidemia is higher among individuals with other comorbidities, such as obesity, abdominal obesity, and diabetes than among those with no comorbidities.[29] In general, the Asian population maintained relatively lower cholesterol levels compared with white Western populations as reported in the international Dyslipidemia Interventional Study II (DYSYS II).[30,31] One characteristic feature of Asia is the high prevalence of hypertriglyceridemia and low HDL cholesterolemia compared with Western populations.[32] In the Korean National Health and Nutritional Examination Survey from 1998 to 2010, hypertriglyceridemia and low HDL cholesterolemia are more common than hypercholesterolemia.[27]

The ACC/AHA published new guidelines in 2013 on the management of cholesterol levels.[33] This guideline no longer targeted specific lipid goals. Instead, it emphasized the administration of high-potency statin therapy instead of "treat to target" goals for LDL-C levels. The concept of "lower is better" for LDL-C levels was replaced by the "more is better" approach to statin therapy.[34] The 2016

ESC/European Atherosclerosis Society (EAS) guidelines made it clear that an LDL-C goal of <70 mg/dL should be achieved, or at least 50% reduction of the baseline LDL-C level in very high-risk patients.[35] However, most Asian guidelines maintained the target LDL-C concentration based on the level of CVD risk factors. Although 2013 ACC/AHA treatment guideline is beneficial by simplifying the criteria for statin administration to "four statin benefit groups,"[33] the 2013 ACC/AHA treatment guidelines could not be directly applied in Asia, as it did not reflect individual differences in drug responses by uniformly recommending a moderate-to-high dose of statin for all patients without a specific LDL-C target level, did not clearly examine the benefits and adverse reactions of high-dose statin administration, and may overestimate CVD risk in Asia. Especially the lipid goal of 50% LDL-C reduction by high-potency statins as recommended in 2013 ACC/AHA guidelines probably received high reluctance.[36] Also, compared with North Americans and Europeans, Asian patients reported having superior statin responsiveness and lower LDL-C levels.[37,38] The plasma levels of statins were higher, and the half-life of the statins was longer after a given dose of any statin[39]. Therefore, the usual recommended doses of statins were lower in Asian guidelines, for instance, atorvastatin 40 mg/day instead of 80 mg/day.[40]

Key elements of the pharmacologic treatment for dyslipidemia are generally the same as 2016 European guidelines. Patients with established CVDs are classified as a very high-risk group, and the treatment goal is to lower LDL-C levels to <70 mg/dL (<100 mg/dL in Japanese guidelines[41]) or by 30%−50% from the baseline level for secondary prevention. Patients with two or more major risk factors other than LDL-C are classified as a moderate risk group, and are recommended to administer statin if the LDL-C concentration is ≥ 120−130 mg/dL for primary prevention. Patients with one or fewer major risk factors other than LDL-C are classified as low-risk group, and statin treatment in this population is recommended for LDL-C concentrations ≥160 mg/dL. When the triglyceride level is between 200 and 499 mg/dL, the primary treatment goal is to lower the LDL-C to below the target on the basis of the calculated CV risk and the secondary goal is to lower non-HDL-C to below the target by therapeutic lifestyle modification and statin therapy. When fasting triglyceride concentrations are still >200 mg/dL despite achieving the target LDL-C goal through therapeutic lifestyle modification and statin therapy, triglyceride lowering drug therapy such as fibrates or omega-3 fatty acids can be used, especially in high-risk and very high-risk groups.[42,43] Similarly, the primary treatment goal for low HDL cholesterolemia is to lower the LDL-C to the target level. To increase HDL-C while lowering the LDL-C to the target, therapeutic lifestyle modification, such as smoking cessation, weight loss, and exercise, should be concurrently performed. It is still debated whether dyslipidemia treatment has long-term beneficial effects on vascular stiffness.[44] However, statin treatment has been reported to improve vascular stiffness the in short-term.[45]

Diabetes mellitus

Type 2 diabetes mellitus (T2DM) is becoming a global health threat owing to its increasing prevalence worldwide.[46] Although the prevalence of diabetes is increasing globally, the situation is particularly alarming in Asia. Two Asian countries, China and India, are home to the largest number of patients with diabetes in the world.[47] Three other Asian countries, Indonesia, Japan, and Bangladesh, are also ranked among the countries with the highest number of patients with diabetes worldwide.[48] In case of South Korea, the prevalence of diabetes among adults 30 years or older was 14.4%; however, when the analysis was limited to adults older than 65 years, the prevalence of diabetes was even higher (29.8%), meaning that one in three Koreans 65 years or older had diabetes.[49] Given the increasing prevalence of obesity and the rapid adoption of a Westernized lifestyle in most Asian countries (especially developing countries), the diabetes epidemic will likely continue to impose a burden on public health systems across Asia.[50]

T2DM develops in East Asian patients at a lower mean BMI compared with those of European descent. At any given BMI, East Asians have a greater amount of body fat and a tendency to visceral adiposity.[51] Greater visceral adiposity can lead to increased fatty acid influx to the liver, altered adipokine production, fatty liver, and hepatic insulin resistance.[52] In Asian patients, diabetes develops at a younger age and is characterized by early β cell dysfunction in the setting of insulin resistance, with many requiring early insulin treatment.[53] T2DM in Asian population tends to occur approximately three years earlier than Western population.[54] The increase in the prevalence and decrease in the age of onset of diabetes in young Asian generations may be explained by the increasing prevalence of obesity and abundant nutrition, including during the intrauterine period: that is, "the thrifty genotype" hypothesis.[55] In developed countries, T2DM affects mainly those older than 65 years, as dietary patterns and energy intake have not changed dramatically in the past decades. Although Asians are not accustomed to Western dietary patterns, most developing countries in Asia accept these as markers of economic development. The younger generations in Asian developing countries are born in relative wealth compared with their parents and, although they retain their parents' genetic background, they usually have access to an abundantly nutritional diet throughout their lives.[56]

Besides lifestyle factors, Asians are known for dysfunctional pancreatic insulin secretory function.[57] A study performed in South Koreans suggested that impaired insulin secretion was induced by insufficient pancreatic

β-cell mass, functional defects within β-cells themselves, or a combination of both. They reported a linear correlation between β-cell mass and BMI in patients with T2DM, suggesting the possibility of reduced insulin secretory function in Asians due to lower BMI and, thus, smaller β-cell mass.[58] Also, there was possibility that Asians have a higher risk of developing diabetes due to genetic defects affecting insulin secretory function and β-cell mass. Several T2DM loci, including KCNQ1, were first discovered in Asians and meta-analysis of East Asian studies identified eight novel loci for T2DM; most of these variants were predicted to influence the risk of T2DM by affecting insulin secretion.[59]

Asian individuals with diabetes are at increased risk of microvascular complications and albuminuria compared with Caucasian first reported in the WHO Multinational Study of Vascular Disease in Diabetes.[60] These patterns of higher microvascular complications in Asians compared with Caucasians were replicated across multiple studies. In a cross-sectional study involving 32,308 patients with T2DM from 33 countries, Asian diabetic patients had the highest prevalence of microalbuminuria as well as macroalbuminuria.[61] In the Action in Diabetes and Vascular Disease (ADVANCE) study, patients with T2DM from Asia had a higher incidence of renal complications and ischemic stroke but a lower risk of coronary artery disease than their counterparts in Eastern Europe.[62] Although, the exact mechanisms underlying these distinctive patterns remain unknown, more intensive risk factor control especially hypertension will be necessary in Asian diabetic population to prevent microvascular complications.

As it is well known that several chronic complications can occur owing to poor glycemic control, long-term glycemic control is important not only in the prevention of diabetic complication but also in the management of combined risk factors such as hypertension and dyslipidemia. In the Kumamoto study in Japan and the UK Prospective Diabetes Study (UKPDS) study showed that intensive glycemic control proved to be effective in preventing microvascular complications.[63,64] In the Kumamoto study, the intensive glucose control group targeting HbA1c <7% decreased retinopathy by 69%, nephropathy by 70%, and improved nerve conduction velocity. Most Asian guidelines recommended glycemic target as HbA1c concentration <6.5% to 7%.[65,66] However, the glycemic control is largely suboptimal worldwide. The mean baseline HbA1c was higher in India (8.6%), the Middle East and Latin America (both, 8.5%) compared with those in East Asia and Europe (7.7% and 7.9%).[67] Even in East Asian countries, for example, South Korea, the control rate, defined by an HbA1c level <6.5%, was only 25.1%, which

was relatively low considering the high awareness and treatment rates.[49] Even if the target HbA1c level was defined as <7.0%, the control rate remained 50%.[29,68]

Life style modification

Nonpharmacologic therapy or lifestyle modification, such as adoption of a healthy diet, increasing exercise, smoking cessation, and moderation of alcohol intake, has shown great ability to lower BP and is strongly recommended in all patients with hypertension and also in population with BP ranged 120−139/80−89 mmHg.[69]

Asians generally have a higher salt intake than Westerners.[70] Recent studies indicate that salt consumption remains high throughout the Asia−Pacific region in countries including Australia (9.6 g/day),[71] China (9.1 g/day),[72] Korea (10 g/day),[73] Japan (11 g/day),[23] and India (9.45−10.41 g/day).[74] These estimated intakes are almost double the WHO's recommended maximum daily salt intake of 5 g/day. The main source of salt in Asians is spices, vegetables, and grains.[75,76] Excessive salt intake is associated with significantly increased BP and the progression of target organ damage.[77,78] Salt intake is more closely correlated with central hemodynamics than peripheral hemodynamics of the brachial artery in patients with hypertension.[79] Salt intake predominantly influences central BP, which is implicated in the development of arterial stiffening. It is noteworthy, therefore, that measuring brachial BP is likely to underestimate the detrimental effects of salt intake on central BP.[80] High sodium intake was positively linked to subsequent vascular stiffness measured by brachial-ankle pulse wave velocity (baPWV) and carotid intima-media thickness levels in South Korean adults.[81] High salt intake may also increase the risk of stroke and CVD independently of the effects of elevated BP, a hypothesis that has been supported by research demonstrating that dietary sodium alters vascular endothelial function independently of systolic BP changes.[82] Reducing dietary sodium effectively reduces systolic BP in Asian patients.[83,84] The daily recommended amount of salt in Asian guidelines is less than 6 g (sodium (g) × 2.5).[69] Substitution of normal salt with reduced sodium, high potassium salt has been shown to significantly reduce BP in Chinese patients with hypertension.[83] Reducing dietary sodium may be particularly effective in reducing systolic BP in older patients.[85]

BP increases with increasing BMI and waist circumference in Asian subjects.[86,87] Obesity was defined as a BMI equal to or higher than 25 kg/m^2, according to the Asia−Pacific Region definition.[88] Over the past 10 years, the prevalence of obesity in Asia markedly increased. For example in South Korea, the prevalence of obesity in the total population was 29.7% in 2009, which increased to

35.7% in 2018.[89] As a result, the prevalence of obesity was 45.4% in men and 26.5% in women, showing a higher prevalence in men than in women. The prevalence of abdominal obesity similarly increased over the past 10 years in Korean adults, with prevalence rates of 23.8% in the total population, 28.1% in men, and 18.2% in women recorded in 2018. The impact of obesity on hypertension appears to be elevated in Asian subjects compared with Western subjects[90]; a BMI of 25 kg/m^2 in Asians has a similar impact on prehypertension and hypertension as a BMI of 30 kg/m^2 in Western individuals.[91,92] Obesity and associated metabolic syndrome are becoming more common in Asian regions.[93] Both of these conditions increase salt sensitivity.[94] Hence, Asians with high salt intake or salt sensitivity may experience increases in BP if they are overweight or only mildly obese. Conversely, the combination of weight reduction with exercise, moderation of alcohol consumption, and reduction of salt intake has synergistic effects on BP. A report on data from 1.2 million Koreans revealed that the risk of death from any cause was lowest among patients with a BMI of 23.0−24.9 kg/m^2 and recommended a BMI of less than 25 kg/m^2.[95] In cohorts of East Asians, including Chinese, Japanese, and Koreans, the lowest risk of death was seen among persons with a BMI of 22.6−27.5.[96] A waist circumference of less than 90 cm for men and 85 cm for women is recommended for Asian individuals.[97]

Table 32.1 shows the specific characteristics of CV risk and their relevant guidelines in East Asia. Compared to those of the United States and Europe, East Asian have higher stroke incidence and mortality but lower CVD incidence and mortality. However, In India and South and Middle East Asia, they have higher CVD and stroke incidence and mortality than those of East Asia and the United States and Europe. Insulin resistance and cental obesity is key difference between East Asians and South Asians.

Role of vascular markers in Asian cardiovascular prevention guidelines

There was no consensus for the role of vascular markers in the risk prediction models. Recently, Japan Brachial-Ankle Pulse Wave Velocity Individual Participant Data Meta-Analysis of Prospective Studies (J-BAVELs) suggested steno-stiffness approach for CVD risk assessment in primary prevention using the interarm BP difference, the ankle-brachial index, and brachial-ankle PWV, showing improvement of the risk assessment.[98] As a result, there were no specific indications for the vascular markers in Asian CV prevention guidelines. However, the recently published Japanese Society of Hypertension Guidelines introduced the implication of vascular markers.[23] The carotid artery intima-media thickness is considered as unsuitable as an indicator for evaluation of exacerbation/improvement of the risk following changes in condition or treatment, whereas ABI measurement is highly recommended in high-risk patients. Both cfPWV and baPWV have been shown to improve the evaluation results of existing risk models, with the improvement of the prognostic ability larger when baPWV was used in the low-risk group.[99] cfPWV may be useful when measured in cases at moderate or higher risk.[100] baPWV may be applicable to risk assessment also in low-risk cases, but there is a need of verifying the medicoeconomic efficiency of its

TABLE 32.1 Asian characteristics of cardiovascular risk and their relevant guidelines.

	Characteristics	Guidelines
Hypertension	■ More blood pressure dependent CVD, particularly stroke ■ Predominant isolated systolic hypertension	■ Target BP, initially less than 140/90 followed by 130/80 mmHg when tolerated
Dyslipidemia	■ Higher prevalence of dyslipidemia, relatively low cholesterol and high triglyceride and low HDL-cholesterol in serum	■ Prominent LDL-C lowering effect with statin and therefore the lower dose of statin needed ■ Emphasis on therapeutic lifestyle modification
Diabetes	■ Relatively lower body weight, but more visceral fat ■ Young age-onset of diabetes ■ Dysfunctional pancreatic insulin secretion ■ Increased comorbidity	■ Early intervention of lifestyle modification ■ Strict control of concomitant risk factors
Lifestyles	■ Still high salt intake ■ Rapidly growing obesity	■ Education ■ Early intervention of therapeutic lifestyle modification

BP, blood pressure; *CVD*; cardiovascular disease; *HDL-cholesterol*, high density lipoprotein-cholesterol; *LDL-C*, low density lipoprotein-cholesterol.
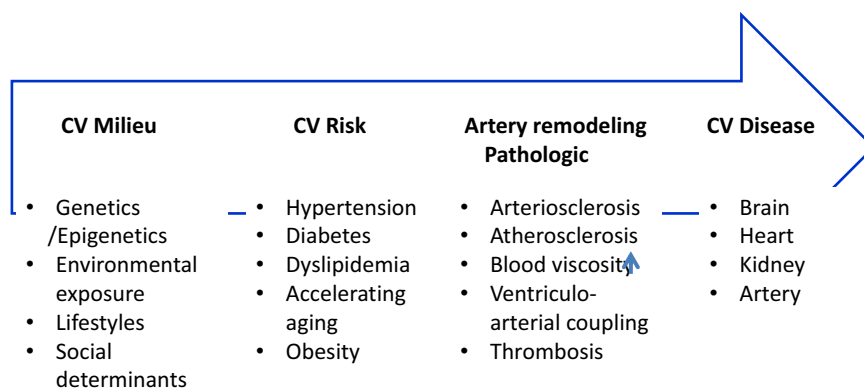
measurement, and its measurement may be useful in patients aged 50 and over or patients having risk factors other than BP. Although the guideline mentioned potential usefulness as a prognostic indicator, there were no specific recommendations for the cardio-ankle vascular index, pulse wave analysis, or endothelial function test. Also, the guideline recommended to conduct vascular marker evaluation upon stabilization of BP after the start of antihypertensive treatment rather than before starting treatment.

Perspective for the prevention of cardiovascular risk in Asia

One of characteristic feature of Asia is rapid "Population aging."[101,102] Regarding vascular health, it is particularly important, because vascular aging—related medial degeneration is the dominant factor associated with increased arterial stiffness (arteriosclerosis) more than the narrowing of the artery (atherosclerosis) in the Asian population.[103] Asian populations may have a particular predisposition to increased central aortic pulse pressure.[104] Age-related changes in arterial mechanical properties increased arterial stiffness and wave reflection are themselves potent and independent risk factors for CV diseases.[105] More importantly, CV risk factors often form a vicious cycle in CV complications. For example, salt intake has an independent effect on arterial wall properties contributing to increased arterial stiffness with age[106] which in turn increases pulse pressure. Urinary salt excretion, a surrogate for intake, is higher among the obese and the elderly.[107] More vigorous CV prevention strategies to cut the vicious cycle should be implemented for Asian populations. Moreover, since most CV risk factors ultimately lead to CV disease through pathologic artery remodeling, the prevention or reversal of pathologic artery remodeling itself should be a central component of prevention strategies (Fig. 32.1).

References

1. Zhou BF, Stamler J, Dennis B, et al. Nutrient intakes of middle-aged men and women in China, Japan, United Kingdom, and United States in the late 1990s: the INTERMAP study. **J Hum Hypertens**. 2003; 17(9):623−630. https://doi.org/10.1038/sj.jhh.1001605. Epub 2003/09/19. PubMed PMID: 13679952; PubMed Central PMCID: PMCPMC6561109.

2. Shimamoto K, Fujita T, Ito S, et al. Impact of blood pressure control on cardiovascular events in 26,512 Japanese hypertensive patients: the Japan Hypertension Evaluation with Angiotensin II Antagonist Losartan Therapy (J-HEALTH) study, a prospective nationwide observational study. **Hypertens Res**. 2008; 31(3):469−478. https://doi.org/10.1291/hypres.31.469. Epub 2008/05/24. PubMed PMID: 18497466.

3. Arima H, Murakami Y, Lam TH, et al. Effects of prehypertension and hypertension subtype on cardiovascular disease in the Asia-Pacific Region. **Hypertension**. 2012; 59(6):1118−1123. https://doi.org/10.1161/HYPERTENSIONAHA.111.187252. Epub 2012/05/02. PubMed PMID: 22547441.

4. Ueshima H. Explanation for the Japanese paradox: prevention of increase in coronary heart disease and reduction in stroke. **J Atherosclerosis Thromb**. 2007; 14(6):278−286. https://doi.org/10.5551/jat.e529. Epub 2008/01/05. PubMed PMID: 18174657.

5. Ishikawa Y, Ishikawa J, Ishikawa S, et al. Prehypertension and the risk for cardiovascular disease in the Japanese general population: the jichi medical school cohort study. **J Hypertens**. 2010; 28(8):1630−1637. https://doi.org/10.1097/HJH.0b013e32833a8b9f. Epub 2010/07/22. PubMed PMID: 20647859.

6. Goff Jr DC, Lloyd-Jones DM, Bennett G, et al. 2013 ACC/AHA guideline on the assessment of cardiovascular risk: a report of the American College of Cardiology/American heart association task force on practice guidelines. **Circulation**. 2014; 129(25 Suppl 2):S49−S73. https://doi.org/10.1161/01.cir.0000437741.48606.98. Epub 2013/11/14. PubMed PMID: 24222018.

7. Jung KJ, Jang Y, Oh DJ, et al. The ACC/AHA 2013 pooled cohort equations compared to a Korean Risk Prediction Model for atherosclerotic cardiovascular disease. **Atherosclerosis**. 2015; 242(1):367−375. https://doi.org/10.1016/j.atherosclerosis.2015.07.033. Epub 2015/08/11. PubMed PMID: 26255683.

FIGURE 32.1 Projection of cardiovascular (CV) milieu to CV disease through pathologic vascular remodeling. Social determinants include economics, education, occupation, and healthcare access.

8. Chia YC, Lim HM, Ching SM. Validation of the pooled cohort risk score in an Asian population - a retrospective cohort study. **BMC Cardiovascular Disorders**. 2014; 14:163. https://doi.org/10.1186/1471-2261-14-163. Epub 2014/11/21. PubMed PMID: 25410585; PubMed Central PMCID: PMCPMC4246627.

9. Chia YC, Gray SY, Ching SM, Lim HM, Chinna K. Validation of the Framingham general cardiovascular risk score in a multiethnic Asian population: a retrospective cohort study. **BMJ Open**. 2015; 5(5):e007324. https://doi.org/10.1136/bmjopen-2014-007324. Epub 2015/05/21. PubMed PMID: 25991451; PubMed Central PMCID: PMCPMC4442208.

10. Williams B, Mancia G, Spiering W, et al. 2018 ESC/ESH Guidelines for the management of arterial hypertension. **Eur Heart J**. 2018; 39(33):3021−3104. https://doi.org/10.1093/eurheartj/ehy339. Epub 2018/08/31. PubMed PMID: 30165516.

11. Lau KK, Wong YK, Chan YH, et al. Prognostic implications of surrogate markers of atherosclerosis in low to intermediate risk patients with type 2 diabetes. **Cardiovasc Diabetol**. 2012; 11:101. https://doi.org/10.1186/1475-2840-11-101. Epub 2012/08/21. PubMed PMID: 22900680; PubMed Central PMCID: PMCPMC3444371.

12. WHO. Global Health Observatory. Prevalence of raised blood pressure: situations and trends. http://www.who.int/gho/ncd/risk_factors/blood_pressure_prevalence_text/en/. (accessed 15 April 2020).

13. Kim HC, Ihm SH, Kim GH, et al. 2018 Korean Society of Hypertension guidelines for the management of hypertension: part I-epidemiology of hypertension. **Clin Hypertens**. 2019; 25:16. https://doi.org/10.1186/s40885-019-0121-0. Epub 2019/08/08. PubMed PMID: 31388451; PubMed Central PMCID: PMCPMC6670210.

14. Chung N, Baek S, Chen MF, et al. Expert recommendations on the challenges of hypertension in Asia. **Int J Clin Pract**. 2008; 62(9):1306−1312. https://doi.org/10.1111/j.1742-1241.2008.01838.x. Epub 2008/07/23. PubMed PMID: 18643931.

15. Perkovic V, Huxley R, Wu Y, Prabhakaran D, MacMahon S. The burden of blood pressure-related disease: a neglected priority for global health. **Hypertension**. 2007; 50(6):991−997. https://doi.org/10.1161/HYPERTENSIONAHA.107.095497. Epub 2007/10/24. PubMed PMID: 17954719.

16. Sauvaget C, Ramadas K, Thomas G, Thara S, Sankaranarayanan R. Prognosis criteria of casual systolic and diastolic blood pressure values in a prospective study in India. **J Epidemiol Community Health**. 2010; 64(4):366−372. https://doi.org/10.1136/jech.2008.086777. Epub 2009/08/21. PubMed PMID: 19692728.

17. Li J, Xu C, Sun Z, et al. Prevalence and risk factors for isolated untreated systolic hypertension in rural Mongolian and Han populations. **Acta Cardiol**. 2008; 63(3):389−393. https://doi.org/10.2143/AC.63.3.1020317. Epub 2008/07/31. PubMed PMID: 18664031.

18. Park JB, Kario K, Wang JG. Systolic hypertension: an increasing clinical challenge in Asia. **Hypertens Res**. 2015; 38(4):227−236. https://doi.org/10.1038/hr.2014.169. Epub 2014/12/17. PubMed PMID: 25503845; PubMed Central PMCID: PMCPMC4396396.

19. Asia Pacific Cohort Studies C. The impact of cardiovascular risk factors on the age-related excess risk of coronary heart disease. **Int J Epidemiol**. 2006; 35(4):1025−1033. https://doi.org/10.1093/ije/dyl058. Epub 2006/04/04. PubMed PMID: 16581818.

20. JATOS Study Group. Principal results of the Japanese trial to assess optimal systolic blood pressure in elderly hypertensive patients (JATOS). **Hypertens Res**. 2008; 31(12):2115−2127. https://doi.org/10.1291/hypres.31.2115. PubMed PMID: 19139601.

21. Group SR, Wright Jr JT, Williamson JD, et al. A randomized trial of intensive versus standard blood-pressure control. **N Engl J Med**. 2015; 373(22):2103−2116. https://doi.org/10.1056/NEJMoa1511939. PubMed PMID: 26551272; PubMed Central PMCID: PMCPMC4689591.

22. Ogihara T, Saruta T, Rakugi H, et al. Target blood pressure for treatment of isolated systolic hypertension in the elderly: valsartan in elderly isolated systolic hypertension study. **Hypertension**. 2010; 56(2):196−202. https://doi.org/10.1161/HYPERTENSIONAHA.109.146035. PubMed PMID: 20530299.

23. Umemura S, Arima H, Arima S, et al. The Japanese society of hypertension guidelines for the management of hypertension (JSH 2019). **Hypertens Res**. 2019; 42(9):1235−1481. https://doi.org/10.1038/s41440-019-0284-9. Epub 2019/08/04. PubMed PMID: 31375757.

24. Joint Committee for Guideline R. 2018 Chinese guidelines for prevention and treatment of hypertension-A report of the revision committee of Chinese guidelines for prevention and treatment of hypertension. **J Geriatr Cardiol**. 2019; 16(3):182−241. https://doi.org/10.11909/j.issn.1671-5411.2019.03.014. Epub 2019/05/14. PubMed PMID: 31080465; PubMed Central PMCID: PMCPMC6500570 During the revision of this guideline, AstraZeneca Investment (China) Co., Ltd., Bayer Health Care Co., Ltd., Beijing Double-Crane Pharmaceutical Co., Ltd., Sinopharm Holding Distribution Co., Ltd., Hanhui Pharmaceutical Co., Ltd., Hangzhou MSD Pharmaceutical Co., Ltd., Lepu Pharmaceutical Technology Co., Ltd., Merck Serono Co., Ltd., Sanofi (Hangzhou) Pharmaceutical Co., Ltd., Shenzhen Salubris Pharmaceutical Co., Ltd., Servier (Tianjin) Pharmaceutical Co., Ltd., Tianjin Tanabe Pharmaceutical Co., Ltd., Tibet Kangzhe Pharmaceutical Development Co., Ltd., Nanjing Chia Tai Tianqing Pharmaceutical Co., Ltd., Jiangsu Simcere Pharmaceutical Co., Ltd., Beijing Nuohe Xinkang Gene Technology Co., Ltd., and Beijing Precision Health Management of Hypertension & Angiocardiopathy Co., Ltd. supported the conferences of revision, but did not participate in or influence the guideline's academic content and evidence review. The guideline remains independent.

25. Park JS, Shin JH, Park JB, et al. Relationship between arterial stiffness and variability of home blood pressure monitoring. **Medicine (Baltim)**. 2020; 99(30):e21227. https://doi.org/10.1097/MD.0000000000021227. Epub 2020/08/15. PubMed PMID: 32791697; PubMed Central PMCID: PMCPMC7387033.

26. Antza C, Vazakidis P, Doundoulakis I, et al. Masked and white coat hypertension, the double trouble of large arteries: a systematic review and meta-analysis. **J Clin Hypertens**. 2020; 22(5):802−811. Epub 2020/05/02. 10.1111/jch.13876. PubMed PMID: 32356941.

27. Rhee EJ, Kim HC, Kim JH, et al. 2018 Guidelines for the management of dyslipidemia. **Korean J Intern Med (Korean Ed)**. 2019; 34(4):723−771. https://doi.org/10.3904/kjim.2019.188. Epub 2019/07/06. PubMed PMID: 31272142; PubMed Central PMCID: PMCPMC6610190.

28. Park JH, Lee MH, Shim JS, et al. Effects of age, sex, and menopausal status on blood cholesterol profile in the Korean population. **Korean Circ J**. 2015; 45(2):141−148. https://doi.org/10.4070/

kcj.2015.45.2.141. Epub 2015/03/27. PubMed PMID: 25810736; PubMed Central PMCID: PMCPMC4372980.

29. Rhee EJ. Prevalence and current management of cardiovascular risk factors in Korean adults based on fact sheets. **Endocrinol Metab (Seoul)**. 2020; 35(1):85−94. https://doi.org/10.3803/EnM.2020.35.1.85. Epub 2020/03/25. PubMed PMID: 32207267; PubMed Central PMCID: PMCPMC7090302.

30. Poh KK, Ambegaonkar B, Baxter CA, et al. Low-density lipoprotein cholesterol target attainment in patients with stable or acute coronary heart disease in the Asia-Pacific region: results from the Dyslipidemia International Study II. **Eur J Prev Cardiol**. 2018; 25(18):1950−1963. https://doi.org/10.1177/2047487318798927. Epub 2018/09/11. PubMed PMID: 30198749.

31. Ferrieres J, De Ferrari GM, Hermans MP, et al. Predictors of LDL-cholesterol target value attainment differ in acute and chronic coronary heart disease patients: results from DYSIS II Europe. **Eur J Prev Cardiol**. 2018; 25(18):1966−1976. https://doi.org/10.1177/2047487318806359. Epub 2018/10/20. PubMed PMID: 30335504.

32. Rashid S, Sniderman A, Melone M, et al. Elevated cholesteryl ester transfer protein (CETP) activity, a major determinant of the atherogenic dyslipidemia, and atherosclerotic cardiovascular disease in South Asians. **Eur J Prev Cardiol**. 2015; 22(4):468−477. https://doi.org/10.1177/2047487314528461. Epub 2014/03/25. PubMed PMID: 24659026.

33. Stone NJ, Robinson JG, Lichtenstein AH, et al. 2013 ACC/AHA guideline on the treatment of blood cholesterol to reduce atherosclerotic cardiovascular risk in adults: a report of the American College of Cardiology/American Heart Association Task Force on Practice Guidelines. **Circulation**. 2014; 129(25 Suppl 2):S1−S45. https://doi.org/10.1161/01.cir.0000437738.63853.7a. Epub 2013/11/14. PubMed PMID: 24222016.

34. Wang Y, Yan BP, Tomlinson B, Lee VW. Is lipid goal one-size-fits-all: a review of evidence for recommended low-density lipoprotein treatment targets in Asian patients. **Eur J Prev Cardiol**. 2019; 26(14):1496−1506. https://doi.org/10.1177/2047487319843077. Epub 2019/04/27. PubMed PMID: 31023098.

35. Catapano AL, Graham I, De Backer G, et al. 2016 ESC/EAS guidelines for the management of dyslipidaemias. **Eur Heart J**. 2016; 37(39):2999−3058. https://doi.org/10.1093/eurheartj/ehw272. Epub 2016/08/28. PubMed PMID: 27567407.

36. Setia S, Fung SS, Waters DD. Doctors' knowledge, attitudes, and compliance with 2013 ACC/AHA guidelines for prevention of atherosclerotic cardiovascular disease in Singapore. **Vasc Health Risk Manag**. 2015; 11:303−310. https://doi.org/10.2147/VHRM.S82710. Epub 2015/06/18. PubMed PMID: 26082642; PubMed Central PMCID: PMCPMC4461017.

37. Lee CW, Kang SJ, Ahn JM, et al. Comparison of effects of atorvastatin (20 mg) versus rosuvastatin (10 mg) therapy on mild coronary atherosclerotic plaques (from the ARTMAP trial). **Am J Cardiol**. 2012; 109(12):1700−1704. https://doi.org/10.1016/j.amjcard.2012.01.399. Epub 2012/03/24. PubMed PMID: 22440123.

38. Matsuzaki M, Kita T, Mabuchi H, et al. Large scale cohort study of the relationship between serum cholesterol concentration and coronary events with low-dose simvastatin therapy in Japanese patients with hypercholesterolemia. **Circ J**. 2002; 66(12):1087−1095. https://doi.org/10.1253/circj.66.1087. Epub 2002/12/25. PubMed PMID: 12499611.

39. Liao JK. Safety and efficacy of statins in Asians. **Am J Cardiol**. 2007; 99(3):410−414. https://doi.org/10.1016/j.amjcard.2006.08.051. Epub 2007/01/31. PubMed PMID: 17261409; PubMed Central PMCID: PMCPMC2651637.

40. Miyauchi K, Ray K. A review of statin use in patients with acute coronary syndrome in Western and Japanese populations. **J Int Med Res**. 2013; 41(3):523−536. https://doi.org/10.1177/0300060513476428. Epub 2013/04/10. PubMed PMID: 23569015.

41. Kinoshita M, Yokote K, Arai H, et al. Japan atherosclerosis society (JAS) guidelines for prevention of atherosclerotic cardiovascular diseases 2017. **J Atherosclerosis Thromb**. 2018; 25(9):846−984. https://doi.org/10.5551/jat.GL2017. Epub 2018/08/24. PubMed PMID: 30135334; PubMed Central PMCID: PMCPMC6143773.

42. Bhatt DL, Steg PG, Miller M, et al. Cardiovascular risk reduction with icosapent ethyl for hypertriglyceridemia. **N Engl J Med**. 2019; 380(1):11−22. https://doi.org/10.1056/NEJMoa1812792. Epub 2018/11/13. PubMed PMID: 30415628.

43. Group AS, Ginsberg HN, Elam MB, et al. Effects of combination lipid therapy in type 2 diabetes mellitus. **N Engl J Med**. 2010; 362(17):1563−1574. https://doi.org/10.1056/NEJMoa1001282. Epub 2010/03/17. PubMed PMID: 20228404; PubMed Central PMCID: PMCPMC2879499.

44. Sahebkar A, Pecin I, Tedeschi-Reiner E, Derosa G, Maffioli P, Reiner Z. Effects of statin therapy on augmentation index as a measure of arterial stiffness: a systematic review and meta-analysis. **Int J Cardiol**. 2016; 212:160−168. https://doi.org/10.1016/j.ijcard.2016.03.010. Epub 2016/04/04. PubMed PMID: 27038725.

45. Gepner AD, Lazar K, Hulle CV, Korcarz CE, Asthana S, Carlsson CM. Effects of simvastatin on augmentation index are transient: outcomes from a randomized controlled trial. **J Am Heart Assoc**. 2019; 8(20):e009792. https://doi.org/10.1161/JAHA.118.009792. Epub 2019/10/15. PubMed PMID: 31607205; PubMed Central PMCID: PMCPMC6818042.

46. Hu FB. Globalization of diabetes: the role of diet, lifestyle, and genes. **Diabetes Care**. 2011; 34(6):1249−1257. https://doi.org/10.2337/dc11-0442. Epub 2011/05/28. PubMed PMID: 21617109; PubMed Central PMCID: PMCPMC3114340.

47. Yang JJ, Yu D, Wen W, et al. Association of diabetes with all-cause and cause-specific mortality in Asia: a pooled analysis of more than 1 million participants. **JAMA Netw Open**. 2019; 2(4):e192696. https://doi.org/10.1001/jamanetworkopen.2019.2696. Epub 2019/04/20. PubMed PMID: 31002328; PubMed Central PMCID: PMCPMC6481439.

48. Ramachandran A, Ma RC, Snehalatha C. Diabetes in Asia. **Lancet**. 2010; 375(9712):408−418. https://doi.org/10.1016/S0140-6736(09)60937-5. Epub 2009/10/31. PubMed PMID: 19875164.

49. Kim BY, Won JC, Lee JH, et al. Diabetes fact sheets in Korea, 2018: an appraisal of current status. **Diabetes Metab J**. 2019; 43(4):487−494. https://doi.org/10.4093/dmj.2019.0067. Epub 2019/07/25. PubMed PMID: 31339012; PubMed Central PMCID: PMCPMC6712228.

50. Nanditha A, Ma RC, Ramachandran A, et al. Diabetes in Asia and the pacific: implications for the global epidemic. **Diabetes Care**. 2016; 39(3):472−485. https://doi.org/10.2337/dc15-1536. Epub 2016/02/26. PubMed PMID: 26908931.

51. Yoon KH, Lee JH, Kim JW, et al. Epidemic obesity and type 2 diabetes in Asia. **Lancet**. 2006; 368(9548):1681−1688. https://doi.org/10.1016/S0140-6736(06)69703-1. Epub 2006/11/14. PubMed PMID: 17098087.

52. Unger RH, Clark GO, Scherer PE, Orci L. Lipid homeostasis, lipotoxicity and the metabolic syndrome. **Biochim Biophys Acta**. 2010; 1801(3):209−214. https://doi.org/10.1016/j.bbalip.2009.10.006. Epub 2009/12/02. PubMed PMID: 19948243.

53. Ma RC, Chan JC. Type 2 diabetes in East Asians: similarities and differences with populations in Europe and the United States. **Ann N Y Acad Sci**. 2013; 1281:64−91. https://doi.org/10.1111/nyas.12098. Epub 2013/04/05. PubMed PMID: 23551121; PubMed Central PMCID: PMCPMC3708105.

54. Yeung RO, Zhang Y, Luk A, et al. Metabolic profiles and treatment gaps in young-onset type 2 diabetes in Asia (the JADE programme): a cross-sectional study of a prospective cohort. **Lancet Diabetes Endocrinol**. 2014; 2(12):935−943. https://doi.org/10.1016/S2213-8587(14)70137-8. Epub 2014/08/02. PubMed PMID: 25081582.

55. Sellayah D, Cagampang FR, Cox RD. On the evolutionary origins of obesity: a new hypothesis. **Endocrinology**. 2014; 155(5):1573−1588. https://doi.org/10.1210/en.2013-2103. Epub 2014/03/13. PubMed PMID: 24605831.

56. Rhee EJ. Diabetes in Asians. **Endocrinol Metab (Seoul)**. 2015; 30(3):263−269. https://doi.org/10.3803/EnM.2015.30.3.263. Epub 2015/10/06. PubMed PMID: 26435131; PubMed Central PMCID: PMCPMC4595349.

57. Fukushima M, Suzuki H, Seino Y. Insulin secretion capacity in the development from normal glucose tolerance to type 2 diabetes. **Diabetes Res Clin Pract**. 2004; 66(Suppl 1):S37−S43. https://doi.org/10.1016/j.diabres.2003.11.024. Epub 2004/11/27. PubMed PMID: 15563978.

58. Yoon KH, Ko SH, Cho JH, et al. Selective beta-cell loss and alpha-cell expansion in patients with type 2 diabetes mellitus in Korea. **J Clin Endocrinol Metabol**. 2003; 88(5):2300−2308. https://doi.org/10.1210/jc.2002-020735. Epub 2003/05/03. PubMed PMID: 12727989.

59. Cho YS, Chen CH, Hu C, et al. Meta-analysis of genome-wide association studies identifies eight new loci for type 2 diabetes in east Asians. **Nat Genet**. 2011; 44(1):67−72. https://doi.org/10.1038/ng.1019. Epub 2011/12/14. PubMed PMID: 22158537; PubMed Central PMCID: PMCPMC3582398.

60. Lee ET, Lu M, Bennett PH, Keen H. Vascular disease in younger-onset diabetes: comparison of European, Asian and American Indian cohorts of the WHO multinational study of vascular disease in diabetes. **Diabetologia**. 2001; 44(Suppl 2):S78−S81. https://doi.org/10.1007/pl00002943. Epub 2001/10/06. PubMed PMID: 11587054.

61. Parving HH, Lewis JB, Ravid M, Remuzzi G, Hunsicker LG, investigators D. Prevalence and risk factors for microalbuminuria in a referred cohort of type II diabetic patients: a global perspective. **Kidney International**. 2006; 69(11):2057−2063. https://doi.org/10.1038/sj.ki.5000377. Epub 2006/04/14. PubMed PMID: 16612330.

62. Clarke PM, Glasziou P, Patel A, et al. Event rates, hospital utilization, and costs associated with major complications of diabetes: a multicountry comparative analysis. **PLoS Medicine**. 2010; 7(2):e1000236. https://doi.org/10.1371/journal.pmed.1000236. Epub 2010/02/27. PubMed PMID: 20186272; PubMed Central PMCID: PMCPMC2826379.

63. Ohkubo Y, Kishikawa H, Araki E, et al. Intensive insulin therapy prevents the progression of diabetic microvascular complications in Japanese patients with non-insulin-dependent diabetes mellitus: a randomized prospective 6-year study. **Diabetes Res Clin Pract**. 1995; 28(2):103−117. https://doi.org/10.1016/0168-8227(95)01064-k. Epub 1995/05/01. PubMed PMID: 7587918.

64. Holman RR, Paul SK, Bethel MA, Matthews DR, Neil HA. 10-year follow-up of intensive glucose control in type 2 diabetes. **N Engl J Med**. 2008; 359(15):1577−1589. https://doi.org/10.1056/NEJMoa0806470. Epub 2008/09/12. PubMed PMID: 18784090.

65. Kim MK, Ko SH, Kim BY, et al. 2019 clinical practice guidelines for type 2 diabetes mellitus in Korea. **Diabetes Metab J**. 2019; 43(4):398−406. https://doi.org/10.4093/dmj.2019.0137. Epub 2019/08/24. PubMed PMID: 31441247; PubMed Central PMCID: PMCPMC6712226.

66. Haneda M, Noda M, Origasa H, et al. Japanese clinical practice guideline for diabetes 2016. **Diabetol Int**. 2018; 9(1):1−45. https://doi.org/10.1007/s13340-018-0345-3. Epub 2019/01/04. PubMed PMID: 30603347; PubMed Central PMCID: PMCPMC6224875.

67. Brath H, Paldanius PM, Bader G, Kolaczynski WM, Nilsson PM. Differences in glycemic control across world regions: a post-hoc analysis in patients with type 2 diabetes mellitus on dual anti-diabetes drug therapy. **Nutr Diabetes**. 2016; 6(7):e217. https://doi.org/10.1038/nutd.2016.25. Epub 2016/07/05. PubMed PMID: 27376699; PubMed Central PMCID: PMCPMC4973138.

68. Shin JY. Trends in the prevalence and management of diabetes in Korea: 2007−2017. **Epidemiol Health**. 2019; 41:e2019029. https://doi.org/10.4178/epih.e2019029. Epub 2019/07/20. PubMed PMID: 31319658; PubMed Central PMCID: PMCPMC6702122.

69. Lee HY, Shin J, Kim GH, et al. 2018 Korean Society of Hypertension Guidelines for the management of hypertension: part II-diagnosis and treatment of hypertension. **Clin Hypertens**. 2019; 25:20. https://doi.org/10.1186/s40885-019-0124-x. Epub 2019/08/08. PubMed PMID: 31388453; PubMed Central PMCID: PMCPMC6670135.

70. Strazzullo P, D'Elia L, Kandala NB, Cappuccio FP. Salt intake, stroke, and cardiovascular disease: meta-analysis of prospective studies. **BMJ**. 2009; 339:b4567. https://doi.org/10.1136/bmj.b4567. Epub 2009/11/26. PubMed PMID: 19934192; PubMed Central PMCID: PMCPMC2782060.

71. Land MA, Neal BC, Johnson C, Nowson CA, Margerison C, Petersen KS. Salt consumption by Australian adults: a systematic review and meta-analysis. **Med J Aust**. 2018; 208(2):75−81. https://doi.org/10.5694/mja17.00394. Epub 2018/02/02. PubMed PMID: 29385968.

72. Hipgrave DB, Chang S, Li X, Wu Y. Salt and sodium intake in China. **J Am Med Assoc**. 2016; 315(7):703−705. https://doi.org/10.1001/jama.2015.15816. Epub 2016/02/18. PubMed PMID: 26881375.

73. Kim YC, Koo HS, Kim S, Chin HJ. Estimation of daily salt intake through a 24-hour urine collection in Pohang, Korea. **J Kor Med Sci**. 2014; 29(Suppl 2):S87−S90. https://doi.org/10.3346/jkms.2014.29.S2.S87. Epub 2014/10/16. PubMed PMID: 25317022; PubMed Central PMCID: PMCPMC4194289.

74. Johnson C, Praveen D, Pope A, et al. Mean population salt consumption in India: a systematic review. **J Hypertens**. 2017; 35(1):3−9. https://doi.org/10.1097/HJH.0000000000001141. Epub 2016/10/19. PubMed PMID: 27755388.

75. 2010 Korean Natrional Health Statistics. **2010 Korean National Health and Nutrition Examination Survey**. 2010.

76. Rhee MY, Shin SJ, Park SH, Kim SW. Sodium intake of a city population in Korea estimated by 24-h urine collection method. **Eur J Clin Nutr**. 2013; 67(8):875−880. https://doi.org/10.1038/ejcn.2013.87. PubMed PMID: 23632748.

77. Kawano Y, Ando K, Matsuura H, et al. Report of the working group for dietary salt reduction of the Japanese society of hypertension: (1) rationale for salt restriction and salt-restriction target level for the management of hypertension. **Hypertens Res**. 2007; 30(10):879−886. https://doi.org/10.1291/hypres.30.879. Epub 2007/12/01. PubMed PMID: 18049018.

78. Nagata C, Takatsuka N, Shimizu N, Shimizu H. Sodium intake and risk of death from stroke in Japanese men and women. **Stroke**. 2004; 35(7):1543−1547. https://doi.org/10.1161/01.STR.0000130425.50441.b0. Epub 2004/05/15. PubMed PMID: 15143292.

79. Park S, Park JB, Lakatta EG. Association of central hemodynamics with estimated 24-h urinary sodium in patients with hypertension. **J Hypertens**. 2011; 29(8):1502−1507. https://doi.org/10.1097/HJH.0b013e3283486311. Epub 2011/06/15. PubMed PMID: 21666493; PubMed Central PMCID: PMCPMC4535170.

80. Starmans-Kool MJ, Stanton AV, Xu YY, Mc GTSA, Parker KH, Hughes AD. High dietary salt intake increases carotid blood pressure and wave reflection in normotensive healthy young men. **J Appl Physiol**. 2011; 110(2):468−471. https://doi.org/10.1152/japplphysiol.00917.2010. Epub 2010/11/23. PubMed PMID: 21088211.

81. Jung S, Kim MK, Shin J, et al. High sodium intake and sodium to potassium ratio may be linked to subsequent increase in vascular damage in adults aged 40 years and older: the Korean multi-rural communities cohort (MRCohort). **Eur J Nutr**. 2019; 58(4):1659−1671. https://doi.org/10.1007/s00394-018-1712-3. Epub 2018/05/16. PubMed PMID: 29761317.

82. Jablonski KL, Racine ML, Geolfos CJ, et al. Dietary sodium restriction reverses vascular endothelial dysfunction in middle-aged/older adults with moderately elevated systolic blood pressure. **J Am Coll Cardiol**. 2013; 61(3):335−343. https://doi.org/10.1016/j.jacc.2012.09.010. Epub 2012/11/13. PubMed PMID: 23141486; PubMed Central PMCID: PMCPMC3549053.

83. Zhou B, Wang HL, Wang WL, Wu XM, Fu LY, Shi JP. Long-term effects of salt substitution on blood pressure in a rural north Chinese population. **J Hum Hypertens**. 2013; 27(7):427−433. https://doi.org/10.1038/jhh.2012.63. Epub 2012/12/21. PubMed PMID: 23254595.

84. He FJ, Marciniak M, Visagie E, et al. Effect of modest salt reduction on blood pressure, urinary albumin, and pulse wave velocity in white, black, and Asian mild hypertensives. **Hypertension**. 2009; 54(3):482−488. https://doi.org/10.1161/HYPERTENSIONAHA.109.133223. Epub 2009/07/22. PubMed PMID: 19620514.

85. He J, Gu D, Chen J, et al. Gender difference in blood pressure responses to dietary sodium intervention in the GenSalt study. **J Hypertens**. 2009; 27(1):48−54. https://doi.org/10.1097/hjh.0b013e328316bb87. Epub 2009/01/17. PubMed PMID: 19145767; PubMed Central PMCID: PMCPMC2882679.

86. Lee HS, Park YM, Kwon HS, et al. Factors associated with control of blood pressure among elderly people diagnosed with hypertension in a rural area of South Korea: the Chungju metabolic disease cohort study (CMC study). **Blood Pres**. 2010; 19(1):31−39. https://doi.org/10.3109/08037050903424117. Epub 2009/11/26. PubMed PMID: 19929285.

87. Kawamoto R, Kohara K, Tabara Y, Miki T. High prevalence of prehypertension is associated with the increased body mass index in community-dwelling Japanese. **Tohoku J Exp Med**. 2008; 216(4):353−361. https://doi.org/10.1620/tjem.216.353. Epub 2008/12/09. PubMed PMID: 19060450.

88. Consultation WHOE. Appropriate body-mass index for Asian populations and its implications for policy and intervention strategies. **Lancet**. 2004; 363(9403):157−163. https://doi.org/10.1016/S0140-6736(03)15268-3. Epub 2004/01/17. PubMed PMID: 14726171.

89. Nam GE, Kim YH, Han K, et al. Obesity fact sheet in Korea, 2018: data focusing on waist circumference and obesity-related comorbidities. **J Obes Metab Syndr**. 2019; 28(4):236−245. https://doi.org/10.7570/jomes.2019.28.4.236. Epub 2020/01/08. PubMed PMID: 31909366; PubMed Central PMCID: PMCPMC6939699.

90. Kario K. Proposal of a new strategy for ambulatory blood pressure profile-based management of resistant hypertension in the era of renal denervation. **Hypertens Res**. 2013; 36(6):478−484. https://doi.org/10.1038/hr.2013.19. Epub 2013/03/22. PubMed PMID: 23514717.

91. Ishikawa Y, Ishikawa J, Ishikawa S, et al. Prevalence and determinants of prehypertension in a Japanese general population: the jichi medical school cohort study. **Hypertens Res**. 2008; 31(7):1323−1330. https://doi.org/10.1291/hypres.31.1323. Epub 2008/10/30. PubMed PMID: 18957802.

92. Greenlund KJ, Croft JB, Mensah GA. Prevalence of heart disease and stroke risk factors in persons with prehypertension in the United States, 1999-2000. **Arch Intern Med**. 2004; 164(19):2113−2118. https://doi.org/10.1001/archinte.164.19.2113. Epub 2004/10/27. PubMed PMID: 15505124.

93. Kubo M, Hata J, Doi Y, Tanizaki Y, Iida M, Kiyohara Y. Secular trends in the incidence of and risk factors for ischemic stroke and its subtypes in Japanese population. **Circulation**. 2008; 118(25):2672−2678. https://doi.org/10.1161/CIRCULATIONAHA.107.743211. Epub 2008/12/25. PubMed PMID: 19106389.

94. Chen J, Gu D, Huang J, et al. Metabolic syndrome and salt sensitivity of blood pressure in non-diabetic people in China: a dietary intervention study. **Lancet**. 2009; 373(9666):829−835. https://doi.org/10.1016/S0140-6736(09)60144-6. Epub 2009/02/19. PubMed PMID: 19223069; PubMed Central PMCID: PMCPMC2822441.

95. Jee SH, Sull JW, Park J, et al. Body-mass index and mortality in Korean men and women. **N Engl J Med**. 2006; 355(8):779−787. https://doi.org/10.1056/NEJMoa054017. Epub 2006/08/24. PubMed PMID: 16926276.

96. Zheng W, McLerran DF, Rolland B, et al. Association between body-mass index and risk of death in more than 1 million Asians. **N Engl J Med**. 2011; 364(8):719−729. https://doi.org/10.1056/NEJMoa1010679. Epub 2011/02/25. PubMed PMID: 21345101; PubMed Central PMCID: PMCPMC4008249.

97. Kim MK, Lee WY, Kang JH, et al. 2014 clinical practice guidelines for overweight and obesity in Korea. **Endocrinol Metab (Seoul)**. 2014; 29(4):405−409. https://doi.org/10.3803/EnM.2014.29.4.405. Epub 2015/01/07. PubMed PMID: 25559568; PubMed Central PMCID: PMCPMC4285036.

98. Tomiyama H, Ohkuma T, Ninomiya T, et al. Steno-stiffness approach for cardiovascular disease risk assessment in primary prevention. **Hypertension**. 2019; 73(3):508−513. https://doi.org/10.1161/HYPERTENSIONAHA.118.12110. Epub 2019/01/15. PubMed PMID: 30636553.

99. Ohkuma T, Ninomiya T, Tomiyama H, et al. Brachial-ankle pulse wave velocity and the risk prediction of cardiovascular disease: an individual participant data meta-analysis. **Hypertension**. 2017; 69(6):1045−1052. https://doi.org/10.1161/HYPERTENSIONAHA.117.09097. Epub 2017/04/26. PubMed PMID: 28438905.

100. Ben-Shlomo Y, Spears M, Boustred C, et al. Aortic pulse wave velocity improves cardiovascular event prediction: an individual participant meta-analysis of prospective observational data from 17,635 subjects. **J Am Coll Cardiol**. 2014; 63(7):636−646. https://doi.org/10.1016/j.jacc.2013.09.063. Epub 2013/11/19. PubMed PMID: 24239664; PubMed Central PMCID: PMCPMC4401072.

101. Cheng ST, Lum T, Lam LC, Fung HH. Hong Kong: embracing a fast aging society with limited welfare. **Gerontol**. 2013; 53(4):527−533. https://doi.org/10.1093/geront/gnt017. Epub 2013/03/27. PubMed PMID: 23528290.

102. Eggleston KTS. **Aging Asia: The Economic and Social Implications of Rapid Demographic Change in China, Japan, and South Korea**. Stanford, CA: APARC Books; 2010.

103. Avolio AP, Chen SG, Wang RP, Zhang CL, Li MF, O'Rourke MF. Effects of aging on changing arterial compliance and left ventricular load in a northern Chinese urban community. **Circulation**. 1983; 68(1):50−58. https://doi.org/10.1161/01.cir.68.1.50. Epub 1983/07/01. PubMed PMID: 6851054.

104. Avolio A. Genetic and environmental factors in the function and structure of the arterial wall. **Hypertension**. 1995; 26(1):34−37. https://doi.org/10.1161/01.hyp.26.1.34. Epub 1995/07/01. PubMed PMID: 7607729.

105. Cheng HM, Park S, Huang Q, et al. Vascular aging and hypertension: implications for the clinical application of central blood pressure. **Int J Cardiol**. 2017; 230:209−213. https://doi.org/10.1016/j.ijcard.2016.12.170. Epub 2017/01/04. PubMed PMID: 28043670.

106. Avolio AP, Deng FQ, Li WQ, et al. Effects of aging on arterial distensibility in populations with high and low prevalence of hypertension: comparison between urban and rural communities in China. **Circulation**. 1985; 71(2):202−210. https://doi.org/10.1161/01.cir.71.2.202. Epub 1985/02/01. PubMed PMID: 3965165.

107. Seko C, Odani K, Wada S, et al. Characteristic dietary habits associated with high values of estimated 24-hours urinary sodium excretion and sodium-to-potassium ratio assessed by age group among the residents of a rural town in Japan. **Clin Exp Hypertens**. 2019; 42:1−11. https://doi.org/10.1080/10641963.2019.1693587. Epub 2019/11/22. PubMed PMID: 31747813.

This page intentionally left blank

Arterial stiffness for cardiovascular risk stratification in clinical practice

Dimitrios Terentes-Printzios and Charalambos Vlachopoulos
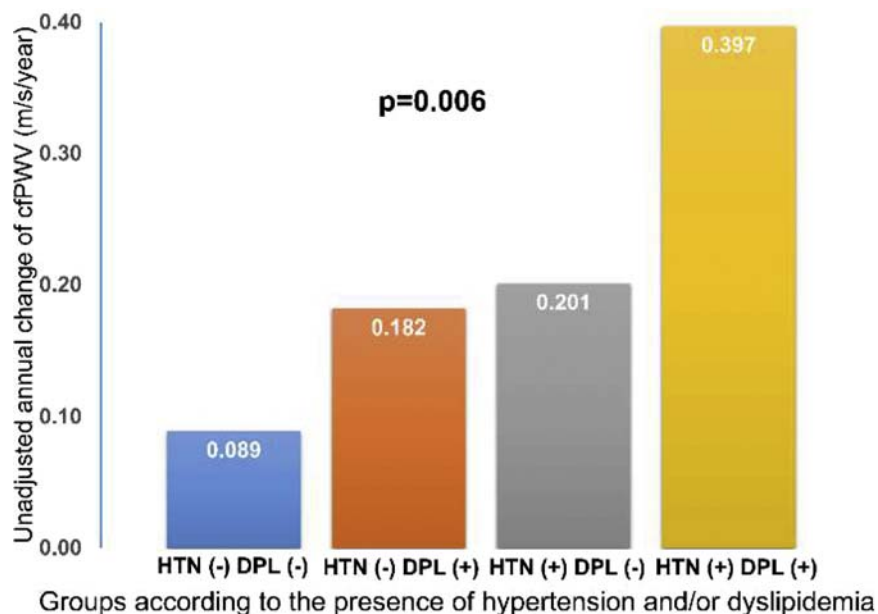
First Department of Cardiology, Hippokration Hospital, Medical School, National and Kapodistrian University of Athens, Athens, Greece

Introduction

Biological markers or biomarkers are valuable tools in prediction of risk. Some traditional individual risk factors, or other proposed biomarkers can fluctuate over time and their values, recorded at the time of risk assessment, may not reflect their true impact on the arterial wall. Arterial biomarkers have the advantage that they can better integrate both the cumulative effect of a traditional risk factor on the arterial wall over a long period of time and the synergistic effects from risk factor combinations (Fig. 33.1).[1] Before a biomarker can be introduced as a surrogate endpoint in clinical practice, important conditions/criteria must be fulfilled.[2,3] According to the American Heart Association (AHA),[4] these criteria (and the relevant questions that need to be answered) are:

1. Proof of concept: Do novel biomarker levels differ between subjects with and without outcome?
2. Prospective validation: Does the novel biomarker predict the development of future outcomes in a prospective cohort or nested case-cohort study?
3. Incremental value: Does it add predictive information over and above established, standard risk markers?
4. Clinical utility: Does it change predicted risk sufficiently to change recommended therapy?

FIGURE 33.1 Unadjusted mean annual change of carotid-femoral pulse wave velocity according to the presence of hypertension and/or dyslipidemia. *DPL*, dyslipidemia; *HTN*, hypertension. *P* value by ANOVA. *Modified from Terentes-Printzios D, Vlachopoulos C, Xaplanteris P, et al. Cardiovascular risk factors accelerate progression of vascular aging in the general population: results from the CRAVE study (cardiovascular risk factors affecting vascular age).* **Hypertension.** *2017;70:1057−1064.*

5. Clinical outcomes: Does the use of the novel biomarker improve clinical outcomes, especially when tested in a randomized clinical trial?
6. Cost-effectiveness: Does the use of the biomarker improve clinical outcomes sufficiently to justify the additional costs?
   Further, there is requirement of three additional criteria (not present in the AHA scientific statement) to be fulfilled for a biomarker to qualify as clinical surrogate endpoint:
7. Ease of use; this will allow widespread application.
8. Methodological consensus
9. Reference values, or, at least, cut-off values to allow for practical implementation.

Arterial stiffness

Predictive value: Clearly, since the predictive role of a certain biomarker for future events is the cornerstone of its clinical usefulness, prospective survival studies are warranted as an early step for its clinical applicability. A considerable number of studies have examined the ability of arterial stiffness to predict the risk of future fatal and nonfatal cardiovascular events (myocardial infarction [MI], stroke, revascularization, aortic syndromes, and peripheral vascular events) and total mortality (Table 33.1, Fig. 33.2) and the list is growing. At a critical point of the accumulation of studies, we performed a meta-analysis in which we pooled the aortic pulse wave velocity (PWV) data for 15,877 subjects from 17 available published studies who were followed up for a mean of 7.7 years.[5] Several populations, such as patients with hypertension, diabetes, end-stage renal disease (ESRD), and coronary artery disease, and subjects from the general population or ethnic minorities were included in that analysis. Aortic stiffness emerged as a strong predictor of future CV events and all-cause mortality. An increase in aortic PWV by 1 m/s corresponded to an age-, sex-, and risk factor–adjusted risk increase of 14%, 15%, and 15% in total CV events, CV mortality, and all-cause mortality, respectively. Importantly, the predictive ability of arterial stiffness is higher in subjects with a higher baseline CV risk, such as renal disease. The results of this meta-analysis were confirmed by a subsequent meta-analysis with individual data of 17,635 subjects, which also importantly added that reclassification was significant for those at intermediate risk (13% for 10-year CVD risk) and in younger subjects (Fig. 33.3).[6,7] Importantly, the latter delineates the group of patients (intermediate risk) that would benefit more from the clinical implementation of PWV.

A closer look at the studies reveals considerable heterogeneity in study design, methodology, and endpoints. This heterogeneity is two-faced. It vividly demonstrates the wide applicability of arterial stiffness measurements in various populations and underlying diseases. On the other hand, it identifies that techniques and conclusions specific to one patient group cannot be used interchangeably. Therefore, there is a need to answer specific questions based on the available prospective data. These questions are:

1. How was arterial stiffness measured?
2. In which populations was arterial stiffness predictive of future events?
3. Which cut-off should be used to identify patients at high risk?
4. Which future endpoints are more closely related to arterial stiffness measurements?
5. What is the effect of blood pressure (BP)/antihypertensive treatment at the time of measurement?

Measurement of arterial stiffness: The techniques of assessing aortic PWV include invasive measurements (considered to be the gold standard), tonometry (the most popular noninvasive technique), oscillometry (either single or two sites), imaging techniques (including MRI and echocardiography), photoplythesmography and, finally, use of estimated values of PWV (derived either by equations or machine learning methods using hemodynamic data or pulse wave form characteristics). For a more comprehensive review regarding methods to assess arterial stiffness, please refer to Chapters 1–4, and 7. Based on the review of the current literature, the large body of evidence stems from two-sites tonometry measurements and thus this should be considered as the first choice for use in clinical practice, despite its inherent technical difficulties (relatively time-consuming in a busy outpatient clinic, need for exposure of the groin, challenges in obese subjects, and availability). However, in an ever-changing world that everything needs to be faster and easier it is possible that alternative techniques might also rise high in user preference. As far as the predictive role is concerned, these techniques should be compared to the current gold standards. In such an effort, recently Hametner et al.[8] compared in patients undergoing coronary angiography the predictive role of invasive PWV, formula-based PWV (calculated by age and BP), and an estimated PWV (by a model incorporating age, central systolic BP, and pulse waveform characteristics) showing comparable predictive effects. Although these results are promising toward the applicability of these alternative techniques, studies comparing them with the two-site tonometry technique in low-to-intermediate cardiovascular risk populations are warranted. Moreover, it should be noted that formula-based PWV estimations based on only age and BPs do not represent genuine individual measurements, but rather mathematical transformations that incorporate the prognostic information contained in age and BP values.

Study population: Historically, the earliest studies included patients belonging to high-risk groups, such as ESRD (Table 33.1). Progressively, studies extended to other patient groups, such as hypertensive, diabetic, or

TABLE 33.1 Overview of studies on the association between aortic pulse wave velocity and clinical events with at least 300 subjects.

Author, year, country/study name	Population-sample size	Age (years)	Follow-up duration	Systolic blood pressure and diastolic blood pressure in mmHg (mean, standard deviation)	Events	Aortic pulse wave velocity in m/s (mean, standard deviation), measurement method	Aortic pulse wave velocity cut-off (high vs. low)
Avramoski et al. (2016), Northern Macedonia[61]	General population (n = 558)	56.2 ± 11.6	36 months	N.a.	17 CV deaths	9.21 ± 1.98, Doppler	>9.4 m/s
Bastos et al. (2010), Portugal[62]	Hypertensives (n = 1200)	51 ± 12	8.2 ± 3.0 years	N.a.	62 deaths and 152 nonfatal CV events	N.a., Complior	N.a.
Benetos et al. (2012), France and Italy, PARTAGE[63]	Elderly (n = 1126)	88 ± 5	2 years	138(17) 73(9)	247 deaths and 228 major CV events	14.3 ± 5.1, PulsePen	Per 1 m/s and terttiles
BLSA (2014) unpub., USA[6]	General population (n = 334)	53.9 ± 17.1	6.4 ± 3.1 years	124.4(17.6) 79.7(9.5)	50 all-cause deaths	6.4 (5.1−8.3), Doppler	No
Boutouyrie et al. (2002), France[64]	Hypertension (n = 1045)	51 ± 12	5.7 years	156(25) 93(16)	53 coronary events, 97 CV events	11.5 ± 3.5, Complior	>12.3 m/s (upper tertile)
Cardoso et al. (2013), Brazil[65]	High-risk type 2 diabetic patients (n = 565)	60.4 ± 9.5	5.75 years	148(24) 85(13)	88 total CV events and 72 all-cause deaths	9.6 ± 2.1, Complior	>10 m/s
Cardoso et al. (2019), Brazil[66]	Resistant hypertensives (n = 891)	68.7 ± 11.5	7.8 years	160(27) 85(18)	138 patients had a CV events (123 major adverse CV event) and 142 patients died (91 CV death)	9.1 ± 1.9, Complior	>11 m/s (corrected at 10 m/s)
Chirinos et al. (2014), USA, CRIC[43]	Subjects free of HF (n = 2602)	59.9 ± 11.1	3.5 years	126.7(21.8) 70.1(12.4)	154 first hospital admissions for HF	9.7, SphygmoCor	>10.3 m/s (upper tertile)
Choi et al. (2007), South Korea[67]	Chest pain patients (n = 497)	57.7 ± 10.1	2.6 years	134(21) 82(13)	1 death, 0 CV death, 120 CV events	N.a., Invasive	>12.5 m/s (upper tertile)
Cooper et al. (2016), USA, Framingham[68]	General population (n = 4547)	51 ± 11	8.6 years (median)	121(17) 75(10)	232 new CV events	8.4 ± 2.7, Tonometer	≥9.2 m/s (upper quartile)
Cruickshank et al. (2002), United Kingdom[69]	DM (n = 394) and community controls (n = 174)	60 ± 10	10.7 years	DM: 144.5/78.5 Control: 139.6/79.3	DM: 179 deaths Controls: 40 deaths	DM: 11.6 ± 3.8 Control: 10.0 ± 2.7, Doppler	1 m/s increase
Dahle et al. (2015), Norway[70]	Renal transplant recipients (n = 1040)	52.3 ± 14.3	4.2 years (median)	135.5(17.2) 83.9(10.9)	82 deaths	10.1 ± 3.3, SphygmoCor	≥12 m/s (upper quartile)

Continued

TABLE 33.1 Overview of studies on the association between aortic pulse wave velocity and clinical events with at least 300 subjects.—cont'd

Author, year, country/study name	Population-sample size	Age (years)	Follow-up duration	Systolic blood pressure and diastolic blood pressure in mmHg (mean, standard deviation)	Events	Aortic pulse wave velocity in m/s (mean, standard deviation), measurement method	Aortic pulse wave velocity cut-off (high vs. low)
Fortier et al. (2015), Canada[71]	Patients on dialysis (n = 310)	67 (56−76)	29 months	135.5(17.2) 83.9(10.9)	146 deaths	13.52 ± 4.07, Complior	Per 1 m/s
Girerd et al. (2012), France[72]	Hypertension work-up patients (n = 498)	51.2 ± 13.8	5.0 ± 2.8 years	Daytime: 155.6(21.1) 94.6(13.4)	51 participants either died (n = 22) or had a major CV event	9.3 ± 2.4 (real distance), Complior	>12 m/s
Hametner et al. (2021), Austria[8]	High-risk patients with suspected coronary artery disease undergoing invasive angiography (n = 1040)	63	1565 days (median)	142 (126−160) 68 (62−76)	24% of the patients reached the combined end point (108 deaths, 37 MI, 32 strokes and 77 unplanned coronary revascularizations; 254 total)	8.6 (7.2−10.3) invasive PWV estimated PWV, formula-based PWV	Per 1-SD
Han et al. (2016),[73] China	Individuals with mildly impaired renal function (n = 1499)	61.4	4.8 years	128.1(17.3) 77.3(10.0)	99 major adverse CV events	11.1, Complior SP	≥12 m/s
Holewijn et al. (2014),[74] Netherlands	General population (n = 1367)	46.33 ± 13.76	3.8 years	128.4(15.4) 78.1(10.4)	71 CV events	9.8, SphygmoCor	Men ≥11.2 m/s and women ≥11.0 m/s
Kaolawanich et al. (2020),[75] Thailand	Patients referred for adenosine stress cardiac MRI as part of the diagnosis and risk stratification of CAD (n = 520)	68.9 ± 10.6	46.5 months (median)	136.8(19.9) 72.9 (12.0)	116 (22.3%) composite endpoint of all-cause mortality, ACS, de novo or decompensated HF, revascularization, and stroke	10.54 (7.86−13.89) MRI	≥10.54 m/s (median)
Karras et al. (2012), France, Nephro Test Study[76]	Patients with CKD (n = 439)	59.8 ± 14.5	4.67 years	135(21) 73(11)	53 deaths and 69 fatal (20) or nonfatal (44) CV events	11.9 ± 3.4, Complior	≥12 m/s
Kavousi et al. (2012), Netherlands, Rotterdam Study[77]	Asymptomatic community-dwelling participants (n = 5933)	69.1 ± 8.5	6.8 years (median)	143.3(21.3) 77.0(11.2)	347 first CAD events	12.6 (10.9, 14.8) Complior	≥6.4 m/s aged 45−54 years and ≥ 8.1 m/s aged ≥55 years

Study	Population	Age (years)	Follow-up	SBP/DBP (mmHg)	Events	PWV, device	Threshold
Kim et al. (2019), USA, ARIC[78]	Participants (66–90 years) without CVD (n = 3034)	75 ± 5	4.4 years	130.7(17.4) 67.0(10.3)	168 incident CVD events and 244 deaths	11.2 (3.3–23.2) (median, range), Tonometer	>11.2 m/s (2 highest quartiles)
Laurent (2001), France[79]	Hypertension (n = 1980)	50 ± 13	9.3 years	148(22) 89(14)	107 deaths, 46 CV deaths	11.5 ± 3.4, Complior	Per 5 m/s
Maldonado et al. (2011), Portugal[80]	General population (n = 2200)	46.33 ± 13.76	21.42 ± 10.76 months	142.3(21.1) 84.3(12.3)	47 major CV events	10.05 ± 2.03, Complior	>95th percentile adjusted to age and gender
Maroules et al. (2014), USA, Dallas Heart Study[81]	General population (n = 2122)	44 ± 10	7.8 ± 1.5 years	126(17) DBP:N.a.	153 CV events	4.9 ± 3.0 Arch PWV by MRI	N.a. (upper quartile)
Matschkal et al. (2019), Germany, ISAR Study[82]	Hemodialysis patients (n = 344)	69.3 (median)	36 months	24h-SBP/DBP 123.6 ± 16.5 73.6 ± 11.8 Office-SBP/DBP 132.5 ± 19.8 80.5 ± 14.0	89 deaths (35 CV deaths)	24 h-PWV: 9.8 (7.9–11.2) Office-PWV: 10.0 (8.0–11.5), Mobil-O-Graph 24 h-PWA	Tertiles Thresholds (24h-PWV) 9.1 m/s for all-cause mortality and 9.3 m/s for cardiovascular mortality
Mattace-Raso (2006), Netherlands, Rotterdam Study[83]	Community-based adults (n = 2835)	71.7 ± 6.7	4–9 years	143(21) 75(10)	352 deaths, 156 CV events	13.3 ± 23.8 m/s, Complior	Men: >14.6 m/s; women: >14.2 m/s (upper tertile)
Mitchell et al. (2010), Germany[84]	Renal transplant recipients (n = 330)	51.4 ± 0.75	3.87 ± 0.7 years	149(20) 83(11)	16 deaths	9.1 ± 3.3, Sphygmocor	>10 m/s (upper tertile)
Mitchell et al. (2010), USA, Framingham[36]	General population (n = 2232)	63 ± 12	7.8 years	127(20) 74(10)	151 CV events	9.3 (7.8–11.8) median (interquartile range), Tonometer	>9.3 m/s (median)
Niiranen et al. (2017),[85] USA, Framingham	General population (n = 2114)	60 ± 10	12.6 years	127(19) 74(10)	248 first CVD events	9.9 ± 3.4, Tonometer	Sex- and 5-year age-specific medians
Ohishi et al. (2011),[86] Japan	Hypertensives (n = 531)	61.7 ± 12.3	7 ± 3 years	140.4(18.2) 82.3(11.8)	57 strokes, 44 CV disease and 53 deaths	9.1 ± 1.8 FCP-4731 (pressure-sensitive transducer)	Mean value 11.3 (upper quartile)
Ohyama et al. (2017),[87] USA MESA	General population (n = 3527)	62 ± 10	10 years	126(22) 72(11)	456 CV events	7.4 (5.6–10.2), Arch PWV by MRI	45–54 years: ≥ 6.4 m/s and aged ≥55 years: ≥ 8.1 m/s

TABLE 33.1 Overview of studies on the association between aortic pulse wave velocity and clinical events with at least 300 subjects.—cont'd

Author, year, country/study name	Population-sample size	Age (years)	Follow-up duration	Systolic blood pressure and diastolic blood pressure in mmHg (mean, standard deviation)	Events	Aortic pulse wave velocity in m/s (mean, standard deviation), measurement method	Aortic pulse wave velocity cut-off (high vs. low)
Pandey et al. (2017), USA, Health ABC[88]	General population without prevalent HF (n = 2290)	73.7 ± 2.9	11.4 years	136.4(20.9) DBP:N.a.	390 HF events	9.0, Doppler	Mean 13.3 m/s (upper tertile), cut-off n.a.
Pannier et al. (2005), France[25]	ESRD (n = 305)	53.1 ± 16.2	5.8 years	155(28) 83.7(16.4)	96 CV deaths	11.1 ± 3.1, Complior	Upper tertile
Pannier et al. (2014) unpub., France[6]	ESRD (n = 1875)	49.5 ± 11.7	12.8 ± 1.3 years	141.9(19.7) 87.3(13.1)	79 deaths, 13 CV deaths, 9 CAD, 13 CV disease, 4 strokes	9.2 (8.1−10.6), Complior	N.a.
Pereira et al. (2013), Portugal[89]	Hypertensives (n = 1133)	51.05 ± 12.64	2 years	150.9(20.9) 88.6(11.6)	21 strokes	10.72 ± 2.04, Complior	>95th percentile adjusted to age and gender
Regnault et al. (2014), Multi-centre (41 in 12 countries), EPHESUS[90]	Subjects with acute MI, EF <40% and HF (n = 306)	61 ± 11	16 months	118(16) 74(9)	28 all-cause deaths, 64 CV deaths/hospitalizations and 26 CV deaths	12.0 ± 3.1, Complior	Per 1 m/s
Ryliškytė et al. (2019), Lithuania[91]	Middle-aged MetS subjects without overt CVD (n = 2728)	53.9 ± 6.2	3.9 ± 1.7 years	149 (17) 89 (11)	83 (3%) patients had at least one cardiovascular event	8.8 ± 1.6, Vasera VS-1000	Per 1 m/s
Scandale et al. (2020), Italy[92]	Screening of peripheral arterial disease (n = 398)	68 ± 9	5.4 years	138 (21) 80 (10)	47 deaths	10.4 ± 2.6, Sphygmocor	>10 m/s
Sehestedt et al. (2010),[93] Denmark	Population-based sample (n = 1968)	53	12.8 years (median)	124(17) 80(10)	81 CV deaths	10 Piezoelectric pressure transducers	>12 m/s (upper tertile)
Shokawa et al. (2005), USA[25]	Japanese-Americans living in Hawaii (n = 492)	63.7 ± 8.8	10 years	135.9(20.4) 79.3(9.6)	43 deaths, 14 CV deaths	9.7 ± 1.9, MCG400	>9.9 m/s (optimal cut-off by ROC curve)
Sutton-Tyrrell (2005), USA, Health ABC[94]	Community-based old adults (n = 2488)	73.7 ± 2.9	4.6 years	136.4(20.7) 71.9(11.5)	265 deaths, 111 CV deaths, 616 CV events	9.0 ± 3.9, Doppler	>8.4 m/s men; >7.9 m/s women (age-specific median)

Terai et al. (2008), Japan[95]	Hypertension (n = 676)	62 ± 12	4.8 years	140(18) 83(12)	22 deaths, 88 CV events	9.0 ± 0.6, FCP-4731 device	>8.8 m/s (median)
Tougaard et al. (2020), Denmark[96]	Type 1 DM (n = 633)	54 ± 13	6.2 years (median)	132 (15) 93 (10)	90 (14%) had a decline in eGFR of ≥30%, 19 (3%) developed ESRD, 81 (13%) experienced a CV event, 48 (8%) died, and 112 (18%) had the composite renal end point of decline in eGFR, ESRD, or death	10.4 ± 3.3 Sphygmocor	Per 1 SD (3.3 m/s) increase Quartiles (>12.3, upper quartile)
Townsend et al. (2018), USA, CRIC[97]	CKD patients (n = 2795)	59.9 ± 10.8	4.9 ± 2.1 years	128.8(22.7) 70.5(13.0)	394 deaths	9.7, SphygmoCor	>10.3 m/s (upper tertile)
Van Sloten et al. (2014), Netherlands Hoorn Study[26]	Population-based cohort (n = 579)	67	7.6 years (median)	142(21) 82(11)	130 participants had a CV event and 96 died	10.6, Echo of arterial diameters through time (distension curves)	>12 m/s (upper tertile)
Vasan et al. (2019), USA, Framingham[98]	General population (n = 5803)	49 ± 15	10.3 years (median)	120 (16) 75 (10)	297 CV events	8.1 ± 2.7 Tonometer	Per 1-SD
Vavruch et al. (2015), Sweden[99]	Type 2 DM (n = 720)	61 ± 3	6 years (median)	137(16) 80(10)	57 died or were hospitalized for CAD	10.3 ± 2.1, SphygmoCor	Per 1 m/s
Verbeke et al. (2011), France[100]	Renal transplant recipients (n = 512)	52.4	5 years	135 80	20 fatal and 75 nonfatal CV events	9.4, Sphygmocor	>10 m/s (upper tertile)
Verbeke et al. (2011), France, CORD[101]	Prevalent dialysis patients (n = 1084)	62	2 years (median)	147 79	234 deaths and 91 nonfatal CV events	10.2, Sphygmocor	>12 m/s (upper tertile)
Vlachopoulos et al. (2014), Greece[102]	Erectile dysfunction (n = 383)	56	4.7 ± 1.9 years	137(19) 85(10)	24 major adverse cardiac events	8.3, Complior	>8.8 m/s (upper tertile)
Vongsanim et al. (2021), Thailand[103]	Hemodialysis patients (n = 383)	67.7 (median)	61.1 months	146.6 (27.5) DBP:N.a.	229 deaths	8.9 (median), Arteriograph	Per 1 m/s and >10 m/s
Wadström et al. (2019), Sweden, Malmö Diet Cancer study[104]	General population (n = 2718)	72 (median)	6.05 years (mean)	136(17) 76(9)	269 major adverse CV events	8.6 (median), Sphygmocor	>8.6 m/s (median)

TABLE 33.1 Overview of studies on the association between aortic pulse wave velocity and clinical events with at least 300 subjects.—cont'd

Author, year, country/study name	Population-sample size	Age (years)	Follow-up duration	Systolic blood pressure and diastolic blood pressure in mmHg (mean, standard deviation)	Events	Aortic pulse wave velocity in m/s (mean, standard deviation), measurement method	Aortic pulse wave velocity cut-off (high vs. low)
Wang et al. (2010), Taiwan[37]	General population (n = 1272)	52 ± 13	15 years	139(23) DBP:N.a.	225 deaths, 64 CV deaths	9.5 ± 2.3 (men) and 9.5 ± 2.5 (women), Doppler	2.3 m/s increase (men); 2.5 m/s increase (women)
Weir-McCall et al. (2018), United Kingdom, CaPS[105]	General population (n = 825)	72.3 ± 3.9	8.5 years (median)	141.4(19.4) 74.2(11.2)	154 major adverse CV events (79 fatal)	11.6 ± 2.9, SphygmoCor	Per 1 SD
Wijkman et al. (2016), Sweden, CARDIPP[106]	Type 2 DM (n = 627)	60.5 (58.0−63.0)	7.9 years (median)	138(15) 81(10)	45 CV events	10.4 (9.0−11.5), SphygmoCor	≥10.8 m/s (upper tertile) and per 1 m/s
Willum-Hansen et al. (2006), Denmark[107]	General population (n = 1678)	40−70 years	9.4 years	130(18) 81(10)	62 CV deaths, 154 CV events	11.3 ± 3.4, Piezoelectric pressure transducers	>13.1 m/s (upper quintile)
Zhang et al. (2013), France, PROTEGER[108]	Elderly patients (n = 331)	87 ± 7	378 days	136.2(20.5) DBP:N.a.	117 deaths	14.4 ± 3.6, Complior	Per 1 m/s
Zuo et al. (2018), China[109]	Hypertensive patients (n = 675)	61 ± 9	25 ± 4 months	141(20) 81(12)	59 total events and 4 all-cause deaths (47 CV events or CV deaths)	12.7 ± 3.1, Complior SP	Per 1 SD (3 m/s)

BLSA, Baltimore Longitudinal Study of Aging; *CAD,* coronary artery disease; *CKD,* chronic kidney disease; *CV,* cardiovascular; *DBP,* diastolic blood pressure; *DM,* diabetes mellitus; *EF,* ejection fraction; *ESRD,* end-stage renal disease; *HF,* heart failure; *MI,* myocardial infarction; *N.a.,* not available; *PWV,* pulse wave velocity; *ROC,* receiver-operator characteristic; *SBP,* systolic blood pressure; *SD,* standard deviation; *Unpub.,* unpublished.

Number of subjects investigated in studies on the prognostic role of aortic pulse wave velocity around the world
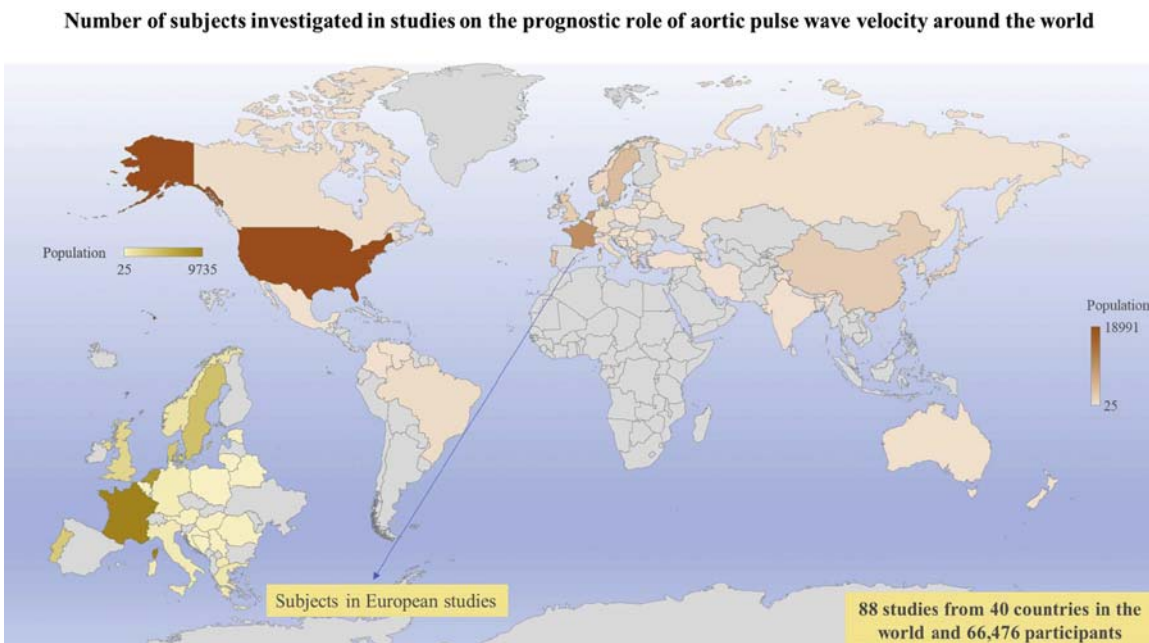
FIGURE 33.2 Distribution and number of subjects investigating the prognostic role of pulse wave velocity worldwide up until the end of 2019.
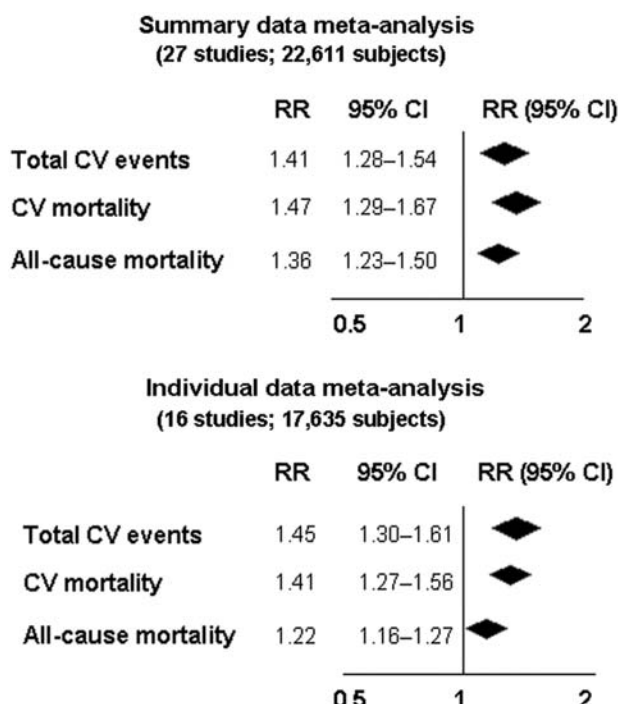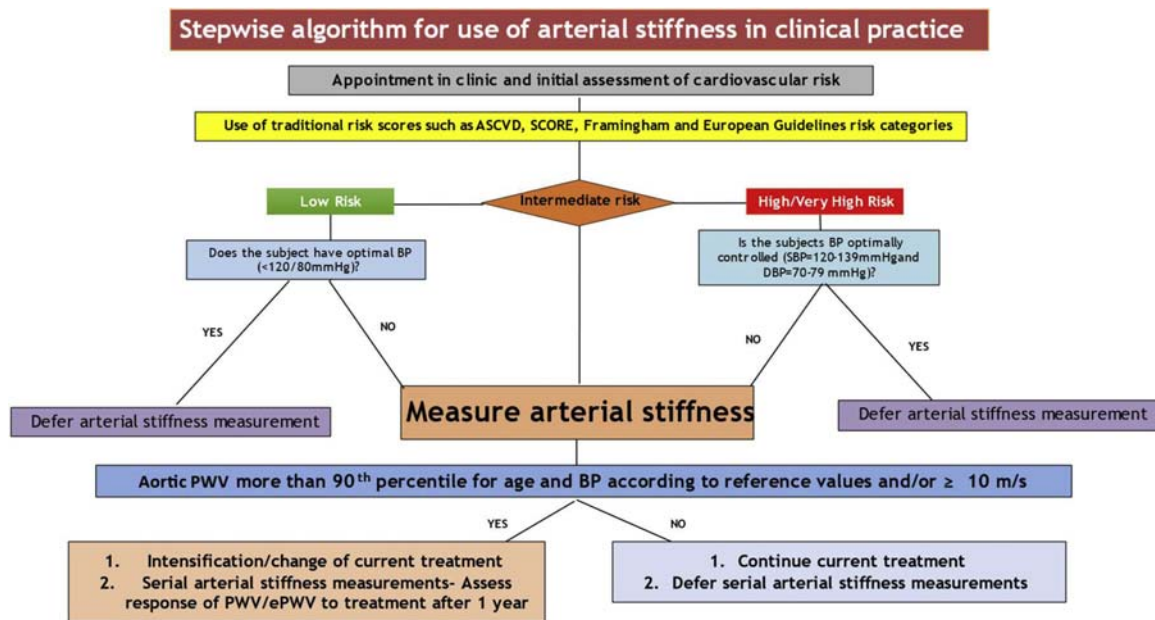
FIGURE 33.3 Relative risks (RRs) and 95% confidence intervals (CIs) for a 1-SD increase in aortic pulse wave velocity (aPWV) and total cardiovascular (CV) events, CV mortality, and all-cause mortality according to summary data meta-analysis. *Modified from Vlachopoulos, et al. J Am Coll Cardiol. 2014.*

coronary artery disease patients, and subsequently, to the general population. As PWV is a measure of arteriosclerosis, the use of subjects prone to these pathological entities (ESRD, hypertension, and diabetes) was the appropriate first step. Interestingly though, PWV provided evidence of its predictive role in other populations as well, including patients with heart failure, acute coronary syndromes, or inflammatory diseases, thus providing a useful tool for risk stratification in other disease states. In a diagnostic arena overflown with diagnostic modalities, the real conundrum from all these data is which one of these populations would benefit the most from having PWV as an addition risk stratification tool. It appears that individuals who would benefit the most are, apart from patients with hypertension or renal insufficiency those who, according to office-based evaluation with available risk calculators (Framingham, European SCORE, Atherosclerotic CVD) belong to the intermediate risk category. Additionally, measurement of PWV could provide incremental prognostic information in individuals belonging to a low-risk category but with the presence of risk factors, such as family history of early onset of CVD, substantially elevated single risk factor, elevated estimates of arterial biomarkers, such as increased SAGE risk score (systolic BP, age, fasting glucose and estimated glomerular filtration rate [eGFR]), and estimated pulse wave velocity (ePWV), and novel risk factors (Fig. 33.4 and 33.5).

Cut-off: Unfortunately, studies have used different measurement techniques and cut-offs to identify subjects with increased arterial stiffness. The proposed cut-off by the European Society of Cardiology (ESC) Guidelines at 10 m/s is a rough estimate in order to provide clinicians with an easy to remember number.[9,10] However, is this solution supported by evidence and has it provided help

FIGURE 33.4   Algorithmic approach of the use of measurement of pulse wave velocity in the clinical practice.

FIGURE 33.5   SAGE score chart according to the four constituents of the score. Combinations of risk factors resulting in a SAGE score equal or higher than eight are marked in orange color and indicate a high probability of elevated arterial stiffness (PWV>10 m/s). Combinations or risk factors resulting in a SAGE score of less than eight are marked in green and indicate a low probability of elevated arterial stiffness. *Modified from Xaplanteris, et al. J Hypert. 2019.*

into the introduction of PWV into clinical practice? In the studies, cut-offs range usually from 8 to 13 m/s, while even the individual data meta-analysis of many of these studies[6] did not provide any cut-off confirming the difficulties and

oversimplification of such an approach. A more elaborate method has been recently proposed with the introduction of EVA and the use of an estimation of vascular age based on PWV and its comparison to the true age of each

participant.[11] This approach seems more suitable as it incorporates the effects of age, BP, and treatment in the identification of patients at high CV risk, but is hampered by the more cumbersome estimation process. It seems reasonable that a cut-off based on the PWV reference values for certain age, BP, and treatment might be the best solution, but this remains to be proven in future studies.

Endpoints: The fact that arterial stiffness is predictive of CV events is largely expected since it is pathophysiologically important for both arterial and overall CV performance. PWV is a BP-dependent biomarker and thus has a strong correlation with endpoints, such as stroke and other cardiovascular events (including heart failure). Interestingly though, arterial stiffness is predictive also for all-cause mortality, with 45%−50% of deaths attributed to noncardiac causes. This important finding should be emphasized and further scrutinized. Although pathophysiological explanations are not readily identifiable, this could reflect the existence of common pathogenetic mechanisms, such as aging, inflammation, and oxidative stress, over a wide range of conditions.

Effect of BP/antihypertensive treatment: When gauging cardiovascular risk with PWV, it is essential to take into account the BP and whether patient is on antihypertensive treatment. One cut-off value does not fit all, and this is especially important in patients with optimal BP levels, or hypertensives with well-controlled BP with antihypertensive treatment. This has not been properly addressed in the prospective studies but data from ePWV showed that the predictive value of ePWV equal or more than 10 m/s was significantly higher in untreated rather than treated patients in the Paris cohort.[12] Also, from a post hoc analysis of the Systolic Blood Pressure Intervention Trial (SPRINT), intensive treatment was superior to standard treatment only when it was accompanied with a response in ePWV at the first year, while, within the standard group, those with an ePWV response had improved all-cause mortality.[13]

Inclusion in clinical recommendations and guidelines: Based on the available data to date, we believe that inclusion of arterial stiffness by guidelines on the disease prevention is justified. European recommendations have been rather favorable.[2,9,10] The current recommendation of the European Society of Hypertension/ESC hypertension guidelines is IIb (i.e., "may be used"). Accumulating evidence, increased clinical integration, and awaited data on PWV as a plausible treatment target (SPARTE trial [Stratégie de Prévention Cardiovasculaire Basée sur la Rigidité Arterielle])[14] may require reappraisal of level of recommendation in the near future.

Estimated PWV: When actual measurement of PWV is not feasible, additional approaches that could aid integration into clinical practice have been tested. One is based on the determination of reference values for carotid-femoral PWV: an estimated aortic PWV is derived by relevant equations that take into account age and BP. Despite its dependence on these two parameters, ePWV was shown to be predictive of future events and improved risk prediction over traditional risk scores.[12,13] The other strategy employs a simple clinical score (SAGE score) that predicts high aortic PWV values based on widely available clinical variables (systolic BP, age, glucose, and eGFR) and can prioritize actual measurement of aortic PWV in those with high score.[15] Both approaches can ultimately result in greater evidence accumulation and appreciation of the clinical role of aortic stiffness.
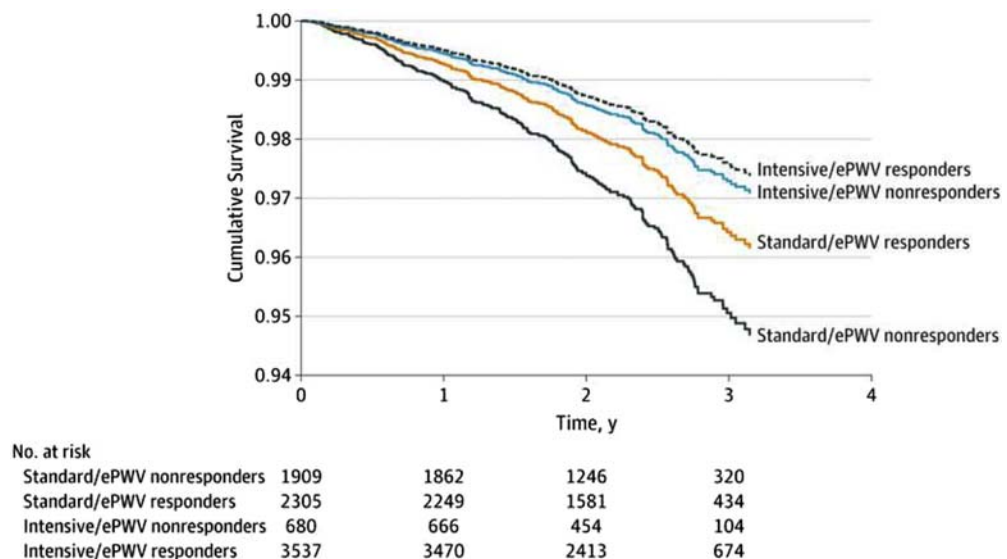
Association with intermediate endpoints: Apart for the (preferred) hard endpoints, arterial stiffness has been associated with intermediate ones. In patients with essential hypertension, indexes of large-artery stiffness indicate the presence and extent of atherosclerotic disease and correlate with CV risk estimates as assessed by the Framingham risk score.[16] Aortic PWV is associated with left ventricular (LV) hypertrophy,[17] while it is an independent marker of cognitive impairment,[18] cerebral blood flow, and cerebrovascular reactivity[19] and correlates with silent small vessel cerebral disease.[20] Furthermore, carotid-femoral PWV is an independent predictor of coronary flow reserve[21] and renal function, as assessed by eGFR[22] and microalbuminuria.[23]

Arterial stiffness as a therapeutic target: From the therapeutic standpoint, aortic stiffness appears as a worthwhile treatment target. However, to date, there is only one study in patients with ESRD showing that improvement in outcome was mediated through an improvement in aortic stiffness.[24] Despite the similar reduction in pressure, only survivors experienced a reduction in aortic stiffness, whereas nonsurvivors exhibited an increase in PWV. Interestingly, in a hypothesis-generating study, we showed in a post hoc analysis from data of the SPRINT trial that patients in the standard treatment arm that had an effective ePWV reduction at 1 year had an improved survival independently of the reduction in systolic BP (Fig. 33.6).[13] Undoubtedly, more studies are needed and soon-to-revealed studies, such as the SPARTE study, will further clarify the role of PWV as a therapeutic target.[14]

Additional indices of arterial stiffness: It should be stressed that results supporting the role of arterial stiffness as an appealing biomarker are at this stage valid for aortic PWV (an index of regional arterial stiffness) only and are not necessarily expandable to indices of local arterial stiffness (aortic, carotid, and femoral) or systemic arterial stiffness. Regarding other indices of regional arterial stiffness, carotid-radial PWV is unlikely to have predictive value,[25] while data are accumulating on local stiffness parameters, such as carotid and femoral[26]; for these, reference values are now available.[27,28]

Accumulating evidence on brachial-ankle PWV (baPWV) appear convincing. baPWV capitalizes on the assumption that it evaluates a large part of the arterial pathway. It has shown an independent and incremental predictive role for future events[29−31] and a considerable number of patients (up to 25%) can be reclassified as an individual-data meta-analysis showed that also can predict

FIGURE 33.6 Combined effect of treatment allocation and response of estimated pulse wave velocity (ePWV) to treatment on all-cause death. *Modified from Vlachopoulos C, Terentes-Printzios D, Laurent S, et al. Association of estimated pulse wave velocity with survival: a secondary analysis of SPRINT. JAMA Netw Open. 2019;2:e1912831.*

the incidence of hypertension and ESRD. Subjects with values over 18 m/s are considered of high risk, whereas it has been suggested that subjects <60 years with values over 14 m/s should be counseled toward lifestyle modification.[32]

Central pressure and wave reflection indices

Central pressure waveforms, either directly measured, or estimated noninvasively from peripheral pressure waveforms have resurged into the forefront of research of hypertension in the last three decades as many devices have incorporated them in their measurement. Apart from the classic values of central systolic, diastolic, and pulse pressures, measurement of the central pressure waveform can provide clinically useful information beyond BP measured in the brachial artery, such as the quantification of wave reflections with aortic augmentation index (AIx) and pulse pressure amplification. Please refer to Chapters 2, 3 and 11 for a more extensive discussion of wave reflections and its impact on the pressure waveform. In this Chapter we will mainly focus on the central pressures and wave reflections as assessed by the aortic AIx and not to other waveform related indices such as reflection magnitude and backward wave amplitude.

Predictive value: Central (aortic and carotid) pressures are pathophysiologically more relevant than peripheral pressures for the pathogenesis of cardiovascular disease[33,34] and according to accumulating clinical evidence, this could be translated into a significant predictive role for future cardiovascular events. While several studies have shown an ability of central pressures and indices to predict future events, findings have not always been consistent (Table 33.2). We[35] meta-analyzed 11 longitudinal studies that had employed measures of central hemodynamics and had followed 5648 subjects for a mean follow-up of 45 months. The age- and risk factor−adjusted pooled relative risk (RR) of total CV events was 1.14 (95% CI 1.06−1.22) for a 10 mmHg increase of central pulse pressure. Furthermore, a 10% increase of central AIx was associated with an RR of 1.38 (95% CI 1.19−1.61) for all-cause mortality. When three more studies[36-38] that were published after the respective meta-analysis were included (a total of 9093 subjects and mean follow-up of 54.9 months), the RRs of total CV events were 1.12 (95% CI 1.03−1.21) for a 10 mmHg increase of central pulse pressure, and 1.30 (95% CI 1.10−1.55) for a 10% absolute increase of central AIx. Furthermore, a 10% increase of central AIx was associated with an RR of 1.33 (95% CI 1.17−1.51) for all-cause mortality.

As with arterial stiffness, taking a closer look at the studies, it is easy to observe a large degree of heterogeneity in several aspects of study design, methodology, and endpoints. So, there is a need to provide answers to specific questions based on the available prospective data:

1. How was central waveform derived?
2. How closely related were the central pressures to peripheral pressures and was central pressure's predictive ability independent of peripheral pressures?
3. In which populations were central pressures predictive of future events?
4. Which cut-off should be used to identify patients at high risk?

TABLE 33.2 Overview of large studies (more than 100 subjects) up to 2021 on the association between measured central pressures and clinical endpoints.

Author, year	Population-sample size	Age (years)	Follow-up duration (longitudinal studies)	Index	Events	Central indices versus peripheral blood pressures[a]
Safar et al. (2002)[110,111]	ESRD (n = 180)	54 ± 16	52 ± 36 months	Carotid SBP, PP, PPA	Deaths and CV deaths	Central better
Chirinos et al. (2005)	CAD or nonobstructive coronary atherosclerosis (n = 297)	63.8 ± 10.3	40 ± 14 months	Aortic PP, AP, AIx	Deaths and CV events	Central better
Weber et al. (2005)[53]	CAD/angioplasty (n = 262)	65 ± 10	24 months	AIx@75	Deaths and CV events	Central better
Williams et al. (2006)[53]	Hypertensives (n = 2199)	62.8 ± 8.2	Up to 4 years	Central SBP, PP, AIx, PPA	CV events and procedures plus renal impairment	Similar
Dart et al. (2006)[112]	Elderly female hypertensives (n = 484)	72 ± 5	49 months (median)	Carotid SBP, PP, AIx	CV events	Peripheral better
Roman et al. (2007)[113]	American Indians free of CVD (n = 2403)	63.5 ± 7.5	58 ± 16 months	Aortic SBP, PP	Deaths, CV deaths, and CV events	Central better
Jankowski et al. (2008)[114]	Subjects undergoing nonemergency coronary angiography (n = 1109)	52.7 ± 19.2	52.7 ± 19.2 months	Aortic PP	Deaths, CV deaths, and CV events	Central better
Pini et al. (2008)[115]	Community-dwelling individuals 65 years (n = 398)	73 ± 6	94 ± 24 months	Aortic SBP, PP, AIx	Deaths, CV deaths, and CV events	Central better
Mitchell et al. (2010)[36]	General population (n = 2232)	63 ± 12	7.8 years	Carotid AIx, PPA, carotid PP	CV events	Central indices not anymore significant when adjusted for RFs
Wang et al. (2010)[37]	General population (n = 1272)	52 ± 13	15 years	Carotid SBP, PP, AP, AIx, RWTT, RI, Pi, Pf, and Pb	Deaths, CV deaths	Central better
Weber et al. (2010)[38]	Males undergoing coronary angiography (n = 520)	64.0 (54−71.5)	49 months	Aortic AIx, Aix@75, pulse wave transit time	Deaths and CV events	Central better
Manisty et al. (2010)[116]	Hypertensives (n = 259)	63.9 ± 7.4	5.9 years	Log WRI (wave reflection index), carotid SBP, PP, AIx, Pb/Pf	CV events	Only WRI and carotid PP (not in multivariable model) were significant
Huang et al. (2011)[117]	Normotensives or untreated hypertensives (n = 1014)	52 ± 13	15 years	Central SBP, PP	Deaths, CV deaths	Central better
Verbeke et al. (2011)[100]	Renal transplant recipients (n = 512)	52.4	5 years	Central SBP, PP, AP, Aix	Fatal and nonfatal CV events	Central better
Benetos et al. (2012)[63]	Elderly (n = 1126)	88 ± 5	2 years	PPA	Deaths and major CV events	PPA better than peripheral

TABLE 33.2 Overview of large studies (more than 100 subjects) up to 2021 on the association between measured central pressures and clinical endpoints.—cont'd

Author, year	Population-sample size	Age (years)	Follow-up duration (longitudinal studies)	Index	Events	Central indices versus peripheral blood pressures[a]
Weber et al. (2012)[118]	Subjects undergoing coronary angiography (n = 725)	64	1399 days	Central SBP, PP, AP, AIx, AIx@75, RM, Pb, Pf, RI	CV events	Central better
Karras et al. (2012)[76]	Patients with CKD (n = 439)	59.8 ± 14.5	4.67 years	Carotid PP	Deaths and fatal or nonfatal CV events	Peripheral better
Sung et al. (2012)[119]	Acute HF (n = 120)	72 ± 14	601 days (median)	Carotid SBP, PP AP, AIx, AIx@75, Pf, Pb	66 adverse CV events	Central better
Ishisone et al. 2013[120]	General population (n = 973)	59	7.8 years	Central SBP	All-cause deaths, CV events	Central BP not significant
Janner et al. (2013)[121]	General population (n = 3073)	58	6.5 years	AIx, central SBP, PP	All-cause deaths, CV events	Central BPs not adjusted for peripheral BPs
Cheng et al. (2013)[122]	General population (n = 2501)	53.6 ± 12.0	10 years	Central SBP, PP	All-cause deaths, CV deaths, stroke deaths	Central better
Huang et al. (2013)[123]	Patients for elective PCI (n = 448)	70 ± 12	41.8 ± 15.4 months	Central PP	CV events, death	Central BPs not adjusted for peripheral BPs
Zhang et al. (2013)[108]	Elderly patients (n = 331)	87 ± 7	378 days	Central SBP, PP, PPA	Deaths	Nonsignificant
Chirinos et al. (2014)[43]	Subjects free of HF (n = 2602)	59.9 ± 11.1	3.5 years	Central SBP, PP, AIx, AIx@75	First hospital admissions for HF	Peripheral better
Holewijn et al. (2014)[74]	General population (n = 1367)	46.33 ± 13.76	3.8 years	Central SBP, AP, Aix	CV events	Not anymore significant when adjusted for risk factors, except from CAP in men
Kals et al. (2014)[124]	Symptomatic peripheral arterial disease (n = 117)	62	4.1 ± 2.2 years	Central SBP, PP, AP, AIx, AIx@75, PPA	Fatal events	Peripheral better
Theilade et al. (2014)[125]	Type 1 DM patients (n = 636)	54 ± 13	2.8 years (median)	Central SBP, PP, SEVR	Deaths or ESRD	Only SEVR was significant
Fortier et al. (2015)[71]	Patients on dialysis (n = 310)	67 (56−76)	29 months	Central SBP, PP, AIx, AIx@75, Pf, Pb, RM, SEVR	Deaths	Similar
Narayan et al. (2015)[126]	Elderly hypertensives (n = 838)	72	49 months (median)	Carotid SBP, PP, AIx, PPA, reservoir wave parameters	Fatal and nonfatal stroke and MI	Peripheral better

Wassertheurer et al. (2015)[127]	CKD stages 2−4 (*n* = 159)	59.9 ± 15.2	42 months	Aortic SBP	Deaths	Central better
Chuang et al. (2016)[128]	General population (*n* = 2033)	56	9.81 years	Central SBP	Strokes	Not adjusted for peripheral BPs
Laugesen et al. (2016)[129]	Subjects undergoing coronary angiography (*n* = 21,908)	63	3.7 years (median)	Aortic SBP	Stroke, MI, and deaths	Peripheral better
Mitchell et al. (2016)[130]	General population (*n* = 2183)	63 ± 12	7.4 years (median)	Central SBP, PP, AIx, PPA	CV events	Nonsignificant in multivariable models
Sun et al. (2016)[131]	Subjects undergoing coronary angiography (*n* = 325)	55 ± 12	2 years	Aortic PP, AIx@75	Adverse CV events	Peripheral better, AIx@75 significant
Chen et al. (2017)[132]	Subjects undergoing coronary angiography (*n* = 334)	63.1 ± 10.3	3 years	Aortic PP	CV events	Central better
Sarafidis et al. (2017)[133]	Hemodialysis patients (*n* = 170)	63.76 ± 14.32	28.1 ± 11.2 months	48h ambulatory central SBP, PP, AIx@75	Deaths and CV events	Central PP better
Vlachopoulos et al. (2017)[134]	Erectile dysfunction (*n* = 398)	56	6.5 years	Aortic SBP, PP, AIx	Major adverse cardiac events	Central better, no adjustment for peripheral BPs
Cremer et al. (2018)[135]	Hypertensives (*n* = 703)	51.5 ± 13.6	112.5 ± 70 months	24h central PP, PPA, amplification	CV events	Central better
Eguchi et al. (2018)[136]	Treated hypertensives (*n* = 3566)	66.0 ± 10.9	5 years (median)	SBP2, PP2 (estimates of central pressures)	CV events	Central better
Guajardo et al. (2018)[137]	ESRD (*n* = 131)	56 ± 13 (overall)	420 days (median)	Central SBP, PP, AIx@75	Events (deaths, CV hospitalizations)	Nonsignificant
Nair et al. (2018)[138]	ESRD (*n* = 623)	56.7 ± 8.9	6 months	Central SBP, PP, PPA	CV events and death	Not adjusted for peripheral BPs
Rahman et al. (2018)[139]	CKD (*n* = 2875)	60	5.5 years	Central SBP, PP, AIx, AIx@75, PPA	CV events and all-cause deaths	Peripheral better
Sluyter et al. (2018)[140]	General population in randomized study (*n* = 3566)	66	4.6 years (median)	Central BP variability parameters	CV events	Central better
Zuo et al. (2018)[109]	Treated hypertensives (*n* = 675)	61 ± 9	25 ± 4 months	Central SBP, PP, AP, AIx, AIx@75, PPA	CV events	Central better
Ryliškytė et al. (2019)[91]	Middle-aged MetS subjects without overt CVD (*n* = 2728)	53.9 ± 6.2	3.9 ± 1.7 years	AIx@75	CV events	AIx@75 significant
Vasan et al. (2019)[98]	General population (*n* = 5803)	49 ± 15	10.3 years (median)	Central PP, MAP	CV events	Central PP significant not adjusted for peripheral BPs

TABLE 33.2 Overview of large studies (more than 100 subjects) up to 2021 on the association between measured central pressures and clinical endpoints.—cont'd

Author, year	Population-sample size	Age (years)	Follow-up duration (longitudinal studies)	Index	Events	Central indices versus peripheral blood pressures[a]
Ndrepepa et al. (2019)[141]	Patients with STEMI (n = 1384)	62.5 ± 12.1	6.1 years (median)	Invasive central PP	All-cause mortality	U-shaped association between central PP and the risk of mortality (attenuated after adjustment)
Mukai et al. (2019)[142]	Patients with CKD stage 5 (n = 261)	56 (median)	25 months (median)	AIx	CV and all-cause mortality	AIx significant
Wu et al. (2020)[143]	Hypertensives undergoing percutaneous intervention (n = 1184)	66	228 weeks	Invasive aortic PP	CV events	Not adjusted for peripheral BPs
Tynjälä et al. (2020)[144]	Type 1 DM (n = 906)	54 ± 13	8.2 years (median)	AIx, central pressures	Cardiovascular and/or diabetes-related mortality	Central pressures and AIx significant, no adjustment for peripheral BPs
Huang et al. (2020)[145]	General population (n = 5608)	54.2	4.1 years (median)	Central PP, SBP	CV events	Central PP/SBP not significant after adjustment for peripheral BPs
Dong et al. (2020)[146]	General population (n = 8710)	50.1 (mean)	6.36 years (median)	Central SBP/PP	CV events	Central pressures better than peripheral BPs but no adjustment
Scandale et al. (2020)[92]	Screening of peripheral arterial disease (n = 398)	68 ± 9	5.4 years	AIx@75	All-cause mortality	Not significant
Lamarche et al. (2021)[147]	Participants of CARTaGENE without CVD or antihypertensive medication (n = 13,461)	52	8.75 years (median)	Central SBP	Major CV events	Central SBP significant after adjustment for peripheral BPs

AIx, augmentation index; *AIx@75*, augmentation index corrected for a heart rate of 75 bpm.; *AP*, augmented pressure; *BP*, blood pressure; *CAD*, coronary artery disease; *CKD*, chronic kidney disease; *CVD*, cardiovascular disease; *DM*, diabetes mellitus; *ESRD*, end-stage renal disease; *FU*, follow-up; *HF*, heart failure; *MI*, myocardial infarction; *Pb*, backward pressure amplitude; *PCI*, percutaneous coronary intervention; *Pf*, forward pressure amplitude; *Pi*, incident pressure wave height; *PP*, pulse pressure; *PPA*, pulse pressure amplification (brachial-carotid); *RF*, risk factors; *RI*, reflection index; *RM*, reflection magnitude; *RWTT*, reflected wave transit time; *SBP*, systolic blood pressure; *SEVR*, subendocardial viability ratio.
[a]"better" denotes numerically larger RR, not necessarily tested in a statistically adjusted statistical test.

Measurement/estimation of central pressure waveform/central pressures: The techniques of assessing central hemodynamic indices include invasive measurements (considered to be the gold-standard), tonometry (the most popular noninvasive technique), oscillometry (either single- or two-sites), imaging techniques (including echocardiography), photoplethysmography, and finally use of estimated values of central pressures (derived mainly by equations, and more recently, by machine learning techniques).[34] Based on the review of the current literature, the large body of evidence stems from tonometry measurements and thus this technique could the first choice for use in clinical practice, despite its inherent technical limitations (use of peripheral pressures measured in other arterial segments to derive the central pressure waveform through a transfer function). All approaches have their advantages and disadvantages. Some are limited by methodological shortcomings. Unquestionably, all should be rigorously and carefully validated with a standardized method before commercialization.[39] Central pressures may be more easily adopted by the clinician compared to calculated indices, such as AIx and pulse pressure amplification, but, on the other hand, they may be more prone to error since they rely on the (in)accuracy of the cuff measurement.[40] The development of 24-h measurement of central BP is appealing. It remains to be investigated whether the 24-h values have better predictive ability for future events and target organ damage than single measurements of central BPs or peripheral BPs[41] as already has been shown for 24-h ambulatory peripheral BPs compared to single office BPs. For a more extensive discussion of ambulatory measurement of central aortic pressures and pulsatile hemodynamics, the reader is referred to Chapter 8.

Correlation of central pressures and peripheral pressures: A crucial issue to be addressed is whether central indices have a predictive ability over and above peripheral pressures. This can be difficult since central pressures are usually derived by peripheral pressures, and their correlation is extremely high (correlation coefficient of approximately 0.9). Despite this strong correlation between them, it seems that when central pressures are measured properly,[39] they can be at least as good or even better than peripheral pressures. According to our meta-analysis, AIx has a predictive value independent of peripheral pressures, whereas central pulse pressure has a marginally better predictive value compared to peripheral BP ($P = .057$). This marginal but existent superiority of central BPs was supported by a recent large individual-data meta-analysis in 22,433 subjects from 15 studies,[42] where although the predictive ability for MI was similar for central and peripheral systolic BP, there was a statistically significant superiority of central BP compared to peripheral BP for the prediction of stroke, especially in subjects below 61 years. However, it must be acknowledged that so far there are no

published data of an improved reclassification with the use of central BP with the inclusion of peripheral BP in the model.

Study populations: The majority of the studies have been conducted in hypertensive subjects and patients with renal dysfunction. Further, as wave reflection indices have been strongly correlated with atherosclerosis and inflammation, studies on patients on high underlying risk have also been conducted. Finally, the pathophysiological close relationship of the central pressure waveform with heart failure makes it a very attractive biomarker both for the prediction of incident HF,[43,44] as well as for predicting events in patients with HF. Undoubtedly, there is room for further refinement since the degree of pressure amplification toward the periphery is variable, depending on several factors including age, gender, and heart rate. Further, an extension of predictive ability over and above brachial BP in a wider range of populations and disease states is mandatory. Lastly, it should be noted that evidence for a specific central pressure component or index does not necessarily apply to the others.

Cut-off: The publication of reference values has been a facilitation for the implementation of central BPs in clinical practice.[45] Unfortunately, studies have used different measurement techniques and cut-offs (when used) to identify subjects with increased central pressures. Guidelines have not adopted any single cut-off for central pressures, but it has been proposed by several studies that a value of 130/90 mmHg might be the ideal cut-off for prediction of events.[46]

Association with intermediate endpoints: In a recent meta-analysis, central BP was shown to be slightly, but consistently superior to the peripheral BP in predicting end-organ damage, such as carotid intima-media thickness, PWV and LV mass index, except for albuminuria.[47] Increased aortic AIx is associated with coronary artery disease.[48] In fact, in young patients with suspected coronary artery disease, increased wave reflections can discriminate patients with coronary artery disease from those without. The late systolic augmentation of the central pressure waveform is associated with an increase in LV mass index independent of age and mean BP,[49] and carotid systolic pressure is an independent determinant of LV wall thickness.[50] Moreover, central pressure is also more closely related to other important cardiovascular intermediate endpoints, such as vascular hypertrophy, the extent of carotid atherosclerosis.[51] Higher carotid pressure augmentation in older individuals has been linked to increased flow pulsations entering the cerebral circulation, which may increase the risk of cerebral microvascular damage.[52]

Central pressures as a therapeutic target: Despite similar effects on brachial pressure, antihypertensive drugs have differential effects on central pressure, and this may explain the superiority of arterial vasodilating drugs in

outcome trials. In the Conduit Artery Function Evaluation study, a substudy of the Anglo-Scandinavian Cardiac Outcomes Trial, a higher treatment-related decrease of central pulse pressure, that was not evident in brachial pressure measurements, was independently associated with clinical benefit and reduced cardiovascular events.[53] Other studies have also shown that endpoints related to organ damage can be predicted by indices of central hemodynamics after therapy. Aortic and radial AIx, as well as amplification of the pulse between central and radial arteries, were superior to conventional cuff measures in predicting a reduction in LV mass during antihypertensive therapy.[54] Furthermore, the reduction in carotid wall diameter and hypertrophy with antihypertensive treatment was related to carotid pulse pressure, but not to mean BP.[55] The pREterax in regression of Arterial Stiffness in a contrOlled double-bliNd (REASON) trial, which compared a perindopril/indapamide combination against atenolol, showed that normalization of brachial systolic BP is achieved with a significantly greater reduction of carotid systolic BP after a 12-month treatment with the combination.[56] In this study, compared with atenolol, the perindopril/indapamide combination was associated with a greater fall in LV mass, and this was related to carotid but not brachial BP.[57]

Whether central pressures can provide superior results compared to peripheral BP should they were the guide of therapy instead of the latter[2] awaits confirmation. In this direction, in two recent small studies in which central BP in hypertensives[58] and AIx in heart failure[59] were used as therapeutic targets there were modest but clinically apparent benefits for the patients. Specifically, in the first case measurement of central pressures led to decrease in the number of antihypertensive medications used, as well as to a marginal improvement in reduction of LV mass; in the second case, there was a slight improvement in exercise capacity.

Conclusions/future perspectives

Both cfPWV and central pressures have convincingly shown their ability to predict future cardiovascular events and could provide crucial prognostic information especially in younger individuals at intermediate risk and with borderline office or 24h BP values.[60] Measurement of cfPWV seems to be able to integrate the long-term deleterious effects of various cardiovascular risk factors[1] and principally of increased BP, overcoming the inherent shortcomings of BP detection that stem from its large variability even in 24 h readings. Also, cfPWV provides an easily accessible window toward the possible hypertension-related target organ damage. Contrary to central pressures that need to prove their worth beyond the closely to them correlated peripheral BPs, cfPWV has no other major competitors that can describe better the vascular damage caused by risk factors and aging.

However, the journey toward clinical implementation and larger adaptation from guidelines is still long and full of challenges. First, ongoing and future large randomized controlled studies need to confirm the clinical utility of cfPWV in decision-making by providing robust evidence of its ability to guide therapy and improve prognosis. Second, this should be done in a relatively simple and cost-effective manner so that the regulatory authorities will give the green light for its further clinical implementation by providing reimbursement for its measurement. Finally, what seems reasonable but still remains to be seen is that the experts in the field should provide a clear and collective proposal to the nonexperts on the field that would clearly state what physicians should measure and how in order to avoid confusion and alienation from the biomarker. It seems that such a coalition is feasible and based on the promising results on cfPWV the above-mentioned scenario seems to be closer than ever.

References

1. Terentes-Printzios D, Vlachopoulos C, Xaplanteris P, et al. Cardiovascular risk factors accelerate progression of vascular aging in the general population: results from the CRAVE study (cardiovascular risk factors affecting vascular age). **Hypertension**. 2017; 70:1057−1064.
2. Vlachopoulos C, Xaplanteris P, Aboyans V, et al. The role of vascular biomarkers for primary and secondary prevention. A position paper from the European Society of Cardiology Working Group on peripheral circulation: endorsed by the Association for Research into Arterial Structure and Physiology (Artery) Society. **Atherosclerosis**. 2015; 241:507−532.
3. Townsend RR, Wilkinson IB, Schiffrin EL, et al. Recommendations for improving and standardizing vascular research on arterial stiffness: a scientific statement from the American heart association. **Hypertension**. 2015; 66:698−722.
4. Hlatky MA, Greenland P, Arnett DK, et al. American Heart Association expert panel on subclinical atherosclerotic D, emerging risk F and the stroke C. Criteria for evaluation of novel markers of cardiovascular risk: a scientific statement from the American Heart Association. **Circulation**. 2009; 119:2408−2416.
5. Vlachopoulos C, Aznaouridis K, Stefanadis C. Prediction of cardiovascular events and all-cause mortality with arterial stiffness: a systematic review and meta-analysis. **J Am Coll Cardiol**. 2010; 55:1318−1327.
6. Ben-Shlomo Y, Spears M, Boustred C, et al. Aortic pulse wave velocity improves cardiovascular event prediction: an individual participant meta-analysis of prospective observational data from 17,635 subjects. **J Am Coll Cardiol**. 2014; 63:636−646.
7. Vlachopoulos C, Aznaouridis K, Stefanadis C. Aortic stiffness for cardiovascular risk prediction: just measure it, just do it!. **J Am Coll Cardiol**. 2014; 63:647−649.
8. Hametner B, Wassertheurer S, Mayer CC, Danninger K, Binder RK, Weber T. Aortic pulse wave velocity predicts cardiovascular events and mortality in patients undergoing coronary angiography: a comparison of invasive measurements and noninvasive estimates. **Hypertension**. 2021; 77:571−581.

9. Mancia G, Fagard R, Narkiewicz K, et al. 2013 ESH/ESC guidelines for the management of arterial hypertension: the task force for the management of arterial hypertension of the European Society of Hypertension (ESH) and of the European Society of Cardiology (ESC). **Eur Heart J**. 2013; 34:2159−2219.

10. Williams B, Mancia G, Spiering W, et al. 2018 ESC/ESH Guidelines for the management of arterial hypertension. **Eur Heart J**. 2018; 39:3021−3104.

11. Bruno RM, Nilsson PM, Engstrom G, et al. Early and supernormal vascular aging: clinical characteristics and association with incident cardiovascular events. **Hypertension**. 2020; 76:1616−1624.

12. Greve SV, Blicher MK, Kruger R, et al. Estimated carotid-femoral pulse wave velocity has similar predictive value as measured carotid-femoral pulse wave velocity. **J Hypertens**. 2016; 34:1279−1289.

13. Vlachopoulos C, Terentes-Printzios D, Laurent S, et al. Association of estimated pulse wave velocity with survival: a secondary analysis of SPRINT. **JAMA Netw Open**. 2019; 2:e1912831.

14. Stephane L, Gilles C, Michel A, et al. Protocol of the SPARTE study: a strategy for preventing cardiovascular and renal events based on ARTErial stiffness. **Artery Res**. 2020; 26:250−260.

15. Xaplanteris P, Vlachopoulos C, Protogerou AD, et al. A clinical score for prediction of elevated aortic stiffness. **J Hypertens**. 2019; 37:339−346.

16. Blacher J, Asmar R, Djane S, London GM, Safar ME. Aortic pulse wave velocity as a marker of cardiovascular risk in hypertensive patients. **Hypertension**. 1999; 33:1111−1117.

17. Toprak A, Reddy J, Chen W, Srinivasan S, Berenson G. Relation of pulse pressure and arterial stiffness to concentric left ventricular hypertrophy in young men (from the Bogalusa Heart Study). **Am J Cardiol**. 2009; 103:978−984.

18. van Sloten TT, Protogerou AD, Henry RM, Schram MT, Launer LJ, Stehouwer CD. Association between arterial stiffness, cerebral small vessel disease and cognitive impairment: a systematic review and meta-analysis. **Neurosci Biobehav Rev**. 2015; 53:121−130.

19. Jefferson AL, Cambronero FE, Liu D, et al. Higher aortic stiffness is related to lower cerebral blood flow and preserved cerebrovascular reactivity in older adults. **Circulation**. 2018; 138:1951−1962.

20. Henskens LH, Kroon AA, van Oostenbrugge RJ, et al. Increased aortic pulse wave velocity is associated with silent cerebral small-vessel disease in hypertensive patients. **Hypertension**. 2008; 52:1120−1126.

21. Nichols WW, Denardo SJ, Davidson JB, Huo T, Bairey Merz CN, Pepine CJ. Association of aortic stiffness and wave reflections with coronary flow reserve in women without obstructive coronary artery disease: an ancillary study from the National Heart, Lung, and Blood Institute-sponsored Women's Ischemia Syndrome Evaluation (WISE). **Am Heart J**. 2015; 170:1243−1254.

22. Schillaci G, Pirro M, Mannarino MR, et al. Relation between renal function within the normal range and central and peripheral arterial stiffness in hypertension. **Hypertension**. 2006; 48:616−621.

23. Mule G, Cottone S, Cusimano P, et al. The association of micro-albuminuria with aortic stiffness is independent of C-reactive protein in essential hypertension. **Am J Hypertens**. 2009; 22:1041−1047.

24. Guerin AP, Blacher J, Pannier B, Marchais SJ, Safar ME, London GM. Impact of aortic stiffness attenuation on survival of patients in end-stage renal failure. **Circulation**. 2001; 103:987−992.

25. Pannier B, Guerin AP, Marchais SJ, Safar ME, London GM. Stiffness of capacitive and conduit arteries: prognostic significance for end-stage renal disease patients. **Hypertension**. 2005; 45:592−596.

26. van Sloten TT, Schram MT, van den Hurk K, et al. Local stiffness of the carotid and femoral artery is associated with incident cardiovascular events and all-cause mortality: the Hoorn study. **J Am Coll Cardiol**. 2014; 63:1739−1747.

27. Bossuyt J, Engelen L, Ferreira I, et al. Van Bortel LM and Reference Values for Arterial Measurements C. Reference values for local arterial stiffness. Part B: femoral artery. **J Hypertens**. 2015; 33:1997−2009.

28. Engelen L, Bossuyt J, Ferreira I, et al. Boutouyrie P and Reference Values for Arterial Measurements C. Reference values for local arterial stiffness. Part A: carotid artery. **J Hypertens**. 2015; 33:1981−1996.

29. Vlachopoulos C, Aznaouridis K, Terentes-Printzios D, Ioakeimidis N, Stefanadis C. Prediction of cardiovascular events and all-cause mortality with brachial-ankle elasticity index: a systematic review and meta-analysis. **Hypertension**. 2012; 60:556−562.

30. Tomiyama H, Koji Y, Yambe M, et al. Brachial – ankle pulse wave velocity is a simple and independent predictor of prognosis in patients with acute coronary syndrome. **Circ J**. 2005; 69:815−822.

31. Ohkuma T, Ninomiya T, Tomiyama H, et al. Brachial-ankle pulse wave velocity and the risk prediction of cardiovascular disease: an individual participant data meta-analysis. **Hypertension**. 2017; 69:1045−1052.

32. Tomiyama H, Matsumoto C, Shiina K, Yamashina A. Brachial-ankle PWV: current status and future directions as a useful marker in the management of cardiovascular disease and/or cardiovascular risk factors. **J Atheroscler Thromb**. 2016; 23:128−146.

33. Agabiti-Rosei E, Mancia G, O'Rourke MF, et al. Central blood pressure measurements and antihypertensive therapy: a consensus document. **Hypertension**. 2007; 50:154−160.

34. McEniery CM, Cockcroft JR, Roman MJ, Franklin SS, Wilkinson IB. Central blood pressure: current evidence and clinical importance. **Eur Heart J**. 2014; 35:1719−1725.

35. Vlachopoulos C, Aznaouridis K, O'Rourke MF, Safar ME, Baou K, Stefanadis C. Prediction of cardiovascular events and all-cause mortality with central haemodynamics: a systematic review and meta-analysis. **Eur Heart J**. 2010; 31:1865−1871.

36. Mitchell GF, Hwang SJ, Vasan RS, et al. Arterial stiffness and cardiovascular events: the Framingham heart study. **Circulation**. 2010; 121:505−511.

37. Wang KL, Cheng HM, Sung SH, et al. Wave reflection and arterial stiffness in the prediction of 15-year all-cause and cardiovascular mortalities: a community-based study. **Hypertension**. 2010; 55:799−805.

38. Weber T. Arterial stiffness, wave reflections, and diabetes: a bidirectional relationship? **Am J Hypertens**. 2010; 23:1047−1048.

39. Sharman JE, Avolio AP, Baulmann J, et al. Validation of non-invasive central blood pressure devices: ARTERY Society task force consensus statement on protocol standardization. **Eur Heart J**. 2017; 38:2805−2812.

40. Picone DS, Schultz MG, Otahal P, et al. Accuracy of cuff-measured blood pressure: systematic reviews and meta-analyses. **J Am Coll Cardiol**. 2017; 70:572−586.

41. Argyris AA, Weber T, Protogerou AD. Aortic ambulatory blood pressure monitoring and target organ damage: are the data really conflicting? **Am J Hypertens**. 2018; 31:1260−1262.

42. McEniery C. **Central Blood Pressure and Cardiovascular Risk: An Individual Participant Meta-Analysis of Prospective Observational Data From 22,433 Subjects**. Vol. 65. 2015:A1464.

43. Chirinos JA, Khan A, Bansal N, et al. Arterial stiffness, central pressures, and incident hospitalized heart failure in the chronic renal insufficiency cohort study. **Circ Heart Fail**. 2014; 7:709−716.

44. Chirinos JA, Kips JG, Jacobs Jr DR, et al. Arterial wave reflections and incident cardiovascular events and heart failure: MESA (Multiethnic Study of Atherosclerosis). **J Am Coll Cardiol**. 2012; 60:2170−2177.

45. Herbert A, Cruickshank JK, Laurent S, Boutouyrie P, Reference Values for Arterial Measurements C. Establishing reference values for central blood pressure and its amplification in a general healthy population and according to cardiovascular risk factors. **Eur Heart J**. 2014; 35:3122−3133.

46. Cheng HM, Chuang SY, Sung SH, et al. Derivation and validation of diagnostic thresholds for central blood pressure measurements based on long-term cardiovascular risks. **J Am Coll Cardiol**. 2013; 62:1780−1787.

47. Kollias A, Lagou S, Zeniodi ME, Boubouchairopoulou N, Stergiou GS. Association of central versus brachial blood pressure with target-organ damage: systematic review and meta-analysis. **Hypertension**. 2016; 67:183−190.

48. Weber T, Auer J, O'Rourke MF, et al. Arterial stiffness, wave reflections, and the risk of coronary artery disease. **Circulation**. 2004; 109:184−189.

49. Hashimoto J, Imai Y, O'Rourke MF. Indices of pulse wave analysis are better predictors of left ventricular mass reduction than cuff pressure. **Am J Hypertens**. 2007; 20:378−384.

50. Roman MJ, Ganau A, Saba PS, Pini R, Pickering TG, Devereux RB. Impact of arterial stiffening on left ventricular structure. **Hypertension**. 2000; 36:489−494.

51. Boutouyrie P, Bussy C, Lacolley P, Girerd X, Laloux B, Laurent S. Association between local pulse pressure, mean blood pressure, and large-artery remodeling. **Circulation**. 1999; 100:1387−1393.

52. Hirata K, Yaginuma T, O'Rourke MF, Kawakami M. Age-related changes in carotid artery flow and pressure pulses: possible implications for cerebral microvascular disease. **Stroke**. 2006; 37:2552−2556.

53. Williams B, Lacy PS, Thom SM, et al. Investigators C, Anglo-Scandinavian Cardiac Outcomes Trial I, Committee CS and Writing C. Differential impact of blood pressure-lowering drugs on central aortic pressure and clinical outcomes: principal results of the Conduit Artery Function Evaluation (CAFE) study. **Circulation**. 2006; 113:1213−1225.

54. Hashimoto J, Imai Y, O'Rourke MF. Monitoring of antihypertensive therapy for reduction in left ventricular mass. **Am J Hypertens**. 2007; 20:1229−1233.

55. Boutouyrie P, Bussy C, Hayoz D, et al. Local pulse pressure and regression of arterial wall hypertrophy during long-term antihypertensive treatment. **Circulation**. 2000; 101:2601−2606.

56. London GM, Asmar RG, O'Rourke MF, Safar ME, Investigators RP. Mechanism(s) of selective systolic blood pressure reduction after a low-dose combination of perindopril/indapamide in hypertensive subjects: comparison with atenolol. **J Am Coll Cardiol**. 2004; 43:92−99.

57. de Luca N, Asmar RG, London GM, O'Rourke MF, Safar ME, Investigators RP. Selective reduction of cardiac mass and central blood pressure on low-dose combination perindopril/indapamide in hypertensive subjects. **J Hypertens**. 2004; 22:1623−1630.

58. Sharman JE, Marwick TH, Gilroy D, Otahal P, Abhayaratna WP, Stowasser M, Value of Central Blood Pressure for GMoHSI. Randomized trial of guiding hypertension management using central aortic blood pressure compared with best-practice care: principal findings of the BP GUIDE study. **Hypertension**. 2013; 62:1138−1145.

59. Borlaug BA, Olson TP, Abdelmoneim SS, et al. A randomized pilot study of aortic waveform guided therapy in chronic heart failure. **J Am Heart Assoc**. 2014; 3:e000745.

60. Chirinos JA, Segers P, Hughes T, Townsend R. Large-artery stiffness in health and disease: JACC state-of-the-art review. **J Am Coll Cardiol**. 2019; 74:1237−1263.

61. Avramovski P, Avramovska M, Sikole A. Bone strength and arterial stiffness impact on cardiovascular mortality in a general population. **J Osteoporos**. 2016; 2016:7030272.

62. Bastos JM, Bertoquini S, Polonia J. Prognostic significance of ambulatory arterial stiffness index in hypertensives followed for 8.2 years: its relation with new events and cardiovascular risk estimation. **Rev Port Cardiol**. 2010; 29:1287−1303.

63. Benetos A, Gautier S, Labat C, et al. Mortality and cardiovascular events are best predicted by low central/peripheral pulse pressure amplification but not by high blood pressure levels in elderly nursing home subjects: the PARTAGE (Predictive Values of Blood Pressure and Arterial Stiffness in Institutionalized Very Aged Population) study. **J Am Coll Cardiol**. 2012; 60:1503−1511.

64. Boutouyrie P, Tropeano AI, Asmar R, et al. Aortic stiffness is an independent predictor of primary coronary events in hypertensive patients: a longitudinal study. **Hypertension**. 2002; 39:10−15.

65. Cardoso CR, Ferreira MT, Leite NC, Salles GF. Prognostic impact of aortic stiffness in high-risk type 2 diabetic patients: the Rio deJaneiro Type 2 Diabetes Cohort Study. **Diabetes Care**. 2013; 36:3772−3778.

66. Cardoso CRL, Salles GC, Salles GF. Prognostic impact of aortic stiffness in patients with resistant hypertension. **Hypertension**. 2019; 73:728−735.

67. Choi CU, Park EB, Suh SY, et al. Impact of aortic stiffness on cardiovascular disease in patients with chest pain: assessment with direct intra-arterial measurement. **Am J Hypertens**. 2007; 20:1163−1169.

68. Cooper LL, Palmisano JN, Benjamin EJ, et al. Microvascular function contributes to the relation between aortic stiffness and cardiovascular events: the Framingham heart study. **Circ Cardiovasc Imaging**. 2016; 9.

69. Cruickshank K, Riste L, Anderson SG, Wright JS, Dunn G, Gosling RG. Aortic pulse-wave velocity and its relationship to mortality in diabetes and glucose intolerance: an integrated index of vascular function? **Circulation**. 2002; 106:2085−2090.

70. Dahle DO, Eide IA, Asberg A, et al. Aortic stiffness in a mortality risk calculator for kidney transplant recipients. **Transplantation**. 2015; 99:1730−1737.

71. Fortier C, Mac-Way F, Desmeules S, et al. Aortic-brachial stiffness mismatch and mortality in dialysis population. **Hypertension**. 2015; 65:378−384.

72. Girerd N, Legedz L, Paget V, et al. Outcome associations of carotid-femoral pulse wave velocity vary with different measurement methods. **Am J Hypertens**. 2012; 25:1264−1270.

73. Han J, Wang X, Ye P, et al. The predictive value of arterial stiffness on major adverse cardiovascular events in individuals with mildly impaired renal function. **Clin Interv Aging**. 2016; 11:1175−1181.

74. Holewijn S, den Heijer M, Kiemeney LA, Stalenhoef AF, de Graaf J. Combining risk markers improves cardiovascular risk prediction in women. **Clin Sci (Lond)**. 2014; 126:139−146.

75. Kaolawanich Y, Boonyasirinant T. Incremental prognostic value of aortic stiffness in addition to myocardial ischemia by cardiac magnetic resonance imaging. **BMC Cardiovasc Disord**. 2020; 20:287.

76. Karras A, Haymann JP, Bozec E, et al. Large artery stiffening and remodeling are independently associated with all-cause mortality and cardiovascular events in chronic kidney disease. **Hypertension**. 2012; 60:1451−1457.

77. Kavousi M, Elias-Smale S, Rutten JH, et al. Evaluation of newer risk markers for coronary heart disease risk classification: a cohort study. **Ann Intern Med**. 2012; 156:438−444.

78. Kim ED, Ballew SH, Tanaka H, Heiss G, Coresh J, Matsushita K. Short-term prognostic impact of arterial stiffness in older adults without prevalent cardiovascular disease. **Hypertension**. 2019; 74:1373−1382.

79. Laurent S, Boutouyrie P, Asmar R, et al. Aortic stiffness is an independent predictor of all-cause and cardiovascular mortality in hypertensive patients. **Hypertension**. 2001; 37:1236−1241.

80. Maldonado J, Pereira T, Polonia J, et al. Arterial stiffness predicts cardiovascular outcome in a low-to-moderate cardiovascular risk population: the EDIVA (Estudo de DIstensibilidade VAscular) project. **J Hypertens**. 2011; 29:669−675.

81. Maroules CD, Khera A, Ayers C, et al. Cardiovascular outcome associations among cardiovascular magnetic resonance measures of arterial stiffness: the Dallas heart study. **J Cardiovasc Magn Reson**. 2014; 16:33.

82. Matschkal J, Mayer CC, Sarafidis PA, et al. Comparison of 24-hour and office pulse wave velocity for prediction of mortality in hemodialysis patients. **Am J Nephrol**. 2019; 49:317−327.

83. Mattace-Raso FU, van der Cammen TJ, Hofman A, et al. Arterial stiffness and risk of coronary heart disease and stroke: the Rotterdam Study. **Circulation**. 2006; 113:657−663.

84. Mitchell A, Opazo Saez A, Kos M, Witzke O, Kribben A, Nurnberger J. Pulse wave velocity predicts mortality in renal transplant patients. **Eur J Med Res**. 2010; 15:452−455.

85. Niiranen TJ, Kalesan B, Larson MG, et al. Aortic-brachial arterial stiffness gradient and cardiovascular risk in the community: the Framingham heart study. **Hypertension**. 2017; 69:1022−1028.

86. Ohishi M, Tatara Y, Ito N, et al. The combination of chronic kidney disease and increased arterial stiffness is a predictor for stroke and cardiovascular disease in hypertensive patients. **Hypertens Res**. 2011; 34:1209−1215.

87. Ohyama Y, Ambale-Venkatesh B, Noda C, et al. Aortic arch pulse wave velocity assessed by magnetic resonance imaging as a predictor of incident cardiovascular events: the MESA (Multi-Ethnic study of atherosclerosis). **Hypertension**. 2017; 70:524−530.

88. Pandey A, Khan H, Newman AB, et al. Arterial stiffness and risk of overall heart failure, heart failure with preserved ejection fraction, and heart failure with reduced ejection fraction: the health ABC study (health, aging, and body composition). **Hypertension**. 2017; 69:267−274.

89. Pereira T, Maldonado J, Pereira L, Conde J. Aortic stiffness is an independent predictor of stroke in hypertensive patients. **Arq Bras Cardiol**. 2013; 100:437−443.

90. Regnault V, Lagrange J, Pizard A, et al. Opposite predictive value of pulse pressure and aortic pulse wave velocity on heart failure with reduced left ventricular ejection fraction: insights from an Eplerenone Post-Acute Myocardial Infarction Heart Failure Efficacy and Survival Study (EPHESUS) substudy. **Hypertension**. 2014; 63:105−111.

91. Ryliskyte L, Navickas R, Serpytis P, et al. Association of aortic stiffness, carotid intima-media thickness and endothelial function with cardiovascular events in metabolic syndrome subjects. **Blood Press**. 2019; 28:131−138.

92. Scandale G, Dimitrov G, Recchia M, et al. Arterial stiffness and 5-year mortality in patients with peripheral arterial disease. **J Hum Hypertens**. 2020; 34:505−511.

93. Sehestedt T, Jeppesen J, Hansen TW, et al. Risk prediction is improved by adding markers of subclinical organ damage to SCORE. **Eur Heart J**. 2010; 31:883−891.

94. Sutton-Tyrrell K, Najjar SS, Boudreau RM, et al. Elevated aortic pulse wave velocity, a marker of arterial stiffness, predicts cardiovascular events in well-functioning older adults. **Circulation**. 2005; 111:3384−3390.

95. Terai M, Ohishi M, Ito N, et al. Comparison of arterial functional evaluations as a predictor of cardiovascular events in hypertensive patients: the Non-Invasive Atherosclerotic Evaluation in Hypertension (NOAH) study. **Hypertens Res**. 2008; 31:1135−1145.

96. Tougaard NH, Theilade S, Winther SA, et al. Carotid-femoral pulse wave velocity as a risk marker for development of complications in type 1 diabetes mellitus. **J Am Heart Assoc**. 2020; 9:e017165.

97. Townsend RR, Anderson AH, Chirinos JA, et al. Association of pulse wave velocity with chronic kidney disease progression and mortality: findings from the CRIC study (chronic renal insufficiency cohort). **Hypertension**. 2018; 71:1101−1107.

98. Vasan RS, Short MI, Niiranen TJ, et al. Interrelations between arterial stiffness, target organ damage, and cardiovascular disease outcomes. **J Am Heart Assoc**. 2019; 8:e012141.

99. Vavruch C, Lanne T, Fredrikson M, Lindstrom T, Ostgren CJ, Nystrom FH. Serum leptin levels are independently related to the incidence of ischemic heart disease in a prospective study of patients with type 2 diabetes. **Cardiovasc Diabetol**. 2015; 14:62.

100. Verbeke F, Marechal C, Van Laecke S, et al. Aortic stiffness and central wave reflections predict outcome in renal transplant recipients. **Hypertension**. 2011; 58:833−838.

101. Verbeke F, Van Biesen W, Honkanen E, et al. Prognostic value of aortic stiffness and calcification for cardiovascular events and mortality in dialysis patients: outcome of the calcification outcome in renal disease (CORD) study. **Clin J Am Soc Nephrol**. 2011; 6:153−159.

102. Vlachopoulos C, Ioakeimidis N, Aznaouridis K, et al. Prediction of cardiovascular events with aortic stiffness in patients with erectile dysfunction. **Hypertension**. 2014; 64:672−678.

103. Vongsanim S, Davenport A. The association between peri-dialytic pulse wave velocity measurements and hemodialysis patient mortality. **Hemodial Int**. 2021; 25:71−77.

104. Nilsson Wadstrom B, Fatehali AH, Engstrom G, Nilsson PM. A vascular aging index as independent predictor of cardiovascular events and total mortality in an elderly urban population. **Angiology**. 2019; 70:929−937.

105. Weir-McCall JR, Brown L, Summersgill J, et al. Development and validation of a path length calculation for carotid-femoral pulse wave velocity measurement: a TASCFORCE, SUMMIT, and caerphilly collaborative venture. **Hypertension**. 2018; 71:937−945.

106. Wijkman M, Lanne T, Ostgren CJ, Nystrom FH. Aortic pulse wave velocity predicts incident cardiovascular events in patients with type 2 diabetes treated in primary care. **J Diabet Complicat**. 2016; 30:1223−1228.

107. Willum-Hansen T, Staessen JA, Torp-Pedersen C, et al. Prognostic value of aortic pulse wave velocity as index of arterial stiffness in the general population. **Circulation**. 2006; 113:664−670.

108. Zhang Y, Protogerou AD, Iaria P, Safar ME, Xu Y, Blacher J. Prognosis in the hospitalized very elderly: the PROTEGER study. **Int J Cardiol**. 2013; 168:2714−2719.

109. Zuo J, Chang G, Tan I, Butlin M, Chu SL, Avolio A. Central aortic pressure improves prediction of cardiovascular events compared to peripheral blood pressure in short-term follow-up of a hypertensive cohort. **Clin Exp Hypertens**. 2018:1−8.

110. Safar ME, Blacher J, Pannier B, et al. Central pulse pressure and mortality in end-stage renal disease. **Hypertension**. 2002; 39:735−738.

111. Chirinos JA, Zambrano JP, Chakko S, et al. Aortic pressure augmentation predicts adverse cardiovascular events in patients with established coronary artery disease. **Hypertension**. 2005; 45:980−985.

112. Dart AM, Gatzka CD, Kingwell BA, et al. Brachial blood pressure but not carotid arterial waveforms predict cardiovascular events in elderly female hypertensives. **Hypertension**. 2006; 47:785−790.

113. Roman MJ, Devereux RB, Kizer JR, et al. Central pressure more strongly relates to vascular disease and outcome than does brachial pressure: the Strong Heart Study. **Hypertension**. 2007; 50:197−203.

114. Jankowski P, Kawecka-Jaszcz K, Czarnecka D, et al. Aortic Blood P and Survival Study G. Pulsatile but not steady component of blood pressure predicts cardiovascular events in coronary patients. **Hypertension**. 2008; 51:848−855.

115. Pini R, Cavallini MC, Palmieri V, et al. Central but not brachial blood pressure predicts cardiovascular events in an unselected geriatric population: the ICARe Dicomano Study. **J Am Coll Cardiol**. 2008; 51:2432−2439.

116. Manisty C, Mayet J, Tapp RJ, et al. Wave reflection predicts cardiovascular events in hypertensive individuals independent of blood pressure and other cardiovascular risk factors: an ASCOT (Anglo-Scandinavian Cardiac Outcome Trial) substudy. **J Am Coll Cardiol**. 2010; 56:24−30.

117. Huang CM, Wang KL, Cheng HM, et al. Central versus ambulatory blood pressure in the prediction of all-cause and cardiovascular mortalities. **J Hypertens**. 2011; 29:454−459.

118. Weber T, Wassertheurer S, Rammer M, Haiden A, Hametner B, Eber B. Wave reflections, assessed with a novel method for pulse wave separation, are associated with end-organ damage and clinical outcomes. **Hypertension**. 2012; 60:534−541.

119. Sung SH, Yu WC, Cheng HM, et al. Excessive wave reflections on admission predict post-discharge events in patients hospitalized due to acute heart failure. **Eur J Heart Fail**. 2012; 14:1348−1355.

120. Ishisone T, Koeda Y, Tanaka F, Sato K, Nagano M, Nakamura M. Comparison of utility of arterial stiffness parameters for predicting cardiovascular events in the general population. **Int Heart J**. 2013; 54:160−165.

121. Janner JH, Godtfredsen NS, Ladelund S, Vestbo J, Prescott E. High aortic augmentation index predicts mortality and cardiovascular events in men from a general population, but not in women. **Eur J Prev Cardiol**. 2013; 20:1005−1012.

122. Chang CC, Sung SH, Yu WC, Cheng HM, Chen CH. Night-time electromechanical activation time, pulsatile hemodynamics, and discharge outcomes in patients with acute heart failure. **ESC Heart Fail**. 2015; 2:184−193.

123. Huang SS, Huang PH, Leu HB, Wu TC, Lin SJ, Chen JW. Association of central pulse pressure with contrast-induced nephropathy and clinical outcomes in patients undergoing coronary intervention. **J Hypertens**. 2013; 31:2187−2194.

124. Kals J, Lieberg J, Kampus P, Zagura M, Eha J, Zilmer M. Prognostic impact of arterial stiffness in patients with symptomatic peripheral arterial disease. **Eur J Vasc Endovasc Surg**. 2014; 48:308−315.

125. Theilade S, Hansen TW, Rossing P. Central hemodynamics are associated with cardiovascular disease and albuminuria in type 1 diabetes. **Am J Hypertens**. 2014; 27:1152−1159.

126. Narayan O, Davies JE, Hughes AD, et al. Central aortic reservoir-wave analysis improves prediction of cardiovascular events in elderly hypertensives. **Hypertension**. 2015; 65:629−635.

127. Wassertheurer S, Baumann M. Assessment of systolic aortic pressure and its association to all cause mortality critically depends on waveform calibration. **J Hypertens**. 2015; 33:1884−1888. discussion 1889.

128. Chuang SY, Cheng HM, Bai CH, Yeh WT, Chen JR, Pan WH. Blood pressure, carotid flow pulsatility, and the risk of stroke: a community-based study. **Stroke**. 2016; 47:2262−2268.

129. Laugesen E, Knudsen ST, Hansen KW, et al. Invasively measured aortic systolic blood pressure and office systolic blood pressure in cardiovascular risk assessment: a prospective cohort study. **Hypertension**. 2016; 68:768−774.

130. Mitchell GF, Hwang SJ, Larson MG, et al. Transfer function-derived central pressure and cardiovascular disease events: the Framingham Heart Study. **J Hypertens**. 2016; 34:1528−1534.

131. Sun T, Cheng Y, Wang S, Tao Y, Zhao ZJA. Invasive aortic augmentation index could predict the adverse events in patients without established coronary heart disease. **Angiol Open Access**. 2016; 4:2.

132. Chen G, Bliden KP, Chaudhary R, et al. Central aortic pulse pressure, thrombogenicity and cardiovascular risk. **J Thromb Thrombolysis**. 2017; 44:223−233.

133. Sarafidis PA, Loutradis C, Karpetas A, et al. Ambulatory pulse wave velocity is a stronger predictor of cardiovascular events and all-cause mortality than office and ambulatory blood pressure in hemodialysis patients. **Hypertension**. 2017; 70:148−157.

134. Vlachopoulos C, Ioakeimidis N, Rokkas K, et al. Central haemodynamics and prediction of cardiovascular events in patients with erectile dysfunction. **Am J Hypertens**. 2017; 30:249−255.

135. Cremer A, Boulestreau R, Gaillard P, Laine M, Papaioannou G, Gosse P. Twenty-four-hour central pulse pressure for cardiovascular events prediction in a low-cardiovascular-risk population: results from the bordeaux cohort. **J Am Heart Assoc**. 2018; 7.

136. Eguchi K, Miyashita H, Takenaka T, et al. High central blood pressure is associated with incident cardiovascular events in treated hypertensives: the ABC-J II Study. **Hypertens Res**. 2018; 41:947−956.

137. Guajardo I, Ayer A, Johnson AD, et al. Sex differences in vascular dysfunction and cardiovascular outcomes: the cardiac, endothelial function, and arterial stiffness in ESRD (CERES) study. **Hemodial Int**. 2018; 22:93−102.

138. Nair R, Nair S, Vinayakumar D, et al. Central aortic pressure indices and cardiovascular risk factors: demographic, clinical, and prognostic characterization. **Heart India**. 2018; 6:102−107.

139. Rahman M, Hsu JY, Desai N, et al. Central blood pressure and cardiovascular outcomes in chronic kidney disease. **Clin J Am Soc Nephrol**. 2018; 13:585−595.

140. Sluyter JD, Camargo Jr CA, Lowe A, Scragg RKR. Pulse rate variability predicts atrial fibrillation and cerebrovascular events in a large, population-based cohort. **Int J Cardiol**. 2019; 275:83−88.

141. Ndrepepa G, Cassese S, Kufner S, et al. U-shaped association of central pulse pressure with long-term prognosis after ST-segment elevation myocardial infarction. **Heart Ves**. 2019; 34:1104−1112.

142. Mukai H, Svedberg O, Lindholm B, et al. Skin autofluorescence, arterial stiffness and Framingham risk score as predictors of clinical outcome in chronic kidney disease patients: a cohort study. **Nephrol Dial Transplant**. 2019; 34:442−448.

143. Wu HP, Lin MJ. Central aortic pressure and long-term outcome in hypertensive patients undergoing percutaneous coronary intervention. **Sci Rep**. 2020; 10:17420.

144. Tynjala A, Forsblom C, Harjutsalo V, Groop PH, Gordin D, Finn-Diane Study G. Arterial stiffness predicts mortality in individuals with type 1 diabetes. **Diabetes Care**. 2020; 43:2266−2271.

145. Huang QF, Aparicio LS, Thijs L, et al. Cardiovascular end points and mortality are not closer associated with central than peripheral pulsatile blood pressure components. **Hypertension**. 2020; 76:350−358.

146. Dong Y, Jiang L, Wang X, et al. Central rather than brachial pressures are stronger predictors of cardiovascular outcomes: a longitudinal prospective study in a Chinese population. **J Clin Hypertens**. 2020; 22:623−630.

147. Lamarche F, Agharazii M, Madore F, Goupil R. Prediction of cardiovascular events by type I central systolic blood pressure: a prospective study. **Hypertension**. 2021; 77:319−327.

This page intentionally left blank

Role of the heart and arterial tree in physiologic adjustments during exercise

Wesley K. Lefferts[1,2], Elizabeth C. Lefferts[1,2], Brooks A. Hibner[1] and Bo Fernhall[1]

[1]University of Illinois at Chicago, Chicago, IL, United States; [2]Iowa State University, Ames, IA, United States

Aerobic exercise challenges the cardiovascular system to increase oxygen and nutrient delivery to the active skeletal muscle to meet their increase in energy requirements. To do so, a highly integrated response (depicted in Fig. 34.1) is elicited by the cardiovascular system to increase blood flow to specific tissues while also maintaining blood pressure. This chapter examines the intense demands of aerobic exercise and how the heart and pulmonary, central, and peripheral arteries work in concert to meet the dramatic increase in blood flow demand at the working skeletal muscle.

Cardiac output

Exercise is dependent on the ability of the heart to increase cardiac output and match the metabolic demands of the working tissue. Cardiac output increases five- to eightfold from rest to heavy exercise depending on exercise training status (Fig. 34.2). The magnitude of increase in cardiac output during exercise matches exercise intensity, as increased oxygen demand is met with increased blood flow. The ability to increase cardiac output is dependent on (1) compensatory increases in heart rate, (2) increases in stroke volume, and (3) a prioritizing of left ventricular (LV) work to overcome the load presented by the vasculature (described by ventricular-vascular coupling).
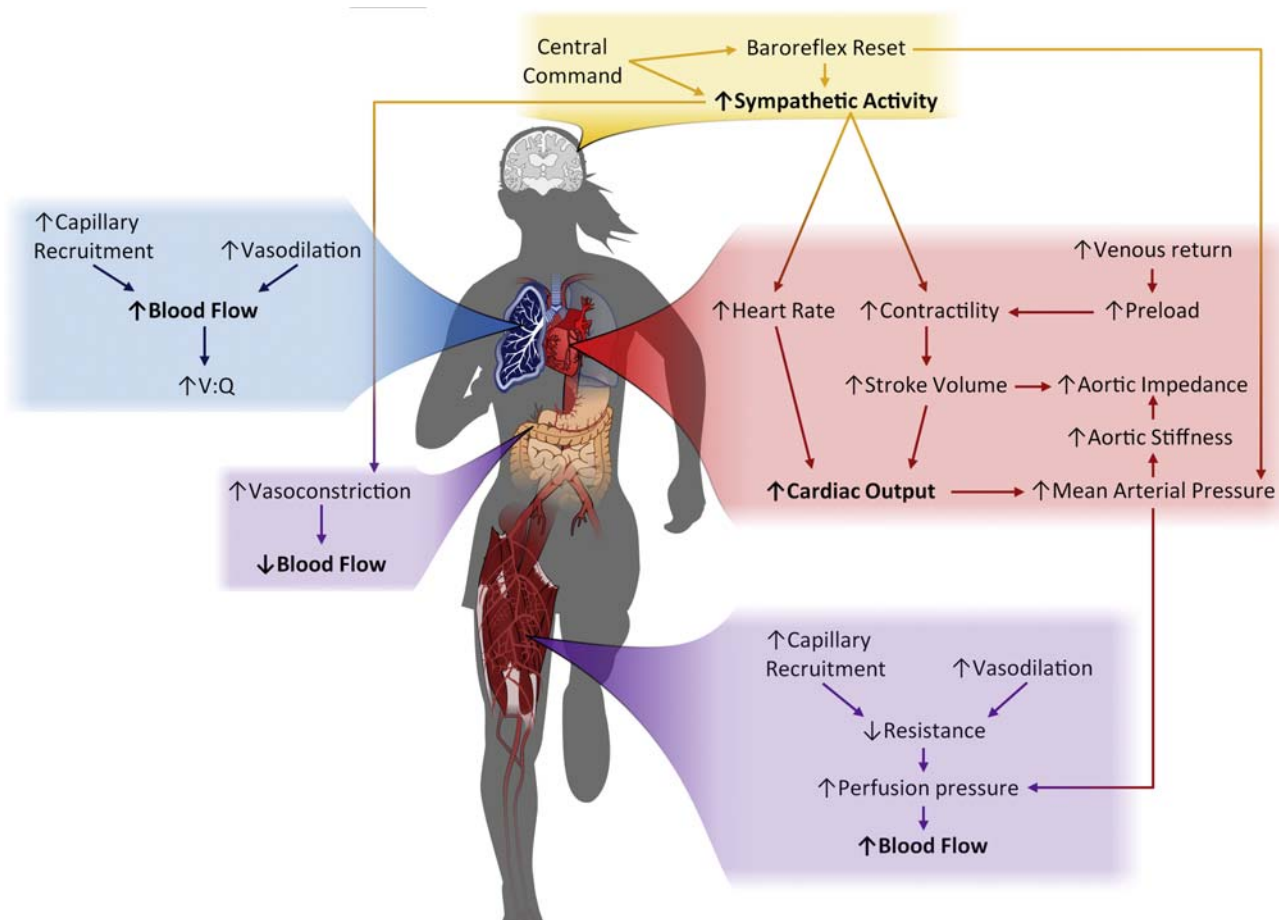
Heart rate response during exercise

Heart rate increases linearly during exercise in an intensity-dependent manner and eventually plateaus at maximal exercise intensity (Fig. 34.2). Heart rate is critical to exercise-induced increases in cardiac output, particularly during moderate-to-high intensity exercise. Increases in heart rate during exercise occur via redundant direct and indirect (i.e., reflex-driven) pathways resulting in greater sympathetic nerve activity (neural) and catecholamine release (hormonal).
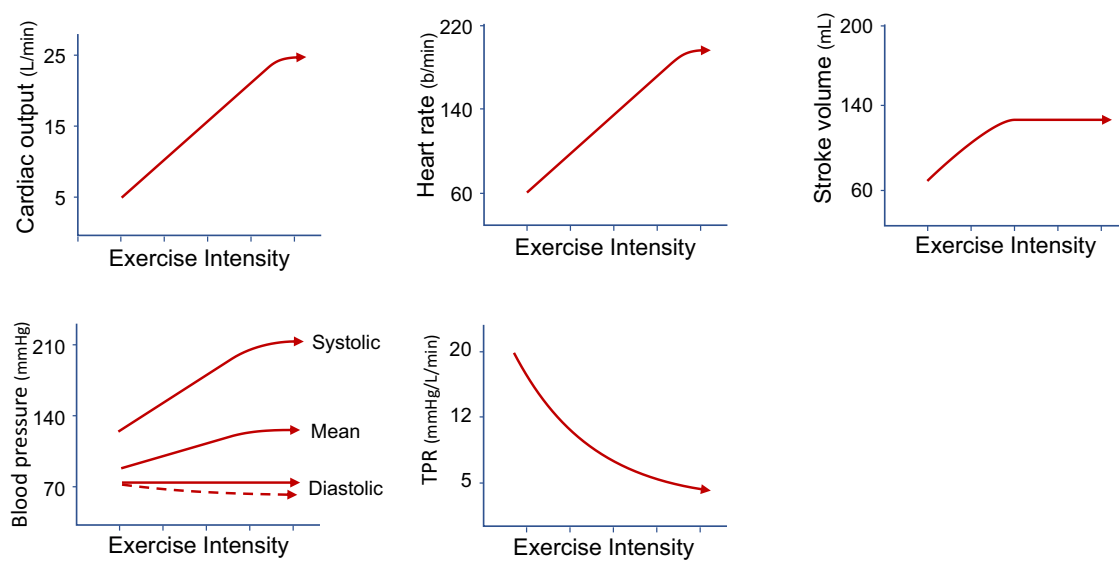
Initial increases in heart rate with exercise occur due to withdrawal of parasympathetic outflow to the heart and subsequent increases in sympathetic activation (Fig. 34.3). When the motor cortex in the brain elicits the contraction of peripheral skeletal muscles, a simultaneous coordinated response is initiated from the cardiovascular control center in the medulla. This coordinated response is known as central command and is responsible for initial increases in heart rate via parasympathetic withdrawal and sympathetic activation.[1–3] Central command is a feedforward mechanism that increases activation based on perceived effort and can be independent of actual muscle activation and force production.[4,5]

The exercise pressor reflex is an important peripheral feedback mechanism contributing to the increase in heart rate during exercise. The exercise pressor reflex involves both the mechanoreflex and chemoreflex from the periphery (Fig. 34.3). Muscle contraction elicits mechanical (muscle length and tension) and chemical stimuli (metabolic by-products) that activate the mechanoreflex and chemoreflex, respectively.[6,7] While the mechanoreflex is immediately activated by muscle contraction, the chemoreflex is delayed due to the time required for metabolites to accumulate. The mechano- and chemoreflex activate group III (thinly myelinated) and group IV (unmyelinated) afferent nerve fibers within the skeletal muscle and increase neural discharge frequency to the central nervous system. In response, the central nervous system increases sympathetic nerve activity, which increases heart rate.[6,8,9] The exercise pressor reflex remains active throughout exercise, providing continuous feedback to the cardiovascular control center and modulation of autonomic activity.[10,11]
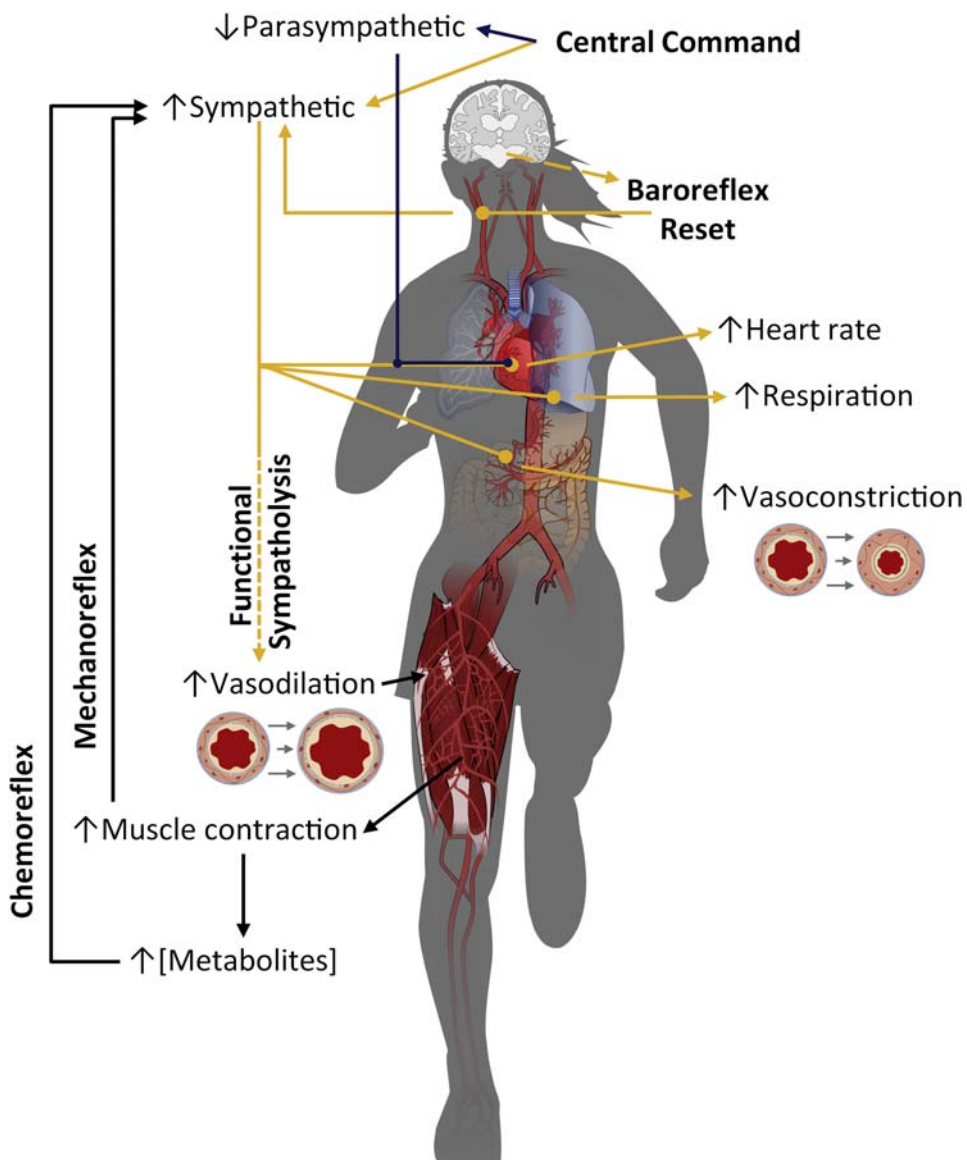
Heart rate additionally increases during exercise via the direct effects of catecholamines and the Bainbridge reflex (also known as atrial reflex). Catecholamines (epinephrine and norepinephrine) released from the adrenal medulla (and

FIGURE 34.1   Overview of the cardiovascular adjustments during aerobic exercise necessary to increase sympathetic nervous system activity, cardiac output, and increase and redistribute blood flow to the lungs and active muscle.

FIGURE 34.2   Theoretical changes in components of cardiac output, total peripheral resistance, and blood pressure during aerobic exercise. *TPR*, total peripheral resistance.

FIGURE 34.3 Overview of autonomic nervous system adjustments during aerobic exercise and its role in blood flow redistribution.

from synaptic spillover for norepinephrine) assist the neural input to the heart to increase heart rate during exercise, particularly at moderate and high intensities. The impact of catecholamines on heart rate is dependent on β-adrenergic receptor sensitivity.[12] Downregulation or desensitization of β-adrenergic receptors (as occurs in aging and disease) blunts the typical heart rate response during exercise.[12,13] The Bainbridge reflex may also support increases in heart rate during exercise. This reflex is triggered by stretch receptors in the atria that detect increases in venous pressure (as would occur with an increase in venous return during exercise, discussed further below), and results in sympathetic-driven increases in heart rate. Together, central command, the exercise pressor reflex, catecholamine release, and the Bainbridge reflex act in concert to elevate heart rate during

exercise, thereby supporting increases in cardiac output necessary to match blood flow requirements in the active tissue.

Stroke volume response during exercise

The amount of blood ejected per heart beat (stroke volume) may increase 2-fold from rest to moderate exercise (Fig. 34.2).[14] Stroke volume increases until light to moderate (40%−50% VO_2 max) intensity after which it plateaus.[15] The stroke volume response during aerobic exercise is the result of synergistic changes in preload, contractility (inotropy), afterload, and ventricular filling time.

During upright exercise, the volume of blood available for ventricular filling (i.e., preload) increases owing to

synergistic changes in venous return, atrial contraction, and ventricular relaxation. Venous return increases during exercise as blood is mobilized through the venous network by the skeletal muscle pump, abdominothoracic pump, and sympathetic-mediated arterial and venous vasoconstriction.[16–20] The vasoconstriction imposed in the splanchnic (liver, gastrointestinal tract, pancreas, and spleen) and renal circulation reallocates a large volume of blood as exercise intensity increases, with these regions receiving ∼25% of cardiac output at rest and only ∼3% of cardiac output during maximal exercise.[21] Increases in end-diastolic volume during the initial stage of upright exercise are further supported by increased contractility of the atria, forcing a larger volume of blood from the atria into the ventricle in late diastole.[22] Additionally, diastolic relaxation of the ventricle (lusitropic function) is improved during exercise with the rapid untwisting of the ventricle.[23–25] The rapid untwisting of the ventricle decreases ventricular pressure quickly and increases the filling pressure gradient, creating a "suction-like" force that enhances ventricular filling and aids in maintenance of stroke volume as heart rate increases (discussed further below).

Increases in end-diastolic volume during early stages of upright exercise stretch the myocardium and result in a more forceful ventricular contraction, following the Frank Starling relationship.[26] This end-diastolic volume-driven increase in contractility is further augmented by increased sympathetic activity to the myocardium. Contractility additionally increases owing to the Bowditch effect, whereby increases in heart rate alter calcium handling within myocardial muscle fibers, enhancing actin–myosin interaction and thus, contractility.[27] Greater ventricular contractility reduces the volume of blood remaining at end systole (i.e., end-systolic volume). Ultimately, these complementary mechanisms enhance the contractile function of the heart during exercise and play a role in both increasing stroke volume and maintaining stroke volume at high heart rates.[28]

The ability of the ventricles to eject blood (i.e. increase stroke volume) is dependent on the amount of pressure they must generate to overcome the pressure in the main arteries (pulmonary trunk for the right ventricle and aorta for the left ventricle). As described in more detail below, in spite of the increased cardiac output during exercise, aerobic exercise only produces a modest increase in mean arterial pressure, owing to arteriolar vasodilation in exercising muscle, which normally reduces total peripheral resistance (despite vasoconstriction elsewhere), thus preventing substantial exercise-induced increases in afterload. The impact of afterload on the heart during exercise is described in more detail in the next section. Even modest increases in afterload can be compensated for by via cardiac inotropy and the Anrep effect,[29–31] whereby an acute increase in afterload enhances ventricular contractility. Taken together,
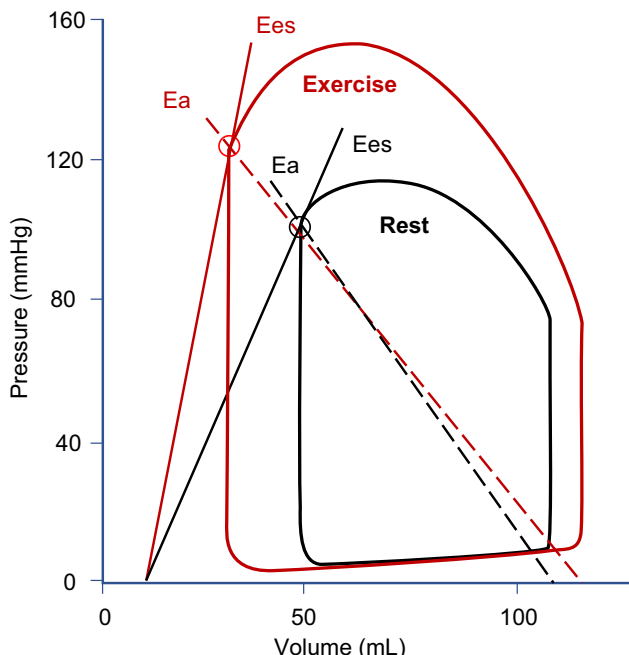
the net increase in preload and contractility, and reduced afterload during exercise ensure increases in stroke volume as part of a concerted approach to augment cardiac output at lower exercise intensities.

Initial increases in stroke volume slow and plateau at moderate to vigorous exercise intensities. This plateau in stroke volume is related to the reduced diastolic duration from the increase in heart rate with increasing exercise intensity. The faster heart rate, and thus shorter diastolic duration, reduces ventricular filling time and causes end-diastolic volume to plateau or slightly decrease as exercise intensity increases.[15] As such, initial, synergistic changes in preload, contractility, and afterload that serve to increase stroke volume become somewhat limited at moderate to higher intensity exercise by heart rate–mediated reductions in filling time, thereby preventing further increases in stroke volume.

Ventricular-vascular coupling

The ability of the cardiovascular system to match the demands of exercise depend on the left ventricle overcoming the load imposed by the arterial system to increase cardiac output. This dynamic interaction between the left ventricle and the arterial system is known as ventricular-vascular coupling[32] (explored more in-depth in Chapters 13–17). Ventricular-vascular coupling is traditionally measured by representing the heart and the arterial system as coupled elastances. In this setting, elastance is defined by the change in pressure for a given change in volume,[33] as illustrated for the ventricle with pressure volume loops acquired at different preloads (Fig. 34.4). The slope of the change in end-systolic pressure to end-systolic volume is a measure of contractility and represents ventricular elastance (Ees). The negative slope between end-systolic pressure and end-diastolic volume is arterial elastance (Ea), meant to represent total arterial load imposed on the ventricle. The ratio of arterial elastance to ventricular elastance (Ea/Ees) has been used to quantify ventricular-vascular coupling and provides a measurement of the interaction between the cardiac and arterial system.[2] This method of coupling assessment has inherent limitations (as discussed in detail in Chapter 15), but to date has been the most widely used method used to assess ventricular-vascular coupling during exercise.

Optimal ventricular-vascular coupling at rest results in a balanced cardiovascular system such that the system provides optimal transfer of blood without excessive changes in pressure. Thus, under resting conditions, the cardiovascular system is an efficient or coupled system that prioritizes energetic efficiency over cardiac work.[34] During exercise, however, the interaction between the ventricle and vasculature becomes uncoupled as energetic efficiency is sacrificed to favor greater cardiac work.[35,36] Indeed, cardiac

FIGURE 34.4 Theoretical changes in left ventricular pressure-volume relations at rest and during aerobic exercise. *Ea*, arterial elastance; *Ees*, ventricular elastance.

work (partially signified by stroke work, the area within the pressure-volume loop) increases during exercise owing to increased contractility (ejection fraction) and thus, stroke volume. The widening of the pressure-volume loop (i.e., increase in stroke volume) during exercise also demonstrates the changes in both ventricular and arterial elastance. Contractility and stroke volume increase during exercise, thereby reducing end systolic volume and increasing end systolic pressure. As such, both ventricular (end systolic pressure/end systolic volume) and arterial elastance (end systolic pressure/stroke volume) increase during exercise; but ventricular elastance increases to a greater degree to overcome arterial load, thus supporting increases in cardiac output. These changes subsequently impact the Ea/Ees coupling ratio.[35–38] The increase in ventricular elastance has led to both reductions[35,36] and maintenance of the Ea/Ees ratio during exercise,[37,38] depending on the simultaneous magnitude of change in Ea. Reductions in the Ea/Ees ratio (increases in efficiency of the heart during exercise) are blunted with age, suggesting an inability to attain maximal stroke work[36] among older individuals. The traditional elastance model of ventricular-vascular coupling is not without its limitations.[39] True arterial load is best characterized using pressure-flow relationships or aortic input impedance. While this method is not often used during exercise, optimal coupling would theoretically occur when greatest ejection (highest flow) occurs at frequencies where impedance is lowest. Increased heart rate during

exercise shifts the first harmonic of flow to a frequency where impedance modulus is lowest.[40,41] Exercise-induced increases in heart rate optimally couple the heart and arterial systems by aligning the greatest ejection with the lowest aortic impedance, thereby improving ventricular performance. Ultimately, redundant mechanisms increase heart rate and stroke volume during exercise which shifts the balance between ventricular performance and vascular load to prioritize increases in cardiac output into the pulmonary and central vasculature for oxygenation and distribution to the active tissue.

Exercise hemodynamics
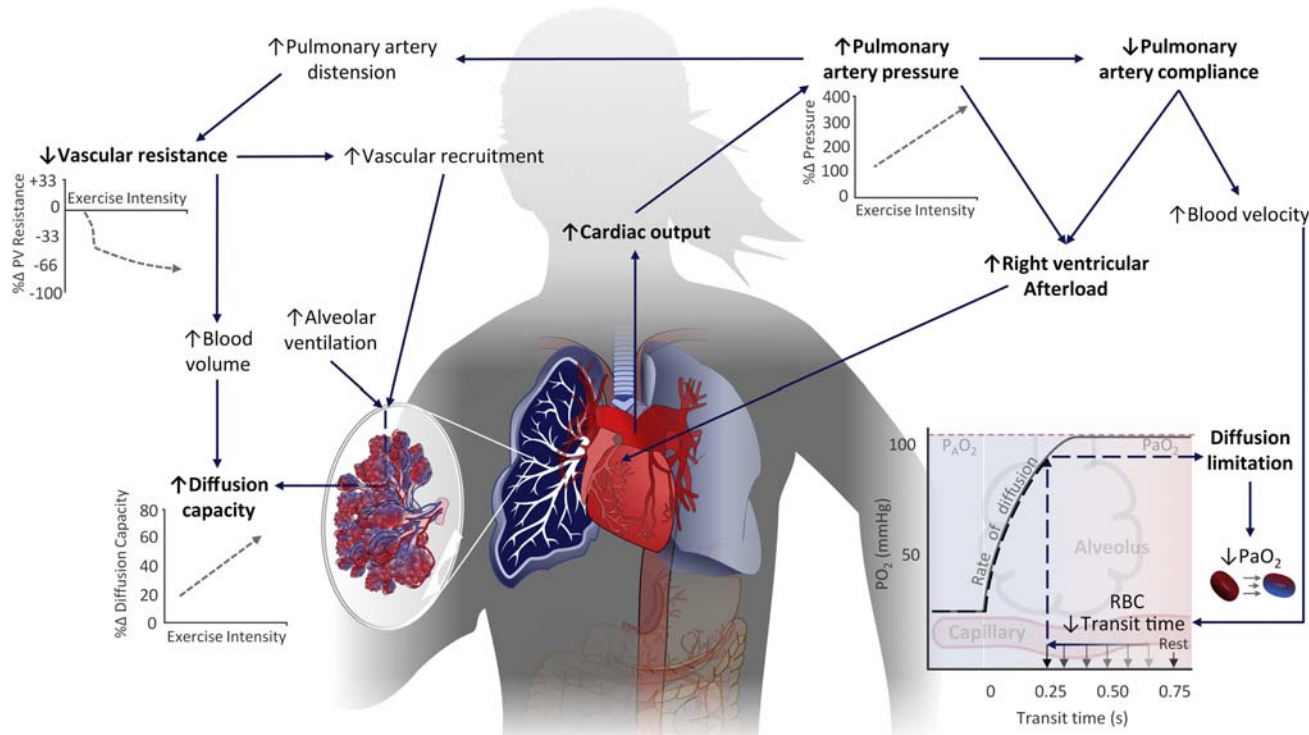
Increases in cardiac output must be balanced between the left and right sides of the heart during exercise. This co-ordinated effort ensures adequate oxygenation of pulmonary arterial blood and subsequent transportation to specific active regions of the body. Thus, while the pulmonary circulation and vasculature differ considerably from the systemic circulation both anatomically and physiologically, they must respond in concert to adequately support efficient oxygenation of arterial blood and oxygen delivery to exercising muscle.

Pulmonary hemodynamics during exercise

The pulmonary circulation is designed as a low-pressure system, reflected in the anatomical design of both the right heart and the vasculature. Considering the pressure in the pulmonary circulation is about 1/20th of that on the systemic side, it is not surprising that both the right ventricle and the pulmonary vasculature are thin walled and highly compliant at rest. The pulmonary circulatory system is not as adaptive as the systemic circulation to accommodate the high levels of blood flow observed during intense and/or prolonged exercise; however, it serves a vital function to increase oxygenation of deoxygenated blood for transport to peripheral tissues. The discussion below will highlight the effect of aerobic exercise on the hemodynamics of pulmonary circulatory function as depicted in Fig. 34.5.

Pulmonary arterial pressure and resistance during exercise

Mean pulmonary artery pressure (PAP) increases from rest to high-intensity exercise (Fig. 34.5).[42–47] PAP can approach over 40 mmHg in young healthy adults but may increase to ∼46 mmHg among older (>50 years) adults.[46] PAP may be even greater during exercise among highly trained individuals, owing to the relationship between

FIGURE 34.5 Overview of pulmonary vascular hemodynamic adjustments during aerobic exercise in response to an increase in cardiac output. Graphs depict theoretical changes with increases in exercise intensity. P_AO_2, partial pressure of oxygen in alveoli; PaO_2, partial pressure of oxygen in arterial blood; PO_2, partial pressure of oxygen; *PV*, pulmonary vascular; *RBC*, red blood cell; *V:Q*, ventilation-perfusion mismatch. *Adapted from Coffman KE, Carlson AR, Miller AD, Johnson BD, Taylor BJ. The effect of aging and cardiorespiratory fitness on the lung diffusing capacity response to exercise in healthy humans.* **J Appl Physiol** *(1985). 2017;122:1425−1434; Dempsey JA. Respiratory determinants of exercise limitation: focus on phrenic afferents and the lung vasculature.* **Clin Chest Med**. *2019; 40:331−342.*

cardiac output and PAP (discussed below).[43] Increases in PAP during exercise reflect adjustments in its constituents: cardiac output, pulmonary vascular resistance, and left atrial pressure, where:

$$PAP = (cardiac\ output \times pulmonary\ vascular\ resistance) + left\ atrial\ pressure.$$

Ultimately, substantial changes in cardiac output, coupled with increases in left atrial pressure, offset modest reductions in pulmonary vascular resistance, thus increasing PAP during exercise.

Increases in cardiac output appear linearly related to changes in PAP during exercise.[42−47] Moreover, PAP does not change between workloads when cardiac output is not altered.[48,49] Theoretically, the relationship between PAP and cardiac output may be curvilinear due to the low distensibility of the pulmonary arteries, since the relationship between pressure and distension is nonlinear.[50] The distensibility of the pulmonary vasculature, however, is limited and may explain why most studies have found a linear relationship between PAP and cardiac output.[42−47] Increases in PAP during exercise are also related to left atrial pressure. Left atrial pressure (assessed as pulmonary

artery wedge pressure) increases in a linear manner with cardiac output during incremental exercise.[43,46] Thus, increases in cardiac output and left atrial pressure contribute to increased PAP during exercise.

Vascular resistance decreases rapidly with initiation of exercise in the pulmonary circulation, similar to responses observed in the systemic circulation. The rapid fall in pulmonary vascular resistance, however, seemingly plateaus at cardiac outputs ∼7−10 L/min, with only a small additional reduction or no change until maximal exercise.[43,44] This plateau in pulmonary vascular resistance (approximately −Δ66%) at a low cardiac output is considerably different from the consistent, large reductions in resistance within the systemic circulation (approximately −Δ300%) with increasing exercise intensity. The limited reduction in pulmonary vascular resistance compared to the systemic circulation is likely related to the relatively "fixed" size of the pulmonary vascular system and its limited ability to vasodilate. The initial fall in pulmonary vascular resistance is thus attributed to pulmonary vascular recruitment coupled with distention of the pulmonary resistance vessels in response to increased blood flow.[43,51] Following the initial reductions in pulmonary vascular

resistance, pulmonary vessel recruitment is usually maximized and the slow gradual decline in vascular resistance is a function of the limited (1%−2%) distensibility of the pulmonary arterial bed (discussed further below)[43,51,52] Taken together, increases in PAP during exercise partially reflects increases in cardiac output and left atrial pressure, but is also driven by the limited vasodilatory reserve and vessel distensibility that attenuates reductions in pulmonary vascular resistance during exercise.

Pulmonary blood volume expansion, diffusion capacity, and pulmonary artery distensibility during exercise

Increases in cardiac output and PAP during exercise doubles the pulmonary arterial blood volume in an approximately linear manner from rest to maximal exercise. Theoretically, the blood volume expansion during exercise enhances ventilation—perfusion coupling when matched with sympathetic-mediated increases in minute ventilation and downstream alveolar ventilation.[43,53] This is accompanied by a linear increase in lung diffusing capacity and alveolar-capillary membrane conductance from rest to maximal exercise. Interestingly, aging reduces both lung diffusing capacity and alveolar-capillary membrane conductance but does not alter the rate of increase during exercise compared to young individuals.[53] Ultimately, while increasing pulmonary arterial blood volume is necessary and beneficial during exercise, this expansion of blood volume reveals structural limitations within the pulmonary vasculature that can influence exercise hemodynamics.

Increases in blood volume in the pulmonary circulation during exercise are primarily accommodated via distention of the arterial wall. The distension of the pulmonary vasculature reduces pulmonary arterial distensibility and compliance,[48,54] and increases pulmonary arterial stiffness during exercise (Fig. 34.5).[55] This blood volume—mediated shift in compliance and stiffness increases with exercising intensity and likely indicates a "mechanical constraint" of the pulmonary arterial bed to increased blood flow, and this constraint contributes to the increase in pressure with increased cardiac output during exercise. This "stiffening" of the pulmonary arterial bed during acute exercise may contribute to increased right ventricular afterload and reduced stroke volume in older populations.[48] However, the stiffening of the arterial bed may also contribute to an increase in flow velocity, especially in highly trained individuals who exhibit very high cardiac output which can decrease red blood cell transit time in highly trained individuals.

Limitations in both pulmonary arterial wall distensibility and vasodilation during substantial increases in cardiac output and increased pressure (e.g., highly trained
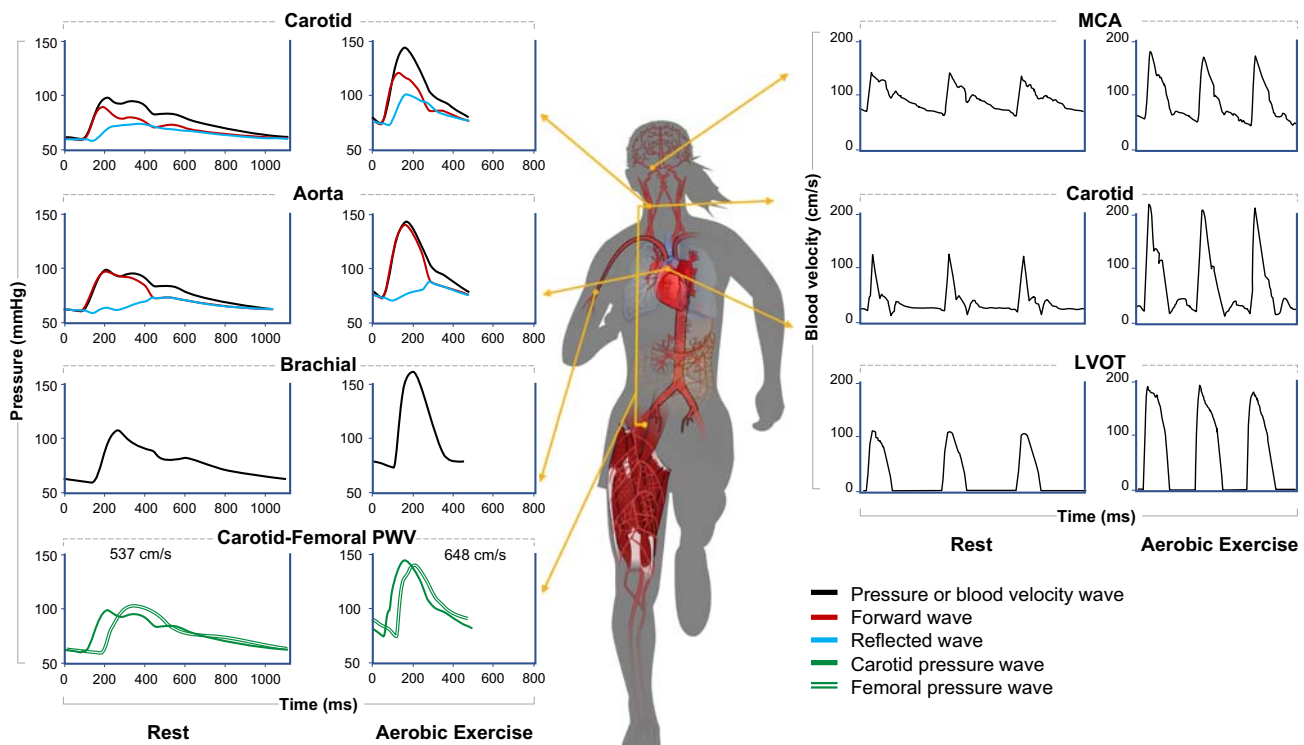
individuals during exercise) increases blood velocity through the pulmonary vasculature.[43,56] The accelerated speed of red blood cells through the pulmonary circulation reduces red blood cell transit time at the level of the capillary-alveolus interface.[43,56] Although red blood cell transit time may only decrease by ∼25% from rest to a maximal cardiac output of 20 L/min for a normal healthy sedentary or moderately active person, the reduction in transit time at a cardiac output of 30 L/min for a highly trained endurance athlete would be ∼50%.[43] This substantial decrease in capillary transit time at high cardiac outputs/blood velocities can lead to diffusion limitation, whereby oxygen does not have sufficient time to fully diffuse and equilibrate during the transient interaction between alveolus and red blood cell.[43,56] The "incomplete loading" of oxygen from the alveolus to the red blood cells results in a widening of the alveolar-arterial oxygen difference and arterial hypoxemia. As such, oxygen desaturation to levels of 85%−90% is not uncommon among highly trained endurance athletes.[57,58] Ultimately, while the PAP-driven expansion of blood volume in the pulmonary circulation during exercise is necessary to increase oxygenation of arterial blood, it pushes the limits of the pulmonary artery structure and function and may present challenges under certain exercise conditions.

Central hemodynamics during exercise

The central vasculature serves as a highway during exercise, facilitating transportation of oxygenated blood from the heart downstream to the peripheral vasculature where blood flow is directed to metabolically active tissue. Exercise-induced changes in cardiac output and peripheral redistribution of blood flow result in an expansion of pulse pressure and modest increase in mean pressure. This section will discuss the hemodynamic mechanisms driving central blood pressure and blood pressure amplification during exercise and their effects on hemodynamic pulsatility, arterial stiffness, and characteristic impedance, as depicted in Fig. 34.6.

Mean arterial pressure

Mean arterial pressure in the systemic circulation must increase during exercise in order to establish an adequate pressure gradient to drive adequate blood flow to active tissue (Fig. 34.2). This occurs through offsetting changes in systolic and diastolic pressure. Increases in systolic blood pressure during exercise are driven by increased stroke volume. The concomitant increase in mean arterial pressure during aerobic exercise is relatively modest. Cardiac-driven increases in systolic pressure are accompanied by peripheral vasodilation and reductions in total peripheral resistance (thereby maintaining or decreasing diastolic blood

FIGURE 34.6 Example central blood pressure, pulse wave dynamics, and blood velocity responses during moderate intensity aerobic exercise (60% heart rate reserve; heart rate ∼135 b/min, semirecumbent cycle ergometer) in a 30-year-old female. *LVOT*, left ventricular outflow tract; *MCA*, middle cerebral artery; *PWV*, pulse wave velocity.

pressure). The blood pressure response to exercise is highly variable and dependent on underlying cardiovascular disease, fitness, sex, age, and exercise intensity.[59,60] On average, peak systolic blood pressure during exercise ranges from ∼165 mmHg in young adults to ∼190 mmHg in older adults,[59] with exaggerated blood pressure responses linked to underlying cardiovascular disease.[60] Increases in systolic pressure >200 mmHg during maximal exercise among aerobically trained individuals may not be pathological in nature but solely reflect very high cardiac output and stroke volume.[61] The regulation of the blood pressure response to exercise is highly dependent on the exercise pressor reflex (discussed previously in the context of heart rate), arterial baroreflex, and compensatory autonomic control during exercise (Fig. 34.3).

Carotid and aortic baroreceptors are responsive to stretch and operate under a negative feedback loop to intricately control beat-by-beat arterial pressure. At rest, distension of the arterial wall from high pressure stretches the baroreceptors and initiates afferent nerve discharge. These afferent signals trigger subsequent efferent signals from the brainstem, increasing parasympathetic outflow and reducing sympathetic outflow, leading to reductions in heart rate and total peripheral resistance, ultimately decreasing blood pressure back to its original set point value. During exercise, the arterial baroreflex maintains its

role in regulating blood pressure but is reset by central command to operate around a higher exercise-induced blood pressure.[62-66] The upward and rightward resetting of the baroreflex occurs in an intensity-dependent manner from rest to heavy exercise and adjusts to greater sensitivity toward preventing excessive increases in blood pressure during exercise.[66-68] Interestingly, the regulation of arterial pressure is highly dependent on alterations in vascular tone and subsequent changes in total peripheral resistance. At rest, ∼25% of baroreflex-mediated changes in arterial pressure are achieved through changes in cardiac output. With increasing exercise intensity, however, baroreflex control of arterial pressure becomes almost entirely reliant on changes in total peripheral resistance.[69,70] Ultimately, baroreflex-mediated regulation of cardiac output and peripheral resistance contribute to changes in pulse wave dynamics in the central vasculature during exercise.

Central pressure and pulse wave dynamics

Left ventricular contraction generates a forward traveling compression wave, which increases central systolic pressure and drives flow. Exercise-induced increases in contractility increase the magnitude of the forward traveling compression wave generated by the left ventricle (Fig. 34.6).[71] This increase in forward wave energy appears to largely explain

exercise-induced increases in central systolic pressure, rather than increases in wave reflection.[71] The amount of wave reflection, relative to the forward wave (i.e., wave reflection magnitude) appears maintained during aerobic exercise,[71] despite substantial peripheral vasodilation. Our recent unpublished observations indicate reductions in wave reflection magnitude at the aorta during aerobic exercise (see representative data in Fig. 34.6, aortic reflection magnitude rest 32%, during exercise 18%). Emerging data appear to concur with this observation, suggesting reflection magnitude decreases among young, healthy adults despite increased forward wave magnitude and shortened reflected wave transit time.[72] Although reductions in wave reflection magnitude may relate to peripheral dilation of vasculature at the working muscle, the integrated wave reflection response during exercise is undoubtedly complicated by concomitant vasoconstriction at nonexercising tissue, large artery stiffening, constructive interference between upper and lower body wave reflections, and poor retrograde transmission of reflected pulse waves (i.e., reflected wave entrapment/dissipation).[73,74] As such, changes in aortic wave reflections during exercise remain an active area of investigation, and the mechanisms governing changes in wave reflection during exercise may differ by population, exercise modality, and intensity.

The contribution of pulse wave reflection to central systolic pressure (i.e., augmentation pressure/index) generally decreases during aerobic exercise.[75−78] It should be highlighted that augmentation index is a relatively poor index of wave reflection, thus reductions in augmentation index during exercise may reflect changes in heart rate and pattern of ventricular ejection rather than wave reflection per se.[77] Reductions in augmentation index during exercise appear attenuated with age, with older adults exhibiting increases in augmentation pressure and left ventricle wasted-pressure effort, and attenuated reductions in augmentation index during aerobic exercise.[75] As such, pulse wave reflection may contribute to increases in central systolic pressure during exercise when combined with age-related aortic stiffening and impaired functional sympatholysis that may alter the speed and magnitude of pulse wave reflection, respectively.[75] Ultimately, changes in cardiac chronotropy and central vascular pulse wave dynamics act to maximize flow output and transmission of forward-traveling pulse waves during exercise while minimizing wave reflection contributions to central systolic blood pressure. These mechanisms governing central blood pressure during aerobic exercise have further effects on the degree of blood pressure amplification traveling from the central to peripheral vasculature.

Pulse pressure amplification

The blood pressure waveform is distorted as it travels from the central to peripheral vasculature within the nonuniform viscoelastic arterial system.[79] This "distortion" manifests as an amplification of the blood pressure waveform, or an amplification of pulse pressure, while traveling distally, downstream.[74,79] Pulse pressure amplification occurs primarily owing to an increase in systolic blood pressure, with minimal changes in diastolic and mean pressure.[79] Data indicate that peripheral pulse pressure increases to a greater degree than central pulse pressure (i.e., greater pulse pressure amplification) during aerobic exercise,[75−78,80,81] although this is not universal.[82,83] Pulse pressure amplification increases during low-intensity exercise (i.e., 45% age-estimated maximal heart rate) and does not increase further during moderate- (50%−60% age-estimated maximal heart rate) or higher-intensity exercise (70% −80% age-estimated maximal heart rate).[75,77,84] These increases in pulse pressure amplification during exercise likely stem from changes in heart rate, reducing the potential contribution of wave reflection to central systolic pressure.[77]

Increases in pulse pressure amplification during aerobic exercise may be attenuated in older adults compared to young and middle-aged adults[75]; however, this is not universal[80] and may depend on presence of cardiovascular disease risk factors.[78] The degree of pulse pressure amplification during exercise also appears dependent on where peripheral blood pressure is assessed (i.e., at nonworking vs. active musculature). Pulse pressure amplification during exercise increases to inactive musculature (i.e., brachial artery during lower-body exercise),[85] while amplification at the level of working muscle may be attenuated[82] owing to local vasodilatory control in the working limb. Indeed, increases in pulse pressure amplification are attenuated when local vasodilator stimuli (e.g., heat, reactive hyperemia) are applied on top of an exercise stimulus.[81,86] While central pulse wave dynamics appear to minimize pulse pressure expansion in the central compared to peripheral vasculature, increases in pulse pressure ultimately relate to the manner in which blood flow is transmitted downstream.

Blood flow pulsatility

Blood flow in the arterial tree is inherently pulsatile (i.e., discontinuous) with greater blood velocity/flow occurring during systole than diastole. Blood flow pulsatility is linked with pulsatile pressure (i.e., pulse pressure) and forward pulse wave energy. As such, exercise-induced increases in pulse pressure and forward pulse wave energy are accompanied by concomitant increases in the degree of blood velocity pulsatility during aerobic exercise.[87−90] This has primarily been examined within the cerebral vasculature owing to growing links between hemodynamic pulsatility and brain health[91] and the implications of exercise on the brain.[92,93] Both extracranial (common carotid artery)[89] and intracranial (middle/anterior cerebral artery)[87,88,90] blood velocity pulsatility increase during aerobic exercise (Fig. 34.6). The mechanism governing the increase in cerebrovascular pulsatile blood flow may be multifactorial in

nature. Increased cerebral blood flow pulsatility during exercise could relate to downstream vasoconstriction via sympathetic activation and catecholamine release;[88] however, it remains plausible that local cerebral metabolic activity constrains sympathetic-mediated vasoconstriction (i.e., sympatholysis) within the cerebral vasculature.[94] Increases in pulse pressure and its effect on cerebral blood velocity may be a more likely explanation of exercise-induced increases in cerebral blood flow pulsatility.[90,95] Indeed, diastolic cerebral blood flow may decrease during exercise because of an inability of dynamic cerebral autoregulation to buffer the rapid decrease in pressure that occurs in diastole.[90] These reductions in diastolic velocity, concomitant with increases in systolic velocity[87] and forward pulse wave energy, likely explain increases in cerebral blood velocity pulsatility during exercise. Chronic exposure to pulsatile blood flow is linked with damage to sensitive vascular beds, such as the brain and kidney,[96] although causal data remain elusive. Importantly, there is no evidence that transient increases in pulsatility associated with exercise increases risk of accumulating such damage; rather, participation in exercise training is likely protective for organs like the brain.[92,93,97]

Large artery stiffness and characteristic impedance

Acute aerobic exercise increases the stiffness of the large elastic arteries (i.e., aorta, carotid; Fig. 34.6). Much of the literature to date has focused on the aorta, documenting significant increases in both proxy estimates (e.g., time to reflection)[71,76,77] and direct measures (e.g., pulse wave velocity) of aortic stiffness.[82,98−100] Aortic stiffness appears to increase during low and moderate-intensity aerobic exercise by roughly 1.0−1.5 m/s on average across studies. Similar observations have been made at the carotid artery, with reduced distensibility (i.e., increased stiffness) during aerobic exercise.[101] The exact hemodynamic mechanisms driving acute increases in large artery stiffness during exercise are likely multifaceted, and may include:

(A) Increases in mean and pulse pressure in the central vasculature, which would shift the pressure load burden within the artery wall from elastin to collagen,[102,103] functionally stiffening the vessel during exercise.[100] In support of this, reductions in aortic time to pulse wave reflection (Tr; a proxy of aortic stiffness) is associated with increases in mean pressure during aerobic exercise.[77]

(B) Increases in heart rate during exercise would shorten diastole and alter the time available for mechanical recoil of the artery wall.[104] The rate of diameter change lags behind reductions in pressure during diastole owing to vascular hysteresis and the nonlinear pressure-diameter relationship in the viscoelastic large arteries.[40,105] The magnitude of this delay appears dependent on the amplitude of stretch (imposed by pulse pressure).[105] As such, the shortened diastole imposed by exercise-induced elevations in heart rate likely prevents complete recoil of the aorta walls, thereby stiffening the vessel.

(C) Increases in sympathetic activity during exercise may directly modulate aortic stiffness,[106,107] although this is still debated.[108]

Ultimately, increases in large artery stiffness during exercise may alter large artery characteristic impedance. Changes in large artery characteristic impedance during aerobic exercise are still somewhat unclear. Early work suggested aortic characteristic impedance was maintained during aerobic exercise, despite increases in aortic stiffness.[100] Maintenance of characteristic impedance in this setting would require a roughly 10% increase in aortic diameter to offset the effect of increased aortic stiffness during exercise.[100] Work in canine models indicates that while aortic characteristic impedance is maintained during exercise in young animals, it increases during exercise in aged animals and impacts left ventricle performance.[109] Increases in distension pressure during exercise would tend to increase aortic diameter[109] while also stiffening the aorta owing to the preferential loading of collagen within the wall. Age-related dilation of the aorta[110] may limit further increases in diameter with exercise-mediated increases in distension pressure, thereby contributing to increased characteristic impedance during exercise with aging. Additional work is necessary to fully elucidate how aortic stiffness, diameter, and characteristic impedance respond during exercise, particularly since current data do not suggest aortic diameter increases during exercise. Indeed, imaging data obtained via MRI during exercise that report reductions, rather than increases, in ascending and proximal descending aorta cross-sectional area during exercise.[98] Cumulatively, changes in aortic stiffness, aortic characteristic impedance and pulsatile hemodynamics appear to largely be a consequence of cardiac adjustments to exercise. Taken together, the central hemodynamic response during exercise reflects complementary changes within the heart and peripheral vasculature that act to minimize arterial contributions to the already augmented workload of the left ventricle during exercise, supporting increases in blood flow for redistribution to working tissue.

Blood flow redistribution

Increasing blood flow to meet the metabolic demand of working cardiac and skeletal muscle is one of the major challenges faced by the cardiovascular system during exercise. Increased blood flow delivers necessary oxygen and nutrients to active tissues, removes metabolic by-products, and is proportional to the oxygen requirement by the active tissue.[111,112] Cardiac output increases dramatically with exercise and blood flow is preferentially redistributed away

from inactive tissue to highly active tissue. One major contributor to the redistribution is the highly malleable splanchnic and renal vasculature. Splanchnic and renal blood flow is dramatically reduced to ~25% of resting values during high intensity exercise and is compensated by a large increase in oxygen extraction.[21,113,114] Subsequent redistribution of the splanchnic/renal blood volume results in large increases in absolute blood flow in the coronary vasculature and active muscle beds, with ~85% of cardiac output directed to the active muscle during peak exercise.[21,113] This redistribution of blood flow away from less active tissue during exercise facilitates a dramatic and critical increase in blood flow to active skeletal muscle and tissue. The redistribution of blood flow that ultimately supports metabolic processes and muscular work necessary for exercise is largely dependent on the reciprocal actions of systemic sympathetic activation and local regulation of blood flow.

Total peripheral resistance and functional sympatholysis

Blood flow is inversely related to total peripheral resistance. During exercise, the cardiovascular control center increases sympathetic nerve activity which serves to increase total peripheral resistance (Fig. 34.3). The increased sympathetic activity, however, does not have a systemic effect. Sympathetic activity causes vasoconstriction in inactive tissue; however, in active skeletal muscle, the metabolite build-up and release of local vasodilators attenuates the sympathetic vasoconstriction by interfering with α-adrenergic receptor vasoconstriction.[115] This mechanism has been deemed functional sympatholysis.[116] This balancing act between sympathetic-vasoconstriction and functional sympatholysis increases total peripheral resistance in the inactive tissue and decreases total peripheral resistance in the active tissue, thus contributing to blood flow redistribution. This concept of blood flow regulation is critical because (1) without partial vasoconstriction, total peripheral resistance would dramatically fall and result in a mean arterial pressure too low to maintain perfusion pressure, (2) without local vasodilation, skeletal muscle would not receive adequate blood flow for metabolic exchange, and (3) without redistribution, much of the increased cardiac output would be delivered to tissues which do not need it, therefore reducing the arteriovenous O_2 gradient essentially indicating an inefficient use of the cardiac output. As exercise intensity increases, the attenuation of sympathetic vasoconstrictor tone is increased suggesting functional sympatholysis occurs in an intensity-dependent manner;[117] however, there is not a complete attenuation of all sympathetic activity at the level of the active muscle.[118,119] This phenomenon allows blood flow to reach the metabolically active muscle without

compromising blood pressure control. In order to maintain adequate arterial pressure when large muscle mass is working though, some vasoconstriction is imposed which reduces perfusion of the active muscle.[120] Thus sympathetic-mediated vasoconstriction is critical in maintaining arterial pressure in the face of functional sympatholysis and local vasodilation that give rise to increased blood flow during exercise.
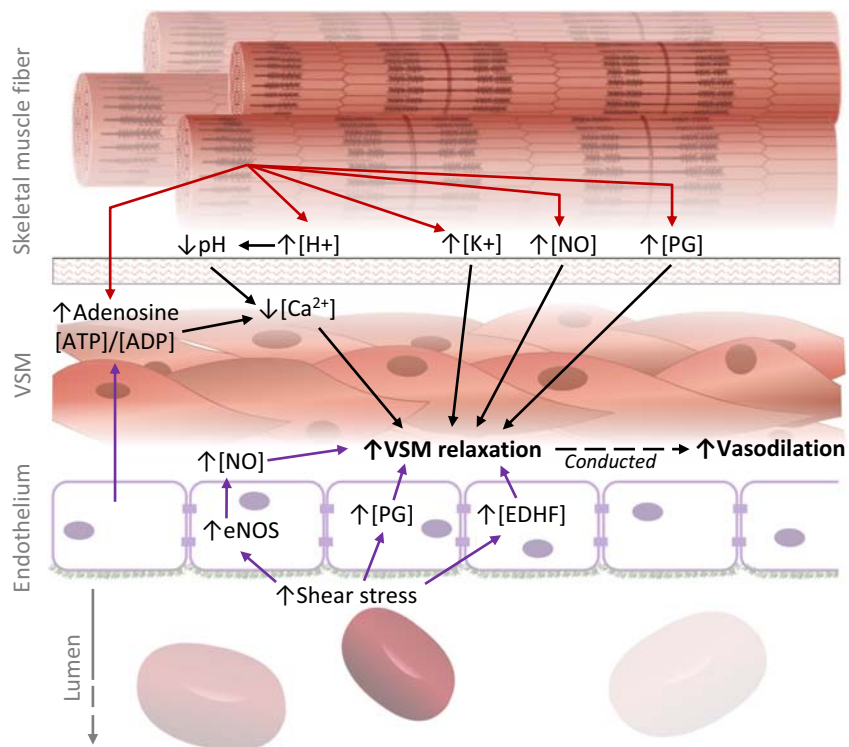
Exercise hyperemia

Blood flow increases to active skeletal muscle almost immediately following a single contraction. This quick and timely response is due to both rapid vasodilation and the mechanical effects of muscle contraction.[121−123] The initiation and maintenance of exercise hyperemia (i.e., increased blood flow) is largely due to vasodilation in the microcirculation, with minor contribution from the skeletal muscle pump, rather than increased pressure, as mean arterial pressure only increases modestly during aerobic exercise. Large conduit arteries, such as the femoral and brachial arteries, are also capable of vasodilating during exercise; however, this is not a functionally significant change for the regulation of blood flow. Exercise hyperemia is thus a coordinated response of the vasculature in and around the skeletal muscle and is successfully initiated and maintained by vasoactive substances, conducted vasodilation, and flow-mediated dilation.

Vasoactive substances

Local vasodilation is caused by chemical substances released from the muscle (e.g., nitric oxide, prostaglandins, adenosine, lactate, K^+), endothelium (e.g., nitric oxide, adenosine, K^+, ATP, prostaglandins), and red blood cells (e.g., ATP, nitric oxide) (See reviews[113,124]; overview presented in Fig. 34.7). The magnitude of vasodilatory substance release appears intensity-dependent, with higher intensities eliciting a greater vasodilatory stimulus and larger reduction in total peripheral resistance. Several redundant mechanisms exist through which vasodilation can occur within the microcirculation and increase local blood flow.

Muscle contraction changes the surrounding environment (i.e., lowers pH) and initiates production of several substances within the muscle itself that induce vasodilation, such as nitric oxide, prostaglandins, lactate, hydrogen ions, potassium, and adenosine. The production of ATP and muscular contraction leads to an accumulation of metabolites and byproducts that alter the environment within the muscle, which traditional dogma suggests cause vasodilation.[125] Indeed, exercise-induced increases in lactate, potassium,[126,127] and adenosine,[128] and decreases in pH[129] have been proposed to influence local regulation of blood flow and vasodilation. Nitric oxide and prostacyclin are

FIGURE 34.7   Overview of local regulation of vasodilation at metabolically active tissue during exercise. *ADP*, adenosine diphosphate; *ATP*, adenosine triphosphate; Ca^{2+}, calcium; *EDHF*, endothelial-derived hyperpolarizing factor; *eNOS*, endothelial nitric oxide synthase; *H+*, hydrogen; *K+*, potassium; *NO*, nitric oxide; *PG*, prostaglandins; *VSM*, vascular smooth muscle.

also two proposed central vasodilators given that each is stimulated by several vasodilator compounds and mechanical stimuli, as discussed below.[130] Unfortunately, determining which vasodilator is the largest contributor to exercise hyperemia is experimentally difficult owing to the inherent redundancy. As such, no single vasodilator has currently been shown to contribute >30% of the vasodilatory response to exercise, suggesting local vasodilation during exercise involves multiple vasoactive substances. Indeed, while lactate and pH modify vasodilation, they do not solely determine exercise hyperemia.[126,129] However, adenosine (by itself or as ADP or ATP) is considered one of the stronger vasodilator substances released by the exercising skeletal muscle owing to strong correlations between adenosine concentration and leg blood flow during exercise.[128] Endogenous nitrate is also converted to nitrite and ultimately nitric oxide, particularly during hypoxia, implicating another pathway by which vasodilation is induced in active muscle.[124,131] The individual importance of these chemical and metabolic substances within the active muscle is complicated by their complex interplay as part of the integrated exercise hyperemic response. Ultimately, the complex interaction between vasodilators and redundant mechanisms within the vasculature system is critical to maintain blood flow and thus nutrient delivery and waste removal during exercise.

Conducted vasodilation

Adequate vasodilation of the feed arteries is necessary to achieve adequate perfusion pressure to the downstream terminal arterioles where the highest resistance to flow occurs.[132] Interestingly, the local vasodilator response initiated in the smallest arterioles proximal to the capillaries is conducted upstream to larger feed arteries. Thus, initial distal arteriolar vasodilation spreads proximally through the vasculature via cell-to-cell communication between neighboring smooth muscle and endothelial cells. This upstream transmission of vasodilation is termed conducted vasodilation.[133,134] Conducted vasodilation is a complex and highly integrated process that ensures upstream resistance decreases and blood flow increases to facilitate downstream/local metabolic exchange during exercise.

Flow-mediated vasodilation

The initial increase in blood flow with exercise is driven by local vasodilatory factors; however, sustained vasodilation during exercise is additionally linked to the effect of increased blood flow on the endothelium. Increased local blood flow during exercise from local vasodilators and conducted vasodilation produces a frictional force (i.e., shear stress) on endothelial cells. Elevated shear stress

results in increased production of endothelial nitric oxide synthase (which synthesizes nitric oxide) and other vaso-active molecules (e.g., nitric oxide, prostacyclin, and endothelial-derived hyperpolarizing factor).[113,130] The response of the endothelial cells to the shear stress is termed flow-mediated vasodilation and is important for maintenance of increased blood flow during exercise.

Mechanical actions of the muscle

Exercise hyperemia is also minimally contributed to by muscle contraction. Muscle contraction influences both the arterial and venous circulation. When the muscle contracts, arterial blood flow is temporarily reduced or cut-off. When the muscle relaxes, however, blood flow increases. This increased flow influences shear stress on the vessel, leading to a flow-mediated dilation and increased nitric oxide and prostacyclin release. In the venous circulation, muscle contraction leads to a pumping effect where venous return is enhanced and subsequently perfusion due to the magnified pressure gradient. This concept is referred to as the skeletal muscle pump. The mechanical compression of muscle contraction squeezes blood toward the heart by taking advantage of the inherent composition and structure of the veins. Each contraction-induced compression of the highly compliant venous walls forces blood flow toward the heart, with one-way valves preventing backflow (contributing to increased preload, discussed in cardiac output). This movement of blood volume from the nearby venous bed increases the pressure gradient in the capillary bed. As the muscle relaxes, the expanded pressure gradient leads to an increase in muscle blood flow. Given the rhythmic nature of muscle contractions during dynamic exercise, mechanical contraction of skeletal muscle does not limit overall blood flow to the active skeletal muscles.

Cardiovascular limitations to exercise

Aerobic exercise capacity is dependent on an integrated response that facilitates the intake, delivery, and consumption of oxygen. The Fick principle describes oxygen consumption as the product of oxygen delivery (cardiac output: heart rate, stroke volume) and oxygen extraction at the working muscle (arterial-venous oxygen content difference).[135] The magnitude of each of these variables can increase determining the upper limit of whole-body oxygen consumption (i.e., VO_2 max). The ability of the cardiovascular system to deliver oxygenated blood to working tissues during whole body exercise, however, can become limited at different steps throughout the oxygen pathway. Whether exercise is limited by central (cardiac output) or peripheral (muscle) mechanisms is highly debated within the literature. The limiting mechanism is likely dependent on several factors such as exercise training status, age, and/

or chronic conditions. Potential mechanisms limiting oxygen consumption, and thus exercise capacity, have been reviewed extensively elsewhere[136,137] but will be summarized here within the context of (1) pulmonary diffusing and oxygen carrying capacity, (2) cardiac output, and (3) skeletal muscle oxygen extraction.

Oxygen delivery depends on the arterial oxygen content, which is determined in part by pulmonary diffusion capacity. Attenuated increases in pulmonary diffusion capacity during exercise would reduce oxygen content in arterial blood and are associated with reduced exercise capacity.[53] Indeed, pulmonary diffusion capacity may limit exercise in certain populations vulnerable to exercise-induced diffusion limitation (e.g., highly trained athletes, chronic obstructive pulmonary disease patients).[56,136] In this setting, exercise capacity can be improved by supplementing with oxygen to offset exercise-induced hypoxemia.[138−140] In young, healthy individuals, however, pulmonary diffusion capacity does not limit exercise and increasing arterial oxygen content via hyperoxia does not necessarily increase oxygen consumption.[141,142] Red blood cell mass is an additional contributor to exercise capacity owing to its direct influence on arterial oxygen content. Greater red blood cell mass increases hemoglobin content (the transporter of oxygen in the blood), which augments oxygen-carrying capacity and thus, oxygen delivery.[137] While the arterial oxygen content (via pulmonary diffusion capacity or red blood cell mass) can influence exercise capacity in certain populations, it is likely less limiting in generally healthy populations.

Increased delivery of oxygen to the working tissue can only be accomplished by augmenting blood flow via cardiac output. Traditional dogma suggests that cardiac output (and specifically stroke volume) is the primary physiological determinant of exercise capacity in most adults.[137] Cardiac output has been estimated to account for 70% −85% of the limitation in exercise capacity.[136] Consequently, an inability to increase cardiac work (and decrease ventricular-vascular coupling) during exercise is associated with reduced oxygen consumption,[143] and may be related to impaired ventricular vascular coupling at rest (higher ratio owing to greater ventricular elastance)[144−146] which reduces functional reserve during exercise.[35−38] Alternatively, the pulmonary circulation and right ventricle may become limiting in certain environments/populations[43,53] such as aging and elite athletes. Older adults and highly trained athletes may exhibit substantial increases in pulmonary artery stiffness during exercise, owing to age-related elevation of resting artery stiffness and extreme increases in cardiac output (for athletes)/PAP during exercise, respectively. These large increases in pulmonary artery stiffness augment right ventricular afterload, thereby limiting stroke volume[48] and cardiac output during high intensity exercise.[43] As such, elevated pulmonary artery

stiffness is associated with reduced exercise capacity in certain populations.[54] Additionally, increased respiratory muscle work during high intensity exercise may create a "steal" phenomenon whereby competition between respiratory and skeletal muscle blood flow reduces oxygen delivery to locomotor muscles and limits exercise capacity.[147] Cumulatively, left or right ventricular limitations that impair increases in cardiac output may limit the ability to perform aerobic exercise.

Oxygen delivery to the periphery does not guarantee extraction by the active tissue. Exercise capacity may therefore be dependent on the ability of the mitochondria to extract and use oxygen during exercise. Although early data suggested oxygen extraction is maximized (extracting ∼88% of arterial oxygen content) at the active muscle during heavy whole-body exercise,[136] more recent data suggest oxygen consumption among untrained individuals appears limited by mitochondrial oxygen demand, rather than oxygen supply (e.g., cardiac output).[135] It is evident that the role of the periphery in limiting exercise capacity requires further research to determine the magnitude of its contribution. In summary, multiple mechanisms throughout the oxygen cascade can limit aerobic exercise capacity and may differ based on environment, age, sex, and clinical conditions.

Summary

Aerobic exercise requires a complex, coordinated response from the cardiovascular system to ensure adequate blood flow to metabolically active tissue and maintenance of blood pressure. The complementary cardiac and vascular responses during exercise act to minimize vascular contributions to the already prioritized increase in cardiac work during exercise. Increases in cardiac output are directed to metabolically active and away from inactive vascular beds through reciprocal actions of the sympathetic nervous system and local regulators of blood flow. Blood flow to skeletal muscle is maximized through multiple, redundant vasodilatory mechanisms that can be conducted upstream to ensure adequate oxygen delivery and removal of metabolic waste. Ultimately, the highly integrated cardiovascular response can become limiting at multiple levels of oxygen intake (pulmonary circulation), delivery (cardiac output, blood flow distribution), and use (mitochondrial O_2 extraction); however, the limiting factors may vary by population, modality, and environment.

Examining cardiovascular adjustments during exercise remains a formidable challenge owing to experimental/methodological constraints that are inherent with exercise (e.g., intense movement, physiological noise). Emerging methodologies and innovative research designs are making measurement of cardiovascular responses during exercise more achievable, lending optimism to the prospect of gaining new insight into the mechanisms and regulation of cardiovascular hemodynamics during exercise. Future work is still necessary to better understand clinical implications for cardiovascular adjustments to aerobic exercise and the degree to which responses differ in clinical populations with limited cardiovascular function or exercise capacity. Future work delineating the coupling of pulmonary circulation and right heart function with left heart function and impact on myocardial work and cardiac output is needed. Additional work is necessary to better interrogate changes in large artery characteristic impedance, artery stiffness, and upper/lower body pulse wave reflection during exercise. Further examination of ventricular-vascular coupling during exercise in health and disease requires use of pressure-flow relationships and aortic input impedance, rather than reliance on elastance which is not sensitive to pulsatile load.[39] Finally, the impact of sex, race, and ethnicity on the integrative cardiovascular response to aerobic exercise needs to be better understood. Although the mechanisms governing vasodilatory responses during exercise are redundant and complex, additional work seeking to understand limiting factors within specific chronic diseases may help inform therapeutic treatments.

References

1. Goodwin GM, McCloskey DI, Mitchell JH. Cardiovascular and respiratory responses to changes in central command during isometric exercise at constant muscle tension. **J Physiol**. 1972; 226:173−190.
2. Krogh A, Lindhard J. The regulation of respiration and circulation during the initial stages of muscular work. **J Physiol**. 1913; 47:112−136.
3. Williamson JW, Fadel PJ, Mitchell JH. New insights into central cardiovascular control during exercise in humans: a central command update. **Exp Physiol**. 2006; 91:51−58.
4. Williamson JW, McColl R, Mathews D, Ginsburg M, Mitchell JH. Activation of the insular cortex is affected by the intensity of exercise. **J Appl Physiol (1985)**. 1999; 87:1213−1219.
5. Williamson JW, McColl R, Mathews D, Mitchell JH, Raven PB, Morgan WP. Brain activation by central command during actual and imagined handgrip under hypnosis. **J Appl Physiol (1985)**. 2002; 92:1317−1324.
6. Alam M, Smirk FH. Observations in man upon a blood pressure raising reflex arising from the voluntary muscles. **J Physiol**. 1937; 89:372−383.
7. Secher NH, Amann M. Human investigations into the exercise pressor reflex. **Exp Physiol**. 2012; 97:59−69.
8. Rowell LB, Hermansen L, Blackmon JR. Human cardiovascular and respiratory responses to graded muscle ischemia. **J Appl Physiol**. 1976; 41:693−701.
9. Bell MP, White MJ. Cardiovascular responses to external compression of human calf muscle vary during graded metaboreflex stimulation. **Exp Physiol**. 2005; 90:383−391.
10. Amann M, Blain GM, Proctor LT, Sebranek JJ, Pegelow DF, Dempsey JA. Group III and IV muscle afferents contribute to

ventilatory and cardiovascular response to rhythmic exercise in humans. **J Appl Physiol (1985)**. 2010; 109:966−976.

11. Amann M, Runnels S, Morgan DE, et al. On the contribution of group III and IV muscle afferents to the circulatory response to rhythmic exercise in humans. **J Physiol**. 2011; 589:3855−3866.

12. Leosco D, Parisi V, Femminella GD, et al. Effects of exercise training on cardiovascular adrenergic system. **Front Physiol**. 2013; 4:348.

13. Rockman HA, Koch WJ, Lefkowitz RJ. Seven-transmembrane-spanning receptors and heart function. **Nature**. 2002; 415:206−212.

14. Smith DL, Fernhall B. **Advanced Cardiovascular Exercise Physiology**. Champaign, IL: Human Kinetics; 2011:139−162.

15. Rowland T. Echocardiography and circulatory response to progressive endurance exercise. **Sports Med**. 2008; 38:541−551.

16. Smith DL, Fernhall B. **Advanced Cardiovascular Exercise Physiology**. Champaign, IL: Human Kinetics; 2011.

17. Joyce W, Wang T. How cardiac output is regulated: August Krogh's proto-Guytonian understanding of the importance of venous return. **Comp Biochem Physiol A Mol Integr Physiol**. 2020; 253:110861.

18. Miller JD, Pegelow DF, Jacques AJ, Dempsey JA. Skeletal muscle pump versus respiratory muscle pump: modulation of venous return from the locomotor limb in humans. **J Physiol**. 2005; 563:925−943.

19. Magder S. Venous mechanics of contracting gastrocnemius muscle and the muscle pump theory. **J Appl Physiol (1985)**. 1995; 79:1930−1935.

20. Anrep GV, von Saalfeld E. The blood flow through the skeletal muscle in relation to its contraction. **J Physiol**. 1935; 85:375−399.

21. Rowell LB. **Human Cardiovascular Control**. New York, New York: Oxford University Press; 1993.

22. Channer KS, Jones JV. The contribution of atrial systole to mitral diastolic blood flow increases during exercise in humans. **J Physiol**. 1989; 411:53−61.

23. Notomi Y, Martin-Miklovic MG, Oryszak SJ, et al. Enhanced ventricular untwisting during exercise: a mechanistic manifestation of elastic recoil described by Doppler tissue imaging. **Circulation**. 2006; 113:2524−2533.

24. Stöhr EJ, González-Alonso J, Shave R. Left ventricular mechanical limitations to stroke volume in healthy humans during incremental exercise. **Am J Physiol Heart Circ Physiol**. 2011; 301:H478−H487.

25. Doucende G, Schuster I, Rupp T, et al. Kinetics of left ventricular strains and torsion during incremental exercise in healthy subjects: the key role of torsional mechanics for systolic-diastolic coupling. **Circ Cardiovasc Imaging**. 2010; 3:586−594.

26. Katz AM. Ernest Henry Starling, his predecessors, and the "Law of the Heart". **Circulation**. 2002; 106:2986−2992.

27. Matsubara I, Yagi N, Endoh M. Behaviour of myosin projections during the staircase phenomenon of heart muscle. **Nature**. 1978; 273:67.

28. Rowland T, Unnithan V, Fernhall B, Baynard T, Lange C. Left ventricular response to dynamic exercise in young cyclists. **Med Sci Sports Exerc**. 2002; 34:637−642.

29. Nichols CG, Hanck DA, Jewell BR. The Anrep effect: an intrinsic myocardial mechanism. **Can J Physiol Pharmacol**. 1988; 66:924−929.

30. Reil JC, Reil GH, Kovács Á, et al. CaMKII activity contributes to homeometric autoregulation of the heart: a novel mechanism for the Anrep effect. **J Physiol**. 2020; 598:3129−3153.

31. Sarnoff SJ, Mitchell JH, Gilmore JP, Remensnyder JP. Homeometric autoregulation in the heart. **Circ Res**. 1960; 8:1077−1091.

32. Ikonomidis I, Aboyans V, Blacher J, et al. The role of ventricular-arterial coupling in cardiac disease and heart failure: assessment, clinical implications and therapeutic interventions. A consensus document of the European Society of Cardiology Working Group on Aorta & Peripheral Vascular Diseases, European Association of Cardiovascular Imaging, and Heart Failure Association. **Eur J Heart Fail**. 2019; 21:402−424.

33. Sunagawa K, Maughan WL, Burkhoff D, Sagawa K. Left ventricular interaction with arterial load studied in isolated canine ventricle. **Am J Physiol**. 1983; 245:H773−H780.

34. Chantler PD, Lakatta EG, Najjar SS. Arterial-ventricular coupling: mechanistic insights into cardiovascular performance at rest and during exercise. **J Appl Physiol (1985)**. 2008; 105:1342−1351.

35. Asanoi H, Kameyama T, Ishizaka S, Sasayama S. [Ventriculo-arterial coupling during aerobic and anaerobic exercise in normal subjects]. **J Cardiol**. 1990; 20:423−429.

36. Najjar SS, Schulman SP, Gerstenblith G, et al. Age and gender affect ventricular-vascular coupling during aerobic exercise. **J Am Coll Cardiol**. 2004; 44:611−617.

37. Cote AT, Bredin SS, Phillips AA, et al. Left ventricular mechanics and arterial-ventricular coupling following high-intensity interval exercise. **J Appl Physiol (1985)**. 2013; 115:1705−1713.

38. Fahs CA, Rossow LM, Yan H, et al. Resting and post exercise arterial-ventricular coupling in endurance-trained men and women. **J Hum Hypertens**. 2013; 27:552−556.

39. Chirinos JA, Rietzschel ER, Shiva-Kumar P, et al. Effective arterial elastance is insensitive to pulsatile arterial load. **Hypertension**. 2014; 64:1022−1031.

40. Nichols WW, O'Rourke MF. **McDonald's Blood Flow in Arteries. Theoretical, Experimental and Clinical Principles**. 5th ed. London: Hodder Arnold; 2005.

41. O'Rourke MF, Taylor MG. Input impedance of the systemic circulation. **Circ Res**. 1967; 20:365−380.

42. Bellofiore A, Dinges E, Naeije R, et al. Reduced haemodynamic coupling and exercise are associated with vascular stiffening in pulmonary arterial hypertension. **Heart**. 2017; 103:421−427.

43. Dempsey JA. Respiratory determinants of exercise limitation: focus on phrenic afferents and the lung vasculature. **Clin Chest Med**. 2019; 40:331−342.

44. Esfandiari S, Wright SP, Goodman JM, Sasson Z, Mak S. Pulmonary artery wedge pressure relative to exercise work rate in older men and women. **Med Sci Sports Exerc**. 2017; 49:1297−1304.

45. Kane GC, Sachdev A, Villarraga HR, et al. Impact of age on pulmonary artery systolic pressures at rest and with exercise. **Echo Res Pract**. 2016; 3:53−61.

46. Kovacs G, Berghold A, Scheidl S, Olschewski H. Pulmonary arterial pressure during rest and exercise in healthy subjects: a systematic review. **Eur Respir J**. 2009; 34:888−894.

47. Vriz O, Argiento P, D'Alto M, et al. Increased pulmonary vascular resistance in early stage systemic hypertension: a resting and exercise stress echocardiography study. **Can J Cardiol**. 2015; 31:537−543.

48. Buchan TA, Wright SP, Esfandiari S, et al. Pulmonary hemodynamic and right ventricular responses to brief and prolonged exercise in middle-aged endurance athletes. **Am J Physiol Heart Circ Physiol**. 2019; 316:H326−h334.

49. Esfandiari S, Wolsk E, Granton D, et al. Pulmonary arterial wedge pressure at rest and during exercise in healthy adults: a systematic review and meta-analysis. **J Card Fail**. 2019; 25:114−122.

50. Naeije R, Vanderpool R, Dhakal BP, et al. Exercise-induced pulmonary hypertension: physiological basis and methodological concerns. **Am J Respir Crit Care Med**. 2013; 187:576−583.

51. Lewis GD, Bossone E, Naeije R, et al. Pulmonary vascular hemodynamic response to exercise in cardiopulmonary diseases. **Circulation**. 2013; 128:1470−1479.

52. Reeves JT, Linehan JH, Stenmark KR. Distensibility of the normal human lung circulation during exercise. **Am J Physiol Lung Cell Mol Physiol**. 2005; 288:L419−L425.

53. Coffman KE, Carlson AR, Miller AD, Johnson BD, Taylor BJ. The effect of aging and cardiorespiratory fitness on the lung diffusing capacity response to exercise in healthy humans. **J Appl Physiol (1985)**. 2017; 122:1425−1434.

54. Kang KW, Chang HJ, Kim YJ, et al. Cardiac magnetic resonance imaging-derived pulmonary artery distensibility index correlates with pulmonary artery stiffness and predicts functional capacity in patients with pulmonary arterial hypertension. **Circ J**. 2011; 75:2244−2251.

55. Forouzan O, Warczytowa J, Wieben O, François CJ, Chesler NC. Non-invasive measurement using cardiovascular magnetic resonance of changes in pulmonary artery stiffness with exercise. **J Cardiovasc Magn Reson**. 2015; 17:109.

56. Dempsey JA, Hanson PG, Henderson KS. Exercise-induced arterial hypoxaemia in healthy human subjects at sea level. **J Physiol**. 1984; 355:161−175.

57. Dempsey JA, La Gerche A, Hull JH. Is the healthy respiratory system built just right, overbuilt, or underbuilt to meet the demands imposed by exercise? **J Appl Physiol (1985)**. 2020; 129:1235−1256.

58. Dempsey JA, McKenzie DC, Haverkamp HC, Eldridge MW. Update in the understanding of respiratory limitations to exercise performance in fit, active adults. **Chest**. 2008; 134:613−622.

59. Sabbahi A, Arena R, Kaminsky LA, Myers J, Phillips SA. Peak blood pressure responses during maximum cardiopulmonary exercise testing: reference standards from FRIEND (Fitness Registry and the Importance of Exercise: A National Database). **Hypertension**. 2018; 71:229−236.

60. Schultz MG, La Gerche A, Sharman JE. Blood pressure response to exercise and cardiovascular disease. **Curr Hypertens Rep**. 2017; 19:89.

61. Tanaka H, Bassett Jr DR, Turner MJ. Exaggerated blood pressure response to maximal exercise in endurance-trained individuals. **Am J Hypertens**. 1996; 9:1099−1103.

62. Bevegård BS, Shepherd JT. Circulatory effects of stimulating the carotid arterial stretch receptors in man at rest and during exercise. **J Clin Invest**. 1966; 45:132−142.

63. Fadel PJ, Ogoh S, Watenpaugh DE, et al. Carotid baroreflex regulation of sympathetic nerve activity during dynamic exercise in humans. **Am J Physiol Heart Circ Physiol**. 2001; 280:H1383−H1390.

64. Joyner MJ. Baroreceptor function during exercise: resetting the record. **Exp Physiol**. 2006; 91:27−36.

65. Papelier Y, Escourrou P, Gauthier JP, Rowell LB. Carotid baroreflex control of blood pressure and heart rate in men during dynamic exercise. **J Appl Physiol (1985)**. 1994; 77:502−506.

66. Potts JT, Shi XR, Raven PB. Carotid baroreflex responsiveness during dynamic exercise in humans. **Am J Physiol**. 1993; 265:H1928−H1938.

67. Norton KH, Gallagher KM, Smith SA, Querry RG, Welch-O'Connor RM, Raven PB. Carotid baroreflex function during prolonged exercise. **J Appl Physiol (1985)**. 1999; 87:339−347.

68. Raven PB, Fadel PJ, Ogoh S. Arterial baroreflex resetting during exercise: a current perspective. **Exp Physiol**. 2006; 91:37−49.

69. Fadel PJ. Arterial baroreflex control of the peripheral vasculature in humans: rest and exercise. **Med Sci Sports Exerc**. 2008; 40:2055−2062.

70. Ogoh S, Fadel PJ, Nissen P, et al. Baroreflex-mediated changes in cardiac output and vascular conductance in response to alterations in carotid sinus pressure during exercise in humans. **J Physiol**. 2003; 550:317−324.

71. Schultz MG, Davies JE, Roberts-Thomson P, Black JA, Hughes AD, Sharman JE. Exercise central (aortic) blood pressure is predominantly driven by forward traveling waves, not wave reflection. **Hypertension**. 2013; 62:175−182.

72. Stock JM, Chirinos JA, Edwards DG. Lower-body dynamic exercise reduces wave reflection in healthy young adults. **Exp Physiol**. 2021; 106:1720−1730.

73. Davies JE, Alastruey J, Francis DP, et al. Attenuation of wave reflection by wave entrapment creates a "horizon effect" in the human aorta. **Hypertension**. 2012; 60:778−785.

74. Hope SA, Tay DB, Meredith IT, Cameron JD. Waveform dispersion, not reflection, may be the major determinant of aortic pressure wave morphology. **Am J Physiol Heart Circ Physiol**. 2005; 289:H2497−H2502.

75. Martin JS, Casey DP, Gurovich AN, Beck DT, Braith RW. Association of age with timing and amplitude of reflected pressure waves during exercise in men. **Am J Hypertens**. 2011; 24:415−420.

76. Sharman JE, McEniery CM, Campbell R, et al. Nitric oxide does not significantly contribute to changes in pulse pressure amplification during light aerobic exercise. **Hypertension**. 2008; 51:856−861.

77. Sharman JE, McEniery CM, Campbell RI, Coombes JS, Wilkinson IB, Cockcroft JR. The effect of exercise on large artery haemodynamics in healthy young men. **Eur J Clin Invest**. 2005; 35:738−744.

78. Sharman JE, McEniery CM, Dhakam ZR, Coombes JS, Wilkinson IB, Cockcroft JR. Pulse pressure amplification during exercise is significantly reduced with age and hypercholesterolemia. **J Hypertens**. 2007; 25:1249−1254.

79. Avolio AP, Van Bortel LM, Boutouyrie P, et al. Role of pulse pressure amplification in arterial hypertension: experts' opinion and review of the data. **Hypertension**. 2009; 54:375−383.

80. Casey DP, Nichols WW, Braith RW. Impact of aging on central pressure wave reflection characteristics during exercise. **Am J Hypertens**. 2008; 21:419−424.

81. Rowell LB, Brengelmann GL, Blackmon JR, Bruce RA, Murray JA. Disparities between aortic and peripheral pulse pressures induced by upright exercise and vasomotor changes in man. **Circulation**. 1968; 37:954−964.

82. Kroeker EJ, Wood EH. Comparison of simultaneously recorded central and peripheral arterial pressure pulses during rest, exercise and tilted position in man. **Circ Res**. 1955; 3:623−632.

83. Sharman JE, Lim R, Qasem AM, et al. Validation of a generalized transfer function to noninvasively derive central blood pressure during exercise. **Hypertension**. 2006; 47:1203−1208.

84. Holland DJ, Sacre JW, McFarlane SJ, Coombes JS, Sharman JE. Pulse wave analysis is a reproducible technique for measuring central blood pressure during hemodynamic perturbations induced by exercise. **Am J Hypertens**. 2008; 21:1100−1106.

85. Lacy PS, Brunel P, Baschiera F, Botha J, Williams B. Effects of exercise on central aortic pressure before and after treatment with renin-angiotensin system blockade in patients with hypertension. **J Renin Angiotensin Aldosterone Syst**. 2015; 16:1052−1060.

86. Bevegård BS, Shepherd JT. Reaction in man of resistance and capacity vessels in forearm and hand to leg exercise. **J Appl Physiol**. 1966; 21:123−132.

87. Alwatban MR, Liu Y, Perdomo SJ, et al. TCD cerebral hemodynamic changes during moderate-intensity exercise in older adults. **J Neuroimaging**. 2020; 30:76−81.

88. Heckmann JG, Hilz MJ, Mück-Weymann M, Neundörfer B. Transcranial Doppler sonography-ergometer test for the non-invasive assessment of cerebrovascular autoregulation in humans. **J Neurol Sci**. 2000; 177:41−47.

89. Jiang ZL, Yamaguchi H, Tanaka H, et al. Blood flow velocity in the common carotid artery in humans during graded exercise on a treadmill. **Eur J Appl Physiol Occup Physiol**. 1995; 70:234−239.

90. Ogoh S, Fadel PJ, Zhang R, et al. Middle cerebral artery flow velocity and pulse pressure during dynamic exercise in humans. **Am J Physiol Heart Circ Physiol**. 2005; 288:H1526−H1531.

91. Mitchell GF, van Buchem MA, Sigurdsson S, et al. Arterial stiffness, pressure and flow pulsatility and brain structure and function: the Age, Gene/Environment Susceptibility–Reykjavik study. **Brain**. 2011; 134:3398−3407.

92. Tarumi T, Zhang R. The role of exercise-induced cardiovascular adaptation in brain health. **Exerc Sport Sci Rev**. 2015; 43:181−189.

93. Tarumi T, Zhang R. Cerebral blood flow in normal aging adults: cardiovascular determinants, clinical implications, and aerobic fitness. **J Neurochem**. 2018; 144:595−608.

94. Brassard P, Tymko MM, Ainslie PN. Sympathetic control of the brain circulation: appreciating the complexities to better understand the controversy. **Auton Neurosci**. 2017; 207:37−47.

95. Jørgensen LG, Perko G, Secher NH. Regional cerebral artery mean flow velocity and blood flow during dynamic exercise in humans. **J Appl Physiol (1985)**. 1992; 73:1825−1830.

96. Mitchell GF. Aortic stiffness, pressure and flow pulsatility, and target organ damage. **J Appl Physiol (1985)**. 2018; 125:1871−1880.

97. Barnes JN, Corkery AT. Exercise improves vascular function, but does this translate to the brain? **Brain Plast**. 2018; 4:65−79.

98. Bal-Theoleyre L, Lalande A, Kober F, et al. Aortic function's adaptation in response to exercise-induced stress assessing by 1.5T MRI: a pilot study in healthy volunteers. **PLoS One**. 2016; 11:e0157704.

99. Keith LJ, Rattigan S, Keske MA, Jose M, Sharman JE. Exercise aortic stiffness: reproducibility and relation to end-organ damage in men. **J Hum Hypertens**. 2013; 27:516−522.

100. Murgo JP, Westerhof N, Giolma JP, Altobelli SA. Effects of exercise on aortic input impedance and pressure wave forms in normal humans. **Circ Res**. 1981; 48:334−343.

101. Studinger P, Lénárd Z, Kováts Z, Kocsis L, Kollai M. Static and dynamic changes in carotid artery diameter in humans during and after strenuous exercise. **J Physiol**. 2003; 550:575−583.

102. Armentano RL, Levenson J, Barra JG, et al. Assessment of elastin and collagen contribution to aortic elasticity in conscious dogs. **Am J Physiol**. 1991; 260:H1870−H1877.

103. Townsend RR, Wilkinson IB, Schiffrin EL, et al. Recommendations for improving and standardizing vascular research on arterial stiffness: a scientific statement from the American Heart Association. **Hypertension**. 2015; 66:698−722.

104. Mangoni AA, Mircoli L, Giannattasio C, Ferrari AU, Mancia G. Heart rate-dependence of arterial distensibility in vivo. **J Hypertens**. 1996; 14:897−901.

105. Dobrin PB. Mechanical properties of arteries. **Physiol Rev**. 1978; 58:397−460.

106. Holwerda SW, Luehrs RE, DuBose L, et al. Elevated muscle sympathetic nerve activity contributes to central artery stiffness in young and middle-age/older adults. **Hypertension**. 2019; 73:1025−1035.

107. Swierblewska E, Hering D, Kara T, et al. An independent relationship between muscle sympathetic nerve activity and pulse wave velocity in normal humans. **J Hypertens**. 2010; 28:979−984.

108. Mäki-Petäjä KM, Wilkinson IB, Nichols WW. Letter by Mäki-Petäjä et al Regarding Article "Elevated Muscle Sympathetic Nerve Activity Contributes to Central Artery Stiffness in Young and Middle-Age/Older Adults". **Hypertension**. 2019; 74:e31−e32.

109. Yin FC, Weisfeldt ML, Milnor WR. Role of aortic input impedance in the decreased cardiovascular response to exercise with aging in dogs. **J Clin Invest**. 1981; 68:28−38.

110. Mitchell GF, Conlin PR, Dunlap ME, et al. Aortic diameter, wall stiffness, and wave reflection in systolic hypertension. **Hypertension**. 2008; 51:105−111.

111. Corcondilas A, Koroxenidis GT, Shepherd JT. Effect of a brief contraction of forearm muscles on forearm blood flow. **J Appl Physiol**. 1964; 19:142−146.

112. Saltin B. Metabolic fundamentals in exercise. **Med Sci Sports**. 1973; 5:137−146.

113. Joyner MJ, Casey DP. Regulation of increased blood flow (hyperemia) to muscles during exercise: a hierarchy of competing physiological needs. **Physiol Rev**. 2015; 95:549−601.

114. Rowell LB, Blackmon JR, Kenny MA, Escourrou P. Splanchnic vasomotor and metabolic adjustments to hypoxia and exercise in humans. **Am J Physiol**. 1984; 247:H251−H258.

115. Hansen J, Sander M, Thomas GD. Metabolic modulation of sympathetic vasoconstriction in exercising skeletal muscle. **Acta Physiol Scand**. 2000; 168:489−503.

116. Remensnyder JP, Mitchell JH, Sarnoff SJ. Functional sympatholysis during muscular activity. Observations on influence of carotid sinus on oxygen uptake. **Circ Res**. 1962; 11:370−380.

117. Tschakovsky ME, Sujirattanawimol K, Ruble SB, Valic Z, Joyner MJ. Is sympathetic neural vasoconstriction blunted in the vascular bed of exercising human muscle? **J Physiol**. 2002; 541:623−635.

118. Buckwalter JB, Clifford PS. The paradox of sympathetic vasoconstriction in exercising skeletal muscle. **Exerc Sport Sci Rev**. 2001; 29:159−163.

119. Buckwalter JB, Mueller PJ, Clifford PS. Sympathetic vasoconstriction in active skeletal muscles during dynamic exercise. **J Appl Physiol (1985)**. 1997; 83:1575−1580.

120. Secher NH, Clausen JP, Klausen K, Noer I, Trap-Jensen J. Central and regional circulatory effects of adding arm exercise to leg exercise. **Acta Physiol Scand**. 1977; 100:288−297.

121. Saunders NR, Tschakovsky ME. Evidence for a rapid vasodilatory contribution to immediate hyperemia in rest-to-mild and mild-to-moderate forearm exercise transitions in humans. **J Appl Physiol (1985)**. 2004; 97:1143−1151.

122. Tschakovsky ME, Sheriff DD. Immediate exercise hyperemia: contributions of the muscle pump vs. rapid vasodilation. **J Appl Physiol (1985)**. 2004; 97:739−747.

123. Tschakovsky ME, Shoemaker JK, Hughson RL. Vasodilation and muscle pump contribution to immediate exercise hyperemia. **Am J Physiol**. 1996; 271:H1697−H1701.

124. Clifford PS, Hellsten Y. Vasodilatory mechanisms in contracting skeletal muscle. **J Appl Physiol (1985)**. 2004; 97:393−403.

125. Gaskell WH. On the tonicity of the heart and blood vessels. **J Physiol**. 1880; 3:48−92.16.

126. Lott ME, Hogeman CS, Vickery L, Kunselman AR, Sinoway LI, MacLean DA. Effects of dynamic exercise on mean blood velocity and muscle interstitial metabolite responses in humans. **Am J Physiol Heart Circ Physiol**. 2001; 281:H1734−H1741.

127. Juel C, Pilegaard H, Nielsen JJ, Bangsbo J. Interstitial K(+) in human skeletal muscle during and after dynamic graded exercise determined by microdialysis. **Am J Physiol Regul Integr Comp Physiol**. 2000; 278:R400−R406.

128. Hellsten Y, Maclean D, Rådegran G, Saltin B, Bangsbo J. Adenosine concentrations in the interstitium of resting and contracting human skeletal muscle. **Circulation**. 1998; 98:6−8.

129. Street D, Bangsbo J, Juel C. Interstitial pH in human skeletal muscle during and after dynamic graded exercise. **J Physiol**. 2001; 537:993−998.

130. Hellsten Y, Nyberg M, Jensen LG, Mortensen SP. Vasodilator interactions in skeletal muscle blood flow regulation. **J Physiol**. 2012; 590:6297−6305.

131. Piknova B, Park JW, Kwan Jeff Lam K, Schechter AN. Nitrate as a source of nitrite and nitric oxide during exercise hyperemia in rat skeletal muscle. **Nitric Oxide**. 2016; 55−56:54−61.

132. Lash JM. Contribution of arterial feed vessels to skeletal muscle functional hyperemia. **J Appl Physiol (1985)**. 1994; 76:1512−1519.

133. Segal SS, Duling BR. Propagation of vasodilation in resistance vessels of the hamster: development and review of a working hypothesis. **Circ Res**. 1987; 61:Ii20−I25.

134. Segal SS, Welsh DG, Kurjiaka DT. Spread of vasodilatation and vasoconstriction along feed arteries and arterioles of hamster skeletal muscle. **J Physiol**. 1999; 516(Pt 1):283−291.

135. Gifford JR, Garten RS, Nelson AD, et al. Symmorphosis and skeletal muscle VO2 max : in vivo and in vitro measures reveal differing constraints in the exercise-trained and untrained human. **J Physiol**. 2016; 594:1741−1751.

136. Bassett Jr DR, Howley ET. Limiting factors for maximum oxygen uptake and determinants of endurance performance. **Med Sci Sports Exerc**. 2000; 32:70−84.

137. Joyner MJ, Dominelli PB. Central cardiovascular system limits to aerobic capacity. **Exp Physiol**. 2020. https://doi.org/10.1113/EP088187.

138. Rooyackers JM, Dekhuijzen PN, Van Herwaarden CL, Folgering HT. Training with supplemental oxygen in patients with COPD and hypoxaemia at peak exercise. **Eur Respir J**. 1997; 10:1278−1284.

139. Davidson AC, Leach R, George RJ, Geddes DM. Supplemental oxygen and exercise ability in chronic obstructive airways disease. **Thorax**. 1988; 43:965−971.

140. Powers SK, Lawler J, Dempsey JA, Dodd S, Landry G. Effects of incomplete pulmonary gas exchange on VO2 max. **J Appl Physiol (1985)**. 1989; 66:2491−2495.

141. Roca J, Agusti AG, Alonso A, et al. Effects of training on muscle O2 transport at VO2max. **J Appl Physiol (1985)**. 1992; 73:1067−1076.

142. Cardús J, Marrades RM, Roca J, et al. Effects of F(I)O2 on leg VO2 during cycle ergometry in sedentary subjects. **Med Sci Sports Exerc**. 1998; 30:697−703.

143. Fournier SB, Donley DA, Bonner DE, Devallance E, Olfert IM, Chantler PD. Improved arterial-ventricular coupling in metabolic syndrome after exercise training: a pilot study. **Med Sci Sports Exerc**. 2015; 47:2−11.

144. Chen C-H, Nakayama M, Nevo E, Fetics BJ, Maughan WL, Kass DA. Coupled systolic-ventricular and vascular stiffening with age. **J Am Coll Cardiol**. 1998; 32:1221−1227.

145. Kass DA. Ventricular arterial stiffening: integrating the pathophysiology. **Hypertension**. 2005; 46:185−193.

146. Kawaguchi M, Hay I, Fetics B, Kass DA. Combined ventricular systolic and arterial stiffening in patients with heart failure and preserved ejection fraction: implications for systolic and diastolic reserve limitations. **Circulation**. 2003; 107:714−720.

147. Sheel AW, Boushel R, Dempsey JA. Competition for blood flow distribution between respiratory and locomotor muscles: implications for muscle fatigue. **J Appl Physiol (1985)**. 2018; 125:820−831.

Chapter 35

Invasive hemodynamic assessments during exercise: normal patterns and clinical value

Kazunori Omote, Yogesh N.V. Reddy and Barry A. Borlaug

Mayo Clinic, Rochester, MN, United States

Introduction

Exertional dyspnea is one of the commonest symptoms for which medical evaluation is sought, but dyspnea may develop from a number of causes. Cardiac catheterization provides direct assessment for evidence of heart failure (HF), but resting hemodynamics are often normal in ambulatory patients with early stage HF.[1] Common and simple stressors such as saline loading can provide some value but are inferior to exercise testing.[2] Noninvasive cardiopulmonary exercise testing (CPET) provides valuable information on gas exchange and aerobic capacity but may not discern cardiac from noncardiac sources of dyspnea.[1,3] Invasive exercise hemodynamics provides the most robust and direct method to evaluate the causes for exercise intolerance and serves as the gold standard to confirm or refute the presence of HF or pulmonary hypertension (PH).[1,3–5] In this chapter we will review the emerging utility of invasive exercise physiology assessment in modern clinical practice.

Role for invasive hemodynamics in diagnostic ambiguity

The diagnosis of HF is often challenging because symptoms or signs of HF commonly overlap with other conditions.[5] HF can be defined objectively as the inability of the heart to perfuse the body without pathological increases in filling pressure during rest or exertion. The diagnosis of HF therefore relies upon the demonstration of elevated filling pressures, on the basis of either physical examination, radiography, natriuretic peptide levels, or echocardiography data. Certain symptoms such as orthopnea and paroxysmal nocturnal dyspnea are highly specific for HF, while more

common symptoms of dyspnea and fatigue are more sensitive but less specific. Echocardiography often provides valuable information including assessments of ventricular structure and function and valve disease but is less accurate to assess right- and left-filling pressures, particularly in an earlier or milder stage of HF where hemodynamics become abnormal only during exertion.[3,6] When these tests are inconclusive, invasive hemodynamic assessments, which have the ability to directly assess ventricular filling pressures, pulmonary arterial pressures, cardiac output (CO), pulmonary vascular resistance (PVR), and measures of O_2 transport and utilization, provides much greater accurate information for diagnosing HF. The insertion of an arterial catheter can also provide continuous arterial pressure measurements in a peripheral artery during exercise, which are valuable to assess arterial resistive and pulsatile hemodynamics, as well as ventricular–arterial interactions, during exercise.

Physiology of invasive hemodynamic assessment

HF is defined hemodynamically as an inability of the heart to pump blood to the body at a rate commensurate with its needs or to do so at the cost of elevated filling pressures.[7] This definition applies to both HF with reduced ejection fraction (HFrEF) and HF with preserved ejection fraction (HFpEF), and indeed, invasive hemodynamics studies have shown that both HF phenotypes share similar elevations in right heart filling pressure (right atrial pressure [RAP]) and left heart filling pressure (pulmonary capillary wedge pressure [PCWP] and left ventricular [LV] end-diastolic pressure [LVEDP]).[8,9] These hemodynamic perturbations
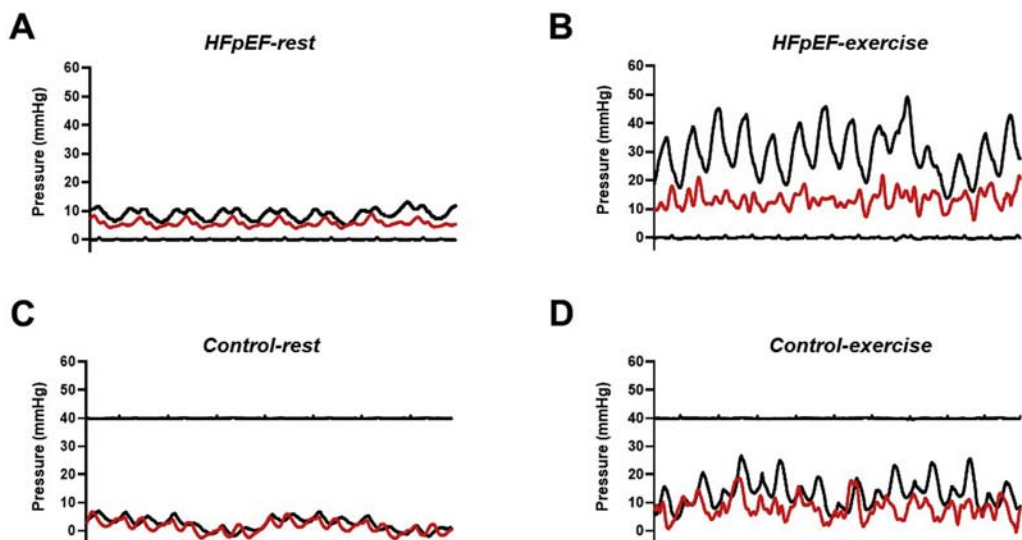
are correlated with dyspnea severity, pulmonary limitations, impairment in aerobic capacity, and associated with increased risk of mortality in HF.[10−14] Noninvasive modalities such as echocardiography are specific when frankly abnormal but frequently have low sensitivity to identify elevated filling pressures at rest or during exertion.[3,6] Despite clinical euvolemia, normal natriuretic peptide levels, echocardiography, and normal resting filling pressures at rest, patients may show a number of hemodynamic changes during exercise (Figs. 35.1 and 35.2). Given its definitive and comprehensive nature, invasive CPET has emerged as the gold standard test to assess cardiac filling pressures.[1,3]

Assessment of left-sided filling pressures
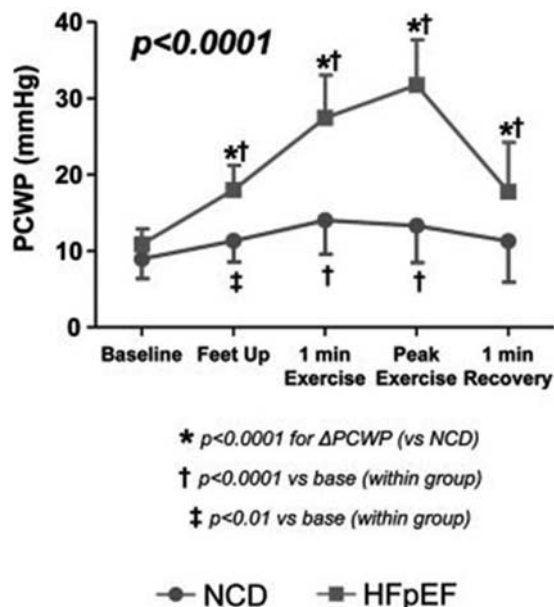
The determination of left-sided filling pressures (PCWP or LVEDP) is clinically important because it allows estimation of pulmonary venous pressure as it relates to dyspnea and PH, but also used clinically as an estimate of LV preload. Preload can be defined by the magnitude of distention or stretching of ventricular myocytes before the onset of contraction, which dictates the extent of myofiber shortening in the subsequent contraction according to Frank−Starling principle.[4] The PCWP or LVEDP is a useful surrogate for preload and correlates with the LV end-diastolic volume [LVEDV] which determines end-diastolic myofiber stretch. Filling pressures for any preload (LVEDV) are determined by both the compliance properties of the myocardium and extrinsic pericardial restraint mediated by the right heart and pericardium. The PCWP reflects the LVEDV reasonably well at lower filling pressures but as the PCWP increases

there is a weaker correlation between PCWP and preload due to the impact of pericardial restraint increasing the PCWP through an external compressive contract force without contributing to end-diastolic myocyte stretch. LV transmural pressure (LVTMP), which reflects LV preload independent of right heart congestion and pericardial restraint, can be estimated by subtracting extrinsic pericardial pressure (estimated from RA pressure) from the PCWP.[3,15−17] Determination of how much of the PCWP elevation is due to pericardial interaction as opposed to LV filling is particularly important during exercise where pericardial interaction may play an increasingly important role due to the acute heart dilation from an acute increase in venous return.

Regardless of mechanism, the risk of pulmonary congestion increases with acute increases in pulmonary venous and left-sided filling pressures. Notably, Reddy et al.[18] reported that the development of lung congestion assessed by lung ultrasound during exercise was significantly associated with exertional elevations in PCWP and left atrial (LA) stiffness in well-compensated ambulatory patients with HFpEF. On the other hand, patients with established HF often display increased LV filling pressure at rest, but the correlation between pulmonary venous pressure and lung congestion may be surprisingly weak. This is because many HF patients develop adaptations that allow them to tolerate even marked elevations of LA pressure without developing clinical or radiographic lung congestion.[19−22] The pulmonary adaptation to increased PCWP in HF is believed to be caused by reduced capillary filtration due to basal membrane thickening, enhanced alveolar fluid clearance, and increased lymphatic drainage.[23] Melenovsky and colleauges[24] demonstrated that pulmonary

FIGURE 35.1   Typical right atrial pressure (RAP; red) and pulmonary capillary wedge pressure (PCWP; black) tracings in a patient with HFpEF at rest (A) and with exercise (B) and in a control patient at respective states (C and D). *HFpEF*, heart failure with preserved ejection fraction.

FIGURE 35.2 PCWP increased to a greater extent in HFpEF compared with NCD with feet up and during exercise. PCWP returned to baseline almost immediately in recovery. *HFpEF*, heart failure with preserved ejection fraction; *NCD*, noncardiac dyspnea; *PCWP*, pulmonary capillary wedge pressure. *Figure adapted with permission from Borlaug BA, Nishimura RA, Sorajja P, Lam CS, Redfield MM. Exercise hemodynamics enhance diagnosis of early heart failure with preserved ejection fraction. Circ Heart Fail. 2010;3:588−595.*

congestion in patients with established HF is associated with increased PVR and reduced PA compliance, suggesting that lung congestion itself may contribute to PH severity in advanced HF.

Right atrial pressure

HF is characterized by neurohumoral activation and sodium retention that leads to excessive fluid accumulation in the systemic and pulmonary circulations, which coupled with abnormalities in right heart-pulmonary artery coupling results in elevation of right-sided filling pressures reflected by the RAP.[25] RAP is also a surrogate marker for pericardial pressure,[17] so when RAP and PCWP both become elevated in tandem to very high levels, this suggests that the heart has filled to the point at which the pericardium restrains further filling, and there is enhanced diastolic ventricular interaction (DVI) with the right heart and pericardium driving the PCWP elevation.[26] This is a distinct hemodynamic signature in patients with HF and a key reason for measuring RAP continuously throughout exercise testing. Patients with HF and elevated RAP are more likely to develop lung congestion during exercise, due to the combined effects of increased fluid filtration caused by high PCWP and reduced pulmonary lymphatic drainage due to central venous hypertension.[18]

Concept of pericardial restraint

The elastic pericardium exerts a compressive contact force on the surface of the myocardium that becomes more substantial when heart volume increases, as can occur in many forms of HF including HFrEF, HFpEF, and patients with pulmonary arterial hypertension (PAH).[26] Pericardial restraint plays an important role in determining hemodynamics, LV preload and ventricular function. For example, total heart enlargement and cardiomegaly in HFpEF in particular with right heart enlargement creates the substrate for increased pericardial restraint and DVI, where the right heart influences the left in parallel.[27] When DVI is enhanced, left heart filling pressures can be elevated disproportionate to the degree of LV diastolic stiffness and LVEDV is lower than expected (i.e., LVEDP and LVEDV become uncoupled), resulting in failure to augment CO through failure of Frank−Starling reserve.[28] This phenomenon is also commonly observed in patients with severe tricuspid regurgitation (TR) as well, where exertional right heart filling pressure elevation may mediate decreases in left heart filling during exercise despite increases in left-sided "filling" pressures.[15] Similar physiology has also been observed in a subset of patients with HFrEF where LV filling pressures and RAP increase in a 1:1 ratio, with no further enhancement in stroke volume (SV), owing to the restraining effects of the pericardium that prevent additional preload recruitment.[29,30]

Measurement of flow

The Fick principle

The Fick principle enables measurement of CO from directly measured O_2 consumption (VO_2) together with blood sampling to measure O_2 contents obtained from a systemic artery and PA to calculate arterial-venous O_2 content difference (AVO_2 diff). The Fick principle states that uptake of oxygen in blood by the lung (mL/min) is equal to the product of the AVO_2 diff of the oxygen and the blood flow to the lung. Therefore, if the arterial O_2 content, venous O_2 content and oxygen consumption are measured, the CO can then be calculated. A 4 Fr to 6 Fr radial arterial cannula is used to measure arterial blood pressure and allow sampling of arterial blood gases. Simultaneous PA blood samples are obtained to measure systemic and mixed venous O_2 contents ($= O_2$ saturation $\times$ hemoglobin $\times$ 1.34). AVO_2 diff is calculated from systemic arterial and PA O_2 contents. Oxygen consumption can be directly measured at the mouth at rest and during exercise using a metabolic cart. CO is calculated by using the direct Fick equation ($CO = VO_2/AVO_2$ diff). SV can be calculated as the quotient of CO and heart rate.

CO assessment using VO$_2$ measured versus assumed

Many clinical laboratories do not have the ability to directly measure VO$_2$, and therefore instead rely on regression equations to estimate what the directly measured VO$_2$ would be, usually based predominantly upon body size. However, these regression equations have substantial error, and with differing metabolic needs such as obesity or systemic illness, there can be great deviation from estimated VO$_2$.[31−33] Thus, use of directly measured VO$_2$ should be performed when the Fick method is utilized for CO assessment. If VO$_2$ cannot be measured, thermodilution CO is preferred.

Thermodilution CO

Thermodilution is a form of the indicator dilution method, in which a bolus of cold saline is injected rapidly via the proximal port of the right heart catheter into the RA. The injectate mixes with blood and the change in temperature over time is recorded at the thermal sensor located at the distal portion of the right heart catheter. The area under this curve of change in temperature over time is calculated, which is inversely related to CO. This method can assess CO without blood gas data and expired gases analyses and therefore has advantages in the absence of directly measured VO$_2$. However, there are several limitations to thermodilution CO limiting its application compared to the direct Fick method with directly measured VO$_2$.[34] In cases with low CO, blood is rewarmed by the walls of the cardiac chambers and surrounding tissue, resulting in overestimation in CO estimation. The back and forth flow across the tricuspid valve in severe TR can result in underestimation of CO.[35] In patients with atrial fibrillation, irregular heart rates and cycle lengths can result in variability in thermodilution CO estimates. In the presence of a left to right shunt, the thermodilution CO represents the total pulmonary blood flow including the left to right shunt and therefore differs from Fick CO perfusing the systemic circulation.[36] Furthermore, errors in measuring thermodilution CO may be introduced by technical errors, such as increase injection temperature, an inappropriate injection speed, or lower injection volume. Variability may be high between injections, particularly when attempted during exercise, where Fick CO represents the preferred method.

Vascular load

The determination of vascular load of the circulatory system relies on modeling the circulation in terms of assuming steady state or pulsatile flow. Quantifying load assuming the circulation is nonpulsatile provides a measure of mean systemic vascular resistance (SVR). As discussed in Chapters 15−17, this measure of load fails to account for pulsatile loading conditions and provides an incomplete description of vascular loading.
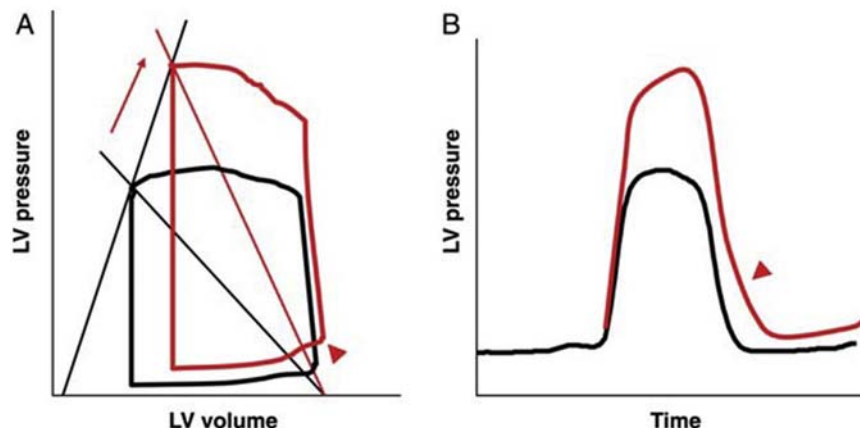
Systemic vascular load

SVR is determined by dividing mean arterial pressure minus central venous pressure (CVP) and CO, converted to standard units. Pulsatile arterial load may be assessed in a general way by the central aortic pulse pressure (PP = systolic blood pressure-diastolic blood pressure), effective arterial elastance (Ea), and total arterial compliance (TAC). Ea is a lumped measure of the total stiffness of the arterial system, which is assessed by end-systolic central blood pressure/SV.[37] Ea is most strongly related to SVR and is also influenced by heart rate. TAC is an approximation of the pressure−volume relationship for the lumped arterial system. Although multiple methods exist to assess TAC (as detailed in Chapter 3), it is usually estimated as SV index/central PP in the catheterization laboratory.[38]
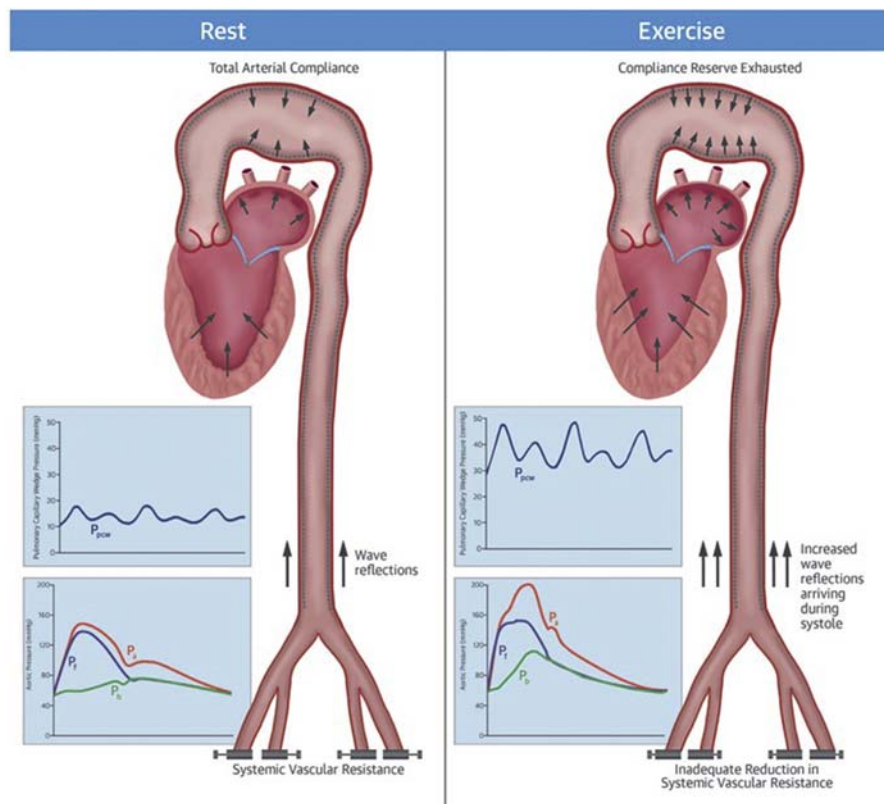
Ventricular and vascular stiffening increase with aging and comorbidity (e.g., hypertension and/or diabetes) and are abnormally elevated in patients with HFpEF. Acute afterload elevation in the setting of ventricular−arterial stiffening causes greater increase in blood pressure, which may then feedback to further impair diastolic relaxation, leading to dramatic increases in filling pressures during exercise (Fig. 35.3).[39] Many patients such as those with HFpEF may manifest arterial reserve limitations only during exercise. Reddy et al.[40] compared indices of arterial stiffness and pulsatile hemodynamics (both steady state and pulsatile load) at rest and during exercise in subjects with HFpEF and hypertensive control subjects (who themselves display vascular stiffening) to examine their relationships to cardiac hemodynamics and determine whether exertional arterial stiffening can be mitigated by inorganic nitrite. This study concluded that arterial load in HFpEF were similar to those in hypertensive control subjects at rest, but during submaximal exercise, HFpEF subjects displayed higher Ea index and reduced TAC index and at peak exercise there was greater reflected wave burden compared to control subjects. Importantly, these pulsatile arterial loads were directly correlated with higher LV filling pressures and depressed CO reserve (Fig. 35.4).[40] This pulsatile load increase appeared to be partially treatable with inorganic nitrite, as measures of wave reflection and arterial loading were improved following nitrite as compared to placebo.

Pulmonary vascular load

In patients with HF and chronic elevations in LA pressure, there may be structural vascular remodeling and changes in PA tone leading to increases in PVR and reductions in PA

FIGURE 35.3 (A) Combined ventricular−arterial stiffening in heart failure with preserved ejection fraction may lead to dramatic elevations in blood pressure with afterload increase (*red arrow*). This feeds back to increase LV end-diastolic pressures (*arrowhead*), by altering the slope or position of the diastolic pressure−volume relation, and/or (B) by prolonging LV pressure decay during isovolumic relaxation (*arrowhead*). *Figure adapted with permission from Borlaug BA, Paulus WJ. Heart failure with preserved ejection fraction: pathophysiology, diagnosis, and treatment.* **Eur Heart J.** *2011;32:670−679.*

FIGURE 35.4 At rest (left panel), the aortic pressure waveform, P_a (orange) is shown as a composite of the forward wave, P_f (blue) and reflected wave, P_b (green).Wave reflections, which develop at the points of impedance mismatch along the arterial tree, are reflected back to the aorta causing systolic pressure augmentation. Total arterial compliance, which reflects the ability of the arteries to store blood during systole without untoward elevation in pressure, is not significantly compromised, and pulmonary capillary wedge pressure (PCWP) is near normal. During exercise (right panel), venous return and cardiac output increase. Stiffening of the aorta, along with a lack of small vessel vasodilation in the periphery (inadequate reduction in systemic vascular resistance), augments pressure wave reflections, P_b (green) and pressure augmentation of the central aorta during mid to late systole. Total arterial compliance reserve becomes saturated, such that increases in stroke volume cause greater elevation in aortic pulse pressure, further augmenting left ventricular load. These changes are then correlated with pathologic increases in PCWP that promote symptoms of dyspnea, and impairment in forward cardiac output reserve, limiting oxygen transfer to the body. *Figure adapted with permission from Reddy YNV, Andersen MJ, Obokata M, et al. Arterial stiffening with exercise in patients with heart failure and preserved ejection fraction.* **J Am Coll Cardiol.** *2017;70:136−148.*

compliance. Increases in PCWP preferentially increase pulsatile RV loading by reducing compliance greater for any increase in resistance. Pulmonary vascular disease (PVD) commonly coexists with HF, can also worsen PH for any degree of LA pressure elevation. Given that the RV is highly sensitive to afterload, PH is an important contributor to RV dysfunction in HF in part due to pulsatile RV loading.[41,42]

Assessment during exercise

Normal range of resting and exercise value

In order to interpret the data from an invasive CPET, it is important to recognize the normal response to exercise. Normal ranges of resting and exercise values are shown in Table 35.1.[43] With the onset of exercise, there is an increase in venous return to the heart mediated by the combined actions of the skeletal muscle and respiratory pumps, together with sympathetic-mediated venoconstriction that shifts blood from the capacitance veins to the central circulation. The heart must cope with this increase in venous return by enhancing diastolic relaxation and suction. However, there is diastolic reserve limitation during exercise in patients with HFpEF (Fig. 35.5).[4] When venous return exceeds output, there is central congestion. This develops in the lungs in isolated left HF, and in the right heart in patients with PH in the absence of left HF or other causes of right HF. The increase in filling pressures is often exacerbated by pericardial restraint and DVI as total heart volume increases. This effect is greater in patients with obesity, right heart dilatation, and atrial fibrillation.

The duties of the LV are fundamentally to keep the lungs dry by filling to an adequate preload volume without pathologic increase in LA pressure, and to pump blood to the body at a rate commensurate with its metabolic needs, reflected by total body VO_2. This latter component is one area were invasive CPET provides an advantage against other modalities: the ability to measure both O_2 delivery and consumption in tandem. In health, studies dating back over 50 years have showed that CO increases with respect to VO_2 by a ratio of 6:1.[44,45] The lower limit of normal may be higher with supine exercise, as some studies have shown that HF-free controls have higher CO reserve with respect to VO_2.[7,46] Further study is required to define the lower limits of normal with supine exercise. By measuring the change in VO_2 (in mL/min) during exercise, one can determine what the expected change in CO should be, if the heart is adequately performing its duty as a pump.

Preforming an exercise hemodynamic study

Setup

In the catheterization laboratory under mild sedation while lying supine, access is obtained in the right internal jugular vein followed by placement of a 9 Fr sheath (Arrow, Morrisville, NC). Access is also obtained in the right radial artery using a 4–6 Fr catheter. Solid state pressure transducers are leveled at mid-chest. A 7 Fr balloon-tipped catheter (Balloon wedge, Arrow, Morrisville, NC) is advanced to the RA. In our laboratory, a 2 Fr micromanometer is then advanced to the tip of the balloon-tipped catheter and balanced to the
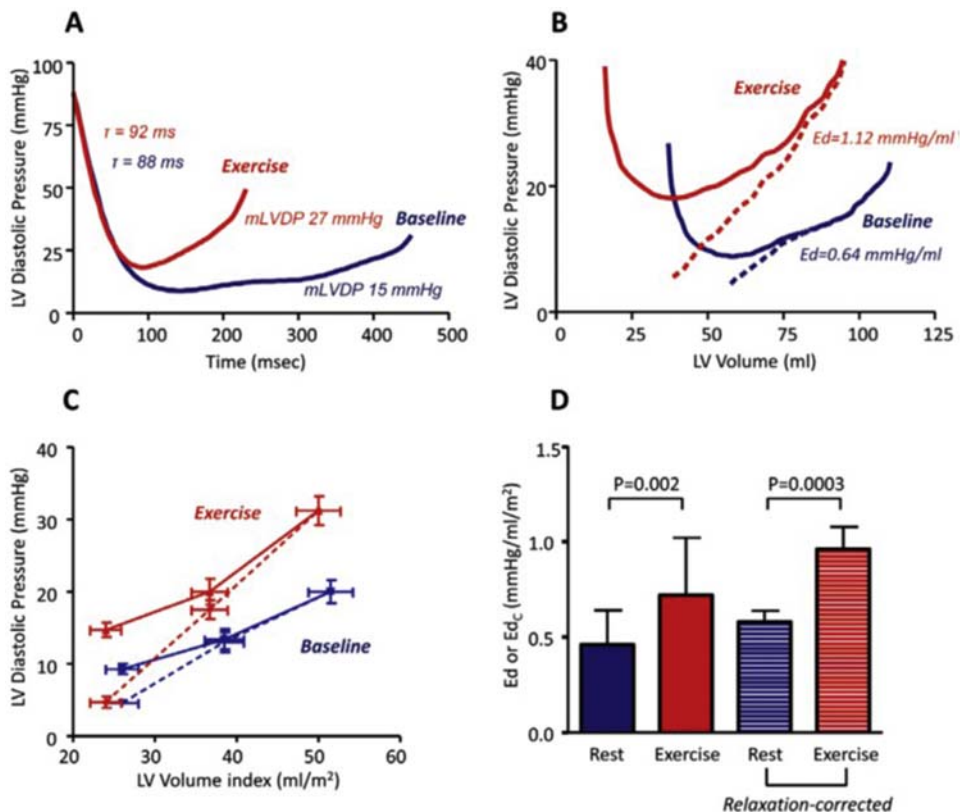
TABLE 35.1 Normal range of resting and exercise values.[43]

	Normal resting values	Normal exercise values	Comments
RAP (mmHg)	0–6	<15	Normal range with exercise not well-defined
Mean PA (mmHg)	≤20	<30 with TPR<3 WU[a]	Often >30 above age 50 years in normal adults, but not with high TPR
PA/CO slope (mmHg/L/min)	–	<3	Less established for supine exercise
PCWP (mmHg)	<15	<25	Some references indicate normal resting values of <12 or <15; >20 during exercise may be abnormal in patients <50 years of age
PCWP/CO slope (mmHg/L/min)	–	<2	Less established for supine exercise
PVR (WU)	<2–3	<2–3	True normal <2 WU but clinical risk increases >3 WU; PVR should drop with exercise normally
CI/CO (L/min*m² or L/min)	2.2–4.0 (L/min[a]m²)	>4.8*ΔVO₂ (L/min)	Expected increase in CO is 6 mL/min for each 1 mL/min increase in VO₂[b]

[a]TPR, total pulmonary resistance, defined by mean PA pressure divided by CO.
[b]Predicted cardiac output reserve is equal to 6*ΔVO₂. Cardiac output reserve is then calculated as observed minus rest CO divided by predicted cardiac output reserve. This ratio has been referred to as the exercise factor and should be 0.8 or 80%.
Table adapted with permission from Jain CC, Borlaug BA. Performance and interpretation of invasive hemodynamic exercise testing. **Chest.** 2020.

FIGURE 35.5 Diastolic reserve limitations during exercise in patients with heart failure with preserved ejection fraction (HFpEF). (A) In a typical HFpEF patient, there is dramatic elevation in mean left ventricular diastolic pressure (mLVDP) during exercise associated with limited hastening of isovolumic relaxation (reduction in the time constant of relaxation, τ). Inadequate relaxation reserve during exercise is coupled with an acute shift upward and to the left in the diastolic pressure-volume relationship, with an increase in operant diastolic elastance (Ed) as shown in an example patient (B) and in group data (C and D). The *solid lines/bar graphs* show raw unadjusted pressure-volume data and the *dashed lines/hashed bar graphs* show elastance data corrected for the effects of incomplete relaxation. *Figure adapted with permission from Borlaug BA. Mechanisms of exercise intolerance in heart failure with preserved ejection fraction. **Circ J**. 2014;78:20–32.*

mean fluid-filled catheter. The reason for the micro-manometer is the poor frequency response of the fluid-filled catheter, which becomes limiting during exercise in particular. CVP is measured continuously through the sidearm of the 9 Fr jugular sheath, taking care to assure that distal sheath pressure is equal to direct RA pressure. Transthoracic echocardiography may also be performed simultaneously with catheterization to evaluate for ventricular function, valve disease, and lung congestion. Pressures in the RA, PA, RV, and PCWP were measured at end-expiration using the mean of ≥ 3 beats. PCWP position is confirmed via appearance on fluoroscopy, characteristic waveforms, and wedge saturation $\geq 94\%$, with mean pressure taken at mid-A wave. In our laboratory, CO is determined by the Fick method from directly measured VO_2 (MedGraphics, St. Paul, MN) together with blood sampling to measure O_2 contents and pO_2 obtained from the radial artery and PA to calculate AVO_2diff. The protocol for the procedure is summarized in Box 35.1.[43]

Supine versus upright
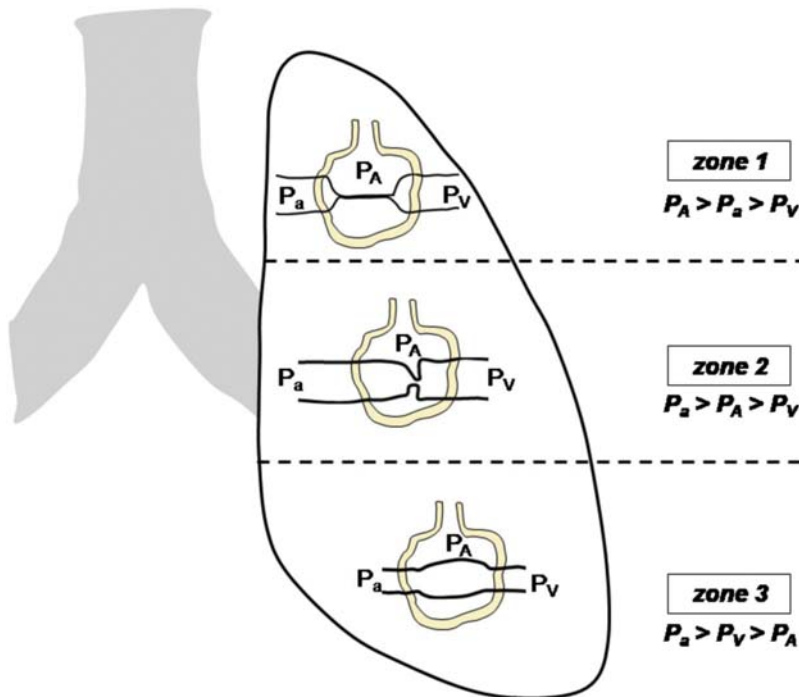
Invasive CPET can be performed in either the supine or upright positions. While our catheter laboratory performs studies either way, our preferred approach is to utilize supine exercise, where venous return is maximized, increasing the sensitivity to detect diastolic reserve impairments. Normal ranges are also more familiar in the supine position, which is how cardiac catheterization has been performed since first introduced in the 1940s. It is important to recognize that RA, PA, and PCWP pressures are higher in the supine position as compared to upright. However, prior studies have shown that the changes with exercise are similar in both positions, as are changes in the relationships between PA and PCWP.[47,48] Of note, PVR falls more with upright exercise, particularly at low levels of exercise. With upright exercise there may be greater ringing artifact (fluctuations due to catheter movement) and catheter whip, as well as greater variability in PCWP when measured in different West zones (Box 35.2)[49] which is less relevant to supine exercise.[50]

BOX 35.1 Setup for Invasive CPET.[43]

1. Obtain access into the right internal Jugular (IJ) vein (9 Fr sheath) and right radial artery (e.g., 4 Fr monitoring line).
2. Start measurement of oxygen consumption (VO_2) for calculation of Fick cardiac output through mouthpiece or tight-fitting mask. This expired gas analysis continues throughout the remainder of the case.
3. Prepare and flush 7 Fr balloon wedge (BW) with a micromanometer (MM, 2 Fr) advanced through a sidearm.
4. Insert BW into the right atrium. Level the MM to the fluid-filled catheter and obtain right atrial pressure (RAP).
5. Transduce and record pressures from the radial arterial line, the right IJ sheath (RAP), and the BW at each stage.
6. Pass BW into the right ventricle. Verify no drift in the MM, and then record pressure.
7. Pass BW into the pulmonary artery (PA). Verify no drift in the MM and record pressures. Obtain blood gas samples from the PA, SVC (to rule out left to right shunt) and radial arterial line simultaneously. Annotate the time of blood sampling to correspond with the expired gas analysis for Fick output.
8. With flush on, advance BW in the PCWP position. Confirm PCWP position with waveform analysis, fluoroscopic appearance, and saturation >94%. Transduce pressure, verifying no drift in the MM, and record pressures.
9. Place feet into cycle ergometer pedals. After 30 s with feet up, take records while in PCWP position.
10. Begin exercise protocol (20 W). The duration of this stage is 3 min for tests without simultaneous imaging and 5 min if imaging is being performed to allow adequate time for image acquisition. After 2–4 min, pressure data and blood samples obtained as in the baseline phase.
11. Advance to next stage, in older adults with dyspnea, we generally use 20 W stage increments (3 min each) until peak.
12. Measurements of PCWP, PA, RAP, and arterial pressure tracings and arterial/PA blood samples 30 s prior to stage end for each incremental stage. Obtain Borg scores for perceived dyspnea and exertion at each stage.
13. When perceived patient effort reaches maximal tolerated effort (i.e., Borg perceived effort score >16, Borg dyspnea score >6), repeat steps 11 and 12. Confirmatory evidence of maximal effort includes respiratory exchange ratio >1.05.
14. Once all measurements obtained, stop exercise. Recovery pressure records taken at 1 min postexercise.
15. Remove patient's feet from the bike pedals and remove BW catheter from the sheath after all information obtained. Remove access sites per usual protocol.

BOX 35.2 The concept of West zones.

The lung is divided into three zones as described above. In each of zones, the magnitude of pulmonary artery pressure (P_a), pulmonary venous pressure (P_V), and alveolar pressure (P_A) are different. P_A exceeds both P_a and P_V in Zone 1. In Zone 2, where arterial exceeds alveolar but alveolar exceeds venous. Most zones in the supine position are called Zone 3, where both P_a and P_V exceed P_A. With upright exercise, venous pressure can be very low at the apex of the lungs, creating Zone 2 conditions. In that case, vascular pressure is not be measuring but rather alveolar pressure.

Measurement of pressures

End-expiration versus respiratory averaged

All pressures should be measured at end-expiration, which is when intrapleural pressure is closest to zero, lungs are at functional reserve capacity, and there is minimal airflow impacting intracardiac pressures. During exercise, some have advocated for use of pressures averaged over the entire respiratory rather than end-expiration, and this has advantages in patients with obstructive lung disease in whom intrinsic positive end-expiratory pressure (auto-PEEP) develops. For such patients where changes in intrathoracic pressure are dramatic and considered to contribute to elevated intravascular pressures, pressures averaged over the respiratory cycle may more accurately account for the effect of intrathoracic pressure and auto-PEEP compared to end-expiratory pressure. However, for the vast majority of patients without these conditions, end-expiratory values can be readily obtained and accurately reflect the transmural hydrostatic pressure in the pulmonary veins and capillaries. In these patients using pressure averaged throughout the respiratory cycle can underestimate transmural pressure due to the effect of inspiration falsely lowering measured pressures. Indeed, end-expiration PCWP was found to display a stronger relationship with the development of lung congestion as compared to PCWP averaged over the respiratory cycle.[18]

Cardiac output reserve

Invasive CPET also enables the assessment of CO reserve, which requires measurement of CO and oxygen consumption in tandem. Conventionally, CO is considered to increase by 6 mL for every 1 mL increase in whole-body oxygen consumption if the heart is adequately performing its duty as a pump as described above. Thus, if VO_2 increases from 250 mL per minute at rest to 1250 mL per minute at peak exercise (1000 mL/min), a 6 L per minute increase in CO is expected. Values <80% of this level are considered to indicate impairment in CO reserve, which is frequently observed in both HFrEF and HFpEF.[7,46,51,52] Subtle abnormalities in resting contractility in patients with HFpEF become dramatic during stress because of the inability to enhance systolic function that attenuates the increase in SV during exercise to limit CO reserve. Although resting LV ejection fraction (LVEF), SV, and CO are generally normal in HFpEF, the ability to enhance those with exercise relative to metabolic needs is impaired.

Added value of simultaneous exercise echocardiography

Exercise echocardiography provides valuable information including assessments of ventricular and valve structure and function. It is particularly useful to discriminate causes of the prominent V wave in the PCWP tracing that is commonly observed in patients with HF, which may be related to poor LA compliance or worsening mitral regurgitation. In the absence of significant mitral regurgitation, it suggests that the large V wave would be more a reflection of increased LA stiffness, as is commonly observed in patients with HF.[53] Furthermore, one advantage of echocardiography is the ability to perform simultaneous lung ultrasound, which enables evaluation of increases in pulmonary congestion during exercise.[18] Echocardiography with short axis imaging also allows determination of the degree of pericardial restraint with LV underfilling which can be estimated from the degree of LV collapse and eccentricity index resulting in a more D-shaped LV and septum. A higher eccentricity index and more collapsed LV for a given PCWP elevation reflects a greater degree of pericardial restraint. For these reasons, we often perform concurrent echocardiography during invasive CPET. Echocardiography also allows for the measurement of time-resolved blood flow velocity across the LV outflow tract, which in tandem with estimated central aortic pressures, can provide comprehensive assessments of arterial properties and ventricular—arterial interactions (as detailed in Chapters 3 and 17).

Clinical utility in the evaluation of suspected heart failure

HFpEF

Diagnostic uncertainty

In contrast to HFrEF, the diagnosis of HFpEF is challenging because ejection fraction is normal, cardiac congestion is difficult to evaluate noninvasively, and many patients display hemodynamic abnormalities only during exercise.[1,3,18] Despite normal resting hemodynamics, HFpEF patients develop cardiac injury and an impairment in myocardial function that worsen with exercise, leading to marked elevation in pulmonary vascular pressures that causes lung congestion, altered breathing mechanics and dyspnea.[5]

To diagnose HFpEF, clinical history, physical examination, and imaging tests are essential, but in patients with stable HFpEF or early stage HFpEF, current measures are poorly sensitive (Table 35.2).[54] Regarding blood tests, plasma natriuretic peptide levels increase in response to elevations in cardiac wall stress, which is related to chamber dimension and distending pressure. However, compared with patients with HFrEF, patients with HFpEF have lower wall stress owing to a smaller cavity size and thicker ventricular walls.[55] Many patients with HFpEF have normal distending cardiac pressures at rest and increased distending pressures only during exercise when the patient becomes symptomatic. Therefore, resting plasma natriuretic peptide levels are substantially lower in patients with HFpEF than in patients with HFrEF and are indeed often normal. For these reasons, the diagnosis of HFpEF can be often challenging.

TABLE 35.2 Clinical, laboratory and imaging predictors of HFpEF.[54]

Parameters	Odds ratio	C-statics	Sensitivity (%)	Specificity (%)	P value
Clinical					
Age >60 years	6.20	0.704	80	60	<.0001
Obesity	3.46	0.651	65	65	<.0001
Grade II obesity or higher[a]	4.02	0.615	35	88	<.0001
Chronic kidney disease stage 3 or higher	3.38	0.584	26	90	<.0001
Hypertension	5.33	0.664	86	47	<.0001
Atrial fibrillation	12.35	0.652	35	96	<.0001
Diabetes mellitus	2.80	0.579	28	88	.0003
Prediabetes or diabetes	2.82	0.624	55	70	<.0001
Laboratory					
NT- proBNP >125 pg/mL	3.74	0.649	77	53	<.0001
NT- proBNP >275 pg/mL	4.82	0.680	59	77	<.0001
NT- proBNP >450 pg/mL	4.93	0.657	46	85	<.0001
Electrocardiography					
First degree AV block	1.92	0.532	15	92	.006
PR interval per millisecond	1.02	0.644	69	56	<.0001
Pacemaker	21.30	0.560	13	99	<.0001
Chest radiography					
Cardiomegaly	7.56	0.601	24	96	<.0001
Pleural effusion	4.96	0.537	9	98	.002
Echocardiography					
Global longitudinal strain <16%	2.10	0.591	62	56	.0004
LV hypertrophy	2.55	0.570	26	88	.0006
LA volume index >30 mL/m^2	5.65	0.704	70	71	<.0001
E/e′ ratio >9	5.23	0.687	78	59	<.0001
E/e′ ratio >13	5.20	0.661	46	86	<.0001
Septal e′ velocity <7 cm/s	2.90	0.619	48	76	<.0001
PASP >35 mmHg	5.05	0.657	46	86	<.0001
RV fractional area change <48%	4.88	0.673	39	88	<.0001
TAPSE <21 mm	3.69	0.637	46	81	<.0001
Qualitative RV dysfunction	4.26	0.578	22	94	<.0001
Qualitative RV dilatation	3.45	0.598	32	88	<.0001

AV, atrioventricular; *HFpEF*, heart failure with preserved ejection fraction; *LA*, left atrial; *LV*, left ventricular; *NT-proBNP*, N- terminal pro-B-type natriuretic peptide; *PASP*, pulmonary artery systolic pressure; *RV*, right ventricular; *TAPSE*, tricuspid annular plane systolic excursion.
[a]*Defined as a BMI $\geq$35 kg/m^2.*
Table adapted with permission from Reddy YNV, Carter RE, Obokata M, Redfield MM, Borlaug BA. A simple, evidence-based approach to help guide diagnosis of heart failure with preserved ejection fraction. **Circulation.** 2018;138:861−870.

Evaluation of specific phenotypes
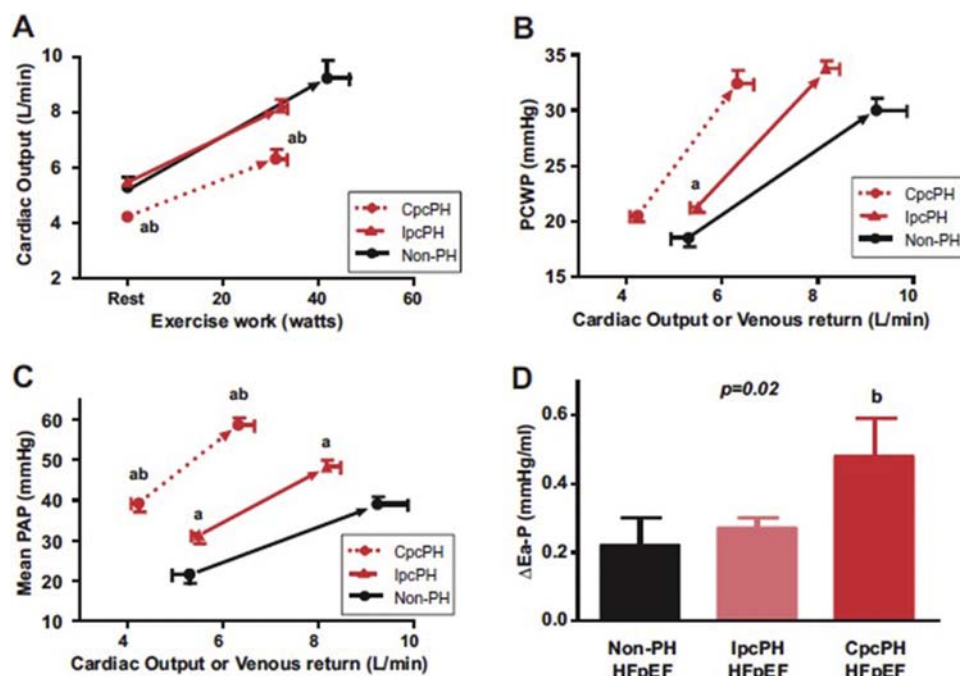
HFpEF is a heterogeneous syndrome. Clinical trials to date have not identified a treatment that improves the prognosis of people with HFpEF,[5,56] but phenotyping patients into pathophysiologically homogeneous groups may enable better targeting of treatment.[57]

Obesity has reached epidemic proportions worldwide and is a common finding in people with HFpEF (60% −75%).[5] Obesity has many deleterious effects on the cardiovascular system, mediated by changes in volume status, cardiac loading, energy substrate utilization, tissue metabolism, and systemic inflammation, which are believed to promote disease progression such as HFpEF. Several studies have reported that obesity was associated with more adverse hemodynamic measures, poorer RV function, increased volume retention, greater ventricular interaction, reduced exercise capacity and efficiency, greater symptom severity, increased vulnerability to kidney dysfunction, and poorer quality of life.[58−62] Furthermore, obesity is related to reduced natriuretic peptide levels in plasma as a result of increased clearance via natriuretic peptide receptors in adipocytes[63] as well as with a reduction in cardiac chamber distention owing to heightened pericardial restraint.[59] These distinctions suggest that obesity may be considered as a specific HFpEF phenotype. Exercise testing is often

necessary not only to unmask the diagnosis of HFpEF in these individuals but also can identify unique pathophysiological impairments including enhanced DVI and increased pulmonary vascular burden which may have therapeutic implications.

PH is common and contributes to increased morbidity and mortality in patients with HFpEF. Lam and colleagues demonstrated that echo-estimated PH was very common in HFpEF, present in greater than 80% of stable outpatients. For each 10 mmHg increase in estimated systolic PA pressures, there was a 30% increased risk of death.[64] PH in HFpEF may be caused by high downstream PCWP, increased impedance to flow through the pulmonary vessels, or both. The former has been termed isolated postcapillary PH (IpcPH) and the latter combined post- and precapillary PH (CpcPH).[65]

Gorter et al.[28] evaluated and compared cardiovascular structure, function, and reserve capacity in patients with non-PH-HFpEF, IpcPH-HFpEF, and CpcPH-HFpEF by performing invasive hemodynamic CPET. Exercise capacity was reduced in HFpEF patients with PH, evidenced by lower workload achieved and decreased peak VO$_2$. CO increased similarly with exercise in non-PH and IpcPH-HFpEF but was lower for any exercise workload in CpcPH-HFpEF (Fig. 35.6A). While all groups displayed
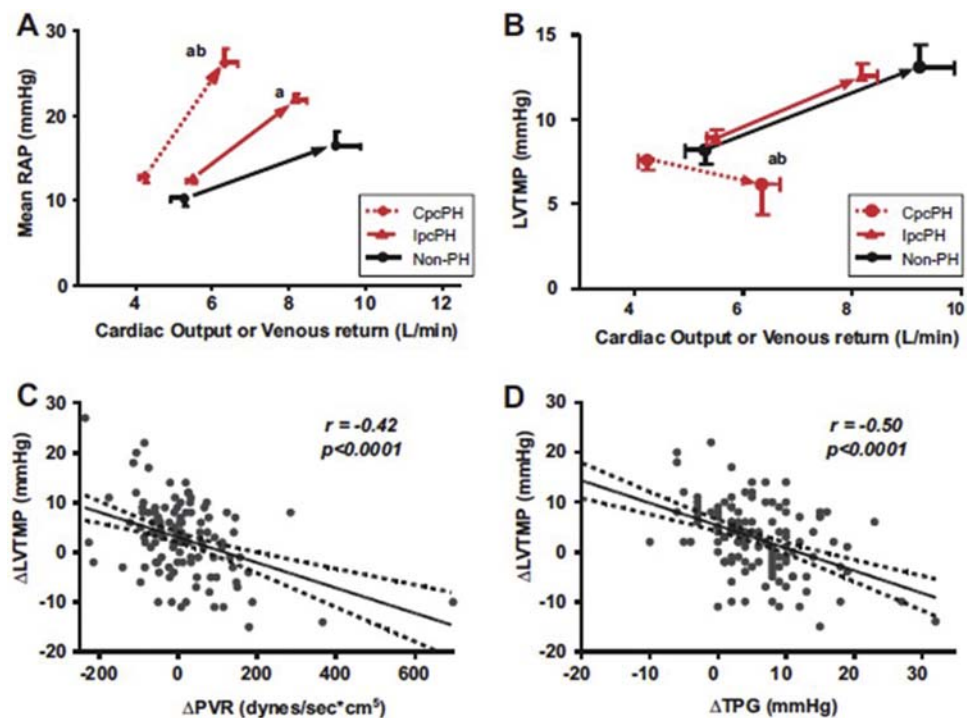
FIGURE 35.6   (A) Baseline and peak exercise for cardiac output. (B−C) PCWP and mean PAP and as a function of venous return. (D) As compared to both non-PH- and IpcPH-HFpEF, CpcPH-HFpEF patients displayed greater increase in pulmonary arterial elastance (Ea) during exercise a $P < .05$ versus non-PH-HFpEF; and b $P < .05$ versus IpcPH-HFpEF. *CpcPH*, combined post- and precapillary pulmonary hypertension; *HFpEF*, heart failure with preserved ejection fraction; *IpcPH*, isolated postcapillary pulmonary hypertension; *PAP*, pulmonary artery pressure; *PCWP*, pulmonary capillary wedge pressure; *PH*, pulmonary hypertension. *Figure adapted with permission from Gorter TM, Obokata M, Reddy YNV, Melenovsky V, Borlaug BA. Exercise unmasks distinct pathophysiologic features in heart failure with preserved ejection fraction and pulmonary vascular disease.* **Eur Heart J.** *2018;39:2825−2835.*
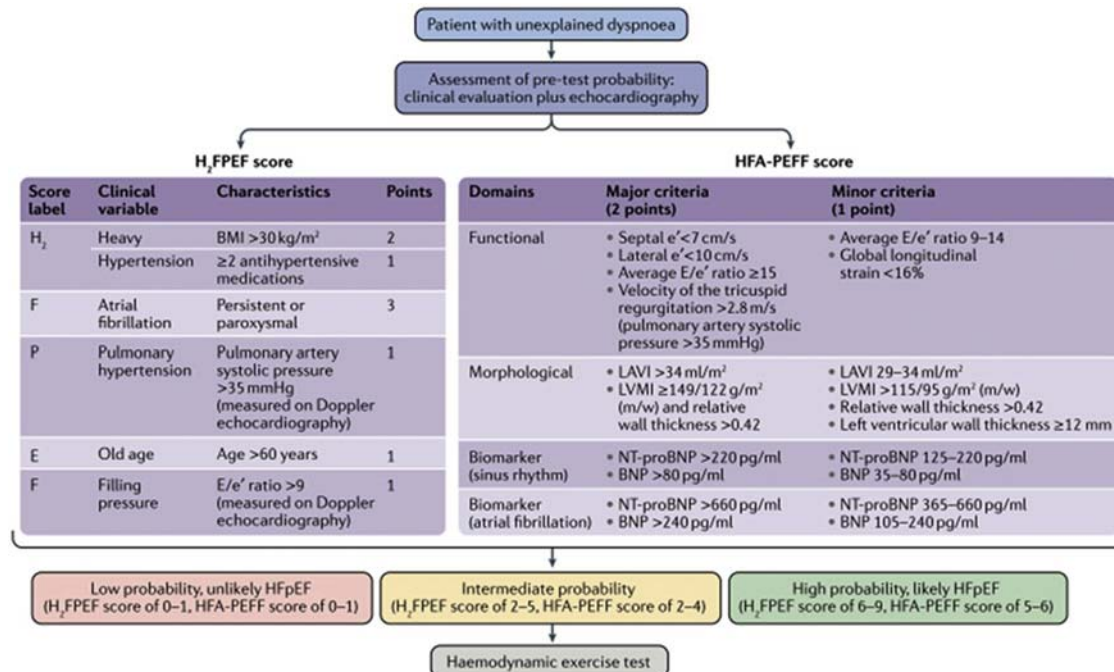
similar absolute increases in PCWP with exercise, PCWP elevation occurred at lesser CO in CpcPH-HFpEF (Fig. 35.6B). Pulmonary artery pressures increased in all groups with exercise, but the greatest increases were observed in the CpcPH group, with higher pressures relative to blood flow (Fig. 35.6C). Patients in the CpcPH-HFpEF group experienced greater reduction in PA compliance on exercise along with higher exercise PVR and pulmonary artery elastance, in keeping with impaired pulmonary vascular reserve (Fig. 35.6D). Furthermore, recent studies reported that many patients with HFpEF also have coexisting PVD, which could also contribute to worsen PVR.[28,66–69] Patients with HFpEF and PH display worse pulmonary vascular load with impaired RV reserve, which is associated with poorer exercise capacity and worse clinical outcomes.[28,69] In patients with early stages of HFpEF, this may become manifest exclusively by abnormal pulmonary vasodilation during exercise. It has been proposed that these patients with HFpEF represent a unique HFpEF phenotype with enhanced ventricular interaction and pericardial restraint with LV underfilling and limited SV reserve during exercise (Fig. 35.7). HFpEF patients with this phenotype may share biological overlap with PAH,[70,71] which is defined by high PA pressure but normal PCWP.

The LA plays a key role in HFpEF progression. In the early stage of HFpEF, it may compensate for LV diastolic dysfunction through its booster function as an important barrier between the LV and the pulmonary circulation, but with prolonged LV dysfunction, there is LA dilatation, resulting in LA mechanical failure.[56] LA strain assessed by speckle tracking globally reflects atrial function, remodeling and distensibility components that become progressively more impaired in the setting of chronic LV diastolic dysfunction, as in patients with HFpEF. Notably, a previous study[53] showed that LA reservoir strain and LA compliance allow for discrimination of HFpEF from noncardiac dyspnea with similar or greater accuracy as compared to commonly used echocardiographic parameters of diastolic function. Therefore, LA volume contraction or failure to dilate could contribute to pulmonary venous hypertension and unfavorable symptoms in patients with HFpEF.

FIGURE 35.7 Ventricular interdependence with exercise in heart failure with preserved ejection fraction and pulmonary vascular disease. (A) Increase in venous return during exercise was associated with more dramatic increase in RAP in CpcPH-HFpEF compared to the other HFpEF groups. (B) While patients with non-PH-HFpEF and IpcPH-HFpEF displayed an increase in LVTMP, CpcPH-HFpEF patients developed a paradoxical decrease in LVTMP as venous return to the right heart increased during exercise. (C−D) The reduction in LVTMP was increased as exercise pulmonary vascular resistance and TPG increased, indicating that left heart underfilling was directly related to the severity of pulmonary vascular disease. a $P < .05$ versus Non-PH-HFpEF; and b $P < .05$ versus IpcPH-HFpEF. *CpcPH*, combined post- and precapillary pulmonary hypertension; *IpcPH*, isolated postcapillary pulmonary hypertension; *LVTMP*, left ventricular transmural pressure; *PH*, pulmonary hypertension; *PVR*, pulmonary vascular resistance; *RAP*, right atrial pressure; *TPG*, transpulmonary gradient. *Figure adapted with permission from Gorter TM, Obokata M, Reddy YNV, Melenovsky V, Borlaug BA. Exercise unmasks distinct pathophysiologic features in heart failure with preserved ejection fraction and pulmonary vascular disease.* **Eur Heart J.** *2018;39:2825−2835.*

FIGURE 35.8 Diagnostic Approach for HFpEF. In the patient with unexplained dyspnea, assessment of the pretest probability that HFpEF is present is first performed via clinical, echocardiographic, and laboratory testing. Two scoring systems have been developed for this purpose: the H_2FPEF score[54] (left) and the HFA−PEFF[72] (right). With either system, patients deemed at high and low probability are generally diagnosed as having or not having HFpEF, respectively, without further testing. In patients with intermediate probability of HFpEF, hemodynamic exercise testing is needed, which can be performed using cardiac catheterization or stress echocardiography. *BNP*, B-type natriuretic peptide; *LAVI*, left atrial volume index; *LVMI*, left ventricular mass index, *NT-pro BNP*, N-terminal pro-B-type natriuretic peptide. *Figure adapted with permission from Borlaug BA. Evaluation and management of heart failure with preserved ejection fraction.* **Nat Rev Cardiol.** *2020.*

Bayesian approach can guide decision to refer for invasive assessment

In the patient with unexplained dyspnea, assessment of the pretest probability of HFpEF is first performed by clinical, echocardiographic, and laboratory testing. In the past two years, two scoring systems have been developed approaches for the diagnostic work-up of HFpEF: the H_2FPEF score[54] and the HFA−PEFF score[72] (Fig. 35.8). With either system, patients deemed at high and low probability are generally diagnosed as having or not having HFpEF, respectively, without further testing. In patients with intermediate probability of HFpEF, hemodynamic exercise testing is needed, which can be performed using cardiac catheterization or stress echocardiography. If exercise Doppler echo is clearly negative test, no further testing would be required, but its result is positive or equivocal, we need to consider invasive exercise test for diagnosis.[3]

HFrEF

Value in determining cardiac component of limitation

In patients with HFrEF undergoing evaluation for advanced therapies, bringing the sophisticated expired gas analysis techniques of CPET together with invasive exercise hemodynamics evaluation can determine the severity of the cardiac component of limitation compared to peripheral abnormalities beyond the heart. A previous study[46] reported that both CO response to exercise and peak exercise VO_2 were independently associated with worse clinical outcome in ambulatory patients with chronic HF who had been referred for cardiac transplantation. In contrast, there are a well-characterized subset of HFrEF patients where peripheral abnormalities are prominent,[73] and conceptually such patients may have relatively preserved CO reserve and likely derive less benefit from advanced HF therapies such as transplantation.[74] Invasive CPET may provide greater insight into the selection for potential heart transplantation candidates, although the conventional selection criteria of candidates for cardiac transplantation had limited by resting hemodynamics, echocardiography, and NYHA functional classification so far. Thus, invasive CPET has been expected to be used as a robust method to determine cardiac component of limitation even in HFrEF.

Degree of pulmonary hypertension, RV dysfunction

PH in HFrEF is initially felt to be a reflection of passive elevation in downstream PCWP, but in some patients, sustained elevation PCWP leads to pulmonary vascular remodeling and changes in pulmonary arterial tone leading to increases in PVR and reductions in PA compliance. In an

invasive hemodynamics assessment, Schwartzenberg et al[8] showed that PA mean pressure and PCWP were similar in subjects with HFpEF and HFrEF. Exercise markedly elevates RV afterload through increases in downstream PCWP and PA mean pressures. RV preload also increases by exercise via greater increases in CO and venous return from peripheral. In this study, PA mean pressure and resistance were largely reversible with intravenous sodium nitroprusside, suggesting that there is a substantial reactive component.

RV dysfunction from increased RV afterload is a major cause of morbidity and mortality in all HF cohorts. The pulmonary circulation and the afterload are very different from the systemic circulation. PH and pulmonary fibrosis do not significantly change the hyperbolic dependence between PVR and compliance.[42] This fixed relationship helps explain the difficulty of reducing total RV afterload by therapies that have a modest impact on mean PVR. Higher PCWP appears to enhance net RV afterload by elevating pulsatile, relative to resistive load and may contribute to RV dysfunction.

PAH

Utility in atypical PAH

The term PH is sometimes confused with what used to be called PAH, defined by high PA pressure but normal LV filling pressure. This is now referred to by consensus as Group 1 PH.[65] Group 1 PH is different disorder than HFpEF with IpcPH, but increasing evidence suggests that it has many similarities to HFpEF with CpcPH.[68,70,75] Recently, Opitz and colleagues identified a group out of registry patients with special characteristics who have hemodynamic criteria for PAH as well as more than three risk factors of clinical features of HFpEF.[71] They named this group as "atypical PAH." This group of patients responded less well to pulmonary vasoactive therapy when compared with Group 1 PH (PAH), but better than the registry patients who met criteria for HFpEF with PH. As such, the authors suggested that "atypical PAH" exists as part of a disease continuum between Group 1 PH (PAH) and PH associated with HFpEF. Further support for this disease continuum hypothesis, comes from Assad and colleagues, who recently reported that subjects with CpcPH display genes and biological pathways in the lung known to contribute to "PAH" pathophysiology.[70] Exercise testing uncouples occult left heart disease in these subjects with atypical PAH many of whom have risk factors for HFpEF, and such identification may help predict possible response to therapy.

Valve disease

Paradoxical LG AS
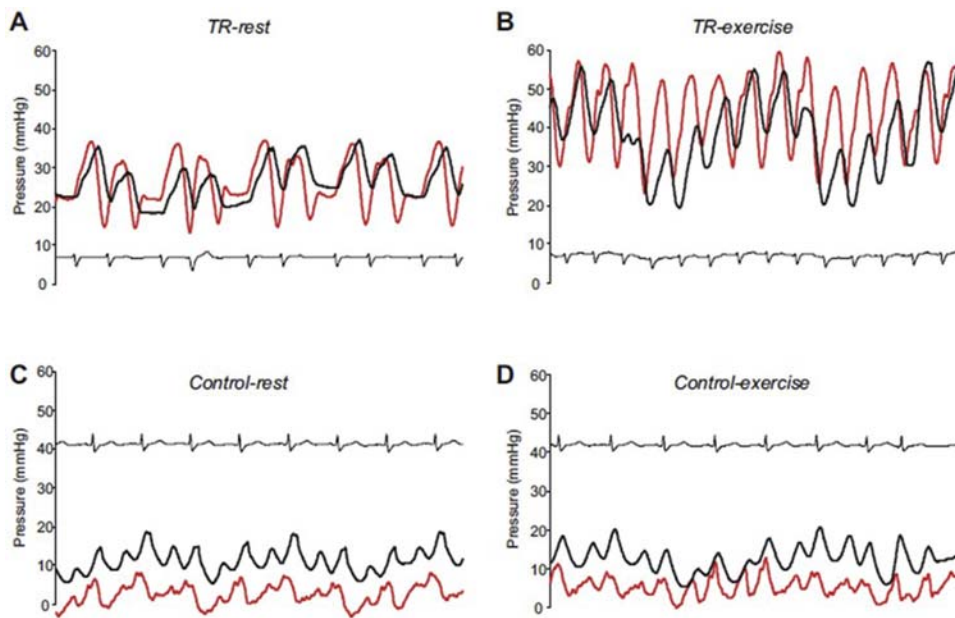
Severe aortic stenosis (AS) is usually diagnosed on the basis of both an aortic valve effective orifice area (EOA) $\leqq 1.0$ cm^2 (or $\leqq 0.6$ cm^2/m^2 converted to standard units) and a mean transvalvular pressure gradient $\geqq 40$ mmHg. However, low CO (e.g., SV index <35 mL/m^2) may lead to an important reduction in transvalvular pressure gradients even if the stenosis is very severe. There are some patients with severe AS on the basis of EOA might develop a restrictive physiology, resulting in low CO and lower than expected transvalvular pressure gradients despite the presence of a preserved LVEF (e.g., LVEF $>50\%$), what is called "Paradoxical LG AS." Paradoxical LG AS accounts for 10%−25% of patients with severe AS and is characterized by pronounced LV concentric remodeling, small LV cavity size, and a restrictive physiology leading to impaired LV filling pressure, altered myocardial function and is associated with poor prognosis.[76−81]

A recent study found that paradoxical LG AS display elevated arterial afterload (lower total arterial compliance and greater effective arterial elastance) compared with patients with high gradient severe AS and moderate AS.[82] In this study, nitroprusside reduced afterload and reducing LV filling pressures in patients with paradoxical LG severe AS. Furthermore, an inverse relationship between baseline SV index and change in SV index with afterload reduction was observed, which could reclassify to moderate AS in 25% of patients. The findings suggest that heightened sensitivity to afterload is a significant contributor to LG AS pathophysiology. Reduction of afterload might be a useful method to increase flow and distinguish between true severe and pseudo severe AS in patients with paradoxical LG AS. The importance of arterial low in LG AS is discussed in more detail in Chapter 37.

Severe TR with pericardial restraint

TR is a common valvular lesion that is usually caused by ventricular and annular dilation. Patients with TR are often asymptomatic, but with more advanced disease, patients complain of exertional fatigue, edema, and anorexia. The cause of exercise intolerance in patients with TR is complex. To clarify the cause of impaired exercise tolerance in patients with TR, invasive CPET is a robust method. Andersen et al.[15] demonstrated that impaired exercise capacity in patients with TR who had no evidence of left heart disease and PVD was related to an inability to adequately increase CO relative to metabolic needs, coupled with elevated systemic and pulmonary venous pressures assessed by invasive CPET. This impairment in perfusion is coupled with abnormal increases in PCWP that is related to right heart congestion and DVI rather than a primary left heart lesion because LVTMP dropped with exercise, consist with inadequate LV preload, despite elevated left-sided filling pressure (Fig. 35.9).[3,15−17] When RV and pericardial pressures are low, LVEDP (and PCWP) accurately reflects true LV preload (LVEDV). However, when there is right heart overload and pericardial restraint, LVEDP and LVEDV become uncoupled. This phenomenon is commonly observed in HF patients, wherein

FIGURE 35.9   Typical RAP (red) and PCWP (black) tracings in a patient with severe TR at rest (A) and with exercise (B) and in a control patient at respective states (C and D). Note the prominent C−V waves with absent × descent (ventricularized waveforms) and near-equalization of right and left heart pressures in the TR patient. During inspiration, there is no drop in RAP (Kussmaul sign) despite reduction in PCWP associated with the drop in intrathoracic pressure, such that the transmural pressure gradient becomes transiently negative. In the control patient, PCWP and RAP are normal at rest and with exercise, and PCWP consistently exceeds RAP. *PCWP*, pulmonary capillary wedge pressure; *RAP*, right atrial pressure; *TR*, tricuspid regurgitation. *Figure adapted with permission from Andersen MJ, Nishimura RA, Borlaug BA. The hemodynamic basis of exercise intolerance in tricuspid regurgitation.* **Circ Heart Fail.** *2014;7:911−917.*

reduction in right-sided venous return may increase LV stroke work.

More advanced assessment

Peripheral O_2 utilization

Peak VO_2 is limited in equal parts by peripheral O_2 utilization (AVO_2 diff) as well as CO.[83] As such, enhanced peripheral O_2 distribution, utilization, and extraction (i.e., AVO_2 diff reserve) during exercise plays an equally important role as CO reserve in maximizing achieved VO_2. Although the heart increases its output during exercise, this enhanced flow needs to be distributed to tissues where perfusion is most needed, which is achieved by regional vasodilation in skeletal muscle and vasoconstriction in nonexercising regions such as the skin, splanchnic beds, and kidneys.[4] In patients with HF, there are some who are predominantly limited by peripheral factors, even when the EF is low. Accordingly, combining expired gas analysis techniques of CPET together with invasive exercise hemodynamics evaluation and direct arterial and venous blood sampling provides the direct method to evaluate both CO and peripheral O_2 utilization (AVO_2 diff), which can detect these causes for exercise intolerance.

Ventilation and expired gas analysis
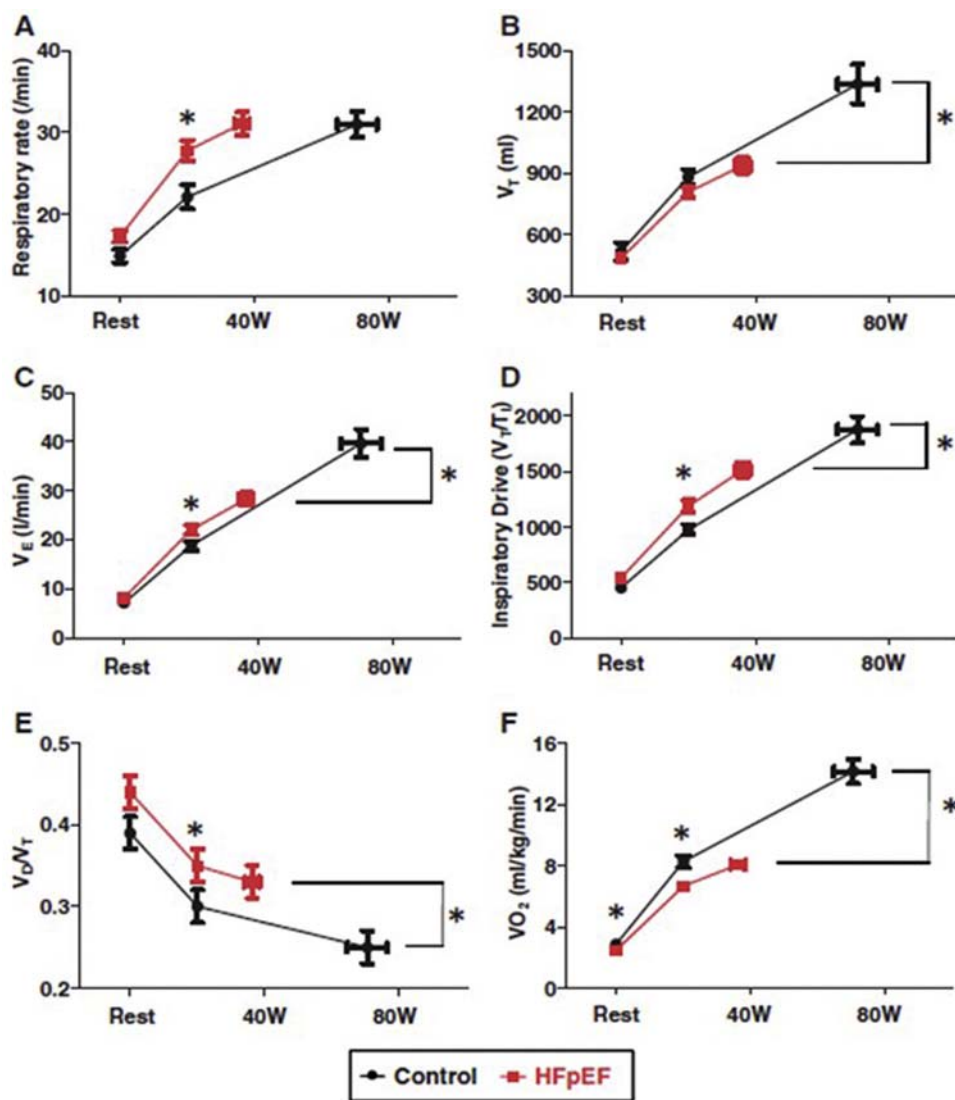
Breath-by-breath VO_2, carbon dioxide production (VCO_2), tidal volume (V_T), minute ventilation (V_E), respiratory rate, minute ventilation ($V_E = V_T \times$ respiratory rate), and inspiratory time (T_I) can be measured throughout the invasive CPET to quantify functional capacity. Objective effort is estimated by the respiratory exchange ratio ($RER = VCO_2/VO_2$). Ventilatory efficiency is assessed by the slope of V_E to VCO_2, and ventilatory drive is assumed by the ratio of V_T to T_I. Pulmonary dead space (V_D) is the volume that does not participate in gas exchange, and the sum of anatomical dead space (conduit airways such as the mouth and trachea) and alveolar dead space. The ratio of dead space ventilation to tidal volume (V_D/V_T) is determined from the modified alveolar gas equation. Obokata et al.[13] demonstrated that elevation in left heart filling pressure with exercise is correlated with worse symptoms, greater ventilatory drive, more tachypneic breathing, impaired ventilation, and worse exercise capacity in HFpEF (Figs. 35.10 and 35.11).
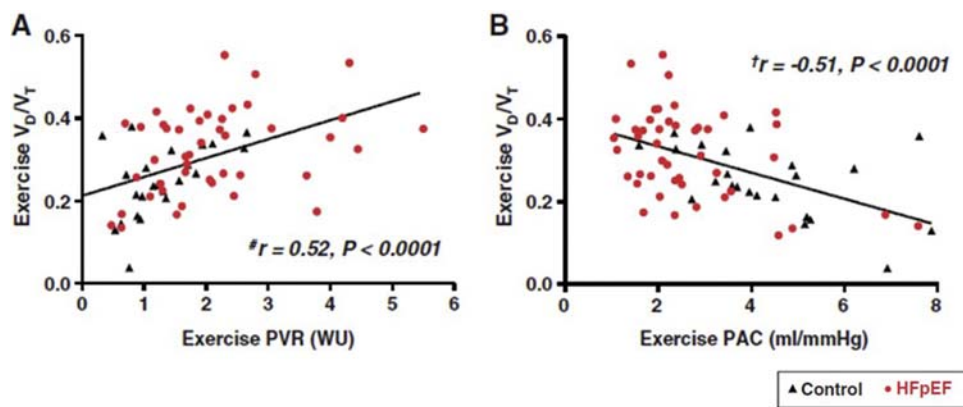
Conclusion

Invasive CPET combines the robust expired gas analysis capabilities of CPET with the definitive assessments of pressure, flow, and resistance from cardiac catheterization, providing the most robust evaluation of exertional intolerance available in clinical practice. This chapter summarizes the performance and proper interpretation of invasive CPET, which relies upon careful integration of pressure waveforms, blood gas data, expired gas analysis, and assessments of O_2 transport. Given the comprehensive nature

FIGURE 35.10 Baseline, low-level (20 W) and peak exercise for (A) respiratory rate, (B) tidal volume (V_T), (C) minute ventilation (V_E), (D) inspiratory drive [tidal volume/inspiration time (V_T/T_I)], (E) dead space ventilation relative to tidal volume (V_D/V_T), and (F) peak oxygen consumption in heart failure with preserved ejection fraction and control subjects. *$P < .05$ between groups. *Figure adapted with permission from Obokata M, Olson TP, Reddy YNV, Melenovsky V, Kane GC, Borlaug BA. Haemodynamics, dyspnoea, and pulmonary reserve in heart failure with preserved ejection fraction.* **Eur Heart J.** *2018;39:2810–2821.*

FIGURE 35.11 Correlation of peak V_D/V_T ratio with peak pulmonary vascular resistance, pulmonary arterial compliance. *Figure adapted with permission from Obokata M, Olson TP, Reddy YNV, Melenovsky V, Kane GC, Borlaug BA. Haemodynamics, dyspnoea, and pulmonary reserve in heart failure with preserved ejection fraction.* **Eur Heart J.** *2018;39:2810–2821.*

of these assessments and excellent safety profile, invasive CPET has emerged as the gold standard method to evaluate patients with potential HF.

References

1. Borlaug BA, Nishimura RA, Sorajja P, Lam CS, Redfield MM. Exercise hemodynamics enhance diagnosis of early heart failure with preserved ejection fraction. **Circ Heart Fail**. 2010; 3:588−595.

2. Andersen MJ, Olson TP, Melenovsky V, Kane GC, Borlaug BA. Differential hemodynamic effects of exercise and volume expansion in people with and without heart failure. **Circ Heart Fail**. 2015; 8:41−48.

3. Obokata M, Kane GC, Reddy YN, Olson TP, Melenovsky V, Borlaug BA. Role of diastolic stress testing in the evaluation for heart failure with preserved ejection fraction: a simultaneous invasive-echocardiographic study. **Circulation**. 2017; 135:825−838.

4. Borlaug BA. Mechanisms of exercise intolerance in heart failure with preserved ejection fraction. **Circ J**. 2014; 78:20−32.

5. Borlaug BA. Evaluation and management of heart failure with preserved ejection fraction. **Nat Rev Cardiol**. 2020; 17:559−573.

6. Nauta JF, Hummel YM, van der Meer P, Lam CSP, Voors AA, van Melle JP. Correlation with invasive left ventricular filling pressures and prognostic relevance of the echocardiographic diastolic parameters used in the 2016 ESC heart failure guidelines and in the 2016 ASE/EACVI recommendations: a systematic review in patients with heart failure with preserved ejection fraction. **Eur J Heart Fail**. 2018; 20:1303−1311.

7. Abudiab MM, Redfield MM, Melenovsky V, et al. Cardiac output response to exercise in relation to metabolic demand in heart failure with preserved ejection fraction. **Eur J Heart Fail**. 2013; 15:776−785.

8. Schwartzenberg S, Redfield MM, From AM, Sorajja P, Nishimura RA, Borlaug BA. Effects of vasodilation in heart failure with preserved or reduced ejection fraction implications of distinct pathophysiologies on response to therapy. **J Am Coll Cardiol**. 2012; 59:442−451.

9. van Heerebeek L, Borbely A, Niessen HW, et al. Myocardial structure and function differ in systolic and diastolic heart failure. **Circulation**. 2006; 113:1966−1973.

10. Cooper LB, Mentz RJ, Stevens SR, et al. Hemodynamic Predictors of heart failure morbidity and mortality: fluid or flow? **J Card Fail**. 2016; 22:182−189.

11. Damman K, van Deursen VM, Navis G, Voors AA, van Veldhuisen DJ, Hillege HL. Increased central venous pressure is associated with impaired renal function and mortality in a broad spectrum of patients with cardiovascular disease. **J Am Coll Cardiol**. 2009; 53:582−588.

12. Dorfs S, Zeh W, Hochholzer W, et al. Pulmonary capillary wedge pressure during exercise and long-term mortality in patients with suspected heart failure with preserved ejection fraction. **Eur Heart J**. 2014; 35:3103−3112.

13. Obokata M, Olson TP, Reddy YNV, Melenovsky V, Kane GC, Borlaug BA. Haemodynamics, dyspnoea, and pulmonary reserve in heart failure with preserved ejection fraction. **Eur Heart J**. 2018; 39:2810−2821.

14. Reddy YNV, Olson TP, Obokata M, Melenovsky V, Borlaug BA. Hemodynamic correlates and diagnostic role of cardiopulmonary exercise testing in heart failure with preserved ejection fraction. **JACC Heart Fail**. 2018; 6:665−675.

15. Andersen MJ, Nishimura RA, Borlaug BA. The hemodynamic basis of exercise intolerance in tricuspid regurgitation. **Circ Heart Fail**. 2014; 7:911−917.

16. Belenkie I, Dani R, Smith ER, Tyberg JV. Effects of volume loading during experimental acute pulmonary embolism. **Circulation**. 1989; 80:178−188.

17. Tyberg JV, Taichman GC, Smith ER, Douglas NW, Smiseth OA, Keon WJ. The relationship between pericardial pressure and right atrial pressure: an intraoperative study. **Circulation**. 1986; 73:428−432.

18. Reddy YNV, Obokata M, Wiley B, et al. The haemodynamic basis of lung congestion during exercise in heart failure with preserved ejection fraction. **Eur Heart J**. 2019; 40:3721−3730.

19. Chakko S, Woska D, Martinez H, et al. Clinical, radiographic, and hemodynamic correlations in chronic congestive heart failure: conflicting results may lead to inappropriate care. **Am J Med**. 1991; 90:353−359.

20. Clark AL, Cleland JG. Causes and treatment of oedema in patients with heart failure. **Nat Rev Cardiol**. 2013; 10:156−170.

21. Mahdyoon H, Klein R, Eyler W, Lakier JB, Chakko SC, Gheorghiade M. Radiographic pulmonary congestion in end-stage congestive heart failure. **Am J Cardiol**. 1989; 63:625−627.

22. Ware LB, Matthay MA. Clinical practice. Acute pulmonary edema. **N Engl J Med**. 2005; 353:2788−2796.

23. Gheorghiade M, Follath F, Ponikowski P, et al. Assessing and grading congestion in acute heart failure: a scientific statement from the acute heart failure committee of the heart failure association of the European Society of Cardiology and endorsed by the European Society of Intensive Care Medicine. **Eur J Heart Fail**. 2010; 12:423−433.

24. Melenovsky V, Andersen MJ, Andress K, Reddy YN, Borlaug BA. Lung congestion in chronic heart failure: haemodynamic, clinical, and prognostic implications. **Eur J Heart Fail**. 2015; 17:1161−1171.

25. Dzau VJ, Colucci WS, Hollenberg NK, Williams GH. Relation of the renin-angiotensin-aldosterone system to clinical state in congestive heart failure. **Circulation**. 1981; 63:645−651.

26. Borlaug BA, Reddy YNV. The role of the pericardium in heart failure: implications for pathophysiology and treatment. **JACC Heart Fail**. 2019; 7:574−585.

27. Guazzi M, Borlaug BA. Pulmonary hypertension due to left heart disease. **Circulation**. 2012; 126:975−990.

28. Gorter TM, Obokata M, Reddy YNV, Melenovsky V, Borlaug BA. Exercise unmasks distinct pathophysiologic features in heart failure with preserved ejection fraction and pulmonary vascular disease. **Eur Heart J**. 2018; 39:2825−2835.

29. Dauterman K, Pak PH, Maughan WL, et al. Contribution of external forces to left ventricular diastolic pressure. Implications for the clinical use of the Starling law. **Ann Intern Med**. 1995; 122:737−742.

30. Janicki JS. Influence of the pericardium and ventricular interdependence on left ventricular diastolic and systolic function in patients with heart failure. **Circulation**. 1990; 81:Iii15−20.

31. Dehmer GJ, Firth BG, Hillis LD. Oxygen consumption in adult patients during cardiac catheterization. **Clin Cardiol**. 1982; 5:436−440.

32. Fakler U, Pauli C, Hennig M, Sebening W, Hess J. Assumed oxygen consumption frequently results in large errors in the determination of cardiac output. **J Thorac Cardiovasc Surg**. 2005; 130:272−276.

33. Kendrick AH, West J, Papouchado M, Rozkovec A. Direct Fick cardiac output: are assumed values of oxygen consumption acceptable? **Eur Heart J**. 1988; 9:337−342.

34. Nadeau S, Noble WH. Limitations of cardiac output measurements by thermodilution. **Can Anaesth Soc J**. 1986; 33:780−784.

35. Cigarroa RG, Lange RA, Williams RH, Bedotto JB, Hillis LD. Underestimation of cardiac output by thermodilution in patients with tricuspid regurgitation. **Am J Med**. 1989; 86:417−420.

36. Obokata M, Reddy YNV, Shah SJ, et al. Effects of interatrial shunt on pulmonary vascular function in heart failure with preserved ejection fraction. **J Am Coll Cardiol**. 2019; 74:2539−2550.

37. Kelly RP, Ting CT, Yang TM, et al. Effective arterial elastance as index of arterial vascular load in humans. **Circulation**. 1992; 86:513−521.

38. Chemla D, Hébert JL, Coirault C, et al. Total arterial compliance estimated by stroke volume-to-aortic pulse pressure ratio in humans. **Am J Physiol**. 1998; 274:H500−H505.

39. Borlaug BA, Paulus WJ. Heart failure with preserved ejection fraction: pathophysiology, diagnosis, and treatment. **Eur Heart J**. 2011; 32:670−679.

40. Reddy YNV, Andersen MJ, Obokata M, et al. Arterial stiffening with exercise in patients with heart failure and preserved ejection fraction. **J Am Coll Cardiol**. 2017; 70:136−148.

41. Obokata M, Reddy YNV, Melenovsky V, Pislaru S, Borlaug BA. Deterioration in right ventricular structure and function over time in patients with heart failure and preserved ejection fraction. **Eur Heart J**. 2019; 40:689−697.

42. Tedford RJ, Hassoun PM, Mathai SC, et al. Pulmonary capillary wedge pressure augments right ventricular pulsatile loading. **Circulation**. 2012; 125:289−297.

43. Jain CC, Borlaug BA. Performance and interpretation of invasive hemodynamic exercise testing. **Chest**. 2020; 158:2119−2129.

44. Astrand PO, Cuddy TE, Saltin B, Stenberg J. Cardiac output during submaximal and maximal work. **J Appl Physiol**. 1964; 19:268−274.

45. Beck KC, Randolph LN, Bailey KR, Wood CM, Snyder EM, Johnson BD. Relationship between cardiac output and oxygen consumption during upright cycle exercise in healthy humans. **J Appl Physiol**. 2006; 101:1474−1480.

46. Chomsky DB, Lang CC, Rayos GH, et al. Hemodynamic exercise testing. A valuable tool in the selection of cardiac transplantation candidates. **Circulation**. 1996; 94:3176−3183.

47. Mizumi S, Goda A, Takeuchi K, et al. Effects of body position during cardiopulmonary exercise testing with right heart catheterization. **Physiol Rep**. 2018; 6:e13945.

48. Thadani U, Parker JO. Hemodynamics at rest and during supine and sitting bicycle exercise in normal subjects. **Am J Cardiol**. 1978; 41:52−59.

49. West JB, Dollery CT, Naimark A. Distribution OF blood flow IN isolated lung; relation to vascular and alveolar pressures. **J Appl Physiol**. 1964; 19:713−724.

50. Stampfer M, Epstein SE, Beiser GD, Braunwald E. Exercise in patients with heart disease. Effects of body position and type and intensity of exercise. **Am J Cardiol**. 1969; 23:572−576.

51. Borlaug BA, Kane GC, Melenovsky V, Olson TP. Abnormal right ventricular-pulmonary artery coupling with exercise in heart failure with preserved ejection fraction. **Eur Heart J**. 2016; 37:3293−3302.

52. Epstein SE, Beiser GD, Stampfer M, Robinson BF, Braunwald E. Characterization of the circulatory response to maximal upright exercise in normal subjects and patients with heart disease. **Circulation**. 1967; 35:1049−1062.

53. Reddy YNV, Obokata M, Egbe A, et al. Left atrial strain and compliance in the diagnostic evaluation of heart failure with preserved ejection fraction. **Eur J Heart Fail**. 2019; 21:891−900.

54. Reddy YNV, Carter RE, Obokata M, Redfield MM, Borlaug BA. A simple, evidence-based approach to help guide diagnosis of heart failure with preserved ejection fraction. **Circulation**. 2018; 138:861−870.

55. Borlaug BA, Redfield MM. Diastolic and systolic heart failure are distinct phenotypes within the heart failure spectrum. **Circulation**. 2011; 123:2006−2013. Discussion 2014.

56. Borlaug BA. The pathophysiology of heart failure with preserved ejection fraction. **Nat Rev Cardiol**. 2014; 11:507−515.

57. Shah SJ, Kitzman DW, Borlaug BA, et al. Phenotype-specific treatment of heart failure with preserved ejection fraction: a multiorgan roadmap. **Circulation**. 2016; 134:73−90.

58. Miller WL, Borlaug BA. Impact of obesity on volume status in patients with ambulatory chronic heart failure. **J Card Fail**. 2020; 26:112−117.

59. Obokata M, Reddy YNV, Pislaru SV, Melenovsky V, Borlaug BA. Evidence supporting the existence of a distinct obese phenotype of heart failure with preserved ejection fraction. **Circulation**. 2017; 136:6−19.

60. Reddy YNV, Lewis GD, Shah SJ, et al. Characterization of the obese phenotype of heart failure with preserved ejection fraction: a RELAX trial Ancillary study. **Mayo Clin Proc**. 2019; 94:1199−1209.

61. Reddy YNV, Obokata M, Testani JM, et al. Adverse renal response to decongestion in the obese phenotype of heart failure with preserved ejection fraction. **J Card Fail**. 2020; 26:101−107.

62. Reddy YNV, Rikhi A, Obokata M, et al. Quality of life in heart failure with preserved ejection fraction: importance of obesity, functional capacity, and physical inactivity. **Eur J Heart Fail**. 2020; 22:1009−1018.

63. Wang TJ, Larson MG, Levy D, et al. Impact of obesity on plasma natriuretic peptide levels. **Circulation**. 2004; 109:594−600.

64. Lam CS, Roger VL, Rodeheffer RJ, Borlaug BA, Enders FT, Redfield MM. Pulmonary hypertension in heart failure with preserved ejection fraction: a community-based study. **J Am Coll Cardiol**. 2009; 53:1119−1126.

65. Galiè N, Humbert M, Vachiery JL, et al. 2015 ESC/ERS guidelines for the diagnosis and treatment of pulmonary hypertension: the joint task force for the diagnosis and treatment of pulmonary hypertension of the European Society of Cardiology (ESC) and the European Respiratory Society (ERS): endorsed by: association for European Paediatric and Congenital Cardiology (AEPC), International Society for heart and lung transplantation (ISHLT). **Eur Heart J**. 2016; 37:67−119.

66. Borlaug BA, Obokata M. Is it time to recognize a new phenotype? Heart failure with preserved ejection fraction with pulmonary vascular disease. **Eur Heart J**. 2017; 38:2874−2878.

67. Fayyaz AU, Edwards WD, Maleszewski JJ, et al. Global pulmonary vascular remodeling in pulmonary hypertension associated with heart failure and preserved or reduced ejection fraction. **Circulation**. 2018; 137:1796−1810.

68. Hoeper MM, Lam CSP, Vachiery JL, et al. Pulmonary hypertension in heart failure with preserved ejection fraction: a plea for proper phenotyping and further research. **Eur Heart J**. 2017; 38:2869−2873.

69. Vanderpool RR, Saul M, Nouraie M, Gladwin MT, Simon MA. Association between hemodynamic markers of pulmonary hypertension and outcomes in heart failure with preserved ejection fraction. **JAMA Cardiol**. 2018; 3:298−306.

70. Assad TR, Hemnes AR, Larkin EK, et al. Clinical and biological insights into combined post- and pre-capillary pulmonary hypertension. **J Am Coll Cardiol**. 2016; 68:2525−2536.

71. Opitz CF, Hoeper MM, Gibbs JS, et al. Pre-capillary, combined, and post-capillary pulmonary hypertension: a pathophysiological continuum. **J Am Coll Cardiol**. 2016; 68:368−378.

72. Pieske B, Tschöpe C, de Boer RA, et al. How to diagnose heart failure with preserved ejection fraction: the HFA-PEFF diagnostic algorithm: a consensus recommendation from the Heart Failure Association (HFA) of the European Society of Cardiology (ESC). **Eur Heart J**. 2019; 40:3297−3317.

73. Esposito F, Mathieu-Costello O, Shabetai R, Wagner PD, Richardson RS. Limited maximal exercise capacity in patients with chronic heart failure: partitioning the contributors. **J Am Coll Cardiol**. 2010; 55:1945−1954.

74. Reddy YNV, Obokata M, Haykowsky MJ, Borlaug BA. Skeletal muscle compensation for cardiac muscle insufficiency in heart failure and reduced ejection fraction. **Circ Heart Fail**. 2018; 11:e004714.

75. Assad TR, Brittain EL, Wells QS, et al. Hemodynamic evidence of vascular remodeling in combined post- and precapillary pulmonary hypertension. **Pulm Circ**. 2016; 6:313−321.

76. Cramariuc D, Cioffi G, Rieck AE, et al. Low-flow aortic stenosis in asymptomatic patients: valvular-arterial impedance and systolic function from the SEAS Substudy. **JACC Cardiovasc Imaging**. 2009; 2:390−399.

77. Dumesnil JG, Pibarot P, Carabello B. Paradoxical low flow and/or low gradient severe aortic stenosis despite preserved left ventricular ejection fraction: implications for diagnosis and treatment. **Eur Heart J**. 2010; 31:281−289.

78. Hachicha Z, Dumesnil JG, Bogaty P, Pibarot P. Paradoxical low-flow, low-gradient severe aortic stenosis despite preserved ejection fraction is associated with higher afterload and reduced survival. **Circulation**. 2007; 115:2856−2864.

79. Herrmann S, Störk S, Niemann M, et al. Low-gradient aortic valve stenosis myocardial fibrosis and its influence on function and outcome. **J Am Coll Cardiol**. 2011; 58:402−412.

80. Lancellotti P, Magne J, Donal E, et al. Clinical outcome in asymptomatic severe aortic stenosis: insights from the new proposed aortic stenosis grading classification. **J Am Coll Cardiol**. 2012; 59:235−243.

81. Minners J, Allgeier M, Gohlke-Baerwolf C, Kienzle RP, Neumann FJ, Jander N. Inconsistent grading of aortic valve stenosis by current guidelines: haemodynamic studies in patients with apparently normal left ventricular function. **Heart**. 2010; 96:1463−1468.

82. Lloyd JW, Nishimura RA, Borlaug BA, Eleid MF. Hemodynamic response to nitroprusside in patients with low-gradient severe aortic stenosis and preserved ejection fraction. **J Am Coll Cardiol**. 2017; 70:1339−1348.

83. Haykowsky MJ, Brubaker PH, John JM, Stewart KP, Morgan TM, Kitzman DW. Determinants of exercise intolerance in elderly heart failure patients with preserved ejection fraction. **J Am Coll Cardiol**. 2011; 58:265−274.

This page intentionally left blank

Chapter 36

Arterial stiffness and pulsatile hemodynamics in heart failure

Julio A. Chirinos[1,2]

[1]*University of Pennsylvania Perelman School of Medicine, Hospital of the University of Pennsylvania and Perelman Center for Advanced Medicine, Philadelphia, PA, United States;* [2]*Ghent University, Ghent, Belgium*

Introduction

Heart Failure (HF) is an important clinical and public health problem in developed countries. In the United States, HF affects ∼6 million American adults ≥20 years of age[1] and is associated with high mortality, poor quality of life, and important societal costs.[2]
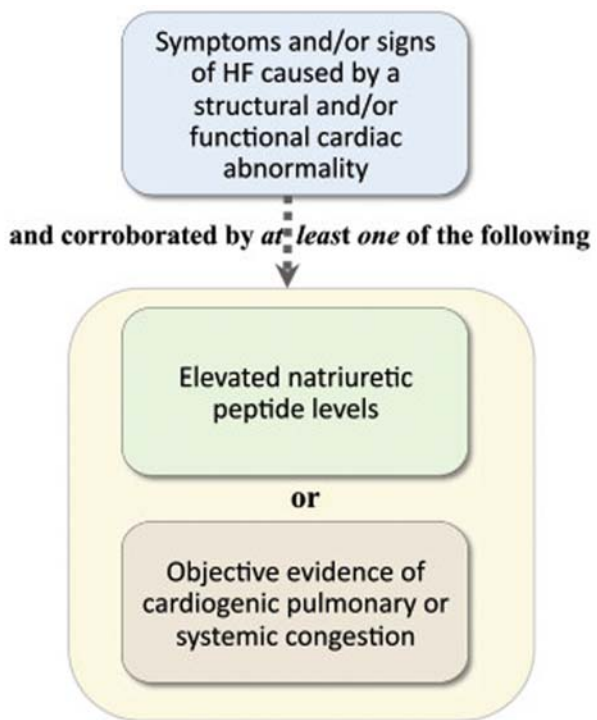
Given the growing burden of HF, understanding mechanistic abnormalities that contribute to the pathophysiology of HF and that can be targeted with therapy is important.[3,4] Arterial load exerts a profound impact on left ventricular (LV) structure and function. Assessments of pulsatile arterial hemodynamics have provided important insights into the pathophysiology of LV remodeling and fibrosis, myocardial dysfunction, and failure. Moreover, pulsatile arterial load may interact with the distal microvasculature, promoting microvascular dysfunction and impaired oxygen delivery to peripheral skeletal muscle, all of which contribute to exercise intolerance in HF. Arterial pulsatile hemodynamic mechanisms likely contribute to the frequent presence of HF comorbidities, such as chronic kidney disease and dementia (see Chapters 40 and 41), particularly in patients with HF with preserved ejection fraction (HFpEF).

Arterial load, particularly increased late systolic load from arterial wave reflections, represents an increasingly recognized mechanistic abnormality with an established causal link to LV maladaptive remodeling and dysfunction in experimental models. Similarly, prominent arterial wave reflections have been shown to correlate with LV remodeling (both hypertrophy and fibrosis), LV and left atrial (LA) dysfunction, and incident HF risk in humans. Wave reflections may be susceptible to modification by pharmacologic interventions, which could have important implications for HF prevention and treatment. This chapter is largely based on recent reviews of the topic by the author and collaborators,[5−8] and discusses our current knowledge of the role of pulsatile arterial hemodynamics in HF, including HF with reduced ejection fraction (HFrEF) and HFpEF. This chapter does not deal with pulmonary arterial load and its role in pulmonary hypertension and right ventricular dysfunction, which are discussed in detail in Chapters 55−58.

Heart failure: definition and classification

HF has classically been defined according to its pathophysiology as a syndrome resulting from an inability of the heart to pump enough blood to meet the body's needs or to do so at the expense of elevated LV filling pressures. Such definition, although conceptually attractive, has a number of theoretical and practical limitations.[9] Similarly, operational HF case definitions used in epidemiologic and clinical research are highly varied and can be discordant. Recently, the Heart Failure Society of America (HFSA), the HF Association of the European Society of Cardiology (HFA-ESC), and the Japanese HF Society (JHFS) released a document proposing a Universal Definition and Classification of HF.[9] The proposed universal definition of HF (Fig. 36.1) is based on symptoms and or signs of HF caused by a structural and/or functional cardiac abnormality, as determined by an EF of <50%, abnormal cardiac chamber enlargement, early diastolic atrioventricular inflow to annular tissue velocity ratio (E/e′) >15 (a marker of elevated ventricular filling pressures), moderate/severe ventricular hypertrophy, or moderate/severe valvular obstructive or regurgitant lesion. This should be corroborated by at least one of the following:

FIGURE 36.1 **Universal definition of heart failure according to the** Heart Failure Society of America (HFSA), the HF Association of the European Society of Cardiology (HFA-ESC), and the Japanese HF Society (JHFS). *Reproduced from reference Bozkurt B, Coats A, Tsutsui H. Universal definition and classification of heart failure.* **J Card Fail**. *2021.*

(1) Elevated natriuretic peptide levels, or;
(2) Objective evidence of cardiogenic pulmonary or systemic congestion by diagnostic modalities, such as imaging (e.g., by chest radiograph or elevated filling pressures by echocardiography) or hemodynamic measurements (e.g., right heart catheterization, pulmonary artery catheter) at rest or with provocation (e.g., exercise).

HF can be classified according to several different criteria, including the stage of the disease continuum, the severity of symptoms or functional limitation, its etiology (for example, ischemic/nonischemic, valvular, hypertensive, infiltrative, peripartum, viral myocarditis chemotherapy-induced cardiomyopathy), or the LV EF category. The recent HFSA/HFA-ESC/JHFS document also standardized the definition and subclassification of HF according to EF categories and provided a revised classification of the stages of HF (Fig. 36.2).[9] Briefly, the revised stages of the HF continuum include:

- Stage A ("at risk" for HF): Patients at risk for HF, but without current or prior symptoms or signs of HF and without structural cardiac changes or elevated biomarkers of heart disease (particularly, natriuretic peptide levels). This category includes patients with

hypertension, atherosclerotic cardiovascular disease, diabetes, obesity, known exposure to cardiotoxins, a positive family history of cardiomyopathy or genetic cardiomyopathy.
- Stage B (Pre-HF): Patients without current or prior symptoms or signs of HF, but who exhibit at least one of the following: structural heart disease (such as LV hypertrophy, cardiac chamber enlargement, ventricular wall motion abnormalities, myocardial tissue abnormalities, or valvular heart disease), abnormal cardiac function such as reduced left or right ventricular systolic function, diastolic dysfunction and/or evidence of increased filling pressures, elevated natriuretic peptide or cardiac troponin levels (especially in the setting of exposure to cardiotoxins).
- Stage C HF: Patients with current or prior symptoms and/or signs of HF caused by a structural and/or functional cardiac abnormality.
- Stage D (Advanced) HF: Severe symptoms and/or signs of HF at rest, recurrent hospitalizations despite guideline-directed medical therapy, refractory or intolerant to guideline-directed medical therapy, requiring advanced therapies such as consideration for cardiac transplantation, mechanical circulatory support, or palliative care.
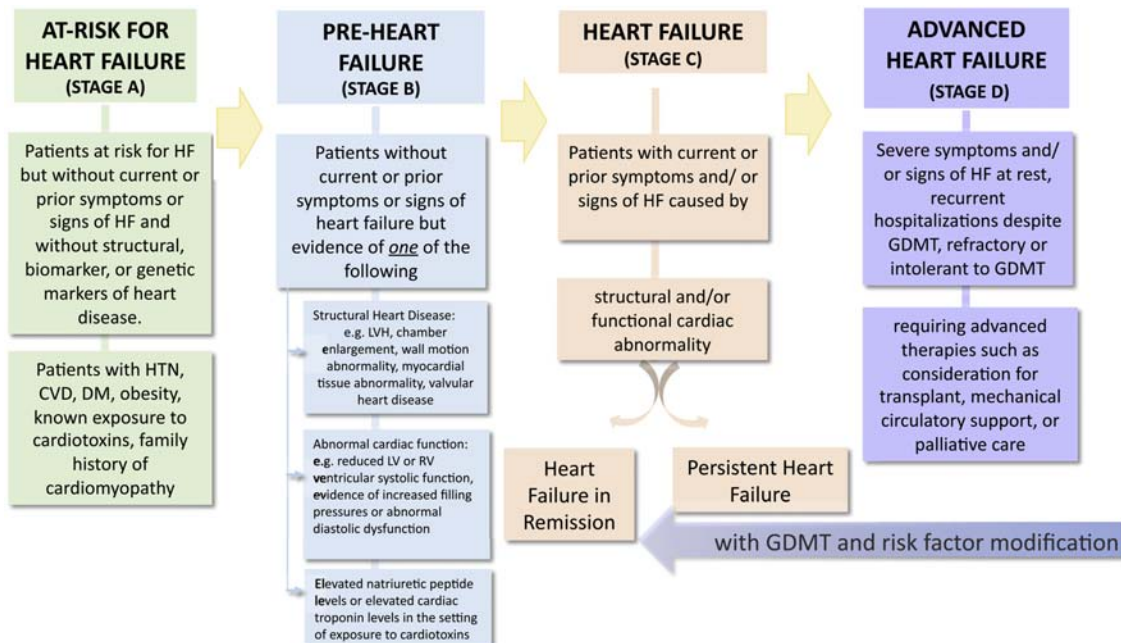
The document also endorses the widely used New York Heart Association (NYHA) functional classification to characterize the symptoms and functional capacity of patients with symptomatic (Stage C) or advanced (Stage D) HF. The NYHA functional classification system categorizes HF on a scale of I to IV, as follows:

- Class I, no limitation of physical activity.
- Class II, slight limitation of physical activity.
- Class III, marked limitation of physical activity.
- Class IV, symptoms occur even at rest and discomfort with any physical activity.

Finally, the document also proposed a revised classification of HF according to LV EF, as follows:

- HF with reduced EF (HFrEF): HF with LV EF $\leq 40\%$.
- HF with mildly reduced EF (HFmrEF): HF with LV EF of $41\%-49\%$.
- HF with preserved EF (HFpEF): HF with LV EF $\geq 50\%$.
- HF with improved EF (HFimpEF): HF with a baseline LV EF $\leq 40\%$, a ≥ 10-point increase from baseline LV EF, and a second measurement of LV EF of $>40\%$.

This chapter deals predominantly with studies of arterial stiffness and pulsatile hemodynamics in stage C–D HF (typically including patients with NYHA classes II–IV). We will also discuss the role of increased large artery stiffness and adverse pulsatile hemodynamics in promoting

FIGURE 36.2 Stages in the development and progression of HF. *CVD*, cardiovascular disease; *DM*, diabetes mellitus; *HTN*, hypertension. *Reproduced from reference Bozkurt B, Coats A, Tsutsui H. Universal definition and classification of heart failure.* **J Card Fail**. *2021.*

LV remodeling and dysfunction prior to the onset of HF symptoms (i.e., stage B HF). Discussions regarding large artery stiffness and pulsatile hemodynamics in conditions that define Stage A HF (i.e., conditions placing patients at risk for HF, such as diabetes, hypertension, obesity, and atherosclerotic cardiovascular disease) are discussed in Chapters 29, 30, 38, 39, 49, and 52−54. Regarding the proposed classification by LV EF, we will largely focus on HFpEF and HFrEF, since the literature regarding arterial stiffness and pulsatile hemodynamics in HFimpEF and HFmrEF is very limited at present.

The arterial tree in HF

For didactic purposes, the chapter discusses the role of the aorta first, followed by the more distal muscular arteries (in the context of the role of arterial wave reflections) and finally, the microvasculature, in HF. We will then briefly discuss the therapeutic implications of pulsatile load in patients with HFrEF and HFpEF.

The aorta in HF
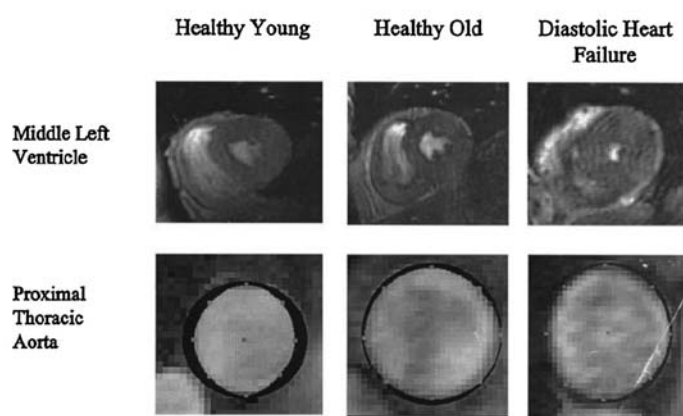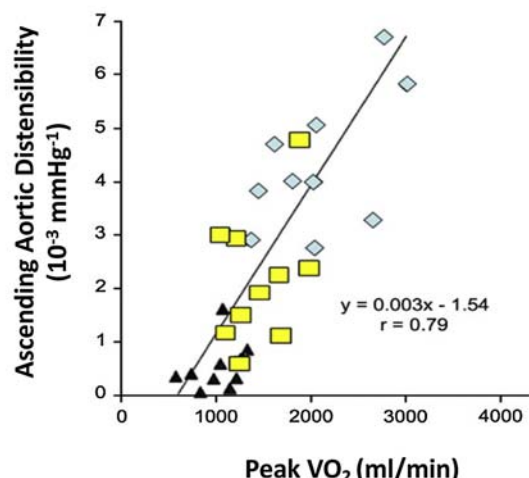
As described throughout this book, the aorta plays an important hemodynamic role. The proximal aortic geometry and wall material properties determine the aortic root characteristic impedance (Zc), which in turn represents the arterial pulsatile load to the LV in the absence of wave reflections, as discussed in detail Chapters 1, 3, 10 and 17.

Aortic Zc is a dominant factor as a determinant of pulsatile load in early systole, prior to the arrival of wave reflections originating in more distal arterial segments.[5,8,10−14] A small aortic diameter, a stiff aortic wall, or both, can determine an increased Zc and pulsatile load from the aortic root. Moreover, an increased aortic wall stiffness causes an increased aortic pulse wave velocity (PWV) which leads to a premature arrival of wave reflections to the LV during mid-to-late systole, as will be discussed in more detail in later sections of this chapter.

The aorta in HFpEF
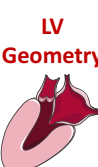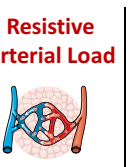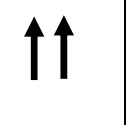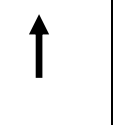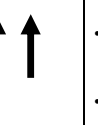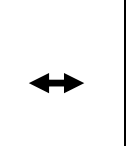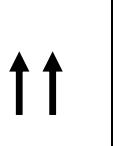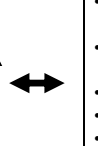
It has long been known that proximal aortic stiffness is increased in HFpEF. Hundley et al. demonstrated that patients with HFpEF exhibit a significant reduction in the cardiac cycle-dependent change in ascending aortic area and distensibility, assessed with magnetic resonance imaging (MRI), compared to young or old control healthy participants (Fig. 36.3A). Moreover, thoracic aortic distensibility was strongly correlated with aerobic exercise capacity measured as peak exercise oxygen consumption (VO$_2$; Fig. 36.3B).[15] This correlation persisted after adjustment for age and sex. Patients with HFpEF also exhibited increased ascending aortic wall thickness in this study.

More recently, Weber et al.[16] assessed pulsatile arterial function and invasively measured aortic PWV among patients with dyspnea and a preserved LV ejection fraction.

FIGURE 36.3 (A) Short-axis magnetic resonance images of the left ventricle (LV) acquired at the midpapillary muscle level at end systole (top row) and the magnitude component of the phase-contrast images of the ascending thoracic aorta (bottom row) from a participant in each of the three patient groups (healthy young, healthy old and HFpEF (i.e., "diastolic heart failure"), in the study by Hundley et al.[15] The myocardium is gray, and the blood pool within the cavity is white in the images of the LV. The blackened silhouettes on the images of the aorta represent the difference in aortic area between end-diastole and end-systole. Cardiac cycle-dependent changes in aortic area and aortic distensibility decreased with advancing age and were most reduced in older participants with HFpEF. (B) Relation between peak volume of oxygen (VO₂) and proximal thoracic aortic distensibility (vertical axis) for healthy young participants (blue diamonds), healthy old participants (yellow squares), and patients with HFpEF (black triangles). *Modified from reference Hundley WG, Kitzman DW, Morgan TM, et al. Cardiac cycle-dependent changes in aortic area and distensibility are reduced in older patients with isolated diastolic heart failure and correlate with exercise intolerance.* **J Am Coll Cardiol**. 2001; 38:796–802.

In this study, the presence or absence of HFpEF was established based on invasively derived filling pressures and natriuretic peptide levels. Pulse pressure, aortic PWV, and measures of arterial wave reflections were higher in patients with HFpEF. Moreover, this study suggested that adding measures of aortic stiffness and pulsatile arterial hemodynamics can improve the diagnosis of HFpEF in this clinical setting, although the latter point requires further validation.

Whereas the above studies in HFpEF indicate an overall increase in aortic stiffness in this population, it is important to remember that there is substantial phenotypic heterogeneity among patients with HFpEF, some of which may be driven by specific comorbidities. Chirinos et al. assessed the role of diabetes mellitus on LV and arterial structure and function in patients with established HFpEF.[17] It was demonstrated that, despite few differences in clinical characteristics, diabetic participants with HFpEF exhibited a much greater LV mass index and indexed extracellular volume measured by T1 mapping MRI (a measure of diffuse LV interstitial expansion), as well as pronounced aortic stiffening, as demonstrated by a markedly increased carotid-femoral PWV and proximal aortic Zc, relative to nondiabetic HFpEF participants. Diabetic participants also exhibited other features of adverse pulsatile hemodynamics, including increased forward wave amplitude, backward wave amplitude, and oscillatory power.

Interestingly, adverse pulsatile hemodynamics were also evident in 24-h ambulatory monitoring in the diabetic group, despite the absence of significant differences in 24-h systolic blood pressure between the groups.

Another comorbidity that may impact the arterial HFpEF phenotype is chronic obstructive pulmonary disease (COPD). Jain et al.[18] compared key cardiovascular phenotypes between patients with COPD, HFpEF, or both, using MRI and arterial tonometry to assess cardiac structure and function, pulsatile hemodynamics, and thoracic aortic stiffness. Participants with HFpEF and COPD demonstrated a more concentric LV geometry, a greater LV mass, and LV extracellular volume, as well as greater thoracic aortic PWV and aortic Zc. These results indicated that individuals with comorbid HFpEF and COPD have a greater degree of systemic large artery stiffening, LV remodeling, and LV fibrosis than those with either condition alone.

Although diabetes and COPD are common comorbidities in HFpEF, a wide range of relevant demographic and comorbidity factors can affect the phenotypic heterogeneity of the HFpEF population. These factors include older age, female sex, history of hypertension, obesity, atrial fibrillation, and coronary artery disease, among others.[19,20] Patients with HFpEF also have highly variable underlying cardiac structural and functional abnormalities.[21] Therefore, more formal approaches to characterizing the

phenotypic heterogeneity in HFpEF are advantageous to discern specific mechanistic abnormalities in various subgroups of patients. A useful approach is cluster analysis, which applies empirical statistical and/or machine learning techniques designed to detect naturally occurring subgroups of patients, maximizing within-group similarities and between-group differences on the basis of multiple measurable characteristics.[22−25] Clustering approaches can provide a potentially valuable way to identify discrete subphenotypes (or "phenogroups") of HFpEF patients, and have been applied in various studies.[23−25] Cohen et al. recently assessed large artery stiffness and related phenotypes in HFpEF phenogroups identified among participants enrolled in the Treatment of Preserved Cardiac Function Heart Failure With an Aldosterone Antagonist Trial (TOPCAT). Using latent class analysis, a well-established clustering technique, the study identified three distinct clinical phenogroups, which exhibited clear differences in clinical features, circulating biomarker profiles, cardiac structure and function, large artery stiffness (assessed via carotid-femoral PWV in a subgroup of participants), prognosis, and response to randomized spironolactone therapy, as follows (Fig. 36.4):

- Phenogroup 1 ("Younger with mild symptoms") exhibited younger age, higher smoking prevalence, preserved functional class, and the least evidence of LV hypertrophy and large artery stiffening. It is unclear if phenogroup 1 constituted individuals with genuine HFpEF, or whether it was composed predominantly by individuals with noncardiac causes of dyspnea. A noncardiac cause of dyspnea (such as lung disease) was supported by the observation that phenogroup 1 exhibited the highest prevalence of smoking and highest levels of MMP-9 (a protein involved in respiratory tract remodeling and known to be elevated in individuals with asthma and COPD).[26]
- Phenogroup 2 ("Older with stiff arteries, small LVs, and AF") was characterized by the oldest mean age and the highest prevalence of female sex and atrial fibrillation. This phenogroup also exhibited normotrophic or even hypotrophic concentric LV remodeling, LA enlargement, and markedly increased large artery stiffness. Phenogroup 2 demonstrated the highest levels of several markers of innate immunity, which have been previously associated with vascular injury as well as aging.[27] This phenogroup also exhibited the highest

FIGURE 36.4 Summary of biomarker, echocardiographic, vascular, and clinical differences across the three identified HFpEF phenogroups. *Afib*, atrial fibrillation; *CKD*, chronic kidney disease; *NAFLD*, nonalcoholic fatty liver disease; *NYHA*, New York Heart Association. *Modified from reference Cohen JB, Schrauben SJ, Zhao L, et al. Clinical phenogroups in heart failure with preserved ejection fraction: detailed phenotypes, prognosis, and response to spironolactone.* **JACC Heart Fail.** *2020; 8:172−184.*

levels of osteoprotegerin, which is a regulator of tissue calcification that has been linked with increased large artery stiffness, independent of atherosclerotic disease.[28]

- Phenogroup 3 ("Obese, diabetic with advanced symptoms") demonstrated a very high prevalence of obesity and diabetes, as well as chronic kidney disease, concentric LV hypertrophy, echocardiographic signs of high LV filling pressures, high renin, and biomarkers of tumor necrosis factor-alpha-mediated inflammation, liver fibrosis, and tissue remodeling. This phenogroup demonstrated evidence of increased large artery stiffness and pulsatile load, but not of resistive arterial load (i.e., microvascular resistance). This phenogroup exhibited the greatest functional impairment and most severe symptoms, with the highest risk of the primary endpoint of cardiovascular death, HF hospitalization, or aborted cardiac arrest. Interestingly, spironolactone randomized therapy appeared to selectively benefit participants in phenogroup 3.

Overall, these findings suggested distinct disease mechanisms across clinical phenogroups of HFpEF, which may benefit from targeted therapeutic interventions. Further studies are required to characterize more detailed measures of aortic stiffness and pulsatile arterial load in various HFpEF phenogroups.

The aorta in HFrEF

Increased aortic stiffness is also important in HFrEF. Pepine et al. reported an increase in invasively measured aortic Zc, among patients with nonischemic cardiomyopathy compared to age-matched control participants.[29] In this study, evidence of increased wave reflections was also found among HFrEF participants. Rerkpattanapipat et al.[30] examined patients with HFrEF as well as age matched and younger control participants. The investigators measured aortic distensibility using MRI and quantified aerobic exercise capacity (VO_2) using ergometry with expired gas analysis. In this study, patients with HFrEF exhibited a markedly decreased distensibility of the ascending aorta and increased aortic wall thickness. Aortic distensibility was strongly and significantly correlated with peak VO_2, and the correlation remained after adjusting for age and LV ejection fraction.[30] Reduced abdominal aortic distensibility was also reported by Giannattasio et al. among patients with HFrEF compared to age- and sex-matched controls.[31]

Interestingly, although aortic stiffening clearly has the potential to contribute to systolic LV dysfunction, some data support a bidirectional relationship, by which LV dysfunction may also result in secondary aortic abnormalities leading to increased pulsatile load. In a canine model of LV dysfunction induced by rapid pacing, Eaton et al. demonstrated that aortic Zc increased in response to LV

systolic dysfunction and this preceded changes in systemic vascular resistance.[32] In another study using a similar canine model, Khan et al. demonstrated that the aortic changes in response to a reduced LV systolic function were due to a change in geometry (smaller diameter and thicker wall), rather to changes in the material properties of the wall (stress-strain stiffness), suggesting that under-expansion of the aorta by a reduced stroke volume may play an important role.[33] This phenomenon may partially explain the reduced distensibility and increased aortic wall thickness reported in humans with HFrEF by Rerkpattanapipat et al.[30]

Large artery stiffness as a predictor of incident HF

Large artery stiffness predicts the incidence of new-onset HF. In the Framingham cohort, carotid-femoral PWV was associated with an increased risk of incident HF over approximately 10 years, and was associated with both incident HFpEF and HFrEF.[34] In the recent CAVI-J study, which included 2932 participants aged 40−74 years in Japan, an increased cardio-ankle vascular index (a metric strongly influenced by large artery stiffness) was associated with HF hospitalization over a ∼5 year follow-up period.[35] Although the direct causal contribution of aortic stiffening on HF risk remains to be quantified in humans, multiple mechanisms link aortic stiffening to the pathogenesis of LV dysfunction and HF. Whether reducing aortic stiffness using specific therapeutic interventions can reduce the risk of HF remains to be determined.

Large artery stiffness as a predictor of outcomes in established HF

In advanced HFrEF, a lower pulse pressure can be associated with a worse prognosis. In these patients, a low pulse pressure is due to a very poor LV function and small stroke volume. In patients with less severe HFrEF, the relationship may become direct, since in these patients, pulse pressure is more reflective of arterial stiffness and increased pulsatile afterload. In HFpEF, the relationship between pulse pressure and outcomes tends to be direct (a higher pulse pressure being associated with a worse prognosis). In some studies, patients with the lowest pulse pressure also have a worse prognosis, likely due to a small stroke volume, despite a preserved EF due to pronounced concentric remodeling and a small LV cavity.

Given the important confounding effect of LV structure and function on pulse pressure, more direct measurements of large artery stiffness are likely to be informative. An increase in carotid-femoral PWV, aortic PWV or brachial-ankle PWV has been shown to be related to the risk of HF hospitalization, CV, and all-cause mortality in HF patients, regardless of EF.[36,37]

Arterial wave reflection in heart failure

Every beat, the LV generates a pulse wave that travels forward in the arteries and gets partially reflected at sites of impedance mismatch, such as points of branching or changes in wall diameter or material properties along the arterial tree. Innumerable reflections merge into a discrete reflected wave, which travels back to the heart.[12,13,38] Of note, the source of wave reflections is not necessarily the same as the resistance microvasculature, which determines mean arterial pressure.[12,13,38] Therefore, it is possible to modify wave reflections without affecting mean pressure, and vice versa. Important sources of wave reflection include arterial bifurcations, the tapering of the aorta, sites of tortuosity or focal wall stiffening, and/or narrowing in conduit arteries, as well as more distal arterial segments.[12,13,38]
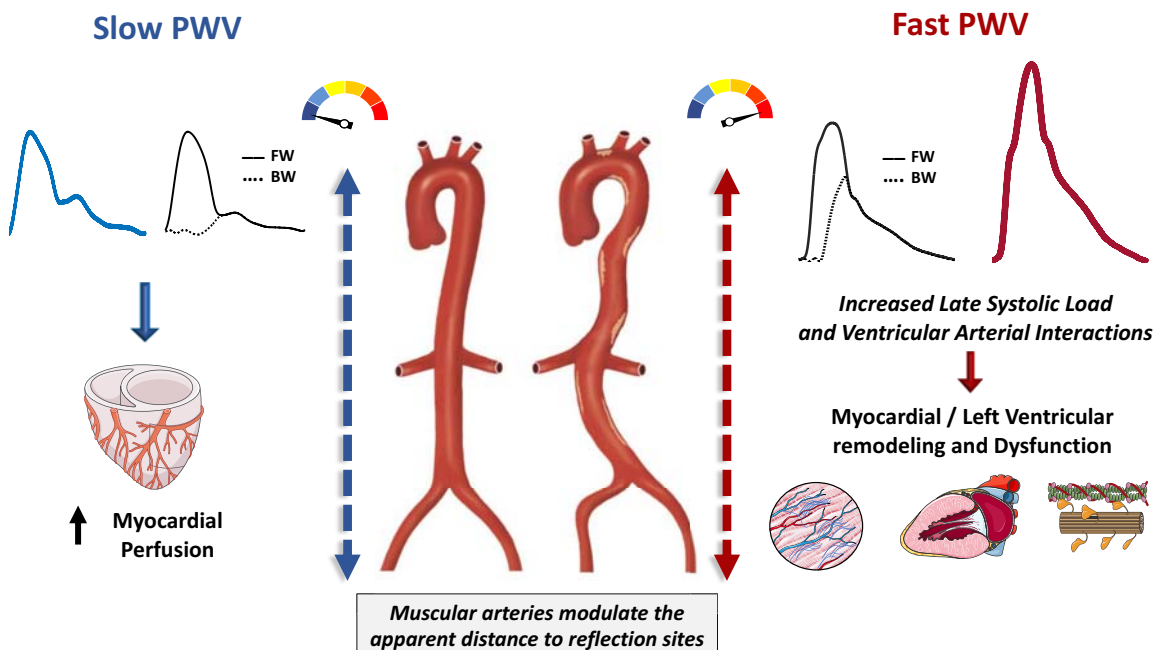
The time of arrival of the reflected wave to the proximal aorta is strongly dependent on the PWV of conduit vessels, particularly the aorta, which transmits forward and backward traveling waves from and toward the LV, respectively.[38–41] Stiffer aortas, which exhibit greater PWV, conduct forward and backward traveling waves at greater velocities and therefore promote an earlier arrival of wave reflections to the LV (Fig. 36.5).[10,12,38,42,43] As a consequence of the aortic stiffening that occurs with aging

and various disease states, the hemodynamic effects of wave reflections shift from diastole to systole, with prominent effects during mid-to-late systole in older adults,[38,42] particularly in women[12,13,42,44–47] and in patients with HFpEF.[16,48,49] In these conditions, wave reflection can have a substantial impact on the LV loading sequence (increasing mid/late relative to early systolic load), as discussed in detail in Chapter 16.

Despite the key role of the aorta as a determinant of reflected wave transit time, it is useful to consider the role of wave reflection along with muscular artery function, given that the latter can modulate the timing and magnitude of wave reflection for any given aortic PWV (Fig. 36.5). Moreover, muscular arterial function represents a readily modifiable target for pharmacologic interventions. However, it should be emphasized that, as mentioned above, wave reflections occur throughout the arterial tree, including the aorta, intermediate-sized conduit arteries, and more distal arterial segments.

Wave reflection and LV hypertrophy

As discussed in various other sections of this book, exaggerated mid-to-late systolic pulsatile load from arterial wave reflections can lead to LV remodeling. For any given level of systolic (peak) blood pressure, prominent

FIGURE 36.5 Cardiac Consequences of Arterial Stiffening and premature wave reflection. Earlier arrival of wave reflections favor a loss of coronary perfusion pressure on one hand, and increased mid-to-late systolic load on the other, due to a shift of wave reflection arrival from diastole to systole. In populations with stiff aortas, muscular artery function may become a key determinant of the apparent distance to reflection sites and thus the effects of wave reflections on the central aorta, for any given PWV. *BW*, backward wave; *FW*, forward wave; *PWV*, pulse wave velocity. *Reproduced from Chirinos JA, Segers P, Hughes T, Townsend R. Large-artery stiffness in health and disease: JACC state-of-the-art review.* **J Am Coll Cardiol**. *2019; 74:1237−1263.*

mid-to-late systolic loading has been shown to exert deleterious effects on LV structure and function in animal models and has been associated with LV hypertrophy in humans, as discussed in more detail in Chapter 16.[38,50,51] Aortic constriction studies in rats[50] that induced early versus late systolic load demonstrated a causal effect of late systolic loading on LV hypertrophy and fibrosis, despite identical peak LV pressure levels. In humans, changes in wave reflection magnitude occurring during antihypertensive therapy predicted regression of LV mass independently of blood pressure reduction.[52] A relationship between reflection magnitude (approximated from measured pressure and an assumed physiologic flow waveform) and LV mass has been reported in large community-based studies that included normotensive and hypertensive individuals.[45,53] Finally, in patients with repaired aortic coarctation, reflection magnitude estimated from the ascending aortic distension waveform and measured aortic flow using MRI was independently associated with LV hypertrophy.[54] When interpreted in the context of available animal data, available human studies support a role for wave reflections in the development of LV hypertrophy, independent of absolute blood pressure levels. Also consistent with animal data implicating wave reflection in the development of LV fibrosis, a relationship between reflection magnitude and LV diffuse interstitial fibrosis has been reported in patients with severe aortic stenosis undergoing aortic valve replacement.[55] Whether this relationship is present in other forms of severe LV pressure overload (i.e., in the absence of aortic stenosis) in humans remains unclear.

Effect of mid-to-late systolic load on LV diastolic dysfunction

Multiple animal studies have demonstrated the deleterious effect of mid-to-late systolic load on LV relaxation.[51,56−60] Hori et al. used a canine model of aortic clamping and demonstrated that, for a given increase in peak systolic LV pressure, mid-to-late systolic loading interventions prolonged the time constant of diastolic LV relaxation much more than early loading. Gillebert et al.[51] studied the effect of the timing of systolic load in a canine model using rapid balloon inflations in the ascending aorta at different times during ejection (inducing either early systolic load or mid-to-late systolic load), demonstrating that, for a given increase in peak systolic LV pressure, mid-to-late systolic loading prolonged *tau* much more than early systolic inflation.[51] These results are consistent with several other animal studies[57−62] as discussed further in Chapter 16.

Consistent with available animal studies demonstrating a cause-effect relationship between mid-to-late systolic load and impaired LV relaxation, human studies have shown that indices of wave reflections and/or mid-to-late systolic

myocardial wall stress (MWS) are independently associated with diastolic dysfunction,[48,61,63−72] LA remodeling and dysfunction,[65,73,74] decreased longitudinal LV systolic function (despite preserved EF),[67,75] and elevated brain natriuretic peptide levels.[66,71,76,77]

The effect of mid-to-late systolic load on LV relaxation and remodeling may relate to differential cellular processes in different phases of ejection. During early ejection, active development of fiber cross-bridges occurs in the electrically activated myocardium and peak MWS develops,[78] which is followed by a transition from contraction to relaxation.[67,69,78−80] Before this transition, active cross-bridge formation takes place and loading increases the number of interacting cross-bridges (cooperative activity), a physiological mechanism that favors matching of the number of cross-bridges with systolic load.[51,81] However, when increased load occurs after the onset of myocardial relaxation, the number of interacting cross-bridges can no longer adapt, resulting in a mismatch between the number of cross-bridges and load, increasing the stress on individual cross-bridges and decreasing cross-bridge cycling. However, more complex interplays between cross-bridge recruitment, cooperative activity, cross-bridge inactivation, and cross-bridge cycling rate are likely at play.[69,70,79,81]

As discussed in detail in Chapter 16, under normal conditions MWS rapidly decreases during mid-systole as a result of the geometric reconfiguration induced by early systolic LV ejection, resulting in a shift of the LV pressure-stress relation that favors lower MWS levels for any given LV pressure.[78] This shift protects the cardiomyocytes against late systolic load, but may be impaired in LV hypertrophy or LV systolic dysfunction. The resulting mismatch between early and late systolic load may result in impaired shortening-deactivation in cardiomyocytes.[69] The phenomenon of shortening-deactivation (which is associated with reduced calcium sensitivity of the contractile apparatus) decreases force development after early systolic rapid shortening, and increases the relaxation rate of muscle.[69,70] This represents a perfect "match" to the normal physiology (i.e., markedly reduced MWS in mid-to-late systole), because sustained myocardial force development in this period is unnecessary to preserve fiber shortening and LV ejection against the load imposed by wave reflections. However, in the presence of contractile abnormalities that compromise early ejection, the mid-systolic dynamic geometric reconfiguration of the LV that favors a reduced MWS relative to pressure is impaired. In these conditions, shortening-deactivation does not operate fully, such that force development continues or increases in mid-to-late systole.[69,70] However, much remains to be learned about the molecular pathways that mediate malignant effects of late systolic load at the cellular level, and this should be the focus of future research.

Arterial wave reflection and the risk of incident HF
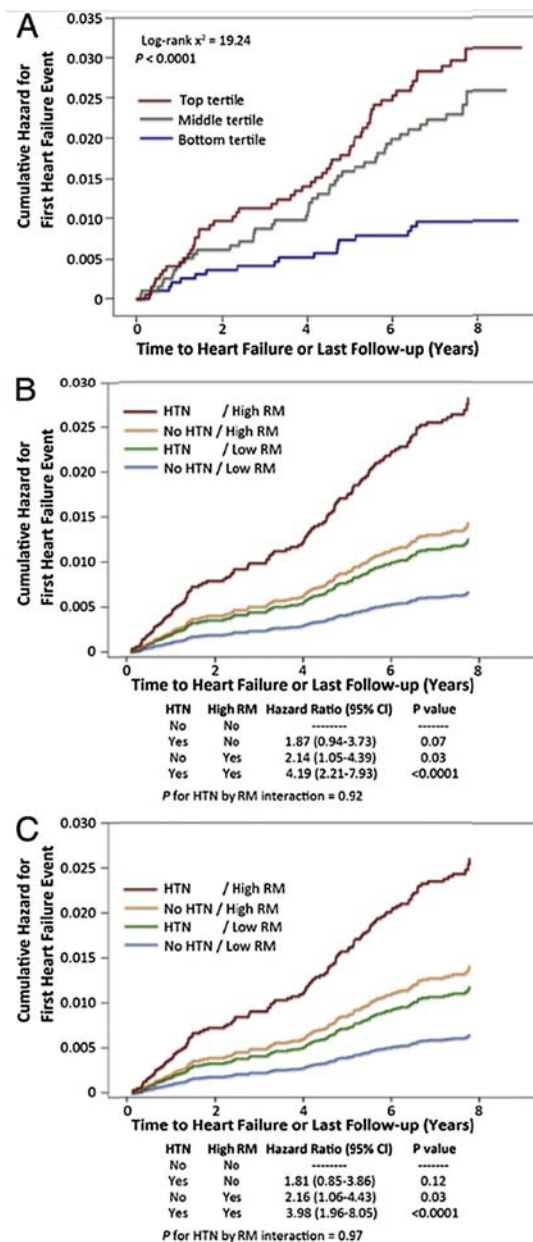
Wave reflection magnitude has been shown to strongly predict new onset HF among 5934 participants in the Multiethnic Study of Atherosclerosis (MESA), who were free of clinically apparent cardiovascular disease at baseline (Fig. 36.6). During 7.61 years of follow-up (and after adjustment for systolic and diastolic blood pressure, age, gender, body mass index, diabetes, ethnicity, antihypertensive medication use, total and HDL-cholesterol, current smoking, heart rate, and glomerular filtration rate), reflection magnitude strongly predicted HF (Hazard ratio per 10% - increase = 2.69; 95% CI = 1.79−4.04; $P < .0001$) and was a stronger predictor than blood pressure and all other modifiable risk factors listed above. When we stratified the population based on the presence or absence of hypertension and the presence or absence of high reflection magnitude (Fig. 36.6B and C), we found that, compared to nonhypertensive subjects with low reflection magnitude (lowest risk category), hazard ratios for hypertensive subjects with low reflection magnitude, nonhypertensive subjects with high reflection magnitude and hypertensive subjects with high reflection magnitude were 1.81 (95% CI = 0.85−3.86), 2.16 (95% CI = 1.04−4.43), and 3.98 (95% CI = 1.96−8.05), respectively.

Furthermore, we assessed the strength of the association between reflection magnitude and incident HF using multiple parameters. Reflection magnitude was associated with the largest Wald statistic of all predictors (including age), the greatest reduction in Akaike's information and Bayesian information criteria (indicating improvement in model fit). With the exception of age, a nonmodifiable risk factor, reflection magnitude was associated with the greatest net reclassification improvement for prediction of HF. Therefore, reflection magnitude was a robust and strong predictor of incident HF in this cohort after adjustment for other known predictors. In the same population, systemic vascular resistance, total arterial compliance, and effective arterial elastance (E_A) did not predict HF.[83] A limitation of this study is the utilization of a synthetic flow approach that approximates reflection magnitude. Further studies are required to assess the association between reflection magnitude and incident HFpEF versus HFrEF.

Hemodynamic role of the microvasculature in HF

The microvasculature as a determinant of LV load

The resistive load imposed by small arterioles throughout the body is the main determinant of the so called "effective arterial elastance" (E_A), which represents the arterial load in the pressure−volume plane (see Chapter 15). Whereas

FIGURE 36.6 (A) Cumulative hazard for heart failure among subjects stratified according to tertiles of reflection magnitude (RM). (B) Hazard function for incident of heart failure in subjects stratified according to the presence or absence of hypertension (prevalence: 45%) or reflection magnitude above ("high" RM) or below ("low" RM) the 55th percentile (prevalence of "high" RM: 45%), adjusted for other significant heart failure predictors. (C) Analogous hazard functions after further adjustment for ethnicity, antihypertensive medication use, total-cholesterol, HDL-cholesterol, current smoking, glomerular filtration rate, and heart rate. *Reproduced with permission from Chirinos JA, Kips JG, Jacobs DR, Jr, et al. Arterial wave reflections and incident cardiovascular events and heart failure: MESA (Multiethnic Study of Atherosclerosis).* **J Am Coll Cardiol**. *2012; 60:2170−2177.*

effective arterial elastance is a misnomer (since it bears little relation with arterial stiffness or pulsatile arterial load), E_A does impact the LV EF for any given LV
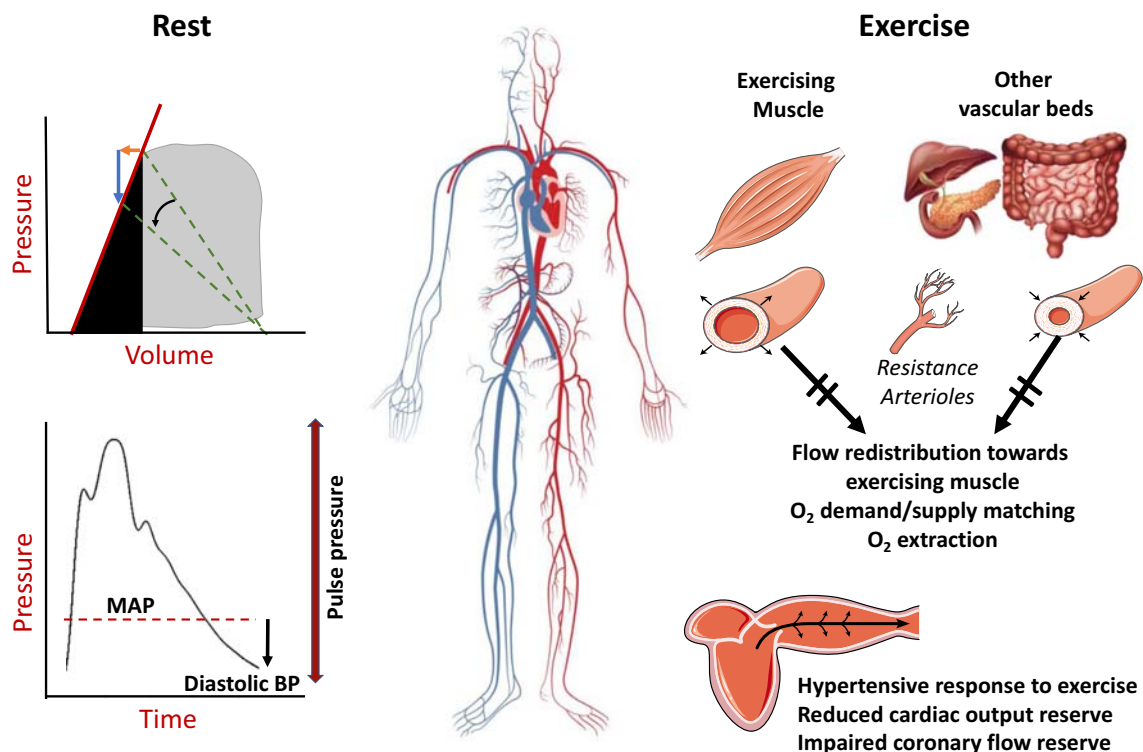
end-systolic stiffness (the gold-standard load-independent parameter of LV contractility). For an in-depth discussion of ventricular–arterial coupling in the pressure–volume plane, please refer to Chapter 15.

In the setting of marked reductions in LV contractility and LV end-systolic stiffness (as occurs in HFrEF), a high E_A can contribute to an impaired energetic efficiency of the ventricular–arterial system. In this setting, substantial reductions in SVR, with consequent reductions in E_A with the use of arteriolar vasodilators can improve ventricular–arterial coupling, stroke volume, and the energetic state of the failing LV.

In HFpEF (which by definition is accompanied by a normal LV EF and a normal to high LV end-systolic stiffness), the pressure–volume plane is much less informative regarding the variability in energetic aspects of ventricular–arterial coupling, but it does provide some insights into ventricular–arterial interactions. In particular,

in the setting of a high E_A, increased LV systolic stiffness can be necessary to preserve the ejection fraction (thus being implicit in HFpEF), but this results in increased blood pressure lability.[84] In the setting of increased LV end-systolic stiffness, a given reduction in E_A (which as mentioned above is primarily influenced by systemic vascular resistance) will lead to a proportionally greater blood pressure decrease versus a stroke volume increase (Fig. 36.7). Furthermore, an increased LV systolic stiffness at rest will impair the LV chamber contractile reserve (and stroke volume reserve) during exercise. This is particularly problematic in this condition because patients with HFpEF demonstrate an impaired microvascular vasodilatory reserve during exercise, which thus limits the exercise-induced reduction in E_A.[85–88]

This constellation of abnormalities presents a unique challenge for vasoactive therapeutic strategies in HFpEF because important reductions in systemic vascular

FIGURE 36.7 Role of microvascular hemodynamic function in hemodynamics at rest and during exercise. At rest (left panels), the ventricular–arterial system of patients with HFpEF is characterized by increased LV systolic stiffness (i.e., increased E_{ES}, upper left panel, red line). Therefore, any therapeutic intervention that reduces vascular resistance at rest (black curved arrow) (which is the key arterial determinant of "effective arterial elastance," represented in green lines) will induce a large pressure decrease (blue arrow) relative to the increase in stroke volume (orange arrow). Furthermore, given the presence of stiff conduit arteries and premature wave reflections that augment systolic, rather than diastolic aortic pressure, a reduction in mean arterial pressure may decrease diastolic arterial pressure excessively (left lower panel), leading to a reduction of perfusion pressure in key organs. During exercise (right panels), however, a reduction in vascular resistance is essential. A combination of vasoconstriction in most vascular beds (splanchnic vasculature, nonexercising muscle, etc) along with vasodilation in exercising muscle (local functional sympatholysis) is key for the optimization the cardiac output distribution and oxygen supply-demand matching in the periphery. In addition, the lack of reduction in SVR during exercise increases LV load and contributes to the limitation in cardiac output reserve. Microvascular function is also essential for enhancing coronary perfusion during exercise. However, pulsatile hemodynamics also affect myocardial oxygen demand (workload) and supply (diastolic perfusion pressure) during exercise (see text). *DBP*, diastolic blood pressure; *MAP*, mean arterial pressure.

resistance in this population may result in important side effects (such as dizziness and hypotension). However, enhancing vasodilatory reserve (i.e., a selective reduction in systemic vascular resistance with exercise) is a logical goal to enhance aerobic capacity, as discussed below.

Effects of peripheral microvascular function on exercise capacity

In addition to the role of vasodilatory reserve on arterial load and ventricular—arterial interactions during exercise, an abnormal vasodilatory response has profound implications for peripheral oxygen delivery and utilization (Fig. 36.7). Vasodilatory responses during exercise mediate the peripheral redistribution of blood flow to working muscle tissue, which is a key component of the normal hemodynamic response to exercise,[89] and depends on local vasodilatory mechanisms within locomotive muscle, allowing it to advantageously compete with other vascular beds for the available cardiac output.[89] This is a highly suitable adaptive response to balance oxygen supply and demand, given the marked increase in metabolic demands imposed by active skeletal muscle contraction.[89,90] Skeletal muscle vasodilation during exercise allows the local vasculature to overcome humoral and reflex-mediated vasoconstriction.[89] In particular, exercise is accompanied by systemic sympathetic activation, and "functional sympatholysis" must occur in exercising muscle to overcome the intense systemic sympathetic vasoconstrictive response. Based on these principles and experimental evidence, it follows that impaired microvascular responses within skeletal muscle can have important adverse consequences for oxygen extraction, creating a marked imbalance between oxygen delivery and demand in muscle, ultimately resulting in a large oxygen deficit, accentuated intracellular metabolic perturbations, and enhanced glycogenolysis even at low levels of activity.[89]

The importance of flow distribution *within* muscle should also be noted, given that blood flow within active muscles is not homogeneous, but greater in highly oxidative muscles, which require greater vasodilatation.[91,92] Hypoxic vasodilation favors preferential vasodilation in tissues with high oxidative capacity, which seems important to optimize the matching of oxygen supply and demand.[89,90] Finally, microvascular vasodilation in skeletal muscle during exercise is important to washout metabolites (such as hydrogen ions), preventing an excessive afferent stimulus for metaboreflex responses which result in sympathetic activation and vasoconstriction.

Given the important role of the peripheral microvasculature in HF, various studies have assessed exercise-induced vasodilatory responses in HFrEF and HFpEF, as discussed below.

- *Peripheral vasodilatory reserve in HFrEF*: Sullivan et al.[93] compared hemodynamic and metabolic responses to maximal upright bicycle exercise between participants with HFrEF and healthy controls. In this study, mean arterial pressure was not different between the two groups at rest or at matched submaximal work rates, whereas leg vascular resistance was higher in patients compared with normal subjects at rest, submaximal, and maximal exercise. Patients with HFrEF also demonstrated increased leg oxygen extraction and lactate production accompanied by a decreased leg oxygen consumption during exercise. These findings were consistent with impaired local vasodilation leading to leg hypoperfusion in HFrEF, which was associated with decreased leg oxygen utilization (despite increased leg oxygen extraction) and anaerobic skeletal muscle metabolism. Barrett-O' Keefe et al.[94] compared the hemodynamic responses to small muscle mass exercise (static-intermittent handgrip and dynamic single-leg knee-extension) between HFrEF patients and age-matched control subjects. These exercise interventions induce activation of a small amount of muscle mass that does not provoke significant central cardiopulmonary stress, thus better isolating peripheral responses. The investigators demonstrated that despite similar increases in mean arterial pressure during exercise, HFrEF patients exhibited an attenuated increase in arm and leg blood flow. Whereas the former was evident only at high workloads, the latter was present across all work rates, albeit with more substantial attenuations at higher intensities. Wilson et al.[95] reported that the impaired local vasodilatory reserve may be limited to HFrEF patients with a markedly reduced aerobic capacity, whereas impaired cardiac output reserve is a contributor to reduced blood flow in HFrEF, regardless of aerobic capacity. Although the majority of available studies indicate an attenuation in exercising limb perfusion attributable to impairments in peripheral vasodilatory capacity in HFrEF, some data argue against the presence of impaired peripheral vasodilation in this condition.[96] This may be related to a small sample size and/or the heterogeneity in the etiology or severity of HFrEF in different studies.

- *Peripheral vasodilatory reserve in HFpEF*: Although an impaired systemic vasodilatory reserve in HFpEF was reported long ago by Borlaug et al.,[87] thus providing indirect evidence of impaired local vasodilation in exercising muscle, few studies have specifically assessed local skeletal muscle vasodilatory reserve in this condition. Using cardiovascular magnetic resonance imaging during submaximal exercise, Punta-wangkoon et al. reported a reduction in superficial

femoral artery blood flow upon cessation of supine cycling exercise in HF patients (including both HFpEF and HFrEF) compared to healthy controls, despite similar flow in the ascending and descending aorta. These differences, consistent with an impaired blood flow distribution attributable to reduced local conductance (the inverse of resistance) in exercising skeletal muscle in HF, persisted after adjustment for LV EF. Lee et al.[97] compared leg blood flow during dynamic, single leg knee-extensor exercise between HFpEF patients and healthy controls and reported a lower leg vascular conductance at high but not low workloads in HFpEF, which resulted in reduced local blood flow despite similar mean arterial pressure between the groups. Similarly, Ratchford et al.[98] concomitantly evaluated brachial artery blood flow during progressive intermittent handgrip exercise (at 15%, 30%, and 45% of maximal voluntary contraction) among individuals with HFpEF and control overweight individuals with hypertension. In this study, systemic stroke volume and cardiac output were not different between groups across exercise intensities, whereas forearm blood flow was significantly lower ($\sim 20-40\%$) in individuals with HFpEF at higher exercise intensities (30% and 45% of maximum voluntary contraction), and forearm vascular conductance was $\sim 20\%$ lower in HFpEF only at the highest exercise intensity. Overall, these studies support the presence of an attenuation in the vasodilatory response in muscle during exercise in HFpEF, particularly at higher exercise intensities, which is sufficient to induce hypoperfusion of skeletal muscle and is likely to contribute to exercise intolerance in this condition.

The relationship between microvascular dysfunction and adverse central pulsatile hemodynamics remains unclear. On one hand, it is possible that long-term adverse central pulsatile hemodynamics may contribute to microvascular damage in skeletal muscle, although this is less likely than in other organs given the relatively high vascular resistance of the skeletal muscle microvasculature at rest. On the other hand, common risk factors and biochemical pathways may impact vasodilatory responses and pulsatile arterial hemodynamics, and these may represent both mechanistic links between macrovascular and microvascular dysfunction in HFpEF and suitable targets for therapy, as will be discussed later in this chapter. Regardless of whether mechanisms leading to microvascular and macrovascular dysfunction in HFpEF are interrelated, it is clear that both can contribute to the syndrome in general and to impaired exercise capacity in particular, given the important role of pulsatile arterial load on the LV at rest and during exercise.[5,7,99]

Role of the coronary microcirculation

Abnormalities of the coronary microcirculation are increasingly recognized determinants of myocardial function.[100-103] Myocardial blood flow must increase during exercise to match the metabolic demands of the myocardium. Myocardial blood flow occurs predominantly in diastole given the compression of the coronary microvasculature that occurs during systolic myocardial contraction. Impaired myocardial microvascular reserve may impair diastolic myocardial perfusion during exercise, worsening myocardial function and exercise intolerance. Resting myocardial blood flow and flow reserve in response to various stimuli are determined by a complex set of factors, including myocardial tissue architecture, coronary microvascular resistance, and importantly, aortic root pulsatile hemodynamics (see Chapter 18).[5,6]

In patients with a normal LV ejection fraction, normal epicardial perfusion, and risk factors for HFpEF, a decreased myocardial flow reserve is associated with diastolic dysfunction, increased LV filling pressures, and abnormal LA function.[104] Moreover, patients with established HFpEF exhibit myocardial microvascular rarefaction and impaired coronary flow reserve.[100,103,105] Kato et al. assessed coronary flow reserve responses to adenosine among 163 HFpEF patients and found that an impaired response was associated with the risk of all-cause death and hospitalization due to HF exacerbation during a median follow-up of 4.1 years.[106]

Inflammation has been proposed as a key determinant of coronary microvascular dysfunction in HFpEF, but a direct causal link remains to be proven.[107,108] Moreover, microvascular dysfunction in the coronary bed likely represents a component of systemic microvascular dysfunction. More research is required to understand the determinants and the implications of coronary microvascular dysfunction in HFpEF. Finally, the relative role of microvascular rarefaction, abnormal vasodilatory responses in small vessels, and aortic pulsatile hemodynamics as determinants of abnormal coronary flow reserve in HFpEF requires further study.

Coronary flow reserve also seems to be important in HFrEF. Canneti et al. demonstrated an impairment in coronary blood flow reserve in response to adenosine among patients with idiopathic dilated cardiomyopathy despite normal epicardial coronary arteries.[109] Similarly, Morales et al. demonstrated that myocardial blood flow reserve in response to dipyridamole was depressed in patients with idiopathic dilated cardiomyopathy even the in absence of overt HF.[110]

An important aspect neglected by the studies mentioned above is the role of aortic root pulsatile hemodynamics. As discussed in detail in Chapter 18, the diastolic pressure-time integral is a key determinant of coronary blood flow,

given that it represents the driving pressure promoting perfusion across the coronary microvascular bed. Coronary blood flow is directly related to the aortic diastolic pressure-time integral, for any given coronary microvascular resistance and coronary sinus/right atrial pressure. Therefore, coronary flow reserve (assessed via coronary sinus flow measurements) or myocardial flow reserve (assessed via perfusion techniques such as positron emission tomography or MRI perfusion imaging) cannot be equated to coronary microvascular dilatory reserve. Adverse aortic pulsatile hemodynamics can clearly impact the diastolic pressure-time integral and therefore reduce coronary blood flow independently of microvascular rarefaction or vasodilation. Specifically, large artery stiffening and low total arterial compliance will determine a steep pressure decay during diastole,[111] as the arterial volume decreases due to diastolic blood flow to the venous circulation across the systemic capillary bed. Similarly, wave reflections that shift from diastole to systole as a result of a short reflected-wave transit time, fail to augment diastolic pressure and thus coronary perfusion. Despite the importance of these hemodynamic factors as determinants of coronary blood flow, available studies have not separated them from true coronary microvascular resistance and vasodilatory coronary reserve. The extent to which aortic root hemodynamics versus coronary microvascular function are involved in the abnormal coronary/myocardial flow reserve abnormalities in HFpEF described above remains to be determined, but it should be recognized that increased large artery stiffness and wave reflections may conspire with coronary microvascular dysfunction to impair coronary flow, particularly during exercise (in which diastolic duration is shortened). Optimizing aortic root pulsatile hemodynamics may thus represent a suitable therapeutic approach to improve myocardial oxygen supply and demand in HF. A detailed discussion regarding the role of aortic root pulsatile hemodynamics as a determinant myocardial blood supply can be found in Chapter 18.

Macrovascular-microvascular cross-talk: role of large arterial pulsatile hemodynamics in microvascular dysfunction and HFpEF comorbidities

There is an increasing recognition of the role of large artery stiffness and abnormal arterial pulsatile hemodynamics on microvascular disease, which is relevant for the damage of target organs such as the brain, the kidney, and possibly, the liver, and endocrine pancreas.[43,112−116] Cognitive dysfunction/dementia, renal dysfunction, and diabetes are highly prevalent in HFpEF, and can significantly influence prognosis.[117−121]

Aortic stiffening and increased wave reflections have important adverse consequences on microvascular pressure and flow. Conduit arteries normally exert a powerful cushioning function, which results in nearly steady flow in the microvasculature despite the intermittent LV ejection. Aortic stiffening results in a loss of this cushioning function and promotes increased pulsatility in the microvasculature. Peripheral vascular resistance, largely imposed by small arteries, governs the amount of mean capillary flow for any given mean arteriovenous pressure gradient (which in turn, depends mostly on mean arterial pressure). Given that mean pressure varies minimally throughout the arterial system, differences in vascular resistance primarily determine the vastly different flow rates seen in various vascular beds. Since resistance is highly correlated with arteriolar tone, it is thought that in low-resistance, high-flow vascular beds, a low precapillary arteriolar tone allows for greater transmission of proximal pulsatility into the capillaries, resulting in increased pulsatile pressure (barotrauma) and pulsatile flow (with excessive pulsatile shear forces). In contrast, the high arteriolar tone in high-resistance vascular beds uncouples the proximal pulsations from the distal capillaries, which are more effectively protected from excessive pulsatility.

Consistent with these principles, accumulating evidence links cerebral microvascular disease and renal disease with increased aortic stiffness.[43,112,114,115] Similarly, the pancreatic islets exhibit very high flow per gram of tissue, and thus low-resistance high-flow physiology.[122] Recent evidence indeed suggests a role for large artery stiffening in the development of diabetes, although a causal link remains speculative at present.[123−125]

Vascular beds with increased resistance (such as skeletal muscle) are relatively (but not entirely) protected from increased central pulsatility. Increased large artery stiffness is also associated with impaired microvascular dysfunction (postischemic vasodilation) in the forearm vascular bed.[113] As discussed above, axial skeletal muscle microvascular function (vasodilatory reserve) is key for exercise-induced vasodilation, flow redistribution, and oxygen extraction during exercise, and is impaired in HFrEF and HFpEF, although its mechanistic link with large artery hemodynamics remains unclear.

Wave reflections are also important for microvascular dysfunction. Wave reflections from the lower body increase central (aortic) pressure pulsatility and thus promote microvascular pulsatility in target organs such as the brain. A more controversial issue is the role of local wave reflection at the aortic-carotid interface, which has been suggested to protect the brain. This is based on the observation that aging is associated with a disproportionate increase in aortic stiffness relative to muscular arterial
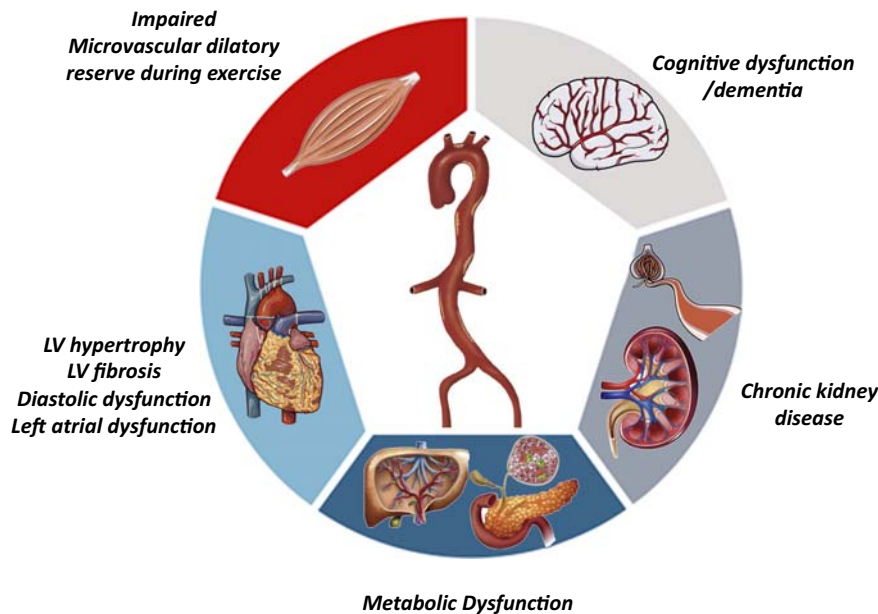
stiffness, promoting impedance matching and a reduction in wave reflection in first-order arterial bifurcations in older adults.[114] Loss of wave reflection proximal to target organs (such as at the aorta-carotid interface) has thus been proposed as a mechanism for excessive pulsatile power transmission to the distal circulation. However, impedance matching is not only dependent on wall stiffness, but strongly dependent on vessel size.[126] Therefore, despite substantial differences in PWV between the aorta and muscular arteries, optimization of the size ratio between parent and daughter vessels in the arterial tree[126] optimizes impedance matching in individual first order bifurcations even before the aorta stiffens with age and disease. The configuration of parent and daughter arterial branches, which appears perfectly designed to favor forward energy transmission, is also responsible for the fact that reflections at single bifurcations tend to be quite small, relative to the composite reflected wave arising from the sum of millions of tiny reflections elsewhere. For example, it has been reported that 90% of reflection coefficient values at the aorta-carotid interface were between 0% and 15%,[114] corresponding to power transmission coefficients as high as 97.75%−100%, indicating that such reflections return as little as 0%−2.75% of the pulsatile energy to the parent branch. It is also worth noting that reflections at a single interface tend to increase pulse (and systolic) pressure in the distal branches, which is in principle, deleterious to target organs.

Despite these considerations, some investigators propose an important role of discrete reflections at the entry of low-resistance vascular beds, which requires serious consideration and further study. A recent study by Haidar et al. indicated that a reduced impedance gradient between the proximal aorta and the common carotid arteries leads to a predominant increase in the local flow transmission coefficient despite the low overall reflection coefficient of the bifurcation. Another important factor suggested to play a key role in energy penetration to the brain is the relative impedances of the parent branch (proximal aorta), carotid branches, and distal aortic segments, coupled with distal carotid bed reflections and re-reflections.[127] Interestingly, this study indicated that reflections arising from the distal carotid circulation and re-reflection of these waves at the carotid origin can reduce pulsatile power transmitted into the cerebral vasculature. This is due to the fact that re-reflections at the carotid origin are "open" reflections; that is, reflections arising from the distal carotid circulation, travel down the common carotid in a retrograde direction, and encounter a high-to-low impedance change at its origin from the arch. Open reflection changes the sign of waves and thus results in compression waves being re-reflected at the interface as forward-traveling suction waves that reduce pulsatile pressure and flow (see Chapters 1, 3 and 11).

Despite the potential protective role of local reflections at the aortic-carotid interface and within the cerebral vasculature, it is also important to note that most wave reflections arise from locations distal to the upper body first-order bifurcations and in fact, the larger reflected wave returning from arterial locations distal to the aortic arch penetrates the carotid artery as a "forward" wave (thus increasing pressure and flow in the carotid bed).[43,128] The innumerable reflections from arterial locations distal to the aortic arch form a larger composite reflected wave, which thus demonstrates a larger reflection coefficient, and carries a larger amount of reflected power than the single reflection at the aorta-carotid interface. Furthermore, impedance matching at the aortic-carotid interface may paradoxically promote the penetration of the reflected wave returning from the lower body into the carotid territory. Interestingly, arteries upstream of the cerebral microvasculature appear to attenuate high-frequency flow pulsations (such as those contained in the early systolic carotid flow peak produced by the initial cardiac contraction), much more effectively than low-frequency oscillations (such as those contained in the reflected wave returning from the lower body).[43,128] Therefore, the pulsatile energy from reflected waves arising in the lower body appears to more effectively penetrate into the cerebral microvasculature.[43,128]

Clearly, wave reflections cannot be simply categorized as benign or malignant events for target organs such as the brain, but its origin and interaction with local hemodynamics must be carefully considered. However, the preponderance of evidence suggests that the bulk of systemic wave reflections arising in places other than target organs themselves can be deleterious to target organs via their effects on central pressure pulsatility. Interestingly, vasodilators that reduce wave reflection (such as calcium channel blockers) have been shown to reduce cognitive decline in older adults with systolic hypertension.[43,112,129] This effect on cognitive function is not true for all antihypertensive agents, and is likely independent on the effects of these drugs on brachial blood pressure.

Aortic stiffness and abnormal pulsatile arterial hemodynamics are also deleterious for the kidney, as discussed in detail in Chapter 40. The loss of renal autoregulation (because of altered myogenic tone) is a feature of aging, hypertension, and diabetes,[130−133] all of which are commonly present in patients with HF. Loss of autoregulation favors the transmission of higher pulsatile pressure and flow to the renal microcirculation, leading to glomerulosclerosis. Available data suggest that systemic wave reflections are also deleterious to the kidney, which is expected to the degree that they increase aortic pressure pulsatility.[134] Measures of wave reflection have been shown to predict a poor prognosis in patients with established renal disease.[135,136] Similarly, augmentation index is positively associated with a faster progression of

FIGURE 36.8   Role of arterial hemodynamic dysfunction in HF and HF comorbidities. Abnormal macrovascular and microvascular hemodynamic dysfunction promotes LV diastolic dysfunction, LV maladaptive remodeling (hypertrophy, fibrosis), and causes a reduced vasodilatory reserve during exercise, which in turn impairs coronary flow, peripheral flow redistribution, oxygen delivery, and extraction in exercising muscle. Abnormal pulsatile arterial hemodynamics also contribute to microvascular disease in the brain and the kidney (dementia, chronic kidney disease, which are frequently encountered comorbidities in HF, particular older patients with HFpEF).

established kidney disease,[137,138] and backward wave amplitude is independently associated with a lower glomerular filtration rate[139] and with faster renal function decline over time in the general population, even after adjustment for forward wave amplitude.[140] Furthermore, measures of wave reflection correlate positively with renal resistive index (a measure of renal microvascular dysfunction).[141]

In summary, a host of arterial hemodynamic abnormalities may play a role into the pathophysiology of LV remodeling, dysfunction, abnormal myocardial oxygen supply and demand, exercise intolerance, and the frequent presence of some comorbidities (Fig. 36.8). The arterial tree, therefore, represents an important therapeutic target in patients with HF.

Therapeutic implications

Although modifying aortic wall stiffness represents a high priority goal, the chronic material changes in the aortic wall, including elastin breakdown and degradation, collagen and elastin cross-linking, fibrosis and calcification, impose a formidable challenge for substantial modifications of aortic wall stiffness with short-term pharmacologic interventions. Implantable mechanical interventions to modify arterial pulsatility represent an interesting area of investigation that could be applied in HF, but these are currently in early stages of preclinical development.[142]

Relatively few studies have assessed the impact of pharmacologic interventions on aortic wall stiffness and pulsatile hemodynamics in HF, as discussed below.

Spironolactone

Spironolactone has been studied in both HFpEF and HFrEF. In a randomized controlled trial comparing spironolactone (25 mg/d) versus placebo in elderly patients with stable HFpEF and controlled blood pressure, Upadhya et al. demonstrated that spironolactone therapy for nine months reduced BP but did not improve exercise capacity, quality of life, LV mass, or large artery stiffness.[143] Interestingly, this contrasts with earlier findings by Edwards et al. in a population of patients with chronic kidney disease and LV hypertrophy but not established HF, in which randomized spironolactone therapy (25 mg/d for 40 weeks) significantly reduced carotid-femoral PWV and ascending aortic distensibility.[144] However, it is unclear to what extent the latter results were related to the reduction in mean arterial pressure observed in that trial. Among TOPCAT HFpEF participants enrolled in the Americas, the rates of the primary outcome (a composite of cardiovascular death, aborted cardiac arrest, or hospitalization for the management of HF), as well as individual secondary outcomes (cardiovascular death, and hospitalization for HF) were significantly reduced by spironolactone.[145] However, spironolactone has multiple systemic effects and it is

unclear to what extent any potential benefit of this intervention is mediated by effects on the arterial tree. Similarly, although mineralocorticoid receptor antagonism is clearly beneficial in stage C HFrEF,[146] the extent to which this benefit is mediated by arterial effects is unknown. A more detailed discussion of the effects of mineralocorticoid receptor antagonists on arterial stiffness can be found in Chapter 50.

Vasodilators

The important role of muscular arteries in modulating wave reflection and pulsatile load to the LV suggests that targeting muscular arteries may be a viable therapeutic strategy in HF. Nitric oxide (NO) is an endogenous regulator of wave reflection. Unfortunately, most exogenous NO donors and vasoactive agents exhibit nonselectivity for muscular arteries, producing predominant reductions in arteriolar tone and thus SVR. As described above, this can be beneficial in HFrEF due to the reduced LV end-systolic stiffness, which coupled with a high E_A can contribute to an impaired energetic efficiency of the ventricular—arterial system. In this setting, reductions in SVR, with consequent reductions in E_A induced by arteriolar vasodilators, can improve ventricular—arterial coupling, stroke volume, and the energetic state of the failing LV without markedly affecting mean arterial pressure.[5,8,11] Indeed, various agents that have shown beneficial effects in HFrEF (hydralazine, organic nitrates, angiotensin converting enzyme inhibitors, angiotensin receptor blockers) exert arteriolar vasodilatory effects and may reduce wave reflection, although it is unclear to what extent their beneficial effects are due to various hemodynamic versus neurohormonal factors, particularly for the case of renin-angiotensin-aldosterone system antagonists. A more detailed discussion regarding the effects of commonly used vasodilators on arterial stiffness and arterial hemodynamics can be found in Chapter 49.

In contrast to HFrEF, in which arteriolar vasodilation coupled with effects on muscular arteries can be beneficial, the arterial hemodynamic characteristics of HFpEF dictate a set of much more specific "ideal" characteristics for a hemodynamic intervention, namely, one that: (1) Reduces wave reflections and mid-to-late systolic load at rest (which could improve diastolic function and exert long-term, "disease-modifying" effects on LV maladaptive remodeling); (2) Does not significantly reduce mean arterial or systemic vascular resistance at rest, avoiding hypotension; (3) Enhances exercise-induced vasodilation (reduction in SVR) to reduce LV afterload during exercise; (4) Has selectivity for enhancing local vasodilation in hypoxic/acidotic environments, in order to match blood flow to metabolic demands (i.e., directing blood flow to exercising muscle); (5) Does not vasodilate low-resistance

microvascular beds (target organs), due to their vulnerability to the prominent central pulsatility seen in this older population.
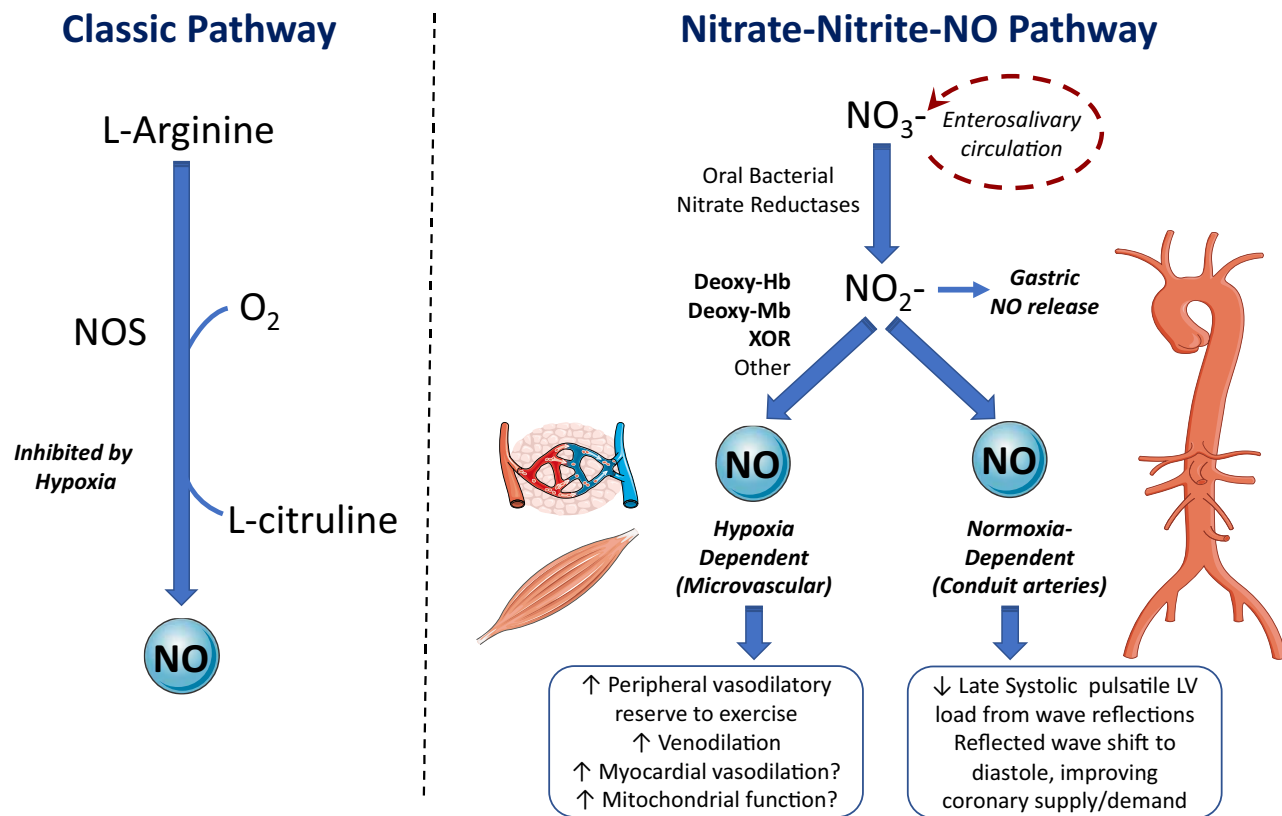
NO donors

NO is a key regulator of various cardiac and peripheral physiologic adaptations to exercise. Two major pathways exist for the production of NO in the cardiovascular system: the classic, NO-synthase dependent pathway, and the more recently recognized nitrate-nitrite-NO pathway (Fig. 36.9).[147]

In the classic pathway, NO synthases (NOSs) catalyze the formation of NO from L-arginine and molecular oxygen. In the nitrate-nitrite-NO pathway, inorganic nitrate (derived from dietary ingestion or from the oxidation of endogenous NO) undergoes a regulated two-step reduction process (nitrate→nitrite→NO). Nitrate (NO_{3-}) is actively concentrated and secreted by the salivary glands and subsequently absorbed in the gastrointestinal tract with high bioavailability (>90%). With each enterosalivary cycle, a small proportion of nitrate is reduced to nitrite (NO_{2-}) by oral cavity commensal bacteria. Some reduction of nitrite to NO occurs in the acid pH of the stomach, with the remainder nitrite undergoing systemic absorption. Circulating nitrite is an immediate precursor to NO.

Nitrite reduction to NO occurs under particular conditions: (a) via hypoxia-dependent reduction, catalyzed by deoxy-hemoglobin, deoxy-myoglobin, xanthine oxidoreductase, and other nitrite reductases; (b) via a more recently described normoxia-dependent reduction pathway that operates in the wall of conduit muscular systemic arteries[148] (Fig. 36.9). Therefore, the nitrate-nitrite-NO pathway mediates a series of effects via normoxic vasodilation of conduit muscular arteries[148] (which thus operates both at rest and during exercise and reduces wave reflection)[99,148–150] in combination with selective microvascular dilation in hypoxic/acidotic conditions (such as occurs in exercising muscle)[147,149,151,152] that seem ideal to improve the prevalent arterial hemodynamic abnormalities in HFpEF. Moreover, inorganic nitrate, in contrast to organic nitrate, does not significantly vasodilate the cerebral vasculature or increase the amount of hydraulic energy transmitted into the carotid artery in HFpEF.[151,153]

Interestingly, two separate studies have recently demonstrated that patients with HFpEF exhibit a reduced circulating NO metabolite pool[154,155] (composed largely of nitrate and to a lesser extent, nitrite), which may limit the activity of this pathway. Exogenous inorganic nitrate supplementation is being investigated as a therapeutic approach in HFpEF. However, there are significant challenges related to the pharmacokinetic and side effect profile of various preparations. Whereas the administration of nitrite (the main "active" NO donor in this pathway) is

Classic Pathway

L-Arginine

NOS

O_2

Inhibited by Hypoxia

L-citruline

NO

Nitrate-Nitrite-NO Pathway

NO_3- *Enterosalivary circulation*

Oral Bacterial Nitrate Reductases

Deoxy-Hb Deoxy-Mb XOR Other

NO_2- → *Gastric NO release*

NO

NO

Hypoxia Dependent (Microvascular)

Normoxia- Dependent (Conduit arteries)

↑ Peripheral vasodilatory reserve to exercise
↑ Venodilation
↑ Myocardial vasodilation?
↑ Mitochondrial function?

↓ Late Systolic pulsatile LV load from wave reflections Reflected wave shift to diastole, improving coronary supply/demand

FIGURE 36.9 The classic NOS-dependent NO pathway (left), and the nitrate-nitrite-NO pathway (right). *Reproduced with permission from Chirinos JA. The nitrate-nitrite-NO pathway as a novel therapeutic target in heart failure with reduced ejection fraction.* ***J Card Fail****. 2018; 24:74−77.*

possible, nitrite has a very short half-life ($\sim$35−40 min), potentially leading to important waxing and waning of hemodynamic effects, which may activate counter-regulatory responses. In the INDIE HFpEF trial, inhaled inorganic nitrite administered thrice daily for four weeks failed to improve peak oxygen consumption, daily activity levels assessed by accelerometry, quality of life, functional class, cardiac filling pressures assessed by echocardiography, or NT-pro brain natriuretic peptide levels.[156] In contrast to the very short half-life of inorganic nitrite, oral inorganic nitrate has a half-life of $\sim$5−8 h, allowing for steady-state pharmacokinetics with thrice daily adminstration.[151,153] Small trials have demonstrated acute or short term effects of inorganic nitrate on peak exercise capacity and submaximal exercise endurance in HFpEF.[149,153,157] In the single-dose study by Zamani et al., the reduction in measures of wave reflection correlated with the improvement in peak VO$_2$. The main disadvantage of oral nitrate is the variable activation to nitrite by mouth bacteria. An ongoing trial (KNO$_3$CK OUT HFpEF) is assessing the potential efficacy of orally administered potassium nitrate in HFpEF. A more detailed discussion of the nitrate-nitrite-NO pathway can be found in Chapter 51.

Interestingly, organic nitrates do not share the ideal vasoactive characteristics exhibited by inorganic nitrate. In contrast to inorganic nitrate, organic nitrates in HFpEF: (1) induce a less consistent reduction in wave reflection; (2) can markedly reduce mean arterial pressure at rest; (3) lack the selective vasodilatory effect during exercise in exercising muscle; (4) exert prominent cerebrovascular vasodilatory effects, which account for the high incidence of headaches (and may also expose the already susceptible cerebrovascular microvasculature to excessive pressure and flow pulsatility); (5) induce tolerance or pseudotolerance; (6) increase oxidative stress.[151,158,159] In a recent multi-center trial, isosorbide mononitrate reduced outpatient activity in a dose-dependent manner in this population.[160] In another trial,[161] isosorbide dinitrate, with or without hydralazine, failed to improve wave reflections, LV remodeling or the 6-minute walk distance in HFpEF. Furthermore, in the isosorbide dinitrate-hydralazine arm, an increase in wave reflections at 24 weeks was seen, which was associated with worsened 6-minute walk distance and an increased myocardial T1 (assessed by MRI T1 mapping), suggesting adverse interstitial remodeling/fibrosis. In both trials, organic nitrates were poorly tolerated. This is in contrast with available studies with inorganic nitrate which suggest a better tolerability profile.[147,149,151,153,157,162−164]

Inorganic nitrate may also have therapeutic potential in HFrEF.[165] It has been shown to increase skeletal muscle

power[166] and to improve exercise tolerance[167] in two previous studies in nonischemic cardiomyopathy, as well as a trial in patients with predominantly nonischemic cardiomyopathy,[168] whereas Hirai et al.[169] reported no effect on exercise capacity in a male population of predominantly ischemic cardiomyopathy. Further research and larger trials are necessary to determine the potential efficacy and therapeutic role of inorganic nitrate in HFrEF.

Soluble guanylate cyclase stimulators/activators

The binding of NO to soluble guanylate cyclase (sGC) (the primary acceptor and sensor of NO) boosts the enzymatic activity of sGC to catalyze the conversion of guanosine triphosphate into inorganic pyrophosphate and cyclic guanosine monophosphate. The latter then acts on downstream effectors, to regulate multiple physiological processes in the cell.[170] The VICTORIA trial demonstrated that vericiguat, a novel oral soluble guanylate cyclase stimulator, reduced the risk of death from cardiovascular causes or hospitalization for HF in patients with HF and an LV EF <45%, although formal evaluations of the effect of this medication on central hemodynamics in humans are lacking.[171] A recent study assessed the central pulsatile hemodynamic effects of vericiguat in hypertensive dogs.[172] It was found that vericiguat did not exert significant effects on mean arterial pressure or diastolic blood pressure. In contrast, parameters of arterial wave reflection exhibited significant reductions starting from the first hour of administration. Significant dose-dependent reductions in reflection magnitude and augmentation index were seen, with minimal effects detected on forward wave amplitude (which changed only with high doses). This study demonstrates that sGC stimulation can reduce wave reflection even at doses that do not reduce blood pressure, likely via effects on muscular arteries rather than resistance arterioles. The extent to which this effect mediates its benefits in HFrEF remains unknown.

Importantly, sGC stimulators (including vericiguat) have not proven effective in improving quality of life or peak aerobic exercise capacity in HFpEF.[173,174] Whereas the recent study in hypertensive dogs mentioned above suggests that sGC stimulation can produce some of the desirable hemodynamic effects for the HFpEF population (1 and 2 above), it is unlikely that sGC stimulators exhibit exercise-induced selective effects that may be key to improve exercise hemodynamics. sGC stimulators are discussed in more detail in Chapter 51.

Neprilysin inhibitors
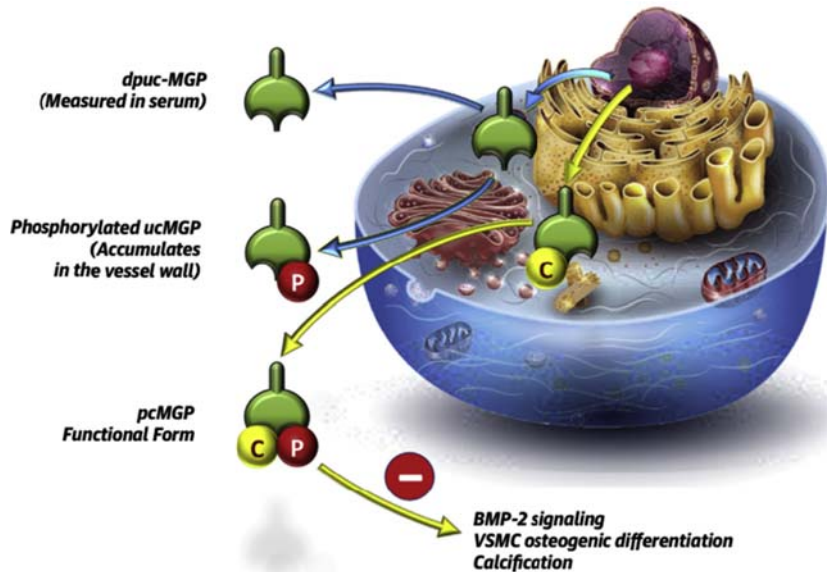
Neprilysin inhibitors represent another important drug class with relevant hemodynamic effects in HF, which work by blocking the action of neprilysin, a membrane metallo-

endopeptidase that cleaves natriuretic peptides, glucagon, glucagon-like peptide-1, bradykinin, substance P, neurotensin, oxytocin, enkephalins, angiotensin I, endothelin-1, adrenomedullin, amyloid β, and others. Sacubitril/valsartan (formerly called LCZ696) consists of an ARB, valsartan, and a neprilysin inhibitor, sacubitril, in a 1:1 molecular ratio.[174] The PARADIGM Heart Failure trial demonstrated that sacubitril/valsartan was superior to enalapril in reducing the risk of death and hospitalization for HF in HFrEF.[175] In contrast, the PARAGON trial demonstrated that sacubitril-valsartan did not reduce the risk of hospitalization for HF and death from cardiovascular causes among patients with HF and an LV EF ≥ 45%. However, in prespecified subgroup analyses, there was suggestion of heterogeneity with possible benefit with sacubitril-valsartan in patients with lower EF (45%−57%) and in women. Interestingly, in the latter trial, pulse pressure was significantly lower in the sacubitril/valsartan group compared with the valsartan group one year after randomization. Moreover, pulse pressure was an independent predictor of cardiovascular events in this trial.

The EVALUATE-HF study was specifically designed to compare the effect combined angiotensin-neprilysin inhibition with sacubitril-valsartan versus enalapril on changes in central aortic stiffness in patients with HFrEF, and demonstrated no significant difference in the primary end point of change from baseline to 12 weeks in ascending aortic Zc.[176,177] In a subsequent analysis of the data which examined effects of treatment on aortic Zc at 4 and 12 weeks after randomization, treatment with sacubitril-valsartan was associated with a greater acute (postdose) reduction in aortic Z_c compared to enalapril. The investigators also found evidence of effect modification by LV EF, such that in the lower LV EF group (LV EF<40%), there was evidence of an acute, postdose reduction in Z_c in the sacubitril-valsartan group, with no evidence of effect modification by sex, which was proposed as a possible contributor to the favorable clinical outcomes seen in the PARADIGM-HF study. In the higher LV EF group (LV EF ≥ 40%), there was evidence of effect modification by sex, with evidence for a reduction in Z_c in women only, which persisted throughout the dosing interval and remained significant after further adjustment for baseline and change in mean pressure, consistent with a pressure-independent favorable effect of sacubitril-valsartan on aortic Z_c. Importantly, however, the high LV EF group in this study is unlikely to represent true HFpEF, but more likely HF with midrange EF or recovered LV EF. Finally, none of these analyses reported effects on wave reflection, which is a key phenotype in both HFpEF and HFrEF.

The matrix gla protein pathway

Matrix gla protein (MGP) is a small secretory protein produced by chondrocytes and vascular smooth muscle

FIGURE 36.10 Vitamin K-dependent Matrix Gla protein (MGP) maturation. MGP maturation requires vitamin K and leads to the formation of pc-MGP (phosphorylated, carboxylated MGP), which is a strong inhibitor of vascular calcification via inhibition of bone morphogenetic protein 2 (BMP-2) signaling and vascular smooth muscle cell (VSMC) osteogenic-differentiation. Vitamin K deficiency in the vascular wall leads to the formation of uncarboxylated (uc-) MGP (which accumulates in the vessel wall) and dephosphorylated, uncarboxylated (dpuc-)MGP, which can be measured in serum. *MGP*, matrix gla protein.

cells (VSMCs).[178] Its inactive form, dephospho-uncarboxylated MGP (dp-ucMGP), must undergo serial posttranslational carboxylation and phosphorylation to become active (Fig. 36.10). Active MGP is a potent inhibitor of arterial calcification by inhibiting bone morphogenetic protein-2-induced osteogenic differentiation of VSMCs, and via calcium phosphate scavenging. Carboxylation of MGP is dependent upon the availability of vitamin K in the vascular wall.[178] Vascular vitamin K deficiency appears to occur at lower thresholds of severity than those leading to coagulopathy and can be completely unapparent on standard clinical testing. Since dp-uc-MGP (inactive MGP) is secreted into the circulation, it represents a circulating biomarker of vascular vitamin K availability/deficiency. An increase in circulating dp-uc-MGP has been shown to be independently associated with increased large artery stiffness in various populations, including the general population,[179,180] adults with diabetes,[181] hypertension,[182] chronic kidney disease,[183] and HF with preserved or reduced ejection fraction.[184] It has been shown that warfarin inhibits MGP carboxylation/activation and is a potent promoter of vascular calcification in animal models. Hasmath et al. demonstrated that warfarin is associated with increased large artery stiffness in HF, and this relationship was dependent on the relationship between warfarin use and dp-uc-MGP.[184] With the current availability of novel oral anticoagulants that, in contrast to warfarin, do not interfere with vitamin K-dependent carboxylation, it may be possible to target MGP with vitamin K2

supplementation in HF. Whether this will represent a useful approach to improve outcomes in this patient population remains to be determined.

Conclusions

Compelling evidence from animal and human studies strongly suggest that large artery stiffness and pulsatile arterial hemodynamics (particularly increased and/or premature wave reflections) represent key phenotypes and relevant therapeutic targets in HF. In addition to their impact on the LV, increased aortic stiffness and abnormal pulsatile hemodynamics are linked to microvascular disease in the brain, the kidney, and other extracardiac organs, and are thus relevant for common HF comorbidities that impact the clinical course of HF. Reductions in large artery stiffness and/or improvements in pulsatile hemodynamics may be involved in the benefit seen with various available agents in HF. However, comprehensive hemodynamic profiling in large studies or randomized trials has been rather limited to date, and should be more widely applied in future studies.

Acknowledgments

References

1. Virani SS, Alonso A, Aparicio HJ, et al. Heart disease and stroke statistics-2021 update: a report from the American Heart Association. **Circulation**. 2021; 143:e254−e743.

2. Heidenreich PA, Albert NM, Allen LA, et al. Forecasting the impact of heart failure in the United States: a policy statement from the American heart association. **Circ Heart Fail**. 2013; 6(3):606−619.

3. Pandey A, Shah SJ, Butler J, et al. Exercise intolerance in older adults with heart failure with preserved ejection fraction: JACC state-of-the-art review. **J Am Coll Cardiol**. 2021; 78:1166−1187.

4. Shah SJ, Borlaug BA, Kitzman DW, et al. Research priorities for heart failure with preserved ejection fraction: national heart, lung, and blood institute working group summary. **Circulation**. 2020; 141:1001−1026.

5. Chirinos JA. Deep phenotyping of systemic arterial hemodynamics in HFpEF (Part 2): clinical and therapeutic considerations. **J Cardiovasc Transl Res**. 2017; 10:261−274.

6. Chirinos JA. Deep phenotyping of systemic arterial hemodynamics in HFpEF (Part 1): physiologic and technical considerations. **J Cardiovasc Transl Res**. 2017; 10:245−259.

7. Chirinos JA, Sweitzer N. Ventricular-arterial coupling in chronic heart failure. **Card Fail Rev**. 2017; 3:12−18.

8. Weber T, Chirinos JA. Pulsatile arterial haemodynamics in heart failure. **Eur Heart J**. 2018; 39:3847−3854.

9. Bozkurt B, Coats A, Tsutsui H, Abdelhamid M. Universal definition and classification of heart failure. **J Card Fail**. 2021; 27(4):387−413.

10. Chirinos JA. Arterial stiffness: basic concepts and measurement techniques. **J Cardiovasc Transl Res**. 2012; 5:243−255.

11. Chirinos JA. Ventricular-arterial coupling: invasive and non-invasive assessment. **Artery Res**. 2013; 7.

12. Chirinos JA, Segers P. Noninvasive evaluation of left ventricular afterload: part 1: pressure and flow measurements and basic principles of wave conduction and reflection. **Hypertension**. 2010; 56:555−562.

13. Chirinos JA, Segers P. Noninvasive evaluation of left ventricular afterload: part 2: arterial pressure-flow and pressure-volume relations in humans. **Hypertension**. 2010; 56:563−570.

14. Chirinos JA, Segers P, Hughes T, Townsend R. Large-artery stiffness in health and disease: JACC state-of-the-art review. **J Am Coll Cardiol**. 2019; 74:1237−1263.

15. Hundley WG, Kitzman DW, Morgan TM, et al. Cardiac cycle-dependent changes in aortic area and distensibility are reduced in older patients with isolated diastolic heart failure and correlate with exercise intolerance. **J Am Coll Cardiol**. 2001; 38:796−802.

16. Weber T, Wassertheurer S, O'Rourke MF, et al. Pulsatile hemodynamics in patients with exertional dyspnea: potentially of value in the diagnostic evaluation of suspected heart failure with preserved ejection fraction. **J Am Coll Cardiol**. 2013; 61:1874−1883.

17. Chirinos JA, Bhattacharya P, Kumar A, et al. Impact of diabetes mellitus on ventricular structure, arterial stiffness, and pulsatile hemodynamics in heart failure with preserved ejection fraction. **J Am Heart Assoc**. 2019; 8:e011457.

18. Jain S, Obeid MJ, Yenigalla S, et al. Impact of chronic obstructive pulmonary disease in heart failure with preserved ejection fraction. **Am J Cardiol**. 2021; 149:47−56.

19. Owan TE, Hodge DO, Herges RM, Jacobsen SJ, Roger VL, Redfield MM. Trends in prevalence and outcome of heart failure with preserved ejection fraction. **N Engl J Med**. 2006; 355:251−259.

20. Lee DS, Gona P, Vasan RS, et al. Relation of disease pathogenesis and risk factors to heart failure with preserved or reduced ejection fraction: insights from the framingham heart study of the national heart, lung, and blood institute. **Circulation**. 2009; 119:3070−3077.

21. Shah AM, Pfeffer MA. The many faces of heart failure with preserved ejection fraction. **Nat Rev Cardiol**. 2012; 9:555−556.

22. Chirinos JA, Lanfear DE. Embracing the long road to precision medicine. **Circ Heart Fail**. 2018; 11:e005089.

23. Kao DP, Lewsey JD, Anand IS, et al. Characterization of subgroups of heart failure patients with preserved ejection fraction with possible implications for prognosis and treatment response. **Eur J Heart Fail**. 2015; 17:925−935.

24. Shah SJ, Katz DH, Selvaraj S, et al. Phenomapping for novel classification of heart failure with preserved ejection fraction. **Circulation**. 2015; 131:269−279.

25. Cohen JB, Schrauben SJ, Zhao L, et al. Clinical phenogroups in heart failure with preserved ejection fraction: detailed phenotypes, prognosis, and response to spironolactone. **JACC Heart Fail**. 2020; 8:172−184.

26. Grzela K, Litwiniuk M, Zagorska W, Grzela T. Airway remodeling in chronic obstructive pulmonary disease and asthma: the role of matrix metalloproteinase-9. **Arch Immunol Ther Exp**. 2016; 64:47−55.

27. Puntmann VO, Taylor PC, Mayr M. Coupling vascular and myocardial inflammatory injury into a common phenotype of cardiovascular dysfunction: systemic inflammation and aging - a mini-review. **Gerontology**. 2011; 57:295−303.

28. Zagura M, Serg M, Kampus P, et al. Association of osteoprotegerin with aortic stiffness in patients with symptomatic peripheral artery disease and in healthy subjects. **Am J Hypertens**. 2010; 23:586−591.

29. Pepine CJ, Nichols WW, Conti CR. Aortic input impedance in heart failure. **Circulation**. 1978; 58:460−465.

30. Rerkpattanapipat P, Hundley WG, Link KM, et al. Relation of aortic distensibility determined by magnetic resonance imaging in patients > or =60 years of age to systolic heart failure and exercise capacity. **Am J Cardiol**. 2002; 90:1221−1225.

31. Giannattasio C, Achilli F, Failla M, et al. Radial, carotid and aortic distensibility in congestive heart failure: effects of high-dose angiotensin-converting enzyme inhibitor or low-dose association with angiotensin type 1 receptor blockade. **J Am Coll Cardiol**. 2002; 39:1275−1282.

32. Eaton GM, Cody RJ, Binkley PF. Increased aortic impedance precedes peripheral vasoconstriction at the early stage of ventricular failure in the paced canine model. **Circulation**. 1993; 88:2714–2721.

33. Khan Z, Millard RW, Gabel M, Walsh RA, Hoit BD. Effect of congestive heart failure on in vivo canine aortic elastic properties. **J Am Coll Cardiol**. 1999; 33:267–272.

34. Tsao CW, Lyass A, Larson MG, et al. Relation of central arterial stiffness to incident heart failure in the community. **J Am Heart Assoc**. 2015; 4.

35. Miyoshi T, Ito H, Shirai K, et al. Predictive value of the cardio-ankle vascular index for cardiovascular events in patients at cardiovascular risk. **J Am Heart Assoc**. 2021; 10:e020103.

36. Regnault V, Lagrange J, Pizard A, et al. Opposite predictive value of pulse pressure and aortic pulse wave velocity on heart failure with reduced left ventricular ejection fraction: insights from an Eplerenone Post-Acute Myocardial Infarction Heart Failure Efficacy and Survival Study (EPHESUS) substudy. **Hypertension**. 2014; 63:105–111.

37. Meguro T, Nagatomo Y, Nagae A, et al. Elevated arterial stiffness evaluated by brachial-ankle pulse wave velocity is deleterious for the prognosis of patients with heart failure. **Circ J**. 2009; 73:673–680.

38. Nichols WWORM, Vlachopoulos C. **McDonald's Blood Flow in Arteries. Theoretical, Experimental and Clinical Principles**. 6 ed. Hodder Arnold; 2011.

39. Mitchell GF. Arterial stiffness and wave reflection in hypertension: pathophysiologic and therapeutic implications. **Curr Hypertens Rep**. 2004; 6:436–441.

40. Mitchell GF. Clinical achievements of impedance analysis. **Med Biol Eng Comput**. 2009; 47:153–163.

41. Nichols WW, O'Rourke MF. McDonald's blood flow in arteries. **In: Theoretical, Experimental and Clinical Principles**. 5 ed. Oxford University Press; 2005.

42. Phan TS, Li JK, Segers P, et al. Aging is associated with an earlier arrival of reflected waves without a distal shift in reflection sites. **J Am Heart Assoc**. 2016; 5.

43. Nichols WWORM, Vlachopoulos C. **McDonald's Blood Flow in Arteries: Theoretical, Experimental and Clinical Principles**. 6th ed. Hodder Arnold; 2011.

44. Townsend RR, Wilkinson IB, Schiffrin EL, et al. Recommendations for improving and standardizing vascular research on arterial stiffness: a scientific statement from the American Heart Association. **Hypertension**. 2015; 66:698–722.

45. Zamani P, Bluemke DA, Jacobs Jr DR, et al. Resistive and pulsatile arterial load as predictors of left ventricular mass and geometry: the multi-ethnic study of atherosclerosis. **Hypertension**. 2015; 65:85–92.

46. Zamani P, Jacobs Jr DR, Segers P, et al. Reflection magnitude as a predictor of mortality: the multi-ethnic study of atherosclerosis. **Hypertension**. 2014; 64:958–964.

47. Chirinos JA, Kips JG, Roman MJ, et al. Ethnic differences in arterial wave reflections and normative equations for augmentation index. **Hypertension**. 2011; 57:1108–1116.

48. Weber T, O'Rourke MF, Ammer M, Kvas E, Punzengruber C, Eber B. Arterial stiffness and arterial wave reflections are associated with systolic and diastolic function in patients with normal ejection fraction. **Am J Hypertens**. 2008; 21:1194–1202.

49. Marechaux S, Samson R, van Belle E, et al. Vascular and microvascular endothelial function in heart failure with preserved ejection fraction. **J Card Fail**. 2016; 22:3–11.

50. Kobayashi S, Yano M, Kohno M, et al. Influence of aortic impedance on the development of pressure-overload left ventricular hypertrophy in rats. **Circulation**. 1996; 94:3362–3368.

51. Gillebert TC, Lew WY. Influence of systolic pressure profile on rate of left ventricular pressure fall. **Am J Physiol**. 1991; 261:H805–H813.

52. Hashimoto J, Westerhof BE, Westerhof N, Imai Y, O'Rourke MF. Different role of wave reflection magnitude and timing on left ventricular mass reduction during antihypertensive treatment. **J Hypertens**. 2008; 26:1017–1024.

53. Booysen HL, Woodiwiss AJ, Sibiya MJ, et al. Indexes of aortic pressure augmentation markedly underestimate the contribution of reflected waves toward variations in aortic pressure and left ventricular mass. **Hypertension**. 2015; 65:540–546.

54. Quail MA, Short R, Pandya B, et al. Abnormal wave reflections and left ventricular hypertrophy late after coarctation of the aorta repair. **Hypertension**. 2017; 69(3):501–509.

55. Chirinos JA, Akers SR, Schelbert E, et al. Arterial properties as determinants of left ventricular mass and fibrosis in severe aortic stenosis: findings from ACRIN PA 4008. **J Am Heart Assoc**. 2019; 8:e03742.

56. Hori M, Inoue M, Kitakaze M, et al. Loading sequence is a major determinant of afterload-dependent relaxation in intact canine heart. **Am J Physiol**. 1985; 249:H747–H754.

57. Gaasch WH, Blaustein AS, Adam D. Myocardial relaxation IV: mechanical determinants of the time course of left ventricular pressure decline during isovolumic relaxation. **Eur Heart J**. 1980; 1:7.

58. Yano M, Kohno M, Konishi M, Takahashi T, Seki K, Matsuzaki M. Influence of left ventricular regional nonuniformity on afterload-dependent relaxation in intact dogs. **Am J Physiol**. 1994; 267:H148–H154.

59. Wu MS, Chang CY, Chang RW, Chang KC. Early return of augmented wave reflection impairs left ventricular relaxation in aged Fisher 344 rats. **Exp Gerontol**. 2012; 47:680–686.

60. Schafer S, Fiedler VB, Thamer V. Afterload dependent prolongation of left ventricular relaxation: importance of asynchrony. **Cardiovasc Res**. 1992; 26:631–637.

61. Yano M, Kohno M, Kobayashi S, et al. Influence of timing and magnitude of arterial wave reflection on left ventricular relaxation. **Am J Physiol Heart Circ Physiol**. 2001; 280:H1846–H1852.

62. Ishizaka S, Asanoi H, Wada O, Kameyama T, Inoue H. Loading sequence plays an important role in enhanced load sensitivity of left ventricular relaxation in conscious dogs with tachycardia-induced cardiomyopathy. **Circulation**. 1995; 92:3560–3567.

63. Fukuta H, Ohte N, Wakami K, et al. Impact of arterial load on left ventricular diastolic function in patients undergoing cardiac catheterization for coronary artery disease. **Circ J**. 2010; 74:1900–1905.

64. Borlaug BA, Melenovsky V, Redfield MM, et al. Impact of arterial load and loading sequence on left ventricular tissue velocities in humans. **J Am Coll Cardiol**. 2007; 50:1570–1577.

65. Peterson VR, Woodiwiss AJ, Libhaber CD, Raymond A, Sareli P, Norton GR. Cardiac diastolic dysfunction is associated with aortic wave reflection, but not stiffness in a predominantly young-to-middle-aged community sample. **Am J Hypertens**. 2016; 29:1148–1157.

66. Goto T, Ohte N, Fukuta H, Wakami K, Tani T, Kimura G. Relationship between effective arterial elastance, total vascular resistance, and augmentation index at the ascending aorta and left ventricular diastolic function in older women. **Circ J**. 2013; 77:123–129.

67. Chirinos JA, Segers P, Rietzschel ER, et al. Early and late systolic wall stress differentially relate to myocardial contraction and relaxation in middle-aged adults: the Asklepios study. **Hypertension**. 2013; 61:296−303.

68. Fujimoto N, Onishi K, Tanabe M, et al. Nitroglycerin improves left ventricular relaxation by changing systolic loading sequence in patients with excessive arterial load. **J Cardiovasc Pharmacol**. 2005; 45:211−216.

69. Gu H, Li Y, Fiok H, et al. Reduced first-phase ejection fraction and sustained myocardial wall stress in hypertensive patients with diastolic dysfunction. **Hypertension**. 2017; 69(4):633−640.

70. Chirinos JA. Deciphering systolic-diastolic coupling in the intact heart. **Hypertension**. 2017; 69.

71. Kaji Y, Miyoshi T, Doi M, et al. Augmentation index is associated with B-type natriuretic peptide in patients with paroxysmal atrial fibrillation. **Hypertens Res**. 2009; 32:611−616.

72. Canepa M, Alghatrif M, Strait JB, et al. Early contribution of arterial wave reflection to left ventricular relaxation abnormalities in a community-dwelling population of normotensive and untreated hypertensive men and women. **J Hum Hypertens**. 2014; 28:85−91.

73. Jaroch J, Rzyczkowska B, Bociaga Z, et al. Arterial-atrial coupling in untreated hypertension. **Blood Press**. 2015; 24:72−78.

74. Jaroch J, Rzyczkowska B, Bociaga Z, et al. Relationship of carotid arterial functional and structural changes to left atrial volume in untreated hypertension. **Acta Cardiol**. 2016; 71:227−233.

75. Russo C, Jin Z, Takei Y, et al. Arterial wave reflection and subclinical left ventricular systolic dysfunction. **J Hypertens**. 2011; 29:574−582.

76. Kimura K, Tomiyama H, Matsumoto C, et al. Correlations of arterial stiffness/central hemodynamics with serum cardiac troponin T and natriuretic peptide levels in a middle-aged male worksite cohort. **J Cardiol**. 2015; 66:135−142.

77. Sakuragi S, Maruo T, Taniguchi M, et al. Radial augmentation index associated with increase in B-type natriuretic peptide in patients with hypertension. **Int J Cardiol**. 2008; 130:414−419.

78. Chirinos JA, Segers P, Gupta AK, et al. Time-varying myocardial stress and systolic pressure-stress relationship: role in myocardial-arterial coupling in hypertension. **Circulation**. 2009; 119:2798−2807.

79. Solomon SB, Nikolic SD, Frater RW, Yellin EL. Contraction-relaxation coupling: determination of the onset of diastole. **Am J Physiol**. 1999; 277:H23−H27.

80. Chirinos JA, Segers P, Gillebert TC, et al. Arterial properties as determinants of time-varying myocardial stress in humans. **Hypertension**. 2012; 60:64−70.

81. Gillebert TC, Leite-Moreira AF, De Hert SG. Load dependent diastolic dysfunction in heart failure. **Heart Fail Rev**. 2000; 5:345−355.

82. Chirinos JA, Kips JG, Jacobs Jr DR, et al. Arterial wave reflections and incident cardiovascular events and heart failure: MESA (Multiethnic Study of Atherosclerosis). **J Am Coll Cardiol**. 2012; 60:2170−2177.

83. Zamani P, Lilly SM, Segers P, et al. Pulsatile load components, resistive load and incident heart failure: the multi-ethnic study of atherosclerosis (MESA). **J Card Fail**. 2016; 22:988−995.

84. Kass DA. Ventricular arterial stiffening: integrating the pathophysiology. **Hypertension**. 2005; 46:185−193.

85. Borlaug BA, Olson TP, Lam CS, et al. Global cardiovascular reserve dysfunction in heart failure with preserved ejection fraction. **J Am Coll Cardiol**. 2010; 56:845−854.

86. Ennezat PV, Lefetz Y, Marechaux S, et al. Left ventricular abnormal response during dynamic exercise in patients with heart failure and preserved left ventricular ejection fraction at rest. **J Card Fail**. 2008; 14:475−480.

87. Borlaug BA, Melenovsky V, Russell SD, et al. Impaired chronotropic and vasodilator reserves limit exercise capacity in patients with heart failure and a preserved ejection fraction. **Circulation**. 2006; 114:2138−2147.

88. Lee JF, Barrett-O'Keefe Z, Garten RS, et al. Evidence of microvascular dysfunction in heart failure with preserved ejection fraction. **Heart**. 2016; 102:278−284.

89. Poole DC, Hirai DM, Copp SW, Musch TI. Muscle oxygen transport and utilization in heart failure: implications for exercise (in)tolerance. **Am J Physiol Heart Circ Physiol**. 2012; 302:H1050−H1063.

90. Umbrello M, Dyson A, Feelisch M, Singer M. The key role of nitric oxide in hypoxia: hypoxic vasodilation and energy supply-demand matching. **Antioxidants Redox Signal**. 2013; 19(14):1690−1710.

91. Muller-Delp JM. Aging-induced adaptations of microvascular reactivity. **Microcirculation**. 2006; 13:301−314.

92. Poole DC, Ferreira LF. Oxygen exchange in muscle of young and old rats: muscle-vascular-pulmonary coupling. **Exp Physiol**. 2007; 92:341−346.

93. Sullivan MJ, Knight JD, Higginbotham MB, Cobb FR. Relation between central and peripheral hemodynamics during exercise in patients with chronic heart failure. Muscle blood flow is reduced with maintenance of arterial perfusion pressure. **Circulation**. 1989; 80:769−781.

94. Barrett-O'Keefe Z, Lee JF, Berbert A, et al. Hemodynamic responses to small muscle mass exercise in heart failure patients with reduced ejection fraction. **Am J Physiol Heart Circ Physiol**. 2014; 307:H1512−H1520.

95. Wilson JR, Martin JL, Schwartz D, Ferraro N. Exercise intolerance in patients with chronic heart failure: role of impaired nutritive flow to skeletal muscle. **Circulation**. 1984; 69:1079−1087.

96. Esposito F, Wagner PD, Richardson RS. Incremental large and small muscle mass exercise in patients with heart failure: evidence of preserved peripheral haemodynamics and metabolism. **Acta Physiol**. 2015; 213:688−699.

97. Lee JF, Barrett-O'Keefe Z, Nelson AD, et al. Impaired skeletal muscle vasodilation during exercise in heart failure with preserved ejection fraction. **Int J Cardiol**. 2016; 211:14−21.

98. Ratchford SM, Clifton HL, La Salle DT, et al. Cardiovascular responses to rhythmic handgrip exercise in heart failure with preserved ejection fraction. **J Appl Physiol**. 2020; 129:1267−1276.

99. Reddy YNV, Andersen MJ, Obokata M, et al. Arterial stiffening with exercise in patients with heart failure and preserved ejection fraction. **J Am Coll Cardiol**. 2017; 70:136−148.

100. Mohammed SF, Hussain S, Mirzoyev SA, Edwards WD, Maleszewski JJ, Redfield MM. Coronary microvascular rarefaction and myocardial fibrosis in heart failure with preserved ejection fraction. **Circulation**. 2015; 131:550−559.

101. Sucato V, Evola S, Novo G, et al. Angiographic evaluation of coronary microvascular dysfunction in patients with heart failure and preserved ejection fraction. **Microcirculation**. 2015; 22:528−533.

102. Giamouzis G, Schelbert EB, Butler J. Growing evidence linking microvascular dysfunction with heart failure with preserved ejection fraction. **J Am Heart Assoc**. 2016; 5.

103. Kato S, Saito N, Kirigaya H, et al. Impairment of coronary flow reserve evaluated by phase contrast cine-magnetic resonance imaging in patients with heart failure with preserved ejection fraction. **J Am Heart Assoc**. 2016; 5.

104. Konerman MC, Greenberg JC, Kolias TJ, et al. Reduced myocardial flow reserve is associated with diastolic dysfunction and decreased left atrial strain in patients with normal ejection fraction and epicardial perfusion. **J Card Fail**. 2018; 24:90–100.

105. AbouEzzeddine OF, Kemp BJ, Borlaug BA, et al. Myocardial energetics in heart failure with preserved ejection fraction. **Circ Heart Fail**. 2019; 12:e006240.

106. Kato S, Fukui K, Kodama S, et al. Cardiovascular magnetic resonance assessment of coronary flow reserve improves risk stratification in heart failure with preserved ejection fraction. **J Cardiovasc Magn Reson**. 2021; 23:112.

107. Franssen C, Chen S, Unger A, et al. Myocardial microvascular inflammatory endothelial activation in heart failure with preserved ejection fraction. **JACC Heart Fail**. 2016; 4:312–324.

108. Paulus WJ, Tschope C. A novel paradigm for heart failure with preserved ejection fraction: comorbidities drive myocardial dysfunction and remodeling through coronary microvascular endothelial inflammation. **J Am Coll Cardiol**. 2013; 62:263–271.

109. Canetti M, Akhter MW, Lerman A, et al. Evaluation of myocardial blood flow reserve in patients with chronic congestive heart failure due to idiopathic dilated cardiomyopathy. **Am J Cardiol**. 2003; 92:1246–1249.

110. Morales MA, Neglia D, L'Abbate A. Reduction of myocardial blood flow reserve in idiopathic dilated cardiomyopathy without overt heart failure and its relation with functional indices: an echo-Doppler and positron emission tomography study. **J Cardiovasc Med**. 2008; 9:778–782.

111. Hashimoto J, Ito S. Central diastolic pressure decay mediates the relationship between aortic stiffness and myocardial viability: potential implications for aortosclerosis-induced myocardial ischemia. **J Hypertens**. 2017; 35:2034–2043.

112. O'Rourke MF, Safar ME. Relationship between aortic stiffening and microvascular disease in brain and kidney: cause and logic of therapy. **Hypertension**. 2005; 46:200–204.

113. Mitchell GF, Vita JA, Larson MG, et al. Cross-sectional relations of peripheral microvascular function, cardiovascular disease risk factors, and aortic stiffness: the Framingham Heart Study. **Circulation**. 2005; 112:3722–3728.

114. Mitchell GF, van Buchem MA, Sigurdsson S, et al. Arterial stiffness, pressure and flow pulsatility and brain structure and function: the age, gene/environment susceptibility–Reykjavik study. **Brain**. 2011; 134:3398–3407.

115. Woodard T, Sigurdsson S, Gotal JD, et al. Mediation analysis of aortic stiffness and renal microvascular function. **J Am Soc Nephrol**. 2015; 26:1181–1187.

116. Chirinos JA. Large artery stiffness, microvascular function, and cardiovascular risk. **Circ Cardiovasc Imaging**. 2016; 9.

117. Damman K, Solomon SD, Pfeffer MA, et al. Worsening renal function and outcome in heart failure patients with reduced and preserved ejection fraction and the impact of angiotensin receptor blocker treatment: data from the CHARM-study programme. **Eur J Heart Fail**. 2016; 18:1508–1517.

118. Parissis JT, Ikonomidis I, Rafouli-Stergiou P, et al. Clinical characteristics and predictors of in-hospital mortality in acute heart failure with preserved left ventricular ejection fraction. **Am J Cardiol**. 2011; 107:79–84.

119. Gurwitz JH, Magid DJ, Smith DH, et al. Contemporary prevalence and correlates of incident heart failure with preserved ejection fraction. **Am J Med**. 2013; 126:393–400.

120. Chamberlain AM, St Sauver JL, Gerber Y, et al. Multimorbidity in heart failure: a community perspective. **Am J Med**. 2015; 128:38–45.

121. Campbell RT, McMurray JJ. Comorbidities and differential diagnosis in heart failure with preserved ejection fraction. **Heart Fail Clin**. 2014; 10:481–501.

122. Chirinos JA. Large artery stiffness and new-onset diabetes. **Circ Res**. 2020; 127:1499–1501.

123. Muhammad IF, Borne Y, Ostling G, et al. Arterial stiffness and incidence of diabetes: a population-based cohort study. **Diabetes Care**. 2017; 40:1739–1745.

124. Yasuno S, Ueshima K, Oba K, et al. Is pulse pressure a predictor of new-onset diabetes in high-risk hypertensive patients?: a subanalysis of the Candesartan Antihypertensive Survival Evaluation in Japan (CASE-J) trial. **Diabetes Care**. 2010; 33:1122–1127.

125. Mengyi Zheng XZ, Chen S, Song Y, Zhao Q, Gao X, Wu S. Arterial stiffness preceding diabetes: a longitudinal study. **Circ Res**. 2020; 127(12):1491–1498.

126. Li JK. Dominance of geometric over elastic factors in pulse transmission through arterial branching. **Bull Math Biol**. 1986; 48:97–103.

127. Haidar MA, van Buchem MA, Sigurdsson S, et al. Wave reflection at the origin of a first-generation branch artery and target organ protection: the AGES-Reykjavik study. **Hypertension**. 2021; 77:1169–1177.

128. Hirata K, Yaginuma T, O'Rourke MF, Kawakami M. Age-related changes in carotid artery flow and pressure pulses: possible implications for cerebral microvascular disease. **Stroke**. 2006; 37:2552–2556.

129. Forette F, Seux ML, Staessen JA, et al. Birkenhager WH and systolic hypertension in europe I. The prevention of dementia with antihypertensive treatment: new evidence from the systolic hypertension in Europe (Syst-Eur) study. **Arch Intern Med**. 2002; 162:2046–2052.

130. Christensen PK, Hansen HP, Parving HH. Impaired autoregulation of GFR in hypertensive non-insulin dependent diabetic patients. **Kidney Int**. 1997; 52:1369–1374.

131. Hill GS, Heudes D, Bariety J. Morphometric study of arterioles and glomeruli in the aging kidney suggests focal loss of autoregulation. **Kidney Int**. 2003; 63:1027–1036.

132. Palmer BF. Disturbances in renal autoregulation and the susceptibility to hypertension-induced chronic kidney disease. **Am J Med Sci**. 2004; 328:330–343.

133. Hill GS, Heudes D, Jacquot C, Gauthier E, Bariety J. Morphometric evidence for impairment of renal autoregulation in advanced essential hypertension. **Kidney Int**. 2006; 69:823–831.

134. Hashimoto J, Ito S. Aortic blood flow reversal determines renal function: potential explanation for renal dysfunction caused by aortic stiffening in hypertension. **Hypertension**. 2015; 66:61–67.

135. Verbeke F, Marechal C, Van Laecke S, et al. Aortic stiffness and central wave reflections predict outcome in renal transplant recipients. **Hypertension**. 2011; 58:833−838.

136. London GM, Blacher J, Pannier B, Guerin AP, Marchais SJ, Safar ME. Arterial wave reflections and survival in end-stage renal failure. **Hypertension**. 2001; 38:434−438.

137. Takenaka T, Mimura T, Kanno Y, Suzuki H. Qualification of arterial stiffness as a risk factor to the progression of chronic kidney diseases. **Am J Nephrol**. 2005; 25:417−424.

138. Taal MW, Sigrist MK, Fakis A, Fluck RJ, McIntyre CW. Markers of arterial stiffness are risk factors for progression to end-stage renal disease among patients with chronic kidney disease stages 4 and 5. **Nephron Clin Pract**. 2007; 107:c177−c181.

139. Sibiya MJ, Woodiwiss AJ, Booysen HL, et al. Reflected rather than forward wave pressures account for brachial pressure-independent relations between aortic pressure and end-organ changes in an African community. **J Hypertens**. 2015; 33:2083−2090.

140. Hsu JJ, Katz R, Chirinos JA, Jacobs Jr DR, Duprez DA, Peralta CA. Arterial wave reflections and kidney function decline among persons with preserved estimated glomerular filtration rate: the multi-ethnic study of atherosclerosis. **J Am Soc Hypertens**. 2016; 10:438−446.

141. Stea F, Sgro M, Faita F, et al. Relationship between wave reflection and renal damage in hypertensive patients: a retrospective analysis. **J Hypertens**. 2013; 31:2418−2424.

142. Stefanov F, Sayed S, Delassus P, Bouchier-Hayes J. **WaveGraft−A Novel Endovascular Device Concept for Restoring the Natural Arterial Cushioning Effect**. Artery20 Virtual Conference Atlantis Press; 2020.

143. Upadhya B, Hundley WG, Brubaker PH, Morgan TM, Stewart KP, Kitzman DW. Effect of spironolactone on exercise tolerance and arterial function in older adults with heart failure with preserved ejection fraction. **J Am Geriatr Soc**. 2017; 65:2374−2382.

144. Edwards NC, Steeds RP, Stewart PM, Ferro CJ, Townend JN. Effect of spironolactone on left ventricular mass and aortic stiffness in early-stage chronic kidney disease: a randomized controlled trial. **J Am Coll Cardiol**. 2009; 54:505−512.

145. Pfeffer MA, Claggett B, Assmann SF, et al. Regional variation in patients and outcomes in the treatment of preserved cardiac function heart failure with an aldosterone antagonist (TOPCAT) trial. **Circulation**. 2015; 131:34−42.

146. Yancy CW, Jessup M, Bozkurt B, et al. 2017 ACC/AHA/HFSA focused update of the 2013 ACCF/AHA Guideline for the Management of Heart Failure: a report of the American college of Cardiology/American Heart Association Task Force on Clinical Practice Guidelines and the Heart Failure Society of America. **Circulation**. 2017; 136:e137−e161.

147. Vanderpool R, Gladwin MT. Harnessing the nitrate-nitrite-nitric oxide pathway for therapy of heart failure with preserved ejection fraction. **Circulation**. 2015; 131:334−336.

148. Omar SA, Fok H, Tilgner KD, et al. Paradoxical normoxia-dependent selective actions of inorganic nitrite in human muscular conduit arteries and related selective actions on central blood pressures. **Circulation**. 2015; 131:381−389. discussion 389.

149. Zamani P, Rawat D, Shiva-Kumar P, et al. The effect of inorganic nitrate on exercise capacity in heart failure with preserved ejection fraction. **Circulation**. 2015; 131:371−380. discussion 380.

150. Chirinos JA, Londono-Hoyos F, Zamani P, et al. Effects of organic and inorganic nitrate on aortic and carotid haemodynamics in heart failure with preserved ejection fraction. **Eur J Heart Fail**. 2017; 19:1507−1515.

151. Chirinos JA, Zamani P. The nitrate-nitrite-NO pathway and its implications for heart failure and preserved ejection fraction. **Curr Heart Fail Rep**. 2016; 13:47−59.

152. Colburn TD, Ferguson SK, Holdsworth CT, Craig JC, Musch TI, Poole DC. Effect of sodium nitrite on local control of contracting skeletal muscle microvascular oxygen pressure in healthy rats. **J Appl Physiol**. 2017; 122:153−160.

153. Zamani P, Tan V, Soto-Calderon H, et al. Pharmacokinetics and pharmacodynamics of inorganic nitrate in heart failure with preserved ejection fraction. **Circ Res**. 2017; 120:1151−1161.

154. Chirinos JA, Akers SR, Trieu L, et al. Heart failure, left ventricular remodeling, and circulating nitric oxide metabolites. **J Am Heart Assoc**. 2016; 5.

155. Zamani P, French B, Brandimarto JA, et al. Effect of heart failure with preserved ejection fraction on nitric oxide metabolites. **Am J Cardiol**. 2016; 118:1855−1860.

156. Borlaug BA, Anstrom KJ, Lewis GD, et al. Effect of inorganic nitrite vs placebo on exercise capacity among patients with heart failure with preserved ejection fraction: the INDIE-HFpEF randomized clinical trial. **J Am Med Assoc**. 2018; 320:1764−1773.

157. Eggebeen J, Kim-Shapiro DB, Haykowsky M, et al. One week of daily dosing with beetroot juice improves submaximal endurance and blood pressure in older patients with heart failure and preserved ejection fraction. **JACC Heart Fail**. 2016; 4:428−437.

158. Chirinos JAL-HF, Beraun M, Haines P, et al. Effects of organic and inorganic nitrate on aortic and carotid hemodynamics in heart failure and preserved ejection fraction. **Circulation**. 2016; 134:1.

159. Iversen HK. Experimental headache in humans. **Cephalalgia**. 1995; 15:281−287.

160. Redfield MM, Anstrom KJ, Levine JA, et al. Isosorbide mononitrate in heart failure with preserved ejection fraction. **N Engl J Med**. 2015; 373:2314−2324.

161. Zamani PAS, Soto-Calderon H, Beraun M, et al. Isosorbide dinitrate, with or without hydralazine, does not reduce wave reflections, LV hypertrophy, or myocardial fibrosis in HFpEF. **J Am Heart Assoc**. 2017; 6.

162. Borlaug BA, Koepp KE, Melenovsky V. Sodium nitrite improves exercise hemodynamics and ventricular performance in heart failure with preserved ejection fraction. **J Am Coll Cardiol**. 2015; 66:1672−1682.

163. Borlaug BA, Melenovsky V, Koepp KE. Inhaled sodium nitrite improves rest and exercise hemodynamics in heart failure with preserved ejection fraction. **Circ Res**. 2016; 119:880−886.

164. Simon MA, Vanderpool RR, Nouraie M, et al. Acute hemodynamic effects of inhaled sodium nitrite in pulmonary hypertension associated with heart failure with preserved ejection fraction. **JCI Insight**. 2016; 1:e89620.

165. Chirinos JA. The nitrate-nitrite-NO pathway as a novel therapeutic target in heart failure with reduced ejection fraction. **J Card Fail**. 2018; 24:74−77.

166. Coggan AR, Leibowitz JL, Spearie CA, et al. Acute dietary nitrate intake improves muscle contractile function in patients with heart failure: a double-blind, placebo-controlled, randomized trial. **Circ Heart Fail**. 2015; 8:914−920.

167. Kerley CP, O'Neill JO, Reddy Bijjam V, Blaine C, James PE, Cormican L. Dietary nitrate increases exercise tolerance in patients with non-ischemic, dilated cardiomyopathy-a double-blind, randomized, placebo-controlled, crossover trial. **J Heart Lung Transplant**. 2016; 35:922−926.

168. Coggan AR, Broadstreet SR, Mahmood K, et al. Dietary nitrate increases VO_2 peak and performance but does not alter ventilation or efficiency in patients with heart failure with reduced ejection fraction. **J Card Fail**. 2018; 24:65−73.

169. Hirai DM, Zelt JT, Jones JH, et al. Dietary nitrate supplementation and exercise tolerance in patients with heart failure with reduced ejection fraction. **Am J Physiol Regul Integr Comp Physiol**. 2017; 312:R13−R22.

170. Kang Y, Liu R, Wu JX, Chen L. Structural insights into the mechanism of human soluble guanylate cyclase. **Nature**. 2019; 574:206−210.

171. Armstrong PW, Pieske B, Anstrom KJ, et al. Vericiguat in patients with heart failure and reduced ejection fraction. **N Engl J Med**. 2020; 382:1883−1893.

172. Boden KSP, Roessig P, Vogel J, Chirinos JA, Mondritzki T. Vericiguat improves aortic wave reflection parameters in a new preclinical model of hypertension. **Circ Heart Fail**. 2021. https://doi.org/10.1161/CIRCHEARTFAILURE.121.008735.

173. Armstrong PW, Lam CSP, Anstrom KJ, et al. Effect of vericiguat vs placebo on quality of life in patients with heart failure and preserved ejection fraction: the VITALITY-HFpEF randomized clinical trial. **J Am Med Assoc**. 2020; 324:1512−1521.

174. Udelson JE, Lewis GD, Shah SJ, et al. Effect of praliciguat on peak rate of oxygen consumption in patients with heart failure with preserved ejection fraction: the CAPACITY HFpEF randomized clinical trial. **J Am Med Assoc**. 2020; 324:1522−1531.

175. McMurray JJ, Packer M, Desai AS, et al. Angiotensin-neprilysin inhibition versus enalapril in heart failure. **N Engl J Med**. 2014; 371:993−1004.

176. Desai AS, Solomon SD, Shah AM, et al. Effect of sacubitril-valsartan vs enalapril on aortic stiffness in patients with heart failure and reduced ejection fraction: a randomized clinical trial. **J Am Med Assoc**. 2019; 322:1077−1084.

177. Mitchell GF, Solomon SD, Shah AM, et al. Hemodynamic effects of sacubitril-valsartan versus enalapril in patients with heart failure in the EVALUATE-HF study: effect modification by left ventricular ejection fraction and sex. **Circ Heart Fail**. 2021; 14:e007891.

178. Schurgers LJ, Uitto J, Reutelingsperger CP. Vitamin K-dependent carboxylation of matrix Gla-protein: a crucial switch to control ectopic mineralization. **Trends Mol Med**. 2013; 19:217−226.

179. Pivin E, Ponte B, Pruijm M, et al. Inactive matrix gla-protein is associated with arterial stiffness in an adult population-based study. **Hypertension**. 2015; 66:85−92.

180. Mayer Jr O, Seidlerova J, Wohlfahrt P, et al. Desphospho-uncarboxylated matrix Gla protein is associated with increased aortic stiffness in a general population. **J Hum Hypertens**. 2016; 30:418−423.

181. Sardana M, Vasim I, Varakantam S, et al. Inactive matrix gla-protein and arterial stiffness in type 2 diabetes mellitus. **Am J Hypertens**. 2017; 30:196−201.

182. Chirinos JA, Sardana M, Syed AA, et al. Aldosterone, inactive matrix gla-protein, and large artery stiffness in hypertension. **J Am Soc Hypertens**. 2018; 12(9):681−689.

183. Puzantian H, Akers SR, Oldland G, et al. Circulating dephospho-uncarboxylated matrix gla-protein is associated with kidney dysfunction and arterial stiffness. **Am J Hypertens**. 2018; 31:988−994.

184. Hashmath Z, Lee J, Gaddam S, et al. Vitamin K status, warfarin use, and arterial stiffness in heart failure. **Hypertension**. 2019; 73:364−370.

This page intentionally left blank

Chapter 37

Ventricular–arterial coupling and arterial load in aortic valve disease

Ezequiel Guzzetti, Nancy Côté, Marie-Annick Clavel and Philippe Pibarot
Institut Universitaire de Cardiologie et de Pneumologie de Québec / Québec Heart & Lung Institute, Laval University, Québec City, QC, Canada

Introduction

A harmonious anatomical and functional interrelation between the left ventricle (LV), the aortic valve, and the aorta is key to ensure both adequate blood flow and driving pressure to ensure perfusion to all body organs.[1] Any abnormality—congenital or acquired—of the LV myocardium, LV outflow tract, aortic valve, aortic root, or arteries may compromise the complex anatomical and functional coupling between these components which, ultimately, may lead to heart failure and death. In recent years, there has been important progress in noninvasive advanced cardiovascular imaging (Doppler echocardiography, multidetector computed tomography [MDCT], and cardiovascular magnetic resonance [CMR]), which coupled with hemodynamic modeling, will allow for detailed assessments of ventriculo–valvular–arterial coupling in both health and disease. The purpose of this chapter is to describe the morphological and functional interplay between the LV, the aortic valve, and the aorta and its implications with regards to the diagnosis and treatment of aortic valve disease.

Anatomical interaction between the LV, aortic valve, and aortic root

Anatomical interrelation between the LV outflow tract, aortic valve, and aortic root
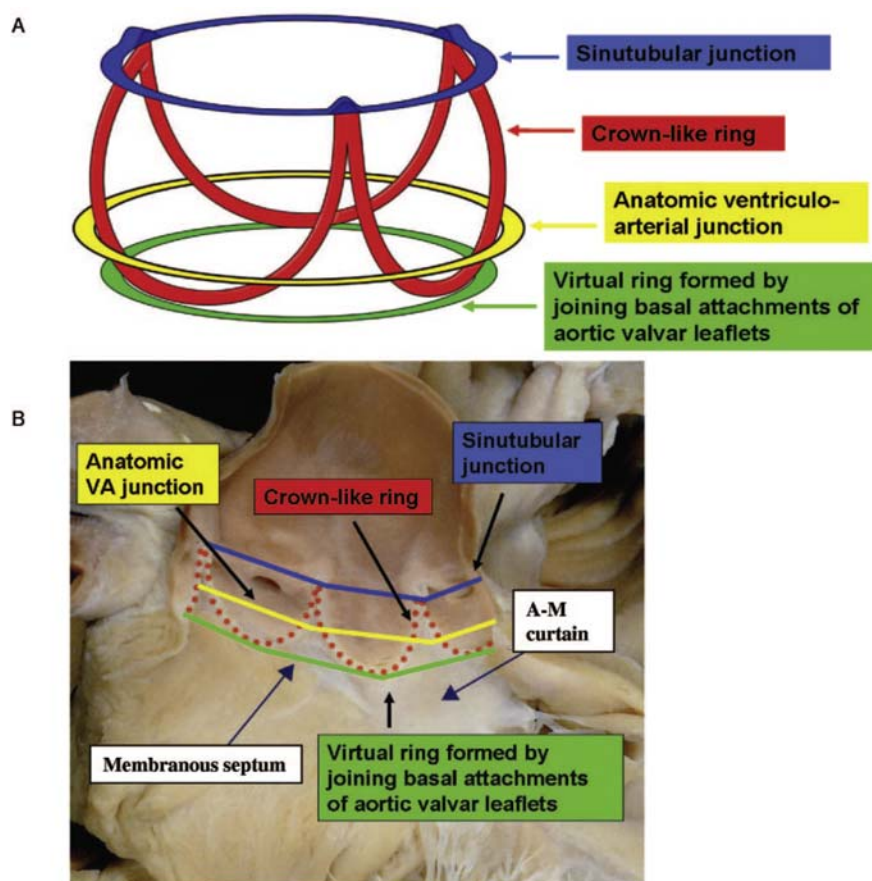
The aortic valve is composed of three semilunar leaflets that are attached to the aortic root. Thus, the aortic root can be divided by the semilunar attachment of the leaflets into supravalvular and subvalvular components (Fig. 37.1).[2] The supravalvular component is represented by the three sinuses of Valsalva, two of which host a coronary ostium. The flow vortices created in the sinuses reduce mechanical stress on the aortic leaflets and support coronary blood flow.[3] Hence, effacement of the sinuses may impair coronary flow and increase the mechanical stress and ensuing structural degeneration of aortic valve leaflets.

The subvalvular component consists in the LV outflow tract, which is surrounded by both myocardium and fibrous tissue. Under each commissure of the leaflets lies one of the three interleaflet triangles, which are, in fact, extensions of the LV outflow tract and reach the level of the sinotubular junction in the area of the commissures. The triangle between the left and noncoronary sinuses forms a part of the mitro-aortic curtain that leads to the anterior mitral leaflet. The triangle between the right and noncoronary sinuses forms part of the membranous septum.[4] This area is of particular importance during aortic valve procedures (especially transcatheter aortic valve replacement [TAVR]), as injury at this level can lead to conduction abnormalities, which may require the implantation of a permanent pacemaker.[5]

Due to their semilunar configuration, the leaflets of the aortic valve are attached in crown-like fashion with a basal ring at the bottom of leaflet insertion, i.e., the aortic "annulus" and an upper ring at the level of the sinotubular junction (Fig. 37.1). The aortic annulus that is measured clinically by echocardiography, MDCT, or CMR for diagnostic or therapeutic purposes (e.g., selection of valve size for transcatheter aortic valve implantation) corresponds to the circle at the base of the crown formed by the leaflets.[6] However, the aortic annulus is not a real and distinct anatomic entity, as it does not correspond to the basal contour of the aortic valve, which is not circular but rather has a tripoint crown shape. Furthermore, the aortic annulus is a dynamic structure, with larger and more circular cross-sectional area during systole than diastole.[7] Ultimately, the aortic annulus represents the landing zone of most TAVR devices, and thus its accurate measurement is essential to determine the size of the prosthetic valve to be implanted.[6]

FIGURE 37.1 Anatomy of the LV outflow tract, aortic valve, and aortic root. (A) Three-dimensional arrangement of the aortic root, which contains three circular "rings," but with the leaflets suspended within the root in crown-like fashion. (B) The leaflets have been removed from this specimen of the aortic root, showing the location of the three rings relative to the crown-like hinges of the leaflets. *A-M*, aortic–mitral; *VA*, ventriculo–arterial. *Adapted with permission from Piazza N, de Jaegere P, Schultz C, Becker AE, Serruys PW, Anderson RH. Anatomy of the aortic valvar complex and its implications for transcatheter implantation of the aortic valve.* **Circ Cardiovasc Interv**. *2008; 1:74–81.*
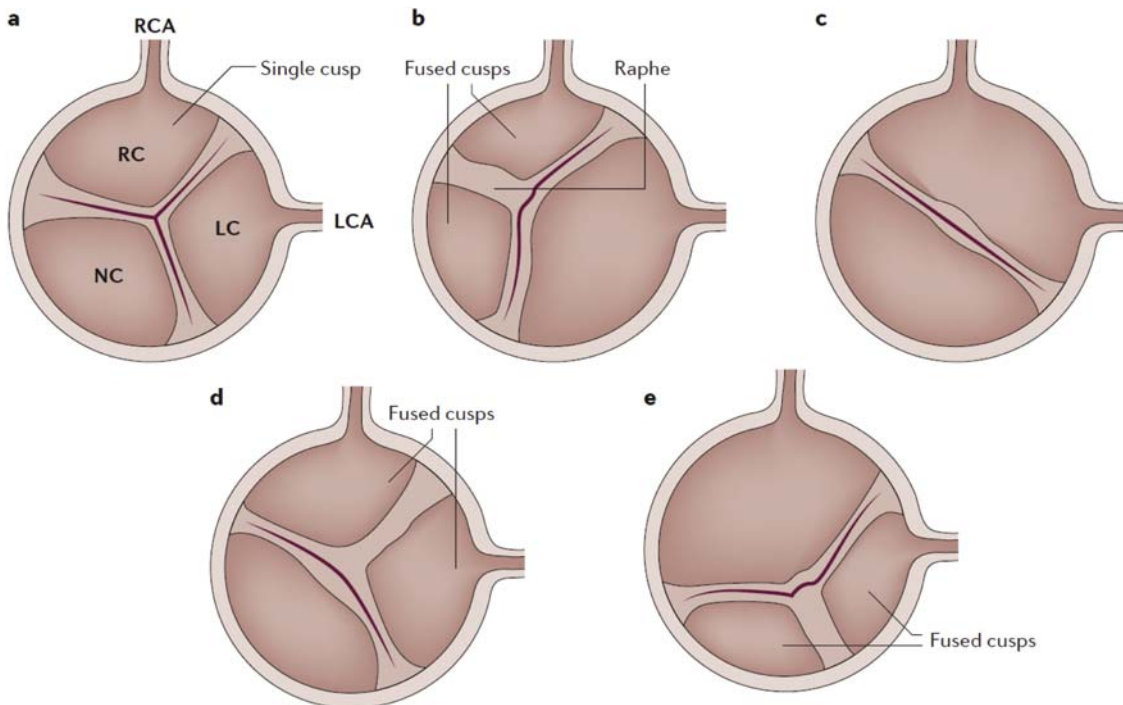
Bicuspid aortic valve and aortopathy

The normal architecture of the aortic valve is a 3-cusp (tricuspid or trileaflet) configuration. However, some subjects may have a bicuspid, unicuspid, or quadricuspid configuration. Bicuspid aortic valve (BAV) is the most common congenital heart defect, affecting 1%–2% of the population and three men for one woman.[8,9] All combination of cusps fusion with and without raphe are theoretically possible, but the most common types are fusion of the right and left coronary leaflets (60%) and fusion of the right and the noncoronary leaflets (35%) (Fig. 37.2).[10] Despite the evidence of an autosomal dominant pattern of BAV inheritance with variable expression and incomplete penetrance in families, the genetic determinants of BAV are far from being elucidated.[11,12] Patients with BAV have a high risk of developing aortic valve dysfunction, i.e., stenosis and/or regurgitation, and show a higher rate of progression of aortic stenosis (AS) than those with trileaflet (tricuspid) aortic valves.[13] The lifetime risk of aortic valve replacement for AS in subjects with BAV is about 50%.

BAV has been associated with other congenital defects, and in particular aorta dilation, aneurysm, and dissection.[9]

The link between BAV and aorta dilation/aneurism is likely multifactorial with a genetic basis and a possible impact of flow pattern induced by BAV type (Fig. 37.3, – A).[14] The eccentric aortic blood flow generated by the BAV increases the radial forces and thus the stress on the aortic wall, thus causing a dilation of the aortic root.[12,15] This phenomenon is more pronounced in patients with BAV and AS (Fig. 37.3, Panel B).[12] On the other hand, the genetic basis for aortic dilation is supported by the fact that aortopathy is often present in relatives of patients with BAV. The structural support and elasticity of the aorta are achieved by alternating layers of elastic lamellae and smooth-muscle cells (Fig. 37.3, Panel C). In subjects with a trileaflet aortic valve, the smooth-muscle cells in the aorta are secured to the adjacent elastin and collagen matrix by fibrillin 1 microfibrils. The aorta of subjects with a bicuspid valve may be deficient in fibrillin 1, which causes a disruption of the histological architecture of the aortic wall whereby smooth muscle cells detach, leading to weakened structural integrity and reduced elasticity of the aorta.[12] Disruption of the histologic architecture of the aortic wall has also been observed in subjects with bicuspid valves in the absence of any identifiable genetic or mechanical explanation.

FIGURE 37.2 Comparison of tricuspid and bicuspid aortic valve structures. Schematic representation of a normal—tricuspid—aortic valve with the three cusps (A), a bicuspid valve with right noncoronary cusp fusion and one raphe (the line of union between the fused cups) (B), a bicuspid valve with fusion of the right and left coronary cusps and no raphe (C), a bicuspid valve with right−left coronary cusp fusion and one raphe (D), and a bicuspid valve with fusion of the left and noncoronary cups and one raphe (E). *LC*, left coronary; *LCA*, left coronary artery; *NC*, noncoronary; *RC*, right coronary; *RCA*, right coronary artery. *Reproduced with permission from Lindman BR, Clavel MA, Mathieu P, et al. Calcific aortic stenosis.* **Nat Rev Dis Primers**. *2016; 2:16006.*

Functional interaction between the left ventricle, aortic valve, and aorta

Ventriculo−valvulo−arterial coupling
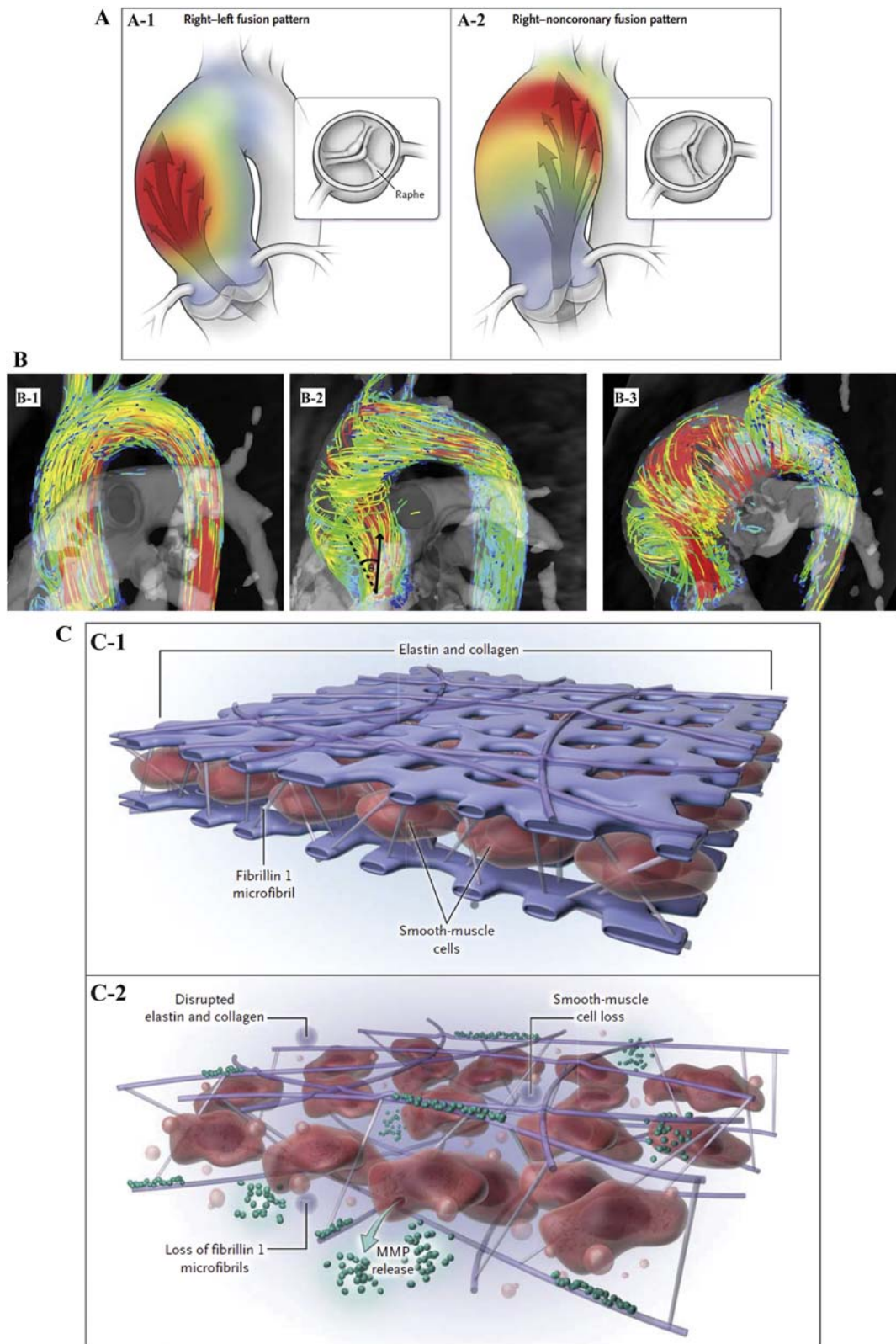
The dynamic interaction between the heart and the systemic circulation allows the cardiovascular system to be efficient in providing adequate cardiac output and arterial pressures to ensure adequate organ perfusion in different physiological conditions, such as rest and exercise. The cardiovascular system indeed works better when the heart and the arterial system are coupled.[16] The ventriculo−arterial coupling is achieved by the continuous modulation of the arterial system compliance and resistance with respect to LV systolic performance, and this physiological process is key to maintain adequate LV stroke volume and cardiac output.[17] Because LV stroke volume depends on myocardial contractility and loading conditions (i.e., preload and afterload), any myocardial, valvular, and arterial dysfunction can lead to ventriculo−arterial decoupling with resulting decrease in LV myocardial contractility, stroke volume, cardiac output, and organ perfusion,[16,18,19]

One approach to quantify ventriculo−arterial coupling is via the ratio of the effective arterial elastance (Ea) to the ventricular elastance (Ees) measured on the LV pressure−volume loop (Fig. 37.4, panel A).[17,20] Ea is calculated as the ratio of the end-systolic pressure to the LV stroke volume and is usually considered a measure of the arterial hemodynamic load imposed on the LV. Ees describes the maximal pressure that can be developed by the ventricle at any given LV volume. Ees is an index of myocardial contractility that is relatively insensitive to changes in preload, afterload, and heart rate. The Ea/Ees ratio is useful to evaluate the mechanical efficiency of the cardiovascular system and the interaction between cardiac performance and systemic vascular function. An unbalance between Ea and Ees as reflected by an increase or decrease in the Ea/Ees ratio may lead to heart failure. The main limitation of this approach to assess ventriculo−arterial coupling is that Ea is merely a function of systemic vascular resistance and heart rate and is insensitive to pulsatile arterial load.[21,22] Hence, Ea is not an optimal and comprehensive metric of true arterial load. Assessment of ventricular−arterial coupling in the pressure−volume plane is discussed in detail in Chapter 15.

Impact of aortic stenosis on ventriculo−arterial coupling

AS is the most common disease of the aortic valve. In AS, the LV afterload is increased and as a consequence, the LV stroke volume is reduced and the LV peak systolic pressure

FIGURE 37.3   Morphological and pathophysiological features of aortopathy in subjects with a bicuspid aortic valve. Panel A shows the fusion configuration of the aortic-valve cusps lays the foundation for changes in aortic wall shear stress and the resultant flow pattern. In the right—left fusion pattern (A-1), the jet is directed toward the right anterior wall of the ascending aorta, where it travels in a right-handed helical direction to promote

and end-diastolic pressures are increased (Fig. 37.4, panel C). The stroke work, which is the area enclosed within the LV pressure—volume loop, is increased. With advanced severity of AS, Ea increases and Ees decreases resulting in a marked augmentation of the Ea/Ees ratio and ventriculo—arterial "decoupling." A ratio >1.0 is a marker for the development of heart failure.

Ea is calculated from the LV end-systolic pressure and therefore is influenced by arterial load but does not include the valvular load per se. This valvular load is negligible in patients with a normal aortic valve but is markedly increased in patients with severe AS. To estimate the true total (i.e., arterial + valvular) hemodynamic load that the LV is facing in patients with AS, one can calculate the valvulo—arterial impedance, which is the ratio of the LV peak systolic pressure to the stroke volume index (Figs. 37.5B and 37.6).[23,24] The LV systolic pressure can be estimated noninvasively by Doppler echocardiography by adding the mean transvalvular gradient to the systolic blood pressure. The rationale for using the stroke volume index rather than the unindexed stroke volume as in the Ea is that a small-size subject may have a much smaller stroke volume than a large-size subject but nonetheless similar arterial and LV pressures. The valvulo—arterial impedance represents the valvular and arterial factors that oppose ventricular ejection by dissipation of the mechanical energy developed by the LV. As opposed to Ea, this parameter also includes the valvular load (i.e., the mean transvalvular gradient) and it accounts for the interindividual variability in body size. Valvulo—arterial impedance values > 4.5 mmHg/ml m^2 have been shown to provide incremental value to predict symptoms, heart failure, and mortality in patients with AS.[24,25]

The stroke volume index is a good surrogate marker of the ventriculo—arterial coupling and of the overall performance of the cardiovascular system in patients with AS (Fig. 37.6). Several studies and metaanalyses reported that a low flow state defined as a stroke volume index <35 mL/ m^2 (or <40 mL/m^2 in men and <32 mL/m^2 in women[26]) is a powerful predictor of outcomes in patients with AS both before and after aortic valve replacement.[27,28] Although

from a mechanistic standpoint, it may be interesting to measure Ea, Ees, and Ea/Ees ratio in patients with AS, from a practical standpoint, however, it may be preferable and easier to measure the valvulo—arterial impedance (i.e., a marker of the true total LV hemodynamic load) and the stroke volume index (i.e., a downstream marker of ventriculo—arterial decoupling). These two parameters can easily be measured in the echocardiography laboratory and have shown to correlate well with invasive measurements.[29]
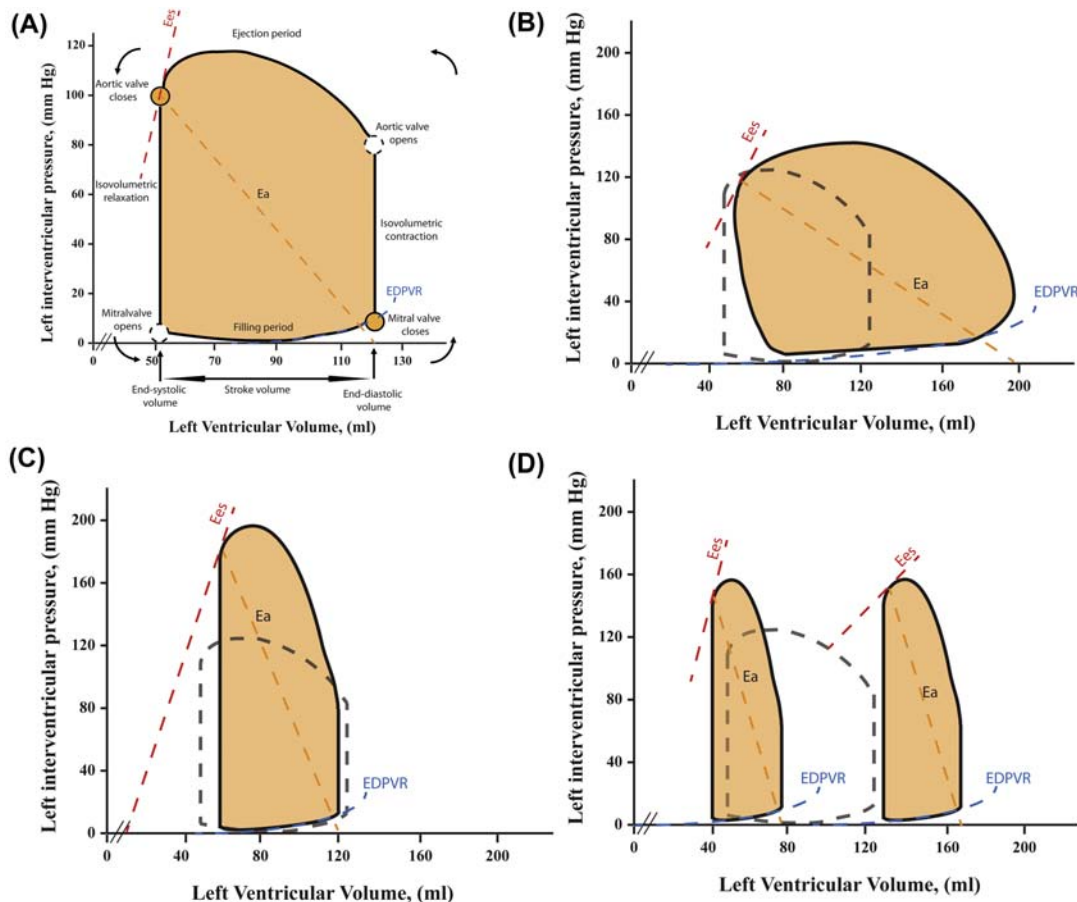
Impact of aortic regurgitation on ventriculo—arterial coupling

Aortic valve regurgitation (AR) causes a volume overload in the LV as well as in the arterial system. In patients with AR, the LV end-diastolic volume is markedly increased due to the enhanced ventricular filling. In the compensated phase of the disease, the LV contractility increases as a result of the increased preload and the Frank—Starling mechanism and the LV end-systolic volume is only slightly increased (Fig. 37.4, panel B).[30] As a consequence, the LV stroke volume, LV stroke work, and LV systolic pressure increase. The Ea/Ees ratio is decreased compared to normal. In the decompensation phase of the disease, the LV end-systolic volume increases markedly, the LV contractility drops, and thus the LV stroke volume and systolic pressure fall. Furthermore, the arterial load (Ea) is increased. As a consequence, the Ea/Ees ratio increases and there is ventriculo—arterial decoupling.

Interaction between LV outflow tract and aortic valve

When the blood flow passes through the aortic valve, there is a contraction of the flow and for that reason, the valve anatomic orifice area (AOA) is always larger than the valve EOA, which represents the cross-sectional area of the vena contracta (i.e., smallest section) of the transvalvular flow jet (Fig. 37.5, panel A; Fig. 37.6).[31,32] In the situation of a normal aortic valve, there is no or minimal flow contraction

---

dilatation predominantly of the ascending aorta. In the pattern with fusion of the right and noncoronary cusps (A-2), the jet is directed toward the posterior wall of the aorta, whereby the pattern of wall shear stress it causes may promote aortic dilatation within the proximal arch. Panel B shows the flow patterns in bicuspid aortic valve disease. (B-1) Normal flow pattern, (B-2) right-handed helical flow, and (B-3) left-handed helical flow. The systolic flow angle (θ) is demonstrated in B-2: the angle between the aortic midline (dashed) and the instantaneous mean flow vector at peak systole (*arrow*). Panel C shows the structural support and elasticity are afforded to the aorta by means of alternating layers of elastic lamellae and smooth-muscle cells. At the histologic level, the smooth-muscle cells in the aorta in persons with tricuspid valves are secured to the adjacent elastin and collagen matrix by fibrillin 1 microfibrils (C-1). The aorta in persons with bicuspid valves may be deficient in fibrillin 1. This deficiency culminates in a disrupted architecture whereby smooth muscle cells detach, accompanied by a surge in local levels of matrix metalloproteinases (MMPs), leading to loss of integrity in the extracellular matrix and the accumulation of apoptotic cells. These events may lead to an aorta with weakened structural integrity and reduced elasticity (C-2). *Panels A and C Reproduced with permission from Verma S, Siu SC. Aortic dilatation in patients with bicuspid aortic valve.* **N Engl J Med**. *2014; 370:1920—1929; Panel B Reproduced with permission from Bissell MM, Hess AT, Biasiolli L, et al. Aortic dilation in bicuspid aortic valve disease: flow pattern is a major contributor and differs with valve fusion type.* **Circ Cardiovasc Imag**. *2013; 6:499—507.*
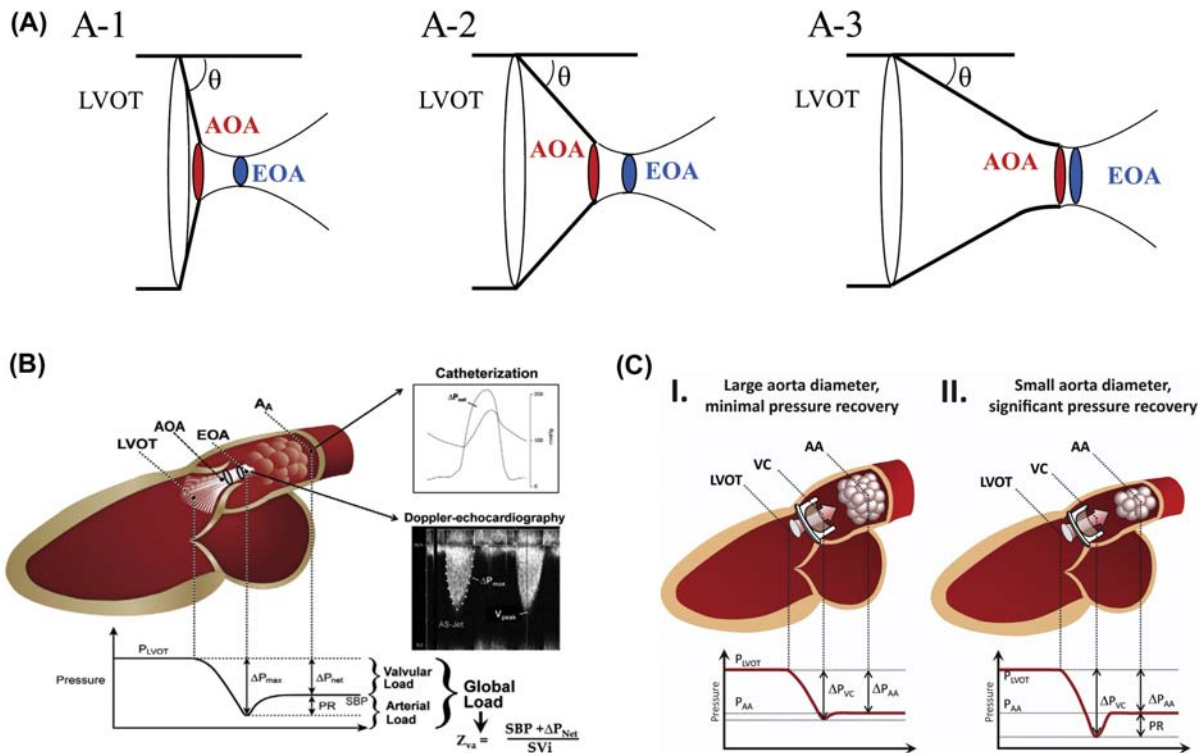
FIGURE 37.4   (Central Figure): Ventriculo—valvulo—arterial coupling, assessed in the pressure—volume plane, in normal condition, aortic regurgitation, and aortic stenosis. This figure shows the LV pressure—volume loops for different situations including normal condition (A), severe aortic regurgitation (B), severe aortic stenosis with high gradient (C), paradoxical (preserved LV ejection fraction) and classical (reduced LV ejection fraction) low-flow, low-gradient aortic stenosis (C). The dashed pressure—volume loop on Panels B—D represents the loop in normal condition. *AS*, aortic stenosis; *Ea*, arterial elastance; *EDPVR*, end-diastolic pressure—volume relationship; *Ees*, ventricular elastance (end-systolic pressure—volume relationship).

at the level of the aortic valve and thus the EOA is almost equal to the AOA. In this situation both the AOA and EOA are normal and there is no or minimal pressure drop and thus energy loss across the aortic valve. However, in the presence of AS, the AOA is reduced because of the fibro-calcific remodeling of the valve leaflets and the EOA is further reduced compared to the AOA because of significant flow contraction that occurs downstream of the valve orifice. The transvalvular pressure gradient and thus the LV pressure overload are essentially determined by the EOA and the smaller the EOA the larger are the gradients and, ultimately, the LV pressure overload (Fig. 37.6). The accurate assessment of the hemodynamic severity of the valvular stenosis is crucial for clinical decision-making in patients with AS. The severity of AS is generally determined by measuring the pressure gradient across the valve or, preferably the EOA, since it is less flow-dependent (Fig. 45.5B). The EOA can be measured either by Doppler echocardiography with the use of the continuity

equation or by left heart catheterization with the Gorlin formula.[33] The AOA can be measured by planimetry of the valve orifice visualized by echocardiography, MDCT, or CMR.
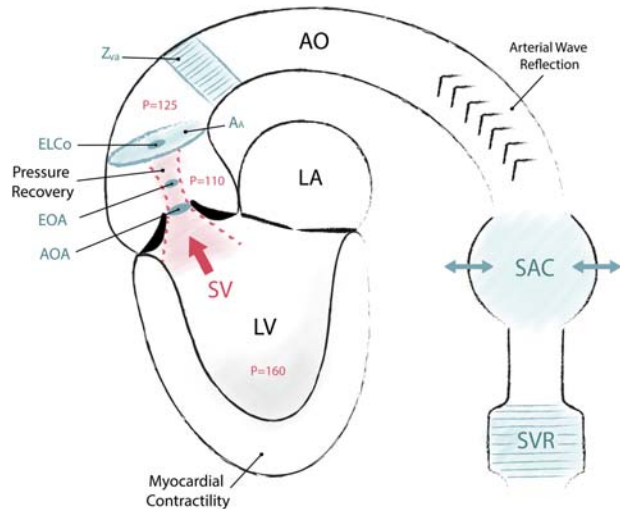
The main factors that influence the flow contraction coefficient, i.e., the ratio of EOA/AOA, are the shape and size of the LVOT and the magnitude of the LV outflow (Fig. 37.5, panel A; Fig. 37.6). A decrease in stroke volume and transvalvular flow results in more pronounced flow contraction and thus in a smaller EOA relative to the AOA.[34] A larger LVOT cross section and/or an LVOT shape with abrupt transition from LVOT to AOA (i.e., flat valve inflow shape) are associated with greater flow contraction.[31,35,36] On the other hand, smaller LVOT size or funnel-shaped LVOT allows more progressive convergence of the flow toward the valve orifice and thus less flow contraction downstream of the valve. Interestingly, in up to 75% of patients with AS LVOT has an hourglass (i.e., diameter at the annulus higher than 5—10 mm below) and

FIGURE 37.5 **Flow contraction and pressure recovery at the level of the aortic valve.** Panel A shows the flow contraction that occurs downstream of the aortic valve. The flow contraction is more pronounced when the valve aperture angle θ is larger and so the valve inflow is flatter (A-1) compared to smaller angle and funnel shape inflow (A-2 and A-3). The flow contraction coefficient (CC = EOA/AOA) is close to 0.6 and so the effective orifice area is much smaller than the anatomic orifice area when θ is close to 90 degrees and it increases up 1.0 when θ is < 20 degrees. In such case, there is little flow contraction and the EOA is similar to the AOA. Hence, for the same AOA (i.e., size of aortic valve orifice), the EOA (minimal cross section of the transvalvular flow) and thus the transvalvular pressure gradient and LV pressure overload may vary significantly depending on the valve inflow shape. *LVOT*, Left ventricular outflow tract. Panel B shows the evolution of blood flow and pressure across the LVOT, aortic valve, and ascending aorta during systole. When the blood flow contracts to pass through a stenotic orifice (i.e., the anatomic orifice area [AOA]), a portion of the potential energy of the blood, namely, pressure, is converted into kinetic energy, namely, velocity, thus resulting in a pressure drop and acceleration of flow. Downstream of the vena contracta (i.e., the effective orifice area [EOA]), a large part of the kinetic energy is irreversibly dissipated as heat because of flow turbulences. The remaining portion of the kinetic energy that is reconverted back to potential energy is called the "pressure recovery" (PR). The global hemodynamic load imposed on the left ventricle results from the summation of the valvular load and the arterial load. This global load can be estimated by calculating the valvulo—arterial impedance. In patients with medium or large size ascending aorta, the impedance can be calculated with the standard Doppler mean gradient in place of the net mean gradient. *AA*, cross-sectional area of the aorta at the level of the sinotubular junction; ΔP_{max}, maximum transvalvular pressure gradient recorded at the level of vena contracta (i.e., mean gradient measured by Doppler); ΔP_{net}, net transvalvular pressure gradient recorded after pressure recovery (i.e., mean gradient measured by catheterization); *LVOT*, left ventricular outflow tract; P_{LVOT}, pressure in the LVOT; *SBP*, systolic blood pressure; *SVi*, stroke volume index; *Vpeak*, peak aortic jet velocity; *Zva*, valvuloarterial impedance. Panel C shows the pressure recovery phenomenon in prosthetic heart valves in patients with large aorta diameter (I, minimal pressure recovery) and small aorta diameter (II, significant pressure recovery). *Panel A Adapted from Garcia D, Kadem L. What do you mean by aortic valve area: geometric orifice area, effective orifice area, or gorlin area?* **J Heart Valve Dis**. *2006; 15:601—608; Panel B Reproduced with permission from Pibarot P, Dumesnil JG. Improving assessment of aortic stenosis.* **J Am Coll Cardiol**. *2012; 60:169—180; Panel C Adapted with permission from Durko AP, Head SJ, Pibarot P, et al. Characteristics of surgical prosthetic heart valves and problems around labeling: a document from the European Association for Cardio-Thoracic Surgery (EACTS)-The Society of Thoracic Surgeons (STS)-American Association for Thoracic Surgery (AATS) valve labelling task force.* **J Thorac Cardiovasc Surg**. *2019; 158:1041—1054.*

this has a significant impact on SVi and AVA estimations.[37] Depending on the conditions of LV flow and LVOT size and shape, the contraction coefficient may vary between 0.6 and 1.0 and thus major differences may be observed between AOA and EOA.[31,34—36] Hence, it is preferable to use the EOA rather the AOA to assess the hemodynamic severity of the aortic valve stenosis. In the clinical setting, the EOA can be measured either by Doppler echocardiography with the use of the continuity equation or by left heart catheterization with the Gorlin formula. CMR provides unique capabilities to measure flow using phase-contrast imaging[38,39] without doing geometric (such as a circular LVOT which is known to be elliptic) or fluid dynamics (such as a flat flow profile which in practice is skewed) assumptions as compared to continuity equation by echocardiography. The underlying principles of

FIGURE 37.6 Ventriculo—arterial coupling and valvulo—arterial load in aortic valve disease. This figure illustrates the interplay between the left ventricular, valvular, and arterial anatomic and hemodynamic factors in the context of aortic valve stenosis. The flow ejected by the left ventricle during systole contracts to pass through the stenotic aortic valve. This flow contraction occurs, in large part, within the LV outflow tract but increases further downstream to the valve. This is why the effective orifice area (EOA, i.e., cross section of the vena contracta of the transvalvular flow) is smaller than the anatomic orifice area (AOA) at the level of the valve. The EOA is the main determinant of the pressure loss or pressure gradient (50 mmHg in this case) that occurs between the LV outflow tract and the vena contracta and that results in a pressure overload ($P = 160$ mmHg in this case) on the left ventricle. Downstream to the vena contracta, a portion of the kinetic energy of the flow jet is, however, reconverted into potential energy, i.e., pressure. This pressure recovery phenomenon is more important when the ratio between the EOA and the cross-sectional area of the ascending aorta (AA) is high because in this context, there is less flow turbulences downstream to the valve and thus less energy (pressure) loss. Because of the pressure recovery (+15 mmHg in this case), the blood pressure in the ascending aorta (125 mmHg) is higher than at the level of the vena contracta (110 mmHg). The systemic arterial compliance (SAC) is in large part determined by the compliance of the aorta and large arteries, whereas the systemic vascular resistance (SVR) is mainly determined by the small arteries. A reduction in SAC causes a faster reflection of arterial waves from the periphery, which may contribute to increase the aortic and then the LV systolic pressure. Hence, reduced SAC and increased SVR contribute to increase the pulsatile (SAC) and steady (SVR) components of the arterial impedance and thus of the afterload imposed on the LV. In patients with aortic stenosis and concomitant hypertension, the LV is facing a double load, i.e., a valvular load because of the valve stenosis and an arterial load because of the reduced SAC and/or increased SVR. The valvulo—arterial impedance (Zva) encompasses these factors and reflects the overall hemodynamic burden imposed by the aortic valve, the aorta, and the arterial system on the LV. The increase in LV afterload related to the increase in Zva leads to reduced myocardial contractility and ventricular—arterial uncoupling, which, in turn, cause a reduction in stroke volume (SV).

through-plane phase-contrast MRI relies on the acquisition of flow-sensitizing bipolar gradients. Flow volume is measured by the acquisition of a cross-sectional image of the vessel or area of interest. Fluid velocity can then be calculated for every pixel covering the region of interest, which in turn represents a voxel of a given thickness (often 5 mm or more). The flow corresponds to the product of every pixel fluid velocity multiplied by every pixel area. Total flow is derived by the summation of all pixel flow covering the area of interest.[40,41] Though phase-contrast CMR can be considered the noninvasive gold standard for stroke volume estimations, a recent study by our group showed that Doppler echocardiography provides comparable stroke volumes versus phase-contrast CMR.[37] However, phase-contrast CMR is known to underestimate velocity—time integrals and peak velocities. This is due to its lower temporal resolution in relation to Doppler, difficulties in finding the exact perpendicular through plane (position and angle) of the vena contracta and voxel averaging of flow velocity.[38] Thus, even though some studies have shown the feasibility of AVA calculation by CMR,[42,43] a recent metaanalysis has confirmed that CMR estimation of effective orifice area cannot be compared to that of Doppler echocardiography.[44] Time-resolved three-directional velocity encoded phase-contrast-CMR (i.e., 4D-flow)[45,46] can overcome many of these limitations and has a promising role in assessing blood flow and blood—vessel interactions, such as energy loss, kinetic energy, and shear stress.[45—47] Therefore, CMR (and especially 4D flow) will represent an important step toward improving the understanding of the complexities of ventriculo—valvulo—arterial coupling.[48] The main limitations of 4D flow phase-contrast MRI are the long acquisition times need to encode velocities in three dimensions, and its temporal resolution, which remains limited even with very long acquisition times.

Interaction between aorta and aortic valve in aortic valve disease

Aortic stenosis

Effacement of sinotubular junction

The size and geometry of the aortic root and ascending aorta may have an impact on the aortic valve mechanics and hemodynamics. In particular, a recent study reported that effacement of the sinotubular junction is independently associated with faster AS progression.[49] Indeed, this abnormality of the aortic root geometry may increase mechanical stress of aortic valve leaflets and disturb the flow pattern at the aortic surface of the valve leaflets, which may, in turn, alter the mechanobiology of the valve and promote disease initiation or progression.

Pressure recovery

When the blood flow contracts to pass through a stenotic orifice, a portion of the potential energy of the blood, i.e., pressure, is converted into kinetic energy, i.e., velocity,

thus resulting in a pressure drop and acceleration of flow (Figs. 37.5B and 37.6). Downstream of the vena contracta, the flow jet reexpands and decelerates. Given that the total energy must remain constant, the kinetic energy is converted back into potential energy, i.e., blood velocity decreases, whereas blood pressure increases. However, this energy conversion is not complete in the context of an abrupt obstruction such as an aortic valve stenosis because the sudden expansion of the flow jet downstream of the vena contracta generates flow turbulences. As a result of these turbulences, a large part of the kinetic energy is irreversibly dissipated as heat. The remaining portion of the kinetic energy that is reconverted back to potential energy is called the "pressure recovery" (Figs. 37.5B and 37.6). The extent of this pressure recovery essentially depends on the relationship between the size of the valve orifice and the size of the aorta.[50–52] The smaller the valve EOA relative to the size of the aorta, the more flow turbulences will occur and the less energy will be available to be recovered as pressure. Hence, the extent of pressure recovery generally becomes clinically relevant in patients with smaller aortas, i.e., with an aorta diameter at the sinotubular junction ≤ 30 mm, and especially in those with mild, moderate, or moderate-to-severe AS.[50–54] Patients with a large aneurysm of the ascending aorta have no pressure recovery and therefore have a larger energy loss for a given valve EOA. Congenital bicuspid AS is often associated with dilation of the ascending aorta, which may reduce the extent of pressure recovery and thereby increase the energy loss at the level of the aortic valve/root. The same considerations should be taken into account in the case of aortic prostheses (Fig. 37.5C).[55]

Doppler-echocardiographic measurements rely on the maximum velocity or gradient measured across the aortic valve at the level of the vena contracta (Fig. 37.5B). On the other hand, catheterization measurements are generally performed at a few centimeters downstream of the valve, where the pressure is fully recovered. As a result, the pressure gradient recorded by catheterization, which corresponds to the "recovered" or "net" pressure gradient, is generally lower than the Doppler gradient, which corresponds to the maximum gradient recorded at the level of the vena contracta.[33] Likewise, EOA by the Gorlin formula is derived from recovered pressures such that its value is higher than EOA derived by the continuity equation, which measures the actual area occupied by flow at the valvular level. Hence, the extent of pressure recovery and thus the discrepancies between Doppler and catheter measurements are more important in patients with smaller aortas and/or with mild, moderate, or moderate-to-severe AS. Nonetheless, these discrepancies can in large part be reconciled by taking into account the pressure recovery phenomenon. To

this effect, one can calculate the "energy loss coefficient" (ELCo), a new parameter proposed by Garcia et al. that adjusts the Doppler EOA for the size of the aorta in order to take into account the pressure recovery (Fig. 37.6):[5]

$$ELCo = (EOA \times A_A)/(A_A - EOA)$$

where A_A is the cross-sectional area of the aorta measured at about 1 cm downstream of the sinotubular junction. This energy loss coefficient is easily measurable by Doppler echocardiography and is more or less equivalent to the catheter EOA calculated with the use of the Gorlin formula. Several studies have demonstrated that the energy loss coefficient is superior to the Doppler EOA in predicting the actual energy loss and the occurrence of LV dysfunction and adverse outcomes in patients with AS.[50,56] Not accounting for pressure recovery in patients with small aortas may lead to overestimation of severity by Doppler echocardiography and unwarranted investigations or interventions.

Pressure recovery also occurs downstream of surgical or transcatheter prosthetic valves that are used to replace the disease native aortic valve. It is important to make a distinction between the pressure recovery phenomenon that may occur with any type of native or prosthetic aortic valve versus the localized high gradient phenomenon that occurs within the central orifice of the bileaflet mechanical valves. As for the native aortic valve, the magnitude of pressure recovery is higher in patients with a small aorta. Furthermore, recent studies suggest that pressure recovery may be relatively more important in prosthetic valves versus native disease aortic valves and in transcatheter versus surgical bioprosthetic aortic valves.[57–59]

Interaction between hypertension and AS

Arterial hemodynamics, and, in particular arterial compliance, may also interact with the diagnosis of AS. Hypertension may contribute to increase the LV afterload and therefore lead to a decrease in LV contractility, stroke volume, and transvalvular flow.[60–62] Given that the transvalvular pressure gradient is highly flow dependent, any decrease in flow may substantially reduce the gradient (i.e., low-flow, low-gradient pattern) and thereby lead to an underestimation of stenosis severity. Hence, when hypertension and AS coexist, there is a decrease in flow that leads to a "pseudo-normalization" of gradient and also blood pressure with ensuing underestimation of both AS severity and hypertension severity.[63] In contrast to the gradient, the EOA measured in a hypertensive patient may yield to an overestimation of stenosis severity. Indeed, although less flow dependent than the gradient, the EOA may nonetheless decrease with decreasing flow rate and may thus be "pseudo-severe."[60,61]

It has also been suggested that a reduction in arterial compliance, which is frequent in patients with bicuspid AS or in older patients with trileaflet, AS may cause a decrease in the gradient, independently of transvalvular flow (Fig. 37.6).[64,65] Indeed, faster and earlier reflection of arterial wave from the periphery may blunt the transvalvular gradient. This phenomenon may, at least in part, be responsible for some of the discordant grading (i.e., small EOA with low gradient) situations observed in patients with AS and normal flow rate. Hence, in patients with hypertension, it is recommended to reassess severity after normalization of blood pressure.

Systemic arterial hypertension is associated with faster progression of aortic valve calcification and stenosis.[66] This association may be explained, at least in part, by the increased mechanical stress on aortic valve leaflets and by the disturbed flow transaortic flow patterns caused by hypertension.

Aortic regurgitation

Aortic regurgitation can result from abnormalities of the aortic valve leaflets or from dilation of the aortic root. When the aortic leaflets are involved, there is frequently a destructive process occurring such as infective endocarditis, rheumatic heart disease, or degenerative valvular disease. Any disease process that results in dilation of the aortic root (i.e., Marfan's syndrome, BAV, etc.) may cause a tethering of the leaflets and thus a lack of coaptation in diastole. Similarity with the Carpentier's mitral classification, aortic regurgitation caused by leaflet tethering is often referred as type I.[67] Dilatation can affect the ascending aorta starting from the sinotubular junction (Type IA) or can present as an aneurysm of the entire aortic root with dilation of the aortic annulus, the sinuses of Valsalva and the sinotubular junction (Type IB). Surgical treatment is different in both types, consisting in a supracoronary tube graft sutured above the aortic root without need for coronary arteries reimplantation in the type IA, while in type IB, the entire aortic root is replaced, and the coronary ostia reimplanted, the native aortic valve being spared if its leaflets are normal.

Interaction between aorta, aortic valve, and LV in AS

The pathophysiology of heart failure in AS is essentially determined by the extent of imbalance between the increase in LV hemodynamic load due to the valvular obstruction and/or concomitant arterial hypertension, on the one hand, and the capacity of the LV to overcome this increase in load both at rest and during exercise, on the other hand (Figs. 37.4 and 37.6). In patients with calcific AS, several factors may lead to an unbalance between Ea and Ees and thus to ventriculo−arterial decoupling.

First, the aortic valve obstruction contributes to increase in the LV afterload. In response to pressure overload, the LV generally develops concentric remodeling. This is an adaptive process whereby the increase in wall thickness tends to stabilize the wall tension. This adaptive process is initially useful to maintain myocardial contractility and systolic function. However, with progression to more advanced stages of AS, LV hypertrophy is not able to compensate for the increase in afterload and myocardial contractility decreases due to afterload mismatch. Furthermore, because of the major LV pressure overload and the pronounced LV hypertrophy, the coronary perfusion declines, whereas the myocardial oxygen demand increases, thus leading to repetitive myocardial ischemia. These processes in turn induce dysfunction and then apoptosis of myocytes and development of myocardial fibrosis, which leads to reduced LV myocardial contractility (decrease in Ees) and compliance (increase in LV end-diastolic pressure). Hence, in the more advanced stages of the disease, patients develop LV diastolic and systolic dysfunction, which eventually progress to heart failure. Therefore, AS is currently considered a disease of both the valve and the myocardium.[68] The myocardial response of the LV to AS has a major impact on the presence of symptoms and clinical outcomes, but the timing and type of LV remodeling is not predictable for the individual patient and is influenced by other load-independent factors such as the metabolic milieu. Advanced cardiac imaging has greatly contributed to the understanding of the complex interaction between the increased afterload (both valvular due to AS and vascular due to increased peripheral resistance and aortic impedance) and the myocardial consequences (LV hypertrophy, adverse remodeling, myocardial fibrosis, and, ultimately, decreased contractility).[69] However, the amount on which decreased LVEF is secondary to increased afterload (*"afterload mismatch",* therefore relieved by AVR) or to intrinsic myocardial damage has proven to be difficult to assert. Several echocardiographic and CMR imaging biomarkers of early "subclinical" systolic dysfunction (e.g., LVEF 50%−59%, decreased global longitudinal strain, midwall focal fibrosis and increased extracellular volume) are being currently tested in randomized clinical trials as markers for an earlier intervention

in asymptomatic stages (EVoLVeD, NCT03094143; EARLY-TAVR, NCT03042104).[70] Furthermore, the interaction of a nonsevere increase in afterload (moderate AS) with an already failing LV has been shown to be associated with worse outcomes and, therefore, an early intervention might be of benefit. This hypothesis is currently being tested in the TAVR-UNLOAD randomized clinical trial (NCT02661451).[71]
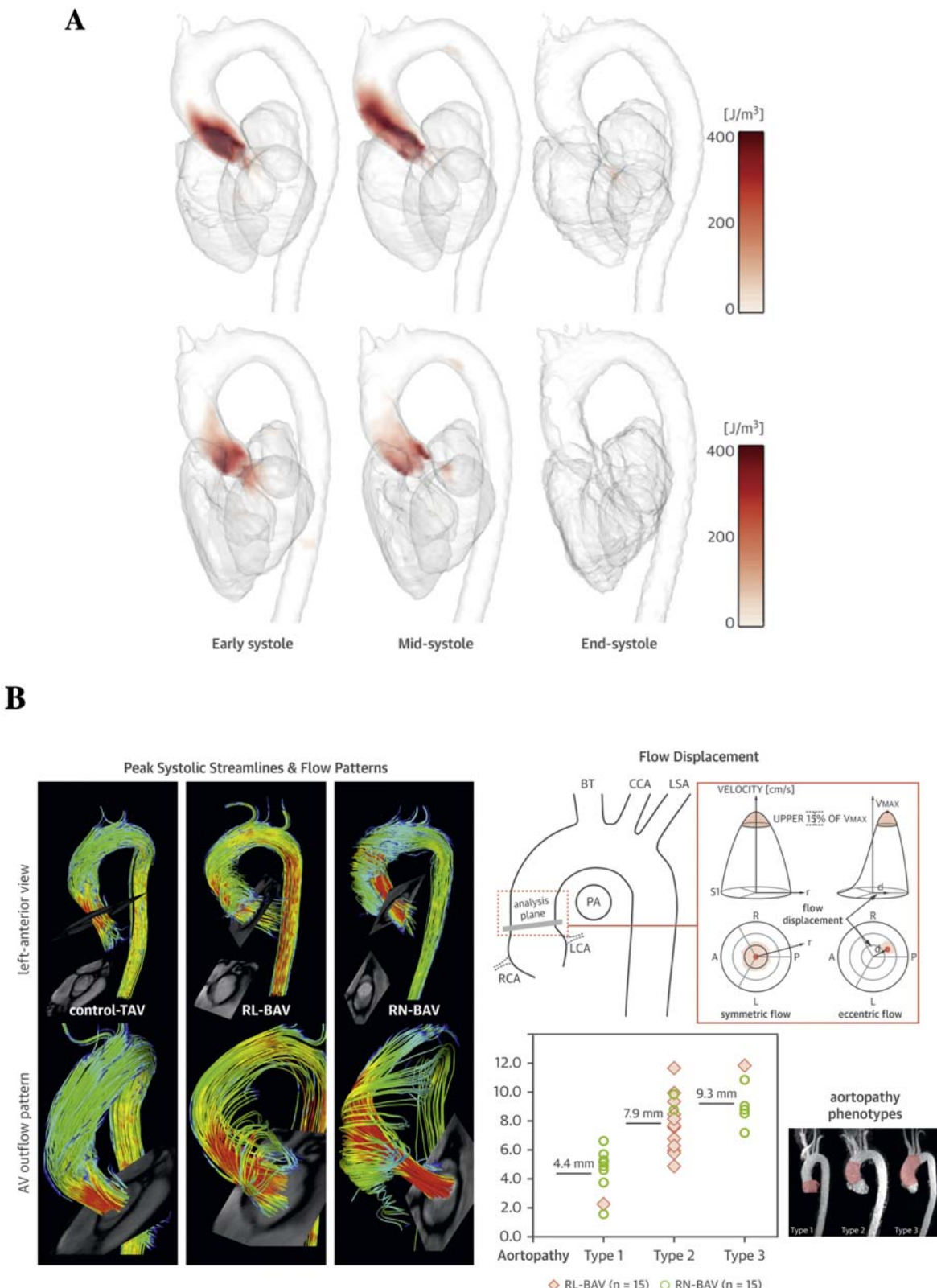
Second, patients with calcific AS are generally older and thus frequently have reduced arterial compliance and associated systolic hypertension.[23,66,72] As a matter of fact, hypertension, and particularly systolic hypertension, is highly prevalent (30%—70%) in patients with AS.[23,72] These patients thus often have increased Ea as a result of concomitant reduced arterial compliance and increased vascular resistance.[16,73] Because the LV of these patients is facing a double (i.e., valvular + arterial) hemodynamic load, they are predisposed to the development of symptoms, LV dysfunction, and heart failure (Fig. 37.6).[23,24,72,74] To this effect, Antonini-Canterin et al. also reported that symptoms of AS develop at an earlier stage (i.e., nonsevere) of the valvular stenosis in hypertensive patients compared to normotensive ones.[74] LV dysfunction may also develop at a lower degree of AS severity in patients with concomitant hypertension.[23,24] Recent studies also suggest that hypertension may accelerate the progression of the severity of AS per se.[66,75] Finally, the presence of hypertension is associated with a twofold increase in the risk of all-cause mortality in patients with AS.[72,75] Once again, advanced cardiac imaging (and especially 4D-Flow CMR) allows to noninvasively assess arterial physiology, such as aortic pulse wave velocity,[76] wall shear stress,[77] and advanced hemodynamic measures such as vorticity and helicity, flow displacement, pressure gradients, viscous energy loss, and turbulent kinetic energy (Fig. 37.7).[45] Furthermore, the combination of valvular (AS) and vascular (increased peripheral vascular resistance, increased or premature wave reflection, and/or decreased vascular compliance) hemodynamic load cumulate to increase LV afterload and, thus, the degree of LV hypertrophy and myocardial fibrosis.[73] Hence, it is crucial to optimize diagnosis and treatment of systemic arterial hypertension in patients with aortic valve disease.

Third, Ees is often reduced in AS patients, thus further contributing to the increase in Ea/Ees ratio, ventriculo—arterial decoupling, and heart failure. The main factors responsible for the decline in Ees in AS are **(i)** LV afterload mismatch and associated decrease in myocardial contractility related to the disproportionate increase in LV afterload (resulting from AS and frequent concomitant hypertension) relative to LV performance; **(ii)** Impaired LV contractility due to concomitant coronary artery disease—which is also frequent in the elderly population with AS, myocardial fibrosis[78] or concomitant cardiac amyloidosis.[79]

The ventricular—arterial decoupling ultimately results in a decline in LV ejection and stroke volume, which yields to heart failure symptoms.[80,81] Furthermore, in these conditions of low flow state, the transvalvular gradient, which is highly flow dependent, may decrease and thus underestimate the actual severity of the stenosis.[80,82] Dobutamine stress echocardiography may be useful to confirm the stenosis severity in these patients with low LV ejection fraction, low-flow, low-gradient AS (Fig. 37.4). However, the recent advent of MDCT aortic valve calcium quantification has revolutionized AS evaluation in the last years. It requires an ECG-gated, noncontrast acquisition with low radiation (<1 mSv). Quantification relies on the Agatston method using semiautomated software and provides a flow-independent quantitative assessment of AS anatomical severity. Details on the scan protocol, quantitative analysis, and caveats have been recently published.[83] AVC quantification has excellent reproducibility and performance for AS severity assessment and has consistently proven to be of incremental prognostic value in several studies.[84,85] Furthermore, it has been incorporated into ESC/EACTS guidelines to be used in patients with symptomatic, discordant grading AS and both reduced (<50%) and preserved LVEF (≥50%).[86] Due to sex differences in AS pathophysiology (women present with more fibrosis and less calcification than men[87]), specific cutoffs defining severe AS differ for women (≥1200 Agatston Units [AU]) and men (≥2000 AU).

However, the majority of patients with severe AS develop symptoms prior to decline in LV ejection fraction. In these patients, the symptoms are mainly related to the development of LV diastolic dysfunction and increased LV filling pressures. When it becomes severe and evolves toward restrictive pattern, LV diastolic dysfunction can even cause a low-flow, low-gradient phenotype but with preserved LV ejection. This entity is named "paradoxical" low-flow, low-gradient AS and it corresponds to the "heart failure with preserved LV ejection fraction, i.e., HFpEF" form of AS, whereas the classical low-flow, low-gradient with low LVEF described above represents the "heart failure with reduced LV ejection fraction, i.e., HFrEF" form (Fig. 37.4).[80,82] As mentioned previously, in patients with

FIGURE 37.7 Cardiovascular magnetic resonance 4D flow for assessment of advanced hemodynamic measures. Panel A: Turbulent kinetic energy (in Joules/m^3) in a patient with AS (top) and a healthy volunteer (bottom). Panel B: 3D flow visualization of streamlines (left panel) and flow displacement (right panel)—a semiquantitative measurement of flow eccentricity—in patients with tricuspid and bicuspid aortic valves with right-left and right-noncoronary cusp fusion. Different flow patterns showed association with specific types of aortopathy. Panel C: Average of 3D wall shear stress in healthy controls (A), dilation of the aorta with tricuspid aortic valve (B) and aortic stenosis (C). *Panels A—C Reproduced with permission from Garcia J, Barker AJ, Markl M. The role of imaging of flow patterns by 4D flow MRI in aortic stenosis. **JACC Cardiovasc Imag**. 2019; 12:252—266.*
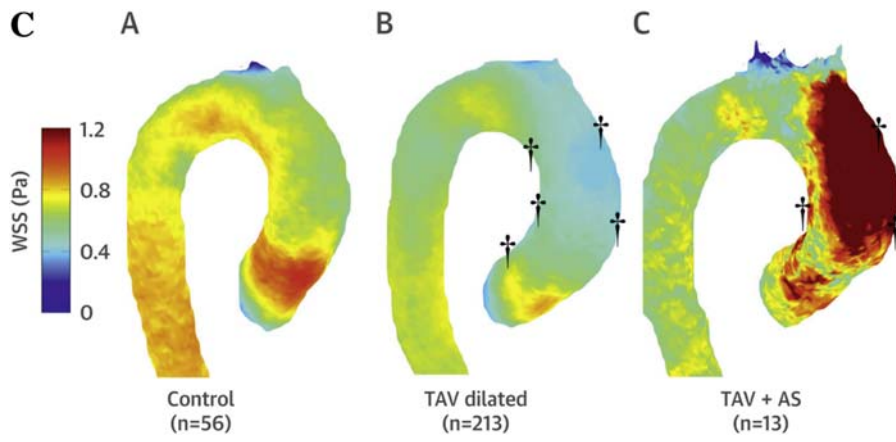
FIGURE 37.7 cont'd

paradoxical low-flow, low-gradient AS, quantitation of aortic valve calcium burden by CT may be used to confirm stenosis severity.
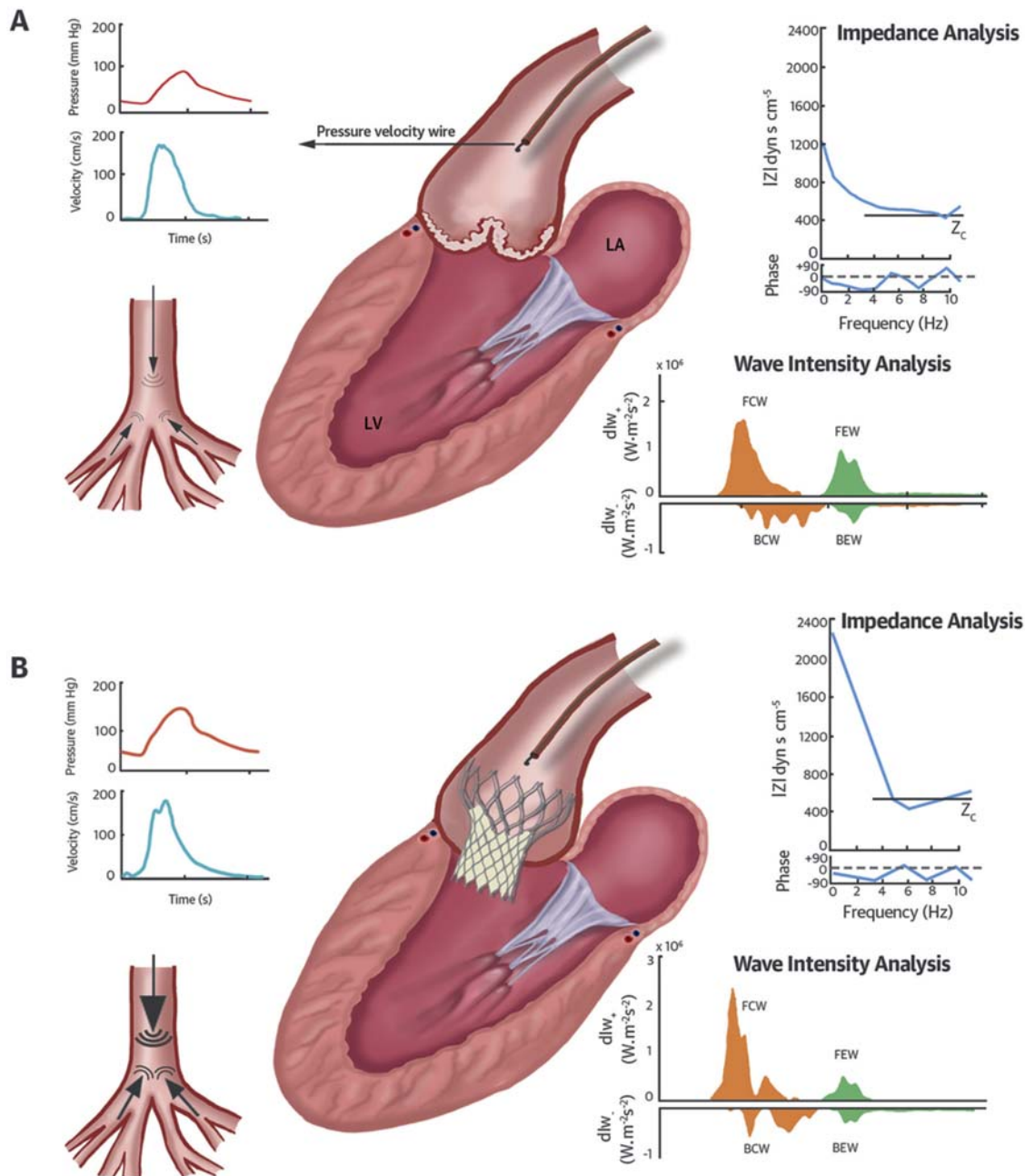
Impact of arterial load following aortic valve replacement

Aortic valve replacement addresses the aortic valve disease per se and therefore corrects the valvular hemodynamic load imposed on the LV. However, this procedure does not correct the arterial abnormalities associated with the aortic valve disease, if any (Fig. 37.8). New onset or a worsening of arterial hypertension is frequently observed following aortic valve replacement.[88,89] This intriguing phenomenon may be related to the increase in stroke volume and cardiac output resulting from the LV afterload reduction achieved by the valve replacement procedure. The postprocedural increase in flow may lead to an increase in systemic arterial pressure and may therefore unmask a preexisting hypertensive disease in patients with severe AS, low flow state, and thus pseudo-normal arterial pressure prior to the procedure. Furthermore, Yotti et al. reported that aortic valve replacement may be associated with an acute worsening of the arterial load in patients with severe AS (Fig. 37.8).[88] Indeed, the valvular obstruction may dampen forward and backward compression waves in the arterial tree of these patients. An acute relief, by aortic valve replacement, of this valvular obstruction and of the associated dampening effect may actually result in an increase in the arterial load, and particularly of its pulsatile component. This may, in turn, limit the benefit of the valve procedure on the reduction of LV afterload and thus on the postprocedural regression of LV hypertrophy and improvement of patient's functional status. Several studies reported that abnormal arterial properties and increased arterial load are important determinant of i) the persistence of LV hypertrophy,

ventriculo—arterial uncoupling, and low-flow state; ii) suboptimal improvement in functional capacity and quality of life; iii) persistent or recurrent heart failure; and iv) mortality following aortic valve replacement.[73,89—91] In particular, systemic arterial compliance is often abnormal in patients with severe calcific AS and appears to be the most important contributor to postprocedural outcomes. Given that patients with severe AS are often in low flow state both before and after aortic valve replacement, increased pulsatile arterial load, rather than blood pressure, may be a target for adjunctive medical therapy to improve outcomes after TAVR.[89]

Conclusion

Optimal anatomical and functional interplay between the LV, the aortic valve, and the aorta is essential to maintain adequate blood flow and pressure, and thus adequate organ perfusion (Fig. 37.6). Any abnormality in the anatomy or the function of any of these three entities may cause a ventriculo—arterial decoupling, which may in turn lead to heart failure. The assessment of the ventriculo—valvulo—arterial coupling may thus help to identify patients with ventricular, valvular, or arterial diseases being at risk for the development of heart failure and also to reconcile discordant situations such as i) EOA being smaller than the AOA in patients with AS; ii) the concomitance of a small EOA with a low gradient in patients with low-flow or normal-flow AS; iii) the underestimation of AS severity in patients with concomitant arterial hypertension; iv) and the development of LV dysfunction in patients with nonsevere AS or AR but concomitant arterial hypertension. Advanced cardiac imaging, and especially 4D-CMR, has a fundamental role in assessing the complex interaction between the LV, aortic valve (stenotic and/or regurgitant), and the arterial system.

FIGURE 37.8   Changes in arterial load following transcatheter aortic valve replacement in patients with severe AS. Panels A and B: Aortic impedance and wave intensity analysis are shown in a patient before (A) and after (B) transcatheter aortic valve replacement (TAVR). Aortic systolic and pulse pressures increased after TAVR. Fourier decomposition of the simultaneous aortic pressure and velocity signals shows that SVR and the first three harmonic frequencies of the impedance spectrum (Z) increase after TAVR. Wave intensity analysis was used to separate total wave intensity into contributions from the forward (dIwþ) and backward (dIw-) traveling waves. Compression waves (salmon) increase pressure, and expansion waves (green) decrease aortic pressure. The forward compression wave (FCW) increases immediately after TAVR. *BCW*, backward compression wave; *BEW*, backward expansion wave; *dIw*, wave intensity; *FEW*, forward expansion wave; *LA*, left atrium; *LV*, left ventricle; *SVR*, systemic vascular resistance. Panel C: Boxplots and individual value plots (patients showing a decrease [salmon] or increase [blue] in SVI after TAVR) show values of mean pressure gradient, systolic blood pressure, peak left ventricular pressure, and stroke volume index (SVI) in 23 patients with severe AS before and after TAVR.

References

1. Sunagawa K, Maughan WL, Sagawa K. Optimal arterial resistance for the maximal stroke work studied in isolated canine left ventricle. **Circ Res**. 1985; 56:586–595.

2. Piazza N, de Jaegere P, Schultz C, Becker AE, Serruys PW, Anderson RH. Anatomy of the aortic valvar complex and its implications for transcatheter implantation of the aortic valve. **Circ Cardiovasc Interv**. 2008; 1:74–81.

3. Yoganathan AP, He Z, Casey Jones S. Fluid mechanics of heart valves. **Annu Rev Biomed Eng**. 2004; 6:331–362.

4. Anderson RH. Clinical anatomy of the aortic root. **Heart**. 2000; 84:670–673.

5. Jilaihawi H, Zhao Z, Du R, et al. Minimizing permanent pacemaker following repositionable self-expanding transcatheter aortic valve replacement. **JACC Cardiovasc Interv**. 2019; 12:1796–1807.

6. Ng VG, Hahn RT, Nazif TM. Planning for success: pre-procedural evaluation for transcatheter aortic valve replacement. **Cardiol Clin**. 2020; 38:103–113.

7. Murphy DT, Blanke P, Alaamri S, et al. Dynamism of the aortic annulus: effect of diastolic versus systolic CT annular measurements on device selection in transcatheter aortic valve replacement (TAVR). **J Cardiovasc Comput Tomogr**. 2016; 10:37–43.

8. Basso C, Boschello M, Perrone C, et al. An echocardiographic survey of primary school children for bicuspid aortic valve. **Am J Cardiol**. 2004; 93:661–663.

9. Michelena HI, Khanna AD, Mahoney D, et al. Incidence of aortic complications in patients with bicuspid aortic valves. **J Am Med Assoc**. 2011; 306:1104–1112.

10. Lindman BR, Clavel MA, Mathieu P, et al. Calcific aortic stenosis. **Nat Rev Dis Primers**. 2016; 2:16006.

11. Michelena HI, Prakash SK, Della Corte A, et al. Bicuspid aortic valve: identifying knowledge gaps and rising to the challenge from the international bicuspid aortic valve consortium (BAVCon). **Circulation**. 2014; 129:2691–2704.

12. Verma S, Siu SC. Aortic dilatation in patients with bicuspid aortic valve. **N Engl J Med**. 2014; 370:1920–1929.

13. Shen M, Tastet L, Capoulade R, et al. Effect of bicuspid aortic valve phenotype on progression of aortic stenosis. **Eur Heart J Cardiovasc Imag**. 2020; 21:727–734.

14. Mathieu P, Bossé Y, Huggins GS, et al. The pathology and pathobiology of bicuspid aortic valves: state of the art and novel research perspective. **J Pathol Clin Res**. 2015; 1:195–206.

15. Bissell MM, Hess AT, Biasiolli L, et al. Aortic dilation in bicuspid aortic valve disease: flow pattern is a major contributor and differs with valve fusion type. **Circ Cardiovasc Imag**. 2013; 6:499–507.

16. Chirinos JA, Segers P, Hughes T, Townsend R. Large-artery stiffness in health and disease: JACC state-of-the-art review. **J Am Coll Cardiol**. 2019; 74:1237–1263.

17. Sunagawa K, Maughan WL, Burkhoff D, Sagawa K. Left ventricular interaction with arterial load studied in isolated canine ventricle. **Am J Physiol**. 1983; 245:H773–H780.

18. Chirinos JA, Segers P. Noninvasive evaluation of left ventricular afterload: part 2: arterial pressure-flow and pressure-volume relations in humans. **Hypertension**. 2010; 56:563–570.

19. Panzer J, De Somer F, Segers P, De Wolf D, Bove T. Effect of aortic stiffness versus stenosis on ventriculo-arterial interaction in an experimental model of coarctation repair. **Eur J Cardio Thorac Surg**. 2020; 58:1206–1215.

20. Suga H. Time course of left ventricular pressure-volume relationship under various enddiastolic volume. **Jpn Heart J**. 1969; 10:509–515.

21. Townsend RR, Wilkinson IB, Schiffrin EL, et al. Recommendations for improving and standardizing vascular research on arterial stiffness: a scientific statement from the American Heart Association. **Hypertension**. 2015; 66:698–722.

22. Chirinos JA, Rietzschel ER, Shiva-Kumar P, et al. Effective arterial elastance is insensitive to pulsatile arterial load. **Hypertension**. 2014; 64:1022–1031.

23. Briand M, Dumesnil JG, Kadem L, et al. Reduced systemic arterial compliance impacts significantly on left ventricular afterload and function in aortic stenosis: implications for diagnosis and treatment. **J Am Coll Cardiol**. 2005; 46:291–298.

24. Hachicha Z, Dumesnil JG, Pibarot P. Usefulness of the valvuloarterial impedance to predict adverse outcome in asymptomatic aortic stenosis. **J Am Coll Cardiol**. 2009; 54:1003–1011.

25. Harada K, Saitoh T, Tanaka J, Shibayama K, Berdejo J, Shiota T. Valvuloarterial impedance (Zva), but not aortic stenosis severity, predicts syncope in aortic stenosis. **Circ Cardiovasc Imag**. 2013; 6:1024–1031.

26. Guzzetti E, Poulin A, Annabi MS, et al. Transvalvular flow, sex, and survival after valve replacement surgery in patients with severe aortic stenosis. **J Am Coll Cardiol**. 2020; 75:1897–1909.

27. Hachicha Z, Dumesnil JG, Bogaty P, Pibarot P. Paradoxical low flow, low gradient severe aortic stenosis despite preserved ejection fraction is associated with higher afterload and reduced survival. **Circulation**. 2007; 115:2856–2864.

28. Dayan V, Vignolo G, Magne J, Clavel MA, Mohty D, Pibarot P. Outcome and impact of aortic valve replacement in patients with preserved LV ejection fraction and low gradient aortic stenosis: a meta-analysis. **J Am Coll Cardiol**. 2015; 66:2594–2603.

29. Stanberry L, Ahmed A, Sorajja P, Cavalcante JL, Gossl M. Invasive versus non-invasive assessment of valvuloarterial impedance in severe aortic stenosis. **Open Heart**. 2020; 7.

30. Devlin WH, Petrusha J, Briesmiester K, Montgomery D, Starling MR. Impact of vascular adaptation to chronic aortic regurgitation on left ventricular performance. **Circulation**. 1999; 99:1027–1033.

31. Garcia D, Kadem L. What do you mean by aortic valve area: geometric orifice area, effective orifice area, or gorlin area? **J Heart Valve Dis**. 2006; 15:601–608.

32. Pibarot P, Larose É. What our eyes see is not necessarily what our heart feels. **Cardiology**. 2008; 109:122–125.

33. Abbas AE, Pibarot P. Hemodynamic characterization of aortic stenosis states. **Cathet Cardiovasc Interv**. 2019; 93:1002–1023.

34. Kadem L, Rieu R, Dumesnil JG, Durand LG, Pibarot P. Flow-dependent changes in Doppler-derived aortic valve effective orifice area are real and not due to artifact. **J Am Coll Cardiol**. 2006; 47:131–137.

35. Gilon D, Cape EG, Handschumacher MD, et al. Effect of three-dimensional valve shape on the hemodynamics of aortic stenosis: three-dimensional echocardiograpic stereolithography and patient studies. **J Am Coll Cardiol**. 2002; 40:1479–1486.

36. Weyman AE, Scherrer-Crosbie M. Aortic stenosis: physics and physiology–what do the numbers really mean? **Rev Cardiovasc Med**. 2005; 6:23–32.

37. Guzzetti E, Capoulade R, Tastet L, et al. Estimation of stroke volume and aortic valve area in patients with aortic stenosis: a comparison of echocardiography versus cardiovascular magnetic resonance. **J Am Soc Echocardiogr**. 2020; 33:953–963 e5.

38. Kilner PJ, Gatehouse PD, Firmin DN. Flow measurement by magnetic resonance: a unique asset worth optimising. **J Cardiovasc Magn Reson**. 2007; 9:723−728.

39. Nayak KS, Nielsen JF, Bernstein MA, et al. Cardiovascular magnetic resonance phase contrast imaging. **J Cardiovasc Magn Reson**. 2015; 17:71.

40. Lotz J, Meier C, Leppert A, Galanski M. Cardiovascular flow measurement with phase-contrast MR imaging: basic facts and implementation. **Radiographics**. 2002; 22:651−671.

41. Nayak KS, Nielsen J-F, Bernstein MA, et al. Cardiovascular magnetic resonance phase contrast imaging. **J Cardiovasc Magn Reson**. 2015; 17.

42. Caruthers SD, Lin SJ, Brown P, et al. Practical value of cardiac magnetic resonance imaging for clinical quantification of aortic valve stenosis: comparison with echocardiography. **Circulation**. 2003; 108:2236−2243.

43. Garcia J, Kadem L, Larose É, Clavel MA, Pibarot P. Comparison between cardiovascular magnetic resonance imaging and transthoracic Doppler echocardiography for the estimation of valve effective orifice area in patients with aortic stenosis. **J Cardiovasc Magn Reson**. 2011; 13:25.

44. Woldendorp K, Bannon PG, Grieve SM. Evaluation of aortic stenosis using cardiovascular magnetic resonance: a systematic review & meta-analysis. **J Cardiovasc Magn Reson**. 2020; 22:45.

45. Garcia J, Barker AJ, Markl M. The role of imaging of flow patterns by 4D flow MRI in aortic stenosis. **JACC Cardiovasc Imag**. 2019; 12:252−266.

46. Archer GT, Elhawaz A, Barker N, et al. Validation of four-dimensional flow cardiovascular magnetic resonance for aortic stenosis assessment. **Sci Rep**. 2020; 10:10569.

47. Jamalidinan F, Hassanabad AF, Francois CJ, Garcia J. Four-dimensional-flow magnetic resonance imaging of the aortic valve and thoracic aorta. **Radiol Clin N Am**. 2020; 58:753−763.

48. Bhuva AN, D'Silva A, Torlasco C, et al. Non-invasive assessment of ventriculo-arterial coupling using aortic wave intensity analysis combining central blood pressure and phase-contrast cardiovascular magnetic resonance. **Eur Heart J Cardiovasc Imag**. 2020; 21:805−813.

49. Capoulade R, Teoh JG, Bartko PE, et al. Relationship between proximal aorta morphology and progression rate of aortic stenosis. **J Am Soc Echocardiogr**. 2018; 31:561−569.e1.

50. Garcia D, Pibarot P, Dumesnil JG, Sakr F, Durand LG. Assessment of aortic valve stenosis severity: a new index based on the energy loss concept. **Circulation**. 2000; 101:765−771.

51. Baumgartner H, Steffenelli T, Niederberger J, Schima H, Maurer G. Overestimation of catheter gradients by Doppler ultrasound in patients with aortic stenosis: a predictable manifestation of pressure recovery. **J Am Coll Cardiol**. 1999; 33:1655−1661.

52. Garcia D, Dumesnil JG, Durand LG, Kadem L, Pibarot P. Discrepancies between catheter and Doppler estimates of valve effective orifice area can be predicted from the pressure recovery phenomenon: practical implications with regard to quantification of aortic stenosis severity. **J Am Coll Cardiol**. 2003; 41:435−442.

53. Gjertsson P, Caidahl K, Svensson G, Wallentin I, Bech-Hanssen O. Important pressure recovery in patients with aortic stenosis and high Doppler gradients. **Am J Cardiol**. 2001; 88:139−144.

54. Guzzetti E, Clavel MA, Pibarot P. Usefulness of the energy loss index in the adjudication of low-gradient aortic stenosis severity. **Eur Heart J Cardiovasc Imag**. 2020; 21:616−618.

55. Durko AP, Head SJ, Pibarot P, et al. Characteristics of surgical prosthetic heart valves and problems around labeling: a document from the European Association for Cardio-Thoracic Surgery (EACTS)-The Society of Thoracic Surgeons (STS)-American Association for Thoracic Surgery (AATS) valve labelling task force. **J Thorac Cardiovasc Surg**. 2019; 158:1041−1054.

56. Bahlmann E, Gerdts E, Cramariuc D, et al. Prognostic value of energy loss index in asymptomatic aortic stenosis. **Circulation**. 2013; 127:1149−1156.

57. Abbas AE, Mando R, Hanzel G, Goldstein J, Shannon F, Pibarot P. Hemodynamic principles of prosthetic aortic valve evaluation in the transcatheter aortic valve replacement era. **Echocardiography**. 2020; 37:738−757.

58. Abbas AE, Mando R, Hanzel G, et al. Invasive versus echocardiographic evaluation of transvalvular gradients immediately post-transcatheter aortic valve replacement. **Circ Cardiovasc Interv**. 2019; 12:e007973.

59. Abbas AE, Hanzel G, Shannon F, et al. Post-TAVR trans-aortic valve gradients: echocardiographic versus invasive measurements. **Struct Heart**. 2019; 3:348−350.

60. Kadem L, Dumesnil JG, Rieu R, Durand LG, Garcia D, Pibarot P. Impact of systemic hypertension on the assessment of aortic stenosis. **Heart**. 2005; 91:354−361.

61. Little SH, Chan KL, Burwash IG. Impact of blood pressure on the Doppler echocardiographic assessment of aortic stenosis severity. **Heart**. 2007; 93:848−855.

62. Eleid MF, Nishimura RA, Sorajja P, Borlaug BA. Systemic hypertension in low gradient severe aortic stenosis with preserved ejection fraction. **Circulation**. 2013; 128:1349−1353.

63. Pibarot P, Dumesnil JG. Improving assessment of aortic stenosis. **J Am Coll Cardiol**. 2012; 60:169−180.

64. Kadem L, Garcia D, Durand LG, Rieu R, Dumesnil JG, Pibarot P. Value and limitations of the peak-to-peak gradient for the evaluation of aortic stenosis. **J Heart Valve Dis**. 2006; 15:609−616.

65. Clavel MA, Messika-Zeitoun D, Pibarot P, et al. The complex nature of discordant severe calcified aortic valve disease grading: new insights from combined Doppler-echocardiographic and computed tomographic study. **J Am Coll Cardiol**. 2013; 62:2329−2338.

66. Tastet L, Capoulade R, Clavel MA, et al. Systolic hypertension and progression of aortic valve calcification in patients with aortic stenosis: results from the PROGRESSA study. **Eur Heart J Cardiovasc Imag**. 2017; 18:70−78.

67. le Polain de Waroux JB, Pouleur AC, Goffinet C, et al. Functional anatomy of aortic regurgitation: accuracy, prediction of surgical repairability, and outcome implications of transesophageal echocardiography. **Circulation**. 2007; 116:I264−I269.

68. Dweck MR, Boon NA, Newby DE. Calcific aortic stenosis: a disease of the valve and the myocardium. **J Am Coll Cardiol**. 2012; 60:1854−1863.

69. Treibel TA, Badiani S, Lloyd G, Moon JC. Multimodality imaging markers of adverse myocardial remodeling in aortic stenosis. **JACC Cardiovasc Imag**. 2019; 12:1532−1548.

70. Bing R, Everett RJ, Tuck C, et al. Rationale and design of the randomized, controlled early valve replacement guided by biomarkers of left ventricular decompensation in asymptomatic patients with severe aortic stenosis (EVOLVED) trial. **Am Heart J**. 2019; 212:91−100.

71. Pibarot P, Messika-Zeitoun D, Ben-Yehuda O, et al. Moderate aortic stenosis and heart failure with reduced ejection fraction: can imaging guide us to therapy? **JACC Cardiovasc Imag**. 2019; 12:172−184.

72. Rieck AE, Cramariuc D, Boman K, et al. Hypertension in aortic stenosis: implications for left ventricular structure and cardiovascular events. **Hypertension**. 2012; 60:90–97.

73. Chirinos JA, Akers SR, Schelbert E, et al. Arterial properties as determinants of left ventricular mass and fibrosis in severe aortic stenosis: findings from ACRIN PA 4008. **J Am Heart Assoc**. 2019; 8:e03742.

74. Antonini-Canterin F, Huang G, Cervesato E, et al. Symptomatic aortic stenosis: does systemic hypertension play an additional role? **Hypertension**. 2003; 41:1268–1272.

75. Capoulade R, Clavel MA, Mathieu P, et al. Impact of hypertension and renin-angiotensin system inhibitors in aortic stenosis. **Eur J Clin Invest**. 2013; 43:1262–1272.

76. Houriez-Gombaud-Saintonge S, Mousseaux E, Bargiotas I, et al. Comparison of different methods for the estimation of aortic pulse wave velocity from 4D flow cardiovascular magnetic resonance. **J Cardiovasc Magn Reson**. 2019; 21:75.

77. von Knobelsdorff-Brenkenhoff F, Karunaharamoorthy A, Trauzeddel RF, et al. Evaluation of aortic blood flow and wall shear stress in aortic stenosis and its association with left ventricular remodeling. **Circ Cardiovasc Imag**. 2016; 9:e004038.

78. Papanastasiou CA, Kokkinidis DG, Kampaktsis PN, et al. The prognostic role of late gadolinium enhancement in aortic stenosis: a systematic review and meta-analysis. **JACC Cardiovasc Imag**. 2020; 13:385–392.

79. Ternacle J, Krapf L, Mohty D, et al. Aortic stenosis and cardiac amyloidosis: JACC review topic of the week. **J Am Coll Cardiol**. 2019; 74:2638–2651.

80. Clavel MA, Magne J, Pibarot P. Low-gradient aortic stenosis. **Eur Heart J**. 2016; 37:2645–2657.

81. Migliore RA, Adaniya ME, Barranco M, et al. Ventricular-arterial coupling in severe aortic stenosis: relation with symptoms and heart failure. **Rev Argent Cardiol**. 2016; 84:304–309.

82. Pibarot P, Dumesnil JG. Low-flow, low-gradient aortic stenosis with normal and depressed left ventricular ejection fraction. **J Am Coll Cardiol**. 2012; 60:1845–1853.

83. Pawade T, Sheth T, Guzzetti E, Dweck MR, Clavel MA. Why and how to measure aortic valve calcification in patients with aortic stenosis. **JACC Cardiovasc Imag**. 2019; 12:1835–1848.

84. Clavel MA, Pibarot P, Messika-Zeitoun D, et al. Impact of aortic valve calcification, as measured by MDCT, on survival in patients with aortic stenosis: results of an international registry study. **J Am Coll Cardiol**. 2014; 64:1202–1213.

85. Pawade T, Clavel MA, Tribouilloy C, et al. Computed tomography aortic valve calcium scoring in patients with aortic stenosis. **Circ Cardiovasc Imag**. 2018; 11:e007146.

86. Baumgartner H, Falk V, Bax JJ, et al. 2017 ESC/EACTS guidelines for the management of valvular heart disease: the task force for the management of valvular heart disease of the European Society of Cardiology (ESC) and the European Association for Cardio-Thoracic Surgery (EACTS). **Eur Heart J**. 2017; 38:2739–2791.

87. Simard L, Côté N, Dagenais F, et al. Sex-related discordance between aortic valve calcification and hemodynamic severity of aortic stenosis: is valvular fibrosis the explanation? **Circ Res**. 2017; 120:681–691.

88. Yotti R, Bermejo J, Gutierrez-Ibanes E, et al. Systemic vascular load in calcific degenerative aortic valve stenosis: insight from percutaneous valve replacement. **J Am Coll Cardiol**. 2015; 65:423–433.

89. Lindman BR, Otto CM, Douglas PS, et al. Blood pressure and arterial load after transcatheter aortic valve replacement for aortic stenosis. **Circ Cardiovasc Imag**. 2017; 10.

90. Cramariuc D, Gerdts E, Segadal L. Impact of hypertension on left ventricular hypertrophy regression and exercise capacity in patients operated for aortic valve stenosis. **Scand Cardiovasc J**. 2006; 40:167–174.

91. Pibarot P, Salaun E, Dahou A, et al. Echocardiographic results of transcatheter versus surgical aortic valve replacement in low-risk patients: the PARTNER 3 trial. **Circulation**. 2020; 141:1527–1537.

This page intentionally left blank

Chapter 38

Arterial stiffness and atherosclerosis: mechanistic and pathophysiologic interactions

Kazuomi Kario[1,2]

[1]*Division of Cardiovascular Medicine, Department of Medicine, Jichi Medical University School of Medicine, Shimotsuke, Tochigi, Japan;* [2]*The Hypertension Cardiovascular Outcome Prevention and Evidence in Asia (HOPE Asia) Network, Tokyo, Japan*

Introduction

There are two common types of arterial disease: atherosclerosis triggered by endothelial damage and stiffness of the large arteries (which is linked to small artery remodeling). Atherosclerosis is primarily associated with, and promoted by, the presence of metabolic risk factors (e.g., dyslipidemia, diabetes mellitus),[1,2] whereas arterial stiffness is closely associated with aging and hypertension.[3] Large artery stiffness is an important contributor to atherosclerotic cardiovascular disease (CVD) and to microvascular disease, which in turn plays a role in renal and cerebrovascular disease.[4]

Vascular failure: interaction between atherosclerosis and arterial stiffness
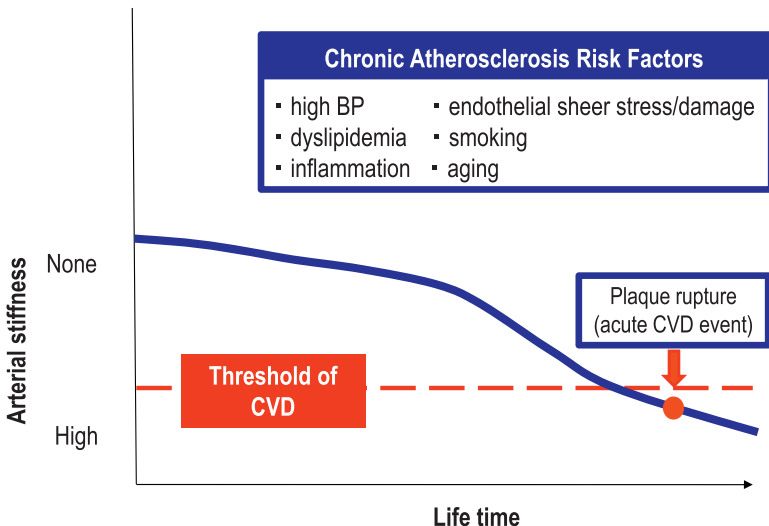
Progressive atherosclerosis is characterized by accumulation of inflammatory cells, lipids, fibrous elements, and calcification in the wall of larger arteries, resulting in progressive narrowing of the vessel lumen.[5,6] This narrowing reduces the ability of arteries to deliver oxygen-rich blood to important organs like the heart and brain. Endothelial dysfunction, which reflects the inability of the vascular endothelium to maintain homeostasis, plays a fundamental role in the development of atherosclerosis.[2,7–11]

A reduction in the ability of an artery to expand and contract in response to pressure changes is known as arterial stiffening.[5] This progressive phenomenon occurs as a result of the thickening and stiffening of the wall material (arteriosclerosis),[6,12,13] and is closely associated with age and hypertension.[3] From an early age, blood pressure (BP)-related stress on the arterial wall may initiate endothelial

cell damage that contributes to the atherosclerotic process (Fig. 38.1).[14] Thus, endothelial dysfunction might represent the first step in the pathophysiology of atherosclerosis, prior to the development of arterial stiffness.[15] However, endothelial dysfunction and arterial stiffness may develop simultaneously, or arterial stiffness may even occur before endothelial dysfunction.[15] At later stages (and older ages), the circumferential force of BP and resulting stretch of the arterial wall may trigger rupture of an atherosclerotic plaque or the arterial wall, resulting in the occurrence of an atherothrombotic CVD event (Fig. 38.1).[14]

Significant relationships between endothelial dysfunction and arterial stiffness have been reported in longitudinal studies.[16] A study of Japanese patients with treated hypertension found a significant association between endothelial dysfunction (based on flow-mediated vasodilatation of the brachial artery) and longitudinal progression of arterial stiffness (determined using brachial-ankle pulse wave velocity [baPWV]).[2] However, the potential mechanisms linking arterial stiffness and atherosclerosis have not been widely studied to date.[17] Increasing arterial stiffness is associated with increases in systolic BP (SBP) and pulse pressure. Higher SBP increases afterload leading to left ventricular (LV) hypertrophy, and lower diastolic BP (DBP) decreases coronary perfusion. Both of these effects contribute to myocardial ischemia and coronary atherosclerosis. Increased pulse pressure is associated with damage of the blood–brain barrier, contributing to cerebral atherosclerosis. In addition, arterial stiffness directly or indirectly contributes to vascular remodeling, progression of atheroma, endothelial dysfunction, accumulation of extracellular matrix, oxidative stress, and plaque rupture.[17] Furthermore, risk factors for atherosclerosis (e.g., hypertension, diabetes,

dyslipidemia, smoking, inflammation, etc.) are also risk factors for arterial stiffness, contributing to the high cardiovascular (CV) morbidity and mortality associated with these conditions.

Pulse wave velocity and atherosclerosis

Perhaps the most widely studied and most commonly used measure of arterial stiffness studied to date is pulse wave velocity (PWV).[18,19] This parameter reflects segmental arterial elasticity. Increasing arterial stiffness is associated with an increase in the propagation speed of the pulse wave generated by contraction of the left ventricle.[15] There are two approaches to evaluating PWV: carotid-femoral (cf) PWV (which is a measure of aortic stiffness) and baPWV (which provides an indication of stiffness in both the aorta and peripheral muscular arteries). PWV is determined to a large extent by BP and age, and is also influenced by genetics, CV risk factors, and the presence and extent of atherosclerosis.[20–29]

There is a large body of evidence for significant associations between PWV and the presence of atherosclerosis in coronary, cerebral, and carotid arteries.

In coronary arteries

In symptomatic patients, both cfPWV and baPWV have been significantly associated with the presence and severity of invasively assessed coronary artery disease (CAD).[23,30–37] Similar associations have been reported in patients with type 2 diabetes mellitus. In one of these studies, coronary plaques with unfavorable characteristics were more prevalent in asymptomatic patients with well-controlled type 2 diabetes compared with healthy controls. In addition, the presence of coronary plaques was significantly and independently associated with baseline cfPWV, independent of age, sex, diabetes, and BP.[38]

Studies of middle-aged adults without CAD reported a link between baPWV and atherosclerosis (based on the presence of coronary artery calcification).[21,39–42] These data highlight the potential for evaluation of arterial stiffness to identify the presence of subclinical atherosclerosis, facilitating early intervention to reduce the risk of atherosclerosis progressing to overt CAD, and prevent the clinical adverse events that occur in patients with symptomatic CAD.

In cerebral arteries

Data from population studies and patients with hypertension highlight a link between baPWV or cfPWV and the presence of cerebral small vessel disease, including cerebral microbleeds, white matter hyperintensity, or lacunar infarction.[25,43–48] These subclinical manifestations of cerebral atherosclerosis are common in older populations and are recognized as important risk factors for cognitive impairment and stroke.[49,50] PWV has also been associated with the longitudinal progression of cognitive decline in the elderly.[51,52]

In patients with ischemic stroke, it has been reported that baPWV is significantly correlated with calcification or stenosis of cerebral arteries.[53,54] In addition, baPWV increases the risk of cerebral infarction, above and beyond the risk associated with traditional risk factors, including hypertension, diabetes, dyslipidemia, and fasting blood glucose.[55] However, not all studies have reported these positive associations. One cross-sectional study of 66 patients with stroke found that baPWV was not independently associated with an increased risk of stroke, white matter hyperintensity, or cerebral microbleeds after adjustment for potential confounders (e.g., hypertension).[56] However, this was a small study, and the majority of currently available data support an association between PWV and cerebral atherosclerosis.

In the carotid artery

Intima-media thickness (IMT) in the carotid artery is generally considered an atherosclerotic marker, and has been associated with the occurrence of both stroke and CAD.[57,58] Carotid IMT has shown a positive linear correlation with cfPWV in general population studies,[59–62] and in patients with hypertension[63] or diabetes.[61] In addition, data from cross-sectional or longitudinal studies show an association between baPWV and increased carotid IMT or formation of atherosclerotic plaques in the carotid artery in community-based populations,[64,65] and in patients with hypertension,[66] cerebral artery thrombosis,[67] end-stage kidney disease,[68] or type 2 diabetes mellitus.[69] Again, the majority of data support a relationship between PWV and carotid atherosclerosis, but one study showed that only cfPWV (not baPWV) was significantly associated with carotid IMT in a general population.[59]

Cardio-ankle vascular index and atherosclerosis

The cardio-ankle vascular index (CAVI) is a newer measure that provides information on arterial stiffness from its origin at the aorta to the ankle.[70] There is a linear increase in CAVI with age[71–74] but, in contrast to PWV, CAVI is largely independent of BP.[70,75] Data from a study conducted in Japan showed a statistically significant positive correlation between IMT of the carotid artery and CAVI in patients with essential hypertension, suggesting that CAVI may be a useful marker for evaluating atherosclerosis in this patient group.[76] CAVI is also significantly associated with the degree of coronary artery calcification and stenosis in asymptomatic subjects,[77] and may therefore be useful as a screening tool to reveal the subclinical atherosclerotic burden in symptom-free individuals. It has been suggested that a CAVI of ≥ 8.0 might be associated with subclinical arterial stiffening and/or subclinical atherosclerosis, and CAVI ≥ 9.0 seems to be associated with an increased CV risk based on currently available data.[15] However, caution needs to be exercised when applying CAVI cutoff values in the general population due to a lack of longitudinal data from population-based studies.[15]

Support for an association between arterial stiffness determined using CAVI and atherosclerosis comes from the growing body of evidence highlighting the relationship between CAVI and future CV events.[78–84] In addition, CAVI appears to add value to the coronary artery calcium score for the assessment of future CVD risk.[78] Longitudinal assessment of CAVI showed that the incidence of CVD events over a mean 2.9 years of follow-up was significantly lower in patients/subjects/individuals who did versus did not show an improvement in CAVI over the first 6 months.[82]

Other arterial stiffness parameters

Several other parameters can provide data on arterial stiffness.[85] These include the beta stiffness index of the carotid artery evaluated by carotid ultrasound and aortic stiffness evaluated by magnetic resonance imaging (MRI). Increased arterial stiffness detected using these measures reflects an increase in both structural stiffness due to changes in the matrix (smooth muscle cell hypertrophy, increased collagen, decreased elastin, and fibrosis) and functional stiffness due to neurohumoral activation (activation of sympathetic nervous system, renin–angiotensin–aldosterone system, endothelin system, etc.). The stiffness parameter beta reflects arterial stiffness without the influence of BP,[86] and was used in the development of CAVI.

Another potential measurement that may be related to arterial stiffness is reflection magnitude (RM), which is defined as the ratio of the amplitude of the backward wave to that of the forward wave.[87–89] RM is determined by the structure and function of the total arterial tree, including the central aorta and peripheral arteries of different diameters. Rather than a stiffness index per se, pronounced wave reflections interact with high aortic stiffness (PWV) such that in the presence of a stiff aorta (high PWV), they increment LV afterload, whereas in the presence of an elastic aorta (low PWV), they increase coronary perfusion pressure. Wave RM has been shown to be a strong predictor of incident heart failure (HF) and CV events in prospective studies in older populations (which tend to have stiff aortas).[87,88]

Interaction between vascular disease and hemodynamic stress

The prognostic significance of arterial stiffness is likely to be due, at least in part, to the adverse hemodynamic effects associated with stiffened arteries, including increased systolic load and decreased myocardial perfusion pressure.[5] Increases in large artery stiffening with advancing age increase the pressure required to generate blood flow (known as characteristic impedance), resulting in impaired ventricular:vascular coupling.[90] This accounts for the marked increases in systolic pressure and pulse pressure as age increases, and the associated increase in ventricular load, which contributes to the development of HF, especially HF with preserved ejection fraction.[91–94]

Hemodynamic factors influence several aspects of vascular physiology and play an important role in vascular homeostasis, meaning that they contribute to the development of vascular pathologies, including atherosclerosis.[95] Local flow hemodynamics (e.g., endothelial sheer stress) and inflammatory mechanisms both contribute to localized alterations in the endothelium that progress to atherosclerosis.[96] The preferential localization of atherosclerotic plaques at branches and sharp bends in the arterial system is indicative of an important role for hemodynamics in the development of atherosclerosis.[97]

By definition, BP is associated with cyclic physical stress on the CV system, including continuous vertical

physical force on arterial walls.[98] The shape of the pulse wave changes based on cardiac function and vascular tone and differs between central and peripheral arterial sites.[98] Exaggerated BP surges place strain on the CV system, especially in the presence of stiffened arteries. The synchronization of a variety of BP surges with different time phases and triggers (resonance hypothesis of BP surge)[99] is likely to be particularly problematic in terms of increasing hemodynamic stress and impact on atherosclerotic vessels, and is a potential mechanism for triggering of CV events.[85] Exaggerated BP surges occur more frequently in the morning compared with other times of the day because baroreflex sensitivity is reduced in the morning due to increased central sympathetic activation at this time.[85]

SHATS: a proposed novel clinical entity

The term systemic hemodynamic atherothrombotic syndrome (SHATS) has been proposed to describe an age-related and synergistic vicious cycle of hemodynamic stress and vascular disease (Fig. 38.2).[85,100,101] A synergistic combination of different forms of BP variability (BPV) and hemodynamic stress related to vascular disease forms the basis of the SHATS concept. This approach also separates the role of physical hemodynamic stress from other CV risk factors (e.g., hyperglycemia, dyslipidemia, and inflammatory processes.).[101]

The clinical manifestations of SHATS including common CV conditions such as stroke, CAD, and HF; small artery disease and microvascular disease–related conditions such as dementia, chronic kidney disease (CKD), and retinopathy are also closely linked with SHATS (Fig. 38.3).

Mechanisms and evidence

BP variability

Increasing arterial stiffness due to aging and in the presence of hypertension is closely associated with BPV, including
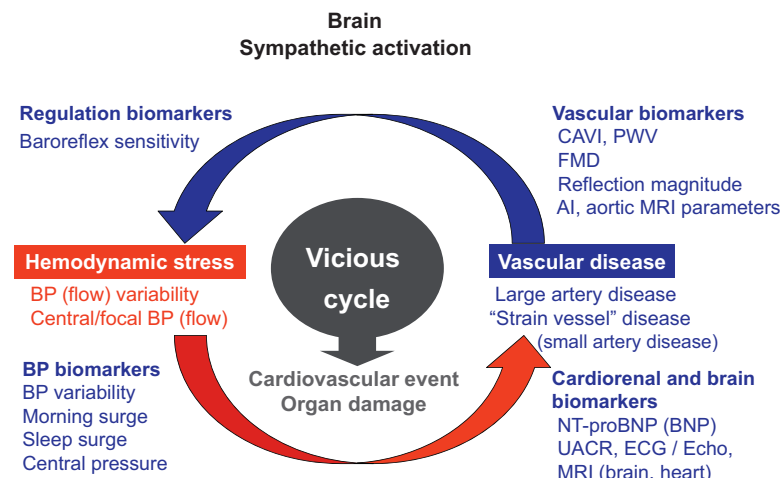
the morning BP surge.[102] Variability in BP is seen across a variety of timeframes (beat-by-beat, diurnal, day-by-day, visit-to-visit, and yearly). BP also varies based on different environmental stimuli (e.g., temperature, humidity, light level, etc.) and by season (being higher in winter and lower in summer).[103] BPV increases with increasing age, and although most forms are related, the magnitude of variability differs between individuals.[104–107] Growing evidence suggests that each type of BPV is associated with organ damage and CVD.[103,106–108] The synergistic resonance hypothesis suggests that various forms of BPV could coincide to generate a large dynamic surge in BP, which in turn would trigger CV events, especially in high-risk patients with arterial stiffening (Fig. 38.4).[99,109]
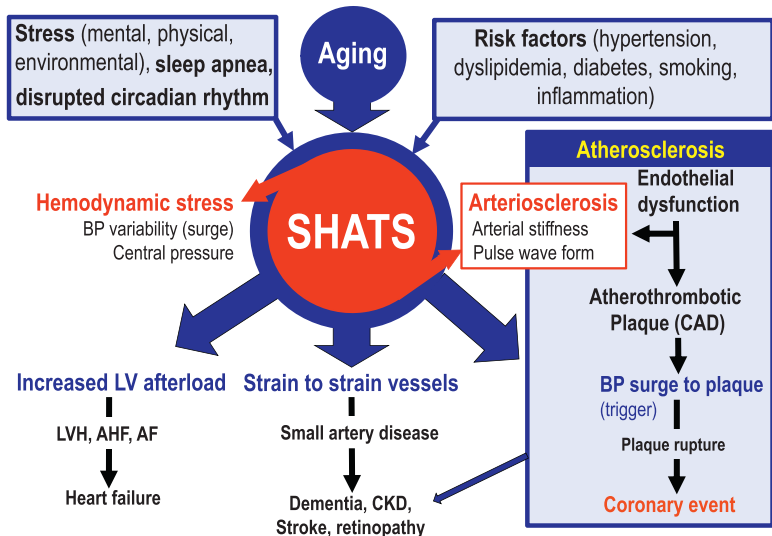
Hemodynamic factors

The hemodynamic stress of SHATS refers to the combination of BP-related circumferential stress and blood flow–related shear stress. This means that BP is the most important hemodynamic component of SHATS.[100] BP represents the continuous physical force transmitted to cardiac and arterial walls by cyclic cardiac contractions. Even when SBP and DBP values are the same, there may be different continuous waveform shapes in each cycle that produce different stress on the CV system. Cardiac function and vascular tone influence the shape of pressure waveforms, and differ based on location of atherosclerotic plaques (e.g., central CV system or peripheral sites).
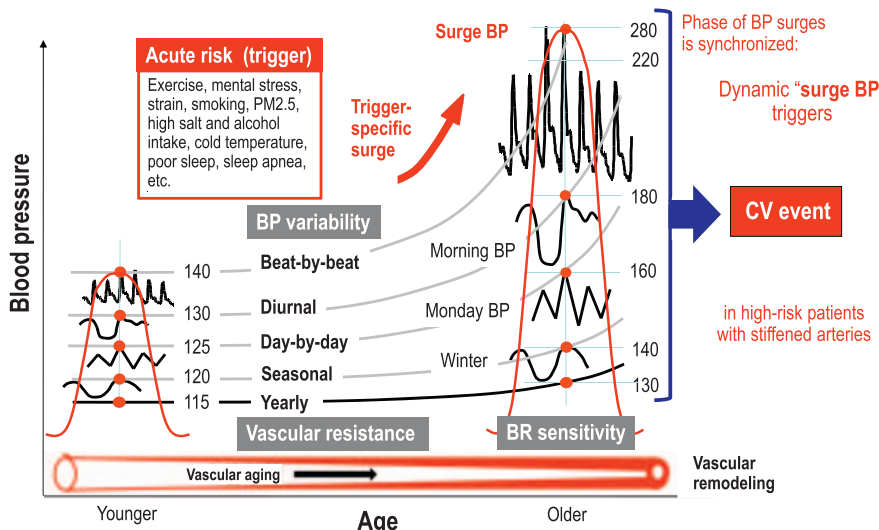
SHATS is characterized by increased LV afterload via high aortic stiffness and a reduced transit time of reflected pulse waves. Therefore, reflected waves arrive at the heart in systole, while the left ventricle is ejecting blood, increasing late systolic LV afterload. Increased LV afterload, particularly late systolic load from wave reflections, promotes chronic LV hypertrophy,[110,111] diastolic dysfunction,[112–114] and atrial dysfunction,[115] and is associated with an increased risk of HF.[87,116] Acutely elevated

FIGURE 38.2 Systemic hemodynamic atherothrombotic syndrome (SHATS)—acceleration of the risk of cardiovascular events and organ damage via a vicious cycle of hemodynamic stress and vascular disease. *AI*, augmentation index; *BP*, blood pressure; *CAVI*, cardio-ankle vascular index; *ECG*, electrocardiography; *Echo*, echocardiography; *FMD*, flow-medicated dilatation; *MRI*, magnetic resonance imaging; *NT-proBNP*, N-terminal pro-brain natriuretic peptide; *PWV*, pulse wave velocity; *UACR*, urinary albumin/creatinine ratio. *Reproduced, with permission, from Kario K, Chirinos JA, Townsend RR, et al. Systemic hemodynamic atherothrombotic syndrome (SHATS) - coupling vascular disease and blood pressure variability: proposed concept from Pulse of Asia.* **Prog Cardiovasc Dis**. *2020;63(1):22–32.*

**Brain
Sympathetic activation**

Regulation biomarkers
Baroreflex sensitivity

Vascular biomarkers
CAVI, PWV
FMD
Reflection magnitude
AI, aortic MRI parameters

Hemodynamic stress
BP (flow) variability
Central/focal BP (flow)

Vicious cycle

Vascular disease
Large artery disease
"Strain vessel" disease
(small artery disease)

**Cardiovascular event
Organ damage**

BP biomarkers
BP variability
Morning surge
Sleep surge
Central pressure

Cardiorenal and brain biomarkers
NT-proBNP (BNP)
UACR, ECG / Echo,
MRI (brain, heart)

FIGURE 38.3   Relationships between the systemic hemodynamic atherothrombotic syndrome (SHATS) and cardiovascular events. Hemodynamic stress, atherosclerosis, and arterial stiffness combine to form a vicious cycle driving the development of cardiovascular disease. *AHF*, acute heart failure; *AF*, atrial fibrillation; *BP*, blood pressure; *CAD*, coronary artery disease; *CKD*, chronic kidney disease; *LV*, left ventricle; *LVH*, left ventricular hypertrophy. *Adapted, with permission, from Kario K, Chirinos JA, Townsend RR, et al. Systemic hemodynamic atherothrombotic syndrome (SHATS) - coupling vascular disease and blood pressure variability: proposed concept from Pulse of Asia.* **Prog Cardiovasc Dis**. *2020;63(1):22−32.*

FIGURE 38.4   Resonance hypothesis of surge blood pressure (BP) to trigger cardiovascular (CV) events. Dynamic surge BP is produced by the synchronized resonance of a variety of different BP surges, each with different time phase. *BR*, baroreflex; *PM2.5*, particulate matter 2.5 μm or less in diameter. *Reproduced, with permission from Kario.* **Am J Hypertens**. *2016;29:14−16.*

LV afterload secondary to exaggerated BP surges increases LV pressure and may contribute to triggering acute HF in high-risk patients with stiff arteries and LV hypertrophy.

Systemic BP-dependent hemodynamic stress affects the microcirculation, and could therefore contribute to age-related microcirculatory disease, including white matter disease (predisposing to dementia, depression, and falls in the elderly),[117,118] cardiac diseases such as microvascular angina and HF with preserved ejection fraction,[119] and CKD.[120]

Vascular component

Large arterial atherosclerosis with arterial stiffness is the central vascular component of SHATS. Stiffened conduit arteries (e.g., the aorta) do not properly absorb the power of the pulse (BP surge), and this is therefore transmitted to peripheral atherothrombotic plaques, resulting in plaque rupture and triggering atherothrombotic events such as myocardial infarction and stroke.

Microvascular disease in strain vessels also plays a key role in SHATs. Even in the absence of a large artery atherosclerotic plaque, exaggerated BP surge that is not absorbed at the conduit arteries is transmitted to small arteries anatomically exposed to high pressure that must maintain strong vascular tone in order to dampen the penetration of large pressure gradients from large arteries to the capillaries (known as strain vessels).[121] The higher wall strain on these strain vessels is partly due to their size, stiffness, and maladaptive remodeling, and from branching at a right angle from relatively larger arteries. Stiffness in

larger arteries influences the burden on strain vessels, meaning that focal pressure on the proximal portion of a strain vessel is higher when large artery stiffness is increased. Silent cerebral infarct (SCI) and clinical cerebral hemorrhage and infarction occur most often in the area of small perforating arteries (e.g., the lenticulostriate and paramedian pontine arteries) and are particularly common in elderly patients with hypertension. SCI (especially multiple SCIs), detected using brain MRI, are more prevalent in patients with versus without an exaggerated morning BP surge.[122] Burden on strain vessels also occurs in the glomerular afferent arterioles of juxtamedullary nephrons—the nearer the large artery (arcuate artery), the greater the pressure overload in afferent arterioles of the glomeruli.[121] The filtration of albumin into the urinary space is higher in the "deep" glomeruli, those nearest the arcuate arteries of the outer medulla.[121]

Role in organ damage and cardiovascular events

Even in patients without clinically overt atherosclerotic CVD events and small artery disease, small artery remodeling impairs autoregulation of blood flow to the microcirculation and organs. There is evidence that SHATS makes an important contribution to increasing the risk of CVD events or organ damage. For example, in elderly patients, increased office BPV and arterial stiffness (based on PWV and/or stiffness of the carotid artery) had a synergistic negative effect on cognitive function.[123] In the Japan Morning Surge-1 study on the effect of alpha blockade on urinary albumin excretion in 404 elderly patients with hypertension, albuminuria was significantly reduced when home BP decreased.[124] In addition, those with decreased PWV had a greater reduction in albuminuria than those with increased PWV.[124] This suggests that decreases in both BP and arterial stiffness are necessary to ameliorate organ damage.

In a recent study, SHATS was defined as simultaneous occurrence of target organ damage in the heart (LVH), carotid artery (IMT >0.9 mm and/or presence of a plaque in the common carotid artery), and the kidney (based on estimated glomerular filtration rate). Subjects with versus without SHATS had a higher prevalence of "very stiff artery" (PWV >10 m/s; 84.9 vs. 64.3%, $P < .01$) and used more antihypertensive medications.[125] For a similar level of office BP, patients with SHATS had higher 24-hour SBP and DBP, smaller nighttime SBP fall, and a twofold higher prevalence of the riser pattern of nocturnal BP (48.2 vs. 20.2%, $P < .001$) compared to those without SHATS. "Very stiff artery" and abnormal BPV were significant, independent, and strong predictors of SHATS.[125]

One of the key components of SHATS, arterial stiffness, appears to play an important role in the development of structural heart disease, including LV diastolic dysfunction,[126−128] LV hypertrophy,[129] and left atrial enlargement.[130−132] Hypertension, another important factor in SHATS, is also a risk factor for structural heart disease, especially LV hypertrophy as a marker of cardiac damage.[133]

Proposed diagnostic score

The SHATS concept provides the opportunity to assess BPV and arterial disease as a strategy to identify changes and intervene early to ameliorate progression to hypertension in younger patients or to end-organ damage and CVD events in older patients. However, there is currently no consensus on how to define or diagnose the severity of SHATS. The first step toward achieving this was the development of a proposed SHATS score[134] based on the above data suggesting that BP, hemodynamic alterations, and vascular disease play a central role in the vicious cycle of events that accelerates organ damage and triggers CVD events. The overall score includes a BP score and a vascular score, which are multiplied to calculate the SHATS score.[134] This reflects the synergistic effects of BP/BPV and vascular disease on organ damage and CVD events.

The BP score includes the following measures: office, home, and ambulatory SBP and systolic BPV, and/or the presence of atrial fibrillation (seen as the extreme manifestation of complete hemodynamic variability of BP and blood flow).[134] The inclusion of BPV measures reflects the significant associations reported between these measures and CVD risk, independent of average office BP.[135−138]

The vascular score depends on the presence of clinically overt CVD, asymptomatic CVD based on test of arterial structure or function, and/or microvascular disease. Clinically overt CVD includes stroke, CAD, HF, aortic stenosis, cognitive dysfunction, and both symptomatic and asymptomatic peripheral artery disease/aortic dissection.[134] The number of these conditions present is used to determine the CVD score, while the number of abnormal vascular test findings is used to calculate the asymptomatic CVD score. The following five components are determined to inform the vascular score: pulse pressure, ankle-brachial index or the presence of carotid plaque; arterial stiffness based on CAVI, baPWV, or cfPWV), abnormal cardiac findings (e.g., LV hypertrophy determined using echocardiography or elevated N-terminal probrain natriuretic peptide level); and other abnormalities such as reduced flow-mediated dilatation of the brachial artery, renal artery stenosis, or white matter lesion, SCI or microbleeds assessed by brain MRI. The microvascular disease score includes the presence of diabetes-related CKD and/or small artery retinopathy.

Minimum requirements to calculate the SHATS score are the following tests used in clinical practice: 1) Measurement of office BP; 2) Measurement of out-of-office (home or ambulatory) BP; 3) Measurement of large artery stiffness (using CAVI, cfPWV, or baPWV); 4) A basic cardiac evaluation (ECG); and 5) Blood (glucose, creatinine) and urine (albuminuria/proteinuria) analysis.[134]

The SHATS score has been developed with the goal of improving individualized patient management to prevent CV events. However, it requires validation before widespread use in clinical practice can be recommended.

Potential treatment strategies

To obtain the greatest benefit, the goal would be to detect and reduce the risk of SHATS in its early phase. SHATS precedes hypertension in younger adults and therefore earlier detection of SHATS and lifestyle modification before the development of HTN is important for the prevention of future CVD. In older patients with advanced SHATS, surge BP could trigger CVD events. Therefore, more strict control of BP and returning BPV to a normal circadian rhythm (including suppression exaggerated BP surge) should contribute to the prevention of CVD events.

Strategies to reduce the risk of SHATS should concentrate on preventing or interrupting the synergistic vicious cycle involving BPV and vascular disease. There is a range of international guidelines to inform evidence-based approaches to reducing high BP.[139−145] In addition to reducing BP levels, maintenance/restoration of adequate dipping status of nocturnal BP, and reducing exaggerated BP surge(s) are important components of achieving "perfect 24-hour BP control."[14] Morning home BP is closely associated with CVD (including both stroke and CAD),[146] especially in those with high CVD risk,[147] and therefore is an important target in managing SHATS. Achieving 24-hour BP control with well-controlled morning BP requires the use of long-acting antihypertensive agents, use of split or bedtime drug dosing, and/or combination therapy.[148] Inclusion of a long-acting calcium channel blocker would be useful because this reduces BPV.[149,150] In addition, the combination of a long-acting calcium channel blocker and an angiotensin receptor blocker has been shown to effectively reduce PWV as well as ambulatory and home BPV.[151] For patients with both hypertension and diabetes, treatment with a sodium−glucose co-transporter-2 (SGLT2) inhibitor effectively reduces morning and 24-hour BP, regardless of baseline glucose control status.[152] In addition, renal denervation may reduce 24-hour BP, including nighttime and morning BP.[153] However, the efficacy of renal denervation remains unclear and requires further study.

In contrast to the well-documented approaches to managing hypertension, there are currently no specific pharmacologic approaches to improve subclinical vascular disease (particularly large artery stiffening). However, a strategy that involves management of multiple risk factors and interventions based on current evidence-based therapies (such as statins and glucose-lowering drugs that reduce the risk of atherosclerotic CVD [e.g., glucagon-like peptide 1 agonist] and/or HF [e.g., SGLT2 inhibitors] in diabetes) may attenuate the progression of SHATS. There is not yet any specific evidence for use of antiplatelets and/or anticoagulants in SHATS, but data from the use of these agents for the primary or secondary prevention of CVD events in high-risk individuals based on standard clinical risk factors suggest that they may have a role in SHATS. However, a substantial proportion of the current burden of CVD may not be attributable to these standard CVD risk factors. Evolution of knowledge around the phenotyping of SHATS will require the design and implementation of new trials to assess the potential benefits of targeting early-stage, asymptomatic vascular disease, even when clinical factors might not suggest the need for intervention. In addition, the search for specific strategies that reduce large artery stiffening with age should be aggressively pursued.

Conclusion

There is a rapidly growing body of evidence for interactions between arterial stiffness, atherosclerosis, and hemodynamics as important contributors to CVD and cerebrovascular events. The SHATS syndrome combines these three important pathologies and provides a mechanistic link between arterial stiffness and CVD events. Evaluation of SHATS offers the possibility of early intervention to reduce CV risk and the occurrence of outcome events such as stroke and CAD. However, it remains to be determined whether assessment and monitoring of vascular failure (including arterial stiffness and vascular disease such as atherosclerosis) and early intervention based on this information will facilitate improvements in CV prognosis. This needs to be investigated in appropriately designed randomized clinical trials, and the resulting data used to inform future treatment approaches and evidence-based guidelines.

Acknowledgments

References

1. Kabutoya T, Hoshide S, Ogata Y, Iwata T, Eguchi K, Kario K. The time course of flow-mediated vasodilation and endothelial dysfunction in patients with a cardiovascular risk factor. **J Am Soc Hypertens**. 2012; 6(2):109−116.
2. Tomiyama H, Ishizu T, Kohro T, et al. Longitudinal association among endothelial function, arterial stiffness and subclinical organ damage in hypertension. **Int J Cardiol**. 2018; 253:161−166.

3. Laurent S, Boutouyrie P. The structural factor of hypertension: large and small artery alterations. **Circ Res**. 2015; 116(6):1007−1021.

4. Chirinos JA. Large artery stiffness, microvascular function, and cardiovascular risk. **Circ Cardiovasc Imag**. 2016; 9(12).

5. Cecelja M, Chowienczyk P. Role of arterial stiffness in cardiovascular disease. **JRSM Cardiovasc Dis**. 2012; 1(4).

6. Lusis AJ. Atherosclerosis. **Nature**. 2000; 407(6801):233−241.

7. Widlansky ME, Gokce N, Keaney Jr JF, Vita JA. The clinical implications of endothelial dysfunction. **J Am Coll Cardiol**. 2003; 42(7):1149−1160.

8. Landmesser U, Hornig B, Drexler H. Endothelial function: a critical determinant in atherosclerosis? **Circulation**. 2004; 109(21 Suppl 1):Ii27−33.

9. Bonetti PO, Lerman LO, Lerman A. Endothelial dysfunction: a marker of atherosclerotic risk. **Arterioscler Thromb Vasc Biol**. 2003; 23(2):168−175.

10. Stary HC, Chandler AB, Dinsmore RE, et al. A definition of advanced types of atherosclerotic lesions and a histological classification of atherosclerosis. A report from the Committee on Vascular Lesions of the Council on Arteriosclerosis, American Heart Association. **Arterioscler Thromb Vasc Biol**. 1995; 15(9):1512−1531.

11. Deanfield JE, Halcox JP, Rabelink TJ. Endothelial function and dysfunction: testing and clinical relevance. **Circulation**. 2007; 115(10):1285−1295.

12. Lee HY, Oh BH. Aging and arterial stiffness. **Circ J**. 2010; 74(11):2257−2262.

13. Cavalcante JL, Lima JA, Redheuil A, Al-Mallah MH. Aortic stiffness: current understanding and future directions. **J Am Coll Cardiol**. 2011; 57(14):1511−1522.

14. Kario K. **Essential Manual on Perfect 24-hour Blood Pressure Management from Morning to Nocturnal Hypertension: Up-to-Date for Anticipation Medicine**. Japan: Wiley Publishing; 2018.

15. Tanaka A, Tomiyama H, Maruhashi T, et al. Physiological diagnostic criteria for vascular failure. **Hypertension**. 2018; 72(5):1060−1071.

16. Roca F, Iacob M, Remy-Jouet I, Bellien J, Joannides R. Evidence for a role of vascular endothelium in the control of arterial wall viscosity in humans. **Hypertension**. 2018; 71(1):143−150.

17. Kim HL, Kim SH. Pulse wave velocity in atherosclerosis. **Front Cardiovasc Med**. 2019; 6:41.

18. O'Rourke MF, O'Brien C, Edelman ER. Arterial stiffening in perspective: advances in physical and physiological science over centuries. **Am J Hypertens**. 2016; 29(7):785−791.

19. Townsend RR, Wilkinson IB, Schiffrin EL, et al. Recommendations for improving and standardizing vascular research on arterial stiffness: a scientific statement from the American Heart Association. **Hypertension**. 2015; 66(3):698−722.

20. Vlachopoulos C, Xaplanteris P, Aboyans V, et al. The role of vascular biomarkers for primary and secondary prevention. A position paper from the European Society of Cardiology Working Group on peripheral circulation: endorsed by the Association for Research into Arterial Structure and Physiology (Artery) Society. **Atherosclerosis**. 2015; 241(2):507−532.

21. Nam HJ, Jung IH, Kim J, et al. Association between brachial-ankle pulse wave velocity and occult coronary artery disease detected by multidetector computed tomography. **Int J Cardiol**. 2012; 157(2):227−232.

22. Matsumoto M, Inoue K, Moriki A. Associations of brachial-ankle pulse wave velocity and carotid atherosclerotic lesions with silent cerebral lesions. **Hypertens Res**. 2007; 30(9):767−773.

23. Kim JH, Rhee MY, Kim YS, et al. Brachial-ankle pulse wave velocity for the prediction of the presence and severity of coronary artery disease. **Clin Exp Hypertens**. 2014; 36(6):404−409.

24. Imanishi R, Seto S, Toda G, et al. High brachial-ankle pulse wave velocity is an independent predictor of the presence of coronary artery disease in men. **Hypertens Res**. 2004; 27(2):71−78.

25. Ochi N, Tabara Y, Igase M, et al. Silent cerebral microbleeds associated with arterial stiffness in an apparently healthy subject. **Hypertens Res**. 2009; 32(4):255−260.

26. Saji N, Kimura K, Shimizu H, Kita Y. Association between silent brain infarct and arterial stiffness indicated by brachial-ankle pulse wave velocity. **Intern Med**. 2012; 51(9):1003−1008.

27. Terentes-Printzios D, Vlachopoulos C, Xaplanteris P, et al. Cardiovascular risk factors accelerate progression of vascular aging in the general population: results from the CRAVE study (cardiovascular risk factors affecting vascular age). **Hypertension**. 2017; 70(5):1057−1064.

28. van Popele NM, Mattace-Raso FU, Vliegenthart R, et al. Aortic stiffness is associated with atherosclerosis of the coronary arteries in older adults: the Rotterdam study. **J Hypertens**. 2006; 24(12):2371−2376.

29. Cecelja M, Jiang B, Keehn L, et al. Arterial stiffening is a heritable trait associated with arterial dilation but not wall thickening: a longitudinal study in the twins UK cohort. **Eur Heart J**. 2018; 39(24):2282−2288.

30. Chae MJ, Jung IH, Jang DH, et al. The brachial ankle pulse wave velocity is associated with the presence of significant coronary artery disease but not the extent. **Korean Circ J**. 2013; 43(4):239−245.

31. Chiha J, Mitchell P, Gopinath B, et al. Prediction of coronary artery disease extent and severity using pulse wave velocity. **PloS One**. 2016; 11(12):e0168598.

32. Chung CM, Yang TY, Lin YS, et al. Relation of arterial stiffness assessed by brachial-ankle pulse wave velocity to complexity of coronary artery disease. **Am J Med Sci**. 2014; 348(4):294−299.

33. Duman OO, Goldeli O, Gursul E, Baris N, Ozpelit E, Simsek MA. The value of aortic pulse wave velocity in predicting coronary artery disease diagnosis and severity. **Acta Cardiol**. 2015; 70(3):315−322.

34. Hofmann B, Riemer M, Erbs C, et al. Carotid to femoral pulse wave velocity reflects the extent of coronary artery disease. **J Clin Hypertens**. 2014; 16(9):629−633.

35. Xiong Z, Zhu C, Zheng Z, et al. Relationship between arterial stiffness assessed by brachial-ankle pulse wave velocity and coronary artery disease severity assessed by the SYNTAX score. **J Atherosclerosis Thromb**. 2012; 19(11):970−976.

36. Bechlioulis A, Vakalis K, Naka KK, et al. Increased aortic pulse wave velocity is associated with the presence of angiographic coronary artery disease in overweight and obese patients. **Am J Hypertens**. 2013; 26(2):265−270.

37. Kim HL, Jin KN, Seo JB, et al. The association of brachial-ankle pulse wave velocity with coronary artery disease evaluated by coronary computed tomography angiography. **PloS One**. 2015; 10(4):e0123164.

38. Funck KL, Laugesen E, Ovrehus K, et al. Increased high-risk coronary plaque burden is associated with arterial stiffness in patients with type 2 diabetes without clinical signs of coronary artery disease: a computed tomography angiography study. **J Hypertens**. 2017; 35(6):1235−1243.

39. Torii S, Arima H, Ohkubo T, et al. Association between pulse wave velocity and coronary artery calcification in Japanese men. **J Atherosclerosis Thromb**. 2015; 22(12):1266−1277.

40. Vishnu A, Choo J, Wilcox B, et al. Brachial-ankle pulse wave velocity is associated with coronary calcification among 1131 healthy middle-aged men. **Int J Cardiol**. 2015; 189:67−72.

41. Lee JY, Ryu S, Lee SH, et al. Association between brachial-ankle pulse wave velocity and progression of coronary artery calcium: a prospective cohort study. **Cardiovasc Diabetol**. 2015; 14:147.

42. Cainzos-Achirica M, Rampal S, Chang Y, et al. Brachial-ankle pulse wave velocity is associated with coronary calcium in young and middle-aged asymptomatic adults: the Kangbuk Samsung health study. **Atherosclerosis**. 2015; 241(2):350−356.

43. Brandts A, van Elderen SG, Westenberg JJ, et al. Association of aortic arch pulse wave velocity with left ventricular mass and lacunar brain infarcts in hypertensive patients: assessment with MR imaging. **Radiology**. 2009; 253(3):681−688.

44. Henskens LH, Kroon AA, van Oostenbrugge RJ, et al. Increased aortic pulse wave velocity is associated with silent cerebral small-vessel disease in hypertensive patients. **Hypertension**. 2008; 52(6):1120−1126.

45. King KS, Chen KX, Hulsey KM, et al. White matter hyper-intensities: use of aortic arch pulse wave velocity to predict volume independent of other cardiovascular risk factors. **Radiology**. 2013; 267(3):709−717.

46. Rosano C, Watson N, Chang Y, et al. Aortic pulse wave velocity predicts focal white matter hyperintensities in a biracial cohort of older adults. **Hypertension**. 2013; 61(1):160−165.

47. Zhai FF, Ye YC, Chen SY, et al. Arterial stiffness and cerebral small vessel disease. **Front Neurol**. 2018; 9:723.

48. Zhang J, Li Y, Wang Y, et al. Arterial stiffness and asymptomatic intracranial large arterial stenosis and calcification in hypertensive Chinese. **Am J Hypertens**. 2011; 24(3):304−309.

49. Pantoni L. Cerebral small vessel disease: from pathogenesis and clinical characteristics to therapeutic challenges. **Lancet Neurol**. 2010; 9(7):689−701.

50. Wardlaw JM, Smith EE, Biessels GJ, et al. Neuroimaging standards for research into small vessel disease and its contribution to ageing and neurodegeneration. **Lancet Neurol**. 2013; 12(8):822−838.

51. Li X, Lyu P, Ren Y, An J, Dong Y. Arterial stiffness and cognitive impairment. **J Neurol Sci**. 2017; 380:1−10.

52. Taniguchi Y, Fujiwara Y, Nofuji Y, et al. Prospective study of arterial stiffness and subsequent cognitive decline among community-dwelling older Japanese. **J Epidemiol**. 2015; 25(9):592−599.

53. Kim J, Cha MJ, Lee DH, et al. The association between cerebral atherosclerosis and arterial stiffness in acute ischemic stroke. **Atherosclerosis**. 2011; 219(2):887−891.

54. Park KY, Kim YB, Moon HS, Suh BC, Chung PW. Association between cerebral arterial calcification and brachial-ankle pulse wave velocity in patients with acute ischemic stroke. **Eur Neurol**. 2009; 61(6):364−370.

55. Yokokawa H, Goto A, Watanabe K, Yasumura S. Evaluation of atherosclerosis-associated factors and pulse wave velocity for predicting cerebral infarction: a hospital-based, case-control study in Japan. **Intern Med J**. 2007; 37(3):161−167.

56. Choi JC, Lee JS, Kang SY, Kang JH, Bae JM, Lee DH. Limitation of brachial-ankle pulse wave velocity in assessing the risk of stroke: importance of instantaneous blood pressure. **Cerebrovasc Dis**. 2009; 27(5):417−425.

57. Nambi V, Chambless L, Folsom AR, et al. Carotid intima-media thickness and presence or absence of plaque improves prediction of coronary heart disease risk: the ARIC (Atherosclerosis Risk in Communities) study. **J Am Coll Cardiol**. 2010; 55(15):1600−1607.

58. O'Leary DH, Polak JF, Kronmal RA, Manolio TA, Burke GL, Wolfson Jr SK. Carotid-artery intima and media thickness as a risk factor for myocardial infarction and stroke in older adults. Cardiovascular Health Study Collaborative Research Group. **N Engl J Med**. 1999; 340(1):14−22.

59. Lu Y, Zhu M, Bai B, et al. Comparison of carotid-femoral and brachial-ankle pulse-wave velocity in association with target organ damage in the community-dwelling elderly Chinese: the Northern Shanghai study. **J Am Heart Assoc**. 2017; 6(2).

60. Shen L, Wu W, You B, Gao H, Wang C, Liu Y. Relationship between pulse wave velocity and carotid atherosclerosis in geriatric people. **Cerebrovasc Dis**. 2011; 32(Suppl 1):16−20.

61. Taniwaki H, Kawagishi T, Emoto M, et al. Correlation between the intima-media thickness of the carotid artery and aortic pulse-wave velocity in patients with type 2 diabetes. Vessel wall properties in type 2 diabetes. **Diabetes Care**. 1999; 22(11):1851−1857.

62. Zureik M, Temmar M, Adamopoulos C, et al. Carotid plaques, but not common carotid intima-media thickness, are independently associated with aortic stiffness. **J Hypertens**. 2002; 20(1):85−93.

63. Sumbul HE, Koc AS, Demirtas D. Increased carotid-femoral pulse wave velocity and common carotid artery intima-media thickness obtained to assess target organ damage in hypertensive patients are closely related. **Clin Exp Hypertens**. 2019; 41(5):466−473.

64. Joo HJ, Cho SA, Cho JY, et al. Brachial-ankle pulse wave velocity is associated with composite carotid and coronary atherosclerosis in a middle-aged asymptomatic population. **J Atherosclerosis Thromb**. 2016; 23(9):1033−1046.

65. Yang Y, Fan F, Kou M, et al. Brachial-ankle pulse wave velocity is associated with the risk of new carotid plaque formation: data from a Chinese community-based cohort. **Sci Rep**. 2018; 8(1):7037.

66. Zhao XX, Liu J, Zhao H, Zhou Y, Li L, Wang H. The effect of cardiovascular risk factors on the carotid intima-media thickness in an old-aged cohort with hypertension: a longitudinal evolution with 4-year follow-up of a random clinical trial. **Clin Exp Hypertens**. 2019; 41(1):49−57.

67. Tomonori T, Keiko S, Shinkichi H, Yoji N, Akira T. Carotid atherosclerosis and arterial peripheral pulse wave velocity in cerebral thrombosis. **J Clin Neurosci**. 2006; 13(1):45−49.

68. Munakata M, Sakuraba J, Tayama J, et al. Higher brachial-ankle pulse wave velocity is associated with more advanced carotid atherosclerosis in end-stage renal disease. **Hypertens Res**. 2005; 28(1):9−14.

69. Masugata H, Senda S, Yoshikawa K, et al. Relationships between echocardiographic findings, pulse wave velocity, and carotid atherosclerosis in type 2 diabetic patients. **Hypertens Res**. 2005; 28(12):965−971.

70. Shirai K, Utino J, Otsuka K, Takata M. A novel blood pressure-independent arterial wall stiffness parameter; cardio-ankle vascular index (CAVI). **J Atherosclerosis Thromb**. 2006; 13(2):101−107.

71. Takaki A, Ogawa H, Wakeyama T, et al. Cardio-ankle vascular index is a new noninvasive parameter of arterial stiffness. **Circ J**. 2007; 71(11):1710−1714.

72. Namekata T, Suzuki K, Ishizuka N, Shirai K. Establishing baseline criteria of cardio-ankle vascular index as a new indicator of arteriosclerosis: a cross-sectional study. **BMC Cardiovasc Disord**. 2011; 11:51.

73. Choi SY, Oh BH, Bae Park J, Choi DJ, Rhee MY, Park S. Age-associated increase in arterial stiffness measured according to the cardio-ankle vascular index without blood pressure changes in healthy adults. **J Atherosclerosis Thromb**. 2013; 20(12):911−923.

74. Wen W, Luo R, Tang X, et al. Age-related progression of arterial stiffness and its elevated positive association with blood pressure in healthy people. **Atherosclerosis**. 2015; 238(1):147−152.

75. Hayashi K, Yamamoto T, Takahara A, Shirai K. Clinical assessment of arterial stiffness with cardio-ankle vascular index: theory and applications. **J Hypertens**. 2015; 33(9):1742−1757. discussion 1757.

76. Okura T, Watanabe S, Kurata M, et al. Relationship between cardio-ankle vascular index (CAVI) and carotid atherosclerosis in patients with essential hypertension. **Hypertens Res**. 2007; 30(4):335−340.

77. Park JB, Park HE, Choi SY, Kim MK, Oh BH. Relation between cardio-ankle vascular index and coronary artery calcification or stenosis in asymptomatic subjects. **J Atherosclerosis Thromb**. 2013; 20(6):557−567.

78. Chung SL, Yang CC, Chen CC, Hsu YC, Lei MH. Coronary artery calcium score compared with cardio-ankle vascular index in the prediction of cardiovascular events in asymptomatic patients with type 2 diabetes. **J Atherosclerosis Thromb**. 2015; 22(12):1255−1265.

79. Gohbara M, Iwahashi N, Sano Y, et al. Clinical impact of the cardio-ankle vascular index for predicting cardiovascular events after acute coronary syndrome. **Circ J**. 2016; 80(6):1420−1426.

80. Kusunose K, Sato M, Yamada H, et al. Prognostic implications of non-invasive vascular function tests in high-risk atherosclerosis patients. **Circ J**. 2016; 80(4):1034−1040.

81. Laucevicius A, Ryliskyte L, Balsyte J, et al. Association of cardio-ankle vascular index with cardiovascular risk factors and cardiovascular events in metabolic syndrome patients. **Medicina**. 2015; 51(3):152−158.

82. Otsuka K, Fukuda S, Shimada K, et al. Serial assessment of arterial stiffness by cardio-ankle vascular index for prediction of future cardiovascular events in patients with coronary artery disease. **Hypertens Res**. 2014; 37(11):1014−1020.

83. Sato Y, Nagayama D, Saiki A, et al. Cardio-ankle vascular index is independently associated with future cardiovascular events in outpatients with metabolic disorders. **J Atherosclerosis Thromb**. 2016; 23(5):596−605.

84. Kubota Y, Maebuchi D, Takei M, et al. Cardio-ankle vascular index is a predictor of cardiovascular events. **Artery Res**. 2011; 5(3):91−96.

85. Kario K. Hemodynamic arteriosclerotic syndrome - a vicious cycle of hemodynamic stress and vascular disease. **J Clin Hypertens**. 2018; 20(6):1073−1077.

86. Hayashi K. Experimental approaches on measuring the mechanical properties and constitutive laws of arterial walls. **J Biomech Eng**. 1993; 115(4b):481−488.

87. Chirinos JA, Kips JG, Jacobs Jr DR, et al. Arterial wave reflections and incident cardiovascular events and heart failure: MESA (Multiethnic Study of Atherosclerosis). **J Am Coll Cardiol**. 2012; 60(21):2170−2177.

88. Wang KL, Cheng HM, Sung SH, et al. Wave reflection and arterial stiffness in the prediction of 15-year all-cause and cardiovascular mortalities: a community-based study. **Hypertension**. 2010; 55(3):799−805.

89. Westerhof BE, Guelen I, Westerhof N, Karemaker JM, Avolio A. Quantification of wave reflection in the human aorta from pressure alone: a proof of principle. **Hypertension**. 2006; 48(4):595−601.

90. Williams B, Cockcroft JR, Kario K, et al. Effects of sacubitril/valsartan versus olmesartan on central hemodynamics in the elderly with systolic hypertension: the PARAMETER study. **Hypertension**. 2017; 69(3):411−420.

91. Mitchell GF, Izzo Jr JL, Lacourcière Y, et al. Omapatrilat reduces pulse pressure and proximal aortic stiffness in patients with systolic hypertension: results of the conduit hemodynamics of omapatrilat international research study. **Circulation**. 2002; 105(25):2955−2961.

92. Desai AS, Mitchell GF, Fang JC, Creager MA. Central aortic stiffness is increased in patients with heart failure and preserved ejection fraction. **J Card Fail**. 2009; 15(8):658−664.

93. Lam CS, Gona P, Larson MG, et al. Aortic root remodeling and risk of heart failure in the Framingham Heart study. **JACC Heart Fail**. 2013; 1(1):79−83.

94. Pepine CJ, Nichols WW, Conti CR. Aortic input impedance in heart failure. **Circulation**. 1978; 58(3 Pt 1):460−465.

95. Otero-Cacho A, Aymerich M, Flores-Arias MT, et al. Determination of hemodynamic risk for vascular disease in planar artery bifurcations. **Sci Rep**. 2018; 8(1):2795.

96. Zaromytidou M, Siasos G, Coskun AU, et al. Intravascular hemodynamics and coronary artery disease: new insights and clinical implications. **Hellenic J Cardiol**. 2016; 57(6):389−400.

97. Caro CG, Fitz-Gerald JM, Schroter RC. Atheroma and arterial wall shear. Observation, correlation and proposal of a shear dependent mass transfer mechanism for atherogenesis. **Proc R Soc Lond B Biol Sci**. 1971; 177(1046):109−159.

98. Kario K. Systemic hemodynamic atherothrombotic syndrome and resonance hypothesis of blood pressure variability: triggering cardiovascular events. **Korean Circ J**. 2016; 46(4):456−467.

99. Kario K. New insight of morning blood pressure surge into the triggers of cardiovascular disease-synergistic resonance of blood pressure variability. **Am J Hypertens**. 2016; 29(1):14−16.

100. Kario K, Chirinos JA, Townsend RR, et al. Systemic hemodynamic atherothrombotic syndrome (SHATS) - coupling vascular disease and blood pressure variability: proposed concept from Pulse of Asia. **Prog Cardiovasc Dis**. 2020; 63(1):22−32.

101. Kario K. Systemic hemodynamic atherothrombotic syndrome: a blind spot in the current management of hypertension. **J Clin Hypertens**. 2015; 17(5):328−331.

102. Pucci G, Battista F, Anastasio F, Schillaci G. Morning pressor surge, blood pressure variability, and arterial stiffness in essential hypertension. **J Hypertens**. 2017; 35(2):272−278.

103. Kario K. Prognosis in relation to blood pressure variability: pro side of the argument. **Hypertension**. 2015; 65(6):1163−1169. discussion 1169.

104. Kario K. Evidence and perspectives on the 24-hour management of hypertension: hemodynamic biomarker-initiated 'anticipation medicine' for zero cardiovascular event. **Prog Cardiovasc Dis**. 2016; 59(3):262−281.

105. Kario K, Tomitani N, Kanegae H, et al. Development of a new ICT-based multisensor blood pressure monitoring system for use in hemodynamic biomarker-initiated anticipation medicine for cardiovascular disease: the national IMPACT program project. **Prog Cardiovasc Dis**. 2017; 60(3):435−449.

106. Webb AJS, Mazzucco S, Li L, Rothwell PM. Prognostic significance of blood pressure variability on beat-to-beat monitoring after transient ischemic attack and stroke. **Stroke**. 2018; 49(1):62−67.

107. Wei FF, Li Y, Zhang L, et al. Beat-to-beat, reading-to-reading, and day-to-day blood pressure variability in relation to organ damage in untreated Chinese. **Hypertension**. 2014; 63(4):790−796.

108. Parati G, Ochoa JE, Lombardi C, Bilo G. Assessment and management of blood-pressure variability. **Nat Rev Cardiol**. 2013; 10(3):143−155.

109. Kario K. Hemodynamic biomarker-initiated anticipation medicine in the future management of hypertension. **Am J Hypertens**. 2017; 30(3):226−228.

110. Hashimoto J, Westerhof BE, Westerhof N, Imai Y, O'Rourke MF. Different role of wave reflection magnitude and timing on left ventricular mass reduction during antihypertensive treatment. **J Hypertens**. 2008; 26(5):1017−1024.

111. Zamani P, Bluemke DA, Jacobs Jr DR, et al. Resistive and pulsatile arterial load as predictors of left ventricular mass and geometry: the multi-ethnic study of atherosclerosis. **Hypertension**. 2015; 65(1):85−92.

112. Weber T, Chirinos JA. Pulsatile arterial haemodynamics in heart failure. **Eur Heart J**. 2018; 39(43):3847−3854.

113. Chirinos JA, Segers P, Rietzschel ER, et al. Early and late systolic wall stress differentially relate to myocardial contraction and relaxation in middle-aged adults: the Asklepios study. **Hypertension**. 2013; 61(2):296−303.

114. Chirinos JA, Segers P, Raina A, et al. Arterial pulsatile hemodynamic load induced by isometric exercise strongly predicts left ventricular mass in hypertension. **Am J Physiol Heart Circ Physiol**. 2010; 298(2):H320−H330.

115. Chirinos JA, Phan TS, Syed AA, et al. Late systolic myocardial loading is associated with left atrial dysfunction in hypertension. **Circ Cardiovasc Imag**. 2017; 10(6):e006023.

116. Chirinos JA, Segers P, Duprez DA, et al. Late systolic central hypertension as a predictor of incident heart failure: the multi-ethnic study of atherosclerosis. **J Am Heart Assoc**. 2015; 4(3):e001335.

117. Hybels CF, Pieper CF, Payne ME, Steffens DC. Late-life depression modifies the association between cerebral white matter hyperintensities and functional decline among older adults. **Am J Geriatr Psychiatr**. 2016; 24(1):42−49.

118. Srikanth V, Beare R, Blizzard L, et al. Cerebral white matter lesions, gait, and the risk of incident falls: a prospective population-based study. **Stroke**. 2009; 40(1):175−180.

119. Pries AR, Reglin B. Coronary microcirculatory pathophysiology: can we afford it to remain a black box? **Eur Heart J**. 2017; 38(7):478−488.

120. Zafrani L, Ince C. Microcirculation in acute and chronic kidney diseases. **Am J Kidney Dis**. 2015; 66(6):1083−1094.

121. Ito S, Nagasawa T, Abe M, Mori T. Strain vessel hypothesis: a viewpoint for linkage of albuminuria and cerebro-cardiovascular risk. **Hypertens Res**. 2009; 32(2):115−121.

122. Kario K, Pickering TG, Umeda Y, et al. Morning surge in blood pressure as a predictor of silent and clinical cerebrovascular disease in elderly hypertensives: a prospective study. **Circulation**. 2003; 107(10):1401−1406.

123. Nagai M, Hoshide S, Nishikawa M, Masahisa S, Kario K. Visit-to-visit blood pressure variability in the elderly: associations with cognitive impairment and carotid artery remodeling. **Atherosclerosis**. 2014; 233(1):19−26.

124. Matsui Y, Eguchi K, Shibasaki S, et al. Impact of arterial stiffness reduction on urinary albumin excretion during antihypertensive treatment: the Japan morning Surge-1 study. **J Hypertens**. 2010; 28(8):1752−1760.

125. Scuteri A, Rovella V, Alunni Fegatelli D, Tesauro M, Gabriele M, Di Daniele N. An operational definition of SHATS (Systemic Hemodynamic Atherosclerotic Syndrome): role of arterial stiffness and blood pressure variability in elderly hypertensive subjects. **Int J Cardiol**. 2018; 263:132−137.

126. Chow B, Rabkin SW. The relationship between arterial stiffness and heart failure with preserved ejection fraction: a systemic meta-analysis. **Heart Fail Rev**. 2015; 20(3):291−303.

127. Mizuguchi Y, Oishi Y, Tanaka H, et al. Arterial stiffness is associated with left ventricular diastolic function in patients with cardiovascular risk factors: early detection with the use of cardio-ankle vascular index and ultrasonic strain imaging. **J Card Fail**. 2007; 13(9):744−751.

128. Namba T, Masaki N, Matsuo Y, et al. Arterial stiffness is significantly associated with left ventricular diastolic dysfunction in patients with cardiovascular disease. **Int Heart J**. 2016; 57(6):729−735.

129. Miyoshi T, Doi M, Hirohata S, et al. Cardio-ankle vascular index is independently associated with the severity of coronary atherosclerosis and left ventricular function in patients with ischemic heart disease. **J Atherosclerosis Thromb**. 2010; 17(3):249−258.

130. Janwanishstaporn S, Boonyasirinant T. Correlation between aortic stiffness and left atrial volume index in hypertensive patients. **Clin Exp Hypertens**. 2016; 38(2):160−165.

131. Lantelme P, Laurent S, Besnard C, et al. Arterial stiffness is associated with left atrial size in hypertensive patients. **Arch Cardiovasc Dis**. 2008; 101(1):35−40.

132. Osawa K, Nakanishi R, Miyoshi T, et al. Correlation of arterial stiffness with left atrial volume index and left ventricular mass index in young adults: evaluation by coronary computed tomography angiography. **Heart Lung Circ**. 2019; 28(6):932−938.

133. Yildiz M, Oktay AA, Stewart MH, Milani RV, Ventura HO, Lavie CJ. Left ventricular hypertrophy and hypertension. **Prog Cardiovasc Dis**. 2020; 63(1):10−21.

134. Kario K. Systemic hemodynamic atherothrombotic syndrome (SHATS): diagnosis and severity assessment score. **J Clin Hypertens**. 2019; 21(7):1011−1015.

135. Kario K. Orthostatic hypertension-a new haemodynamic cardiovascular risk factor. **Nat Rev Nephrol**. 2013; 9(12):726−738.

136. Muntner P, Whittle J, Lynch AI, et al. Visit-to-visit variability of blood pressure and coronary heart disease, stroke, heart failure, and mortality: a cohort study. **Ann Intern Med**. 2015; 163(5):329−338.

137. Ohkuma T, Woodward M, Jun M, et al. Prognostic value of variability in systolic blood pressure related to vascular events and premature death in type 2 diabetes mellitus: the ADVANCE-ON study. **Hypertension**. 2017; 70(2):461−468.

138. Rothwell PM, Howard SC, Dolan E, et al. Prognostic significance of visit-to-visit variability, maximum systolic blood pressure, and episodic hypertension. **Lancet**. 2010; 375(9718):895−905.

139. National Institute for Health and Care Excellence. **Hypertension: Clinical Management of Primary Hypertension in Adults**. Clinical guideline 127; 2011. Available from: https://www.nice.org.uk/guidance/cg127/chapter/1-guidance. Accessed December , 2016.

140. Nerenberg KA, Zarnke KB, Leung AA, et al. Hypertension Canada's 2018 guidelines for diagnosis, risk assessment, prevention, and treatment of hypertension in adults and children. **Can J Cardiol**. 2018; 34(5):506−525.

141. Parati G, Stergiou G, O'Brien E, et al. European Society of Hypertension practice guidelines for ambulatory blood pressure monitoring. **J Hypertens**. 2014; 32(7):1359−1366.

142. Sharman JE, Howes FS, Head GA, et al. Home blood pressure monitoring: Australian expert consensus statement. **J Hypertens**. 2015; 33(9):1721−1728.

143. Umemura S, Arima H, Arima S, et al. The Japanese society of hypertension guidelines for the management of hypertension (JSH 2019). **Hypertens Res**. 2019; 42(9):1235−1481.

144. Whelton PK, Carey RM, Aronow WS, et al. 2017 ACC/AHA/AAPA/ABC/ACPM/AGS/APhA/ASH/ASPC/NMA/PCNA guideline for the prevention, detection, evaluation, and management of high blood pressure in adults: executive summary: a report of the American College of Cardiology/American Heart Association Task Force on Clinical Practice Guidelines. **J Am Coll Cardiol**. 2018; 71(19):2199−2269.

145. Williams B, Mancia G, Spiering W, et al. 2018 ESC/ESH guidelines for the management of arterial hypertension: the task force for the management of arterial hypertension of the European Society of Cardiology and the European Society of Hypertension. **J Hypertens**. 2018; 36(10):1953−2041.

146. Kario K, Saito I, Kushiro T, et al. Home blood pressure and cardiovascular outcomes in patients during antihypertensive therapy: primary results of HONEST, a large-scale prospective, real-world observational study. **Hypertension**. 2014; 64(5):989−996.

147. Kario K, Iwashita M, Okuda Y, et al. Morning home blood pressure and cardiovascular events in Japanese hypertensive patients. **Hypertension**. 2018; 72(4):854−861.

148. Wang JG, Kario K, Chen CH, et al. Management of morning hypertension: a consensus statement of an Asian expert panel. **J Clin Hypertens**. 2018; 20(1):39−44.

149. Matsui Y, O'Rourke MF, Hoshide S, Ishikawa J, Shimada K, Kario K. Combined effect of angiotensin II receptor blocker and either a calcium channel blocker or diuretic on day-by-day variability of home blood pressure: the Japan combined treatment with Olmesartan and a calcium-channel blocker versus olmesartan and diuretics randomized efficacy study. **Hypertension**. 2012; 59(6):1132−1138.

150. Webb AJ, Fischer U, Mehta Z, Rothwell PM. Effects of antihypertensive-drug class on interindividual variation in blood pressure and risk of stroke: a systematic review and meta-analysis. **Lancet**. 2010; 375(9718):906−915.

151. Zhang Y, Agnoletti D, Safar ME, Blacher J. Effect of antihypertensive agents on blood pressure variability: the Natrilix SR versus candesartan and amlodipine in the reduction of systolic blood pressure in hypertensive patients (X-CELLENT) study. **Hypertension**. 2011; 58(2):155−160.

152. Kario K, Okada K, Kato M, et al. 24-hour blood pressure-lowering effect of an SGLT-2 inhibitor in patients with diabetes and uncontrolled nocturnal hypertension: results from the randomized, placebo-controlled SACRA study. **Circulation**. 2019; 139(18):2089−2097.

153. Kario K, Bohm M, Mahfoud F, et al. Twenty-four-hour ambulatory blood pressure reduction patterns after renal denervation in the SPYRAL HTN-OFF MED trial. **Circulation**. 2018; 138(15):1602−1604.

Chapter 39

Arterial stiffness and pulsatile hemodynamics in coronary artery disease and other forms of atherosclerotic vascular diseases

Junichiro Hashimoto

Miyagi University of Education Medical Center, Sendai, Miyagi, Japan

Introduction

Many acute cardiovascular events occur in the presence of atherosclerotic lesions in arteries responsible for vital organ perfusion. For early prevention of cardiovascular diseases, numerous efforts have been made to clinically evaluate atherosclerosis noninvasively. The various evaluation methods include the local assessments of intimal (stenotic) plaques and the regional or systemic assessments of arterial stiffness, since this can be a consequence of atherosclerosis. Strictly speaking, however, atherosclerosis and arteriosclerosis (assessed as arterial stiffness) are distinct entities (Table 39.1); they are different from each other in terms of pathology (i.e., intimal thickening vs. medial degeneration)

and distribution (i.e., local vs. systemic). Since atherosclerosis (at least in the initial stage) may be patchy throughout the large arteries, not all atherosclerotic plaques necessarily influence actual stiffness measures until they become thickened, confluent, and calcified. For instance, studies disagree about aortic distensibility in patients with hypercholesterolemia (a major risk factor for atherosclerosis). Some studies of young patients have reported reduced distensibility,[1] whereas other studies of older patients showed opposite results,[2] indicating that the involvement of atherosclerosis in arterial stiffening differs considerably according to whether it is in the early or late stage. Despite their different pathologies, however, atherosclerosis and arteriosclerosis coincide in most cases

TABLE 39.1 Traditional view of arteriosclerosis and atherosclerosis.

	Arteriosclerosis	Atherosclerosis
Mainly affected arterial wall layer	Media of elastic arteries	Intima of elastic and muscular arteries
Predilection site	Diffuse	Focal (bifurcation, high curvature)
Arterial lumen	Dilatation	Stenosis/occlusion
Pathology	Elastic fracture/degeneration	Lipid accumulation/inflammation
Hemodynamic etiology	Tensile stress	Shear stress
Main risk factors	Age/hypertension	Age/hypercholesterolemia/diabetes/smoking
Reversibility	−	± (Stabilization +)
Wall stiffness	↑	↑ or →

and have common risk factors, such as older age. From a hemodynamic point of view, diffuse arteriosclerosis (specifically, the stiffening of large arteries) leads to substantial changes in systemic hemodynamics. These changes are represented by an increase in central systolic pressure and a decrease in diastolic pressure, which affect local hemodynamics in organs and tissues perfused by these arteries. When arteries are narrowed by atherosclerosis, local hemodynamics can be impaired and relevant tissues underperfused, leading to end-organ ischemia or infarction. These findings indicate a clinically inextricable link between atherosclerosis and arterial stiffness.

This chapter addresses the roles of aortic stiffness and pulsatile hemodynamics in various atherosclerotic diseases, including coronary artery disease (CAD), peripheral artery disease (PAD), and stroke. This chapter is focused on (a) the clinical and epidemiological evidence regarding associations between aortic stiffness/hemodynamics indices and atherosclerotic diseases and (b) potential underlying mechanisms responsible for these associations.

Coronary artery disease

Clinical evidence

CAD is the leading cause of mortality and morbidity worldwide.[3] CAD has various risk factors, including age, smoking, hypertension, diabetes, and hypercholesterolemia. In addition to these traditional risk factors, further focus has recently been directed toward arterial stiffness and pulsatile hemodynamics.

Several studies have shown associations between aortic stiffness and CAD. Cross-sectional studies have demonstrated that carotid-femoral pulse wave velocity (PWV), which is the gold standard for noninvasive measures of aortic stiffness,[4] and PWV index, which is calculated as ([measured PWV−theoretical PWV]/theoretical PWV), are associated with the extent and severity of stenotic lesions detected by coronary angiography.[5,6] In addition, prospective studies have shown that carotid-femoral PWV is a predictor of primary coronary and total cardiovascular events, independent of conventional risk factors.[7−10] Furthermore, in recent years, the prognostic significance of aortic stiffness for cardiovascular events has been evaluated based on other PWV measures, rather than the traditional carotid-femoral PWV. In the Multi-Ethnic Study of Atherosclerosis (MESA), aortic arch PWV was assessed using magnetic resonance imaging (MRI) in 3527 participants, and it was found to be predictive of cardiovascular (including coronary) events during the 10-year follow-up of middle-aged individuals.[11] In another study, a 48-h PWV was estimated in 170 hemodialysis patients by an ambulatory blood pressure monitor, and was shown to predict

cardiovascular events (including fatal/nonfatal myocardial infarction and coronary revascularization) during the median follow-up period of 26 months.[12] That study[12] also showed that ambulatory PWV was a stronger predictor of cardiovascular events than brachial resting or ambulatory blood pressure, suggesting that arterial stiffness does have an impact on the risk for cardiovascular events. However, as discussed in Chapter 7, estimations of PWV via single-site cuff measurements are problematic and may be confounded by various factors.

There is increasing evidence regarding the significance of central pulsatile hemodynamics in CAD. Nishijima et al.[13] were the first to report a cross-sectional observation that aortic pulse pressure, but not mean arterial pressure, was higher in patients with CAD, indicating the importance of the pulsatile, rather than steady, component of central pressure as a CAD risk. Weber et al.[14] showed that the aortic augmentation index (AIx) and augmented pressure correlated with the presence and severity of coronary stenotic lesions in patients suspected of CAD, suggesting the involvement of peripheral wave reflection in coronary atherosclerosis progression.

Prospective studies have repeatedly demonstrated the involvement of aortic pulsatile hemodynamics in the prognosis of CAD.[15] Most of the studies have shown indices of pulse wave reflection (e.g., aortic AIx, augmented pressure, and reflection magnitude) to be independent predictors of major adverse cardiovascular events (such as myocardial infarction, coronary restenosis, and death) in patients with CAD,[16−20] emphasizing the potential relevance of peripheral wave reflection to CAD progression. In addition, some studies attempting to compare the predictive ability between aortic and brachial pressures have revealed that aortic pressure is a better predictor of cardiovascular events than conventional brachial pressure. For instance, Chirinos et al.[21] showed that higher aortic but not brachial pulse pressure, as well as lower diastolic pressure, were significantly associated with an increased risk of major adverse cardiovascular events (unstable angina pectoris, myocardial infarction, coronary revascularization, stroke, and death) in a CAD cohort. Jankowski et al.[22] demonstrated that aortic pulse pressure, but neither brachial pulse pressure nor mean arterial pressure, was predictive of cardiovascular events (myocardial infarction, stroke, cardiac arrest, heart transplantation, myocardial revascularization, and death) in CAD patients. In the MESA cohort, Chirinos et al.[20] showed that lower pulse pressure amplification (i.e., radial/aortic pulse pressure ratio) was associated with a higher incidence of cardiovascular events (including myocardial infarction, angina, stroke, and cardiovascular death) in a general population. This clearly indicates that the predictive ability of aortic pulse pressure is independent of peripheral pulse pressure.

The evidence mentioned above indicates that aortic stiffening and widened pulse pressure are closely related to the development and progression of CAD. Together with a recent finding that the combination of higher carotid-femoral PWV and wider central pulse pressure were associated with a considerably higher incidence of cardiovascular disease than either alone,[23] aortic stiffening and increased pressure pulsatility may have synergistic adverse impacts on CAD.

Mechanism

Atherosclerotic narrowing of the large coronary arteries is the main cause of CAD. Formation of atheromatous plaques with or without thrombus or calcification narrows the coronary artery lumen, reduces blood flow downstream of the stenotic lesions, and induces myocardial ischemia, which leads to coronary events. Besides atherosclerotic CAD, other etiologies for ischemic heart disease include coronary vasospasm and microvascular dysfunction, which are usually diagnosed when the epicardial coronary arteries appear structurally normal on conventional coronary angiography. The common pathophysiology to atherosclerotic and nonatherosclerotic CAD is the presence of abnormalities in coronary hemodynamics.

Coronary arteries have characteristic structures and hemodynamics. Anatomically, the coronary arteries branch off vertically from the central aorta. Hemodynamically, coronary flow occurs mostly during diastole. These structural and hemodynamic features suggest that diastolic lateral pressure in the central aorta is an important determinant of coronary flow.

Aortic stiffness plays a major role in determining coronary hemodynamics.[24] Stiffening of the elastic aorta leads to an increase in systolic blood pressure, a decrease in diastolic blood pressure, and, consequently, a widening of pulse pressure. The elevation of aortic systolic pressure increases left ventricular afterload, resulting in an increase in myocardial oxygen demand. Peripheral wave reflection enhanced by aortic stiffening can cause the extra left ventricular workload to maintain the cardiac outflow against the reflected waves, and such wasted left ventricular effort contributes to an increase in systolic tension-time index and compensatory development of left ventricular hypertrophy.[25,26] The reduction of aortic diastolic pressure leads to a decrease in coronary perfusion pressure and myocardial oxygen supply. Such an imbalance between myocardial oxygen supply and demand resulting from central hemodynamic alterations may account for the predisposition of hypertensive patients (particularly those with isolated systolic hypertension) to CAD.[27]

Despite such a theoretical basis for the relationship between increased aortic stiffness and decreased coronary blood flow, direct in vivo evidence has been scarce on any aorto-coronary relationship until relatively recently. Previous experimental studies have shown conflicting results; some have associated arterial stiffness with reduced coronary flow,[28] while others have associated it with increased coronary flow.[29] However, subsequent clinical studies in humans have consistently reported a significant contribution of aortic stiffening to decreased coronary flow. For instance, in patients undergoing percutaneous coronary intervention, aortic PWV was related to resting and hyperemic coronary blood flow irrespective of the presence of stenosis.[30] In another study of patients with CAD, the aortic PWV and central (carotid) pulse pressure were inversely correlated with the time to myocardial ischemia during a treadmill test.[31] Nelson et al.[32] recently used intracoronary Doppler flow measurement and noninvasive cardiovascular MRI to confirm significant associations between aortic stiffening with reduced resting and hyperemic coronary blood flow among patients with minor angiographic coronary disease. That study also showed that aortic pulse pressure was inversely associated with hyperemic coronary blood flow and coronary flow velocity reserve.[32]

The influence of central hemodynamics on coronary hemodynamics has been assessed noninvasively using the subendocardial viability ratio (SEVR), also known as the Buckberg index.[33,34] The SEVR is calculated on the basis that the aortic systolic pressure-time integral (SPTI, the area under the aortic pressure curve during systole) represents the myocardial oxygen demand,[35] and that the aortic diastolic pressure-time integral (DPTI) represents the myocardial blood supply; therefore, the ratio of the latter to the former represents the myocardial oxygen supply/demand balance. Buckberg et al. showed that there was no significant difference between the subepicardial and subendocardial blood flow when the SEVR (i.e., the ratio of DPTI/SPTI) exceeded 1.0. When the SEVR was below 0.8, the subendocardial muscle was underperfused relative to the subepicardial muscle.[34] Barnard et al. determined that subendocardial ischemia became apparent on ECG when the SEVR fell below 0.45 in normal hearts.[36] Subendocardial ischemia can occur at an even higher SEVR with large increases in left ventricular mass or dilatation, and therefore, the critical value of 0.8 may be considered reasonable.[37] The SEVR reflects coronary flow reserve in hypertensive patients with normal coronary arteries.[38]
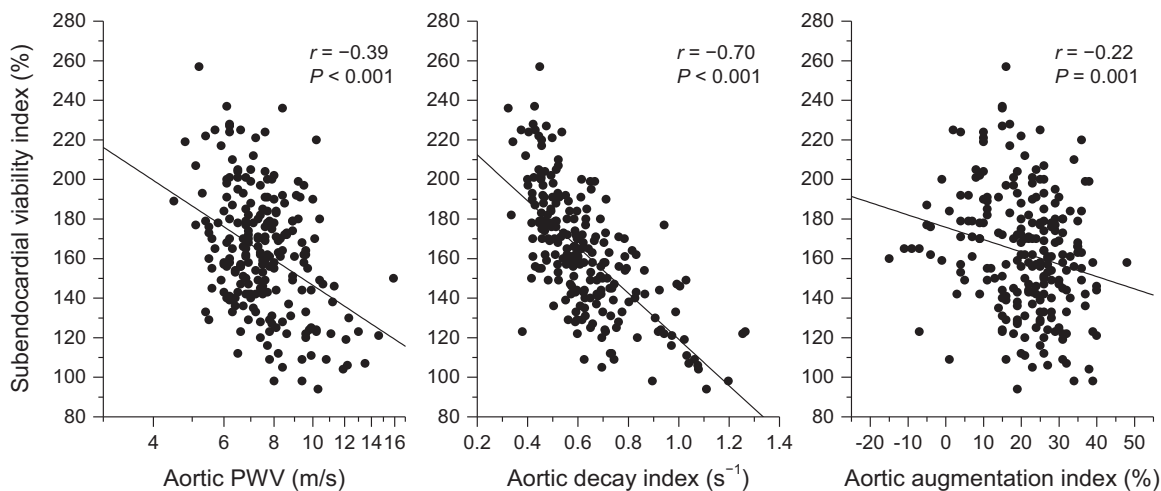
The SEVR is determined by not only ejection duration (heart rate) and aortic mean diastolic/systolic pressure ratio but also age and sex. An epidemiological study of 3682 healthy volunteers showed that the SEVR decreased with aging in both men and women, but women consistently had lower SEVRs than men at all ages.[39] These data indicate that age-related arteriosclerosis predisposes elderly people to myocardial ischemia and also supports the fact that

women are more prone to ischemic episodes as they get older, even in the absence of significant stenosis on coronary angiography (i.e., syndrome X).[40]

Several studies have reported significant associations between the SEVR and aortic stiffness and wave reflection. Guelen et al.[41] demonstrated that, in a general population of 2490 older adults, aortic SPTI increased, whereas DPTI decreased with increasing aortic carotid-femoral PWV and, accordingly, the SEVR decreased with aortic stiffening. In a study of cardiology outpatients, Namasivayam et al.[42] showed that both incident and reflected waves were strong predictors of tension-time index (i.e., the product of SPTI and heart rate), but only the reflected wave was associated with a longer ejection duration. They also reported greater independent contributions of incident waves (as measured by the incident pressure wave height) and reflected waves (as measured by augmented pressure) to lowering SEVRs.[39] A recent study extended these findings by using the SEVR in 222 hypertensive patients without CAD and confirmed significant inverse associations of aortic PWV and AIx with the SEVR.[43] Notably, this study[43] revealed an additional finding that the exponential decay of aortic pressure during diastole, a marker of total arterial compliance,[44] was correlated with the SEVR ($r = -0.70$, $P < .001$) more closely than with the aortic PWV or AIx (Fig. 39.1). In mediation analysis, the association between higher PWV and lower SEVR was indirect and mediated through faster aortic diastolic pressure decay, indicating that the impairment of myocardial viability secondary to aortic stiffening resulted from accelerated diastolic exponential decay of central blood pressure. In addition, the rapid decline of blood pressure during diastole was a characteristic of hypertensive patients with stiff aorta.[43]

Taken together, these findings suggest that the faster the diastolic pressure decay, the lower the SEVR becomes, thus predisposing hypertensive patients to ischemic heart disease.

The evidence mentioned above indicates that abnormalities in central pulsatile hemodynamics are a key initiator of myocardial ischemia, even in the absence of coronary stenosis. On the other hand, major adverse coronary events are also attributable to local (i.e., coronary) atherosclerosis progression and plaque instability. To date, however, evidence for the potential association between aortic stiffness and coronary atherosclerosis is limited. A possible association between arterial stiffness and coronary artery calcification (which may not only cause luminal narrowing but could also contribute to "stable" plaques) has varied among different study samples, such as a general population[45] and renal transplant recipients.[46] A recent prospective study of patients with type-2 diabetes demonstrated an association between baseline aortic PWV and low-density noncalcified plaque volume on computed tomography coronary angiography 5 years later.[47] Local stiffness measured as coronary PWV may be "lower" in patients with acute coronary syndromes versus stable CAD, even when aortic PWVs do not differ.[48] In addition, while higher PWV is associated with carotid intraplaque hemorrhage (i.e., a sign of vulnerable plaques) in the general population,[49] its potential involvement with coronary plaques is currently unclear. Finally, although brachial pulse pressure (as an indicator of pulsatile tensile stress) is independently associated with carotid plaque ulceration,[50] it remains to be determined whether aortic pulsatile pressure triggers coronary plaque rupture. Further studies are necessary to clarify these important issues.

FIGURE 39.1 Relationships between aortic function measures and subendocardial viability index in patients with hypertension.[42] Aortic decay index (λ) is calculated as $P(t) = P_0 e^{-\lambda t}$, where $P(t)$ is the pressure at the time from the end of systole (t), P_0 the estimated pressure at end systole, by regarding diastolic pressure curve as a monoexponential decay.

The reader is referred to Chapter 18 for a comprehensive review of the hemodynamic determinants of myocardial supply and demand.

Peripheral artery disease

Clinical evidence

PAD is mainly caused by the progression of atherosclerosis in the arteries of the lower extremities. A world database recently estimated that 237 million people (5.6%) aged >25 years had PAD in 2015.[51] PAD is linked to a significantly increased risk of cardiovascular morbidity and mortality as well as disability, and it is the third most common clinical manifestation of atherosclerosis, after CAD and stroke.[52]

Several studies have investigated arterial stiffness indices in patients with PAD. Most of the studies have demonstrated that aortic AIx and pulse pressure are higher in patients with PAD than in controls.[53−55] Such alterations in central hemodynamics are related to lower limb function; higher AIx and lower round-trip travel time of pulse waves (i.e., earlier return of the reflected waves) are associated with decreased walking ability in PAD patients.[56] Furthermore, revascularization of peripheral artery stenosis with percutaneous transluminal angioplasty contributes to a significant reduction in AIx.[57] In contrast to AIx, the relationship between aortic PWV and PAD is more complex and likely depends on the severity of PAD. Some studies have shown that when PAD is diagnosed as an ankle-brachial pressure index (ABI) of <0.9, the PAD patients as a whole have significantly increased carotid-femoral PWV compared with subjects without PAD.[58,59] However, in cases of critical limb ischemia with more advanced arterial obstruction, the carotid-femoral PWV is decreased, although the AIx is increased.[55]

Mechanism
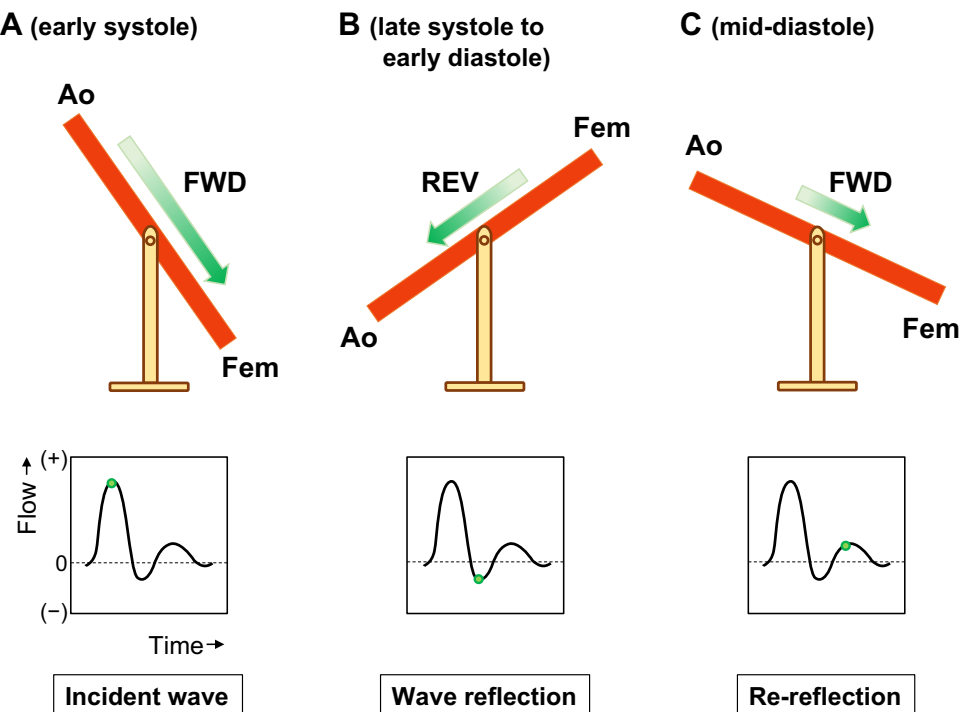
There is ample evidence for an inverse correlation between aortic AIx and ABI in patients with and without PAD.[60−62] This suggests that the presence of lower extremity atherosclerotic disease increases wave reflection or, alternatively, increased wave reflection (and arterial stiffness) may increase the risk of developing lower extremity PAD. The former may be explained on the basis that (1) atherosclerosis itself can increase arterial stiffness[58] and then hasten pulse wave propagation and reflection, and (2) arterial obstructions and atherosclerotic bifurcations create larger impedance mismatches at sites closer to the normal sites, which causes an increase in and premature return of wave reflection.

In patients with PAD, the incidence of CAD is reported to be extremely high, and the long-term prognosis depends on the presence and severity of CAD. As mentioned previously, aortic stiffening and earlier return of wave reflection lead to faster aortic diastolic pressure decay and thereby lower SEVR,[43] which may account for a predisposition of patients with PAD to CAD. This assumption is consistent with the fact that lower ABI in PAD patients is associated with lower SEVR, as well as higher AIx.[60] These alterations in central hemodynamics are also likely to have adverse impacts on other target organs, resulting in markedly increased risks of cerebral artery disease and renal artery stenosis in patients with PAD.[52]
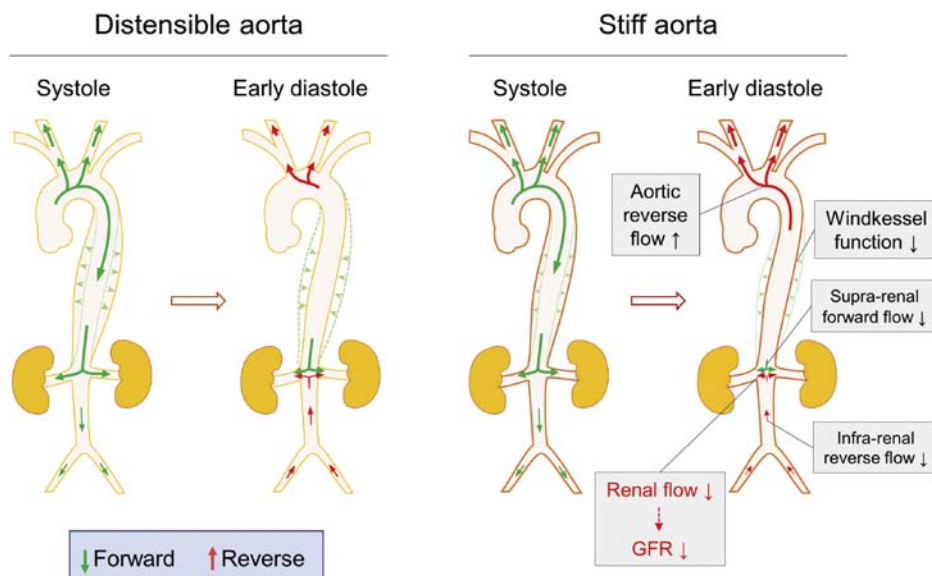
Normally, the flow waveform of the lower extremities is triphasic with a systolic forward flow, early diastolic reverse flow, and mid-diastolic forward flow (Fig. 39.2).[63,64] In advanced PAD, however, the flow waveform is monophasic without diastolic flow reversal; this loss of flow reversal is attributed to compensatory reduction in peripheral vascular resistance. In the case of milder atherosclerosis, the flow waveform may become biphasic, since the recoil function of the elastic and muscular arteries is lost.[63] A study on pulsatile flow waveforms of the femoral artery in hypertensive patients without PAD revealed that the reverse/forward flow index is inversely correlated with aortic PWV and AIx, and positively correlated with aorta-to-femoral pulse pressure amplification.[63] This finding indicates that aortic stiffening and a reduced aorta-to-leg pressure gradient attenuate femoral diastolic flow reversal (Fig. 39.2).[64] A similar flow reversal has been observed throughout the infra-renal aorta and iliac arteries, and diastolic reverse flow is considered essential for blood supply to internal organs, including the kidneys.[65] Specifically for the kidneys, both the forward flow from the suprarenal aorta and the reverse flow from the infrarenal aorta generate the total inflow into the renal arteries in early diastole (Fig. 39.3),[65,66] and the infrarenal aortic (as estimated from the femoral) flow reversal determines the intrarenal diastolic flow.[67] Therefore, it seems likely that the disappearance of diastolic flow reversal due to lower extremity artery atherosclerosis will cause hypoperfusion in the kidney as well as the pelvic organs, which will lead to functional impairments.[63] In addition, a reduced mid-diastolic forward flow (typically seen as a biphasic pattern of the femoral flow) resulting from aortic stiffening[63] could contribute to a decrease in total blood flow into the lower extremities and hence predispose patients to PAD.[68]

Caution is required when using carotid-femoral PWV to evaluate aortic stiffness in patients with PAD. In the case of critical limb ischemia, even if a markedly attenuated PWV is observed, it may not be attributable to a true reduction in aortic stiffness, but rather to a decrease in distending pressure distal to arterial stenosis (e.g., due to aortoiliac disease). In this regard, the ratio of aortic pulse pressure to PWV may be helpful in diagnosing advanced PAD.[55]

FIGURE 39.2 Hypothetical mechanism for the association between alternate pressure gradients and bidirectional (triphasic) flow at the femoral artery (seesaw theory).[63] *Ao* indicates aorta; *Fem*, femoral artery; *FWD*, forward flow; *REV*, reverse flow. Upper panels: The slope of the seesaw (shown in red) represents pressure gradient, and the *arrow* (in green) represents flow velocity and direction. Changes in pressure gradient and flow velocity are shown in chronological order from early systole (A) late systole/early diastole (B) to mid-diastole (C) Middle panels: Femoral flow waveform is depicted in time domain, with the horizontal *dotted line* as zero flow. The *green circle* represents femoral flow at the corresponding time. Lower panels indicate main hemodynamic events.

FIGURE 39.3 Estimated aortic, carotid, renal, and femoral blood flow patterns during systole and early diastole in the case of distensible aorta (left) and stiff aorta (right).[66] Aortic forward and reverse flows are depicted as *arrows* in terms of magnitude and direction. *Light green arrows* represent Windkessel function of descending thoracic aorta.

Aortic calcification

Clinical evidence

As mentioned above, several previous studies have investigated the associations between aortic stiffness and local atherosclerosis in coronary and lower extremity arteries. However, atherosclerosis is a systemic but patchy disease; thus, the presence of plaque in one area might not equate to its presence in another. As such, studies examining the link between arteriosclerosis and atherosclerosis have also included the aorta itself.

In the Rotterdam Study of elderly subjects,[58] atherosclerosis of the abdominal aorta was determined by assessing the calcified deposits on a plain radiograph. The results showed that an increased number of aortic calcified plaques was associated with a higher carotid-femoral PWV.[58] A study of healthy volunteers also confirmed a significant association between aortic PWV (but not AIx) and aortic calcification, which was quantified as aortic calcium content observed from high-resolution computed tomography.[69] In patients with chronic kidney disease, a strong positive association between aortic calcification and stiffness is well recognized.[70,71] In a recent prospective study investigating annual changes in brachial-ankle PWV and aortic calcium score, increased aortic calcification was found to be an independent determinant of greater progression of arterial stiffness in healthy middle-aged men.[72]

Compared with calcified plaques, the association between noncalcified atheromatous plaques and aortic stiffness is less obvious. A heritability study of female twins used combined computed tomography and MRI to demonstrate that, whereas there was an independent significant association between aortic PWV and calcification mediated by genetic factors, aortic PWV was not linked to plaque score.[73] An autopsy study that examined the relationship between premortem carotid-femoral PWV and postmortem plaque scores of systemic large arteries showed only a weak correlation, which was independent of age and blood pressure.[74] A recent magnetic resonance study of subjects without clinical symptoms of cardiovascular disease failed to find an independent association between total arterial compliance (the ratio of pulse pressure to indexed stroke volume) and atherosclerotic stenosis of systemic large arteries.[75]

Mechanism

Aortic stiffening has generally been thought to result primarily from structural degeneration of elastic fibers in the medial layer, which is accompanied by an increase in collagen fibers, ground substance, and often calcium deposition. Given the evidence mentioned above,[58,69−72] aortic calcification is causally linked to aortic stiffness and can be proposed as an additional mechanism for aortic

stiffening. Aortic calcification is pathologically classifiable into two types: (1) intimal calcification attributable to advanced atherosclerotic plaques and (2) medial calcification attributable to arteriosclerosis. The reported lack of association between early-stage (noncalcified) atheromatous plaques and stiffness[73] suggests that aortic stiffness is determined by calcification rather than by plaque burden alone. Accordingly, aortic stiffening is likely to be due to medial more than intimal calcification.[76]

However, it is also possible that aortic calcification is a consequence, rather than a cause, of aortic stiffening. Hypertension (which often accompanies aortic stiffening) is associated with increased, and faster progression of, calcification.[77] This association is theoretically explicable on the basis that increased repetitive tensile stress resulting from aortic stiffening accelerates elastic degeneration of the aortic wall, thereby contributing to aortic calcification. If this is the case, the prognostic significance of aortic calcification for predicting cardiovascular disease[77] is likely a result of adverse hemodynamic effects with respect to pulsatile load on the heart and arteries, where plaque rupture may cause thrombosis and tissue infarction. The potential mechanisms by which aortic pulsatile hemodynamics cause aortic plaque instability and thrombosis in patients with a stiff aorta will be discussed in the next section of *Stroke and Cerebrovascular Disease*.

Stroke and cerebrovascular disease

Clinical evidence

Stroke is the second leading cause of death worldwide and is responsible for excessive loss of disability-adjusted life years. Although age-standardized mortality rates decreased sharply from 1990 to 2016, the decrease in age-standardized incidence has been less steep, indicating that the burden of stroke remains high.[78]

Associations between aortic stiffness and stroke have been investigated in many previous studies. Cross-sectional, case−control studies have shown greater aortic stiffness in patients with acute ischemic stroke.[79,80] Longitudinal prospective studies have shown aortic PWV to be predictive of stroke mortality.[8,81,82] Laurent et al.[81] reported that each 1-SD (4 m/s) increase in carotid-femoral PWV was associated with a relative risk increase of 1.72 for fatal stroke. A metaanalysis of 16 prospective studies confirmed the significant predictive ability, independent of conventional risk factors, of aortic PWV for stroke events.[10] Aortic PWV is also a predictor of functional outcome in patients after ischemic stroke.[83]

Arterial stiffness is related not only to major stroke events but also to cerebral small vessel disease. Increased PWV was found in asymptomatic individuals[84−87] as well as those with symptomatic[88] lacunar stroke. Patients with

lacunar stroke are likely to have higher aortic PWV than patients with large-artery atherosclerotic, cardioembolic, or cryptogenic stroke.[89] Higher aortic PWV is also associated with the presence of white matter hyperintensities (WMHs), whether qualified using the Fazekas scale or quantified using hyperintensity volume.[85−87,90−93] In two prospective studies, baseline aortic PWV was shown to be independently predictive of WMH volume after 7−10 years.[94,95] Aortic PWV is also cross-sectionally associated with cerebral microbleeds[90] and enlarged perivascular (Virchow−Robin) spaces.[96]

These microvascular brain lesions (WMHs, lacunar infarcts, microbleeds, and enlarged perivascular spaces) are closely linked to cognitive impairment. In addition, a number of studies have reported a cross-sectional relationship between increased aortic stiffness and cognitive decline using mini-mental state examination scores.[97,98] Longitudinal studies have also shown that aortic stiffness is associated with faster rates of cognitive decline[99,100] and can be predictive of mild cognitive impairment and dementia.[101]

Analogous to aortic stiffness, measures of central hemodynamics have also been considered to be predictive of, and significantly associated with, stroke. A cross-sectional study demonstrated higher aortic AIx in patients with acute ischemic stroke than in control subjects.[88] Several prospective studies have shown that central pulse pressure and AIx predict cardiovascular events, including major (mostly large vessel) stroke, and their predictive abilities can be more precise than, or independent of, brachial blood pressure.[18,22,102,103]

Recent focus on central hemodynamics has been directed toward the prediction of asymptomatic small vessel diseases in the brain. Kearney-Schwartz et al.[104] were the first to report aortic AIx as an independent correlate of the severity of WMHs when they were assessed using the Fazekas scale, and this finding was confirmed by subsequent studies.[105,106] Shrestha et al. showed central systolic pressure to be associated with WMH severity independent of carotid plaque score.[107] Radial late systolic pressure (an estimate of aortic systolic pressure)[108] and central pulse pressure[86] are associated with silent lacunar infarcts. Aortic AIx can serve as a potential predictor of short-term outcomes (e.g., length of stay in hospital) after acute ischemic stroke, due largely to lacunar infarction.[109]

Central hemodynamic measures can predict brain function. Aortic pulse pressure and AIx were correlated with memory speed in healthy volunteers.[110] A cross-sectional observation of the Framingham Heart study showed that wider central pulse pressure was associated with lower logical memory-delayed scores.[85] In a prospective survey of the Framingham cohort, higher baseline central pulse pressure (as well as carotid-femoral PWV)

was associated with greater progression of neurocognitive decline, independent of the WMH volume.[111]

Mechanism

Cerebrovascular disease can be classified into macrovascular and microvascular types. Macrovascular (large vessel) stroke is generally attributable to atherothrombotic lesions in the carotid, cerebral, or vertebral arteries, or to thromboembolism of cardiac origin. Macrovascular stroke occurs frequently in the cortical regions that are perfused from the outside by branches arising from the pial arterial plexus. In contrast, microvascular stroke (including lacunar stroke, branch atheromatous disease, and intracerebral hemorrhage) occurs more often in the deep regions that are perfused from the inside out by short penetrating branches, which arise directly from the large cerebral arteries and circle of Willis.
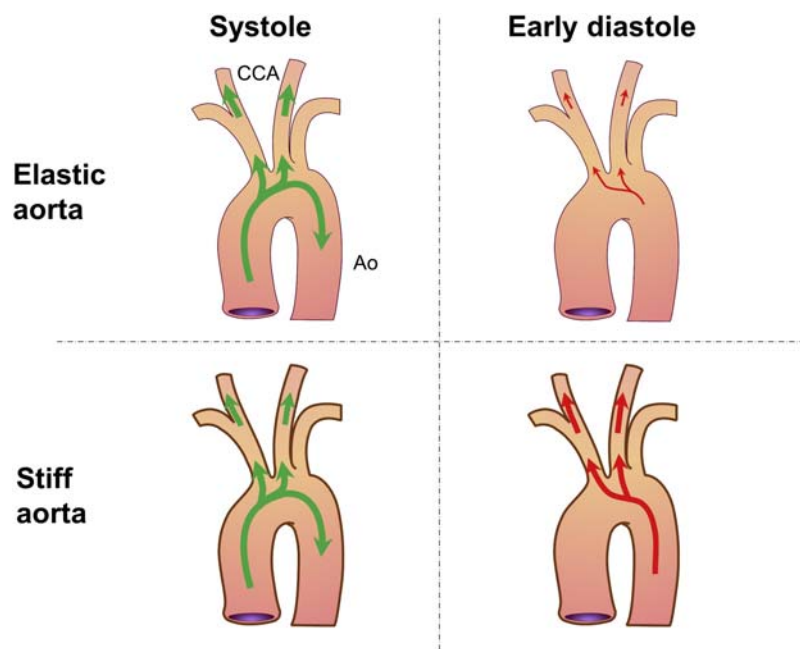
One of the main mechanisms for macrovascular stroke is thromboembolism secondary to atheromatous plaque rupture in the carotid, cerebral, or vertebral arteries. Increased pulsatile stress may be responsible for plaque vulnerability and disruption,[112] given that pulse pressure is independently associated with carotid plaque ulceration.[50] Aortic stiffness is also likely related to this mechanism by increasing the central (carotid) pulse pressure. The second mechanism is cardiogenic embolism attributable to atrial fibrillation. A prospective study demonstrated that a wider central pulse pressure and higher AIx are associated with an increased risk of new-onset atrial fibrillation,[113] suggesting a potential involvement of central hemodynamics and peripheral wave reflection in triggering the development of embolic stroke.

Previously, as many as 25% of all ischemic strokes have been considered to be from unknown causes ("cryptogenic"). However, the current understanding is that most cases of cryptogenic stroke are attributable to embolic stroke of an undetermined source.[114] Potential embolic sources include minor-risk heart disease (e.g., aortic valve stenosis), covert paroxysmal atrial fibrillation, cancer-related emboli, arteriogenic emboli, and paradoxical embolism (e.g., due to the right-to-left shunt via patent foramen ovale). Arteriogenic emboli have generally been attributed to nonstenotic (<50% diameter stenosis) atherosclerotic plaques in the carotid arteries, vertebral arteries, ascending aorta, or an aortic arch proximal to the origin of the supra-aortic arteries. Recent evidence, however, indicates that even the descending thoracic aorta (which is distal to the origin of the supra-aortic arteries) is a potential source for embolism.[115] Such a retrograde plaque embolism can occur[116] because the proximal descending aorta has flow reversal in early diastole,[117] which can transport detached plaques from the descending aorta or

aortic arch to the supra-aortic arteries.[116] Of further importance, it was found that aortic stiffening (which might be exacerbated by atherosclerotic plaque lesions) increases aortic flow reversal, which can prompt any mobile complex plaques to detach from the aortic wall and increase the risk that they will flow into the supra-aortic arteries (Fig. 39.4).[117] It is also possible that degenerated aortas exhibit complex vortices that may include caudal to cranial flow in the arch or proximal descending aorta even during systole,[118] which could also trigger thrombus formation and retrograde embolism. In addition, greater aortic flow reversal contributes to a reduction in glomerular filtration rate,[66] which is recognized as a strong risk factor for stroke. There is also solid evidence that aortic atherosclerosis is one of the leading causes of embolic stroke,[119] and aortic complex plaques are much more prevalent in the descending aorta than in the ascending aorta or aortic arch.[120] Recent investigations have demonstrated that cryptogenic stroke patients more often have large vulnerable plaques in the aortic arch and descending aorta than control subjects,[121] and aortic retrograde flow markedly increases in stroke patients with concomitant complex plaques in the proximal descending aorta.[121] Taken together, further investigation is needed to establish the clinical importance of retrograde plaque embolism as a cause of cryptogenic stroke.

Similar to macrovascular stroke, microvascular cerebral diseases are attributed to aortic stiffening and altered central hemodynamics, but the underlying mechanisms may be different. The deep perforating arteries, which are responsible for subcortical lacunar infarcts and WMHs, directly branch off of the large cerebral arteries. These short, small arteries are exposed to the high pulsatile pressure of the large arteries and are therefore particularly vulnerable to cyclic tensile stress. Moreover, like the kidney,[67] the brain requires high-flow, low-resistance (and low-impedance[122]) arterial properties because of its high metabolic demands. This inevitably exposes its fragile microvessels to torrential, highly pulsatile flow from the large arteries upstream.[24] Such high pressure and flow pulsations may predispose patients to microvascular injury in the subcortical areas, which can subsequently lead to tissue damage, and finally to hypoperfusion. White matter is more susceptible to hypoperfusion because it is far less vascularized and receives less perfusion than the gray matter.

Large-artery (aorta and carotid artery) stiffening increases pressure and flow pulsations, both of which are transmitted deeply into the cerebral microvasculature, can cause microvascular baro- and trauma from excessive shear forces, respectively, leading to lacunar infarction or microbleeding in the basal ganglia. Microvascular trauma may also cause extravascular fluid exudation and
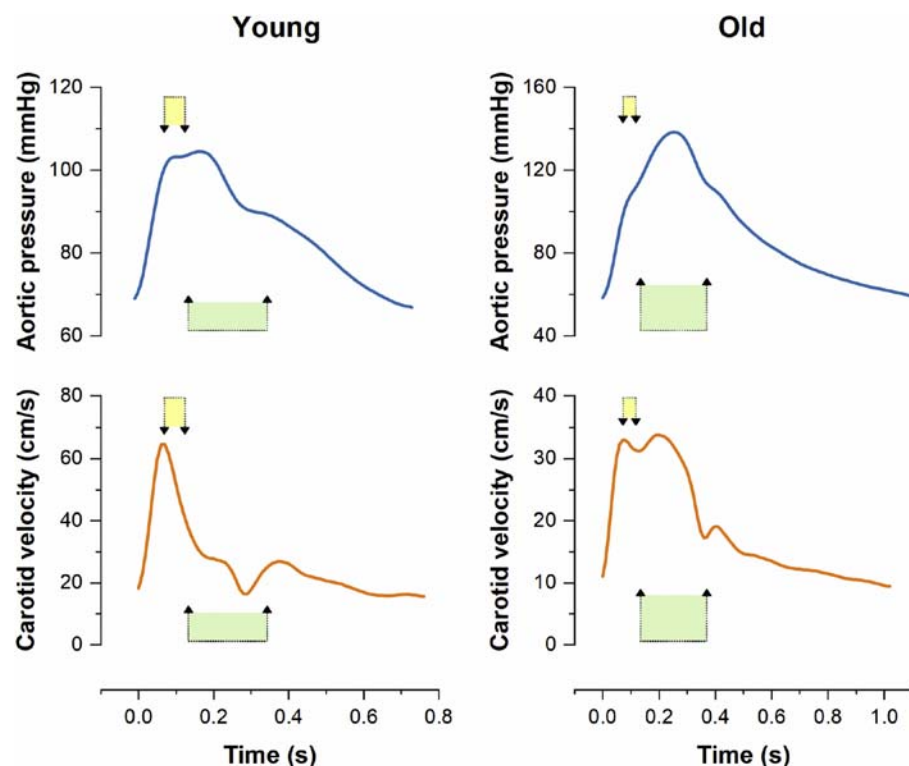
FIGURE 39.4 Association between aortic stiffness and flow dynamics in systole (left) and early diastole (right).[117] *Green* and *red arrows* represent forward and reverse flows, respectively. Thickness and length of *arrow lines* indicate flow intensity. *Ao* indicates aorta; *CCA*, common carotid artery.

perivascular tissue edema, resulting in WMHs.[93,123] In fact, the pulsatility index (a measure of flow pulsation) of the middle cerebral artery is independently associated with WMH, along with aortic stiffness.[124] Recent studies have emphasized the pathogenic influence of peripheral pressure wave reflection on increasing the flow as well as pressure pulsations in the cerebral vasculature. Pressure wave reflection from the lower body penetrates the brain as a forward wave, this increasing pressure and flow in the carotid and brain circulation. Such influence of wave reflection becomes more marked with advancing age (Fig. 39.5). Furthermore, impedance matching at the aortic–carotid interface (due to aortic stiffening) paradoxically promotes the penetration of the reflected wave returning from the lower body into the carotid arteries.[125] Late systolic augmentation of the carotid flow, which is determined by aortic stiffness and aortic pressure augmentation,[126] was found to be associated with the presence and severity of WMHs (Fig. 39.6).[106] In addition, flow AIx was more predictive of WMHs than the pressure AIx.[106] The flow peak in early systole markedly attenuates while traveling from the extracranial to intracranial arteries but, in contrast, the flow peak or shoulder in late systole (which is augmented by pressure wave reflection) remains unchanged throughout the arterial path.[126,127] This suggests that the late, rather than early, systolic peak of the carotid artery is an indicator of intracerebral flow pulsation. The importance of the late systolic peak flow is also supported by the finding that intracranial (including middle cerebral and basilar) artery flow waveform (recorded with transcranial Doppler ultrasound) resembles the central aortic pressure waveform,[122] in which the late systolic peak is generally more prominent than the early systolic peak.
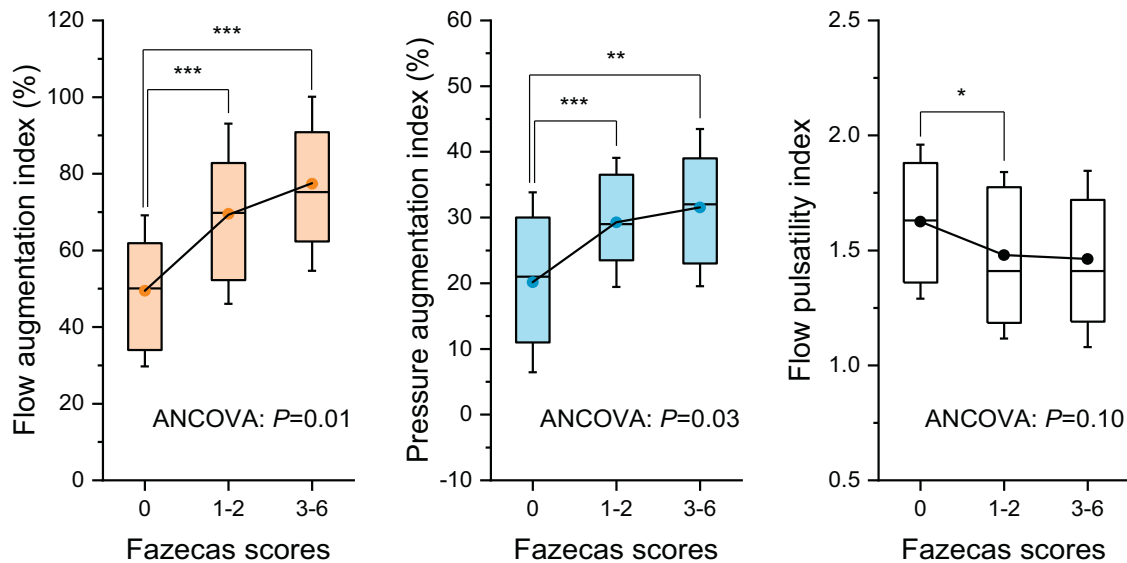
The presence of cerebral small vessel disease may account for the relationship between aortic stiffening and cognitive impairment. In fact, one study showed a direct association between higher aortic PWV and lower memory function to attenuate when WMHs and cerebrovascular resistance were regarded as mediators in pathway analysis.[128] However, it is also possible that the relationship between aortic stiffness and cognitive dysfunction appears even before overt small vessel disease develops, if cerebral blood flow is decreased. A recent study has reported greater aortic stiffening relative to lower regional cerebral blood flow in cognitively normal older adults, especially individuals with increased genetic predisposition for Alzheimer's disease.[129]

The above-mentioned discussion has focused mainly on aortic stiffness, as measured by carotid-femoral PWV. A recent metaanalysis claimed that carotid stiffness, as

FIGURE 39.5 Aortic pressure and carotid velocity pulse waveforms in young (left) and old (right) subjects.[106] The early *double down arrow* (in yellow) represents the suggested influence of wave reflection from the upper body, and the later *double up arrow* (in green) wave reflection from the lower part of the body. The length and interval of the *double arrows* indicate the estimated intensity and duration of wave reflection, respectively.

FIGURE 39.6 Association between carotid hemodynamic measures and white matter hyperintensities (WMH).[103] WMH was classified using Fazekas scale into three groups: none (0), mild (1−2), and moderate-to-severe (3−6) WMH. ANCOVA indicates analysis of covariance adjusted by potential covariates. ***$P < .001$, **$P = .01$, *$P = .03$.

assessed by ultrasound, is associated with incident stroke independent of aortic stiffness, and carotid stiffness can improve stroke risk prediction beyond aortic PWV.[130] In addition, measurement of carotid-cerebral PWV may be useful to detect segment atherosclerosis between the common carotid artery and ipsilateral middle cerebral artery,[131] which is the most frequent cause of anterior circulation ischemic stroke. Further studies are needed to clarify the clinical usefulness and pathophysiological implications of these local stiffness measurements for stroke prediction and prevention.

Although not directly related to atherosclerosis, some of the mechanisms discussed above are also relevant for cognitive dysfunction associated with aortic stiffening, which is discussed in more detail in Chapter 41.

Perspectives

In conclusion, aortic stiffness and central hemodynamics are deeply involved in the pathophysiological mechanisms of atherosclerotic diseases. Current data imply that destiffening therapy and antihypertensive therapy may have the potential to ameliorate central hemodynamic abnormalities and improve the long-term prognosis of patients with systemic atherosclerotic diseases. The reported contribution of aortic calcification to arterial stiffness indicates that anticalcification therapy may also be a potential therapeutic modality for preventing aortic stiffening. Future investigations are needed to clarify whether these therapies can contribute to the stabilization or regression of atheromatous plaques and to the restoration of blood flow into target organs.

References

1. Lehmann ED, Watts GF, Fatemi-Langroudi B, Gosling RG. Aortic compliance in young patients with heterozygous familial hypercholesterolaemia. **Clin Sci**. 1992; 83:717−721.
2. Lehmann ED, Watts GF, Gosling RG. Aortic distensibility and hypercholesterolaemia. **Lancet**. 1992; 340:1171−1172.
3. Collaborators GBDCD. Global, regional, and national age-sex-specific mortality for 282 causes of death in 195 countries and territories, 1980-2017: a systematic analysis for the global burden of disease study 2017. **Lancet**. 2018; 392:1736−1788.
4. Townsend RR, Wilkinson IB, Schiffrin EL, et al. Recommendations for improving and standardizing vascular research on arterial stiffness: a scientific statement from the American Heart Association. **Hypertension**. 2015; 66:698−722.
5. Covic A, Haydar AA, Bhamra-Ariza P, Gusbeth-Tatomir P, Goldsmith DJ. Aortic pulse wave velocity and arterial wave reflections predict the extent and severity of coronary artery disease in chronic kidney disease patients. **J Nephrol**. 2005; 18:388−396.
6. Yannoutsos A, Ahouah M, Dreyfuss Tubiana C, Topouchian J, Safar ME, Blacher J. Aortic stiffness improves the prediction of both diagnosis and severity of coronary artery disease. **Hypertens Res**. 2018; 41:118−125.
7. Boutouyrie P, Tropeano AI, Asmar R, et al. Aortic stiffness is an independent predictor of primary coronary events in hypertensive patients: a longitudinal study. **Hypertension**. 2002; 39:10−15.
8. Mattace-Raso FU, van der Cammen TJ, Hofman A, et al. Arterial stiffness and risk of coronary heart disease and stroke: the Rotterdam study. **Circulation**. 2006; 113:657−663.
9. Vlachopoulos C, Aznaouridis K, Stefanadis C. Prediction of cardiovascular events and all-cause mortality with arterial stiffness: a systematic review and meta-analysis. **J Am Coll Cardiol**. 2010; 55:1318−1327.
10. Ben-Shlomo Y, Spears M, Boustred C, et al. Aortic pulse wave velocity improves cardiovascular event prediction: an individual

participant meta-analysis of prospective observational data from 17,635 subjects. **J Am Coll Cardiol**. 2014; 63:636−646.

11. Ohyama Y, Ambale-Venkatesh B, Noda C, et al. Aortic arch pulse wave velocity assessed by magnetic resonance imaging as a predictor of incident cardiovascular events: the MESA (multi-ethnic study of atherosclerosis). **Hypertension**. 2017; 70:524−530.

12. Sarafidis PA, Loutradis C, Karpetas A, et al. Ambulatory pulse wave velocity is a stronger predictor of cardiovascular events and all-cause mortality than office and ambulatory blood pressure in hemodialysis patients. **Hypertension**. 2017; 70:148−157.

13. Nishijima T, Nakayama Y, Tsumura K, et al. Pulsatility of ascending aortic blood pressure waveform is associated with an increased risk of coronary heart disease. **Am J Hypertens**. 2001; 14:469−473.

14. Weber T, Auer J, O'Rourke MF, et al. Arterial stiffness, wave reflections, and the risk of coronary artery disease. **Circulation**. 2004; 109:184−189.

15. Hashimoto J, Ito S. Central blood pressure and prediction of cardiovascular events. **Curr Hypertens Rev**. 2012; 8:108−113.

16. Ueda H, Hayashi T, Tsumura K, Yoshimaru K, Nakayama Y, Yoshikawa J. The timing of the reflected wave in the ascending aortic pressure predicts restenosis after coronary stent placement. **Hypertens Res**. 2004; 27:535−540.

17. Weber T, Auer J, O'Rourke MF, et al. Increased arterial wave reflections predict severe cardiovascular events in patients undergoing percutaneous coronary interventions. **Eur Heart J**. 2005; 26:2657−2663.

18. Chirinos JA, Zambrano JP, Chakko S, et al. Aortic pressure augmentation predicts adverse cardiovascular events in patients with established coronary artery disease. **Hypertension**. 2005; 45:980−985.

19. Weber T, O'Rourke MF, Lassnig E, et al. Pulse waveform characteristics predict cardiovascular events and mortality in patients undergoing coronary angiography. **J Hypertens**. 2010; 28:797−805.

20. Chirinos JA, Kips JG, Jacobs Jr DR, et al. Arterial wave reflections and incident cardiovascular events and heart failure: MESA (multi-ethnic study of atherosclerosis). **J Am Coll Cardiol**. 2012; 60:2170−2177.

21. Chirinos JA, Zambrano JP, Chakko S, et al. Relation between ascending aortic pressures and outcomes in patients with angiographically demonstrated coronary artery disease. **Am J Cardiol**. 2005; 96:645−648.

22. Jankowski P, Kawecka-Jaszcz K, Czarnecka D, et al. Pulsatile but not steady component of blood pressure predicts cardiovascular events in coronary patients. **Hypertension**. 2008; 51:848−855.

23. Niiranen TJ, Kalesan B, Mitchell GF, Vasan RS. Relative contributions of pulse pressure and arterial stiffness to cardiovascular disease. **Hypertension**. 2019; 73:712−717.

24. O'Rourke MF, Hashimoto J. Mechanical factors in arterial aging: a clinical perspective. **J Am Coll Cardiol**. 2007; 50:1−13.

25. Hashimoto J, Watabe D, Hatanaka R, et al. Enhanced radial late systolic pressure augmentation in hypertensive patients with left ventricular hypertrophy. **Am J Hypertens**. 2006; 19:27−32.

26. Hashimoto J, Nichols WW, O'Rourke MF, Imai Y. Association between wasted pressure effort and left ventricular hypertrophy in hypertension: influence of arterial wave reflection. **Am J Hypertens**. 2008; 21:329−333.

27. Franklin SS, Chow VH, Mori AD, Wong ND. The significance of low DBP in US adults with isolated systolic hypertension. **J Hypertens**. 2011; 29:1101−1108.

28. Watanabe H, Ohtsuka S, Kakihana M, Sugishita Y. Decreased aortic compliance aggravates subendocardial ischaemia in dogs with stenosed coronary artery. **Cardiovasc Res**. 1992; 26:1212−1218.

29. Saeki A, Recchia F, Kass DA. Systolic flow augmentation in hearts ejecting into a model of stiff aging vasculature. Influence on myocardial perfusion-demand balance. **Circ Res**. 1995; 76:132−141.

30. Leung MC, Meredith IT, Cameron JD. Aortic stiffness affects the coronary blood flow response to percutaneous coronary intervention. **Am J Physiol Heart Circ Physiol**. 2006; 290:H624−H630.

31. Kingwell BA, Waddell TK, Medley TL, Cameron JD, Dart AM. Large artery stiffness predicts ischemic threshold in patients with coronary artery disease. **J Am Coll Cardiol**. 2002; 40:773−779.

32. Nelson AJ, Puri R, Nicholls SJ, et al. Aortic distensibility is associated with both resting and hyperemic coronary blood flow. **Am J Physiol Heart Circ Physiol**. 2019; 317:H811−H819.

33. Buckberg GD, Fixler DE, Archie JP, Hoffman JI. Experimental subendocardial ischemia in dogs with normal coronary arteries. **Circ Res**. 1972; 30:67−81.

34. Buckberg GD, Towers B, Paglia DE, Mulder DG, Maloney JV. Subendocardial ischemia after cardiopulmonary bypass. **J Thorac Cardiovasc Surg**. 1972; 64:669−684.

35. Sarnoff SJ, Braunwald E, Welch Jr GH, Case RB, Stainsby WN, Macruz R. Hemodynamic determinants of oxygen consumption of the heart with special reference to the tension-time index. **Am J Physiol**. 1958; 192:148−156.

36. Barnard RJ, MacAlpin R, Kattus AA, Buckberg GD. Ischemic response to sudden strenuous exercise in healthy men. **Circulation**. 1973; 48:936−942.

37. Hoffman JI, Buckberg GD. The myocardial oxygen supply:demand index revisited. **J Am Heart Assoc**. 2014; 3:e000285.

38. Tsiachris D, Tsioufis C, Syrseloudis D, et al. Subendocardial viability ratio as an index of impaired coronary flow reserve in hypertensives without significant coronary artery stenoses. **J Hum Hypertens**. 2012; 26:64−70.

39. Namasivayam M, McEniery CM, Wilkinson IB, et al. Different effects of vascular aging on ischemic predisposition in healthy men and women. **Hypertension**. 2018; 72:1294−1300.

40. Johnson BD, Shaw LJ, Pepine CJ, et al. Persistent chest pain predicts cardiovascular events in women without obstructive coronary artery disease: results from the NIH-NHLBI-sponsored Women's Ischaemia Syndrome Evaluation (WISE) study. **Eur Heart J**. 2006; 27:1408−1415.

41. Guelen I, Mattace-Raso FU, van Popele NM, et al. Aortic stiffness and the balance between cardiac oxygen supply and demand: the rotterdam study. **J Hypertens**. 2008; 26:1237−1243.

42. Namasivayam M, Adji A, O'Rourke MF. Influence of aortic pressure wave components determined noninvasively on myocardial oxygen demand in men and women. **Hypertension**. 2011; 57:193−200.

43. Hashimoto J, Ito S. Central diastolic pressure decay mediates the relationship between aortic stiffness and myocardial viability: potential implications for aortosclerosis-induced myocardial ischemia. **J Hypertens**. 2017; 35:2034−2043.

44. Messerli FH, Frohlich ED, Ventura HO. Arterial compliance in essential hypertension. **J Cardiovasc Pharmacol**. 1985; 7(Suppl 2):S33−S35.

45. Torii S, Arima H, Ohkubo T, et al. Association between pulse wave velocity and coronary artery calcification in Japanese men. **J Atheroscler Thromb**. 2015; 22:1266−1277.

46. Strozecki P, Serafin Z, Adamowicz A, Flisinski M, Wlodarczyk Z, Manitius J. Coronary artery calcification and large artery stiffness in renal transplant recipients. **Adv Med Sci**. 2015; 60:240−245.

47. Funck KL, Laugesen E, Ovrehus K, et al. Increased high-risk coronary plaque burden is associated with arterial stiffness in patients with type 2 diabetes without clinical signs of coronary artery disease: a computed tomography angiography study. **J Hypertens**. 2017; 35:1235−1243.

48. Harbaoui B, Courand PY, Cividjian A, Lantelme P. Development of coronary pulse wave velocity: new pathophysiological insight into coronary artery disease. **J Am Heart Assoc**. 2017; 6.

49. Selwaness M, van den Bouwhuijsen Q, Mattace-Raso FU, et al. Arterial stiffness is associated with carotid intraplaque hemorrhage in the general population: the Rotterdam study. **Arterioscler Thromb Vasc Biol**. 2014; 34:927−932.

50. Lovett JK, Howard SC, Rothwell PM. Pulse pressure is independently associated with carotid plaque ulceration. **J Hypertens**. 2003; 21:1669−1676.

51. Song P, Rudan D, Zhu Y, et al. Global, regional, and national prevalence and risk factors for peripheral artery disease in 2015: an updated systematic review and analysis. **Lancet Glob Health**. 2019; 7:e1020−e1030.

52. Norgren L, Hiatt WR, Dormandy JA, et al. Inter-society consensus for the management of peripheral arterial disease (TASK II). **J Vasc Surg**. 2007; 45(Suppl S):S5−S67.

53. Catalano M, Scandale G, Carzaniga G, et al. Aortic augmentation index in patients with peripheral arterial disease. **J Clin Hypertens**. 2014; 16:782−787.

54. Zahner GJ, Gruendl MA, Spaulding KA, et al. Association between arterial stiffness and peripheral artery disease as measured by radial artery tonometry. **J Vasc Surg**. 2017; 66:1518−1526.

55. Brand M, Woodiwiss AJ, Michel F, Booysen HL, Veller MG, Norton GR. A mismatch between aortic pulse pressure and pulse wave velocity predicts advanced peripheral arterial disease. **Eur J Vasc Endovasc Surg**. 2013; 46:338−346.

56. Brewer LC, Chai HS, Bailey KR, Kullo IJ. Measures of arterial stiffness and wave reflection are associated with walking distance in patients with peripheral arterial disease. **Atherosclerosis**. 2007; 191:384−390.

57. Jacomella V, Shenoy A, Mosimann K, Kohler MK, Amann-Vesti B, Husmann M. The impact of endovascular lower-limb revascularisation on the aortic augmentation index in patients with peripheral arterial disease. **Eur J Vasc Endovasc Surg**. 2013; 45:497−501.

58. van Popele NM, Grobbee DE, Bots ML, et al. Association between arterial stiffness and atherosclerosis: the Rotterdam study. **Stroke**. 2001; 32:454−460.

59. Catalano M, Scandale G, Carzaniga G, et al. Increased aortic stiffness and related factors in patients with peripheral arterial disease. **J Clin Hypertens**. 2013; 15:712−716.

60. Mosimann K, Jacomella V, Thalhammer C, et al. Severity of peripheral arterial disease is associated with aortic pressure augmentation and subendocardial viability ratio. **J Clin Hypertens**. 2012; 14:855−860.

61. Khaleghi M, Kullo IJ. Aortic augmentation index is associated with the ankle-brachial index: a community-based study. **Atherosclerosis**. 2007; 195:248−253.

62. Eldrup N, Sillesen H, Prescott E, Nordestgaard BG. Ankle brachial index, C-reactive protein, and central augmentation index to identify individuals with severe atherosclerosis. **Eur Heart J**. 2006; 27:316−322.

63. Hashimoto J, Ito S. Pulse pressure amplification, arterial stiffness, and peripheral wave reflection determine pulsatile flow waveform of the femoral artery. **Hypertension**. 2010; 56:926−933.

64. Hashimoto J. Central hemodynamics and target organ damage in hypertension. **Tohoku J Exp Med**. 2014; 233:1−8.

65. Bogren HG, Buonocore MH. Blood flow measurements in the aorta and major arteries with mr velocity mapping. **J Magn Reson Imaging**. 1994; 4:119−130.

66. Hashimoto J, Ito S. Aortic blood flow reversal determines renal function: potential explanation for renal dysfunction caused by aortic stiffening in hypertension. **Hypertension**. 2015; 66:61−67.

67. Hashimoto J, Ito S. Central pulse pressure and aortic stiffness determine renal hemodynamics: pathophysiological implication for microalbuminuria in hypertension. **Hypertension**. 2011; 58:839−846.

68. Suzuki E, Kashiwagi A, Nishio Y, et al. Increased arterial wall stiffness limits flow volume in the lower extremities in type 2 diabetic patients. **Diabetes Care**. 2001; 24:2107−2114.

69. McEniery CM, McDonnell BJ, So A, et al. Aortic calcification is associated with aortic stiffness and isolated systolic hypertension in healthy individuals. **Hypertension**. 2009; 53:524−531.

70. Guerin AP, London GM, Marchais SJ, Metivier F. Arterial stiffening and vascular calcifications in end-stage renal disease. **Nephrol Dial Transplant**. 2000; 15:1014−1021.

71. Toussaint ND, Lau KK, Strauss BJ, Polkinghorne KR, Kerr PG. Associations between vascular calcification, arterial stiffness and bone mineral density in chronic kidney disease. **Nephrol Dial Transplant**. 2008; 23:586−593.

72. Guo J, Fujiyoshi A, Willcox B, et al. Increased aortic calcification is associated with arterial stiffness progression in multiethnic middle-aged men. **Hypertension**. 2017; 69:102−108.

73. Cecelja M, Hussain T, Greil G, et al. Multimodality imaging of subclinical aortic atherosclerosis: relation of aortic stiffness to calcification and plaque in female twins. **Hypertension**. 2013; 61:609−614.

74. Sawabe M, Takahashi R, Matsushita S, et al. Aortic pulse wave velocity and the degree of atherosclerosis in the elderly: a pathological study based on 304 autopsy cases. **Atherosclerosis**. 2005; 179:345−351.

75. Weir-McCall JR, Lambert M, Gandy SJ, et al. Systemic arteriosclerosis is associated with left ventricular remodeling but not atherosclerosis: a TASCFORCE study. **J Cardiovasc Magn Reson**. 2018; 20:7.

76. Niederhoffer N, Lartaud-Idjouadiene I, Giummelly P, Duvivier C, Peslin R, Atkinson J. Calcification of medial elastic fibers and aortic elasticity. **Hypertension**. 1997; 29:999−1006.

77. Iribarren C, Sidney S, Sternfeld B, Browner WS. Calcification of the aortic arch: risk factors and association with coronary heart disease, stroke, and peripheral vascular disease. **J Am Med Assoc**. 2000; 283:2810−2815.

78. Collaborators GBDS. Global, regional, and national burden of stroke, 1990-2016: a systematic analysis for the global burden of disease study 2016. **Lancet Neurol**. 2019; 18:439−458.

79. Sugioka K, Hozumi T, Sciacca RR, et al. Impact of aortic stiffness on ischemic stroke in elderly patients. **Stroke**. 2002; 33:2077−2081.

80. Saeed S, Waje-Andreassen U, Fromm A, et al. Early vascular aging in young and middle-aged ischemic stroke patients: the Norwegian stroke in the young study. **PLoS One**. 2014; 9, e112814.

81. Laurent S, Katsahian S, Fassot C, et al. Aortic stiffness is an independent predictor of fatal stroke in essential hypertension. **Stroke**. 2003; 34:1203−1206.

82. Sutton-Tyrrell K, Najjar SS, Boudreau RM, et al. Elevated aortic pulse wave velocity, a marker of arterial stiffness, predicts cardiovascular events in well-functioning older adults. **Circulation**. 2005; 111:3384−3390.

83. Gasecki D, Rojek A, Kwarciany M, et al. Aortic stiffness predicts functional outcome in patients after ischemic stroke. **Stroke**. 2012; 43:543−544.

84. Hashimoto J, Aikawa T, Imai Y. Large artery stiffening as a link between cerebral lacunar infarction and renal albuminuria. **Am J Hypertens**. 2008; 21:1304−1309.

85. Tsao CW, Seshadri S, Beiser AS, et al. Relations of arterial stiffness and endothelial function to brain aging in the community. **Neurology**. 2013; 81:984−991.

86. Mitchell GF, van Buchem MA, Sigurdsson S, et al. Arterial stiffness, pressure and flow pulsatility and brain structure and function: the Age, Gene/Environment Susceptibility (AGES)-Reykjavik study. **Brain**. 2011; 134:3398−3407.

87. Henskens LH, Kroon AA, van Oostenbrugge RJ, et al. Increased aortic pulse wave velocity is associated with silent cerebral small-vessel disease in hypertensive patients. **Hypertension**. 2008; 52:1120−1126.

88. Tuttolomondo A, Di Sciacca R, Di Raimondo D, et al. Arterial stiffness indexes in acute ischemic stroke: relationship with stroke subtype. **Atherosclerosis**. 2010; 211:187−194.

89. Wohlfahrt P, Krajcoviechova A, Jozifova M, et al. Large artery stiffness and carotid flow pulsatility in stroke survivors. **J Hypertens**. 2014; 32:1097−1103.

90. Poels MM, Zaccai K, Verwoert GC, et al. Arterial stiffness and cerebral small vessel disease: the Rotterdam Scan Study. **Stroke**. 2012; 43:2637−2642.

91. Coutinho T, Turner ST, Kullo IJ. Aortic pulse wave velocity is associated with measures of subclinical target organ damage. **JACC Cardiovasc Imaging**. 2011; 4:754−761.

92. Palta P, Sharrett AR, Wei J, et al. Central arterial stiffness is associated with structural brain damage and poorer cognitive performance: the aric study. **J Am Heart Assoc**. 2019; 8:e011045.

93. Maillard P, Mitchell GF, Himali JJ, et al. Aortic stiffness, increased white matter free water, and altered microstructural integrity: a continuum of injury. **Stroke**. 2017; 48:1567−1573.

94. Rosano C, Watson N, Chang Y, et al. Aortic pulse wave velocity predicts focal white matter hyperintensities in a biracial cohort of older adults. **Hypertension**. 2013; 61:160−165.

95. King KS, Chen KX, Hulsey KM, et al. White matter hyperintensities: use of aortic arch pulse wave velocity to predict volume independent of other cardiovascular risk factors. **Radiology**. 2013; 267:709−717.

96. Riba-Llena I, Jimenez-Balado J, Castane X, et al. Arterial stiffness is associated with basal ganglia enlarged perivascular spaces and cerebral small vessel disease load. **Stroke**. 2018; 49:1279−1281.

97. Hanon O, Haulon S, Lenoir H, et al. Relationship between arterial stiffness and cognitive function in elderly subjects with complaints of memory loss. **Stroke**. 2005; 36:2193−2197.

98. Watson NL, Sutton-Tyrrell K, Rosano C, et al. Arterial stiffness and cognitive decline in well-functioning older adults. **J Gerontol A Biol Sci Med Sci**. 2011; 66:1336−1342.

99. Scuteri A, Tesauro M, Appolloni S, Preziosi F, Brancati AM, Volpe M. Arterial stiffness as an independent predictor of longitudinal changes in cognitive function in the older individual. **J Hypertens**. 2007; 25:1035−1040.

100. Zeki Al Hazzouri A, Newman AB, Simonsick E, et al. Pulse wave velocity and cognitive decline in elders: the health, aging, and body composition study. **Stroke**. 2013; 44:388−393.

101. Pase MP, Beiser A, Himali JJ, et al. Aortic stiffness and the risk of incident mild cognitive impairment and dementia. **Stroke**. 2016; 47:2256−2261.

102. Roman MJ, Devereux RB, Kizer JR, et al. Central pressure more strongly relates to vascular disease and outcome than does brachial pressure: the Strong Heart Study. **Hypertension**. 2007; 50:197−203.

103. Pini R, Cavallini MC, Palmieri V, et al. Central but not brachial blood pressure predicts cardiovascular events in an unselected geriatric population: the ICARe Dicomano Study. **J Am Coll Cardiol**. 2008; 51:2432−2439.

104. Kearney-Schwartz A, Rossignol P, Bracard S, et al. Vascular structure and function is correlated to cognitive performance and white matter hyperintensities in older hypertensive patients with subjective memory complaints. **Stroke**. 2009; 40:1229−1236.

105. Nakano T, Munakata A, Shimaura N, Asano K, Ohkuma H. Augmentation index is related to white matter lesions. **Hypertens Res**. 2012; 35:729−732.

106. Hashimoto J, Westerhof BE, Ito S. Carotid flow augmentation, arterial aging, and cerebral white matter hyperintensities. **Arterioscler Thromb Vasc Biol**. 2018; 38:2843−2853.

107. Shrestha I, Takahashi T, Nomura E, et al. Association between central systolic blood pressure, white matter lesions in cerebral mri and carotid atherosclerosis. **Hypertens Res**. 2009; 32:869−874.

108. Ochi N, Kohara K, Tabara Y, et al. Association of central systolic blood pressure with intracerebral small vessel disease in Japanese. **Am J Hypertens**. 2010; 23:889−894.

109. Soiza RL, Davie MM, Williams DJ. Use of the augmentation index to predict short-term outcome after acute ischemic stroke. **Am J Hypertens**. 2010; 23:737−742.

110. Pase MP, Pipingas A, Kras M, et al. Healthy middle-aged individuals are vulnerable to cognitive deficits as a result of increased arterial stiffness. **J Hypertens**. 2010; 28:1724−1729.

111. Tsao CW, Himali JJ, Beiser AS, et al. Association of arterial stiffness with progression of subclinical brain and cognitive disease. **Neurology**. 2016; 86:619−626.

112. Falk E, Shah PK, Fuster V. Coronary plaque disruption. **Circulation**. 1995; 92:657−671.

113. Shaikh AY, Wang N, Yin X, et al. Relations of arterial stiffness and brachial flow-mediated dilation with new-onset atrial fibrillation: the Framingham Heart Study. **Hypertension**. 2016; 68:590−596.

114. Hart RG, Diener HC, Connolly SJ. Embolic strokes of undetermined source: support for a new clinical construct–authors' reply. **Lancet Neurol**. 2014; 13:967.

115. Harloff A, Strecker C, Dudler P, et al. Retrograde embolism from the descending aorta: visualization by multidirectional 3d velocity mapping in cryptogenic stroke. **Stroke**. 2009; 40:1505−1508.

116. Harloff A, Simon J, Brendecke S, et al. Complex plaques in the proximal descending aorta: an underestimated embolic source of stroke. **Stroke**. 2010; 41:1145−1150.

117. Hashimoto J, Ito S. Aortic stiffness determines diastolic blood flow reversal in the descending thoracic aorta: potential implication for retrograde embolic stroke in hypertension. **Hypertension**. 2013; 62:542−549.

118. Chirinos JA. Echocardiographic assessment of large artery stiffness. **J Am Soc Echocardiogr**. 2016; 29:1117−1121.

119. Kronzon I, Tunick PA. Aortic atherosclerotic disease and stroke. **Circulation**. 2006; 114:63−75.

120. Meissner I, Khandheria BK, Sheps SG, et al. Atherosclerosis of the aorta: risk factor, risk marker, or innocent bystander? A prospective population-based transesophageal echocardiography study. **J Am Coll Cardiol**. 2004; 44:1018−1024.

121. Wehrum T, Guenther F, Vach W, et al. Aortic atherosclerosis determines increased retrograde blood flow as a potential mechanism of retrograde embolic stroke. **Cerebrovasc Dis**. 2017; 43:132−138.

122. Kim MO, Li Y, Wei F, et al. Normal cerebral vascular pulsations in humans: changes with age and implications for microvascular disease. **J Hypertens**. 2017; 35:2245−2256.

123. Wardlaw JM, Valdes Hernandez MC, Munoz-Maniega S. What are white matter hyperintensities made of? Relevance to vascular cognitive impairment. **J Am Heart Assoc**. 2015; 4:001140.

124. Webb AJ, Simoni M, Mazzucco S, Kuker W, Schulz U, Rothwell PM. Increased cerebral arterial pulsatility in patients with leukoaraiosis: arterial stiffness enhances transmission of aortic pulsatility. **Stroke**. 2012; 43:2631−2636.

125. Chirinos JA. Large artery stiffness, microvascular function, and cardiovascular risk. **Circ-Cardiovasc Imag**. 2016; 9.

126. Hirata K, Yaginuma T, O'Rourke MF, Kawakami M. Age-related changes in carotid artery flow and pressure pulses: possible implications for cerebral microvascular disease. **Stroke**. 2006; 37:2552−2556.

127. de Roos A, van der Grond J, Mitchell G, Westenberg J. Magnetic resonance imaging of cardiovascular function and the brain: is dementia a cardiovascular-driven disease? **Circulation**. 2017; 135:2178−2195.

128. Cooper LL, Woodard T, Sigurdsson S, et al. Cerebrovascular damage mediates relations between aortic stiffness and memory. **Hypertension**. 2016; 67:176−182.

129. Jefferson AL, Cambronero FE, Liu D, et al. Higher aortic stiffness is related to lower cerebral blood flow and preserved cerebrovascular reactivity in older adults. **Circulation**. 2018; 138:1951−1962.

130. van Sloten TT, Sedaghat S, Laurent S, et al. Carotid stiffness is associated with incident stroke: a systematic review and individual participant data meta-analysis. **J Am Coll Cardiol**. 2015; 66:2116−2125.

131. Fu X, Liu Q, Zeng X, Huang S, Huang R, Gao Q. Association between cerebral arterial stiffness and large artery atherosclerosis in acute ischemic stroke. **J Stroke Cerebrovasc Dis**. 2018; 27:2993−3000.

This page intentionally left blank

Arterial stiffness and pulsatile hemodynamics in renal disease

Raymond R. Townsend

Perelman School of Medicine, University of Pennsylvania Health System, Philadelphia, PA, United States

Importance of kidney disease

Roughly one adult in seven has impaired kidney function relative to their age.[1] Kidney function is estimated by combining a serum creatinine level with age, gender, and race to calculate the estimated glomerular filtration rate (eGFR).[2] Currently (*c.2020*) an eGFR less than 60 mL/min/1.73 m^2 is considered the lower limit of normal, and values <60 reflect impaired kidney function.[3] Kidney disease is important for two reasons. First, when the kidney function declines to a level that causes symptoms ("uremia"), in the absence of undergoing dialysis or kidney transplantation, a person will die. Although dialysis is commonly undertaken, it is expensive, averaging about $90,000 (USD) per year in 2018 (https://pharm.ucsf.edu/kidney/need/statistics accessed July 2020). Transplantation is the preferred therapy when a patient losses kidney function to the point of end-stage kidney disease (ESKD), but there is an imbalance here since about 100,000 patients reach ESKD each year, but only 20−21,000 people are transplanted each year and waiting times for a kidney transplant can exceed 5 years.[4] Second, kidney function impairment enhances the likelihood of cardiovascular events,[5] particularly hospitalized heart failure,[6] adding further burden to the individual suffering with kidney disease, and the public health economic burden of caring for this population. Consequently, an understanding of the factors involved in kidney disease progression is critical to the development of intervention studies that can mitigate the otherwise relentless progression of kidney function loss that happens to most patients with chronic kidney disease (CKD).

Unique features of the kidney circulation

The consequences of increased arterial stiffness for an organ like the kidney are likely to be selectively amplified because of characteristics that require the kidney to filter a large volume of blood continuously. In most tissues, the microcirculation is protected from the increased pulsatility attending large artery stiffening by "upstream" arterial/arteriolar constriction. The kidney, however, has a much lower inherent vascular resistance and the pulsatile nature of the large artery pressure profile penetrates deep into the kidney microcirculation.[7,8] To understand the transmission of energy contained in the large artery pulse wave, and how it may be transmitted into the kidney circulation, Woodard and colleagues in the AGES-Reykjavik Study used magnetic resonance (MR) imaging and mediation analysis.[9] This study used a *pulsatility index*, defined as the maximum minus the minimum (i.e., the amplitude) of the flow waveform divided by the mean flow in the kidney artery as ascertained from the MR imaging. They observed that large artery stiffening was associated with greater transfer of pulsatile energy into the kidneys and an associated drop out of renal vessels (rarefaction). They also noted an elevation in renal vascular resistance in this cross-sectional study

which correlated with reduced kidney function. These findings link plausibly to the idea that as the aorta stiffens, the impedance mismatching between the aortic and renal vessels results in less local wave reflection, fostering damage to the kidney microcirculatory apparatus, especially the glomeruli. The result is further impairment in the filtration function of the glomeruli, adding to kidney function loss.

Another unique feature of the kidney circulation is the distribution of glomeruli in the cortex, where a subpopulation (of roughly 10%) is situated deep in the cortex at the corticomedullary junction. This location may be particularly vulnerable to vascular strain as shown in elegant work by Ito and colleagues in Japan.[10] Since the arcuate arteries traverse the corticomedullary area, the pressure wave should be higher in the more proximal segments of the branches leading to the nearby deepest glomeruli, potentially transmitting more energy, differentially, to these deeper juxtamedullary glomeruli via their afferent arterioles. The afferent arterioles in these juxtamedullary glomeruli are also quite short, and need to generate high vascular tone to protect their downstream glomeruli. The consequences of hypertension and diabetes, which take a toll on the afferent arterioles serving these glomeruli through reducing their "gatekeeper" function, result in glomerular damage, including

albuminuria. They have labeled this a "strain vessel hypothesis," and given that a similar vascular situation exists in the brain/eye and the coronary circulation, the emergence of albuminuria may be a signal linking the known associations of CKD to the brain,[11] retina,[12] and coronary[13] circulations potentially mediated through strain vessel damage in patients with CKD.

Role of known factors for chronic kidney disease progression

Unlike cardiovascular disease (CVD), fewer risk factors are known to be significantly associated with CKD occurrence and progression. Blood pressure elevation was among the first factors associated with the development of ESKD.[14] Diabetes contributes both to the occurrence of CKD and the rate at which kidney function is lost.[15] Increasing levels of urine protein excretion are also associated with a faster decline in kidney function.[16] In addition, the recent identification of the APOL1 disease alleles helps to explain the greater susceptibility to more rapid kidney function in patients of African descent.[17,18]

In recent years, more attention has been given to pulsatile hemodynamics and arterial stiffness in CKD which will be the basis for the balance of this chapter.[19]

In depth box for clinicians: unique features of the interactions between hemodynamics and the kidney

Although protection of the heart and brain from hypertension-mediated damage has been a consistent finding in hypertension trials, there is far less data guiding clinical practice on preserving kidney function. Surprisingly perhaps, there are little data to support the concept that treating elevated BP prevents kidney disease. Moreover, once kidney failure is established, recent trials like SPRINT have shown that more aggressive BP reduction does not translate into less need for dialysis or kidney transplantation. Why is this so? One reason to consider is that unlike the heart or the brain, the kidneys are located below the heart level, and when a person is sitting or standing, they experience higher levels of BP than the heart or the brain because the column of blood in the aorta contributes to the pressure that the kidneys "see." The peculiar nature of the kidney circulation that offers a very low resistance to blood flow in the interest of cleaning the circulation through filtering high volumes of blood occurs in a situation disadvantaged by exposure to these high pressures. The delicate filtration mechanism in the glomeruli of the kidney are scrupulously protected by the afferent arteriole. However, aging, diabetes, salt sensitivity, and perhaps obesity reduce the vigilance of the afferent arteriole protective effects, and these are groups that are susceptible to kidney failure. As described in the text, a clue to the afferent arteriolar failure is the presence of elevated protein, particularly albumin, in the urine. In our experience in the CRIC Study, proteinuria is the most impressive independent risk factor for the rate at which kidney failure progresses. Drugs which reduce the urinary protein losses also seem to favorably affect large artery stiffness. Furthering our understanding of the interactions of large artery stiffness, pressure wave reflection, and afferent arteriolar responsiveness represents a logical research initiative with a promise of substantial public health benefit.

Clinical epidemiology of large artery stiffness in chronic kidney disease

Cross-sectional findings

General populations with kidney measurements

A representative general population of 1291 people incorporated measures of large artery stiffness and in their cross-sectional study, Mourad and colleagues evaluated the relationship between kidney function using serum creatinine,[20] and PWV measured with the Complior © device.[21] They noted a direct correlation between increasing large artery stiffness and measures of decreasing kidney function, but only in the tertile with the lowest kidney function.

Chronic kidney disease—not on dialysis

In a Taiwanese study of established CKD patients, Wang and colleagues conducted measurements of carotid-femoral pulse wave velocity (cfPWV) using the Sphygmocor device,[22] and measurements of kidney function using the Cockcroft-Gault equation.[23,24] They observed an increase in cfPWV from an average value of 8.4 m/s in NKF Stage 1−2 kidney function, to values of 10.1 m/s in stages 3−4 and 11.6 m/s in stage 5.

The largest study to date of arterial stiffness measurements in nondialysis CKD patients is the NIH-funded Chronic Renal Insufficiency Cohort.[25] cfPWV measurements were incorporated into an annual visit of participants enrolled in this study beginning in 2005. The first publication from the CRIC study in 2564 CKD participants showed an average cfPWV of 9.5 m/s in a population ranging in age from 21 to 75 years.[26] More than one third of the CRIC participants had a cfPWV higher than 10 m/s, the level considered clinically important for future CVD events in the European guidance document.[27] Diabetes, present in roughly half the participants, contributed about 2 m/s greater cfPWV when matched for age with nondiabetic participants. This study also showed that for every 10 mL/min/1.73 m^2 decrement in eGFR, there was an increase of 0.4 m/s in cfPWV.

Chronic kidney disease—on dialysis (endstage kidney disease/end-stage renal disease)

In the Hemodialysis Patients treated with Atenolol or Lisinopril (HD-PAL) study,[28] Agarwal and colleagues measured aortic PWV using an echo-Doppler technique.[29] In hemodialysis patients with an average age of 52 years, they observed a mean aortic PWV of 7.0−7.2 m/s and found that atenolol was more effective than lisinopril on reducing arterial stiffness, but this was mediated by a reduction of BP and not an independent effect.

Several European Centers have studied aortic stiffness in hemodialysis patients,[30,31] including children on hemodialysis.[32] The often cited study of Pannier and colleagues from Paris evaluated 305 subjects aged 53 years at first study using carotid-femoral tonometry.[33] The mean aortic PWV was 11 ± 3 m/s. Their study also showed that while it was possible to also measure carotid-radial and femoral-dorsalis pedis PWV, these measures were not predictive of CV survival, while the aortic PWV was clearly (and impressively) so. This study settled the issue of which vascular bed to study prospectively in patients with kidney disease.

The work of Levin and colleagues[34] from Vancouver, Canada in peritoneal dialysis (PD) patients reveals a substantial spectrum of cfPWV, which was measured using the Sphygmocor device.[35] In their study of 50 PD patients, the overall cfPWV was about 10 m/s, but ranged from average values of about 8 m/s in those with a mean age of 48 years to more than 12 m/s for those with a mean age of 68 years.

An impressive number of cohorts have obtained cross-sectional and longitudinal evaluations of LAS in kidney disease including NephroTEST[36]; Hoorn[37]; Chronic Renal Insufficiency Standards Implementation Study (CRISIS)[38]; Age, Gene/Environment Susceptibility-Reykjavik Stud (AGES-Reykjavik)[39]; Taiwan[40]; Tokyo[41]; and Tohoku.[42]

Longitudinal studies (see Table 40.1)
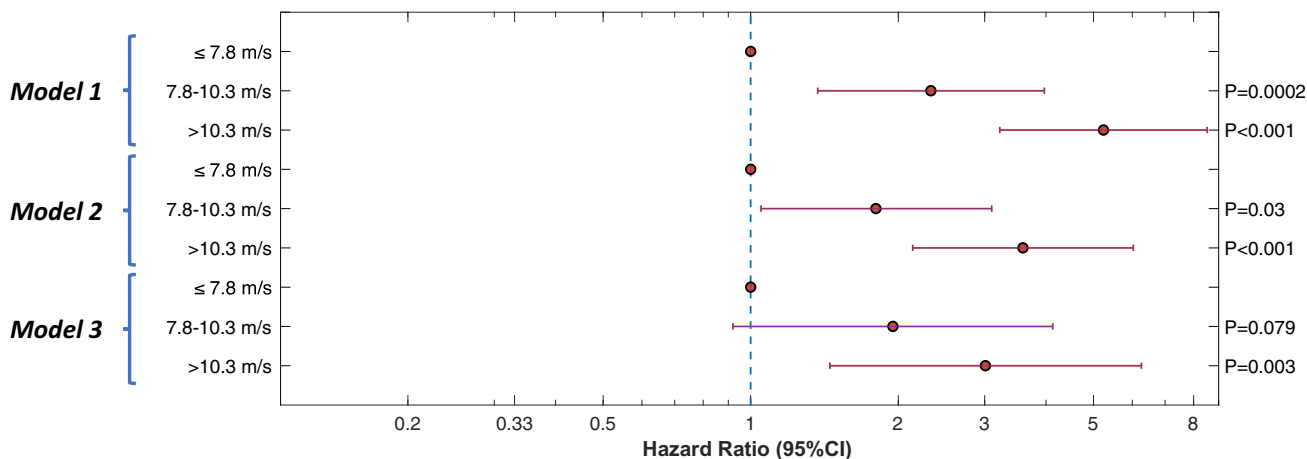
Increased arterial stiffness enhances the risks of death and the likelihood of CVD events, and contributes to a sharper decline in renal function in established CKD. The dramatic study of Pannier cited previously noted a marked reduction in survival in hemodialysis patients with the highest tertile of cfPWV.[33] In the Vlachopoulos meta-analysis, 4 of the 17 longitudinal studies of arterial stiffness in human cohorts enrolled patients exclusively with ESKD.[43] In that meta-analysis, hazard ratios for patients on dialysis with higher PWV values ranged from 2 to 4x the referent population for CV events and reduced survival. Arterial stiffness is clearly linked to reduced survival and likely a significant component of the marked disparity in longevity between a dialysis patient compared with an age matched non-CKD control.[44]

In the CRIC Study, we were able to measure cfPWV using the Sphygmocor © device in 12 enrolling centers in the United States.[25] We successfully obtained measurements on 2795 CRIC participants who underwent yearly assessment of kidney function for 4−5.5 years after their PWV measurement.[47] CRIC recruitment was specifically designed to encourage the participation of diabetic and black patients.[49] In our cfPWV Study, we observed that among our initial 2795 participants, 394 participants died during the 5.4 years of follow up for this outcome. We also observed that 504 participants reached ESKD (defined as

TABLE 40.1 Examples of longitudinal studies of arterial stiffness in established kidney disease cohorts.

Author year	n	Age ± SD	Method/ Device	%F	F/U duration (years)	Deaths	CV events	ESKD events	Comments
Blacher (1999)[45]	241	52 ± 16	Doppler	39%	6.0	73	48	N/A	ESKD only
Briet (2011)[36]	180	60 ± NR	Wall track and complior		3.5	10	NR	41	Increased carotid circumferential wall strain predicted GFR loss, cfPWV did not predict GFR change
Pannier (2005)[33]	305	53 ± 16	Complior	38%	5.8	96 (all CVD)	NR	N/A	End-stage renal disease only; aortic PWV predictive, but not PWV in arm or leg
Shoji (2001)[46]	265	55 ± 11	PWV-200	59%	5.3	81	NR	N/A	ESKD only; diabetics fared worse than non-DM
Townsend (2018)[47]	2795	60 ± 11	Sphygmocor	45%	4–5	394	NR	504	CKD not on dialysis; Tertiles of PWV predicted death and ESKD
Zoungas (2007)[48]	207	55 ± 13	Millar SPT-301	33%	3.6	17	65	N/A	ESKD only

cfPWV, carotid-femoral pulse wave velocity; *CKD*, chronic kidney disease; *DM*, diabetes mellitus; *ESKD*, end-stage kidney disease; *F*, female; *GFR*, glomerular filtration rate; *N/A*, not applicable; *NR*, not reported; *PWV*, pulse wave velocity.

FIGURE 40.1 Figure shows a horizontal bar graph depicting hazard ratios (with 95% CI) of carotid-femoral pulse wave velocity (PWV) tertiles in participants with chronic kidney disease for the outcome of first hospitalized heart failure in the CRIC Study. A PWV of less than or equal to 7.8 m/s is the referent group in all three models. Model 1 is the unadjusted HR for the heart failure outcome. Model 2 is HR of the heart failure outcome adjusted for age, race, sex, and enrollment site in the CRIC Study. Model 3 adjusted for diabetes mellitus, proteinuria, the presence of chronic obstructive pulmonary disease, mean arterial pressure, heart rate, high-density lipoprotein (HDL)-cholesterol, low-density lipoprotein (LDL)-cholesterol, body mass index, triglycerides, history of myocardial infarction (MI)/revascularization, current smoking, hemoglobin, human recombinant erythropoietin use, angiotensin-converting enzyme inhibitor use, beta blocker use, calcium channel blocker use, history of hypertension, fasting glucose, and serum albumin. *Adapted from Chirinos, J.A., et al., Arterial stiffness, central pressures and incident hospitalized heart failure in the chronic renal insufficiency cohort (CRIC) study.* **Circ Heart Fail.** *2014; 7(5):709−716.*

starting dialysis or receiving a kidney transplant) during the 4.1 years of follow up for this outcome. We noted that both the mean arterial pressure (MAP) and the cfPWV each had independent contributions to these outcomes. In an earlier study in CRIC, we studied 2602 participants who were free of heart failure at the time of cfPWV Study and noted that cfPWV was a significant and independent predictor of incident hospitalized heart failure in the CRIC Study participants (Fig. 40.1).[6] We observed a hazard ratio of 1.95 [0.92, 4.13; 95% CI] for the middle tertile of cfPWV (>7.8 m/s and <10.3 m/s), and 3.01 [1.45, $8 = 6.26$] for the highest tertile of cfPWV (>10.3 m/s) adjusted for diabetes mellitus, proteinuria, the presence of chronic obstructive pulmonary disease, MAP, heart rate, HDL-cholesterol, LDL-cholesterol, body mass index, triglycerides, history of MI/revascularization, current smoking, hemoglobin, human recombinant erythropoietin use, angiotensin-converting enzyme (ACE) inhibitor use, beta blocker use, calcium channel blocker use, history of hypertension, fasting glucose, and serum albumin.

Summarizing, large artery stiffness, as reflected in measurements of PWV is independently predictive of kidney function loss, ESKD, and interval CVD events. The high prevalence of diabetes in CKD populations, and the accelerated vascular aging that attends CKD, especially in patients with diabetes, are likely contributors to this phenomenon.[50] Mechanisms stiffening the large arteries in CKD are covered after the next section on pulsatility.

Clinical pulsatility indices and kidney function

Several indices exist that evaluate maximal, minimal, and mean flow parameters in the kidney circulation using either ultrasound or MR imaging. Ultrasound studies are more established, and most of the pulsatility literature on kidney function is ultrasound based.

Pulsatility index

Pulsatility is an inherent property of the circulatory system. It reflects the vulnerability differential across vascular regions, in which energy in the more proximal (upstream) vasculature enters into the (downstream) microcirculation, ideally at a desirable mean pressure, with the goal of providing adequate perfusion. An early paper describing the ultrasound-derived pulsatility index appeared in 1974.[51] The basic calculation of the pulsatility index ciphers (the peak systolic flow velocity minus the minimal diastolic flow velocity) divided by the mean flow velocity. An example of the usage of the pulsatility index was cited previously in this chapter using MR imaging.[9] The mechanisms by which pulsatility promotes vascular damage in an organ like the kidney result from a reduction in the mismatch of impedance between the aorta and the kidney circulation, which reduces wave reflection, enhances flow pulsatility, and promotes damage to and loss of the kidney

microcirculation, especially the glomeruli.[19] This, in turn, results in a decrement in kidney function.

Resistive index

A resistive index (RI) is also available which is calculated by subtracting the end-diastolic velocity from the peak systolic velocity, and then dividing that by the peak systolic velocity.[52] The interlobar and the arcuate arterial beds in the kidney are the insonation target in this measurement, and a commonly used normal range is 0.50−0.70 (it is a ratio, thus unitless).

It was initially hoped that the RI would predict benefit from interventions like percutaneous renal artery angioplasty, and be useful in patient selection for that invasive procedure.[53] In this high profile study, Radermacher and colleagues observed that an RI of >0.8 indicated a reduced likelihood of benefit following successful intervention on the main renal artery in terms of ultimate BP reduction, and stabilization or improvement of kidney function. Other studies have not found this to be the case,[54,55] for reasons which include the challenge of assessing the three-dimensional aspects of threatened blood flow inferred by a two dimensional arteriogram image.[56]

The use of the renal RI is more common, at least in this author's experience, compared with the pulsatility index. It is, however, often misinterpreted as being a proxy for kidney arterial "resistance," which it is not, despite the name.[57] What it does reflect is the influence of systemic hemodynamics, particularly that of the central aorta, on the kidney circulation.[42]
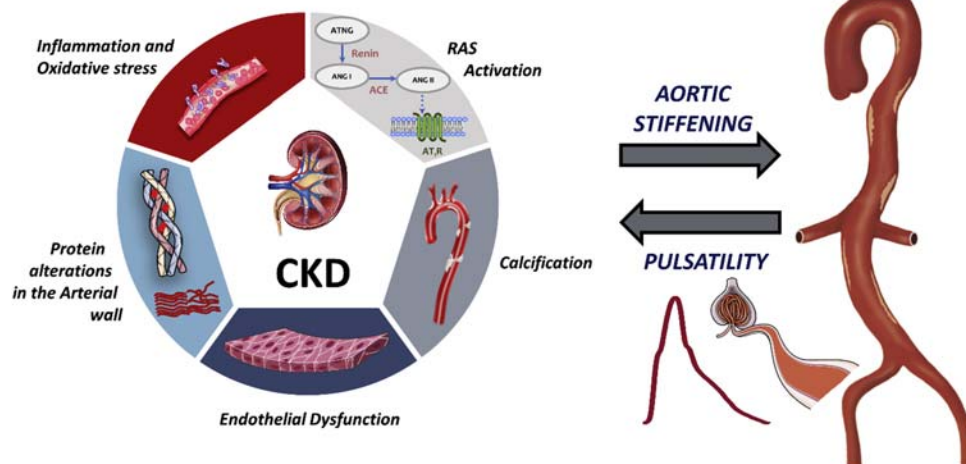
The use of the renal RI has a niche in kidney transplant care, where a number of findings have emerged over the years. Renal RI is a proxy for central hemodynamics in the kidney transplant recipient, and is more reflective of the milieu of the kidney transplant *recipient* rather than the *donor*,[58,59] and when the renal RI increases in conjunction with kidney allograft dysfunction, it is predictive of antibody-mediated rejection.[60]

Mechanisms of increased arterial stiffness in chronic kidney disease

The multitude of excretory and hormonal functions that are part of normal kidney function, when impaired or absent, underscore the complex nature of the influence of the kidney on large artery health. Moreover, most of the aberrations that occur as kidney function declines have bidirectional effect wherein the loss of kidney function worsens their influence and the resultant LAS increase in turn, continues to more kidney function loss (see Fig. 40.2).

Vascular calcification

Large vessel calcification has an adverse effect on arterial stiffness.[61] The increase in stiffness, in turn, promotes a greater pulse pressure which contributes to the pathophysiology of the vessel wall calcification processes, thus perpetuating a vicious cycle.[62] Both CKD and diabetes are marked by increased vascular calcification.[63] The mechanisms leading to vascular calcification in CKD involve a

FIGURE 40.2 Figure shows bidirectional relationship of processes within (or related to) kidney disease promoting large artery stiffness and, in turn the result of increased large arterial stiffening on kidney function in patients with chronic kidney disease. See text for details.

deranged bone-mineral axis with the result that vascular smooth muscle cells take on the phenotype of osteochondrogenic cells, a process worsened by elevated glucose and lipid levels, elevated phosphorous and aldosterone concentrations that characterize the CKD patient.[64] When vascular calcification is present, it markedly enhances the CV risk of patients with this profile, particularly in the presence of end stage renal disease.[65] At this time, there are no treatments to reverse calcification in humans, though the use of pyrophosphate in an animal model of uremia associated vascular calcification was promising,[66] and accession of the clinicaltrials.gov Website using the search term "vascular calcification" returned 75 results (accessed July 2020), thus, this may change in the near future.

Renin system activation

Increased renin system activity generates additional angiotensin-II, which in turn contributes to vasoconstriction, inflammation (superoxides), vascular remodeling, and increased production and release of aldosterone.[67–69] Many years of use of blockers of the renin system have demonstrated the potential benefit of ACE inhibitors, angiotensin receptor blockers (ARBs), and mineralocorticoid receptor antagonists in managing patients with CKD.[70] The use of ACE-inhibitors and ARBs may not necessarily reduce aldosterone concentration[71] and rationale exists for combining MRAs with these agents if the patient's potassium level can tolerate the combination.[72]

Changes in vessel wall proteins

There are two key proteins in the vascular smooth muscle, elastin and collagen. Elastin proteins have good recoil, but poor load bearing function.[73] Collagens have excellent load bearing, but poor recoil.[74] The combination of both protein types results in a desirable balance of recoil and load bearing in health. In CKD there is an accelerated fragmentation and loss of elastin, and an increase in the relative amount of collagen.[67] Additionally, there is increased cross linking of collagen which reduces its turnover in the vessel wall.[75] An increase in the activity of tissue matrix metalloproteinase (MMP) activity in CKD promotes greater elastin and collagen turnover, resulting in disarray of the extracellular matrix.[76] In particular, MMPs have been shown to be upregulated in the internal mammary artery of patients with CKD,[77] and in the kidney arteries of patients on dialysis compared with the levels in kidney donors,[78] and MMPs are felt to contribute in particular to the loss of elastin. As elastin is lost and collagen gained, the large artery wall becomes stiffer.[79] Specific chemical inhibition of MMPs as well as exercise are potential tools in altering MMP activity (Table 40.2).

Advanced glycation endproducts

Similar to the section immediately prior, the cross-linkage occurring within collagen proteins in the vessel wall contributes to larger artery stiffness, and another pathway by which this happens is through the nonenzymatic glycation of carbonyl products with cross linking, particularly at lysine residues in protein[80]. Such cross linking restricts the ability of inherent process to turn over collagen protein, leading to a build-up of collagen with increasing stiffness as the result. AGEs accumulate more rapidly in the kidneys of those with diabetic nephropathy—and more so with declining renal function.[81] AGEs are both generated by the kidney, in addition to settling within the kidney in diabetic and nondiabetic kidney diseases.[82] Hope remains for a nontoxic compound to be deployed in humans either blocking the generation of AGE or blocking the receptors for AGE (RAGE).[83,84]

TABLE 40.2 Potential interventions to reduce large artery stiffness in chronic kidney disease.

Process	Goal	Possible Rx
Increased pulsatility	Reduce pulsatility	Renin system blockade (angiotensin-converting enzyme—inhibitor, angiotensin-II receptor blockers)
Vascular calcification	Reduce calcium deposition	Vitamin K supplements, magnesium supplements, and pyrophosphate supplements
Metalloproteinase	Preserve elastin content	Doxycycline
Endothelial dysfunction	Improve vasodilation	Aerobic exercise and nitrates
Oxidative stress	Reduce reactive oxygen species generation; improve mitochondrial function	N-acetyl-cysteine supplements (in dialysis patients)
Glycation endproducts	Reduce formation of AGE or block the receptor for AGE	Green tea extract, sirtuin-1, and pyridoxamine

AGE, advanced glycation endproduct; *CKD*, chronic kidney disease; *LAS*, large artery stiffness; *Rx*, treatment.

Endothelial dysfunction

The ability of the endothelium of vessel, particularly in response to shear stress, to secrete nitric oxide (NO) and potentiate vascular smooth muscle relaxation is an important means to regulate blood flow in health.[85] The reduction in, or loss of, this capacity is termed endothelial dysfunction and is a recognized component of the vascular dysfunction attendant to CKD.[86] Endothelial dysfunction promotes large artery stiffness, particularly in CKD.[87] A principal mechanism of this endothelial dysfunction, but by no means the only mechanism, is the accumulation of asymmetric dimethyl-arginine (ADMA) in the circulation due to reduced renal excretion as kidneys fail.[88] ADMA accumulation interferes with intracellular mechanisms that free NO from arginine residues. We and others have shown that aerobic exercise improves endothelial function in CKD and also improves aortic pressure waveforms.[89]

Inflammation/oxidative stress

Chronic inflammation, characterized by increased circulating levels of inflammatory biomarkers, is part of the CKD profile,[90] particularly when co-morbidities like rheumatoid arthritis, and lupus are present.[91] Positron emission tomographic scanning using fluorodeoxyglucose has been used to investigate the presence of inflammation in the aortic wall, which in turn is associated with increased aortic stiffness.[92] Inflammation-mediated damage to vascular wall proteins like elastin reduces this component in aortic compliance, and healing phases of inflammation may deposit calcium in the vessel wall contributing yet further to large artery stiffening.[93] In the CRIC Study, we showed there were significant cross-sectional associations between elevated levels of inflammatory biomarkers and large artery stiffness.[94]

Oxidative stress also affects large artery wall function, particularly in CKD.[95] We have shown, for example, that specific inhibition of NADPH oxidases restores impaired cutaneous vasodilation in CKD.[96] However, a recent Cochrane review on this topic indicates that although administration of antioxidants in human CKD does no harm, it achieves little significant benefit on CVD endpoints, with the exception of dialysis patients, in which there was some encouraging outcome data.[97]

Therapies

One of the more significant problems in the study of large artery stiffness in humans has been the challenge of disentangling an intervention designed to improve stiffness from the simple hemodynamic benefit of lowering BP itself. This was addressed in the AHA Science Statement on arterial stiffness in humans.[98] In Table 40.2 are some examples of proposed therapies to possibly improve large artery stiffness in CKD. I suggest the reader consult www.clinicaltrials.gov, and enter either a keyword like "advanced glycation" or a compound like "green tea" in the site search box, since there is literally daily turnover of listings on this website. However, to date (August 2020), and to the best of the author's knowledge, there is no FDA-approved product or intervention specifically indicated to improve large artery stiffness in patients with CKD. A timely meta-analysis of destiffening therapies in dialysis patients evaluating pharmacologic approaches mainly for treating disordered bone-mineral metabolism (vitamin D, phosphate binders), or hypertension (CCB, RAS inhibitors), found mixed results and expressed concern over the low quality of many studies.[99] Similarly, a meta-analysis of nondrug therapies from the same group noted that lowering dialysate calcium concentration, careful volume management, and promoting intradialytic exercise also seem to improve large artery stiffness, however, again it is difficult to separate stiffness findings from that of systolic BP reduction.[100]

References

1. Hsu RK, Powe NR. Recent trends in the prevalence of chronic kidney disease: not the same old song. **Curr Opin Nephrol Hypertens**. 2017; 26(3):187−196.
2. Levey AS, Coresh J, Greene T, et al. Using standardized serum creatinine values in the modification of diet in renal disease study equation for estimating glomerular filtration rate. **Ann Intern Med**. 2006; 145(4):247−254.
3. Cirillo M, Lombardi C, Mele AA, Marcarelli F, Bilancio G. A population-based approach for the definition of chronic kidney disease: the CKD Prognosis Consortium. **J Nephrol**. 2012; 25(1):7−12.
4. System, U.S.R.D., 2019 USRDS annual data report: epidemiology of kidney disease in the United States, N.I.o.D.a.D.a.K.D. National Institutes of Health, Editor. 2019: Bethesda, MD.
5. Go AS, Chertow GM, Fan D, McCulloch CE, Hsu C-Y. Chronic kidney disease and the risks of death, cardiovascular events, and hospitalization. **N Engl J Med**. 2004; 351(13):1296−1305.
6. Chirinos JA, Khan AM, Bansal N, et al. Arterial stiffness, central pressures and incident hospitalized heart failure in the chronic renal insufficiency cohort (CRIC) study. **Circ Heart Fail**. 2014; 7(5):709−716.
7. O'Rourke M. Arterial stiffness, systolic blood pressure, and logical treatment of arterial hypertension. **Hypertension**. 1990; 15(4):339−347.
8. Salvi P, Parati G. Chronic kidney disease: arterial stiffness and renal function–a complex relationship. **Nat Rev Nephrol**. 2015; 11(1):11−13.
9. Woodard T, Sigurdsson S, Gotal JD, et al. Mediation analysis of aortic stiffness and renal microvascular function. **J Am Soc Nephrol**. 2015; 26(5):1181−1187.
10. Ito S, Nagasawa T, Abe M, Mori T. Strain vessel hypothesis: a viewpoint for linkage of albuminuria and cerebro-cardiovascular risk. **Hypertens Res**. 2009; 32(2):115−121.

11. Sandsmark DK, Messe SR, Zhang X, et al. Proteinuria, but not eGFR, predicts stroke risk in chronic kidney disease: chronic renal insufficiency cohort study. **Stroke**. 2015; 46(8):2075−2080.

12. Lee MK, Han K-D, Lee J-H, et al. Normal-to-mildly increased albuminuria predicts the risk for diabetic retinopathy in patients with type 2 diabetes. **Sci Rep**. 2017; 7(1):11757.

13. de Chickera SN, Bota SE, Kuwornu JP, et al. Albuminuria, reduced kidney function, and the risk of ST - and non-ST-segment-elevation myocardial infarction. **J Am Heart Assoc**. 2018; 7(20):e009995.

14. Klag MJ, Whelton PK, Randall BL, Neaton JD, Brancati FL, Stamler J. End-stage renal disease in African-American and white men. 16-year MRFIT findings. **J Am Med Assoc**. 1997; 277(16):1293−1298.

15. Susztak K, Bottinger EP. Diabetic nephropathy: a frontier for personalized medicine. **J Am Soc Nephrol**. 2006; 17(2):361−367.

16. Jafar TH, Stark PC, Schmid CH, et al. Proteinuria as a modifiable risk factor for the progression of non- diabetic renal disease. **Kidney Int**. 2001; 60(3):1131−1140.

17. Rostand SG, Brown G, Kirk KA, Rutsky EA, Dustan HP. Renal insufficiency in treated essential hypertension. **N Engl J Med**. 1989; 320:684−688.

18. Freedman BI, Kopp JB, Langefeld CD, et al. The apolipoprotein L1 (APOL1) gene and nondiabetic nephropathy in African Americans. **J Am Soc Nephrol**. 2010; 21(9):1422−1426.

19. Mitchell GF. Aortic stiffness, pressure and flow pulsatility, and target organ damage. **J Appl Physiol (1985)**. 2018; 125(6):1871−1880.

20. Mourad JJ, Pannier B, Blacher J, et al. Creatinine clearance, pulse wave velocity, carotid compliance and essential hypertension. **Kidney Int**. 2001; 59(5):1834−1841.

21. Pereira T, Maldonado J. Comparative study of two generations of the Complior device for aortic pulse wave velocity measurements. **Blood Press Monit**. 2010; 15(6):316−321.

22. Stea F, Bozec E, Millaseau S, Khettab H, Boutouyrie P, Laurent S. Comparison of the Complior Analyse device with Sphygmocor and Complior SP for pulse wave velocity and central pressure assessment. **J Hypertens**. 2014; 32(4):873−880.

23. Cockcroft DW, Gault MH. Prediction of creatinine clearance from serum creatinine. **Nephron**. 1976; 16:31−41.

24. Wang MC, Tsai WC, Chen JY, Huang JJ. Stepwise increase in arterial stiffness corresponding with the stages of chronic kidney disease. **Am J Kidney Dis**. 2005; 45(3):494−501.

25. Feldman HI, Appel LJ, Chertow GM, et al. The chronic renal insufficiency cohort (CRIC) study: design and methods. **J Am Soc Nephrol**. 2003; 14(7 Supple 2):S148−S153.

26. Townsend RR, Wimmer NJ, Chirinos JA, et al. Aortic PWV in chronic kidney disease: a CRIC ancillary study. **Am J Hypertens**. 2010; 23(3):282−289.

27. Van Bortel LM, Laurent S, Boutouyrie P, et al. Expert consensus document on the measurement of aortic stiffness in daily practice using carotid-femoral pulse wave velocity. **J Hypertens**. 2012; 30(3):445−448.

28. Georgianos PI, Agarwal R. Effect of lisinopril and atenolol on aortic stiffness in patients on hemodialysis. **Clin J Am Soc Nephrol**. 2015; 10(4):639−645.

29. Lehmann ED, Riley WA, Clarkson P, Gosling RG. Non-invasive assessment of cardiovascular disease in diabetes mellitus. **Lancet**. 1997; 350(Suppl 1):SI14−S19.

30. Guerin AP, Blacher J, Pannier B, Marchais SJ, Safar ME, London GM. Impact of aortic stiffness attenuation on survival of patients in end-stage renal failure. **Circulation**. 2001; 103(7):987−992.

31. London GM, Marchais SJ, Guerin AP. Arterial stiffness and function in end-stage renal disease. **Adv Chronic Kidney Dis**. 2004; 11(2):202−209.

32. Covic A, Mardare N, Gusbeth-Tatomir P, et al. Increased arterial stiffness in children on haemodialysis. **Nephrol Dial Transplant**. 2006; Vol. 21:729−735.

33. Pannier B, Guerin AP, Marchais SJ, Safar ME, London GM. Stiffness of capacitive and conduit arteries: prognostic significance for end-stage renal disease patients. **Hypertension**. 2005; 45(4):592−596.

34. Tang M, Romann A, Chiarelli G, et al. Vascular stiffness in incident peritoneal dialysis patients over time. **Clin Nephrol**. 2012; 78(4):254−262.

35. Davies JM, Bailey MA, Griffin KJ, Scott DJ. Pulse wave velocity and the non-invasive methods used to assess it: Complior, SphygmoCor, Arteriograph and Vicorder. **Vascular**. 2012; 20(6):342−349.

36. Briet M, Collin C, Karras A, et al. Arterial remodeling associates with CKD progression. **J Am Soc Nephrol**. 2011; 22(5):967−974.

37. Hermans MM, Henry R, Dekker JM, et al. Estimated glomerular filtration rate and urinary albumin excretion are independently associated with greater arterial stiffness: the Hoorn Study. **J Am Soc Nephrol**. 2007; 18(6):1942−1952.

38. Eddington H, Sinha S, Li E, et al. Factors associated with vascular stiffness: cross-sectional analysis from the chronic renal insufficiency standards implementation study. **Nephron Clin Pract**. 2009; 112(3):c190−c198.

39. Huang N, Foster MC, Mitchell GF, et al. Aortic stiffness and change in glomerular filtration rate and albuminuria in older people. **Nephrol Dial Transplant**. 2017; 32(4):677−684.

40. Chen SC, Chang JM, Liu WC, et al. Brachial-ankle pulse wave velocity and rate of renal function decline and mortality in chronic kidney disease. **Clin J Am Soc Nephrol**. 2011; 6(4):724−732.

41. Tomiyama H, Tanaka H, Hashimoto H, et al. Arterial stiffness and declines in individuals with normal renal function/early chronic kidney disease. **Atherosclerosis**. 2010; 212(1):345−350.

42. Hashimoto J, Ito S. Central pulse pressure and aortic stiffness determine renal hemodynamics: pathophysiological implication for microalbuminuria in hypertension. **Hypertension**. 2011; 58(5):839−846.

43. Vlachopoulos C, Aznaouridis K, Stefanadis C. Prediction of cardiovascular events and all-cause mortality with arterial stiffness: a systematic review and meta-analysis. **J Am Coll Cardiol**. 2010; 55(13):1318−1327.

44. Sarnak MJ, Levey AS. Cardiovascular disease and chronic renal disease: a new paradigm. **Am J Kidney Dis**. 2000; 35(4:Suppl 1):S117−S131.

45. Blacher J, Guerin AP, Pannier B, Marchais SJ, Safar ME, London GM. Impact of aortic stiffness on survival in end-stage renal disease. **Circulation**. 1999; 99(18):2434−2439.

46. Shoji T, Emoto M, Shinohara K, et al. Diabetes mellitus, aortic stiffness, and cardiovascular mortality in end-stage renal disease. **J Am Soc Nephrol**. 2001; 12(10):2117−2124.

47. Townsend R, Anderson AH, Chirinos JA, et al. Association of pulse wave velocity with chronic kidney disease progression and

mortality: findings from the CRIC study. **Hypertension**. 2018; 71(6):1101−1107.

48. Zoungas S, Cameron JD, Kerr PG, et al. Association of carotid intima-medial thickness and indices of arterial stiffness with cardiovascular disease outcomes in CKD. **Am J Kidney Dis**. 2007; 50(4):622−630.

49. Lash JP, Go AS, Appel LJ, et al. Chronic Renal Insufficiency Cohort (CRIC) Study: baseline characteristics and associations with kidney function. **Clin J Am Soc Nephrol**. 2009; 4(8):1302−1311.

50. Nilsson PM, Boutouyrie P, Laurent S. Vascular aging: a tale of EVA and ADAM in cardiovascular risk assessment and prevention. **Hypertension**. 2009; 54(1):3−10.

51. Gosling RG, King DH. Arterial assessment by Doppler-shift ultrasound. **Proc R Soc Med**. 1974; 67(6 Pt 1):447−449.

52. Di Nicolo P, Granata A. Renal Resistive Index: not only kidney. **Clin Exp Nephrol**. 2017; 21(3):359−366.

53. Radermacher J, Chavan A, Bleck J, et al. Use of Doppler ultrasonography to predict the outcome of therapy for renal-artery stenosis. **N Engl J Med**. 2001; 344(6):410−417.

54. Zeller T, Frank U, Muller C, et al. Predictors of improved renal function after percutaneous stent-supported angioplasty of severe atherosclerotic ostial renal artery stenosis. **Circulation**. 2003; 108(18):2244−2249.

55. Zeller T, Muller C, Frank U, et al. Stent angioplasty of severe atherosclerotic ostial renal artery stenosis in patients with diabetes mellitus and nephrosclerosis. **Catheter Cardiovasc Interv**. 2003; 58(4):510−515.

56. Zeller T. Renal artery stenosis: epidemiology, clinical manifestation, and percutaneous endovascular therapy. **J Interv Cardiol**. 2005; 18(6):497−506.

57. O'Neill WC. Renal resistive index: a case of mistaken identity. **Hypertension**. 2014; 64(5):915−917.

58. Krumme B, Grotz W, Kirste G, Schollmeyer P, Rump LC. Determinants of intrarenal Doppler indices in stable renal allografts. **J Am Soc Nephrol**. 1997; 8(5):813−816.

59. Heine GH, Gerhart MK, Ulrich C, Kohler H, Girndt M. Renal Doppler resistance indices are associated with systemic atherosclerosis in kidney transplant recipients. **Kidney Int**. 2005; 68(2):878−885.

60. Naesens M, Heylen L, Lerut E, et al. Intrarenal resistive index after renal transplantation. **N Engl J Med**. 2013; 369(19):1797−1806.

61. London GM. Mechanisms of arterial calcifications and consequences for cardiovascular function. **Kidney Int Suppl (2011)**. 2013; 3(5):442−445.

62. Tsao CW, Pencina KM, Massaro JM, et al. Cross-sectional relations of arterial stiffness, pressure pulsatility, wave reflection, and arterial calcification. **Arterioscler Thromb Vasc Biol**. 2014; 34(11):2495−2500.

63. Yannoutsos A, Bahous SA, Safar ME, Blacher J. Clinical relevance of aortic stiffness in end-stage renal disease and diabetes: implication for hypertension management. **J Hypertens**. 2018; 36(6):1237−1246.

64. Shao JS, Cai J, Towler DA. Molecular mechanisms of vascular calcification: lessons learned from the aorta. **Arterioscler Thromb Vasc Biol**. 2006; 26(7):1423−1430.

65. Rennenberg RJ, Kessels AG, Schurgers LJ, van Engelshoven JM, de Leeuw PW, Kroon AA. Vascular calcifications as a marker of increased cardiovascular risk: a meta-analysis. **Vasc Health Risk Manag**. 2009; 5(1):185−197.

66. Chue CD, Edwards NC, Davis LJ, Steeds RP, Townend JN, Ferro CJ. Serum phosphate but not pulse wave velocity predicts decline in renal function in patients with early chronic kidney disease. **Nephrol Dial Transplant**. 2011; 26(8):2576−2582.

67. Chue CD, Townend JN, Steeds RP, Ferro CJ. Arterial stiffness in chronic kidney disease: causes and consequences. **Heart**. 2010; 96(11):817−823.

68. Schalekamp MA, Schalekamp-Kuyken MP, de Moor-Fruytier M, Meininger T, Vaandrager-Kranenburg DJ, Birkenhager WH. Interrelationships between blood pressure, renin, renin substrate and blood volume in terminal renal failure. **Clin Sci Mol Med**. 1973; 45(4):417−428.

69. Greene EL, Kren S, Hostetter TH. Role of aldosterone in the remnant kidney model in the rat. **J Clin Invest**. 1996; 98(4):1063−1068.

70. Ku E, Lee BJ, Wei J, Weir MR. Hypertension in CKD: core curriculum 2019. **Am J Kidney Dis**. 2019; 74(1):120−131.

71. Bomback AS, Klemmer PJ. The incidence and implications of aldosterone breakthrough. **Nat Clin Pract Nephrol**. 2007; 3(9):486−492.

72. Mehdi UF, Adams-Huet B, Raskin P, Vega GL, Toto RD. Addition of angiotensin receptor blockade or mineralocorticoid antagonism to maximal angiotensin-converting enzyme inhibition in diabetic nephropathy. **J Am Soc Nephrol**. 2009; 20(12):2641−2650.

73. Avolio A, Jones D, Tafazzoli-Shadpour M. Quantification of alterations in structure and function of elastin in the arterial media. **Hypertension**. 1998; 32(1):170−175.

74. Chen ML, Ruberti JW, Nguyen TD. Increased stiffness of collagen fibrils following cyclic tensile loading. **J Mech Behav Biomed Mater**. 2018; 82:345−354.

75. Chiang C. The use of bone turnover markers in chronic kidney disease-mineral and bone disorders. **Nephrology**. 2017; 22(Suppl 2):11−13.

76. Jacob MP. Extracellular matrix remodeling and matrix metalloproteinases in the vascular wall during aging and in pathological conditions. **Biomed Pharmacother**. 2003; 57(5−6):195−202.

77. Chung AW, Booth AD, Rose C, Thompson CR, Levin A, van Breemen C. Increased matrix metalloproteinase 2 activity in the human internal mammary artery is associated with ageing, hypertension, diabetes and kidney dysfunction. **J Vasc Res**. 2008; 45(4):357−362.

78. Chung AW, Yang HHC, Kim JM, et al. Upregulation of matrix metalloproteinase-2 in the arterial vasculature contributes to stiffening and vasomotor dysfunction in patients with chronic kidney disease. **Circulation**. 2009; 120(9):792−801.

79. Deplano V, Boufi M, Gariboldi V, et al. Mechanical characterisation of human ascending aorta dissection. **J Biomech**. 2019; 94:138−146.

80. Reiser K, McCormick RJ, Rucker RB. Enzymatic and nonenzymatic cross-linking of collagen and elastin. **FASEB J**. 1992; 6(7):2439−2449.

81. Makita Z, Radoff S, Rayfield EJ, et al. Advanced glycosylation end products in patients with diabetic nephropathy. **N Engl J Med**. 1991; 325(12):836−842.

82. Bohlender JM, Franke S, Stein G, Wolf. Advanced glycation end products and the kidney. **Am J Physiol Renal Physiol**. 2005; 289(4):F645−F659.

83. Goh SY, Cooper ME. Clinical review: the role of advanced glycation end products in progression and complications of diabetes. **J Clin Endocrinol Metab**. 2008; 93(4):1143−1152.

84. Win MT, Yamamoto Y, Munesue S, et al. Regulation of RAGE for attenuating progression of diabetic vascular complications. **Exp Diabetes Res**. 2012; 2012:894605.

85. Gibbons GH. Endothelial function as a determinant of vascular function and structure: a new therapeutic target. **Am J Cardiol**. 1997; 79(5A):3−8.

86. Martens CR, Edwards DG. Peripheral vascular dysfunction in chronic kidney disease. **Cardiol Res Pract**. 2011; 2011:267257.

87. Satoh M. Endothelial dysfunction as an underlying pathophysiological condition of chronic kidney disease. **Clin Exp Nephrol**. 2012; 16(4):518−521.

88. Roumeliotis S, Mallamaci F, Zoccali C. Endothelial dysfunction in chronic kidney disease, from biology to clinical outcomes: a 2020 update. **J Clin Med**. 2020; 9(8).

89. Kirkman DL, Ramick MG, Muth BJ, et al. Effects of aerobic exercise on vascular function in nondialysis chronic kidney disease: a randomized controlled trial. **Am J Physiol Renal Physiol**. 2019; 316(5):F898−F905.

90. Amdur RL, Feldman HI, Dominic EA, et al. Use of measures of inflammation and kidney function for prediction of atherosclerotic vascular disease events and death in patients with CKD: findings from the CRIC study. **Am J Kidney Dis**. 2019; 73(3):344−353.

91. Maki-Petaja KM, Hall FC, Booth AD, et al. Rheumatoid arthritis is associated with increased aortic pulse-wave velocity, which is reduced by anti-tumor necrosis factor-alpha therapy. **Circulation**. 2006; 114(11):1185−1192.

92. Joly L, Djaballah W, Koehl G, et al. Aortic inflammation, as assessed by hybrid FDG-PET/CT imaging, is associated with enhanced aortic stiffness in addition to concurrent calcification. **Eur J Nucl Med Mol Imaging**. 2009; 36(6):979−985.

93. Aikawa E, Aikawa M, Libby P, et al. Arterial and aortic valve calcification abolished by elastolytic cathepsin S deficiency in chronic renal disease. **Circulation**. 2009; 119(13):1785−1794.

94. Peyster E, Chen J, Feldman HI, et al. Inflammation and arterial stiffness in chronic kidney disease: findings from the CRIC study. **Am J Hypertens**. 2017; 30(4):400−408.

95. Lacolley P, Regnault V, Laurent S. Mechanisms of arterial stiffening: from mechanotransduction to epigenetics. **Arterioscler Thromb Vasc Biol**. 2020; 40(5):1055−1062.

96. DuPont JJ, Ramick MG, Farquhar WB, Townsend RR, Edwards DG. NADPH oxidase-derived reactive oxygen species contribute to impaired cutaneous microvascular function in chronic kidney disease. **Am J Physiol Renal Physiol**. 2014; 306(12):F1499−F1506.

97. Jun M, Venkataraman V, Razavian M, et al. Antioxidants for chronic kidney disease. **Cochrane Database Syst Rev**. 2012; 10:CD008176.

98. Townsend RR, Wilkinson IB, Schiffrin EL, et al. Recommendations for improving and standardizing vascular research on arterial stiffness: a scientific statement from the American heart association. **Hypertension**. 2015; 66(3):698−722.

99. Rodriguez RA, Spence M, Hae R, Agharazii M, Burns KD. Pharmacologic therapies for aortic stiffness in end-stage renal disease: a systematic review and meta-analysis. **Can J Kidney Health Dis**. 2020; 7:2054358120906974.

100. Rodriguez RA, Hae R, Spence M, Shea B, Agharazii M, Burns KD. A systematic review and meta-analysis of nonpharmacologic-based interventions for aortic stiffness in end-stage renal disease. **Kidney Int Rep**. 2019; 4(8):1109−1121.

This page intentionally left blank

Arterial stiffness, pulsatile hemodynamics, and the vascular contributions to dementia

M.L. Meyer[1] and T.M. Hughes[2]

[1]Department of Emergency Medicine, School of Medicine, University of North Carolina at Chapel Hill, Chapel Hill, NC, United States; [2]Department of Internal Medicine, Wake Forest School of Medicine, Winston-Salem, NC, United States

Introduction
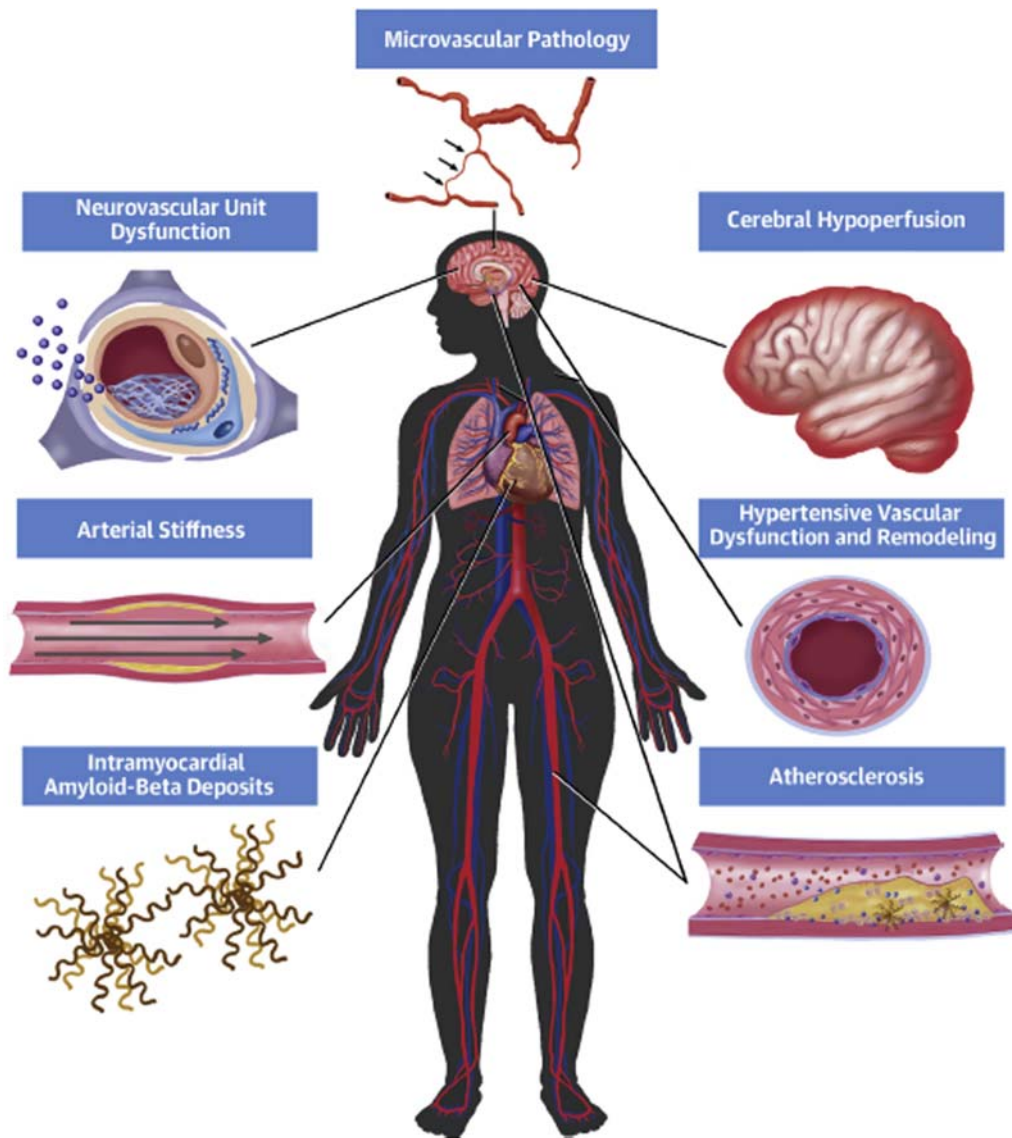
Central arterial stiffness results in hemodynamic changes throughout the arterial tree and has marked effects on distal end-organs, such as the kidneys and brain. In fact, the brain pulsates with every beat of the heart.[1] Consistent perfusion of the brain is orchestrated at various levels by the sympathetic and neuromuscular tone controlling heart rate and arterial compliance, systemic blood pressure and resistance, and cerebral autoregulation. It only takes a bout of acute tachycardia induced by aerobic exercise or pre-syncope induced by orthostatic hypotension to appreciate the essential role of hemodynamics in proper functioning of the central nervous system. Chronic effects of hemodynamic insufficiency and excessive pulsatile force attributed to central arterial stiffness may be less apparent but far more insidious especially in late life.

Arterial stiffness is recognized as a vascular risk factor for age-related cognitive disorders including Alzheimer's disease (AD) and related dementias (ADRD). As previous chapters note, arterial stiffness is an age-related vascular disorder that is accelerated by cardiometabolic disorders like hypertension and diabetes. Notably, both hypertension and diabetes are identified as key modifiable risk factors for ADRD.[2]

Cognitive impairment is a clinical syndrome characterized by quantifiable deficits in cognitive performance in one or more cognitive domain with or without subjective cognitive concerns and functional impairments. At the level of dementia, functional impairments affect activities of daily living. The clinical presentation of cognitive decline along with neuroimaging biomarkers, biofluid assays, and ultimately neuropathological study of the brain are used to inform the etiology of dementia. AD and ADRD are distinct from vascular dementia in clinical presentation and underlying neuropathology. While vascular dementia is characterized by infarction, stroke, and acute, precipitous declines in cognitive function, AD is characterized by the development of hallmark AD pathology (β-amyloid [Aβ] and phosphorylated tau [p-tau]) and neurodegeneration, preceding by years and decades the insidious decline in cognitive performance over time. Yet, the vast majority of individuals with probable AD also have evidence of vascular pathology. Less than half (41%) of AD is attributable to the hallmark AD pathology[3] and the majority (75%) of probable AD have vascular pathology, especially cerebral infarction.[4] Recently, the term "Vascular Contributions to Cognitive Impairment and Dementia (VCID)" was developed to describe the broad field of research considering the role of a range of vascular risk and vascular lesions on cognition in the context of ADRD and is now used broadly by the American Heart Association,[5] the Alzheimer's Association,[6] and the NIH.[7]

The heterogeneity of ADRD pathology/etiology and the importance of VCID has implications for prevention and precision medicine. This is especially important in diverse populations as there may be ethnic/race differences in the prevalence of vascular comorbidities that may explain some of the reported excess risk for ADRD among Hispanic and African American older adults.[8] Although various vascular etiologies/pathways are important contributors to VCID and ADRD risk (Fig. 41.1),[9] this chapter will review and critique the evidence that arterial stiffness is a risk factor for reduced cognitive function and dementia through its

FIGURE 41.1   Vascular changes associated with Alzheimer's disease and related dementias. Age-related vascular changes across the cerebral vasculature and outside the brain are exacerbated in Alzheimer's disease. Intracranial and extracranial atherosclerosis, reduced cerebral microvascular density, cerebral amyloid angiopathy, and neurovascular unit dysfunction, together with large artery stiffening and hypertensive vascular remodeling, changes in heart function, and a procoagulant state, contribute to important reductions in cerebrovascular blood flow. Aβ may play a contributory role in these vascular changes. *Reprinted from Cortes-Canteli M, Iadecola C. Alzheimer's disease and vascular aging: JACC focus seminar.* **J Am Coll Cardiol**. *2020; 75(8):942−951, with permission from Elsevier.*

associations with various cerebral pathologies underlying age-related cognitive decline and ADRD. In this chapter, we primarily focus the review of epidemiologic studies evaluating central and aortic arterial stiffness to ADRD. Although arterial stiffness can be measured by various modalities, the majority of studies to date measure central stiffness using aortic and carotid-femoral (cf) pulse wave velocity (PWV). We note throughout where confirmatory and novel evidence from other modalities (cardiac magnetic resonance imaging (MRI), phase contract cerebral blood flow MRI, and carotid ultrasound) when available. The second part of this chapter links this evidence with other lines of supporting research and evaluates the sum total in a causal framework linking arterial stiffness to ADRD.

Review of studies linking arterial stiffness to Alzheimer's disease and related dementias

Arterial stiffness and cognitive impairment

Higher arterial stiffness is consistently associated with mild cognitive impairment (MCI) and dementia in most studies.[10−15] In one study of individuals with MCI, higher

cfPWV was associated with the conversion to dementia.[16] While most prior studies distinguished between a primary etiology of cerebrovascular disease and AD dementia, the two pathologies often overlap and most dementias in the elderly are a mix of both.[17] A meta-analysis report showed that PWV was higher among those with cerebrovascular disease compared to those with AD dementia or controls,[13] although these analyses pooled studies that used heterogeneous methods of cerebrovascular disease and AD dementia diagnostic classification, cross-sectional designs, and different PWV methods, as well as studies reporting on brachial-ankle PWV (baPWV). In the Atherosclerosis Risk in Communities Neurocognitive Study (ARIC-NCS) among 3550 White participants, higher cfPWV was associated with the prevalence of dementia and higher central pulse pressure (cPP) was associated with the prevalence of dementia and MCI.[18]

At this time, there are only three prospective, population-based studies on arterial stiffness, measured at one point in time, and risk of ADRD. The first showed an association of higher cfPWV with the 10-year incidence of MCI in all study participants (n = 1101) and with the incidence of all-cause dementia among those without diabetes.[19] The other prospective evaluation did not detect an association between cfPWV and the risk of cerebrovascular disease or dementia in 3714 participants after a mean follow-up of 4.4 years, although the number of cases of cerebrovascular disease was small (11 incident cases) and MCI was not ascertained.[12] Lastly, in the Cardiovascular Health Study (n = 356), higher cfPWV was associated with 15-year incidence of dementia.[20] As discussed in subsequent sections, the evidence of an association between arterial stiffness, cognitive function, brain imaging, and biomarker hallmarks of AD supports the evidence of an association of arterial stiffness with MCI and ADRD.

Arterial stiffness and cognitive function
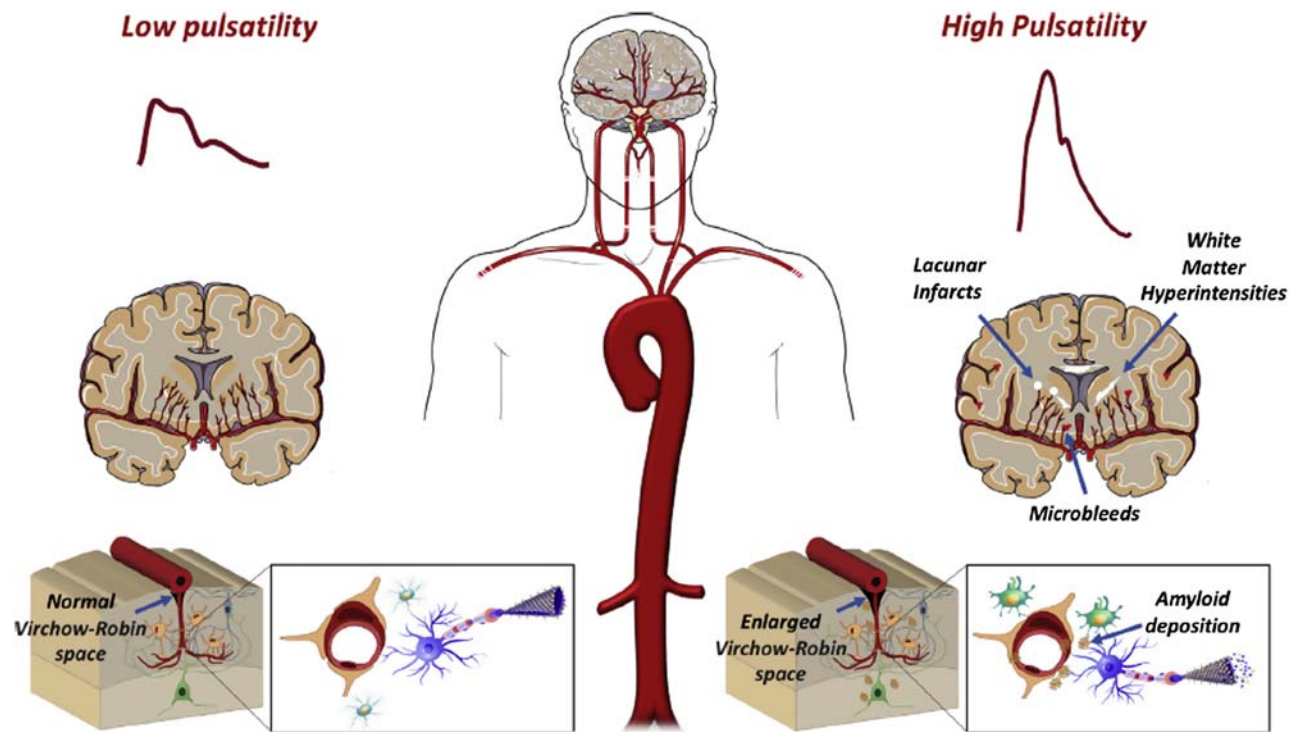
Arterial stiffness is associated with reduced cognitive function in both community-based studies[21−26] and in systematic reviews and meta-analyses.[10,27−29] Few longitudinal studies on global cognitive function are available.[12,30,31] Among older adults in nursing homes, increasing tertiles of cfPWV at baseline were associated with greater one-year cognitive decline in Mini-Mental Status Examination (MMSE) scores (n = 873),[30] and baseline values of cfPWV and pulse pressure amplification were higher among those with a two-year decline of >3 points in MMSE (n = 682).[31] In contrast, the Rotterdam Study (n = 2767) found no association of cfPWV with decline in MMSE during a mean follow-up of 4.4 years.[12] These studies relied on the MMSE, whereas specific domains of cognition might be more sensitive to increased cfPWV and cPP.[12,21,23,25]

Declines in domains of executive function and psychomotor speed/attention are often related to cerebrovascular injury whereas declines in memory typically reflect neurodegenerative damage to the brain.[5] Extant reports indicate that arterial stiffness is more consistently associated with tests of executive function,[25,32] suggesting arterial stiffness and pulsatility most likely act through vascular processes rather than neurodegenerative processes. In the ARIC-NCS Study (n = 3703), cfPWV associated with lower executive function/processing speed and general cognition, but not with memory or language.[33] In contrast, cfPWV and cPP were associated with lower memory scores, but not with processing speed or executive function in a community-based cohort (n = 668).[23] Longitudinally, cfPWV was associated with seven-year global cognitive decline and phonemic fluency, but was not significantly associated with other domain-specific measures of memory, reasoning, and semantic fluency in the Whitehall II study (n = 4300).[34] In the Framingham Offspring Cohort (n = 1223), cfPWV was associated with a 6.4-year increase in Trail Making Test Part B minus Part A test (worse executive function), but not was not associated with change in Similarities test, a measure of executive function/abstract reasoning.[35] When evaluating other cognitive domains, higher cfPWV was associated with a three-year decline in psychomotor speed, and perceptual speed, but was not associated with verbal memory (n = 552).[25]

In the latest meta-analysis, higher PWV was associated with lower global cognitive function, executive function, and memory in cross-sectional studies, whereas in longitudinal studies, PWV was associated with reduced global cognitive function and executive function, but not with change in memory.[36] The discrepancies in the literature may be attributable to differences in the tests of domain-specific cognitive function, measures of arterial stiffness, cross-sectional designs, and study populations. Harmonization of cognitive function measures would facilitate a more direct comparison of the association of arterial stiffness and cognitive function across studies. Further, the inclusion of imaging biomarkers of ADRD continue to advance our understanding of the cerebral pathology underlying associations between arterial stiffness and cognitive function.

Arterial stiffness and brain structural abnormalities on magnetic resonance imaging

Arterial stiffness is consistently associated with macrostructural and microstructural brain abnormalities and cerebral small vessel disease before the development of ADRD (Fig. 41.2). Arterial stiffness is associated with reduced gray matter volumes and indicators of cerebral small vessel disease, quantified by white matter

FIGURE 41.2 Arterial stiffness and age-related changes in the brain commonly seen in Alzheimer disease and related dementias. These changes include declines in cerebral perfusion to the gray matter, evidence of multiple forms of cerebral small vessel disease (lacunar infarcts [*white circles*], white matter hyperintensities [*white streaks*], cerebral microbleed [*red triangles*], enlarged perivascular [Virchow-Robin] spaces), loss of brain volume, and β-amyloid deposition in the brain (*brown plaques*). Such changes are suspected to affect the integrity of the white matter and neurovascular unit. *Reprinted from Chirinos JA, Segers P, Hughes T, Townsend R, Large-artery stiffness in health and disease: JACC state-of-the-art review.* **J Am Coll Cardiol**. *2019; 74(9):1237−1263, with permission from Elsevier.*

hyperintensities (WMHs), and morphologic abnormalities on MRI (reviewed in Table 41.1 and Concept Box), such as microbleeds and lacunar infarcts in individuals with hypertension,[37−40] community-based samples,[23,24,37,41] and in meta-analyses.[10,29]

WMH is the most often reported form of cerebral small vessel disease reported in the literature and most commonly and consistently associated with arterial stiffness. In the community-based Age, Gene/Environment Susceptibility−Reykjavik cohort study (n = 668), cfPWV and cPP were cross-sectionally associated with the presence of subcortical infarcts and cfPWV was associated with a higher WMH volume.[23] In the ARIC-NCS Study (n = 1255), cfPWV was associated with WMH volume, smaller brain volume, and smaller AD signature region volumes.[33] Arterial stiffness is related to WMH in middle-aged adults.[42,43] In the Framingham Third Generation Cohort Study, cfPWV was associated with larger lateral ventricular volumes in 759 participants 30−45 years old and with white matter injury in 1129 participants 45−65 years old.[42] Two longitudinal studies have shown an association between higher cfPWV and a higher burden of WMH.[44,45] The first of these showed a positive association of cfPWV and WMH volume, with a stronger magnitude of effect among Black older adults compared to White older adults (n = 303; 41% Black).[44] The prospective Dallas Heart Study (n = 1270) reported that aortic arch PWV was associated with WMH volume measured seven years later, and estimated that a 1% increase in aortic arch PWV (m/s) corresponds to a 0.3% increase in WMH volume.[45] In contrast in the Framingham Offspring Cohort (n = 1118), cfPWV was not associated with 6.4-year change in total cerebral brain volume or WMH volume.[35] Additionally, higher carotid artery stiffness was associated with higher WMH volume 20 years later in the ARIC-NCS Study (n = 1402).[46]

Arterial stiffness is consistently related to WMH,[47,48] especially in the periventricular[49−51] and to a lesser extent deep white matter.[49,51] Arterial stiffness appears to show particular specificity for WM tracts susceptible to age-related damage,[44] likely contributing to WMH in areas of the brain that are directly supplied by the deep cerebral circulation. Furthermore, the arterial border zone of the cerebral white matter (watershed) is particularly sensitive to cerebral hemodynamic abnormalities and increased pulsatility.[52]

Changes in white matter integrity are thought to occur prior to visible WMH.[53] The microstructural integrity of

TABLE 41.1 Summary of the imaging and cognitive data related to arterial stiffness.

Dementia-related pathology and functional measures	Modality	Strength of evidence
Macrostructural biomarkers		
Atrophy (e.g., gray matter volume)	T1 MRI	●
White matter hyperintensities	FLAIR MRI	●●●
Periventricular	FLAIR MRI	●●●
Subcortical	FLAIR MRI	●●
Large infarcts	DWI MRI	●●
Lacunes	FLAIR MRI	●●
Cortical microinfarcts	DWI MRI	NA
Cerebral microbleeds	GRE/SWI MRI	●
Enlarged perivascular spaces	T2/FLAIR MRI	●●
β-amyloid	PET or CSF	●●●
Tau	PET or CSF	●●
Other proteinopathies (e.g., TDP-43, α-synuclein)	NA	NA
Microstructural biomarkers		
Fractional anisotropy	DWI MRI	●●
Radial diffusivity	DWI MRI	●●●
Myelin fraction	DWI MRI	●
Free water	DWI MRI	●●
Neurite density	DWI MRI	NA
Functional biomarkers		
Cerebral blood flow	ASL/BOLD MRI	●●
Cerebrovascular reactivity	ASL MRI challenge	●●
Cognitive function		
Global cognitive performance	Cognitive testing	●●●
Executive function	Cognitive testing	●●●
Memory	Cognitive testing	●●●
Speed of processing	Cognitive testing	●●
Attention	Cognitive testing	●

Evidence: ● low; ●● moderate; ●●● strong; *ASL*, arterial spin labeling; *BOLD*, blood oxygen level dependent; *DWI*, diffusion-weighted imaging; *FLAIR*, fluid-attenuated inversion recovery; *GRE*, gradient-recalled echo; *NA*, not available; *SWI*, susceptibility-weighted imaging.

white matter can be measured using diffusion tensor imaging (DTI) by MRI. Higher mean diffusivity (MD) and lower fractional anisotropy (FA), indicating axonal damage, and demyelination signifies lower white matter microstructural integrity, which could lead to WMH. Arterial stiffness is associated with loss of integrity in various age-related regions in both middle-aged[54] and older adults.[43,55,56] In 54 cognitively unimpaired elderly individuals, cfPWV was associated with DTI measures of white matter microstructure, including FA and radial diffusivity (axonal organization/degeneration), but not with myelin volume fraction (myelination).[55] In the ARIC-NCS Study (n = 1484), cfPWV was associated with lower FA and higher MD even after adjustment for WMH volume.[57] In the Framingham Offspring and Third Generation cohorts (n = 1903), cfPWV was found to be associated with higher free water, particularly in the WM fed by the middle cerebral artery, and lower FA.[54] The relationship between central arterial stiffness and white matter integrity may be focal, localized to individual tracts, but detectable in

multiple ethnic groups.[44,57] These studies suggest that arterial stiffness effects WM integrity before the development of WMH.

Despite the numerous studies of arterial stiffness and white matter, few have included gray matter volume or density, which is the outermost layer of the brain and consists primarily of neuronal cell bodies. Studies among community-based populations are conflicting, as cfPWV was associated with lower gray matter density in one study (n = 1903),[54] not associated in another (n = 303),[44] and one showed that carotid pulsatility index, not cfPWV, was associated with lower gray matter volume (n = 668).[23] Similarly, among patients with arterial disease, carotid stiffness was associated with lower cortical gray matter volume (n = 526), but not with the four-year progression of cortical gray matter volume (n = 308).[58] Future studies should assess both white and gray matter to fully characterize the association of arterial stiffness and brain volumes.

The associations of arterial stiffness with other indicators of cerebral small vessel disease, such as lacunes and microbleeds,[47] are inconsistent. As lacunes represent small ischemic lesions, the associations with arterial stiffness seem less than direct and more likely to be mediated by prothrombotic comorbidities common to both. The exception would be for subcortical lacunes, which may present from generalized hypoxia. The inconsistent relationship with arterial stiffness and cerebral microbleeds may be attributable to differential associations with location of the microbleeds, with deep and infratentorial being associated rather than lobar regions.[47] Microbleeds are thought to hemosiderin-laden macrophages in perivascular tissue, consistent with vascular leakage of blood cells. Further, microbleeds are linked to vascular amyloid deposition especially when present outside of the white matter.[59] When extensively seen in the parietal lobe, they indicate presence of cerebral amyloid angiopathy (CAA). As discussed below, arterial stiffness is associated with cerebral Aβ deposition and the presence of microbleeds in older adults.[48]

General enlargement of perivascular spaces is associated with other morphological features of cerebral small vessel disease, including WMH and lacunes, but not atrophy.[60] Arterial stiffness is associated with the presence of enlarged perivascular spaces among 782 individuals with hypertension[40] and community-based samples of older adults, particularly in the basal ganglia.[47] One of the described functions of perivascular spaces is to drain interstitial fluid back to circulation. However, when the aorta is stiff, a high pulsatility wave is transmitted to end-organ vascular beds forcing small arteries to adapt to higher flows, which might facilitate the interstitial fluid leakage.[40]

	Recent small subcortical infarct	White matter hyperintensity	Lacune	Perivascular space	Cerebral microbleed	White matter diffusion	Cerebral blood flow	Cerebrovascular reactivity
Example image								
Imaging modality	Diffusion Weighted Imaging (DWI)	Fluid-Attenuated Inversion Recovery (FLAIR)	Fluid-Attenuated Inversion Recovery (FLAIR)	T2 and T1/FLAIR	Susceptibility Weighted Imaging (SWI) or T2*	Diffusion Tensor Imaging (DTI)	Arterial Spin Labeling (ASL) Blood-Oxygen-Level-Dependent (BOLD)	Difference of ASL pre- and post-challenge

This concept box details the magnetic resonance imaging (MRI)-based *macrostructural, microstructural*, and *hemodynamic* measures used to study the vascular contributions to dementia, as described below.

Macrostructural measures[59]

Recent small subcortical infarcts are occlusions of a single, deep perforating brain artery and is likely a consequence of cerebral small vessel disease.

White matter hyperintensities (WMHs), also known as Leukoaraiosis, are brain lesions with increased brightness when identified on MRI using fluid-attenuated inversion recovery (FLAIR) sequences.

Lacunes are small (3 mm and about 15 mm in diameter) fluid-filled cavities in the white matter or basal ganglia consistent with a previous acute small subcortical infarct or hemorrhage in the territory of one perforating arteriole. Lacunes are frequently observed coincidentally on imaging in older people, often not clearly associated with discrete neurological symptoms.

Perivascular spaces are also known as Virchow−Robin spaces, are fluid-filled spaces that follow the typical course of a vessel as it goes through gray or white matter.

Cerebral microbleeds are small hypointense lesions that are visible on paramagnetic-sensitive MRI sequences. These lesions are most commonly located in the cortico-subcortical junction, and deep gray or white matter in the cerebral lobes, brainstem, and cerebellum. Cerebral microbleeds are associated with other forms of cerebral small vessel disease, cerebral amyloid angiopathy, and Alzheimer's disease.

Microstructural measures

White matter diffusion is restricted (anisotropic flow) along nerve fibers and myelin of the white matter. Unrestricted (isotropic) flow can indicate areas of reduced microstructural integrity and freely diffusing water indicative of neuroinflammation. Diffusion imaging enables the assessment of microstructural integrity of the white matter and gray matter through several diffusion metrics.

Hemodynamic measures

Cerebral blood flow is remarkably constant under a normal physiological state. Cerebral blood flow is regulated by cardiac output, aortic distensibility, pulsatile pressure gradient along arteries, and cerebral autoregulation. It is also subject to the development of arteriopathies, such as arterial stenosis, atherosclerosis, and arterial stiffness.

Cerebrovascular reactivity is the response to a functional challenge (e.g., exercise, hypercapnia, and orthostatics) and is a measure cerebral autoregulation.

Association of arterial stiffness and Alzheimer's disease biomarkers

Emerging studies show associations of vascular risk factors with biomarkers of Aβ and p-tau, which are hallmarks of AD pathology that precede atrophy and onset of cognitive impairment.[61] Biomarkers of Aβ and tau aggregation measured by positron emission tomography (PET) represent the burden of AD pathology. In contrast, biofluid levels of ADRD biomarkers provide insight into the concentration of hallmark AD pathology (Aβ, p-tau), neurodegeneration (total tau (t-tau)), synaptic dysfunction (e.g., neurogranin), neuro-axonal injury (e.g., neurofilament light), neuroinflammation (e.g., YKL-40), and more. Arterial stiffness is associated with the extent and progression of cerebral Aβ plaques burden quantified by PET imaging in older adults without dementia, but may differ by vascular bed assessed.[48,62] While central aortic PWV is inconsistently associated with the extent of Aβ burden at a single time point, one study suggests that cfPWV appears to be most strongly associated with the accumulation of Aβ over time.[62] In contrast, markers of peripheral arterial stiffness (baPWV and carotid stiffness) appear to be more strongly associated with the extent Aβ in the brain.[48,62] Associations between arterial stiffness and Aβ burden have been replicated in a diverse cohort, and appear to be consistent across White and Black older adults (n = 320).[48] Currently, there are limited data available directly linking arterial stiffness and tau pathology and neurogenerative processes, the other hallmark of AD pathology. Tau PET imaging is beginning to associate vascular risk factors with tau aggregation in the brain.[63] Among older adults in their eighth decade of life, greater aortic stiffness measured by cardiac MRI is associated with higher cerebrospinal fluid levels of neurodegenerative (phosphorylated and total tau, neurogranin, and neuroinflammatory markers (YKL-40).[64] More studies are needed to further characterize the association of arterial stiffness and Aβ and tau aggregation and the role of arterial stiffness in the development of cognitive impairment and dementia (Fig. 41.3).
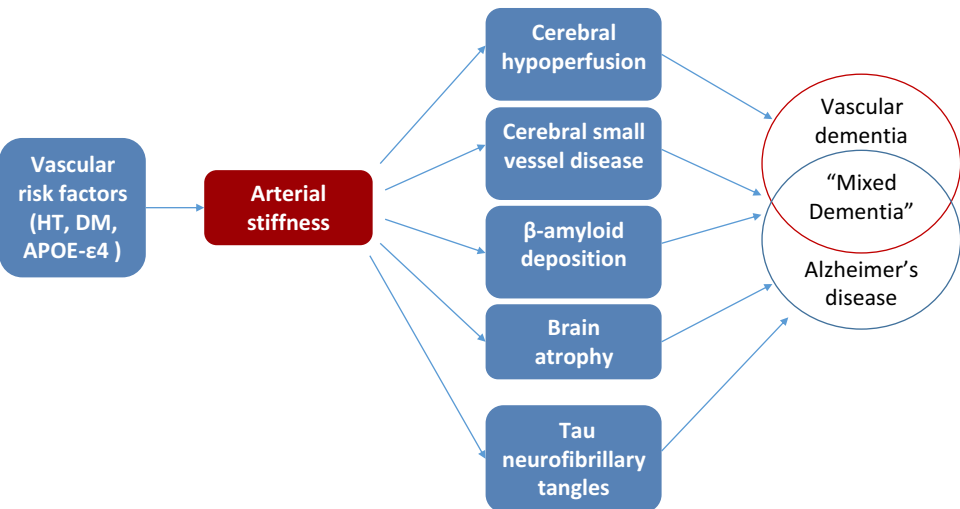
Assessing evidence of the association between arterial stiffness and dementia

As discussed herein, there is mounting evidence that age-related arterial stiffening is associated with the various forms of dementia pathology from cerebral small vessel disease to Aβ deposition to risk for cognitive decline and dementia. The accumulating literature warrants reflection on the potential causal role of arterial stiffness in ADRD through promotion of dementia related neuropathology and cognitive decline. Applying The Bradford Hill Criteria[65] framework to assess the evidence of association for the potential role of arterial stiffness in dementia, we see moderate and consistent evidence linking arterial stiffness to dementia through its related pathology.

Strength of evidence—As detailed above, the strength of associations between arterial stiffness, cerebral small vessel disease, cognitive impairment, and ADRD are of modest strength and follow the proposed causal pathway for the vascular contributions to ADRD depicted in Fig. 41.3.

Consistency of evidence—Measures of arterial stiffness show strong consistency for their relationships with specific dementia-related phenotypes, cognitive impairment, and structural abnormalities in the brain. There are, of course, limitations to this evidence. First, heterogeneity in results are apparent across methods used to measure arterial stiffness. Some inconsistent results may be attributed to variable measurement error across methods used to measure arterial stiffness (e.g., cfPWV, baPWV, cardiac MRI, and carotid ultrasound). In contrast, the vascular bed at which arterial stiffness is assessed could provide physiologic information about the proximity of each measure to cerebral hemodynamics, as well as the extension of arterial stiffness gradient.

A second major limitation of the current studies resides in the homogeneity of populations studied. Most of the studies to date have focused on individuals of European decent. This is an important public health issue given that

FIGURE 41.3   Conceptual model of the association between arterial stiffness and brain aging. *APOE-ε4*, Apolipoprotein E epsilon 4 allele; *DM*, diabetes mellitus; *HT*, hypertension.

underrepresented groups in the United States have not only a greater burden of subclinical cardiovascular disease, including arterial stiffness,[66] but also a greater risk for ADRD.[67–70] Racial and ethnic differences exist in vascular[71,72] and metabolic disorders,[73] apolipoprotein E epsilon 4 allele (*APOE-ε4*) frequencies,[74,75] Aβ deposition,[76] and the prevalence and incidence of ADRD.[77–80] A recent multiethnic autopsy study revealed that the brains of African-Americans with AD had more severe evidence of cerebral arteriosclerosis and atherosclerosis, more "mixed dementia" pathology, and less "pure AD" pathology than the brains of matched White counterparts.[81] Cardiovascular disease risk factor profiles differ for African-Americans[82] and Hispanics[83] compared to Whites.[84] Yet, the effects of these differential risk factor profiles have not been well studied in AD. Some studies report up to twice the prevalence of AD in African-Americans compared to Whites,[85,86] and lower pathologic thresholds for cognitive impairment in African-Americans[87] and Hispanics.[88] Taken together, these studies suggest that underrepresented groups are at greater risk for subclinical vascular disease, cardiovascular disease events, and ADRD. Further studies of arterial stiffness and brain aging are needed in diverse populations.

Biologic gradient—Most studies finding significant relationships between arterial stiffness and dementia pathology and risk for dementia employ linear models as a base for dose response relationships. While various thresholds for abnormal arterial stiffness have been proposed for different age groups (e.g., >12 m/s[89] or >10 m/s[90] for cfPWV), studies that report linear models of arterial stiffness and continuous outcomes (e.g., cognitive performance, brain volumes) find monotonic relationships. It should be noted that these published thresholds were developed for

cardiovascular events, dependent upon the age of the reference population, may represent statistical artifact rather than biology, and have not been validated for brain outcomes.

Specificity of evidence—The breadth of observed relationships of arterial stiffness with dementia-related pathology underscores the challenge to relate arterial stiffness to a complex, multifactorial disease such as ADRD in a causal framework. The predominant hypothesis is that arterial stiffness directly relates the pulsatile force of left ventricular function and systemic hypertension to deliver excess pulsatile force in the peripheral organs with dire vascular consequences to blood flow in the extensive microvasculature structure of the kidneys and brain. Arterial stiffness transmits unabated pulsatile flow along the carotid and vertebral arteries and deeper into the cerebral microvasculature with purported effects: microhemorrhages,[38] endothelial denudation, and thrombosis.[91,92] Neuroimaging biomarkers of cerebrovascular damage related to arterial stiffness are in primarily three forms: (1) excess pulsatile force delivered to the brain resulting in various form of gross cerebral small vessel disease[60]; (2) axonal damage in white matter; and (3) hypoperfusion of microvasculature particularly harmful in watershed regions. Arterial stiffness is associated with abnormalities in ADRD biomarkers of cerebral blood flow, cerebral small vessel disease, and AD pathology purported to precede cognitive dysfunction. Therefore, it may be difficult to isolate and attribute a single cerebral pathology associated with arterial stiffness. Further, more regional specificity in neuroimaging or neuropathologic outcomes are needed on studies of arterial stiffness in the vascular contributions to dementia to inform highly susceptible brain regions for endpoints in clinical trials.

Temporality—The evidence to date supports a chain of evidence linking arterial stiffness to cerebral hemodynamic

changes and structural abnormalities indicative of cerebral small vessel disease and AD pathology that are proposed to precede cognitive impairment by years and even decades. This suggest that cerebral effects of age-related arterial stiffness begin early in the lifecourse before they culminate in late-life cognitive impairment. Yet, the majority of the data available linking arterial stiffness to related dementia pathology are cross-sectional in design. Measures of carotid arterial stiffness accurately predict WMH burden 20 years later.[46] Several longitudinal studies show that arterial stiffness is associated with accelerated cognitive decline in various cognitive domains[34,93,94] and the risk for incident cognitive impairment.[19] While future studies are needed to provide support for temporal changes in arterial stiffness relative to changes in dementia pathology and cognition, the long subclinical phase of both age-related disorders of arterial stiffness and dementia pathogenesis add to the complexity of establishing temporal evidence.

Biologic plausibility—Dementia is a complex and multifactorial neurocognitive disorder with as many etiologies as there are subtypes. Accordingly, the vascular contributions to dementia are also multifaceted and correspond to various forms of cerebrovascular pathology evident in the brain, from ischemic and hemorrhagic stroke to evidence of cerebral small vessel disease.[7] Similarly, arterial stiffness is not only associated with the clinical syndrome of dementia but also multiple structural changes in the brain prior to onset of cognitive symptoms. It is important to note that the current research suggests that arterial stiffness is less likely to be related to vascular dementia, which is more often characterized by infarction, stroke, and acute, precipitous declines in cognitive function. While arterial stiffness does increase the risk for stroke,[95] is more closely related to cerebral small vessel disease and the insidious onset of cognitive symptoms characteristic of ADRD.
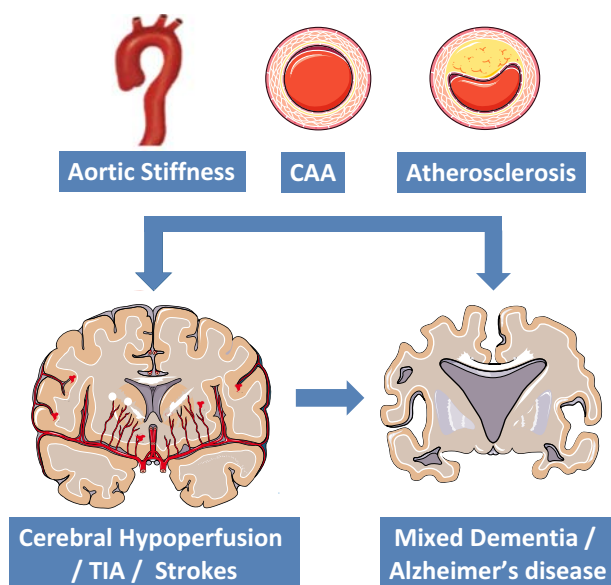
Increased arterial stiffness is posited to contribute to cerebral microvascular damage,[96] cognitive impairment, and dementia by reducing mean cerebral blood flow and increasing pulsatile stress in the brain (Fig. 41.3). Large elastic arteries, such as the aorta, absorb and dampen pulsatile flow, creating a steady flow to smaller resistance vessels incapable of absorbing pulsatile energy. As a consequence of arterial stiffening, higher pulsatility reaches the smaller resistance vessels in the brain, a high-flow, low-impedance organ particularly sensitive to excessive pressure and flow pulsatility.[91] With accelerated vascular aging, higher pulsatility reaches further into the cerebral vasculature,[97] promoting microvascular remodeling and impairing oxygen delivery to tissue (i.e., perfusion of the brain).[98] Chronic cerebral hypoperfusion and repeated occurrences of microvascular ischemia may lead to tissue damage[38,52,99] that is associated with cognitive decline and ADRD.[100–103] The primary sites for cerebrovascular damage from excess pulsatility delivered by arterial stiffness is

seen in various forms of cerebral small vessel disease[104] observed in the white matter and basal ganglia.[33,47]

The excess pulsatility to the cerebral vasculature also impairs cerebral autoregulatory mechanisms, a combination of myogenic, autonomic, and metabolic mechanisms of the cerebral circulation to maintain vascular resistance and perfusion.[105] Although cerebral autoregulation is not fully understood, it is characterized by cerebral blood flow and cerebrovascular reactivity. Indeed, cerebrovascular reactivity is lower in individuals with hypertension, with greater arterial stiffness,[106] and with MCI.[106,107]

Additional pathways contributing to cognitive decline and dementia associated with cerebral hypoperfusion have been proposed.[108,109] Cerebral blood flow is constant in a normal physiological state; however, individuals with ADRD and vascular dementia have lower mean cerebral blood flow and higher pulsatile flow velocity in middle cerebral arteries, compared with those with normal cognition.[110] The effect of arterial stiffness on cerebral blood flow increases the risk for subclinical brain infarction and incident stroke.[111] Central arterial stiffness, measured by PWV[112] and cPP[113] are associated with these hemodynamic alterations in the middle cerebral artery, as further links between arterial stiffness and cerebral microvascular damage, cognitive impairment, and ADRD.

Coherence of evidence—Novel preclinical murine models create central arterial stiffness through the following: hypertensive murine models; carotid artery calcification by direct injection of calcium chloride to the adventitia of the carotid artery; as well as elastin and fibrillin-1 haploinsufficiency. When crossed with transgenic AD mouse models, these novel models reveal mechanistic insights into the role of arterial stiffness and excess pulsatility in increased neuroinflammation, endothelial dysfunction, microvascular disease, neurodegeneration, Aβ production, and reduced Aβ clearance. (For informative review, see Winder, Reeve, and Walker).[114] In microvascular models of human cerebral vascular endothelial cells, pulsatile stretch modulates Aβ generation and secretion and activates endothelial inflammatory pathways,[115] supporting the role of excess vascular pulsatility in Aβ pathogenesis. In mouse models, cerebral arterial pulsatility contributes to blood−brain barrier breakdown and paravascular fluid exchange,[116] potentially increasing infiltration of solutes into the brain and inhibiting Aβ clearance from the brain along paravascular pathways.[117] Further evidence shows that the pulse wave may drive pulsatile flow of interstitial fluid,[118] suggesting that arterial stiffening may impair the clearing of interstitial waste, including Aβ, from the aged brain. Impairing clearance of soluble Aβ may contribute to aggregation of Aβ in the vessel wall, clinically termed CAA. Since CAA often occurs with the AD hallmark parenchymal Aβ plaques in individuals with AD,[119] CAA is an emerging

FIGURE 41.4 Functional effects of amyloid-beta (Aβ). Vascular Aβ deposition, called cerebral amyloid angiopathy (CAA), induces functional changes (vascular stiffening) and promotes vascular inflammation and atherosclerosis, all of which leads to cerebral hypoperfusion and associated dementias (mixed dementia and AD). *Modified from Stakos DA, Stamatelopoulos K, Bampatsias D, et al. The Alzheimer's disease amyloid-beta hypothesis in cardiovascular aging and disease: JACC focus seminar. J Am Coll Cardiol. 2020; 75:952−967.*

marker of risk for cerebral small vessel disease, vascular cognitive impairment, and AD. Cerebral arteries from older adults exhibit arteriosclerotic markers, reduced mechanical compliance, loss of elastin, and CAA.[120] The association of arterial stiffness with increased arterial pulsatility Aβ production and reduced clearance of interstitial waste may constitute a feed-forward cycle whereby Aβ deposition increases cerebral arterial stiffness leading to neurodegeneration (Fig. 41.4). These mechanisms provide support for an association between arterial stiffness and dementia pathogenesis.

Analogy—While arterial stiffness is associated with various aspects of ADRD when accounting for potential confounders (e.g., age, blood pressure, hypertension, and diabetes), it is plausible that arterial stiffness simply represents some residual aspect of accelerated vascular aging in the body or brain, but does not impart direct effects on the brain. Additionally, hemodynamic factors and arterial stiffness could have shared pathways contributing to ADRD, making it difficult to identify direct effects. As hypertensive models demonstrate, central arterial stiffness is both a potential cause and consequence of hypertension. Further, metabolic disorders such as glucose dysregulation, insulin resistance, metabolic syndrome, and diabetes increase the risk for hypertension and arterial stiffness.[121] Both of which are risk factors for ADRD and increase vascular pathology and therefore the vascular contributions to dementia.

Applying causal effects to blood pressure, hypertension, and diabetes is challenging because they represent complex multifactorial traits. Blood pressure level is determined by just two variables: peripheral vascular resistance and cardiac output. It exhibits a Gaussian distribution in the general population indicating that it is the net effect of a multitude of independent factors each with a small cumulative effect.[122] The same can be said for the multitude of factors regulating peripheral resistance. Principal and most proximal of these is arterial stiffness. It can be argued that arterial stiffness better relates hemodynamics to distal organ systems.

Similarly, arterial stiffness and atherosclerosis are interrelated forms of vascular pathology that makes disentangling the two difficult. Arterial stiffness and changes in vascular structure can occur from and be accelerated by atherosclerosis, which is a major risk factor for stroke.[123] Atherosclerotic plaques deposited in the media of the carotid wall changes both the regional blood flow and the local stiffness, and the calcification of atherosclerotic plaques imaged by computed tomography (CT). Several studies show that CT-assessed coronary calcification is associated with cerebral atrophy on MRI, poorer cognitive performance,[124,125] and worse microstructural integrity.[126] These relationships appear to be evident with both the extracranial and intracranial arteries.[127] Intracranial atherosclerosis is a confirmed, strong risk factor for dementia[128]; however, the presence of intracranial atherosclerotic plaque or stenosis is not associated with brain Aβ deposition.[129] Future studies will have to confirm this apparent lack of association between atherosclerotic disease and dementia pathology.

The presence of regional carotid atherosclerosis alone may be a risk factor for AD and dementia through its contributions to cerebrovascular disease. In fact, AD cases have a greater degree of cerebral artery (circle of Willis) occlusion than controls, and there was a positive correlation between the degree of arterial stenosis and neurofibrillary tangle score.[130] Regional atherosclerosis can be imaged by carotid ultrasound, CT, and MRI. Carotid ultrasound is routinely used to identify carotid plaques, identify vascular occlusions, and measure carotid intima media thickness (IMT). Greater IMT of the carotid and brachiocephalic trunk are associated with deep subcortical WMH[131] and brain infarcts.[104,123] Studies that relate both atherosclerosis (via IMT and plaques) and arterial stiffness (via PWV) to cerebral small vessel disease show arterial stiffness to be more strongly related to cerebral small vessel disease than atherosclerosis measures.[104]

Finally, it should be recognized that the gene encoding *APOE* and the function of ApoE is a risk factor for developing cardiovascular disease, arterial stiffness, and ADRD. Proper function of ApoE interrupts a mechanically driven feed-forward loop that increases the expression of

collagen-I, fibronectin, and lysyl oxidase in response to substratum stiffening.[132] Inefficiency of ApoE function is expressed with inheritance of the APOE-ε4, which is also the primary genetic risk factor for AD. Limited studies suggested a shared risk of APOE-ε4 may modify the relationship between arterial stiffness, cognitive decline, and AD. APOE-ε4 status modified the association of arterial stiffness (carriers worse)[133] and pulse pressure (noncarriers worse)[134] with cognitive function, but not with arterial stiffness and dementia.[20]

More deeply phenotyped and multifactorial studies of arterial stiffness and ADRD are needed to disentangle the relationships between arterial stiffness, atherosclerosis, APOE, and ADRD biomarkers.

Experimental evidence—Ultimately, experimental evidence is necessary to prove or refute causality. There are currently no randomized clinical trials aimed specifically at reducing arterial stiffness to prevent cognitive decline, dementia, or dementia-related pathology. The closest supporting evidence comes from the SPRINT MIND trial comparing intensive systolic blood pressure lowering (<120 mmHg) to standard treatment target for systolic (<140 mmHg) to risk of developing dementia and MCI. Intensive treatment of systolic blood pressure lowered PWV,[135] the risk for incident cognitive impairment,[136] and reduced the rate of WMH progression.[137] This suggests that improving hemodynamic risk factors could reduce the risk of cognitive impairment and cerebral small vessel disease. Future studies specifically targeting arterial stiffness should be sufficiently powered to cognitive and brain outcomes. Agents developed to target arterial stiffness or microvascular function may blunt or mitigate the effects arterial stiffness on cerebral health. Arterial stiffening is largely age-related, but also modifiable. Arterial de-stiffening[138] is an active area of research in blood pressure control[139,140] and lifestyle interventions such as habitual physical activity.[141–145] In addition to physical activity, weight loss, smoking cessation, salt reduction,[144] and dietary interventions[141] have been reported to reduce arterial stiffness. Neuroendocrine-directed therapies in development may reduce arterial stiffness. These include pharmacologic therapies targeting the renin—angiotensin system, natriuretic peptides, insulin modulators, as well as novel therapies that target advanced glycation end products and arterial fibrosis. Randomized clinical trials of arterial stiffness reduction and risk of ADRD are needed to provide experimental evidence for arterial stiffness as a modifiable target for cognitive impairment and ADRD.

Conclusions

This chapter reviewed and summarized the current state of evidence linking arterial stiffness to clinical evidence of ADRD biomarkers (cerebral hemodynamics, cerebral small vessel disease, neuroinflammation, neurodegeneration, Aβ deposition, and tau hyperphosphorylation), cognitive decline, and the risk for dementia, especially in older adults in the eighth and ninth decades of life who are at greatest risk for ADRD. These observations are supported by mechanisms detailed in biologic models linking arterial stiffness to neuroinflammation, neurodegeneration, and accelerated cerebral pathology, as well as evidence from clinical trials that aggressively reducing blood pressure slows small vessel disease and cognitive decline. Further, arterial stiffness is not only associated with forms of cerebral pathology related to ADRD but also the co-occurrence of cerebral small vessel disease and Aβ deposition most commonly seen in vast majority of age-related dementias that make up ADRD. Finally, the evidence to date posits that arteriosclerosis, but not atherosclerosis, as prime therapeutic target for the prevention of VCID and ADRD, by preserving structural integrity of the brain. The breadth and depth of observational data linking arterial stiffness to dementia warrants more detailed examination of relationships between the progression of arterial stiffness and specific aspects of dementia-related pathology, as well as clinical trials to directly test the purported relationships that place arterial stiffness at a nexus of vascular disorders and dementia-related pathologies commonly seen in older adults.

References

1. Terem I, Ni WW, Goubran M, et al. Revealing sub-voxel motions of brain tissue using phase-based amplified MRI (aMRI). **Magn Reson Med**. 2018; 80:2549−2559.
2. Montine TJ, Koroshetz WJ, Babcock D, et al. Recommendations of the Alzheimer's disease-related dementias conference. **Neurology**. 2014; 83:851−860.
3. Boyle PA, Yu L, Leurgans SE, et al. Attributable risk of Alzheimer's dementia attributed to age-related neuropathologies. **Ann Neurol**. 2019; 85:114−124.
4. Kapasi A, DeCarli C, Schneider JA. Impact of multiple pathologies on the threshold for clinically overt dementia. **Acta Neuropathologica**. 2017; 134:171−186.
5. Gorelick PB, Scuteri A, Black SE, et al. Vascular contributions to cognitive impairment and dementia: a statement for healthcare professionals from the american heart association/american stroke association. **Stroke**. 2011; 42:2672−2713.
6. Snyder HM, Corriveau RA, Craft S, et al. Vascular contributions to cognitive impairment and dementia including Alzheimer's disease. **Alzheim Dement**. 2015; 11:710−717.
7. Corriveau RA, Bosetti F, Emr M, et al. The science of vascular contributions to cognitive impairment and dementia (VCID): a framework for advancing research priorities in the cerebrovascular biology of cognitive decline. **Cell Mol Neurobiol**. 2016; 36:281−288.
8. Filshtein TJ, Dugger BN, Jin LW, et al. Neuropathological diagnoses of demented hispanic, black, and non-hispanic white decedents seen at an Alzheimer's disease center. **J Alzheim Dis**. 2019; 68:145−158.

9. Power MC, Mormino E, Soldan A, et al. Combined neuropathological pathways account for age-related risk of dementia. **Ann Neurol**. 2018; 84:10−22.

10. Singer J, Trollor JN, Baune BT, Sachdev PS, Smith E. Arterial stiffness, the brain and cognition: a systematic review. **Ageing Res Rev**. 2014; 15:16−27.

11. Hanon O, Haulon S, Lenoir H, et al. Relationship between arterial stiffness and cognitive function in elderly subjects with complaints of memory loss. **Stroke**. 2005; 36:2193−2197.

12. Poels MM, van Oijen M, Mattace-Raso FU, et al. Arterial stiffness, cognitive decline, and risk of dementia: the Rotterdam study. **Stroke**. 2007; 38:888−892.

13. Rabkin SW, Jarvie G. Comparison of vascular stiffness in vascular dementia, Alzheimer dementia and cognitive impairment. **Blood Press**. 2011; 20:274−283.

14. Riba-Llena I, Nafria C, Filomena J, et al. High daytime and night-time ambulatory pulse pressure predict poor cognitive function and mild cognitive impairment in hypertensive individuals. **J Cerebr Blood Flow Metabol**. 2016; 36:253−263.

15. Dhoat S, Ali K, Bulpitt CJ, Rajkumar C. Vascular compliance is reduced in vascular dementia and not in Alzheimer's disease. **Age Ageing**. 2008; 37:653−659.

16. Rouch L, Cestac P, Sallerin B, et al. Pulse wave velocity is associated with greater risk of dementia in mild cognitive impairment patients. **Hypertension**. 2018; 72:1109−1116.

17. Grinberg LT, Heinsen H. Toward a pathological definition of vascular dementia. **J Neurol Sci**. 2010; 299:136−138.

18. Meyer ML, Palta P, Tanaka H, et al. Association of central arterial stiffness and pressure pulsatility with mild cognitive impairment and dementia: the atherosclerosis risk in Communities study-neurocognitive study (ARIC-NCS). **J Alzheim Dis**. 2017; 57:195−204.

19. Pase MP, Beiser A, Himali JJ, et al. Aortic stiffness and the risk of incident mild cognitive impairment and dementia. **Stroke**. 2016; 47(9):2256−2261. https://doi.org/10.1161/STROKEAHA.116.013508. Epub 2016 Aug 4. PMID: 27491735. PMCID: PMC4995162.

20. Cui C, Sekikawa A, Kuller LH, et al. Aortic stiffness is associated with increased risk of incident dementia in older adults. **J Alzheim Dis**. 2018; 66:297−306.

21. Waldstein SR, Rice SC, Thayer JF, Najjar SS, Scuteri A, Zonderman AB. Pulse pressure and pulse wave velocity are related to cognitive decline in the Baltimore Longitudinal Study of Aging. **Hypertension**. 2008; 51:99−104.

22. Elias MF, Robbins MA, Budge MM, Abhayaratna WP, Dore GA, Elias PK. Arterial pulse wave velocity and cognition with advancing age. **Hypertension**. 2009; 53:668−673.

23. Mitchell GF, van Buchem MA, Sigurdsson S, et al. Arterial stiffness, pressure and flow pulsatility and brain structure and function: the Age, Gene/Environment Susceptibility–Reykjavik study. **Brain**. 2011; 134:3398−3407.

24. Tsao CW, Seshadri S, Beiser AS, et al. Relations of arterial stiffness and endothelial function to brain aging in the community. **Neurology**. 2013; 81:984−991.

25. Watson NL, Sutton-Tyrrell K, Rosano C, et al. Arterial stiffness and cognitive decline in well-functioning older adults. **J Gerontol Ser A Biol Sci Med Sci**. 2011; 66:1336−1342.

26. Rensma SP, Stehouwer CDA, Van Boxtel MPJ, et al. Associations of arterial stiffness with cognitive performance, and the role of microvascular dysfunction: the Maastricht study. **Hypertension**. 2020; 75:1607−1614.

27. Zeki Al Hazzouri A, Yaffe K. Arterial stiffness and cognitive function in the elderly. **J Alzheim Dis**. 2014; 42(Suppl 4):S503−S514.

28. Pase MP, Herbert A, Grima NA, Pipingas A, O'Rourke MF. Arterial stiffness as a cause of cognitive decline and dementia: a systematic review and meta-analysis. **Intern Med J**. 2012; 42:808−815.

29. van Sloten TT, Protogerou AD, Henry RM, Schram MT, Launer LJ, Stehouwer CD. Association between arterial stiffness, cerebral small vessel disease and cognitive impairment: a systematic review and meta-analysis. **Neurosci Biobehav Rev**. 2015; 53:121−130.

30. Benetos A, Watfa G, Hanon O, et al. Pulse wave velocity is associated with 1-year cognitive decline in the elderly older than 80 years: the PARTAGE study. **J Am Med Dir Assoc**. 2012; 13:239−243.

31. Watfa G, Benetos A, Kearney-Schwartz A, et al. Do arterial hemodynamic parameters predict cognitive decline over a period of 2 years in individuals older than 80 years living in nursing homes? The PARTAGE study. **J Am Med Dir Assoc**. 2015; 16:598−602.

32. Pase MP, Stough C, Grima NA, et al. Blood pressure and cognitive function: the role of central aortic and brachial pressures. **Psychol Sci**. 2013; 24:2173−2181.

33. Palta P, Sharrett AR, Wei J, et al. Central arterial stiffness is associated with structural brain damage and poorer cognitive performance: the ARIC study. **J Am Heart Assoc**. 2019; 8:e011045.

34. Araghi M, Shipley MJ, Wilkinson IB, et al. Association of aortic stiffness with cognitive decline: Whitehall II longitudinal cohort study. **Eur J Epidemiol**. 2020; 35(9):861−869. https://doi.org/10.1007/s10654-019-00586-3. Epub 2019 Nov 27 PMID: 31776832. PMCID: PMC7441227.

35. Tsao CW, Himali JJ, Beiser AS, et al. Association of arterial stiffness with progression of subclinical brain and cognitive disease. **Neurology**. 2016; 86:619−626.

36. Alvarez-Bueno C, Cunha PG, Martinez-Vizcaino V, et al. Arterial stiffness and cognition among adults: a systematic review and meta-analysis of observational and longitudinal studies. **J Am Heart Assoc**. 2020; 9:e014621.

37. Poels MM, Zaccai K, Verwoert GC, et al. Arterial stiffness and cerebral small vessel disease: the Rotterdam Scan Study. **Stroke**. 2012; 43:2637−2642.

38. Henskens LH, Kroon AA, van Oostenbrugge RJ, et al. Increased aortic pulse wave velocity is associated with silent cerebral small-vessel disease in hypertensive patients. **Hypertension**. 2008; 52:1120−1126.

39. Henskens LH, van Oostenbrugge RJ, Kroon AA, de Leeuw PW, Lodder J. Brain microbleeds are associated with ambulatory blood pressure levels in a hypertensive population. **Hypertension**. 2008; 51:62−68.

40. Riba-Llena I, Jiménez-Balado J, Castañé X, et al. Arterial stiffness is associated with basal ganglia enlarged perivascular spaces and cerebral small vessel disease load. **Stroke**. 2018; 49:1279−1281.

41. Hughes TM, Kuller LH, Barinas-Mitchell EJM, et al. Pulse wave velocity is associated with β-amyloid deposition in the brains of very elderly adults. **Neurology**. 2013; 81(19):1711−1718. https://doi.org/10.1212/01.wnl.0000435301.64776.37. Epub 2013 Oct 16. PMID: 24132374. PMCID: PMC3812104.

42. Pase MP, Himali JJ, Mitchell GF, et al. Association of aortic stiffness with cognition and brain aging in young and middle-aged adults: the Framingham Third generation cohort study. **Hypertension**. 2016; 67:513−519.

43. Maillard P, Mitchell GF, Himali JJ, et al. Aortic stiffness, increased white matter free water, and altered microstructural integrity: a continuum of injury. **Stroke**. 2017; 48:1567−1573.

44. Rosano C, Watson N, Chang Y, et al. Aortic pulse wave velocity predicts focal white matter hyperintensities in a biracial cohort of older adults. **Hypertension**. 2013; 61:160−165.

45. King KS, Chen KX, Hulsey KM, et al. White matter hyperintensities: use of aortic arch pulse wave velocity to predict volume independent of other cardiovascular risk factors. **Radiology**. 2013; 267:709−717.

46. de Havenon A, Wong KH, Elkhetali A, McNally JS, Majersik JJ, Rost NS. Carotid artery stiffness accurately predicts white matter hyperintensity volume 20 Years later: a secondary analysis of the atherosclerosis risk in the community study. **Am J Neuroradiol**. 2019; 40:1369−1373.

47. Zhai FF, Ye YC, Chen SY, et al. Arterial stiffness and cerebral small vessel disease. **Front Neurol**. 2018; 9:723.

48. Hughes T, Wagenknecht L, Craft S, et al. Arterial stiffness and dementia pathology: atherosclerosis risk in Communities (ARIC)-PET study. **Neurology**. 2018; 90.

49. Brandts A, van Elderen SG, Westenberg JJ, et al. Association of aortic arch pulse wave velocity with left ventricular mass and lacunar brain infarcts in hypertensive patients: assessment with MR imaging. **Radiology**. 2009; 253:681−688.

50. Ohmine T, Miwa Y, Yao H, et al. Association between arterial stiffness and cerebral white matter lesions in community-dwelling elderly subjects. **Hypertens Res**. 2008; 31:75−81.

51. Shrestha I, Takahashi T, Nomura E, et al. Association between central systolic blood pressure, white matter lesions in cerebral MRI and carotid atherosclerosis. **Hypertens Res**. 2009; 32:869−874.

52. Pantoni L, Garcia JH. Pathogenesis of leukoaraiosis: a review. **Stroke**. 1997; 28:652−659.

53. Maillard P, Carmichael O, Fletcher E, Reed B, Mungas D, DeCarli C. Coevolution of white matter hyperintensities and cognition in the elderly. **Neurology**. 2012; 79:442−448.

54. Maillard P, Mitchell GF, Himali JJ, et al. Effects of arterial stiffness on brain integrity in young adults from the Framingham heart study. **Stroke**. 2016; 47:1030−1036.

55. Badji A, Noriega de la Colina A, Karakuzu A, et al. Arterial stiffness and white matter integrity in the elderly: a diffusion tensor and magnetization transfer imaging study. **Neuroimage**. 2019; 186:577−585.

56. Tarumi T, de Jong DLK, Zhu DC, et al. Central artery stiffness, baroreflex sensitivity, and brain white matter neuronal fiber integrity in older adults. **Neuroimage**. 2015; 110:162−170.

57. Wei J, Palta P, Meyer ML, et al. Aortic stiffness and white matter microstructural integrity assessed by diffusion tensor imaging: the ARIC-NCS. **J Am Heart Assoc**. 2020; 9:e014868.

58. Jochemsen HM, Muller M, Bots ML, et al. Arterial stiffness and progression of structural brain changes: the SMART-MR study. **Neurology**. 2015; 84:448−455.

59. Cullen KM, Kocsi Z, Stone J. Microvascular pathology in the aging human brain: evidence that senile plaques are sites of microhaemorrhages. **Neurobiol Aging**. 2006; 27:1786−1796.

60. Wardlaw JM, Smith EE, Biessels GJ, et al. Neuroimaging standards for research into small vessel disease and its contribution to ageing and neurodegeneration. **Lancet Neurol**. 2013; 12:822−838.

61. Jack Jr CR, Bennett DA, Blennow K, et al. NIA-AA Research Framework: toward a biological definition of Alzheimer's disease. **Alzheim Dement**. 2018; 14:535−562.

62. Hughes TM, Kuller LH, Barinas-Mitchell EJ, et al. Arterial stiffness and beta-amyloid progression in nondemented elderly adults. **JAMA Neurol**. 2014; 71:562−568.

63. Vemuri P, Lesnick TG, Przybelski SA, et al. Age, vascular health, and Alzheimer disease biomarkers in an elderly sample. **Ann Neurol**. 2017; 82:706−718.

64. Moore EE, Liu D, Li J, et al. Association of aortic stiffness with biomarkers of neuroinflammation, synaptic dysfunction, and neurodegeneration. **Neurology**. 2021; 97(4):e329−e340. https://doi.org/10.1212/WNL.0000 000000012257. Epub 2021 May 24 PMID: 34031194. PMCID: PMC8362359.

65. Hill AB. The environment and disease: association or causation? **Proc R Soc Med**. 1965; 58:295−300.

66. Schutte AE, Kruger R, Gafane-Matemane LF, Breet Y, Strauss-Kruger M, Cruickshank JK. Ethnicity and arterial stiffness. **Arterioscler Thromb Vasc Biol**. 2020; 40:1044−1054.

67. Plassman BL, Langa KM, Fisher GG, et al. Prevalence of dementia in the United States: the aging, demographics, and memory study. **Neuroepidemiology**. 2007; 29:125−132.

68. Kuller LH, Lopez OL, Newman A, et al. Risk factors for dementia in the cardiovascular health cognition study. **Neuroepidemiology**. 2003; 22:13−22.

69. Ferri CP, Prince M, Brayne C, et al. Global prevalence of dementia: a Delphi consensus study. **Lancet**. 2005; 366:2112−2117.

70. Hebert LE, Weuve J, Scherr PA, Evans DA. Alzheimer disease in the United States (2010-2050) estimated using the 2010 census. **Neurology**. 2013; 80:1778−1783.

71. Stern R, Tattersall MC, Gepner AD, et al. Sex differences in predictors of longitudinal changes in carotid artery stiffness: the Multi-Ethnic Study of Atherosclerosis. **Arterioscler Thromb Vasc Biol**. 2015; 35:478−484.

72. Gepner AD, Tedla Y, Colangelo LA, et al. Progression of carotid arterial stiffness with treatment of hypertension over 10 years: the multi-ethnic study of atherosclerosis. **Hypertension**. 2017; 69:87−95.

73. Bahrami H, Kronmal R, Bluemke DA, et al. Differences in the incidence of congestive heart failure by ethnicity: the multi-ethnic study of atherosclerosis. **Arch Intern Med**. 2008; 168:2138−2145.

74. Mahley RW, Rall Jr SC. Apolipoprotein E: far more than a lipid transport protein. **Annu Rev Genom Hum Genet**. 2000; 1:507−537.

75. Crean S, Ward A, Mercaldi CJ, et al. Apolipoprotein E epsilon4 prevalence in Alzheimer's disease patients varies across global populations: a systematic literature review and meta-analysis. **Dement Geriatr Cognit Disord**. 2011; 31:20−30.

76. Gottesman RF, Schneider AL, Zhou Y, et al. The ARIC-PET amyloid imaging study: brain amyloid differences by age, race, sex, and APOE. **Neurology**. 2016; 87:473−480.

77. Heyman A, Fillenbaum G, Prosnitz B, Raiford K, Burchett B, Clark C. Estimated prevalence of dementia among elderly black and white community residents. **Arch Neurol**. 1991; 48:594−598.

78. Gurland BJ, Wilder DE, Lantigua R, et al. Rates of dementia in three ethnoracial groups. **Int J Geriatr Psychiatr**. 1999; 14:481−493.

79. Tang MX, Cross P, Andrews H, et al. Incidence of AD in African-Americans, Caribbean Hispanics, and Caucasians in northern Manhattan. **Neurology**. 2001; 56:49−56.

80. Demirovic J, Prineas R, Loewenstein D, et al. Prevalence of dementia in three ethnic groups: the South Florida program on aging and health. **Ann Epidemiol**. 2003; 13:472−478.

81. Barnes LL, Leurgans S, Aggarwal NT, et al. Mixed pathology is more likely in black than white decedents with Alzheimer dementia. **Neurology**. 2015; 85:528−534.

82. Chin AL, Negash S, Hamilton R. Diversity and disparity in dementia: the impact of ethnoracial differences in Alzheimer disease. **Alzheim Dis Assoc Disord**. 2011; 25:187−195.

83. Qian J, Wolters FJ, Beiser A, et al. APOE-related risk of mild cognitive impairment and dementia for prevention trials: an analysis of four cohorts. **PLoS Med**. 2017; 14:e1002254.

84. Goel A, Maroules CD, Mitchell GF, et al. Ethnic difference in proximal aortic stiffness: an observation from the Dallas heart study. **JACC Cardiovasc Imaging**. 2017; 10:54−61.

85. Shirai K, Utino J, Otsuka K, Takata M. A novel blood pressure-independent arterial wall stiffness parameter; cardio-ankle vascular index (CAVI). **J Atherosclerosis Thromb**. 2006; 13:101−107.

86. Manly JJ, Tang MX, Schupf N, Stern Y, Vonsattel JP, Mayeux R. Frequency and course of mild cognitive impairment in a multiethnic community. **Ann Neurol**. 2008; 63:494−506.

87. Howell JC, Watts KD, Parker MW, et al. Race modifies the relationship between cognition and Alzheimer's disease cerebrospinal fluid biomarkers. **Alzheim Res Ther**. 2017; 9:88.

88. Burke SL, Rodriguez MJ, Barker W, et al. Relationship between cognitive performance and measures of neurodegeneration among hispanic and white non-hispanic individuals with normal cognition, mild cognitive impairment, and dementia. **J Int Neuropsychol Soc**. 2018; 24:176−187.

89. Mancia G, De Backer G, Dominiczak A, et al. Management of Arterial Hypertension of the European Society of H and European Society of C. 2007 Guidelines for the Management of Arterial Hypertension: The Task Force for the Management of Arterial Hypertension of the European Society of Hypertension (ESH) and of the European Society of Cardiology (ESC). **J Hypertens**. 2007; 25:1105−1187.

90. Van Bortel LM, Laurent S, Boutouyrie P, et al. Expert consensus document on the measurement of aortic stiffness in daily practice using carotid-femoral pulse wave velocity. **J Hypertens**. 2012; 30:445−448.

91. Hashimoto J, Aikawa T, Imai Y. Large artery stiffening as a link between cerebral lacunar infarction and renal albuminuria. **Am J Hypertens**. 2008; 21:1304−1309.

92. O'Rourke MF, Hashimoto J. Mechanical factors in arterial aging: a clinical perspective. **J Am Coll Cardiol**. 2007; 50:1−13.

93. Hajjar I, Goldstein FC, Martin GS, Quyyumi AA. Roles of arterial stiffness and blood pressure in hypertension-associated cognitive decline in healthy adults. **Hypertension**. 2016; 67:171−175.

94. Zeki Al Hazzouri A, Newman AB, Simonsick E, et al. Pulse wave velocity and cognitive decline in elders: the Health, Aging, and Body Composition study. **Stroke**. 2013; 44:388−393.

95. Sugioka K, Hozumi T, Sciacca RR, et al. Impact of aortic stiffness on ischemic stroke in elderly patients. **Stroke**. 2002; 33:2077−2081.

96. Bateman GA. Pulse wave encephalopathy: a spectrum hypothesis incorporating Alzheimer's disease, vascular dementia and normal pressure hydrocephalus. **Med Hypotheses**. 2004; 62:182−187.

97. Zarrinkoob L, Ambarki K, Wahlin A, et al. Aging alters the dampening of pulsatile blood flow in cerebral arteries. **J Cerebr Blood Flow Metabol**. 2016; 36:1519−1527.

98. Mitchell GF. Effects of central arterial aging on the structure and function of the peripheral vasculature: implications for end-organ damage. **J Appl Physiol**. 2008; 105:1652−1660.

99. O'Rourke MF. Arterial aging: pathophysiological principles. **Vasc Med**. 2007; 12:329−341.

100. Bozzali M, Padovani A, Caltagirone C, Borroni B. Regional grey matter loss and brain disconnection across Alzheimer disease evolution. **Curr Med Chem**. 2011; 18:2452−2458.

101. Eckerstrom C, Olsson E, Klasson N, et al. High white matter lesion load is associated with hippocampal atrophy in mild cognitive impairment. **Dement Geriatr Cognit Disord**. 2011; 31:132−138.

102. Gili T, Cercignani M, Serra L, et al. Regional brain atrophy and functional disconnection across Alzheimer's disease evolution. **J Neurol Neurosurg Psychiatry**. 2011; 82:58−66.

103. Grambaite R, Reinvang I, Selnes P, et al. Pre-dementia memory impairment is associated with white matter tract affection. **J Int Neuropsychol Soc**. 2011; 17:143−153.

104. Zhang K, Jiang Y, Wang Y, et al. Associations of arterial stiffness and carotid atherosclerosis with cerebral small vessel disease in a rural community-based population. **J Atherosclerosis Thromb**. 2020; 27:922−933.

105. Yang SH, Liu R. Chapter 10 - cerebral autoregulation. In: Caplan LR, Biller J, Leary MC, et al., eds. **Primer on Cerebrovascular Diseases**. 2nd ed. San Diego: Academic Press; 2017:57−60.

106. Jefferson AL, Cambronero FE, Liu D, et al. Higher aortic stiffness is related to lower cerebral blood flow and preserved cerebrovascular reactivity in older adults. **Circulation**. 2018; 138:1951−1962.

107. Beishon L, Haunton VJ, Panerai RB, Robinson TG. Cerebral hemodynamics in mild cognitive impairment: a systematic review. **J Alzheim Dis**. 2017; 59:369−385.

108. Ruitenberg A, den Heijer T, Bakker SL, et al. Cerebral hypoperfusion and clinical onset of dementia: the Rotterdam Study. **Ann Neurol**. 2005; 57:789−794.

109. de la Torre JC. Alzheimer's disease is a vasocognopathy: a new term to describe its nature. **Neurol Res**. 2004; 26:517−524.

110. Sabayan B, Jansen S, Oleksik AM, et al. Cerebrovascular hemodynamics in Alzheimer's disease and vascular dementia: a meta-analysis of transcranial Doppler studies. **Ageing Res Rev**. 2012; 11:271−277.

111. Ben-Shlomo Y, Spears M, Boustred C, et al. Aortic pulse wave velocity improves cardiovascular event prediction: an individual participant meta-analysis of prospective observational data from 17,635 subjects. **J Am Coll Cardiol**. 2014; 63:636−646.

112. Kwater A, Gasowski J, Gryglewska B, Wizner B, Grodzicki T. Is blood flow in the middle cerebral artery determined by systemic arterial stiffness? **Blood Press**. 2009; 18:130−134.

113. Pase MP, Grima NA, Stough C, Scholey A, Pipingas A. Association of pulsatile and mean cerebral blood flow velocity with age and neuropsychological performance. **Physiol Behav**. 2014; 130:23−27.

114. Winder NR, Reeve EH, Walker AE. Large artery stiffness and brain health: insights from animal models. **Am J Physiol Heart Circ Physiol**. 2021; 320(1):H424−H431. https://doi.org/10.1152/ajpheart.00696.2020. Epub 2020 Nov 8. PMID: 33164578. PMCID: PMC7847068.

115. Gangoda SVS, Avadhanam B, Jufri NF, et al. Pulsatile stretch as a novel modulator of amyloid precursor protein processing and associated inflammatory markers in human cerebral endothelial cells. **Sci Rep**. 2018; 8:1689.

116. Weller RO, Djuanda E, Yow HY, Carare RO. Lymphatic drainage of the brain and the pathophysiology of neurological disease. **Acta Neuropathol**. 2009; 117:1−14.

117. Iliff JJ, Wang M, Liao Y, et al. A paravascular pathway facilitates CSF flow through the brain parenchyma and the clearance of interstitial solutes, including amyloid beta. **Sci Transl Med**. 2012; 4:147ra111.

118. Iliff JJ, Wang M, Zeppenfeld DM, et al. Cerebral arterial pulsation drives paravascular CSF-interstitial fluid exchange in the murine brain. **J Neurosci**. 2013; 33:18190−18199.

119. Bourassa P, Tremblay C, Schneider JA, Bennett DA, Calon F. Beta-amyloid pathology in human brain microvessel extracts from the parietal cortex: relation with cerebral amyloid angiopathy and Alzheimer's disease. **Acta Neuropathol**. 2019; 137(5):801−823. https://doi.org/10.1007/s00401-019-01967-4. Epub 2019 Feb 7. PMID: 30729296. PMCID: PMC6483878.

120. Fonck E, Feigl GG, Fasel J, et al. Effect of aging on elastin functionality in human cerebral arteries. **Stroke**. 2009; 40:2552−2556.

121. Hughes TM, Craft S. The role of insulin in the vascular contributions to age-related dementia. **Biochim Biophys Acta**. 2016; 1862:983−991.

122. Padmanabhan S, Caulfield M, Dominiczak AF. Genetic and molecular aspects of hypertension. **Circ Res**. 2015; 116:937−959.

123. Touboul PJ, Labreuche J, Vicaut E, Amarenco P, Investigators G. Carotid intima-media thickness, plaques, and Framingham risk score as independent determinants of stroke risk. **Stroke**. 2005; 36:1741−1745.

124. Rosano C, Naydeck B, Kuller LH, Longstreth Jr WT, Newman AB. Coronary artery calcium: associations with brain magnetic resonance imaging abnormalities and cognitive status. **J Am Geriatr Soc**. 2005; 53:609−615.

125. Vidal JS, Sigurdsson S, Jonsdottir MK, et al. Coronary artery calcium, brain function and structure: the AGES-Reykjavik Study. **Stroke**. 2010; 41:891−897.

126. Bos D, Vernooij MW, Elias-Smale SE, et al. Atherosclerotic calcification relates to cognitive function and to brain changes on magnetic resonance imaging. **Alzheim Dement J Alzheim Assoc**. 2012; 8:S104−S111.

127. Selkoe DJ. Alzheimer's disease: genes, proteins, and therapy. **Physiol Rev**. 2001; 81:741−766.

128. Dolan H, Crain B, Troncoso J, Resnick SM, Zonderman AB, Obrien RJ. Atherosclerosis, dementia, and Alzheimer disease in the Baltimore longitudinal study of aging cohort. **Ann Neurol**. 2010; 68:231−240.

129. Gottesman RF, Mosley TH, Knopman DS, et al. Association of intracranial atherosclerotic disease with brain β-amyloid deposition: secondary analysis of the ARIC study. **JAMA Neurol**. 2019; 77:350−357.

130. Roher AE, Esh C, Kokjohn TA, et al. Circle of willis atherosclerosis is a risk factor for sporadic Alzheimer's disease. **Arterioscler Thromb Vasc Biol**. 2003; 23:2055−2062.

131. Isa K, Sakima A, Sakima H, Nakachi K, Kinjyo K, Ohya Y. Association between the intima-media thickness of the brachiocephalic trunk and white matter hyperintensity in brain MRI. **Hypertens Res**. 2013; 36:980−984.

132. Kothapalli D, Liu SL, Bae YH, et al. Cardiovascular protection by ApoE and ApoE-HDL linked to suppression of ECM gene expression and arterial stiffening. **Cell Rep**. 2012; 2:1259−1271.

133. Cambronero FE, Liu D, Neal JE, et al. APOE genotype modifies the association between central arterial stiffening and cognition in older adults. **Neurobiol Aging**. 2018; 67:120−127.

134. Werhane ML, Thomas KR, Edmonds EC, et al. Differential effect of APOE ε4 status and elevated pulse pressure on functional decline in cognitively normal older adults. **J Alzheim Dis**. 2018; 62:1567−1578.

135. Program abstracts from the 21st International Association of Gerontology and Geriatrics (IAGG) World Congress. **Innov Aging**. 2017; 1:1−1452.

136. Group SMIftSR, Williamson JD, Pajewski NM, et al. Effect of intensive vs standard blood pressure control on probable dementia: a randomized clinical trial. **J Am Med Assoc**. 2019; 321:553−561.

137. Group SMIftSR, Nasrallah IM, Pajewski NM, et al. Association of intensive vs standard blood pressure control with cerebral white matter lesions. **J Am Med Assoc**. 2019; 322:524−534.

138. Chen Y, Shen F, Liu J, Yang GY. Arterial stiffness and stroke: de-stiffening strategy, a therapeutic target for stroke. **Stroke Vasc Neurol**. 2017; 2:65−72.

139. Koumaras C, Tzimou M, Stavrinou E, et al. Role of antihypertensive drugs in arterial 'de-stiffening' and central pulsatile hemodynamics. **Am J Cardiovasc Drugs**. 2012; 12:143−156.

140. Laurent S, Boutouyrie P, Vascular Mechanism C. Dose-dependent arterial destiffening and inward remodeling after olmesartan in hypertensives with metabolic syndrome. **Hypertension**. 2014; 64:709−716.

141. Sacre JW, Jennings GL, Kingwell BA. Exercise and dietary influences on arterial stiffness in cardiometabolic disease. **Hypertension**. 2014; 63:888−893.

142. Hawkins M, Gabriel KP, Cooper J, Storti KL, Sutton-Tyrrell K, Kriska A. The impact of change in physical activity on change in arterial stiffness in overweight or obese sedentary young adults. **Vasc Med**. 2014; 19:257−263.

143. Ashor AW, Lara J, Siervo M, Celis-Morales C, Mathers JC. Effects of exercise modalities on arterial stiffness and wave reflection: a systematic review and meta-analysis of randomized controlled trials. **PLoS One**. 2014; 9:e110034.

144. Pucci G, Battista F, Schillaci G. Aerobic physical exercise and arterial de-stiffening: a recipe for vascular rejuvenation? **Hypertens Res**. 2012; 35:964−966.

145. Montero D, Vinet A, Roberts CK. Effect of combined aerobic and resistance training versus aerobic training on arterial stiffness. **Int J Cardiol**. 2015; 178:69−76.

146. Stakos DA, Stamatelopoulos K, Bampatsias D, et al. The Alzheimer's disease amyloid-beta hypothesis in cardiovascular aging and disease: JACC focus seminar. **J Am Coll Cardiol**. 2020; 75:952−967.

This page intentionally left blank

Arterial stiffness and pulsatile hemodynamics in pregnancy and pregnancy-related vascular complications

Stella S. Daskalopoulou

Fonds de recherche du Québec – Santé – Boursier Clinicien – Senior, Director, Vascular Health Unit, Department of Medicine, Division of Internal Medicine, McGill University Health Centre, McGill University, Montreal, QC, Canada

In healthy pregnancies, physiological changes occur to meet the increased metabolic demands of both the mother and the fetus. These maternal adaptations ensure adequate uteroplacental circulation for fetal growth and development. Early in the first trimester, the maternal cardiovascular system undergoes a complex series of vascular and hematological alterations; systemic vasodilation and increased vascular compliance occur, leading to decreased systemic vascular resistance to accommodate the increase in cardiac output (CO) and plasma volume. These changes result in a characteristic high-volume, low-resistance circulation.[1] Failure to accommodate the increased demands of gestation due to vascular maladaptation leads to vascular complications, such as preeclampsia (PrE), which can have devastating consequences for both mother and fetus.

Below, we will elaborate on the physiological changes that occur during healthy, uncomplicated pregnancy, followed by a discussion of pregnancy-related vascular complications, with a particular focus on PrE. Specifically, we will provide an overview of typical physiological changes in CO, blood volume, blood pressure (BP), vascular remodeling and resistance, and arterial stiffness within both contexts, followed by a discussion of the beneficial effects of exercise in enhancing cardiovascular adaptations in pregnancy.

Healthy pregnancy

Blood volume and hematological changes

Pregnancy is a state of circulatory volume expansion and vasodilation involving considerable orchestration of several physiologic processes. Plasma volume increases progressively throughout gestation, starting at around 6–8 weeks, with the steepest increase observed during the second trimester. Plasma volume continues to increase in the third trimester to a pooled maximum increase of over 1 L. Overall, plasma volume typically increases by about 45%–50% above nonpregnancy levels (varying from 20% to 100%), with expansion being proportional to fetal growth.[2–4] This increase is critical to maintaining sufficient circulating blood volume and pressure for uteroplacental perfusion and accommodating the oxygen requirements of maternal organs and the growing fetus.[2]

During pregnancy, there is systemic and renal artery vasodilation; the latter leading to a 50% increase in renal plasma flow and glomerular filtration rates by the end of the first trimester.[5] Vasodilation leads to a cardiovascular system that is underfilled. This underfilling is compensated by an activation of the sympathetic nervous system and an increase in CO, renin–angiotensin–aldosterone system (RAAS) activity, and plasma volume.[6] Indeed, early in pregnancy the sympathetic activity is elevated, with enhanced maternal baroreceptor reflex sensitivity and decreased responsiveness to α-adrenergic stimulation.[7] Additionally, in order to maintain BP and retain salt and water during pregnancy, there is increased activation of the RAAS system. Aldosterone activates the mineralocorticoid receptor, which plays an important role in the growth and development of the placenta and fetus.[8]

Stimulation of the RAAS in the second and third trimester leads to a net increase in exchangeable sodium of approximately 1000 mg. Conversely, relaxin, a hormone produced by the corpus luteum, decidua, and placenta, triggers thirst and antidiuretic hormone secretion, leading to water retention that is greater than the sodium retention induced by RAAS.[8,9] Furthermore, progesterone acts on the

mineralocorticoid receptor as an aldosterone antagonist to prevent sodium retention and hypokalemia. Overall, the physiologic changes of pregnancy lead to hyponatremic hypoosmolar hypervolemia. In the third trimester, maternal plasma atrial natriuretic peptide levels increase by 40%, with a rise of 148% over the mean nonpregnant level noted during the first week postpartum, suggesting that atrial natriuretic peptide may be involved in postpartum diuresis.[10]

It is noteworthy that a significant increase in red blood cell production occurs during pregnancy, leading to a red blood cell mass increase of up to 40%.[11] Human placental lactogen (human chorionic somatomammotropin) enhances the production of erythropoietin, responsible for effective erythropoiesis. Although both plasma volume and red blood cell mass increase, there is a proportionally greater increase in plasma volume, leading to hemodilution and pseudoanemia with generally no change in mean corpuscular volume or mean corpuscular hemoglobin concentration.[6]

Cardiac output

CO is the product of heart rate (HR) and stroke volume (SV), calculated by the formula: $CO = HR \times SV$. CO is dependent on HR, heart contractility, preload, and afterload.[12] In normal pregnancy, CO increases with maternal weight, and decreases with maternal age.[11] The greatest increase in CO is observed at the beginning of the first trimester, and continues to increase up to the end of the second trimester.[13−17] CO remains stable after the second trimester, with a possible small decline toward the end of pregnancy.[13−17] In an uncomplicated singleton pregnancy, CO can increase by 30%−50% by the 24th gestational week, with a further increase of 15% observed in twin pregnancies.

In early pregnancy, increases in CO occur primarily in association with elevated SV. Later in pregnancy, the increase in CO is thought to be predominantly due to increased HR.[11] HR increases gradually throughout pregnancy, peaking in the third trimester, where an increase of 10−20 beats per minute (bpm), or 20%−25% over the baseline HR, is noted.[16] A recent metaanalysis demonstrated that the mean HR of healthy pregnant women significantly increased by 7.6 bpm (95% Confidence Interval [CI] 1.8−13.4) between 10 and 40 weeks'gestation.[18] SV also shows a gradual increase up to the end of the second trimester, where it then remains constant or decreases in the third trimester. Shortly after delivery, CO declines rapidly followed by a more gradual decrease over the next few weeks, reaching prepregnancy levels around 6 weeks postpartum.

Interestingly, myocardial contractility and ejection fraction do not appear to change during pregnancy.[19] Both echocardiography and cardiac magnetic resonance can be used to assess CO, SV, and cardiac function in pregnancy.[11] Typically, there is mild four-chamber dilatation with transient mild regurgitation of all valves, except for the aortic valve. Studies conducted in the third trimester and postpartum performed by both modalities demonstrated an increase in left ventricular end-diastolic volume, left ventricular mass, and CO during pregnancy, which subsequently resolved within 12 weeks postpartum; however, these values were underestimated by echocardiography when compared to cardiac magnetic resonance.[19] Indeed, cardiac magnetic resonance imaging evaluates left ventricular volumes more accurately than echocardiography and is also safe in pregnancy, as demonstrated by data from Ducas et al. and others.[19−21]
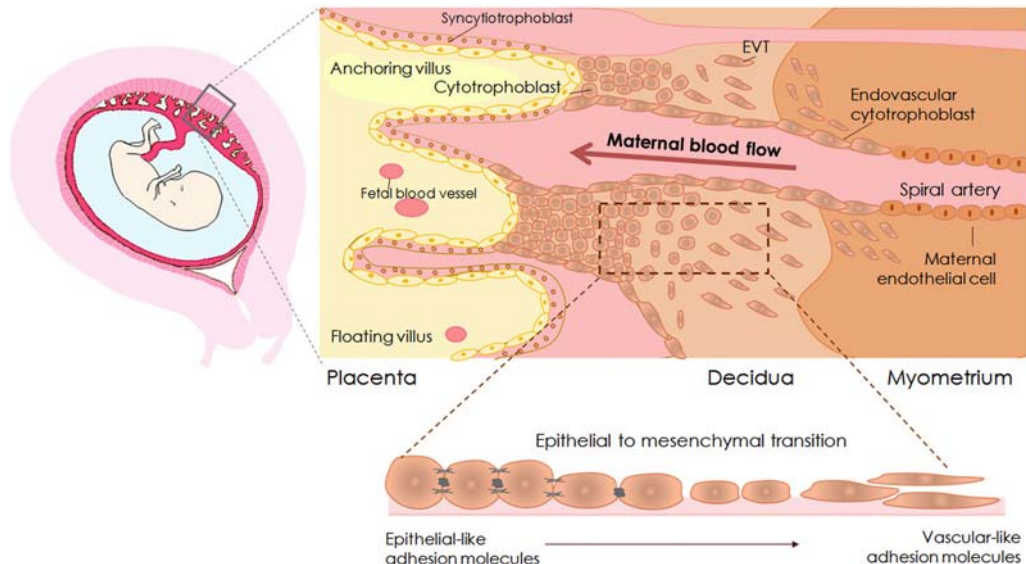
Vascular remodeling and vascular resistance
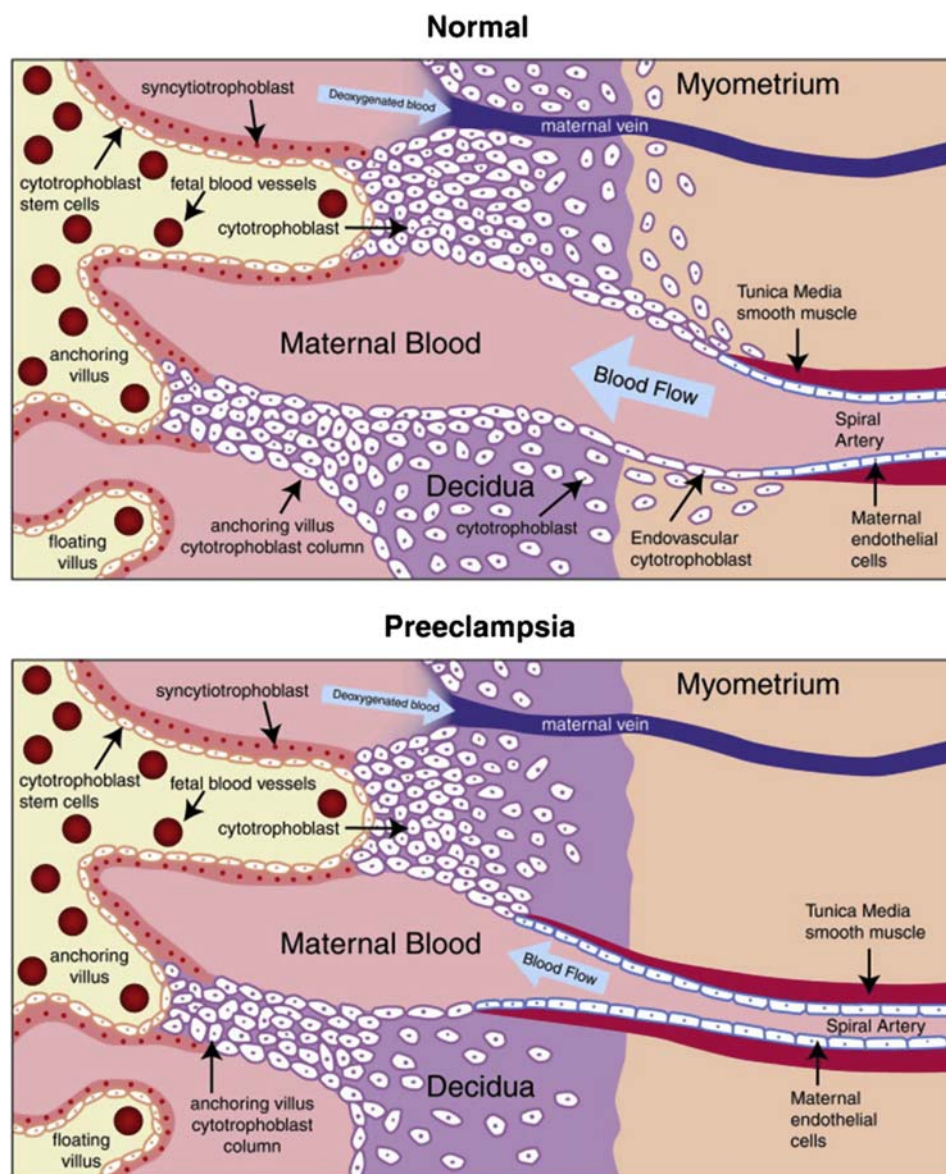
Arteries are highly adaptive structures that accommodate large increases in blood volume during pregnancy, redistributing blood flow to the growing fetus through vascular remodeling and vasodilation (Figs. 42.1 and 42.2).[22,23] Specifically, the vascular endothelium of the uterine arteries can increase its capacity to produce vasodilators to multiple agonists though increased expression of key mediators.[24]

Temporary vascular remodeling is primarily mediated by upregulation of vascular endothelial growth factors (VEGFs), including placental growth factor (PlGF). Upregulated by placental hormones, including the human chorionic gonadotropin hormone, the VEGF family of hormones promotes angiogenesis and maintenance of endothelial cell function during gestation.[25,26] These hormones increase to double their normal levels during early gestation and tend to decrease after placentation (13−16 weeks). Mediated by VEGF and PlGF, the uteroplacental unit undergoes angiogenesis and vasculogenesis. As a result, the uterine artery increases in length by 300%−500%, predominantly in the first trimester. Furthermore, high levels VEGF and PlGF lead to an increase in skin capillary density (by 13%) in the second trimester. Given that capillary beds contribute to 10%−15% of the total peripheral resistance, this results in a decrease in vascular resistance.

Conversely, soluble fms-like tyrosine kinase 1 (sFlt-1) is the nonmembrane-associated splice variant of VEGF receptor-1 (VEGFR-1) and is antiangiogenic (Fig. 42.3).[23] Specifically, sFlt-1 binds VEGF and PlGF, thus blocking their angiogenic effects on VEGFR-1. sFlt-1 is secreted by the placenta, and is thus increased in normal pregnancy. It progressively rises, with a greater increase observed in the third trimester, triggering a decline in VEGF and PlGF bioavailability in preparation for delivery. The ratio of sFlt-1/PlGF is an important clinical indicator of angiogenic status in pregnancy.[27]
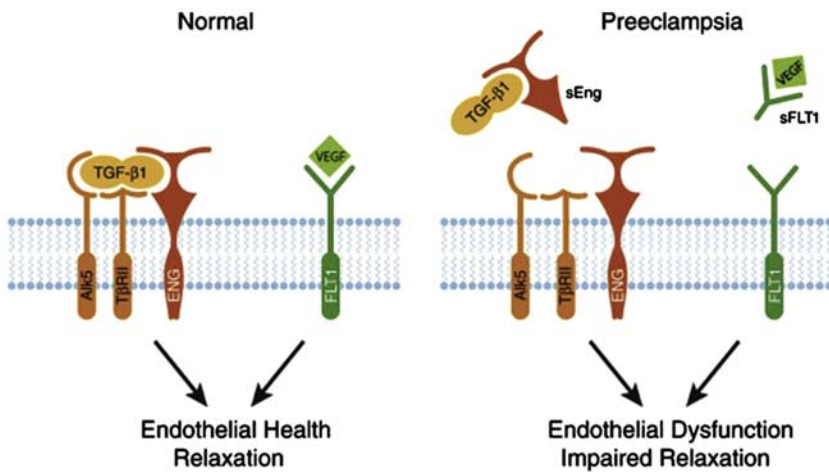
FIGURE 42.1 Cytotrophoblast invasion of uterine spiral arteries in a normal pregnancy. Extravillous trophoblast cells (EVTs) transform into invasive cells through a partial epithelial—mesenchymal transition in which epithelial-like adhesion molecules are replaced by vascular-like adhesion molecules. EVT migrations occur through the decidua until reaching the inner third of the myometrium to invade the maternal spiral artery. Optimal EVT invasion is required to adapt the maternal vasculature to pregnancy and maintain blood flow to the placenta. *Reproduced from Garrido-Gómez T, Castillo-Marco N, Cordero T, Simón C. Decidualization resistance in the origin of preeclampsia.* Am J Obstet Gynecol. *2020.*

FIGURE 42.2 A schematic of placental vascular remodeling in health (upper panel) and in disease—preeclampsia (lower panel). Exchange of oxygen, nutrients, and waste products between the fetus and the mother depends on adequate placental perfusion by maternal spiral arteries. Blood from the intervillous space is returned to the mother's circulation via spiral maternal veins noted above. In normal placental development, cytotrophoblasts of fetal origin invade the maternal spiral arteries, transforming them from small-caliber resistance vessels to high-caliber capacitance vessels capable of providing adequate placental perfusion to sustain the growing fetus. During the process of vascular invasion, the cytotrophoblasts undergo a transformation from an epithelial to an endothelial phenotype, a process referred to as "pseudovasculogenesis" (upper panel). In preeclampsia, cytotrophoblasts fail to adopt an invasive endothelial phenotype. Instead, invasion of the spiral arteries is shallow, and they remain small-caliber, resistance vessels (lower panel). This is thought to lead to placental ischemia and secretion of antiangiogenic factors. *Reproduced from Karumanchi SA, Rana S, Taylor RN. Angiogenesis and Preeclampsia. 4th ed. Amsterdam: Elsevier; 2015:113—132.*

FIGURE 42.3 Soluble fms-like tyrosine kinase (sFlt-1) and soluble endoglin (sEng) causes endothelial dysfunction by antagonizing vascular endothelium growth factor (VEGF) and transforming growth factor-β (TGF-β) signaling. There is mounting evidence that VEGF and TGF-β are required to maintain endothelial health in several tissues including the kidney and perhaps the placenta. During normal pregnancy, vascular homeostasis is maintained by physiological levels of VEGF and TGF-β signaling in the vasculature. In preeclampsia, excess placental secretion of sFlt-1 and sEng (two endogenous circulating antiangiogenic proteins) inhibits VEGF and TGF-β1 signaling, respectively, in the vasculature. This results in endothelial cell dysfunction, including decreased prostacyclin, nitric oxide production, and release of procoagulant proteins. *Reproduced from Karumanchi SA, Rana S, Taylor RN. Angiogenesis and Preeclampsia. 4th ed. Amsterdam: Elsevier; 2015:113−132.*

Vasodilation of the maternal vasculature is mediated by hormonal and hemodynamic alterations. Estrogen, progesterone, and relaxin are implicated in dilation and relaxation of the muscular layer of the maternal arterial walls.[28] Relaxin levels, in particular, increase and peak at the end of the first trimester, then decrease to a lower level for the rest of gestation. Relaxin can cause endothelium-dependent vasodilation, affecting small arterial vessel resistance. Interestingly, women with higher levels of relaxin and progesterone early in gestation had lower systolic BP (SBP) in the second and third trimesters of pregnancy, while higher diastolic BP (DBP) in the third trimester was noted in women with lower relaxin levels.[29]

Systemic vasodilation with increased vascular compliance can be detected early in gestation (at 5−8 weeks). Systemic vascular resistance decreases substantially in the first trimester, reaching a nadir in the middle of the second trimester. Increased nitric oxide (NO), prostacyclin, endothelium-derived hyperpolarizing factor, estrogen, progesterone, and relaxin are thought to mediate these effects.[24,29] Consequently, systemic vascular resistance is reduced by 35%−40% from baseline, and return to prepregnancy levels approximately 2 weeks postpartum. The decrease in systemic vascular resistance compensates for the gestational increase in blood volume and CO, thus preventing an increase or even leading to a decrease in BP. However, while a drop in vascular resistance occurs throughout the body, a disproportionately large drop in vascular resistance is observed in the uterine circulation. The outcome is a greater proportion of CO being directed toward the uteroplacental unit to meet the needs of the growing fetus.[24]

During early pregnancy, endothelial function is improved, as assessed by increased flow-mediated vasodilation (FMD—the ability of a large conduit artery to dilate in response to a shear stress stimulus), decreased nonspecific vasodilation by glyceryl trinitrate, and endothelium-dependent skin microvascular reactivity to acetylcholine.[30] Interestingly, birth weight has also been shown to correlate positively with maternal endothelial function (as assessed by skin microcirculatory responses to acetylcholine and sodium nitroprusside).[31] Endothelial cells play a critical role in the redistribution of blood flow during pregnancy to accommodate the growing fetus. Endothelial cells are particularly responsive to hemodynamic shear stress, thus regulating blood flow.[32] Increased shear stress, due to elevated CO and blood volume, leads to a progressive increase in endothelial-dependent NO release throughout gestation, causing decreased peripheral resistance and vasodilation.[32] Specifically, the myometrial uterine spiral arteries show a threefold increase in NO synthase activity leading to an increase in the diameter of uterine arteries, which doubles by midpregnancy and then plateaus. This results in redistribution of up to 12% of the CO to the uteroplacental unit.[33] Interestingly, inhibition of NO synthase in pregnant women leads to greater vasoconstriction when compared to nonpregnant women.[33] In healthy pregnancies, the uterine arteries are remodeled from small muscular, high-resistance, coiled vessels to large capacitance vessels of low-resistance, promoting greater blood flow toward the placenta compared to other areas of the uterus.[34] During this process, there appears to be no significant change in the collagen and elastin arrangement. Vasodilation of the uterine arteries occurs through outward hypertrophic remodeling. As a result of these processes, by the end of pregnancy, blood flow in the uterine arteries more than doubles, with the uterus getting approximately 20% of the woman's prepregnancy blood supply.

Blood pressure

In healthy pregnancy, increases in vascular compliance and distensibility start in the first trimester. As a result, decreases in BP occur, including peripheral SBP, DBP, mean arterial pressure (MAP), and central BPs, with a relatively larger decrease in DBP and MAP than SBP. Central BPs are significantly lower than peripheral BPs; this difference between central and peripheral BPs has been shown to be most pronounced in the first-half of gestation, decreases in the third trimester and reaches its lowest point in the postpartum period.[35]

Typically, arterial pressures steadily reduce to a nadir during the second trimester, reaching 5–10 mmHg below preconception levels.[16] The majority of this reduction is observed by 6–8 weeks gestation.[16] Visit-to-visit BP variability increases from the second to the third trimester. BPs increase during the third trimester and return to near preconception levels after delivery.[16] A recent metaanalysis demonstrated that the mean SBP was lowest at around 10 weeks of gestation (110.4 mmHg, 95% CI 108.5–112.3) and significantly increased by 5.6 mmHg (95% CI 4.0–7.2) at 40 weeks. Mean DBP was lowest at 21 weeks of gestation (65.9 mmHg, 95% CI 64.2–67.7) and significantly increased by 6.9 mmHg (6.2–7.5) at 40 weeks.[18] Several longitudinal studies have also shown that when compared with women with a normal prepregnancy body mass index (BMI), women with BMI over 25 kg/m^2 have significantly higher BPs in the first trimester, which remain elevated throughout pregnancy and postpartum.[36,37]

Hormones also play an important role in modulation of BP during normal pregnancy. It is well established that estrogen affects the RAAS and modulates angiotensin II sensitivity. Indeed, estrogen decreases renin, angiotensin-converting enzyme (ACE), *angiotensin* II type 1 (*AT1*) *receptor* density, and the NADPH oxidase subunits Nox1 and Nox2, whereas it increases angiotensinogen, ACE2, AT2 receptor density, and endothelial NO synthase.[38–40] Altogether, these alterations favor the vasodilatory branch of the RAAS, leading to lower BP levels.

Arterial stiffness

Pulse wave velocity (PWV), a measure of pulse wave speed through the vascular system, is measured as the ratio of the total distance traveled to the transit time of the pulse waveform. As discussed in detail in Chapters 1, 3, and 7, PWV depends on the functional and structural features of arteries, which are related to their intrinsic elastic properties. Stiffer arteries propagate pulse waves faster. In pregnancy, alterations in arterial stiffness occur due to changes in vascular structure, NO bioavailability and responsiveness, and/or sympathetic vasoconstriction.[33,41] Carotid-femoral PWV (cfPWV) reflects the elasticity of the central, elastic arteries and is considered the gold standard measure of large artery stiffness from a clinical and epidemiological standpoint. While normal and reference values for cfPWV have been proposed for nonpregnant individuals,[42] cross-sectional comparisons of pregnant and nonpregnant women suggest that these reference values may not apply to pregnant women.[17,30,43,44]

Few studies[16,17,30,43–51] have assessed arterial stiffness parameters longitudinally across gestation (Table 42.1). Of those, only seven studies[16,17,30,43,44,46,50] followed the same group of women for repeated measurements, while the rest recruited women with normal pregnancies at varied gestational ages. Consistent with decreased peripheral vascular resistance, most available studies have demonstrated a U-shaped relationship between cfPWV and gestational age, with a nadir in midpregnancy[30,43] or in the third trimester.[50] It is estimated that the decrease is approximately 6%–13% when compared with nonpregnant counterparts.[33] Osman et al. reported a cubic relationship of cfPWV with gestational age ($P = .002$), with cfPWV reaching a nadir around 17–20 weeks gestation (7.27 m/s from 7.50 m/s at 13 weeks), increasing to a peak at 35 weeks gestation (8.33 m/s), and subsequently declining again toward term (8.02 m/s).[17] Franz et al. reported a similar cubic relationship, with the lowest cfPWV values noted at 20 weeks' gestation and the peak values at 35 weeks ($P = .015$). However, other authors have noted that the decrease in cfPWV was nonsignificant in the first[45] or second trimesters.[16,47,48] The postpartum cfPWV value was evaluated in six studies with conflicting results; when compared with the end of pregnancy measurement, three studies reported the cfPWV to be slightly elevated at 7 weeks,[43] 12 weeks postpartum (5.4 m/s vs. 6.7 m/s),[50] and 9 months postpartum.[30] Conversely, a nonsignificant decrease in cfPWV has also been reported at 3–6 months postpartum when compared with end of pregnancy measurements.[44] Furthermore, others have demonstrated that postpartum cfPWV values remained at a similar level to the second or third trimester when measured at 7 weeks[47] or at 14–17 weeks postpartum.[16] Thus, based on current limited evidence, there is no consensus as to the direction of cfPWV changes postpartum, and whether the values are similar or greater to those of nonpregnant women.

Similar mixed findings have been reported for carotid-radial PWV (crPWV), a measure of muscular (medium-sized) artery stiffness. It was reported to decrease in the second trimester by 6%–11%,[33] while it was shown to increase by the end of pregnancy, either to above nonpregnant levels[30] or similar to first trimester values.[47] Still others report no difference in crPWV with gestation and no significant difference between pregnant and nonpregnant women.[48]

TABLE 42.1 Longitudinal studies assessing arterial stiffness and hemodynamic parameters throughout healthy pregnancy and postpartum.

First author, year	Population	Design	Method	Metrics	Gestational timepoints	Results
Osman, 2017	Low-risk, healthy pregnant women with singleton pregnancy, n = 30	Longitudinal (same women followed prospectively)	Oscillometric (Arteriograph®); NICOM device	cfPWV, brAIx, aoAIx, MAP, CO	11−13, 20−22, 26−28, 32−34, and 37−40 weeks	cfPWV reached lowest value at 17 weeks, then increased to a peak at 35 weeks ($P = .002$); brAIx and aoAIx reduced during early pregnancy, reaching a nadir at 28 weeks and increasing toward 40 weeks ($P = .001$, .002, respectively); MAP increased from T_2 to term ($P = .023$); CO rose to a peak at 28 weeks before declining to term ($P < .001$)
Iacobaeus, 2017	Healthy nulliparous women with singleton pregnancy, n = 52	Longitudinal (same women followed prospectively)	Oscillometric (Omron 705IT); applanation tonometry; flow-mediated dilatation (FMD)	cfPWV, crPWV, AIx75, MAP, CBP, FMD	11−14, 22−24, 32−34, and 9 months postpartum	MAP and CBP decreased in T_1 and T_2 followed by an increase in T_3 ($P < .001$); adjusted cfPWV decreased during pregnancy and rose at term ($P < .001$); crPWV followed a similar pattern but rose above nonpregnant levels in T_3 ($P < .01$); AIx75 significantly reduced during pregnancy and rose at term ($P < .001$); FMD significantly increased during pregnancy ($P < .05$)
Pandey, 2014	Women with, normotensive, healthy, singleton pregnancies, n = 137; age-matched nonpregnant controls, n = 35	Longitudinal (different women at different gestational ages)	Oscillometric (PeriScope)	cfPWV, baPWV, CBP, AIx	12−14, 20−24, and 32−36 weeks	Central SBP, AP, and CPP greater in T_1 than in nonpregnant controls ($P < .05$), yet decreased to comparable levels in T_2 and increased again in T_3; baPWV lower in T_1 than in controls ($P = .0001$) then increased in T_2 and T_3 to level similar to controls; no significant change in cfPWV; AIx was higher in T_1 than in controls, decreased to a nadir in T_2, then rose again to a peak in T_3 ($P < .0001$)
Khalil, 2009	Healthy women with singleton pregnancy, n = 541	Longitudinal (different women at different gestational ages; 45 followed across all trimesters)	Applanation tonometry	AIx75, CBP, MAP	8−13, 14−26^{+0}, 26^{+1}−39 weeks (cross-sectional); 12, 23 and 32 weeks (longitudinal)	No significant differences in AP or AIx75 across pregnancy (cross-sectional); AP and AIx75 decreased significantly from T_1 to T_2, then rose again in T_3 ($P < .001$) (longitudinal); MAP rose significantly in T_3 ($P = .015$)
Smith, 2004	Normotensive pregnant women, n = 53; nonpregnant women, n = 10	Longitudinal (same women followed prospectively)	Applanation tonometry	AIx, CBP	17−20, 25−28, and 33−36 weeks	AIx and CBP were lower in pregnant compared to nonpregnant women ($P < .05$); AIx decreased from T_2 to T_3 ($P < .01$)

Franz, 2013	Healthy pregnant women, n = 53	Longitudinal (same women followed prospectively)	Oscillometric (TensioClinic TL1 Arteriograph)	cfPWV, AIx	11–13, 14–16, 19–21, 24–26, 29–30, 33–35, 37–38, and 3–6 months postpartum	Significant AIx decrease from T_1 to end of T_2 and increase from T_3 to postpartum ($P = .041$ and $P < .001$, respectively); cfPWV values lowest at 20 weeks gestation and peaked at 35 weeks ($P = .015$)
Gomez, 2016	Women with low-risk, singleton uncomplicated pregnancy, n = 63	Longitudinal (different women at different gestational ages; 11 followed across all trimesters)	Applanation tonometry	cfPWV, crPWV, AIx, CBP, MAP, SEVR, PPA	7–13, 14–17, 18–21, 22–25, 26–29, 30–33, 34–40, and 6.5 weeks postpartum	MAP ($P = .04$) and CPP ($P = .03$) decreased during pregnancy; PPA and crPWV decreased in T_2, then increased steadily until delivery ($P = .01$ and $.04$, respectively); PPA sharply decreased postpartum ($P = .01$); AIx and SEVR significantly increased postpartum ($P = .03$ and $.02$, respectively); no differences in cfPWV, AIx, SEVR, or CBP across pregnancy
Macedo, 2008	Women with normal singleton pregnancies, n = 193; nonpregnant controls, n = 23	Cross-sectional	Applanation tonometry	cfPWV, crPWV, AIx, CBP, MAP	11–41 weeks (all 3 trimesters)	Pregnant women had lower MAP ($P = .01$), CPP ($P = .03$), central SBP ($P = .001$), central DBP ($P = .008$), and AIx ($P < .001$); metrics changed significantly with gestation, reaching nadir at midpregnancy ($P = .001$ to 0.02); cfPWV and crPWV not significantly different across pregnancy or compared with controls
Robb, 2009	Healthy primigravida women with uncomplicated singleton pregnancy, n = 22	Longitudinal (same women followed prospectively)	Applanation tonometry	cfPWV, crPWV, AIx75, CBP, MAP	16, 24, 32, 37, and 7 weeks postpartum	AIx75 rose from 16 weeks to term ($P < .01$) and remained elevated postpartum ($P = .0002$); cfPWV rose from 24 to 7 weeks postpartum ($P = .0008$); crPWV rose from 24 weeks to term ($P < .05$) and remained similar postpartum ($P = .07$); MAP and CBP increased from 24 weeks to term ($P < .0001$)
Mahendru, 2014	Normal pregnant women with previous healthy pregnancies, n = 54	Longitudinal (same women followed prospectively)	Applanation tonometry; Innocor® inert gas rebreathing technique	cfPWV, AIx, CBP, MAP, CO	Preconception; 6–7, 23–24, 32–34, and 14–17 weeks postpartum	Adjusted change in cfPWV not significant; AIx, MAP, and central SBP reached nadir in T_2 and increased in T_3 and postpartum ($P < .001$); AIx significantly higher postpartum than preconception ($P = .01$); postpartum central SBP remained significantly lower than at preconception ($P < .001$); CO peaked in T_2 ($P = .001$), returned to baseline postpartum

TABLE 42.1 Longitudinal studies assessing arterial stiffness and hemodynamic parameters throughout healthy pregnancy and postpartum.—cont'd

First author, year	Population	Design	Method	Metrics	Gestational timepoints	Results
Mersich, 2005	Normotensive pregnant women, n = 12	Longitudinal (same women followed prospectively)	Echo—wall tracking; applanation tonometry	cfPWV, AIx, β stiffness index, carotid CC, carotid DC, MAP	12, 20, 33, and 13 weeks postpartum	Carotid DC and CC decreased and β stiffness increased during pregnancy and reversed after delivery ($P < .05$); cfPWV and AIx decreased from T_1 to T_3, then increased in postpartum period ($P < .05$); no significant changes in MAP
Fujime, 2012	Healthy women with normal singleton pregnancies, n = 830	Longitudinal (different women at different gestational ages; 69 followed across all trimesters)	Applanation tonometry	AIx75, central SBP	12−14, 17−20, 23−27, and 34−36 weeks (cross-sectional); 12−14, 23−27, 34−36 weeks, within a few days of delivery and 4 weeks postpartum (longitudinal)	AIx75 and central SBP decreased to a nadir around midpregnancy ($P < .05$), then increased to T_1 levels toward term and continued rising after delivery ($P < .05$)

AIx75, augmentation index corrected for a heart rate of 75 beats per minute; *aoAIx*, aortic augmentation index; *AP*, augmentation pressure; *baPWV*, brachial-ankle PWV; *BrAIx*, brachial augmentation index; *CBP*, central blood pressure; *CC*, compliance coefficient; *cfPWV*, carotid-femoral PWV; *CO*, cardiac output; *CPP*, central pulse pressure; *crPWV*, carotid-radial PWV; *DBP*, diastolic blood pressure; *DC*, distensibility coefficient; *MAP*, mean arterial pressure; *PPA*, pulse pressure amplification; *SBP*, systolic blood pressure; *SEVR*, subendocardial viability ratio; T_1, first trimester; T_2, second trimester; T_3, third trimester.

As discussed in detail in Chapters 3, 8, and 11, the propagative and reflective properties of the arterial tree can be assessed with pulse wave analysis. Specifically, augmentation index (AIx) is a measure of pulse wave reflection, and as such depends on the diameter and elasticity of the small muscular arteries/arterioles at the major sites of pulse wave reflection. AIx is estimated to decrease by 3%–15% in pregnancy,[33] and to be negatively associated with birth weight.[31] The majority of studies have shown a nadir in AIx midpregnancy[16,30,43,45,46,48,49,51] or at the end of the second trimester,[17,44] while one study showed that the lowest AIx was noted in the third trimester.[50] Of note, a study by Khalil et al. in 541 women recruited at different gestational ages noted no significant difference in AIx standardized to a HR of 75 bpm (AIx75) or augmentation pressure (AP) across the three trimesters; however, when 45 of those pregnant women were assessed prospectively once per trimester, a significant decrease in AIx75 was noted in the second trimester (23–24 weeks).[46] That same study also demonstrated that there was no difference in AIx75 or AP in any trimester throughout pregnancy between Caucasian and Afro-Caribbean ethnic groups. Furthermore, in a cross-sectional study of 830 pregnant women who were recruited at different trimesters, a similar nadir was shown in AIx75 in midpregnancy; this association was confirmed in 69 of the women who were followed longitudinally.[51] Seven studies assessed AIx postpartum between 4 weeks and 9 months[16,30,43,44,47,50,51]; compared with third trimester AIx values, the postpartum AIx was significantly higher in five of these studies,[16,30,44,47,51] significantly lower in one study,[50] and no different in another one.[43] These postpartum AIx values were significantly higher than the first trimester value in four studies[30,44,47,51] and no different in two other studies.[16,50] In the only study that assessed AIx from preconception to postpartum prospectively in the same group of women, the AIx adjusted for HR reduced to a nadir in the second trimester and rose above preconception values postpartum.[16] Some debate also exists as to whether AIx is increased or decreased during early pregnancy with respect to nonpregnant controls,[45,48,49] as normative values of AIx across gestation are not available. Of note, there is no evidence of significant diurnal variability for the majority of arterial stiffness parameters, including cfPWV and pulse wave analysis, suggesting that their measurements do not need be performed at a specific time of day.[52]

Other important hemodynamic indices have also been assessed during pregnancy. Pulse pressure amplification, a measure of the progressive increase in pulse pressure from central to peripheral arteries, was found to decrease early in the second trimester (14–17 weeks) followed by a steady increase until delivery ($P = .01$), and finally a sharp decrease at 7 weeks postpartum ($P = .01$).[47] The subendocardial viability ratio was not found to change during pregnancy but significantly increased at 7 weeks postpartum.[47]

Several mechanisms have been proposed to explain the decrease in arterial stiffness in early and midpregnancy. As previously discussed, there is a gradual reduction in total peripheral resistance despite a gradual increase in CO. This occurs in response to vasodilation of the peripheral vasculature and structural remodeling to accommodate the volume expansion of pregnancy.[33] These changes could be due to the alterations of vasoactive substances, such as NO, prostacyclin, endothelium-derived hyperpolarizing factor, estrogen, progesterone, and relaxin.[24,29] This state of high flow-low resistance circulation is accompanied by increased aortic compliance and distensibility, providing optimal coupling between the heart and the vasculature. In late pregnancy, the increased arterial stiffness from midpregnancy to term could be due to the inhibition of NO, increased CO, and increased circulatory volume.[17]

Importantly, vascular compliance and distensibility may vary depending on the vascular bed. For example, aortic compliance and distensibility increases gradually from the first to the third trimester, along with an increase in its diameter, by about 12%; the aortic compliance and distensibility decrease postpartum compared to late gestation.[50] On the other hand, in order to protect the cerebral circulation from excessive blood flow/volume during pregnancy, carotid compliance and distensibility have been shown to decrease from the first to third trimester of pregnancy, coupled with reduced arterial baroreceptor reflex sensitivity.[53] The arterial smooth muscle cells express both estrogen receptors (causing vasodilation and decreased production of collagen) and angiotensin II receptors (causing vasoconstriction). Given that the relative density of these receptors on the vascular smooth muscle varies in different segments of the arterial tree, it can produce contraction in the carotid artery and relaxation in other arteries, such as the aorta, which has been shown to have higher density of estrogen receptors. Therefore, although the carotid artery increases in diameter during pregnancy, it may gradually become up to 30% stiffer compared to the aorta. Indeed, it has previously been shown that the carotid end-diastolic diameter is increased by 8% across pregnancy, while the pulsatile distension is decreased by 23%; consequently, strain is decreased by 28%.[50] Therefore, compliance and distensibility change approximately in parallel. These alterations were found to reverse in the postpartum period; however, it may take over 6 months for the aortic diameter and 3 months for the carotid artery diameter to return to prepregnancy levels.

Pregnancy complications

Pregnancy acts as a natural cardiometabolic "stress test" that can reveal underlying predispositions to vascular dysfunction.[54] Pregnancy complications are most likely to manifest in the late stages of pregnancy, with the demands

of the growing fetus steadily increasing throughout gestation. In this context, PrE, a common hypertensive disorder of pregnancy (HDP), is a progressive multisystem syndrome characterized by systemic endothelial dysfunction. Other HDPs include gestational hypertension, chronic hypertension, and PrE superimposed chronic hypertension. HDPs remain leading causes of maternal and neonatal morbidity and mortality worldwide,[55] affecting as many as 10% of pregnancies and contributing to 343,000 maternal and around 1.5 million fetal and neonatal deaths annually.[56–58] The health burden imposed by HDPs extends beyond pregnancy, as afflicted women are at significantly increased cardiovascular risk in the postpartum period and later in life.[59,60] Importantly, HDP incidence is on the rise, given the obesity and diabetes epidemic, as well as more advanced maternal age in recent years to accommodate career and life choices.

PrE is the most severe form of HDP, occurring in 5%–8% of pregnancies annually worldwide. It typically manifests as new onset or worsening of hypertension, new-onset proteinuria, and/or signs and symptoms of end-organ dysfunction after the 20th week of gestation.[61] While the majority of PrE cases occur in late gestation (late-onset PrE), approximately 10% occur before 34 weeks, termed early-onset PrE. The latter typically represents a more severe form of PrE, with greater placental dysfunction and a higher risk for maternal and fetal complications.[62] PrE occurring after the 37th week is called term PrE, while before the 37th week preterm PrE. In 5% of cases, PrE is diagnosed postpartum.[63] Diagnosis of PrE is also associated with an increased risk of premature cardiovascular disease, at a relative risk of 2.0 for mild PrE (95% CI 1.8–2.2) and up to 9.5 for severe PrE (4.5–20.3). Women with a history of PrE have a 3.7-fold increased risk (2.7–5.1) of chronic hypertension and a 1.8-fold increased risk of developing type 2 diabetes (1.3–2.6) within 10 years postpartum. The risk for developing hypertension is increased >3.5-fold after mild PrE and >6-fold after severe PrE.[64–68]

Given that PrE is a heterogeneous syndrome, multiple pathways have been proposed for both the causal and exacerbating factors leading to maternal vascular dysfunction. Below, we present changes occurring during pregnancy complicated with HDPs, with a particular focus on PrE.

Blood volume

Plasma volume expansion occurs gradually across gestation but is lower in pregnancies complicated by pregnancy-induced hypertension, PrE, or fetal growth restriction than in healthy pregnancy, and hemoconcentration is often present. According to a metaanalysis, plasma volume is significantly lower by 13% than in healthy pregnancies in the third trimester. Specifically, a 0.8 L volume expansion is noted in PrE (total increase of 32% in the third trimester) as opposed to the >1 L volume expansion seen in healthy pregnancies (a 45% increase in the third trimester).[2] It appears that the decrement in volume precedes the onset of hypertension.

The role of the RAAS and intrarenal renin–angiotensin system (iRAS) is complex in PrE, with several different theories proposed. It has been suggested that abnormal placental development causes dysregulated expression of the placental RAS through oversecretion of renin and other proteins/angiotensin peptides by the placenta released into the maternal circulation.[5] Shallow placentation and alterations in uteroplacental perfusion in PrE are also accompanied by increased levels of AT1 receptor autoantibodies, which act as agonists on the AT1 receptor. These molecules, or their combination, may cause activation of maternal iRAS and failure of the circulating RAAS to be activated and respond to the homeostatic demands.[5] As such, plasma concentrations of angiotensin II are reduced in PrE, largely due to reduced active octapeptide angiotensin. There is correspondingly enhanced pressor sensitivity to angiotensin II in PrE. Plasma aldosterone concentrations (PACs) are also reduced in PrE compared with normal pregnancy. The reduction is proportionally less than that of plasma renin activity and plasma renin concentration (PRC), and thus the PAC:PRC ratio rises.[69] Overall, compared with the increase in RAAS components in normotensive pregnancy, the circulating levels of renin, Angiotensin I, Angiotensin II, Angiotensin (1–7), and aldosterone are much lower, with little fluctuation in ACE levels.[70] In sum, most components of the circulating RAAS are downregulated in PrE and the condition associates with a relatively low degree of RAAS activity compared to normal pregnancy.[71]

Cardiac output

CO has divergently been described as decreased, unchanged, and increased in this disease. It has been suggested that PrE is characterized by variations in hemodynamic status, ranging from a hyperdynamic high-CO–low-resistance state with increased left ventricular function in the preclinical phase of PrE to a low-CO–high-resistance vasoconstrictive state with decreased left ventricular function during PrE.[72] However, conflicting results have been reported. Specifically, it was shown that those who subsequently developed PrE without small for gestational age infants had increased CO and MAP at 11–14 gestational weeks compared to a control group.[73] Increased CO was also shown by others when measured at 24–40 weeks in cases of PrE but without fetal growth restriction.[74] Conversely, others have observed that women who subsequently developed PrE have decreased CO and

increased total peripheral resistance, even before conception, when compared with healthy pregnancies.[75]

Most studies report that cardiovascular adaptations are compromised in PrE, including a 13% reduction in plasma volume expansion and decreased CO (5.5 ± 1.5 vs. 6.2 ± 1.9 L/min)[2,76]; central venous and pulmonary wedge pressures are also reduced and may vary inversely with the severity of the disease.[77] Moreover, higher impedance to flow in the uterine arteries is inversely related to gestational age at delivery.[72] Furthermore, it has been demonstrated that CO in PrE is significantly lower in the early-onset PrE (<34 weeks) compared with late-onset PrE ($\geq$34 weeks)[78] and is positively associated with birth weight.[74]

The evidence on HR is equally mixed. Lower HR in the third trimester with a lower SV have been reported in PrE and gestational hypertension.[79] The SV index has also been shown to be reduced by a mean of 9.7% between early- and late-onset PrE.[80] Conversely, others have observed no significant differences in HR between women with PrE and gestational age-matched healthy controls as well as between early- and late-onset PrE groups.[81] HR variability has been shown to be higher in PrE groups compared to healthy pregnant controls, although not consistently in the literature; HR variability and baroreceptor reflex sensitivity were found to be significantly higher in late-onset PrE compared to gestational age-matched controls, but not between early-onset PrE and controls.[81] A study performing 24-h ambulatory BP monitoring suggested that the odds of developing an HDP increased by 1.5 times for every 1 bpm increase in the 24-h ambulatory BP monitor HR, when measured at 14−24 weeks' gestation. This became nonsignificant at 24−32 weeks and was reversed by 33 weeks to delivery.[82]

In general, it is thought that sympathetic activity is greater in PrE and gestational hypertension than in healthy pregnancy and in nonpregnant women with hypertension.[83] Although a decrease in baroreceptor reflex sensitivity is also seen in healthy pregnancy, this is further impaired in PrE.[81,83] Interestingly, PrE appears to be associated with decreased vagal control of the heart.[81−83] More broadly, sympathetic overdrive and adrenergic receptor−induced vasoconstriction are elevated in PrE.
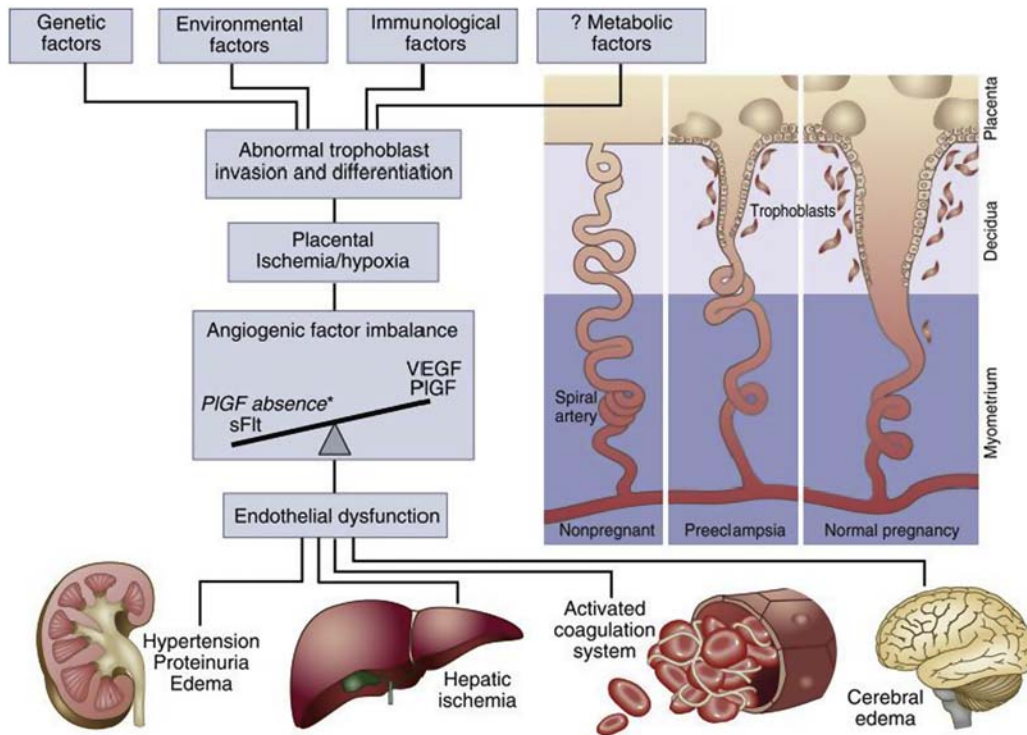
Finally, evidence suggests that PrE is associated with abnormal cardiac geometry.[84,85] Women who subsequently develop PrE show evidence of left ventricular concentric remodeling at midgestation. Importantly, reduced SV, diastolic dysfunction, and left ventricular remodeling can occur before clinical manifestations of PrE and are most affected in severe and early-onset PrE.[1,84] Indeed, women who develop preterm PrE exhibit a high resistance−low volume hemodynamic state and demonstrate asymptomatic left ventricular diastolic or systolic dysfunction as well as segmental impaired myocardial relaxation at midgestation.[85] Both early and late PrE are characterized by increased left ventricular

mass and relative wall thickness. However, concentric hypertrophy and diastolic dysfunction are significantly more prevalent in early- rather than late-onset PrE.[86] Furthermore, longitudinal, radial, and circumferential strain are significantly worsened in women with PrE compared to those with gestational hypertension or without HDP; however, their ejection fraction is not significantly different, unless there is decompensation.[80,87,88] Autopsy data have shown that, compared with deaths in pregnancy from other causes, there is a 10-fold prevalence of myocardial contraction band necrosis in PrE cases.[80]

Vascular remodeling and vascular resistance

Although PrE symptoms typically appear in the second-half of pregnancy, disease processes can be detected in the first trimester. PrE has been associated with the failure of the maternal cardiovascular system to undergo normal adaptations (Figs. 42.2 and 42.4).[23,89] As such, insufficient remodeling of the uteroplacental arteries results in a 21%−42% increase in uterine artery resistance in women who develop PrE, leading to a reduction in uterine blood flow, which can be observed as early as 16 weeks' gestation.[33] To this end, an increased uterine artery pulsatility index in the second trimester is correlated with an increased risk of PrE. Together, these changes lead to abnormal placentation, angiogenic imbalance, and maternal vascular dysfunction, which are implicated in the development of PrE and alter the delivery of blood, oxygen, and nutrients to the fetus, which can impair fetal growth and development.[33]

Due to inadequate remodeling of the spiral arteries, the myometrial segments retain vasoreactivity, leading to intermittent placental perfusion and a cascade of events that result in PrE.[90,91] Postulated mechanisms include imbalance in the bioavailability and activity of endothelium-derived contracting and relaxing factors and oxidative stress.[92] Consistent with ischemia-reperfusion injury, fluctuating oxygen supplies result in oxidative stress−induced endothelial dysfunction.[93] Although reactive oxygen species are required and upregulated for normal physiology during gestation, an imbalance of oxidative species and antioxidative defense mechanisms are implicated in PrE.[94] As a result, a decrease in NO bioavailability and the associated endothelial dysfunction occur such that endothelial-dependent vasodilation is reduced without concurrent changes to endothelial-independent vasodilation. Furthermore, hormonal alterations and exaggerated immune and systemic inflammatory responses occur with production of proinflammatory cytokines (tumor necrosis factor-α, interleukin [IL]-6, and IL-17) and a decrease in antiinflammatory cytokine (IL-10, IL-4) levels.[95] Moreover, it appears that, unlike in healthy pregnancies, increased sensitivity to angiotensin II and vasoconstrictor

FIGURE 42.4 The current understanding of the pathogenesis of preeclampsia. *PlGF*, placental growth factor; *sFlt*, soluble fms-like tyrosine kinase; *VEGF*, vascular endothelium growth factor. *Reproduced from Almaani SJ. Placental growth factor in pre-eclampsia: friend or foe?* Kidney Int. 2019;95:730—732.

responses are enhanced in PrE.[91] To this end, placenta-derived factors, including antiangiogenic factors, microparticles, and cell-free nucleic acids, are released into the maternal circulation and act on the vascular wall to modify the secretory capacity of endothelial cells that alter the responsiveness of vascular smooth muscle cells to constricting and relaxing stimuli.[92] Indeed, the trophoblastic stress caused by placental hypoperfusion and hypoxia triggers excess release of sFlt-1 at the placental surface into the circulation (Fig. 42.3).[23,91] Up to a threefold increase in sFlt-1 has been noted in PrE, resulting in up to a 90% decrease in VEGF and PlGF.[33] Together, this imbalance of angiogenic/antiangiogenic factors negatively affects angiogenesis and placentation in PrE.[96] It is noteworthy that the sFlt-1/PlGF ratio correlates with severity of PrE, while a greater reduction in PlGF is associated with early-onset PrE.[97,98] A sFlt-1:PlGF ratio of 38 or lower has been shown to have a negative predictive value (no occurrence of PrE) of 99.3% in the subsequent week, and thus can be used as a cutoff value to predict the short-term absence of PrE.[99]

Hormonal alterations associated with PrE also play an important role in vascular remodeling. Estrogen levels have been shown to be decreased by 30%—40% in PrE, contributing to the observed endothelial dysfunction.[33,100] Low estradiol (E2) levels reduce angiogenesis and vasculogenesis, leading to insufficient placental development and maternofetal exchange,[100] in turn, leading to lower E2 levels and triggering a vicious circle between hormonal imbalance and disrupted implantation. Both severe and mild PrE have been associated with low E2 concentrations. In pregnancy complicated by PrE and/or fetal growth restriction, lower placental aromatization and E2 levels and higher progesterone inactivation have been noted.[101] Indeed, E2 and progesterone levels have been shown to be significantly reduced in PrE at the time of diagnosis compared to gestation-matched normotensive pregnant women.[102] However, relaxin levels in women with PrE do not seem to be significantly different from that of healthy pregnancies during the third trimester, at delivery, and up to 2 weeks postpartum.[103,104]

It is generally believed that PrE is associated with increased total peripheral resistance, while aortic diameter is inversely proportional to total peripheral resistance.[33,92] As such, the aortic diameter in pregnancies complicated with hypertension is lower compared to healthy pregnancies; however, this is not consistent in the literature. Contrary to this principle, the carotid artery's diameter is up to 20% larger in women with PrE in the third trimester; this increase is related to the severity of PrE and is greater in early- versus late-onset PrE.[105] The increased diameter of the carotid artery is accompanied by a decrease in its

compliance. Furthermore, carotid intima—media thickness has been shown to be increased by up to 10% in women with PrE, a finding that endures postpartum. These alterations in the carotid artery seem to be proportional to BP.[33] In contrast, the resting diameter of the brachial artery has been found to decrease or remain unchanged in PrE.[33] At the microcirculatory level, a decrease in the density of skin capillaries of up to 17% has been noted in women who develop PrE.[106,107] This decrease may precede the development of PrE and may persist up to 15 weeks postpartum. These microcirculatory alterations further contribute to the increased vascular resistance and decreased peripheral blood flow observed in PrE.[106,107]

PrE is a very complex disorder and manifests with different patterns. For example, PrE that occurs earlier in gestation and is associated with fetal growth restriction is likely related to low CO, low inotropy, and high peripheral vascular resistance,[108] while cases of later and term gestation PrE involve babies who tend to be larger, and there is a predominantly high CO, low peripheral vascular resistance, and increased intravascular volume in midgestation.[109] Moreover, early- and late-onset PrE are both characterized by increased total vascular resistance at term.[110]

Blood pressure

Altered BP trajectories in gestation have been reported in women who develop HDP (gestational hypertension and PrE), whereby SBP and DBP are higher throughout pregnancy compared to normotensive women. Specifically, unlike women with healthy pregnancies, women with HDP have generally stable BPs during the first-half of pregnancy, which then increase until delivery.[111] Indeed, in 13,016 women from the Avon Longitudinal Study of Parents and Children, the rate of change in SBP and DBP from 18 weeks' gestation onward was higher in women with PrE compared to women with healthy pregnancies.[112] While DBP increases by about 7% between midgestation and delivery in women with healthy pregnancies, this increment is around 12%—15% in those with HDPs.[111] Additionally, greater BP variability, especially systolic coefficient of variation, in the second to third trimester is independently associated with higher odds of severe hypertension and PrE.[113]

Similarly, MAP has demonstrated an increasing trend from the second trimester onwards in both early- and late-onset types of PrE; in early-onset PrE, its highest value was observed at 20 weeks of gestation compared to a control group. Whereas in late-onset PrE, absolute MAP and increases in MAP were higher from 20 to 27 weeks and 28—37 weeks into gestation compared to controls. Further, while an increment of 5% in MAP was noted in women with healthy pregnancies, this was observed to be increased by 13% in those with late-onset PrE.[111]

Nonsevere hypertension in pregnancy is defined as an SBP of 140—159 mmHg and/or DBP 80—109 mmHg, while severe is characterized as SBP $\geq$160 mmHg and/or DBP$\geq$ 110 mmHg.[114] Notably, when measured in the first trimester (8—11 weeks), the incidence of PrE was found to be significantly higher, in a graded manner, in women with high-normal BP (clinic SBP: 120—129 mmHg and DBP <80 mmHg), temporary hypertension (clinic BP $\geq$140/90 mmHg, with clinic BP <140/90 mmHg in midgestation), white coat hypertension, high BP (clinic SBP: 130—139 mmHg and/or DBP: 80—89 mmHg), and chronic hypertension than in normotensive women.[115] In a recent cohort study analyzing data of 137, 389 pregnancies, it was found that using the lower diagnostic threshold for hypertension recommended in the 2017 ACC/AHA guideline (130/80 mmHg) increased the prevalence of chronic and gestational hypertension, markedly improved the appropriate identification of women who would go on to develop PrE, and was associated with improved identification of adverse fetal/neonatal risk.[114]

As previously stated, PrE significantly increases the risk of chronic hypertension later in life, which increases with increasing severity of PrE.[64–68] Interestingly, longitudinal assessment of PrE revealed that $\approx$50% of women have persistent hypertension and increased rates of nocturnal, ambulatory, and masked hypertension at 12 weeks postpartum.[1]

Arterial stiffness

Increased systemic arterial stiffness and wave reflection have been reported among women with HDP.[116–118] In a systematic review, our group has demonstrated that PrE is associated with increased arterial stiffness during and after pregnancy, more so than gestational hypertension.[116] Our metaanalyses showed that a significant weighted mean increase of 1.04 m/s in cfPWV was noted at the time of PrE diagnosis, as well as a sizable 15% increase in AIx.[116] The magnitude of the increase in arterial stiffness appears to be greater in early-onset PrE and is proportional to the severity of PrE.[116,119,120]

The limited number of longitudinal studies with data preceding PrE onset generally showed that arterial stiffness and wave reflection parameters were increased as early as 11 weeks among pregnant women who subsequently developed PrE and remained elevated throughout pregnancy compared to healthy pregnant women or women with gestational or chronic hypertension (Table 42.2).[118,121] More severe PrE was associated with a greater increase in arterial stiffness. Furthermore, women who developed gestational diabetes mellitus were also shown to have increased arterial stiffness starting in the first trimester compared to healthy controls.[122] Specifically, cfPWV has been shown to be increased in PrE pregnancies

TABLE 42.2 Longitudinal studies assessing arterial stiffness and hemodynamic parameters throughout pregnancy subsequently complicated with preeclampsia and postpartum.

First author, year	Population	Design	Method	Metric	Gestational timepoints	Results
Franz, 2013	Healthy pregnant women, n = 19; women presenting with PrE, n = 21	Longitudinal cohort trial	Oscillometric (TensioClinic TL1 Arteriograph)	cfPWV, AIx	Onset of disease (mean 28 (early-onset) and 36 (late-onset) weeks) and 3—6 months postpartum	No differences in cfPWV during pregnancy; AIx significantly greater in early- and late-onset PrE during pregnancy ($P < .001$); cfPWV ($P = .006$) and AIx ($P = .001$) elevated in early-onset PrE postpartum; no differences between late-onset PrE and controls postpartum
Robb, 2009	Healthy primigravida women with uncomplicated singleton pregnancy, n = 22; singleton primigravida women with PrE, n = 15	Longitudinal	Applanation tonometry	cfPWV, crPWV, AIx75, CBP, MAP	At diagnosis (mean 30 (early-onset) and 38 (late-onset) weeks) and 7 weeks postpartum	All metrics greater in both PrE groups ($P \leq .01$); cfPWV, AIx75, CBP, and MAP remained elevated 7 weeks postpartum ($P \leq .02$)
Khalil, 2010	High-risk women with singleton pregnancy, n = 252 (42 PrE)	Nested case—control	Applanation tonometry	AIx75	11—13 weeks	AIx75 significantly higher in all PrE, early-onset PrE and PrE + SGA compared to controls ($P \leq .002$)
Khalil, 2014	High-risk women with singleton pregnancy, n = 245 (44 PrE)	Prospective longitudinal	Oscillometric (Arteriograph, TensioMed Ltd.)	cfPWV, AIx, aortic SBP	11—13 weeks and every 4 weeks until delivery	cfPWV, AIx, and aortic SBP significantly higher in the preterm PrE group ($P \leq .033$), but not in the term PrE group
Savvidou, 2011	Healthy women with singleton pregnancy, n = 140 (29 PrE)	Prospective	Applanation tonometry	cfPWV, crPWV, AIx75, MAP, CBP, T1R	22—24 weeks	Adjusted cfPWV/crPWV, MAP, and CBP higher and T1R lower in PrE group ($P \leq .02$); adjusted AIx75 not significantly different between PrE and non-PrE groups; adjusted cfPWV not different between early- and late-onset PrE
Khalil, 2012	Women with singleton pregnancy, n = 6947 (181 PrE)	Longitudinal	Oscillometric (Arteriograph, TensioMed Ltd.)	cfPWV, AIx75, aortic SBP	11—13 weeks	Significantly greater cfPWV, AIx75, and aortic SBP in PrE ($P < .0001$)

Khalil, 2009	Low-risk women with singleton pregnancy, n = 210 (14 PrE)	Prospective longitudinal	Applanation tonometry	AIx75, MAP	11–13 weeks	AIx75 had a detection rate of 79% for all PrE and 88% for early-onset PrE, with an FPR of 11%; no differences in MAP
Carty, 2014	High-risk pregnant women, n = 140 (17 PrE)	Longitudinal	Applanation tonometry, peripheral arterial tonometry	AIx75, peripheral AIx, CBP	16 and 28 weeks; 6–9 months postpartum	Central DBP higher in PrE at week 16 ($P = .013$); no difference in other metrics
Katsipi, 2014	High-risk pregnant women, n = 118 (21 PrE)	Longitudinal	Doppler ultrasound	cfPWV, MAP	22–26 weeks	cfPWV showed a detection rate of all PrE of 81% and of early-onset PrE of 82% at a fixed 10% FPR; MAP elevated in PrE ($P < .01$)
Khalil, 2012	Women with singleton pregnancy, n = 6814 (337 PrE + SGA and 48 SGA)	Prospective longitudinal	Oscillometric (Arteriograph, TensioMed Ltd.)	cfPWV, AIx75, aortic SBP	11–13 weeks	In PrE + SGA, AIx75, and aortic SBP were increased ($P \leq .001$) but not cfPWV; no differences between SGA and controls

AIx75, augmentation index corrected for a heart rate of 75 beats per minute; *CBP*, central blood pressure; *cfPWV*, carotid-femoral pulse wave velocity; *DBP*, diastolic blood pressure; *FPR*, false-positive rate; *MAP*, mean arterial pressure; *PrE*, preeclampsia; *SBP*, systolic blood pressure; *SGA*, small for gestational age; *T1R*, timing of the reflected wave.

by approximately 20% (1 m/s) above normotensive pregnant values and remain elevated at 7 weeks postpartum; importantly, this increase was shown to be independent of BP values.[33,43,123–126] Only two studies measured cfPWV in the first trimester of pregnancy, one showed that cfPWV was significantly higher in those destined to develop PrE and the other noted a significant increase only in early-onset PrE.[126,127] Another small study (n = 20, three developed PrE) also found a significant increase in brachial PWV in the first trimester using ultrasound.[128]

When measured in the second trimester, cfPWV was found to be significantly increased by 17%[124] or 30% (10.2 ± 1.9 m/s vs. 7.2 ± 1.1 m/s)[125] in women who subsequently developed PrE compared with healthy pregnancies. It was also shown that for every 1 m/s increase in cfPWV, there was a 3.9-fold (95% CI 2.2–7.0) increased risk for PrE, which was even higher when an increase in sFlt-1 levels was also considered.[125]

Limited evidence suggests an increase in crPWV of around 10%–15% above healthy pregnancy values can be detected in the third trimester in women with PrE, with no difference postpartum.[33,43,123] The difference in central versus peripheral PWV could be due to the fact that the aorta undergoes more adverse adaptations in PrE, while the brachial artery structures remain generally unaltered.[33]

Measures of wave reflection have also shown unique changes in complicated pregnancy. AIx may be increased by up to 20% in PrE, although there is no universal agreement.[124,129] The four studies that measured AIx/AIx75 in the first trimester showed that these parameters were increased in women destined to develop PrE,[126,127,130,131] although one study found that this increase was significant only for preterm PrE.[126] However, studies that measured AIx later in pregnancy (in the second[124] or second and third[129] trimester) showed no significant difference between those who did and did not develop PrE, while some evidence suggests that AIx remains elevated up to 6 months postpartum.[43,44] These mixed results highlight the lack of systematic research in this area and the need for more comprehensive examinations of arterial stiffness and wave reflection parameters during and after pregnancy.

Overall, in a metaanalysis of a limited number of eligible studies that assessed arterial stiffness and wave reflection parameters, it was shown that, in the first trimester, mean AIx75 was significantly higher in the PrE group, with an estimated standardized mean difference (SMD) of 0.90 [95% CI 0.07–1.73; $P = .034$]. In the second trimester, the PrE group had significantly higher cfPWV with an estimated SMD of 1.26 m/s (95% CI 0.22–2.30; $P = .018$).[121]

Interestingly, one study that measured AIx, cfPWV, and central SBP throughout high-risk pregnancies found the arterial stiffness measures to be significantly higher only in the preterm PrE group from 16 weeks onwards, but not in the term PrE group, and the difference increased with gestational age.[126]

A study of high-risk pregnant women by our group demonstrated that arterial stiffness was significantly increased throughout pregnancy and that a first-trimester 1 m/s increase in cfPWV was associated with 64% increased odds of developing PrE ($P < .05$), while a 1 m/s increase in time to wave reflection (T_{1R}) was associated with 11% decreased odds for PrE ($P < .01$) (unpublished data). Furthermore, a changepoint in cfPWV and crPWV was detected at 14–17 weeks gestation, at which time cfPWV started increasing in women who developed PrE but decreasing in women who did not; at 22–25 weeks' gestation, a 1.2 m/s difference in cfPWV was observed. Furthermore, women who subsequently developed PrE showed an increase in AIx at 18–21 weeks that was not seen in women who did not develop PrE until 30–33 weeks.[132] This study further highlighted the importance of changes in arterial stiffness early in pregnancy.

Regarding early-onset versus late-onset PrE, all markers of arterial stiffness and hemodynamics have been shown to be elevated at the time of PrE diagnosis compared to healthy pregnancies,[116,117] with two studies showing no significant differences between the different types of PrE.[43,44] While there are limited studies examining postpartum measurements, one group showed that all measures except crPWV remained elevated 7 weeks postpartum in both types of PrE,[43] while others showed that cfPWV and AIx were elevated 3–6 months postpartum only in early-onset PrE,[44] or that PWA parameters were not significantly different 6–9 months postpartum from the values during pregnancy.[129] When cfPWV measurements were performed in the second trimester, prior to PrE onset, they were found to be either similar in early- and late-onset PrE[124] or significantly higher in early-onset PrE.[125] Overall, evidence suggests that the early-onset PrE shows more significant alterations in arterial stiffness, but more studies are needed to confirm the differences between the two types.

In terms of prediction of early- versus late-onset PrE, AIx75 had a prediction rate of 79% for all PrE cases and 88% for early-onset PrE in the first trimester, while MAP was not found to be predictive.[131] Measurement of PWV, among other markers in the second trimester, showed that cfPWV had the highest prediction rate, at 81% for all PrE cases and 82% for early-onset PE; when combined with sFlt-1 measurements, these rates increased to 90% and 92%, respectively.[125] To this end, a study of high-risk pregnant women by our group has demonstrated that a combination of arterial stiffness and wave reflection indices (cfPWV, AIx75, and T_{1R}) measured between 10 and 13 weeks' gestation predicted PrE earlier and with greater accuracy than BP, ultrasound indices, and/or angiogenic

biomarkers alone. The area under the curve of arterial stiffness, BP, ultrasound indices, and angiogenic biomarkers was 0.84, 0.68, 0.66, and 0.64, respectively (unpublished data). Importantly, we found that BP had a sensitivity of 14% for PrE prediction, whereas that of arterial stiffness was 36%, demonstrating the clinical value of these measurements.

Peripheral vascular stiffness and resistance in women with PrE has been associated with decreased resting blood flow,[133] decreased capillary density,[107] and impaired vascular compliance and endothelial function. A meta-analysis has demonstrated that women who develop PrE have reduced FMD not only at the time of diagnosis but also prior to diagnosis in the first or second trimester compared to controls.[134] Moreover, women who subsequently developed PrE had similar FMD values at 16–19 weeks compared to 24–28 weeks, indicating that, unlike in healthy pregnancy, PrE is linked to a failure of endothelial function to improve.[135] Furthermore, FMD values were shown to be up to 75% lower in women with PrE in the third trimester. Interestingly, the impaired FMD values remained up to 3 years postpartum, thus contributing to increased future cardiovascular risk.[33]

It is also clinically relevant that increased arterial wave reflections may affect fetal growth in pregnant women even in the absence of hypertension. Specifically, a significant inverse association between AIx and AIx75 and birth weight has been suggested.[136] Furthermore, an increase of 1 m/s in cfPWV was associated with a decrease in birth weight centiles by 17.6% and a catch-up growth after birth of 22.3% in weight centiles, independent of MAP; this association was even stronger for pulse pressure.[137] However, these associations are not universally noted; a large study measuring AIx and PWV in the first trimester observed no difference in these parameters in women who subsequently delivered small for gestational age infants versus unaffected controls, unless PrE was also present.[138]

Overall, in contrast to women with healthy pregnancies, women with PrE appear to have an impaired vascular response to hemodynamic changes that occur during pregnancy. As such, arterial stiffness and vascular resistance may be early indicators of PrE development.

Fetal growth restriction

Fetal growth restriction (previously termed intrauterine growth restriction) has also been independently associated with increased markers of arterial stiffness and impaired vessel hemodynamics. Pregnant women destined to develop fetal growth restriction exhibited decreased SV and CO, as well as increased peripheral vascular resistance compared to their healthy counterparts.[139] Furthermore, in women who went on to develop fetal growth restriction, but not superimposed PrE, AIx75 was significantly elevated.[140]

Moreover, aortic AIx75 was found to be the only significant independent determinant of birth weight in a cohort of pregnant women with chronic hypertension.[140]

Pregnancies complicated by fetal growth restriction had greater MAP and reactive hyperemia index, measured in the second or third trimester, than unaffected controls.[141] In high-risk pregnant women followed longitudinally from the first to third trimesters, unaffected pregnancy was associated with reduced vascular resistance and increased CO until midpregnancy, while pregnancies complicated by fetal growth restriction showed no change across gestation with lower CO and higher peripheral vascular resistance. Fetal growth restriction is thus linked to a persistent failure of maternal hemodynamic adaptation in pregnancy.[142]

It has been noted that screening and predictive tools for fetal growth restriction tend to underperform in high-risk groups compared with general pregnant populations.[143] Hemodynamic indices which have shown independent predictive potential for fetal growth restriction when measured in the first trimester in high-risk women include peripheral vascular resistance, and to a greater extent, CO.[143]

Exercise in pregnancy

Due to concerns and uncertainty around the safety of pharmacological regimens in pregnancy, there is currently a lack of specific treatments to prevent pregnancy complications. Thus, prevention of pregnancy complications through lifestyle modification is that much more essential to ensuring a healthy pregnancy. Physical exercise, in particular, appears to enhance the beneficial adaptations that occur in healthy pregnancy.

Overall, placental angiogenesis and endothelial function are enhanced in women who are active prior and during pregnancy compared to those who are not.[33] Indeed, regular aerobic training in the year before conception and/or during early pregnancy (up to 24 weeks of gestation) has been found to decrease the overall risk of developing HDPs by 30%; specifically, risk of gestational hypertension was reduced by 20%–40%, and PrE by 20%–60%.[33,144,145] Prepregnancy physical activity in general was associated with a 28% reduced risk of PrE for every 1 hour of physical activity per day, plateauing at 5–6 h per week, while leisure-time physical activity in early pregnancy decreased the risk of PrE by 17% for every hour per day with no plateau. Higher intensity activity and increased walking in early pregnancy were also beneficial and reduced PrE risk.[146] In patients with diagnosed PrE, supervised training was shown to lower BP and proteinuria over time.[145] The beneficial effects of exercise on PrE have been further examined in a transgenic mouse model, where exercise training both before and during gestation led to normalization of MAP, proteinuria, cardiac hypertrophy, vascular reactivity, and placental VEGF expression.[146]

Regular exercise also reduces the risk of gestational diabetes by 20%−40%; it has been shown to ameliorate glycemic control and reduce insulin resistance (improve skeletal muscle insulin sensitivity) and leptin levels in both normal weight and obese women.[144,146−148] Exercise and physical activity, in general, during pregnancy can prevent excessive gestational weight gain and have been shown to improve lipid profiles.[146,148] Additionally, regular exercise has been associated with reductions in preterm birth by 20%−50% and the risk of large-for-gestational-age infants, or macrosomia, by 30%−50%. The odds of having a small newborn were not found to be affected by exercise.[148,149]

Exercise in early pregnancy enhances placentation by enabling the invasion and proliferation of trophoblast cells, in part through changes in perfusion pressure and oxygen supply. Exercise may be beneficial to placental growth and vascular development as brief bouts of mild hypoxia and a reduction in placental perfusion may promote cell proliferation and angiogenesis.[33] The increase in shear stress produces a state of hyperemia, while an increase of blood flow during exercise results in improved endothelial function.[150] Indeed, repeated bouts of exercise effectively improve vascular function (a) directly by exerting shear forces on the vascular wall, which activates endothelial NO synthase (eNOS) and reduces NAD(P)H oxidase activity, decreasing reactive oxygen species and increasing NO bioavailability and (b) indirectly through the release of antiinflammatory and anabolic mediators in response to increased energy demands from muscles.[33,145,151,152] To this end, a significant increase in FMD during the third trimester of pregnancy has been observed in pregnant women who participated in controlled exercise programs.[153]

Exercise may also lead to improved antiangiogenic/angiogenic balance, with an approximately 40% decrease in sFlt-1 and approximately 50% increase in PlGF and VEGF in active versus inactive pregnant women. Exercise was also found to improve placental vessel formation and density without affecting placental size.[33] Regular weight-bearing exercise in pregnancy lowers the level of plasma proinflammatory cytokine tumor necrosis factor-α, and reduces oxidative stress through reduction of lipid peroxidation and thromboxane levels, while increasing iron-binding capacity, antioxidant enzyme levels, and prostacyclin.[145,146]

The evidence on the effect of exercise on arterial stiffness and vessel hemodynamics is limited. In a prospective cohort study, control brachial-ankle PWV (baPWV) at 1 month after delivery was significantly higher than the control baPWV in the early second trimester, while baPWV remained essentially the same in healthy pregnant women who performed vigorous exercise three or more times per week. These results indicate a relative decrease in arterial stiffness after healthy pregnancy associated with exercise.[154] Lastly, a randomized controlled trial found that regular aerobic exercise starting in the second trimester lasting 16 weeks led to greater cardiorespiratory fitness, lower HR at rest, and 44% greater FMD at the end of the intervention than that observed in a control group without regular aerobic activity, as assessed by the 6-min walk test and VO_{2max}.[153]

Worldwide guidelines encourage women without contraindication to begin or continue regular moderate intensity exercise during pregnancy, recommending 60−150 min/week.[33,145] The majority of pregnant women currently do not reach this target and continue to be inactive, especially as the pregnancy progresses.[145] Regular moderate intensity exercise during pregnancy is safe and the beneficial effects are numerous for the mother and developing fetus.

Concluding remarks

The complexity of changes during gestation and in HDP (and particularly PrE) have not allowed to fully unravel the physiology of pregnancy and the pathophysiology of its complications. Overall, it is accepted that during healthy pregnancy there is systemic vasodilation and decreased vascular resistance to accommodate the increase in blood volume and CO and meet the metabolic needs of the growing fetus. These changes lead to a U-shaped curve in BPs, arterial stiffness, and wave reflection, reaching a nadir in the second trimester. In contrast, in HDP and particularly in PrE, there are relatively lower increases in blood volume and CO, with marked elevation in peripheral vascular resistance, leading to continuous increases in BPs as well as in arterial stiffness and wave reflection throughout pregnancy.

Pregnancy is a cardiometabolic "stress test" that can uncover vascular abnormalities that manifest later in life as hypertension, diabetes, and premature cardiovascular disease. In this context, HDP and PrE constitute sex-specific, pregnancy-related cardiovascular disorders that share similar risk factors and have similar long-term adverse cardiovascular outcomes as the conventional cardiovascular disease. Therefore, it is important to accurately predict and prevent HDP from happening. To this end, the optimization of health care to prevent and treat women with HDPs continues to be a top priority on the global health agenda.[155] The American Heart Association in its "Effectiveness-Based Guidelines for the Prevention of Cardiovascular Disease in Women" recommends including a history of pregnancy complications as part of the cardiovascular risk evaluation and screening of women.

At present, there are no accurate clinical tools to predict early HDP and PrE. Arterial stiffness and hemodynamic parameters hold promise and they should be systematically investigated as early predictive tools for HDP and PrE.

Currently, the evidence examining arterial stiffness and hemodynamic alterations, although encouraging, is still sparse; limited number of studies of typically small sample sizes, mainly cross-sectional study designs, methodological differences, and measurement at different timepoints do not allow to capture the continuum of acute vascular changes that occur during the short timeline of pregnancy. Furthermore, first trimester or postpartum baselines may underestimate the magnitude of pregnancy and HDP-related changes. Prospective studies from preconception to postpartum, as well as identification of reference and normative values of arterial stiffness and hemodynamic parameters, will help reveal the magnitude of cardiovascular maladaptations during pregnancy and their long-term cardiovascular effects.

Thus, more comprehensive investigations to establish the ability of arterial stiffness and hemodynamics to predict early and accurately HDP and PrE are necessary. As such, arterial stiffness−related parameters may serve to address the current lack of effective and accurate screening methods for predicting HDP and PrE risk in early pregnancy with the potential to ultimately be incorporated into obstetric clinical practice.

References

1. Thilaganathan B, Kalafat E. Cardiovascular system in preeclampsia and beyond. **Hypertension**. 2019; 73:522−531.

2. de Haas S, Ghossein-Doha C, van Kuijk SM, van Drongelen J, Spaanderman ME. Physiological adaptation of maternal plasma volume during pregnancy: a systematic review and meta-analysis. **Ultrasound Obstet Gynecol**. 2017; 49:177−187.

3. Rodger M, Sheppard D, Gándara E, Tinmouth A. Haematological problems in obstetrics. **Best Pract Res Clin Obstet Gynaecol**. 2015; 29:671−684.

4. Aguree S, Gernand AD. Plasma volume expansion across healthy pregnancy: a systematic review and meta-analysis of longitudinal studies. **BMC Pregnancy Childbirth**. 2019; 19:508.

5. Lumbers ER, Delforce SJ, Arthurs AL, Pringle KG. Causes and consequences of the dysregulated maternal renin-angiotensin system in preeclampsia. **Front Endocrinol**. 2019; 10:563.

6. Soma-Pillay P, Nelson-Piercy C, Tolppanen H, Mebazaa A. Physiological changes in pregnancy. **Cardiovasc J Afr**. 2016; 27:89−94.

7. Leduc L, Wasserstrum N, Spillman T, Cotton DB. Baroreflex function in normal pregnancy. **Am J Obstet Gynecol**. 1991; 165:886−890.

8. Scaife PJ, Mohaupt MG. Salt, aldosterone and extrarenal Na(+) -sensitive responses in pregnancy. **Placenta**. 2017; 56:53−58.

9. Cheung KL, Lafayette RA. Renal physiology of pregnancy. **Adv Chron Kidney Dis**. 2013; 20:209−214.

10. Castro LC, Hobel CJ, Gornbein J. Plasma levels of atrial natriuretic peptide in normal and hypertensive pregnancies: a meta-analysis. **Am J Obstet Gynecol**. 1994; 171:1642−1651.

11. Sanghavi M, Rutherford JD. Cardiovascular physiology of pregnancy. **Circulation**. 2014; 130:1003−1008.

12. Vincent JL. Understanding cardiac output. **Crit Care**. 2008; 12:174.

13. Robson SC, Hunter S, Boys RJ, Dunlop W. Serial study of factors influencing changes in cardiac output during human pregnancy. **Am J Physiol**. 1989; 256:H1060−H1065.

14. Bader RA, Bader ME, Rose DF, Braunwald E. Hemodynamics at rest and during exercise in normal pregnancy as studies by cardiac catheterization. **J Clin Invest**. 1955; 34:1524−1536.

15. Duvekot JJ, Peeters LL. Maternal cardiovascular hemodynamic adaptation to pregnancy. **Obstet Gynecol Surv**. 1994; 49:S1−S14.

16. Mahendru AA, Everett TR, Wilkinson IB, Lees CC, McEniery CM. A longitudinal study of maternal cardiovascular function from preconception to the postpartum period. **J Hypertens**. 2014; 32:849−856.

17. Osman MW, Nath M, Khalil A, Webb DR, Robinson TG, Mousa HA. Longitudinal study to assess changes in arterial stiffness and cardiac output parameters among low-risk pregnant women. **Pregnancy Hypertens**. 2017; 10:256−261.

18. Loerup L, Pullon RM, Birks J, et al. Trends of blood pressure and heart rate in normal pregnancies: a systematic review and meta-analysis. **BMC Med**. 2019; 17:167.

19. Ducas RA, Elliott JE, Melnyk SF, et al. Cardiovascular magnetic resonance in pregnancy: insights from the cardiac hemodynamic imaging and remodeling in pregnancy (CHIRP) study. **J Cardiovasc Magn Reson**. 2014; 16:1.

20. Stewart RD, Nelson DB, Matulevicius SA, et al. Cardiac magnetic resonance imaging to assess the impact of maternal habitus on cardiac remodeling during pregnancy. **Am J Obstet Gynecol**. 2016; 214:640.e1−640.e6.

21. Romagano M, Louis-Jacques A, Quinones J, et al. Is there a role for cardiac magnetic resonance imaging during pregnancy? **J Matern Fetal Neonatal Med**. 2020; 33:558−563.

22. Garrido-Gómez T, Castillo-Marco N, Cordero T, Simón C. Decidualization resistance in the origin of preeclampsia. **Am J Obstet Gynecol**. 2020; S0002-9378(20)31130-3.

23. Karumanchi SA, Rana S, Taylor RN. **Angiogenesis and Preeclampsia**. 4th ed. Amsterdam: Elsevier; 2015:113−132.

24. Boeldt DS, Bird IM. Vascular adaptation in pregnancy and endothelial dysfunction in preeclampsia. **J Endocrinol**. 2017; 232:R27−R44.

25. Zygmunt M, Herr F, Münstedt K, Lang U, Liang OD. Angiogenesis and vasculogenesis in pregnancy. **Eur J Obstet Gynecol Reprod Biol**. 2003; 110(Suppl 1):S10−S18.

26. Lamarca B. Endothelial dysfunction. An important mediator in the pathophysiology of hypertension during pre-eclampsia. **Minerva Ginecol**. 2012; 64:309−320.

27. Lecarpentier É, Vieillefosse S, Haddad B, et al. Placental growth factor (PlGF) and sFlt-1 during pregnancy: physiology, assay and interest in preeclampsia. **Ann Biol Clin**. 2016; 74:259−267.

28. Napso T, Yong HEJ, Lopez-Tello J, Sferruzzi-Perri AN. The role of placental hormones in mediating maternal adaptations to support pregnancy and lactation. **Front Physiol**. 2018; 9:1091.

29. Kristiansson P, Wang JX. Reproductive hormones and blood pressure during pregnancy. **Hum Reprod**. 2001; 16:13−17.

30. Iacobaeus C, Andolf E, Thorsell M, et al. Longitudinal study of vascular structure and function during normal pregnancy. **Ultrasound Obstet Gynecol**. 2017; 49:46−53.

31. Khan F, Mires G, Macleod M, Belch JJ. Relationship between maternal arterial wave reflection, microvascular function and fetal growth in normal pregnancy. **Microcirculation**. 2010; 17:608−614.

32. Rodríguez I, González M. Physiological mechanisms of vascular response induced by shear stress and effect of exercise in systemic and placental circulation. **Front Pharmacol**. 2014; 5:209.

33. Skow Rachel J, King Emily C, Steinback Craig D, Davenport Margie H. The influence of prenatal exercise and pre-eclampsia on maternal vascular function. **Clin Sci**. 2017; 131:2223−2240.

34. Brosens IA, Robertson WB, Dixon HG. The role of the spiral arteries in the pathogenesis of preeclampsia. **Obstet Gynecol Annu**. 1972; 1:177−191.

35. Szczepaniak-Chicheł L, Markwitz W, Tykarski A. Difference between central and peripheral blood pressure in healthy and hypertension-complicated pregnancy. **Blood Press Monit**. 2016; 21:103−110.

36. Grindheim G, Estensen ME, Langesaeter E, Rosseland LA, Toska K. Changes in blood pressure during healthy pregnancy: a longitudinal cohort study. **J Hypertens**. 2012; 30:342−350.

37. Gaillard R, Bakker R, Willemsen SP, Hofman A, Steegers EA, Jaddoe VW. Blood pressure tracking during pregnancy and the risk of gestational hypertensive disorders: the Generation R Study. **Eur Heart J**. 2011; 32:3088−3097.

38. Te Riet L, van Esch JH, Roks AJ, van den Meiracker AH, Danser AH. Hypertension: renin-angiotensin-aldosterone system alterations. **Circ Res**. 2015; 116:960−975.

39. Di Giosia P, Giorgini P, Stamerra CA, Petrarca M, Ferri C, Sahebkar A. Gender differences in epidemiology, pathophysiology, and treatment of hypertension. **Curr Atheroscler Rep**. 2018; 20:13.

40. Tadic M, Cuspidi C, Grassi G, Ivanovic B. Gender-specific therapeutic approach in arterial hypertension - challenges ahead. **Pharmacol Res**. 2019; 141:181−188.

41. Townsend RR, Wilkinson IB, Schiffrin EL, et al. Recommendations for improving and standardizing vascular research on arterial stiffness: a scientific statement from the American heart association. **Hypertension**. 2015; 66:698−722.

42. Reference Values for Arterial Stiffness' Collaboration. Determinants of pulse wave velocity in healthy people and in the presence of cardiovascular risk factors: 'establishing normal and reference values'. **Eur Heart J**. 2010; 31:2338−2350.

43. Robb AO, Mills NL, Din JN, et al. Influence of the menstrual cycle, pregnancy, and preeclampsia on arterial stiffness. **Hypertension**. 2009; 53:952−958.

44. Franz MB, Burgmann M, Neubauer A, et al. Augmentation index and pulse wave velocity in normotensive and pre-eclamptic pregnancies. **Acta Obstet Gynecol Scand**. 2013; 92:960−966.

45. Pandey AK, Siwach S, Sangwan V, Sharma S, Das A. Assessment of maternal vascular stiffness indices in three trimesters of normal pregnancy. **Indian J Physiol Pharmacol**. 2014; 58:196−204.

46. Khalil A, Jauniaux E, Cooper D, Harrington K. Pulse wave analysis in normal pregnancy: a prospective longitudinal study. **PLoS One**. 2009; 4:e6134.

47. Gomez YH, Hudda Z, Mahdi N, et al. Pulse pressure amplification and arterial stiffness in low-risk, uncomplicated pregnancies. **Angiology**. 2016; 67:375−383.

48. Macedo ML, Luminoso D, Savvidou MD, McEniery CM, Nicolaides KH. Maternal wave reflections and arterial stiffness in normal pregnancy as assessed by applanation tonometry. **Hypertension**. 2008; 51:1047−1051.

49. Smith SA, Morris JM, Gallery ED. Methods of assessment of the arterial pulse wave in normal human pregnancy. **Am J Obstet Gynecol**. 2004; 190:472−476.

50. Mersich B, Rigó Jr J, Besenyei C, Lénárd Z, Studinger P, Kollai M. Opposite changes in carotid versus aortic stiffness during healthy human pregnancy. **Clin Sci (Lond)**. 2005; 109:103−107.

51. Fujime M, Tomimatsu T, Okaue Y, et al. Central aortic blood pressure and augmentation index during normal pregnancy. **Hypertens Res**. 2012; 35:633−638.

52. Osman MW, Leone F, Nath M, et al. Diurnal variation and repeatability of arterial stiffness and cardiac output measurements in the third trimester of uncomplicated pregnancy. **J Hypertens**. 2017; 35:2436−2442.

53. Visontai Z, Lenard Z, Studinger P, Rigo Jr J, Kollai M. Impaired baroreflex function during pregnancy is associated with stiffening of the carotid artery. **Ultrasound Obstet Gynecol**. 2002; 20:364−369.

54. Williams D. Pregnancy: a stress test for life. **Curr Opin Obstet Gynecol**. 2003; 15:465−471.

55. Brown MA, Lindheimer MD, de Swiet M, Van Assche A, Moutquin JM. The classification and diagnosis of the hypertensive disorders of pregnancy: statement from the International Society for the Study of Hypertension in Pregnancy (ISSHP). **Hypertens Pregnancy**. 2001; 20:Ix−xiv.

56. Say L, Chou D, Gemmill A, et al. Global causes of maternal death: a WHO systematic analysis. **Lancet Glob Health**. 2014; 2:e323−e333.

57. World Health Organization. **WHO Recommendations for Prevention and Treatment of Pre-eclampsia and Eclampsia**. 2011.

58. von Dadelszen P, Magee LA. Preventing deaths due to the hypertensive disorders of pregnancy. **Best Pract Res Clin Obstet Gynaecol**. 2016; 36:83−102.

59. Smith GN, Pudwell J, Walker M, Wen SW. Ten-year, thirty-year, and lifetime cardiovascular disease risk estimates following a pregnancy complicated by preeclampsia. **J Obstet Gynaecol Can**. 2012; 34:830−835.

60. Andersgaard AB, Acharya G, Mathiesen EB, Johnsen SH, Straume B, Øian P. Recurrence and long-term maternal health risks of hypertensive disorders of pregnancy: a population-based study. **Am J Obstet Gynecol**. 2012; 206:143.e1−143.e8.

61. Magee LA, Pels A, Helewa M, Rey E, von Dadelszen P. Diagnosis, evaluation, and management of the hypertensive disorders of pregnancy: executive summary. **J Obstet Gynaecol Can**. 2014; 36:416−441.

62. Lisonkova S, Joseph KS. Incidence of preeclampsia: risk factors and outcomes associated with early- versus late-onset disease. **Am J Obstet Gynecol**. 2013; 209:544.e1−544.e12.

63. Sibai BM. Etiology and management of postpartum hypertension-preeclampsia. **Am J Obstet Gynecol**. 2012; 206:470−475.

64. Bellamy L, Casas JP, Hingorani AD, Williams DJ. Pre-eclampsia and risk of cardiovascular disease and cancer in later life: systematic review and meta-analysis. **Br Med J**. 2007; 335:974.

65. Lykke JA, Langhoff-Roos J, Sibai BM, Funai EF, Triche EW, Paidas MJ. Hypertensive pregnancy disorders and subsequent cardiovascular morbidity and type 2 diabetes mellitus in the mother. **Hypertension**. 2009; 53:944−951.

66. McDonald SD, Malinowski A, Zhou Q, Yusuf S, Devereaux PJ. Cardiovascular sequelae of preeclampsia/eclampsia: a systematic review and meta-analyses. **Am Heart J**. 2008; 156:918−930.

67. Mongraw-Chaffin ML, Cirillo PM, Cohn BA. Preeclampsia and cardiovascular disease death: prospective evidence from the child health and development studies cohort. **Hypertension**. 2010; 56:166−171.

68. Ahmed R, Dunford J, Mehran R, Robson S, Kunadian V. Pre-eclampsia and future cardiovascular risk among women: a review. **J Am Coll Cardiol**. 2014; 63:1815−1822.

69. Brown MA, Wang J, Whitworth JA. The renin-angiotensin-aldosterone system in pre-eclampsia. **Clin Exp Hypertens**. 1997; 19:713−726.

70. Yang J, Shang J, Zhang S, Li H, Liu H. The role of the renin-angiotensin-aldosterone system in preeclampsia: genetic polymorphisms and microRNA. **J Mol Endocrinol**. 2013; 50:R53−R66.

71. Verdonk K, Visser W, Van Den Meiracker AH, Danser AH. The renin-angiotensin-aldosterone system in pre-eclampsia: the delicate balance between good and bad. **Clin Sci (Lond).** 2014; 126:537−544.

72. De Paco C, Kametas N, Rencoret G, Strobl I, Nicolaides KH. Maternal cardiac output between 11 and 13 weeks of gestation in the prediction of preeclampsia and small for gestational age. **Obstet Gynecol**. 2008; 111:292−300.

73. Khaw A, Kametas NA, Turan OM, Bamfo JE, Nicolaides KH. Maternal cardiac function and uterine artery Doppler at 11-14 weeks in the prediction of pre-eclampsia in nulliparous women. **BJOG**. 2008; 115:369−376.

74. Tay J, Foo L, Masini G, et al. Early and late preeclampsia are characterized by high cardiac output, but in the presence of fetal growth restriction, cardiac output is low: insights from a prospective study. **Am J Obstet Gynecol**. 2018; 218:517.e1−517.e12.

75. Foo FL, Mahendru AA, Masini G, et al. Association between pre-pregnancy cardiovascular function and subsequent preeclampsia or fetal growth restriction. **Hypertension**. 2018; 72:442−450.

76. Lang RM, Pridjian G, Feldman T, Neumann A, Lindheimer M, Borow KM. Left ventricular mechanics in preeclampsia. **Am Heart J**. 1991; 121:1768−1775.

77. Lindheimer MD, Katz AI. Preeclampsia: pathophysiology, diagnosis, and management. **Annu Rev Med**. 1989; 40:233−250.

78. Valensise H, Vasapollo B, Gagliardi G, Novelli GP. Early and late preeclampsia: two different maternal hemodynamic states in the latent phase of the disease. **Hypertension**. 2008; 52:873−880.

79. Guy GP, Ling HZ, Garcia P, Poon LC, Nicolaides KH. Maternal cardiac function at 35-37 weeks' gestation: prediction of pre-eclampsia and gestational hypertension. **Ultrasound Obstet Gynecol**. 2017; 49:61−66.

80. Cong J, Fan T, Yang X, Shen J, Cheng G, Zhang Z. Maternal cardiac remodeling and dysfunction in preeclampsia: a three-dimensional speckle-tracking echocardiography study. **Int J Cardiovasc Imaging**. 2015; 31:1361−1368.

81. Weber TM, Lackner HK, Roessler A, et al. Heart rate variability and baroreceptor reflex sensitivity in early- versus late-onset pre-eclampsia. **PLoS One**. 2017; 12:e0186521.

82. Booker CJ, Dodson WC, Kunselman AR, Repke JT, Legro RS. Twenty-four-hour ambulatory blood pressure monitor heart rate: a potential marker for gestational hypertension in at-risk women. **Am J Perinatol**. 2012; 29:339−346.

83. Moors S, Staaks KJJ, Westerhuis M, et al. Heart rate variability in hypertensive pregnancy disorders: a systematic review. **Pregnancy Hypertens**. 2020; 20:56−68.

84. Castleman JS, Ganapathy R, Taki F, Lip GY, Steeds RP, Kotecha D. Echocardiographic structure and function in hypertensive disorders of pregnancy: a systematic review. **Circ Cardiovasc Imaging**. 2016; 9.

85. Melchiorre K, Sutherland G, Sharma R, Nanni M, Thilaganathan B. Mid-gestational maternal cardiovascular profile in preterm and term pre-eclampsia: a prospective study. **BJOG**. 2013; 120:496−504.

86. Borges VTM, Zanati SG, Peraçoli MTS, et al. Maternal left ventricular hypertrophy and diastolic dysfunction and brain natriuretic peptide concentration in early- and late-onset pre-eclampsia. **Ultrasound Obstet Gynecol**. 2018; 51:519−523.

87. Shahul S, Rhee J, Hacker MR, et al. Subclinical left ventricular dysfunction in preeclamptic women with preserved left ventricular ejection fraction: a 2D speckle-tracking imaging study. **Circ Cardiovasc Imaging**. 2012; 5:734−739.

88. Dennis AT. Transthoracic echocardiography in women with pre-eclampsia. **Curr Opin Anaesthesiol**. 2015; 28:254−260.

89. Almaani SJ. Placental growth factor in pre-eclampsia: friend or foe? **Kidney Int**. 2019; 95:730−732.

90. Hung TH, Skepper JN, Charnock-Jones DS, Burton GJ. Hypoxia-reoxygenation: a potent inducer of apoptotic changes in the human placenta and possible etiological factor in preeclampsia. **Circ Res**. 2002; 90:1274−1281.

91. Chaiworapongsa T, Chaemsaithong P, Yeo L, Romero R. Pre-eclampsia part 1: current understanding of its pathophysiology. **Nat Rev Nephrol**. 2014; 10:466−480.

92. Goulopoulou S, Davidge ST. Molecular mechanisms of maternal vascular dysfunction in preeclampsia. **Trends Mol Med**. 2015; 21:88−97.

93. Granger DN, Kvietys PR. Reperfusion injury and reactive oxygen species: the evolution of a concept. **Redox Biol**. 2015; 6:524−551.

94. Sulistyowati S. The role of oxidative stress in the pathogenesis of pre-eclampsia. **Pregnancy Hypertens**. 2014; 4:244.

95. Cornelius DC. Preeclampsia: from inflammation to immunoregulation. **Clin Med Insights Blood Disord**. 2018; 11, 1179545x17752325.

96. Powe CE, Levine RJ, Karumanchi SA. Preeclampsia, a disease of the maternal endothelium: the role of antiangiogenic factors and implications for later cardiovascular disease. **Circulation**. 2011; 123:2856−2869.

97. Lecarpentier E, Tsatsaris V. Angiogenic balance (sFlt-1/PlGF) and preeclampsia. **Ann Endocrinol**. 2016; 77:97−100.

98. Torry DS, Wang HS, Wang TH, Caudle MR, Torry RJ. Pre-eclampsia is associated with reduced serum levels of placenta growth factor. **Am J Obstet Gynecol**. 1998; 179:1539−1544.

99. Zeisler H, Llurba E, Chantraine F, et al. Predictive value of the sFlt-1:PlGF ratio in women with suspected preeclampsia. **N Engl J Med**. 2016; 374:13−22.

100. Berkane N, Liere P, Oudinet JP, et al. From pregnancy to pre-eclampsia: a key role for estrogens. **Endocr Rev**. 2017; 38:123−144.

101. Baud O, Berkane N. Hormonal changes associated with intra-uterine growth restriction: impact on the developing brain and future neurodevelopment. **Front Endocrinol**. 2019; 10:179.

102. Wan J, Hu Z, Zeng K, et al. The reduction in circulating levels of estrogen and progesterone in women with preeclampsia. **Pregnancy Hypertens**. 2018; 11:18−25.

103. Szlachter BN, Quagliarello J, Jewelewicz R, Osathanondh R, Spellacy WN, Weiss G. Relaxin in normal and pathogenic pregnancies. **Obstet Gynecol**. 1982; 59:167−170.

104. Lafayette RA, Hladunewich MA, Derby G, Blouch K, Druzin ML, Myers BD. Serum relaxin levels and kidney function in late

pregnancy with or without preeclampsia. **Clin Nephrol**. 2011; 75:226−232.

105. Stergiotou I, Crispi F, Valenzuela-Alcaraz B, Bijnens B, Gratacos E. Patterns of maternal vascular remodeling and responsiveness in early- versus late-onset preeclampsia. **Am J Obstet Gynecol**. 2013; 209:558.e1−558.e14.

106. Antonios TF, Nama V, Wang D, Manyonda IT. Microvascular remodelling in preeclampsia: quantifying capillary rarefaction accurately and independently predicts preeclampsia. **Am J Hypertens**. 2013; 26:1162−1169.

107. Nama V, Manyonda IT, Onwude J, Antonios TF. Structural capillary rarefaction and the onset of preeclampsia. **Obstet Gynecol**. 2012; 119:967−974.

108. Gagliardi G, Tiralongo GM, LoPresti D, et al. Screening for preeclampsia in the first trimester: role of maternal hemodynamics and bioimpedance in non-obese patients. **Ultrasound Obstet Gynecol**. 2017; 50:584−588.

109. Lees C, Ferrazzi E. Relevance of haemodynamics in treating preeclampsia. **Curr Hypertens Rep**. 2017; 19:76.

110. Lucovnik M, Lackner HK, Papousek I, et al. Systemic vascular resistance and endogenous inhibitors of nitric oxide synthesis in early- compared to late-onset preeclampsia: preliminary findings. **Hypertens Pregnancy**. 2017; 36:276−281.

111. Mayrink J, Souza RT, Feitosa FE, et al. Mean arterial blood pressure: potential predictive tool for preeclampsia in a cohort of healthy nulliparous pregnant women. **BMC Pregnancy Childbirth**. 2019; 19:460.

112. Macdonald-Wallis C, Lawlor DA, Fraser A, May M, Nelson SM, Tilling K. Blood pressure change in normotensive, gestational hypertensive, preeclamptic, and essential hypertensive pregnancies. **Hypertension**. 2012; 59:1241−1248.

113. Jieyu L, Yingying C, Tian G, et al. Visit-to-visit blood pressure variability is associated with gestational hypertension and preeclampsia. **Pregnancy Hypertens**. 2019; 18:126−131.

114. Bello NA, Zhou H, Cheetham TC, et al. Prevalence of hypertension among pregnant women when using the 2017 American College of Cardiology/American Heart Association Blood Pressure Guidelines and Association with maternal and fetal outcomes. **JAMA Netw Open**. 2021; 4:e213808.

115. Ohkuchi A, Hirashima C, Arai R, et al. Temporary hypertension and white coat hypertension in the first trimester as risk factors for preeclampsia. **Hypertens Res**. 2019; 42:2002−2012.

116. Hausvater A, Giannone T, Sandoval YH, et al. The association between preeclampsia and arterial stiffness. **J Hypertens**. 2012; 30:17−33.

117. Rönnback M, Lampinen K, Groop PH, Kaaja R. Pulse wave reflection in currently and previously preeclamptic women. **Hypertens Pregnancy**. 2005; 24:171−180.

118. Tihtonen KM, Kööbi T, Uotila JT. Arterial stiffness in preeclamptic and chronic hypertensive pregnancies. **Eur J Obstet Gynecol Reprod Biol**. 2006; 128:180−186.

119. Avni B, Frenkel G, Shahar L, Golik A, Sherman D, Dishy V. Aortic stiffness in normal and hypertensive pregnancy. **Blood Press**. 2010; 19:11−15.

120. Oylumlu M, Oylumlu M, Yuksel M, et al. A simple method for the assessment of arterial stiffness in pre-eclamptic patients. **Clin Exp Hypertens**. 2014; 36:531−537.

121. Osman MW, Nath M, Breslin E, et al. Association between arterial stiffness and wave reflection with subsequent development of placental-mediated diseases during pregnancy: findings of a systematic review and meta-analysis. **J Hypertens**. 2018; 36:1005−1014.

122. Foo FL, McEniery CM, Lees C, Khalil A. Assessment of arterial function in pregnancy: recommendations of the International Working Group on maternal hemodynamics. **Ultrasound Obstet Gynecol**. 2017; 50:324−331.

123. Kaihura C, Savvidou MD, Anderson JM, McEniery CM, Nicolaides KH. Maternal arterial stiffness in pregnancies affected by preeclampsia. **Am J Physiol Heart Circ Physiol**. 2009; 297:H759−H764.

124. Savvidou MD, Kaihura C, Anderson JM, Nicolaides KH. Maternal arterial stiffness in women who subsequently develop pre-eclampsia. **PLoS One**. 2011; 6:e18703.

125. Katsipi I, Stylianou K, Petrakis I, et al. The use of pulse wave velocity in predicting pre-eclampsia in high-risk women. **Hypertens Res**. 2014; 37:733−740.

126. Khalil A, Garcia-Mandujano R, Maiz N, Elkhouli M, Nicolaides KH. Longitudinal changes in maternal hemodynamics in a population at risk for pre-eclampsia. **Ultrasound Obstet Gynecol**. 2014; 44:197−204.

127. Khalil A, Akolekar R, Syngelaki A, Elkhouli M, Nicolaides KH. Maternal hemodynamics at 11-13 weeks' gestation and risk of pre-eclampsia. **Ultrasound Obstet Gynecol**. 2012; 40:28−34.

128. Hale SA, Badger GJ, McBride C, Magness R, Bernstein IM. Pre-pregnancy vascular dysfunction in women who subsequently develop hypertension during pregnancy. **Pregnancy Hypertens**. 2013; 3:140−145.

129. Carty DM, Neisius U, Rooney LK, Dominiczak AF, Delles C. Pulse wave analysis for the prediction of preeclampsia. **J Hum Hypertens**. 2014; 28:98−104.

130. Khalil A, Cowans NJ, Spencer K, Goichman S, Meiri H, Harrington K. First-trimester markers for the prediction of pre-eclampsia in women with a-priori high risk. **Ultrasound Obstet Gynecol**. 2010; 35:671−679.

131. Khalil AA, Cooper DJ, Harrington KF. Pulse wave analysis: a preliminary study of a novel technique for the prediction of pre-eclampsia. **BJOG**. 2009; 116:268−276. discussion 276-7.

132. Phan K, Schiller I, Dendukuri N, et al. A longitudinal analysis of arterial stiffness and wave reflection in preeclampsia: identification of changepoints. **Metabolism**. 2021; 120 (accepted).

133. Bowyer L, Brown MA, Jones M. Forearm blood flow in preeclampsia. **BJOG**. 2003; 110:383−391.

134. Weissgerber TL, Milic NM, Milin-Lazovic JS, Garovic VD. Impaired flow-mediated dilation before, during, and after preeclampsia: a systematic review and meta-analysis. **Hypertension**. 2016; 67:415−423.

135. Brandão AH, Pereira LM, Gonçalves AC, Reis ZS, Leite HV, Cabral AC. Comparative study of endothelial function and uterine artery Doppler velocimetry between pregnant women with or without preeclampsia development. **J Pregnancy**. 2012; 2012:909315.

136. Tomimatsu T, Fujime M, Kanayama T, et al. Maternal arterial stiffness in normotensive pregnant women who subsequently deliver babies that are small for gestational age. **Eur J Obstet Gynecol Reprod Biol**. 2013; 169:24−27.

137. Elvan-Taspinar A, Franx A, Bots ML, Koomans HA, Bruinse HW. Arterial stiffness and fetal growth in normotensive pregnancy. **Am J Hypertens**. 2005; 18:337−341.

138. Khalil A, Sodre D, Syngelaki A, Akolekar R, Nicolaides KH. Maternal hemodynamics at 11-13 weeks of gestation in pregnancies delivering small for gestational age neonates. **Fetal Diagn Ther**. 2012; 32:231−238.

139. Roberts LA, Ling HZ, Poon LC, Nicolaides KH, Kametas NA. Maternal hemodynamics, fetal biometry and Doppler indices in pregnancies followed up for suspected fetal growth restriction. **Ultrasound Obstet Gynecol**. 2018; 52:507−514.

140. Tomimatsu T, Fujime M, Kanayama T, et al. Abnormal pressure-wave reflection in pregnant women with chronic hypertension: association with maternal and fetal outcomes. **Hypertens Res**. 2014; 37:989−992.

141. Sharabi-Nov A, Kumar K, Fabjan Vodušek V, et al. Establishing a differential marker profile for pregnancy complications near delivery. **Fetal Diagn Ther**. 2020; 47:471−484.

142. Stott D, Papastefanou I, Paraschiv D, Clark K, Kametas NA. Longitudinal maternal hemodynamics in pregnancies affected by fetal growth restriction. **Ultrasound Obstet Gynecol**. 2017; 49:761−768.

143. Stott D, Bolten M, Salman M, Paraschiv D, Clark K, Kametas NA. Maternal demographics and hemodynamics for the prediction of fetal growth restriction at booking, in pregnancies at high risk for placental insufficiency. **Acta Obstet Gynecol Scand**. 2016; 95:329−338.

144. Davenport MH, Ruchat S-M, Poitras VJ, et al. Prenatal exercise for the prevention of gestational diabetes mellitus and hypertensive disorders of pregnancy: a systematic review and meta-analysis. **Br J Sports Med**. 2018; 52:1367−1375.

145. Witvrouwen I, Mannaerts D, Van Berendoncks AM, Jacquemyn Y, Van Craenenbroeck EM. The effect of exercise training during pregnancy to improve maternal vascular health: focus on gestational hypertensive disorders. **Front Physiol**. 2020; 11.

146. Aune D, Saugstad OD, Henriksen T, Tonstad S. Physical activity and the risk of preeclampsia: a systematic review and meta-analysis. **Epidemiology**. 2014; 25:331−343.

147. Wiebe HW, Boulé NG, Chari R, Davenport MH. The effect of supervised prenatal exercise on fetal growth: a meta-analysis. **Obstet Gynecol**. 2015; 125:1185−1194.

148. da Silva SG, Ricardo LI, Evenson KR, Hallal PC. Leisure-time physical activity in pregnancy and maternal-child health: a systematic review and meta-analysis of randomized controlled trials and cohort studies. **Sports Med**. 2017; 47:295−317.

149. Davenport MH, Meah VL, Ruchat S-M, et al. Impact of prenatal exercise on neonatal and childhood outcomes: a systematic review and meta-analysis. **Br J Sports Med**. 2018; 52:1386−1396.

150. Roberts CK, Vaziri ND, Barnard RJ. Effect of diet and exercise intervention on blood pressure, insulin, oxidative stress, and nitric oxide availability. **Circulation**. 2002; 106:2530−2532.

151. Uematsu M, Ohara Y, Navas JP, et al. Regulation of endothelial cell nitric oxide synthase mRNA expression by shear stress. **Am J Physiol**. 1995; 269:C1371−C1378.

152. Pyke KE, Tschakovsky ME. The relationship between shear stress and flow-mediated dilatation: implications for the assessment of endothelial function. **J Physiol**. 2005; 568:357−369.

153. Ramírez-Vélez R, Aguilar de Plata AC, Escudero MM, et al. Influence of regular aerobic exercise on endothelium-dependent vasodilation and cardiorespiratory fitness in pregnant women. **J Obstet Gynaecol Res**. 2011; 37:1601−1608.

154. Kawabata I, Nakai A, Sekiguchi A, Inoue Y, Takeshita T. The effect of regular exercise training during pregnancy on postpartum brachial-ankle pulse wave velocity, a measure of arterial stiffness. **J Sports Sci Med**. 2012; 11:489−494.

155. Khan KS, Wojdyla D, Say L, Gülmezoglu AM, Van Look PF. WHO analysis of causes of maternal death: a systematic review. **Lancet**. 2006; 367:1066−1074.

This page intentionally left blank

Chapter 43

Arterial stiffness and pulsatile hemodynamics in pediatric populations

Andrew H. Tran[1,2] and Elaine M. Urbina[3,4]

[1]The Heart Center, Nationwide Children's Hospital, Columbus, OH, United States; [2]The Ohio State University, Columbus, OH, United States; [3]Division of Cardiology, Cincinnati Children's Hospital Medical Center, Cincinnati, OH, United States; [4]University of Cincinnati, Cincinnati, OH, United States

Introduction

Measures of arterial stiffness have been measured in adults for many years resulting in a large body of literature and established normal values for many parameters. Contrasting this, the study of arterial stiffness in children has received less attention and data are limited on normal values. One of the difficulties with studying arterial stiffness in children is the change in arterial physiology with growth. Aortic length progressively increases in childhood until reaching adult proportions, which affects the wave reflection sites. In addition to changes in aortic length, structural aortic changes occur during development. As discussed in Chapters 7 and 19 in detail, elastin is a major structural component of large arteries, with elastogenesis starting at mid-gestation and continuing after birth until adolescence.[1,2] This means that essentially no de novo elastin fibers are made during adulthood. The most elastic the aorta will be is during childhood with subsequent increasing stiffness as the integrity of the elastin fibers degrade over time. These physiologic changes over time make studying arterial stiffness in children a unique and interesting challenge. In this chapter, we present the currently available literature on arterial stiffness in children, encompassing various disease states and measurement modalities.

Vascular effects of various disease states

Obesity

Pulse wave velocity

Obesity increases the risk for comorbidities even during childhood.[3] The effects of obesity also extend to aortic stiffness, with obese children having increased aortic stiffness compared to lean children.[4–6] A recent large meta-analysis of 15 studies found that 10 out of the 12 studies measuring central pulse wave velocity (PWV) and all of the studies that evaluated carotid and aortic β-stiffness demonstrated higher values in obese children compared to controls.[4] The studies measured central PWV in various ways including assessment of carotid-femoral PWV (cfPWV), Doppler ultrasound of the aorta, or local PWV measured at the carotid artery. Another meta-analysis also found that PWV was higher in obese children compared to nonobese children but found no significant differences in Augmentation Index (AIx).[5] A significant limitation is that PWV was also measured in various ways in the included studies encompassing assessment of cfPWV, carotid-radial PWV (crPWV), Doppler ultrasound of the aorta, upper and lower limb PWV measured by Doppler ultrasound and photoplethysmography, or local PWV measured at the carotid artery. Cardiac magnetic resonance imaging (MRI) may be an even more sensitive technique to evaluate obesity-related arterial stiffening in youth. Caterini et al. found that mean aortic PWV by cardiac MRI was higher in obese/overweight youth compared to controls despite no differences in cfPWV measurements by applanation tonometry.[7] Sletner et al. examined the relative contributions of fat mass and lean mass and found that increasing lean mass attenuated the effect of fat mass on cfPWV such that subjects with the lowest cfPWV had low fat mass and high lean mass. These findings suggest that lean mass may have a vascular protective effect.[8]

Pulse wave analysis

Available studies regarding the effect of obesity on arterial wave reflections in children are mixed. A large multiethnic

study found that AIx was significantly higher in obese youth compared to lean controls.[9] However, a study examining African-American youth found no differences in AIx between obese youth versus lean controls.[10] Another study found that AIx was significantly lower in obese children compared to lean controls but noted that the forward pulse wave amplitude (Pf) and backward pulse wave amplitude (Pb) of the aortic pressure wave were significantly higher in obese children.[11] Pierce et al. also found that Pf was significantly higher in obese children compared to lean controls but saw no difference in AIx or Pb between groups.[12] It is possible that the difference in conclusions regarding AIx, Pf, and Pb between the studies can be explained the various age ranges of the studies. Urbina et al. had the largest age range and included subjects up to 24 years old[9] whereas Castro et al. had the youngest subjects with a mean age of approximately 10 years.[11] The differences between studies may be related to the well-known changes in arterial wave reflections over time as subjects age and progress toward adulthood. Nevertheless, it appears that arterial wave reflections are altered in obese subjects, suggesting vascular changes in this condition.

Distensibility

Arterial distensibility appears to decrease in states of obesity. Overweight children have significantly decreased carotid distensibility compared to normal weight children.[13] To our knowledge, no studies of aortic distensibility and obesity in children currently exist. However, in a study of predominantly normal weight subjects, Mikola et al. found that systolic blood pressure (SBP) and low-density lipoprotein cholesterol (LDL-C) were independent determinants of aortic distensibility while body mass index (BMI), SBP, LDL-C, and homeostasis model of insulin resistance influenced carotid distensibility.[14] Brachial distensibility was also decreased in obese children when compared to lean controls.[9] Adding to these findings, adolescents and young adults classified as severely obese exhibited significantly lower brachial distensibility compared to subjects classified in the nonsevere obesity category.[15] Indeed, Whincup et al. found that as measures of adiposity increase, brachial distensibility decreases, and that the effects of adiposity on brachial distensibility emerge around 13−15 years of age.[16] The findings of these various studies are important because they suggest that increasing obesity leads to further impaired arterial distensibility and that these effects worsen with age even during the pediatric period.

Global measures

Global measures of arterial function such as pulse pressure (PP) and stroke volume (SV) are also affected by obesity. SV is increased in obese children[11,17] and adults[17] compared to normal weight subjects. If necessary, correction of SV using BSA can be performed in order to remove the expected effect of body size in measurements.[17] PP is also increased in obese children. Chandramohan et al. examined NHANES data from 1988 to 1994 and found that obesity was associated with increased PP with waist circumference, rather than BMI, being a significant predictor of PP.[18] Zachariah et al. reexamined NHANES data more recently including data up to 2008 and found that PP has increased over time paralleling the increase in childhood obesity.[19]

Dyslipidemia

Pulse wave velocity

Dyslipidemia influences PWV in children. Riggio et al. evaluated children with elevated LDL-C and found that they had significantly increased local PWV measured at the carotid artery compared to controls.[20] A more recent study of youth with familial hypercholesterolemia (FH) using cardiac MRI showed significantly increased ascending-to-descending aortic PWV.[21] However, other studies of subjects with familial hypercholesterolemia (FH) involving greater age ranges (adults and children) showed no differences in ascending-to-descending PWV as assessed by cardiac MRI[22] or in cfPWV as assessed by applanation tonometry.[23] Differences in outcomes of PWV between the studies may be explained partially by differences in method of measuring PWV, but the predominance of adult subjects in the latter two studies may suggest possible age-related changes in PWV. Triglyceride to HDL-C ratio (TG:HDL-C) also influences cfPWV with cfPWV increasing across TG/HDL-C tertiles.[24] Taken together, the above studies show the impact of dyslipidemia on large artery stiffness even in children.

Pulse wave analysis

The impact of dyslipidemia on arterial wave reflections in children has been less well studied. However, children with elevated LDL-C had significantly higher AIx compared to controls.[20] Additionally, triglyceride levels were found to be an independent determinant of AIx,[25] and children in the highest tertile of TG:HDL-C had significantly higher AIx compared to the lowest tertile.[24]

Distensibility

The effect of dyslipidemia on arterial distensibility is mixed. Multiple studies show that lipid levels are independent determinants of arterial distensibility.[14,16,24] LDL-C levels were noted to be associated with both aortic and carotid distensibility[14] while another study found that total cholesterol and LDL-C were inversely related to brachial distensibility in youth.[16] Brachial distensibility was also noted to decrease across increasing TG:HDL-C tertiles.[24]

These studies primarily looked at the general pediatric population. However, studies specifically examining youth with FH show a more nuanced picture. Lehmann et al. studied young FH patients (age <24 years) and found a significantly more compliant aorta when assessed by ultrasound compared to controls even after correction for age and sex.[26] LDL-C:HDL-C ratio and duration of disease were independent predictors of aortic compliance in this study. Evaluation of FH subjects by cardiac MRI support these findings of increased aortic compliance as Tran et al. found significantly increased aortic distensibility in adolescents with FH and Soljanlahti et al. found a trend toward significance in increased aortic compliance in their study including adults and children with FH. On the other hand, Aggoun et al. found decreased carotid compliance and distensibility in children with FH as assessed by ultrasound.[27] The varied findings between studies are important as they highlight decreased distensibility in the carotid and brachial arteries but *increased* distensibility in the aorta in the setting of hypercholesterolemia in children. By adulthood, this effect disappears with aortic distensibility in FH subjects being significantly higher than normolipidemic controls.[28]

Global measures

Study of global measures of arterial function in children with dyslipidemia are scarce. Adult data reveal significantly higher central PP in hypercholesterolemic subjects compared to normolipidemic controls.[29] While specific SV data for hypercholesterolemic children is unavailable, there was no difference in ventricular function in two cardiac MRI studies of FH subjects compared to norms.[21,22]

Hypertension

Pulse wave velocity

Hypertension is associated with increased PWV in children. Kulsum-Mecci et al. studied 159 children and found that cfPWV was increased in children with hypertension, obesity, or those with both hypertension and obesity compared to controls.[30] The differences seen in the hypertensive group were independent of obesity. Another study found that obese children with hypertension had significantly higher PWV estimated by oscillometry compared to lean controls and obese children without hypertension[31] suggesting that blood pressure has an effect on arterial stiffness beyond that explained by obesity alone. Incremental increases in blood pressure also appear to be associated with PWV elevation (estimated by oscillometry) with PWV rising for each unit of increase in SBP or DBP independent of BMI.[32] However, these studies are limited since oscillometry is not a reliable method to estimate

PWV. In another study, cfPWV (a well-validated measure of large artery stiffness) also exhibited increases across blood pressure categories in normotensive to prehypertensive to hypertensive youth.[33]

Pulse wave analysis

Measures of arterial wave reflections appear to be worse in hypertensive children than normotensive youth. When comparing AIx across blood pressure categories of normotensive, prehypertensive, and hypertensive youth, there was a significant increase in AIx between groups with increasing blood pressure.[33] Differences in AIx are also seen when comparing central blood pressures. Adolescents and young adults (16−24 years) with high central blood pressure (but normal peripheral blood pressure) had higher AIx compared to subjects with normal central blood pressures.[25]

Contrasting the above studies, Wójtowicz et al. found no significant difference in AIx between lean controls, obese subjects without hypertension, and obese subjects with hypertension.[31] No difference in AIx was also seen in a study by Garcia-Espinosa et al., but Pf and Pb were significantly higher in the high blood pressure group compared to normotensive controls.[34] A later follow-up study from the same group found that high blood pressure was associated with higher Pf, Pb, and AIx.[35]

Distensibility

Arterial distensibility is impaired in states of elevated blood pressure. Brachial distensibility was significantly lower in a graded fashion when compared between hypertensive to prehypertensive to normotensive youth.[33] Adolescents and young adults with higher central blood pressure but normal peripheral blood pressure also exhibited similar findings of lower brachial distensibility when compared to controls with normal central blood pressure.[25] Adding to these findings, both SBP[13] and diastolic blood pressure[16] were found to be independent determinants of arterial distensibility.

Global measures

Global measures of arterial function such as PP are increased in high blood pressure states in children. Children with high blood pressure were found to have significantly higher peripheral and central PP values compared to normotensive youth.[34,35] Furthermore, youth with isolated systolic high normal blood pressure and systolic hypertension had significantly higher peripheral and central blood pressure compared to normotensive controls.[36] Subjects classified as having high central blood pressure also exhibit higher peripheral and central PPs compared to normotensive subjects.[25]

Diabetes

Pulse wave velocity

Large artery vascular changes are present in children with diabetes mellitus. Differences in PWV are evident between type 1 diabetic (T1D) subjects and controls across measurement modalities such as tonometry[37,38] and oscillometry.[39] When compared to nondiabetic controls, T1D adolescents and young adults had significantly higher cfPWV even after adjusting for cardiovascular risk factors such as blood pressure, adiposity, lipid levels, and microalbuminuria.[37] Another study found significantly higher crPWV in T1D subjects compared to controls.[38] While cfPWV was higher in T1D subjects in this study, it did not reach statistical significance.

Large artery vascular changes are also present in subjects with Type 2 diabetes (T2D). Shah et al. evaluated the arterial stiffness of young adults with youth-onset T2D and found increased arterial stiffness in approximately half of the subjects.[40] PWV was significantly higher in the T2D group compared to lean controls. Treatment assignment for T2D between metformin, metformin + intensive lifestyle intervention, or metformin + rosiglitazone did not predict arterial stiffness.

Contrasting the findings in subjects with T1D and T2D, subjects with prediabetes do not appear to have significant large artery changes compared to controls. Shah et al. compared the vascular health of 102 obese youth with prediabetes to 139 obese youth without prediabetes. While the prediabetic obese youth had higher carotid intima-media thickness and lower brachial distensibility, there was no significant difference in PWV between the two groups.

Diabetes duration and insulin resistance influence arterial stiffness. crPWV, cfPWV, and lower extremity PWV in diabetic youth at five year follow-up were significantly higher than their baseline values.[41] Putarek et al. found that diabetic disease duration was the strongest independent determinant of arterial stiffness with BMI, blood pressure, and HbA1c also influencing local PWV measured at the carotid artery.[42] Diabetes duration was also a significant determinant of PWV in another large pediatric study of 1809 T1D youth[43] which also found that subjects with a HbA1c ≥9% had significantly higher crPWV, cfPWV, and lower extremity PWV compared to youth with lower HbA1c. Adding to these findings, Shah et al. found that lower insulin sensitivity was associated with a higher rate of change in cfPWV in their study of diabetic youth.[44]

Pulse wave analysis

Arterial wave reflections are altered in diabetic children. Multiple studies of T1D subjects found significantly higher AIx in T1D youth and young adults compared to nondiabetic controls.[37,39,43] Shah et al. found similar findings in T2D subjects.[40] These subjects diagnosed with T2D as children had vascular assessment obtained as young adults (mean age 20.8 ± 2.5 years). AIx was significantly higher in the T2D subjects when compared to obese nondiabetic controls. Prediabetic youth did not show significantly higher AIx compared to nondiabetic youth in contrast to the aforementioned studies in T1D and T2D subjects.[45] Similar findings are seen in studies of T1D[37,42] and T2D subjects[40] with significantly lower arterial distensibility and compliance compared to controls. MRI evaluation of T2D diabetic youth found a trend toward significance in decreased aortic distensibility compared to controls.[46] Insulin resistance appeared to contribute to distensibility as the children in the lowest two tertiles of insulin resistance had significantly lower descending aortic strain and distensibility.

Global measures

Studies of global measures of vascular health in diabetic children are very limited. Dost et al. studied peripheral PP data of 46,737 children with T1D in Germany and found that peripheral PP in T1D was significantly higher than the nondiabetic control population.[47] Notably, diabetes duration, insulin dose, BMI, age, and male sex were independent determinants of PP in this study. Suláková et al. also evaluated children with T1D but used ambulatory blood pressure monitor data to find that diabetic subjects with white coat hypertension or true hypertension had significantly higher PP compared to normotensive diabetic subjects.[48] These findings suggest that diabetic subjects have impaired arterial health especially in the setting of concurrent cardiovascular risk factor such as hypertension.

Other conditions

Individuals with congenital heart disease (CHD) demonstrate abnormal large artery characteristics. Multiple studies have shown that PWV is significantly higher in subjects with Tetralogy of Fallot (TOF) compared to controls both before[49] and after[49−51] repair. Similar findings are seen in children after heart transplantation[52] and transposition of the great arteries (TGAs).[51,53] Subjects with aortic coarctation (CoA) have significantly higher PWV after repair both during childhood[51] and as adults[54] compared to controls. Measures of pulse wave analysis (PWA) are also abnormal with significantly higher AIx in adult subjects with cyanotic CHD[55] and children with TOF after repair.[50] Adult subjects with repaired with CoA had higher central SBP and lower arterial compliance compared to controls,[54] and children with TGA had higher central SBP compared to controls[53] though no difference in central SBP was found in children with TOF after repair.[53] The findings described above are important because they demonstrate that individuals with CHD have impaired arterial health even after repair which

may put them at increased risk above and beyond their CHD. However, there is evidence that physical activity may lower PWV in subjects with CHD.[56] Therapies to address these large artery impairments in individuals with CHD deserve more exploration. For a detailed review regarding arterial stiffness and pulsatile hemodynamics in CHD, the reader is referred to Chapter 47.

Renal disease is also known to affect arterial health. Children with end-stage renal disease (ESRD) requiring dialysis have significantly higher PWV[57,58] and aortic AIx[58] compared to controls. These findings persist when comparing measurements before and after dialysis[58] and continue to be elevated even 6 months after renal transplantation[59] suggesting that the vascular changes that occur in ESRD are more structural rather than functional. Acute cases of renal disease can also cause elevations in PWV that normalize after resolution of renal disease as seen in children with poststreptococcal glomerulonephritis.[60] Contrasting the findings of the previous studies, children with mild to moderate chronic kidney disease do not appear to have significant differences compared to reference values[61] or controls.[62] However, PWV does not appear to be linked merely to glomerular filtration rate as children with nephrotic syndrome but normal renal function had significantly higher PWV compared to controls. Instead, differences in arterial parameters may be explained by blood pressure.[62,63] The changes in arterial stiffness seen in children with renal disease are important to note as adult data in ESRD subjects demonstrate that PWV is an independent predictor of all-cause and CV mortality.[64]

Arterial parameters are altered in numerous other disease states. AIx is increased in subjects with cystic fibrosis,[65] and PWV is higher in adults with childhood asthma compared to nonasthmatic subjects.[66] Pulmonary arterial hypertension influences aortic stiffness with significantly higher PWV and decreased distensibility in subjects versus controls.[67] Kawasaki disease subjects have significantly increased PWV compared to controls,[68–70] and PWV was lower and AIx higher in sickle cell disease patients.[71] Subjects with Turner syndrome and bicuspid aortic valve had decreased aortic distensibility but no difference in PWV compared to controls in one study[72] whereas another study found significantly higher PWV and lower distensibility versus controls.[73] The variety of these studies demonstrates how large artery parameters can provide information regarding possible cardiovascular risk across a range of disease conditions.

Methods and normal values in children

General principles regarding methods of measurement of arterial stiffness in vivo are discussed in Chapter 7. This section deals with aspects unique or particularly relevant to measurements in children.

Pulse wave velocity

Similar to adults, measurement of PWV can be obtained through various methods. cfPWV can be assessed by placing tonometers or ultrasound probes over the carotid and femoral regions and using ECG tracings to determine the pulse time delay between measurement points with the R wave as a reference point. Another approach is to use a tonometer over the carotid and a blood pressure cuff over the thigh. To approximate the distance the pulse travels, the measured carotid-to-femoral distance can be multiplied by 80% or the sternal notch-to-carotid distance can be subtracted from the notch-to-femoral distance.[74] Brachial-ankle PWV can be assessed using blood pressure cuffs on both arms and ankles with the distance from the brachial artery to the ankle calculated by height and pulse time delay directly computed.[74] Aortic flow measurements and direct aortic measurements can also be performed using cardiac MRI to determine aortic PWV. Sinus arrhythmia in children can be a challenge when measuring the pulse wave using tonometry, and usage of the thigh cuff in assessing cfPWV may not be as accurate for children as for adults. Use of calipers in determining pulse wave distance in obese children helps to improve accuracy. The faster heart rate in children can also impact readings and depending on the age of the patient, sedation may be required for PWV measurement using MRI.

Large datasets of normative data are available in adults providing thresholds to define clinical abnormality. However, these large datasets are not available in children. The European Network for Noninvasive Investigation of Large Arteries published a large dataset of normal PWV values in 2010.[75] This study spanned eight European countries and included 11,092 subjects to determine reference values. Because the centers involved in the study obtained cfPWV through applanation tonometry using a variety of devices, measurements were then standardized prior to generating reference values. Ages were classified by decade for these values: <30, $30-39$, $40-49$, $50-59$, $60-69$, and ≥70 years. While the study included some pediatric patients (age range $15-97$ years), these patients were in the adolescent age range and the proportion of the subjects aged <18 years in the study was not specified. Nevertheless, this large study demonstrated that PWV increases progressively with age and that those in the <30 year age category had a mean (±2 SD) cfPWV of 6.2 (4.7–7.6) and median (10–90 percentile) cfPWV of 6.1 (5.3–7.1).
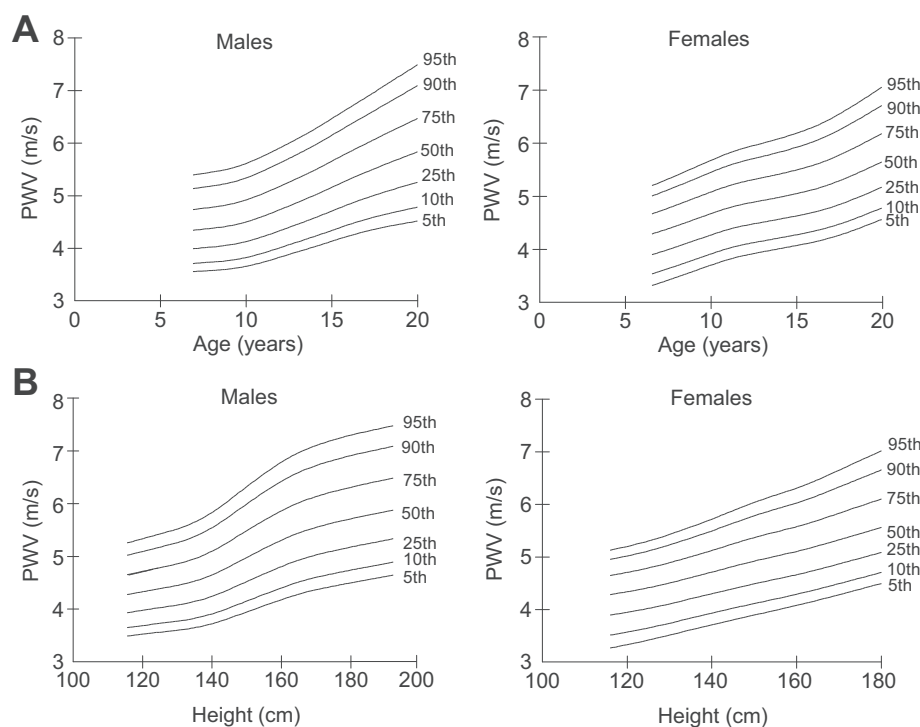
In adults, a PWV cut-off of 10 m/s was proposed, above which there is an increased risk for cardiovascular events.[76]

Unlike adult guidelines, there is no set threshold value for PWV in children as there are no longitudinal data sets tying the measurements in children to hard outcomes. There have been multiple attempts at defining age- and sex-specific reference values in children and adolescents.[77−84] However, these studies used varying techniques and devices in measuring PWV such that determining a standard set of values is difficult.
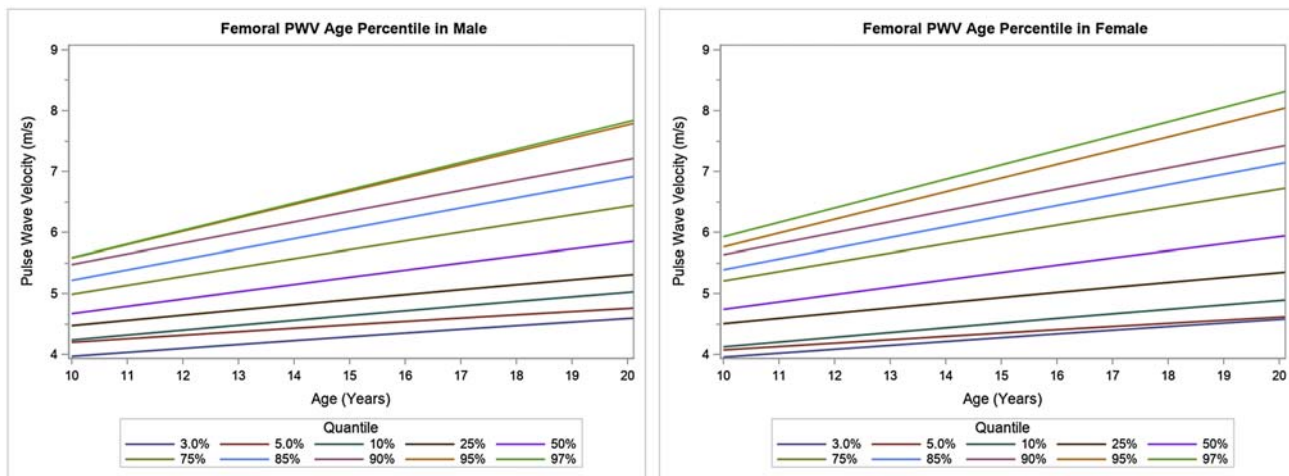
Applanation tonometry

Applanation tonometry is considered the gold standard noninvasive method of measuring PWV. The largest study in children thus far using this method was performed by Reusz et al. in 2010.[78] In this study, age- and sex-specific percentile curves were developed form measurements performed on 1008 children and adolescents measured by applanation tonometry using the PulsePen device (Fig. 43.1). cfPWV increased with age though values were similar in both boys and girls in the first two age quartiles. In the third and fourth age quartiles, cfPWV increased for boys more than for girls; however, this effect disappeared when subjects were matched for age and height. cfPWV also increased with increasing height. The population for the study consisted of Hungarian, Italian, and Algerian children so this should be considered when generalizing these values for other races/ethnicities. The Reusz et al.
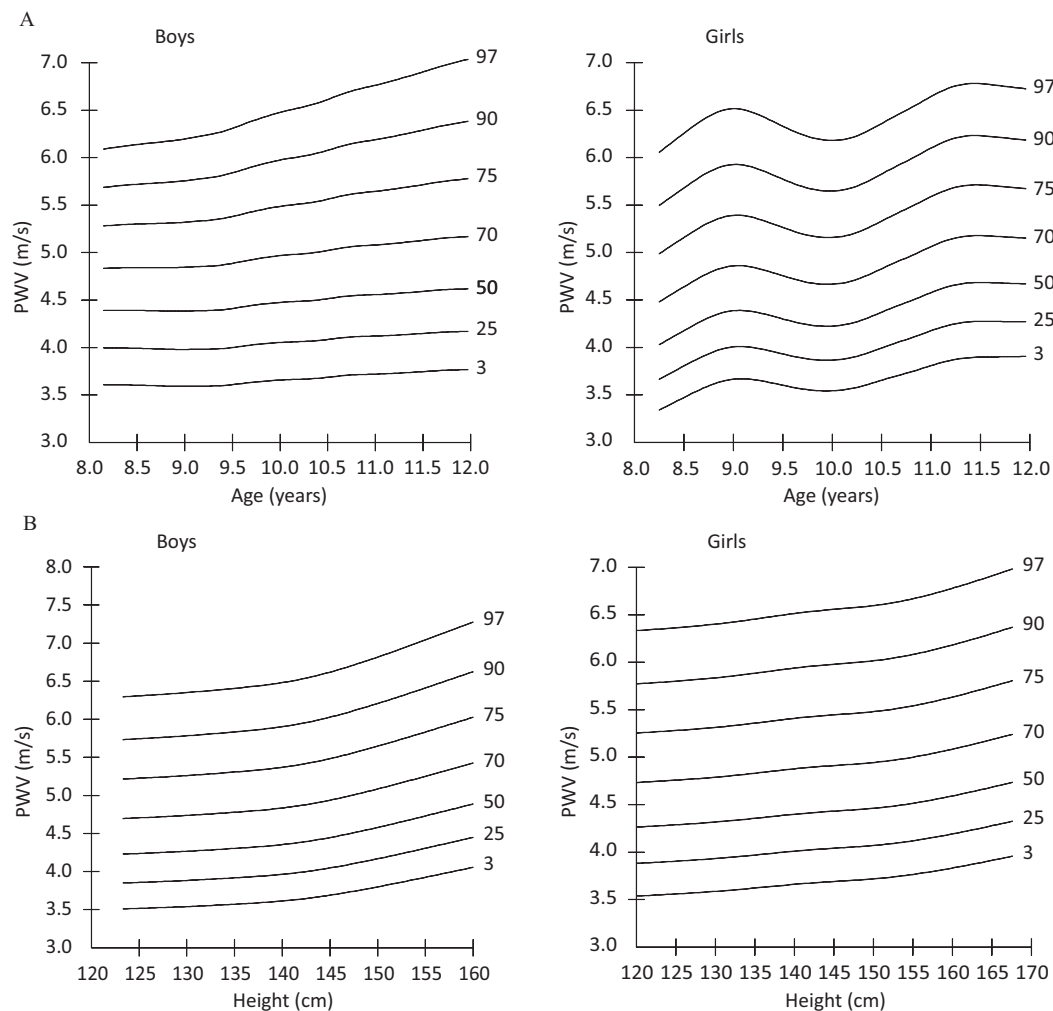
values are similar to American data adapted from Urbina et al. (unpublished data) (Fig. 43.2).[6] The 50th percentile curve is similar in both studies, but the 5th and 95th percentile curves are slightly higher in the Urbina et al. data. A smaller study by Curcio et al. used applanation tonometry to obtained cfPWV in Uruguayan children.[85] Similarly to Reusz et al., the authors found that cfPWV was similar in boys and girls during the prepubescent age range but that PWV increased more in boys after that period. Mora-Urda et al. also used applanation tonometry to measure cfPWV and create percentile curves for healthy Spanish children aged 8−11 years based on 350 subjects (Fig. 43.3).[80] Compared to the percentiles curves by Reusz et al. and Urbina et al., the 50th percentile curves are similar, but the 90th and 97th percentile curves are slightly higher. Additionally, there is a mild decrease in cfPWV in girls around age 10 years in the Mora-Urda et al. study that is not evident in the Reusz et al. curves. When comparing cfPWV by height, the values from Mora-Urda et al. rise with increasing height similarly to the values from the Reusz et al. study. The 50th percentile curves for boys and girls are similar at the shorter heights but are less in the Mora-Urda et al. study with increasing height. Boys and girls at the 90th percentile of height in the Mora-Urda et al. study have higher cfPWV at shorter heights but then are similar at 160 cm to values from Reusz et al.

FIGURE 43.1 Carotid-femoral pulse wave velocity (PWV) percentile curves assessed by applanation tonometry using PulsePen device according to age (A) and height (B). Subjects were from Hungary, Italy, and Algeria. *Reprinted by permission from Wolters Kluwer Health, Inc. Reusz GS, Cseprekal O, Temmar M, et al. Reference values of pulse wave velocity in healthy children and teenagers. **Hypertension**. 2010; 56:217−224. https://doi.org/10.1161/HYPERTENSIONAHA.110.152686.*

FIGURE 43.2 Carotid-femoral pulse wave velocity (PWV) percentile curves by applanation tonometry using SphygmoCor device according to age. Subjects were from the United States. *Unpublished data adapted from Urbina EM, Kimball TR, Khoury PR, Daniels SR, Dolan LM. Increased arterial stiffness is found in adolescents with obesity or obesity-related type 2 diabetes mellitus.* **J Hypertension**. *2010; 28:1692−1698.* https://doi.org/10.1097/HJH.0b013e32833a6132.
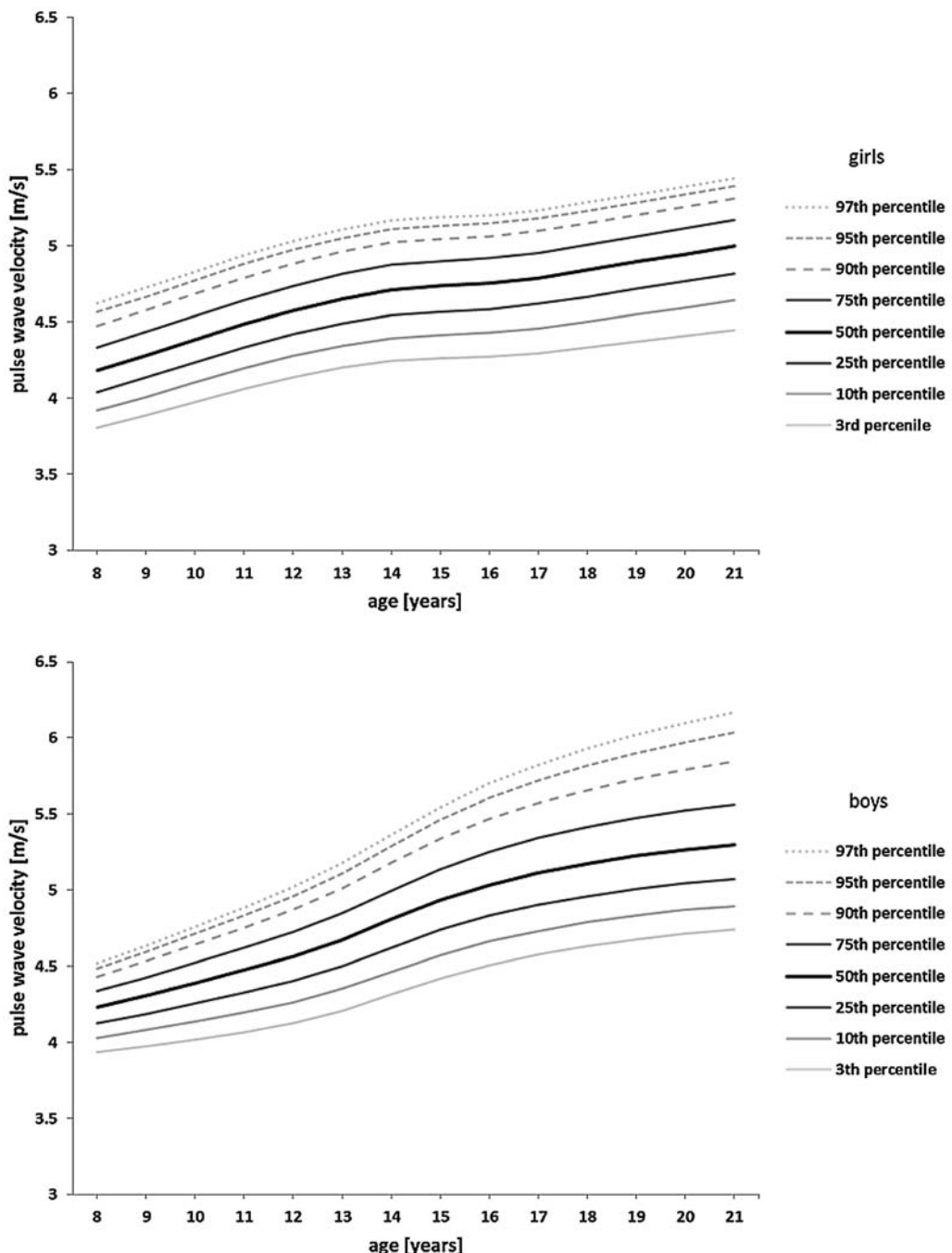
FIGURE 43.3 Carotid-femoral pulse wave velocity (cfPWV) percentile curves by applanation tonometry using SphygmoCor device according to sex and age (A) and height (B) in healthy children (N = 277). Subjects were from Spain. *Reprinted by permission from John Wiley and Sons. Mora-Urda AI, Molina MDCB, Mill JG. Montero-López P. Carotid-femoral pulse wave velocity in healthy Spanish children: reference percentile curves.* **J Clinic Hypertens**. *2017; 19:227−234.* https://doi.org/10.1111/jch.12899.
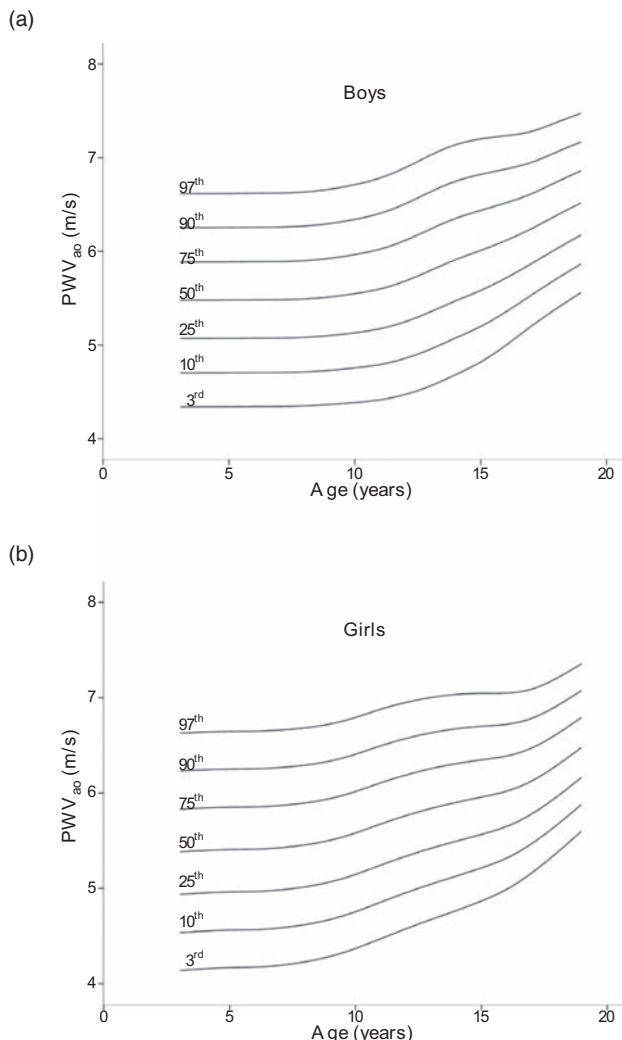
Oscillometric devices

Oscillometric devices for measuring PWV have also become popular due to relative ease of use compared to applanation tonometry.[81–84] Two German studies used the Vicorder device to determine cfPWV in a pediatric cohort using a carotid and femoral cuff[82] and a combined group of adults and children using a carotid plethysmograph and a femoral cuff.[86] Elmenhorst et al. studied German children with the Mobil-O-Graph, which use a single brachial cuff, to measure PWV in 1445 subjects (Fig. 43.4). The authors found that while PWV increased with age and height, there were different trajectories between boys and girls that were potentially explained by different growth patterns. Two other large studies used the Arteriograph device to determine normal values with Hidvégi et al. obtaining PWV measurements in 3374 Hungarian children (Fig. 43.5)[81] and Diaz et al. measuring PWV in 1000 Argentinean children

FIGURE 43.4   Pulse wave velocity percentile curves by brachial oscillometry using Mobil-O-Graph device according to age, displayed separately for girls and boys. *Reprinted from Elmenhorst J, Hulpke-Wette M, Barta C, Dalla Pozza R, Springer S, Oberhoffer R. Percentiles for central blood pressure and pulse wave velocity in children and adolescents recorded with an oscillometric device.* **Atherosclerosis.** *238:9–16, Copyright 2015, with permission from Elsevier.* https://doi.org/10.1016/j.atherosclerosis.2014.11.005.

(a)

(b)

FIGURE 43.5 Pulse wave velocity smoothed percentile curves by brachial oscillometry using Arteriograph device according to age for boys (A) and girls (B). *Reprinted by permission from Wolters Kluwer Health, Inc. Hidvégi EV, Illyés M, Benczúr B, et al. Reference values of aortic pulse wave velocity in a large healthy population aged between 3 and 18 years.* **J Hypertens**. *2012; 30:2314−2321. https://doi.org/10.1097/HJH.0b013e328359562c.*

(Fig. 43.6).[84] The 50th percentile values from Diaz et al. and Hidvégi et al. are similar, but the 90th and 10th percentile lines are slightly higher in the Hidvégi et al. study. The percentile curves obtained by Elmenhorst et al. are lower overall than the other two studies which may be a function of using the Mobil-O-Graph device instead of the Arteriograph. Despite the availability of normative data from these methods, it should be noted that single site oscillometry is not a reliable method to estimate aortic PWV.

Cardiac magnetic resonance imaging

Cardiac MRI measures of PWV in children are limited. Voges et al. used MRI flow data to develop normative curves for aortic PWV in children and young adults

(Fig. 43.7).[77] In addition to using a different modality, the PWV measurements obtained in this study were of the aortic arch only (ascending-to-descending aorta) which may contribute to the overall lower measurements compared to PWV values by applanation tonometry or oscillometry. Additionally, the study was relatively small (n = 71) compared to studies measuring PWV by applanation tonometry or oscillometry.

Sex-specific differences in pulse wave velocity
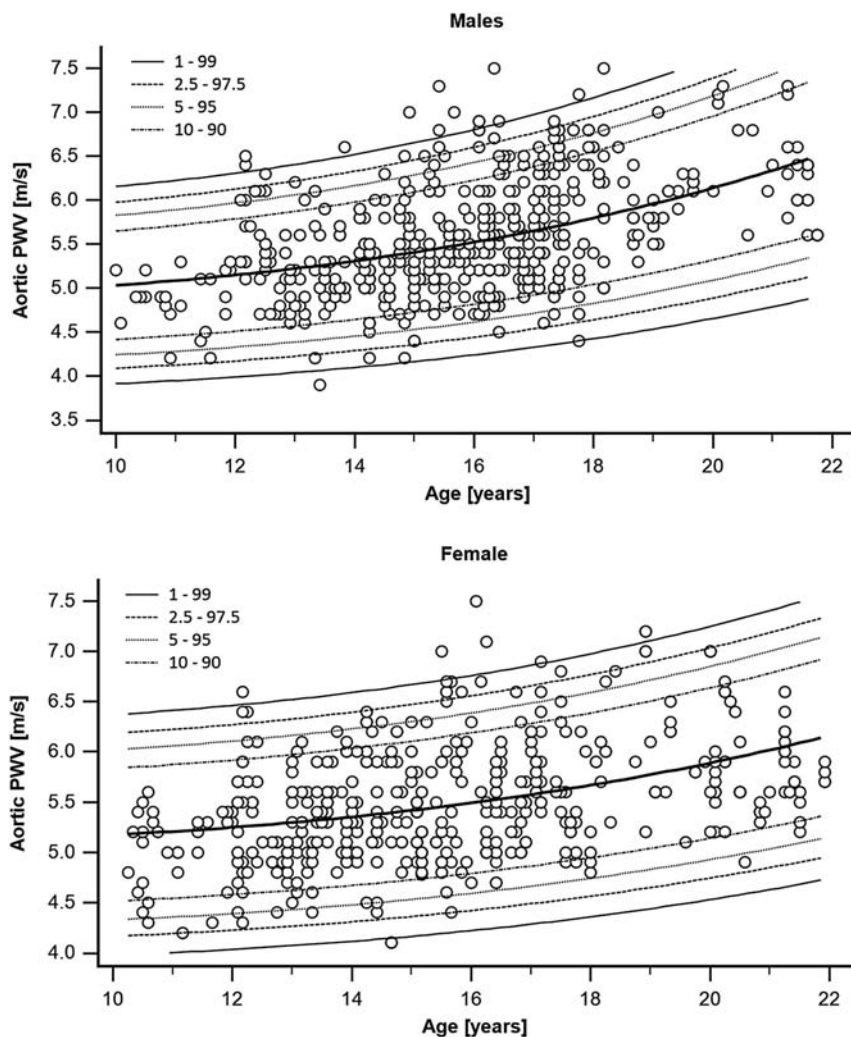
In prepubescent children, there appears to be no difference in PWV between males and females. However, after puberty, PWV is higher in males. These findings have been replicated in multiple studies encompassing PWV measurements by applanation tonometry[78] and oscillometry[82−84] though one large oscillometric study found no significant difference in PWV values between sexes.[81] The higher PWV values in males after puberty can be explained by the overall greater height and weight at those ages compared to females.[78,83,84] Indeed when subjects were matched by age and height[78] or by age, anthropometric values, and hemodynamic values,[84] no sex-specific differences were evident.

Race-specific differences in pulse wave velocity
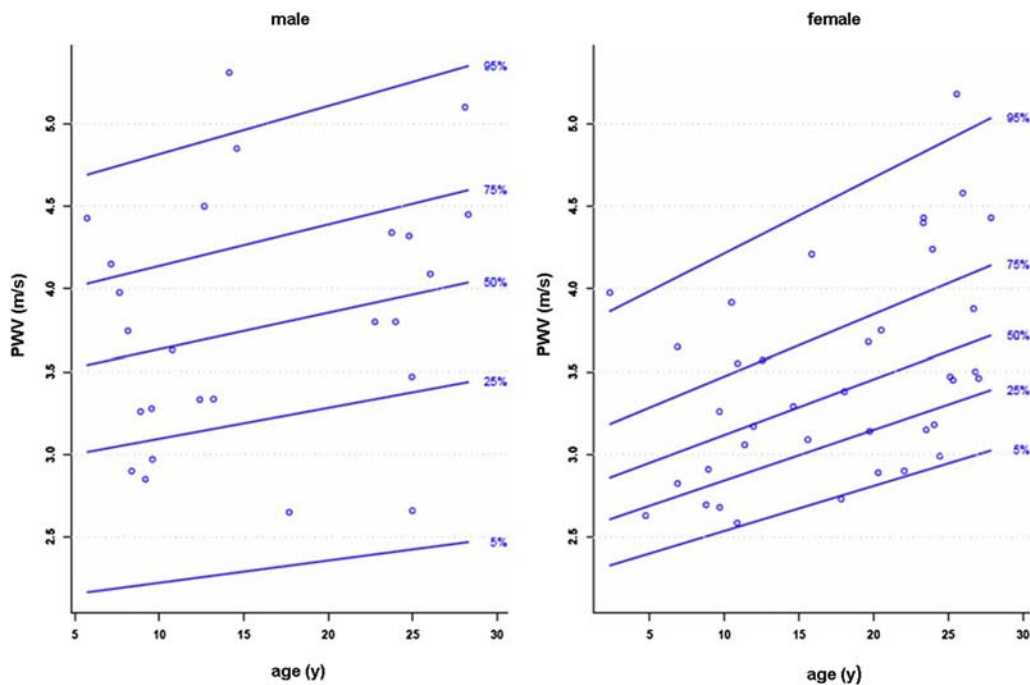
cfPWV in African-American men has been noted to be higher compared to cfPWV measurements in white men.[87] These findings are mirrored in children as well with Lefferts et al. comparing cfPWV by applanation tonometry in 54 African-American children compared to 54 white children.[88] While the African-American children were taller and heavier than the white children, cfPWV was higher in the African-American children even after multivariable adjustment that included height. A large study of 791 children by Zaniqueli et al. studied Brazilian children and adolescents comparing the cfPWV by applanation tonometry in Blacks (n = 211) versus Non-Blacks (n = 560).[89] There was no difference in cfPWV between groups during the prepubescent time period, but cfPWV was significantly higher in blacks during the pubescent and postpubescent phases after adjustment for sex, age, height, BMI, SBP, and heart rate.

Conclusions about pulse wave velocity normal values

Measurement of arterial stiffness in youth is now established as a robust method for evaluating CV risk, but there is still a lack of normative data across age, population, and device. More research into defining this normative data is needed before arterial stiffness can be incorporated into care for pediatric patients.

FIGURE 43.6 Age-specific Aortic pulse wave velocity (PWV) percentiles in male population (n = 560) and female population (n = 440). *Reprinted by permission from Taylor & Francis Ltd, http://www.tandfonline.com. Díaz A, Zócalo Y, Bia D, Sabino F, Rodríguez V, Cabrera Fischer EI. Reference intervals of aortic pulse wave velocity assessed with an oscillometric device in healthy children and adolescents from Argentina.* **Clin Exp Hypertens**. *2019; 41:101−112. https://doi.org/10.1080/10641963.2018.1445754.*
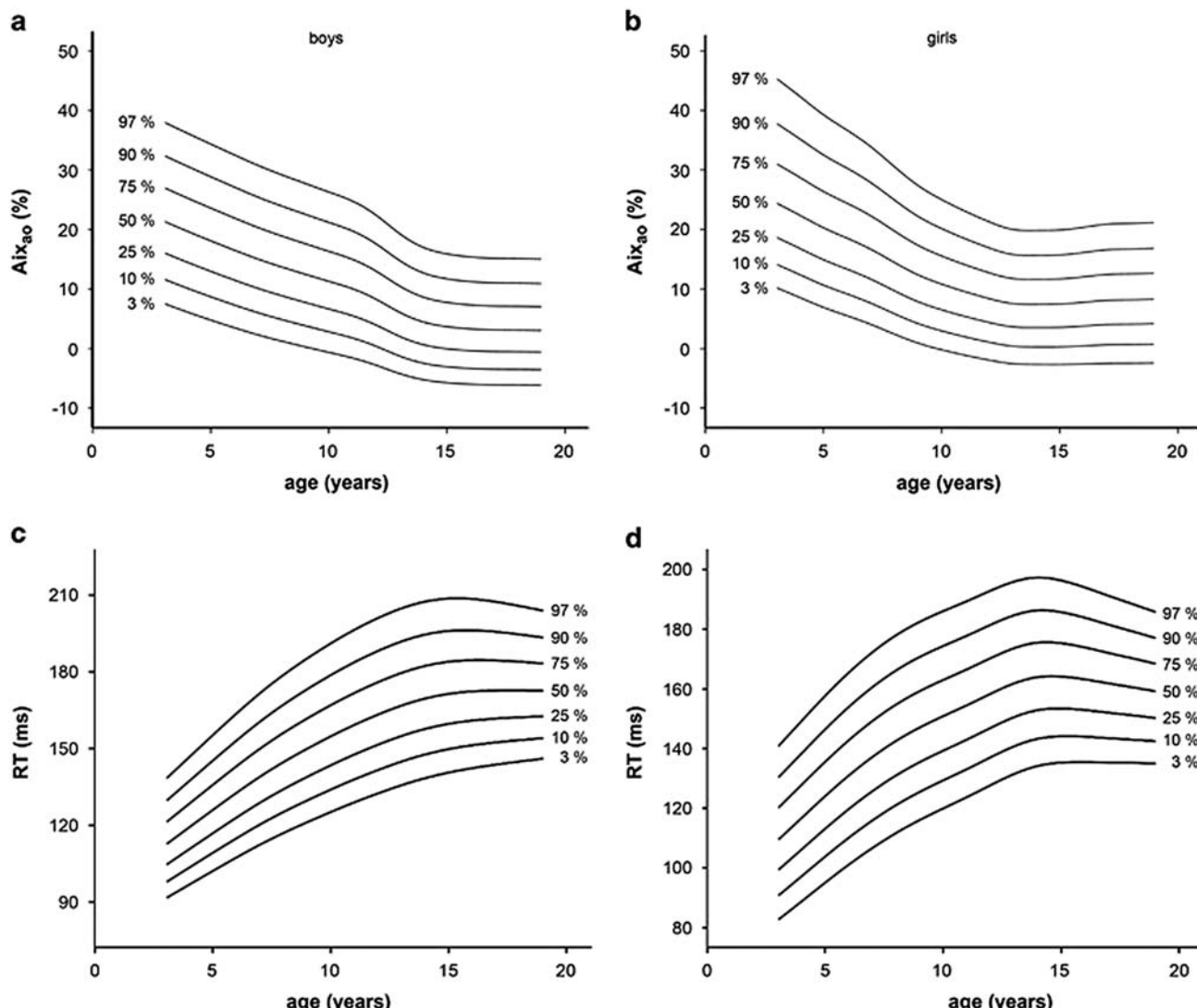
FIGURE 43.7 Gender-specific reference percentiles for pulse wave velocity (PWV) in the aortic arch assessed by cardiac magnetic resonance imaging (MRI). *Reprinted by permission from Springer Nature. Voges I, Jerosch-Herold M, Hedderich J, et al. Normal values of aortic dimensions, distensibility, and pulse wave velocity in children and young adults: a cross-sectional study.* **J Cardiovasc Magn Reson**. *2012; 14:77. https://doi.org/10.1186/1532-429X-14-77.*

Pulse wave analysis

PWA is typically obtained in children, similarly to adults, by using oscillometric or tonometric devices to determine the central arterial PP waveform. However, invasive measurement of the central waveform by cardiac catheterization is also performed. Using the central PP waveform, augmentation index and other parameters such as augmentation pressure (AP), component waveforms (Pf, Pb), and central blood pressure can be determined as measures of arterial health. The faster heart rate in children and heart rate variability with respiration (sinus arrhythmia) can make measurements challenging in children. Additionally, it may be more technically challenging to take radial artery measurements using a tonometer due to the smaller size of the artery. Appropriate cuff sizing for younger children is another potential challenge as the devices are typically designed for adults.

More robust literature exists in children for reference values of augmentation index whereas there are no established reference values for Pf or Pb. Murakami et al. assessed AIx by direct cardiac catheterization measurements in Japanese subjects and found that AIx was highest in infancy and early childhood and that it steadily decreased until approximately age 15 years when values then plateaued and then increased afterward in early adulthood.[90] These findings were confirmed using oscillometry by Hidvegi et al. in a large study of 4619 Hungarian subjects (age range 3−18 years) with AIx decreasing from early childhood until subjects reached puberty.[91] Return time of the systolic wave reflection was also found to be shorter in younger children due to shorter aortic length. This finding explains the greater AIx values in younger children as the sooner return of the systolic wave reflection results in greater wave augmentation. Reference curves for AIx from Hidvegi et al. are shown in Fig. 43.8.

FIGURE 43.8 Smoothed percentile curves from 3rd to 97th of aortic augmentation index (Aix$_{ao}$) and return time (RT) related with age for boys (A and C) and girls (B and D). *Reprinted by permission from Springer Nature. Hidvégi EV, Illyés M, Molnár FT, Cziráki A. Influence of body height on aortic systolic pressure augmentation and wave reflection in childhood.* **J Hum Hypertens.** *2015; 9:495−501.* https://doi.org/10.1038/jhh.2014.118.

Diaz et al. also determined normal AIx values in children but used applanation tonometry in a large study of 1038 Argentinean subjects (age range 5−22 years).[92] Their findings mirrored those of Murakami et al. and Hidvégi et al. with reference curves shown in Fig. 43.9. AIx values for girls were higher than in boys for both studies. It is important to note the different racial/ethnic backgrounds of the subjects in the previously mentioned studies when attempting to generalize findings to other races/ethnicities.

Distensibility
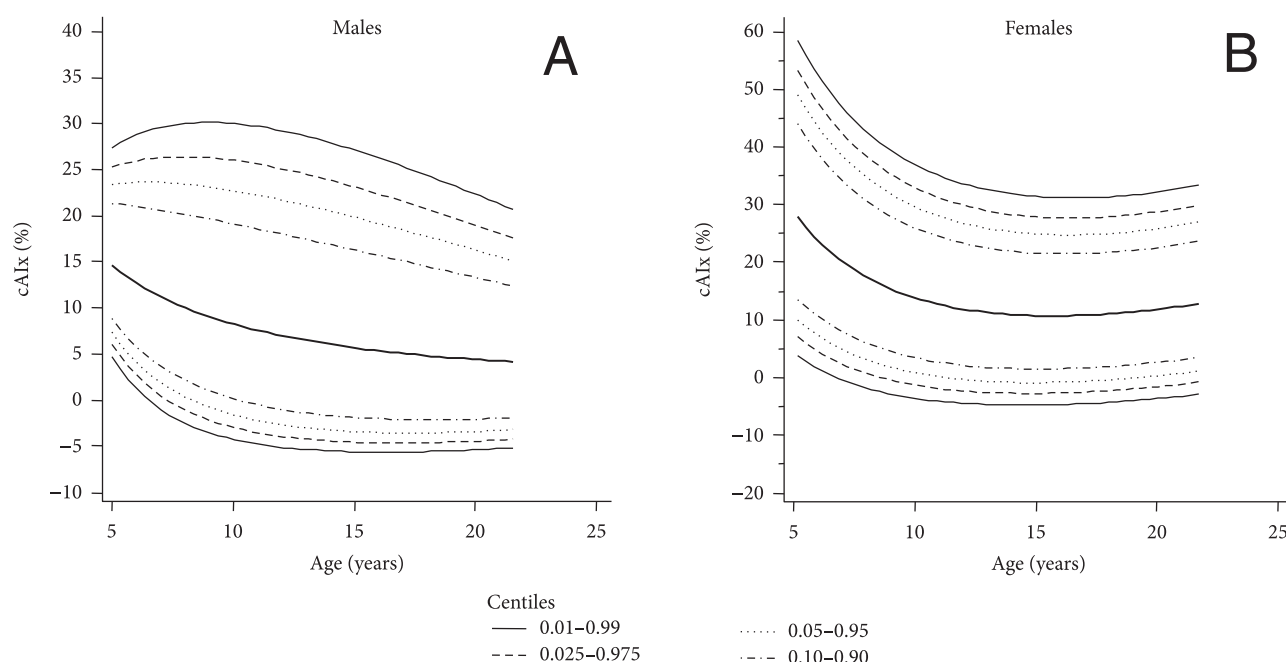
Arterial distensibility can be assessed through multiple methods ranging from oscillometry, ultrasound, and MRI. Challenges in children with these methods are similar to those seen in determining PWV and PWA and include difficulty with correct cuff sizing due to younger/smaller subjects, children having faster heart rates and potential sinus arrhythmia, technical challenges of children having smaller arteries and potentially having more compressible arteries, and the possible need for sedation if using MRI.

Reference data for arterial distensibility in children exist for ultrasound and MRI modalities. Doyon et al. created sex-specific reference charts for carotid distensibility coefficient determined by ultrasound that are normalized to age using data from 1051 children (age range 6−18 years). The general trend appears to be that carotid distensibility decreases with age in both boys and girls (Fig. 43.10G and H). The authors noted that age- and sex-specific differences
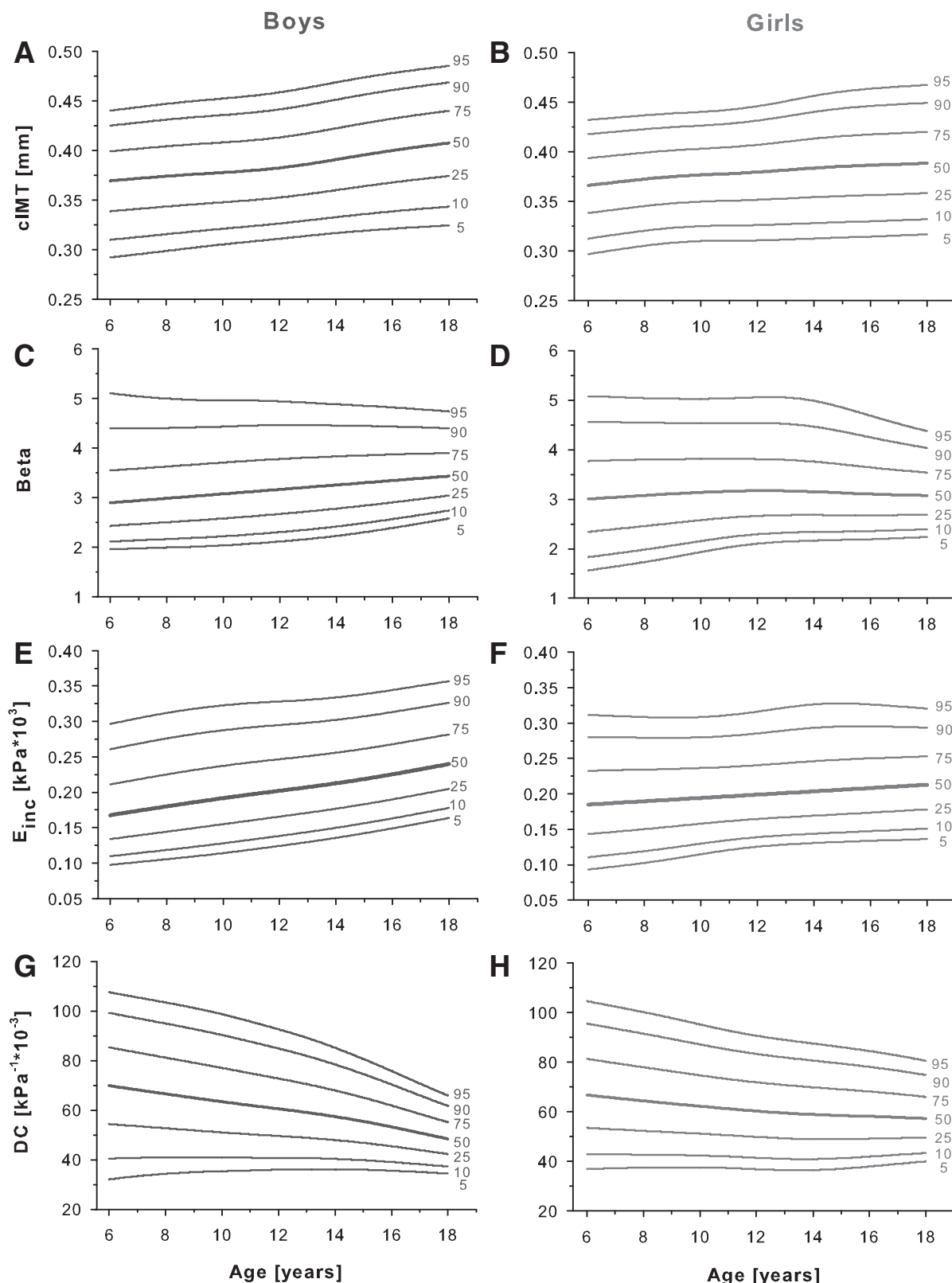
started to appear at age 15 years and with carotid distensibility for boys decreasing more steeply than girls after that age.

Mikola et al. assessed carotid and abdominal aortic distensibility longitudinally in children by ultrasound and found that distensibility was significantly lower in boys compared to girls in both regions and that distensibility significantly decreased with age. Measurements were taken at 11, 13, 15, 17, and 19 years of age.[93] However, when adjusted for PP, the differences between sexes disappeared suggesting that PP may be driving the differences rather than arterial diameter.
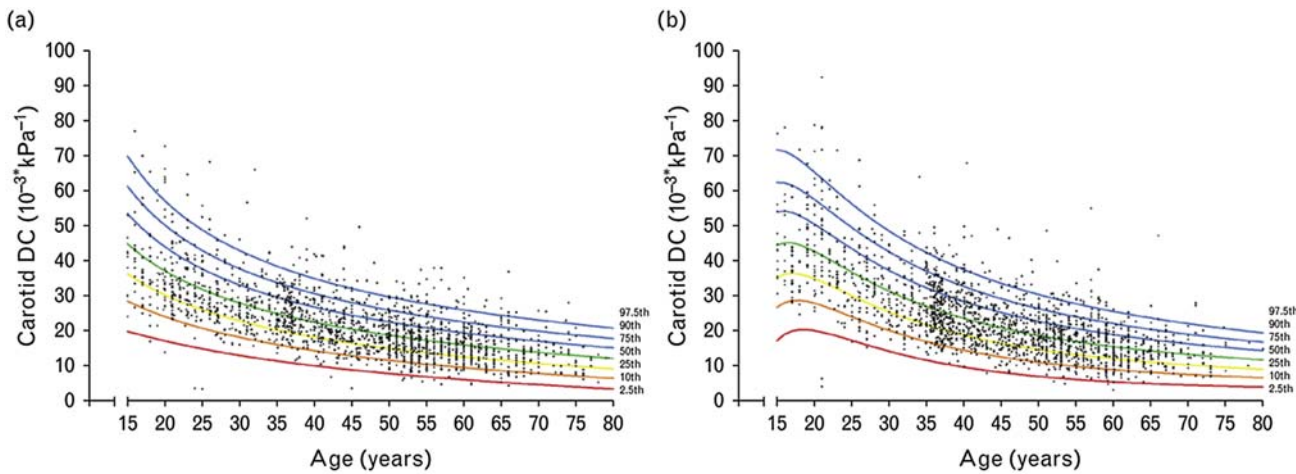
Engelen et al. compiled carotid distensibility coefficient values assessed by echo-tracking across 24 studies to create age- and sex-specific reference curves from 3601 healthy individuals.[94] While the majority of the data were of adult subjects, data from late adolescents were included and can be seen in Fig. 43.11. The same group also compiled data from seven studies with femoral artery distensibility values to create age-specific reference curves from 1489 healthy individuals.[95] Again, the majority of the data were from adults but data from late adolescents were also included. Contrasting the findings of the carotid distensibility coefficient data, femoral artery distensibility appears to be stable over time without major changes until the 6th decade of life. When comparing the carotid distensibility coefficient values between the Doyon et al. study and the Engelen et al. data, the carotid distensibility coefficient values were higher overall for both males and females in the Doyon

FIGURE 43.9 Age-specific central (aortic) augmentation index (cAIx) percentiles corresponding to male cohort (n = 576) (A) and female cohort (n = 462) (B) of children and adolescents. *Reprinted by permission through the Creative Commons Attribution License. Diaz A, Zócalo Y, Bia D, Cabrera Fischer E. Reference intervals of central aortic blood pressure and augmentation index assessed with an oscillometric device in healthy children, adolescents, and young adults from Argentina.* **Int J Hypertens**. *2018; 2018:1469651. https://doi.org/10.1155/2018/1469651.*

FIGURE 43.10 Sex-specific percentile curves for carotid intima-media thickness (cIMT, mm; A and B), β (C and D), incremental modulus of elasticity (Einc, kPa $\times 10^3$; E and F), and distensibility coefficient (DC, kPa^{-1} $\times 10^{-3}$; G and H) according to age. *Reprinted by permission from Wolters Kluwer Health, Inc. Doyon A, Kracht D, Bayazit AK, et al. Carotid artery intima-media thickness and distensibility in children and adolescents: reference values and role of body dimensions.* **Hypertension.** *2013; 62:550−556.* https://doi.org/10.1161/HYPERTENSIONAHA.113.01297.
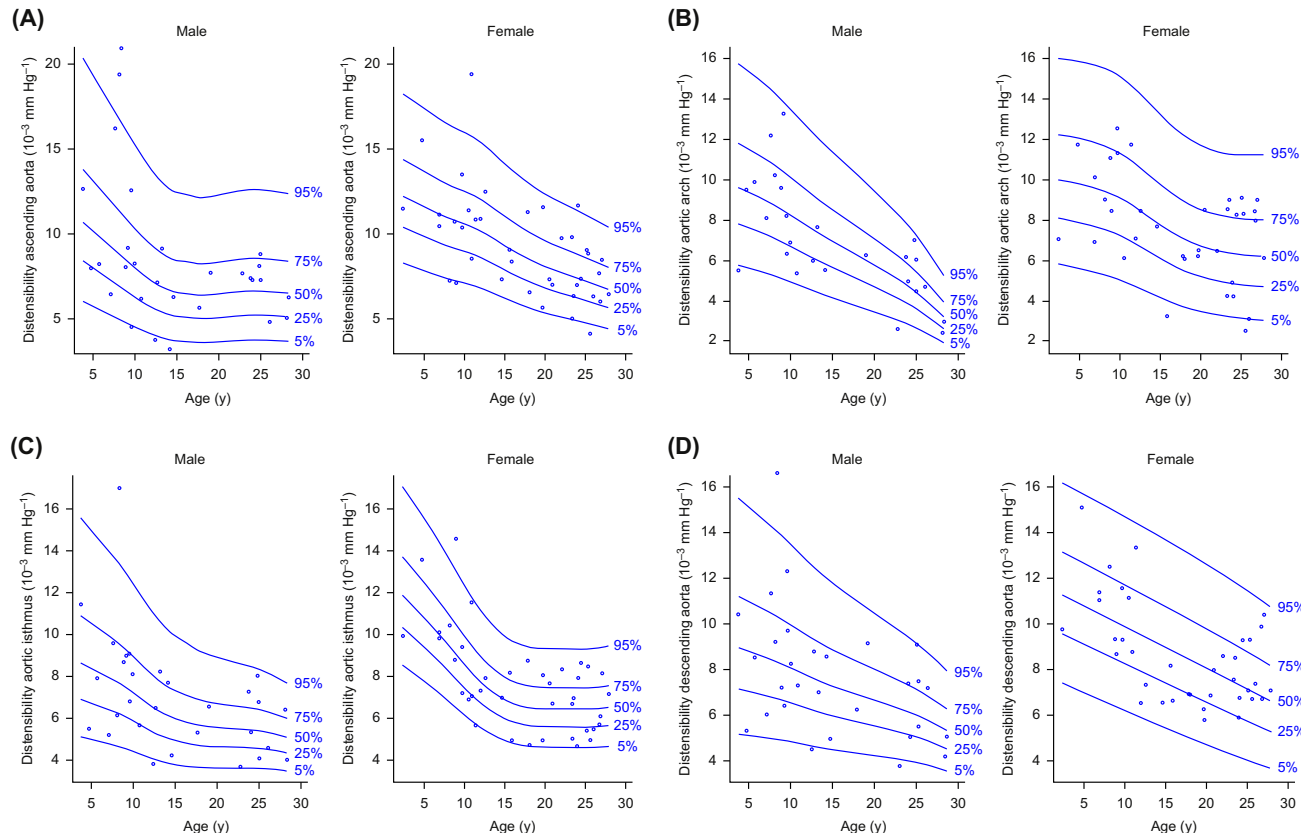
FIGURE 43.11   Age-specific percentiles of carotid DC in the healthy subpopulation. (A) men; (B) women. *DC*, distensibility coefficient. *Reprinted by permission from Wolters Kluwer Health, Inc. Engelen L, Bossuyt J, Ferreira I, et al. Reference values for local arterial stiffness. Part A: carotid artery. **J Hypertens**. 2015; 33:1981−1996. https://doi.org/10.1097/HJH.0000000000000654.*

et al. study. These differences may be explained by the use of ultrasound to measure distensibility in Doyon et al. group versus the echo-tracking technique used in the Engelen et al. study.

Cardiac MRI data are limited regarding reference values of aortic distensibility in children. However, Voges et al.

created gender-specific reference percentiles for aortic distensibility in multiple regions of the aorta as seen in Fig. 43.12.[96] While distensibility decreases with increasing age similarly to the findings by ultrasound, the ascending aortic distensibility in males appears to decrease more drastically with age compared to that seen in females, and
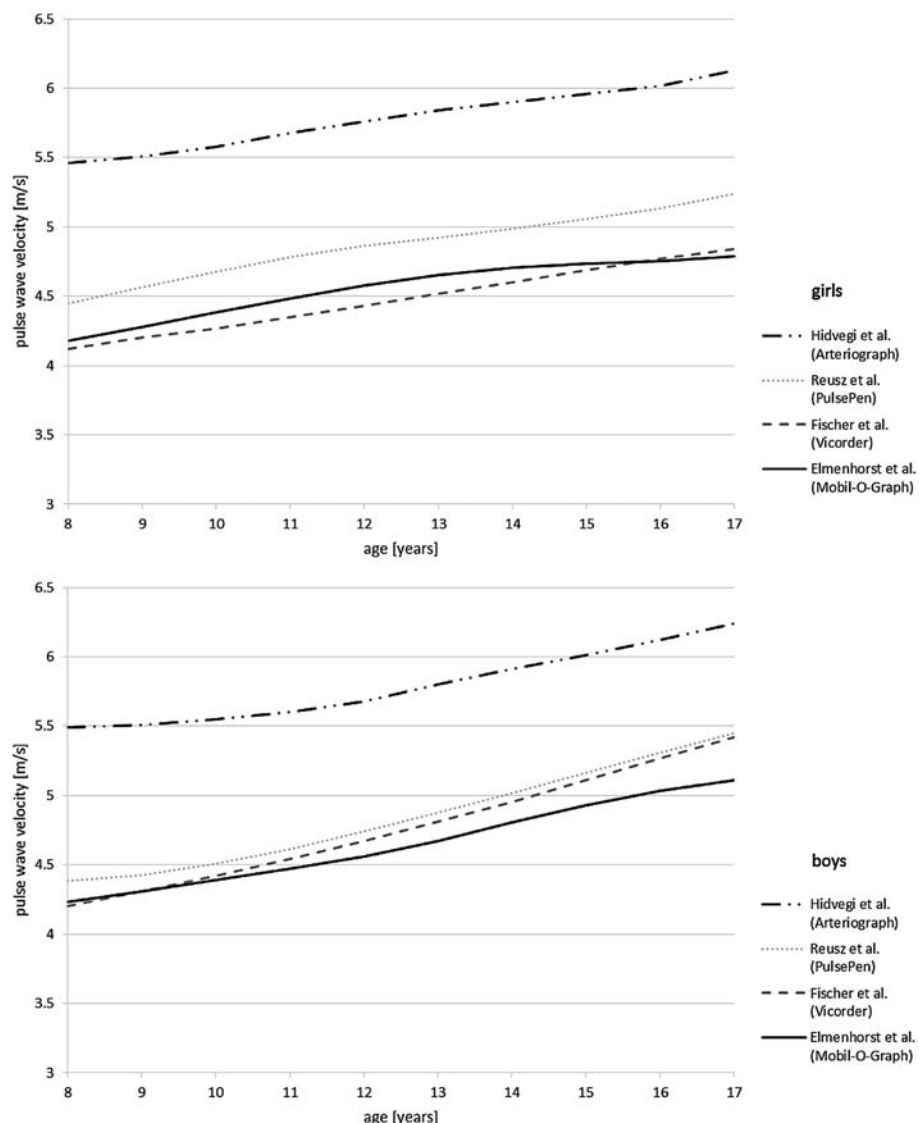
FIGURE 43.12   Gender-specific reference percentiles for aortic distensibility at four locations: (A) ascending aorta, (B) aortic arch, (C) aortic isthmus, and (D) descending aorta above the diaphragm. *Reprinted by permission from Springer Nature. Voges I, Jerosch-Herold M, Hedderich J, et al. Normal values of aortic dimensions, distensibility, and pulse wave velocity in children and young adults: a cross-sectional study. **J Cardiovasc Magn Reson**. 2012; 14:77. https://doi.org/10.1186/1532-429X-14-77.*

the aortic isthmus distensibility undergoes a steeper decline in both males and females compared to the aortic arch and descending aortic regions.

Future directions

As more advanced and direct methods of assessing arterial health have been developed such as PWV, PWA, and arterial distensibility, global measures of arterial health such as PP are used less often in favor of the other modalities mentioned above. As demonstrated in this text, while there are some pediatric data on reference values for measures of arterial health, they are limited in comparison to adult data. More normative data are needed across race,

sex, and ethnicity in children to provide better understanding of normal differences. Calibration of measurements between devices for children is also an area of potential focus as this will allow easier conversion/comparison of readings for patients. Some of the considerable differences in PWV by device can be seen in Fig. 43.13. Additionally, longitudinal data of arterial measures in children are needed to show what normal change in arterial stiffness is in children. The need for accurate assessment of arterial health in children remains with the hope that increased and better normative data will allow use of these measures to more accurately risk stratify patients with CV risk factors and be a tool toward helping children live longer, healthier lives.

FIGURE 43.13   Comparison between the 50th percentiles for pulse wave velocity (PWV) obtained with different devices (Arteriograph [79], PulsePen [76], Vicorder [80], and Mobil-O-Graph [81]) displayed separately for girls and boys. *Reprinted from Elmenhorst J, Hulpke-Wette M, Barta C, Dalla Pozza R, Springer S, Oberhoffer R. Percentiles for central blood pressure and pulse wave velocity in children and adolescents recorded with an oscillometric device.* **Atherosclerosis**. *238:9−16, Copyright 2015, with permission from Elsevier.* https://doi.org/10.1016/j.atherosclerosis.2014.11.005.

References

1. Cocciolone AJ, Hawes JZ, Staiculescu MC, Johnson EO, Murshed M, Wagenseil JE. Elastin, arterial mechanics, and cardiovascular disease. **Am J Physiol Heart Circ Physiol**. 2018; 315(2):H189−h205.

2. Wagenseil JE, Mecham RP. Vascular extracellular matrix and arterial mechanics. **Physiol Rev**. 2009; 89(3):957−989.

3. Expert Panel on Integrated Guidelines for Cardiovascular Health and Risk Reduction in Children and Adolescents, National Heart Lung, and Blood Institute. Expert panel on integrated guidelines for cardiovascular health and risk reduction in children and adolescents: summary report. **Pediatrics**. 2011; 128(Suppl 5):S213−S256.

4. Cote AT, Phillips AA, Harris KC, Sandor GGS, Panagiotopoulos C, Devlin AM. Obesity and arterial stiffness in children: systematic review and meta-analysis. **Arterioscler Thromb Vasc Biol**. 2015; 35(4):1038−1044.

5. Hudson LD, Rapala A, Khan T, Williams B, Viner RM. Evidence for contemporary arterial stiffening in obese children and adolescents using pulse wave velocity: a systematic review and meta-analysis. **Atherosclerosis**. 2015; 241(2):376−386.

6. Urbina EM, Kimball TR, Khoury PR, Daniels SR, Dolan LM. Increased arterial stiffness is found in adolescents with obesity or obesity-related type 2 diabetes mellitus. **J Hypertens**. 2010; 28(8):1692−1698.

7. Caterini JE, Banks L, Wells GD, et al. Magnetic resonance imaging reveals elevated aortic pulse wave velocity in obese and overweight adolescents. **Clin Obes**. 2017; 7(6):360−367.

8. Sletner L, Mahon P, Crozier SR, et al. Childhood fat and lean mass: differing relations to vascular structure and function at age 8 to 9 years. **Arterioscler Thromb Vasc Biol**. 2018; 38(10):2528−2537.

9. Urbina EM, Kimball TR, Khoury PR, Daniels SR, Dolan LM. Increased arterial stiffness is found in adolescents with obesity or obesity-related type 2 diabetes mellitus. **J Hypertens**. 2010; 28(8):1692−1698.

10. Pierce GL, Zhu H, Darracott K, et al. Arterial stiffness and pulse-pressure amplification in overweight/obese African-American adolescents: relation with higher systolic and pulse pressure. **Am J Hypertens**. 2013; 26(1):20−26.

11. Castro JM, Garcia-Espinosa V, Curcio S, et al. Childhood obesity associates haemodynamic and vascular changes that result in increased central aortic pressure with augmented incident and reflected wave components, without changes in peripheral amplification. **Int J Vasc Med**. 2016; 2016:3129304.

12. Pierce GL, Pajaniappan M, DiPietro A, Darracott-Woei ASK, Kapuku GK. Abnormal central pulsatile hemodynamics in adolescents with obesity: higher aortic forward pressure wave amplitude is independently associated with greater left ventricular mass. **Hypertension**. 2016; 68(5):1200−1207.

13. Banach AM, Peralta-Huertas J, Livingstone K, et al. Arterial distensibility is reduced in overweight pre- and early pubescent children. **Eur J Pediatr**. 2010; 169(6):695−703.

14. Mikola H, Pahkala K, Niinikoski H, et al. Cardiometabolic determinants of carotid and aortic distensibility from childhood to early adulthood. **Hypertension**. 2017; 70(2):452−460.

15. Shah AS, Dolan LM, Khoury PR, Gao Z, Kimball TR, Urbina EM. Severe obesity in adolescents and young adults is associated with subclinical cardiac and vascular changes. **J Clin Endocrinol Metab**. 2015; 100(7):2751−2757.

16. Whincup PH, Gilg JA, Donald AE, et al. Arterial distensibility in adolescents: the influence of adiposity, the metabolic syndrome, and classic risk factors. **Circulation**. 2005; 112(12):1789−1797.

17. de Simone G, Devereux RB, Daniels SR, et al. Stroke volume and cardiac output in normotensive children and adults. Assessment of relations with body size and impact of overweight. **Circulation**. 1997; 95(7):1837−1843.

18. Chandramohan G, Kalantar-Zadeh K, Kermah D, Go SC, Vaziri ND, Norris KC. Relationship between obesity and pulse pressure in children: results of the National Health and Nutrition Survey (NHANES) 1988-1994. **J Am Soc Hypertens**. 2012; 6(4):277−283.

19. Zachariah JP, Graham DA, de Ferranti SD, Vasan RS, Newburger JW, Mitchell GF. Temporal trends in pulse pressure and mean arterial pressure during the rise of pediatric obesity in US children. **J Am Heart Assoc**. 2014; 3(3):e000725.

20. Riggio S, Mandraffino G, Sardo MA, et al. Pulse wave velocity and augmentation index, but not intima-media thickness, are early indicators of vascular damage in hypercholesterolemic children. **Eur J Clin Invest**. 2010; 40(3):250−257.

21. Tran A, Burkhardt B, Tandon A, et al. Pediatric heterozygous familial hypercholesterolemia patients have locally increased aortic pulse wave velocity and wall thickness at the aortic root. **Int J Cardiovasc Imaging**. 2019; 35(10):1903−1911.

22. Soljanlahti S, Autti T, Vuorio AF, Keto P, Turtola H, Lauerma K. Aorta of young and middle-aged heterozygous familial hypercholesterolemia patients shows no functional or morphological impairment assessed by MRI. **Vasc Health Risk Manag**. 2008; 4(4):923−929.

23. Ershova AI, Meshkov AN, Rozhkova TA, et al. Carotid and aortic stiffness in patients with heterozygous familial hypercholesterolemia. **PLoS One**. 2016; 11(7):e0158964.

24. Urbina EM, Khoury PR, McCoy CE, Dolan LM, Daniels SR, Kimball TR. Triglyceride to HDL-C ratio and increased arterial stiffness in children, adolescents, and young adults. **Pediatrics**. 2013; 131(4):e1082−1090.

25. Totaro S, Khoury PR, Kimball TR, Dolan LM, Urbina EM. Arterial stiffness is increased in young normotensive subjects with high central blood pressure. **J Am Soc Hypertens**. 2015; 9(4):285−292.

26. Lehmann ED, Watts GF, Fatemi-Langroudi B, Gosling RG. Aortic compliance in young patients with heterozygous familial hypercholesterolaemia. **Clin Sci.** 1992; 83(6):717−721.

27. Aggoun Y, Bonnet D, Sidi D, et al. Arterial mechanical changes in children with familial hypercholesterolemia. **Arterioscler Thromb Vasc Biol**. 2000; 20(9):2070−2075.

28. Pitsavos C, Toutouzas K, Dernellis J, et al. Aortic stiffness in young patients with heterozygous familial hypercholesterolemia. **Am Heart J**. 1998; 135(4):604−608.

29. Wilkinson IB, Prasad K, Hall IR, et al. Increased central pulse pressure and augmentation index in subjects with hypercholesterolemia. **J Am Coll Cardiol**. 2002; 39(6):1005−1011.

30. Kulsum-Mecci N, Goss C, Kozel BA, Garbutt JM, Schechtman KB, Dharnidharka VR. Effects of obesity and hypertension on pulse wave velocity in children. **J Clin Hypertens**. 2017; 19(3):221−226.

31. Wójtowicz J, Łempicka A, Łuczyński W, et al. Central aortic pressure, arterial stiffness and echocardiographic parameters of children with overweight/obesity and arterial hypertension. **Adv Clin Exp Med**. 2017; 26(9):1399−1404.

32. Kochli S, Endes K, Steiner R, et al. Obesity, high blood pressure, and physical activity determine vascular phenotype in young children. **Hypertension**. 2019; 73(1):153−161.

33. Urbina EM, Khoury PR, McCoy C, Daniels SR, Kimball TR, Dolan LM. Cardiac and vascular consequences of pre-hypertension in youth. **J Clin Hypertens**. 2011; 13(5):332−342.

34. Garcia-Espinosa V, Curcio S, Marotta M, et al. Changes in central aortic pressure levels, wave components and determinants associated with high peripheral blood pressure states in childhood: analysis of hypertensive phenotype. **Pediatr Cardiol**. 2016; 37(7):1340−1350.

35. Zocalo Y, Castro JM, Garcia-Espinosa V, et al. Forward and backward aortic components and reflection indexes in children and adolescents: determinants and role in high pressure states. **Curr Hypertens Rev**. 2018; 14(2):137−153.

36. Lurbe E, Torro MI, Alvarez-Pitti J, Redon P, Redon J. Central blood pressure and pulse wave amplification across the spectrum of peripheral blood pressure in overweight and obese youth. **J Hypertens**. 2016; 34(7):1389−1395.

37. Shah AS, Wadwa RP, Dabelea D, et al. Arterial stiffness in adolescents and young adults with and without type 1 diabetes: the SEARCH CVD study. **Pediatr Diabetes**. 2015; 16(5):367−374.

38. Bradley TJ, Slorach C, Mahmud FH, et al. Early changes in cardiovascular structure and function in adolescents with type 1 diabetes. **Cardiovasc Diabetol**. 2016; 15:31.

39. Terlemez S, Bulut Y, Ünüvar T, Tokgöz Y, Eryilmaz U, Çelik B. Evaluation of arterial stiffness in children with type 1 diabetes using the oscillometric method. **J Diabetes Complicat**. 2016; 30(5):864−867.

40. Shah AS, El Ghormli L, Gidding SS, et al. Prevalence of arterial stiffness in adolescents with type 2 diabetes in the TODAY cohort: relationships to glycemic control and other risk factors. **J Diabetes Complicat**. 2018; 32(8):740−745.

41. Alman AC, Talton JW, Wadwa RP, et al. Inflammation, adiposity, and progression of arterial stiffness in adolescents with type 1 diabetes: the SEARCH CVD Study. **J Diabetes Complicat**. 2018; 32(11):995−999.

42. Putarek K, Banfic L, Pasalic M, Krnic N, Spehar Uroic A, Rojnic Putarek N. Arterial stiffness as a measure of cardiovascular risk in obese adolescents and adolescents with diabetes type 1. **J Pediatr Endocrinol Metab**. 2018; 31(12):1315−1323.

43. Urbina EM, Isom S, Bell RA, et al. Burden of cardiovascular risk factors over time and arterial stiffness in youth with type 1 diabetes mellitus: the SEARCH for diabetes in youth study. **J Am Heart Assoc**. 2019; 8(13):e010150.

44. Shah AS, Black S, Wadwa RP, et al. Insulin sensitivity and arterial stiffness in youth with type 1 diabetes: the SEARCH CVD study. **J Diabetes Complicat**. 2015; 29(4):512−516.

45. Shah AS, Gao Z, Urbina EM, Kimball TR, Dolan LM. Prediabetes: the effects on arterial thickness and stiffness in obese youth. **J Clin Endocrinol Metab**. 2014; 99(3):1037−1043.

46. McCulloch MA, Mauras N, Canas JA, et al. Magnetic resonance imaging measures of decreased aortic strain and distensibility are proportionate to insulin resistance in adolescents with type 1 diabetes mellitus. **Pediatr Diabetes**. 2015; 16(2):90−97.

47. Dost A, Molz E, Krebs A, et al. Pulse pressure in children and adolescents with type 1 diabetes mellitus in Germany and Austria. **Pediatr Diabetes**. 2014; 15(3):236−243.

48. Suláková T, Janda J, Cerná J, Janštová V, Feber J. Assessment of arterial stiffness from ambulatory blood pressure monitoring in children with diabetes mellitus type-1 (DMT1). **J Hum Hypertens**. 2012; 26(6):357−364.

49. Saiki H, Kojima T, Seki M, Masutani S, Senzaki H. Marked disparity in mechanical wall properties between ascending and descending aorta in patients with tetralogy of Fallot. **Eur J Cardio Thorac Surg**. 2012; 41(3):570−573.

50. Cheung YF, Ou X, Wong SJ. Central and peripheral arterial stiffness in patients after surgical repair of tetralogy of Fallot: implications for aortic root dilatation. **Heart**. 2006; 92(12):1827−1830.

51. Mivelaz Y, Leung MT, Zadorsky MT, De Souza AM, Potts JE, Sandor GG. Noninvasive assessment of vascular function in postoperative cardiovascular disease (coarctation of the aorta, tetralogy of Fallot, and transposition of the great arteries). **Am J Cardiol**. 2016; 118(4):597−602.

52. Klinge A, Allen J, Murray A, O'Sullivan J. Increased pulse wave velocity and blood pressure in children who have undergone cardiac transplantation. **J Heart Lung Transplant**. 2009; 28(1):21−25.

53. Hock J, Häcker AL, Reiner B, et al. Functional outcome in contemporary children and young adults with tetralogy of Fallot after repair. **Arch Dis Child**. 2019; 104(2):129−133.

54. Quail MA, Short R, Pandya B, et al. Abnormal wave reflections and left ventricular hypertrophy late after coarctation of the aorta repair. **Hypertension**. 2017; 69(3):501−509.

55. Trojnarska O, Szczepaniak-Chicheł L, Gabriel M, et al. Arterial stiffness and arterial function in adult cyanotic patients with congenital heart disease. **J Cardiol**. 2017; 70(1):62−67.

56. Boyes NG, Stickland MK, Fusnik S, et al. Physical activity modulates arterial stiffness in children with congenital heart disease: a CHAMPS cohort study. **Congenit**. 2018; 13(4):578−583.

57. Dursun I, Poyrazoglu HM, Gunduz Z, et al. The relationship between circulating endothelial microparticles and arterial stiffness and atherosclerosis in children with chronic kidney disease. **Nephrol Dial Transplant**. 2009; 24(8):2511−2518.

58. Covic A, Mardare N, Gusbeth-Tatomir P, et al. Increased arterial stiffness in children on haemodialysis. **Nephrol Dial Transplant**. 2006; 21(3):729−735.

59. Aoun B, Lorton F, Wannous H, Lévy B, Ulinski T. Aortic stiffness in ESRD children before and after renal transplantation. **Pediatr Nephrol**. 2010; 25(7):1331−1336.

60. Yu MC, Yu MS, Yu MK, Lee F, Huang WH. Acute reversible changes of brachial-ankle pulse wave velocity in children with acute poststreptococcal glomerulonephritis. **Pediatr Nephrol**. 2011; 26(2):233−239.

61. Savant JD, Betoko A, Meyers KEC, et al. Vascular stiffness in children with chronic kidney disease. **Hypertension**. 2017; 69(5):863−869.

62. Sinha MD, Keehn L, Milne L, Sofocleous P, Chowienczyk PJ. Decreased arterial elasticity in children with nondialysis chronic kidney disease is related to blood pressure and not to glomerular filtration rate. **Hypertension**. 2015; 66(4):809−815.

63. Hsu C-N, Lu P-C, Lo M-H, Lin IC, Tain Y-L. The association between nitric oxide pathway, blood pressure abnormalities, and cardiovascular risk profile in pediatric chronic kidney disease. **Int J Mol Sci**. 2019; 20(21).

64. Blacher J, Guerin AP, Pannier B, Marchais SJ, Safar ME, London GM. Impact of aortic stiffness on survival in end-stage renal disease. **Circulation**. 1999; 99(18):2434−2439.

65. Kartal Öztürk G, Conkar S, Eşki A, Gülen F, Keskinoğlu A, Demir E. Evaluation of increased arterial stiffness in pediatric patients with cystic fibrosis by augmentation index and pulse wave velocity analysis. **Pediatr Pulmonol**. 2020; 55:1147−1153.

66. Sun D, Li X, Heianza Y, et al. History of asthma from childhood and arterial stiffness in asymptomatic young adults: the Bogalusa heart study. **Hypertension**. 2018; 71(5):928−936.

67. Schäfer M, Ivy DD, Abman SH, et al. Apparent aortic stiffness in children with pulmonary arterial hypertension: existence of vascular Interdependency? **Circ Cardiovasc Imaging**. 2017; 10(2).

68. Schäfer M, Truong U, Ivy DD, et al. Children with kawasaki disease present elevated stiffness of great arteries: phase-contrast MRI study. **J Magn Reson Imaging**. 2018; 48(5):1228−1236.

69. Nakagawa R, Kuwata S, Kurishima C, et al. Arterial stiffness in patients after Kawasaki disease without coronary artery involvement: assessment by performing brachial ankle pulse wave velocity and cardio-ankle vascular index. **J Cardiol**. 2015; 66(2):130−134.

70. Benschop L, Schalekamp-Timmermans S, Roeters van Lennep JE, Jaddoe VWV, Steegers EAP, Ikram MK. Cardiovascular risk factors track from mother to child. **J Am Heart Assoc**. 2018; 7(19):e009536.

71. Ranque B, Menet A, Boutouyrie P, et al. Arterial stiffness impairment in sickle cell disease associated with chronic vascular complications: the Multinational African CADRE study. **Circulation**. 2016; 134(13):923−933.

72. De Groote K, Devos D, Van Herck K, et al. Increased aortic stiffness in prepubertal girls with Turner syndrome. **J Cardiol**. 2017; 69(1):201−207.

73. Devos DGH, De Groote K, Babin D, et al. Proximal aortic stiffening in Turner patients may be present before dilation can be detected: a segmental functional MRI study. **J Cardiovasc Magn Reson**. 2017; 19(1):27.

74. Chirinos JA, Segers P, Hughes T, Townsend R. Large-artery stiffness in health and disease: JACC state-of-the-art review. **J Am Coll Cardiol**. 2019; 74(9):1237−1263.

75. Reference Values for Arterial Stiffness Collaboration. Determinants of pulse wave velocity in healthy people and in the presence of cardiovascular risk factors: 'establishing normal and reference values'. **Eur Heart J**. 2010; 31(19):2338−2350.

76. Van Bortel LM, Laurent S, Boutouyrie P, et al. Expert consensus document on the measurement of aortic stiffness in daily practice using carotid-femoral pulse wave velocity. **J Hypertens**. 2012; 30(3):445−448.

77. Voges I, Jerosch-Herold M, Hedderich J, et al. Normal values of aortic dimensions, distensibility, and pulse wave velocity in children and young adults: a cross-sectional study. **J Cardiovasc Magn Reson**. 2012; 14:77.

78. Reusz GS, Cseprekal O, Temmar M, et al. Reference values of pulse wave velocity in healthy children and teenagers. **Hypertension**. 2010; 56(2):217−224.

79. Niboshi A, Hamaoka K, Sakata K, Inoue F. Characteristics of brachial-ankle pulse wave velocity in Japanese children. **Eur J Pediatr**. 2006; 165(9):625−629.

80. Mora-Urda AI, Molina MD, Mill JG, Montero-Lopez P. Carotid-femoral pulse wave velocity in healthy Spanish children: reference percentile curves. **J Clin Hypertens**. 2017; 19(3):227−234.

81. Hidvegi EV, Illyes M, Benczur B, et al. Reference values of aortic pulse wave velocity in a large healthy population aged between 3 and 18 years. **J Hypertens**. 2012; 30(12):2314−2321.

82. Fischer DC, Schreiver C, Heimhalt M, Noerenberg A, Haffner D. Pediatric reference values of carotid-femoral pulse wave velocity determined with an oscillometric device. **J Hypertens**. 2012; 30(11):2159−2167.

83. Elmenhorst J, Hulpke-Wette M, Barta C, Dalla Pozza R, Springer S, Oberhoffer R. Percentiles for central blood pressure and pulse wave velocity in children and adolescents recorded with an oscillometric device. **Atherosclerosis**. 2015; 238(1):9−16.

84. Diaz A, Zocalo Y, Bia D, Sabino F, Rodriguez V, Cabrera FEI. Reference intervals of aortic pulse wave velocity assessed with an oscillometric device in healthy children and adolescents from Argentina. **Clin Exp Hypertens**. 2019; 41(2):101−112.

85. Curcio S, Garcia-Espinosa V, Arana M, et al. Growing-related changes in arterial properties of healthy children, adolescents, and young adults Nonexposed to cardiovascular risk factors: analysis of gender-related differences. **Int J Hypertens**. 2016; 2016:4982676.

86. Muller J, Oberhoffer R, Barta C, Hulpke-Wette M, Hager A. Oscil-lometric carotid to femoral pulse wave velocity estimated with the Vicorder device. **J Clin Hypertens**. 2013; 15(3):176−179.

87. Heffernan KS, Jae SY, Wilund KR, Woods JA, Fernhall B. Racial differences in central blood pressure and vascular function in young men. **Am J Physiol Heart Circ Physiol**. 2008; 295(6): H2380−H2387.

88. Lefferts WK, Augustine JA, Spartano NL, Atallah-Yunes NH, Heffernan KS, Gump BB. Racial differences in aortic stiffness in children. **J Pediatr**. 2017; 180:62−67.

89. Zaniqueli D, Alvim RO, Luiz SG, Oliosa PR, de Sa Cunha R, Mill JG. Ethnicity and arterial stiffness in children and adolescents from a Brazilian population. **J Hypertens**. 2017; 35(11):2257−2261.

90. Murakami T, Takeda A, Takei K, et al. Aortic pressure wave reflection in children. **Hypertens Res**. 2010; 33(3):225−228.

91. Hidvégi EV, Illyés M, Molnár FT, Cziráki A. Influence of body height on aortic systolic pressure augmentation and wave reflection in childhood. **J Hum Hypertens**. 2015; 29(8):495−501.

92. Diaz A, Zócalo Y, Bia D, Cabrera Fischer E. Reference intervals of central aortic blood pressure and augmentation index assessed with an oscillometric device in healthy children, adolescents, and young adults from Argentina. **Int J Hypertens**. 2018; 2018:1469651.

93. Mikola H, Pahkala K, Rönnemaa T, et al. Distensibility of the aorta and carotid artery and left ventricular mass from childhood to early adulthood. **Hypertension**. 2015; 65(1):146−152.

94. Engelen L, Bossuyt J, Ferreira I, et al. Reference values for local arterial stiffness. Part A: carotid artery. **J Hypertens**. 2015; 33(10):1981−1996.

95. Bossuyt J, Engelen L, Ferreira I, et al. Reference values for local arterial stiffness. Part B: femoral artery. **J Hypertens**. 2015; 33(10):1997−2009.

96. Voges I, Jerosch-Herold M, Hedderich J, et al. Normal values of aortic dimensions, distensibility, and pulse wave velocity in children and young adults: a cross-sectional study. **J Cardiovasc Magn Reson**. 2012; 14:77, 77.

Aortopathies and arteriopathies

Reed E. Pyeritz

Perelman School of Medicine, University of Pennsylvania Health System, Philadelphia, PA, United States

Introduction

Disorders primarily affecting large and medium caliber arteries, the aorta, or both can arise in people of all ages, from fetuses to the elderly. Except in severely affected individuals, the age of onset is typically overestimated due to a failure to diagnose earlier. Some of these disorders occur or are influenced because of strong environmental and other conditions, such as smoking, hypertension, and lipidopathies. While genetic factors usually play a role in the modulation of blood pressure and cholesterol levels, the focus of this chapter is on genetic conditions that primarily cause arteriopathies and aortopathies (Box 44.1).

BOX 44.1 Human genetic complement

Nuclear DNA

6.4 billion nucleotides arranged on 23 pairs of chromosomes. There are 22 pairs of autosomes (numbered 1−22) and two sex chromosomes, X and Y. Females have two X chromosomes and males have an X and a Y.

The genome consists of all of this nuclear DNA. All of these sequences are arrayed when whole genome sequencing is performed.

The exome consists of the DNA that encodes approximately 22,000 genes, the exons (coding sequences) and introns (sequences between each exon). The exons constitute 1.5%−2% of the nuclear DNA. When exome sequencing is performed, only these sequences are examined.

Mitochondrial DNA

Each cell has multiple mitochondria in its cytoplasm. Each mitochondrion has multiple copies of a small, circular chromosome composed of 16,569 nucleotide pairs that encode 37 genes. Mitochondria, utilizing its own genes and some encoded by the nuclear chromosomes, are essential for oxidative metabolism.

Three decades or so ago, anyone with a dilated ascending aorta, especially if there was a positive family history, was labeled as "Marfan syndrome," which led to an inflated estimate of the prevalence of this condition and inaccurate expectations as to the prognosis of each patient. Since then, not only is there improved understanding of true Marfan syndrome, but that many dozens of genes are, individually, associated with arteriopathies and aortopathies. Fortunately, what we learned about the medical and surgical management of aortic disease in Marfan syndrome generally applies to aortopathies due to most genes.

What is meant by the term "genetic" is a trait primarily caused by a pathogenic variant (previously termed a "mutation") in one gene. The term "hereditary" refers to a condition or predisposition that is due to a genetic variant that is, or can be, evident in multiple members of the same family. While all hereditary disorders are genetic, the reverse is not necessarily the case. Disorders may not be identified as hereditary because of small families or minimal clinical information of previous generations. Autosomal recessive and X-linked conditions may appear as isolated cases in a family because people with only one of two copies of the aberrant gene show no clinical effects. In the case of autosomal dominant conditions not recognized as hereditary, the affected person will have unaffected parents (or more distant relatives) because the pathogenic variant arose for the first time in the patient, typically in the oocyte or spermatocyte that led to his or her fertilization. For example, at least one-quarter of patients with Marfan syndrome have parents neither of whom has the pathogenic variant in *FBN1* present in the patient. Of course, nonpaternity can confuse this interpretation (Box 44.2).

Several other terms deserve note. "Phenotype" refers to the outward manifestations of a genetic variant while "genotype" is the specific variant (a change in a single or multiple nucleotides) that causes the condition. "Genetic heterogeneity" refers to multiple pathogenic variants that cause the same condition. These multiple variants can be

Textbook of Arterial Stiffness and Pulsatile Hemodynamics in Health and Disease. https://doi.org/10.1016/B978-0-323-91391-1.00044-3
707

within the same gene (intragenic) or in more than one gene (intergenic). For example, only variants in *FBN1* cause Marfan syndrome, but there are more than a 1000 of them. On the other hand, multiple variants in at least two genes (*TGFBR1* and *TGFBR2*) cause Loeys−Dietz syndrome, which reflects both intra- and intergenic heterogeneity. "Variability" defines differences in phenotype among people with the same genotype, often relatives. Variability can be due to multiple causes, such as differences in age of expression of the phenotype, influences of one or more other genes, even environmental factors. "Nonpenetrance" is one end of the spectrum of variability, in which a person with a clearly pathogenic variant does not show any manifestations. All of these concepts are highly relevant to both the investigation and management of arteriopathies and aortopathies.

Last, "natural history" and "clinical history" are often used interchangeably but should be distinguished. Natural history defines the evolution of a phenotype if no therapy, effective or not, is employed for a specific trait. On the other hand, clinical history refers to how the phenotype is altered by therapy. For example, the clinical history of ascending aortic disease in Marfan syndrome has been remarkably altered by medical and surgical therapy. However, the improved life span has resulted in the emergence of a host of features (such as sleep apnea, cardiomyopathy, and central adiposity) that expand the scope of natural history.[1]

Approaches to defining the genetic contributions to arterial and aortic disease

Two general approaches are employed to define how variation in one or more genes determine a particular disease. These are defined as "phenotype first" and "genotype first." In the former, a specific disease, well characterized and readily identifiable, is the basis for searching for pathogenic variation in a specific gene or genes that are causative. One of the first such successes was identification in 1991 of variants in the gene for fibrillin-1, *FBN1*, as causative of the Marfan syndrome.[2] Since then, dozens of successes have been achieved, often by first understanding the pathology and protein defects of the arterial lesion and then systematically examining the genes that encode the relevant proteins. Another example is the vascular form of Ehlers−Danlos syndrome for which mutations in *COL3A1* were identified based on the known importance of type 3 collagen in the arterial wall. As more genes predisposing to thoracic aortic disease are discovered, then they can be assessed for pathogenic variants in patients.[3]

The more recent but expanding approach is defined as "genotype first." Here one, several, many or all genes are examined for pathogenic variants, which are then associated with a specific disorder. For example, we examined patients in the Penn Medicine Biobank for one of a dozen pathogenic variants in *FBN1* and found that ** subjects had such a variant.[4] Only two of these subjects had been diagnosed with Marfan syndrome, but many of the others had thoracic aortic disease. Variations in all genes can be determined by sequencing the 1.5%−2% of the genome known to encode proteins, termed whole exome sequencing. Increasingly, because of markedly improved and rapid techniques, the entire 6.4 billion nucleotides that comprise our 23 pairs of chromosomes are being sequenced, whole genome sequencing. Then, many programs[5] that screen any variation from "normal" are used to assess whether it is likely to be harmful. Likely pathogenic variants are then screened for their association with a

phenotype of interest. Because of statistical applications to large databases, such as biobanks, potential causes of specific diseases can be established. For example, all pathogenetic variants in large numbers of subjects in a biobank can be identified and the phenotypes of people with each variant can be investigated to understand if they have a disease for which the cause is undetermined.[5,6] The genetic cause of a specific Mendelian condition can be searched. Alternatively, a common phenotype, such as type A aortic dissection can be examined based on appropriate ICD-10 codes in a biobank. The results can include specific genetic variants predisposing to type A dissection either in specific Mendelian conditions or in subjects without a known underlying condition.

Pathogenic mechanisms

Four major classes of proteins are abnormal in arteriopathies and aortopathies: extracellular, transmembrane, cytoplasmic, and nuclear. These result in conditions that affect many organs or mainly one. These disorders are typically classified as connective tissue disorders, smooth muscle disorders, and signaling disorders. Some conditions that have been classified as connective tissue disorders, the Marfan syndrome termed that for half a century, are now recognized as resulting primarily from defects in signaling. As a general example, vascular smooth muscle function is the principal determinant of arterial contraction. Mutations in a number of genes, for example, *FBN1* and *ACTA2*, disrupt the mechanosensing of the elastin-contractile unit. This can result in numerous downstream detrimental effects that lead to aortic aneurysm and dissection.[7] As an example, some variants increase aortic stiffness, which increases the rate of sinuses of Valsalva dilatation and poor outcomes in Marfan syndrome.[8]

Arteriopathies with limited aortic involvement

Arterial aneurysms and dissections appear in young people in the absence of any obvious syndrome. Occasionally, relatives have the same disorders, so a strong genetic component to cause is likely. For example, people, usually women, can present with bilateral carotid or vertebral artery dissections. In some cases, there is a family history of similarly affected relatives. To date, screening for pathogenic variants in genes known to cause aortic conditions is likely uninformative. Such conditions are ideal for a genotype-first approach.

A few Mendelian conditions are associated with arteriopathy (Table 44.1). Most are rare, with the exception of hereditary hemorrhagic telangiectasia (HHT) which occurs in about 1 in 5000.

The diagnosis of HHT is established by documenting three or the following four signs: recurrent epistaxis, mucocutaneous telangiectases, pulmonary arteriovenous malformations, and a family history of HHT.[9] Finding a pathogenic variant in *ENG*, *ACVRL1*, or *SMAD4* confirms the diagnosis.[10] In HHT, the telangiectases are connections between arterials and venules bypassing capillaries. In addition, however, patients are at risk for arterial aneurysms and arteriovenous malformations in the nervous system (brain and spinal cord) and arteriopathy in the liver. Pulmonary AVMs are the most common serious problem, but when diagnosed can be treated by embolization of the feeding artery.[11]

TABLE 44.1 Arteriopathies typically with minimal aortic involvement.

Disorder	OMIM entry[a]
ANGPTL6 associated intracranial aneurysm	609336
Cerebral arteriopathy	125310; 600142; 616719
Cutis laxa	614437
Hereditary hemorrhagic telangiectasia	600376; 601101; 6105506; 6155506; 175050; 187300
Moyamoya disease	252350; 300845; 603277; 604910; 613768; 61402; 615750; 615761
PHACE association	606519
Polycystic kidney disease 1 and 2	173900; 613095
Sneddon syndrome	182410
Spontaneous dissection of the internal carotid artery	147820
Vascular Ehlers–Danlos syndrome	130050

[a]Number of disorder in On-line Mendelian in Man (omim.org; accessed October 17, 2020).

Vascular Ehlers—Danlos syndrome is a serious but fortunately uncommon autosomal dominant condition due to pathogenic variants in *COL3A1*, the gene encoding type 3 collagen, an important component of skin and the walls of muscular arteries, the intestine, and the uterus.[12,13] Any of the latter can spontaneously rupture, with pregnancy being the only predisposing condition. Other than keeping blood pressure as low as reasonable, there is no effective therapy, although beta-adrenergic blockade and inhibiting oxytocin or androgen effects are still being investigated.[14] Occasionally the aorta minimally dilates. Dissection of the aorta or peripheral arteries is not associated with histopathology showing medial degeneration.

Disorders that primarily involve the aorta with arterial involvement

The most common and well-known of these conditions in the Marfan syndrome. Diagnosis is based on findings in multiple organ systems and pathogenic variants in *FBN1*, the gene encoding the connective tissue protein fibrillin-1.[2,15] Patients are typically disproportionately tall of stature, develop deformity of the anterior chest and vertebral column, are prone to dislocation of the ocular lens, and have enlargement of the lumbosacral spinal canal (dural ectasia). At least 50% have mitral valve prolapse, and mitral regurgitation often develops. Aortic dilatation begins in the sinuses of Valsalva, is typically gradually progressive and rarely progresses above the proximal ascending aorta. With increasing diameter, the valve attachments are stretched with the development of aortic regurgitation. Most important, as the diameter increases so does the risk of a type A dissection. This can be prevented with a prophylactic valve-sparing ascending aortic replacement. The appropriate diameter for recommending repair varies, with a dimension of 45 mm if the family history includes relatives with dissection at early ages, a rapidly increasing dimeter (>5 mm in a year), or a diameter >50 mm. As soon as the diagnosis of Marfan syndrome is made, oral beta-adrenergic blockade or angiotensin receptor blockade should be stared. Patients should be counseled to avoid vigorous exertion (especially isometric) and contact sports. The mitral valve should be assessed because of the high prevalence of prolapse and regurgitation. About 10% of acute dissections are type B and is the most common form in peripartum women. Today, acute dissection remains the most common cause of premature death.

The recommendations of beta-adrenergic blockade, restricting exertion and contact sports, and prophylactic ascending aortic repair were developed in patients diagnosed with Marfan syndrome in the 1970s and 1980s. Angiotensin receptor blockade is equally effective as beta-adrenergic blockade.[16] Subsequently, more than two dozen

TABLE 44.2 Aortopathies with arterial involvement.

Disorder	OMIM entry[a]
Loeys—Dietz syndrome	609168; 610168; 613795; 614816; 615582
Marfan syndrome	154700
Williams—Beuren syndrome	194050

[a]*Number of disorder in On-line Mendelian in Man (omim.org; accessed 3 Dec 2021).*

genetic predispositions to aortic disease like that in Marfan syndrome have been defined (Table 44.2), and more are sure to follow. However, the approaches to reducing aortic dilatation and the risk of dissection delineated from Marfan syndrome are completely appropriate today.

Involvement of other arteries in Marfan syndrome most often occurs as a result of aortic dissection. However, primary dilatation or frank aneurysms of aortic branches can occur, so it is wise to image the vascular system from the neck to the pelvis in an adult at least once.

Some of the other aortopathies listed in Table 44.2 are syndromic (the various Loeys—Dietz syndromes and some mutations in *ACAT2*), while others involve mainly the aorta. All are autosomal dominant. While management of the aortic disease is the same as in Marfan syndrome, based on the specific gene and pathogenic variant surveillance and treatment need to be more aggressive. Variants at one specific codon in *ACTA2*, normally encoding an arginine at position 179, lead to more rapidly progressive aortic disease and involvement in other arteries.[17] In most of these disorders, peripheral arteries may be involved as in Marfan syndrome. In most, including the Marfan syndrome, arteries may be unusually tortuous.[18] Additionally, shining a bright light through the distal phalanges of the hand (transillumination) often reveals both vascular tortuosity and dilatations. These tend to correlate with the severity of the arteriopathy and are invariably asymptomatic.[19]

The underlying causes involve components of the extracellular matrix or vascular smooth muscle and signaling pathways such as for TGF-β. Knowing the genetic variant underlying aortic disease in a particular patient enables predicting the course of their condition and the diagnosis of disease, often undetected, in relatives. Additionally, understanding how a signaling pathway is involved may lead to the development of specific therapies, such as angiotensin receptor blockade.

Disorders that primarily affect the aorta

The most common cause of dilatation of the ascending aorta is its association with bicuspid aortic valve (BAV). Postductal coarctation may also occur. The aortic valve,

ascending aorta, and periductal aorta all derive from the same embryologic origin. Rarely do the sinuses of Valsalva, which are distinct embryologically, dilate. The severity of ascending aortic dilatation may not correlate with the severity of the aortic valve pathology.[20] In most instances, the dilatation of the aorta is not as rapidly progressive or prone to dissection as in the Marfan syndrome.[21] Because transthoracic (i.e., standard) echocardiography often does not visualize the midascending aorta, patients with BAV should have a CT or MR of the thorax to establish if dilatation is present, and if so, to be followed by an adequate imaging modality. The histopathology of the aortic wall typically shows medial degeneration, indistinguishable from MFS.

About one-quarter of patients with BAV give a family history of a relative with BAV or at least aortic valve disease. Thus, a strong genetic predisposition must be contributory. Despite this evidence, there has been surprisingly little success in defining specific genes with pathogenic variants that cause BAV.

Concern about the possible diagnosis of MFS is a common reason for referral to medical genetics clinics. Many such probands have one or more features of MFS but fail to meet strict criteria. The acronym MASS represents common (but not essential) involvement of the mitral valve, the aorta, the skin, and the skeleton.[22]

MVP as an echocardiographic entity occurs in perhaps 2.5% of the general population, is more common among women, and is more common in adolescence and young adulthood than in childhood or old age. MVP is an autosomal dominant trait in many families. Based on standard transthoracic echocardiographic evaluation, two classes of MVP can be defined: those with abnormal leaflet motion but normal leaflet morphology; and those with both prolapse and thickening of the leaflets, which correlates with the degree of myxomatous degeneration. The latter is sometimes termed primary MVP; is typical of the MVP in most heritable disorders of connective tissue, including MASS phenotype; and is more likely to be associated with clinical complications. In some people, MVP is associated with deformity of the chest wall or the vertebral column, or both. These patients also often have an aortic root dimension near or slightly above the upper limit of normal for age and body surface area (but no dissection or apparent progressive enlargement), myopia (but by definition no ectopia lentis), joint hypermobility (in addition to pectus excavatum and scoliosis), pneumothorax, and striae atrophicae. Some probands have a family history of similarly affected relatives. Thus, the MASS phenotype is not Marfan syndrome, although in some instances it certainly resembles what one would expect a mild variant of MFS to be. The MASS phenotype seemingly has a good prognosis, with the worst manifestation being a predisposition to progressive MVP and mitral regurgitation. Whether and how "familial

TABLE 44.3 Disorders affecting primarily the aorta.

Disorder	OMIM entry[a]
Bicuspid aortic valve	109730; 190198; 314400; 614823; 618496
MASS phenotype	157700
Tuberous sclerosis 2	613254
Turner syndrome and X-linked Alport syndrome	301050

[a]Number of disorder in On-line Mendelian in Man (omim.org; accessed 3 Dec 2021).

MVP" and MASS phenotype should be distinguished have not been clarified (Table 44.3).

The MASS phenotype is likely heterogeneous in etiology, hence the term "phenotype," rather than syndrome. A very few patients with a mutation in *FBN1* qualify for a MASS phenotype diagnosis. One example is a patient with a mutation that results in little abnormal fibrillin monomer and is close to a null allele. In general, mutations near the 3′-terminus of *FBN1*, little expression of the mutant allele, and in vitro deposition of fibrillin in the ECM greater than 70% of normal are all associated with a milder MFS-like phenotype. However, other patients with missense mutations near the 3′ end of *FBN1* have had a severe, classic MFS phenotype. Meanwhile, other pedigrees that could be characterized as MASS are not linked to *FBN1*. Moreover, three loci for familial MVP have been mapped, Xq28, 13q31.3−q32.1, and 16p11.2−p12.1.

Precision medicine

Many factors go into determining who receives what therapy when. From a purely phenotypic perspective, issues such as age, gender, effectiveness of pharmacologic therapies, even institutional expertise can be major factors. For example, in the absence of useful genetic markers for BAV, these factors are major determinants of choosing the vessel diameter at which to recommend replacement of the ascending aorta.[23]

Understanding the genetic cause, the pathogenic mechanism, or both can lead to the development of a targeted therapy for a specific disease. For example, beta-adrenergic blockade was used for decades to reduce dP/dt in Marfan syndrome, learning that a defect in TGFβ signally is the pathogenic mechanism led to angiotensin-receptor blockade as an alternative therapy.[16] As another example, the arteriopathy in vascular Ehlers−Danlos was always assumed to be a straightforward connective tissue disorder resulting in weakness of the vessel wall. Recently, however, attenuation of androgen and oxytocin signaling was discovered to reduce vascular risk.[14]

References

1. Pyeritz RE. Marfan syndrome: improved clinical history results in expanded natural history. **Genet Med**. 2019; 21:1683−1690.

2. Dietz HC, Cutting GR, Pyeritz RE, et al. Marfan syndrome caused by a recurrent de novo missense mutation in the fibrillin gene. **Nature**. 1991; 352:337−339.

3. Wolford BN, Hornsby WE, Guo D, et al. Clinical implications of identifying pathogenic variants in individuals with thoracic aortic dissection. **Circ Genom Precis Med**. 2019; 12:e002476.

4. Damrauer SM, Hardie K, Kember RL, et al. FBN1 coding variants and nonsyndromic aortic disease. **Circ Genom Precis Med**. 2019; 12:e002454.

5. Turro E, Astle WJ, Megy K, et al. Whole-genome sequencing of patients with rare diseases in a national health system. **Nature**. 2020; 583:96−102.

6. Wise AL, Manolio TA, Mensah GA, et al. Genomic medicine for undiagnosed diseases. **Lancet**. 2019; 394:533−540.

7. Pinard A, Jones GT, Milewicz DM. Genetics of thoracic and abdominal aortic diseases. **Circ Res**. 2019; 124:588−606.

8. Selamet Tierney ES, Levine JC, Sleeper LA, et al. Influence of aortic stiffness on aortic-root growth rate and outcome in patients with the Marfan syndrome. **Am J Cardiol**. 2018; 121:1094−1101.

9. Faughnan ME, Palda VA, Garcia-Tsao G, et al. International guidelines for the diagnosis and management of hereditary haemorrhagic telangiectasia. **J Med Genet**. 2011; 48:73−87.

10. Shovlin CL, Simeoni I, Downes K, et al. Mutational and phenotypic characterization of hereditary hemorrhagic telangiectasia. **Blood**. 2020; 136:1907−1918.

11. Trerotola SO, Pyeritz RE. PAVM embolization: an update. **AJR Am J Roentgenol**. 2010; 195:837−845.

12. Pepin M, Schwarze U, Superti-Furga A, Byers PH. Clinical and genetic features of Ehlers-Danlos syndrome type IV, the vascular type. **N Engl J Med**. 2000; 342:673−680.

13. Ritelli M, Rovati C, Venturini M, et al. Application of the 2017 criteria for vascular Ehlers-Danlos syndrome in 50 patients ascertained according to the Villefranche nosology. **Clin Genet**. 2020; 97(2):287−295.

14. Bowen CJ, Calderon Giadrosic JF, Burger Z, et al. Targetable cellular signaling events mediate vascular pathology in vascular Ehlers-Danlos syndrome. **J Clin Invest**. 2020; 130:686−698.

15. Loeys BL, Dietz HC, Braverman AC, et al. The revised Ghent nosology for the Marfan syndrome. **J Med Genet**. 2010; 47:476−485.

16. Lacro RV, Dietz HC, Sleeper LA, et al. Atenolol versus losartan in children and young adults with Marfan's syndrome. **N Engl J Med**. 2014; 371:2061−2071.

17. Regalado ES, Mellor-Crummey L, De Backer J, et al. Clinical history and management recommendations of the smooth muscle dysfunction syndrome due to ACTA2 arginine 179 alterations. **Genet Med**. 2018; 20:1206−1215.

18. Morris SA, Orbach DB, Geva T, Singh MN, Gauvreau K, Lacro RV. Increased vertebral artery tortuosity index is associated with adverse outcomes in children and young adults with connective tissue disorders. **Circulation**. 2011; 124:388−396.

19. Pyeritz R. Transillumination of the digits in aortopathies. **Am J Med Genet**. 2021. https://doi.org/10.1002/ajmg.a.62495.

20. Roman MJ, Pugh NL, Devereux RB, et al. Aortic dilatation associated with bicuspid aortic valve: relation to sex, hemodynamics, and valve morphology (the national heart lung and blood institute-sponsored national registry of genetically triggered thoracic aortic aneurysms and cardiovascular conditions). **Am J Cardiol**. 2017; 120:1171−1175.

21. Guala A, Rodriguez-Palomares J, Dux-Santoy L, et al. Influence of aortic dilation on the regional aortic stiffness of bicuspid aortic valve assessed by 4-dimensional flow cardiac magnetic resonance: comparison with Marfan syndrome and degenerative aortic aneurysm. **JACC Cardiovasc Imaging**. 2019; 12:1020−1029.

22. Glesby MJ, Pyeritz RE. Association of mitral valve prolapse and systemic abnormalities of connective tissue. A phenotypic continuum. **J Am Med Assoc**. 1989; 262:523−528.

23. Nissen AP, Truong VTT, Alhafez BA, et al. Surgical repair of bicuspid aortopathy at small diameters: clinical and institutional factors. **J Thorac Cardiovasc Surg**. 2020; 159:2216−2226 e2.

Chapter 45

Arterial stiffness and pulsatile hemodynamics in thoracic aortopathies

Jasjit Rooprai[1] and Thais Coutinho[2]

[1]Department of Medicine, University of Toronto, Toronto, ON, Canada; [2]Division of Cardiology, Division of Cardiac Prevention & Rehabilitation, University of Ottawa Heart Institute, Ottawa, ON, Canada

List of abbreviations

BAV bicuspid aortic valve
cfPWV carotid-femoral pulse wave velocity
EDS Ehlers—Danlos syndrome
FTAAD Familial thoracic aortic aneurysms and dissections
HTN hypertension
LDS Loeys—Dietz Syndrome
MFS Marfan syndrome
MMP matrix metalloproteinase
TAA thoracic aortic aneurysm
VSMCs vascular smooth muscle cells

Aortopathy refers to a family of structural pathologies of the aorta, which can have life-threatening consequences. These include aortic aneurysm, dissection, rupture, penetrating aortic ulcer, aortic intramural hematoma, and aortitis. For epidemiological and clinical purposes, diseases of the aorta are typically categorized as involving the thoracic and/or abdominal segments of the vessel. For the purpose of this chapter, we will focus on thoracic aortic aneurysms (TAAs) given that most studies have focused on this segment.

Epidemiology and sex differences of thoracic aortic disease
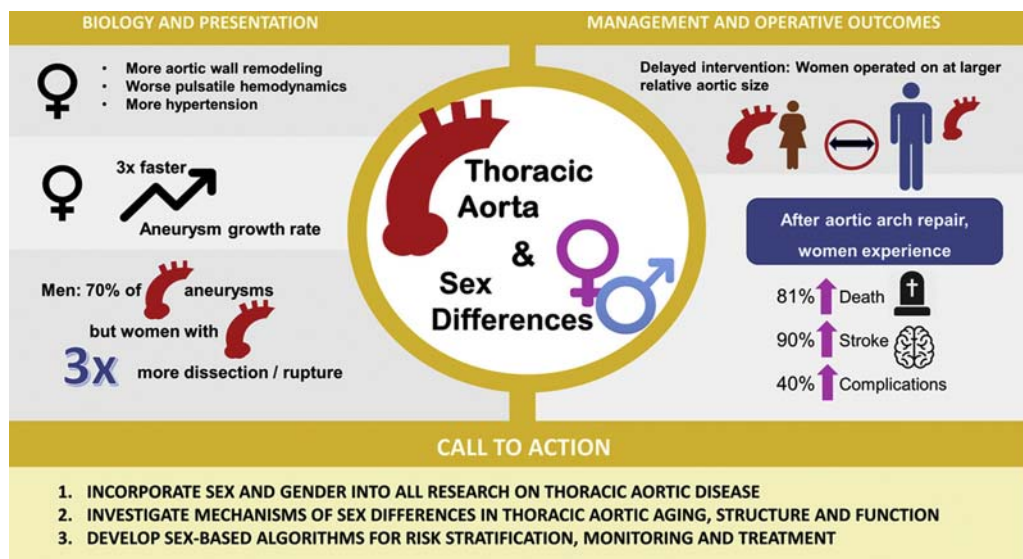
TAAs are clinically silent conditions associated with high morbidity and mortality when complicated by acute aortic syndromes.[1–4] Most TAAs can be broadly categorized as being degenerative or heritable in nature. Patients with degenerative aortic aneurysms are typically older, and commonly have atherosclerotic risk factors, particularly hypertension (HTN). HTN has the highest population-attributable risk for acute aortic syndromes,[5] and is present in over two-thirds of patients with TAA (61%—78%).[6,7]

TAAs identified in younger patients are commonly associated with a number of heritable/genetic disorders, including bicuspid aortic valves (BAVs), Marfan's syndrome, familial TAA, Loeys—Dietz, Turner and Ehlers—Danlos syndrome (EDS) (vascular form).[8] Other etiologies, such as aortitis, posttraumatic or mycotic, are rare.

Given its predominantly silent nature, it is difficult to precisely estimate the incidence and prevalence of TAA. According to the published data, the annual incidence of TAA is estimated to be 5.6—10.4 cases per 100,000 patient-years.[6,9] However, these numbers are undoubtedly underestimated, given the lack of screening strategies for TAA and the fact that most TAAs are discovered incidentally (1% of all imaging studies).[10] Recent population data from Canada[11,12] and Sweden[13] suggest that incidence of thoracic aortic disease (aneurysms and dissections) has increased over the past decade, especially in women, which may relate to the aging population and the increased utilization of imaging techniques.

All in all, the incidence of ruptured aortic aneurysm reported in the literature is approximately 5—10 per 100,000 person-years, and that of aortic dissection is estimated to be 2—4 per 100,000 person-years.[14] However, similarly to TAA statistics, the incidence of acute aortic syndromes is also underestimated and expected to be 3—5 times higher than reported,[15] since individuals who die suddenly from these conditions are often misclassified as dying from heart attacks or strokes,[16–19] and 60% of cases of aortic dissection are missed clinically and first identified at autopsy.[20] Importantly, contemporary mortality rates of nondissected TAA and of acute aortic syndromes parallel those of other known and more commonly recognized killers such as heart disease and cancer.[12]

It is important to highlight the observed sex differences in thoracic aortopathies (Fig. 45.1).[21,22] Similar risk factors for

FIGURE 45.1   Sex differences in thoracic aortic aneurysms and dissections. Sex differences exist in the epidemiology, biology, management and outcomes of patients with thoracic aortic disease. *Adapted, with permission, from Chung J, Coutinho T, Chu MWA, Ouzounian M. Sex differences in thoracic aortic disease: a review of the literature and a call to action.* **J Thorac Cardiovasc Surg.** *2020; 160:656−660.*

developing TAA exist for men and women,[23] including age, HTN, atherosclerosis, and genetic factors/family history. However, while TAAs are 2−4 times more prevalent in men than women,[24] women with this condition carry a significantly worse prognosis.[21,24−26] Compared to men, women with TAA have twice as fast aneurysm growth rates,[25] three times higher risk of acute aortic syndromes[27−30] and 40% higher mortality. In addition, acute aortic syndromes occur at smaller aneurysm sizes in women than men, despite correction of aneurysm size to body size.[27] Further, prognosis is also worse for women undergoing TAA repair, who experience 81% higher mortality and 90% higher risk of stroke as compared to their male counterparts.[26]

Causes for these sex differences remain incompletely understood. The lower TAA prevalence in women may be partly due to the protective effects of estrogen during the reproductive years, which is believed to mediate its protective effect on the aorta through modulating matrix metalloproteinases (MMPs).[31] MMPs are enzymes that play an important role in arterial wall remodeling and have been shown to predispose to aortic aneurysm formation and dissection. The activity of MMPs is mainly regulated by tissue inhibitors of metalloproteinases (TIMPs).[32] It has been found that high levels of circulating estrogen protect against aortic aneurysm formation by reducing inflammation and MMP activity in aortic tissue.[33] While it is true that women with TAA tend to be older and harbor more comorbidities than men with TAA, the aforementioned sex differences in outcomes are independent of age, body size, and comorbidities. However, one study that included aortic specimens from men and women undergoing elective TAA repair has demonstrated greater MMP and lower TIMP

activity, indicating greater extracellular matrix (ECM) remodeling in the arterial wall, in women.[34] This was reflected in stiffer aortic walls in women than men.[34] Thus, it is possible that while women may be naturally protected against aortic aneurysm development, those that go on to develop a TAA may have greater burden of disease and remodeling in the aortic wall, which, in turn, may contribute to the worse aortic-related outcomes in women.

Clinical management of thoracic aortic aneurysm

Among patients with TAA, the risk of acute aortic syndromes is influenced by a number of factors including patient characteristics (age, sex, HTN, history of smoking, family history of aortic disease) and disease-related factors (aortic size, rate of aneurysm growth, connective tissue disorder, BAV, among others). Clinical management consists of blood pressure control for those who are hypertensive, beta-blocker or angiotensin-receptor blocker for those with Marfan syndrome, and yearly imaging surveillance with expectant management until critical aneurysm size is met.[8,35,36] As such, clinical management centers upon the absolute size of the aneurysm in light of the etiology and location of aortic disease, with recommended TAA size cut-offs for surgical repair based on these characteristics, and a watchful-waiting approach with serial imaging surveillance for those not yet meeting TAA surgical size criteria. While this strategy is adequate for many patients, it is imperfect, as several individuals suffer acute aortic syndromes with aneurysm sizes that are smaller than the guideline-recommended cut-offs for prophylactic

surgery.[30,37] Additionally, individuals experience different rates of aneurysm expansion and aortic complications despite having similar aneurysm sizes. These findings highlight the fact that aneurysm size alone fails to capture all of the complexity of the aorta, and motivate us to turn our attention to novel aortic parameters to better understand disease activity, risk and prognosis among TAA patients.

Histopathological links between thoracic aortic aneurysms and arterial aging

Aging plays a major role in the process of aortic disease.[38] Arterial aging is the age-associated change in arterial structure and function,[39] and is reflected in aortic stiffness and measures of aortic function. With aging, and even in the absence of aortopathy, aortic lumen increases, while the thickness of the arterial wall triples between the ages of 20 and 90 years, mainly due to intimal and subintimal thickening.[39]

As discussed in detail in Chapter 19, with increasing age, the repetitive pulsatile stress imposed upon the aorta by the beating left ventricle over time leads to fatigue and breakdown of the elastic fibers in the aortic wall. These fibers consist primarily of the structural protein elastin (90%) as well as elastin-associated glycoproteins (10%) including fibrillins. In arterial aging, there is an accelerated depletion of elastin and deposition of collagen as a result of the repetitive cyclic stress (i.e., arterial wall distension and elastic recoil)[39,40] (Fig. 45.2).
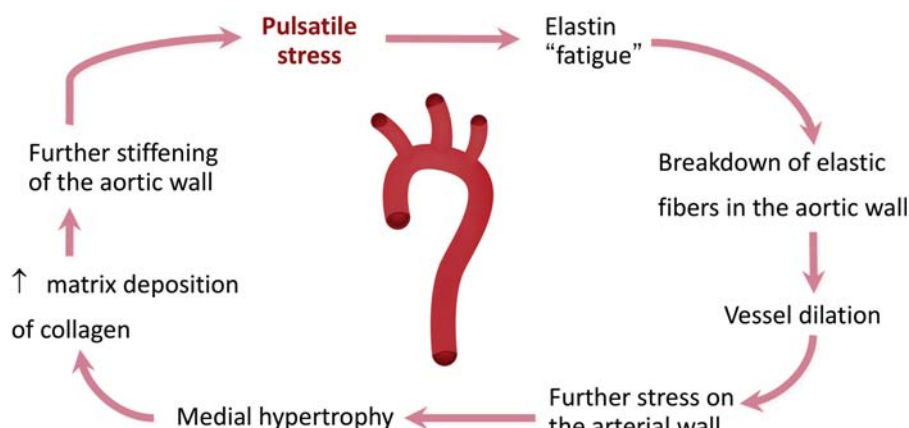
By disrupting this elastic architecture, this normal "wear and tear" of the aortic wall due to aging causes increased aortic stiffness and wall stress[41−44] and decreased aortic ability to buffer the pulsatile pressure generated by the heart. Importantly, loss of elastic fiber integrity reduces

aortic resilience, which allows the artery to dilate uniformly with aging.[45] Importantly, the process of age-related aortic stiffening is not a passive process, but involves multiple active mechanisms, discussed in detail in Section III of this textbook (Chapters 19−25).
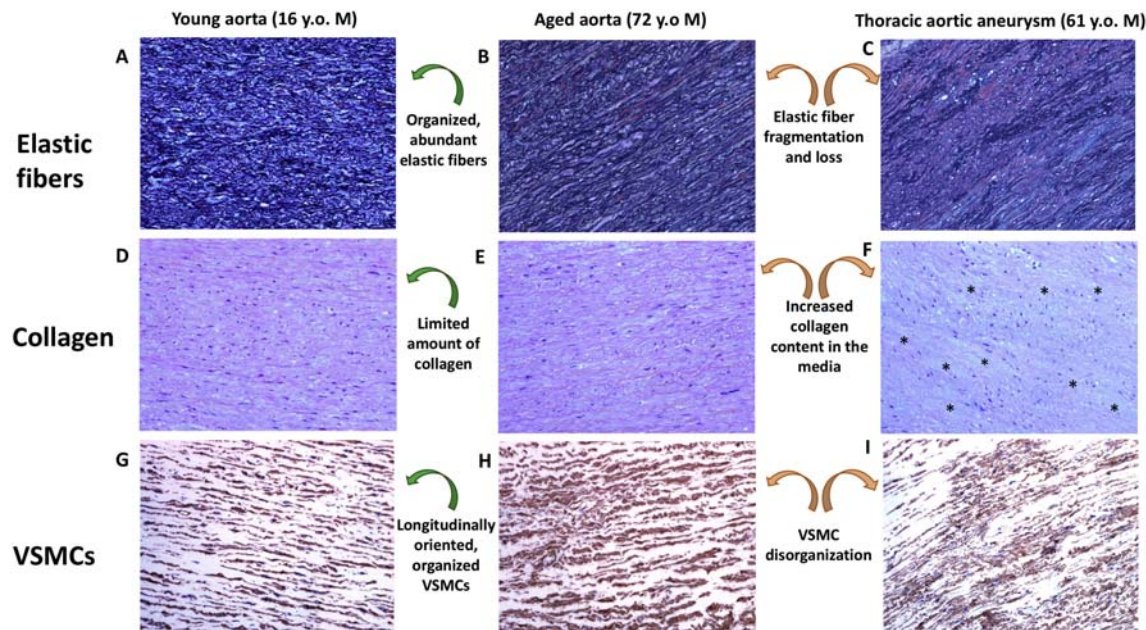
The aging process also affects the vascular smooth muscle cells (VSMCs) in the aortic wall. It has been demonstrated that aging promotes VSMC proliferation, migration, and apoptosis, in addition to a phenotypic change leading to a secretory behavior by the aortic VSMCs, which in turn promote vessel inflammation, calcification and further alterations in the ECM.[46] These changes cause additional alterations to aortic wall structure, further impairing pressure-buffering function. The role of VMCs in aortic stiffening is discussed in detail in Chapter 22.

Aneurysms are characterized by the localized yet permanent dilatation and weakening of the arterial wall.[47] Its underlying pathophysiology is multifactorial: inflammation of the aortic wall, modulation of the ECM, apoptosis of VSMCs, complex atherosclerosis, and oxidative stress.[48] Importantly, several of the structural abnormalities observed in histological examination of TAAs closely resemble those observed in aged, stiff aortas (Fig. 45.3). For example, the main histological findings of human TAA specimens include elastic fiber thinning, disorganization, fragmentation and loss; medial fibrosis (collagen deposition); and VSMC disorganization.[49] The main difference is that such histological abnormalities found in TAA tend to be focal, more severe, and occur at younger ages as compared to the normal arterial aging process.[50] As such, experts have suggested that TAA represents a focal, accelerated aging of a segment of the aortic wall.[45]

Importantly, the loss of elastic fiber integrity that occurs with both natural aging and TAA allows the wall to dilate either uniformly, as in aging when the loss is diffuse or locally, as in TAAs when the loss is focal. Realizing the

FIGURE 45.2 Arterial aging and aortic stiffness. With the repetitive stretch and recoil of the aorta over the years, there is fatigue of the elastic fibers in the aortic wall. This pulsatile stress leads to a series of structural alterations in the aortic wall's extracellular matrix that culminates with elastic fiber disruption, wall fibrosis (collagen deposition), and vessel remodeling. This promotes aortic wall stiffness and exacerbates pulsatile stress. This process occurs naturally with aging but is exacerbated in the presence of hypertension, cardiovascular risk factors, renal insufficiency, and systemic inflammatory conditions.

FIGURE 45.3   Structural similarities between natural aortic aging and thoracic aortic aneurysms. This figure demonstrates the structural alterations of the aortic wall that occur as a result of natural arterial aging (middle panels) and a thoracic aortic aneurysm (right-sided panels). Notably, even though the patient with a thoracic aortic aneurysm (TAA) is a decade younger than elderly patient without an aneurysm, he displayed even greater disruptions to aortic wall architecture and composition, suggesting exacerbated and accelerated arterial aging associated with the thoracic aortic aneurysm. These structural alterations are expected to lead to abnormalities in aortic stiffness, function, and pulsatile arterial hemodynamics. (A) Movat Pentachrome stain in an autopsy aortic specimen of a 16-year-old male who died of noncardiovascular causes. Elastic fibers are seen stained in black, and are abundant, intact and organized in the wall of a young, healthy aorta. (B) Movat Pentachrome stain from a 72-year-old male's aorta, demonstrating some sparsity and mild fragmentation of elastic fibers as compared to the young aorta specimen from panel A. (C) Movat Pentachrome stain from a surgical aortic specimen from a 61-year-old male with TAA. Note the significant fragmentation and sparsity of elastic fibers, leading to substantial disruption of arterial wall architecture. (D) Hematoxylin phloxine saffron (HPS) stain in the aortic specimen from the same 16-year-old male as in panel A. The areas stained in light blue, corresponding to collagen deposition in the extracellular matrix (ECM), are minimal. (E) HPS stain in the same aortic specimen from the 72-year-old male as in panel (B). Note the increase in the portions stained in light blue, corresponding to increased ECM collagen. (F) Hematoxylin and eosin stain from the same 61-year old male with TAA as in panel C. There is a substantial increase in ECM collagen deposition, highlighted by the *. (G) Muscle actin immunohistochemistry stain of the 16-year-old male's aorta. Vascular smooth muscle cells (VSMCs) are seen stained in dark red, and their nuclei are stained in blue. In this young aorta, the VSMCs and their nuclei are well organized along the aortic wall. (H) Muscle actin immunohistochemistry stain of the aged aorta (72-year-old male), demonstrating VSMC hypertrophy, distortion, and mild disorganization of the cells and their nuclei. (I) Muscle actin immunohistochemistry of a TAA in the 61-year-old male. There is extreme disorganization of VSMCs and their nuclei in the TAA wall, and the white "empty" spaces between the VSMCs represent areas of increased collagen and glycosaminoglycan deposition. *Images courtesy of Dr. John Veinot, Department of Pathology & Laboratory Medicine, The Ottawa Hospital − Ottawa, ON, Canada.*

close similarities between structural aortic alterations occurring in natural aging and in TAAs, and understanding the hemodynamic consequences resulting from aortic aging, we anticipate a significant potential for evaluating the hemodynamic consequences of aortic aging in the clinical evaluation of patients with TAA.

Aortic wall structure, aortic stiffness, and arterial biomechanics in thoracic aortic aneurysm

In animal models studying aortic aneurysm formation, blockade of plasmin formation by overexpression of plasminogen activator inhibitor-1 prevents the formation of aneurysms and aortic rupture by inhibiting MMP activation.[50] Aneurysm rupture correlates with an increase in MMP levels, local overexpansion of tissue inhibitor of MMPs can prevent aneurysmal degeneration and rupture,[51] confirming that enhanced and deleterious matrix remodeling contribute to structure alterations in the aortic wall, rendering it prone to dilation and rupture.

Per Laplace's law, wall tension (T) equals pressure (P) multiplied by radius (R), or $T = PR$. Aneurysm formation increases wall tension, causing further expansion of the aneurysmal segment.[52,53] As the aorta enlarges, distensibility of the aortic wall decreases.[52,53] At a diameter of 6 cm in size, the tensile limit is reached, and at this point, the aorta loses its natural elasticity and becomes a relatively rigid tube.[52,53] As a result, the aneurysmal aortic wall cannot further "stretch" during systole, so the critically enlarged aorta stays rigid and thus the full energy of the pulse wave is translated into wall stress.[52,53] This results in the enlarged aorta demonstrating lower distensibility and

higher wall stress, which may predispose to dissections as a result.[52,53] Fig. 45.4 illustrates a conceptual framework highlighting the potentially incremental effects of changes in aortic diameter and hemodynamics in increasing dissection risk.
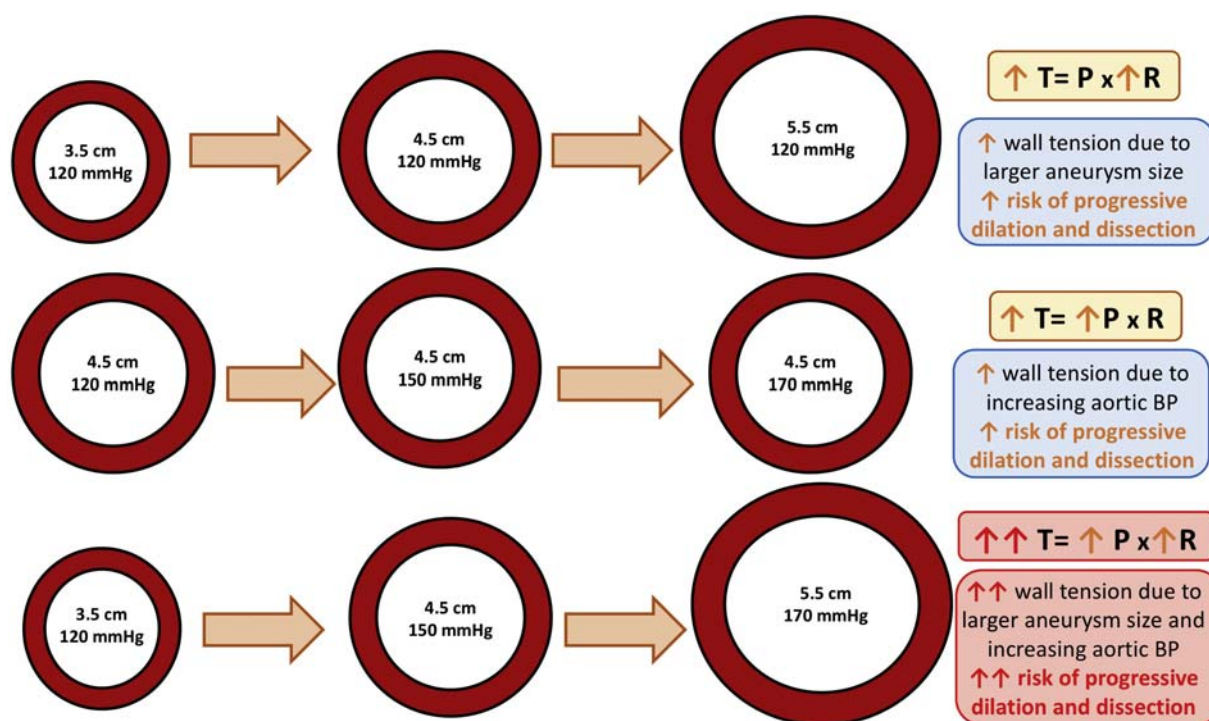
Based on the histopathological similarities between arterial aging and TAAs outlined in Section 3, it is possible that similar hemodynamic derangements observed as a consequence of an aged aorta may be observed in thoracic aneurysmal disease. This has been demonstrated in several forms of thoracic aortopathy, as summarized below.

Marfan syndrome

For a discussion of general concepts regarding genetic aortopathy, the reader is referred to Chapter 44. Marfan syndrome (MFS) is an autosomal dominant disorder caused by mutations in the FBN1 gene coding for a large glyco-protein called fibrillin-1.[54] Fibrillin-1 is a protein that forms one of the major components of microfibrils of elastin and is found at the periphery of elastic fibers in the medial layer of the ascending aorta.[52,54] The mutations in MFS result in a decrease in the amount of elastin in the aortic wall and a loss of elastin's normally highly organized structure.[55] As a consequence, the Marfan aorta exhibits abnormal elastic properties, including lower aortic distensibility[55–57] and greater aortic wall stiffness[58,59] than non-Marfan controls. As a result of these alterations in distensibility and stiffness, aortic pressure-buffering function is impaired in MFS, evidenced by the higher central pulse pressure and lower pulse pressure amplification in this population as compared to controls.[60] In addition, the age-related increases in aortic pulse wave velocity (the gold-standard measure of arterial stiffness and the hallmark of arterial aging) were greater in MFS patients as compared to non-Marfan controls.[61,62] Importantly, given their correlation with aortic wall structure and health, measures of aortic elasticity at baseline are associated with aneurysm growth rate in MFS. In a study of 608 people with MFS, above-median aortic root elastic modulus (assessed by transthoracic echocardiography) was associated with faster root growth, and top quartile aortic root elastic modulus was associated with greater risk of a composite outcome that included aortic root surgery, aortic dissection or death.[63]

Given the reported benefits of atenolol and losartan in curbing aneurysm expansion in patients with MFS, these two medications have been compared in a small randomized clinical trial in terms of their effects on the

FIGURE 45.4 Role of aortic size and pressure on wall tension and possible aortic dissection risk. Conceptual framework demonstrating the potentially incremental effects of aneurysm size and aortic pressure on potential risk of progressive aortic dilation and dissection resulting from increased wall tension. Larger aneurysms with the greatest alterations in aortic wall structure, resulting in impaired aortic pressure-buffering function and increased central blood pressure, may have the highest risk for progressive aneurysm expansion and aortic dissection. This conceptual framework illustrates the need to consider both aortic size and aortic hemodynamics to improve estimation of disease activity and risk of acute aortic syndromes in patients with thoracic aortic aneurysms. *BP*, blood pressure.

biomechanical properties of the aorta. Although there were group imbalances in terms of participant sex and baseline aortic root size, the main finding was that losartan therapy led to more favorable changes in measures of aortic stiffness (pulse wave velocity) and pulsatile arterial hemodynamics (aortic impedance, total arterial compliance) as compared to Atenolol.[64] These findings highlight measures of aortic stiffness and pulsatile hemodynamics as potential therapeutic targets in MFS patients with TAA.

Loeys−Dietz syndrome

Although MFS has been most vastly studied, alterations in aortic stiffness and pulsatile hemodynamics have also been reported in individuals with other heritable forms of aortopathy, helping prove the concept that the deleterious structural alterations in the aortic wall that simulate the natural aging process may be responsible for hemodynamic abnormalities in this population. Among patients with Loeys−Dietz syndrome (LDS), an autosomal dominant disease characterized by mutations in transforming growth factor beta receptor 1 or 2, there is increased transforming growth factor beta signaling[65] in the arterial walls, which culminates in disorganization of elastic fibers and enhanced deposition of collagen in the aortic media (again, similar to the processes observed with natural aging, but in these cases occurring much earlier in life, and in an exacerbated fashion).[65] Unlike MFS, literature reporting arterial hemodynamic alterations in LDS is scant. In a study of 31 patients with heritable aortopathies that included five participants with LDS, aortic distensibility and strain (estimated with transthoracic echocardiography) was lower in aortopathy patients as compared to controls, even when their aortas were not dilated.[66] Aortopathy patients with dilated aortic root had the worse values of aortic distensibility and strain.

Familial thoracic aortic aneurysms and dissections

Familial thoracic aortic aneurysms and dissection (FTAAD) describes a spectrum of heritable disorders associated with aortopathy in the absence of identifiable syndromes or other characteristic phenotypical features. Several gene mutations have been reported in FTAAD, including SMAD3, ACTA2, MYH11, MYLK, and PRKG1. Description of aortic specimens from individuals with FTAAD caused by MYH11 mutation also demonstrates focal medial degeneration, with increased proteoglycans, decreased elastic fibers, and disorganized VSMCs.[67] Similarly, in six individuals with FTAAD due to ACTA2 mutation, aortic tissue examination showed loss of elastic fibers, marked medial smooth muscle cell proliferation, and increased proteoglycan accumulation.[68] At the time of writing of this chapter, human hemodynamic data from FTAAD remain extremely scant. In a study of eight asymptomatic subjects with a mutation of the MYH11 gene but without aortic aneurysms, MRI-derived aortic compliance and distensibility were significantly lower, and aortic pulse wave velocity was higher when compared to 21 controls without this mutation.[69]

Bicuspid aortic valve

BAV is the most common form of congenital heart disease, affecting 0.5%−2.0% of the population. As a result, aortopathy associated with BAV is the most common form of heritable aortopathy. Being relatively common, BAV aortopathy has benefited from abundant research with regards to aortic elasticity and hemodynamics. The body of available data is fairly concordant in identifying abnormal aortic material properties and adverse pulsatile hemodynamics in patients with BAV. Similar to what was described above for MFS, LDS, and FTAAD, histological examination of BAV-TAA also demonstrates varying degrees of elastic fiber fragmentation and smooth muscle cell abnormalities,[70] also resembling abnormalities found in the naturally aged aorta. Importantly, advanced histological abnormalities in BAV-TAA can be found even when the aorta is not severely dilated,[70] confirming the notion that the absolute size of the aorta is an imperfect predictor of aortic wall disease and subsequent risk. Another important observation is that, in BAV-TAA, the greatest severities of aortic wall histological abnormalities were found in younger individuals,[70,71] giving rise to the notion that the arterial age may be more relevant than chronological age for understanding TAA disease activity and risks.

These structural abnormalities of the aortic wall in BAV predispose patients to impaired aortic biomechanics and function. Compared to individuals with TAA but who have trileaflet aortic valves, aortas from BAV-TAA have greater collagen-related stiffness.[72] Perhaps as a result of this, the elastic module of BAV-TAA aortas has been shown to be higher than in trileaflet aortic valve TAA and in normal aortas, translating into greater wall stiffness in BAV-TAA.[72] The aortic energy loss, a size-independent measure defined as hysteresis normalized to total stored strain energy, represents the relative amount of energy absorbed by the aorta during the cardiac cycle. Higher energy loss highlights greater aortic inefficiency in expanding to act as a capacitor during systole, and in recoiling to return the stored energy to the circulation in diastole. The aortic energy loss correlates with elastin and collagen composition in the aortic wall, increasing with lower elastin and greater collagen content.[72] As such, aortic energy loss directly reflects aortic health by corresponding to the aorta's pressure-buffering function and efficiency in performing Windkessel functions. Aortic energy loss is higher in BAV-TAA than in normal aortas, reflecting abnormal aortic

pressure-buffering function in BAV aneurysms, but not as high as in trileaflet aortic valve TAAs, who have the greatest aortic energy loss and, therefore, the worst aortic function.[72]

The BAV-TAA abnormalities in aortic stiffness and aortic function identified in the fundamental studies above have also been demonstrated in clinical studies that have used imaging techniques to estimate aortic stiffness and hemodynamics. Even in the absence of an aneurysm, the aortas of patients with BAV already display lower distensibility and higher stiffness index, estimated by transthoracic echocardiography, as compared to controls with trileaflet aortic valves.[73,74] In addition, lower aortic distensibility and higher stiffness index correlate with larger aneurysm sizes in BAV.[74] Among 50 BAV patients, 28% of whom had dilated ascending aortas, carotid-femoral pulse wave velocity (cfPWV), central augmentation index, and central pulse pressure were higher, whereas pulse pressure amplification was lower than in age- and sex-matched trileaflet aortic valve controls without aortopathy.[75]

There appears to be a gradient of aortic hemodynamic abnormalities based on clinical involvement of the aorta in patients with BAV. As demonstrated by the aforementioned studies, measures of aortic stiffness and function are abnormal in BAV patients when compared to trileaflet aortic valve controls. But even within the group of BAV subjects, further deterioration of aortic function is observed based on degree of aortic involvement. In 32 men with BAV, 16 of whom also had a TAA, cfPWV, augmentation index, central systolic, and pulse pressures were higher, and pulse pressure amplification was lower among patients with BAV-TAA as compared to those with BAV alone, despite similar ages, body sizes, and brachial blood pressures.[76] BAV-TAA participants also exhibited greater circulating levels of matrix metalloproteinase-2 (MMP-2) than those with BAV alone, likely reflecting a greater degree of adverse arterial wall remodeling among those with an aneurysm.

Measures of aortic stiffness and pulsatile arterial hemodynamics also appear to carry potential to serve as gauges for disease activity and risk in BAV. We have previously shown that higher cfPWV, aortic characteristic impedance (Z_c) and amplitude of the forward pressure wave (P_f), and lower total arterial and proximal aortic compliances are independently associated with faster TAA expansion among individuals with BAV.[77] Subsequently, Longobardo and colleagues evaluated 47 BAV patients who underwent echocardiographic evaluation of ascending aorta longitudinal strain (LS), finding that lower aortic LS was independently associated with progressive aortic dilation and need for aortic surgery after a 48 ± 11 month follow-up.[78]

Turner's syndrome

Turner's syndrome is a genetic disorder caused by the presence of a single X chromosome (typically 45X0), and associated with cardiovascular abnormalities in approximately half of affected patients.[79] Although aortic dissection is relatively uncommon in Turner's syndrome,[79] at least one predisposing factor to aortic dissection including BAV, HTN, or aortic coarctation is present in 90% of patients. A few patients with Turner's syndrome also have dilation of aortic root, although the true prevalence is unknown. Aortic root diameters have been shown to be significantly larger for Turner's syndrome patients with 45XO karyotype (complete absence of the second X chromosome in all cells), as compared to those with either mosaic (when some cells have a second X chromosome, and some do not), isochromosome (when one of the X chromosomes is composed of mirror images of one of the arms of the chromosome, resulting in deletion of the opposite arm) or deletion (when the individual has two X chromosomes, but one of them has a deletion) forms of the disorder, and to controls.[80] These differences were observed despite similar body sizes among groups. Aortic dilation has been reported as present in 29%[81]−46%[81] of TS patients. It appears that abnormalities of aortic function may be most prominent among Turner's syndrome patients with some degree of aortopathy, confirming the link between aortic pathology and aortic function. Aortic distensibility, assessed by echocardiography, has been reported to be significantly lower in Turner's syndrome patients with aortic dilation as compared to those with normal aortas, and controls without Turner's syndrome or TAA.[81] Similarly, Turner's syndrome patients who have aortic coarctation have much lower MRI-derived descending aorta distensibility than age-matched female controls and Turner's syndrome patients without coarctation.[82] In this study, lower aortic distensibility in Turner's syndrome resulted in higher central systolic blood pressure.

Ehlers−Danlos syndrome

Patients with vascular EDS (EDS type IV) have very different aortic pathology as compared to MFS, BAV, FTAAD, and LDS. Instead of disruption of elastic fiber integrity promoting collagen deposition in the aortic wall, as seen in other heritable aortopathies, vascular EDS is an autosomal dominant condition characterized by mutation in the gene encoding type III procollagen (COL3A1), which leads to deficits in the most abundant type of collagen found in the aorta's ECM. This results in excessive vessel fragility and predisposition to rupture. In contrast to MFS, vascular EDS most often involves the descending thoracic

and abdominal portions of the aorta and can be complicated by arterial rupture even in the absence of vessel dilation. As could be expected by the different type of insult to the aortic wall, it appears that EDS leads to normal to increased arterial elasticity. In a study of 12 individuals with EDS from six families, four of whom had vascular EDS, EDS participants did not have different aortic or carotid pressure strain elastic modulus or beta stiffness index as compared to controls.[83] Conversely, in a study of 60 EDS patients (eight of whom had vascular EDS), patients with this condition had lower cfPWV when compared to age-based reference values from normal subjects.[84]

Degenerative aortopathy

Patients with degenerative TAAs are typically older, with high prevalence of HTN and other cardiovascular risk factors. Considering the significant similarities between natural aortic aging and pathological alterations of the aortic wall in TAAs, perhaps degenerative thoracic aortopathy may represent the ultimate manifestation of aortic aging. By adding further structural disruptions to an aortic wall that may already be abnormal from aging, patients with degenerative TAAs may exhibit the greatest abnormalities in measures of aortic health and function. Concordant to this hypothesis, in a recent study, Chung et al. performed extensive biomechanical testing of human aortic tissue and demonstrated that S_d, the force required to mechanically tear apart the aortic sample, was the lowest among dissected aortas, and lower in patients with non-dissected TAAs with trileaflet aortic valves (91% of whom had degenerative TAAs) than in patients with nondissected BAV-TAA.[72] In the same study, the authors also showed that aortic energy loss is much higher in the trileaflet TAA patients (again, 91% of whom had degenerative aneurysms) than in BAV-TAA and nonaneurysm controls, and that aortic energy loss was inversely correlated with S_d. The interpretation of these findings is that degenerative TAAs have the greatest disruption to elastin/collagen balance in the wall, leading to the greatest impairments to the aorta's pressure-buffering function and the highest susceptibility to dissection.

In a separate biomechanical study, surgical aortic specimens from 26 subjects with degenerative TAA (average aneurysm size: 59 ± 3 mm) were examined and compared to fresh postmortem control aortic specimens from 15 age-matched individuals without aortopathy.[85] TAA specimens had lower elastin density in the aortic wall when compared to control aortas, as well as lower wall thickness and failure strain values, and higher peak elastic modulus. Failure stress (i.e., tensile strength) was not different between TAA and control aortic specimens. These findings confirm that aortas affected by degenerative TAA have greater structural disruption to wall architecture (lower elastin fiber density) and are considerably stiffer than aortas of age-matched control subjects, once again highlighting the accelerated vascular aging affecting the aortic wall of patients with aortopathy. In addition, since the tensile strength of TAAs does not appear to be different than that of unaffected aortas, with only weak negative correlations between maximum aneurysm diameter and tensile strength, findings from this study also corroborate the notion that aneurysm size (the universally acknowledged criterion considered for prophylactic surgical intervention) may not be the most representative parameter for the quality of aortic tissue. Rather, the rupture risk of TAAs (in the case of this study, degenerative TAAs) may be better ascribed to the increased wall stresses caused by tissue stiffening and vessel enlargement. Importantly, and particularly relevant for degenerative TAAs (whose main risk factor is HTN), a study that focused on the effects of HTN and wall stiffness found that stiffer TAAs were correlated with the most altered distribution of wall stress, and an acute change of peripheral vascular resistance could significantly increase the risk of rupture for a stiffer aneurysm.[86]

Measures of aortic stiffness and pulsatile hemodynamic as markers of disease activity and thoracic aortic aneurysm—related risk

The natural history of TAA is one of slow expansion with an increasing risk of aortic dissection as the aorta enlarges. The rate of aneurysm growth gives insights into disease activity, highlighting potential adverse processes occurring in an unstable aortic wall that ultimately promotes growth. Expansion rates range from 0.1 to 1.0 cm per year, depending upon TAA etiology diameter and location within the aorta.[1−3,87−89] A recent meta-analysis reported that the average TAA expansion rate is ∼0.60 mm/year, being faster for those with BAV (∼0.76 mm/year) and those with trileaflet aortic valves (∼0.34 mm/year).[90] Although sex-based data have historically lacked, we have demonstrated that TAA expansion is twice as fast in women than men, which seems to be unique to individuals with degenerative forms of TAA.[25]

Given the direct links between aortic wall structural and functional abnormalities, leading to accelerated vascular aging and alterations in the aorta's mechanical properties in the presence of TAA, it is reasonable to consider that alterations in aortic function (aortic stiffness and pulsatile hemodynamics) may present a window to better understand aortic health, disease activity, and risk (Fig. 45.5).

At the time of writing of this chapter, this remains a relatively new area for research but with significant potential to positively impact the field. To date, a few studies have evaluated the role of measures of aortic stiffness and

FIGURE 45.5 Potential mechanisms linking aortic stiffness, central blood pressure, and pulsatile arterial load to thoracic aortic aneurysm expansion. The compliance and pressure-buffering function of the aorta are intrinsically linked to the health of its wall. According to this premise, it is possible that thoracic aortic aneurysm patients with more active disease in the wall (i.e., greater degree of inflammation, elastic fiber disruption, and matrix remodeling) may be identified by greater aortic stiffness and impaired pressure-buffering capacity. This, in turn, marks an individual whose aneurysm is more likely to expand over time, and highlights a window to identify disease activity, increase surveillance, and develop targeted therapies to control the disease. *cfPWV*, carotid-femoral pulse wave velocity; *PP*, pulse pressure; *SBP*, systolic blood pressure. *Adapted, with permission, from Boczar KE, Boodhwani M, Beauchesne L, et al. Aortic stiffness, central blood pressure, and pulsatile arterial load predict future thoracic aortic aneurysm expansion. **Hypertension**. 2021; 77:126−134.*

hemodynamics as potential predictors of aneurysm size, expansion or acute aortic syndromes. Research from our group has focused on noninvasive assessment of aortic stiffness (cfPWV), central blood pressure, and pulsatile hemodynamics (assessed with pressure-flow analyses that integrate pressure data from arterial applanation tonometry with flow and volume data from transthoracic echocardiography, as described in detail in Chapters 1−3). In an initial cross-sectional study, we demonstrated that aortic stiffness, measured by cfPWV, as well as measures of higher pulsatile arterial load (central systolic blood pressure, central pulse pressure, proximal aortic compliance global reflection coefficient, and reflected pressure wave amplitude in univariable analyses; central systolic blood pressure and global reflection coefficient retained statistical significance in multivariable analyses) are correlated with larger aneurysm sizes in women, but not in men,[91] suggesting a greater role for aortic structural and functional abnormalities in women with TAA. In accordance to his topic, in a retrospective evaluation, we have shown that greater aortic stiffness (cfPWV) is independently associated

with a faster rate of aneurysm growth, and that this association is stronger in women than men.[92] Also in a retrospective analysis, we focused on the subgroup of participants who had a TAA associated with a BAV and showed that a stiffer aorta (higher cfPWV) with higher measures of pulsatile arterial load (higher aortic characteristic impedance and forward pressure wave amplitude, as well as lower proximal aortic, and total arterial compliances) was associated with faster aneurysm expansion rates in the BAV-TAA population.[77]
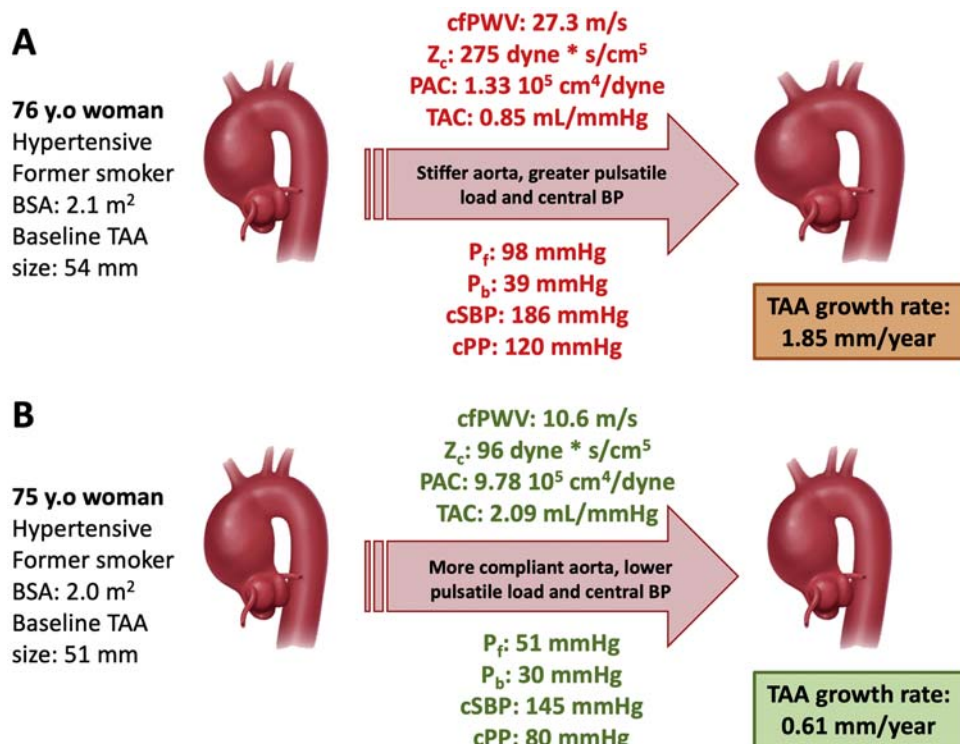
In prospective studies that have included participants with all TAA etiologies (58% degenerative TAA, 42% heritable TAA with the majority having a BAV), we have demonstrated the independent value of baseline aortic stiffness and aortic function assessment for the evaluation of future aneurysm growth. Higher aortic stiffness (cfPWV) and greater pulsatile arterial load (higher central systolic and pulse pressures, amplitude of the forward and reflected pressure waves, and lower total arterial compliance) at baseline were not only independently associated with faster TAA expansion in the future, but some of the hemodynamic

measures (namely cfPWV, forward pressure wave amplitude, and central pulse pressure) were even stronger correlates of future TAA growth than the current clinical standard of care (aneurysm size).[93] Fig. 45.6 illustrates a comparison of two real-life examples of patients with similar clinical characteristics and baseline TAA sizes, but with very different aortic stiffness and pulsatile hemodynamic measures, resulting in different rates of aneurysm expansion.

Further, it appears that undertaking an aortic evaluation that takes into account both aortic size and function may be a superior strategy for assessment of TAA disease activity, as the combination of aneurysm size with variables reflecting aortic stiffness and pulsatile hemodynamics were more strongly associated with future TAA expansion than aneurysm size or aortic function measures alone.[94] This is directly in line with the concepts proposed in Fig. 45.4, whereby combined abnormalities of aortic diameter and hemodynamics/pressure have potential to cause the greatest increases in aortic wall tension, which, in turn, may lead to unstable aneurysmal disease.

The role of assessing the aorta's function and elastic properties has also been demonstrated in the specific population of patients with TAA due to MFS. In a study of 78 unoperated MFS patients who underwent aortic stiffness and distensibility assessment by MRI, both larger aortic diameter and lower aortic distensibility were found to be independent predictors of future aneurysm expansion.[95] In this study, a 10^{-3} mmHg^{-1} decrease in aortic distensibility was associated with a fourfold increase in the risk of experiencing progressive aortic dilation, independent of baseline aortic diameter. Most recently, a separate study of 117 unoperated MFS patients followed patients prospectively after MRI, showing that lower proximal aorta LS at baseline was independently associated with faster aneurysm growth rate in the future, and aortic events (composite of aortic dissection and elective aortic surgery).[96] Confirming the notion that including information about aortic health/function/elasticity improves risk stratification in TAA (in this case, in MFS-TAA), the authors compared the receiver-operating characteristic curves for aortic diameter alone (C-statistic: 0.80), aortic LS alone (C-statistic: 0.74), and a full model that included age, sex, aortic diameter, and aortic LS (C-statistic: 0.95) in the prediction of aortic events, demonstrating that combining aortic size and function is better than each parameter alone in this prediction.

FIGURE 45.6 Comparison of two patients with similar clinical characteristics and baseline thoracic aortic aneurysm (TAA) sizes, but with different rates of aneurysm expansion. Despite similar age, clinical characteristics, and baseline aneurysm sizes, Patient A has a stiffer aorta, with greater pulsatile load and central pulse pressure (cPP) leading to faster aneurysm expansion compared to Patient B who has a more compliant aorta (albeit, with the same baseline aneurysm size). This highlights the fact that measures of aortic stiffness, central blood pressure, and pulsatile arterial load could potentially be clinically useful office-based markers for TAA risk assessment and determination of disease activity in TAA. *BSA*, body surface area; *cfPWV*, carotid-femoral pulse wave velocity; *cSBP*, central systolic blood pressure; *PAC*, proximal aortic compliance; *Pb*, reflected pressure wave amplitude; *Pf*, forward pressure wave amplitude; *TAC*, total arterial compliance; *Zc*, characteristic impedence of the aorta. *Adapted, with permission, from Boczar KE, Boodhwani M, Beauchesne L, et al. Aortic stiffness, central blood pressure, and pulsatile arterial load predict future thoracic aortic aneurysm expansion.* **Hypertension**. *2021; 77:126−134.*

When it comes to assessing disease activity and risk in TAA, it also makes sense to include HTN as a potential prognostic factor in patients with this condition. Arterial HTN is the greatest population-attributable risk factor leading to the development of TAAs.[97–99] Being highly prevalent among TAA patients, HTN is a predictor of acute aortic syndromes in these patients and negatively influences their overall survival.[7,97,98,100,101] Importantly, HTN increases hemodynamic forces on the ascending aorta.[102] In these cases, the aortic VSMC's mechanosensing is stressed by the increased forces on the wall, leading to misperceptions of high stress as low stress and resulting in maladaptive remodeling.[102,103] Importantly, wall stress increases almost linearly with systolic blood pressure.[104,105] Thus, controlling HTN is particularly important in TAA in order to reduce aortic wall stress[104] and, in turn, target disease prevention.[45,103] Understanding the importance of HTN in TAA, we must acknowledge that HTN is typically diagnosed based on brachial blood pressure, which does not perfectly reflect central blood pressure and may better predict cardiovascular events.[106] To address this, we have prospectively studied patients with TAA and found that occult central HTN (i.e., central systolic blood pressure ≥ 130 mmHg in the presence of brachial blood pressure < 140 mmHg and no previous clinical diagnosis of HTN) is relatively common, affecting 15% of TAA patients.[107] Furthermore, among all patients, while baseline brachial BP was not associated with aneurysm size or aneurysm growth, higher central blood systolic and pulse pressures were independently associated with larger aneurysms among those without a clinical diagnosis of HTN, and with faster future aneurysm expansion in all participants regardless of previous HTN diagnosis. Similar to our findings, in the aforementioned study of 117 MFS-TAA, brachial blood pressure was not included in multivariable statistical models for prediction of aortic growth and aortic events, as it was not associated with these outcomes.[96] Therefore, although HTN diagnosed by brachial artery measurement remains an important risk factor for TAA and acute aortic syndromes, it appears that central BP and central HTN may carry even higher potential for improving risk stratification of TAA patients. In addition, central blood pressure may present a viable therapeutic target aimed at controlling TAA expansion and complications, which remains amenable to testing in clinical trials.

Conclusions and future directions

Thoracic aortopathies are silent killers of increasing prevalence. Despite this, TAA remains an understudied condition with suboptimal management strategies that rely on an imperfect parameter (aortic size) for decision-making, followed by a watchful waiting until an irreversible abnormality occurs and either culminates in a catastrophic

outcome (acute aortic syndrome) or in prophylactic surgical repair. In the present chapter, we demonstrated the similarities between natural aortic aging and TAA (considered by some as an accelerated, focal aging of the affected segment of aortic wall), the resulting aortic functional and hemodynamic abnormalities associated with thoracic aortopathy, and the role of alterations in aortic stiffness and hemodynamics on aneurysm growth and aortic events.

Although this research field is relatively young, existing evidence highlights a significant role for incorporating measures of function (aortic stiffness, central blood pressure, and pulsatile hemodynamics) into clinical practice to better assess a patient's disease activity and aneurysm-related risk. By affording a window into the evolving fundamental biology of TAA expansion, measures of aortic function may provide an early indication of when adverse events are occurring in the aortic wall, presenting the opportunity to intervene on susceptible patients before experiencing excessive dilation and having to resort to surgery to correct an irreversible abnormality. This is key for development of new therapies for TAA, as there is a potential for these aortic function measures to be used toward identifying patients that would benefit from novel biological therapies directed toward the unstable aortic wall. Further, aortic function measures may be used to personalize a surveillance plan for patients, suggesting closer imaging follow-up and earlier prophylactic surgery for those with faster predicted growth or higher risk of aortic events, and longer imaging intervals and delayed surgical intervention for those with slower predicted growth or lower risk of events. This will optimize utilization of healthcare resources. By moving from standard size cutoffs to a personalized assessment based on a combination of individual characteristics, aortic size, and function, TAA care will be brought into the realm of precision medicine, with significant potential to improve outcomes. To achieve this, additional studies are needed to develop and validate TAA risk prediction algorithms, and to test biological interventions aimed at containing disease activity and preventing progressive aneurysm dilation.

References

1. Davies RR, Gallo A, Coady MA, et al. Novel measurement of relative aortic size predicts rupture of thoracic aortic aneurysms. **Ann Thorac Surg**. 2006; 81:169−177.
2. Elefteriades JA. Natural history of thoracic aortic aneurysms: indications for surgery, and surgical versus nonsurgical risks. **Ann Thorac Surg**. 2002; 74:S1877−S1880. discussion S1892-8.
3. Kuzmik GA, Sang AX, Elefteriades JA. Natural history of thoracic aortic aneurysms. **J Vasc Surg**. 2012; 56:565−571.
4. Milewicz DM, Guo DC, Tran-Fadulu V, et al. Genetic basis of thoracic aortic aneurysms and dissections: focus on smooth muscle cell contractile dysfunction. **Ann Rev Genom Hum Genet**. 2008; 9:283−302.

5. Landenhed M, Engstrom G, Gottsater A, et al. Risk profiles for aortic dissection and ruptured or surgically treated aneurysms: a prospective cohort study. **J Am Heart Assoc**. 2015; 4.

6. Bickerstaff LK, Pairolero PC, Hollier LH, et al. Thoracic aortic aneurysms: a population-based study. **Surgery**. 1982; 92:1103−1108.

7. Chan KK, Rabkin SW. Increasing prevalence of hypertension among patients with thoracic aorta dissection: trends over eight decades–a structured meta-analysis. **Am J Hypertens**. 2014; 27:907−917.

8. Boodhwani M, Andelfinger G, Leipsic J, et al. Canadian Cardiovascular Society position statement on the management of thoracic aortic disease. **Can J Cardiol**. 2014; 30:577−589.

9. Clouse WD, Hallett Jr JW, Schaff HV, Gayari MM, Ilstrup DM, Melton 3rd LJ. Improved prognosis of thoracic aortic aneurysms: a population-based study. **J Am Med Assoc**. 1998; 280:1926−1929.

10. van Walraven C, Wong J, Morant K, Jennings A, Jetty P, Forster AJ. Incidence, follow-up, and outcomes of incidental abdominal aortic aneurysms. **J Vasc Surg**. 2010; 52, 282-289 e1-2.

11. Lodewyks CL, Prior HJ, Hiebert BM, et al. A province-wide analysis of the epidemiology of thoracic aortic disease: incidence is increasing in a sex-specific way. **Can J Cardiol**. 2020; 36:1729−1738.

12. McClure RS, Brogly SB, Lajkosz K, Payne D, Hall SF, Johnson AP. Epidemiology and management of thoracic aortic dissections and thoracic aortic aneurysms in Ontario, Canada: a population-based study. **J Thorac Cardiovasc Surg**. 2018; 155:2254−2264 e4.

13. Smedberg C, Steuer J, Leander K, Hultgren R. Sex differences and temporal trends in aortic dissection: a population-based study of incidence, treatment strategies, and outcome in Swedish patients during 15 years. **Eur Heart J**. 2020; 41:2430−2438.

14. Huynh TT, Starr JE. Diseases of the thoracic aorta in women. **J Vasc Surg**. 2013; 57, 11S-7S.

15. Anagnostopoulos C. **Diagnosis of Aortic Dissection**. Baltimore, MD: University Park Press; 1975.

16. Elefteriades JA, Barrett PW, Kopf GS. Litigation in nontraumatic aortic diseases–a tempest in the malpractice maelstrom. **Cardiology**. 2008; 109:263−272.

17. von Kodolitsch Y, Schwartz AG, Nienaber CA. Clinical prediction of acute aortic dissection. **Arch Intern Med**. 2000; 160:2977−2982.

18. Spittell PC, Spittell Jr JA, Joyce JW, et al. Clinical features and differential diagnosis of aortic dissection: experience with 236 cases (1980 through 1990). **Mayo Clin Proc**. 1993; 68:642−651.

19. Fradet G, Jamieson WR, Janusz MT, Ling H, Miyagishima RT, Munro AI. Aortic dissection: current expectations and treatment. Experience with 258 patients over 20 years. **Can J Surg**. 1990; 33:465−469.

20. Huynh N, Thordsen S, Thomas T, et al. Clinical and pathologic findings of aortic dissection at autopsy: review of 336 cases over nearly 6 decades. **Am Heart J**. 2019; 209:108−115.

21. Chung J, Coutinho T, Chu MWA, Ouzounian M. Sex differences in thoracic aortic disease: a review of the literature and a call to action. **J Thorac Cardiovasc Surg**. 2020; 160:656−660.

22. Boczar K, Coutinho T. Sex considerations in aneurysm formation, progression and outcomes. **Can J Cardiol**. 2018; 34:362−370.

23. Lo RC, Schermerhorn ML. Abdominal aortic aneurysms in women. **J Vasc Surg**. 2016; 63:839−844.

24. Olsson C, Thelin S, Stahle E, Ekbom A, Granath F. Thoracic aortic aneurysm and dissection: increasing prevalence and improved outcomes reported in a nationwide population-based study of more than 14,000 cases from 1987 to 2002. **Circulation**. 2006; 114:2611−2618.

25. Cheung K, Boodhwani M, Chan KL, Beauchesne L, Dick A, Coutinho T. Thoracic aortic aneurysm growth: role of sex and aneurysm etiology. **J Am Heart Assoc**. 2017; 6.

26. Chung J, Stevens LM, Ouzounian M, et al. Sex-related differences in patients undergoing thoracic aortic surgery. **Circulation**. 2019; 139:1177−1184.

27. Nienaber CA, Fattori R, Mehta RH, et al. Gender-related differences in acute aortic dissection. **Circulation**. 2004; 109:3014−3021.

28. Davies RR, Goldstein LJ, Coady MA, et al. Yearly rupture or dissection rates for thoracic aortic aneurysms: simple prediction based on size. **Ann Thorac Surg**. 2002; 73:17−27. discussion 27-8.

29. Juvonen T, Ergin MA, Galla JD, et al. Prospective study of the natural history of thoracic aortic aneurysms. **Ann Thorac Surg**. 1997; 63:1533−1545.

30. Pape LA, Tsai TT, Isselbacher EM, et al. Aortic diameter >or = 5.5 cm is not a good predictor of type A aortic dissection: observations from the International Registry of Acute Aortic Dissection (IRAD). **Circulation**. 2007; 116:1120−1127.

31. Galis ZS, Khatri JJ. Matrix metalloproteinases in vascular remodeling and atherogenesis: the good, the bad, and the ugly. **Circ Res**. 2002; 90:251−262.

32. Papazafiropoulou A, Tentolouris N. Matrix metalloproteinases and cardiovascular diseases. **Hippokratia**. 2009; 13:76−82.

33. Wu XF, Zhang J, Paskauskas S, Xin SJ, Duan ZQ. The role of estrogen in the formation of experimental abdominal aortic aneurysm. **Am J Surg**. 2009; 197:49−54.

34. Sokolis DP, Iliopoulos DC. Impaired mechanics and matrix metalloproteinases/inhibitors expression in female ascending thoracic aortic aneurysms. **J Mech Behav Biomed Mater**. 2014; 34:154−164.

35. Erbel R, Aboyans V, Boileau C, et al. 2014 ESC Guidelines on the diagnosis and treatment of aortic diseases: document covering acute and chronic aortic diseases of the thoracic and abdominal aorta of the adult. The Task Force for the Diagnosis and Treatment of Aortic Diseases of the European Society of Cardiology (ESC). **Eur Heart J**. 2014; 35:2873−2926.

36. Kabra A, Neri L, Weiner H, Khalil Y, Matsumura ME. Carotid intima-media thickness assessment in refinement of the Framingham Risk Score: can it predict ST-elevation myocardial infarction? A pilot study. **Echocardiography**. 2013; 30:1209−1213.

37. Kim EK, Choi SH, Sung K, et al. Aortic diameter predicts acute type A aortic dissection in patients with Marfan syndrome but not in patients without Marfan syndrome. **J Thorac Cardiovasc Surg**. 2014; 147:1505−1510.

38. Groenink M, Langerak SE, Vanbavel E, et al. The influence of aging and aortic stiffness on permanent dilation and breaking stress of the thoracic descending aorta. **Cardiovasc Res**. 1999; 43:471−480.

39. Najjar SS, Scuteri A, Lakatta EG. Arterial aging: is it an immutable cardiovascular risk factor? **Hypertension**. 2005; 46:454−462.

40. O'Rourke MF, Safar ME, Dzau V. The cardiovascular continuum extended: aging effects on the aorta and microvasculature. **Vasc Med**. 2010; 15:461−468.

41. Bruel A, Oxlund H. Changes in biomechanical properties, composition of collagen and elastin, and advanced glycation endproducts of the rat aorta in relation to age. **Atherosclerosis**. 1996; 127:155−165.

42. Bader H. Dependence of wall stress in the human thoracic aorta on age and pressure. **Circ Res**. 1967; 20:354−361.

43. Dobrin PB. Mechanical properties of arteries. **Physiol Rev**. 1978; 58:397−460.

44. Spina M, Garbisa S, Hinnie J, Hunter JC, Serafini-Fracassini A. Age-related changes in composition and mechanical properties of the tunica media of the upper thoracic human aorta. **Arteriosclerosis**. 1983; 3:64−76.

45. Humphrey JD, Schwartz MA, Tellides G, Milewicz DM. Role of mechanotransduction in vascular biology: focus on thoracic aortic aneurysms and dissections. **Circ Res**. 2015; 116:1448−1461.

46. Monk BA, George SJ. The effect of ageing on vascular smooth muscle cell behaviour–A mini-review. **Gerontology**. 2015; 61:416−426.

47. Boese AC, Kim SC, Yin KJ, Lee JP, Hamblin MH. Sex differences in vascular physiology and pathophysiology: estrogen and androgen signaling in health and disease. **Am J Physiol**. 2017; 313:H524−H545.

48. Makrygiannis G, Courtois A, Drion P, Defraigne JO, Kuivaniemi H, Sakalihasan N. Sex differences in abdominal aortic aneurysm: the role of sex hormones. **Ann Vasc Surg**. 2014; 28:1946−1958.

49. Halushka MK, Angelini A, Bartoloni G, et al. Consensus statement on surgical pathology of the aorta from the Society for Cardiovascular Pathology and the Association for European Cardiovascular Pathology: II. Noninflammatory degenerative diseases - nomenclature and diagnostic criteria. **Cardiovasc Pathol**. 2016; 25:247−257.

50. Allaire E, Hasenstab D, Kenagy RD, Starcher B, Clowes MM, Clowes AW. Prevention of aneurysm development and rupture by local overexpression of plasminogen activator inhibitor-1. **Circulation**. 1998; 98:249−255.

51. Allaire E, Forough R, Clowes M, Starcher B, Clowes AW. Local overexpression of TIMP-1 prevents aortic aneurysm degeneration and rupture in a rat model. **J Clin Investig**. 1998; 102:1413−1420.

52. Goldfinger JZ, Halperin JL, Marin ML, Stewart AS, Eagle KA, Fuster V. Thoracic aortic aneurysm and dissection. **J Am Col Cardiol**. 2014; 64:1725−1739.

53. Koullias G, Modak R, Tranquilli M, Korkolis DP, Barash P, Elefteriades JA. Mechanical deterioration underlies malignant behavior of aneurysmal human ascending aorta. **J Thorac Cardiovasc Surg**. 2005; 130:677−683.

54. Isselbacher EM. Thoracic and abdominal aortic aneurysms. **Circulation**. 2005; 111:816−828.

55. Schafer M, Browne LP, Truong U, et al. Aortic stiffness in adolescent Turner and Marfan syndrome patients. **Eur J Cardio Thorac Surg**. 2018; 54:926−932.

56. Adams JN, Brooks M, Redpath TW, et al. Aortic distensibility and stiffness index measured by magnetic resonance imaging in patients with Marfan's syndrome. **Br Heart J**. 1995; 73:265−269.

57. Jeremy RW, Huang H, Hwa J, McCarron H, Hughes CF, Richards JG. Relation between age, arterial distensibility, and aortic dilatation in the Marfan syndrome. **Am J Cardiol**. 1994; 74:369−373.

58. Baumgartner D, Baumgartner C, Matyas G, et al. Diagnostic power of aortic elastic properties in young patients with Marfan syndrome. **J Thorac Cardiovasc Surg**. 2005; 129:730−739.

59. Hirata K, Triposkiadis F, Sparks E, Bowen J, Wooley CF, Boudoulas H. The Marfan syndrome: abnormal aortic elastic properties. **J Am Coll Cardiol**. 1991; 18:57−63.

60. Grillo A, Salvi P, Marelli S, et al. Impaired central pulsatile hemodynamics in children and adolescents with Marfan syndrome. **J Am Heart Assoc**. 2017; 6.

61. Salvi P, Grillo A, Marelli S, et al. Aortic dilatation in Marfan syndrome: role of arterial stiffness and fibrillin-1 variants. **J Hypertens**. 2018; 36:77−84.

62. Westenberg JJ, Scholte AJ, Vaskova Z, et al. Age-related and regional changes of aortic stiffness in the Marfan syndrome: assessment with velocity-encoded MRI. **J Magn Reson Imaging**. 2011; 34:526−531.

63. Selamet Tierney ES, Levine JC, Sleeper LA, et al. Influence of aortic stiffness on aortic-root growth rate and outcome in patients with the Marfan syndrome. **Am J Cardiol**. 2018; 121:1094−1101.

64. Sandor GG, Alghamdi MH, Raffin LA, et al. A randomized, double blind pilot study to assess the effects of losartan vs. atenolol on the biophysical properties of the aorta in patients with Marfan and Loeys-Dietz syndromes. **Int J Cardiol**. 2015; 179:470−475.

65. Van Hemelrijk C, Renard M, Loeys B. The Loeys-Dietz syndrome: an update for the clinician. **Curr Opin Cardiol**. 2010; 25:546−551.

66. Akazawa Y, Motoki N, Tada A, et al. Decreased aortic elasticity in children with Marfan syndrome or Loeys-Dietz syndrome. **Circ J**. 2016; 80:2369−2375.

67. Pannu H, Tran-Fadulu V, Papke CL, et al. MYH11 mutations result in a distinct vascular pathology driven by insulin-like growth factor 1 and angiotensin II. **Hum Mol Genet**. 2007; 16:2453−2462.

68. Guo DC, Pannu H, Tran-Fadulu V, et al. Mutations in smooth muscle alpha-actin (ACTA2) lead to thoracic aortic aneurysms and dissections. **Nat Genet**. 2007; 39:1488−1493.

69. Lalande A, Khau Van Kien P, Walker PM, et al. Compliance and pulse wave velocity assessed by MRI detect early aortic impairment in young patients with mutation of the smooth muscle myosin heavy chain. **J Magn Reson Imaging**. 2008; 28:1180−1187.

70. Leone O, Biagini E, Pacini D, et al. The elusive link between aortic wall histology and echocardiographic anatomy in bicuspid aortic valve: implications for prophylactic surgery. **Eur J Cardio Thorac Surg**. 2012; 41:322−327.

71. Forsell C, Bjorck HM, Eriksson P, Franco-Cereceda A, Gasser TC. Biomechanical properties of the thoracic aneurysmal wall: differences between bicuspid aortic valve and tricuspid aortic valve patients. **Ann Thorac Surg**. 2014; 98:65−71.

72. Chung JC, Wong E, Tang M, et al. Biomechanics of aortic dissection: a comparison of aortas associated with bicuspid and tricuspid aortic valves. **J Am Heart Assoc**. 2020; 9:e016715.

73. Huang FQ, Le Tan J. Pattern of aortic dilatation in different bicuspid aortic valve phenotypes and its association with aortic valvular dysfunction and elasticity. **Heart Lung Circ**. 2014; 23:32−38.

74. Nistri S, Grande-Allen J, Noale M, et al. Aortic elasticity and size in bicuspid aortic valve syndrome. **Eur Heart J**. 2008; 29:472−479.

75. Shim CY, Cho IJ, Yang WI, et al. Central aortic stiffness and its association with ascending aorta dilation in subjects with a bicuspid aortic valve. **J Am Soc Echocardiogr**. 2011; 24:847−852.

76. Tzemos N, Lyseggen E, Silversides C, et al. Endothelial function, carotid-femoral stiffness, and plasma matrix metalloproteinase-2 in men with bicuspid aortic valve and dilated aorta. **J Am Coll Cardiol**. 2010; 55:660−668.

77. Rooprai J, Boodhwani M, Beauchesne L, et al. Thoracic aortic aneurysm growth in bicuspid aortic valve patients: role of aortic

stiffness and pulsatile hemodynamics. **J Am Heart Assoc**. 2019; 8:e010885.

78. Longobardo L, Carerj S, Bitto A, et al. Bicuspid aortic valve and aortopathy: novel prognostic predictors for the identification of high-risk patients. **Eur Heart J Cardiovasc Imaging**. 2021; 22:808−816.

79. Sybert VP. Cardiovascular malformations and complications in Turner syndrome. **Pediatrics**. 1998; 101:E11.

80. Allen DB, Hendricks SA, Levy JM. Aortic dilation in Turner syndrome. **J Pediatr**. 1986; 109:302−305.

81. Sharma J, Friedman D, Dave-Sharma S, Harbison M. Aortic distensibility and dilation in Turner's syndrome. **Cardiol Young**. 2009; 19:568−572.

82. Wen J, Trolle C, Viuff MH, et al. Impaired aortic distensibility and elevated central blood pressure in Turner Syndrome: a cardiovascular magnetic resonance study. **J Cardiovasc Magn Reson**. 2018; 20:80.

83. Sonesson B, Hansen F, Lanne T. The mechanical properties of elastic arteries in Ehlers-Danlos syndrome. **Eur J Vasc Endovasc Surg**. 1997; 14:258−264.

84. Miller AJ, Schubart JR, Sheehan T, Bascom R, Francomano CA. Arterial elasticity in Ehlers-Danlos syndromes. **Genes**. 2020; 11.

85. Iliopoulos DC, Kritharis EP, Giagini AT, Papadodima SA, Sokolis DP. Ascending thoracic aortic aneurysms are associated with compositional remodeling and vessel stiffening but not weakening in age-matched subjects. **J Thorac Cardiovasc Surg**. 2009; 137:101−109.

86. Campobasso R, Condemi F, Viallon M, Croisille P, Campisi S, Avril S. Evaluation of peak wall stress in an ascending thoracic aortic aneurysm using FSI simulations: effects of aortic stiffness and peripheral resistance. **Cardiovasc Eng Technol**. 2018; 9:707−722.

87. Griepp RB, Ergin MA, Lansman SL, Galla JD, Pogo G. The natural history of thoracic aortic aneurysms. **Semin Thorac Cardiovasc Surg**. 1991; 3:258−265.

88. Bonser RS, Pagano D, Lewis ME, et al. Clinical and patho-anatomical factors affecting expansion of thoracic aortic aneurysms. **Heart**. 2000; 84:277−283.

89. Dapunt OE, Galla JD, Sadeghi AM, et al. The natural history of thoracic aortic aneurysms. **J Thorac Cardiovasc Surg**. 1994; 107:1323−1332. discussion 1332-3.

90. Guo MH, Appoo JJ, Saczkowski R, et al. Association of mortality and acute aortic events with ascending aortic aneurysm: a systematic review and meta-analysis. **JAMA Netw Open**. 2018; 1:e181281.

91. Jue J, Boodhwani M, Beauchesne L, et al. Greater aortic stiffness and pulsatile arterial load are associated with larger thoracic aortic aneurysm size in women. **Circulation**. 2019; 139:1124−1126.

92. Boczar KE, Cheung K, Boodhwani M, et al. Sex differences in thoracic aortic aneurysm growth. **Hypertension**. 2019; 73:190−196.

93. Boczar KE, Boodhwani M, Beauchesne L, et al. Aortic stiffness, central blood pressure, and pulsatile arterial load predict future thoracic aortic aneurysm expansion. **Hypertension**. 2021; 77:126−134.

94. Zhu T, Boodhwani M, Beauchesne L, et al. Combining aortic size with measures of aortic stiffness and pulsatile hemodynamics enhances prediction of future thoracic aortic aneurysm expansion (Abstract). **Eur Heart J**. 2019; 40.

95. Nollen GJ, Groenink M, Tijssen JG, Van Der Wall EE, Mulder BJ. Aortic stiffness and diameter predict progressive aortic dilatation in patients with Marfan syndrome. **Eur Heart J**. 2004; 25:1146−1152.

96. Guala A, Teixido-Tura G, Rodriguez-Palomares J, et al. Proximal aorta longitudinal strain predicts aortic root dilation rate and aortic events in Marfan syndrome. **Eur Heart J**. 2019; 40:2047−2055.

97. Ince H, Nienaber C. Etiology, pathogenesis and management of thoracic aortic aneurysm. **Nat Clin Pract Cardiovasc Med**. 2007; 4:418−427.

98. LeMaire S, Russell L. Epidemiology of thoracic aortic dissection. **Nat Rev Cardiol**. 2011; 8:103−113.

99. Rabkin S, Mathewson A, Tate R. Predicting risk of ischemic heart disease and cerebrovascular disease from systolic and diastolic blood pressures. **Ann Intern Med**. 1978; 88:342−345.

100. Pape LA, Tsai T, Isselbacher EM, et al. Aortic diameter ≥ 5.5 cm is not a good predictor of type a aortic dissection: observations from the International Registry of Acute Aortic Dissection (IRAD). **Circulation**. 2007; 116:1120−1127.

101. Joyce J, Fairbairn J, Kincaid O. Aneurysms of the thoracic aorta: a clinical study with special reference to prognosis. **Circulation**. 1964; 29:176−181.

102. Milewicz D, Prakash S, Ramirez F. Therapeutics targeting drivers of thoracic aortic aneurysms and acute aortic dissections: insights from predisposing genes and mouse models. **Annu Rev Med**. 2017; 68:51−67.

103. Humphrey J, Milewicz D, Tellides G. Dysfunctional mechano-sensing in aneurysms. **Science**. 2014; 344:477−479.

104. Rabkin S, Janusz M. Aortic wall stress in hypertension and ascending thoracic aortic aneurysms: implications for antihypertensive therapy. **High Blood Pres Cardiovasc Prev**. 2013; 20:265−271.

105. Okamoto R, Xu H, Kouchoukos N. The influence of mechanical properties on wall stress and distensibility of the dilated ascending aorta. **J Thorac Cardiovasc Surg**. 2003; 126:842−850.

106. Roman MJ, Devereux R, Kizer JR, et al. Central pressure more strongly relates to vascular disease and outcome than does brachial pressure the strong heart study. **Hypertension**. 2007:197−203.

107. Rooprai J, Boodhwani M, Beauchesne L, et al. Central hypertension in apparently normotensive patients with thoracic aortic aneurysms: prevalence and association with aneurysm expansion. **Am J Hypertens**. March 24, 2021. https://doi.org/10.1093/ajh/hpaa183 (Online ahead of print).

Arterial stiffness and pulsatile hemodynamics in congenital heart disease

Michael A. Quail

Department of Pediatric Cardiology, Great Ormond Street Hospital for Children and University College London, London, United Kingdom

Background

Congenital heart disease (CHD) is any developmental malformation of the heart or great vessels. Involvement of the aorta is common and may occur in isolation (coarctation or interruption of the aortic arch) or in association with more complex abnormalities such as hypoplastic left heart. Aortic involvement (usually dilatation) may also complicate forms of CHD traditionally considered to be limited to the right heart, such as tetralogy of Fallot (TOF).
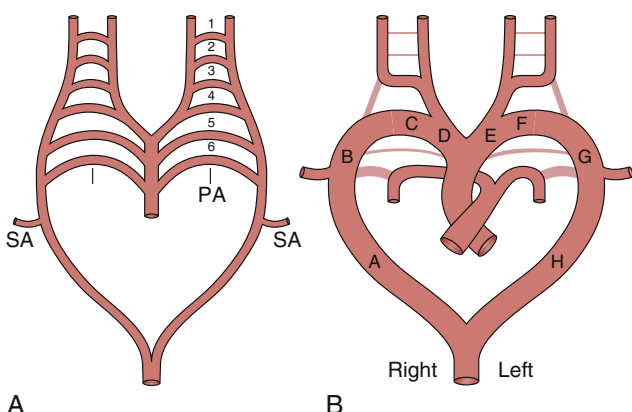
Normal aortic morphology

The normal aorta is a spiral structure, arising above the aortic valve and ascending in a cranial and rightward direction. At the level of the right pulmonary artery, the *ascending aorta* spirals leftward and posteriorly, adopting a transverse orientation. The *transverse aorta* passes to the left of the trachea and is morphologically divided into proximal and distal portions. The *proximal transverse aorta* gives rise to the innominate and left common carotid arteries (LCCAs), and the *distal transverse aorta* gives rise to the left subclavian artery (LSA). In normal fetal life, the aorta and left pulmonary artery (or pulmonary trunk) are connected by the arterial duct (ductus arteriosum), a vessel which facilitates a physiological bypass of the lungs, redirecting right ventricular cardiac output to the descending aorta. The *aortic isthmus* is the region of insertion of the ductus arteriosus into the aorta and is usually located on the under surface of the aorta in the vicinity of the LSA. Distal to the aortic isthmus, the *proximal descending aorta* spirals caudally toward the diaphragm passing leftward to the vertebral bodies.

Aortic development

The aortic arch and pulmonary trunk, together with the main branches, are evolutionarily related to six pairs of arterial arches which exist in embryological life. The aortic arches represent the blood supply to the embryological pharyngeal (branchial) arches. Remodeling of these transient symmetrical arch arteries into the definitive adult left-sided aortic arch pattern involves the asymmetrically programmed regression and persistence of specific arch arteries. This process involves signaling between the endothelial cells lining the pharyngeal arch arteries, neural crest cell−derived smooth muscle and mesenchyme, and the endoderm; disruption of this process is believed to contribute to congenital abnormalities of the aortic arch.[1,2]

The embryological aortic arches partially encircle the pharynx to connect the ventral aorta to the paired dorsal aortas, which are joined to the future descending aorta. Edwards originally proposed a simplified embryonic double arch system (Fig. 46.1A and B) which can assist understanding the morphological variations which can occur.[3−5] Once the third paired arches have developed, the first and second paired arches disappear. The cephalic extension of the ventral and dorsal aorta beyond the fourth arch becomes the common carotid (portion of ventral aorta between third and fourth arches), internal carotid (cephalic extension of ventral aorta beyond third arch), and external carotid (third arch and cephalic extension of dorsal aorta) arteries, respectively, on each side. The dorsal aortas between the third and fourth arches regress. The part of the ventral aorta proximal to the fourth arch on the right becomes the brachiocephalic artery (segment D, Fig. 46.1B), and on the left it becomes the future aortic arch between the

FIGURE 46.1 (A) The basic pattern of the six pairs of primitive aortic arches with the position of the primary pulmonary arteries (PA) and subclavian arteries (SA) also indicated. (B) The embryonic double arch system is formed by the fourth arches and the dorsal aortas of both sides. The various lettered segments may persist or disappear in different configurations of the great arteries.

right brachiocephalic and LCCAs (segment E, Fig. 46.1B). The fourth arch on the left side becomes the future aortic arch between the LCCA and the origin of the future LSA (segment F, Fig. 46.B), and on the right it forms the origin of the future right subclavian artery (segment C, Fig. 46.1B). The fifth paired arches usually disappear but may persist. The lateral portion of the left sixth arch forms the ductus arteriosus, and the medial portions of both sixth arches form the origins of the pulmonary arteries. The seventh intersegmental arteries migrate cephalad to form the future subclavian arteries (see Fig. 46.1A). Ultimately, the spiral septation of the ventral aorta, or common arterial trunk, provides for separation of the pulmonary trunk from the ascending aorta.

In normal development, we observe the disappearance of segment A (see Fig. 46.1B) of the dorsal aorta and distal part of the right sixth arch while the distal part of the left sixth arch persists as the arterial duct, thus giving rise to a left aortic arch. Atresia or persistence of various segments can give rise to morphological aortic variations (see Fig. 46.2), some of which may result in vascular rings with compression of the trachea or esophagus.

Coarctation of the aorta and interrupted aortic arch
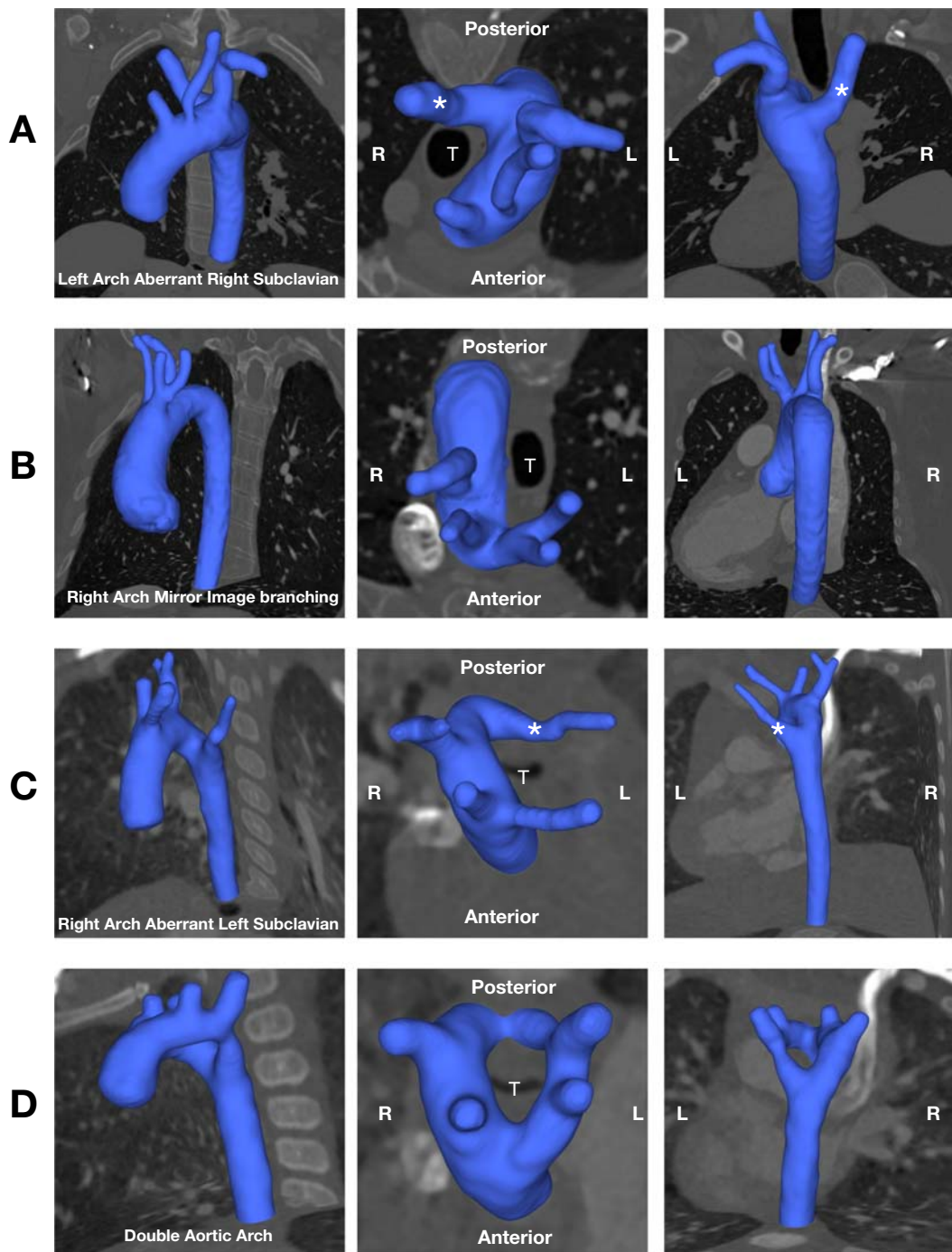
Coarctation of the aorta is a form of aortic obstruction, characterized by narrowing at the level of the aortic isthmus. The prevalence is 2.9 per 10,000 births and globally it represents 3.6% of all CHD (Table 46.1).[6] The condition is more common in boys, with a 2:1 sex ratio. Morphologically, this lesion is a localized intraluminal projection of a "shelf" from the posterior or lateral wall of the isthmus in the region of the ductus arteriosus.

Coarctation is also often associated with a variable degree of hypoplasia of the transverse arch. As the ductus arteriosus closes, the degree of aortic obstruction becomes progressively more severe, resulting in reduced systemic perfusion, acutely increased afterload, and cardiogenic shock. Initial medical treatment includes resuscitation and initiation of intravenous prostaglandin therapy to maintain or restore ductal patency. Definitive surgical treatment requires resection of the narrowed aortic isthmus, with end-to-end anastomosis or patch angioplasty using the LSA or prosthetic patch material. Rarely a primary percutaneous balloon angioplasty or endovascular stenting is performed. Antenatal diagnosis is difficult but can identify a proportion of infants with features suggestive of coarctation, who can be stabilized prior to clinical deterioration by commencing prostaglandin therapy at birth. Less severe forms of isthmus narrowing, or those with an extensive collateral supply may present later in life, sometimes with resistant arterial hypertension (Fig. 46.3). A collateralized circulation is not developed at the time of birth because the aorta is not obstructed in utero, but may develop in those with less severe obstruction over weeks and months. Coarctation may occur in combination with other forms of CHD, most notably bicuspid aortic valve in approximately 50% of patients (conversely coarctation occurs in approximately 5% of patients with bicuspid valves). Turner syndrome is the most frequent chromosomal abnormality associated with coarctation. This, together with the male preponderance suggests an X-chromosome dosage effect.[7,8]

Interrupted aortic arch (IAA) is characterized by complete luminal discontinuity in the aortic arch; it is morphologically subdivided according to the location of the interruption. Type A is interrupted at the level of the aortic isthmus, after the LSA (20%); Type B is interrupted in the distal transverse arch between the left common carotid and LSA (75%), Fig. 46.4; and Type C is interrupted in the proximal transverse arch, between the innominate artery and left common carotid (5%). IAA is a developmentally different entity to coarctation and is more frequently associated with other complex cardiac lesions and genetic abnormalities. The prevalence of IAA is 0.4 per 10,000 births, and it represents 0.6% of all CHD (Table 46.1).[6] DiGeorge syndrome (22q11 deletion) is the most frequently associated chromosomal abnormality. IAA shares medical and surgical management strategies with coarctation but has a higher rate of reintervention.[9,10]

Hypertension after coarctation repair

Large studies published in the late 1980s and early 1990s identified an emerging problem among patients who had undergone surgical repair of coarctation—a very high prevalence of hypertension, Table 46.2. An increased rate of hypertension also appears likely for IAA, despite limited

FIGURE 46.2 Aortic arch morphological variations. (A) Left aortic arch with aberrant right subclavian artery (0.5% of population). There is persistence of segment A with atresia of segment B and C (see Fig. 46.1B). (B) Right aortic arch with mirror image branching caused by atresia of segment H (see Fig. 46.1B), is seen in 2%−3% of the population. (C) Right aortic arch with aberrant left subclavian artery is due to the absence of the fourth arch on the left side (segments F and G, Fig. 46.1B) with persistence of segments A and H. The aberrant left subclavian artery has a retroesophageal course and forms an incomplete vascular ring if the arterial duct is right sided. However, in the presence of a left-sided arterial duct connecting the origin of the aberrant subclavian artery to the left pulmonary artery, the vascular ring becomes complete. (D) Double aortic arch (DAA) is the most common cause of tracheoesophageal compression. Here, persistence of segment A (see Fig. 46.1B) will result in a DAA completely encircling the trachea and esophagus, sometimes leading to severe obstruction. Each aortic arch gives rise to respective common carotid and subclavian arteries.

TABLE 46.1 Prevalence and percentages of common forms of congenital heart disease.

Congenital heart disease subtype	Prevalence of congenital heart disease subtype per 1000 (95% confidence interval)	Percentage of congenital heart disease subtype, % (95% confidence interval)
Ventricular septal defect	3.07 (2.85−3.31)	35.6 (33.9−37.3)
Atrial septal defect	1.44 (1.22−1.69)	15.4 (13.5−17.4)
Patent ductus arteriosus	1.00 (0.80−1.23)	10.2 (8.5−12.0)
Pulmonary stenosis	0.55 (0.49−0.61)	6.2 (5.7−6.8)
Tetralogy of Fallot	0.36 (0.33−0.39)	4.4 (4.1−4.8)
Transposition of the great arteries	0.30 (0.27−0.32)	3.8 (3.4−4.2)
Atrioventricular septal defect	0.29 (0.27−0.32)	3.6 (3.3−3.9)
Coarctation of the aorta	0.29 (0.26−0.31)	3.6 (3.3−3.9)
Interrupted aortic arch	0.04 (0.03−0.05)	0.6 (0.4−0.8)

Adapted from Liu Y, Chen S, Zühlke L, et al. Global birth prevalence of congenital heart defects 1970-2017: updated systematic review and meta-analysis of 260 studies. **Int J Epidemiol** 2019; 48:455−463.

data. A recent systematic review has estimated the prevalence of hypertension in adults following coarctation repair as 32.5% (range 25%−68%),[a] which is significantly higher than expected for equivalent groups of teenagers and young adults without coarctation.[11] By contrast, the estimated UK prevalence of hypertension is: 1% between 16 and 24years; 11% between 15 and 34years; and 18% between 35 and 44 years of age (*BHF statistics compendium 2019*). In the USA, the prevalence of hypertension among 18−39 year olds is 7.5% (*CDC 2015−16*).[12]

A large contemporary study from Sweden using a national registry (n = 653), found hypertension in 53% of adult patients, raising the possibility earlier studies have underestimated the extent of the problem.[13] Similarly high levels were also reported recently by Lee et al.[14] in a large single center study of 834 patients. Systemic hypertension was present in 57% (375/661) and prehypertension in a further 13% (83/661) of patients. Risk factors for elevated blood pressure included age, sex, and age at repair and residual coarctation. Thirty-six percent of patients (289/796) were on at least one antihypertensive medication. Hypertension was found to be difficult to treat; multiple medications were required in 10% (2 mediations), 4% (3 medications), 2% (4 medications), and 0.3% (5 medications) of patients. It is of great concern that only 18% (50/279) of patients on antihypertensive medication were normotensive.

The average age of repair in studies covering the period 1960−1980 was significantly older than current practice. However, a trend toward earlier coarctation repair was already emerging at this time: Koller et al.[15] reported that
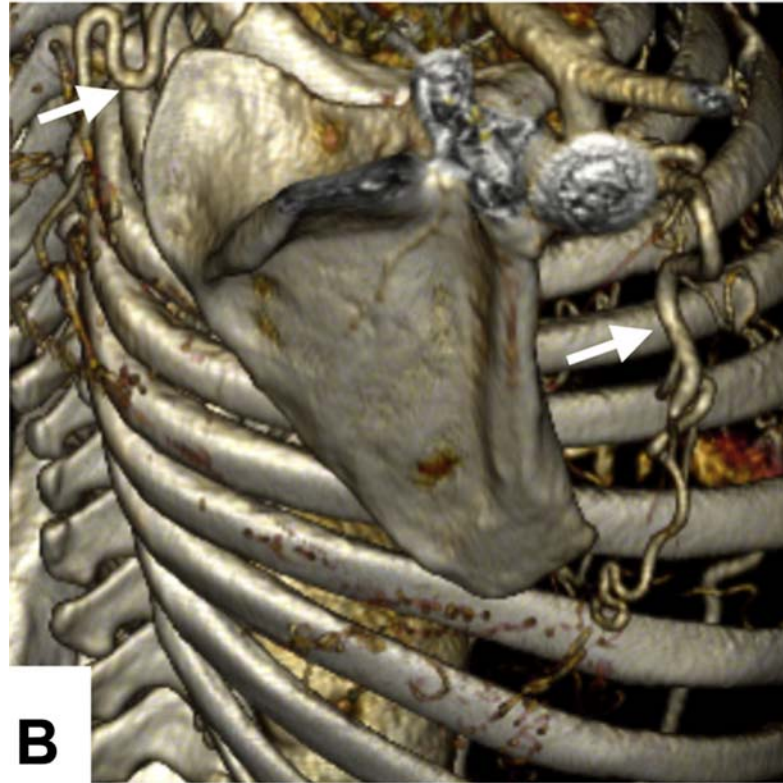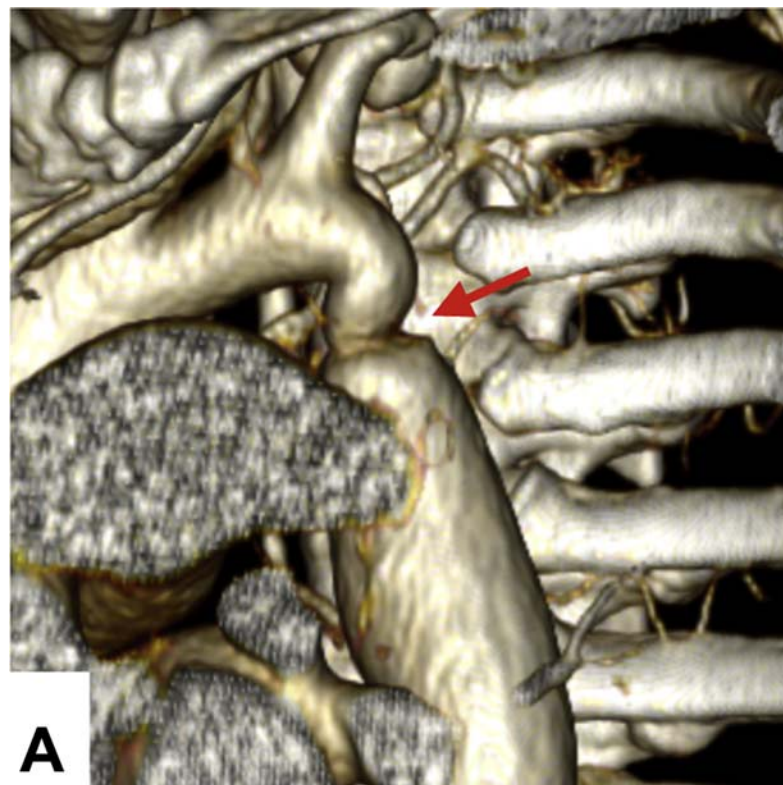
the percentage of patients operated before age two years of age doubled from 12% in the period 1961−70, to 26% in 1971−80. In a contemporary cohort (Great Ormond Street Hospital for Children, 2004−20), the median age of repair was 25 days (IQR eight days−six months), with 83% of infants repaired under two years (unpublished data from author's institution).

The trend to earlier coarctation repair was facilitated by two major developments in CHD practice during the 1970s and 1980s. First, infants with severe coarctation could now be resuscitated and stabilized using prostaglandin infusions to dilate the ductus arteriosus, thus providing the first effective emergency therapy for duct-dependent cardiac lesions.[16−19] The second important development was the ability to more easily diagnose infants with arch obstruction noninvasively by the proliferation of echocardiography.[20]

An understanding of the evolution of clinical practice during the latter part of the 20th century is important because many patients with severe coarctation died in infancy and are underrepresented in early studies. Samples in earlier studies are therefore dominated by groups of patients who survived infancy (due to less severe disease) but had been exposed to a hypertensive ascending aorta (and cerebrovascular circulation) for many years prior to repair. Optimism that early repair may mitigate the high prevalence arose from an observation that younger patients appeared to have a lower prevalence of hypertension.[15,21,22]

Unfortunately, the view that earlier surgery would completely mitigate the increased risk of hypertension has not been realized. A large study of children by O'Sullivan et al.[23] showed that approximately 30% of the cohort operated on in infancy (median age of 2.6 months [IQR 0.5−48 months]) had significantly elevated blood pressure, based on either office or ambulatory readings, when followed up at a mean age of 12 years. Unpublished data from

[a] The age of patients at time of assessment in published studies is variable, but typically less than 40years. There is also considerable variability in the definition of hypertension and inclusion of patients with some degree of residual obstruction.

FIGURE 46.3 Computed tomography (CT) aortogram from adult patient with unrepaired coarctation of the aorta. (A) Narrowed aortic isthmus (*red arrow*). (B) Arterial collaterals on right lateral chest wall and back (*white arrows*). (C) Arterial collaterals on anterior chest wall and abdomen.
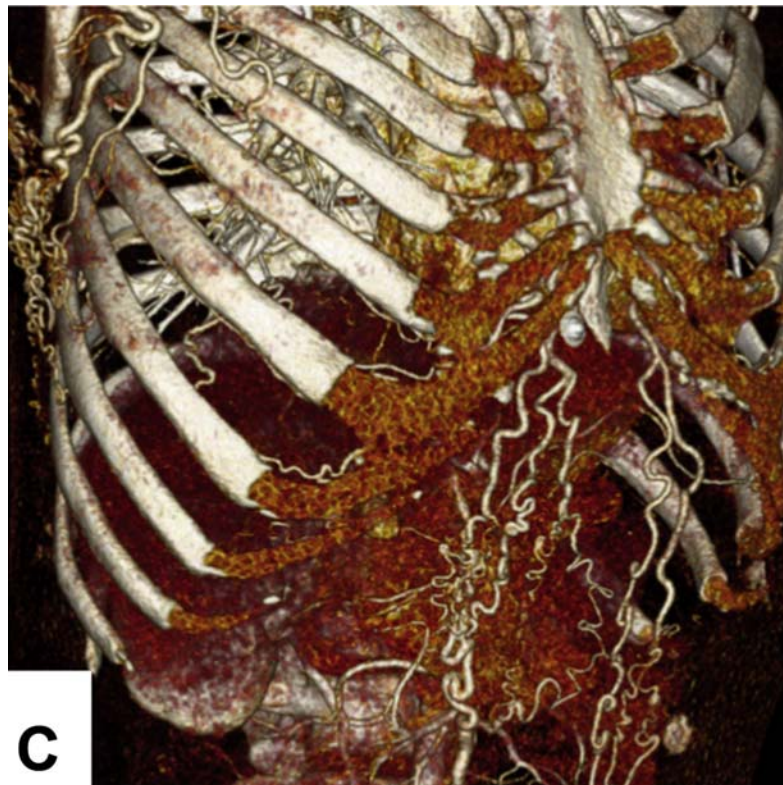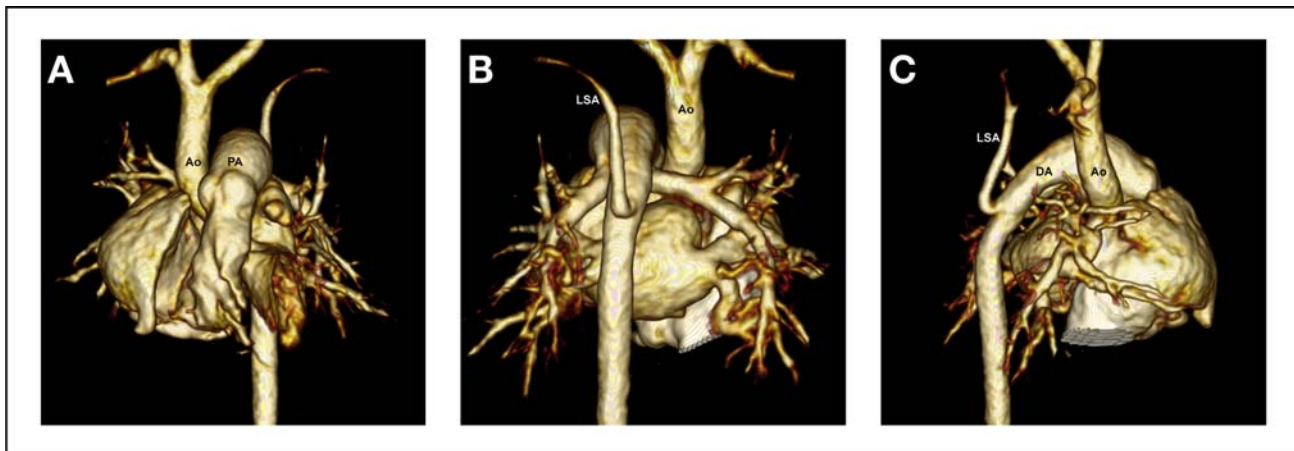
FIGURE 46.3 cont'd.

the author's institution indicate that approximately 20% of children aged 5−7 years after successful neonatal coarctation repair have prehypertension (systolic and diastolic blood pressure >90th centile), Fig. 46.5. These data suggest that even in an era of very early coarctation repair, patients without arch obstruction remain at increased risk for hypertension. Such hemodynamic abnormalities manifest even in early childhood, but unfortunately the underlying mechanisms are unclear.

Cardiovascular morbidity

Patients with repaired coarctation of the aorta exhibit higher rates of cardiovascular disease.[21,24−28] A systematic review
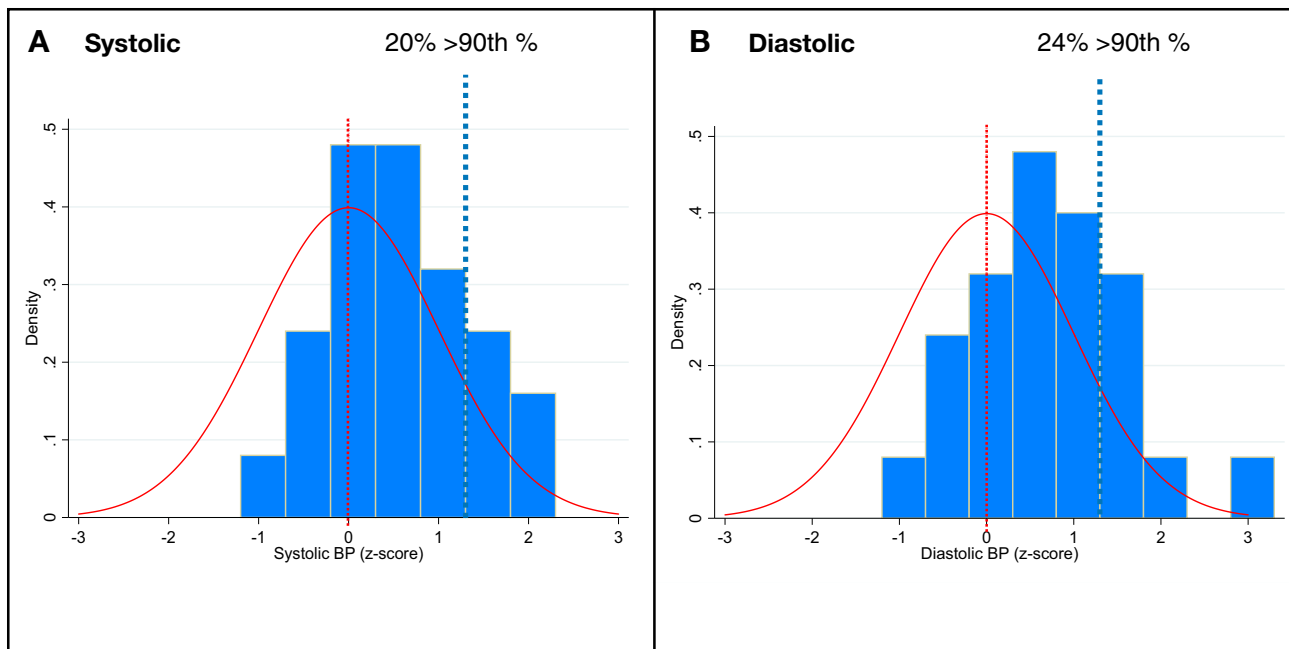
FIGURE 46.4 Computed tomography (CT) aortogram from a neonate with unrepaired Type B interruption of the aortic arch, (interruption of the distal transverse arch between the left common carotid and left subclavian artery). (A) Anterior projection showing the relationship between aorta (Ao) and pulmonary artery (PA), note the absence of the distal transverse aorta. (B) Posterior projection showing origin of left subclavian artery (LSA) from the descending aorta. (C) Lateral projection showing ductus arteriosus (DA) connecting pulmonary artery and descending aorta.

TABLE 46.2 Prevalence of Hypertension in large observational studies of coarctation and interrupted aortic arch.

Author	Year of study	Sample size	Definition of HTN (mmHg)	Residual gradient excluded	Age at operation (year)	Mean follow up (year)	HTN (%)
Coarctation							
Koller (EHJ)[15]	1987	362	>18 year ≥ 140/90; <18 year ≥ 95th centile for age	No	17.7	10.4	25
Presbitero (BHJ)[24]	1987	226	>30 year ≥ 160/95; 19−30 ≥ 150/90	Yes	20	20	36
Cohen (Circ)[21]	1989	646	≥150/90	No	16	20	25
Brouwer (JTCVS)[22]	1994	120	≥160/90	No	15.5	32	25
Seirafi (ATS)[126]	1998	176	>18 year ≥ 160/90; <18 year ≥ 90th centile for age	No	0.9	7.5	17
O'Sullivan (Heart)[23]	2002	119	Casual ≥95th centile for normal pop; ABP = mean > 95th centile for age.	Yes	0.2	9.5	30
Toro-Salazar (AJC)[25]	2002	274	Casual ≥95th centile for age or drug treatment for hypertension.	No	10.3	29.8	34
Vriend (EHJ)[127]	2005	73	Mean ABP systolic ≥135 ± diastolic ≥85	Yes	8.1	21.7	45
Hager (JTCVS)[128]	2007	245[a]	Drug treatment for hypertension, mean ABP systolic ≥133 ± diastolic ≥78	Yes	10.4	19.5	55
Roifman (Circ)[30]	2012	616	Registry data (1983−2005) ICD-9 codes for hypertension	No	—	—	45
Choudhary (Heart)[129]	2015	140	≥140/90 on two separate occasions	No	5	26	42
Rinnström (AJC)[13]	2016	653	≥140/90 or drug treatment for hypertension (Swedish registry)	No	9.5	27.4	53
Lee (Heart)[14]	2019	834	≥140/90 or drug treatment for hypertension	No	4	27	57
Interrupted aortic arch							
Hussein (JTCVS)[9]	2010	112	>133/78	No	6 days	18	12

ABP, ambulatory blood pressure; *HTN*, Hypertension.
[a]Subset of patients without obstruction.

FIGURE 46.5   Childhood blood pressure in 25 children, mean age 5.8 (SD one year) who underwent neonatal coarctation repair in 2012−14. (A) Distribution of casual systolic blood pressure (SBP), compared to normal distribution according to age and height, 20% had SBP >90th centile. (B) Distribution of diastolic blood pressure (DBP), compared to normal distribution of age and height, 24% had DBP >90th centile.

found a disappointing survival rate of 87.4% at a mean age of 40 years in patients with aortic coarctation, with a particularly increased risk of cerebrovascular events and myocardial infarction.[29] Recent data by Lee et al. in a sample of 834 patients report overall survival of 99%, 88%, and 65% at 30, 50, and 70 years of age, respectively. Survival was significantly reduced compared with a matched normal population (standardized mortality ratio: 3.20, log-rank: $P < .001$).[14] A study by Roifman et al.[30] used registry data to compare patients with coarctation to patients with a repaired ventricular septal defect (VSD). Those with coarctation had higher rates of congestive heart failure (14.8% vs. 7.4%; $P < .0001$), stroke (5.6% vs. 2.6%; $P < .0001$), coronary artery disease (4.9% vs. 3.5%; $P = .04$), and peripheral vascular disease (13.1% vs. 2.7%; $P = .0001$). The authors found that the increased risk of cardiovascular morbidity appeared due, at least in part, to a higher burden of "traditional" cardiovascular risk factors, including hypertension and dyslipidaemia which were disproportionately higher in patients with coarctation.

Pickard et al.[31] examined the relationship between coarctation repair and cerebrovascular events in a cross-sectional study utilizing the US National Inpatient Sample database from 2005 to 2014. Among 4,894,582 stroke discharges, 207 had a diagnosis of coarctation. After adjusting for potential confounders, coarctation patients had strokes at significantly younger age compared with others: 18.9 years younger for all-cause stroke ($P < .001$), 15.9 years younger for ischemic stroke ($P < .001$), and 28.5 years younger for hemorrhagic stroke ($P < .001$). The authors found an increased rate of diabetes in patients with coarctation and confirmed the high prevalence of hypertension.

These concerning data highlight the need for close cardiovascular surveillance of coarctation patients, with mitigation of cardiac risk factors to prevent cardiovascular morbidity and mortality.

They also raise an important question: why are patients at risk of hypertension following successful aortic repair? We will explore this question in the following sections.

Abnormalities of pulsatile hemodynamics

Arterial stiffness—regional effects

Several studies, in the 1990s and 2000s, showed an association between abnormal arterial stiffness and hypertension in patients with coarctation.[32−35] These findings have been extensively replicated and strongly support a role for increased arterial stiffness as a key explanatory variable underlying the increased rates of hypertension in coarctation.[36−40]

In 1997, Xu et al.[41] used intravascular ultrasound at the time of cardiac catheterization to measure the aortic stiffness in patients with coarctation. The authors appear to be the first group to suggest regional variation in arterial stiffness in the aorta of patients with coarctation, showing increased stiffness in the aorta proximal to the coarctation. However, data from this study suggest an important role for different segmental loading conditions. Following balloon dilatation of coarctation, there was a reduction in distal compliance and distensibility as a result of increased distal pressure. This finding demonstrates the influence of loading conditions on stiffness metrics, which is especially problematic in patients with residual coarctation.

In 2001, de Divitiis et al.[33] reported muscular artery stiffness metrics in coarctation patients (n = 64, mean age = 19 ± 9.9; median age at repair = 4 months) and controls (n = 45, mean age = 20 ± 8.1). The authors reported abnormal brachial-radial pulse wave velocity (PWV), but normal femoral-dorsalis PWV. This PWV finding was replicated in a slightly larger study by the same group in 2003. Which also showed a relationship between ambulatory BP and increased LV mass.[32]

Asymmetric upper-lower body stiffness has been reported across different ages, levels of blood pressure, and method of ascertainment.[37,42–44] However, the role of different segmental loading conditions has not been sufficiently resolved.

It remains an unanswered question whether the increased proximal stiffness is congenital or acquired. However, data from children suggest that the phenomenon occurs early.[43,45]

Central pressure and total arterial compliance

It is well recognized that brachial systolic blood pressure (SBP) usually overestimates central SBP due to patient specific pressure augmentation, and there is some evidence that central SBP is a better predictor of cardiovascular risk.[46] Limited data exist on the correct assessment of central blood pressure in CHD, especially in the presence of regional variations in stiffness which may affect pulse pressure amplification.

One approach to estimate central aortic blood pressure is to use cardiovascular magnetic resonance (CMR)-derived area-time data in the ascending aorta, calibrated to brachial mean and diastolic pressure using an exponential model of the pressure-area relationship.[47] This method avoids the use of a generalized transfer function, which may not be valid in patients following coarctation repair.[48]

The possibility of CMR-derived central pressure and simultaneous aortic flow makes it feasible to possible to perform a comprehensive, noninvasive, assessment of central arterial hemodynamics. A single breath-hold flow acquisition with simultaneous oscillometric blood pressure provides data to calculate: central aortic pressure, systemic vascular resistance (SVR) (MAP/cardiac index); total arterial compliance (TAC) (2-element Windkessel model using central pulse pressure and aortic flow); PWV/characteristic impedance (Bramwell–Hill equation, using delta area and pulse pressure); and wave intensity analysis (WIA).

Quail et al.[49] used this technique in a study of coarctation patients (median age = 22 years; IQR 20–28) without arch obstruction and representative of those repaired in the 1990s. These patients were slightly older at repair than current cohorts (described above): median age at repair was 4.0 months (IQR 0.5–48.2 months); 68% had their repair <2 years of age. The main findings of this study were that compared to healthy controls, patients with repaired coarctation showed evidence of an aortopathy associated with elevated central SBP, decreased TAC, increased ascending aorta local PWV and increased backwards compression waves (BCWs), without differences in aortic root characteristic impedance (due to an increased aortic root size). Despite similar brachial blood pressure, central SBP was on average 6 mmHg higher in patients.

Conflicting data have arisen in studies using the SphygmoCor device to assess central hemodynamics using radial applanation tonometry. Swan et al.[40] measured central blood pressure in postcoarctation repair patients and normal volunteers, and in contrast to the study by Quail et al.,[49] no difference was observed in c-SBP. However, this may be partly due to their exclusion of any patient with high brachial artery blood pressure. By contrast, Szczepaniak-Chicheł et al.[50] studied 85 patients with repaired coarctation and found higher c-SBP, PWV, and augmentation index. Unfortunately, despite the many advantages of such devices, the validity of a generalized transfer function in patients with CHD remains uncertain. In particular, generalized transfer functions may not adequately control for the abnormal wave reflections that may be present in patients postcoarctation repair.[48,51]

Murakami and Takeda recruited 20 patients following coarctation or IAA repair and age-matched controls who had not undergone aortic surgery. Aortic pressure was measured invasively during cardiac catheterization. Compared to controls, patient with arch repairs had higher SBP (105.2 ± 12.2 vs. 94.7 ± 11.7 mmHg, P = .0018) and pulse pressure (40.4 ± 7.2 vs. 32.7 ± 5.3 mmHg, P = .0004). Patients also had increased augmentation index (27.5 ± 15.4 vs. −3.47 ± 8.8%, P < .0001), suggesting increased wave reflection.

Data from the preceding chapter sections indicate that hypertension manifests prematurely in patients with coarctation as a consequence of early aortic stiffening. However, the hemodynamic abnormalities are not limited to increased pressure and aortic stiffness, but also other elements of aortic input impedance which are less frequently considered, such as aortic wave reflections.

Aortic wave reflections

Experimental occlusion of the thoracic aorta in animals has been shown to result in partial reflection of the early systolic forward compression wave, thereby increasing ventricular afterload.[52–55] Similar findings have also been observed in humans with unrepaired coarctation at the time of cardiac catheterization and surgery.[54]

After surgical repair of coarctation, the presence of increased wave reflection has been inferred based on abnormal augmentation index or semiquantitative assessment of aortic flow curves.[38,40,56,57] However, augmentation index may not be a reliable index of wave reflection, since it

has a major dependence on both aortic wave speed, forward wave amplitude, and left ventricular function. Unfortunately very few studies have investigated simultaneous pressure and flow relationships.[58]
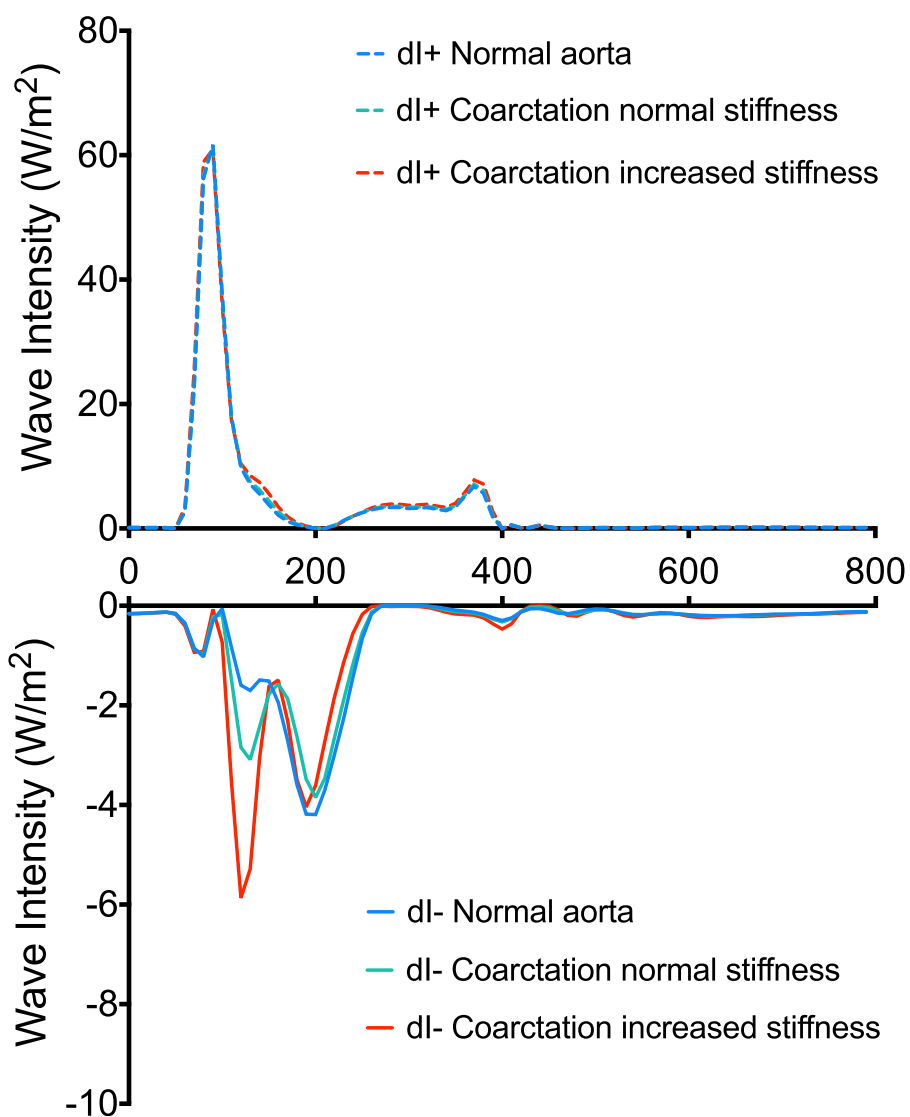
Recently, it has been shown that WIA can be performed noninvasively using image-based measures of arterial distension and blood flow.[49,59−61] The initial implementation by Feng and Khir relied on ultrasound imaging; however, phase contrast magnetic resonance (PCMR) can also provide accurate measures of distension and flow (see Chapters 2 and 4).[62] Unfortunately, high temporal resolution data are necessary to accurately assess wave speed, and this conventionally requires long free breathing acquisitions which may be associated with image blurring due to bulk motion of the aortic root through the imaging plane.[63]

Using high temporal resolution PCMR in the ascending aorta, Quail et al. performed WIA using flow (Q) and area (A) waves.[49] The authors found that patients with coarctation had evidence of higher BCWs compared to controls, and that the magnitude of the BCW was an important explanatory variable of LV mass in the sample. It is speculated that these reflections arise from reflection sites in repaired the aortic arch. To support this thesis, one-dimensional (1D) computer models were used to simulate the repaired aortic arch: First, the diameter of a segment in the descending aorta was reduced by 25% to mimic a mild residual aortic coarctation, while maintaining the normal distensibility. Second, the stiffness of the narrowed section was increased by five orders of magnitude to mimic the effect of a stiffened coarctation repair zone. Using this model, the authors observed an increase in backwards reflections in mild coarctation which was significantly increased in the presence of a stiffened segment (Fig. 46.6). These data are in keeping with the more sophisticated FSI modeling study by Taelman et al.[64]

Mynard et al.[65] have performed detailed experimental and computer modeling studies of wave reflection in

FIGURE 46.6 A validated one-dimensional (1D) model of the systemic vascular tree was used to explore differences in wave reflection between controls and patients following coarctation repair. The model solves the 1D Navier–Stokes equations and provides pressure and flow waveforms along the arterial tree. The model was run using a time-varying elastance model for the heart on its upstream boundary, such that simulated waves originate from the interaction of the pumping heart in the arterial tree. Apart from the baseline condition (Blue) using default parameters for the model (default lengths, inlet and outlet diameters, and arterial distensibility), two additional scenarios were simulated. First, the diameter of a segment in the descending aorta was reduced by 25% to mimic a mild residual aortic coarctation, while maintaining the normal distensibility (Green). Second, the stiffness of the narrowed section was increased by five orders of magnitude to mimic the effect of a stiffened coarctation repair zone (Red). Positive (dI+) and Negative wave intensity (dI−) in 1D simulation. Units of wave intensity are conventional W/m². Note scale of dI− increased relative to dI+ to assist visualization. In the coarctation models, increased backward compression waves are observed, which increase in magnitude in the presence of stiffened segment.

coarctation with particular reference to the effects of wave reflection on the cerebral circulation. Their study investigated the hypothesis that the BCW is not only reflected back toward the heart but also partially transmitted into cerebral circulation. The authors measured simultaneous pressure and flow in the aorta and brachiocephalic trunk (BCT) of eight sheep with surgically induced coarctation of two severities: (A) 10 mmHg and (B) 25 mmHg mean pressure increase in ascending aorta. Using wave power analysis,[66] it was shown that aortic constriction produced not only an aortic BCW, but also a second forward compression wave in the BCT that augmented pressure and flow after the initial forward compression wave, which increased with increasing coarctation severity.

In further mathematical and computational analyses, the authors investigated the effects of altering the stiffness of the head and neck vessels to examine the influence on wave transmission to the cerebrovascular system and on LV load. The authors discovered that stiffer or smaller head and neck vessels (i.e., with lower admittance, which is the inverse of impedance) had two important effects: (1) Greater transmission of FCW from the ascending aorta to aortic isthmus, and also greater reflection of BCW from the aortic isthmus to ascending aorta. Both of these mechanisms would tend to increase the impact of wave reflection on LV load; (2) Increased transmission of waves toward the brain with increased aortic stiffness was reversed or ameliorated when stiffness in the head and neck branches was also increased. Although this reduced peak flow pulsatility in the carotid artery, it increased pulse pressure and flow pulsatility in the middle cerebral artery.

This group complemented this experimental work with an observational study of head and neck wave reflection in patients with coarctation. Kowalski et al.[67] showed that coarctation subjects had higher brachial and central SBP ($P = .04$), with lower aortic compliance and increased characteristic impedance (Z_c). Aortic distensibility was the only independent predictor of central aortic SBP on multivariable analysis. In agreement with their modeling work, carotid forward compression wave power was higher and was negatively correlated with aortic compliance ($r^2 = 0.42$, $P < .001$) and distensibility ($r^2 = 0.37$, $P = .001$) in coarctation subjects. Although carotid intima-media thickness was higher ($P < .001$), carotid biomechanics were no different.

In contrast to Quail et al.,[49] aortic wave power and wave reflection indices were not different in control and coarctation patients. The reasons for this difference could be related to factors such as differing imaging modalities (magnetic resonance imaging vs. ultrasound) and acquisition locations (ascending aorta vs. transverse aortic arch), or more likely—differences in patient characteristics which are typical in the coarctation literature. Another possibility is different carotid stiffness in the samples which could

affect reflection to the ascending aorta according to their modeling study. Increased aorto-carotid transmission of wave energy following surgical repair of aortic coarctation may contribute to the high rates of cerebrovascular disease in this group. This work contributed substantially to our understanding of possible biomechanical mechanisms of cerebrovascular disease in coarctation patients.

Geometric considerations

Aortic arch obstruction

Residual aortic arch obstruction (residual or recurrent stenosis at the repair site) can occur in patients with coarctation and results in increased proximal aortic pressure. A contemporary study found arch obstruction in 15% of patients using a conventional definition of a Doppler-derived peak gradient >25 mmHg.[68] However, studies which have specifically excluded patients with residual obstruction still demonstrate an increased risk of hypertension (Table 46.2).
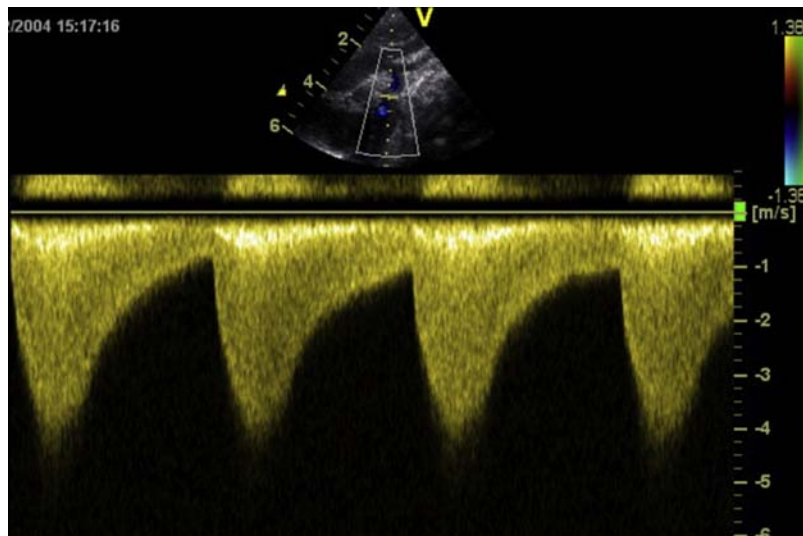
Arch obstruction can be identified using routine clinical assessments, including clinical imaging (Doppler echocardiography or cross-sectional imaging) or clinical measurements (brachial-ankle BP gradient). An interesting phenomenon in echocardiographic imaging of native or recurrent coarctation is the presence of continuous diastolic flow distal to the coarctation site (Fig. 46.7). The pattern is traditionally ascribed by cardiologists to the severity of the stenosis. However, the phenomenon is better understood in terms of a Windkessel, with consideration given to both the resistance of the coarctation and the proximal aortic compliance.[69] Conceptualized in this way, the presence of diastolic flow is related to the RC time constant. Patients with severe stenosis but significantly reduced proximal compliance may not manifest this echocardiographic finding, due to a lower RC time constant and more rapid diastolic pressure decay.

Abnormal aortic shape without obstruction has also been implicated as a significant mediator of increased load after coarctation repair.[38,39] Quenelle et al. found that persistent, mild aortic arch hypoplasia, even in the absence of an arm-leg SBP difference at rest, is also associated with late systemic hypertension.[70] Acute arch angulation (the gothic arch) has also been proposed as an important determinant of increased load and hypertension.[38,39] In particular, the gothic arch has been associated with exercise hypertension and abnormal flow profiles that are suggestive of increased wave reflections.[38,39] However, other studies have demonstrated no relationship between shape and exercise hemodynamics.[71]

Types of repair

As described briefly in the background section, aortic coarctation may be repaired via a number of surgical techniques, including end-to-end anastomoses (with

FIGURE 46.7 Continuous wave Doppler flow profile in the proximal descending aorta in a patient with unrepaired coarctation of the aorta (closed ductus arteriosus). There is increased velocity and continuous antegrade flow in diastole which is related to the severity of the stenosis and the compliance of the proximal aorta.

variable augmentation of the transverse arch, so-called extended end-to-end anastomosis), subclavian flap aortoplasty (the subclavian artery is used to augment the narrowed isthmus), or prosthetic material patch repairs (e.g., Dacron, GoreTex). Each of these approaches will affect the aortic geometry and regional stiffness. While it is possible that variation in surgical strategy may influence hypertension risk, the evidence for this is currently limited.[72] A recent prospective study compared vascular phenotypes in patients treated by either surgery, balloon dilatation, or endovascular stenting, and found no significant group differences.[73]

Three-dimensional shape and hemodynamics

The analysis of complex three-dimensional (3D) shape is difficult; the aorta is a curved tube with continuous variation in curvature and radius along its length.[74,75] Unfortunately, the coarctation literature suffers from evaluations of aortic shape which are often qualitative (i.e., identification of a gothic arch) or overly simplistic (i.e., simple height/width ratios). This may be why several studies have produced contradictory results regarding the link between shape and hemodynamic parameters.[71] Curvature and "shape" are often conflated with most definitions of abnormal shape actually relating to curvature. Using principal component analysis, Quail et al.[76] recently analyzed the relationship between the two components of 3D shape (curvature and radius) and pulsatile hemodynamics including wave reflections. Using this methodology, the authors found no association between principle components of curvature and abnormal wave reflection, suggesting that the so-called Gothic arch is less important than suggested by other groups. By contrast, principle components of radius were associated with the magnitude of the BCW.

Specifically, a large ascending aorta (associated with bicuspid valves), transverse arch hypoplasia, and a relatively smaller descending aorta were all associated with an increased magnitude of BCW.

The fact that curvature does not significantly influence wave reflections is not surprising from a mechanical point of view. The wave lengths of pressure and flow waves are in the order of meter, much larger than the geometrical dimensions of the aorta and its bends and curves. This explains why arterial wave dynamics are very well described using 1D formulations of the momentum equations.[77]

What causes the arterial abnormalities arise in coarctation?

In the previous sections, we have explored the data which show that patients with repaired coarctation have a very high prevalence of hypertension, and this appears to be due to an underlying vasculopathy characterized by reduced TAC, increased ascending aorta PWV, and pathological wave reflections.

However, it is still unexplained why patients develop this vasculopathy, given successful early repair of coarctation. In order to effectively reduce the excess cardiovascular risk in this population, it is important that this question is answered, although currently there are little explanatory data.

Congenital stiffness or control of systemic vascular resistance?

A commonly held view is that the aorta in coarctation is congenitally noncompliant. While this is a possibility, it is difficult to separate from transient abnormalities of arterial function in the perioperative period.[43,45]

Unpublished data from the author's institution showed a 20% incidence of prehypertension (casual SBP and DBP >90th centile) in 5—7-year-old children. These children had proportional elevations in SBP and DBP (and thus increased mean pressure, rather than pulse pressure), likely due to higher SVR. This pattern contrasts with older patients, in whom the predominant hemodynamic mechanism of hypertension is reduced TAC with normal SVR, characterized by a widened pulse pressure and a stiff aorta.[49]

The presence of elevated SVR is strongly suggestive of abnormal renal and autonomic control mechanisms. Infants with coarctation are at increased risk of renal injury at the time of aortic surgery due to either preoperative cardiogenic shock or renal ischemia due to aortic cross clamp.[78–80] Unfortunately, there are no long-term studies assessing the relationship with incident hypertension.

A role for autonomic dysfunction in coarctation is suggested by the presence of abnormal stress responses in patients with coarctation, in particular during exercise.[34,58,71,81] However, the underlying mechanisms are unclear, and could include the effect of increased stroke volume in a system with markedly reduce TAC. Alternatively, abnormal autonomic control mechanisms may be operating in children following coarctation repair.[28,82–84] Reasons for afferent baroreflex dysfunction in coarctation include abnormal antenatal baroreflex development (developmental programming), vagal nerve injury (aortic arch manipulation), or injury to descending inhibitory pathways due to subclinical spinal ischemia during aortic cross clamp.[65,66]

Evidence for neurohumoral abnormalities is suggested by a study of children by Hauser et al.[85] The cardiovascular response to the sympathomimetic, isoprenaline, is characterized by an increased heart rate and a reduction in blood pressure due to vasodilation. In a study of children with repaired coarctation (mean age 11.3 ± 6 years), 20% experienced a "paradoxical" increase in BP to isoprenaline. These children also had an elevated plasma renin activity response to exercise and high rates of early, transient, postoperative hypertension. These data suggest that abnormal responses to physiological stress in late childhood may be mediated by abnormal activity of the RAS and autonomic nervous system.

Assessment of endothelial function by flow-mediated dilatation has featured heavily in many studies of coarctation and has suggested the presence of endothelial dysfunction in patients,[33,34] as summarized in Table 46.3. However a recent careful study of contemporary patients, including half who had a diagnosis of hypertension, demonstrated no abnormalities of endothelial dysfunction by either reactive hyperemia or circulating endothelial progenitor cells.[86]

Evolution to vasculopathy—inflammation and biomechanics

Although congenital stiffness, renal, autonomic or neurohumoral abnormalities could explain the initiation of hypertension in coarctation, they do not fully explain the increased rate of aortic stiffening with age in coarctation, Fig. 46.8.

Inflammation is emerging as an important risk factor for the development of large artery stiffness and hypertension. In the general adult population and in other specific disease groups, systemic inflammation is associated with increased large artery stiffness.[87–93]

Conventionally, hypertensive vascular remodeling has been ascribed to smooth muscle cell hypertrophy and medial collagen deposition by these cells.[94] However, there is a growing body of knowledge that points to inflammation within the adventitia as a significant and perhaps even the principal contributor to pathological hypertensive remodeling.[95–97] The underlying idea is that adventitial inflammation switches the normal adaptive response to hypertension (increased wall thickness) to an exaggerated and maladaptive process.[98,99]

Variation in a child's systemic inflammatory state may potentiate maladaptive remodeling caused by elevated blood pressure in coarctation. Acute inflammatory stimuli in coarctation may include SIRS due to surgery or cardiogenic shock, or chronic inflammation due to renal dysfunction.[100–102] Additional variability in childhood systemic inflammation has many causes, including infections/vaccinations, obesity, psychological stress, and poverty.[103–106]

Both systemic and aortic inflammations have also been described in adults after coarctation repair; however, their role in the development of aortic stiffness is unclear.[45,86,107–110] While increased inflammatory biomarkers have been reported, there has not been an unambiguous relationship demonstrated with either hypertension or stiffness, Table 46.1.

Vascular abnormalities in other forms of congenital heart disease

Compared to coarctation of the aorta, the literature related to other forms of CHD is sparse.

Tetralogy of fallot

TOF is the most common form of *cyanotic* CHD, occurring in 36 per 10,000 live births. Morphologically the principal defect of this condition is anterocephalad deviation of the muscular outlet septum resulting in the tetrad of, VSD, pulmonary outflow tract obstruction, overriding aorta, and right ventricular hypertrophy. Complete repair of TOF was devised over 50 years ago and can result in complete intracardiac repair in early infancy. However, despite excellent short- and medium-term survival rates, the 30-year actuarial survival for patients repaired before their fifth birthday is 90% of the expected survival rate and the annualized risk of death triples in the third postoperative decade.[111,112]

TABLE 46.3 Selected studies of inflammatory and vascular function biomarkers in coarctation of the aorta.
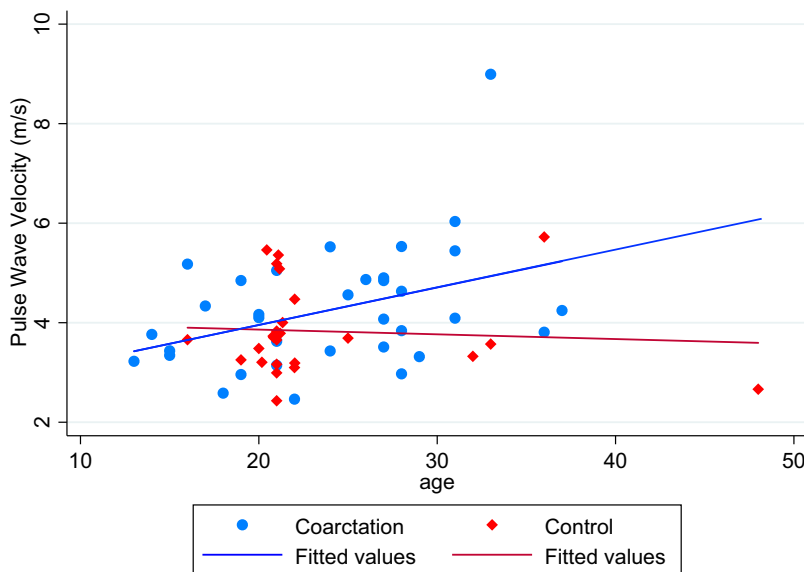
Study	Year	Type of study	Biomarkers	Vascular biomarkers	Disease status	Mean age	Cases, N (% males)	Pulse wave velocity	Pressure	Aix	Other vascular	Serum findings	Notes
Brili (atherosclerosis)[109]	2005	Case-control	IL-1b, IL-6, sVCAM-1, sICAM-1, E-Selectin	Flow mediated-dilatation (FMD)	Normotensive coarctation patients, age operation 17.7 years	29.9	15 (30%)				Higher IMT and lower carotid distensibility in coarctation versus control. Lower FMD in coarctation versus control	Coarctation versus control: higher sICAM-1, higher sVCAM-1, higher IL-1b, higher E-selectin. (No difference, CRP, fibrinogen, IL-6)	No explicit linear relationships between serum inflammation and stiffness metrics
Osmancik (Endothelium)[130]	2006	Case-control (pediatric)	IL-6, sE-Selectin, sL-Selectin, sICAM-1		Mean age at operation 7.7 years (3–12.8). Pre- and postoperative samples		17 (82%)					sICAM-1 higher in coarctation than controls at 10 months. No differences pre- or postoperative in adhesion molecules or IL-6.	Postoperative samples 10 months after surgery
Brili (JACC)[108]	2008	Randomized cross-over trial: Ramipril 5 mg/day four weeks	IL-1b, IL-6, sCD40L, sVCAM-1, CRP	Flow mediated-dilatation (FMD)	Normotensive coarctation patients, age operation 13.4 years	27.3	20 (65%)		Reduced systolic pressure with ramipril versus control: 110 versus 121 mmHg		Improved flow-mediated dilatation with ramipril	Reduced: IL-6, IL-1b, sVCAM and sCD40L with ramipril	
Brili (Heart)[131]	2012	Open-label: atorvastatin 10 mg/day four weeks	IL-1b, IL-6, sVCAM-1	Flow mediated-dilatation (FMD)	24% hypertensive in atrovastatin arm, age repair 10 years	31.4	17 (60%)	—	—	—	Improved flow-mediated dilatation with atorvastatin		Reduction in IL-1b and sVCAM-1 in atorvastatin

Study	Year	Design	Biomarkers	Vascular method	Population							
Mizia-Stec (IJC)[110]	2012	Case-control	Asymmetric dimethylarginine (ADMA), hsCRP	Flow-mediated dilatation (FMD), intima-media thickness, PWV	47% hypertensive, age operation 11.1 years.	34.1	62 (60%)	Higher pulse wave velocity (PWV) in patients than controls (higher PWV in hypertensive cases)		Lower FMD in patients versus controls, higher IMT in hypertensive coarctation	ADMA and CRP higher in hypertensive patients than not-hypertensive (also higher than controls)	Inverse linear relationship between ADMA and FMD. No relationship with CRP (personal communication with author)
Moutafi (IJC)[132]	2012	Case-control	IL-1b, IL-6, sVCAM-1, sICAM-1, E-Selectin, IL-10, Endothelin-1, TNF-alpha	Flow mediated dilatation (FMD), Sphygmocor: PWV, Aix	Mean systolic blood pressure (SBP) 130 ± 19 mmHg, age operation 7.4 years	25.3	19 (47%)		Higher AIx in patients versus controls	Lower FMD in patients versus controls, lower aortic distensibility and higher stiffness index in patients versus controls	Higher inflammatory markers in patient than controls (except IL-6, sFAS, ET1 and TNF-alpa)	No explicit linear relationships between serum inflammation and stiffness metrics
Moutafi (IJC)[133]	2014	Case-control (pediatric)	IL-10, IL-6, TNF-alpha, sFAS, Endothelin-1, sICAM-1, sVCAM-1, E-Selectin			9.1	10 (60%)			No differences in aortic distensibility or stiffness between cases and controls	Elevated IL-10, IL-6, TNF-alpha and sFas in patients. No differences in endothelin-1 or soluble adhesion markers	
Radke (Heart)[86]	2014	Case-control	IL-6, IL-8, ICAM-1, VCAM1, MCP1, VEGF. Circulating endothelial progenitor cells	Peripheral arterial tonometry	50% hypertensive. Mean age at operation seven years	35	20 (80%)			No differences in peripheral tonometry or EPCs between hypertensive and normotensive patients	Only MCP-1 higher in patients compared to controls	

Continued

TABLE 46.3 Selected studies of inflammatory and vascular function biomarkers in coarctation of the aorta.—cont'd

Study	Year	Type of study	Biomarkers	Vascular biomarkers	Disease status	Mean age	Cases, N (% males)	Pulse wave velocity	Pressure	Aix	Other vascular	Serum findings	Notes
Wybraniec (JASH)[134]	2014	Case-control	Renalase, CRP	Sphygmocor: PWV, AIx. Intima-media thickness	Dacron patch repair. 42% hypertensive. Median age at operation 10 years.	33	50 (62%)	Higher PWV in hypertensive cases	Inverse correlation between renalase and pulse pressure			Higher CRP in cases than controls. Significant association between CRP and diagnosis of hypertension: OR 1.13 (1.03—1.23) [per 1 mg/L increase in CRP]	
Brili (IJC)[42]	2016	Case-control	TGF-beta, IL-6	Sphygmocor: PWV, AIx			17	Higher carotid-radial, but not carotid-femoral PWV in coarctation				Elevated TGF-beta and IL-6 in coarctation	No explicit linear relationships between serum inflammation and stiffness metrics
Brili (Circ Imaging)[107]	2018	Case-control	18-FDG PET-CT, Spyhgmocor	Sphygmocor: PWV, AIx	Normotensive coarctation patients	—	15	No relationship with PWV and TBR	Higher target to background ratio (TBR) associated with higher mean pressure	No relationship between Aix and TBR	Higher TBR in coarctation patients (particularly bicuspid valve) than controls. Descending aorta highest TBR	Correlation between IL-6 and TBR	Control group treated for lymphoma
Rog (Acta Cardiologica)[135]	2018	Case-control	Fibrinogen, hsCRP	Sphygmocor: PWV, AIx	Mean SBP 137 ± 16 mmHg. Median age at operation 8.7 years	27.5	58 (62%)	Higher PWV in hypertensive coarctation. Correlation between PWV and fibrinogen ($r = 0.31$, $P = .039$)	Higher central SBP in patients than controls	Higher AIx in patients versus controls		CRP and fibrinogen higher in coarctation than controls	No association of PWV with hsCRP

FIGURE 46.8 Relationship between pulse wave velocity and age in patients with coarctation repaired in infancy <1 year (Blue), compared with healthy controls (Red). Significant linear relationship between covariates for coarctation group ($P = .02$). Nonsignificant association for control group ($P = .7$). *Unpublished data from Quail MA, Short R, Pandya B, et al. Abnormal wave reflections and left ventricular hypertrophy late after coarctation of the aorta repair.* **Hypertension** *2017; 69:501−509.*

In addition to the right ventricular lesions of TOF, it is also increasingly recognized that these patients have an increased risk of progressive aortic root dilatation.[113] Risk factors for progressive aortic dilation include the presence of pulmonary atresia, right aortic arch, history of an aortopulmonary shunt, male sex, and the presence of a 22q11 deletion[114]; pregnancy does not appear to be associated with a significantly increased risk of progression or aortic events.[115] Current data indicate that the risk of aortic dissection is less than for other forms of connective tissue disease.[116] However, aortic root and valve surgery may be required when accompanied by significant aortic regurgitation.

Histological studies of the aortic wall in TOF have highlighted degeneration of the tunica media of the aorta (including fibrosis, fragmentation of elastic fibers, and loss of smooth muscle cells) as an important cause of aortic root dilatation.[117,118] Abnormal aortic distensibility has also been described in children and adults with both repaired and unrepaired TOF (Table 46.4).[119,120]

Senzaki et al. has performed the most detailed assessment of aortic pulsatile hemodynamics in TOF.[58] In this study, simultaneous aortic pressure and flow data were acquired using a high-fidelity pressure transducer and a catheter-mounted flow velocity probe at the time of cardiac catheterization to calculate aortic impedance in patients and controls. Flow velocity was converted to flow volume using echocardiographic measurements of the sinutubular junction.

TOF patients had larger aortic diameters than controls: 18.8 mm (SD 4.8) versus 15.8 mm (SD 3.6). Patients had similar systolic, but lower diastolic and mean blood pressures. In patients compared to controls, there was higher impedance modulus at heart frequency (Z_1; 204 vs. 151 dyn s/cm^5.m^2; $P < .05$) and higher Z_c (average impedance moduli at 3−10 Hz; 158 vs. 105 dyn s.cm^{-5}.m^2; $P < .05$). Patients had an overall stiffer vasculature as assessed by TAC (0.93 vs. 1.24 mL/mmHg/m^2; $P < .05$) and PWV (5.6 vs. 4.2 m/s; $P < .05$). Interestingly, patients also had evidence of increased wave reflection as measured as the ratio between the peak amplitudes of forward and backward pressure waves (0.21 vs. 0.16; $P < .05$). There was a nonsignificant trend to higher SVR in TOF. The authors reported a significant inverse correlation between cardiac index and measures of pulsatile load.

These data are interesting as they show abnormalities of pulsatile hemodynamics in the absence of hypertension in TOF. Left ventricular dysfunction is common in TOF. In retrospective unpublished data from the author's institution, 13% of patients (53/408) have at least mild LV systolic dysfunction on CMR imaging (LVEF <55%). However, while indices of LV systolic function are frequently abnormal, they are infrequently severe (<3%). The reasons for impaired LV function in TOF are poorly understood but are likely multifactorial. One possible explanation, at least in part, could be abnormal pulsatile hemodynamics arising as a consequence of abnormal aortic biomechanics.

Other forms of congenital heart disease

Abnormalities of arterial biomechanics have been described in several other forms of CHD (including transposition of the great arteries [Table 46.4] and in single ventricle CHD), but their clinical significance remains uncertain.[121−125]

TABLE 46.4 Selected studies of arterial stiffness in patients with tetralogy of fallot and transposition of the great arteries.

Author	Year	CHD	Sample size	Age at study (years)	Finding
Grotenhuis (Heart)[136]	2009	Tetralogy of Fallot (TOF)	16	31	Reduced aortic elasticity (pulse wave velocity [PWV] and aortic root distensibility)
Cheung (Heart)[137]	2006	TOF	31	15.3	Increased heart-femoral PWV in patients
Senzaki (Heart)[58]	2012	TOF	36		Invasive haemodynamcis: Increased aortic characteristic impedance and PWV; Reduced total arterial compliance; higher aortic wave reflection;
Seki (EJCTS)[120]	2012	TOF	37	1	Prior to corrective surgery. Invasive hemodynamics: Increased PWV
Murakami (ATS)[122]	2000	TGA—arterial switch	15	4.5	Reduced distensibility in "neo-aortic root" (Sinus and STJ). Normal distensibility ascending and descending aorta
Mersich (Hypertension)[123]	2006	TGA—atrial and arterial switch	34 atrial; 14 arterial	13.2 (atrial); 8.1 (arterial)	Increased carotid beta stiffness index in both atrial switch and arterial switch patients
Grotenhuis (Radiology)[121]	2000	TGA—arterial switch	15	16	Reduced distensibility in "neo-aortic root" (STJ). Increased PWV (transit time)

Conclusions

In this chapter, we have discussed the abnormalities of arterial stiffness and pulsatile hemodynamics in patients with CHD, with a particular focus on coarctation of the aorta. There is an extensive body of evidence showing that coarctation is associated with excessive cardiovascular morbidity and mortality compared to the normal population or other forms of CHD. Abnormalities in vascular function appear in early life and are associated with the development of a vasculopathy characterized by elevated blood pressure, reduced arterial compliance, increased stiffness (particularly the proximal aorta), and pathological wave reflections. This latter phenomenon increases LV afterload with resultant hypertrophy and emerging evidence suggests a role in the pathogenesis of cerebrovascular events. There are important knowledge gaps: Why does this vasculopathy develop?; Is the increased risk of cardiovascular mortality associated with hypertension only, or are more complex hemodynamic abnormalities such as wave reflections involved?; Can medical therapies be used to attenuate wave reflections and reduce afterload? Finally, it is vital that we begin to better understand the hemodynamic abnormalities in order to develop rational treatments to prevent their development and associated complications.

References

1. Snider P, Olaopa M, Firulli AB, Conway SJ. Cardiovascular development and the colonizing cardiac neural crest lineage. **TheScientificWorldJournal**. 2007; 7.
2. Neeb Z, Lajiness JD, Bolanis E, Conway SJ. Cardiac outflow tract anomalies. **WIREs Dev Biol**. 2013; 2:499−530.
3. Edwards J. Malformations of the aortic arch system manifested as vascular rings. **Lab Invest**. 1952; 2:56−75.
4. Edwards JE. Anomalies of the derivatives of the aortic arch system. **Med Clin**. 1948; 32:925.
5. Moes CF, Freedom RM. Rare types of aortic arch anomalies. **Pediatr Cardiol**. 1993; 14:93−101.
6. Liu Y, Chen S, Zühlke L, et al. Global birth prevalence of congenital heart defects 1970-2017: updated systematic review and meta-analysis of 260 studies. **Int J Epidemiol**. 2019; 48:455−463.
7. Bondy C, Bakalov VK, Cheng C, Olivieri L, Rosing DR, Arai AE. Bicuspid aortic valve and aortic coarctation are linked to deletion of the X chromosome short arm in Turner syndrome. **J Med Genet**. 2013; 50:662−665.
8. Moosmann J, Uebe S, Dittrich S, Rüffer A, Ekici AB, Toka O. Novel loci for non-syndromic coarctation of the aorta in sporadic and familial cases. **PLoS One**. 2015; 10:e0126873−e.
9. Hussein A, Iyengar AJ, Jones B, et al. Twenty-three years of single-stage end-to-side anastomosis repair of interrupted aortic arches. **J Thorac Cardiovasc Surg**. 2010; 139:942−949.

10. Jegatheeswaran A, McCrindle BW, Blackstone EH, et al. Persistent risk of subsequent procedures and mortality in patients after interrupted aortic arch repair: a Congenital Heart Surgeons' Society study. **J Thorac Cardiovasc Surg**. 2010; 140:1059−1075.e2.

11. Canniffe C, Ou P, Walsh K, Bonnet D, Celermajer D. Hypertension after repair of aortic coarctation–a systematic review. **Int J Cardiol**. 2013; 167:2456−2461.

12. Fryar CD, Ostchega Y, Hales CM, Zhang G, Kruszon-Moran D. Hypertension Prevalence and Control Among Adults: United States, 2015-2016.

13. Rinnström D, Dellborg M, Thilén U, et al. Hypertension in adults with repaired coarctation of the aorta. **Am Heart J**. 2016; 181:10−15.

14. Lee MG, Babu-Narayan SV, Kempny A, et al. Long-term mortality and cardiovascular burden for adult survivors of coarctation of the aorta. **Heart**. 2019; 105:1190−1196.

15. Koller M, Rothlin M, Senning A. Coarctation of the aorta: review of 362 operated patients. Long-term follow-up and assessment of prognostic variables. **Eur Heart J**. 1987; 8:670−679.

16. Freed MD, Heymann MA, Lewis AB, Roehl SL, Kensey RC. Prostaglandin E1 infants with ductus arteriosus-dependent congenital heart disease. **Circulation**. 1981; 64:899−905.

17. Elliott R, Starling M, Neutze J. Medical manipulation of the ductus arteriosus. **Lancet**. 1975; 305:140−142.

18. Olley P, Coceani F, Bodach E. E-type prostaglandins: a new emergency therapy for certain cyanotic congenital heart malformations. **Circulation**. 1976; 53:728−731.

19. Heymann MA, Berman Jr W, Rudolph AM, Whitman V. Dilatation of the ductus arteriosus by prostaglandin E1 in aortic arch abnormalities. **Circulation**. 1979; 59:169−173.

20. Smallhorn JF, Huhta JC, Adams PA, Anderson RH, Wilkinson JL, Macartney FJ. Cross-sectional echocardiographic assessment of coarctation in the sick neonate and infant. **Br Heart J**. 1983; 50:349−361.

21. Cohen M, Fuster V, Steele PM, Driscoll D, McGoon DC. Coarctation of the aorta. Long-term follow-up and prediction of outcome after surgical correction. **Circulation**. 1989; 80:840−845.

22. Brouwer RM, Erasmus ME, Ebels T, Eijgelaar A. Influence of age on survival, late hypertension, and recoarctation in elective aortic coarctation repair. Including long-term results after elective aortic coarctation repair with a follow-up from 25 to 44 years. **J Thorac Cardiovasc Surg**. 1994; 108:525−531.

23. O'Sullivan JJ, Derrick G, Darnell R. Prevalence of hypertension in children after early repair of coarctation of the aorta: a cohort study using casual and 24 hour blood pressure measurement. **Heart**. 2002; 88:163−166.

24. Presbitero P, Demarie D, Villani M, et al. Long term results (15-30 years) of surgical repair of aortic coarctation. **Br Heart J**. 1987; 57:462−467.

25. Toro-Salazar OH, Steinberger J, Thomas W, Rocchini AP, Carpenter B, Moller JH. Long-term follow-up of patients after coarctation of the aorta repair. **Am J Cardiol**. 2002; 89:541−547.

26. Tanous D, Benson LN, Horlick EM. Coarctation of the aorta: evaluation and management. **Curr Opin Cardiol**. 2009; 24:509−515.

27. Cokkinos DV, Leachman RD, Cooley DA. Increased mortality rate from coronary artery disease following operation for coarctation of the aorta at a late age. **J Thorac Cardiovasc Surg**. 1979; 77:315−318.

28. Hanson E. Coarctation of the aorta. A long-term follow-up study after surgery. **Scand J Thorac Cardiovasc Surg Suppl**. 1980;(Suppl 24):1−31.

29. Verheugt CL, Uiterwaal CSPM, Grobbee DE, Mulder BJM. Long-term prognosis of congenital heart defects: a systematic review. **Int J Cardiol**. 2008; 131:25−32.

30. Roifman I, Therrien J, Ionescu-Ittu R, et al. Coarctation of the aorta and coronary artery disease: fact or fiction? **Circulation**. 2012; 126:16−21.

31. Pickard SS, Gauvreau K, Gurvitz M, et al. Stroke in adults with coarctation of the aorta: a national population-based study. **J Am Heart Assoc**. 2018; 7:e009072.

32. de Divitiis M, Pilla C, Kattenhorn M, et al. Ambulatory blood pressure, left ventricular mass, and conduit artery function late after successful repair of coarctation of the aorta. **J Am Coll Cardiol**. 2003; 41:2259−2265.

33. de Divitiis M, Pilla C, Kattenhorn M, et al. Vascular dysfunction after repair of coarctation of the aorta: impact of early surgery. **Circulation**. 2001; 104:I165−I170.

34. Gardiner HM, Celermajer DS, Sorensen KE, et al. Arterial reactivity is significantly impaired in normotensive young adults after successful repair of aortic coarctation in childhood. **Circulation**. 1994; 89:1745−1750.

35. Ong CM, Canter CE, Gutierrez FR, Sekarski DR, Goldring DR. Increased stiffness and persistent narrowing of the aorta after successful repair of coarctation of the aorta: relationship to left ventricular mass and blood pressure at rest and with exercise. **Am Heart J**. 1992; 123:1594−1600.

36. Kenny D, Polson JW, Martin RP, et al. Relationship of aortic pulse wave velocity and baroreceptor reflex sensitivity to blood pressure control in patients with repaired coarctation of the aorta. **Am Heart J**. 2011; 162:398−404.

37. Ou P, Celermajer DS, Jolivet O, et al. Increased central aortic stiffness and left ventricular mass in normotensive young subjects after successful coarctation repair. **Am Heart J**. 2008; 155:187−193.

38. Ou P, Celermajer DS, Raisky O, et al. Angular (Gothic) aortic arch leads to enhanced systolic wave reflection, central aortic stiffness, and increased left ventricular mass late after aortic coarctation repair: evaluation with magnetic resonance flow mapping. **J Thorac Cardiovasc Surg**. 2008; 135:62−68.

39. Ou P, Mousseaux E, Celermajer DS, et al. Aortic arch shape deformation after coarctation surgery: effect on blood pressure response. **J Thorac Cardiovasc Surg**. 2006; 132:1105−1111.

40. Swan L, Kraidly M, Vonder Muhll I, Collins P, Gatzoulis MA. Surveillance of cardiovascular risk in the normotensive patient with repaired aortic coarctation. **Int J Cardiol**. 2010; 139:283−288.

41. Xu J, Shiota T, Omoto R, et al. Intravascular ultrasound assessment of regional aortic wall stiffness, distensibility, and compliance in patients with coarctation of the aorta. **Am Heart J**. 1997; 134:93−98.

42. Brili S, Antonopoulos AS, Oikonomou E, et al. Impairment of arterial elastic properties and elevated circulating levels of transforming growth factor-beta in subjects with repaired coarctation of aorta. **Int J Cardiol**. 2016; 207:282−283.

43. Vogt M, Kühn A, Baumgartner D, et al. Impaired elastic properties of the ascending aorta in newborns before and early after successful coarctation repair: proof of a systemic vascular disease of the pre-stenotic arteries? **Circulation**. 2005; 111:3269−3273.

44. Voges I, Kees J, Jerosch-Herold M, et al. Aortic stiffening and its impact on left atrial volumes and function in patients after successful coarctation repair: a multiparametric cardiovascular magnetic reso-nance study. **J Cardiovasc Magn Reson**. 2016; 18:56.

45. Lombardi KC, Northrup V, McNamara RL, Sugeng L, Weismann CG. Aortic stiffness and left ventricular diastolic function in children following early repair of aortic coarctation. **Am J Car-diol**. 2013; 112:1828−1833.

46. McEniery CM, Cockcroft JR, Roman MJ, Franklin SS, Wilkinson IB. Central blood pressure: current evidence and clinical importance. **Eur Heart J**. 2014; 35:1719−1725.

47. Quail MA, Steeden JA, Knight D, Segers P, Taylor AM, Muthurangu V. Development and validation of a novel method to derive central aortic systolic pressure from the MR aortic distension curve. **J Magn Reson Imaging**. 2014; 40:1064−1070.

48. Hope SA, Meredith IT, Cameron JD. Arterial transfer functions and the reconstruction of central aortic waveforms: myths, controversies and misconceptions. **J Hypertens**. 2008; 26:4−7.

49. Quail MA, Short R, Pandya B, et al. Abnormal wave reflections and left ventricular hypertrophy late after coarctation of the aorta repair. **Hypertension**. 2017; 69:501−509.

50. Szczepaniak-Chicheł L, Trojnarska O, Mizia-Stec K, et al. Augmentation of central arterial pressure in adult patients after coarctation repair. **Blood Press Monit**. 2011; 16:22−28.

51. Hope SA, Hughes AD. Drug effects on the mechanical properties of large arteries in humans. **Clin Exp Pharmacol Physiol**. 2007; 34:688−693.

52. Khir AW, Parker KH. Wave intensity in the ascending aorta: effects of arterial occlusion. **J Biomech**. 2005; 38:647−655.

53. Kobayashi S, Yano M, Kohno M, et al. Influence of aortic imped-ance on the development of pressure-overload left ventricular hy-pertrophy in rats. **Circulation**. 1996; 94:3362−3368.

54. O'Rourke MF, Cartmill TB. Influence of aortic coarctation on pul-satile hemodynamics in the proximal aorta. **Circulation**. 1971; 44:281−292.

55. Van Den Bos GC, Westerhof N, Elzinga G, Sipkema P. Reflection in the systemic arterial system: effects of aortic and carotid occlusion. **Cardiovasc Res**. 1976; 10:565−573.

56. Murakami T, Takeda A. Enhanced aortic pressure wave reflection in patients after repair of aortic coarctation. **Ann Thorac Surg**. 2005; 80:995−999.

57. Agnoletti G, Bonnet C, Bonnet D, Sidi D, Aggoun Y. Mid-term effects of implanting stents for relief of aortic recoarctation on systemic hypertension, carotid mechanical properties, intimal medial thickness and reflection of the pulse wave. **Cardiol Young**. 2005; 15:245−250.

58. Senzaki H, Iwamoto Y, Ishido H, et al. Ventricular-vascular stiff-ening in patients with repaired coarctation of aorta: integrated pathophysiology of hypertension. **Circulation**. 2008; 118:S191−S198.

59. Biglino G, Steeden JA, Baker C, et al. A non-invasive clinical application of wave intensity analysis based on ultrahigh temporal resolution phase-contrast cardiovascular magnetic resonance. **J Cardiovasc Magn Reson**. 2012; 14:57.

60. Feng J, Khir AW. Determination of wave speed and wave separation in the arteries using diameter and velocity. **J Biomech**. 2010; 43:455−462.

61. Quail M, Knight D, Steeden J, Taylor A, Muthurangu V. Novel magnetic resonance wave intensity analysis in pulmonary hyper-tension. **J Cardiovasc Magn Reson**. 2014; 16:P252.

62. Li Y, Borlotti A, Hickson SS, McEniery CM, Wilkinson IB, Khir AW. Using magnetic resonance imaging measurements for the determination of local wave speed and arrival time of reflected waves in human ascending aorta. **Conf Proc**. 2010; 2010:5153−5156.

63. Quail MA, Steeden JA, Taylor AM, Muthurangu V. The effect of temporal resolution on mr assessment of pulse wave velocity. **Ar-tery Res**. 2013; 7:157−158.

64. Taelman L, Bols J, Degroote J, et al. Differential impact of local stiffening and narrowing on hemodynamics in repaired aortic coarc-tation: an FSI study. **Med Biol Eng Comput**. 2016; 54:497−510.

65. Mynard JP, Kowalski R, Cheung MM, Smolich JJ. Beyond the aorta: partial transmission of reflected waves from aortic coarctation into supra-aortic branches modulates cerebral hemodynamics and left ventricular load. **Biomech Model Mechanobiol**. 2017; 16(2):635−650. https://doi.org/10.1007/s10237-016-0842-x. Epub 2016 Oct 11.

66. Mynard JP, Smolich JJ. Novel wave power analysis linking pressure-flow waves, wave potential, and the forward and backward components of hydraulic power. **Am J Physiol Heart Circ Physiol**. 2016; 310:H1026−H1038.

67. Kowalski R, Lee MGY, Doyle LW, et al. Reduced aortic distensi-bility is associated with higher aorto-carotid wave transmission and central aortic systolic pressure in young adults after coarctation repair. **J Am Heart Assoc**. 2019; 8:e011411.

68. Lee MG, Allen SL, Kawasaki R, et al. High prevalence of hyper-tension and end-organ damage late after coarctation repair in normal arches. **Ann Thorac Surg**. 2015; 100:647−653.

69. DeGroff CG, Orlando W, Shandas R. Insights into the effect of aortic compliance on Doppler diastolic flow patterns seen in coarc-tation of the aorta: a numeric study. **J Am Soc Echocardiogr**. 2003; 16:162−169.

70. Quennelle S, Powell AJ, Geva T, Prakash A. Persistent aortic arch hypoplasia after coarctation treatment is associated with late sys-temic hypertension. **J Am Heart Assoc**. 2015; 4.

71. Ntsinjana HN, Biglino G, Capelli C, et al. Aortic arch shape is not associated with hypertensive response to exercise in patients with repaired congenital heart diseases. **J Cardiovasc Magn Reson**. 2013; 15:101.

72. Kenny D, Polson JW, Martin RP, et al. Surgical approach for aortic coarctation influences arterial compliance and blood pressure con-trol. **Ann Thorac Surg**. 2010; 90:600−604.

73. Martins JD, Zachariah J, Tierney ESS, et al. Impact of treatment modality on vascular function in coarctation of the aorta: the LOVE COARCT study. **J Am Heart Assoc**. 2019; 8:e011536.

74. Bruse JL, Khushnood A, McLeod K, et al. How successful is suc-cessful? Aortic arch shape after successful aortic coarctation repair correlates with left ventricular function. **J Thorac Cardiovasc Surg**. 2017; 153:418−427.

75. Bruse JL, McLeod K, Biglino G, et al. A statistical shape modelling framework to extract 3D shape biomarkers from medical imaging data: assessing arch morphology of repaired coarctation of the aorta. **BMC Med Imaging**. 2016; 16:40.

76. Quail MA, Segers P, Steeden JA, Muthurangu V. The aorta after coarctation repair - effects of calibre and curvature on arterial haemodynamics. **J Cardiovasc Magn Reson**. 2019; 21:22.

77. Milnor WR. **Hemodynamics**. 2nd ed. Baltimore: Williams & Wilkins; 1989.

78. Jang WS, Kim W-H, Choi K, et al. Incidence, risk factors and clinical outcomes for acute kidney injury after aortic arch repair in paediatric patients. **Eur J Cardio Thorac Surg**. 2014; 45:e208−e214.

79. Han WK, Waikar SS, Johnson A, et al. Urinary biomarkers in the early diagnosis of acute kidney injury. **Kidney Int**. 2008; 73:863−869.

80. Bennett M, Dent CL, Ma Q, et al. Urine NGAL predicts severity of acute kidney injury after cardiac surgery: a prospective study. **Clin J Am Soc Nephrol**. 2008; 3:665−673.

81. Swan L, Goyal S, Hsia C, Hechter S, Webb G, Gatzoulis MA. Exercise systolic blood pressures are of questionable value in the assessment of the adult with a previous coarctation repair. **Heart**. 2003; 89:189−192.

82. Lee MGY, Hemmes RA, Mynard J, et al. Elevated sympathetic activity, endothelial dysfunction, and late hypertension after repair of coarctation of the aorta. **Int J Cardiol**. 2017; 243:185−190.

83. Polson JW, McCallion N, Waki H, et al. Evidence for cardiovascular autonomic dysfunction in neonates with coarctation of the aorta. **Circulation**. 2006; 113:2844−2850.

84. Kenny D, Polson JW, Martin RP, et al. Relationship of aortic pulse wave velocity and baroreceptor reflex sensitivity to blood pressure control in patients with repaired coarctation of the aorta. **Am Heart J**. 2011; 162:398−404.

85. Hauser M, Kuehn A, Wilson N. Abnormal responses for blood pressure in children and adults with surgically corrected aortic coarctation. **Cardiol Young**. 2000; 10:353−357.

86. Radke RM, Diller GP, Duck M, et al. Endothelial function in contemporary patients with repaired coarctation of aorta. **Heart**. 2014; 100:1696−1701.

87. Booth A, Wallace S, McEniery C, Brown J, Jayne D, Wilkinson I. Inflammation and arterial stiffness in systemic vasculitis: a model of vascular inflammation. **Arthritis Rheum**. 2004; 50:581−588.

88. Mäki-Petäjä KM, Elkhawad M, Cheriyan J, et al. Anti-tumor necrosis factor-α therapy reduces aortic inflammation and stiffness in patients with rheumatoid arthritis. **Circulation**. 2012; 126:2473−2480.

89. Sabit R, Bolton CE, Edwards PH, et al. Arterial stiffness and osteoporosis in chronic obstructive pulmonary disease. **Am J Respir Crit Care Med**. 2007; 175:1259−1265.

90. Yasmin, McEniery CM, Wallace S, et al. Matrix metalloproteinase-9 (MMP-9), MMP-2, and serum elastase activity are associated with systolic hypertension and arterial stiffness. **Arterioscler Thromb Vasc Biol**. 2005; 25:372.

91. Yasmin, McEniery CM, Wallace S, Mackenzie IS, Cockcroft JR, Wilkinson IB. C-reactive protein is associated with arterial stiffness in apparently healthy individuals. **Arterioscler Thromb Vasc Biol**. 2004; 24:969−974.

92. Jain S, Khera R, Corrales−Medina VF, Townsend RR, Chirinos JA. Inflammation and arterial stiffness in humans. **Atherosclerosis**. 2014; 237:381−390.

93. Mäki-Petäjä KM, Wilkinson IB. Inflammation and large arteries: potential mechanisms for inflammation-induced arterial stiffness. **Artery Res**. 2012; 6:59−64.

94. Sehgel NL, Sun Z, Hong Z, et al. Augmented vascular smooth muscle cell stiffness and adhesion when hypertension is superimposed on aging. **Hypertension**. 2015; 65:370−377.

95. Lehoux S. Adventures in the adventitia. **Hypertension**. 2016; 67:836−838.

96. Wu J, Thabet SR, Kirabo A, et al. Inflammation and mechanical stretch promote aortic stiffening in hypertension through activation of p38 mitogen-activated protein kinase. **Circ Res**. 2014; 114:616−625.

97. Eberth JF, Gresham VC, Reddy AK, Popovic N, Wilson E, Humphrey JD. Importance of pulsatility in hypertensive carotid artery growth and remodeling. **J Hypertens**. 2009; 27:2010.

98. Latorre M, Bersi MR, Humphrey JD. Computational modeling predicts immuno-mechanical mechanisms of maladaptive aortic remodeling in hypertension. **Int J Eng Sci**. 2019; 141:35−46.

99. Bersi MR, Bellini C, Wu J, Montaniel KRC, Harrison DG, Humphrey JD. Excessive adventitial remodeling leads to early aortic maladaptation in angiotensin-induced hypertension. **Hypertension**. 2016; 67:890−896.

100. Kohsaka S, Menon V, Lowe AM, et al. Systemic inflammatory response syndrome after acute myocardial infarction complicated by cardiogenic shock. **Arch Intern Med**. 2005; 165:1643−1650.

101. Boehne M, Sasse M, Karch A, et al. Systemic inflammatory response syndrome after pediatric congenital heart surgery: incidence, risk factors, and clinical outcome. **J Card Surg**. 2017; 32:116−125.

102. Silverstein DM. Inflammation in chronic kidney disease: role in the progression of renal and cardiovascular disease. **Pediatr Nephrol**. 2009; 24:1445−1452.

103. Visser M, Bouter LM, McQuillan GM, Wener MH, Harris TB. Elevated C-reactive protein levels in overweight and obese adults. **JAMA**. 1999; 282:2131−2135.

104. Cote AT, Phillips AA, Harris KC, Sandor GGS, Panagiotopoulos C, Devlin AM. Obesity and arterial stiffness in children. **Arterioscler Thromb Vasc Biol**. 2015; 35:1038−1044.

105. Hiura M, Kikuchi T, Nagasaki K, Uchiyama M. Elevation of serum C-reactive protein levels is associated with obesity in boys. **Hypertens Res**. 2003; 26:541−546.

106. Broyles ST, Staiano AE, Drazba KT, Gupta AK, Sothern M, Katzmarzyk PT. Elevated C-reactive protein in children from risky neighborhoods: evidence for a stress pathway linking neighborhoods and inflammation in children. **PLoS One**. 2012; 7:e45419.

107. Brili S, Oikonomou E, Antonopoulos AS, et al. 18F-Fluorodeoxyglucose positron emission tomography/computed tomographic imaging detects aortic wall inflammation in patients with repaired coarctation of aorta. **Circ Cardiovasc Imaging**. 2018; 11:e007002.

108. Brili S, Tousoulis D, Antoniades C, et al. Effects of ramipril on endothelial function and the expression of proinflammatory cytokines and adhesion molecules in young normotensive subjects with successfully repaired coarctation of aorta: a randomized cross-over study. **J Am Coll Cardiol**. 2008; 51:742−749.

109. Brili S, Tousoulis D, Antoniades C, et al. Evidence of vascular dysfunction in young patients with successfully repaired coarctation of aorta. **Atherosclerosis**. 2005; 182:97−103.

110. Mizia-Stec K, Trojnarska O, Szczepaniak-Chichel L, et al. Asymmetric dimethylarginine and vascular indices of atherosclerosis in patients after coarctation of aorta repair. **Int J Cardiol**. 2012; 158:364−369.

111. Murphy JG, Gersh BJ, Mair DD, et al. Long-term outcome in patients undergoing surgical repair of tetralogy of Fallot. **N Engl J Med**. 1993; 329:593−599.

112. Nollert G, Fischlein T, Bouterwek S, Bohmer C, Klinner W, Reichart B. Long-term survival in patients with repair of tetralogy of Fallot: 36-year follow-up of 490 survivors of the first year after surgical repair. **J Am Coll Cardiol**. 1997; 30:1374−1383.

113. Yetman AT, Graham T. The dilated aorta in patients with congenital cardiac defects. **J Am Coll Cardiol**. 2009; 53:461−467.

114. Niwa K. Aortic root dilation in tetralogy of Fallot long-term after repair–histology of the aorta in tetralogy of Fallot: evidence of intrinsic aortopathy. **Int J Cardiol**. 2005; 103:117−119.

115. Cauldwell M, Quail MA, Smith GS, et al. Effect of pregnancy on ventricular and aortic dimensions in repaired tetralogy of Fallot. **J Am Heart Assoc**. 2017; 6:e005420.

116. Zanjani KS, Niwa K. Aortic dilatation and aortopathy in congenital heart diseases. **J Cardiol**. 2013; 61:16−21.

117. Niwa K, Perloff JK, Bhuta SM, et al. Structural abnormalities of great arterial walls in congenital heart disease: light and electron microscopic analyses. **Circulation**. 2001; 103:393−400.

118. Tan JL, Davlouros PA, McCarthy KP, Gatzoulis MA, Ho SY. Intrinsic histological abnormalities of aortic root and ascending aorta in tetralogy of Fallot. **Circulation**. 2005; 112:961−968.

119. Cheung YF, Ou X, Wong SJ. Central and peripheral arterial stiffness in patients after surgical repair of tetralogy of Fallot: implications for aortic root dilatation. **Heart**. 2006; 92:1827−1830.

120. Seki M, Kurishima C, Saiki H, et al. Progressive aortic dilation and aortic stiffness in children with repaired tetralogy of Fallot. **Heart Ves**. 2014; 29:83−87.

121. Grotenhuis HB, Ottenkamp J, Fontein D, et al. Aortic elasticity and left ventricular function after arterial switch operation: MR imaging—initial experience. **Radiology**. 2008; 249:801−809.

122. Murakami T, Nakazawa M, Momma K, Imai Y. Impaired distensibility of neoaorta after arterial switch procedure. **Ann Thorac Surg**. 2000; 70:1907−1910.

123. Mersich B, Studinger P, Lenard Z, Kadar K, Kollai M. Transposition of great arteries is associated with increased carotid artery stiffness. **Hypertension**. 2006; 47:1197−1202.

124. Saiki H, Kurishima C, Masutani S, Senzaki H. Cerebral circulation in patients with Fontan circulation: assessment by carotid arterial wave intensity and stiffness. **Ann Thorac Surg**. 2014; 97:1394−1399.

125. Biglino G, Giardini A, Ntsinjana HN, Schievano S, Hsia TY, Taylor AM. Ventriculoarterial coupling in palliated hypoplastic left heart syndrome: noninvasive assessment of the effects of surgical arch reconstruction and shunt type. **J Thorac Cardiovasc Surg**. 2014; 148:1526−1533.

126. Seirafi PA, Warner KG, Geggel RL, Payne DD, Cleveland RJ. Repair of coarctation of the aorta during infancy minimizes the risk of late hypertension. **Ann Thorac Surg**. 1998; 66:1378−1382.

127. Vriend JW, Mulder BJ. Late complications in patients after repair of aortic coarctation: implications for management. **Int J Cardiol**. 2005; 101:399−406.

128. Hager A, Kanz S, Kaemmerer H, Schreiber C, Hess J. Coarctation Long-term Assessment (COALA): significance of arterial hypertension in a cohort of 404 patients up to 27 years after surgical repair of isolated coarctation of the aorta, even in the absence of restenosis and prosthetic material. **J Thorac Cardiovasc Surg**. 2007; 134:738−745. e2.

129. Choudhary P, Canniffe C, Jackson D, Tanous D, Walsh K, Celermajer D. Late outcomes in adults with coarctation of the aorta. **Heart**. 2015; 101:1190−1195.

130. Osmancik P, Bocsi J, Hambsch J, Schneider P, Tárnok A. Soluble endothelial adhesion molecule concentration in patients with aortic coarctation. **Endothelium**. 2006; 13:353−358.

131. Brili S, Tousoulis D, Antonopoulos AS, et al. Effects of atorvastatin on endothelial function and the expression of proinflammatory cytokines and adhesion molecules in young subjects with successfully repaired coarctation of aorta. **Heart**. 2012; 98:325−329.

132. Moutafi AC, Alissafi T, Chamakou A, et al. Neurohormonal activity and vascular properties late after aortic coarctation repair. **Int J Cardiol**. 2012; 159:211−216.

133. Moutafi AC, Alissafi T, Chryssanthopoulos S, et al. Neurohormones, cytokines, and aortic function in children with repaired coarctation of the aorta. **Int J Cardiol**. 2014; 172:e26−e27.

134. Wybraniec MT, Mizia-Stec K, Trojnarska O, et al. Low plasma renalase concentration in hypertensive patients after surgical repair of coarctation of aorta. **J Am Soc Hypertens**. 2014; 8:464−474.

135. Róg B, Okólska M, Dziedzic-Oleksy H, et al. Arterial stiffness in adult patients after coarctation of aorta repair and with bicuspid aortic valve. **Acta Cardiologica**. 2019; 74:517−524.

136. Grotenhuis HB, Ottenkamp J, de Bruijn L, et al. Aortic elasticity and size are associated with aortic regurgitation and left ventricular dysfunction in tetralogy of Fallot after pulmonary valve replacement. **Heart**. 2009; 95:1931−1936.

137. Cheung YF, Ou X, Wong SJ. Central and peripheral arterial stiffness in patients after surgical repair of tetralogy of Fallot: implications for aortic root dilatation. **Heart**. 2006; 92:1827−1830.

Chapter 47

Infection and arterial stiffness

Vicente F. Corrales–Medina[1] and Julio A. Chirinos[2,3]

[1]Department of Medicine, Division of Infectious Diseases at the University of Ottawa, The Ottawa Hospital Research Institute, Centre for Infection, Immunity and Inflammation (CI3) at the University of Ottawa, Ottawa, ON, Canada; [2]University of Pennsylvania Perelman School of Medicine, Hospital of the University of Pennsylvania and Perelman Center for Advanced Medicine, Philadelphia, PA, United States; [3]Ghent University, Ghent, Belgium

Introduction

Acute infections can perturb the cardiovascular system acutely and are also associated with increased cardiovascular risk in the long-term. Patients with chronic infections are also at increased risk of cardiovascular disease. In this chapter, using sepsis as model for acute infection, and infection with the human immunodeficiency virus (HIV) as model for chronic infection, we discuss the association between infections and the cardiovascular system and explore the potential role of arterial stiffness in these relationships.

Arterial stiffness and sepsis

Sepsis is a life-threatening multiorgan dysfunction caused by a dysregulated host response to infection.[1] The pathophysiological cascade of sepsis starts when an invading pathogen (bacteria, virus, or fungus) is recognized by the innate immune system and triggers the generation and release of inflammatory mediators that while promoting an immune response against the infecting agent, can also have detrimental effects on several body organs. A detailed discussion of the molecular, cellular, and regulatory pathways of sepsis, as well as the range of organ involvement and treatment strategies in this condition are beyond the scope of this Chapter, and the reader can refer to published reviews on this topic.[2] The circulatory system is preeminently affected in sepsis, and cardiovascular abnormalities are a hallmark of this syndrome. In this section, we will discuss our current understanding of the circulatory responses to sepsis, how arterial stiffness could influence this paradigm, the current experimental and clinical evidence of a relationship between sepsis and arterial stiffness, and the potential mechanisms underlying this association.

Effect of sepsis on the circulatory system

Short term

In the prevailing model of the effect of sepsis on the circulatory system, the acute septic inflammatory response leads to the synthesis and release of inflammatory mediators (tumor necrosis factor, interleukin [IL]-1, IL-6, IL-8, IL-12, IL-18, interferon γ, prostaglandins [PGs], and matrix-metalloproteases [MMPs], among others) and toxic oxidative and nitrosative intermediates into the blood, and the adhesion of platelets and leukocytes to the endothelium.[3,4] The net result is vascular smooth muscle dilation and disruption of the supportive structures of the vascular endothelium, including the cell cytoskeleton (actin), intercellular adhesion molecules (tight junctions), and an array of supportive proteins. These effects produce dilation of the "resistance" vessels (i.e., vessels with predominant vascular smooth muscle wall architecture like small arteries and arterioles) and capillary "leakage" (with outflow of intravascular proteins and plasma fluid) into the extravascular space, both leading to a drop in the peripheral vascular resistance and effective preload, progressively challenging the conservation of adequate blood pressures.[3,5] Compounding these effects is the development of a form of nonischemic sepsis-induced cardiomyopathy characterized by ventricular dilatation, reduced ventricular contractility, and both right and left systolic and diastolic dysfunction.[6,7] In its most advanced stages, sepsis results in a form of shock that is poorly responsive to plasma volume expansion and the administration of vasopressor and inotropic agents, and that shows poor tolerance to fluid challenges. Increased serum markers of myocardial injury (i.e., cardiac troponin) are present in a majority of patients with sepsis and they are associated with increased sepsis mortality.[8]

The mechanisms underlying this sepsis-induced cardiomyopathy are not well understood but appear to involve excessive formation of nitric oxide (NO), reactive oxygen species and nitrogen radicals, mitochondrial dysfunction, transcriptional and metabolic changes, direct cardiotoxicity from bacterial products and inflammatory molecules, and ischemic damage due to mismatches between the metabolic demands of the myocardium and the coronary blood supply (i.e., "supply/demand mismatch").[6,7,9,10] Sepsis-associated myocardial dysfunction can affect both systolic and diastolic function, and it is present in a majority of patients with sepsis.[11] Given the circulatory and metabolic demands of sepsis and the effect of sepsis on myocardial function, it is not surprising that sepsis is one of the most common precipitants of new-onset or acutely decompensated heart failure,[12,13] and that sepsis carries a particularly poor prognosis in patients with preexisting diagnosis of heart failure.[14,15] However, the relationship between sepsis and new onset heart failure is confounded by the need for aggressive fluid resuscitation, which often leads to a markedly positive sodium and water balance over short periods of time, particularly in critically ill patients.

The incidence of acute myocardial infarction during sepsis is difficult to ascertain due to the difficulty of distinguishing between true myocardial infarction and nonischemic sepsis-induced myocardial injury, and the changing criteria for defining myocardial infarction in clinical research.[16] Contemporary reports suggest that myocardial infarction complicates the course of about 4% to 8% of patients with severe sepsis.[17,18] A similar incidence of myocardial infarction has been reported in patients with pneumonia.[19–21] The mechanisms contributing to the increased risk of myocardial infarction during sepsis and associated states (i.e., pneumonia) are largely unknown, but infection driven increased systemic and coronary inflammatory activity, and dominant prothrombotic conditions, among others, have been proposed as potential contributors.[22–24]

Intermediate and long term

In the last decade, a growing body of literature suggests that the effects of sepsis and other sepsis-related conditions such as pneumonia on the circulatory system are not limited to the short-term but can extend for months and years after an index septic/infectious episode. Epidemiologic studies show that new-onset heart failure can occur in as many as 13% of sepsis survivors by year 2 after their index sepsis episode.[25] Compared to nonhospitalized and hospitalized controls without sepsis, the risk of heart failure in sepsis survivors over 7 years after their index sepsis episode is increased by 43% and 48%, respectively.[26] Likewise, among elderly survivors of pneumonia requiring hospitalization, about 10% develop new-onset heart failure in the first year after the index pneumonia episode.[27] Compared to elderly controls without pneumonia, the risk of new-onset heart failure in pneumonia survivors is increased by about sevenfold between 30 and 90 days after the index infection, about threefold between 90 days and 1 year, and almost twofold between 1 and 5 years post-pneumonia.[27] An increased long-term risk of new-onset heart failure after pneumonia has also been observed in other age-groups.[28]

Both sepsis and pneumonia survivors also remain at high risk of myocardial infarction and stroke.[29] Epidemiologic studies of sepsis survivors suggest a one-year post-sepsis incidence of stroke and myocardial infarction of 18% and 9%, respectively.[30] Similar to the risk of HF, the risk of myocardial infarction in sepsis survivors over 7 years of follow-up after their index episode of sepsis and relative to nonhospitalized and hospitalized controls was increased by 22% and 14%, respectively. Among elderly survivors of pneumonia, the cumulative incidence of (composite) myocardial infarction or stroke is 12% at 30 days after pneumonia, 13% at 90 days and 18% at 1 year.[31] Compared to controls without pneumonia, the risk of myocardial infarction or stroke in elderly survivors of pneumonia with severe sepsis is increased by about fivefold in the first 30 days postinfection, two- to threefold between 1 month and 1 year postpneumonia, and about onefold afterward and up to 10 years.[31] An increased long-term risk of myocardial infarction and stroke after pneumonia has also been observed in other age-groups.[30,31]

Sepsis and arterial stiffness

Mostly neglected in the pathophysiologic model of the acute circulatory effects of sepsis discussed above, is the role of the larger elastic conduit arterial vessels and the ventricle-arterial pulsatile interactions in the septic state. In the current model, the circulatory system is conceived as a pump-driven, one-way system of blood flow in which the hemodynamic effects of the pulsatile nature of the cardiac cycle and the mechanical properties of the arteries that accommodate the blood ejected by the heart in each heartbeat are largely overlooked. However, as discussed throughout this textbook, the arterial tree imparts afterload to the left ventricle, and arterial structure and function directly impact both steady and pulsatile left ventricular afterload. Microvascular and muscular artery dysfunction in sepsis could interact with large artery stiffness to produce adverse patterns of left ventricular afterload that may contribute to cardiac complications both during sepsis and after recovery from the acute septic episode.

Animal studies on sepsis and arterial stiffness

In rabbits, injection of lipopolysaccharide (LPS, the major component of the outer membrane of gram-negative bacteria) induces reduction of endothelium-mediated relaxation of the aorta in the context of a severe-sepsis type of response.[32] In another swine LPS-induced sepsis model, LPS infusion produces, within an overall hypotensive hyperdynamic septic-shock type of response, acute reversal of the usual pulse pressure (PP) amplification (from aortic to radial or femoral arteries), and reduced total arterial compliance increased aortic characteristic impedance (Zc) (Table 47.1).[33] Interestingly, these adverse large artery changes occurred despite a reduction in blood pressure. There are no animal studies examining long-term effects of sepsis on arterial stiffness.

Human studies on sepsis and arterial stiffness

Concordant with the animal models above, a challenge with the *Salmonella typhi* capsular polysaccharide vaccine in healthy volunteers resulted in acute increase of the carotid-femoral PVW by 0.43 m/s, but a reduction in the augmentation index (by 5%) at 8 h postchallenge. The latter effect was thought to result from a reduction in the magnitude of wave reflection at peripheral sites secondary to peripheral vasodilation.[34] In a study of 45 septic patients (median age 67 years; interquartile range 54−75), the median carotid-femoral pulse wave velocity (PWV) was 14.6 (8.1−24.7) m/s when measured within 24h of admission compared to 12 m/s, the reference value for hypertensive individuals ≥70 years old (with or without history of dyslipidemia and/or smoking). In this study, however, carotid-femoral PWV did not correlate with the progression of multiple organ failure, (before or after adjustment for vasopressor use), or with improvement in the subgroup of patients who had cardiovascular instability at baseline. Nonetheless, Cox regression and survival analyses (including age, APACHE II, and baseline SOFA score) showed shorter hospital survival time for patients with

carotid-femoral pulse wave velocity >24.7 m/s (HR = 9.45, 95% CI 1.24−72.2; P = .03).[35,36] This cutoff corresponds to a very high value of carotid-femoral PWV, indicating marked large artery stiffening. Another study of 21 patients with sepsis found a significant increase in their cardio-ankle vascular index (CAVI) after 1 week of treatment, with no significant change in blood pressure, relative to the measurements at their presentation to the emergency department before initiation of guideline-directed therapy for sepsis (7.9 ± 2.4 at presentation vs. 9.6 ± 1.8 at 1 week, P < .001). The magnitude of CAVI increase posttreatment correlated with initial serum levels of procalcitonin, a biomarker associated with inflammation, bacterial infections, and infection severity. In this study, there was no association between CAVI and a systemic inflammatory response syndrome score, prevalence of hypertension and diabetes, type of infection or treatment.[37] There are no human studies examining long-term effects of sepsis on arterial stiffness. Interestingly however, the long-term incidence of new-onset heart failure after recovery from sepsis is not significantly different between survivors that exhibit left ventricular dysfunction during sepsis and survivors whose left ventricular function remained preserved, thus suggesting that factors other than myocardial injury during the acute septic state can contribute to the elevated long-term risk of cardiovascular morbidity postsepsis.[25]

Potential mechanisms for an effect of sepsis on arterial stiffness

Infections can produce acute inflammatory changes in human aortic cells. In an in-vitro model, *Staphylococcus aureus* induced several inflammatory responses in human aortic endothelial cells including cyclooxygenase-2 expression, PGE_2 secretion, and PGE_2/ IL-6/matrix metallopeptidase-9 (MMP-9)-dependent cell migration.[38] Infection with influenza virus in Apo-E deficient mice induced the expression of MMP-13 in aortic atherosclerotic plaques.[39] Administration of the Streptococcus pyogenes Phospholipase A_2 to mice acutely upregulates the

TABLE 47.1 Derived aortic hemodynamic parameters in a porcine model of endotoxemia.

Parameter	Baseline	Endotoxemia	ANOVA
	Mean ± SD	Mean ± SD	Baseline to endotoxemia
Z	1.5 ± 0.6	2.7 ± 1.2	P = .0003; F = 23.5
R	10.7 ± 3.3	6.9 ± 3.5	P = .004; F = 11.9
C	34 ± 11	20 ± 18	P = .02; F = 5.8

n = 19. *Z*, input impedance (mmHg.min/L); (mmHg·min/L); *R*, resistance; and *C*, compliance (mL/mmHg).
Adapted from Hatib F, Jansen JR, Pinsky MR. Peripheral vascular decoupling in porcine endotoxic shock. **J Appl Physiol**. 2011; 111(3):853−860.

transcription of the cell adhesion molecules ICAM1 and VCAM1 and their aortas.[40] In humans, white blood cell count, a marker of systemic inflammatory activity that is very sensitive to acute infections, correlates with increased brachial-ankle PWV.[41] The increase in carotid-femoral PWV after vaccination with *Salmonella typhi* capsular polysaccharide described in the previous sections correlated with increases in inflammatory markers such as C-reactive protein, IL-6, and MMP-9, and interestingly, pretreatment with aspirin blunted these effects.[34] In animal models, a septic insult results in an inflammatory infiltration of the aortic wall that continues well after the septic episode has resolved and into the long-term.[42] Therefore, it seems likely that sepsis can affect the function and structure of conduit arterial vessels and that inflammation is the main driver of this effect. However, the putative specific mechanisms by which the inflammatory response in sepsis would affect arterial stiffness (i.e., elastin degradation, smooth muscle dysfunction, endothelial dysfunction, extracellular tissue matrix remodeling, cellular inflammatory infiltration, etc.) remain to be studied in detail.

Can alterations of the human microbiome by antibiotics used to treat acute infections affect the associations between sepsis and cardiovascular phenotypes?
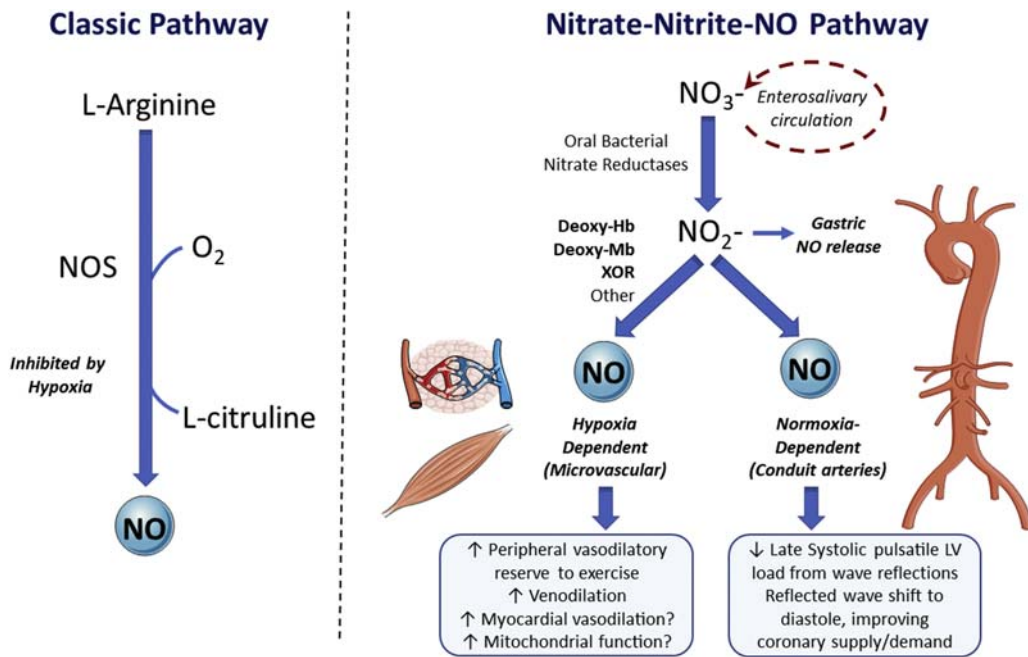
The historical view of the interaction between microbes (bacteria, viruses, and/or fungi) and humans is of a constant battle in which microbes try to establish infection in our bodies and we try to eliminate them from our system. However, over the last two decades, we have come to realize that because of human/microbe coevolution, a large variety (in the trillions) of microbial communities reside in our bodies in a symbiotic manner, primarily in the gastro-intestinal tract. This large collection of resident microbes (and their genes) is referred to as the "human microbiome" and has the human gastrointestinal tract as its primary anatomical residence.[43] Rather than a mere co-existence, the relationship between the human body and the microbiome is dynamic and bidirectional where internal (i.e., age, hormonal changes, inherited genes, among others) and external factors (diet and antibiotics, among others) can affect the composition of the microbiome, and the make-up of the microbiome is also capable of affecting body physiological functions such as immune, metabolic, and vascular functions, among others.[43] Relative to arterial stiffness, for example, Menni et al.[44] demonstrated, in adult middle-aged female twins, that arterial stiffness (measured by carotid-femoral PWV) is inversely correlated with gut microbiome diversity and with the abundance of specific bacterial taxa (mainly from the Ruminococcaceae family). Because (*a*) these bacteria have been linked to lower levels of gut derived endotoxemia in mice; (*b*) experimentally

induced endotoxemia is known to increase inflammatory cytokines in humans; and (*c*) persistent low-grade systemic inflammatory activity is associated with increased arterial stiffness; it has been hypothesized that an association between the composition of the gut microbiome and arterial stiffness could be mediated, at least in part, by the effect of the microbiome make-up on the background systemic inflammatory activity of humans.[45]

The make-up of the oral microbiome could also affect arterial stiffness via the increased or decreased bacterial metabolism of nitrates. In humans, NO formation occurs via two pathways: (1) The L-arginine-NO pathway (where NO synthases [NOS] catalyze the formation of NO from L-arginine and O2), and (2) the nitrate-nitrite-NO pathway (NOS-independent; Fig. 47.1).[46]

In the nitrate-nitrite-NO pathway, inorganic nitrate reaches the oral cavity from (*a*) dietary nitrate (from vegetables such as leafy greens, beets, among others); and (*b*) salivary nitrate (actively taken off the circulation and concentrated in the saliva by the salivary glands).[46] In the oral cavity, bacteria of the oral resident microbiome reduce nitrate to nitrite. Nitrite and remaining nitrate are then swallowed and almost fully absorbed in the intestine (>90% bioavailability). Nitrite in blood is then directly reduced to NO in reactions catalyzed by several molecules, particularly deoxygenated myoglobin[47] and hemoglobin.[48] Meanwhile, ~75% of circulating nitrate (coming from intestinal absorption and from being the stable end-metabolite of NO) is excreted in urine and the rest is taken-up by the salivary glands to continue the cycle just described.[46] Mammalian cells are thought to be incapable of reducing nitrate to nitrite; therefore, reduction of nitrate to nitrite by the oral microbiome is the limiting step in this pathway. NO is known to decrease the vascular tone of resistance vessels and coronary and brachial conduit arteries, and more recent evidence suggests that higher NO blood levels from oral nitrate supplementation can also functionally reduce the hemodynamic effects of stiffened larger vessels, probably via modulation of smooth muscle tone.[49,50]

Antibiotics are the mainstay treatment for acute infections including sepsis. Since antibiotics, depending on their class, have important effects on the composition of the intestinal microbiome,[51] it is possible that they could also affect putative associations between the human microbiome and arterial stiffness. For example, Dougall et al.[52] demonstrated that pretreatment with amoxicillin (a beta-lactam antibiotic with high activity against *Veillonella sp.*, the most important nitrate-reducing bacterial taxa of the mouth) reduces the concentration of salivary nitrite by 40% after a loading dose of potassium nitrate (Fig. 47.2). Thus, if an association existed between oral nitrite production levels and arterial stiffness, it could be affected significantly by the administration of antibiotics. These considerations

FIGURE 47.1   The classic NOS-dependent NO pathway (left), and the nitrate-nitrite-NO pathway (right). *Deoxy-Hb*, deoxy-hemoglobin; *Deoxy-Mb*, deoxy-myoglobin; *NOS*, nitric oxide synthase; *XOR*, xanthine oxidoreductase. *Reproduced from Chirinos JA, 2018,* **J Card Fail***, 24(4); 74−77.*

are even more relevant when current evidence suggests that alterations of the intestinal microbiome induced by antibiotics can be lasting and long-term.[51]

Finally, it is important to acknowledge that any association between the composition of the intestinal microbiome and arterial stiffness is likely complex, and that the effect of antibiotics on this relationship, given the differences among them in terms of antibacterial spectrum, intestinal absorption, and other factors, need not to be consistent in only one direction. For example, treatment of older mice (20− 24 months of age) with a cocktail of very broad spectrum nonabsorbable antibiotics including ampicillin, neomycin, metronidazole, and vancomycin produced a decrease in their aortic PWV to levels that were no longer different from those of control young mice (8−10 weeks of age).[53]

Arterial stiffness and human immunodeficiency virus infection

Once invariably fatal, infection with HIV has evolved into a more chronic condition in which combination antiretroviral therapy (CART) can effectively suppress viral replication and extend the life expectancy of people living with HIV (PLHIV) to levels that approach the general population.[54,55] As a consequence, age-related noncommunicable conditions like cardiovascular diseases are becoming an increasing burden for PLHIV.[56] Indeed, while death rates associated with cardiovascular diseases in the general population and some high risk groups (like people with inflammatory polyarthropaties) are decreasing, these rates
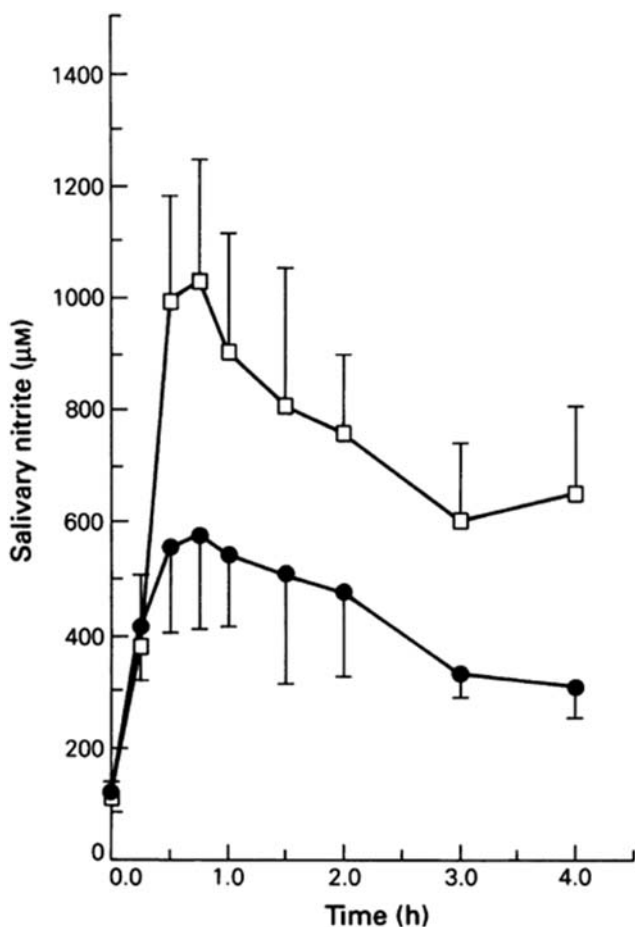
continue to rise in PLHIV (Fig. 47.3).[57] It is estimated that by the year 2030, 73% of PLHIV will be ≥50 years of age, and 78% of them will have cardiovascular disease.[58] In this section, we discuss the burden of cardiovascular disease, including coronary artery disease and heart failure in PLHIV, review the evidence suggesting increased risk of arterial stiffening in this population and the potential mechanisms in this relationship.

Myocardial infarction in people living with human immunodeficiency virus

Although myocardial infarction is not directly related to arterial stiffness, since it is a consequence of atherosclerotic disease of the coronary vessels, it is useful to review its epidemiology in PLHIV, to better understand the burden of cardiovascular disease in this population. Moreover, some mechanisms of arterial disease may be common to conduit muscular arteries and proximal elastic large arteries.

Epidemiological studies have consistently demonstrated a 0.5- to one-fold increased risk of myocardial infarction in PLHIV compared to uninfected individuals, even after adjustment for other known cardiovascular risk factors (including smoking, which is particularly prevalent in this population).[59−62] The magnitude of this excess risk of MI associated with HIV infection is comparable to other major traditional risk factors (Fig. 47.4).[59,60,63]

The excess MI-risk attributable to HIV is higher in patients whose infection is suboptimally controlled (as measured by lower CD4 cell counts and higher detectable
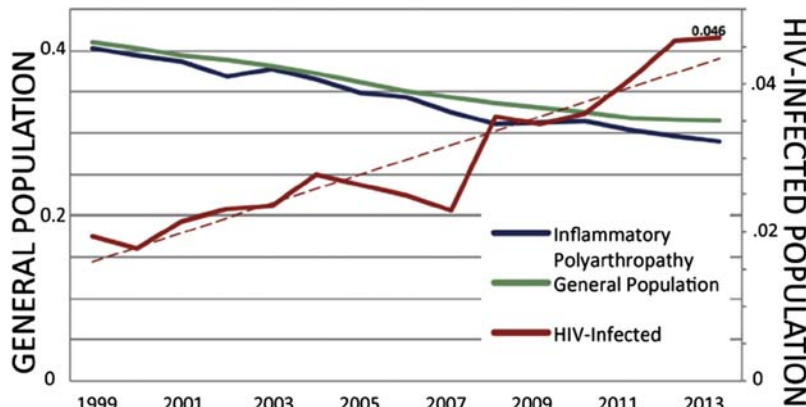
FIGURE 47.2 Mean salivary nitrate concentration (±s.e. mean) after ingestion of potassium nitrate (200 mg) showing the significantly lower levels attained after a two-day course of amoxycillin (●) when compared with control (□) in healthy male volunteers. *Reproduced from Dougall HT, Smith L, Duncan C, Benjamin N. The effect of amoxycillin on salivary nitrite concentrations: an important mechanism of adverse reactions? Br J Clin Pharmacol. 1995; 39(4):460–462.*

levels of viral copies of HIV in blood) and in those that interrupt CART.[64,65] Nonetheless, excess risk of MI is still present (at around 0.5-fold higher) even among PLHIV that achieve undetectable viral levels (<500 viral copies/ml) in blood with treatment.[59] Data suggest that MI risk is also increased in "elite controllers," a unique population of PLHIV (<1% of them) able to suppress HIV replication below detectable levels in blood without CART, but the magnitude of this excess risk is not well defined.[66] A primary mechanism for the increased risk of MI attributable to HIV infection is thought to be persistent immune dysregulation. PLHIV with lower nadir CD4 cell counts before initiation of CART are at higher risk of MI.[67] PLHIV exhibit higher levels of CRP compared to uninfected individuals, and increasing levels of HIV viral load correlate positively with IL-6 levels in this population.[68,69] Higher CRP and IL-6 are both independently associated with
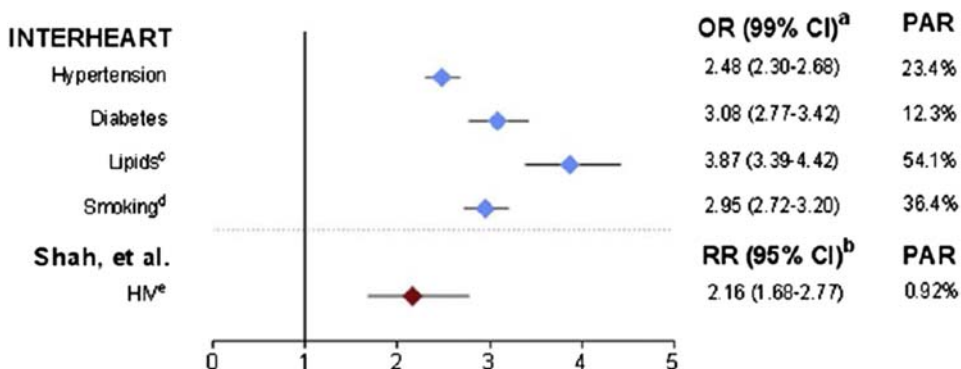
greater MI-risk in PLHIV.[70,71] In addition to smoking being highly prevalent among PLHIV,[61,62] some studies suggest a magnified effect of smoking on MI-risk in the setting of HIV infection with approximately three of four MIs among PLHIV being associated with ever smoking compared to only one of four MIs among uninfected controls.[72] Dyslipidemia, hypertension, and diabetes are also more prevalent in PLHIV, and this observation has been linked to CART use.[73–75] Some specific antiretrovirals have also been associated with increased MI-risk in PLHIV, independent of traditional cardiovascular risk factors. Antiretrovirals belonging to the protease-inhibitors class, especially those approved before the early 2000s, have been associated with about 10% increase in the risk of myocardial infarction per year of use.[76–78] The newer protease-inhibitors atazanavir and darunavir appear to carry significantly less cardiovascular risk than their older counterparts with atazanavir appearing to have the safest cardiovascular risk profile.[77] Abacavir, another antiretroviral belonging to the nucleoside reverse transcriptase inhibitors class has also been linked, although inconsistently, to a higher risk of myocardial infarction.[79,80] However, both early protease inhibitors and abacavir are no longer preferred agents in contemporary CART regimens.[81] Integrase inhibitors, a newer class of antiretroviral agents are associated with favorable lipid profiles but also increased risk of obesity and their overall effect on MI-risk and in the context of CART regimens with other antiretroviral classes is to be characterized.[82–84]

Heart failure in people living with human immunodeficiency virus

In the pre-CART era, AIDS-related dilated cardiomyopathy, often accompanied by pericardial involvement, affected as many as one-third of AIDS patients.[85,86] This disorder appeared to be secondary to direct myocardial invasion by HIV, opportunistic infections of the myocardium by other pathogens, and also inflammation and autoimmunity.[85,87] However, with the wide adoption and ever earlier initiation of CART, AIDS-related dilated cardiomyopathy has become rare in developed countries.[88] Nevertheless, PLHIV appear to still remain at higher risk of developing HF even when CART is widely available.[89–94] Over the last decade, several large studies have consistently documented a HF-risk increase in PLHIV compared to uninfected controls (Table 47.2).[89–95] The magnitude of this HIV-associated HF-risk increase has varied between 0.3- and 1.5-fold among studies, it has been demonstrated in both predominantly male[89,91–95] and female populations,[90] and it has shown independence from coronary heart disease (prevalent or incident),[89–95] traditional cardiovascular risk factors,[89–95] and makers of socioeconomic status and access to health care.[92,93,95,96] Importantly, while

FIGURE 47.3 Proportionate mortality for cardiovascular disease of all deaths within the general population, inflammatory polyarthropathy population, and human immunodeficiency virus (HIV)-infected population. *Reproduced from Feinstein MJ, Bahiru E, Achenbach C, et al. Patterns of cardiovascular mortality for HIV-infected adults in the United States: 1999 to 2013.* **Am J Cardiol**. *2016; 117(2):214−220.*

FIGURE 47.4 Cardiovascular risk of HIV compared to traditional risk factors. Because ORs can give inflated estimates of risk when the outcome is common, it is likely that the RRs of traditional risk factors in the INTERHEART study are smaller and thus closer to that of HIV. [a]Risk of acute MI, adjusted for age, sex, and smoking. Adjustment for confounders was limited to those available in the primary studies. [b]Risk of ASCVD (CVD, stroke, or MI). [c]High ApoB/ApoA1 ratio. [d]OR (99% CI) for current smoking; PAR for any smoking. [e]PAR for 2015 using prevalence data for HIV for the 15- to 49-year-old group. *Apo*, apolipoprotein; *ASCVD*, atherosclerotic cardiovascular disease; *CVD*, cardiovascular disease; *HIV*, human immunodeficiency virus; *MI*, myocardial infarction; *OR*, odds ratio; *PAR*, population attributable risk; *RR*, risk ratio. *Reproduced from Hsue PY, Waters DD. Time to recognize HIV infection as a major cardiovascular risk factor.* **Circulation**. *2018; 138(11):1113−1115.*

most of these studies used administrative data codes for the ascertainment of HF diagnosis,[89−92,94] one study used a centralized adjudication protocol involving objective clinical, laboratory, radiographic, and pharmacy criteria.[93] Compared to uninfected controls with HF, PLHIV with HF also have higher risk of hospitalization, rehospitalization (after an index HF hospital admission), sudden cardiac death, and cardiovascular and overall mortality, and lower CD4 counts, higher viral loads and lower LV ejection fraction are associated with worse outcomes.[94,97−101] Depression appears to have a synergistic effect with HIV infection in increasing HF risk.[91]

The contribution of the different phenotypes of HF (i.e., HF with reduced ejection fraction [HFrEF] and HF with preserved ejection fraction [HFpEF]) to the burden of PLHIV is still not well characterized. A large study (31,523 subjects) of predominantly (97%) male PLHIV without prior history of

cardiac disease found 941 cases of newly diagnosed HF (defined by the new documentation of one or more inpatient or two or more outpatient ICD.9 codes consistent with HF) over a mean follow-up of seven years. After extracting EF values from clinical notes using an automated extraction application, of these 941 cases, 284 (30%) were classified as HFpEF (EF ≥50%), 142 (15%) as borderline HFpEF (EF ≥40% and <50%), and 380 (41%) as HFrEF (EF <40%); another 135 (14%) did not EF ascertained. Relative to uninfected controls, the adjusted risks of HFpEF, borderline HFpEF and HFrEF were increased by 21%, 37%, and 61%, respectively (Table 47.2). The risk of HFrEF was particularly elevated (by 2.6-fold) among PLHIV younger than 40 years at baseline.[94] In another study of only women with prevalent HF of mean age of 59 years, HFpEF comprised 71% and 63% of cases among PLHIV (n = 1388) and controls (n = 13,781), respectively

TABLE 47.2 Studies of heart failure risk in people living with HIV (PLHIV).

Study, year of publication (ref)	Country in which the study was done	Population	Outcome	Follow-up time	Adjusted risk of HF attributable to HIV infection
Butt et al., 2011[89]	USA	2391 veteran PLHIV and 6095 veteran uninfected controls All men Median age in both groups, 48 years old No prior diagnosis of coronary heart disease or heart failure	New diagnosis of heart failure defined as new documentation of one or more inpatient or two or more outpatient ICD-9 codes 425.xx or 428.xx	Median of 7.3 years	HR 1.8 (95% CI 1.4−2.4)
Womack et al., 2014[90]	USA	710 veteran PLHIV and 1477 veteran uninfected controls All women Median age 44 years old in both groups No prior diagnosis of coronary heart disease or heart failure	New diagnosis of heart failure defined as new documentation of one or more inpatient or two or more outpatient ICD-9 codes 428.xx, 429.3, 402.01, 402.11, 402.91, and 425.xx	Median of 6.0 years	IRR 2.5 (95% CI 1.5−4.5)
White et al., 2015[91]	USA	26,908 veteran PLHIV (19% with major depression diagnosis) and 54,519 veteran uninfected controls (16% with major depression diagnosis) ∼97% male in both groups Mean age 48 years old in both groups No prior diagnosis of heart failure, coronary heart disease, or stroke/transient ischemic attack	New diagnosis of heart failure defined as new documentation of ICD-9 codes 428.xx, 429.3, 402.01, 402.11, 402.91, and 425.xx	Median of 5.8 years	PLHIV without depression, HR 1.3 (95% CI 1.2−1.4) PLHIV with depression, HR 1.68 (1.45−1.95)
Al-Kindi et al., 2016[92]	USA	36,400 PLHIV and 12,208,430 uninfected controls 68% of PLHIV and 41% of controls were male 93% of PHLIV and 73% of controls were <65 years old	Prevalence of heart failure defined by the umbrella term "heart failure" in the platform Explorys (Cleveland, Ohio, USA) that uses ICD codes, systemized nomenclature of medicine—clinical terms (SNOMED-CT), logical observation identifiers names and codes and RxNorm	Not applicable	RR 1.7 (95% CI 1.6−1.7)
Freiberg et al., 2017[94]	USA	31,523 veteran PLHIV and 66,492 veteran controls 97% male in both groups Mean age 48 years old in both groups No prior diagnosis of heart failure, coronary heart disease, or stroke/transient ischemic attack	New diagnosis of heart failure defined as new documentation of one or more inpatient or two or more outpatient ICD-9 codes 428.xx, 402.01, 402.11, 402.91, 404.01, 404.03, 404.11, 404.13, 404.91, and 404.93. EF was ascertained using an automated extraction application from clinical notes	Median of 7.1 years	HR 1.4 (95% CI 1.0−1.4) for HFpEF HR 1.2 (95% CI 1.1−1.7) for borderline HFpEF HR 1.6 (95% CI 1.4−1.9) for borderline HFrEF

Feinstein et al., 2018[93]	USA	4640 PLHIV and 4250 uninfected controls ~80% male in both groups Mean age 40 years old in both groups No prior diagnosis of heart failure Baseline prevalence of coronary heart disease 5% in both groups	New diagnosis of heart failure, centrally adjudicated by physicians based on clinical and laboratorial criteria	Mean of 5.6 years	HR 2.1 (95% CI 1.4–3.2)
Yen et al., 2019[95]	Taiwan	24,153 PLHIV (72% on CART) and 96,612 uninfected controls 94% male in both groups Mean age 32 years old in both groups No prior diagnosis of heart failure	New diagnosis of heart failure defined as new documentation of one or more inpatient or three or more outpatient ICD-9 codes 428.xx	Mean of 5.8 years	HR 1.5 (95% CI 1.3–1.8)
Prasada et al., 2020[96]	USA	2715 PLHIV and 19,358 uninfected controls 85% males in PLHIV and 43% in controls Mean age 43 years old in PLHIV and 49 years old in controls No prior diagnosis of heart failure	New diagnosis of heart failure defined as new documentation of an unspecified set of ICD.9 codes associated with heart failure	Median of 3.6 years	HR 1.3 (95% CI 1.0–1.7)

ICD-9 denotes International Classification of Diseases, Ninth Revision. HR denotes hazard ratio. IRR denotes incidence rate ratio. RR denotes relative risk. HFpEF denotes heart failure with preserved ejection fraction, EF ≥50%. Borderline HFpEF, ≥40%–49%. HFrEF denotes heart failure with reduced ejection fraction, EF <40%.

($P = .44$). Although left ventricular ejection fractions were similar between groups, HIV-infected women had wider QRS (113.19 vs. 97.20 ms; $P < .0001$) and higher pulmonary artery systolic pressure (49.12 vs. 39.10 mm Hg; $P < .0001$). HIV + women also had higher rates of HF hospitalization, longer HF hospitalizations, lowers rates of optimal pharmacological therapy for HFrEF, and higher rates of all-cause and cardiovascular mortality.[101] A meta-analysis of studies of cardiac function in PLHIV observed a shift toward lower prevalence of systolic dysfunction in more recent reports and in settings of wide availability of CART.[102] In another meta-analysis of 11 studies of paucisymptomatic PLHIV without clinical cardiovascular disease, the pooled incidence of diastolic dysfunction among 2242 participants (mean age, 42 years) was 43.4% (95% CI: 31.7%−55.0%) compared to only 8.3% (95% CI: 2.2−14.3) for systolic dysfunction.[103] For reference, the prevalence of diastolic dysfunction in the general population aged 45−55 years is estimated at ∼6%.[104,105] In studies where LV mass is assessed, PLHIV without clinical HF consistently show larger masses than uninfected controls.[106−110] However, differentiation between eccentric versus concentric LV hypertrophy was not clear. All in all, current data appear to signal to HFrEF being more prominent among male PLHIV and HFpEF more prominent in female PLHIV. However, given the high prevalence of subclinical diastolic dysfunction in PLHIV, and as this population continues to age, it is likely that HFpEF will continue to take a more prominent role overall.

An association between persistent immune dysregulation and increased risk of HF in PLHIV, similar to the case of MI risk in this population, has also been proposed though its supportive evidence is less robust. Among 5098 PLHIV participating in a trial of intermittent versus continuous use of CART, serum levels of IL-6, high sensitivity CRP, and D-dimer were associated with an increased risk of a composite endpoint of cardiovascular disease that included cardiovascular death, nonfatal myocardial infarction, nonfatal stroke, congestive heart failure, coronary revascularization, coronary artery disease requiring drug treatment, and peripheral arterial disease.[71] Otherwise, we could not find reports documenting associations between inflammatory markers and specific HF risk in PLHIV. Several studies also suggest that PLHIV, even when well controlled with CART and without clinical heart failure, have increased myocardial inflammation, interstitial fibrosis and steatosis as measured by cardiac magnetic resonance.[111−114] However, the exact contribution of these abnormalities to the excess HF risk of PLHIV is not well defined. There is a relative paucity of data about the influence of CART on HF risk. One study suggested that the excess risk of HF associated with HIV decreases over time as the duration of CART increases.[95] The use of tenofovir, an antiretroviral of the nucleotide reverse transcriptase

inhibitor class, has been associated with lower incidence of HF whereas the use of antiretrovirals of the protease inhibitor class has been linked to lower left ventricular ejection fraction, higher pulmonary artery systolic pressure, and increased mortality and readmission rates after a hospitalization for acute decompensated HF in PLHIV.[115] Overall the effect of CART on HF risk is still unclear.

Human immunodeficiency virus infection and arterial stiffness

In two small studies from 2005 to 2008, Schillaci et al.[116,117] found that PLHIV that were either CART-naive or already receiving CART, had higher carotid-femoral PWV than uninfected controls. Since then, several subsequent reports, also mostly with small sample sizes, have delivered inconsistent results on this topic, with some studies finding increased aortic stiffness in PLHIV compared uninfected controls,[116−128] while others did not.[129−139] Reports have also been conflicting regarding the impact of CART on arterial stiffness as some studies found a negative impact of CART on PWV,[118,119,125,132,139] whereas others did not.[120,126,131,134] This divergence in findings could well be explained by the small sample sizes of these studies and also the remarkable heterogeneity among them including, but not limited to, the sex and age composition of their groups, their geographic setting, the time since HIV diagnosis in their PLHIV cohorts, the techniques used to account for the central blood pressure, the arterial segments used for the measurement of PWV (some including muscular arterial segments), the exposure to CART among PLHIV participants, the duration and composition of the CART regimens, the degree of immunodeficiency reached before CART was initiated, the degree of immune recovery with CART, and the techniques and equipment used to measure PWV (Table 47.3). Several studies also claimed the assessment of PWV in PLHIV but did not specify the arterial paths for their measurements and thus, they are difficult to interpret.[140−143]

Studies that investigated other specific determinants of PWV in PLHIV showed that factors that have been associated with arterial stiffness in the general population, such as age, blood pressure, smoking, body mass index, dyslipidemia and metabolic syndrome, are also primary determinants of arterial stiffness in PLHIV.[116−120,122−125,129−131,133,136−139] The magnitude of the effect of the metabolic syndrome on arterial stiffness seems especially magnified in PLHIV.[123,139] Among factors specific to HIV infection, lower nadir T-CD4+ cell counts (i.e., before initiation of CART), ongoing immune dysregulation, and duration of exposure to CART also seem to be associated with PWV in PLHIV.[118−120,123,126,127,132,136,139] Overall, however, the preponderance of data suggests that the burden of

TABLE 47.3 Studies of arterial stiffness in people living with HIV (PLHIV).

Study, country, year (ref)	Population	Measurement instrument	Findings	Significance	Factors associated with PWV in PLHIV
Schillaci et al., Italy, 2005[116]	**32 PLHIV** (78% men, mean age 41 ± 8, mean BMI 25 ± 4, all on CART) 32 uninfected controls (78% men, mean age 41 ± 8, mean BMI 25 ± 3)	SphygmoCor Vx (AtCor Medical, West Ryde, NSW, Australia)	Mean cfPWV in PLHIV, 7.6 ± 1.1 m/s Mean cfPWV in uninfected controls, 6.8 ± 1.2 m/s	$P = .015$	Age, duration of CART
Schillaci et al., Italy, 2008[117]	**39 PLHIV, CART naive** (67% men, mean age 37 ± 8, mean BMI 23 ± 3) 28 uninfected controls (67% men, mean age 37 ± 7, mean BMI 25 ± 3)	SphygmoCor Vx (AtCor Medical, West Ryde, NSW, Australia)	Mean cfPWV in PLHIV, CART naive, 7.5 ± 1.4 m/s Mean cfPWV in uninfected controls, 6.7 ± 1.1 m/s	$P = .001$	Age, mean arterial pressure, serum gamma-glutamyl transpeptidase, HIV infection
Vlachopoulos et al., Greece, 2009[129]	**51 PLHIV, CART naive** (92% men, mean age 33 ± 8, mean BMI 24 ± 3) 35 uninfected controls (89% men, mean age 33 ± 8, mean BMI 27 ± 5)	Complior SP (Artech Medical, Pantin, France)	Mean cfPWV in PLHIV, CART naive, 6.4 ± 0.8 m/s Mean cfPWV in uninfected controls, 6.3 ± 1.0 m/s	0.74	Age, BMI, aortic systolic and diastolic blood pressure, brachial systolic and diastolic blood pressure, hs-CRP, and LDL-cholesterol
Lekakis et al., Greece, 2009[118]	**22 PLHIV, CART naive** (all men, mean age 40 ± 13, mean BMI 23 ± 3) **34 PLHIV, CART exposed** (96% men, mean age 40 ± 14, mean BMI 23 ± 2) 28 uninfected hypertensive controls (96% men, mean age 41 ± 13, mean BMI 24 ± 3) 28 uninfected normotensive controls (96% men, mean age 40 ± 12, mean BMI 24 ± 3)	Complior SP (Artech Medical, Pantin, France)	Mean cfPWV in PLHIV, CART naive and CART exposed, 8.1 ± 1.4 m/s Mean cfPWV in uninfected normotensive controls, 6.7 ± 1.1 m/s Mean cfPWV in PLHIV, CART naive and CART exposed, 8.1 ± 1.4 m/s Mean cfPWV in uninfected hypertensive controls, 9.0 ± 1.0 m/s Mean cfPWV in PLHIV, CART naive, 7.5 ± 1.3 m/s Mean cfPWV in PLHIV, CART exposed, 8.4 ± 1.4 m/s Mean cfPWV in PLHIV, CART exposed, 8.4 ± 1.4 m/s Mean cfPWV in uninfected hypertensive controls, 9.0 ± 1.0 m/s Mean cfPWV in PLHIV, CART naive, 7.5 ± 1.3 m/s Mean cfPWV in uninfected normotensive controls, 6.7 ± 1.1 m/s	$P = .03$ $P = .01$ $P = .03$ $P = .25$ $P = .03$	Mean or diastolic blood pressure, serum cholesterol, serum triglycerides, CART duration, protease-inhibitor use, and nucleoside reverse transcript inhibitor use

Continued

TABLE 47.3 Studies of arterial stiffness in people living with HIV (PLHIV).—cont'd

Study, country, year (ref)	Population	Measurement instrument	Findings	Significance	Factors associated with PWV in PLHIV
Charakida et al., UK, 2009[119]	**35 PLHIV, CART naive** (63% men, mean age 10 ± 3, median BMI z score 0.62 [IQR, −1.32−0.38]) **48 PLHIV, CART exposed** (62% men, mean age 11 ± 3, median BMI z score −0.18 (IQR, −0.81−0.69]) 59 uninfected controls (47% men, mean age 12 ± 3, median BMI z score −0.20 (IQR, −0.46−1.04])	SphygmoCor (AtCor Medical, West Ryde, NSW, Australia)	Mean crPWV in PLHIV, CART naive and CART exposed, 7.5 ± 1.3 m/s Mean crPWV in uninfected controls, 7.0 ± 1.1 m/s Mean crPWV in PLHIV, CART naive, 7.2 ± 0.9 m/s Mean crPWV in PLHIV, CART exposed, 7.8 ± 1.5 m/s Mean crPWV in PLHIV, CART naive, 7.2 ± 0.9 m/s Mean crPWV in uninfected controls, 7.0 ± 1.1 m/s	$P = .03$ $P = .04$ No significant difference (P value not provided)	Systolic blood pressure, serum cholesterol, HIV infection disease severity (as per CDC guidelines), and CART use
Zeng et al., China, 2010[120]	**41 PLHIV, CART naive** (63% men, mean age 37 ± 9, median age 37 [range 25−76], mean BMI 26 ± 4) **41 PLHIV, CART exposed** (59% men, median age 39 [range 21−70], mean BMI 22 ± 3) 43 uninfected controls (67% men, mean age 39 ± 4, mean BMI 24 ± 4)	BP-203RPE II (Nihon Colin, Japan)	Mean haPWV (one-point) in PLHIV, CART naive, 13.6 ± 1.2 m/s Mean haPWV (one-point) in uninfected controls, 12.7 ± 1.9 m/s Mean haPWV (one-point) in PLHIV, CART naive, 13.6 ± 1.2 m/s Mean haPWV (one-point) in PLHIV, CART exposed, 12.8 ± 1.8 m/s	$P = .01$ $P = .03$	Age, current smoking, and CART use
Ferraioli et al., Italy, 2012[130]	**54 PLHIV** (67% men, median age 46 [IQR 42−54], median BMI 25 [IQR 23−27], ±4, 96% on CART) 54 uninfected controls (67% men, median age 48 [IQR 38−54], median BMI 25 [IQR 23−28])	ProSound α 10 (Aloka, Tokio, Japan)	Median cPWV in PLHIV, 5.8 (IQR 5.0−6.5) Median cPWV in uninfected controls, 5.8 (IQR 5.3−6.4)	$P = .89$	Age
Eira et al., Brazil, 2012[121]	**28 PLHIV, CART naive** (61% men, mean age for men 42 ± 2, mean age for women 43 ± 2; mean BMI for men 25 ± 1, mean BMI for women 28 ± 7) **28 PLHIV, CART exposed** (71% men, mean age for men 45 ± 2, mean age for women 42 ± 2; mean BMI for men 25 ± 1, mean BMI for women 26 ± 4) 44 uninfected diabetic controls (48% men, mean age for men 46 ± 1, mean age for women 52 ± 1; mean BMI for men 30 ± 1, mean BMI for women 31 ± 5) 30 uninfected nondiabetic controls (53% men, mean age for men 42 ± 2, mean age for women 43 ± 2; mean BMI for men 32 ± 3, mean BMI for women 27 ± 5)	Complior SP (Artech Medical, Pantin, France)	Mean cfPWV in uninfected nondiabetic controls, 8.6 (95% CI 8.1−9.1) m/s Mean PWV in PLHIV, CART naive, 8.8 (95% CI 8.2−9.4) m/s Mean cfPWV in uninfected nondiabetic controls, 8.6 (95% CI 8.1−9.1) m/s Mean PWV in uninfected diabetic controls, 9.9 (95% CI 9.4−10.3) m/s Mean cfPWV in uninfected nondiabetic controls, 8.6 (95% CI 8.1−9.1) m/s Mean PWV in PLHIV, CART exposed, 9.7 (95% CI 9.1−10.3) m/s	No significant difference (P value not provided) $P < .01$ $P < .01$	Not reported

Monteiro et al., Brazil, 2012[131]	**261 PLHIV** (58% men, mean age 42 ± 8, mean BMI 24 ± 4, 89% on CART) 82 uninfected controls (33% men, mean age 42 ± 11, mean BMI 27 ± 4)	Complior SP (Artech Medical, Pantin, France)	Mean cfPWV in PLHIV, 7.9 ± 1.5 m/s Mean cfPWV in uninfected controls, 7.8 ± 1.5 m/s	No significant difference (P value not provided)	Age, male sex, blood pressure
Maloberti et al., Italy, 2013[132]	**36 PLHIV, CART naive** (81% men, mean age 41 ± 8, BMI 25 ± 5) **72 PLHIV, CART exposed** (83% men, mean age 47 ± 8, BMI 24 ± 3) 224 uninfected controls (74% men, mean age 45 ± 7, BMI 25 ± 3)	SphygmoCor Vx (AtCor Medical, West Ryde, NSW, Australia)	Mean cfPWV in PLHIV, CART naive, 9.9 ± 1.3 m/s Mean cfPWV in PLHIV, CART exposed, 10.8 ± 1.9 m/s Mean cfPWV in PLHIV, CART naive, 9.9 ± 1.3 m/s Mean cfPWV in uninfected controls, 9.3 ± 1.2 m/s Mean cfPWV in PLHIV, CART exposed, 10.8 ± 1.9 m/s Mean cfPWV in uninfected controls, 9.3 ± 1.2 m/s	No significant difference (P value not provided) No significant difference (P value not provided) P = .02	CART exposure
Ngatchou et al., Cameroon, 2013[122]	**108 PLHIV, CART naive** (24% men, mean age 39 ± 11, mean BMI 25 ± 12) 96 uninfected controls (29% men, mean age 41 ± 12, mean BMI 28 ± 6)	SphygmoCor v6.1 (AtCor Medical, West Ryde, NSW, Australia)	Mean cfPWV in CART naive PLHIV, 7.5 ± 2.2 m/s Mean cfPWV in uninfected controls, 6.9 ± 1.7 m/s	P = .02	Age and serum LDL-cholesterol
Echevarría et al., France, 2014[133]	**174 PLHIV** (84% men, median age 47 [IQR, 42%−52%, 32% with BMI >25, 94% on CART) 80 uninfected controls (79% men, median age 46 [IQR, 41%−52%, 43% with BMI >25)	Complior SP (Artech Medical, Pantin, France)	Median cfPWV in PLHIV, 8.0 (IQR, 7.0−9.2) m/s Median cfPWV in uninfected controls, 7.1 (IQR, 6.4−7.7) m/s	No significant difference (P value not provided)	Diastolic blood pressure and serum triglycerides
Rider et al., UK, 2014[123]	**73 PLHIV without metabolic syndrome** (80% men, mean age 44 ± 10; mean BMI 25 ± 4, 84% on CART) **17 PLHIV with metabolic syndrome** (82% men, mean age 48 ± 8; mean BMI 30 ± 6, 94% on CART) 92 uninfected controls without metabolic syndrome (53% men, mean age 45 ± 10; mean BMI 25 ± 4) 44 uninfected controls with metabolic syndrome (77% men, mean age 49 ± 11; mean BMI 33 ± 7)	MRI	Mean taPWV in PLHIV with metabolic syndrome, 7.4 ± 2.4 Mean taPWV in PLHIV without metabolic syndrome, 6.2 ± 1.9 Mean taPWV in PLHIV without metabolic syndrome, 6.2 ± 1.9 Mean taPWV in uninfected controls with metabolic syndrome, 6.7 ± 1.9 Mean taPWV in PLHIV without metabolic syndrome and PLHIV with metabolic syndrome were 15%−38% higher than uninfected controls without metabolic syndrome (crude numbers not reported) Mean taPWV in PLHIV without metabolic syndrome and uninfected controls with metabolic syndrome were 16%−20% higher than uninfected controls without metabolic syndrome (crude numbers not reported)	P < .05 P = .94 P < .05 (comparison) P < .05 (comparison)	Age, systolic blood pressure and CART exposure

TABLE 47.3 Studies of arterial stiffness in people living with HIV (PLHIV).—cont'd

Study, country, year (ref)	Population	Measurement instrument	Findings	Significance	Factors associated with PWV in PLHIV
Lemogoum et al., Cameroon, 2014[124]	**238 PLHIV**, (24% men, mean age 40 ± 11, mean BMI 25 ± 9, 55% on CART) 96 uninfected controls (29% men, mean age 41 ± 12, mean BMI 28 ± 6)	Complior SP (Artech Medical, Pantin, France)	Mean cfPWV in PLHIV, 7.3 ± 1.9 m/s Mean cfPWV in uninfected controls, 6.9 ± 1.7 m/s	$P = .037$	Body weight, serum LDL-cholesterol, serum HDL-cholesterol, serum non-HDL-cholesterol
Fourie et al., South Africa, 2015[134]	**78 PLHIV, CART naive** (35% men, mean age 48 ± 1, mean BMI 24 ± 1) **66 PLHIV, CART exposed** (26% men, mean age 49 ± 1, mean BMI 22 ± 1) 165 uninfected controls (41% men, mean age 50 ± 1, mean BMI 24 ± 0.5)	Complior SP (Artech Medical, Pantin, France)	Mean cdPWV in CART naive PLHIV, 8.6 (95% CI, 8.2–9.0) Mean cdPWV in CART exposed PLHIV, 8.5 (95% CI, 8.0–8.9) Mean cdPWV in uninfected controls, 8.8 (95% CI, 8.5–9.0)	No significant difference (P value not provided)	Not reported
Maloberti et al., Italy, 2015[135]	**94 PLHIV** (83% men, mean age 44 ± 6, mean BMI 24 ± 4, 67% on CART) 37 uninfected controls (76% men, mean age 45 ± 8, mean BMI 25 ± 3)	SphygmoCor Vx system (AtCor Medical, Sydney, NSW, Australia)	Mean cfPWV in PLHIV, 7.5 (no measure of variability provided) Mean cfPWV in uninfected controls, 7.4 (no measure of variability provided)	P = not significant (no actual value provided)	Not reported
Maia-Leite et al., France, 2016[136]	**133 PLHIV** (92% men, mean age 48 ± 8, median BMI 24 [IQR, 21–25], 99% on CART) 135 uninfected controls (91% men, mean age 48 ± 9, median BMI 26 [IQR, 23–29])	Complior SP (Artech Medical, Pantin, France)	Median cfPWV in PLHIV, 7.5 (IQR, 6.7–8.4) m/s Median cfPWV in uninfected controls, 7.5 (IQR, 6.6–8.4) m/s	$P = .64$	Age, mean arterial pressure, nadir CD4+ T-cell count <200 cells/uL
Msoka et al., Tanzania, 2016[125]	**47 PLHIV, CART naive** (23% men, mean age 45 ± 6; mean BMI 25 ± 4) **34 PLHIV on CART** (18% men, mean age 45 ± 4; mean BMI 25 ± 4) 40 uninfected controls (63% men, mean age 45 ± 5; mean BMI 26 ± 4)	SphygmoCor (AtCor Medical, Itasca, IL USA)	Mean cfPWV in PLHIV, CART naive and on CART, 7.7 ± 1.7 m/s Mean cfPWV in uninfected controls, 7.0 ± 1.2 m/s Mean cfPWV in PLHIV, CART naive, 7.3 ± 1.5 m/s Mean cfPWV in uninfected controls, 7.0 ± 1.2 m/s Mean cfPWV in PLHIV, CART naive, 7.3 ± 1.5 m/s Mean cfPWV in PLHIV on CART, 8.2 ± 1.8 m/s	$P = .039$ $P = .401$ $P = .017$	Age and time since HIV infection diagnosis
Eckard et al., US, 2017[137]	**101 PLHIV** (64% men, median age 20 [IQR, 17–23], median BMI 22 [IQR, 19–25], all on CART) 86 prospective uninfected controls (59% men, median age 19 [IQR, 14–23], median BMI 23 [IQR, 18–28])	SphygmoCor (AtCor Medical, Itasca, IL USA)	Median cfPWV in PLHIV, 5.7 (IQR, 5.2–6.3) m/s Median cfPWV in uninfected controls, 5.7 (IQR, 4.9–6.25) m/s	$P = .81$	Male sex, systolic blood pressure, alcohol use

Study	Population	Device	Results	Statistics	Adjustment variables
Moreira et al., Brazil, 2018[138]	**644 PLHIV** (58% men, median age 44 [IQR, 36–51], median BMI 24 [IQR, 22–28], 89% on CART) 105 prospective uninfected controls (35% men, median age 44 [IQR, 36–55], median BMI 28 [IQR, 24–31]) 14,873 retrospective uninfected controls (46% men, median age 51 [IQR, 45–58], median BMI 27 [IQR, 24–30])	Complior SP (Artech Medical, Paris, France)	Median cfPWV in PLHIV, 8.48 (IQR, 7.66–9.40) m/s Median cfPWV in retrospective uninfected controls, 9 (IQR, 8.10–10.20) m/s Median cfPWV in PLHIV, 8.48 (IQR, 7.66–9.40) m/s Median cfPWV in prospective uninfected controls, 8.70 (IQR, 7.90–10.20) m/s	$\beta = -0.05$, (95% CI, -0.23–0.12; $P = .52$) for the weighted association of HIV infection with cf PWV $\beta = 0.10$, (95% CI, -0.10 -0.31; $P = .32$) for the weighted association of HIV infection with cf PWV	Age, family history of sudden death, systolic blood pressure, diastolic blood pressure, hypertension, antihypertension medication use, serum triglycerides, waist to hip ratio
Msoka et al., Tanzania, 2018[139]	**32 PLHIV without metabolic syndrome, CART naive** (28% male, mean age 44 ± 6; mean BMI 24 ± 4) **42 PLHIV without metabolic syndrome on CART** (29% male, mean age 46 ± 5; mean BMI 23 ± 4) **16 PLHIV with metabolic syndrome, CART naive** (13% men, mean age 47 ± 5; mean BMI 27 ± 3) **12 PLHIV with metabolic syndrome on CART** (25% men, mean age 47 ± 4; mean BMI 29 ± 4) 39 uninfected controls without metabolic syndrome (69% men, mean age 45 ± 3; mean BMI 25 ± 4) 10 uninfected controls without metabolic syndrome (50% men, mean age 45 ± 4; mean BMI 30 ± 5)	SphygmoCor (AtCor Medical, Itasca, IL USA)	No difference in cfPWV between PLHIV (all included) and controls (all included)—data not shown Mean cfPWV in PLHIV, CART naive, 7.1 ± 1.9 m/s Mean aPWV in PLHIV on CART, 7.9 ± 1.9 m/s Mean cfPWV in participants (PLHIV and controls) without metabolic syndrome, 7.1 ± 1.3 m/s Mean cfPWV in participant (PLHIV and controls) with metabolic syndrome, 8.3 ± 1.6 m/s No difference in cfPWV among PLHIV CART naive without metabolic syndrome, PLHIV on CART without metabolic syndrome, and controls without metabolic syndrome—data not shown cfPWV in PLHIV on CART with metabolic syndrome was 25% higher than uninfected controls with metabolic syndrome—data not shown cfPWV in PLHIV on CART with metabolic syndrome was 21% higher than PLHIV CART naive with metabolic syndrome—data not shown cfPWV in PLHIV on CART with metabolic syndrome was higher than PLHIV on CART without metabolic syndrome—data not shown Mean cfPWV in PLHIV, CART naive with metabolic syndrome, 7.7 ± 1.3 m/s Mean cfPWV in PLHIV, CART naive without metabolic syndrome, 7.1 ± 1.6 m/s cfPWV was similar in controls with and without metabolic syndrome—data not shown	N.A $P = .008$ $P < .001$ $P = .464$ $P = .018$ $P = .023$ $P = .009$ $P = .139$ $P = .590$	Age, mean arterial pressure, duration of CART, metabolic syndrome

Continued

TABLE 47.3 Studies of arterial stiffness in people living with HIV (PLHIV).—cont'd

Study, country, year (ref)	Population	Measurement instrument	Findings	Significance	Factors associated with PWV in PLHIV
Kelly et al., Malawi, 2019[126]	**279 PLHIV**, (56% men, median age 37 [IQR 31−43], median BMI 20 [IQR 18−22], CART naive at enrollment) 110 uninfected controls (40% men, median age 35 [IQR 31−41], median BMI 22 [IQR 20−25])	Vicorder device (Skidmore Medical, London, UK)	Mean cfPWV in PLHIV at baseline 7.54 m/s (95% CI, 7.36−7.72 m/s) Mean cfPWV in control at baseline 7.19 m/s (95% CI, 6.92−7.45 m/s) Mean cfPWV in PLHIV at 10 weeks of CART 7.41 m/s (95% CI, 7.21−7.61 m/s) Median cfPWV in controls, 7.15 m/s (95% CI, 6.89−7.41 m/s) Mean cfPWV in PLHIV at 22 weeks of CART 7.20 m/s (95% CI, 7.02−7.39 m/s) Median cfPWV in controls, 7.32 m/s (95% CI, 7.05−7.58 m/s) Mean cfPWV in PLHIV at 44 weeks of CART 7.24 m/s (95% CI, 7.04−7.45 m/s) Median cfPWV in controls, 7.21 m/s (95% CI, 6.93−7.50 m/s)	$P = .07$ $P = .02$ $P = .46$ $P = .59$	Persistence of initially high proportion of PD-1+ CD8+ T cells
Toribio et al., US, 2020[127]	**34 PLHIV** (all women, mean age 52 ± 4; mean BMI 32 ± 7; 59% on CART) 34 uninfected controls (all women; mean age 52 ± 4; mean BMI 32 ± 7)	MRI	Mean taPWV in PLHIV: 8.6 ± 1.3 m/s Mean taPWV in controls: 6.5 ± 1.3 m/s	$P < .0001$	sCD163 levels
Martínez-Ayala et al., Mexico, 2020	**51 PLHIV** (90% men, mean age 33 ± 10, mean BMI 23 ± 4, CART naive) 51 uninfected controls (86% men, mean age 32 ± 10, mean BMI 25 ± 3)	PulsePen (Diatechne, Milan, Italy)	Median cfPWV in PLHIV 7.4 m/s (IQR, 0.12 m/s) Median cfPWV in controls 6.8 m/s IQR, 0.12 m/s	$P < .01$	Not reported

BMI, body mass index; *CART*, combination antiretroviral therapy; *cdPWV*, carotid-dorsalis pedis PWV; *cfPWV*, carotid-femoral PWV; *cPWV*, carotid (local, one-point) PWV; *crPWV*, carotid-radial PWV; *haPWV*, heart-ankle PWV; *PLHIV*, people living with HIV; *PWV*, pulse wave velocity; *taPWV*, thoracic aorta PWV. Several studies that did not specify the arterial paths for the measurement of PWV were not included.[140−143]

traditional risk factors for vascular aging are the major determinants of arterial stiffness in PLHIV, and that immune alterations more specific to HIV infection play a less important role.

Chronic inflammatory activity in the vascular walls of conduit arteries has been proposed as a mechanism for accelerated "aging" of these vessels and resultant increased arterial stiffness.[144,145] Few studies have assessed aortic inflammation in PLHIV using positron emission tomography. Four studies by Subramanian et al.[146] (27 PLHIV recruited prospectively and 27 historic uninfected controls), Taglieri et al.[147] (20 PLHIV recruited prospectively and 20 prospective uninfected controls), Lawal et al.[148] (121 PLHIV and121 uninfected controls, both historical), and Longenecker et al. (55 PLHIV and 19 uninfected controls, both groups prospectively recruited) found that compared to uninfected controls, PLHIV had a significant increase (though marginal) in aortic inflammation even when their infection was well controlled on CART and differences in traditional cardiovascular risks factors were accounted for. However, another study by Knudsen et al.[149] did not corroborate this finding. In 12 PLHIV naive to antiretroviral therapy, commencement of CART did not translate in meaningful changes in aortic inflammation at six months post-CART initiation despite effective HIV viral suppression.[150]

Hence, a putative association between HIV infection and increased arterial stiffness and its mechanisms, let alone its clinical implications, remain poorly defined and they should be the focus of future research.

Conclusion

A robust body of epidemiological evidence demonstrates that cardiovascular disease is a significant contributor to the morbidity and mortality associated with acute and chronic infections. For the case of acute infections, cardiovascular disease not only complicates the course of infected patients in the short term but also in the long term, after the infection has clinically resolved. The biological pathways driving these associations are poorly understood. Furthermore, regarding the association between acute infections and cardiovascular disease, the mechanistic framework under which this relationship has been approached has mostly neglected any putative role of arterial stiffness and pulsatile hemodynamics. For the association between chronic infections like infection by HIV and cardiovascular disease, studies on the role of arterial stiffness and pulsatile hemodynamics are limited by small sample sizes, methodological shortfalls, and lack of standardization. A higher awareness of the importance of arterial stiffness and pulsatile hemodynamics in cardiovascular disease among clinicians and researches, the simplification of their surrogate measures, and the standardization of measuring instruments

should greatly facilitate the characterization of the role of arterial stiffness and pulsatile hemodynamics in the relationship between infections and cardiovascular disease in future studies.

References

1. Singer M, Deutschman CS, Seymour CW, et al. The third international consensus definitions for sepsis and septic shock (Sepsis-3). **JAMA**. 2016; 315(8):801−810.
2. Gotts JE, Matthay MA. Sepsis: pathophysiology and clinical management. **BMJ**. 2016; 353:i1585.
3. Hotchkiss RS, Moldawer LL, Opal SM, Reinhart K, Turnbull IR, Vincent JL. Sepsis and septic shock. **Nat Rev Dis Prim**. 2016; 2:16045.
4. Martin G, Asensi V, Montes AH, et al. Role of plasma matrix-metalloproteases (MMPs) and their polymorphisms (SNPs) in sepsis development and outcome in ICU patients. **Sci Rep**. 2014; 4:5002.
5. Angus DC, van der Poll T. Severe sepsis and septic shock. **N Engl J Med**. 2013; 369(9):840−851.
6. Martin L, Derwall M, Al Zoubi S, et al. The septic heart: current understanding of molecular mechanisms and clinical implications. **Chest**. 2019; 155(2):427−437.
7. Ehrman RR, Sullivan AN, Favot MJ, et al. Pathophysiology, echocardiographic evaluation, biomarker findings, and prognostic implications of septic cardiomyopathy: a review of the literature. **Crit Care**. 2018; 22(1):112.
8. Frencken JF, Donker DW, Spitoni C, et al. Myocardial injury in patients with sepsis and its association with long-term outcome. **Circ Cardiovasc Qual Outcomes**. 2018; 11(2):e004040.
9. Alhamdi Y, Neill DR, Abrams ST, et al. Circulating pneumolysin is a potent inducer of cardiac injury during pneumococcal infection. **PLoS Pathog**. 2015; 11(5):e1004836.
10. Frencken JF, van Baal L, Kappen TH, et al. Myocardial injury in critically ill patients with community-acquired pneumonia. A cohort study. **Ann Am Thorac Soc**. 2019; 16(5):606−612.
11. Pulido JN, Afessa B, Masaki M, et al. Clinical spectrum, frequency, and significance of myocardial dysfunction in severe sepsis and septic shock. **Mayo Clin Proc**. 2012; 87(7):620−628.
12. Logeart D, Isnard R, Resche-Rigon M, et al. Current aspects of the spectrum of acute heart failure syndromes in a real-life setting: the OFICA study. **Eur J Heart Fail**. 2013; 15(4):465−476.
13. Alon D, Stein GY, Korenfeld R, Fuchs S. Predictors and outcomes of infection-related hospital admissions of heart failure patients. **PLoS One**. 2013; 8(8):e72476.
14. Vaduganathan M, Patel RB, Michel A, et al. Mode of death in heart failure with preserved ejection fraction. **J Am Coll Cardiol**. 2017; 69(5):556−569.
15. Walker AMN, Drozd M, Hall M, et al. Prevalence and predictors of sepsis death in patients with chronic heart failure and reduced left ventricular ejection fraction. **J Am Heart Assoc**. 2018; 7(20):e009684.
16. Thygesen K, Alpert JS, Jaffe AS, et al. Fourth universal definition of myocardial infarction (2018). **J Am Coll Cardiol**. 2018; 72(18):2231−2264.
17. Shah M, Patnaik S, Maludum O, et al. Mortality in sepsis: comparison of outcomes between patients with demand ischemia, acute

myocardial infarction, and neither demand ischemia nor acute myocardial infarction. **Clin Cardiol**. 2018; 41(7):936–944.

18. Allou N, Brulliard C, Valance D, et al. Obstructive coronary artery disease in patients hospitalized for severe sepsis or septic shock with concomitant acute myocardial infarction. **J Crit Care**. 2016; 32:159–164.

19. Corrales-Medina VF, Suh KN, Rose G, et al. Cardiac complications in patients with community-acquired pneumonia: a systematic review and meta-analysis of observational studies. **PLoS Med**. 2011; 8(6):e1001048.

20. Corrales-Medina VF, Musher DM, Wells GA, Chirinos JA, Chen L, Fine MJ. Cardiac complications in patients with community-acquired pneumonia: incidence, timing, risk factors, and association with short-term mortality. **Circulation**. 2012; 125(6):773–781.

21. Violi F, Cangemi R, Falcone M, et al. Cardiovascular complications and short-term mortality risk in community-acquired pneumonia. **Clin Infect Dis**. 2017; 64(11):1486–1493.

22. Corrales-Medina VF, Madjid M, Musher DM. Role of acute infection in triggering acute coronary syndromes. **Lancet Infect Dis**. 2010; 10(2):83–92.

23. Corrales-Medina VF, Musher DM, Shachkina S, Chirinos JA. Acute pneumonia and the cardiovascular system. **Lancet**. 2013; 381(9865):496–505.

24. Violi F, Cangemi R, Calvieri C. Pneumonia, thrombosis and vascular disease. **J Thromb Haemost**. 2014; 12(9):1391–1400.

25. Vallabhajosyula S, Jentzer JC, Geske JB, et al. New-onset heart failure and mortality in hospital survivors of sepsis-related left ventricular dysfunction. **Shock**. 2018; 49(2):144–149.

26. Ou SM, Chu H, Chao PW, et al. Long-term mortality and major adverse cardiovascular events in sepsis survivors. A nationwide population-based study. **Am J Respir Crit Care Med**. 2016; 194(2):209–217.

27. Corrales-Medina VF, Taljaard M, Yende S, et al. Intermediate and long-term risk of new-onset heart failure after hospitalization for pneumonia in elderly adults. **Am Heart J**. 2015; 170(2):306–312.

28. Eurich DT, Marrie TJ, Minhas-Sandhu JK, Majumdar SR. Risk of heart failure after community acquired pneumonia: prospective controlled study with 10 years of follow-up. **BMJ**. 2017; 356:j413.

29. Musher DM, Abers MS, Corrales-Medina VF. Acute infection and myocardial infarction. **N Engl J Med**. 2019; 380(2):171–176.

30. Yende S, Linde-Zwirble W, Mayr F, Weissfeld LA, Reis S, Angus DC. Risk of cardiovascular events in survivors of severe sepsis. **Am J Respir Crit Care Med**. 2014; 189(9):1065–1074.

31. Corrales-Medina VF, Alvarez KN, Weissfeld LA, et al. Association between hospitalization for pneumonia and subsequent risk of cardiovascular disease. **J Am Med Assoc**. 2015; 313(3):264–274.

32. Leclerc J, Pu Q, Corseaux D, et al. A single endotoxin injection in the rabbit causes prolonged blood vessel dysfunction and a procoagulant state. **Crit Care Med**. 2000; 28(11):3672–3678.

33. Hatib F, Jansen JR, Pinsky MR. Peripheral vascular decoupling in porcine endotoxic shock. **J Appl Physiol**. 2011; 111(3):853–860.

34. Vlachopoulos C, Dima I, Aznaouridis K, et al. Acute systemic inflammation increases arterial stiffness and decreases wave reflections in healthy individuals. **Circulation**. 2005; 112(14):2193–2200.

35. Kazune S, Grabovskis A, Cescon C, Strike E, Vanags I. Association between increased arterial stiffness and clinical outcomes in patients with early sepsis: a prospective observational cohort study. **Intensive Care Med Exp**. 2019; 7(1):26.

36. Reference Values for Arterial Stiffness Collaboration. Determinants of pulse wave velocity in healthy people and in the presence of cardiovascular risk factors: 'establishing normal and reference values'. **Eur Heart J**. 2010; 31(19):2338–2350.

37. Nagayama D, Imamura H, Endo K, et al. Marker of sepsis severity is associated with the variation in cardio-ankle vascular index (CAVI) during sepsis treatment. **Vasc Health Risk Manag**. 2019; 15:509–516.

38. Tsai MH, Wu CH, Lin WN, et al. Infection with *Staphylococcus aureus* elicits COX-2/PGE2/IL-6/MMP-9-dependent aorta inflammation via the inhibition of intracellular ROS production. **Biomed Pharmacother**. 2018; 107:889–900.

39. Lee HS, Noh JY, Shin OS, Song JY, Cheong HJ, Kim WJ. Matrix metalloproteinase-13 in atherosclerotic plaque is increased by influenza A virus infection. **J Infect Dis**. 2020; 221(2):256–266.

40. Oda M, Domon H, Kurosawa M, et al. Streptococcus pyogenes Phospholipase A2 induces the expression of adhesion molecules on human umbilical vein endothelial cells and aorta of mice. **Front Cell Infect Microbiol**. 2017; 7:300.

41. Lee YJ, Lee JW, Kim JK, et al. Elevated white blood cell count is associated with arterial stiffness. **Nutr Metab Cardiovasc Dis**. 2009; 19(1):3–7.

42. Kaynar AM, Yende S, Zhu L, et al. Effects of intra-abdominal sepsis on atherosclerosis in mice. **Crit Care**. 2014; 18(5):469.

43. Lynch SV, Pedersen O. The human intestinal microbiome in health and disease. **N Engl J Med**. 2016; 375(24):2369–2379.

44. Menni C, Lin C, Cecelja M, et al. Gut microbial diversity is associated with lower arterial stiffness in women. **Eur Heart J**. 2018; 39(25):2390–2397.

45. Laurent S, Bruno RM. Gut microbiome composition, a third player in the inflammation-arterial stiffness relationship. **Eur Heart J**. 2018; 39(25):2398–2400.

46. Lundberg JO, Weitzberg E, Gladwin MT. The nitrate-nitrite-nitric oxide pathway in physiology and therapeutics. **Nat Rev Drug Discov**. 2008; 7(2):156–167.

47. Totzeck M, Hendgen-Cotta UB, Luedike P, et al. Nitrite regulates hypoxic vasodilation via myoglobin-dependent nitric oxide generation. **Circulation**. 2012; 126(3):325–334.

48. Gladwin MT, Kim-Shapiro DB. The functional nitrite reductase activity of the heme-globins. **Blood**. 2008; 112(7):2636–2647.

49. Zamani P, Bluemke DA, Jacobs Jr DR, et al. Resistive and pulsatile arterial load as predictors of left ventricular mass and geometry: the multi-ethnic study of atherosclerosis. **Hypertension**. 2015; 65(1):85–92.

50. Blekkenhorst LC, Bondonno NP, Liu AH, et al. Nitrate, the oral microbiome, and cardiovascular health: a systematic literature review of human and animal studies. **Am J Clin Nutr**. 2018; 107(4):504–522.

51. Shaw LP, Bassam H, Barnes CP, Walker AS, Klein N, Balloux F. Modelling microbiome recovery after antibiotics using a stability landscape framework. **ISME J**. 2019; 13(7):1845–1856.

52. Dougall HT, Smith L, Duncan C, Benjamin N. The effect of amoxycillin on salivary nitrite concentrations: an important mechanism of adverse reactions? **Br J Clin Pharmacol**. 1995; 39(4):460–462.

53. Brunt VE, Gioscia-Ryan RA, Richey JJ, et al. Suppression of the gut microbiome ameliorates age-related arterial dysfunction and oxidative stress in mice. **J Physiol**. 2019; 597(9):2361–2378.

54. Samji H, Cescon A, Hogg RS, et al. Closing the gap: increases in life expectancy among treated HIV-positive individuals in the United States and Canada. **PLoS One**. 2013; 8(12):e81355.

55. Teeraananchai S, Kerr SJ, Amin J, Ruxrungtham K, Law MG. Life expectancy of HIV-positive people after starting combination anti-retroviral therapy: a meta-analysis. **HIV Med**. 2017; 18(4):256−266.

56. Trickey A, May MT, Vehreschild J, et al. Cause-specific mortality in HIV-positive patients who survived ten years after starting antiretroviral therapy. **PLoS One**. 2016; 11(8):e0160460.

57. Feinstein MJ, Bahiru E, Achenbach C, et al. Patterns of cardiovascular mortality for HIV-infected adults in the United States: 1999 to 2013. **Am J Cardiol**. 2016; 117(2):214−220.

58. Smit M, Brinkman K, Geerlings S, et al. Future challenges for clinical care of an ageing population infected with HIV: a modelling study. **Lancet Infect Dis**. 2015; 15(7):810−818.

59. Freiberg MS, Chang CC, Kuller LH, et al. HIV infection and the risk of acute myocardial infarction. **JAMA Intern Med**. 2013; 173(8):614−622.

60. Shah ASV, Stelzle D, Lee KK, et al. Global burden of atherosclerotic cardiovascular disease in people living with HIV: systematic review and meta-analysis. **Circulation**. 2018; 138(11):1100−1112.

61. Helleberg M, Afzal S, Kronborg G, et al. Mortality attributable to smoking among HIV-1-infected individuals: a nationwide, population-based cohort study. **Clin Infect Dis**. 2013; 56(5):727−734.

62. Helleberg M, May MT, Ingle SM, et al. Smoking and life expectancy among HIV-infected individuals on antiretroviral therapy in Europe and North America. **AIDS**. 2015; 29(2):221−229.

63. Hsue PY, Waters DD. Time to recognize HIV infection as a major cardiovascular risk factor. **Circulation**. 2018; 138(11):1113−1115.

64. Lang S, Mary-Krause M, Simon A, et al. HIV replication and immune status are independent predictors of the risk of myocardial infarction in HIV-infected individuals. **Clin Infect Dis**. 2012; 55(4):600−607.

65. Strategies for Management of Antiretroviral Therapy Study G, El-Sadr WM, Lundgren J, et al. CD4+ count-guided interruption of antiretroviral treatment. **N Engl J Med**. 2006; 355(22):2283−2296.

66. Crowell TA, Gebo KA, Blankson JN, et al. Hospitalization rates and reasons among HIV elite controllers and persons with medically controlled HIV infection. **J Infect Dis**. 2015; 211(11):1692−1702.

67. Silverberg MJ, Leyden WA, Xu L, et al. Immunodeficiency and risk of myocardial infarction among HIV-positive individuals with access to care. **J Acquir Immune Defic Syndr**. 2014; 65(2):160−166.

68. Reingold J, Wanke C, Kotler D, et al. Association of HIV infection and HIV/HCV coinfection with C-reactive protein levels: the fat redistribution and metabolic change in HIV infection (FRAM) study. **J Acquir Immune Defic Syndr**. 2008; 48(2):142−148.

69. Kuller LH, Tracy R, Belloso W, et al. Inflammatory and coagulation biomarkers and mortality in patients with HIV infection. **PLoS Med**. 2008; 5(10):e203.

70. Triant VA, Meigs JB, Grinspoon SK. Association of C-reactive protein and HIV infection with acute myocardial infarction. **J Acquir Immune Defic Syndr**. 2009; 51(3):268−273.

71. Duprez DA, Neuhaus J, Kuller LH, et al. Inflammation, coagulation and cardiovascular disease in HIV-infected individuals. **PLoS One**. 2012; 7(9):e44454.

72. Rasmussen LD, Helleberg M, May MT, et al. Myocardial infarction among Danish HIV-infected individuals: population-attributable fractions associated with smoking. **Clin Infect Dis**. 2015; 60(9):1415−1423.

73. Triant VA, Lee H, Hadigan C, Grinspoon SK. Increased acute myocardial infarction rates and cardiovascular risk factors among patients with human immunodeficiency virus disease. **J Clin Endocrinol Metab**. 2007; 92(7):2506−2512.

74. Brown TT, Cole SR, Li X, et al. Antiretroviral therapy and the prevalence and incidence of diabetes mellitus in the multicenter AIDS cohort study. **Arch Intern Med**. 2005; 165(10):1179−1184.

75. Grunfeld C, Pang M, Doerrler W, Shigenaga JK, Jensen P, Feingold KR. Lipids, lipoproteins, triglyceride clearance, and cytokines in human immunodeficiency virus infection and the acquired immunodeficiency syndrome. **J Clin Endocrinol Metab**. 1992; 74(5):1045−1052.

76. Group DADS, Friis-Moller N, Reiss P, et al. Class of antiretroviral drugs and the risk of myocardial infarction. **N Engl J Med**. 2007; 356(17):1723−1735.

77. Ryom L, Lundgren JD, El-Sadr W, et al. Cardiovascular disease and use of contemporary protease inhibitors: the D:A:D international prospective multicohort study. **Lancet HIV**. 2018; 5(6):e291−e300.

78. Mulligan K, Grunfeld C, Tai VW, et al. Hyperlipidemia and insulin resistance are induced by protease inhibitors independent of changes in body composition in patients with HIV infection. **J Acquir Immune Defic Syndr**. 2000; 23(1):35−43.

79. Group DADS, Sabin CA, Worm SW, et al. Use of nucleoside reverse transcriptase inhibitors and risk of myocardial infarction in HIV-infected patients enrolled in the D:A:D study: a multi-cohort collaboration. **Lancet**. 2008; 371(9622):1417−1426.

80. Ding X, Andraca-Carrera E, Cooper C, et al. No association of abacavir use with myocardial infarction: findings of an FDA meta-analysis. **J Acquir Immune Defic Syndr**. 2012; 61(4):441−447.

81. Department of Health and Human Services. Panel on Antiretroviral Guidelines for Adults and Adolescents. Guidelines for the Use of Antiretroviral Agents in Adults and Adolescents with HIV. https://clinicalinfo.hiv.gov/sites/default/files/inline-files/AdultandAdo-lescentGL.pdf. Accessed January 6, 2021.

82. Martinez E, Larrousse M, Llibre JM, et al. Substitution of raltegravir for ritonavir-boosted protease inhibitors in HIV-infected patients: the SPIRAL study. **AIDS**. 2010; 24(11):1697−1707.

83. Gatell JM, Assoumou L, Moyle G, et al. Immediate versus deferred switching from a boosted protease inhibitor-based regimen to a dolutegravir-based regimen in virologically suppressed patients with high cardiovascular risk or age >/=50 years: final 96-week results of the NEAT022 study. **Clin Infect Dis**. 2019; 68(4):597−606.

84. Shah S, Hill A. Risks of metabolic syndrome and diabetes with integrase inhibitor-based therapy. **Curr Opin Infect Dis**. 2021; 34(1):16−24.

85. Sani MU. Myocardial disease in human immunodeficiency virus (HIV) infection: a review. **Wien Klin Wochenschr**. 2008; 120(3−4):77−87.

86. Thienemann F, Sliwa K, Rockstroh JK. HIV and the heart: the impact of antiretroviral therapy: a global perspective. **Eur Heart J**. 2013; 34(46):3538−3546.

87. Kaplan RC, Hanna DB, Kizer JR. Recent insights into cardiovascular disease (CVD) risk among HIV-infected adults. **Curr HIV/AIDS Rep**. 2016; 13(1):44−52.

88. Bijl M, Dieleman JP, Simoons M, van der Ende ME. Low prevalence of cardiac abnormalities in an HIV-seropositive population on antiretroviral combination therapy. **J Acquir Immune Defic Syndr**. 2001; 27(3):318−320.

89. Butt AA, Chang CC, Kuller L, et al. Risk of heart failure with human immunodeficiency virus in the absence of prior diagnosis of coronary heart disease. **Arch Intern Med**. 2011; 171(8):737−743.

90. Womack JA, Chang CC, So-Armah KA, et al. HIV infection and cardiovascular disease in women. **J Am Heart Assoc**. 2014; 3(5):e001035.

91. White JR, Chang CC, So-Armah KA, et al. Depression and human immunodeficiency virus infection are risk factors for incident heart failure among veterans: Veterans Aging Cohort Study. **Circulation**. 2015; 132(17):1630−1638.

92. Al-Kindi SG, ElAmm C, Ginwalla M, et al. Heart failure in patients with human immunodeficiency virus infection: epidemiology and management disparities. **Int J Cardiol**. 2016; 218:43−46.

93. Feinstein MJ, Steverson AB, Ning H, et al. Adjudicated heart failure in HIV-infected and uninfected men and women. **J Am Heart Assoc**. 2018; 7(21):e009985.

94. Freiberg MS, Chang CH, Skanderson M, et al. Association between HIV infection and the risk of heart failure with reduced ejection fraction and preserved ejection fraction in the antiretroviral therapy era: results from the veterans aging cohort study. **JAMA Cardiol**. 2017; 2(5):536−546.

95. Yen YF, Ko MC, Yen MY, et al. Human immunodeficiency virus increases the risk of incident heart failure. **J Acquir Immune Defic Syndr**. 2019; 80(3):255−263.

96. Prasada S, Rivera A, Nishtala A, et al. Differential associations of chronic inflammatory diseases with incident heart failure. **JACC Heart Fail**. 2020; 8(6):489−498.

97. Erqou S, Jiang L, Choudhary G, et al. Heart failure outcomes and associated factors among veterans with human immunodeficiency virus infection. **JACC Heart Fail**. 2020; 8(6):501−511.

98. Brouch D, Tashtish N, Di Felice C, Longenecker CT, Al-Kindi SG. Human immunodeficiency virus infection and risk of heart failure rehospitalizations. **Am J Cardiol**. 2019; 124(8):1232−1238.

99. Alvi RM, Neilan AM, Tariq N, et al. The risk for sudden cardiac death among patients living with heart failure and human immunodeficiency virus. **JACC Heart Fail**. 2019; 7(9):759−767.

100. Alvi RM, Afshar M, Neilan AM, et al. Heart failure and adverse heart failure outcomes among persons living with HIV in a US tertiary medical center. **Am Heart J**. 2019; 210:39−48.

101. Janjua SA, Triant VA, Addison D, et al. HIV infection and heart failure outcomes in women. **J Am Coll Cardiol**. 2017; 69(1):107−108.

102. Erqou S, Lodebo BT, Masri A, et al. Cardiac dysfunction among people living with HIV: a systematic review and meta-analysis. **JACC Heart Fail**. 2019; 7(2):98−108.

103. Cerrato E, D'Ascenzo F, Biondi-Zoccai G, et al. Cardiac dysfunction in pauci symptomatic human immunodeficiency virus patients: a meta-analysis in the highly active antiretroviral therapy era. **Eur Heart J**. 2013; 34(19):1432−1436.

104. Redfield MM, Jacobsen SJ, Burnett Jr JC, Mahoney DW, Bailey KR, Rodeheffer RJ. Burden of systolic and diastolic ventricular dysfunction in the community: appreciating the scope of the heart failure epidemic. **JAMA**. 2003; 289(2):194−202.

105. Lam CS, Lyass A, Kraigher-Krainer E, et al. Cardiac dysfunction and noncardiac dysfunction as precursors of heart failure with reduced and preserved ejection fraction in the community. **Circulation**. 2011; 124(1):24−30.

106. Hsue PY, Hunt PW, Ho JE, et al. Impact of HIV infection on diastolic function and left ventricular mass. **Circ Heart Fail**. 2010; 3(1):132−139.

107. Grandi AM, Nicolini E, Giola M, et al. Left ventricular remodelling in asymptomatic HIV infection on chronic HAART: comparison between hypertensive and normotensive subjects with and without HIV infection. **J Hum Hypertens**. 2012; 26(10):570−576.

108. Secemsky EA, Scherzer R, Nitta E, et al. Novel biomarkers of cardiac stress, cardiovascular dysfunction, and outcomes in HIV-infected individuals. **JACC Heart Fail**. 2015; 3(8):591−599.

109. Fontes-Carvalho R, Mancio J, Marcos A, et al. HIV patients have impaired diastolic function that is not aggravated by anti-retroviral treatment. **Cardiovasc Drugs Ther**. 2015; 29(1):31−39.

110. Ntusi N, O'Dwyer E, Dorrell L, et al. HIV-1-Related cardiovascular disease is associated with chronic inflammation, frequent pericardial effusions, and probable myocardial edema. **Circ Cardiovasc Imaging**. 2016; 9(3):e004430.

111. Holloway CJ, Ntusi N, Suttie J, et al. Comprehensive cardiac magnetic resonance imaging and spectroscopy reveal a high burden of myocardial disease in HIV patients. **Circulation**. 2013; 128(8):814−822.

112. Thiara DK, Liu CY, Raman F, et al. Abnormal myocardial function is related to myocardial steatosis and diffuse myocardial fibrosis in HIV-infected adults. **J Infect Dis**. 2015; 212(10):1544−1551.

113. Luetkens JA, Doerner J, Schwarze-Zander C, et al. Cardiac magnetic resonance reveals signs of subclinical myocardial inflammation in asymptomatic HIV-infected patients. **Circ Cardiovasc Imaging**. 2016; 9(3):e004091.

114. Zanni MV, Awadalla M, Toribio M, et al. Immune correlates of diffuse myocardial fibrosis and diastolic dysfunction among aging women with human immunodeficiency virus. **J Infect Dis**. 2020; 221(8):1315−1320.

115. Alvi RM, Neilan AM, Tariq N, et al. Protease inhibitors and cardiovascular outcomes in patients with HIV and heart failure. **J Am Coll Cardiol**. 2018; 72(5):518−530.

116. Schillaci G, De Socio GV, Pirro M, et al. Impact of treatment with protease inhibitors on aortic stiffness in adult patients with human immunodeficiency virus infection. **Arterioscler Thromb Vasc Biol**. 2005; 25(11):2381−2385.

117. Schillaci G, De Socio GV, Pucci G, et al. Aortic stiffness in untreated adult patients with human immunodeficiency virus infection. **Hypertension**. 2008; 52(2):308−313.

118. Lekakis J, Ikonomidis I, Palios J, et al. Association of highly active antiretroviral therapy with increased arterial stiffness in patients infected with human immunodeficiency virus. **Am J Hypertens**. 2009; 22(8):828−834.

119. Charakida M, Loukogeorgakis SP, Okorie MI, et al. Increased arterial stiffness in HIV-infected children: risk factors and antiretroviral therapy. **Antivir Ther**. 2009; 14(8):1075−1079.

120. Zeng Y, Ye YC, Luo L, et al. Premature atherosclerosis in patients with acquired immunodeficiency syndrome. **Chin Med J (Engl)**. 2010; 123(23):3396−3399.

121. Eira M, Bensenor IM, Dorea EL, Cunha RS, Mill JG, Lotufo PA. Potent antiretroviral therapy for human immunodeficiency virus infection increases aortic stiffness. **Arq Bras Cardiol**. 2012; 99(6):1100−1107.

122. Ngatchou W, Lemogoum D, Ndobo P, et al. Increased burden and severity of metabolic syndrome and arterial stiffness in treatment-naive HIV+ patients from Cameroon. **Vasc Health Risk Manag**. 2013; 9:509−516.

123. Rider OJ, Asaad M, Ntusi N, et al. HIV is an independent predictor of aortic stiffness. **J Cardiovasc Magn Reson**. 2014; 16:57.

124. Lemogoum D, Ngatchou W, Van De Borne P, et al. Cardiometabolic phenotype and arterial stiffness in HIV-positive black African patients. **Open J Prev Med**. 2014; 4:182−192.

125. Msoka T, Van Guilder G, Smulders Y, van Furth M, Bartlett J, van Agtmael M. Antiretroviral treatment and time since HIV-1 diagnosis are associated with large artery stiffness in sub-Saharan African HIV-1 patients. **Artery Res**. 2016; 16:34−41.

126. Kelly C, Mwandumba HC, Heyderman RS, et al. HIV-related arterial stiffness in Malawian adults is associated with the proportion of PD-1-expressing CD8+ T cells and reverses with antiretroviral therapy. **J Infect Dis**. 2019; 219(12):1948−1958.

127. Toribio M, Awadalla M, Cetlin M, et al. Brief report: vascular dysfunction and monocyte activation among women with HIV. **J Acquir Immune Defic Syndr**. 2020; 85(2):233−238.

128. Martinez-Ayala P, Alanis-Sanchez GA, Gonzalez-Hernandez LA, et al. Aortic stiffness and central hemodynamics in treatment-naive HIV infection: a cross-sectional study. **BMC Cardiovasc Disord**. 2020; 20(1):440.

129. Vlachopoulos C, Sambatakou H, Tsiachris D, et al. Impact of human immunodeficiency virus infection on arterial stiffness and wave reflections in the early disease stages. **Artery Res**. 2009; 3(3):104−110.

130. Ferraioli G, Tinelli C, Maggi P, et al. Arterial stiffness evaluation in HIV-positive patients: a multicenter matched control study. **AJR Am J Roentgenol**. 2011; 197(5):1258−1262.

131. Monteiro P, Miranda-Filho DB, Bandeira F, et al. Is arterial stiffness in HIV-infected individuals associated with HIV-related factors? **Braz J Med Biol Res**. 2012; 45(9):818−826.

132. Maloberti A, Giannattasio C, Dozio D, et al. Metabolic syndrome in human immunodeficiency virus-positive subjects: prevalence, phenotype, and related alterations in arterial structure and function. **Metab Syndr Relat Disord**. 2013; 11(6):403−411.

133. Echeverria P, Bonjoch A, Molto J, et al. Pulse wave velocity as index of arterial stiffness in HIV-infected patients compared with a healthy population. **J Acquir Immune Defic Syndr**. 2014; 65(1):50−56.

134. Fourie CM, Schutte AE, Smith W, Kruger A, van Rooyen JM. Endothelial activation and cardiometabolic profiles of treated and never-treated HIV infected Africans. **Atherosclerosis**. 2015; 240(1):154−160.

135. Maloberti A, Dozio D, Betelli M, et al. Brachial and central blood pressure in HIV-infected subjects. **Hypertens Res**. 2015; 38(6):405−412.

136. Maia-Leite LH, Catez E, Boyd A, et al. Aortic stiffness aging is influenced by past profound immunodeficiency in HIV-infected individuals: results from the EVAS-HIV (EValuation of Aortic Stiffness in HIV-infected individuals). **J Hypertens**. 2016; 34(7):1338−1346.

137. Eckard AR, Raggi P, Ruff JH, et al. Arterial stiffness in HIV-infected youth and associations with HIV-related variables. **Virulence**. 2017; 8(7):1265−1273.

138. Moreira RC, Mill JG, Grinsztejn B, et al. HIV infection is not associated with aortic stiffness. Traditional cardiovascular risk factors are the main determinants-cross-sectional results of INI-ELSA-BRASIL. **J Acquir Immune Defic Syndr**. 2018; 78(1):73−81.

139. Msoka TF, Van Guilder GP, Smulders YM, van Furth M, Bartlett JA, van Agtmael MA. Association of HIV-infection, anti-retroviral treatment and metabolic syndrome with large artery stiffness: a cross-sectional study. **BMC Infect Dis**. 2018; 18(1):708.

140. Papita AM, Albu A, Fodor D, Bondor C, Itu C, Carstina D. Markers of preclinical vascular disease and left ventricular diastolic dysfunction in patients with HIV infection. **Med Ultrason**. 2012; 14(1):10−18.

141. Gleason Jr RL, Caulk AW, Seifu D, et al. Current Efavirenz (EFV) or ritonavir-boosted lopinavir (LPV/r) use correlates with elevate markers of atherosclerosis in HIV-infected subjects in Addis Ababa, Ethiopia. **PLoS One**. 2015; 10(4):e0117125.

142. Kooij KW, Schouten J, Wit FW, et al. Difference in aortic stiffness between treated middle-aged HIV type 1-infected and uninfected individuals largely explained by traditional cardiovascular risk factors, with an additional contribution of prior advanced immunodeficiency. **J Acquir Immune Defic Syndr**. 2016; 73(1):55−62.

143. Kuilder JS, Idris NS, Grobbee DE, et al. Association between human immunodeficiency virus infection and arterial stiffness in children. **Eur J Prev Cardiol**. 2017; 24(5):480−488.

144. Sun Z. Aging, arterial stiffness, and hypertension. **Hypertension**. 2015; 65(2):252−256.

145. Jain S, Khera R, Corrales-Medina VF, Townsend RR, Chirinos JA. Inflammation and arterial stiffness in humans. **Atherosclerosis**. 2014; 237(2):381−390.

146. Subramanian S, Tawakol A, Burdo TH, et al. Arterial inflammation in patients with HIV. **J Am Med Assoc**. 2012; 308(4):379−386.

147. Taglieri N, Bonfiglioli R, Bon I, et al. Pattern of arterial inflammation and inflammatory markers in people living with HIV compared with uninfected people. **J Nucl Cardiol**. 2021. https://doi.org/10.1007/s12350-020-02522-5.

148. Lawal IO, Ankrah AO, Popoola GO, Lengana T, Sathekge MM. Arterial inflammation in young patients with human immunodeficiency virus infection: a cross-sectional study using F-18 FDG PET/CT. **J Nucl Cardiol**. 2019; 26(4):1258−1265.

149. Knudsen A, Hag AM, Loft A, et al. HIV infection and arterial inflammation assessed by (18)F-fluorodeoxyglucose (FDG) positron emission tomography (PET): a prospective cross-sectional study. **J Nucl Cardiol**. 2015; 22(2):372−380.

150. Zanni MV, Toribio M, Robbins GK, et al. Effects of antiretroviral therapy on immune function and arterial inflammation in treatment-naive patients with human immunodeficiency virus infection. **JAMA Cardiol**. 2016; 1(4):474−480.

This page intentionally left blank

Chapter 48

Arterial stiffness, hemodynamics, and microvascular complications in conditions characterized by low arterial pulsatility

Barry J. McDonnell[1], William K. Cornwell, III[2] and Eric J. Stöhr[1,3]

[1]Cardiovascular Physiology Research Group, Cardiff School of Sport & Health Sciences, Cardiff Metropolitan University, Cardiff, United Kingdom;
[2]Department of Medicine-Cardiology, University of Colorado Anschutz Medical Campus, Aurora, CO, United States; [3]Department of Medicine,
Division of Cardiology, Columbia University Irving Medical Center, New York, NY, United States

Introduction

In the mammalian cardiovascular system, pressure and flow oscillations across a single cardiac cycle are generally referred to as "pulsatility." To distinguish between different types of pulsatility, several different terms exist. Pulsatility related to oscillations in blood *pressure* is often quantified as pulse pressure (PP). PP is calculated as the difference between systolic and diastolic pressure of the arterial pressure waveform and can be influenced by variations in stroke volume and compliance of the large arteries. Conversely, pulsatility related to oscillations in blood *flow* is commonly quantified as the pulsatility index (PI). The PI describes the relationship between the peak systolic flow velocity and the end-diastolic velocity, normalized to the prevailing mean flow velocity. It should be noted that although PP and PI have similar biological origins, there are many instances when these are not interchangeable and specificity of terminology when describing pulsatility is always advised.
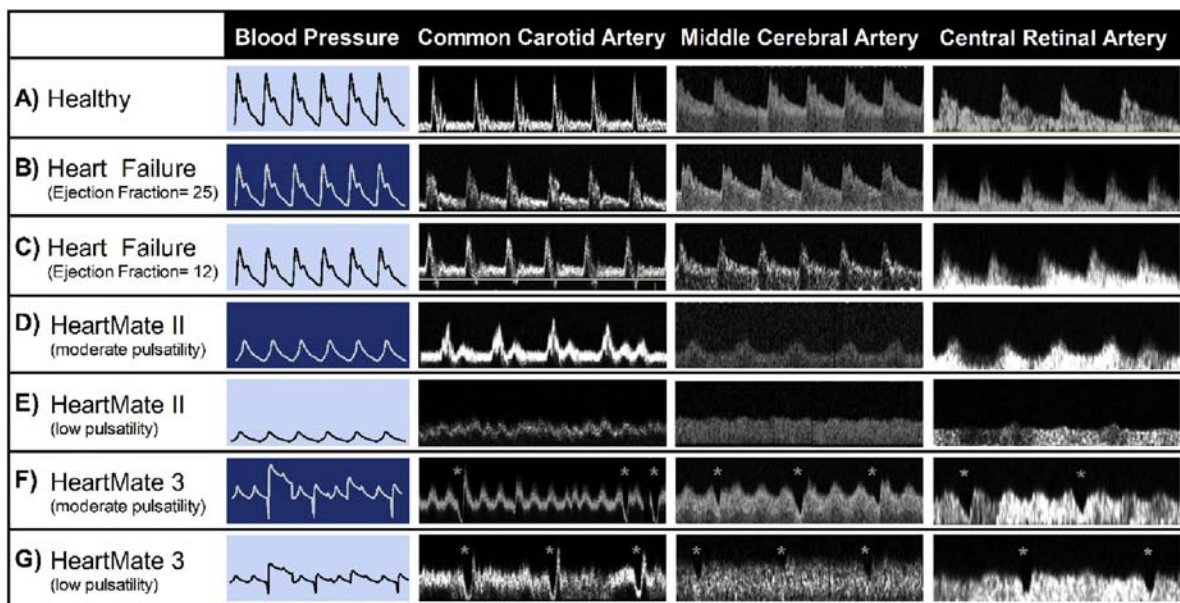
A large body of literature has shown that both high PP and high PI are associated with large artery stiffness, altered hemodynamics (e.g., turbulent flow patterns), and microvascular complications. Specifically, increased PP and PI have been shown to relate to microvascular complications and end-organ damage in healthy aging and disease, including diabetes and end-stage renal disease.[1–3]

Unfortunately, literature describing how the arterial network and cardiovascular system interact and react to continuous, *low* PP and PI is limited. Yet, the in vivo investigation of the effects of low PP and PI is possible in patients implanted with a continuous-flow left ventricular assist device (LVAD). Studying LVAD patients can therefore expand our understanding of the effects of altered PP and PI by identifying the impact of low PP and PI on the macro- and microcirculation.

Over the course of the last 25 years, different pulsatile and continuous-flow LVAD systems have been developed.[4]

The main role of such implantable devices is to support the failing heart and improve the peripheral circulation while patients wait for a donor heart for transplantation (termed bridge-to-transplant therapy), or as a permanent therapy in patients who do not meet the criteria for heart transplantation (termed destination therapy).

There are different models of mechanical pumps used. The majority of LVAD systems used today are considered continuous-flow pumps (continuous output of blood volume, characterized with predominantly low oscillations between systolic and diastolic flow and pressures). However, these different LVAD models have drastically different mechanical interactions with the blood, they output blood volume using different pump settings (e.g., at different pump speeds) and produce different hemodynamic profiles in the macro- and microcirculation. See Fig. 48.1 below.

FIGURE 48.1   **Hemodynamic profiles.** (A) In healthy individuals, the PP and PI are clearly present across the whole body, from the macrocirculation (here, carotid artery) to the microcirculation (here, central retinal artery). (B, C) In heart failure, PP is slightly reduced as reflected by the lower oscillations in blood pressure. However, PI in the macro- and microcirculation is maintained. (D, E) LVAD patients implanted with the continuous-flow HeartMate II have a much lower PP and PI. (F, G) Although HeartMate 3 patients also have a reduced PP and PI, the "artificial pulse" can interrupt the continuous flow. Because the "artificial pulse" is not synchronized with the native heartbeat, sometimes it creates marked oscillations in the macro- and microcirculation (represented by *), while at other times it has much less of an affect. This makes the PP and PI waveforms of HeartMate 3 patients unpredictable, and hence increases the difficulty in measuring blood pressure and interpreting the biological impact of the "artificial pulse."

Low pulsatile hemodynamics in continuous-flow left ventricular assist device therapy

In the sections below, the physiological and clinical consequences of living with continuous-flow LVADs will be described and evaluated.

Clinically, the implantation of an LVAD significantly improves survival for appropriate candidates with advanced heart failure.[5,6] Although LVADs are successful at achieving their aims of unloading the left ventricle (LV) of a failing heart and restoring the cardiac output to normal levels at rest, patients implanted with such devices often present with increased rates of microvascular complications (e.g., stroke, gastrointestinal (GI) bleeding, and cerebral microbleeds). These complications are likely caused by the combined effects of a chronically failing heart with a powerful, continuous-flow LVAD that transmits low pulsatile pressure and flow to the microcirculation. The cardiac output generated by both the native heart and the LVAD is characterized by a low pulsatile pressure and flow profile in the ascending aorta. These low pulsatile pressure and flow hemodynamics dramatically impact on how the cardiovascular system regulates itself and interacts with such low oscillations, in a bid to maintain systemic homeostasis.

Acute and chronic consequences of these low pulsatile oscillations may determine the degree of large artery stiffening and the hemodynamic energy transmitted to the microcirculation.

Because of their different LVAD settings and the altered hemodynamic profile of the cardiac output, important differences in PP and PI can be observed between commonly implanted LVADs. Fig. 48.1 highlights some of the variability in hemodynamics that may have a role in determining the magnitude and severity of both macro- and microvascular complications in LVAD patients.

Importantly, recent clinical trials have revealed significant differences in device therapy—associated outcomes, with the newest generation of LVADs, the HeartMate 3 devices, achieving a significantly better clinical outcome than the HeartMate II.[5,6] Potential reasons for this clinical benefit have been proposed, including the reduction of the mechanical shear between the metal bearings and blood (achieved by the combination of a lower pump speed, wider bore size, and the introduction of an "artificial pulse" that washes out the mechanical components of the pump), and a consequently lower von Willebrand factor degradation.[7] Automated modulations in pump speed, which occur at a frequency of 0.5Hz (every 2 seconds), create what is known as the "artificial pulse". These pump modulations

may provide some pulsatility to the periphery, but further study is warranted to determine the degree to which this "artificial pulse" simulates normal physiology. Because the occurrence of the artificial pulse is not synchronized with the native heart rate, the resultant pressure and flow dynamics are not entirely predictable (see Fig. 48.1F and G). However, to date, superiority of HeartMate 3 over the HeartMate II devices in lowering specific microvascular complications (e.g., rates of GI bleeding and hemorrhagic stroke) has not been shown.

Before discussing the impact of low pulsatile pressure and flow on microvascular complications, the next section will address the consequences of low PP and PI on the macrocirculation which plays an important role in dampening or transmitting the central hemodynamics to the peripheral microcirculation.

Effects of low pressure and flow pulsatility on the macrocirculation

In conditions like the LVAD therapy described in the previous section, the low pulsatile pressure and flow are already present at the level of the ascending aorta. Consequently, the entre circulation, from the central elastic arteries to the microvessels, is affected. Sections Sympathetic nerve activity, vascular remodeling, and aortic stiffness, Endothelial dysfunction, and Blood pressure below describe the different effects of low pressure and flow pulsatility of LVAD patients on the macrocirculation.

Sympathetic nerve activity, vascular remodeling, and aortic stiffness

Because of a reduced systolic blood pressure in advanced heart failure patients, the baroreflex is often chronically activated via the baroreceptors located in the central macrocirculation. In accordance, the increased sympathetic activity has been shown to maintain arterial perfusion pressures via increasing vascular resistance as heart failure with reduced ejection fraction progresses. Similarly, data in LVAD patients reveal a markedly elevated muscle sympathetic nerve activity attributed to the missing pulsatile stretch of the baroreceptors (because the low arterial oscillations caused by the weak native heart and the continuous flow of the LVAD create an extremely low PP and PI). Importantly, it has been shown that acute restoration of rhythmical distension of the baroreceptors through alterations of LVAD speed settings (i.e., increasing the pulsatile nature of the flow and pressure output) can lower SNA in LVAD patients.[8] These data suggest that the low PP and/or PI play an important role in the overall cardiovascular regulation, and that restoring PP and/or PI to optimal levels

may reduce future bleeding complications in LVAD patients.[9,10] It should be noted that while previous pulsatile LVAD systems did not present with high levels of GI bleeding when compared to continuous-flow LVADs, they did present with increased risk of stroke. Therefore, creating optimal pulsatile pressure and flow for these LVAD patients may be essential for reducing overall risk. Since increased SNA induces vascular remodeling of large and small arteries in non-LVAD patients, it can be postulated that the high SNA reported in LVAD patients may have long-term consequences on subsequent macro- and microvascular complications.[11]

Unfortunately, due to the inability to accurately measure pressure oscillations within many LVAD patients, measuring arterial stiffness independent of blood pressure during LVAD therapy is very challenging, if not impossible. Therefore, several studies have used the methodological approach to compare heart failure patients before LVAD surgery and shortly after orthotopic heart transplant (OHT).

Indeed, it has been shown that patients on LVAD therapy have higher aortic stiffness compared to heart failure patients not on LVAD support.[12] These findings were further described by a reduced smooth muscle content and an increased collagen content of ascending aorta tissue samples, harvested during transplant after only 7 months on LVAD therapy. LVAD patients may thus experience dramatic aortic stiffening as a result of major structural remodeling compared to heart failure patients not on LVAD therapy. In addition, more recent evidence suggests that aortic stiffness index [aSI: ln(systolic/diastolic pressures) to (relative change in diameter)] does not increase in all LVAD patients, highlighting a differential macrovascular response to continuous-flow therapy.[13,14] The reasons for such disparate responses may be attributed to the duration of LVAD support, differential pharmacological therapy, and the individual LVAD settings (mostly pump speed). Moreover, the same data highlighted that composite outcome (reported as GI bleeding, pump thrombosis, and stroke) was highest in those patients where aSI increased while on LVAD therapy, compared to those patients where aSI did not increase or even decreased. As such, this study emphasizes the potentially important link between increased arterial stiffness and microvascular complications.

One point that must not be ignored is the probable impact of the severity of heart failure and duration prior to LVAD implantation, as well as the potential effects of the duration of LVAD therapy, which may influence how and to what extent continuous flow interacts with an already diseased cardiovascular system, and thus impacts on the macro- and microcirculation.

Endothelial dysfunction

In addition to increased sympathetic nerve activity, accelerated vascular remodeling, and arterial stiffness, patients with continuous-flow LVADs have been shown to have greater levels of endothelial dysfunction compared to heart failure patients with reduced ejection fraction.[15] Since endothelial dysfunction is associated with high cardiovascular risk, understanding the extent and reasons behind this endothelial dysfunction in LVAD patients is critical.[16] In a non-LVAD population, the cyclical changes in blood flow and pressures create an optimal shear stress on the endothelial layer of the arteries, stimulating the release of endothelial-derived nitric oxide (NO), which is necessary for smooth muscle relaxation, dilatation, and regulation of arterial stiffness.[17] In continuous-flow LVAD patients, it has been proposed that the low PI results in a decreased stimulation of the endothelium and thus a lower NO, with a subsequent reduction in dynamic endothelial responsiveness and increased arterial stiffness.[18]

One approach used to determine endothelial function is a standardized test termed flow-mediated dilatation (FMD). Typically, the degree of endothelial dysfunction and therefore FMD is predominantly associated with NO release, or to a lesser extent, the release of prostacyclin and endothelial-derived hyperpolarizing factor.[19,20] Unsurprisingly, FMD is lower in continuous-flow LVAD patients compared to patients implanted with pulsatile LVAD systems that are no longer in use.[15] These findings highlight the critical cyclical role that pressure and flow oscillations play in regulating NO release and maintaining endothelial function in LVAD patients. Moreover, the interconnections between the native heart, LVAD speed settings, and device differences may produce different magnitudes of pulsatility (see Fig. 48.1) and subsequent degree of endothelial dysfunction. Since endothelial dysfunction and NO production are associated with increasing arterial stiffness, it is acceptable to suggest that these links may play a role in determining the degree of arterial stiffness observed in LVAD patients and the associated risk of GI bleeding and stroke.

With the introduction of the third generation of LVAD devices (HM3), more studies are needed to investigate the impact of the "artificial pulse" of this system on the development and progression of endothelial dysfunction and arterial stiffness. These much-needed data will elucidate if the "artificial pulse" is even present across the macro- and microcirculation of LVAD patients, and whether it creates enough of an oscillatory swing to stimulate an increased NO release from the endothelial layer and maintain endothelial function.
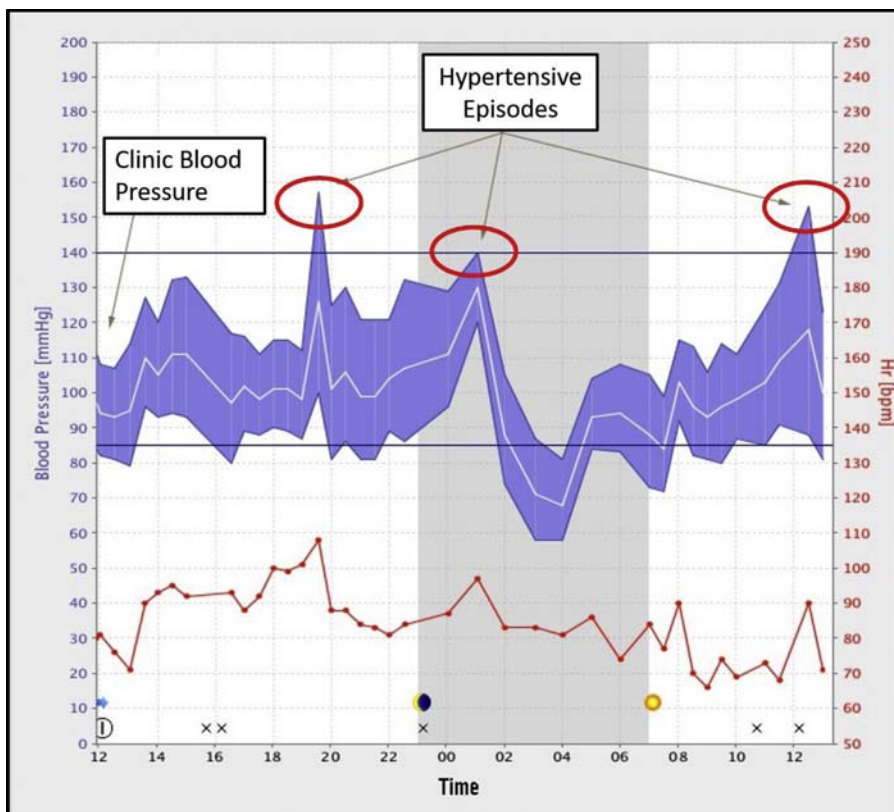
Given the impact of LVADs on the macrocirculation, it is reasonable to expect that the observed impact of continuous flow and low pulsatility on large artery endothelial dysfunction may also be apparent within the microcirculation. Investigating microcirculatory endothelial dysfunction in specific peripheral organs (e.g., the brain and GI tract) may provide future mechanisms linked to clinical microcirculatory outcome in LVAD patients.

Blood pressure

As already stated, a baroreceptor-mediated rise in SNA increases peripheral vascular tone and contributes to the maintenance of mean arterial pressure (in the face of a reduced systolic BP) observed in LVAD patients. However, due to the absence of detectable pressure oscillations in the majority of LVAD patients, the ability to accurately measure blood pressure is often lacking. The inability to accurately measure systolic and diastolic blood pressure and therefore PP in LVAD patients means that decision-making in relation to optimizing treatment may often be suboptimal. When oscillometric devices fail to capture a blood pressure in the clinic, an alternative of using Doppler to attempt to record a measurement of pressure is often used. Importantly, there has been debate as to what pressure the Doppler method measures (mean arterial pressure vs. systolic pressure). Thus, its interpretation in clinical practice is uncertain. The aforementioned lack of oscillations makes it a critical issue in providing informed treatment for hypertension in patients on continuous-flow LVAD therapy. Importantly, LVAD patients have been shown to have a lower threshold of blood pressure−associated CV risk and outcome compared to that of other populations. For example, the risk of stroke is increased above a relatively low systolic blood pressure ∼101 mmHg, compared to >140 mmHg in typical hypertensive populations.[21−24] Therefore, continuous-flow LVAD patients may be at high risk of stroke due to the inability of their macrovasculature to regulate and maintain a blood pressure below 101mmHg. Moreover, risk of stroke could also be influenced by levels of anticoagulation and levels of v-WF deficiency in these patients. In addition, higher levels of blood pressure may also lead to higher risk of thrombus formation in the LVAD device due to increased stasis from a lowered driving pressure from the system.

The current inability to record and accurately measure blood pressure−related clinical issues in the majority of LVAD patients poses a serious challenge for our understanding. Importantly, these issues are exacerbated in HM3 patients who have a chaotic blood flow and pressure profile due to the artificial pulse (see Fig. 48.1F and G). The chaotic waveform further complicates an accurate blood pressure measurements. At present, there are no commercially available, noninvasive, oscillometric systems that can accurately measure and record blood pressure in HM3 patients. This causes significant challenges during clinical

FIGURE 48.2 The 24-hour blood pressure profile and variability (inclusive of highlighted hypertensive episodes) of a HMII LVAD patient. The figure above describes the blood pressure profile of the HMII LVAD patient over 24 h, with hypertensive episodes circled in red.

follow-up when attempting to measure and treat high blood pressure and reduce microvascular complications.

Importantly, 24-h recordings of ambulatory blood pressure of HMII patients have revealed several blood pressure surges throughout the 24-hour period (see Fig. 48.2). Due to the fact that LVAD patients are already at high risk of stroke at systolic blood pressure levels above 101 mmHg, evidence to show an inability to buffer systolic blood pressure surges >140 mmHg over a 24-h period, could mean that the LVAD patient is potentially at higher risk of microvascular insults during such hypertensive episodes.

Consequences of low pressure and flow pulsatility on the microcirculation

The previous sections have highlighted the impact of low pulsatility hemodynamics from the implanted device on the large arteries. Moreover, the clinical data indicate that the third-generation LVAD, the HM3, is associated with overall improved clinical outcomes. However, there are some remaining clinical challenges that seem to be as problematic with the HM3 as with the HM II. This indicates that the technological advances of the HM3, including the intermittent "artificial pulse," have not sufficiently resolved the circulatory complications in LVAD patients. Several

major complications mentioned above persist even in the third-generation LVAD patients, including right heart failure (27%−32% of patients), GI bleeding (27%), stroke (10%−19%), respiratory failure (22%−24%), and a reduced exercise capacity that is minimally improved from the pre-LVAD heart failure state. In the following paragraphs, we discuss the potential role of microcirculatory disruption in relation to these complications and the possible pharmacological management, before summarizing the potential mechanisms involved.

At present, it seems conceivable that the low pulsatile hemodynamics are a systemic phenomenon, as evidenced by the lower pulsatility across the whole circulation. Recent studies have revealed that the reduced arterial pulsatility of LVAD patients implanted with both the second- and third-generation devices can be seen in the large, intermediate-sized conduit arteries as well as the microcirculation.[25] Of great importance is the observation that the reduction in pulsatility from the aorta and carotid arteries to the middle cerebral and central retinal artery of healthy individuals is halved again in LVAD patients.[25] These findings demonstrate the extent to which the microcirculation of LVAD patients may be impacted. Yet, our current knowledge also suggests that these hemodynamics may have a differential impact on the microcirculation of different end organs, given the varied complications mentioned above.

Right heart failure and respiratory complications

Right heart function is important for the circulatory function of patients with LVADs and may itself produce some microcirculatory complications in the lungs. Studies that acutely changed the LVAD pump speed highlighted the relationship between an unloading of the LV and an overloading of the right ventricle (RV).[26] Unloading the LV to an end-diastolic volume less than 260 mL will increase the volumetric load on the RV and vice versa. This may indicate why a significant portion of LVAD patients experience severe right heart complications, in particular in the postoperative period. Ultrasound of the right heart has revealed some important hemodynamic shifts in LVAD patients and has the potential to inform the clinician about early changes in pulmonary artery pulsatility index as well as of right ventricular dysfunction.[26,27] Whether the altered RV hemodynamics are directly linked to the respiratory complications remains to be elucidated. Phenomena like the exercise-induced arterial hypoxemia in LVAD patients (see below for more details) do suggest that there is a circulatory problem in the lungs, which could either relate to an increased transit time of blood (caused by a volume overload) or to direct respiratory issues.[28]

Cerebrovascular complications

In the brain, microcirculatory complications are alarmingly high, with a reported prevalence of 97% of LVAD patients with cortical microbleeds.[29] It is likely that the LVAD itself, and the continuous-flow more precisely, causes such widespread pathophysiologic changes that predispose to microvascular complications. Yet, the kidneys, which are known to be particularly sensitive to altered hemodynamics, are less affected than other organs (in particular when considering the confounding influence of declining muscle mass in the estimation of glomerular filtration rate).[5,30] Despite a concerted effort of the LVAD research community, the mechanisms associated with microcirculatory complications in the brain remain elusive. This is in part the case because of the technical challenges of measuring the microcirculatory hemodynamics in the different target organs. MRI assessments are not possible during LVAD support, and other imaging techniques have their own limitations. Equally, ultrasound has been used successfully to determine hemodynamics in the cerebral circulation, namely the middle cerebral artery.[25] The typical investigation of the middle cerebral artery is, however, not representative of the cerebral *micro*circulation. MRI investigations immediately before LVAD implantation and after OHT have revealed important insights into the cerebral microcirculation as discussed above. But the lack of data on the cerebral microcirculation *during* LVAD support presents a major

gap of knowledge in the LVAD community. Given the close anatomic relationship between the eye and the cerebral circulation, the use of ultrasound to detect flow dynamics and pulsatility in the central retinal artery (diameter range of ∼140–180 μm) of LVAD patients may significantly advance our current knowledge in this area. At present, it is not known whether the HeartMate 3 creates a similar transmission of hemodynamics from the macro- to the microcirculation. Furthermore, the impact of the "artificial pulse" on the macrocirculation and its transmission into the microcirculation remains unknown, and more research is required to assess cerebrovascular, macro- and microcirculatory dynamics in patients with contemporary LVADs.

Gastrointestinal bleeding

For the GI tract, the noninvasive hemodynamic assessment is particularly problematic, since the clinical interventions in response to suspected or overt GI bleeding may worsen the patients' prognosis.[31,32] Studies have shown that the high prevalence of GI bleeding in LVAD patients is associated with angiodysplasia and arterio-venous (AV) malformations.[31,32] Because of the similar prevalence of GI bleeding in HeartMate II and HeartMate 3 patients, the "artificial pulse" of the HM3 does not seem to have had a positive impact. Consequently, the exact mechanisms associated with GI bleeding in LVAD patients remain unknown. However, uncontrolled hypervolemia, increased sympathetic state (known to affect the GI tract), a neurohormonal axis related to AV malformations, and/or the reduced pressure and flow pulsatility could influence the integrity of the GI microcirculation and clinical presentation of GI bleeding. Equally, it is possible that the right heart failure discussed above may cause a backflow into the GI tract that could manifest as microcirculatory complications and ultimately angiodysplasia and GI bleeding.[33,34]

Interestingly, GI bleeding is also prevalent in severe aortic stenosis, suggesting a more general link between altered cardiac output dynamics and GI bleeding across different patient groups. Furthermore, a common complication in LVAD patients is aortic insufficiency, which can lead to aortic regurgitation similar to severe aortic stenosis.[35] However, it is important to acknowledge that the arterial hemodynamics of aortic stenosis are more pulsatile than those of LVAD patients, and that the angiodysplasia of LVAD patients has its own distinct phenotype.[36–38] Instead, the hemodynamics of patients with severe aortic stenosis may actually be more similar to those of advanced heart failure patients *prior* to LVAD implantation. Consequently, the microcirculatory complications experienced during chronic heart failure have the potential to prime the microcirculation and predispose the patients to the above-mentioned complications when the hemodynamics are suddenly altered to a hypervolemic, low-pulsatile state during LVAD support.
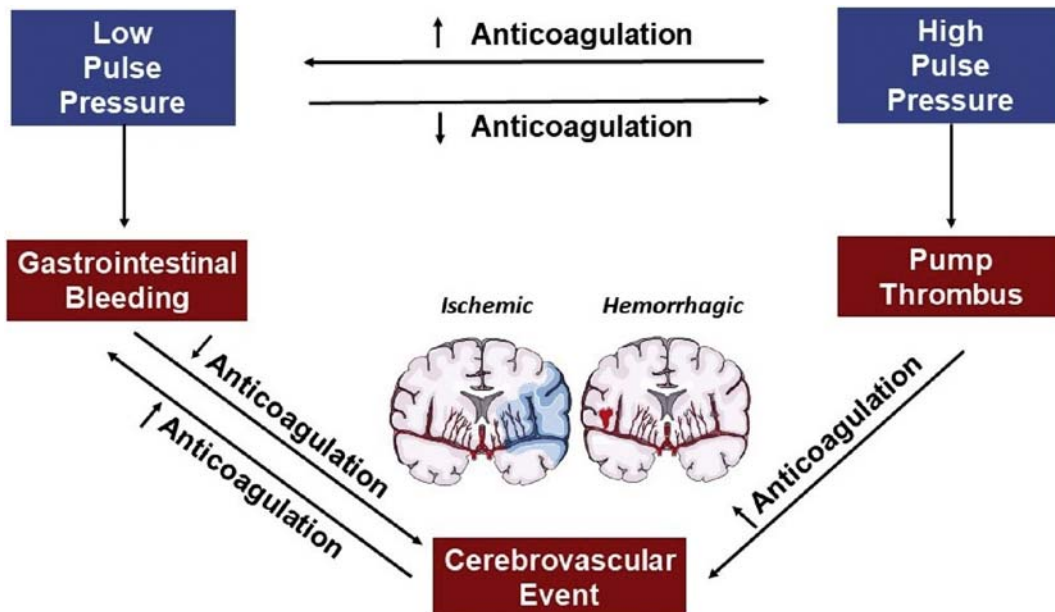
Pharmacological decision-making in relation to PP and PI in LVAD patients

Historically, stroke has been the primary cause of death among heart failure patients supported by LVAD from 6 to 24 months of support.[39] The reasons for this are multifactorial and related to comorbidities, medication effects, a prothrombotic state, and other LVAD-related complications that result from chronic exposure to a nonphysiologic pulse.[8,40,41] These factors work together in an almost synergistic fashion to increase the risk of cerebrovascular events.[40] As demonstrated in Fig. 48.3 below, reductions in PP increase the risk of GI bleeding,[42] and reductions in strength of anticoagulation subsequent to a bleeding event substantially increase the risk of pump thrombus formation or an ischemic stroke. Hypertension may increase the risk of pump thrombus formation by nearly threefold, which increases the risk of subsequent stroke. Therefore, careful and personalized medication considerations are required when treating such patients. Potential application of measuring localized flow PI may help inform pharmacological decision-making in the future.

Finally, it is noteworthy that more than one-fourth of LVAD patients experience a device-related infection over time,[43] which independently increases the risk of stroke, possibly as a result of formation of mycotic aneurysms from bacterial seeding.[44]

Left ventricular assist device therapy and exercise capacity

Despite normalization of a resting cardiac output following implantation of an LVAD, patients suffer from severe and persistent reductions in functional exercise capacity. However, the mechanisms related to the reduced exercise capacity and the consequences for the microcirculation are not clear. It has been shown that subjective assessments of quality-of-life and the severity of heart failure improve following LVAD implantation.[45] However, objective metrics such as the maximal oxygen uptake (VO_2max) obtained during cardiopulmonary exercise testing fail to improve and typically remain in the range of 12–15 mL/kg/min, even up to 1 year after device implantation.[46–48] The ability of current-generation LVADs to augment flow during exercise is limited and as such, delivery of oxygenated blood to exercising muscle largely depends on the intrinsic contractility of the native LV.[47,49,50] Considering that the absolute workload and 6-min walk distance mildly improve during LVAD therapy, the lack of a clear increase in VO_2max may be attributable to longstanding skeletal muscle microcirculatory issues. Severe deconditioning of the skeletal musculature because of a long history of chronic heart failure may be one reason, thereby possibly affecting mitochondrial density, mitochondrial respiration, and the energetic efficiency of different muscle fiber types. Equally, the dramatically low PP

FIGURE 48.3 The complex and sensitive interactions between low pulse pressure, high pulse pressure, anticoagulation treatment, and microvascular complications of LVAD patients. Lines show the interconnections between blood pressures, GI bleeding or Pump thrombus and cerebrovascular events when anticoagulation therapy is increased or decreased. *Figure modified and changed from source Cornwell III WK, Ambardekar AV, Tran T, et al. Stroke incidence and impact of continuous-flow left ventricular assist devices on cerebrovascular physiology. Stroke. 2019; 50:542–548.*

and PI in the microcirculation may affect capillary recruitment and O_2 kinetics in the capillaries, which is supported by the observation that LVAD patients experience exercise-induced arterial hypoxemia at low cardiac outputs.[28] Furthermore, exercise among patients with heart failure may be limited by pulmonary, peripheral vascular, autonomic or musculoskeletal abnormalities, and it is not clear by any means that LVAD implantation improves these organ systems.[46] Finally, the pump itself is a denervated machine with no biofeedback mechanisms in place and, as such, does not participate in autonomic/exercise presser reflexes that otherwise facilitate the body's response to exercise, including the regulation of arteriolar and capillary diameter and tone.

Conclusions

It is clear that low pulsatility has detrimental consequences on the macro- and microcirculation that is as serious a problem as excessive pulsatility. However, the role of low pulsatility in LVAD patients must be interpreted and discussed in relation to many interconnecting factors. Such factors include pharmacological treatment regimens, pump speed settings, hypervolemia, O_2 uptake, and the severity of underlying cardiac and vascular disease states pre-implantation. Further studies are needed to understand the direct role of low pressure and flow pulsatility in affecting macro- and microcirculatory health, which will likely substantially advance our general understanding of arterial physiology and circulatory regulation.

References

1. Mitchell GF, van Buchem MA, Sigurdsson S, et al. Arterial stiffness, pressure and flow pulsatility and brain structure and function: the age, gene/environment susceptibility–Reykjavik study. **Brain**. 2011; 134:3398−3407.
2. UK Prospective Diabetes Study Group. Tight blood pressure control and risk of macrovascular and microvascular complications in type 2 diabetes: UKPDS 38. UK Prospective Diabetes Study Group. **BMJ**. 1998; 317:703−713.
3. Safar ME, Blacher J, Pannier B, et al. Central pulse pressure and mortality in end-stage renal disease. **Hypertension**. 2002; 39:735−738.
4. Gopinathannair R, Cornwell WK, Dukes JW, Ellis CR, Hickey KT, Joglar JA, Pagani FD, Roukoz H, Slaughter MS, Patton KK. Device therapy and arrhythmia management in left ventricular assist device recipients: A scientific statement from the American Heart Association. **Circulation**. 2019; 139(20):e967−e989.
5. Mehra MR, Goldstein DJ, Uriel N, et al. Two-year outcomes with a magnetically levitated cardiac pump in heart failure. **N Engl J Med**. 2018; 378:1386−1395.
6. Mehra MR, Uriel N, Naka Y, et al. A fully magnetically levitated left ventricular assist device - final report. **N Engl J Med**. 2019; 380(17):1618−1627.
7. Netuka I, Kvasnicka T, Kvasnicka J, et al. Evaluation of von Willebrand factor with a fully magnetically levitated centrifugal continuous-flow left ventricular assist device in advanced heart failure. **J Heart Lung Transplant**. 2016; 35:860−867.
8. Cornwell 3rd WK, Tarumi T, Stickford A, et al. Restoration of pulsatile flow reduces sympathetic nerve activity among individuals with continuous-flow left ventricular assist devices. **Circulation**. 2015; 132:2316−2322.
9. Stöhr EJ, McDonnell BJ, Colombo PC, Willey JZ. CrossTalk proposal: blood flow pulsatility in left ventricular assist device patients is essential to maintain normal brain physiology. **J Physiol**. 2019; 597:353−356.
10. Cornwell W, Tarumi T, Lawley J, Ambardekar AV. CrossTalk opposing view: blood flow pulsatility in left ventricular assist device patients is NOT essential to maintain normal brain physiology. **J Physiol**. 2019; 597(2):357−359.
11. Holwerda SW, Luehrs RE, DuBose L, et al. Elevated muscle sympathetic nerve activity contributes to central artery stiffness in young and middle-age/older adults. **Hypertension**. 2019; 73:1025−1035.
12. Ambardekar AV, Hunter KS, Babu AN, Tuder RM, Dodson RB, Lindenfeld J. Changes in aortic wall structure, composition, and stiffness with continuous-flow left ventricular assist devices: a pilot study. **Circ Heart Fail**. 2015; 8:944−952.
13. Rosenblum H, Pinsino A, Demmer RT, et al. Increased aortic stiffness is associated with higher rates of stroke, GI-bleeding and pump thrombosis in continuous-flow left ventricular assist device patients. **J Heart Lung Transplant**. 2018; 37.
14. Mackenzie IS, Wilkinson IB, Cockcroft JR. Assessment of arterial stiffness in clinical practice. **QJM**. 2002; 95:67−74.
15. Witman MA, Garten RS, Gifford JR, et al. Further peripheral vascular dysfunction in heart failure patients with a continuous-flow left ventricular assist device: the role of pulsatility. **JACC Heart Fail**. 2015; 3:703−711.
16. Shimbo D, Grahame-Clarke C, Miyake Y, et al. The association between endothelial dysfunction and cardiovascular outcomes in a population-based multi-ethnic cohort. **Atherosclerosis**. 2007; 192:197−203.
17. Wilkinson IB, MacCallum H, Cockcroft JR, Webb DJ. Inhibition of basal nitric oxide synthesis increases aortic augmentation index and pulse wave velocity in vivo. **Br J Clin Pharmacol**. 2002; 53:189−192.
18. Nakano T, Tominaga R, Nagano I, Okabe H, Yasui H. Pulsatile flow enhances endothelium-derived nitric oxide release in the peripheral vasculature. **Am J Physiol Heart Circ Physiol**. 2000; 278:H1098−H1104.
19. Moncada S, Radomski MW, Palmer RM. Endothelium-derived relaxing factor. Identification as nitric oxide and role in the control of vascular tone and platelet function. **Biochem Pharmacol**. 1988; 37:2495−2501.
20. Stoner L, Erickson ML, Young JM, et al. There's more to flow-mediated dilation than nitric oxide. **J Atheroscler Thromb**. 2012; 19:589−600.
21. Pinsino A, Castagna F, Zuver AM, et al. Prognostic implications of serial outpatient blood pressure measurements in patients with an axial continuous-flow left ventricular assist device. **J Heart Lung Transplant**. 2019; 38:396−405.
22. Teuteberg JJ, Slaughter MS, Rogers JG, et al. The HVAD left ventricular assist device: risk factors for neurological events and risk mitigation strategies. **JACC Heart Fail**. 2015; 3:818−828.

23. Najjar SS, Slaughter MS, Pagani FD, et al. An analysis of pump thrombus events in patients in the HeartWare ADVANCE bridge to transplant and continued access protocol trial. **J Heart Lung Transplant**. 2014; 33:23−34.

24. Nassif ME, Tibrewala A, Raymer DS, et al. Systolic blood pressure on discharge after left ventricular assist device insertion is associated with subsequent stroke. **J Heart Lung Transplant**. 2015; 34:503−508.

25. Stöhr EJ, Ji R, Akiyama K, et al. HM3 patients do not have an increased pulsatility in large, muscular or microcirculatory arteries. **J Heart Lung Transplant**. 2020; 39.

26. Addetia K, Uriel N, Maffessanti F, et al. 3D morphological changes in LV and RV during LVAD ramp studies. **JACC Cardiovasc Imaging**. 2018; 11:159−169.

27. Kang G, Ha R, Banerjee D. Pulmonary artery pulsatility index predicts right ventricular failure after left ventricular assist device implantation. **J Heart Lung Transplant**. 2016; 35:67−73.

28. Koerber DM, Rosenbaum AN, Olson TP, et al. Exercise-induced hypoxemia predicts heart failure hospitalization and death in patients supported with left ventricular assist devices. **Int J Artif Organs**. 2020; 43:165−172.

29. Yoshioka D, Okazaki S, Toda K, et al. Prevalence of cerebral microbleeds in patients with continuous-flow left ventricular assist devices. **J Am Heart Assoc**. 2017; 6:10.

30. Pinsino A, Mondellini GM, Royzman EA, et al. Cystatin C- versus creatinine-based assessment of renal function and prediction of early outcomes among patients with a left ventricular assist device. **Circ Heart Fail**. 2020; 13:e006326.

31. Axelrad JE, Faye AS, Pinsino A, et al. Endoscopic algorithm for management of gastrointestinal bleeding in patients with continuous flow LVADs: a prospective validation study. **J Card Fail**. 2020; 26:324−332.

32. Axelrad JE, Pinsino A, Trinh PN, et al. Limited usefulness of endoscopic evaluation in patients with continuous-flow left ventricular assist devices and gastrointestinal bleeding. **J Heart Lung Transplant**. 2018; 37:723−732.

33. Gurvits GE. Gastrointestinal hemorrhage in left ventricular assist device patients: red scare or pressure from the right? **Dig Dis Sci**. 2018; 63:1381−1383.

34. Tomizawa Y, Tanaka A, Kitahara H, et al. Preoperative right-sided cardiac congestion is associated with gastrointestinal bleeding in patients with continuous-flow left ventricular assist devices. **Dig Dis Sci**. 2018; 63:1518−1524.

35. Bouabdallaoui N, El-Hamamsy I, Pham M, et al. Aortic regurgitation in patients with a left ventricular assist device: a contemporary review. **J Heart Lung Transplant**. 2018; 37:1289−1297.

36. Madhwal S, Yesenko S, Kim ES, Park M, Begelman SM, Gornik HL. Manifestations of cardiac disease in carotid duplex ultrasound examination. **JACC Cardiovasc Imaging**. 2014; 7:200−203.

37. Birks EJ. Stopping LVAD bleeding: a piece of the puzzle. **Circ Res**. 2017; 121:902−904.

38. Kang J, Hennessy-Strahs S, Kwiatkowski P, et al. Continuous-flow LVAD support causes a distinct form of intestinal angiodysplasia. **Circ Res**. 2017; 121:963−969.

39. Kirklin JK, Pagani FD, Kormos RL, et al. Eighth annual INTERMACS report: special focus on framing the impact of adverse events. **J Heart Lung Transplant**. 2017; 36:1080−1086.

40. Cornwell III WK, Ambardekar AV, Tran T, et al. Stroke incidence and impact of continuous-flow left ventricular assist devices on cerebrovascular physiology. **Stroke**. 2019; 50:542−548.

41. Markham DW, Fu Q, Palmer MD, et al. Sympathetic neural and hemodynamic responses to upright tilt in patients with pulsatile and nonpulsatile left ventricular assist devices. **Circ Heart Fail**. 2013; 6:293−299.

42. Wever-Pinzon O, Selzman CH, Drakos SG, et al. Pulsatility and the risk of nonsurgical bleeding in patients supported with the continuous-flow left ventricular assist device HeartMate II. **Circ Heart Fail**. 2013; 6:517−526.

43. Gordon RJ, Weinberg AD, Pagani FD, et al. Prospective, multicenter study of ventricular assist device infections. **Circulation**. 2013; 127:691−702.

44. Aggarwal A, Gupta A, Kumar S, et al. Are blood stream infections associated with an increased risk of hemorrhagic stroke in patients with a left ventricular assist device? **Am Soc Artif Intern Organs J**. 2012; 58:509−513.

45. Rogers JG, Aaronson KD, Boyle AJ, et al. Continuous flow left ventricular assist device improves functional capacity and quality of life of advanced heart failure patients. **J Am Coll Cardiol**. 2010; 55:1826−1834.

46. Buchanan C, Kanwar M, Cockcroft JR, McDonnell B, Stohr EJ, Cornwell 3rd WK. Bionic women and men - Part 4: cardiovascular, cerebrovascular and exercise responses among patients supported with left ventricular assist devices. **Exp Physiol**. 2020; 105:763−766.

47. Sailer C, Edelmann H, Buchanan C, et al. Impairments in blood pressure regulation and cardiac baroreceptor sensitivity among heart failure patients suppported with continuous-flow left ventricular assist devices. **Circ Heart Fail**. 2021; 14(1):e007448.

48. Leibner ES, Cysyk J, Eleuteri K, El-Banayosy A, Boehmer JP, Pae WE. Changes in the functional status measures of heart failure patients with mechanical assist devices. **Am Soc Artif Intern Organs J**. 2013; 59:117−122.

49. Jung MH, Houston B, Russell SD, Gustafsson F. Pump speed modulations and sub-maximal exercise tolerance in left ventricular assist device recipients: a double-blind, randomized trial. **J Heart Lung Transplant**. 2017; 36:36−41.

50. Tran T, Muralidhar A, Hunter K, et al. Right ventricular function and cardiopulmonary performance among heart failure patients supported by durable mechanical circulatory support devices. **J Heart Lung Transplant**. 2021; 40(2):128−137.

This page intentionally left blank

Therapeutic approaches to improve arterial stiffness and pulsatile hemodynamics

This page intentionally left blank

Chapter 49

Effects of common antihypertensive treatments on pulsatile arterial hemodynamics

Yi-Bang Cheng and Ji-Guang Wang

National Research Centre for Translational Medicine, Centre for Epidemiological Studies and Clinical Trials, Shanghai Key Laboratory of Hypertension, The Shanghai Institute of Hypertension, Department of Hypertension, Ruijin Hospital, Shanghai Jiao Tong University School of Medicine, Shanghai, Shanghai, China

Introduction

When the blood flows from the central large elastic aorta to peripheral smaller muscular arteries, systolic blood pressure (BP) increases, without significant changes in diastolic BP and mean arterial pressure, resulting in widened pulse pressure. Although brachial BP highly correlates with central BP, substantial individual discrepancies between central and peripheral BP exist. Some studies have shown that the strength of the associations between target organ damage and systolic BP and pulse pressure was stronger for the central than brachial arteries. In a meta-analysis of 11 studies that included 5648 subjects followed up for 3.8 years, central pulse pressure showed borderline superiority to brachial pulse pressure in the prediction of cardiovascular events.[1]

Several previous studies have shown that various classes of antihypertensive drugs may have different treatment effects. The Conduit Artery Function Evaluation study,[2] a substudy of the Anglo-Scandinavian Cardiac Outcomes Trial (ASCOT), showed that amlodipine/perindopril was more efficacious than atenolol/thiazide in reducing central systolic BP and pulse pressure by 4.3 mm Hg (95% confidence interval [CI], 3.3 to 5.4) and 3 mm Hg (95% CI, 2.1 to 3.9), respectively, despite similar brachial BP reductions in the two groups. In addition, central pulse pressure was significantly associated with the risk of the composite outcome of total cardiovascular events and procedures and development of renal impairment.[2] The cardiovascular benefits of amlodipine and perindopril based regimen observed in ASCOT[3] might have resulted at least in part

from their effect on central BP, although other hemodynamic effects (such as reduced BP variability) might have been involved as well.[4] There is therefore a growing interest in central BP as a target of treatment in hypertension.

In this review article, we summarize the evidence on the effect of pharmaceutical- or device-based cardiovascular therapeutics on pulsatile arterial hemodynamics. We discuss (1) whether antihypertensive drug treatment reduced arterial wave reflections; (2) whether the newer agents, such as renin-angiotensin-aldosterone (RAS) inhibitors and calcium-channel blockers (CCBs), were more efficacious than the older ones, such as diuretics, β-blockers, and α-blockers; (3) whether the even newer agents, such as vasodilating β-blockers and angiotensin receptor neprilysin inhibitors (ARNIs), were more efficacious than their respective comparators, i.e., non-vasodilating β-blockers and angiotensin receptor blockers (ARBs), respectively. In addition, we also studied device-based antihypertensive therapy for its effects on central hemodynamics.

Antihypertensive drug classes and their mechanisms of action

Current hypertension guidelines recommend several classes of antihypertensive agents for the treatment of hypertension, such as angiotensin-converting enzyme (ACE) inhibitors, ARBs, β-blockers, dihydropyridine CCBs, and thiazide diuretics. These agents reduce BP via different modes of action. ACE inhibitors and ARBs block the RAS

system by inhibiting ACE and blocking the angiotensin II type 1 receptor, respectively. β-blockers reduce BP by inhibiting activation of the sympathetic nervous system, and reducing heart rate and myocardial contractility. Newer β-blockers show ancillary vasodilatory properties, which may play a part in BP lowering. Dihydropyridine CCBs dilate arteries, especially arterioles, and reduce BP by constricting calcium channels on vascular smooth muscle cells. Diuretics exert antihypertensive effects on the kidneys via enhancing electrolytes and water excretion and regulating body fluid volume. Several other classes of antihypertensive agents are also recommended on special conditions or for patients with resistant hypertension, such as α_1-blockers, central sympatholytic agents, loop diuretics, nondihydropyridine CCBs, potassium sparing diuretics (aldosterone receptor antagonists and others), direct vasodilators, and so on. Direct renin inhibitors and ARNIs still have limited availability but can also be used in the treatment of hypertension on various clinical conditions (Fig. 49.1).

Data acquisition, extraction, and analysis
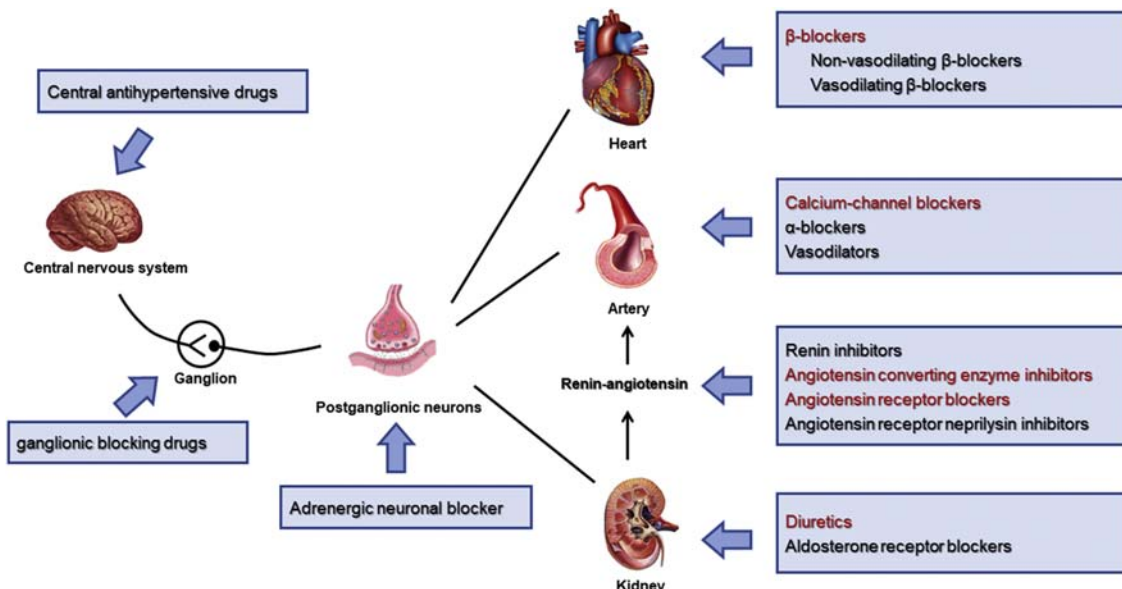
We searched the PubMed, Embase, and Cochrane Central Register of Controlled Trials for randomized controlled trials that tested antihypertensive treatment with central arterial hemodynamics as an outcome measure. The search key terms included "central pressure," "aortic pressure," "carotid pressure," "pulse amplification," "central-to-peripheral pulse pressure ratio," "augmentation index (AI)," "antihypertensive drug," "antihypertensive treatment," and "antihypertensive agent." We limited our search to studies published in English in peer-reviewed journals up to

September 2020. We checked the reference lists of review articles and original studies identified by the electronic search to find other potentially eligible studies.

We identified 140 published studies meeting the above criteria. We excluded 70 studies because of less than four weeks of follow-up time (n = 9), uncontrolled or self-controlled design (n = 4), nonrandomized subgroup analyses (n = 7), dose-dependent study (n = 2) or crossover design (n = 45), or ambulatory central BP as outcome (n = 3). We further excluded 29 studies because of combination antihypertensive therapy (n = 6), within class drug comparison (n = 13), actively controlled trials between RAS inhibitors, ARNI, CCBs, and vasodilating β-blockers comparison (n = 7), or without central BP mean values (n = 1) or 95% confidence intervals (n = 2). Thus, a total of 41 studies were eventually included in the present overview.

These 41 trials[5−45] included 13 trials that compared antihypertensive drugs with placebo[6−10,12,13,15,17] or "usual care,"[4,10,13,15] and 20 trials that compared RAS inhibitors[8,18−23,26−34] (n = 16) or CCBs[20,24,25,35,36] (n = 5) with diuretics,[8,18−20,24,25,33−35] β-blockers[20−22,26−32,36] or an α-blocker,[23] or compared vasodilating with non-vasodilating β-blockers[22,37−43] (n = 8), or ARNI with ARB[44,45] (n = 2). We additionally identified four device-based therapy trials[46−49] for the treatment effect of either renal sympathetic denervation (RDN)[46] or continuous positive airway pressure (CPAP)[47−49] on central pressure and AI.

We based our analysis on summary statistics reported in the literature. For central arterial hemodynamics, we extracted the means and standard deviations for the experimental and control groups separately, at baseline and during follow-up, and if available in the published report,

FIGURE 49.1 Main classes of antihypertensive agents and mechanism of action. Drug classes in red color are those recommended by the current hypertension guidelines.

also changes over time. We extracted measurement information on the techniques used to assess arterial hemodynamics. We searched for specifications about the BP measuring device and other methods for BP measurement, arterial sites, and the algorithm for AI estimation.

For each comparison within each trial, we calculated the absolute difference in the mean changes over time in central systolic BP (mm Hg), central pulse pressure (mm Hg), augmentation pressure (mm Hg) and AI (%) between the experimental and control groups. The pooled effect for each grouping of trials was derived from the point estimate for each separate trial weighted by the inverse of the variance $(1/SE^2)$. Heterogeneity of effect sizes was tested across trials using the χ^2 test. If trials were homogeneous $(P < .10)$, a fixed-effects model was used to calculate pooled effect sizes. Otherwise, a random-effects model was applied to calculate overall differences. Net treatment effects on central pressure and AI were determined by subtracting the mean change in the experimental group from the corresponding mean change in the control group. We ran all aforementioned computations and statistical analyses in Stata version 15 (Stata Corp LP, College Station, Texas, USA).

Antihypertensive drugs versus placebo or no-treatment

This part of our analysis included 13 studies with 635 participants, of whom 415 (65.4%) had been randomized in nine double-blind trials and 220 (34.6%) in four studies with an open design (Table 49.1). Active antihypertensive treatment consisted of an ACEI in three trials (n = 165),[5−7] an ARB in three trials (n = 186),[8−10] an aldosterone receptor antagonist in two trials (n = 102),[11,12] a renin inhibitor in two trials (n = 49),[12,13] a diuretic in one trial (n = 40),[8] and a vasodilating β-blocker in three trials (n = 129).[15−17] Klingbeil's study[8] contributed two groups to the present overview, valsartan or hydrochlorothiazide versus placebo. The weighted mean changes in central systolic and diastolic BP across the nine trials[5,7,8,10−16] were −6.9 mm Hg (95% CI, −9.9 to −3.7, $P < .001$) and −4.1 mm Hg (95% CI, −5.7 to −2.5, $P < .001$), respectively. The weighted mean changes were −2.0 mm Hg (95% CI, −3.5 to −0.6, $P = .007$) in augmentation pressure across five trials,[5,7,8,13,15] and −5.2% (−9.1 to −1.3, $P < .001$) in AI across 10 trials.[5−11,14,15,17]

Renin-angiotensin-aldosterone inhibitors and calcium-channel blockers versus diuretics, β-blockers, and α-blockers

London and colleagues conducted a controlled, blinded study to compare perindopril and nitrendipine on their effects on arterial hemodynamics in patients on chronic hemodialysis.[50] The results showed that 12 months of treatment with ACEI and CCB had similar effects on AI and carotid BP. A series of subsequent studies investigated the central hemodynamic effects of vasoactive antihypertensive agents.[2,8,18−45,51]

The following REASON study[51] revealed that in 471 hypertensive participants followed for 12 months, the indapamide and perindopril combination decreased brachial systolic BP and pulse pressure significantly more than atenolol, with an adjusted between-group difference of −6.02 mm Hg (95% CI, −8.90 to −3.14) and −5.57 mm Hg (95% CI, −7.70 to −3.44), respectively. Similar adjusted between-group differences were observed for central systolic BP [−12.52 mm Hg (95% CI, −17.97 to −7.08)] and pulse pressure [−10.34 mm Hg (95% CI, −14.12 to −6.56)], and for carotid [−5.57% (95% CI, −10.77 to −0.36)] and aortic AI [−5.17% (95% CI, −7.74 to −2.61)].

Taking all the 20 trials together (Table 49.2),[8,18−36] newer antihypertensive agents consisted of an ACEI in seven trials (n = 854),[18−23] an ARB in eight trials (n = 1123),[8,26−32] a renin inhibitor in three trials (n = 197),[22,33,34] and a CCB in five trials (n = 490).[20,24,25,35,36] Compared with diuretics, β-blockers or α-blockers, the differences in the changes in central systolic BP were statistically significant for ACEIs by −3.4 mm Hg (95% CI, −5.9 to −0.9, $P = .008$), for ARBs by −4.1 mm Hg (95% CI, −6.0 to −2.2, $P < .001$), for renin inhibitors by −6.7 mm Hg (95% CI, −7.8 to −5.5, $P < .001$), and for CCBs by −5.6 mm Hg (95% CI, −8.2 to −3.0, $P < .001$). No significant heterogeneity was noticed within the four comparisons ($P \geq .24$). The weighted mean changes were −5.6 mm Hg (95% CI, −6.5 to −4.8, $P < .001$) in central systolic BP across the 20 trials[8,18−36] and −3.3 mm Hg (95% CI, −5.0 to −1.6, $P < .001$) in pulse pressure across 12 studies.[8,18−20,22,24,26,28,30−32,35] The weighted mean changes were −3.4 mm Hg (−5.3 to −1.4, $P < .001$) in augmentation pressure across five trials[8,20,24,27,35] and −6.1% (−7.9 to −4.3, $P < .001$) in AI across 18 trials.[8,19−25,27−36]

Vasodilating versus nonvasodilating β-blockers

β-blockers have been shown to increase central systolic BP or decrease central-to-peripheral BP amplification through slowing heart rate and increasing peripheral vasoconstriction. However, β-blockers are usually classified into three generations: the first-generation nonselective β-blockers, the second-generation cardioselective (selective β1-blockade) agents, and the third-generation agents with ancillary vasodilating action, via the release of nitric oxide and antioxidative, β2-agonistic, and calcium entry blocking effects (Table 49.3).[52] The

TABLE 49.1 Trials of antihypertensive drugs versus placebo or no-treatment.

First author	Year	Blinding	Patients	No. of patients	Treatment	Arterial site	Device	Algorithm[a]	Measurements	Follow-up
Angiotensin converting enzyme inhibitors										
Dart AM[5]	2001	Open	HT	111	Perindopril	Radial	PWV medical	P2/P1	cBP, AP, and AI	12 w
Tsang TSM[6]	2006	Double	Isolated diastolic dysfunction	21	Quinapril	Radial	SphygmoCor	(P2 − P1)/PP	AI	12 m
Shahin Y[7]	2013	Double	Intermittent claudication	33	Ramipril	Radial	SphygmoCor	(P2 − P1)/PP	cBP, AP, and AI	24 w
Angiotensin receptor blockers										
Klingbeil AU[8]	2002	Double	HT	60	Valsartan	Radial	SphygmoCor	P2/P1	cBP, AP, and AI	6 w
Mitchell GF[9]	2006	Double	Heart failure	64	Candesartan	Carotid	Cardiovascular engineering	(P2 − P1)/PP	AI	6/14 m
Peters CD[10]	2014	Double	Hemodialysis	82	Irbesartan	Radial	SphygmoCor	(P2 − P1)/PP	cBP and AI	1 y
Aldosterone receptor blockers										
Boesby L[11]	2013	Open	CKD	51	Eplerenone	Radial	SphygmoCor	(P2 − P1)/PP	cBP and AI	24 w
Kalizki T[12]	2017	Double	Resistant HT	51	Eplerenone	Radial	SphygmoCor	−	cBP	26 w
Renin inhibitors										
Calhoun D[13]	2017	Double	Diabetes	21	Aliskiren	Radial	SphygmoCor	−	cBP and AP	3 m
Hwang JW[14]	2018	Open	Marfan syndrome	28	Aliskiren	Radial	SphygmoCor	(P2 − P1)/PP @HR75	cBP and AI	24 w
Diuretic										
Klingbeil AU[8]	2002	Double	HT	60	HCTZ	Radial	SphygmoCor	P2/P1	cBP, AP, and AI	6 w
Vasodilating β-blockers										
Davis JT[15]	2013	Double	Pre-HT	50	Nebivolol	Radial	SphygmoCor	(P2 − P1)/PP	cBP, AP, and AI	8 w
Werner TJ[16]	2013	Open	HT	30	Nebivolol	Carotid	Cardiovascular engineering	−	cBP	12 w
Kandavar R[17]	2015	Double	Pre-HT	34	Nebivolol	Radial	Omron	P2/P1@HR75	AI	8 w

Studies are listed in the order of the year of publication per category. *AI*, augmentation index; *AP*, augmentation pressure; *cBP*, central blood pressure; *CKD*, chronic kidney disease; *HCTZ*, hydrochlorothiazide; *HT*, hypertension; *m*, months; *w*, weeks; *y*, years.

[a]Augmentation index was calculated either by the ratio of the second peak (P2) to the first peak (P1) of the central blood pressure wave, or by augmentation pressure (P2−P1) divided by pulse pressure (PP), expressed in percent. @HR75 indicated that augmentation index was adjusted by heart rate at 75 bpm.

TABLE 49.2 Renin-angiotensin-aldosterone inhibitors and calcium-channel blockers versus diuretics, β-blockers, and α-blockers.

First author	Year	Blinding	Patients	No. of patients	Treatment	Arterial site	Device	Algorithm[a]	Measurements	Follow-up
ACEIs versus diuretics										
Dart AM[18]	2007	Open	HT	479	ACEI versus diuretic	Carotid	Millar	—	cBP	4 y
Jiang XJ[19]	2007	Double	HT	101	Enalapril versus indapamide	Radial	SphygmoCor	(P2 − P1)/PP	cBP and AI	8 w
Mackenzie IS[20]	2009	Double	HT	28	Perindopril versus bendrofluazide	Radial	SphygmoCor	(P2 − P1)/PP	cBP, AP, and AI	10 w
ACEIs versus β-blockers										
Chen CH[21]	1995	Double	HT	79	Fosinopril versus atenolol	Carotid	Millar	(P2 − P1)/PP	AI	8 w
Mackenzie IS[20]	2009	Double	HT	32	Perindopril versus atenolol	Radial	SphygmoCor	(P2 − P1)/PP	cBP, AP, and AI	10 w
Koumaras C[22]	2014	Unknown	HT	37	Quinapril versus atenolol	Radial	SphygmoCor	(P2 − P1)/PP	cBP and AI	10 w
Koumaras C[22]	2014	Unknown	HT	37	Quinapril versus nebivolol	Radial	SphygmoCor	(P2 − P1)/PP	cBP and AI	10 w
ACEIs versus α-blockers										
Jekell A[23]	2017	Double	HT	61	Doxazosin versus ramipril	Radial	SphygmoCor	(P2 − P1)/PP	cBP and AI	12 w
ARBs versus diuretics										
Klingbeil AU[8]	2002	Double	HT	40	Valsartan versus HCTZ	Radial	SphygmoCor	P2/P1	cBP, AP, and AI	6 w
ARBs versus β-blockers										
Ariff B[26]	2006	Double	HT	88	Candesartan versus atenolol	Carotid	Millar	—	cBP	52 w
Schneider MP[27]	2008	Double	HT	156	Irbesartan versus atenolol	Radial	SphygmoCor	(P2 − P1)/PP	cBP, AP, and AI	18 m
Boutouyrie P[28]	2010	Open	HT	393	Valsartan versus atenolol	Radial	SphygmoCor	(P2 − P1)/PP	cBP and AI	24 w
Radchenko GD[29]	2013	Open	HT	59	Losartan versus bisoprolol	Radial	SphygmoCor	(P2 − P1)/PP	cBP and AI	6 m
Choi MH[30]	2018	Double	Ischaemic stroke	70	Valsartan versus atenolol	Radial	Omron	(P2 − P1)/PP	cBP and AI	12 w
Choi MH[30]	2018	Double	Ischaemic stroke	70	Fimasartan versus atenolol	Radial	Omron	(P2 − P1)/PP	cBP and AI	12 w
Kim EJ[31]	2014	Open	HT	182	Losartan versus carvedilol	Radial	Hanbyul Meditech	(P2−P1)/PP	cBP and AI	24 w
Vitale C[32]	2012	Double	HT	65	Irbesartan versus nebivolol	Radial	SphygmoCor	(P2 − P1)/PP	cBP and AI	8 w

Continued

TABLE 49.2 Renin-angiotensin-aldosterone inhibitors and calcium-channel blockers versus diuretics, β-blockers, and α-blockers.—cont'd

First author	Year	Blinding	Patients	No. of patients	Treatment	Arterial site	Device	Algorithm[a]	Measurements	Follow-up
Renin inhibitors versus diuretics										
Kubota Y[33]	2013	Open	HT	30	Aliskiren versus HCTZ	Radial	Omron	P2/P1	cBP and AI	12 w
Miyoshi T[34]	2017	Open	HT	97	Aliskiren versus trichlormethiazide	Radial	Omron	P2/P1	cBP and AI	24 w
Renin inhibitors versus β-blockers										
Koumaras C[22]	2014	Unknown	HT	35	Aliskiren versus atenolol	Radial	SphygmoCor	(P2 − P1)/PP	cBP and AI	10 w
Koumaras C[22]	2014	Unknown	HT	35	Aliskiren versus nebivolol	Radial	SphygmoCor	(P2 − P1)/PP	cBP and AI	10 w
CCBs versus diuretics										
Ghiadoni L[35]	2017	Open	Metabolic syndrome	76	Lercanidipine versus HCTZ	Radial	SphygmoCor	(P2 − P1)/PP@HR75	cBP, AP, and AI	24 w
Mackenzie IS[20]	2009	Double	HT	27	Lercanidipine versus bendrofluazide	Radial	SphygmoCor	(P2 − P1)/PP	cBP, AP, and AI	10 w
Matsui Y[24]	2009	Open	HT	207	Azelnidipine versus HCTZ	Radial	SphygmoCor	(P2 − P1)/PP	cBP, AP, and AI	24 w
Doi M[25]	2010	Open	HT	37	Azelnidipine versus trichlormethiazide	Radial	Omron	P2/P1	cBP and AI	6 m
CCBs versus β-blockers										
Mackenzie IS[20]	2009	Double	HT	31	Lercanidipine versus atenolol	Radial	SphygmoCor	(P2 − P1)/PP	cBP, AP, and AI	10 w
Webster LM[36]	2017	Open	HT in pregnancy	112	Nifedipine versus labetalol	Brachial	Arteriograph	(P2 − P1)/PP	cBP and AI	130 d

Studies are listed in the order of the year of publication per category. *AI*, augmentation index; *AP*, augmentation pressure; *cBP*, central blood pressure; *d*, days; *HCTZ*, hydrochlorothiazide; *HT*, hypertension; *m*, months; *w*, weeks; *y*, years.

[a]Augmentation index was calculated either by the ratio of the second peak (P2) to the first peak (P1) of the central blood pressure wave, or by augmentation pressure (P2−P1) divided by pulse pressure (PP), expressed in percent. @HR75 indicated that augmentation index was adjusted by heart rate at 75 bpm.

TABLE 49.3 Pharmacological effects of various vasodilating β-blockers.

Drugs	Selective β1-blockade (vs. β2)	α-Blockade	Vasodilating actions
Celiprolol	√	√	Activate β2-adrenoceptors, and release nitric oxide and ANP
Nebivolol	√	−	Release nitric oxide
Nipradilol	−	√	Contain the nitric dioxide radicals in chemical structure
Carvedilol	−	√	Release nitric oxide, and antioxidative action
Carteolol	−	−	Activate β2-adrenoceptors, and release nitric oxide
Bucindolol	−	√	Activate β2-adrenoceptors, and release AMP
Betaxolol	√	−	Block Ca^{2+} entry
Bopindolol	−	−	Activate β2-adrenoceptors, and release nitric oxide
Bevantolol	√	√	Block Ca^{2+} entry
Dilevalol	−	−	Activate β2-adrenoceptors
Tilisolol	−	−	Activate ATP-sensitive K^+ channel

ANP, atrial natriuretic peptide; *AMP*, adenosine 5′-monophosphate.

third-generation β-blockers may behave differently from nonvasodilating β-blockers. A total of eight trials[22,37–43] compared vasodilating with nonvasodilating β-blockers on central hemodynamics (Table 49.4). Vasodilating compared to nonvasodilating β-blockers reduced central systolic BP and AI significantly with a weighted mean difference of −2.3 mm Hg (95% CI, −4.6 to 0.03, $P = .053$) and −2.1% (95% CI, −3.9 to −0.3, $P = .02$), respectively. The effect seemed less pronounced than RAS inhibitors and CCBs, probably because of the stroke volume enhancement of β-blockers.[53,54]

Angiotensin receptor neprilysin inhibitor versus angiotensin receptor blocker

Neprilysin is a neutral endopeptidase that degrades several potentially beneficial vasoactive peptides, including natriuretic peptides, bradykinin, and adrenomedullin. Two parallelly conducted randomized, double-blind studies compared ARNI with olmesartan on central pulsatile waves in hypertensive patients with arterial stiffness represented by high pulse pressure. The PARAMETER study[44] revealed that sacubitril/valsartan reduced central aortic systolic BP (primary outcome) greater than olmesartan [between-treatment difference: −3.7 mm Hg (95% CI, −6.4 to −0.9), $P = .01$] after 12-week treatment. Similar results were observed at 12-week treatment in the secondary outcomes, including central aortic pulse pressure (−2.4 mm Hg, $P < .012$) and mean 24-hour ambulatory central aortic systolic BP (−3.6 mm Hg, $P < .001$). However, these pressures were similar between the two groups after 52-week treatment, probably because in the olmesartan group more subjects required add-on antihypertensive therapy than the

sacubitril/valsartan group (47% vs. 32%, $P < .002$). Indeed, Schmieder found that sacubitril/valsartan reduced central aortic pulse pressure to a greater extent than olmesartan (−3.5 mm Hg, $P = .01$) after 52-week treatment, with similar add-on treatment of amlodipine (17.5% *vs.* 29.8%, $P = .12$).[45] Of note, left ventricular mass index was reduced more in the sacubitril/valsartan group, and the between-group difference was marginally significant after adjustment for systolic BP ($P = .0529$).[45]

Organic and inorganic nitrates, soluble guanylyl cyclase stimulators and cyclic guanosine monophosphate (cGMP)-binding phosphodiesterase (PDE5) inhibitors

The production of nitric oxide is important to the vasodilation in muscular arteries through cGMP-mediated processes. Organic and inorganic nitrates cause vasodilation, presumably by enzymatic degradation or conversion to nitric oxide. Soluble guanylyl cyclase (sGC) was the primary receptor for nitric oxide. PDE5 was a cGMP-specific hydrolase. Both sGC stimulators and PDE5 inhibitors regulate vasodilation by increasing the intracellular cGMP concentration. The hemodynamic effects of these agents are discussed in detail in Chapter 52.

Device-based antihypertensive therapy

RDN has proven renal safety in trials and might be efficacious in treating resistant hypertension. In a prospective study,[46] arterial stiffness was assessed by the fingertip tonometry-derived AI at baseline and three-month

TABLE 49.4 Vasodilating versus nonvasodilating β-blockers.

First author	Year	Blinding	Patients	No. of patients	Treatment	Arterial site	Device	Algorithm[a]	Measurements	Follow-up
Mahmud A[37]	2008	Single	HT	40	Nebivolol versus metoprolol	Radial	SphygmoCor	(P2 − P1)/PP	cBP and AI	4 w
Briasoulis A[38]	2013	Single	Diabetes	61	Nebivolol versus metoprolol	Radial	SphygmoCor	P2/P1 @HR75	cBP and AI	26 w
Kampus P[39]	2011	Double	HT	80	Nebivolol versus metoprolol	Radial	SphygmoCor	(P2 − P1)/PP	cBP and AI	52 w
Kandavar R[40]	2011	Unknown	HT	40	Nebivolol versus metoprolol	Unknown	Omron	P2/P1@HR75	cBP and AI	8 w
Shah NK[41]	2011	Open	HT	41	Carvedilol versus atenolol	Radial	SphygmoCor	(P2 − P1)/PP	cBP and AI	4 w
Studinger P[42]	2013	Open	HT	39	Nebivolol versus metoprolol	Brachial	Omron	(P2 − P1)/PP	cBP and AI	3 m
Studinger P[42]	2013	Open	HT	39	Carvedilol versus metoprolol	Brachial	Omron	(P2 − P1)/PP	cBP and AI	3 m
Koumaras C[22]	2014	Unknown	HT	34	Nebivolol versus atenolol	Radial	SphygmoCor	(P2 − P1)/PP	cBP and AI	10 w
Eguchi K[43]	2015	Open	HT	101	Celiprolol versus bisoprolol	Radial	Omron	P2/P1	cBP and AI	12 w

AI, augmentation index; *cBP*, central blood pressure; *HT*, hypertension; *m*, months; *w*, weeks.
[a]Augmentation index was calculated either by the ratio of the second peak (P2) to the first peak (P1) of the central blood pressure wave, or by augmentation pressure (P2−P1) divided by pulse pressure (PP), expressed in percent. @HR75 indicated that augmentation index was adjusted by heart rate at 75 bpm.

follow-up in 40 patients treated with RDN and 10 controls. RDN significantly reduced AI (30.6 ± 23.8 *vs.* $22.7 \pm 22.4\%$, $P = .002$), and the heart rate adjusted AI (22.4 ± 21.6 *vs.* $14.4 \pm 20.7\%$, $P = .002$). Changes in heart rate-adjusted AI were not correlated with BP components, indicating that RDN may function, beyond antihypertensive effect, via the regulation of smooth muscle tone or arterial wall composition.[55]

CPAP is a standard therapy for symptomatic obstructive sleep apnea (OSA), and has been reported to reduce brachial BP. In a randomized crossover trial, 44 patients with resistant hypertension and severe OSA were treated with CPAP or sham CPAP for 3 weeks and crossed over afterwards to the alternative ventilation regimen.[47] In comparison with the sham CPAP, CPAP showed a decrease in central and peripheral systolic/diastolic BP by $-4.4/-4.0$ mm Hg and $-4.6/-3.4$ mm Hg, respectively. In a longer intervention period of 8 weeks, similar reductions in central and peripheral BP were observed. Time to reflection on the pulse wave was improved with CPAP compared to the sham CPAP (3.7 ms, $P = .01$), without any between-group difference in AI.[48] In a three parallel groups trial, 139 adults with obesity and moderate and severe OSA were randomized to CPAP and weight loss alone or both for 24 weeks.[49] Only patients in the CPAP and weight loss combination group showed significant reductions in central systolic BP by 7.4 mm Hg ($P = .004$). None of these treatments significantly changed central pulse pressure, pulse pressure amplification, AI, or carotid-femoral pulse wave velocity. The effect of CPAP on central pressure seemed to be mediated by changes in mean arterial pressure rather than central pulse pressure or arterial stiffness.

Conclusions and perspectives

This review showed some efficacy of pharmaceutical- or device-based cardiovascular therapeutics on arterial hemodynamics, and confirmed divergent effects of various classes of antihypertensive drugs on central BP and AI. Nonetheless, none of the currently available antihypertensive treatments selectively or preferentially reduced central BP over and above their brachial BP lowering effect.

The mechanisms for these treatment effects remained under investigation. Because of the less central BP lowering effect of nonvasodilating β-blockers, heart rate and vasodilation or vasoconstriction must play a major role in the modulation of central hemodynamics. Indeed, in a meta-regression analysis,[56] we previously found that slowing heart rate may to a large extent explain the less efficacy of β-blockers versus the other classes of antihypertensive drugs. However, because of the divergent effects of vasodilating versus nonvasodilating β-blockers, vasoactive property must also play an important part of the central hemodynamic regulation. Studies on the I_f inhibitor ivabradine provided

further evidence. In a randomized, placebo-controlled, crossover, double-blind study in 12 normotensive patients with stable coronary artery disease, sinus heart rate ≥ 70 beats per minute and background β-blocker therapy, ivabradine treatment for 3 weeks reduced heart rate (-15.8 ± 7.7 *vs.* 0.3 ± 5.8 beats per minute, $P = .001$) and increased left ventricular ejection time (18.5 ± 17.8 *vs.* 2.8 ± 19.3 ms, $P = .074$) and diastolic perfusion time (215.6 ± 105.3 *vs.* -3.0 ± 55.8 ms, $P = .0005$), but did not significantly increase central systolic BP (-4.0 ± 9.6 *vs.* 2.4 ± 12.0 mm Hg, $P = .13$) or AI ($-0.8 \pm 10.0\%$ *vs.* $0.3 \pm 7.6\%$, $P = .87$).[57] Taken these evidence together, it is probably the interaction between heart rate and vasoactive property that determine the extent of central pressure augmentation from wave reflections. This hypothesis may be tested in future animal experiments as well as human research.

At present, there is no direct evidence regarding the clinical relevance of central hemodynamics for decision-making in the management of hypertension and cardiovascular prevention. It is therefore imperative to run adequately powered outcome trials to investigate whether central pressure and wave reflection are clinically useful in guiding antihypertensive treatment and other cardiovascular therapeutic approaches for the prevention of cardiovascular events.

References

1. Vlachopoulos C, Aznaouridis K, Stefanadis C. Prediction of cardiovascular events and all-cause mortality with arterial stiffness: a systematic review and meta-analysis. **J Am Coll Cardiol**. 2010; 55(13):1318−1327.
2. Williams B, Lacy PS, Thom SM, et al. Differential impact of blood pressure-lowering drugs on central aortic pressure and clinical outcomes: principal results of the Conduit Artery Function Evaluation (CAFE) study. **Circulation**. 2006; 113(9):1213−1225.
3. Dahlöf B, Sever PS, Poulter NR, et al. Prevention of cardiovascular events with an antihypertensive regimen of amlodipine adding perindopril as required versus atenolol adding bendroflumethiazide as required, in the Anglo-Scandinavian Cardiac Outcomes Trial-Blood Pressure Lowering Arm (ASCOT-BPLA): a multicentre randomised controlled trial. **Lancet**. 2005; 366(9489):895−906.
4. Rothwell PM, Howard SC, Dolan E, et al. Prognostic significance of visit-to-visit variability, maximum systolic blood pressure, and episodic hypertension. **Lancet**. 2010; 375(9718):895−905.
5. Dart AM, Reid CM, McGrath B, et al. Effects of ACE inhibitor therapy on derived central arterial waveforms in hypertension. **Am J Hypertens**. 2001; 14(8 Pt 1):804−810.
6. Tsang TS, Barnes ME, Abhayaratna WP, et al. Effects of quinapril on left atrial structural remodeling and arterial stiffness. **Am J Cardiol**. 2006; 97(6):916−920.
7. Shahin Y, Cockcroft JR, Chetter IC. Randomized clinical trial of angiotensin-converting enzyme inhibitor, ramipril, in patients with intermittent claudication. **Br J Surg**. 2013; 100(9):1154−1163.
8. Klingbeil AU, John S, Schneider MP, et al. AT1-receptor blockade improves augmentation index: a double-blind, randomized, controlled study. **J Hypertens**. 2002; 20(12):2423−2428.

9. Mitchell GF, Arnold JM, Dunlap ME, et al. Pulsatile hemodynamic effects of candesartan in patients with chronic heart failure: the CHARM Program. **Eur J Heart Fail**. 2006; 8(2):191−197.

10. Peters CD, Kjaergaard KD, Jensen JD, et al. No significant effect of angiotensin II receptor blockade on intermediate cardiovascular end points in hemodialysis patients. **Kidney Int**. 2014; 86(3):625−637.

11. Boesby L, Elung-Jensen T, Strandgaard S, et al. Eplerenone attenuates pulse wave reflection in chronic kidney disease stage 3-4–a randomized controlled study. **PLoS One**. 2013; 8(5):e64549.

12. Kalizki T, Schmidt BMW, Raff U, et al. Low dose-eplerenone treatment decreases aortic stiffness in patients with resistant hypertension. **J Clin Hypertens**. 2017; 19(7):669−676.

13. NCT01349114. **Effect of the Direct Renin Inhibitor Aliskiren on Endothelial Function and Arterial Stiffness in Diabetic Subjects**; 2012. clinicaltrialsgov/ct2/show/NCT01349114.

14. Hwang JW, Kim EK, Jang SY, et al. Comparison of the effect of aliskiren versus negative controls on aortic stiffness in patients with Marfan syndrome under treatment with atenolol. **Rev Esp Cardiol**. 2018; 71(9):743−749.

15. Davis JT, Pasha DN, Khandrika S, et al. Central hemodynamics in prehypertension: effect of the beta-adrenergic antagonist nebivolol. **J Clin Hypertens**. 2013; 15(1):69−74.

16. Werner TJ, Boutagy NE, Osterberg KL, et al. Singular and combined effects of nebivolol and lifestyle modification on large artery stiffness in hypertensive adults. **Ther Adv Cardiovasc Dis**. 2013; 7(6):285−292.

17. Kandavar R, Fernandez C, Sander GE, et al. Digital plethysmography and arginine metabolism in prehypertension: effect of nebivolol therapy. **J Clin Hypertens**. 2015; 17(1):14−19.

18. Dart AM, Cameron JD, Gatzka CD, et al. Similar effects of treatment on central and brachial blood pressures in older hypertensive subjects in the Second Australian National Blood Pressure Trial. **Hypertension**. 2007; 49(6):1242−1247.

19. Jiang XJ, O'Rourke MF, Zhang YQ, et al. Superior effect of an angiotensin-converting enzyme inhibitor over a diuretic for reducing aortic systolic pressure. **J Hypertens**. 2007; 25(5):1095−1099.

20. Mackenzie IS, McEniery CM, Dhakam Z, et al. Comparison of the effects of antihypertensive agents on central blood pressure and arterial stiffness in isolated systolic hypertension. **Hypertension**. 2009; 54(2):409−413.

21. Chen CH, Ting CT, Lin SJ, et al. Different effects of fosinopril and atenolol on wave reflections in hypertensive patients. **Hypertension**. 1995; 25(5):1034−1041.

22. Koumaras C, Tziomalos K, Stavrinou E, et al. Effects of renin-angiotensin-aldosterone system inhibitors and beta-blockers on markers of arterial stiffness. **J Am Soc Hypertens**. 2014; 8(2):74−82.

23. Jekell A, Kalani M, Kahan T. The effects of alpha 1-adrenoceptor blockade and angiotensin converting enzyme inhibition on central and brachial blood pressure and vascular reactivity: the doxazosin-ramipril study. **Heart Ves**. 2017; 32(6):674−684.

24. Matsui Y, Eguchi K, O'Rourke MF, et al. Differential effects between a calcium channel blocker and a diuretic when used in combination with angiotensin II receptor blocker on central aortic pressure in hypertensive patients. **Hypertension**. 2009; 54(4):716−723.

25. Doi M, Miyoshi T, Hirohata S, et al. Combination therapy of calcium channel blocker and angiotensin II receptor blocker reduces augmentation index in hypertensive patients. **Am J Med Sci**. 2010; 339(5):433−439.

26. Ariff B, Zambanini A, Vamadeva S, et al. Candesartan- and atenolol-based treatments induce different patterns of carotid artery and left ventricular remodeling in hypertension. **Stroke**. 2006; 37(9):2381−2384.

27. Schneider MP, Delles C, Klingbeil AU, et al. Effect of angiotensin receptor blockade on central haemodynamics in essential hypertension: results of a randomised trial. **J Renin Angiotensin Aldosterone Syst**. 2008; 9(1):49−56.

28. Boutouyrie P, Achouba A, Trunet P, et al. Amlodipine-valsartan combination decreases central systolic blood pressure more effectively than the amlodipine-atenolol combination: the EXPLOR study. **Hypertension**. 2010; 55(6):1314−1322.

29. Radchenko GD, Sirenko YM, Kushnir SM, et al. Comparative effectiveness of a fixed-dose combination of losartan + HCTZ versus bisoprolol + HCTZ in patients with moderate-to-severe hypertension: results of the 6-month ELIZA trial. **Vasc Health Risk Manag**. 2013; 9:535−549.

30. Choi MH, Lee JS, Lee SE, et al. Central and cerebral haemodynamic changes after antihypertensive therapy in ischaemic stroke patients: a double-blind randomised trial. **Sci Rep**. 2018; 8(1):1556.

31. Kim EJ, Song WH, Lee JU, et al. Efficacy of losartan and carvedilol on central hemodynamics in hypertensives: a prospective, randomized, open, blinded end point, multicenter study. **Hypertens Res**. 2014; 37(1):50−56.

32. Vitale C, Marazzi G, Iellamo F, et al. Effects of nebivolol or irbesartan in combination with hydrochlorothiazide on vascular functions in newly-diagnosed hypertensive patients: the NINFE (Nebivololo, Irbesartan Nella Funzione Endoteliale) study. **Int J Cardiol**. 2012; 155(2):279−284.

33. Kubota Y, Takahashi H, Asai K, et al. The influence of a direct renin inhibitor on the central blood pressure. **J Nippon Med Sch**. 2013; 80(1):25−33.

34. Miyoshi T, Murakami T, Sakuragi S, et al. Comparable effect of aliskiren or a diuretic added on an angiotensin II receptor blocker on augmentation index in hypertension: a multicentre, prospective, randomised study. **Open Heart**. 2017; 4(1):e000591.

35. Ghiadoni L, Bruno RM, Cartoni G, et al. Combination therapy with lercanidipine and enalapril reduced central blood pressure augmentation in hypertensive patients with metabolic syndrome. **Vascul Pharmacol**. 2017; 92:16−21.

36. Webster LM, Myers JE, Nelson-Piercy C, et al. Labetalol versus nifedipine as antihypertensive treatment for chronic hypertension in pregnancy: a randomized controlled trial. **Hypertension**. 2017; 70(5):915−922.

37. Mahmud A, Feely J. Beta-blockers reduce aortic stiffness in hypertension but nebivolol, not atenolol, reduces wave reflection. **Am J Hypertens**. 2008; 21(6):663−667.

38. Briasoulis A, Oliva R, Kalaitzidis R, et al. Effects of nebivolol on aortic compliance in patients with diabetes and maximal renin angiotensin system blockade: the EFFORT study. **J Clin Hypertens**. 2013; 15(7):473−479.

39. Kampus P, Serg M, Kals J, et al. Differential effects of nebivolol and metoprolol on central aortic pressure and left ventricular wall thickness. **Hypertension**. 2011; 57(6):1122−1128.

40. Kandavar R, Higashi Y, Chen W, et al. The effect of nebivolol versus metoprolol succinate extended release on asymmetric dimethylarginine in hypertension. **J Am Soc Hypertens**. 2011; 5(3):161−165.

41. Shah NK, Smith SM, Nichols WW, et al. Carvedilol reduces aortic wave reflection and improves left ventricular/vascular coupling: a

comparison with atenolol (CENTRAL Study). **J Clin Hypertens**. 2011; 13(12):917−924.

42. Studinger P, Tabák ÁG, Chen CH, et al. The effect of low-dose carvedilol, nebivolol, and metoprolol on central arterial pressure and its determinants: a randomized clinical trial. **J Clin Hypertens**. 2013; 15(12):910−917.

43. Eguchi K, Hoshide S, Kario K. Effects of celiprolol and bisoprolol on blood pressure, vascular stiffness, and baroreflex sensitivity. **Am J Hypertens**. 2015; 28(7):858−867.

44. Williams B, Cockcroft JR, Kario K, et al. Effects of sacubitril/valsartan versus olmesartan on central hemodynamics in the elderly with systolic hypertension: the PARAMETER Study. **Hypertension**. 2017; 69(3):411−420.

45. Schmieder RE, Wagner F, Mayr M, et al. The effect of sacubitril/valsartan compared to olmesartan on cardiovascular remodelling in subjects with essential hypertension: the results of a randomized, double-blind, active-controlled study. **Eur Heart J**. 2017; 38(44):3308−3317.

46. Hering D, Lambert EA, Marusic P, et al. Renal nerve ablation reduces augmentation index in patients with resistant hypertension. **J Hypertens**. 2013; 31(9):1893−1900.

47. Litvin AY, Sukmarova ZN, Elfimova EM, et al. Effects of CPAP on "vascular" risk factors in patients with obstructive sleep apnea and arterial hypertension. **Vasc Health Risk Manag**. 2013; 9:229−235.

48. Hoyos CM, Yee BJ, Wong KK, et al. Treatment of sleep apnea with CPAP lowers central and peripheral blood pressure independent of the time-of-day: a randomized controlled study. **Am J Hypertens**. 2015; 28(10):1222−1228.

49. Jain S, Gurubhagavatula I, Townsend R, et al. Effect of CPAP, weight loss, or CPAP plus weight loss on central hemodynamics and arterial stiffness. **Hypertension**. 2017; 70(6):1283−1290.

50. London GM, Pannier B, Guerin AP, et al. Cardiac hypertrophy, aortic compliance, peripheral resistance, and wave reflection in end-stage renal disease. Comparative effects of ACE inhibition and calcium channel blockade. **Circulation**. 1994; 90(6):2786−2796.

51. Asmar RG, London GM, O'Rourke ME, et al. Amelioration of arterial properties with a perindopril-indapamide very-low-dose combination. **J Hypertens Suppl**. 2001; 19(4):S15−S20.

52. Toda N. Vasodilating beta-adrenoceptor blockers as cardiovascular therapeutics. **Pharmacol Ther**. 2003; 100(3):215−234.

53. Cockcroft J. Nebivolol: a review. **Expert Opin Pharmacother**. 2004; 5(4):893−899.

54. Metra M, Giubbini R, Nodari S, et al. Differential effects of beta-blockers in patients with heart failure: a prospective, randomized, double-blind comparison of the long-term effects of metoprolol versus carvedilol. **Circulation**. 2000; 102(5):546−551.

55. Hao Z, Jiang X, Sharafeih R, et al. Stimulated release of tissue plasminogen activator from artery wall sympathetic nerves: implications for stress-associated wall damage. **Stress**. 2005; 8(2):141−149.

56. Ding FH, Li Y, Li LH, et al. Impact of heart rate on central hemodynamics and stroke: a meta-analysis of beta-blocker trials. **Am J Hypertens**. 2013; 26(1):118−125.

57. Dillinger JG, Maher V, Vitale C, et al. Impact of ivabradine on central aortic blood pressure and myocardial perfusion in patients with stable coronary artery disease. **Hypertension**. 2015; 66(6):1138−1144.

This page intentionally left blank

Chapter 50

Pharmacologic approaches to reduce arterial stiffness

Marina Cecelja and Phil Chowienczyk

British Heart Foundation Centre, King's College London, Department of Clinical Pharmacology, St Thomas' Hospital, London, United Kingdom

Introduction

Given the physiological importance of aortic stiffening and its association with clinical events and mortality, there has been intense interest as to whether it can be prevented or reversed. Reduction of blood pressure leads to an immediate reduction in arterial stiffness as measured by carotid-femoral PWV, but this is probably mediated in large part by an indirect effect to reduce the distension of the arterial wall and/or an alteration of tone in the vascular smooth muscle of the aorta and large arteries. The various biologic pathways that lead or contribute to large artery stiffening are discussed in detail in Chapters 19−25. The effects of common vasoactive drugs on arterial stiffness and pulsatile hemodynamics are discussed in Chapter 49. This chapter will focus on pharmacological therapies that have a specific effect to reduce large artery stiffness via an action on the structure of the arterial wall. These mostly target the extracellular matrix in the media layer of large arteries (Fig. 50.1).

We first discuss potential therapeutic targets for arterial destiffening and preclinical studies of destiffening, to then focus on clinical studies.

Potential therapeutic targets for arterial destiffening: preclinical studies
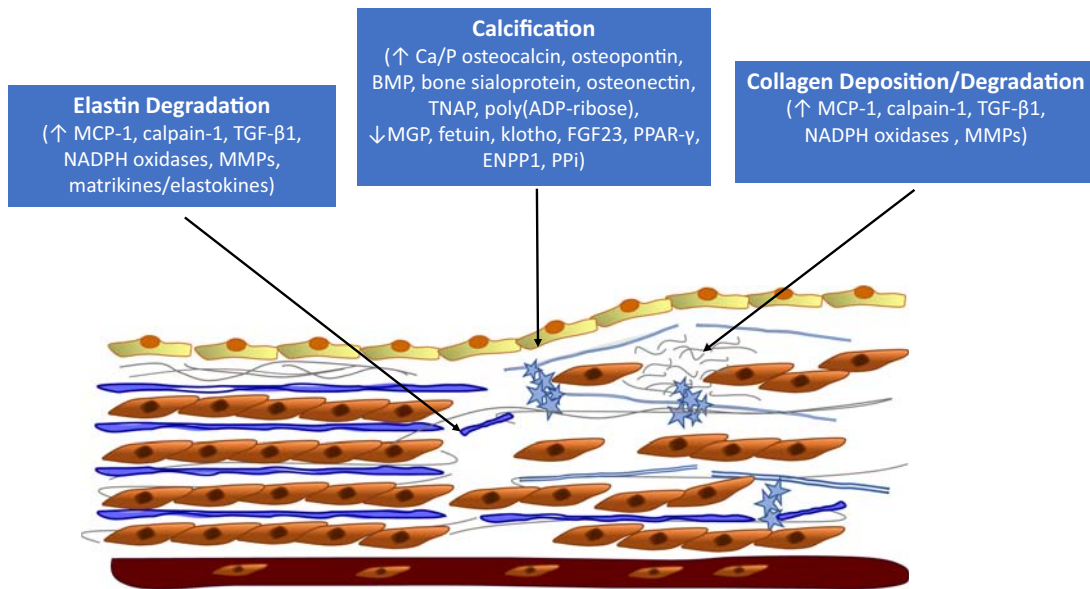
Inflammation and oxidative stress

Various mechanisms may underlie the association between inflammation and oxidative stress and arterial stiffening, including elastin degradation (Chapter 19), collagen accumulation, and medial calcification (Chapter 21).[1,2] Inflammation (Chapter 20) is thought to be induced by vascular and other stressors which initiate inflammatory processes through transcription factors and other downstream signaling molecules. A phenotypic shift in vascular
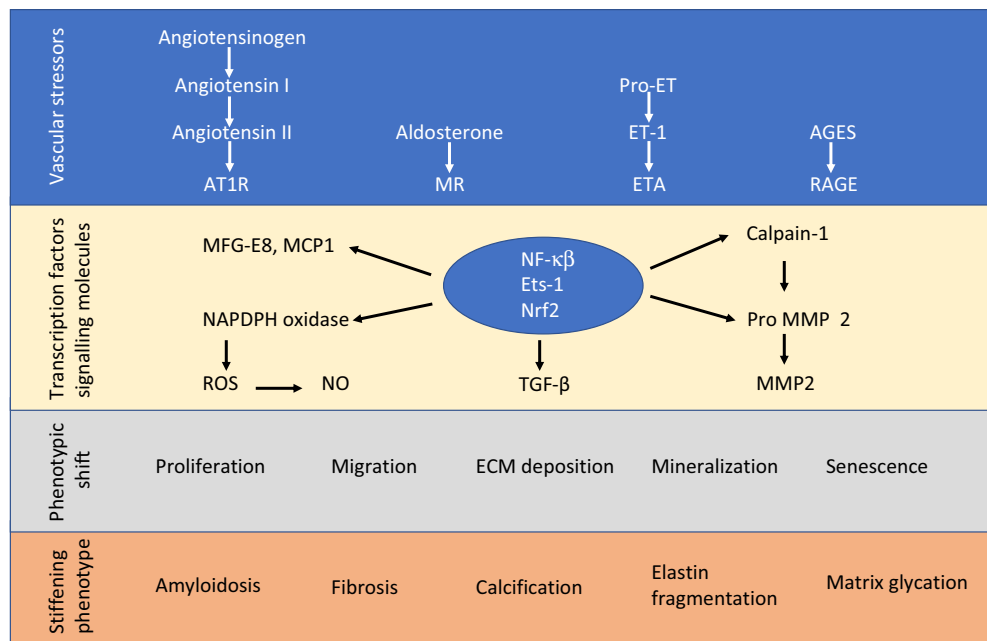
smooth muscles cells is involved (Chapter 22) which leads to their proliferation, migration, deposition of collagen within the extracellular matrix, and calcification of this matrix. This leads to the final vascular stiffening phenotype that may involve elastin fragmentation, deposition of collagen and amyloid, fibrosis, glycation and cross-linking of matrix components, and calcification (Fig. 50.2).

In young rats, chronic infusion of angiotensin II increases the activation of inflammatory transcription factors within the arterial wall[3] inducing a proinflammatory signaling profile characterized by an increase in monocyte chemoattractant protein-1, calpain-1, transforming growth factor-β1 (TGF-β1), and also increased expression of matrix metalloproteinase-2 (MMP-2) and oxidative stress[4] which collectively increase arterial stiffness. Increased TGF-β1 signaling leads to increased synthesis of collagen by vascular smooth muscle cells (VSMCs)[5] and increased expression of MMP-2, which degrades elastin within the arterial wall further contributing to arterial stiffness.[6] In normotensive male rats, inhibition of angiotensin-converting enzyme inhibits proinflammatory molecules and age-associated arterial stiffening.[7]

A further consequence of the proinflammatory state is increased oxidative stress as characterized by increased NADPH oxidases that interact synergistically with inflammation.[8] Excess NADPH oxidase activity leads to increased arterial superoxide levels and inactivation of nitric oxide (NO),[9] alongside inadequate upregulation of cellular antioxidant defenses.[10] In mice, resveratrol, a polyphenol that activates the deacetylase sirtuin-1 (and also inhibits mTOR pathways as described below[11]), prevented an increase in vascular inflammation and oxidative stress induced by a high fat high sucrose diet as well as preventing an increase in aortic stiffness.[12] Administration of SRT1720, a sirtuin-1-specific activator, effectively reversed diet-induced aortic stiffness alongside stimulation of

FIGURE 50.1 Structural change in the arterial wall driving arterial stiffening is thought to involve elastin degradation, collagen deposition, and calcification in the media of the arterial wall. *BMP*, bone morphogenic protein; *Ca*, calcium; *ENPP1*, ectonucleotide pyrophosphatase/phosphodiesterase 1; *FGF23*, fibroblast growth factor 23; *MCP-1*, monocyte chemoattractant protein-1; *MGP*, matrix gla protein; *MMPs*, matrix metalloproteinases; *NADPH*, nicotinamide adenine dinucleotide phosphate oxidase; *P*, phosphate; *PPAR-γ*, peroxisome proliferator−activated receptor gamma; *PPi*, pyrophosphatase inhibitor; *TGF-β*, transforming growth factor beta; *TNAP*, tissue nonspecific alkaline phosphatase.

FIGURE 50.2 Vascular and other stressors including angiotensin II, aldosterone, endothelin, and advanced glycosylation end products generate inflammation through transcription factors and downstream signaling molecules. These include calpain-1, MMPs, MCP-1, and TGF-β1 and NADPH oxidase. Activation of calpain-1, MMPs, TGF-β1, and NADPH oxidase increases oxidative stress and NO bioavailability decreases. There is a phenotypic shift in vascular smooth muscle cell that leads to proliferation, migration, deposition of collagen in the extracellular matrix, mineralization, and senescence. This leads to the final phenotype of stiffening in which there is deposition of amyloid, collagen, elastin fragmentation, fibrosis, calcification, and matrix glycation. *ETA*, endothelin-1 receptor A; *ET-1*, endothelin-1; *Ets-1*, v-ets erythroblastosis virus E26 oncogene homolog 1; *MCP-1*, monocyte chemoattractant protein-1; *MFG-E8*, milk fat globule epidermal growth factor-8; *MMPs*, matrix metalloproteinases; *MR*, aldosterone/mineralocorticoid receptor; *NADPH oxidase*, nicotinamide adenine dinucleotide phosphate oxidase; *NF-κB*, nuclear factor kappa-light-chain enhancer of activated B cells; *Nrf-2*, NF-E2-related factor 2; *NO*, nitric oxide; *TGF-β*, transforming growth factor beta.

antiinflammatory and antioxidant pathways.[12] These findings have also been replicated in nonhuman primates on high caloric diets.[13] Sirtuin activity can also be increased by nicotinamide mononucleotide. In old mice with increased arterial stiffness, supplementation with nicotinamide mononucleotide reduces arterial stiffness alongside a reduction in markers of oxidative stress and increase in elastin and inhibition of collagen.[14]

Vascular mitochondrial oxidative stress, another source of vascular oxidative stress, is associated with excessive production of mitochondria-derived reactive oxygen species (mtROS) produced as a result of cellular metabolism. Mice deficient in mitochondrial antioxidant protein manganese superoxide dismutase (SOD2) exhibit arterial stiffening.[1] mtROS may promote stiffening through several pathways including redox-related alterations in matrix protein turnover altering the breakdown of collagen and elastin.[15–17] A consequence of increased mtROS is mitochondrial DNA damage, which in turn drives maturation of proinflammatory cytokines.[15,18,19] In male mice, the mitochondria-targeted antioxidant MitoQ, which lowers mitochondrial oxidative stress, prevented age-associated increases in aortic pulse wave velocity in old (27 month) but not in young (6 months) mice. MitoQ did not affect collagen expression or cytokine expression but did partially preserve elastin expression.[20] Curcumin, a naturally occurring polyphenol found in the spice turmeric, has been associated with reduced oxidative stress. In old (26–28 month) C57BL6/N mice supplementation with curcumin restored large artery stiffness to levels similar to that seen in young (4–6 month) mice, ameliorating age-associated oxidative stress and collagen deposition.[21]

Conditions of low cellular energy which can be induced by selective nutrient deprivation, exercise or hypoxia, are associated with increased oxidative stress. They activate adenosine monophosphate (AMP)-activated protein kinase (AMPK) which then phosphorylates a diverse number of targets to direct cell metabolism toward adenosine triphosphate (ATP) generating catabolic pathways such as fatty acid oxidation, autophagy, and glucose utilization and away from ATP-consuming anabolic pathways (e.g., fatty acid, lipid and protein synthesis, and cell growth and proliferation).[22] mTOR kinase, part of two multiprotein complexes, mTORC1 and mTORC2, is a kinase which when activated (for example, by insulin and growth factors) regulates ATP-consuming anabolic pathways and suppresses ATP-generating catabolic pathways.[22] In mice, aging is associated with increased mTOR activation,[23] whereas downregulation of mTORC1 in genetically modified murine models[24] and via pharmaceutical interventions has been associated with an increased lifespan.[25] Rapamycin may inhibit mTOR and in mice fed a rapamycin supplemented or control diet for 6–8 weeks, age-related increases in mTOR activation were inhibited by

rapamycin. In old mice (30 months), rapamycin inhibited NADPH oxidase expression and superoxide production which were comparable to that of young (4 months) mice. Importantly, an age-associated increase in aortic stiffness evidenced by higher pulse wave velocity in old compared to young mice was inhibited and collagen content reduced by treatment with rapamycin.[23] These potential antiaging properties of rapamycin have led to interest in developing less toxic analogues of rapamycin that could be used in clinical studies.[26] The findings that drugs which act to reduce oxidative stress and increase lifespan also reduce arterial stiffness are consistent with calorie restriction successfully prolonging lifespan and reducing arterial stiffness in animal models.[27]

Vascular calcification

Calcification of the vessel wall contributes to increased arterial stiffness.[28] Mechanisms that lead to vascular calcification are discussed in detail in Chapter 21. Briefly, vascular calcification is now known to be an active process resembling osteogenesis in which VSMCs undergo osteogenic differentiation, losing their contractility markers (αSM0actin and α-SM22) and expressing many of the proteins associated with bone formation including osteocalcin, osteopontin, bone morphogenic protein (BMP), bone sialoprotein, osteonectin, and collagen.[29] These proteins often accumulate in areas of metabolically active calcification and have a high binding affinity for calcium salts. The phenotypic shift of VSMC seems to be induced by various conditions which include a proinflammatory environment[30,31] and oxidative stress.[32,33] Osteogenically differentiated VSMCs also release apoptotic bodies and matrix vesicles into the extracellular matrix which serves as nucleation sites for accumulation of hydroxyapatite crystals.[34,35] In healthy individuals, precipitation of calcium in tissue is inhibited by regulatory factors including matrix gla protein (MGP), fetuin, klotho, and fibroblast growth factor 23 (FGF23). It is likely that initiation and progression of calcification is dependent on complex cellular interactions between promoters and inhibitors of calcification and the exact mechanism of mineral nucleation is not fully elucidated. Collagen is the predominant extracellular matrix component around which mineralization occurs.[36] However, as discussed in detail in Chapter 19, elastin degradation also promotes calcification through elastin-derived soluble peptides (matrikines or elastokines) which can also activate VSMC osteogenic differentiation,[37] and increase matrix affinity for nucleating mineral deposition.[38]

Rat and mouse animal models of vascular calcification fall into two predominant categories: naturally occurring age-dependent calcification (e.g., DBA2 mice and polycystic kidney disease) or calcification induced by various interventions.[39] Treatment with large doses of vitamin D
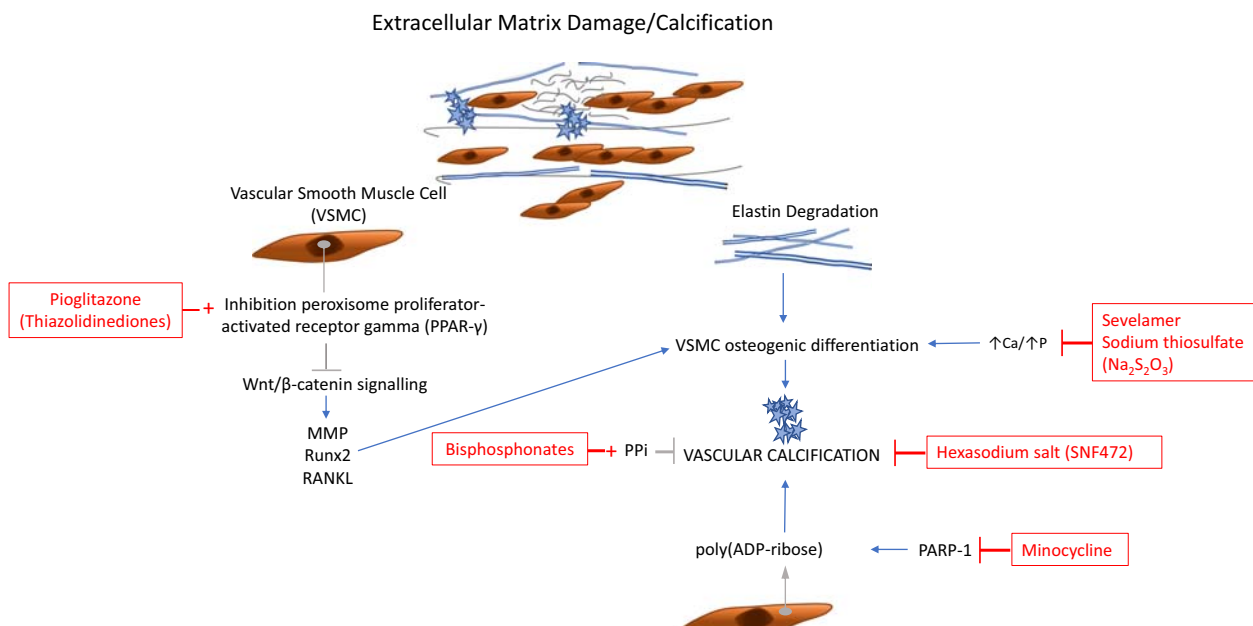
and nicotine, for example, leads to a proinflammatory state, medial calcification, and increased wall stiffness. The potential interplay between inflammation and calcification in this model is illustrated by a study in which pioglitazone, which is thought to have antiinflammatory actions via activation of peroxisome proliferator–activated receptor gamma (PPAR-γ), reduced medial calcification alongside a reduction in inflammatory markers, elastin fragmentation, and arterial stiffness.[40] Several genetically modified mouse models are characterized by calcification and include those leading to alterations in matrix gla protein, osteopontin, and ectonucleotide pyrophosphatase/phosphodiesterase-1 (ENPP1). ENPP1 converts ATP into adenosine 5′-monophosphate (AMP) and pyrophosphate (PPi), an endogenous inhibitor of hydroxyapatite formation. PPi is hydrolyzed by tissue-nonspecific alkaline phosphatase (TNAP) and overexpression of TNAP is associated with vascular calcification. Mutations in ATP-binding cassette C6 (ABCC6) mouse models lead to vascular calcification through incompletely understood mechanisms but which are likely to include regulation of PPi. Findings by Ziegler et al.[41] suggest that ABCC6 acts in concert with ENPP1 to regulate PPi.

Actions of PPAR-γ inhibitors and other drugs that may have more specific effects to prevent calcification are summarized in Fig. 50.3.

Bisphosphonates probably have multiple actions to inhibit arterial calcification: acting as a nonhydrolyzable analogue of PPi and a TNAP inhibitor (in $Abcc6^{-/-}$ mice they attenuate the development and progression of vascular calcification[42]), blocking apatite crystal formation,[43] inhibiting metalloproteinases,[44] and inhibiting expression of tumor necrosis factor-α, which promotes osteoblastic differentiation of vascular cells.[45] They can be metabolized by phagocytes into nonhydrolyzable adenine-containing analogues of ATP,[46] which inhibit adenine nucleotide translocase, promoting the activation of caspase-3 and leading to apoptosis of macrophages and osteoclasts.[47]

In chronic kidney disease, hyperphosphatemia and a raised serum calcium–phosphate product is associated with vascular calcification. The potential importance of the calcium–phosphate product is illustrated by a study in uremic rats fed on a high phosphorus diet for 6 months, treated with a calcium-containing phosphate blocker and sevelamer, a noncalcium containing phosphate blocker. Even though both treatment regiments effectively reduced phosphate levels, only sevelamer-treated rats reduced vascular calcification.[48] Sodium thiosulfate ($Na_2S_2O_3$) has antioxidant properties[49] and chelates calcium to form soluble calcium thiosulfate complexes.[50] Pasch et al.[51] found that uremic rats treated with thiosulfate did not develop aortic calcification compared to untreated control rats; this was associated with increased urinary calcium excretion and reduced bone strength. Preclinical studies of a hexasodium salt (SNF472) with the active ingredient myo-inositol hexaphosphate (IP6) which binds to sites of hydroxyapatite crystals have demonstrated reduced development of calcification[52] and reduced progression of established calcification in uremic and nonuremic rodent models of calcification.[53]

FIGURE 50.3 Pathways of extracellular matrix damage and calcification. *Ca*, calcium; *MMP*, matrix metalloproteinase; *PARP-1*, poly (ADP-ribose)-1; *P*, phosphate; *PPi*, pyrophosphatase inhibitor; *RANKL*, Receptor activator of nuclear factor kappa-b ligand; *Runx2*, Runt-related transcription factor 2.

Another potentially exciting therapeutic target for vascular calcification and stiffening is poly(ADP-ribose) (PAR) which is a posttranslational polymer of two or more ADP-ribose units added to proteins by the enzymes PAR polymerases (PARPs) in a process called PARylation. PAR is found in developing fetal bone and the dominant PARPs are expressed in response to oxidative stress.[54,55] Muller et al.[56] showed that PAR can generate calcified spherical particles and bone-like calcification of collagen fibrils. Importantly, in a uraemic rat model, treatment with minocycline (a widely used antibiotic, 5–50 mg/hg), which directly inhibits PARP-1, reduced calcification in the aorta, femoral and carotid arteries. This is a potentially exciting area that could be directly translated into human clinical pharmacology since minocycline is widely used as an antibiotic in humans and has low toxicity. However, it can cause gastrointestinal disturbances, photosensitivity reactions, and rarely more serious side effects that may limit long-term use. Other related tetracycline antibiotics which may also inhibit PARP-1 are also in human use.

Elastase inhibitors and extracellular matrix metalloproteases

Extracellular matrix components, particularly elastin and collagen, are fundamental structural components of large arteries. Pathological processes relating to these structural proteins, such as elastin fragmentation/degradation, collagen accumulation, and cross-linking, are thought to be key mechanisms underlying age-related arterial stiffening.[1] As discussed above, elastin degradation may also promote calcification by activating VSMC osteogenic differentiation.[37] As discussed in more detail in Chapter 19, elastin can be degraded by proteolytic enzymes with "elastase-like" activity including serine and cysteine (cathepsins) proteases and MMPs.[57] MMPs are proteins which are involved in the breakdown of the extracellular matrix and their activity is increased in aged vascular cells.[58,59] Tissue inhibitors of MMPs (TIMPs) are likely to play a role in regulating extracellular matrix components. In a rat aneurysm model, local application of TIMP-1 preserved elastin in the media and prevented aneurysm rupture.[28] MMPs also activate TGF-β1[31] further contributing to a proinflammatory vascular state. In 16-month-old rats, administration of a broad-spectrum MMP inhibitor, PD166739, reduced age-associated arterial proinflammatory signaling, reduced elastic fiber degeneration and collagen deposition, and prevented the age-associated increase in blood pressure (consistent with a reduction in stiffening).[31] Other inhibitors of MMP include zinc chelators, marimastat, and the antibiotic doxycycline.[60] In hypertensive rats, doxycycline favorably altered the ratio of MMP-2 to TIMP-2, preventing hypertension and arterial wall thickening.[61] In a "two-kidney one clip" hypertensive rat model, doxycycline

reduced MMP-2 and prevented a rise in blood pressure.[62] In male Wistar rats, where calcification was induced with warfarin and vitamin D, doxycycline prevented calcification,[63] but may also have had actions through PARP-1 inhibition as discussed above. Not all studies with doxycycline have been positive: in a spontaneously hypertensive rat model, even though doxycycline improved structural alterations, blood pressure and PWV were not affected.[64]

Micro-RNAs

Micro-RNAs (miRNAs) are small (19–25 nucleotide long) noncoding posttranscriptional regulators of gene expression that have been implicated in the regulation of most biological processes including arterial stiffness.[65] miR-765, miR-1185, miR-181b, and miR-21, in particular, have been implicated in arterial stiffness.[66,67] Although the exact mechanisms by which miRNA signaling pathways modulate arterial stiffness are unclear, reduction of miR-181b expression is associated with activation of the TGF-β pathway, inflammation, accumulation of collagen, and arterial stiffening.[68] Deletion of the microRNA-degrading complex that degrades miR-181b prevented arterial stiffening associated with chronic high salt intake in mice.[65] miRNA may also play a central role in VSMC phenotype modulation and/or vascular relaxation. Experimental data investigating whether pharmacological intervention of miRNA signaling pathways could lead to a reduction of arterial stiffness are limited. In uremic dilute-brown agouti 2 (DBA/2) mice susceptible to high-phosphate diet–induced calcification, intravenous injections of a synthetic miR-142-3p mimic restored acetylcholine induced smooth muscle relaxation but showed no effect on vascular calcification.[69]

Mineralocorticoid receptor antagonism

Mineralocorticoid steroid hormones, such as aldosterone, are secreted in response to an increase in extracellular potassium ion concentration or activation of the renin–angiotensin system. Mineralocorticoid receptor (MR) activation by aldosterone regulates blood pressure by modulating renal sodium reabsorption and body fluid volume through myogenic tone, vasoconstriction, and redox signaling.[70] In addition to its traditional role as a blood pressure regulator, MRs are now increasingly recognized as playing a role in arterial stiffness independently of blood pressure regulation. MR activation may have profibrotic actions mediated by multiple mechanisms including oxidative stress, inflammation, and associated increase in connective tissue growth factor, MMP-2, and BMP-4.[71] In animal models, MR expression in VSMCs increases with increasing age.[72] MR activation activates NADPH oxidase-dependent superoxide production and inactivation of

NO.[9,73] MR antagonists (MRA) reverse this with a reduction in NADPH oxidase activity, reduction in superoxide formation, and improvement in NO bioavailability.[74] In mice fed a high fat/high sugar western diet, administration of the MRA spironolactone for 4 months prevented stiffening, inflammation, and fibrosis[75] without a change in mean arterial pressure or heart rate.[75] In spontaneously hypertensive rats, 4-month treatment with spironolactone prevented collagen accumulation in the presence of a small antihypertensive effect.[76] In old normotensive rats, 8-week treatment with spironolactone reduced arterial collagen and elastin densities alongside a reduction in arterial stiffness compared to placebo-treated animals.[77] These changes occurred independently of any change in intraarterial blood pressure and arterial wall thickness. In a rat model of chronic kidney disease, treatment with finerenone, a novel nonsteroidal potent MRA, lowered arterial stiffness in parallel with a change in collagen and elastin organization, reduction in MMP-2, MMP-9, and oxidative stress.[78] Low intracellular potassium in VSMC is associated with a prolonged increment of intracellular calcium linked to osteogenic differentiation of VSMC.[79] In an apolipoprotein-E deficient mouse model, Sun et al.[79] demonstrated that dietary potassium supplementation attenuated vascular calcification and aortic stiffness. Elevation of intracellular potassium by mineralocorticoid receptor antagonism could, therefore, be another mechanism through which these agents may influence arterial stiffening.

Amyloid-β and arterial stiffness

In humans, amyloid protein known as medin, which binds to tropoelastin, is deposited in the media of the aged arterial wall.[80] This has raised interest in the possibility that amyloid deposition in the arteries and brain is a mechanism to explain the association between arterial stiffness and cognitive decline. However, it should be remembered that both of these processes are strongly age-dependent and there are other potential mechanisms to explain the association such as the susceptibility of the cerebral microvasculature to high pulsatile pressure induced by arterial stiffening. There have been limited animal studies on the role of amyloid in arterial stiffening as most animal models do not naturally accumulate amyloid-β.[81]

Clinical studies on aortic and large artery destiffening

Clinical studies on arterial stiffness have largely focused on existing drugs that have established indications for conditions known to relate to cardiovascular disease and may also reduce arterial stiffness through various mechanisms. In addition, there have been a few studies on drugs specifically designed to reduce stiffness. Most studies have used a measure of pulse wave velocity (PWV) over a pathway that incorporates the aorta, usually carotid-femoral PWV (cfPWV) but with some including additional conduit pathways such as brachial-ankle PWV (baPWV). Some studies have used other measurements thought to relate in part to arterial stiffness such as augmentation index. With the recognition that the latter is influenced by many factors other than arterial stiffness, this review concentrates mainly on PWV data.

Drugs inhibiting the renin−angiotensin−aldosterone system and mineralocorticoid antagonists

Angiotensin II and aldosterone may promote inflammation and fibrosis within the arterial wall and there has been interest in whether antihypertensive drugs that inhibit the renin−angiotensin−aldosterone system (RAAS) such as angiotensin-converting enzyme inhibitors (ACEis), angiotensin receptor blockers (ARBs), and mineralocorticoid receptor antagonists (MRAs) may have a specific action to reduce arterial stiffness. Evaluation of this in clinical studies is complicated by the fact that these drugs also relax vascular smooth muscle and reduce blood pressure. Elastic properties of the arterial wall are dependent on stretch of the wall which may transfer load from highly elastic components such as elastin to stiffer components such as collagen. Stretch is dependent on ambient blood pressure and therefore any intervention that lowers blood pressure would be expected to lower stiffness by an indirect action. Similarly, relaxation of smooth muscle within the wall of the aorta may modulate stiffness independent of any action on wall structure. Thus, although almost all studies of antihypertensive drugs show a reduction in cfPWV, interest has been in comparing effects at comparable levels of blood pressure reduction. One metaanalysis suggested that ACEi do have a small but significant blood pressure−independent action to lower cfPWV and baPWV[82] but others have shown no specific effect.[83,84] MRA may have a more specific effect to inhibit fibrosis in the arterial wall and one well-controlled trial examining effects of spironolactone on cfPWV in patients with early chronic kidney disease demonstrated a blood pressure independent effect of spironolactone to reduce cfPWV.[85] However, this was not confirmed in the recent Vasera trial comparing spironolactone to doxazosin.[86]

Statins and other lipid lowering therapy

Although the etiology of arterial stiffening differs from that of atherosclerosis, there may be some overlap between the two pathologies and statins have pleiotropic effects including antiinflammatory and antioxidant effects that could reduce arterial stiffening. Results of RCT involving

statins have been somewhat discordant. However, two relatively recent metaanalyses have been performed which both suggest a modest positive effect to lower cfPWV.[87,88] The most recent identified 11 RCT in which treatments with and without statins were compared involving 573 individuals. This demonstrated modest 6.8% [95% CI 1.8−11.7] reduction in cfPWV.[87] There was significant heterogeneity between studies but the effect was independent of change in blood pressure. There is little relationship between cfPWV and low-density lipoprotein cholesterol (LCL-C) or ratio of LDL-C to high-density lipoprotein cholesterol (HDL-C) in epidemiological studies[89] and in the interventional studies with statins no relationship between change in cfPWV and that in LDL-C was seen[87] suggesting effects may be more likely to be due to pleiotropic effects of statins. However, in an observational study in which ezetimbe or a PCSK9 inhibitor was added to high dose statin therapy in patients with familial hypercholesterolaemia achieving a large range of reduction of low-density lipoprotein cholesterol (LDL-C), an improvement in PWV was seen which correlated with the change in LDL-C.[90] Thus, the mechanism by which statins and other lipid lowering drugs may reduce PWV remains uncertain.

Antioxidant vitamins and vitamin B12/folate supplementation

Clinical trials examining effects of antioxidant vitamins include early trials of vitamins C, E, A, and beta-carotene. These were performed in small numbers of individuals and although a metaanalysis suggested a small but significant positive effect on various measures of arterial stiffness including cfPWV,[91] the finding that supplementation with these vitamins does not reduce cardiovascular risk (or may increase risk)[92,93] raises the question as to whether this positive finding with regard to effects on arterial stiffness was due to publication bias and there has been little enthusiasm for further large studies. However, it should be noted that lack of efficacy of conventional antioxidant vitamins to reduce cardiovascular risk or arterial stiffness does not necessarily disprove the importance of oxidative stress since these vitamins are weak antioxidants which may not decease oxidative stress at a cellular level.[94]

Elevated homocysteine is associated with increased cardiovascular risk[95] and increased arterial stiffness[96] and alongside trials to determine if homocysteine lowering therapy with vitamin B12 and folic acid decreases cardiovascular risk, effects of this supplementation on PWV have been examined. A number of small studies have been positive. However, in a substudy of the B-PROOF study involving supplementation of 569 elderly individuals with B12/folic acid for 2 year, achieving a lowering of homocysteine of 3.6 µmol/L in the active treatment group, there was no significant effect of homocysteine lowering on cfPWV.[97] This trial is notable for being one of the few relatively long-term clinical trials of an intervention to lower cfPWV.

Antidiabetic drugs and advanced glycosylation end-product breakers

Presence of type 2 diabetes is associated with increased arterial stiffness,[98] and with the recognition that antidiabetic drugs may differ in their effects on cardiovascular outcomes, there has been interest in whether these drugs influence arterial stiffness. However, studies have been predominantly exploratory with small sample size (typically <50 patients) and not all have been controlled or randomized. A metaanalysis suggests that dipeptidyl peptidase-4 (DPP-4) inhibitors and glucagon-like peptide-1 receptor agonists (GLP-1 RA) have modest effects to lower PWV.[99] However, there was significant heterogeneity between studies. In a randomized controlled cross-over study, the selective sodium−glucose cotransporter 2 inhibitor empagliflozin resulted in a reduction in measures of central blood pressure and a small but significant reduction in an indirect estimate of PWV.[100] Hypertension and diabetes are associated with the accumulation of advanced glycation end products (AGEs) formed from nonenzymatic cross-links between glucose and amino groups on proteins. These accumulate in the extracellular matrix to cause stiffening and also bind to AGE receptors (RAGEs) to generate oxidative stress and inflammation and increase stiffness as described above (Fig. 50.2). Preclinical experimental studies in animals using AGE cross-link breakers show an impressive reduction of arterial stiffening and improvement in hemodynamics. A notable early RCT using the cross-link breaker ALT-177 (alagebrium) in hypertensive patients with high pulse pressure demonstrated a reduction in pulse pressure. However, this was a relatively small study and there was no significant reduction in cfPWV.[101] Despite some positive findings in open label uncontrolled studies,[102,103] subsequent RCTs have been largely negative. No benefit was seen in exercise tolerance or secondary measures of cardiac function in patients with heart failure.[104] Another randomized controlled study in healthy, previously sedentary seniors showed no effect on hemodynamics, LV geometry, or exercise capacity. However, it did show a modestly favorable effect on age-associated LV stiffening (measured from LV pressure−volume curves obtained from echocardiography and right heart catheterization during modulation of preload).[105] Thus, while a well-powered RCT remains to be performed to address effects of cross-link breakers on arterial stiffness, these negative results underline the difficulty in extrapolating from experimental animal studies to clinical studies.

Antiinflammatory drugs

Given the evidence for the role of inflammation and inflammatory cytokines in arterial stiffening and preclinical studies indicating a positive effect of antiinflammatory drugs on arterial stiffening, there has been much interest in the biological therapies for inflammation, that are markedly effective in reducing the clinical burden of diseases such as inflammatory arthritidies,[106] inflammatory bowel,[107] and skin disease.[108] Studies on arterial stiffness have been mainly in these cohorts of patients in whom there is a clinical indication for an antiinflammatory drug and most involving biological agents inhibiting tumor necrosis factor-α or various interleukins. Early studies reported positive effects in uncontrolled studies[109] but later RCTs have been largely negative. A recent systematic review identified 22 studies comparing effects of TNFα biologics on arterial stiffness mostly assessing cfPWV but only four of these were RCT and all of the RCT were negative.[110] A discrepancy between uncontrolled and randomized trials on various measures of subclinical atherosclerosis and arteriosclerosis was a common finding, suggestive of significant publication bias toward positive studies.[110]

Drugs targeting arterial calcification and bone mineral metabolism

Arterial calcification is particularly prevalent in patients with end-stage renal disease (ESRD) who exhibit accelerated stiffening strongly predictive of poor clinical outcome.[111] It is characterized by low plasma concentrations of vitamin D, raised parathyroid hormone, and hyperphosphatemia. In small cohort studies of patients with CKD and ESRD not all of which have been randomized and controlled, there is no consistent evidence of benefit from vitamin D analogues and calcimimetics that act as allosteric modulators of the calcium signaling receptor (CaS).[112] Treatment of hyperphosphatemia with sevelamer attenuates progression of aortic calcification in hemodialysis patients[113] and one small cohort study has suggested that sevelamer decreases PWV in hemodialysis patients without affecting blood pressure. A limitation of this study, however, was the lack of control for baseline calcium and phosphorus.[114] In kidney transplant patients the immunosuppressant sirolimus reduced arterial stiffness alongside a reduction in blood pressure, but effects on calcification were not measured and effects were postulated to be due to inhibition of mTOR.[115] Renal disease is associated with vitamin K deficiency, and in an open uncontrolled trial in patients with renal transplants, vitamin K2 supplementation reduced cfPWV.[116] A new molecule SNF472 inhibits the development and progression of ectopic calcification by binding to the growth sites of hydroxyapatite (HAP) crystals and has been shown to inhibit the progression of arterial calcification in ESRD patients on haemodialysis.[117] In the general population and in specific groups there is some evidence that vitamin D may have a beneficial effect on cfPWV but only in individuals who are vitamin D deficient.[118] Bisphosphonates have been shown to retard vascular calcification in patients with ESRD but there have been few studies on arterial stiffness with no consistent effects to reduce PWV.[119]

Summary

In summary, most clinical studies of interventions to lower PWV through a blood pressure−independent mechanism are negative or at best show small effects. It might therefore be concluded that arterial stiffening is largely irreversible. This may be true but epidemiological evidence does suggest that accelerated age-related stiffening can be prevented. It is notable that age-related stiffening takes place over decades. A major limitation of clinical trials to date is that these have been of relatively short duration. A major challenge for the future, therefore, is to perform well-controlled adequately powered trials over the long term.

Conclusion

Inflammation, oxidative stress, and calcification are implicated in structural change of the arterial wall leading to arterial stiffening. Preclinical studies suggest that this can be reversed through a number of potential interventions including antiinflammatory therapies, MRA antagonists, inhibitors of vascular calcification, collagen cross-linking inhibitors, elastase/elastin-related peptide signaling inhibition, and miRNAs. Clinical trials to date have been limited by small cohort size and short-term duration. The challenge for the future is to perform well-controlled adequately powered trials over the long term.

References

1. Chirinos JA, Segers P, Hughes T, Townsend R. Large-artery stiffness in health and disease: JACC state-of-the-art review. **J Am Coll Cardiol**. 2019; 74:1237−1263.
2. Wang M, Jiang L, Monticone RE, Lakatta EG. Proinflammation: the key to arterial aging. **Trends Endocrinol Metab**. 2014; 25:72−79.
3. Wang M, Khazan B, Lakatta EG. Central arterial aging and angiotensin II signaling. **Curr Hypertens Rev**. 2010; 6:266−281.
4. Montezano AC, Nguyen Dinh Cat A, Rios FJ, Touyz RM. Angiotensin II and vascular injury. **Curr Hypertens Rep**. 2014; 16:431.
5. Wang M, Zhao D, Spinetti G, et al. Matrix metalloproteinase 2 activation of transforming growth factor-beta1 (TGF-beta1) and TGF-beta1-type II receptor signaling within the aged arterial wall. **Arterioscler Thromb Vasc Biol**. 2006; 26:1503−1509.
6. Yasmin, McEniery CM, Wallace S, et al. Matrix metalloproteinase-9 (MMP-9), MMP-2, and serum elastase activity are associated with

systolic hypertension and arterial stiffness. **Arterioscler Thromb Vasc Biol**. 2005; 25:372.

7. Michel JB, Heudes D, Michel O, et al. Effect of chronic ANG I-converting enzyme inhibition on aging processes. II. Large arteries. **Am J Physiol**. 1994; 267:R124−R135.

8. Holmstrom KM, Finkel T. Cellular mechanisms and physiological consequences of redox-dependent signalling. **Nat Rev Mol Cell Biol**. 2014; 15:411−421.

9. Adler A, Messina E, Sherman B, et al. NAD(P)H oxidase-generated superoxide anion accounts for reduced control of myocardial O_2 consumption by NO in old Fischer 344 rats. **Am J Physiol Heart Circ Physiol**. 2003; 285:H1015−H1022.

10. Donato AJ, Eskurza I, Silver AE, et al. Direct evidence of endothelial oxidative stress with aging in humans: relation to impaired endothelium-dependent dilation and upregulation of nuclear factor-kappaB. **Circ Res**. 2007; 100:1659−1666.

11. Liu M, Wilk SA, Wang A, et al. Resveratrol inhibits mTOR signaling by promoting the interaction between mTOR and DEPTOR. **J Biol Chem**. 2010; 285:36387−36394.

12. Fry JL, Al Sayah L, Weisbrod RM, et al. Vascular smooth muscle sirtuin-1 protects against diet-induced aortic stiffness. **Hypertension**. 2016; 68:775−784.

13. Mattison JA, Wang M, Bernier M, et al. Resveratrol prevents high fat/sucrose diet-induced central arterial wall inflammation and stiffening in nonhuman primates. **Cell Metab**. 2014; 20:183−190.

14. de Picciotto NE, Gano LB, Johnson LC, et al. Nicotinamide mononucleotide supplementation reverses vascular dysfunction and oxidative stress with aging in mice. **Aging Cell**. 2016; 15:522−530.

15. Lakatta EG. Arterial and cardiac aging: major shareholders in cardiovascular disease enterprises: Part III: cellular and molecular clues to heart and arterial aging. **Circulation**. 2003; 107:490−497.

16. Vendrov AE, Vendrov KC, Smith A, et al. NOX4 NADPH oxidase-dependent mitochondrial oxidative stress in aging-associated cardiovascular disease. **Antioxid Redox Signal**. 2015; 23:1389−1409.

17. Zhou RH, Vendrov AE, Tchivilev I, et al. Mitochondrial oxidative stress in aortic stiffening with age: the role of smooth muscle cell function. **Arterioscler Thromb Vasc Biol**. 2012; 32:745−755.

18. Zhou R, Yazdi AS, Menu P, Tschopp J. A role for mitochondria in NLRP3 inflammasome activation. **Nature**. 2011; 469:221−225.

19. Sanada F, Taniyama Y, Muratsu J, et al. Source of chronic inflammation in aging. **Front Cardiovasc Med**. 2018; 5:12.

20. Gioscia-Ryan RA, Battson ML, Cuevas LM, Eng JS, Murphy MP, Seals DR. Mitochondria-targeted antioxidant therapy with MitoQ ameliorates aortic stiffening in old mice. **J Appl Physiol**. 2018; 124:1194−1202.

21. Fleenor BS, Sindler AL, Marvi NK, et al. Curcumin ameliorates arterial dysfunction and oxidative stress with aging. **Exp Gerontol**. 2013; 48:269−276.

22. Kazyken D, Magnuson B, Bodur C, et al. AMPK directly activates mTORC2 to promote cell survival during acute energetic stress. **Sci Signal**. 2019; 12.

23. Lesniewski LA, Seals DR, Walker AE, et al. Dietary rapamycin supplementation reverses age-related vascular dysfunction and oxidative stress, while modulating nutrient-sensing, cell cycle, and senescence pathways. **Aging Cell**. 2017; 16:17−26.

24. Johnson SC, Rabinovitch PS, Kaeberlein M. mTOR is a key modulator of ageing and age-related disease. **Nature**. 2013; 493:338−345.

25. Harrison DE, Strong R, Sharp ZD, et al. Rapamycin fed late in life extends lifespan in genetically heterogeneous mice. **Nature**. 2009; 460:392−395.

26. Lamming DW, Ye L, Sabatini DM, Baur JA. Rapalogs and mTOR inhibitors as anti-aging therapeutics. **J Clin Invest**. 2013; 123:980−989.

27. Edwards AG, Donato AJ, Lesniewski LA, Gioscia RA, Seals DR, Moore RL. Life-long caloric restriction elicits pronounced protection of the aged myocardium: a role for AMPK. **Mech Ageing Dev**. 2010; 131:739−742.

28. Dao HH, Essalihi R, Bouvet C, Moreau P. Evolution and modulation of age-related medial elastocalcinosis: impact on large artery stiffness and isolated systolic hypertension. **Cardiovasc Res**. 2005; 66:307−317.

29. Demer LL. Vascular calcification and osteoporosis: inflammatory responses to oxidized lipids. **Int J Epidemiol**. 2002; 31:737−741.

30. Moe SM, Chen NX. Inflammation and vascular calcification. **Blood Purif**. 2005; 23:64−71.

31. Wang M, Zhang J, Telljohann R, et al. Chronic matrix metalloproteinase inhibition retards age-associated arterial proinflammation and increase in blood pressure. **Hypertension**. 2012; 60:459−466.

32. Mody N, Parhami F, Sarafian TA, Demer LL. Oxidative stress modulates osteoblastic differentiation of vascular and bone cells. **Free Radic Biol Med**. 2001; 31:509−519.

33. Yildiz M. Arterial distensibility in chronic inflammatory rheumatic disorders. **Open Cardiovasc Med J**. 2010; 4:83−88.

34. Kim KM. Calcification of matrix vesicles in human aortic valve and aortic media. **Fed Proc**. 1976; 35:156−162.

35. Reynolds JL, Joannides AJ, Skepper JN, et al. Human vascular smooth muscle cells undergo vesicle-mediated calcification in response to changes in extracellular calcium and phosphate concentrations: a potential mechanism for accelerated vascular calcification in ESRD. **J Am Soc Nephrol**. 2004; 15:2857−2867.

36. You AYF, Bergholt MS, St-Pierre JP, et al. Raman spectroscopy imaging reveals interplay between atherosclerosis and medial calcification in the human aorta. **Sci Adv**. 2017; 3:e1701156.

37. Duca L, Floquet N, Alix AJ, Haye B, Debelle L. Elastin as a matrikine. **Crit Rev Oncol Hematol**. 2004; 49:235−244.

38. Basalyga DM, Simionescu DT, Xiong W, Baxter BT, Starcher BC, Vyavahare NR. Elastin degradation and calcification in an abdominal aorta injury model: role of matrix metalloproteinases. **Circulation**. 2004; 110:3480−3487.

39. Herrmann J, Babic M, Tolle M, van der Giet M, Schuchardt M. Research models for studying vascular calcification. **Int J Mol Sci**. 2020; 21.

40. Gaillard V, Casellas D, Seguin-Devaux C, et al. Pioglitazone improves aortic wall elasticity in a rat model of elastocalcinotic arteriosclerosis. **Hypertension**. 2005; 46:372−379.

41. Ziegler SG, Ferreira CR, MacFarlane EG, et al. Ectopic calcification in pseudoxanthoma elasticum responds to inhibition of tissue-nonspecific alkaline phosphatase. **Sci Transl Med**. 2017; 9.

42. Chen Y, Zhao X, Wu H. Arterial stiffness: a focus on vascular calcification and its link to bone mineralization. **Arterioscler Thromb Vasc Biol**. 2020; 40:1078−1093.

43. Lomashvili KA, Monier-Faugere MC, Wang X, Malluche HH, O'Neill WC. Effect of bisphosphonates on vascular calcification and bone metabolism in experimental renal failure. **Kidney Int**. 2009; 75:617−625.

44. Buga GM, Griscavage JM, Rogers NE, Ignarro LJ. Negative feedback regulation of endothelial cell function by nitric oxide. **Circ Res**. 1993; 73:808−812.

45. Tintut Y, Patel J, Parhami F, Demer LL. Tumor necrosis factor-α promotes in vitro calcification of vascular cells via the cAMP pathway. **Circulation**. 2000; 102:2636−2642.

46. Rogers MJ, Gordon S, Benford HL, et al. Cellular and molecular mechanisms of action of bisphosphonates. **Cancer**. 2000; 88:2961−2978.

47. Lehenkari PP, Kellinsalmi M, Napankangas JP, et al. Further insight into mechanism of action of clodronate: inhibition of mitochondrial ADP/ATP translocase by a nonhydrolyzable, adenine-containing metabolite. **Mol Pharmacol**. 2002; 61:1255−1262.

48. Cozzolino M, Staniforth ME, Liapis H, et al. Sevelamer hydrochloride attenuates kidney and cardiovascular calcifications in long-term experimental uremia. **Kidney Int**. 2003; 64:1653−1661.

49. Pouyatos B, Gearhart C, Nelson-Miller A, Fulton S, Fechter L. Oxidative stress pathways in the potentiation of noise-induced hearing loss by acrylonitrile. **Hear Res**. 2007; 224:61−74.

50. Yatzidis H. Absence or decreased endogenous thiosulfaturia: a cause of recurrent calcium nephrolithiasis. **Int Urol Nephrol**. 2004; 36:587−589.

51. Pasch A, Schaffner T, Huynh-Do U, Frey BM, Frey FJ, Farese S. Sodium thiosulfate prevents vascular calcifications in uremic rats. **Kidney Int**. 2008; 74:1444−1453.

52. Grases F, Sanchis P, Perello J, et al. Effect of crystallization inhibitors on vascular calcifications induced by vitamin D: a pilot study in Sprague-Dawley rats. **Circ J**. 2007; 71:1152−1156.

53. Ferrer MD, Ketteler M, Tur F, et al. Characterization of SNF472 pharmacokinetics and efficacy in uremic and non-uremic rats models of cardiovascular calcification. **PLoS One**. 2018; 13:e0197061.

54. Schreiber V, Dantzer F, Ame JC, de Murcia G. Poly(ADP-ribose): novel functions for an old molecule. **Nat Rev Mol Cell Biol**. 2006; 7:517−528.

55. Brunyanszki A, Szczesny B, Virag L, Szabo C. Mitochondrial poly(ADP-ribose) polymerase: the Wizard of Oz at work. **Free Radic Biol Med**. 2016; 100:257−270.

56. Muller KH, Hayward R, Rajan R, et al. Poly(ADP-Ribose) links the DNA damage response and biomineralization. **Cell Rep**. 2019; 27:3124−3138 e13.

57. Robert L, Robert AM, Jacotot B. Elastin-elastase-atherosclerosis revisited. **Atherosclerosis**. 1998; 140:281−295.

58. Wang M, Takagi G, Asai K, et al. Aging increases aortic MMP-2 activity and angiotensin II in nonhuman primates. **Hypertension**. 2003; 41:1308−1316.

59. Wang M, Zhang J, Jiang LQ, et al. Proinflammatory profile within the grossly normal aged human aortic wall. **Hypertension**. 2007; 50:219−227.

60. Benjamin MM, Khalil RA. Matrix metalloproteinase inhibitors as investigative tools in the pathogenesis and management of vascular disease. **Exp Suppl**. 2012; 103:209−279.

61. Castro MM, Rizzi E, Figueiredo-Lopes L, et al. Metalloproteinase inhibition ameliorates hypertension and prevents vascular dysfunction and remodeling in renovascular hypertensive rats. **Atherosclerosis**. 2008; 198:320−331.

62. Guimaraes DA, Rizzi E, Ceron CS, et al. Doxycycline dose-dependently inhibits MMP-2-mediated vascular changes in 2K1C hypertension. **Basic Clin Pharmacol Toxicol**. 2011; 108:318−325.

63. Bouvet C, Moreau S, Blanchette J, de Blois D, Moreau P. Sequential activation of matrix metalloproteinase 9 and transforming growth factor beta in arterial elastocalcinosis. **Arterioscler Thromb Vasc Biol**. 2008; 28:856−862.

64. Susic D, Frohlich ED. Increased collagen, per se, may not affect left ventricular function in spontaneously hypertensive rats. **Ochsner J**. 2011; 11:241−245.

65. Tuday E, Nomura Y, Ruhela D, et al. Deletion of the microRNA-degrading nuclease, translin/trax, prevents pathogenic vascular stiffness. **Am J Physiol Heart Circ Physiol**. 2019; 317:H1116−H1124.

66. Liao YC, Wang YS, Hsi E, Chang MH, You YZ, Juo SH. MicroRNA-765 influences arterial stiffness through modulating apelin expression. **Mol Cell Endocrinol**. 2015; 411:11−19.

67. Deng H, Song Z, Xu H, et al. MicroRNA-1185 promotes arterial stiffness though modulating VCAM-1 and E-selectin expression. **Cell Physiol Biochem**. 2017; 41:2183−2193.

68. Hori D, Dunkerly-Eyring B, Nomura Y, et al. miR-181b regulates vascular stiffness age dependently in part by regulating TGF-beta signaling. **PLoS One**. 2017; 12:e0174108.

69. Ketszeri M, Kirsch A, Frauscher B, et al. MicroRNA-142-3p improves vascular relaxation in uremia. **Atherosclerosis**. 2019; 280:28−36.

70. Kim SK, McCurley AT, DuPont JJ, et al. Smooth muscle cell-mineralocorticoid receptor as a mediator of cardiovascular stiffness with aging. **Hypertension**. 2018; 71:609−621.

71. Gorini S, Kim SK, Infante M, et al. Role of aldosterone and mineralocorticoid receptor in cardiovascular aging. **Front Endocrinol**. 2019; 10:584.

72. Krug AW, Allenhofer L, Monticone R, et al. Elevated mineralocorticoid receptor activity in aged rat vascular smooth muscle cells promotes a proinflammatory phenotype via extracellular signal-regulated kinase 1/2 mitogen-activated protein kinase and epidermal growth factor receptor-dependent pathways. **Hypertension**. 2010; 55:1476−1483.

73. Keidar S, Kaplan M, Pavlotzky E, et al. Aldosterone administration to mice stimulates macrophage NADPH oxidase and increases atherosclerosis development: a possible role for angiotensin-converting enzyme and the receptors for angiotensin II and aldosterone. **Circulation**. 2004; 109:2213−2220.

74. Sartorio CL, Fraccarollo D, Galuppo P, et al. Mineralocorticoid receptor blockade improves vasomotor dysfunction and vascular oxidative stress early after myocardial infarction. **Hypertension**. 2007; 50:919−925.

75. DeMarco VG, Habibi J, Jia G, et al. Low-dose mineralocorticoid receptor blockade prevents western diet-induced arterial stiffening in female mice. **Hypertension**. 2015; 66:99−107.

76. Benetos A, Lacolley P, Safar ME. Prevention of aortic fibrosis by spironolactone in spontaneously hypertensive rats. **Arterioscler Thromb Vasc Biol**. 1997; 17:1152−1156.

77. Lacolley P, Safar ME, Lucet B, Ledudal K, Labat C, Benetos A. Prevention of aortic and cardiac fibrosis by spironolactone in old normotensive rats. **J Am Coll Cardiol**. 2001; 37:662−667.

78. Gil-Ortega M, Vega-Martin E, Martin-Ramos M, et al. Finerenone reduces intrinsic arterial stiffness in Munich Wistar Fromter rats, a genetic model of chronic kidney disease. **Am J Nephrol**. 2020; 51:294−303.

79. Sun Y, Byon CH, Yang Y, et al. Dietary potassium regulates vascular calcification and arterial stiffness. **JCI Insight**. 2017; 2.

80. Larsson A, Malmstrom S, Westermark P. Signs of cross-seeding: aortic medin amyloid as a trigger for protein AA deposition. **Amyloid**. 2011; 18:229−234.

81. Winder NR, Reeve EH, Walker AE. Large artery stiffness and brain health: insights from animal models. **Am J Physiol Heart Circ Physiol**. 2021; 320:H424−H431.

82. Mallareddy M, Parikh CR, Peixoto AJ. Effect of angiotensin-converting enzyme inhibitors on arterial stiffness in hypertension: systematic review and meta-analysis. **J Clin Hypertens**. 2006; 8:398−403.

83. Shahin Y, Khan JA, Chetter I. Angiotensin converting enzyme inhibitors effect on arterial stiffness and wave reflections: a meta-analysis and meta-regression of randomised controlled trials. **Atherosclerosis**. 2012; 221:18−33.

84. Li X, Chang P, Wang Q, et al. Effects of angiotensin-converting enzyme inhibitors on arterial stiffness: a systematic review and meta-analysis of randomized controlled trials. **Cardiovasc Ther**. 2020; 2020:7056184.

85. Edwards NC, Steeds RP, Stewart PM, Ferro CJ, Townend JN. Effect of spironolactone on left ventricular mass and aortic stiffness in early-stage chronic kidney disease: a randomized controlled trial. **J Am Coll Cardiol**. 2009; 54:505−512.

86. Mills CE, Govoni V, Faconti L, et al. A randomised, factorial trial to reduce arterial stiffness independently of blood pressure: proof of concept? The VaSera trial testing dietary nitrate and spironolactone. **Br J Clin Pharmacol**. 2020; 86:891−902.

87. D'Elia L, La Fata E, Iannuzzi A, Rubba PO. Effect of statin therapy on pulse wave velocity: a meta-analysis of randomized controlled trials. **Clin Exp Hypertens**. 2018; 40:601−608.

88. Upala S, Wirunsawanya K, Jaruvongvanich V, Sanguankeo A. Effects of statin therapy on arterial stiffness: a systematic review and meta-analysis of randomized controlled trial. **Int J Cardiol**. 2017; 227:338−341.

89. Cecelja M, Chowienczyk P. Dissociation of aortic pulse wave velocity with risk factors for cardiovascular disease other than hypertension: a systematic review. **Hypertension**. 2009; 54:1328−1336.

90. Mandraffino G, Scicali R, Rodriguez-Carrio J, et al. Arterial stiffness improvement after adding on PCSK9 inhibitors or ezetimibe to high-intensity statins in patients with familial hypercholesterolemia: a Two-Lipid Center Real-World Experience. **J Clin Lipidol**. 2020; 14:231−240.

91. Ashor AW, Siervo M, Lara J, Oggioni C, Mathers JC. Antioxidant vitamin supplementation reduces arterial stiffness in adults: a systematic review and meta-analysis of randomized controlled trials. **J Nutr**. 2014; 144:1594−1602.

92. Myung SK, Ju W, Cho B, et al. Efficacy of vitamin and antioxidant supplements in prevention of cardiovascular disease: systematic review and meta-analysis of randomised controlled trials. **BMJ**. 2013; 346:f10.

93. Miller 3rd ER, Pastor-Barriuso R, Dalal D, Riemersma RA, Appel LJ, Guallar E. Meta-analysis: high-dosage vitamin E supplementation may increase all-cause mortality. **Ann Intern Med**. 2005; 142:37−46.

94. McCall MR, Frei B. Can antioxidant vitamins materially reduce oxidative damage in humans? **Free Radic Biol Med**. 1999; 26:1034−1053.

95. Wald DS, Law M, Morris JK. Homocysteine and cardiovascular disease: evidence on causality from a meta-analysis. **BMJ**. 2002; 325:1202.

96. Bortolotto LA, Safar ME, Billaud E, et al. Plasma homocysteine, aortic stiffness, and renal function in hypertensive patients. **Hypertension**. 1999; 34:837−842.

97. van Dijk SC, Enneman AW, Swart KM, et al. Effects of 2-year vitamin B12 and folic acid supplementation in hyper-homocysteinemic elderly on arterial stiffness and cardiovascular outcomes within the B-PROOF trial. **J Hypertens**. 2015; 33:1897−1906. Discussion 1906.

98. De Angelis L, Millasseau SC, Smith A, et al. Sex differences in age-related stiffening of the aorta in subjects with type 2 diabetes. **Hypertension**. 2004; 44:67−71.

99. Batzias K, Antonopoulos AS, Oikonomou E, et al. Effects of newer antidiabetic drugs on endothelial function and arterial stiffness: a systematic review and meta-analysis. **J Diabetes Res**. 2018; 2018:1232583.

100. Striepe K, Jumar A, Ott C, et al. Effects of the selective sodium-glucose cotransporter 2 inhibitor empagliflozin on vascular function and central hemodynamics in patients with type 2 diabetes mellitus. **Circulation**. 2017; 136:1167−1169.

101. Kass DA, Shapiro EP, Kawaguchi M, et al. Improved arterial compliance by a novel advanced glycation end-product crosslink breaker. **Circulation**. 2001; 104:1464−1470.

102. Little WC, Zile MR, Kitzman DW, Hundley WG, O'Brien TX, Degroof RC. The effect of alagebrium chloride (ALT-711), a novel glucose cross-link breaker, in the treatment of elderly patients with diastolic heart failure. **J Card Fail**. 2005; 11:191−195.

103. Zieman SJ, Melenovsky V, Clattenburg L, et al. Advanced glycation endproduct crosslink breaker (alagebrium) improves endothelial function in patients with isolated systolic hypertension. **J Hypertens**. 2007; 25:577−583.

104. Hartog JW, Willemsen S, van Veldhuisen DJ, et al. Effects of alagebrium, an advanced glycation endproduct breaker, on exercise tolerance and cardiac function in patients with chronic heart failure. **Eur J Heart Fail**. 2011; 13:899−908.

105. Fujimoto N, Hastings JL, Carrick-Ranson G, et al. Cardiovascular effects of 1 year of alagebrium and endurance exercise training in healthy older individuals. **Circ Heart Fail**. 2013; 6:1155−1164.

106. Luchetti MM, Benfaremo D, Gabrielli A. Biologics in inflammatory and immunomediated arthritis. **Curr Pharm Biotechnol**. 2017; 18:989−1007.

107. Rawla P, Sunkara T, Raj JP. Role of biologics and biosimilars in inflammatory bowel disease: current trends and future perspectives. **J Inflamm Res**. 2018; 11:215−226.

108. Veilleux MS, Shear NH. Biologics in patients with skin diseases. **J Allergy Clin Immunol**. 2017; 139:1423−1430.

109. Maki-Petaja KM, Hall FC, Booth AD, et al. Rheumatoid arthritis is associated with increased aortic pulse-wave velocity, which is reduced by anti-tumor necrosis factor-alpha therapy. **Circulation**. 2006; 114:1185−1192.

110. Knowles L, Nadeem N, Chowienczyk PJ. Do anti-tumour necrosis factor-alpha biologics affect subclinical measures of atherosclerosis and arteriosclerosis? A systematic review. **Br J Clin Pharmacol**. 2020; 86:837−851.

111. Blacher J, Guerin AP, Pannier B, Marchais SJ, Safar ME. Impact of aortic stiffness on survival in end-stage renal disease. **Circulation**. 1999; 99:2434−2439.

112. Rodriguez RA, Spence M, Hae R, Agharazii M, Burns KD. Pharmacologic therapies for aortic stiffness in end-stage renal disease: a systematic review and meta-analysis. **Can J Kidney Health Dis**. 2020; 7, 2054358120906974.

113. Chertow GM, Burke SK, Raggi P. Sevelamer attenuates the progression of coronary and aortic calcification in hemodialysis patients. **Kidney Int**. 2002; 62:245−252.

114. Othmane TH, Bakonyi G, Egresits J, et al. Effect of sevelamer on aortic pulse wave velocity in patients on hemodialysis: a prospective observational study. **Hemodial Int**. 2007; 11(Suppl 3):S13−S21.

115. Joannides R, Monteil C, de Ligny BH, et al. Immunosuppressant regimen based on sirolimus decreases aortic stiffness in renal transplant recipients in comparison to cyclosporine. **Am J Transplant**. 2011; 11:2414−2422.

116. Mansour AG, Hariri E, Daaboul Y, et al. Vitamin K2 supplementation and arterial stiffness among renal transplant recipients-a single-arm, single-center clinical trial. **J Am Soc Hypertens**. 2017; 11:589−597.

117. Raggi P, Bellasi A, Sinha S, et al. Effects of SNF472, a novel inhibitor of hydroxyapatite crystallization in patients receiving hemodialysis - subgroup analyses of the CALIPSO trial. **Kidney Int Rep**. 2020; 5:2178−2182.

118. Chen NC, Hsu CY, Mao PC, Dreyer G, Wu FZ, Chen CL. The effects of correction of vitamin D deficiency on arterial stiffness: a systematic review and updated meta-analysis of randomized controlled trials. **J Steroid Biochem Mol Biol**. 2020; 198:105561.

119. Caffarelli C, Montagnani A, Nuti R, Gonnelli S. Bisphosphonates, atherosclerosis and vascular calcification: update and systematic review of clinical studies. **Clin Interv Aging**. 2017; 12: 1819−1828.

Organic and dietary nitrates, inorganic nitrite, nitric oxide donors, and soluble guanylate cyclase stimulation

Kevin O'Gallagher and Andrew James Webb

Department of Clinical Pharmacology, School of Cardiovascular Medicine and Sciences, King's College London British Heart Foundation Centre, St. Thomas' Hospital, London, United Kingdom

Part 1: introduction

First described as endothelium-derived relaxing factor (EDRF),[1,2] over the last four decades nitric oxide (NO) has been identified as a key signaling molecule in the cardiovascular system and multiple other organ systems. The importance of the discovery and identification of NO as EDRF is reflected by the award of 1998 Nobel Prize in Medicine to Furchgott, Murad, and Ignarro.[3]

NO is a free radical gas, with a half-life in the circulation of ~ 20 ms[4]. In humans, it is produced via two key pathways: the "L-arginine-nitric oxide pathway" as originally described by Moncada[5] and the more recently discovered nitrate-nitrite-NO pathway.[6] The latter significantly impacted our understanding of the role of inorganic nitrate and nitrite in relation to the cardiovascular system from inert by-products of NO oxidation (at physiological concentrations) to important sources of NO,[7,8] and will be considered in a later section.
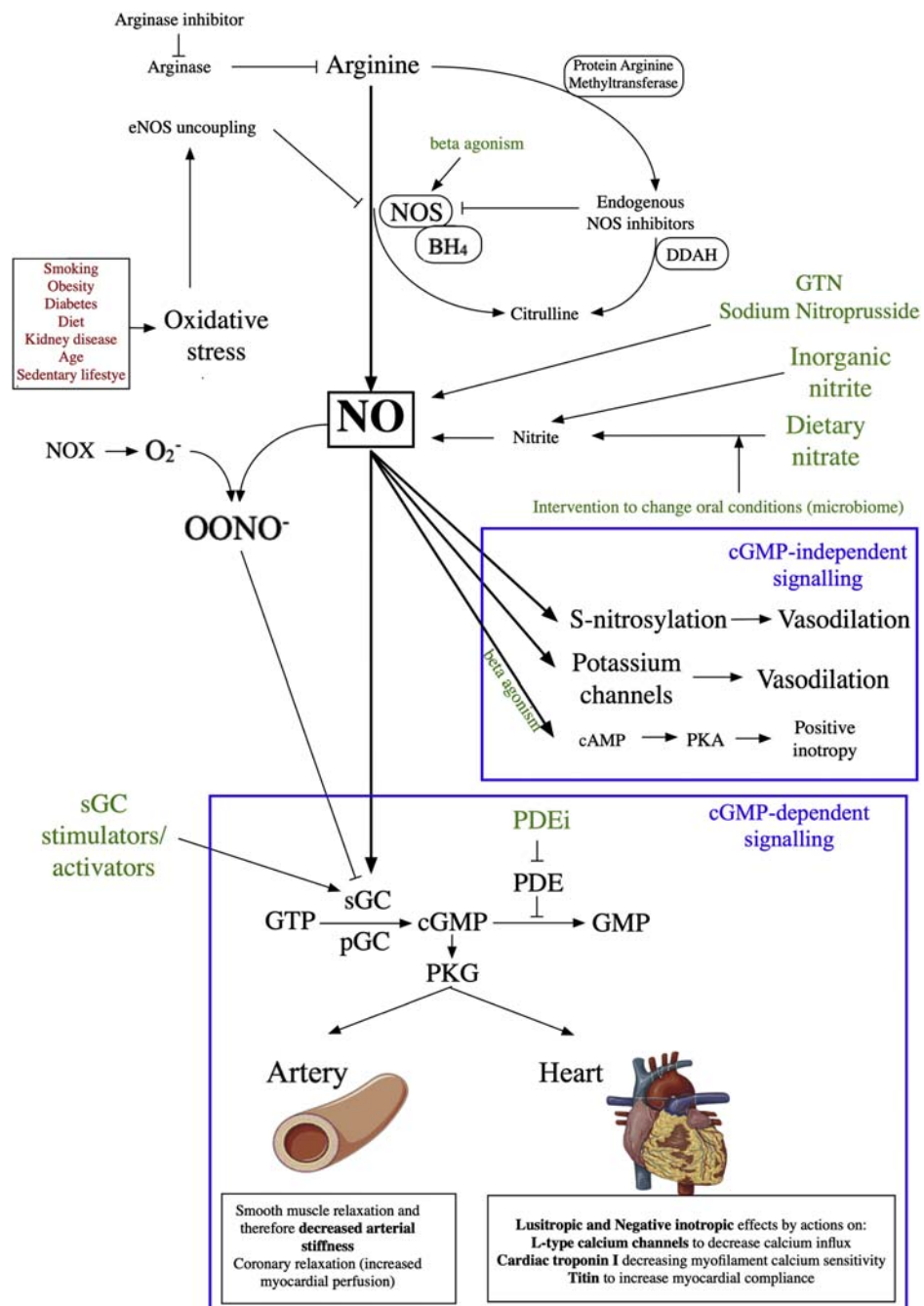
The L-arginine-NO pathway involves the generation of NO via the conversion of L-arginine to L-citrulline by heme- and flavin-containing nitric oxide synthase (NOS) enzymes[9] in a process that requires dimerism of the NOS enzyme and the presence of the co-factors tetrahydrobiopterin (BH$_4$), NADPH, and O$_2$.[10] Three NOS isoenzymes have been identified in humans: endothelial (eNOS), neuronal (nNOS), and inducible (iNOS). eNOS and nNOS are constitutively expressed and have distinct roles in the regulation of cardiovascular function. This is in contrast to iNOS, which is a major player in the host response to infection and inflammation. While the production of NO by eNOS and nNOS is Ca^{2+}/calmodulin-dependent, production of NO by iNOS continues until the enzyme is degraded, generating higher local concentrations of NO.[11]

Nitric oxide signaling in the vasculature and vasodilatation

NO's role as a signaling molecule in the vasculature occurs primarily in a paracrine fashion, i.e., NO produced by NOS (eNOS in the vascular endothelium, nNOS in nitrergic nerves) diffuses into the vascular smooth muscle cell, whereby it binds to the heme moiety of soluble guanylate cyclase (sGC). This in turn leads to the activation of cyclic guanosine monophosphate (cGMP) and subsequently protein kinase G (PKG), resulting in relaxation of the smooth muscle cell with consequent vasodilatation. Additionally, s-nitrosylation (the NO-mediated modification of cysteine residues in proteins) affords a mechanism by which NO can exert a number of effects, including vasodilatation, in a cGMP-independent manner. Examples include NO's effect on calcium-dependent potassium channels in vascular smooth muscle[12] and the vasodilatory actions of the nitrosothiol S-nitrosoglutathione.[13] The pathways of cardiovascular NO signaling are illustrated in Fig. 51.1.
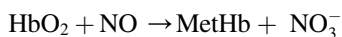
In the healthy human vasculature, eNOS and nNOS have relatively distinct roles: nNOS is responsible for basal regulation of microvascular tone (and therefore systemic vascular resistance and peripheral blood pressure[14]) and the vasodilatory response to mental stress,[15] while eNOS is responsible for the dilatory response to increased shear stress or agonist stimulation.[16,17] The L-arginine-NO pathway also mediates the vasodilatory response of beta-2-agonism, as demonstrated in the human forearm.[18]

There are potential limiting factors to the ability of NO to diffuse from the vascular endothelium to adjacent smooth muscle. Firstly, as noted above, the half-life of NO is approximately 20 ms in whole blood, due to NO's status as a reactive oxygen species (ROS). This innate reactivity limits
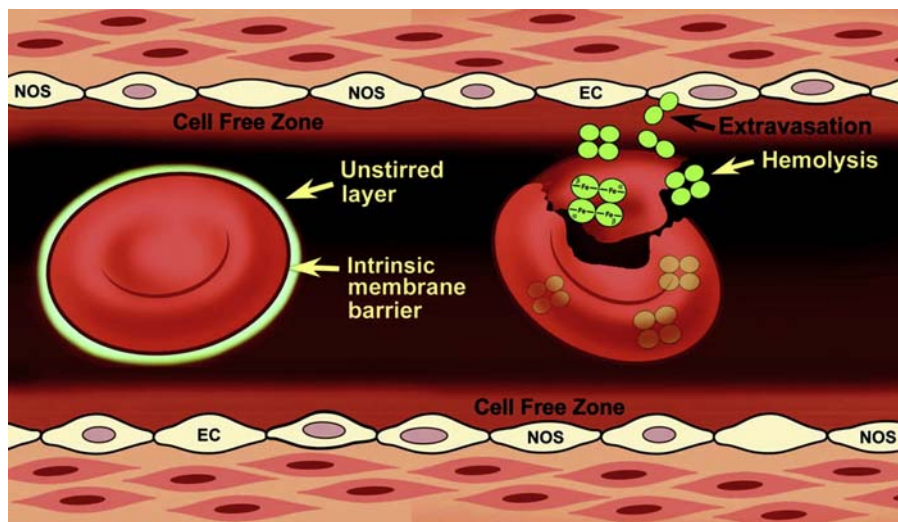
FIGURE 51.1 Cardiovascular nitric oxide signaling: pathways to vasodilatation, myocardial relaxation, central and peripheral hemodynamic changes. Green items indicate therapeutic interventions. *BH$_4$*, tetrahydrobiopterin; *cGMP*, cyclic guanosine monophosphate; *DDAH*, dimethylarginine dimethy-laminohydrolase; *eNOS*, endothelial NOS; *GTN*, glyceryl trinitrate; *NOS*, nitric oxide synthase; *NOX*, NADPH oxidase; *PDE*, phosphodiesterase; *PDEi*, PDE inhibitor; *PKG*, subsequently protein kinase G; *sGC*, soluble guanylate cyclase. *Original drawing by Kevin O'Gallagher and Andrew Webb.*

NO to diffusion from adjacent cells rather than being transported in blood as free NO. Secondly, NO is avidly scavenged by hemoglobin in both its deoxy- and oxy-hemoglobin forms. The reaction of NO with oxyhemoglobin to produce methemoglobin and inorganic nitrate is described below:

$$HbO_2 + NO \rightarrow MetHb + NO_3^-$$

As pointed out by Kim-Shapiro et al. in their review,[19] this presents an apparent paradox: NO is produced by the vascular endothelium in extremely close proximity to a substance (the blood) which would prevent it enacting its role in relaxation of vascular smooth muscle, especially as any NO concentration gradient would, in fact, favor

FIGURE 51.2 Factors involved in mitigating nitric oxide scavenging by RBCs. *Reproduced from Kim-Shapiro DB, Schechter AN, Gladwin MT. Unraveling the reactions of nitric oxide, nitrite, and hemoglobin in physiology and therapeutics.* Arterioscler Thromb Vasc Biol. *2006;26:697−705.*

diffusion *away* from the vascular smooth muscle cell and into the bloodstream to be scavenged (see Fig. 51.2).

Several mechanisms have been described which limit NO scavenging by Hb and therefore ensure that eNOS-derived NO can indeed diffuse from the vascular endothelium into the vascular smooth muscle and initiate relaxation. Firstly, hemoglobin is encapsulated within the erythrocyte, which decreases the magnitude of scavenging when compared with free Hb.[20] Secondly, due to the dynamics of blood flow within the vessel, there exists a "cell-free layer" in the blood immediately adjacent to the vascular endothelium (faster blood flow velocity in the middle of the vessel lumen leads to a pressure gradient within the vessel and relative concentration of erythrocytes in the middle of the vessel), resulting in a "barrier" between free NO and erythrocytes. Thirdly, in a moving/mixing fluid (in this case the blood), there exists an "unstirred layer"[21] around a cell membrane (in this case the erythrocyte membrane) in which there is static fluid, i.e., a region adjacent to a cell membrane when there is low flow, which, like the cell-free layer, acts as a barrier to diffusion.

Deonikar et al.[22] modeled the concentrations of NO from endothelium-derived NO in the luminal subregions representing the RBC rich core and cell-free zone (CFZ), and the abluminal regions including endothelium, interstitial space, smooth muscle cell later, nonperfused tissue, and parenchymal tissue perfused with capillaries in larger arterioles (200 μm) and smaller arterioles (50 μm) as shown in Fig. 51.3.

Notably, there was an important effect of flow velocity. As the flow increased from 0.1 to 4 cm/s, the NO concentration in the CFZ increased up to eightfold. Also, Chen X et al. identified an important role for the glycocalyx.[23] While the modeling suggested that the presence of RBCs in
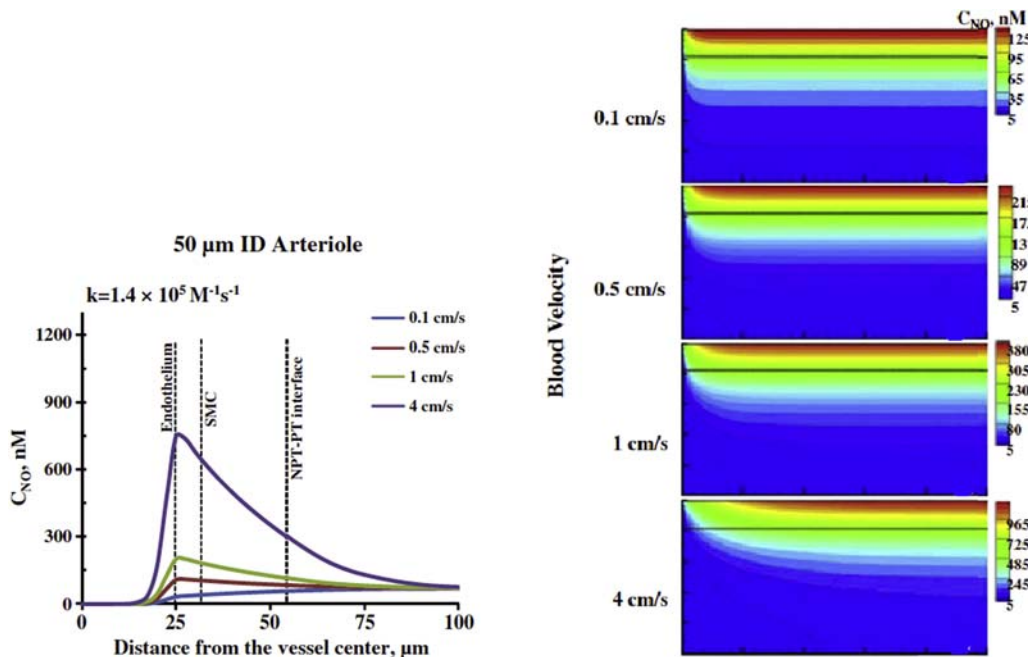
the boundary layer near the endothelium had a larger effect on NO than on O_2 transport, as the thickness of the glycocalyx increased, scavenging of NO by hemoglobin decreased, such that the presence versus absence of RBCs equated to a difference in glycocalyx thickness of ∼0.8 μm (see Fig. 6 from Chen X et al.,[23] https://journals.physiology.org/doi/full/10.1152/japplphysiol.00633.2005 [free access]).

The effect of nitric oxide on cardiac function

NO exerts an effect on cardiovascular function in a number of ways. From a vascular point of view, its role in the regulation of systemic arterial hemodynamics[14,17,24] affects cardiac loading conditions. NO also regulates cardiac function via a direct myocardial effect, through both paracrine (NO from the coronary endothelium[16]) and autocrine (NOS enzymes expressed within cardiomyocytes[25]) processes.

Endothelial paracrine regulation of left ventricular function

NO released from vascular (and endocardial) endothelium exerts a paracrine effect on cardiac function, while NO generated within cardiomyocytes exerts an autocrine effect.[26] The paracrine effect has been demonstrated in both animal preparations and in human in vivo experiments using substance P (a known stimulator of eNOS-derived NO release).[27] Disruption of NO signaling can have deleterious effects on cardiac function. In dogs, prolonged NOS inhibition with L-NAME resulted in decreased LV compliance and markers of cardiac efficiency, with additional changes to LV afterload.[28]

FIGURE 51.3 Nitric oxide concentration profiles across and relationship to blood velocity. The left-hand panel shows [NO] across all the regions (including *NPT*, nonperfused tissue; *PT*, parenchymal tissue; and *SMC*, smooth muscle cell later) of an arteriole (50 μm internal diameter) at the end of the arteriolar segments, plotted as a function of distance from the vessel center and increasing blood velocity range from 0.1 cm/s (lowest trace) to 4 cm/s (top trace). The right-hand panel shows [NO] in the vascular lumen of an arteriole (50 μm internal diameter, 500 μm length) with an NO−RBC reaction rate constant of 0.2×10^{-5} M^{-1}/s, and increasing blood velocity range from 0.1 to 4 cm/s from the top to the bottom panel. NO availability in the vascular lumen cell-free zone (CFZ) increased with increase in blood velocity. *Adapted from Deonikar P, Kavdia M. A computational model for nitric oxide, nitrite and nitrate biotransport in the microcirculation: effect of reduced nitric oxide consumption by red blood cells and blood velocity.* Microvasc Res. *2010;80:464−476.*

Effects of nitric oxide signaling at the myocardial level

In the myocardium, there is subcellular localization of NOS isoenzymes (eNOS localized to caveolae,[29] nNOS to sarcoplasmic reticulum[30]), which allows NO to have varying effects on myocardial function, including contractility.[31]

NO stimulation of sGC results in increased levels of intracellular cGMP; see Fig. 51.1. cGMP in turn stimulates PKG. Through PKG-mediated phosphorylation of L-type calcium channels[32] (decreasing calcium influx) and cardiac troponin I (decreasing myofilament calcium sensitivity[33]), NO exerts a negatively inotropic effect. Conversely, in response to stimulation by beta-agonism,[34] nNOS-derived NO can exert a positively inotropic effect, via cAMP-mediated protein kinase A action on ryanodine receptors and phospholamban, which has the net result of increasing sarcoplasmic reticulum calcium release.[31] In addition to sGC, cGMP is also produced in an NO-independent fashion by a membrane-bound guanylate cyclase isoform known as particulate guanylate cyclase which acts as a receptor for natriuretic peptides.

Interaction with phosphodiesterase

Phosphodiesterases (PDE) are a family of cyclic nucleotide-hydrolyzing enzymes, which play a key role in the regulation of second messenger signaling. cGMP interacts with members of the phosphodiesterase (PDE) family in a number of ways. PDE5 hydrolyzes cGMP to 5′ GMP, therefore regulating NO-mediated PKG activity by exerting an inhibitor effect on cGMP. PDE5 inhibitors were initially developed as potential therapies for coronary artery disease, but are currently established as effective treatments for erectile dysfunction[35] and pulmonary arterial hypertension.[36]

At the level of the cardiomyocyte, PDE5 inhibition promotes negative inotropic effects. By increasing cGMP levels, PDE5 inhibition promotes increased PKG-mediated phosphorylation of both L-type calcium channels (decreasing calcium influx) and also troponin I (decreasing myofilament sensitivity), thus opposing beta-adrenergic stimulation. In mice, PDE5 inhibition with sildenafil blunts LV hypertrophic remodeling in response to transverse arterial constriction and reverses existing LV hypertrophy, all in the context of increased PKG-1 activity.[37]

PDE2 and PDE3 provide a mechanism by which cGMP (and therefore NO signaling) interacts with cAMP (and

therefore adrenergic signaling). PDE2 is cGMP stimulated, acting to hydrolyze cAMP, therefore inhibiting its activity.[38] Conversely, PDE3 hydrolysis of cAMP is competitively inhibited by cGMP, by virtue of PDE3 having a higher substrate affinity for cGMP than cAMP.

Accordingly, inhibition of PDE2 improves NO signaling in animal models of pulmonary hypertension and pressure overload-induced heart failure,[39,40] while cilostazol, a PDE3 inhibitor, induces arterial dilation and reactivity through both endothelium dependent and independent mechanisms.[41−43]

While endogenously produced NO has important effects on the vasculature, targeted delivery of NO to the vasculature has proved challenging given its extremely short half-life. Thus, the strategy of prolonging its effects with PDE inhibitors as described above.

PDE inhibition has been studied as a potential therapy in heart failure with preserved ejection fraction (HFpEF). In addition to beneficial effects on RV function, sildenafil improves left sided hemodynamics,[44] however the RELAX trial (n = 216) failed to demonstrate any improvement in exercise capacity from sildenafil treatment in HFpEF patients.[45]

An alternative approach to increase intravascular NO is via the use of nitrates which are metabolized to NO as discussed in the next section.

Part 2: organic nitrates
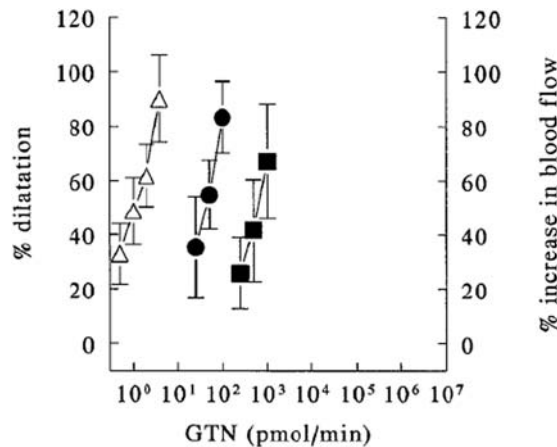
Organic nitrates are usually laboratory synthesized chemicals. A notable exception is ethyl nitrite, which is formed in the human stomach following ingestion of lettuce (dietary nitrate as a source of nitrite as described below) and red wine or whisky (ethanol),[46−48] with potent vasodilatory properties.

Clinically, organic nitrates are used in a number of conditions. For example, acute administration of glyceryl trinitrate (GTN) is effective for the relief of angina caused by myocardial ischemia, for hypertensive emergencies, and for acute heart failure.[49] In combination with hydralazine, organic nitrates (isosorbide dinitrate) have been shown to reduce mortality and improve outcomes in African Americans with HFrEF.[50] However, in HFpEF organic nitrates did not improve quality of life (QOL) or outpatient physical activity.[51] Regular/chronic administration of isosorbide mononitrate (ISMN) is useful for relief of angina. The use of nitrates is limited by their side effect profile (headaches), interactions with other vasodilator medications,[52] and tachyphylaxis. As further discussed in Chapter 36, in patients with HFpEF, inorganic nitrate therapy seems to be associated with particular high incidence of side effects, including headaches and dizziness.[50,53]

Pulsatile hemodynamic effects of organic nitrates

GTN and amyl nitrite were identified as antianginals and treatments for elevated arterial pressure (and heart failure) identified through palpation or sphygmographic recording of the arterial pulse in the late 19th century by Broadbent (1875) and Murrell (1879), respectively.[54,55] In response, Mahomed, who had modified and improved the sphygmograph at Guy's Hospital (where the co-author to this Chapter, A.W. runs hypertension clinics), highlighted the significance of a modifiable functional component of high arterial tension, as opposed to fixed structural changes in the arterial wall.[56] However, as GTN was not found to consistently lower brachial blood pressure (systolic or diastolic) as estimated by the occlusive cuff method of Scipione Riva Rocci in 1896,[57] interest in its use for chronic hypertension waned. The relationship between the effects of GTN on arterial waveform, different vessel types and effect on aortic versus brachial systolic pressure were not fully appreciated until over a century later, as reviewed and further investigated by Jiang et al.[58]

As initially described by Winbury M et al., in the coronary circulation in 1969,[59] organic nitrates were further characterized as being selective for conduit versus resistance arteries by Barba et al.[60]; see Fig. 51.4.

FIGURE 51.4 Arteriovenous profiles of dilators. Dilator responses of dorsal hand veins (Δ; n = 6; left axis), the radial artery (●; n = 4; left axis), and the forearm resistance bed (■; n = 4−5; right axis) to local infusions of glyceryl trinitrate. Allowing for the approximately 50-fold differences in blood flow between dorsal hand veins and the forearm arterial bed, these results suggest that nitric oxide donors are approximately equipotent in dorsal hand veins and the radial artery and 10-fold less potent in the resistance vasculature. *Reproduced from Figure 1A from Barba G, Mullen MJ, Donald A, MacAllister RJ. Determinants of the response of human blood vessels to nitric oxide donors in vivo.* J Pharmacol Exp Ther. *1999;289:1662−1668.*
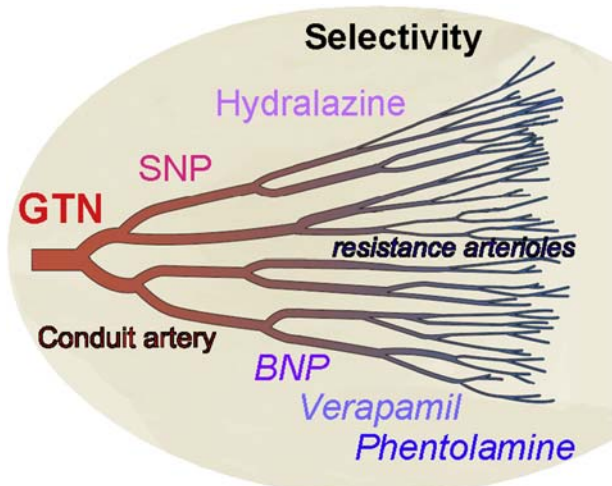
In a recent study utilizing the human forearm model, Fok et al. assessed changes in conduit (radial) artery diameter (measured by ultrasound) in response to intrabrachial infusion of various vasodilators.[61] Fig. 1 from that article[61] (free access: https://www.ahajournals.org/doi/10.1161/HYPERTENSIONAHA.112.198788?url_ver=Z39.88-2003&rfr_id=ori:rid:crossref.org&rfr_dat=cr_pub%20%200pubmed) shows that for the same degree of effect on resistance arterioles (assessed by forearm blood flow [FBF]), GTN, had the largest effect on conduit artery dilatation, followed by sodium nitroprusside (SNP): these agents are metabolized to NO or donate/release NO, respectively, suggesting selectivity for larger (conduit) arteries versus smaller (resistance) arterioles, via a mechanism relating to NO. By comparison, the other vasodilators, such as alpha-adrenergic blockers (phentolamine) and calcium channel blockers (verapamil) had little or no effect on conduit arteries but were highly effective at increasing FBF (resistance arterioles). We have summarized these comparative differences in selectivity in Fig. 51.5. In addition, changes in local PWV in the conduit arteries and impedance (Zc) were closely correlated with changes in radial artery diameter.[61]

Key evidence to explain the hemodynamic effects of organic nitrates is provided in the Jiang et al. paper mentioned above.[58] By assessing the effect of increasing doses of GTN patches on peripheral and central (aortic) blood pressure, the investigators identified GTN's related

effects on aortic augmentation pressure (AP) and ejection duration. While GTN only decreased brachial blood pressure at the highest dose, it decreased aortic pressures (systolic blood pressure [SBP], pulse pressure, and augmentation index) at all doses, which was considered to be due to a selective effect on conduit versus resistance vessels.

A subsequent study by Pauca et al., using invasive measures of aortic pressure, found that the decrease in central aortic systolic and pulse pressures is attributable to its effect on peripheral conduit arteries: GTN acts to dilate conduit vessels therefore decreasing aortic wave reflections.[62] These results are consistent with the current clinical uses of organic nitrates: they are effective at dilating conduit arteries, e.g., the epicardial coronaries and are therefore an effective antianginal therapy (however the main mechanism is via venous dilatation with decreased preload and therefore LV wall stress). At low doses they are relatively ineffective at dilating resistance arterioles, therefore restricting their use as antihypertensive agents (at least with respect to peripheral BP), unless at high doses, e.g., via an intravenous infusion for hypertensive crises.

A further complementary insight into the mechanism of GTN was provided by Cecelja M et al. in the Twins UK Study. Here the ∼10 mmHg increase in central pulse pressure over a decade in 411 female twins was accounted for mainly by an increase in AP. GTN (in a subsample, n = 42) transiently "reversed this decade of aging"—decreasing the cPP by 10 mmHg; this was entirely by decreasing the AP.[63] Gu et al. recently developed a novel echocardiographic parameter, the first-phase ejection fraction (EF1), which is the fraction of left ventricular volume ejected from the start of systole to the time of the first peak in left ventricular pressure (corresponding to the time of maximal ventricular shortening).[64] The EF1 was found to be diminished in patients with hypertension and diastolic dysfunction: a pattern of sustained myocardial contraction, which preserves systolic ejection fraction but at the expense of impairing diastolic function was identified. Moreover, EF1 was improved by GTN, as was diastolic function, with the onset of ventricular relaxation also being hastened. The hemodynamic effects of organic nitrates and the other NO-related therapeutics, to be discussed below, are summarized in Table 51.1.

FIGURE 51.5 Illustration of relative vasodilatory selective actions for conduit versus resistance arterioles. *BNP*, B-natriuretic peptide; *GTN*, Nitroglycerin; and *SNP*, sodium nitroprusside. *Based on the findings from Fok Fok H, Jiang B, Clapp B, Chowienczyk P. Regulation of vascular tone and pulse wave velocity in human muscular conduit arteries: selective effects of nitric oxide donors to dilate muscular arteries relative to resistance vessels.* Hypertension. *2012;60:1220—1225. Blood vessels drawing adapted from Lundberg JO, Weitzberg E, Gladwin MT. The nitrate-nitrite-nitric oxide pathway in physiology and therapeutics.* Nat Rev Drug Discov. *2008;7:156—167.*

Part 3: inorganic nitrite

Early pharmacological studies of nitrite on arterial tension/waveform

Considerable interest in the cardiovascular effects of pharmacologically administered sodium and potassium nitrite developed shortly after Broadbent (1875) and Murrell (1879) had explored the effects of the organic nitrates, as described above,[54,55] and partly in the search for other agents given the short duration of action of amyl nitrite for

TABLE 51.1 Effects of nitric oxide—related therapeutics on hemodynamics, pulsatility, and arterial stiffness in humans.

	Vasodilation: small arterioles	Vasodilation: medium conduit arteries/wave reflecton	Stiffness: large artery aorta (PWV) (independent of BP)	Peripheral SBP / DBP	Central SBP	Heart (LVEDP)	Pulsatility: carotid AP, AIx
Organic nitrate (oral, iv, i.a.)	↑	↑↑↑	⇔	↓↓ *tol / ↓/⇔	↓↓↓	↓	↓
Inorganic nitrite/dietary nitrate (oral, inhaled, iv, i.a.)	Normoxia ↑ / Hypoxia ↑↑↑	↑↑↑↑ / ↑	⇔	↓↓ / ↓	↓↓↓	↓	↓
SNP (iv. i.a.)	↑↑	↑↑	?	↓↓	↓↓↓	↓	?
sGC stimulators/activators (oral, iv)	? ↑	?	?	↓↓	?	?	?

*tol, tolerance; *Aix*, augmentation index; *AP*, augmentation pressure; *DBP*, diastolic blood pressure; *i.a.*, intra-arterial; *iv*, intravenous; *LVEDP*, left ventricular end-diastolic pressure; *PWV*, pulse wave velocity; *SBP*, systolic blood pressure; *sGC*, soluble guanylate cyclase; *SNP*, sodium nitroprusside

the treatment of angina, as reviewed by Butler and Feelisch.[65] Reichert and Mitchell in 1880 showed that intravenous doses of potassium nitrite reduced arterial blood pressure in cats and dogs, while orally administered potassium nitrite was found to have effects on pulse rate and character in humans.[66] Five years later, Leech published an extensive series of sphygmographs in the British Medical Journal in 1885[67] demonstrating while the onset of action of nitrite on the arterial waveform was delayed (6—10 min) relative to that of nitroglycerine (2 min), the durations of action of sodium and potassium nitrite were more prolonged (strongly for 2.5 h, altogether for 4—5 h) than those produced by nitroglycerine (marked for 30—45 min, detectable for 2.5—3 h) and both were longer than amyl nitrite (10—20 min). This helped fuel the ongoing interest in the use of (inorganic) nitrite as a potentially superior drug, which then appeared in Materia Medica, was manufactured by Squibb in 1906, and was available as an injectable solution for vasospasm and hypertension in the 1920s.

Ben Densham, from King's College London (where this Chapter's co-authors are based), described in experiments performed in the cat fore- and hindlimb in 1927 "A species of 'unlocking effect' of the hydrogen ion on the vasodilator action of sodium nitrite and acetyl choline…" and "A specific adjuvant action of the lactate ion on the vasodilator action of sodium nitrite…,"[68] thus identifying the role of lower pH in the physiological responses to nitrite.

While Furchgott and Bhadrakom explored nitrite's vasodilatory potential in high concentrations with isolated strips of rabbit aorta in 1953[69] by that time, nitrite's clinical use had declined, due to its side effects and the availability of other agents, including longer-acting organic nitrates.

Reevaluation of nitrite in the "nitric oxide era"

Some 27 years after Furchgott's studies on nitrite in rabbit aorta, he discovered EDRF, which was followed by its identification as NO, see Palmer, Ferrrige and Moncada.[1,2] Against the huge amount of interest in NO, inorganic nitrite was considered to be "an inert oxidative end product of endogenous NO metabolism" in 1993 by Moncada and Higgs[5] and thus lack physiological effects. Even with the demonstration by Zweier in 1995 that nitrite is reduced to bioavailable NO during ischemia-reperfusion in the isolated perfused Langendorff rat heart,[70] nitrite appeared to have a deleterious effect and interest in nitrite waned again. Coupled with concerns about the potential to cause cancer (discussed below), nitrite was considered at worse toxic, and at best inactive. Interest in nitrite was not restored until this century, with the finding of cardiovascular effects under physiological conditions[71] in addition to beneficial effects under ischemic/hypoxic conditions.[72] This led to a proliferation of studies exploring nitrite's physiological role and therapeutic potential in a range of disease states.

Nitrite is formed endogenously in cells from the oxidation of NOS-derived NO by cytochrome C oxidase in mitochondria,[73] in the circulation by ceruloplasmin in plasma,[74] and in the gastrointestinal tract from the reduction of inorganic (including dietary) nitrate in the saliva,[75,76] by bacterial nitrate reductases (though nitrite

thus generated was not originally thought to be absorbed systemically, as discussed further in inorganic nitrate section below). Nitrite is now proposed to comprise the largest vascular storage pool of NO.[71]
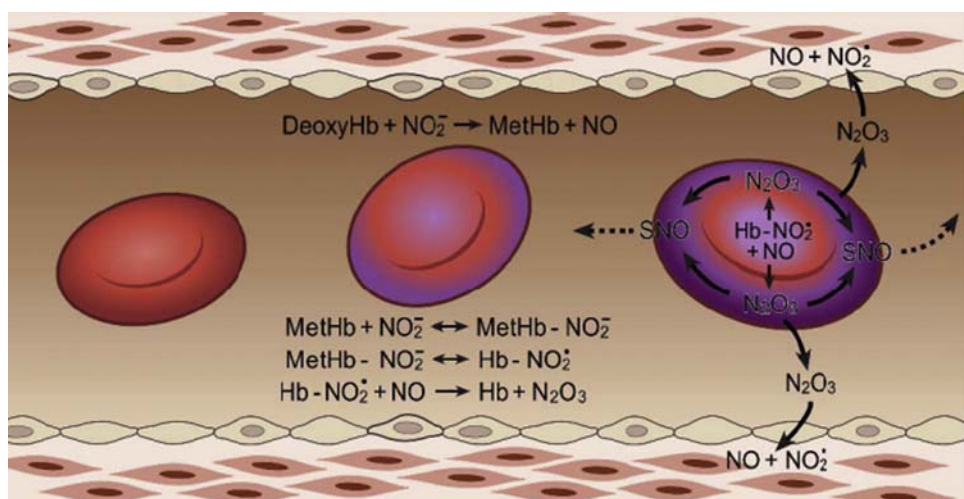
Recent assessment of vascular effects of nitrite

Blood flow studies in the human forearm allow observation of the effect of drugs on small resistance arteriolar function. Following intra-arterial infusion of a drug (via brachial artery cannulation), the effect on resistance arterioles is observed by measuring the change in estimated forearm blood volume, a technique known as forearm venous occlusion plethysmography. Although an initial study by Lauer et al. did not demonstrate any increase in FBF (representing small resistance arterioles) in response to an intrabrachial infusion of sodium nitrite (n = 3),[77] a landmark study by Cosby et al. found that infusion of supraphysiological and near-physiological concentrations of nitrite did increase FBF.[71] Vasodilatation was enhanced during handgrip exercise, and, the rate of NO formation was enhanced with lower oxygen saturations in ex vivo experiments, suggesting that nitrite bioactivation is regulated by a hypoxia-dependent mechanism. Maher et al. went on to show that at several doses, the nitrite-induced increase in FBF was enhanced under hypoxia conditions (vs. normoxia).[78] Nitrite is therefore recognized as a hypoxia-dependent dilator of small resistance arterioles, and this is entirely consistent with the proposed mechanism of nitrite bioactivation, such as deoxyHb and xanthine oxidase, which are hypoxia-dependent mechanisms.[7] On this point, however, the key question has been, how does the NO formed from nitrite/catalyzed by deoxyHb in the
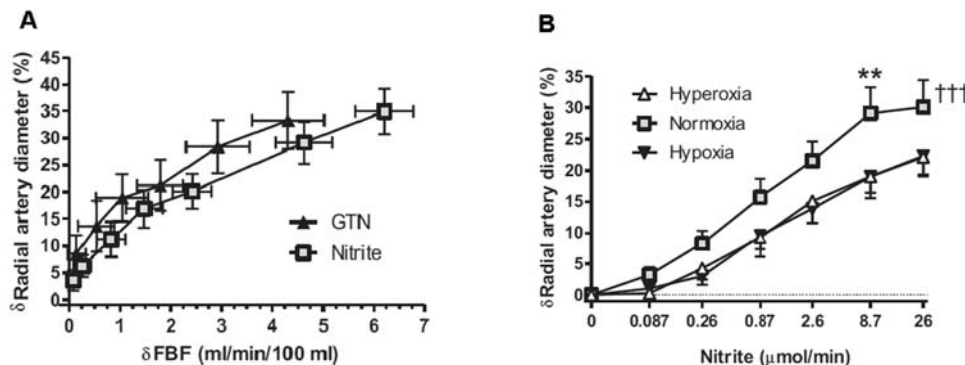
RBC escape scavenging by Hb/the RBC to reach the vessel wall and effect vasodilatation? Basu et al. proposed a mechanism via dinitrogen trioxide formation (N_2O_3), which is a small and uncharged molecule with a greater diffusion coefficient than NO and the capacity to readily form vasodilating nitrosothiols; see Fig. 51.6.[79]

The human forearm model can also be used to assess conduit artery function through 2D ultrasound assessment of radial artery diameter, which we performed simultaneously with FBF. With ∼100% arterial hemoglobin oxygen saturation in healthy volunteers, nitrite would not be expected to result in vasodilatation in conduit vessels, as this would not support reduction of nitrite to NO and NO is rapidly oxidized to nitrite and nitrate. However, we found pronounced radial artery dilatation following intrabrachial infusion.[80] Moreover, this was relatively greater than the effect on FBF, suggesting a selective dilatory effect of nitrite on medium-sized conduit arteries. Indeed, the degree of selectivity almost matched that of GTN (see Fig. 51.7A)—the most selective larger artery (i.e., of medium sized conduit arteries) dilator yet identified, as we have described above.[61]

Furthermore, the impact of hypoxia was opposite in the radial (conduit) artery compared to resistance arterioles: nitrite's vasodilatory effect was maximal in normoxia and inhibited by hypoxia (and by hyperoxia); see Fig. 51.7B.[80] Given this surprising finding, identifying the precise mechanism has proven challenging. However, nitrite infusion was associated with local forearm increases in cGMP production, albeit collected in the returning venous circulation; thus, while this supported generation of NO from nitrite, to what extent this occurred in the radial artery was not clear. We also showed that the use of raloxifene to

FIGURE 51.6   Model of nitrite- and Hb-mediated N_2O_3 export and nitrosation. Hemoglobin deoxygenation (purple) occurs preferentially at the submembrane of the red blood cell as it traverses the arteriole. Nitrite reacts with deoxyHb to make MetHb and NO. Much of this NO binds to hemes of deoxyHb or undergoes dioxygenation to form nitrate and MetHb from oxyHb. MetHb binds nitrite to form an adduct with some Fe(II)−NO2 character (Hb−NO2). This species reacts quickly with NO to form N2O3, which can diffuse out of the red cell, later forming NO and effecting vasodilation and/or forming nitrosothiols (SNOs). Low-molecular-weight nitrosothiols may contribute to exportable vasodilatory activity. *Reproduced from Figure 7 from Basu S, Grubina R, Huang J, et al. Catalytic generation of N_2O_3 by the concerted nitrite reductase and anhydrase activity of hemoglobin. Nat Chem Biol. 2007;3:785−794.*
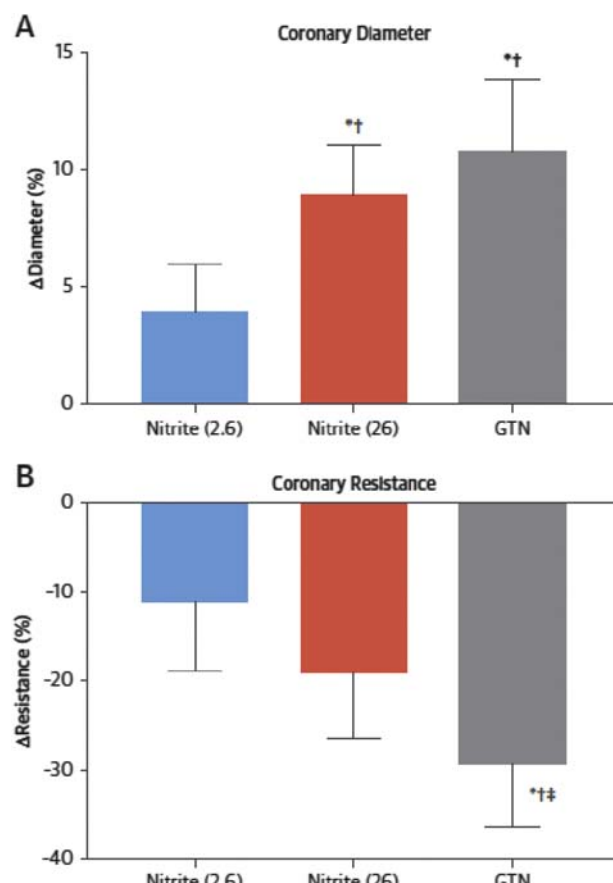
FIGURE 51.7 Changes in radial artery diameter (%) with intrabrachial infusions of (A) sodium nitrite and glyceryl trinitrate (GTN) versus change in forearm blood flow (FBF) at incremental dose steps of nitrite (0.087−87 μmol/min) and GTN (0.013−4.4 nmol/min); (B) sodium nitrite (0.087−26 μmol/min; n = 8) randomized crossover study under conditions of systemic hypoxia, normoxia, and hyperoxia on the change in radial artery diameter during. **P < .01 versus hypoxia; †††P < .001 versus hypoxia and hyperoxia. *Reproduced from Figures 3C and 7 from Omar SA, Fok H, Tilgner KD, et al. Paradoxical normoxia-dependent selective actions of inorganic nitrite in human muscular conduit arteries and related selective actions on central blood pressures. Circulation. 2015;131:381−389; Discussion 389.*

inhibit aldehyde oxidase (AO)—an important producer of ROS in humans, enhanced nitrite-induced dilatation. Since hypoxia, as well as hyperoxia, predisposes to ROS production, this provides indirect evidence for varying dilatory responses in light of the prevailing levels of oxygenation.
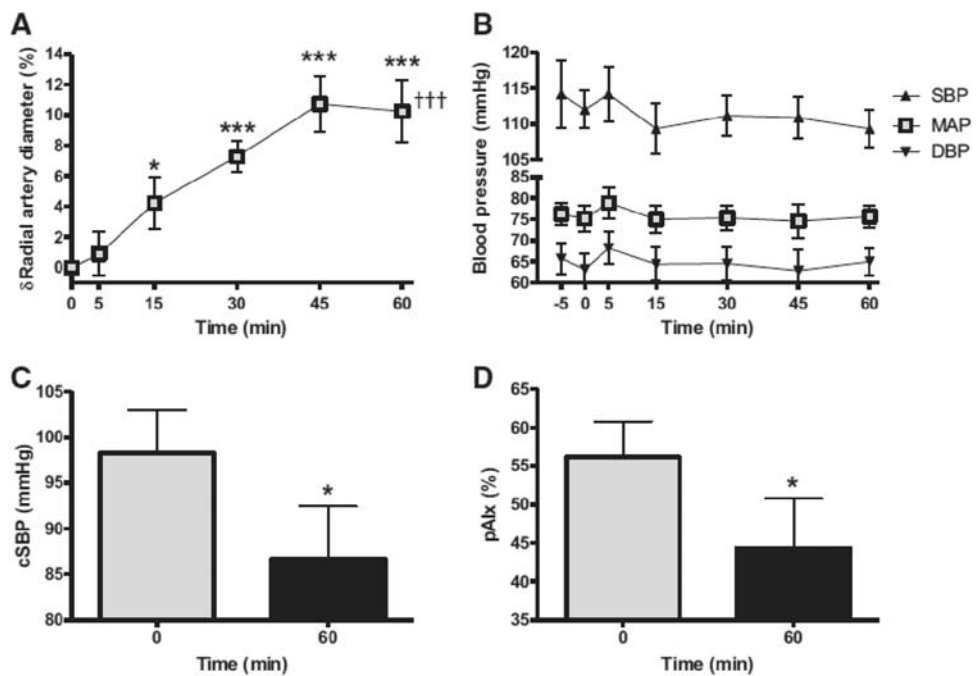
We have also demonstrated nitrite's selectivity for conduit over resistance arteries in human coronary arteries. Intracoronary infusion of sodium nitrite demonstrates a dose-dependent dilatory effect on epicardial (conduit) coronary arteries, but without any significant effect on coronary blood flow or coronary artery resistance (which reflect resistance arteriolar function)—despite being observed in the metabolically active (beating) heart[81]; see Fig. 51.8. The effect of nitrite was compared to that of GTN, which dilated epicardial coronary arteries, but also increased coronary flow and decreased coronary resistance. These findings suggest that nitrite was at least as selective for large versus small vessels as GTN.

When given via an intravenous infusion, inorganic nitrite causes systemic vasodilatation of conduit arteries—i.e., the radial artery by ∼11%, and a decrease in central (aortic) systolic blood pressure (and augmentation index, AIx),[80] without effect on peripheral brachial systolic blood pressure (or on FBF/small resistance artery dilatation); see Fig. 51.9.

The finding described above is consistent with nitrite's selectivity for conduit arteries, given the similar relationship described for GTN.[58,62] The benefit of a circulating pool of nitrite is its stability in whole blood. Nitrite has a half-life following intravenous infusion in vivo of approximately 50 min[82,83] compared to the extremely short half-life of molecular NO (∼20 ms).[4] This disparity in half-life therefore allows effective delivery of the NO precursor nitrite to the target tissue, whereby local reduction yields bioactive NO.

FIGURE 51.8 Changes in (A) Coronary Artery Diameter, (B) Coronary resistance with intracoronary infusions of nitrite (2.6 mmol/min "Nitrite (2.6)") and nitrite (26 mmol/min "Nitrite (26)"), and glyceryl trinitrate (GTN; (1 μg/min)). Data are mean ± SEM. *P < .05 versus baseline; †P < .05 versus nitrite (2.6 mmol/min); ‡P < .05 versus nitrite (26 mmol/min). *Reproduced from O'Gallagher K, Khan F, Omar SA, et al. Inorganic nitrite selectively dilates epicardial coronary arteries. J Am Coll Cardiol. 2018;71:363−364.*

FIGURE 51.9   Effect of intravenous sodium nitrite (8.7 μmol/min over 60 min) on (A) change in radial artery diameter (%) in the contralateral arm (B) peripheral brachial blood pressure (BP) measurements (systolic BP [SBP], mean arterial pressure [MAP], or diastolic BP [DBP]), (C) central SBP (cSBP), and (D) peripheral augmentation index (pAIx) performed before and after the 60-minute infusion of sodium nitrite. Data are shown as mean - ± SEM (n = 9, A and B; n = 7, C and D). *$P < .05$, **$P < .01$ versus baseline; †††$P < .001$ overall. *Reproduced from Figure 8 from Omar SA, Fok H, Tilgner KD, et al. Paradoxical normoxia-dependent selective actions of inorganic nitrite in human muscular conduit arteries and related selective actions on central blood pressures.* Circulation. *2015;131:381−389; Discussion 389.*

The effect of inorganic nitrite on the cardiovascular system—ventricular hemodynamics

Limited animal and human data exist to describe the effect of nitrite on cardiac function. In the rat heart, nitrite exerts a concentration-dependent lusitropic effect[84] and augments the Frank Starling response[85] in an NO and cGMP/PKG-dependent, but NOS-independent manner. Nitrite's effect on the human heart has been studied in HFpEF, in which it improves ventricular performance during exercise (a greater increase in cardiac output with exercise vs. placebo),[86] as well as decreasing aortic wave reflections and inducing improvements in arterial elastance[87]; see below.

Clinical applications of inorganic nitrite

The therapeutic role of inorganic nitrite has been extensively studied in a number of conditions in which dysfunctional or dysregulated NO signaling has been demonstrated, including ischemia-reperfusion injury (IRI)[88−91] and cerebral vasospasm following subarachnoid hemorrhage (SAH).[92−94] Although not directly relevant to the theme of this text, the current lack of definitive RCT evidence for therapeutic use of nitrite in IRI and SAH highlights the difficulty often seen in therapeutic translation from "bench to bedside."

More relevant to the theme of arterial stiffness and pulsatile hemodynamics is nitrite's effect in conditions such

as arterial hypertension and HFpEF, as discussed in Chapter 36. HFpEF is of particular relevance to the therapeutic potential of nitrite in that it is a disease that is both associated with dysfunctional NO signaling on a cellular basis (eNOS uncoupling,[95] decreased myocardial PKG activity,[96] and decreased phosphorylation of cytoskeletal proteins[96,97]) while also on a systems basis being associated with abnormalities in arterial stiffness and pulsatile hemodynamics. For these and other reasons (such as lack of tolerance, Table 51.1), nitrite would appear to be an attractive therapy to target the key pathophysiological abnormalities in HFpEF.

Mechanistic studies have demonstrated the potential beneficial effects of nitrite in HFpEF, with benefits on resting hemodynamics[98] and also following exercise.[99] In the INDIE-HFpEF trial, however, inhaled nitrite failed to improve exercise capacity in patients with HFpEF compared to placebo,[100] nor did it improve any of the secondary endpoints (QOL, activity levels, ventricular filling pressures, or biomarkers). It has been suggested that the short half-life of nitrite (∼50 min) is the key reason why the findings of acute dosing were not confirmed with a four-week course of inhaled nitrite. It may also be that inhaled nitrite is more akin to local rather than systemic dosing.

There are several limitations of the current evidence base for inorganic nitrite in HFpEF. For example, on a mechanistic level, it is not clear whether systemic delivery of nitrite acts solely via changing cardiac loading conditions or whether there is a direct myocardial effect. Furthermore, on a

therapeutic level, although dietary nitrate—in contrast to organic nitrates—has been shown to improve exercise capacity in patients with HFpEF, there is a lack of placebo-controlled data to suggest that the effects seen with acute dosing persist with extended duration of therapies.

Part 4: inorganic (dietary) nitrate

Discovery of the inorganic nitrate-nitrite-NO pathway and its cardiovascular relevance

The medicinal purposes of nitrate have been utilized as early as the ninth century, when the Chinese documented the ability of wall saltpetre (calcium nitrate) to relieve "acute heart pains, and cold in the hands and feet".[101] However, the nitrate-nitrite-NO pathway was not realized and described as such until 2008[6]; see Fig. 51.10.

The nitrate-nitrite-NO pathway (which includes the enterosalivary circulation) describes the two-step process by which NO is produced from orally ingested, and endogenously produced, inorganic nitrate (NO_3^-), via inorganic nitrite (NO_2^-). Inorganic nitrate is readily absorbed by the upper gastrointestinal tract with a bioavailability of $\sim$100%,[102,103] peak plasma [nitrate], Cmax is achieved from $\sim$60 to 90 min, with a half-life of 5—8 h in the circulation.[104,105] Approximately 25% is concentrated in the salivary glands, with the majority of the remainder being excreted via the kidneys.[106] Following salivary secretion into the oral cavity, nitrate is reduced to nitrite, mainly by strict anaerobes (e.g., *Veillonella species*) and by facultative anaerobic bacteria (*Actinomyces odontolyticus* and *Rothia mucilaginosa*) on the posterior surface of the tongue[107] resulting in a salivary nitrite concentration >1000 times the plasma nitrite concentration.[108]

A proportion of the nitrite in swallowed saliva is subsequently converted in the acidic stomach environment in a nonenzymatic fashion to NO, i.e., nitrite disproportionation via nitrous oxide and dinitrogen trioxide[109] (which is also a mechanism of NO generation from nitrite in ischemic tissues, where the local pH is low[70,110]). However, at physiological and dietary-derived concentrations, nitrite was not originally thought to be absorbed systemically, e.g., with no increase in plasma nitrite concentrations found in 2003 following lettuce ingestion,[111] and therefore would lack physiological effect. With high pharmacological doses of nitrite, it was easier to demonstrate that it entered the circulation (due to absorption across the upper gastrointestinal tract) as shown in 2009.[112] Lundberg and Govoni showed in 2004 that ingested nitrate did result in an increase in plasma (nitrite).[108]

Dietary nitrate and blood pressure

The functional effect of dietary nitrate was initially revealed by Larsen et al. who found a decrease in diastolic blood pressure following three days of sodium nitrate ingestion in healthy volunteers in 2006.[113] We demonstrated in 2008 that a single ingestion of beetroot juice by healthy volunteers, as a source of dietary nitrate, acutely decreased systolic and diastolic blood pressure with peak effects from approximately 2—3 h, in parallel with the peak increase in plasma [nitrite].[105] The importance of the salivary conversion of nitrate to nitrite was demonstrated by the finding that if subjects spit rather than swallow their saliva (and therefore expel salivary nitrite), the rise in plasma nitrite associated with ingestion of dietary nitrate is abolished[108] as is the blood pressure-lowering effect.[105] The term "nitrate-nitrite-NO pathway" was thus coined in 2008.[6] Since, besides beetroot, green leafy vegetables are a rich source of dietary nitrate, and they are widely consumed in Mediterranean and Japanese diets which are associated with greater longevity and diminished cardiovascular disease, it has been proposed that nitrate is a key component of a healthy diet and accounts for the blood pressure lowering and other cardiovascular benefits, for example, as demonstrated in the DASH study,[114]
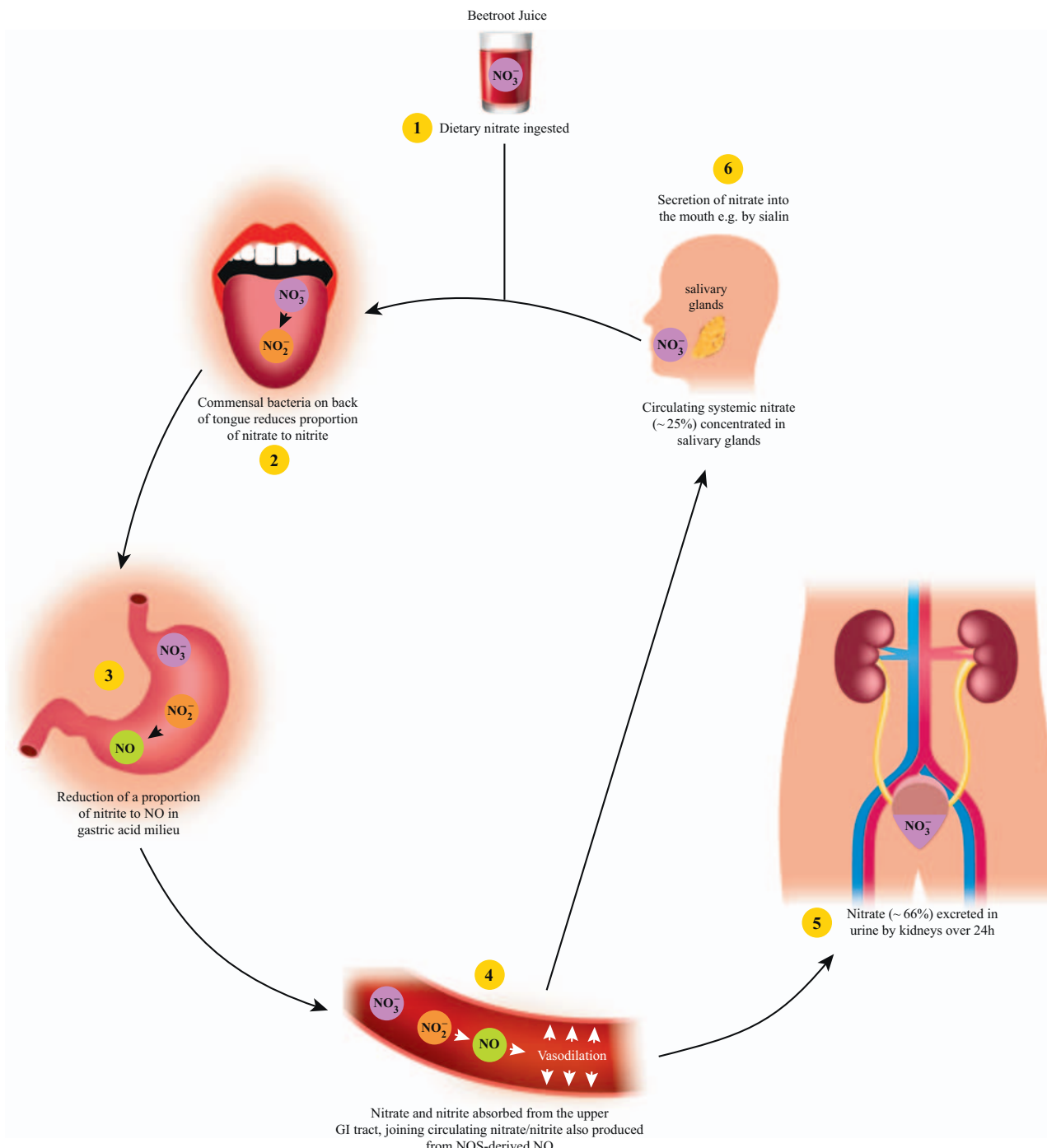
Besides spitting, the nitrate-nitrite-NO pathway may be interrupted by mouthwash such as chlorhexidine, which reduces the amount of nitrate-reducing bacteria on the posterior surface of the tongue (by 80% for bacterial counts from tongue scrapings), almost abolishing the increase in salivary [nitrite] and plasma [nitrite] in healthy volunteers, following an oral nitrate load.[115] Furthermore, under basal conditions with low-normal dietary nitrate intake, chlorhexidine increases systolic and diastolic blood pressure in healthy volunteers from the first day, and throughout a seven-day period of mouthwash use.[116] This highlights the potential implications of widespread mouthwash use on blood pressure and other cardiovascular parameters in the population.

A number of recent meta-analyses have been performed to address the overall effect of inorganic nitrate on BP. The findings of these analyses suggest that, for interventions of up to 15 days duration, inorganic nitrate supplementation is associated with a significant decrease in SBP of $\sim$4 mmHg.[117] A similar magnitude of effect on SBP was seen in a later meta-analysis of studies with an intervention duration of 1 week or more; however, the effect was only significant for clinic BP measurements, with no significant BP changes observed in studies using ambulatory and/or home BP monitoring.[118]

Dietary nitrate and arterial stiffness/pulse wave velocity

In addition to blood pressure, several studies have shown that inorganic nitrate improves arterial stiffness. This was first demonstrated in healthy volunteers by Bahra et al.,[119] whereby aortic pulse wave velocity (aPWV) was decreased by $\sim$0.3 m/s following potassium nitrate (8 mmol) ingestion ($P < .01$), associated with an almost 5 mmHg decrease

FIGURE 51.10 The nitrate-nitrite-NO pathway. *Based on an original drawing by Andres Jaramillo Moyano and Andrew Webb.*

in SBP.[119] Similarly, in patients with grade 1 hypertension, Ghosh et al. found that beetroot juice ($\sim$3.5 mmol nitrate) decreased aPWV by $\sim$0.8 m/s at 3h, again associated with a $\sim$10 mmHg decrease in SBP.[120] Velmurugan et al. showed that in a double-blind parallel group placebo-controlled study in 69 patients with hypercholesterolemia that the effect was maintained following a six-week course

of dietary nitrate (250 mL of beetroot juice/day), with a $\sim$0.2 m/s decrease in aPWV accompanied by a $\sim$4 mmHg decrease in SBP.[121] While as in the previous studies, these differences in PWV were only significant for before and after the active intervention, and not versus control, there was in this placebo-controlled study also a decrease in augmentation index between groups (-3.9%). In each of

the above studies with dietary nitrate, the decrease in aPWV was measured using the Vicorder device and was in the context of a decrease in blood pressure. However, whether dietary nitrate's effect on aPWV is all due to the change in BP, or whether it is possible to alter aPWV independently of BP (i.e., via effects on the arterial wall), and over a longer period was not clear. Therefore, we tested this in our "Vasera study," with Kennedy Cruickshank, a factorial design study in which we randomized 126 patients with hypertension and with Type 2 diabetes (T2DM), or at risk of T2DM (mainly BMI >27) to six months' active nitrate-containing beetroot juice or placebo nitrate-depleted beetroot juice and either spironolactone or doxazosin.[122,123] As two previous studies in patients with T2DM by Gilchrist and colleagues had not identified a blood pressure-lowering effect of dietary nitrate,[124,125] we were not anticipating a decrease in BP with the nitrate versus placebo in this cohort; this would allow comparison of any difference in arterial stiffness in the absence of any difference in BP, but we were also assessing arterial stiffness using cardio-ankle vascular index (CAVI) a nominally BP-independent measure. Indeed, nitrate did not decrease peripheral brachial BP versus placebo beetroot juice, and there were no differences in CAVI. Instead, dietary nitrate resulted in a significant decrease in central aortic SBP by ∼2.6 mmHg. Given the lack of effect on brachial BP, this represented a selective decrease in central BP, which is consistent with our previous findings described above with inorganic nitrite (selectively reducing central BP), with the associated mechanism of normoxia-dependent conduit artery dilation.[80] Therefore, dietary nitrate and inorganic nitrite may have their main effects on medium-sized conduit arteries in normoxia, associated with decreases in central aortic BP, rather than an effect on large artery (aortic stiffness) per se. For spironolactone versus doxazosin, there were also no differences between them in their effects on decreasing BP (as intended in the design of the study) but also no significant differences in CAVI (infact, CAVI was borderline lower for doxazosin than spironolactone). Thus, our data suggest that it is possible to alter aortic stiffness independently of BP and eluding to a role for sympathetic (nor)-adrenergic tone in regulation of large arterial stiffness, mechanisms which are supported by subsequent work by Faconti et al.[126] Here we used lower-limb venous occlusion (LVO; a similar intervention to lower-body negative pressure) which reduced mean arterial BP (by ∼1.8 mmHg) in 70 patients with hypertension but increases sympathetic activity (reflected by an increase in heart rate variability; HRV) and found that LVO elevated aortic and carotid-femoral PWV by ∼0.8 and ∼0.7 m/s, respectively. By comparison, device-guided breathing decreased BP, sympathetic tone/HRV and PWV by ∼1.2 m/s, exceeding

nifedipine's effect on PWV ∼0.7 m/s, despite the latter's greater effect on BP (but lack of effect on HRV).

Several other studies have been performed investigating pulsatile hemodynamics and arterial stiffness with dietary nitrate. For example, Liu et al. performed a study in 26 healthy volunteers (albeit with average BMI in the overweight range 25.4 [range 19.1−30.4]) with acute dosing with a spinach-rich meal (220 mg nitrate) which improved pulsatile hemodynamics (it reduced pulse pressure and SBP, but not DBP) but showed only a trend to improvement in carotid-femoral PWV (cfPWV).[127] The same group (Bondonno et al.) performed a crossover RCT assessing the effect of seven days' high-nitrate (>300 mg nitrate) versus seven days' low nitrate diet in 38 patients with high-normal blood pressure, who were on average in the overweight range BMI 27.1 (range 20.6−37.0): there was no effect on SBP or DBP or cfPWV (SphygmoCor).[128] Kim et al., studied 13 healthy postmenopausal women (Aged 63 ± 1 year; BMI 25.4 ± 1.4 [SEM]) and found that acute administration of nitrate-rich beetroot juice decreased peripheral and central (aortic) systolic and mean blood pressures, and increased pulse pressure augmentation, but had no effect on cfPWV, AP, or AIx; SphygmoCor).[129]

Whether age influences the hemodynamic responses before and after dietary nitrate was investigated by Hughes W. et al., who found that beetroot juice (nitrate 9.4 mmol) decreased aortic augmentation index (AIx@75 bpm; SphygmoCor) in 14 healthy young adults (aged ∼25 year) despite AIx@75 already being negative: from −4.3% at baseline to −8.8%, but did not decrease AIx in 12 healthy older normotensive individuals (aged ∼64 year; baseline AIx ∼28%), despite decreasing peripheral and central BP in both groups.[130] Walker M et al. studied 15 healthy older men of similar age (mean 69 years old, mean BMI 26.6) in an acute double blind randomized crossover study with a similar dose of dietary nitrate (800 mg) as beetroot juice, and found an improvement in AIx75 versus placebo, but no effect on BP or PWV.[131] The results of larger, longer intervention studies are awaited, such as the NITRATE-TOD study, a randomized, double-blind, placebo-controlled trial investigating the effects of inorganic nitrate in hypertension-induced target organ damage, in which reduction in PWV and central BP are primary outcomes along with change in LV mass.[132]

Augmentation index was also assessed in 17 patients with HFpEF (mean age 65.5 ± 8.9 years) in the randomized, double-blind, crossover study by Zamani et al.,[133] as discussed in Chapter 36. In brief, here a single dose of nitrate-rich beetroot juice (nitrate 12.9 mmol) significantly decreased AIx and systemic vascular resistance (vs. placebo), in parallel with the accompanying increases in total work performed, cardiac output, and peak oxygen

consumption (peak VO_2) during supine-cycle maximal-effort cardiopulmonary exercise tests. Chirinos and colleagues also tested the effects of organic and inorganic nitrates on carotid as well as aortic hemodynamics, using carotid tonometry in two separate studies (one being the above study by Zamani et al.) in patients with HFpEF.[134] Sublingual GTN (0.4 mg) (n = 26) produced marked vasodilation in the carotid territory, decreasing carotid bed vascular resistance, and carotid characteristic impedance, and while it diminished the real component of the reflection coefficient in the first harmonic, GTN lacked effect in the second harmonic and increased the third harmonic. These first three harmonics contain most of the pulsatile energy which is transmitted to the brain. This was also in the face of a significant ∼13 mmHg drop in central SBP, without a significant decrease in pulse pressure. Hence, GTN exhibited risks of hypotension and produced excessive brain vasodilation/without decreasing the arterial pulsatile load on the left ventricle. By contrast, oral dietary inorganic nitrate (n = 16) in the form of 12.9 mmol nitrate-rich beetroot juice, more consistently decreased central arterial wave reflections—across all three lower harmonics, without decreasing carotid vascular resistance, carotid characteristic impedance, or BP. Further analysis revealed that GTN significantly elevated total transmission, from the aorta to the carotid, of hydraulic power by ∼50% and energy penetration by ∼33%, with reciprocal losses in aortic hydraulic power and energy.[135] These findings may underpin GTN's common adverse effects such as headaches and highlight concerns of increased pulsatile hemodynamic stress of the cerebral microcirculation in HFpEF. Dietary nitrate lacked such deleterious effects. Additionally, inorganic nitrate, but not GTN, improved the Buckberg index (ratio of diastolic to systolic pressure-time integrals[136]). This suggests that inorganic nitrate, but not GTN, improves the relationship between pulsatile hemodynamics and myocardial oxygen supply:demand matching. While the study found that GTN reduced central systolic blood pressure, but inorganic nitrate had no significant effect, this was carried out in 16 patients, comparing BPs only at ∼2.5h postjuice ingestion in patients with an elevated BMI 34.4 (SD 3.5). As we have described above, several other studies in varied patient/participant groups provide evidence that inorganic nitrate/beetroot juice lowers central SBP both acutely, and, for example, in our study with chronic ingestion over six months, among others.[122,123,129,137−139] Moreover, a very recent meta-analysis by Li et al. provides further confirmatory support from 47 trials with 1101 participants which used repeated dosing of nitrate over at least three days, with overall significant effects on decreasing: peripheral SBP by ∼3 mmHg, peripheral DBP ∼1.5 mmHg, central SBP ∼1.6 mmHg, central DBP ∼2 mmHg; while for PWV there was a borderline effect −0.24 m/s (95% CIs −0.50,

0.01; $P = .06$) along with borderline effects on AIx and 24h SBP and DBP.[140]

The above data highlight several important differences between organic and inorganic nitrates in the context of HFpEF. The ventricular and arterial dysfunction and stiffening seen in HFpEF renders patients susceptible to hypotension in the setting of excessive peripheral vasodilatation. Given inorganic nitrate/nitrite's relatively selective action on conduit versus microvascular arteries (and theoretically central over peripheral BP) in normoxia as well, this confers a potential advantage versus organic nitrate. Furthermore, in exercising tissues (local hypoxia), the effect of inorganic nitrate/nitrite on the microvasculature may enhance blood flow to exercising muscles. An additional, likely related and potentially beneficial cardiac effect that we identified, was that dietary nitrate (beetroot juice) ingestion over six months decreased left ventricular end-diastolic and end-systolic volumes by ∼5% (vs. placebo) in our Vasera study.[141]

Inorganic nitrate and angina

A number of studies have assessed the effect of inorganic nitrate on angina. In the "Inorganic Nitrate in Angina Study," 600 mg sodium nitrate for 7−10 days increased plasma [nitrate] and [nitrite] in 70 patients with stable angina, associated with a trend to an increase in time-to- 1 mm ST depression on treadmill testing and significantly increased total exercise time by ∼16 s versus double blind placebo.[142] The NITRATE-OCT study is an ongoing randomized-double-blind, placebo-controlled trial testing the effect of six months' nitrate-containing versus nitrate-depleted beetroot juice on vascular function, platelet reactivity and coronary restenosis (the primary outcome measure, assessed by quantitative coronary angiography and optical coherence tomography; OCT) in 246 patients undergoing percutaneous coronary intervention for stable angina.[143]

Limitations of organic and dietary/inorganic nitrates

In the published literature regarding inorganic nitrate, it is common to see comparisons with organic nitrate in which the limitations of organic nitrate are listed.[144] Key examples of such limitations include: the rapid development of tolerance; side effects such as headache; and the tendency of organic nitrates to induce a state of endothelial dysfunction.[145,146] Indeed, in the NEAT-HF study, organic nitrate actually worsened activity levels in patients with HFpEF, a finding that has been attributed to endothelial dysfunction due to ISMN,[51] or could be related to its side effect profile from nonselective hemodynamic effects (including brain vasodilation and hypotension) as discussed above.

Although dietary nitrate is often considered synonymous with beetroot juice, nutritional studies may consider a range of green leafy vegetables as dietary nitrate. In such studies, calculation of daily dietary nitrate intake may involve calculation of the total amount of dietary nitrate using participant food diaries. Estimations such as this are highly prone to error. Beetroot juice as dietary nitrate has issues with palatability. In a recent study, we asked volunteers to give concentrated beetroot juice a score for taste on a scale of 0 to 10 (0 for disgusting, 10 for delicious). The average score for concentrated beetroot juice (diluted in water) was only 4 out of 10[147] (of note in this particular study, taste was improved by mixing the beetroot juice with golden grapefruit juice, a combination which potentiated beetroot juice's effect on lowering SBP and pulse pressure). This is in addition to discoloration of urine and stool due to beetroot which, although harmless, may be distressing to patients. While most studies to date suggest that individuals taking inorganic nitrate (and nitrite) do not develop tolerance, a recent study in which 20 patients with hypertension and metabolic syndrome took sodium nitrite for 12 weeks has suggested that tolerance to inorganic nitrite may indeed occur (the BP-lowering effect was sustained for the first 10 weeks, but not present at week 12).[148] Also, a recent, relatively large study in 231 patients with hypertension, found no overall effect on ambulatory blood pressure of nitrate pills (300 mg nitrate), or leafy green vegetables containing 300 mg nitrate versus low-nitrate vegetables or placebo pills taken daily over five weeks.[149]

These data are in contrast to the other studies described above, with long term evidence from our findings of the (central) BP-lowering effect of dietary nitrate is seen at 6 months.[122] Further studies are required to assess whether this effect is consistently seen with longer term treatment with nitrite and also whether a similar phenomenon is seen with dietary nitrate.

As is discussed in detail later in this chapter (Part 6), the pathophysiology of some disease states involves abnormalities in the redox state of sGC which becomes NO-unresponsive. This may therefore decrease the effectiveness of any therapies, organic and inorganic nitrates included, that act via NO signaling.

Safety concerns regarding dietary nitrate and inorganic nitrite

Although inorganic nitrate is not associated with the side-effects commonly seen with organic nitrates, e.g., headache, acute side effects can occur, depending on mode of delivery. For example, as noted above, approximately 10% of patients who receive oral sodium nitrate experience gastrointestinal side effects such as nausea, vomiting, and/or abdominal discomfort.[142]

Methaemoglobinaemia (oxidation of hemoglobin to methemoglobin which lacks oxygen-carrying capacity) is considered to be a possible side effect of treatment with inorganic nitrate/nitrite; however, the doses used in clinical studies have not resulted in clinically significant methaemoglobinaemia (generally considered as a methemoglobin level of greater than 5%−10%).

The most concerning potential adverse effect of dietary nitrate is perhaps also the most contentious, i.e., whether or not consumption of dietary nitrate causes gastrointestinal malignancy. Definitive data are absent with some studies suggesting a positive association yet others suggesting that higher levels of dietary nitrate are associated with *decreased* incidence of malignancy.[150−153] The conflicting data may be due to different effects from dietary inorganic nitrate (beetroot, green leafy vegetables which may confer a protective effect) versus inorganic nitrate and nitrite used as both food preservative in curing meats and as a colorant, which may be harmful. This tension is reflected in the guidance from the International Agency for Research on Cancer guidance that it is nitrate/nitrite consumed under "conditions that result in endogenous nitrosation" that is probably carcinogenic to humans, rather than dietary nitrate/nitrite in themselves.

Part 5: nitric oxide donors
Sodium nitroprusside

In current cardiovascular clinical practice, the role of SNP is largely restricted to hypertensive crises and is used less frequently than in the past. Nonetheless, SNP displays some interesting characteristics which provide further insights related to NO physiology and deserves a brief mention here. For example, in the rabbit heart, SNP exerts a negatively inotropic effect in a cGMP-mediated manner, disproportionately decreasing myocardial oxygen consumption and consequently increasing economy of cardiac muscle contraction.[153] In humans, SNP (like GTN and inorganic nitrite) demonstrates relative selectivity for conduit over resistance arteries.[61] When delivered via the intracoronary route, SNP decreases LVEDP, heart rate, and the time to end-systole (i.e., hastens the onset of diastole), while increasing the LV end-diastolic volume.[154] Indeed, such studies utilizing intracoronary SNP were the first to suggest a direct myocardial effect of NO.

Part 6: soluble guanylate cyclase
The role of soluble guanylate cyclase in the cardiovascular system

As we have described above, sGC is a key component in NO signal transduction, generating cGMP in the presence of NO stimulation. Vascular disease, e.g., hypertension, is associated with decreased expression and activity of sGC.[155−157]

Dysfunctional soluble guanylate cyclase signaling

sGC is itself under redox regulation[158] and exists in both reduced, heme-containing and oxidized, heme-free forms. Heme-free sGC is unresponsive to NO. In the setting of oxidative stress, free radicals such as peroxynitrite oxidize sGC, resulting in an increased proportion of oxidized, heme-free sGC. A concept has emerged which hypothesizes pathological "NO resistance" within cardiovascular disease states such that oxidative stress results not only in a free radical-induced decrease in NO bioavailability, but also in a peroxynitrite-induced decrease in sGC function via an increased proportion of NO-unresponsive oxidized sGC.[159]

Drugs that target soluble guanylate cyclase

Two main classes of drugs exist that target sGC directly: the sGC *stimulators* and the sGC *activators*.

Soluble guanylate cyclase stimulators

sGC stimulators (e.g., Riociguat, Vericiguat) act in both an NO-dependent and NO-independent manner. They have both the ability to directly stimulate heme-containing sGC[160,161] and also to sensitize sGC to low concentrations of NO. In the clinical setting, riociguat improves exercise tolerance in pulmonary arterial hypertension.[162,163]

Following phase II studies of Vericiguat,[164] the VIC-TORIA trial was the first large scale RCT assessing the effect of vericiguat in HF.[165] In this study, in patients with symptomatic HFrEF (NYHA II−IV, EF<45%) vericiguat decreased the composite endpoint of cardiovascular death and first hospitalization for HF. Side effects of vericiguat included symptomatic hypotension, syncope, and anemia.

In a placebo-controlled, double-blind phase IIb trial exploring the effects of vericiguat in 789 patients with HFpEF, vericiguat failed to improve the primary end points of function, symptoms, and QOL.[166]

Soluble guanylate cyclase activators

Cinaciguat is an *sGC activator* which binds to the heme pocket of heme-free sGC.[167] It has been studied in patients with acute decompensated heart failure. Initial studies suggested that an intravenous infusion of cinaciguat was associated with favorable effects on cardiac loading, but with hypotension as a frequent adverse effect.[168,169] However, the COMPASS series of randomized controlled trials were halted early due to an excess of (nonfatal) hypotension and an absence of effect of cinaciguat on either cardiac index or symptom burden (all in the context of difficulty in patient recruitment).[170]

Nitroxyl

In addition to the sGC stimulators and activators, nitroxyl has an NO-like effect on sGC, triggering cGMP-dependent signaling. Nitroxyl (HNO) is the protonated, reduced form of NO,[171,172] with vasodilator[173] and positive inotropic effects,[174] which does not develop tolerance.[175] While the positive inotropic effects of nitroxyl are sGC-independent, experimental work in mice suggests that the vasodilatory effect is mediated by sGC signaling; nitroxyl's vasodilatory effect is abolished by the sGC inhibitor 1H-[1,2,4]oxadiazolo-[4,3-a]quinoxaline-1-one (ODQ) and is absent in sGC knockout mice.[176] In humans in vivo (patients with systolic heart failure), nitroxyl decreases cardiac filling pressures, with a decrease in systemic vascular resistance and increase in cardiac output.[177]

Conclusions and future directions

In conclusion, therapeutic strategies targeted at NO signaling are of value (or potential value) in addressing arterial stiffness and abnormal pulsatile hemodynamics and associated conditions.

However, therapies for chronic pathology such as arterial stiffness, hypertension, and heart failure necessarily need to be long-term therapies. Therefore, future clinical studies focused on chronic conditions will require longer durations of treatment to be studied, reflecting the chronic nature of treatment that would be required in the relevant condition. While organic nitrates have been studied for decades, the field of inorganic nitrate/nitrite therapeutics is still in the process of progressing to large scale, long-duration randomized control trials, a step that will be necessary if these approaches are to become widely adopted in clinical practice. Following recent studies such as our Vasera study with 126 patients treated for six months,[178,179] and Sundqvist et al., with 231 patients treated for five weeks,[149] the results of several ongoing studies are awaited. These include the studies described above: NITRATE-OCT,[143] NITRATE-TOD (target organ damage and central BP/PWV in 160 patients with hypertension treated for 4 months),[132] and also NITRATE-CIN (prevention of contrast-induced nephropathy with five days' nitrate in 640 patients with acute coronary syndrome)[180] and the KNO3CK OUT HFpEF (Effect of KNO_3 Compared to KCl on Oxygen UpTake in HFpEF) in 76 patients, assessing the effects of a six-week' potassium nitrate administration on aerobic capacity.[181] This requirement for longer and larger trials is true for the other therapeutic strategies discussed in this chapter. In addition to the need for such trials, further study of the complex mechanisms relating to the biochemistry, (patho)-physiology, pharmacology, and hemodynamics are required. The figure by Vanderpool and Gladwin,[182] available free access (https://www.ahajournals.org/doi/10.1161/CIRCULATIONAHA.114.014149?url_ver=Z39.88-2003&rfr_id=ori:rid:crossref.org&rfr_dat=cr_pub%20%200pubmed), provides a summary of how the nitrate-nitrite-NO pathway influences central and peripheral hemodynamics and how this relates to potentially beneficial effects in HFpEF pathophysiology.

References

1. Furchgott RF, Zawadzki JV. The obligatory role of endothelial cells in the relaxation of arterial smooth muscle by acetylcholine. **Nature**. 1980; 288:373−376.

2. Palmer RM, Ferrige AG, Moncada S. Nitric oxide release accounts for the biological activity of endothelium-derived relaxing factor. **Nature**. 1987; 327:524−526.

3. Smith O. Nobel prize for NO research. **Nat Med**. 1998; 4:1215.

4. Crawford JH, Isbell TS, Huang Z, et al. Hypoxia, red blood cells, and nitrite regulate NO-dependent hypoxic vasodilation. **Blood**. 2006; 107:566−574.

5. Moncada S, Higgs A. The L-arginine-nitric oxide pathway. **N Engl J Med**. 1993; 329:2002−2012.

6. Lundberg JO, Weitzberg E, Gladwin MT. The nitrate-nitrite-nitric oxide pathway in physiology and therapeutics. **Nat Rev Drug Discov**. 2008; 7:156−167.

7. Khatri J, Mills CE, Maskell P, Odongerel C, Webb AJ. It is rocket science - why dietary nitrate is hard to 'beet'! Part I: twists and turns in the realization of the nitrate-nitrite-NO pathway. **Br J Clin Pharmacol**. 2017; 83:129−139.

8. Mills CE, Khatri J, Maskell P, Odongerel C, Webb AJ. It is rocket science - why dietary nitrate is hard to 'beet'! Part II: further mechanisms and therapeutic potential of the nitrate-nitrite-NO pathway. **Br J Clin Pharmacol**. 2017; 83:140−151.

9. Forstermann U, Sessa WC. Nitric oxide synthases: regulation and function. **Eur Heart J**. 2012; 33:829−837, 837a-837d.

10. Kwon NS, Nathan CF, Gilker C, Griffith OW, Matthews DE, Stuehr DJ. L-citrulline production from L-arginine by macrophage nitric oxide synthase. The ureido oxygen derives from dioxygen. **J Biol Chem**. 1990; 265:13442−13445.

11. MacMicking J, Xie QW, Nathan C. Nitric oxide and macrophage function. **Annu Rev Immunol**. 1997; 15:323−350.

12. Bolotina VM, Najibi S, Palacino JJ, Pagano PJ, Cohen RA. Nitric oxide directly activates calcium-dependent potassium channels in vascular smooth muscle. **Nature**. 1994; 368:850−853.

13. Lima B, Forrester MT, Hess DT, Stamler JS. S-nitrosylation in cardiovascular signaling. **Circ Res**. 2010; 106:633−646.

14. Shabeeh H, Khan S, Jiang B, et al. Blood pressure in healthy humans is regulated by neuronal NO synthase. **Hypertension**. 2017; 69:970−976.

15. Khan SG, Melikian N, Shabeeh H, et al. The human coronary vasodilatory response to acute mental stress is mediated by neuronal nitric oxide synthase. **Am J Physiol Heart Circ Physiol**. 2017; 313:H578−H583.

16. Seddon M, Melikian N, Dworakowski R, et al. Effects of neuronal nitric oxide synthase on human coronary artery diameter and blood flow in vivo. **Circulation**. 2009; 119:2656−2662.

17. Seddon MD, Chowienczyk PJ, Brett SE, Casadei B, Shah AM. Neuronal nitric oxide synthase regulates basal microvascular tone in humans in vivo. **Circulation**. 2008; 117:1991−1996.

18. Dawes M, Chowienczyk PJ, Ritter JM. Effects of inhibition of the L-arginine/nitric oxide pathway on vasodilation caused by beta-adrenergic agonists in human forearm. **Circulation**. 1997; 95:2293−2297.

19. Kim-Shapiro DB, Schechter AN, Gladwin MT. Unraveling the reactions of nitric oxide, nitrite, and hemoglobin in physiology and therapeutics. **Arterioscler Thromb Vasc Biol**. 2006; 26:697−705.

20. Liao JC, Hein TW, Vaughn MW, Huang KT, Kuo L. Intravascular flow decreases erythrocyte consumption of nitric oxide. **Proc Natl Acad Sci USA**. 1999; 96:8757−8761.

21. Barry PH, Diamond JM. Effects of unstirred layers on membrane phenomena. **Physiol Rev**. 1984; 64:763−872.

22. Deonikar P, Kavdia M. A computational model for nitric oxide, nitrite and nitrate biotransport in the microcirculation: effect of reduced nitric oxide consumption by red blood cells and blood velocity. **Microvasc Res**. 2010; 80:464−476.

23. Chen X, Jaron D, Barbee KA, Buerk DG. The influence of radial RBC distribution, blood velocity profiles, and glycocalyx on coupled NO/O$_2$ transport. **J Appl Physiol**. 2006; 100:482−492.

24. Stamler JS, Loh E, Roddy MA, Currie KE, Creager MA. Nitric oxide regulates basal systemic and pulmonary vascular resistance in healthy humans. **Circulation**. 1994; 89:2035−2040.

25. Balligand JL, Kelly RA, Marsden PA, Smith TW, Michel T. Control of cardiac muscle cell function by an endogenous nitric oxide signaling system. **Proc Natl Acad Sci USA**. 1993; 90:347−351.

26. Shah AM, MacCarthy PA. Paracrine and autocrine effects of nitric oxide on myocardial function. **Pharmacol Ther**. 2000; 86:49−86.

27. Paulus WJ, Vantrimpont PJ, Shah AM. Paracrine coronary endothelial control of left ventricular function in humans. **Circulation**. 1995; 92:2119−2126.

28. Post H, d'Agostino C, Lionetti V, et al. Reduced left ventricular compliance and mechanical efficiency after prolonged inhibition of NO synthesis in conscious dogs. **J Physiol**. 2003; 552:233−239.

29. Feron O, Saldana F, Michel JB, Michel T. The endothelial nitric-oxide synthase-caveolin regulatory cycle. **J Biol Chem**. 1998; 273:3125−3128.

30. Xu KY, Huso DL, Dawson TM, Bredt DS, Becker LC. Nitric oxide synthase in cardiac sarcoplasmic reticulum. **Proc Natl Acad Sci USA**. 1999; 96:657−662.

31. Barouch LA, Harrison RW, Skaf MW, et al. Nitric oxide regulates the heart by spatial confinement of nitric oxide synthase isoforms. **Nature**. 2002; 416:337−339.

32. Yang L, Liu G, Zakharov SI, Bellinger AM, Mongillo M, Marx SO. Protein kinase G phosphorylates Cav1.2 alpha1c and beta2 subunits. **Circ Res**. 2007; 101:465−474.

33. Layland J, Li JM, Shah AM. Role of cyclic GMP-dependent protein kinase in the contractile response to exogenous nitric oxide in rat cardiac myocytes. **J Physiol**. 2002; 540:457−467.

34. Vielma AZ, Leon L, Fernandez IC, Gonzalez DR, Boric MP. Nitric oxide synthase 1 modulates basal and beta-adrenergic-stimulated contractility by rapid and reversible redox-dependent S-nitrosylation of the heart. **PLoS One**. 2016; 11:e0160813.

35. Boolell M, Allen MJ, Ballard SA, et al. Sildenafil: an orally active type 5 cyclic GMP-specific phosphodiesterase inhibitor for the treatment of penile erectile dysfunction. **Int J Impot Res**. 1996; 8:47−52.

36. Galie N, Ghofrani HA, Torbicki A, et al. Simonneau G and sildenafil use in pulmonary arterial hypertension study G. Sildenafil citrate therapy for pulmonary arterial hypertension. **N Engl J Med**. 2005; 353:2148−2157.

37. Takimoto E, Champion HC, Li M, et al. Chronic inhibition of cyclic GMP phosphodiesterase 5A prevents and reverses cardiac hypertrophy. **Nat Med**. 2005; 11:214−222.

38. Michie AM, Lobban M, Muller T, Harnett MM, Houslay MD. Rapid regulation of PDE-2 and PDE-4 cyclic AMP phosphodiesterase

activity following ligation of the T cell antigen receptor on thymocytes: analysis using the selective inhibitors erythro-9-(2-hydroxy-3-nonyl)-adenine (EHNA) and rolipram. **Cell Signal**. 1996; 8:97−110.

39. Baliga RS, Preedy MEJ, Dukinfield MS, et al. Phosphodiesterase 2 inhibition preferentially promotes NO/guanylyl cyclase/cGMP signaling to reverse the development of heart failure. **Proc Natl Acad Sci USA**. 2018; 115:E7428−E7437.

40. Bubb KJ, Trinder SL, Baliga RS, et al. Inhibition of phosphodiesterase 2 augments cGMP and cAMP signaling to ameliorate pulmonary hypertension. **Circulation**. 2014; 130:496−507.

41. Yamashiro K, Milsom AB, Duchene J, et al. Alterations in nitric oxide and endothelin-1 bioactivity underlie cerebrovascular dysfunction in ApoE-deficient mice. **J Cereb Blood Flow Metab**. 2010; 30:1494−1503.

42. Nakamura K, Ikomi F, Ohhashi T. Cilostazol, an inhibitor of type 3 phosphodiesterase, produces endothelium-independent vasodilation in pressurized rabbit cerebral penetrating arterioles. **J Vasc Res**. 2006; 43:86−94.

43. Li H, Hong DH, Son YK, et al. Cilostazol induces vasodilation through the activation of Ca(2+)-activated K(+) channels in aortic smooth muscle. **Vascul Pharmacol**. 2015; 70:15−22.

44. Guazzi M, Vicenzi M, Arena R, Guazzi MD. Pulmonary hypertension in heart failure with preserved ejection fraction: a target of phosphodiesterase-5 inhibition in a 1-year study. **Circulation**. 2011; 124:164−174.

45. Redfield MM, Chen HH, Borlaug BA, et al. Effect of phosphodiesterase-5 inhibition on exercise capacity and clinical status in heart failure with preserved ejection fraction: a randomized clinical trial. **J Am Med Assoc**. 2013; 309:1268−1277.

46. Rocha BS, Gago B, Barbosa RM, Cavaleiro C, Laranjinha J. Ethyl nitrite is produced in the human stomach from dietary nitrate and ethanol, releasing nitric oxide at physiological pH: potential impact on gastric motility. **Free Radic Biol Med**. 2015; 82:160−166.

47. Gago B, Nystrom T, Cavaleiro C, et al. The potent vasodilator ethyl nitrite is formed upon reaction of nitrite and ethanol under gastric conditions. **Free Radic Biol Med**. 2008; 45:404−412.

48. Takahama U, Tanaka M, Hirota S. Transformation of ethyl alcohol to ethyl nitrite in acidified saliva: possibility of its occurrence in the stomach. **Arch Biochem Biophys**. 2008; 475:135−139.

49. Cotter G, Metzkor E, Kaluski E, et al. Randomised trial of high-dose isosorbide dinitrate plus low-dose furosemide versus high-dose furosemide plus low-dose isosorbide dinitrate in severe pulmonary oedema. **Lancet**. 1998; 351:389−393.

50. Taylor AL, Ziesche S, Yancy C, et al. Combination of isosorbide dinitrate and hydralazine in blacks with heart failure. **N Engl J Med**. 2004; 351:2049−2057.

51. Redfield MM, Anstrom KJ, Levine JA, et al. Isosorbide mononitrate in heart failure with preserved ejection fraction. **N Engl J Med**. 2015; 373:2314−2324.

52. Webb DJ, Freestone S, Allen MJ, Muirhead GJ. Sildenafil citrate and blood-pressure-lowering drugs: results of drug interaction studies with an organic nitrate and a calcium antagonist. **Am J Cardiol**. 1999; 83:21C−28C.

53. Zamani P, Akers S, Soto-Calderon H, et al. Isosorbide dinitrate, with or without hydralazine, does not reduce wave reflections, left ventricular hypertrophy, or myocardial fibrosis in patients with heart failure with preserved ejection fraction. **J Am Heart Assoc**. 2017; 6.

54. Murrell. Nitroglycerin as a remedy for angina pectoris. **Lancet**. 1879; 1:80−81.

55. Broadbent W. The pulse: its diagnostic prognostic and therapeutic indications. **Lancet**. 1875; ii:901−907.

56. Cameron JS, Hicks J. Frederick Akbar Mahomed and his role in the description of hypertension at Guy's Hospital. **Kidney Int**. 1996; 49:1488−1506.

57. Riva R. Un Nuovo sfigmomanometro. **Gazz Med di Torino**. 1896; 47:981−1001.

58. Jiang XJ, O'Rourke MF, Jin WQ, et al. Quantification of glyceryl trinitrate effect through analysis of the synthesised ascending aortic pressure waveform. **Heart**. 2002; 88:143−148.

59. Winbury MM, Howe BB, Hefner MA. Effect of nitrates and other coronary dilators on large and small coronary vessels: an hypothesis for the mechanism of action of nitrates. **J Pharmacol Exp Ther**. 1969; 168:70−95.

60. Barba G, Mullen MJ, Donald A, MacAllister RJ. Determinants of the response of human blood vessels to nitric oxide donors in vivo. **J Pharmacol Exp Ther**. 1999; 289:1662−1668.

61. Fok H, Jiang B, Clapp B, Chowienczyk P. Regulation of vascular tone and pulse wave velocity in human muscular conduit arteries: selective effects of nitric oxide donors to dilate muscular arteries relative to resistance vessels. **Hypertension**. 2012; 60:1220−1225.

62. Pauca AL, Kon ND, O'Rourke MF. Benefit of glyceryl trinitrate on arterial stiffness is directly due to effects on peripheral arteries. **Heart**. 2005; 91:1428−1432.

63. Cecelja M, Jiang B, Spector TD, Chowienczyk P. Progression of central pulse pressure over 1 decade of aging and its reversal by nitroglycerin a twin study. **J Am Coll Cardiol**. 2012; 59:475−483.

64. Gu H, Li Y, Fok H, et al. Reduced first-phase ejection fraction and sustained myocardial wall stress in hypertensive patients with diastolic dysfunction: a manifestation of impaired shortening deactivation that links systolic to diastolic dysfunction and preserves systolic ejection fraction. **Hypertension**. 2017; 69:633−640.

65. Butler AR, Feelisch M. Therapeutic uses of inorganic nitrite and nitrate: from the past to the future. **Circulation**. 2008; 117:2151−2159.

66. ET Reichert SM. On the physiological action of potassium nitrite. **Am J Med Sci**. 1880; 156:158−180.

67. Leech JA. Changes in sleep duration and recreational screen time among Canadians, 1998-2010. **J Sleep Res**. 2017; 26:202−209.

68. Densham B. The adjuvant action of the lactate ion on the vasodilator effect of sodium nitrite. **J Physiol**. 1927; 63:175−179.

69. Furchgott RF, Bhadrakom S. Reactions of strips of rabbit aorta to epinephrine, isopropylarterenol, sodium nitrite and other drugs. **J Pharmacol Exp Ther**. 1953; 108:129−143.

70. Zweier JL, Wang P, Samouilov A, Kuppusamy P. Enzyme-independent formation of nitric oxide in biological tissues. **Nat Med**. 1995; 1:804−809.

71. Cosby K, Partovi KS, Crawford JH, et al. Nitrite reduction to nitric oxide by deoxyhemoglobin vasodilates the human circulation. **Nat Med**. 2003; 9:1498−1505.

72. Webb A, Bond R, McLean P, Uppal R, Benjamin N, Ahluwalia A. Reduction of nitrite to nitric oxide during ischemia protects against myocardial ischemia-reperfusion damage. **Proc Natl Acad Sci USA**. 2004; 101:13683−13688.

73. Torres J, Sharpe MA, Rosquist A, Cooper CE, Wilson MT. Cytochrome c oxidase rapidly metabolises nitric oxide to nitrite. **FEBS Lett**. 2000; 475:263−266.

74. Shiva S, Wang X, Ringwood LA, et al. Ceruloplasmin is a NO oxidase and nitrite synthase that determines endocrine NO homeostasis. **Nat Chem Biol**. 2006; 2:486−493.

75. Tannenbaum SR, Sinskey AJ, Weisman M, Bishop W. Nitrite in human saliva. Its possible relationship to nitrosamine formation. **J Natl Cancer Inst**. 1974; 53:79−84.

76. Tannenbaum SR, Weisman M, Fett D. The effect of nitrate intake on nitrite formation in human saliva. **Food Cosmet Toxicol**. 1976; 14:549−552.

77. Lauer T, Preik M, Rassaf T, et al. Plasma nitrite rather than nitrate reflects regional endothelial nitric oxide synthase activity but lacks intrinsic vasodilator action. **Proc Natl Acad Sci USA**. 2001; 98:12814−12819.

78. Maher AR, Milsom AB, Gunaruwan P, et al. Hypoxic modulation of exogenous nitrite-induced vasodilation in humans. **Circulation**. 2008; 117:670−677.

79. Basu S, Grubina R, Huang J, et al. Catalytic generation of N_2O_3 by the concerted nitrite reductase and anhydrase activity of hemoglobin. **Nat Chem Biol**. 2007; 3:785−794.

80. Omar SA, Fok H, Tilgner KD, et al. Paradoxical normoxia-dependent selective actions of inorganic nitrite in human muscular conduit arteries and related selective actions on central blood pressures. **Circulation**. 2015; 131:381−389. Discussion 389.

81. O'Gallagher K, Khan F, Omar SA, et al. Inorganic nitrite selectively dilates epicardial coronary arteries. **J Am Coll Cardiol**. 2018; 71:363−364.

82. Dejam A, Hunter CJ, Tremonti C, et al. Nitrite infusion in humans and nonhuman primates: endocrine effects, pharmacokinetics, and tolerance formation. **Circulation**. 2007; 116:1821−1831.

83. Pluta RM, Oldfield EH, Bakhtian KD, et al. Safety and feasibility of long-term intravenous sodium nitrite infusion in healthy volunteers. **PLoS One**. 2011; 6:e14504.

84. Pellegrino D, Shiva S, Angelone T, Gladwin MT, Tota B. Nitrite exerts potent negative inotropy in the isolated heart via eNOS-independent nitric oxide generation and cGMP-PKG pathway activation. **Biochim Biophys Acta**. 2009; 1787:818−827.

85. Angelone T, Gattuso A, Imbrogno S, Mazza R, Tota B. Nitrite is a positive modulator of the Frank-Starling response in the vertebrate heart. **Am J Physiol Regul Integr Comp Physiol**. 2012; 302:R1271−R1281.

86. Borlaug BA, Koepp KE, Melenovsky V. Sodium nitrite improves exercise hemodynamics and ventricular performance in heart failure with preserved ejection fraction. **J Am Coll Cardiol**. 2015; 66:1672−1682.

87. Reddy YNV, Andersen MJ, Obokata M, et al. Arterial stiffening with exercise in patients with heart failure and preserved ejection fraction. **J Am Coll Cardiol**. 2017; 70:136−148.

88. Zweier JL. Measurement of superoxide-derived free radicals in the reperfused heart. Evidence for a free radical mechanism of reperfusion injury. **J Biol Chem**. 1988; 263:1353−1357.

89. Ingram TE, Fraser AG, Bleasdale RA, et al. Low-dose sodium nitrite attenuates myocardial ischemia and vascular ischemia-reperfusion injury in human models. **J Am Coll Cardiol**. 2013; 61:2534−2541.

90. Jones DA, Pellaton C, Velmurugan S, et al. Randomized phase 2 trial of intracoronary nitrite during acute myocardial infarction. **Circ Res**. 2015; 116:437−447.

91. Siddiqi N, Neil C, Bruce M, et al. Intravenous sodium nitrite in acute ST-elevation myocardial infarction: a randomized controlled trial (NIAMI). **Eur Heart J**. 2014; 35:1255−1262.

92. Pluta RM, Dejam A, Grimes G, Gladwin MT, Oldfield EH. Nitrite infusions to prevent delayed cerebral vasospasm in a primate model of subarachnoid hemorrhage. **J Am Med Assoc**. 2005; 293:1477−1484.

93. Fathi AR, Pluta RM, Bakhtian KD, Qi M, Lonser RR. Reversal of cerebral vasospasm via intravenous sodium nitrite after subarachnoid hemorrhage in primates. **J Neurosurg**. 2011; 115:1213−1220.

94. Oldfield EH, Loomba JJ, Monteith SJ, et al. Safety and pharmacokinetics of sodium nitrite in patients with subarachnoid hemorrhage: a phase IIa study. **J Neurosurg**. 2013; 119:634−641.

95. Franssen C, Chen S, Unger A, et al. Myocardial microvascular inflammatory endothelial activation in heart failure with preserved ejection fraction. **JACC Heart Fail**. 2016; 4:312−324.

96. van Heerebeek L, Hamdani N, Falcao-Pires I, et al. Low myocardial protein kinase G activity in heart failure with preserved ejection fraction. **Circulation**. 2012; 126:830−839.

97. Zile MR, Baicu CF, Ikonomidis JS, et al. Myocardial stiffness in patients with heart failure and a preserved ejection fraction: contributions of collagen and titin. **Circulation**. 2015; 131:1247−1259.

98. Borlaug BA, Melenovsky V, Koepp KE. Inhaled sodium nitrite improves rest and exercise hemodynamics in heart failure with preserved ejection fraction. **Circ Res**. 2016; 119:880−886.

99. Simon MA, Vanderpool RR, Nouraie M, et al. Acute hemodynamic effects of inhaled sodium nitrite in pulmonary hypertension associated with heart failure with preserved ejection fraction. **JCI Insight**. 2016; 1:e89620.

100. Borlaug BA, Anstrom KJ, Lewis GD, et al. Effect of inorganic nitrite vs placebo on exercise capacity among patients with heart failure with preserved ejection fraction: the INDIE-HFpEF randomized clinical trial. **J Am Med Assoc**. 2018; 320:1764−1773.

101. Gladwin MT, Schechter AN, Kim-Shapiro DB, et al. The emerging biology of the nitrite anion. **Nat Chem Biol**. 2005; 1:308−314.

102. Florin TH, Neale G, Cummings JH. The effect of dietary nitrate on nitrate and nitrite excretion in man. **Br J Nutr**. 1990; 64:387−397.

103. van Velzen AG, Sips AJ, Schothorst RC, Lambers AC, Meulenbelt J. The oral bioavailability of nitrate from nitrate-rich vegetables in humans. **Toxicol Lett**. 2008; 181:177−181.

104. McKnight GM, Smith LM, Drummond RS, Duncan CW, Golden M, Benjamin N. Chemical synthesis of nitric oxide in the stomach from dietary nitrate in humans. **Gut**. 1997; 40:211−214.

105. Webb AJ, Patel N, Loukogeorgakis S, et al. Acute blood pressure lowering, vasoprotective, and antiplatelet properties of dietary nitrate via bioconversion to nitrite. **Hypertension**. 2008; 51:784−790.

106. Wagner DA, Schultz DS, Deen WM, Young VR, Tannenbaum SR. Metabolic fate of an oral dose of 15N-labeled nitrate in humans: effect of diet supplementation with ascorbic acid. **Cancer Res**. 1983; 43:1921−1925.

107. Doel JJ, Benjamin N, Hector MP, Rogers M, Allaker RP. Evaluation of bacterial nitrate reduction in the human oral cavity. **Eur J Oral Sci**. 2005; 113:14−19.

108. Lundberg JO, Govoni M. Inorganic nitrate is a possible source for systemic generation of nitric oxide. **Free Radic Biol Med**. 2004; 37:395−400.

109. Lundberg JO, Weitzberg E, Lundberg JM, Alving K. Intragastric nitric oxide production in humans: measurements in expelled air. **Gut**. 1994; 35:1543−1546.

110. Samouilov A, Kuppusamy P, Zweier JL. Evaluation of the magnitude and rate of nitric oxide production from nitrite in biological systems. **Arch Biochem Biophys**. 1998; 357:1−7.

111. Pannala AS, Mani AR, Spencer JP, et al. The effect of dietary nitrate on salivary, plasma, and urinary nitrate metabolism in humans. **Free Radic Biol Med**. 2003; 34:576−584.

112. Hunault CC, van Velzen AG, Sips AJ, Schothorst RC, Meulenbelt J. Bioavailability of sodium nitrite from an aqueous solution in healthy adults. **Toxicol Lett**. 2009; 190:48−53.

113. Larsen FJ, Ekblom B, Sahlin K, Lundberg JO, Weitzberg E. Effects of dietary nitrate on blood pressure in healthy volunteers. **N Engl J Med**. 2006; 355:2792−2793.

114. Appel LJ, Moore TJ, Obarzanek E, et al. A clinical trial of the effects of dietary patterns on blood pressure. DASH Collaborative Research Group. **N Engl J Med**. 1997; 336:1117−1124.

115. Govoni M, Jansson EA, Weitzberg E, Lundberg JO. The increase in plasma nitrite after a dietary nitrate load is markedly attenuated by an antibacterial mouthwash. **Nitric Oxide**. 2008; 19:333−337.

116. Kapil V, Haydar SM, Pearl V, Lundberg JO, Weitzberg E, Ahluwalia A. Physiological role for nitrate-reducing oral bacteria in blood pressure control. **Free Radic Biol Med**. 2013; 55:93−100.

117. Siervo M, Lara J, Ogbonmwan I, Mathers JC. Inorganic nitrate and beetroot juice supplementation reduces blood pressure in adults: a systematic review and meta-analysis. **J Nutr**. 2013; 143:818−826.

118. Ashor AW, Lara J, Siervo M. Medium-term effects of dietary nitrate supplementation on systolic and diastolic blood pressure in adults: a systematic review and meta-analysis. **J Hypertens**. 2017; 35:1353−1359.

119. Bahra M, Kapil V, Pearl V, Ghosh S, Ahluwalia A. Inorganic nitrate ingestion improves vascular compliance but does not alter flow-mediated dilatation in healthy volunteers. **Nitric Oxide**. 2012; 26:197−202.

120. Ghosh SM, Kapil V, Fuentes-Calvo I, et al. Enhanced vasodilator activity of nitrite in hypertension: critical role for erythrocytic xanthine oxidoreductase and translational potential. **Hypertension**. 2013; 61:1091−1102.

121. Velmurugan S, Gan JM, Rathod KS, et al. Dietary nitrate improves vascular function in patients with hypercholesterolemia: a randomized, double-blind, placebo-controlled study. **Am J Clin Nutr**. 2016; 103:25−38.

122. Mills CE, Govoni V, Faconti L, et al. A randomised, factorial trial to reduce arterial stiffness independently of blood pressure: proof of concept? The VaSera trial testing dietary nitrate and spironolactone. **Br J Clin Pharmacol**. 2020; 86:891−902.

123. Mills CE, Govoni V, Faconti L, et al. Reducing arterial stiffness independently of blood pressure: the VaSera trial. **J Am Coll Cardiol**. 2017; 70:1683−1684.

124. Gilchrist M, Winyard PG, Aizawa K, Anning C, Shore A, Benjamin N. Effect of dietary nitrate on blood pressure, endothelial function, and insulin sensitivity in type 2 diabetes. **Free Radic Biol Med**. 2013; 60:89−97.

125. Shepherd AI, Wilkerson DP, Dobson L, et al. The effect of dietary nitrate supplementation on the oxygen cost of cycling, walking performance and resting blood pressure in individuals with chronic obstructive pulmonary disease: a double blind placebo controlled, randomised control trial. **Nitric Oxide**. 2015; 48:31−37.

126. Faconti L, Farukh B, McNally R, Webb A, Chowienczyk P. Arterial stiffness can be modulated by pressure-independent mechanisms in hypertension. **J Am Heart Assoc**. 2019; 8:e012601.

127. Liu AH, Bondonno CP, Croft KD, et al. Effects of a nitrate-rich meal on arterial stiffness and blood pressure in healthy volunteers. **Nitric Oxide**. 2013; 35:123−130.

128. Bondonno CP, Liu AH, Croft KD, et al. Short-term effects of nitrate-rich green leafy vegetables on blood pressure and arterial stiffness in individuals with high-normal blood pressure. **Free Radic Biol Med**. 2014; 77:353−362.

129. Kim DJ, Roe CA, Somani YB, et al. Effects of acute dietary nitrate supplementation on aortic blood pressures and pulse wave characteristics in post-menopausal women. **Nitric Oxide**. 2019; 85:10−16.

130. Hughes WE, Ueda K, Treichler DP, Casey DP. Effects of acute dietary nitrate supplementation on aortic blood pressure and aortic augmentation index in young and older adults. **Nitric Oxide**. 2016; 59:21−27.

131. Walker MA, Bailey TG, McIlvenna L, Allen JD, Green DJ, Askew CD. Acute dietary nitrate supplementation improves flow mediated dilatation of the superficial femoral artery in healthy older males. **Nutrients**. 2019; 11.

132. Lau CWZ, Hamers AJP, Rathod KS, et al. Randomised, double-blind, placebo-controlled clinical trial investigating the effects of inorganic nitrate in hypertension-induced target organ damage: protocol of the NITRATE-TOD study in the UK. **BMJ Open**. 2020; 10:e034399.

133. Zamani P, Rawat D, Shiva-Kumar P, et al. Effect of inorganic nitrate on exercise capacity in heart failure with preserved ejection fraction. **Circulation**. 2015; 131:371−380. Discussion 380.

134. Chirinos JA, Londono-Hoyos F, Zamani P, et al. Effects of organic and inorganic nitrate on aortic and carotid haemodynamics in heart failure with preserved ejection fraction. **Eur J Heart Fail**. 2017; 19(11):1507−1515. https://doi.org/10.1002/ejhf.885. Epub 2017 May 25.

135. Londono-Hoyos F, Zamani P, Beraun M, Vasim I, Segers P, Chirinos JA. Effect of organic and inorganic nitrates on cerebrovascular pulsatile power transmission in patients with heart failure and preserved ejection fraction. **Physiol Meas**. 2018; 39:044001.

136. Buckberg GD, Fixler DE, Archie JP, Hoffman JI. Experimental subendocardial ischemia in dogs with normal coronary arteries. **Circ Res**. 1972; 30:67−81.

137. Kukadia S, Dehbi HM, Tillin T, Coady E, Chaturvedi N, Hughes AD. A double-blind placebo-controlled crossover study of the effect of beetroot juice containing dietary nitrate on aortic and brachial blood pressure over 24 h. **Front Physiol**. 2019; 10:47.

138. Jovanovski E, Bosco L, Khan K, et al. Effect of spinach, a high dietary nitrate source, on arterial stiffness and related hemodynamic measures: a randomized, controlled trial in healthy adults. **Clin Nutr Res**. 2015; 4:160−167.

139. Rammos C, Hendgen-Cotta UB, Sobierajski J, Bernard A, Kelm M, Rassaf T. Dietary nitrate reverses vascular dysfunction in older adults with moderately increased cardiovascular risk. **J Am Coll Cardiol**. 2014; 63:1584−1585.

140. Li D, Nishi SK, Jovanovski E, et al. Repeated administration of inorganic nitrate on blood pressure and arterial stiffness: a systematic review and meta-analysis of randomized controlled trials.

J **Hypertens**. 2020; 38(11):2122−2140. https://doi.org/10.1097/HJH.0000000000002524.

141. Faconti L, Mills CE, Govoni V, et al. Cardiac effects of 6 months' dietary nitrate and spironolactone in patients with hypertension and with/at risk of type 2 diabetes, in the factorial design, double-blind, randomized controlled VaSera trial. **Br J Clin Pharmacol**. 2019; 85:169−180.

142. Schwarz K, Singh S, Parasuraman SK, et al. Inorganic nitrate in angina study: a randomized double-blind placebo-controlled trial. **J Am Heart Assoc**. 2017; 6.

143. Rathod KS, Jones DA, Van-Eijl TJ, et al. Randomised, double-blind, placebo-controlled study investigating the effects of inorganic nitrate on vascular function, platelet reactivity and restenosis in stable angina: protocol of the NITRATE-OCT study. **BMJ Open**. 2016; 6:e012728.

144. Omar SA, Artime E, Webb AJ. A comparison of organic and inorganic nitrates/nitrites. **Nitric Oxide**. 2012; 26:229−240.

145. Gori T, Mak SS, Kelly S, Parker JD. Evidence supporting abnormalities in nitric oxide synthase function induced by nitroglycerin in humans. **J Am Coll Cardiol**. 2001; 38:1096−1101.

146. Caramori PR, Adelman AG, Azevedo ER, Newton GE, Parker AB, Parker JD. Therapy with nitroglycerin increases coronary vasoconstriction in response to acetylcholine. **J Am Coll Cardiol**. 1998; 32:1969−1974.

147. O'Gallagher K, Borg Cardona S, Hill C, et al. Grapefruit juice enhances the systolic blood pressure-lowering effects of dietary nitrate-containing beetroot juice. **Br J Clin Pharmacol**. 2021; 87:577−587.

148. Hughan KS, Levine A, Helbling N, et al. Effects of oral sodium nitrite on blood pressure, insulin sensitivity, and intima-media arterial thickening in adults with hypertension and metabolic syndrome. **Hypertension**. 2020; 76(3):866−874. https://doi.org/10.1161/HYPERTENSIONAHA.120.14930. Epub 2020 Aug 3.

149. Sundqvist ML, Larsen FJ, Carlstrom M, et al. A randomized clinical trial of the effects of leafy green vegetables and inorganic nitrate on blood pressure. **Am J Clin Nutr**. 2020; 111:749−756.

150. Eichholzer M, Gutzwiller F. Dietary nitrates, nitrites, and N-nitroso compounds and cancer risk: a review of the epidemiologic evidence. **Nutr Rev**. 1998; 56:95−105.

151. Knekt P, Jarvinen R, Dich J, Hakulinen T. Risk of colorectal and other gastro-intestinal cancers after exposure to nitrate, nitrite and N-nitroso compounds: a follow-up study. **Int J Cancer**. 1999; 80:852−856.

152. Song P, Wu L, Guan W. Dietary nitrates, nitrites, and nitrosamines intake and the risk of gastric cancer: a meta-analysis. **Nutrients**. 2015; 7:9872−9895.

153. Hunlich M, Hasenfuss G. Effects of the NO donor sodium nitroprusside on oxygen consumption and energetics in rabbit myocardium. **Basic Res Cardiol**. 2009; 104:359−365.

154. Paulus WJ, Vantrimpont PJ, Shah AM. Acute effects of nitric oxide on left ventricular relaxation and diastolic distensibility in humans. Assessment by bicoronary sodium nitroprusside infusion. **Circulation**. 1994; 89:2070−2078.

155. Bauersachs J, Bouloumie A, Mulsch A, Wiemer G, Fleming I, Busse R. Vasodilator dysfunction in aged spontaneously hypertensive rats: changes in NO synthase III and soluble guanylyl cyclase expression, and in superoxide anion production. **Cardiovasc Res**. 1998; 37:772−779.

156. Ruetten H, Zabel U, Linz W, Schmidt HH. Downregulation of soluble guanylyl cyclase in young and aging spontaneously hypertensive rats. **Circ Res**. 1999; 85:534−541.

157. Kloss S, Bouloumie A, Mulsch A. Aging and chronic hypertension decrease expression of rat aortic soluble guanylyl cyclase. **Hypertension**. 2000; 35:43−47.

158. Shah RC, Sanker S, Wood KC, Durgin BG, Straub AC. Redox regulation of soluble guanylyl cyclase. **Nitric Oxide**. 2018; 76:97−104.

159. Gladwin MT. Deconstructing endothelial dysfunction: soluble guanylyl cyclase oxidation and the NO resistance syndrome. **J Clin Invest**. 2006; 116:2330−2332.

160. Stasch JP, Becker EM, Alonso-Alija C, et al. NO-independent regulatory site on soluble guanylate cyclase. **Nature**. 2001; 410:212−215.

161. Becker EM, Alonso-Alija C, Apeler H, et al. NO-independent regulatory site of direct sGC stimulators like YC-1 and BAY 41-2272. **BMC Pharmacol**. 2001; 1:13.

162. Ghofrani HA, Galie N, Grimminger F, et al. Riociguat for the treatment of pulmonary arterial hypertension. **N Engl J Med**. 2013; 369:330−340.

163. Rubin LJ, Galie N, Grimminger F, et al. Riociguat for the treatment of pulmonary arterial hypertension: a long-term extension study (PATENT-2). **Eur Respir J**. 2015; 45:1303−1313.

164. Gheorghiade M, Greene SJ, Butler J, et al. Effect of vericiguat, a soluble guanylate cyclase stimulator, on natriuretic peptide levels in patients with worsening chronic heart failure and reduced ejection fraction: the SOCRATES-REDUCED randomized trial. **J Am Med Assoc**. 2015; 314:2251−2262.

165. Armstrong PW, Pieske B, Anstrom KJ, et al. Vericiguat in patients with heart failure and reduced ejection fraction. **N Engl J Med**. 2020; 382:1883−1893.

166. Armstrong PW, Lam CSP, Anstrom KJ, et al. Effect of vericiguat vs placebo on quality of life in patients with heart failure and preserved ejection fraction: the VITALITY-HFpEF randomized clinical trial. **J Am Med Assoc**. 2020; 324:1512−1521.

167. Evgenov OV, Pacher P, Schmidt PM, Hasko G, Schmidt HH, Stasch JP. NO-independent stimulators and activators of soluble guanylate cyclase: discovery and therapeutic potential. **Nat Rev Drug Discov**. 2006; 5:755−768.

168. Lapp H, Mitrovic V, Franz N, et al. Cinaciguat (BAY 58-2667) improves cardiopulmonary hemodynamics in patients with acute decompensated heart failure. **Circulation**. 2009; 119:2781−2788.

169. Erdmann E, Semigran MJ, Nieminen MS, et al. Cinaciguat, a soluble guanylate cyclase activator, unloads the heart but also causes hypotension in acute decompensated heart failure. **Eur Heart J**. 2013; 34:57−67.

170. Gheorghiade M, Greene SJ, Filippatos G, et al. Cinaciguat, a soluble guanylate cyclase activator: results from the randomized, controlled, phase IIb COMPOSE programme in acute heart failure syndromes. **Eur J Heart Fail**. 2012; 14:1056−1066.

171. Flores-Santana W, Salmon DJ, Donzelli S, et al. The specificity of nitroxyl chemistry is unique among nitrogen oxides in biological systems. **Antioxid Redox Signal**. 2011; 14:1659−1674.

172. Fukuto JM, Cisneros CJ, Kinkade RL. A comparison of the chemistry associated with the biological signaling and actions of nitroxyl (HNO) and nitric oxide (NO). **J Inorg Biochem**. 2013; 118:201−208.

173. Favaloro JL, Kemp-Harper BK. The nitroxyl anion (HNO) is a potent dilator of rat coronary vasculature. **Cardiovasc Res**. 2007; 73:587−596.

174. Gao WD, Murray CI, Tian Y, et al. Nitroxyl-mediated disulfide bond formation between cardiac myofilament cysteines enhances contractile function. **Circ Res**. 2012; 111:1002−1011.

175. Irvine JC, Favaloro JL, Widdop RE, Kemp-Harper BK. Nitroxyl anion donor, Angeli's salt, does not develop tolerance in rat isolated aortae. **Hypertension**. 2007; 49:885−892.

176. Zhu G, Groneberg D, Sikka G, et al. Soluble guanylate cyclase is required for systemic vasodilation but not positive inotropy induced by nitroxyl in the mouse. **Hypertension**. 2015; 65:385−392.

177. Sabbah HN, Tocchetti CG, Wang M, et al. Nitroxyl (HNO): a novel approach for the acute treatment of heart failure. **Circ Heart Fail**. 2013; 6:1250−1258.

178. Mills CE, Govoni V, Faconti L, et al. Reducing arterial stiffness independently of blood pressure. The VaSera trial. **J Am Coll Cardiol**. 2017; 70:1683−1684.

179. Faconti L, Mills CE, Govoni V, et al. Cardiac effects of 6 months' dietary nitrate and spironolactone in patients with hypertension and with/at risk of type 2 diabetes, in the factorial design, double-blind, randomised-controlled, VaSera trial. **Br J Clin Pharmacol**. 2019; 85:169−180.

180. Beirne AM, Mitchelmore O, Palma S, et al. NITRATE-CIN study: protocol of a randomized (1:1) single-center, UK, double-blind placebo-controlled trial testing the effect of inorganic nitrate on contrast-induced nephropathy in patients undergoing coronary angiography for acute coronary syndromes. **J Cardiovasc Pharmacol Ther**. 2021, 1074248421000520.

181. Chirinos JA, Zamani P. The nitrate-nitrite-NO pathway and its implications for heart failure and preserved ejection fraction. **Curr Heart Fail Rep**. 2016; 13:47−59.

182. Vanderpool R, Gladwin MT. Harnessing the nitrate-nitrite-nitric oxide pathway for therapy of heart failure with preserved ejection fraction. **Circulation**. 2015; 131(4):334−336.

Further reading

1. Mirvish SS. Role of N-nitroso compounds (NOC) and N-nitrosation in etiology of gastric, esophageal, nasopharyngeal and bladder cancer and contribution to cancer of known exposures to NOC. **Cancer Lett**. 1995; 93:17−48.

Effect of exercise training and weight loss on arterial stiffness and pulsatile hemodynamics

Gary L. Pierce[1], Kevin S. Heffernan[2] and Kevin P. Davy[3]

[1]University of Iowa, Iowa City, IA, United States; [2]Syracuse University, Syracuse, NY, United States; [3]Virginia Tech, Blacksburg, VA, United States

Introduction

The large elastic central arteries, including the aorta and common carotid arteries, stiffen with advancing age in humans even in the absence of significant cardiovascular disease (CVD) risk factor burden. Both aortic and carotid stiffness are robust predictors of future CVD morbidity and mortality independent of blood pressure and other cardiovascular risk factors.[1,2] Higher large central artery stiffness is associated with numerous pathological conditions associated with older age including isolated systolic hypertension, heart failure, orthostatic hypotension, myocardial ischemia, chronic kidney disease, cognitive impairment, and cerebral white matter lesions, the latter three conditions likely from penetration of damaging excessive pulsatile pressure into the microcirculation of these high flow target organs.[3] The rate of increase of aortic stiffness, in particular, over the lifespan can be accelerated in the presence of hypertension,[4] whereas other traditional risk factors such as dyslipidemia, smoking, and glucose appear to have a more modest or minor influence with advancing age.[5] In contrast, high levels of habitual aerobic physical activity (PA)[6,7] and cardiorespiratory fitness (CRF)[8-12] are associated with an attenuated age-related increase in central artery stiffness among middle-age/older (MA/O) adults without hypertension. However, the benefits of habitual aerobic PA and high CRF on aortic stiffness are largely absent among MA/O adults with treated and treatment-naïve hypertension,[13-17] although carotid artery stiffness appears to be more modifiable.[18] Interestingly, in contrast to habitual aerobic PA or structured aerobic exercise training, heavy volume/intensity resistance exercise training (RET) may cause increases in central artery stiffness,[19-22] whereas moderate intensity RET appears to not have adverse effects and may even be

beneficial.[23,24] Finally, obesity is associated with higher central artery stiffness and weight (body fat) loss is generally associated with reductions in central artery stiffness among MA/O adults; in this setting, the change in stiffness appears to be associated with abdominal visceral fat.[25,26] This chapter will discuss the evidence for the beneficial effects of aerobic PA/aerobic exercise training, RET, and weight gain and loss on central artery stiffness in young and MA/O adults with and without hypertension.
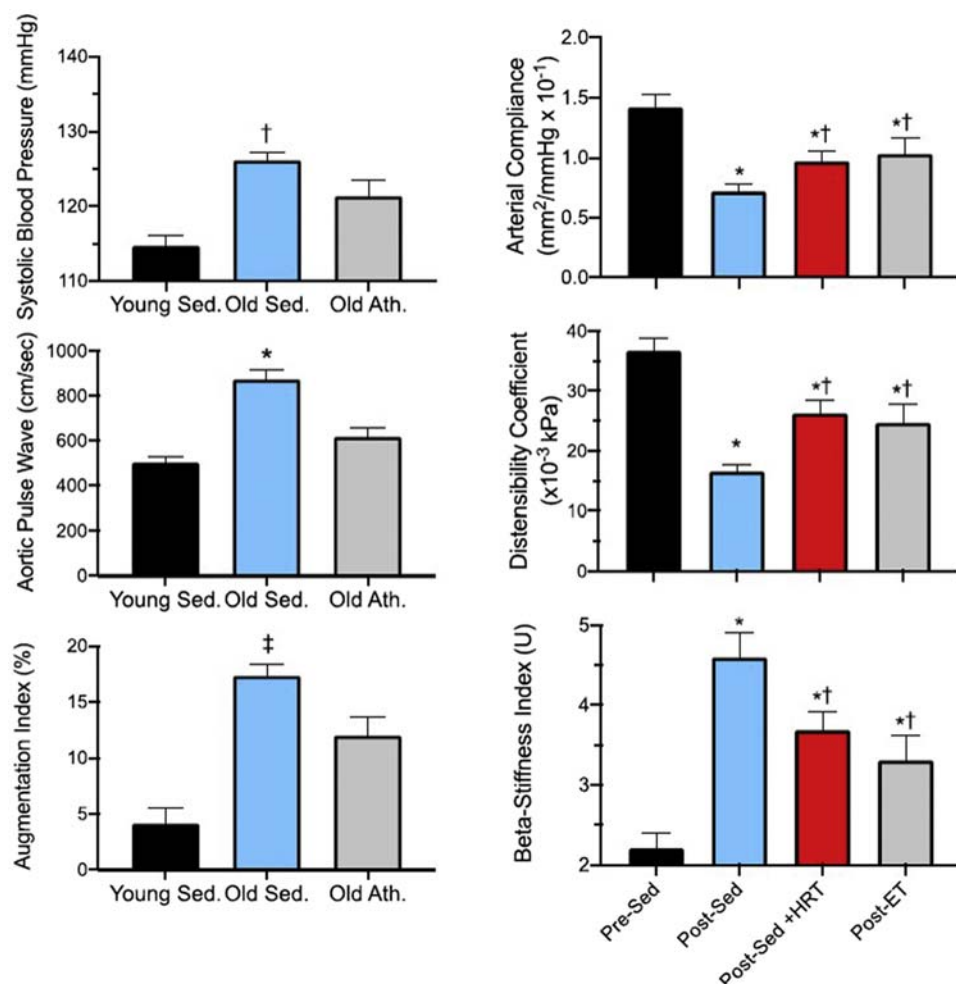
Effect of high cardiorespiratory fitness and habitual aerobic PA on central artery stiffness and pulsatile hemodynamics with aging

Given the strong relation between higher central artery stiffness and CVD risk[1,2] and the inverse association between higher CRF and high PA with lower CVD morbidity and mortality,[27-31] it reasons that maintaining higher CRF and levels of aerobic PA with advancing age would have a favorable effect of attenuating age-related central artery stiffening compared with lower CRF and physical inactivity. To test this hypothesis investigators have conducted cross-sectional studies of MA/O adults without hypertension who have been performing moderate-to-vigorous habitual aerobic exercise 5–6 days/week, typically "master's athletes" competing in competitive endurance events and comparing them to physically inactive, age- and sex-matched adults. Thus, these endurance-trained MA/O adults maintain a higher CRF than the physically inactive adults and in most studies demonstrate a complete or partial prevention of the age-related increase in aortic and/or carotid artery stiffness. In the first such study, Vaitkevicius

et al.[8] demonstrated that Doppler flow−acquired aortic pulse wave velocity (PWV) was significantly lower among MA/O men and women who had been engaging in vigorous endurance exercise for multiple years compared with physically inactive age-matched adults, and this was in the absence of any differences in blood pressure between groups (see Fig. 52.1). Also, aortic PWV did not differ between the endurance-trained MA/O and younger adults, consistent the idea that high CRF from chronic moderate-to-vigorous aerobic exercise, abrogated the age-related elevation in aortic stiffness among physically inactive MA/O men. Furthermore, maximal CRF, measured as the rate of oxygen consumption at maximal exercise (VO$_2$max), was inversely correlated with aortic PWV and the relation was strongest among older men >70 years of age. Thus, these data suggest that high CRF from habitual moderate/vigorous aerobic exercise in middle- to older age, or perhaps other factors associated with higher CRF (e.g., genetics, low adiposity), blunt the age-related elevation in aortic stiffness in MA/O men without hypertension.

Numerous other cross-sectional studies since have confirmed these findings related to aortic stiffness in both MA/O men and postmenopausal women who perform moderate-to-vigorous aerobic exercise.[9,11,32] Similar age- and aerobic exercise training status-cross-sectional findings in MA/O men and women have also been reported with carotid artery compliance or β-stiffness index.[10,33,34] Moreover, these beneficial alterations in central artery stiffness associated with high CRF appear to be largely independent of lower blood pressure and less CVD risk factor burden. Although these studies suggest a favorable direct effect of repeated bouts of aerobic exercise and/or high CRF on the elastic properties of the arterial wall, other lifestyle or unmeasured biological and social factors (e.g., healthy diet, low inflammation, higher socioeconomic status, etc.) in individuals with high CRF may have also contributed in part to lower aortic stiffness. Interestingly, in a study by Moreau et al.[33] physically inactive post-menopausal women on hormone replacement therapy demonstrated similar carotid artery compliance and

FIGURE 52.1 Left panel: Bar graphs of systolic blood pressure (upper), aortic pulse wave velocity (middle), and augmentation index (lower) are compared among young sedentary, old sedentary, and old athletic adults by analysis of variance. Values are mean ± SEM. A, SBP: †old sedentary different from young sedentary controls $P < .01$; B, APWV: *old sedentary controls differ from young sedentary controls and older athletes at $P < .001$; C, AGI%: ‡all groups differ at $P < .001$. Right panel: Carotid arterial compliance (top), arterial distensibility coefficient (middle), and beta-stiffness index (lower) of women in the cross-sectional study. *$P < .001$ versus Sed; †*Pre*, premenopausal; *Post*, postmenopausal; *HRT*, hormone replacement therapy; *ET*, endurance training. *Left panel: Vaitkevicius PV, Fleg JL, Engel JH, et al. Effects of age and aerobic capacity on arterial stiffness in healthy adults.* **Circulation**. *1993; 88:1456−1462 with permission. Right panel: Moreau KL, Gavin KM, Plum AE, Seals DR. Oxidative stress explains differences in large elastic artery compliance between sedentary and habitually exercising post-menopausal women.* **Menopause**. *2006; 13:951−958 with permission.*

β-stiffness index as endurance-trained postmenopausal women who were not on hormone replacement, although carotid compliance/stiffness was not back to levels of young premenopausal women (see Fig. 52.1). Given the potential adverse health effects of prolonged hormone replacement therapy on increased risk of breast cancer[35] and lack of CVD benefit in randomized, controlled trials,[36–38] habitual aerobic exercise may be a valuable alternative therapeutic strategy to improve central artery stiffness in estrogen-deficient postmenopausal women.

Because many MA/O adults cannot perform the high volume of moderate-to-vigorous aerobic exercise as endurance-trained master's athletes, it is important to determine whether daily occupational and leisure levels of PA may lower central artery stiffness among MA/O adults in the community.[6,7] In this regard, among a cohort of multiethnic older community-dwelling adults, moderate and higher volumes of PA (computed from duration, frequency, and intensity of PA) expressed as metabolic equivalents (METs) in minutes/week from the self-report Baecke PA Questionnaire, were associated with lower carotid-femoral PWV compared with no PA in models adjusted for age, sex, education, race-center, smoking status, and mean arterial pressure.[7] Indeed, those with moderate and high volume of aerobic PA demonstrated −0.30 and −0.38 m/s slower carotid-femoral PWV, respectively, compared with no PA, consistent with the idea that aortic stiffening is less prominent in more physically active MA/O adults. Interestingly, low volume of aerobic PA was not associated with a lower aortic stiffness indicating that at least a moderate volume of PA may be required to destiffen the aorta in older adults. In a subsample of the cohort who maintained a high volume of PA between study visits 1 and 3 (∼6 years), the favorable relation with carotid-femoral PWV was even larger with a reduction of −0.73 m/s. Moreover, these results were maintained after further adjustment for presence of hypertension (which was present in ∼3/4 of the cohort) but was attenuated when adjusted for prevalence of diabetes. These data suggest that persistent high volume of PA from middle age into older age has a favorable association with slower aortic stiffness progression even if hypertension is present but perhaps not diabetes.

In one of the only longitudinal studies performed to date investigating whether moderate-to-vigorous PA can alter the progression of aortic stiffness, Ahmadi-Abhari et al.[6] studied change in carotid-femoral PWV over 5 years among MA/O adults from the Whitehall II cohort consisting of >4300 participants. Using questionnaire-based estimates of PA over the previous 4 weeks and converted to METs at two visits between 4 and 6 years apart, activities were stratified into mild (<3 METS), moderate (3–5.9 METS), or vigorous (≥6 METS) PA and then expressed as weekly total PA in MET-h/week. Importantly, the authors

also collected data on sedentary time spent sitting at home (watching television, sitting at desk) or at work/commuting. They found that adults with higher baseline levels of PA (i.e., more MET-h/week) had slower carotid-femoral PWV compared with low levels PA, but that baseline total PA was not associated with change in carotid-femoral PWV over the subsequent 5-year follow-up. Interestingly, each additional hour of moderate-to-vigorous PA at baseline was associated with a −0.02 m/s smaller increase in carotid-femoral PWV compared with the average 5-year increase of +0.76 m/s, suggesting that moderate-to-vigorous PA (e.g., sports, cycling, swimming, mowing) and not mild PA (e.g., gardening, housework) was necessary to attenuate the rise in aortic stiffness from age 65 to 70 years. In the longitudinal analysis, participants who *increased* their PA over the 5-year follow-up demonstrated a smaller increase in carotid-femoral PWV compared with those who did not increase PA (+0.60 vs. +0.76 m/s, P for trend <0.001). Importantly, adults who *decreased* their PA over the 5-year follow-up had larger increases in carotid-femoral PWV compared with those who did not increase PA (+0.85 vs. +0.76 m/s, *P* for trend <.001) confirming that becoming more inactive was associated with accelerated age-related aortic stiffening. Furthermore, with each additional hour of leisure-time sitting a larger increase in carotid-femoral PWV over 5 years was observed independent of total PA. Taken together, engaging in and sustaining moderate-to-vigorous PA with advancing age possibly slows the progressive stiffening of the aorta independent of most conventional CVD risk factors, but mild levels of PA such as housework, gardening, and leisure walking may not be protective. Furthermore, reductions in PA, in particular excessive sitting, was associated with accelerated aortic stiffening over the 5 years indicating that adopting sedentary behaviors among MA/O adults should be avoided.

An important finding from these previous studies is that they suggest that low levels of PA is not sufficient to reduce aortic stiffness. However, these studies are limited by reliance on self-report of PA via questionnaires that can be less reliable and lead to misclassification of magnitude of PA, particularly quantifying light PA that tends to be unstructured activities of daily living (e.g., housework, gardening, etc.).[39] To address these limitations, PA accelerometers have been employed in some studies to better characterize the relation between volume and intensity of PA and central artery stiffness. In this regard, studies using uniaxial accelerometers confirm self-report studies that "light" PA is not sufficient to alter aortic stiffness in older men and postmenopausal women.[40,41] However, uniaxial accelerometers can underestimate light PA because horizontal movements are not detected. Therefore, in a study using triaxial accelerometers that measure movements in three dimensions, Gando et al.[42] investigated whether

higher amounts of "light" PA over 14 days was associated with lower aortic stiffness in a cross-sectional cohort of 538 healthy, nonsmoking young (age <40 years), middle-aged (age 40−59 years), and older (age ≥60 years) men and women. Importantly, they also considered the influence of CRF (from directly measured VO_2max) on whether PA alters aortic stiffness differently in individuals with high versus low CRF. They observed that time spent in "light" PA was longer, but time spent in vigorous PA was shorter, among MA/O compared with the young adults. Importantly, older adults who performed high amounts of "light" PA demonstrated slower carotid-femoral PWV compared with older adults who performed low amounts of "light" PA (8.8 vs. 9.5 m/s, $P < .05$) which remained significant after adjusting for sex and for moderate and vigorous PA, but this same effect was not found among young or middle-aged adults. However, the older adults with higher levels of "light" PA also had lower mean blood pressure (−6 mmHg) and higher CRF than the "low" PA group, but the model did not adjust for these important confounders. Thus, it is possible that disparities in blood pressure and CRF could explain the differences in carotid-femoral PWV between high and low amounts of "low" PA. Furthermore, the finding that light and moderate PA predicted carotid-femoral PWV in the older adults was driven by the relation among the unfit (i.e., low CRF) older adults because there was no relation between "light" PA and carotid-femoral PWV among the older adults with high CRF. Taken together, these data suggest that CRF may moderate the relation between PA and aortic stiffness, particularly in older adults who have low CRF. This finding has important implications because older unfit adults may more easily incorporate light PA into daily activities rather than initiate organized moderate-to-vigorous exercise training at a level sufficient to increase CRF.

Effect of aerobic exercise interventions on central artery stiffness and pulsatile hemodynamics in young and MA/O adults with and without hypertension

Effects of aerobic exercise on aortic stiffness among normotensive MA/O adults. An important question that cannot be answered by cross-sectional studies is whether an aerobic exercise training intervention initiated by previously sedentary MA/O adults without hypertension can reverse or improve (decrease) aortic and/or carotid artery stiffness. Results from intervention studies have been mixed largely because the studies differ in mode, intensity, and frequency of exercise training, consist of small sample sizes, some lack of control groups and randomization, consist of a short duration of the intervention (3−4 months) or do not adjust for changes in blood pressure.[43−47] In

addition, the results differ depending on whether aortic or carotid artery stiffness is the primary outcome.[10,18,33] For example, Hayashi et al.[43] found that 16 weeks of walking/jogging in middle-aged normotensive men reduced carotid-femoral PWV by 0.5 m/s and increased carotid artery compliance by 30%, in the absence of any changes in femoral-posterior tibial PWV and femoral artery compliance (i.e., peripheral muscular artery stiffness). However, the lack of adjustment for the 3 mmHg reduction in mean arterial pressure and no randomized, parallel-time control group makes it difficult to conclude that the observed changes were mediated by reductions in passive elastic properties of the arterial wall rather than just distending pressure (see Table 52.1). In a study of 35 middle-aged women randomly assigned to aerobic exercise, resistance exercise or a nonexercise control group for 12 weeks, Yoshizawa et al.[44] found a −0.4 m/s reduction in carotid-femoral PWV in the aerobic exercise group after 12 weeks along with a 9% increase in VO_2max, in the absence of changes in carotid-femoral PWV after resistance exercise or nonexercise time control. However, this small change in carotid-femoral PWV after aerobic exercise was not significantly more than the resistance exercise group and was not adjusted for the 3 mmHg decrease in mean arterial pressure, again suggesting that the decrease in distending pressure and not wall stiffness likely explains the results (see Table 52.1). Lastly, in a randomized, controlled trial, 48 previously inactive older adults without hypertension were randomized to 12 months of aerobic exercise or nonexercise control in combination with or without advanced-glycation end-product cross-link breaker alagebrium.[47] They reported that no change was observed in carotid-femoral PWV among the aerobic exercise alone or combination with alagebrium groups, despite a 15% increase in CRF. Although it is possible the total volume of exercise required to increase CRF in healthy older adults is less than what is required to reduce aortic stiffness, it is possible that aortic stiffness may not be modifiable in older healthy adults age >65 years. Alternatively, it is plausible that more frequent exercise than three sessions per week and/or longer than 1 year is required to induce clinically meaningful reductions in aortic stiffness in previously inactive older (>70 years of age) adults (see Table 52.1). In this regard, Shibata et al.[12] investigated this question of frequency in a cross-sectional cohort of older adults (mean age 70 years) who had performed a consistent frequency of aerobic exercise training for at least 20 years. Participants were stratified based on frequency: <2 days/week ("sedentary"), 2−3 days/week ("casual exercisers"), 4−5 days/week ("committed exercisers"), and 6−7 days/week ("Master's athletes"). They found that carotid-femoral PWV was lower in the "committed exercisers" compared with "casual exercisers" suggesting that 4−5 days/week was the minimal frequency required to

TABLE 52.1 Randomized and nonrandomized intervention studies of effects of aerobic exercise training in middle-aged and/or older nonhypertensive adults on carotid-femoral pulse wave velocity (upper panel) or carotid artery β-stiffness index (lower panel).

					Aerobic exercise program											
Study (year)	n (male/female)	Age (years)	Randomization	Control group(s)	Frequency (days/week)	Duration/session (min)	Intensity	Duration (weeks)	Mode	% δV0$_2$max	Pre-CFPWV (m/sec)	Post-CFPWV (m/sec)	δCFPWV (m/sec)	P < .05 versus baseline	δMAP (mm/Hg) versus baseline	Adjusted for δMAP
Hayashi et al. (2005)	20 (10/10)	50 ± 3	No	None	3−4	45	60%−75% HRR	16	Walk/jog	+13%	9.4 ± 3.4	8.7 ± 3.2	−0.6	Yes	−3	No
Yosizawa et al. (2009)	35 (0/35)	32−59	Yes	Resistance ex (n = 11) or non-exercise (n = 12)	2	30	60%−70% VO$_2$max	12	Cycling	+9%	n/a	n/a	−0.4	Yes	−3	No
Oudegeest et al. (2013)	44 (25/19)	70 ± 4	Yes	Nonexercise (n = 22) +/− alagebrium (n = 22)	3	30	70%−85% HRR	48	Cycling	+15%	11.0 ± 3.2	11.4 ± 2.6	+0.4	No	−2.3	No
Study (year)	n (male/female)	Age (years)	Randomization	Control group(s)	Frequency (days/week)	Duration/session (min or kcal)	Intensity	Duration (weeks)	Mode	% δV0$_2$max	Pre-carotid β-stiffness (U)	Post-carotid β-stiffness (AU)	%δ carotid β-stiffness	P < .05 versus baseline	δMAP (mm/Hg) versus baseline	Adjusted for δMAP
Tanaka et al. (2000)	20 (20/0)	53 ± 2	No	None	5.3 ± 0.2	42 ± 1	73 ± 1% HRmax	13.5 ± 1	Walking	+5%	3.0 ± 0.2	2.4 ± 0.2	−23%	Yes	0	No
Moreau et al. (2003)	12 (0/12)	63 ± 2	No	None	4.9 ± 0.5	40 ± 2	70 ± 1% HRmax	13.1 ± 1	Walking	+6%	n/a	n/a	−25%	Yes	−1	No
Sugawara et al. (2006)	17 (0/17)	59 ± 6	Yes	Moderate intensity, 40% HRR (n = 8)	3−5	180 −300 kcal	70% HHR	13−14	Cycling	n/a	12.3 ± 4.6	8.2 ± 3.6	−33%	Yes	+3	Yes

Data are mean ± SD or (95% CI); HTN, hypertension; HRmax, heart rate maximum; *CFPWV*, carotid-femoral pulse wave velocity; *HRR*, heart rate reserve; *MAP*, mean arterial pressure; *n/a*, not available; *RT*, resistance training; *VT*, ventilatory threshold.
Note: Studies were only included if casual/office MAP was reported or could be computed from systolic and diastolic pressure reported pre- versus postexercise intervention.

attain the destiffening benefits of habitual aerobic exercise and that there was no added benefit with 6−7 days per week (no difference with Master's athletes). Interestingly, carotid artery β-stiffness index was lower among the "casual exercisers" compared with the "committed exercisers" indicating that less frequent aerobic exercise (2−3 days/ week vs. 4−5 days/week) appears sufficient to attenuate carotid artery, but not aortic, stiffness among older adults.

Taken together, these studies reveal that short-term (3−4 months) aerobic exercise interventions in middle-aged adults result in small reductions in carotid-femoral PWV but may be a result of concomitant decreases in blood pressure, and longer (12 months) aerobic exercise 3 days/week among older adults without hypertension have little effect, suggesting that longer duration and/or higher frequency of exercise per week is likely required to alter age-related aortic stiffness. Importantly, a critical component of the beneficial effects of habitual aerobic exercise on aortic stiffness appear to be that a minimum threshold of 4−5 days/week is obligatory that was not achieved in the aforementioned intervention studies.

Effect of aerobic exercise on carotid artery stiffness among normotensive middle-aged/older adults. In contrast to inconsistent findings related to aortic stiffness, common carotid artery stiffness appears to be more amenable to shorter duration interventions of habitual aerobic exercise. Tanaka et al. [10] studied MA/O healthy men before and after a 3-month aerobic exercise intervention consisting of walking 4−6 days/week (see Table 52.1). Although there was no significant increase in VO$_2$max after 3 months of training, carotid artery compliance increased 25% and carotid β-stiffness index decreased 20% to levels similar with MA/O endurance athletes but not back to levels of young adults, and this occurred in the absence of any changes in CVD risk factors such as body fat%, blood pressure, and cholesterol fasting glucose. Moreau et al.[33] conducted a similar aerobic exercise intervention design that resulted in significant 20% increase in maximal treadmill test time and 6% improvement in VO$_2$max in previously physically inactive postmenopausal women who had previously taken, but not currently using, hormone replacement therapy (see Table 52.1). They reported that carotid compliance was similarly increased 40% and carotid β-stiffness was reduced 25% after 3 months of training. Importantly, carotid artery elastic properties in the postmenopausal women after the exercise intervention were reversed back to levels of young premenopausal women similar to the previous study in MA/O men. Furthermore, Sugawara et al.[40] found similar 27% reductions in carotid artery β-stiffness in postmenopausal women after both a moderate and vigorous intensity of aerobic exercise training for 12 weeks. Together, these data suggest that carotid artery stiffness is very amenable to change after moderate, short duration aerobic exercise training among both MA/O men and postmenopausal women, and that are not explained by improvements in CVD risk factors.
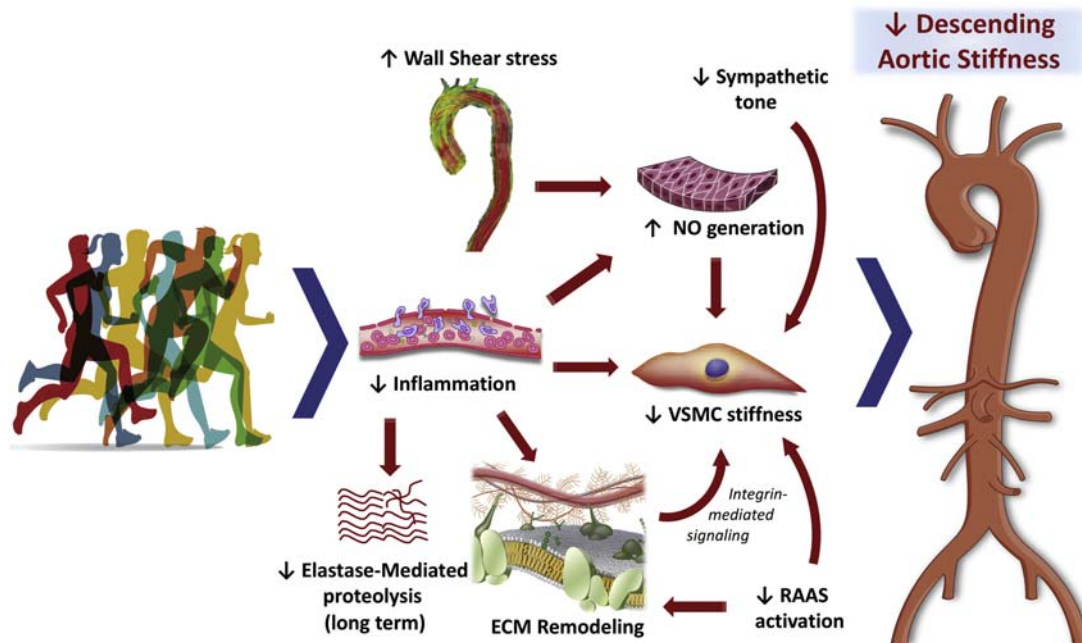
Potential mechanisms for selective improvements in carotid and aortic stiffness among healthy middle-aged/ older adults. The mechanisms for the observed consistent improvements in carotid artery compliance/stiffness but not aortic stiffness in healthy MA/O adults in response to aerobic exercise interventions are unknown. Higher carotid artery stiffness is modulated at least in part by reduced nitric oxide bioavailability[48] and augmented sympathetic nervous system mediated α-adrenergic vasoconstriction.[49,50] Therefore, the selective favorable adaptation in the carotid arteries versus aorta in response to aerobic exercise training may be related in part to reductions in tonic α-adrenergic tone and/or augmentation of nitric oxide−mediated endothelial function, or "functional stiffness" of the carotid arteries that is absent in the aorta. In addition, the small blood pressure−dependent changes or lack of change in aortic stiffness in intervention studies among MA/O adults may also be related to the regional differences in the relative content of elastin and VSMCs in the aorta. In this regard, the proximal ascending aorta has higher elastin content relative to the more VSMC content of the carotid arteries, therefore passive elastic "intrinsic" stiffness in the aorta may be less amenable to change than the "functional stiffness"of the carotid arteries in response to short-term aerobic exercise training among older adults. Consistent with this idea, a detailed study of young and middle-aged adults who initiated a 6-month running program to complete a marathon race demonstrated regional differences in improvements in proximal ascending aorta versus descending thoracic and abdominal aorta measured by MRI.[51] Specifically, following the running program there was no change in the distensibility of the proximal ascending aorta, whereas there was an increase in both the proximal descending and distal distending aorta that was at least partially independent of reductions in mean arterial pressure. Thus, these data suggest that more distal aortic segment, which consists of more VSMCs and less elastin in the medial wall compared with the proximal ascending aorta,[52] may be more amenable to favorable alterations in wall stiffness over the short 6-month duration than the ascending elastic aorta. Thus, similar to the common carotid artery, the more muscular descending aorta perhaps is responsive to short-term aerobic exercise training via favorable reductions in VSMC tone/stiffness from either enhanced nitric oxide−mediated endothelial function and/ or less sympathetic nerve adrenergic vasoconstrictor tone, whereas the more elastic proximal ascending aorta does not adapt in this short-term intervention.[53] One possible mechanism may be repeated bouts of augmented wall shear stress in the distal aortic segments during repeated bouts of aerobic exercise leading to regional differences in stiffness of ascending and descending aortic segments. In addition,

regions of enhanced wall shear stress are associated with reduced vascular inflammation, oxidative stress, renin—angiotensin aldosterone activation, extracellular matrix remodeling (elastin and collagen ratio), and elastin proteolysis of elastin lamellae (see Fig. 52.2).[53]

Finally, rodent models provide some insight into the mechanisms by which habitual aerobic exercise potentially modifies age-related aortic or carotid stiffness in older humans.[54,55] Indeed, late-life initiated voluntary wheel running in old mice for 10 weeks ($\sim$1–3 km per day) results in decreases in collagen-1, advanced glycation end-products, oxidative stress, TGF-β, and calcification in the absence of alterations in medial elastin in aorta or carotid arteries.[54,55] However, it should be noted that these late-life initiated, short-term exercise interventions in older mice demonstrate more robust reductions in aortic PWV than in normotensive older humans.[54–56] Thus, the structural and elastic properties of the older mouse aorta appear much more amenable to late-life aerobic exercise; therefore, extrapolating cellular mechanisms in aorta from rodents to humans should be done with caution.

Effect of aerobic exercise interventions on aortic and carotid stiffness among MA/O adults with hypertension. The presence of hypertension is not only associated with higher aortic stiffness (matched for age and blood pressure)[57] but also with an accelerated *rate* of increase in aortic stiffness with advancing age even after adjusting for antihypertensive medications.[4] However, elevated aortic stiffness may precede the development of hypertension suggesting a bidirectional relation between central artery stiffness and hypertension.[58,59] In this regard, it reasons that initiating habitual aerobic exercise among MA/O adults with hypertension may result in reductions in blood pressure and subsequently central artery stiffness, or conversely, exercise may lead to decreases in central artery stiffness and then subsequently blood pressure. Although the direction of this cause and effect pathway is difficult to dissect, intervention studies that have investigated the effects of aerobic exercise training on aortic or carotid stiffness among MA/O adults with treatment-naïve or treated hypertension have largely been ineffective with a few exceptions (see Table 52.2). The earliest study to test this

FIGURE 52.2 Exercise increases aortic blood flow and wall shear stress (WSS), which is normally greater in the descending aorta and can be preferentially affected by lower-extremity exercise (such as running). WSS in turn enhances endothelial nitric oxide (NO) generation, which decreases vascular smooth muscle cell (VSMC) tone/stiffness. Reductions in sympathetic nervous system and renin—angiotensin—aldosterone system (RAAS) activation, which have been reported with exercise training, could also affect VSMC tone/stiffness. Given the greater content of VSMCs in distal aortic segments, VSMC stiffness is more likely to affect descending versus ascending aortic wall stiffness. Aerobic exercise also appears to reduce systemic inflammation, although it is unclear to what extent this is independent of changes in adiposity. Reduced inflammation may have downstream effects on oxidative stress, extracellular matrix composition, and elastase-mediated proteolysis; however, reduced elastin degradation is unlikely to explain changes over 6 months. Changes in other components of the extracellular matrix (ECM) may also affect VSMC stiffness through integrin—cytoskeletal interactions. However, the key molecular mediators of the exercise-related effect on large artery stiffness remain to be identified and represent an important area for future research. *Chirinos JA. The run against arterial aging. J Am Coll Cardiol. 2020 Jan 7;75:72–75. with permission.*

TABLE 52.2 Randomized and nonrandomized studies of effects of continuous aerobic exercise training in middle-aged and/or older adults with prehypertension and/or hypertension on carotid-femoral pulse wave velocity (CFPWV) or carotid artery β-stiffness index.

| | | | | | | | Aerobic exercise program | | | | | | | | | | | |
Study (year)	n (male/female)	Age (years)	Pre HTN or HTN	On anti-HTN meds?	Rando-mization	Control group	Frequency (days/week)	Dura-tion/session (min)	Intensity	Dura-tion (weeks)	Aerobic exercise mode	% δV0₂max	Pre-CFPWV (m/sec)	Post-CFPWV (m/sec)	δCFPW-V (m/sec)	P < .05 versus. bseline	δMAP (mm/Hg) versus baseline	Adjust-ed for δMAP
Ferrier et al. (2001)	20 (10/10)	64 ± 7	Stage 1 HTN	No	Yes	Nonexercise (n = 20)	3	40	65% HRR	8	Cycling	13.5%	11.5 ± 2.8	11.5 ± 1.9	0	No	0	No
Seals et al. (2001)	14 (14/0)	62 ± 9	PreHTN/Stage 1 HTN	No	Yes	Na + restriction (n = 11)	5.8 ± 1.1	40 ± 4	70% HRmax	12	Walking	5.2%	8.8 ± 2.9	8.7 ± 1.9	−0.15	No	−3.8	No
Stew-art et al. (2005)	40 (21/19)	63 (62, 65)	PreHTN/Stage 1 HTN	No	Yes	Nonexercise (n = 53)	3	45	60%−90% HRmax	26	Walk/Cy-cle/Step	16.4%	9.0 (8.2, 9.9)	10.1 (7.9, 12.6)	1.1	No	−4.3	No
Collier et al. (2008)	15 (10/5)	50 ± 2	PreHTN/Stage 1 HTN	No	Yes	RT (n = 15)	3	30	65% V02peak	4	Walking	n/a	12.1 ± 3.1	11.1 ± 3.1	−1.0	Yes	−3.2	No
Gui-mar-aes et al. (2010)	16 (9/7)	50 ± 8	Stage 1 HTN controlled	Yes	Yes	Interval (n = 26), non-exercise (n = 13)	3	40	60% HRR	16	Walking	n/a	10.2 ± 1.2	10.0 ± 1.8	−0.2	No	−4.6	No
Madd-en et al. (2013)	25 (13/12)	69 ± 5	HTN (+T2DM and dyslipidemia)	Yes	Yes	Nonexercise (n = 27)	3	40	60%−75% HRR	24	Walk/Cycle	14.0%	13.4 ± 3.5	12.2 ± 3.6	−1.2	No	−5.6	No
Fantin et al. (2012)	21 (0/21)	68 ± 6	Normal BP (n = 11) and HTN (n = 10)	Yes	No	None	2	60	Up to 75% HRR 4 min @VT: 1 min	24	Walking	n/a	13.2 ± 2.5	11.9 ± 2.1	−1.3	Yes	−5.6	Yes
Vogel et al. (2013)	n = 71 (36/35)	66 ± 7	Normal BP (n = 44); HTN (n = 27)	Yes	No	None	2	30 (6 × 5 -min bouts)	@90% max power	9	Cycling	19.6%	10.9 ± 3.0	10.8 ± 2.8	−0.1	No	−7.0	Yes
Study (year)	n (male/female)	Age (years)	Pre HTN or HTN	On anti-HTN meds?	Rando-mization	Control group	Frequency (days/week)	Dura-tion/ses-sion (min)	Intensity	Dura-tion (weeks)	Aerobic exercise mode	% δV0₂max	Pre-carotid β- stiffness (U)	Post-carotid β-stiffness (AU)	%δ ca-rotid β-stiffness	P < .05 versus. baseline	δMAP (mm/Hg) versus baseline	Adjust-ed for δMAP
Nual-nim et al. (2012)	43 (11/32)	58 ± 2	Pre-HTN (n = 24)	No	Semi-random	Nonexercise (n = 19)	3−4	40−45	70%−75% HRR	12	Swimming	2.6% (NS)	n/a	n/a	−12%	Yes	−7.0	No

Data are mean ± SD or (95% CI); *CFPWV*, carotid-femoral pulse wave velocity; *Hrmax*, heart rate maximum; *HRR*, heart rate reserve; *HTN*, hypertension; *n/a*, not available; *NS*, non-significant; *RT*, resistance training; *VT*, ventilatory threshold. Note: Studies were only included if casual/office MAP was reported or could be computed from systolic and diastolic pressure reported pre-versus post-exercise intervention.

hypothesis, Ferrier et al.[14] randomized 10 MA/O adults with treatment-naïve stage 1 systolic hypertension to 8 weeks of moderate intensity cycling exercise and then crossed-over to 8 weeks of sedentary activity. As expected, the group with stage I hypertension had significantly higher BP, carotid-femoral PWV, aortic characteristic impedance and lower systemic arterial compliance at baseline compared with age-matched control adults without hypertension. Although cycling exercise training resulted in a 13% in VO_2max, there was no change in any of the expressions of central artery stiffness suggesting that elastic properties of the central arteries are resistant to improvement in older adults with hypertension. Seals et al.[13] randomized 35 healthy postmenopausal women with treatment-naïve pre- or stage 1 systolic hypertension to either 3 months of moderate intensity walking exercise, or moderate dietary sodium restriction (~1200 mg/day sodium reduction). Although the exercise group exhibited a significant increase in maximal treadmill time/work consistent with a physiological training effect, they found no change in carotid-femoral PWV or 24-h ambulatory systolic BP after 3 months of aerobic exercise. In contrast, 3 months of sodium restriction resulted in a significant decrease in carotid-femoral PWV and carotid augmentation index that was associated with significant decreases in casual and 24-h ambulatory systolic BP. Thus, these data indicate that moderate sodium restriction has a more powerful influence on lowering aortic stiffness and wave reflection than 3 months of habitual aerobic exercise among postmenopausal women with untreated hypertension (see Table 52.2). Similarly, Stewart et al.[15] randomized MA/O adults with treatment-naïve stage 1 systolic or diastolic hypertension 6 months of either combined aerobic or resistance training or usual care control. Despite a small reduction in diastolic blood pressure and 16% increase in VO_2max in the exercise group compared with controls, there was no significant change in Doppler flow−acquired aortic PWV after 6 months (see Table 52.2).

In contrast to the aforementioned negative studies, Collier et al.[60] reported that carotid-femoral PWV was reduced ~1 m/s after 4 weeks of aerobic exercise but increased ~1.7 m/s after 4 weeks of resistance training group in a randomized study of middle-aged adults with treatment-naïve pre- or stage 1 hypertension despite both aerobic exercise and resistance training groups demonstrating a 3−4 mmHg reduction in mean arterial pressure (see Table 52.2). Although the mechanisms for the divergent results in aortic stiffness in this study are unclear, it may have been related to differences in sympathetic nerve activity activation to the heart and α-adrenergic tone of central elastic and muscular arteries, because heart rate was reduced in the aerobic exercise group and increased in the resistance exercise group and sympathetic nerve activity is known to modulate central elastic artery tone in addition to

heart rate.[49] Lastly, Fantin et al.[45] studied 21 older women (~1/2 of whom were treated for hypertension) before and after a 6 month walking exercise program 2 times/week. They reported a −0.75 m/s reduction in carotid-femoral PWV that remained significant after adjusting for changes in mean arterial pressure. Interestingly, much of the change was driven by the subset of women with hypertension (n = 11) because they exhibited a larger decrease in carotid-femoral PWV (−1.29 m/s) than the normotensive women (−0.40 m/s). However, given the small sample with poorly controlled hypertension (systolic BP = 156 mmHg), lack of a randomized control group or information related to the timing of antihypertensive medication dosing, the overall effects of aerobic exercise program are difficult to interpret (see Table 52.2). Nonetheless, the preponderance of the evidence of the current prospective, randomized intervention studies suggest that habitual aerobic exercise training in the form of walking/jogging or cycling initiated in MA/O adults with treated or treatment-naïve hypertension has small or no beneficial effects on reducing aortic stiffness.

CRF and aortic stiffness in MA/O adults with hypertension. As noted, these intervention studies often result in small or no changes in CRF suggesting that perhaps a greater exercise stimulus is necessary to raise VO_2max to a greater extent to modify aortic stiffness. Contrary to this hypothesis, in a cross-sectional study, Kraft et al.[16] found that aortic PWV, measured by MRI of the descending aorta, did not differ between "high fit" and "low fit" middle-aged adults with hypertension but "high fit" adults without hypertension demonstrated the expected lower aortic PWV compared with "low fit" adults. In accordance, aortic PWV was correlated with VO_2max only among the middle-aged adults without hypertension and not those with hypertension; and this was true for both younger (<50 years) or older participants suggesting that CRF does not modulate aortic stiffness with hypertension present. Moreover, those treated with antihypertensive medications exhibited the expected lower systolic and diastolic blood pressure than the treatment-naïve group, but the groups did not differ in aortic PWV indicating that current antihypertensive drugs that lower blood pressure do not necessarily modify the elastic wall properties of the aorta.

Non−weight-bearing exercise (swimming) and central artery stiffness among MA/O adults with hypertension. Although most of the exercise intervention studies employing continuous exercise protocols in MA/O adults with hypertension have employed typical walking or cycling exercise interventions, they also have reported exclusively on aortic stiffness. Other modalities popular with MA/O adults such as swimming have not been studied extensively nor have many focused on local carotid artery stiffness, compliance, or distensibility. In this regard, Nualnim et al.[18] randomly assigned 43 healthy MA/O

adults with prehypertension or untreated stage 1 hypertension to 12 weeks of swimming exercise or control. The swimming exercise group exhibited an impressive 9 mmHg reduction in casual and 24-h ambulatory systolic blood pressure with a concomitant 21% increase in carotid artery compliance in the absence of any changes in carotid AIx. Interestingly, these changes occurred in the absence of any changes in VO$_2$max, body weight/fat, or other CVD risk factors and the increase in carotid compliance was not correlated with the reduction in blood pressure. Thus, 12 weeks of habitual swimming exercise appears to result in clinically meaningful reductions in blood pressure and improvements in carotid artery stiffness in previously inactive MA/O adults with untreated stage 1 hypertension (see Table 52.2). Although it remains unknown if swimming exercise reduces aortic stiffness, given the low impact and non−weight-bearing advantages of swimming, this exercise might be a feasible option for MA/O adults with hypertension to destiffen central arteries who have orthopedic or mobility issues that limit performing weight-bearing exercise.

Effect of resistance exercise training on large central artery stiffness and central pulsatile hemodynamics

Engaging in habitual RET (also known as strength training) confers numerous systemic health effects beyond those afforded by aerobic/endurance exercise alone. In addition to favorable effects on musculoskeletal health (i.e., bone health, muscle mass, muscular strength), RET has favorable effects on metabolism, insulin sensitivity, inflammation, and overall cardiovascular health.[61] Numerous metaanalyses now support the idea that dynamic RET (when performed as recommended by the American College of Sports Medicine for general muscular fitness—operationally defined as 2−3 days/week, 8−15 repetitions for major muscle groups performed at a moderate-to-vigorous intensity or 60%−70% of 1RM) favorably lowers blood pressure.[62,63] Reductions in blood pressure are comparable to that seen with traditional aerobic/endurance exercise with most studies noting ∼4 mmHg reductions in systolic and diastolic blood pressures in adults with hypertension and prehypertension and reductions of ∼3 mmHg in normotensive adults.[64] At a population level, this modest level of blood pressure reduction translates to decreases in coronary artery disease risk by 5%−9%, stroke risk by 8%−14%, and all-cause mortality risk by 4%.[64] As such, several professional medical societies such as the American College of Sports Medicine and the American Heart Association recommend RET for cardiovascular health promotion.[65−67] Despite the favorable effect of habitual RET on measures of CVD risk, controversy still remains regarding the effects of this exercise modality on

vascular health, because some studies have reported that heavy volume/intensity RET may cause increases in carotid artery and aortic stiffness.[19−21] Therefore, this section will explore the effect of habitual RET on large central artery stiffness and central pulsatile hemodynamics. There are now 50+ studies on this very topic with several systematic reviews and metaanalyses.[68] This section will attempt to offer a thematic overview of seminal studies, key findings that have advanced this area of research, commentary on potential implications of findings, mechanisms, and future directions.
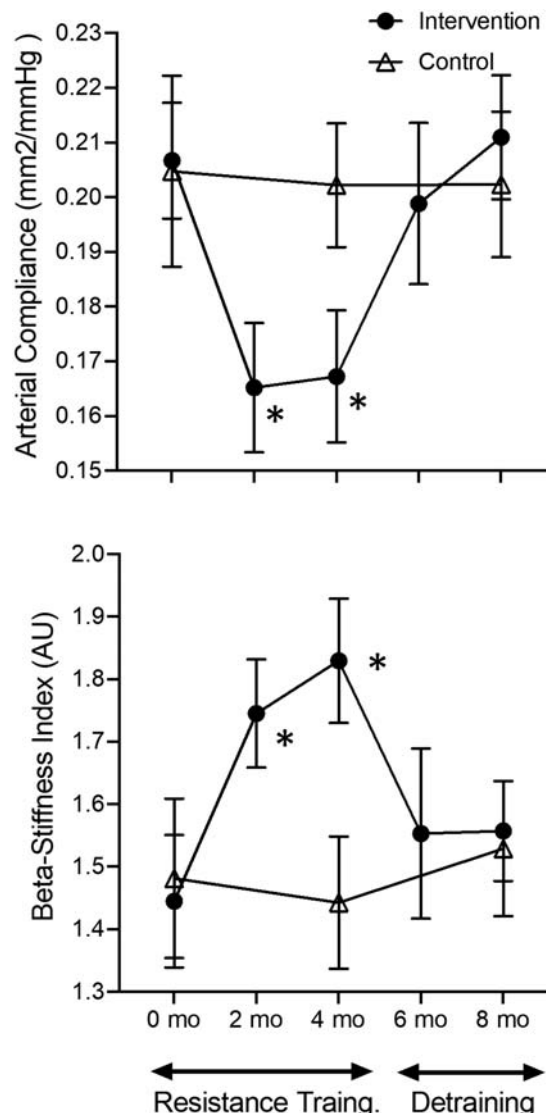
RET and large central artery stiffness. Among the first to explore the effect of habitual RET on large central artery stiffness and pulsatile hemodynamics, Bertovic et al.[21] performed an expansive vascular and hemodynamic assessment on 19 strength-trained men, comparing them with age-matched controls (mean 26 years of age). All participants were healthy and nonsmokers and strength-trained adults were not concomitantly performing aerobic exercise and were not using anabolic agents. Both groups enjoyed a moderately high level of CRF (above average—good) as evidenced by a VO$_2$max of ∼41−44 mL/kg/min. Overall, the authors found that the strength athletes had higher brachial and carotid pulse pressure coupled with lower systemic arterial compliance, higher input and characteristic impedance, and higher aortic β-stiffness and elastic modulus. Aortic geometry was similar between groups as well as carotid-femoral PWV, wave reflection magnitude, relative left ventricular mass, and left ventricular function (i.e., fractional shortening, E/A ratio, and deceleration time). Thus, the habitual strength-trained individuals had greater pulsatile blood pressure that was likely a result of greater proximal aortic stiffness and impedance that was not revealed by carotid-femoral PWV. Authors concluded that the group differences in proximal aortic stiffness were likely of structural origin, alluding to the possibility that chronic elevations in central pulsatile load may cause proximal aortic remodeling and changes in vessel wall composition with increases in smooth muscle and collagen at the expense of elastin. Interestingly, the differences in afterload did not equate to alterations in relative left ventricular mass or function. In summary, this seminal study incorporating numerous measures of central artery stiffness and pulsatile hemodynamics obtained from pressure-flow measures and wave separation analyses raised a provocative question—what are the clinical implications of such large artery adaptations with regard to CVD risk? Twenty years later, the answer to this question posed by Bertovic is still unclear.

In 2003, Miyachi et al.[19] extended the work by Bertovic by studying both young and middle-aged habitually resistance-trained and untrained men (n = 62 total) and incorporated a several measures of large central artery stiffness. Overall, there were no differences in common carotid artery compliance between younger sedentary and

resistance-trained adults. But compared to middle-aged sedentary controls, middle-aged resistance-trained individuals had lower carotid compliance and higher carotid augmentation index. Interestingly, middle-aged resistance-trained individuals also had higher carotid intima-medial thickness (IMT) and left ventricular mass and there were associations between carotid compliance with IMT and a left ventricular hypertrophy index (a ratio of left ventricular wall thickness to left ventricular internal end-diastolic diameter). Miyachi and colleagues reiterated that the clinical significance of the greater age-associated decline in large artery compliance in RET athletes was unclear, in light of the fact that other studies reported that habitually strength-trained adults do not have higher carotid-femoral PWV.[69,70] Indeed, additional studies confirmed RET-trained adults may have increased proximal aortic stiffness[71] and carotid stiffness,[72] findings that have also been extended specifically to women.[73]

Although cross-sectional studies are informative, they are limited because they do not allow for testing of direct exposure to the stimulus. In this regard, Miyachi et al.[20] followed up with the first randomized intervention study to examine the effect of RET on large central artery stiffness in young and middle-aged men (n = 28) (see Fig. 52.3). Fourteen previously untrained men underwent 4 months of RET (3 days per week). After the intervention, there were significant reductions in carotid artery compliance and parenthetically significant increases in carotid β-stiffness in the absence of changes in carotid augmentation index. Making these findings even more compelling, after a 4-month detraining epoch (i.e., removal of the resistance exercise stimulus), carotid artery compliance and stiffness returned completely back to baseline values. There were also significant increases in left ventricular mass following RET and changes in carotid compliance were strongly associated with changes in left ventricular mass. The authors highlighted that their findings supported those of previous cross-sectional studies. However, the authors also stressed that the volume, frequency, and intensity used in their intervention study was greater than the recommended dosage for general health and muscular fitness and questioned whether such an approach would be appropriate for older and clinical high-risk populations. Thus, the clinical relevance of these findings remained to be determined.

This pivotal study generated considerable conversation and debate and instigated several immediate follow-up investigations. How could a mode of exercise with numerous health benefits possibly be detrimental to large central artery buffering reserve and thus cardiovascular function? Over the next few years, additional studies were conducted. A few supported that RET increased large central artery stiffness,[22] while others emerged noting no negative effect on large central artery stiffness.[23,24,74,75] Over the past 15 years, well over 20 studies have been done on this topic.

FIGURE 52.3 Changes in (A) carotid arterial compliance (top) and (B) carotid β-stiffness index in the resistance training intervention group (black circles) and control group (white triangles). Values are mean ± SEM. *$P < .05$ versus baseline; †$P < .05$ versus resistance training period (2 and 4 month values). *Miyachi M, Donato AJ, Yamamoto K, et al. Greater age-related reductions in central arterial compliance in resistance-trained men.* **Hypertension**. *2003; 41:130−135 with permission.*

Results from well-done meta-analyses with stringent but slightly variable inclusion criteria have concluded the following (presented in chronological order):

1. Higher volume/intensity RET may increase large central artery stiffness in younger individuals with lower baseline stiffness values but may not affect large central artery stiffness in MA/O individuals with higher baseline stiffness (derived from 8 RCTs including 193 participants).[76]
2. RET has no effect on large central artery stiffness (14 studies involving 278 participants) in healthy adults with/without obesity/overweight and prehypertension.[77]

3. RET has no effect on large central artery stiffness in adults with CVD (2 studies involving 27 participants).[78]
4. RET has no effect on large central artery stiffness in adults at risk for CVD (13 RCTs including 651 participants with established CVD risk factors).[79]
5. RET has no effect (favorable or detrimental) on large central artery stiffness in healthy adults (10 studies involving 310 participants).[80]
6. RET has no effect on large artery stiffness in adults with hypertension (2 studies involving 28 participants).[81]

In summary, there is a growing body of evidence that contradicts earlier findings of negative effects of RET on large central artery stiffness. Most contemporary studies note that RET does not increase large central artery stiffness (and may even reduce arterial stiffness in select studies) in a variety of healthy and clinical populations, regardless of participant characteristics, training volume, or load.[82–86] The reason for the marked vascular heterogeneity in intraindividual responses to RET is unknown and will be addressed below.

RET and central pulsatile hemodynamics. As alluded to in the previous section, initial cross-sectional studies suggested that habitually resistance exercise-trained adults may have increased central pulsatile hemodynamics. Bertovic et al. noted increased carotid wave reflection magnitude (determined from wave separation analysis) and Miyachi et al. noted increased carotid augmentation index in those engaging in habitual RET.[19,21] In general, far fewer cross-sectional studies have explored central pulsatile hemodynamics in strength-trained individuals with aforementioned studies noting differences with RET status and others noting no differences.[70]

For intervention studies, the literature is as similarly inconsistent for the effects of RET on central hemodynamic pulsatility as it is for the effects of RET on large central artery stiffness. Miyachi et al. were among the first to explore the effect of RET on global wave reflections and noted no change in carotid augmentation index following RET in men. Soon after, Cortez–Cooper et al.[22] found that higher intensity RET increased carotid augmentation index in women. Subsequent studies revealed no effect of RET on augmentation index either when assessed from direct carotid pressure waveforms or from synthesized aortic pressure waveforms using radial tonometry and a generalized transfer function.[74,87] Accordingly, recent metaanalyses have concluded that RET has no effect on augmentation index.[77,78]

Relying exclusively in augmentation index to infer change in wave reflections is not without limitation. For example, RET may result in slight decreases in heart rate and there is a well-known inverse association between heart rate and augmentation index.[88] Many studies report augmentation index as a contrived measure standardized to an arbitrary heart rate of 75 bpm (based on an early cardiac pacing study performed in a small sample).[88] Augmentation index also suffers from what Dr. Gary Mitchell refers to as the "tip of the iceberg" effect.[89] That is, based on the timing of wave reflections and the magnitude of the forward wave, the augmented pressure used to calculate augmentation index may not be truly reflective of wave reflection magnitude. As such, the American Heart Association encourages use of wave separation analyses wherever possible when assessing central pulsatile load and wave reflection magnitude.[90] In this regard, Heffernan et al.[91] explored the effect of a 12-week randomized RET intervention on measures of central pulsatile hemodynamics in a small group of adults with prehypertension and hypertension (n = 11). Compared with a nonexercise control group (n = 10), RET resulted in significant reductions in both brachial and aortic blood pressure in the absence of changes in augmentation index derived from pulse contour analysis or backward pressure wave amplitude derived from wave separation analysis. Interestingly, there were reductions in forward pressure wave amplitude and reservoir wave pressure. Taken together within the context of the broader literature, RET does not appear to have a detrimental effect on central pulsatile hemodynamics including wave reflection.

Potential reasons for discrepancies in the literature on RET and arterial stiffness. RET imposes a very different stress on the cardiovascular system than aerobic exercise and can be conceptualized as a series of static muscular contractions performed dynamically. Although aerobic exercise induces a volume load on the heart and vasculature, resistance exercise imposes a pressure load. Classic findings from MacDougall et al.[92] found that dual-leg leg press performed at near maximal effort can result in brachial pressures exceeding 320/250 mmHg (with some individuals recording systolic and diastolic pressures >400/300 mmHg). This pressor response with subsequent effects on large central artery stiffness can vary with amount of muscle mass activated, lower- versus upper-body exercise, static/isometric versus concentric versus eccentric muscle contraction, timing and composition of last meal, intrinsic muscular strength, and breathing technique/incorporation of a Valsalva maneuver.[93–95] Moreover, the arterial response may also vary based on phase of menstrual cycle and use of hormonal contraceptives in women, although this is not a universal finding.[96,97] Thus, the "same" exercise stimulus can be quite different across individuals.

There is also physiological plausibility for interindividual biological variability in response to RET. Unlike animal studies showing that aerobic exercise can affect arterial structural wall components and stiffness,[54,98] there are no such data to support that RET results in passive (structural) changes to vessel wall material properties (i.e., changes in extracellular matrix components elastin or

collagen composition). Changes in large central artery stiffness with RET may be related in part to active (functional) changes in VSMC tone.[99,100] In animal models, up to half of total aortic wall stiffness is attributable to active stiffness of the VSMCs.[101] Dynamic changes in VSMC plasticity may explain disparate reports in the literature regarding the effects of RET on large central artery stiffness. Excessive increases in blood pressure coupled with Valsalva maneuver exposes the aorta to unique cycles of both static and cyclic stretch and strain. Habitual exposure of the aorta to such hemodynamic perturbations may alter VSMC stiffness as a means of regulating cellular mechanotransduction (i.e., VSMC-ECM interactions redistributing tensile forces across elastin and collagen) as a defense mechanism to "normalize" wall stress and prevent dissection or aneurysm.[101,102] Indeed, the "tensegrity hypothesis" implies that cell stiffness must increase in proportion with the level of the tensile stress.[101]

Select studies note increased sympathetic modulation and elevations in norepinephrine concentrations following RET[103]; an effect that may be attenuated with habituation.[104] Acute hypertension from resistance exercise may possibly cause endothelial damage[105−107] and result in increases in the vasoconstrictor molecule endothelin-1.[108,109] Large central arteries have their own blood supply (vasa vasorum) and neural supply (nervi vasorum). Thus, vasoactive peptide-mediated and/or neurally mediated VSMC contraction and cross-bridge cycling could alter vessel wall (Young's) elastic modulus and increase PWV. Changes in VSMC stiffness may contribute to overall changes in large central artery stiffness with RET. In support of this possibility, studies that note elevations in central artery stiffness with habitual RET also note associations with increases in IMT,[19] and studies in vivo support that changes in VSMC tone can manifest as changes in vessel wall IMT.[110]

Implications and future directions for RET and central artery stiffness. In general, habitually strength-trained individuals do not experience increased incidence of hypertensive CVD and enjoy a typical lifespan (although not the extended lifespan conferred by aerobic/endurance training).[111,112] Structure and functionality of target organs susceptible to hemodynamic pulsatility stemming from age- or disease-associated increases in large central artery stiffness remain preserved with RET. When surveying risk for CVD, one can look to the outcome of the lifestyle behavior (i.e., strength) rather than the behavior itself (i.e., self-reported strength training). In this regard, Dankel et al. [113] demonstrated that strength is a more important predictor of all-cause mortality than self-reported strength training. Indeed, muscular strength is cardioprotective[114] and is inversely associated with aortic stiffness and carotid IMT and extramedia thickness.[115−117] Muscular strength is also associated with lower risk of developing obesity, metabolic syndrome, incident hypertension, sudden cardiac death, and CVD mortality.[114,118−126] Parenthetically, lower muscular strength is a significant predictor of the development of heart failure

and CVD events later in life, independently of CRF.[127−129] Moreover, muscle mass is inversely associated with large central artery stiffness and augmentation index.[130−132] Thus, the "by-products" of strength training do not appear to be associated with detrimental cardiovascular adaptations.

In summary, it appears that RET has negligible adverse effects on large central artery stiffness and hemodynamic pulsatility in most individuals. However, large interindividual variation and observations of increases in large central artery stiffness and hemodynamic pulsatility in select studies cannot and should not be dismissed. Whether such changes confer increased risk (or resiliency) for CVD will need to be scrutinized. Attention to the effects of aging, sex, and ethnic/racial influence on variation will be required. Finally, given that RET is suggested as one part of a general exercise prescription that includes aerobic exercise and flexibility, both of which may reduce large central artery stiffness,[81,133,134] studies that explore the intersection of these exercise modalities for optimal vascular health will be needed.

Effect of obesity, weight loss, and weight gain on central arterial stiffness

Obesity is a major public health problem and the United States has the highest prevalence among high-income countries. The prevalence of obesity reached 42.4% and severe obesity 9.2% in 2017−18.[135] Current projections indicate 50% of the population will have obesity and one in four Americans will have severe obesity by 2030.[136] In addition, obesity is associated with a poor quality of life[137] and reduced life expectancy.[138] In turn, obesity-related illnesses place a significant burden on the economy by increasing rates of health care usage and associated costs.[139] Obesity increases the risk of CVD[140] and the increasing prevalence is contributing the rising adverse CVD mortality trends.[141] Importantly, the association of obesity with CVD is complex and highly dependent on the accumulation of visceral and ectopic fat.[142] The accumulation of visceral fat is associated with a clustering of CVD risk factors termed the "metabolic syndrome" and an increased risk of major adverse CVD outcomes even in the absence of general obesity.[143]

One mechanism by which obesity, particularly visceral obesity, increases CVD risk is by increasing stiffness of central elastic arteries. In this regard, the results of numerous studies suggest that obesity accelerates age-related central artery stiffening[144−148]; the relation between adiposity and arterial stiffness is evident throughout the nonobese range. Importantly, long duration obesity does not appear to be necessary to increase large central artery stiffening as the relation between obesity and arterial stiffness is evident even in young children.[149] Moreover, the location of the excess adiposity, such as visceral versus subcutaneous depots, also contributes to the degree of central artery stiffness among individuals with obesity.

Interindividual variability in central arterial stiffness among individuals of similar age. There is considerable variability in large central artery stiffening among individuals of similar age such that some display levels of central arterial stiffness resembling that of much older individuals and vice versa.[8] Indeed, aortic PWV can vary as much as fourfold among individuals of similar age. Visceral fat accumulation may be an important source of interindividual variability in central artery stiffness where it is more closely associated with visceral fat than other measures of total or regional adiposity.[144−148] The latter may be related, at least in part, to the clustering of cardiometabolic risk factors as well as the accumulation of certain ectopic fat depots (e.g., perivascular fat) in individuals with visceral obesity.[142] As such, the accumulation of body fat, particularly in the abdominal visceral depot, accelerates age-related central arterial stiffening and this can manifest across the age range.[150]
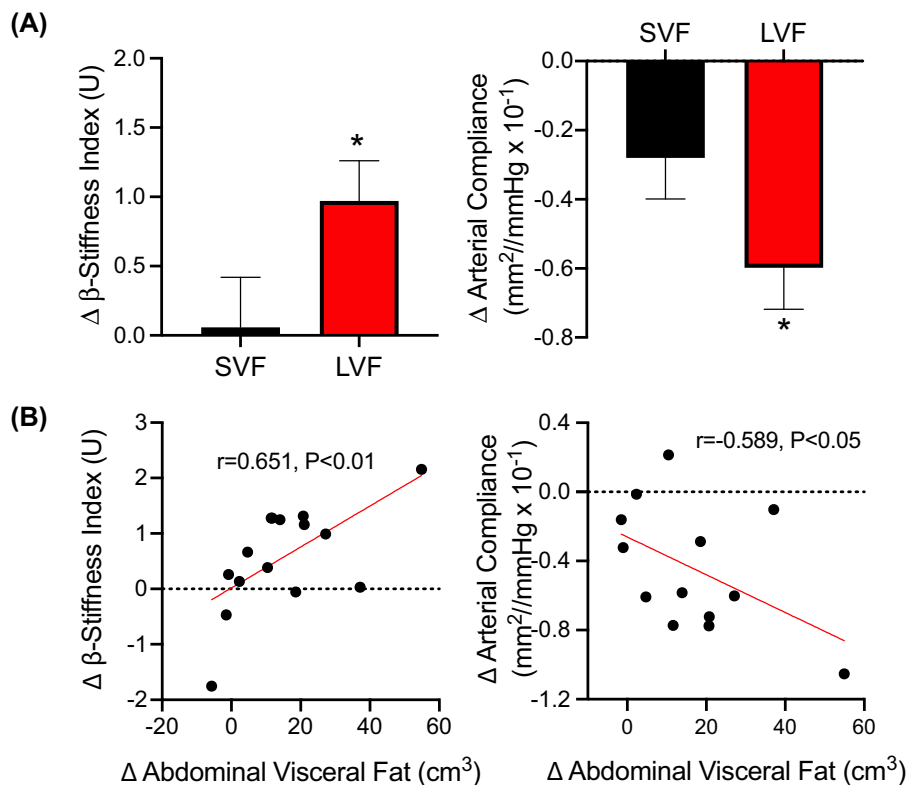
Visceral obesity, the metabolic syndrome, and arterial stiffness. MA/O adults are disproportionately affected by visceral obesity and the metabolic syndrome[151] that amplifies the increasing risk of CVD associated with advancing age. The presence of visceral obesity in MA/O adults is associated with higher levels of central artery stiffness compared with those with general obesity.[147] The closer association of central artery stiffness with visceral adiposity in MA/O adults may be related, at least in part, to

their correspondingly higher levels of blood pressure, circulating glucose, triglycerides, and lower HDL cholesterol,[152] i.e., the risk factors that comprise the metabolic syndrome. Furthermore, these metabolic syndrome risk factors that interact synergistically to increase in central artery stiffness among older adults.[152] In this regard, central artery stiffness can be considered a time-integrated index of an individual's risk factor exposure over time. Indeed, a healthy weight and favorable levels of CVD risk factors are consistent correlates of low carotid-femoral PWV (i.e., healthy vascular aging) in large cohorts.[153,154]

Weight change and central artery stiffness. Weight gain and loss are associated with increases and decreases in central artery stiffness, respectively.[155] Consistent with these observations, experimental weight gain over a period of 6−8 weeks resulted in increases in carotid artery β-stiffness index in young men with healthy weight at baseline. Importantly, the degree of carotid artery stiffening (and reduction in compliance) appears to be determined, in part, by the accumulation of visceral fat (see Fig. 52.4).[25]

Therapeutic weight loss can improve many CVD risk factors and, in many cases, can occur with a modest amount (5%−10%) of weight loss.[156] Weight loss via caloric restriction also reduces aortic stiffness in individuals with obesity across a wide age range.[157] A systematic review and meta-analysis concluded that weight loss achieved by caloric restriction with or without concomitant exercise,

FIGURE 52.4 (A) Change in carotid β-stiffness index (left panel) and change in carotid artery compliance (right panel) following weight gain in subjects with smaller and larger increases in visceral fat. (B) Relation between changes in abdominal visceral fat and changes in carotid β-stiffness left panel) and changes in arterial compliance (right panel) in pooled sample. *Orr JS, Gentile CL, Davy BM and Davy KP. Large artery stiffening with weight gain in humans: role of visceral fat accumulation.* **Hypertension**. *2008; 51:1519−1524 with permission.*

pharmacological intervention, or bariatric surgery was effective in reducing central artery stiffness.[157] Interestingly, caloric restriction plus exercise does not appear to reduce central artery stiffness more than caloric restriction alone.[158] In general, greater weight loss was associated with larger reductions in central artery stiffness irrespective of the mode of weight loss. The duration of weight loss does not clearly impact central artery stiffness as long as weight loss is maintained. Reductions in blood pressure with weight loss tend to be correlated with the decreases in aortic or carotid-femoral PWV, but this finding is inconsistent. Indeed, reductions in central artery stiffness with calorie restriction-induced weight loss have been observed in MA/O adults but the reductions were not correlated with reductions in mean arterial pressure.[26] Interestingly, these decreases in central artery stiffness (both carotid artery β-stiffness index and aortic PWV) were correlated with reductions in abdominal visceral fat. Furthermore, obstructive sleep apnea (OSA), a common comorbidity of severe obesity, is associated with elevated CVD risk, and short-term treatment of OSA with continuous positive airway pressure (CPAP) is associated with reductions in carotid-femoral PWV.[159,160] In contrast, in obese adults with OSA, randomization to 24 weeks of CPAP, caloric-restriction weight loss or combination weight loss plus CPAP (resulting in 6% weight loss), did not result in any change in carotid-femoral PWV in the combination weight loss plus CPAP group despite a significant reduction in central systolic and mean arterial blood pressure. Thus, future studies will need to test whether greater weight loss with longer duration CPAP is likely necessary to lower central artery stiffness among adults with severe obesity and OSA.

Mechanisms and consequences of age- and obesity-related large central artery stiffness. The mechanisms responsible for obesity-related central artery stiffening have not been completely elucidated but elastin fragmentation, collagen cross-linking, and the accumulation of advanced glycation end-products have all been implicated.[161] The mechanisms that contribute to central arterial stiffness with aging have been considered to occur earlier with obesity consistent with the idea of acceleration of age-related arterial stiffening.[162] As with aging, changes in the expression, organization, and function of the structural proteins comprising the medial layer contribute to stiffening of the aorta and carotid arteries in obesity. Remodeling of the extracellular matrix in the medial layer of the aorta and carotid arteries is characterized by collagen cross-linking, elastin fragmentation and degradation, and the formation of advanced glycation end-products.[163] Inflammation and oxidative stress appear to be primary underlying mechanisms.[164] Perivascular adipose tissue, an important source of inflammatory cytokines and oxidative stress, has been implicated in obesity-related arterial

stiffening.[164] Impaired endothelium-dependent dilation and elevated sympathetic nerve activity can contribute to both acute and chronic central artery stiffening by increasing VSMC tone.[49,165] In addition, reduced nitric oxide bioavailability, resulting from inflammation and oxidative stress, and transglutaminase-2 activity promote collagen cross-linking.[162] Activation of the sympathetic and renin—angiotensin systems also exacerbate extracellular matrix remodeling, endothelial dysfunction, vasoconstrictor tone, and carotid artery wall thickening.[164,166]

The association between obesity and hypertension is well documented.[167] Although activation of the renin—angiotensin and sympathetic nervous systems as well as a rightward shift in the renal pressure—natriuresis relation have been well described, the role of arterial stiffening in obesity-associated hypertension has not been systematically studied in humans. However, arterial stiffening occurs rapidly and precedes the increase in systolic blood pressure in mice fed a high-fat, high-sugar diet.[162] Carotid-femoral PWV increased after 1 month, whereas systolic blood pressure did not increase until after 6 months of consuming the high-fat, high-sugar diet. The latter was accompanied by increases in the aortic expression of the inflammatory cytokines tumor necrosis factor-α, monocyte chemoattractant protein-1, and macrophage inflammatory protein-1α and markers of oxidative stress. Impaired endothelium-dependent dilation of aortic rings isolated from the mice was evident after 2 months of consuming the diet and associated with an increase in transglutaminase-2 in aortic lysates. Weight loss reduced central artery stiffness and systolic blood pressure within 2 months of return mice to their chow diet. Markers of inflammation and oxidative stress, endothelium-dependent dilation, and transglutaminase-2 were also reduced following weight loss. Taken together with the observations that central artery stiffness is present in normotensive adults with obesity[26] and precedes the development of hypertension in MA/O humans,[58,59,168] these findings suggest large central artery stiffening may contribute to and precede the development of obesity hypertension.

Obesity-related central artery stiffening is associated with excessive pulsatile arterial load which lead to left ventricular hypertrophy and impaired diastolic function.[3] Indeed, in adolescents and young adults with obesity, augmented aortic forward wave pressure amplitude was a strong predictor of higher left ventricular mass index.[169] In turn, impaired diastolic function in obesity may contribute to the link between large central artery stiffening and HFpEF.[170] However, the impact of visceral obesity on the hemodynamic consequences of large central artery stiffening is not well studied. Nevertheless, the increase in pulsatile pressure with increasing adiposity would increase the transmission of excess pulsatile into the vulnerable microcirculations of the brain and kidney.[3] The increased

exposure of capillaries to pulsatile pressure and flow results in remodeling of the microcirculation to reduce cerebrovascular reactivity and repeated episodes of ischemia and tissue damage. In the brain, this microvascular damage and remodeling may be a link between arterial stiffness, white matter lesions, and cognitive impairment in obesity.[171] Similarly, increased flow pulsatility penetration in the kidney may damage small arteries and glomeruli in the renal cortex and impair function. The impact of large central artery stiffening and its hemodynamic consequence on target organ damage in obesity requires further study.

In summary, total and abdominal visceral adiposity contribute importantly to interindividual variability in age-related central artery stiffness. Weight maintenance is an important strategy for avoiding accelerated arterial stiffening and its adverse clinical sequelae. Future studies are needed to better understand the mechanisms and consequences of accelerated central artery stiffening associated with excess total and visceral adiposity so that targeted therapeutics can be developed. In addition, more information is needed on how to effectively implement and utilize measurements of central artery stiffness in clinical practice to improve risk stratification.

References

1. Ben-Shlomo Y, Spears M, Boustred C, et al. Aortic pulse wave velocity improves cardiovascular event prediction: an individual participant meta-analysis of prospective observational data from 17,635 subjects. **J Am Coll Cardiol**. 2014; 63:636−646.

2. van Sloten TT, Sedaghat S, Laurent S, et al. Carotid stiffness is associated with incident stroke: a systematic review and individual participant data meta-analysis. **J Am Coll Cardiol**. 2015; 66:2116−2125.

3. Mitchell GF. Aortic stiffness, pressure and flow pulsatility, and target organ damage. **J Appl Physiol**. 2018; 125:1871−1880.

4. AlGhatrif M, Strait JB, Morrell CH, et al. Longitudinal trajectories of arterial stiffness and the role of blood pressure: the Baltimore Longitudinal Study of Aging. **Hypertension**. 2013; 62:934−941.

5. McEniery CM, Yasmin, Maki-Petaja KM, et al. The impact of cardiovascular risk factors on aortic stiffness and wave reflections depends on age: the Anglo-Cardiff Collaborative Trial (ACCT III). **Hypertension**. 2010; 56:591−597.

6. Ahmadi-Abhari S, Sabia S, Shipley MJ, et al. Physical activity, sedentary behavior, and long-term changes in aortic stiffness: the Whitehall II study. **J Am Heart Assoc**. 2017; 6.

7. Tanaka H, Palta P, Folsom AR, et al. Habitual physical activity and central artery stiffening in older adults: the Atherosclerosis Risk in Communities study. **J Hypertens**. 2018; 36:1889−1894.

8. Vaitkevicius PV, Fleg JL, Engel JH, et al. Effects of age and aerobic capacity on arterial stiffness in healthy adults. **Circulation**. 1993; 88:1456−1462.

9. Tanaka H, DeSouza CA, Seals DR. Absence of age-related increase in central arterial stiffness in physically active women. **Arterioscler Thromb Vasc Biol**. 1998; 18:127−132.

10. Tanaka H, Dinenno FA, Monahan KD, Clevenger CM, DeSouza CA, Seals DR. Aging, habitual exercise, and dynamic arterial compliance. **Circulation**. 2000; 102:1270−1275.

11. Pierce GL, Casey DP, Fiedorowicz JG, et al. Aortic pulse wave velocity and reflecting distance estimation from peripheral waveforms in humans: detection of age- and exercise training-related differences. **Am J Physiol Heart Circ Physiol**. 2013; 305:H135−H142.

12. Shibata S, Fujimoto N, Hastings JL, et al. The effect of lifelong exercise frequency on arterial stiffness. **J Physiol**. 2018; 596:2783−2795.

13. Seals DR, Tanaka H, Clevenger CM, et al. Blood pressure reductions with exercise and sodium restriction in postmenopausal women with elevated systolic pressure: role of arterial stiffness. **J Am Coll Cardiol**. 2001; 38:506−513.

14. Ferrier KE, Waddell TK, Gatzka CD, Cameron JD, Dart AM, Kingwell BA. Aerobic exercise training does not modify large-artery compliance in isolated systolic hypertension. **Hypertension**. 2001; 38:222−226.

15. Stewart KJ, Bacher AC, Turner KL, et al. Effect of exercise on blood pressure in older persons: a randomized controlled trial. **Arch Intern Med**. 2005; 165:756−762.

16. Kraft KA, Arena R, Arrowood JA, Fei DY. High aerobic capacity does not attenuate aortic stiffness in hypertensive subjects. **Am Heart J**. 2007; 154:976−982.

17. Guimaraes GV, Ciolac EG, Carvalho VO, D'Avila VM, Bortolotto LA, Bocchi EA. Effects of continuous vs. interval exercise training on blood pressure and arterial stiffness in treated hypertension. **Hypertens Res**. 2010; 33:627−632.

18. Nualnim N, Parkhurst K, Dhindsa M, Tarumi T, Vavrek J, Tanaka H. Effects of swimming training on blood pressure and vascular function in adults >50 years of age. **Am J Cardiol**. 2012; 109:1005−1010.

19. Miyachi M, Donato AJ, Yamamoto K, et al. Greater age-related reductions in central arterial compliance in resistance-trained men. **Hypertension**. 2003; 41:130−135.

20. Miyachi M, Kawano H, Sugawara J, et al. Unfavorable effects of resistance training on central arterial compliance: a randomized intervention study. **Circulation**. 2004; 110:2858−2863.

21. Bertovic DA, Waddell TK, Gatzka CD, Cameron JD, Dart AM, Kingwell BA. Muscular strength training is associated with low arterial compliance and high pulse pressure. **Hypertension**. 1999; 33:1385−1391.

22. Cortez-Cooper MY, DeVan AE, Anton MM, et al. Effects of high intensity resistance training on arterial stiffness and wave reflection in women. **Am J Hypertens**. 2005; 18:930−934.

23. Cortez-Cooper MY, Anton MM, Devan AE, Neidre DB, Cook JN, Tanaka H. The effects of strength training on central arterial compliance in middle-aged and older adults. **Eur J Cardiovasc Prev Rehabil**. 2008; 15:149−155.

24. Casey DP, Beck DT, Braith RW. Progressive resistance training without volume increases does not alter arterial stiffness and aortic wave reflection. **Exp Biol Med**. 2007; 232:1228−1235.

25. Orr JS, Gentile CL, Davy BM, Davy KP. Large artery stiffening with weight gain in humans: role of visceral fat accumulation. **Hypertension**. 2008; 51:1519−1524.

26. Dengo AL, Dennis EA, Orr JS, et al. Arterial destiffening with weight loss in overweight and obese middle-aged and older adults. **Hypertension**. 2010; 55:855−861.

27. Wei M, Kampert JB, Barlow CE, et al. Relationship between low cardiorespiratory fitness and mortality in normal-weight, overweight, and obese men. **JAMA**. 1999; 282:1547−1553.

28. Sui X, LaMonte MJ, Blair SN. Cardiorespiratory fitness and risk of nonfatal cardiovascular disease in women and men with hypertension. **Am J Hypertens**. 2007; 20:608−615.

29. Blair SN, Kampert JB, Kohl 3rd HW, et al. Influences of cardiorespiratory fitness and other precursors on cardiovascular disease and all-cause mortality in men and women. **JAMA**. 1996; 276:205−210.

30. Blair SN, Kohl 3rd HW, Paffenbarger Jr RS, Clark DG, Cooper KH, Gibbons LW. Physical fitness and all-cause mortality. A prospective study of healthy men and women. **JAMA**. 1989; 262:2395−2401.

31. Evenson KR, Stevens J, Thomas R, Cai J. Effect of cardiorespiratory fitness on mortality among hypertensive and normotensive women and men. **Epidemiology**. 2004; 15:565−572.

32. Gates PE, Tanaka H, Graves J, Seals DR. Left ventricular structure and diastolic function with human ageing. Relation to habitual exercise and arterial stiffness. **Eur Heart J**. 2003; 24:2213−2220.

33. Moreau K, Donato A, Seals D, DeSouza C, Tanaka H. Regular exercise, hormone replacement therapy, and the age-related decline in carotid arterial compliance in healthy women. **Cardiovasc Res**. 2003; 57:861−868.

34. Moreau KL, Gavin KM, Plum AE, Seals DR. Oxidative stress explains differences in large elastic artery compliance between sedentary and habitually exercising postmenopausal women. **Menopause**. 2006; 13:951−958.

35. Col NF, Pauker SG, Goldberg RJ, et al. Individualizing therapy to prevent long-term consequences of estrogen deficiency in postmenopausal women. **Arch Intern Med**. 1999; 159:1458−1466.

36. Hulley S, Grady D, Bush T, et al. Randomized trial of estrogen plus progestin for secondary prevention of coronary heart disease in postmenopausal women. Heart and Estrogen/progestin Replacement Study (HERS) Research Group. **J Am Med Assoc**. 1998; 280:605−613.

37. Rossouw JE, Anderson GL, Prentice RL, et al. Risks and benefits of estrogen plus progestin in healthy postmenopausal women: principal results from the Women's Health Initiative randomized controlled trial. **J Am Med Assoc**. 2002; 288:321−333.

38. Herrington DM, Reboussin DM, Brosnihan KB, et al. Effects of estrogen replacement on the progression of coronary-artery atherosclerosis. **N Engl J Med**. 2000; 343:522−529.

39. Shephard RJ. Limits to the measurement of habitual physical activity by questionnaires. **Br J Sports Med**. 2003; 37:197−206. Discussion 206.

40. Sugawara J, Otsuki T, Tanabe T, Hayashi K, Maeda S, Matsuda M. Physical activity duration, intensity, and arterial stiffening in postmenopausal women. **Am J Hypertens**. 2006; 19:1032−1036.

41. Kozakova M, Palombo C, Mhamdi L, et al. Habitual physical activity and vascular aging in a young to middle-age population at low cardiovascular risk. **Stroke**. 2007; 38:2549−2555.

42. Gando Y, Yamamoto K, Murakami H, et al. Longer time spent in light physical activity is associated with reduced arterial stiffness in older adults. **Hypertension**. 2010; 56:540−546.

43. Hayashi K, Sugawara J, Komine H, Maeda S, Yokoi T. Effects of aerobic exercise training on the stiffness of central and peripheral arteries in middle-aged sedentary men. **Jpn J Physiol**. 2005; 55:235−239.

44. Yoshizawa M, Maeda S, Miyaki A, et al. Effect of 12 weeks of moderate-intensity resistance training on arterial stiffness: a randomised controlled trial in women aged 32-59 years. **Br J Sports Med**. 2009; 43:615−618.

45. Fantin F, Rossi A, Morgante S, et al. Supervised walking groups to increase physical activity in elderly women with and without hypertension: effect on pulse wave velocity. **Hypertens Res**. 2012; 35:988−993.

46. Vogel T, Lepretre PM, Brechat PH, et al. Effect of a short-term intermittent exercise-training programme on the pulse wave velocity and arterial pressure: a prospective study among 71 healthy older subjects. **Int J Clin Pract**. 2013; 67:420−426.

47. Oudegeest-Sander MH, Olde Rikkert MG, Smits P, et al. The effect of an advanced glycation end-product crosslink breaker and exercise training on vascular function in older individuals: a randomized factorial design trial. **Exp Gerontol**. 2013; 48:1509−1517.

48. Sugawara J, Komine H, Hayashi K, et al. Effect of systemic nitric oxide synthase inhibition on arterial stiffness in humans. **Hypertens Res**. 2007; 30:411−415.

49. Holwerda SW, Luehrs RE, DuBose L, et al. Elevated muscle sympathetic nerve activity contributes to central artery stiffness in young and middle-age/older adults. **Hypertension**. 2019; 73:1025−1035.

50. Sugawara J, Komine H, Hayashi K, et al. Reduction in alpha-adrenergic receptor-mediated vascular tone contributes to improved arterial compliance with endurance training. **Int J Cardiol**. 2009; 135:346−352.

51. Bhuva AN, D'Silva A, Torlasco C, et al. Training for a first-time marathon reverses age-related aortic stiffening. **J Am Coll Cardiol**. 2020; 75:60−71.

52. Schlatmann TJ, Becker AE. Histologic changes in the normal aging aorta: implications for dissecting aortic aneurysm. **Am J Cardiol**. 1977; 39:13−20.

53. Chirinos JA. The run against arterial aging. **J Am Coll Cardiol**. 2020; 75:72−75.

54. Fleenor BS, Marshall KD, Durrant JR, Lesniewski LA, Seals DR. Arterial stiffening with ageing is associated with transforming growth factor-beta1-related changes in adventitial collagen: reversal by aerobic exercise. **J Physiol**. 2010; 588:3971−3982.

55. Gioscia-Ryan RA, Clayton ZS, Fleenor BS, et al. Late-life voluntary wheel running reverses age-related aortic stiffness in mice: a translational model for studying mechanisms of exercise-mediated arterial de-stiffening. **Geroscience**. 2021; 43:423−432.

56. Pierce GL. Aortic stiffness in aging and hypertension: prevention and treatment with habitual aerobic exercise. **Curr Hypertens Rep**. 2017; 19:90.

57. Avolio AP, Deng FQ, Li WQ, et al. Effects of aging on arterial distensibility in populations with high and low prevalence of hypertension: comparison between urban and rural communities in China. **Circulation**. 1985; 71:202−210.

58. Kaess BM, Rong J, Larson MG, et al. Aortic stiffness, blood pressure progression, and incident hypertension. **J Am Med Assoc**. 2012; 308:875−881.

59. Najjar SS, Scuteri A, Shetty V, et al. Pulse wave velocity is an independent predictor of the longitudinal increase in systolic blood pressure and of incident hypertension in the Baltimore Longitudinal Study of Aging. **J Am Coll Cardiol**. 2008; 51:1377−1383.

60. Collier SR, Kanaley JA, Carhart Jr R, et al. Effect of 4 weeks of aerobic or resistance exercise training on arterial stiffness, blood flow and blood pressure in pre- and stage-1 hypertensives. **J Hum Hypertens**. 2008; 22:678−686.

61. McLeod JC, Stokes T, Phillips SM. Resistance exercise training as a primary countermeasure to age-related chronic disease. **Front Physiol**. 2019; 10:645.

62. de Sousa EC, Abrahin O, Ferreira ALL, Rodrigues RP, Alves EAC, Vieira RP. Resistance training alone reduces systolic and diastolic blood pressure in prehypertensive and hypertensive individuals: meta-analysis. **Hypertens Res**. 2017; 40:927−931.

63. MacDonald HV, Johnson BT, Huedo-Medina TB, et al. Dynamic resistance training as stand-alone antihypertensive lifestyle therapy: a meta-analysis. **J Am Heart Assoc**. 2016; 5.

64. Pescatello LS, MacDonald HV, Lamberti L, Johnson BT. Exercise for hypertension: a prescription update integrating existing recommendations with emerging research. **Curr Hypertens Rep**. 2015; 17:87.

65. Arnett DK, Blumenthal RS, Albert MA, et al. 2019 ACC/AHA guideline on the primary prevention of cardiovascular disease: executive summary: a report of the American College of Cardiology/ American heart Association task force on clinical practice guidelines. **J Am Coll Cardiol**. 2019; 74:1376−1414.

66. Garber CE, Blissmer B, Deschenes MR, et al. Quantity and quality of exercise for developing and maintaining cardiorespiratory, musculoskeletal, and neuromotor fitness in apparently healthy adults: guidance for prescribing exercise. **Med Sci Sports Exerc**. 2011; 43:1334−1359.

67. Pescatello LS, Buchner DM, Jakicic JM, et al. Physical activity to prevent and treat hypertension: a systematic review. **Med Sci Sports Exerc**. 2019; 51:1314−1323.

68. Figueroa A, Okamoto T, Jaime SJ, Fahs CA. Impact of high- and low-intensity resistance training on arterial stiffness and blood pressure in adults across the lifespan: a review. **Pflugers Arch**. 2019; 471:467−478.

69. Morra EA, Zaniqueli D, Rodrigues SL, et al. Long-term intense resistance training in men is associated with preserved cardiac structure/function, decreased aortic stiffness, and lower central augmentation pressure. **J Hypertens**. 2014; 32:286−293.

70. Heffernan KS, Jae SY, Echols GH, Lepine NR, Fernhall B. Arterial stiffness and wave reflection following exercise in resistance-trained men. **Med Sci Sports Exerc**. 2007; 39:842−848.

71. Vitarelli A, Capotosto L, Placanica G, et al. Comprehensive assessment of biventricular function and aortic stiffness in athletes with different forms of training by three-dimensional echocardiography and strain imaging. **Eur Heart J Cardiovasc Imaging**. 2013; 14:1010−1020.

72. Kawano H, Nakagawa H, Onodera S, Higuchi M, Miyachi M. Attenuated increases in blood pressure by dynamic resistance exercise in middle-aged men. **Hypertens Res**. 2008; 31:1045−1053.

73. Hayashi K, Sugawara J, Aizawa K, et al. Arterial elastic property in young endurance and resistance-trained women. **Eur J Appl Physiol**. 2008; 104:763−768.

74. Heffernan KS, Fahs CA, Iwamoto GA, et al. Resistance exercise training reduces central blood pressure and improves microvascular function in African American and white men. **Atherosclerosis**. 2009; 207:220−226.

75. Rakobowchuk M, McGowan CL, de Groot PC, et al. Effect of whole body resistance training on arterial compliance in young men. **Exp Physiol**. 2005; 90:645−651.

76. Miyachi M. Effects of resistance training on arterial stiffness: a meta-analysis. **Br J Sports Med**. 2013; 47:393−396.

77. Ashor AW, Lara J, Siervo M, Celis-Morales C, Mathers JC. Effects of exercise modalities on arterial stiffness and wave reflection: a systematic review and meta-analysis of randomized controlled trials. **PLoS One**. 2014; 9:e110034.

78. Zhang Y, Qi L, Xu L, et al. Effects of exercise modalities on central hemodynamics, arterial stiffness and cardiac function in cardiovascular disease: systematic review and meta-analysis of randomized controlled trials. **PLoS One**. 2018; 13:e0200829.

79. Evans W, Willey Q, Hanson ED, Stoner L. Effects of resistance training on arterial stiffness in persons at risk for cardiovascular disease: a meta-analysis. **Sports Med**. 2018; 48:2785−2795.

80. Ceciliato J, Costa EC, Azevedo L, Sousa JC, Fecchio RY, Brito LC. Effect of resistance training on arterial stiffness in healthy subjects: a systematic review and meta-analysis. **Curr Hypertens Rep**. 2020; 22:51.

81. Lopes S, Afreixo V, Teixeira M, et al. Exercise training reduces arterial stiffness in adults with hypertension: a systematic review and meta-analysis. **J Hypertens**. 2021; 39:214−222.

82. Au JS, Oikawa SY, Morton RW, Macdonald MJ, Phillips SM. Arterial stiffness is reduced regardless of resistance training load in young men. **Med Sci Sports Exerc**. 2017; 49:342−348.

83. Werner TJ, Pellinger TK, Rosette VD, Ortlip AT. Effects of a 12-week resistance training program on arterial stiffness: a randomized controlled trial. **J Strength Cond Res**. 2019 Aug 15. https://doi.org/10.1519/JSC.0000000000003331. Online ahead of print.

84. Hildreth KL, Schwartz RS, Vande Griend J, Kohrt WM, Blatchford PJ, Moreau KL. Effects of testosterone and progressive resistance exercise on vascular function in older men. **J Appl Physiol**. 2018; 125:1693−1701.

85. Fernandez-del-Valle M, Gonzales JU, Kloiber S, Mitra S, Klingensmith J, Larumbe-Zabala E. Effects of resistance training on MRI-derived epicardial fat volume and arterial stiffness in women with obesity: a randomized pilot study. **Eur J Appl Physiol**. 2018; 118:1231−1240.

86. Jones LM, Stoner L, Baldi JC, McLaren B. Circuit resistance training and cardiovascular health in breast cancer survivors. **Eur J Cancer Care**. 2020; 29:e13231.

87. Casey DP, Pierce GL, Howe KS, Mering MC, Braith RW. Effect of resistance training on arterial wave reflection and brachial artery reactivity in normotensive postmenopausal women. **Eur J Appl Physiol**. 2007; 100:403−408.

88. Wilkinson IB, MacCallum H, Flint L, Cockcroft JR, Newby DE, Webb DJ. The influence of heart rate on augmentation index and central arterial pressure in humans. **J Physiol**. 2000; 525(Pt 1):263−270.

89. Mitchell GF. Triangulating the peaks of arterial pressure. **Hypertension**. 2006; 48:543−545.

90. Townsend RR, Wilkinson IB, Schiffrin EL, et al. Recommendations for improving and standardizing vascular research on arterial stiffness: a scientific statement from the American heart association. **Hypertension**. 2015; 66:698−722.

91. Heffernan KS, Yoon ES, Sharman JE, et al. Resistance exercise training reduces arterial reservoir pressure in older adults with prehypertension and hypertension. **Hypertens Res**. 2013; 36:422−427.

92. MacDougall JD, Tuxen D, Sale DG, Moroz JR, Sutton JR. Arterial blood pressure response to heavy resistance exercise. **J Appl Physiol**. 1985; 58:785−790.

93. Heffernan KS, Jae SY, Edwards DG, Kelly EE, Fernhall B. Arterial stiffness following repeated Valsalva maneuvers and resistance

exercise in young men. **Appl Physiol Nutr Metab**. 2007; 32:257−264.

94. Heffernan KS, Rossow L, Jae SY, Shokunbi HG, Gibson EM, Fernhall B. Effect of single-leg resistance exercise on regional arterial stiffness. **Eur J Appl Physiol**. 2006; 98:185−190.

95. Augustine J, Tarzia B, Kasprowicz A, Heffernan KS. Effect of a single bout of resistance exercise on arterial stiffness following a high-fat meal. **Int J Sports Med**. 2014; 35:894−899.

96. Augustine JA, Nunemacher KN, Heffernan KS. Menstrual phase and the vascular response to acute resistance exercise. **Eur J Appl Physiol**. 2018; 118:937−946.

97. Okamoto T, Kobayashi R, Sakamaki-Sunaga M. Effect of resistance exercise on arterial stiffness during the follicular and luteal phases of the menstrual cycle. **Int J Sports Med**. 2017; 38:347−352.

98. Padilla J, Ramirez-Perez FI, Habibi J, et al. Regular exercise reduces endothelial cortical stiffness in western diet-fed female mice. **Hypertension**. 2016; 68:1236−1244.

99. Lacolley P, Regnault V, Avolio AP. Smooth muscle cell and arterial aging: basic and clinical aspects. **Cardiovasc Res**. 2018; 114:513−528.

100. Nicholson CJ, Singh K, Saphirstein RJ, et al. Reversal of aging-induced increases in aortic stiffness by targeting cytoskeletal protein-protein interfaces. **J Am Heart Assoc**. 2018; 7.

101. Lacolley P, Regnault V, Segers P, Laurent S. Vascular smooth muscle cells and arterial stiffening: relevance in development, aging, and disease. **Physiol Rev**. 2017; 97:1555−1617.

102. Black JM, Stohr EJ, Shave R, Esformes JI. Influence of exercise training mode on arterial diameter: a systematic review and meta-analysis. **J Sci Med Sport**. 2016; 19:74−80.

103. Pratley R, Nicklas B, Rubin M, et al. Strength training increases resting metabolic rate and norepinephrine levels in healthy 50- to 65-yr-old men. **J Appl Physiol**. 1994; 76:133−137.

104. Saito M, Iwase S, Hachiya T. Resistance exercise training enhances sympathetic nerve activity during fatigue-inducing isometric handgrip trials. **Eur J Appl Physiol**. 2009; 105:225−234.

105. Buchanan CE, Kadlec AO, Hoch AZ, Gutterman DD, Durand MJ. Hypertension during weight lifting reduces flow-mediated dilation in nonathletes. **Med Sci Sports Exerc**. 2017; 49:669−675.

106. de Oliveira GV, Mendes Cordeiro E, Volino-Souza M, Rezende C, Conte-Junior CA, Silveira Alvares T. Flow-mediated dilation in healthy young individuals is impaired after a single resistance exercise session. **Int J Environ Res Public Health**. 2020; 17.

107. Jurva JW, Phillips SA, Syed AQ, et al. The effect of exertional hypertension evoked by weight lifting on vascular endothelial function. **J Am Coll Cardiol**. 2006; 48:588−589.

108. Otsuki T, Maeda S, Iemitsu M, et al. Effects of athletic strength and endurance exercise training in young humans on plasma endothelin-1 concentration and arterial distensibility. **Exp Biol Med**. 2006; 231:789−793.

109. Tagawa K, Ra SG, Kumagai H, et al. Effects of resistance training on arterial compliance and plasma endothelin-1 levels in healthy men. **Physiol Res**. 2018; 67:S155−S166.

110. Thijssen DH, Scholten RR, van den Munckhof IC, Benda N, Green DJ, Hopman MT. Acute change in vascular tone alters intima-media thickness. **Hypertension**. 2011; 58:240−246.

111. Sarna S, Kaprio J, Kujala UM, Koskenvuo M. Health status of former elite athletes. The Finnish experience. **Aging**. 1997; 9:35−41.

112. Kettunen JA, Kujala UM, Kaprio J, et al. All-cause and disease-specific mortality among male, former elite athletes: an average 50-year follow-up. **Br J Sports Med**. 2015; 49:893−897.

113. Dankel SJ, Loenneke JP, Loprinzi PD. Determining the importance of meeting muscle-strengthening activity guidelines: is the behavior or the outcome of the behavior (strength) a more important determinant of all-cause mortality? **Mayo Clin Proc**. 2016; 91:166−174.

114. Artero EG, Lee DC, Ruiz JR, et al. A prospective study of muscular strength and all-cause mortality in men with hypertension. **J Am Coll Cardiol**. 2011; 57:1831−1837.

115. Fahs CA, Heffernan KS, Ranadive S, Jae SY, Fernhall B. Muscular strength is inversely associated with aortic stiffness in young men. **Med Sci Sports Exerc**. 2010; 42:1619−1624.

116. Fahs CA, Thiebaud RS, Rossow LM, Loenneke JP, Bemben DA, Bemben MG. Relationships between central arterial stiffness, lean body mass, and absolute and relative strength in young and older men and women. **Clin Physiol Funct Imaging**. 2018; 38:676−680.

117. Karabinus JA, DeBlois JP, Keller A, Glasgow AC, Barreira TV, Heffernan KS. The inverse association of muscular strength with carotid intima-media and extra-media thickness in women. **Int J Sports Med**. 2021; 42:419−424.

118. Garcia-Hermoso A, Cavero-Redondo I, Ramirez-Velez R, et al. Muscular strength as a predictor of all-cause mortality in an apparently healthy population: a systematic review and meta-analysis of data from approximately 2 million men and women. **Arch Phys Med Rehabil**. 2018; 99:2100−2113 e5.

119. Jackson AW, Lee DC, Sui X, et al. Muscular strength is inversely related to prevalence and incidence of obesity in adult men. **Obesity**. 2010; 18:1988−1995.

120. Jimenez-Pavon D, Brellenthin AG, Lee DC, Sui X, Blair SN, Lavie CJ. Role of muscular strength on the risk of sudden cardiac death in men. **Mayo Clin Proc**. 2019; 94:2589−2591.

121. Laukkanen JA, Voutilainen A, Kurl S, Isiozor NM, Jae SY, Kunutsor SK. Handgrip strength is inversely associated with sudden cardiac death. **Mayo Clin Proc**. 2020; 95:825−828.

122. Jurca R, Lamonte MJ, Barlow CE, Kampert JB, Church TS, Blair SN. Association of muscular strength with incidence of metabolic syndrome in men. **Med Sci Sports Exerc**. 2005; 37:1849−1855.

123. Maslow AL, Sui X, Colabianchi N, Hussey J, Blair SN. Muscular strength and incident hypertension in normotensive and pre-hypertensive men. **Med Sci Sports Exerc**. 2010; 42:288−295.

124. McGrath RP, Vincent BM, Lee IM, Kraemer WJ, Peterson MD. Handgrip strength, function, and mortality in older adults: a time-varying approach. **Med Sci Sports Exerc**. 2018; 50:2259−2266.

125. Patel AV, Hodge JM, Rees-Punia E, Teras LR, Campbell PT, Gapstur SM. Relationship between muscle-strengthening activity and cause-specific mortality in a large US cohort. **Prev Chronic Dis**. 2020; 17:E78.

126. Ruiz JR, Sui X, Lobelo F, et al. Association between muscular strength and mortality in men: prospective cohort study. **BMJ**. 2008; 337:a439.

127. Andersen K, Rasmussen F, Held C, Neovius M, Tynelius P, Sundstrom J. Exercise capacity and muscle strength and risk of vascular disease and arrhythmia in 1.1 million young Swedish men: cohort study. **BMJ**. 2015; 351:h4543.

128. Lindgren M, Aberg M, Schaufelberger M, et al. Cardiorespiratory fitness and muscle strength in late adolescence and long-term risk of

early heart failure in Swedish men. **Eur J Prev Cardiol**. 2017; 24:876−884.

129. Timpka S, Petersson IF, Zhou C, Englund M. Muscle strength in adolescent men and risk of cardiovascular disease events and mortality in middle age: a prospective cohort study. **BMC Med**. 2014; 12:62.

130. Sampaio RA, Sewo Sampaio PY, Yamada M, et al. Arterial stiffness is associated with low skeletal muscle mass in Japanese community-dwelling older adults. **Geriatr Gerontol Int**. 2014; 14(Suppl 1):109−114.

131. Loenneke JP, Fahs CA, Heffernan KS, Rossow LM, Thiebaud RS, Bemben MG. Relationship between thigh muscle mass and augmented pressure from wave reflections in healthy adults. **Eur J Appl Physiol**. 2013; 113:395−401.

132. Abbatecola AM, Chiodini P, Gallo C, et al. Pulse wave velocity is associated with muscle mass decline: health ABC study. **Age**. 2012; 34:469−478.

133. Kato M, Nihei Green F, Hotta K, et al. The efficacy of stretching exercises on arterial stiffness in middle-aged and older adults: a meta-analysis of randomized and non-randomized controlled trials. **Int J Environ Res Public Health**. 2020; 17.

134. Zhang Y, Miyai N, Abe K, et al. Muscle mass reduction, low muscle strength, and their combination are associated with arterial stiffness in community-dwelling elderly population: the Wakayama Study. **J Hum Hypertens**. 2021; 35:446−454.

135. Hales CM, Carroll MD, Fryar CD, Ogden CL. **Prevalence of Obesity and Severe Obesity Among Adults: United States, 2017-2018**. NCHS Data Brief; 2020:1−8.

136. Heidenreich PA, Trogdon JG, Khavjou OA, et al. Forecasting the future of cardiovascular disease in the United States: a policy statement from the American Heart Association. **Circulation**. 2011; 123:933−944.

137. Kolotkin RL, Andersen JR. A systematic review of reviews: exploring the relationship between obesity, weight loss and health-related quality of life. **Clin Obes**. 2017; 7:273−289.

138. Berrington de Gonzalez A, Hartge P, Cerhan JR, et al. Body-mass index and mortality among 1.46 million white adults. **N Engl J Med**. 2010; 363:2211−2219.

139. Tremmel M, Gerdtham UG, Nilsson PM, Saha S. Economic burden of obesity: a systematic literature review. **Int J Environ Res Public Health**. 2017; 14.

140. Piche ME, Poirier P, Lemieux I, Despres JP. Overview of epidemiology and contribution of obesity and body fat distribution to cardiovascular disease: an update. **Prog Cardiovasc Dis**. 2018; 61:103−113.

141. Adair T, Lopez AD. The role of overweight and obesity in adverse cardiovascular disease mortality trends: an analysis of multiple cause of death data from Australia and the USA. **BMC Med**. 2020; 18:199.

142. Neeland IJ, Ross R, Despres JP, et al. Visceral and ectopic fat, atherosclerosis, and cardiometabolic disease: a position statement. **Lancet Diabetes Endocrinol**. 2019; 7:715−725.

143. Choi D, Choi S, Son JS, Oh SW, Park SM. Impact of discrepancies in general and abdominal obesity on major adverse cardiac events. **J Am Heart Assoc**. 2019; 8:e013471.

144. Danias PG, Tritos NA, Stuber M, Botnar RM, Kissinger KV, Manning WJ. Comparison of aortic elasticity determined by cardiovascular magnetic resonance imaging in obese versus lean adults. **Am J Cardiol**. 2003; 91:195−199.

145. Resnick LM, Militianu D, Cunnings AJ, Pipe JG, Evelhoch JL, Soulen RL. Direct magnetic resonance determination of aortic distensibility in essential hypertension: relation to age, abdominal visceral fat, and in situ intracellular free magnesium. **Hypertension**. 1997; 30:654−659.

146. Strasser B, Arvandi M, Pasha EP, Haley AP, Stanforth P, Tanaka H. Abdominal obesity is associated with arterial stiffness in middle-aged adults. **Nutr Metab Cardiovasc Dis**. 2015; 25:495−502.

147. Sutton-Tyrrell K, Newman A, Simonsick EM, et al. Aortic stiffness is associated with visceral adiposity in older adults enrolled in the study of health, aging, and body composition. **Hypertension**. 2001; 38:429−433.

148. Wildman RP, Mackey RH, Bostom A, Thompson T, Sutton-Tyrrell K. Measures of obesity are associated with vascular stiffness in young and older adults. **Hypertension**. 2003; 42:468−473.

149. Cote AT, Phillips AA, Harris KC, Sandor GG, Panagiotopoulos C, Devlin AM. Obesity and arterial stiffness in children: systematic review and meta-analysis. **Arterioscler Thromb Vasc Biol**. 2015; 35:1038−1044.

150. Zebekakis PE, Nawrot T, Thijs L, et al. Obesity is associated with increased arterial stiffness from adolescence until old age. **J Hypertens**. 2005; 23:1839−1846.

151. Park YW, Zhu S, Palaniappan L, Heshka S, Carnethon MR, Heymsfield SB. The metabolic syndrome: prevalence and associated risk factor findings in the US population from the Third National Health and Nutrition Examination Survey, 1988-1994. **Arch Intern Med**. 2003; 163:427−436.

152. Scuteri A, Najjar SS, Muller DC, et al. Metabolic syndrome amplifies the age-associated increases in vascular thickness and stiffness. **J Am Coll Cardiol**. 2004; 43:1388−1395.

153. Niiranen TJ, Lyass A, Larson MG, et al. Prevalence, correlates, and prognosis of healthy vascular aging in a western community-dwelling cohort: the framingham heart study. **Hypertension**. 2017; 70:267−274.

154. Nilsson PM, Laurent S, Cunha PG, et al. Characteristics of healthy vascular ageing in pooled population-based cohort studies: the global Metabolic syndrome and Artery REsearch Consortium. **J Hypertens**. 2018; 36:2340−2349.

155. Wildman RP, Farhat GN, Patel AS, et al. Weight change is associated with change in arterial stiffness among healthy young adults. **Hypertension**. 2005; 45:187−192.

156. Magkos F, Fraterrigo G, Yoshino J, et al. Effects of moderate and subsequent progressive weight loss on metabolic function and adipose tissue biology in humans with obesity. **Cell Metab**. 2016; 23:591−601.

157. Petersen KS, Blanch N, Keogh JB, Clifton PM. Effect of weight loss on pulse wave velocity: systematic review and meta-analysis. **Arterioscler Thromb Vasc Biol**. 2015; 35:243−252.

158. Balkestein EJ, van Aggel-Leijssen DP, van Baak MA, Struijker-Boudier HA, Van Bortel LM. The effect of weight loss with or without exercise training on large artery compliance in healthy obese men. **J Hypertens**. 1999; 17:1831−1835.

159. Drager LF, Bortolotto LA, Figueiredo AC, Krieger EM, Lorenzi GF. Effects of continuous positive airway pressure on early signs of atherosclerosis in obstructive sleep apnea. **Am J Respir Crit Care Med**. 2007; 176:706−712.

160. Litvin AY, Sukmarova ZN, Elfimova EM, et al. Effects of CPAP on "vascular" risk factors in patients with obstructive sleep apnea and arterial hypertension. **Vasc Health Risk Manag**. 2013; 9:229−235.

161. Lakatta E, Levy D. Arterial and cardiac aging: major shareholders in cardiovascular disease enterprises: Part I: aging arteries: a "set up" for vascular disease. **Circulation**. 2003; 107:139−146.

162. Weisbrod RM, Shiang T, Al Sayah L, et al. Arterial stiffening precedes systolic hypertension in diet-induced obesity. **Hypertension**. 2013; 62:1105−1110.

163. O'Rourke M. Arterial stiffness, systolic blood pressure, and logical treatment of arterial hypertension. **Hypertension**. 1990;15:339−347.

164. Aroor AR, Jia G, Sowers JR. Cellular mechanisms underlying obesity-induced arterial stiffness. **Am J Physiol Regul Integr Comp Physiol**. 2018; 314:R387−R398.

165. Hijmering ML, Stroes ES, Olijhoek J, Hutten BA, Blankestijn PJ, Rabelink TJ. Sympathetic activation markedly reduces endothelium-dependent, flow-mediated vasodilation. **J Am Coll Cardiol**. 2002; 39:683−688.

166. Holwerda SW, Luehrs RE, DuBose LE, Majee R, Pierce GL. Sex and age differences in the association between sympathetic outflow and central elastic artery wall thickness in humans. **Am J Physiol Heart Circ Physiol**. 2019; 317:H552−H560.

167. Davy KP. The global epidemic of obesity: are we becoming more sympathetic? **Curr Hypertens Rep**. 2004; 6:241−246.

168. Liao D, Arnett DK, Tyroler HA, et al. Arterial stiffness and the development of hypertension. The ARIC study. **Hypertension**. 1999; 34:201−206.

169. Pierce GL, Pajaniappan M, DiPietro A, Darracott-Woei ASK, Kapuku GK. Abnormal central pulsatile hemodynamics in adolescents with obesity: higher aortic forward pressure wave amplitude is independently associated with greater left ventricular mass. **Hypertension**. 2016; 68:1200−1207.

170. Rozenbaum Z, Topilsky Y, Khoury S, Pereg D, Laufer-Perl M. Association of body mass index and diastolic function in metabolically healthy obese with preserved ejection fraction. **Int J Cardiol**. 2019; 277:147−152.

171. Buie JJ, Watson LS, Smith CJ, Sims-Robinson C. Obesity-related cognitive impairment: the role of endothelial dysfunction. **Neurobiol Dis**. 2019; 132:104580.

This page intentionally left blank

Chapter 53

Dietary salt and arterial stiffness

David G. Edwards and William B. Farquhar

Department of Kinesiology and Applied Physiology, University of Delaware, Newark, DE, United States

Introduction

Dietary sodium restriction is widely considered an important lifestyle modification to control blood pressure (BP) in individuals with hypertension with many organizations worldwide providing information on the benefits of reducing sodium in the diet. Although the increase in sodium consumption in our diets occurred ∼5000−10,000 years ago with the advent of agriculture and farming, the deleterious effects of salt were appreciated long ago by Chinese physician Huang Ti Nei Ching Su Wein in ∼1700 BC who said "therefore if large amounts of salt are taken, the pulse will stiffen and harden" (translated by Wan Ping AD 762).[1]

The average salt intake in most countries is approximately 8−10 g/day (or 3200−4000 mg/day of sodium)[2,3] far higher than our paleolithic ancestors who consumed less than 1g of salt per day.[4] Salt intake is an important factor in the development of hypertension.[5,6] Salt sensitivity of BP, an increase in BP going from a low salt to a high salt diet, is more common in older adults and African Americans.[7,8] Both normotensive and hypertensive individuals can be salt sensitive.[9] Salt sensitivity predicts future hypertension in normotensive individuals[10] and is associated with increased mortality in both normotensive and hypertensive adults.[9,10] While there is a large proportion of the population for which high salt intake will raise BP, the majority of young individuals are normotensive and salt resistant. There is evidence that high salt is detrimental beyond its effect on BP. For example, in the Trials of Hypertension, the long-term risk of cardiovascular events was reduced by dietary sodium reduction with very small changes in BP (SBP-1.7 mmHg, DBP-0.8 mmHg).[11] We will review the effects of dietary salt on BP as well as its BP independent effects in this chapter with an overall focus on arterial stiffness.

Salt vs. Sodium

The major source of sodium in the diet is salt (~90%).

The terms salt and sodium are often used interchangeably.

Salt comprises 40% sodium and 60% chloride based on mass.

1 gram of sodium = 2.5 grams of salt

Dietary salt and blood pressure

There is a large body of literature demonstrating a causal relation between dietary salt intake and BP (see He et al. 2019[12] for recent extensive review). Epidemiological studies have demonstrated a direct association between salt intake and BP.[13−15] Randomized trials of salt reduction have also demonstrated a decline in BP that varied depending on the group studied.[12] In studies where participants were assigned differing levels of salt intake, a dose response relation between salt intake and BP has been shown.[16,17] A number of meta-analyses have been conducted that demonstrate a reduction in BP with salt restriction.[18−21]

Increased dietary salt intake likely leads to increased BP through multiple mechanisms. In the setting of reduced renal function such as aging, an increase in BP may be required to excrete excess sodium in the setting of suppressed RAAS on high salt.[22] Extracellular fluid volume expansion also occurs to buffer the increase in plasma sodium that occurs with changes in salt intake.[23]

Additionally, there are direct BP independent effects of high salt on the vasculature, heart, and inflammation that can affect BP and over the long term will contribute to an increase in BP. The BP independent effects of salt will be discussed more fully below.

Dietary salt and cardiovascular outcomes

Although the focus of this chapter is on the role that dietary salt may have in arterial stiffness and related measures, it is important to briefly consider the association of dietary salt with cardiovascular outcomes. The appropriate level of salt consumption remains a highly debated area; however, there is plenty of evidence that high salt consumption is associated with poor cardiovascular outcomes, with global estimates of over 1.5 million cardiovascular deaths linked to increased BP due to high salt intake.[24] There is a large body of literature on the association between BP, an important cardiovascular disease risk factor, and dietary salt from both observational studies and randomized controlled trials.[25] Many studies have demonstrated a linear relation between dietary sodium intake and poor outcomes, whereas others have identified a "J" or "U"-shaped relation between dietary sodium intake and risk, suggesting an optimal range of sodium intake in the 3000−5000 mg/day range (for example, see References 26,27).

In the Trials of Hypertension Prevention (TOHP) phase 1 and 2, sodium intake was assessed using multiple 24-hour urinary sodium (24hU-Na$^+$) samples, and prehypertensive individuals were followed for 15 years in TOHP 1 and 10 years in TOHP 2. A 17% increase in CV events was found for every 1000 mg/day increase in sodium, and there was no evidence of a J-shaped association.[28] The findings were confirmed in an analysis of postsurveillance TOHP.[29] TOHP is considered representative of the general US population as the median 24hU-Na$^+$ excretion was 3630 mg/day. Similar results have been found in patients with kidney disease. Mills et al.[30] investigated the association between the average of three urinary 24hU-Na$^+$ excretion collections and clinical CV events in data from the Chronic Renal Insufficiency Cohort (CRIC) Study. There was a significant linear association between Na$^+$ excretion and CV events, and the cumulative incidence of CV events were greater in the highest quartile of sodium excretion compared with the lowest quartile.

As discussed elsewhere,[31,32] errors in study design and statistical power have contributed to some of the controversy generated by studies finding a "J" or "U"-shaped relation between sodium consumption and CV outcomes. One reason for the discrepancies in results is likely due to the estimation of dietary sodium intake.[12,33] A variety of methods have been used to estimate sodium intake including food frequency questionnaires, 24-h recall, and spot or overnight urine collection; however, a single 24hU-Na$^+$ may not be satisfactory as data have suggested that at least four collections are needed to reliably quantify dietary sodium intake.[34] Recently, He and colleagues[33] examined TOHP follow up data. They compared sodium intake assessed by measured 24hU-Na$^+$ excretion (average of three to seven measures during the trial) and estimations using three different formulas, Kawasaki,[35] Tanaka,[36] and INTERSALT.[37] Over a median follow-up of 24 years, they found that all estimated values of sodium intake were systematically biased with an overestimation at lower values and underestimation at high values. There was a significant linear relation between measured sodium intake and mortality, whereas there appeared to be a "J" or "U"-shaped relation with mortality for all the formula estimates of sodium intake. These findings highlight the importance of measuring sodium intake accurately when assessing the relation with outcomes and that commonly used estimates are inappropriate to use when assessing the relation between sodium intake and mortality. The biased estimates of sodium intake help explain the J-shaped findings in some cohort studies that are inconsistent with efforts to reduce sodium intake.[12,33]

Blood pressure independent effects of dietary salt

An awareness of the detrimental effects of dietary salt apart from raising BP is not new,[38−40] and studies of the independent effects of salt have increased over last 10 years. Dietary salt has been demonstrated to adversely affect a number of organs and systems independent of BP (Fig. 53.1). While some of these effects may initially occur independent of BP, they may lead to increased salt sensitivity and/or hypertension later in life. We briefly described some of these effects below with a greater focus on the adverse vascular effects and in particular on endothelial function.

Heart

As described above, high dietary salt is associated with poor CV outcomes. Dietary salt has been shown to have deleterious effects on the heart, and in some studies, these effects have been demonstrated to be independent of BP. Urinary sodium excretion has been shown to be independently associated with left ventricular (LV) mass in both normotensive and hypertensive individuals.[41−45] The risk of heart failure is increased in overweight individuals in the highest quartile of sodium intake compared to the lowest quartile even after correction for a number of variables

FIGURE 53.1 Blood pressure independent effects of dietary sodium. There is evidence that dietary salt has deleterious effects independent of, or in addition to, its effects on blood pressure.

including and BP.[46] In a three-year study of patients who underwent treatment of essential hypertension, 24-h urinary sodium was positively related with LV mass at baseline and at the end of the study, independent of age, sex, and systolic BP.[47] The change in LV mass in response to treatment was positively correlated with the changes in systolic BP, urinary sodium, and plasma aldosterone concentration.[47] The association with aldosterone suggests a potential role for a lack of aldosterone suppression on a high salt diet on LV mass.[47]

Inflammation

Excess dietary salt may result in end organ damage, including vascular damage/dysfunction, as a result of inflammation and an exacerbated immune response. High salt diets can promote inflammation through macrophages and proinflammatory T cells.[48–50] T cells exposed to high sodium polarize into proinflammatory TH17 cells producing inflammatory cytokines such as IL-17 that worsen experimental autoimmune disease and promote hypertension.[49,51] Isolevuglandins (IsoLGs), highly reactive lipid oxidation products,[52] have been shown to accumulate in dendritic cells (DCs), promoting T cell activation and hypertension.[53] Sodium stimulates IsoLG-adduct formation in DCs which leads to activation of NADPH oxidase and superoxide formation.[54] High salt intake is also associated with changes in the gut microbiome, which may partly mediate the inflammatory effects of high salt. High salt reduces *Lactobacillus* spp. (a loss of which has been shown to be proinflammatory) and increases TH17 cells.[55,56] A high-salt diet resulted in increased intestinal and vascular inflammation and the formation of IsoLG-adducts in DCs and IL-17A production by T cells in mice.[57] Taken together there is evidence for an inflammatory effect of high salt. The role of changes in the microbiome as a mediator of the immune response to high salt requires additional studies in humans.

Arteries

Endothelial function

An increase in basal NO synthesis occurs as a result of short term high salt intake that helps facilitate sodium excretion.[58,59] However, high salt reduces stimulated NO synthesis which has implications for local blood flow regulation.[39] A reduction in NO synthesis may also play a role in dietary salt-induced increases in arterial stiffness, as discussed below. There are a number of studies in rodents demonstrating that high salt leads to an impairment in endothelial function without a change in BP. Studies in spontaneously hypertensive rats, normotensive Wistar-Kyoto rats, and Sprague–Dawley rats, have demonstrated adverse vascular effects of high salt on the vasculature prior to an increase in BP.[60–62] Further, aortic and mesenteric endothelial function is impaired in Sprague–Dawley rats by high salt without an increase BP.[63–65] Deleterious effects of high salt on the vasculature have also been observed in mice.[66]

Studies in humans have reported findings consistent with the studies in rodents. A high salt diet reduced the vasoconstrictor response to L-NMMA, an eNOS inhibitor, in healthy, normotensive men, indicating lower basal NO synthesis induced by high salt intake.[67] One way to investigate the effects of salt intake on endothelial function independent of BP is to manipulate salt intake in normotensive individuals who are salt resistant. Seven days of a high salt diet impaired brachial artery flow mediated dilation (FMD), a measure of conduit artery endothelial function, in salt resistant individuals (defined as 24-h MAP $\leq$ 5 mmHg between low and high salt diets).[68] A high salt also reduced cutaneous vasodilation in response to local heating, a measure of microvascular function[69] which has been shown to be largely mediated by endothelial-derived NO.[70,71] These studies provide evidence that high salt impairs endothelial function in normotensive adults

without altering BP. Interestingly, the effects of high salt on FMD appear to be similar in salt resistant and salt sensitive individuals.[72] There may be sex differences in the vascular response to alterations in salt intake, with women potentially less sensitive to the vascular effects of high salt[73,74]; however, more work is needed in this area.
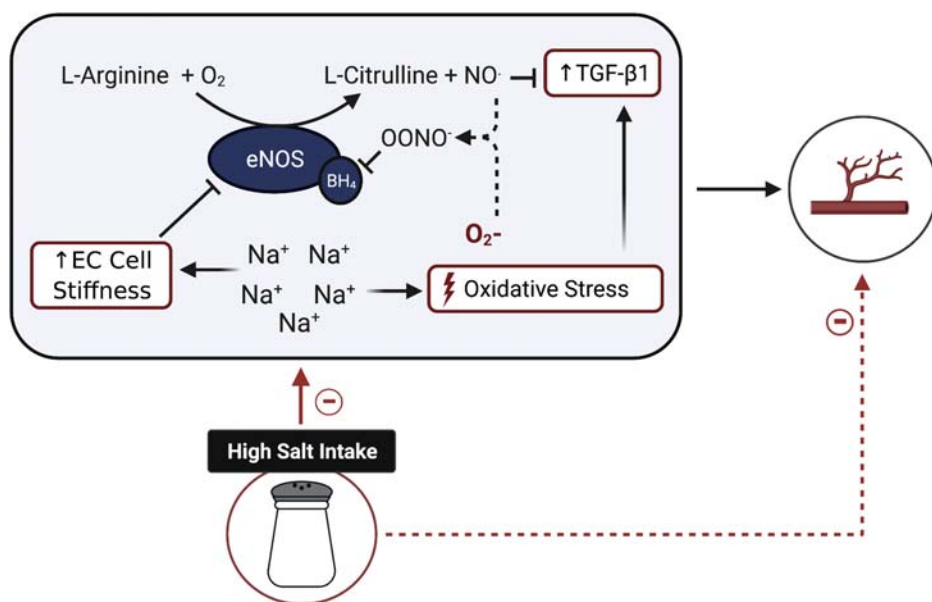
High salt has also been shown to have an adverse effect on vascular function in groups that are at a higher risk for cardiovascular disease. A low salt diet has been shown to improve brachial artery FMD and reduce BP compared to a usual diet in overweight and obese normotensive adults.[75] Because BP was also reduced, it is unclear if there are direct beneficial effects of salt reduction on endothelial function in this study. However, a modest reduction of dietary salt of 3 g/day improved FMD in normotensive overweight and obese individuals independent of BP.[76] There is also evidence that a lower salt diet has beneficial effects on endothelial function in middle age and older adults with elevated BP. Middle-aged and older adults with elevated systolic BP who habitually consumed a low salt diet had a higher FMD compared to a group that consumed higher salt.[77] Dietary sodium restriction in a similar group of middle aged and older adults with moderately elevated systolic BP (130–159 mmHg) improved both brachial artery FMD and the forearm blood flow response to acetylcholine.[78] Although there was a reduction in systolic BP (~12 mmHg), the improvement in endothelial function was still evident after correcting for BP providing evidence that the improvement in endothelial function as a result of sodium restriction occurred independent from the reduction in BP.

Potential mechanisms of reduced endothelial function by high salt (Fig. 53.2)

Oxidative stress

A well-known mechanism of reduced bioavailability of NO occurs through the rapid reaction of NO with elevated levels of superoxide, reducing NO bioavailability, and resulting in the formation of peroxynitrite ($OONO^-$). An increase in oxidative stress as a result of excess superoxide production appears to be a primary mechanism by which high dietary salt impairs endothelial function. Studies in rodents provide evidence that higher levels of superoxide occur as a result of a high salt diet in resistance arteries[63–65] and venules.[63,64] A high salt diet also decreases stimulated NO production as a result of increased reactive oxygen species (ROS).[64,65] Human studies provide additional evidence to support a role for oxidative stress as a mechanism for salt-induced declines in endothelial function as a result of high salt intake.[69,78,79] Local infusion of ascorbic acid reversed the salt-induced impairment in cutaneous vasodilation in normotensive salt resistant subjects.[69] Systemic infusion of ascorbic acid improved both conduit and resistance vessel endothelial function in middle age and older adults with elevated SBP on a normal salt diet, but had no effect following dietary salt restriction.[78] ROS may also result in the oxidation of tetrahydrobiopterin (BH_4), a critical cofactor for eNOS, leading to reduced NO synthesis and generation of superoxide by eNOS. A high salt diet reduced BH_4 levels as a result of BH_4 oxidation in rodents,[80] and oral supplementation of BH_4 improved both conduit and resistance vessel function in middle age and

FIGURE 53.2 Proposed mechanisms by which high salt intake leads to impaired endothelial function/reduced nitric oxide (NO) bioavailability. NO bioavailability is decreased due to reaction of NO with O_2 to form peroxynitrite ($OONO^-$); oxidation of endothelial nitric oxide synthase (eNOS) cofactor tetrahydrobiopterin reducing NO synthesis; and an increase in endothelial cell stiffness which leads to decreased synthesis of NO. Oxidative stress also leads to increased TGF-β which is no longer suppressed by NO.

older adults on a normal salt diet but had no effect following dietary salt restriction.[78]

As described above, superoxide appears to be the primary ROS mediating the impairment of endothelial function on a high salt diet.[65,66] There is evidence that superoxide production is increased on a high salt diet by NADPH oxidase,[64,65] xanthine oxidase,[64,65] and eNOS[66] via uncoupling. The role of NADPH oxidase has received the most attention. The NADPH oxidase inhibitor, apocynin, has been shown to restore vasodilation in mesenteric arteries of rats on a high salt diet.[65] Additionally, NADPH oxidase protein expression has been shown to be increased in the femoral arteries of rats on a high salt diet.[81] Studies in humans also support a role for NADPH oxidase in salt induced increases in ROS. Apocynin ameliorated the salt-induced declines in cutaneous vasodilation in response to both local heating[79] and acetylcholine[82] in normotensive adults. Taken together, it appears that NADPH oxidase is a likely source of ROS as a result of high dietary salt intake.

Oxidative stress as a result of high salt may be related to reduced endogenous antioxidant capacity in addition to increased ROS production. Superoxide dismutase (SOD) is important for scavenging superoxide and is located in both the cytosol (SOD-1) and the mitochondria (SOD-2). High salt diets have been shown to reduce SOD expression and activity.[83,84] Inhibition of SOD-1 in rats on a high salt diet resulted in an attenuated increase in superoxide suggesting that SOD activity or expression was already reduced on the high salt diet.[84] Circulating SOD activity has been found to be greater on a low salt compared to normal salt diet in middle aged and older adults with elevated BP;[78] however, additional investigations are needed to understand the role of reduced SOD in dietary salt-induced declines in vascular function. The mechanism by which salt reduces SOD may be due, at least in part, to the suppression of angiotensin II (Ang II) that occurs as a result of a high salt diet. Sub-pressor doses of Ang II prevented oxidative stress and endothelial dysfunction when given to rodents on a high salt diet.[85,86]

Endothelial cell stiffening

A high salt diet may directly affect endothelial function by altering endothelial cell stiffness. Cell culture studies have shown that increased extracellular sodium stiffens endothelial cells and reduces NO synthesis.[87] This effect is dependent on the presence of physiologic levels of aldosterone and can be inhibited by amiloride which inhibits the epithelial sodium channel (ENaC).[87] The abundance of ENaC present on endothelial cells is increased by elevated extracellular sodium levels.[88] Additionally, excess sodium damages the endothelial glycocalyx (eGC)[89] which allows for increased sodium to enter endothelial cells via ENaC and stiffens cells.[88,90] Damage to the eGC also allows for

monocyte adhesion and inflammation further reducing endothelial function.[91] High extracellular sodium levels disturb the eGC, increase ENaC abundance, stiffen endothelial cells, and reduce NO synthesis;[90] however, the role the eGC and ENac channels on vessel function during high salt in humans has yet to be investigated.

Brain and sympathetic outflow

Cerebrovascular function also appears to be adversely affected by high dietary salt. Epidemiologic evidence suggests that high salt intake is associated with increased mortality from stroke,[92,93] and data from rodent studies have shown that a high salt diet impairs cerebrovascular function via oxidative stress and inflammation.[94,95] Further, autoregulation, the ability of the brain to maintain blood flow in the face of changing BP, has also been shown to be impaired in rodents on a high salt diet.[96] In addition to adverse effects on cerebrovascular function, there is evidence that high salt may increase sympathetic responsiveness. Sympathetic nerve activity is enhanced by elevations in plasma and cerebrospinal fluid sodium concentration leading to an increase in BP in rodents.[97,98] One human study has demonstrated that a high salt diet increases cerebrospinal fluid sodium concentration[99] and BP in hypertensives. Also, there is evidence that a high salt diet alters cardiovagal baroreflex sensitivity in healthy adults.[100] Additional work is needed in humans including clinical populations to fully elucidate the role of sympathetic activation in the deleterious effects of high salt.

Dietary salt and arterial stiffness

An increase in arterial stiffness leads to an increase in LV systolic load, which contributes to ventricular remodeling, and an increase in pulsatile flow into the microcirculation, which contributes to target organ damage.[101] Data from the Framingham Heart Study indicate that aortic stiffness, as assessed by carotid-femoral PWV (cfPWV), was associated with BP progression and incident hypertension.[102] This study and others suggest arterial stiffness is a cause of hypertension rather than a consequence.[102–105] Measures of arterial stiffness have been shown to be predictors of cardiovascular events in clinical populations[106–109] as well as in apparently healthy subjects.[110] Understanding the role of dietary salt as a mediator of arterial stiffness is of clinical importance. It is appreciated that there is a BP-independent effect of dietary salt on arterial stiffness[40] and recent evidence suggests an increase in arterial stiffness partly mediates the effect of a high salt diet on systolic BP.[111]

As described above, a high salt impairs vascular function through a number of mechanisms, and these same mechanisms may affect the structure and function of large elastic arteries in addition to more distal conduit and

resistance vessels. Several studies using rodent models of hypertension have shown that arterial structure is altered by high dietary salt, and that this effect is independent of BP.[40] For example, increased salt intake in spontaneously hypertensive rats resulted in thickening of the aortic media and excess collagen content during the initial time period when BP was not altered.[112,113]
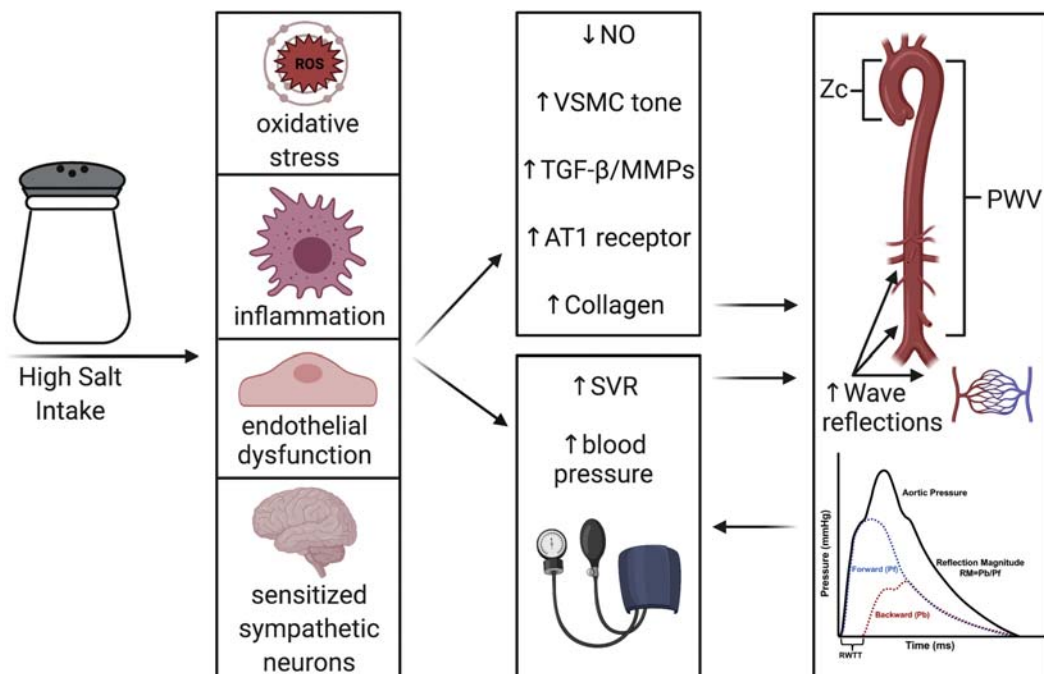
Lower dietary salt intake has been shown to reduce arterial stiffness in hypertensive humans.[114,115] A cross-sectional study in Chinese populations provided the first human data to support a BP independent effect of salt on arterial stiffness.[116] In a study of two groups of Chinese populations, aortic arch-femoral PWV was lower in a rural population that consumed lower salt compared to an urban population that consumed higher salt when the groups were compared at similar BPs.[116] Additional evidence for BP independent effect of salt on arterial stiffness comes from a study that compared a group of normotensive adults who had followed a low salt diet and a control group who consumed a regular diet. When each of the groups were divided into three age groups (2–19, 29–44, 45–66 years), there was a marked increase in aortic arch-femoral PWV across age in the control group but not in the low salt group, and aortic arch-femoral PWV was greater in the middle age and older control groups despite no differences in BP between diets.[117]

A number of studies have examined the effect of reduced dietary salt or dietary salt loading on arterial stiffness. These studies have generally been smaller, and the results have been inconsistent.[76,115,118–121] The duration of interventions has varied from one to six weeks, and those that found improvements in arterial stiffness typically found that BP changed as well. Recently, D'Elia and colleagues[122] performed a systematic review and meta-analysis of the randomized controlled trials of dietary salt and arterial stiffness as assessed by cfPWV. In their pooled analysis, lower salt intake was associated with a significantly lower cfPWV compared to higher salt conditions. Pooled analysis of the effect of salt restriction on BP from the same studies showed a significant reduction in both systolic and diastolic BP on low salt compared to the higher salt condition. Interestingly, further analysis revealed that the changes in BP did not influence the relation between low salt and cfPWV suggesting a BP independent effect of salt on arterial stiffness.

Potential mechanisms of increased arterial stiffness by high salt

Arterial stiffness appears to be increased as a result of high salt due to both BP dependent and independent mechanisms (Fig. 53.3). In many studies of dietary salt, there is a concomitant change in BP along with changes in stiffness; however, the recent meta-analysis by D'Elia and colleagues suggests that the benefits of low salt on arterial stiffness go beyond any benefit from lowering BP.[122] The BP independent mechanisms by which dietary salt increases arterial stiffness are likely due to a combined effect of oxidative stress, inflammation, and endothelial dysfunction. Elevated sympathetic activation as a result of sensitized sympathetic neurons may also play a role. A reduction in NO and an

FIGURE 53.3 Proposed mechanisms by which high salt intake leads to an increase in arterial stiffness. High salt induces oxidative stress, inflammation, endothelial dysfunction, and sensitization of sympathetic neurons that lead to an increase in arterial stiffness through both BP dependent and independent mechanisms. In addition to increased arterial stiffness, alterations in wave reflection amplitude and timing further increase the load on the heart.

increase in vascular smooth muscle cell (VSMC) tone can result in a functional increase in stiffness. Endothelial dysfunction and a reduced bioavailability of NO occur in the setting of high salt diet primarily as a result of oxidative stress and endothelial cell stiffening as described above. Inhibition of NO synthesis has been shown to increase arterial stiffness[123,124] thus salt-induced endothelial dysfunction likely plays a role in increasing arterial stiffness. Endothelial cell stiffness may also contribute to overall vascular stiffness however this requires investigation.

Sympathetic neurons are sensitized by high salt as discussed above, and there is a growing appreciation that the sympathetic nervous system can modulate arterial stiffness.[125] In rodent models, α-adrenergic stimulation results in aortic VSMC proliferation and hypertrophy,[126] and sympathetic innervation increases VSMC contractile protein expression.[127] In humans resting muscle sympathetic nerve activity (MSNA) was positively correlated with cfPWV.[128] Studies utilizing lower body negative pressure to stimulate an increase in sympathetic activity without a change in MAP have found that an acute increase in MSNA is associated with an acute increase in arterial stiffness.[128–130] Dietary salt induced alterations in sympathetic activity may influence arterial stiffness, through both BP dependent and independent mechanisms; however, this remains to be determined. Acute increases in plasma osmolality have been shown to increase plasma norepinephrine levels and MSNA;[131,132] however, the long-term effects of a high salt diet on sympathetic activity have yet to be elucidated.

Inflammation as a result of high salt can increase cytokines and ROS contributing to the decrease in NO bioavailability[133,134] and increase in arterial stiffness. Inflammation and oxidative stress can also result in structural changes to the arterial wall by altering the equilibrium between matrix metalloproteinases (MMPs) and their inhibitors, tissue inhibitors of metalloproteinases.[135] Acute inflammation induced by *Salmonella typhi* vaccination increased MMP-9 levels in association with PWV.[136] MMP 2 and 9 correlated positively with aortic PWV in hypertensive individuals.[137] Dietary sodium intake has been shown to be related to carotid structure and stiffness as well as MMP-9 in hypertension.[138] Interestingly, the associations between dietary salt intake and carotid diameter and stiffness were independent of BP.

Structural alterations to the vasculature as a result of high salt are also due to the profibrotic effects of transforming growth factor-β (TGF-β).[139] Endothelial production of TGF-β has been shown to increase following 7 days of a high salt diet without an increase in BP.[59] Although basal levels of NO production may be increased short-term by high salt, via TGF-β signaling, and may help reduce the negative effect of TGF-β initially,[58,59] endothelial function and stimulated NO synthesis are reduced by high salt intake as described above. Therefore, high salt diets may lead to increased arterial stiffness due to increased and unrestrained TGF-β as a result of high salt induced reductions in NO bioavailability. This effect may be even greater in clinical populations with already impaired endothelial function.[140] Local RAAS signaling may also be an important determinant of collagen content as a result of high salt. Angiotensin II receptor type 1 (AT1) has been shown to be increased by high salt and AT1 blockade during high salt attenuates aortic collagen accumulation.[141]

Dietary salt and pulsatile load

A consequence of increased arterial stiffness and altered timing and magnitude of wave reflection as a result of high salt can lead to an increase in pulsatile load on the LV. High salt diets impair endothelial function which has the potential to alter wave reflection from the periphery and along with increased arterial stiffness increase the pulsatile load on the heart.[142] High dietary salt consumption may increase pulsatile load on the heart, which can lead to LV hypertrophy and ultimately heart failure.[143,144] Wave reflections can arrive back at the heart while the LV is still ejecting blood in mid-to-late systole.[145] Wave reflections thus increase the systolic workload of the LV and can profoundly impact the LV loading sequence. Data from animal studies indicate that late systolic loading from wave reflections promotes LV hypertrophy in rats and diastolic dysfunction in dogs.[146,147] In humans, reflected wave amplitude is independently associated with LV hypertrophy in the general population.[144] Additionally, the reduction of wave reflection has been shown to correlate with regression of LV mass independent of BP reduction.[148] Wave reflections/late systolic load have also been associated with diastolic dysfunction in humans, and to the presence of heart failure with preserved ejection fraction.[149–151] Further, the magnitude of wave reflection strongly predicted the new onset of heart failure in the Multiethnic Study of Atherosclerosis participants who were free from CV disease.[143] Therefore, the relation between a high salt diet and poor cardiovascular outcomes may be, at least in part, due to increased pulsatile load on the LV.

Cross-sectional data provides evidence that dietary salt increases measures of pulsatile load. In a study of black adults from Johannesburg, urinary sodium excretion was related to pulsatile load (forward wave amplitude, pressure augmentation, and augmentation index) and these relations persisted after controlling for MAP.[152] In hypertensive adults, 24-h urinary sodium excretion was independently associated with central pulse pressure (PP), augmented pressure, augmentation index, and PP amplification.[153] Once again, these findings occurred while controlling for MAP, suggesting the effects of sodium are independent of steady state pressure. In a crossover design comparing low and high salt diets, a high salt diet resulted in an increase in both forward and reflected wave

amplitudes in young and middle-aged normotensive adults.[154] Reflection magnitude, or the ratio of the reflected wave to the forward wave, has also been shown to be increased by high salt.[155] It has recently been reported that 24-hour urinary Na^+/K^+ was independently associated with characteristic impedance and that this explained the relation between 24-hour urinary Na^+/K^+ and pulse or systolic pressure.[156] Taken together there is a growing body of evidence suggesting that high salt results in an increase in components of pulsatile load which may partly explain the association between a high salt diet and LV hypertrophy as well as poor cardiovascular outcomes.

Lifestyle and dietary salt
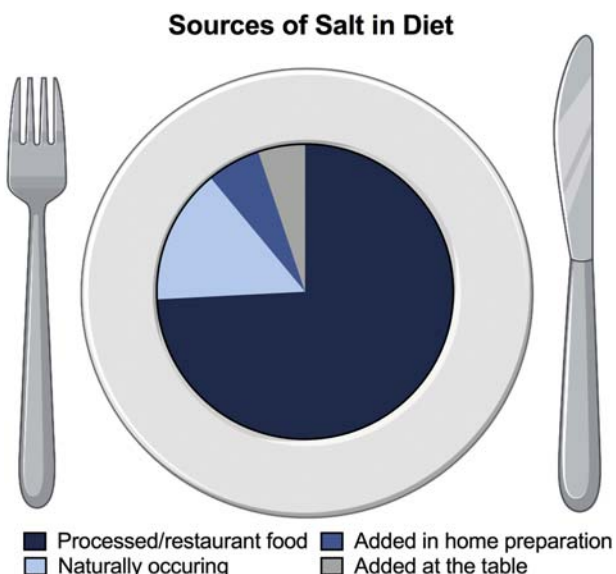
Worldwide dietary salt intake is greater than that recommended by a number of organizations including the World Health Organization as previously mentioned. A small percentage (less than 10%) of Americans is able to abide by the dietary sodium recommendations put forth in the Dietary Guidelines for Americans.[157,158] The primary source of salt in the diet comes from processed food and meals prepared in restaurants[159] with many American exceeding the daily sodium recommendation in a single meal eaten at a restaurant (Fig. 53.4).[160,161] It is extremely difficult to get individuals to reduce their salt intake therefore other lifestyle factors may be important to consider in order to combat the deleterious effects of salt.

Sources of Salt in Diet

- Processed/restaurant food
- Added in home preparation
- Naturally occuring
- Added at the table

FIGURE 53.4 Sources of salt in the diet. The majority of salt consumed in the diet comes from processed and restaurant food. *Adapted from Harnack LJ, Cogswell ME, Shikany JM, et al. Sources of sodium in US adults from 3 geographic regions. **Circulation**. 2017; 135(19):1775−1783.*

Potassium
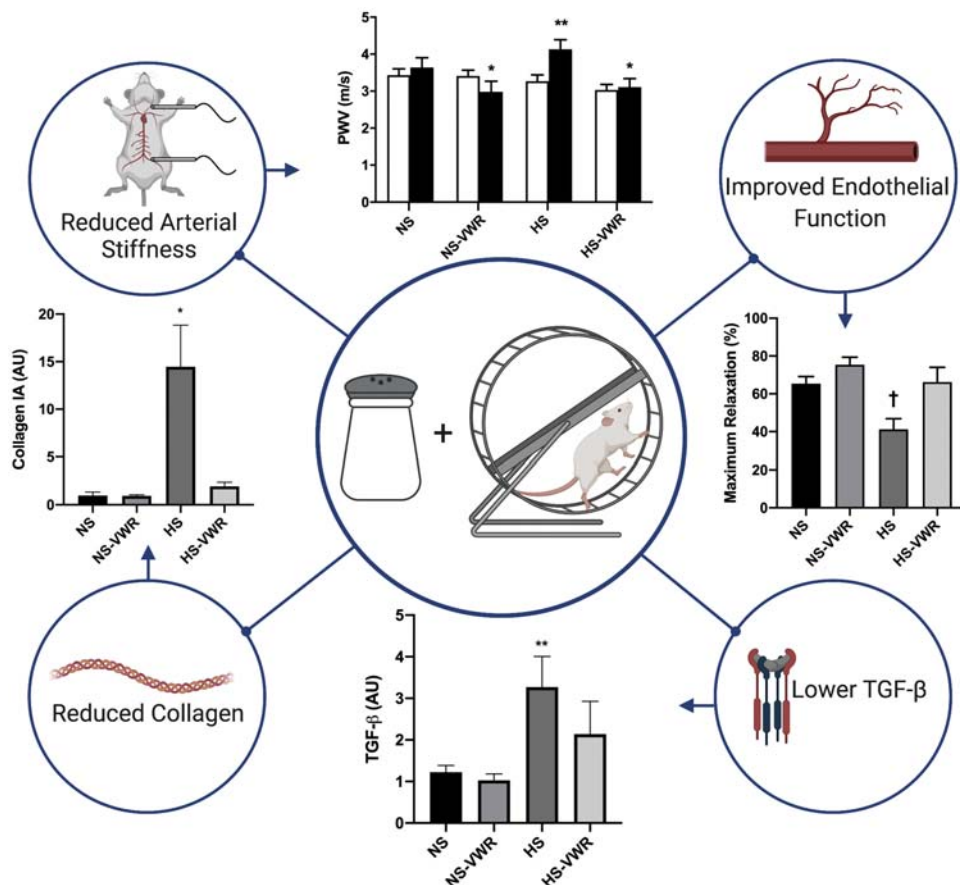
An individual's background diet may be important in modulating the effects of high salt. When high salt is consumed in the setting of a DASH diet that is high in fruit and vegetables and low in dairy fat, it results in lower BP compared to a standard diet that is high in salt.[17,162] The effect may be mediated, at least in part, by higher potassium intake in a DASH diet. There is evidence from large trials that a higher urinary sodium to potassium excretion ratio is associated with increased risk of cardiovascular disease[163,164] suggesting that the interaction of sodium and potassium consumption may be important. Potassium supplementation has been shown to reduce BP[165] and substituting a portion of dietary salt with potassium chloride has been shown to lower BP and reduce the incidence of hypertension.[166] However, there are limited studies of vascular function and potassium consumption. Potassium can soften endothelial cells and increase NO synthesis as demonstrated in cell studies[167] and increased dietary potassium has been shown to inhibit vascular production of TGF-β in rats fed a high salt diet.[168] Recently, endothelial function, as measured by brachial artery FMD, was not reduced on a high salt diet that was also high in potassium providing evidence that potassium may counteract the deleterious effect of salt on the vasculature.[169] Additional studies are warranted to examine the interaction of potassium and sodium on vascular function and in particular arterial stiffness.

Exercise/physical activity

Exercise and/or physical activity has many known beneficial effects including reduced cardiovascular morbidity and mortality.[170,171] The beneficial effects of exercise on arterial stiffness are reviewed elsewhere but are important to consider here in the context of a high salt diet. Exercise has the opposite effect in most instances to dietary salt when it comes to the vasculature, where salt has a deleterious effect exercise has a positive effect. There is a large body of literature that demonstrates improvements in both endothelial function and arterial stiffness from exercise. In aging there is a reduction in endothelial function and an increase in arterial stiffness whereas exercise improves or maintains vascular function.[172] It stands to reason then that exercise may counteract the deleterious effects of salt. In a recent set of studies in rats consuming a high salt diet, Guers and colleagues have demonstrated that voluntary wheel running prevented the negative effects of salt on both endothelial function and arterial stiffness[81,173](Fig. 53.5). Voluntary wheel running resulted in lower aortic TGF-β and collagen content on a high salt diet compared to high salt without voluntary running. This resulted in lower aortic pulse wave velocity. Importantly, these effects were observed without any changes in BP indicating that the positive effects of voluntary wheel running occurred independent of BP.

FIGURE 53.5 The effects of voluntary wheel running with a high salt diet. Voluntary wheel running has been shown to prevent a decline in endothelial function and increase in arterial stiffness in rats fed a high salt diet.[81,173] The lack of increase in arterial stiffness was associated with lower TGF-β and aortic collagen content.[173]

Studies in humans are needed to understand whether exercise or physical activity may be able to counteract high salt in humans.

Conclusion

Worldwide dietary salt intake is high, and excess dietary sodium is associated with increased cardiovascular disease risk and all-cause mortality. High dietary salt intake can lead to increased BP; however, there are BP independent effects of high salt on vascular function, in particular, endothelial function and arterial stiffness. The consequences of dietary salt induced alterations in endothelial function and arterial stiffness include increased pulsatile load on the LV. Endothelial dysfunction and increased arterial stiffness are predictors of cardiovascular disease and data from Framingham indicate that both are associated with incident hypertension.[102] Therefore, reducing excess dietary salt should be considered important for overall vascular health in addition to BP. Lifestyle changes, such as a diet high in potassium and/or exercise, may counteract the deleterious effects of high salt. This may be important as a reduction in salt consumption is difficult to achieve for most individuals.

References

1. Meneton P, Jeunemaitre X, Wardener HE, Macgregor GA. Links between dietary salt intake, renal salt handling, blood pressure, and cardiovascular diseases. **Physiol Rev**. 2005; 85(2):679−715.
2. Powles J, Fahimi S, Micha R, et al. Global, regional and national sodium intakes in 1990 and 2010: a systematic analysis of 24 h urinary sodium excretion and dietary surveys worldwide. **BMJ Open**. 2013; 3(12):e003733.
3. Thout SR, Santos JA, McKenzie B, et al. The Science of Salt: updating the evidence on global estimates of salt intake. **J Clin Hypertens**. 2019; 21(6):710−721.
4. Eaton SB, Konner M. Paleolithic nutrition. **N Engl J Med**. 1985; 312(5):283−289.
5. Graudal NA, Hubeck-Graudal T, Jurgens G. Effects of low sodium diet versus high sodium diet on blood pressure, renin, aldosterone, catecholamines, cholesterol, and triglyceride. **Cochrane Database Syst Rev**. 2011;(11):CD004022.
6. He FJ, Li J, Macgregor GA. Effect of longer-term modest salt reduction on blood pressure. **Cochrane Database Syst Rev**. 2013; 4: CD004937.
7. Weinberger MH. Salt sensitivity of blood pressure in humans. **Hypertension**. 1996; 27(3 Pt 2):481−490.
8. Luft FC, Miller JZ, Grim CE, et al. Salt sensitivity and resistance of blood pressure. Age and race as factors in physiological responses. **Hypertension**. 1991; 17(1 Suppl):I102−I108.

9. Weinberger MH. Salt sensitivity is associated with an increased mortality in both normal and hypertensive humans. **J Clin Hypertens**. 2002; 4(4):274−276.

10. Weinberger MH, Fineberg NS. Sodium and volume sensitivity of blood pressure. Age and pressure change over time. **Hypertension**. 1991; 18(1):67−71.

11. Cook NR, Cutler JA, Obarzanek E, et al. Long term effects of dietary sodium reduction on cardiovascular disease outcomes: observational follow-up of the trials of hypertension prevention (TOHP). **BMJ**. 2007; 334(7599):885−888.

12. He FJ, Tan M, Ma Y, MacGregor GA. Salt reduction to prevent hypertension and cardiovascular disease: JACC state-of-the-art review. **J Am Coll Cardiol**. 2020; 75(6):632−647.

13. Intersalt: an international study of electrolyte excretion and blood pressure. Results for 24 hour urinary sodium and potassium excretion. Intersalt Cooperative Research Group. **BMJ**. 1988; 297(6644):319−328.

14. Zhou BF, Stamler J, Dennis B, et al. Nutrient intakes of middle-aged men and women in China, Japan, United Kingdom, and United States in the late 1990s: the INTERMAP study. **J Hum Hypertens**. 2003; 17(9):623−630.

15. Khaw KT, Bingham S, Welch A, et al. Blood pressure and urinary sodium in men and women: the Norfolk Cohort of the European Prospective Investigation into Cancer (EPIC-Norfolk). **Am J Clin Nutr**. 2004; 80(5):1397−1403.

16. MacGregor GA, Markandu ND, Sagnella GA, Singer DR, Cappuccio FP. Double-blind study of three sodium intakes and long-term effects of sodium restriction in essential hypertension. **Lancet**. 1989; 2(8674):1244−1247.

17. Sacks FM, Svetkey LP, Vollmer WM, et al. Effects on blood pressure of reduced dietary sodium and the dietary approaches to stop hypertension (DASH) diet. DASH-sodium Collaborative Research group. **N Engl J Med**. 2001; 344(1):3−10.

18. He FJ, Li J, Macgregor GA. Effect of longer term modest salt reduction on blood pressure: cochrane systematic review and meta-analysis of randomised trials. **BMJ**. 2013; 346:f1325.

19. Aburto NJ, Ziolkovska A, Hooper L, Elliott P, Cappuccio FP, Meerpohl JJ. Effect of lower sodium intake on health: systematic review and meta-analyses. **BMJ**. 2013; 346:f1326.

20. Graudal NA, Hubeck-Graudal T, Jürgens G. Effects of low-sodium diet vs. high-sodium diet on blood pressure, renin, aldosterone, catecholamines, cholesterol, and triglyceride (cochrane review). **Am J Hypertens**. 2012; 25(1):1−15.

21. Graudal NA, Hubeck-Graudal T, Jurgens G. Effects of low sodium diet versus high sodium diet on blood pressure, renin, aldosterone, catecholamines, cholesterol, and triglyceride. **Cochrane Database Syst Rev**. 2017; 4(4):Cd004022.

22. Mimran A, Ribstein J, Jover B. Aging and sodium homeostasis. **Kidney Int Suppl**. 1992; 37:S107−S113.

23. He FJ, Markandu ND, Sagnella GA, MacGregor GA. Effect of salt intake on renal excretion of water in humans. **Hypertension**. 2001; 38(3):317−320.

24. Mozaffarian D, Fahimi S, Singh GM, et al. Global sodium consumption and death from cardiovascular causes. **N Engl J Med**. 2014; 371(7):624−634.

25. Mancia G, Oparil S, Whelton PK, et al. The technical report on sodium intake and cardiovascular disease in low- and middle-income countries by the joint working group of the World Heart Federation, the European Society of Hypertension and the European Public Health Association. **Eur Heart J**. 2017; 38(10):712−719.

26. Mente A, O'Donnell M, Rangarajan S, et al. Associations of urinary sodium excretion with cardiovascular events in individuals with and without hypertension: a pooled analysis of data from four studies. **Lancet**. 2016; 388(10043):465−475.

27. Stolarz-Skrzypek K, Kuznetsova T, Thijs L, et al. Fatal and nonfatal outcomes, incidence of hypertension, and blood pressure changes in relation to urinary sodium excretion. **JAMA**. 2011; 305(17): 1777−1785.

28. Cook NR, Appel LJ, Whelton PK. Lower levels of sodium intake and reduced cardiovascular risk. **Circulation**. 2014; 129(9):981−989.

29. Cook NR, Appel LJ, Whelton PK. Sodium intake and all-cause mortality over 20 Years in the trials of hypertension prevention. **J Am Coll Cardiol**. 2016; 68(15):1609−1617.

30. Mills KT, Chen J, Yang W, et al. Sodium excretion and the risk of cardiovascular disease in patients with chronic kidney disease. **JAMA**. 2016; 315(20):2200−2210.

31. Farquhar WB, Edwards DG, Jurkovitz CT, Weintraub WS. Dietary sodium and health: more than just blood pressure. **J Am Coll Cardiol**. 2015; 65(10):1042−1050.

32. Cobb LK, Anderson CA, Elliott P, et al. Methodological issues in cohort studies that relate sodium intake to cardiovascular disease outcomes: a science advisory from the American Heart Association. **Circulation**. 2014; 129(10):1173−1186.

33. He FJ, Ma Y, Campbell NRC, MacGregor GA, Cogswell ME, Cook NR. Formulas to estimate dietary sodium intake from spot urine alter sodium-mortality relationship. **Hypertension**. 2019; 74(3):572−580.

34. Lerchl K, Rakova N, Dahlmann A, et al. Agreement between 24-hour salt ingestion and sodium excretion in a controlled environment. **Hypertension**. 2015; 66(4):850−857.

35. Kawasaki T, Itoh K, Uezono K, Sasaki H. A simple method for estimating 24 h urinary sodium and potassium excretion from second morning voiding urine specimen in adults. **Clin Exp Pharmacol Physiol**. 1993; 20(1):7−14.

36. Tanaka T, Okamura T, Miura K, et al. A simple method to estimate populational 24-h urinary sodium and potassium excretion using a casual urine specimen. **J Hum Hypertens**. 2002; 16(2): 97−103.

37. Brown IJ, Dyer AR, Chan Q, et al. Estimating 24-hour urinary sodium excretion from casual urinary sodium concentrations in Western populations: the INTERSALT study. **Am J Epidemiol**. 2013; 177(11):1180−1192.

38. de Wardener HE, MacGregor GA. Harmful effects of dietary salt in addition to hypertension. **J Hum Hypertens**. 2002; 16(4): 213−223.

39. Boegehold MA. The effect of high salt intake on endothelial function: reduced vascular nitric oxide in the absence of hypertension. **J Vasc Res**. 2013; 50(6):458−467.

40. Safar ME, Thuilliez C, Richard V, Benetos A. Pressure-independent contribution of sodium to large artery structure and function in hypertension. **Cardiovasc Res**. 2000; 46(2):269−276.

41. van der Westhuizen B, Schutte AE, Gafane-Matemane LF, Kruger R. Left ventricular mass independently associates with 24-hour sodium excretion in young masked hypertensive adults: the African-PREDICT study. **Int J Cardiol**. 2019; 276:218−223.

42. Rodriguez CJ, Bibbins-Domingo K, Jin Z, Daviglus ML, Goff Jr DC, Jacobs Jr DR. Association of sodium and potassium

intake with left ventricular mass: coronary artery risk development in young adults. **Hypertension**. 2011; 58(3):410−416.

43. Jin Y, Kuznetsova T, Maillard M, et al. Independent relations of left ventricular structure with the 24-hour urinary excretion of sodium and aldosterone. **Hypertension**. 2009; 54(3):489−495.

44. Schmieder RE, Messerli FH, Garavaglia GE, Nunez BD. Dietary salt intake. A determinant of cardiac involvement in essential hypertension. **Circulation**. 1988; 78(4):951−956.

45. Liebson PR, Grandits G, Prineas R, et al. Echocardiographic correlates of left ventricular structure among 844 mildly hypertensive men and women in the Treatment of Mild Hypertension Study (TOMHS). **Circulation**. 1993; 87(2):476−486.

46. He J, Ogden LG, Bazzano LA, Vupputuri S, Loria C, Whelton PK. Dietary sodium intake and incidence of congestive heart failure in overweight US men and women: first National Health and Nutrition Examination Survey Epidemiologic Follow-up Study. **Arch Intern Med**. 2002; 162(14):1619−1624.

47. du Cailar G, Fesler P, Ribstein J, Mimran A. Dietary sodium, aldosterone, and left ventricular mass changes during long-term inhibition of the renin-angiotensin system. **Hypertension**. 2010; 56(5):865−870.

48. Wu C, Yosef N, Thalhamer T, et al. Induction of pathogenic TH17 cells by inducible salt-sensing kinase SGK1. **Nature**. 2013; 496(7446):513−517.

49. Kleinewietfeld M, Manzel A, Titze J, et al. Sodium chloride drives autoimmune disease by the induction of pathogenic TH17 cells. **Nature**. 2013; 496(7446):518−522.

50. Zhang W-C, Zheng X-J, Du L-J, et al. High salt primes a specific activation state of macrophages, M(Na). **Cell Res**. 2015; 25(8):893−910.

51. Foss JD, Kirabo A, Harrison DG. Do high-salt microenvironments drive hypertensive inflammation? **Am J Physiol Regul Integr Comp Physiol**. 2017; 312(1):R1−r4.

52. Iyer RS, Ghosh S, Salomon RG. Levuglandin E2 crosslinks proteins. **Prostaglandins**. 1989; 37(4):471−480.

53. Kirabo A, Fontana V, de Faria AP, et al. DC isoketal-modified proteins activate T cells and promote hypertension. **J Clin Invest**. 2014; 124(10):4642−4656.

54. Barbaro NR, Foss JD, Kryshtal DO, et al. Dendritic cell amiloride-sensitive channels mediate sodium-induced inflammation and hypertension. **Cell Rep**. 2017; 21(4):1009−1020.

55. Elijovich F, Laffer CL, Sahinoz M, Pitzer A, Ferguson JF, Kirabo A. The gut microbiome, inflammation, and salt-sensitive hypertension. **Curr Hypertens Rep**. 2020; 22(10):79.

56. Wilck N, Matus MG, Kearney SM, et al. Salt-responsive gut commensal modulates TH17 axis and disease. **Nature**. 2017; 551(7682):585−589.

57. Ferguson JF, Aden LA, Barbaro NR, et al. High dietary salt-induced dendritic cell activation underlies microbial dysbiosis-associated hypertension. **JCI Insight**. 2019; 5(13).

58. Ying WZ, Aaron KJ, Sanders PW. Transforming growth factor-beta regulates endothelial function during high salt intake in rats. **Hypertension**. 2013; 62(5):951−956.

59. Ying WZ, Sanders PW. Dietary salt increases endothelial nitric oxide synthase and TGF-beta1 in rat aortic endothelium. **Am J Physiol**. 1999; 277(4 Pt 2):H1293−H1298.

60. Frohlich ED, Chien Y, Sesoko S, Pegram BL. Relationship between dietary sodium intake, hemodynamics, and cardiac mass in SHR and WKY rats. **Am J Physiol**. 1993; 264(1 Pt 2):R30−R34.

61. Matavelli LC, Zhou X, Varagic J, Susic D, Frohlich ED. Salt loading produces severe renal hemodynamic dysfunction independent of arterial pressure in spontaneously hypertensive rats. **Am J Physiol Heart Circ Physiol**. 2007; 292(2):H814−H819.

62. Yu HC, Burrell LM, Black MJ, et al. Salt induces myocardial and renal fibrosis in normotensive and hypertensive rats. **Circulation**. 1998; 98(23):2621−2628.

63. Lenda DM, Boegehold MA. Effect of a high-salt diet on oxidant enzyme activity in skeletal muscle microcirculation. **Am J Physiol Heart Circ Physiol**. 2002; 282(2):H395−H402.

64. Lenda DM, Sauls BA, Boegehold MA. Reactive oxygen species may contribute to reduced endothelium-dependent dilation in rats fed high salt. **Am J Physiol Heart Circ Physiol**. 2000; 279(1):H7−H14.

65. Zhu J, Huang T, Lombard JH. Effect of high-salt diet on vascular relaxation and oxidative stress in mesenteric resistance arteries. **J Vasc Res**. 2007; 44(5):382−390.

66. Nurkiewicz TR, Boegehold MA. High salt intake reduces endothelium-dependent dilation of mouse arterioles via superoxide anion generated from nitric oxide synthase. **Am J Physiol Regul Integr Comp Physiol**. 2007; 292(4):R1550−R1556.

67. Tzemos N, Lim PO, Wong S, Struthers AD, MacDonald TM. Adverse cardiovascular effects of acute salt loading in young normotensive individuals. **Hypertension**. 2008; 51(6):1525−1530.

68. DuPont JJ, Greaney JL, Wenner MM, et al. High dietary sodium intake impairs endothelium-dependent dilation in healthy salt-resistant humans. **J Hypertens**. 2013; 31(3):530−536.

69. Greaney JL, DuPont JJ, Lennon-Edwards SL, Sanders PW, Edwards DG, Farquhar WB. Dietary sodium loading impairs microvascular function independent of blood pressure in humans: role of oxidative stress. **J Physiol**. 2012; 590(Pt 21):5519−5528.

70. Kellogg Jr DL, Zhao JL, Wu Y. Endothelial nitric oxide synthase control mechanisms in the cutaneous vasculature of humans in vivo. **Am J Physiol Heart Circ Physiol**. 2008; 295(1):H123−H129.

71. Bruning RS, Santhanam L, Stanhewicz AE, et al. Endothelial nitric oxide synthase mediates cutaneous vasodilation during local heating and is attenuated in middle-aged human skin. **J Appl Physiol**. 2012; 112(12):2019−2026.

72. Matthews EL, Brian MS, Ramick MG, Lennon-Edwards S, Edwards DG, Farquhar WB. High dietary sodium reduces brachial artery flow-mediated dilation in humans with salt-sensitive and salt-resistant blood pressure. **J Appl Physiol**. 2015; 118(12):1510−1515.

73. Eisenach JH, Gullixson LR, Kost SL, Joyner MJ, Turner ST, Nicholson WT. Sex differences in salt sensitivity to nitric oxide dependent vasodilation in healthy young adults. **J Appl Physiol**. 2012; 112(6):1049−1053.

74. Lennon-Edwards S, Ramick MG, Matthews EL, Brian MS, Farquhar WB, Edwards DG. Salt loading has a more deleterious effect on flow-mediated dilation in salt-resistant men than women. Nutrition, metabolism, and cardiovascular diseases. **Nutr Metabol Cardiovasc Dis**. 2014; 24(9):990−995.

75. Dickinson KM, Keogh JB, Clifton PM. Effects of a low-salt diet on flow-mediated dilatation in humans. **Am J Clin Nutr**. 2009:485−490.

76. Dickinson KM, Clifton PM, Keogh JB. A reduction of 3 g/day from a usual 9 g/day salt diet improves endothelial function and decreases endothelin-1 in a randomised cross_over study in normotensive

overweight and obese subjects. **Atherosclerosis**. 2014; 233(1):32–38.

77. Jablonski KL, Gates PE, Pierce GL, Seals DR. Low dietary sodium intake is associated with enhanced vascular endothelial function in middle-aged and older adults with elevated systolic blood pressure. **Therap Adv Cardiovasc Dis**. 2009; 3(5):347–356.

78. Jablonski KL, Racine ML, Geolfos CJ, et al. Dietary sodium restriction reverses vascular endothelial dysfunction in middle-aged/ older adults with moderately elevated systolic blood pressure. **J Am Coll Cardiol**. 2013; 61(3):335–343.

79. Ramick MG, Brian MS, Matthews EL, et al. Apocynin and Tempol ameliorate dietary sodium-induced declines in cutaneous microvascular function in salt-resistant humans. **Am J Physiol Heart Circ Physiol**. 2019; 317(1):H97–h103.

80. Nurkiewicz TR, Wu G, Li P, Boegehold MA. Decreased arteriolar tetrahydrobiopterin is linked to superoxide generation from nitric oxide synthase in mice fed high salt. **Microcirculation**. 2010; 17(2):147–157.

81. Guers JJ, Kasecky-Lardner L, Farquhar WB, Edwards DG, Lennon SL. Voluntary wheel running prevents salt-induced endothelial dysfunction: role of oxidative stress. **J Appl Physiol**. 2019; 126(2):502–510.

82. Alba BK, Stanhewicz AE, Dey P, Bruno RS, Kenney WL, Alexander LM. Controlled feeding of an 8-d, high-dairy cheese diet prevents sodium-induced endothelial dysfunction in the cutaneous microcirculation of healthy, older adults through reductions in superoxide. **J Nutr**. 2020; 150(1):55–63.

83. Durand MJ, Lombard JH. Low-dose angiotensin II infusion restores vascular function in cerebral arteries of high salt-fed rats by increasing copper/zinc superoxide dimutase expression. **Am J Hypertens**. 2013; 26(6):739–747.

84. Lenda DM, Boegehold MA. Effect of a high salt diet on microvascular antioxidant enzymes. **J Vasc Res**. 2002; 39(1):41–50.

85. Zhu J, Drenjancevic-Peric I, McEwen S, et al. Role of superoxide and angiotensin II suppression in salt-induced changes in endothelial Ca^{2+} signaling and NO production in rat aorta. **Am J Physiol Heart Circ Physiol**. 2006; 291(2):H929–H938.

86. McEwen ST, Schmidt JR, Somberg L, Cruz Lde L, Lombard JH. Time-course and mechanisms of restored vascular relaxation by reduced salt intake and angiotensin II infusion in rats fed a high-salt diet. **Microcirculation**. 2009; 16(3):220–234.

87. Oberleithner H, Riethmuller C, Schillers H, MacGregor GA, de Wardener HE, Hausberg M. Plasma sodium stiffens vascular endothelium and reduces nitric oxide release. **Proc Natl Acad Sci USA**. 2007; 104(41):16281–16286.

88. Korte S, Wiesinger A, Straeter AS, Peters W, Oberleithner H, Kusche-Vihrog K. Firewall function of the endothelial glycocalyx in the regulation of sodium homeostasis. **Pflugers Arch**. 2012; 463(2):269–278.

89. Oberleithner H, Peters W, Kusche-Vihrog K, et al. Salt overload damages the glycocalyx sodium barrier of vascular endothelium. **Pflugers Arch Eur J Physiol**. 2011; 462(4):519–528.

90. Kusche-Vihrog K, Jeggle P, Oberleithner H. The role of ENaC in vascular endothelium. **Pflugers Arch Eur J Physiol**. 2014; 466(5):851–859.

91. Schierke F, Wyrwoll MJ, Wisdorf M, et al. Nanomechanics of the endothelial glycocalyx contribute to Na+-induced vascular inflammation. **Sci Rep**. 2017; 7(1):46476.

92. Perry IJ, Beevers DG. Salt intake and stroke: a possible direct effect. **J Hum Hypertens**. 1992; 6(1):23–25.

93. Nagata C, Takatsuka N, Shimizu N, Shimizu H. Sodium intake and risk of death from stroke in Japanese men and women. **Stroke**. 2004; 35(7):1543–1547.

94. Cosic A, Jukic I, Stupin A, et al. Attenuated flow-induced dilatation of middle cerebral arteries is related to increased vascular oxidative stress in rats on a short-term high salt diet. **J Physiol**. 2016; 594(17):4917–4931.

95. Faraco G, Brea D, Garcia-Bonilla L, et al. Dietary salt promotes neurovascular and cognitive dysfunction through a gut-initiated TH17 response. **Nat Neurosci**. 2018; 21(2):240–249.

96. Allen LA, Schmidt JR, Thompson CT, Carlson BE, Beard DA, Lombard JH. High salt diet impairs cerebral blood flow regulation via salt-induced angiotensin II suppression. **Microcirculation**. 2019; 26(3):e12518.

97. Stocker SD, Lang SM, Simmonds SS, Wenner MM, Farquhar WB. Cerebrospinal fluid hypernatremia elevates sympathetic nerve activity and blood pressure via the rostral ventrolateral medulla. **Hypertension**. 2015; 66(6):1184–1190.

98. Simmonds SS, Lay J, Stocker SD. Dietary salt intake exaggerates sympathetic reflexes and increases blood pressure variability in normotensive rats. **Hypertension**. 2014; 64(3):583–589.

99. Kawano Y, Yoshida K, Kawamura M, et al. Sodium and noradrenaline in cerebrospinal fluid and blood in salt-sensitive and non-salt-sensitive essential hypertension. **Clin Exp Pharmacol Physiol**. 1992; 19(4):235–241.

100. Babcock MC, Brian MS, Watso JC, et al. Alterations in dietary sodium intake affect cardiovagal baroreflex sensitivity. **Am J Physiol Regul Integr Comp Physiol**. 2018; 315(4). R688-r95.

101. Townsend RR, Wilkinson IB, Schiffrin EL, et al. Recommendations for improving and standardizing vascular research on arterial stiffness. **Hypertension**. 2015; 66(3):698–722.

102. Kaess BM, Rong J, Larson MG, et al. Aortic stiffness, blood pressure progression, and incident hypertension. **JAMA**. 2012; 308(9):875–881.

103. Dernellis J, Panaretou M. Aortic stiffness is an independent predictor of progression to hypertension in nonhypertensive subjects. **Hypertension**. 2005; 45(3):426–431.

104. Najjar SS, Scuteri A, Shetty V, et al. Pulse wave velocity is an independent predictor of the longitudinal increase in systolic blood pressure and of incident hypertension in the Baltimore Longitudinal Study of Aging. **J Am Coll Cardiol**. 2008; 51(14):1377–1383.

105. Takase H, Dohi Y, Toriyama T, et al. Brachial-ankle pulse wave velocity predicts increase in blood pressure and onset of hypertension. **Am J Hypertens**. 2011; 24(6):667–673.

106. Laurent S, Boutouyrie P, Asmar R, et al. Aortic stiffness is an independent predictor of all-cause and cardiovascular mortality in hypertensive patients. **Hypertension**. 2001; 37(5):1236–1241.

107. Laurent S, Katsahian S, Fassot C, et al. Aortic stiffness is an independent predictor of fatal stroke in essential hypertension. **Stroke**. 2003; 34(5):1203–1206.

108. Blacher J, Safar ME, Guerin AP, Pannier B, Marchais SJ, London GM. Aortic pulse wave velocity index and mortality in end-stage renal disease. **Kidney Int**. 2003; 63(5):1852–1860.

109. Blacher J, Pannier B, Guerin AP, Marchais SJ, Safar ME, London GM. Carotid arterial stiffness as a predictor of

cardiovascular and all-cause mortality in end-stage renal disease. **Hypertension**. 1998; 32(3):570−574.

110. Mattace-Raso FU, van der Cammen TJ, Hofman A, et al. Arterial stiffness and risk of coronary heart disease and stroke: the Rotterdam Study. **Circulation**. 2006; 113(5):657−663.

111. Siriopol D, Covic A, Iliescu R, et al. Arterial stiffness mediates the effect of salt intake on systolic blood pressure. **J Clin Hypertens**. 2018; 20(11):1587−1594.

112. Limas C, Westrum B, Limas CJ, Cohn JN. Effect of salt on the vascular lesions of spontaneously hypertensive rats. **Hypertension**. 1980; 2(4):477−489.

113. Partovian C, Benetos A, Pommiès JP, Mischler W, Safar ME. Effects of a chronic high-salt diet on large artery structure: role of endogenous bradykinin. **Am J Physiol**. 1998; 274(5):H1423−H1428.

114. Gates PE, Tanaka H, Hiatt WR, Seals DR. Dietary sodium restriction rapidly improves large elastic artery compliance in older adults with systolic hypertension. **Hypertension**. 2004; 44(1):35−41.

115. Todd AS, Macginley RJ, Schollum JB, et al. Dietary salt loading impairs arterial vascular reactivity. **Am J Clin Nutr**. 2010; 91(3):557−564.

116. Avolio AP, Deng FQ, Li WQ, et al. Effects of aging on arterial distensibility in populations with high and low prevalence of hypertension: comparison between urban and rural communities in China. **Circulation**. 1985; 71(2):202−210.

117. Avolio AP, Clyde KM, Beard TC, Cooke HM, Ho KK, O'Rourke MF. Improved arterial distensibility in normotensive subjects on a low salt diet. **Arteriosclerosis**. 1986; 6(2):166−169.

118. He FJ, Marciniak M, Visagie E, et al. Effect of modest salt reduction on blood pressure, urinary albumin, and pulse wave velocity in white, black, and Asian mild hypertensives. **Hypertension**. 2009; 54(3):482−488.

119. Pimenta E, Gaddam KK, Oparil S, et al. Effects of dietary sodium reduction on blood pressure in subjects with resistant hypertension: results from a randomized trial. **Hypertension**. 2009; 54(3):475−481.

120. Jablonski KL, Fedorova OV, Racine ML, et al. Dietary sodium restriction and association with urinary marinobufagenin, blood pressure, and aortic stiffness. **Clin J Am Soc Nephrol**. 2013; 8(11):1952−1959.

121. Gijsbers L, Dower JI, Mensink M, Siebelink E, Bakker SJ, Geleijnse JM. Effects of sodium and potassium supplementation on blood pressure and arterial stiffness: a fully controlled dietary intervention study. **J Hum Hypertens**. 2015; 29(10):592−598.

122. D'Elia L, Galletti F, La Fata E, Sabino P, Strazzullo P. Effect of dietary sodium restriction on arterial stiffness: systematic review and meta-analysis of the randomized controlled trials. **J Hypertens**. 2018; 36(4):734−743.

123. Wilkinson IB, MacCallum H, Cockcroft JR, Webb DJ. Inhibition of basal nitric oxide synthesis increases aortic augmentation index and pulse wave velocity in vivo. **Br J Clin Pharmacol**. 2002; 53(2):189−192.

124. Stewart AD, Millasseau SC, Kearney MT, Ritter JM, Chowienczyk PJ. Effects of inhibition of basal nitric oxide synthesis on carotid-femoral pulse wave velocity and augmentation index in humans. **Hypertension**. 2003; 42(5):915−918.

125. Nardone M, Floras JS, Millar PJ. Sympathetic neural modulation of arterial stiffness in humans. **Am J Physiol Heart Circ Physiol**. 2020; 319(6):H1338−H1346.

126. Zhang H, Faber JE. Trophic effect of norepinephrine on arterial intima-media and adventitia is augmented by injury and mediated by different alpha1-adrenoceptor subtypes. **Circ Res**. 2001; 89(9):815−822.

127. Damon DH. Sympathetic innervation promotes vascular smooth muscle differentiation. **Am J Physiol Heart Circ Physiol**. 2005; 288(6):H2785−H2791.

128. Holwerda SW, Luehrs RE, DuBose L, et al. Elevated muscle sympathetic nerve activity contributes to central artery stiffness in young and middle-age/older adults. **Hypertension**. 2019; 73(5):1025−1035.

129. Nardone M, Incognito AV, Millar PJ. Evidence for pressure-independent sympathetic modulation of central pulse wave velocity. **J Am Heart Assoc**. 2018; 7(3).

130. Bock JM, Hughes WE, Casey DP. Age-associated differences in central artery responsiveness to sympathoexcitatory stimuli. **Am J Hypertens**. 2019; 32(6):564−569.

131. Farquhar WB, Wenner MM, Delaney EP, Prettyman AV, Stillabower ME. Sympathetic neural responses to increased osmolality in humans. **Am J Physiol Heart Circ Physiol**. 2006; 291(5):H2181−H2186.

132. Farquhar WB, Paul EE, Prettyman AV, Stillabower ME. Blood pressure and hemodynamic responses to an acute sodium load in humans. **J Appl Physiol**. 2005; 99(4):1545−1551.

133. Gunnett CA, Lund DD, McDowell AK, Faraci FM, Heistad DD. Mechanisms of inducible nitric oxide synthase-mediated vascular dysfunction. **Arterioscler Thromb Vasc Biol**. 2005; 25(8):1617−1622.

134. Yoshizumi M, Perrella MA, Burnett Jr JC, Lee ME. Tumor necrosis factor downregulates an endothelial nitric oxide synthase mRNA by shortening its half-life. **Circ Res**. 1993; 73(1):205−209.

135. Jain S, Khera R, Corrales−Medina VF, Townsend RR, Chirinos JA. Inflammation and arterial stiffness in humans. **Atherosclerosis**. 2014; 237(2):381−390.

136. Vlachopoulos C, Dima I, Aznaouridis K, et al. Acute systemic inflammation increases arterial stiffness and decreases wave reflections in healthy individuals. **Circulation**. 2005; 112(14):2193−2200.

137. Yasmin, McEniery CM, Wallace S, et al. Matrix metalloproteinase-9 (MMP-9), MMP-2, and serum elastase activity are associated with systolic hypertension and arterial stiffness. **Arterioscler Thromb Vasc Biol**. 2005; 25(2):372.

138. Ferreira-Sae MCS, Cipolli JAA, Cornélio ME, et al. Sodium intake is associated with carotid artery structure alterations and plasma matrix metalloproteinase-9 upregulation in hypertensive adults. **J Nutr**. 2011; 141(5):877−882.

139. Sanders PW. Vascular consequences of dietary salt intake. **Am J Physiol Ren Physiol**. 2009; 297(2):F237−F243.

140. Kanbay M, Chen Y, Solak Y, Sanders PW. Mechanisms and consequences of salt sensitivity and dietary salt intake. **Curr Opin Nephrol Hypertens**. 2011; 20(1):37−43.

141. Nickenig G, Strehlow K, Roeling J, Zolk O, Knorr A, Böhm M. Salt induces vascular AT_1 receptor overexpression in vitro and in vivo. **Hypertension**. 1998; 31(6):1272−1277.

142. Chirinos JA, Townsend R. Sodium, potassium, and target organ damage: a case for central hemodynamics. **Hypertension**. 2010; 56(4):578−580.

143. Chirinos JA, Kips JG, Jacobs Jr DR, et al. Arterial wave reflections and incident cardiovascular events and heart failure: MESA

(Multiethnic Study of Atherosclerosis). **J Am Coll Cardiol**. 2012; 60(21):2170−2177.

144. Zamani P, Bluemke DA, Jacobs Jr DR, et al. Resistive and pulsatile arterial load as predictors of left ventricular mass and geometry: the multi-ethnic study of atherosclerosis. **Hypertension**. 2015; 65(1):85−92.

145. Chirinos JA, Segers P. Noninvasive evaluation of left ventricular afterload: part 2: arterial pressure-flow and pressure-volume relations in humans. **Hypertension**. 2010; 56(4):563−570.

146. Gillebert TC, Lew WY. Influence of systolic pressure profile on rate of left ventricular pressure fall. **Am J Physiol**. 1991; 261(3 Pt 2):H805−H813.

147. Kobayashi S, Yano M, Kohno M, et al. Influence of aortic impedance on the development of pressure-overload left ventricular hypertrophy in rats. **Circulation**. 1996; 94(12):3362−3368.

148. Hashimoto J, Westerhof BE, Westerhof N, Imai Y, O'Rourke MF. Different role of wave reflection magnitude and timing on left ventricular mass reduction during antihypertensive treatment. **J Hypertens**. 2008; 26(5):1017−1024.

149. Chirinos JA, Segers P, Rietzschel ER, et al. Early and late systolic wall stress differentially relate to myocardial contraction and relaxation in middle-aged adults: the Asklepios study. **Hypertension**. 2013; 61(2):296−303.

150. Weber T, O'Rourke MF, Ammer M, Kvas E, Punzengruber C, Eber B. Arterial stiffness and arterial wave reflections are associated with systolic and diastolic function in patients with normal ejection fraction. **Am J Hypertens**. 2008; 21(11):1194−1202.

151. Weber T, Wassertheurer S, O'Rourke MF, et al. Pulsatile hemodynamics in patients with exertional dyspnea: potentially of value in the diagnostic evaluation of suspected heart failure with preserved ejection fraction. **J Am Coll Cardiol**. 2013; 61(18):1874−1883.

152. Redelinghuys M, Norton GR, Scott L, et al. Relationship between urinary salt excretion and pulse pressure and central aortic hemodynamics independent of steady state pressure in the general population. **Hypertension**. 2010; 56(4):584−590.

153. Park S, Park JB, Lakatta EG. Association of central hemodynamics with estimated 24-h urinary sodium in patients with hypertension. **J Hypertens**. 2011; 29(8):1502−1507.

154. Muth BJ, Brian MS, Chirinos JA, Lennon SL, Farquhar WB, Edwards DG. Central systolic blood pressure and aortic stiffness response to dietary sodium in young and middle-aged adults. **J Am Soc Hypertens**. 2017; 11(10):627−634.

155. Starmans-Kool MJ, Stanton AV, Xu YY, Mc GTSA, Parker KH, Hughes AD. High dietary salt intake increases carotid blood pressure and wave reflection in normotensive healthy young men. **J Appl Physiol**. 2011; 110(2):468−471.

156. Mmopi KN, Norton GR, Bello H, et al. Increased aortic characteristic impedance explains relations between urinary Na^+/K^+ and pulse or systolic blood pressure. **Hypertension**. 2020; 75(5):1260−1270.

157. Quader ZS, Zhao L, Gillespie C, et al. Sodium intake among persons aged ≥2 Years - United States, 2013−2014. **MMWR Morb Mortal Wkly Rep**. 2017; 66(12), 324-238.

158. Bailey RL, Parker EA, Rhodes DG, et al. Estimating sodium and potassium intakes and their ratio in the American diet: data from the 2011-2012 NHANES. **J Nutr**. 2015; 146(4):745−750.

159. Harnack LJ, Cogswell ME, Shikany JM, et al. Sources of sodium in US adults from 3 geographic regions. **Circulation**. 2017; 135(19):1775−1783.

160. Byrd K, Almanza B, Ghiselli RF, Behnke C, Eicher-Miller HA. Reported action to decrease sodium intake is associated with dining out frequency and use of menu nutrition information among US adults. **J Acad Nutr Diet**. 2018; 118(5):824−835.

161. Auchincloss AH, Leonberg BL, Glanz K, Bellitz S, Ricchezza A, Jervis A. Nutritional value of meals at full-service restaurant chains. **J Nutr Educ Behav**. 2014; 46(1):75−81.

162. Juraschek SP, Miller 3rd ER, Weaver CM, Appel LJ. Effects of sodium reduction and the DASH diet in relation to baseline blood pressure. **J Am Coll Cardiol**. 2017; 70(23):2841−2848.

163. O'Donnell MJ, Yusuf S, Mente A, et al. Urinary sodium and potassium excretion and risk of cardiovascular events. **J Am Med Assoc**. 2011; 306(20):2229−2238.

164. Cook NR, Obarzanek E, Cutler JA, et al. Joint effects of sodium and potassium intake on subsequent cardiovascular disease: the Trials of Hypertension Prevention follow-up study. **Arch Intern Med**. 2009; 169(1):32−40.

165. Whelton PK, He J, Cutler JA, et al. Effects of oral potassium on blood pressure. Meta-analysis of randomized controlled clinical trials. **J Am Med Assoc**. 1997; 277(20):1624−1632.

166. Bernabe-Ortiz A, Sal YRVG, Ponce-Lucero V, et al. Effect of salt substitution on community-wide blood pressure and hypertension incidence. **Nat Med**. 2020; 26(3):374−378.

167. Oberleithner H, Callies C, Kusche-Vihrog K, et al. Potassium softens vascular endothelium and increases nitric oxide release. **Proc Natl Acad Sci USA**. 2009; 106(8):2829−2834.

168. Ying WZ, Aaron K, Wang PX, Sanders PW. Potassium inhibits dietary salt-induced transforming growth factor-beta production. **Hypertension**. 2009; 54(5):1159−1163.

169. Smiljanec K, Mbakwe A, Ramos Gonzalez M, Farquhar WB, Lennon SL. Dietary potassium attenuates the effects of dietary sodium on vascular function in salt-resistant adults. **Nutrients**. 2020; 12(5).

170. Maessen MF, Verbeek AL, Bakker EA, Thompson PD, Hopman MT, Eijsvogels TM. Lifelong exercise patterns and cardiovascular health. **Mayo Clin Proc**. 2016; 91(6):745−754.

171. Hamer M, O'Donovan G, Stamatakis E. Association between physical activity and sub-types of cardiovascular disease death causes in a general population cohort. **Eur J Epidemiol**. 2019; 34(5):483−487.

172. Seals DREF. Adolph Distinguished Lecture: the remarkable anti-aging effects of aerobic exercise on systemic arteries. **J Appl Physiol**. 2014; 117(5):425−439.

173. Guers JJ, Farquhar WB, Edwards DG, Lennon SL. Voluntary wheel running attenuates salt-induced vascular stiffness independent of blood pressure. **Am J Hypertens**. 2019; 32(12):1162−1169.

Chapter 54

Role of arterial stiffness and central hemodynamics in personalized medicine in hypertension

Hao-Min Cheng[1,2,3], Shao-Yuan Chuang[4], Shih-Hsien Sung[1,5] and Chen-Huan Chen[1,2,6]

[1]Department of Medicine, National Yang Ming Chiao Tung University College of Medicine, Taipei, Taiwan; [2]Institute of Public Health and Community Medicine Research Center, National Yang Ming Chiao Tung University College of Medicine, Taipei, Taiwan; [3]Center for Evidence-based Medicine, Taipei Veterans General Hospital, Taipei, Taiwan; [4]Institute of Population Health Science, National Health Research Institutes, Miaoli, Taiwan; [5]Department of Medicine, Taipei Veterans General Hospital, Taipei, Taiwan; [6]Department of Medical Education, Taipei Veterans General Hospital, Taipei, Taiwan

Introduction

Hypertension is the most important risk factor in the global burden of disease.[1] Despite the advances in the treatment of hypertension, hypertension control remains a big challenge to every country in the world and there is substantial variation across countries in the rate of hypertension control.[2,3] Patients with hypertension are different from one another and thus may respond differently to the same treatment.[4] The well-recognized heterogeneity in the etiology and pathophysiology of hypertension defines the various hypertension phenotypes[5,6] and may provide an opportunity for the personalization of hypertension management.[4]

Increased arterial stiffness causes an increase in blood pressure pulsatility so systolic blood pressure (SBP) rises and diastolic blood pressure (DBP) falls when mean arterial blood pressure keeps unchanged.[7−9] Increased wave reflection magnitude results in an increase in central pressure augmentation in systole in the presence of increased arterial stiffness.[7−9] Therefore, progressive increase in arterial stiffness and wave reflections due to vascular aging inevitably causes the progressive rise in SBP and pulse pressure (PP), and thus the increased prevalence of hypertension with age.[9] Thus, increased arterial stiffness and adverse central pulsatile hemodynamics can be the cause as well as the consequence of hypertension.[10,11]

In this chapter, we attempt to review the roles of arterial stiffness and central pulsatile hemodynamics in the pathogenesis of hypertension phenotypes (Table 54.1), the effects of currently available antihypertensive medications on arterial stiffness and central pulsatile hemodynamics (Table 54.3), and the usefulness of noninvasive measurements of arterial stiffness and central pulsatile hemodynamics in the diagnosis and management of the various hypertension phenotypes (Table 54.4). For the purpose of this review, measures of arterial stiffness include carotid-femoral pulse wave velocity (CFPWV),[72] brachial-ankle pulse wave velocity (BAPWV),[73] and parameters of reservoir function calculated from the carotid pressure waveform analyzed according to the reservoir-wave model[9,74]; measures of central pulsatile hemodynamics include ascending aorta pulse wave velocity (AAPWV),[75] characteristic impedance of aorta (Zc),[12,15] central SBP,[76] central PP,[77] augmentation index (cAI),[77] carotid augmented pressure (Pa),[77] amplitude of the backward wave decomposed from carotid artery pressure wave (Pb),[77] reflection magnitude (RM),[77] PP amplification,[78] and excess pressure integral (XSPI) (Fig. 54.1).[79]
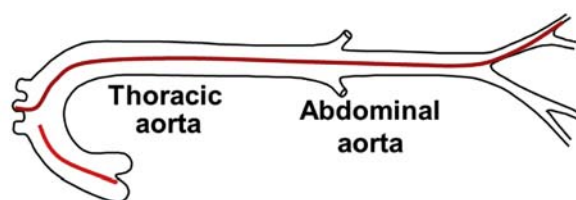
TABLE 54.1 Clinical phenotypes described in the chapter.

Abbreviation	Phenotype	Definition
ISH	Isolated systolic hypertension	ISH is defined by an elevated SBP in the presence of a normal or low DBP, and is therefore always characterized by a high PP
IDH	Isolated diastolic hypertension	IDH is defined by an elevated DBP in the presence of a normal or low SBP
ICH	Isolated central hypertension	Isolated central hypertension (ICH) has been identified as central hypertension in the presence of normal brachial blood pressure (SBP<140 mmHg and DBP<90 mmHg)
IBH	Isolated brachial hypertension	Isolated brachial hypertension (IBH) as brachial hypertension in the presence of normal central blood pressure with the proposed central blood pressure threshold of 130/90 mm Hg
	White coat hypertension	White coat hypertension is referred to an untreated condition, while blood pressure is elevated in the office but normal when measured by home blood pressure monitoring or 24-h ambulatory blood pressure monitoring
	Masked hypertension	Masked hypertension is characterized by normal office blood pressure but elevated out-of-office blood pressure measures
INH	Isolated nocturnal hypertension	Isolated nocturnal hypertension is defined as a nighttime SBP>120 mm Hg or DBP>70 mm Hg and a daytime blood pressure <135/85 mm Hg through the use of 24-h ambulatory blood pressure monitoring
Exaggerated BPV	Exaggerated blood pressure variability	An abnormal increase in BPV

BPV, blood pressure variability; *DBP*, diastolic blood pressure; *SBP*, systolic blood pressure.

FIGURE 54.1 Measures of arterial stiffness and central pulsatile hemodynamics. *AAPWV*, ascending aorta pulse wave velocity; *BAPWV*, brachial-ankle pulse wave velocity; *cAI*, carotid augmentation index; *CFPWV*, carotid-femoral pulse wave velocity; *Pa*, carotid augmented pressure; *Pb*, amplitude of the backward wave decomposed from carotid pressure wave; *PP*, pulse pressure; *RM*, reflection magnitude; *SBP*, systolic blood pressure; *XSPI*, excess pressure integral; *Zc*, characteristic impedance of aorta.

Isolated systolic hypertension in the elderly

Isolated systolic hypertension (ISH) is the most common form of hypertension among both untreated and inadequately treated hypertensive individuals aged 50 years or older.[80–82] ISH is conceptually defined by an elevated SBP in the presence of a normal or low DBP, and is therefore always characterized by a high PP. ISH is strongly associated with increased cardiovascular disease morbidity and mortality,[83,84] and antihypertensive treatment in the elderly with ISH significantly reduces the risk of adverse cardiovascular events.[85–87]

Arterial stiffness and central pulsatile hemodynamics in ISH in the elderly

Patients with ISH are characterized by a marked increase in arterial stiffness[12–14,88–92] and Zc,[12,15] a moderately increase in wave reflections,[12] a marked increase in central SBP and central PP,[15] and a mildly increased total peripheral resistance (TPR) (Table 54.2).[12]

Large artery stiffening associated with vascular aging is the most important pathophysiological determinant of ISH

TABLE 54.2 Roles of arterial stiffness and central pulsatile hemodynamics in the pathogenesis of hypertension phenotypes

	Arterial stiffness	Central pulsatile hemodynamics			TPR
	CFPWV, BAPWV, total arterial compliance, five parameters from reservoir-wave analysis	AAPWV Zc	Wave reflections: XSPI cAI AP RM RI Pf Pb Reflection coefficient Amplification of SBP or PP	Central BP: cSBP cPP	
ISH in the elderly	↑↑↑[12−14]	↑↑↑[12,15]	↑↑[12]	↑↑↑[15]	↑[12]
ISH in the youth: spurious hypertension	↔[16]	N/A	↓[16−19]	↔[19]	↔[17,18]
ISH in the youth	↑[17,18]	↑↑[20]	↔[18]	↑[16−18]	↑[20]
IDH	↔[21]	↔[20]	N/A	↔[21]	↑↑↑[20]
ICH	N/A	N/A	N/A	↑↑↑[22−24]	N/A
IBH	N/A	N/A	N/A	↔[22−24]	N/A
WCH	↑↑↑[25−28]	N/A	↑↑↑[25,26]	↑↑[25,26]	N/A
MKH	↑↑↑[26,29,30]	N/A	N/A	↔[26]	N/A
INH	↑↑[31−34]	N/A	↑[34]	↑[32]	N/A
Exaggerated BPV	↑[34,35]	N/A	↑↑[35]	↑↑[36]	↔[35]

↑, ↑↑, ↑↑↑, different degree of increase; ↓, ↓↓, ↓↓↓, different degree of decrease; ↔, no change; *BPV*, blood pressure variability; *IBH*, isolated brachial hypertension; *ICH*, isolated central hypertension; *IDH*, isolated diastolic hypertension; *INH*, isolated nocturnal hypertension; *ISH*, isolated systolic hypertension; *MKH*, masked hypertension; *N/A*, not available; *WCH*, white coat hypertension.

and the age-dependent increase in PP.[9,13,72] Invasive aortic input impedance analysis from elderly subjects with ISH demonstrated that Zc was 107% higher, the first harmonic of impedance moduli (influenced by wave reflection) was 57% higher, TPR was 44% higher, and the first impedance moduli minimum was shifted to a higher frequency, when compared to age-matched normotensive subjects.[12] The changes in impedance spectra among ISH patients indicate that the aorta and large arteries have become stiffer and facilitate an earlier return of pulse wave reflection in systole.[12]

However, other studies indicate that elevated PP in ISH is primarily attributable to elevated Zc and reduced effective diameter of the proximal aorta,[15] implying that aortic function plays an active role in the pathophysiology of ISH.[15]

An increase in TPR may indicate a decrease in the cross-sectional area of the peripheral vascular bed and a decline in endothelial function associated with vascular aging.[12,13] The marked increase in arterial stiffness in ISH offsets the increase in DBP that would have been expected from an increase in TPR.[12]

Usefulness of noninvasive measurement of arterial stiffness and central pulsatile hemodynamics in the diagnosis of ISH in the elderly

Current diagnosis of ISH is based solely on blood pressure readings taken from an upper-arm cuff blood pressure method.[5,93] Diagnostic blood pressure thresholds of ISH may vary with the current definitions of hypertension (elevated SBP and/or DBP).[5,6] Thus, in Europe, ISH is defined as SBP ≥140 mmHg and DBP <90 mmHg,[6] whereas the current cut-points for ISH are SBP ≥130 mmHg and DBP<80 mmHg in the United States.[5]

Usefulness of noninvasive measurement of arterial stiffness and central pulsatile hemodynamics in the treatment of ISH in the elderly

The relative effectiveness of antihypertensive therapies on arterial stiffness and central pulsatile hemodynamics is summarized in Table 54.3. All six classes of antihypertensive medications are variably effective in improving arterial stiffness, Zc, wave reflections, central blood pressure, and TPR (Table 54.3). However, current standard antihypertensive medications largely act through reductions in TPR or cardiac output and probably do not change the intrinsic material properties of the arterial wall.[94] A comprehensive understanding of the molecular mechanisms of large artery stiffening may help develop novel therapies to improve the material properties of the arterial wall.[94]

Patients with ISH usually have a limited response to renal denervation.[6] Measurement of CFPWV may be useful in identifying a subset of ISH patients who would respond to the renal denervation therapy.[64] It remains to be demonstrated that measurements of arterial stiffness and central pulsatile hemodynamics is useful in drug titration and monitoring of treatment efficacy for elderly ISH patients (Table 54.4).

Prognostic value of noninvasive measurements of arterial stiffness and central pulsatile hemodynamics in ISH in the elderly

CFPWV is currently considered the clinical and epidemiologic gold standard metric of large artery stiffness[95] and an increase in CFPWV (>10 m/s) in patients with hypertension is considered an indicator of hypertension-mediated cardiovascular target organ damage in some hypertension treatment guidelines.[5,6] Several studies have demonstrated the additive prognostic value of CFPWV above and beyond traditional risk factors (Table 54.4).[6,96] However, since CFPWV was more strongly related to the risk of coronary heart disease and stroke in younger subjects, it is expected that the prognostic value of CFPWV would decline in the elderly ISH patients.[96] Therefore, routine use of CFPWV measurements in elderly ISH patients is not recommended for routine practice.[6] The prognostic value of other measures of arterial stiffness and central pulsatile hemodynamics in patients ISH remains to be determined in future studies.

Isolated systolic hypertension in the young

From puberty to mid-life, SBP increases steeply during childhood, reaches a plateau phase between 20 and 40 years, and then increases subsequently,[97−99] whereas DBP displays a cubic trajectory with a plateau-like behavior followed by a decline as age increases.[97] Therefore, at the population level, PP values may be high around the age of 20 years and low in the age range between 20 and 40 years.[100−103] The transient physiological elevation of SBP and PP detected in some young adults may reach the criteria of ISH and create an innocent condition called pseudo or spurious systolic hypertension of youth whose central blood pressure is normal.[97,104] However, an increase in CFPWV has been found in about 20% of the young individuals with ISH.[17] Moreover, obesity,

TABLE 54.3 Pharmacological interventions targeting arterial stiffness and central pulsatile hemodynamics.

	Arterial stiffness		Central pulsatile hemodynamics		TPR
	CFPWV, BAPWV, total arterial compliance, five parameters from reservoir-wave analysis	AAPWV Zc	Wave reflections: XSPI cAI AP RM RI Pf Pb Reflection coefficient	Central BP: cSBP cPP	
ACEI/ARB	↓↓[37,38]	N/A	↓↓[37,39]	↓↓[40−42]	↓[43]
Beta-blocker	↔[44] or ↓[38,39]	N/A	↔[38,45] or ↑[39]	↔[40,42,46] or ↑[39]	↔[47]
CCB	Low dose ↑, high dose ↓[48], ↓[39,49−52]	↓[51]	↓[39]	↔[42,53] or ↓[39]	↓[54]
Diuretics	↓[55]	N/A	↔[39]	↓[55] or ↔[42] or ↑[39]	↓[47]
Alpha-blocker	↓[56] or ↔[57]	N/A	↔[45]	↓[42]	↓[58]
Spironolactone	↓↓[59−62]	N/A	↓[57]	↓[61]	↓[63]

↑, ↑↑, ↑↑↑, different degree of increase; ↓, ↓↓, ↓↓↓, different degree of decrease; ↔, no change; *N/A*, not available.

TABLE 54.4 Usefulness of arterial stiffness and central pulsatile hemodynamics in the diagnosis and management of hypertension.

		Treatment			
	Diagnosis	Drug selection	Drug titration	Monitoring treatment efficacy	Prognosis Risk stratification
ISH	N[6]	Y[64]	N/A	N/A	Y[6]
ISH in the youth	Y[6]	N/A	N/A	N/A	Y[6]
IDH	N[20]	N[20]	N[20]	N[20]	N[20]
ICH	Y[22−24]	N/A	N/A	N/A	Y[22−24]
IBH	Y[22−24]	N/A	N/A	N/A	N/A
WCH	Y[65]	N/A	Y[25,66]	Y[25,66]	Y[25]
MKH	Y[26,30]	N/A	Y[26,30]	Y[26,30]	N/A
INH	N[67]	N/A	N/A	N/A	Y[68]
Exaggerated BPV	Y[69]	N/A	N/A	N/A	Y[70,71]

BPV, blood pressure variability; *IBH*, isolated brachial hypertension; *ICH*, isolated central hypertension; *IDH*, isolated diastolic hypertension; *INH*, isolated nocturnal hypertension; *ISH*, isolated systolic hypertension; *MKH*, masked hypertension; *N*, no, not useful; *N/A*, not available, unknown; *WCH*, white coat hypertension; *Y*, yes, useful.

metabolic disturbances, and white coat hypertension have often been documented to be associated with ISH in the young.[105,106] ISH is the most common form of hypertension in adolescents and young adults.[107] However, whether ISH in the young implies a worse outcome and requires antihypertensive treatment remains controversial and future clinical trials will elucidate if a benefit can be achieved with pharmacological treatment in some subgroups with associated risk factors and/or high central blood pressure.[97]

Arterial stiffness and central pulsatile hemodynamics in ISH in the young

Current evidence suggests two main phenotypes of ISH in the young, one is spurious systolic hypertension, the other is ISH with increased cardiovascular risk (Fig. 54.2). Young subjects with spurious systolic hypertension are characterized by normal arterial stiffness,[16] reduced wave reflections,[16−19] normal central blood pressure,[19] increased stroke volume,[17,18] and normal TPR (Table 54.2).[17,18] Young subjects with ISH and increased cardiovascular risk are characterized by increased arterial stiffness,[17,18] increased Zc,[20] normal wave reflections,[18] increased central blood pressure,[16−18] and increased TPR.[20] They are also characterized by a smaller difference between central and peripheral SBP, i.e., a reduced PP amplification, presumably from a smaller stiffness gradient between central and peripheral arteries.[97]

Usefulness of noninvasive measurements of arterial stiffness and central pulsatile hemodynamics in the diagnosis of ISH in the young

Similar to ISH in the elderly, the diagnosis of ISH in the young is based solely on blood pressure readings taken
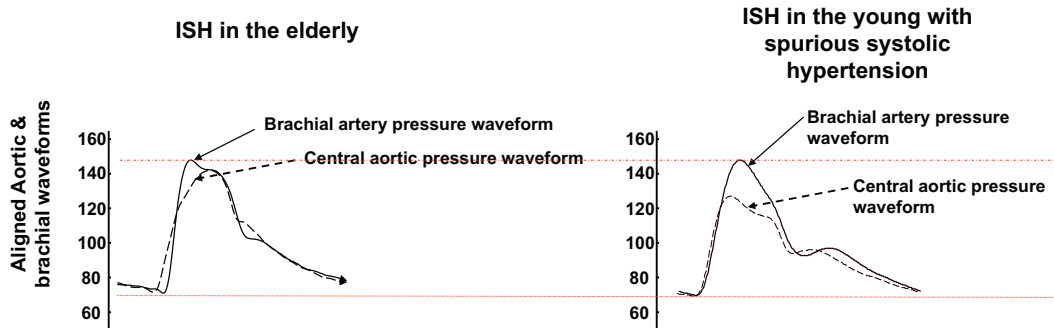
FIGURE 54.2 Brachial and central aortic pressure waveforms of subjects with isolated systolic hypertension (ISH).

from an upper-arm cuff blood pressure method.[5,93] However, measurement of central blood pressure or CFPWV may be useful in identifying different phenotypes of ISH in the young (Table 54.4).[16−19]

Usefulness of noninvasive measurements of arterial stiffness and central pulsatile hemodynamics in the treatment of ISH in the young

On the basis of currently available evidence, young individuals with ISH should receive recommendations on lifestyle modification.[6] Although measurements of arterial stiffness and central blood pressure may be useful in identifying the high risk phenotype of ISH in the young, it is unclear whether they should receive drug treatment.[6,97] There is no evidence to support the usefulness of noninvasive measurement of arterial stiffness and central hemodynamics in drug titration and monitoring of treatment efficacy in the treatment of ISH in young ISH subjects (Table 54.4). However, to the degree that measurements of arterial stiffness or central hemodynamics can identify young individuals with ISH who are at higher risk of adverse outcomes (see next section), these measurements may identify young individuals who require a more aggressive therapeutic approach; this should be the focus of further research.

Prognostic value of noninvasive measurement of arterial stiffness and central pulsatile hemodynamics in ISH in the young

According to prospective data from the Chicago Heart Association Detection Project, young men with ISH had a CV risk similar to that of individuals with high-normal blood pressure.[83] Since ISH in younger adults appears to be a heterogeneous condition, noninvasive measurements of CFPWV and/or central blood pressure may aid in discriminating high from low cardiovascular risk (Table 54.4).[17]

Isolated diastolic hypertension

Isolated diastolic hypertension (IDH) is common in young adults and may represent the early stage of hypertension development.[108,109] Increased TPR and decreased stroke volume are the major hemodynamic features for IDH[20] and obesity is one of the major risk factors.[108,110] In persons with IDH, cardiovascular disease risk is apparently being driven by DBP elevation.[111] DBP and IDH drive coronary risk in younger subjects, whereas SBP is the predominant risk indicator in older people.[112] However, whether IDH is associated with an increased cardiovascular disease risk remains inconsistent.[111,113]

Arterial stiffness and central pulsatile hemodynamics in IDH

According to the Dallas Heart Study of 2001 untreated participants 18−64 years of age, subjects with IDH had similar Zc and ascending aortic PWV (AAPWV), when compared to those with optimal blood pressure or prehypertension.[20] Subjects with IDH had decreased aortic compliance when compared to those with optimal blood pressure (Table 54.2).[20]

Usefulness of arterial stiffness and central pulsatile hemodynamics in the diagnosis of IDH

The diagnosis of IDH is based solely on blood pressure readings taken from an upper-arm cuff blood pressure method.[5,93] Diagnostic blood pressure thresholds for IDH may vary with the current definitions of hypertension (elevated SBP and/or DBP).[5,6] Thus, in Europe, IDH would be defined as SBP<140 mmHg and DBP≥90 mmHg,[6] whereas the current cut-points for IDH would be SBP<130 mmHg and DBP≥80 mmHg in the United States.[5,111]

Usefulness of arterial stiffness and central pulsatile hemodynamics in the treatment of IDH

Active treatment reduced the relative risk of major vascular events by 27% among patients with ISH, by 28% among those with IDH, and by 32% among those with systolic−diastolic hypertension.[114] Currently, there has been no evidence of differences in the magnitude of the effects of treatment among different types of hypertension. Therefore, blood pressure lowering is likely to provide a similar level of protection against major vascular events for patients with IDH as for those with ISH and systolic−diastolic hypertension (Table 54.4).[114]

Prognostic value of arterial stiffness and central pulsatile hemodynamics in IDH

Currently, there is no evidence suggesting the association of measures of arterial stiffness and central pulsatile hemodynamics with future cardiovascular events in patients with IDH.

Isolated central hypertension and isolated brachial hypertension

Central blood pressure refers to blood pressure readings measured from the central aorta or common carotid

arteries.[115,116] Hypertension is almost always diagnosed according to blood pressure measurement obtained from the brachial arteries, which highly correlates with central blood pressure.[117] Because the individual discrepancies between central and brachial blood pressure may be substantial and highly variable and may be magnified during hemodynamic changes or after pharmacological interventions,[117] brachial blood pressure readings cannot serve as direct substitutes for their central counterpart.[118] Accumulating evidence has suggested that central blood pressure may be more relevant than peripheral blood pressure in predicting target organ damage and cardiovascular outcomes.[76] Central blood pressure can now be measured noninvasively, including using convenient cuff-based central blood pressure monitors.[116] Hypertension diagnosed by central blood pressure readings and the proposed central blood pressure threshold of 130/90 mm Hg is designated as central hypertension, as opposed to the conventional brachial hypertension.[119] Central hypertension has been characterized by a greater discriminatory power for long-term events than brachial hypertension.[119] Accordingly, isolated central hypertension (ICH) has been identified as central hypertension in the presence of normal brachial blood pressure (SBP<140 mmHg and DBP<90 mmHg), and isolated brachial hypertension (IBH) as brachial hypertension in the presence of normal central blood pressure.[22,119] In a recent study from Taiwan, the national weighted prevalence rates of ICH and IBH were 7.35% and 0.30%, respectively.[22] Hypertension detection using a conventional brachial blood pressure approach may underestimate the prevalence of hypertension and result in a less effective hypertension control.[22]

Arterial stiffness and central pulsatile hemodynamics in ICH and IBH

Subjects with ICH have an elevated central blood pressure. The major determinants of central blood pressure are arterial stiffness and wave reflections, the dominant hemodynamic manifestations of vascular aging.[9] Subjects with IBH have not been characterized, except those in the subgroup of ISH in the young adults.[107,120] In the subgroup of ISH and normal central blood pressure, the high elasticity of the vascular tree may play a mechanistic role in the youth.[120] Most subjects with IBH have IDH, which is a consequence of an increase in TPR.[121]

Usefulness of arterial stiffness and central pulsatile hemodynamics in the diagnosis of ICH and IBH

Diagnosis of ICH or IBH requires measurements of brachial and central blood pressure. The various central blood pressure measuring devices can be broadly

categorized into two types. Type I device purports to give an estimate of central blood pressure relative to measured brachial blood pressure, and Type II device purports to estimate the intraarterial central blood pressure.[122] The prevalence of ICH and IBH may vary according to the central blood pressure measuring devices.[22,23]

Usefulness of arterial stiffness and central pulsatile hemodynamics in the treatment of ICH and IBH

Currently, there is no evidence suggesting the usefulness of arterial stiffness and central pulsatile hemodynamics in the treatment of ICH or IBH. Whether ICH should be treated remains an important area of future research.

Prognostic value of arterial stiffness and central pulsatile hemodynamics in ICH and IBH

Subjects with ICH may have a cardiovascular risk profile equivalent to that of those with stage 1 brachial hypertension but significantly worse than those with prehypertension.[22] Currently, there is no evidence suggesting the association of measures of arterial stiffness and central pulsatile hemodynamics with future cardiovascular events in patients with ICH or IBH.

White coat hypertension

White coat hypertension is referred to an untreated condition, while blood pressure is elevated in the office but normal when measured by home blood pressure monitoring or 24-h ambulatory blood pressure monitoring.[5,6] Although white coat hypertension is associated with less target organ damage and adverse cardiovascular events than sustained hypertension,[123] white coat hypertension should not be considered prognostically benign.[25,124] Even if the out-of-office blood pressure in white coat hypertension is normal, by definition, it is generally higher than that in normotensive subjects.[25,26] This may partly explain the associated target organ damage and increased risk of mortality in white coat hypertension.[125−127] However, whether or not patients with white coat hypertension should receive antihypertensive medications remains debatable.[6]

Arterial stiffness and central pulsatile hemodynamics in white coat hypertension

The white coat effect is positively related to arterial stiffness.[27] A metaanalysis of 20 studies has demonstrated a significant increase of arterial stiffness, indexed by CFPWV in adults with white coat hypertension, when compared to the normotensives.[28] But there was no

significant difference in CFPWV between white coat hypertension and sustained hypertension.[25,26,128] Subjects with white coat hypertension may also have higher central aortic pressure and wave reflections compared to subjects with normotension, indicating the presence of significant vascular aging and/or dysfunction.[25,26,29]

Usefulness of noninvasive measurements of arterial stiffness and central pulsatile hemodynamics in the diagnosis of white coat hypertension

Out-of-office blood pressure measurements are needed to confirm the diagnosis of white coat hypertension. Arterial stiffness and central hemodynamics are probably not distinguishable between subjects with white coat hypertension and sustained hypertension.[25,26,128] Mestanik et al. proposed a potential role of corrected cardio-ankle vascular index to differentiate white coat hypertension from sustained hypertension in overweight adolescent boys.[65] However, this approach has not been independently validated.

Usefulness of noninvasive measurement of arterial stiffness and central pulsatile hemodynamics in the treatment of white coat hypertension

Although the indications of pharmacological intervention in white coat hypertension have not yet been determined, white coat hypertension does independently correlate with subclinical target organ damage, including carotid intima-media thickness, albuminuria, glomerular filtration rate, left ventricular hypertrophy, as well as incident cardiovascular events.[25,29,129] Since the white coat effect has been associated with arterial stiffness, wave reflections, and target organ damage,[25,66] noninvasive measurements of arterial stiffness and central hemodynamics may be helpful to identify subjects at risk of developing target organ damage, who may benefit from early pharmacological therapy.

Prognostic value of noninvasive measurements of arterial stiffness and central pulsatile hemodynamics in white coat hypertension

An epidemiologic study of 1257 never-been-treated individuals has shown that subjects with white coat hypertension and increased wave reflection, indexed by AIx or Pb, exhibit adverse clinical outcomes similar to those with sustained hypertension.[25] The results may encourage the clinical application of noninvasive measurements of arterial stiffness and central pulsatile hemodynamics in white coat hypertension for further risk stratification and tailored therapy.

Masked hypertension

Subjects with masked hypertension are characterized by normal office blood pressure but elevated out-of-office blood pressure measures.[5,6] Masked hypertension prevails in untreated subjects. In the Jackson Heart Study of African Americans, one-third of the study population had masked hypertension at a time when the mean office blood pressure was normal.[130] In addition, masked hypertension has been consistently accompanied by a greater degree of target organ damage and a higher risk of cardiac events and stroke than those with normotension or prehypertension.[29,130,131] Masked uncontrolled hypertension was even associated with a greater risk of death than sustained uncontrolled hypertension.[132] A specific challenge is to recognize masked hypertension early by ambulatory or home blood pressure monitoring, followed by medical therapy, especially when office blood pressure is in the high-normal range.[6]

Arterial stiffness and central pulsatile hemodynamics in masked hypertension

Although office blood pressure is normal in masked hypertension, it has been generally observed that masked hypertension is characterized by increased arterial stiffness, central blood pressure, and wave reflection, when compared with normotension.[26,29,30] A metaanalysis of seven studies and 2352 patients has further indicated that arterial stiffness in patients with masked hypertension is similar to that in white coat hypertension.[128] In addition, masked hypertension has significantly lower central blood pressure and wave reflection, when compared with white coat hypertension or sustained hypertension.[26]

Usefulness of noninvasive measurements of arterial stiffness and central pulsatile hemodynamics in the diagnosis of masked hypertension

Out-of-office blood pressure measurements are needed to confirm the diagnosis of masked hypertension. Patients with masked hypertension have normal office blood pressure but increased arterial stiffness, wave refection, and central blood pressure, when compared with normotensives.[26,30] Measures of arterial stiffness and/or central pulsatile hemodynamics may indicate the presence of masked hypertension in subjects with normal office blood pressure. This may identify individuals among whom further study of out-off-office blood pressure should be implemented.

Usefulness of noninvasive measurements of arterial stiffness and central pulsatile hemodynamics in the treatment of masked hypertension

The noninvasive measurement of arterial stiffness and central pulsatile hemodynamics could be helpful for the early detection of masked hypertension and to facilitate antihypertensive treatment.[26,30] Both arterial stiffness and wave reflection indices could serve as potential therapeutic targets, in addition to the home blood pressure measures. This remains to be assessed in future studies.

Prognostic value of noninvasive measurements of arterial stiffness and central pulsatile hemodynamics in masked hypertension

Currently, there is no direct evidence demonstrating an association between measures of arterial stiffness and central pulsatile hemodynamics and future cardiovascular events in patients with masked hypertension. Patients with masked hypertension are considered to have a cardiovascular risk equivalent to that of sustained hypertension. Since measures of arterial stiffness and central blood pressure have been associated with mortality or adverse cardiovascular events in patients with sustained hypertension,[117,133] similar prognostic value could be expected in patients with masked hypertension.

Isolated nocturnal hypertension

Isolated nocturnal hypertension (INH) is a relatively newly proposed hypertension phenotype (first formally described in 2007), which is defined as a nighttime SBP$\geq$120 mm Hg or DBP$\geq$70 mm Hg and a daytime blood pressure $<$135/85 mm Hg through the use of 24-h ambulatory blood pressure monitoring.[31,32,68] INH has been related to atherosclerosis and target organ damages and independently predicted cardiovascular events.[32,33,68] The incidence of INH varies slightly among different ethnic groups; Asians and blacks have less nocturnal blood pressure dipping than whites.[31]

Arterial stiffness and central pulsatile hemodynamics in INH

A systematic review summarized the evidence on the association between INH and subclinical target organ damage.[32] INH was associated with higher ambulatory arterial stiffness index, BAPWV, cAI in a Chinese study,[31] but not associated with increased arterial stiffness or left ventricular mass index in a Swedish study. The existing evidence shows that there may be a weak relationship between INH and arterial stiffness and central pulsatile hemodynamics.

The inconsistent results suggest that arterial stiffness and pulsatile hemodynamics may be involved in but not the primary mechanism responsible for development of INH.[32,34]

Usefulness of noninvasive measurements of arterial stiffness and central pulsatile hemodynamics in the diagnosis of INH

Since INH can only be diagnosed by blood pressure measurements during sleep, it is suggested that ambulatory blood pressure monitoring should be applied more widely in clinical practice. However, one recent study further investigated the reproducibility of the diagnosis of INH,[67] and concluded that INH and isolated daytime hypertension are both poorly reproducible phenotypes. They also suggested that 24-h ambulatory blood pressure monitoring should be primarily used to identify individuals with daytime hypertension and/or nocturnal hypertension, but not INH or isolated daytime hypertension. In other words, INH and isolated daytime hypertension are both poorly reproducible and not stable phenomena over the short term.
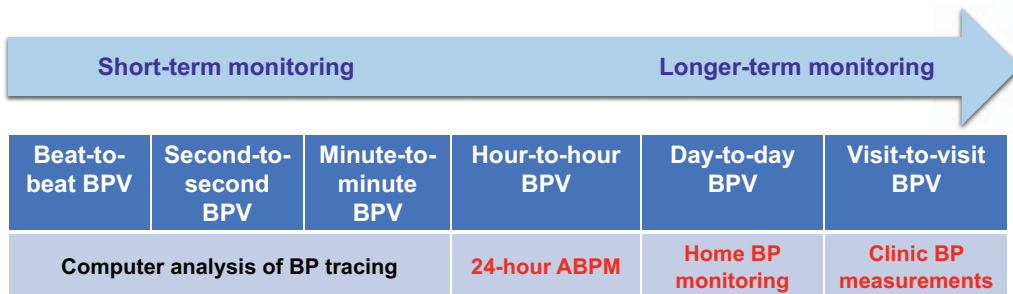
Prognostic value of noninvasive measurements of arterial stiffness and central pulsatile hemodynamics in INH

It has been repeatedly demonstrated that night-time blood pressure is superior to the daytime blood pressure in the prediction of cardiovascular outcomes.[68,134] INH has been associated with an increased risk of cardiovascular disease events and mortality.[31,135] Currently, there are no available studies assessing the association of measures of arterial stiffness and central pulsatile hemodynamics with future cardiovascular events in patients with INH. Whether these hemodynamic measures can provide prognostic value in patients with INH needs to be further explored. Future clinical studies should also address the benefit of specifically lowering the night-time blood pressure in patients with INH.

Exaggerated blood pressure variability

Blood pressure fluctuations, also coined as blood pressure variability (BPV), constitute a complex phenomenon. BPV has usually been considered a physiological indicator reflecting autonomic nerve function and arterial compliance.[136,137] It can also be used as a risk predictor for cardiovascular and cerebrovascular events in patients with hypertension and cardiovascular diseases, and an index for evaluating the efficacy of antihypertensive medications.

BPV can be classified into short-term BPV and long-term BPV according to the length of time of BP recordings (Fig. 54.3). Short-term fluctuations in blood

Short-term monitoring				Longer-term monitoring	
Beat-to-beat BPV	Second-to-second BPV	Minute-to-minute BPV	Hour-to-hour BPV	Day-to-day BPV	Visit-to-visit BPV
Computer analysis of BP tracing			24-hour ABPM	Home BP monitoring	Clinic BP measurements

FIGURE 54.3 Various measures of blood pressure variability derived from different blood pressure measuring techniques. *ABPM*, ambulatory BP monitoring; *BP*, blood pressure; *BPV*, BP variability.

pressure often occur within a 24 h period, including beat-to-beat, minute-to-minute, hour-to-hour, and day-to-night changes; long-term substantial variations in blood pressure have usually been shown to occur over more prolonged periods of time, including days, weeks, months, seasons, and even years.[138,139] A variety of methods have been utilized to measure BPV.[140] In particular, BPVs in SBP, DBP, or PP quantified by using the average real variability (ARV) index from 24-h ambulatory BP monitoring have been associated with cardiovascular outcomes independent of absolute BP levels.[141,142] ARV is calculated by the following formula:

$$ARV = |BP_{K+1} - BP_K|$$

k ranges from 1 to n − 1 and w is the time interval between BP_K and BP_{K+1}. n is the number of blood pressure readings.

Previous animal studies have demonstrated that the degree of fluctuation in blood pressure is closely related to the target organ damage.[139] Recent studies pointed out that the abnormal increase in BPV (exaggerated BPV) can add to the damage to target organs caused by blood pressure itself, and that the exaggerated BPV is an independent risk factor of target organs damages, and the prognostic value of BPV in hypertensive subjects has been extensively investigated.[141] However, the relevant mechanism of exaggerated BPV has not been fully understood.[35,36,138,139,143]

Arterial stiffness and central pulsatile hemodynamics in exaggerated BPV

It has been demonstrated that decreased arterial compliance (as measured by changes in CFPWV) is significantly related to exaggerated BPV in the American and Asian populations.[138] However, a recent study found that in the groups of normotensive and treated hypertensive patients, CFPWV was independently associated with average real variability of 24-h DBP (ARVd) but not average real variability of 24-h SBP (ARVs).[35] It has been further revealed that ARVd but not ARVs was significantly

associated with cardiovascular mortality independently of 24-h SBP in the hypertensive patients.[69] In addition, this study also uncovered that the association of amplitude of the decomposed backward pressure (Pb) with measures of the short-term BPV was stronger than that of CFPWV, cardiac output, or TPR.[35] On the other hand, TPR was not associated with ARVd or ARVs.

Usefulness of noninvasive measurement of arterial stiffness and central pulsatile hemodynamics in the diagnosis of exaggerated BP variability

Recent studies have indicated that increased arterial stiffness may be a pathological mechanism contributing to long-term BPV. The Multiethnic Study of Atherosclerosis has demonstrated that a reduction in aortic distensibility and arterial elasticity was associated with a higher visit-to-visit BPV,[139,144] but whether similar associations exist between CFPWV or other vascular measures and exaggerated visit-to-visit BPV remains to be investigated.[144,145]

Prognostic value of noninvasive measurement of arterial stiffness and central pulsatile hemodynamics in exaggerated BP variability

The definition and measurement of BPV have certain complexity, such as BPV with different time intervals and the difference in data recording methods and the analytic methods. Therefore, in patients with exaggerated BPV, whether the measures of arterial stiffness and central hemodynamics can be used to predict these patients' outcomes remains to be determined.[69] Nevertheless, short-term BPV including all indices of SBP variability with 24-h measurements has been associated with aortic stiffness as measured by CFPWV.[70] Future studies are required to demonstrate whether such associations can be used to predict outcomes of these patients with exaggerated BPV.

Summary and conclusion

In personalized medicine, understanding patients' unique personal profiles is important to inform clinical decisions. In this chapter, we present available evidence relating to several important hypertension phenotypes, including ISH, IDH, ICH, IBH, white coat hypertension, masked hypertension, INH, and exaggerated BPV. Despite using the mechanical biomarkers of arterial stiffness and central pulsatile hemodynamics might be beneficial in the detection, evaluation, treatment, and prevention of hypertension, evidence for these hypertension phenotypes is not yet widely available. However, emerging evidence has suggested the vital role of CFPWV and central pulsatile hemodynamics especially in predicting the prognosis of hypertensive patients.

In the process of vascular aging, the increase in arterial stiffness and wave reflections causes a corresponding increase in SBP and PP.[9] As the possible cause and the consequence of hypertension, it can be anticipated that arterial stiffness and adverse central pulsatile hemodynamics should play a critical role in the management of hypertension and its diverse and distinct phenotypes, including diagnosis, prognosis, and treatment monitoring. More efforts are encouraged to study the usefulness of these mechanical biomarkers in personalized medicine in hypertension.

References

1. Collaborators GBDRF. Global, regional, and national comparative risk assessment of 84 behavioural, environmental and occupational, and metabolic risks or clusters of risks for 195 countries and territories, 1990-2017: a systematic analysis for the global burden of disease study 2017. **Lancet**. 2018; 392:1923−1994.

2. Collaboration NCDRF. Long-term and recent trends in hypertension awareness, treatment, and control in 12 high-income countries: an analysis of 123 nationally representative surveys. **Lancet**. 2019; 394:639−651.

3. Chow CK, Gupta R. Blood pressure control: a challenge to global health systems. **Lancet**. 2019; 394:613−615.

4. Melville S, Byrd JB. Personalized medicine and the treatment of hypertension. **Curr Hypertens Rep**. 2019; 21:13.

5. Whelton PK, Carey RM, Aronow WS, et al. 2017 ACC/AHA/ AAPA/ABC/ACPM/AGS/APHA/ASH/ASPC/NMA/PCNA guideline for the prevention, detection, evaluation, and management of high blood pressure in adults: a report of the American College of Cardiology/American Heart Association Task Force on Clinical Practice Guidelines. **J Am Coll Cardiol**. 2018; 71:e127−e248.

6. Williams B, Mancia G, Spiering W, et al. 2018 ESC/ESH guidelines for the management of arterial hypertension. **Eur Heart J**. 2018; 39:3021−3104.

7. Mitchell GF. Arterial stiffness and hypertension: chicken or egg? **Hypertension**. 2014; 64:210−214.

8. Humphrey JD, Harrison DG, Figueroa CA, Lacolley P, Laurent S. Central artery stiffness in hypertension and aging: a problem with cause and consequence. **Circ Res**. 2016; 118:379−381.

9. Cheng HM, Park S, Huang Q, et al. Vascular aging and hypertension: implications for the clinical application of central blood pressure. **Int J Cardiol**. 2017; 230:209−213.

10. Kaess BM, Rong J, Larson MG, et al. Aortic stiffness, blood pressure progression, and incident hypertension. **J Am Med Assoc**. 2012; 308:875−881.

11. Najjar SS, Scuteri A, Shetty V, et al. Pulse wave velocity is an independent predictor of the longitudinal increase in systolic blood pressure and of incident hypertension in the baltimore longitudinal study of aging. **J Am Coll Cardiol**. 2008; 51:1377−1383.

12. Nichols WW, Nicolini FA, Pepine CJ. Determinants of isolated systolic hypertension in the elderly. **J Hypertens Suppl**. 1992; 10:S73−S77.

13. Wallace SM, Yasmin, McEniery CM, et al. Isolated systolic hypertension is characterized by increased aortic stiffness and endothelial dysfunction. **Hypertension**. 2007; 50:228−233.

14. Yasmin, McEniery CM, Wallace S, et al. Matrix metalloproteinase-9 (mmp-9), mmp-2, and serum elastase activity are associated with systolic hypertension and arterial stiffness. **Arterioscler Thromb Vasc Biol**. 2005; 25:372.

15. Mitchell GF, Lacourciere Y, Ouellet JP, et al. Determinants of elevated pulse pressure in middle-aged and older subjects with uncomplicated systolic hypertension: the role of proximal aortic diameter and the aortic pressure-flow relationship. **Circulation**. 2003; 108:1592−1598.

16. Hulsen HT, Nijdam ME, Bos WJ, et al. Spurious systolic hypertension in young adults; prevalence of high brachial systolic blood pressure and low central pressure and its determinants. **J Hypertens**. 2006; 24:1027−1032.

17. Eeftinck Schattenkerk DW, van Gorp J, Vogt L, Peters RJ, van den Born BH. Isolated systolic hypertension of the young and its association with central blood pressure in a large multi-ethnic population. The helius study. **Eur J Prev Cardiol**. 2018; 25:1351−1359.

18. McEniery CM, Yasmin, Wallace S, et al. Increased stroke volume and aortic stiffness contribute to isolated systolic hypertension in young adults. **Hypertension**. 2005; 46:221−226.

19. O'Rourke MF, Vlachopoulos C, Graham RM. Spurious systolic hypertension in youth. **Vasc Med**. 2000; 5:141−145.

20. Yano Y, Neeland IJ, Ayers C, et al. Hemodynamic and mechanical properties of the proximal aorta in young and middle-aged adults with isolated systolic hypertension: the dallas heart study. **Hypertension**. 2017; 70:158−165.

21. Nakagomi A, Imazeki F, Nishimura M, et al. Central blood pressure and pulse wave velocity in young and middle-aged Japanese adults with isolated systolic hypertension. **Hypertens Res**. 2020; 43:207−212.

22. Chuang SY, Chang HY, Cheng HM, Pan WH, Chen CH. Prevalence of hypertension defined by central blood pressure measured using a type ii device in a nationally representative cohort. **Am J Hypertens**. 2018; 31:346−354.

23. Yu S, Xiong J, Lu Y, et al. The prevalence of central hypertension defined by a central blood pressure type i device and its association with target organ damage in the community-dwelling elderly Chinese: the northern shanghai study. **J Am Soc Hypertens**. 2018; 12:211−219.

24. Rouxinol-Dias A, Araujo S, Silva JA, Barbosa L, Polonia J. Association between ambulatory blood pressure values and central aortic pressure in a large population of normotensive and hypertensive patients. **Blood Press Monit**. 2018; 23:24–32.

25. Sung SH, Cheng HM, Wang KL, et al. White coat hypertension is more risky than prehypertension: important role of arterial wave reflections. **Hypertension**. 2013; 61:1346–1353.

26. Scuteri A, Morrell CH, Orru M, et al. Gender specific profiles of white coat and masked hypertension impacts on arterial structure and function in the sardinia study. **Int J Cardiol**. 2016; 217:92–98.

27. de Simone G, Schillaci G, Chinali M, Angeli F, Reboldi GP, Verdecchia P. Estimate of white-coat effect and arterial stiffness. **J Hypertens**. 2007; 25:827–831.

28. Cai P, Peng Y, Wang Y, Wang X. Effect of white-coat hypertension on arterial stiffness: a meta-analysis. **Medicine (Baltim)**. 2018; 97:e12888.

29. Tientcheu D, Ayers C, Das SR, et al. Target organ complications and cardiovascular events associated with masked hypertension and white-coat hypertension: analysis from the dallas heart study. **J Am Coll Cardiol**. 2015; 66:2159–2169.

30. Antza C, Doundoulakis I, Stabouli S, Tziomalos K, Kotsis V. Masked hypertensives: a disguised arterial stiffness population. **J Clin Hypertens**. 2019; 21:1473–1480.

31. Li Y, Staessen JA, Lu L, Li L-H, Wang G-L, Wang J-G. Is isolated nocturnal hypertension a novel clinical entity? Findings from a Chinese population study. **Hypertension**. 2007; 50:333–339.

32. O'Flynn AM, Madden JM, Russell AJ, Curtin RJ, Kearney PM. Isolated nocturnal hypertension and subclinical target organ damage: a systematic review of the literature. **Hypertens Res**. 2015; 38:570–575.

33. Kario K. Perfect 24-h management of hypertension: clinical relevance and perspectives. **J Hum Hypertens**. 2017; 31:231–243.

34. Liu Z, Hesse C, Curry TB, et al. Ambulatory arterial stiffness index is not correlated with the pressor response to laboratory stressors in normotensive humans. **J Hypertens**. 2009; 27:763.

35. Hsu P-F, Cheng H-M, Sung S-H, et al. Hemodynamic determinants of the short-term blood pressure variability: differential roles of arterial stiffness and wave reflection. **Am J Hypertens**. 2017; 30:256–263.

36. Kario K. Orthostatic hypertension—a new haemodynamic cardiovascular risk factor. **Nat Rev Nephrol**. 2013; 9:726.

37. Shahin Y, Khan JA, Chetter I. Angiotensin converting enzyme inhibitors effect on arterial stiffness and wave reflections: a meta-analysis and meta-regression of randomised controlled trials. **Atherosclerosis**. 2012; 221:18–33.

38. Pannier BM, Guerin AP, Marchais SJ, London GM. Different aortic reflection wave responses following long-term angiotensin-converting enzyme inhibition and beta-blocker in essential hypertension. **Clin Exp Pharmacol Physiol**. 2001; 28:1074–1077.

39. Protogerou AD, Stergiou GS, Vlachopoulos C, Blacher J, Achimastos A. The effect of antihypertensive drugs on central blood pressure beyond peripheral blood pressure. Part II: evidence for specific class-effects of antihypertensive drugs on pressure amplification. **Curr Pharmaceut Des**. 2009; 15:272–289.

40. Dhakam Z, McEniery CM, Cockcroft JR, Brown MJ, Wilkinson IB. Atenolol and eprosartan: differential effects on central blood pressure and aortic pulse wave velocity. **Am J Hypertens**. 2006; 19:214–219.

41. Morgan T, Lauri J, Bertram D, Anderson A. Effect of different antihypertensive drug classes on central aortic pressure. **Am J Hypertens**. 2004; 17:118–123.

42. Manisty CH, Hughes AD. Meta-analysis of the comparative effects of different classes of antihypertensive agents on brachial and central systolic blood pressure, and augmentation index. **Br J Clin Pharmacol**. 2013; 75:79–92.

43. Alyavi A, Uzokov J. Treatment of stable angina pectoris: focus on the role of calcium antagonists and ace inhibitors. **Ont Health Technol Assess Ser**. 2017; 15:1–12.

44. Niu W, Qi Y. A meta-analysis of randomized controlled trials assessing the impact of beta-blockers on arterial stiffness, peripheral blood pressure and heart rate. **Int J Cardiol**. 2016; 218:109–117.

45. Protogerou AD, Blacher J, Aslangul E, et al. Gender influence on metabolic syndrome's effects on arterial stiffness and pressure wave reflections in treated hypertensive subjects. **Atherosclerosis**. 2007; 193:151–158.

46. Protogerou A, Blacher J, Stergiou GS, Achimastos A, Safar ME. Blood pressure response under chronic antihypertensive drug therapy: the role of aortic stiffness in the reason (preterax in regression of arterial stiffness in a controlled double-blind) study. **J Am Coll Cardiol**. 2009; 53:445–451.

47. Lund-Johansen P. Hemodynamic response: decrease in cardiac output vs reduction in vascular resistance. **Hypertension**. 1983; 5:III49.

48. Andreadis E, Sfakianakis M, Tsourous G, et al. Differential impact of angiotensin receptor blockers and calcium channel blockers on arterial stiffness. **Int Angiol**. 2010; 29:266.

49. Asmar RG, Benetos A, Chaouche-Teyara K, Raveau-Landon CM, Safar ME. Comparison of effects of felodipine versus hydrochlorothiazide on arterial diameter and pulse-wave velocity in essential hypertension. **Am J Cardiol**. 1993; 72:794–798.

50. Ishimitsu T, Numabe A, Masuda T, et al. Angiotensin-ii receptor antagonist combined with calcium channel blocker or diuretic for essential hypertension. **Hypertens Res**. 2009; 32:962–968.

51. Matsui Y, Eguchi K, O'Rourke MF, et al. Differential effects between a calcium channel blocker and a diuretic when used in combination with angiotensin ii receptor blocker on central aortic pressure in hypertensive patients. **Hypertension**. 2009; 54:716–723.

52. Ichihara A, Kaneshiro Y, Takemitsu T, Sakoda M. Effects of amlodipine and valsartan on vascular damage and ambulatory blood pressure in untreated hypertensive patients. **J Hum Hypertens**. 2006; 20:787–794.

53. Tsai J-P, Wang J-H, Chen M-L, Yang C-F, Chen Y-C, Hsu B-G. Association of serum leptin levels with central arterial stiffness in coronary artery disease patients. **BMC Cardiovasc Disord**. 2016; 16:80.

54. Paterno Marchioli C. P4559 assess of angiotensin receptor blockers therapy associated to mineralocorticoid receptor antagonists or to calcium channel blockers plus hydrochlorothiazide according central haemodynamic parameters. **Eur Heart J**. 2019; 40:ehz745.

55. Alem M, Milia P, Muir S, Lees K, Walters M. Comparison of the effects of diuretics on blood pressure and arterial stiffness in patients with stroke. **J Stroke Cerebrovasc Dis**. 2008; 17:373–377.

56. Cypiene A, Laucevicius A, Venalis A, et al. Non-invasive assessment of arterial stiffness indices by applanation tonometry and pulse wave analysis in patients with rheumatoid arthritis treated with tnf-

alpha blocker remicade (infliximab). **Proc West Pharmacol Soc**. 2007; 50:119.

57. Mahmud A. Reducing arterial stiffness and wave reflection−quest for the holy grail? **Artery Res**. 2007; 1:13−19.

58. Das S, Kumar P, Kiran U, Airan B. Alpha blockers: a relook at phenoxybenzamine. **J Pract Cardiovasc Sci**. 2017; 3:11.

59. Liu Y, Dai S, Liu L, Liao H, Xiao C. Spironolactone is superior to hydrochlorothiazide for blood pressure control and arterial stiffness improvement: a prospective study. **Medicine**. 2018; 97.

60. Kithas PA, Supiano MA. Spironolactone and hydrochlorothiazide decrease vascular stiffness and blood pressure in geriatric hypertension. **J Am Geriatr Soc**. 2010; 58:1327−1332.

61. Nikolic SB, Wilson R, Hare JL, Adams MJ, Edwards LM, Sharman JE. Spironolactone reduces aortic stiffness via blood pressure-dependent effects of canrenoate. **Metabolomics**. 2014; 10:105−113.

62. Xeni J. **The Effect of Spironolactone on Cerebral Blood Flow and Cognition**. 2018.

63. Ramsay LE. **Department of Therapeutics, Royal Hallamshire Hospital**. sheffield, uk: Hormone antagonists; 2019:335.

64. Fengler K, Rommel KP, Hoellriegel R, et al. Pulse wave velocity predicts response to renal denervation in isolated systolic hypertension. **J Am Heart Assoc**. 2017; 6.

65. Mestanik M, Jurko A, Spronck B, et al. Improved assessment of arterial stiffness using corrected cardio-ankle vascular index (cavi0) in overweight adolescents with white-coat and essential hypertension. **Scand J Clin Lab Invest**. 2017; 77:665−672.

66. Maseko MJ, Woodiwiss AJ, Libhaber CD, Brooksbank R, Majane OH, Norton GR. Relations between white coat effects and left ventricular mass index or arterial stiffness: role of nocturnal blood pressure dipping. **Am J Hypertens**. 2013; 26:1287−1294.

67. Abdalla M, Goldsmith J, Muntner P, et al. Is isolated nocturnal hypertension a reproducible phenotype? **Am J Hypertens**. 2016; 29:33−38.

68. Fan H-Q, Li Y, Thijs L, et al. Prognostic value of isolated nocturnal hypertension on ambulatory measurement in 8711 individuals from 10 populations. **J Hypertens**. 2010; 28:2036−2045.

69. Hsu P-F, Cheng H-M, Wu C-H, et al. High short-term blood pressure variability predicts long-term cardiovascular mortality in untreated hypertensives but not in normotensives. **Am J Hypertens**. 2016; 29:806−813.

70. Schillaci G, Bilo G, Pucci G, et al. Relationship between short-term blood pressure variability and large-artery stiffness in human hypertension: findings from 2 large databases. **Hypertension**. 2012; 60:369−377.

71. Avolio AP, Xu K, Butlin M. Effect of large arteries on blood pressure variability. **In: 2013 35th Annual International Conference of the IEEE Engineering in Medicine and Biology Society (EMBC)**. 2013:4078−4081.

72. Laurent S, Cockcroft J, Van Bortel L, et al. Expert consensus document on arterial stiffness: methodological issues and clinical applications. **Eur Heart J**. 2006; 27:2588−2605.

73. Vlachopoulos C, Aznaouridis K, Terentes-Printzios D, Ioakeimidis N, Stefanadis C. Prediction of cardiovascular events and all-cause mortality with brachial-ankle elasticity index: a systematic review and meta-analysis. **Hypertension**. 2012; 60:556−562.

74. Wang JJ, O'Brien AB, Shrive NG, Parker KH, Tyberg JV. Time-domain representation of ventricular-arterial coupling as a windkessel and wave system. **Am J Physiol Heart Circ Physiol**. 2003; 284:H1358−H1368.

75. Redheuil A, Kachenoura N, Bollache E, et al. Left ventricular and proximal aorta coupling in magnetic resonance imaging: aging together? **Am J Physiol Heart Circ Physiol**. 2019; 317:H300−H307.

76. Wang KL, Cheng HM, Chuang SY, et al. Central or peripheral systolic or pulse pressure: which best relates to target organs and future mortality? **J Hypertens**. 2009; 27:461−467.

77. Wang KL, Cheng HM, Sung SH, et al. Wave reflection and arterial stiffness in the prediction of 15-year all-cause and cardiovascular mortalities: a community-based study. **Hypertension**. 2010; 55:799−805.

78. Hashimoto J, Ito S. Pulse pressure amplification, arterial stiffness, and peripheral wave reflection determine pulsatile flow waveform of the femoral artery. **Hypertension**. 2010; 56:926−933.

79. Huang JT, Cheng HM, Yu WC, et al. Value of excess pressure integral for predicting 15-year all-cause and cardiovascular mortalities in end-stage renal disease patients. **J Am Heart Assoc**. 2017; 6.

80. Franklin SS, Jacobs MJ, Wong ND, L'Italien GJ, Lapuerta P. Predominance of isolated systolic hypertension among middle-aged and elderly us hypertensives: analysis based on National Health and Nutrition Examination Survey (NHANES) III. **Hypertension**. 2001; 37:869−874.

81. Chuang SY, Cheng HM, Chou P, Chen CH. Prevalance of isolated systolic hypertension and the awareness, treatment, and control rate of hypertension in kinmen. **ACS**. 2006; 22:83−90.

82. Chou P, Chen CH, Chen HH, Chang MS. Epidemiology of isolated systolic hypertension in pu-li, taiwan. **Int J Cardiol**. 1992; 35:219−226.

83. Yano Y, Stamler J, Garside DB, et al. Isolated systolic hypertension in young and middle-aged adults and 31-year risk for cardiovascular mortality: the chicago heart association detection project in industry study. **J Am Coll Cardiol**. 2015; 65:327−335.

84. Staessen JA, Gasowski J, Wang JG, et al. Risks of untreated and treated isolated systolic hypertension in the elderly: meta-analysis of outcome trials. **Lancet**. 2000; 355:865−872.

85. Prevention of stroke by antihypertensive drug treatment in older persons with isolated systolic hypertension. Final results of the systolic hypertension in the Elderly Program (SHEP). SHEP Cooperative Research Group. **J Am Med Assoc**. 1991; 265:3255−3264.

86. Staessen JA, Fagard R, Thijs L, et al. Randomised double-blind comparison of placebo and active treatment for older patients with isolated systolic hypertension. The systolic hypertension in europe (syst-eur) trial investigators. **Lancet**. 1997; 350:757−764.

87. Liu L, Wang JG, Gong L, Liu G, Staessen JA. Comparison of active treatment and placebo in older Chinese patients with isolated systolic hypertension. Systolic hypertension in China (syst-China) collaborative group. **J Hypertens**. 1998; 16:1823−1829.

88. Reference Values for Arterial Stiffness C. Determinants of pulse wave velocity in healthy people and in the presence of cardiovascular risk factors: 'Establishing normal and reference values'. **Eur Heart J**. 2010; 31:2338−2350.

89. Avolio AP, Chen SG, Wang RP, Zhang CL, Li MF, O'Rourke MF. Effects of aging on changing arterial compliance and left ventricular load in a northern Chinese urban community. **Circulation**. 1983; 68:50−58.

90. Avolio AP, Deng FQ, Li WQ, et al. Effects of aging on arterial distensibility in populations with high and low prevalence of hypertension: comparison between urban and rural communities in China. **Circulation**. 1985; 71:202−210.

91. Engelen L, Bossuyt J, Ferreira I, et al. Reference values for local arterial stiffness. Part A: carotid artery. **J Hypertens**. 2015; 33:1981−1996.

92. Bossuyt J, Engelen L, Ferreira I, et al. Reference values for local arterial stiffness. Part B: femoral artery. **J Hypertens**. 2015; 33:1997−2009.

93. Williams B, Mancia G, Spiering W, et al. 2018 ESC/ESH guidelines for the management of arterial hypertension: the task force for the management of arterial hypertension of the european society of cardiology and the european society of hypertension. **J Hypertens**. 2018; 36:1953−2041.

94. Chirinos JA, Segers P, Hughes T, Townsend R. Large-artery stiffness in health and disease: JACC state-of-the-art review. **J Am Coll Cardiol**. 2019; 74:1237−1263.

95. Van Bortel LM, Laurent S, Boutouyrie P, et al. Expert consensus document on the measurement of aortic stiffness in daily practice using carotid-femoral pulse wave velocity. **J Hypertens**. 2012; 30:445−448.

96. Ben-Shlomo Y, Spears M, Boustred C, et al. Aortic pulse wave velocity improves cardiovascular event prediction: an individual participant meta-analysis of prospective observational data from 17,635 subjects. **J Am Coll Cardiol**. 2014; 63:636−646.

97. Palatini P, Rosei EA, Avolio A, et al. Isolated systolic hypertension in the young: a position paper endorsed by the european society of hypertension. **J Hypertens**. 2018; 36:1222−1236.

98. O'Rourke MF, Adji A. Pressure paradox: high pulse pressure and low mean pressure are favorable features in young adults. **Hypertension**. 2017; 70:493−495.

99. Saladini F, Fania C, Mos L, Mazzer A, Casiglia E, Palatini P. Office pulse pressure is a predictor of favorable outcome in young- to middle-aged subjects with stage 1 hypertension. **Hypertension**. 2017; 70:537−542.

100. Shen W, Zhang T, Li S, et al. Race and sex differences of long-term blood pressure profiles from childhood and adult hypertension: the bogalusa heart study. **Hypertension**. 2017; 70:66−74.

101. Franklin SS, Gustin W, Wong ND, et al. Hemodynamic patterns of age-related changes in blood pressure. The framingham heart study. **Circulation**. 1997; 96:308−315.

102. Ayer JG, Harmer JA, Marks GB, Avolio A, Celermajer DS. Central arterial pulse wave augmentation is greater in girls than boys, independent of height. **J Hypertens**. 2010; 28:306−313.

103. McEniery CM, Yasmin, McDonnell B, et al. Central pressure: variability and impact of cardiovascular risk factors: the anglo-cardiff collaborative trial ii. **Hypertension**. 2008; 51:1476−1482.

104. Mahmud A, Feely J. Spurious systolic hypertension of youth: fit young men with elastic arteries. **Am J Hypertens**. 2003; 16:229−232.

105. Grebla RC, Rodriguez CJ, Borrell LN, Pickering TG. Prevalence and determinants of isolated systolic hypertension among young adults: the 1999-2004 us national health and nutrition examination survey. **J Hypertens**. 2010; 28:15−23.

106. Palatini P, Saladini F, Mos L, Fania C, Mazzer A, Casiglia E. Clinical characteristics and risk of hypertension needing treatment in young patients with systolic hypertension identified with ambulatory monitoring. **J Hypertens**. 2018; 36:1810−1815.

107. McEniery CM, Franklin SS, Cockcroft JR, Wilkinson IB. Isolated systolic hypertension in young people is not spurious and should be treated: pro side of the argument. **Hypertension**. 2016; 68:269−275.

108. Yeh CJ, Pan WH, Jong YS, Kuo YY, Lo CH. Incidence and predictors of isolated systolic hypertension and isolated diastolic hypertension in taiwan. **J Formos Med Assoc**. 2001; 100:668−675.

109. Fang J, Madhavan S, Cohen H, Alderman MH. Isolated diastolic hypertension. A favorable finding among young and middle-aged hypertensive subjects. **Hypertension**. 1995; 26:377−382.

110. Asgari S, Khalili D, Mehrabi Y, Kazempour-Ardebili S, Azizi F, Hadaegh F. Incidence and risk factors of isolated systolic and diastolic hypertension: a 10 year follow-up of the tehran lipids and glucose study. **Blood Press**. 2016; 25:177−183.

111. McGrath BP, Kundu P, Daya N, et al. Isolated diastolic hypertension in the UK biobank: comparison of acc/aha and esc/nice guideline definitions. **Hypertension**. 2020; 76:699−706.

112. Li Y, Wei FF, Wang S, Cheng YB, Wang JG. Cardiovascular risks associated with diastolic blood pressure and isolated diastolic hypertension. **Curr Hypertens Rep**. 2014; 16:489.

113. McEvoy JW, Daya N, Rahman F, et al. Association of isolated diastolic hypertension as defined by the 2017 acc/aha blood pressure guideline with incident cardiovascular outcomes. **J Am Med Assoc**. 2020; 323:329−338.

114. Arima H, Anderson C, Omae T, et al. Effects of blood pressure lowering on major vascular events among patients with isolated diastolic hypertension: the perindopril protection against recurrent stroke study (progress) trial. **Stroke**. 2011; 42:2339−2341.

115. Nichols WW, O'Rourke MF, Vlachopoulos C. **Mcdonald's Blood Flow in Arteries: Theoretic, Experimental and Clinical Principles**. London: Arnold; 2011.

116. Cheng HM, Chuang SY, Sung SH, et al. 2019 consensus of the taiwan hypertension society and taiwan society of cardiology on the clinical application of central blood pressure in the management of hypertension. **Acta Cardiol Sin**. 2019; 35:234−243.

117. Williams B, Lacy PS, Thom SM, et al. Differential impact of blood pressure-lowering drugs on central aortic pressure and clinical outcomes: principal results of the conduit artery function evaluation (cafe) study. **Circulation**. 2006; 113:1213−1225.

118. Herbert A, Cruickshank JK, Laurent S, Boutouyrie P, Reference Values for Arterial Measurements Collaboration. Establishing reference values for central blood pressure and its amplification in a general healthy population and according to cardiovascular risk factors. **Eur Heart J**. 2014; 35:3122−3133.

119. Cheng HM, Chuang SY, Sung SH, et al. Derivation and validation of diagnostic thresholds for central blood pressure measurements based on long-term cardiovascular risks. **J Am Coll Cardiol**. 2013; 62:1780−1787.

120. Lurbe E, Redon J. Isolated systolic hypertension in young people is not spurious and should be treated: con side of the argument. **Hypertension**. 2016; 68:276−280.

121. Liu F, Adi D, Xie X, et al. Prevalence of isolated diastolic hypertension and associated risk factors among different ethnicity groups in xinjiang, China. **PLoS One**. 2015; 10:e0145325.

122. Sharman JE, Avolio AP, Baulmann J, et al. Validation of non-invasive central blood pressure devices: artery society task force consensus statement on protocol standardization. **Eur Heart J**. 2017; 38:2805−2812.

123. Ohkubo T, Kikuya M, Metoki H, et al. Prognosis of "masked" hypertension and "white-coat" hypertension detected by 24-h

ambulatory blood pressure monitoring 10-year follow-up from the ohasama study. **J Am Coll Cardiol**. 2005; 46:508−515.

124. Mancia G, Facchetti R, Bombelli M, Grassi G, Sega R. Long-term risk of mortality associated with selective and combined elevation in office, home, and ambulatory blood pressure. **Hypertension**. 2006; 47:846−853.

125. Strandberg TE, Salomaa V. White coat effect, blood pressure and mortality in men: prospective cohort study. **Eur Heart J**. 2000; 21:1714−1718.

126. Gustavsen PH, Hoegholm A, Bang LE, Kristensen KS. White coat hypertension is a cardiovascular risk factor: a 10-year follow-up study. **J Hum Hypertens**. 2003; 17:811−817.

127. Puato M, Palatini P, Zanardo M, et al. Increase in carotid intima-media thickness in grade i hypertensive subjects: white-coat versus sustained hypertension. **Hypertension**. 2008; 51:1300−1305.

128. Antza C, Vazakidis P, Doundoulakis I, et al. Masked and white coat hypertension, the double trouble of large arteries: a systematic review and meta-analysis. **J Clin Hypertens**. 2020; 22:802−811.

129. Wojciechowska W, Stolarz-Skrzypek K, Olszanecka A, et al. Subclinical arterial and cardiac damage in white-coat and masked hypertension. **Blood Press**. 2016; 25:249−256.

130. Diaz KM, Veerabhadrappa P, Brown MD, Whited MC, Dubbert PM, Hickson DA. Prevalence, determinants, and clinical significance of masked hypertension in a population-based sample of african americans: the jackson heart study. **Am J Hypertens**. 2015; 28:900−908.

131. Brguljan-Hitij J, Thijs L, Li Y, et al. International Database on Ambulatory Blood Pressure in Relation to Cardiovascular Outcome I. Risk stratification by ambulatory blood pressure monitoring across JNC classes of conventional blood pressure. **Am J Hypertens**. 2014; 27:956−965.

132. Spannella F, Filipponi A, Giulietti F, et al. Prognostic role of masked and white-coat hypertension: 10-year mortality in treated elderly hypertensives. **J Hum Hypertens**. 2019; 33:741−747.

133. Laurent S, Boutouyrie P, Asmar R, et al. Aortic stiffness is an independent predictor of all-cause and cardiovascular mortality in hypertensive patients. **Hypertension**. 2001; 37:1236−1241.

134. Yang W-Y, Melgarejo JD, Thijs L, et al. Association of office and ambulatory blood pressure with mortality and cardiovascular outcomes. **JAMA**. 2019; 322:409−420.

135. Li Y, Wang JG. Isolated nocturnal hypertension: a disease masked in the dark. **Hypertension**. 2013; 61:278−283.

136. Avolio A. Central aortic blood pressure and management of hypertension: confirmation of a paradigm shift? **Hypertension**. 2013; 62:1005−1007.

137. Task Force Members. 2013 ESH/ESC guidelines for the management of arterial hypertension: the task force for the management of arterial hypertension of the European Society of Hypertension (ESH) and of the European Society of Cardiology (ESC). **Eur Heart J**. 2013; 34:2159−2219.

138. Parati G, Ochoa JE, Lombardi C, Bilo G. Assessment and management of blood-pressure variability. **Nat Rev Cardiol**. 2013; 10:143.

139. Höcht C. Blood pressure variability: prognostic value and therapeutic implications. **ISRN Hypertens**. 2013; 2013:398485.

140. Sogunuru GP, Kario K, Shin J, et al. Morning surge in blood pressure and blood pressure variability in asia: evidence and statement from the hope asia network. **J Clin Hypertens**. 2019; 21:324−334.

141. Mena LJ, Felix VG, Melgarejo JD, Maestre GE. 24-hour blood pressure variability assessed by average real variability: a systematic review and meta-analysis. **J Am Heart Assoc**. 2017; 6.

142. Huang JT, Cheng HM, Yu WC, Lin YP, Sung SH, Chen CH. Increased nighttime pulse pressure variability but not ambulatory blood pressure levels predicts 14-year all-cause mortality in patients on hemodialysis. **Hypertension**. 2019; 74:660−668.

143. Nagai M, Hoshide S, Dote K, Kario K. Visit-to-visit blood pressure variability and dementia. **Geriatr Gerontol Int**. 2015; 15:26−33.

144. Shimbo D, Shea S, McClelland RL, et al. Associations of aortic distensibility and arterial elasticity with long-term visit-to-visit blood pressure variability: the multi-ethnic study of atherosclerosis (mesa). **Am J Hypertens**. 2013; 26:896−902.

145. Aznaouridis K, Vlachopoulos C, Protogerou A, Stefanadis C. Ambulatory systolic−diastolic pressure regression index as a predictor of clinical events: a meta-analysis of longitudinal studies. **Stroke**. 2012; 43:733−739.

This page intentionally left blank

Arterial stiffness and pulsatile hemodynamics in the pulmonary circulation

This page intentionally left blank

Pulsatile hemodynamics and ventricular–arterial interactions in the pulmonary circulation: physiologic concepts

Berend E. Westerhof, Anton Vonk Noordegraaf and Masafumi Fukumitsu

Department of Pulmonary Medicine, Amsterdam Universitair Medische Centra, Vrije Universiteit Amsterdam, Amsterdam Cardiovascular Sciences, Amsterdam, the Netherlands

Introduction

The pulmonary circulation can be described in much the same way as the systemic circulation, with static measures such as mean pressure, cardiac output (CO), and vascular resistance, and with pulsatile hemodynamics, such as systolic and diastolic pressures, pressure wave reflection, and frequency-domain analysis. That being said, many differences between the systemic and pulmonary circulations can be identified. Structure and function may differ, but similar approaches can be taken for its characterization.

Physiologically, the properties of the right ventricle (RV) and the arterial load can be described in two ways[1]: (1) by the intrinsic characteristics (for example, pulmonary vascular resistance (PVR) and pulmonary arterial compliance (PAC), and RV contractility and RV diastolic stiffness) and (2) by the system characteristics, determined by the interaction between the RV and arterial load (for example, pulmonary artery pressure (PAP), CO, and RV ejection fraction, EF). In clinical practice, the latter parameters are commonly used; however, correct interpretation of data requires an adequate understanding of the former parameters.

In this chapter, we will describe measurements in the pulmonary cardiovascular system (the system characteristics) which assess the combined effect of heart and vascular load.[2] Based on the measurements, the RV and the vasculature can be characterized (the intrinsic characteristics), from the pressure-flow relation, and the pressure-volume relation, respectively.[1]

Measurements in the pulmonary circulation
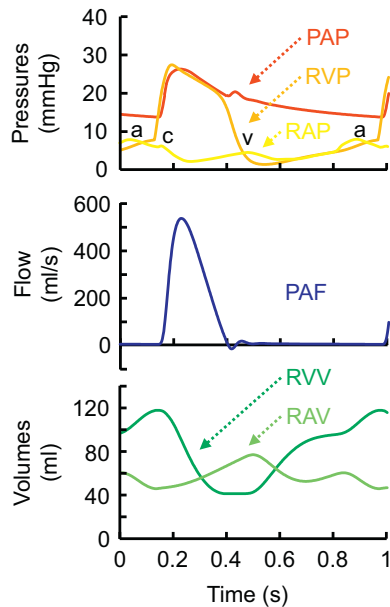
Pressures in the pulmonary system

Noninvasive measurement of pressures in the pulmonary circulation is not possible. Right heart catheterization (RHC) is highly invasive; however, it provides a wealth of data.[3] Care must be taken though to obtain reliable measurements.[4,5] RHC is the recommended method to assess pulmonary hypertension.[6]

For RHC, a pulmonary artery (PA) catheter, sometimes called a Swan-Ganz catheter eponymous of its inventors,[7] is used. After being inserted in the jugular (sometimes femoral, antecubital or brachial) vein, the balloon at the tip of the catheter allows it to "go with the flow," floating toward the heart, entering through the right atrium (RA), continuing to the RV, and finally into the PA. A Wiggers diagram of pressures and volumes in the pulmonary circulation is given in Fig. 55.1.[8] With multiple lumen catheters, it is possible to measure pressures at these sites simultaneously providing detailed information on the right side of the heart and its load.

Right atrial pressure as a function of time

In right atrial pressure (RAP) and in central venous pressure (CVP, which is similar since the connection between central veins and the RA is open), characteristic features can be distinguished, comparable to left atrial pressure (LAP).[9] With RA contraction (P-top in the ECG), an a-wave

FIGURE 55.1 Wiggers diagram of pulmonary hemodynamics, based on simulations with the Aplysia CardioVascular Lab 2020 (Aplysia Medical AB, Stockholm, Sweden).[8] Top: pulmonary artery pressure (PAP), right atrial pressure (RAP), and right ventricular pressure (RVP). Middle: pulmonary artery flow (PAF). Bottom: right atrial volume (RAV) and right ventricular volume (RVV). For detailed descriptions, see the text.

appears in RAP, which drops (the x-descent) with an interruption caused by the closing of the tricuspid valve when the RV starts to contract (just after the R-top in the ECG). Some of the RV pressure (RVP) may be transmitted to the RA by the bulging of the tricuspid valve (between the RA and the RV) into the RA, visible as the c-wave in the x-descent of RAP. The contraction of the RV stretches the RA, causing RAP decrease to its minimum value, after which the passive filling of the RA starts accompanied by an increasing RAP. When the RV relaxes further and RVP drops below RAP, the tricuspid valve opens, causing a decline of RAP, visible as the y-descent of the v-peak.[9] As long as the tricuspid valve is open, RAP and RVP are essentially equal. RAP is an important risk factor in PH.[6,10]

Right ventricular pressure as a function of time

The RVP shows a gradual increase during ventricular diastole, with a final increase in pressure at end-diastole caused by contraction of the RA. RVP systole is characterized by a steep increase, and a steep fall at the end of RV contraction. RVP is an important determinant of RV wall stress (or wall tension) together with volume (radius) and wall thickness according to Laplace's law.[11] The shape of the RV complicates the calculation of RV wall stress and tension, however, can be approximated.[12] RV wall stress and tension (see also Chapter 56 Pulmonary arterial load

and ventriculararterial coupling in pulmonary hypertension") are relevant in the understanding of progression of RV adaptation in PH.[13]

Pulmonary artery pressure as a function of time

PAP starts to increase when the pulmonary valves open, after which RVP and PAP increase and then fall together.[9] When the pulmonary valves close, RVP continues to drop quickly, while PAP falls much slower because of the Windkessel function of the pulmonary circulation. Systolic and diastolic PAP are referred to as sPAP and dPAP.

Pulmonary artery wedge pressure

By wedging the PA catheter into a branch of the PAs, or by inflating the balloon at the tip, flow in the trajectory downstream is stopped.[14] In this manner, the vasculature forms an extension of the catheter, allowing to determine the pressure at the outflow of the pulmonary system, i.e., LAP.[15] Thus, pulmonary artery wedge pressure (PAWP) or pulmonary artery occlusion pressure provides valuable information over the pressure drop over the pulmonary vasculature, called transpulmonary pressure gradient. This transpulmonary pressure gradient is usually quantified by mean PAP (mPAP) minus PAWP (determined at end-expiration when intrathoracic pressure is closest to atmospheric pressure). A historical name is pulmonary capillary wedge pressure (PCWP) which suggested that capillary pressure was measured by occlusion or catheter wedging. Now it is generally accepted that LAP is assessed[15] and PCWP is no longer used.[16] The estimation of capillary pressure is described in the next section.

Pulmonary capillary pressure

It has been suggested that pulmonary capillary pressure PCP may be estimated from the decay of the pressure after inflating the catheter-tip balloon. Several methods have been proposed, involving fitting of exponential functions, looking for an inflection point in the decay, or extrapolating part of the decay.[17–19] PCP is relevant in the pathophysiology of pulmonary edema.[20,21]

Flow measurements in the pulmonary system

Cardiac output

A Swan-Ganz catheter has a thermistor some 3 cm behind the tip, which is placed in the PA. Through a proximal port of the catheter, cold saline can be injected into the RA, where it is mixed. Downstream in the PA, the temperature change caused by the cold saline represents an indicator dilution ("thermo-dilution") curve, from which CO can be estimated[22–24] with the Stewart (1893)–Hamilton (1932) equation.[25,26]

Pulmonary artery flow

The pulsatile flow velocity (Fig. 55.1) into the PA can be measured by echocardiography or by through-plane phase-contrast MRI. With the former technique, the area of the outflow tract is needed so that flow velocity (cm/s) can be transformed to volume flow (cm^3/s, corresponding to mL/s). With through-plane phase-contrast MRI, the volume flow is obtained (usually at the main PA) by summing the flow across all pixels in a cross-sectional anatomic representation (each pixel representing a three-dimensional voxel); for each voxel, the volume flow is computed as their cross-sectional area (i.e., pixel size) times their flow velocity. Stroke volume (SV) can then be obtained by time integration of volume flow, the area under the flow curve giving volume in ml. Velocity measurement with Doppler echocardiography is sensitive to the insonation angle. Conversion of velocity to volume flow is sensitive to errors in the quantification of the outflow area, particularly when area is determined from a squared radius. For a detailed discussion regarding technical aspects of flow measurements using Doppler echocardiography and phase-contrast MRI, the reader is referred to Chapters 2 and 4.

Volume measurements of the right heart

Echocardiography

Many relevant measures can be obtained from volume measurements of the RV, such as chamber sizes, SV, and EF. Several length related quantifications can be obtained as well, like RV fractional area change, longitudinal strain, and tricuspid annular plane systolic excursion.[6] Measuring the volume of the RV with echocardiography is difficult because of its complicated shape; therefore, results should be interpreted carefully.[27] A great advantage of echocardiography is its wide availability at the bedside.

Cardiac MRI

If available, volumes of the RV are ideally measured with cardiac MRI (CMRI).[28–30] Recently it has been proposed that CMRI-derived volume measurements are not inferior to invasive pressure measurements for the risk assessment of PH patients.[31]

Conductance catheter

The conductance catheter measures changes in ventricular volume with a series of ring-shaped electrodes. A small high frequency current is injected by the outer electrodes, and the voltage that is sensed over the inner electrodes is a measure of conductance, which in turn is related to blood volume.[32]

The SV determined by the conductance catheter needs to be calibrated with separate (e.g., thermodilution) measurements. Although developed for the LV, with the assumption that the shape of the ventricle can be described by a sphere or an ellipse,[33] it has been used for the RV as well.

Right atrial volume as a function of time

With the contraction of the RA at the end of ventricular diastole, volume decreases (Fig. 55.1); after the start of ventricular systole, and closing of the tricuspid valve, volume increases again. When ventricular systole ends and the tricuspid valve opens again, the volume stored in the RA translocates to the RV.

Right ventricular volume as a function of time

The volume of the RV is increased to its maximal value by the contraction of the RA just before ventricular systole (Fig. 55.1). With opening of the pulmonary valves and ejection, RV volume rapidly decreases. After closing of the tricuspid valve, and opening of the tricuspid valve, the volume in the RA is distributed to the RV.

The pulmonary vasculature

Anatomy and function of the pulmonary vasculature

The requirements for the geometry of the pulmonary vasculature are optimal gas exchange, thus maximum of contract area between blood and air, in a minimum of space. These requirements are met by a network with branching in rapid succession.[34,35] Typically, each mother vessel (except for the pulmonary trunk) branches into three daughter vessels. This is unlike the arrangement in the systemic circulation, that is optimized for the transport of blood, with limited loss of pressure, over relatively large distances, to the branches that supply specific tissues or organs. The arrangement of the pulmonary vasculature results in unique characteristics which will be discussed later (see "*Arterial time constant*").

The pulmonary system is connected in series with the systemic circulation. This layout allows the pulmonary circulation to operate at much lower pressures, while transporting the same flow as the systemic tree. To make this possible, the PVR is much lower than systemic vascular resistance.

mPAP is built up by the pressure resulting from PVR times CO, plus the outflow pressure of the pulmonary vasculature, i.e., LAP. LAP contributes a large proportion to mPAP when compared to the systemic counterpart. While RAP (the outflow pressure of the systemic tree) is around 2–6 mmHg, LAP is some 5–15 mmHg, quite considerable since a normal mPAP is 10–20 mmHg[36]
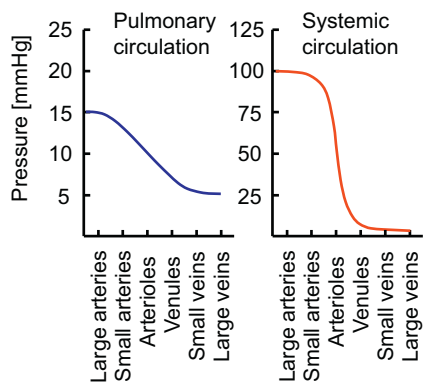
(see "Normal values in the pulmonary circulation" in this chapter). When calculating PVR from (mPAP−LAP)/CO it is clear that LAP contributes substantially and cannot be neglected in the calculation. For instance, if mPAP were 15 mmHg and LAP 5 mmHg, not taking the latter into account could result in an error of some 50%. In comparison, systemic mean arterial pressure is around 95 mmHg, thus neglecting an RAP of 2−6 mmHg in the calculation of systemic vascular resistance (SVR) results in an error close to 5%, which is negligible compared to the errors associated with the determination of CO (order of 30%).[22,37]

Resistance in the pulmonary circulation is not predominantly located in the arteries as in the systemic circulation, but is distributed over the system, resulting in a more gradual pressure drop (Fig. 55.2).[38−40]

While in the systemic circulation the pressure has decreased to approximately CVP beyond the capillaries, in the pulmonary circulation some pressure drop occurs behind the capillaries, suggesting that part of the PVR is located on the venous side.[41] Indeed, some 40% of PVR was reported to be contributed by the veins in an animal study.[39] Data reported by Chazova et al.[42] in health and PH suggest that indeed changes in the veins may increase PVR. In that sense, the term "pre-capillary PH," indicating PH related to vascular changes (as opposed to "post-capillary PH," which implicates elevated LA pressure as the cause (see Chapter 56)) could be considered confusing.

In the pulmonary circulation, compliance is more evenly spread over arteries and veins when compared to the systemic circulation. In the former the compliance in the veins is only 2 times larger compared to arterial compliance.[43] In the latter, compliance in the veins is some 20 times larger than in the arteries.[9]

Pressure and flow in the pulmonary capillaries are pulsatile,[44,45] and pulsatility was proposed to play a role in capillary recruitment[46] and in gas exchange.[47] Modeling studies confirm the pulsatility of pressure and flow,[48] and

further suggested flow pulsatility passes more or less unchanged through the microcirculation, while pressure pulsatility is reduced.[48] The effect of left atrial contraction on pressure and flow pulsatility was confirmed but considered secondary.[48] The pulsatility relative to mean capillary flow is reduced in advanced pulmonary hypertension.[49] Pulmonary endothelial dysfunction has been related to a lack of pulsatility.[50]
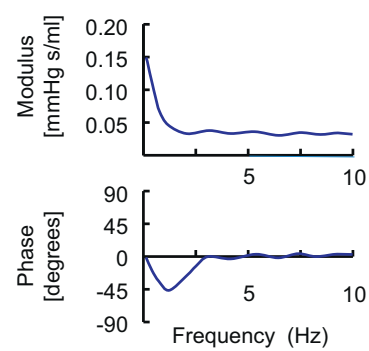
Descriptions of the pulmonary vascular load

Frequency domain

The vascular load can be fully described by calculating the input impedance. This is done in the frequency domain, pressure and flow as a function of time can be transformed to functions of frequency by the Fourier transform.[11] This transform yields a static term (also called DC term, from "direct current") and pulsatile terms (AC terms, from "alternating current") at the "harmonics" of the signal. The first harmonic is heart rate (HR), higher harmonics are multiples. Hemodynamic signals are adequately described by harmonics up to 10 times the heart rate. The static components of pressure and flow are mPAP and CO, respectively.

By using Ohm's law in the frequency domain, the input impedance (Fig. 55.3) is calculated by dividing the Fourier transforms of pressure and flow.[51−53]

The DC term (or zeroth harmonic) of the input impedance gives PVR. The steep drop in the modulus (magnitude) of the impedance and the negative phase after the zeroth harmonic are caused by the effect of the PAC on the pulsatile pressure−flow relation. For higher frequencies, the impedance levels out, and the phase returns to zero, indicating that the impedance behaves like a resistance. This is the characteristic impedance (Zc), which is determined by the characteristics of the proximal PA and describing the interaction of acceleration and deceleration of blood with a compliant vessel. To obtain Zc from the

FIGURE 55.2 Pressure drop in the pulmonary and systemic circulation. In the pulmonary system the decrease in pressure is more distributed over all vessels, even over the veins, while in the systemic circulation the largest pressure drop is seen in the arterioles.[11,38−40]

FIGURE 55.3 The input impedance of the pulmonary vascular load. The aspect is similar to the input impedance of the systemic vasculature, but the magnitude is lower.

input impedance spectrum (the "frequency method," see also Chapter 56), the average of the moduli of the higher frequencies (for example, 4th to 10th harmonics) is calculated. For lower harmonics, the phase is not (close to) zero, thus the impedance is not "real" (it has an "imaginary" part); for higher frequencies, the power of the signals is low, thus the signal-to-noise ratio becomes insufficient. A detailed review of the input impedance of the pulmonary circulation was written by Lammers et al.[54]

Windkessel description

The Windkessel model provides a useful simplification of the pulmonary arterial system.[55−57] The three-element Windkessel follows the frequency-domain description the input impedance well, thereby providing the values of PVR, PAC and Zc. The two-element follows the input impedance less well but can still be used for the estimation of compliance and of the arterial time constant, both discussed later.[56−58] Since the Windkessel model are "lumped" (or 0-dimensional) models, wave travel is not incorporated.

Pulmonary vascular resistance

As mentioned, PVR represents the "0th harmonic" of the input impedance; in practice it is calculated by using Ohm's law for hemodynamics

$$PVR = \frac{mPAP - PAWP}{CO} \qquad (55.1)$$

where mPAP−PAWP is the transpulmonary pressure gradient. In the field of pulmonology, often CO is expressed in l/min, together with the pressure gradient in mmHg, the units of PVR are mmHg·min/L or Wood units. When PAWP is not known or neglected, an approximation of PVR can be made which is called total pulmonary resistance (TPR):

$$TPR = \frac{mPAP}{CO} \qquad (55.2)$$

Note that in both calculations mean values are used, so oscillatory effects are not included. PVR is about a factor $10^{59−61}$ lower than the systemic vascular resistance (see sections "Differences between the systemic and pulmonary circulation" and "Normal values in the pulmonary circulation" of this chapter).

Pulmonary arterial compliance

PAC is defined as a change in volume (ΔV) for a given change in pressure (ΔP) in an experimentally isolated arterial segment filled with liquid.[59] In clinical practice, the most accurate PAC would be estimated using a 2-element Windkessel model,[58] which consists of resistance and

compliance.[60] Using measured flow waveform and resistance, arterial compliance that best predicts pulse pressure (PP) is obtained. A simpler method to estimate PAC is SV/PP,[61] assuming that there is no peripheral outflow (1-element Windkessel). In the hypothetical system to mimic an isolated arterial segment, SV is a change in volume and PP is a change in pressure. However, the end of the system is open, and therefore blood leaves the vascular bed during ejection, reducing the increase in vascular volume. SV/PP overestimates the true PAC derived from a 2-Windkessel model by 60%−80%.[56,57] Compared to the systemic circulation, accurately determining compliance in the pulmonary circulation may be even more difficult because resistive and compliant vessels overlap.[62]

PAC is 3 (or more) times higher[63−65] than systemic arterial compliance (see sections "Differences between the systemic and pulmonary circulation" and "Normal values in the pulmonary circulation" of this chapter).

Characteristic impedance

Zc is defined as input impedance in the absence of wave reflection.[59] While input impedance is represented by both moduli and phase, Zc is usually considered in terms of modulus only because the phase of Zc is close to zero. In the clinical setting, Zc can be obtained by the following two methods: (1) averaged moduli of input impedance at the higher frequencies (for example, the 4th to 10th harmonics, see the "Frequency domain" section) where fluctuations induced by reflections have settled (so-called the "frequency-domain method")[59] and 2) the slope of pressure−flow relationship in the early systole when wave reflection effects are minimal (so-called the "time-domain method")[66] (see also Chapter 56). The time-domain method avoids the complex mathematical processes such as the Fourier transform required for the frequency-domain method. On the other hand, the time-domain method needs the identification of a linear segment in the pressure−flow loops, which may carry some arbitrariness.[67] Nonetheless, if pertinently carried out, the two methods mostly show only small differences.[67]

Zc is dependent on the geometrical and mechanical properties of elastic arteries and blood viscosity,[11,59] which can be given as

$$Zc = \sqrt{\frac{\rho Eh}{2\pi^2 r^5}} \qquad (55.3)$$

where ρ: the density of blood, E: elastic modulus of proximal arteries, h: wall thickness, r: luminal radius.[11,59,68] Therefore, Zc is larger when the proximal arteries are stiffer (increasing elastic modulus), but smaller when the arteries dilate (increasing radius or cross-sectional area). The effect of Zc on the wave shape is explained in Chapter 56.

Wave reflection

In the very compliant arterial vasculature of the pulmonary circulation, wave reflection is much less pronounced than in the systemic circulation.[69] As a result, the pressure wave shape approaches a flow wave shape in appearance.[70] The differences in the pressure wave shape of the PAP and aortic pressure can be explained by wave reflection. When nitroprusside (a systemic vasodilator) is given (less wave reflection), the aortic pressure wave takes on a flowlike shape similar to PAP in the normal state, while the PAP becomes more like aortic pressure when serotonin is administered (which induces pulmonary vasoconstriction and more wave reflection) as shown in Fig. 55.4.

In Chapter 56, the increased relevance of pulse wave reflection in PH is discussed.

Relation of pressure levels

In the pulmonary circulation, sPAP and dPAP are proportional to mPAP in normal subjects and patients with several types of PH.[74–76]

$$sPAP = 1.61 \times mPAP \qquad (55.4)$$

$$dPAP = 0.62 \times mPAP \qquad (55.5)$$

The relations are shown in Fig. 55.5.[76]

The proportionality approximates the golden ratio which could be the connecting factor.[77] If, for two numbers a and b, it holds that $(a + b)/a = a/b$, then a and b are related by the golden ratio φ. From this relation it follows that $\varphi = (1 + \sqrt{5})/2$: $\varphi \approx 1.618$, $1/\varphi \approx 0.618$. The golden ratio is found in many instances in nature, e.g., describing the arrangement of flower petals and the shape of the nautilus shell. Since antiquity the golden ratio, also called "the divine proportion," has been used in art and architecture.

From the golden ratio it follows that $PP = sPAP - dPAP = 1.618 \cdot mPAP - 0.618 \cdot mPAP = 1.0 \cdot mPAP$. The proportionality allows clinical physicians to estimate mPAP and dPAP from echocardiography measured sPAP (i.e., RV systolic pressure)[76,78] (Fig. 55.5). Since the pressure levels are closely related, in pulmonary hypertension there is no "isolated systolic hypertension" as known from the systemic circulation.

Arterial time constant

The "time constant (τ)" is a term that is perhaps more common in the fields of physics and engineering. In cardiovascular physiology, the time constant explains the elapsed time for the pressure in the vascular system to decay to 37% ($\approx 1/e$, e being the Euler's number, approximately equal to 2.718; the base of the natural logarithm) of its initial value when the arterial inflow is zero. Both a large resistance and a large compliance result in a long τ: a high compliance means a large storage of volume; a high resistance limits the outflow. Both are associated with a slow drop in pressure. The time constant in pulmonary vasculature can be determined in two ways: (1) from the diastolic PA pressure decay and (2) as the product of PVR and PAC (PVR × PAC).
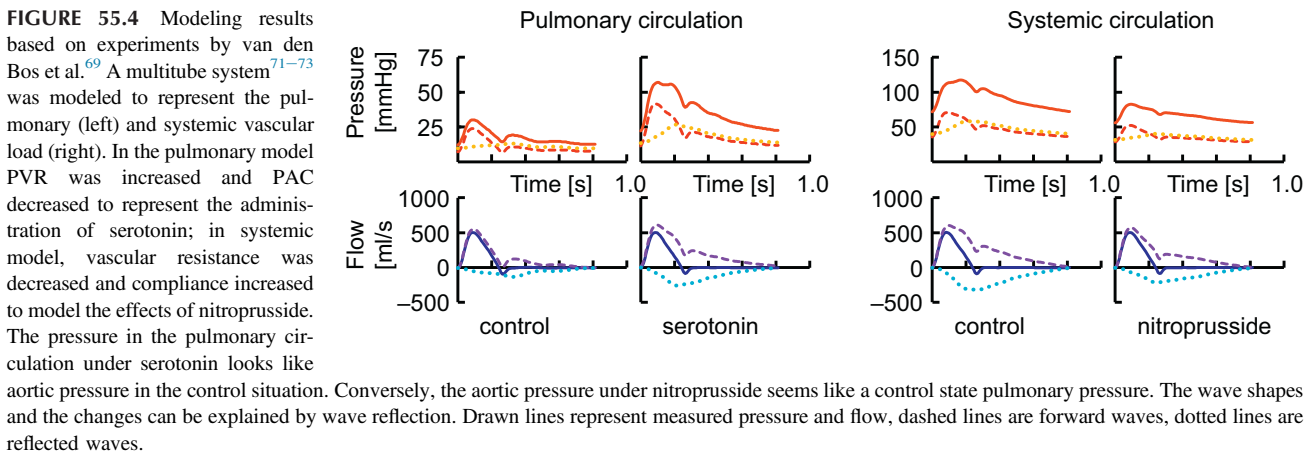
Diastolic PA pressure decay can provide the time constant as follows.
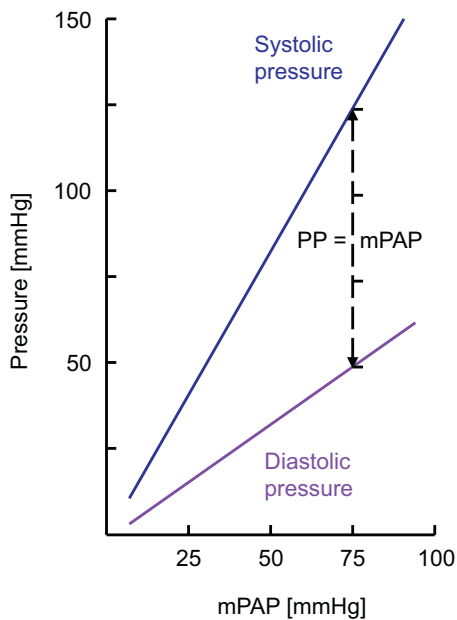
$$PAP(t) = PAPes \times e^{-t/\tau} + PAWP \qquad (55.6)$$

where PAPes is PA end-systolic pressure when the pulmonary valve closes, and τ is the time constant. As time elapses after the valve closes ($t \rightarrow \infty$), PA pressure declines asymptotically to PAWP. In this method, pressure waves are required for obtaining the time constant.

Alternatively, a simpler method to derive time constant is the product of PVR and PAC (i.e., PVR × PAC). This method is based on a 2-element Windkessel model, where PVR and PAC are connected in a parallel configuration (called RC-circuit in electrical terms, in this case a first-order low pass filter system; the time constant is often called RC-time).
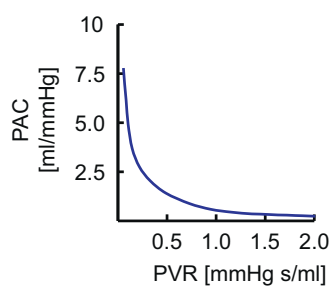
A remarkable finding is that the RC-time is constant in the pulmonary circulation, that was established by Lankhaar et al. in patients with pulmonary arterial hypertension as well as chronic thromboembolic pulmonary

FIGURE 55.4 Modeling results based on experiments by van den Bos et al.[69] A multitube system[71–73] was modeled to represent the pulmonary (left) and systemic vascular load (right). In the pulmonary model PVR was increased and PAC decreased to represent the administration of serotonin; in systemic model, vascular resistance was decreased and compliance increased to model the effects of nitroprusside. The pressure in the pulmonary circulation under serotonin looks like aortic pressure in the control situation. Conversely, the aortic pressure under nitroprusside seems like a control state pulmonary pressure. The wave shapes and the changes can be explained by wave reflection. Drawn lines represent measured pressure and flow, dashed lines are forward waves, dotted lines are reflected waves.

FIGURE 55.5 Systolic and diastolic pressure are proportional to mean pressure (*drawn lines*) in the pulmonary circulation.[74—76] The relation is such that the difference between systolic and diastolic pressure, PP, is approximately equal to mPAP. In the figure, the dashed line indicates a PP of 75 mmHg, at an mPAP of 75 mmHg.

hypertension (Fig. 55.6).[57,79] Reuben had already reported an inverse relation between PVR and PAC in 1971.[49] It is probably brought about by the unique structure of the pulmonary circulation, where resistance (Fig. 55.2) and compliance are evenly distributed over the vasculature.[80] Only 20% of PAC is found in the proximal PAs, while 80% distributed in the peripheral PAs.[81] In comparison, in the systemic circulation 60% located in the aorta.[58] Also, when one lung was removed, the RC-time remained the same, while R doubled but C halved.[81] Thus, PVR and PAC have a tight inverse relationship in the form of a hyperbola (Fig. 55.6).[57,79] These unique vascular properties in the pulmonary circulation have been suggested to explain the fixed pressure relations (see "Relation of pressure levels").[82]

FIGURE 55.6 In the pulmonary circulation, the product of resistance (PVR) and compliance (PAC) is constant, so that PAC as function of PVR shows a hyperbolic relation. PAC is reduced with increasing PVR.[57,79]

The right ventricle

Anatomy and function of the right ventricle

Ventricular anatomy

The RV is the most anterior part of the heart, located behind the sternum. It shares muscle layers with the LV, around which it is wrapped, giving the RV a crescent shape in transaction.[83] Seen from the side it has a triangular shape. Besides muscle layers, the RV and LV also share the pericardium and the septum. These anatomical features have as a consequence that the RV and LV continually interact (discussed in "Ventricular interaction").

Ventricular function

Although the function of the RV has been known since Harvey,[83] its relevance has been underestimated for a long time. Partly this is related to animal experiments that showed that circulation could be maintained by the LV alone. However, the left—right cooperation between the ventricles was disrupted when the pericardium was opened.[83] Moreover, the importance of the RV emerges from the astonishing way in which it is able to adapt to elevated pressure. Before birth, the RV contributes importantly to pressure and CO in the systemic circulation (while the pulmonary circulation is largely bypassed).[9,84,85] During exercise,[86,87] and also in the presence of continuously elevated afterload as in PH (see Chapter 56), the RV is able to cope with large increases in pressure.[78]

Descriptions of the right ventricular function

Ventricular pressure—volume relation

The ventricular pressure—volume relation (PV-relation, or PV-diagram/loop) has become the standard tool to describe the function of the RV,[88] and to obtain load-independent quantifications of systolic chamber function and diastolic stiffness, as well as insights about the energetic efficiency of the RV. The pump function graph gives some of the same information in a different representation, with the advantage that ventricular volume is not required, but CO or SV.[11,89—91]

To construct a PV-diagram, RVP and volume as a function of time are needed (see "Measurements in the pulmonary circulation"). When pressure is plotted against volume, time aspects are no longer evident; however, the loop runs in a counterclockwise manner, demonstrating that energy is generated by the RV (chamber volume decreases, while the RV generates pressure as a result muscle contraction, and receives volume while muscles are relaxed).

The area of the PV-loop is called stroke work and represents the external work of the ventricle. For further information on the pressure volume plane, we refer the

reader to Chapter 15; for further information regarding the work and energy consumption of the RV, we refer the reader to Chapter 56.

When looking at the PV-loop (Fig. 55.7), filling of the ventricle commences at the lowest left point, with the co-ordinates volume at the beginning of diastole (Vbd, which is the same as the end-systolic volume, Ves, when valves are competent) and pressure at the beginning of diastole (Pbd). With the increase of volume, the pressure increases slightly, until maximal volume is reached: end-diastolic volume (Ved) and end-diastolic pressure (Ped). When the RV starts to contract, pressure increases rapidly, first without a change in volume (the isovolumic contraction phase), until pressure at the beginning of systole is reached (Pbs) and the pulmo-nary valve opens. Pressure increases further and then de-clines, while the heart is ejecting, thus RV volume decreases. When RVP falls below PAP, the pulmonary valve closes: end-systolic pressure (Pes), and volume is at its lowest: end-systolic volume (Ves, which is the same as Vbd). Pressure in the RV drops rapidly (without changes in volume: the iso-volumic relaxation phase) until Pbd and the cycle repeats. The difference between maximal and minimal RV volume (Ved−Ves) equals SV.
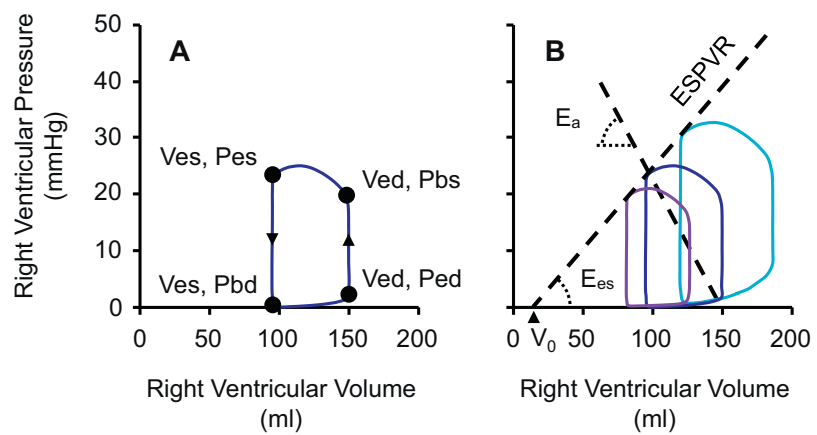
Pressure divided by volume has the units of elastance, and several elastances can be quantified and be made visible in the PV-diagram. The elastance of the ventricle varies over the cardiac cycle, elastance is low (compliance is high) in dias-tole (allowing filling of the ventricle with little increase in pressure) and elastance is high in systole (causing a pressure increase and ventricular ejection). The changes in elastance can be represented by the slope of a line that hinges around a point on the volume axis, called V_0 (or V_d for dead volume), which is the theoretical volume of the ventricle with zero pressure. During the cardiac cycle, the slope of the line in-creases little during diastolic filling, increases steeply with systole, is maximal at end-systole, then rapidly decreases. The elastance as a function of time has been described by Senzaki et al. for the LV.[94]
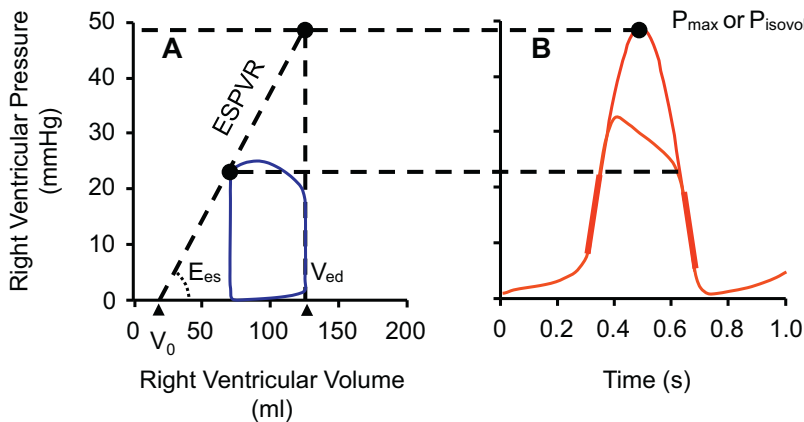
End-systolic elastance

The maximal slope of the elastance line is of great interest, as it is a load-independent measure of chamber contractility. This maximal slope is called end-systolic elastance (Ees, Fig. 55.7). Since V_0 is not known in practice, other points on this line should be found so to determine its slope. This can be approached by changing the preload of the RV, e.g., by vena cava occlusion. With less preload available to the RV, Ved, and Ped will decrease (Fig. 55.7), and with that, SV will be reduced, and Ves and Pes will descend along the line that describes the contractility of the RV.[92,93] The slope of the line, however, remains the same independent of the preload changes. Several loops can be obtained during the preload reduction and connecting the end-systolic pressure−volume points allows for constructing the end-systolic pressure−volume relation (ESPVR), the slope of which is, as mentioned, Ees. The assumption that the ESPVR is a straight line is a simplification that can cause errors depending on the amount and direction of the preload changes. This has con-sequences for the determination of Ees and of V_0,[95] as was demonstrated in the systemic circulation[95] and discussed in the pulmonary circulation.[96]

The construction of the ESPVR requires simultaneous measurement of ventricular pressure and volume (e.g., with the conductance catheter), and an intervention to change preload, which is usually not feasible, although a Valsalva maneuver has been used.[97] As an alternative to the multiple-loop method, a single beat method has been proposed by Sunagawa et al.,[98] extended by Senzaki et al.[94] and validated for the RV by Brimioulle et al.[99] Nonetheless, many caveats known from studies on the systemic circulation[100] and recently discussed for the pulmonary circulation[101] should be kept in mind. The single beat method assumes that the maximal pressure that can be reached by the RV, without ejecting, can the approximated by extrapolating the iso-volumic contraction phase and isovolumic relaxation phase with a sine curve (Fig. 55.8). The maximal pressure of the sine is called Pmax, or Pisovol, since an isovolumic contraction is

FIGURE 55.7 (A) The pressure−volume diagram of the RV. Filling commences at the point labeled Ves, Pbd: end-systolic volume and pressure at the beginning of diastole. Maximal volume is reached at Ved, Ped: end-diastolic volume and end-diastolic pressure. The isovolumic contraction phase ends in Ved, Pbs: same volume, pressure at the beginning of systole. Ejection starts and continues to Ves, Pes: end-systolic volume, as mentioned, and end-systolic pressure. Pressure falls with no change in volume, the isovolumic relaxation phase. When pressure turns Pbd again, the loop is closed. (B) When the preload of the RV changes, differing loops are generated. The end-systolic pres-sure−volume relation (ESPVR) is the line that can be drawn through the end-systolic pressure−volume points. The slope of the ESPVR is called end-systolic elastance (Ees), a measure of the contractility of the RV.[92,93]

FIGURE 55.8 The single beat method (A) to determine Ees uses a fit of a sine wave to the isovolumic contraction and isovolumic relaxation phases of RVP as a function of time (B), assuming it describes the pressure in the RV when it cannot eject. The maximal pressure of the isovolumic contraction is Pmax (also called Pisovol or Piso). In the pressure—volume plane (A), the isovolumic contraction is represented by a dashed vertical line (only pressure increase, no volume change) going up to Pmax. Then, the ESPVR can be determined by from the two points Ved, Pmax, and Ves, Pes. Ees (and V_0) can now be calculated.

mimicked. An isovolumic contraction in the PV-diagram would be represented by an increase to Pmax without a change in volume (volume remains equal to Ved) (Fig. 55.8, left panel, right dashed line). Together with the end-systolic pressure—volume point of one PV-loop, the slope of the ESPVR can be determined and thus contractility:

Ees = (Pmax − Pes)/(Ved − Ves) = (Pmax − Pes)/SV. Instead of Pes, often mPAP is used since it can be more readily and reliably obtained.
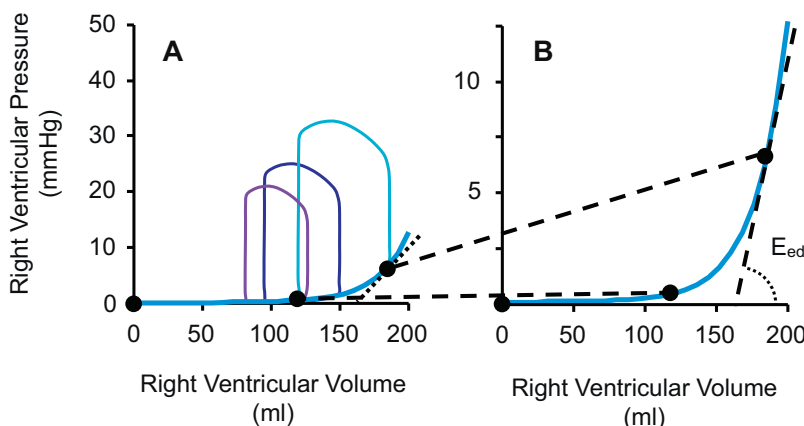
Arterial elastance

A convenient heart-independent description of load that can be plotted in the PV-diagram is arterial elastance (Ea).[102] It is the slope of a line that is defined by the ratio Pes/SV (Fig. 55.7). Although Ea has the units of elastance, it has nothing to do with the elastance (or its reciprocal value PAC) of the pulmonary vasculature.[102] In fact, it is related to the heart-independent load description TPR, but without HR (which is absent in the PV-diagram). After all, TPR is mPAP/CO; since CO = SV·HR, TPR = mPAP/(SV·HR), and as we have seen that instead of Pes, mPAP can be used,[87,103−105]   Ea = Pes/SV ≈ mPAP/SV.   Thus, Ea = TPR·HR. That Ea is a nonpulsatile description of load can also be appreciated from the fact that a steady

pressure is used (Ees or mPAP) and not a ΔP such as PP which is used for the calculation of PAC from SV/PP (see section "Pulmonary arterial compliance"). Besides this theoretical demonstration that Ea is a representation of nonpulsatile load, modeling approaches[106] and cohort studies demonstrate the same.[107] From the strong dependency on heart rate it follows that it (as well as diastolic and systolic duration) is required to remain constant.[100] As discussed, the contribution of downstream pressure (PAWP) to mPAP is relatively important compared to the role of CVP in the systemic circulation. Therefore, neglecting PAWP in the calculation of Ea is a point of concern, that has not yet been resolved.

End-diastolic elastance

Like systolic function, diastolic function of the RV can be determined from the PV-diagram, by assessing the lower part of the loop (Fig. 55.9, left panel). Ideally, again preload changes are imposed, resulting in several different loops. From the end-diastolic points, an end-diastolic pressure—volume relation (EDPVR) can be constructed. The slope of the EDPVR at the end-diastolic pressure—volume point represents the stiffness, called end-diastolic elastance (Eed) of the RV. Eed the reveals much pressure is needed to fill

FIGURE 55.9 Multiple loops in the pressure—volume plane (A) give insight in the end-diastolic elastance of the RV.[93] Multiple loops however are difficult to obtain. The single beat method to determine Eed uses an exponential function (giving pressure as function of volume) to approximate the EDPVR. The following pressure—volume points are used: 0, 0; Ves, Pbd (end-systolic volume equaling begin-diastolic volume, and begin-diastolic pressure); and Ved, Ped (end-diastolic volume, and end-diastolic pressure, see also Fig. 55.7). In (B), these points and the fit are shown on an expanded scale. In the end-diastolic point, the tangent to the exponential curve is drawn (A: *dotted*; B: *dashed*). The slope in (Eed, Ped) can be calculated as measure of end-diastolic elastance Eed from the derivative of the exponential function.[103,104]

the RV to the Ved. The relation between pressure and volume of the passive RV is highly nonlinear, steeply increasing for high volumes. Eed can be affected by disease[103] (see Chapter 56).

Calculating Eed from multiple loops[93] gives the most reliable results, however, these are difficult to obtain. Therefore, also a single beat method to determine Eed is being used[103,104] (Fig. 55.9). Fitting an exponential function through the points (0,0), (Ees, Pes), and (Eed, Ped), the EDPVR can be approximated, and from the derivative of the function the slope in (Eed, Ped) can be calculated. The exponential used to describe the pressure–volume relation is $P = \alpha[\exp(\beta V) - 1]$, with P and V being pressure and volume, and α and β curve-fitting constants, β represents a diastolic stiffness constant. The derivative of the function is $dP/dV = \alpha\beta \times \exp(\beta V)$; filling in Ved gives the slope in that point, thus $Eed = \alpha\beta \times \exp(\beta Ved)$.[103,104] Both β as well as Eed are used to describe diastolic RV stiffness, Eed specifically when the RV is maximally filled.

Ventricular interaction

The interaction between the RV and the LV[108] is determined by the circuitry (being connected in series, "series interaction") and by the shared anatomy[109] ("parallel interaction," also called "direct interdependence" or "direct interaction"). In series interaction, the contribution of (elevated) LAP to PAP "passive backward transmission of left-sided filling pressures")[110] is of relevance, particularly in left-sided failure. In addition, the (reduction of) CO of the one ventricle is important since it determines the CO of the other ventricle.[111]

In normal physiology, the effect of the LV on the RV is much greater than vice versa. In PH (see Chapter 56), leftward septal bowing caused by a prolonged RV contraction time of the RV[112] hampers LV filling.[111]

Ventriculoarterial coupling

Maximal power or efficiency: energetic coupling

Ventriculoarterial coupling is a term that is often used broadly to describe interactions between the RV and its vascular load. Here we intend RV coupling to relate to the concept that the RV is working in a way such that maximal external power is produced, or in a way that efficiency is highest. These need not be identical but are close in practice.[11] Mean output power is calculated from mPAP times CO. Input power can be calculated from oxygen consumption.[113] The ratio of output power and input power is efficiency.[11]

As mentioned earlier in this chapter ("Ventricular pressure-volume relation"), the area of the PV-loop represents the external work of the ventricle. The pressure–

volume area enclosed by the ESPVR, the EDPVR, and the isovolumic contraction limb (dashed vertical line in Fig. 55.8) is related to cardiac oxygen consumption.[114] In PH, higher RV contractility and ventricular dilatation will thus increase pressure–volume area, see Chapter 56.

Ventriculoarterial coupling determined from the pressure–volume relation

For the LV it has been shown that external work to the arterial load is maximized when the ventricular and arterial elastances are equal, thus the ratio Ees/Ea = 1; while for Ees/Ea = 2, maximal efficiency is reached.[115] It has been proposed that the ventricle adapts to its load, in pulmonary hypertension Ea increases and Ees follows suit by increasing contractility and ventricular wall thickness.[78] As long as coupling is preserved, SV can be maintained. In the end stage of pulmonary hypertension, the ventricle uncouples, and SV is reduced. Uncoupling is associated with increased ventricular volumes and increased wall stress.[13]

Surrogate measures of ventriculoarterial coupling in the pressure–volume plane

Since Ees = (Pmax − Pes)/SV, and since Ea = Pes/SV, the Ees/Ea ratio is a pressure-only relation: Ees/Ea = (Pmax − Pes)/Pes. A volume-only approach would be of interest since it could be obtained noninvasively. As described earlier in this chapter, Ees can also be calculated from Pes/(Ves − V$_0$); together with Ea the ratio is then Ees/Ea = [Pes/(Ves − V$_0$)]/[Pes/SV] = SV/(Ves − V$_0$). It has been suggested to neglect V$_0$, giving Ees/Ea ≈ SV/Ves.[116,117] However, V$_0$ is not negligible, particularly not in patients with a dilated RV.[118] Moreover, SV/Ves is inversely related to RV EF. After all, EF = SV/Ved, and Ves = Ved − SV   thus,   SV/Ves = SV/(Ved − SV). Dividing numerator and denominator by Ved, we get [SV/Ved]/(Ved/Ved − SV/Ved) = EF/(1 − EF). This simplified volume-only approach gives no information over and above EF; furthermore, it has not been shown to represent coupling. See also Chapter 56.

Differences between the systemic and pulmonary circulation

Here we list some marked differences between the systemic and pulmonary circulations (Table 55.1).

Normal values in the pulmonary circulation

Normal values for pressures of pulmonary circulation and volumes and intrinsic characteristics of the pulmonary cardiovascular system are collected in Table 55.2.

TABLE 55.1 Differences between the systemic and pulmonary circulations.

Systemic	Pulmonary
Aorta forms a central reservoir: Most of the compliance is situated in the aorta	Arteries form a distributed reservoir: compliance is distributed over the arteries
Venous compliance 20 times larger than arterial compliance (much storage in veins)	Venous compliance 2 times larger than arterial compliance (little storage in veins)
One main artery with branching according to organ site and need (wide or narrow, long or short: e.g., kidneys receive 20%—25% of CO which is accommodated by short wide arteries, while the bronchial arteries are relatively long and narrow, only some 1—2% of CO needs to be transported)	From two main pulmonary arteries, branching into three daughter vessels (each of comparable diameter)
Many arteries are accompanied by 2 veins: the approximate ratio of veins:arteries = 2:1 (except for the largest vessels, where the ratio = 1:1, e.g., descending aorta and inferior vena cava)	Most of the arteries have 1 accompanying vein: overall the ratio of veins:arteries = 1:1 (except for the largest vessels, where the ratio = 2:1, e.g., two left and two right pulmonary veins and one left and one right pulmonary artery)
Little resistance in supplying arteries and collecting veins. Main pressure-drop over arterioles of organ/tissue	Resistance is more gradually increasing in the supplying arteries toward the arterioles, and more gradually decreasing in collecting veins. Little pressure-drop over arterioles
Hypoxic vasodilatation	Hypoxic vasoconstriction

TABLE 55.2 Normal values.

Pressures	Middle	Min	Max
Systolic pulmonary pressure (sPAP, mmHg)	22	16	32
Diastolic pulmonary pressure (dPAP, mmHg)	9	6	13
Mean pulmonary pressure (mPAP, mmHg)	14	10	20
Pulmonary artery wedge pressure (PAWP, mmHg)	10	5	15
Systolic right ventricular pressure (sRVP, mmHg)	22	16	32
(End) Diastolic right ventricular pressure (dRVP, mmHg)	7	2	10
Right atrial pressure (RAP, mmHg)	4	2	6
Volumes			
Right ventricular end-systolic volume (Ves, mL)	55	10	100
Right ventricular end-diastolic volume (Ved, mL)	140	60	220
Right ventricular ejection fraction (EF, %)	60	45	75
Intrinsic characteristics			
Pulmonary vascular resistance (PVR, mmHg·s/mL)	0.1	0.055	0.18
Pulmonary arterial compliance (PAC, mL/mmHg)	4	—	12
Characteristic impedance (Zc, mmHg·s/mL)	0.017	—	—
End-systolic elastance (Ees, mmHg/ml)	1.3	—	—
End-diastolic elastance (Eed, mmHg/mL)	0.2	—	—

The values in the table are based on several studies.[3,51,63,80,83,103,119—123]

Summary

In this chapter, we described physiologic concepts to understand the pulmonary circulation. Based on measurements, we looked at pulsatile and static hemodynamics, and derived descriptions of the cardiovascular system and ventricular–arterial interaction.

It is useful to distinguish between system characteristics, determined by the interaction between the RV and arterial load, which can typically be obtained by measurement of pressure, flow, or volume, e.g., PAP, CO, or EF. Intrinsic characteristics can be obtained by combining measurements, e.g., PVR and input impedance from PA pressure and flow, or Ees and Eed from RVP and volume.

Therefore, we started by describing measurements relevant to the pulmonary circulation (system characteristics). These measurements allowed us to determine intrinsic characteristics, the heart-independent vascular load, and the load-independent RV function. Finally, by combining intrinsic characteristics of the heart (Ees) and its vascular load (Ea), coupling could be defined: the condition in which ventricular–arterial interaction is optimally efficient.

Several features unique to the pulmonary circulation were discussed, such as the golden ratio relation between pressure levels and the constant RC-time and ended with a listing of differences between pulmonary and systemic circulation, and a collection of normal values of the pulmonary hemodynamics and the cardiovascular system.

References

1. Vonk Noordegraaf A, Chin KM, Haddad F, et al. Pathophysiology of the right ventricle and of the pulmonary circulation in pulmonary hypertension: an update. **Eur Respir J**. 2019; 53.
2. Stergiopulos N, Meister JJ, Westerhof N. Determinants of stroke volume and systolic and diastolic aortic pressure. **Am J Physiol**. 1996; 270:H2050–H2059.
3. Rosenkranz S, Preston IR. Right heart catheterisation: best practice and pitfalls in pulmonary hypertension. **Eur Respir Rev**. 2015; 24:642–652.
4. D'Alto M, Dimopoulos K, Coghlan JG, Kovacs G, Rosenkranz S, Naeije R. Right heart catheterization for the diagnosis of pulmonary hypertension: controversies and practical issues. **Heart Fail Clin**. 2018; 14:467–477.
5. Kovacs G, Avian A, Pienn M, Naeije R, Olschewski H. Reading pulmonary vascular pressure tracings. How to handle the problems of zero leveling and respiratory swings. **Am J Respir Crit Care Med**. 2014; 190:252–257.
6. Galie N, Humbert M, Vachiery JL, et al. 2015 ESC/ERS guidelines for the diagnosis and treatment of pulmonary hypertension: the joint task force for the diagnosis and treatment of pulmonary hypertension of the European Society of Cardiology (ESC) and the European respiratory Society (ERS): endorsed by: Association for European Paediatric and Congenital Cardiology (AEPC), International Society for Heart and Lung Transplantation (ISHLT). **Eur Respir J**. 2015; 46:903–975.
7. Swan HJ, Ganz W, Forrester J, Marcus H, Diamond G, Chonette D. Catheterization of the heart in man with use of a flow-directed balloon-tipped catheter. **N Engl J Med**. 1970; 283:447–451.
8. Broome M, Maksuti E, Bjallmark A, Frenckner B, Janerot-Sjoberg B. Closed-loop real-time simulation model of hemodynamics and oxygen transport in the cardiovascular system. **Biomed Eng Online**. 2013; 12:69.
9. Boron WF, Boulpaep EL. **Medical Physiology**. Elsevier Health Sciences; 2008.
10. D'Alonzo GE, Barst RJ, Ayres SM, et al. Survival in patients with primary pulmonary hypertension. Results from a national prospective registry. **Ann Intern Med**. 1991; 115:343–349.
11. Westerhof N, Stergiopulos N, Noble NIM, Westerhof BE. **Snapshots of Hemodynamics**. 3rd ed. ed. Springer; 2018.
12. Arts T, Bovendeerd PH, Prinzen FW, Reneman RS. Relation between left ventricular cavity pressure and volume and systolic fiber stress and strain in the wall. **Biophys J**. 1991; 59:93–102.
13. Westerhof BE, Saouti N, van der Laarse WJ, Westerhof N, Vonk Noordegraaf A. Treatment strategies for the right heart in pulmonary hypertension. **Cardiovasc Res**. 2017; 113:1465–1473.
14. Peacock AJ, Naeije R, Rubin LJ. **Pulmonary Circulation: Diseases and Their Treatment**. 4th ed. CRC Press; 2016.
15. Luchsinger PC, Seipp Jr HW, Patel DJ. Relationship of pulmonary artery-wedge pressure to left atrial pressure in man. **Circ Res**. 1962; 11:315–318.
16. Cope DK, Allison RC, Taylor AE. A simple method to determine pulmonary capillary-pressure. **Anesthesiology**. 1987; 67:866–868.
17. Holloway H, Perry M, Downey J, Parker J, Taylor A. Estimation of effective pulmonary capillary pressure in intact lungs. **J Appl Physiol Respir Environ Exerc Physiol**. 1983; 54:846–851.
18. Cope DK, Grimbert F, Downey JM, Taylor AE. Pulmonary capillary pressure: a review. **Crit Care Med**. 1992; 20:1043–1056.
19. Pellett AA, Johnson RW, Morrison GG, Champagne MS, deBoisblanc BP, Levitzky MG. A comparison of pulmonary arterial occlusion algorithms for estimation of pulmonary capillary pressure. **Am J Respir Crit Care Med**. 1999; 160:162–168.
20. Cope DK, Allison RC, Parmentier JL, Miller JN, Taylor AE. Measurement of effective pulmonary capillary pressure using the pressure profile after pulmonary artery occlusion. **Crit Care Med**. 1986; 14:16–22.
21. Souza R, Amato MB, Demarzo SE, et al. Pulmonary capillary pressure in pulmonary hypertension. **Crit Care**. 2005; 9:R132–R138.
22. Truijen J, Westerhof BE, Kim YS, et al. The effect of haemodynamic and peripheral vascular variability on cardiac output monitoring: thermodilution and non-invasive pulse contour cardiac output during cardiothoracic surgery. **Anaesthesia**. 2018; 73:1489–1499.
23. Conway J. Clinical assessment of cardiac output. **Eur Heart J**. 1990; 11(Suppl I):148–150.
24. Conway J, Lund-Johansen P. Thermodilution method for measuring cardiac output. **Eur Heart J**. 1990; 11(Suppl I):17–20.
25. Stewart GN. Researches on the circulation time in organs and on the influences which affect it: parts I.—III. **J Physiol**. 1893; 15:1–89.
26. Hamilton WF, Moore JW, Kinsman JM, Spurling RG. Studies on the circulation. IV. Further analysis of the injection method, and of changes in hemodynamics under physiological and pathological conditions. **Am J Physiol**. 1932; 99:534–551.

27. Rudski LG, Lai WW, Afilalo J, et al. Guidelines for the echocardiographic assessment of the right heart in adults: a report from the American Society of Echocardiography endorsed by the European Association of Echocardiography, a registered branch of the European Society of Cardiology, and the Canadian Society of Echocardiography. **J Am Soc Echocardiogr**. 2010; 23:685—713. quiz 786-8.

28. van de Veerdonk MC, Marcus JT, Bogaard HJ, Vonk Noordegraaf A. State of the art: advanced imaging of the right ventricle and pulmonary circulation in humans (2013 Grover Conference series). **Pulm Circ**. 2014; 4:158—168.

29. Vonk-Noordegraaf A, van Wolferen SA, Marcus JT, et al. Noninvasive assessment and monitoring of the pulmonary circulation. **Eur Respir J**. 2005; 25:758—766.

30. Mauritz GJ, Kind T, Marcus JT, et al. Progressive changes in right ventricular geometric shortening and long-term survival in pulmonary arterial hypertension. **Chest**. 2012; 141:935—943.

31. van der Bruggen CE, Handoko ML, Bogaard HJ, et al. The value of hemodynamic measurements or cardiac magnetic resonance imaging in the follow-up of patients with idiopathic pulmonary arterial hypertension. **Chest**. 2021; 159:1575—1585.

32. Baan J, van der Velde ET, de Bruin HG, et al. Continuous measurement of left ventricular volume in animals and humans by conductance catheter. **Circulation**. 1984; 70:812—823.

33. Shigemi K, Fuke S, Une D, et al. Physiological insights of recent clinical diagnostic and therapeutic technologies for cardiovascular diseases. **J Physiol Sci**. 2017; 67:655—672.

34. Horsfield K. Morphometry of the small pulmonary arteries in man. **Circ Res**. 1978; 42:593—597.

35. Huang W, Yen RT, McLaurine M, Bledsoe G. Morphometry of the human pulmonary vasculature. **J Appl Physiol**. 1996; 81:2123—2133.

36. Galie N, Humbert M, Vachiery JL, et al. 2015 ESC/ERS guidelines for the diagnosis and treatment of pulmonary hypertension: the joint task force for the fiagnosis and treatment of pulmonary hypertension of the European Society of Cardiology (ESC) and the European respiratory Society (ERS): endorsed by: Association for European Paediatric and Congenital Cardiology (AEPC), International Society for Heart and Lung Transplantation (ISHLT). **Eur Heart J**. 2016; 37:67—119.

37. Jansen JR, Schreuder JJ, Settels JJ, Kloek JJ, Versprille A. An adequate strategy for the thermodilution technique in patients during mechanical ventilation. **Intensive Care Med**. 1990; 16:422—425.

38. Bhattacharya J, Nanjo S, Staub NC. Micropuncture measurement of lung microvascular pressure during 5-HT infusion. **J Appl Physiol Respir Environ Exerc Physiol**. 1982; 52:634—637.

39. Hakim TS, Kelly S. Occlusion pressures vs. micropipette pressures in the pulmonary circulation. **J Appl Physiol**. 1989; 67:1277—1285.

40. Michel RP, Hakim TS, Freeman CR. Distribution of pulmonary vascular resistance in experimental fibrosis. **J Appl Physiol**. 1988; 65:1180—1190.

41. Brody JS, Stemmler EJ, DuBois AB. Longitudinal distribution of vascular resistance in the pulmonary arteries, capillaries, and veins. **J Clin Invest**. 1968; 47:783—799.

42. Chazova I, Loyd JE, Zhdanov VS, Newman JH, Belenkov Y, Meyrick B. Pulmonary artery adventitial changes and venous involvement in primary pulmonary hypertension. **Am J Pathol**. 1995; 146:389—397.

43. Engelberg J, Dubois AB. Mechanics of pulmonary circulation in isolated rabbit lungs. **Am J Physiol**. 1959; 196:401—414.

44. Lee GD, Dubois AB. Pulmonary capillary blood flow in man. **J Clin Invest**. 1955; 34:1380—1390.

45. Chrispin AR, Steiner RE. Pulsatile flow in the pulmonary circulation: a cinefluoroscopic study. **Br Heart J**. 1964; 26:592—599.

46. Presson Jr RG, Baumgartner Jr WA, Peterson AJ, Glenny RW, Wagner Jr WW. Pulmonary capillaries are recruited during pulsatile flow. **J Appl Physiol**. 2002; 92:1183—1190.

47. Bidani A, Flumerfelt RW, Crandall ED. Analysis of effects of pulsatile capillary blood-flow and volume on gas-exchange. **Resp Physiol**. 1978; 35:27—42.

48. Wiener F, Morkin E, Skalak R, Fishman AP. Wave propagation in pulmonary circulation. **Circ Res**. 1966; 19:834.

49. Reuben SR. Compliance of the human pulmonary arterial system in disease. **Circ Res**. 1971; 29:40—50.

50. Khambadkone S, Li J, de Leval MR, Cullen S, Deanfield JE, Redington AN. Basal pulmonary vascular resistance and nitric oxide responsiveness late after Fontan-type operation. **Circulation**. 2003; 107:3204—3208.

51. Murgo JP, Westerhof N. Input impedance of the pulmonary arterial system in normal man. Effects of respiration and comparison to systemic impedance. **Circ Res**. 1984; 54:666—673.

52. Huez S, Brimioulle S, Naeije R, Vachiery JL. Feasibility of routine pulmonary arterial impedance measurements in pulmonary hypertension. **Chest**. 2004; 125:2121—2128.

53. Hunter KS, Lee PF, Lanning CJ, et al. Pulmonary vascular input impedance is a combined measure of pulmonary vascular resistance and stiffness and predicts clinical outcomes better than pulmonary vascular resistance alone in pediatric patients with pulmonary hypertension. **Am Heart J**. 2008; 155:166—174.

54. Lammers S, Scott D, Hunter K, Tan W, Shandas R, Stenmark KR. Mechanics and function of the pulmonary vasculature: implications for pulmonary vascular disease and right ventricular function. **Compr Physiol**. 2012; 2:295—319.

55. Westerhof N, Lankhaar JW, Westerhof BE. The arterial Windkessel. **Med Biol Eng Comput**. 2009; 47:131—141.

56. Segers P, Brimioulle S, Stergiopulos N, et al. Pulmonary arterial compliance in dogs and pigs: the three-element windkessel model revisited. **Am J Physiol**. 1999; 277:H725—H731.

57. Lankhaar JW, Westerhof N, Faes TJ, et al. Quantification of right ventricular afterload in patients with and without pulmonary hypertension. **Am J Physiol Heart Circ Physiol**. 2006; 291:H1731—H1737.

58. Stergiopulos N, Segers P, Westerhof N. Use of pulse pressure method for estimating total arterial compliance in vivo. **Am J Physiol**. 1999; 276:H424—H428.

59. Vlachopoulos C, O'Rourke M, Nichols WW. **McDonald's Blood Flow in Arteries: Theoretical, Experimental and Clinical Principles**. CRC Press; 2011.

60. Frank O. Die Grundform des arteriellen pulses. **Z Biol**. 1899; 37:483—526.

61. Chemla D, Hebert JL, Coirault C, et al. Total arterial compliance estimated by stroke volume-to-aortic pulse pressure ratio in humans. **Am J Physiol**. 1998; 274:H500—H505.

62. Vanden Eynden F, Bove T, Chirade ML, Van Nooten G, Segers P. Measuring pulmonary arterial compliance: mission impossible?

Insights from a novel in vivo continuous-flow based experimental model. **Pulm Circ**. 2018; 8.

63. Thenappan T, Prins KW, Pritzker MR, Scandurra J, Volmers K, Weir EK. The critical role of pulmonary arterial compliance in pulmonary hypertension. **Ann Am Thorac Soc**. 2016; 13:276−284.

64. Mahapatra S, Nishimura RA, Sorajja P, Cha S, McGoon MD. Relationship of pulmonary arterial capacitance and mortality in idiopathic pulmonary arterial hypertension. **J Am Coll Cardiol**. 2006; 47:799−803.

65. Pellegrini P, Rossi A, Pasotti M, et al. Prognostic relevance of pulmonary arterial compliance in patients with chronic heart failure. **Chest**. 2014; 145:1064−1070.

66. Li JK. Time domain resolution of forward and reflected waves in the aorta. **IEEE Trans Biomed Eng**. 1986; 33:783−785.

67. Westerhof N, Segers P, Westerhof BE. Wave separation, wave intensity, the reservoir-wave concept, and the instantaneous wave-free ratio: presumptions and principles. **Hypertension**. 2015; 66:93−98.

68. Wang Z, Chesler NC. Pulmonary vascular wall stiffness: an important contributor to the increased right ventricular afterload with pulmonary hypertension. **Pulm Circ**. 2011; 1:212−223.

69. van den Bos GC, Westerhof N, Randall OS. Pulse wave reflection: can it explain the differences between systemic and pulmonary pressure and flow waves? A study in dogs. **Circ Res**. 1982; 51:479−485.

70. Naeije R, Huez S. Reflections on wave reflections in chronic thromboembolic pulmonary hypertension. **Eur Heart J**. 2007; 28:785−787.

71. Westerhof N, Bosman F, De Vries CJ, Noordergraaf A. Analog studies of the human systemic arterial tree. **J Biomech**. 1969; 2:121−143.

72. Westerhof BE, van Gemert MJC, van den Wijngaard JP. Pressure and flow relations in the systemic arterial tree throughout development from newborn to adult. **Front Pediatr**. 2020; 8:251.

73. van den Wijngaard JP, Siebes M, Westerhof BE. Comparison of arterial waves derived by classical wave separation and wave intensity analysis in a model of aortic coarctation. **Med Biol Eng Comput**. 2009; 47:211−220.

74. Chemla D, Castelain V, Humbert M, et al. New formula for predicting mean pulmonary artery pressure using systolic pulmonary artery pressure. **Chest**. 2004; 126:1313−1317.

75. Syyed R, Reeves JT, Welsh D, Raeside D, Johnson MK, Peacock AJ. The relationship between the components of pulmonary artery pressure remains constant under all conditions in both health and disease. **Chest**. 2008; 133:633−639.

76. Handoko ML, De Man FS, Oosterveer FP, Bogaard HJ, Vonk-Noordegraaf A, Westerhof N. A critical appraisal of transpulmonary and diastolic pressure gradients. **Physiol Rep**. 2016; 4.

77. Chemla D, Boulate D, Weatherald J, et al. Golden ratio and the proportionality between pulmonary pressure components in pulmonary arterial hypertension. **Chest**. 2019; 155:991−998.

78. Vonk Noordegraaf A, Westerhof BE, Westerhof N. The relationship between the right ventricle and its load in pulmonary hypertension. **J Am Coll Cardiol**. 2017; 69:236−243.

79. Lankhaar JW, Westerhof N, Faes TJ, et al. Pulmonary vascular resistance and compliance stay inversely related during treatment of pulmonary hypertension. **Eur Heart J**. 2008; 29:1688−1695.

80. Slife DM, Latham RD, Sipkema P, Westerhof N. Pulmonary arterial compliance at rest and exercise in normal humans. **Am J Physiol**. 1990; 258:H1823−H1828.

81. Saouti N, Westerhof N, Helderman F, et al. RC time constant of single lung equals that of both lungs together: a study in chronic thromboembolic pulmonary hypertension. **Am J Physiol Heart Circ Physiol**. 2009; 297:H2154−H2160.

82. Kind T, Faes TJ, Vonk-Noordegraaf A, Westerhof N. Proportional relations between systolic, diastolic and mean pulmonary artery pressure are explained by vascular properties. **Cardiovasc Eng Technol**. 2011; 2:15−23.

83. Haddad F, Hunt SA, Rosenthal DN, Murphy DJ. Right ventricular function in cardiovascular disease, part I: anatomy, physiology, aging, and functional assessment of the right ventricle. **Circulation**. 2008; 117:1436−1448.

84. McGovern M, Miletin J. Cardiac output monitoring in oreterm infants. **Front Pediatr**. 2018; 6:84.

85. de Boode WP. Advanced hemodynamic monitoring in the neonatal intensive care unit. **Clin Perinatol**. 2020; 47:423−434.

86. Kovacs G, Berghold A, Scheidl S, Olschewski H. Pulmonary arterial pressure during rest and exercise in healthy subjects: a systematic review. **Eur Respir J**. 2009; 34:888−894.

87. Spruijt OA, de Man FS, Groepenhoff H, et al. The effects of exercise on right ventricular contractility and right ventricular-arterial coupling in pulmonary hypertension. **Am J Respir Crit Care Med**. 2015; 191:1050−1057.

88. Maughan WL, Shoukas AA, Sagawa K, Weisfeldt ML. Instantaneous pressure-volume relationship of the canine right ventricle. **Circ Res**. 1979; 44:309−315.

89. Elzinga G, Westerhof N. How to quantify pump function of the heart. The value of variables derived from measurements on isolated muscle. **Circ Res**. 1979; 44:303−308.

90. Elzinga G, Westerhof N. Pump function of the feline left heart: changes with heart rate and its bearing on the energy balance. **Cardiovasc Res**. 1980; 14:81−92.

91. Overbeek MJ, Lankhaar JW, Westerhof N, et al. Right ventricular contractility in systemic sclerosis-associated and idiopathic pulmonary arterial hypertension. **Eur Respir J**. 2008; 31:1160−1166.

92. Suga H, Sagawa K, Shoukas AA. Load independence of the instantaneous pressure-volume ratio of the canine left ventricle and effects of epinephrine and heart rate on the ratio. **Circ Res**. 1973; 32:314−322.

93. Rommel KP, von Roeder M, Oberueck C, et al. Load-independent systolic and diastolic right ventricular function in heart failure with preserved ejection fraction as assessed by resting and handgrip exercise pressure-volume loops. **Circ Heart Fail**. 2018; 11:e004121.

94. Senzaki H, Chen CH, Kass DA. Single-beat estimation of end-systolic pressure-volume relation in humans. A new method with the potential for noninvasive application. **Circulation**. 1996; 94:2497−2506.

95. Kass DA, Beyar R, Lankford E, Heard M, Maughan WL, Sagawa K. Influence of contractile state on curvilinearity of in situ end-systolic pressure-volume relations. **Circulation**. 1989; 79:167−178.

96. Naeije R, Brimioulle S, Dewachter L. Biomechanics of the right ventricle in health and disease. **Pulm Circ**. 2014; 4:395−406.

97. Tedford RJ, Mudd JO, Girgis RE, et al. Right ventricular dysfunction in systemic sclerosis-associated pulmonary arterial hypertension. **Circ Heart Fail**. 2013; 6:953—963.

98. Sunagawa K, Yamada A, Senda Y, et al. Estimation of the hydromotive source pressure from ejecting beats of the left ventricle. **IEEE Trans Biomed Eng**. 1980; 27:299—305.

99. Brimioulle S, Wauthy P, Ewalenko P, et al. Single-beat estimation of right ventricular end-systolic pressure-volume relationship. **Am J Physiol Heart Circ Physiol**. 2003; 284:H1625—H1630.

100. Chirinos JA. Ventricular—arterial coupling: invasive and non-invasive assessment. **Artery Res**. 2013; 7:2—14.

101. Philip JL, Chesler NC. Know your limitations: assumptions in the single-beat method for estimating right ventricular-pulmonary vascular coupling. **Am J Respir Crit Care Med**. 2018; 198:707—709.

102. Sunagawa K, Maughan WL, Burkhoff D, Sagawa K. Left ventricular interaction with arterial load studied in isolated canine ventricle. **Am J Physiol**. 1983; 245:H773—H780.

103. Trip P, Rain S, Handoko ML, et al. Clinical relevance of right ventricular diastolic stiffness in pulmonary hypertension. **Eur Respir J**. 2015; 45:1603—1612.

104. Vanderpool RR, Pinsky MR, Naeije R, et al. RV-pulmonary arterial coupling predicts outcome in patients referred for pulmonary hypertension. **Heart**. 2015; 101:37—43.

105. Gerges M, Gerges C, Pistritto AM, et al. Pulmonary hypertension in heart failure. Epidemiology, right ventricular function, and survival. **Am J Respir Crit Care Med**. 2015; 192:1234—1246.

106. Segers P, Stergiopulos N, Westerhof N. Relation of effective arterial elastance to arterial system properties. **Am J Physiol Heart Circ Physiol**. 2002; 282:H1041—H1046.

107. Chirinos JA, Rietzschel ER, Shiva-Kumar P, et al. Effective arterial elastance is insensitive to pulsatile arterial load. **Hypertension**. 2014; 64:1022—1031.

108. Belenkie I, Smith ER, Tyberg JV. Ventricular interaction: from bench to bedside. **Ann Med**. 2001; 33:236—241.

109. Janicki JS, Weber KT. The pericardium and ventricular interaction, distensibility, and function. **Am J Physiol**. 1980; 238:H494—H503.

110. Rosenkranz S, Gibbs JS, Wachter R, De Marco T, Vonk-Noordegraaf A, Vachiery JL. Left ventricular heart failure and pulmonary hypertension. **Eur Heart J**. 2016; 37:942—954.

111. Gan C, Lankhaar JW, Marcus JT, et al. Impaired left ventricular filling due to right-to-left ventricular interaction in patients with pulmonary arterial hypertension. **Am J Physiol Heart Circ Physiol**. 2006; 290:H1528—H1533.

112. Marcus JT, Gan CT, Zwanenburg JJ, et al. Interventricular mechanical asynchrony in pulmonary arterial hypertension: left-to-right delay in peak shortening is related to right ventricular overload and left ventricular underfilling. **J Am Coll Cardiol**. 2008; 51:750—757.

113. Wong YY, Westerhof N, Ruiter G, et al. Systolic pulmonary artery pressure and heart rate are main determinants of oxygen consumption in the right ventricular myocardium of patients with idiopathic pulmonary arterial hypertension. **Eur J Heart Fail**. 2011; 13:1290—1295.

114. Suga H, Yasumura Y, Nozawa T, Futaki S, Igarashi Y, Goto Y. Prospective prediction of O_2 consumption from pressure-volume area in dog hearts. **Am J Physiol**. 1987; 252:H1258—H1264.

115. Sunagawa K, Maughan WL, Sagawa K. Optimal arterial resistance for the maximal stroke work studied in isolated canine left ventricle. **Circ Res**. 1985; 56:586—595.

116. Sanz J, Garcia-Alvarez A, Fernandez-Friera L, et al. Right ventriculo-arterial coupling in pulmonary hypertension: a magnetic resonance study. **Heart**. 2012; 98:238—243.

117. Vanderpool RR, Rischard F, Naeije R, Hunter K, Simon MA. Simple functional imaging of the right ventricle in pulmonary hypertension: can right ventricular ejection fraction be improved? **Int J Cardiol**. 2016; 223:93—94.

118. Trip P, Kind T, van de Veerdonk MC, et al. Accurate assessment of load-independent right ventricular systolic function in patients with pulmonary hypertension. **J Heart Lung Transplant**. 2013; 32:50—55.

119. Saouti N, Westerhof N, Postmus PE, Vonk-Noordegraaf A. The arterial load in pulmonary hypertension. **Eur Respir Rev**. 2010; 19:197—203.

120. Stevens GR, Garcia-Alvarez A, Sahni S, Garcia MJ, Fuster V, Sanz J. RV dysfunction in pulmonary hypertension is independently related to pulmonary artery stiffness. **JACC Cardiovasc Imaging**. 2012; 5:378—387.

121. Lorenz CH, Walker ES, Morgan VL, Klein SS, Graham Jr TP. Normal human right and left ventricular mass, systolic function, and gender differences by cine magnetic resonance imaging. **J Cardiovasc Magn Reson**. 1999; 1:7—21.

122. Milnor WR, Conti CR, Lewis KB, O'Rourke MF. Pulmonary arterial pulse wave velocity and impedance in man. **Circ Res**. 1969; 25:637—649.

123. Dell'Italia LJ, Walsh RA. Application of a time varying elastance model to right ventricular performance in man. **Cardiovasc Res**. 1988; 22:864—874.

This page intentionally left blank

Chapter 56

Pulmonary arterial load and ventricular–arterial coupling in pulmonary hypertension

Masafumi Fukumitsu, Anton Vonk Noordegraaf and Berend E. Westerhof

Department of Pulmonary Medicine, Amsterdam Universitair Medische Centra, Vrije Universiteit Amsterdam, Amsterdam Cardiovascular Sciences, Amsterdam, the Netherlands

Introduction

Definition of pulmonary hypertension

Pulmonary hypertension (PH) is a pathophysiological disorder that is characterized as increased pulmonary artery (PA) pressure. In the 2015 European Society of Cardiology (ESC)/the European Respiratory Society (ERS) guidelines for the diagnosis and treatment of PH, PH is defined by a mean pulmonary artery pressure (mPAP) ≥25 mmHg at rest, measured via right heart catheterization (RHC),[1] although a new lower threshold (mPAP >20 mmHg) has been recently proposed at the sixth World Symposium on PH.[2] Based on the "downstream" pressure (left atrial pressure, represented by pulmonary artery wedge pressure, PAWP), PH is hemodynamically classified into precapillary PH and postcapillary PH. In the current guidelines, precapillary PH describes PH with PAWP ≤15 mmHg, and postcapillary PH is PH with PAWP >15 mmHg.[1]

The pathophysiological process behind the development of PH can depend on several underlying etiologies. From the viewpoint of pathophysiological characteristics, the clinical classification distinguishes PH into the following five groups (Table 56.1), group-1: pulmonary arterial hypertension (PAH); group-2: PH due to left heart diseases (LHDs); group-3: PH due to lung diseases and/or hypoxia; group-4: chronic thromboembolic PH (CTEPH) and other PA obstruction; group-5: PH with unclear and/or multifactorial mechanisms.[1] Although these five groups have pathologically distinct etiologies, all of the groups can induce severe PH, where the right ventricle (RV) function deteriorates as a consequence of increased arterial loading.[3,4] Most importantly, right-sided heart failure is the main cause of death in patients with PH.[3–6] Consequently, it is essential to establish the pathophysiological mechanisms by which the pulmonary arterial load compromises RV function in PH.

TABLE 56.1 Clinical classification of pulmonary hypertension from 2015 European Society of Cardiology/European Respiratory Society guideline.

1. Pulmonary arterial hypertension
    1.1. Idiopathic
    1.2. Heritable
    1.3. Drug and toxins induced
    1.4 Associated with
        1.4.1. Connective tissue disease
        1.4.2. Human immunodeficiency virus (HIV) infection
        1.4.3. Portal hypertension
        1.4.4. Congenital heart disease
        1.4.5. Schistosomiasis

1′ Pulmonary veno-occlusive disease and/or pulmonary capillary hemangiomatosis

1″ Persistent pulmonary hypertension of the newborn

2. Pulmonary hypertension due to left heart disease

3. Pulmonary hypertension due to lung disease and/or hypoxia

4. Chronic thromboembolic pulmonary hypertension and other pulmonary artery obstructions

5. Pulmonary hypertension with unclear and/or multifactorial mechanisms

The properties of pulmonary arterial load and right ventricular function
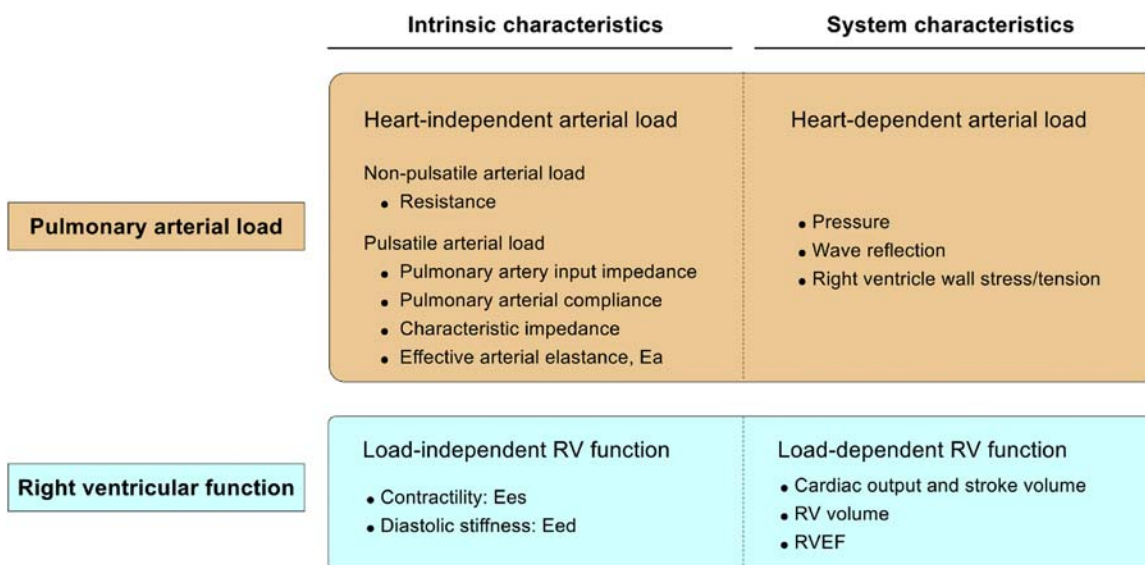
To understand the pulmonary arterial load and RV function, the terms should be described correctly. The properties of arterial load and RV function can be described in two ways (Fig. 56.1), using (1) the intrinsic characteristics and (2) the system characteristics.[7] The intrinsic characteristics of the arterial load and the RV function are "independent," and insensitive to each other. The intrinsic characteristics of arterial load (vascular properties) can be determined from the PA pressure-flow relationship, and those of RV function are given by RV pressure-volume relationship. Interaction between the intrinsic characteristics of arterial load and RV function yields the system characteristics, for example, cardiac output (CO) and RV ejection fraction (RVEF) (Fig. 56.1).

The intrinsic characteristics of arterial load (vascular properties) are called "heart-independent," and the system characteristics of arterial load are called "heart-dependent" (further referred to as heart-independent or heart-dependent arterial load). The heart-independent arterial load includes pulmonary vascular resistance (PVR), total pulmonary arterial compliance (PAC), characteristic impedance of the proximal arteries (Zc), and effective arterial elastance (Ea), implicitly assuming that heart rate (a ventricular variable) is constant. On the other hand, the heart-dependent arterial load is provided by pressure (mean, systolic and diastolic pressure, and pulse pressure),

wave reflection (magnitude and timing of reflected waves), and RV wall stress/tension (Fig. 56.1).

The intrinsic characteristics of RV function are also called "load-independent," and the system characteristics are called "load-dependent" (further referred to as load-independent or load-dependent RV function). The load-independent RV function is represented by RV contractility (represented by end-systolic RV pressure-volume relationship) and diastolic stiffness (represented by end-diastolic RV pressure-volume relationship). Load-dependent RV function includes CO, stroke volume (SV), RV volumes (RV end-diastolic volume [RVEDV] and RV end-systolic volume [RVESV]), and RVEF.

In clinical practice, the heart-dependent load (PA pressure) and the load-dependent RV function (CO and RVEF) are more commonly used; however, we have to be careful when interpreting these parameters because a change in PA pressure or in CO cannot always be attributed to a change in pulmonary vasculature or the RV. For example, whereas the RV is in a hyper-contractile state, decreased RVEF and CO are present in patients with PAH.[8] The exact interpretation requires a sufficient understanding of the heart-independent load and the load-independent RV function. This chapter explains (1) properties of pulmonary arterial load and (2) properties of the RV function in terms of intrinsic and system characteristics, and describes (3) the mechanisms of how the RV adapts to increased pulmonary arterial load in PH.

FIGURE 56.1 The properties of pulmonary arterial load and right ventricular function. The pulmonary arterial load and right ventricular functions are characterized by their intrinsic characteristics. System characteristics are derived from cardiopulmonary interaction. *Ea*, pulmonary effective arterial elastance; *RV*, right ventricle; *Ees*, end-systolic right ventricular elastance; *Eed*, end-diastolic right ventricular elastance; *RVEF*, right ventricular ejection fraction.

Pulmonary arterial load in pulmonary hypertension

Heart-independent arterial load

The heart-independent load describes the intrinsic characteristic of the arterial load, represented by PVR, total PAC, characteristic impedance of the proximal arteries (Zc), and effective arterial elastance (Ea). In the human body, the ventricle ejects blood into the vascular bed beat-by-beat, which generates arterial pressure and flow waves. Since waves are the signals which vary in time, the description of vascular properties should include not only the nonpulsatile (steady) but also pulsatile (dynamic) state. Thus, the heart-independent arterial load is further classified into nonpulsatile load and pulsatile load.

Nonpulsatile arterial load: pulmonary vascular resistance

The nonpulsatile arterial load is a vascular property in a nonpulsatile state without the emergence of waves, which is given by resistance at 0 Hz. In clinical practice, physicians can assess nonpulsatile load using PVR or total pulmonary resistance (TPR), calculated by mean values of pressure and flow. PVR is calculated as (mPAP−PAWP)/CO, where mPAP is mean pulmonary arterial pressure. CO corresponds to mean flow per one minute. TPR is calculated as mPAP/CO.

PVR represents hydraulic resistance which covers the whole pulmonary vasculature: the main trunk of pulmonary arteries, small arteries, capillaries, and veins. In PH, PVR increases as a consequence of vascular remodeling. While a 50% increase in vascular resistance in systemic hypertension is considered exceptional, PVR increases by four times or more in PH.[9] Although PVR is undoubtedly the simplest and most widely used description of arterial load, it captures only nonpulsatile load and thus ignores pulsatile load. Indeed, a reduction in PVR is not associated with improved RV function and clinical prognosis in patients with PH.[5] Thus, PVR does not provide a complete description of RV loading in PH.

Pulsatile arterial load

Pulmonary arterial input impedance

The pulsatile arterial load is nonnegligible when we treat patients with PH. Assessment of pulsatile arterial load requires an adequate understanding of pressure and flow "waves," which are generated by the heartbeat. As discussed in detail in Chapters 1 and 3, based on the magnitude and cycle length of these waves, pressure and flow waveforms can be converted to pressure and flow spectrum in the frequency domain. Physiologically, pulsatile loading can be described most completely by pulmonary arterial input impedance, which is calculated as P(f)/F(f) at each frequency, where P(f): pressure spectrum at each frequency, F(f): flow spectrum at each frequency. PA input impedance describes the vascular properties at each frequency, which consists of magnitude and phase (Fig. 56.2). Assessment of PA input impedance is feasible in clinical settings;[10,11] however, the interpretation is not straightforward for most clinicians. In this regard, the derivatives of pulmonary arterial input impedance, for example, total PAC, Ea (heart-independent load, heart rate remaining constant), and wave reflection and wall stress (heart-dependent load) may be more practical and more intuitive to understand pulsatile loading in PH. In Chapter 55, the derivation of PAC was described; here we focus on its pathological changes in PH.
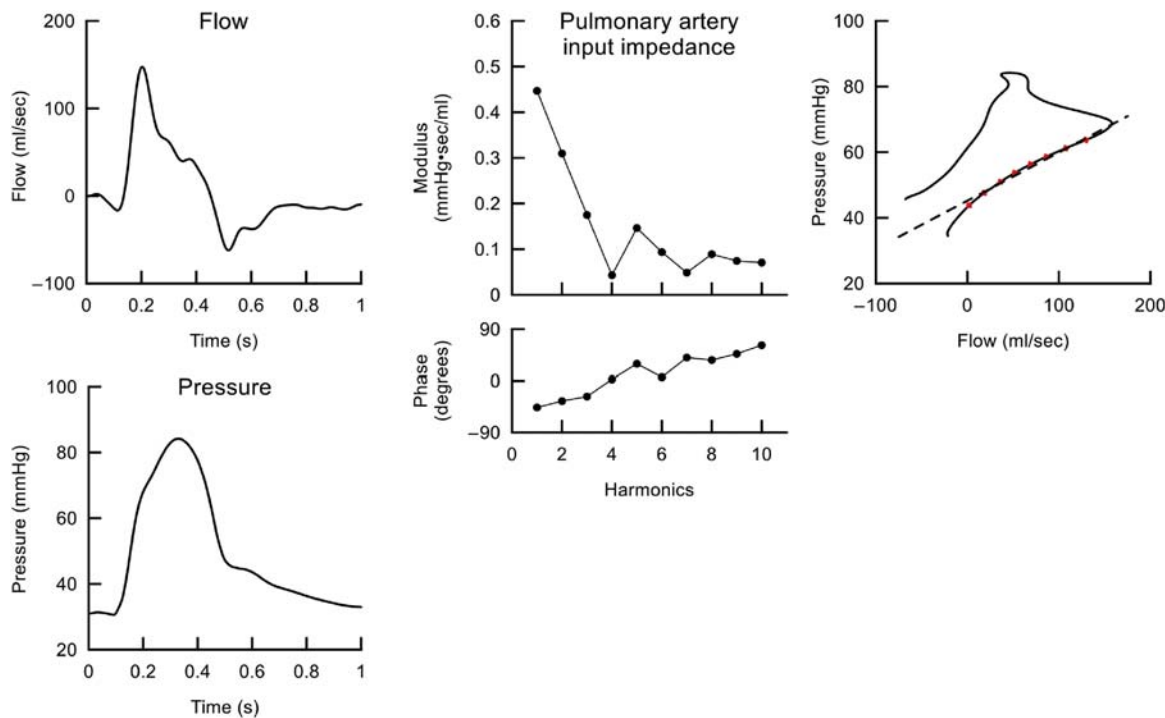
Pulmonary arterial compliance

PAC is the most used parameter to evaluate pulsatile load for patients with PH. When PAC is estimated from SV/PP, PAC is 4.0 mmHg/mL in control subjects;[12] however, PAC decreases to 30−40% (1.2−1.6 mmHg/mL) in patients with precapillary PH.[13−15] While in the systemic circulation, 60% of arterial compliance resides in the proximal aorta,[16] PAC is distributed mainly to small peripheral pulmonary vessels rather than proximal large arteries. Proximal arterial compliance estimated by magnetic resonance imaging (MRI) accounts for only 20% of total PAC for the whole pulmonary vascular bed.[14]
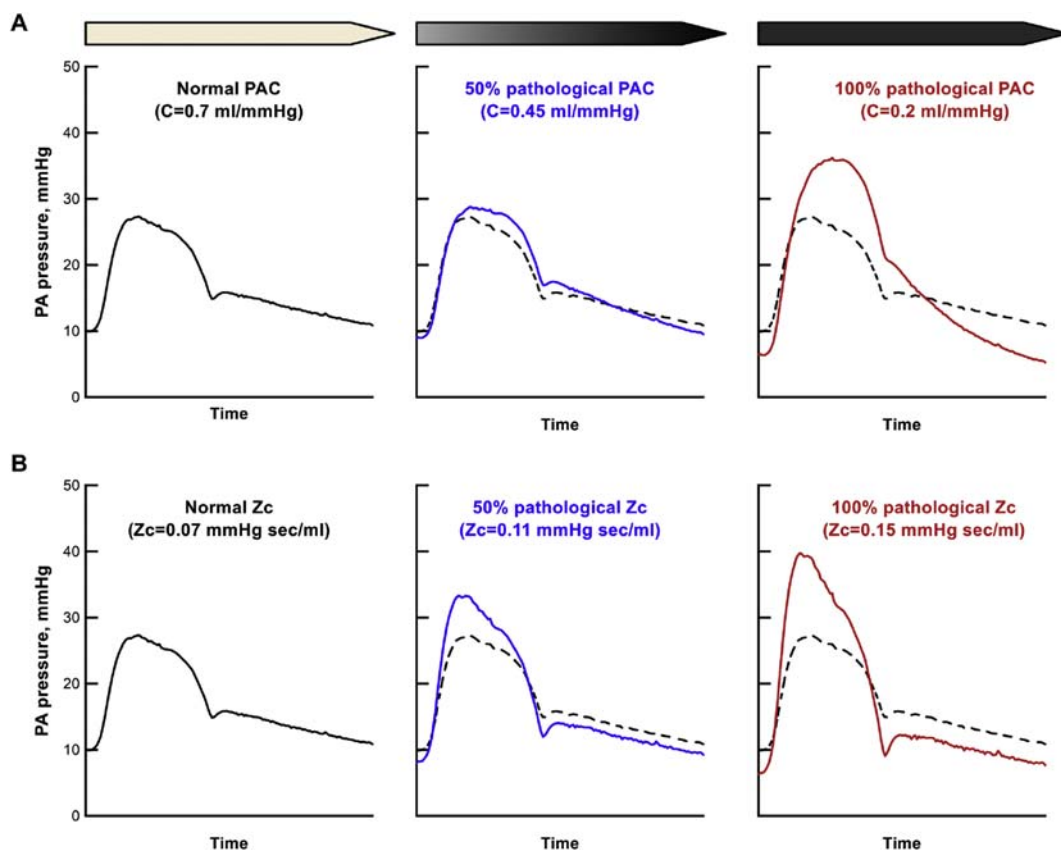
In patients with postcapillary PH, PAC derived from SV/PP can be altered by PAWP. When PVR is given as 3.0 Wood units, PAC decreases from 3.34 mmHg/mL to 1.65 mmHg/mL (50% decrease) and to 0.82 mmHg/mL (25% decrease), if PAWP increases from 0 to 25 mmHg−50 mmHg, respectively.[17] Since PAC has an inverse relationship with PVR[18] (see Chapter 55, and the section below: "Time constant of the pulmonary circulation"), PAC is reduced with increasing PVR.[12,13] Decreased PAC changes PA pressure waveform and increases systolic PAP (sPAP) independently of PVR (Fig. 56.3). Increased PA (or RV) pressure elevates RV wall stress (see section "Right ventricle wall stress/tension"). Decreased PAC is associated with exercise intolerance and clinical adverse events in patients with PH.[19−22] PAC is the key pulsatile load for the management of patients with PH.

Time constant of the pulmonary circulation

The time constant of the pulmonary circulation (which equals PVR×PAC, as discussed in detail in Chapter 55) is similar in healthy individuals and patients with PAH and CTEPH, and even after treatment.[12,13] PVR×PAC for the single lung equals to that of both lungs together.[14]

FIGURE 56.2 Pulmonary artery flow and pressure waveforms and pulmonary arterial input impedance. Pulmonary artery input impedance represents the pulmonary pressure-flow relationship at each frequency (or harmonic). Pulmonary artery input impedance consists of modulus and phase. Characteristic impedance is obtained by (1) averaged modulus in the range of high frequencies or harmonics (for example: 4th to 10th harmonics) (frequency-method) or (2) a slope of pressure-flow relationship in the early systole (time-domain method).

FIGURE 56.3 Effect of (A) pulmonary arterial compliance (PAC) and (B) characteristic impedance of the proximal arteries (Zc) on pulmonary artery pressure waveform. Data are simulation data using three-element Windkessel arterial model, which is constructed from a preclinical study of Fukumitsu. et al.[108] (A) When only PAC is decreased, PA pressure is increased, with its peak occurring in later systole. (B) When only Zc is increased from normal to pathological value of pulmonary hypertension, PA pressure is elevated steeply with its peak remaining in early systole. Both Zc and PAC alter PA pressure waves independently. Since resistance is unchanged, mean PA pressure remains a normal value in this simulation.

Although there is still a debate whether PVR×PAC is unchanged in patients with proximal obstruction of the pulmonary arteries,[23,24] a larger cohort study shows the inverse relationship of PVR and PAC in a wide range of severity of PH.[17] Of note, PVR×PAC is sensitive to pulmonary venous pressure (mean PAWP)[17]: in the calculation of PVR, PAWP is taken into account, but in the estimation of PAC from SV/PP, it is not (see Chapter 55, the SV/PP method to estimate PAC assumes that there is no outflow from the system). Therefore, the PVR×PAC product is influenced by PAWP. A more direct measurement of the time constant by analyses of the diastolic PA pressure decay (Fig. 56.4) would give an answer and reveal the effect of PAWP on the time constant in PH.[25]

The inverse relationship of PVR and PAC provides practically important insights to physicians. The change in PAC is more noticeable than the change in PVR in patients with early-stage of PH,[12] while in the more advanced-stage of PH, change in PVR is greater than that of PAC (Fig. 56.4). Therefore, PAC may be more suitable to detect the early stage of PH before an increase in PVR is marked.

Characteristic impedance of the proximal arteries

Characteristic impedance of the proximal arteries (an abbreviation is Zc) is not commonly used in clinical practice. However, Zc is important to describe the pulsatile arterial load, because Zc has the two relevant clinical implications: (1) Zc represents the vascular properties of the proximal PA, and (2) Zc plays a central role in wave reflection (see "wave reflection: wave separation analysis and wave intensity analysis").

Zc is defined as input impedance in the absence of wave reflection and can be determined in the frequency-domain (from the higher frequency range, see Chapter 55) or in
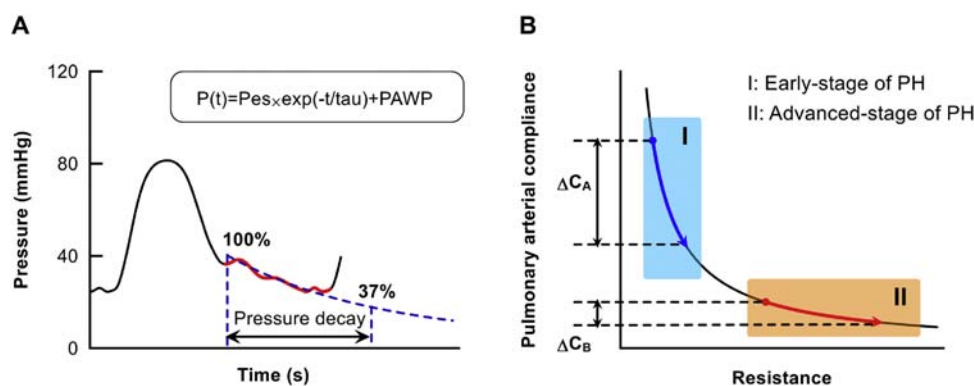
the time domain from the slope of the early systolic part of the pressure-flow relationship (Figure 56.2)[26,27]; see Chapters 1, 3 and 55. For large vessels, the Zc is a real number (whereas for smaller vessels, Zc should be described in the frequency domain with a modulus and phase).

Zc is determined by the geometry and mechanical properties of elastic arteries,[27,28] and is larger for stiffer arteries, but smaller when the arteries dilate. In clinical measurements, Zc increases 2.5- to sixfold with the development of various types of PH.[10,12,29,30]

When only Zc is increased experimentally in the systemic circulation, peak aortic pressure (systolic aortic pressure) reaches larger values and occurs earlier in the ejection period.[31] When we extrapolate this to the pulmonary circulation, increasing Zc augments pulsatile loading with an elevation in sPAP, even if PVR or PAC remains unchanged (Fig. 56.3). Given the fact that sPAP determines RV wall stress during systole (see section "Right ventricular wall stress/tension"), increased Zc would impact the RV function in PH.

Effective arterial elastance

Effective arterial elastance (an abbreviation is Ea) is a ventricle-independent measure of arterial function in the ventricular pressure-volume diagram.[32] One should bear in mind that in this pressure-volume plane description, heart rate is assumed constant. As shown in Chapter 55, heart rate is a major determinant of Ea.[33,34] Suga et al. described the ventricular contractility independent of arterial loading as the slope of the ventricular end-systolic pressure-volume relationship (ESPVR) (see section "Right ventricular contractility").[35] To understand how well the ventricle is coupled with the arterial load, the function of the arterial system is represented as "effective" arterial elastance in

FIGURE 56.4 Time constant of pulmonary circulation. (A) Calculation of time constant using diastolic pulmonary artery pressure decay. Time constant (τ) can be estimated by fitting measured pulmonary artery (PA) pressure during diastole to PAP(t) = PAPes × exp(−t/τ) + PAWP, where PAPes is end-systole PA pressure and PAWP is mean PA wedge pressure. (B) The pulmonary vascular resistance (resistance)—pulmonary arterial compliance (PAC) relationship. In early stage pulmonary hypertension (PH), the change of PAC is more readily noticed than that in resistance. In advanced-stage PH, the change of resistance is more easily detectable, while that of PAC is small.
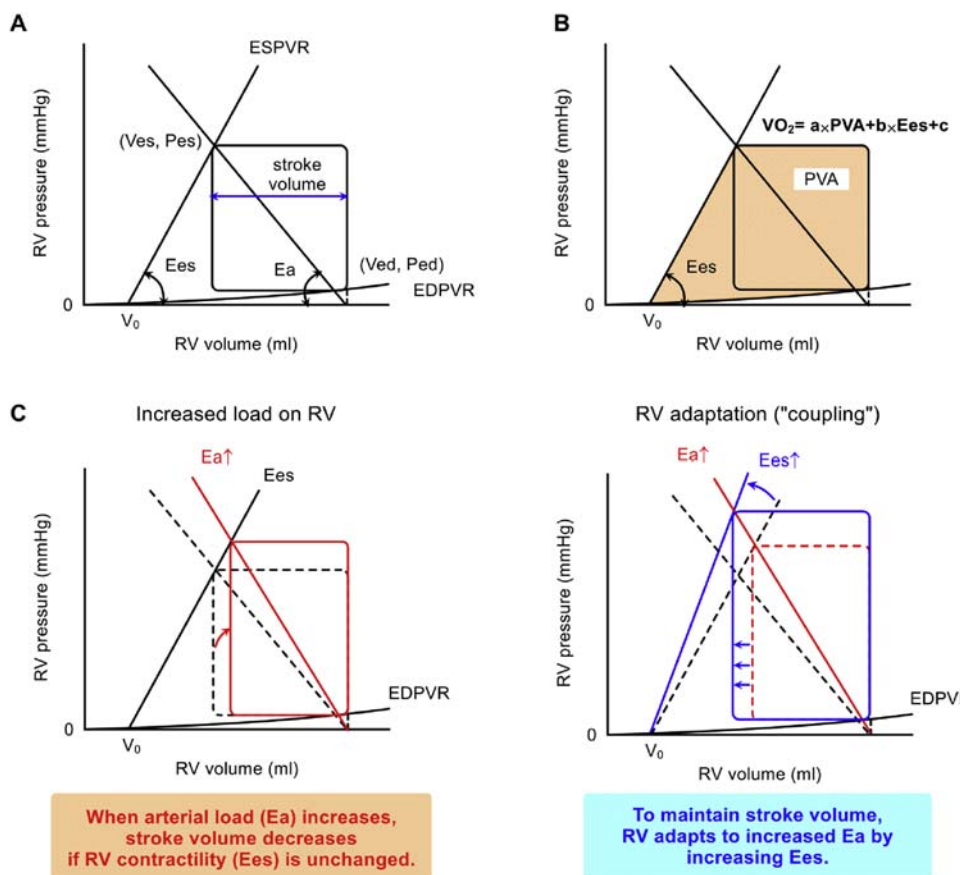
terms of its end-systolic pressure-SV relationship as follows.[32]

$$Ea = \frac{Pes}{SV} \quad (56.1)$$

where Pes: end-systolic ventricular pressure, SV: stroke volume (Fig. 56.5A). The slope of the arterial Pes-SV relationship is neither the physical elastance nor arterial compliance, but functions as "effective" arterial elastance.[32] For the systemic circulation, it was shown by mathematical modeling[34] as well as in a large cohort[33] that Ea is insensitive to the pulsatile load, but tightly related to vascular resistance. In this Chapter 56, Ea is introduced in the section of "pulsatile load", because Ea is given using arterial input impedance approximated by a three-element Windkessel model, as follows.

$$Ea = \frac{Zc + R}{ts + \tau[1 - exp(-td/\tau)]} \quad (56.2)$$

where Zc: characteristic impedance, R: peripheral resistance, ts: duration of ejection, td: duration of diastole, τ: time constant of the diastolic pressure artery decay.[32] Thus, increased arterial compliance decreases Ea only mildly, and since Ea increases markedly with increases in peripheral resistance,[32] resistance is the major determinant of Ea. In most clinical studies on pulmonary circulation, Ea is examined as (1) mPAP/SV[8,36−38] or (2) sPAP/SV.[39] Both are based on the assumption that Pes can be approximated to mPAP or sPAP. However, these approximations should be used carefully because Pes is underestimated by mPAP in higher pressure ranges.[40]

FIGURE 56.5 The concept of the pressure-volume loop (PV-loop). (A) The slope of ventricular end-systole pressure-volume relationship (ESPVR) is Ees, and the volume axis intercept of ESPVR line is V_0. The slope of the arterial end-systole pressure-volume relationship is Ea. End-systolic ventricular volume is given by the interaction between these two lines. Stroke volume is the difference between end-diastole ventricular volume (Ved, the x-axis value of the lower right corner of the PV loop) and end-systole ventricular volume (Ves, the x-axis value of the higher left corner of the PV loop). The ventricular end-diastole pressure-volume relationship is given as EDPVR curve. (B) Pressure-volume area (PVA) is the area circumscribed by (1) the EDPVR line, (2) the PDPVR curve, and (3) the systolic segment of the pressure-volume trajectory in the PV-loop (colored pink). PVR is one of the determinants of oxygen myocardial consumption. (C) (left) When Ea increases in pulmonary hypertension (PH), the intersection of the two lines shifts upward (Ves increases and Pes is elevated). If Ees is unchanged, stroke volume decreases (right). To maintain stoke volume, the RV increases Ees so that x-axis of the intersection remains unchanged (blue line and loop).

Ea may increase by four- to fivefold in patients with precapillary PH,[8,36] and also by two- to fivefold in patients with LHD.[38,39,41] Since Ea determines SV by interacting with Ees, increased Ea reduces SV if Ees does not increase in parallel (Fig. 56.5C). Thus, the RV needs to increase Ees to maintain SV. Both Ea and Ees are given in terms of their Pes-SV relationships (with the same unit of mmHg/ml), and therefore the ratio of Ees to Ea represents how well the RV remains coupled with increased arterial load in PH (see section "the right ventricular-pulmonary artery coupling: Ees/Ea"). Increased Ea is associated with clinical adverse outcomes in patients with postcapillary PH.[39]

As described, Ea is a concept proposed initially in the systemic circulation where down-stream pressure (i.e., central venous pressure) is negligible. On the other hand, in pulmonary circulation, down-stream pressure (PAWP) is not negligible relative to Pes even in normal conditions. It is not yet established whether or not PAWP can be ignored to calculate Ea in the pulmonary circulation. A new approach to estimate Ea by subtracting PAWP was proposed by the researchers who have originally developed Ea in systemic circulation.[42] They noted that their proposal does not diminish prior findings of Ea in PH, but this approach may provide additional insight regarding the role of PAWP on the load to the RV. Further investigations would be expected.

Heart-dependent arterial load

Pulmonary artery pressure (mean, systolic, and diastolic pressure)

PA pressure is a heart-dependent description of arterial load. Owing to Ohm's law, mPAP is simply determined by the product of PVR and CO (mean flow per one minute). mPAP can increase fourfold in PH, while systemic hypertension is considered severe with a 25% increase in mean arterial pressure.[26] Just as mPAP, pressure waves are determined by not only the arterial properties (resistance, arterial compliance, and characteristic impedance) but also the ventricular function (ventricular contractility and diastolic stiffness).[43] For example, sPAP is augmented when PVR and characteristic impedance are increased, PAC is reduced, and RV contractility is enhanced. All these changes are involved in the development of PH.

As described in Chapter 55, in the pulmonary circulation, sPAP and diastolic PAP are proportional to mPAP in normal subjects and patients with several types of PH.[44–46] According to these relations, RV systolic pressure of 40 mmHg would best estimate mPAP of 25 mmHg as an indication of the presence of PH by the current guidelines.[1]

Wave reflection: wave separation analysis and wave intensity analysis

As discussed in detail in Chapters 1, 3 and 11, pressure and flow waves are generated by the cardiac ejection and are transmitted over the elastic arteries into the vasculature with a certain wave speed toward. These waves reflect at all discontinuities in the arterial trees and then return to the ventricle. The discontinuities include pathological sites; for example, where vessels are disrupted or abruptly narrowing. Physiologically (or functionally), the discontinuities can be explained by the mismatch of input impedance. Namely, wave reflections occur at the vascular sites where input impedance increases from a lower value (at normal or large vessels) to a higher value (at disrupted or narrowing vessels). Or, vice versa: when vessels widen (input impedance decreases from a higher to a lower value), negative wave reflections appear ("open reflections").

The normal pulmonary circulation is characterized by a low resistance and high compliance with little wave reflection.[47] When reflections are absent, pressure and flow waves would have the same wave shape. Indeed, PA pressure and flow are quite similar in normal physiological conditions.[47] In patients with PH, however, shapes of pressure and flow waves are different from each other. PA flow waves show a steep deceleration during systole, which coincides with pressure augmentation.[12] The deceleration of flow waves and augmentation of pressure waves is indicative of exaggerated wave reflection returning to the RV during systole.

Measured pressure and flow waves consist of forward and backward (reflected) waves. Clinically, there are two approaches to derive forward and backward waves: (1) wave separation analysis (WSA) and (2) wave intensity analysis (WIA). Both WSA and WIA methods can accomplish wave separation, using characteristic impedance. A difference is that the WSA method uses measured pressure and flow, while the WIA method is applied for time derivatives of pressure and flow.

In WSA, forward and backward pressure can be derived as:

$$Pf = \frac{Pm + Fm \times Zc}{2} \tag{56.3}$$

$$Pb = \frac{Pm - Fm \times Zc}{2} \tag{56.4}$$

where P: pressure, F: flow, and f: forward, b: backward, and m: measured, respectively.[48]

In WIA, forward and backward pressure are introduced as:

$$dPf = \frac{dPm + dFm \times Zc}{2} \tag{56.5}$$

$$dPb = \frac{dPm - dFm \times Zc}{2} \tag{56.6}$$

where dP: time derivative of pressure, dF: time derivative of flow, and f: forward, b: backward, and m: measured, respectively.[49,50] Integration of WIA-obtained forward and backward waves yields WSA-obtained waves.[51,52] With the use of the WSA or WIA, we can investigate wave reflection, in terms of (1) the magnitude and timing of backward waves, and (2) wave speed (pulse wave

velocity: PWV). The magnitude of forward and backward waves depends on both the heart and arterial load. On the other hand, the timing of backward waves and PWV are less affected by the RV function because of the relation:

$$PWV = \frac{Zc \times A}{\rho} \tag{56.7}$$

where A: area of elastic arteries and ρ is blood density. This means that PWV depends on the properties of elastic arteries, but less on the heart. This section of heart-dependent loading includes the timing of backward waves and PWV for the convenience of explanation of wave reflection. Please be reminded that the return time of the reflected wave, which can be found by WSA or WIA, is determined by the vasculature. When looking at inflection points of measured pressure or flow, timing as well as the shapes of forward and reflected waves (which are the results of the interaction of heart and vessels) have an influence. Inflection points may thus be not directly related to timing aspects.[53,54]
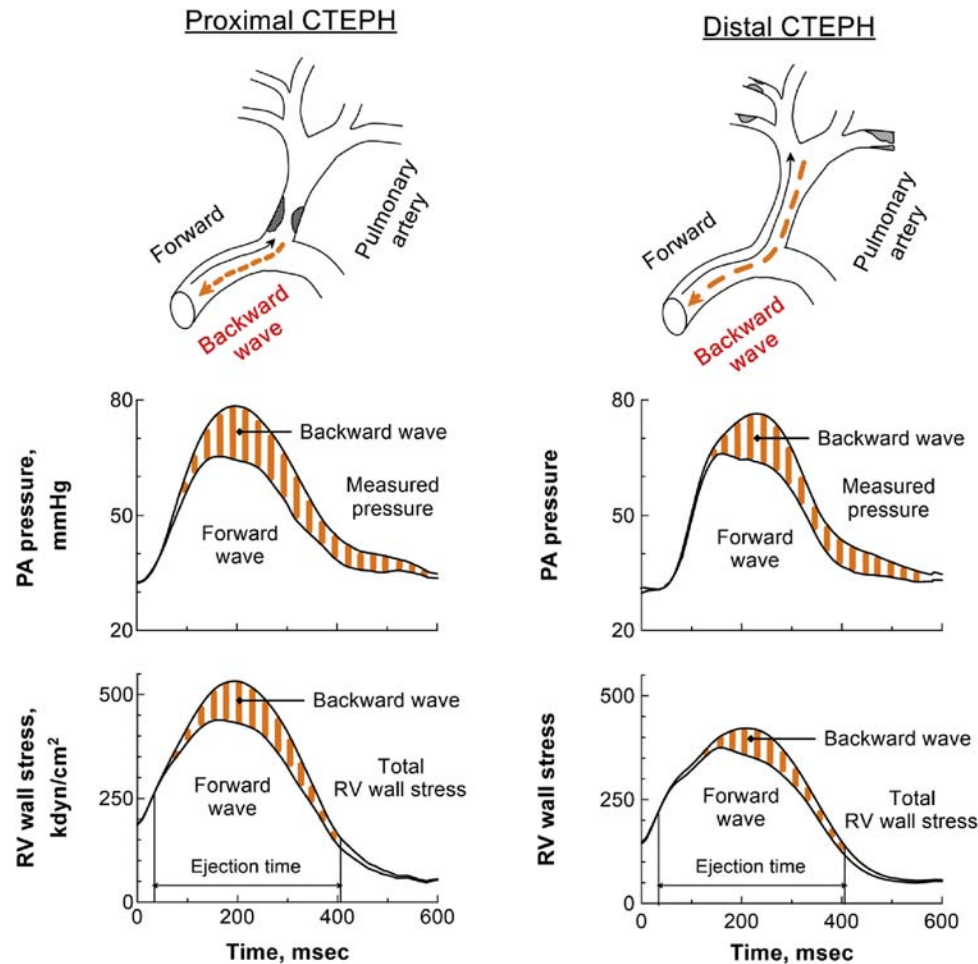
In PH, backward waves five to six times larger than normal return to the RV.[55-58] A preclinical study using a PH animal model indicates that, as the peripheral pulmonary arteries are narrowed, the magnitude of backward waves becomes larger.[59]

Furthermore, backward waves return earlier in PH.[57,58] In a PH animal model, wave transmission time from the RV to the reflection point was smaller than normal animals.[59] Early return of backward waves in PH can be explained by (1) increased wave speed or (2) a location of a reflection point close to the RV.[47] Since stiffer proximal arteries can increase PWV (see Eq. 56.11), the PWV is accelerated by two to four times in patients with PH compared with controls.[55,57] In addition, proximal site of reflection is also a cause for early return of backward waves. In CTEPH patients with proximal pathological lesions, the RV is exposed to earlier backward waves than in patients with distal lesions.[60]

The early return of backward waves may increase mechanical stress on the RV (Fig. 56.6). RV wall stress/tension over the cardiac cycle depends on the RV volume (radius) and pressure, which means that wall stress is large when pressure and volume are large (see "Right ventricular wall stress/tension"). Early return of backward waves increases wall stress/tension considerably, and compromises RV function (RV dilatation and hypertrophy).[60] Since the time

FIGURE 56.6 Early return of backward waves increases right ventricular (RV) mechanical stress. Backward waves return sooner in chronic thromboembolic pulmonary hypertension (CTEPH) patients with proximal obstructive lesions, than those with distal lesions. Backward waves add pressure to the forward wave (orange, middle) and elevate RV mechanical stress (orange, bottom) according to RV volume when backward waves arrive back to the RV.
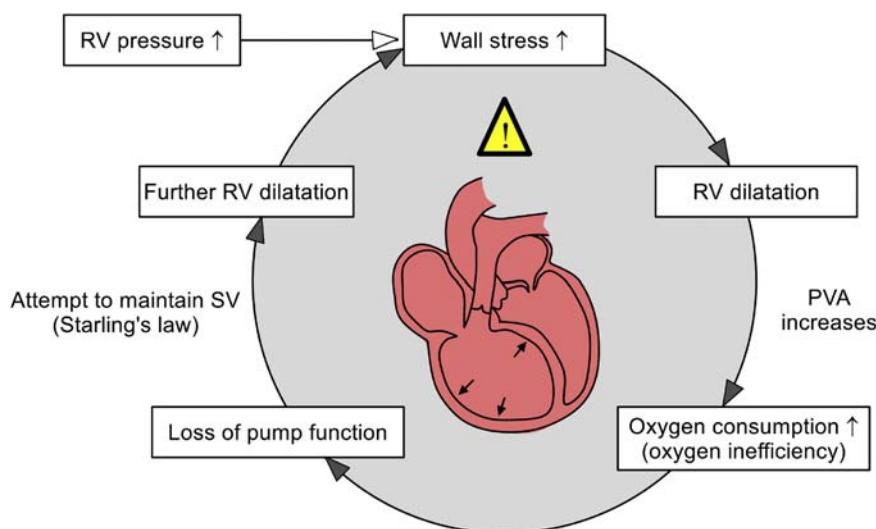
of wave transmission is not taken into account by lumped-parameter models such as a three-element Windkessel model,[61] early return of wave reflection might become a relevant addition to complement a description of arterial load in PH. Owing to the complexity of applying the WSA and WIA methods, simpler methods are used in clinical practice based on the analysis of: (1) pressure waves: increased augmentation index[62,63] and (2) flow waves: a notch of flow velocity.[64,65] Both are based on the concept that backward pressure waves add to forward pressure waves, while backward flow waves subtract from forward flow waves.[26] The shape of the pressure waves may differentiate PAH from CTEPH: CTEPH is characterized by a larger augmentation index and shorter reflection time than PAH.[62,63] An abnormal shape of flow waves is also useful to estimate an incidence of backward waves in PH.[64,65] In particular, a mid-systolic notch of flow waves is associated with poor RV function assessed by echocardiography (e.g., tricuspid annular plane systolic excursion [TAPSE] and RV fractional area change [RVFAC]).[65]

Right ventricular wall stress/tension

RV wall stress (tension) is a time-varying load imposed on the cardiac muscle.[66] RV wall stress (tension) is an important load parameter determined by an interaction of the RV and pulmonary arterial system. Increased wall stress (tension) induces oxygen inefficiency, resulting in loss of pump function.[67,68] Wall stress (tension) cannot be measured directly, but can be estimated by pressure, volume (radius), and wall thickness, based on Laplace's law:[27]

$$\text{wall stress} = \frac{(\text{pressure} \times \text{radius})}{\text{wall thickness}} \quad (56.8)$$

$$\text{wall tension} = \text{pressure} \times \text{radius} \quad (56.9)$$

which means that wall stress is directly proportional to pressure and volume, and inversely to wall thickness. In the presence of elevated pressure, the RV increases wall thickness in an attempt to attenuate increased wall stress. Ultimately, loss of pump function with a decrease in CO occurs as a consequence of increased wall stress. While the RV dilates to maintain CO, larger RV volume further increases wall stress (tension). Wall stress (tension) plays a central role in the vicious cycle of development of RV failure in PH (Fig. 56.7).[67] RV wall stress was increased by approximately fourfold in patients with precapillary PH.[69,70] Increased RV wall stress was associated with mortality in a cohort combined with pre- and postcapillary PH.[71] The foremost way to break this vicious cycle is to reduce wall stress. Lowering pressure is crucial, and also targeting volume overload by diuretics is effective in decreasing wall stress. Although wall stress might not be used for routine monitoring for PH treatment, N-terminal B-type natriuretic peptide (NT-proBNP) may become a surrogate marker to assess wall stress in clinical practice.[69,72]

The right ventricular function in pulmonary hypertension

Load-independent right ventricular function

Right ventricular contractility: end-systolic elastance

Increased RV contractility is an essential adaptation of the RV to cope with increased arterial loading in PH.[25] The gold standard measure of ventricular contractility is end-systolic elastance of the ventricle (Ees), which represents the maximum elastance of the ventricle during a cardiac cycle. Ees is determined as the slope of the ESPVR in the diagram of

FIGURE 56.7 Right ventricular (RV) response to increased wall stress. Increased RV pressure elevates RV wall stress, which induces RV dilatation. RV dilatation increases pressure-volume area (PVA) (see Fig. 56.5). As a consequence, the RV results in oxygen consumption and loss of pump function. To maintain stroke volume, according to the Starling's law, the RV further dilates, however, increased RV volume (radius) further increases RV wall stress.

PV-loops,[35] requiring both ventricular pressure and volume over cardiac cycles at different loading conditions (see Chapter 55). Clinical studies of PH have applied the conductance catheter technique into the RV for investigation of PV loops.[15,73−75] Preload interventions, for example, vena cava obstruction[35,76] or a Valsalva maneuver,[15] are required for this so-called "multiple-beat method" (Fig. 56.8). In clinical studies, therefore, a simpler method (so-called "single-beat method"), not requiring PV-loops analysis or preload interventions, is applied to estimate Ees.[77] Of the measured ventricular pressure curves, the isovolumic phases are extrapolated to a hypothetical isovolumic contraction curve if the pulmonary valve would not open. This extrapolation gives the peak isovolumic pressure (Pmax), and thereby Ees can be calculated by (Pmax−Pes)/SV (Fig. 56.8). The single-beat method was originally developed for the LV, but this concept was validated into the RV by an animal model with PH,[78] and thereafter applied to the patients with PAH.[79] Although it has been discussed whether single-beat method gives a precise estimation of Pmax even in patients with severe PH,[25] it was found that the single-beat method accurately estimates an Ees-related factor (Ees/Ea) derived from the multiple-beat method in patients with moderate to severe PH.[80]

Pes/ESV was proposed as the possible simplest estimation of Ees, assuming that hypothetical volume at zero pressure (V_0) on the PV-loops diagram is negligible.[81−83] It might be a convenient measure in daily clinical practice, not requiring RV pressure curves. However, it should be noted that Pes/ESV differs from true Ees derived from the single-beat method because V_0 is not equal to zero.[84] Particularly, V_0 becomes larger as RV dilates. Thus, Pes/ESV gives much lower values than true Ees in patients with moderate to severe PH, not reflecting RV contractility.[84]

When Ea is elevated, the RV increases Ees to preserve the Ees/Ea ratio and maintain the SV (see "Cardiac output and stroke volume"). Ees is increased fourfold in precapillary PH,[8,36] and two- to threefold in PH due to LHD,[38,41] both reflecting that the RV is in a hypercontractile state in PH. Interestingly, the response of Ees may differ depending on the etiologies of PH even if these are categorized into the same group. In group-1, both idiopathic PAH and systemic sclerosis-associated PH (SSc-PH) Ees increases against the augmented Ea; however, the increase in Ees is relatively modest in SSc-PH. Ees in SSc-PH remains at only one-third of that seen in idiopathic PAH though the RV is exposed to the same loading (Ea, PVR, and PAC).[15] The insufficient increase of Ees results in poorer RV-PA coupling (given as Ees/Ea) in SSc-PH than idiopathic PAH.[15]
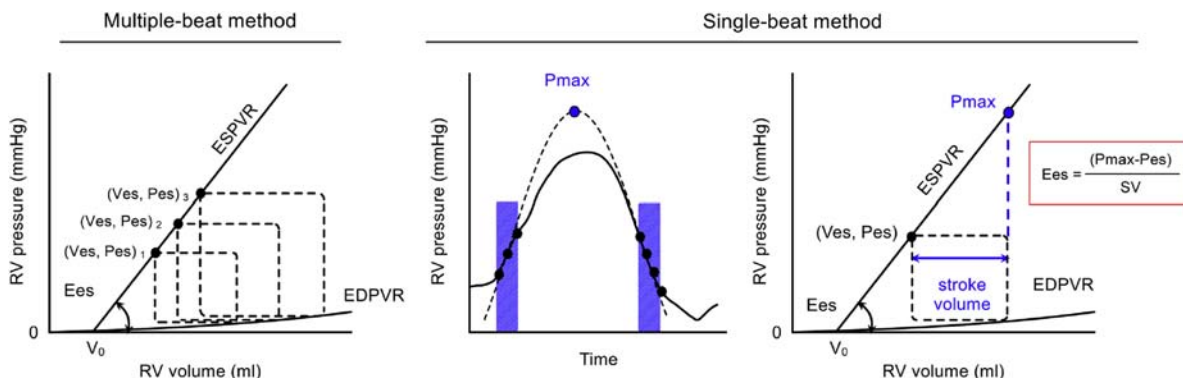
While the RV may properly adapt to increased load at rest in PH, the RV may have no exertional contractile reserve to deal with the further increase in arterial load.[85] Exercise increases pulmonary arterial load (Ea), but the RV cannot sufficiently augment Ees during exercise in PH, resulting in deterioration of RV-PA coupling.[85] Consequently, PH is characterized as a poor increase in SV during exercise than that in normal subjects.

Several limitations should be kept in mind when analyzing coupling in the pressure-volume plane, for which we refer to excellent reviews by, e.g., Chirinos et al.[86,87] For Ees, the crossing with the volume axis of the ESPVR, V_0 should not be neglected.[25] Moreover, the ESPVR is assumed to be a straight line which is a simplification.[88,89] When determining Ea, it is assumed that heart rate (and diastolic and systolic duration) remains constant.[86] Further, it should be remembered that Ea is a measure of non-pulsatile load and is hardly related to PAC.[33,34,86]

Right ventricular diastolic stiffness: end-diastolic elastance

RV diastolic stiffness gives an important load-independent description of RV function. The RV is stiffened with

FIGURE 56.8 Calculation of right ventricular (RV) end-systolic pressure-volume relationship (ESPVR). Multiple-beat method (left): the ESPVR line is estimated using multiple pressure-volume loops with different preload conditions. Single-beat method (right): peak isovolumic pressure is estimated by an extrapolated sine curve (dash line) from the isovolumic phase (blue zone). Using the estimated Pmax and measured end-systolic RV volume and pressure (Ves, Pes), the slope of ESPVR can be calculated.

hypertrophy, fibrosis, and specific biological alterations, such as reduced titin phosphorylation.[90] RV diastolic stiffness is determined by the end-diastolic pressure-volume relationship (EDPVR) curve in the diagram of PV-loops, so-called end-diastolic elastance, Eed[36] (Fig. 56.5A). While Ees is the maximum elastance of the ventricle (see "Right ventricular contractility"), Eed is the minimum elastance, which corresponds to the mechanical properties of a fully relaxed ventricle at end-diastole.

Eed is calculated using multiple PV-loops with preload intervention.[76] Alternatively, Eed can be estimated by fitting an exponential curve to the diastolic portion of PV-loops, with the formula $P = \alpha[\exp(\beta V) - 1]$, where P: RV pressure, α: curve-fitting constant, β: diastolic stiffness constant, V: RV volume. α and β are estimated based on the following three pressure points, (1) pressure at the beginning of diastole, (2) pressure at end-diastole, and (3) the origin (0,0).[36,37] Using α and β, Eed is given as $Eed = \alpha\beta \times \exp(\beta Ved)$, where Ved: end-diastolic volume (Fig. 56.5A).

Eed is increased two- to fourfold in several types of PH,[36,76] which means that the RV is stiffened in PH more than normal subjects. The stiffness of the RV during exercise is similar to resting values in normal subjects, but in PH due to LHD, the RV becomes stiffer during exercise.[76] Increased Eed, but not Ees or Ea, deteriorates right atrial function, which in turns contributes to backward central venous flow and systemic congestion.[91,92] Higher RV stiffness (increased Eed) is closely correlated with disease severity[90] and clinical adverse events.[36]

Load-dependent right ventricular function

Cardiac output and stroke volume

CO is determined by SV×HR. Since SV depends on the interaction of the heart and vascular systems, the diagram of PV loops may help understanding how SV or CO is determined when the RV is exposed to increased arterial load in PH. In the PV-loops diagram, SV is determined by the ratio of Ees to the sum of Ees and Ea as:

$$SV = \frac{Ees}{Ees + Ea}(Ved - V_0) \qquad (56.10)$$

where Ved is end-diastolic volume, and V_0 is volume at zero pressure determined as the volume axis intercept of the ventricular ESPVR (Fig. 56.5A).[93] This equation shows that when Ea is increased, the RV needs to enhance its contractility Ees, otherwise SV is not maintained (Fig. 56.5C). When Ees is not enhanced sufficiently, the RV needs to dilate to maintain SV (a dilated RV, with similar shortening of the muscle fibers, produces a somewhat larger output). When SV is maintained, but V_0 and EDV increase in tandem, thus the entire loop shifting to the right, EF will be lower, since the SV is a smaller

proportion of the EDV. The time course of decreasing SV with RV dilatation reflects the progress of PH since progressive PH is characterized by more dilated RV with lower RVEF and SV over time, compared with stable PH.[94]

The hemodynamic parameter which best reflects treatment efficacy is SV: an increase in SV indicates a better coupling of the RV to its load and is associated with a favorable outcome.[95–97] Note that higher CO or SV is not equal to more exaggerated RV contractility after treatment. A sufficient reduction in arterial load (Ea) can increase SV, releasing the RV from the hypercontractile status, as shown in Eq. (56.10).

Right ventricular volume and ejection fraction

Functional imaging parameters derived by cardiac MRI or echocardiography are categorized as load-dependent function.[7] RV volume, i.e., EDV and ESV, provide anatomical information of the RV itself; however, these are determined by not only RV function but also by preload and pulmonary arterial properties (afterload). For example: when the RV contractility (Ees) does not change, increased Ea can augment ESV because ESV is determined by the point of intersection of Ea with Ees (Fig. 56.5C). Likewise, RVEF is also a load-dependent RV function, which is calculated as SV/RVEDV or (RVEDV−RVESV)/RVEDV. As already indicated in the section of "Cardiac output and stroke volume," the RV adapts to PH by dilatation such that the SV is maintained.[94] In other words, even if SV is maintained adequately, severe PH is accompanied by a larger RVEDV, resulting into lower RVEF. Lower RVEF at diagnosis is associated with adverse clinical outcomes in PH, irrespective of PVR.[5] In addition, insufficient increase in RVEF after treatment but, interestingly, not a reduction in PVR, is related to adverse clinical events.[5] Undoubtedly, RVEF is a key tool to assess the progression of PH; however, RVEF should be interpreted carefully because RVEF is neither an accurate parameter of "RV contractility" nor "RV−PA coupling." Since RVEF = SV/EDV, RVEF is determined by several parameters as follows:

$$RVEF = \frac{Pes}{ESV} \times \frac{1}{Ea} \times \frac{ESV}{EDV} \qquad (56.11)$$

where Ea is defined by Pes/SV. Since Ees should not be approximated as Pes/ESV[84] (see "Right ventricular contractility"), RVEF is not a direct measure of contractility or coupling.

Echocardiographic measures

Echocardiography is one of the most widely used tools in daily practice. Whereas the diagnosis of PH should be conducted based on RHC,[1] echocardiography is useful to assess disease severity and improvement after treatment.

The ESC/ERS guidelines proposed several echocardiographic measures; for example, RV chamber sizes, RVFAC (%FAC), the magnitude of tricuspid regurgitation, the LV eccentricity index, the RV longitudinal systolic strain/strain rate, and TAPSE.[1] Owing to the unusual and complex shape of the RV, the echocardiographic measurements are mostly angle-dependent and qualitative.[98] Both RV function and arterial load affect these echocardiographic measures.[98] In the same way as RV volume and RVEF, echocardiographic measures are improved by a reduction in arterial load after treatment.
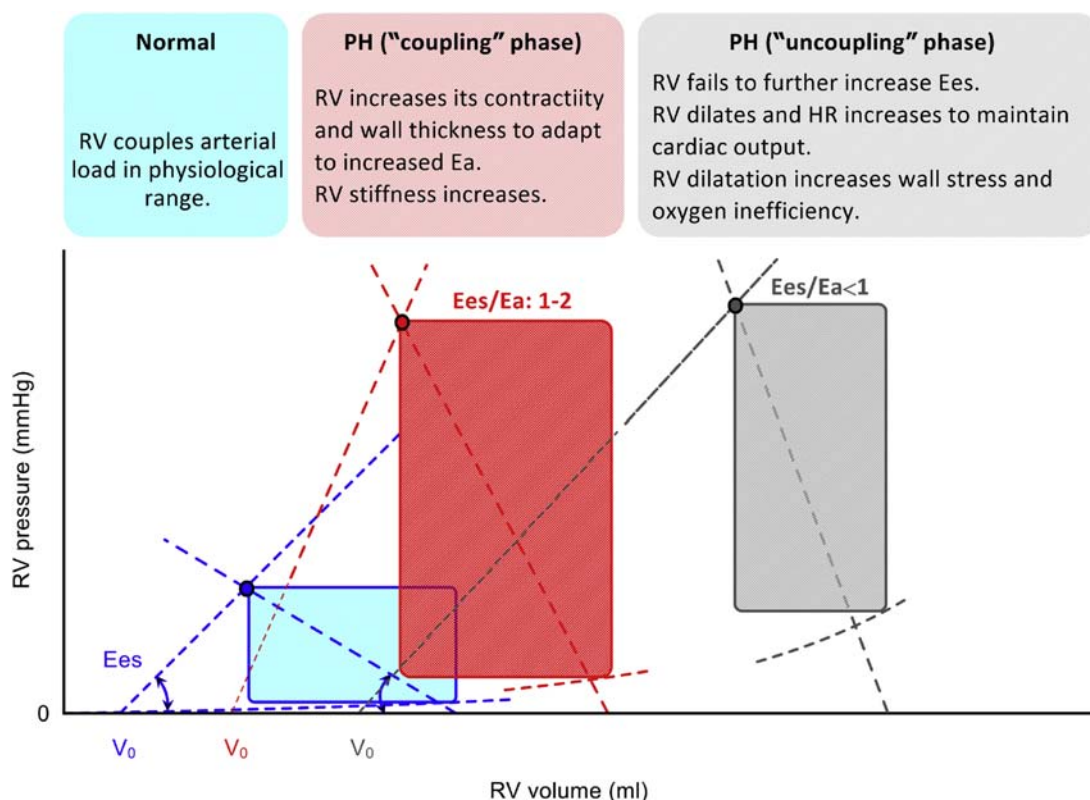
The cardiovascular interaction in pulmonary hypertension

The right ventricle—pulmonary artery coupling: Ees/Ea

Most of the clinical parameters (for example, CO and RVEF) are determined by the interaction between the RV and the arterial load. To interpret these parameters precisely, the "intrinsic" properties of the RV and arterial loading (for example, RV contractility and diastolic stiffness and arterial elastance) should be understood correctly. We define coupling of the RV with arterial loading as the ratio of RV contractility to arterial elastance (Ees/Ea). While "coupling" is often used in a much broader sense to describe the interaction between heart and vasculature, in the context of this chapter we use coupling in the narrow sense of the Ees/Ea ratio (see also section "The properties of pulmonary arterial load and right ventricular function" where we defined intrinsic characteristics and system characteristics).[7] Cardiac performance depends on Ees/Ea, and this ratio is a measure of energy transfer from the heart to the arteries. Based on animal experiments investigating the LV,[93,99] an Ees/Ea ratio between 1 and 2 is considered to be in the normal range. This range reflects the maximum stroke work with minimizing myocardial oxygen consumption,[99] as explained in more detail in Chapters 15 and 55. Further discussions of the advantages and limitations of the use of coupling and efficiency can be found in the literature.[86]

In the relatively early stage of PH, the RV enhances its contractility by four- to fivefold to adapt to increased arterial loading. During this phase (so-called "coupling phase"), Ees/Ea is maintained above 1, and SV is preserved (Fig. 56.9). Since increased contractility is attributed to increased RV mass (hypertrophy), increased RV diastolic stiffness is also observed during the coupling phase.[36] However, when PH further advances, the hypertrophic

FIGURE 56.9 Right ventricular (RV) pressure-volume (PV) loops in control (blue), pulmonary hypertension (PH) with maintained RV-pulmonary artery (PA) coupling (early stage, red) and PH with RV-PA uncoupling (late stage, gray). *Ees*, the slope of end-systolic RV pressure-volume loop; *Ea*, arterial elastance; V_0, hypothetical RV volume at zero pressure.

process is insufficient for enhancing Ees in proportion to further increases in Ea, resulting in a decline in Ees/Ea.[36] During this phase (so-called "uncoupling phase"), the RV dilates to maintain SV (Fig. 56.9). HR also increases to compensate for the reduced SV, since CO=HR×SV. The "uncoupling" is critical for patients with PH. Decreased Ees/Ea, particularly lower than 0.7−0.8, is associated with adverse events in patients with PH.[36,80]

The framework of PV-loops provides insight not only in RV-PA coupling but also in myocardial oxygen consumption. Myocardial oxygen consumption per one heartbeat (VO_2) is described as:

$$VO_2 = a \times PVA + b \times Ees + c \qquad (56.12)$$

where PVA: systolic pressure-volume area, a, b, c: constant value.[100] PVA is the area circumscribed by the ESPVR line, the EDPVR curve, and the systolic limb of the PV-loops trajectory (Fig. 56.5B). Thus, hyper RV contractility and ventricular dilatation will increase PVA, resulting in increased myocardial oxygen consumption (Fig. 56.9). When the PH treatment decreases PA pressure and RV volume and attenuates the enhanced Ees, it contributes to an attenuation of the increased myocardial oxygen consumption and to a more effective RV function.

Right ventricle volumetric adaptation and wall stress

Wall stress/tension is a concept different from Ea to describe the ventricular loading. While Ea is an "effective" arterial elastance with a unit of mmHg/mL,[32] wall stress represents mechanical force imposed on a unit area of cardiac muscle, whose unit is dyne/cm^2 (dyne/cm for wall tension). As indicated in the section of "Right ventricular wall stress/tension," wall stress will increase when ventricular pressure and/or volume are large, both of which increase oxygen consumption. While myocardial oxygen consumption is increased as a consequence of increased wall stress in PH, oxygen supply is limited in PH.[68,101,102] Oxygen inefficiency induces loss of pump function, and ultimately RV failure. In an attempt to maintain CO, the RV needs to dilate particularly during the uncoupling phase; however, the ventricular dilatation further increases wall stress[67] (Fig. 56.7). Once wall stress augments and RV dilatation occurs, the RV is in a vicious cycle of increased wall stress (Fig. 56.7). Lowering pressure is the most reasonable approach to release the RV from the vicious cycle of wall stress, and guarantees long-term survival in PH.

Left ventricle–right ventricle interaction

The RV has little impact on the LV under normal physiological conditions; however, the interaction between the RV and the LV should not be ignored in PH. In PH, increased RV wall stress/tension prolongs RV contraction, resulting in asynchrony between the RV and LV contraction. The RV continues to contract while the LV is already in the diastolic phase. Therefore, the peak of the RV shortening occurs later than that of the LV shortening.[103] As a consequence, the ventricular septum bows leftward, impairing LV filling.[104] The importance of this hampering of LV filling is illustrated by the fact that in PH, SV does not correlate to RVEDV, but correlates positively to LVEDV.[104] Furthermore, the LV EDV provides prognostic information in addition to RV volume.[5,105] In PH, LV cardiomyocytes are atrophic, and cardiomyocyte contractile function is impaired.[106] As a result, severe LV dysfunction becomes apparent when RV afterload is largely reduced, for example, by lung transplantation.[107]

Summary

This chapter shows the adaptation of the RV to increased arterial load in PH. The pathological changes in arterial load and the RV function, and the adaptation of the RV to increased arterial load in PH are summarized as below.

- The heart-independent arterial load is increased in PH: PVR increases to fourfold, PAC decreases to 30% −40% of controls, Zc increases to 2.5- to sixfold, and Ea increases to four- to fivefold. As a result, the heart-dependent load (for example, pressure and wall stress/tension) is also elevated by the interaction of the load-independent heart function (Ees and Eed).
- Load-independent heart function is altered in PH. Ees (contractility) is increased to two- to fourfold, and Eed (diastolic stiffness) is also increased to 2 ∼ four-fold. When interpreting load-dependent heart function (for example, RV volume, RVEF, and CO), we should keep in mind that these parameters are determined by not only the RV but also the arterial load. Since the RV is under hyper-contractile state in PH, reduced RVEF and CO are not always equal to impaired contractility of the RV.
- The RV couples to increased arterial load (Ea) by increasing Ees. During the "coupling phase," the ratio of Ees to Ea is maintained between 1 and 2; here we use coupling only in this strict sense, although the term may be used in different manners. Since increased Ees largely depends on RV hypertrophy, if the hypertrophic process is not successful, Ees/Ea is below 1 ("uncoupling phase"). During the uncoupling phase, the RV needs to dilate to maintain SV. However, the dilatation increases myocardial oxygen consumption and further elevates wall stress/tension. In the advanced stage of PH, the RV is exposed to higher wall stress with oxygen inefficiency.

References

1. Galie N, Humbert M, Vachiery JL, et al. 2015 ESC/ERS guidelines for the diagnosis and treatment of pulmonary hypertension: the Joint Task Force for the Diagnosis and Treatment of Pulmonary Hypertension of the European Society of Cardiology (ESC) and the European Respiratory Society (ERS): endorsed by: Association for European Paediatric and Congenital Cardiology (AEPC), International Society for Heart and Lung Transplantation (ISHLT). **Eur Respir J**. 2015; 46:903−975.

2. Simonneau G, Montani D, Celermajer DS, et al. Haemodynamic definitions and updated clinical classification of pulmonary hypertension. **Eur Respir J**. 2019; 53.

3. Ghio S, Gavazzi A, Campana C, et al. Independent and additive prognostic value of right ventricular systolic function and pulmonary artery pressure in patients with chronic heart failure. **J Am Coll Cardiol**. 2001; 37:183−188.

4. Gorter TM, van Veldhuisen DJ, Bauersachs J, et al. Right heart dysfunction and failure in heart failure with preserved ejection fraction: mechanisms and management. Position statement on behalf of the Heart Failure Association of the European Society of Cardiology. **Eur J Heart Fail**. 2018; 20:16−37.

5. van de Veerdonk MC, Kind T, Marcus JT, et al. Progressive right ventricular dysfunction in patients with pulmonary arterial hypertension responding to therapy. **J Am Coll Cardiol**. 2011; 58:2511−2519.

6. Delcroix M, Lang I, Pepke-Zaba J, et al. Long-term outcome of patients with chronic thromboembolic pulmonary hypertension: results from an international prospective registry. **Circulation**. 2016; 133:859−871.

7. Vonk Noordegraaf A, Chin KM, Haddad F, et al. Pathophysiology of the right ventricle and of the pulmonary circulation in pulmonary hypertension: an update. **Eur Respir J**. 2019; 53.

8. Spruijt OA, de Man FS, Groepenhoff H, et al. The effects of exercise on right ventricular contractility and right ventricular-arterial coupling in pulmonary hypertension. **Am J Respir Crit Care Med**. 2015; 191:1050−1057.

9. Shigemi K, Fuke S, Une D, et al. Physiological insights of recent clinical diagnostic and therapeutic technologies for cardiovascular diseases. **J Physiol Sci**. 2017; 67:655−672.

10. Huez S, Brimioulle S, Naeije R, Vachiery JL. Feasibility of routine pulmonary arterial impedance measurements in pulmonary hypertension. **Chest**. 2004; 125:2121−2128.

11. Hunter KS, Lee PF, Lanning CJ, et al. Pulmonary vascular input impedance is a combined measure of pulmonary vascular resistance and stiffness and predicts clinical outcomes better than pulmonary vascular resistance alone in pediatric patients with pulmonary hypertension. **Am Heart J**. 2008; 155:166−174.

12. Lankhaar JW, Westerhof N, Faes TJ, et al. Quantification of right ventricular afterload in patients with and without pulmonary hypertension. **Am J Physiol Heart Circ Physiol**. 2006; 291:H1731−H1737.

13. Lankhaar JW, Westerhof N, Faes TJ, et al. Pulmonary vascular resistance and compliance stay inversely related during treatment of pulmonary hypertension. **Eur Heart J**. 2008; 29:1688−1695.

14. Saouti N, Westerhof N, Helderman F, et al. RC time constant of single lung equals that of both lungs together: a study in chronic thromboembolic pulmonary hypertension. **Am J Physiol Heart Circ Physiol**. 2009; 297:H2154−H2160.

15. Tedford RJ, Mudd JO, Girgis RE, et al. Right ventricular dysfunction in systemic sclerosis-associated pulmonary arterial hypertension. **Circ Heart Fail**. 2013; 6:953−963.

16. Stergiopulos N, Segers P, Westerhof N. Use of pulse pressure method for estimating total arterial compliance in vivo. **Am J Physiol**. 1999; 276:H424−H428.

17. Tedford RJ, Hassoun PM, Mathai SC, et al. Pulmonary capillary wedge pressure augments right ventricular pulsatile loading. **Circulation**. 2012; 125:289−297.

18. Reuben SR. Compliance of the human pulmonary arterial system in disease. **Circ Res**. 1971; 29:40−50.

19. Mahapatra S, Nishimura RA, Sorajja P, Cha S, McGoon MD. Relationship of pulmonary arterial capacitance and mortality in idiopathic pulmonary arterial hypertension. **J Am Coll Cardiol**. 2006; 47:799−803.

20. Malhotra R, Dhakal BP, Eisman AS, et al. Pulmonary vascular distensibility predicts pulmonary hypertension severity, exercise capacity, and survival in heart failure. **Circ Heart Fail**. 2016; 9.

21. Dupont M, Mullens W, Skouri HN, et al. Prognostic role of pulmonary arterial capacitance in advanced heart failure. **Circ Heart Fail**. 2012; 5:778−785.

22. Miller WL, Grill DE, Borlaug BA. Clinical features, hemodynamics, and outcomes of pulmonary hypertension due to chronic heart failure with reduced ejection fraction: pulmonary hypertension and heart failure. **JACC Heart Fail**. 2013; 1:290−299.

23. MacKenzie Ross RV, Toshner MR, Soon E, Naeije R, Pepke-Zaba J. Decreased time constant of the pulmonary circulation in chronic thromboembolic pulmonary hypertension. **Am J Physiol Heart Circ Physiol**. 2013; 305:H259−H264.

24. Pagnamenta A, Vanderpool R, Brimioulle S, Naeije R. Proximal pulmonary arterial obstruction decreases the time constant of the pulmonary circulation and increases right ventricular afterload. **J Appl Physiol**. 2013; 114:1586−1592.

25. Vonk Noordegraaf A, Westerhof BE, Westerhof N. The relationship between the right ventricle and its load in pulmonary hypertension. **J Am Coll Cardiol**. 2017; 69:236−243.

26. Vlachopoulos C, O'Rourke M, Nichols WW. **McDonald's Blood Flow in Arteries: Theoretical, Experimental and Clinical Principles**. CRC Press; 2011.

27. Westerhof N, Stergiopulos N, Noble NIM, Westerhof BE. **Snapshots of Hemodynamics**. 3rd ed. ed. Springer; 2018.

28. Wang Z, Chesler NC. Pulmonary vascular wall stiffness: an important contributor to the increased right ventricular afterload with pulmonary hypertension. **Pulm Circ**. 2011; 1:212−223.

29. Yin FC, Guzman PA, Brin KP, et al. Effect of nitroprusside on hydraulic vascular loads on the right and left ventricle of patients with heart failure. **Circulation**. 1983; 67:1330−1339.

30. Laskey WK, Ferrari VA, Palevsky HI, Kussmaul WG. Pulmonary artery hemodynamics in primary pulmonary hypertension. **J Am Coll Cardiol**. 1993; 21:406−412.

31. Sunagawa K, Maughan WL, Sagawa K. Stroke volume effect of changing arterial input impedance over selected frequency ranges. **Am J Physiol**. 1985; 248:H477−H484.

32. Sunagawa K, Maughan WL, Burkhoff D, Sagawa K. Left ventricular interaction with arterial load studied in isolated canine ventricle. **Am J Physiol**. 1983; 245:H773−H780.

33. Chirinos JA, Rietzschel ER, Shiva-Kumar P, et al. Effective arterial elastance is insensitive to pulsatile arterial load. **Hypertension**. 2014; 64:1022−1031.

34. Segers P, Stergiopulos N, Westerhof N. Relation of effective arterial elastance to arterial system properties. **Am J Physiol Heart Circ Physiol**. 2002; 282:H1041—H1046.

35. Suga H, Sagawa K, Shoukas AA. Load independence of the instantaneous pressure-volume ratio of the canine left ventricle and effects of epinephrine and heart rate on the ratio. **Circ Res**. 1973; 32:314—322.

36. Trip P, Rain S, Handoko ML, et al. Clinical relevance of right ventricular diastolic stiffness in pulmonary hypertension. **Eur Respir J**. 2015; 45:1603—1612.

37. Vanderpool RR, Pinsky MR, Naeije R, et al. RV-pulmonary arterial coupling predicts outcome in patients referred for pulmonary hypertension. **Heart**. 2015; 101:37—43.

38. Gerges M, Gerges C, Pistritto AM, et al. Pulmonary hypertension in heart failure. Epidemiology, right ventricular function, and survival. **Am J Respir Crit Care Med**. 2015; 192:1234—1246.

39. Tampakakis E, Shah SJ, Borlaug BA, et al. Pulmonary effective arterial elastance as a measure of right ventricular afterload and its prognostic value in pulmonary hypertension due to left heart disease. **Circ Heart Fail**. 2018; 11:e004436.

40. Tello K, Richter MJ, Axmann J, et al. More on single-beat estimation of right ventriculo-arterial coupling in pulmonary arterial hypertension. **Am J Respir Crit Care Med.** 2018; 198:816—818.

41. Wright SP, Groves L, Vishram-Nielsen JKK, et al. Elevated pulmonary arterial elastance and right ventricular uncoupling are associated with greater mortality in advanced heart failure. **J Heart Lung Transplant**. 2020; 39:657—665.

42. Brener MI, Burkhoff D, Sunagawa K. Effective arterial elastance in the pulmonary arterial circulation: derivation, assumptions, and clinical applications. **Circ Heart Fail**. 2020; 13:e006591.

43. Stergiopulos N, Meister JJ, Westerhof N. Determinants of stroke volume and systolic and diastolic aortic pressure. **Am J Physiol**. 1996; 270:H2050—H2059.

44. Chemla D, Castelain V, Humbert M, et al. New formula for predicting mean pulmonary artery pressure using systolic pulmonary artery pressure. **Chest**. 2004; 126:1313—1317.

45. Syyed R, Reeves JT, Welsh D, Raeside D, Johnson MK, Peacock AJ. The relationship between the components of pulmonary artery pressure remains constant under all conditions in both health and disease. **Chest**. 2008; 133:633—639.

46. Handoko ML, De Man FS, Oosterveer FP, Bogaard HJ, Vonk-Noordegraaf A, Westerhof N. A critical appraisal of transpulmonary and diastolic pressure gradients. **Physiol Rep**. 2016; 4.

47. Naeije R, Huez S. Reflections on wave reflections in chronic thromboembolic pulmonary hypertension. **Eur Heart J**. 2007; 28:785—787.

48. Westerhof N, Sipkema P, van den Bos GC, Elzinga G. Forward and backward waves in the arterial system. **Cardiovasc Res**. 1972; 6:648—656.

49. Parker KH, Jones CJ. Forward and backward running waves in the arteries: analysis using the method of characteristics. **J Biomech Eng**. 1990; 112:322—326.

50. Khir AW, O'Brien A, Gibbs JS, Parker KH. Determination of wave speed and wave separation in the arteries. **J Biomech**. 2001; 34:1145—1155.

51. Westerhof N, Segers P, Westerhof BE. Wave separation, wave intensity, the reservoir-wave concept, and the instantaneous wave-free ratio: presumptions and principles. **Hypertension**. 2015; 66:93—98.

52. van den Wijngaard JP, Siebes M, Westerhof BE. Comparison of arterial waves derived by classical wave separation and wave intensity analysis in a model of aortic coarctation. **Med Biol Eng Comput**. 2009; 47:211—220.

53. Westerhof BE, Westerhof N. Uniform tube models with single reflection site do not explain aortic wave travel and pressure wave shape. **Physiol Meas**. 2018; 39:124006.

54. Westerhof BE, Westerhof N. Magnitude and return time of the reflected wave: the effects of large artery stiffness and aortic geometry. **J Hypertens**. 2012; 30:932—939.

55. Quail MA, Knight DS, Steeden JA, et al. Noninvasive pulmonary artery wave intensity analysis in pulmonary hypertension. **Am J Physiol Heart Circ Physiol**. 2015; 308:H1603—H1611.

56. Schafer M, Wilson N, Ivy DD, et al. Noninvasive wave intensity analysis predicts functional worsening in children with pulmonary arterial hypertension. **Am J Physiol Heart Circ Physiol**. 2018; 315:H968—H977.

57. Lau EM, Abelson D, Dwyer N, Yu Y, Ng MK, Celermajer DS. Assessment of ventriculo-arterial interaction in pulmonary arterial hypertension using wave intensity analysis. **Eur Respir J**. 2014; 43:1804—1807.

58. Su J, Manisty C, Parker KH, et al. Wave intensity analysis provides novel insights into pulmonary arterial hypertension and chronic thromboembolic pulmonary hypertension. **J Am Heart Assoc**. 2017; 6.

59. Fukumitsu M, Kawada T, Shimizu S, Turner MJ, Uemura K, Sugimachi M. Wave reflection correlates with pulmonary vascular wall thickening in rats with pulmonary arterial hypertension. **Int J Cardiol**. 2017; 249:396—401.

60. Fukumitsu M, Westerhof BE, Ruigrok D, et al. Early return of reflected waves increases right ventricular wall stress in chronic thromboembolic pulmonary hypertension. **Am J Physiol Heart Circ Physiol**. 2020; 319:H1438—H1450.

61. Westerhof N, Lankhaar JW, Westerhof BE. The arterial Windkessel. **Med Biol Eng Comput**. 2009; 47:131—141.

62. Castelain V, Herve P, Lecarpentier Y, Duroux P, Simonneau G, Chemla D. Pulmonary artery pulse pressure and wave reflection in chronic pulmonary thromboembolism and primary pulmonary hypertension. **J Am Coll Cardiol**. 2001; 37:1085—1092.

63. Nakayama Y, Nakanishi N, Hayashi T, et al. Pulmonary artery reflection for differentially diagnosing primary pulmonary hypertension and chronic pulmonary thromboembolism. **J Am Coll Cardiol**. 2001; 38:214—218.

64. Kitabatake A, Inoue M, Asao M, et al. Noninvasive evaluation of pulmonary hypertension by a pulsed Doppler technique. **Circulation**. 1983; 68:302—309.

65. Arkles JS, Opotowsky AR, Ojeda J, et al. Shape of the right ventricular Doppler envelope predicts hemodynamics and right heart function in pulmonary hypertension. **Am J Respir Crit Care Med**. 2011; 183:268—276.

66. Sagawa K. **Cardiac Contraction and the Pressure-Volume Relationship**. Oxford University Press; 1988.

67. Westerhof BE, Saouti N, van der Laarse WJ, Westerhof N, Vonk Noordegraaf A. Treatment strategies for the right heart in pulmonary hypertension. **Cardiovasc Res**. 2017; 113:1465—1473.

68. Wong YY, Westerhof N, Ruiter G, et al. Systolic pulmonary artery pressure and heart rate are main determinants of oxygen consumption in the right ventricular myocardium of patients with idiopathic

pulmonary arterial hypertension. **Eur J Heart Fail**. 2011; 13:1290−1295.

69. Uchiyama N, Yuasa T, Miyata M, et al. Correlation of right ventricular wall stress with plasma B-type natriuretic peptide levels in patients with pulmonary hypertension. **Circ J**. 2019; 83:1278−1285.

70. Addetia K, Sebag IA, Marelli A, et al. Right ventricular end-diastolic wall stress: does it impact on right atrial size, and does it differ in right ventricular pressure vs volume loading conditions? **Can J Cardiol**. 2013; 29:858−865.

71. Annone U, Bocchino PP, Marra WG, et al. Echocardiographic estimation of right ventricular wall tension: haemodynamic comparison and long-term follow-up. **Pulm Circ**. 2019; 9.

72. Vonk Noordegraaf A, Westerhof N. Right ventricular ejection fraction and NT-proBNP are both indicators of wall stress in pulmonary hypertension. **Eur Respir J**. 2007; 29:622−623.

73. Hsu S, Houston BA, Tampakakis E, et al. Right ventricular functional reserve in pulmonary arterial hypertension. **Circulation**. 2016; 133:2413−2422.

74. Tello K, Wan J, Dalmer A, et al. Validation of the tricuspid annular plane systolic excursion/systolic pulmonary artery pressure ratio for the assessment of right ventricular-arterial coupling in severe pulmonary hypertension. **Circ Cardiovasc Imaging**. 2019; 12:e009047.

75. Tello K, Dalmer A, Vanderpool R, et al. Cardiac magnetic resonance imaging-based right ventricular strain analysis for assessment of coupling and diastolic function in pulmonary hypertension. **JACC Cardiovasc Imaging**. 2019; 12:2155−2164.

76. Rommel KP, von Roeder M, Oberueck C, et al. Load-independent systolic and diastolic right ventricular function in heart failure with preserved ejection fraction as assessed by resting and handgrip exercise pressure-volume loops. **Circ Heart Fail**. 2018; 11:e004121.

77. Sunagawa K, Yamada A, Senda Y, et al. Estimation of the hydro-motive source pressure from ejecting beats of the left ventricle. **IEEE Trans Biomed Eng**. 1980; 27:299−305.

78. Brimioulle S, Wauthy P, Ewalenko P, et al. Single-beat estimation of right ventricular end-systolic pressure-volume relationship. **Am J Physiol Heart Circ Physiol**. 2003; 284:H1625−H1630.

79. Kuehne T, Yilmaz S, Steendijk P, et al. Magnetic resonance imaging analysis of right ventricular pressure-volume loops: in vivo validation and clinical application in patients with pulmonary hypertension. **Circulation**. 2004; 110:2010−2016.

80. Richter MJ, Peters D, Ghofrani HA, et al. Evaluation and prognostic relevance of right ventricular-arterial coupling in pulmonary hypertension. **Am J Respir Crit Care Med**. 2020; 201:116−119.

81. Sanz J, Garcia-Alvarez A, Fernandez-Friera L, et al. Right ventriculo-arterial coupling in pulmonary hypertension: a magnetic resonance study. **Heart**. 2012; 98:238−243.

82. Vanderpool RR, Rischard F, Naeije R, Hunter K, Simon MA. Simple functional imaging of the right ventricle in pulmonary hypertension: can right ventricular ejection fraction be improved? **Int J Cardiol**. 2016; 223:93−94.

83. Namasivayam M, Hayward CS, Muller DWM, Jabbour A, Feneley MP. Ventricular-vascular coupling ratio is the ejection fraction in disguise. **J Am Soc Echocardiogr**. 2019; 32:791.

84. Trip P, Kind T, van de Veerdonk MC, et al. Accurate assessment of load-independent right ventricular systolic function in patients with pulmonary hypertension. **J Heart Lung Transplant**. 2013; 32:50−55.

85. Spruijt OA, Bogaard HJ, Vonk-Noordegraaf A. Assessment of right ventricular responses to therapy in pulmonary hypertension. **Drug Discov Today**. 2014; 19:1246−1250.

86. Chirinos JA. Ventricular−arterial coupling: invasive and non-invasive assessment. **Artery Res**. 2013; 7:2−14.

87. Chirinos JA, Sweitzer N. Ventricular-arterial coupling in chronic heart failure. **Card Fail Rev**. 2017; 3:12−18.

88. Lankhaar JW, Rovekamp FA, Steendijk P, et al. Modeling the instantaneous pressure-volume relation of the left ventricle: a comparison of six models. **Ann Biomed Eng**. 2009; 37:1710−1726.

89. Kass DA, Beyar R, Lankford E, Heard M, Maughan WL, Sagawa K. Influence of contractile state on curvilinearity of in situ end-systolic pressure-volume relations. **Circulation**. 1989; 79:167−178.

90. Rain S, Handoko ML, Trip P, et al. Right ventricular diastolic impairment in patients with pulmonary arterial hypertension. **Circulation**. 2013; 128:2016−2025, 1-10.

91. Tello K, Dalmer A, Vanderpool R, et al. Right ventricular function correlates of right atrial strain in pulmonary hypertension: a combined cardiac magnetic resonance and conductance catheter study. **Am J Physiol Heart Circ Physiol**. 2020; 318:H156−H164.

92. Marcus JT, Westerhof BE, Groeneveldt JA, Bogaard HJ, de Man FS, Vonk Noordegraaf A. Vena cava backflow and right ventricular stiffness in pulmonary arterial hypertension. **Eur Respir J**. 2019; 54.

93. Sunagawa K, Maughan WL, Sagawa K. Optimal arterial resistance for the maximal stroke work studied in isolated canine left ventricle. **Circ Res**. 1985; 56:586−595.

94. van de Veerdonk MC, Marcus MJT, Westerhof N, et al. Signs of right ventricular deterioration in clinically stable patients with pulmonary arterial hypertension. **Chest**. 2015; 147:1063−1071.

95. Nickel N, Golpon H, Greer M, et al. The prognostic impact of follow-up assessments in patients with idiopathic pulmonary arterial hypertension. **Eur Respir J**. 2012; 39:589−596.

96. Galie N, Jansa P, Pulido T, et al. SERAPHIN haemodynamic substudy: the effect of the dual endothelin receptor antagonist macitentan on haemodynamic parameters and NT-proBNP levels and their association with disease progression in patients with pulmonary arterial hypertension. **Eur Heart J**. 2017; 38:1147−1155.

97. Weatherald J, Boucly A, Chemla D, et al. Prognostic value of follow-up hemodynamic variables after initial management in pulmonary arterial hypertension. **Circulation**. 2018; 137:693−704.

98. Rudski LG, Lai WW, Afilalo J, et al. Guidelines for the echocardiographic assessment of the right heart in adults: a report from the American Society of Echocardiography endorsed by the European Association of Echocardiography, a registered branch of the European Society of Cardiology, and the Canadian Society of Echocardiography. **J Am Soc Echocardiogr**. 2010; 23:685−713. quiz 786-8.

99. Hayashida K, Sunagawa K, Noma M, Sugimachi M, Ando H, Nakamura M. Mechanical matching of the left ventricle with the arterial system in exercising dogs. **Circ Res**. 1992; 71:481−489.

100. Suga H, Yasumura Y, Nozawa T, Futaki S, Igarashi Y, Goto Y. Prospective prediction of O_2 consumption from pressure-volume area in dog hearts. **Am J Physiol**. 1987; 252:H1258−H1264.

101. Vogel-Claussen J, Skrok J, Shehata ML, et al. Right and left ventricular myocardial perfusion reserves correlate with right ventricular

function and pulmonary hemodynamics in patients with pulmonary arterial hypertension. **Radiology**. 2011; 258:119−127.

102. van Wolferen SA, Marcus JT, Westerhof N, et al. Right coronary artery flow impairment in patients with pulmonary hypertension. **Eur Heart J**. 2008; 29:120−127.

103. Marcus JT, Mauritz GJ, Kind T, Vonk-Noordegraaf A. Interventricular mechanical dyssynchrony in pulmonary arterial hypertension: early or delayed strain in the right ventricular free wall? **Am J Cardiol**. 2009; 103:894−895.

104. Gan C, Lankhaar JW, Marcus MJT, et al. Impaired left ventricular filling due to right-to-left ventricular interaction in patients with pulmonary arterial hypertension. **Am J Physiol Heart Circ Physiol**. 2006; 290:H1528−H1533.

105. Altmayer SP, Patel AR, Addetia K, Gomberg-Maitland M, Forfia PR, Han Y. Cardiac MRI right ventricle/left ventricle (RV/LV) volume ratio improves detection of RV enlargement. **J Magn Reson Imaging**. 2016; 43:1379−1385.

106. Manders E, Bogaard HJ, Handoko ML, et al. Contractile dysfunction of left ventricular cardiomyocytes in patients with pulmonary arterial hypertension. **J Am Coll Cardiol**. 2014; 64:28−37.

107. Gupta S, Torres F, Bollineni S, Mohanka M, Kaza V. Left ventricular dysfunction after lung transplantation for pulmonary arterial hypertension. **Transplant Proc**. 2015; 47:2732−2736.

108. Fukumitsu M, Kawada T, Shimizu S, Turner MJ, Uemura K, Sugimachi M. Effects of proximal pulmonary artery occlusion on pulsatile right ventricular afterload in rats. **Circ J**. 2016; 80:2010−2018.

This page intentionally left blank

Chapter 57

Biologic mechanisms and consequences of pulmonary artery stiffening in pulmonary hypertension

Alexis M. Corcoran[1,a], Rakhshinda Rehman[1,a], Marcy Maracle[2], Piera Sosa[3], Paul B. Dieffenbach[1,b] and Laura E. Fredenburgh[1,b]

[1]Division of Pulmonary and Critical Care Medicine, Department of Medicine, Brigham and Women's Hospital, Boston, MA, United States; [2]Schulich School of Medicine and Dentistry, Western University, London, ON, Canada; [3]Meharry Medical College, Nashville, TN, United States

Pulmonary vascular stiffening and mechanobiological feedback in PH pathogenesis

Pulmonary hypertension

Pulmonary hypertension (PH), defined as an elevated mean arterial pressure in the pulmonary arterial (PA) circulation, is a serious and potentially life-threatening condition arising pathologically as a consequence of pulmonary vascular remodeling.[1] Common pathological features of this condition include endothelial dysfunction, inflammation, matrix deposition, increased smooth muscle cell (SMC) contractility, altered cellular metabolism, and amplified vascular cell proliferation, all resulting in both increased pulmonary vascular stiffening and elevated pulmonary vascular resistance (PVR).[2] Although these changes are initially spread heterogeneously throughout the pulmonary circulation and remain clinically silent, progressive disease manifests as exertional dyspnea, hypoxemia, and increased workload on the right ventricle (RV).[3] Severe disease leads to right heart failure and death. At present, treatment options are limited to pulmonary vasodilator therapies, and even these agents have not been found to be helpful for many common etiologies of PH.[4] These limitations have elicited extensive clinical research into potential targets to disrupt and reverse the vascular remodeling process.

Pulmonary vascular stiffening in clinical studies

PA stiffness has become increasingly appreciated as an important disease marker that correlates with disease severity, functional status, and PH mortality.[2] Noninvasive measures of proximal pulmonary vascular stiffness or global PA capacitance have been associated with mortality in pediatric pulmonary arterial hypertension (PAH) patients, idiopathic PAH (iPAH) cohorts, scleroderma-associated PH, and PH in the setting of heart failure.[5−10] Many of these studies showed that pulmonary vascular stiffness measures were better predictors of mortality than typically measured resistance indices,[6,9,10] with particular prognostic utility in patients with normal PVR.[5,9,10]

It is not surprising that PA stiffness measures provide prognostic information, as arterial stiffening is the primary determinant of pulsatile afterload in the RV (as discussed in detail in Chapters 55 and 56), contributing approximately 23% of the RV workload.[11] In contrast with the systemic circulation, vessels throughout the pulmonary vascular tree contribute to vascular capacitance and pulsatile afterload,[12,13] with proximal large arteries contributing only 15%−25% of the total oscillatory load.[14] Global measures of vascular stiffness thus carry information about the status of vessels throughout the pulmonary tree, unlike resistance measures that are primarily impacted by changes in small arteries.

These clinical data and physiologic principles suggest that typical clinical evaluation of PH without assessment of pulmonary vascular stiffness will yield an incomplete portrait of the disease. Several investigators have therefore examined stiffness as a determinant of functional status,

---

[a] These authors contributed equally to this work.
[b] These authors contributed equally to this work.

particularly in early PH. Hunter and colleagues examined pulmonary vascular input impedance during right heart catheterization in a PAH cohort and found that increased input impedance was a better predictor of clinical worsening than PVR index alone.[15] MRI-derived measures of proximal PA stiffness have been shown to be better predictors of poor functional status on 6-minute walk test than standard resistive measures[16] and are also altered early in disease.[17] During cardiopulmonary exercise testing, decreased global PA distensibility predicts patients with known or subsequently diagnosed PH at a time when they had normal resting hemodynamics.[18] In a different cohort of patients with mixed etiologies of PH, PA distensibility was a good independent predictor of peak oxygen consumption in multivariable analysis.[19] These clinical observations offer strong supportive evidence that pulmonary vascular stiffening is an important early marker of disease activity and a clinically important contributor to PH morbidity and mortality.
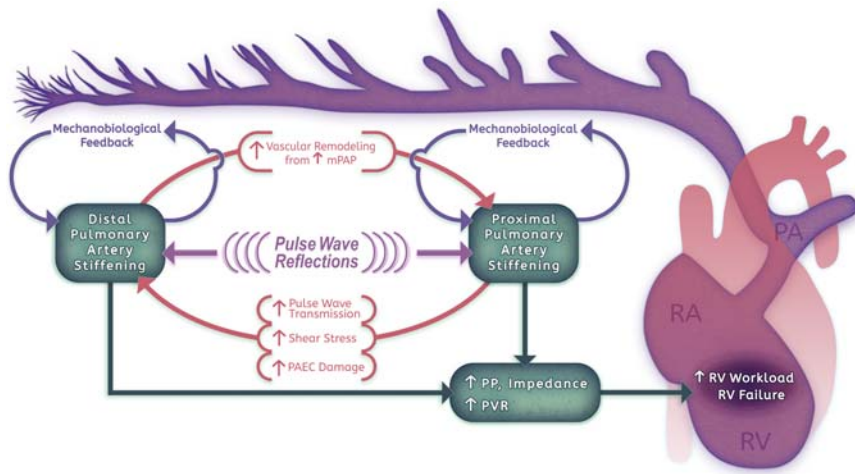
Pathophysiology of pulmonary vascular stiffening in disease progression

Pathophysiologic data from humans and animal PH models have steadily accumulated in favor of a critical role for PA stiffening as an early driver of disease. Stiffening of the proximal pulmonary vasculature amplifies pulse-wave transmission to the distal pulmonary arteries, and can result in inflammation, shear stress, endothelial injury, and smooth muscle remodeling.[20,21] Distal pulmonary vascular stiffening and muscularization increase the mean vascular pressures and result in large vessel remodeling including wall thickening, dilation, and alterations in extracellular matrix (ECM).[13,22] On a cellular level, changes in pulmonary vascular stiffness in either location can alter gene expression and cellular behaviors to promote proliferation and metabolic changes, increased cytoskeletal tension, and matrix alterations that reinforces local cell-matrix stiffness, a process that has been termed mechanobiological feedback.[23–25] The net result of these macroscopic and microscopic reinforcing feedback loops is pathologic progression from early pulmonary vascular stiffening toward increasingly severe vascular remodeling, increased RV afterload, and development of clinical disease.

Although often explained as a later response to changes in the resistance vessels, seminal work in PH models has demonstrated changes in the stiffness and structure of proximal pulmonary vessels at early stages of PH pathogenesis. Foundational work by Meyrick and Reid in the rat hypoxia model noted increased PA diameter and doubling of the elastic lamina thickness at 3–10 days post-exposure.[26] Further work in this model found increased collagen and hydroxyproline synthesis within 3–5 days that correlated with a doubling in stiffness throughout the

PA tree by pressure–volume loop analysis.[27,28] Ex vivo testing of mouse PAs after 1–2 weeks of hypoxia exposure also showed an increase in elastic modulus and thickening of collagen and elastin in the PA wall.[29] In the monocrotaline (MCT) rat model, the Rabinovitch laboratory found early disruption in the internal elastic lamina and high elastase activity within days after injection, weeks before hemodynamic changes.[30] Hints of distal pulmonary vascular stiffening were also seen by Meyrick and Reid, who noted muscularization of intraacinar PAs at day 3 after hypoxia or Crotolaria exposure.[31] This neomuscularization has more recently been found to arise from distal migration and proliferation of SMC progenitor cells.[32] Using atomic force microscopy to directly measure passive mechanical properties of frozen tissues, Liu et al. found a 1.5-2-fold increase in PA stiffness in the media of small vessels within 1 week of pathologic stimuli in both the MCT and sugen/hypoxia rat PH models.[24] Direct flow and pressure measurements from the main PA in vivo in the MCT model also demonstrate this early stiffening, indicating an early and linear decrease in compliance throughout the disease process before the development of a nonlinear change in resistance properties.[33]

Stiffness of the proximal pulmonary vasculature is determined in large part by the composition of the ECM proteins in the laminae of the vessel wall. The most prominent of these proteins are elastin, allowing flexibility, and collagen, providing strength.[27,28] Studies have shown that vascular remodeling occurring from PH correlates with inflammatory cell accumulation, elastin breakdown, collagen production, and vessel dilation.[34] The findings of elastin degradation and collagen accumulation correlate well with ex vivo biaxial strain testing of human PH tissue, which demonstrate collagen-predominant mechanics regardless of strain conditions.[35] Proximal pulmonary vasculature stiffening affects distal vessels by augmenting pulse wave transmission and generating high pulsatile flow distally (Fig. 57.1).[20,21,36] Studies on the effects of flow pulsatility on the endothelium and underlying smooth muscle have demonstrated alterations in nitric oxide (NO), prostaglandin-F1α, and endothelin production, increased expression of leukocyte adhesion molecules, and alterations in smooth muscle contractile proteins,[20,21,36] all of which contribute to distal remodeling. At the same time, early distal vessel stiffening and muscularization from these and other pathogenic processes will increase circumferential stress in the proximal pulmonary vessels due to pulse wave reflections and pressure-induced dilation.[13] Locally, the change in pulmonary vascular stiffness at the cellular level activates mechanotransduction pathways including integrins, cytoskeleton-associated kinases, mechanosensitive calcium channels, and nuclear transducers to increase expression of matrix proteins and cross-linking enzymes,[24,25] alter metabolism,[37] downregulate vasodilatory

FIGURE 57.1 **Pulmonary arterial stiffening in the pathogenesis of pulmonary hypertension.** Proximal and distal pulmonary arterial (PA) stiffening and stiffness-dependent mechanobiological feedback loops, which propagate pulmonary vascular remodeling, play a key role in the pathobiology of pulmonary hypertension (PH). Proximal PA stiffening may amplify pulse wave transmission to the distal pulmonary vasculature resulting in increased shear stress and injury to pulmonary artery endothelial cells (PAEC), inflammation, and vascular cell remodeling behaviors that drive distal PA stiffening. Distal PA stiffening can promote increased mean PA pressures (mPAP), leading to large PA vessel wall thickening, dilation, and extracellular matrix (ECM) alterations which drive proximal PA stiffening. Together, this crosstalk between proximal and distal PA stiffening leads to increased pulse pressure (PP) and impedance and elevated pulmonary vascular resistance (PVR) which increase right ventricular (RV) workload and ultimately may lead to RV failure in PH. *Modified from Dieffenbach PB, Maracle M, Tschumperlin DJ, Fredenburgh LE. Mechanobiological feedback in pulmonary vascular disease.* **Front Physiol**. *2018; 9:951.*

prostanoids,[24,25] and drive proliferation, all reinforcing vascular remodeling through mechanobiological feedback (Fig. 57.2).[2] In the remainder of this chapter, we will focus on these molecular pathways that drive stiffness-mediated signaling, and how targeting these pathways may offer the potential to disrupt mechanobiological feedback and pathologic pulmonary vascular remodeling in PH.
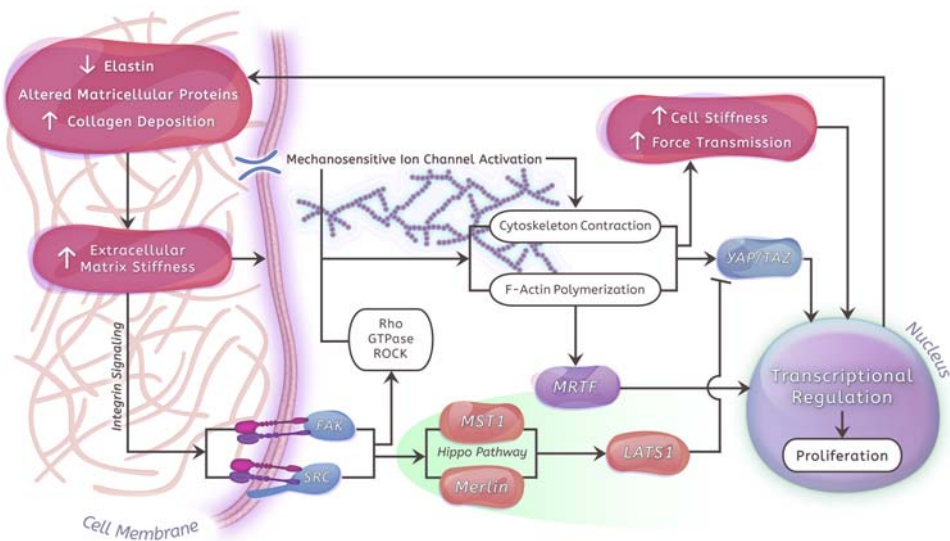
Regulation of smooth muscle contractility and tone

In the absence of disease, contractility of arterial smooth muscle regulates PA luminal diameter, thereby maintaining normal pressures and adequate blood flow throughout the pulmonary vasculature. In the setting of PH, several pathogenic stimuli, including PA stiffening, can lead to dysregulation of pulmonary artery smooth muscle cell (PASMC) contractile function, including increased tone and impaired relaxation, through a variety of mechanisms. PH leads to well-described dysregulation of the endothelial-derived mediators of arterial stiffness, NO and endothelin-1 (ET-1), which induce smooth muscle vasodilation and vasoconstriction, respectively.[38,39] Throughout the vascular tree, high pulsatility flow (HPF) increases ET-1 expression and decreases endothelial nitric oxide synthase (eNOS)-derived NO production, which enhance PA tone and lead to increased vascular resistance and stiffness. Increased proximal PA stiffness leads to further pulsatile flow and propagates the dysfunction deeper into the pulmonary

vascular tree. Additionally, HPF upregulates expression of contractile proteins such as α-smooth-muscle actin (α-SMA) and smooth muscle myosin heavy chain.[21,40,41] This may lead to hyperactive pulmonary vascular smooth muscle contractility leading to sustained abnormal vasoconstriction and thereby contributing to PH progression.[42]

During PH pathogenesis, several molecular pathways are activated to enhance vasoconstriction via increased phosphorylation of myosin light chain (MLC). Canonically, adrenergic stimulation activates myosin light chain kinase (MLCK) and induces PASMC contraction by activating calcium-dependent channels in the endoplasmic reticulum to increase cytosolic Ca^{2+} concentration ($[Ca^{2+}]$).[41] Several mechanosensitive calcium channels have been shown to play a role in enhancing MLCK activation and vasoconstriction in response to mechanical signals. In particular, the channels TRPV4, TRPM7, and TRPC6 have been shown to be significantly upregulated in iPAH PASMC compared with control cells,[43] and correlate with increased cytoplasmic calcium in response to shear stress. In animal models, hypoxia-induced TRPV4 expression correlates with increased vascular tone and TRPV4 deficiency attenuates hypoxia-induced pulmonary vascular remodeling in mice, indicating a significant role for these stiffness-dependent ion channels in PH pathobiology.[44]

An alternative regulatory mechanism that enhances SMC tone includes inhibition of MLC phosphatase (MLCP), which counteracts the effects of MLCK. The most well-studied mechanism of MLCP inhibition is the

FIGURE 57.2   Molecular mechanisms of mechanobiological feedback in pulmonary hypertension. Increased extracellular matrix stiffness activates mechanotransduction pathways, which promote vascular cell proliferation and pulmonary vascular remodeling and amplify pulmonary vascular stiffening in a mechanobiological feedback loop in pulmonary hypertension (PH). Key molecular pathways include integrins, cytoskeleton-associated kinases, mechanosensitive calcium channels, and nuclear transducers such as myocardin-related transcription factors (MRTF) and the Hippo pathway downstream effectors Yes-associated protein (YAP) and transcriptional coactivator with PDZ-binding motif (TAZ). Matrix stiffness regulates activation of integrin signaling and key intracellular mechanosensors, focal adhesion kinase (FAK) and steroid receptor coactivator (Src), which can activate Rho GTPase and its downstream target Rho-associated protein kinase (ROCK) and increase pulmonary artery smooth muscle cell contraction. FAK and Src also regulate the Hippo pathway and when activated may suppress Merlin, leading to inactivation of MST1/2 and LATS1/2 and promoting nuclear translocation of YAP/TAZ. When activated, nuclear YAP/TAZ bind to transcription factors to drive mechanical signaling leading to enhanced proliferation and apoptosis resistance in pulmonary vascular cells. Stiffness-induced F-actin polymerization and stress fiber formation also liberates MRTF from G-actin cytoplasmic complexes allowing it to translocate to the nucleus where it regulates smooth muscle cell contractile genes which contribute to vascular remodeling in PH. *Modified from Dieffenbach PB, Maracle M, Tschumperlin DJ, Fredenburgh LE. Mechanobiological feedback in pulmonary vascular disease.* **Front Physiol**. *2018; 9:951.*

RhoA/ROCK pathway, which plays an important role in the development of vascular diseases.[45] RhoA GTPase is activated by FAK and Src downstream of matrix stiffness-induced activation of integrin signaling (Fig. 57.2) (discussed in more detail below), as well as vasoconstriction-activated G-protein coupled receptors. RhoA GTPase then activates its downstream target RhoA-associated protein kinase (ROCK), which inhibits MLCP and leads to enhanced SMC contraction. RhoA is particularly important for sustaining enhanced tone and SMC contractility in the setting of decreasing cytosolic $[Ca^{2+}]$, and disruption of this process with Rho kinase inhibitors has been shown to be highly effective at decreasing vasoconstriction and contraction.[41,46] Treatment with the ROCK inhibitor fasudil has been found to suppress both MCT-induced PH and hypoxia-induced PH in rodents,[47,48] and has had modest success in early clinical trials in PAH.[49]

Myocardin-related transcription factors (MRTFs) are emerging as a key link between gene expression changes and stiffness-driven cellular activation in PH and fibrotic lung disease. These stiffness-dependent transcription factors are fundamental constituents of a profibrotic mechanobiological feedback loop downstream of ECM stiffness and RhoA/ROCK (Fig. 57.2).[50,51] MRTFs form complexes with monomeric soluble G-actin, sequestering them in the cytoplasm. With increased mechanical stress or migration, G-actin becomes polymerized into F-actin filaments and forms stress fibers, releasing MRTFs from cytoplasmic complexes and allowing for their nuclear translocation. There, MRTFs act as cofactors for serum response factor to modulate expression of a transcriptional program central to SMC contractile machinery[50,52,53] including α-SMA,[54] which may drive pulmonary vascular remodeling in PH. MRTFs have also been linked to activation of inflammatory responses in SMCs, endothelial cells, and myofibroblasts, and are known to be downstream effectors of profibrotic signaling.[2] Inhibition of MRTF-A using shRNA reduced collagen deposition and significantly attenuated the development of PH in hypoxia-exposed rats.[55]

Proliferation

At the cellular level, one of the most striking effects of ECM stiffness is the development of a hyperproliferative phenotype in PASMC and pulmonary artery endothelial cells (PAEC), which may contribute to the medial hypertrophy, neointimal formation, and plexiform lesions observed in PAH. This is nicely illustrated in vitro, where

human PASMC and PAEC demonstrate exaggerated proliferation and enhanced matrix production when grown on stiff matrices (mimicking remodeled PAs) compared with soft matrices mimicking physiologic PA stiffness.[24] This is accompanied by transcriptional changes in mechanosensitive genes which serve to further amplify proliferation and pulmonary vascular remodeling in a self-sustaining mechanobiological feedback loop.[24,25] The feed-forward loop initiated by stiffness-induced pulmonary vascular cell activation has led to investigation of matrix alterations and proproliferative mechanotransduction pathways as potential early contributors to PH pathogenesis.

Under homeostatic conditions, the ECM is regulated by a balance of proteolytic enzymes and their endogenous tissue inhibitors. In PAH, this balance becomes disrupted, leading to increased collagen production, deposition, and cross linkage. Increased deposition of type I, III, and IV collagen is observed in animal models of PH, and type III collagen levels correlate with severity and rapidity of disease progression in PAH.[56,57] Following increases in collagen deposition, ECM components such as tenascin-C (Tn-C), fibronectin, and serine elastases may accumulate in pulmonary arteries of PAH patients.[58,59] Tn-C is an ECM glycoprotein that is known to play a pivotal role in regulating cell adhesion, and whose expression correlates with PASMC proliferation in PAH.[58] Fibronectin, a key integrin ligand, is upregulated in intimal lesions and plays a role in medial smooth muscle remodeling in PAH.[60] These matrix alterations lead to increased stiffness in the intravascular and perivascular regions, particularly in smaller pulmonary vascular beds.[34] In proximal PAs and small arteries that contain an elastic lamina, serine elastases, which are upregulated in PAH and colocalize with pathological neointimal lesions, play a key role in vascular mechanics.[61] This accumulation of collagen and degradation of elastin by serine elastases result in lower arterial compliance and increased PA stiffness.[62] On a cellular level, elastin fragmentation promotes PASMC remodeling through liberation of matrix-bound mitogens and exposure of novel integrin binding sites.[63–65] Inhibition of serine elastases can lead to regression of progressive medial PA hypertrophy in culture ex vivo[66] and has been shown to attenuate pulmonary vascular remodeling in PH models.[67–70]

Alterations in levels of matrix metalloproteinases (MMPs) and their endogenous inhibitors, tissue inhibitors of metalloproteinases (TIMPs), can also increase extracellular stiffness in PAH.[71] MMPs are a family of zinc-dependent endopeptidases that reduce matrix stiffness by degrading ECM proteins including collagen and elastin.[72] MMPs also influence endothelial and SMC migration, proliferation, and contraction, and thus play an important role in vascular tissue remodeling in PAH. Under normal conditions, MMP levels are regulated by TIMPs, and the MMP/TIMP ratio is essential for maintaining ECM homeostasis.[73] In PAH, this normal MMP/TIMP balance becomes disrupted, leading to changes in ECM environments (Fig. 57.2). MMP-2 and MMP-9, the most efficient MMPs at degrading collagen, have been associated with vascular SMC activation and neointimal formation in arterial tissue remodeling in PAH,[74–76] and are increased in PASMC from iPAH patients.[63] MMP-9 levels have also been to found to correlate with disease severity in PAH.[14,57] In addition, MMP-3, which is likely to be a critical regulator of arterial stiffness due to its interactions with most major matrix components, is significantly reduced in human iPAH cells.[71,77] TIMP-1 and TIMP-2 are also increased in iPAH[71] and may be indicative of active vascular remodeling and reflect clinically relevant markers of disease and outcome in PAH.[57] While several animal models of PH suggest roles for MMP-2, MMP-9, and MMP-3 in disease pathogenesis,[78,79] studies of other MMP subtypes differ across animal models used, making it difficult to determine their roles in PAH from animal models alone.[14] Further work is needed to precisely delineate the roles of different MMP and TIMP subtypes in regulating ECM stiffness and PH pathogenesis.

Changes in ECM stiffness are transmitted intracellularly by integrins (Fig. 57.2), which act as both signaling receptors and physically connect the ECM to the cytoskeleton.[80] Upon binding to the ECM, most notably fibronectin, integrins connect to the intracellular actomyosin system via linking proteins such as talin and vinculin, initiating downstream mechanosignaling.[81] In animal models, increased expression of α_1-, α_8-, and α_v-integrins and decreased expression of α_5- and β_1-integrins has been observed in PAs from hypoxia-exposed and MCT-treated rats.[82] Activation of MMPs also leads to accumulation of $\alpha_v\beta_3$ integrin, which interacts with many ECM ligands including fibronectin, collagen, and several MMP substrates.[63] Several studies have demonstrated that $\alpha_v\beta_3$ integrin is associated with increased SMC proliferation and migration as well as decreased SMC apoptosis,[83,84] suggesting an important role for $\alpha_v\beta_3$ integrin in mediating stiffness-induced vascular cell activation and remodeling in PH.

When integrins are activated, their cytoplasmic domains associate with focal adhesions (FAs), which directly transmit forces between the ECM and the cytoskeleton. These forces are also translated into signaling pathways via mechanotransduction. The steroid receptor coactivator (Src) family of tyrosine kinases and focal adhesion kinase (FAK) are two important proteins that are activated and recruited by ligand-bound integrins to FAs and modulate cytoskeletal proteins via mechanotransduction (Fig. 57.2).[14,85,86] Increased activation of FAK and Src has been observed in PAH PASMC and are associated with enhanced proliferation and migration.[87–90] Inhibition of

either FAK and Src activation has been shown to attenuate experimental PH in rodent models,[87,88] suggesting potential roles for FAK and Src in driving stiffness-dependent pulmonary vascular remodeling in PAH.

The Hippo pathway has emerged as playing a critical role in mediating the effects of ECM stiffness on vascular remodeling phenotypes in PAH, particularly via the homologous transcriptional coactivators, Yes-associated protein (YAP) and transcriptional coactivator with PDZ-binding motif (TAZ) (Fig. 57.2). Canonically, Hippo signaling suppresses cell proliferation by inactivating YAP/TAZ, which promote downstream proproliferative and antiapoptotic signaling pathways. Hippo pathway component FERM domain-containing tumor suppressor NF2 (neurofibromatosis type 2)/Merlin activates MST1/2 and serine-threonine kinases LATS1/2 which leads to sequestration of YAP/TAZ in the cytoplasm for degradation.[91−93] Increased ECM stiffness and enhanced integrin signaling through FAK and Src may downregulate the Hippo pathway by suppressing Merlin, leading to inactivation of MST1/2 and LATS1/2, and nuclear translocation of YAP/TAZ. Nuclear accumulation of YAP/TAZ activates a transcriptional program that may promote a hyperproliferative and apoptosis-resistant phenotype in PASMC and PAEC in PAH. While the Hippo pathway is the canonical YAP/TAZ regulator, there may also be relevant YAP/TAZ phosphorylation-independent modifiers of YAP/TAZ localization, including ECM rigidity, strain, and shear stress.[94]

Nuclear YAP/TAZ target a number of promoter-specific transcription factors to drive mechanical signaling, including the transcriptional enhancer activator domain (TEAD) family, which promote cellular proliferation and survival.[93] Upregulation of YAP/TAZ activity in response to matrix stiffness promotes collagen deposition and cross-linking, and is necessary for the development of stiffness-dependent vascular remodeling in PH.[23,25] This demonstrates the potential for a pathological positive feedback loop between YAP/TAZ upregulation and ECM stiffness. Promising in vivo studies have shown that pharmacological inhibition of YAP/TAZ leads to significant reductions in pulmonary vascular stiffness, RV pressures, and RVH in animal models of PH.[95]

In addition to the Hippo pathway, the transforming growth factor-β (TGF-β)/bone morphogenetic protein (BMP) pathway contributes to proliferative phenotypes in PAH. Bone morphogenetic protein type 2 receptor (BMPR2), a TGF-β receptor, is particularly relevant as mutations in the BMPR2 gene are present in 70% of heritable PAH cases and underly many cases of iPAH.[96] Loss of BMPR2 function promotes PASMC proliferation via altered TGF-β1 signaling. In addition to enhancing PASMC proliferation, exaggerated TGF-β1 signaling may regulate many cellular responses including inflammation,
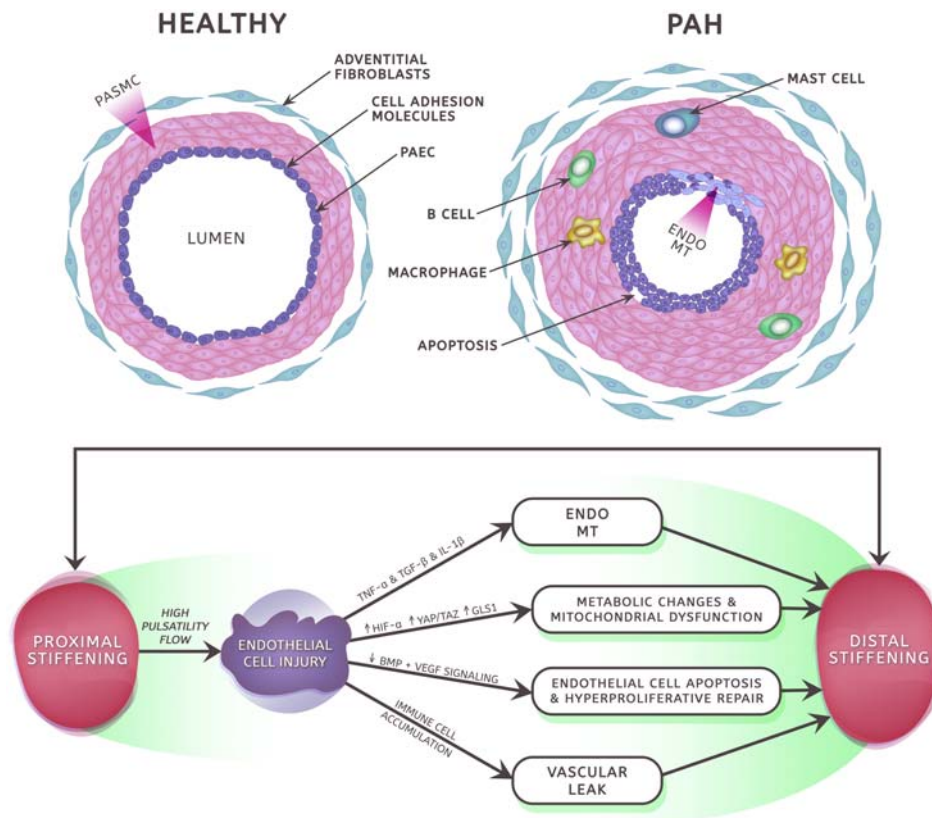
angiogenesis, and migration, many of which are altered in PAH.[97] Recent studies have sought to understand the role of BMPR2 mutations in PAH development, particularly as the penetrance of PAH in families with BMPR2 mutations is only around 20%. While loss of BMP signaling induces PASMC hyperproliferation, disruption of BMPR2 increases apoptosis in PAEC in PAH.[98] PAEC transfected with mutant BMPR2 demonstrate enhanced apoptosis and release more TGF-β compared with control cells.[99] Disruption of normal TGF-β signaling is communicated via paracrine signaling from PAEC and leads to increased PASMC proliferation.[99,100] Similarly, HPF that mimics PAH environments in vitro has been found to increase PAEC apoptosis and TGF-β release (Fig. 57.3) and induce PASMC proliferation.[99]

Matrix stiffness has also been shown to alter endothelial responses to vascular endothelial growth factor (VEGF).[101,102] VEGF and its receptor 2 (VEGFR-2) regulate proper endothelial cell (EC) differentiation and function, and their signaling may be affected by ECM stiffness in PAH. Inhibition of VEGFR-2 with SU5416 initially causes PAEC apoptosis, but is followed by hyperproliferation of the remaining apoptosis-resistant PAEC in the setting of increased shear stress[103] and hypoxia leading to development of plexiform lesions in vivo.[104] Further studies are required to elucidate the effects of PA stiffness on BMP/TGF-β and VEGF signaling, as well as crosstalk between BMP/TGF-β, VEGF, and the Hippo pathway in driving stiffness-induced vascular remodeling in PAH.

Inflammation and endothelial dysfunction

Ongoing investigation into PAH pathogenesis has frequently highlighted a role for inflammatory signaling. Both innate immune cells and adaptive immune lymphocytes are found in the interstitium and tertiary lymphoid tissue around remodeled vessels in human PAH and rodent PH models.[105] Furthermore, many inflammatory cytokines, such as IL-1β, IL-2, IL-4, IL-6, IL-8, IL-10, IL-12, p70, and tumor necrosis factor-α (TNF-α), are more highly expressed in PAH patients compared to controls.[106] Not surprisingly, there is extensive crosstalk between inflammation, endothelial dysfunction, and vascular stiffness. Inflammation-induced vascular leak and edema can lead to arterial stiffening and increased tone prior to collagen deposition and fibrosis, while altered blood flow and matrix characteristics due to vessel stiffening can enhance inflammatory cell migration and inflammatory signaling.[107]

Matrix stiffness is a critical mediator of endothelial barrier characteristics due to its impact on cell−cell and cell-matrix adhesion properties. In stiff ECM environments, ECs have punctate expression of VE cadherin, a principle cell−cell junction protein, as compared to on softer matrix,

FIGURE 57.3 **Biological mechanisms and effects of pulmonary arterial stiffening in endothelial cells in pulmonary hypertension.** Proximal pulmonary arterial (PA) stiffening increases flow pulsatility in the distal vasculature which may cause endothelial injury leading to pulmonary artery endothelial cell (PAEC) apoptosis, vascular leak, and hyperproliferative repair in pulmonary hypertension (PH). Stiffness-induced endothelial barrier disruption allows for immune cell infiltration and increased expression of inflammatory cytokines including tumor necrosis factor (TNF)-α, transforming growth factor (TGF)-β, and interleukin (IL)-1β, which may promote endothelial to mesenchymal transition (EndoMT). Bone morphogenetic protein (BMP) and vascular endothelial growth factor (VEGF) signaling may modulate endothelial cell responses to PA stiffness-induced alterations in flow and endothelial injury and may promote hyperproliferative repair in PH. Metabolic reprogramming and mitochondrial dysfunction may also occur in PAEC in PH with a shift from oxidative phosphorylation to glycolysis, which is dependent on hypoxia-induced factor (HIF)-1α. Matrix stiffness activates YAP/TAZ which may promote HIF-1α stabilization as has been observed in cancer cells, although further study is necessary in PH. Stiffness-induced YAP/TAZ activation upregulates glutaminase 1 (GLS1), which promotes glutaminolysis and drives hyperproliferation in pulmonary vascular cells. Together, these stiffness-induced endothelial responses drive pulmonary vascular remodeling and propagate distal and proximal PA stiffening in a mechanobiological feedback loop.

where VE−cadherin junctions are continuous between ECs.[108] Stiffness also increases EC permeability through Rho force transmission via enhancing EC actomyosin-mediated contractility.[109] Increased intracellular contractile function leads to cell edge retraction and disruption of tight junctions, which subsequently allows for infiltration of circulating immune cells (Fig. 57.3).[110] Consequently, ECs grown on stiff matrix have enhanced leukocyte transmigration, increased expression of inflammatory cytokines, and higher induction of leukocyte adhesion molecules in response to inflammatory stimuli such as TNF-α or lipopolysaccharide.[111,112] The synergistic effects of inflammation on vascular remodeling are also demonstrated by the induction of fibronectin, collagen 1, and lysyl oxidase,[112] which contribute to progressive matrix stiffening.

Early pulmonary vascular stiffening in PH also induces inflammation through alterations in vascular flow characteristics and subsequent endothelial injury (Fig. 57.3). Like most endothelial stressors, HPF and shear-induced injury can lead to expression of endothelial adhesion molecules and induction of cytokines that enhance inflammatory cell recruitment.[105] Nuclear factor-kappa B (NF-κB) is a transcription factor known to be involved in flow-mediated inflammatory responses in endothelial cells,[113−115] and has been found to be strongly activated early and continuously by high-pulsatility flow[36] and mechanical stretch.[116] In vivo, NF-κB contributes to vascular inflammation by recruiting leukocytes to perivascular regions of PAs during vascular remodeling.[117] Inhibition of NF-κB attenuates peri-vascular inflammation, development of PH, and RVH

in rodent models.[117,118] One of the key proinflammatory cytokines regulated by NF-κB is IL-6, which has been found to be increased and associated with mortality in PAH.[106] Overexpression of IL-6 in the lung leads to spontaneous PH and RVH development in mice, which is exacerbated by hypoxia and leads to occlusive neointimal angioproliferative lesions composed of T cells and endothelial cells.[119] IL-6 and other inflammatory cytokines have also been shown to drive PASMC proliferation[120] and contribute to endothelial to mesenchymal transition (EndoMT),[121] likely further enhancing vascular stiffening in PH (Fig. 57.3). This crosstalk between inflammation and pulmonary vascular stiffening is an important contributor to PH pathophysiology that would benefit from further investigation.

Endothelial to mesenchymal transition

EndoMT is emerging as another phenotype which may contribute to endothelial dysfunction and vascular remodeling in PAH,[121,122] and may be dependent on ECM stiffness. ECs in the pulmonary vasculature normally act as a barrier between blood components such as inflammatory cells and tissues and remain in a monolayer comprising the vessel wall. In PAH, inflammatory processes and altered TGF-β/BMPR2 signaling have been shown to compromise this barrier and contribute to the induction of mesenchymal markers, intimal thickening, and medial migration of endothelial cells, a process known as EndoMT (Fig. 57.3).[121] In vitro, EndoMT is stimulated by increased TGF-β receptor signaling from TGF-β and cytokines leading to migration and further decreased barrier integrity in PAEC.[121,123]

During EndoMT, PAEC become elongated and lose EC-specific adhesion proteins that help maintain barrier integrity such as CD31/PECAM-1 and VE-cadherin.[124,125] These PAEC then detach from the endothelial layer and change their morphologic characteristics. They take on a more mesenchymal-like phenotype with increased collagen deposition and α-SMA expression. BMPR2 signaling has been shown to attenuate EndoMT phenotypes, and cells with BMPR2 mutations have enhanced EndoMT induction.[97,126] In animal models of PH, hypoxia has been shown to increase expression of transcriptional drivers of EndoMT.[122,127] In vitro, inflammatory cytokines IL-1β, IL-6, TNF-α, and reactive oxygen species (ROS) induce EndoMT through TGF-β pathway activation, indicating that inflammatory signaling promotes EndoMT. ET-1 has synergistic effects with TGF-β and cytokines in inducing EndoMT, which is of interest given the role of ET-1 in proximal pulmonary artery stiffening.[128] In addition, HPF has been shown to induce EndoMT and activate adventitial fibroblasts.[129]

YAP/TAZ signaling has been implicated in EndoMT in the cardiovascular system, with downregulation of YAP disrupting EndoMT in vitro and in vivo, leading to cardiac cushion defects in EC-specific YAP knockout mice.[130] EndoMT can also be induced by canonical Wnt signaling. In a myocardial infarction model and using lineage tracing, one group demonstrated that the Wnt pathway was activated in α-SMA-positive mesenchymal cells derived from ECs.[131] In vitro, activation of canonical Wnt signaling was associated with induction of mesenchymal markers and reduction in endothelial markers in endothelial cells.[131] Furthermore, TGF-β1-induced EndoMT in aortic valvular endothelial cells was enhanced in cells grown on stiff substrates and was accompanied by increased nuclear localization of β-catenin.[132] Further research is needed to determine the role of ECM stiffness and the Hippo pathway, as well as crosstalk with Wnt signaling, in driving EndoMT in PAH.

Angiogenesis

Vascular stiffness may also contribute to PH pathogenesis via upregulation of proangiogenic signaling.[108,133] Circulating levels of VEGF are elevated in PAH patients and VEGF and VEGFR-2 are both robustly expressed in pulmonary vascular neointimal lesions.[134] Leukocyte recruitment in PAH may lead to release of many proangiogenic factors that induce resident vascular cells to initiate new vessel growth.[135–137]

Several groups have demonstrated that MMPs, in addition to modulating ECM, regulate angiogenesis. MMP-9, which is increased in PAH patients, regulates the bioavailability of VEGF and has been shown to increase angiogenesis in metastatic cancer.[138,139] MMP-13 also stimulates VEGF secretion and promotes tumor angiogenesis through FAK signaling.[140] Membrane-bound MMP-14 regulates localization of VEGFR-2 on the cell surface and is required for increased angiogenesis in cancer.[108,141] MMP-2 is also localized at the cell surface during angiogenesis by interactions with integrin αvβ3, which, along with other αv integrins, are known to be overexpressed on the EC surface of newly forming vessels.[142] Studies in solid tumors have also found that increased Rho/ROCK-dependent cytoskeletal tension in ECs allow for capillary network formation.[143]
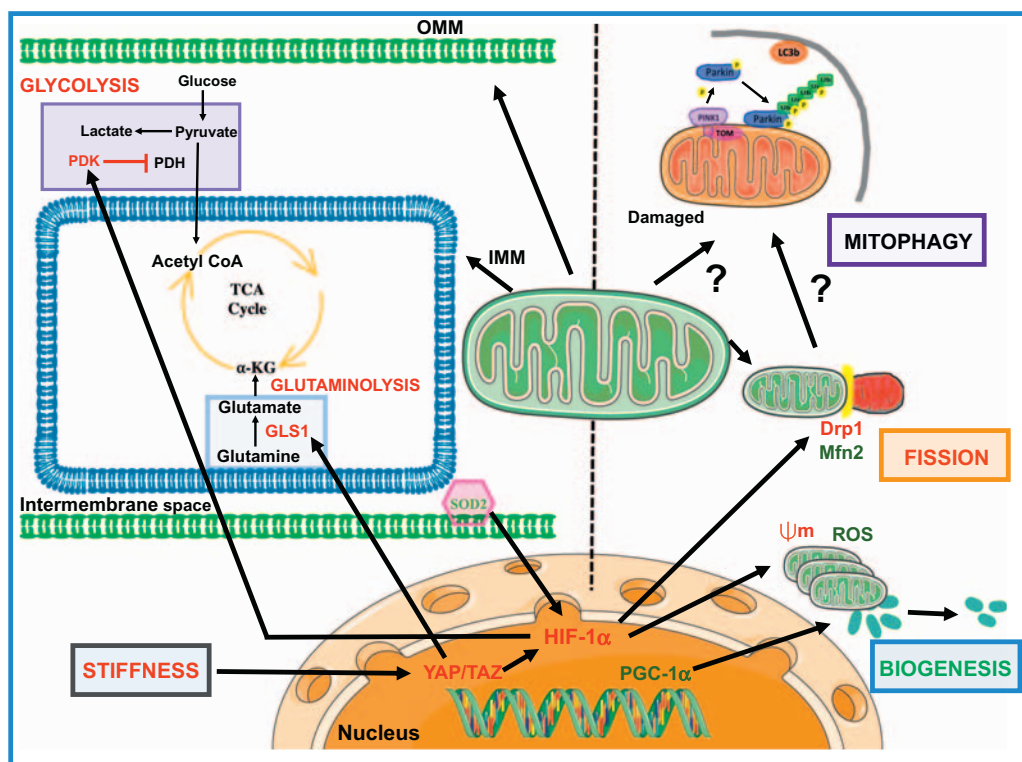
Hippo pathway mechanotransduction has also been associated with angiogenesis downstream of VEGF signaling. VEGFR activation inhibits MST1/MST2 and LATS1/LATS2, thus indirectly upregulating YAP/TAZ.[144] YAP/TAZ likely play a critical role in vascular sprouting, branching, and angiogenesis, as EC-specific YAP/TAZ knockout mice are embryonically lethal with heart and vascular malformations.[145] In addition, YAP knockdown

results in defective EC tubular network formation.[146] One of the key transcriptional regulatory targets of YAP in ECs is angiopoietin-2 (Ang-2), a vascular growth factor secreted by ECs at active remodeling sites that demonstrates context-specific regulation of angiogenesis.[144,146] The interactions between YAP/TAZ, VEGF, and Ang-2 and their in vivo consequences suggest an important role for stiffness and YAP/TAZ signaling in the regulation of angiogenesis; however, the crosstalk and effects on vascular remodeling in PAH has not yet been clearly established. While many studies demonstrate the role of stiffness-associated signaling and angiogenesis in the field of oncology, further work is needed to determine how

mechanotransduction contributes to regulation of angiogenesis in PAH pathobiology.

Metabolic reprogramming and mitochondrial dysregulation

Metabolic reprogramming, also called the Warburg effect, refers to the shift from oxidative phosphorylation to aerobic glycolysis in order to meet cellular energy requirements (Fig. 57.4).[147] Abnormalities in metabolic reprogramming have been increasingly recognized as pathologic contributors to many diseases including asthma, obesity, diabetes, chronic obstructive pulmonary disease, PAH, and

FIGURE 57.4 Vascular stiffness and mitochondrial dysfunction in pulmonary arterial hypertension. Metabolic reprogramming and mitochondrial dysfunction are increasingly recognized as contributing to the pathobiology of pulmonary arterial hypertension (PAH) with a shift from glucose oxidation to glycolysis (Warburg effect). Stabilization of the transcription factor HIF-1α leads to upregulation of PDK, PDH inactivation, and inhibition of pyruvate conversion to acetyl-CoA. Stiffness-induced YAP/TAZ activation may play a role in HIF-1α stabilization in PAH, as has been observed in malignant cells. Stiffness-mediated YAP/TAZ activation also enhances GLS1-dependent glutaminolysis, replenishing the TCA cycle metabolite α-ketoglutarate which may contribute to amino acid and nucleic acid biosynthesis in hyperproliferative pulmonary vascular cells. Other mitochondrial abnormalities in PAH include an increase in the mitochondrial membrane potential (Ψm), alteration in mitochondrial-derived ROS generation, reduced mitochondrial biogenesis (decreased PGC-1α), and enhanced mitochondrial fission/fragmentation (increased Drp1, decreased Mfn2). Much less is known about mitophagy, the process of removing damaged mitochondria, in PAH and whether it may contribute to reduced mitochondrial mass and pulmonary vascular remodeling phenotypes. While it is unknown whether vascular stiffness regulates mitochondrial dynamics in PAH, YAP has been shown to modulate expression of Drp1 and regulate mitochondrial fission and mitochondrial membrane potential during myofibroblast differentiation. Further study is needed to elucidate the effects of pulmonary vascular stiffening on mitochondrial quality control and metabolic dysfunction in PAH. *Acetyl-CoA*, acetyl coenzyme A; *α-KG*, α-ketoglutarate; *Drp1*, dynamin-related protein 1; *GLS1*, glutaminase 1; *HIF-1α*, hypoxia-induced factor-1α; *IMM*, inner mitochondrial membrane; *LC3B*, microtubule-associated protein 1 light chain-3B; *Mfn2*, mitofusin 2; *OMM*, outer mitochondrial membrane; *P*, phosphoryl group; *PDH*, pyruvate dehydrogenase; *PDK*, pyruvate dehydrogenase kinase; *PGC-1α*, Peroxisome proliferator-activated receptor-γ coactivator 1α; *PINK1*, PTEN-induced kinase 1; *ROS*, reactive oxygen species; *SOD2*, superoxide dismutase 2; *TAZ*, transcriptional co-activator with PDZ-binding motif; *TCA*, tricarboxylic acid; *TOM*, translocase of the outer membrane; *Ub*, ubiquitin; *YAP*, Yes-associated protein; *Ψm*, mitochondrial membrane potential. Red text denotes pathways that are increased in PAH, while green text indicates pathways that are downregulated in PAH.

particularly malignancies.[148,149] Given the known changes in proliferative capacity and dedifferentiation that occur during PAH pathogenesis, it is perhaps unsurprising that the Warburg effect has been consistently found in arterial vascular cells in PAH patients and rodent PH models.[150] Endothelial cells engineered to overexpress BMPR2 mutations found in patients with hereditary PAH also demonstrate increased glycolysis and the Warburg effect in culture, indicating that this reprogramming may be an important "first hit" in PAH pathogenesis.[151]

Enhanced glycolysis is well-established downstream of hypoxia-induced factor-1α (HIF-1α) activation in the setting of hypoxia, but the mechanism of Warburg activation under normoxic conditions in pulmonary vascular cells during PAH pathogenesis has been less understood until recently. An early clue was the effectiveness of the pyruvate dehydrogenase kinase (PDK) inhibitor dichloroacetate (DCA) in driving PAH-derived PASMC apoptosis and partially reversing PH in animal models.[152] PDK is a direct target of HIF-1α (Fig. 57.4), and implied likely HIF-1α stabilization during normoxic pulmonary vascular remodeling, a finding that was subsequently verified.[152] There is some evidence that superoxide dismutase 2 (SOD2) deficiency, which has been seen in human PAH and pulmonary vascular cells, may be a key underlying contributor to HIF-1α stabilization, and likely underlies spontaneous PH observed in fawn-hooded rats.[153] Although understudied in PH, TAZ forms a complex with HIF-1α in the nucleus,[154−156] and HIF-1α and TAZ act synergistically as reciprocal coactivators in breast cancer cells.[154] YAP has also been found to be essential for HIF-1α stabilization in the setting of malignancy.[157] It is therefore highly plausible that HIF-1α stabilization in the absence of hypoxia is, in some part, promoted by stiffness-dependent YAP/TAZ activation, but further study is needed to confirm this hypothesis.

Enhanced glycolysis has a profound effect on cellular metabolic activity, most directly via decreased flux through the electron transport chain, generating high membrane potentials and decreased mitochondrial ROS production that alter multiple mitochondrial functions (Fig. 57.4). Mitochondrial dynamics, including biogenesis, fission/fusion, and turnover (mitophagy), remain understudied in PH. One intriguing line of research from the Archer group has demonstrated fragmentation of mitochondria associated with an increase in one of the major proteins controlling mitochondrial fission, dynamin-related protein 1 (Drp1). Inhibition of Drp1 using a small molecule inhibitor or siDrp1 leads to antiproliferative, proapoptotic effects in vitro and partially ameliorates PH in murine models.[158] Intriguingly, the mechanism of Drp1 activation in this setting is unknown, but YAP activity at least appears to indirectly regulate Drp1 in developing myoblasts,[159] again suggesting a possible connection to stiffness-dependent

mechanotransduction. Further study on mitochondrial dynamics in the setting of pulmonary vascular stiffening and early PH pathogenesis will hopefully provide a clearer sense of how these two pathogenic phenotypes intersect.

In proliferating cells with enhanced glycolysis, mitochondrial activity via the tricarboxylic acid (TCA) cycle is still required to facilitate production of amino acids and nucleic acids. Increased TCA activity, which has been observed in human PAH lungs,[160] leads to upregulation of metabolic pathways for TCA intermediates. One such pathway is glutaminolysis, which converts glutamine into the TCA cycle metabolite α-ketoglutarate. Recent work has shown that the key enzyme in this process, glutaminase 1 (GLS1), is activated by increased vascular stiffness via a YAP/TAZ-mediated pathway in pulmonary vascular cells (Fig. 57.4).[37] Pharmacological inhibition of either YAP or GLS1 attenuates increases in right ventricular systolic pressure (RVSP) and pulmonary vascular remodeling in the MCT-induced PH model in rats.[37] Enhanced glutaminolysis has also been observed in the RV in experimental PH, and inhibition of glutaminolysis has been shown to attenuate RV cardiomyocyte hypertrophy and restore normal glucose oxidation.[161] This evidence strongly suggests that targeting mechanical signaling may have a significant impact on metabolic derangements observed in PAH. These intriguing links between mitochondrial dynamics, metabolic reprogramming, and mechanotransduction are summarized in Fig. 57.4.

Targeting PA stiffness and mechanotransduction in PH

Accumulating evidence has demonstrated that early PA stiffening is a major driver of vascular remodeling in PH by promoting mechanical signaling in pulmonary vascular cells. Inhibition of early ECM remodeling, pulmonary vascular stiffening, and mechanotransduction attenuates vascular remodeling and development of PH in preclinical models. Therapeutic targeting of ECM remodeling and mechanotransduction pathways has the potential to intercept mechanobiological feedback and arrest or reverse PA stiffness-induced vascular remodeling in PH (Table 57.1).

Inhibition of serine elastase with elafin reduces ECM accumulation and has shown promising results in preclinical PH models[69,162]; it is currently being evaluated in early-phase clinical trials. In addition to increased collagen deposition, enhanced collagen cross-linking, which contributes to ECM remodeling and pulmonary vascular stiffening, may be a potential novel mechanobiological target in PH. Lysyl oxidases (LOX) are key collagen cross-linking enzymes upregulated in PAH and experimental PH,[163] and inhibition of their activity with BAPN prevents ECM remodeling and attenuates PH in rodent models.[23,37,163] While no studies to date have evaluated LOX inhibitors in

TABLE 57.1 Potential mechanobiological therapeutic targets in pulmonary hypertension.

Mechanosensitive target	Drug/Molecular target	Preclinical	Clinical trial
ECM remodeling			
Serine elastase inhibitor	SC-39026, SC-37698, M249314, ZD0892	Attenuates/reverses hypoxia- and MCT-induced PH in rats[67,68,70]	
	Elafin	Reverses sugen/hypoxia-induced PH in rats; elafin transgenic mice protected from hypoxia-induced PH[69,162]	Phase 1 (NCT03522935)
Lysyl oxidase (LOX) inhibitor	β-aminopropionitrile (BAPN)	Prevents/rescues hypoxia-induced PH in mice[23,163]; attenuates MCT-induced PH in rats[37]	
	PXS-5505 (Pharmaxis)		Phase 2 (myelofibrosis)
Lysyl oxidase-like 2 (LOXL2) inhibitor	LOXL2 small molecule inhibitor (Pharmaxis)		Phase 2 planned (NASH, cardiac fibrosis, idiopathic pulmonary fibrosis [IPF])
	Simtuzumab (LOXL2 monoclonal antibody)		Negative phase 2 in IPF[164]
Transglutaminase-2 (TG2)	ERW1041E (TG2 inhibitor)	Attenuates ECM remodeling and RVSP but not RVH in mouse sugen/hypoxia model[165,166]; hypoxia-induced PH attenuated in VSMC-specific TG2 knockout mice[a]	
	ZED1227		Phase 2 (celiac disease)
TGF-β signaling	TGF-β receptor I (ALK5) inhibitor SD-208, TGF-β antibody T9429	Attenuates MCT-induced PH in rats[167,168]	
	TGFBRII-Fc (TGF-β1/3 ligand trap)	Attenuates MCT-induced PH and sugen/hypoxia- induced PH in rats and sugen/hypoxia-induced PH in mice, improves established PH in rats induced by MCT and sugen/hypoxia[169]	
	ACTRIIA-Fc (GDF8/11 and activin ligand trap)	Attenuates PH development and improves established PH induced by MCT and sugen/hypoxia in rats[170]	
	Sotatercept (GDF8/11 and activin ligand trap)		Phase 2 trial showed improvement in PVR and 6-minute walk distance at 24 weeks in PAH patients (NCT03496207, NCT03738150)[171,172]; phase 3 in PAH (NCT04576988)
Mechanosensors			
FAK	PF-573228, FAK siRNA	Inhibits MCT-induced PH in rats[88]	
	GSK-2256098		Phase 2 in pancreatic cancer (NCT02428270)
	Defactinib (VS-6063)		Phase 1 in advanced pancreatic cancer (NCT02546531), phase 1/2a in advanced solid malignancies (NCT02758587)

TABLE 57.1 Potential mechanobiological therapeutic targets in pulmonary hypertension.—cont'd

Mechanosensitive target	Drug/Molecular target	Preclinical	Clinical trial
Rho/ROCK	Fasudil	Attenuates MCT-induced PH in rats and hypoxia-induced PH in mice[47,48]; reduced hypoxia-induced PH in VSMC-specific ROCK2^{+/−} mice[b]	Short-term IV use reduces PVR and mPAP, may improve outcomes in right heart failure and severe PH[49]; improves hemodynamics in PH-HFpEF[173]; oral extended formulation (AT-877ER) use for 12 wks improved cardiac index from baseline, no difference in 6-minute walk distance[174]
Transcriptional mechanotransducers			
YAP/TAZ	Verteporfin	Attenuates MCT-induced PH in rats[37]	FDA-approved for IV use in photo-dynamic therapy of age-related macular degeneration
MRTF-A	MRTF-A shRNA	Attenuates hypoxia-induced PH in rats[55]	
miRNA-130/301	miR-130/301 inhibition (Short-130)	Reduces ECM expression, YAP activity, RVSP, and RVH in MCT-treated rats; attenuates vascular stiffening in sugen/hypoxia model in mice[23]	
Metabolism mediators			
Glutaminase inhibitors	C968, CB-839	Prevents/reverses MCT-induced PH in rats[37]	Telaglenastat (CB-839) in phase 1/2 clinical trials in advanced lung cancer (NCT03831932, NCT04250545, NCT04265534) and other solid malignancies (NCT02071862)

[a]*Liu B, Wang D, Luo E, Hou J, Qiao Y, Yan G, Wang Q, Tang C. Role of TG2-mediated SERCA2 serotonylation on hypoxic pulmonary vein remodeling.* **Front Pharmacol**. *2019; 10:1611.*
[b]*Shimizu T, Fukumoto Y, Tanaka S, Satoh K, Ikeda S, Shimokawa H. Crucial role of ROCK2 in vascular smooth muscle cells for hypoxia-induced pulmonary hypertension in mice.* **Arterioscler Thromb Vasc Biol**. *2013; 33:2780–2791.*

patients with PH, a Phase 2 trial of simtuzumab, a monoclonal antibody against lysyl oxidase-like 2 (LOXL2), showed no significant improvement in progression-free survival in patients with idiopathic pulmonary fibrosis (IPF).[164] A LOX inhibitor PXS-5505 is in Phase 2 trials for myelofibrosis and a small molecule inhibitor of LOXL2 is currently being developed for study in nonalcoholic steatohepatitis (NASH), cardiac fibrosis, and IPF. Tissue transglutaminase (TG2), which promotes cross-linking of ECM proteins with serotonin and leads to increased ECM stability and tissue rigidity,[175] is emerging as another potential mechanobiological target in PH. TG2 expression and activity are upregulated in rodent models of PH[165,176] and TG2 inhibition with ERW1041E reduces ECM production and attenuates RVSP in the sugen hypoxia model in mice.[165,166] While a Phase 2 trial of the oral TG2 inhibitor ZED1227 is underway in celiac disease, TG2 inhibitors have yet to be studied in PH or fibrotic diseases.

Integrins relay critical mechanical information from the ECM to key intracellular mechanosensors such as FAK, Src, and Rho/ROCK, and downstream transcriptional mechanotransducers such as YAP/TAZ and MRTF-A, all of which may be potential mechanobiological targets in PH. Integrin signaling also activates latent TGF-β,[177] which drives EndoMT and leads to further matrix stiffening and amplification of pulmonary vascular remodeling in PH. Small molecule inhibitors of different integrins are under investigation in fibrotic diseases with an ongoing Phase 2a trial of a dual selective αvβ6/αvβ1 integrin inhibitor, PLN-74809, in IPF (NCT04072315). While integrins have been less well-studied in PH, small molecular inhibitors of TGF-β signaling have been shown to be beneficial in animal PH models.[167,168] Most recently, a selective TGF-β 1/3 ligand trap has been shown to attenuate and reverse established PH in experimental models.[169] Furthermore, treatment with a ligand trap targeting ACTRIIA ligands activin and GDF8/11 attenuated established PH and inhibited pulmonary vascular cell proliferation via inhibition of Smad 2/3 activation.[170] Preliminary results from a Phase 2 trial (PULSAR) of the human ACTRIIA-Fc analog sotatercept

in PAH were recently reported,[171,172] showing improvement in PVR and 6-minute walk distance at 24 weeks. A Phase 3 trial of sotatercept in PAH (NCT04576988) is planned.

Inhibition of the downstream mechanosensor FAK with pharmacological inhibitors or siRNA has been shown to attenuate MCT-induced PH[88] and preclinical lung fibrosis.[178] While no clinical studies have evaluated FAK inhibition in PAH, several Phase 2 trials evaluating small molecule inhibitors of FAK are underway in pancreatic cancer and other advanced solid malignancies. Inhibition of the Rho/ROCK pathway with fasudil has also shown promise in experimental PH models[47,48] and clinical trials evaluating its short-term use.[49,173,174] Intravenous (IV) fasudil has been shown to acutely reduce PVR and mean pulmonary arterial pressures (mPAP) in patients with PAH[49] and PH due to left ventricular heart failure with preserved ejection fraction (PH-HFpEF),[173] although the effects of long-term fasudil use remain understudied. A small trial of an oral extended release formulation of fasudil (AT-877ER) in PAH patients for 12 weeks showed modest improvement in cardiac index, although did not significantly improve 6-minute walk distance.[174]

Stiffness-dependent activation of transcriptional regulators, such as YAP/TAZ and MRTF, play a key role in driving transcriptional programs that promote vascular cellular remodeling and have therefore emerged as potential mechanobiological targets in PAH. Knockdown of MRTF-A has been shown to attenuate hypoxia-induced increases in RVSP, pulmonary vascular remodeling, ECM expression, and RVH in rats.[55] MRTFs are also of interest as potential targets in fibrosis and pancreatic cancer; however, studies remain preclinical to date. YAP/TAZ are powerful effectors of mechanical signaling in pulmonary vascular cells and have recently shown promise in experimental PH. Pharmacological inhibition of YAP with verteporfin, an FDA-approved photosensitizer for treatment of age-related macular degeneration, reduced PA stiffening, RVSP, and RVH in MCT-treated rats.[37] In addition, inhibition of miRNA 130/301 reduced ECM deposition, YAP activation, and attenuated PH in MCT-treated rats in a YAP/TAZ-miRNA 130/301-ECM feedback loop.[23] Furthermore, treatment with a GLS1 inhibitor prevented YAP/TAZ-dependent activation of GLS1 and in doing so, both attenuated PH development and reversed established PH in MCT-treated rats.[37] The glutaminase inhibitor telaglenastat is currently being studied in Phase 1/2 trials in advanced lung cancer and other solid malignancies, and may be a promising therapeutic in human PAH. In addition to agents which inhibit YAP/TAZ-TEAD interactions such as verteporfin, a number of small molecules have been found to inhibit upstream activation of YAP/TAZ, including statins,[179] and dopamine receptor D1 agonists such as dihydrexidine, which selectively inhibits YAP/TAZ activation

in fibroblasts and reverses experimental lung and liver fibrosis.[180] Development of small molecule inhibitors of YAP/TAZ activity is an active area of research, particularly in the oncology field,[181] with significant potential for therapeutic applications in fibrosis and PAH.

Conclusion

Accumulating evidence demonstrates that early PA stiffening drives vascular cell activation via upregulation of mechanosensitive molecular pathways that promote further vascular remodeling, matrix stiffening, and progression of disease in PAH. Recent studies have begun to elucidate the mechanisms by which pulmonary vascular cells sense and transduce signals from the micromechanical environment to drive transcriptional responses which promote pathologic vascular remodeling in PAH. Therapeutics that intercept this mechanobiological feedback loop, whether directed at ECM remodeling or the downstream signaling pathways that are activated in response to alterations in the matrix microenvironment, may have potential to halt or reverse vascular remodeling in PAH (Table 57.1). Further research is needed to more thoroughly delineate the key mechanotransduction pathways activated in pulmonary vascular cells in response to PA stiffening in order to identify optimal targets for mechanotherapeutic targeting in PAH.

References

1. Farber HW, Miller DP, Poms AD, et al. Five-year outcomes of patients enrolled in the REVEAL registry. **Chest**. 2015; 148:1043−1054.

2. Dieffenbach PB, Maracle M, Tschumperlin DJ, Fredenburgh LE. Mechanobiological feedback in pulmonary vascular disease. **Front Physiol**. 2018; 9:951.

3. Tuder RM, Archer SL, Dorfmuller P, et al. Relevant issues in the pathology and pathobiology of pulmonary hypertension. **J Am Coll Cardiol**. 2013; 62:D4−D12.

4. Thomas CA, Anderson RJ, Condon DF, de Jesus Perez VA. Diagnosis and management of pulmonary hypertension in the modern era: insights from the 6th world symposium. **Pulm Ther**. 2020; 6:9−22.

5. Ploegstra MJ, Brokelman JGM, Roos-Hesselink JW, et al. Pulmonary arterial stiffness indices assessed by intravascular ultrasound in children with early pulmonary vascular disease: prediction of advanced disease and mortality during 20-year follow-up. **Eur Heart J Cardiovasc Imaging**. 2018; 19:216−224.

6. Mahapatra S, Nishimura RA, Sorajja P, Cha S, McGoon MD. Relationship of pulmonary arterial capacitance and mortality in idiopathic pulmonary arterial hypertension. **J Am Coll Cardiol**. 2006; 47:799−803.

7. Gan CT, Lankhaar JW, Westerhof N, et al. Noninvasively assessed pulmonary artery stiffness predicts mortality in pulmonary arterial hypertension. **Chest**. 2007; 132:1906−1912.

8. Campo A, Mathai SC, Le Pavec J, et al. Hemodynamic predictors of survival in scleroderma-related pulmonary arterial hypertension. **Am J Respir Crit Care Med**. 2010; 182:252−260.

9. Pellegrini P, Rossi A, Pasotti M, et al. Prognostic relevance of pulmonary arterial compliance in patients with chronic heart failure. **Chest**. 2014; 145:1064−1070.

10. Tampakakis E, Shah SJ, Borlaug BA, et al. Pulmonary effective arterial elastance as a measure of right ventricular afterload and its prognostic value in pulmonary hypertension due to left heart disease. **Circ Heart Fail**. 2018; 11:e004436.

11. Saouti N, Westerhof N, Helderman F, et al. Right ventricular oscillatory power is a constant fraction of total power irrespective of pulmonary artery pressure. **Am J Respir Crit Care Med**. 2010; 182:1315−1320.

12. Saouti N, Westerhof N, Postmus PE, Vonk-Noordegraaf A. The arterial load in pulmonary hypertension. **Eur Respir Rev**. 2010; 19:197−203.

13. Wang Z, Chesler NC. Pulmonary vascular wall stiffness: an important contributor to the increased right ventricular afterload with pulmonary hypertension. **Pulm Circ**. 2011; 1:212−223.

14. Bloodworth NC, West JD, Merryman WD. Microvessel mechanobiology in pulmonary arterial hypertension: cause and effect. **Hypertension**. 2015; 65:483−489.

15. Hunter KS, Lee PF, Lanning CJ, et al. Pulmonary vascular input impedance is a combined measure of pulmonary vascular resistance and stiffness and predicts clinical outcomes better than pulmonary vascular resistance alone in pediatric patients with pulmonary hypertension. **Am Heart J**. 2008; 155:166−174.

16. Kang KW, Chang HJ, Kim YJ, et al. Cardiac magnetic resonance imaging-derived pulmonary artery distensibility index correlates with pulmonary artery stiffness and predicts functional capacity in patients with pulmonary arterial hypertension. **Circ J**. 2011; 75:2244−2251.

17. Sanz J, Kariisa M, Dellegrottaglie S, et al. Evaluation of pulmonary artery stiffness in pulmonary hypertension with cardiac magnetic resonance. **JACC Cardiovasc Imaging**. 2009; 2:286−295.

18. Lau EM, Chemla D, Godinas L, et al. Loss of vascular distensibility during exercise is an early hemodynamic marker of pulmonary vascular disease. **Chest**. 2016; 149:353−361.

19. Malhotra R, Dhakal BP, Eisman AS, et al. Pulmonary vascular distensibility predicts pulmonary hypertension severity, exercise capacity, and survival in heart failure. **Circ Heart Fail**. 2016; 9.

20. Li M, Scott DE, Shandas R, Stenmark KR, Tan W. High pulsatility flow induces adhesion molecule and cytokine mRNA expression in distal pulmonary artery endothelial cells. **Ann Biomed Eng**. 2009; 37:1082−1092.

21. Scott D, Tan Y, Shandas R, Stenmark KR, Tan W. High pulsatility flow stimulates smooth muscle cell hypertrophy and contractile protein expression. **Am J Physiol Lung Cell Mol Physiol**. 2013; 304:L70−L81.

22. Birukova AA, Tian X, Cokic I, Beckham Y, Gardel ML, Birukov KG. Endothelial barrier disruption and recovery is controlled by substrate stiffness. **Microvasc Res**. 2013; 87:50−57.

23. Bertero T, Cottrill KA, Lu Y, et al. Matrix remodeling promotes pulmonary hypertension through feedback mechanoactivation of the YAP/TAZ-miR-130/301 circuit. **Cell Rep**. 2015; 13:1016−1032.

24. Liu F, Haeger CM, Dieffenbach PB, et al. Distal vessel stiffening is an early and pivotal mechanobiological regulator of vascular remodeling and pulmonary hypertension. **JCI Insight**. 2016; 1.

25. Dieffenbach PB, Haeger CM, Coronata AMF, et al. Arterial stiffness induces remodeling phenotypes in pulmonary artery smooth muscle cells via YAP/TAZ-mediated repression of cyclooxygenase-2. **Am J Physiol Lung Cell Mol Physiol**. 2017; 313:L628−L647.

26. Meyrick B, Reid L. The effect of continued hypoxia on rat pulmonary arterial circulation. An ultrastructural study. **Lab Invest**. 1978; 38:188−200.

27. Poiani GJ, Tozzi CA, Yohn SE, et al. Collagen and elastin metabolism in hypertensive pulmonary arteries of rats. **Circ Res**. 1990; 66:968−978.

28. Tozzi CA, Christiansen DL, Poiani GJ, Riley DJ. Excess collagen in hypertensive pulmonary arteries decreases vascular distensibility. **Am J Respir Crit Care Med**. 1994; 149:1317−1326.

29. Kobs RW, Muvarak NE, Eickhoff JC, Chesler NC. Linked mechanical and biological aspects of remodeling in mouse pulmonary arteries with hypoxia-induced hypertension. **Am J Physiol Heart Circ Physiol**. 2005; 288:H1209−H1217.

30. Todorovich-Hunter L, Dodo H, Ye C, McCready L, Keeley FW, Rabinovitch M. Increased pulmonary artery elastolytic activity in adult rats with monocrotaline-induced progressive hypertensive pulmonary vascular disease compared with infant rats with nonprogressive disease. **Am Rev Respir Dis**. 1992; 146:213−223.

31. Meyrick B, Reid L. Development of pulmonary arterial changes in rats fed Crotalaria spectabilis. **Am J Pathol**. 1979; 94:37−50.

32. Sheikh AQ, Misra A, Rosas IO, Adams RH, Greif DM. Smooth muscle cell progenitors are primed to muscularize in pulmonary hypertension. **Sci Transl Med**. 2015; 7:308ra159.

33. Gerringer JW, Wagner JC, Velez-Rendon D, Valdez-Jasso D. Lumped-parameter models of the pulmonary vasculature during the progression of pulmonary arterial hypertension. **Physiol Rep**. 2018; 6.

34. Lammers SR, Kao PH, Qi HJ, et al. Changes in the structure-function relationship of elastin and its impact on the proximal pulmonary arterial mechanics of hypertensive calves. **Am J Physiol Heart Circ Physiol**. 2008; 295:H1451−H1459.

35. Rogers NM, Yao M, Sembrat J, et al. Cellular, pharmacological, and biophysical evaluation of explanted lungs from a patient with sickle cell disease and severe pulmonary arterial hypertension. **Pulm Circ**. 2013; 3:936−951.

36. Li M, Tan Y, Stenmark KR, Tan W. High pulsatility flow induces acute endothelial inflammation through overpolarizing cells to activate NF-κB. **Cardiovasc Eng Technol**. 2013; 4:26−38.

37. Bertero T, Oldham WM, Cottrill KA, et al. Vascular stiffness mechanoactivates YAP/TAZ-dependent glutaminolysis to drive pulmonary hypertension. **J Clin Invest**. 2016; 126:3313−3335.

38. Haynes WG, Noon JP, Walker BR, Webb DJ. Inhibition of nitric oxide synthesis increases blood pressure in healthy humans. **J Hypertens**. 1993; 11:1375−1380.

39. Spratt JC, Goddard J, Patel N, Strachan FE, Rankin AJ, Webb DJ. Systemic ETA receptor antagonism with BQ-123 blocks ET-1 induced forearm vasoconstriction and decreases peripheral vascular resistance in healthy men. **Br J Pharmacol**. 2001; 134:648−654.

40. Scott-Drechsel D, Su Z, Hunter K, Li M, Shandas R, Tan W. A new flow co-culture system for studying mechanobiology effects of pulse flow waves. **Cytotechnology**. 2012; 64:649−666.

41. Nagaoka T, Morio Y, Casanova N, et al. Rho/Rho kinase signaling mediates increased basal pulmonary vascular tone in chronically hypoxic rats. **Am J Physiol Lung Cell Mol Physiol**. 2004; 287:L665−L672.

42. Archer SL, London B, Hampl V, et al. Impairment of hypoxic pulmonary vasoconstriction in mice lacking the voltage-gated potassium channel Kv1.5. **FASEB J**. 2001; 15:1801−1803.

43. Song S, Yamamura A, Yamamura H, et al. Flow shear stress enhances intracellular Ca^{2+} signaling in pulmonary artery smooth muscle cells from patients with pulmonary arterial hypertension. **Am J Physiol Cell Physiol**. 2014; 307:C373−C383.

44. Yang XR, Lin AH, Hughes JM, et al. Upregulation of osmomechanosensitive TRPV4 channel facilitates chronic hypoxia-induced myogenic tone and pulmonary hypertension. **Am J Physiol Lung Cell Mol Physiol**. 2012; 302:L555−L568.

45. Noda M, Yasuda-Fukazawa C, Moriishi K, et al. Involvement of rho in GTPγS-induced enhancement of phosphorylation of 20 kDa myosin light chain in vascular smooth muscle cells: inhibition of phosphatase activity. **FEBS Lett**. 1995; 367:246−250.

46. Sakurada S, Okamoto H, Takuwa N, Sugimoto N, Takuwa Y. Rho activation in excitatory agonist-stimulated vascular smooth muscle. **Am J Physiol Cell Physiol**. 2001; 281:C571−C578.

47. Abe K, Shimokawa H, Morikawa K, et al. Long-term treatment with a Rho-kinase inhibitor improves monocrotaline-induced fatal pulmonary hypertension in rats. **Circ Res**. 2004; 94:385−393.

48. Abe K, Tawara S, Oi K, et al. Long-term inhibition of Rho-kinase ameliorates hypoxia-induced pulmonary hypertension in mice. **J Cardiovasc Pharmacol**. 2006; 48:280−285.

49. Zhang Y, Wu S. Effects of fasudil on pulmonary hypertension in clinical practice. **Pulm Pharmacol Ther**. 2017; 46:54−63.

50. Huang J, Elicker J, Bowens N, et al. Myocardin regulates BMP10 expression and is required for heart development. **J Clin Invest**. 2012; 122:3678−3691.

51. Esnault C, Stewart A, Gualdrini F, et al. Rho-actin signaling to the MRTF coactivators dominates the immediate transcriptional response to serum in fibroblasts. **Genes Dev**. 2014; 28:943−958.

52. Small EM, Thatcher JE, Sutherland LB, et al. Myocardin-related transcription factor-A controls myofibroblast activation and fibrosis in response to myocardial infarction. **Circ Res**. 2010; 107:294−304.

53. Scharenberg MA, Pippenger BE, Sack R, et al. TGF-β-induced differentiation into myofibroblasts involves specific regulation of two MLK1 isoforms. **J Cell Sci**. 2014; 127:1079−1091.

54. Zabini D, Granton E, Hu Y, et al. Loss of SMAD3 promotes vascular remodeling in pulmonary arterial hypertension via MRTF disinhibition. **Am J Respir Crit Care Med**. 2018; 197:244−260.

55. Yuan Z, Chen J, Chen D, et al. Megakaryocytic leukemia 1 (MLK1) regulates hypoxia induced pulmonary hypertension in rats. **PLoS One**. 2014; 9:e83895.

56. Estrada KD, Chesler NC. Collagen-related gene and protein expression changes in the lung in response to chronic hypoxia. **Biomech Model Mechanobiol**. 2009; 8:263−272.

57. Safdar Z, Tamez E, Chan W, et al. Circulating collagen biomarkers as indicators of disease severity in pulmonary arterial hypertension. **JACC Heart Fail**. 2014; 2:412−421.

58. Jones PL, Rabinovitch M. Tenascin-C is induced with progressive pulmonary vascular disease in rats and is functionally related to increased smooth muscle cell proliferation. **Circ Res**. 1996; 79:1131−1142.

59. Rabinovitch M. Pathobiology of pulmonary hypertension. Extracellular matrix. **Clin Chest Med**. 2001; 22:433−449. viii.

60. Mitani Y, Ueda M, Komatsu R, et al. Vascular smooth muscle cell phenotypes in primary pulmonary hypertension. **Eur Respir J**. 2001; 17:316−320.

61. Kim YM, Haghighat L, Spiekerkoetter E, et al. Neutrophil elastase is produced by pulmonary artery smooth muscle cells and is linked to neointimal lesions. **Am J Pathol**. 2011; 179:1560−1572.

62. Sun Z. Aging, arterial stiffness, and hypertension. **Hypertension**. 2015; 65:252−256.

63. Chelladurai P, Seeger W, Pullamsetti SS. Matrix metalloproteinases and their inhibitors in pulmonary hypertension. **Eur Respir J**. 2012; 40:766−782.

64. Thompson K, Rabinovitch M. Exogenous leukocyte and endogenous elastases can mediate mitogenic activity in pulmonary artery smooth muscle cells by release of extracellular-matrix bound basic fibroblast growth factor. **J Cell Physiol**. 1996; 166:495−505.

65. Kafienah W, Buttle DJ, Burnett D, Hollander AP. Cleavage of native type i collagen by human neutrophil elastase. **Biochem J**. 1998; 330(Pt 2):897−902.

66. Cowan KN, Jones PL, Rabinovitch M. Elastase and matrix metalloproteinase inhibitors induce regression, and tenascin-C antisense prevents progression, of vascular disease. **J Clin Invest**. 2000; 105:21−34.

67. Maruyama K, Ye CL, Woo M, et al. Chronic hypoxic pulmonary hypertension in rats and increased elastolytic activity. **Am J Physiol**. 1991; 261:H1716−H1726.

68. Ye CL, Rabinovitch M. Inhibition of elastolysis by SC-37698 reduces development and progression of monocrotaline pulmonary hypertension. **Am J Physiol**. 1991; 261:H1255−H1267.

69. Zaidi SH, You XM, Ciura S, Husain M, Rabinovitch M. Overexpression of the serine elastase inhibitor elafin protects transgenic mice from hypoxic pulmonary hypertension. **Circulation**. 2002; 105:516−521.

70. Cowan KN, Heilbut A, Humpl T, Lam C, Ito S, Rabinovitch M. Complete reversal of fatal pulmonary hypertension in rats by a serine elastase inhibitor. **Nat Med**. 2000; 6:698−702.

71. Lepetit H, Eddahibi S, Fadel E, et al. Smooth muscle cell matrix metalloproteinases in idiopathic pulmonary arterial hypertension. **Eur Respir J**. 2005; 25:834−842.

72. Overall CM, Lopez-Otin C. Strategies for MMP inhibition in cancer: Innovations for the post-trial era. **Nat Rev Cancer**. 2002; 2:657−672.

73. Wang X, Khalil RA. Matrix metalloproteinases, vascular remodeling, and vascular disease. **Adv Pharmacol**. 2018; 81:241−330.

74. Novotna J, Herget J. Possible role of matrix metalloproteinases in reconstruction of peripheral pulmonary arteries induced by hypoxia. **Physiol Res**. 2002; 51:323−334.

75. Ambalavanan N, Nicola T, Li P, et al. Role of matrix metalloproteinase-2 in newborn mouse lungs under hypoxic conditions. **Pediatr Res**. 2008; 63:26−32.

76. Li XQ, Wang HM, Yang CG, Zhang XH, Han DD, Wang HL. Fluoxetine inhibited extracellular matrix of pulmonary artery and inflammation of lungs in monocrotaline-treated rats. **Acta Pharmacol Sin**. 2011; 32:217−222.

77. Wilhelm SM, Collier IE, Kronberger A, et al. Human skin fibroblast stromelysin: structure, glycosylation, substrate specificity, and differential expression in normal and tumorigenic cells. **Proc Natl Acad Sci USA**. 1987; 84:6725−6729.

78. Flamant M, Placier S, Dubroca C, et al. Role of matrix metalloproteinases in early hypertensive vascular remodeling. **Hypertension**. 2007; 50:212−218.

79. Atli O, Ilgin S, Ergun B, Burukoglu D, Musmul A, Sirmagul B. Matrix metalloproteinases are possible targets in monocrotaline-induced pulmonary hypertension: investigation of anti-remodeling effects of alagebrium and everolimus. **Anatol J Cardiol**. 2017; 17:8−17.

80. Katsumi A, Naoe T, Matsushita T, Kaibuchi K, Schwartz MA. Integrin activation and matrix binding mediate cellular responses to mechanical stretch. **J Biol Chem**. 2005; 280:16546−16549.

81. Sun Z, Guo SS, Fassler R. Integrin-mediated mechanotransduction. **J Cell Biol**. 2016; 215:445−456.

82. Umesh A, Paudel O, Cao YN, Myers AC, Sham JS. Alteration of pulmonary artery integrin levels in chronic hypoxia and monocrotaline-induced pulmonary hypertension. **J Vasc Res**. 2011; 48:525−537.

83. Bendeck MP, Irvin C, Reidy M, et al. Smooth muscle cell matrix metalloproteinase production is stimulated via αvβ3 integrin. **Arterioscler Thromb Vasc Biol**. 2000; 20:1467−1472.

84. Merklinger SL, Jones PL, Martinez EC, Rabinovitch M. Epidermal growth factor receptor blockade mediates smooth muscle cell apoptosis and improves survival in rats with pulmonary hypertension. **Circulation**. 2005; 112:423−431.

85. Cooper J, Giancotti FG. Integrin signaling in cancer: mechanotransduction, stemness, epithelial plasticity, and therapeutic resistance. **Cancer Cell**. 2019; 35:347−367.

86. Tschumperlin DJ. Mechanotransduction. **Compr Physiol**. 2011; 1:1057−1073.

87. Liu P, Gu Y, Luo J, et al. Inhibition of Src activation reverses pulmonary vascular remodeling in experimental pulmonary arterial hypertension via Akt/mTOR/HIF-1α signaling pathway. **Exp Cell Res**. 2019; 380:36−46.

88. Paulin R, Meloche J, Courboulin A, et al. Targeting cell motility in pulmonary arterial hypertension. **Eur Respir J**. 2014; 43:531−544.

89. Pullamsetti SS, Berghausen EM, Dabral S, et al. Role of Src tyrosine kinases in experimental pulmonary hypertension. **Arterioscler Thromb Vasc Biol**. 2012; 32:1354−1365.

90. Jeong K, Kim JH, Murphy JM, et al. Nuclear focal adhesion kinase controls vascular smooth muscle cell proliferation and neointimal hyperplasia through GATA4-mediated cyclin D1 transcription. **Circ Res**. 2019; 125:152−166.

91. Serrano I, McDonald PC, Lock F, Muller WJ, Dedhar S. Inactivation of the Hippo tumour suppressor pathway by integrin-linked kinase. **Nat Commun**. 2013; 4:2976.

92. Dong J, Feldmann G, Huang J, et al. Elucidation of a universal size-control mechanism in *Drosophila* and mammals. **Cell**. 2007; 130:1120−1133.

93. Halder G, Dupont S, Piccolo S. Transduction of mechanical and cytoskeletal cues by YAP and TAZ. **Nat Rev Mol Cell Biol**. 2012; 13:591−600.

94. Dupont S, Morsut L, Aragona M, et al. Role of YAP/TAZ in mechanotransduction. **Nature**. 2011; 474:179−183.

95. Bertero T, Cottrill KA, Annis S, et al. A YAP/TAZ-miR-130/301 molecular circuit exerts systems-level control of fibrosis in a network of human diseases and physiologic conditions. **Sci Rep**. 2015; 5:18277.

96. Machado RD, Southgate L, Eichstaedt CA, et al. Pulmonary arterial hypertension: a current perspective on established and emerging molecular genetic defects. **Hum Mutat**. 2015; 36:1113−1127.

97. Rol N, Kurakula KB, Happe C, Bogaard HJ, Goumans MJ. TGF-β and BMPR2 signaling in PAH: two black sheep in one family. **Int J Mol Sci**. 2018; 19.

98. Teichert-Kuliszewska K, Kutryk MJ, Kuliszewski MA, et al. Bone morphogenetic protein receptor-2 signaling promotes pulmonary arterial endothelial cell survival: implications for loss-of-function mutations in the pathogenesis of pulmonary hypertension. **Circ Res**. 2006; 98:209−217.

99. Yang X, Long L, Reynolds PN, Morrell NW. Expression of mutant BMPR-II in pulmonary endothelial cells promotes apoptosis and a release of factors that stimulate proliferation of pulmonary arterial smooth muscle cells. **Pulm Circ**. 2011; 1:103−110.

100. McCaffrey TA, Du B, Consigli S, et al. Genomic instability in the type II TGF-β1 receptor gene in atherosclerotic and restenotic vascular cells. **J Clin Invest**. 1997; 100:2182−2188.

101. LaValley DJ, Zanotelli MR, Bordeleau F, Wang W, Schwager SC, Reinhart-King CA. Matrix stiffness enhances VEGFR-2 internalization, signaling, and proliferation in endothelial cells. **Converg Sci Phys Oncol**. 2017; 3.

102. Sack KD, Teran M, Nugent MA. Extracellular matrix stiffness controls VEGF signaling and processing in endothelial cells. **J Cell Physiol**. 2016; 231:2026−2039.

103. Sakao S, Taraseviciene-Stewart L, Lee JD, Wood K, Cool CD, Voelkel NF. Initial apoptosis is followed by increased proliferation of apoptosis-resistant endothelial cells. **FASEB J**. 2005; 19:1178−1180.

104. Taraseviciene-Stewart L, Kasahara Y, Alger L, et al. Inhibition of the VEGF receptor 2 combined with chronic hypoxia causes cell death-dependent pulmonary endothelial cell proliferation and severe pulmonary hypertension. **FASEB J**. 2001; 15:427−438.

105. Kuebler WM, Bonnet S, Tabuchi A. Inflammation and autoimmunity in pulmonary hypertension: is there a role for endothelial adhesion molecules? (2017 Grover Conference Series). **Pulm Circ**. 2018; 8.

106. Soon E, Holmes AM, Treacy CM, et al. Elevated levels of inflammatory cytokines predict survival in idiopathic and familial pulmonary arterial hypertension. **Circulation**. 2010; 122:920−927.

107. Rabinovitch M, Guignabert C, Humbert M, Nicolls MR. Inflammation and immunity in the pathogenesis of pulmonary arterial hypertension. **Circ Res**. 2014; 115:165−175.

108. Bordeleau F, Mason BN, Lollis EM, et al. Matrix stiffening promotes a tumor vasculature phenotype. **Proc Natl Acad Sci USA**. 2017; 114:492−497.

109. Krishnan R, Klumpers DD, Park CY, et al. Substrate stiffening promotes endothelial monolayer disruption through enhanced physical forces. **Am J Physiol Cell Physiol**. 2011; 300:C146−C154.

110. Savai R, Pullamsetti SS, Kolbe J, et al. Immune and inflammatory cell involvement in the pathology of idiopathic pulmonary arterial hypertension. **Am J Respir Crit Care Med**. 2012; 186:897−908.

111. Karki P, Birukova AA. Substrate stiffness-dependent exacerbation of endothelial permeability and inflammation: mechanisms and potential implications in ALI and PH (2017 Grover Conference Series). **Pulm Circ**. 2018; 8.

112. Mambetsariev I, Tian Y, Wu T, et al. Stiffness-activated GEF-H1 expression exacerbates LPS-induced lung inflammation. **PLoS One**. 2014; 9:e92670.

113. Davis ME, Grumbach IM, Fukai T, Cutchins A, Harrison DG. Shear stress regulates endothelial nitric-oxide synthase promoter activity through nuclear factor κB binding. **J Biol Chem**. 2004; 279:163−168.

114. Orr AW, Hahn C, Blackman BR, Schwartz MA. PAK signaling regulates oxidant-dependent NF-κB activation by flow. **Circ Res**. 2008; 103:671−679.

115. Petzold T, Orr AW, Hahn C, Jhaveri KA, Parsons JT, Schwartz MA. Focal adhesion kinase modulates activation of NF-κB by flow in endothelial cells. **Am J Physiol Cell Physiol**. 2009; 297:C814−C822.

116. Smedlund K, Tano JY, Vazquez G. The constitutive function of native TRPC3 channels modulates vascular cell adhesion molecule-1 expression in coronary endothelial cells through nuclear factor κB signaling. **Circ Res**. 2010; 106:1479−1488.

117. Farkas D, Alhussaini AA, Kraskauskas D, et al. Nuclear factor κB inhibition reduces lung vascular lumen obliteration in severe pulmonary hypertension in rats. **Am J Respir Cell Mol Biol**. 2014; 51:413−425.

118. Li L, Wei C, Kim IK, Janssen-Heininger Y, Gupta S. Inhibition of nuclear factor-κB in the lungs prevents monocrotaline-induced pulmonary hypertension in mice. **Hypertension**. 2014; 63:1260−1269.

119. Steiner MK, Syrkina OL, Kolliputi N, Mark EJ, Hales CA, Waxman AB. Interleukin-6 overexpression induces pulmonary hypertension. **Circ Res**. 2009; 104:236−244, 228pp. following 244.

120. Courboulin A, Tremblay VL, Barrier M, et al. Kruppel-like factor 5 contributes to pulmonary artery smooth muscle proliferation and resistance to apoptosis in human pulmonary arterial hypertension. **Respir Res**. 2011; 12:128.

121. Good RB, Gilbane AJ, Trinder SL, et al. Endothelial to mesenchymal transition contributes to endothelial dysfunction in pulmonary arterial hypertension. **Am J Pathol**. 2015; 185:1850−1858.

122. Stenmark KR, Frid M, Perros F. Endothelial-to-mesenchymal transition: an evolving paradigm and a promising therapeutic target in PAH. **Circulation**. 2016; 133:1734−1737.

123. Ranchoux B, Antigny F, Rucker-Martin C, et al. Endothelial-to-mesenchymal transition in pulmonary hypertension. **Circulation**. 2015; 131:1006−1018.

124. Tzima E, Irani-Tehrani M, Kiosses WB, et al. A mechanosensory complex that mediates the endothelial cell response to fluid shear stress. **Nature**. 2005; 437:426−431.

125. Dejana E, Vestweber D. The role of VE-cadherin in vascular morphogenesis and permeability control. **Prog Mol Biol Transl Sci**. 2013; 116:119−144.

126. Hopper RK, Moonen JR, Diebold I, et al. In pulmonary arterial hypertension, reduced BMPR2 promotes endothelial-to-mesenchymal transition via HMGA1 and its target Slug. **Circulation**. 2016; 133:1783−1794.

127. Mammoto T, Muyleart M, Konduri GG, Mammoto A. Twist1 in hypoxia-induced pulmonary hypertension through transforming growth factor-β-Smad signaling. **Am J Respir Cell Mol Biol**. 2018; 58:194−207.

128. Wermuth PJ, Li Z, Mendoza FA, Jimenez SA. Stimulation of transforming growth factor-β 1-induced endothelial-to-mesenchymal transition and tissue fibrosis by endothelin-1 (ET-1): a novel profibrotic effect of ET-1. **PLoS One**. 2016; 11:e0161988.

129. Elliott WH, Tan Y, Li M, Tan W. High pulsatility flow promotes vascular fibrosis by triggering endothelial EndMt and fibroblast activation. **Cell Mol Bioeng**. 2015; 8:285−295.

130. Zhang H, von Gise A, Liu Q, et al. YAP1 is required for endothelial to mesenchymal transition of the atrioventricular cushion. **J Biol Chem**. 2014; 289:18681−18692.

131. Aisagbonhi O, Rai M, Ryzhov S, Atria N, Feoktistov I, Hatzopoulos AK. Experimental myocardial infarction triggers canonical Wnt signaling and endothelial-to-mesenchymal transition. **Dis Model Mech**. 2011; 4:469−483.

132. Zhong A, Mirzaei Z, Simmons CA. The roles of matrix stiffness and β-catenin signaling in endothelial-to-mesenchymal transition of aortic valve endothelial cells. **Cardiovasc Eng Technol**. 2018; 9:158−167.

133. Carmeliet P, Jain RK. Molecular mechanisms and clinical applications of angiogenesis. **Nature**. 2011; 473:298−307.

134. Voelkel NF, Gomez-Arroyo J. The role of vascular endothelial growth factor in pulmonary arterial hypertension. The angiogenesis paradox. **Am J Respir Cell Mol Biol**. 2014; 51:474−484.

135. Coussens LM, Raymond WW, Bergers G, et al. Inflammatory mast cells up-regulate angiogenesis during squamous epithelial carcinogenesis. **Genes Dev**. 1999; 13:1382−1397.

136. Schaper W, Ito WD. Molecular mechanisms of coronary collateral vessel growth. **Circ Res**. 1996; 79:911−919.

137. Corliss BA, Azimi MS, Munson JM, Peirce SM, Murfee WL. Macrophages: an inflammatory link between angiogenesis and lymphangiogenesis. **Microcirculation**. 2016; 23:95−121.

138. Deryugina EI, Quigley JP. Tumor angiogenesis: MMP-mediated induction of intravasation- and metastasis-sustaining neovasculature. **Matrix Biol**. 2015; 44−46:94−112.

139. Huang H. Matrix metalloproteinase-9 (MMP-9) as a cancer biomarker and MMP-9 biosensors: Recent advances. **Sensors**. 2018; 18.

140. Kudo Y, Iizuka S, Yoshida M, et al. Matrix metalloproteinase-13 (MMP-13) directly and indirectly promotes tumor angiogenesis. **J Biol Chem**. 2012; 287:38716−38728.

141. Eisenach PA, Roghi C, Fogarasi M, Murphy G, English WR. MT1-MMP regulates VEGF-A expression through a complex with VEGFR-2 and Src. **J Cell Sci**. 2010; 123:4182−4193.

142. Weis SM, Cheresh DA. Alphav integrins in angiogenesis and cancer. **Cold Spring Harb Perspect Med**. 2011; 1:a006478.

143. Ghosh K, Thodeti CK, Dudley AC, Mammoto A, Klagsbrun M, Ingber DE. Tumor-derived endothelial cells exhibit aberrant Rho-mediated mechanosensing and abnormal angiogenesis in vitro. **Proc Natl Acad Sci USA**. 2008; 105:11305−11310.

144. Azad T, Janse van Rensburg HJ, Lightbody ED, et al. A LATS biosensor screen identifies VEGFR as a regulator of the Hippo pathway in angiogenesis. **Nat Commun**. 2018; 9:1061.

145. Kim J, Kim YH, Kim J, et al. YAP/TAZ regulates sprouting angiogenesis and vascular barrier maturation. **J Clin Invest**. 2017; 127:3441−3461.

146. Choi HJ, Zhang H, Park H, et al. Yes-associated protein regulates endothelial cell contact-mediated expression of angiopoietin-2. **Nat Commun**. 2015; 6:6943.

147. Vander Heiden MG, Cantley LC, Thompson CB. Understanding the Warburg effect: the metabolic requirements of cell proliferation. **Science**. 2009; 324:1029−1033.

148. Faubert B, Solmonson A, DeBerardinis RJ. Metabolic reprogramming and cancer progression. **Science**. 2020:368.

149. Zhao H, Dennery PA, Yao H. Metabolic reprogramming in the pathogenesis of chronic lung diseases, including BPD, COPD, and pulmonary fibrosis. **Am J Physiol Lung Cell Mol Physiol**. 2018; 314:L544−L554.

150. Izquierdo-Garcia JL, Arias T, Rojas Y, et al. Metabolic reprogramming in the heart and lung in a murine model of pulmonary arterial hypertension. **Front Cardiovasc Med**. 2018; 5:110.

151. Fessel JP, Hamid R, Wittmann BM, et al. Metabolomic analysis of bone morphogenetic protein receptor type 2 mutations in human

pulmonary endothelium reveals widespread metabolic reprogramming. **Pulm Circ**. 2012; 2:201−213.

152. McMurtry MS, Bonnet S, Wu X, et al. Dichloroacetate prevents and reverses pulmonary hypertension by inducing pulmonary artery smooth muscle cell apoptosis. **Circ Res**. 2004; 95:830−840.

153. Archer SL, Marsboom G, Kim GH, et al. Epigenetic attenuation of mitochondrial superoxide dismutase 2 in pulmonary arterial hypertension: a basis for excessive cell proliferation and a new therapeutic target. **Circulation**. 2010; 121:2661−2671.

154. Xiang L, Gilkes DM, Hu H, et al. HIF-1α and TAZ serve as reciprocal co-activators in human breast cancer cells. **Oncotarget**. 2015; 6:11768−11778.

155. Xiang L, Gilkes DM, Hu H, et al. Hypoxia-inducible factor 1 mediates TAZ expression and nuclear localization to induce the breast cancer stem cell phenotype. **Oncotarget**. 2014; 5:12509−12527.

156. Bendinelli P, Maroni P, Matteucci E, Luzzati A, Perrucchini G, Desiderio MA. Hypoxia inducible factor-1 is activated by transcriptional co-activator with PDZ-binding motif (TAZ) versus WWdomain-containing oxidoreductase (WWOX) in hypoxic microenvironment of bone metastasis from breast cancer. **Eur J Cancer**. 2013; 49:2608−2618.

157. Ma B, Chen Y, Chen L, et al. Hypoxia regulates Hippo signalling through the SIAH2 ubiquitin E3 ligase. **Nat Cell Biol**. 2015; 17:95−103.

158. Marsboom G, Toth PT, Ryan JJ, et al. Dynamin-related protein 1-mediated mitochondrial mitotic fission permits hyperproliferation of vascular smooth muscle cells and offers a novel therapeutic target in pulmonary hypertension. **Circ Res**. 2012; 110:1484−1497.

159. Huang S, Wang X, Wu X, et al. YAP regulates mitochondrial structural remodeling during myoblast differentiation. **Am J Physiol Cell Physiol**. 2018; 315:C474−C484.

160. Zhao Y, Peng J, Lu C, et al. Metabolomic heterogeneity of pulmonary arterial hypertension. **PLoS One**. 2014; 9:e88727.

161. Piao L, Fang YH, Parikh K, Ryan JJ, Toth PT, Archer SL. Cardiac glutaminolysis: a maladaptive cancer metabolism pathway in the right ventricle in pulmonary hypertension. **J Mol Med**. 2013; 91:1185−1197.

162. Nickel NP, Spiekerkoetter E, Gu M, et al. Elafin reverses pulmonary hypertension via caveolin-1-dependent bone morphogenetic protein signaling. **Am J Respir Crit Care Med**. 2015; 191:1273−1286.

163. Nave AH, Mizikova I, Niess G, et al. Lysyl oxidases play a causal role in vascular remodeling in clinical and experimental pulmonary arterial hypertension. **Arterioscler Thromb Vasc Biol**. 2014; 34:1446−1458.

164. Raghu G, Brown KK, Collard HR, et al. Efficacy of simtuzumab versus placebo in patients with idiopathic pulmonary fibrosis: a randomised, double-blind, controlled, phase 2 trial. **Lancet Respir Med**. 2017; 5:22−32.

165. DiRaimondo TR, Klock C, Warburton R, et al. Elevated transglutaminase 2 activity is associated with hypoxia-induced experimental pulmonary hypertension in mice. **ACS Chem Biol**. 2014; 9:266−275.

166. Penumatsa KC, Toksoz D, Warburton RR, et al. Transglutaminase 2 in pulmonary and cardiac tissue remodeling in experimental pulmonary hypertension. **Am J Physiol Lung Cell Mol Physiol**. 2017; 313:L752−L762.

167. Megalou AJ, Glava C, Oikonomidis DL, et al. Transforming growth factor-β inhibition attenuates pulmonary arterial hypertension in rats. **Int J Clin Exp Med**. 2010; 3:332−340.

168. Zaiman AL, Podowski M, Medicherla S, et al. Role of the TGF-β/Alk5 signaling pathway in monocrotaline-induced pulmonary hypertension. **Am J Respir Crit Care Med**. 2008; 177:896−905.

169. Yung LM, Nikolic I, Paskin-Flerlage SD, Pearsall RS, Kumar R, Yu PB. A selective transforming growth factor-β ligand trap attenuates pulmonary hypertension. **Am J Respir Crit Care Med**. 2016; 194:1140−1151.

170. Yung LM, Yang P, Joshi S, et al. ACTRIIA-Fc rebalances activin/GDF versus BMP signaling in pulmonary hypertension. **Sci Transl Med**. 2020; 12.

171. Badesch DB, McLaughlin V, Gibbs S, et al. Sotatercept for the treatment of pulmonary arterial hypertension. **ATS 2020 Virtual**; 2020. https://conference.thoracic.org/program/session-information/virtual-clinical-trials.php.

172. Badesch D, Gibbs S, Gomberg-Maitland M, et al. PULSAR: a phase 2, randomized, double-blind, placebo-controlled study to assess the efficacy and safety of sotatercept (ACE-011) when added to standard of care (SOC) for treatment of pulmonary arterial hypertension (PAH). **Eur Respir J**. 2019; 54(Suppl. 63):PA4750.

173. Zhang X, Zhang X, Wang S, et al. Effects of fasudil on patients with pulmonary hypertension associated with left ventricular heart failure with preserved ejection fraction: a prospective intervention study. **Can Respir J**. 2018; 2018:3148259.

174. Fukumoto Y, Yamada N, Matsubara H, et al. Double-blind, placebo-controlled clinical trial with a Rho-kinase inhibitor in pulmonary arterial hypertension. **Circ J**. 2013; 77:2619−2625.

175. Eckert RL, Kaartinen MT, Nurminskaya M, et al. Transglutaminase regulation of cell function. **Physiol Rev**. 2014; 94:383−417.

176. Wei L, Warburton RR, Preston IR, et al. Serotonylated fibronectin is elevated in pulmonary hypertension. **Am J Physiol Lung Cell Mol Physiol**. 2012; 302:L1273−L1279.

177. Shi M, Zhu J, Wang R, et al. Latent TGF-β structure and activation. **Nature**. 2011; 474:343−349.

178. Lagares D, Busnadiego O, Garcia-Fernandez RA, et al. Inhibition of focal adhesion kinase prevents experimental lung fibrosis and myofibroblast formation. **Arthritis Rheum**. 2012; 64:1653−1664.

179. Sorrentino G, Ruggeri N, Specchia V, et al. Metabolic control of YAP and TAZ by the mevalonate pathway. **Nat Cell Biol**. 2014; 16:357−366.

180. Haak AJ, Kostallari E, Sicard D, et al. Selective YAP/TAZ inhibition in fibroblasts via dopamine receptor D1 agonism reverses fibrosis. **Sci Transl Med**. 2019; 11.

181. Crawford JJ, Bronner SM, Zbieg JR. Hippo pathway inhibition by blocking the YAP/TAZ-TEAD interface: a patent review. **Expert Opin Ther Pat**. 2018; 28:867−873.

Chapter 58

Therapeutic approaches to improve pulmonary arterial load and right ventricular–pulmonary arterial coupling

Michael J. Bashline[1] and Marc A. Simon[2]

[1]*Division of Cardiology, Department of Medicine, University of Pittsburgh, Pittsburgh, PA, United States;* [2]*Division of Cardiology, Department of Medicine, University of California, San Francisco (UCSF), San Francisco, CA, United States*

Introduction

The prevalence of heart failure continues to remain an epidemic on a global scale, especially throughout the United States, contributing to an elevated mortality and morbidity within the healthcare system. Significant advancements have been made that resulted in an improvement in mortality and reduction of hospitalizations for patients with heart failure with reduced ejection fraction (HFrEF) since the implementation of guideline directed medical therapy (GDMT).[1] Furthermore, research has continued to produce trials that support the use of newer agents that provide incremental benefit in this specific patient population, including SGLT-2 inhibitors and oral guanylate cyclase stimulators.[2,3] However, less success has been made with right ventricular (RV) failure, despite the increasing recognition of importance as the presence of RV dysfunction or failure is among the strongest predictors of outcome for patients with precapillary pulmonary hypertension (PH) as well as in left-sided heart failure.[4,5] While several explanations are possible including numerous etiologies with different pathophysiologic mechanisms, another reason is likely due to the physiology of the pulmonary circulation and the unique loading forces that the RV encounters.

This chapter will first review the pathophysiology of RV dysfunction and eventual failure, and then will briefly expand upon RV afterload. A current approach to managing RV dysfunction and failure will be presented, focusing on strategies to improve RV performance by reducing afterload. The most common conditions that contribute to an increase in RV afterload will be reviewed, including PH due to pulmonary arterial hypertension (PAH) and heart failure with preserved ejection fraction (HFpEF) while emphasizing the available treatment options and novel therapies under current investigation.

Right ventricular dysfunction and failure
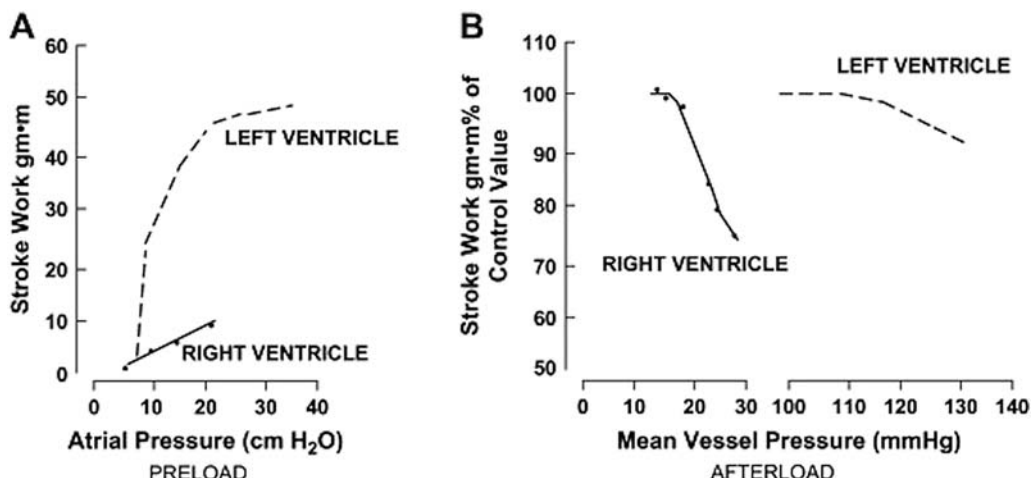
Response to normal loading conditions

Due to the inherent differences between the structure and anatomy of the RV and left ventricle (LV), the response to alterations in preload and afterload are dramatically dissimilar. The LV can tolerate abrupt increases in afterload, but has difficulty handling abrupt increases in preload. In contrast, the thin-walled, highly compliant nature of the RV can accommodate changes in preload but cannot tolerate abrupt increases in afterload.[6] Therefore, the highly compliant RV allows for significant increases in end-diastolic volume (EDV) without significant increases in the end-diastolic pressure (EDP) (Fig. 58.1).[6–8]

According to the law of LaPlace, wall tension (σ) is proportional to the pressure (P) times the radius (r), divided by the wall thickness (h).

$$\sigma \propto \frac{P * r}{h}$$

Thus, wall tension is greater in the RV during conditions that raise afterload or preload given that the RV has a thinner wall (h) and dilates easily, resulting in an increased cavity radius (r) during contraction.[9]

FIGURE 58.1 *Left panel*: Effects of an increase in preload on the left ventricle (LV) compared with the right ventricle (RV). RV is more compliant as demonstrated by large changes in stroke work with little changes in atrial pressure. *Right panel*: Effect of an increase in afterload on the LV compared with the RV. A small increase in afterload results in a large reduction RV stroke work which is in contrast to smaller reductions in LV stroke work. *Reproduced from Chan CM.* **Clin Chest Med**. *2008; 29:661−76. Copyright 2008, with permission from Elsevier.*

Pathophysiology of acute right heart failure

Acute failure of the RV is either due to the result of an abrupt increase in afterload, or a sudden decrease in contractility/RV performance. A common cause of an abrupt increase in afterload is pulmonary embolism (PE), while RV infarction or acute, fulminant myocarditis of the RV are the common etiologies of reduced contractility.[10] As mentioned above, the RV is less equipped to tolerate an abrupt rise in afterload and results in a decline in RV stroke volume (SV) without a corresponding increase in RV systolic pressure. Without adequate contractility, the RV will not be able to generate a sufficient SV to maintain cardiac output (CO) to the LV, which ultimately leads to cardiogenic shock.

Pathophysiology of chronic right heart failure
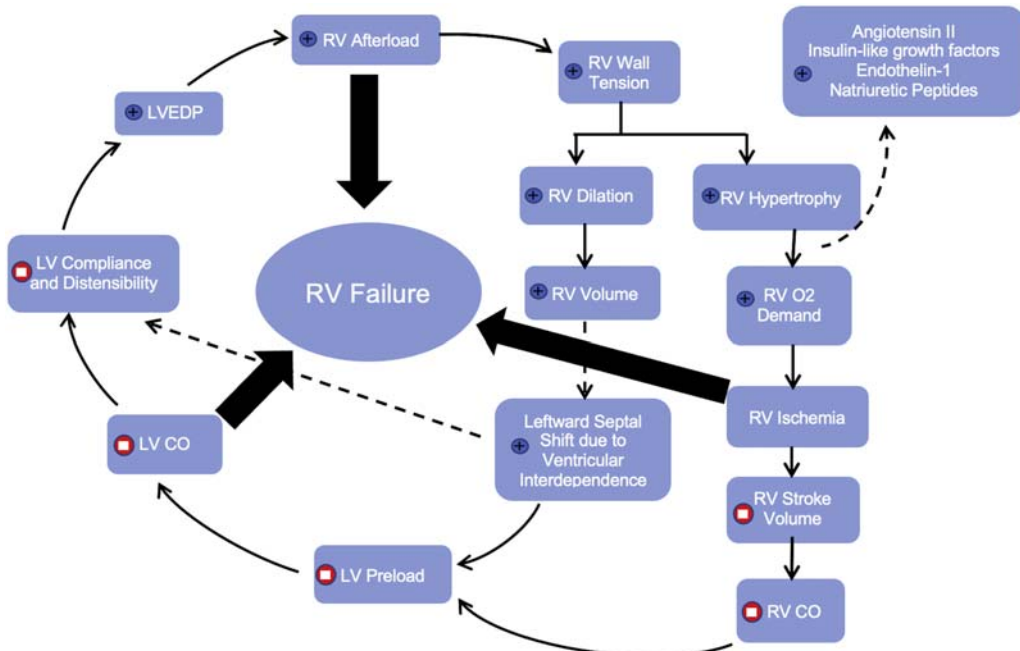
There are a variety of clinical conditions, including myocardial ischemia, PH, left-sided heart failure, valvular heart disease, cardiomyopathies, and congenital heart disease, that can lead to RV dysfunction over time. Regardless of the underlying etiology, RV dysfunction often starts with myocyte hypertrophy and chamber dilation in response to an increased wall stress which permits the RV to generate a higher RV systolic pressure and EDV. RV hypertrophy involves an increase in size via sarcomere synthesis and extracellular matrix expansion via fibrosis that is mediated by an overexpression of growth factors including angiotensin II, insulin-like growth factor I, natriuretic peptides, and endothelin 1 that seem to be uniquely expressed in the RV.[11,12] Furthermore, there is growing evidence that these biochemical signaling pathways that lead to RV remodeling are unique when compared to the remodeling pathways

present in the LV. This is likely due to the unique physiology of the RV and pulmonary vascular circulation, as well as a distinct embryological origin in comparison to the LV.[13,14] While these pathways are initially a compensatory adaptation of the RV in response to increase in wall stress, continued tension will eventually lead to a decompensated state in which RV contractility becomes uncoupled from the pulmonary vascular circulation. In this phase, the RV is unable to generate a high enough RV systolic pressure to maintain CO.[6,15–17]

Interventricular interdependence also may contribute to RV dysfunction. Normally, LV EDP is greater than the RV EDP, and thus the septum shifts toward the RV during diastole. However, in situations that cause an elevation in RV afterload, the RV EDP can exceed the LV EDP and the interventricular septum shifts toward the LV during diastole, which results in a reduction in LV filling and a subsequent decrease in CO.[7,18,19] Fig. 58.2 is a diagram that illustrates the complex pathways and mechanisms that intersect to lead to RV failure.

The components of right ventricular afterload

In order to understand the various treatment options available to reduce RV afterload and improve RV myocardial performance, a brief understanding of the components that represent afterload must be described. Afterload by definition represents the impedance to blood flow that the ventricle encounters during systole. There are two components to RV afterload: resistance which is the steady-state opposition to flow, and forces related to the pulsatile nature of blood flow. Pulmonary vascular

FIGURE 58.2   Schematic illustrating the complex pathophysiology that results in a negative feedback loop and eventual RV failure. *CO*, cardiac output; *LVEDP*, left ventricular end-diastolic pressure.

resistance (PVR), which can be obtained invasively via right heart catheterization (RHC), is defined as the change in pressure from entry to exit of the pulmonary vasculature (also known as the transpulmonary gradient [TPG]), and is defined as the difference between the mean pulmonary artery pressure [mPAP] and the pulmonary artery wedge pressure [PAWP] divided by to CO:

$$PVR = \frac{TPG}{CO} = \frac{(mPAP - PAWP)}{CO}$$

However, PVR is a steady-state measurement, rather than representing the time-varying load during ventricular systole, and thus ignores the pulsatile components of load. The pulsatile component of RV afterload is substantial, representing up to one-third to one-half of the total hydraulic load encountered by the RV.[20]

While PVR can be obtained via RHC, it is more difficult to accurately measure the pulsatile components that contribute to RV afterload. Several studies have shown a correlation between the pulsatile load and pulmonary arterial compliance (C_{PA}) which is estimated as the RV SV divided by the PA pulse pressure (PP), defined as the difference between systolic pulmonary artery pressure (sPAP) and diastolic pulmonary artery pressure (dPAP). However, this method does not take into account the presence of wave reflections.[21–23]
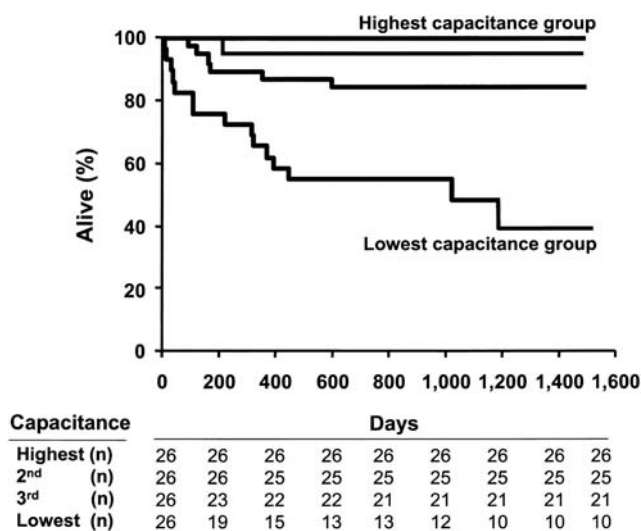
$$C_{PA} = \frac{SV}{PP} = \frac{SV}{sPAP - dPAP}$$

Considering PVR in isolation as a measure of load not only neglects approximately one-third to one-half of the RV afterload but also several recent trials that have found an association between C_{PA} and mortality or cardiac hospitalizations in patients with PH due to heart failure with preserved ejection fraction (PH-HFpEF). C_{PA} has also been shown to be an independent risk factor for mortality in patients with idiopathic PAH (Fig. 58.3).[22,24,25]

The gold standard for assessing RV afterload is the pulmonary vascular impedance (PVZ) which incorporates the steady-state load and pulsatile load, including the wave reflections that the RV encounters.[20,26,27] PVZ is technically challenging to measure, which explains its limited use clinically, as it represents the ratio of pressure to flow waves in the frequency domain, and thus requires performing a fast Fourier transform to obtain the sinusoidal components of the pressure and flow waves via a method that has been validated by several prior studies.[28,29] Chapters 1 and 7 include detailed discussion regarding the derivation and interpretation of input impedance spectra.

Approach to the management of right ventricular failure

The approach to RV dysfunction and failure continues to represent a challenging dilemma for physicians as management depends on the underlying etiology, yet the presence of RV failure is an independent risk factor for

FIGURE 58.3   Kaplan–Meier survival curve in a population with idiopathic pulmonary arterial hypertension depicting higher percent survival with time in the highest capacitance group, and the lowest percent survival with time in the lowest capacitance group. *Reproduced from Mahapatra S. J Am Coll Cardiol. 2006; 47:793–803. Copyright 2006, with permission from Elsevier.*

mortality regardless of etiology. Despite this, several broad themes exist that are common to management, including optimization of preload and volume status, maintenance of perfusion, improvement of contractility, and neurohormonal modulation. An additional approach revolves around therapeutic agents that target reducing the afterload, which will be the focus of the next section. While each of these approaches to management will be presented separately, it is important to remember that a combination of strategies is often required for the optimal treatment of RV dysfunction/failure, and applying one of these management strategies will often impact the others. Fig. 58.4 illustrates each of these themes in the pathway of RV failure and the corresponding therapies that will be discussed.

Optimization of preload and volume status

The importance of optimizing volume status, or preload, was illustrated in the CHAMPION trial which showed a 37% reduction in heart failure–related hospitalizations using CardioMEMS, an implantable hemodynamic monitor placed in the distal pulmonary artery, to guide volume management.[30] However, this trial included patients with HFrEF, and did not report on the degree of RV dysfunction/failure present. Physiologically, this principle is illustrated by the Frank–Starling curve which depicts how changes in preload affect SV. The Frank–Starling curve for the RV tends to be much flatter in comparison to the LV, owing to the highly compliant nature of the RV, implying that RV contractility changes less over a wide range of right atrial filling pressures.[6–8]
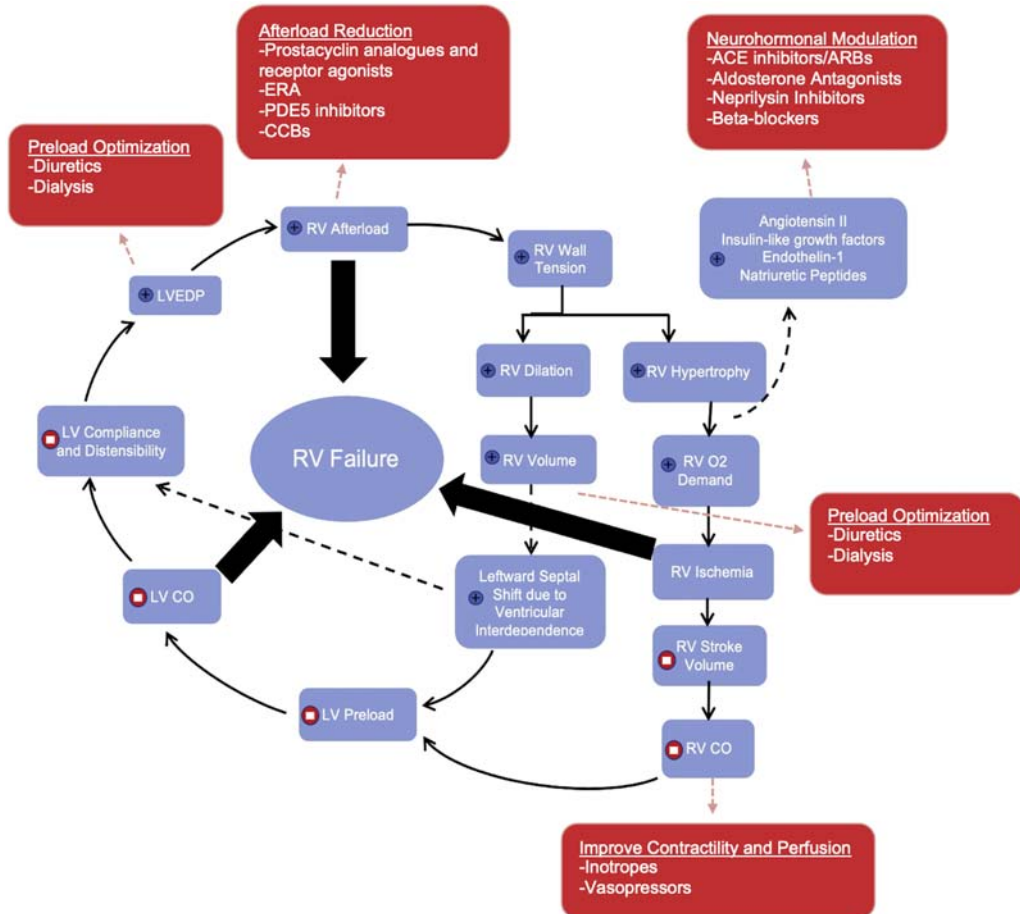
RV afterload is usually increased in the vast majority of cases where RV dysfunction/failure is present, and in the presence of RV dysfunction is frequently accompanied by volume overload (increased preload). Therefore, reducing preload is important to reduce RV dilatation, free wall tension, and septal shifting that can impair LV filling.[31] Presentation of volume overload due to RV failure is often an insidious process that eventually results in lower extremity and scrotal edema, hepatic congestion, and ascites. Furthermore, an elevated right atrial pressure can lead to renal congestion resulting in acute kidney injury and activation of the sympathetic nervous system and the renin-angiotensin-aldosterone axis, with the degree of severity linked to poorer outcomes.[32–34]

Given the consideration above, diuretics remain one of the hallmark treatment options, with an estimated 75% of patients with chronic RV dysfunction/failure requiring a daily dosing regimen.[35] While guidelines do not recommend a specific diuretic, most clinicians use bumetanide over furosemide, due its higher oral bioavailability, which is often advantageous due to the presence of bowel wall edema in these patients.[36,37] Patients admitted to the hospital often require large doses of intravenous diuretics, and often require combination therapy with thiazide diuretics for sequential nephron blockage of sodium reabsorption.[38] Among patients that fail to respond to diuretic doses, renal replacement therapies including intermittent hemodialysis or continuous veno-venous ultrafiltration may be considered to remove intravascular volume. While there have not been any trials examining the role of these therapies in isolated RV failure, the CARRESS-HF trial included patients with left-sided or biventricular failure and compared a stepwise approach of a diuretic regimen to ultrafiltration. Ultrafiltration was associated with more adverse events, worsening renal function, and no change in weight.[39] However, a more recent meta-analysis suggested that ultrafiltration was safe and effective at reducing body weight without increase risk of renal injury and may even reduce admissions.[40] Due to the conflicting evidence, early use of renal-replacement is often not recommended at this time.

A concurrent strategy used to maintain an optimal preload state is fluid and salt restriction. Current guidelines recommend limiting sodium intake to <2 g/day and a fluid restriction of 1.5–2 L/day.[1]

Maintaining myocardial perfusion

Decreased myocardial perfusion in RV failure is often due to two separate mechanisms: RV myocardial oxygen supply-demand mismatch causing an increase in oxygen extraction or decreased systemic CO resulting from hypotension. As discussed previously, wall tension increases in response to either a decrease in contractility due to RV infarction or increase in afterload which initially results in

FIGURE 58.4   Schematic revealing where available therapeutic agents act in the pathway that leads to right ventricular (RV) failure. *ACE*, angiotensin converting enzyme; *ARBs*, angiotensin receptor blockers; *CCBs*, calcium-channel blockers; *CO*, cardiac output; *ERA*, endothelin-1 receptor antagonists; *LVEDP*, left ventricular end-diastolic pressure; *PDE5*, phosphodiesterase-5.

adaptive changes to the RV including dilation and eventual hypertrophy. These changes require an increase in myocardial oxygen delivery.[6,41,42] While reperfusion with percutaneous coronary interventions is the mainstay treatment for restoring perfusion in patients with RV ischemia or infarction, optimizing preload, afterload, and contractility will help reduce myocardial oxygen demand.

Systemic hypotension resulting from impaired RV CO can be seen in severe cases of RV failure, which often necessitates the use of inotropic support with addition of vasopressor agents if hypotensive. The use of inotropes to improve contractility will be discussed in the next section. Norepinephrine, an alpha and beta receptor agonist, tends to be the preferred vasopressor agent in patients with cardiogenic shock, when compared to dopamine and epinephrine.[43,44] In a small analysis of patients with septic shock, norepinephrine was associated with an improvement in RV myocardial oxygen delivery, as well as an increase in PVR, although there was no adverse effect on RV contractility.[45] Epinephrine was shown to improve RV

contractility in a different small analysis in patients with septic shock, but its use was limited by arrhythmias.[46] Therefore, norepinephrine seems to be the vasopressor agent of choice, although some clinicians still favor the use of epinephrine or dopamine due to their mild inotropic properties. It is important to recognize that the major drawback of all these vasopressor agents is that they will further increase ventricular afterload. Therefore, these agents should be used with the sole goal of maintaining a mean arterial pressure to ensure adequate CO to vital organs.[6,10,17] Vasopressin, which binds to V1 receptors on vascular smooth muscle cells, at low doses (0.01−0.03 U/ min) can cause pulmonary vasodilation via endothelial nitric oxide stimulation, but its use clinically for this is limited by a frequent need for higher doses.[47,48]

Improving contractility

Contractility is a measure of the strength of ventricular contraction, or inotropy, and represents an intrinsic

property of the ventricular myofibers. The gold standard measurement of ventricular function is end-systolic elastance (E_{es}) which is derived from the end-systolic pressure-volume relationship on the pressure-volume (PV) loop. E_{es} is a load-independent measure of myocardial contractility, but clinically it is often interchanged with CO, although they should not be equated as CO is a load dependent measure of ejection.[18,49] As mentioned in the prior section, inotropic therapy should be considered for known or suspected low CO states which manifests clinically as signs of worsening end-organ perfusion and inadequate response to diuretics. The ultimate goal is to augment myocardial contractility and RV SV while optimizing EDV and EDP.

Milrinone, a phosphodiesterase 3 inhibitor, and dobutamine, a beta-receptor agonist, represent the two most common inotropic agents used clinically. As a class, they both have inotropic and vasodilator properties and thus can worsen or precipitate hypotension which may necessitate use of a vasopressor agent in conjunction, and direct comparisons of these two drugs have shown similar outcomes with a potential to induce arrhythmias.[50,51] Milrinone is generally not recommended in isolated RV failure as the vasodilator properties may result in cardiovascular collapse. In such cases, vasopressors with inotropic properties, such as norepinephrine, are preferred.[6,52,53] Regardless of the agent selected, the goal should strictly be for short-term administration as chronic use is associated with increased mortality.[54,55]

Levosimendan is a myocardial calcium sensitizer and vasodilator agent that is currently unavailable in the United States. Several smaller studies in patients with decompensated right-sided heart failure have shown favorable improvements in hemodynamics via a dose-dependent increase in CO and SV that is associated with a reduction in PAWP. In addition, it appears to have some effect on the pulmonary vascular circulation by reducing PVR and TPG and is currently being investigated in patients with right-sided heart failure due to PH-HFpEF (NCT03541603).[56-59]

Neurohormonal modulation

Dysregulated neurohormonal pathways are one of the main mechanisms of heart failure that pharmacologic agents have had success targeting. These agents include the use of β-blockers, angiotensin-converting enzyme (ACE) inhibitors and angiotensin receptor blockers (ARBs), mineralocorticoid receptor antagonists (MRAs), and neprilysin inhibitors. While these agents have been shown to reduce the incidence of heart failure hospitalizations and improve mortality with the administration of these agents in patients with left-sided heart failure (HFrEF), the role of these agents in right-sided heart failure is less clear.

β-blockers, such as metoprolol succinate, carvedilol, and bisoprolol, remain the cornerstone in treatment of patients with HFrEF by improving LV ejection fraction and mortality.[1] In brief, the mechanisms are thought to be secondary to inhibition of altered sympathetic stimulation mediated by the renin-angiotensin-aldosterone system (RAAS), decrease in preload, and decrease in myocardial oxygen demand. There are preclinical data from several studies that demonstrated direct benefit in RV function, exercise capacity, mortality, and reduction in fibrosis in rat models that had RV failure secondary to PH mediated by monocrotaline and Sugen-hypoxia.[60-62] However, these results have yet to translate into human clinical trials with most reporting no benefit or even potential harm including one small RCT in PAH patients treated with bisoprolol which demonstrated significant reductions in heart rate, cardiac index, and 6-minute walk time.[63] Not all β-blockers are equivalent, however. For example, nebivolol was shown to reduce PA smooth muscle cell proliferation and proinflammatory cytokines while increasing nitric oxide release in comparison to metoprolol.[64] Currently, β-blockers are not recommended for use in RV failure unless indicated for a concurrent comorbidity, such as left-sided HFrEF.

Similar to β-blockers, the use of ACE inhibitors and ARBs for treatment of RV failure is controversial. By suppressing the RAAS, these agents reduce sympathetic stimulation and reduce the progression of myocardial hypertrophy and fibrosis.[65] To date, trials have shown that ACE inhibitors increase RV filling time in patients with concurrent HFrEF, ARBs have been shown to attenuate RV dysfunction after myocardial infarction in animal models and improve RV-arterial coupling in animals with PAH. However, these trials were small and other trials have shown no clear hemodynamic benefits and an increased risk of hypotension.[17,66-68] Therefore, ACE inhibitors and ARBs are not recommended for use in RV failure unless indicated for a concurrent comorbidity. MRAs such as aldosterone have been shown to improve pulmonary vascular remodeling and reduce PA pressure, but no effect has been shown on RV function, which may suggest that its beneficial effects are secondary to afterload reduction.[69] Interestingly, retrospective analyses of the ARIES-1 and ARIES-2 trials suggest that patients treated with combination of ambrisentan, an endothelin type-A receptor inhibitor, and spironolactone had improved 6-minute walk times and a greater reduction in brain natriuretic peptide levels when compared to ambrisentan alone.[70] Thus, current trials with spironolactone are being conducted in patients with PAH (NCT01712620) and with chronic right heart failure (NCT03344159).

Sacubitril/valsartan is one of the newer agents available for the treatment of left-sided heart failure. It acts by combining the ARB mechanism of action of valsartan with

sacubitril, which is a neprilysin inhibitor that prevents the breakdown of natriuretic peptides. It was studied in patients with HFrEF and shown to have a reduction in all-cause mortality, cardiovascular mortality, and heart failure hospitalizations when compared to the ACE inhibitor, enalapril.[71] While there are limited data for patients with RV failure, a recently published trial suggests that this agent may prevent maladaptive RV remodeling via reduction of hypertrophy, afterload, prevention of RV-PA uncoupling, and prevention of myocardial stiffness in Sprague−Dawley rat model that had main PA banded.[72] Another preclinical trial demonstrated a significant reduction in RV pressure, RV hypertrophy, collagen content, PA pressures, and decreased pulmonary vascular wall thickness compared to valsartan alone and placebo in mice with PH.[73] Therefore, sacubitril/valsartan remains a promising agent for the treatment of RV failure.

Therapies targeting right ventricular afterload

This section will provide an overview of the different therapeutic approaches that reduce RV afterload. To accomplish this, a brief review of the relationship between resistance and compliance in the pulmonary vascular system (including resistance-compliance curves and ventricular−vascular coupling) will be provided, in order to fully understand the mechanisms of action and some of the current limitations of available therapeutic options. Other chapters in this textbook provide a more detailed discussion of pulsatile hemodynamics and ventricular−arterial interactions in the pulmonary circulation in general (Chapter 55), and in PH in particular (Chapter 56).

The most common cause of an increase in RV afterload is PH, which includes a wide spectrum of disorders with a common end result being an elevated PVR. PH is defined by a mean PA pressure >20 mmHg with a PVR ≥3 Wood units on RHC.[74] Table 58.1 lists an updated clinical classification of PH accordingly.

The majority of this section will focus on the various treatment agents available for Group 1 PAH, while the rest will explore the challenges associated with managing Group 2 PH.

Relationship between resistance and compliance

We earlier outlined the two components of afterload as PVR, which represents the steady-state load, and C_{PA}, which represents the pulsatile load. While these two components are conceptually two separate entities, they are dependent upon each other and changes in one factor will impact the other; this is particularly true in the pulmonary circulation. A dynamic, inverse relationship is present between these two factors that explains the treatment responses to pharmacologic agents that reduce afterload. The product of resistance (R) and compliance (C) is closely related to time constant (τ), or RC time, of diastolic pressure decay.[75] An inverse, hyperbolic relationship between the two has been shown to be relatively constant in patients with PH regardless of etiology and treatment.[76,77] The hyperbolic resistance−compliance relationship explains why patients with severe PH will require a much larger reduction in resistance when compared to patients with mild PH to achieve the same reduction in RV afterload. These patients with severe PH are on the right side of the RC curve, and thus reducing PVR has minimal impact on compliance. In contrast, patients with mild PH are located on the left side of the RC curve, and the same net reduction in PVR will have a more profound improvement in compliance (Fig. 58.5).

It also follows from this curve that a reduction in resistance will only affect the steady-state load in severe PH, whereas the same reduction will affect the steady-state and pulsatile load in mild PH.[76,78]

Ventricular−vascular coupling

The RV and the pulmonary vascular system work together as a cohesive unit rather than two separate entities, and the combination together is known as ventricular−vascular (RV−PA) coupling.[79] The most widely used approach to assess RV−PA coupling has been via the PV plane. For the application of this paradigm, the gold standard method of obtaining key parameters is via measurements of PV loops under varying loading conditions. In the PV plane, RV contractility is best represented by the slope of the end-systolic pressure volume relationship, and its slope is known as the end-systolic elastance (E_{es}), while RV afterload is best represented by the ratio of end-systolic pressure to SV, which is also known as E_a. The heart and pulmonary vascular system attempt to work under a state of maximal efficiency, and thus tries to maintain a ratio of 1.5−2. Normally, as the afterload in the pulmonary vasculature increases, the RV will first increase the contractility to match the corresponding increase in afterload. Initially, the RV will be able to compensate and maintain the ratio of 1.5−2 via adaptative mechanisms such as RV hypertrophy, but after a prolonged period of time, RV dilation occurs leading to an uncoupled state of the RV-PA unit with a ratio below 1.5.[80,81] Fig. 58.6 provides an example of the RV in a normal state, a normal, but compensated state, and an uncoupled state.

TABLE 58.1 Updated clinical classification of pulmonary hypertension.

Group 1: Pulmonary arterial hypertension (PAH)

(1) Idiopathic PAH
(2) Heritable PAH
(3) Drug-or-toxin-induced PAH
(4) PAH associated with:
   - Connective tissue disease
   - HIV infection
   - Portal hypertension
   - Congenital heart disease
   - Schistosomiasis
(5) PAH long-term responders to calcium channel blockers
(6) PAH with overt features of venous/capillaries (PVOD/PCH) involvement
(7) Persistent PH of the newborn syndrome

Group 2: PH due to left heart disease

(1) PH due to heart failure with preserved LVEF
(2) PH due to heart failure with reduced LVEF
(3) Valvular heart disease
(4) Congenital/acquired cardiovascular conditions leading to postcapillary pH

Group 3: PH due to lung disease and/or hypoxia

(1) Obstructive lung disease
(2) Restrictive lung disease
(3) Other lung disease with mixed restrictive/obstructive pattern
(4) Hypoxia without lung disease
(5) Developmental lung disorders

Group 4: PH due to pulmonary artery obstructions

(1) Chronic thromboembolic PH
(2) Other pulmonary artery obstructions

Group 5: PH with unclear and/or multifactorial mechanisms
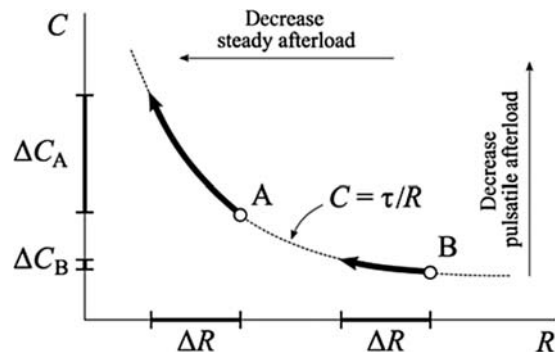
(1) Hematological disorders
(2) Systemic and metabolic disorders
(3) Others
(4) Complex congenital heart disease

LVEF, left ventricular ejection fraction; *PCH*, pulmonary capillary hemangiomatosis; *PVOD*, pulmonary-veno-occlusive disease.
Adapted from Simonneau G. Eur Respir J. 2019.

Clinically, this is useful as it could be used to monitor the response of pulmonary vasodilator therapy on RV function or provide clinicians with a more accurate way of assessing RV dysfunction compared to conventional noninvasive methods. However, the acquisition of PV loops requires an invasive procedure and specialized costly equipment, limiting its performance to a few research centers. To overcome this limitation, several noninvasively derived parameters have been proposed as surrogates to E_{es}/E_a. The ratio of SV/ESV has been shown to be related to E_{es}/E_a and highly predictive of outcomes in PH.[82–84] SV/ESV can be measured with cardiac MRI or 3D echocardiography. The ratio of tricuspid annular plane systolic excursion to pulmonary artery systolic pressure as measured from echocardiography has also been shown to be a surrogate for E_{es}/E_a that also correlates with clinical outcomes in PH.[85] Such noninvasive estimates of RV−PA coupling may be useful for following treatment for PH and RV failure.
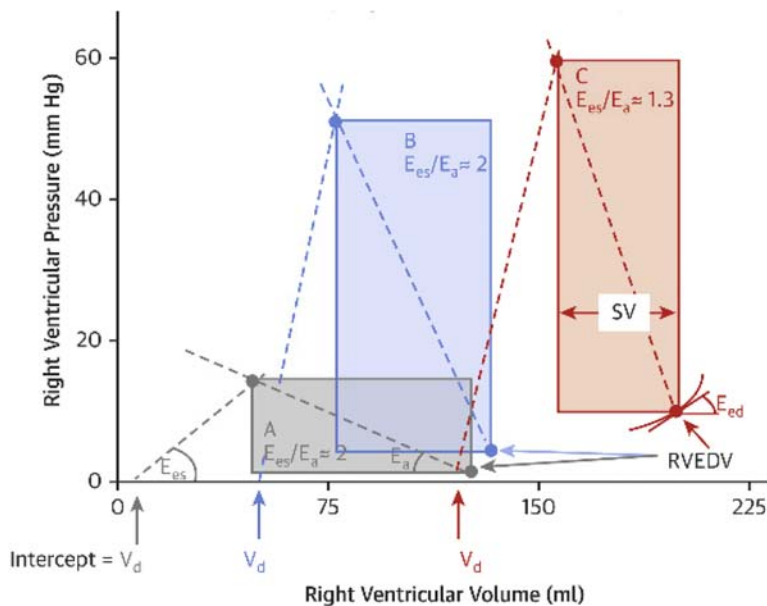
FIGURE 58.5 RC curve of two patients, *A* and *B*. Patient *A* has a low resistance, *R*, and patient *B* has a higher *R* or more severe PH. Reducing *R* in patient *A*, (ΔR), will result in a greater improvement in compliance, ΔC_A, compared with the same ΔR in patient *B*. *Reproduced from Lankhaar JW.* **Eur Heart J**. *2008; 29:1688−95. Copyright 2008, with permission from Oxford University Press.*

Therapeutic agents for treatment of pulmonary arterial hypertension
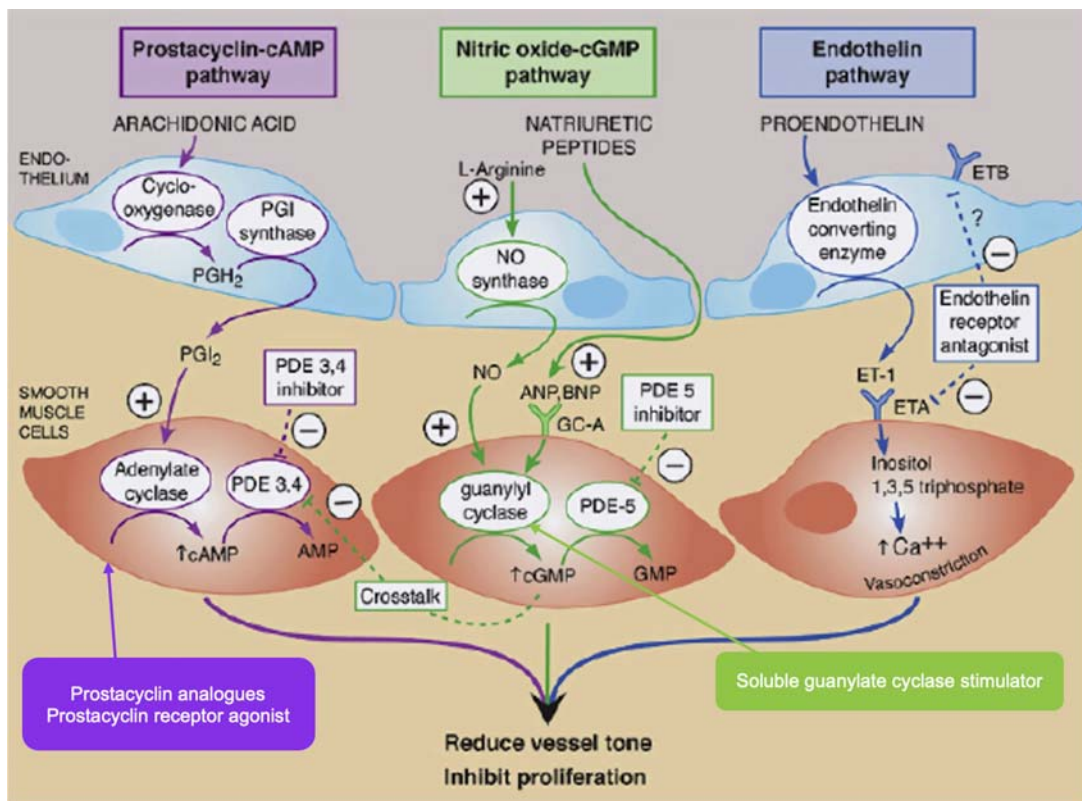
Group 1 PH, also referred to as PAH, is defined by a mean PA pressure >20 mmHg, PCWP ≤15 mmHg, and PVR ≥3 Wood units and due to a wide spectrum of disorders including idiopathic, familial, connective tissue disorders, HIV infection, and congenital heart disease.[74] While the exact pathophysiology has yet to be fully described, vasoconstriction, vascular remodeling of the pulmonary vessel wall, endothelial cell dysfunction, inflammation, and thrombosis in situ are all thought to be implicated, resulting in an elevated PVR.[86] Chronic alterations in these parameters lead to dysregulation of key vascular mediators such as nitric oxide, prostacyclin, and endothelin-1 which are the targets of the available therapeutic agents for the treatment of Group 1 PAH. Fig. 58.7 illustrates the key pathways of these hormones and the corresponding therapeutic agents that target them.

Prostacyclin analogues and prostacyclin receptor agonists are some of the most effective therapeutic agents currently available. Prostacyclin is a potent vasodilator that is produced by endothelial cells that works by stimulating the production of cyclic adenosine monophosphate (cAMP), inhibits growth of vascular smooth muscle cells, and is a powerful platelet aggregation inhibitor.[87,88] Epoprostenol is a synthetic prostacyclin with a half-life on an order of minutes which requires continuous intravenous administration. This agent has been extensively studied in patients with idiopathic PAH (IPAH) and PAH due to connective tissue disease revealing an improvement in WHO functional class, exercise capacity, and improvement in hemodynamics by causing a reduction in mean PA pressure and PVR, with an improvement in CO, and is the

FIGURE 58.6 Representative PV loops of the RV under different loading conditions. *Box A* (gray), shows an RV PV loop under optimal loading conditions with E_{es}/E_a ratio = 2. In *box B* (blue), RV afterload increased, but the RV contractility was able to compensate to maintain a normal E_{es}/E_a ratio. *Box C* (red) shows uncoupling of the RV-PA unit after further increases in RV afterload. *Reproduced from Vonk Noordegraaf A.* **J Am Coll Cardiol**. *2017; 69:236−243. Copyright 2017, with permission from Elsevier.*

FIGURE 58.7   Diagram illustrating the three major pathways that available therapeutic agents target. Prostacyclin analogues and prostacyclin receptor agonists target the prostacyclin pathway, while PDE5 inhibitors and soluble guanylate cyclase stimulators act on the nitric oxide pathway, and endothelin receptor antagonists block the endothelin pathway. *Reproduced and modified from Hirschtritt, M.* **Trans Comb Ther Pulm Arter Hypertens**. *2008. Copyright 2008, with permission from Springer Nature.*

only treatment available that has been shown to reduce mortality in IPAH.[89,90] For example, when compared to administration of conventional oral therapy at that time for patients with IPAH which included diuretics, supplemental oxygen, and oral vasodilators such as calcium channel blockers (CCBs), administration of epoprostenol was associated with improvement in quality of life metrics, average increase in 6 minute walk distance (6MWD) by 32 m, reduced mPAP by average of 8%, and reduced PVR by average of 21% when compared to baseline values. These hemodynamic benefits resulted in improvement in RV function, which was assessed by an average increase in SV of 6.2 ± 2.2 mL, and average increase in cardiac index of 0.3 ± 0.1 L/min/m^2 in the epoprostenol group.[90] Epoprostenol is often initiated at a low dose (2−4 ng/kg/min), and in an intensive care unit setting, can be titrated upwards by 2 ng/kg/min every few hours to achieve the optimal dose which is patient dependent and ultimately limited due to such as systemic hypotension, high output heart failure, flushing, headache, diarrhea, and muscle/joint aches. The main drawback with this agent is the need for permanent central venous access which greatly increases the risk of infection, pump malfunction, or drug interruption which can lead to a rebound increase in afterload if stopped abruptly and withheld for a long enough period of time.[91] Epoprostenol has been associated with worse outcomes in left-sided heart failure, and is therefore not indicated in this patient population.[92]

Iloprost and treprostinil are prostacyclin analogues that have the benefit of having a longer half-life. Iloprost is delivered via inhalation, while treprostinil is approved in formulations for IV, SQ, inhaled, and PO administration. Both iloprost and treprostinil have similar hemodynamic benefits when compared to epoprostenol. Administration of iloprost resulted in significant improvements in 6MWD of 36.4 m and an average reduction in mPAP of 4.6 ± 9.3 mmHg, and average reduction in PVR of

239 ± 279 dynes*sec*cm^{-5} from baseline values when compared to a placebo.[93] The benefits of continuous subcutaneous treprostinil was first illustrated in an RCT in 2002 that showed an improvement in median 6MWD of 16 m, and an average reduction in mPAP of 2.3 ± 0.5 mmHg, and average reduction in pulmonary vascular index (PVRI) of 3.5 ± 0.6 Wood units/m^2 from baseline values. An improvement in RV function was demonstrated by an average increase in CI of 0.12 ± 0.04 L/min/m2.[94] Inhaled treprostinil was associated with a median improvement in 6MWD of 18 m, while administration of the oral formulation was recently shown to delay clinical progression (defined as death form any cause, hospitalization for worsening PAH, disease progression, initiation of inhaled or infused prostacyclin therapy, or unsatisfactory clinical response) in patients already on oral monotherapy.[95–97] The IV formulation was shown to increase mean 6MWD by 125 m and result in a reduction in mPAP by 17% and PVRI by 50%, while increasing CI by 56% that was sustained up to 48 weeks in a multicenter, prospective trial.[98]

The most recent agent in the prostacyclin class is selexipag which is an oral prostacyclin IP receptor agonist, which is chemically distinct from prostacyclin. Selexipag has been reported to reduce PVR by 30.3% after 17 weeks in a phase 2 proof-of-concept study, improve WHO functional class, and reduce the composite endpoint of death from any cause or complication related to PAH according to the GRIPHON trial.[99,100] However, it should be noted that there was a significant increase in rates of medication discontinuation in patients on selexipag due to adverse effects including headache, diarrhea, nausea, and jaw pain.[99]

Phosphodiesterase type 5 (PDE5) inhibitors (sildenafil and tadalafil) reduce the enzymatic breakdown of cyclic guanosine monophosphate (cGMP), and thus increase NO levels leading to pulmonary vasodilation. Both agents have been shown to improve exercise capacity, quality of life, improve pulmonary hemodynamics by causing a reduction in mPAP and PVR, and reduce time to clinical worsening.[101–104] The SUPER trial was a double-blind, RCT that compared administration of sildenafil to a placebo and demonstrated significantly increased mean 6MWD of 45, 46, and 50 m from to baseline for 20 mg, 40 mg, and 80 mg doses of sildenafil, respectively. All sildenafil doses yielded significant hemodynamic benefits in a dose-dependent manner with a reduction in mPAP (4.7 mmHg, for 80 mg dose), PVR (261 dynes*sec*cm^{-5}), and increase in CI (0.37 L/min/m^2).[105] The SUPER-2 trial showed that the improvements in 6MWD were sustained for up to three years.[103] In addition to targeting the increased afterload, a smaller study has shown that sildenafil can improve RV

contractility in heart preparations and in individual cardiomyocytes.[106] Systemic vasodilation is the main side effect of this class of drugs which can cause systemic hypotension, headache, gastrointestinal disturbances, and muscle/joint aches. Sildenafil has been associated with worse outcomes in left-sided valvular heart disease, and thus its use is not indicated in this population.[107]

Riociguat is an oral soluble guanylate cyclase stimulant that enhances cGMP production, rather than inhibit its breakdown like the PDE5 inhibitors. Riociguat has shown beneficial effects in the PAH population in the PATENT-1 and PATENT-2 trials.[108,109] After 12 weeks when riociguat was compared to placebo, patients had a significant improvement in 6MWD as demonstrated by a mean increase in 30 m from baseline, reduction in mPAP of 4 ± 8 mmHg and PVR of 223 ± 260 dynes*sec*cm^{-5}, improvement in CO of 1 ± 1 L/min, and improvement in time to clinical worsening. This agent is also FDA approved for treatment of inoperable or persistent chronic thromboembolic pulmonary hypertension (CTEPH) and was shown to improve 6MWD by a mean of 39 m, reduce PVR by 226 dynes*sec*cm^{-5}, and improve functional class in this patient population.[110]

Endothelin-1 not only has a direct vasoconstrictor effect on the pulmonary vasculature but also can cause vascular smooth muscle cell proliferation leading to fibrosis, via endothelin receptor type A while endothelin receptor type B mediates endothelin-1 clearance.[111] Thus, therapeutic agents that modulate these receptors are attractive options, and include the nonselective receptor blockers macitentan and bosentan, while ambrisentan is a selective receptor A blocker. Ambrisentan has been analyzed in two RCTs (AIRES-1 and AIRES-2) in patients with moderate-severe IPAH and PAH due to connective tissue disorders (WHO functional class II–III) and found that ambrisentan delayed disease progression and clinical worsening, while improving exercise tolerance as demonstrated by a mean increase in 6MWD of 59 m, Borg dyspnea scale, WHO functional class, and quality of life compared to placebo.[112,113] Other trials have shown similar benefits with bosentan and macitentan, but due to the selective endothelin receptor type A effects of ambrisentan, this agent is often the initial choice. Endothelin receptor antagonists (ERAs) have also been shown to improve RV function as assessed by cardiac MRI in one study that demonstrated an increase in RV EF of $4.6 \pm 10.7\%$, LV EF of $3.6 \pm 9.8\%$, RV SV index 4.9 ± 10.5 mL/m^2, and improvement in CI of 0.33 ± 0.72 L/min/m^2 compared to placebo.[114] Furthermore, COMPASS 3 trial, which studied the use of bosentan $\pm$ sildenafil, found that cardiac MRI correlated strongly with RHC parameters at baseline, including a strong correlation between RVEDV: LVEDV, and a strong inverse

correlation between RVEDV:LVEDV to SVR:PVR.[115] The main adverse effects of this class include peripheral edema as well as hepatotoxicity causing elevated transaminase levels. However, the actual risk of hepatotoxicity for these agents, especially for ambrisentan, is quite small as this concern stemmed from the use of sitaxsentan which was withdrawn from the market following cases of severe hepatotoxicity. Bosentan has also been associated with worse outcomes in left-sided heart failure, so the use of ERAs as a class is not currently approved.[116]

CCBs currently have a limited role in the treatment of PAH since the development of newer, more effective therapeutic agents, but it still does have a niche for patients with a positive vasoreactivity test. CCBs cause smooth muscle relaxation leading to vasodilation in the pulmonary vascular circulation, but also causes systemic vasodilation and can lead to hypotension. In a vasoreactivity test, patients are administered a short acting pulmonary vasodilator, usually nitric oxide, epoprostenol, or adenosine, with a positive test defined as a reduction in mean PA pressure ≥ 10 mmHg to a value ≤ 40 mmHg without a significant reduction in MAP and unchanged CO. These patients potentially benefit from a short trial of three to four months of a high dose nifedipine, amlodipine, or diltiazem. Similar to the use of oral anticoagulation, vasoreactivity testing should not be performed in all patients with PAH, as it seems to have its greatest benefit in patients with IPAH, familial PAH, or PAH due to drugs or toxins, and little to no benefit in PAH due to connective tissue disorders, HIV, or portopulmonary hypertension.[117] Its increasingly recognized that among those patients that undergo vasoreactivity testing, only about 10%–20% of them will test positive, and out of those patients, an even smaller percentage will be able to tolerate the CCBs due to side effects and/or not require an additional agent due to progression of disease.[118]

Traditionally, anticoagulation was considered an essential therapy for all patients with PAH due to the increased risk of intrapulmonary vascular thrombosis, high prevalence of vascular thrombotic lesions in postmortem studies, and risk of hemodynamic collapse in this patient population with early studies suggesting possible benefit.[119–121] However, the overall data are inconclusive with recent trials suggesting no benefit of anticoagulation and even potential harm in patients with PAH secondary to connective tissue diseases.[122] There is a strong consensus that anticoagulation should therefore be avoided in patients with PAH secondary to connective tissue diseases, and the general trend is shifting toward avoiding anticoagulation unless there is a separate indication. If anticoagulation is to be used without a separate indication, it is recommended that it only be added for patients with idiopathic PAH (IPAH), familial PAH, or PAH due to anorexigens because the data show the most potential benefit in these groups.

Approach to the treatment of pulmonary arterial hypertension

While there is a number of different therapeutic agents available for the treatment of PAH as noted above, the approach to management of PAH can be quite nuanced and dependent on a number of different factors, with which a PAH specialist or center is able to assist. Once a diagnosis of PAH has been made by RHC, the patient should be classified into a low-risk, intermediate-risk, or high-risk category. There are several risk scoring systems with considerable data, including French Pulmonary Hypertension Network, 2015 ESC/ERS guidelines risk classification table, and REVEAL 2.0 which is shown in Fig. 58.8.[123–125]
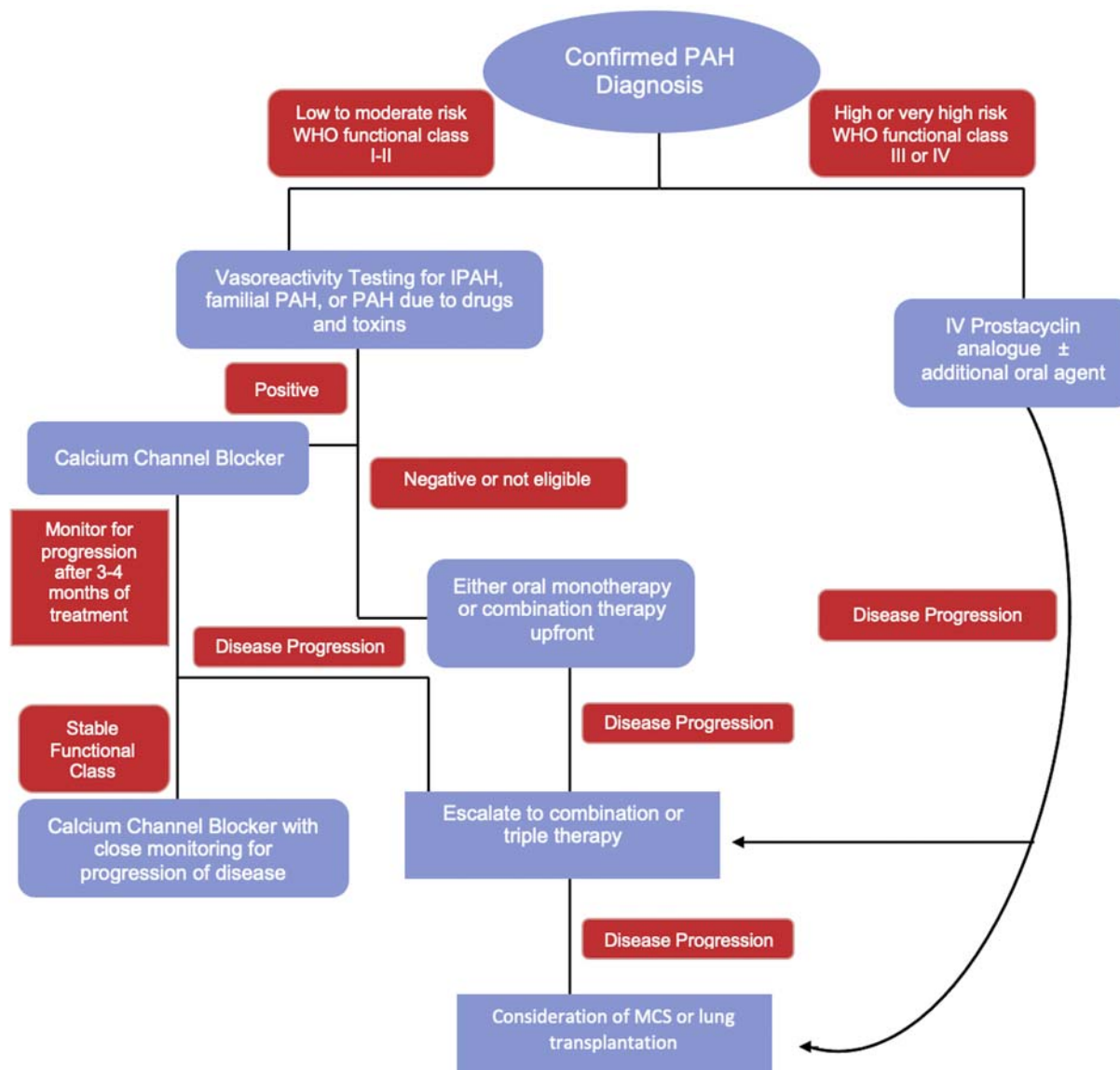
These systems have highlighted the need to treat patients more aggressively to a goal of attaining the low-risk category in order to preserve RV function and improve clinical outcomes. The scores all include a measure of RV function and/or afterload. Fig. 58.9 depicts a proposed algorithm in the management of PAH based off of patient's baseline risk as well as WHO functional class.

In general, it is reasonable to consider vasoreactivity testing in patients whom are classified as low-to-moderate risk with WHO functional class I–III symptoms, only if they have IPAH, familial PAH or PAH due to drugs or toxins.[117] If positive, CCB monotherapy can be initiated for a short trial of 3–4 months to monitor for therapeutic response, which is defined as a same or improved hemodynamic response than what was seen on initial vasoreactivity testing, and usually a mean PA pressure <30 mmHg. As mentioned before, only about 5% of patients will fall into this category, so vasoreactivity testing is becoming less common.[118]

Patients typically present with functional limitation and intermediate or high-risk features since PH can be a challenging diagnosis with an average delay of two years to diagnosis.[74] This has underscored the need for early diagnosis. Patients are commonly considered either average or moderate-risk with either WHO functional class II or III symptoms. The main approach to management in this patient population involves upfront combination therapy, rather than monotherapy. The two classes of drugs that are often selected include an ERA along with a PDE5 inhibitor. The combination of ambrisentan and tadalafil was shown in the AMBITION trial to be associated with a 50% reduction in rate of clinical failure (mainly driven by decreased hospitalizations) as well improved exercise capacity.[126] Other drug combinations studied include tadalafil + bosentan, macitentan + sildenafil, selexipag + ERA.[99,127] Interestingly, there are data suggesting that the combination of sildenafil + bosentan is not beneficial which may be related to drug interactions.[128] Some clinicians argue for a staggered initiation with one agent added at a time in short succession,

FIGURE 58.8 REVEAL 2.0 risk calculator. A score 0−7 is considered low risk and is associated with a predicted one-year survival of ≥95%, 8 is considered average risk and is associated with a predicted one-year survival of 90% to <95%, 9 is considered moderate risk and is associated with a predicted one-year survival of 85% to <90%, 10−11 is considered high risk and is associated with a predicted one-year survival of 70% to <85%, and ≥12 is considered very high risk and is associated with a predicted one-year survival <70%. *Reproduced from Benza, RL. **Chest**. 2019; 2:323−337. Copyright 2019, with permission from Elsevier.*

FIGURE 58.9 A simplified algorithm for management of pulmonary arterial hypertension (PAH) based off of REVEAL 2.0 risk score and WHO functional class symptoms. *MCS*, Mechanical circulatory support.

which provides clinicians with the benefit of being able to accurately monitor response to adverse reactions of a specific agent while assessing treatment response, while data from the large RCTs seem to suggest that upfront, low-dose combination therapy is equally safe and effective.[126]

Patients considered high or very high-risk with WHO functional class III or IV symptoms are often treated initially with monotherapy in the parenteral prostacyclin analogue class with eventual goal of getting patient on combination therapy or even triple therapy.[123] Parenteral prostacyclin analogues are the most potent vasodilators available with immediate benefits often appreciated, which makes these agents useful in the ICU setting in patients with cardiogenic shock due to RV failure from PAH.

Intravenous epoprostenol was shown to improve mortality in patients with IPAH.[90]

With the exception of one trial of intravenous epoprostenol in IPAH and a few meta-analyses involving the parenteral prostacyclin analogues, these PH agents improve hemodynamics and exercise capacity while reducing progression of clinical worsening, but data on mortality are lacking. There have been few outcome-driven trials due to the number of patients required in a rare disease. More recent trials involving clinical outcomes such as GRIPHON and SERAPHIN utilized composite endpoints of clinical worsening.[99,127] Despite being some of the largest trials in PAH ever performed, it was not feasible to power these trials for mortality. It is also unknown if these therapeutic

agents would improve mortality in asymptomatic patients, or in patients with mild PH. The EDITA trial was a double-blinded, placebo-controlled RCT that studied the effect of initiating ambrisentan in patients with PAH due to systemic sclerosis with a mildly elevated mean PA pressure between 21 and 24 mmHg at rest or >30 mmHg with exercise. At six months, there was no significant different in mean PA pressures; however, patients treated with ambrisentan had a significant improvement in CI at rest of 0.36 ± 0.66 L/min/m^2 and with exercise of 0.7 ± 0.81 L/min/m^2, and reduction in PVR at rest of 0.70 ± 0.78 Wood units and with exercise of 0.84 ± 0.48 Wood units.[129]

More recently, upfront triple therapy has been studied. A small, retrospective pilot study of PAH patients looked at initiation of the combination of intravenous epoprostenol, bosentan, and sildenafil. Out of 19 patients, 17 (89%) were WHO functional class I or II, and 100% of the patients were alive at 3 years.[130] More recently, the TRITON study compared triple therapy with selexipag, macitentan, and tadalafil versus macitentan and tadalafil. While there was no difference in primary outcome of PVR, 6MWD, or N-terminal pro-brain natriuretic peptide levels, at 26 weeks, there was a nonsignificant 41% reduction in risk of disease progression in the triple therapy group suggesting a signal for improved long-term outcomes.[131] This treatment approach requires further study.

Of note, one of the ways to determine success of treatment is through monitoring change in PVR, which as mentioned before, ignores the pulsatile load that affects the RV. PA compliance has been shown to a more accurate predictor of mortality than PVR and often declines early in the disease process prior to any change in PVR.[132,133] For example, pulmonary vascular compliance has been shown to be a better predictor for long-term response to CCBs in patients with IPAH with positive vasoreactivity testing compared to PVR.[134] Thus, measuring the pulsatile load either invasively or via PA compliance might allow us to detect PH earlier and more accurately monitor treatment response.

Creation of palliative right-to-left shunts

The idea of creating a right-to-left shunt for treatment of PH and/or RV failure stems from anecdotal evidence demonstrating that patients with severe PAH whom had a patent foramen ovale (PFO) lived longer compared to those patients without a PFO, as well as in patients with Eisenmenger physiology having a lower right atrial pressure and higher CO compared to patients without Eisenmenger physiology.[135,136] Mechanistically, this occurs as blood is able to bypass the lungs and instead travel through a shunt at the interatrial level, thus increasing systemic CO while

also reducing RV pressure and unloading the RV. Blood is able to travel right-to-left due to the increased right-sided pressures that are greater than the left-sided pressures. However, this comes at a cost of worsening systemic arterial oxygen saturation as blood is shunted away from the lungs into the systemic circulation.

Balloon atrial septostomy is the most common procedure that utilizes this technique and involves perforating the septum at the interatrial level, and using balloons of increasing sizes in a "step-by-step" manner while measuring hemodynamic variables to ensure reduction in right-sided pressures and improvement in CO. The size of the shunt is ultimately limited by a drop in systemic arterial saturation of >10% from baseline or increased in LVEDP >18 mmHg.[137] An alternative procedure is called a Potts anastomosis which creates a surgical anastomosis between the left PA and the aorta, and thus mimics a patent ductus arteriosus. The main benefit of this method is that it does not lead to arterial oxygen desaturation in the upper part of the body and thus would have more oxygen to supply the brain and coronary arteries. Despite these theoretic benefits, this procedure is technically challenging to perform non-invasively and has almost exclusively been studied in small trials in children, and thus lacks the long-term data of balloon atrial septostomy.[137,138] An interatrial shunt device that is implanted transcutaneously via a catheter-based approach is being investigated for the treatment of PAH (NCT03838445).

Current guidelines recommend balloon atrial septostomy in patients with severe PAH who have refractory right-sided failure despite maximally tolerated medical therapy either for palliative purposes or as a bridge to transplantation. Contraindications to performing this procedure include patients with baseline arterial oxygen saturation <85%, patients with LV dysfunction or Group 2 PH, or patients with baseline right atrial pressure >20 mmHg since this will likely lead to acute pulmonary edema upon creation of the shunt.[123]

Approach to treatment of group 2 pulmonary hypertension

Group 2 PH, which is due to left-sided heart disease including HFrEF, HFpEF, valvular disease, etc., may be isolated postcapillary PH or combined pre- and post-capillary PH. Isolated postcapillary PH is defined as a mPAP >20 mmHg with PAWP >15 mmHg, and a PVR <3 Wood units. Combined pre- and postcapillary PH is defined as a mPAP >20 mmHg with PAWP >15 mmHg, but a PVR ≥3 Wood units. This is an important distinction, as this population exhibits an increased mortality and a phenotype that is more similar to PAH.[74,139,140]

Management of Group 2 PH focuses on treating the underlying etiology. For example, in patients with HFrEF, this often means diuretics to reduce the wedge pressure along with GDMT medications that have been shown to improve mortality. Agents that target a reduction in afterload via pulmonary vasodilation have yielded no benefit until recently. However, recently the VICTORIA trial demonstrated that vericiguat, an oral guanylate cyclase inhibitor, significantly reduced the composite endpoint of cardiovascular death and time to first heart failure hospitalization compared to placebo in patients with HFrEF, without an impact on mortality.[2] Vericiguat likely has multiple effects on the systemic vasculature, pulmonary vasculature, myocardium, and other organs, such that the extent to which pulmonary vascular effects are responsible for the improved outcomes seen in this trial is unclear.

Patients with PH associated with HFpEF (PH-HFpEF) represent a unique population that is much more challenging to manage as there are currently no approved therapeutic agents that have been shown to improve mortality in patients with HFpEF. Several possible explanations for a lack of benefit include different pathophysiologic mechanisms that lead to develop of HFpEF, rather than neurohormonal dysfunction that is prominent in HFrEF, and belief that HFpEF compromises a wide range of different phenotypes that might require a more personalized treatment strategy.[141] PH is not only a common complication of patients with HFpEF, but it is also an independent predictor of hospitalization and mortality.[25] Impairment in nitric oxide bioavailability is thought to play a role in the development of LV diastolic dysfunction and increased PA pressure, but trials using isosorbide mononitrate and inhaled sodium nitrite have not yielded positive results.[142,143] One possible reason is that the study population included patients with HFpEF rather than patients with PH-HFpEF. This may also have been associated with the neutral findings of the INDIE trial of inhaled sodium nitrite despite multiple earlier single center studies showing improvements in hemodynamics including PA compliance and impedance spectra, as well as functional capacity.[142,144−146] However, the very short half-life of inhaled sodium nitrite ($\sim$35 min) combined with the administration regimen (three times/day) in the INDIE trial may have been related to the failure of this preparation. Ongoing studies with orally administered inorganic nitrate (which has a half-life of several hours) are ongoing. A detailed discussion of agents that target the nitrate-nitrite-NO pathway can be found in Chapter 51; a detailed discussion of the role of these agents in HFpEF

can be found in Chapter 36. Finally, there are ongoing clinical trials that are examining the role of riociguat (NCT02744339) and tadalafil in patients with PH-HFpEF (2017-003688-37).

Advanced therapeutic options for treatment of right venrticular failure

Up to this point, various pharmacologic therapies have been presented with the goal of optimizing RV performance by modifying preload, contractility, perfusion, and afterload. However, there are occasions when the RV will continue to fail despite exhaustion of all possible medical and pharmacologic therapies, such as RV infarct, postcardiotomy ventricular failure, or RV failure after placement of a left ventricular assist device (LVAD). It is at this point, that advanced therapeutic options should be discussed, which include the use of mechanical circulatory support (MCS) devices and heart transplantation. Two major barriers to the use of the various MCS devices are the lack of durable, long-term options and, in the case of biventricular failure, the need for concurrent LV support. RV MCS devices work by reducing right-sided filling pressures while improving RV CO and therefore increasing LV preload. If the patient has concurrent LV failure, increasing the preload to the left side of the heart will result in acute pulmonary edema and the patient will continue to have low systemic perfusion.

One of the most commonly used MCS devices for RV failure is the RP Impella (Abiomed Inc, Danvers, MA), which is a percutaneous microaxial-flow device that sits in the RA and delivers blood to the PA, thus bypassing the RV. It can provide up to 4 L/min of additional flow while decreasing RA pressure, increasing right-sided CO, and increases preload to the left-side of the heart, thus improving systemic perfusion.[147] It does not have an oxygenator present, so is not effective for patients with severe PH who also have concurrent hypoxia. The RECOVER RIGHT trial demonstrated an improvement in RA pressure and cardiac index while also permitting weaning of inotropes and vasopressors in patients with acute RV infarct or postcardiotomy.[148] Common adverse effects include vascular access complications, including hematoma or dissection, as well as hemolysis.

Right ventricular assist devices (RVADs) have a similar mechanism to the RP Impella and include the TandemHeart RVAD (TandemLife, Pittsburgh, PA) and the Protek Duo cannula. These devices are an extracorporeal centrifugal-flow pump that has an inflow cannula in the RA that

bypasses blood externally before returning to the outflow cannula that is located in the PA. The RVADs are not only capable of providing RV support up to 4.5 L/min but are also able to have an oxygenator added to the circuit, and thus can be used for patients with an acute PE or decompensated, severe PH.[17,147] Studies have shown an improvement in RA and PA pressures, improvement in CO and RV stroke work, and improvement in oxygenation.[147] Common adverse effects include vascular access complications, bleeding, and thrombosis.

Venoarterial extracorporeal membrane oxygenation (VA-ECMO) displaces venous blood from the RA across an oxygenator and returns it to the arterial circulation. Unlike the RVADs, VA-ECMO will increase LV afterload due to the increase in blood return to the arterial circulation and can cause worsening cardiogenic shock and acute pulmonary edema if the patient also has LV dysfunction. In these instances, it is often necessary to implant an additional MCS device, such as an Impella device or intra-aortic balloon pump to help unload the LV and reduce left-sided filling pressures. Adverse events associated with ECMO include bleeding, thromboembolism, and vessel injury.[10,147]

As briefly mentioned above, MCS for RV failure is currently only designed for short-term use unlike the LVADs which have been approved for destination therapy. Thus, careful consideration must be taken among a multidisciplinary heart team, including heart failure specialists, interventional cardiologists, and cardiothoracic surgeons, prior to implantation as they are typically reserved for either a short-term bridge to recovery or bridge to transplantation. Currently, the CentriMag pump (St. Jude, Minneapolis, MN), an extracorporeal centrifugal-flow pump, is the longest duration support device available and is approved for use up to 30 days. Future studies are examining the feasibility of more durable RV support devices and include the HeartWare MVAD, the Circulite Synergy device, and the Syncardia total artificial heart (Syncardia Systems, LLC, Tucson, AZ).[149−151]

Emerging therapeutic options

Given the high morbidity and mortality associated with RV failure, there remains a strong need for novel therapeutic agents that target unique pathways contributing to RV dysfunction. As the severity of PH worsens, the RV will begin to dilate leading to left-to-right asynchrony, which can be visualized by septal bowing in early LV diastole on echocardiography. The RV volume will shift toward the relaxed LV leading to septal bowing, but this allows the pulmonary valve to close while the RV is still contracting

leading to increase in oxygen consumption and a decrease in early LV diastolic filling.[152,153] Therefore, it has been postulated that cardiac right-to-left resynchronization therapy by pacing the RV earlier might be beneficial for patients with severe PH and evidence of RV dilation and septal bowing. While cardiac resynchronization therapy is currently approved for patients with HFrEF and a wide QRS morphology in an effort to improve LV systolic dysfunction, data are limited in this patient population, mainly occurring in experimental animal models and one small trial in patients with CTEPH in which RV pacing reduced asynchrony, increased RV contractility, and improved LV diastolic filling time and SV.[154,155]

One of the mechanisms that is thought to contribute to RV dysfunction is activation of the RAAS and excess sympathetic tone. As discussed previously, while this pathway is important in the pathophysiology of HFrEF and inhibition of this pathway via ACE inhibitors or ARBs have resulted in an improvement in LVEF and mortality, these agents have had mixed results in isolated RV failure. Nevertheless, an emerging therapeutic option consists of directly blocking the excess sympathetic tone and bypassing the RAAS, via performing PA denervation. This is a minimally invasive catheter-based procedure that utilizes radiofrequency ablation to eliminate the PA baroreceptors located between the distal main trunk and ostial left branch, thus reducing sympathetic tone.[156,157] The benefits of PA denervation were studied in the PADN-5 trial which compared PA denervation to sildenafil plus a sham procedure in patients with combined pre- and postcapillary PH and found that PA denervation group had a higher 6MWD and lower PVR at 6 months.[158] Similar hemodynamic findings were shown in animal models with Group 1 PAH, and a clinical trial is planned (NCT02835950).[159]

Several other pharmacologic agents that are currently being investigated include antioxidant agents that target reactive oxygen species (ROS), fatty acid oxidation inhibitors, and antiinflammatory agents.[69,160] Studies to date with these agents have been limited to animal models or small clinical trials with the only randomized controlled trial being the use of trimetazidine, a fatty acid oxidation inhibitor, for patients post percutaneous coronary intervention which did not show any benefit, although this trial did not examine the benefits in isolated RV infarct.[161] Thus, further clinical trials are needed studying patients with RV failure and/or PH before widespread use will be adopted. Table 58.2 reviews the different therapeutic options along with brief description of mechanism of action and supporting trial data that has been discussed in this chapter.

TABLE 58.2 Overview of main therapeutic agents along with mechanism of action discussed throughout chapter.

Therapeutic agents	Mechanism of action	Trials
Diuretics		
• Furosemide • Torsemide • Bumetanide • Dialysis	Optimization of preload to improve RV stroke volume, reduce RV dilatation, reduce RV free wall tension	CARRESS-HF: Diuretics versus dialysis[39]
Vasopressors		
• Norepinephrine • Epinephrine • Dopamine • Vasopressin • Phenylephrine	- Increase perfusion by increasing blood pressure but may increase RV afterload - Epinephrine has some inotropic effect at low-dose - Vasopressin can cause pulmonary vasodilation via endothelial nitric oxide stimulation at low doses	Norepinephrine[45] Epinephrine[46] Vasopressin[47]
Inotropes		
• Dobutamine • Milrinone • Levosimendan	- Dobutamine: beta 1 and 2 receptor agonist - Milrinone: phosphodiesterase 3 inhibitor and often preferred agent due to mild pulmonary vasodilation properties - Levosimendan: myocardial calcium sensitizer	Levosimendan[56–59] Dobutamine and milrinone[6]
Neurohormonal modulation		
Beta-blockers (metoprolol succinate, carvedilol, bisoprolol, and nebivolol)	- Either selectively block beta-1 or 2 receptors, or nonselective blockade of both - Decrease in altered stimulation mediated by RAAS - Decrease in preload and decrease myocardial oxygen demand - Nebivolol may reduce PA smooth muscle proliferation	60,62 Bisoprolol[61,63] Nebivolol[64]
ACE inhibitors and ARBs	Blocks RAAS by either blocking angiotensin receptors or by inhibiting angiotensin converting enzyme	17,66–68
Mineralocorticoid receptor antagonist (aldosterone)	- Blocks aldosterone receptors to suppress RAAS stimulation - May also reduce afterload when combined with ambrisentan (AIRES trial)	ARIES trial[70] Use in PAH (NCT01712620) Use in RV failure (NCT03344159)
Sacubitril/valsartan	- ARB with a neprilysin inhibitor that inhibits breakdown of natriuretic peptides - May prevent maladaptive remodeling	72,73
Prostacyclin analogues and prostacyclin receptor agonists		
• Epoprostenol (IV) • Iloprost (Inhaled) • Treprostinil (IV, SQ, inhaled, PO) • Selexipag (PO)	- Either mimic prostacyclin or acts on receptor to increase production of prostacyclin which then increases production of cAMP and leads to vasodilation - Reduces mPAP and PVR; improves 6MWD and CO/CI - Epoprostenol improves mortality in IPAH	Epoprostenol[89,90,92] Iloprost[93] Treprostinil[94–98] Selexipag in GRIPHON trial[99,100]
Phosphodiesterase 5 inhibitors		
• Sildenafil • Tadalafil	- Reduces enzymatic breakdown of cGMP and increase levels of NO leading to pulmonary vasodilation - Reduces mPAP and PVR; improves 6MWD and CO/CI	Tadalafil[101] Sildenafil[102–107]
Oral soluble guanylate cyclase		
Riociguat	- Enhances cGMP production Also has benefit in Group 4 PH - Reduces mPAP and PVR; improves 6MWD and CO/CI	PAH[108,109] Group 4 PH[110]
Endothelin receptor antagonists		
• Ambrisentan • Bosentan • Macitentan	- Ambrisentan: receptor A blocker → blocks production of endothelin-1 - Bosentan and macitentan: receptor A and B blockers → blocks of production of endothelin-1 but also blocks clearance of endothelin-1 - Reduces mPAP and PVR; improves 6MWD and CO/CI	Ambrisentan[70,112,113] Bosentan in COMPASS 3[115]

TABLE 58.2 Overview of main therapeutic agents along with mechanism of action discussed throughout chapter.—cont'd

Therapeutic agents	Mechanism of action	Trials
Calcium channel blockers		
• Nifedipine, amlodipine, or diltiazem	- Blocks calcium channels leading to vasodilation - Need to be vasoreactivity testing positive to get benefit	117,118
Palliative right-to-left shunts		
• Balloon atrial septostomy • Potts anastomosis	- Creates a shunt at atrial level to improve CO while reducing RV pressure - Will cause hypoxia as a result so generally reserved for palliative cases - Potts anastomosis creates a shunt between left PA and aorta; does not cause hypoxia	Balloon atrial septostomy[135–137] Potts anastomosis[138] Transcutaneous interatrial shunt (NCT03838445)
RV resynchronization therapy		
	Paces RV earlier in order to reduce RV oxygen consumption and promote cardiac synchrony	154,155
PA nerve denervation		
	Eliminate the PA baroreceptors located between the distal main trunk and ostial left branch to reduce sympathetic tone that contributes to altered RV remodelling	PADN-5 Trial[158] 159 NCT02835950
Fatty acid oxidation inhibitors and antiinflammatory agents		
	- Reduce inflammation and inhibit production of fatty acid metabolism to reduce myocardial oxygen consumption	69,160 Trimetazidine[161]

6MWD, 6 minute walk distance; *cAMP*, cyclic adenosine monophosphate; *cGMP*, cyclic guanosine monophosphate; *CI*, cardiac index; *CO*, cardiac output; *IPAH*, idiopathic pulmonary arterial hypertension; *mPAP*, mean pulmonary artery pressure; *NO*, nitric oxide; *PA*, pulmonary artery; *PVR*, pulmonary vascular resistance; *RAAS*, renin-angiotensin aldosterone system.

Conclusion

In conclusion, it is important to recognize and treat RV failure as it remains a strong predictor of mortality in patients with heart failure due to left-sided dysfunction and PH. Management requires optimization of several different parameters, including preload, contractility, myocardial perfusion, and afterload. As our understanding of the RV continues to grow, there is a push to better incorporate our understanding of the components of RV afterload that contribute to RV dysfunction (including pulsatile components, including wave reflections) into the design of agents that target these mechanisms in effort to improve outcomes.

References

1. Yancy CW, Jessup M, Bozkurt B, et al. ACC/AHA/HFSA focused update of the 2013 ACCF/AHA guideline for the management of heart failure: a report of the American College of Cardiology/American Heart Association Task Force on Clinical Practice Guidelines and the Heart Failure Society of America. **J Card Fail**. 2017; 23:628−651.

2. Armstrong PW, Pieske B, Anstrom KJ, et al. Vericiguat in patients with heart failure and reduced ejection fraction. **N Engl J Med**. 2020; 382:1883−1893.

3. McMurray JJV, Docherty KF, Jhund PS. Dapagliflozin in patients with heart failure and reduced ejection fraction. **N Engl J Med**. 2020; 382:973.

4. Ghio S, Gavazzi A, Campana C, et al. Independent and additive prognostic value of right ventricular systolic function and pulmonary artery pressure in patients with chronic heart failure. **J Am Coll Cardiol**. 2001; 37:183−188.

5. Fine NM, Chen L, Bastiansen PM, et al. Outcome prediction by quantitative right ventricular function assessment in 575 subjects evaluated for pulmonary hypertension. **Circ Cardiovasc Imaging**. 2013; 6:711−721.

6. Ventetuolo CE, Klinger JR. Management of acute right ventricular failure in the intensive care unit. **Ann Am Thorac Soc**. 2014; 11:811−822.

7. Greyson CR. The right ventricle and pulmonary circulation: basic concepts. **Rev Esp Cardiol**. 2010; 63:81−95.

8. Maughan WL, Shoukas AA, Sagawa K, Weisfeldt ML. Instantaneous pressure-volume relationship of the canine right ventricle. **Circ Res**. 1979; 44:309−315.

9. Yin FC. Ventricular wall stress. **Circ Res**. 1981; 49:829−842.

10. Konstam MA, Kiernan MS, Bernstein D, et al. Evaluation and management of right-sided heart failure: a scientific statement from the American Heart Association. **Circulation**. 2018; 137:e578–e622.

11. Modesti PA, Vanni S, Bertolozzi I, et al. Different growth factor activation in the right and left ventricles in experimental volume overload. **Hypertension**. 2004; 43:101–108.

12. Bogaard HJ, Abe K, Vonk Noordegraaf A, Voelkel NF. The right ventricle under pressure: cellular and molecular mechanisms of right-heart failure in pulmonary hypertension. **Chest**. 2009; 135:794–804.

13. Urashima T, Zhao M, Wagner R, et al. Molecular and physiological characterization of RV remodeling in a murine model of pulmonary stenosis. **Am J Physiol Heart Circ Physiol**. 2008; 295:H1351–H1368.

14. Zaffran S, Kelly RG, Meilhac SM, Buckingham ME, Brown NA. Right ventricular myocardium derives from the anterior heart field. **Circ Res**. 2004; 95:261–268.

15. Haddad F, Doyle R, Murphy DJ, Hunt SA. Right ventricular function in cardiovascular disease, part II: pathophysiology, clinical importance, and management of right ventricular failure. **Circulation**. 2008; 117:1717–1731.

16. Peacock AJ, Naeije R, Rubin LJ. **Pulmonary Circulation : Diseases and Their Treatment**. 4th ed. Boca Raton: CRC Press, Taylor & Francis Group; 2016.

17. Simon MA. Assessment and treatment of right ventricular failure. **Nat Rev Cardiol**. 2013; 10:204–218.

18. Hines R. Right ventricular function and failure: a review. **Yale J Biol Med**. 1991; 64:295–307.

19. Weyman AE, Wann S, Feigenbaum H, Dillon JC. Mechanism of abnormal septal motion in patients with right ventricular volume overload: a cross-sectional echocardiographic study. **Circulation**. 1976; 54:179–186.

20. Grant BJ, Lieber BB. Clinical significance of pulmonary arterial input impedance. **Eur Respir J**. 1996; 9:2196–2199.

21. Finkelstein SM, Collins VR, Cohn JN. Arterial vascular compliance response to vasodilators by Fourier and pulse contour analysis. **Hypertension**. 1988; 12:380–387.

22. Mahapatra S, Nishimura RA, Sorajja P, Cha S, McGoon MD. Relationship of pulmonary arterial capacitance and mortality in idiopathic pulmonary arterial hypertension. **J Am Coll Cardiol**. 2006; 47:799–803.

23. Weinberg CE, Hertzberg JR, Ivy DD, et al. Extraction of pulmonary vascular compliance, pulmonary vascular resistance, and right ventricular work from single-pressure and Doppler flow measurements in children with pulmonary hypertension: a new method for evaluating reactivity: in vitro and clinical studies. **Circulation**. 2004; 110:2609–2617.

24. Al-Naamani N, Preston IR, Paulus JK, Hill NS, Roberts KE. Pulmonary arterial capacitance is an important predictor of mortality in heart failure with a preserved ejection fraction. **JACC Heart Fail**. 2015; 3:467–474.

25. Vanderpool RR, Saul M, Nouraie M, Gladwin MT, Simon MA. Association between hemodynamic markers of pulmonary hypertension and outcomes in heart failure with preserved ejection fraction. **JAMA Cardiol**. 2018; 3:298–306.

26. Hunter KS, Lee PF, Lanning CJ, et al. Pulmonary vascular input impedance is a combined measure of pulmonary vascular resistance and stiffness and predicts clinical outcomes better than pulmonary vascular resistance alone in pediatric patients with pulmonary hypertension. **Am Heart J**. 2008; 155:166–174.

27. Milnor WR. Arterial impedance as ventricular afterload. **Circ Res**. 1975; 36:565–570.

28. Brimioulle S, Maggiorini M, Stephanazzi J, Vermeulen F, Lejeune P, Naeije R. Effects of low flow on pulmonary vascular flow-pressure curves and pulmonary vascular impedance. **Cardiovasc Res**. 1999; 42:183–192.

29. Huez S, Brimioulle S, Naeije R, Vachiery JL. Feasibility of routine pulmonary arterial impedance measurements in pulmonary hypertension. **Chest**. 2004; 125:2121–2128.

30. Givertz MM, Stevenson LW, Costanzo MR, et al. Pulmonary artery pressure-guided management of patients with heart failure and reduced ejection fraction. **J Am Coll Cardiol**. 2017; 70:1875–1886.

31. Skhiri M, Hunt SA, Denault AY, Haddad F. [Evidence-based management of right heart failure: a systematic review of an empiric field]. **Rev Esp Cardiol**. 2010; 63:451–471.

32. British Cardiac Society Guidelines and Medical Practice Commitee and approved by the British Thoracic Society and the British Society of Rheumatology. Recommendations on the management of pulmonary hypertension in clinical practice. **Heart**. 2001; 86(Suppl 1):I1–I13.

33. Damman K, van Deursen VM, Navis G, Voors AA, van Veldhuisen DJ, Hillege HL. Increased central venous pressure is associated with impaired renal function and mortality in a broad spectrum of patients with cardiovascular disease. **J Am Coll Cardiol**. 2009; 53:582–588.

34. Mullens W, Abrahams Z, Francis GS, et al. Importance of venous congestion for worsening of renal function in advanced decompensated heart failure. **J Am Coll Cardiol**. 2009; 53:589–596.

35. Nickel NP, O'Leary JM, Brittain EL, et al. Kidney dysfunction in patients with pulmonary arterial hypertension. **Pulm Circ**. 2017; 7:38–54.

36. Brater DC, Day B, Burdette A, Anderson S. Bumetanide and furosemide in heart failure. **Kidney Int**. 1984; 26:183–189.

37. Cook JA, Smith DE, Cornish LA, Tankanow RM, Nicklas JM, Hyneck ML. Kinetics, dynamics, and bioavailability of bumetanide in healthy subjects and patients with congestive heart failure. **Clin Pharmacol Ther**. 1988; 44:487–500.

38. Felker GM, Lee KL, Bull DA, et al. Diuretic strategies in patients with acute decompensated heart failure. **N Engl J Med**. 2011; 364:797–805.

39. Bart BA, Goldsmith SR, Lee KL, et al. Ultrafiltration in decompensated heart failure with cardiorenal syndrome. **N Engl J Med**. 2012; 367:2296–2304.

40. Chen HY, Chou KJ, Fang HC, et al. Effect of ultrafiltration versus intravenous furosemide for decompensated heart failure in cardiorenal syndrome: a systematic review with meta-analysis of randomized controlled trials. **Nephron**. 2015; 129:189–196.

41. Dell'Italia LJ. The right ventricle: anatomy, physiology, and clinical importance. **Curr Probl Cardiol**. 1991; 16:653–720.

42. Foschi M, Di Mauro M, Tancredi F, et al. The dark side of the moon: the right ventricle. **J Cardiovasc Dev Dis**. 2017; 4.

43. De Backer D, Biston P, Devriendt J, et al. Comparison of dopamine and norepinephrine in the treatment of shock. **N Engl J Med**. 2010; 362:779–789.

44. Levy B, Clere-Jehl R, Legras A, et al. Epinephrine versus norepinephrine for cardiogenic shock after acute myocardial infarction. **J Am Coll Cardiol**. 2018; 72:173−182.

45. Schreuder WO, Schneider AJ, Groeneveld AB, Thijs LG. Effect of dopamine vs norepinephrine on hemodynamics in septic shock. Emphasis on right ventricular performance. **Chest**. 1989; 95:1282−1288.

46. Le Tulzo Y, Seguin P, Gacouin A, et al. Effects of epinephrine on right ventricular function in patients with severe septic shock and right ventricular failure: a preliminary descriptive study. **Intensive Care Med**. 1997; 23:664−670.

47. Leather HA, Segers P, Berends N, Vandermeersch E, Wouters PF. Effects of vasopressin on right ventricular function in an experimental model of acute pulmonary hypertension. **Crit Care Med**. 2002; 30:2548−2552.

48. Zamanian RT, Haddad F, Doyle RL, Weinacker AB. Management strategies for patients with pulmonary hypertension in the intensive care unit. **Crit Care Med**. 2007; 35:2037−2050.

49. Weidemann F, Jamal F, Sutherland GR, et al. Myocardial function defined by strain rate and strain during alterations in inotropic states and heart rate. **Am J Physiol Heart Circ Physiol**. 2002; 283:H792−H799.

50. Aranda Jr JM, Schofield RS, Pauly DF, et al. Comparison of dobutamine versus milrinone therapy in hospitalized patients awaiting cardiac transplantation: a prospective, randomized trial. **Am Heart J**. 2003; 145:324−329.

51. Movsesian M, Stehlik J, Vandeput F, Bristow MR. Phosphodiesterase inhibition in heart failure. **Heart Fail Rev**. 2009; 14:255−263.

52. Chen EP, Bittner HB, Davis Jr RD, Van Trigt 3rd P. Milrinone improves pulmonary hemodynamics and right ventricular function in chronic pulmonary hypertension. **Ann Thorac Surg**. 1997; 63:814−821.

53. Colucci WS, Wright RF, Jaski BE, Fifer MA, Braunwald E. Milrinone and dobutamine in severe heart failure: differing hemodynamic effects and individual patient responsiveness. **Circulation**. 1986; 73:III175−I183.

54. O'Connor CM, Gattis WA, Uretsky BF, et al. Continuous intravenous dobutamine is associated with an increased risk of death in patients with advanced heart failure: insights from the Flolan International Randomized Survival Trial (FIRST). **Am Heart J**. 1999; 138:78−86.

55. Packer M, Carver JR, Rodeheffer RJ, et al. Effect of oral milrinone on mortality in severe chronic heart failure. The PROMISE Study Research Group. **N Engl J Med**. 1991; 325:1468−1475.

56. Follath F, Cleland JG, Just H, et al. Efficacy and safety of intravenous levosimendan compared with dobutamine in severe low-output heart failure (the LIDO study): a randomised double-blind trial. **Lancet**. 2002; 360:196−202.

57. Kivikko M, Lehtonen L, Colucci WS. Sustained hemodynamic effects of intravenous levosimendan. **Circulation**. 2003; 107:81−86.

58. Nieminen MS, Akkila J, Hasenfuss G, et al. Hemodynamic and neurohumoral effects of continuous infusion of levosimendan in patients with congestive heart failure. **J Am Coll Cardiol**. 2000; 36:1903−1912.

59. Russ MA, Prondzinsky R, Carter JM, et al. Right ventricular function in myocardial infarction complicated by cardiogenic shock:

60. improvement with levosimendan. **Crit Care Med**. 2009; 37:3017−3023.

60. Bogaard HJ, Natarajan R, Mizuno S, et al. Adrenergic receptor blockade reverses right heart remodeling and dysfunction in pulmonary hypertensive rats. **Am J Respir Crit Care Med**. 2010; 182:652−660.

61. de Man FS, Handoko ML, van Ballegoij JJ, et al. Bisoprolol delays progression towards right heart failure in experimental pulmonary hypertension. **Circ Heart Fail**. 2012; 5:97−105.

62. Perros F, de Man FS, Bogaard HJ, et al. Use of beta-blockers in pulmonary hypertension. **Circ Heart Fail**. 2017; 10.

63. van Campen JS, de Boer K, van de Veerdonk MC, et al. Bisoprolol in idiopathic pulmonary arterial hypertension: an explorative study. **Eur Respir J**. 2016; 48:787−796.

64. Perros F, Ranchoux B, Izikki M, et al. Nebivolol for improving endothelial dysfunction, pulmonary vascular remodeling, and right heart function in pulmonary hypertension. **J Am Coll Cardiol**. 2015; 65:668−680.

65. Te Riet L, van Esch JH, Roks AJ, van den Meiracker AH, Danser AH. Hypertension: renin-angiotensin-aldosterone system alterations. **Circ Res**. 2015; 116:960−975.

66. Henein MY, O'Sullivan CA, Coats AJ, Gibson DG. Angiotensin-converting enzyme (ACE) inhibitors revert abnormal right ventricular filling in patients with restrictive left ventricular disease. **J Am Coll Cardiol**. 1998; 32:1187−1193.

67. Nguyen QT, Colombo F, Clement R, Gosselin H, Rouleau JL, Calderone A. AT1 receptor antagonist therapy preferentially ameliorated right ventricular function and phenotype during the early phase of remodeling post-MI. **Br J Pharmacol**. 2003; 138:1485−1494.

68. Therrien J, Provost Y, Harrison J, Connelly M, Kaemmerer H, Webb GD. Effect of angiotensin receptor blockade on systemic right ventricular function and size: a small, randomized, placebo-controlled study. **Int J Cardiol**. 2008; 129:187−192.

69. Zelt JGE, Chaudhary KR, Cadete VJ, Mielniczuk LM, Stewart DJ. Medical therapy for heart failure associated with pulmonary hypertension. **Circ Res**. 2019; 124:1551−1567.

70. Maron BA, Waxman AB, Opotowsky AR, et al. Effectiveness of spironolactone plus ambrisentan for treatment of pulmonary arterial hypertension (from the [ARIES] study 1 and 2 trials). **Am J Cardiol**. 2013; 112:720−725.

71. McMurray JJ, Packer M, Desai AS, et al. Angiotensin-neprilysin inhibition versus enalapril in heart failure. **N Engl J Med**. 2014; 371:993−1004.

72. Sharifi Kia D, Benza E, Bachman TN, Tushak C, Kim K, Simon MA. Angiotensin receptor-neprilysin inhibition attenuates right ventricular remodeling in pulmonary hypertension. **J Am Heart Assoc**. 2020:e015708.

73. Clements RT, Vang A, Fernandez-Nicolas A, et al. Treatment of pulmonary hypertension with angiotensin II receptor blocker and neprilysin inhibitor sacubitril/valsartan. **Circ Heart Fail**. 2019; 12:e005819.

74. Simonneau G, Montani D, Celermajer DS, et al. Haemodynamic definitions and updated clinical classification of pulmonary hypertension. **Eur Respir J**. 2019; 53.

75. Milnor WR. **Hemodynamics**. Baltimore: Williams & Wilkins; 1982.

76. Lankhaar JW, Westerhof N, Faes TJ, et al. Pulmonary vascular resistance and compliance stay inversely related during treatment of pulmonary hypertension. **Eur Heart J**. 2008; 29:1688−1695.

77. Lankhaar JW, Westerhof N, Faes TJ, et al. Quantification of right ventricular afterload in patients with and without pulmonary hypertension. **Am J Physiol Heart Circ Physiol**. 2006; 291:H1731−H1737.

78. Sniderman AD, Fitchett DH. Vasodilators and pulmonary arterial hypertension: the paradox of therapeutic success and clinical failure. **Int J Cardiol**. 1988; 20:173−181.

79. O'Rourke MF, Yaginuma T, Avolio AP. Physiological and pathophysiological implications of ventricular/vascular coupling. **Ann Biomed Eng**. 1984; 12:119−134.

80. Sunagawa K, Maughan WL, Sagawa K. Optimal arterial resistance for the maximal stroke work studied in isolated canine left ventricle. **Circ Res**. 1985; 56:586−595.

81. Vonk-Noordegraaf A, Haddad F, Chin KM, et al. Right heart adaptation to pulmonary arterial hypertension: physiology and pathobiology. **J Am Coll Cardiol**. 2013; 62:D22−D33.

82. Breeman KTN, Dufva M, Ploegstra MJ, et al. Right ventricular-vascular coupling ratio in pediatric pulmonary arterial hypertension: a comparison between cardiac magnetic resonance and right heart catheterization measurements. **Int J Cardiol**. 2019; 293:211−217.

83. Brewis MJ, Bellofiore A, Vanderpool RR, et al. Imaging right ventricular function to predict outcome in pulmonary arterial hypertension. **Int J Cardiol**. 2016; 218:206−211.

84. Vanderpool RR, Pinsky MR, Naeije R, et al. RV-pulmonary arterial coupling predicts outcome in patients referred for pulmonary hypertension. **Heart**. 2015; 101:37−43.

85. Tello K, Wan J, Dalmer A, et al. Validation of the tricuspid annular plane systolic excursion/systolic pulmonary artery pressure ratio for the assessment of right ventricular-arterial coupling in severe pulmonary hypertension. **Circ Cardiovasc Imaging**. 2019; 12:e009047.

86. Humbert M, Sitbon O, Simonneau G. Treatment of pulmonary arterial hypertension. **N Engl J Med**. 2004; 351:1425−1436.

87. Clapp LH, Finney P, Turcato S, Tran S, Rubin LJ, Tinker A. Differential effects of stable prostacyclin analogs on smooth muscle proliferation and cyclic AMP generation in human pulmonary artery. **Am J Respir Cell Mol Biol**. 2002; 26:194−201.

88. Moncada S, Gryglewski R, Bunting S, Vane JR. An enzyme isolated from arteries transforms prostaglandin endoperoxides to an unstable substance that inhibits platelet aggregation. **Nature**. 1976; 263:663−665.

89. Badesch DB, Tapson VF, McGoon MD, et al. Continuous intravenous epoprostenol for pulmonary hypertension due to the scleroderma spectrum of disease. A randomized, controlled trial. **Ann Intern Med**. 2000; 132:425−434.

90. Barst RJ, Rubin LJ, Long WA, et al. A comparison of continuous intravenous epoprostenol (prostacyclin) with conventional therapy for primary pulmonary hypertension. **N Engl J Med**. 1996; 334:296−301.

91. Rich S, McLaughlin VV. The effects of chronic prostacyclin therapy on cardiac output and symptoms in primary pulmonary hypertension. **J Am Coll Cardiol**. 1999; 34:1184−1187.

92. Califf RM, Adams KF, McKenna WJ, et al. A randomized controlled trial of epoprostenol therapy for severe congestive heart failure: the Flolan International Randomized Survival Trial (FIRST). **Am Heart J**. 1997; 134:44−54.

93. Olschewski H, Simonneau G, Galie N, et al. Inhaled iloprost for severe pulmonary hypertension. **N Engl J Med**. 2002; 347:322−329.

94. Simonneau G, Barst RJ, Galie N, et al. Continuous subcutaneous infusion of treprostinil, a prostacyclin analogue, in patients with pulmonary arterial hypertension: a double-blind, randomized, placebo-controlled trial. **Am J Respir Crit Care Med**. 2002; 165:800−804.

95. Benza RL, Seeger W, McLaughlin VV, et al. Long-term effects of inhaled treprostinil in patients with pulmonary arterial hypertension: the Treprostinil Sodium Inhalation Used in the Management of Pulmonary Arterial Hypertension (TRIUMPH) study open-label extension. **J Heart Lung Transplant**. 2011; 30:1327−1333.

96. McLaughlin VV, Benza RL, Rubin LJ, et al. Addition of inhaled treprostinil to oral therapy for pulmonary arterial hypertension: a randomized controlled clinical trial. **J Am Coll Cardiol**. 2010; 55:1915−1922.

97. White RJ, Jerjes-Sanchez C, Bohns Meyer GM, et al. Combination therapy with oral treprostinil for pulmonary arterial hypertension. A double-blind placebo-controlled clinical trial. **Am J Respir Crit Care Med**. 2020; 201:707−717.

98. Benza RL, Tapson VF, Gomberg-Maitland M, Poms A, Barst RJ, McLaughlin VV. One-year experience with intravenous treprostinil for pulmonary arterial hypertension. **J Heart Lung Transplant**. 2013; 32:889−896.

99. Sitbon O, Channick R, Chin KM, et al. Selexipag for the treatment of pulmonary arterial hypertension. **N Engl J Med**. 2015; 373:2522−2533.

100. Simonneau G, Torbicki A, Hoeper MM, et al. Selexipag: an oral, selective prostacyclin receptor agonist for the treatment of pulmonary arterial hypertension. **Eur Respir J**. 2012; 40:874−880.

101. Galie N, Brundage BH, Ghofrani HA, et al. Pulmonary arterial H and response to tadalafil study G. Tadalafil therapy for pulmonary arterial hypertension. **Circulation**. 2009; 119:2894−2903.

102. Singh TP, Rohit M, Grover A, Malhotra S, Vijayvergiya R. A randomized, placebo-controlled, double-blind, crossover study to evaluate the efficacy of oral sildenafil therapy in severe pulmonary artery hypertension. **Am Heart J**. 2006; 151:851 e1−5.

103. Rubin LJ, Badesch DB, Fleming TR, et al. Long-term treatment with sildenafil citrate in pulmonary arterial hypertension: the SUPER-2 study. **Chest**. 2011; 140:1274−1283.

104. Sastry BK, Narasimhan C, Reddy NK, Raju BS. Clinical efficacy of sildenafil in primary pulmonary hypertension: a randomized, placebo-controlled, double-blind, crossover study. **J Am Coll Cardiol**. 2004; 43:1149−1153.

105. Galie N, Ghofrani HA, Torbicki A, et al. Sildenafil citrate therapy for pulmonary arterial hypertension. **N Engl J Med**. 2005; 353:2148−2157.

106. Nagendran J, Archer SL, Soliman D, et al. Phosphodiesterase type 5 is highly expressed in the hypertrophied human right ventricle, and acute inhibition of phosphodiesterase type 5 improves contractility. **Circulation**. 2007; 116:238−248.

107. Bermejo J, Yotti R, Garcia-Orta R, et al. Sildenafil for improving outcomes in patients with corrected valvular heart disease and persistent pulmonary hypertension: a multicenter, double-blind, randomized clinical trial. **Eur Heart J**. 2018; 39:1255−1264.

108. Ghofrani HA, Galie N, Grimminger F, et al. Riociguat for the treatment of pulmonary arterial hypertension. **N Engl J Med**. 2013; 369:330−340.

109. Rubin LJ, Galie N, Grimminger F, et al. Riociguat for the treatment of pulmonary arterial hypertension: a long-term extension study (PATENT-2). **Eur Respir J**. 2015; 45:1303−1313.

110. Ghofrani HA, D'Armini AM, Grimminger F, et al. Riociguat for the treatment of chronic thromboembolic pulmonary hypertension. **N Engl J Med**. 2013; 369:319−329.

111. Benigni A, Remuzzi G. Endothelin antagonists. **Lancet**. 1999; 353:133−138.

112. Galie N, Olschewski H, Oudiz RJ, et al. Ambrisentan for the treatment of pulmonary arterial hypertension: results of the ambrisentan in pulmonary arterial hypertension, randomized, double-blind, placebo-controlled, multicenter, efficacy (ARIES) study 1 and 2. **Circulation**. 2008; 117:3010−3019.

113. Oudiz RJ, Galie N, Olschewski H, et al. Long-term ambrisentan therapy for the treatment of pulmonary arterial hypertension. **J Am Coll Cardiol**. 2009; 54:1971−1981.

114. Peacock AJ, Crawley S, McLure L, et al. Changes in right ventricular function measured by cardiac magnetic resonance imaging in patients receiving pulmonary arterial hypertension-targeted therapy: the EURO-MR study. **Circ Cardiovasc Imaging**. 2014; 7:107−114.

115. Benza RL, Raina A, Gupta H, et al. Bosentan-based, treat-to-target therapy in patients with pulmonary arterial hypertension: results from the COMPASS-3 study. **Pulm Circ**. 2018; 8, 2045893217741480.

116. Packer M, McMurray J, Massie BM, et al. Clinical effects of endothelin receptor antagonism with bosentan in patients with severe chronic heart failure: results of a pilot study. **J Card Fail**. 2005; 11:12−20.

117. Montani D, Savale L, Natali D, et al. Long-term response to calcium-channel blockers in non-idiopathic pulmonary arterial hypertension. **Eur Heart J**. 2010; 31:1898−1907.

118. Sitbon O, Humbert M, Jais X, et al. Long-term response to calcium channel blockers in idiopathic pulmonary arterial hypertension. **Circulation**. 2005; 111:3105−3111.

119. Fuster V, Steele PM, Edwards WD, Gersh BJ, McGoon MD, Frye RL. Primary pulmonary hypertension: natural history and the importance of thrombosis. **Circulation**. 1984; 70:580−587.

120. Johnson SR, Mehta S, Granton JT. Anticoagulation in pulmonary arterial hypertension: a qualitative systematic review. **Eur Respir J**. 2006; 28:999−1004.

121. Olsson KM, Delcroix M, Ghofrani HA, et al. Anticoagulation and survival in pulmonary arterial hypertension: results from the Comparative, Prospective Registry of Newly Initiated Therapies for Pulmonary Hypertension (COMPERA). **Circulation**. 2014; 129:57−65.

122. Preston IR, Roberts KE, Miller DP, et al. Effect of Warfarin treatment on survival of patients with pulmonary arterial hypertension (PAH) in the registry to evaluate early and long-term PAH disease management (REVEAL). **Circulation**. 2015; 132:2403−2411.

123. Galie N, Humbert M, Vachiery JL, et al. ESC/ERS guidelines for the diagnosis and treatment of pulmonary hypertension: the joint task force for the diagnosis and treatment of pulmonary hypertension of the European Society of Cardiology (ESC) and the European Respiratory Society (ERS): Endorsed by: Association for European Paediatric and Congenital Cardiology (AEPC), International Society for Heart and Lung Transplantation (ISHLT). **Eur Respir J**. 2015; 46:903−975.

124. Benza RL, Gomberg-Maitland M, Elliott CG, et al. Predicting survival in patients with pulmonary arterial hypertension: the REVEAL risk score calculator 2.0 and comparison with ESC/ERS-Based risk assessment strategies. **Chest**. 2019; 156:323−337.

125. Humbert M, Sitbon O, Chaouat A, et al. Pulmonary arterial hypertension in France: results from a national registry. **Am J Respir Crit Care Med**. 2006; 173:1023−1030.

126. Galie N, Barbera JA, Frost AE, et al. Initial use of ambrisentan plus tadalafil in pulmonary arterial hypertension. **N Engl J Med**. 2015; 373:834−844.

127. Pulido T, Adzerikho I, Channick RN, et al. Macitentan and morbidity and mortality in pulmonary arterial hypertension. **N Engl J Med**. 2013; 369:809−818.

128. McLaughlin V, Channick RN, Ghofrani HA, et al. Bosentan added to sildenafil therapy in patients with pulmonary arterial hypertension. **Eur Respir J**. 2015; 46:405−413.

129. Pan Z, Marra AM, Benjamin N, et al. Early treatment with ambrisentan of mildly elevated mean pulmonary arterial pressure associated with systemic sclerosis: a randomized, controlled, double-blind, parallel group study (EDITA study). **Arthritis Res Ther**. 2019; 21:217.

130. Sitbon O, Jais X, Savale L, et al. Upfront triple combination therapy in pulmonary arterial hypertension: a pilot study. **Eur Respir J**. 2014; 43:1691−1697.

131. Chin KM, Stibon O, Doelberg M, et al. **Efficacy and Safety of Initial Triple Oral versus Initial Double Oral Combination Therapy in Patients with Newly Diagnosed Pulmonary Arterial Hypertension (PAH): Results of the Randomized Controlled TRITON Study**. American Thoracic Society International Conference 2020; 2020. Session B27 - Up-To-Date PAH Assessment and Management.

132. Tampakakis E, Shah SJ, Borlaug BA, et al. Pulmonary effective arterial elastance as a measure of right ventricular afterload and its prognostic value in pulmonary hypertension due to left heart disease. **Circ Heart Fail**. 2018; 11:e004436.

133. Thenappan T, Prins KW, Pritzker MR, Scandurra J, Volmers K, Weir EK. The critical role of pulmonary arterial compliance in pulmonary hypertension. **Ann Am Thorac Soc**. 2016; 13:276−284.

134. Cheng XL, He JG, Liu ZH, et al. Pulmonary vascular capacitance is associated with vasoreactivity and long-term response to calcium channel blockers in idiopathic pulmonary arterial hypertension. **Lung**. 2016; 194:613−618.

135. Hopkins WE, Ochoa LL, Richardson GW, Trulock EP. Comparison of the hemodynamics and survival of adults with severe primary pulmonary hypertension or Eisenmenger syndrome. **J Heart Lung Transplant**. 1996; 15:100−105.

136. Rozkovec A, Montanes P, Oakley CM. Factors that influence the outcome of primary pulmonary hypertension. **Br Heart J**. 1986; 55:449−458.

137. Sandoval J, Gomez-Arroyo J, Gaspar J, Pulido-Zamudio T. Interventional and surgical therapeutic strategies for pulmonary arterial hypertension: beyond palliative treatments. **J Cardiol**. 2015; 66:304−314.

138. Esch JJ, Shah PB, Cockrill BA, et al. Transcatheter Potts shunt creation in patients with severe pulmonary arterial hypertension: initial clinical experience. **J Heart Lung Transplant**. 2013; 32:381−387.

139. Miller WL, Grill DE, Borlaug BA. Clinical features, hemodynamics, and outcomes of pulmonary hypertension due to chronic heart failure with reduced ejection fraction: pulmonary hypertension and heart failure. **JACC Heart Fail**. 2013; 1:290−299.

140. Vachiery JL, Tedford RJ, Rosenkranz S, et al. Pulmonary hypertension due to left heart disease. **Eur Respir J**. 2019; 53.

141. Parikh KS, Sharma K, Fiuzat M, et al. Heart failure with preserved ejection fraction expert panel report: current controversies and implications for clinical trials. **JACC Heart Fail**. 2018; 6:619−632.

142. Borlaug BA, Anstrom KJ, Lewis GD, et al. Effect of inorganic nitrite vs placebo on exercise capacity among patients with heart failure with preserved ejection fraction: the INDIE-HFpEF randomized clinical trial. **J Am Med Assoc**. 2018; 320: 1764−1773.

143. Redfield MM, Anstrom KJ, Levine JA, et al. Isosorbide mononitrate in heart failure with preserved ejection fraction. **N Engl J Med**. 2015; 373:2314−2324.

144. Simon MA, Vanderpool RR, Nouraie M, et al. Acute hemodynamic effects of inhaled sodium nitrite in pulmonary hypertension associated with heart failure with preserved ejection fraction. **JCI Insight**. 2016; 1:e89620.

145. Bashline MJ, Bachman TN, Helbling NL, Nouraie M, Gladwin MT, Simon MA. The effects of inhaled sodium nitrite on pulmonary vascular impedance in patients with pulmonary hypertension associated with heart failure with preserved ejection fraction. **J Card Fail**. 2020; 26:654−661.

146. Borlaug BA, Melenovsky V, Koepp KE. Inhaled sodium nitrite improves rest and exercise hemodynamics in heart failure with preserved ejection fraction. **Circ Res**. 2016; 119:880−886.

147. Kapur NK, Esposito ML, Bader Y, et al. Mechanical circulatory support devices for acute right ventricular failure. **Circulation**. 2017; 136:314−326.

148. Anderson MB, Goldstein J, Milano C, et al. Benefits of a novel percutaneous ventricular assist device for right heart failure: the prospective RECOVER RIGHT study of the Impella RP device. **J Heart Lung Transplant**. 2015; 34:1549−1560.

149. Connellan MIA, Robson D, Granger E, Dhital K, Spratt P. The HeartWare transvalvular miniature ventricular assist device used for right ventricular support. **J Heart Lung Transplant**. 2013; 32.

150. Cook JA, Shah KB, Quader MA, et al. The total artificial heart. **J Thorac Dis**. 2015; 7:2172−2180.

151. Klotz S, Meyns B, Simon A, et al. Partial mechanical long-term support with the CircuLite Synergy pump as bridge-to-transplant in congestive heart failure. **Thorac Cardiovasc Surg**. 2010; 58(Suppl 2):S173−S178.

152. Gan C, Lankhaar JW, Marcus JT, et al. Impaired left ventricular filling due to right-to-left ventricular interaction in patients with pulmonary arterial hypertension. **Am J Physiol Heart Circ Physiol**. 2006; 290:H1528−H1533.

153. Handoko ML, Lamberts RR, Redout EM, et al. Right ventricular pacing improves right heart function in experimental pulmonary arterial hypertension: a study in the isolated heart. **Am J Physiol Heart Circ Physiol**. 2009; 297:H1752−H1759.

154. Hardziyenka M, Surie S, de Groot JR, et al. Right ventricular pacing improves haemodynamics in right ventricular failure from pressure overload: an open observational proof-of-principle study in patients with chronic thromboembolic pulmonary hypertension. **Europace**. 2011; 13:1753−1759.

155. Westerhof BE, Saouti N, van der Laarse WJ, Westerhof N, Vonk Noordegraaf A. Treatment strategies for the right heart in pulmonary hypertension. **Cardiovasc Res**. 2017; 113:1465−1473.

156. Chen SL, Zhang FF, Xu J, et al. Pulmonary artery denervation to treat pulmonary arterial hypertension: the single-center, prospective, first-in-man PADN-1 study (first-in-man pulmonary artery denervation for treatment of pulmonary artery hypertension). **J Am Coll Cardiol**. 2013; 62:1092−1100.

157. Le T, Makar C, Morway P, Hoftman N, Umar S. Pulmonary artery denervation: a novel treatment modality for pulmonary hypertension. **J Thorac Dis**. 2019; 11:1094−1096.

158. Zhang H, Zhang J, Chen M, et al. Pulmonary artery denervation significantly increases 6-min walk distance for patients with combined pre- and post-capillary pulmonary hypertension associated with left heart failure: the PADN-5 study. **JACC Cardiovasc Interv**. 2019; 12:274−284.

159. Chen SL, Zhang YJ, Zhou L, et al. Percutaneous pulmonary artery denervation completely abolishes experimental pulmonary arterial hypertension in vivo. **EuroIntervention**. 2013; 9:269−276.

160. Groeneveldt JA dMFS, Westerhof BE. The right treatment for the right ventricle. **Curr Opin Pulm Med**. 2019; 25:410−417.

161. Ferrari RF,I, Fox K, Challeton JP, et al. Efficacy and safety of trimetazidine after percutaneous coronary intervention (ATPCI): a randomized double-blind, placebo-controlled trial. **Lancet**. 2020; 396(10254):830−838.

Index

TEXTBOOK OF
ARTERIAL STIFFNESS AND PULSATILE HEMODYNAMICS IN HEALTH AND DISEASE

VOLUME 2

Edited by

Julio A. Chirinos, MD, PhD, FAHA, FESC

Associate Professor of Medicine; Director, Arterial Hemodynamics and Cardiac Imaging Quantification Core Laboratory; Co-Director, Training Program in Cardiovascular Biology and Medicine, Clinical/Translational Science; Adjunct Faculty, Center for Magnetic Resonance and Optical Imaging. University of Pennsylvania Perelman School of Medicine, USA

Most biology-oriented books misinterpret or lack an in-depth discussion of key biophysical aspects of arterial stiffness and pulsatile arterial hemodynamics. A proper understanding of the field requires both biologic/clinical and biophysical/bioengineering knowledge which *Textbook of Arterial Stiffness and Pulsatile Hemodynamics in Health and Disease* provides in a comprehensive yet simplified manner. The resource is organized into five parts covering principles, physiology, biologic pathways, clinical implications, and therapeutics and provides a thorough overview of the field, presenting complex engineering concepts in a way that those in life science and medicine can more easily understand.

Textbook of Arterial Stiffness and Pulsatile Hemodynamics in Health and Disease includes detailed illustrations and advanced bioengineering concepts presented in boxes for the reader who wants more in-depth biophysical knowledge. This is a must-have reference for students, researchers, and clinicians interested in learning more about this rapidly growing field.

Key features

- Provides a comprehensive review of the clinical implications of arterial stiffness and pulsatile hemodynamics and its role in human disease
- Incorporates mathematical principles explained in a conceptual manner without complicated formulas
- Features chapter contributions from leading international researchers and clinicians